



TMS 2012

141st Annual Meeting & Exhibition



SEE PG. 2

March 11 - 15, 2012
Walt Disney World
Swan and Dolphin Resort • Orlando, Florida

FINAL PROGRAM

***“Linking Science and Technology
for Global Solutions”***

www.tms.org/TMS2012



LEARN • NETWORK • ADVANCE



MATERIALS INNOVATION

@TMS

Full Speed Ahead: Materials Innovation @ TMS Launches at TMS 2012

Join TMS in celebrating the launch of its new strategic initiative focused on accelerating the discovery, development, and deployment of materials systems and processes: Materials Innovation @ TMS.

What you experience at TMS 2012 is just the beginning of what Materials Innovation @ TMS can offer you. For the latest news on Materials Innovation @ TMS programs, resources, and activities, visit our website at materialsinnovation.tms.org.

Materials Innovation @ TMS Learning and Networking Opportunities

TMS 2012 Annual Meeting of the Membership

“Fueling Growth and Fostering Innovation”

Featuring the Official Membership Introduction of Materials Innovation @ TMS

Sunday, March 11: 7-8 p.m.

Walt Disney World Dolphin Resort—Southern II

Materials Innovation Gallery (See page 9 of this program for details.)

A showcase of ideas, techniques, and principles that can potentially transform the future of materials and manufacturing innovation.

TMS 2012 Exhibition * Booth 441

Open during regular Exhibition hours, starting at noon on Monday, March 12.

Special Plenary Session (See page 14 of this program for details.)

“Reaching New Heights: Materials Innovation in the Aerospace Industry”

Wednesday, March 14, 2-3:45 p.m.

Walt Disney World Dolphin Resort—Northern E2

2012 Federal Funding Workshop and Reception (See page 14 of this program for details.)

“Funding Opportunities to Advance the Materials Genome Initiative”

4 p.m.: Panel Discussion

5:15-6 p.m.: Networking Reception with Panelists

Walt Disney World Dolphin Resort—Northern C

Preview TMS’s New Open Access Journal (See page 9 of this program for details.)

Integrating Materials and Manufacturing Innovation (IMMI).

Opportunities to interact with IMMI editor, Chuck Ward, will be available during the conference.

For more information:

Stop by the Materials Innovation @ TMS Information Center located at the TMS Member Welcome Center .

Welcome to the TMS 2012 Annual Meeting & Exhibition!



Dear Colleagues & Friends!

As president of TMS, I offer a warm welcome to our members, society guests, exhibitors, and all other attendees who have gathered here in sunny Orlando, Florida for our 141st annual conference.

While compelling technical programming takes center stage at TMS2012, this meeting will offer a full menu of special events and new incentives for building our future with the TMS Foundation.

We are also introducing a new TMS2012 mobile application for smart phone users that will keep all conference information at your fingertips. See page 2 for more details about this amazing conference tool!

There are also a number of events planned this week to launch our new strategic initiative, Materials Innovation @ TMS, focused on accelerating the discovery, development, and deployment of materials systems and processes. I encourage you to browse the Materials Innovation Gallery at the Exhibition (Page 9), attend the plenary session, "Reaching New Heights: Materials Innovation in the Aerospace Industry," (Page 20) and participate in the other Materials Innovation @ TMS activities highlighted in this program.

Here is a brief synopsis of the other valuable offerings at TMS2012:

Technical Program & Poster Session – Nearly 70 symposia will present the research of some of the world's most distinguished materials scientists and engineers. Technical areas to be covered include: Advanced Characterization, Modeling and Materials Performance; High Performance Materials; Light Metals: Aluminum, Magnesium, and Titanium; Materials and Society: Energy and Sustainable Production; Materials Processing and Production; and Nanoscale and Amorphous Materials.

Networking – Second only to the technical programming offered at TMS2012 are the invaluable networking opportunities. By attending TMS2012 you reap the countless benefits of connecting with colleagues from around the world in person!

Awards Presentation – Honoring outstanding colleagues will be even more exciting with the TMS-AIME Awards Banquet at the World ShowPlace Pavilion East Hall in EPCOT. The banquet will conclude with an amazing fireworks display, "Disney IllumiNations: Reflections of Earth."

Special Lectures – Compelling research and food for thought is on the agenda when you choose to attend a luncheon lecture, plenary session or presentation. See page 22 for more information.

Student Events – TMS realizes the future of the society and profession lies in its student members. Visit the Student Poster contest or enjoy the spirit of competition at the Materials Bowl, sponsored by Alcoa, all day Sunday. Details on student events are on page 28.

Continuing Education – Feel the power of knowledge. TMS2012 features compelling courses and workshops designed to enhance your conference experience.

Welcome to TMS2012 in warm and wonderful Orlando, Florida! Be prepared for the ultimate conference experience.

Sincerely,

Garry Warren

Table of Contents

Registration	2	Networking & Social Events	24
Meeting Policies	2	Honors & Awards	26
Schedule of Events.....	3	Student Activities.....	28
Maps.....	17	Proceedings	30
Materials Innovation	20	TMS Leadership	31
Lectures & Luncheons	22	Exhibit Directory	33
Award-Winning Speakers	23	Technical Program.....	47

MEETING INFORMATION




TMS 2012

141st Annual Meeting & Exhibition

MEETING INFORMATION

Full Conference Registration

Your full conference registration includes a collected proceedings CD and your badge ensures admission to each of these events:

- Technical & Poster sessions
- Student Poster Contest
- Women in Science Breakfast Lecture (pre-registrants only) 
- Admission to TMS Materials Bowl Championship
- Three-day pass to TMS2012 Exhibition
- President's Welcoming Reception (located in the Exhibit Hall)
- Happy Hour Reception (located in the Exhibit Hall)

Internet Options

Free wireless service will be available in the Author's Coffee area located in **Atlantic B Hall** in the **Dolphin Hotel** Monday through Thursday.

Username: **TMSWireless**

Password: **tms2012ame**

(case sensitive, use all lower case)

CyberCenter Internet work stations, sponsored by Stellar Materials Inc., will be available in the exhibit hall located in the Pacific Room of the Dolphin Resort during regular show hours.

NEW! TMS2012 Mobile Application

TMS is pleased to offer this new mobile application available for the 2012 Annual Meeting and Exhibition. Attendees will be able to easily download this free conference tool from the **Apple iTunes Store for you iPhone or iPad** and through the **Android Marketplace**

Features:

- Latest programming schedule
- Interactive exhibit map
- Hotel information
- Speaker information
- Evaluations
- Schedule changes via Push Notifications (when not using application)
- Much more!



Through the application you will also be able to organize and track those events you wish to attend by building a "My Schedule" list plus quickly narrow current presentations with the "What's on Now?" feature.

To download the TMS Mobile Application, search "TMS Annual Meeting" in your respective device store.

Policies

Badges

All attendees must wear registration badges at all times during the conference to ensure admission to events included in the paid fee such as technical sessions, exhibition and receptions. "Exhibit Only" badges provide exclusive admittance to the show floor for events in the exhibit hall. "Guest" badges are for spouses or companions of registered attendees and used as identification only. "Guest" and "Exhibit Only" attendees may not attend technical sessions.

Refunds

The deadline for all refunds was February 15, 2012. No refunds will be issued at the conference. Fees and tickets are nonrefundable.

Photography Notice

By registering for this conference, all attendees acknowledge that they may be photographed by TMS personnel while at events and that those photos may be used for promotional purposes.

Audio/Video Recording Policy

TMS reserves the right to all audio and video reproductions of presentations at TMS sponsored meetings. Recording of sessions (audio, video, still photography, etc.) intended for personal use, distribution, publication, or copyright without the express written consent of TMS and the individual authors is strictly prohibited. Contact TMS Technical Programming at (724) 776-9000, ext. 212 to obtain a copy of the waiver release form.

Americans With Disabilities Act




TMS strongly supports the federal Americans with Disabilities Act (ADA) which prohibits discrimination against, and promotes public accessibility for, those with disabilities. In support of, and in compliance with ADA, we ask those requiring specific equipment or services to contact TMS Meeting Services in advance.

Cell Phone Use

In consideration of attendees and presenters, TMS kindly requests that you minimize disturbances by setting all cell phones or PDAs on "silent" while in meeting rooms.

Recycling

Discard badges and programs in the bins located in the Registration area.

Be materials-minded.  Join TMS in reducing, reusing and recycling.

Schedule of Events

as of February 23, 2012

TMS Meetings & Events are scheduled on the following days, times and locations:

Key: **D** Dolphin Hotel **S** Swan Hotel

FUNCTION	TIME	LOCATION	ROOM	ACCESS*
Saturday, March 10, 2012				
Exhibit Move-In	8:00 AM to 5:00 PM	D	Pacific	O

Committee Meetings				
Professional Registration Writers Workshop and Committee Meeting	9:00 AM to 5:00 PM	S	Peacock 1	R
TMS Foundation Board of Trustees Meeting	2:00 PM to 5:00 PM	D	President's Suite #200097	R
Professional Registration Committee Dinner	6:00 PM to 8:00 PM	S	Peacock 2	R

FUNCTION	TIME	LOCATION	ROOM	ACCESS*
Sunday, March 11, 2012				

All Conference Events				
Registration	7:00 AM to 6:00 PM	D	Atlantic	O
TMS Member Welcome Center <i>Materials Innovation at TMS Info Center, Visit Orlando, Visit San Antonio, and TMS Housing Representatives available through Thursday, March 15</i>	7:00 AM to 6:00 PM	D	Atlantic	O
TMS Foundation Center	7:00 AM to 6:00 PM	D	Atlantic	O
Exhibit Move-In	8:00 AM to 5:00 PM	D	Pacific	O
General & Student Poster Sessions Set-Up	12:00 PM to 5:00 PM	D	Atlantic	O
Young Leader Meet the Candidate Poster Session	6:30 PM to 8:00 PM	D	Southern I	O
<i>Poster Set-Up</i>	12:00 PM to 6:00 PM	D	Southern I	O
TMS Programming Support Center	2:00 PM to 5:00 PM	D	Atlantic	O

* O - Open to all attendees **T** - Ticketed Event
 R - Restrictions Apply **T1** - Pre-Registration Ticket Required
T2 - Ticket Required, can be purchased/picked up at door

MEETING INFORMATION



TMS 2012

141st Annual Meeting & Exhibition

Schedule of Events

as of February 23, 2012

Key: **D** Dolphin Hotel **S** Swan Hotel

Special Presentations				
Short Course: Electrowinning and Electrorefining of Copper and Zinc	8:30 AM to 4:00 PM	D	Europe 2	T
Short Course: Integrated Computational Materials Education	8:30 AM to 4:00 PM	D	Europe 3	T
Short Course: Process Energy Modeling: Spreadsheets and Beyond	8:30 AM to 4:00 PM	D	Europe 6	T
Short Course: Estimation of Slag Properties	8:30 AM to 4:30 PM	D	Europe 10	T
Workshop: Lead Free Solders	9:00 AM to 4:30 PM	D	Asia 3	T1
Short Course/Workshop Breaks, Lunch	10:30 AM to 3:00 PM	D	Asia 4 & 5	T
Volunteer Leadership Program Leadership Materials: Tools to Build Your Career	1:00 PM to 4:00 PM	D	Northern A4	R
ABET Refresher Training	3:00 PM to 5:00 PM	S	Sandpiper	R
TMS Meeting of the Membership	7:00 PM to 8:00 PM	D	Southern II	O

* O - Open to all attendees
R - Restrictions Apply

T - Ticketed Event

T1 - Pre-Registration Ticket Required

T2 - Ticket Required, can be purchased/picked up at door

MEETING INFORMATION

Meet the Candidate Employment Poster Session

Sunday, March 11 • 6:30 to 8 p.m. • Dolphin Hotel, Atlantic Room

Organized by the TMS Young Leaders Committee, this new TMS event is designed to create networking opportunities for young professionals that will allow them to connect with potential employers for post-doctoral, full-time, or faculty positions. Candidates will present a poster to potential employers from various universities, industries, and national labs.

Visit the San Antonio, Texas Booth...site of TMS2013

Next to the Visit Orlando Concierge booth in the TMS Member Welcome Center Located in the Dolphin Hotel Atlantic Hall



Schedule of Events

as of February 23, 2012

Key:  Dolphin Hotel

 Swan Hotel


Committee Meetings				
TMS Financial Planning Committee	7:00 AM to 9:30 AM	S	Parrot 1	R
Professional Registration Leadership Committee	8:00 AM to 10:00 AM	S	Teal	R
TMS Board of Directors Meeting	9:30 AM to 1:30 PM	S	Lark	R
REWAS Organizing Committee	10:00 AM to 11:30 AM	S	Peacock 1	R
Recycling and Environmental Technologies Committee	12:00 PM to 1:30 PM	S	Toucan 1	O
Accreditation Committee	12:30 PM to 2:30 PM	S	Toucan 2	R
Aluminum Processing Committee	1:30 PM to 2:30 PM	S	Parrot 1	O
Magnesium Committee	1:30 PM to 3:00 PM	S	Pelican 2	O
TMS Nominating Committee	2:00 PM to 3:00 PM	S	Parrot 2	R
Aluminum Committee	2:00 PM to 4:00 PM	S	Lark	O
Materials Characterization Committee	3:00 PM to 5:00 PM	S	Macaw 1	O
Program Committee	3:00 PM to 5:00 PM	S	Heron	R
Public and Governmental Affairs Committee	3:30 PM to 5:00 PM	S	Macaw 2	R
Nanomaterials Committee	4:00 PM to 5:00 PM	D	Europe 4	O
Thin Films and Interfaces Committee	4:00 PM to 5:00 PM	S	Pelican 2	O
PRICM 8 International Organizing Committee	4:00 PM to 6:00 PM	S	Parrot 2	R
LMD Council	4:30 PM to 6:00 PM	S	Ibis	R
Pyrometallurgy Committee	4:30 PM to 6:00 PM	S	Toucan 1	O
Content Development and Dissemination Committee	5:00 PM to 7:00 PM	S	Parrot 1	R
Nanomechanical Behaviors Materials Behavior Committee	5:45 PM to 6:45 PM	S	Toucan 2	O
Mechanical Behaviors of Materials Committee	7:00 PM to 8:30 PM	S	Toucan 2	O
Alloy Phases Committee	7:30 PM to 9:30 PM	S	Mockingbird	O
Phase Transformations Committee	7:30 PM to 9:30 PM	S	Toucan 1	O

* O - Open to all attendees

R - Restrictions Apply

 T - Ticketed Event

 T1 - Pre-Registration Ticket Required

 T2 - Ticket Required, can be purchased/picked up at door



TMS 2012

141st Annual Meeting & Exhibition

Schedule of Events

as of February 23, 2012

Key: **D** Dolphin Hotel **S** Swan Hotel

Student Events

Materials Bowl	12:00 PM to 8:30 PM	D	Southern V	O
Elimination Rounds	12:00 PM to 3:00 PM			
Championship Round	8:00 PM to 8:30 PM			
Student Network Mixer	8:30 PM to 10:30 PM	D	Southern III	T2

Social Functions

Fellows and Invited Guests Reception	4:30 PM to 6:30 PM	D	Northern C	R
New Member/Young Leader Reception	5:00 PM to 6:00 PM	D	Southern IV	T2

* O - Open to all attendees

R - Restrictions Apply

T - Ticketed Event

T1 - Pre-Registration Ticket Required

T2 - Ticket Required, can be purchased/picked up at door

MEETING INFORMATION

TMS ANNUAL MEETING OF THE MEMBERSHIP

Sunday, March 11 • 7 to 8 p.m. • Dolphin Southern II

Don't miss this important membership engagement opportunity—highlighted by the official introduction of **Materials Innovation @ TMS**, the society's newest strategic initiative.

Also planned:

- Preview of new projects and programs for 2012
- TMS's most recent accomplishments — including publication of its latest energy materials report on behalf of the U.S. Department of Energy
- TMS's recent and expected financial performance

Speakers:

- Garry Warren.....2011 TMS President
- Wolfgang Schneider.....2012 TMS President
- Stanley M. Howard.....TMS Financial Planning Officer
- Warren H. HuntTMS Executive Director

Member Welcome Center

Dolphin Hotel, Atlantic Hall • Daily

Sunday: 7 a.m. to 6 p.m. • Monday: 7 a.m. to 6 p.m. • Tuesday: 7 a.m. to 5:30 p.m.

Wednesday: 7 a.m. to 5:00 p.m. • Thursday: 7 a.m. to 3:30 p.m.

Learn and gather information about your membership, volunteering with TMS, the TMS Foundation, and all of our upcoming events and activities! Discover all TMS can offer as, "Your Professional Partner for Career Advancement".

Schedule of Events

as of February 23, 2012

Key: **D** Dolphin Hotel

S Swan Hotel

FUNCTION	TIME	LOCATION	ROOM	ACCESS*
Monday, March 12, 2012				
All Conference Events				
Exhibit Move-In	7:00 AM to 11:00 AM	D	Pacific	
Author's Coffee	7:00 AM to 8:00 AM	D	Atlantic	R
Registration	7:00 AM to 6:00PM	D	Atlantic	O
TMS Member Welcome Center	7:00 AM to 6:00 PM	D	Atlantic	O
TMS Foundation Center	7:00 AM to 6:00 PM	D	Atlantic	O
TMS Programming Support Center	7:00 AM to 5:00 PM	D	Atlantic	O
Technical Symposia	8:30 AM to 6:00 PM	See Technical Program for complete schedule and symposia locations		
General Poster Session (Authors Present)	5:00 PM to 6:30 PM	D	Atlantic	O
<i>Poster Set Up</i>	7:00 AM to 8:00 AM	D	Atlantic	O
Materials Innovation at TMS Gallery	12:00 PM to 6:30 PM	D	Pacific	O
TMS 2012 Exhibition	12:00 PM to 6:30 PM	D	Pacific	O
President's Welcoming Reception	5:00 PM to 6:30 PM	D	Pacific	O

Special Presentations				
2012 Aluminum Plenary: "Aluminum Technology 2020: A Look Ahead"	8:00 AM to 12:00 PM	D	Southern III	O
Congressional Fellow Informational Meeting	1:00 PM to 2:00 PM	S	Parrot 2	O
IOMMMS Global Materials Forum: Materials In a Green Economy: An International Perspective	2:00 PM to 6:30 PM	D	Northern A4	O
Emeritus Professor George D.W. Smith Honorary Dinner	6:30 PM to 8:00 PM	S	Lark	T
Randall M. German Honorary Dinner	6:30 PM to 8:00 PM	S	Toucan	T
Rob Ritchie Honorary Dinner	6:30 PM to 8:00 PM	S	Osprey 1	T
Dinner in Memory of Patrick Veyssiere	6:30 PM to 8:00 PM	S	Osprey 2	T
T.T. Chen Honorary Dinner	6:30 PM to 8:00 PM	D	Northern B	T

* O - Open to all attendees

R - Restrictions Apply

T - Ticketed Event

T1 - Pre-Registration Ticket Required

T2 - Ticket Required, can be purchased/picked up at door

MEETING INFORMATION



TMS 2012

141st Annual Meeting & Exhibition

Schedule of Events

as of February 23, 2012

Key: **D** Dolphin Hotel **S** Swan Hotel

Committee Meetings				
MetTrans A Board of Review	7:00 AM to 8:00 AM	S	Toucan	R
Process Technology & Modeling Committee	7:00 AM to 8:00 AM	D	Europe 8	O
Membership and Student Development Committee	8:45 AM to 10:00 AM	D	Europe 4	R
TMS Past Presidents	11:00 AM to 1:00 PM	S	Teal	R
EPD Council	12:00 PM to 2:00 PM	D	Asia 5	R
Superalloys Programming Committee	12:00 PM to 2:00 PM	S	Heron	R
ICME Committee	12:30 PM to 2:00 PM	S	Peacock	O
EMPMD Council	12:30 PM to 2:00 PM	D	Europe 7	R
Powder Materials Committee	12:30 PM to 2:00 PM	D	Europe 4	O
Springer TMS-ASM Strategic Planning	2:00 PM to 5:00 PM	S	Egret	R
TMS-ASM Leadership Meeting	3:45 PM to 4:45 PM	D	President's Suite #200097	R
REWAS Committee	4:30 PM to 6:00 PM	D	Peacock	R
Energy Conversion and Storage Committee	5:00 PM to 6:00 PM	D	Europe 4	O
Superalloys Organizing Committee	5:00 PM to 7:00 pm	S	Heron	R
Chemistry and Physics of Materials Committee	5:30 PM to 6:30 PM	D	Europe 8	O
IOMMMS Committee	5:30 PM to 6:30 PM	D	Northern A4	O
Nuclear Materials Committee	5:30 PM to 7:00 PM	S	Swan 1	O
Advanced Characterization Testing and Simulation Committee	5:45 PM to 6:45 PM	S	Parrot 1	O
Composite Materials Committee	5:45 PM to 6:45 PM	S	Parrot 2	O
Surface Engineering Committee	6:00 PM to 7:00 PM	S	Macaw 1	O
Biomaterials Committee	6:00 PM to 7:00 PM	D	Europe 4	O
Hydrometallurgy and Electrometallurgy Committee	6:00 PM to 7:00 PM	D	Oceanic 5	O
Materials and Society Committee	6:00 PM to 8:00 PM	S	Peacock	O
Technical Division Chairs Meeting	6:30 PM to 8:30 PM	S	Teal	R
Magnetic Materials Committee	8:00 PM to 9:00 PM	D	Europe 10	O

* O - Open to all attendees
R - Restrictions Apply

T - Ticketed Event

T1 - Pre-Registration Ticket Required

T2 - Ticket Required, can be purchased/picked up at door

MEETING INFORMATION

2012 Aluminum Plenary:

Aluminum Industry Technology 2020, A Look Ahead

Monday, March 12 • 8:30 a.m. to Noon • Dolphin Hotel, Southern III

Schedule of Events

as of February 23, 2012

Key: **D** Dolphin Hotel

S Swan Hotel

Student Events				
Student Poster Contest — Preliminary Judging	5:00 PM to 6:30 PM	D	Atlantic	O
Poster Set Up	7:00 AM to 8:00 AM	D	Atlantic	O

Social Functions				
Women in Science Breakfast	7:00 AM to 8:00 AM	D	Northern B	T
TMS & ASM Board of Trustees Social	8:30 PM to 9:30 PM	D	Northern E4	R

* O - Open to all attendees

T - Ticketed Event

R - Restrictions Apply

T1 - Pre-Registration Ticket Required

T2 - Ticket Required, can be purchased/picked up at door

IOMMMS Global Materials Forum: Materials in a Green Economy: An International Perspective, Monday, March 12 • 2 p.m. • Dolphin Hotel, Northern A4

Ten presentations, including an invited talk by AIME President Brajendra Mishra, "The Role of Materials Recycling in Economic Sustainability", will be offered.



MATERIALS INNOVATION GALLERY

Monday, March 12 through Wednesday, March 14
TMS2012 Exhibition Hall - Dolphin Hotel, Pacific Room

Welcome to TMS's showcase of ideas on how the techniques and principles that form the foundation for Materials Innovation @ TMS can potentially transform the development and deployment of advanced materials. A special feature of the TMS 2012 Exhibition, the Gallery has been designed to provide a visually compelling glimpse of how these concepts can potentially transform the future of materials and manufacturing innovation. You'll also have the opportunity to learn about the array of resources that are being offered as part of Materials Innovation @ TMS — highlighted by a preview of *Integrating Materials and Manufacturing Innovation (IMMI)*, TMS's new, peer-reviewed Open Access publication.

The Materials Innovation Gallery will be open throughout the conference during regular exhibition hours, so stop by often!

MEETING INFORMATION



WORLDWIDE PROJECTS AND EXPERIENCE

The Next Generation of Process Control & Automation:

FLOGEN

Managing the Present - Inventing the Future

- Iron & Steel
- Non-Ferrous Metals
- Precious Metals
- Materials Recycling

Increase Productivity - Decrease Cost - Protect Environment

www.flogen.com • secretary@flogen.com • 1-514-344-8786 • 1-877-2-FLOGEN

Schedule of Events










as of February 23, 2012

Key:  Dolphin Hotel

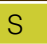



 Swan Hotel

FUNCTION	TIME	LOCATION	ROOM	ACCESS*
Tuesday, March 13, 2012				

All Conference Events

Author's Coffee	7:00 AM to 8:00 AM		Atlantic	R
Registration	7:00 AM to 5:30 PM		Atlantic	O
TMS Member Welcome Center	7:00 AM to 5:30 PM		Atlantic	O
TMS Foundation Center	7:00 AM to 5:30 PM		Atlantic	O
General Poster Session Gallery	7:00 AM to 5:30 PM		Atlantic	O
TMS Programming Support Center	7:00 AM to 5:00 PM		Atlantic	O
Technical Symposia	8:30 AM to 6:00 PM	See Technical Program for complete schedule and symposia locations		
TMS 2012 Exhibition	10:30 AM to 6:00 PM		Pacific	O
Materials Innovation at TMS Gallery	10:30 AM to 6:00 PM		Pacific	O
Happy Hour Reception	5:00 PM to 6:00 PM		Pacific	O

Special Presentations

Young Leaders Tutorial Luncheon	12:00 PM to 2:00 PM		Osprey 1	 T
EPD/MPMD Luncheon: Institute of Metals/ Robert Franklin Mehl Award featuring Subra Suresh	12:00 PM to 2:15 PM		Northern C	 T

Committee Meetings


Electronic Packaging and Interconnection Materials Committee	7:00 AM to 8:00 AM		Parrott	O
MetTrans B Board of Review	7:00 AM to 8:00 AM		Toucan	R
MPMD Council	7:00 AM to 9:00 AM		Peacock	R
Honors and Professional Recognition Committee	7:30 AM to 8:30 AM		Teal	R
Young Leaders Business Committee	9:00 AM to 10:30 AM		Toucan	R
TMS-FEMS Leadership Meeting	9:00 AM to 10:00 AM		President's Suite #200097	R
Springer Editorial Manager Orientation	12:00 PM to 1:00 PM		Peacock	R
SMD Council	12:00 PM to 2:00 PM		Parrott	R
Education Committee	12:30 PM to 2:00 PM		Toucan	R

* O - Open to all attendees

R - Restrictions Apply

 T - Ticketed Event

 T1 - Pre-Registration Ticket Required

 T2 - Ticket Required, can be purchased/picked up at door



TMS 2012

141st Annual Meeting & Exhibition

Schedule of Events

as of February 23, 2012

Key: **D** Dolphin Hotel **S** Swan Hotel

TMS-MetSoc Leadership Meeting	2:00 PM to 3:00 PM	D	President's Suite #200097	R
TMS Executive Committee	3:00 PM to 4:00 PM	D	President's Suite #200097	R
Energy Committee	5:00 PM to 6:00 PM	S	Parrott	O
Computational Materials Science and Engineering Committee	5:30 PM to 6:30 PM	S	Lark	O
Refractory Metals Committee	5:30 PM to 6:30 PM	S	Sandpiper	O
High Temperature Alloys Committee	5:30 PM to 7:00 PM	S	Peacock	O
Solidification Committee	6:00 PM to 7:00 PM	S	Teal	O
Titanium Committee	6:00 PM to 7:00 PM	D	Oceanic 3	O
Shaping and Forming Committee	6:00 PM to 8:00 PM	D	Oceanic 8	O
Corrosion and Environmental Effects Committee	6:30 PM to 7:30 PM	S	Lark	O

Student Events

Student Poster Contest- Best of Show Judging	10:30 AM to 11:30 AM	D	Atlantic	O
Student Career Forum	3:00 PM to 5:00 PM	S	Osprey 2	O

Social Functions

TMS-AIME Awards Reception	6:00 PM to 6:45 PM		EPCOT	T1
Shuttles will transport ticketed attendees to EPCOT	5:30 PM to 6:30 PM	D	Europe Foyer	T1
TMS-AIME Awards Banquet	6:45 PM to 10:00 PM		EPCOT	T1
Shuttles will transport attendees to Swan, Dolphin, Caribbean Beach, and Coronado Springs Resorts	9:15 PM to 9:45 PM		EPCOT	T1

* O - Open to all attendees
R - Restrictions Apply

T - Ticketed Event

T1 - Pre-Registration Ticket Required

T2 - Ticket Required, can be purchased/picked up at door

MEETING INFORMATION

Searching for Volunteer Opportunities?

TMS Technical Committees need your expertise!

Learn how by attending Technical Committee Meetings at TMS2012. Most meetings are open to all guests. See the Calendar of Events for sessions, times & locations.

Our volunteers are priceless.

Foundation Booth

Dolphin Hotel – Atlantic Room • Daily



Sunday: 7 a.m. to 6 p.m. • Monday: 7 a.m. to 6 p.m. • Tuesday: 7 a.m. to 5:30 p.m.
Wednesday: 7 a.m. to 3:30 p.m. • Thursday: 7 a.m. to 3:30 p.m.

PREMIUM ITEMS DONATION PROGRAM*

Help the TMS Foundation continue to support these society-building initiatives:

- Young Leaders Program
- Materials & Society (*Past projects include: TMS- Engineers Without Borders-USA Mali, Africa Project Partnership*)
- Vittorio DeNora Prize for Environmental Improvements in Metallurgical Industries
- TMS Scholarship Program

Receive these items for donations of the following correlating amounts:



\$10 – TMS Pin



\$25 – TMS Umbrella



\$50 -- Periodic Table Mug



\$250 – Apple TV



\$500 – Kindle Fire



\$1,000 – iPad

**The Premium Item Donation Program will run through April 15.*

Disney Drawings

Enter to win Disney Park Hopper passes through a daily drawing held for the duration of the conference. Simply drop your business card off at the Foundation Booth.



TMS 2012

141st Annual Meeting & Exhibition

Schedule of Events

as of February 23, 2012

Key: **D** Dolphin Hotel **S** Swan Hotel

FUNCTION	TIME	LOCATION	ROOM	ACCESS*
----------	------	----------	------	---------

Wednesday, March 14, 2012

All Conference Events

Author's Coffee	7:00 AM to 8:00 AM	D	Atlantic	R
Registration	7:00 AM to 5:00 PM	D	Atlantic	O
TMS Member Welcome Center	7:00 AM to 5:00 PM	D	Atlantic	O
TMS Foundation Center	7:00 AM to 5:00 PM	D	Atlantic	O
TMS Programming Support Center	7:00 AM to 5:00 PM	D	Atlantic	O
Poster Tear Down	3:00 PM to 5:00 PM	D	Atlantic	O
General Poster Session	7:00 AM to 3:00 PM	D	Atlantic	O
Poster Session Tear Down	3:00 PM to 5:00 PM	D	Atlantic	O
Technical Symposia	8:30 AM to 6:00 PM	See Technical Program for complete schedule and symposia locations		
Materials Innovation at TMS Gallery	10:30 AM to 3:30 PM	D	Pacific	O
TMS 2012 Exhibition	10:30 AM to 3:00 PM	D	Pacific	O

Special Presentations

LMD Luncheon	12:00 PM to 2:00 PM	S	Osprey	T
Materials Innovation Plenary Session	2:00 PM to 3:45 PM	D	Northern E2	O
Federal Funding Workshop & Reception	4:00 PM to 6:00 PM	D	Northern C	O

MEETING INFORMATION

Special Plenary Session:

Reaching New Heights: Materials Innovation in the Aerospace Industry

Wednesday, March 14 • Dolphin Hotel, Northern E2

New materials development is at a crucial stage of evolution, with Integrated Computational Materials Engineering (ICME) and new data sharing breakthroughs paving the way to remarkable time and cost reductions in product deployment. Through a series of compelling case studies, this program offers insights that can be applied to many aspects of product manufacturing, with significant impact on economic security and the race to heightened competitiveness.

Federal Funding Workshop and Reception

“Funding Opportunities to Advance the Materials Genome Initiative”

Panel Discussion: 4 p.m. • Reception: 5:15 to 6 p.m.

Wednesday, March 14 • Dolphin Hotel, Northern C

Don't miss this highly interactive session on funding opportunities related to the U.S. Materials Genome Initiative (MGI), as presented by program leaders from an array of federal funding agencies. Networking reception sponsored by the Georgia Institute of Technology.

Schedule of Events

as of February 23, 2012

Key: **D** Dolphin Hotel

S Swan Hotel

Committee Meetings				
TMS Board of Directors	8:00 AM to 11:30 AM	S	Lark	O
Graduate Student Advisory Council	9:00 AM to 10:00 AM	S	Toucan	R
Ni-Co 2013 Organizing Committee	12:00 PM to 1:30 PM	S	Sandpiper	R
Met Trans B Editorial Meeting	1:00 PM to 3:00 PM	S	Parrot 2	R
TMS-SME Leadership Meeting	3:30 PM to 4:30 PM	D	President's Suite #200097	R
Women in Materials Science and Engineering Committee	4:00 PM to 5:00 PM	D	Asia 5	R
Materials and Manufacturing Leaders Summit Reception & Dinner	6:00 PM to 9:00 PM	D	Northern D	R

* O - Open to all attendees
R - Restrictions Apply

T - Ticketed Event

T1 - Pre-Registration Ticket Required

T2 - Ticket Required, can be purchased/picked up at door

MEETING INFORMATION



CIVIL INFRASTRUCTURE

COMMUNICATIONS

MINING & METALS

OIL, GAS & CHEMICALS

POWER

Bechtel is proud to support TMS 2012:
TMS's 141st Annual Meeting and Exhibition

With a 'can-do' attitude, Bechtel achieves what others don't even attempt, and we proudly stand by everything we do.

For more information on Bechtel, visit bechtel.com

A history of delivering ground breaking projects

Shaping tomorrow together





TMS 2012

141st Annual Meeting & Exhibition

Schedule of Events

as of February 23, 2012

Key: **D** Dolphin Hotel **S** Swan Hotel

FUNCTION	TIME	LOCATION	ROOM	ACCESS*
----------	------	----------	------	---------

Thursday, March 15, 2012

All Conference Events

Author's Coffee	7:00 AM to 8:00 AM	D	Atlantic	R
Registration	7:00 AM to 3:30 PM	D	Atlantic	O
TMS Member Welcome Center	7:00 AM to 3:30 PM	D	Atlantic	O
TMS Foundation Center	7:00 AM to 3:30 PM	D	Atlantic	O
TMS Programming Support Center	7:00 AM to 3:30 PM	D	Atlantic	O
Technical Symposia	8:30 AM to 6:00 PM	See Technical Program for complete schedule and symposia locations		
Registration Satellite Desk	3:30 PM to 5:00 PM	D	Convention Foyer	O
TMS Programming Support Center	3:30 PM to 5:00 PM	D	Convention Foyer	O

Committee Meetings

Materials and Manufacturing Leaders Summit	8:00 AM to 4:30 PM	D	Northern D	R
Materials and Manufacturing Leader Summit Lunch	12:00 PM to 1:00 PM	D	Northern E2	R

* O - Open to all attendees

R - Restrictions Apply

T - Ticketed Event

T1 - Pre-Registration Ticket Required

T2 - Ticket Required, can be purchased/picked up at door

MEETING INFORMATION



TAR ALLIANCE

TAR ALLIANCE LLC

1/1 Umova Str., Gorlovka,
Donetsk region, 84609
Ukraine

Tel.: +380 (6242) 4-41-66, 4-02-57

Fax: +380 (62) 206-78-15

e-mail: info@taralliance.com

http:// www.taralliance.com

TAR ALLIANCE LLC is the largest processor of Coal Tar in Ukraine. We supply binder pitch and various coal tar distillates to customers in Europe, Asia, Africa and the Americas.

Walt Disney World Swan & Dolphin Resort Map



Restaurants

- 1 Shula's Steak House
- 2 Lobby Lounge
- 3 Cabana Bar and Beach Club
- 4 Picabu
- 5 The Fountain
- 6 Todd English's bluezoo
- 7 Fresh Mediterranean Market

Other

- 8 Lobby / Front Desk
- 9 Concierge
- 10 Disney Guest Services
- 11 Business Center
- 12 Shipping Desk
- 13 Shopping
- 14 Health Club
- 15 Camp Dolphin
- 16 Guest Laundry
- 17 Game Room
- 18 Mandara Spa

Outdoor

- 19 Disney Shuttle Bus
- WT Disney Water Taxi
- 20 Grotto Pool and Beach
- WP Whirlpools
- 21 Children's Playground
- 22 Cabana Beach Hut
- 23 Pacific Terrace
- 24 Cabana Deck
- 25 Lap Pool
- 26 Spring Pool
- 27 Kiddie Pool
- SA Smoking Area



Restaurants

- A Splash Grill
- B Splash Terrace
- C Garden Grove
- D Kimonos
- E Java Bar
- F IL Mulino New York Trattoria

Other

- G Lobby / Front Desk
- H Concierge / Disney Guest Services / Japanese Hospitality Desk
- I Business Center / Shipping Desk
- J Convention Registration Desk
- K Shopping
- L Health Club
- M Game Room
- N Bakery Display

Outdoor

- O Disney Shuttle Bus
- WT Disney Water Taxi
- P Lake Terrace
- Q Swan Terrace
- R Lap Pool
- WP Whirlpool
- S Crescent Terrace
- T Osprey Terrace 1
- U Osprey Terrace 2
- SA Smoking Area

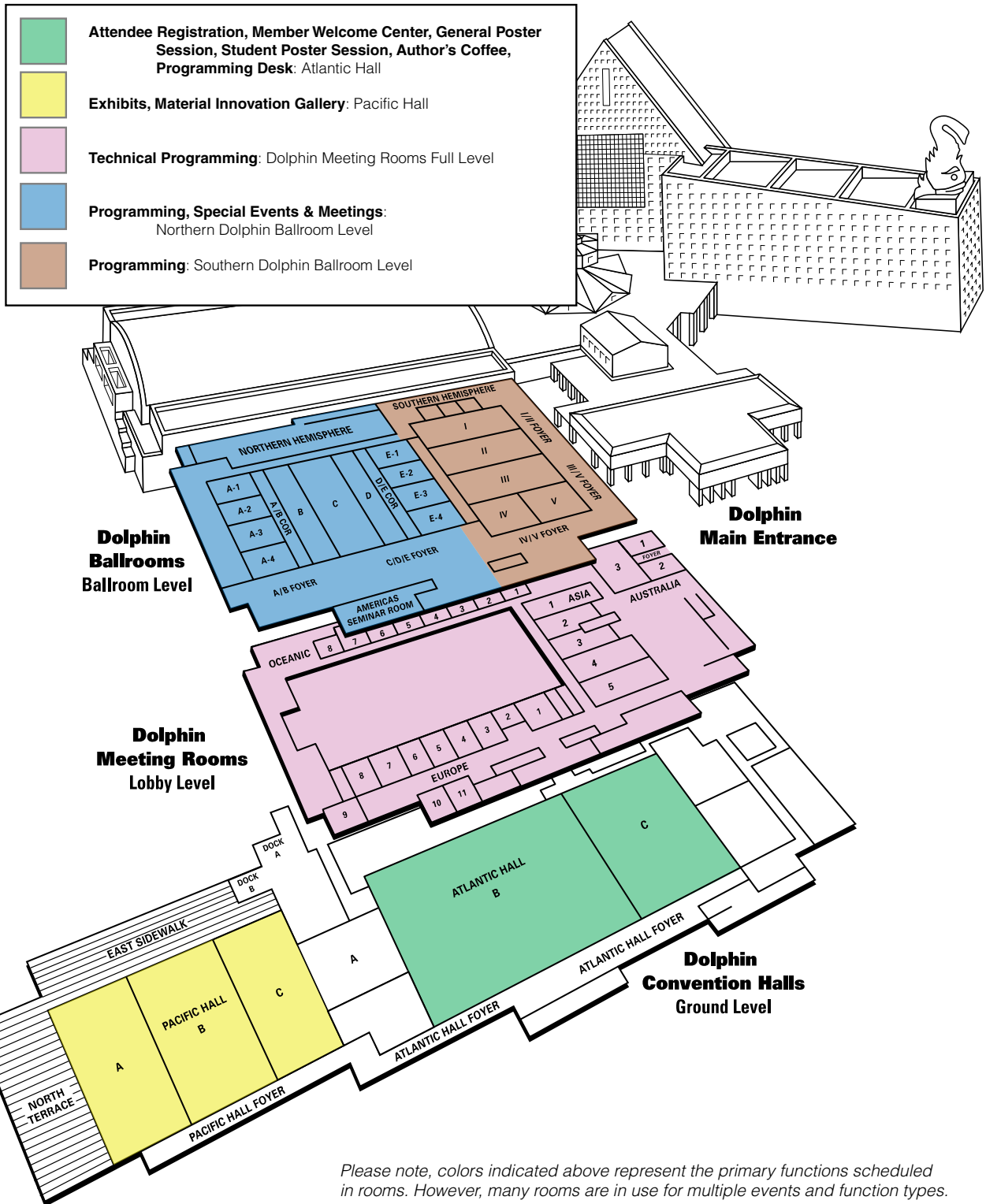
MEETING INFORMATION



TMS 2012

141st Annual Meeting & Exhibition

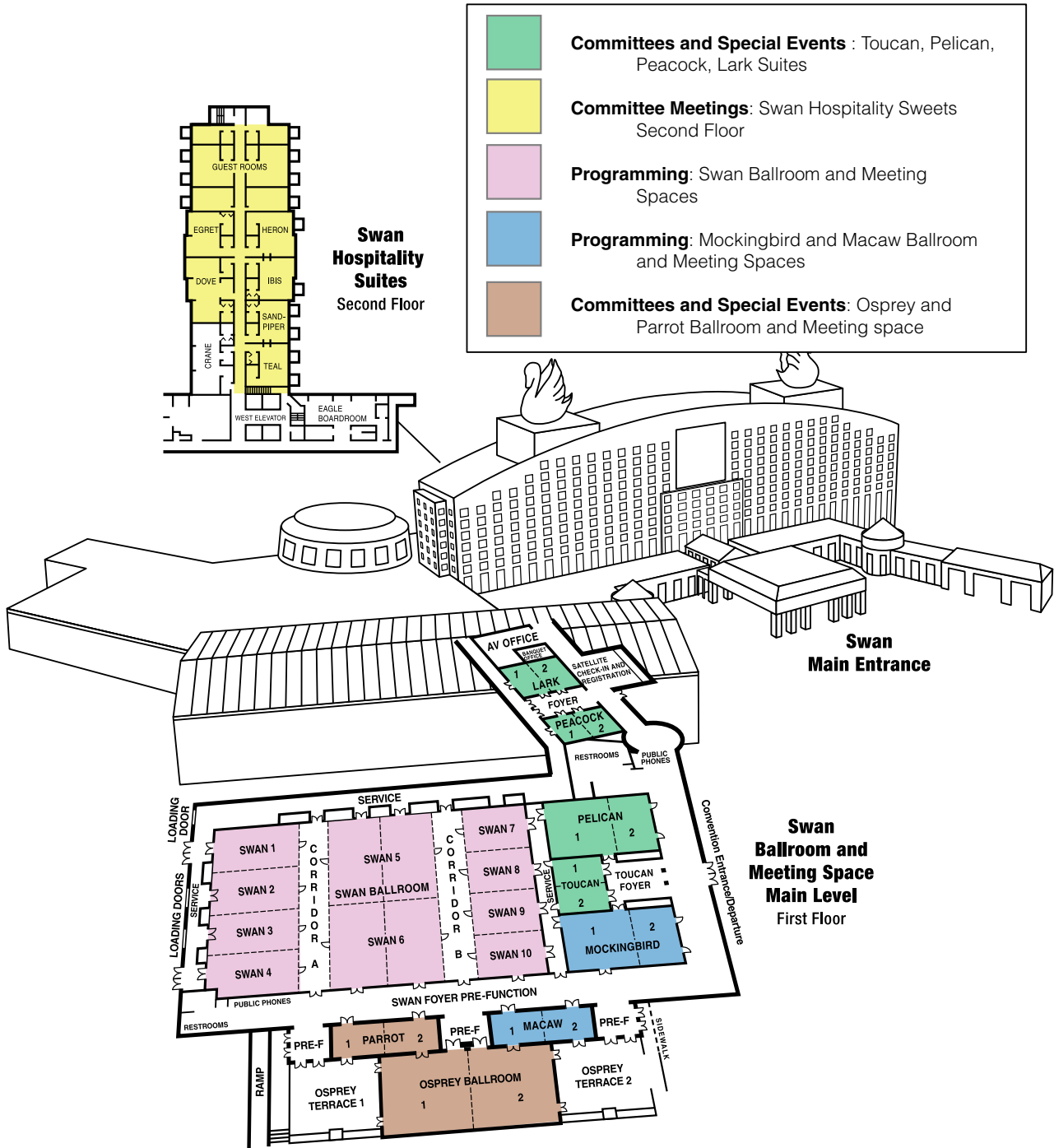
Dolphin Hotel Map



MEETING INFORMATION

Please note, colors indicated above represent the primary functions scheduled in rooms. However, many rooms are in use for multiple events and function types. Please refer to the Schedule of Events for detailed locations and times.

Swan Hotel Map



Please note, colors indicated above represent the primary functions scheduled in rooms. However, many rooms are in use for multiple events and function types. Please refer to the Schedule of Events for detailed locations and times.

Special Plenary • Reaching New Heights: Materials Innovation in the Aerospace Industry

Wednesday, March 14 • 2 p.m. to 3:45 p.m.
Dolphin Hotel, Northern E2

The aerospace industry is a demonstrated leader in materials innovation and acceleration. Through a series of compelling case studies, this program offers insights that can be applied to many aspects of product manufacturing, with significant impact on economic security and the race to heightened competitiveness. (Presented in cooperation with *Integrating Materials and Manufacturing Innovation (IMMI)* TMS's new Open Access journal.)

Moderator: Charles Ward, Chief, Metals, Ceramics, & Nondestructive Evaluation Division, U.S. Air Force Research Laboratory; Editor, *Integrating Materials and Manufacturing Innovation*

TOPICS AND SPEAKERS:



James Warren

Leader, Thermodynamics and Kinetics Group, Metallurgy Division National Institute of Standards and Technology; Technology Advisor to the Director on the Materials Genome

Topic: Materials Genome Initiative

The Materials Genome Initiative (MGI) is a new, multi-stakeholder effort to develop an infrastructure for accelerating advanced materials discovery and deployment in the United States. This talk will provide a brief introduction to the MGI, and set the stage for the case studies discussed in this session.



Robert E. Schafrik

General Manager, Materials and Process Engineering Department GE Aviation

Topic: ICME: Promise and Future Directions

GE Aviation has been engaged in various aspects of integrated computational materials engineering (ICME) for 10 years, driven primarily by the desire to implement new materials development within half the standard time. To accomplish this, a close relationship with design engineering and supply chain has been established.



Charles Kuehmann

President and CEO
QuesTek Innovations LLC

Topic: Lessons Learned from the Trenches and Implications on ICME and the MGI

The Materials Genome Initiative challenges innovation in materials modeling and engineering methods, enabling new materials to reach commercial application in half the time of current capabilities. In this new paradigm, a specific engineering problem must dictate the priorities for developing MGI-and ICME-related modeling, tools and data, not the other way around.



Michael Dudzik,

Vice President Science & Technology,
Washington Operations, Lockheed Martin Corporation

Rick Barto, Program Manager, Advanced Technology Laboratory, Lockheed Martin Corporation



Topic: Enabling the Era of Hybrid Materials – A Tipping Point of Change

The ongoing state-of-the-art transition in the field of materials science, from metal alloys to composites to hybrid materials, offers the aerospace market unique design solutions to meet ever demanding requirements in product manufacturing cost reduction, system performance enhancement, and total lifecycle sustainability. A review of recent successes achieved through better utilization of computational physics, material data management, certification, and the manufacturing supply chain will be presented.

Materials Innovation @ TMS is TMS's new strategic initiative. The following programs have been developed as part of this effort.

Federal Funding Workshop & Reception

Funding Opportunities to Advance the Materials Genome Initiative

(Organized by the TMS Public and Governmental Affairs Committee)

Wednesday, March 14

Panel Discussion: 4 p.m. • Reception: 5:15 p.m.

Dolphin Hotel, Northern C

This highly interactive session will examine funding opportunities related to the Materials Genome Initiative (MGI), as presented by program leaders from an array of federal funding agencies. Panelists will provide an overview of current MGI activities in their agencies and present a look to the future, with significant time for questions from the audience. Continue the dialogue during the networking reception, sponsored by the Georgia Institute of Technology, designed to promote one-on-one conversation with the panelists.

TOPICS AND SPEAKERS



Diana Farkas,

Program Director, Condensed Matter and Materials Theory, Division of Materials Research National Science Foundation

Topic: Looking for Transformative Approaches for the Materials Genome Initiative



Diana Bauer

Director of the Office of Economic Analysis U.S. Department of Energy

Topic: New Efforts on Computational Materials



Julie Christodoulou

Director, Naval Materials Division Office of Naval Research

Topic: Basic Research Challenge in Materials



Michael Caton

Senior Materials Research Engineer Materials & Manufacturing Directorate Air Force Research Laboratory

Topic: Advancing Superalloys

Don't Miss These Other Materials Innovation @ TMS Opportunities

Materials Innovation Gallery: Browse a visually compelling showcase of ideas—developed as a special feature of the TMS 2012 Exhibition—on implementing materials innovation principles, techniques, and concepts. (See page 9 for details.)

Preview of *Integrating Materials and Manufacturing Innovation (IMMI)*: Learn more about TMS's new Open Access journal that combines peer review rigor with enhanced digital content to rapidly share knowledge and learning on innovations, from materials discovery through manufacturing. Opportunities to interact with the *IMMI* editor, Chuck Ward, will be presented throughout the conference.

Annual Meeting of the Membership: Start your conference by attending this important membership engagement opportunity—highlighted by the official introduction of **Materials Innovation @ TMS**, (See page 6 for details.)

For additional information, stop by the Materials Innovation @ TMS Information Center at the TMS Member Welcome Center or visit our website at materialsinnovation.tms.org.



TMS 2012

141st Annual Meeting & Exhibition

Lectures & Luncheons

Extraction & Processing Division Distinguished Lecturer-Plenary Session
International Smelting Technology Symposium
(Incorporating the 6th Advances in Sulfide Smelting Symposium)

Monday, March 12 • 8:40 a.m.
Dolphin Hotel, Northern A3



Speaker: **Theo Lehner**,
Boliden Mineral AB, Sweden

Topic: Conservation & Development: Industrial Learning in Non-Ferrous Smelting

About the Topic: This lecture will present thoughts and experience on the following issues in Non-Ferrous Smelting: conservation and its corollary waste; development; industrial learning curves. Waste occurs in many shapes, be it losses of material, loss of health, loss of ability or knowledge. Development in non-ferrous smelting over the last decades has changed many a flow sheet, but also ended many projects. Operations have adapted to new processes and new conditions.

Young Leaders Tutorial Luncheon Lecture

Tuesday, March 13 • Noon
Swan Hotel, Northern C



Speaker: **Michael Demkowicz**,
Massachusetts Institute of Technology, USA

Topic: Becoming a Better Scientist by Learning the History of Science

About the Topic: A scientist educated in the current curricula finds it difficult to defend scientific perspectives to skeptical non-scientists. He will propose that this educational gap be filled by making the history of science part of the typical science curriculum. In this talk, Demkowicz will present several topics from the history of science that could serve as case studies to be incorporated into such a class.

Light Metals Division Luncheon Lecture

Wednesday, March 14 • Noon
Swan Hotel, Osprey



Speaker: **Diana Bauer**,
Director of the Office of Economic Analysis, U.S. Department of Energy's Office of Policy and International Affairs.

Topic: The Department of Energy's 2011 Critical Materials Strategy

About the Topic: Bauer will present an overview of the DOE's Critical Materials Strategy.

Invited Talks



Speaker: **Brajendra Mishra**,
AIME President, a professor at the Colorado School of Mines and 2006 TMS President

Brajendra Mishra will present two talks:

IOMMMS Global Materials Forum: Materials in a Green Economy: An International Perspective Symposium

Monday, March 12 • 2:10 to 2:30 p.m.
Dolphin Hotel North A4

Presentation Title: The Role of Materials Recycling in Economic Sustainability.

Integrative Materials Design: Performance and Sustainability Symposium

Tuesday, March 13 • 11:05 a.m.
Dolphin Hotel Europe 2

MEETING INFORMATION

Award-Winning Speakers

Extraction & Processing Division/Materials Processing & Manufacturing Joint Division Luncheon and Institute of Metals/ Robert Franklin Mehl Award Lecture

Tuesday, March 13 • Noon
Swan Hotel, Northern C



Speaker: **Subra Suresh**,
Director of the U.S. National
Science Foundation (NSF)

Topic: Nanomechanics of Engineered and Biological Materials

Vittorio de Nora Prize Lecture

Tuesday, March 13 • 11:25 a.m.
Dolphin Hotel, Europe 5



Speakers: **Antoine Allanore**,
Massachusetts Institute of Technology, USA; and



James Yurko,
Electrolytic Research Corporation,
USA

Topic: Development of Electrometallurgical Processes for 21st Century Metal Extraction

About the Topic: This presentation will first briefly present some existing extraction methods, in particular electrometallurgical ones, pointing-out the advantages and issues related to the current state-of-the art. The second part of the talk will present how breakthrough electrochemical processes have recently been developed to adapt to environmental and energy constraints, taking the example of low- and high-temperature electrochemical extraction processes scaled-up for transition and light metals.

2012 Shri Ram Arora Award

Wednesday, March 14 • 3 p.m.
Swan Hotel, Pelican 2



Speaker: **Anjali Sharma**,
University of Delhi

Topic: Novel Sensor Structure of SnO₂ Thin Film Integrated with Catalytic Micro-Discs for the Detection of Trace Level NO₂ Gas

About the Topic: An improvement in the sensing response, response time and recovery time could be attributed to the spill-over of sensing gas molecules over the uncovered surface of SnO₂ thin films by WO₃ micro-discs catalyst.

JIM International Scholar Award Winner

Tuesday, March 13 • 8:30 a.m.
Dolphin Hotel, Southern II



Speaker: **Noritaka Saito**,
Kyushu University

Topic: Effect of Shear Stress on Crystallization Behavior of Mold Flux for Continuous Casting

About the Topic: This presentation will focus on how modern steelmaking involves handling slags and fluxes mostly in the temperature region between liquidus and solidus, to fully exploit their functional capabilities and the various methods researchers have developed to study the crystallization behavior of them.



TMS 2012

141st Annual Meeting & Exhibition

Networking & Social Events

Student Mixer

Sunday, March 11 • 8:30 10:30 p.m.
Dolphin Hotel, Southern III


Meet and mingle with the next generation of materials scientists and engineers as peer mentors in an informal social setting.

President's Welcoming Reception

Monday, March 12 • 5 to 6:30 p.m.
Dolphin Resort, Pacific Room

Gather with 2011 TMS President Garry Warren and colleagues for an informal social event in the exhibition hall.

Honorary & Memorial Dinners

All honorary dinners will be held Monday, March 12. Tickets are needed for admission to these events and may be purchased at the Registration Desk in Dolphin Resort, Atlantic Room. 

T.T. Chen Honorary Dinner

6:30 to 8 p.m. • Dolphin Resort, Northern B Room

Emeritus Professor George D.W. Smith Honorary Dinner

6:30 to 8 p.m. • Swan Resort, Lark Room

Robert Ritchie Honorary Dinner

6:30 to 8 p.m. • Swan Resort, Osprey 1

Randall M. German Honorary Dinner

6:30 to 8 p.m. • Swan, Toucan Room

Dinner in Memory of Patrick Veysseyre

6:30 to 8 p.m. • Swan, Osprey 2

MEETING INFORMATION

One Source

Expertise in Bauxite Mining & Refining, Calcination, & Smelting

High Performance for Alumina Handling Systems

Every day, worldwide, our equipment crushes, conveys, grinds, digests, clarifies, precipitates, stores, and calcinates bauxite to produce alumina. Combining the respected brand names of MÖLLER, KOCH-MVT, FULLER-TRAYLOR, EIMCO, DORR-OLIVER, KREBS, and ABON, FLSmidth offers a broad range of equipment and processes while increasing recoveries, lowering energy consumption, and providing proven reliability.

For more information, visit us at www.flsmidth.com





Some stories stay alive long after the theatre lights come up. If this can could talk, it would recite its own series of gripping endings. And you can be certain the aluminium you see today will be starring elsewhere tomorrow.

Hydro – Infinite ideas in aluminium.

www.hydro.com



HYDRO

141st TMS-AIME Annual Awards Banquet

including Dinner, Awards Presentation, and Installation of the 2012 President

**Tuesday, March 13,
World ShowPlace Pavilion, EPCOT**

TMS will honor the best among the materials science & engineering community. Incoming 2012 TMS President Wolfgang Schneider will also be recognized and will present his vision for the new year. This year, the banquet will be held in the **World ShowPlace Pavilion in EPCOT** and will include a **Disney fireworks display, "IllumiNations: Reflections of Earth,"** to close the event. **Shuttles will board at 5:30 p.m. outside of the Europe Ballrooms Foyer on the Lobby/3rd Level of the Dolphin Hotel and depart for EPCOT at 5:45 p.m.**

Attendees are reminded to wear their name badges and bring their banquet tickets in order to board the busses and gain admittance to the **EPCOT World Showplace**. For guests needing assistance, a shuttle will be available for transport to the private area.

Following the banquet, TMS staff and Walt Disney World Guides will direct guests to the **Italy Pavilion Dock** for the fireworks show and accompanying dessert. Shuttles will meet guests behind the Italy Pavilion for transport back to the Swan and Dolphin, the Coronado Springs, and the Caribbean Beach Resorts at the conclusion of **IllumiNations**.

ADVANCE TICKETS ARE REQUIRED FOR THIS LIMITED SEATING EVENT. 



**Wolfgang Schneider,
2012 TMS President**

About the 2012 TMS President

Wolfgang Schneider is the head of the research and development center of Hydro Aluminum Rolled Products Business in Bonn, Germany and is also a professor of metallurgy at the Technical University of Berlin. A TMS member since 1996, Schneider's vision for his presidency is growing the mission of TMS, with more emphasis on professional development.

"During my presidency, my focus will be on innovation that can expand the product and service portfolio of TMS. One specific area I feel requires more attention is our professional education strategy. I would also like to see more emphasis on the technical agenda and volunteer structure with the focus on technical divisions and committees, which are responsible for the major programming activities of TMS." Schneider received his Dipl.-Ing. degree in foundry technology, as well as his doctorate in metallurgy, from the Technical University of Berlin. He has published more than 140 technical papers and is named as an inventor in nine patents.

As a member of the Society, Schneider served as chair of the TMS Light Metals Division from 2007-2010 and on the TMS Board of Directors from 2003 to 2006 in the membership development area. He has also volunteered in various other capacities for TMS since 1997. His service included: Cast Shop Technology Symposium subject chair, Aluminum Committee chair, Strategic Advisory Committee member, and Nominating Committee member. Schneider has also received several Society awards, including the TMS Light Metals Award in both 1990 and 1995. He has been active in a number of other societies, such as the German Society of Material Science DGM and the German Foundrymen Society VDG.



Society Awards presented by 2011 TMS President Garry Warren

Garry W. Warren is professor in the Department of Metallurgical and Materials Engineering, and Director of the Materials Science Program at the University of Alabama, Tuscaloosa. He is active in the TMS Extraction & Processing Division (EPD) and has served in numerous capacities. Warren has also served at the society level on the TMS Programming Committee, the TMS Financial Planning Committee, the TMS Publications Coordinating Committee, and the TMS Board of Directors.

SOCIETY AWARDS

TMS Fellows Class of 2012

Ian Baker

Sherman Fairchild Professor of Engineering,
Dartmouth University

David Dunand

James and Margie Krebs
Professor, Northwestern University

Sung-Kwon Kang

Research staff, IBM Corporation

Pradeep Rohatgi

Professor, University of Wisconsin

Alexander Scott Distinguished
Service Award

Ramana Reddy

University of Alabama

Application to Practice Award

Mark Taylor

University of Auckland

Brimacombe Medalist(s)

Robert Hyers

University of Massachusetts

Paul Krajewski

General Motors Company

Zi-Kui Liu

Pennsylvania State University

Bruce Chalmers Award

A. Lindsay Greer

University of Cambridge

Cyril Stanley Smith Award

Mats Hillert

Royal Institute of Technology

Early Career Faculty Fellow Award

Michael Demkowicz

Massachusetts Institute of
Technology

Educator Award

Marc DeGraef

Carnegie Mellon University

Institute of Metals/Robert Franklin

Mehl Award

Subra Suresh

National Science Foundation

Morris Cohen Award

Michael Ashby

University of Cambridge

Shri Ram Arora Award

Anjali Sharma

University of Delhi

Vittorio de Nora Prize for
Environmental Improvements in
Metallurgical Industries

Antoine Allanore

Massachusetts Institute of
Technology

James Yurko

Electrolytic Research Corp.

DIVISION AWARDS

*Presented at technical
division-related events.*

**Electronic, Magnetic &
Photonic Materials Division**

Distinguished Scientist/Engineer

KN Mani Subramanian

Michigan State University

Distinguished Service

Srinivas Chada

Power-One Renewable Energy
Solutions

John Bardeen Award

John William Morris, Jr.

University of California

JEM Best Paper

Joyelle J. Harris

Exponent Failure Analysis
Associates

**Extraction & Processing
Division**

EPD Distinguished Lecturer

Theodor Lehner

Boliden Mineral AB

EPD Distinguished Service

Tzong Chen

CANMET-MMSL

Technology Award

Jiann-Yang "Jim" Hwang

Xiang Sun

Xiaodi Huang

Michigan Technological University

141st TMS-AIME Annual Awards Banquet

including Dinner, Awards Presentation, and Installation of the 2012 President

DIVISION AWARDS

Science Award

James. E. Miller

Richard B. Diver

Nathan P. Siegel

Eric N. Coker

Andrea Ambrosini

Daniel E. Dedrick

Mark D. Allendorf

Anthony H. McDaniel

Gary L. Kellogg

Roy E. Hogan

Ken S. Chen

Ellen B. Stechel

Sandia National Labs

Light Metals Division

Distinguished Service Award

Eric Nyberg

Pacific Northwest National Lab

Technology Award

Mark Taylor

University of Auckland

Light Metals Award

Xiangwen Wang

Garry Tarcy

Eliezer Batista

Geff Wood

Alcoa Inc

Aluminum Reduction Technology
Award

Feng Naixiang

Northeastern University

Tian Yingfu

Chongqing Tiantai Aluminum

Industry Co Ltd

Peng Jianping

Wang Yaowu

Qi Xiquan

Tu Ganfeng

Northeastern University

Bauxite & Alumina Award

Lucy Martin

Steven Howard

Bechtel Australia Pty Ltd

Electrode Technology for Aluminum
Production Award

Olivier Trempe

Daniel Larouche

Michel Guillot

Mario Fafard

Universite Laval

Donald Ziegler

Alcoa Inc

Warren Peterson Cast Shop for
Aluminum Production Award

Dmitry Eskin

Brunel University

Mehdi Lalpoor

Delft University of Technology/

Materials Innovation Inst (M2i)

Laurens Katgerman

Delft University of Technology

Energy Best Paper – Professional
Award

Peter Loutzenhiser

Anastasia Stamatian

ETH Zurich

Willy Villasmil

Anton Meier

Paul Scherrer Institute

Energy Best Paper – Student Award

Peng Li

Qing-bo Yu

Qin Qin

Northeastern University

JOM Best Paper Award

Pascal Coursol

Patrick Coulombe

Serge Gosselin

Dany Lavoie

Aluminerie Alouette

Jean-Marc Simard

Exaprom

Jerry Marks

J. Marks and Associates

Sylvain Fardeau

Rio Tinto Alcan

Energy Best Paper

Peter G. Loutzenhiser

Anastasia Stamatian

Aldo Steinfeld

ETH Zurich

Willy Villasmil

Anton Meier

Paul Scherrer Institute

Magnesium Best Paper -

Application Award

Kazutaka Okamoto

Hitachi Research Lab

Masato Sasaki

Norikazu Takashi

Hitachi

Qudong Wang

Yan Gao

Dongdi Yin

Changjiang Chen

Shanghai Jiao Tong University

Magnesium Best Paper -
Fundamental Research Award

Kiran Solanki

Mehul Bhatia

Arizona State University

Amitava Moitra

Mississippi State University

Magnesium Best Paper -
Student Award

Lennart Stutz

Helmholtz-Zentrum Geesthacht

GmbH

Jan Bohlen

Dietmar Letzig

Karl Kainer

GKSS Forschungszentrum

Geesthacht GmbH

Materials Processing & Manufacturing Division

Distinguished Scientist/Engineer
Award

John Morral

Ohio State University

Distinguished Service

Joy Forsmark

Ford Motor Company

Structural Materials Division

Distinguished Scientist/Engineer
Award

Yuntian Zhu

North Carolina State University

Distinguished Service Award

Eric Taleff

University of Texas

JOM Best Paper Award

Scott Hollister

University of Michigan



AIME Awards Presented by Brajendra Mishra

Brajendra Mishra is president of The American Institute of Mining, Metallurgical, and Petroleum Engineers. A member of TMS since 1992, Mishra served as president in 2006. He is a professor of metallurgical and materials engineering and the associate director of the Kroll Institute for Extractive Metallurgy and the Advanced Coatings and Surface Engineering Laboratory, Colorado School of Mines. He is also the associate director of the National Science Foundation Industry-University Cooperative Research Center for Resource, Recovery and Recycling.

AIME AWARDS

AIME Henry DeWitt Smith
Scholarship

Jennifer Carter

The Ohio State University

Eric Gratz

Boston University

Karem Tello

Colorado School of Mines

Mengtao Xie

Illinois Institute of Technology

AIME Honorary Membership

David Laughlin

Carnegie Mellon University

AIME Champion H. Mathewson
Award

Adam L. Pilchak

U.S. Air Force Research Laboratory

Robert E.A. Williams

James C. Williams

The Ohio State University

AIME Rossiter W. Raymond
Memorial Award

David Rowenhorst

Alexis Lewis

Naval Research Laboratory

Robert Lansing Hardy Award

Andrew Minor

University of California

STUDENT AWARDS

2011 ASCE Alfred Noble Prize

Markus Buehler

Raffaella Paparcone

Massachusetts Institute of
Technology

Graduate Outstanding Student Paper

First Place: **Zhinan An**

University of Tennessee

Second Place: **Indranil Lahiri**

Florida International University

Undergraduate Outstanding Student
Paper

First Place: **Sumit Goenka**

Carnegie Mellon University

Second Place: **Tasha Totten**

Washington State University

TMS J. Keith Brimacombe

Presidential Scholarship

Rachel Garrick

University of Illinois

**Young Leader Professional
Development Award Winners**

EMPMD Young Leader Professional
Development

Chao-Hong Wang

National Chung Cheng University

Ashwin Ramasubramaniam

University of Massachusetts

EPD Young Leader Professional
Development

John Carpenter

Los Alamos National Lab

Soobhankar Pati

Metal Oxygen Separation

Technologies

LMD Young Leader Professional
Development

Qizhen Li

University of Nevada

Pretesh Patel

Light Metals Research Center

OTHER AWARDS

MPMD Young Leader Professional
Development

Nathan Mara

Los Alamos National Lab

Kantesh Balani

Indian Institute of Technology

SMD Young Leader Professional
Development

Nima Rahbar

University of Massachusetts

Clarissa Yablinsky

University of Wisconsin

Young Leader International Scholar
Award

Douglas Spearot

University of Arkansas



TMS 2012

141st Annual Meeting & Exhibition

Student Activities

Sunday

TMS2012 Materials Bowl

Noon to 8:30 p.m. • Dolphin Hotel, Southern IV
Elimination Rounds – Noon to 3 p.m.
Final Championship Round – 8:00 p.m.

Student teams compete for cash prizes and earn the right to take home the traveling trophy after conquering three rounds of intense, materials science-based questions.

Student Mixer

8:30 to 10:30 p.m. • Dolphin Hotel, Southern III

Put on your dancing shoes to meet and mingle with peers in an informal social setting.

Monday

Poster Contest Judging

5 to 6:30 p.m. • Dolphin Hotel, Atlantic

Tuesday

Best of Show Judging – Ribbon Presentation

10:30 to 11:30 a.m. • Dolphin Hotel, Atlantic

Career Forum

3 to 5 p.m. • Swan Hotel, Osprey 2

Organized by the TMS Young Leader Committee, this session will feature speakers from a variety of materials science backgrounds and career stages who discuss how to navigate a career path to ultimate goals.

Career Panel

Julia Greer,
Cal Tech

Eric Brown,
Los Alamos National
Laboratory

Frank DelRio,
NIST

Alpesh Shukla,
Lawrence Berkeley National
Laboratory

Paul Ohodnicki,
National Energy Technology
Laboratory

Jud Ready,
Georgia Tech

George T. "Rusty" Gray III,
Los Alamos National
Laboratory

Eric Schmidt,
V&M Star

Frank Balle
University of Kaiserslautern

Chris Weinberger,
Sandia National Laboratory

SPECIAL INFORMATIONAL SESSION: Congressional Science and Engineering Fellowship Program

Monday, March 12 • 1 to 2 p.m.
Swan Hotel, Parrot 2 Room

Speakers:



Jennifer Nekuda Malik

2011-2012 TMS/MRS Congressional Science and Engineering Fellow

Topic: Engineering Public Policy: Science in Government



Edward Herderick

2009-2010 TMS/MRS/ACerS Congressional Science and Engineering Fellow

Topic: The Transition from PhD candidate to Congressional Staffer to Engineer in the Materials Industry

Have you ever considered learning about the field of science policy in the U.S. Senate and House of Representatives?

The TMS/MRS Congressional Fellowship Program offers an amazing opportunity for scientists at all stages of their careers to spend a year as a special legislative assistant in the United States Congress in Washington, DC.

TMS2012 offers a snapshot of this experience via this informational session featuring testimonials from Jennifer Nekuda Malik, current Fellow, who is a staff member on the Senate Energy and Natural Resources Committee, and Edward Herderick, who served on the staff of Ohio Senator Sherrod Brown during his Fellowship. The pair will discuss their day-to-day agenda, education, and benefits to their personal career advancement. An opportunity for questions and discussion will follow.

MEETING INFORMATION

Mark Your Calendar

Upcoming Meetings

TMS provides numerous opportunities for advancing research and collaboration on the latest technology through a series of diverse conferences and workshops. For the ultimate in professional development and networking, make the face-to-face connections at these events designed to engage the materials science and engineering community.

For more information visit the [TMS Meetings and Events page at www.tms.org/Meetings/meetings_events.aspx](http://www.tms.org/Meetings/meetings_events.aspx).



2012 Near Net Shape Manufacturing Workshop

April 11-13, 2012

iWireless Center, Moline, Illinois • USA

13th International Conference on Aluminum Alloys (ICAA -13)

June 3-7, 2012

Carnegie Mellon University • Pittsburgh, Pennsylvania

2012 NanoNuclear Workshop

June 5-7, 2012

Gaithersburg Marriott Washingtonian Center, Gaithersburg, Maryland

International Conference on 3D Materials Science 2012

July 8-12, 2012

Seven Springs Mountain Resort • Seven Springs, Pennsylvania

2012 Methods for 3D Microstructural Studies Workshop

July 13-14, 2012

Carnegie Mellon University • Pittsburgh, Pennsylvania

TMS 2012 Industrial Aluminum Electrolysis Course: The Definitive Theory and Practice of Primary Aluminum Production

September 9-14, 2012

Rio Tinto Alcan • Jonquiere, Quebec, Canada

Superalloys 2012: The 12th International Symposium on Superalloys

September 9-13, 2012

Seven Springs Mountain Resort • Champion, Pennsylvania

Materials Science & Technology 2012 Conference & Exhibition

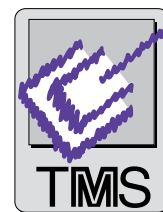
October 7-11, 2012

Pittsburgh, Pennsylvania

TMS 2013: Linking Science and Technology for Global Solutions

March 3-7, 2013

San Antonio, Texas



TMS

The Valuable Resource that Keeps on Giving...

TMS 2012 Annual Meeting Proceedings

The following stand-alone book titles and supplemental proceedings will be available:

- 3rd International Symposium on High Temperature Metallurgical Processing
- CFD Modeling and Simulation in Materials Processing
- Characterization of Minerals, Metals, and Materials
- Electrometallurgy 2012
- Energy Technology 2012
- EPD Congress 2012
- International Smelting Technology Symposium
- Light Metals 2012
- Magnesium Technology 2012
- TMS2012 Supplemental Proceedings: Volume 1: Materials Processing and Interfaces
- TMS2012 Supplemental Proceedings: Volume 2: Materials Properties, Characterization, and Modeling
- T.T. Chen Honorary Symposium on Hydrometallurgy, Electrometallurgy and Materials Characterization

Attendees may purchase books at the Wiley booth located adjacent to the Member Welcome area outside the exhibit hall.

Don't Miss These TMS-Wiley Book Author Events!

Meet an authority on materials processing applications, Arthur E. Morris, coauthor of *Handbook on Material and Energy Balance Calculations in Materials Processing, Third Edition*. Purchase a signed copy of his book for a special show price of \$99.95.*

Take a look at engineering education today—with an eye to tomorrow—with Diran Apelian, coeditor of *Shaping Our World: Engineering Education for the 21st Century*. Buy a signed copy of his book for a special show price of \$35.*

Stop by the Wiley booth in the registration area for more information.

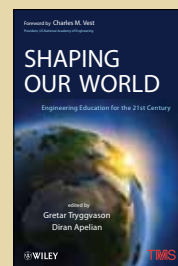
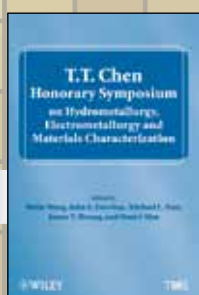
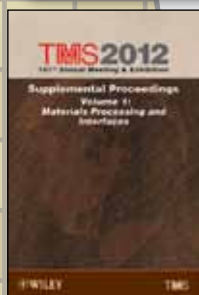
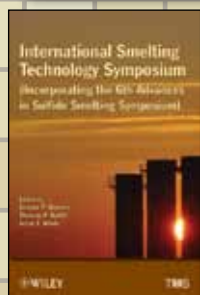
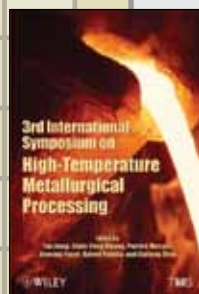
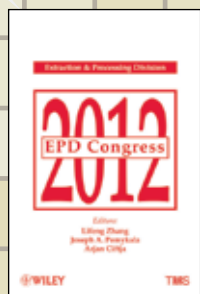
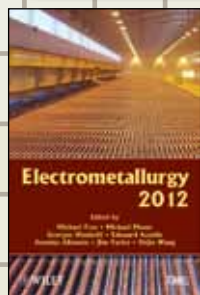
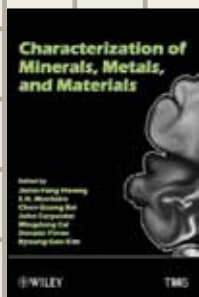
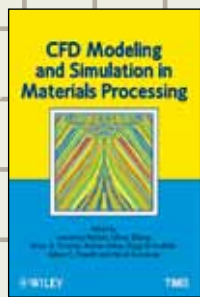
Author Signing Hours:

Morris: Monday, March 12, 2 to 3 p.m.

Apelian: Tuesday, March 13, Noon to 1 p.m.

Cookies and coffee will be served!

*Discount available only at the TMS2012 Annual Meeting.



TMS 2011-2012 Leadership Executive Committee

President:

Garry Warren

University of Alabama – Tuscaloosa, USA

Past President:

George T. “Rusty” Gray III

Los Alamos National Laboratory, USA

Vice President:

Wolfgang Schneider

Hydro Aluminum Rolled Products GMBH, Germany

Elizabeth A. Holm

Sandia National Laboratory, USA (Incoming)

Financial Planning Officer:

Stanley Howard

South Dakota School of Mines and Technology, USA

Robert W. Hyers

University of Massachusetts, USA (Incoming)

Functional Area Directors

Membership & Student Development:

Ellen K. Cerreta

Los Alamos National Laboratory, USA

David Bahr

Washington State University, USA (Incoming)

Programming:

Hani Henein

University of Alberta, Canada

Neville Moody

Sandia National Laboratory, USA (Incoming)

Professional Development:

David Shifler

Office of Naval Research, USA

Content Development and Dissemination Committee:

William J. “Jud” Ready

Georgia Institute of Technology, USA

Carl Cady

Los Alamos National Laboratory, USA

Public and Governmental Affairs:

Kevin J. Hemker

Johns Hopkins University, USA

Technical Division Directors

Electronic, Magnetic & Photonic Materials:

Srinivas Chada

Power-One Renewable Energy, USA

Extraction & Processing:

Adrian Deney

Praxair, Inc., USA

Materials Processing & Manufacturing:

James W. Sears

South Dakota School of Mines and Technology, USA

Light Metals:

John N. Hryn

Argonne National Laboratory, USA

Structural Materials:

Dennis M. Dimiduk

United States Air Force Research Laboratory

AROUND THE WORLD.
WE ARE WHERE YOU NEED US.



SUPERIOR PRODUCTS CUSTOM ENGINEERED
FOR YOUR DEMANDING APPLICATIONS

Making the largest precast shapes for quicker installations
for
MegaBrix™ Furnaces
or any of the following applications



SIFCA® Skim Tools



Sicon Tap Out Troughs



SIFCA® Impellers

Refractory Technology | Engineering | Precast | Installation

WWW.WAHLREF.COM
800.837.WAHL

Linked in facebook



Coming soon!
Exo-Fuse.com

TMS 2012
141st Annual Meeting & Exhibition

26th EXHIBITION

March 11-15, 2012 • Swan & Dolphin Resort
Orlando, Florida

Exhibit Hours

Monday, March 12.....	12 p.m. - 6:30 p.m.
Tuesday, March 13.....	10:30 a.m. - 6:00 p.m.
Wednesday, March 14.....	10:30 a.m. - 3:00 p.m.

Table of Contents

Exhibiting Companies.....	34
Exhibit Floor Plan.....	35
Products & Services Index.....	36
Company Descriptions.....	38
Sponsors.....	Inside Back Cover



TMS 2012

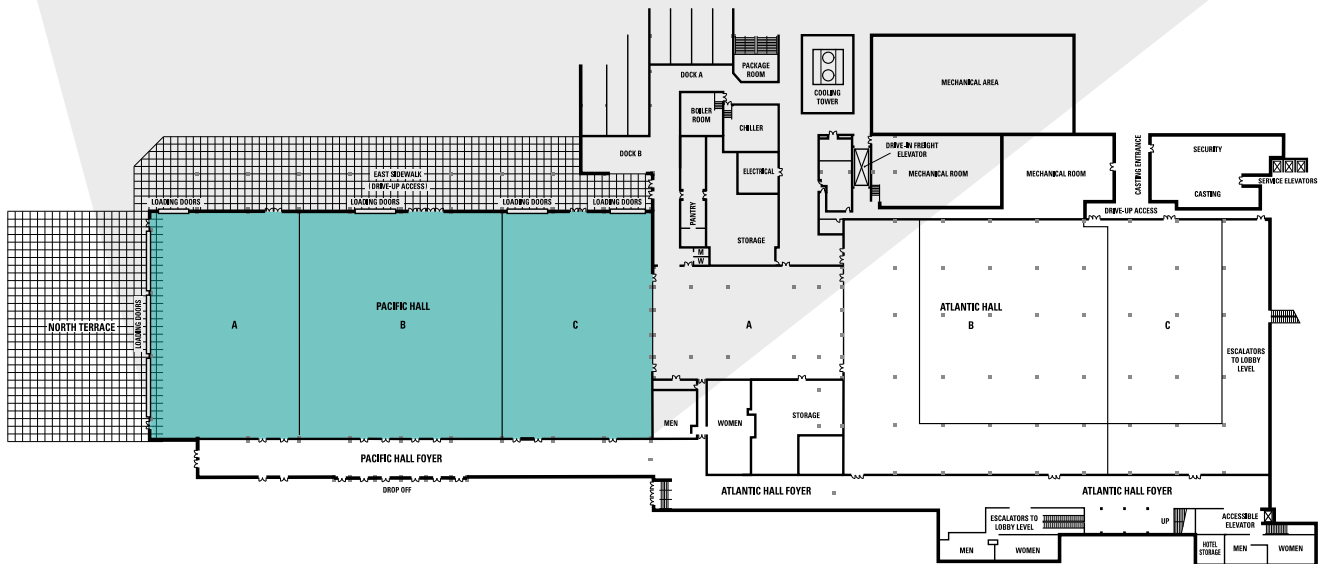
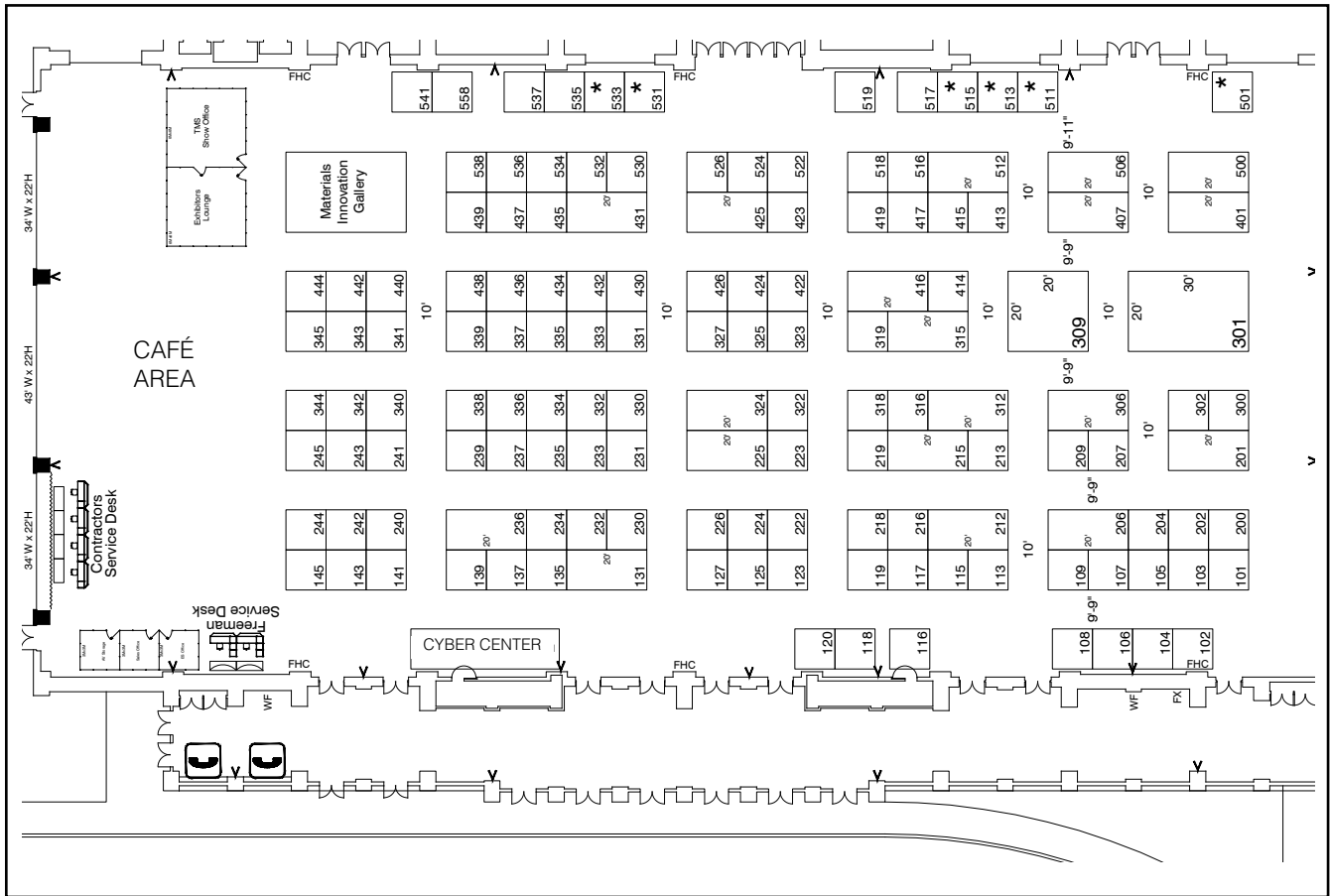
141st Annual Meeting & Exhibition

Exhibiting Companies

(as of January 30, 2012)

Company	Booth number	Company	Booth number
ABB Inc.	300	Harper International	236
Across International	113	Hencon BV	102
Advanced Dynamics Corp., Ltd.	101	Hysitron	416
Advanced Scientific Technology & Management Research Institute	226	ICE Publishing	500
Almeq Norway AS	506	InfoSol Inc.	224
Aluminium International Today (Quartz)	105	Innovatherm GmbH + Co., KG	213
Aluminium Network.com	417	International Aluminium Journal	235
Astrium North America	333	Jordan Valley Semiconductor	107
ATR	316	Kempe International	315
AUMUND Foerdertechnik	501	Light Metal Age	216
Beijing Antaike Information Development Co., Ltd	332	Linde LLC	120
Big C: Dino-Lite Scopes	340	LP Royer, Inc.	204
Boreal Laser	319	Magneco/Metrel, Inc.	322
Brochot	200	Maney Publishing	232
Buss AG	116	Materials Innovation Gallery	441
Buss ChemTech and Laeis	431	Mecfor	430
CA Picard International	415	Metallurgical & Materials Society of CIM	230
Chongqing Runji Alloy Co., LTD. / Okaya (U.S.A.), Inc.	323	Micro Materials Ltd.	432
CIMM	426	Moduloc Ltd., a Rotalec company	434
Claudius Peters	318	MTI Corp.	330
CMI Novacast Inc.	131	MTS Systems Corp.	331
Colt International	104	Nanovea	511
CompuTherm LLC	518	National Filter Media Corporation	519
CSM Instruments	231	Nederman	339
Cytec Industries, Inc.	512	Netsch	327
Daifuku Webb Co/Webb Aluminum	312	NFC - China Nonferrous Metal Industry	425
Danieli Corus Technical Services	115	NIST/Measurement Services Division	222
Dubai Aluminium Co., Inc.	517	NKM Noell GmbH	306
EBSD Analytical	233	Olympus Innov-X	422
EDAX Inc.	218	Opsis	419
EGYPTANODE	424	Outotec Ltd.	309
Eirich Machines, Inc.	522	Parker Hannifin	206
Energoprom	202	Photron Inc.	335
Farra Engineering, Ltd.	526	Precision Light and Air Ltd.	105
Fives Solios	407	Proto Manufacturing	123
FL Smidth	225	RHI AG	516
Gannon University	139	Riedhammer GmbH	513
Gautschi Engineering GmbH	212	Rio Tinto Alcan	301
GE Aviation	207	Sente Software Ltd.	338
GES	219	SLM Co., Ltd.	240
Gillespie + Powers, Inc.	324	STAS	302
GLAMA Maschinenbau GmbH	201	Sunstone	215
GNA alutech, Inc.	103	Techmo Car	413
Goodfellow Corporation	341	Tenova Core	334
Gouda Refractories	414	Thermo Scientific	423
Guangxi Bama Zhengyu Titanium Industry Co., Ltd.	209	Thermo-Calc Software	223
		Tri-State Refractories Corp.	239
		UES, Inc.	108
		University of Central Florida AMPAC	119
		Westmoreland Advanced Materials, LLC	325
		York Linings Intl. Inc.	401

Floor Plan of Dolphin Convention Halls





TMS 2012

141st Annual Meeting & Exhibition

Products & Services Index

Aluminum, Magnesium, & Titanium

ABB Inc.	# 300
Advanced Dynamics Corp., Ltd.	# 101
Aluminium Network.com	# 417
Boreal Laser	# 319
Brochot	#200
Buss AG	# 116
Buss ChemTech and Laeis	# 431
CIMM	# 426
Colt International	# 104
CompuTherm LLC	# 518
Danieli Corus Technical Services	# 115
Dubai Aluminium Co., Inc.	# 517
EBSD Analytical.	# 233
EDAX Inc.	# 218
Fives Solios	# 407
FL Smidth	# 225
GES	# 219
GLAMA Maschinenbau GmbH	# 201
Goodfellow Corporation	# 341
Hencon BV	# 102
Light Metal Age	# 216
LP Royer, Inc.	# 204
Mecfor	# 430
Metallurgical & Materials Society of CIM.	# 230
Nederman	# 339
NFC - China Nonferrous Metal Industry	# 425
Outotec Ltd.	# 309
RHI AG	# 516
Rio Tinto Alcan	# 301
STAS	# 302
Techmo Car	# 413
Thermo-Calc Software.	# 223
Tri-State Refractories Corp.	# 239

Advanced Characterization, Modeling & Materials Performance

ABB Inc.	# 300
ATR	# 316
CompuTherm LLC	# 518
CSM Instruments.	# 231
EBSD Analytical.	# 233
EDAX Inc.	# 218
FL Smidth	# 225
GE Aviation	# 207
GLAMA Maschinenbau GmbH	# 201
Hysitron	# 416
ICE Publishing.	# 500
Jordan Valley Semiconductor	# 107
Maney Publishing	# 232
Micro Materials Ltd	# 432

MTS Systems Corp	# 331
Nanovea	# 511
NIST/Measurement Services Division	# 222
Olympus Innov-X.	# 422
STAS	# 302
Thermo Scientific	# 423
Thermo-Calc Software.	# 223
University of Central Florida AMPAC.	# 119

High Performance Materials

ATR	# 316
Chongqing Runji Alloy Co., LTD. /	
Okaya (U.S.A.), Inc	# 323
CIMM.	# 426
CompuTherm LLC	# 518
EBSD Analytical.	# 233
GE Aviation	# 207
GES	# 219
Goodfellow Corporation	# 341
Gouda Refractories	# 414
Harper International	# 236
LP Royer, Inc.	# 204
Maney Publishing	# 232
MTS Systems Corp	# 331
Parker Hannifin	# 206
RHI AG	# 516
SLM Co., Ltd	# 240
Sunstone	# 215

Materials & Society: Energy & Sustainable Production

Boreal Laser	# 319
EDAX Inc.	# 218
Guangxi Bama Zhengyu Titanium	
Industry Co., Ltd	# 209
ICE Publishing.	# 500
Metallurgical & Materials Society of CIM.	# 230
Nederman	# 339
Olympus Innov-X.	# 422
Outotec Ltd.	# 309
Rio Tinto Alcan	# 301
SLM Co., Ltd	# 240
Sunstone	# 215

Materials Processing and Production

Advanced Dynamics Corp., Ltd.	# 101
Aluminium International Today (Quartz)	# 105
AUMUND Foerdertechnik	# 501
Big C: Dino-Lite Scopes	# 340

Boreal Laser	# 319
Buss AG	# 116
Buss ChemTech and Laeis	# 431-433
CA Picard International	# 415
Chongqing Runji Alloy Co., LTD. /	
Okaya (U.S.A.), Inc	# 323
CIMM	# 426
Claudius Peters	# 318
Colt International	# 104
Cytec Industries, Inc.	# 512
EGYPTANODE	# 424
Farra Engineering, Ltd.	# 526
FL Smidth	# 225
GE Aviation	# 207
Goodfellow Corporation	# 341
Harper International	# 236
Hencon BV	# 102
Hysitron	# 416
Kempe International	# 315
Light Metal Age	# 216
Maney Publishing	# 232
Mecfor	# 430
Metallurgical & Materials Society of CIM.	# 230
MTS Systems Corp	# 331

Nanovea	# 511
Nederman	# 339
NKM Noell GmbH	# 306
Olympus Innov-X	# 422
Outotec Ltd.	# 309
Parker Hannifin	# 206
RHI AG	# 516
Rio Tinto Alcan	# 301
SLM Co., Ltd	# 240
STAS	# 302
Sunstone	# 215
Techmo Car	# 413
Thermo-Calc Software	# 223
University of Central Florida AMPAC	# 119

Nanoscale & Amorphous Materials

ABB Inc.	# 300
CSM Instruments	# 231
Hysitron	# 416
ICE Publishing	# 500
University of Central Florida AMPAC	# 119



© - ALSTOM - Being

COMMITTING FOR TOMORROW

A global leader in equipment and services for the power generation, power transmission and rail transport markets, Alstom has placed sustainable growth at the centre of its strategy, by developing innovative, environmentally friendly technologies. Each day, Alstom's employees, spread throughout more than 70 countries, work to make our future better.

www.alstom.com

We are Shaping the future





TMS 2012

141st Annual Meeting & Exhibition

Company Descriptions

ABB Inc.

ABB Analytical Measurements designs, manufactures and markets high-performance analytical system solutions and spectroradiometers for petroleum, chemical, life sciences, academic, semiconductor, metallurgy and remote sensing/aerospace markets. Building on more than 39 years of experience in analytical instrumentation, ABB has established itself as a worldwide leader in inclusion and hydrogen measurements in liquid aluminum. The company offers a complete range of analytical solutions to the aluminum industry: AISCAN™ hydrogen analyzer, LiMCA inclusion analyzer, Prefil®-Footprinter melt cleanliness analyzer, PoDFA inclusion identification and quantification analysis. ABB also offers metallographic analysis service for its customers.

Booth #300

Almeq Norway AS

ALMEQ Norway AS is an engineering and marketing company for a wide range of equipment and services to aluminium smelters worldwide.

The long term objective for the company is to be a leading supplier of own equipment as well as an export marketing partner for other well accepted manufacturers of machines and equipment for the primary aluminium smelters worldwide.

Booth #506

Across International

Founded and based in New Jersey, United States, Across International supplies crystal substrates, laboratory equipment, in the area of heat treatment and material processing for universities, research facilities and labs. We have more than 15 years of industrial manufacturing experience in drying ovens, ball mills, lab furnaces, pellet presses and pressing dies.

Our goal is to build up business partnerships with friends around the world. We provide quantity discounts and will reply to your requests within the same business day; 100% customer satisfaction is always our first priority.

Booth #113

Aluminium International Today

Aluminium International Today is the aluminium industry's leading international publication reporting on aluminium production and processing. Founded in 1989, it provides a wealth of technical features aimed at equipping producers and processors with information on latest developments. Added to this is a digest of industry news, contracts, events, new technology and conference reports. Supported by the Aluminium Federation in the UK, Aluminium International Today publishes six times a year in English plus two Chinese issues and two Russian issues. E-mail aluminium@quartzltd.com and visit www.aluminiumtoday.com.

Booth #105

Advanced Dynamics Corp., Ltd.

For over four decades, Advanced Dynamics (ADCL) has supplied our global customer base with state-of-the-art material handling systems for carbon plants and cast houses.

Our handling technology includes fully automated or semi-automated equipment for anode handling and cleaning, aluminum ingot and T-Bar handling, sawing and packaging systems. We also have experience in specialty systems for the magnesium, copper, zinc, steel and lead industries.

Booth #101

AluminiumNetwork.com

A Global Network for the Primary Aluminium Industry, AluminiumNetwork.com is your internet-based portal to supply and support you with a wide range of services; your meeting place with like-minded partners who can assist in improving your business and accelerate your project.

The main focus of aluminiumnetwork.com is the primary aluminium industry and it is aimed particularly at:

- Primary producers
- Suppliers of raw materials or intermediates
- Equipment suppliers
- Providers of services, including consulting services and project support.

Booth #417

ADCL is a one-stop shop for your material handling needs including mechanical and controls engineering, fabrication, assembly, test and commissioning. Whether you need a new system or upgrades to existing systems or simply individual pieces of equipment, we can help improve your company's productivity. Remember, "Our ingenuity delivers productivity" when you think of ADCL for your next project.

Advanced Scientific Technology & Management Research Institute

Booth #226

The AluminiumNetwork.com Consultants / Freelancers data base is the perfect source for independent expertise in all of the engineering disciplines, from alumina through to primary aluminum production, including all the support functions of the process. By providing a global platform, AluminiumNetwork.com is THE place to meet with Consultants and Freelancers within the primary aluminum industry. The clients of AluminiumNetwork.com will have access to the Consultants and Freelancers database and will be able to select their required need by qualification and skills.

Please visit www.AluminiumNetwork.com for detailed information.

Company Descriptions

Astrium North America

Astrium North America is a U.S. based company specializing in program and project management, software engineering, external carrier development and integration services, experiment and payload processing, life and physical sciences hardware and flight simulation and training for the international space community.

ATR

The ATR National Scientific User Facility offers materials science engineers and scientists the opportunity to test materials in an irradiation environment and perform analyses on the irradiated specimens. Capabilities available include three test reactors and a host of post irradiation examination facilities across the United States. Non-proprietary research is cost-free to U.S. university led teams.

Access to facilities is through a solicitation and review process: The kinds of research solicited include, but are not limited to, advanced materials for high performance reactor systems, understanding light water reactor core materials including austenitic steels and nickel alloys, determining properties of material joints after exposure to a neutron irradiation environment and the applicability of nanostructured materials to radiation resistant applications.

To learn more about ATR NSUF, please visit our website at: <http://atrnsuf.inl.gov>.

AUMUND Foerdertechnik

With their proven track record in materials handling and storage from mineral processing to hot materials handling the AUMUND Group offers engineered and cost effective solutions for the primary aluminium production process.

Controlled cooling and clean handling of bath material in the primary aluminium smelting process with the AUMUND Cooling conveyor for hot bath material:

- Economical and efficient handling
- Defined cooling from 850°C down to below 100°C
- Drastic reduction of HF emission through controlled suction
- Improved environmental and health conditions
- Reduced investment and operating cost

AUMUND's head office is located in Rheinberg, Germany. E-mail at metallurgy@aumund.de. Contact Person/Designation: Matthias Moritz / General Manager

Booth #333

Beijing Antaike Information Development Co., Ltd

Booth #332

Beijing Antaike Information Development Co., Ltd, relying on the industrial status and background of China Non ferrous Metals Industry Information Center, focuses on researching and analyzing the production, consumption, market, management, and industrial policies of non ferrous metals industry and uses the information within the industry to push forward the overall development of the industry. We provide information and consultancy services for global metals markets, and the construction of enterprise information technology as well as their brand promotion. engineering and production of special mobile and stationary equipment for the aluminium and non ferrous metals industry. The full range of purpose designed machines covers different types of equipment performing a large number of operations in pot-rooms, rodding shops and cast-houses. The Company's aim is to provide the most innovative, rational, cost effective and user friendly technical solutions. Among the most significant families of mobile equipment are the Tapping Vehicles, Anode Transporters, Crucible Transporters and Tilters, Alumina/ AlF₃ Feeding Vehicles, Furnace Charging Vehicles and Furnace Tending Vehicles, Multipurpose Anode Changers and Crust Breakers. Beside its line of stationary equipment such as Crucible Cleaning Machines, the Crucible Tilting stations and the Anode Butts Cleaning Stations.

Big C: Dino-Lite Scopes

Booth #340

Big C offers the Dino-Lite Portable Digital Microscope, which provides high-quality microscopy video interfacing to PC and MAC with clear and steady imaging and 10X–200X magnification. The included software "DinoCapture" makes it easy and convenient to take snapshots, record videos, manipulate images, and save and e-mail discoveries. It is a single lens device with diverse applications.



Company Descriptions

Boreal Laser Booth #319

Boreal Laser makes GasFinder laser based toxic and hazardous gas detectors that are used in a variety of open path (ambient, environmental and safety), stack, vent and process monitoring applications. Portable GasFinders are light, battery operated and easy to set up and use. Multiple path/point GasFinder MC systems can monitor up to eight paths or points with a single analyzer. Both portable and fixed GasFinders are self-calibrating, robust, reliable and maintenance free. GasFinders benefits also include fast one second response, lack of interference from other gases and low cost of ownership. GasFinders are currently available for hydrogen fluoride (HF), hydrogen chloride (HCl), hydrogen sulfide (H₂S), ammonia (NH₃), methane (CH₄), carbon dioxide (CO₂), hydrogen cyanide (HCN), ethylene (C₂H₄) and acetylene (C₂H₂). Typical applications include Aluminum smelting, Refineries (esp. HF Alkylation), Petrochemical and Chemical Plants, Gas Production and Processing, Green House Gas applications, plus Bricks and Ceramics.

Brochot

Booth #200

Brochot SA is the descendent of a very old industrial company going back to the early 19th Century. The Brochot family remained the owners until 1986, when it was bought by its present management.

During the years 1986 to 1992 the new owners were to develop the firm both internally and by external acquisitions along two lines:

- Increasing its sub-contracting work, a thriving activity at the time
- Developing the range of equipment for the production of primary aluminium BROCHOT concentrated on developing and rounding out its know-how in the design and building of special equipment for industry, in the automated "meddle mechanical" area.

Despite having skills and references in other sectors, such as the motor and railway and printing industries, for several years BROCHOT has, for several years seen the bulk of its turnover come from companies producing primary aluminium and magnesium.

Buss AG

Booth #116

Buss AG is an established Swiss manufacturer of value-added mixing and kneading systems for various applications.

The genuine Buss Kneader technology, developed by Buss AG in 1945, has meanwhile made its mark in the aluminium and other industries. Today, more than 2500 BUSS Kneaders are in operation worldwide, 250 thereof in the continuous production of carbon pastes.

For nearly 60 years, the Buss Kneader has been the benchmark for reliable and cost-effective mixing of anode pastes. Now Buss AG is proud to present a new Kneader generation, the four-flighted KX series, designed for even more intensive mixing and micro-dispersion at considerably higher output rates and lower investment cost.

The genuine Buss Kneader technology is the best choice for a reliable low production cost and customer approved production of high quality anodes.

Buss ChemTech and Laeis

Booth #431

Buss ChemTech AG (BCT):

as the world leader in equipment supply and technologies for the aluminium industry based on 60 years experience, offers high developed and fully dedicated applications for Anode manufacturing and Aluminium Fluoride production, covering:

- Modular and fully continuous running Green Anode Plants, e.g. the KAS Carbon Plant in Pavlodar
- Pitch Melting Plants based on unique, highly efficient function incl. appropriate storage
- BCT Paste Kneader with latest major improvements, the most efficient paste preparation application
- Coke Preheater, Paste Cooler and Hydraulic Anode Press integrated to the process

BCT is providing original parts and worldwide on-site support for all maintenance, operating and process aspects to ensure you an efficient and reliable production.

Since September 2011, Buss ChemTech is joining KRESTA Industries, a private owned industrial group with 700 employees, own fabrication facilities and full EPC services. A further step to successfully serve our customers with guaranteed solutions.

www.buss-ct.com

LAEIS GmbH:

offers hydraulic presses MEGA 2500/1600 AV for production of prebaked anodes. These presses are modifications of the renowned HPF presses, supplied more than 600 times to different industries, optimally adapted to anode production requirements. With die areas up to 1800 x 850 mm² and filling depth up to 1400 mm practically all anode formats can be produced. A vacuum system provides for optimal densification and even density distribution over the whole anode volume. The special weighing and mould filling system together with the sophisticated press control guarantees extremely high accuracy and reproducibility of anode weight and height. Depending on anode formats, production capacity is up to 50-60 t/h in a single line. The remarkably lower forming temperature results in higher green strength, avoids a separate water cooling and reduces the emission of PAH and other pitch volatiles.

www.laeis.eu

Company Descriptions

CA Picard International

Booth #415

C.A. PICARD is specialized in manufacturing of high quality wear parts for continuous kneaders for the manufacture of green anodes for the primary aluminum industry.

PICARD manufactures kneading teeth, wearing plates / liners and screw flights out of high wear resistant qualities.

Chongqing Runji Alloy Co., LTD. / Okaya (U.S.A.), Inc

Booth #323

We specialize in producing all kinds of alloying tablets. We are continuing to improve, modernize and expand our company's production capacity in order to increase productivity and efficiency. Our acquisition of the largest Mn ore mines in Jingxi County, Guangxi province of China, has increased our capacity to more than 3 million tons and our new production line of Mn flakes has also been completed with an annual capacity of 30,000 tons. With the development of these programs along with our state-of-the-art production management, technologies and facilities, we can guarantee enough raw material supply at very competitive price levels while maintaining our high level of quality.

Information about our partners: Okaya (U.S.A.), Inc. is an international trading house that provides representation in North America for Chongqing Runji Alloy Company, LTD. This partnership is an example of Okaya's expansion of our business domain from its core area of iron and steel to various related fields of business. We can also perform marketing, logistics and processing functions to fulfill our role as the "Best Global Sourcing Partner". As an independent trading company with a high level of flexibility, Okaya will continue to propose insightful and creative business opportunities by looking at various areas with a broad perspective. Also visit us online at www.okaya.co.jp/en

TMS 2012 MARCH 11-15, 2012 • ORLANDO, FL
141ST ANNUAL MEETING AND EXHIBITION

CARBONE SAVOIE
LEADER IN CATHODIC SOLUTIONS FOR THE ALUMINIUM INDUSTRY

 CARBONE SAVOIE



Company Descriptions

CIMM

Booth #426

As the company certified by ISO9001:2008 and international projects contractor accredited by P.R.China, CIMM GROUP is a healthy and fast growing integrated multinational corporation professionally engaged in providing technology, engineering, manufacturing, trade and EPC service in fields of aluminium and steel, minerals, metals and metallurgy, cement and construction, refinery and petrochemical, ports and shipyards, oil and gas, power generation and transmission, green resource, and energy, etc.

CIMM GROUP is also the leading raw material and equipments supplier for aluminium smelters. Some of the products are aluminium fluoride and cryolite, anode, cathode, silicon metals, refractory, insulation bricks, silicon nitride bonded silicon carbide blocks, CPC, aluminium tablets, etc. and some of equipments are Pot Tending Machine, Stacking Crane, Furnace Tending Assembly, Aluminium Ladle cleaning Machine, Vibration Machine, Anode Clamp, Crush Breaker and assorted Spare Parts, etc., which have been supplied to overseas markets to establish good and steady relationships with Australia, Brazil, India, Russia, Middle East, Kazakhstan, Europe, USA, etc. The supplied products have a great reputation among our customers. CIMM GROUP is always committed to be a trustworthy business partner.

Claudius Peters

Booth #318

In the field of materials handling and processing, from stockyard, pneumatic conveying, silo, clinker cooler, grinding mill and packing & dispatch systems, Claudius Peters are experts in the Cement, Coal, Alumina, Gypsum and Bulk Handling industries.

Claudius Peters Projects GmbH, Germany and Claudius Peters Technologies SAS France are part of the Technologies Division of Claudius Peters Group GmbH, headquartered in Buxtehude, near Hamburg, with regional offices in the Americas, Europe, China and the Far East, offering turnkey and semi-turnkey systems.

The group's other principal division, Aerospace, is engaged in the manufacture of aircraft parts for the European Airbus programme. Claudius Peters Group GmbH is a wholly owned subsidiary of Langley Holdings plc, a privately controlled UK engineering group.

CMI Novacast Inc

Booth #131

CMI Novacast Inc. is a privately held company founded in 1972 as Cast Metals International by Paul R. Gouwens. At that time, it was a consulting firm endeavoring to introduce new technologies to the United States from foreign countries. One of the companies introduced was GAAA of Lyon, France. GAAA was in the business of producing electromagnetic pumps for metering of molten metal.

GAAA opened an office in Elk Grove Village, Illinois, in 1973 to service the North American market. GAAA was purchased by Novatome in 1978, and in 1981 the French government nationalized Novatome with the requirement that all work in aluminum cease. At that time, Cast Metals International changed its name to CMI Novacast Inc. and took over the production and sale of the pumps as designed by Novatome.

CMI Novacast's commitment to all customers is to deliver the most reliable, predictable, and high-performance low pressure or gravity casting system in the industry.

Colt International

Booth #104

Colt is a global supplier and manufacturer of natural and mechanical ventilation systems.

The principal activity of Colt is the supply of specialist products and systems in the field of building services with particular emphasis on gravity ventilation and the environmental control of industrial and commercial buildings. Especially for the aluminum industries, Colt is supplier of

- Static Roof Ventilators for reduction area and anode bake building
- Controllable Air intake louvers for air intake in the basement of reduction, anode bake buildings and cast houses
- Claustra Wall , manufactured from reinforced fiber plastic
- Pot hoods/covers for pots.

MISSION STATEMENT: Our vision is to make the world a better place in which to live and work by helping to make the environment associated with buildings healthy, safe, productive and comfortable.

CompuTherm LLC

Booth #518

CompuTherm, LLC, expertise in thermodynamics and kinetics, develops computational tools for industrial applications in the broad field of materials science and engineering. The products of CompuTherm include the Pandat software and thermodynamic databases for numerous alloy systems, such as Al-, Ni-, Ti-, Mg-, Fe- based alloys. These products are currently used by hundreds of users worldwide. Pandat is a powerful software package for the calculation of multi-component, multi-phase equilibrium and related properties. In addition to the phase diagram calculation and optimization modules,

a precipitation module and a diffusion module are currently being developed in the framework of the Pandat software. In the past 15 years, CompuTherm has collaborated with academic and industrial partners and has worked on many government-sponsored projects. CompuTherm also develops tailor-made software and databases for specific applications, provides consulting services to materials industries and collaborates with other institutions working on challenging programs with potential commercial payoffs.

Company Descriptions

CSM Instruments

CSM Instruments has been leader in the development of instruments for advanced materials testing for over thirty years.

CSM Instruments offers a wide range of instruments and testing services for surface mechanical properties characterization, including: Hardness Testers, Scratch Testers and Tribometers. 3D-imaging options are available with the ConScan or AFM objective. CSM Instruments manufactures standalone instruments as well as testing modules that can be combined together on an automated platform.

Additionally, we have a thorough sample testing service and demonstration laboratory in Boston, MA where you can send us your samples for evaluation or take a firsthand look at our instruments.

Booth #231

Cytec Industries, Inc.

Cytec collaborates with mining companies to optimize their operations through the delivery of innovative chemical technologies. We utilize our superior application expertise to develop solutions based on our customer's specific needs. We offer technologies that:

- Decrease the cost of operations
- Provide better recovery and selectivity
- Process difficult ores
- Prevent or limit employee's exposure to hazards
- Optimize the use of natural resources
- Minimize waste and re-tooling
- Do not require on-staff scientists or engineers

Cytec is committed to partnering with our customers to meet their needs. Our network of technical staff provides on-site technical assistance worldwide. We are dedicated to on-time delivery, even to the worlds harder to reach areas. Our unique approach to servicing our customers has made Cytec the leading provider of reagents to the mining industry.

Booth #512




Connecting with the World through Carbon

WITH THE PRIDE OF CARBON

SK-B[®]
Since 1973

World Best Graphitized Cathode Block from Kyoto, Japan

SEC CARBON, LIMITED

<http://sec-carbon.com>

SK-B[®] is a registered trade mark of SEC Carbon, Limited.



TMS 2012

141st Annual Meeting & Exhibition

Company Descriptions

2012 EXHIBITION DIRECTORY

Daifuku Webb Co/Webb Aluminum

Booth #312

Daifuku Webb Company is a recognized leader in the field of engineered material handling systems and equipment. Our full line of integrated material handling products are computer controlled to efficiently automate rod/anode assembly, and green or baked anode operations.

Our product line includes:

- Automatic Guided Vehicles
- Power and free conveyors
- Roller conveyors
- Heavy-duty chain conveyors
- Automated Storage and Retrieval Systems
- Custom designed automation equipment

From raw materials handling and transport to anode, molten metal, and cast ingot handling to automated storage of work-in-process and finished product, Daifuku Webb Company has nearly 50 years of material handling and control experience in the Aluminum Industry.

Danieli Corus Technical Services

Booth #115

Using proven technology, Danieli Corus helps clients in the primary metals industry achieve maximum performance. We bring reliability, economic benefits and minimized emissions to aluminium producers world-wide.

Based on specialized know-how and vast experience, Danieli Corus offers engineering and contracting services as well as consultancy at all levels of development. Danieli Corus is a client-focused, solutions-driven company. It offers an integrated approach to all aspects essential to success in an increasingly competitive global industry.

Danieli Corus provides efficient, cost-effective and versatile scrubbing technologies for the aluminium smelting industry. We are best known for our proprietary dry scrubbing technology, incorporating the patented vertical radial injection (VRI) system, for the control of emissions from potlines, carbon anode baking furnaces and green carbon plants. Danieli Corus also commissioned the two largest wet scrubbers ever built at an aluminum smelter for the reduction of sulfur emissions from the potlines.

Today, based on our proprietary dry scrubbing technology and our versatile wet scrubbing technology, numerous fume and gas treatment plants have been built for primary aluminium smelters around the world.

Dubai Aluminium Co., Inc.

Booth #517

Dubai Aluminium ("DUBAL") owns and operates one of the world's largest single-site primary aluminium smelters. The DUBAL complex, built on an 480-hectare site in Jebel Ali, Dubai, comprises a one million mtpa smelter, a 2,350 MW power station (at 30°C), a large carbon plant, extensive casting operations (1.267 million mtpa), a water desalination plant and other facilities.

High quality aluminium products are made in three main forms: foundry alloy for the automotive industry; extrusion billet for construction, transport and industrial applications plus billets for forging processes in automotive industries; and high purity aluminium for the electronics and aerospace industries. More than 300 customers are served in at least 45 countries worldwide, predominantly in the Far East, Europe, the ASEAN region, the MENA region and North America. A quality-focused, customer-centered and innovation-drive organization, DUBAL holds ISO 9001, ISO/TS 16949, ISO 14001, ISO/IEC 27001, ISO/IEC 20000-1, and OHSAS 18001 certification.

DUBAL also owns 50% of Emirates Aluminium ("EMAL") in Al Taweelah, Abu Dhabi, where Phase I with a smelter capacity of 750,000 mtpa was fully commissioned by the end of 2010. EMAL Phase II is currently under construction. With a view to securing its alumina requirements, DUBAL has invested actively in greenfield bauxite/alumina projects in Republic of Guinea, Brazil, Cameroon and India. These projects are in various stages of development.

DUBAL's in-house developed, proprietary reduction cell technologies, DX Technology and DX+ Technology (operating at 380 kA and 420 kA respectively), currently rank among the best reduction technologies available. DX Technology has already been installed at industrial scale at DUBAL (40 cells) and EMAL Phase I (756 cells); while DX+ Technology has been specified for EMAL Phase II (444 cells).

EBSD Analytical

Booth #233

EBSD Analytical provides advanced microstructural materials characterization services using EBSD/EDS/SEM techniques. We specialize in providing texture, grain size, ODF, grain boundary analysis, and phase ID including elemental composition. With over 16 years experience in EBSD, you can trust that the results we provide will be of the highest quality.

Company Descriptions

EDAX Inc.

EDAX is a leading provider of innovative materials characterization systems encompassing Energy Dispersive Spectrometry (EDS), Wavelength Dispersive Spectrometry (WDS), Electron Backscatter Diffraction (EBSD) and Micro X-ray Fluorescence (XRF).

EDAX's two TEAM™ analysis systems, TEAM™ EDS and TEAM™ Pegasus are both easy to use and offer Smart Features, which provide analytical intelligence to enable users to easily obtain exceptional results. TEAM™ EDS is the industry's most advanced EDS Analysis System. The newly released TEAM™ Pegasus is a world class materials characterization solution, providing users with both crystal structure and elemental composition results in one easy-to-use EBSD/EDS package. In addition the Orbis micro-XRF elemental analyzer provides small and micro-spot analysis and mapping.

EDAX also offers camera and detector solutions to meet all your analysis needs.

EDAX develops the best solutions for micro- and nano-characterization, where elemental and/or structural information is required, making analysis easier and more accurate. www.edax.com

EGYPTANODE

EgyptAnode is a merchant coke calcining and baked carbon anode production facility, aiming to produce high quality carbon materials to be used in the aluminium industry worldwide. EgyptAnode is set to build its own calciners as a 1st phase of its project, with a 300,000 MT capacity of high quality calcined coke (Anode & Fuel grade) with start-up scheduled in 3rd Quarter 2013, while the anode production is scheduled to be in 2015.

The facility is located in Suez, Egypt, on the Southern entrance of the Suez Canal, on the Red Sea, and a short distance from Egypt's Mediterranean ports, giving it an ideal location to the Middle East market, Europe, and the Americas.

Eirich Machines, Inc.

Eirich Machines designs, manufactures and supplies batch and continuous machinery and systems for the processing of raw materials, compounds, waste and residues in a wide range of industries. Our complete line of products for mixing, agglomerating, pelletizing, grinding, granulating and plasticizing range from laboratory size units to 250 ft³ capacity machines. Eirich High Intensity Mixers can also be equipped with vacuum. The results of this process technology are synonymous worldwide for some outstanding achievements in the solution of problems in diverse applications.

Booth #218

Energoprom Group

Energoprom Group is one of the most efficient companies of non-raw material sector of the Russian economy, runs business globally and supplies more than 50% of its production to the world market.

The Group is the fifth largest world producers of carbon and graphite products.

The main activity - production of high technological electrode, cathode and other carbon and graphite products for steel, aluminum, ferroalloy, silicon, chemical, nuclear and engineering industries.

The Group includes five companies: NovoCherkassk, Novosibirsk, Chelyabinsk Electrode Plants, Doncarb Graphite and Aviauglerod, which are located in close proximity to consumers.

Farra Engineering, Ltd.

Farra Engineering is a New Zealand based company that in conjunction with aluminium smelters in New Zealand and Australia has developed two machines to increase efficiency and safety in the carbon bake plants.

The Pit Maintenance Unit (PMU) provides easy and safe access to the bake pits for routine maintenance, utilizing one or two traversing cages that lower down into the pits. The unit can service up to 8 pits before simply relocating via the overhead crane and the beautifully balanced single point lifting attachment on the unit. To complement this we have developed a Flue Wall Building Station (FWBS) that allow tradesmen to safely and efficiently build the brick flue walls from an elevated platform, utilizing four interconnected rack and pinion drives to keep the flue wall rock steady and perfectly level. The wall drops down after every completed row of bricks and once fully completed it is easily removed for subsequent installation in the bake pits.

Our PMU's are installed in most recent new builds including Qatalum and Emirates Aluminium in the Middle East and the FWBS in the Hydro smelter at Kurri Kurri in Australia.

Booth #522

Booth #202

Booth #526



TMS 2012

141st Annual Meeting & Exhibition

Company Descriptions

Fives Solios

Booth #407

FIVES SOLIOS is one of the companies of Fives, a major International Group, with considerable experience in industrial engineering and management of large projects all over the world. Fives Solios is specifically dedicated to the Aluminium Industry and develops innovative solutions in order to comply with more and more stringent environmental standards while increasing safety and reliability. Fives Solios most particularly works on reducing energy consumption in its process technologies.

- Reduction: Gas Treatment Centers on electrolysis pots and Bath Processing Units.
- Carbon: High Capacity Green Anode Plants, Pitch storage and processing, Liquid Pitch Marine Terminal, Firing & Control Systems for anode baking furnaces, and Fume Treatment Centers on anode baking furnaces.
- Casthouse Area: Melting and Holding furnaces including water cooling systems as well as integration of downstream casting machines, Heat Treatment furnaces for rolling mills and associated control systems.
www.fivesgroup.com

FLSmidth

Booth #225

FLSmidth is your major equipment supplier from Bauxite Mining and Refining through Calcination and Smelting. Every day, worldwide, our equipment crushes, conveys, grinds, digests, clarifies, precipitates, stores, and calcinates bauxite to produce alumina. Combining the respected brand names of MÖLLER, KOCH-MVT, FULLER-TRAYLOR, WEMCO, EIMCO, DORR-OLIVER, PNEUMAPRESS, KREBS, ABON, RAHCO, CEntry, Conveyor Engineering and Raptor, FLSmidth offers a broad range of equipment and processes while increasing recoveries, lowering energy consumption, and providing proven reliability. We also offer metallurgical testing utilizing the expertise of FLSmidth Dawson's metallurgical laboratories. FLSmidth is your One Source, One Partner providing integrated solutions that will save you valuable time on your project schedule!

2012 EXHIBITION DIRECTORY



Solid leadership in a constantly *changing* world.

With a global reach spanning six continents, Koppers is a leading integrated producer of carbon compounds and treated wood products essential to many world industries.

True leadership begins with Koppers employees. We embrace safety, health, environmental stewardship and personal integrity in everything we do and in every product we produce. We give back to our communities in so many ways and we don't just talk sustainability, *we live it.*

To learn more about our standards of leadership, visit us at www.koppers.com.



436 Seventh Avenue Pittsburgh, PA 15219-1800
www.koppers.com

Company Descriptions

Gannon University

Booth #139

Founded in 1925 in Erie, Pennsylvania, Gannon University is a comprehensive Catholic institution that encourages the professional and personal growth of its students through a holistic education. Gannon University offers an Online Master's in Engineering Management (MS-EM) degree designed to help professional engineers put their careers on track for increased responsibility as an engineering manager or project director. The online engineering management program curriculum blends the best in advanced engineering studies and advanced coursework in business. Engineering professionals who complete Gannon University's MS-EM are poised to assume additional leadership responsibilities to advance their career.

Gautschi Engineering GmbH Booth #212

Gautschi Engineering GmbH is a leading supplier of equipment for primary aluminum casthouses and recycling plants.

The product range of Gautschi™ includes:

- Melting – and holding furnaces
- Pusher-type furnaces for rolling slab
- Homogenizing furnaces for extrusion billet and rolling slab
- Multiple chamber furnaces for coil and foil annealing
- Single coil annealing furnaces
- Horizontal D.C. casting plants
- Open mould ingot casting and stacking plants
- Vertical D.C. Casters for extrusion billet and rolling slab
- AIR GLIDE® and AIRSOL VEIL® mould technology

GE Aviation

Booth # 207

GE Aviation is the world's leading producer of large and small jet engines for commercial and military aircraft. We also supply aircraft-derived engines for marine applications and provide aviation services. GE Aviation's technological excellence, supported by continuing substantial investments in research and development, has been the foundation of growth, and helps to ensure quality products for customers.

GES

Booth #219

GES, supplying quality graphite to various industries for over 25 years, represents some of the leading graphite producers worldwide. The fine grain extruded, molded and iso-molded grades cover three distinct grain sizes. Offerings include cathode blocks, rods for molten metal pump shafts and support posts, large block for pump bases, and rounds for rotor heads. GES provides competitive pricing, technical support, and convenient warehousing to meet your needs. Our Technical Sales personnel will be available in our booth to discuss your application and which grades will meet your requirements.

Gillespie + Powers, Inc.

Booth #324

A Corporation engaged in the design, supply, installation, and maintenance of industrial aluminum melting and process furnaces, refractory systems, acid-proof construction, and specialty refractories, as in waste incineration.

GLAMA Maschinenbau GmbH

Booth #201

GLAMA has designed and built heavy-duty Equipment for Aluminium pot rooms, cast houses and anode rodding shops throughout the world for more than 50 years. The following type of equipment is available:

- Anode Changing Vehicles
- Hammer Crustbreakers
- Tapping Trucks
- Anode Pallet Transporters
- Furnace Charging Machines
- Furnace Tending Machines
- Ladle Charging Trucks
- Butt Cleaning Manipulators
- Coil Lift Trucks
- Molten Metal Carriers

GLAMA's experience of many years of producing machines with a unique combination of advanced control and rugged, reliable construction is evident in the several hundred machines now in service. GLAMA equipment withstands the heat, dust, vibration and battering of heavy industry while delivering precise handling performance.

More details: www.glama.de

GNA alutech, Inc.

Booth #103

A comprehensive range of equipment and unsurpassed reliability and efficiency are at the heart of GNA alutech's success. Leading aluminum works all over the world rely on GNA alutech products and technologies, proof of the company's capacity to respond to the multiple needs and stringent requirements of its clients.



Company Descriptions

Goodfellow Corporation

Booth #341

Goodfellow supplies small quantities of metals, alloys, ceramics and polymers to meet the research, development and specialist product requirements of science industry worldwide.

The company offers two distinct services:

The first meets the needs of those customers who require small quantities of our standard catalog products for immediate shipment.

The second is for those who require larger quantities or further processing of the company's standard products, or who need products which fall within our general supply capabilities.

Our web catalog lists a comprehensive range of materials in many forms including rods, wires, tubes and foils. There is no minimum order quantity and items are in stock ready for immediate shipment worldwide with no extra shipping charge. Custom made items are available to special order.

Visit Goodfellow Corporation at website: www.goodfellowusa.com or e-mail info@goodfellowusa.com

Gouda Refractories

Booth #414

Gouda Refractories is an innovative refractory producer (refractory bricks, castables, mortar, self-flowing castables, complex pre-cast shapes) with global experience and a long track record of supplying superior quality refractories all over the world, combined with innovative installation technology for more than 100 years.

Gouda Refractories develops, manufactures, sells and installs top quality refractory linings. Gouda's solutions play an important role in, non-ferrous metal (mainly aluminium), petrochemical, environmental and energy industries. Based on an industry-oriented structure and highly competent employees, Gouda Refractories guarantees an optimal support which results in efficiency and reduction of refractory cost. Gouda Refractories supplies total solutions to customers which are cost effective, state of the art, and reliable. Gouda's R&D department is conducted in close co-operation with its customers and renowned research institutes. Gouda's quality assurance is based on the international ISO 9001 standard.

Guangxi Bama Zhengyu Titanium Industry Co., Ltd

Booth #209

Guangxi Bama Zhengyu Titanium Industry Co., Ltd is a professional manufacturer of Aluminum master alloys and Aluminum alloying additives in China. We always take innovation as the power of development. We are highly professional, well educated, diligent and full of vigor. In principle of good honesty, equality and mutual benefits, we always keep the modest and prudential attitude, develop more new products, make more friends globally, and provide our customers with qualified products and good service.

Harper International

Booth #236

Harper International is a global leader in complete thermal processing solutions, as well as technical services essential for the production of advanced materials. Harper serves advanced, cutting-edge material markets with custom-engineered thermal processing systems. Our support to these emerging industries begins in early stages of research and development, whether at corporate R&D centers, universities, government institutions, or start-ups. Harper is a partner through the entire development process assisting in the scale up and commercialization of advanced materials that will change our everyday lives. One thing you won't see at Harper is a cookie cutter line of products that we work to fit into your requirements. We specialize in first-of-a-kind solutions using our exceptional depth and breadth of knowledge. Harper's culture is one of real ingenuity and creativity – we are constantly challenging ourselves to craft the best-engineered technology solutions for our customers' needs.

Company Descriptions

Hencon BV

Hencon provides a complete range of heavy duty vehicles and vacuum technology solutions for aluminium smelters, aluminium foundries, light metal producers, industrial plants and mining applications. Originally a Dutch company, we developed a broad experience in the supply of solutions for customers in the light metal industry. With our solutions we want to make the difference for our customers and commit ourselves to measurable cost savings. Therefore we design machines that are safe to use and easy to operate and maintain. While at the same time our company is committed to offering you the support you require to make your business a success.

We think global and act local. This resulted in the unique concept of business units of Hencon on your doorstep: such as our service and production plants in the Netherlands, Russia, South Africa, Mozambique and India up to today.

Our goal is to offer our customers solutions to enable them to strive for continuous operating excellence in the lower cost curve of the industry.

With Hencon, you select a partner who has over 55 years of experience in the industry. We translate this knowledge into a durable partnership that shows commitment, creativity and entrepreneurship, in order to make our customers excel.

Whenever you would have questions about vacuum technology solutions, transport equipment and plant logistics; feel free to contact us for:

- Feasibility studies
- Know-how and analyses
- Training
- Support
- New equipment
- Maintenance solutions

Hencon offers tailor-made solutions with a clear eye for your specific needs and production processes. Combined with our know-how, we make the difference with solutions that offer you value for money.

Our clients can be found worldwide in the following countries: Argentina, Australia, Bahrain, Belgium, Brazil, Canada, China, Czech Republic, Denmark, Egypt, France, Germany, Greece, Hungary, Iceland, India, Indonesia, Cameroon, Mexico, Montenegro, Mozambique, Netherlands, New Zealand, Norway, Oman, Poland, Qatar, Romania, Russian Federation, Saudi Arabia, Slovakia, Slovenia, South Africa, Spain, Sweden, Switzerland, Turkey, United Arab Emirates, United Kingdom, United States of America and Venezuela.

Booth #102

Hysitron

As world leader in nanomechanical test instruments, Hysitron is dedicated to providing next-generation testing solutions for nanoscale mechanical characterization. Hysitron's nanomechanical test instruments provide in-situ SPM imaging in addition to the quantitative measurement of multiple mechanical properties, including hardness, modulus, fracture toughness, interfacial adhesion, and wear resistance. Our instruments feature a full suite of advanced complementary techniques, including nanoDMA® III to continuously obtain elastic-plastic and viscoelastic properties of materials as a function of indentation depth, frequency, and time. Additional Hysitron hybrid techniques include nanoECR® for simultaneous electrical and mechanical property measurements, Modulus Mapping for high resolution property mapping, and elevated temperature testing to determine material properties at operating or processing temperatures. Stop by our booth to see how the industry-leading TI 950 TriboIndenter redefines the world of nanomechanical testing. Hysitron will also be showcasing the PI 95 and PI 85 PicoIndenter®, truly quantitative depth-sensing indenters capable of in-situ observation during testing inside a TEM and SEM.

Booth #416

ICE Publishing

Booth #500

ICE Science is the new flagship journal collection from ICE Publishing inspiring fresh thinking on how breakthrough research can be practically applied to make energy, materials and medicines ever more efficient and effective. Launching with a series of full-color, bi-monthly journals in 2012, the collection aims to deliver a truly holistic overview of each scientific discipline, bringing together communities that traditionally work in silos to ensure important discoveries and applications are accessible to all those in the field. The first two editions of 'Bioinspired, Biomimetic and Nanobiomaterials', 'Emerging Materials Research' and 'Nanomaterials and Energy' are available free on our booth.

ICE Publishing is the publishing division of the Institution of Civil Engineers (ICE). We produce a wide range of publications sharing expert advice, leading research and best practice. With a history of making research in engineering and allied sciences practically useful since 1836, we offer a unique breadth of experience.



Company Descriptions

InfoSol Inc.

Booth #224

InfoSol is a leading provider of Business Intelligence solutions. With an in-house product development team and partnerships with other leading Business Intelligence solutions providers around the world, InfoSol offers the "best in class" and most innovative add-on solutions. These solutions include InfoBurst for Automated Report and Dashboard Bursting/Publishing, along with Intelligent Cache Query for optimal Xcelsius dashboard performance and scalability.

Having more than fifteen years experience in providing end-to-end Business Intelligence applications, InfoSol sees beyond the data to deliver visionary solutions that inspire.

Innovatherm GmbH + Co., KG

Booth #213

Innovatherm is the competent partner and the world market leader in anode baking technology. As a subsidiary of the LINGL Company, innovatherm operates in the aluminium industry, providing full service in combustion technology for reconstruction, fine tuning and optimization of existing anode baking furnaces as well as new furnaces including dry adsorption fume treatment plants.

For this purpose, Innovatherm has developed excellent process technologies and concepts with mathematical models, special components for the combustion like burners and gas valves, and future oriented control philosophies for optimal process management as well. For best results these concepts are custom-tailored to maximize plant safety, efficiency and economics.

Latest products established in the market are:

- ProBake Advanced Firing Systems for anode baking furnaces
- ProClean Fume Treatment Plants for the aluminium industry
- ProCast Supervisory Control Systems for primary and secondary Casthouses incl. charging management, target alloy calculation and melting optimization

International Aluminium Journal

Booth #235

International ALUMINIUM Journal deals with all facets of aluminium's value chain from the production of the metal via its processing through to recycling. The editorial focus is on smelting and semis production including the suppliers of plant, equipment and technology. Consideration is given to economic, technical and environmental/ecological topics as well as other aspects that affect the metal and its product applications in the different target markets. Aluminium relevant research articles from companies and institutes are also published. The publication is thus of particular interest to smelters and remelters, semis producers, foundries, fabricators and converters, metal traders, semis stock holders and research facilities. International ALUMINIUM Journal is circulated in over 40 countries worldwide – made in Germany, distributed to the world. Published by Giesel Verlag GmbH; visit www.alu-web.de and www.giesel.de.

Jordan Valley Semiconductor

Booth #107

Jordan Valley is the leaders in X-ray metrology for semiconductors and thin films, with a range of products to suit all needs. Our products range from fully automated systems for specialist semiconductor fabs (JVX range) through to diffractometers for compound semi manufacturers (QC3, QC-Velox and QC-RT) and state of the art general research diffractometers (D1).

With the acquisition of Bede Scientific in 2008, Jordan Valley has over 30 years experience in a wide range of X-ray metrology methods including X-ray diffraction (XRD), X-ray reflectivity (XRR), high resolution XRD (HRXRD), X-ray Fluorescence (XRF) and X-ray topography (XRT). The systems are designed to be simple to use yet powerful enough to perform the most demanding measurements. Automation of the alignment, measurement and analysis is available on all systems to remove the necessity of highly trained operators being required for routine measurements. The simulation software (RADS, REFS) is generally regarded as the industry leader for HRXRD and XRR analysis.

Jordan Valley systems are installed in major semi manufacturers production lines, R&D labs, LED manufacturers, GaAs and InP production lines as well as many universities and research institutes worldwide.

Company Descriptions

Kempe International

Booth #315

Kempe is the largest provider of asset and maintenance services in the aluminium smelting industry and has the most extensive product range for the aluminium smelting industry and is one of the top five global suppliers.

Kempe is currently supplying the Anode Rodding Shop and Anode Handling System for Ma'aden Aluminium and the Bath Treatment Plants for Hindalco Mahan & Aditya Smelters. We have recently installed the CBF4 Anode Handling & Transfer System at Boyne Smelters.

Kempe works for 30 smelters in 21 countries across 7 regions – Australasia, Middle East, Africa, Asia, Europe, North America, and South America. Kempe has in-house manufacturing in Australia, China, UAE & Mozambique.

Kempe has more than 2,000 employees globally, which includes in-house construction crews & equipment.

Kempe will be available at TMS to discuss potential client requirements in the various areas of aluminium smelting including – Anode Handling & Cleaning, Rodding Shops, Bath Removal (hot & cold), Bath Cooling & Processing, and other Carbon, Potroom and Casthouse equipment.

Light Metal Age

Booth #216

Light Metal Age is the pre-eminent magazine of the light metal world. In 2012, we are pleased to celebrate our 70th anniversary of publication, covering primary production and semi fabrication of the light metals aluminum, titanium, and magnesium. Circulation is international and goes to primary and secondary smelters; casthouses; extrusion operations; rolling mills; sheet, rod, and wire mills; and foundries. Coverage of associated metal processes and equipment includes DC casting, surface technologies such as anodizing, furnaces and melting, degassing and filtration, automation and instrumentation, and handling. Recipients are executives, general managers, plant managers, technicians, metallurgists, chemists, and engineers responsible for fabrication, production, and operations.

Light Metal Age also produces select article archive content on CDs, including the Titanium Article Archive (Nov. 1945 – Aug. 2009) and the Magnesium Article Archive (May 1943 – August 2011), as well as the Aluminum Extrusion Article Archive (July 1943 – April 2011). For more information, visit Light Metal Age on the web at www.lightmetalage.com.

Linde LLC

Booth #120

Linde, a leading global industrial gases company, provides industry-leading portfolio solutions for the aluminum industry ranging from gases and equipment to process consulting and services. These solutions enable our customers to increase productivity, lower fuel consumption and other costs and reduce emissions.

We offer dedicated applications for every step in the aluminum process chain, all designed to help you reduce fuel consumption and emissions, and improve quality:

- Low-temperature oxyfuel melting technologies to increase the melt rate, cut energy costs and reduce emissions
- Refining to improve the quality of the final product by purging the melt with gases to remove hydrogen, non-metallic inclusions and unwanted trace elements
- Heat treatment in the form of annealing in a protective nitrogen atmosphere to reduce oxidation and discoloration
- Extrusion cooling and shrouding with liquid nitrogen to raise production rates, improve surface finish and increase die lifetime.

LP Royer, Inc.

Booth #204

For all workers in the metallurgical industry, L.P. Royer is your "one stop" supplier for specialized and innovative safety footwear since 1934, visit us and see "THE SMELTER BOOT". The XPAN® soling technology, unique to L.P. Royer in North America, adds to the mix to bring you a lighter dual density rubber sole that protect from heat and extreme cold and offer superior traction, shock absorption and durability. With our wide range of adapted protection including internal and external metatarsal protection, nonmagnetic toe protection you will find the best style for you. L.P. Royer products meet CSA, ASTM CE marking quality standards.

Maney Publishing

Booth #232

Maney delivers a personalized service to authors, societies, readers and libraries for the publishing and international dissemination of high quality, peer-reviewed scholarly research.

Specializing in print and electronic journal publishing, Maney is committed to technical and editorial innovation combined with traditional values of quality and collaboration.

Maney publishes an impressive collection of highly regarded, peer-reviewed journals covering both niche and general topics in materials science and engineering. Coverage ranges from fundamental research to engineering application and from the extraction and refining of minerals to the characterization, processing and fabrication of materials and their performance in service.



Company Descriptions

Materials Innovation Gallery Booth

#441

Welcome to TMS's showcase of ideas on how the techniques and principles that form the foundation for Materials Innovation @ TMS—the Society's exciting new strategic initiative—can revolutionize the design, development and deployment of advanced materials.

Browse the gallery of scientific and technical posters and displays that present "materials innovation in action." Network with individuals and companies who offer tools, support, and services that can enable you to implement these approaches within your own organization or team. Learn about the array of resources and opportunities that are being offered as part of Materials Innovation @ TMS. A special feature of the TMS 2012 Exhibition, the Materials Innovation Gallery will be open throughout the conference during regular exhibit hours, so stop by often!

Materials Innovation @ TMS is focused on significantly reducing the time and costs associated with materials development through the advancement of a seamless and dynamic innovation infrastructure that unifies and streamlines design and manufacturing processes. The Materials Innovation Gallery

has been designed to provide a visually compelling glimpse of how these concepts can potentially transform the future of materials and manufacturing innovation.

Mecfor Booth

#430

For the last 15 years, we have design and manufactured specialized equipment for the Aluminum production sector. We are present in many countries worldwide and part of the 4 or 5 worldwide manufacturers, thus the only one in America. Our main products are, crucible carriers, anode carriers, anode grooving, descaling robots, skimming stations, mobile equipment for loading, custom made specialized equipment.

Metallurgical & Materials Society of CIM

Booth #230

We are a world class Canadian organization that serves society and the needs of professionals in the global metallurgy and materials community. The purpose of MetSoc is to serve our members, society and others involved in the research, development and application of the science and technologies for the environmentally responsible extraction, fabrication, utilization and recycling of metals and materials

Anode Baking Furnace



- Refractory Bricks & Special Shapes (Low Creep 42% to 55% Al₂O₃)
- Heat & Air Setting Refractory Mortars
- Precast Prefired Monoblocks for Flue Walls
- Burner Blocks & Roof Anchors

Aluminium Melting/Holding & Reverberatory Furnaces


- Phosphate Bonded Non-wetting Bricks & Mortars (upto 85% Al₂O₃)
- Chemical Bonded Ramming Refractory for Repair Lining
- High Alumina Bricks & Mortars (42 to 60% Al₂O₃)
- Non-wetting Castables for Metal Contact Lining

Hot Metal Transfer Ladles

- Non-wetting Monolithics Lining
- Thermal Shock Resistant High Alumina Brick Lining

REFRACTORY SOLUTIONS FOR THE ALUMINIUM INDUSTRY




Aluminium Cast House

- Monolithic Lining for Degasser
- Wear Resistant Precast Prefired Shapes & In-situ Castables for Metal Conveying Line

Aluminium Pot Cell

- Dry Impervious Material
- High Strength Castable Material (Claycrete Al)
- Castable C 640
- Clayburn Bedding Mix

DRI-BARRIER MIX® INSTALLATION



30D, Jawaharlal Nehru Road, Kolkata - 700 016, India
Tel. : +91 33 2249 6507

Works : Ipitata Nagar, Dhenkanal - 759013, Odisha, India
Tel. : +91 6762 228071, 228928, E-mail : mktg@nilachal.in

www.nilachal.in

Company Descriptions

Micro Materials Ltd

Booth #432

Micro Materials Ltd (MML) - A wealth of mechanical property measurements in one instrument: The NanoTest Vantage system carries out a range of nanomechanical property measurements:

- Nanoindentation
- Nano-scratch and wear
- Nano-impact and fatigue
- Nano-fretting

Optimize material properties under true "in-service" conditions: The instrument can operate under a range of environmental conditions: high temperature up to 750 C, in liquids, and under non-ambient gases.

Unique capability: The high temperature testing module allows testing of a sample heated up to temperatures of 750 C. The patented MML nano-impact and fatigue system affords unrivalled information on fracture and fatigue behavior.

A trusted manufacturer: Established in 1988, MML's global customer base includes leading research institutes such as MIT, Cambridge and Oxford Universities.

Details from: Denise Hoban, International Business Development Director, denise@micromaterials.co.uk or www.micromaterials.co.uk

Moduloc Ltd, a Rotaloc company

Booth #434

- Engineered Solutions for the Metals Industry
- Industrial Sensors and Measurement Systems
- Laser Based Measurement Systems of hot or cold product for length, width or positioning
- Industrial Part Marking and Reading Solutions
- Digital Laser Level Counters
- Industrial Vision Systems
- Hot Metal Detectors
- Wireless Safety and Radio Remote Control
- Material Handling Solutions

MTI Corp

Booth #330

MTI Corporation, founded in 1994 by a group of material researchers from MIT and UC Berkeley, has now become the leading manufacturer of oxide crystals and substrates in the world, thanks to venture capital from Silicon Valley. MTI continues to develop new crystal substrates and maintain high quality of its single crystal substrates. MTI is equipped with the latest state of the art instruments, which allow achievement of the highest standard. We strive continuously to keep pace with customers' increasing demands on super-smoothness, super-flatness, and super-cleanliness. In 2000, by popular demand, MTI started to manufacture precision bench-top machines for material processing, analysis, and crystal wafer containers.

MTI currently operates three production factories in China. This allows for the possibility of providing high quality and low cost precision machines for material research and R&D Labs, including: low speed cutting saw, wire diamond saw, auto polishing machine, high temperature oven, tube furnace, X-Ray crystal orientation machine, and Mini XRD, as well as complete set of equipments for research of rechargeable battery materials. Simple to operate, low cost, and commitment to our customers is our priority. MTI strives to become the world's leader in bench-top machines for material lab.

MTS Systems Corp

Booth #331

Engineers and researchers worldwide rely on MTS for the testing technology and expertise required to support the research, development and production of advanced metals, composites and ceramics. Reliable, high-performance MTS solutions are deployed across a diversity of industries such as aerospace, power generation, civil engineering and automotive, accurately and efficiently meeting the most demanding materials testing requirements.

The MTS portfolio is engineered to address a full spectrum of materials testing requirements - from tension/compression to fracture mechanics to complex multi-axial fatigue studies at elevated temperatures. This portfolio features: high-performance servohydraulic, static-hydraulic and electromechanical testing systems; versatile, high-resolution controls; proven application software; precision accessories; robust environmental simulation systems; and unmatched service and support.

Explore the MTS booth and discover how innovative MTS test solutions and decades of industry expertise can optimize the effectiveness and efficiency of your materials research, development and production programs.

Nanovea

Booth #511

Nanovea designs and manufacture Profilometers, Mechanical Testers & Tribometers to combine the most advanced testing capabilities in the industry: Scratch Adhesion, Indentation Hardness, Wear Friction & 3D Non-Contact Metrology at Nano, Micro & Macro range. Unlike other manufactures Nanovea also provides Laboratory Services, offering clients availability to the latest technology and optimal results through improvements in material testing standards.



Company Descriptions

National Filter Media Corporation Booth #519

At National Filter Media we take pride that we are one of the world's oldest and largest providers of air pollution control and liquid filtration products. NFM has achieved success by adhering to the same business principles practiced since the firm was founded in 1906. We believe in building partnerships with our customers and in earning their business every day. The technology has changed since 1906, but our commitment remains the same. We want to be long term partners with our customers.

Nederman Booth #339

Nederman has been in business since 1944 and is one of the world's leading companies supplying products and services to protect our environment. The new headquarters in Thomasville, NC and sales/manufacturing in Westland, MI and Reno, NV bring even greater capabilities to design, manufacture, install and service our products nationwide, providing you with complete turnkey solutions.

Our new product offering includes systems for the extraction and filtration of dust, gas, smoke, and automobile exhaust fumes, equipment for industrial cleaning, as well as at source extraction equipment and clamp-together ducting.

Netzsch Booth #327

Thermal analysis, calorimetry, thermal properties, & contract testing services; DSC, DTA, TGA, STA (Simultaneous DSC/DTA-TGA) from cryogenic to +2400C, evolved gas analysis by coupled FTIR, MS, and a new GC-MS system, adiabatic reaction calorimeters (ARC & APTAC) to measure thermal & pressure properties of exothermic chemical reactions, new MMC 274 tabletop reaction calorimeter, dilatometers, thermal conductivity, thermal diffusivity by laser flash & xenon flash to +2800C, DMA, TMA, and DEA - dielectric analysis for in-situ thermoset cure monitoring.

NFC - China Nonferrous Metal Industry Booth #425

China Nonferrous Metal Industry's Foreign Engineering & Construction Co., Ltd. (NFC) was founded in 1983. It is a state-controlled holding company listed on Shenzhen Stock Exchange in 1997. As a China leading enterprise engaged in general contracting of overseas nonferrous metal (particularly aluminum, copper, zinc and etc.) projects and resources development, it covers a wide spectrum from technical assistance, engineering design, equipment manufacturing, construction, supervision, installation and training to mining, beneficiation, smelting, processing and etc. It is also listed on ENR as one of the top 225 international contractors for consecutive years. With competitive edges in technology and rich experience in EPC contracting, NFC has consistently

been dedicated to global nonferrous metal industry. NFC is capable and willing to work with world partners by providing a portfolio of services including technologies, equipment supply and management.

NIST/Measurement Services Division Booth #222

NIST Standard Reference Materials supports accurate and compatible measurements by certifying and providing over 1300 Standard Reference Materials with well-characterized composition or properties, or both. SRMs are used to perform instrument calibrations as part of overall quality assurance programs, verify the accuracy of specific measurements and support the development of new measurement methods. The Standard Reference Data Group has provided well-documented numeric data to scientists and engineers for use in technical problem-solving, research, and development. The Calibration Services are designed to help the makers and users of precision instruments achieve high levels of measurement quality and productivity.

NKM Noell GmbH Booth #306

NNSC has built a strong technical force based on specialists who individually have up to 25 years experience in Primary Aluminium Industry for Potroom as well for Carbon Area, being the only independent equipment supplier.

For more than 40 years on the market through its constitutive companies, with more than 1,000 cranes in operation worldwide, NNSC is developing its mission for the Primary Aluminium Smelters and Nuclear plants:

- To be a global supplier of handling systems, process equipment and solutions,
- To integrate the client's process objectives in the design of the products through a continuous flow of mutual exchange.

Olympus Innov-X Booth #422

Olympus Innov-X provides portable handheld X-Ray Fluorescence (HHXRF) analyzers for simple, non-destructive sorting of challenging grade separations, alloy chemistry and grade ID in seconds. They provide highly specific material chemistry to rapidly and accurately identify pure metals and alloy grades. HHXRFs allow for testing of literally thousands of types of materials anywhere, anytime. For scrap recycling applications, our HHXRFs provide reliable ID in 1-2 seconds for most grades. They are designed for durability – to withstand the tough processing environment. Our HHXRFs are used for fast, reliable alloy sorting and analysis for a wide variety of ferrous and non-ferrous material. We provide optimized HHXRF configurations for cost-effective analysis when time is of the essence and when materials cannot be transported, damaged, or altered. Our X-5000 Mobile XRF analyzers offer maximum portable power with a closed beam configuration

Company Descriptions

and large touch screen interface.

Opsis

Booth #419

Opsis is a worldwide supplier of gas monitoring systems for process control applications, industrial continuous emission monitoring and ambient air quality and fence-line monitoring.

Systems use open path UV-DOAS, FTIR and laser diode TDL technologies. Monitoring solutions are provided as integrated systems including gas measurements, additional sensors such as flow and temperature and software applications for reporting and networking.

Opsis systems have been implemented in applications in a wide range of industries globally, including aluminum smelters, power plants, incinerators, cement plants and sulfuric acid production plants.

The Opsis system does not need to extract any sample of the gas making it effective to measure reactive components such as ammonia, and strong acids. Same is applicable in case gas condition is either extremely corrosive or hot, or both.

Gaseous components that can be measured include, for example: SO₂, SO₃, NO_x, CO, CO₂, H₂O, NH₃, HCL, HF, CL₂, CLO₂, HCHO, BTX, O₃, Hg, HgTot. Measurements are certified under TUV, MCERTS and EPA.

A worldwide network of skilled distributor companies is available for sales and support. Opsis is a ISO 9001 and ISO 17025 certified company.

Outotec Ltd.

Booth #309

Outotec develops and provides technology solutions for the sustainable use of Earth's natural resources. As the global leader in minerals and metals processing technology, Outotec has developed several breakthrough technologies. Outotec serves the light metals industries including the provision of cutting-edge alumina refineries and aluminum smelters. The company has over 50 years experience helping customers worldwide in both segments of the aluminum process to reach their goals. What sets Outotec apart from its competition?

They are there to help their customers from start to finish in terms of plant design, and they customize solutions to fit a client's specific needs. Outotec's processes and equipment have become industry standards and their references stretch back decades – a track record that has led to their current reputation as a leading innovative technology partner. The company also offers innovative solutions for the chemical industry, industrial water treatment and the utilization of alterna-

tive energy sources.

Parker Hannifin

Booth #206

Parker is the world's leading diversified manufacturer of motion and control technologies and systems. Parker provides precision engineered solutions for a variety of commercial mobile, industrial and aerospace markets. We design and manufacture optimal systems using fluid connectors, hydraulics, pneumatics, instrumentation, refrigeration, filters, electromechanical components, and seals required in motion control systems. Parker's experience in the aluminum industry spans more than 40 years. Parker has equipped machinery in all phases of aluminum production including smelters, casters and extruders through grinders, rolling mills and strip processing lines, etc.

Photron Inc.

Booth #335

Photron offers a wide range of high-speed cameras; from HD resolution to 2,000 frames per second (fps), through dual miniature heads providing 2K fps for real time image processing, to the world's fastest mega pixel high speed camera providing reduced resolution to over one and a half million fps.

Precision Light and Air Ltd.

Booth #105

Precision Light and Air (PLA) is an Australian based industrial instrumentation manufacturer specializing in process analyzers for mining and metals industries. These analyzers are particularly suited for high temperature and high scale applications as in alumina and nickel refineries. Our flag ship Smartdiver is regarded as the industry standard for measuring mud level, clarity, interface and tank profiles in the most hostile operating environments. Other analyzers supplied globally by PLA include non-nuclear density gauges, slurry liquor phase density refractometers, inline ceramic conductivity meters and suspended solids meters. With a support team ranking second to none, PLA remains a premier solution provider in industry.



Company Descriptions

Proto Manufacturing

Booth #123

PROTO Manufacturing is a leading provider of portable and laboratory based x-ray diffraction systems and services including:

- X-ray diffraction residual stress measurement
- X-ray diffraction retained austenite and nitride analysis
- Laue single crystal orientation systems
- Custom powder diffraction systems
- Fine focus and micro focus x-ray tubes
- Electropolishers

PROTO Manufacturing also provides measurement services through its laboratories in the United States, Canada and Japan. Visit online at <http://www.protoxrd.com> or by e-mail at xrdlab@protoxrd.com.

RHI AG

Booth #516

Refractory competence for the non ferrous metals industry: RHI is the world's leading supplier of high-grade ceramic refractory products and services. As a reliable and competent partner it is our constant aim to add value to the process of our customers by achieving the best price/performance ratio with our refractory system solutions.

The comprehensive program of products and services ranges from basic and non-basic mixes and bricks to prefabricated products, slide gate plates, purging plugs, as well as computer simulations like CFD or FEM. We also offer special machines, repair systems and technical equipment used to install refractory products into the various production units of the non ferrous metals industry. Our metallurgists are active around the globe and cooperate with renowned research facilities and universities to support the improvement of metallurgical processes and furnace integrity.

Riedhammer GmbH

Booth #513

Since 1924 dedicated to the design and construction of furnace plants for carbon products (OPEN as well as CLOSED type), RIEDHAMMER is presently the only independent supplier worldwide being able to deliver complete solutions and technology for baking of anodes, cathodes, electrodes and special carbon products. More than 85 years of experience and know-how guarantee a high economic efficiency and reliability of the plants. In total RIEDHAMMER has executed more than 300 bake furnace projects in 25 countries. Our reference list includes major global players in the production of primary aluminum with pre-baked technology as well as top suppliers of cathodes and electrodes respectively for the aluminum and steel industry.

Rio Tinto Alcan

Booth #301

Global leader in the aluminium industry

Building on more than a century of experience and expertise, Rio Tinto Alcan is a global leader in the aluminium industry. We supply high quality bauxite, alumina and aluminium worldwide and our AP smelting technology is the industry benchmark. Our enviable hydroelectric power position delivers significant competitive advantages in today's carbon constrained world. Rio Tinto Alcan is the aluminium product group of Rio Tinto, a leading international business involved in each stage of metal and mineral production. The Group is listed on the London Stock Exchange and Australian Securities Exchange under the symbol RIO. Rio Tinto's major products are aluminium, copper, diamonds, coal, iron ore, uranium, gold and industrial minerals.

Sente Software Ltd.

Booth #338

We offer materials-focused software products for modeling the behavior and properties of complex alloys. The thermodynamic databases produced by Thermotech set the standard for the prediction of equilibrium and non-equilibrium structures in multi-component commercial alloys. Our latest product, JMat-Pro, is a unique software program for predicting phase transformations, physical/mechanical properties and solidification properties for complex alloys. It provides fast and robust calculations that have been extensively validated to ensure sound predictions of the properties. Our software combines industrial relevance with realistic physical models and user-friendly interfaces that work with "real" materials which are multi-component in nature and exhibit complex behavior. www.jmatpro.com.

SLM Co., Ltd

Booth #240

We are an Aluminium Master Alloys Manufacturer located in Korea. Our company is specialized in Grain Refiners(AlTiB Alloys), Modifiers(AlSr Alloys) and Other Aluminium Alloys such as AlTi, AlB, AlV, AlMg, AlMn etc. We produce aluminium alloys in various forms such as Rod in coil, Cut Rod, Bar and Plate.

We have been producing high quality of Aluminium Master Alloys for 19 years and we export to over 20 countries. We supply high quality materials at competitive price.

We are looking for distributors now. Please visit our stand!

Company Descriptions

STAS

Booth #302

STAS is a Canadian based company specialized in the fabrication of process technologies for the aluminium industry.

The company has over 20 years experience, with clients on all continents. Most of STAS' sales activities are managed from STAS' head office in Canada, with a network of well known agents in specific countries or geographical areas. STAS is a world leader in providing various equipment designed to improve productivity and the quality of molten aluminium.

Three main product lines are available:

1. Casthouse technologies, which include the Alcan Compact Degasser (ACD), the Rotary Flux Injector (RFI), the Inert Gas Dross Cooler (IGDC), the Deep Bed Filter (DBF) and the Treatment of Aluminium in Crucible (TAC).

2. Crucible cleaning shops, which include crucible cleaning systems, crucible preheating systems, and siphon tube cleaners and preheaters.

3. Pot room and rodding shop equipment, which include fume hoods to reduce HF emissions, anode positioning systems, anode stub inspection systems and anode butt inspection systems.

Sunstone

Booth #215

Sunstone Development Co., Ltd. ("Sunstone") is the largest anode exporter and one of the largest merchant anode manufacturers in China. It owns and operates two anode production facilities with an annual capacity of 520,000 metric tons. More than half of Sunstone's annual capacity is exported to more than 20 aluminium smelters in as many countries. Sunstone provides anodes to aluminium smelters in North America, Europe, Russia and the Middle East. The company holds ISO 9001, ISO 14001 and OHSAS 18001 certifications.

Other products and services supplied by Sunstone include calcined petroleum coke, cathode blocks, anode paste, cold ramming paste, anode slot sawing machinery, anode cleaning machinery, pot shells, anode yokes and other various equipment used by the aluminium industry.

Our company's mission is:

- To be the world's largest merchant anode manufacturer and supplier. To provide the highest quality integrated solutions and project management for the global electrolytic aluminium industry.
- To be recognized as the company with the "Best Practice" in the comprehensive utilization of resources in the prebaked anode industry.
- To be recognized as the company with the most environmentally friendly and energy efficient process that produces innovative and technologically superior anodes.

Techmo Car

Booth #413

Techmo is an Italian independent company focused in the engineering and production of special mobile and stationary equipment for the aluminium and non ferrous metals industry. The full range of purpose designed machines covers different types of equipment performing a large number of operations in pot-rooms, rodding shops and cast-houses. The Company's aim is to provide the most innovative, rational, cost effective and user friendly technical solutions. Among the most significant families of mobile equipment are the Tapping Vehicles, Anode Transporters, Crucible Transporters and Tilters, Alumina/ AIF₃ Feeding Vehicles, Furnace Charging Vehicles and Furnace Tending Vehicles, Multipurpose Anode Chargers and Crust Breakers. Beside its line of purposed designed vehicles, Techmo provides a number of stationary equipment such as Crucible Cleaning Machines, the Crucible Tilting stations and the Anode Butts Cleaning Stations.

Tenova Core

Booth #334

Tenova Core is a worldwide leader in the supply of loose carbonaceous material calciners based on rotary hearth technology. These furnaces are used for the processing of petroleum coke, coal, formed coke briquettes and various other carbon based products. Tenova Core also provides a wide range of heat treating, reheating and specialty furnaces as well as technical and spare parts services. Booth Personnel: Thomas Walsh, Bill Barraclough, Bert Mangold; visit Tenova Core online at www.tenovacore.com.

Thermo Scientific

Booth #423

Thermo Scientific product portfolio provides world-class solutions for analytical microscopists. See the QuasOr EBSD system and experience the seamless integration of EDS, WDS and EBSD in the NORAN System 7 X-ray microanalysis system. Also see our EDXRF, WDXRF/XRD and OES products for materials characterization in terms of qualitative and quantitative elemental/phase composition.

Thermo-Calc Software

Booth #223

Thermo-Calc Software is a leading developer of software and databases for calculations involving computational thermodynamics and diffusion controlled simulations. Thermo-Calc is a powerful tool for performing thermodynamic calculations for multicomponent systems. Calculations are based on thermodynamic databases produced by expert evaluation of experimental data. Databases are available for Al, Mg, steels, Ni-superalloys, Ti, solders and other materials. Programming interfaces are available which enable Thermo-Calc to be called directly from in-house developed software or MatLab. DICTRA is used for accurate simulations of diffusion in multicomponent alloys. TC-PRISMA is a new software package for the simulation of precipitation kinetics in multicomponent alloys.



Company Descriptions

Tri-State Refractories Corp.

Booth #239

Tri-State Refractories is a full service contractor specializing in the Aluminum Industry. We offer turn key projects for Carbon Bake Furnaces, Aluminum Holding and Melters, De Laq Furnaces, Rotary Furnaces, Pot Lining, and most other requirements for plant operations. We also have maintenance contracts in place with Rio Tinto Alcan and Alcoa doing multi task type work throughout these facilities.

UES, Inc.

Booth #108

UES, Inc. is an innovative science and technology company that provides its industry and government customers with superior research and development expertise. We create products and services from our technology breakthroughs and successfully commercialize them.

RoboMet.3D™ is a fully automated, serial sectioning system that generates two-dimensional data for three-dimensional reconstruction. Robo-Met.3D enables more time for data analysis and characterization and ensures repeatable and accurate data is collected in an efficient and cost-effective manner.

Additional areas of expertise for UES include materials science, metallurgy, ceramics, processing science, modeling and simulation, surface engineering, materials characterization, biotechnology, sensor development and nanomaterials.

University of Central Florida AMPAC Booth #119

The Advanced Materials Processing and Analysis Center (AMPAC) located at the University of Central Florida is an interdisciplinary research and education center for materials science and engineering. AMPAC excels in the development, processing and characterization of advanced materials, addressing a broad range of civilian and defense applications including energy, microelectronics, nanotechnology, sensors and actuators, biomaterials, lasers and propulsion. AMPAC administers the Materials Science and Engineering Graduate Program, a nationally ranked academic program. AMPAC is also home to the Materials Characterization Facility (MCF), a user facility with state-of-the-art electron microscopy, ion spectroscopy, x-ray analysis and much more. AMPAC also maintains the Advanced Microfabrication Facility, a class 1000 cleanroom facility for the fabrication and testing of semiconductor devices, thin films and more.

Westmoreland Advanced Materials, LLC

Booth #325

Westmoreland Advanced Materials manufactures a full line of premium refractory castables. In addition, the company provides innovative refractory technology for the aluminum industry. WAM® AL II is a truly unique, non-wetting corundum resistant refractory castable developed specifically for the aluminum industry. This family of products provides for all metal contact needs including a non-penetrable insulating product, a high strength/high density product, a gunning product and maintenance and repair products. Customers using this technology in aluminum metal processing applications have measured and documented energy savings up to 46%, maintenance savings of at least 50% and have reduced down times to 8% of typical.

If you process aluminum metal come visit us at booth #325 and learn how we can improve your processing efficiency and your cost to produce product.

York Linings Intl. Inc.

Booth #401

York Linings Inc. is a market leader in the design and installation of refractory linings in all major industries. We incorporate our own in-house experience and technology with that of the major refractory suppliers to provide our clients with an installed product that will provide the best lining performance in their specific industry.

YLI have been involved in many major Aluminum smelting plants in the United States and Overseas. Major projects include New Carbon Bake Furnaces, Reduction Cells, Cathode Sealing, Metal Holding Furnaces and Plant maintenance.

YLI are committed to deliver a quality Refractory project, meeting the high levels of design criteria, safety standards and schedule requirements for today's industrial climate, providing best results for the future of your facility.

TMS2012

141st Annual Meeting & Exhibition

Program At-A-Glance	2
Monday AM	11
Monday PM.....	63
Tuesday AM.....	137
Tuesday PM.....	213
Wednesday AM	293
Wednesday PM	372
Thursday AM.....	445
Thursday PM	502
Posters.....	523
Index	589



TMS 2012

141st Annual Meeting & Exhibition

	Day	AM or PM	Room	Page
			(D) Dolphin / (S) Swan	
2012 Aluminum Plenary				
"Aluminum Industry Technology 2020, A Look Ahead"	Mon	AM	Southern III (D)	II
2012 Functional and Structural Nanomaterials: Fabrication, Properties, Applications and Implications				
Carbon Nanomaterials	Mon	AM	Pelican 1 (S)	12
Nanomaterials for Information Technology	Mon	PM	Pelican 1 (S)	63
0-Dimensional Nanomaterials	Tues	AM	Pelican 1 (S)	137
1-Dimensional Nanomaterials and ZnO	Tues	PM	Pelican 1 (S)	213
Nanomaterials for Energy Technology	Wed	AM	Pelican 1 (S)	293
Structural Nanomaterials	Wed	PM	Pelican 1 (S)	372
Joint Session with "2012 Symposium on Surface and Heterostructures ..."	Thurs	AM	Pelican 1 (S)	445
2012 Symposium on Surfaces and Heterostructures at Nano- or Micro-Scale and Their Characterization, Properties, and Applications				
Heterostructure Growth and Characterization	Mon	AM	Pelican 2 (S)	13
Carbon Nanomaterials and Heterostructures	Mon	PM	Pelican 2 (S)	65
Surfaces, Deposition, and Coatings	Tues	AM	Pelican 2 (S)	138
Energy and Catalysis	Tues	PM	Pelican 2 (S)	215
I-Energy II-Magnetic Materials III-Chemical Sensing and Surfaces	Wed	AM	Pelican 2 (S)	294
I-Chemical Sensing and Devices II-Biomaterials and Applications	Wed	PM	Pelican 2 (S)	374
3rd International Symposium on High Temperature Metallurgical Processing				
High Efficiency New Metallurgical Technology	Mon	AM	Southern II (D)	14
Reduction and Titanium Production	Mon	PM	Southern II (D)	66
Basic Research of Metallurgical Process	Tues	AM	Southern II (D)	139
Alloy and Materials Preparation	Tues	PM	Southern II (D)	217
Sintering and Synthesis	Wed	AM	Southern II (D)	296
Energy and Environment	Wed	PM	Southern II (D)	376
Treatment and Recycling of Solid Slag/Wastes	Thurs	AM	Southern II (D)	446
Pelletizing and Raw Materials Processing	Thurs	PM	Southern II (D)	502
Advances in Surface Engineering: Alloyed and Composite Coatings				
Session-I	Mon	AM	Macaw 1 (S)	16
Session-II	Mon	PM	Macaw 1 (S)	68
Session-III	Tues	AM	Macaw 1 (S)	141
Session-IV	Tues	PM	Macaw 1 (S)	218
Session-V	Wed	AM	Macaw 1 (S)	297
Alumina and Bauxite				
Bauxite Digestion	Mon	PM	Northern E3 (D)	70
Red Mud Bauxite Residue	Tues	AM	Northern E3 (D)	143
Hydrate Precipitation, Calcination and Environment	Tues	PM	Northern E3 (D)	219
Energy and Processing Alternative Rawmaterials	Wed	AM	Northern E3 (D)	298
Aluminium Processing				
Rolling	Mon	PM	Europe 1 (D)	71
General	Tues	AM	Europe 1 (D)	144
Casting	Tues	PM	Europe 1 (D)	221
Aluminum Alloys: Fabrication, Characterization and Applications				
Development and Application	Mon	AM	Northern E1 (D)	17
Solidification	Mon	PM	Northern E1 (D)	72
Thermal Mechanical Processing	Tues	AM	Northern E1 (D)	145
Solutioning and Aging Behaviours	Tues	PM	Northern E1 (D)	222
Material Characterization	Wed	AM	Northern E1 (D)	300
Emerging Technologies	Wed	PM	Northern E1 (D)	377

	Day	AM or PM	Room	Page
			(D) Dolphin / (S) Swan	
Aluminum Reduction Technology				
Environment I	Mon	PM	Southern III (D)	74
Energy Saving	Tues	AM	Southern III (D)	147
Anode Effect, Process Control.....	Tues	PM	Southern III (D)	224
Cell Fundamentals, Phenomena and Alternatives I	Tues	PM	Northern E4 (D)	225
Cell Technology and Operation.....	Wed	AM	Southern III (D)	301
Environment II	Wed	PM	Southern III (D)	380
Cell Fundamentals, Phenomena and Alternatives II	Wed	PM	Northern E4 (D)	378
Modelling I	Thurs	AM	Southern III (D)	449
Modelling II and Measurement	Thurs	PM	Southern III (D)	503
Equipment	Thurs	AM	Europe 1 (D)	448
Atomistic Effects in Migrating Interphase Interfaces - Recent Progress and Future Study				
Interfacial Structure with Small Misfit.....	Mon	AM	Europe 3 (D)	18
Interfacial Structure with Large Misfit and Deformation-induced Migration	Mon	PM	Europe 3 (D)	75
Kinetics of Phase Transformations in Ferrous Alloys	Tues	AM	Europe 3 (D)	148
Interface Migration and Alloy Partitioning	Tues	PM	Europe 3 (D)	226
Modelling and Mechanisms of Interface Migration	Wed	AM	Europe 3 (D)	303
Roles of Interface on Microstructure Development.....	Wed	PM	Europe 3 (D)	381
Battery Recycling				
Session I	Thurs	AM	Europe 4 (D)	450
Biological Materials Science Symposium				
Bio-Inspired Materials: Mechanics and Design.....	Mon	AM	Swan 7 (S)	20
Mechanical Behavior of Biological Materials	Mon	PM	Swan 7 (S)	76
Biological and Bio-Inspired Materials I: Hard Biomaterials	Tues	AM	Swan 7 (S)	149
Biological and Bio-Inspired Materials II: Hard Biomaterials.....	Tues	PM	Swan 7 (S)	227
Biological and Bio-Inspired Materials III: Soft Biomaterials	Wed	AM	Swan 7 (S)	304
Biological and Bio-Inspired Materials IV: Soft Biomaterials	Wed	PM	Swan 7 (S)	382
Bio-Inspired Materials: Implants and Devices.....	Thurs	AM	Swan 7 (S)	451
Bulk Metallic Glasses IX				
Alloy Development and Application	Mon	AM	Swan 6 (S)	21
Alloy Development and Mechanical Properties	Mon	PM	Swan 6 (S)	78
Structures and Mechanical Properties I	Tues	AM	Swan 6 (S)	151
Structures and Mechanical Properties II	Tues	PM	Swan 6 (S)	229
Fatigue and Corrosion	Wed	AM	Swan 6 (S)	305
Simulation and Modeling	Wed	PM	Swan 6 (S)	384
Mechanical and Other Properties.....	Thurs	AM	Swan 6 (S)	453
Structures and Other Properties I.....	Thurs	AM	Swan 1 (S)	455
Other Related Alloys and Properties	Thurs	PM	Swan 6 (S)	504
Structures and Other Properties II.....	Thurs	PM	Swan 1 (S)	506
Cast Shop for Aluminum Production				
Grain Refinement and Castings	Tues	AM	Northern A4 (D)	153
Furnace	Tues	PM	Northern A4 (D)	231
Dross and Melt Quality Control.....	Wed	AM	Northern A4 (D)	308
Direct-Chill Casting and Microstructures	Wed	PM	Northern A4 (D)	386
CFD Modeling and Simulation in Materials Processing				
CFD Modeling in Materials Processing I	Mon	AM	Asia 4 (D)	23
CFD Modeling in Materials Processing II	Mon	PM	Asia 4 (D)	80
Modeling of Melting and Remelting Processes	Tues	AM	Asia 4 (D)	154
Modeling of Casting and Solidification Processes I.....	Tues	PM	Asia 4 (D)	232
Modeling of Casting and Solidification Processes II.....	Wed	AM	Asia 4 (D)	309
Electromagnetic and Ultrasonic Processing of Materials	Wed	PM	Asia 4 (D)	387
Modeling of Steelmaking Processes	Thurs	AM	Oceanic 6 (D)	457



TMS 2012

141st Annual Meeting & Exhibition

	Day	AM or PM	Room	Page
			(D) Dolphin / (S) Swan	
Characterization of Minerals, Metals, and Materials				
Characterization of Ferrous Metals I	Mon	AM	Asia 2 (D)	24
Characterization of Non-Ferrous Materials.....	Mon	PM	Asia 2 (D)	81
Characterization of Minerals and Ceramics.....	Tues	AM	Asia 2 (D)	156
Characterization Technologies.....	Tues	PM	Asia 2 (D)	233
Characterization of Environmental and Construction Materials.....	Wed	AM	Asia 2 (D)	310
Characterization of Energy, Electronic and Optical Materials.....	Wed	PM	Asia 2 (D)	388
Characterization of Carbon and Soft Materials	Thurs	AM	Asia 2 (D)	459
Characterization of Light Metals	Thurs	AM	Europe 6 (D)	461
Characterization of Ferrous Metals II	Thurs	PM	Europe 6 (D)	508
Computational Thermodynamics and Kinetics				
In honor of Dr. Long-Qing Chen, EMPMD Outstanding Scientist: Session I.....	Mon	AM	Australia 3 (D)	26
In honor of Dr. Long-Qing Chen, EMPMD Outstanding Scientist: Session II.....	Mon	PM	Australia 3 (D)	83
Thermodynamics	Tues	AM	Australia 3 (D)	160
Phase-field Simulations in Alloys I.....	Tues	AM	Asia 5 (D)	158
Diffusion Coefficients.....	Tues	PM	Australia 3 (D)	235
Phase-field Simulations in Alloys II.....	Tues	PM	Asia 5 (D)	237
Molecular Dynamics: Potentials and Simulations	Wed	AM	Australia 3 (D)	312
Oxides, Steels, and Nuclear Materials	Wed	AM	Asia 5 (D)	314
Cluster Expansion, Kinetic Monte Carlo, and First-principles.....	Wed	PM	Australia 3 (D)	390
Interfaces.....	Thurs	AM	Australia 3 (D)	462
Defects and Properties of Cast Metals				
Metal Cleanliness	Mon	AM	Oceanic 4 (D)	27
Porosity.....	Mon	PM	Oceanic 4 (D)	84
Hot Tearing	Tues	AM	Oceanic 4 (D)	162
Solidification Structure and Segregation	Tues	PM	Oceanic 4 (D)	239
Ductility, Creep, Stress and Cracks.....	Wed	AM	Oceanic 4 (D)	316
Novel Processes and Applications	Wed	PM	Oceanic 4 (D)	392
Deformation, Damage, and Fracture of Light Metals and Alloys				
Session I.....	Mon	PM	Northern A2 (D)	86
Session II.....	Tues	AM	Northern A2 (D)	163
Session III.....	Tues	PM	Northern A2 (D)	241
Session IV	Wed	AM	Northern A2 (D)	317
Session V.....	Wed	PM	Northern A2 (D)	393
Electrode Technology for Aluminium Production				
Paste Plant Design and Improvement	Mon	PM	Americas Seminar (D)	87
Bake Oven Design and Improvement.....	Tues	AM	Americas Seminar (D)	164
Carbon Materials for Anode and Cathode.....	Tues	PM	Americas Seminar (D)	242
Characterization of Anode Materials	Wed	AM	Americas Seminar (D)	318
Characterization of Cathode Materials	Wed	PM	Americas Seminar (D)	394
Inert Anode and Wetttable Cathode Materials.....	Thurs	AM	Americas Seminar (D)	464
Electrometallurgy 2012				
Session I.....	Mon	PM	Europe 5 (D)	88
Session II.....	Tues	AM	Europe 5 (D)	165
Session III.....	Tues	PM	Europe 5 (D)	244
Session IV	Wed	AM	Europe 5 (D)	320
Emeritus Professor George D.W. Smith Honorary Symposium				
Atom Probe Tomography	Mon	AM	Mockingbird 2 (S)	29
Novel Materials and Aluminium Alloys.....	Mon	PM	Mockingbird 2 (S)	90
Steels I.....	Tues	AM	Mockingbird 2 (S)	167
Steels II and Superalloys.....	Tues	PM	Mockingbird 2 (S)	245

	Day	AM or PM	Room	Page
			(D) Dolphin / (S) Swan	
Energy Nanomaterials				
Li-ion Batteries	Mon	AM	Swan 3 (S).....	30
Li-ion Batteries and Beyond	Mon	PM	Swan 3 (S).....	92
Photovoltaics I	Tues	AM	Swan 3 (S).....	168
Photovoltaics II	Tues	PM	Swan 3 (S).....	247
Supercapacitors.....	Wed	AM	Swan 3 (S).....	321
Thermoelectrics and Thermal Transport	Wed	PM	Swan 3 (S).....	395
Fuel Cells, Hydrogen Storage, and Wind Energy	Thurs	AM	Swan 3 (S).....	465
Catalysts and Photocatalysts	Thurs	PM	Swan 3 (S).....	510
Energy Technologies and Carbon Dioxide Management				
CO2 Management	Wed	PM	Europe 8 (D)	396
Energy Technologies.....	Thurs	AM	Europe 8 (D)	467
Waste Heat Recovery	Thurs	PM	Europe 8 (D)	511
Fatigue and Corrosion Damage in Metallic Materials: Fundamentals, Modeling and Prevention				
Fundamentals of Fatigue Damage and Modeling.....	Mon	AM	Oceanic 6 (D)	31
Fatigue Property-microstructure Relationships and Crack Growth.....	Mon	PM	Oceanic 6 (D)	93
Fatigue Life Prediction and Enhancement.....	Tues	AM	Oceanic 6 (D)	169
Fatigue Behaviors at Elevated Temperature	Tues	PM	Oceanic 6 (D)	248
Fatigue and Corrosion Interaction and Materials Corrosion	Wed	AM	Oceanic 6 (D)	323
Materials Corrosion and Prevention	Wed	PM	Oceanic 6 (D)	398
Federal Funding Workshop				
Panel Discussion	Wed	PM	Northern C (D)	399
From Macro to Nano, Understanding Mechanical Behavior across Length Scales: A Structural Materials Division Symposium in Honor of Robert Ritchie				
Biological and Bioinspired Materials Science.....	Mon	AM	Mockingbird 1 (S)	33
Fatigue.....	Mon	PM	Mockingbird 1 (S)	95
Amorphous and Nanocrystalline Materials	Tues	AM	Mockingbird 1 (S)	171
Small Scale Mechanical Behavior and Theory	Tues	PM	Mockingbird 1 (S)	250
Environmental Effects and Hydrogen Embrittlement.....	Wed	AM	Mockingbird 1 (S)	324
Deformation and Fracture.....	Wed	PM	Mockingbird 1 (S)	400
Mechanical Behavior of Novel Materials.....	Thurs	AM	Mockingbird 1 (S)	468
Integrating and Leveraging Collaborative Efforts for ICME Education				
Session I.....	Wed	AM	Europe 2 (D)	326
Integrative Materials Design: Performance and Sustainability				
Processing and Properties of Traditional and Novel Matls. at Ambient and High Temps. I	Mon	AM	Europe 2 (D)	34
Processing and Properties of Traditional and Novel Matls. at Ambient and High Temps. II	Mon	PM	Europe 2 (D)	97
Processing and Properties of Adv. Steels & Sustainable Design, Life-Cycle Analyses, and Recy. ..	Tues	AM	Europe 2 (D)	172
Advances in ICME & Residual Stress Considerations in Design.....	Tues	PM	Europe 2 (D)	251
International Smelting Technology Symposium (Incorporating the 6th Advances in Sulfide Smelting Symposium)				
Plenary Session	Mon	AM	Northern A3 (D).....	35
Smelter Design, Construction, Commissioning and Operation	Mon	PM	Northern A3 (D).....	98
Current and Emerging Smelting Technologies.....	Tues	AM	Northern A3 (D).....	174
Pretreatment and Recycling Processes	Tues	PM	Northern A3 (D).....	253
Fundamentals: Thermodynamics, Phase Equilibria, and Kinetics.....	Wed	AM	Northern A3 (D).....	327
Pyrometallurgical Process Modeling, Control & Instrumentation.....	Wed	PM	Northern A3 (D).....	401
IOMMMS Global Materials Forum: Materials in a Green Economy: An International Perspective				
Session I.....	Mon	PM	Northern A4 (D).....	99



TMS 2012

141st Annual Meeting & Exhibition

	Day	AM or PM	Room	Page
			(D) Dolphin / (S) Swan	
Magnesium Technology 2012				
Plenary Session	Mon	AM	Southern IV (D)	36
High Temperature Processing and Properties	Wed	PM	Southern V (D)	404
Alloy and Microstructural Design	Wed	AM	Southern V (D)	328
Processing-Microstructure-Property Relationships I	Thurs	AM	Southern IV (D)	472
Energy and Biomedical/Primary Production	Thurs	PM	Southern V (D)	513
Casting and Solidification	Wed	AM	Southern IV (D)	330
Primary Production	Mon	PM	Southern V (D)	103
Corrosion and Coating	Wed	PM	Southern IV (D)	402
Deformation Mechanisms	Mon	PM	Southern IV (D)	101
Advanced Processing and Joining	Thurs	AM	Southern V (D)	470
Processing-Microstructure-Property Relationships II	Thurs	PM	Southern IV (D)	514
Magnetic Materials for Energy Applications II				
Permanent Magnets for Energy Applications	Tues	AM	Europe 10 (D)	175
Magnetocaloric and Magnetostrictive Materials	Wed	AM	Europe 10 (D)	331
Power Conversion and Microstructural Effects	Thurs	AM	Europe 10 (D)	473
Materials and Fuels for the Current and Advanced Nuclear Reactors				
Nuclear Fuels - Modeling	Mon	AM	Swan 2 (S)	37
Nuclear Fuels - Characterization	Mon	PM	Swan 2 (S)	104
Nuclear Fuels	Tues	AM	Swan 2 (S)	176
Structural Materials I	Tues	PM	Swan 2 (S)	254
Structural Materials II	Wed	AM	Swan 2 (S)	333
Structural Materials - Characterization	Wed	PM	Swan 2 (S)	407
Modeling I	Wed	PM	Swan 4 (S)	405
Structural Materials - Irradiation Studies I	Thurs	AM	Swan 2 (S)	476
Modeling II	Thurs	AM	Swan 4 (S)	475
Structural Materials - Irradiation Studies II	Thurs	PM	Swan 2 (S)	517
General	Thurs	PM	Swan 4 (S)	515
Materials Design Approaches and Experiences III				
Material Design Tools	Mon	PM	Europe 11 (D)	106
High Strength High Toughness Steels	Tues	AM	Europe 11 (D)	178
Non-ferrous Alloys and Processes	Tues	PM	Europe 11 (D)	256
Superalloys	Wed	AM	Europe 11 (D)	334
High Strength Steels	Wed	PM	Europe 11 (D)	409
Joining and Microstructure-Property Relationships	Thurs	AM	Europe 11 (D)	478
Materials in Clean Power Systems VII: Clean Coal-, Hydrogen Based-Technologies, and Fuel Cells				
Fuel Cells	Tues	AM	Europe 8 (D)	179
Materials for Hydrogen Production, Separation, and Storage	Tues	PM	Europe 8 (D)	257
Materials for Clean Coal Technologies, Turbines	Wed	AM	Europe 8 (D)	335
Materials Processing Fundamentals				
Process Metallurgy of Metals	Mon	AM	Oceanic 8 (D)	39
Physical Metallurgy of Steel	Mon	PM	Oceanic 8 (D)	107
Application of Microwave, Magnet, Laser and Plasma Technology	Tues	AM	Oceanic 8 (D)	181
Metallurgy of Non-Ferrous Metals	Tues	PM	Oceanic 8 (D)	259
Materials Research in Microgravity				
Session I	Mon	AM	Asia 3 (D)	40
Session II	Mon	PM	Asia 3 (D)	109
Session III	Tues	AM	Asia 3 (D)	182
Session IV	Tues	PM	Asia 3 (D)	260
Session V	Wed	AM	Asia 3 (D)	337
Session VI	Wed	PM	Asia 3 (D)	410

	Day	AM or PM	Room	Page
			(D) Dolphin / (S) Swan	
Mechanical Behavior at Nanoscale I				
In-situ Technique on Deformation Process	Mon	AM	Asia 1 (D)	41
Atomistic Modeling on Deformation Mechanisms	Mon	PM	Asia 1 (D)	110
Deformation Mechanisms at Nanoscale	Tues	AM	Asia 1 (D)	183
Nanowires, Pillar, Multilayers and Nanocrystalline	Tues	PM	Asia 1 (D)	261
Deformation/strength at Nanoscale and Li-induced Deformation	Wed	AM	Asia 1 (D)	338
Nanomechanical Experiment and Modeling	Wed	PM	Asia 1 (D)	411
Thin Film and Multilayers	Thurs	AM	Asia 1 (D)	480
Mechanical Behavior Related to Interface Physics				
Grain Boundaries: Experiment and Modeling	Mon	AM	Oceanic 1 (D)	43
Interface Evolution under Mechanical Loading: Experiment, Char., and Theoretical Modeling	Mon	PM	Oceanic 1 (D)	112
Microscopic Characterization of Interface Mechanical Response	Tues	AM	Oceanic 1 (D)	185
Structure and Mechanical Behavior of Amorphous and Crystalline Nanocomposites	Tues	PM	Oceanic 1 (D)	263
Interface Structures: Characterization, Theory, and Modeling	Wed	AM	Oceanic 1 (D)	340
Deformation Mechanisms in Nanoscale Materials	Wed	PM	Oceanic 1 (D)	413
Dynamic Response of Interfaces: Experiment and Modeling	Thurs	AM	Oceanic 1 (D)	482
Mechanical Performance of Materials for Current and Advanced Nuclear Reactors				
Mechanical Behavior of Reactor Materials	Mon	AM	Swan 1 (S)	45
Mechanical and Small-Scale Testing of Reactor Materials	Mon	PM	Swan 1 (S)	113
Characterization and Modeling of Dislocation Structures in Nuclear Materials	Tues	AM	Swan 1 (S)	187
Characterization and Modeling of Microstructural Evolution in Nuclear Materials	Tues	PM	Swan 1 (S)	265
Irradiation and Testing of Fuels and Cladding Materials	Wed	AM	Swan 1 (S)	341
Irradiation Performance of Advanced and Model Alloys	Wed	PM	Swan 1 (S)	415
Minerals, Metals and Materials under Pressure				
Damage and Microstructure	Wed	PM	Europe 7 (D)	416
Phase Transformations and Microstructure	Thurs	AM	Europe 7 (D)	483
New Materials and Properties	Thurs	PM	Europe 7 (D)	519
Nanocomposites				
Mechanical Behavior and Modelling of Nanocomposites	Mon	AM	Swan 8 (S)	46
Processing of Nanocomposites I	Mon	PM	Swan 8 (S)	115
Energetic & Catalytic Nanocomposites	Tues	AM	Swan 8 (S)	188
Nanocomposites for Energy Transport, Harvesting and Storage	Wed	PM	Swan 8 (S)	418
Nanocomposites for Magnetic and Dielectric Applications	Wed	AM	Swan 8 (S)	343
Nanocomposite Interfaces and Characterization	Tues	PM	Swan 8 (S)	266
Processing of Nanocomposites II	Thurs	AM	Swan 8 (S)	485
Neutron and X-Ray Studies of Advanced Materials V: Centennial				
Von Laue, Bragg and Diffraction Centennial	Mon	AM	Southern 1 (D)	48
In Honor of Dr. Gabrielle Long	Mon	PM	Southern 1 (D)	116
In Honor of Prof. G. Kostorz	Tues	AM	Southern 1 (D)	190
Dislocations, Strains, Deformation I	Tues	PM	Southern 1 (D)	268
Alloys, Correlations, Phase Transitions	Wed	AM	Southern 1 (D)	345
Local Structure from Diffraction	Wed	AM	Northern E4 (D)	347
Three Dimensional Studies	Wed	PM	Southern 1 (D)	419
Dislocations, Strains, Deformation II	Thurs	AM	Southern 1 (D)	486
New Advances in Synthesis, Characterization, and Application of Layered Double Hydroxides				
Session I	Thurs	AM	Oceanic 2 (D)	489
Pb-Free Solders and Other Materials for Emerging Interconnect and Packaging Technologies				
Studies of Mechanical Properties and Effects of Current I	Mon	AM	Swan 9 (S)	50
Studies of Mechanical Properties and Effects of Current II	Mon	PM	Swan 9 (S)	118
Effects of Ultrafine Joints and Alloy/microstructure Relationships	Tues	AM	Swan 9 (S)	192
Alternative Interconnects and Harsh Environmental Influences	Tues	PM	Swan 9 (S)	270
Solder Alloy Design for Challenging Applications	Wed	AM	Swan 9 (S)	349
Whisker Growth in Tin and Related Solder Alloys	Wed	PM	Swan 9 (S)	422
Physical Property Effects and Responses to Current	Thurs	AM	Swan 9 (S)	491



TMS 2012

141st Annual Meeting & Exhibition

	Day	AM or PM	Room	Page
			(D) Dolphin / (S) Swan	
Phase Stability, Phase Transformations, and Reactive Phase Formation in Electronic Materials XI				
Solder-related Reliability Issues	Mon	AM	Swan 10 (S)	51
Phase Equilibria and Transformations of the Pb-free Solders and Thermoelectric Materials	Mon	PM	Swan 10 (S)	120
Interfacial Reactions of the Pb-free Solder Joints	Tues	AM	Swan 10 (S)	194
General Issues in Microelectronics	Tues	PM	Swan 10 (S)	272
Phase Transformations and Deformation in Magnesium Alloys				
Phase Transformations and Deformation	Tues	AM	Southern V (D)	196
Deformation Twinning and Texture	Tues	PM	Southern V (D)	274
Processing to Control Morphology and Texture in Magnetic Materials				
Processing to Enhance Performance in Rare Earth Permanent Magnets	Mon	PM	Europe 10 (D)	122
Role of Magnetic Fields and Texturing to Improved Magnetic Materials	Tues	PM	Europe 10 (D)	275
Thin Films and Applications	Wed	PM	Europe 10 (D)	423
Production, Recovery and Recycling of Rare Earth Metals				
Session I	Thurs	PM	Europe 4 (D)	520
Radiation Effects in Ceramic Oxide and Novel LWR Fuels				
Experimental Characterization of Radiation Damage in Uranium Fuel and Surrogate Materials	Tues	PM	Macaw 2 (S)	277
Computational Modeling of Defect Evolution under Irradiation	Wed	AM	Macaw 2 (S)	351
Effects of Radiation on Thermal Transport and Fuel Performance	Wed	PM	Macaw 2 (S)	424
Randall M. German Honorary Symposium on Sintering and Powder-Based Materials				
Sintering Theory and Practice	Mon	AM	Oceanic 2 (D)	53
Current Activated and Conventional Sintering	Mon	PM	Oceanic 2 (D)	123
Powder Technology	Tues	AM	Oceanic 2 (D)	197
Powder Processing and Consolidation I	Tues	PM	Oceanic 2 (D)	278
Powder Processing and Consolidation II	Wed	AM	Oceanic 2 (D)	353
Powder Processing and Consolidation III	Wed	PM	Oceanic 2 (D)	426
Reaching New Heights: Materials Innovation in the Aerospace Industry				
Session I	Wed	PM	Northern E2 (D)	428
Recent Developments in Biological, Electronic, Functional and Structural Thin Films and Coatings				
Process-Properties-Performance Correlations I	Wed	AM	Swan 10 (S)	354
Process-Properties-Performance Correlations II	Wed	PM	Swan 10 (S)	428
Applications to Bio, Energy and Electronic Systems	Thurs	AM	Swan 10 (S)	492
Process-Properties-Performance Correlations III	Thurs	PM	Swan 10 (S)	521
Recycling General Sessions				
Metals	Tues	AM	Europe 4 (D)	198
Electronics	Tues	PM	Europe 4 (D)	280
Building Materials	Wed	AM	Europe 4 (D)	355
Waste Utilization	Wed	PM	Europe 4 (D)	430
Refractory Metals 2012				
W and Mo Alloys Structure, Microstructure and Properties	Wed	AM	Mockingbird 2 (S)	357
Alloy Predictions and Synthesis Oxidation and Corrosion	Wed	PM	Mockingbird 2 (S)	431
Science and Engineering of Light Metal Matrix Nanocomposites and Composites				
Metal Matrix Nanocomposites	Mon	AM	Macaw 2 (S)	54
Nanocomposites and Composites	Mon	PM	Macaw 2 (S)	125
Metal Matrix Composites	Tues	AM	Macaw 2 (S)	200
Solar Cell Silicon				
Silicon Production	Mon	PM	Europe 7 (D)	126
Refining and Characterization	Tues	AM	Europe 7 (D)	202

	Day	AM or PM	Room	Page
			(D) Dolphin / (S) Swan	
Solid-State Interfaces II: Toward an Atomistic-Scale Understanding of Structure, Properties, and Behavior through Theory and Experiment				
Atomic Level Structures, Compositions, and General Methods.....	Mon	AM	Oceanic 7 (D)	56
Morphological Stability	Mon	PM	Oceanic 7 (D)	128
Interface Interaction with Defects	Tues	AM	Oceanic 7 (D)	203
Mechanical Properties.....	Tues	PM	Oceanic 7 (D)	281
Non-metallic Interfaces, Electronic Structures.....	Wed	AM	Oceanic 7 (D)	358
Grain-boundaries and Triple Junctions	Wed	PM	Oceanic 7 (D)	433
Interface Dynamics, Oxidation.....	Thurs	AM	Oceanic 7 (D)	494
Stochastic Methods in Materials Research				
Session I.....	Tues	PM	Europe 7 (D)	282
Session II.....	Wed	AM	Europe 7 (D)	360
Symposium in Memory of Patrick Veysseyre: Understanding the Mechanisms Controlling Plastic Flow				
Dislocations Organization.....	Mon	AM	Europe 6 (D)	58
Plastic Flow	Mon	PM	Europe 6 (D)	129
Screw Dislocations-lattice Friction.....	Tues	AM	Europe 6 (D)	205
Intermetallic Alloys.....	Tues	PM	Europe 6 (D)	284
Nanograined Materials	Wed	AM	Europe 6 (D)	362
Deformation Mechanisms.....	Wed	PM	Europe 6 (D)	434
Titanium: Advances in Processing, Characterization and Properties				
Processing and Process Modeling I	Mon	AM	Oceanic 3 (D)	59
Processing and Process Modeling II	Mon	PM	Oceanic 3 (D)	130
Microstructure Evolution and Characterization I.....	Tues	AM	Oceanic 3 (D)	206
Microstructure Evolution and Characterization II.....	Tues	PM	Oceanic 3 (D)	285
Fatigue of Titanium Alloys.....	Wed	AM	Oceanic 3 (D)	363
Mechanical Properties.....	Wed	PM	Oceanic 3 (D)	436
General Abstracts.....	Thurs	AM	Oceanic 3 (D)	495
T.T. Chen Honorary Symposium on Hydrometallurgy, Electrometallurgy and Materials Characterization				
Plenary Session	Mon	AM	Northern A4 (D)	61
Copper Electrorefining.....	Mon	PM	Oceanic 5 (D)	133
Base Metal Processing.....	Tues	AM	Oceanic 5 (D)	208
Transition Metal Processing.....	Tues	PM	Oceanic 5 (D)	287
Precious Metals, Recycling and the Environment	Wed	AM	Oceanic 5 (D)	365
Processing and Properties I	Wed	PM	Oceanic 5 (D)	438
Characterization	Thurs	AM	Oceanic 5 (D)	497
Processing and Properties II	Thurs	AM	Oceanic 4 (D)	498
Ultrafine Grained Materials VII				
Plenary Session	Mon	AM	Swan 5 (S)	62
Processing-Microstructure-Property Relationships: Al-, Mg- and Ti-Alloys	Tues	PM	Swan 5 (S)	288
Processing-Microstructure-Property Relationships: Fe-, Cu- and High-Entropy Alloys.....	Tues	PM	Swan 4 (S)	291
Young Scientist.....	Wed	PM	Swan 5 (S)	439
Thermal Stability.....	Tues	AM	Swan 5 (S)	211
Applications and Transitions	Thurs	AM	Swan 5 (S)	499
Powder Processing.....	Wed	AM	Swan 5 (S)	368
Deformation Mechanisms.....	Mon	PM	Swan 5 (S)	134
Mechanical Response	Tues	AM	Swan 4 (S)	209
Advanced Analysis Methods	Wed	AM	Swan 4 (S)	366
Ultrasonic Fatigue of Advanced Materials and Systems				
Ultrasonic Fatigue of Metals and Alloys I.....	Wed	AM	Europe 1 (D)	371
Ultrasonic Fatigue of Metals and Alloys II; Very High Cycle Fatigue of Composites and MEMS.....	Wed	PM	Europe 1 (D)	442
Wettability and Interfacial Phenomena between Metals and Ceramic/Refractory Materials				
Session I.....	Wed	PM	Macaw 1 (S)	443



TMS 2012

141st Annual Meeting & Exhibition

	Day	AM or PM	Room	Page
			(D) Dolphin / (S) Swan	
Symposium Poster Sessions				
2012 Functional and Structural Nanomaterials	Mon	PM	Atlantic Hall (D)	523
Alumina and Bauxite.....	Mon	PM	Atlantic Hall (D)	526
Aluminum Alloys: Fabrication, Characterization and Applications	Mon	PM	Atlantic Hall (D)	526
Biological Materials Science Symposium.....	Mon	PM	Atlantic Hall (D)	528
Computational Thermodynamics and Kinetics	Mon	PM	Atlantic Hall (D)	530
Deformation, Damage, and Fracture of Light Metals and Alloys	Mon	PM	Atlantic Hall (D)	532
Magnesium Technology 2012.....	Mon	PM	Atlantic Hall (D)	533
Materials Processing Fundamentals	Mon	PM	Atlantic Hall (D)	539
Materials Research in Microgravity	Mon	PM	Atlantic Hall (D)	540
Mechanical Behavior at Nanoscale I	Mon	PM	Atlantic Hall (D)	542
Mechanical Behavior Related to Interface Physics.....	Mon	PM	Atlantic Hall (D)	547
Nanocomposites.....	Mon	PM	Atlantic Hall (D)	548
Neutron and X-Ray Studies of Advanced Materials V	Mon	PM	Atlantic Hall (D)	549
Pb-Free Solders and Other Materials for Emerging Interconnect and Packaging Technologies	Mon	PM	Atlantic Hall (D)	550
Radiation Effects in Ceramic Oxide and Novel LWR Fuels	Mon	PM	Atlantic Hall (D)	551
Randall M. German Honorary Symposium on Sintering and Powder-Based Materials.....	Mon	PM	Atlantic Hall (D)	552
Recycling General Sessions.....	Mon	PM	Atlantic Hall (D)	552
Refractory Metals 2012	Mon	PM	Atlantic Hall (D)	552
Solid-State Interfaces II	Mon	PM	Atlantic Hall (D)	553
T.T. Chen Honorary Symposium	Mon	PM	Atlantic Hall (D)	554
Ultrafine Grained Materials VII.....	Mon	PM	Atlantic Hall (D)	557
General Poster Session	Mon	PM	Atlantic Hall (D)	562
Student Poster Contests				
Biological Materials Science Student Poster Contest.....	Mon	PM	Atlantic Hall (D)	578
EMPM Student Poster Contest	Mon	PM	Atlantic Hall (D)	579
EPD Student Poster Contest.....	Mon	PM	Atlantic Hall (D)	581
LMD Student Poster Contest.....	Mon	PM	Atlantic Hall (D)	582
MPMD Student Poster Contest.....	Mon	PM	Atlantic Hall (D)	584
SMD Student Poster Contest.....	Mon	PM	Atlantic Hall (D)	585

About TMS Poster Sessions

The TMS 2012 Annual Meeting & Exhibition is pleased to provide a central area for all poster presentations at the conference. This area, located in the Atlantic Hall in the Dolphin Hotel near Registration, will include:

- Individual symposium poster sessions
- General poster session
- Student poster sessions (by division)

Presentation times:

Presenters should plan to be available to discuss their posters on **Monday, March 12, from 5:30 to 6 pm** in conjunction with the **President's Welcoming Reception in the exhibition hall.**

Poster installation and removal:

Presenters may install their posters on **Sunday, March 11, from 12 to 6 pm** and on **Monday, March 12, from 7 to 8 am.**

Presenters may remove their posters beginning at **noon on Wednesday, March 14.** All posters must be removed **before 5 pm on Wednesday.**

2012 Aluminum Plenary: “Aluminum Industry Technology 2020, A Look Ahead ”: Aluminum Industry Technology 2020, A Look Ahead

Sponsored by: The Minerals, Metals and Materials Society, TMS Light Metals Division, TMS: Aluminum Committee, TMS: Aluminum Processing Committee
Program Organizer: Carlos Suarez, Alcoa Maaden JV

Monday AM
March 12, 2012

Room: Southern III
Location: Dolphin Resort

Session Chair: Carlos Suarez, Alcoa

8:30 AM Introductory Comments

8:35 AM

Acceleration of Cell Technology through Breaking Barriers: A Closer look at Innovation by High-Tech Sensor Technology and Energy Recovery Solutions: *Stephan Broek*¹; ¹Hatch Ltd

Today's cell technologies are pushed harder and harder. However, to make the advancement necessary in the future technologies are needed that enables us to look in more detail in how a cell performs. Technical advances in sensor techniques help us learn more of the intimate behavior of cells. Developments today lay the foundation of even more intelligent cell operation in the future. A different trend is advances in the energy recovery potential. As cell become more powerful the opportunity to utilize the waste energy becomes more and more realistic. A brief overview is presented in the status and potential of energy recovery.

9:05 AM

Alumina Technology – Present and Future: *Ender Suvaci*¹; ¹Anadolu University

Alumina has been one of the most widely utilized engineering materials. Besides its use as a precursor for aluminum production, it has been used as an advanced ceramic material which can be tailored to fulfill technological needs. In this presentation, firstly current status of the alumina technology in terms of production methods and material characteristics will be discussed, secondly the current status will be compared with the alumina technology roadmap which was prepared in 2001. In the final part, future of the alumina technology and alumina's possible roles on development of innovative bio and/or nano-technological products will be discussed.

9:35 AM

A Sustainable Production of Primary Aluminum: *Claude Vanvoren*¹; ¹Rio Tinto Alcan

In a carbon and energy constrained world, with dramatically escalating power costs, ever increasing environmental regulations and where access to large power blocks and multi billion capital investments required to build the most competitive smelters becomes increasingly difficult to source, producing Aluminum in a sustainable way, which is already a challenge, will become an industry threat if innovative solutions delivering step change performance improvements are not developed in due time. Presentation will review options which the primary Aluminum industry critically needs to be available for a smelter built in the 2020s.

10:05 AM Break

10:15 AM

Driving Business Technology to Remain Competitive in the Aluminum Business: *Roberto De Andrade*¹; ¹Alcoa Inc

With the slowdown of the economy, aluminum companies respond by delaying technology development and asset expenditures to offset the lower metal prices and lower demand. Prior to these times companies must have strategies in place that will allow them to understand the risks the businesses are taking and prioritizing what equipment expenditures and the technology development programs which must continue on. The future of the industry will also depend on the competence of the organization to advance the production process while driving the aluminum cost down. On the talent front, this will occur through strategic workforce planning, modified selection profiles, accelerated development and organization designs to help facilitate succession planning. The purpose of my paper is to show how technology innovation combined with a vision of being a failure mode driven organization and talented employees can enable aluminum companies to improve operations and remain cost competitive even in tough times.

10:45 AM

Achieving Carbon Neutrality in the Global Aluminum Industry: *Subodh Das*¹; ¹Phinix LLC

The current carbon foot print of the global aluminum industry is estimated at 500 million metric tonnes of carbon dioxide equivalents (CO₂e), representing about 1.7 % of global emissions from all sources. This paper outlines an integrated and quantifiable plan for achieving “carbon neutrality” in the global aluminum industry by advocating several steps such as : using “greener” energy grids, reducing energy intensity of manufacturing processes, deploying products in energy saving applications , diverting material from landfills and urban mining from “aluminum - rich landfills”.

11:15 AM

The Aluminum Story – The Positive Contribution of the Aluminium Industry and its Products to Sustainable Development: *Chris Bayliss*¹; ¹International Aluminium Institute

By working continuously to minimize its environmental impacts and maximize the benefits that its products offer to the world, the aluminium industry is committed to ensuring that aluminium is part of the solution for a sustainable future. The International Aluminium Institute's Aluminium for Future Generation initiative seeks to demonstrate: 1. that the aluminium industry produces responsibly, by mitigating environmental impacts and positively impacting the communities in which it operates; 2. that its products bring a net benefit to society in terms of energy efficiency & emissions reduction, quality of life, health and sustainable development; 3. that at the end of product life, the value of the material, the energy that went into its production and the socio-economic benefit is retained and realised as another product, through collection and recycling or energy recovery.

11:45 AM Panel Discussion

12:05 PM Concluding Comments



TMS 2012

141st Annual Meeting & Exhibition

MONDAY AM

2012 Functional and Structural Nanomaterials: Fabrication, Properties, Applications and Implications: Carbon Nanomaterials

Sponsored by: The Minerals, Metals and Materials Society, TMS Electronic, Magnetic, and Photonic Materials Division, TMS: Nanomaterials Committee

Program Organizers: Jiyoung Kim, University of Texas; David Stollberg, Georgia Tech Research Institute; Seong Jin Koh, University of Texas at Arlington; Nitin Chopra, The University of Alabama; Terry Xu, UNC Charlotte

Monday AM Room: Pelican 1
March 12, 2012 Location: Swan Resort

Session Chairs: Jiyoung Kim, University of Texas at Dallas; Nae Eung Lee, SungKyunKwan University

8:30 AM Introductory Comments

8:45 AM Invited

Graphene -The Route Toward Applications: *Wonbong Choi*¹; ¹Florida International University

Graphene has revolutionized the scientific frontiers in nanoscience and condensed matter physics due to its exceptional electrical, physical and chemical properties. This talk will focus on engineering of graphene and its applications in transparent and flexible display and flexible solar cells. The graphene film was grown by the thermal CVD. Further, the graphene film was functionalized with reactive ion plasma. The doped graphene was characterized as a counter electrode in a dye sensitized solar cells showing ~3.5% efficiency. The graphene film was spin-coated using carbon nanotubes to form the cathode of the field emission device. A phosphor coated graphene-PET film was used as the anode. The device showed good transparency and flexibility apart from offering appreciable emission current. Our efforts on the strategies of manipulation of carbon nanomaterials' interface, growth of large scale graphene and its characterization at nanoscale will be reviewed and critical issues will be highlighted.

9:20 AM

Growth of Low Dimensional Carbon Nanomaterials: *John Boeckl*¹; *Weijie Lu*¹; *William Mitchel*¹; ¹Air Force Research Laboratory

Low dimensional carbon nanostructures have attracted significant interest due to promising applications ranging from high-speed electronics, thermal management, sensing, multi functional structures and beyond. Insight into the growth mechanism of low-dimensional carbon nanomaterials remains a challenge. Metal-free nanocarbon/SiC structures offer an excellent platform to gain a fundamental understanding of carbon nano-materials. In this talk, metal-free nanocarbon/SiC structures are used as a platform to gain a fundamental understanding of the growth mechanisms of CNTs and graphene. We focus on graphene growth on SiC (0 0 0 1) (Si-face) as a model system in comparison with aligned CNT growth on SiC. The experimental growth aspects for graphene growth, including vacuum and ambient growth environments, and growth temperature will be presented, then, proposed decomposition and growth mechanisms are discussed. Example structures based on the growth model for specific applications will be presented.

9:40 AM

Piezoelectric Coated Carbon Nanotubes for Electronic Applications: *David Stollberg*¹; *Austin Mohney*²; ¹Georgia Tech Research Institute; ²Lock Haven University

As electrical devices continue to decrease in size the desire grows to eliminate the need for batteries as power sources. Piezoelectric nanogenerators have proven themselves as a viable means for ambient energy harvesting: Zinc oxide (ZnO) has this the unique property of producing a voltage difference when subjected to mechanical strain. The

objective is an energy harvesting piezoelectric generator that transduces ambient mechanical vibrations into electrical energy. Carbon nanotubes (CNTs) are used as a structural backbone for a ZnO piezoelectric coating and a silver electrode coating. CNTs are chosen for their strong, flexible, and conductive properties. A Schottky diode is created at the interface of the silver electrode and the ZnO coating, rectifying the current output of the piezoelectric-coated nanotubes. Previous devices yielded a maximum current output of 1.2microA. SEM was used to characterize the fabrication process. A Keithley 4200 SCS was used to characterize the power output.

10:00 AM Break

10:15 AM Invited

Engineering Improved Strain Capacity Carbon Nanotube Electrodes on Shape Memory Polymers for Cortical Brain Probes, Cochlear Implants, Flexible Antennas and Multi-Electrode Arrays: *Dustin Simon*¹; *Taylor Ware*¹; *Yael Hanein*²; *Moshe David-Pur*²; *Edward Keefer*³; *Walter Voit*¹; ¹UT Dallas; ²Tel-Aviv University; ³Plexon

A current limitation in the field of flexible electronics is the ability to achieve complex 3-D structures using cost-effective, well-studied photolithographic approaches. A class of dynamic, smart materials called shape memory polymers has been used for interfacing with metallic conductors, to create devices that change in stiffness as a function of temperature or environmental condition. Using the shape memory effect enables standard lithographic processing on these (temporarily) flat surfaces, which then can recover (permanently) to new complex shapes. However, these devices are limited by the strain capacity of the metal electrodes. This work explores the effectiveness of photolithographically patterned carbon nanotube electrodes to scale up and integrate these nanomaterials into functional device architectures and bulk shape memory polymer systems for a variety of engineering applications such as neural brain probes, flexible transistors, flexible antennas, cell culture dishes, cochlear implants and flexible prosthetics.

10:50 AM

Photo-Ignition of Liquid Fuel Spray and Solid Fuel by Carbon Nanotubes: *Alireza Badakhshan*¹; *Stephen Danczyk*²; ¹Jacobs Technology Inc.; ²Air Force Res. Lab

We have studied the ignition of fuel sprays and solid rocket fuels by the photo-ignition of single wall carbon nanotube (SWCNT) with a camera flash. Our investigation includes the effects of O₂ concentration and the presence of solid oxidizers such as ammonium perchlorate (AP) on the minimum ignition energy (MIE) as well as the duration and temperature of the reaction. We have shown that by mixing CNT with other nanoparticles and powdered material, the ignition parameters such as ignition delay, burn temperature, and burn duration can be tailored to meet ignition requirements. This approach in photo-ignition of fuel spray and solid fuel provides a suitable method for ignition of liquid rocket engines and solid rocket motors that is scalable from very small to large rockets. Among the advantages of this photo-ignition approach are; very low weight, low power, robust system, with volumetric distributed ignition capability.

11:10 AM

Boron Carbide Nanowires: Low Temperature Synthesis, Structural and Thermal Conductivity Characterization: *Zhe Guan*¹; *Timothy Gutu*¹; *Juekuan Yang*²; *Yang Yang*²; *Deyu Li*²; *Terry Xu*¹; ¹UNC Charlotte; ²Vanderbilt University

Boron carbide nanowires are synthesized by co-pyrolysis of diborane and methane in a low pressure chemical vapor deposition system at relatively lower temperatures such as 879 °C. Both transverse twins and axial twins are observed from as-synthesized nanowires, which provide additional measures to tune their transport properties for better thermoelectric performance. The thermal conductivity of as-synthesized nanowires is found to be diameter-dependent. The room temperature thermal conductivity of a 55 nm diameter nanowire is 3.78 W m⁻¹ K⁻¹, which is about eight times lower than that of bulk boron carbides.

11:30 AM

Electrical and Mechanical Response of CNT Turfs under Normal Loads: *Anqi Qiu*¹; David Bahr¹; ¹Washington State University

Carbon nanotube turfs; arrays of multiwalled carbon nanotubes with unique electrical and mechanical properties, have potential for dry, electrically conductive adhesives. Nanoindentation and electrical contact resistance testing was used to characterize the properties of CNT turfs. The rate of unloading during nanoindentation impacted the stiffness, while longer time in contact leads to a higher perceived modulus and larger adhesion between the tip and the turf, but also accentuates creep. Electrical properties, such as current density and conductivity, were also evaluated. The electrical conductance stays constant when the tip is held at constant depth. Sweep test determined the turf behaved as a heavily doped semiconductor. The combination of testing methods is used to demonstrate that time dependent behavior is due to movement of tubes beneath the tip, and not relative motion of CNTs to the contact surface. This suggests conductive adhesive applications are viable and will improve over time.

2012 Symposium on Surfaces and Heterostructures at Nano- or Micro-Scale and Their Characterization, Properties, and Applications: Heterostructure Growth and Characterization

Sponsored by: The Minerals, Metals and Materials Society, TMS Electronic, Magnetic, and Photonic Materials Division, TMS Materials Processing and Manufacturing Division, TMS: Energy Conversion and Storage Committee, TMS: Nanomaterials Committee, TMS: Surface Engineering Committee, TMS: Young Leaders Committee, TMS: EMPMD Council

Program Organizers: Nitin Chopra, The University of Alabama; Ramana Reddy, The University of Alabama; Arvind Agarwal, Florida International University; Sandip Harimkar, Oklahoma State University; Jiyoung Kim, University of Texas at Dallas; Christopher Matranga, National Energy Technology Laboratory

Monday AM
March 12, 2012

Room: Pelican 2
Location: Swan Resort

Session Chairs: Nitin Chopra, The University of Alabama; Christopher Matranga, National Energy Technology Laboratory (NETL)

8:30 AM Introductory Comments

8:35 AM Invited

Defining Nanoscale Structure-Property Relationships in Nanowire Heterostructures: *Lincoln Lauhon*¹; ¹Northwestern University

The discovery of new nanoscale structure-property relationships in heterogeneous nanostructures is enabled by techniques that spatially correlate structure/composition with electronic and optical properties. Towards this goal, we pursue correlated imaging studies involving electron microscopy, atom probe tomography (APT), Raman microspectroscopy, and scanning photocurrent microscopy. I will discuss applications of correlated imaging of form and function to nanowire heterostructures and hybrid nanowire-nanoparticle structures of interest in energy harvesting applications. The non-uniform distribution of dopant atoms in Si and Ge nanowires and heterostructures, measured by APT, strongly influences the distribution of majority and minority carriers under electrical biasing and photoexcitation, which are key inputs to models of devices including solar cells. Nanowire and hybrid metal-semiconductor heterostructures strongly influence the absorption of light and the distribution of charge carriers with excess energy that can be extracted for power generation in photovoltaic applications. The talk will highlight recent results from our group and collaborators.

9:10 AM Invited

Challenging the Trade-Offs in Synthesis and Application of Core/Shell Nanocrystal Fluorophores: *Andrew Greytak*¹; ¹University of South Carolina

Core/shell heterostructures have been widely used to increase the brightness of nanocrystal quantum dots (QDs) as fluorophores in two ways: (1) maximizing the quantum yield (QY) through electronic and chemical isolation of the core; and (2) increasing the excitation rate by building a high density of states at energies above the shell bandgap. These two roles for the shell present a potential trade-off in terms of shell material. A wide bandgap shell imposes large barriers for carrier access to the surface but will be less able to contribute to absorption, while a narrower gap shell could participate in light harvesting but may make it harder to achieve high QY. I will present recent work on the development of core/shell QDs with modest band offsets that nonetheless maintain high QY in aqueous solution, and new experiments that explore the limits of alternating layer addition approaches to core/shell nanostructures.

9:45 AM

Anisotropic Evaporation of GaN Nanowires Analyzed Using Atom Probe Tomography: *James Riley*¹; Rodrigo Bernal¹; Qiming Li²; Horacio Espinosa¹; George Wang²; Lincoln Lauhon¹; ¹Northwestern University; ²Sandia National Laboratories

GaN is a promising material for light-emitting diodes (LEDs) but GaN films exhibit numerous dislocations when grown on inexpensive, but lattice-mismatched substrates such as Si. Dislocation-free nanowire heterostructures can be grown at high lattice mismatch, but measurement of dopant incorporation and interface uniformity becomes substantially more challenging in this 3D geometry. We have used atom probe tomography (APT) to analyze the 3D composition of Metal Organic Chemical Vapor Deposition (MOCVD) grown GaN nanowires. Post-APT SEM imaging was used to correlate evaporation features with crystallographic poles. Regions of low Ga+N detection were associated with trajectory effects caused by surface faceting. Furthermore, an area of enhanced N detection was attributed to evaporation from a semipolar surface. The increased N detection in this region causes the overall measured composition to deviate from the expected stoichiometric ratio. This knowledge of spatial variations in apparent stoichiometry is essential to correctly interpret APT data from heterostructures.

10:05 AM

Fabrication of Silicon Nanowires by Metal Nanoparticles Assisted Anisotropic Etching and Their Electron Microscopic Studies: *Wenwu Shi*¹; Laura Phillips¹; Nitin Chopra¹; ¹The University of Alabama

Silicon nanowires possess unique optical and semiconducting properties, and show great potential as solar cell, biological/chemical sensor, and batteries. Anisotropic chemical etching inside strong acids using noble metal nanoparticles could produce large amount, properly aligned silicon nanowires at ambient temperature and pressure within short duration. However, detailed understanding of the growth process is warranted. This study examined the effects of etching duration, temperature, salt type, and acid concentration on the length, morphology, uniformity, and density of nanowires. This fundamental understanding was developed using scanning electron microscopy (SEM), transmission electro spectroscopy (TEM), Raman spectroscopy, and X-ray diffraction (XRD). Of the salt types used, only gold and silver salts produced high quality nanowires after etching, with the silver being the best. This method also allowed for the growth of various morphologies of the Si nanowires with in-situ nanoparticle coatings.

10:20 AM Break

10:30 AM Invited

Hybrid Nanowires for Functional Applications: *Pelagia Gouma*¹; ¹SUNY Stony Brook

Electrospun nanofibers of hybrid materials (polymers, ceramics, metals, biomolecules) are a class of bio-nano-composites that also allow for



TMS 2012

141st Annual Meeting & Exhibition

MONDAY AM

versatile design, ease of manufacturing, and diversity of applications. Both the nanoelectronics and nanomedicine fields will eventually require the integration of protein nanofibers-based design and manufacturing (e.g. nanocircuitry templating, protein structures such as those binding bone to collagen in tissue scaffolding, etc.) and electrospun nanofiber-based synthesis and processing (active components in sensing, actuation, nanocues in templating, drug delivery systems, etc.). This paper provides an overview of the author's research related to hybrid nanowire synthesis and use in specific functional applications. The solution and process parameters that control the morphology and structure of the nanofibrous materials will be discussed and emphasis will be paid on the electrostatic interactions between different types of materials (e.g. organic vs inorganic components) during the electrospinning process.

11:05 AM Invited

Tuning Color by Pore-Depth of Metal-Coated Nanostructured Porous Alumina: Dongxian Zhang¹; Xulongqi Wang¹; Haijun Zhang¹; Yi Ma¹; Jianzhong Jiang¹; ¹Zhejiang University

A simple and effective color-tuning method has been developed by controlling pore-depth of metal-coated porous alumina (PA) template. The mechanism for color tuning in this method was uncovered, which can be used to design colorful complex pattern. A colorful 'World Map' was exhibited on PA template by this method. Such vivid color tuning is predominately due to the interference enhancement of nanostructure. This method has the potential for tuning colors and being widely applied in the fields of nanotechnology, physics and photonics.

11:40 AM Invited

In-Situ TEM Controlled Growth of Silicide in Si Nanowires: Yi-Chia Chou¹; Mark Reuter²; King-Ning Tu³; Eric Stach⁴; Frances Ross²; ¹IBM/Purdue University; ²IBM T. J. Watson; ³University of California Los Angeles; ⁴Purdue University/BNL

Silicides are important for microelectronics, but compared to bulk or thin film reactions, mechanisms and kinetics can be dramatically different in nanoscale structures. In order to quantify these effects, we have used in situ transmission electron microscopy to observe silicidation in Si nanowires. Movies recorded during silicidation show at atomic resolution that homogeneous nucleation of silicide takes place at the center of each Si atomic layer; heterogeneous nucleation is suppressed due to the native oxide. We compare with Si nanowires grown in a UHV transmission electron microscope where metal is deposited without breaking vacuum. Silicidation was observed in real time during annealing and the kinetics measured from movies. The presence of a surface oxide can lead to striking changes in the silicide morphology. We will discuss the degree to which silicide structures can be controlled using oxygen, in particular to form nanowires with silicide at controlled positions along the nanowire.

12:15 PM

Development of ZnO/MgO/p⁺-Si Heterostructures for Pure UV Light Emitting Diode with Carrier Blocking Layer: Byung Oh Jung¹; Ju Ho Lee²; Hyung Koun Cho¹; Jeong Yong Lee²; Ho Seong Lee³; ¹Sungkyunkwan University; ²KAIST; ³Kyungpook National University

ZnO has been considered as candidate material for optical devices alternative to GaN. However, due to the difficulty in obtaining p-ZnO, ZnO emitters utilized the heterojunctions, including p-GaN and SiC. However, ZnO/GaN heterojunction LEDs are economically infeasible. However, the Si substrates based LEDs have stable p-type and cost effective. ZnO can be easily synthesized, leading to the formation of high quality single crystal nanostructure on the Si. For the ZnO/Si, the interface has large band offset because the ZnO has larger band gap energy than Si. Such band offset provides effective hole carrier tunneling effect to the ZnO under forward bias. In this research, the ZnO based UV LEDs including dielectric MgO layers with proper thickness were fabricated on the p⁺-Si substrates. We focus on the thickness effect of inserted MgO layer on the blocking of the carrier flow and the UV emission intensity in the ZnO nanowires.

12:30 PM

The Temperature and Excitation Intensity Effects on the Photoluminescence Spectra of InAs /InP Quantum Dots: Fatiha Besahraoui¹; ¹Oran University

The optoelectronics properties of InAs /InP quantum dots (QDs) are investigated by means of photoluminescence (PL) measurements. The mechanisms of electron-heavy/light hole recombination which is responsible of the PL peaks appearance are explored in this study. The electron-hole recombinations are influenced by the temperature and the laser excitation intensity. The PL signal and its yield are reduced with the increase of temperature. Especially, in high energies range. The PLE measurements are very sensitive to the excitation intensity. From an appropriate value of Laser excitation, the energies levels will be saturated, which favors the light emission. The bands filling is translated by a widening in the PL spectrum towards the high energies range.

3rd International Symposium on High Temperature Metallurgical Processing: High Efficiency New Metallurgical Technology

Sponsored by: The Minerals, Metals and Materials Society, TMS Extraction and Processing Division, TMS: Energy Committee, TMS: Pyrometallurgy Committee

Program Organizers: Tao Jiang, Central South University; Jiann-Yang Hwang, Michigan Technological University; Patrick Masset, TU Freiberg; Onuralp Yuçel, Istanbul Technical University; Rafael Padilla, University of Concepcion; Guifeng Zhou, Wuhan Iron and Steel

Monday AM
March 12, 2012

Room: Southern II
Location: Dolphin Resort

Session Chairs: Tao Jiang, Central South University; Merete Tangstad, Norwegian University of Science and Technology

8:30 AM Introductory Comments

8:40 AM

A Laboratory Investigation of the Reduction of the Siderite Iron Ore to Iron Nugget: Nikolay Panishev¹; Eugene Redin¹; Vladimir Pilshchikov²; ¹Magnitogorsk Iron & Steel Works; ²Hares Engineering GmbH

The Bakal (South Ural, Russia) deposit of iron ore bearing iron carbonate (siderite) with the capacity of more than 1 billion tones belongs to the MMK. This ore cannot be fully processed via blast furnace technology because of high content of MgO. According to the investigations carried out in the USA and Japan in 1999-2004 the ITmk3 technology is a breakthrough in Ironmaking. Reduction, melting and slag removal can be achieved in just 10 min. The main objective of the investigation is to establish optimum operation conditions for the production of iron nuggets from iron carbonate bearing ore via the ITmk3 by means of the lab scale testing. Green pellets were processed via a lab tube (chamber) furnace to simulate RHF conditions. This preliminary test work provides valuable information which may be used for large-scale testing in a commercially sized RHF.

9:00 AM

Composite Agglomeration Process of Iron Ore Fines: Tao Jiang¹; Youming Hu¹; Guanghui Li¹; Yufeng Guo¹; Zhengwei Yu¹; Xiaohui Fan¹; Yuanbo Zhang¹; Yongbin Yang¹; ¹Central South University

Composite agglomeration process (CAP), as an innovative method for preparing blast furnace burden, was developed and has been put into operation in China. CAP is different from traditional agglomeration processes of iron-bearing materials involving sintering and pelletizing. Compared to the traditional agglomeration processes, CAP is characterized by several strengths such as permission of diverse iron-bearing materials in production, obvious improvement of permeability in the feed bed, decreasing the fuel consumption and remarkably increasing

the productivity of sintering machine. Furthermore, the use of the composite agglomerates prepared with CAP is capable of obviating the negative effects caused by the differences in quality of sinter and pellets on the operation of blast furnaces. This paper mainly presents an overview of the principle and applications of CAP.

9:20 AM

Investigation of Pyrometallurgical Nickel Pig Iron (NPI) Production Process from Lateritic Nickel Ores: Onuralp Yucel¹; Ahmet Turan¹; Halil Yildirim¹; ¹Istanbul Technical University

Nickel is mainly used in stainless steel production as ferronickel. In recent years, low grade ferronickel or nickel pig iron (NPI) is used in stainless steel production to reduce expenditure of nickel price. In this study, Turkey East Anatolian region lateritic nickel ores were directly processed by using carbothermal reduction to produce NPI. Firstly the raw lateritic ore that contains 0.9% Ni, 0.054% Co and 2.3% Cr was mixed with metallurgical grade coal at different stoichiometric ratios. The samples were smelted at 1600-1650°C temperature range in a induction furnace for 25 min. In the second experimental set, different process times were investigated varying from 15 to 35 min. Effect of different flux additions to the smelting charge also were examined. The raw material, obtained alloys and slags were analyzed by using XRD (X-Ray Diffractometer), XRF (X-Ray Fluorescence Spectrometer), AAS (Atomic Absorption Spectrometer) and EPMA (Electron Probe Micro Analyzer) techniques.

9:40 AM

Novel Process for Utilizing Low-Grade Manganese Oxide Ores by Sulfur-Based Reduction Roasting-Acid Leaching: Tao Jiang¹; Zhixiong You¹; Yuanbo Zhang¹; Daoxian Duan¹; Guanghui Li¹; ¹Central South University

Manganese is mainly consumed by steel and battery industries. In recent years, high quality manganese oxides are becoming less and less with development of steel and battery industries. It is essential to utilize the low-grade manganese oxides with total manganese below 25%. Conventional pyrometallurgical and hydrometallurgical processes for utilizing pyrolusite are characterized as high production cost and energy consumption, low productivity, serious environmental pollution, etc. In this study, reduction thermodynamic by sulphur of MnO₂ was firstly carried out. Then, a new process of reduction roasting with sulphur followed by acid leaching was developed to recover manganese from very low-grade pyrolusite. Effects of reduction time, S/Mn ratio and leaching parameters were investigated, and a high leaching efficiency above 95% was obtained under optimal conditions.

10:00 AM Break

10:10 AM

Silicon Process Pilot Scale Experiment in a Semi Closed in a 440 kVA Furnace Furnace: Ingeborg Solheim¹; ¹SINTEF Materials and Chemistry

SINTEF Trondheim has carried out several pilot scale silicon process experiments in the past, but always with an open off gas system. In order to test the possibilities in running a semi closed furnace operation, a new off gas hood has been designed and tested. The off gas hood is designed to collect all off gases to gain insight into the phase compositions in the off gas and at the same time have the opportunity to monitor and maintain the charging/stoking of the furnace. The furnace hood has regulation and control of the air inlet into the combustion zone in two different heights. The off gas temperature and composition was continuously monitored and analyzed during the experiment. The presentation will give a description of the pilot scale experiment with setup, equipment and results.

10:30 AM

Slide Gate Systems for Copper Tapping: Klaus Gamweger¹; Andreas Schmid¹; ¹RHI AG

This paper introduces an innovative solution to open and close the tap hole of different furnace types in the copper industry with a slide gate system. Two plates with defined drilled holes are slid against each other,

which enables effective starting and stopping of the copper flow as well as throttling. Typically, the copper is poured via a tap hole into a launder system by rotating the furnace into an appropriate position. Control of the casting rate is also performed in this manner. Or, in case of stationary furnaces the tap hole is opened by oxygen lancing and closed manually with a clay- or copper-cone. These procedures show a lot of disadvantages including splashing, oxygen pick-up, and energy losses as well as a severe danger for the working staff. All these problems can be overcome with an appropriate slide gate system.

10:50 AM

Recovery of Huangmei Limonite by Flash Magnetic Roasting Technique: Wen Chen¹; Xinghua Liu¹; Zeyou Peng¹; Qiulin Wang¹; ¹Changsha Research Institute Of Mining And Metallurgy

Limonite is a collective for iron hydroxide argillaceous materials. It is very difficult to treat due to the wide variation in specific gravity and magnetism and the high argillization rate in the course of grinding and beneficiation. The iron ore in Huangmei, Hubei, China is the typical representative of limonite. If the limonite is processed using conventional physical beneficiation methods (e.g. magnetic separation, gravity separation, flocculation-desliming-flotation, or a combined process of the three), can only be obtained an iron concentrate grade of 51.98% and an iron metal recovery of 86.64%. However, using the technique of flash magnetic roasting—magnetic separation can improve the concentrate grade to 61.03%, iron recovery to 91.17%. This paper describes the tests of recovering limonite by flash magnetic roasting in detail. Key words: limonite; flash magnetic roasting; recovery

11:10 AM

Studies on Alternative Blast Furnace Burden Structure with High Proportion Sinter: Jianjun Fan¹; Guanzhou Qiu¹; Tao Jiang¹; Yufeng Guo¹; Yongbin Yang¹; Meixia Cai²; ¹Central South University; ²Taiyuan Iron and Steel (Group) Co. Ltd

The experiments were conducted on optimizing the blast burden structure so as to replace the original low quality sinter with basicity being around 1.4-1.5. A series of sintering and metallurgical experiments was carried out, the results indicated that the sinter disintegrated seriously with basicity being around 1.4, and after this "turning point", the sintering properties get improved steadily with the increase of sinter basicity. Based on the results, a bold idea was put forward which focused on producing two kinds of sinter with different basicity. Finally an alternative BF burden structure was proposed as following: 44% sinter (Basicity being 1.05)+44% sinter (Basicity being 1.87)+12% pellet, which exhibited better technical indices compared with the original burden structure of 85% sinter (Basicity being 1.4-1.5)+15% pellet.

11:30 AM

Hydrothermal Sulfidation of Carbonate-Hosted Zinc-Lead Ore with Elemental Sulfur: Cunxiong Li¹; Chang WEI¹; ¹Kunming University of Science and Technology

Direct flotation of carbonate hosted zinc-lead ore is characterized by recovery of zinc and lead only around 55% and 50%, respectively. Mineralogical analysis shows that the sample used in the present study is a carbonate hosted zinc-lead ore, with a zinc and lead carbonate content that accounts for 80.14% and 75.63% of the total minerals, respectively. The carbonate hosted zinc-lead ore was hydrothermally sulfidized with elemental sulfur and the experimental data indicated that under the conditions employed up to 75% zinc and 82% lead sulfidation extent were achieved. As a result of pre-sulfidation followed by flotation, the recoveries of zinc and lead into flotation concentrate were over 90%. A flotation concentrate was obtained with 52% Zn and 37% Pb from the materials which was treated by sulfidation.



TMS 2012

141st Annual Meeting & Exhibition

MONDAY AM

Advances in Surface Engineering: Alloyed and Composite Coatings: Session I

Sponsored by: The Minerals, Metals and Materials Society, TMS Materials Processing and Manufacturing Division, TMS: Surface Engineering Committee

Program Organizers: Sandip Harimkar, Oklahoma State University; Srinivasa Bakshi, Indian Institute of Technology Madras; Arvind Agarwal, Florida International University

Monday AM

Room: Macaw 1

March 12, 2012

Location: Swan Resort

Session Chair: To Be Announced

8:30 AM Introductory Comments

8:35 AM Invited

An Overview of Dry Sliding Wear of Two-Phase FeNiMnAl Alloys: *I. Baker*¹; ¹Dartmouth College

This paper presents an overview of the dry sliding wear behavior of two-phase FeNiMnAl alloys tested in different environments, i.e. air, dry oxygen, dry argon and a 5% hydrogen/nitrogen mixture. Pin-on-disk wear tests were performed using FeNiMnAl pins against an yttria-stabilized zirconia counterface. The worn pins and the counterface were examined using a variety of techniques: the near-surfaces of the worn pins were examined using transmission electron microscopy on cross-sectional specimens produced by focused ion beam (FIB) milling; scanning electron microscopy was used to examine the FIBbed pits and the worn surfaces of the pins; debris collected from all the tests was characterized using X-ray diffractometry; and the worn zirconia disk was examined using both optical microscopy and profilometry. Using this combination of techniques it has been possible to understand the wear rates and wear mechanisms for the different alloys in the various test environments.

9:00 AM Invited

CrN-Ag Nanocomposite Coatings: High-Temperature Lubrication through Nanopore Channels: *Daniel Gall*¹; Christopher Mulligan²; Paul Papi¹; Thierry Blanchet¹; ¹Rensselaer Polytechnic Institute; ²Benet Laboratories

A promising approach to achieve high-temperature lubrication and wear protection is the inclusion of a soft noble metal in a hard wear-resistant matrix. Our prototype nanocomposite material system is CrN-Ag, which is co-deposited by reactive sputtering onto steel substrates. A detailed study of the atomistic processes during deposition allows control of the microstructure. In particular, surface diffusion and atomic shadowing effects are exploited to create 1-nm-wide pores (nanopipes) within the CrN matrix which act as channels for Ag lubricant flow during high temperature operation. The key parameter that determines the lubricant transport is the difference in the temperature of layer deposition $T_s = 300\text{--}700\text{ }^\circ\text{C}$ and testing temperature $T_a = 425\text{--}800\text{ }^\circ\text{C}$. This is attributed to the Ag agglomerate size which increases with increasing T_s , reducing the thermodynamic driving force for surface segregation. Ball-on-disk testing against alumina counterfaces shows sustained friction coefficients $=0.2$ at $450\text{--}650\text{ }^\circ\text{C}$.

9:25 AM Invited

Micromechanisms of Failure in Multilayered Hard Coatings of ZrN-Zr and TiAlN-TiN: *Vikram Jayaram*¹; Nisha Verma¹; ¹Indian Institute of Science

Contact damage in hard coatings is a function of coating microstructure, residual stress and the mechanical properties of the constituents as well as the film thickness and substrate's mechanical properties. This talk will describe how multilayering with either similar phases (TiN-AlTiN) or with ductile interlayers (ZrN-Zr) can modify damage modes under indentations. Interfaces between similar phases are able to provide additional modes of deformation that reduce stress concentrations that lead to fracture. On the

other hand, soft layers need to be an optimum thickness which appears to be $\sim 30\text{--}50\text{ nm}$ to avoid interfacial delamination or nitride cracking that is induced by metal plasticity. These observations will be supported by a combination of analytical and finite element modeling of axisymmetric indentations.

9:50 AM

Advances in Surface Engineering for Amorphous Coatings: *Sandip Harimkar*¹; ¹Oklahoma State University

Amorphous alloys represent a new class of advanced materials exhibiting attractive combinations of properties such as high strength/hardness and excellent wear/corrosion resistance. While bulk processing of amorphous alloys is difficult, various binary and multi-component amorphous alloys can be coated using various rapid solidification, solid-state sintering, and electrochemical processes. In this presentation, an overview of processing approaches for coating wear and corrosion resistant amorphous coatings will be presented.

10:10 AM Break

10:25 AM

Metal Matrix Composite Hardfacing by Additive Friction Stir: *Jeffrey Schultz*¹; ¹Schultz-Creehan Holdings, Inc

Additive friction stir (AFS) is a solid-state coating method in which wrought metal is deposited onto metallic substrates. AFS uses shear-induced interfacial heating and plastic deformation to deposit metal and metal matrix composite (MMC) coatings, and the mechanical shearing that occurs at the interface results in a metallurgical bond between the substrate and coating. Al alloys are relatively soft in comparison to other materials used for wear surfaces. However, if the wear resistance of Al alloys can be improved by local surface modification then significant weight reductions could be realized by replacing iron-based materials with Al. Deposition of Al-50 vol% SiC coating onto a MIC 6 substrate was demonstrated using AFS. The deposited MMC coating is approximately twice as hard as the base metal. The MMC-coated surface showed an almost three-fold improvement in the reciprocal wear rate as compared to the base casting when tested under ASTM G65 abrasion testing.

10:45 AM

Multiscale Mechanical and Tribological Behavior of Plasma Sprayed Carbon Nanotube Reinforced Aluminum Composites: *Srinivasa Bakshi*¹; Arvind Agarwal²; ¹Indian Institute of Technology Madras; ²Florida International University

Mechanical and Tribological Properties of CNT reinforced Aluminium have been evaluated at the macro- and nano-scale. Nanoindentation indicated an increase in the elastic modulus by 19% and 39% by the addition of 5 wt.% and 10 wt.% CNTs respectively. Macro-scale compression tests indicated no improvement in the elastic modulus but an increase in the compressive yield strength by 27% and 77% respectively, by addition of 5 wt.% and 10 wt.% CNTs. Nanoscratch testing carried out on the Al-Si matrix with dispersed CNTs indicated a decrease in scratch volume by 34% and 71% for 5 wt.% and 10 wt.% CNTs coating respectively. Macro-scale wear tests indicated a decrease in the wear volume by 68% in case of 5 wt.% CNT coatings but an increase in the wear volume by 15% for the 10 wt.% CNT coating. The variation of the properties at nano and macro scales are discussed.

11:05 AM

Microstructures and Wear Properties of $(\text{Ti}_{1-x}\text{Mo}_x)\text{N}_y$ Hard Coatings: *Shoko Komiyama*¹; Yuji Sutou¹; Junichi Koike¹; Mei Wang²; Takaomi Toihara²; ¹Tohoku University; ²OSG Corporation

TiN films have been widely used in cutting tools and molds. It is recently found by Komiyama et al. that the hardness of Ti-Mo-N films can be increased by precipitation hardening by soft bcc particles [1]. In this study, the effects of the film composition on the microstructures and wear properties of $(\text{Ti}_{1-x}\text{Mo}_x)\text{N}_y$ films were investigated. The films with various compositions were deposited on AISI304 and WC-Co by

RF reactive sputtering using $Ti_{25}Mo_{75}$, $Ti_{50}Mo_{50}$ and $Ti_{75}Mo_{25}$ targets. To deposit nitrides, the mixture of Ar (7.5ccm) and N_2 (0-2.0ccm) gases were introduced. From wear test using carbon steel (S45C) as a counterpart, it was found that a $(Ti_{0.51}Mo_{0.49})N_{0.72}$ film deposited on WC-Co shows excellent wear properties. Transferred materials from the counterpart were hardly observed on the surface of the film. These results suggest that the film has an excellent adhesion resistance. [1] S. Komiyama et al., Materials Transactions, 51 (2010) 1467.

11:25 AM

Wear Resistance of Spray Formed Stainless Steels: *Claudemiro Bolfarini*¹; Leamar Beraldo¹; Conrado Afonso¹; Claudio Kiminami¹; Walter Botta¹; ¹Universidade Federal de São Carlos

This work investigated the microstructure and wear resistance of two spray formed stainless steels, ferritic-AIF with 29% Cr and a superduplex-SDM modified with boron (3.5wt%). The rapid solidification process promoted the formation of a new structure with refined grains and metastable phases. The deposits, weighing about 3.5 kg, were characterized by a combination of optical microscopy, scanning electron microscopy (SEM), hardness test and abrasion test according to ASTM G65-07. The deposits of AIF and SDM presented finer microstructure and higher hardness values when compared to conventionally cast materials. The abrasion resistance of the SDM was higher than the materials tabulated in ASTM G65-07, namely, Stellite 1016 and AISI D2, while the AIF presented an intermediate value between these two materials.

11:45 AM

Use of Thermo-Mechanical Simulator in Studying the Cyclic Oxidation of NiCrAlY Coatings: *Nidhi Rana*¹; R. Jayaganthan¹; Satya Prakash¹; ¹Indian Institute of Technology, Roorkee, India

The MCrAlY coating system has been used in the gas turbine engines to provide the resistance against oxidation and corrosion at the operating temperature of the engine. The cyclic oxidation test of the coatings has been carried out by heating the samples at temperature of 900°C and subsequent cooling so as to simulate the actual operation of the engine. In present work an attempt has been made to use the Thermo-mechanical Simulator for the above study. Various characterisation techniques like X-ray diffraction, Electron microscopy and X-ray elemental mapping has been used to study the presence of different oxide phases, their morphology and elemental composition.

Aluminum Alloys: Fabrication, Characterization and Applications: Development and Application

Sponsored by: The Minerals, Metals and Materials Society, TMS Light Metals Division, TMS: Aluminum Processing Committee
Program Organizers: Subodh Das, Phinix LLC; Tongguang Zhai, University of Kentucky; Zhengdong Long, Kaiser Aluminum

Monday AM
March 12, 2012

Room: Northern E1
Location: Dolphin Resort

Session Chair: Steven Long, Kaiser Aluminum

8:30 AM

Aluminum Welded Blank Applications in the Automotive Industry: *Susan Hartfield-Wunsch*¹; Ravi Verma¹; Blair Carlson¹; ¹General Motors

Aluminum welded blanks (AWB's) are of interest to the automotive industry for applications such as door inner panels to achieve mass reduction over current production steel doors, leading to improved fuel economy. Using an AWB instead of a multi-piece aluminum door inner design provides not only part consolidation, but also improved dimensional performance, and improved door stiffness. In this study, AWB's were evaluated for a midsize car door inner, including laboratory testing and full-scale forming trials. Blanks were fabricated using friction stir welding and laser welding, joining 1.1mm AA5182 to

2.0mm AA5182. The blanks were stamped into door inner panels where local strains and thinning measurements were compared to formability simulation predictions. Weld quality was evaluated with microstructure and microhardness data. Forming results and weld quality evaluation were used to create specification guidelines for AWB's.

8:50 AM

Influence of Stress on Sensitization in Al-Mg Alloys: *William Golumbskie*¹; Jennifer Gaies¹; Mitra Taheri²; ¹Naval Surface Warfare Center, Carderock Division; ²Drexel University

5xxx aluminum alloys are considered sensitized when magnesium precipitates out of solution forming a deleterious β -phase (Mg_2Al_3) around grain boundaries. Current research uses accelerated heat treatments at elevated temperatures in a laboratory setting to simulate sensitization that occurs naturally at lower temperatures and longer times. This approach neglects contributions of stress on the kinetics of β -phase precipitation. Understanding how stress affects sensitization is necessary to ensure that laboratory samples reflect the microstructure and phase stability of naturally sensitized specimens. Test specimens will be loaded at incremental stress levels and exposed to elevated temperatures. Their microstructure and degree of sensitization will be characterized using microscopy coupled with the ASTM G67 test. The findings will be compared to aluminum samples that were sensitized via natural exposure. A key deliverable of this effort is the determination of a combination of time, temperature, stress and environment that best replicate naturally sensitized Al.

9:10 AM

Material Performance of Naturally Sensitized Aluminum 5xxx Alloys: *Angela Whitfield*¹; Daniel Stiles¹; William Golumbskie¹; ¹Naval Surface Warfare Center

Current understanding of the effect of sensitization on 5xxx aluminum mechanical property performance is limited. Sensitization of aluminum in-service has led to severe cracking in marine structures. Degree of sensitization measurements taken near cracks in naturally-sensitized aluminum plates have shown high ($>40 \text{ mg/cm}^2$) levels of sensitization. This effort will examine the degree of sensitization, microstructure, tensile, and fracture toughness of several specimens of naturally sensitized aluminum in an attempt to correlate degree of sensitization with material performance. The resulting data can be used to understand how degree of sensitization degrades performance of aluminum ship structures and can influence maintenance or repair decisions. This study is unique, in that it examines the performance of naturally-sensitized aluminum in lieu of artificially (laboratory) sensitized materials.

9:30 AM

Precipitation of the θ' (Al_2Cu) Phase in Al-Cu-Ag Alloys: *Julian Rosalie*¹; Laure Bourgeois²; Barrington Muddle²; ¹National Institute for Materials Science; ²Monash University

Precipitation of the θ' (Al_2Cu) phase was examined in Al-(1.75-x) at.%Cu-x at.%Ag alloys. In alloys containing trace Ag the θ' precipitates formed T- or cross-shaped arrays of sympathetically-nucleated arrays similar to those reported in binary Al-Cu alloys. However, in alloys with equal atomic levels of copper and silver such arrays were not formed and the θ' plates formed at specific sites on dislocation loops alongside pre-existing γ' ($AlAg_2$) precipitates. The dislocation loops appeared to dissociate at these sites in a manner which would provide a stacking fault that was isostructural with the θ' precipitate. Energy dispersive X-ray (EDX) mapping showed that the dislocation loops were silver-enriched at the sites where the θ' phase eventually precipitated and that a silver atmosphere remained after precipitation of the θ' plates.



TMS 2012

141st Annual Meeting & Exhibition

MONDAY AM

9:50 AM

Using High-Resolution Topographic Imaging to Characterize the Hemming Performance of Automotive Aluminum Alloys: *Mark Stoudt*¹; Joseph Hubbard¹; John Carsley²; Susan Hartfield-Wünsch³; ¹National Institute of Standards and Technology; ²General Motors R&D Center; ³General Motors Technical Center

Flat hemming of aluminum alloys can be problematic due to a lower ductility and fracture resistance that promotes intense strain localization and crack initiation near the apex of the bend. The performance of two-6xxx series aluminum hemming alloys, with and without a ten percent uniaxial pre-strain, was evaluated after bending to a 180-degree angle in a simulated hemming operation. Since the deformed surface is highly dependent on the local microstructural and strain conditions, detailed examinations of the morphologies of the bend apexes from these surfaces revealed substantial details about the character of the deformation produced during hemming. The topographical data were also used to construct high-resolution maps of the strain localization magnitudes. These maps directly quantified the surface conditions required for crack initiation and revealed the specific locations of the most intense surface deformation. The techniques and the observed relationships between the microstructure and the deformed surface shall be discussed.

10:10 AM

Characterization of Electron Beam Deposited Aluminum Alloy 2139: *Milo Kral*¹; Karl Buchanan¹; Craig Brice²; Marcia Domack²; Ravi Shenoy²; William Hofmeister³; ¹University of Canterbury; ²NASA Langley Research Center; ³UT Space Institute

Aluminum 2139 is a Cu-Mg-Ag bearing alloy designed to have a desirable combination of strength and fracture toughness through a large range of plate thicknesses. Electron beam freeform fabrication (EBF3) is an additive manufacturing technique that allows for the creation of near net shape directly from a computer model. Alloy 2139 is an excellent candidate material for EBF3 due to its insensitivity to section size and low mechanical work requirements necessary to achieve peak strength and toughness. This study aims to characterize EBF3 deposited 2139, in the as-deposited state as well as in various heat-treated states. Characterization methods include scanning electron microscopy with electron backscatter diffraction for phase identification and orientation mapping, analytical transmission electron microscopy, differential scanning calorimetry and microhardness mapping. The results of this study will identify the ideal heat treatment for achieving peak strength in EBF3 2139 aluminum alloy.

10:30 AM Break

10:45 AM

Near Net Shaped Casting of 7050 Al Wrought Alloy by CDS Process: Microstructure and Mechanical Properties: *Seyed Giaasiaan*¹; Abbas Khalaf¹; Xiaochun Zeng¹; Sumanth Shankar¹; ¹McMaster University

Controlled diffusion solidification (CDS) involves mixing two precursor alloys at different thermal mass and subsequently casting the resultant mixture into near net shape cast components. The process enables casting of Aluminum wrought alloys into near net shaped components by circumventing the problem of hot tearing by obtaining a non dendritic morphology of the primary Al phase. The study presents the favorable process and alloy parameters to enable sound shaped casting of 7xxx Al wrought alloys (Al-Zn-Mg-Cu) by the CDS process along with the mechanical tensile properties under various heat treatment conditions. The tilt pour gravity casting process was used for this study and the ability to obtain high integrity casting of these alloys with significantly superior strength and ductility of the cast components. In depth microstructure analysis outlining the phased in the cast and heat treated microstructure would also be presented.

11:05 AM

A Study of Stress Effects on η -Phase Precipitation in Al-Mg Alloys Using In-Situ TEM: *Daniel Scotto D'Antuono*¹; Jennifer Gaies²; William Golumbskie²; Mitra Taheri¹; ¹Drexel University; ²Naval Surface Warfare Center

The 5xxx series aluminum-magnesium alloys are non-heat treatable metals commonly found in structural applications due to excellent corrosion resistance and weldability. Despite these strong characteristics these systems are prone to sensitization which leads to failure. Here, magnesium segregates toward grain boundaries and precipitates as Al₃Mg₂ (β -phase). This β -phase renders the alloy susceptible to intergranular and stress corrosion cracking (IGSCC). Aging exposure to medium/high temperatures, corrosive environments, and load contribute to the overall failure. Current studies on 5xxx sensitization have neglected to examine the effects of stress along with temperature on β -phase formation. In this work, the β -phase precipitation mechanism is observed by conducting simultaneous heating and straining experiments using in-situ TEM. This will allow for the determination of the time, temperature, and stress that give rise to the sensitization. Understanding the precipitation of β -phase is necessary to mitigate and prevent its formation and thus reduce the susceptibility of these alloys.

11:25 AM

Effect of Heat Treatment on Silicon in Hypereutectic Al-Si Alloy: *Ying Zhang*¹; ¹Zhengzhou Research Institute of CHALCO

Heat treatment is an efficient way to refine the second-phases in alloys. Refinement is very important to hypereutectic Al-Si alloy, a type of outstanding wear-resistant material, which mechanical properties are always badly damaged by coarse silicon. In this article, morphology and orientation changes of primary and eutectic silicon caused by solution treatment were studied. Integrated thermal analyzer, high temperature metallographic microscope, optical microscope, scanning electronic microscopy and transmission electron microscopy were used. The result shows that the heat treatment can smooth and refine silicon phases, thus increases the tensile strength and elongation. The orientation relationship between silicon and matrix is also changed.

Atomistic Effects in Migrating Interphase Interfaces - Recent Progress and Future Study: Interfacial Structure with Small Misfit

Sponsored by: The Minerals, Metals and Materials Society, TMS Materials Processing and Manufacturing Division, TMS/ASM: Phase Transformations Committee

Program Organizers: Tadashi Furuahara, Institute for Materials Research, Tohoku University; Sudarsanam Babu, Ohio State University; Hatem Zurob, McMaster University; Jian-Feng Nie, Monash University; Wen-Zheng Zhang, Tsinghua University; James Howe, University of Virginia

Monday AM
March 12, 2012

Room: Europe 3
Location: Dolphin Resort

Session Chairs: Tadashi Furuahara, Tohoku University; WenZheng Zhang, Tsinghua University

8:30 AM Introductory Comments Tadashi Furuahara

8:35 AM Invited

Topological Modelling of the Growth and Accommodation of Plate-Shaped Products Formed in Displacive Transformations: *Robert Pond*¹; John Hirth²; ¹University of Exeter; ²Private individual

Both diffusionless (martensitic) and diffusional-displacive transformations can be modelled using the topological method. Here, interfaces are considered to be semi-coherent, with a network of disconnections and dislocations (slip or twinning) superposed on the underlying coherent terrace. The mechanism of transformation is the

motion of disconnections along the interface, so transformation kinetics depend on the mobility of these defects, and the extent of long-range diffusion, if any. The 3-D morphology of a product is determined by the configuration of disconnection loops encircling it. On the broad faces, the defect network compensates the coherency strains, but, towards the edges, longer-range stresses arise. These stresses can be ameliorated by, for example, plastic deformation in the vicinity of the edges, or the coalescence of plate variants in self-accommodating groups. In cases where the matrix and product exhibit common symmetry, internal dislocation walls may be present. Experimental observations consistent with these accommodation mechanisms are discussed.

9:05 AM Invited

Application of Edge-to-Edge Matching Model to Surface Transformation in a Titanium-Chromium Alloy: *Mingxing Zhang*¹; Dong Qiu¹; Patrick Kelly¹; ¹The University of Queensland

The success in applications of the edge-to-edge matching (E2EM) model to crystallography of diffusion-controlled phase transformations in solids, to understanding of the grain refinement mechanism in light metals and to study of the epitaxial growth, quantum dots and nanowires, shows particular importance of the actual atomic matching along the matching rows. However, previous work was done in bulk materials. Phase transformations occurred on the free surface differ from those in the bulk materials because there are less restriction to the formation of new phases, which facilitates the release of strain energy, and surface relief appears on the free surface. The present work reports the recent crystallographic results of surface transformation in a Ti-Cr alloy. The E2EM model is used to understand the formation of surface reliefs. The role of the edge-to-edge atomic matching in reduction of interphase interfacial energy between two phases is also discussed.

9:35 AM

Crystallographic Morphology Evolution in a FCC/BCC System via a Discrete Atom Method: *Dai Fu-Zhi*¹; Wen-Zheng Zhang¹; ¹THU

Phase transformation crystallography evolution in a FCC/BCC system is studied with a discrete atom method proposed by Lee [1995, Scripta Metall.] Isotropic elastic constants and interfacial energy were adopted in the simulation. Morphologies and orientation relationships (ORs) were computed for different precipitate sizes. Small precipitates show a rhombus shape with the N-W OR, while big precipitates are elongate along the invariant line direction, with the direction and OR in a full agreement with the values determined by Dahmen's [1982, Acta Metall.] 2D invariant line model. Application to a Cu-0.20mass%Cr alloy shows the evolution from the N-W OR for small particles to a near K-S OR for big precipitates, which can account for the observations of OR in the early stage of ageing of the same alloy reported in literature.

9:55 AM

Characterization of Alpha/Gamma Interfaces in a Bainitic Microstructure: *Sherri Hadian*¹; Gary Purdy¹; Gianluigi Botton¹; ¹McMaster University

The cementite free bainitic microstructure in a 0.5% C, 1.8% Si and 5% Ni steel, was used to study the interfacial structure of fcc/bcc interfaces. Several facets and their dislocation structure were characterized. Based on observations, the transformation was recognized as an invariant line transformation and consequently the interfacial structure and the mobility of interfaces were discussed as they might be affected by this observation.

10:15 AM Break

10:30 AM Invited

Crystallography, Shape Change and Their Relationship in the Formation of Precipitate Plates/Laths: *Jian-Feng Nie*¹; ¹Monash University

The approach that is based on commensurate edge-on matching of lattice planes is used in the present work to examine the crystallography, shape change and their relationships in the formation of precipitate plates/laths. It is found that many precipitations of the plates/laths, including those that have been conventionally classified as non-displacive, exhibit a significant shear component of the shape strain. In all such precipitations, a shear strain is inevitably associated with interface motion if the coherent or commensurate edge-to-edge matching of lattice plane is to be preserved in the planar interface separating the two lattices. This finding provides some insights into the transformation mechanisms and the nucleation and growth behaviours of precipitate plates/laths. It is conceivable that minimisation of this shear strain, via either self-accommodation or external lattice defects, could be a critical factor in dictating the formation of such precipitates.

11:00 AM

Modelling Morphologies of β' Precipitates in Mg-RE Alloys: *Hong Liu*¹; Yipeng Gao²; Zhe Liu¹; Yunzhi Wang²; Jian-Feng Nie¹; ¹Monash University; ²The Ohio State University

The metastable phase β' is a key strengthening precipitate phase in Mg-RE alloys. Its morphology changes from a nearly spherical shape in Mg-Y-Nd alloys to a lenticular shape in Mg-Gd-Y alloys. In the latter, the broad surface of the lenticular precipitates is nearly parallel to the prismatic planes of the matrix phase and is therefore more effective in strengthening. In this work, we aim to understand the various morphologies of the β' phase in the Mg-RE alloys. The lattice parameters and elastic constants of the β' phase and the interfacial energy of the coherent β' /Mg interface are calculated for various Mg-RE systems by the first-principles approach. Using these parameters as inputs, the equilibrium shape of and the stress field around the β' phase are then determined by the phase field approach. The strengthening effect of β' precipitates having different morphologies are also investigated by phase field model of dislocation-precipitate interactions.

11:20 AM

HRTEM Investigations on Austenite/Ferrite Interfacial Structure in the 2205 Duplex Stainless Steel: *Hung-Wei Yen*¹; Jer-Ren Yang¹; ¹National Taiwan University

The ferrite/austenite interfacial structure always plays a critical role in diffusional austenite-to-ferrite transformation in steels. Unfortunately, undecomposed austenite in the corresponding alloys with diffusional ferrite will transform into bainite or martensite as the alloys cooled down so that it causes difficulty to study the previous interfacial structure. The present study attempts to investigate, by using HRTEM, the interfacial structure of intra- and intergranular austenite form in delta ferrite matrix by diffusional transformation in the 2205 stainless steel. The TEM results indicate the transformation is associated with ledge structure for austenite with and without rational orientation relationship with neighboring ferrite. It is proposed that these ledged interfacial configurations can also occur in diffusional austenite-to-ferrite transformation.



Biological Materials Science Symposium: Bio-Inspired Materials: Mechanics and Design

Sponsored by: The Minerals, Metals and Materials Society, TMS Electronic, Magnetic, and Photonic Materials Division, TMS Structural Materials Division, TMS: Biomaterials Committee
Program Organizers: Nima Rahbar, University of Massachusetts Dartmouth; Candan Tamerler, University of Washington; Po-Yu Chen, University of California, San Diego; Molly Gentleman, Texas A&M University

Monday AM Room: Swan 7
March 12, 2012 Location: Swan Resort

Session Chairs: John Nychka, University of Alberta; Nima Rahbar, University of Massachusetts Dartmouth

8:30 AM Introductory Comments

8:35 AM

Bioinspired Ceramic Coatings: Durability and Potential for Self-Lubricity: *John Nychka*¹; Nathan Lun¹; ¹University of Alberta

Ceramic coatings have been produced on metallic substrates with varying wettability through process optimization of temperature and time. Hydrophilic or near super-hydrophobic coatings are possible, and this presentation will report on investigations of the wettability, durability, and potential for self lubricating qualities when oils are introduced on the surface.

8:55 AM

Structure-Property Relationships of the Natural Multi-Layered Material Systems: *Wayne Hodo*¹; Paul Allison¹; Mei Chandler¹; John Peters¹; Allan Kennedy¹; Rogie Rodriguez²; ¹ERDC; ²University of Puerto Rico - Mayaguez

In this investigation, experiments and modeling were conducted to study the structure and mechanical properties of the alligator gar fish scales to ascertain the possible design principles of the biological armor system. Optical microscope and scanning electron microscope (SEM) images of the cross section of garfish scales revealed a multi-layered structure. Nanoindentation tests correlated to SEM with energy dispersive X-ray (EDX) analysis show that the hardness and modulus exhibit a gradient across the scale's layers when transitioning from one layer to the next instead of discrete variations in mechanical properties between each layer. Microindentation tests were performed at quasi-static loading conditions to examine the fracture and deformation mechanisms of the individual scales due to penetration loading condition. Finite element analysis of garfish scale under microindentation loading shows that the scale's overall property gradient across the layers spreads the deformation which provides delamination resistance at the interfaces.

9:10 AM

Quantum Effects in Interfacial Mechanics of Polymer-Ceramic Hybrid Biomaterials: *Devendra Dubey*¹; *Vikas Tomar*¹; ¹Purdue University

In hierarchical nanocomposite materials (eg. bone, nacre), interfacial interactions between the organic phase (eg. tropocollagen (TC)) and the mineral phase (eg. calcium hydroxyapatite (HAP)) as well as the structural effects arising due to the staggered arrangement, TC mutations, and varied HAP textures significantly affect the strength of such biomaterials. In the present investigation, different idealizations of TC-HAP composite biomaterial system under tensile and compressive loadings are analyzed using explicit three dimensional (3-D) quantum mechanical simulations to develop an understanding of these factors. Analyses show that maximizing the contact area between the TC and HAP phases result in higher interfacial strength as well as higher fracture strength. Analyses based on strength scaling as a function of structural hierarchy reveal that while peak strength follows a multiscaling relation, the fracture strength

does not. The peak strain for failure was found to be independent of the level of structural hierarchy.

9:30 AM Break

9:40 AM Invited

Nonlinear Behavior of Silk Minimizes Damage and Begets Spider Web Robustness from the Molecules Up: *Markus Buehler*¹; Steven Cranford¹; Nicola Pugno¹; Anna Tarakanova¹; ¹Massachusetts Institute of Technology

The behavior of spider webs, ranging from its protein sequence to spiral geometry, has intrigued scientists for centuries. How the role of silk's material behavior, architecture, as well as its failure behavior altogether serve to benefit the integrity of a spider web formation, however, remains unknown. Here we show that the nonlinear material behavior of silk fibers, softening at the yield point to dramatically stiffen during large deformations until point of failure, is what allows for localization of deformation upon loading, and is precisely what makes spider webs robust and extremely resistant to defects, as compared to other linear-elastic or elastic-plastic materials. Through in situ experiments on webs of a European garden spider, we confirm the prediction that locally applied loading results in minimal damage. We further show that under global loads such as wind, the material behavior of silk under small-deformation is crucial to maintaining the web.

10:10 AM Invited

Mechanics of Hierarchical Structures in Bone: *Shashindra Pradhan*¹; *Dinesh Katti*¹; *Kalpna Katti*¹; ¹North Dakota State University

Collagen is the most abundant protein in the human body and provides structural integrity to tissues. A hierarchical organization of collagen exists in bone. The collagen molecule is about 300 nm long and 1.5 nm in diameter. It consists of a triple helical molecular structure consisting of three polypeptide chains. We have studied the role of nonbonded interactions between mineral and collagen on collagen mechanics. We have also investigated molecular level deformation mechanics of full length collagen (300 nm) using steered molecular dynamics (SMD). We report that nonbonded interactions of collagen with mineral as well as with water molecules play significant role on mechanics of collagen. Also, new hierarchical morphologies of collagen are observed in the full length collagen, not seen in short collagen. Multiscale models of fibril level structures are developed using finite element methods. These multiscale simulations provide the necessary framework for robust prediction of human tissue mechanics.

10:40 AM

Phase Field Model of Fracture for Inhomogeneous Materials: *Mark Jhon*¹; Qian Xiao Li¹; ¹Institute of High Performance Computing

Hard biological tissues such as nacre contain many levels of structural hierarchy. One challenge for predicting the mechanical behavior of these materials involves incorporating different levels of structural hierarchy into a mesoscale model. In the present study, we present a phase field model of fracture that incorporates disorder at fine length scales. This is intended to account for randomness in the brick-and-mortar structure of nacre. We find that by introducing disorder in the local stiffness, the apparent toughness of the composite is increased. If spatial correlations in the stiffness are sufficiently large, crack deflection can also be observed.

11:00 AM

A Study of Iatrogenic Fracture Risk in Reduction of Pipkin Fracture-Dislocations of the Hip: *Michael Duffy*¹; *Samar Kalita*²; *Gerald Bertetta*²; *Mark Munro*¹; ¹Orlando Regional Medical Center; ²University of Central Florida

Hip fracture-dislocations are serious injuries that require emergent orthopedic treatment. Iatrogenic femoral neck fracture during closed reduction of hip fracture-dislocations is an unappreciated occurrence. This study evaluated the risk of such fractures during closed reduction of Pipkin fracture-dislocations. 20 specimens (12 male and 8 female), age 54.3-42.4 years, were obtained, radiographed, and prescreened for

abnormalities and bone mineral density (BMD). 18 screened femurs were tested in a tensile tester by randomly assigning them to three groups: native femora, simulated Pipkin I fracture, and simulated Pipkin II fracture. Most specimens failed at the neck. The average failure loads of the native, Pipkin I and Pipkin II specimens were 2501, 2750 and 2787 N, respectively. Statistical analysis, performed with ANOVA, showed no correlation between failure load, BMD, and fracture-type. Closed reduction should be gentle and be attempted under appropriate relaxation to apply the least force to the proximal femur.

Bulk Metallic Glasses IX: Alloy Development and Application

Sponsored by: The Minerals, Metals and Materials Society, TMS Structural Materials Division, TMS/ASM: Mechanical Behavior of Materials Committee

Program Organizers: Peter Liaw, The University of Tennessee; Hahn Choo, The University of Tennessee; Yanfei Gao, The University of Tennessee; Gongyao Wang, University of Tennessee

Monday AM
March 12, 2012

Room: Swan 6
Location: Swan Resort

Session Chairs: Peter Liaw, The University of Tennessee; William Johnson, Keck Laboratory of Engineering

8:30 AM Keynote

Progress in Engineering Applications of Bulk Metallic Glasses: William Johnson¹; ¹University of Tennessee

Bulk metallic glasses with unique combinations of strength, toughness, ductility, and other properties are of increasing interest for a variety of engineering applications as structural and functional materials. Emerging approaches to fabrication of precision net-shape metallic glass hardware such as the recently developed Rapid Discharge Forming method enable fabrication of high performance metallic glass components using methods that parallel those employed to produce widely used polymer plastic parts. The evolution of this processing technology combined with the discovery and optimization of lower cost, high performance, and processable glass forming alloys is expected to lead to accelerated adaption of bulk metallic glasses in a variety of commercial products. The talk presents an overview of this emerging materials/processing technology.

9:00 AM

Glass Formation in a Laser-Glazed Zr-Cu-Ni-Al-Nb Alloy: Brian Welk¹; Hamish Fraser¹; Mark Gibson²; ¹The Ohio State University; ²CSIRO

The present work explores the practical possibilities of using the LENS[®]8482 (laser engineered net shaping) deposition technique, combined with laser-glazing, to evaluate the formation-properties-production of bulk metallic glasses. A Zr-Cu-Ni-Al-Nb alloy was subjected to a number of laser glazing experiments to remelt and rapidly solidify a thin layer. Detailed SEM evaluation was conducted to investigate the microstructural evolution from the base alloy through a semi-solid region to the re-solidified melt pool. A marked transition in the microstructure was observed as a result of phase selection. This provided valuable insight into the scope for microstructure manipulation with alteration of the processing variables. The results obtained thus far indicate that the technique described herein provides a powerful tool for rapid screening of the glass forming potential of compositionally graded alloy bars. Additionally, this technique provided insight into alloy compositions that may produce amorphous matrix composite microstructures for a variety of functional applications.

9:10 AM Invited

Bulk Metallic Glasses: From Fundamentals to Applications: Atakan Peker¹; ¹Washington State University

During the past two decades, Bulk Metallic Glasses (BMG) received an increasing attention from academia and industry. Researchers developed several new alloy formulations, performed extensive structure and property characterization, and end-user engineers explored creative ways to use BMG in various products. Despite all these efforts, the commercial success of BMG is still quite limited. This presentation will give a concise review of these efforts and will consider the underlying issues key to broader success and applications of BMG. Some of these issues are inherent to BMG fundamentals and are difficult challenges to address in the near term. There are also issues, which can be resolved in the near term with better awareness and focused effort by the BMG community. This presentation will focus on these issues and review recent attempts to address such challenges with particular attention to structural applications.

9:30 AM

Fabrication of Microchannels for Micro-Fluidic Applications Using High Frequency Micromachining on an Amorphous Material: Vivek Jain¹; Apurba Sharma¹; Pradeep Kumar¹; ¹Indian Institute of Technology Roorkee

Developments of micron-sized channels and cavities through micromachining techniques have contributed immensely towards advancements in the area of micro-fluidic systems. These microchannels are typically made of silicon, metal, or glass with the size ranging from 1 μm to 1000 μm and often feature circular, rectangular or trapezoidal cross sections. However, precision machining of any feature on an amorphous material is challenging. A high frequency low amplitude micromachining technique is capable of machining high aspect-ratio features on these materials without significantly changing metallurgical, chemical, or physical properties of workpiece material. In the present work, micro ultrasonic machining (micro USM), is employed to create microchannels on glass. The channels produced in the dimensions of 300 μm \times 400 μm \times 500 μm are ideally suited for micro-fluidic applications. The performance of the method while fabricating the microchannels has been evaluated in terms of dimensional errors, flatness, straightness, and surface roughness.

9:40 AM Invited

Development of Porous Metallic Glass Compacts: Ki Buem Kim¹; ¹Sejong University

In this report, a single pulse of 0.1kJ-0.5kJ/0.5g spherical three kinds of metallic glass powder (Cu-Ni-Zr-Ti, Zr-Ti-Cu-Ni-Be and Zr-Al-Ni-Cu alloys) in size range of 90-150 μm at a constant capacitance of 450 μF , was applied to produce the porous metallic glass compacts. Microstructural investigation reveals that fully porous structure was obtained at low input energy (0.1 kJ \sim 0.3 kJ) as similar to pure Ti porous compacts. Moreover, the metallic glassy powder (Zr-Ti-Cu-Ni-Be alloy) with larger supercooled region maintains an amorphous phase without crystallization at higher input energy than metallic glassy powders (Cu-Ni-Zr-Ti and Zr-Al-Ni-Cu alloys). These results suggest that the melting point and supercooled region of the metallic glassy powders are critical factors to fabrication of porous metallic glass compacts without crystallization.

10:00 AM Break

10:15 AM Invited

Bulk Metallic Glasses Form Like Plastics: Jan Schroers¹; ¹Yale University

The metastable nature of BMGs has imposed a barrier to broad commercial adoption, especially where the processing requirements of these alloys conflict with conventional metal processing methods. Research on the crystallization of BMG formers has uncovered novel processing opportunities using thermoplastic forming (TPF), which utilizes the dramatic softening exhibited by a BMG as it approaches its glass transition temperature. This talk introduces such techniques that are unique among metals. Due to the absence of an intrinsic size limitation,



TMS 2012

141st Annual Meeting & Exhibition

MONDAY AM

BMGs can be precision net-shaped on the micro, nano, and even atomic length scale. Furthermore, these length scales can be combined even on complex surfaces. Within TPF, BMGs can be considered high strength material that can be processed like plastics, whereby previously mutually exclusive attributes of materials -processability and performance – can be combined.

10:35 AM Invited

Mechanistic and Thermodynamic Origins of Toughness in Metallic Glasses: *Marios Demetriou*¹; William Johnson¹; Robert Ritchie²; ¹California Institute of Technology; ²University of California, Berkeley

Over the recent years, metallic glasses have evolved at an unusually high rate, far surpassing the development rate of other standard metallic materials used currently in engineering applications. The attributes contributing to their rise are fairly obvious: stronger, harder, and more elastic metal hardware compared to any of the incumbent metals like steel, titanium, and aluminum alloys. Other aspects of their engineering performance however are not quite as universal, and not necessarily as favorable. One such aspect is toughness. Their fracture toughness varies over two orders of magnitude between alloys, from values corresponding to brittle ceramics to tough metals. The acceptance of metallic glasses as widespread engineering materials hinges on our ability to understand and control such broadly-varying fracture toughness. In this presentation, the current understanding of the mechanisms of fracture toughness in metallic glasses will be reviewed, and the chemical and topological origins of these mechanisms will be discussed.

10:55 AM Invited

Recent Research Efforts in Bulk Metallic Glass Matrix Composites at NASA JPL/Caltech: *Douglas Hofmann*¹; ¹NASA JPL/Caltech

In this talk we will review some of the recent research efforts funded by NASA and the Jet Propulsion Laboratory which work towards implementation of metallic glasses and composites into spaceflight hardware. These projects include studying dendrite growth in bulk metallic glass (BMG) composites in the low-gravity environment of the International Space Station, developing BMG shielding for protection from micrometeorites and orbital debris, and fabricating high-performance BMG composite mirrors and structural hardware. The talk will also give a historical perspective of NASA spaceflights performed by the Caltech group and how that relates to industrial development of BMGs as well as currently funded programs and future programs. Processing capabilities at JPL/Caltech will be discussed.

11:15 AM

Glass Forming Ability of the Multi-component Bulk Metallic Glasses: *Anupriya Agrawal*¹; Logan Ward¹; Katharine Flores¹; Wolfgang Windl¹; ¹The Ohio State University

Bulk Metallic Glasses (BMGs) represent a new class of metallic alloys with a wide range of potential applications. Our current work encompasses the development of reliable modeling methods to create realistic multicomponent glass structures, examine their glass forming ability (specifically, the glass transition temperature), and study their mechanical properties as a function of composition using Molecular Dynamics. We studied the glass forming ability in the Cu-Zr-Ti system in the composition ranges Cu₆₀Zr_xTi_{40-x} (x = 5, 10, 20, 30) and Cu₅₀Zr_xTi_{50-x} (x = 5, 7.5, 10, 15, 20, 35, 40) using Embedded Atom Method potentials. The fragility, which we find to be a better measure of glass forming ability, is also calculated within the Green-Kubo formalism. The results predict that a low Ti concentration favors good glass forming ability, which is in excellent agreement with experiment, where an upper limit of ~6-7% of Ti is found for glass formation.

11:25 AM Invited

Effect of Casting Technique on Glass Formation of Bulk Metallic Glasses: *Tao Zhang*¹; ¹Beihang University

The glass-forming ability (GFA) is significant for both scientific research and industry application of bulk metallic glasses (BMGs). However, the

experimental evaluation of GFA for an alloy is still a confusable and arguable problem although the critical diameter (dc) has been provided for a long time as an evaluation parameter of GFA. Recently, we found dc of a certain alloy can be strongly influenced by casting factors, e.g. casting temperature (overheating), casting time (speed) and casting atmosphere (trace gas elements). The proper and careful adoption of optimal casting factors is important for the corrective evaluation of GFA of alloys. Furthermore, we combined some traditional casting techniques with rapid solidification techniques to develop new casting technique for the fabrication of BMGs with special dimension, like super-long bulk glassy rods and micron-scale inner holes, which provide new potential applications of BMGs.

11:45 AM Invited

New Ti-Based Bulk Metallic Glasses for Biomedical Application: *Xidong Hui*¹; Xialiang Zhou¹; Xiaohua Chen¹; Xiongjun Liu¹; Yuan Wu¹; Zhaoping Lu¹; ¹University of Science and Technology Beijing

In this work, new Ti-Zr-Cu-Pd-Sn, Ti-Zr-Cu-Pd-Sn-Hf and Ti-Zr-Cu-Pd-Sn-Hf-Si BMGs were successfully fabricated by copper mold casting method. The compositional feature of this kind of Ti-based BMGs is that they don't contain elements which are harmful to human body (e. g. Be and Ni etc), and the content of Cu is lower than that in Ti₄₀Zr₁₀Cu₃₄Pd₁₄Sn₂. It is shown that these glassy alloys have good thermal stability and wide supercooled liquid regions, resulting in relatively high glass forming ability. The compressive strength and plastic strain of this kind of BMGs reach as high as 2600 MPa and 3.6%. The electrochemical corrosion measurements and immersion tests show that the corrosion resistance properties of these Ti based BMGs are superior to those of Ti₄₀Zr₁₀Cu₃₄Pd₁₄Sn₂, Ti6-Al4-V and 316L stainless steel in NaCl, HCl, NaOH and PBS solutions. It is believed that these Ti-based BMGs are competitive candidates for future biomedical materials applications.

12:05 PM

Effect of Tungsten Reinforcement Particle Sizes on the Fabrication of Hf-Based Metallic Glass Matrix Composites: *Min Ha Lee*¹; Daniel Sordelet²; Jürgen Eckert³; ¹Korea Institute of Industrial Technology; ²Caterpillar Advanced Materials Technology Group; ³IFW Dresden

Due to limitations in decreasing the reinforcement size as well as processing complications, most composites have not achieved uniform nanometer-size scale homogeneity. We investigated the effect of tungsten metal particle sizes from nanometer scale to micrometer scale on the thermal stability and reactivity of uniformly dispersed metal particles in Hf-based metallic glass alloy melt at elevate temperature (1673K). The effect of particle size on solubility is significant for particles less than about 100 nm in radius. In case of fine metal particle with 20 nm in diameter, the solubility of metal remarkably increases around 700% compare to that of coarse metal particle. The mechanisms and kinetics of this dynamic growth of particle are discussed and developing techniques to obtained freezing microstructure of particle reinforced composites using by rapid solidification process was presented.

12:15 PM Invited

Ferromagnetic Fe-Based Bulk Metallic Glasses with Low Glass Transition Temperature and Large Supercooled Liquid Region: *Wei Zhang*¹; Canfeng Fang²; Akihiro Makino³; Akihisa Inoue³; ¹School of Materials Science and Engineering, Dalian University of Technology; ²Institute for Materials Research, Tohoku University; ³WPI, Advanced Institute for Materials Research, Tohoku University

Fe-based bulk metallic glasses (BMGs) have gained considerable attention due to their low material cost and many unique properties, such as excellent soft magnetic properties, high strength, viscous flow workability in the supercooled liquid state, high corrosion resistance, etc. However, most of these Fe-based BMGs show high glass transition temperatures (T_g) or narrow supercooled liquid region (ΔT_x), which hinder their thermoplastic formability. In present work, new ferromagnetic Fe-based BMGs have been synthesized in the (Fe, Ni, Co)-Mo-(P, C, B, Si) alloy

system. The BMGs possess low T_g below 720 K, wide ΔT_x of over 90 K, and high GFA with critical sample diameters of ~4 mm. The alloys also exhibit rather high saturation magnetization of 0.66–0.93 T, low coercive force of 1.47–5.34 A/m, and high compressive yield strength of over 3000 MPa with a distinct plastic strain. In addition, the thermoplastic formability of the BMGs is investigated.

12:35 PM

New Fe-C-Si-B-P-Cu Amorphous and Nanocrystalline Alloys Concurrently Possessing High Glass Forming Ability and Good Soft Magnetic Properties: *Jingen Gao*¹; H.X. Li¹; Y. Wu¹; Z.P. Lu¹; ¹University of Science and Technology Beijing

In order to improve energy saving needed for conservation of environment, the soft magnetic amorphous ribbons applied in the electrical power supplies demand to have high saturation magnetization and large thickness simultaneously. However, obtaining large glass-forming ability (GFA) is always at expense of the saturation magnetization due to alloying nonmagnetic elements substituting Fe. Here we reported our surprising finding that the optimum minor additions of the Cu element which have positive enthalpy of mixing with the main constituent could not only dramatically enhance the GFA but also improve the soft magnetic properties. This surprising finding was realized by tuning formation of the nanosized \square -Fe clusters and annealing conditions. Moreover, the underlying mechanisms for the beneficial effects of the minor Cu doping are also presented.

CFD Modeling and Simulation in Materials Processing: CFD Modeling in Materials Processing I

Sponsored by: The Minerals, Metals and Materials Society, TMS Extraction and Processing Division, TMS Materials Processing and Manufacturing Division, TMS: Process Technology and Modeling Committee, TMS: Solidification Committee
Program Organizers: Laurentiu Nastac, The University of Alabama; Lifeng Zhang, Missouri University of Science and Technology; Brian Thomas, University of Illinois at Urbana-Champaign; Adrian Sabau, Oak Ridge National Lab; Nagy El-Kaddah, The University of Alabama; Adam Powell, Metal Oxygen Separation Technologies, Inc.; Hervé Combeau, Institut Jean Lamour

Monday AM
March 12, 2012

Room: Asia 4
Location: Dolphin Resort

Session Chairs: Lifeng Zhang, Missouri University of Science and Technology; Raj Venuturumilli, Ansys, Inc.

8:30 AM Keynote

Fluid Flow, Solidification and Inclusion Entrapment during Steel Centrifugal Casting Process: *Lifeng Zhang*¹; Edith Martinez¹; Kent Peaslee¹; ¹Missouri University of Science and Technology

The current study investigated the multiphase fluid flow, heat transfer, solidification of the steel, and the motion and entrapment of inclusions during centrifugal casting process using FLUENT software. User-defined functions (UDFs) were developed to add a speed with a value related to the rotation speed and radial distance to the solidified steel, to exert a centrifugal force to the motion of inclusions, and to add the entrapment condition of inclusions at the solidifying shell and export the entrapment locations of inclusion. The calculation shows that there are two peaks of inclusions along the thickness of the produced tube: one at close to outer surface and another one close to the inner surface of the tube. With larger rotation speed, inclusions tend to be entrapped more towards the inner surface. The calculation agrees well with the industrial measurement.

9:00 AM Invited

A Coupled CFD-Thermodynamic-Kinetic Model to Simulate a Gas Stirred Ladle Refining Process: Raj Venuturumilli¹; Pavan Shivaram²; ¹ANSYS, Inc.; ²U.S. Steel Corporation

Dynamics between molten metal and slag in a ladle is of immense interest to the steel industry during steel conditioning through desulphurization and reoxidation reactions in a ladle. Over the years, studies have shown that these processes can be optimized by controlled metal-slag stirring or mixing. For this purpose, argon gas stirring is commonly used. A three dimensional multiphase computational fluid dynamics (CFD) model is developed to study fluid stirring in the ladle. Furthermore, the CFD model is coupled to a thermodynamic and kinetic model to predict the slag-metal interactions. Argon, molten metal and slag are modeled as three separate phases in an Eulerian framework. Desulphurization process in a ladle furnace is among the phenomena studied. The model provides an understanding of the kinetics of the process as well as a means to predict the extent of desulphurization after a given process time.

9:25 AM Invited

A Micro-Macro Model of a PEM Fuel Cell System: *Thiyagarajan Paramadhyalan*¹; Hrushikesh Pimpalgaonkar¹; Suresh Sundarraj¹; ¹General Motors

In this paper, a model of the fuel cell system has been proposed to account for the membrane physics at the micro level which is coupled with the macroscopic flow and mass transport phenomena occurring in a single channel of a PEMFC system. We have developed a novel approach to model the catalyst layer electrochemical processes in a Membrane Electrode Assembly and coupled it with mass transport and fluid flow calculations at the channel level using STAR-CD commercial software. This micro-macro model results of the cell voltage and the current density have been validated with previous literature data. A sensitivity analysis has been carried out to study the effect of the model parameters such as catalyst loading, width of the catalyst layer as well as the channel dimensions and fuel mass flow rate on the overall performance of the PEMFC.

9:50 AM

Mathematical Modelling of Welding Process of Al/Al₂O₃ Nanocomposites Produced by Solidification Route: *Payodhar Padhi*¹; France Behera¹; ¹Konark Institute of Science & Technology

The present study proposes to model of the thermo fluid dynamics of the molten pool created during an arc fusion welding process of aluminium metal matrix Nano composites (MMNCs) produced through solidification route. The aluminium metal matrix nano composites (MMNCs) has been developed by Padhi et al. using solidification process. The said nano composites are subjected to MIG welding. The volume of fluid method and the heat transfer models have been applied using ANSYS R12 to study the welding process. Heat affected zone is not very large compared to the general aluminium alloy welding because of the presence of nano particles. Here nano particles play a major role. During welding, the nano particles present in the weld pool did not settle down since the particles are very fine. The welding joints are very strong compare to the general welding as it behaves like composite.

10:10 AM Break

10:30 AM

Modeling the Effects of Tool Geometries on the Temperature Distributions and Material Flow of Friction Stir Aluminum Welds: Hrushikesh Mohanty¹; Manas Mahapatra¹; Pradeep Kumar¹; P K Jha¹; ¹Indian Institute of Technology Roorkee

During friction stir welding, the tool geometries affect the weld together with the process parameters like welding speed, vertical pressure and tool rotational speed. The present investigation deals with the three dimensional computational fluid dynamics modeling of friction stir welding process considering material flow around the tool, welding speed with respect to tool geometries. Friction stir welding tools with different tool geometries



TMS 2012

141st Annual Meeting & Exhibition

MONDAY AM

were used for the experiments to achieve acceptable aluminum welds. The temperatures near the welds for each tool were experimentally observed. In three dimensional computational fluid dynamics model, temperature dependent material properties of the aluminum alloy was used. Thermal analysis was carried out considering rotational speed, vertical pressure and traverse speed for the tool geometries. The numerically predicted stirring patterns and temperature profiles closely matched with the experimental ones.

10:50 AM

Determination of Heat Transfer Coefficient Distribution at Part Surface during Press Quenching Process Using CFD: Morgan Guardino¹; Soraya Benitez²; *Liang He*¹; Richard D. Sisson¹; ¹Worcester Polytechnic Institute; ²Sikorsky Aircraft

A computational fluid dynamic (CFD) analysis of a gear within a press quench was performed to investigate the effect of oil flow on the heat transfer coefficient (HTC) distribution at the gear surface. A CFD model, built in Fluent within ANSYS Workbench, used an energy and a viscous flow model to calculate the HTC values between the gear and the oil. The results showed where uneven cooling, due to HTC variation, was likely to occur and indicated that a slower oil velocity in this situation caused a larger HTC distribution when compared to a faster flow rate. The results of this model provided insight into the press quenching process and could potentially be used to help improve the heat treatment of the gear.

11:10 AM

Fuzzy Extraction Separation Optimized Process of Tm, Yb and Lu Enriched Oxides by Computer Simulation: Fengli Yang¹; *Sh Yang*¹; Mingzhou Li¹; Changren Tong¹; ¹Jiangxi University of Science and Technology

According to characteristics of Tm, Yb and Lu enriched oxides composition and problems in its traditional extraction separation process, the computer simulation of a optimized fuzzy extraction separation process, in which three products with high purity (>99.99%) could be obtained at same time, was carried out. Distributing curves of every element in both organic and aqueous phases were worked out. Distribution rules of rare earth elements in every stage of the optimized extraction process were studied. The computation results of economical and technical index showed the consumption of the acid and base chemical reagents in the optimized process would be saved more than 30%.

11:30 AM

Understanding Fuming during Metal Refining by CFD: *Jan Erik Olsen*¹; Mari Naess²; Gabriella Tranel²; ¹SINTEF Materials & Chemistry; ²NTNU

Fume produced during metal refining exposes plant operators for disease and health issues. With the motivation to reduce the risk for exposures a CFD model has been developed to better understand the underlying mechanisms and make predictions of potential design modifications. The process considered is gas stirred refining of silicon metal. The model accounts for conservation of mass, momentum and energy by the classical CFD approach. Additionally radiation of heat and species conservation with reactions are included in the model. Results are compared with measurements. It is shown that understanding the flow pattern is important for reducing the fuming rate.

11:50 AM

CFD-Based Modelling on Interfacial Heat Transfer for Water Quenching: *Gang Wang*¹; Yiming Rong¹; ¹Tsinghua University

Water quenching is one of common heat treatment processes with complex physical phenomenon which involves vaporizing, bubbling and convection. The current simulations of liquid quenching processes are conducted by using an average value of heat transfer coefficient obtained from experimental measurement under a strong assumption. A preliminary model for water quenching has been presented in this paper based on multiphase flow theory. The conjugate heat transfer method is used to describe thermal conduction in the simplified workpiece, and

generation, growth and flow of bubbles are modeled by using Eulerian-Eulerian method for the gas-liquid multiphase flow. The simulation result shows the intense variation of heat exchange through the interface between workpiece and liquid and unsteady distribution around the solid surface.

12:10 PM

Mathematical Model of Purges Process at a Heat Treatment Furnace: *Irma Hernández*¹; Jacobo Vargas²; ¹Universidad Autónoma del Estado de México; ²UAEMex

In this work a mathematical model of the purges process at an industrial cylindrical furnace was constructed using CFD, a bi-dimensional nitrogen jet was ejected in the contained air of the furnace. The evolution at the outlet gas composition of the furnace was computed using the commercial software PHOENICS to solve Navier Stokes and the classical k-ε turbulence equations for both, nitrogen and air phases. The results were compared with plant measurements, founding a good agreement. A new geometry for the nozzle was computationally proved with a different velocity profile in the nitrogen purging gas, the computed results presented a major jet expansion for a minor distance from the nozzle and a quickly displacement in the initially contained air at the furnace, it might produce a faster purging process.

Characterization of Minerals, Metals, and Materials: Characterization of Ferrous Metals I

Sponsored by: The Minerals, Metals and Materials Society, TMS Extraction and Processing Division, TMS: Materials Characterization Committee

Program Organizers: Jiann-Yang Hwang, Michigan Technological University; Sergio Montero, State University of North Rio De Janeiro; Chenguang Bai, Chongqing University; John Carpenter, US Department of Energy; Donato Firrao, Politecnico di Torino; Byoung-Gon Kim, Korea Institute of Geoscience & Mineral Resources; Mingdong Cai, Schlumberger

Monday AM
March 12, 2012

Room: Asia 2
Location: Dolphin Resort

Session Chairs: Jian Li, CANMET-MTL; Donato Firrao, Politecnico di Torino

8:30 AM

Characterization of the Microstructure of Compacted Graphite Cast Iron: *Vahid Rastegar*¹; ¹Dalarna University

Characterization of microstructure and revealing dendrites in microstructure and also measuring DAS and distribution of silicon were studied in various pieces of CGI with different mishmetal percentage. Quantitative and qualitative metallography were carried out on various steps of cast samples. Distribution of silicon was studied quantitatively using spot analysis with SEM. Furthermore, effects of two variables (cooling rate and mishmetal percentage) on DAS were investigated. In order to color metallography, samples were plunged into boiling solution of 18% KOH, 9% NaOH and 9% picric acid. It was inferred that the microstructure coloration varies according to the sequence: green, red, yellow, blue, dark brown, light brown as silicon content decreases. After observing dendrites, DAS was measured. In this method, it seems to be possible to predict mechanical properties of CGI by knowing DAS and without any destructive testing. It was concluded that DAS decreases as mishmetal amount increases and it increases as the cooling rate increases.

8:50 AM

EBSDB Analysis of Complex Microstructures of CSP® Processed Low Carbon Micro-Alloyed Steels: *Carl-Peter Reip*¹; Reinhard Flender²; Matthias Frommert²; ¹SMS Siemag AG; ²Salzgitter Mannesmann Forschung GmbH

Today there is a growing demand for strip of superior steels with specifically tailored technological properties. Especially strips of high-strength, micro-alloyed steel grades applied to manufacture longitudinally and spiral-welded pipes are a growth market. Tubes are generally required to have high strength and sufficient toughness values and thus favour specific hot strip microstructures. The correlation of chemical analysis, process parameters and mechanical properties with microstructural features is still a challenging task. During the last decades, scanning electron microscopy (SEM) and electron backscatter diffraction (EBSD) have become useful tools for the characterization of complex microstructures. The EBSD data provides an immense variety of post-processing possibilities, e.g. related to grains, grain boundaries, misorientations or texture. This paper highlights the results of an advanced analysis of microstructures representing industrial produced hot-rolled strips and presents an approach to define and quantify some essential microstructural parameters.

9:10 AM

Empirical Models of Cold Working Effect in Steel Tube Production: *Robert Batson*¹; Jing Zhang¹; ¹University of Alabama

Carbon steel is purchased in coils, slit to width, and fed into electrical resistance welding mills that convert it into round, square, or rectangular structural tubing. The objective of this project was to establish relationships between certain properties (yield, tensile, elongation) of the tube after cold working and those of the flat coil before cold working, and build empirical predictive models from a data base of before-and-after properties provided to us by a tube manufacturer. Using multiple regression analysis, a set of three regression models was built with tube geometry and flat steel properties as the independent variables, and tube physical properties as the dependent variables. These regression models can be used by the manufacturer for prediction of results when coil properties are known, and for computation of ideal coil steel specifications. We provide a sample solution of the latter "inverse problem" using the three equations and Excel Solver.

9:30 AM

Correlation of Cu Precipitation with Austenite Decomposition in a Continuously Cooled Multicomponent Steel: An Atom Probe Tomography Study: *Qingdong Liu*¹; Wenqing Liu¹; Shijin Zhao¹; Qifeng Zeng²; ¹Shanghai University; ²Shanghai Nuclear Engineering Research & Design Institute

The Cu precipitation in continuously cooled multicomponent steel is examined by atom probe tomography. During austenite decomposition, the solutes partitioning behaviors at the migrating ferrite / austenite interphase and the micro-constituents such as dislocation and cementite in the ferrite have a great effect on the nature of Cu precipitation. Both the actual sizes of Cu precipitates and austenite decomposition process correlate with the compositional evolution of Cu precipitates with the different level of Ni and Mn segregation. The partitioning behaviors of solutes atoms at ferrite / austenite interface have an effect on the kinetics of ferrite formation and its final microstructure. The micro-constituents such as dislocation, cementite in ferrite and ferrite / austenite hetero-phase boundary determines the compositional changes of Cu precipitates. The transition bcc Cu precipitates are considered to nucleate through interphase precipitation and grow at crystal defects after being embedded within ferrite.

9:50 AM

Effect of Epsilon Martensite on Low Temperature Tensile Properties of Fe-12Mn and Fe-14Mn Steels: *Jung-Su Kim*¹; Jong Bae Jeon¹; Joong Eun Jung¹; Young Won Chang¹; ¹POSTECH

High manganese steels containing 10 ~ 14% of Mn are now known to exhibit excellent combination of tensile strength and ductility. Their mechanical properties are strongly affected by the deformation-induced martensitic transformation (DIMT) of metastable phases. The present Fe-Mn alloys contained ϵ -martensite formed during prior thermal treatments, which transforms into α' -martensite during the plastic deformation. It is thus important to study the DIMT kinetics of ϵ -martensite in relation to the mechanical properties of these alloys. The transformation kinetics of $\epsilon \rightarrow \alpha'$ has therefore been investigated in this study using the recently proposed kinetics equation by one of the authors to evaluate the stability of ϵ -martensite. The stability of ϵ -martensite phase was found to increase as the test temperature was decreased, contrary to the case of retained austenite being more stable at higher temperatures. This reversed stability-temperature relationship appears to provide an enhanced ductility at lower temperatures exhibited in the present alloys.

10:10 AM Break**10:20 AM**

Microstructural Investigation of Carbon Steel after Hot Rolling to Optimize Complex Hot Forming of Thick Plates: *Gerhard Tober*¹; Okechukwu Anopuo²; Petra Maier¹; ¹University of Applied Sciences Stralsund; ²CORTRONIK GmbH

In this study, an investigation on the microstructure of hot rolled steel S355 was conducted to optimize process parameters of complex forming, which combines rolling and bending. The best sets of parameters are worked out based on homogeneous mechanical properties and microstructure within the varied deformation degree with maximum at $f = 1.14$ on a 25 mm thick plates. Mechanical properties, especially of heavy plates, are strongly influenced by the local deformation degree, strain rate and temperature. Detailed microstructural analyses showed that the ferrite-pearlite band structure recrystallizes near the surface, while maintaining homogeneous microstructure within the deformed work piece. Surface decarburization was also observed and this leads to decrease in hardness. To minimize iron oxide formation which could lead to side cracking, reduction in exposure time to temperature was suggested. On the other hand, temperature reduction below a critical value would risk the accurate forming process.

10:40 AM

Microstructural Characterization of Fe-Mn-C Ternary Alloy under Near-Rapid Solidification: *Wenbin Xia*¹; Rong Yang¹; Changjiang Song¹; Qijie Zhai¹; ¹Shanghai University

This paper focus on the influence of carbon content and cooling rate on the microstructure and phase formation of Fe-Mn-C alloys under near-rapid solidification. When manganese content is about 11wt.%, more ϵ -martensite can be obtained with cooling rate increasing when carbon content is 0.14wt.%, the formed phase changed from a phase to \square phase when 0.74wt.% carbon is added to the samples, and when carbon content up to 2.1wt.%, carbide can be obtained in the sample. A host of stacking fault, which attributes to the strain-induced martensite, can be observed in the sample. The microhardness increased with cooling rate increasing, and under the same cooling rate, the microhardness of samples with 0.14wt.% carbon is highest.

11:00 AM

Effects of Surface Modifications on SCW Corrosion Resistance: *Jian Li*¹; Penttila Sami²; Wenyue Zheng¹; ¹CANMET-MTL; ²VTT

Materials selection for Gen IV supercritical water reactor in-core components faces major challenges due to severe operating condition. Beside high-temperature mechanical properties, SCC and general corrosion resistance of commercially available materials are also major focuses in recent research. Recent reports suggest that certain types of surface modifications are beneficial to SCW corrosion resistance. In this



TMS 2012

141st Annual Meeting & Exhibition

MONDAY AM

study, the effects of surface modifications are investigated, and possible mechanisms for improved corrosion performance are discussed.

11:20 AM

Interface Mass Transfer during the Tribofinishing Process: *Isaias Hilerio*¹; Dulce Medina²; Victor Cortes²; Juan Muñoz²; ¹UAM AZCAPOTZALCO; ²UAM Azcapotzalco

Tribofinishing process is investigated as a means to reach a quality state for the surface treated. For obtain this result is utilized the following combination: Machines, Additives, Abrasives and Pieces to be treated. The machines determines the energy utilized in the process. The additives are utilized to create a superficial tension that permits withdraw material. The abrasives are the components that make the work. During the commented process there occurs a mass transfer at the interface of the piece to be treated and the abrasive charge. It is mentioned the interaction between piece treated and abrasives as an interaction of three bodies. It is shown the evolution of surface roughness to evaluate their quality. This situation is studied for Titanium as a possibility for application in prosthesis. With these results is intended to produce a model of the mass transfer that would allow to have further control in the process.

11:40 AM

Martensitic Meso- and Nanostructures in High-Carbon Low-Alloyed Steels: *Albin Stormvinter*¹; Peter Hedström¹; Annika Borgenstam¹; ¹KTH Royal Inst. of Technology

The martensite morphology of high-carbon low-alloyed steels is commonly described as plate-like and has been studied extensively in the past. However, recently not much attention has been given to characterization of high-carbon martensite. In the present work the SEM-EBSD technique was applied to steels with carbon contents: 0.86, 1.20 and 1.67 mass% C. In contrast to previous works, SEM-EBSD enables characterization through both apparent morphology and crystallography simultaneously. This seems suitable, since although ferrous martensite may appear irrational, it is known to have well-defined crystallographic relationships. In addition, the substructure of the martensite units in the 1.20 and 1.67 mass% C steels was studied by TEM. The results demonstrate that even though the apparent morphology seems plate-like, several unexpected features are found when the meso- and nanostructure are studied in depth. This study has been part of a project to establish a good characterization procedure for martensitic steels.

Computational Thermodynamics and Kinetics: In Honor of Dr. Long-Qing Chen, EMPMD Outstanding Scientist: Session I

Sponsored by: The Minerals, Metals and Materials Society, TMS Electronic, Magnetic, and Photonic Materials Division, TMS Materials Processing and Manufacturing Division, TMS Structural Materials Division, TMS: Alloy Phases Committee, TMS: Chemistry and Physics of Materials Committee, TMS/ASM: Computational Materials Science and Engineering Committee, TMS: Integrated Computational Materials Engineering Committee, TMS/ASM: Phase Transformations Committee, TMS: Process Technology and Modeling Committee

Program Organizers: Zi-Kui Liu, The Pennsylvania State University; Mark Asta, University of California, Berkeley; James Warren, The National Institute of Standards and Technology; Yunzhi Wang, Ohio State University; Raymundo Arroyave, Texas A & M University; Yu Wang, Michigan Tech

Monday AM
March 12, 2012

Room: Australia 3
Location: Dolphin Resort

Session Chairs: Mark Asta, UC Berkeley; Yunzhi Wang, Ohio State

8:30 AM Introductory Comments

8:35 AM Keynote

Phase-Field Modeling of Microstructure Evolution in Elastically Inhomogeneous Systems: *Long Qing Chen*¹; Saswata Bhattacharyya¹; Taewoo Heo¹; Jianjun Wang¹; Qun Li¹; ¹Pennsylvania State University

Essentially all materials in applications are elastically inhomogeneous, i.e., the elastic constants are different in different locations of a solid material. Although for some cases in which the elastic inhomogeneity is small homogeneous modulus approximation is adequate for predicting microstructure evolution during phase transformations, many others require the solution to an elastically elastic inhomogeneous system. Examples include solid materials that contain voids, cracks, and polycrystals. This presentation will provide a brief review of various numerical treatments and their efficiencies of elasticity inhomogeneity within the context of phase-field method, starting from the Khachatryan's theory of microelasticity. Examples of applications to be presented include phase transformations and microstructure evolution in polycrystalline materials, grain boundary motion under the influence of an applied stress, deformation twinning in structural materials, morphology of lithium-rich and lithium-depleted two-phase mixtures in Li-intercalation compounds, and evolution of voids/cracks or crack/domain interactions.

9:05 AM Invited

Phase Field of Prototyping Structural Transformations and Properties in Systems with Long-Range Interaction: *Armen Khachatryan*¹; ¹Rutgers University

Structural transformations in solids results in a strong long range interaction between transformed finite elements. This is the long-range character of this interaction that is responsible for the nano- and submicron heterogeneous structure and for important properties of material. In the structural materials the long-range interaction has a dipole-dipole character. It can be the strain-induced interaction, electrostatic, and manetostatic dipole-dipole interaction or their combination in structural, ferroelectric and ferromagnetic materials. The use of the Phase Field approach, which integrates these interactions, allows us to realistically prototype a spontaneous microstructure evolution and the structure-property relations. It does not require any ad hoc assumptions about a transformation path that would diminish the predicting power of the modeling. This talk presents a review of a current status of the Phase Field of modeling of systems with a long-range interaction.

9:30 AM Invited

Diffusive Molecular Dynamics Simulation of Displacive-Diffusional Coupling in Solid State Processes: Sanket Sarkar¹; William Cox¹; Ju Li²; Yunzhi Wang¹; ¹Ohio State University; ²MIT

In solid processes displacive-diffusional coupling is a rule rather than an exception. For example, curvature driven grain growth may involve coupled tangential (displacive) and normal (diffusional) migration of grain boundaries. Creep deformation often involves conservative and non-conservative motion of dislocations. Mechanistic studies of these processes require modeling capabilities at atomistic length scales but diffusional time scales. In this presentation we review a new computational method called Diffusive Molecular Dynamics (DMD) developed recently, which captures diffusional-displacive evolution of complex microstructures at atomic scale by coarse graining over atomic vibrations and evolving atomic density clouds. Derived in grand canonical ensemble, DMD is a chemical mean-field extension of the variational Gaussian method coupled with master equation for diffusion solved on a moving atomic grid. Several examples involving simultaneous diffusional and displacive processes will be presented, with which we show the importance of sampling the free-energy landscape along coupled displacive-diffusive reaction coordinates.

9:55 AM Break**10:20 AM Invited**

Origin of Negative Thermal Expansion Phenomenon in Solids: Zi-Kui Liu¹; Yi Wang¹; Shun Li Wang¹; ¹The Pennsylvania State University

We show that the negative thermal expansion (NTE) phenomenon originates from the existence of high pressure, small volume phases with higher entropy, with their configurations present in the stable phase matrix through thermal fluctuations, thus exists frequently. Consequently, it extends the platform for designing structures with desired thermal expansion properties whether positive, negative, or zero. The theory is validated for a range of pure elements and compounds and utilized to provide insights to the NTE phenomenon in INVAR and ZrW₂O₈.

10:45 AM Invited

Coherent Precipitation in Ternary Al Alloys: Colin Ophus¹; Maarten de Jong²; Mark Asta²; Marcel Sluiter³; Ulrich Dahmen¹; Velimir Radmilovic⁴; ¹Lawrence Berkeley National Laboratory; ²University of California, Berkeley; ³Delft University of Technology; ⁴University of Belgrade

This talk will discuss recent studies obtained in combining advanced electron microscopy techniques and first-principles calculations in the study of coherent precipitation phenomena in ternary Al-based alloy systems. The studies have been motivated by observations in the Al-Si-Ge and Al-Sc-Li systems. In the former system, it is observed that the precipitation of stable diamond-cubic precipitates are preceded by coherent precipitation of nano-scale coherent precipitates that have a mixed Si-Ge content. The results are analyzed in the framework of a first-principles statistical-thermodynamics treatment that explicitly accounts for elastically-mediated interactions. We further discuss results obtained by combining first-principles-based thermodynamics methods with mean-field models for diffusion-limited precipitate growth in the Al-Sc-Li system. The results explain that the observed, highly monodisperse size distributions for core-shell precipitates in this system arise from capillary effects that can be readily exploited in conventional thermal processing.

11:10 AM Invited

Interplay between Surface Segregation, Ordering, and Adsorption Behavior of Pt-Alloy Surfaces: Wei Chen¹; Chris Wolverton¹; David Schmidt²; William Schneider²; ¹Northwestern University; ²Univ. of Notre Dame

Bimetallic surface alloys are considered a promising type of catalyst for improved activity and selectivity. Understanding surface structure and its effect on catalytic performances plays a critical role in designing catalysts from surface alloys. We have studied the surface structure and ordering of Pt alloys surfaces, such as Pt-Au(111) and Pt-Ti(111), using

a first-principles cluster expansion (CE) based method. Even though the Au-Pt system is phase-separating in the bulk, we find a series of thermodynamically stable, laterally ordered striped structures of AuPt(111) surfaces. In contrast, Pt-Ti(111) subsurface alloys show a strong ordering tendency, in analogy with bulk Pt-Ti alloys. A series of stable ordered Pt-Ti(111) subsurface structures are identified from the two-dimensional (2D) CE. In both cases, we calculate the interplay between metal ordering and segregation at the surface and lateral interactions between adsorbates (O, S, H, and NO) on these surfaces.

11:35 AM Invited

Twin Boundary Behaviors of Magnetic Shape Memory Alloys: Yongmei Jin¹; ¹Michigan Technological University

Twin boundary behaviors of magnetic shape memory alloys are investigated by phase field micromagnetic microelastic model. The simulations show coupled magnetic and elastic domain evolutions under magnetic field, and reveal various aspects of twin boundary behaviors, including pinning effects of twin boundary to magnetic domain wall motion, varying twinning stress with twin volume fraction, different domain evolution pathways depending on the magnitude and direction of external magnetic field, and time-dependent twin boundary motion. The respective contributions from magnetocrystalline anisotropy, twinning strain, magnetostrictive strain, long-range magnetostatic and elastostatic interactions, and twin boundary mobility are analyzed. The findings help explain peculiar domain processes and magnetic field-induced strain behaviors observed in magnetic shape memory alloys.

Defects and Properties of Cast Metals: Metal Cleanliness

Sponsored by: The Minerals, Metals and Materials Society, TMS Materials Processing and Manufacturing Division, TMS: Solidification Committee

Program Organizers: Mark Jolly, University of Birmingham; Brian Thomas, University of Illinois at Urbana-Champaign; Carl Reilly, University of British Columbia

Monday AM
March 12, 2012

Room: Oceanic 4
Location: Dolphin Resort

Session Chairs: John Grandfield, Grandfield Technology Pty Ltd; Daan Majjer, University of British Columbia

8:30 AM Introductory Comments**8:40 AM**

Films and Bifilms – An Update: John Campbell¹; ¹University of Birmingham

It is proposed that bifilms are the only source of cracks generally known as Griffith cracks. Failure modes of cast products involving the creation of porosity, hot tears, cracks and failure modes of solid metals in room temperature tension and high temperature creep (together with cavitation failure in superplastic forming) all appear to be explicable assuming the presence of bifilms. Furthermore, their control over cast microstructures of metals and alloys is profound as a result of the favored precipitation of intermetallics and second phases on the wetted exterior faces of bifilms. Modification of Al-Si alloys and even possibly the structure of cast irons becomes explicable for the first time. The discovery of bifilms promises to revolutionize our understanding of the behavior of cast and wrought engineering metals. Conversely, bifilm-free metals promise unprecedented properties.



TMS 2012

141st Annual Meeting & Exhibition

MONDAY AM

9:00 AM

Fluid Flow and Inclusion Entrapment in the Runner Steel During Ingot Casting: *Lifeng Zhang*¹; Yongfeng Chen¹; Shufeng Yang¹; ¹Missouri University of Science and Technology

This paper studied the nonmetallic inclusions in the steel of an ingot runner. Thermodynamic modeling was performed to study the formation mechanism and sources of inclusions. CFD modeling on fluid flow, heat transfer, solidification of molten steel was carried out and the entrapment of inclusions in runner steel was predicted and compared with the measurement. Al₂O₃-based inclusions were the main ones in the steel samples. MgO/Al₂O₃ mainly stemmed from the lining refractory. The high MnO inclusions in the runner steel came from the runner slag. The effect of natural convection was very important for the cooling and solidification of the steel in the runner. Both the observation and the modeling show that > 50 μm inclusions more accumulated on the upper area in the runner and < 50 μm inclusions dispersed well and more accumulated on the lower area of the runner.

9:20 AM

Modeling of Mould Filling of Low-Pressure Die-Cast Aluminum Alloy Wheels: *Jianglan Duan*¹; Daan Maijer¹; Steve Cockcroft¹; Carl Reilly¹; Ken Nguyen¹; Dominic Au¹; ¹University of British Columbia

As part of a program to understand the influence of die filling on defect formation in low-pressure die-cast aluminum wheels, work has been ongoing toward the development of a thermal-fluid model of the filling process. A transparent planar die section has been built, instrumented and tested using water to explore the role of pressure and venting on the free surface behavior of water and to produce data for validation of the flow aspects of the model. Comparison to the experimental data confirms the model's ability to accurately predict the filling in a planar die and that fill pressure and venting influences the free surface behavior significantly. To examine conditions more similar to the industrial process the material properties of aluminum were input to the model and flow in a periodic section of the production die has been simulated. Once again the fill pressure and venting are found to be critical.

9:40 AM Break

10:00 AM

Quench Sensitivity of 2024, 6063 and 7075: *Engin Tan*¹; Ali Tarakcilar¹; Derya Dispinar²; ¹Pamukkale University; ²University of Istanbul

The influence of quenching temperature during solution heat treatment of 2024, 6063 and 7075 was investigated by means of tensile testing. SEM analyses were carried out on the fracture surfaces. In addition, reduced pressure tests were carried out to correlate the mechanical test results with metal quality. The alloys were received as extruded. SIMA process was applied to achieve spherical grain structure. T6-solution heat treatment was carried out and quenching was done in temperature controlled water bath. Two different quenching temperatures were selected: 20°C and 80°C. The results were analysed by Weibull statistics. It was found that Weibull moduli of all test results were similar for all the alloys and there was a good correlation between bifilm index. Ultimate tensile strengths were high when samples were quenched at 20°C. On the other hand, elongations at fracture were high for the samples quenched at 80°C.

10:20 AM

Effect of Different Casting Parameters on the Cleanliness of High Manganese Steel Ingots Compared to High Carbon Steel: *Petrico von Schweinichen*¹; Zhiye Chen¹; Dieter Senk¹; Alexander Lob¹; ¹RWTH Aachen University, Department of Ferrous Metallurgy, Intzestr. 1, 52072 Aachen, Germany

Nowadays, the demand of excellent steel properties leads to the birth of new steel grades such as high manganese TWIP and TRIP steels which are scientifically investigated in the framework of the SFB 761 "Steel - *ab initio*" in Germany. However, this demand brings new challenges to steel producers with regard to the production of these high-technology products, which are mostly produced by ingot casting. The major defects of casted

ingots like cavity, macro segregation, surface quality and cleanliness as well as as-cast structure and the position of CET are systematically investigated at the RWTH Aachen University. One low alloyed steel and one high manganese alloyed steel with different casting parameters with regard to superheat, casting atmosphere, pouring rate, hot top and stirring conditions have been studied in this paper. The main focus of this research is the investigation of the cleanliness of the ingots of both steel grades.

10:40 AM

Tensile Properties, Porosity and Melt Quality Relation of A356: *Derya Dispinar*¹; Shahid Akhtar²; Arne Nordmark¹; Freddy Syvertsen¹; Marisa Di Sabatino²; Lars Arnberg²; ¹SINTEF Materials and Chemistry; ²NTNU

The movement of liquid aluminium in mould cavity plays a significant role in determining the cast part's quality. Turbulence and entrained defects lower melt quality. What has usually been disregarded is the melt quality of the starting material. If the charge material is of bad quality, the effectiveness of the casting method loses its importance. Therefore, in this work, gravity and counter gravity casting methods were used to cast A356 in a step mould die. Reduced pressure test samples were collected to assess melt quality by means of bifilm index. It was found that although the measured porosity level was lower in LPDC castings, the tensile properties were lower than GDC. In fact, LPDC melt had higher bifilm index than GDC which was the indication of low melt quality. Thus, this investigation has shown that the metal quality has a dominant effect over the mechanical properties than the porosity content.

11:00 AM

Investigation on Non-metallic Inclusions of Q420 Ingots Cast by Bottom Teeming: *Yanzhao Luo*¹; Jiongming Zhang²; Chao Xiao²; Jin Yang²; ¹University of Science & Technology Beijing; ²University of Science & Technology Beijing

For analyzing the composition and morphology of inclusion in the bottom pouring mold cast ingot of Q420 steel, the experimental samples sampled separately at different locations of the ingot were investigated using optical microscope observation, SEM analysis and slim electroanalysis extraction methods. The results showed that the average T.O. in the ingot is about 10ppm at a lower level, indicating that ingot is high purity. The index of microscopic inclusions in the ingot is between 2.09~4.98/mm², the microscopic inclusions in the middle of ingot are less than other parts. The contents of large sized inclusions in the ingot were between 5.7 and 22.5mg/10kg, which composed mainly by SiO₂, Al₂O₃ and a small amount of Na₂O and K₂O. The large sized inclusions were mainly from the mold slag during bottom pouring and its content in the bottom of the ingot is much higher than that in the other parts.

11:20 AM

Tracking the Formation and End Location of Oxides in Orthopaedic Investment Casting Running Systems: *Mark Jolly*¹; Alan Kavanagh²; ¹University of Birmingham; ²Depuy Johnson & Johnson

This work was an investigation into a specific defect identified during the casting of Co-Cr-Mo for human prostheses. A leading cause of such scrap is the presence of sub-surface oxides that are exposed during post-casting machining operations. Their presence on the articulating surface and possible impact on wear and fatigue characteristics of the final product results in the casting being scrapped. Researchers at Birmingham have developed an Oxide Film Entrapment Model (OFEM) tracking algorithm capable of predicting the entrainment of oxides and tracking their movement and final location within simulations performed in the CFD package Flow3D. Validation of the model has been performed using DePuy's existing tree. The number of oxides each casting contained was shown to be dependent on the location of the castings. Metallurgical evaluation of the castings supported this finding. Modifications were made to the tree to reduce possible oxide formation and entrainment events during metal filling.

Emeritus Professor George D.W. Smith Honorary Symposium: Atom Probe Tomography

Sponsored by: The Minerals, Metals and Materials Society, TMS Materials Processing and Manufacturing Division, TMS/ASM: Phase Transformations Committee

Program Organizers: Michael Miller, Oak Ridge National Laboratory; Gregory Olson, Northwestern University and QuesTek Innovations LLC; George Krauss, Colorado School of Mines

Monday AM
March 12, 2012

Room: Mockingbird 2
Location: Swan Resort

Funding support provided by: Oak Ridge National Laboratory; QuesTek Innovations LLC; AMETEK, Inc

Session Chairs: Michael Miller, Oak Ridge National Laboratory; Thomas Kelly, Cameca Instruments, Inc.

8:30 AM Introductory Comments

8:45 AM Keynote

Look Back in Wonder: A Partial View of a Lifetime's Developments in Atom Probe Technology: *Alfred Cerezo*¹; ¹University of Oxford

In the early 80s, atom probe instruments existed in a few specialist laboratories, mainly for metallurgical studies. All-metal designs had been developed, with specimen exchange facilities, and computer data-logging systems. Early experiments with laser pulsing promised to expand the technique to semiconductor materials. Thirty years on, fully-automated 3-dimensional atom probes (3DAPs), which can switch easily between laser and voltage pulsing, are routinely being used in a wide range of laboratories to study an equally wide range of materials. What caused this massive leap forward? The seeds of change were already present in the 2-D elemental maps produced by the imaging atom probe (IAP) which, though less accurate, hinted at the vastly greater information that could be made available. It was using simple position-sensitive detectors in an IAP configuration that produced the first 3DAP data, and encouraged a wave of instrument development that led to our modern instruments.

9:15 AM Keynote

Prospects for Atomic-Scale Tomography: *Thomas Kelly*¹; Michael Miller²; Krishna Rajan³; Simon Ringer⁴; Albina Boresevich²; ¹Cameca Instruments, Inc.; ²Oak Ridge National Laboratory; ³Iowa State University; ⁴University of Sydney

Atomic-scale tomography (AST) may be defined as any technique that provides the precise three-dimensional position and identity of every atom in a "large" structure. Major breakthroughs in microscopy, condensed matter physics, and materials science will occur when this information becomes readily available. In the ultimate expression of AST, vacancies and interstitial atoms would be resolved which would enable a host of dynamic materials processes to be studied. Several experimental approaches are possible that may lead to AST. For example, by combining APT and (S)TEM, the limitations of each technique may be overcome and a robust synergy results. This 3D data could be used to generate many other types of knowledge, such as mechanical, magnetic and electrical properties, through the use of computational modelling techniques. A plan for achieving this goal will be described. Research sponsored by the U.S. DOE- Office of Basic Energy Sciences SHaRE user program [AYB and MKM].

9:45 AM Invited

Recent Developments in Atom Probe Microscopy: From Data to Information and through to Knowledge: *Simon Ringer*¹; ¹The University of Sydney

During public scientific discussion at the 2008 meeting of the international field emission society, Prof. G.D.W. Smith hinted at an

analogy between the notion of 'data mining', such as may be done in the context of extracting information from atom probe data, and the actual endeavour of minerals processing, where the technological stages of geological survey, mining, mineral separation, refinement and smelting processes operate in tandem to create valuable metals and alloys. We use this analogy to explain the impact of Prof. Smith's teaching and research on the research agenda around atom probe microscopy at The University of Sydney. My lecture will focus on our efforts to develop more precise approaches to the tomographic reconstruction, data analysis and recent successes in using atom probe data in first principles calculations that unravel controversies on the origins of certain behaviour in materials.

10:15 AM Break

10:45 AM Invited

APT Applied to MgO-Based Magnetic Tunnel Junctions: *Amanda Peiford-Long*¹; Daniel Schreiber²; David Seidman²; ¹Argonne National Laboratory; ²Northwestern University

The novel properties of magnetic tunnel junctions (MTJs) depend critically on their microstructure and composition, with variations on the atomic scale leading to variations in their properties. In its simplest form a MTJ consists of two ferromagnet layers separated by a nanoscale oxide tunnel barrier. The magnitude of the tunneling electrical current crossing the oxide barrier is a function of the relative orientation of the magnetization in the two ferromagnetic layers, an effect known as tunnel magnetoresistance (TMR). The nature of the oxide / ferromagnetic electrode interfaces is one of the critical parameters that control the magnetotransport properties of the MTJ, such as the spin polarization, tunnel barrier height, and indeed the shape of the tunnel barrier. We have used atom probe tomography and transmission electron microscopy to characterize the buried layers and their interfaces within MTJs to help explain their transport properties.

11:10 AM Invited

Atom Probe Tomography of Thin Films and Interfaces: *David Larson*¹; ¹Cameca Instruments, Inc.

Field ion microscopy and atom probe tomography has been applied to thin films since the early development of each of these instruments. However, a fundamentally limiting problem has always been the capability of fabricate specimens contains thin film regions of interest. Over the past decade or so, specimen fabrication techniques using focused-ion beam instruments with in-situ manipulation has revolutionized preparation of such specimens. Today, a variety of nanoscale thin films (including oxides) with site-specific features may be prepared and analyzed in arbitrary directions using atom probe tomography. APT data reconstruction of such structures, however, is quite complicated and significant work remains in this area. This talk will address the current status of atom probe analysis of thin films and interfaces, using a variety of materials types as examples, and include comparison to simulated structures.

11:35 AM

Atom Probe Studies of Nitride Multilayer Hard Coatings: *Dariusz Tytko*¹; ¹Max-Planck Institut für Eisenforschung

CrN/AlN multilayers having a bilayer thickness in the nanometer range are highly promising as hard coating materials for cutting tools due to their outstanding hardness, wear and oxidation resistance. The hardness of such multilayer hard coatings can be as high as 40 GPa by controlling the interface sharpness and the bilayer period of the multilayers. However, during operation at elevated temperatures such hard coatings undergo significant microstructural changes, which can cause a decrease in hardness. The aim of this study is to elucidate the nanostructural changes of CrN/AlN multilayers upon various thermal treatments and relate them to the mechanical properties. Using RF – magnetron sputtering, CrN/AlN multilayer superlattices with different bilayer periods and compositions were produced. The basic characterization of as-sputtered and annealed multilayers was done using Atom Probe Tomography in conjunction with X-ray diffraction and transmission electron microscopy.



TMS 2012

141st Annual Meeting & Exhibition

MONDAY AM

11:50 AM Invited

Modelling Image Formation in Atom Probe Tomography: *François Vurpillot*¹; ¹GPM UMR 6634

The understanding of image formation in Atom probe Tomography is the direct consequence of the processes of field evaporation, emission and projection of ionised atoms from the "Muller" field emitter (a sharply pointed needle). Basic models of field evaporation are now more than 50 years old. The models are extremely simple and ion trajectories are known to be governed by simple electrostatic relationships. Nevertheless, because since 30 years the complexity of materials analysed with the instrument has gradually increased (from simple metals to heterogeneous materials), these simple ingredients could give rise to various image artefacts. The comprehension of these artefacts and aberrations requires the use of numerical model to improve the fidelity of image reconstruction. This paper will show how the modelling approach could be used to understand the image deformations observed experimentally in alloys, multiphase samples, multilayer samples, or more complex devices.

12:15 PM

Coupled Modeling and Observation of Morphological Change in APT of Multicomponent Materials: *Daniel Haley*¹; George Smith¹; ¹Univeristy of Oxford

We apply combined numerical methods to register and evolve Transmission Electron Microscopy (TEM) observations of interrupted evaporations of Al-Ge alloys. Through multiple tilt-series TEM observation of the morphology of interrupted atom probe evaporated samples, we couple TEM observations to a numerical solution of the boundary motion equations using level set methods. These methods are subsequently used to form the foundation of an experimentally driven, temporally-resolved solution to the electrostatic equation in the tip region. Such a solution allows for the computation of the projection function that occurs as a result of near-atomic scale specimen geometry during the modelled morphological change. This work is conducted with a view to providing and validating a framework for experimentally driven reconstruction of atom probe datasets from inhomogeneous materials.

Energy Nanomaterials: Li-ion Batteries

Sponsored by: The Minerals, Metals and Materials Society, TMS Materials Processing and Manufacturing Division, TMS Structural Materials Division, TMS: Advanced Characterization, Testing, and Simulation Committee, TMS: Nanomechanical Materials Behavior Committee

Program Organizers: Reza Shahbazian-Yassar, Michigan Technological University; Ming Au, Savannah River National Laboratory; Meyya Meyyappan, NASA Ames Research Center

Monday AM
March 12, 2012

Room: Swan 3
Location: Swan Resort

Session Chairs: Reza Shahbazian Yassar, Michigan Technological University; Ming Au, Savannah River National Laboratory

8:30 AM Invited

Advanced Materials for Energy Storage Application: *Ilias Belharouk*¹; ¹Argonne National Laboratory

As lithium-ion batteries continue to be developed for energy storage applications with increasing energy demands, such as electric vehicles, new materials have been developed in efforts to increase the energy density and lower the cost. Lithium-and manganese-enriched oxides recently have received much attention. These materials have overall lithium to transition metal stoichiometry of greater than 1.0 and have greater than half of the relative transition metal composition manganese. These materials are composites of layered LiMO₂ (R m) (M = Ni, Co) and Li₂MnO₃ (C2/m) structures. The paper will provide insights into the structure of the family of Li- and Mn-enriched cathode materials that have shown promise for high capacity Li-ion battery applications.

8:55 AM

Nanoscale Testing of Low Dimensional Materials for Energy Harvesting and Storage: *Reza Shahbazian-Yassar*¹; Hessem Ghassemi¹; Anjana Asthana¹; Yoke Yap¹; ¹Michigan Technological University

Low dimensional materials have received considerable attention for their unique properties in energy storage (batteries) and energy harvesting (nanogenerators) devices. In this presentation, we cover the in-situ studies of Boron Nitride nanotubes (BNNTs), Zinc Oxide nanowires (ZnO NWs), and Silicon nanorods (Si NRs). Size scale effects were observed in ZnO nanowires and were explained by the modification of atomic structure at the nanowire surface. In addition, the rippling and bifurcation of multiwalled BNNTs were observed upon buckling and were quantified in terms of number of walls and nanotube's diameter. We also studied the mechanics of lithiated Si NRs to understand the effect of lithium intercalation into the structure of NRs.

9:10 AM

Nanostructured 3.9 V Triplite Cathode Materials for Li-Ion Batteries: *Prabeer Barpanda*¹; Jean Marie Tarascon²; ¹The University of Tokyo; ²Universite de Picardie Jules Verne

Li-ion batteries empower consumer electronics to (hybrid) electric vehicles. Here, the 3.45 V LiFePO₄ is the most outstanding cathode for its low cost and safety. Benchmarking against LiFePO₄, new cathode materials with higher energy density can be realized by designing novel polyanionic compounds having higher Fe²⁺/Fe³⁺ redox potential. The current work reports a novel 3.9 V (vs Li/Li⁺) triplite nanostructured polyanionic material, namely Li(Fe_{1-x}Mn_x)SO₄F [x=0.01~0.20]. It is a quantum leap in the field of battery showing the highest Fe²⁺/Fe³⁺ redox voltage ever-reported, exceeding that of LiFePO₄ by 450 mV. This novel triplite phase offers excellent reversible capacity of 130 mAh.g⁻¹ with lowest volume change of 0.3%. The local atomic disorder induced by Mn is believed to be at the origin of the triplite structure and 3.9 V Fe redox activity. This recent breakthrough in the Li-ion battery technology [Nature Materials, In Press 2011] will be described in detail.

9:25 AM Invited

A Nanofiber Approach to Advanced Lithium-Ion Battery Materials: *Xiangwu Zhang*¹; ¹North Carolina State University

Among the various existing energy storage technologies, rechargeable lithium-ion batteries have been considered as effective solution to the increasing need for high-energy density electrochemical power sources. Novel electrospun nanofibers with functional properties can dramatically alter surface reaction and charge transport throughout the batteries, causing significant improvement in energy storage efficiency. The design of functional nanofiber materials for alternative energy systems is, therefore, a way to develop a wide range of new technologies for a healthy future. Here, we present our work on the development of advanced functional nanofibers and the integration of these materials into rechargeable lithium-ion batteries to achieve high system performance.

9:50 AM Break

10:10 AM Invited

Carbon-Containing Nanocomposite Materials for Energy Storage: *Gleb Yushin*¹; ¹Georgia Institute of Technology

High power energy storage devices, such as supercapacitors and Li-ion batteries, are critical for the development of zero-emission electrical vehicles, large scale smart grid, and energy efficient cargo ships and locomotives. The energy storage characteristics of supercapacitors and Li-ion batteries are mostly determined by the specific capacities of their electrodes, while their power characteristics are influenced by the maximum rate of the ion transport. The talk will focus on the development of nanocomposite electrodes capable to improve both the energy and power storage characteristics of the state of the art devices. Advanced ultra-high surface area carbons, carbon-polymer, and carbon-metal oxide nanocomposites have been demonstrated to greatly exceed the specific capacitance of traditional electrodes for supercapacitors. Rationally

designed Si-C composites showed up to 8 times higher specific capacity than conventional anodes in Li-ion batteries, and stable performance for over 1000 cycles.

10:35 AM

Nanostructured Metals and Metal Oxides for High Capacity Anodes of Li-Ion Rechargeable Batteries: *Ming Au*¹; Thad Adams¹; ¹Savannah River National Laboratory

The electric vehicles with 300 miles driving range require new batteries with capacity 4-5 times high than today's Li-ion batteries. The metals and metal oxides have the higher theoretic anodic capacity. However, the large volume changes during charge and discharge causes materials pulverization resulting in quick capacity decay. To accommodate the volume change and increase lithium ion mobility in the anodes, the aligned metal nanorods and the nanoporous hollow spheres of the metal oxides were developed. Our anodes made by aligned Al and Si nanorods demonstrated 1000-2000 mAh/g of capacity. By tuning the composition of Si nanorods, their electrochemical cycling life was improved significantly. Our batteries made by the hollow nanoporous spheres of SnO₂ demonstrated 400 mAh/g of capacity in multiply cycles. The good cyclability is contributed to the unique hollow spherical structured of these metal oxides. We will report the details in this presentation.

10:50 AM

Nano-Crystalline Sn/Co-C Alloys Prepared as a High Stable Anode for Lithium Ion Batteries: *Youlan Zou*¹; Xiangyang Zhou¹; Juan Yang¹; Jie Li¹; Jingjing Tang¹; ¹Central South University

A simple hydrolysis synthesis method, united with carbothermal reduction using phenolic resin coated mixed oxides of CoO and SnO₂ as precursor, has been exploited to produce nano-sized Sn/Co-C alloys for lithium ion batteries. Physical and electrochemical properties were investigated by XRD, EDS, SEM, potential-sweep cyclic voltammetry, and galvanostatic charge and discharge tests. The results show that Sn/Co-C alloys with the size range from dozens of to hundreds of nanometer distribute evenly in the carbonaceous substrate. The morphology and granulometric distribution of the Sn/Co-C composites can be controlled by adjusting the heating schedule during carbothermal reduction. It was found that when the activated temperature is 600°C, the Sn/Co-C composite exhibits an initial reversible capacity of 829.4mAh/g at first cycle, decayed to a stable value of 555.9mAh/g after 30 cycles, and coulomb efficiencies of 96% were obtained after the first cycle at 100 mA/g.

11:05 AM

Transmission Electron Microscopy Studies on Lithium Battery Materials III: Effect of Aluminum Substitution in Layered Oxides: *Alpesh Shukla*¹; Thomas Conry¹; Marca Doeff¹; Thomas Richardson¹; ¹Lawrence Berkeley National Laboratory

Layered mixed transition metal oxide materials such as LiNi_xCo_{1-2x}Mn_xO₂ (x=0.33, 0.4) have been extensively investigated as Li-ion battery cathodes to replace LiCoO₂ in consumer electronics and, especially, for potential electric vehicle applications. A further reduction of the Co-content is desirable for cost and environmental reasons. To this end, Al-substitution for Co has been shown to improve both cost and safety aspects of the cathode materials while, notably, enhancing the cycling stability for reasons that are not explicitly known. This work explores the structural effects of Al-substitution in a nanoscale LiNi_{0.45}Co_{0.1-x}Al_xMn_{0.45}O₂ (0=x=0.1) model system through transmission electron microscopy studies. Electron diffraction is used to resolve the unit-cell distortion observed upon Al-substitution in the as-made materials with an average particle size ~50nm. Additionally, the structural changes occurring throughout the cycling life of the parent and substituted cathode materials will be discussed.

11:20 AM

The Effects of Annealing on the Charge-Discharge Characteristics of Eutectic Al-Si Thin Film with Pre-Deposited Al Layer: *Chao-Han Wu*¹; Fei-Yi Hung¹; Truan-Sheng Lui¹; Li-Hui Chen¹; ¹Department of Materials Science and Engineering, National Cheng Kung University

In this study, radio frequency magnetron sputtering was used to prepare 400nm eutectic Al-Si film anodes and the effect of annealing in vacuum on the charge-discharge capacity characteristics at different temperatures are discussed. For the purpose of letting Al-Si film possess the lowest crystallization temperature, the eutectic composition was adopted. The pre-sputtered 40nm Al thin film not only reduced the resistivity of the composite anode film, but also diffused to prevent peeling between the Al-Si films and Cu foils after annealing in the vacuum. The morphology transformation at samples' surface and cross section resulted from annealing at different temperatures and cycling was examined by Focus Ion Beam. Besides, the relationship between cycling performances and other electrochemical characteristics of the Al-Si film anodes was also investigated in this study by Cyclic Voltammetry and Electrochemical AC Impedance Spectroscopy.

Fatigue and Corrosion Damage in Metallic Materials: Fundamentals, Modeling and Prevention: Fundamentals of Fatigue Damage and Modeling

Sponsored by: The Minerals, Metals and Materials Society, TMS Structural Materials Division, TMS/ASM: Mechanical Behavior of Materials Committee

Program Organizers: Tongguang Zhai, University of Kentucky; Zhengdong Long, Kaiser Aluminum; Peter Liaw, University of Tennessee

Monday AM
March 12, 2012

Room: Oceanic 6
Location: Dolphin Resort

Session Chairs: Tongguang Zhai, University of Kentucky; Michael Sangid, Purdue University

8:30 AM Introductory Comments

8:35 AM Invited

Fatigue Modeling - Linking Microstructure to Predictions of Fatigue Crack Initiation: *Michael Sangid*¹; Huseyin Sehitoglu²; ¹Purdue University; ²University of Illinois, Urbana-Champaign

Excessive scatter is observed in the fatigue response of a nickel-based superalloy, U720, which is partly attributed to the variability in the microstructure. There is great interest in linking the microstructure to fatigue properties using a multi-scale approach that focuses on integrating the results of atomic simulations to the continuum level. Our approach is to model the energy of a persistent slip band (PSB) structure and use its stability with respect to dislocation motion as our failure criterion for fatigue crack initiation. Through this methodology, the fatigue life is predicted based on the energy of the PSB, which inherently accounts for the microstructure of the material. From this framework, we construct simulated microstructures based on the measured distributions of grain size, orientation, neighbor information, and grain boundary character, which allows us to calculate fatigue scatter using a deterministic approach. Excellent agreement is shown between the model predictions and experimental data.



TMS 2012

141st Annual Meeting & Exhibition

MONDAY AM

9:00 AM Invited

A FIB Study of the Resistance of Grain Boundaries to Short Fatigue Crack Propagation in Three-Dimensions in High Strength Al Alloys:

*Wei Wen*¹; A. H. W. Ngan²; Tongguang Zhai¹; ¹University of Kentucky; ²University of Hong Kong

Based on the early discovery that the twist component of crack plane deflection across a grain boundary (GB) was the key factor controlling the crack growth in high strength Al alloys, the resistance of the GB to short fatigue crack growth was quantified. Micro-cracks were made with a focus ion beam (FIB) before GBs which have a wide range of α . The measured growth rates of these cracks demonstrated that the resistance of the GB, following a Weibull-type function, increased with α . The study of the crack front advance in 3-D with the aid of the FIB illustrated that the GB could still drag the crack front under the sample surface, though the crack tip on the surface already passed a GB.

9:25 AM Invited

On Crack Initiation and Early Growth of Very-High-Cycle Fatigue for High Strength Steels:

*Youshi Hong*¹; Aiguo Zhao¹; Chengqi Sun¹;

¹Institute of Mechanics, Chinese Academy of Sciences

In the regime of Very-High-Cycle Fatigue (VHCF) for high strength steels, crack initiation and early growth dominate the fatigue life. The process of crack initiation and early growth of high strength steels at VHCF regime almost originates from the interior of the material with fish-eye embracing FGA or ODA. In this paper, fatigue tests on two high strength steels, i.e. a high carbon chromium steel and a medium carbon chromium steel, were performed with rotating bending and ultrasonic fatigue testing machines. The results show the dimensions of FGA and fish-eye as a function of inclusion size and reveal the correlation of the dimensions for FGA and fish-eye with fatigue failure cycles. The results also show the values of stress intensity factor ranges for FGA and fish-eye keep constant with fatigue failure cycles, which was used to estimate the fatigue life of high cycle and VHCF for high strength steels.

9:50 AM

Quantification of Fatigue Weak-Links in 713 Cast Al Alloys:

*Zhiqiang Xu*¹; Xinliang Zang¹; Yanguang Liu¹; Yuanbin Zhang²; Bin Xu²; Tongguang Zhai³; ¹College of Mechanical Engineering, Yanshan University; ²Materials Science and Engineering Department, Shandong Jianzhu University; ³Chemical and Materials Engineering Department, University of Kentucky

By taking into account the effects of pore position in depth and size, the average shear plastic strain amplitude for an applied cyclic stress over a region of 8 mm away from the pore on surface was calculated in 713 cast Al alloys using a finite element analysis method. The pore distribution in the alloy was reconstructed on computer by randomly placing the pores, measured with an optical microscope, in a cube. The average shear plastic strain amplitude around each pore in the surface which was randomly selected in the cube could be subsequently quantified for an applied cyclic stress. Fatigue crack initiation sites were identified from all the pores in the surface by calculating the life of fatigue crack initiation from each of the pores, using an improved Manson-Coffin law. The fatigue weak-link density and strength distribution were obtained and could be regarded as materials properties.

10:15 AM Break

10:25 AM Invited

Fundamental Principle of Cyclic Deformation and Dislocation Evolution in fcc Single Crystals:

*Peng Li*¹; Shouxin Li¹; Zhongguang Wang¹; Zhefeng Zhang¹; ¹Institute of Metal Research

This paper systematically summarized the cyclic deformation behaviors of different kinds of face-centered cubic (fcc) single crystals, including Cu, Ni, Ag, Au, Al, as well as Cu-Al, Cu-Zn and Cu-Ni alloys in attempt to provide a historical perspective of the developments over the last several decades. Combined with plenty of previous research results, the influencing factors of cyclic deformation behaviors can be listed as

follows: temperature, frequency, orientations and stacking fault energy (SFE). Among them, the orientation and SFE are the core factors. Compared with the above two factors, temperature and frequency can be regarded as the extrinsic factors. As the testing temperature increases, the plateau of the cyclic stress-strain (CSS) curves gradually disappears and the saturation resolved shear stress decreases distinctly at low strain amplitudes. However, the increase in frequency does not affect the appearance of the plateau behavior, but the corresponding plateau stress slightly increases.

10:50 AM

Fatigue Interrogating 3D Synthetic Microstructures of Ni-Based Alloys:

*Joseph Tucker*¹; Clayton Stein¹; Lisa Chan²; Albert Cerrone³; Anthony Rollett¹; Anthony Ingraffea³; ¹Carnegie Mellon University; ²EDAX; ³Cornell University

Determining the root cause of decreased fatigue life in Ni-based alloys is a complex problem. Processing, part shape, and application environment all contribute to significant variations. Crack initiation and propagation is first microstructural, leading to a study on grain character. Grain size, orientation, misorientation, NN, substructure, and inclusions collectively affect the likelihood of slip. For instance, forging and heat treating a Ni alloy resulting in as large as grains with little substructure would provide a long dislocation mean free slip length with few obstructions. These types of scenarios are injected into Ni alloy statistical volume elements and tested with crystal plasticity models.

11:10 AM

Modeling Intergranular Crack Growth in a Nickel Based Superalloy:

*Kimberly Maciejewski*¹; Hamouda Ghonem¹; ¹University of Rhode Island

A mechanistic based crack growth model has been developed to simulate intergranular cracking in a polycrystalline Nickel based superalloy at elevated temperatures. The model considers the interactions between creep, fatigue and environment. The bulk material is modeled using a microstructure explicit crystal plasticity model surrounded by an internal state variable type of model. The crack path is described using a cohesive zone approach in which the grain boundary dislocation network is smeared into a Newtonian viscous fluid element. The cohesive laws consider deformation and damage through grain boundary sliding and dynamic embrittlement mechanisms based on the grain boundary dislocation mobility and its evolution due to Oxygen diffusion. The model, in conjunction with experimental results, is utilized to obtain the critical sliding length in both air and vacuum as a function of temperature. This model is then used to study the sensitivity of environment, temperature, precipitate microstructure and grain boundary morphology.

11:30 AM

Investigating Deformation Mechanisms Under Dwell-Fatigue in a Ni-base Superalloy:

*G. B. Viswanathan*¹; Dan Huber²; Sushant Jha¹; Sara Knox³; Ken Bain⁴; Hamish Fraser²; C Woodward¹; ¹Air Force Research Laboratory; ²The Ohio State University; ³Southwestern Ohio Council for Higher Education; ⁴GE Aviation

The ability to resist crack growth at high temperature under hold times is an important design criterion for the new generation superalloys. While the crack nucleation is still an intensely debated issue in these alloys, the mechanism by which stable crack growth occurs also remains unclear. In this study, hold-time stable crack growth studies are conducted in notched samples of Rene104 Ni-base superalloy tested at 1300 with a stress concentration factor 1.7 and a 90 seconds dwell to failure. Thin foils were extracted from specific grains from the fracture surface via focused ion imaging (FIB). TEM analysis showed that depending on the local stress condition (Δk), the deformation substructure within the grains varied from dislocations and stacking faults within the γ matrix to APB coupled dislocations within the γ' precipitates. Based on these observations an attempt is made to elucidate possible operating mechanisms under dwell fatigue conditions in this alloy.

From Macro to Nano, Understanding Mechanical Behavior across Length Scales: A Structural Materials Division Symposium in Honor of Robert Ritchie: Biological and Bioinspired Materials Science

Sponsored by: The Minerals, Metals and Materials Society, TMS Structural Materials Division, TMS/ASM: Mechanical Behavior of Materials Committee, TMS: Biomaterials Committee
Program Organizers: Jamie Kruzic, Oregon State University; Brad Boyce, Sandia National Labs; Reinhold Dauskardt, Stanford University

Monday AM
March 12, 2012

Room: Mockingbird 1
Location: Swan Resort

Session Chairs: Marc Meyers, University of California, San Diego; Markus Buehler, MIT

8:30 AM Introductory Comments

8:35 AM Keynote

Studies of Mechanical Properties of Materials across Length Scales: Subra Suresh¹; ¹Department of Materials Science and Engineering, Massachusetts Institute of Technology

This presentation will provide an overview of research into mechanical properties of materials over the past several decades with a view to assess key advances and remaining challenges. Attention will be devoted to major advances in (a) bridging length scales from the nano- to the macroscopic structures, (b) bringing transformative research from other disciplines, such as genetics and computation, to gain a better understanding of mechanistic processes underlying the mechanical signatures of engineered and living systems, and (c) guiding experiments and engineering practice through advances in computational modeling and simulations. The presentation will also address the unique perspectives that materials science and engineering offer to the coupled mechanical, biochemical and biomedical phenomena in the context of human health and diseases.

9:15 AM

Structural Hierarchies Define Toughness and Defect-Tolerance Despite Simple and Mechanically Inferior Brittle Building Blocks: Markus Buehler¹; ¹Massachusetts Institute of Technology

Mineralized biological materials such as bone, sea sponges or diatoms provide load-bearing and armor functions and universally feature structural hierarchies from nano to macro. Here we report a systematic investigation of the effect of hierarchical structures on toughness and defect-tolerance based on a single and mechanically inferior brittle base material, silica, using a bottom-up approach rooted in atomistic modeling. Our analysis reveals drastic changes in the material crack-propagation resistance (R-curve) solely due to the introduction of hierarchical structures that also result in a vastly increased toughness and defect-tolerance, enabling stable crack propagation over an extensive range of crack sizes. Over a range of up to four hierarchy levels, we find an exponential increase in the defect-tolerance approaching hundred micrometers without introducing additional mechanisms or materials. This presents a significant departure from the defect-tolerance of the base material, silica, which is brittle and highly sensitive even to extremely small nanometer-scale defects.

9:30 AM

Enhanced Energy Dissipation through Size-Dependent Nanoscale Heterogeneity in Bone: Ming Dao¹; ¹MIT

Various mechanisms have been identified in the literature that enhance the strength and toughness of bone. An earlier study showed that nanoscale heterogeneity in bone promotes inelastic energy dissipation during deformation. On the other hand, it is well known that heterogeneity in composite materials may introduce stress concentration and strain localization that can degrade mechanical properties. So, is nanoscale

heterogeneity found in bone good or bad? We have recently quantified both elastic and inelastic heterogeneities of bovine cortical bone with a spatial resolution as low as 100 nm. A characteristic length scale was identified at about 200 nm. Below this length scale, heterogeneity was found to be high and strongly size-dependent; whereas above this length scale, heterogeneity is much less pronounced. Such a size dependence can effectively take advantage of damage tolerance at the nanoscale while limiting stress concentration or strain localization caused by heterogeneity at higher length scales.

9:45 AM

Multiscale Modeling of R-Curve Behaviors in Bone Tissue: Kwai Chan¹; Daniel Nicoletta¹; ¹Southwest Research Institute

The risk of bone fracture increases with age because of a variety of factors that include, among other, decreasing bone quantity and quality. Experimental evidence has indicated that changes in bone microstructure and trace mineralization with age can result in different crack-tip strain field and fracture response, leading to different fracture mechanisms and R-curve behaviors. Age-related embrittlement of bone fracture is associated with higher near-tip strains by lamellar shear and crack deflection at lamellar interfaces in young bone and their absence in the old bone. The different near-tip deformation and fracture behaviors may be related to changes of mineralization in bone tissue with age. In this paper, a multiscale modeling approach is developed to predict the R-curve response of bone tissues by delineating fracture mechanisms that lead to microdamage and ligament bridging. The effects of age and trace mineralization on bone fracture are then examined via the multiscale fracture model.

10:00 AM Break

10:15 AM Keynote

Scale Effects and Hierarchy in Biological Materials: Marc Meyers¹; Po-Yu Chen²; ¹UCSD; ²National Tsing Hua U.

One of the principal differences between biological and synthetic materials is that biological materials are constructed from the bottom up, whereas many synthetic materials are produced in a top-bottom sequence. Synthetic materials benefit from a cornucopia of high temperature synthesis methods not available to biological materials. The ubiquitous presence of water in the extra and intracellular materials is of primary import and dictates, often, the mechanical response. This, and the multifunctionality of biological materials requires structures that often exceed in complexity and hierarchical levels their synthetic counterparts. We illustrate the hierarchical levels, from the nano to the structural scale, for a few biological materials studied by our group: abalone shell, crab exoskeleton, fish scales, and toucan beak and feathers. Funding: NSF DMR Biomaterials and Ceramics Programs

10:55 AM

On the Exceptional Fracture Toughness of Elk Antler Bone: Po-Yu Chen¹; Maximilien Launey²; Joanna McKittrick³; Robert Ritchie⁴; ¹National Tsing Hua University; ²Lawrence Berkeley National Laboratory; ³University of California, San Diego; ⁴University of California, Berkeley

We investigate the fracture toughness of a non-structural bone, namely the elk antler, which has a primary function in combat and is designed for high impact loading without fracture. Antler has lower mineral content compared to mammalian limb bones and consists mainly of young primary osteons due to limited remodeling. In situ mechanical testing under ESEM and micro-CT scans are performed to examine crack propagation in the longitudinal and transverse orientations in compact antler. We find that antler in the transverse orientation is one of the toughest biological materials known, reaching 60 kJ/m². Its resistance to fracture is achieved extrinsically during crack growth by crack deflection/twisting and crack bridging via uncracked ligaments and collagen fibrils. We present an assessment of the toughening mechanisms acting in antler as compared to human cortical bone, and identify an enhanced role of inelastic deformation in antler which further contributes to its intrinsic toughness.



TMS 2012

141st Annual Meeting & Exhibition

MONDAY AM

11:10 AM

Aging-Related Changes in the Plasticity and Toughness of Human Cortical Bone at Multiple Length-Scales: *Elizabeth Zimmermann*¹; Eric Schaible¹; Hrishikesh Bale¹; Holly Barth¹; Simon Tang²; Peter Reichert¹; Bjorn Busse¹; Tamara Alliston²; Joel W Ager III¹; Robert O. Ritchie¹; ¹Lawrence Berkeley National Lab; ²University of California San Francisco

The structure of human cortical bone evolves over a range of length-scales; as this hierarchical structure provides the basis for bone's mechanical properties, each level's contribution to the fracture resistance (from plasticity to crack-tip shielding mechanisms) needs to be evaluated. Although an important reason for the decreased fracture resistance is the loss of bone mass with age (bone quantity), aging-related changes in the structure can occur at multiple length-scales to deteriorate the fracture resistance (bone quality). This study mechanically characterizes different length-scales via small- and wide-angle x-ray scattering/diffraction and fracture toughness measurements of different age groups. On the same bones, structural changes are quantified via crosslinking measurements and x-ray computed tomography. Our results show how aging-related structural changes at differing size-scales can degrade the intrinsic toughness by increased cross-linking suppressing plasticity, as well as the extrinsic toughness of bone by an increased osteonal density limiting the potency of crack-bridging mechanisms.

11:25 AM

Mechanical Behavior in Human Cortical Bone Across Multiple Length Scales: Investigations of Elastic Anisotropy and Damage Accumulation: *Ryan Roeder*¹; Andrew Baumann¹; Travis Turnbull¹; Joshua Gargac¹; David Rudy¹; Justin Deuerling¹; Glen Niebur¹; ¹University of Notre Dame

Elastic properties and fatigue microdamage accumulation in human cortical bone both vary with age, disease, gender, and anatomic location, as governed by complex structure-property relationships across multiple length scales. Variability in experimental measurements of elastic constant magnitudes and anisotropy was shown to be governed primarily by the apatite crystal volume fraction and orientation distribution, respectively, using a specimen-specific, multi-scale micromechanical model. A subsequent multi-scale framework combining specimen-specific micromechanical and micro-finite element models showed that the apatite crystal orientation distribution accounts for the dominant overall transverse anisotropy, while the architecture of intracortical porosity accounts for more subtle variations in tissue orthotropy. Nondestructive and three-dimensional detection of fatigue microdamage was recently enabled using contrast-enhanced micro-computed tomography. Damage initiation and accumulation was shown to be non-uniform, occurring in preferentially in regions of tissue experiencing elevated tensile principal strains due to the whole bone morphology, mode of loading, and intracortical porosity.

Integrative Materials Design: Performance and Sustainability: Processing and Properties of Traditional and Novel Materials at Ambient and High Temperatures I

Sponsored by: The Minerals, Metals and Materials Society, TMS/ASM: Mechanical Behavior of Materials Committee
Program Organizer: Diana A. Lados, Worcester Polytechnic Institute

Monday AM
March 12, 2012

Room: Europe 2
Location: Dolphin Resort

Session Chair: Diana Lados, Worcester Polytechnic Institute

8:30 AM Introductory Comments

8:35 AM Invited

Nanostructured Metals: Synergy between Multiple Scales: *Enrique J. Lavernia*¹; ¹University of California, Davis

Bulk nanostructured materials have matured into a new class of materials with potential structural applications. Successful synthesis of large-scale nanostructured materials is of technological and scientific significance. Technologically, it will be feasible to obtain engineering materials that retain structural and chemical attributes in the nanometer size range. Scientifically, large-scale nanostructured materials will permit systematic investigations of physical and mechanical behavior, as well as novel phenomena. Results from various groups around the world reveal considerable improvements in physical performance as well as interesting deformation phenomena in a variety of nanostructured materials. Increases in strength are commonly documented, ductility, however, appears to scale inversely with strength in these materials. This challenge has been addressed via the introduction of additional size scales that facilitate plasticity during deformation. In this lecture, deformation behavior and underlying mechanisms of several nanostructured metals are discussed to shed light into the fundamental behavior of nanostructured materials.

9:00 AM Invited

Optimization of Mechanical Properties in Ultrafine Grained Lightweight Alloys: *Rajiv Mishra*¹; ¹Missouri University of Science and Technology

For engineering applications, structural materials must possess a balance of static and dynamic properties. Strength, ductility and fatigue life are often critical properties. While ultrafine grained materials (UFG) invariably possess high strength, the level of ductility and fatigue life often limit the applicability. To obtain balanced mechanical response in UFG lightweight alloys, consideration must be given to the details of the microstructure and the microstructure/mechanics intersection. Some examples of change in overall mechanical response in UFG aluminum, magnesium and titanium alloys will be highlighted. The relative role of microstructure and mechanics will be discussed.

9:25 AM Invited

Friction Stir Welding in Aluminum and Magnesium Alloys: Effects of Processing Parameters on Microstructure and Mechanical Properties: *Andrew Biro*¹; Diana Lados¹; ¹WPI

Friction stir welding is a solid-state joining process used in structural and transportation applications where low-density and high-strength requirements dictate the use of light metals including aluminum and magnesium alloys. This study focused on two themes. The first was to optimize processing parameters for welding similar alloys, wrought 6061-6061 aluminum and cast ZE41A-ZE41A magnesium, and to determine the effect of post-weld heat treatments on the microstructures and properties of the welds. The second was to investigate processing parameters for welding dissimilar alloys, wrought aluminum to cast aluminum and

magnesium alloys, specifically 6061-A356 and 6061-ZE41A. In addition, post-weld heat treatments were conducted on the dissimilar welds to determine if and to what degree mechanical properties could be improved over those obtained in as-welded conditions. Fatigue crack growth studies were also conducted on base and welded samples using compact tension specimens, and microstructural effects were analyzed and related to weld performance.

9:50 AM

Sequential Approximate Optimization Based Robust Design of SiC-Si₃N₄ Nanocomposite Microstructures: Gilberto Mejia-Rodriguez¹; Vikas Tomar²; John Renaud³; ¹San Luis Potosi; ²Purdue University; ³University of Notre Dame

A simulation-based robust design optimization methodology to predict the most suitable microstructures of SiC-Si₃N₄ nanocomposites for desired high temperature toughness is presented. The focus is on finding robust nanocomposite microstructures with maximum toughness at two temperatures: 1500°C and 1600°C. Within this context a sequential approximate optimization algorithm under uncertainty is applied to six different test problems addressing different aspects of robust microstructure generation. During optimization, statistical uncertainties inherent to the computational microstructural generation are quantified and introduced in the optimization framework. The results show that the SiC volume fraction, the number of Si₃N₄ grains, the grain size distribution of the Si₃N₄ grains, and the grain size of the SiC grains have varied effects on the microstructure toughness at different temperatures.

10:10 AM Break

10:35 AM Invited

Bulk Metallic Glasses: Highly Processable, High Performance Materials: Jamie Krusic¹; ¹Oregon State University

Bulk metallic glasses (BMGs) are a class of materials with both novel processing characteristics and mechanical properties. Accordingly, BMGs are poised to make major inroads into the design and manufacture of a wide variety of commercial products. The possibility of processing via thermo-plastic forming (TPF) makes BMGs attractive over traditional metals. Advantages of TPF include the ability to process net-shaped components with high dimensional accuracy at low temperature and pressures; thus, there is a large potential for energy and cost saving in manufacturing. The high specific strengths of BMGs coupled with reasonable fracture toughnesses make them attractive for many applications; however, questions of fatigue resistance and durability have slowed their application. More recent research has demonstrated that BMGs can be engineered with good fatigue resistance. This presentation reviews some of the advantageous processing characteristics and mechanical properties of BMGs and explains some of the misconceptions regarding fatigue resistance and durability.

11:00 AM

Characterization of Nickel Rich NiTiHf Shape Memory Alloys for Use as High Temperature Actuators: Daniel Coughlin¹; Glen Bigelow²; Anita Garg²; Ronald Noebe²; Michael Mills¹; ¹Ohio State University; ²NASA Glenn Research Center

The use of shape memory alloys (SMAs) as “smart” structures to eliminate hydraulic and pneumatic actuators can reduce weight, moving parts, and energy cost in many industrial applications, but the need for high temperature SMAs still exists. NiTiHf ternary system exhibit attractive high temperature shape memory properties, including relatively high transformation temperature, and small irrecoverable strain during load-biased and thermal-cycling tests at moderate to high stresses. Two distinct nickel rich compositions, both containing 20at.% Hf and Ti concentrations of 29at.% and 29.7at.%, have been analyzed using TEM in the as-extruded condition and several aging conditions that range from 3hrs at 400°C to 3hrs at 700°C. The strengthening effects due to precipitates formed during aging was measured using isothermal, constant strain rate testing at several temperatures above the austenite finish temperature. A

comparison of the mechanical response and precipitate structure between these NiTiHf alloys and other NiTiX SMAs will be discussed.

11:20 AM Invited

Design of Smart Metal-Matrix Composites for Sustainability and Advanced Performance: Charles Fisher¹; Michele Manuel¹; ¹University of Florida

In an effort to increase reliability and sustainability in complex systems, smart metal-matrix composites with the ability to self-heal are currently under development. Self-healing has the potential to greatly increase the life-cycle of specific components. Designing systems which possess the appropriate processing-structure-property relationships for self-healing, however, can be a difficult undertaking. The multifaceted interaction across multiple length scales yields a very complex issue for composite development. To combat this issue, a systems design approach governed by thermodynamics and empirical models was utilized to aid in the selection of materials with potential for self-healing. This study will present the alloy selection process for a high-specific strength matrix utilizing shape-memory alloy wire reinforcements to aid in self-healing in addition to initial tensile and microstructural characterization of the metal-matrix composite. The authors would like to gratefully acknowledge the support of the National Science Foundation under grant number CMMI-0824352.

11:40 AM

Multi-Scale Design of Open-Cell Aluminum Alloy Foam: Daeyong Kim¹; Ji Hoon Kim¹; Myoung-Gyu Lee²; Jong Kook Lee³; ¹Korea Institute of Materials Science; ²Pohang University of Science and Technology; ³Hyundai Motor Company

Metal foam inserts in the crash member are expected to reduce vehicle weights while maintaining or even increasing the crashworthiness. Due to its complex structure and behavior, however, few works have been reported to design and optimize its structure and performance. In this work, multi-scale methods are used to design the metal foam structures. The 3D structure of an open-cell foam is obtained and analyzed using the X-ray microtomography. Based on the structure information, virtual foam structures are generated by changing the length and orientation of the cell struts. The optimum structure for maximizing the energy absorption is obtained and tested numerically for crashworthiness.

International Smelting Technology Symposium (Incorporating the 6th Advances in Sulfide Smelting Symposium): Plenary Session

Sponsored by: The Minerals, Metals and Materials Society, The Metallurgy and Materials Society of CIM, TMS Extraction and Processing Division, TMS: Pyrometallurgy Committee
Program Organizers: Jerome Downey, Montana Tech of the Univ of Montana; Thomas Battle, Midrex Technologies, Inc.; Jesse White, Elkem Solar Research

Monday AM
March 12, 2012

Room: Northern A3
Location: Dolphin Resort

Session Chair: To Be Announced

8:30 AM Introductory Comments

8:40 AM Keynote

2012 EPD DISTINGUISHED LECTURER: Conservation & Development: Industrial Learning in Non-Ferrous Smelting: Theo Lehner¹; ¹Boliden Mineral AB

The 2012 TMS Annual Meeting hosts The International Smelting Technology Symposium. This makes a metallurgist happy and interested – in at least 4 ways! Our business is truly International: not only by ownership, but also by localizations, global competition, international treaties regulating our operations and not least: friends around the Globe. Smelting calls awake – also after a long life with metallurgy – the curious



TMS 2012

141st Annual Meeting & Exhibition

MONDAY AM

spirits dancing above red hot liquids: whispering sometimes, shouting at other occasions: why don't you understand what is going on in the molten phases below, what is explaining the phenomena observed? Technology allows the engineer to emerge and divide reality quickly into ample boxes to grasp and control. Finally Symposium describes the avenue ahead of us: a forum for continued learning, and it is always equally astonishing how much more there is to be learnt. Our industry has demonstrated impressive industrial learning curves.

9:25 AM

Modernization and New Copper Smelter Project Developments on the Central African Copperbelt: *Timothy Smith*¹; ¹SNC Lavalin

Recent global copper supply and demand factors have, in part, helped to drive a surge of new copper projects within the central African Copperbelt. High copper prices along with issues such as location, by-product cobalt and a regional shortage of sulphuric acid, have provided impetus to investment and rapid development of a cluster of both new and modernized copper smelters to serve local mines. This paper describes these smelter projects and technology developments in the context of the special local factors.

9:55 AM Break

10:10 AM

Developments in DC Arc Smelting Technology in Southern Africa: *Rodney Jones*¹; *Isabel Geldenhuys*¹; *Glen Denton*¹; ¹Mintek

DC arc furnaces are well suited to a number of reductive smelting processes. This technology has been used (initially in southern Africa, but now also elsewhere in the world) for the commercial production of ferrochromium from chromite, the production of titania slag and pig iron from ilmenite, and for the recovery of valuable metals from slags. A further process, currently undergoing commercialisation involves reductive smelting for the production of platinum group metals (PGMs). Some of these processes require the use of other enabling technologies, both for pre-treatment of feed materials, and for making the product more easily handled. An example of this is the use of water atomisation for the production of a powdered metal product for further downstream treatment. This paper describes the development and application of DC arc furnace technology, with a particular emphasis on recent developments.

10:40 AM

Aluminothermic Smelting: A Versatile Process Serving Demanding Markets: *James Robison*¹; ¹Reading Alloys, Inc., an Ametek Company

Aluminothermic ("Thermite") smelting became commercial with the development of tonnage aluminum, and prospered producing metals and alloys with higher cleanliness, consistency and elemental control than competing technologies. We explore the scope of thermite smelting, and metallothermic smelting in general; the thermochemistry of the process, and its advantages and limitations as applied to industrial production. We review currently-produced products of thermite smelting in several forms and a wide range of heat sizes. As these products serve several industries, we will relate the demands of those industries to the requirements imposed on the thermite process, leading to process dynamics and mechanisms to control/alter those dynamics. We review ways to lower the costs of the process by altering process stoichiometry, using other energy sources, and utilizing less costly raw materials while considering effects on product quality and customer requirements. Finally, we examine overall emissions control and waste disposal.

11:10 AM

The Blast Furnace: What Was, What Is, and What Will Be: *Mark Schlesinger*¹; *David Robertson*¹; ¹Missouri University of Science and Technology

The blast furnace is the oldest type of reactor for the production of molten metal from mineral ores. Over eight centuries of development it has become a primary tool for production of metals from oxide ores, and from sintered sulfides. It is particularly important in the production of

pig iron, but is still used to produce other metals, and for the treatment of secondary materials. This presentation will review the development and use of the blast furnace for production of pig iron and other metals, the current state of the art for this technology, and its advantages and limitations.

Magnesium Technology 2012: Plenary Session

Sponsored by: The Minerals, Metals and Materials Society, TMS Light Metals Division, TMS: Magnesium Committee

Program Organizers: Suveen Mathaudhu, U.S. Army Research Office; Wim Sillekens, TNO; Norbert Hort, Helmholtz-Zentrum Geesthacht; Neale Neelameggham, U.S. Magnesium

Monday AM
March 12, 2012

Room: Southern IV
Location: Dolphin Resort

Session Chairs: Suveen Mathaudhu, U.S. Army Research Office; Wim Sillekens, TNO; Norbert Hort, Helmholtz-Zentrum Geesthacht

8:30 AM Introductory Comments

8:45 AM Keynote

Magnesium Alloy Development Using Phase Equilibria Computation and Microstructure Validation: *Alan Luo*¹; *Raja Mishra*¹; *Bob Powell*¹; *Anil Sachdev*¹; ¹General Motors Corporation

This paper summarizes the development of new cast and wrought magnesium alloys using computational thermodynamics and experimental methods. The work illustrates the role of calculated phase diagrams, solidification paths and phases in predicting and interpreting the final microstructure of Mg-Al-Ca and Mg-Al-Sn cast alloy systems and Mg-Al-Mn and Mg-Zn-Ce wrought alloy systems. The Mg-Al-Ca alloys show excellent creep resistance due to the formation of high-temperature (Mg,Al)₂Ca phase. The Mg-Al-Sn alloys are designed for mechanical properties and corrosion resistance by optimizing the Mg₁₇Al₁₂ and Mg₂Sn phases in the microstructure. AM30 (Mg-3Al-0.3Mn) alloy was developed to have significantly improved extrudability and slightly improved mechanical properties compared to AZ31 alloy, due to the absence of low eutectic-point Mg-Al-Zn ternary phases existing in the AM30 alloy. In the Mg-Zn-Ce system, Zn provides strength through solid solution strengthening, while Ce increases the ductility by creating a favorable texture.

9:15 AM Keynote

Research and Application of Mg Alloys for Aerospace: *Donald Shih*¹; ¹The Boeing Company

This keynote presentation will address my perspectives on research, development, and application of Mg alloys in aerospace. Specific focus will be given to the Boeing products.

9:45 AM Keynote

Atoms-to-Grains Corrosion Modeling for Predictive Design of Mg-Alloys: *Santanu Chaudhuri*¹; *Jie Xiao*¹; *Hyunwook Kwak*¹; ¹Washington State University

Development of new Mg-alloys needs greater efforts in systematic evaluation of corrosion protection methods under service environments. A deeper understanding of microscale and nanoscale metallurgy is needed to slow down corrosion. Results from our multiscale model will be presented to demonstrate the power of first-principle theories in predicting the composition-dependent kinetics of corrosion reactions. Our recent results show that the corrosion prevention properties of Mg-alloys can be significantly enhanced by doping rare-earth elements such as Cerium that protects the oxide layer from rapid hydrolysis. Furthermore, we are developing kinetic Monte Carlo and finite-element analysis (FEA) based models to extend the predictions from the atomic length scales to nano-

and microscale models that will include grains and alloy microstructure. The potential for incorporating mechanical and corrosion performance in continuum length scale combined with the insights from first-principles based surface chemical models can have powerful impact on the development of Mg-alloys.

10:15 AM Break

10:30 AM Keynote

Solid State Joining of Magnesium to Steel: *Yuri Hovanski*¹; Michael Santella²; Saamyadeep Jana¹; Hao Yu³; David Field³; Tsung-Yu Pan²; Siva Pilli¹; ¹Pacific Northwest National Laboratory; ²Oak Ridge National Laboratory; ³Washington State University

Friction stir welding and ultrasonic welding techniques were applied to join automotive magnesium alloys to steel sheet. The effect of tooling and process parameters on the post-weld microstructure, texture and mechanical properties was investigated. Static and dynamic loading were utilized to investigate the joint strength of both cast and wrought magnesium alloys including their susceptibility and degradation under corrosive media. The conditions required to produce joint strengths in excess of 75% of the base metal strength were determined, and the effects of surface coatings, tooling and weld parameters on weld properties are presented.

11:00 AM Keynote

Grain Evolution During High Temperature Necking of Magnesium Alloys: *Paul Krajewski*¹; ¹General Motors

Magnesium sheet materials AZ31, AZ61, AM50, ZM21, ZK10, and ZK30 were tested to failure at 350C and 450C at strain rates between 0.001 and 0.3/s. Each of these materials exhibit significant changes in grain structure during deformation, especially in the necked regions of the failed samples. Grain size in the neck is shown to vary with thickness strain and strain rate. At the fastest strain rates, grain size decreases as the strain in the neck increases. At the slower strain rates, very coarse grains are observed at the highest strains. The effect of temperature and alloy will also be presented. The results of this work can be used to help validate models for dynamic recrystallization in magnesium.

11:30 AM Keynote

Production of Wide Shear-Rolled Magnesium Sheet for Part Forming: *David Randman*¹; Bruce Davis¹; Martyn Alderman¹; Govindarajan Muralidharan²; Thomas Muth²; Thomas Watkins²; William Peter²; ¹Magnesium Elektron North America; ²Oak Ridge National Laboratory

In recent years the process of shear rolling has seen considerable study, particularly for heavily textured materials such as magnesium. The goal of this work has been to produce more formable sheet to form parts for industries such as automotive and aerospace. To date, almost all work has been carried out on small strips that are not large enough to produce many useful parts. The current work will discuss the scaling-up of the shear rolling process to generate wider sheet. A mill at the Magnesium Elektron North America plant has been modified to allow shear rolling at a ratio of 1:1.35 on sheets up to 36" wide. Elektron 717 sheets of size 36"x72" have been shear rolled and demonstration automotive parts have been formed by General Motors and Superform USA.

Materials and Fuels for the Current and Advanced Nuclear Reactors: Nuclear Fuels - Modeling

Sponsored by: The Minerals, Metals and Materials Society, TMS Structural Materials Division, TMS/ASM: Corrosion and Environmental Effects Committee, TMS/ASM: Nuclear Materials Committee

Program Organizers: Ramprashad Prabhakaran, Idaho National Laboratory; Dennis Keiser, Idaho National Laboratory; Raul Rebak, GE Global Research

Monday AM
March 12, 2012

Room: Swan 2
Location: Swan Resort

Session Chair: Ramprashad Prabhakaran, Idaho National Laboratory

8:30 AM Invited

3-Dimensional, High-Resolution Modeling of Nuclear Fuel Performance: Pellet Clad Interaction: *Brian Wirth*¹; Derek Gaston²; Jason Hales²; Richard Martineau²; Robert Montgomery³; Y.R. Rashid⁴; Chris Stanek⁵; ¹University of Tennessee; ²Idaho National Laboratory; ³Pacific Northwest National Laboratory; ⁴Anatech Corp.; ⁵Los Alamos National Laboratory

The nuclear fuel operating environment is among the most extreme encountered by any functioning materials system. Fission processes generate high temperatures and high fluxes of energetic particles. The zirconium alloy cladding is exposed to a highly corrosive environment, in addition to numerous mechanical and chemical interaction forces as it serves as the first engineered barrier against the release of radioactive fission products. This presentation will introduce the inherently multiscale nature of irradiation effects in nuclear fuels and cladding materials and then describe an engineering-scale, 3D framework for modeling nuclear fuel performance, with an emphasis on pellet clad interaction. Following a description of the important materials degradation phenomena and the current best effort models to describe them, the presentation will focus on an example demonstrating the capability to the model stress state in a Zirconium alloy fuel clad surrounding a fuel pellet with a missing pellet surface during an operational transient.

9:00 AM

Multiscale Modeling of Reactor Fuel Restructuring: *Michael Tonks*¹; Paul Millett¹; Bulent Biner¹; Liangzhe Zhang¹; Xianming Bai¹; ¹Idaho National Laboratory

Due to temperature and stress gradients, as well as radiation effects, the grain and pore structure of reactor fuel changes significantly during its lifetime. This restructuring in the fuel has a significant impact on thermal conductivity and fission gas release, and therefore is of critical importance when predicting fuel performance. To gain a better understanding of fuel restructuring, we use a combination of atomistic and mesoscale phase field simulations to investigate GB and pore migration and how the two interact. We also compare the effects of stress and temperature gradients. Finally, we demonstrate how this information can be used to improve existing fuel performance materials models.

9:20 AM

Phase-Field Modeling of Pore Migration in Nuclear Fuels Due to a Temperature Gradient: *Liangzhe Zhang*¹; Michael Tonks¹; Paul Millett¹; Bulent Biner¹; Yongfeng Zhang¹; Karthikeyan Chockalingam¹; ¹Idaho National Laboratory

Sintered UO₂ nuclear fuel materials undergo a unique microstructural evolution process during operation. The evolved microstructure is usually characterized by the columnar grains surrounding a large central void, which mainly results from the migration of the initial pores towards the high temperature regions. A quantitative description of the pore migration process is therefore desirable for better understanding and accurate



TMS 2012

141st Annual Meeting & Exhibition

MONDAY AM

predictions of the fuel performance. For this purpose, a phase-field model is developed; in which the kinetics of the migration due to both bulk and surface diffusion is formulated by utilizing fourth order Cahn-Hilliard (CH) equations. The results indicate that the porosities migrate towards the high temperature region owing to the temperature gradient as the driving force, which are consistent with the experimental observations. Furthermore, it is also seen that a pore can also change its shape due to the small variations of temperature profile at its surrounding regions.

9:40 AM

Computational Crystal Plasticity with the Jacobian-Free Newton Krylov Method: *Karthik Chockalingam*¹; Micheal Tonks¹; Paul Millett¹; Bulent Biner¹; ¹Idaho National Laboratory

The primary objective of this work is to study the interaction between grain growth and plastic deformation, focusing on dislocation glide along preferred slip planes. Implicit implementations of crystal plasticity finite element method (CPFEM) are usually solved using Newton's method. However, the inherent non-linearity in the flow rule model that characterizes the crystal slip system deformation makes it difficult to form the exact analytical Jacobian needed by Newton's method. Here we analyze how to circumvent this problem by using Jacobian Free Newton Krylov (JFNK), as it does not require a Jacobian. JFNK is used to solve the system of fully coupled implicit non-linear PDEs by using an approximation to the jacobian, in contrast to the traditional Newton solve thus significantly reducing the computational time. Further studies will be aimed at extending this work in simulating the effects of plasticity on 3-D microstructural evolution to characterize performance of nuclear fuels.

10:00 AM

Thermomechanical Properties Prediction of Complex Heterogeneous Irradiated Nuclear Fuel: *Dongsheng Li*¹; Yulan Li¹; Fei Gao; Ram Devanathan; Xin Sun¹; Mohammed Kahleel¹; ¹Pacific Northwest National Laboratory

Spatial structure and chemical information of irradiated nuclear fuel were obtained by multiple chemical imaging modalities. Synthetic microstructure was reconstructed from metadata set with different signal and resolution. The synthetic microstructure is statistically stable with high resolution and enough components to represent the local and global structure. Simulated behavior from this synthetic microstructure is stable and accurate, comparing with simulation using microstructure information obtained by discrete chemical imaging modality. Correlation function and other statistical representation functions are used in microstructure reconstruction. Efficiency and accuracy in microstructure representation and property prediction were investigated.

10:20 AM Break

10:30 AM

Effect of Di- and Quad-Interstitials on the Diffusivity of Oxygen in UO_{2+x} : *Rakesh Behera*¹; Taku Watanabe¹; David Andersson²; Blas Uberuaga²; Chaitanya Deo¹; ¹Georgia Institute of Technology; ²Los Alamos National Laboratory

Both due to synthesis conditions as well as the evolution of the fuel during burnup, fuels based on urania can be hyper-stoichiometric (UO_{2+x}) during operation. Previously, we characterized the thermophysical properties, in particular diffusivity of oxygen in UO_2 , due to mono- and di-interstitials as a function of stoichiometry. Using density functional theory (DFT), we have predicted that quad-interstitial clusters are more stable than di-interstitials. Thus, this presentation will address the effect of mono-, di-, and quad-interstitials on oxygen transport in UO_{2+x} using kinetic Monte Carlo with inputs from DFT. The predicted diffusivities are compared with the available experimental results. Diffusivity of oxygen interstitials exhibits a non-linear relationship with oxygen non-stoichiometry which can be explained by the formation of defect clusters, their interaction, and their motion. This research is being performed using funding received from the DOE Office of Nuclear Energy's Nuclear Energy University Programs.

10:50 AM

First-Principles Theory of Magnetism, Crystal Field and Phonon Spectrum of UO_2 : *Fei Zhou*¹; Vidvuds Ozolins¹; ¹UCLA

The properties of UO_2 result from rich f-electron physics, including electronic Coulomb interactions, spin-orbit and crystal-field effects, as well as interionic multipolar coupling. However, first-principles modeling of nuclear fuel materials such as UO_2 is often plagued by the problem of inconsistency and disagreement among different theorists and between theory and experiment. In an attempt to address this issue and achieve consistent and accurate theoretical modeling of nuclear fuel materials, we present a comprehensive theoretical study [PRB 83, 085106] of the electronic and structural properties of UO_2 using a combined application of self-consistent LDA+U calculations and a model Hamiltonian. The crystal-field ground states and excitation energies, non-collinear 3-k magnetic ground state and associated lattice distortion are all reproduced in excellent agreement with experiment. Our method also predicts the phonon spectrum of UO_2 with reasonable accuracy. Application of our approach to other oxide fuels such as PuO_2 also shows promising results.

11:10 AM

Investigation of the Stability and Energies of Defect and Defect Clusters In bcc-U Using Atomic Level Simulations: *Priyank Shukla*¹;

Benjamin Beeler¹; Erin Haywar¹; Chaitanya Deo¹; Michael Baskes²; Maria Okuniewski³; ¹Georgia Institute of Technology; ²University of California, San Diego; ³Idaho National Laboratory

Metallic nuclear fuel (U-Zr) exhibits swelling and formation of inert gases during burn-up cycle. We use molecular dynamics simulations to understand the energetics of the vacancy and vacancy cluster formation and arrangement using a recently developed modified embedded atom method interatomic potential for Uranium. First, we vary the number of vacancies in pure bcc Uranium from 1 to 10, and calculate the formation energy for these vacancy clusters. Also, we investigate the effect of inert gases on the physical properties of bcc-U. This work provides fundamental insight with regard to the swelling of bcc-U based nuclear fuel.

11:30 AM

A Semi-Empirical Interatomic Potential for bcc U: *Benjamin Beeler*¹;

Chaitanya Deo¹; Michael Baskes²; Sergey Rashkeev³; Maria Okuniewski³; ¹Georgia Institute of Technology; ²University of California-San Diego; ³Idaho National Laboratory

A Modified Embedded-Atom Method potential is presented for the high temperature body-centered cubic (γ) phase of U. The calculated volume and elastic constants at 0K are in close agreement with previous work. Thermodynamic properties calculated include the melting point, heat capacity, enthalpy of fusion, thermal expansion and volume change on melting. The low temperature mechanical instability of γ U is correctly predicted and investigated as a function of pressure. The mechanical instability is suppressed at pressures greater than 17.23 GPa. Energetics of self-defects in γ U are also investigated at 0K. The vacancy formation energy is calculated to be 1.39 eV and the most energetically favorable interstitial is the $\langle 100 \rangle$ dumbbell, both results in close agreement with previous work. The vacancy formation energy is analyzed as a function of pressure and shows a linear trend, allowing for the calculation of the extrapolated zero pressure vacancy formation energy.

11:50 AM

Influence of Zn on the Thermodynamic Stability in the FeO-Fe₂O₃-NiO System: *Dongwon Shin*¹; Theodore Besmann¹; David Andersson²;

¹Oak Ridge National Laboratory; ²Los Alamos National Laboratory

Phase equilibria will play a controlling role in defining the nature of the Chalk River Unidentified Deposits (CRUD) that form on the surfaces of fuel rods in LWR systems. The deposits are the result of corrosion products of iron, nickel, chromium and other alloying elements dissolved in reactor cooling water from piping and heat exchangers as well as coolant additives i.e., zinc, lithium, and boron. This work aims to add zinc into an existing thermodynamic model of Fe-Cr-Ni-O within the

framework of the Compound Energy Formalism (CEF). Thermodynamic descriptions for constituent systems with zinc have been obtained from the literature and integrated into the existing model. Energetics of Zn containing hypothetical CEF end-members have been calculated from first-principles calculations. Phase diagrams of FeO-Fe₂O₃-NiO with the various ZnO content were computed from the thermodynamic model to illustrate the effect of zinc on the CRUD deposits of nickel ferrites and other phases.

Materials Processing Fundamentals: Process Metallurgy of Metals

Sponsored by: The Minerals, Metals and Materials Society, TMS Extraction and Processing Division, TMS Light Metals Division, TMS: Process Technology and Modeling Committee

Program Organizers: Lifeng Zhang, Missouri University of Science and Technology; Antoine Allanore, MIT; Cong Wang, Saint-Gobain High Performance Materials

Monday AM
March 12, 2012

Room: Oceanic 8
Location: Dolphin Resort

Session Chairs: Lifeng Zhang, Missouri S&T; Antoine Allanore, MIT

8:30 AM Introductory Comments

8:35 AM

A Critical Review of the Modified Froude Number in Ladle Metallurgy: *Krishnakumar Krishnapisharody*¹; Gordon Irons¹; ¹McMaster University

The modeling of gas-liquid plumes in steelmaking ladles has been the subject of many investigations. In most studies, the “modified” Froude number, based on the momentum of the injected gas, has been employed to characterize two-phase plumes. This approach has several shortcomings and is critically reviewed in the present work. Based on an extensive review of previous work and theoretical considerations, it is demonstrated that the injected momentum and consequently, the modified Froude number has no significance to gas blowing operations in Ladle Metallurgy. Instead, an approach based on the “plume” Froude number, previously shown by the authors as the proper form for Froude similarity, is extended as a simpler alternative. Furthermore, the dissipation of the gas momentum in the vicinity of the injector is shown to be consistent with the present analysis.

9:00 AM

Inclusion Characteristics in Stainless Steel Ingots: *Shufeng Yang*¹; *Lifeng Zhang*¹; *Yongfeng Chen*¹; ¹Missouri University of Science and Technology

Inclusions in ingots of the 316L stainless steel casted by two different upgate designs were investigated using SEM and ASPEX with automated feature analysis. The number of high SiO₂ inclusions, MnS inclusions and MnO inclusions was much larger than other types of inclusions and many inclusions in the ingot contained two or three phases. There were much more high SiO₂ and SiO₂-Al₂O₃-CaO inclusions in the samples using a half upgate. The distribution of inclusions was non-uniform in the ingot: more inclusions at the top than other place in the vertical direction, and more inclusions at the side of the ingot in the radial direction.

9:25 AM

FEM Study of Centerline Defect Closure In Large Open-Die Forgings: *Jie Zhou*¹; *Joshua Blacketter*¹; *Philip Nash*¹; ¹Illinois Institute of Technology

Large ingots tend to have internal defects such as shrinkage cavities, which have to be closed at the initial open die forging stage to ensure sound internal quality of forged parts. In this work, two FEM-based software packages, FORGE 3D and DEFORM 3D, were employed to investigate the void closure behavior and the impact of forging parameters on the internal quality of big billet. Several forging variables including feed ratio

and reduction amount were investigated. Especially, the material studied in present work was H13 steel, known to be difficult to forge; therefore, intense attention was paid on the special properties of H13 steel to solve real world problem. Additionally, physical modeling made in selective laser sintering (SLS) machine was used to verify the numerical analysis results. At last, optimal forging practices were propose to produce square and round H13 bars.

9:50 AM

Effect of Mould Taper and Wall Thickness on Steel Ingots Soundness by 3-D Solidification Simulation: *Peng Lan*¹; *Yang Li*¹; *Jiaquan Zhang*¹; *Ruitian Zhang*²; *Jingyuan Wang*²; *Hengyi Zhang*²; ¹Department of Metallurgical Engineering and State Key Laboratory of Advanced Metallurgy, University of Science and Technology Beijing; ²Angang Subsidiary Enterprise Company

For the determination of mould taper and wall thickness, a 3-D numerical model of ingot-mould-hot top system has been made to evaluate the related ingot solidification process and the final soundness. The effect of mould wall thickness and the taper of its hot faces on the thermal history and the as cast structure of steel ingot has been revealed through the numerical simulation. It is shown that the ingot soundness can be improved remarkably by increasing the mould wall thickness, which is possibly beneficial to the mould life as well owning to an improved mould thermal state. The mould taper is vital to the ingot soundness but much less coherent to the mould temperature profiles. Under given casting situations, a larger mould taper can lead to a less intensity of the shrinkage porosities at the top part of ingot.

10:15 AM Break

10:25 AM

Hydrometallurgical Study of Purifying MG Silicon Feedstock for Solar Cells Production: *Yongqiang Liu*¹; *Jilai Xue*¹; *Jun Zhu*¹; ¹University of Science and Technology Beijing

Up-grading silicon feedstock by removing B and metal impurities can improve process efficiency and lower production cost in metallurgical processing for solar cells production. The hydrometallurgical study has been carried out in laboratory through alternative treatments of the metallurgical grade (MG) silicon (< 200 mesh) by using hydrogen peroxide, hydrofluoric acid (4 mol 10/L) and NH₄Cl-NH₄F (30:5) solution. The experiments were usually performed under mechanical agitation at 70°C for 5 hours. ICP-AES analysis showed that B content in MG silicon has reduced by 92.4%, and Fe, Al, and Ca contents by 98.8%, 98.0% and 81%, respectively. Kinetics of the processes was also studied for better understanding of the effects of silicon powder size, acid concentration, leaching or oxidizing time, and so on.

10:50 AM

The Effect of Fe Addition on the Activity of Si in Liquid Cu-Si Alloys: *Yuichi Kato*¹; *Takeshi Yoshikawa*¹; *Kazuki Morita*¹; ¹University of Tokyo

The carbon fiber composite with Cu-Si alloy is a candidate for the next generation brake disks for high-speed trains. The composite can be prepared by vacuum infiltration of Cu-Si alloy into fibrous carbon matrix. During the process, SiC is formed by the reaction between carbon fiber and the alloy, and its excess formation results in the embrittlement of the composite. In order to suppress its formation, Si activity in the alloy should be adequately controlled. Since Fe has a strong affinity for Si, its addition is expected to decrease the activity of Si. In the present work, variation in Si activity of the alloy with Fe addition has been investigated by equilibrating a Cu-Fe-Si alloy with both SiO₂ and graphite under a controlled CO partial pressure. Addition of Fe was found to decrease Si activity in the molten alloy, which was thermodynamically evaluated in terms of the interaction parameter.



TMS 2012

141st Annual Meeting & Exhibition

MONDAY AM

11:15 AM

Thermodynamic Properties of the Silicon Binary Melts: *Jafar Safarian*¹; Leiv Kolbeinsen¹; Merete Tangstad¹; ¹Norwegian University of Science and Technology

Silicon and its binary alloys have several applications in metallurgical, chemical, photovoltaic and semiconductor industries. Silicon goes to its liquid state within its production, refining and when it is alloyed with other elements. Therefore, the characterization of silicon melts thermodynamics is important and useful. The liquidus and activities in several silicon binary systems have been recently calculated by the application of two liquidus constants, which were established using the experimentally determined liquidus data. In the present study, the thermodynamic properties of six silicon binary melts, which are simple eutectics, are calculated by analytical approaches. In this case, the changes in the partial and integral Gibbs free energies and enthalpies of mixing are calculated and compared with the experimental data in literature. The enthalpies are calculated by two methods and the calculation results are compared to the data from the literature. It is shown that thermodynamic properties of silicon binary melts can be accurately predicted without the use of complicated thermodynamic software.

11:40 AM

Minor Element Distributions in Mount Isa Copper Smelter: *Pengfu Tan*¹; ¹Xstrata Copper

Xstrata Copper Smelter at Mount Isa in Australia has operated one copper Isasmelt furnace, two Rotary Holding Furnaces (RHF's), four Peirce-Smith P-S converters, two anode furnaces, one casting wheel, slag crushing and screening plant, and ESP dust recovery plant. During the smelting of copper concentrates, it is important to eliminate deleterious minor elements such as Pb, Zn, As, Sb and Bi, while recover valuable elements such as Au and Ag to copper. The distributions of the minor elements, such as Pb, Zn, As, Bi, Sb, Ni and Co, in Copper Smelter have been presented and discussed. The thermodynamic modeling of those minor element distributions have been compared with the plant data and discussed as well.

Materials Research in Microgravity: Session I

Sponsored by: The Minerals, Metals and Materials Society, TMS Materials Processing and Manufacturing Division, TMS Extraction and Processing Division, TMS: Process Technology and Modeling Committee, TMS: Solidification Committee

Program Organizers: Robert Hyers, University of Massachusetts; Hani Henein, University of Alberta; Valdis Bojarevics, University of Greenwich; James Downey, NASA; Douglas Matson, Tufts University; Achim Seidel, Astrium; Daniela Voss, ESA

Monday AM

March 12, 2012

Room: Asia 3

Location: Dolphin Resort

Session Chair: To Be Announced

8:30 AM Introductory Comments

8:35 AM Invited

Materials Science Experiments under Microgravity - A Review of History, Facilities, and Future Opportunities: *Christian Stenzel*¹; ¹Astrium

Materials science experiments have been a key issue already since the early days of research under microgravity conditions. A microgravity environment facilitates processing of metallic and semiconductor melts without buoyancy driven convection and sedimentation. Hence, crystal growth of semiconductors, solidification of metallic alloys, and the measurement of thermo-physical parameters are the major applications

in the field of materials science making use of these dedicated conditions in space. In the last three decades a large number of successful experiments have been performed, mainly in international collaborations. In parallel, the development of high-performance research facilities and the technological upgrade of diagnostic and stimuli elements have also contributed to providing optimum conditions to perform such experiments. A review of the history of materials science experiments in space focussing on the development of research facilities is given. Furthermore, current opportunities to perform such experiments onboard ISS are described and potential future options are outlined.

9:10 AM

The Materials Science Laboratory

An Opportunity for Materials Processing on Board the ISS

: Petra Neuhaus¹; *Harald Lenski*²; ¹Astrium ; ²Astrium

The Materials Science Laboratory (MSL) is a multi-user facility that supports processing and investigation of materials like metal alloys, semiconductors, and ceramics under weightlessness. MSL was built under a contract of the European Space Agency and is operated since October 2009 as part of NASA's Materials Science Research Rack in the US-Laboratory of the International Space Station. MSL supports various research fields by means of dedicated Furnace Inserts which are exchanged on orbit over the ten years lifetime of the facility. MSL provides a very precise process control, several built-in diagnostics features, and the capability to add experiment specific diagnostics. A series of experiments have meanwhile been successfully executed making use of the Low Gradient Furnace and the Solidification and Quenching Furnace. Two types of experiment cartridges are currently available. However, new cartridge types are under development to broaden the application of the facility.

9:35 AM Invited

Novel Second Generation Inserts for the MSL Aboard ISS: Florian Kargl¹; Christian Stenzel²; *Andreas Meyer*¹; ¹German Aerospace Center (DLR); ²Astrium

The first insert is a high temperature isothermal furnace with a 68mm bore that provides an isothermal zone of 90mm length with less than +2K temperature gradient at 1600°C. It can accommodate a large diameter shear-cell for diffusion experiments on up to six samples simultaneously. The second insert is a compact fully-protected X-ray radiography device. Its total weight is less than 43kg. It consists of a microfocus X-ray source delivering up to 20W at 100kV. It contains a scintillator-based actively-cooled 2D X-ray detector with a total sensor area of 50x50mm at a native pixel resolution of 48µm at 14bit depth and a framerate of 2Hz. The X-ray insert can be used for in-situ studies of e. g. diffusion, solidification, foaming, and granular dynamics. First ground-based shear-cell experiments on metallic alloys using the isothermal furnace are discussed. The results are compared with ground-based in-situ diffusion experiments using the X-ray insert.

10:10 AM Break

10:30 AM Invited

Results of the MICAST Experiments in MSL Onboard the ISS:

*Sonja Steinbach*¹; Lorenz Ratke¹; Sadik Dost²; Robert Erdmann³; Yves Fautrelle⁴; Jacques Lacaze⁵; Andras Roos⁶; Gerhard Zimmermann⁷; ¹DLR; ²University of Victoria; ³University of Arizona; ⁴ENSHMG; ⁵CIRIMAT; ⁶SGMU ; ⁷ACCESS

The ESA-MAP project MICAST performs the first solidification experiments on the ISS in the MSL (Materials Science Laboratory). The MICAST team systematically studies the impact of fluid flow on the as-cast microstructure of industrially relevant Al-Si cast alloys in order to deepen the theoretical understanding of those phenomena and optimize industrial casting processes. Since the influence of fluid flow on the evolution of microstructure cannot be avoided on earth, data from

terrestrial experiments can hardly be used for the verification of models solely based on diffusion which in turn is the prerequisite to elaborate more sophisticated models including fluid flow. Therefore the microgravity environment of the ISS is of special importance to the project. Only there all gravity-induced convections are eliminated and experiments under well defined thermal and controlled fluid flow conditions are possible. The paper gives an overview on recent experimental results and theoretical modelling of the MICAST team.

11:05 AM Invited

Microgravity Melting Experiments: Revealing the Mechanism of Dendritic Growth: Martin Glicksman¹; ¹University of Florida

Sharp interface theories of melting and freezing use capillarity as a boundary condition on the normal fields, which transport the latent heat and/or solute during melting or freezing. Microgravity experiments, to be briefly described, proved that capillarity acts as a real interface field during melting. When this 'missing physics' is added to the theory of dendritic growth, the capillary-induced temperature distribution on the solid-liquid interface provides a two-dimensional energy field, along with appropriate interfacial gradients and heat fluxes. Energy conservation on the interface shows, surprisingly, that the local equilibrium temperature becomes instantaneously unsteady. The details of this unsteadiness depend sensitively upon the interface shape and its energy anisotropy. The LeChatelier Braun principle, a thermodynamic postulate based on the 2nd law of thermodynamics, demands that the interfacial curvature respond to these weak imputed temperature changes with 'negative feedback'. Their response initiates kinematic (deterministic) rotation points on the interface near the dendrite tip. Rotations with favorable chirality then couple with the normal transport field to form dendritic branches. A precision, noise free solver confirms that the predicted interface rotations arise dynamically exactly at the locations specified for various starting shapes. This appears to be the process fundamentally responsible for dendrite formation.

11:40 AM

Phase-Field Simulation of Dendrite Fragmentation: Maziar Aghvami¹; *Christoph Beckermann*¹; ¹University of Iowa

Dendrite fragmentation is an important mechanism for generating new grains during solidification of alloys. It also represents one of the main unknowns in current models of the columnar-to-equiaxed transition in the grain structure of castings. Three-dimensional phase-field simulations are performed of the directional solidification of a binary alloy. Melt convection and movement of solid are neglected so as to simulate a microgravity environment. Fragmentation of the initial dendritic structure is induced by a change in the applied thermal gradient or cooling rate. Parametric studies are performed to investigate the conditions necessary for fragmentation to occur, the rate at which fragmentation proceeds, and the yield of dendrite fragments. The present study represents a first step in developing a general fragmentation model for use in macro-scale simulations of casting processes.

Mechanical Behavior at Nanoscale I: In-situ Technique on Deformation Process

Sponsored by: The Minerals, Metals and Materials Society, TMS Materials Processing and Manufacturing Division, TMS: Nanomechanical Materials Behavior Committee, TMS/ASM: Mechanical Behavior of Materials Committee

Program Organizers: Scott Mao, University of Pittsburgh; Julia R Greer, California Institute of Technology; Jianyu Huang, Center for Integrated Nanotechnologies; Marc Legros, CEMES-CNRS; Ting Zhu, Georgia Institute of Technology

Monday AM
March 12, 2012

Room: Asia 1
Location: Dolphin Resort

Session Chairs: Scott Mao, University of Pittsburgh; Julia Greer, California Institute of Technology

8:30 AM Introductory Comments

8:35 AM Invited

Micro-Compression Testing of Cu: About Single Crystals, Grain Boundaries and Polycrystals: *Gerhard Dehm*¹; Peter Imrich²; Christoph Kirchlechner³; Bo Yang⁴; Christian Motz²; ¹Erich Schmid Institute of Materials Science, Austrian Academy of Sciences and Materials Physics, University of Leoben; ²Erich Schmid Institute of Materials Science, Austrian Academy of Sciences; ³University of Leoben, Materials Physics; ⁴Materials Center Leoben GmbH

Miniaturized compression and tension tests have shed new light on plasticity of single-crystal metals with small volumes. However, the miniaturized tests permit as well to probe the mechanics of grain-boundaries. In the present talk two aspects will be analyzed: Firstly, miniaturized Cu samples with different ratios of grain size to sample diameter will be studied to obtain general information on the impact of grain-boundaries to the strengthening behavior. Secondly, the strength of individual Cu grain-boundaries will be probed. A random large angle grain boundary of a Cu bicrystal is exposed to micro-compression testing, and compared to a Cu twin boundary. Differences and similarities will be analyzed by stress-strain measurements, scanning electron microscopy and micro-Laue diffraction. Acknowledgement: X.H. An S.D. Wu and Z.F. Zhang, Shenyang National Laboratory for Materials Science, Institute of Metal Research, Chinese Academy of Sciences, are acknowledged for supplying the Cu bicrystals.

9:05 AM Invited

On Atomic Resolution In-Situ Electron Microscopy Study of Abnormal Mechanical Properties of Nanowires and Ultra-Thin Layers: *Ze Zhang*¹; X.D. Han²; ¹Department of Materials Science and Engineering, Centre of Electron Microscopy; ²Institute of Microstructure and Properties of Advanced Materials

By applying a tensile or bending strain on low dimensional materials, we developed a special technique which enables an atomic resolution in-situ transmission electron microscopy study of size effects of nanowires or ultra thin layers. For Si-, SiC, and SiO₂ nanowires with two dimensional size confinements, we observed a brittle to ductile transition in contrast with their bulk counterpart with intrinsic brittle nature. The unusual large plasticity appeared via a phase transition from crystalline to amorphous under direct atomic resolution observation. This indicates that these observed strain-induced ductility are diffusion controlled and is more pronounced at nanoscale in these nanowires. From ultra thin Pt metallic layer, we observed a clear evidence of dislocation role concerning the inverse Hall-Petch dependence. Through these studies, we thus provide new routes to study dynamic mechanical properties and their corresponding microstructure evolutions of one-dimensional nanomaterials (crystalline vs. amorphous) under direct atomic scale.



TMS 2012

141st Annual Meeting & Exhibition

MONDAY AM

9:35 AM

Deformation of Gold Nanowires: Elongation Mechanisms and Quantum Conductance: *Lyle Levine*¹; Francesca Tavazza¹; Douglas Smith¹; Anne Chaka¹; Jon Pratt¹; ¹National Institute of Standards and Technology

In situ measurements with unprecedented mechanical stability (2 pm noise floor) combined with several years of density functional theory simulations provide the first comprehensive picture of how individual gold nanowires thin down to single atoms chains during tensile deformation. We will show that Au nanowires deform through a series of distinct transitions between metastable, highly-ordered 3D, 2D and 1D atomic configurations. Discrete jumps in the simulated conductance correlate perfectly with the structural transitions, providing a simple explanation for these previously unexplained phenomena. Excellent agreement between the conductance simulations and experimental results was observed, providing confidence that these predicted structures and transitions reflect the underlying physical reality.

9:55 AM Break

10:05 AM Invited

Size Matters for Deformation Twinning in Single Crystal Metals: *Evan Ma*¹; ¹Johns Hopkins University

This work was performed in collaboration with Qian Yu, Yonghai Yue, Zhiwei Shan, Ju Li, Xiaodong Han, Xiaoxu Huang and Jun Sun. Sample size (d) of deforming single crystal is known to have a major effect on dislocation slip. In contrast, for the other major mechanism of plastic deformation, deformation twinning (DT), the sample size effect is much less understood. Using (in situ) experiments, we have found that the stress required for DT increases drastically with decreasing d of a titanium alloy single crystal, in a Hall-Petch-like relationship. We use a 'stimulated slip' model to explain this size regime. At very small d, a new regime sets in, when dislocation activities are dominated by direct partial (twinning) dislocation emission from surfaces. This leads to an inverse sample size effect. i.e., twinning becomes pronounced while absent at larger d, as illustrated using Cu single crystals over a range of sizes.

10:35 AM

In Situ TEM Observations of Reverse Dislocation Motion upon Unloading of Ultrafine-Grained (UFG) Aluminium Strained in the Microyield Region: *Daniel Caillard*¹; Frederic Mompou¹; Marc Legros¹; Hael Mughrabi²; ¹CNRS; ²University of Erlangen

Ultrafine-grained (UFG) metals produced by Equal Channel Angular Pressing (ECAP) exhibit high strength properties. When strained in the microyield region and subsequently unloaded, such materials also exhibit unusually large inelastic reverse strains. The purpose of the present study is to clarify the reasons for such behavior, by means of in situ transmission electron microscopy experiments, in UFG aluminium produced by ECAP. Sources emitting dislocations which interacted with adjacent grain boundaries (GBs) have been observed. Depending on the character of the dislocations emitted, different behaviors have been observed: i) intensive cross-slip and rapid insertions in GBs for screw and mixed dislocations, and ii) pile-up formation in front of GBs for pure edge dislocations. Upon unloading, the release of stress induces a substantial reverse motion of dislocation pile-ups in case ii). The origin of the inelastic behavior in the bulk material and the possible role of dislocation pile-ups are then discussed.

10:55 AM

Direct Observation of Deformation Behaviors in Nanostructured Ceramic Materials by In Situ Nanoindentation in TEM: *Haiyan Wang*¹; Joon Hwan Lee¹; Amiya Mukherjee²; Xinghang Zhang¹; ¹Texas A&M University; ²UC Davis

At room temperature, in situ nanoindentation experiments in a transmission electron microscope are conducted on nanostructured ceramic materials to reveal their deformation behaviours. The materials include bulk ceramic nanocomposites composed of Al₂O₃ : ZrO₂

: MgAl₂O₄ (AZM), YBa₂Cu₃O_{7-x} (YBCO) thin films and other nanolayered ceramic thin films. In situ dynamic deformation studies show that the AZM nanocomposites undergo the deformation mainly through the grain boundary sliding and rotation of small grains. We observed both plastic and elastic deformations in different sample regions in these multi-phase ceramic nanocomposites at room temperature. Detailed in situ movie analysis on YBCO thin films reveals that twin structures play an important role in deformation and strengthening mechanisms in the films and result in the anisotropic mechanical properties along c-axis and a-axis. This work is funded by the Office of Naval Research (under Dr Lawrence Kabacoff; Contract number: N00014-08-0510).

11:15 AM

Localized Crystal Rotation in Gum Metal at Ideal Strength: *Shigeru Kuramoto*¹; Tadahiko Furuta¹; Daigo Satoyama¹; Elizabeth Withey²; J.W. Morris, Jr.³; ¹Toyota Central R&D Labs., Inc.; ²Lawrence Livermore National Laboratories; ³University of California, Berkeley

Localized crystal rotation in a multifunctional Ti-36Nb-2Ta-3Zr-0.30 alloy (mass%), Gum Metal, was analyzed in the nano-pillar specimens during in situ nano-compression tests. The very small value of C₁₁-C₁₂ in the alloy means that the Peierls stress required for dislocation motion is small. However, the actual deformation strength of the alloy is much higher; the resolved shear stress in nanopillars of the alloy has been reported to approach the ideal shear strength during the compression test. Results of microstructural analyses in various size scales performed so far support that the key basic process of plastic deformation is localized shear deformation accompanied by inhomogeneous crystal lattice rotation. The diffraction patterns after compressive deformation in pillar specimens showed that crystal rotation of as much as 30 degrees occurs continuously in the small deformed area of the pillar specimens. Such crystal rotation will be discussed in relation to the shear orientation and the Schmid factor in the loading direction.

11:35 AM

Stress-Driven Grain Boundary Migration in Ultrafine-Grained Mg Film: *Yong Zhang*¹; John Sharon¹; Kevin Hemker¹; ¹Johns Hopkins University

Stress-driven grain boundary migration and consequent grain growth has been widely observed in face center cubic (fcc) nanocrystalline metals, namely nanocrystalline Al, Ni and Cu. However, no stress-driven grain growth was reported in hexagonal close packed (hcp) nanocrystalline materials. In this work, various stress levels in ultrafine-grained Mg films with 200 nm grain size were achieved by varying the deformation parameters, i.e., strain rate and temperature. Transmission electron microscopy (TEM) studies were used to identify the evolution of grain structure. The results demonstrate that stress-driven grain growth can be activated in hcp Mg with suitable stress, and the grain growth scales with stress as observed in fcc nanocrystalline Al film.

11:55 AM

TEM Studies on Microstructure and Mechanical Properties of Nanotwinned Metals: *Ying Zhang*¹; James Andereg¹; Ryan Ott¹; Mikhail Mendeleev¹; Matthew Kramer¹; ¹Ames Lab

Nanotwinned fcc metals have recently emerged as a particular form of nanoscaled structural materials with uncommonly stable microstructure coupled with enhanced mechanical properties. High-purity copper foils with nano-scale growth twin lamellae are synthesized by means of the pulsed electrodeposition technique from an electrolyte of CuSO₄ and magnetron sputtering system. The microstructure and density of the nanoscaled twins can be controlled by setting up different cathodic square wave pulses periodically for pulsed electrodeposition technique and changing the deposition rate for magnetron sputtering method. A novel Hysitron in-situ transmission electron microscopy (TEM) tensile strain holder is used to measure the stress-strain behavior with concurrent in-situ TEM observations of evolving microstructures on nanotwinned samples. These experiments are being performed in conjunction molecular dynamic

simulations to provide both realistic validation of models and a deeper understanding of fundamental deformation mechanisms in nanotwinned materials.

12:15 PM

Interface Dominated Small Scale Plasticity in a Ni-Based Superalloy:

*Robert Maass*¹; Bin Gan²; Sammy Tin²; Lucas Meza¹; Julia Greer¹;
¹California Institute of Technology; ²Illinois Institute of Technology

Small-scale mechanical behavior of individual constituent phases and interphase boundary-containing nano-pillars made from a Ni-based superalloy was examined by compressive flat punch testing in a nanoindenter. Specimens containing isolated vertical γ/γ' -interfaces with systematically varying coherency were prepared by focused ion beam milling. Microstructure was characterized via side-specific high-resolution TEM and linked to mechanical response as a function of lattice misfit. Attention is focused on the role of misfit dislocations and their influence on flow behavior in two-phase nanopillars as compared with their single crystalline γ and γ' counterparts. Finally, size-affected flow is investigated in the framework of precipitate and interface dominated plasticity at the micron scale.

Mechanical Behavior Related to Interface Physics: Grain Boundaries: Experiment and Modeling

Sponsored by: The Minerals, Metals and Materials Society, TMS Structural Materials Division, TMS Materials Processing and Manufacturing Division, TMS/ASM: Mechanical Behavior of Materials Committee, TMS: Nanomechanical Materials Behavior Committee

Program Organizers: Jian Wang, Los Alamos National Laboratory; Nathan Mara, Los Alamos National Laboratory; Izabela Szlufarska, University of Wisconsin-Madison; Zhiwei Shan, Xi'an Jiaotong University

Monday AM
March 12, 2012

Room: Oceanic 1
Location: Dolphin Resort

Session Chairs: Zhaohui Jin, Shanghai Jiao Tong University; Douglas Irving, North Carolina State University

8:30 AM Keynote

Observations of Stress-Coupled Grain Boundary Migration: John Sharon¹; Frederic Momprou²; Marc Legros²; *Kevin Hemker*¹; ¹Johns Hopkins University; ²CEMES-CNRS

The traditional view of grain boundaries envisions them as mechanically static, immovable structures. Room temperature grain growth in nanocrystalline metals, molecular dynamics simulations, and recently proposed theories of coupled boundary migration all suggest that grain boundaries are not nearly as static as generally assumed. Observations of stress-assisted grain growth will be reviewed and linked to theories of coupled boundary migration by the importance of applied shear stress. In situ experiments designed to investigate the details associated with stress-coupled grain boundary migration will also be presented. These in situ observations are being used to quantify the effect of grain boundary character, morphology, size and connectivity on stress-assisted grain boundary migration. This work was supported by the U.S. Department of Energy under grant number DE-FG02-07ER46437.

9:00 AM Keynote

Atomistic Modeling of Grain Boundary Sliding/Migration and Related Mechanical Behavior in FCC Metals: X.M. Su¹; *Z.H. Jin*¹; P. Gumbsch²; K. Lu³; ¹Shanghai Jiao Tong University; ²Karlsruher Institut für Technologie (KIT); ³Institute of Metal Research (IMR)

Mechanical properties of materials depend on grain boundaries (GBs) or interfaces. Properly introduced GBs in metals may improve the strength, the ductility, or both. It has been long recognized that GB activities

such as sliding and migration play crucial roles. However, to reveal and characterize many details of such plasticity flows, esp. down to the atomic scale, still remains interesting and challenging. With molecular dynamics modeling, we aimed to reveal how tilt and twist GBs slide and/or migrate in fcc metals. We found that, depending on GB structure and mechanical driving force, GB migration and GB sliding involving dislocation emission as well as dislocation-GB interaction may intervene. Besides, the GB mobility not only depends on the driving force but also is temperature and rate limited. These observations suggest correlated GB phenomena and help to clarify the governing deformation mechanisms of nanostructured metals.

9:30 AM

Dislocation Pileups in fcc Aluminum Bicrystals: *Steven Valone*¹; Jian Wang¹; Richard Hoagland¹; Timothy Germann¹; ¹Los Alamos National Laboratory

Materials deformation processes are increasingly approachable through atomistic methods. In one deformation process, dislocation pile-up at a grain boundary, how dislocations transmit through grain boundaries is of intense interest. Here dislocation pile-ups in aluminum bicrystals with several tilt grain boundaries are simulated. Dislocations are initially distributed according to linear elastic estimates from a far-field stress of 40 MPa. The system is propagated for different periods of time, representing different shear rates, with load being incremented every 40 ps. Depending on the details of the grain boundary, a variety of dislocation reflection, transmission and adsorption events can occur. Some boundaries can form steps that propagate to the cell boundaries from dislocation adsorption before transmission occurs. These examples are particularly helpful in understanding the importance the distribution of far-field pinning sites in determining dislocation transmission and macroscopic deformation.

9:45 AM

Molecular Dynamics Simulation of Energy Dissipation at the Liquid/Solid Interface with Slip Boundary Condition: *Kai Huang*¹; Izabela Szlufarska¹; ¹UW-Madison

How mechanical energy is dissipated at a vibrating solid/liquid interface is of great importance for applications in sensor technology and microfluidic devices. For the case of Newtonian liquids with no-slip boundary conditions, continuum-level models have already been developed and validated. Although a number of analytical approaches have been also proposed for the case of slip boundary conditions, it has not been established which theory provides the correct underlying physics because of the difficulty in obtaining slip information directly from experiments. To determine relationships between surface hydrophobicity and energy dissipation at the solid/liquid interface, we performed molecular dynamics simulations of a Quartz Crystal Microbalance (QCM) in the presence of water. By controlling surface chemistry we modify the amount of interfacial slip, which then is directly measured in our simulations. We test existing theoretical models and propose their generalization to relate surface hydrophobicity, slip length, and mechanical damping at the solid/liquid interface.

10:00 AM

Nucleation and Early Growth of Mechanical Deformation Twins in Hexagonal Close-Packed Metals Deformed at Extreme Conditions: *George Kaschner*¹; Stephen Niezgod¹; Rodney McCabe¹; Carlos Tome¹; ¹Los Alamos National Laboratory

In an effort to better understand nucleation and growth of mechanical deformation twins in HCP metals, in particular Zr, we deform samples to small strains at two extreme conditions. The first condition, quasi-static loading at equilibrium liquid nitrogen temperature, has been previously explored by this research team in studies examining larger strains and in the context of strain path change tests. The second condition is more challenging experiment in that we arrest the deformation under high strain rate conditions. We perform statistical analysis of the deformation twins using EBSD and analyze the twin morphology (aspect ratio, thickness, and spacing) as a function of temperature and strain rate. We employ a



TMS 2012

141st Annual Meeting & Exhibition

MONDAY AM

cross-correlation EBSD to analyze local strain fields at the grain boundary/twin interface to determine contributing factors to twin nucleation. Finally, we compare the experimental results with the predictions of our evolving deformation model using parameters of texture, strain rate, and temperature.

10:15 AM Break

10:25 AM Keynote

Coupled Grain Boundary Motion in a Nanocrystalline Grain Boundary Network: Mario Velasco¹; *Helena Van Swygenhoven*¹; Christian Brandl²; Enrique Martinez-Saez²; Alfredo Caro²; ¹Paul Scherrer Institute; ²Los Alamos National Laboratory

Coupled grain boundary motion to shear deformation was simulated in a 3D nanocrystalline Al sample using molecular dynamics. It is shown that in spite of the triple junction constraints around a symmetrical S75(-751) [112] ($\square=23.07^\circ$) tilt boundary, the GB can migrate during the microplastic regime with the same coupling factor as when simulated in a bi-crystal configuration, i.e. the geometric predictions previously seem to be also valid in nanocrystalline structures. After reaching the full plastic regime, dislocations start coming into play changing the grain boundary structure, hindering further coupled motion. The basin-hopping algorithm is used to explore further the effect of structural rearrangement in the triple junctions and the therein-lying implications on the coupled grain boundary motion before the onset of dislocation propagation. The importance of coupled grain boundary motion as a deformation mechanism will be discussed in relation to other mechanism such as dislocation pile-up and grain boundary sliding.

10:55 AM Keynote

Multi-Scale Simulation of the Mechanical Response of Metal/Metal Interfaces in Non-Equilibrium Environments: *Douglas Irving*¹; ¹North Carolina State University

In this talk, I will present our recently developed multi-scale method that couples the solution of electrical and thermal transport equations to an underlying empirical potential molecular dynamics simulation. The method seeks to both correct for the lack of explicit electrons, which impacts the ability to simulate electrical and thermal conductivity with MD, and to also extend the length scale of the simulation. The goal in development of this method is to simulate the response of interfaces exposed to non-equilibrium conditions (Joule Heating). The capabilities of the method will be demonstrated by highlighting our efforts to simulate the complicated environment experienced by interfaces in the electrical contacts of an Au based RF-MEMS switch. Included in this presentation will be our efforts to both extend the efficiency of this method and also extend it to systems that contain non-metallic components between the interfaces. This work is supported by ONR grant N00014-10-1-0402.

11:25 AM

Atomistic Modeling of Structure and Twinning from the {112}KS Cu-Nb Interface: *Keonwook Kang*¹; Jian Wang¹; Irene Beyerlein¹; ¹LANL

Recently, multi-layered Cu-Nb composites were manufactured via a severe plastic deformation technique called accumulative roll-bonding (ARB). TEM analysis showed that the stable ARB interface structure maintains the conventional Kurdjumov-Sachs (KS) orientation, but joins the Cu and Nb crystals at unconventional interface planes: {112}Cu || {112}Nb and $\langle 110 \rangle$ Cu || $\langle 111 \rangle$ Nb. We denote this newly observed ARB KS interface as {112}KS. Twin formation was experimentally observed in copper with an angle of 19.5 degrees from the {112} interface plane. This twin formation is unusual since it does not occur in rolled physical vapor deposited (PVD) nanolayered Cu-Nb composites, where the classical KS {111} Cu || {110} Nb is maintained at the interface. In this study, atomistic simulation is used to explore the atomic interface structure, the intrinsic defect network, and mechanism of twin formation from the {112}KS Cu-Nb interface.

11:40 AM

Phase Separation of Binary Alloy: Effects of Semi-Coherent Interface : *Siu Sin Quek*¹; Rajeev Ahluwalia¹; David Srolovitz¹; ¹Institute of High Performance Computing Singapore

The phase separation (spinodal decomposition) of binary alloys and the effects of elasticity on the microstructure evolution with coherent interfaces had been well studied. For the semi-coherent or incoherent case, continuity of the crystal lattice across the interface is partially or completely lost. Such loss of interface coherency at the interface can occur when the interface induces a strain energy build-up due to the mismatch of lattice constants or when the crystal structures across the interface is completely different. We consider a lattice mismatch between two phases of a binary alloy and examine how plasticity mediates the phase separation and subsequent precipitate coarsening through computational simulation. Cubic anisotropy and inhomogeneous elastic properties are incorporated in our model. Through the interaction of lattice dislocations with the interface, the loss of interface coherency is observed and the microstructure evolution is inadvertently affected. The simulation is carried out via a phase field approach.

11:55 AM

Interface Bond Strength of HIP-Clad Depleted Uranium and 6061-Aluminum: *Manuel Lovato*¹; Cheng Liu¹; William Blumenthal¹; ¹Los Alamos National Laboratory

An experimental study of the interfacial bond strength of thin (0.3 mm) foils of depleted uranium (DU) that were hot-isostatic-press (HIP)-clad within one-inch thick 6061-aluminum were performed as surrogates for low-enriched uranium (LEU) nuclear fuel elements. Mechanical test specimens were prepared with and without pre-cracks along the interface and were loaded under uniaxial tension, nearly pure shear, and in mixed tension-shear loading (45 degrees) at room temperature using 2-D video digital image correlation (DIC) to obtain full-field deformation mapping of the specimen surface perpendicular to the interface and pre-cracks. As expected, pre-cracks introduced using wire electro-discharge machining (EDM) reduced the load required for interface debonding. In addition, bond strength measurements were also made on specimens of 6061-aluminum HIP-clad together without depleted uranium. The high spatial resolution of the DIC strain technique allowed evaluation of local deformation near the interface and the crack growth/debonding response.

Mechanical Performance of Materials for Current and Advanced Nuclear Reactors: Mechanical Behavior of Reactor Materials

Sponsored by: The Minerals, Metals and Materials Society, TMS Structural Materials Division, TMS/ASM: Nuclear Materials Committee

Program Organizers: Nicholas Barbosa, National Institute of Standards & Tech; Greg Oberson, United States Nuclear Regulatory Commission; Matthew Kerr, United States Nuclear Regulatory Commission; Elaine West, Knolls Atomic Power Laboratory; Stuart Maloy, Los Alamos National Laboratory; Osman Anderoglu, LANL

Monday AM
March 12, 2012

Room: Swan 1
Location: Swan Resort

Session Chairs: Nick Barbosa, NIST; Whitney Poling, Colorado School of Mines

8:30 AM

Crack Tip Deformation Mechanisms in hcp Zr with and without Dilute H Impurities: Margarita Ruda¹; Graciela Bertolino²; Diana Farkas³; A. Baruj²; ¹CNEA and Univ. N. del Comahue,; ²CONICET; ³Virginia Tech

We present a study of the atomic scale deformation mechanisms occurring at the crack tip in hcp Zr with and without a dilute amount of H present. Mode I crack propagation was studied using EAM potentials and atomistic simulation techniques. The results show a variety of deformation mechanisms, including twinning and hcp to bcc phase transformations near the crack tip. H impurities were placed at different distances from the crack tip significantly affecting the competition among the various deformation mechanisms involved in the crack propagation process. In particular, the presence of H modified the extent of the hcp to bcc transformation region leading to an increase in ductility in some single crystal configurations.

8:50 AM

Fracture Toughness of 9Cr-1MoV and Thermally Aged Alloy 617 for Advanced Reactor Applications: Randy Nanstad¹; Mikhail Sokolov¹; Xiang (Frank) Chen²; ¹Oak Ridge National Laboratory; ²University of Illinois

Abstract: Nickel-base Alloy 617 is being considered as a structural material for application in the secondary heat exchanger of the New Generation Nuclear Plant, a very high temperature gas-cooled reactor. Thermal aging of Alloy 617 plate and welds is being performed with tensile, Charpy impact, and fracture toughness tests conducted at temperatures to 950°C. Results of testing for thermal aging to 5,300 h have been obtained and are presented; varying effects of thermal aging temperature and time on fracture toughness are observed. The 9Cr-1MoV (Grade 91) ferritic steel is a candidate for structural applications in the sodium fast reactor. Fracture toughness testing of unaged Grade 91 steel has been performed to evaluate specimen size effects in preparation for future testing of the material in the thermally aged condition. Results for material in the mill-annealed and heat treated conditions are presented and show that this heat of Grade 91 steel does not indicate a small specimen bias on the fracture toughness Master Curve reference temperature.

9:10 AM

Influence of Cold Work and Sensitization on Stress Corrosion Cracking of Stainless Steel: Elaine West¹; Nathan Lewis¹; David Morton¹; Bryan Miller²; ¹Knolls Atomic Power Laboratory; ²Bettis Atomic Power Laboratory

The effect of cold work (CW) and sensitization on the stress corrosion cracking (SCC) susceptibility of Type 304 SS was evaluated in high temperature aqueous environments. Experiments were conducted primarily in deaerated water at 550-680°F on ring loaded and active loaded

compact tension specimens with CW levels of 0-28%. Crack growth rates in deaerated water increased as a function of temperature and CW level and decreased with sensitization. In aerated water with 200 ppb sulfate, however, rapid crack growth was measured on a 10% CW sensitized specimen. Transmission electron microscopy (TEM) measurements of grain boundary chromium depletion on sensitized material indicated that the austenite (γ) grain boundaries had chromium concentrations as low as 10.4 wt%, and carbide decoration was observed at both γ/γ and γ/δ -ferrite interfaces. TEM and Electron Backscatter Diffraction analyses were used to characterize the factors promoting crack propagation in the stainless steel specimens.

9:30 AM

Time-Dependent Fatigue Crack Propagation in Ni-Based Solid-Solution-Strengthened Superalloys INCONEL 617 and HAYNES 230: Longzhou Ma¹; Shawoon Roy¹; ¹University of Nevada Las Vegas

Ni-based superalloys INCONEL 617 and HAYNES 230 were subjected to fatigue crack propagation (FCP) tests with sinusoidal and hold time waveform as well as sustained loading crack growth (SLCG) tests at temperatures of 600- 800 Deg.C using the constant stress intensity factor control. The experimental results showed that both alloys displayed the time-dependent FCP behaviors, when a hold time at maximum load of fatigue was imposed. In SLCG tests, both alloys showed the incubation and steady crack growth process. The SLCG rates, da/dt, could be characterized using a thermal activation equation. Toward this end, a general model, based on thermo-dynamic equation, was employed to correlate the FCP rates of alloys at cycle/time-dependent domain.

9:50 AM

Strain Localization During Creep-Fatigue Deformation of Alloy 617: Mark Carroll¹; Laura Carroll¹; Richard Wright¹; ¹Idaho National Laboratory

Alloy 617 is the leading candidate material for the intermediate heat exchanger (IHx) of the Very High Temperature Reactor (VHTR), which will require an alloy capable of operating at temperatures of up to 950°C. In order to provide adequate test data for design Code purposes, numerous strain controlled low-cycle fatigue (LCF) tests with hold times up to 1800 s at peak tensile strain have been conducted at 950°C. Post-test observations reveal that bulk grain boundary damage in the form of intergranular cracking was present in the interior of the creep-fatigue specimens. This bulk cracking was observed throughout the deformed material in distinct grain boundary locations, although the majority of grain boundaries were absent of any observable damage or signs of cavitation. Localized strain fields in the grains adjacent to interior cracks are being investigated using orientation imaging microscopy (OIM) techniques coupled with transmission electron microscopy (TEM) characterization.

10:10 AM Break

10:30 AM

Creep Behaviors of a Nanocluster-Strengthened Ferritic Steel: M Brandes¹; G Daehn¹; M Miller²; M Mills¹; ¹The Ohio State University; ²Oak Ridge National Laboratory

Mechanical-alloyed, nano-ferritic steels represent a class of alloys displaying radiation and creep resistances. Their excellent performance is a result nanoclusters, which have been observed to interact with glide dislocations. Post-mortem, probe-corrected scanning transmission electron imaging has revealed attractive dislocation-nanocluster interactions. The creep behavior of alloy Fe-14YWT has been investigated between 650 and 950°C through creep and monotonic strain rate testing. Significant strain accumulation occurs in the primary regime, and a varying stress dependence is measured in the steady strain regime where $N \sim 1$ at low stress. A new model of the creep response using a modified Kocks-Arghon-Ashby model has been developed and extended to a cellular-automata model. With this approach, it is possible to explain the creep transient behaviors over a wide range of temperature and stress. This research was sponsored by the U.S. Department of Energy, Division of Materials Sciences and Engineering.



TMS 2012

141st Annual Meeting & Exhibition

MONDAY AM

10:50 AM

Creep Deformation Mechanisms in Grade 91 Steel: *Triratna Shrestha*¹; Mehdi Basirat¹; Indrajit Charit¹; Gabriel Potirniche¹; Karl Rink¹; Uttara Sahaym²; ¹University of Idaho; ²Washington State University

Grade 91 (modified 9Cr-1Mo) steel is a candidate material for the pressure vessel of the Very High Temperature Reactor (VHTR). The creep behavior of this steel was studied in the temperature range of 873 K to 1023 K and at a stress range of 35 to 350 MPa. Threshold stress correction of the creep data in the higher stress regime yielded a true stress exponent of 5, indicating the operation of high temperature climb-controlled creep. The estimated threshold stresses displayed strong temperature dependence. The origin of the threshold stress was explained in terms of particle-dislocation attractive interaction. Creep tests in the lower stress regime resulted in a stress exponent of 1, indicating the operation of a Newtonian viscous creep mechanism. Furthermore, the rate-controlling creep mechanisms in both the stress regimes were elucidated with the help of transmission electron microscopy (TEM). The research was supported by the NEUP contract # 42246-59.

11:10 AM

High Temperature Aging Study on Long-Term Aged Alloy 617 and Alloy 230: *Yang Zhao*¹; Kun Mo¹; James Stubbins¹; ¹University of Illinois at Urbana Champaign

Alloy 617 and Alloy 230 are lead structural materials for next generation nuclear power plant (NGNP). Both alloys possess good corrosion resistance and exceptional high-temperature strength. In order to gain a better understanding of the high-temperature degradation process of these materials, long-term (up to 10000 hours) aging experiments have been carried out to investigate the microstructural evolution and mechanical property development for both alloys. In the present study, focus is placed on the alloys aged for 10000 hours. Both alloys softened significantly after aging at 1000°C for 10000 hours. In contrast, the strength of both alloys was maintained when aging at 900°C. Carbide particle growth is known to be a dominant microstructural feature during long-term aging at elevated temperatures. The evolution of the carbide structure is also the major contributor to the changes in mechanical properties. The microstructures are related to the measured changes in mechanical properties.

11:30 AM

High Temperature Creep Studies on Nano Structured Ferritic Alloys: *E. Stergar*¹; M. Salston¹; K. Fields¹; Y. Wu¹; G. R. Odette¹; ¹University of California-Santa Barbara

Nano-structured ferritic alloys (NFAs), which gain their excellent creep and tensile strength from nanometer-scale precipitates, are candidate materials for new generation nuclear and future fusion reactors. NFAs are thermally stable and have good creep strength up to about 800°C. These alloys also manifest remarkable resistance to radiation damage. These attributes are due to an ultrahigh density of Ti-Y-O enriched nano-features (NFs) that provide dispersion strengthening, stabilize dislocation and fine grain structures, reduce excess concentrations of radiation induced defects and trap helium in fine harmless bubbles. The presentation summarizes an extensive database on creep properties of MA957 with different heat treatments as well as other NFAs. Also the mechanical property data is complemented by detailed microstructural characterization studies using high resolution methods like TEM and atom-probe. The results show a significant impact of the thermo-mechanical treatment on the microstructure, precipitate distribution and creep behavior of NFAs.

11:50 AM

Creep Behavior of High Temperature Alloys for Intermediate Heat Exchanger in Next Generation Nuclear Plant: *Xingshuo Wen*¹; Laura Carrol²; Richard Wright²; T. L. (Sam) Sham³; Vijay Vasudevan¹; ¹University of Cincinnati; ²Idaho National Laboratory; ³Oak Ridge National Laboratory

Alloy 617 and 800H were selected as candidate materials for Intermediate Heat Exchanger used in the Next Generation Nuclear Plant with operating temperature in the range of 800 to 950°C and a service life of 60 years.

In this work, creep behavior of alloys 617 and 800H specimens with different grain sizes was studied over the temperatures of 850 to 1050°C and stress levels ranging from 5 to 100MPa. Creep data was analyzed to decipher the various stages, the stress exponents and activation energies were determined and diffusional versus dislocation creep mechanisms were discriminated. Microstructural changes and damage processes following creep were characterized, with special attention given to grain size effects, grain boundary type and structure, second phase precipitates, dislocation structures and void formation. The various results relating the creep behavior to microstructural changes in these alloys will be presented and discussed.

Nanocomposites: Mechanical Behavior and Modelling of Nanocomposites

Sponsored by: The Minerals, Metals and Materials Society, TMS Structural Materials Division, TMS/ASM: Composite Materials Committee

Program Organizers: Garth Wilks, Air Force Research Laboratory; Jonathan Spowart, Air Force Research Laboratory; Meisha Shofner, Georgia Institute of Technology; John Zhanhu Guo, Lamar University

Monday AM
March 12, 2012

Room: Swan 8
Location: Swan Resort

Session Chairs: Jonathan Spowart, Air Force Research Laboratory; Nikhil Gupta, Polytechnic Institute of New York University

8:30 AM

Mechanomodifiable Nanomaterials: Multiscale Computational and Experimental Studies: *Markus Buehler*¹; Steven Cranford¹; Christine Ortiz¹; ¹Massachusetts Institute of Technology

Mutable materials are found widely in biology, characterized by a material's capacity to change its properties under external cues based on directed structural changes at specific material levels. Here we focus on a class of mechanomodifiable materials, which change their mechanical properties such as elasticity, deformability, strength and toughness based on external signals. A hierarchical approach, implemented through coarse-grain molecular modeling, is utilized to develop a powerful framework that can successfully collaborate atomistic theory and simulations with material synthesis and physical experimentation, and facilitate the design of mechanomodifiable structural materials. We review studies of PAA/PAH polymer systems, where a first principles based bottom-up approach is used to predict the structure and mutability of large-scale material properties from the nanoscale up. We demonstrate hierarchical material designs, validated by experimental studies, to realize mechanomodifiable polymer nanotubes and films. Experimental approaches towards the design of adaptable, mutable and active nanomaterials will be presented.

8:50 AM

Compressive Strength of Epoxy- Graphite Nanoplatelets Composites: *H. A. Colorado*¹; A. Wong¹; J M Yang¹; ¹University of California, Los Angeles

Epoxy matrix composites reinforced with Graphite Nanoplatelets (GNPs) at different concentrations have been fabricated in this research. The Epoxy matrix was made with Epon 828 cured with epikure 3055. GNPs were used in two conditions, as received and after being oxidized at high temperature. A planetary Thinky Mixing was used first to mix the Epoxy with the curing agent and then to mix the resulting liquid with the GNPs. The microstructure was identified by using optical and scanning electron microscopes and X-ray diffraction (XRD). Compressive strength was conducted over cylindrical samples of different length. X-ray micro tomography was used to characterize the samples after tested in compression in order to understand the failure modes.

9:10 AM Invited

Graphene Based Composite Materials: *Nikhil Koratkar*¹; ¹Rensselaer Polytechnic Institute

Graphene is a single-atom-thick sheet of sp² hybridized carbon atoms. In this talk, I will describe our process used to synthesize bulk quantities of exfoliated graphene sheets from graphite and the processing techniques used to disperse them in polymer matrices. I will discuss various mechanical properties of these composites including Young's modulus, ultimate tensile strength, fracture toughness, fracture energy, buckling stability, wear and fatigue resistance. Study of Interfacial load transfer at the graphene polymer-matrix interface using Raman spectroscopy will also be presented. I will show that graphene can match the performance of other competing nanofillers such as carbon nanotubes, nano-particles and nanoclays, at 1-2 orders of magnitude lower nanofiller weight fraction. I will discuss the reasons for the superiority of graphene over other forms of nanofiller reinforcement. Finally I will end by discussing the potential of graphene ceramic and graphene metal-matrix composite materials in high performance structural applications.

9:50 AM

Compressive Properties of Polymeric Syntactic Foams at Various Quasi-Static and High Strain Rates: *Vasanth Chakravarthy Shunmugasamy*¹; *Dinesh Pinisetty*¹; *Nikhil Gupta*¹; ¹Polytechnic Institute of New York University

Syntactic foams (SFs) are lightweight composites synthesized by filling a matrix material with hollow particles called microballoons. The use of SFs for weight reduction in marine and aircraft structures makes it necessary to understand their compressive characteristics at various strain rates. The present study attempts to understand the quasi-static and high strain rate compressive characteristics of vinyl ester matrix SFs filled with glass microballoons. A split-Hopkinson pressure bar setup is used for high strain rate testing. The strength is found to be 50–150% higher at high strain rates when compared to quasi-static values for various syntactic foam compositions. Also, a transition in failure pattern is observed from shear cracking under quasi-static loading to failure along the direction of loading with increase in strain rate. Such observations can help in structural design in existing applications and enable new applications.

10:10 AM

Thermal Expansion of Carbon Nanofiber Reinforced Syntactic Foams: *Ronald Poveda*¹; *Sriniket Achar*¹; *Nikhil Gupta*¹; ¹Polytechnic Institute of New York University

Coefficient of thermal expansion (CTE) is an important consideration in several existing applications of composite materials where temperature variations are experienced during their service life. The present study analyzes the effect of carbon nanofibers (CNFs) on the thermal expansion of hollow particle (microballoon) filled composites called syntactic foams. Different CNFs weight fractions are randomly dispersed into syntactic foams and tested using a thermomechanical analyzer. Two types of glass microballoons having wall thickness of 521 and 878 nm are used in 30 and 50 vol.% in syntactic foams. Results show that a combination of CNF and microballoon volume fraction and microballoon wall thickness can be used effectively to tailor the composites' CTE. Turner's and Kerner's models are modified to enable prediction of CTE of hollow particle reinforced composites. The theoretical estimates are in close agreement with the experimental results.

10:30 AM Break**10:50 AM**

Atomistic and Continuum Understanding of the Particle Clustering and Particle Size Effect on the Room and High Temperature Strength of SiCN Nanocomposites: *Vikas Tomar*¹; ¹Purdue University

Silicon Carbide (SiC)-Silicon Nitride (Si₃N₄) nanocomposites are future important high temperature materials. This work presents our recent findings that analyze the effect of morphological variations in second phase SiC particle placement and grain boundary (GB) strength

on the room temperature fracture strength of SiC-Si₃N₄ nanocomposites using continuum analyses based on a mesoscale (~50 nm) cohesive finite element method (CFEM) and using molecular dynamics (MD) based analyses at nanoscale (~15 nm). CFEM and MD analyses have revealed that high strength and relatively small sized SiC particles act as stress concentration sites in Si₃N₄ matrix leading to inter-granular Si₃N₄ matrix cracking as a dominant failure mode. However, the particle's presence does not have a significant effect on the mechanical strength of bicrystalline or nanocrystalline Si₃N₄ phase matrices. The strength of the structures showed an uncharacteristic correlation between the GB thickness and temperature.

11:10 AM

Mechanical Response of the PMMA-CNT Nanocomposite via Molecular Dynamics: *Yae Ji Kim*¹; *Eugenio Jaramillo*²; *Benjamin Haley*¹; *Alejandro Strachan*¹; ¹Purdue University; ²Texas A&M International University

Despite progress in incorporating carbon nanotubes (CNTs) into polymeric matrices, the expected mechanical performance enhancement of the resulting nanocomposites remains unrealized. Progress in this area is hindered by the lack of fundamental understanding of CNT-polymer interactions and the molecular mechanisms that govern the response of the composite. We use large-scale MD simulations to characterize the interface energy between CNTs and poly(methyl methacrylate) surface and bulk as well as the effect of the CNT on the polymer structure. We also characterize the mechanical response of a nanolaminate composite with CNTs at [45/-45] degrees compare their performance with that of bulk PMMA.

11:30 AM

Micromechanical Analysis of Influences of Agglomerated Nanotube Interphase on Effective Material Properties of a Three Phase Piezoelectric Nanocomposit: *Tian Tang*¹; *Paul Wang*¹; ¹Mississippi State University

The focus of the present study is to investigate influences of agglomerated nanotube interphase on effective material properties of a three phase piezoelectric nanocomposite using a recently developed micromechanics framework, namely, variational asymptotic method for unit cell homogenization (VAMUCH). The three phase nanocomposite is composed of PZT-5A fibers and polyimide matrix enhanced with single-wall carbon nanotubes (SWNT). The effects of parameters of agglomerated nanotube interphase (caused by PZT fibers) such as stiffness and volume fraction on effective material properties of nanocomposite were analyzed. For verification, the numerical results were compared with finite element method.

11:50 AM

Effect of Nano-Paper Coating on Flexural Properties of a Fire-Treated Glass Fiber-Reinforced Polyester Composite: *Jamie Skovron*¹; *Jinfeng Zhuge*¹; *Ali Gordon*¹; *Jan Gou*¹; ¹University of Central Florida

Planned aerospace vehicles require materials with high specific strength to withstand thermal shock associated with re-entry. Composites, such as glass fiber-reinforced (GFR) polyester, have rapidly become preferred for high value structural components requiring high specific strength and durability. Their ability to sustain high tensile, impact, etc. has allowed them to be used as light-transmitting panels, fuselages, nose cones, and combustor nozzles. As a part of service conditions, heat flux evolves mechanical properties with exposure time. The effect of including a carbon nano-paper coating on the monotonic flexural properties of a GRP polyester are analyzed. A series of three-point bend experiments was performed on specimen-sized samples of composites subjected to various levels of heat fluxes across numerous exposure times. Analysis of these experiments reveals trends in the deformation mechanisms of these materials near failure. Correlations of flexural modulus, toughness, critical couple are used to develop models for life.



TMS 2012

141st Annual Meeting & Exhibition

MONDAY AM

12:10 PM

Finite Element Modeling of the Nanoscratching of Polymer Surfaces: *William Chirdon*¹; Joshua Rozas¹; ¹University of Louisiana at Lafayette

Modeling of nanoscratching phenomena is important for several material applications. In some applications, scratching is the desired effect of nanofabrication techniques. In other applications, scratching is undesired, as it causes coatings to fail, acts as a mechanism of wear, and can accelerate corrosion. This work uses finite element modeling techniques to investigate the effectiveness of various material models in their ability to model scratch experiments which have been previously published. The material models studied included viscoelasticity, deformation plasticity, elastic/plastic, strain-rate-dependent elastic/plastic, and other mechanical material models. Elastic/plastic models with and without strain-rate dependence were found to be the most robust material models. This work also highlights the importance of the scratching conditions, noting that the material properties that are desirable for resisting a scratching force are different from the desirable material properties for resisting a scratch displacement. Advantages and disadvantages of material models will be discussed.

Neutron and X-Ray Studies of Advanced Materials V: Centennial: Von Laue, Bragg and Diffraction Centennial

Sponsored by: The Minerals, Metals and Materials Society, TMS Structural Materials Division, TMS/ASM: Mechanical Behavior of Materials Committee, TMS: Chemistry and Physics of Materials Committee

Program Organizers: Rozaliya Barabash, Oak Ridge National Laboratory; Xun-Li Wang, Oak Ridge National Laboratory; Gernot Kostorz, ETH Zurich; Lyle Levine, National Institute of Standards and Technology; Peter Liaw, Univ of Tennessee; Yandong Wang, Beijing Institute of Technology; Brent Fultz, California Institute of Technology

Monday AM

March 12, 2012

Room: Southern I

Location: Dolphin Resort

Funding support provided by: Office of Basic Energy Sciences, U.S. Dept. of Energy, Dr. P. Thiyagarajan

Session Chairs: Wolfgang Pantleon, Risoe National Laboratory; Xun-Li Wang, SNS

8:30 AM Keynote

Materials Research with X-Rays: *Gernot Kostorz*¹; ¹ETH Zurich

The year 2012 marks the one hundredth anniversary of the discovery of X-ray diffraction. This is a good reason to look back at the development of X-ray diffraction as a tool in materials science, a discipline that emerged only several decades later. The initial notion of crystalline imperfection as 'mosaicity' survived as a global term even until today. However, the possibility of not only determining the unit cell of a crystalline structure, but also identifying microstructural features down to the atomic level, has inspired many researchers ever since. A few milestones that are (as a personal selection) considered relevant to the development of a deeper understanding of the properties of real materials will be highlighted. The impact of diffraction and scattering of X-rays (complemented by electrons and neutrons) on many advances in materials science is, of course, generally recognized, but may deserve a moment of celebration.

8:55 AM Invited

Diffuse Scattering Resulting from Macromolecular Frustration: *Richard Welberry*¹; ¹Research School of Chemistry

Distinctive diffuse scattering in the form of diffuse rings around Bragg positions has been observed in the diffraction patterns of a crystal of the

N-terminal fragment of the Gag protein from Feline Foamy Virus. It is shown that these are caused by geometric frustration as molecules try to pack on the triangular *bc* mesh of the space group $P6_3$. To explain the strong diffuse scattering the crystal must contain occupational disorder such that each unit cell contains one or other of two different molecular arrangements, **A** and **B**. The frustration arises because the molecular packing prefers neighbouring cells to be **AB** or **BA**. To explain the observation that reciprocal sections $h k 5n l$ where $n = \text{integer}$, contain only Bragg peaks **A** and **B** must be identical molecular arrangements differing only by a translation of $0.2c$. The implications of the disorder for solving the structure of the protein are discussed.

9:15 AM Invited

Residual Strain Measurement by X-Ray and Neutron Diffraction: The First 100 Years: *Philip Withers*¹; ¹University of Manchester

Almost as soon as X-ray Bragg diffraction had been developed as a tool for measuring the lattice spacings of crystals in 1913, its potential for measuring elastic strain was identified in a series of articles in the 1920's. The opportunity to probe the state of elastic strain and hence stress deep inside the bulk of materials had to wait some 50 years until suitable thermal neutron beams became available at research reactors. In the 1990s the high flux and penetrating power of synchrotron x-rays allowed the investigation of residual strains and stresses at the micron scale or sub-second timescales. Each of these beams provided a complementary window into residual stresses for the materials scientist/engineer. In this talk a personal historical perspective of the major developments during the last 100 years is given illustrated by a range of experimental studies made across a large range of scales and engineering applications.

9:35 AM Invited

Inelastic Neutron Scattering Measurements and Calculations of Anharmonic Phonons in fcc Metals: *Brent Fultz*¹; Xiaoli Tang¹; Chen Li¹; ¹California Institute of Technology

Anharmonicity is important in the thermodynamics of solids. Especially at elevated temperatures, anharmonic contributions to the phonon entropy can be a significant fraction of a k_B per atom. We report progress in identifying the sources of non-harmonic behavior, specifically phonon-phonon interactions in the fcc metals Al, Cu, Ag, Au, Pd, Pt. Thermal broadenings of phonon spectra were measured by inelastic neutron scattering on Al, Pd, Pt, and broadenings of individual phonons were measured on a single crystal of Al. The broadenings showed severe "damping" of phonons at moderately high temperatures. Phonon lifetimes at low and high temperatures were calculated using density functional theory combined with second-order perturbation theory, with surprising success. The dominant effects were the kinematical requirements of energy and momentum conservation, not the wavevector-dependence of the cubic anharmonicity itself. Semiquantitative results on phonon damping are possible with a simpler model of cubic anharmonicity.

9:55 AM Invited

Monitoring Strain Path Changes by High Resolution Reciprocal Space Mapping: *Christian Wejdemann*¹; Ulrich Lienert²; Henning Poulsen¹; *Wolfgang Pantleon*¹; ¹Risoe DTU; ²Argonne National Laboratory

The evolution of deformation structures in polycrystalline copper during strain path changes is observed in situ by high resolution reciprocal space mapping with high energy synchrotron radiation. The resolved behavior of a large number of resolved individual subgrains (complemented by conventional x-ray peak profile analysis) allows a distinction between two different regimes during the mechanically transient behavior following the strain path change: below about 0.3% strain, number and orientation of the resolved subgrains changes only slightly while their elastic stresses are significantly altered indicating a microplastic regime during which only the subgrains deform plastically and no yielding occurs in dislocation walls. After reloading to about 0.3% strain, the elastic stresses

of the individual subgrains (having reached the corresponding values of unidirectionally deformed reference specimens) increase only slightly further on - accompanied by occasional appearances of new subgrains, abundant orientation changes and removal of individual existing subgrains.

10:15 AM Break

10:20 AM Invited

Diffraction from Vibrating Crystals: From Ultrasound to Phonons:

*Klaus-Dieter Liss*¹; *Andreas Magerl*²; ¹ANSTO; ²University of Erlangen-Nürnberg

The excitation of ultrasonic waves in perfect crystals can lead to interesting phenomena in neutron and X-ray diffraction, such as peak broadening caused by the lattice gradient, satellite reflections due to the space and time modulated structure, inelastic scattering, and caustics of the beam paths. Furthermore, spatially resolved diffraction on ultrashort time scales leads to the characterization of standing waves and shock waves. White beam Laue section topography is very sensitive to spatial wave field arrangements and shows up the transition between the dynamical and the kinematic theory of diffraction. The presentation reviews the concepts on our older work, gives unpublished experimental results and an outlook to the state-of-the-art and future capabilities of technological development, and their applications in materials science and physics.

10:40 AM Keynote

Real Space Atomic Correlation and Elastic/Inelastic Scattering from Disordered Systems: *Takeshi Egami*¹; ¹University of Tennessee

Traditionally the results of elastic and inelastic neutron or x-ray scattering are presented in the reciprocal space, because the measurements are made as a function of Q, the scattering vector. It also makes sense when the materials studied are crystalline. But for disordered systems it is much more useful to present the results in real space, in terms of the two-body correlation functions. For elastic scattering this is the pair-density function (PDF). For inelastic scattering it corresponds to the dynamic PDF (DPDF). The dynamic structure factor, S(Q,E), of a liquid just shows strongly damped phonons and not much else. But the same data presented as the DPDF shows the atomic dynamics is totally localized to the nearest neighbor. This superlocalization is fundamental in understanding the statistical mechanics of a liquid. This result demonstrates the usefulness of this approach. Work supported by US Department of Energy, Office of Basic Energy Sciences.

11:05 AM Invited

From Closed Packed Metal Structures to Monoclinic SMA and Multiphase Complex Materials: 20 Years of Rietveld Stress-Texture Analyses: *Luca Lutterotti*¹; ¹University of Trento

Until 20 years ago the only available method for texture analysis was to collect pole figures and residual stress measurement were done using the traditional $\sin^2(\psi)$ on single peaks. These methodologies could be applied only to single phase materials with high symmetries. In 1992 the Rietveld method was developed also for texture and residual stresses by measuring several full patterns for a significant number of sample tilting and analyze them including a model for the texture and residual stress effects. Several different models were developed over the years and the method has been used for different scientific problems. The procedure was successfully applied to geological, cultural heritage and material science problems using neutron diffraction in bulk samples or X-ray on thin films and in transmission. Now, complex multiphase materials can be analyzed routinely even if triclinic and monoclinic compounds are present like in the case of NiTi SMA alloys.

11:25 AM Invited

Internal Strain Evolution during Thermomechanical Cycling of NiTi Shape Memory Alloys Investigated Using Neutron Diffraction: *Raj Vaidyanathan*¹; *Othmane Benafan*¹; *Doug Nicholson*¹; *Ron Noebe*²; *Santo Padula*²; *Bjorn Clausen*³; *Don Brown*³; *Sven Vogel*³; ¹UCF; ²NASA Glenn Research Center; ³Los Alamos National Laboratory

In order to engineer stable shape memory alloys for use as actuators, there is a need to understand the internal strain evolution with thermomechanical cycling. We present such a study of the strain evolution with thermomechanical cycling in a binary NiTi alloy. The study reports on in situ neutron diffraction measurements during selected combinations of heating, cooling and loading at Los Alamos National Laboratory as well as ex situ thermomechanical cycling experiments. The in situ neutron diffraction experiments follow the micromechanical and microstructural changes, i.e., texture, strain and phase volume fraction evolution with thermomechanical cycling. Deformation of the cubic austenite phase is also investigated with increasing temperature in order to assess both reversible stress-induced martensite and irreversible retained or residual martensite and plasticity contributions to the strain. The implications of these results for engineering stable shape memory alloys for aerospace applications is presented.

11:45 AM Invited

Small-Angle Scattering with Synchrotron Radiation and Neutrons - Precise Experimental Techniques for Quantitative and Structural Analysis in Chemistry and Physics: *Guenter Goerigk*¹; ¹Helmholtz-Zentrum Berlin

Synchrotron Radiation (SR) provides Small-Angle X-ray Scattering (SAXS) with major improvements, among others the photon flux, allowing the study of samples with only weak small-angle X-ray scattering like diluted chemical solutions or amorphous alloys. Additionally the continuous energy spectrum of SR provides energy tunability in the vicinity of the K- and LIII-absorption edges of most of the elements giving access to an element specific structural and quantitative analysis. From this technique - known as Anomalous Small-Angle X-ray Scattering (ASAXS) - crucial chemical parameters like volume fractions and chemical concentrations can be obtained, which can be correlated to macroscopic or physico-chemical properties. Complementary, Small-Angle Neutron Scattering (SANS) gives access to systems build up by lighter elements especially polymers, suspensions, membranes and moreover by Very Small-Angle Neutron Scattering the structural analysis of Large Scale Structures can be assessed. Different examples from amorphous alloys, soft matter and membrane science are presented.

12:05 PM Keynote

Hard X-ray Microscopy and its Application to Energy Science - Current Studies and Next-Generation Capabilities: *Jörg Maser*¹; *Barry Lai*¹; ¹Argonne National Laboratory

The success of the application of high-resolution, penetrating techniques to the study compositional and structural properties at the nanoscale has spawned the development of a next-generation nanoprobe beamline, the In Situ Nanoprobe, as part of the Upgrade of the Advanced Photon Source. This system provide in-situ capabilities such as heating and cooling, enable study of energy systems such as batteries and processes such as defect formation during materials processing in operando, at currently unavailable spatial resolution. The In-Situ Nanoprobe will provide 1000-fold increased photon flux at a spatial resolution of 50 nm, provide a highest resolution of 20 nm or below, and provide full spectroscopy capabilities for study of most elements in the periodic system. We will present recent materials studies using the Hard X-ray Nanoprobe (Fig. 1), discuss development of our next-generation capabilities, and outline our approach towards APS' goal for hard X-ray focusing to 5 nm.



Pb-Free Solders and Other Materials for Emerging Interconnect and Packaging Technologies: Studies of Mechanical Properties and Effects of Current I

Sponsored by: The Minerals, Metals and Materials Society, TMS Electronic, Magnetic, and Photonic Materials Division, TMS: Electronic Packaging and Interconnection Materials Committee
Program Organizers: Iver Anderson, Ames Laboratory; Sung Kang, IBM; Albert Wu, National Central Univ; Laura Turbini, Research in Motion; Tae-Kyu Lee, Cisco Systems; Govindarajan Muralidharan, Oak Ridge National Lab; John Elmer, Lawrence Livermore National Lab; Yan Li, Intel

Monday AM Room: Swan 9
March 12, 2012 Location: Swan Resort

Session Chair: To Be Announced

8:30 AM Invited

Impact of Sn Grain Orientation and Isothermal Aging on Pd Added Sn-Ag-Cu Solder Interconnect Board Level Mechanical Shock Performance: *Tae-Kyu Lee*¹; Bite Zhou²; Thomas R. Bieler²; Kuo-Chuan Liu¹; ¹Cisco Systems; ²Michigan State University

The mechanical stability of solder joints with Pd added to SnAgCu alloy with different aging conditions was investigated in high G level shock environment. A test vehicle, which has three different strain and shock level condition couples in one board, was used to identify the joint stability and failure modes. The results revealed that the Pd provided stability at the package side interface with an overall shock performance improvement over 40% compared to the SnAgCu alloy without Pd. There is also a dependency on the pad structure on the board side, which implies that the intermetallic at the board side and the package interface have different fracture/failure mechanisms. The effect of Sn grain orientation on shock performance, interconnect stability, and crack path with and without Pd added was investigated and compared with the effect of tin grain orientation in thermomechanical cycling conditions.

8:55 AM Invited

Effect of Temperature Dependant Deformation Characteristics on Thermomechanical Fatigue Reliability of Eutectic Sn-Ag Solder Joints: Deep Choudhuri¹; Andre Lee¹; *K.N. Subramanian*¹; ¹Michigan State University

Results from the monotonic shear loading at different temperatures in the range of -55 to 150°C of eutectic Sn-Ag solder joints with a simple shear strain rate of 10⁻³ s⁻¹ provide a clear explanation for the differences in the thermomechanical fatigue response of such joints subjected to temperature excursions ranging between -55°C to 125°C, and -15°C to 150°C. At very low temperatures regimes the strength of the interfacial Cu₆Sn₅ intermetallic compound layer and the Sn matrix control the monotonic deformation and TMF behavior. However, at higher temperatures the failure mode in both monotonic loading and in TMF is dominated by the Sn-Sn grain boundary sliding/decohesion within the solder matrix. Such observations also explain why significant reduction in the residual shear strength is noted from the very early stages of low temperature regime TMF as compared to that at high temperature regime TMF.

9:20 AM

Stress-Strain Behavior of Lead Free Solder Joints Determined by Digital Image Correlation Techniques: *Golta Khatibi*¹; Martin Lederer¹; Brigitte Weiss¹; Herbert Ipser¹; ¹University of Vienna

Previous investigations on miniaturized solder joints showed a strong increase in their yield and tensile strength with decreasing the gap size. In this study using digital image correlation techniques and FEM simulations the influence of geometrical constraints on stress-strain response of lead-

free solder joints was analyzed. Solder joints of Cu-Sn_{3.5}Ag-Cu with thicknesses between 50µm to 500µm were subjected to tensile loading and the sequences of local strain build-up in the joint area was measured using a VIC3D system. With decreasing the gap size a shift of strain localization from the center of the joints towards the interface region was observed. FEM analysis showed that the interface between the solder and substrate introduces a high triaxiality of stress which reduces the deviatoric stress inside the solder. This effect was more prominent in highly constrained solder joints leading to an increase of strength and a decrease of ductility.

9:40 AM

Effect of Continuous Recrystallization on Pb-Free Solder Joints in Thermo-mechanical Fatigue(TMf): *Liang Yin*¹; Babak Arfaei²; Peter Borgesen²; ¹Universal Instruments Corp; ²Binghamton University

The performance of Pb-free solder joints in TMF depends on the initial microstructure and its subsequent evolution. The fatigue failure of a typical Sn-Ag-Cu joint is commonly observed to involve the recrystallization of beta-Sn across the high strain region of the joint. Recent studies showed the recrystallization occurred through the formation of low-angle grain boundaries and the continuous increase of their misorientations. Random high angle grain boundaries provide sites for damage accumulation, such as grain boundary cracking and cavitation. In this study, the microstructure evolution of Sn-Ag-Cu solder joints was characterized quantitatively by using scanning electron microscopy, polarized light microscopy and imaging processing techniques. The effect of TMF testing parameters, e.g. peak temperature and dwell time, on the levels of recrystallization and strain-enhanced coarsening of secondary precipitates were evaluated and correlated to fatigue crack propagation. Discussions on subgrain/grain rotation and its effect on fatigue crack propagation are presented.

10:00 AM

Influence of Aging on Fatigue Behavior of SnAgCu Solders: *Jonathon Tucker*¹; Dennis Chan¹; Ganesh Subbarayan¹; Carol Handwerker¹; ¹Purdue University

In our prior research we developed the Maximum Entropy Fracture Model (MEFM), a thermodynamically consistent and information theory inspired (non-empirical) damage accumulation theory for ductile solids. Since fracture in SnAgCu solder alloys is known to be highly dependent on grain orientation, the model maximally accounts for uncertainty in the knowledge of the microstructure to describe the risk of fracture for a given applied energy (inelastic dissipation). The model utilizes theoretical arguments from statistical mechanics and continuum thermodynamics to relate probability of fracture to accumulated entropic dissipation. Here, we investigate the effects of isothermal aging on damage accumulation in fatigue cycling testing. A custom-built microscale mechanical tester capable of approximately 10 nm displacement resolution was utilized to carryout isothermal cycling fatigue tests on carefully designed assemblies. The resultant relationship between load drop and accumulated entropic dissipation was used to extract the geometry-independent MEFM damage accumulation parameter for different aging conditions.

10:20 AM Break

10:30 AM

Influence of Solder Microstructure and Intermetallic Layer Thickness on Mechanical Shock Resistance of Pb-free Solder Joints: *K. Yazzie*¹; H. Fei²; H. Jiang²; N. Chawla¹; ¹Materials Science and Engineering, School for Engineering of Matter, Transport, and Energy, Fulton Schools of Engineering, Arizona State University; ²Mechanical and Aerospace Engineering, School for Engineering of Matter, Transport, and Energy, Fulton Schools of Engineering, Arizona State University

Pb-free solder alloys are routinely subjected to mechanical shock and drop conditions in service. These solder alloys are susceptible to dynamic loading. Quantifying the contributions of intermetallic layer thickness and solder microstructure to the mechanical shock behavior of the solder specimen is extremely important and needs to be studied. In this study, dynamic strength of Sn-3.9Ag-0.7Cu solder joints was quantified as

a function of strain rate, solder microstructure, and intermetallic layer thickness. High-speed video and nanoindentation of Sn grains in solder joints was used to measure constitutive data for high-fidelity finite element models. The mechanisms for deformation and the interplay between solder-controlled and intermetallic controlled fracture will be discussed.

10:50 AM

Effects of Crystal Orientation on Recrystallization and Damage in Lead-Free Solders during Thermal Cycling in Low and High Stress Package Designs: *Bite Zhou*¹; Thomas Bieler¹; Tae-Kyu Lee²; Kuo-Chuan Liu²; ¹Michigan State University; ²Cisco Systems, Inc

The stress levels imposed on lead-free solder joints during thermal cycling vary in different package designs. With the same thermal history, solder balls in higher stress packages failed earlier compared to low stress packages. More significant recrystallization and big opening cracks were observed in high stress packages. The effects of Sn crystal orientation on cracking during thermal cycling are compared with packages with different stress levels and discussed in relation to the strain history. A diverse range of Sn crystal orientations were correlated with cracking in high stress packages. Even joints with Sn orientations resistant to cracking during thermal cycling in low stress package (with [001] perpendicular to the interfaces) developed cracks in the high stress package design. Sn crystal orientation evolution in selected solder balls are evaluated using electron backscatter diffraction (EBSD) and differential aperture X-ray microscope (DAXM) for surface and subsurface characteristics.

11:10 AM

Study on Fatigue Mechanism in Pb-Free Solder Joint using Isothermal Shear Fatigue: *Huili Xu*¹; Choong-Un Kim¹; Tae-Kyu Lee²; Hong-Tao Ma²; Kuo-Chuan Liu²; ¹The University of Texas at Arlington; ²Cisco System Incorporation

Prediction of solder joint failure under temperature cycling is a difficult and persisting task in electronics packaging industry because of the continuously changing of solder property caused by dynamic changing of microstructure. To overcome such a difficulty, we conducted series of shear fatigue testing on solder joint and attempt to model the failure rate using known theories. Our investigation reveals that shear fatigue can be successfully modeled by frequency modified Coffin-Manson fatigue theory. However, the success of the model is found to be limited only to a given temperature and cannot be extended to include temperature term. This is related to the change in microstructure dynamics that alters mechanical constraint as well as change in failure location. This paper presents summary of our data, supporting the fatigue model but showing its limitations, along with discussion on their implications especially on the model for thermal cycle fatigue.

11:30 AM

Retarding Electromigration on Lead-Free Solder Joints by Micro-Sized Metal Particle Reinforcements: Limin Ma¹; Yong Zuo¹; Guangchen Xu¹; *Fu Guo*¹; ¹Beijing University of Technology

Although the failure induced by Electromigration(EM) can trigger a large void across the entire cathode interface of solder joints, no effective solutions are presented throughout years of effort on this problem. Here, the composite solder joints are addressed to demonstrate their potential roles on solving the EM issue in the eutectic lead-free solder joints. Micro-sized Ni or Co particles were selected to intentionally add into the solder matrix due to their extensive application as a barrier layer in the under-bump-metallization (UBM) of flip chip solder joints. The ultimate results illustrated that the phase segregation of solder joints induced by EM was significantly inhibited in the composite solder joints during the current stressing, demonstrating the Sn-Ni or Sn-Co IMCs can act as the obstacles to obstruct the movement of dominant diffusion entity along the phase boundaries.

11:50 AM

Effect of Thermomigration on Redistribution and Growth of Intermetallic Compounds in the Sn0.7Cu Solder Bump under Current Stressing: *Wei-Yu Chen*¹; Kwang-Lung Lin¹; ¹National Cheng Kung University

The dissolution and redistribution of Cu₆Sn₅ in the Sn_{0.7}Cu solder bump were observed consecutively with various time intervals under 150°C, 1.0×10⁴ A/cm² of current stressing. The thermal gradients in the vertical (parallel to electron flow) and horizontal directions (normal to the electron flow) were considered to combine the electromigration, induced by electron flow, in a current stressed solder joint. The combined effect of electromigration and thermomigration induces dissolution of Cu₆Sn₅ at the hot side and polarized flux of Cu in the solder bump from the hot side to the cold side. Consequently, the Cu₆Sn₅ recrystallized at the cold side of the solder bump and thus a behavior of the redistribution of the compound. Kinetic analysis indicates that the dissolution of Cu₆Sn₅ at the hot side is dominated by reaction control, while the growth of Cu₆Sn₅ at the cold side follows diffusion control.

Phase Stability, Phase Transformations, and Reactive Phase Formation in Electronic Materials XI: Solder-related Reliability Issues

Sponsored by: The Minerals, Metals and Materials Society, TMS Electronic, Magnetic, and Photonic Materials Division, TMS: Alloy Phases Committee

Program Organizers: Chih-Ming Chen, National Chung Hsing University; Jae-Ho Lee, Hongik University; Ikuo Ohnuma, Tohoku University; Clemens Schmetterer, TU Bergakademie Freiberg; Yee-Wen Yen, National Taiwan University of Science and Technology; Shih-Kang Lin, University of Wisconsin – Madison

Monday AM

March 12, 2012

Room: Swan 10

Location: Swan Resort

Session Chairs: Chih-Ming Chen, National Chung Hsing University; Katsuaki Sukanuma, Osaka University

8:30 AM Invited

Effect of Crystal Orientation on Mechanically Induced Sn Whiskers of Sn-Cu Platings: *Yukiko Mizuguchi*¹; Yosuke Murakami²; Shigetaka Tomiya²; Tadashi Asai³; Tomoya Kiga³; Katsuaki Sukanuma⁴; ¹Sony Corporation, Osaka University; ²Sony Corporation; ³Sony EMCS Corporation; ⁴Osaka University

Mechanically induced Sn whiskers were examined by means of scanning electron microscopy (SEM) and electron backscatter diffraction (EBSD) patterns. The analyses revealed that Sn-Cu grains grew by recrystallization under mechanical stress. The notable feature was frequent twin formations. Most of the twin planes were {301}, and the number of {301} twin boundaries increased about twenty times as many as that of as-deposited platings. The present study clearly shows the first evidence that the mechanically induced Sn whiskers nucleate from twin grains of Sn. The authors will show twin formation plays a key role in the whisker formation. The details are discussed in the presentation.

8:50 AM

Effects of Cu-Bearing Flux on Joint Reliability and Microstructure of Sn-3.5Ag/ENIG Joint: *Hitoshi Sakurai*¹; Youichi Kukimoto²; Chang-Jae Kim¹; Katsuaki Sukanuma¹; ¹Osaka University; ²Harima Chemicals, Inc

The demand for powerful BGA package accelerates the reduction in size of both BGA ball and pad. Therefore, control of the interfacial reaction is important to realize high reliability of small solder joints. In this study, the effects of Cu-bearing flux on joint strength and microstructure of Sn-3.5Ag/ENIG joints with additional heat treatment were investigated. The results of joint strength tests for as-reflowed solder joints showed that Cu-bearing fluxes gave higher joint strength than did flux without



Cu compound. Additionally, the use of flux containing high concentration of Cu compound provided the small reduction rate in joint strength in regard to additional heat treatment. According to the observation of the joint interface obtained by the use of Cu-bearing flux, the growth of a P-rich layer was well suppressed during thermal treatment. The Cu barrier effect by Cu-bearing flux had a significant impact on joint reliability of Sn-3.5Ag/ENIG joint.

9:05 AM

Gold and Palladium Induced Embrittlement Phenomenon in Microbumps Using Au/Pd(P)/Ni(P) Metallization Pads: *Wei-Hsiang Wu¹; Chia-Ming Li¹; Yen-Chen Lin¹; Cheng-En Ho¹; ¹Yuan Ze University*

Thermal reliability of the Au/Pd(P)/Ni(P) tri-layer utilized in microbumps (85 micrometer diameter) was investigated in this study. We found that the surface Au/Pd films would quickly alloy with molten Sn3Ag0.5Cu during soldering and then precipitated significant amounts of AuSn4 and PdSn4 in the solidified Sn matrix, respectively. In the subsequent isothermal aging, these two intermetallic species together with Cu6Sn5 gradually migrated to the solder/Ni(P) interface, forming a mixture layer(s) of AuSn4 + PdSn4 + Cu6Sn5. The driving force for their resettlement is that they can acquire specific amounts of Ni from the Ni(P) substrate, becoming more thermodynamically stable phases. The formation of the multi-compound layer(s) at the interface substantially weakened the interfacial strength, deteriorating the mechanical/electrical reliability of the solder joints. More details regarding the microstructural evolution of AuSn4, PdSn4, and Cu6Sn5 in microbumps will be presented in this talk.

9:20 AM

Inhibiting Cu-Sn Intermetallics by a Pre-Heat Treatment: *Chih-Chia Hu¹; Hsiang-Yao Hsiao¹; Chih Chen¹; ¹National Chiao Tung University*

Copper serves as the most popular under-bump-metal (UBM) in microelectronic packaging industry. During soldering reaction, copper reaction with Sn-based solders to form Cu₆Sn₅ and Cu₃Sn intermetallic compounds (IMCs) very quickly and thus thousands of solder joints form simultaneously in one reflow. Yet, the IMCs are brittle in nature. It will be very beneficial if the Cu-Sn reaction could be inhibited after jointing. We discover a effective approach to inhibit the growth of the Cu-Sn IMCs. By depositing a thin layer of solder on a Cu film and a liquid-state metallurgical reaction at 260 °C for few minutes, the channels between Cu₆Sn₅ IMCs might be closed up. When the sample was jointed to solder afterwards, this layer-type Cu₆Sn₅ IMCs becomes a diffusion barrier for Cu dissolution during additional reflowing, and the growth of the IMCs was retarded.

9:35 AM

Rare-Earth Containing Lead-Free Solders with Enhanced Ductility: *Huxiao Xie¹; Nikhilesh Chawla¹; ¹Arizona State University*

We have previously shown that small additions of the rare-earth (RE) elements to Sn-Ag-Cu alloys (La, Ce, and Y) significantly increase their ductility, without significant loss in the overall strength or creep resistance. We have shown that the unique RE-Sn soft intermetallic (IMC) particles play an important role in the ductility enhancement. Based on these mechanisms, calcium was selected as a potential candidate to increase the ductility of Sn-Ag-Cu lead-free solder. Doping Ca into Sn-rich solder resulted in the formation of CaSn₃ that has the same crystal structure as CeSn₃ and LaSn₃, but possesses a lower melting point. Nanoindentation was used to measure Young's modulus and hardness of CaSn₃. The modulus and hardness are significantly lower than that of RE-Sn and Cu-Sn IMCs formed in Pb-free solders. Finally, the monotonic shear behavior of reflowed Ca-containing Sn-Ag-Cu/Cu lap shear joint was studied and compared to the SAC and RE-containing SAC solder joints.

9:50 AM

Study of Orientation of Solder Grains in Microbumps for 3D IC Packaging: *Han-wen Lin¹; Chih Chen¹; ¹National Chiao Tung University*

As the trend of portable devices strikes the whole world, people want to have more functions on their portable devices. Thus, microprocessors with better performance within the smaller size of packaging are required. So far, the most possible way to fulfill this requirement is 3D IC packaging with Pb-free solder microbumps and through-Si-vias. Many researches have shown that the BCT structure of tin makes different mechanical, electrical properties and failure mechanisms along different axis. However, There are few researches studying the orientation of tin of microbumps, in scale of 20 – 40 μm or even smaller. In this paper, the orientation of Sn and intermetallic compounds (IMCs) in microbumps are examined by EBSD. It is found that when SnAg solder jointed to Cu metallization on both sides, the orientation of Cu₆Sn₅ IMCs is random in the beginning. However, after longer time of reflowing, the merged IMCs became the same orientation.

10:05 AM Break

10:15 AM Invited

Effect of External Strain on Growth of Interfacial Intermetallic Compounds between Sn on Cu Substrate: *Yu-Ting Wang¹; Shin-Nan Li¹; Ming-Tzer Lin¹; ¹National Chung Hsing University*

A four point bend experiments were conducted to study on the effect of substrate strain related to Cu-Sn IMC growth. Two kinds of Tin samples (Matte and Bright) were prepared. 400μm Cu sheet were cut into strips with 27mm in length and 5mm in width as test samples. 35μm tin (Matte or Bright) was deposited on top of copper sheet using electroplating. A set of samples were put into furnace at 200°C and bending strain were applied under tension, compression and no strain. The results on intermetallic formation affected by different strain levels and reflow time were presented. Both of tension and compression strain would affect the Cu-Sn IMC formation. The thickness of IMC was increased when sample under strain and the trend is Compression > Tension > Control. The growth rate of IMC was faster in Bright tin under strain. The IMC structures from different Tin sources present very differently.

10:35 AM

Development and Evaluation of Direct Deposition of Au/Pd(P) Bilayer on the Cu Metallization in Soldering Applications: *Cheng-En Ho¹; T. T. Kuo¹; H. G. Wang¹; C. W. Fan¹; ¹Yuan Ze University*

The Ni-based thin film(s), such as Au/Ni(P) or Au/Pd(P)/Ni(P), is a very common surface finish to treat over the Cu pads in microelectronic packaging applications. The thickness of the Ni(P) usually exceeds 5 μm, and thereby hinders the application in the fine-pitch components. Additionally, there are several reliability concerns induced by the Ni(P), such as black pads and Au- (or Pd-) embrittlement. In order to avoid such reliability concerns, direct deposition of the Au/Pd(P) bilayer on the Cu substrate is being considered and adopted by industry very recently. This study systematically investigates the metallurgy of the solid-state reactions and intermetallic growth kinetics between Sn3Ag0.5Cu and Au/Pd(P)/Cu trilayer with various Pd(P) thicknesses. To quantify mechanical response of the interfacial microstructures, a high-speed ball shear (HSBS) test was conducted in this study. More details regarding the microstructural evolution and mechanical response of various Au/Pd(P) layers will be presented in this talk.

10:50 AM

Effective Suppression of Electromigration-Induced Cu Dissolution by Using a Ag Barrier Layer in Lead-Free Solder Joints: *Chao-hong Wang¹; Han-ting Shen¹; Wei-han Lai¹; ¹National Chung Cheng University*

Electromigration-induced failures are a crucial reliability issue for solder joints in flip-chip technology. The main failure modes are void formation and fast Cu dissolution, leading to a rise in resistance. Under current stressing, electromigration causes a large amount of Cu₆Sn₅ formation in the solder matrix and the considerable consumption of Cu substrate. In

this work, Ag is used as a barrier layer at the solder/Cu interface to inhibit Cu dissolution. The test specimen structure was prepared as Sn/2 μ m Cu/1 μ m Ag/Cu substrate. Without current stressing, the interfacial products were Cu₆Sn₅, AgSn₃, Cu₆Sn₃ and Cu₃Sn. As electron currents passed from Cu substrate to solder, the 2 μ m Cu layer was completely consumed and the formed Cu₆Sn₅ phase dispersed in the solder matrix. The observation of AgSn₃ layer and Cu substrate was similar to that of without current. Hence, Ag can act as an effective diffusion barrier against the Cu dissolution induced by electromigration.

11:05 AM

Driving Force of EM-Induced Cu Dissolution in Cu-Sn Compound: Cheng Tse Lu¹; Cheng-Yi Liu¹; ¹National Central University

Upon current-stressing a Cu/Sn cathode joint interface, the Cu atoms in the Cu-Sn compound layer would experience two major driving forces, which are EM force and difference of Cu chemical potential in the Cu-Sn compound layer and in the Sn solder with deficient Cu solubility. Both forces would simultaneously result in Cu dissolution fluxes from the Cu-Sn compound layer into the Sn joint. In this study, we design a special T-shape solder joint structure to separate this two driving force of EM-induced Cu dissolution in Cu-Sn compound. The current work has demonstrated that the EM-induced deficient Cu solubility in Sn solder is the dominant driving force for the dissolution in the cathode Cu-Sn compound layer under current density of 104 A/cm² at 150 °C.

11:20 AM

Reactive Wetting of Heterogeneous Substrates by Sn-based Solders: Q. Lai¹; L. Zhang¹; J. Shang²; ¹Institute of Metal Research; ²University of Illinois

Reactive wetting of heterogeneous substrates by Sn-based solders were investigated to clarify the mechanisms of reactive wetting in these systems. It was found that the wettability of dual-phase alloys could be made better than that of each component. Over a wide composition range, reactive wetting on dual-phase alloys was shown not to follow the classical Cassie equation. Instead, the contact angle vs. area fraction of the second phase showed a "V"-shape variation and there was an inverse relationship between the contact angle and the phase boundary density. From the observations of wetting processes, it was shown that the excellent wettability of dual-phase alloys resulted from the sharp difference in the dissolution rate between the two phases, which promotes phase boundary grooving at the triple junction and enhances wetting.

11:35 AM

The Cross-Interaction in the Ni/Sn/Cu Sandwich-Type Solder Joint with Electroless Pd Surface Finish: Chi-Pu Lin¹; Chih-Ming Chen¹; ¹National Chung-Hsing University

In modern integrated circuit (IC) packaging, the under bump metallization (UBM) used in flip-chip technologies is often composed of two different types of metal pads. Cu is commonly used as a metallization layer on the printed circuit boards (PCB). Ni has good solderability and is also a good diffusion barrier. Sn is the primary element of the Pb-containing and Pb-free solders, hence the Ni/Sn/Cu sandwich-type structure is often formed in the flip-chip solder joints. Electroless Pd surface finish also has good wetting property and gradually replaces immersion Au in recent years. In this study, the quaternary Ni/Pd/Sn/Cu and Ni/Sn/Pd/Cu systems were prepared by thermal compression and then solid-state aging were performed at 200 °C up to 240h. Cross-interactions in the multi-layered structure were investigated. Morphological evolution, formation, and kinetic behavior of the intermetallic compounds formed by the interfacial reactions were discussed.

11:50 AM

Grain Boundary Penetration of Various Types of Ni Layers by Molten Pb: Chia Yuan Chang¹; C. Robert Kao¹; ¹National Taiwan University

In this study, we investigated the penetration of grain boundary by molten Pb into different Ni-based substrates, including pure Ni, electroplating Ni, and electroless Ni-P. Penetration was observed for all three types of

substrate when these substrates were inserted into molten Pb at 360 °C. Since electroplated Ni has a very small grain size than bulk Ni, liquid Pb not only penetrated the grain boundaries but also resulted in fragmented interface. Molten Pb also penetrate electroless Ni-P even though it is amorphous structure originally, and the penetration depth are more than that of electroplated Ni. This result shows that electroplating Ni exhibits best penetration resistance.

Randall M. German Honorary Symposium on Sintering and Powder-Based Materials: Sintering Theory and Practice

Sponsored by: The Minerals, Metals and Materials Society, TMS Materials Processing and Manufacturing Division, TMS: Powder Materials Committee

Program Organizers: K. Morsi, San Diego State University; Fernand Marquis, Naval Postgraduate School; John Meyer, Iowa State University; Ahmed El-Desouky, San Diego State University; Eugene Olevsky, San Diego State University

Monday AM

March 12, 2012

Room: Oceanic 2

Location: Dolphin Resort

Session Chair: Eugene Olevsky, San Diego State University

8:30 AM Introductory Comments

8:40 AM Keynote

History of Sintering: *Randall German*¹; ¹San Diego State University

Sintering has been used for thousands of years and rediscovered several times. The modern era traces to the early 1900s and is close coupled to basic discoveries in atomic and crystal structure, defect migration, surface energy, and microstructure evolution. This converged in the late 1940s to generate the accepted concepts on how materials sinter. This presentation organizes the timeline for sintering literature to show early concepts were too restrictive. Starting with sintering observations it is possible to sort out how models emerged to explain those observations. Comments are offered on who generated the greatest impact, what applications were most significant, and how a few inspirational leaders and organizations clearly dominated the emergence of sintering theory. Commercial developments were far ahead of theory and that is seen today with the emergence of novel electronic products relying on sintering.

9:10 AM Invited

Grain Growth during Sintering of Nanosized Particles: *Zhigang Fang*¹; Hongtao Wang¹; Vineet Kumar²; ¹University of Utah; ²Kennametal Inc.

Grain growth during sintering of nanosized powders is an issue that is critical for manufacturing of bulk nanocrystalline materials by sintering nanosized powders. In general, it has been found that grains grow rapidly during sintering and it is very difficult to achieve nanoscaled grain sizes in as-sintered state. Although the thermodynamic driving forces for grain growth for nanosized particles are the same as that for micron-sized particles, the kinetics and mechanisms of the grain growth of nano particles during sintering deviate from that of the conventionally known power law relationship. This paper examines the grain growth of nanosized tungsten particles during the early stage of sintering when the relative density of the material is still less than 90%. Linear kinetic behavior of grain growth will be discussed.

9:35 AM Invited

Distortion in a 7xxx Aluminium Alloy Sintered in Nitrogen under Different Flow Patterns: Xini Yuan¹; Ma Qian¹; Saïed Aminossadati¹; Graham Schaffer¹; ¹The University of Queensland

This paper presents an experimental and numerical study of the effects of sample position and gas flow pattern on the distortion that occurs during sintering of a 7xxx aluminium alloy, Al-7Zn-2.5Mg-1Cu. The



TMS 2012

141st Annual Meeting & Exhibition

MONDAY AM

experimental study examines the distortion of three equally spaced compacts during sintering in flowing nitrogen at separation distances ranging from 2 mm to 40 mm. The microstructural evolution in each compact during sintering was characterized using optical and scanning electron microscopy. The surface compositions of the sintered samples were analysed using X-ray photoelectron spectroscopy (XPS) depth profiling. A computational fluid dynamics (CFD) model was developed to investigate the flow pattern surrounding each sample by streamlines corresponding to the experimental conditions. The mechanism of distortion in the Al-7Zn-2.5Mg-1Cu alloy sintered under different sample separation distances is discussed in light of the microstructural observation, composition analysis and CFD modelling results.

10:00 AM Invited

Challenges and Further Developments in Modeling of Sintering: *Eugene Olevsky*¹; ¹San Diego State University

Six possible directions of further developments in modeling of sintering are pointed out, including multi-scale modeling of sintering, development of on-line sintering damage criteria, modeling of nano-powder sintering, modeling of sintering with phase transformations or chemical reactions, modeling of field-assisted sintering, and the development of sintering optimization approaches. Existing theories require a link between the micro-, meso- and macroscopic descriptions of sintering. Certain events occurring at the micro-structure level are not accounted for; those include the phenomena, which are, in particular, important in nano-powders' sintering. Usually, factors of a non-thermomechanical nature are not incorporated in sintering models. Such factors include phase transformations, chemical reactions, influence of sintering atmospheres, and influence of electro-magnetic fields. Rigorous optimization tools are missing in modeling approaches, which could enable the determination of the most favorable initial properties and geometry of the sintered specimen as well as the most advantageous parameters of sintering regimes.

10:25 AM Break

10:40 AM Keynote

Stereological Analysis of Microstructural Evolution during Sintering: *Burton Patterson*¹; ¹University of Florida

Microstructural evolution during sintering is the net result of a number of interacting processes with different driving forces and controlling effects. Following the paths of evolution of 3D microstructural descriptors such as pore and grain boundary surface area per volume and their triple-line of intersection provides insight and shows relationships that may not otherwise be apparent. In liquid phase sintering, growth path envelope analysis of the evolving particle size distribution provides growth and shrinkage rates as a function of initial size class, enabling testing of coarsening models and controlling mechanism. All in all, numerous microstructural characteristics are amenable to quantification via stereological methods for understanding numerous aspects of sintering. This presentation will review useful examples of these analyses.

11:10 AM Invited

A Review on Alloying in Tungsten Heavy Alloys: *Animesh Bose*¹; *Rajendra Sadangi*²; *Randall German*³; ¹Materials Processing, Inc.; ²Rutgers University; ³San Diego State University

This paper will review some of the developments in the area of alloying of tungsten heavy alloys. The review will concentrate on the alloying additions that have been made to the classic liquid phase sintered tungsten heavy alloys primarily based on W-Ni-Fe compositions. The effects of these alloying elements on the microstructure and properties of tungsten heavy alloys will be discussed in this paper. The review will also touch on some of the advantages that these additive modified tungsten heavy alloys yield over conventional tungsten heavy alloys (without the alloying additions), especially the ability to form near net-shaped, high strength, high hardness, heavy alloys without the additional thermo-mechanical treatments needed to attain higher strength and hardness.

11:35 AM Invited

Development of Alternate Materials to Cemented Carbides without Tungsten: *Ken-ichi Takagi*¹; ¹Tokyo City University

Paucity of scarce and unevenly distributed resources such as tungsten has become a crucial issue all over the world. In the field of wear resistant hard materials, development of alternative materials with less or no tungsten is a current research topic. Borides, especially transition metal borides show high hardness, high melting point, etc. and hence borides are well-suited to wear resistant applications. A unique reaction sintering technology named reaction boronizing sintering to form multiple borides coexisting with a metallic binder during liquid phase sintering has been successfully developed as world's first ternary boride base cermets with excellent mechanical properties such as Mo₂FeB₂ and Mo₂NiB₂ base cermets. These boride base cermets containing no tungsten have already been applied to wear resistant applications such as injection molding machine parts, etc. This paper focuses on recent development of alternate materials to cemented carbides without tungsten, especially on the ternary boride base cermets.

Science and Engineering of Light Metal Matrix Nanocomposites and Composites: Metal Matrix Nanocomposites

Sponsored by: The Minerals, Metals and Materials Society, TMS Light Metals Division

Program Organizers: Xiaochun Li, University of Wisconsin-Madison; Alan Luo

Monday AM
March 12, 2012

Room: Macaw 2
Location: Swan Resort

Session Chair: Xiaochun Li, University of Wisconsin-Madison

8:30 AM Introductory Comments

8:35 AM

A Unified Theoretical Model for Nanoparticle and Microparticle Capture by Metal Solidification Front: *Jiaquan Xu*¹; *Lianyi Chen*¹; *Xiaochun Li*¹; ¹University of Wisconsin-Madison

Effective capture of nanoparticles by solidification front is extremely challenging for solidification processing of metal matrix nanocomposites (MMNCs). But there is little theoretical study on nanoparticle capture during metal solidification. This article is to establish a unified theoretical framework for fundamental understanding of nanoparticle and microparticle capture during metal solidification. Nanoscale interactions among particles (micro- and nanoparticles), molten metal, and solidification front were analyzed. Van der Waals and viscous forces were especially studied. Plasma frequencies were introduced to approximate Hamaker constants for various metals. Factors such as thermal conductivity, Gibbs Thomson effect, varying viscosity and possible gas film on surface of nanoparticle were considered. Critical velocity and critical distance for nanoparticle capture were determined. While further study is needed, theoretical predictions from this new model shows promises for particle captures in solidification processing.

8:55 AM

Characterization of Solidification of Nanoparticle enforced Al Using In Situ TEM: *Jorg Wieszorek*¹; *Hasso Weiland*²; *Andreas Kulovits*¹; *Can Liu*¹; ¹University of Pittsburgh; ²Alcoa

Establishing the processing-structure-property relationships in Aluminum matrix nano-composite (Al-NC) requires microstructural analysis methods that can robustly and quantitatively detect the dissimilar nanoparticle reinforcements. This proves challenging for conventional electron microscopy methods, for instance, due to the low contrast resulting in Al-NC for typical reinforcement species, such as Al₂O₃ and SiC nanoparticles or carbon nanotubes. Using transmission electron

microscopy (TEM) studies, inclusive of novel orientation imaging microscopy (OIM), enabled successful analyses of the morphology, size, phase fractions of the Al-matrix grains and the nano-particle dispersions in SiC and Al₂O₃ based Al-NC. In-situ TEM heating studies have been used to monitor effects of the nanoparticles on the microstructural transformations, including melting and solidification, in the Al-NC due to thermal stimulation.

9:15 AM

Interfacial Analysis of CNT Reinforced AZ61 Mg Alloy Composites: *Katsuyoshi Kondoh*¹; Hiroyuki Fukuda¹; Junko Umeda¹; Bunshi Fugetsu²; ¹Osaka University; ²Hokkaido University

In AZ61 Mg alloy composites with multi-walled carbon nanotube (CNT) reinforcements, in-situ formed Al₂MgC₂ compounds at the interface between Mg matrix and CNTs effectively reinforced the interfacial bonding, and enabled tensile loading transfer from the Mg matrix to nanotubes. As a result, the heat treatment at 550°C was obviously effective to synthesis Al₂MgC₂ needle-like compounds and improve the mechanical tensile strength of the composites. It was also clarified that the microstructures and grain orientations of the composite matrix were not significantly influenced by CNT addition.

9:35 AM

Magnesium Nanocomposites Processed by Electromagnetic Acoustic Transduction: *Hunter Henderson*¹; Zachary Bryan¹; Orlando Rios²; Gail Mackiewicz-Ludtka²; Alexander Melin²; George Lopp²; Yu-Min Su²; Michele Manuel¹; ¹University of Florida; ²Oak Ridge National Laboratory

Magnesium (Mg)-based alloys reinforced with ceramic nanoparticles have attained interest for their improvement in strength and ductility, compared to traditional Mg alloys. Among several methods of fabrication, sonication shows promise for scalability to industrial applications. A specialized technique known as Electromagnetic Acoustic Transduction (EMAT), magnetically induced sonication, is evaluated with regard to the dispersion of several particle types in Mg. This technique potentially offers several advantages over traditional melt sonication, including non-contact, higher intensity, and smoother energy distribution. The present study explores the effect of processing parameters on the composite's microstructure. Additionally, radiographic and microscopic techniques are used to evaluate microstructural parameters such as dispersion, particle morphology, and grain size. The authors would like to acknowledge the support of the National Science Foundation (DMR 0845868), National High Magnetic Field Laboratory User Program, and Department of Energy's Energy Efficiency and Renewable Energy Industrial Technologies Program.

9:55 AM

Properties of Aluminum-Graphene Nanocomposites: *Stephen Bartolucci*¹; Joseph Paras¹; Mohammad Rafiee²; Sabrina Lee¹; Javad Rafiee³; Deepak Kapoor¹; Nikhil Koratkar³; ¹US Army ARDEC; ²Rice University; ³Rensselaer Polytechnic Institute

Carbon nanotubes have been studied recently as reinforcement additives for lightweight metal matrices, such as aluminum and magnesium, in order to increase mechanical properties. With the exponential increase in attention given to graphene in current research arenas, we have chosen to study the addition of graphene platelets to an aluminum matrix. Our results have shown a decrease in the mechanical properties performance of the graphene-aluminum nanocomposites as compared to composites made with multi-walled carbon nanotubes. It is believed that aluminum carbide formation plays a central role in the behavior of our graphene composites. Characterization of the composites and explanation of the results will be discussed.

10:15 AM Break

10:30 AM

Biodegradability and Mechanical Performance of Hydroxyapatite Reinforced Magnesium Matrix Nanocomposite: *Chao Ma*¹; Liany Chen¹; Jiaquan Xu¹; Axel Fehrenbacher¹; Yan Li¹; Frank Pfefferkorn¹; Neil Duffie¹; Jing Zheng¹; Xiaochun Li¹; ¹UW-Madison

Magnesium and its alloys have gained significant attention recently in the field of biodegradable medical implant due to its combination of good biodegradability, biocompatibility and mechanical properties. However, magnesium implants are not able to maintain the mechanical integrity under physiological conditions because of the high corrosion rates. In this study, hydroxyapatite (HA) nanoparticles reinforced magnesium matrix nanocomposites are fabricated by friction stir processing (FSP). The microstructure, mechanical properties of the nanocomposites and their in-vivo corrosion properties in simulated body fluid (SBF) were investigated. The results suggest that the mechanical and corrosion properties of the nanocomposites could be effectively controlled by the percentage of HA nanoparticles and the processing parameters.

10:50 AM

Mechanical Properties of A356-CNT Cast Nano Composite Produced by a Special Compocasting Route: *Benyamin Abbasipour*¹; *Behzad Niroumand*¹; Sayed Mahmoud Monirvaghefi¹; ¹Isfahan University of Technology

A356 aluminum alloys reinforced with CNTs were produced by stir casting and compocasting routes and their microstructural characteristics and mechanical properties were examined. In order to alleviate the problems associated with poor wettability, agglomeration and gravity segregation of CNTs in the melt, CNTs were introduced into the melts by injection of CNT deposited aluminum particles as well as raw CNTs. Nickel-phosphorous electroless coating process was employed for uniform co-deposition of CNTs into a Ni-P matrix coated on Aluminum powder. The slurries were subsequently cast at temperatures corresponding to full liquid as well as 0.15 and 0.30 solid fractions. The results showed that addition of CNTs to A356 matrix could significantly refine both fully liquid and semi-solid cast microstructures. Mechanical properties of the samples were also significantly increased by addition of CNTs in the form of CNT deposited aluminum particles.

11:10 AM

Production of Cast AZ91-CNT Nano-Composite by Addition of Ni-P-CNT Coated Magnesium Powder to the Melt: *Mahan Firoozbakht*¹; *Behzad Niroumand*¹; *Behzad Niroumand*¹; Sayed Mahmoud Monirvaghefi¹; ¹Isfahan University of Technology

High agglomeration tendency and poor wettability of CNTs with metallic matrices are the main challenges for using this unique material as the reinforcement in magnesium based composites. In this study, nickel-phosphorous electroless coating process was employed for uniform co-deposition of CNTs into the Ni-P coating on the magnesium powder for the first time. The magnesium powder with the optimum composite coating was then used as the reinforcement and was introduced into the molten AZ91 alloy using stir casting method. Similar composites were also produced with untreated as-purchased CNTs for comparison. It was observed that addition of CNTs dispersed in the electroless coating resulted in refinement of the grain size, reduction in the porosity content and improvement of the hardness and flexural strength. Untreated CNTs were not able to improve the structural and mechanical characteristics of the cast composites to the same extent. This is believed to be due to the more agglomeration, less uniform distribution and poor wettability of the untreated CNTs with the melt compared to those introduced to the melt through the Mg-Ni-P-CNT composite powder.



TMS 2012

141st Annual Meeting & Exhibition

MONDAY AM

11:30 AM

Wear Behavior of Magnesium Matrix Nanocomposites at Room and Elevated Temperature: *Wenzhen Li*¹; ¹Tsinghua University

Magnesium matrix nanocomposite reinforced with nano-sized SiC particles was fabricated by mechanical stirring and high intensity ultrasonic dispersion processing. The dry sliding wear behavior of the magnesium alloy and its nanocomposites were investigated using a ball-on-disc CETR wear testing machine. The test results show that the addition of SiC nanoparticles increased the wear resistance of composites at room and elevated temperature. The wear loss increase as the load increasing as expected and the wear loss of AZ91D is higher than those of its composites at all the loads. The dominative wear mechanisms vary with different load and the load occurring delamination wear can be improved due to SiC nanoparticles strengthening function. Wear test results also showed that the worn stages of AZ91D and its composite include running and stable worn stages, however the acutely worn stages occurs in one hour sliding time.

11:50 AM

Influence of Nanodispersions on Metallurgical Properties and Performance of Cast AlSi Alloys

: *Iman El Mahallawi*¹; Yehia Shash¹; Hoda Abdelkader²; Laila Shehata³; Mohamed Abdelaziz⁴; Asmaa Amer Abdelmegeed³; Joachim Mayer⁵; Alexander Scwedt⁶; ¹Cairo University; ²Helwan University; ³Scientific & Technology Centre of Excellence; ⁴The British University in Egypt; ⁵Gemeinschaftslabor fuer Elektronmikroskopie

The present study aims at developing nano-dispersed cast Al-Si hypo and hyper eutectic alloys with optimised properties and performance in automotive applications. In this work a number of cast samples of A356 and A390 were prepared by rheo-casting in a specially designed and built furnace unit allowing for the addition of the nano-particles into the molten Al-Si alloy with mechanical stirring. The microstructural features and the mechanical properties of the cast samples were investigated, as well as resistance to wear and corrosion in laboratory tests. The results obtained in this work showed improved wear and corrosion resistance of the nano-dispersed alloys, as well as enhancement in the mechanical strength of the nano-dispersed alloys, accompanied by significant increase in the elongation percentage, supported by evidence of refined dendrite arms length, and inter-lamellar spacing.

12:10 PM

Grain Refinement and Mechanical Property Enhancement in As-cast Al-Mg Nanocomposites: *Dake Wang*¹; Michael De Cicco¹; Xiaochun Li¹; ¹University of Wisconsin-Madison

The microstructure and mechanical property after ultrasonic processing were studied in an Al-9Mg matrix with TiC_{0.7}N_{0.3} nanoparticles. The Al-9Mg + TiC_{0.7}N_{0.3}, which had significant nanoparticle incorporation, showed more significant grain refinement and mechanical property enhancement than the Al-9Mg + Al-5Ti-1B alloys. This grain refinement and mechanical property enhancement in 0.2% yield strength, ultimate tensile strength and ductility were maintained when pieces of the original 1.5 vol.% TiC_{0.7}N_{0.3} nanocomposites were added to additional Al-9Mg for the 0.5 vol.% and 0.2 vol.% TiC_{0.7}N_{0.3} nanocomposites. This illustrates the potential of a master nanocomposite approach for metal matrix nanocomposite (MMNC) processing. The nanoparticles probably perform as nucleant catalyst for the α -Al and β -Al₃Mg₂ phase and restrict the grain growth for a refined microstructure. The unusual ductility enhancement is also the result of suppression of pore formation as well as morphology alternation of the intermetallic phase by the nanoparticles.

Solid-State Interfaces II: Toward an Atomistic-Scale Understanding of Structure, Properties, and Behavior through Theory and Experiment: Atomic Level Structures, Compositions, and General Methods

Sponsored by: The Minerals, Metals and Materials Society, TMS Electronic, Magnetic, and Photonic Materials Division, TMS Structural Materials Division, TMS: Chemistry and Physics of Materials Committee, TMS: Nanomechanical Materials Behavior Committee

Program Organizers: Xiang-Yang Liu, Los Alamos National Lab; Douglas Spearot, University of Arkansas; Guido Schmitz, University of Münster; David Seidman, Northwestern University

Monday AM
March 12, 2012

Room: Oceanic 7
Location: Dolphin Resort

Funding support provided by: Los Alamos National Laboratory

Session Chairs: Alan Ardell, National Science Foundation; Xiang-Yang (Ben) Liu, Los Alamos National Lab

8:30 AM Invited

Grain Boundary Complexion Conformations (Equilibrium Interface-Stabilized Phases) in Materials: *Martin Harmer*¹; ¹Lehigh University

A grain boundary complexion is a "phase" that is thermodynamically stabilized by its adjoining grains (Science, 332, 182, 2011). It is chemically and structurally distinct from any bulk phase. Complexion phases can interconvert between well-defined equilibrium structures, which can be represented on complexion phase diagrams analogous to bulk phase diagrams. A progressive series of six possible complexion conformations has been proposed, whereby the discrete number of atomic layers, the layer thickness and the degree of structural/chemical ordering defines the stability of each type of complexion. One well-studied complexion conformation is the equilibrium thickness (1-2nm) intergranular film (IGF). Newly revealed thinner layer complexion conformations include bilayers and trilayers. This talk will present direct evidence obtained by aberration-corrected scanning transmission electron microscopy for the existence of various complexion conformations in metals, ceramics and semiconductors. The findings have important implications to the development of new materials with improved performance by mechanism-informed design.

9:00 AM Invited

Defect Structures of Interphase Boundaries in Metallic Nano-Composites: *Amit Misra*¹; Qiangmin Wei¹; Richard Hoagland¹; Xiang-Yang Liu¹; Dhriti Bhattacharyya²; ¹Los Alamos National Laboratory; ²ANSTO

In nano-composites as the length scale of the constituent phases decreases to below approximately 5 nm, the interphase boundaries begin to dominate the mechanical behavior and radiation damage tolerance. It is therefore crucial to understand the atomic arrangements and defect structures of interphase boundaries in nano-composites. This presentation will review several unusual interface structures that were observed in model systems such as V-Ag and Al-TiN using high-resolution transmission electron microscopy. Atomistic modeling has helped elucidate the mechanisms that give rise to unusual interface structures such as Al layers in twin orientation in Al-TiN, and multiple orientation relationships and tetragonal distortions in V-Ag. This research is supported by DOE, Office of Science, Office of Basic Energy Sciences.

9:30 AM Invited

Structural and Compositional Transitions Across Interfaces in Titanium Alloys (Invited): Soumya Nag¹; Arun Devaraj¹; Robert Williams²; Gopal Viswanathan³; Jaimie Tiley³; Hamish Fraser²; *Rajarshi Banerjee*¹; ¹University of North Texas; ²The Ohio State University; ³Air Force Research Laboratory

The atomic-scale study of solid-solid interfaces in multi-phase multi-component titanium alloys is a challenging but important endeavor. This presentation highlights the coupling of advanced characterization techniques, such as aberration-corrected high resolution transmission electron microscopy (HRTEM and HRSTEM), and atom probe tomography, to address the structural and compositional transition at the atomic scale across solid-solid interfaces in titanium alloys. The specific interfaces to be discussed include the interface between the hcp α precipitates and the bcc β matrix as well as that between the metastable hexagonal ω precipitates and the bcc β matrix. Possible implications of such detailed interface analyses on the solid-solid transformation mechanisms leading to the formation of these precipitates in titanium alloys will also be discussed.

10:00 AM Break

10:10 AM

Gradient Energy, Interfacial Energy and Interface Width: an Example from Ni-Base γ/γ' Alloys: *Alan Ardell*¹; ¹National Science Foundation

A method is presented for calculating the gradient energy, χ , and interface width, δ , from concentration profiles across precipitate-matrix interfaces. This is accomplished provided the interfacial free energy, σ , is known. The relationship between these quantities is $s = 2\chi\Delta X^2/3\delta$, where ΔX is the difference between the solute concentrations in the precipitate and matrix phases. Interfaces between γ and γ' phases from 2 sources are examined. One originates from Monte Carlo simulations of a planar γ/γ' interface in binary Ni-Al alloys and the other from experimental APT measurements across γ/γ' precipitate interfaces in a ternary Ni-Al-Cr alloy. The analysis involves fitting the concentration profiles using the sigmoid function. Meaningful values of χ and δ are obtained even for incomplete profiles, and the magnitudes of χ (typically 10^{-8} to 10^{-10} J/m) compare favorably to those used in phase-field simulations. Free energy is not needed in the analysis.

10:30 AM

Modeling Nickel Surfaces and Grain Boundaries with the Fragment Hamiltonian Model: Helen Telila¹; Susan Atlas²; *Steven Valone*¹; ¹Los Alamos National Laboratory; ²University of New Mexico

Modeling multiple phases, surfaces, and grain boundaries of even an elemental material like nickel within a single atomistic model continues to present challenges. For instance, two separate modified embedded atom method potentials must be invoked to model the pressure and temperature axes of the phase diagrams of iron and zirconium. Here we present a new method of generating atomistic potentials, the Fragment Hamiltonian (FH) model that is aimed at producing a unified model. The FH model holds many similarities to second-moment tight-binding and embedded atom models. In contrast to those two models, the FH model has a second embedding term that contains an effective gap energy that recognizes differences in metallic character among different defects and phases. Both embedding terms contain important coordination dependencies that play an equally important role as the effective gap. Both of these properties are essential for unifying atomistic models.

10:50 AM

Grain Boundary Diagrams: A New Materials Science Tool: *Jian Luo*¹; Xiaomeng Shi¹; Naixie Zhou¹; ¹Clemson University

Recent research to develop grain boundary (GB) “phase” (complexion) diagrams [Shi & Luo, PRB 2011] and relevant experiments are reviewed. HRTEM studies revealed the stabilization of impurity-based, nanometer-thick, quasiliquid, intergranular films below the bulk solidus lines [Luo, Crit. Rev. Solid State Mater. Sci. 2007]. Enhanced diffusion in these films explained a long-standing mystery regarding the origin of “solid-state activated sintering”. Thermodynamic models were developed to construct a preliminary type of GB diagrams – “lambda diagrams”. A computed GB diagram predicted that a retrograde solubility in a binary alloy could lead to a decrease in the GB diffusivity with increasing temperature, and this counterintuitive prediction was experimentally verified [Shi & Luo, PRL 2010]. The correctness and usefulness of these computed GB diagrams were demonstrated. Most recent efforts on (1) extending our models and methods from binary to ternary alloys and (2) modeling discrete GB phases (complexions) are also present and discussed.

11:10 AM

Twin Boundary Structure in Bismuth Telluride: *Douglas Medlin*¹; Q. Ramasse²; C. Spataru¹; N. Yang¹; ¹Sandia National Labs; ²SuperSTEM Laboratory, STFC Daresbury, UK

We investigate the atomic structure of the basal twin boundary in bismuth telluride (Bi_2Te_3), an important thermoelectric material. The basal planes in the perfect Bi_2Te_3 structure are arranged in a repeating sequence of 5-layer wide $\text{Te}^{(1)}\text{-Bi-Te}^{(2)}\text{-Bi-Te}^{(1)}$ packets. Thus, it is possible for the twin interface to be located at one of three distinct locations: the $\text{Te}^{(2)}$ layer, the Bi layer, or the $\text{Te}^{(1)}$ layer. Through HAADF-STEM observations, we show that the twin boundary is terminated at the $\text{Te}^{(1)}$ layer, where the stacking forms a double-layer of Te. Our observations are consistent with *ab initio* calculations. We also analyze the structure of an interfacial step at the basal twin. Through a discussion of the defect crystallography and its relationships to analogous features in face-centered-cubic metals, namely the $\{112\}$ -type interfaces that commonly terminate $\{111\}$ growth and annealing twins, we provide insight concerning the mechanisms of twin formation in Bi_2Te_3 .

11:30 AM

A Dislocation-Based Model for Design of Radiation-Tolerant Nanocomposites: *Aurélien Vattré*¹; Michael Demkowicz²; ¹CEA; ²MIT

A crystallographic model extended by analytical calculations of the elastic energies is used to predict the dislocation structures and energies of heterophase interfaces. Misfit dislocation networks are characterized by accommodating long-range strain with the coherency strain fields in the frame of the anisotropic elasticity. Applying uncertainty quantification and using atomistic simulations, the model is validated for selected interfaces and applied to designing interface interactions with extrinsic point defects. Unexpected interfaces for extreme radiation environment are discussed. This material is based upon work supported as part of the Center for Materials at Irradiation and Mechanical Extremes, an Energy Frontier Research Center funded by the U.S. Department of Energy, Office of Science, Office of Basic Energy Sciences under Award Number 2008LANL1026.



TMS 2012

141st Annual Meeting & Exhibition

Symposium in Memory of Patrick Veyssi re: Understanding the Mechanisms Controlling Plastic Flow: Dislocations Organization

Sponsored by: The Minerals, Metals and Materials Society, TMS Electronic, Magnetic, and Photonic Materials Division, TMS Structural Materials Division

Program Organizers: Georges Saada, LEM CNRS ONERA; Dennis Dimiduk, Air Force Research Laboratory; Hael Mughrabi, University Erlangen-Nuernberg; Haruyuki Inui, Kyoto University

Monday AM

Room: Europe 6

March 12, 2012

Location: Dolphin Resort

Funding support provided by: National Science Foundation

Session Chairs: G. Saada, LEM/CNRS/ONERA; R. Yang, Shenyang National Laboratory for Materials Science

8:30 AM Introductory Comments

8:40 AM Invited

Defect Kinetics on Experimental Timescales Using Atomistic Simulations: Hao Wang¹; David Rodney¹; Dongsheng Xu²; Rui Yang²; ¹INP Grenoble; ²Institute of Metal Research

In his last few years, Patrick Veyssi re got involved in molecular dynamics simulations that give access to the full atomistic details of dislocation/defect interactions. Such simulations are however limited in time and do not allow studying diffusional processes like vacancy migration. For such processes, one needs to explore the configuration space in search of activated states whose energy barriers control the thermally-activated kinetics of defects. We present here a work performed in the context of a project initiated by Patrick Veyssi re, where we studied the long-term evolution of vacancy supersaturations in FCC metals. We employed the Activation-Relaxation Technique in conjunction with kinetic Monte Carlo simulations to reach experimental timescales while retaining atomistic fidelity. Two cases are considered: severe plastic deformation and rapidly quenched metals. The simulations reveal in particular the central role of a specific and so far unidentified cluster, the pentavacancy.

9:20 AM Invited

Atomistic Simulation of the Breaking and Reaction of Dipolar Dislocations under Shear Deformation: Dongsheng Xu¹; Hao Wang¹; Rui Yang¹; David Rodney²; Patrick Veyssi re³; ¹Institute of Metal Research, Chinese Academy of Sciences; ²SIMAP-GPM2, INPG; ³LEM, CNRS-ONERA

The deformation of materials depends not only on the glide of single dislocations, but also on their group behaviors, among which dipolar dislocations play important roles. Molecular dynamics simulations were carried out to investigate the shear deformation of crystals containing dislocation dipoles of various height and density in Al and Cu with fcc and Ti with hcp structure. It was found that the passing and breaking of the dipole depend strongly on its height, and that the corresponding stress for low dipoles exceeds largely the elastic estimation, due to the dislocation reaction. Analysis shows that the resultant structures vary with dipole height, temperature and strain rate. Repeated reactions complicated the defect configuration forming faulted dipoles with 120  zigzagged configuration and loops of various size and shape. The long term evolution of the debris has been investigated with the activation relaxation technique, and the implications to further deformation discussed.

9:40 AM Invited

Dislocation Organisation in Samples of Different Sizes: Yu Lung Chiu¹; ¹University of Birmingham

Dislocation organisation at the early stage of plastic deformation is of interest for understanding the microstructure evolution and mechanical response of materials. This talk will include i) a brief review of dislocation

organisation studies carried out on single crystals of cubic structure; ii) results obtained in a more recent study of dislocation organisation in micro-sized samples; iii) dislocation organisation study using electron tomography.

10:00 AM Break

10:15 AM Invited

Mechanical Behavior and Dislocation Self-Patterning in Fatigued Single Crystalline Silicon: Marc Legros¹; CEMES-CNRS

Fatigue structures and associated mechanical behavior were widely studied in fcc metals, leading to the well known Winter and Mughrabi composite model: characteristic dipolar walls arrange themselves in persistent slip bands (PSBs), that accommodate increasing applied strain at constant stress by invading more crystalline volumes. Dislocation walls produced in fatigued single crystal Si at intermediate temperatures (800-900  C) combine features resembling those of fcc metals and some that have never been observed before: dense dipolar walls separated by low density channels, but a very organized patterning from the early stages of hardening to stress saturation. The associated mechanical behavior is also original, as no stress plateau is observed for a given temperature. Indeed, a softening is observed when the strain amplitude is increased. The thermal activation glide of dislocations in Si and the evolution of wall patterns are combined to explain the link between mechanical behavior and underlying dislocation structures.

10:45 AM Invited

Mechanisms Controlling Plastic Flow of Silicon High Stress: Jacques Rabier¹; ¹CNRS

Patrick Veyssi re has been involved in the study of plastic properties of brittle material under confining pressure below the usual brittle to ductile transition temperature. This includes materials such as semi conductors and oxides with spinel structure. Following one of the first attempts to obtain information about the plasticity of silicon under pressure (1), this paper aims at reviewing how our understanding of the plasticity of silicon has benefited from high pressure experiments, transmission electron microscopy, deformation under pressure in synchrotron beam as well as atomistic and ab initio calculations. Such high stress plasticity experiments have put forward plastic deformation mechanisms involving dislocations with compact core structures rather than expected twinning mechanisms. These mechanisms are likely to control the plasticity of silicon nanostructures as suggested by computer simulations. (1) Plastic deformation of silicon between 300 C and 600 C, J. Castaing, P. Veyssi re, L.P. Kubin, J. Rabier, Phil. Mag. A, 44 (1981) 1407.

11:15 AM Invited

An Extended Kocks-Mecking Approach with an Explicit Role of Cross-Slip on the Balance between Isotropic and Kinematic Hardening: First Application to Solutes in Ferrite: Olivier Bouaziz¹; David Barbier¹; J. D. Embury²; Guillaume Badinier³; ArcelorMittal; ²McMaster University; ³University of British Columbia

Recently, a steel obtained by adding 8% of aluminium in ferrite have been characterized using: - TEM for dislocation structure, - Tensile and Bauschinger tests. By comparison with ferrite without alloying addition, the effects of solutes are: - Increase of the total strain-hardening, - More important Bauschinger effect (kinematic hardening), - Promotion of dislocation slips planarity. If solid solution hardening is one of the most common ways to increase the yield stress of metallic materials, solutes can also change obviously the intensity and the nature of strain-hardening. Surprisingly this last aspect has been poorly discussed in literature and no approach is available to explain completely our observations. An extension of the Kocks-Mecking's approach is proposed taking into account explicitly the role of cross-slip on the balance between isotropic and kinematic hardening and describing the evolution of the planarity of slip. Validations of the new approach are finally presented.

11:20 AM Invited**Low Cycle Fatigue of Copper Single Crystals under Alien Distribution of Dislocations:** *Marek Niewczas*¹; ¹McMaster University

Latent hardening experiments have been carried out on copper single crystals under conditions of low cycle fatigue at 298K, to study behavior of the flow stress and the dislocation substructure in parent and daughter samples. The presaturation region in secondary samples exhibits stage of hardening or softening, determined by the nature of interactions between dislocations of dominant slip system with the preexisting dislocations. This stage is associated with the destabilization and rebuild of old matrix and PSB structure, leading to the collapse of new matrix and formation of new PSB's characteristic of a saturation stage. The flow stress at saturation is a function of crystallographic orientation of single crystals and it is independent on the fatigue history or the type of the preexisting dislocation substructure. Dislocation mechanisms, which may operate under these fatigue conditions that build on Patrick's Veyssi re models for refinement and annihilation of prismatic loops will be discussed.

Titanium: Advances in Processing, Characterization and Properties: Processing and Process Modeling I

Sponsored by: The Minerals, Metals and Materials Society, TMS Structural Materials Division, TMS: Titanium Committee

Program Organizers: Adam Pilchak, US Air Force Research Laboratory; Christopher Szczepanski, US Air Force Research Laboratory; Vasisht Venkatesh, Pratt & Whitney

Monday AM
March 12, 2012

Room: Oceanic 3
Location: Dolphin Resort

Session Chairs: Rodney Boyer, Boeing Company; Vasisht Venkatesh, Pratt & Whitney

8:30 AM Invited**The Evolution of "Beta-Titanium Alloys" for the Aerospace Industry:** *Rodney Boyer*¹; James Williams²; John Fanning³; ¹Boeing Company; ²The Ohio State University; ³TIMET

Beta and metastable-beta titanium alloys have been in production since the early 1960's – an early alloy (Ti-13V-11Cr-3Al) was used extensively on the SR-71 Blackbird. There are two types of metastable beta-alloys, the lean beta-alloys such as Ti-17 and Ti-6-2-4-6 and numerous alloys that are richer in β -stabilizer content such as Ti-15-3. These types may require different processing to optimize their properties. The beta-alloys sometimes offer significant processing advantages, such as the capability for cold rolling. In some instances the forging flow stresses and temperatures are lower. In addition, beta-alloys offer a significant strength advantage over alpha- and alpha/beta- alloys, which has been the primary driver for their use in aerospace applications – where weight savings are a prime consideration. The advantages and disadvantages of beta-alloys will be discussed along with some of their unique characteristics, and the evolution of their applications in the aerospace industry.

9:00 AM Invited**Integrated Computational Materials Engineering: Recent Progress in the Advanced Titanium Microstructure and Modeling Program:** *Michael Glavicic*¹; Rod Boyer²; Tom Broderick³; Fred Cohen⁴; Yunzhi Wang⁵; Fan Zang⁶; Donald Boyce⁷; Wei-Tsu Wu⁸; Ayman Salem⁹; Ron Wallis¹⁰; Vikas Saraf¹¹; Vasisht Venkatesh¹²; Lee Semiatin¹³; ¹Rolls-Royce Corporation; ²The Boeing Company; ³General Electric Aviation; ⁴Pratt & Whitney; ⁵The Ohio State University; ⁶CompuTherm; ⁷Cornell University; ⁸Scientific Forming Technologies; ⁹Materials Resources LLC; ¹⁰Wyman-Gordon; ¹¹ATI Ladish Forging; ¹²TIMET; ¹³Air Force Research Laboratory

A summary of the progress achieved in the Advanced Titanium Microstructure Modeling program funded under the Metals Affordability Initiative (MAI) will be presented. The goal of this program is to develop

computational models that predict location specific microstructure and mechanical properties for wrought titanium alloys through the integration of phase field, crystal plasticity, variant selection, thermodynamic and neural net models into the commercially available finite element software DEFORM. Other topics to be discussed include the use of 2-point statistics in the separation of electron backscatter data (EBSD) into its primary and secondary alpha components and the incorporation of Kearns numbers for the representation of crystallographic texture into neural net models.

9:30 AM**Microstructural Evolution and Mechanical Properties of β -Titanium Ti-10V-2Fe-3Al during Incremental Forming:** *Sven Winter*¹; Sebastian Fritsch¹; Martin F.-X. Wagner¹; ¹Chemnitz University of Technology

Forming of high-strength beta titanium alloys is technologically and scientifically demanding and expensive. One approach to reduce costs is incremental forming by spin extrusion. The advantage of this process is the high utilization of material (80 %) in comparison to deep-hole drilling (40 %). In this study, we investigate the microstructural evolution and the mechanical properties of a Ti-10V-2Fe-3Al hollow shaft formed by spin extrusion, which results in varying stress-strain behavior across the wall thickness. Grain refinement from $>1 \mu\text{m}$ (edge) to $100 \mu\text{m}$ (center) is observed. Subsequent heat treatments can be used to achieve homogeneous properties throughout the shaft's cross section. Even higher strengths are associated with the precipitation of primary α -phase. Our results for the high-strength beta titanium alloy Ti-10V-2Fe-3Al illustrate the potential of spin extrusion, combined with suitable heat treatments, to produce hollow shafts with improved properties at lower costs.

9:50 AM**Low-cost Ultrafine Grained Titanium Sheet Production by Extrusion-Machining:** Kayla Calvert¹; Wilfredo Moscoso²; Mert Efe³; Dinakar Sagapuram³; Srinivasan Chandrasekar³; *Kevin Trumble*³; ¹University of California San Francisco; ²Pontificia Universidad Catolica Madre y Maestra; ³Purdue University

Large Strain Extrusion Machining (LSEM), a single-step deformation technique that exploits large strains of machining and dimensional control of extrusion, is introduced as a low-cost method for the production of commercially pure Grade 2 titanium strips (~2 cm wide and 0.3 mm thick). Cost analysis indicates that LSEM is cost-efficient especially in producing sheet forms of metallic materials having limited workability like titanium, compared to the conventional rolling. TEM investigations revealed that the process is also capable of achieving equiaxed ultrafine grain structures (~200 nm grain size). Crystallographic texture studies suggest that the final deformation texture can be controlled in LSEM through the process parameters. The application of the process to produce superplastic titanium sheet, for which very fine grain size and possibly certain textures are essential factors, looks promising. Economic aspects and scalability of the process to produce wider/thicker sheets will be addressed.

10:10 AM**Microstructure Evolution during Different Thermal Processing in Billet of High-Strength Titanium Base Alloy VT43:** *Anatoliy Yakovlev*¹; Nadezhda Nochovnya¹; ¹All-Russian Scientific Research Institute of Aviation Materials

In the report the new high-strength constructional titanium alloy VT43 based on system Ti-Al-Mo-V-Cr-Nb-Zr-Fe intended for application in welded constructions of hydroaccumulators and capacities is considered. VT43 has high manufacture properties and profitability. Charge for VT43 costs over 20% less than pseudo β alloy VT22 and over 30% less than Ti-10V-2Fe-3Al. The electric power expense while heat treatment ($\alpha+\beta$)-alloy VT43 over 30% less than for VT22 and over 50% for Ti-10V-2Fe-3Al. Processing titanium alloy VT43 in comparison with VT22 and Ti-10V-2Fe-3Al less for 20% and 30% accordingly. Influence of different thermal processing (quenching + aging, high temperature processing + aging) on billets microstructure and mechanical properties of VT43. In this report is shown how high temperature processing + aging at 430-



TMS 2012

141st Annual Meeting & Exhibition

MONDAY AM

520 °C for 10 hours and air cooling provides the best combination of mechanical properties (fine-dispersed intergranular structures), also this processing less county duty (exception of operation of preliminary quenching).

10:30 AM Break

10:40 AM

Crystal Plasticity Finite Element Analysis of Hot Deformation of Ti-6Al-4V with Lamellar Microstructure: *Ayman Salem*¹; Surya Kalidindi²; Jaimie Tiley³; S. Semiatin³; ¹Materials Resources LLC; ²Drexel University; ³Air Force Research Laboratory

A computationally efficient homogenization technique is described to incorporate slip transmission across alpha/beta interfaces in physics-based constitutive modeling of high temperature deformation of Ti-6Al-4V with lamellar microstructure. Each two phase alpha/Beta colony was simulated by a pseudo HCP grain with the orientation of the colony's alpha-phase. Plastic deformation within the HCP grains was assumed to be accommodated by seven independent slip systems. Model parameters were calibrated using measurements from uniaxial compression testing of single colonies at 815 °C. The proposed constitutive equations were incorporated into a Taylor-type crystal plasticity model with a fully implicit time integration scheme implemented in a finite element program (ABAQUS) to predict mechanical behavior and texture evolution under hot working conditions. The methodology provided a practical technique to incorporate slip transmission in physics-based constitutive models that account for anisotropic mechanical behavior and texture evolution in alpha/beta titanium alloys.

11:00 AM

Modeling Superplastic Forming and Diffusion Bonding of Titanium Alloys: *WeiQi Luo*¹; Jae-Bong Yang¹; Ravi Shankar¹; Wei-Tsu Wu¹; Vasisht Venkatesh²; Yoji Kosaka²; Phani Gudipati²; Daniel Sanders³; Larry Hefti³; ¹Scientific Forming Technologies Corporation; ²Titanium Metals Corporation; ³The Boeing Company

Superplastic Forming/Diffusion bonding processes facilitate near-net shape forming of complex aerospace titanium components with considerable cost and weight savings. Optimizing the process variables such as temperature, pressure, time duration, etc., to achieve the desired part configuration and mechanical properties without defects can be challenging. Alpha particle coarsening occurs during this slow process. The particle size affects the flow stress behavior and consequently the stability of the superplastic deformation. The bonding time and contact pressure at the joint are the two important diffusion bonding process parameters. They are, however, location dependent as the contact condition between the sheets and applied pressure continuously evolve during the process. For better predictive capability to address these challenges, the process modeling system DEFORM has been further enhanced under a program funded by the Metals Affordability Initiative. This paper presents the methodology and model validation against the laboratory and shop floor observations.

11:20 AM

Finite Element Analysis of the Anisotropic Behavior of Ti6AL4V during Incremental Sheet Metals Forming: *Kazeem Sanusi*¹; Emad Uheida¹; *Tiaan Oosthuizen*¹; ¹University Of Stellenbosch,

Incremental sheet forming is a manufacturing process that uses a standard smooth-end tool mounted on a numerical controlled multi-axis machine. The tool rotates and follows a circular tool path to progressively deform the clamped metal sheets into the required shape. Titanium alloys have found wide applications in the aerospace and bio-medical industries due to their good strength-to-weight ratio and superior corrosion resistance. It also has good mechanical properties. This paper deals with the finite element analysis of Ti6AL4V based on elastoplastic model using an anisotropic yield criterion and hardening model for the plastic behaviour of titanium alloy. The anisotropic constitutive model is embedded in

ABAQUS for its numerical implementation based on the derivation of the implicit integration algorithm and consistent tangent modulus. The paper will help in understanding the anisotropic behaviour of Ti6AL4V during incremental sheet metals forming since most of the condition and parameter depends on the direction of anisotropic.

11:40 AM

Study on Hot Deformation Behavior of TC4 Titanium Alloy: *Yanling Lu*¹; Sihai Jiao²; Xingtai Zhou¹; Anping Dong³; ¹Shanghai Institute of Applied Physics, Chinese Academy of Sciences; ²Baoshan Iron & Steel Co., LTD.; ³Shanghai Jiao Tong University

Hot compression deformation behavior of TC4 titanium alloy was studied on Thermecmaster-Z simulator in the temperature range 850°C~1150°C and strain rate range 0.5~30s⁻¹. The results show that deformation temperature and strain rate both have significant influence on the flow stress. The flow stress decreases with the increase of deformation temperature, while increases with the increase of strain rate. The deformation mechanism of TC4 alloy exhibit dynamic recovery feature in high temperature. However, in lower temperature, dynamic recrystallization and grain boundary slip behavior may take place. Deformation activation energy values are 862.5 kJ/mol in (α + β) phase region, and 200.6 kJ/mol in β region respectively. Constitutive equations of TC4 alloy described by Zener-Hollomon parameter were formulated. Therefore, a scientific basis is provided for the reasonable choice of thermal parameters of TC4 titanium alloy.

12:00 PM

Evolution of Microstructures and Properties of Ti-44Al-6V-3Nb-0.3Y Alloy after Forging and Rolling: *Yuyong Chen*¹; Hongzhi Niu¹; Shulong Xiao¹; Ping Sun¹; Changjiang Zhang¹; ¹Harbin Institute of Technology

Generally, beta γ-TiAl alloys possess excellent hot deformability and good mechanical properties. In this paper, the evolution of microstructures and tensile properties of Ti-44Al-6V- 3Nb-0.3Y (at. %) alloy after hot forging and rolling were investigated systematically. SEM results indicated that the cast microstructure of current TiAl alloy was completely broken down and refined by forging and rolling. By SEM and TEM measurements, the detailed microstructures and phase composition in the as-forged and as-rolled conditions were characterized and compared. Fully lamellar microstructures of the deformed alloy were obtained by heat treatment of 1330°C/1h/FC + 900°C/10h; Additionally, to assess the effect of microstructure variation on mechanical properties, tensile properties were measured at room temperature and 700°C. It is an extremely effective mean to optimize the microstructures and enhance the mechanical properties of TiAl alloy by hot forging and rolling.

12:20 PM

Effect of Forging on Microstructural Characteristic and Tensile Properties of In-Situ (TiB+TiC)/Ti Composite: *Yuyong Chen*¹; Changjiang Zhang¹; Shulong Xiao¹; Dezhong Wu¹; Hongzhi Niu¹; ¹Harbin Institute of Technology

In this work, 2.5vol. % (TiB+TiC)/Ti composite was prepared by in situ casting route then 1-D forging. The microstructure and tensile properties were presented and discussed. The results indicate that the as cast microstructure can be significantly modified by 1-D forging. After forging, TiB and TiC segregated at the prior β grain boundaries within the as-cast composite tend to fracture and align perpendicular to forging direction. Reduction in aspect ratio of reinforcements and a lath is also observed. 1-D forging can enhance the strength and elongation of as cast composite significantly. However, the increment in strength is quite limited as strain temperature increases to 700 °C. Additionally, Room temperature and high temperature fracture mechanisms are also discussed as well.

T.T. Chen Honorary Symposium on Hydrometallurgy, Electrometallurgy and Materials Characterization: Plenary Session

Sponsored by: The Minerals, Metals and Materials Society, TMS Extraction and Processing Division, TMS: Hydrometallurgy and Electrometallurgy Committee, TMS: Materials Characterization Committee

Program Organizers: Shijie Wang, Rio Tinto Kennecott Utah Copper; J. E. Dutrizac, CANMET; Michael Free, University of Utah; J. Y. Hwang, Michigan Technological University; Daniel Kim, Rio Tinto Kennecott Utah Copper

Monday AM
March 12, 2012

Room: Northern A4
Location: Dolphin Resort

Funding support provided by: Rio Tinto Kennecott Utah Copper, ASARCO, and Freeport McMoRan

Session Chair: Shijie Wang, Rio Tinto Kennecott Utah Copper

8:30 AM

In Honor of Dr. Tzong T. Chen: John Dutrizac¹; *Shijie Wang*²; ¹CANMET-MMSL; ²Rio Tinto Kennecott Utah Copper

A Brief Summary of Dr. T.T. Chen's Career and Accomplishment Will Be Presented.

8:45 AM

A Review of the Behavior and Deposition of Lead, Bismuth, Antimony and Arsenic in Copper Electrorefining: *Michael Moats*¹; Shijie Wang²; Daniel Kim²; ¹University of Utah; ²Rio Tinto Kennecott Utah Copper

The behavior and deposition of lead, arsenic, antimony and bismuth can significantly affect the production of high quality cathode by copper electrorefining. A critical review of research related to these elements is presented along with comparison to industrial data where appropriate. These elements exist predominantly in the anode as complex oxides along the grain boundaries. Upon dissolution, Group 15 elements report both to the electrolyte and slimes while lead essentially enters the slimes. The deposition of the Group 15 elements appear to be influenced by several chemical interactions which are discussed. The effect of these elements on floating slimes and anode passivation is reviewed. Under normal electrorefining conditions, lead, antimony and bismuth are thought to enter the cathode through the encapsulation of slime particles. The literature indicates that arsenic enters the cathode predominantly by electrolyte entrainment. Finally, areas for future research regarding these elements are presented.

9:20 AM Plenary

Technological Overview of Zinc Industry – Now and Future: *Takashi Yoshida*¹; ¹Mitsui Mining & Smelting Co., Ltd

This paper will discuss about recent situation and future of zinc industry from the technical point of view. It includes recent problems faced on zinc industry and technological developments. One of the biggest problems of zinc industry is raw materials. Traditional zinc concentrate becomes much complicated chemical and physical properties. Thus each process faced on various problems. Also secondary resources generated so called recycling process become much important. Recycling is of course very important aspect for sustainable development of society. Secondary raw material includes also very variety of impurities not included or very low level in traditional zinc concentrate. Some problems caused by these impurities. To overcome these problems some technological challenges have been taken place. Details will be discussed in the symposium.

9:55 AM Break

10:15 AM Plenary

The Next Decade in Cu, Ni, Co and Platinum Group Metal Extraction: *Bill Davenport*¹; ¹University of Arizona

Based on recent visits to industrial smelters, refineries, and recycle plants in Africa, Asia, Europe and North America – this paper looks forward to the next decade in Cu, Ni, Co and Pt group metal extraction. It looks specifically at environmental impacts and water and energy requirements – and at technologies for reducing them.

10:50 AM Plenary

The Development of China's Molybdenum Metallurgical Technologies: *Kaixi Jiang*¹; Wang Haipei¹; Zou Xiaoping¹; Zhang Lei¹; Bangsheng Zhang¹; ¹Beijing General Research Institute of Mining and Metallurgy

China plays an important role in the world's molybdenum industry, because both China's mine output and smelter production ranked first in the world. The characteristics of China's molybdenum resources are complex, and molybdenum-nickel ores with carbon, copper-molybdenum ores and wulfenite ores can be found only in China. This paper firstly introduces China's molybdenum resource/reserve situation. Secondly, the status of molybdenum smelting technologies, especially roasting using rotary kilns and multiple-hearth furnaces, is discussed. The practices and the development of some new technologies, such as pressure leaching, solvent extraction, ion exchange and carbon adsorption for molybdenum-nickel ores and low grade molybdenite concentrates are also introduced.

11:25 AM Invited

Some Applications of Molecular Recognition Technology (MRT) to the Mining Industry: *Steven Izatt*¹; Ronald Bruening¹; Neil Izatt¹; ¹IBC Advanced Technologies, Inc.

IBC's Molecular Recognition Technology (MRT) processes selectively extract, recover, and purify a wide range of metals from a variety of process streams. The incorporation of MRT into process flow sheets greatly improves the economics of the processes. MRT separations are effective even at low metal concentrations and in the presence of much greater concentrations of competing species. MRT processes are sustainable, being economically viable, energy efficient, and environmentally friendly as well as having a low carbon footprint. Examples of MRT processes will be presented and discussed involving rhenium, gold, platinum group metals, and other metals of interest to the mining community.



TMS 2012

141st Annual Meeting & Exhibition

MONDAY AM

Ultrafine Grained Materials VII: Plenary Session

Sponsored by: The Minerals, Metals and Materials Society, TMS Structural Materials Division, TMS/ASM: Mechanical Behavior of Materials Committee, TMS: Nanomechanical Materials Behavior Committee, TMS: Shaping and Forming Committee
Program Organizers: Suveen Mathaudhu, U.S. Army Research Office; Xiaoxu Huang, Risø National Laboratory for Sustainable Energy, Technical University of Denmark; Hyoung Seop Kim, POSTECH; Terence Langdon, University of Southern California; Terry Lowe, Manhattan Scientifics, Inc.; Ruslan Valiev, Ufa State Aviation Technical University; Xiaolei Wu, Institute of Mechanics, Chinese Academy of Sciences; Michael Zehetbauer, University of Vienna

Monday AM Room: Swan 5
March 12, 2012 Location: Swan Resort

Session Chairs: Xiaoxu Huang, Risø National Laboratory for Sustainable Energy, Technical University of Denmark; Suveen Mathaudhu, U.S. Army Research Office; Terry Lowe, Manhattan Scientifics, Inc.; Michael Zehetbauer, University of Vienna

8:30 AM Introductory Comments

8:35 AM Keynote

Physics of Grain-Size Effect on Twinning in Nanostructured fcc Metals: *Yuntian Zhu*¹; Xiaolei Wu²; Xiaozhou Liao³; ¹North Carolina State University; ²Institute of Mechanics; ³The University of Sydney

Deformation twinning is an effective approach for enhancing the ductility while at the same time also improves the strength. In this talk, I will present the physics and modeling on the effect of grain size on deformation twinning in nanocrystalline fcc metals. An analytical model based on observed deformation physics, i.e. grain boundary emission of dislocations, will be first presented. The result will be then compared with experimental observation of an optimum grain size range for the formation of deformation twins and the inverse grain-size effect. The physical origin of the observed grain size effect will be delineated.

8:55 AM Invited

Deformation Mechanisms in Nano and Ultrafine Crystalline Nickel: *Marisol Koslowski*¹; ¹Purdue University

Deformation of polycrystalline materials includes mechanisms in the grain interior as well as in the grain boundaries. The competing grain-boundary and dislocation-mediated deformation mechanisms in crystalline Nickel with grain sizes in the range 4 nm to 128 nm are investigated with numerical simulations. We present a three dimensional phase field model that tracks the evolution of grain boundaries and individual dislocations, including the elastic interaction, the core and the stacking fault energies. Our model shows that the transition from Hall-Petch to inverse Hall-Petch as the grain size is reduced cannot be characterized only by the average grain size, but it is also affected by the grain boundary energetics, the grain size distribution and the initial defect concentration. We find that the grain size corresponding to the maximum yield stress (the transition from Hall Petch strengthening with decreasing grain size to inverse Hall Petch) decreases with increasing grain boundary energy.

9:15 AM Invited

Near Surface Nanoscale Structures Produced by Plastic Deformation: *Niels Hansen*¹; Xiaodan Zhang¹; Yukui Gao²; Xiaoxu Huang¹; ¹Risø DTU; ²Beijing Institute of Aeronautical Materials

Hard surface microstructures produced by plastic deformation can improve the fatigue and wear resistance of industrial structures. Such structures have been produced in iron by shot peening and by surface mechanical attrition and characterized by transmission electron microscopy, electron backscattering diffraction and microhardness testing. The structure is subdivided by boundaries forming a lamellar structure. Such a structure

also characterizes samples cold rolled to medium and high strains where the structure is graded with respect to the lamellar spacing with decreases with increasing strain. This dependency can be represented by a power law relationship which allows the strain to be estimated at different depths in the near surface layer and the stress strain relationship to be derived based on the microhardness data. A discussion will focus on the structural evolution in the nanoscale regime and on strengthening mechanisms.

9:35 AM Invited

Strain-Induced Phase Transformations under Compression and Shear in Rotational Diamond Anvil Cell: *Valery Levitas*¹; ¹Iowa State University

Experimental results on phase transformations obtained under compression and large plastic shear of materials in rotational diamond anvil cell (RDAC) are presented. Multiscale (nano-, micro- and macroscales) continuum thermodynamic theory and simulations for strain-induced transformations were developed, which explain a number of mechanochemical phenomena. Specifically, the theory explains why the superposition of plastic shear and high pressure in RDAC leads to: (a) significant reduction (by a factor of 3-5) of transformation pressure and pressure hysteresis, (b) appearance of new phases (in particular, nanostructured), which were not obtained without shear, (c) substitution of reversible transformation by an irreversible one, and (d) strain-controlled kinetics. New phenomenon of phase transformation induced by rotational plastic instability is revealed. It allowed us to reduce the pressure for irreversible phase transformation from rhombohedral to cubic BN from 55 GPa under hydrostatic pressure to 5.6 GPa. Transformation-induced plasticity under pressure and shear is revealed, quantified and modeled.

9:55 AM Invited

Tailoring or Grading Sheet Materials by Using New Concepts in ARB-Processing: *Heinz Werner Höppel*¹; ¹University Erlangen-Nürnberg

The ARB-process is well known to produce UFG sheet materials in larger quantities. Besides, this technique also allows to produce multiphase, tailored or graded sheet materials with promising properties. By an intelligent ARB-processing 3D-architected multiphase materials can be achieved aiming for locally tailored materials properties. It is shown, that the materials properties can be tailored locally by an adopted powder spraying process via the ARB process. Moreover, by using an appropriate post ARB-heat treatment, this technique can also be used to strengthen the sheet material by the formation of intermetallic phases in the sheet. In the talk, microstructural and mechanical properties with respect to the processing parameters will be discussed in detail.

10:15 AM Invited

Analysis of Plastic Flow during High-Pressure Torsion: *Roberto Figueiredo*¹; Maria Teresa Aguilar¹; Paulo Cetlin¹; Terence Langdon²; ¹Federal University of Minas Gerais; ²University of Southern California

It is now established that high-pressure torsion is able to produce bulk nanostructured metallic materials through severe plastic deformation-SPD. This technique produces material with the finest grain structures among all SPD processes. Despite the recent rise in interest, there are many process parameters whose influence on the sample is not clear. For example, some researchers consider the distribution of deformation homogeneous while others report heterogeneity, the hydrostatic stress and the temperature rise due to plastic strain are also not clear. It is thus important to clarify these aspects in order to analyze structure and properties evolution. The present paper reviews the experimental and theoretical results on processing parameters during HPT.

10:35 AM Break

10:50 AM Invited

Microstructure and Microtexture Evolution in Pure Metals after Ultra-High Straining: *Alexander Zhilyaev*¹; Terence Langdon²; ¹School of Engineering Sciences, University of Southampton, Southampton SO17 1BJ, U.K. and Institute for Metals Superplasticity Problems, Russian Academy of Science, 39 Khaturlina, Ufa, 450001 Russia); ²School of

Engineering Sciences, University of Southampton, Southampton SO17 1BJ, U.K. and Departments of Aerospace & Mechanical Engineering and Materials Science, University of Southern California, Los Angeles, CA 90089-1453, U.S.A.

Ultrafine-grained and even nanostructured materials can be manufactured using ultra-high straining by ECAP, HPT, machining and their combinations, such as machining of ECAP specimens, HPT plus ECAP and HPT of machining chips. The report will present recent results of investigations of the microstructure and microtexture of pure copper, nickel and aluminum subjected to different deformation processes to ultimately high imposed strain. Comparison of microstructure, dislocation density and microhardness developed during combinations of different strain paths have been performed. All characteristics have been analyzed by x-ray, transmission and scanning electron microscopy, OIM. Influence of different processing routes is discussed in terms of accumulated strain and microstructure refinement. Saturation in grain refinement is discussed in terms of recovery taking place during ultra-high strain deformation.

11:10 AM Invited

Dilatometry – A Powerful Tool for the Study of Defects in Ultrafine Grained Metals: *Wolfgang Sprengel*¹; Bernd Oberdorfer¹; Eva-Maria Steyskal¹; Roland Würschum¹; ¹Graz University of Technology

Vacancies, dislocations and interfaces are structural defects that are deliberately introduced into solids during grain refinement processes based on severe plastic deformation (SPD). Specific combinations of these defects determine the improved mechanical properties of the obtained ultrafine grained materials. High-precision, non-equilibrium dilatometry, i.e., measurement of the irreversible macroscopic length change upon defect annealing, provides a powerful technique for the characterization and the study of the kinetics of these defects. Dilatometry is applied to determine absolute concentrations of vacancies, to characterize dislocation processes, and to assess grain boundary excess volume in pure, fcc and bcc ultrafine grained metals processed by SPD.

11:30 AM Invited

The Combined Effect of Grain Boundaries and Second Phase Particles on the Flow Stress of Nanocrystalline Metals: *Krzysztof Kurzydłowski*¹; Romuald Dobosz¹; Malgorzata Lewandowska¹; ¹Warsaw University of Technology

Numerical FEM simulations were made to provide an insight into the possible combination of grain boundary and second phase particle strengthening in nanocrystalline metals. Because grain boundary sliding is one of the major deformation mechanisms in these materials special attention was paid to the role of nanoparticles located at the grain boundaries. The results obtained show that second phase particles located at the grain boundaries may contribute to the strengthening process, thereby compensating for the loss of strength brought about by grain boundary sliding. However, the effect of the particles strongly depends on the relative contribution of grain boundary sliding to the overall deformation process. In addition, particles located at grain boundaries under conditions of grain boundary sliding significantly influence the distribution of plastic deformation making it more homogenous. These findings of numerical analyses are well supported by the recent results obtained on a SPD processed aluminium alloy.

11:50 AM Invited

The Super-Strength of Ultrafine-Grained SPD-Processed Alloys Due to Grain Boundary Segregations: *Nariman Enikeev*¹; Xavier Sauvage²; Maxim Murashkin¹; Ruslan Valiev¹; ¹Ufa State Aviation Technical University; ²University of Rouen, Groupe de Physique des Matériaux, CNRS

It is demonstrated that the strength of ultrafine-grained (UFG) alloys produced by severe plastic deformation (SPD) can be increased not only by grain refinement but also by formation of grain boundary (GB) segregations. On the example of several Al alloys it is shown that SPD-induced segregations have unusual morphology (segregation width and concentration of alloying elements) as compared to conventional

GB segregations. This phenomenon is explained by influence of non-equilibrium grain boundaries typical for SPD processed materials on the segregation formation and generation of lattice dislocations from GBs, correspondingly. As result we observed super-strength in UFG alloys, when yield stress values were considerably higher than those predicted by the Hall-Petch relationship extrapolated to the ultrafine grain size range.

12:10 PM Invited

Ultrafine-Grained Shape Memory Alloys: *Thomas Waitz*¹; Clemens Mangler¹; Gerd Steiner¹; Arno Kompatscher¹; Martin Peterlechner²; Wolfgang Pranger³; Thomas Antretter³; Franz Dieter Fischer³; Peter Müllner⁴; ¹University of Vienna; ²University of Muenster; ³University of Leoben; ⁴Boise State University

Grain size can strongly affect the unique thermomechanical properties of shape memory alloys that are based on a martensitic phase transformation. Grain size at the nanoscale can hinder the shape memory effect by suppressing the thermally induced martensitic transformation. However, ultrafine-grained shape memory alloys can show tailored functional properties and enhanced strength. NiTi shape memory alloys, NiTiHf high temperature shape memory alloys and NiMnGa high temperature ferromagnetic shape memory alloys were subjected to severe plastic deformation followed by annealing to achieve grain sizes in the range of several tens to several hundreds of nm. Different pathways of the evolution of the small grains that might involve the formation of an intermediate amorphous phase were encountered. The phase stability and the martensitic morphology of small grains were systematically investigated. Considering a size dependent energy barrier opposing the transformation the results were modelled using the general thermodynamic framework of martensitic phase transformations.

2012 Functional and Structural Nanomaterials: Fabrication, Properties, Applications and Implications: Nanomaterials for Information Technology

Sponsored by: The Minerals, Metals and Materials Society, TMS Electronic, Magnetic, and Photonic Materials Division, TMS: Nanomaterials Committee

Program Organizers: Jiyoung Kim, University of Texas; David Stollberg, Georgia Tech Research Institute; Seong Jin Koh, University of Texas at Arlington; Nitin Chopra, The University of Alabama; Terry Xu, UNC Charlotte

Monday PM
March 12, 2012

Room: Pelican 1
Location: Swan Resort

Session Chairs: David Stollberg, Georgia Tech Research Institute; HyunJung Shin, Kookmin University

2:00 PM Introductory Comments

2:05 PM Invited

In-Situ Studies of High-K/III-V Interfaces for Advanced Electronics: *R.M. Wallace*¹; ¹Department of Materials Science and Engineering, University of Texas at Dallas

A host of new materials are under research to enable the continuation of improved device performance through scaling. Among these, III-V alloy materials such as InGaAs, InGaP, InGaSb and GaN are being studied for advanced logic and power applications. A key component for these systems is the interface between the high-k gate dielectric and the III-V material of choice. This talk will review our recent studies of the physicochemical properties of this interface using in-situ deposition and analytical methods, as well as electrical behavior. We will examine the correlations observed between physical analysis and the electrical behavior, particularly with regard to defects which can generate states that result in Fermi level pinning. This work is supported by the NSF under



TMS 2012

141st Annual Meeting & Exhibition

MONDAY PM

award ECCS-0925844, the AFOSR/AOARD under award FA2386-11-1-4077, the FCRP Materials Structures and Devices (MSD) Center, and the SRC Nanoelectronics Research Initiative and NIST through the Midwest Institute for Nanoelectronics Discovery.

2:40 PM Invited

Stimuli Responsive Field-Effect Transistors Integrated with Nanomaterials: *Nae-Eung Lee*¹; Nguyen Thanh Tien¹; D.-J. Kim¹; I.-Y. Sohn¹; Tran Quang Trung¹; O.J. Yoon¹; ¹Sungkyunkwan university

Stimuli-responsive field-effect transistors (FETs) that are responsive to physical, chemical or biological stimuli are very interesting for various sensing applications due to simplicity of design, fabrication and signal detection. In our work, stimuli-responsive FETs were designed and fabricated by directly incorporating various functional materials as active channel, electrode or gate dielectric layers into the FET structure. In order to enhance the sensitivity of FETs to external stimuli and obtain additional functionalities such as flexibility, transparency, and/or stretchability, nanocomposite films and two-dimensional carbon nanomaterials were employed as gate dielectrics, active channel or electrode in the FET structure. In physically responsive FETs (Physi-FETs), for example, gate dielectric materials with piezoelectricity and pyroelectricity and active channel materials with piezoresistivity were directly incorporated into the FET structure. The generalization of this concept is shown to be applicable to multi-modal sensing of pressure, strain, and IR in the form of flexible physi-FETs.

3:15 PM

Interface Engineering as a Tool to Enhance Efficiencies of Carbon Nanotube Based Devices: *Indranil Lahiri*¹; Wonbong Choi¹; ¹Florida International University

Carbon nanotubes (CNT) are proposed for improved performance of numerous devices – sensors to solar cells and biomedical to electronic devices. However, desired seamless integration, reliable performance and extended device lifetime of CNT-based devices necessitates great structural stability. One of the most critical issues in structural stability is interfacial bonding between CNTs and substrate. To address this vital issue, we present an interface engineered CNT based bulk structure on copper substrate. CNT-substrate bonding is enforced with proper selection of interfacial layer, on various substrates. Such CNT-based structures are applied successfully in cold field emission devices as cathode and in Li-ion batteries as anode. Interface engineering, proposed in this study, is expected to enhance bonding between CNTs and the substrate, contributing towards better structural stability and device life. These newly developed CNT-based electrodes, strongly bonded to Cu current collectors, are anticipated to enhance performance of future electronic and electrochemical devices.

3:30 PM

In-Situ Electrical Studies on Ozone Functionalization of Graphene: *Srikar Jandhyala*¹; Greg Mordt¹; Jiyoung Kim¹; ¹University of Texas at Dallas

It has been reported that ozone (O₃) functionalization allows for conformal deposition of high-quality ALD (atomic layer deposition) Al₂O₃ on graphene surface without damaging it. In this study we have investigated the functionalization mechanisms theoretically using ab-initio calculations and experimentally using in-situ electrical monitoring of transport properties. It is found that the ozone molecules at 300 K are reversibly physisorbed on the surface of graphene and the physisorption bonding is removed immediately after acting as nucleation sites for dielectric deposition. We also performed in-situ studies with H₂O and O₂, two other common oxidants used for deposition of dielectrics using ALD technique. It was found that these species have no significant effect on the charge transport characteristics of graphene at 300 K. This suggests that unlike O₃, H₂O and O₂ have minimal interaction with graphene, which explains the reason for the disability to deposit oxides on graphene using these oxidants.

3:45 PM Break

4:00 PM Invited

Nano-Floating Gate Memory Devices: *Jang-Sik Lee*¹; ¹Kookmin University

In recent decades, memory device technology has advanced through active research and the development of innovative technologies. Single-transistor-type flash memory device is one of the most widely used forms of memory devices because the device structure is simple and the scaling is feasible. Nano-floating gate memory (NFGM) device is a kind of flash memory devices that use nanocrystals as the charge-trapping elements. The use of nanocrystals has advantages over memory devices that rely on other methods, such as discontinuous trap sites and controllable trap levels. Nowadays considerable progress has been made in the field of NFGM devices, and novel application areas have been explored extensively. This presentation focuses on new technologies that are advancing these developments. The discussion highlights recent efforts and research activities regarding the fabrication and characterization of nonvolatile memory devices that use a nanocrystal layer as the charge-trapping element for future device applications.

4:35 PM

Fabrication and Magnetic Properties of Graded Magnetocrystalline Anisotropy Fe(Ni)Pt Nano-Dots: *Bianzhu Fu*¹; Aaron Gin²; James Harrell¹; *Gregory Thompson*¹; ¹University of Alabama; ²Sandia National Laboratories

Increasing magnetic storage densities requires a decrease in the magnetic thin film grain size that then approaches the superparamagnetic limit where the magnetization randomly fluctuates because of thermal energy considerations. The L1₀ phase of FePt has a high magnetocrystalline anisotropy energy, K_u, making it a candidate material for thermally stable magnetization at these nanoscale grain sizes. Unfortunately, its high K_u prevents it from being 'written' with conventional write head field strengths. This presentation will address how compositionally grading FePt with Ni provides the ability to control the K_u enabling switching of the magnetically soft end with stabilization from the magnetically hard end. The films have been epitaxially grown off of MgO substrates, e-beam patterned into an array of nano-dots and magnetically characterized to determine switching field and thermal stability advantages.

4:55 PM

Fabrication of Nanocrystalline InGaZnO Films: The Microstructure and the Device Performance of Their Thin Film Transistors: *Haseok Jeon*¹; Hwayoul Choi¹; Mi Ran Moon¹; Sekwon Na¹; Hyoungsub Kim¹; Hoo-jeong Lee¹; ¹Sungkyunkwan University

In recent years, transparent oxide semiconductors (TAOS) have captivated researchers by offering a combination of several technologically important features high electron mobility, high transparency, the capability for low temperature processing, etc., which makes them an excellent candidate for the active layer of thin film transistors for display applications. Among this class of materials, amorphous IGZO has been the focus of many research and development efforts after its first demonstration as the active layer of TFTs. Here, we fabricated nanocrystalline IGZO films by co-sputtering from InGaO and ZnO targets with a high Zn ratio at an elevated temperature. By combining HRTEM and XRD analysis, we unraveled that the nanocrystalline structure sensitively changed depending on the process conditions (substrate temperature and Zn ratio). Furthermore, measurement of the electrical characteristics of the transistors fabricated from the films disclosed that the microstructure changes induced by substrate heating profoundly influenced the device performance.

5:10 PM

Discovery a Frozen Nano-Domain State in Non-Metallic Ferroelastic System: Yan Ni¹; Zhen Zhang¹; Xiaobing Ren²; ¹Frontier Institute of Science and Technology, Xi'an Jiaotong University; ²National Institute for Materials Science, Japan

A fascinating state which is characterized by frozen nano strain domains has been identified in ferroelastic system as strain glass. It is reported that point defect, e.g. excess Ni in TiNi alloy, drive the crossover from martensite to strain glass. However, all reported strain glass is metallic alloys. Thus, it is a question that is there a strain glass in the ferroelastic ceramics? In present work, we studied the cubic (C) to tetragonal (T) and tetragonal (T) to Orthorhombic(O) transition in CaTiO₃ ceramics with doping La defect. It is found that T-O transition is easier to be suppressed than C-T transition as the concentration of La increases. When the La concentration excess a critical value, a strain glass is found in tetragonal phase and random-distributed nanodomains are observed. In addition, a new phase diagram involving strain glass regime is established for Ca_(1-x)La_{2x/3}TiO₃ ceramics.

2012 Symposium on Surfaces and Heterostructures at Nano- or Micro-Scale and Their Characterization, Properties, and Applications: Carbon Nanomaterials and Heterostructures

Sponsored by: The Minerals, Metals and Materials Society, TMS Electronic, Magnetic, and Photonic Materials Division, TMS Materials Processing and Manufacturing Division, TMS: Energy Conversion and Storage Committee, TMS: Nanomaterials Committee, TMS: Surface Engineering Committee, TMS: Young Leaders Committee, TMS: EMPMD Council

Program Organizers: Nitin Chopra, The University of Alabama; Ramana Reddy, The University of Alabama; Arvind Agarwal, Florida International University; Sandip Harimkar, Oklahoma State University; Jiyoung Kim, University of Texas at Dallas; Christopher Matranga, National Energy Technology Laboratory

Monday PM
March 12, 2012

Room: Pelican 2
Location: Swan Resort

Session Chairs: Ramana Reddy, The University of Alabama; Nitin Chopra, The University of Alabama

2:00 PM Invited

Application of Carbon Nanotubes – Energy to Bioelectronic Sensor: Wonbong Choi¹; Indranil Lahiri¹; Santanu Das¹; Chiwon Kang¹; ¹Florida International University

A wide variety of carbon nanostructures, from zero-dimensional fullerene through one dimensional carbon nanotube to two dimensional graphene, have attracted attention of scientific community worldwide for their exciting properties. C-based nanomaterials have found applications in a vast field – electronics, sensors, biotechnology, energy, structural etc. In Nanomaterials and Device Lab at FIU, we have concentrated our effort in developing new engineering nanomaterials (graphene, carbon nanotubes) and their device applications in the field of energy generation and storage, nanoelectronics, and bio-electronic sensors. This presentation aims to capture those recent research efforts in synthesis and applications of carbon nanotubes in Li-ion battery, bioelectronic sensor and high power field emission.

2:35 PM Invited

Vertically Aligned and Periodically Distributed Carbon Nanotube (CNT) Bundles Grown by a Combination of Laser Interference Ablation and Metal-Catalyzed Chemical Vapor Deposition (CVD): Dajun Yuan¹; Wei Lin¹; Rui Guo¹; C. P. Wong¹; Suman Das¹; ¹Georgia Institute of Technology

Carbon Nanotubes (CNTs) offer attractive anisotropic mechanical, thermal, and electrical properties. Scalable fabrication of CNT bundles is essential to future advances in several applications. Nevertheless, the creation of geometries at sub-micron scales in CNT bundles with existing fabrication methods remains a difficult challenge. Here, we report on the development of a simple, two-step method for fabricating vertically aligned and periodically distributed CNT bundles. The method involves laser interference ablation of an iron film followed by CNT growth through metal-catalyzed chemical vapor deposition (CVD). CNT bundles with sizes ranging from 500 nm to 5 μm in width, and 50 to 200 μm in length, are grown atop the patterned catalyst over areas spanning 5 cm². The CNT bundles exhibit a high degree of control over size, orientation, uniformity, and periodicity. Characterization of the catalyst post-ablation of the CNT bundles is conducted through AFM and SEM.

3:10 PM

Structural Evolution and Growth Mechanism of Hierarchical Heterostructures Comprised of Carbon Nanotubes Decorated with Nanoparticles: Wenwu Shi¹; Nitin Chopra¹; ¹The University of Alabama

We report formation and structural evolution of CNT-nickel/nickel oxide (Ni/NiO) core/shell nanoparticles (CNC) through a simple and single step synthetic approach. High surface-to-volume ratio and aspect ratio of chemical vapor deposition (CVD)-grown CNTs (average diameter ~46±16.4 nm) allowed for the uniform coating with Ni/NiO core/shell nanoparticles (average diameter ~12±2 nm). The crystal structure, morphology, and phases of CNC heterostructures were characterized using high resolution SEM, TEM, XRD, and Raman. Subsequently, as-produced CNC heterostructures were incorporated into polymers and evaluated for their chemical functionality and morphology using FTIR, UV-vis transmittance, SEM, and swelling/shrinking studies. Finally, these heterostructures were further studied for their thermal stability using Raman spectroscopy and XPS studies.

3:30 PM

Synthesis of Porous Graphene Shells with Embedded Noble Metal Nanoparticles: Wenwu Shi¹; Robert Wright¹; Nitin Chopra¹; ¹The University of Alabama

We report the formation of nanowire-nanoparticles heterostructures and their conversion into porous graphene embedded with nanoparticles. Nanowires were synthesized by chemical vapor deposition and noble metal nanoparticles were linked onto these nanowires coating the latter uniformly. These heterostructure were further utilized as catalysts for the growth of porous graphene shells in a chemical vapor deposition process. The synthesized heterostructures were fully characterized with SEM, TEM, EDX, SAED, and Raman spectroscopy. Changes of nanoparticles diameter, nanoparticle density, nanowire diameter after graphene growth were thoroughly studied. These heterostructures were further demonstrated to have unique SERS capability.

3:50 PM

Systematic Studies on the Formation of Graphene on Noble Metal Nanoparticles: Wenwu Shi¹; Nitin Chopra¹; ¹The University of Alabama

Encapsulation of metal nanoparticles into graphene layers could bring multifunctionality and enhanced stability. Herein, we report a detailed systematic study focused on fundamentally understanding the growth of graphene encapsulated noble metal nanoparticles in a chemical vapor deposition process. Different parameters (reaction temperature, duration, H₂ concentration, type of nanoparticles, type of hydrocarbon, hydrocarbon feed speed, plasma oxidation of nanoparticles) were considered to understand the formation mechanism of graphene. The hybrid nanoparticles were characterized by transmission electron



TMS 2012

141st Annual Meeting & Exhibition

MONDAY PM

microscopy and Raman spectroscopy. It was found that oxidation of Au nanoparticles is a prerequisite for the formation of graphene and optimal reaction temperature, H₂ concentration, and hydrocarbon feed rate were identified. It was observed that increase of reaction duration ruptures the graphene shell and result migration of nanoparticles out from graphene shell.

4:05 PM Break

4:20 PM

Evolution of Gold Nanoparticles in a High Temperature Process and Patterned Growth of Graphene Encapsulated Nanoparticles: *Junchi Wu*¹; Larry Summerville¹; Nitin Chopra¹; ¹The University of Alabama

Different sizes and shapes of gold particles were organized on silicon wafer by annealing gold thin films. The nanoparticle patterning was achieved on the silicon wafer by correlating morphology, size, and structure with processing conditions. The crystal structure and optical property of annealed sample was examined by XRD and UV-DRS. Scanning electron microscopy (SEM) was used for morphology and migration study of Au film. During annealing, Au film dewetted the Si surface and migrated to reduce the surface energy, resulting into branched gold islands or particles. These patterned nanoparticles were further utilized for the patterned growth of graphene encapsulated gold nanoparticles.

4:35 PM

Growth Mechanisms of Graphene Encapsulated Nanoparticle and Effect of Catalyst Shape on the Graphene Growth: *Junchi Wu*¹; *Nitin Chopra*¹; ¹The University of Alabama

A systematic study was performed on morphological evolution of gold nanoparticles in both single-step method and seed-growth method. The size, shape, crystallinity, and sample heterogeneity for the nanoparticles were characterized to evaluate the effect of growth parameters. As a next step, gold nanoparticles were surface oxidized used as a catalyst for the growth of graphene shells in a chemical vapor deposition method, resulting in graphene encapsulated gold nanoparticles. The oxidation kinetics of gold nanoparticles was studied. These nanoparticles were characterized by high-resolution transmission electron microscopy (TEM). Oxidation behavior of gold nanoparticles was studied by scanning electron microscopy (SEM) and X-ray photoelectron spectroscopy (XPS). Morphology and aggregation of gold nanoparticles during the CVD growth affected the graphene shells and was studied here. Raman spectroscopy/microscopy were used to evaluate the quality of graphene shells produced and chemical mapping charts were generated to understand the large area growth of these hybrid nanoparticles.

4:50 PM Invited

Defects in Carbon Based Nanostructures: Applications to Novel Morphologies and Device Concepts: *Prabhakar Bandaru*¹; ¹UC, San Diego

Defects in carbon nanotubes can be exploited for the synthesis of interesting coiled structures or in electrodes exhibiting fast electron transfer kinetics. For example, the introduction of disclinations (in terms of pentagonal and heptagonal defects) into graphene sheets can motivate helical structure. In this talk, I will review the influence of defects in determining the electrochemical properties of carbon nanostructures. We have seen that exposure of carbon nanotubes to argon and hydrogen irradiation can be used to either increase/reduce the defect density, through Raman spectroscopy. In cyclic voltammetry (CV) measurements, we have seen that only the Ar treated samples exhibit perfect reversible Nernstian behavior characteristic of ideal electrodes. The application of such studies to novel devices, sensors, capacitors, etc. will be discussed.

5:25 PM Invited

Localized Plasmon Enhancement at Dopant Sites in Graphene: *Stephen Pennycook*¹; *Wu Zhou*¹; *Jaekwang Lee*¹; *Jagjit Nanda*¹; *Socrates Pantelides*²; *Mark Oxley*¹; *Micah Prange*¹; *Juan-Carlos Idrobo*¹; ¹Oak Ridge National Laboratory; ²Vanderbilt University

Using Z-contrast imaging combined with electron energy-loss (EEL) spectrum imaging in scanning transmission electron microscopy (STEM), combined with theoretical simulations, we show that a single point defect can act as an atomic antenna in the petaHertz (10¹⁵ Hz) frequency range. Stable point defect complexes consisting of substitutional Si and N atoms lead to localized surface plasmon resonances at the sub-nanometer scale. We show further that chains of defects could be used to form nanoscale plasmonic waveguides.

3rd International Symposium on High Temperature Metallurgical Processing: Reduction and Titanium Production

Sponsored by: The Minerals, Metals and Materials Society, TMS Extraction and Processing Division, TMS: Energy Committee, TMS: Pyrometallurgy Committee

Program Organizers: Tao Jiang, Central South University; Jiann-Yang Hwang, Michigan Technological University; Patrick Masset, TU Freiberg; Onuralp Yuçel, Istanbul Technical University; Rafael Padilla, University of Concepcion; Guifeng Zhou, Wuhan Iron and Steel

Monday PM
March 12, 2012

Room: Southern II
Location: Dolphin Resort

Session Chairs: Clemens Schmetterer, TU Freiberg; Ting'an Zhang, Northeastern University

2:00 PM

Preparation of Titanium Alloy from Titania-bearing Blast Furnace Slag: *Run Huang*¹; *Chenguang Bai*¹; *Xuewei Lv*¹; *Songli Liu*²; ¹College of Materials Science and Engineering, Chongqing University; ²College of Materials Science and Engineering, Pan Zhihua University

Titanium alloy was prepared from titania-bearing blast furnace slag (Ti-BF slag) by aluminothermic process in an induction furnace. The effects of aluminum amount on the titanium silicon yield and titanium recovery ratio were studied. The phase transformation and chemical composition of the prepared alloy were investigated by X-ray diffractometry (XRD) and X-ray fluorescence (XRF) respectively. It was found that the mass fraction of silicon and aluminum increased with increasing the aluminum amount, however, the mass fraction of titanium increased first and then decreased with increasing the aluminum amount. Furthermore, both the titanium alloy yield and titanium recovery ratio increased with the increase of aluminum amount. The main phases of the alloy were Ti₃Si₂ and AlTi₃. The titanium alloy samples prepared in various conditions had a composition (wt.%): 38–50% Ti, 29–34% Si, 4–11 Al%, 1.6–2.2 Mn%.

2:15 PM

An Overview of Development of Rotary Hearth Furnace and Functions: *Xuefeng She*¹; *Jingsong Wang*¹; *Yihua Han*¹; *Qingguo Xue*¹; ¹University of Science and Technology Beijing

Rotary hearth furnace (RHF) process is summarized in domestic and overseas at the present time. Recent utilization of RHF concerning the part of ironmaking process and recycling of solid wastes have implemented in China, Japan and American. In addition, the conclusions of main functions about RHF process have drawn in three aspects. The first is pretreatment of melting reduction or production of pig iron; the second is disposed of solid wastes from iron and steel plants or nonferrous plants; the last is disposed of special mineral for example vanadium-bearing titanomagnetite, paigeite, laterite etc.

2:30 PM

Basic Research of Direct Pyrolysis Performance of MgCl₂ in Molten State for New Process of Titanium Sponge Production: *Zhang Ting'an*¹; *Lv Guozhi*¹; *Dou Zhihe*¹; *Liu Yan*¹; *Niu Liping*¹; *Zhao Qiuyue*¹; *Sui Lianxu*¹; *He Jicheng*¹; ¹Northeastern University

This paper proposed a new method of Mg and Cl₂ circulation in titanium sponge production by direct pyrolysis of MgCl₂ in Molten State and thermal reduction process of MgO. We aim to study the effects of pyrolysis temperature, pyrolysis time and partial pressure of oxygen on pyrolysis efficiency of MgCl₂ in Molten State, and the crystallite structural transformation of pyrolysis product MgO at different pyrolysis temperature and time by XRD. The experimental results indicate that the pyrolysis temperature and time affect the pyrolysis efficiency obviously, and the reasonable pyrolysis conditions of MgCl₂ in molten state are as follows: pyrolysis temperature 1100°C, pyrolysis time 60 minutes and partial pressure of oxygen 100%. Under this condition, the pyrolysis efficiency get above 95%. The dynamic analysis on pyrolysis reaction of molten magnesium chloride shows that, the reaction is controlled by chemical reaction process with the apparent activation energy $E_a=70.4$ kJ/mol.

2:45 PM

Chlorination of Titania Feedstocks: *Samantha Moodley*¹; *Rauf Eric*²; *Aditya Kale*³; *Cevat Kucukaragoz*²; ¹Exxaro Resources; ²University of the Witwatersrand; ³Mintek

Two titania slags, rutile and synthetic rutile were chlorinated with petroleum coke and CO in a small bubbling fluidized bed reactor. The study aims to identify differences in chlorination mechanism, compare conversion rates, blowover and the chlorination of impurities for the various feedstocks. Chlorination rates were highest at 1000°C; rutile chlorination significantly increases as temperature increases from 800°C to 1000°C. At 1000°C, Slag B has the highest chlorination conversion rate followed by Slag A and rutile. The mechanism for slag and rutile chlorination differs; slag becomes porous with the chlorination of FeO and MnO whilst rutile remains solid. As the porosity of slag particles increases so does its tendency to be elutriated. Ti₂O₃ is oxidized within the early stages of chlorination, it is argued that this takes place during the chlorination of FeO and MnO, Ti₂O₃ not oxidized is rapidly chlorinated.

3:00 PM

Experimental Study on the Pulverization and Reduction Behavior of Sinter in Oxygen Blast Furnace: *Yihua Han*¹; *Jingsong Wang*¹; *Rongzong lan*¹; *Lintao Wang*¹; *Xiaojian Zuo*¹; *Qingguo Xue*¹; ¹University of Science and Technology Beijing

Using the facility of reduction experiment, the low temperature reduction pulverization and reduction behavior of sinter in oxygen blast furnace (OBF) were studied. Through analyzing the results, the difference of pulverization and reduction behavior of sinter in OBF and conventional blast furnace (BF) were discussed. Furthermore, the effect laws of reduction temperature and the content of CO and H₂ on reduction behavior of sinter were studied. Also the controlling step of iron oxide reduction was discussed. The results showed that compared with BF, the low temperature reduction pulverization of sinter became serious at 773K, reduction rate became faster at 1173K, reduction time became less and final reduction degree was increased in OBF. With increasing of H₂ and CO contents, the reduction of sinter was promoted. The reduction process is controlled by interface chemical reaction at the earlier stage and by interface chemical reaction and internal diffusion at the final stage.

3:15 PM

Formation of Ti(C,N) in Blast Furnace Slag Bearing High TiO₂: *Shiwei Ma*¹; *Guibao Qiu*¹; *Qingyu Deng*¹; *Hua Wang*¹; ¹College of Materials Science and Engineering, Chongqing University

The flow properties of the blast furnace slag bearing high TiO₂ at high temperature like the viscosity may change a lot due to the formation of the carbonitride inside, causing serious problems on the separation between the metal and the slag. Therefore, the critical condition of the formation

of Ti(C,N) in blast furnace is vital importance for the ironmaking process with iron ore bearing titania. In this study, the formation of Ti(C,N) in blast furnace and the influences of various factors on the Ti(C,N) formation are investigated by FactSage. It is found that the mass of Ti(C,N) would reach the maximum at 1480 oC, and the product is mainly TiN below 1620 oC, while it is mainly TiC above 1620 oC. The order of the factors by the importance from strong to weak was: temperature, the content of TiO₂ in slag, basicity of slag, the content of MgO and Al₂O₃.

3:30 PM Break

3:40 PM

Modelling of the Thermochemical and Thermophysical Properties of Molten Slags in High Temperature Conversion Processes: A Multiscale Approach: *Yuanyuan Zhang*¹; *Patrick Masset*¹; *Aurélie Jacob*¹; *Clemens Schmetterer*¹; *Ligang Zhang*¹; *Arne Bronsch*¹; *Angus Gray-Weale*¹; ¹TU Bergakademie Freiberg

The modeling of high temperature processes (e.g. gasification, blast furnace process) requires the knowledge of many input parameters. In this work models for slag structure, viscosity and surface tension have been developed for the Al₂O₃-CaO-SiO₂ system with various admixtures of Fe_xO, Na₂O or K₂O. Thermodynamic data were assessed together with the respective phase diagrams using the CALPHAD method, while molecular dynamics provided structural information and viscosity. The obtained information was then used for modeling of the slag surface tension according to the Butler model and a geometric model, as well as for viscosity predictions based on the Einstein-Roscoe-equation. In this contribution the results from the various modeling efforts will be presented and compared to experimental data.

3:55 PM

Research on Carbonthermal Reduction Behavior of Ilmenite: *Yufeng Guo*¹; *Lirong Chen*¹; *Tao Jiang*¹; *Wenjie Weng*¹; *Feng Chen*¹; ¹Central South University

In this paper, the behavior of Panzhihua ilmenite' carbonthermal reduction and its influencing factors under the condition of carbon-burdened were systematically investigated. The results show that under the condition of carbon-burdened, the ilmenite forms into titanium nitride during the reduction process at 1200°C. Carbon-burdened is beneficial to the reduction of iron oxide, but less favorable for the growth of iron grain.

4:10 PM

Study of Reduction Kinetics of Low Grade Hematite Ore: *Tiejun Chun*¹; *Deqing Zhu*¹; *Jian Pan*¹; *Zhao Qiang*¹; ¹Central South University

In this paper, the reduction kinetics of superfine low grade hematite ore was developed. Mineralogy was measured that the ROM ore is of superfine low grade hematite ore type, assaying 27.2wt%Fetotal and with main valuable minerals of hematite occurring at size between 3 to 5µm. The reduction kinetics shows that the reduction reaction rates of pellets with complex additive and without additive are all controlled by diffusion through the product layer. The calculated apparent activation energy of pellets with 12wt% complex additive is 10.15 KJ/mol, dropping 43.9% compared to that of pellets without additive.

4:25 PM

Effect of CaO Addition on Metalthermic Reduction of Strontium Oxide: *Yeliz Demiray*¹; *Onuralp Yücel*¹; ¹Istanbul Technical University

In this present study the effect of CaO addition on Aluminothermic reduction of strontium oxide was investigated. In the experiments SrO which has 99 % purity was used. Al powder addition was selected 100, 200, 300 % of stoichiometric ratio. Effects of CaO addition (100 %, 200 %, 300 % of stoichiometric ratio) on recovering of metallic strontium was investigated. The process temperatures were selected between 1050°C and 1250° C. The final residues were examined for their chemical compositions. XRD, AAS and Flame Photometer devices were used for chemical analysis.



TMS 2012

141st Annual Meeting & Exhibition

MONDAY PM

4:40 PM

Production of ZrB₂ Powders from ZrO₂ Containing Dental Implant

Wastes: *Samet Yilmaz*¹; *Murat Alkan*¹; *Onuralp Yucel*¹; *Bora Derin*¹; ¹Istanbul Technical University

Zirconia based ceramics are used as dental materials more than other ceramics because of their highest mechanical properties. This study covers information about the reuse of dental wastes containing zirconia by self propagating high temperature synthesis (SHS) process. In the first step SHS experiments, different stoichiometric amounts of ZrO₂ containing waste dental implant powders, B₂O₃ obtained through fusing of H₃BO₃ and Mg powders were used. In the second step, SHS products (ZrB₂, MgO, Mg₃B₂O₆, etc.) were leached by using HCl acid solution for the removal of MgO based impurities. Raw materials and the solid products were characterized by using XRD (X-Rays Diffractometer) and AAS (Atomic Absorption Spectrometer) was employed for the analysis of the spent leach solutions. It was found that sub-micron sized zirconium diboride powders without requiring any industrial milling processes, produced by SHS process followed by acid leaching technique.

4:55 PM

Viscosity Evolution of Blast Furnace Slag Bearing Titanium: *Hua Wang*¹; *Guibao Qiu*¹; *Qingyu Deng*¹; *Shiwei Ma*¹; ¹Material Science and Engineering Department, Chongqing University

The flow behavior of the blast furnace slag bearing titanium, like viscosity, play an importance role during the iron-making process with the vanadium-titanium magnetite, which is a very special minerals in Panzhihua, China. The dependency of the viscosity on the chemical composition like TiO₂, Al₂O₃, MgO, binary basicity(CaO/SiO₂), temperature, reaction time were studied. The experiments showed that the viscosity decreased with the increase of TiO₂, MgO content and binary basicity, and it increased with the increase of Al₂O₃ content and temperature. The viscosity showed a slight decrease within 60mins' reaction with graphite crucible, however, it increased rapidly afterwards with the formation of Ti(C, N).

Advances in Surface Engineering: Alloyed and Composite Coatings: Session II

Sponsored by: The Minerals, Metals and Materials Society, TMS Materials Processing and Manufacturing Division, TMS: Surface Engineering Committee

Program Organizers: Sandip Harimkar, Oklahoma State University; Srinivasa Bakshi, Indian Institute of Technology Madras; Arvind Agarwal, Florida International University

Monday PM

March 12, 2012

Room: Macaw 1

Location: Swan Resort

Session Chair: To Be Announced

2:00 PM Introductory Comments

2:05 PM Invited

Understanding the Origins and Evolution of Residual Stress: *Eric Chason*¹; ¹Div of Engineering

During deposition, thin films go through a range of stress states, from compressive to tensile and back again. Understanding the origin of stress is important to enable control of the final stress in the film. We have developed simple analytical models to describe this evolution in terms of a kinetic competition between different mechanisms of stress generation and relaxation. The balance shifts as the microstructure evolves from isolated islands, through coalescence and finally into a uniform film. We will present models for both high mobility and low mobility films which show that the stress depends on the dimensionless parameter D/LR where D is the diffusivity, R is the growth rate and L is the grain size. The model results are compared with real-time measurements of stress using wafer

curvature. We also will present results of stress during sputter deposition to show how surface morphology can influence the stress.

2:30 PM Invited

Elevated Temperature Microstructural Stability of Ni(Cr)-Chromium Carbide Composite Coatings on Stainless Steel: *Graham McCartney*¹; *Yi Ding*¹; *Philip Shipway*¹; ¹University of Nottingham

Ni(Cr)-Cr₃C₂ composite cermet coatings, deposited by HVOF spraying are frequently, used to provide protection against erosion and oxidation at temperatures up to 800°C and are candidate coating materials for power plant components. There has been extensive research on the mechanical and tribological properties at room temperature and elevated temperature of these types of coatings. Additionally, there have been several studies on the microstructural evolution of Ni(Cr)-Cr₃C₂ coatings when exposed to elevated temperature for long periods of time. However, less attention has been given to quantifying the microstructural degradation that occurs due to oxidation at the free surface of the coating and/or interdiffusion between the coating and the substrate alloy. Results on both these aspects of Ni(Cr)-Cr₃C₂ composite coatings deposited onto type 304 stainless steel and held at temperatures in the region of 700 to 800/176C for times ranging from 1 hour to 16 days in air will be presented.

2:55 PM Invited

3-D Focused Ion Beam Serial Sectioning to Determine Solidification and Wear Mechanisms in Adaptive Composites Coatings: *Jon-Erik Mogyonye*¹; *Hamidreza Mohseni*¹; *Sundeep Gopagani*¹; *Junyeon Hwang*¹; *Jamie Tiley*²; *Rajarshi Banerjee*¹; *Thomas Scharf*¹; ¹The University of North Texas; ²Air Force Research Laboratory

Multifunctional, adaptive composite coatings are needed that combine the properties of solid/self-lubrication, high mechanical hardness, and high fracture toughness. We have utilized a Laser Engineered Net Shaping (LENS) process to fabricate a novel Ni/TiC/graphite self-lubricating composite coating for applications that combine these three important properties: graphite phase for solid/self-lubrication and titanium carbide phase for high hardness in a high fracture toughness nickel matrix. Microstructural evolution during solidification and wear were studied with 3-D focused ion beam serial sectioning. Novel insights into surface and subsurface deformation processes and mechanisms include stress-induced tribochemical reactions and structural transformations from microcrystalline graphite to amorphous carbon as well as the formation of a nanocomposite mechanically mixed layer (recrystallized nanocrystalline Ni grains in an amorphous carbon matrix). Another insight into the self-lubricating behavior was how subsurface compressive stresses continually feed primary and eutectic graphite into the mechanically mixed layer. These processes are responsible for improved properties.

3:20 PM

Role of Yttria Stabilized Zirconia on Fracture Toughness of Plasma Sprayed Aluminum Oxide Composite Coatings: *S. Ariharan*¹; *Anup Keshri*²; *Arvind Agarwal*³; *Kantesh Balani*¹; ¹Indian Institute of Technology Kanpur; ²Vellore Institute of Technology; ³Florida International University

Aluminum oxide is used as wear resistant coatings, thermal liners, heaters, crucibles, dielectric systems, biomaterial, etc. But its applications are limited due to their low fracture toughness (~3.2 MPa.m^{0.5}). In this current work, various sizes of YSZ have been incorporated through plasma spraying in Al₂O₃ matrix i.e. (i) pure Al₂O₃, (ii) Al₂O₃ with 20 wt.% YSZ (particle size 30-60 nm), (iii) Al₂O₃ with 20 wt.% YSZ (particle size 0.5µm) and (iv) Al₂O₃ with 20 wt.% YSZ (spray dried). The fracture toughness of plasma sprayed Al₂O₃ with reinforcement of 20 wt.% of nano-YSZ, micro-YSZ and spray dried-YSZ was attained to be 4.18, 3.94 and 4.28 MPa.m^{0.5} respectively (attaining fracture toughness enhancement of 29%, 21% and 34% respectively when compared to that of pure Al₂O₃ ~3.33 MPa.m^{0.5}). Thus, the role of YSZ distribution through its varying size and distribution can strongly affect the toughening obtained in the Al₂O₃ composite coating.

3:40 PM

Microstructure Evolution and Corrosion Behavior in Laser Synthesized Fe-base Amorphous Composite Coating on Structural Steel: *Shravana Katakam*¹; Sameer Paital¹; Narendra Dahotre¹; ¹University of North Texas

Fe-based amorphous materials due to their excellent properties like high corrosion resistance, hardness and wear resistant are promising to produce coatings on different structural materials to enhance the surface properties. In the present study, Laser surface melting was performed on 4130 steel using Fe-Cr-Mo-Y-C-B amorphous powder as a precursor material. In spite of high cooling rates obtained by laser processing, the coating revealed a composite microstructure due to substantial solute redistribution and formation of different heterogeneous nucleation sites, resulting in formation of crystalline phases in the amorphous matrix. A thermal model approach based on COMSOL multi-physics software was developed to estimate the thermal profiles and cooling rates that are responsible for evolution of different microstructures. The corrosion resistant property of the coatings is studied based on the microstructural evolution and an attempt is made to propose a mechanism for the corrosion behavior using XRD, SEM and TEM studies.

4:00 PM Break**4:15 PM**

Structural Coatings in Aluminum Alloy Microtruss Materials: *Bosco Yu*¹; Glenn Hibbard¹; ¹University of Toronto

Incorporating an internal cellular architecture of open space is one strategy to increase the potential functionality of aluminum alloys. Stretch-dominated microtruss cellular architectures, which are designed such that externally applied loads are resolved axially along the internal struts, provide enhanced strength and stiffness at low densities when compared to conventional metal foams. In this study we introduce the idea of using a structural coating to reinforce AA3003 aluminum alloy microtrusses. Because the internal surface area is large and the strut cross-sectional dimensions can be as small as hundreds of microns, only a 40 μm thick hard anodized alumina coating was needed to induce a four-fold increase in compressive strength and a six-fold increase in energy absorption at virtually no additional weight penalty. Backscatter electron microscopy was used to examine the failure mechanisms of the structural coatings and the cores in order to explain such a large change in behaviour.

4:35 PM

Understanding Plasma Spraying of Nano Crystalline Cerium Oxide for SOFC Electrolyte: *Virendra Singh*¹; Robert Draper¹; Shashank Saraf¹; Sudipta Seal¹; ¹University of Central Florida

In the present work three different techniques namely air plasma spray (APS), solution precursor plasma spray (SPPS), and suspension plasma spray (SPS) have been attempted for thin dense coating of CeO₂. During internal injection high temperature and reducing condition in APS vaporizes the agglomerated nano cerium oxide feed stock and drastically reduces the deposition efficiency whereas, external injection improves deposition efficiency. The characteristics of CeO₂ thin coating and challenges prepared by SPS and SPPS were compared with APS. It was found that solution-based deposition could be an alternative for dense coating. Different spray parameters were varied to optimize coating density and deposition efficiency. DSC/TG study was performed to determine the decomposition kinetics of solutions. SEM and TEM studies were carried out for microstructural characterization. XRD and X-ray photoelectron spectroscopy study was performed to understand formation of single phase fluorite structure and the change in oxidation state of cerium, respectively.

4:55 PM

Laser Cladding of High-Performance CPM Tool Steels on Hardened H13 Hot-Work Tool Steel for Automotive Tooling Applications: *Jianyin Chen*¹; Lijue Xue¹; ¹IMI-National Research Council Canada

This paper summarizes our work on laser cladding of high vanadium carbide CPM tool steels including CPM 3V, 9V and 15V onto hardened chromium hot-work H13 tool steel (HRC 52-55) to substantially enhance abrasive wear resistance due to their potentials for fabricating high-performance automotive tooling at affordable cost. The similarities and differences in the morphological characteristics of macro- and microstructures of the CPM coatings obtained by laser cladding were studied using X-ray diffraction (XRD), optical microscope (OM), scanning electron microscope (SEM) and microhardness tester. The implications on the resulting mechanical performance of the laser clad CPM tooling materials were discussed as well.

5:15 PM

Dynamic Annealing Effect during Filtered Cathodic Vacuum Arc Deposition of DLC Coatings: *Feng Ji Li*¹; Sam Zhang¹; Deen Sun²; ¹Nanyang Technological University/School of Mechanical and Aerospace Engineering; ²Singapore Epon Industrial Pte Ltd/PVD Department Plating Division

Demonstrated is the fast deposition of thick DLC coatings of high hardness and yet low residual stress via introducing a titanium (Ti) interlayer. The process makes use of both the unbalanced magnetron sputtering and filtered cathodic vacuum arc (FCVA) deposition. Unbalanced magnetron sputtering is used to deposit a thin Ti layer for bonding and FCVA deposition is used for its high deposition rate of thick and hard diamond-like carbon. The surface morphology, chemistry, bonding structure and mechanical properties of the coatings are examined for such coatings deposited at different substrate bias voltage during FCVA deposition. The results showed that the neutralization effect of the Ti interlayer, back-sputtering and dynamic annealing take place at too high substrate bias voltages.

5:35 PM

Electron Beam Deposited Multilayer Optical Interference Coatings Using Oxide Composites: *Ankush Nayak*¹; N Sahoo²; R Tokas²; Arup Biswas²; Nitin Kamble²; ¹National Institute of Technology Karnataka, Surathkal; ²Bhabha Atomic Research Centre, Mumbai

Optical multilayer interference coatings are not only the key elements/components of the lasers, synchrotron (beam lines), and solar devices but also serve to propagate, deliver and manipulate such radiations for materials science experiments. Composite oxide thin film materials have added several promising dimensions with respect to the design, development and applications of such precision devices. Binary ZrO₂-MgO and ternary ZrO₂-MgO-Al₂O₃ oxide composite thin films have been deposited using electron beam physical vapor deposition (EB-PVD) technique and nano-metric multilayer devices utilizing such films in a regular periodic design have been developed. As a specific objective, a multilayer high-reflection (HR) laser mirror having a narrow bandwidth has been designed and developed for the Nd: YAG second harmonic laser wavelength of 532 nm. These composite thin films and multilayers have been characterized using various microstructural probing techniques.



TMS 2012

141st Annual Meeting & Exhibition

MONDAY PM

Alumina and Bauxite: Bauxite Digestion

Sponsored by: The Minerals, Metals and Materials Society, TMS Light Metals Division, TMS: Aluminum Committee, TMS: Aluminum Processing Committee
Program Organizer: Benny Raahauge, FLSmidth

Monday PM Room: Northern E3
March 12, 2012 Location: Dolphin Resort

Session Chair: Yanli Xie, SONavigation Inc.

2:00 PM

Characterization of Bauxite and its Minerals by Means of Thermoanalytical Methods: *Ekkehard Post*¹; Bob Fidler²; Dorothea Kwiryn²; Doreen Rapp²; ¹NETZSCH Geraetebau GmbH; ²NETZSCH Instruments North America, LLC

Bauxite is the most important metallic ore for the production of aluminum and alumina. With the help of classical thermoanalytical methods such as thermogravimetry (TG), differential scanning calorimetry (DSC) or simultaneous thermal analysis (STA), information on the mineralogical composition and enthalpy values can be obtained. The gaseous products formed during the decomposition processes can be simultaneously detected and identified by means of mass spectrometry or Fourier Transform Infrared Spectroscopy. By means of dilatometry, the thermal expansion or shrinkage can be determined. The Laser Flash Technique yields the thermal diffusivity values of both the raw material and all intermediate phases to the final product. Based on the thermal diffusivity, specific heat and density, the thermal conductivity can then be calculated. With the example of thermoanalytical measurement results on bauxite as well its individual minerals, the most important possibilities of Thermal Analysis for this application field are shown in this paper.

2:20 PM

Study on Application of a New Model for the Kinetics of Diaspore Leaching Process: Li Bao¹; *Ting-An Zhang*²; Anh Nguyen¹; Guozhi Lv¹; Zhihe Dou¹; Yan Liu¹; ¹Northeastern University; ²University of Queensland

The process of leaching diasporic bauxite in sodium aluminate solution is the most popular method to produce alumina in Chinese alumina industry. A new consistent kinetic model for gibbsite leaching process model has been developed in our previous work. This paper aims to study the application of the new model for the diasporic leaching in industrial alkali solution. The model equation was numerically integrated applying the fourth-order Runge-Kutta technique. Nonlinear regression analysis was carried out to estimate the unknown model parameters by comparing numerical solutions with available experimental data. The new model which considers the fractal geometry of the shrinking diasporic particles and the residual aluminium concentration in particles, is more consistent with the leaching process of the diasporic particles distributing in a narrow size range than the particles with the wide range of the size distribution.

2:40 PM

Mechanical Activation of Al-Oxyhydroxide Minerals – Physicochemical Changes, Reactivity and Relevance to Bayer Process: Thomas Alex¹; Rakesh Kumar¹; Sanat Roy²; *Surya Mehrotra*²; ¹National Metallurgical Laboratory (CSIR); ²Indian Institute of Technology, Kharagpur; ³Indian Institute of Technology

Overview of our research on 'structure and reactivity' of gibbsite and boehmite under varied conditions of mechanical activation, e.g. mill type, milling energy and presence of a second phase is presented. Bulk and surface changes induced in the solids by milling are characterized in terms of morphology, particle size distribution, specific surface area and nature of porosity, crystallite size and zeta potential. Results on enhanced amorphisation of gibbsite in presence of a second phase (quartz, hematite

etc), changes in zeta potential of gibbsite due to loss of texture during milling and anomalous decrease in surface area of boehmite during milling are reported. Reactivity of the activated solids in sodium hydroxide and variation in thermal transformation temperatures, is correlated with physicochemical characteristics of the samples and plausible explanation for the observed correlations presented. Significance of the results with specific reference to bauxite and alumina processing in Bayer process is highlighted.

3:00 PM

Research on Mechanically Activated Digestion Performance and Kinetics of Diasporic Bauxite: *Lv Guozhi*¹; Zhang Ting'an¹; Ke Xianyao²; Liu Yan¹; Dou Zhihe¹; Li Yan¹; He Jicheng¹; ¹Northeastern University; ²Shenyang Aluminum & Magnesium Engineering & Research Institute

This paper proposed a "mechanically activated-homogeneous digestion" technology as a strengthening method for diasporic bauxite digestion process of alumina production. Effects of digestion temperature, digestion time and rotary speed on digestion performance of diasporic bauxite were investigated by using "homogeneous digestion" equipment, and the digestion kinetics of diasporic bauxite were researched as well. The results indicate that mechanical activation can greatly improve the digestion performance of diasporic bauxite, and also broaden the size range of raw ore particles. The mechanically activated digestion temperature is 20°C lower than that of direct digestion. The relative digestion rate of alumina gets above 97% when the digestion conditions are temperature 245°C, mechanically activated ball speed 80rpm and holding time 60 minutes. The apparent activation energy of mechanically activated digestion is 57.30kJ/mol, which is 21.09kJ/mol lower than that of direct digestion, and the kinetic equation of mechanically activated digestion is $(1-\eta)^{-1/3}-1=1.5532 \times 10^{-4} \exp(4.764 \times 105/T)t$.

3:20 PM

Mechanochemical Activation to Bauxite: *Fernanda Silva*¹; Carla Barbatto²; Rachel Santos¹; Diego Seixas³; João Sampaio⁴; Marta Medeiros¹; Francisco Garrido¹; ¹IQ/UFRJ; ²COPPETEC; ³IQ/UFRJ-CETEM; ⁴CETEM/MCT

The crystallized layer that compounds the bauxite's geological profile from NE Pará was ore dressed through the processes of crushing, screening, washing and grinding, in order to reach the same size distribution of that in the alumina production industry. After the preparation process, the sample (90%, < 0.21 mm) containing 5.3% reactive silica and 47.2% available alumina was submitted to mechanochemical activation with different kinds of reagents (CaO, Ca(OH)₂, CaCO₃, CaO+HCl, CaSO₄), in different concentrations, which resulted in the formation of a calcium aluminium hydrosilicate (hydrogarnet). This phase was formed in the first 30 min of grinding with the use of CaO and Ca(OH)₂. However, chemical and thermodynamic analysis showed that the principal phase obtained, katoite hydrogarnet, had the largest aluminum content in its chemical composition thus proving that it is not good for the Bayer process once it is not possible to reduce caustic loss.

3:40 PM

Effects of Roasting Pretreatment in Intense Magnetic Field on Digestion Performance of High Iron Bauxite: *Lv Guozhi*¹; Zhang Ting'an¹; Zhang Xuhua¹; Liu Yan¹; Dou Zhihe¹; Li Yan¹; He Jicheng¹; ¹Northeastern University

This paper investigated the changes of phase and apparent morphology under the combined effects of intense magnetic field and temperature field and the effect law of different roasting conditions on the digestion performance of high-iron diasporic and settling performance of the digested slurry. The results indicate that roasting pretreatment under high magnetic field can change the microstructure and improve the digestion performance of bauxite. The reasonable roasting conditions with intense magnetic field for high-iron bauxite are as follows: roasting temperature 500°C, roasting time 60 minutes and magnetic field intensity 9T. The

digestion rate of alumina of the roasted ore is 71.82%, about 20% higher than that of the raw ore and the molecular ratio of digestion liquor is 1.69 under the digestion conditions of temperature 210°C and time 60min. The settling performance of the digested slurry improved obviously after intense magnetic field treatment.

4:00 PM

Effect of Chamosite on Bayer Process of Diasporic Bauxite with High Silica: *Cao Wenzhong*¹; Xun Zhang²; Weiwei Tian²; Hong Zhong³; ¹Environmental and chemical engineering institute, Nanchang university; ²Environmental and Chemical Engineering Institute, Nanchang University; ³Henan Company of Aluminium Corp. of China

Technological investigations were carried out based on the Bayer process. Pre-desilication characteristic of the bauxite, the effects of digestion temperature and retention time, concentration of Na₂O amount of CaO addition on Al₂O₃ digestion efficiency in Bayer process and the settling characteristics of the red mud were determined. The bauxite in the northern region of China is diasporic type with high silica (in 6-15% SiO₂). The main silica minerals in the bauxite are kaolinite and chamosite. The presence of high silica causes high bound-soda losses in the red mud in the Bayer process, but part of silica content in the bauxite was in the form of chamosite, the bound-soda losses could be greatly reduced with chamosite mineral by using Bayer process. Therefore, it is necessary to study digestion characteristics of the special diasporic bauxite and settling separation properties of the red mud by Bayer process.

4:20 PM

The Economical Flexibility for Processing Diasporic Bauxite: *Zhang Baiyong*¹; Zhou Fenglu¹; Guo Shen¹; Liao Xinqin¹; Ma Chaojian¹; Dong Yafeng¹; ¹Chalieco

Until now, the domestic diasporic bauxite resources is the primary supplied bauxite for alumina production, and Bayer, dressing Bayer, sintering, mixed combination and serial combination processes are parallel used to produce alumina product in China. At the same time Chinese diasporic bauxite resources was seriously depleted recently with the greatly increasing of capacity. In this paper, depending on current diasporic bauxite conditions, the raw material, energy consumption and raw materials & fuel cost are studied for different production processes to processing different grade diasporic bauxite, at same time the raw material, energy consumption and raw materials & fuel cost are discussed at same A/S for different processes, in order to provide references to economical usage of Chinese bauxite resources for Chinese alumina industry.

4:40 PM

Turkey Morcukur Bauxite Processing at ETI Aluminium: *Meral Baygul*¹; Sedat Aslan¹; Burak Ozen¹; Serkan Ertugral¹; Carlos Suarez²; ¹Eti Aluminium Co.; ²Hatch Associates Consultant Inc

ETI Aluminium can process nearly 550.000 tons of bauxite and 230.000 Tons of alumina per year. The south region of Turkey produces boehmitic bauxite and various alumina/silica ratio. The reserve of Morcukur Bauxite in this region is about 6.000.000 tons of high reactive silica content. ETI started producing bauxite from the Morcukur deposits in 2007 because of easy handling and lower cost .60.000 tons of Morcukur bauxite have been produced from this mine but could not be used because of red mud settling problems . After XRF, XRD, Goethite/Hematite ratio and Organic content analysis ; and also autoclave efficiency (Parr Reactor) and settling performance tests , 10 % -40 % Morcukur bauxite has been processed in 2011 with a strict laboratory and process control. Results from grinding ,digestion and red mud settling performance in the process and laboratory are discussed in this paper.

Aluminium Processing: Rolling

Sponsored by: The Minerals, Metals and Materials Society, TMS Light Metals Division, TMS: Aluminum Processing Committee
Program Organizers: Kai Karhausen, Hydro Aluminium Rolled Products GmbH; Edward Williams, Alcoa

Monday PM
March 12, 2012

Room: Europe 1
Location: Dolphin Resort

Session Chair: Kai Karhausen, Hydro Aluminium Rolled Products

2:00 PM Introductory Comments

2:05 PM

Implementation of a Combined Work-Hardening, Recovery and Recrystallization Model into a Through-Process-Model for Production of Aluminum Sheet: *Thiemo Brüggemann*¹; Anna Rott²; Volker Mohles²; Günter Gottstein²; Kai Karhausen³; ¹Institute of Physical Metallurgy and Metal Physics; ²Institute of Physical Metallurgy and Metal Physics, RWTH-Aachen University; ³Hydro Aluminium Deutschland GmbH

Coupled optimization of alloys and process chains for aluminum sheet is a major goal of the aluminum industry. Since experimental methods are cost- and time-intensive, simulation tools are used to predict effects of material and process parameter changes on the product. Within this work, using rolling schedules from real production lines, the rolling process is simulated via a thermally coupled roll-gap model. This simulation tool is fully linked to a dislocation density based model, which, according to the calculated state variables, simulates work-hardening, recovery and recrystallization on a parallel timescale. The present model is capable of comprising influences of solute contents, particle radii, their volume fractions, and temperature. This framework is feasible to simulate a whole process chain within minutes and thus offers numerous process optimization trials in a reasonable amount of time. Simulation outcome will be compared to experimental findings and real process results of rolled AA8xxx Aluminum sheets.

2:25 PM

Comparative Microstructure and Texture Evolution in the AA1050 Aluminum Alloy Sheets Produced by DC and CC Methods: *Heber Otomar*¹; Ronald Plaut²; ¹VM - CBA; ²EPUSP

This study aims to compare, on an industrial scale, of the effect of the direct chill (DC) and continuous casting (CC) fabrication processes of AA1050 rolled and annealed sheets. Characterization of their microstructure and texture evolution from the as-cast condition up to the end condition of a deep-drawn cup was carried out. Stamping tests were performed to identify which process presents best performance. Different microstructures were obtained for the studies processes: the DC material was more homogeneous, both in terms of intermetallic distribution and grain size. The mechanical properties of the CC material were slightly higher than those for the DC material. Forming Limit Diagram (FLD) of the homogenized CC material presented the best results.

2:45 PM

Study on Mechanical Properties of 2024 Al Sheet Treated by SMAT and Hot/Cold Rolling: *Ka Po Cheung*¹; San-Qiang Shi¹; Jian Lu²; ¹The Hong Kong Polytechnic University; ²City University of Hong Kong

The strengthening effects of hot/cold rolling and surface mechanical attrition treatment (SMAT) on aluminium alloy were investigated. Before performing the rolling processes, aluminium sheets were treated using SMAT on both sides for 40 min at room temperature. The parameters for the hot/cold rolling process include a range of operating temperature (-200 °C to 480 °C) and percentage of thickness reduction (up to 85%). Then the mechanical properties of rolled samples with different thicknesses were studied. Tensile test results show that the higher the percentage of reduction in thickness, the higher the strength of the rolled samples



TMS 2012

141st Annual Meeting & Exhibition

MONDAY PM

can obtain. Considering the yield and tensile strength, rolling at room temperature with the 80% thickness reduction is the optimum conditions for AA2024-T3 in this article, in which the yield and ultimate tensile strength have been increased by 54% and 79% respectively. It is also found that the ductility was also enhanced according to the operating temperature.

3:05 PM

Effects of Asymmetrical Roll Bonding on Microstructure, Chemical Phases and Property of Copper/Aluminum Clad Sheet: *Xiaobing Li*¹; Guoyin Zu²; Ping Wang³; Rong Xu⁴; ¹School of Materials and Metallurgy, Northeastern University; ²School of Materials and Metallurgy, Northeastern University; ³Key Laboratory of Electromagnetic Processing of Materials, Ministry of Education, Northeastern University; ⁴The State Key Laboratory of Rolling and Automation, Northeastern University

The present paper investigated the morphology and chemical phases of interfacial layer of Copper/Aluminum clad sheet by scanning electrical microscope equipped with energy dispersive X-ray detector and X-ray diffraction, also measured the mechanical property through micro-hardness test. The results are that the interfacial bonding is enhanced and the thickness of interfacial layer increases with mismatch speed ratio rising. The improved interfacial bonding can be found from the tensile fracture. The formation of intermetallic compound (IMC) is promoted by the significant element diffusion at high speed ratio. For sample annealed at 400 °C for 20 min, the formation of IMC is negligible, but the fracture lies between compounds. The micro-hardness on the interface decreases with speed ratio increasing. The study shows that the improvement of microstructure and mechanical property and formation control of IMC of Copper/Aluminum clad sheet can be achieved using asymmetrical roll bonding with high speed ratio.

3:25 PM Question and Answer Period

3:35 PM Break

4:05 PM

Influence of Microstructure Representation on Flow Stress and Grain Size Prediction in A5XXX Alloys: *Johannes Lohmar*¹; Markus Bambach¹; Gerhard Hirt¹; Kai Karhausen²; ¹RWTH Aachen University; ²Hydro Aluminium Rolled Products GmbH

Integrated computational materials engineering is an up to date method for developing and optimizing complete process chains. In the simulation of a process chain, material models play a central role as they capture the response of the material to external process conditions. While much effort is put into their development and improvement, less attention is paid to their implementation, which is problematic because the representation of microstructure in the model has a decisive influence on modeling accuracy and calculation speed. The aim of this paper is to analyze the influence of different microstructure representation concepts on the prediction of flow stress and microstructure evolution when using the same material model. Scalar, tree-based and cluster-based concepts are compared for a multi-stage rolling process of an A5XXX alloy. It was found that implementation influences the predicted flow stress and grain size, in particular in the regime of coupled hardening and softening.

4:25 PM

Influence of Pre-Strain on Formability of AA3XXX Aluminum Alloy: *Yansheng Liu*¹; Xiyu Wen²; Shridas Ningileri¹; ¹SECAT Inc; ²University of Kentucky

Changes in Strain path can impact material behavior. The influences of strain path change on tensile properties of materials have been thoroughly investigated in past decades. Formability is one of the important properties of sheet metals for automotive application. The current investigation focuses on the influence of strain path change on formability of the material. O-temper sheets were pre-strained 15% via different strain paths by rolling in rolling and transverse direction. Olsen and earing cup tests were conducted and compared with the original and two pre-strained samples. Strain distribution were measured by grid etching

method and analyzed by ASAME software. The influences of pre-strain conditions, texture evaluation on formability and mechanical anisotropy were discussed. The result shows that pre-strain via different path has a significant impact on formability.

4:45 PM

From Molten Metal to 3.2 mm Wire for Mechanical Applications: *Giuseppe Marcantoni*¹; ¹Properzi International, Inc.

Aluminium utilization is growing at a steady rate reaching 40 million tons per year considering remelt and semis. Among semis, aluminium rod accounts for approximately 10% of the worldwide consumption, mainly for power transmission. Numerous aluminium alloys have been developed and utilized for various mechanical applications and welding purposes. Many rod alloys are difficult to produce and require highly experienced operators and the most advanced machinery and technical know-how. In the form of wire, from molten metal to 3.2 mm wire, the situation becomes even more critical and only the latest Properzi C.C.W (Continuous Cast Wire) technology provides new possibilities within this industrial field. The Author explores state-of-the-art aluminium rod equipment and the range of application for the C.C.W. technology which allows the production of 1xxx – 2xxx – 3xxx – 4xxx – 5xxx – 6xxx – 7xxx – 8xxx series aluminium alloys for many industrial and specialty applications.

5:05 PM Question and Answer Period

Aluminum Alloys: Fabrication, Characterization and Applications: Solidification

Sponsored by: The Minerals, Metals and Materials Society, TMS Light Metals Division, TMS: Aluminum Processing Committee
Program Organizers: Subodh Das, Phinix LLC; Tongguang Zhai, University of Kentucky; Zhengdong Long, Kaiser Aluminum

Monday PM
March 12, 2012

Room: Northern E1
Location: Dolphin Resort

Session Chair: Hiromi Nagaumi, Suzhou Research Institute for Nonferrous Metals

2:00 PM

Effects of Cu, Mg, and Sr Additions on the Mechanical Properties and Machinability of Near-Eutectic Al-11%Si Casting Alloys: *Yasser Zedan*¹; Agnes Samuel¹; *Fawzy Samuel*¹; Saleh Alkahtani²; ¹UQAC; ²AlKharj University

The effects of Cu (2.25, 3.5%), Mg (0, 0.3, 0.6%) additions, Sr modification, and T6-heat treatment on the mechanical properties and machinability of near eutectic Al-Si cast 396 alloy were studied, using a T6 treatment that provided hardness levels of 110±10 BHN required in commercial Al applications. Increase in Cu/Mg levels has a detrimental effect on drill life. The Mg-free alloy displays the lowest cutting force and moment, producing the highest number of holes drilled. Cooperative precipitation of Al₂Cu, Mg₂Si, Al₂CuMg, and Al₅Si₆Cu₂Mg₈ hardening phases in Mg-containing alloys confer greater strength on the alloy than is the case with only Al₂Cu precipitation in the Mg-free alloy. A comparison of the number of holes drilled in non-modified and Sr-modified alloys (with same Mg and Cu levels) reveals that the Si particle morphology has a noticeable effect in governing the tool life of such Al-Si alloys.

2:20 PM

Evolution of Iron Based Intermetallic Phases in Al-7wt%Si Hypoeutectic Alloy: *Anton Gorny*¹; Sumanth Shankar¹; ¹McMaster University

This study has methodically characterized the iron based intermetallic phases evolving during solidification of Al-Si binary alloys as a function of alloy melt superheat temperature, solidification cooling rate, purity of the initial pure Al and composition of Fe in the alloys. The initial superheat prior to solidification and the cooling rate during solidification played a

significant role in the nature and type of these intermetallic phases evolving in the cast component. Contrary to the predictions of the evolution of only the β (Al,Si,Fe) in these alloys by all commercial thermodynamic phase diagram simulation tools, the dominant phases were mostly metastable intermetallics and significantly vary in nature and type with the process parameters. The results from this study will further enable better design of the Al-Si alloys with an in-depth understanding of the evolution of the intermetallic phases and methodologies to prevent or modify the same in the final cast components.

2:40 PM

A New Approach to Producing Large-Size AA 7055 Aluminum Alloy Ingots: Haitao Zhang¹; Jianzhong Cui¹; Hiromi Nagaumi²; ¹Northeastern University; ²Suzhou Institute for Nonferrous Metals Research

In this paper, Low frequency electromagnetic field and air knife are applied simultaneously to produce large-size AA 7055 aluminum alloy ingots during DC casting. Moreover, the effects of low frequency electromagnetic field and air knife on the macro-physical fields during DC casting and the microstructure and crack in the ingots are studied and analyzed by the numerical and experimental methods. Comparison of the calculated results indicate that applying electromagnetic field can modify the direction and increase the velocity of melt flow and homogenize the distribution of temperature in the sump, and applying air knife can homogenize the distribution of temperature and decrease the stress and strain in the solidified ingots. Further, the microstructure of the billet is refined remarkably and the crack is eliminated by applying electromagnetic field and air knife during DC casting because of modification of the macro-physical fields.

3:00 PM

Thermal Analysis and Microstructures of Modified Grain-Refined Al-7Si-Mg Cast Alloy: Adel Mohamed¹; FH Samuel¹; Saleh Al kahtani¹; ¹UQAC

This article aims to investigate the grain refining response of Sr-modified A356.2 alloy with various Al-Ti, Al-B and Al-Ti-B master alloys at different levels. Thermal analysis was used to evaluate the interactions between Sr and B, and between Sr and Ti. Microstructure was examined using optical microscopy and EPMA technique. Impact properties were evaluated for both as-cast and heat-treated conditions. The results reveal that adding B with levels higher than 0.1% leads to formation of particles containing predominantly B and Sr, such as SrB₆. The Sr-B interaction may postpone grain refinement of the alloy containing 0.02-0.1%B. The addition of Ti and B greatly improves the alloy toughness but only in a fully modified state, and the right type of master alloy and addition levels are used. The toughness of all T6-tempered alloys is significantly higher than those obtained in the as-cast condition, regardless of the type of master alloy used.

3:20 PM

Effect of Solidification Velocity and Hydrogen Content on Porosity in Directionally Solidified A356 Castings: Hengcheng Liao¹; Qigui Wang²; Wan Song¹; Lei Zhao¹; Ran Fan¹; ¹Southeast University; ²GM Global Powertrain Engineering

Micro-focus X-ray technology was utilized to evaluate the influence of solidification velocity and hydrogen content on the volume fraction, number density and sizes of pores in the directionally solidified A356 castings. The results indicate that hydrogen content has a significant influence on porosity formation. When hydrogen content is low, few small irregular-shape pores were observed indicating the dominate impact of solidification shrinkage. While in high hydrogen specimens, many large spherical pores were found. The pore size distribution also shows dual populations. The group of large pores is formed in the liquid far from the solidification front. The group of small pores is formed near the solidification front. When hydrogen content is high, increasing solidification velocity (from 0.1mm/s to 0.2mm/s) not only decreases volume fraction of porosity but also significantly reduces the maximum pore sizes of large pores.

3:40 PM

Grain Refiner for Aluminium-Silicon Sand Casting Alloys: Magdalena Nowak¹; Hari Babu Nadendla¹; ¹Brunel University

Al-Si alloys exhibit large grain structure when Al-Si alloy melt is solidified in sand moulds due to low cooling rate provided by the mould. Ti-based grain refiner is known to be less-effective to refine grain structure of Al-Si alloys due to formation of Ti-Si phase. Recently, we have developed an effective novel grain refiner (NGR) for aluminium-silicon sand casting alloys. Effectiveness of grain size under slow cooling conditions has been investigated. For comparative purposes, a range of sand casting alloys with NGR addition have been produced. The results show that the addition of novel grain refiner reduces the grain and eutectic size significantly for all these alloys at lower cooling rate <0.5 °C/s. As a result of fine primary Al grains, the porosity and elongation in the solidified alloys is notably improved.

4:00 PM Break

4:15 PM

Novel Casting Process of Developing a Carbon Modified Hyper-Eutectic Wear Resistant Aluminum-Silicon Alloy for the Forging Process: Kuldeep Agarwal¹; Rajiv Shivpuri¹; Matthew Blankenhorn²; ¹Ohio State University; ²Aluminastic Corporation

Currently, most Al-Si alloy components are limited to cast structures where their strength and wear capabilities override the additional costs of testing for defects, rejections, and machining. This paper discusses the development of a 20-25% Si alloy based on the 4032 aluminum forging alloy composition that has low density and high wear resistance. To achieve these advantages in hyper-eutectic alloys, the carbon and copper contents are adjusted in the aluminum alloy during melt processing, electric field is used to disperse carbon, and equiaxed particles of primary silicon, carbides and graphite flakes are precipitated during solidification in the Al-Si eutectic. These micro- and nano-particles provide for higher wear resistance, higher modulus and toughness. Characterization is done to relate the different processing parameters and the microstructure formed and the properties obtained. Potential applications of this alloy are in automotive engines including pistons, cylinder heads and connecting rods where wear resistance is important.

4:35 PM

Solidification Analysis of the Hypereutectic Al-Si Alloys with Addition of Cu and Mg Using Neutron Diffraction: Dimitry Sediako¹; Wojciech Kasprzak²; ¹National Research Council Canada; ²MTL-Canmet, NRC

A good understanding of kinetics of solid phases' evolution during solidification of hypereutectic aluminum alloys is a key to controlling the as-cast microstructure and, in turn, enhancing service properties of industrial alloys. A study has been performed to evaluate the solidification kinetics for two hypereutectic Al-18wt%Si alloys with addition of 3wt%Cu and 3wt%Cu+1wt%Mg. This study included thermodynamic calculations of the solidification process using the FactSageTM 6.2 software package, as well as experimental thermal analysis, and neutron diffraction. The study revealed kinetics of solid Al, solid Si (both primary and eutectic), Al₂Cu, and Mg₂Si evolution, as well as an individual effect of Cu and Mg alloying additions on solidification path of the Al-Si system.

4:55 PM

Refinement of Primary and Eutectic Silicon Phases in the Shape Casting of Hyper-Eutectic Al-Si Alloys: Mohammad Shamsuzzoha¹; ¹University of Alabama

The hyper-eutectic Al-Si alloys owing to being of low density materials and of excellent castability are good candidates for aerospace and automobile applications. Our effort over the last few years have demonstrated that such hyper-eutectic Al-Si alloys containing no primary silicon phase, but of eutectic microstructure that assumes nano sized fibrous morphology for the eutectic silicon phase can be grown by directional solidifications. In a further pursuit on this effort, more hyper-eutectic Al-Si alloys containing ultra-refined primary and eutectic silicon



TMS 2012

141st Annual Meeting & Exhibition

MONDAY PM

phases have been grown by a different casting method, which is popularly known as shape casting. The process of fabrications and microstructure of the resulting alloys are presented.

5:15 PM

Analysis of Thermal and Structural Parameters and Microhardness Variations in Different Al-Cu Alloys Directionally Solidified: Carlos M. Rodriguez¹; Adriana E. Candia²; *Carlos E. Schvezov*¹; Mario R. Rosenberger¹; Alicia Ares¹; ¹CONICET/FCEQyN-UNaM; ²FCEQyN-UNaM

The columnar - to - equiaxed transition (CET) was investigated in Al-Cu alloys (Al-1wt%Cu, Al-5wt%Cu, Al-15wt%Cu and Al-33.2wt%Cu) solidified directionally from a chill face in a vertical setup. The CET occurs when the temperature gradient in the melt ahead of the columnar dendrites and the liquid interphase velocity reach critical values. Also, we investigate correlations between microstructural parameters (grain size and dendrite arm spacings) with Vickers microhardness measurements in the directionally solidified samples. We observed that the Vickers microhardness is greater in the equiaxed zone than in the columnar or columnar to equiaxed transition (CET) zone, additionally, is greater on the edges of the samples than in the centre. The grain size and lamellae spacings increase from the columnar to the equiaxed structure. The established correlations were compared with the data in the available literature and the results are discussed.

Aluminum Reduction Technology: Environment I

Sponsored by: The Minerals, Metals and Materials Society, TMS Light Metals Division, TMS: Aluminum Committee, TMS: Aluminum Processing Committee
Program Organizer: Olivier Martin, Rio Tinto Alcan

Monday PM
March 12, 2012

Room: Southern III
Location: Dolphin Resort

Session Chair: Margaret Hyland, Light Metals Research Center

2:00 PM Panel Discussion Organized by Margaret Hyland, Stephan Broek: Environmental challenges for large smelters, - Views of key issues from legislators, Environmental technologies to address Sulfur and Fluoride

3:20 PM Break

3:40 PM

Low Cost Video Emissions Monitoring Technique for Aluminum Smelting Applications: *Michael Gershenson*¹; Neal Dando¹; Nathan Westendorf¹; Steve Lindsay¹; ¹Alcoa

Aluminum smelting plants emit gaseous and particulate fluoride, sulfur dioxide (SO₂), carbon oxides (CO and CO₂), perfluorocarbons CF₄ and C₂F₆, and other by-products of aluminum electrolysis. The fugitive emission intensities for some of these compounds (most notably, fluorides) is strongly correlated with potroom work activities and work practices (e.g., anode change operations, metal tapping practices, pot hood placement, etc.). Therefore, work practice standardization and potroom personnel education regarding the impact of their day-to-day activities on smelter emissions are important components of a comprehensive emission reduction strategy. This work introduces a low-cost video emission monitoring technique utilized at Alcoa that allows overlaying real-time emissions measurements (e.g., HF, SO₂, dust, etc.) on video recordings of specific work activities. The developed capability is used to more effectively and uniformly communicate the impact of work practices on plant environmental performance. Specific examples of high-impact work practices are presented and discussed.

4:00 PM

Electrolytic Cell Gas Cooling Upstream of Treatment Center: Bernard Cloutier¹; Thierry Malard²; El Hani Bouhabila²; Fabienne Virieux³; *Philippe Martineau*; ¹Solios Environnement Inc; ²Solios Environnement SA; ³Fives Solios

The general use of high amperage cells in the last decade has created new challenges for Gas Treatment Centers (GTCs). Aluminum production capacity increases proportionally with the applied electric intensity. This leads to more waste heat by joule's effect which increases the cell outlet gas temperature. The cell gas temperature also depends on the ambient temperature. In hot climate, gas temperature at the cell outlet could exceed 190°C. For such application, it has become necessary to cool the gases before treatment by HF adsorption on alumina in order to protect the filtration media and to improve the overall scrubbing performance on fluorides. Several technologies have been developed and applied in recent years: dilution air cooling, water atomization in the upstream ducts, heat exchangers. The paper will present a technical and economical comparison of the various cooling technologies.

4:20 PM

Jet Induced Boosted Suction System for Roof-Vent Emission Control: New Developments and Perspectives: *Jean-Nicolas Maltais*¹; Michel Meyer¹; Mathieu Leduc¹; Hyacinthe Rollant¹; ¹Rio Tinto Alcan

Reducing fluoride emissions becomes necessary in production growth and/or tightening environmental regulation contexts. Over 40% of the roof vent emissions are generated by the pot during periods with opened pot hoods. These periods are therefore targeted for improvement, which is usually obtained by significantly increasing the pot exhaust flow while the hoods are opened. The Rio Tinto Alcan patented solution: Jet Induced Boosted Suction system, trialed and now rolled-out on AP22 potlines in Tomago, has been scaled up to fit the AP3X technology. This led to the implementation of an industrial demonstration on a 36-pot section in the Alma smelter, including automatic pot hood opening detection. The operational and environmental performance of the system has been evaluated during the trial. In parallel, the design and proof of concept of an AP60 version has taken place in LRF, preparing for future evaluation as part of the AP60 Jonquière project.

4:40 PM

HF Emission Reduction from Anode Butts Using Covered Trays: *Jean-Pierre Gagne*¹; René Minville Minville¹; Neal Dando²; Mike Gershenson²; Steve Lindsay³; Harold Frenette⁴; Alain Moras⁴; Gilles Dufour⁴; ¹STAS; ²Alcoa Technical Center; ³Alcoa TN; ⁴Alcoa Canada, Aluminerie Deschambault

During the production of aluminum from conventional prebake Hall-Héroult electrolysis, anodes have to be replaced on a regular basis. The anode butts are usually placed on uncovered trays for transportation, a practice that contributes to overall hydrogen fluoride (HF) emission. In 2000, anode tray covers developed by Alcoa Deschambault were implemented to significantly reduce fluoride emissions. In 2004, an Alcoa-STAS R&D team developed a second generation of anode tray covers for the new Alcoa Fjardaál plant. In 2009, the Alcoa STAS R&D team designed and fabricated an experimental test garage to allow the accurate full-scale in-plant measurement of temporal HF emissions from cooling anode butts trays. Over the last two years, comparative measurements were performed on covered and uncovered anode trays in a manner to allow estimation of the overall impact of covered trays back to zero time, or removal from the pot. This paper presents results of these studies.

Atomistic Effects in Migrating Interphase Interfaces - Recent Progress and Future Study: Interfacial Structure with Large Misfit and Deformation-induced Migration

Sponsored by: The Minerals, Metals and Materials Society, TMS Materials Processing and Manufacturing Division, TMS/ASM: Phase Transformations Committee

Program Organizers: Tadashi Furuhashi, Institute for Materials Research, Tohoku University; Sudarsanam Babu, Ohio State University; Hatem Zurob, McMaster University; Jian-Feng Nie, Monash University; Wen-Zheng Zhang, Tsinghua University; James Howe, University of Virginia

Monday PM
March 12, 2012

Room: Europe 3
Location: Dolphin Resort

Session Chairs: Robert Pond, University of Exeter; Jian-Feng Nie, Monash University

2:00 PM Invited

Atomistic Structure and Energetics of the θ' (Al_2Cu) – Aluminium Interface: *Laure Bourgeois*¹; Christian Dwyer¹; Matthew Weyland¹; Jian-Feng Nie¹; Barrington Muddle¹; ¹Monash University

The θ' phase is an effective strengthening precipitate in aluminium alloys and a well-known intermediate phase of the textbook decomposition sequence of an Al-Cu solid solution. Yet the atomistic mechanisms of its (notoriously difficult) nucleation and different growth modes remain poorly understood. In this contribution, aberration-corrected scanning transmission electron microscopy observations will be presented for the interfacial structure between aluminium and θ' precipitates in different Al-Cu-based alloys. In particular, we will show that the coherent interface of θ' with aluminium can adopt a structure that differs from that previously assumed based on the bulk crystal structures. These observations, combined with first-principles energetics calculations, demonstrate that this new interfacial structure constitutes an intermediate state in the atomistics of precipitate thickening. We will also present observations on the interaction between Sn and θ' , and suggest potential factors for the beneficial role of Sn additions in promoting the nucleation of θ' .

2:30 PM

Crystallography and Interfacial Energy of $\text{Al}_6(\text{Fe},\text{Mn})$ Dispersoids Precipitated in AA5182 Alloy: *Yanjun Li*¹; Jesper Friis¹; Wenzheng Zhang²; Lars Arnberg³; ¹SINTEF Materials and Chemistry; ²Department of Materials Science and Engineering, Tsinghua University; ³Department of Materials Science and Engineering, NTNU

$\text{Al}_6(\text{Fe},\text{Mn})$ is an important type of dispersoids in non-heat treatable aluminium alloys containing Mn and Fe. In this work, the morphology, habit plane and orientation of $\text{Al}_6(\text{Fe},\text{Mn})$ dispersoids precipitated during homogenization treatment of an AA5182 alloy have been characterized by using transmission electron microscopy. The orientation relationship between the dispersoids and Al matrix has been determined. The habit plane is found to be normal to a set of $\langle 111 \rangle_{\text{Al}}$'s. The interfacial structure at the habit plane of the dispersoids has been studied by atomic simulation and constrained coincidence site lattice (CCSL) analysis. The orientation of the habit plane and the preferential growth direction of the dispersoids can be explained in terms of a relatively high density of near-coincident site lattice points and a good atom-to-atom matching at the interface. Based on the orientation relationship found in the work, a preliminary first-principles calculation of the interfacial energy has been carried out.

2:50 PM

Interfacial Disconnections at Sb_2Te_3 Precipitates in PbTe: Mechanisms of Strain Accommodation and Phase Transformation at a Tetradymite/Rocksalt Telluride Interface: *Douglas Medlin*¹; N. Heinz²; T. Ikeda²; G. Snyder²; ¹Sandia National Labs; ²California Institute of Technology

Understanding the structure and formation mechanisms of interfaces between different telluride phases is important to the development of thermoelectric nanocomposites. Here, we investigate the interfacial structure of tetradymite precipitates in a rocksalt telluride matrix, focusing in particular on plate-like precipitates of Sb_2Te_3 in PbTe. Using high-resolution transmission electron microscopy (HRTEM), we investigate the structure and arrangement of interfacial disconnections—i.e. interfacial steps possessing dislocation character—observed in this system. Our analyses provide insight concerning the roles of these defects in accommodating the large interfacial misfit (6.7%) in this system and in mediating the transformation from the rocksalt to the tetradymite structure. Our observations also suggest how such interfacial disconnections could arise through the dissociation of crystal lattice dislocations that accommodate the misfit on initially flat segments of the interface.

3:10 PM Break

3:30 PM Invited

Interface Facets in Systems with Large Lattice Misfit: *Wenzheng Zhang*¹; Zhangzhi Shi¹; Xiaopeng Yang¹; ¹Tsinghua University

Well-defined facets of precipitates are often considered to have a coherent or semicoherent structure, but usually no coherent region(s) can be sustained if the precipitates have a significantly larger unit cell than that of the matrix. In this work, facets in systems with large lattice misfit are described with a CS-coherent structure (CS = coincidence site(s)). Two conditions are required to form such a structure in a facet: existence of dense CS at least locally and singularity in the secondary dislocation structure if secondary misfit exists. Satisfaction of both conditions in a rational crystal plane yields a rational facet and otherwise an irrational facet. Guidelines are provided to derive geometry of potential facets according to these conditions, with applications to different precipitation systems. The CS-structures are compared with semicoherent and incoherent structures in terms of ratio of near coincidence site in the structure. Migration of different facets is discussed.

4:00 PM

A Study of Plastic Strain Accommodation during Phase Transformation: *Michael Kuba*¹; David Van Aken¹; ¹Missouri University of Science and Technology

An often-overlooked consequence of phase transformations is the volume change. While elastic accommodation of the volume change has been analytically studied, very few studies have addressed the possibility of parent phase plasticity in accommodating the volume change. Acoustic emission is used here to study melting of embedded indium particles to show that dislocation multiplication occurs in the aluminum matrix to accommodate a 2.5% volume change. The geometrically necessary increase in dislocation density was calculated as $4.1 \times 10^{13} \text{ m}^{-2}$ for a dispersion of sub-micron indium particles in an Al-17In alloy. Thermomechanical processing was also used to change the size and distribution of the indium particles to show a difference in acoustic emission signal strength of particles embedded at grain boundaries versus those embedded within the grains. Previous internal friction studies have shown that particles melting at grain boundaries have shorter relaxation times.



TMS 2012

141st Annual Meeting & Exhibition

MONDAY PM

4:20 PM

Grain Rotation and Transformation of Austenite Grains upon Straining of a Si-Alloyed TRIP Assisted Steel: Ganesh Kumar Tirumalasetty¹; Marijn A Van Huis²; Cees Kwakernaak³; Jilt Sietsma³; Wim G Sloof³; Henny W Zandbergen⁴; ¹Materials Innovation Institute (M2i)/ Kavli Institute of Nanoscience, Delft University of Technology; ²Kavli Institute of Nanoscience, Delft University of Technology/EMAT, University of Antwerp; ³Department of Materials Science and Engineering, Delft University of Technology; ⁴Kavli Institute of Nanoscience, Delft University of Technology

Si-alloyed TRIP (transformation induced plasticity) steel was subjected to uni-axial straining experiments in order to assess the role of microstructure on the mechanical stability of austenite grains. Individual austenite grains were monitored before and after straining (up to 20 %) using electron back scattered diffraction (EBSD). Three different types of austenite grains were distinguished with different transformation behaviors. It was found that *twinning austenite grains* and *austenite grains present at grain boundaries* between larger ferrite grains typically transform first, in contrast to *embedded austenite grains* that are completely surrounded by a single ferrite grain. In the latter case, straining leads to rotations of austenite grains within the ferrite matrix before TRIP transformation into martensite occurred. The analysis suggests that in addition to the austenite-martensite transformation, austenite grain rotation is a significant factor contributing to the ductility of these steels.

4:40 PM

Strain Glass Caused by Nano-Scale Randomness -- Strain Glass Transition in Low-Temperature-Aged Ti48.7Ni51.3 Alloy: Yuanchao Ji¹; Xiaobing Ren¹; Xiangdong Ding²; ¹National Institute of Materials Science; ²Los Alamos National Laboratory

Strain glass, a frozen short-range strain-ordered state, has been discovered in many defect-containing ferroelastic/martensitic alloys. Up to now all found strain glass systems have been shown to originate from atomic-scale randomness: randomly distributed point defects. In this study, we report an interesting finding that nano-scale randomness can also lead to the formation of strain glass. The sample under investigation was a Ti48.7Ni51.3 alloy, which undergoes a normal B2-B19' martensitic transition in a precipitation-free state. However, martensitic transformation is suppressed and the sample undergoes a strain glass transition when nano-sized, randomly distributed Ti3Ni4 precipitates (i.e., nano-scale randomness) were introduced into the alloy by a low-temperature aging treatment. The strain glass transition is characterized by a mechanical susceptibility anomaly with frequency-dependence, ergodicity-breaking, and invariance in average structure. The present finding suggests that nano-scale randomness, besides atomic-scale randomness, can create frustration to a ferroelastic system and lead to the formation of strain glass.

Biological Materials Science Symposium: Mechanical Behavior of Biological Materials

Sponsored by: The Minerals, Metals and Materials Society, TMS Electronic, Magnetic, and Photonic Materials Division, TMS Structural Materials Division, TMS: Biomaterials Committee
Program Organizers: Nima Rahbar, University of Massachusetts Dartmouth; Candan Tamerler, University of Washington; Po-Yu Chen, University of California, San Diego; Molly Gentleman, Texas A&M University

Monday PM
March 12, 2012

Room: Swan 7
Location: Swan Resort

Session Chairs: Po-Yu Chen, National Tsing Hua University; Candan Tamerler, University of Washington

2:00 PM Invited

A Model for Diffuse Axonal Injury: K Ramesh¹; ¹Johns Hopkins University

Computational models are often used as a tool to study impact biomechanics. The fidelity of such models relies heavily on an accurate description of the behavior of the materials involved, and the use of an appropriate measure of injury. Diffuse axonal injury (DAI) accounts for a large percentage of deaths due to brain trauma and is characterized by damage to neural axons. We have developed a measure of diffuse axonal injury based on an axonal strain injury criterion. We model the white matter as a nonlinear, anisotropic material, and use diffusion tensor imaging to incorporate the structural orientation of the neural axons into the computational model. We show that the degree of injury that is predicted in a computational model of DAI is highly dependent on the incorporation of the axonal orientation information and the inclusion of anisotropy into the constitutive model for white matter.

2:30 PM

Nanoscale Structural and Mechanical Characterization of Conch Shells: Haoze Li¹; Zhi-Hui Xu¹; Xiaodong Li¹; ¹University of South Carolina

We used conch shells as an example to unveil that the third-order lamellae, which were thought to be signal crystals and the basic building blocks for conch shells, are composed of nanoparticles with diameters ranging from 20 to 45 nm. The nanocomposite third-order lamellae are not brittle, but somewhat ductile. The findings advance our understanding of the mystery of seashells' strengthening and toughening mechanisms, provide additional design guidelines for developing biomimetic materials, and lay a constitutive foundation for modeling of the deformation and fracture of biomaterials.

2:50 PM

Structure and Mechanical Behavior of the Dasyus Novemcinctus Shell: Hongjoo Rhee¹; Mark Horstemeyer¹; ¹Center for Advanced Vehicular Systems, Mississippi State University

Multiscale hierarchical structures, material properties, and mechanical behaviors of the nine-banded armadillo (*Dasyus novemcinctus*) shell were studied to provide fundamental knowledge for understanding biological composite systems. The armadillo's forward and rear shells comprise a sandwich composite structure of functionally gradient material, having relatively denser exterior bony layers and an interior bony network of foam. The band shell revealed a more complicated structure where adjacent bands are partially overlapped and connected with each other to provide flexibility in addition to protection. Compression test results showed a typical nonlinear deformation behavior similar to synthetic foams in which microbuckling is a key inelastic deformation mechanism. A comparison and contrasting study of the structure-property relations

between the armadillo shell and other biological structural materials could provide fundamental understandings for deformation mechanisms which could lead to the development of novel bio-inspired safety system design methodologies.

3:10 PM

Self Healing Characteristics of Human Enamel: *Camilo Rivera*¹; Dwayne Arola¹; Alex Ossa¹; ¹Eafit University

Tooth enamel is the hardest and most highly mineralized substance in the human body. There have been a number of studies dedicated to understand the crack growth resistance characteristics of this hard tissue using microindentation and fracture toughness experiments. These studies have provided an insight towards the main fracture mechanisms of this hard tissue and their correlation with its microstructure. However, there has been limited research aimed at understanding the self-healing characteristics of human enamel, a concept of substantial interest in the field of dentistry and regarding to the potential bioinspiration. This work presents a study of the self-healing ability of “young” human enamel from patients between 18-25 years of age. The apparent fracture toughness and brittleness of enamel were studied by means of microindentation. Microscopic observations revealed that cracks began the healing process immediately after initiation and finished after approximately 48 hours, reaching crack length reductions between 5-15%.

3:30 PM

Modeling Human Eye under Shock Loading: *Nicola Bonora*¹; Luca Esposito¹; Chiara Clemente¹; Tommaso Rossi²; ¹University of Cassino; ²Ospedale Oftalmico di Roma

The mechanical response of biological materials is complex and difficult to be determined experimentally. Anisotropy and visco-elasticplastic behavior make difficult the identification of the effective constitutive response under general stress state. When dealing with dynamic events, such as blunt impact or blast loading, the situation becomes even more complex due to strain rate and pressure dependent effects. Here a calibration procedure for identifying the more appropriate constitutive model to simulate the response of human eye tissues under dynamic loading conditions, is presented. A finite element model for the human eye was developed and constitutive model selection for tissues and the vitreous has been performed base on test data reported in the literature. Using the structural optimizer modFRONTIER, model parameters have been determined simulating the in-vitro instrumented impact experiment reported by Delori et al. (1969). The calibrated material models have been validated under different load rate and state of stress conditions.

3:50 PM Break

4:00 PM Invited

Structure and Mechanical Behavior of Fish Scales: Wen Yang¹; Yen-Shan Lin²; Jianan Li³; Po-Yu Chen⁴; Maria Lopez¹; Vincent Sherman¹; Eugene Olevsky²; *Marc Meyers*¹; ¹University of California, San Diego; ²San Diego State University; ³Shanghai Jiao Tong University; ⁴National Tsing Hua University

Scales provide protection and safeguard of fish from predators. Most scales have the similar constituents as other hard tissues such as bone and teeth, which mainly contain type-I collagen fibers and calcium phosphate-based minerals. The scales of two large fish, *Arapaima gigas* (a large Amazon basin fish) and *Atractosteus spatula* (the largest North American fresh water fish) are characterized mechanically and microstructurally. The *Arapaimas* scales have a laminate composite structure composed of an external mineralized layer and internal lamellae with thickness of 50-60 μm each and composed of collagen fibers with $\sim 1\mu\text{m}$ diameter. The alignment of collagen fibers is consistent in each individual layer but varies from layer to layer, forming a non-orthogonal plywood structure, known as Bouligand stacking. The *Atractosteus* scales are highly mineralized and contain an external ganoin layer and an internal bony layer containing collagen fibers with a thickness of 100~200 nm. Micro and nanoindentation hardness tests were carried out, revealing the

variation in values that provides optimum protection. *Arapaima* scales have a gradually decreasing hardness from external layer to the internal layer, while *Atractosteus* scales have a high hardness in their external layer (ganoin) and a discontinuous drop in internal layer. Tensile and bending testing of both scales carried out in the dry and wet conditions shows that the strength and stiffness are hydration dependent. The structure and mechanical properties are discussed in terms of the protection mechanisms for these fishes.

4:30 PM

Structural and Mechanical Design of Zebra Shark Teeth: Hao-Jen Fang¹; Chang-Yu Sun¹; Yao-Tien Ku¹; *Po-Yu Chen*¹; ¹National Tsing Hua University

The shape and morphology of sharks' teeth vary from species to species depending on their diet. Shark species that feed primarily on soft-bodied prey such as fishes and mammals have needle-like, sometimes serrated teeth for gripping and cutting while those that consume hard shelled mollusks and crustaceans have dense flattened teeth more appropriate for crushing and grinding. In this study, structure and mechanical properties of the teeth of zebra sharks (*Stegostoma fasciatum*) were investigated. Zebra shark have multiple rows and series of tricuspid shaped teeth, forming a crushing surface which are able to crush the sturdiest hard-shelled prey. The teeth consist of a hard external layer of enameloid and tough internal dentine. Nanoindentation and compression tests were performed on the teeth in dry and hydrated conditions. Results were compared with the soft prey-eating great white shark teeth and different functional adaptations and design strategies between the two species were discussed.

4:50 PM

Structure and Mechanical Properties of Alligator Osteoderms: *Irene Chen*¹; Marc Meyers¹; ¹University of California at San Diego

Alligator osteoderms are protective bony-plates embedded underneath the skin on the back of the animal. The osteoderm has a disc-like morphology with a tilted convex ridge at the middle of the plate with depressions on the surface and a porous region in the cross-section. Its main constituents are hydroxyapatite crystals. An abundance of granular mineralization is seen in untreated tissue. With the deproteinization process, SEM images show a series of bundles of mineralized fibrillar structures oriented along the same direction, rather than in a random orientation. The demineralization process was completed by dissolving the minerals on the surface of the osteoderm. The SEM images reveal that the minerals being removed left hollow spaces with honeycomb-like structure and circular geometry of cells of 5 μm in diameter. Mechanical properties (i.e compression and impact) will be discussed. Nano and micro-indentation testings and CT scanning will be performed. Research support by NSF: DMR-1006931

5:10 PM

A Comparative Study of the Compressive Mechanical Properties of Young and Old Bovine Cortical Bone: *Ekaterina Novitskaya*¹; Zherrina Manilay¹; Steve Lee¹; Joanna McKittrick¹; ¹UCSD

The mechanical properties of untreated, demineralized, and deproteinized 18 month and 6 month old cortical bovine femur bones were investigated by compression testing in quasi-static regime in two anatomical directions (longitudinal and transverse). The compressive strength and elastic modulus were found to be smaller for the younger bone. Microstructural features, including the amount of osteonal bone, osteon morphology, and structure of Haversian systems of the samples from two different age groups were studied by optical and scanning electron microscopies. It was found that younger bone has a larger amount of drifting osteons and a higher level of porosity, both characteristics of a faster growing tissue. Energy-dispersive X-ray spectroscopy was applied to the samples from both age groups to measure the difference in mineralization between osteonal and interstitial (woven) bone parts. This research is funded by the National Science Foundation, Division of Materials Research, Ceramics Program (Grant 1006931).



Bulk Metallic Glasses IX: Alloy Development and Mechanical Properties

Sponsored by: The Minerals, Metals and Materials Society, TMS Structural Materials Division, TMS/ASM: Mechanical Behavior of Materials Committee

Program Organizers: Peter Liaw, The University of Tennessee; Hahn Choo, The University of Tennessee; Yanfei Gao, The University of Tennessee; Gongyao Wang, University of Tennessee

Monday PM Room: Swan 6
March 12, 2012 Location: Swan Resort

Session Chairs: C. Liu, Hong Kong Polytechnic University; Y. Yokoyama, Institute for Materials Research

2:00 PM Keynote

Atomic Structures and Mechanical Properties of Bulk Metallic Glasses: C. T. Liu¹; Yong Yang²; X. J. Liu²; ¹City University of Hong Kong; ²Hong Kong Polytechnic University

Because of the lack of long-range periodic lattice structures, the mechanical behavior of bulk metallic glasses (BMGs) is fundamentally different from that of crystalline materials. Thus, the understanding of the mechanical behavior of BMGs with complex amorphous structures is the topic of active research at the present time. In this paper, we will provide a brief review of the recent research findings of unusual mechanical properties of BMGs, including size effect, anelastic deformation behavior, evolution of shear-band embryos, percolation for macroscopic yielding, stability of shear-band propagation, and universal strain for fracture. We intend to explain these unique properties with the atomistic models, involving both tightly-bonded atomic clusters and loosely-bonded free volumes, proposed recently.

2:30 PM

Production and Mechanical Properties of Roll Bonded Bulk Metallic Glass/Aluminium Laminates: Daniel East¹; Mark Gibson¹; Daniel Liang¹; Jian-Feng Nie²; ¹CSIRO; ²Monash University

Hybrid structures combining a high strength brittle material with a soft low strength material have been shown to be a successful method for the improving the toughness and flexural strength of the brittle material. In this study the production of bulk metallic glass and aluminium laminates by a combination of twin roll casting and roll bonding will be presented. The production variables must be such that the BMG retains its amorphous structure and also bonds adequately to the crystalline metal. The effect of rolling conditions on the bonding of BMG to crystalline metal will be presented. The effect of lamellae spacing and size on the impact toughness and flexural strength of the resultant hybrid material will also be presented. The combination of two scalable technologies in twin roll casting and roll bonding may open markets for bulk metallic glass hybrid materials to the sheet materials market.

2:40 PM Invited

Micro-Scale Moldability and Mechanical Properties of Hypoeutectic Zr-Based Metallic Glasses: Sae Takashima¹; T. Yamasaki¹; K. Fujita²; A. R. Yavari³; A. Inoue⁴; Y. Yokoyama⁵; ¹University of Hyogo; ²Ube National College of Technology; ³SIMAP-CNRS; ⁴Tohoku University; ⁵University of Tennessee

Good micro-scale moldability is one of significant advantages of Zr-based bulk metallic glasses (BMGs), whereas the value of viscosity in supercooled liquid state is rather high to compare with Au-, Pd- and Pt-based BMGs. In this study, we tried to use the micro-patterned metallic mold for embossing process of hypoeutectic Zr-based BMG, therefore, we tried to reduce both T_g and viscosity in supercooled liquid state (SCL). As a conclude, we succeeded to found out hypoeutectic BMG with low viscosity of the order of 105 Pas in SCL, and enables to perform the

embossing process for micro patterning by using the tough and long life Ni-W nanocrystalline metallic mold developed by Prof. T Yamasaki. We also examine the mechanical properties of hypoeutectic BMGs exhibiting a low T_g, low viscosity in SCL and wide temperature range of SCL under heating. Good plasticity is also obtained in there hypoeutectic BMGs under tensile loading.

3:00 PM Invited

Structural Order and Density in Bulk Metallic Glass Forming Liquids: Ken Kelton¹; James Bendert¹; Anup Gangopadhyay¹; Nicholas Mauro¹; ¹Washington University

Metallic liquids develop significant short- and medium-range topological and chemical order with supercooling; this is often dominated by icosahedral short-range order (ISRO). Experimental and theoretical studies indicate that this ISRO is intimately associated with the glass transition and raises the nucleation barrier for crystallization, which can favor glass formation. It is reasonable to expect a correlation between the liquid density and this structural ordering, with more ordered and stable liquids having a higher number density. Supporting this, a recent study showed that the density of Cu-Zr glasses showed local maxima at the best glass forming compositions. However, our recent studies show no corresponding maxima in the liquid densities at the liquidus temperatures. Instead, the best glass formers show the largest volume expansion coefficient. Possible reasons for this will be discussed. Supported by NASA (NNX07AK27G & NNX10AU19G) and the National Science Foundation (DMR-08-56199).

3:20 PM Break

3:35 PM Invited

Amorphous Multilayers in the Al-Mn System: Wenjun Cai¹; Shiyun Ruan¹; Christopher Schuh¹; ¹MIT

The lack of work-hardening and rapid strain localization of metallic glasses present a significant limitation upon their application potential. Amorphous/crystalline or amorphous/amorphous composites have the potential to enhance toughness of such amorphous materials without significantly compromising strength. In this work, Al-Mnx/Al-Mny multilayers were electrodeposited using a single bath process in room temperature ionic liquid. By varying the Mn composition between layers, the amorphous phase content in this single system can be systematically modulated, delivering microcomposites of amorphous and nanostructured phases. The microstructures of the multilayered Al-Mn are characterized and nanoindentation and nanoscratch tests are performed to demonstrate the property differential between layers. Control over both the layer structure and the structure within individual layers together offers unique opportunities to optimize multiple properties simultaneously.

3:55 PM Invited

The Role of Cu in an Iron-Based Bulk Metallic Glass: Michael Miller¹; J. Gao²; Y Wu²; Z. Lu²; ¹Oak Ridge National Laboratory; ²University of Science and Technology Beijing

Low cost, iron-based bulk metallic glasses are potential materials for use as transformer cores, as they can be processed to have superior soft magnetic properties to grain-oriented silicon steels and can be cast directly in the final form for the core elements. Doping a soft magnetic Fe_{76-x}C_{7.0}Si_{3.3}B_{3.0}P_{8.7}Cu_x bulk metallic glass alloy with 0.3% Cu dramatically improves the glass forming ability. The roles of Cu (x=0, 0.3 and 0.7 at. % Cu) and the other solutes on the microstructure in the as-spun state and after an isothermal anneal of 0.5 h at 729 K has been investigated by atom probe tomography. The results indicate that the microstructure has phase separated into a fine scale distribution of Fe-rich and Cu-rich precipitates and carbides during annealing. Research supported by ORNL's Shared Research Equipment (SHaRE) User Facility, which is sponsored by the Office of Basic Energy Sciences, U.S. Department of Energy.

4:15 PM**Glass Formation and Properties of Fe- and Co-Based Ternary Bulk Metallic Glasses:** Jianfeng Wang¹; Ran Li¹; Tao Zhang¹; ¹Beihang University

Recently, we developed two families of simply ternary bulk metallic glasses (BMGs), i.e. Fe-P-C and Co-Ta-B alloys. For the Fe-P-C system, the glass-forming range and ability were pinpointed. As a typical sample for the Fe-based BMGs, Fe₈₀P₁₁C₉ alloy show combinative advantages of advanced structural and functional materials with favorable soft-magnetic properties (magnetic polarization of 1.49 T, coercivity of 4 A/m and effective permeability of 11,000 at 1 kHz) and mechanical properties (compressive strength: 3.2 GPa and plasticity: ~1.4%). The ternary Co-Ta-B BMGs show ultrahigh compressive strength of 5.6–6.0 GPa, high specific strength of 639–654 Nm/g, Vickers hardness of 15–16 GPa, and distinct plastic strain of 0.5–1.5%. The strength and the specific strength of the Co-based BMGs are the highest values reported for bulk metallic materials known so far. The possible reasons of the superior mechanical properties related with atomic and electronic structures were clarified.

4:25 PM Invited**Metallic Glass Wireless Biosensors for Pathogen Detection:** Suiqiong Li¹; Shin Horikawa¹; Yating Chai¹; Bryan Chin¹; ¹Auburn University

Metallic glass alloys of the Fe-B and Fe-Ni families display the unique property of magnetostriction. Compared with crystalline materials, these alloys exhibit some of the highest possible elastic-magnetic energy conversion efficiencies and hence make ideal sensors. Recently, free-standing, phage-based biosensors have been fabricated from these alloys. The biosensors are composed of a magnetostrictive resonator that is coated with a bio-molecular recognition element that binds specifically with a target pathogen. Once the biosensor comes into contact with the target pathogen, binding occurs. This causes an increase in the mass of the resonator resulting in a decrease of the biosensor's resonant frequency. These biosensors can be manufactured using standard microelectronics fabrication procedures, resulting in a cost of less than 1/1000 of a cent per biosensor. The potential market for commercial applications of these metallic glass biosensors in food safety, medical and bioterrorism defense is estimated to exceed 50 Billion USD by 2015.

4:45 PM**Metallic Glasses for Electro-Catalytic Applications:** Sundeep Mukherjee¹; Marcelo Carmo¹; Golden Kumar¹; Andre Taylor¹; Jan Schroers¹; ¹Yale University

Materials for catalytic applications require large surface area and desirable chemistry to facilitate the reaction kinetics. Metallic glasses are multi-component alloys that exist in a wide range of chemical compositions and we have recently shown, have tunable nanostructure with large active surface area. Motivated by these characteristics, we have explored the use of a number of metallic glasses as electro-catalysts in direct alcohol fuel cells. We demonstrate that the activity and durability of the metallic-glass nanostructures are superior compared to benchmark catalysts. The activity of these catalysts is further enhanced by de-alloying mediated surface area enhancement. New strategies to develop large surface area nanostructures by accelerated de-alloying will be discussed.

4:55 PM Invited**Impact of Secondary Amorphous Phases on Properties of Metallic Glasses:** Eun Soo Park¹; ¹Seoul National University

The secondary amorphous phases (SAPs) in metallic glasses can be classified into two groups; those in phase separating metallic glasses (PSMGs) and multiple shear planes in pre-deformed metallic glasses. It is our understanding that SAPs in a metallic glass matrix can have a

significant influence on the properties of metallic glasses like secondary phases in crystalline materials. However, there has been no systematic approach to understand the impact of SAPs on these metallic glasses. In this study, we examine the effect of SAPs on properties of various metallic glasses. First, we will provide a systematic discussion of the relationship between SAPs and properties of PSMGs. Second, we will discuss how multiple shear planes work as SAPs in metallic glass matrix based on variation of their properties in pre-deformed metallic glasses. Our results would contribute to a deeper understanding of various roles SAPs play in metallic glass matrix.

5:15 PM**Formation and Magnetic Properties of New CoTiZrCo Bulk Amorphous and Nanocrystalline Composites:** Yang Yuanzheng¹; Qiu Junhua¹; Chen Xianchao¹; Xie Zhiwei¹; ¹Guangdong University of Technology

In this paper, the formation of new copper-based bulk metallic glasses containing some magnetic elements and their magnetic properties were studied. Fully amorphous alloys Cu_{50.4}Ti_{27.1}Zr_{16.2}Co_{6.3} and Cu_{50.9}Ti_{27.4}Zr_{16.4}Co_{5.3} with diameter of 3mm could be successfully prepared. The thermal stability, microstructure, magnetic properties and magnetoresistance effect were detected by DSC, XRD, SEM, VSM and PPMS, respectively. With the heat-treatment temperature increase, the saturated magnetization, Ms of Cu_{50.4}Ti_{27.1}Zr_{16.2}Co_{6.3} alloy increases slightly; while Ms of Cu_{50.9}Ti_{27.4}Zr_{16.4}Co_{5.3} alloy has little change. Besides, Ms of the alloy Cu_{50.9}Ti_{25.4}Zr_{16.4}Co_{5.3}Ni₂ reaches to the maximum value about 17.0emu/g at 470 K for 30min. For the Cu_{50.9}Ti_{27.4}Zr_{16.4}Co_{5.3} alloy hold under 480 K for 60min and Cu_{50.9}Ti_{25.4}Zr_{16.4}Co_{5.3}Ni₂ alloy hold under 470 K for 30min, both of them have no MR effect at temperature 10K. But at 300K, MR effect of the former increases slowly to about 0.4%, while this effect of the latter increases to 1.2% at applied magnetic field about 30kOe.

5:25 PM**Fabrication of Mg-Based Amorphous Composites:** Junhua You¹; ¹Shenyang University of Technology

The microstructures, phase constituents, glass forming ability (GFA) and mechanical properties of Mg-based amorphous composites fabricated by copper casting were investigated by scanning electron microscopy, X-ray diffraction and universal mechanical tester. The results indicate that the second phases can be observed in the amorphous phase of alloy samples. With the adding of different metal elements, the kinds and contents of the second phases are different. The second phases of alloy samples are all the crystal phases, and the crystal phases increase the strength of alloys in different degrees. The compressive strength of (Mg_{58.5}Cu_{30.5}Y₁₁)_{0.9}(Zr₃₅Ti₃₀Be_{27.5}Cu_{7.5})_{0.1} amorphous composites in diameter of 3mm is 953.8MPa.



TMS 2012

141st Annual Meeting & Exhibition

MONDAY PM

CFD Modeling and Simulation in Materials Processing: CFD Modeling in Materials Processing II

Sponsored by: The Minerals, Metals and Materials Society, TMS Extraction and Processing Division, TMS Materials Processing and Manufacturing Division, TMS: Process Technology and Modeling Committee, TMS: Solidification Committee
Program Organizers: Laurentiu Nastac, The University of Alabama; Lifeng Zhang, Missouri University of Science and Technology; Brian Thomas, University of Illinois at Urbana-Champaign; Adrian Sabau, Oak Ridge National Lab; Nagy El-Kaddah, The University of Alabama; Adam Powell, Metal Oxygen Separation Technologies, Inc.; Hervé Combeau, Institut Jean Lamour

Monday PM Room: Asia 4
March 12, 2012 Location: Dolphin Resort

Session Chairs: Adam Powell, Metal Oxygen Separation Technology; Adrian Sabau, Oak Ridge National Lab

2:00 PM Keynote

Multi-Physics Modeling of Molten Salt Transport in Solid Oxide Membrane (SOM) Electrolysis and Recycling of Magnesium: *Adam Powell¹; Soobhankar Pati¹; ¹Metal Oxygen Separation Technologies, Inc.*

Solid Oxide Membrane (SOM) Electrolysis is a new energy-efficient zero-emissions process for producing high-purity magnesium and high-purity oxygen directly from industrial-grade MgO. SOM Recycling combines SOM electrolysis with electrorefining, continuously and efficiently producing high-purity magnesium from low-purity partially oxidized scrap. In both processes, electrolysis and/or electrorefining take place in the crucible, where raw material is continuously fed into the molten salt electrolyte, producing magnesium vapor at the cathode and oxygen at the inert anode inside the SOM. This paper describes a three-dimensional multi-physics finite-element model of ionic current, fluid flow driven by argon bubbling and thermal buoyancy, and heat and mass transport in the crucible. The model predicts the effects of stirring on the anode boundary layer and its time scale of formation, and the effect of natural convection at the outer wall. MOxST has developed this model as a tool for scale-up design of these closely-related processes.

2:25 PM Invited

Numeric Modeling for the Carbothermic Aluminum Process: *David Roha¹; ¹Alcoa*

The high temperatures of the Carbothermic Aluminum Process make observations and measurements of an actual system very difficult. Therefore, from the onset Alcoa has used various numeric models to help us understand the physical phenomena occurring. Thermodynamic and Process codes have been used to predict its performance. Finite Element and CFD codes have been used to compute electric current and the resultant Joule heating. The flow of the molten slag and aluminum metal, which is mainly driven by bubbly flow is simulated using Eulerian/Eulerian multiphase treatment. Convective heat transfer, chemical reaction and sidewall freezing is part of the model. The gaseous headspace above the liquids is modeled separately as a single phase gaseous flow with Lagrangian transport of feed particles. Heat transport is mainly due to radiation through a dusty medium. Back-reaction of Al and Al₂O vapors with CO to form a fine condensate dust is calculated.

2:50 PM Invited

A Coupled CFD-PBE Approach Applied to the Simulation of the Inclusion Behavior in a Steel Ladle: *Jean-Pierre Bellor¹; Valerio De Felice¹; Ismael L. A. Daoud¹; Alain Jardy¹; ¹Institut Jean Lamour*

Gas-stirring ladle treatment of liquid metal has been pointed out for a long time as the processing stage mainly responsible for the inclusion population of specialty steels. A steel ladle is a complex three-phase reactor, where

strongly dispersed inclusions are transported by the turbulent liquid metal / bubbles flow. We have coupled a population balance model with CFD in order to simulate the mechanisms of transport, aggregation, flotation and surface entrapment of inclusions. The simulation results, when applied to an industrial gas-stirring ladle operation, show the efficiency of this modelling approach and allow us to compare the respective roles of these mechanisms on the inclusion removal rate.

3:15 PM Invited

Multiphysics CFD Modeling of a Free Falling Jet during Melt-Blowing Slag Fiberization: *Dimitrios Gerogiorgis¹; Dimitrios Panias¹; Ioannis Paspaliaris¹; ¹National Technical University of Athens (N.T.U.A.)*

Red mud fiberization is a process with remarkable potential, alleviating environmental pressure by transforming an aluminum by-product into marketable products. A promising mineral wool process is molten slag fiberization via an impinging air jet, which avoids mechanical wear and rotating parts. The molten slag which remains after pig iron casting flows out of a heated ladle orifice at high temperature (1600 °C) and adjustable flowrate, forming a free-falling vertical jet which visibly radiates its excessive heat: at a given distance, a high-velocity impinging air jet meets the vertical melt jet perpendicularly (or at an angle), inducing intensive droplet generation and subsequent fiber elongation. This paper focuses on high-fidelity CFD modeling of the molten jet flow under external cooling: the model encompasses all physicochemical phenomena (melt laminar flow, radiative cooling), considering temperature-dependent slag transport properties to understand how operational degrees of freedom (manipulated variables) can be used for process optimization.

3:40 PM Break

4:00 PM

Direct Numerical Simulation of Inclusion Turbulent Deposition at Liquid Metal/Slag Interface: *Arunvady Xayaseh¹; Laurent Joly²; Hervé Duval¹; ¹Laboratoire de Génie des Procédés et Matériaux (LGPM) - Ecole Centrale Paris; ²Département Aérodynamique, Energétique et Propulsion (DAEP) - Institut supérieur de l'aéronautique et de l'espace*

Oxide inclusion transport and capture at liquid metal/slag interface is studied using direct numerical simulation of the liquid flow combined with Lagrangian particle tracking under conditions of one way coupling. The interface is modelled as a non deformable free slip surface. Turbulence is generated by a random forcing in a finite region parallel to the interface. The inclusions are randomly introduced in this region and tracked until their capture at the interface. The body force, the drag force and the forces due to fluid inertia and oxide inertia are taken into account in the inclusion dynamic equation. The effects of the turbulent Reynolds number and of the inclusion characteristics on the deposition velocity are examined. Moreover, the importance of the near surface turbulent events, sweeps and ejections, on the inclusion capture is highlighted.

4:20 PM

A Numerical Simulation of the Influence of Droplet Impact Dynamics on the Microstructure of Plasma Sprayed Coatings: *Jeffrey Yanke¹; Rodney Trice¹; Matthew Krane¹; ¹Purdue Center for Metal Casting Research, School of Materials Engineering, Purdue University*

In plasma sprayed coatings, the impacting droplets' sizes, velocities, and angles of impact are dominant factors in determining the coating structure. To better understand the links between these deposition conditions and coating structure, a numerical model of the interaction of droplets as they are deposited on the substrate was developed. This model employs a volume of fluid method to track the droplet surfaces and the SIMPLER algorithm to solve the momentum equations on a staggered grid. These methods are combined with a novel technique for tracking multiple droplets and a simple solidification model that includes undercooling. This tool is used to investigate the role of deposition conditions on the evolution of the YSZ coating microstructure at the substrate as well as after the deposition of several layers of droplets. In addition, the model predicts the cooling rates of droplets as a function of thickness of the coating.

4:40 PM

CFD Calculation of Nitrogen Gas Quenching for Steel Ring Gears:

*Junsheng Wang*¹; Xuming Su¹; Mei Li¹; Ronald Lucas¹; William Dowling¹; ¹Ford Motor Company

Conjugated (solid/fluid) heat transfer by forced convection through recirculating gas has many practical applications. In this study, we present CFD calculations of gas quenching process during the production of steel ring gears. It is based on the heat conduction equation and $k-\gamma$ equations for turbulence flow solved by a finite volume scheme implemented in Fluent. Comparing to precise measurements of thermal history inside the gears, we found that both convection and radiation must be considered. We devised an approach to incorporate transient heat flux, making this model applicable to process design. Temperature at different locations of the quenching load is not only controlled by quenching velocity and pressure but also determined by the geometry of cooling system. Successful application of CFD model helped optimizing geometry design and operating conditions. In addition, non-uniformity of temperature within a gear was also successfully predicted and coupled to finite element analysis for distortion prediction.

5:00 PM

Numerical Simulation of Erosion Using Computational Fluid Dynamics:

*Harpreet Grewal*¹; Harpreet Singh¹; Anupam Agarwal¹;

¹Indian Institute of Technology Ropar

Erosion related problems in industrial appliances causes huge loss of valuable resources especially due to the presence of solid particles in working medium. Number of erosion models available in the literature; have claimed to predict the erosion response better. In this work, some of these erosion models have been evaluated using finite volume frame work through computational fluid dynamics (CFD) methodology. Three most commonly used experimental test rigs (solid particle and un submerged slurry jet type and pot type) have been simulated and a comparison with the experimental results has been done. The study helps in understanding the effect of fluid medium and flow pattern on the erosion process. The knowledge acquired shows that phenomenological based erosion models give better results considering the wide range of operating parameters. The in-depth study of the flow field shows the possibility that erosion mechanism, being a parameter dependent, could change with location on the same specimen.

5:20 PM

A CFX-based Model of Ironmaking Blast Furnace Considering Layered Cohesive Zone:

*Yansong Shen*¹; Baoyu Guo¹; Aibing Yu¹; Sheng Chew¹; Peter Austin¹; ¹UNSW

A CFX-based mathematical model is developed to describe the flow-heat transfer-chemical reactions behaviours of gas-solid-liquid phases in an ironmaking blast furnace, where the layered cohesive zone is considered explicitly. The typical in-furnace phenomena of an operating blast furnace are simulated in terms of multiphase flow, temperatures, gas composition and reduction degree etc. The effect of different model geometry is investigated by means of comparing the predictions from slot model and sector model. The results indicate that the treatment of layered cohesive zone can naturally predict the in-furnace phenomena of a layered-burden blast furnace. The sector model gives significantly different predictions compared to the slot model. This model offers a cost-effective and easy-transferable tool to understand and optimize blast furnace operation.

5:40 PM

Modelling Pulverized Coal Injection in a Blast Furnace:

*Yansong Shen*¹; Aibing Yu¹; Paul Zulli¹; ¹UNSW

In order to understand the complicated phenomena of pulverized coal injection (PCI) in blast furnace (BF), several mathematical models have been developed, ranging from pulverized coal combustion in a pilot-scale test rig to coal/coke combustion in a real BF. This paper describes these PCI models in aspects of model developments and model applicability in practice. It is indicated that the three PCI models are all able to describe PCI operation qualitatively. The model of coal/coke combustion in a real

BF is more reliable for simulating in-furnace phenomena of PCI operation qualitatively and quantitatively. Such model gives a more reliable burnout prediction over the raceway surface, which could better represent the amount of unburnt char entering the coke bed. These models are useful for understanding the flow-thermo-chemical behaviours and then optimising the PCI operation in practice.

Characterization of Minerals, Metals, and Materials: Characterization of Non-Ferrous Materials

Sponsored by: The Minerals, Metals and Materials Society, TMS Extraction and Processing Division, TMS: Materials Characterization Committee

Program Organizers: Jiann-Yang Hwang, Michigan Technological University; Sergio Montero, State University of North Rio De Janeiro; Chenguang Bai, Chongqing University; John Carpenter, US Department of Energy; Donato Firrao, Politecnico di Torino; Byoung-Gon Kim, Korea Institute of Geoscience & Mineral Resources; Mingdong Cai, Schlumberger

Monday PM

March 12, 2012

Room: Asia 2

Location: Dolphin Resort

Session Chairs: Igor Bunin, Research Institute of Comprehensive Exploitation of Mineral Resources RAS; Byoung-Gon Kim, Korea Institute of Geoscience & Mineral Resources

2:00 PM

Characterization of New Phases in the Ti-Pt System:

*Karem Tello*¹; Anita Garg²; Ronald Noebe²; Michael Kaufman¹; ¹Colorado School of Mines; ²NASA Glenn Research Center

Platinum additions to Nitinol shape memory alloys, SMAs, increase their martensitic transformation temperatures and make them potentially attractive as high temperature SMAs. Unfortunately, the Ti-Pt phase diagram is poorly understood in the range 30-50 at.% Pt making the development of HTSMAs difficult. Alloys in this composition range have been characterized using DTA, SEM and TEM methods and found to frequently contain more than two phases after equilibration treatments; this suggests that interstitial contamination must be complicating the results and should be considered in any phase diagram analyses. Furthermore, two new phases were observed, namely Ti_3Pt_3 and Ti_4Pt_3 the former with a hexagonal structure $P6_3/mcm$, while the latter has not been fully characterized but has a complex and lower-symmetry structure that appears to be structurally related to Ti_3Pt_3 . Attempts to determine the crystal structure of the Ti_4Pt_3 phase have been made using an *ab-initio* approach and the results will be presented.

2:15 PM

Characterization of Sn Whiskering by In Situ Nanoindentation in a Scanning Electron Microscope :

*Nicholas Chapman*¹; Jason Williams¹; Nikhilesh Chawla¹; ¹Arizona State University

The mechanisms for Sn whisker growth in Sn films are still not well known. The presence of a protective oxide has been postulated to control the formation of Sn whiskers from Sn thin films. In this investigation, the effects of oxygen on the degree of whisker formation were studied. We have used an in situ nanoindentation stage inside a scanning electron microscope to introduce local compressive stresses to drive whisker growth on the surface of the Sn thin film. The experiments were conducted under ultra-high vacuum, inert atmosphere, and air. The propensity, location of the whiskers relative to the indentation, and the morphology of the whiskers were controlled by environment and indentation stress. The relationship between stress, oxide on the surface, and whiskering mechanisms will be discussed.



2:30 PM

Columnar Microstructural Architecture in Electron and Laser Beam Melting of Metals and Alloys: *Edwin Martinez¹; Lawrence Murr¹; Sara Gaytan¹; Krista Amato¹; Patrick Shindo¹; Diana Ramirez¹; Francisco Medina¹; Jose Martinez¹; Brenda Machado¹; Ryan Wicker¹; ¹University of Texas at El Paso*

Unlike more conventional directional solidification, electron and laser-beam melting technologies involve building 3D components through layer-by-layer melt/solidification thermal cycling which creates novel, directional microstructural architectures. In this study we compared 3D optical metallographic image composite observations of columnar microstructural architectures in Cu, Co-29-Cr-6Mo-0.2C alloy and Ni-22Cr-9Mo-4Nb (alloy 625) fabricated by electron beam melting (EBM), and Ni-19Cr-19Fe-5Nb-1Al (alloy 718) by selective laser melting (SLM). Cu produced discontinuous columns of Cu₂O precipitates while the Co-base alloy exhibited similar columns of Cr₂₃C₆ precipitates. The alloy 625 produced columns of Ni₃Nb (γ'' -bct) precipitates. All of the EBM-produced columnar microstructure arrays were spaced $\sim 2 \mu\text{m}$. In contrast, the SLM fabricated alloy 718 contained columnar microstructural arrays of Ni₃Nb (γ'') spaced $\sim 0.8 \mu\text{m}$. Columnar grain structures with prominent [200] texture were also observed for these layer fabricated components by XRD analysis, and TEM analysis confirmed precipitate morphologies and crystallographic coincidences.

2:45 PM

Effects of Microstructural Changes on Shape Memory Properties of CuZnNi Shape Memory Alloys: *Sathish S¹; U S Mallik²; Raju T N¹; ¹Dr. Ambedkar Institute of Technology; ²Siddaganga Institute of Technology*

Copper-based shape memory alloys are very sensitive to the thermal effects before and after the transformation, and these effects may cause important changes on crystallographic properties or the other transformation parameters of the alloys. In this study, CuZnNi shape memory alloys in the range of 38- 55 wt. % of Zinc and 0- 15 wt % of nickel, exhibiting β - phase at high temperature and manifesting shape memory effect upon quenching to lower temperatures, were prepared through ingot metallurgy route. The alloys undergo a martensitic transformation upon quenching from β - phase to lower temperatures. CuZnNi alloys were the influence of thermal treatments characterized for their microstructure using optical microscopy, the phases were determined by X-ray diffraction and martensitic transformation behavior by differential scanning calorimetry and shape memory effect. The alloys exhibit good ductility and shape memory effect.

3:00 PM

Effects of Texture and Extrusion Velocity on the High Strain Tensile Behavior of Zr: *Juan Escobedo¹; Ellen Cerreta¹; Carl Trujillo¹; Daniel Martinez¹; Victoria Webster¹; George Gray III¹; ¹Los Alamos National Laboratory*

Dynamic tensile extrusion experiments were conducted to investigate the response of Zr subjected to large plastic strains. The samples were prepared from clock-rolled and annealed, high-purity Zr and tested in two orientations, namely through-thickness (TT) and in-plane (IP). For the TT case the microstructure shows a strong basal (0001) texture. For the IP case, the samples had a nearly (10-10) fiber texture. The substructural and texture evolution were examined by means of electron back scatter diffraction to understand the response of Zr under this integrated loading condition. The results show that the IP samples showed a larger total elongation when compared to the TT cases. Extensive plastic deformation was observed in the IP samples, whereas twinning was the predominant mode of deformation in the TT samples. In both cases, all the specimens tested developed a (10-10) extrusion texture, independent of the initial texture.

3:15 PM Break

3:25 PM

Improvement of Mechanical Properties in Severely Plastically Deformed Ni-Cr Alloy: *Kuk Hyun Song¹; Han Sol Kim¹; Hyun Taek Son¹; Won Yong Kim¹; ¹Korea Institute of Industrial Technology*

We carried out this work to evaluate the grain refining and mechanical properties in alloys that undergo severe plastic deformation (SPD). Conventional rolling (CR) and cross-roll rolling (CRR) were introduced as methods for SPD, and a Ni-20Cr alloy was selected as the experimental material. The materials were cold rolled to 90% thickness reduction and subsequently annealed at 700 °C for 30 min to obtain the fully recrystallized microstructure. The annealed materials after cold rolling were assessed through electron backscattered diffraction (EBSD) analysis to investigate the grain boundary characteristic distributions (GBCDs). The CRR process was more effective than the CR process in developing grain refinement; the grain size decreased from 70 μm in the initial material to 4.2 μm (CR) and 2.4 μm (CRR), respectively. The grain refinement affected mechanical properties such as microhardness, yield, and tensile strength, which were significantly increased relative to the initial material.

3:40 PM

Microstructure Development of Nickel Matrix/Carbide Composites: *Ayodeji Apata¹; ¹Wits*

Vanadium carbide has outstanding tribological behaviour. Despite the attractive properties, industrial application of VC is still limited. Alloy compositions (of at least 99.65% purity) were selected based on the three component binaries. Six $\sim 3\text{g}$ samples were made from the elemental components, and were arc-melted under an argon atmosphere, using Ti as an oxygen-getter. The as-cast and heat treated (at 1000°C for 1000 hours and quenched in water) samples were prepared metallographically. Images and composition analyses were obtained from a LEO1525 SEM with EDX, and X-ray diffraction (XRD) analyses were conducted using a Philips (PW-1810) X-ray diffractometer. SEM examination of the as-cast alloys has identified five phases to date: $\sim\text{V}_8\text{C}_7$, (Ni), $\sim\text{Ni}_2\text{V}$, s and $\sim\text{V}_6\text{C}_5$, which is in agreement with the component binaries. The heat treated samples showed very similar microstructures to the as-cast samples. The observed microstructures suggest the possibility of tailoring VC-Ni alloys for wear control.

3:55 PM

Microstructures and Mechanical Properties of Ni-Base Superalloys Fabricated by Laser and Electron Beam Melting: *K. Amato¹; S.M. Gaytan¹; L.E. Murr¹; P.W. Shindo¹; J. Hernandez¹; S. Collins²; F. Medina²; ¹The University of Texas at El Paso; ²W.M. Keck Center for 3-D innovation*

Ni-base superalloys are used in high-temperature applications due to their high corrosion and oxidation resistance. Directional solidification is a manufacturing method used to improve various properties of the alloys studied including elongation and hardness. Inconel 718 fabricated by electron beam melting is compared to Inconel 625 fabricated by electron beam melting as well and Inconel 718 fabricated by selective laser melting. Samples analyzed by optical metallography (OM), X-ray diffraction (XRD), scanning electron microscopy (SEM), and transmission electron microscopy (TEM) included as-fabricated, fabricated and HIP-ed, and fabricated and annealed cylinders. In all alloys, arrays of γ'' (bct) Ni₃Nb precipitates were observed in γ (fcc) NiCr grains, with columnar grains oriented in the [200] direction, parallel to the build direction. Tensile properties of both alloys are compared to wrought 625 and 718 alloys.

4:10 PM

Processing and Microstructural Control of Copper Foams for Thermal Wick Material Systems: *Keri Ledford*¹; Stephanie Lin²; Jason Nadler¹; ¹Georgia Tech Research Institute; ²Georgia Institute of Technology School of Material Science

Novel processes are being developed to fabricate thin copper thermal wick samples of targeted porous microstructures. Structures of desired porosity, thickness and pore size and distribution are achieved by tailoring the incorporation of sacrificial polymer beads into slurry precursors. The thickness of the final structure is dictated by precisely controllable slurry application methods, such as spin coating. In a subsequent heat treatment, the polymer components thermally decompose, and the remaining copper particles sinter to form a reticulated foam. The resulting microstructures are characterized in terms of porosity, permeability and specific surface area.

4:25 PM

Microstructure and Mechanical Properties of Laser-Deposited Cu-30Ni Alloy: *Guru Dinda*¹; Darryl Menifee¹; Joseph Simpson¹; Ashish Dasgupta¹; Sudip Bhattacharya²; Jyoti Mazumder²; ¹Focus: HOPE; ²University of Michigan

Cu-Ni alloys are extensively used for structures and components exposed to seawater and other marine environments due to their corrosion and biofouling resistance, machinability, and thermal and electrical conductivities. In the present investigation, Cu-30Ni alloy was deposited layer-by-layer on a rolled C71500 (Cu-30Ni) plate by a 5 kW CO₂ laser using Cu-30Ni alloy powder. Mechanical properties of the deposit were evaluated using microhardness and tension tests. Scanning electron microscopy and electron backscatter diffraction techniques were employed to study the microstructural morphology and grain orientation. The lattice parameter and residual strain of the deposit were investigated using X-ray diffraction technique. Hardness and strength of the deposit were found to be lower than Cu-30Ni rolled substrate. Overall, the microstructure was columnar dendrite in nature due to the directional solidification of the melt pool. However, the size and orientation of the dendrites varied with the location of the deposit.

4:40 PM

Deformation Mechanisms at Varying Temperatures in Alloy 718: *Donald McAllister*¹; Ning Zhou¹; Ben Peterson²; Michael Mills¹; ¹The Ohio State University; ²Honeywell Aerospace

The primary deformation mechanisms in a γ' strengthened, Ni-based superalloy, Alloy 718, were investigated at several temperatures. Tensile samples were extracted from the hoop direction of a forged disk and tensile tested to 0.5% plastic strain at strain rates between 0.00005 s⁻¹ and 0.005 s⁻¹. Samples were deformed at 75, 800, and 1200°F. The resulting dislocation and stacking fault structures were observed using transmission electron microscopy (TEM) to determine the dominance of either particle shearing or Orowan looping as the primary interaction between dislocations and the γ' phase at each temperature. Observed deformation mechanisms were compared with computer modeling results based on field dislocation modeling coupled with general stacking fault energies obtained from experiments and ab-initio calculations. The results of this study provide insight into how temperature influences the deformation mechanisms in Alloy 718 and help identify key material parameters which control the critical shear stress of the alloy.

Computational Thermodynamics and Kinetics: In Honor of Dr. Long-Qing Chen, EMPMD Outstanding Scientist: Session II

Sponsored by: The Minerals, Metals and Materials Society, TMS Electronic, Magnetic, and Photonic Materials Division, TMS Materials Processing and Manufacturing Division, TMS Structural Materials Division, TMS: Alloy Phases Committee, TMS: Chemistry and Physics of Materials Committee, TMS/ASM: Computational Materials Science and Engineering Committee, TMS: Integrated Computational Materials Engineering Committee, TMS/ASM: Phase Transformations Committee, TMS: Process Technology and Modeling Committee

Program Organizers: Zi-Kui Liu, The Pennsylvania State University; Mark Asta, University of California, Berkeley; James Warren, The National Institute of Standards and Technology; Yunzhi Wang, Ohio State University; Raymundo Arroyave, Texas A & M University; Yu Wang, Michigan Tech

Monday PM

March 12, 2012

Room: Australia 3

Location: Dolphin Resort

Session Chairs: Yu Wang, MTU; Peter Voorhees, Northwestern University

2:00 PM Invited

Phase Field Modeling and Simulation of Critical Nuclei Morphology: *Qiang Du*¹; ¹Penn State Univ

We present numerical simulations of the critical nuclei morphology in solid state transformations based on the phase field models. Contributions of anisotropic elastic energy are accounted for and we illustrate how they might significantly affect the nuclei morphology. A number of computational issues are also addressed, together with rigorous analysis of the underlying numerical algorithms. This is a joint work with Long-Qing Chen, Lei Zhang and Jingyan Zhang of Penn State.

2:25 PM Invited

Coarsening of Bicontinuous Two-Phase Mixtures: C. Park¹; K. Thornton¹; *Peter Voorhees*²; ¹University of Michigan; ²Northwestern University

We examine the evolution of interfacial morphology produced following phase separation via phase ordering and spinodal decomposition in three-dimensions using phase field simulations. The phase separation process yields completely bicontinuous structures with spatially varying interfacial curvature. We quantify the morphology of these complex microstructures via the interfacial shape distribution, the probability of finding a patch of interface with a given pair of principal curvatures. The time evolution of this distribution is examined in terms of the flow in probability space. We also examine the relationship between the time rate of the change of the mean and Gaussian curvatures, the local normal velocity and its gradient along the interface. Even when the interfacial motion is local, set by the value of the mean curvature at a point, the tangential gradients in the velocity strongly affect the evolution of the curvatures and thus the interfacial morphology evolves in a nonlocal fashion.

2:50 PM Invited

Meso-Scale Phase-Field Simulation of Void Evolution and Swelling in Irradiated Materials: *Shenyang Hu*¹; Yulan Li¹; Charles Henager¹; Richard Kurtz¹; Xin Sun¹; Moe Khaleel¹; ¹PNNL

Prediction of microstructure evolution and thermomechanical property degradation in irradiated materials is critical to the scientific design of fuels and structural components in nuclear reactors. This work will discuss the applications of mesoscale phase-field method in modelling the microstructure and property evolution in irradiated materials. A generic phase-field model is proposed, which takes into account multiple material processes including the generation, diffusion and reaction of defects,

MONDAY PM



TMS 2012

141st Annual Meeting & Exhibition

MONDAY PM

nucleation of second phases, one dimensional motion of interstitials, and long-range elastic interaction. Volumetric swelling, which is one of the important phenomena observed in irradiated materials, is simulated to demonstrate the capability of the model. The temperature dependence of volume swelling is addressed through modelling the effects of defect mobility, defect recombination rate, sink strength on void nucleation and growth kinetics.

3:15 PM Invited

Modeling of Hydride Formation and Fracture in Zirconium: *San-Qiang Shi*¹; ¹The Hong Kong Polytechnic University

Zirconium and its alloys are key structural materials used in the nuclear power industry. In service, these metals are susceptible to a corrosion process that leads to gradual pickup of hydrogen from the environment. At a certain hydrogen concentration level, complicated patterns of hydride precipitates can develop in the alloys, especially around stress concentrators. Hydride formation also involves a large volume expansion which causes plastic deformation around hydrides. Because of the brittleness of these hydrides, the original strength of the alloys can be reduced by orders of magnitude. Experimental results and modeling efforts are reviewed. In particular, phase field modeling of hydride formation and morphology evolution in zirconium will be presented. Major progresses and issues remaining will be summarized. The objective of this effort is to develop computational methodologies to predict realistic three-dimensional morphological evolution of hydride precipitates, and ultimately to predict fracture initiation at hydrides in zirconium alloys.

3:40 PM Break

4:10 PM Invited

Diffuse Interface Field Approach to Modeling and Simulation of Colloid Systems: *Yu Wang*¹; *Tian-Le Cheng*¹; *Paul Millett*²; ¹Michigan Tech; ²Idaho National Laboratory

Based on the conventional Phase Field Method, we present the development of a novel Diffuse Interface Field Approach to modeling and simulation of colloid systems. The model employs diffuse interface fields to describe multiple moving colloidal particles of arbitrary shapes, sizes and configurations, as well as the charge and electric/magnetic dipole properties of the particles. Particle interactions of long-range (electrostatic, magnetostatic) and short-range (mechanical contact, steric repulsion) as well as with fluid interface (capillary force) are taken into account. Evolving microstructures consisting of self-assembling colloid particles and multi-phase fluids with/without applied external field (used to tune long-range interaction forces and control particle microstructures) are simulated without explicitly tracking the arbitrary-shaped particle boundaries and multi-phase fluid interfaces. Simulations are presented to demonstrate the new model's capability and potential to explore processing routes to advanced materials with novel microstructures and improved properties.

4:35 PM Invited

Ostwald Goes to Hollywood: Time-Resolved 3D Study of Microstructural Coarsening by X-Ray Tomography: *Thomas Werz*¹; *Carl Krill*¹; ¹Ulm University

It's not only moviegoers whose imagination has been captured by the 3D revolution in imaging technology — even materials scientists have been swept up in the hype! Their excitement is understandable, given the new possibilities for materials characterization afforded by techniques such as serial sectioning and x-ray microtomography, which offer a 3D view of features heretofore seen only in 2D sections. Moreover, since tomographic imaging occurs nondestructively, time-resolved studies of microstructural evolution are now feasible. We have implemented this strategy in an investigation of Ostwald ripening in the model system Al-5 wt.% Cu. An image segmentation procedure was developed based on the watershed transformation, and correlation routines were written to facilitate the tracking of particle trajectories in time and space. With these

“cutting-room” tools in place, the path has been cleared to shoot a movie of Ostwald ripening and have critics compare it to computer simulations. “X-rays, detector, coarsen!”

5:00 PM Invited

Computational Modeling of Oxidation and Corrosion of Alloys in Complex Environments: *Youhai Wen*¹; *Kaisheng Wu*²; *Long-Qing Chen*³; *Jeff Hawk*¹; ¹National Energy Technology Laboratory; ²NETL/URS; ³Penn State University

Advanced energy systems, such as oxyfuel and ultra-supercritical steam combustion boilers, oxyfuel and hydrogen turbines and advanced gasification systems, will operate at higher temperatures and in complex environments. Due to the complexity of a typical multi-oxidant environment, it is very challenging if not impossible to predict the corrosion product with confidence. The computational approach available is largely based on thermodynamic calculations without any consideration of kinetics effect. To address the kinetic effect, a multi-faceted modeling approach is being developed at NETL/DOE to study oxidation kinetics under different length scales. Some progresses are discussed in this presentation based on results from mean-field and phase-field methods. The computational tools can be used to simulate environmental effect on oxidation behavior.

Defects and Properties of Cast Metals: Porosity

Sponsored by: The Minerals, Metals and Materials Society, TMS Materials Processing and Manufacturing Division, TMS: Solidification Committee

Program Organizers: Mark Jolly, University of Birmingham; Brian Thomas, University of Illinois at Urbana-Champaign; Carl Reilly, University of British Columbia

Monday PM
March 12, 2012

Room: Oceanic 4
Location: Dolphin Resort

Session Chairs: Carl Reilly, UBC; Salem Seifeddine, University of Jonkoping

2:00 PM

Effect of Porosity on Deformation, Damage, and Fracture of Cast Steel: *Christoph Beckermann*¹; *Richard Hardin*¹; ¹University of Iowa

A combined experimental and computational study is performed to investigate the effect of internal shrinkage porosity on the mechanical behavior of cast steel under static loading. Steel plates containing various levels of porosity are cast in a sand mold, machined, and tensile tested until fracture. A significant loss of ductility is observed. Radiographic imaging is used to reconstruct the porosity field in the test specimens. The measured porosity field is then used in a finite-element stress analysis of the tensile tests. The local elastic properties are reduced according to the porosity fraction present and porous metal plasticity theory is used to model the damage due to porosity. Good agreement between measured and predicted stress-strain curves is obtained. The computational model proposed in this study allows for a detailed evaluation of the effect of porosity, including its size, shape and location, on the mechanical performance of a steel casting.

2:25 PM

Detection and Influence of Shrinkage Pores and Non-Metallic Inclusions on Fatigue Life of Cast Aluminum Alloys: *Yakub Tijani*¹; *Andre Heinrietz*¹; *Wolfram Stets*²; *Patrick Voigt*²; ¹Fraunhofer LBF; ²Institut fuer Giessereitechnik

In this work, test bars of cast aluminum alloys EN AC- AlSi8Cu3 and EN AC- AlSi7Mg0.3 were produced with a defined amount of shrinkage pores and oxides. For this purpose a permanent mold with heating and cooling devices for the generation of pores was constructed. The oxides were produced by a contamination of the melt. The specimens and

their corresponding defect distributions were examined and quantified by X-Ray computer tomography (CT) and quantitative metallography respectively. A special test algorithm for the simultaneous image analysis of pores and oxides was developed. The defective samples were examined by fatigue testing. The presence of shrinkage pores causes a lowering of the fatigue strength. The results show that pore volume is not sufficient to characterize the influence of shrinkage pores on fatigue life. A parametric model for the calculation of fatigue life based on the pore parameters obtained from CT scans was implemented. The model accounts for the combined impact of pore location, size and shape on fatigue life reduction.

2:50 PM

Quantifying Fe-Rich Intermetallic Formation and Subsequent Pore Interaction during Solidification of Al Alloys Using *in situ* Synchrotron-Based Tomographic Microscopy: *Chedtha Puncreobutr*¹; André Phillion²; Julie L. Fife³; Peter D. Lee⁴; ¹Imperial College London; ²University of British Columbia; ³Paul Scherrer Institut; ⁴The University of Manchester

The presence of intermetallics and pores in aluminium alloy cast components can often limit final fatigue life. In order to convert these large detrimental phases into a form that is acceptable for engineering applications, an improved understanding of their nucleation and growth mechanisms is required. In this study, ultra-fast synchrotron-based tomographic microscopy (one 3D data set (generated) per second with 3 µm voxels) was performed at the TOMCAT beamline of Swiss Light Source for a range of cooling rates and iron levels in an aluminum alloy (Al-7.5Si-3.5Cu-x-Fe(wt.%)). The nucleation temperatures and growth rates of both the intermetallics and pores were quantified. The interaction of the pores and intermetallics with the primary phase, and each other were also examined. The results illustrate that nucleation/growth of the β-intermetallics is a function of both Fe level and cooling rate. The results are compared to prior experimental results and numerical models.

3:15 PM

An Integrated Methodology for Optimizing Al-Si Diecastings in Automotive Applications Part 1 – Modeling the Influence of Casting Defects: Nicola Gramegna¹; *Franco Bonollo*²; Giulio Timelli²; Stefano Ferraro²; Gianluca Quaglia¹; ¹ENGINSOFT S.p.A.; ²University Of Padova

International standards don't provide useful information about the mechanical properties of aluminum diecasting alloys, but only a value guide. In this part of the work a secondary aluminum alloy is diecast by using a multi-cavity die, to obtain flat specimens for static tensile testing, specimens for fatigue and impact testing, a plate and a specimen for stress corrosion testing. This specimens are used to know the "maximum" mechanical properties of a diecast aluminum alloy used. A microstructural analysis of the samples is made, in order to study the effect of casting defect on mechanical properties. The distribution of gas and shrinkage pores is related with numerical simulation of the multi-cavity die, in order to link the defect content with mechanical properties. A developed quality mapping approach shows how the final properties strongly depend on the position of the casting and the process parameters adopted.

3:40 PM Break

4:00 PM

The Influence of Bismuth on Microstructure and Porosity Formation in Hypoeutectic Aluminium-Silicon Alloys: *Jozef Kasala*¹; Lubomir Caplovic²; Maria Lickova¹; ¹Alexander Dubcek University of Trencin; ²Slovak University of Technology in Bratislava

Multicomponent Al-Si based casting alloys are used for a variety of engineering applications. In order for such alloys to improve manufacturing characteristics, alloy element modifications are being made to further enhance the alloys machinability. In this paper, the effects of additions of bismuth on the microstructure and porosity of the strontium modified aluminium-silicon alloys containing 7 and 10 wt.% silicon were investigated. Microstructures and porosity were observed using optical microscopy, scanning electron microscopy and

electron probe X-ray microanalysis techniques. The results show that a small amount of bismuth has no significant impact on the formation of complex intermetallic phases. The addition of bismuth can counteract the modifying effect of strontium leading to a noticeable coarsening of the eutectic Si particles. It was found that the modification effect of strontium decreases as the amount of bismuth increases. Bismuth additions alters the amount, characteristics, and distribution of porosity in Al-Si castings.

4:25 PM

Relationship between Pores Volume (by Density Measurements) and Pores Area (on Fracture Surfaces) of A356 Fatigue Specimens: *Alessandro Morri*¹; Lorella Ceschini¹; Ingvar Svensson²; Salem Seifeddine²; ¹University of Bologna; ²Jönköping University

The mechanical properties of A356 alloy are largely influenced by the solidification microstructure and especially by defects, such as gas pores, shrinkage cavities and oxide films. For this reason casting simulation software to predict pores volume in complex castings was developed. Few data, however, are available about the relationship between the volume of pores and their distribution on zones of the components where the failure is localized. The aim of this paper was to find a relationship between the pores volume in fatigue specimens (evaluated by density measurement) and the pores area, measured on the fracture surfaces of the same specimens. The preliminary results show that the pores area percentage on the fatigue fracture surfaces can be greater than 10 times the mean volume percentage, so that in samples with 1% in volume of defects, the specimen showed a decrease of the cross section area of about the 10%.

4:50 PM

Non Homogenous Microstructure of Cast Iron Components – Challenge for Fatigue Evaluation of NDT Tested “Defect Free” Components: *Andre Heinrietz*¹; Jens Eufinger¹; Wolfram Stets²; Andreas Sobota²; Herbert Loeblich²; ¹Fraunhofer Institute of Structural Durability and System Reliability LBF; ²Institut fuer Giessereitechnik gGmbH

In order to optimize spheroidal cast iron components for cyclically loaded applications, e.g. for wind mill power plants, the knowledge of the dependence of fatigue on the microstructure is essential to account for the non homogenous fatigue properties of cast components even if it's been tested as “defect free” with NDT methods. These qualities may differ by factor 5 in cycle life although ultimate strengths are equal. In the paper results of a recently finished research project are presented dealing with fatigue investigations of spheroidal cast iron with varying graphite structure, pearlite content and microporosity. Fatigue tests performed on specimens with varying content of microporosity as well as varying size and shape of spheroids are presented. The influence of microporosity in varying fields of spheroids is discussed as well as size effects on fatigue life.

5:15 PM

Fabrication of Ordered Porous Copper Alloy by Continuous Unidirectional Solidification: *Qinglin Jin*¹; Yehua Jiang¹; Rong Zhou¹; ¹Kunming University of Science and Technology

Ordered porous metal (also known as Gasar or lotus-type material) is a new kind of porous material developed in recent years. The most important feature of the fabrication technique for ordered porous metal is unidirectional solidification of a gas saturated melt that causes simultaneous formation of solid metal and gas pores, resulting in long cylindrical pores filled with gas uniformly distributed in solid matrix. In this study, an ordered porous copper and its alloy were fabricated by a continuous unidirectional solidification method under a pressurized hydrogen atmosphere. A theoretical model was developed to relate the porosity, pore size and inter-pore spacing with the casting parameters. The effects of alloying elements (Zn and Ni) on the pore size and pore morphology were discussed by analyzing the solute redistribution at the solidification interface.



TMS 2012

141st Annual Meeting & Exhibition

Deformation, Damage, and Fracture of Light Metals and Alloys: Session I

Sponsored by: The Minerals, Metals and Materials Society, TMS Structural Materials Division, TMS Light Metals Division, TMS/ASM: Mechanical Behavior of Materials Committee
Program Organizers: Qizhen Li, University of Nevada, Reno; Fuqian Yang, Univ. of Kentucky; Ke An, Oak Ridge National Laboratory

Monday PM Room: Northern A2
March 12, 2012 Location: Dolphin Resort

Session Chairs: Qizhen Li, University of Nevada, Reno; Wen-Ming Chien, University of Nevada, Reno

2:00 PM Invited

Strategies for Improving the Strength and Ductility of Nanostructured Light Metals: *Yuntian Zhu*¹; *Yonghao Zhao*²; ¹North Carolina State University; ²Nanjing University of Science and Technology

The strength and ductility of structural materials are frequently inversely related. In other words, high strength is often accompanied by low ductility, and vice versa. Inspection of the scientific literature reveals that this is also the case for nanostructured and ultrafine-grained materials, which are usually strong, but with accompanying low ductility levels. Conventional approaches to improve ductility often yield a loss of strength. This talk presents several approaches that can be effectively implemented to increase the ductility of nanostructured/ultrafine-grained materials while simultaneously improving or at least maintaining their strength. The fundamental mechanisms that underlie the proposed approaches are discussed in this talk.

2:30 PM

Ultrafine Grained Aluminium Alloys: Processes and Superior Properties: *Maxim Murashkin*¹; *Georgiy Raab*¹; *Ruslan Valiev*¹; ¹Ufa State Aviation Technical University

This presentation provides recent results on developments of the processing techniques based on severe plastic deformation (SPD) as applied to age-hardenable and non age-hardenable Al alloys. The unusual mechanical and functional properties of the Al alloys subjected to various SPD methods are presented in terms of the ultrafine-grained microstructure and segregation/precipitation formation in the alloys produced. The outlined 'portrait' of the Al alloys whose microstructure has been modified by SPD also includes such features as very high strength and ductility, fatigue resistance and electroconductivity. Finally, the potential of SPD processing techniques for developing marketable Al products with improved properties is discussed. This research was supported in part by United Company RUSAL.

2:50 PM

Effect of Microalloying with Aluminum or Yttrium on Grain Boundary Damping in Fine-Grained Magnesium: *Hiroyuki Watanabe*¹; *Akira Owashi*²; *Tokuteru Uesugi*²; *Yorinobu Takigawa*²; *Kenji Higashi*²; ¹Osaka Municipal Technical Research Institute; ²Osaka Prefecture University

The damping properties of fine-grained magnesium alloys were measured at elevated temperatures and at low frequencies in order to examine the effect of solid solution alloying on grain boundary relaxation through grain boundary sliding. We chose to examine aluminum and yttrium as alloying elements. The grain sizes of materials examined were ~2 μm irrespective of alloy composition. A sharp increase in damping capacity caused by grain boundary relaxation was observed at above a certain temperature for all materials examined. The temperature at which a sharp increase in damping capacity occurred increased with aluminum content in Mg-Al system. STEM-EDS analyses of the extruded Mg-Al

alloys suggested no notable segregation of aluminum in grain boundaries. Therefore, aluminum is suggested to be effective in suppressing grain boundary relaxation in magnesium alloys. However, yttrium was more effective than aluminum in suppressing grain boundary relaxation.

3:10 PM

Characterization of Ductile Fracture in 5083 Aluminum using Micro Computed X-Ray Tomography: *Caroline Scheck*¹; *Marc Zupan*²; ¹Naval Surface Warfare Center; ²University of Maryland, Baltimore County

Micro-computed X-ray tomography (microCT) has emerged in recent years as a viable non-destructive three-dimensional imaging technique in material science. This technology is applied to characterize secondary Mg particles in plane strain 5083-H116 aluminum specimens whose geometries have been manipulated to create varying stress states (stress triaxiality). The movement of voids initiated during ductile fracture is linked to the measured Mg particle distribution. The tomography-measured Mg particles diameters and distributions are used as experimental inputs for a previously developed theoretical model to non-destructively measure strain to failure. The tomography measured strain to failures show excellent correlation to results obtained from experimental tensile testing and finite element analysis of the specimens.

3:30 PM Break

3:40 PM Invited

Joint Ab-Initio and Experimental Study on the Effects of Rare Earth (RE) Elements on the Stacking Fault Energy and Plasticity of Magnesium Alloys: *Stefanie Sandlöbes*¹; *Martin Friak*¹; *Alexej Dick*¹; *Stefan Zaeferrer*¹; *Jörg Neugebauer*¹; *Dierk Raabe*¹; ¹Max-Planck-Institut

Magnesium and most commercial wrought Magnesium alloys exhibit poor room temperature ductility and mechanical anisotropy caused by sharp basal-type recrystallization textures and limited availability of independent deformation mechanisms. The addition of rare earth (RE) elements in solid solution improves the room temperature ductility of Mg apparently through two mechanisms. First, RE alloying leads to weaker recrystallization textures. Second, such alloys show higher activity of non-basal deformation mechanisms that contribute a <c>-deformation component to the overall crystallographic velocity gradient. These deformation mechanisms are {10-11} <10-12> contraction, {10-11} {10-12} double twinning and pyramidal <c+a> dislocation slip. In particular, pyramidal dislocation slip is essential for the accommodation of strain along the <c>-axis. In this study the mechanisms responsible for the facilitated activation of these out-of-basal plane deformation modes are investigated by complementary transmission electron microscopy (TEM) and density functional theory (DFT) analysis of binary Mg-Y alloys.

4:10 PM

Abnormal Mechanical Properties of Strain Glass Alloys-A Simulation Study: *Dong Wang*¹; *Yunzhi Wang*²; *Xiaobing Ren*³; ¹Xi'an Jiaotong University; ²Ohio State University; ³National Institute for Materials Science

A new glass state was discovered in Ni-Ti alloys [Phys. Rev. Lett 95, (2005) 205702], it was called strain glass because of the existence of randomly distributed strain. Based on our recent strain glass model [Phys. Rev. Lett. 105 (2010) 205702] which assumes that point defects alter the thermodynamic stability of martensite and create local lattice distortion, the transition behavior of a strain glass system under external stress was studied through phase field simulations. The stress-strain hysteresis loops of the strain glass at different temperatures show slim characteristics. Furthermore, the strain-temperature curves upon cooling and heating with different stress values show abnormal properties. At low stress, the systems show gradual and small strain change and can't form long range order martensite upon cooling, the gradual strain increase can compensate the contraction upon cooling—maybe the origin of invar effect of gum metal. These simulation predictions agree well with the experimental observations.

4:30 PM

Warm Forming Simulation of Magnesium Alloy AZ31B Sheets: *Ji Hoon Kim*¹; Daeyong Kim¹; Young-Seon Lee¹; Myoung-Gyu Lee²; R. Wagoner³; ¹Korea Institute of Materials Science; ²Pohang University of Science and Technology; ³The Ohio State University

Magnesium alloy sheets show unique characteristics such as inflected strain hardening, asymmetric behavior in tension and compression, exhaustion of twinning at small strains, particularly at low temperatures, which cannot be described by the conventional constitutive models used for cubic metals. In this work, a practical constitutive model is developed for the magnesium alloy AZ31B sheets and is applied to the warm forming simulations. The unique temperature- and strain history dependent cyclic behavior is accounted for by the use of a novel asymmetrically evolving yield surface in addition to the conventional one, incorporating the coupling between slip and twinning. The developed constitutive model has been implemented into the commercial finite element program Abaqus/Explicit and is used for the warm forming process optimization.

4:50 PM

A Systematic Study of Solute Effects on Strength and Ductility of Mg from First Principles: *Joseph Yasi*¹; Louis Hector²; Dallas Trinkle¹; ¹University of Illinois at Urbana-Champaign; ²General Motors R&D Center

New Mg alloys which can be formed at lower temperatures are of great interest to the transportation industry. Mg is the lightest structural metal at 2/3 the density of Al but has poor room temperature ductility. To have five active slip systems requires increasing non-basal dislocation mobility, and solutes play an important role. We investigate trends in substitutional solute interactions on basal and prismatic slip systems using density functional theory for alkali, alkaline earth, transition metals and rare earths in optimized screw dislocation cores. From this, we predict changes in prismatic cross-slip stress with temperature and solute concentration and observe how solute size and valency modify prismatic slip. We show Ca, K, Na, Sc, Y and Zr soften prismatic slip at low concentrations, allowing for a lower forming temperature.

5:10 PM

A Macroscopic Yield Function Coupled with Crystal Plasticity Theory for Modeling Forming of AZ31 Magnesium Alloy Sheets: *Nitin Chandola*¹; Oana Cazacu¹; Raja Mishra²; Kaan Inal³; ¹University of Florida; ²General Motors; ³University of Waterloo

We present a multi-scale computational tool to use an anisotropic yield function developed by Cazacu et al (2006) to generate yield surfaces for forming simulations of commercial grade AZ31 magnesium alloy sheets. This macro scale model uses input parameters generated using a microstructure based crystal plasticity model that incorporates slip and twinning mechanisms and the accompanying texture evolution. The crystal plasticity model is calibrated and validated at the microstructural level using experimental texture data as well as uniaxial tension and compression data. Both experimental data and crystal plasticity predictions are used to calibrate the macroscopic model. The coupled model is then validated by comparing its predictions of yield stress ratios and strain ratios for up to 10% effective plastic strain with experimental data. We compare the yield surfaces generated by the validated coupled model and the validated crystal plasticity model to assess the robustness and sensitivities of the calibration method.

Electrode Technology for Aluminium Production: Paste Plant Design and Improvement

Sponsored by: The Minerals, Metals and Materials Society, TMS Light Metals Division, TMS: Aluminum Committee, TMS: Aluminum Processing Committee
Program Organizer: Morten Sorlie, Alcoa Norway

Monday PM
March 12, 2012

Room: Americas Seminar
Location: Dolphin Resort

Session Chair: Berthold Hohl, Eirich GmbH & Co KG

2:00 PM Introductory Comments

2:10 PM

Adaptive Fuzzy Controller for Ball Mill in Anode Plant: *Edson Cruz*¹; ¹Albras - Alumínio Brasileiro S.A.

An adaptive controller for keeping a ball mill working stably and efficiently is proposed in this paper. The controller is based on fuzzy logic control strategy by developing a method of adjusting the quantification and proportion factors. The selection of these factors makes a big influence on the static and dynamic performances of the controller. This new control strategy is implemented in Albras Anodo Plants. The controller program was developed with ladder language and runs on programmable logical controller (PLCs) from Allen Bradley. Anode plants are operating with the ball mills which are being controlled by fuzzy controllers, and the noise, that is the control variable is working around the established operation point. The results demonstrate the effectiveness and viability of the system that hereafter will be being implanted in other equipments of the anode plant.

2:35 PM

Use of under Calcined Coke to Produce Baked Anodes for Aluminium Reduction Lines: *Rajesh Garg*¹; *Daniel Sulaiman*¹; ¹Aluminium Bahrain

Anodes produced using under calcined coke (or Low Real Density Coke) reported to have less and homogenous reactivity of all anode components following baking, which results in lower carbon consumption and less carbon dust in pots. Increased butt thickness due to lower carbon consumption provides opportunity for amperage creep in Reduction lines. ALBA has unique arrangement of an in-house coke calcining operation with carbon plants for anode manufacturing. This gives ALBA an added advantage of lower fuel consumption in calciner on use of under calcined coke for anode production. ALBA used this opportunity and a trial batch of under calcined coke was produced at calciner with lower Real Density of 2.03 gm/cc. Anodes manufactured using this under calcined coke were tested in pots for 2-anode cycles. This paper describes about quality of anodes produced using under calcined coke and their performance in pot rooms.

3:00 PM

60 TPH Single Line Green Anode Plant Commissioned at Qatalum: *Christophe Bouche*¹; Bertrand Somnard¹; Sunil Bhajun²; Fabienne Virieux³; ¹Solios Carbone; ²Qatalum; ³Fives Solios

The first single line 60 t/h green anode plant ever was successfully commissioned at the Qatalum smelter. This green anode plant was designed to fulfil the anode requirements of the 585,000 TPY metal capacity smelter. The single process line is based on the Rhodax® technology for dry mix preparation and IMC® technology for the paste mixing/cooling already demonstrated at Sohar Aluminium at 36TPH capacity. For Qatalum, new equipment, including crusher, coke preheating screw, continuous paste mixer/cooler and vibrocompactor, had to be designed, optimized and fine tuned to suit the 60TPH production level without compromising the



TMS 2012

141st Annual Meeting & Exhibition

MONDAY PM

anode quality and the plant reliability. High capacity green anode plants contribute to lower the CAPEX of greenfield or brownfield smelter projects. This paper describes the technical challenges that were met to realize such high production capacity and summarizes the operation performance achieved during one year of industrial production

3:25 PM

Improvement of Anode Paste Quality and Performance of ALCOA Lista: Nils Saue¹; Jon Ystgaard¹; Jon Johannessen¹; Markus Meier²; Raymond Peruchoud²; ¹Alcoa Lista; ²R&D Carbon Ltd.

ALCOA Lista has experienced a severe crisis with up to 100 anode problems per week, mainly occurring as spikes, hanging anode ends, leak in stud holes, vertical cracks and dusting. The anode problems hindered a planned amperage increase. A systematic plant audit conducted by R&D Carbon revealed clear root causes that were responsible for the anode problems. The plant management and operation team swiftly implemented the recommendations of the plant audit and subsequent plant optimization. The major actions included a mixer revamp and adaptations of recipe formulation and mixing conditions. Today, the number of anode problems are down to 10 per week (2.4 in potline 3). The major actions are discussed in this document, which had a significant impact on the plant performance figures (current efficiency, carbon consumption, energy consumption and bubble noise) that eventually allowed a substantial increase of the line current from 120 to 130 kA.

3:50 PM Break

4:10 PM

Baked Anode Quality Improvement through Optimization of Green Anode Plant Ultra Fine Content in Ball Mill Product and Process Parameters: Rajesh Garg¹; Daniel Sulaiman¹; Masood Toorani¹; ¹Aluminium Bahrain

The two long term trends in the aluminum industry that will have the most effect on anode quality requirements are scarcity of good quality calcined coke for anode production and the current creep by pot lines. In ALBA Pot rooms gradually increased line current to increase Aluminium production. Therefore, there was need to improve anode quality and net carbon consumption so that the butts thickness at increased line current was maintained. In ALBA, for given set of raw materials, paste plant process parameters and dry aggregate composition, baked anode density was in the range of 1.580-1.585 g/cm³. With in-house research, baked anode density of 1.600-1.605 g/cm³ was achieved by optimization of ultra fine content in Ball Mill Product, and other process parameters of Green Anode Plant. The paper describes the work done on the optimization of the Paste Plant's dry aggregate recipe & process parameters and results achieved.

4:35 PM

Baked Anode Quality Improvement through Optimization of Green Anode Processing: Xu Haifei¹; Fan Lijun¹; Zhang Yang²; Sun Yi¹; Cui Yinhe¹; ¹SAMI; ²Lanzhou Branch of Chalco

At Lanzhou smelter, there are more than 11 mainly delayed coke suppliers. The range of calcined coke real density was between 1.99 and 2.06kg/cm³, the resistivity was 480- 570 μ Ω.m, and the operating cost of rotary kiln was high due to the short life of tuyere nozzles and chamber lining. The apparent density of green anode was low and the deviation was \pm 0.05kg/cm³ because of variation in the recipe and process parameters. There was so much dust in the cells and the net carbon consumption was about 450kg/t.Al. By blending delayed coke, adjusting calcining process parameters and optimizing the recipe and process parameters of green anode manufacturing, the quality of calcined coke improved. The tuyere nozzles and chamber lining were not distinctly destroyed in the past 8 months, the quantity of dust in the cells has decreased, and the net carbon consumption has reduced to nearly 420 kg/t.Al.

Electrometallurgy 2012: Session I

Sponsored by: The Minerals, Metals and Materials Society, The Metallurgy and Materials Society of CIM, TMS Extraction and Processing Division, TMS: Hydrometallurgy and Electrometallurgy Committee

Program Organizers: Georges Houlachi, Hydro-Quebec; Antoine Allanore, Massachusetts Institute of Technology; Michael Free, University of Utah; Michael Moats, University of Utah; Edouard Asselin, UBC; Shijie Wang, Rio Tinto Kennecott Utah Copper; James Yurko, Materion Brush Beryllium and Composites

Monday PM
March 12, 2012

Room: Europe 5
Location: Dolphin Resort

Session Chairs: Michael Free, University of Utah; Georges Houlachi, Hydro-Quebec

2:00 PM Introductory Comments

2:05 PM

Electrometallurgy – Now and in the Future: Michael Free¹; Michael Moats¹; Tim Robinson²; Georges Houlachi³; Neale Neelameggham⁴; David Creber⁵; George Holywell⁶; Marco Ginatta⁷; ¹University of Utah; ²Republic Anode Fabricators; ³Hydro-Quebec; ⁴ind.LLC; ⁵Rio Tinto Alcan; ⁶Almagi, Inc.; ⁷Ginatta Technologie

Electrolytic processing is used commercially to recover and/or refine metals such as aluminum, copper, magnesium, nickel, and zinc. There are also new and exciting opportunities to utilize electrometallurgy in the production of titanium, lead, and other metals. This paper will review some of the main technologies that are used to produce and refine metals as well as some of the recent advances and directions the electrometallurgy industry is moving to meet the challenges faced now as well as those that are likely to be faced in the future.

2:25 PM

Performance and Commercialization of the Smart Anode, MSATM, for Environmentally Friendly Electrometallurgical Process: Masatsugu Morimitsu¹; ¹Doshisha University

This paper presents the development, performance, and commercialization of the smart anode, MSATM, for electrowinning of non-ferrous metals such as copper, zinc, nickel, and cobalt. The smart anode consists of amorphous oxide catalytic layers formed on a titanium substrate by thermal decomposition. The oxides contain nano-size IrO₂ or RuO₂ particles as the active component. Such oxides can reduce oxygen or chlorine evolution potential and suppress some unwanted side reactions on the anode such as MnOOH, CoOOH, or PbO₂ deposition. These features provide excellent improvement for electrowinning process; cell voltage reduction, no increase in cell voltage with time, no sludge, less maintenance, and others. The smart anode, MSATM, can make the electrometallurgical process more environmentally friendly.

2:45 PM

A Novel Oxygen Evolution Anode for Electrowinning of Non-ferrous Metals: Tian Zhang¹; Masatsugu Morimitsu¹; ¹Doshisha University

This paper presents a novel anode for oxygen evolution in acidic aqueous solutions to produce non-ferrous metals by electrowinning. The method to prepare the anode was thermal decomposition of a precursor solution, and the obtained anode consisted of oxide catalytic layers formed on a titanium substrate, in which the catalytic layer contains nano-oxide particles other than iridium oxide as the active component. The oxygen evolution potential was much lower than commercially available coated titanium anodes using iridium oxide so that the cell voltage with using the novel anode in the electrowinning cells was much reduced.

3:05 PM**Novel DSA® Anode for Electrowinning of Non Ferrous Metals:** *Antonio Antozzi*¹; ¹Industrie De Nora SpA

A new DSA® anode, patent pending, has been tailored for electrowinning of non-ferrous metals (Copper, Nickel, Cobalt, Zinc) by means of a new coating technology, already extensively referenced in the Chlor-alkali world. DSA® anodes are provided with noble-metal electrocatalytic coatings, mainly consisting of iridium-and-ruthenium oxides, obtained by thermal decomposition of their precursor's solutions on titanium substrates. Catalytic activity of a state-of-the-art DSA® anode has been increased by decreasing crystallite size of noble-metals without decreasing the decomposition temperature. It is known in fact below a certain value (400°C) the stability of these oxides, therefore their lifetime, is seriously compromised. Highly active DSA® anodes, having a quasi-amorphous phase, have been obtained at above 450 °C, therefore being not affected by lifetime issues. Advantages: * Improved Lead-free Cathode Product Quality Up to 0.550V, 27.5% power savings compared to industry standard, *Lead-tin-calcium Lead-free-green anodes, *Flexibility in production rate, *Ability to operate at increased Current Density

3:25 PM**Increasing Oxygen Charge Transfer Resistance on the Anode in Copper Electrowinning:** *Reuben Mathew*¹; ¹Laurentian University

Oxygen evolution is the main anode reaction in industrial copper electrowinning. The oxygen bubbles do not conduct electricity, thus increasing the electrolyte resistance. The oxygen bubbles formed at the anode rise to the surface, occupying a larger volume of the electrolyte at the top of the cell than at the bottom. This oxygen bubble concentration gradient contributes to a gradient in electrolyte resistance and consequently a tendency toward uneven current distribution. This phenomenon increases the chance for uneven growth on the cathode and short-circuits, particularly on the lower portions of the cathode. This issue may be ameliorated by increasing the charge transfer resistance for oxygen evolution down the height of the anode. This concept was studied by solving the current distribution for a 2-D model of a copper electrowinning cell using COMSOL.

3:45 PM Break**4:00 PM****Development of a Fully Dynamic Simulation of the Zinc Electrowinning Process:** *Michael Mahon*¹; *Spencer Peng*¹; *Larry Wasik*²; *Akram Alfantazi*¹; ¹University of British Columbia; ²Aurel Systems

A dynamic simulation of a zinc tankhouse would be an effective tool to improve tankhouse production and cost efficiencies. A fully dynamic simulation has potential uses in the design of new tankhouses as well as in the optimization of existing facilities. Equations from previously validated models of a single cell have been adapted to the industrial dynamic process simulation software, CADSIM Plus. Based on the inlet concentration, current density, and electrode setup, the model can predict many parameters, including outlet concentrations, flow rates, current efficiency and energy consumption. Multiple cells are then simulated simultaneously, allowing for an entire tankhouse to be modeled. The finished simulation can be used to dynamically predict the conditions in a zinc tankhouse throughout a timescale. Further applications of this model include, tracking impurity buildup, modeling of recycle streams and the development of new flow regimes within the tankhouse.

4:20 PM**Aqueous Electrodeposition of Molybdenum:** *Thomas Morley*¹; *Leah Penner*²; *Francois Benard*³; *Tom Ruth*¹; *Paul Schaffer*¹; *Stefan Zeisler*¹; *Edouard Asselin*²; ¹TRIUMF; ²UBC; ³BC Cancer Agency Research Centre

A novel method for molybdenum electrodeposition from aqueous electrolytes is presented. Metallic molybdenum is deposited from an acetate solution at near-neutral pH at temperatures not exceeding 50°C. This is the first report of aqueous electrodeposition of Mo to thicknesses well in excess of 1 micrometer. Deposit quality (adherence, morphology and mass) is characterized as a function of pH, electrolyte composition, current density and temperature. The thermodynamics of the process are discussed. Optimal conditions are identified and applications for this new technology are presented.

4:40 PM**Lead Anodes Performance in Nickel Electrowinning:** *Farzad Mohammadi*¹; *Mathew Tunnicliffe*¹; *Paul Nesbit*¹; *Akram Alfantazi*¹; ¹University of British Columbia

Lead and its alloys have always been candidates for anodes in electrowinning plants since they are insoluble in the leach solutions. However, the annual cost of corrosion problems associated with these anodes is millions of dollars. In this study lead-silver and lead-calcium anodes were tested under typical electrowinning conditions and the effects of sulfuric acid and chloride concentrations on the overall corrosion performance of the anode materials were investigated. Corrosion rates of the electrodes were calculated using the discharge plateau (reduction of lead dioxide to lead sulfate) recorded during OCP measurements after galvanostatic experiments at 20 mA.cm⁻², typical for electrowinning plants. SEM images performed after galvanostatic experiments revealed a good agreement between surface morphology of the electrodes and their corrosion rates. Oxygen evolution reaction (OER) rate and overpotential were determined for different electrode material/solution conditions.

5:00 PM**Effect of Different Electrolyte Additives in Zinc Electrowinning Process Using Taguchi Statistical Design Methodology:** *Somayeh Dashti*¹; *Fereshteh Rashchi*¹; *Ehsan Vahidi*¹; ¹University of Tehran

The main goals in zinc electrowinning process are decreasing of power consumption and increasing of current efficiency. In our previous researches, zinc electrowinning using Taguchi method was studied and the optimized conditions (anode composition: Pb-Ag0.5%-Sn2%-Sb1%, current density (A/m²): 500, acid concentration (g/L): 165, temperature: 60°C and zinc ion concentration (g/L): 70) for the process was obtained. In this study, electrowinning of zinc in the presence of different additives in electrolyte was established and Arabic Gum, gelatin, sodium lauryl sulphate (SLS) and 1-hexyl-3-methylimidazolium hydrogen sulfate in five levels using Taguchi method was investigated. The optimum conditions and the most efficient electrolyte for zinc electrowinning were obtained using signal to noise analysis and analysis of variance (ANOVA). As a result, current efficiency and power consumption were shown to be linear function of these factors. Finally, surface morphology of cathodic deposit was studied by scanning electronic microscopy.



TMS 2012

141st Annual Meeting & Exhibition

Emeritus Professor George D.W. Smith Honorary Symposium: Novel Materials and Aluminium Alloys

Sponsored by: The Minerals, Metals and Materials Society, TMS Materials Processing and Manufacturing Division, TMS/ASM: Phase Transformations Committee

Program Organizers: Michael Miller, Oak Ridge National Laboratory; Gregory Olson, Northwestern University and QuesTek Innovations LLC; George Krauss, Colorado School of Mines

Monday PM
March 12, 2012

Room: Mockingbird 2
Location: Swan Resort

Funding support provided by: Oak Ridge National Laboratory; QuesTek Innovations LLC; AMETEK, Inc

Session Chairs: David Larson, Cameca Instruments, Inc.; Alfred Cerezo, Oxford University

2:00 PM Invited

Atom Probe Tomography of Inorganic Materials and Their Devices Using Ultraviolet Laser Atom Probe: *Kazuhiro Hono*¹; Takakatsu Ohkubo¹; ¹National Institute for Materials Science

Recent implementations of pulsed laser to assist field evaporation in atom probe tomography and the advances in the specimen preparation technique using the microsampling focused ion beam (FIB) method broadened the application areas of atom probe tomography to a wide variety of materials including metals, semiconductors, insulators and their devices. In this talk, we will update our recent atom probe studies on 3D nanotomography of various materials of industrial importance including sintered magnets, magnesium alloys, diluted magnetic oxides, lithium metal oxides, and metal/oxide interfaces. We will present features of atom probe tomography obtained using ultraviolet pulsed laser. The impact of the atom probe results to the materials science community will be briefly stated for each application example.

2:25 PM Invited

Microstructure of Cemented Carbides: *Hans-Olof André*¹; ¹Chalmers University of Technology

WC-Co based cemented carbides are primarily used for metal cutting and rock drilling. Seemingly simple – stoichiometric WC grains embedded in a cobalt binder phase - they have a surprisingly complex microstructure, and atom probe microanalysis has been used to investigate phase composition and interfacial chemistry. WC and any cubic carbide MC added (M = Ti, Nb, Ta or Zr) form a hard phase skeleton in which mainly cobalt segregates to WC/WC and WC/MC boundaries in sub-monolayer proportions. Cobalt dissolves W and C to an extent determined by the carbon potential during sintering, and in binder areas a diffusion profile of W (and any added M) is frozen in. Grain growth is determined by the interfacial reaction, and additions of Cr and V give rise to a thin cubic layer at the WC/binder interface, effectively restricting grain growth. Recently we found that WC has a low solubility for many elements.

2:50 PM

Possibility of Electron Beam Damage on the InGaN Well Layers of LED Evaluated by Atom Probe Tomography: *Woo Young Jung*¹; Gil Ho Gu¹; Chan Gyung Park¹; ¹Pohang University of Science and Technology (POSTECH)

GaN-based LEDs usually reveal high internal quantum efficiency (IQE) despite their high threading dislocation density, typically 10^7 - 10^9 /cm². The fluctuation of both indium (In) composition and thickness of InGaN multi-quantum-well (MQW) layers is believed to cause high IQE by

suppressing non-radiative recombination of carriers through the threading dislocations. The fluctuation of In composition is usually analyzed by using either transmission electron microscope (TEM) or atom probe tomography (APT). The important issue on the possibility of electron-induced In fluctuation, however, still remains to be solved. Therefore, in the present study, any possibility of electron-induced In fluctuation in MQW layers has been evaluated by APT. Each APT sample, illuminated within a TEM under various exposure times of high energy electron beam (200keV), has been investigated by APT analysis. Both TEM and APT results will give a clue on the validity of fluctuation of In distribution in InGaN well layers of LED devices.

3:05 PM

From Two to Three Dimensions: the Mutual Benefits of Cross-Sectional Scanning Tunnelling Microscopy and Atom Probe Tomography: *Devin Giddings*¹; Joris Keizer¹; Rian Hamhuis¹; Paul Koenraad¹; ¹Eindhoven University of Technology

The microscopy techniques of cross-sectional scanning tunnelling microscopy (XSTM) and atom probe tomography (APT) both offer atomic-level characterization, yet have wildly different representations. Whilst XSTM is strictly a surface technique, where atoms are imaged directly, with great precision, APT is able to produce a 3D map of a specimen, determining atomic locations through reconstruction. APT has an extremely high mass sensitivity, allowing accurate determination of chemical species of an atom, but XSTM is measuring local electronic properties, able to probe the band structure. By analysing semiconductor nanostructures, such as quantum dots, we are able to juxtapose these two complimentary techniques. This allows us to both benchmark the capabilities of APT against the established XSTM technique and also verify structural composition inferred from planar XSTM images through comparison to the richer volumetric APT view. The unique capabilities of both can be harnessed to achieve a fuller understanding of nanostructural properties.

3:20 PM

Preliminary Investigation of the Microstructure-Property-Processing Relationships in a Series of Co-Cr-Cu-Fe-Ni-Al High Entropy Alloys: *Abraham Munitz*¹; David Diercks¹; Michael Kaufman¹; ¹Colorado School of Mines

High entropy alloys have been developed recently where the entropy of mixing associated with combining multiple components purportedly favors the formation of simple structures (fcc and bcc). In this study, alloys containing equal parts of Co, Cr, Cu, Fe and Ni and varying amounts of Al from 0-30 at. pct. were prepared and examined in their as-cast condition and after various heat treatments using standard methods. The alloys become increasingly complex and harder as the Al content is increased, i.e., the structures solidify dendritically and then undergo one or more solid state reactions some of which appear to occur by spinodal decomposition consistent with previous reports on similar alloys in this six-component space. By combining DTA, heat treatments, microstructural analysis (SEM, TEM and 3DAP) and mechanical property measurements, an attempt will be made to explain the microstructural evolution in this new class of materials and their potential for structural applications.

3:35 PM Break

4:00 PM Invited

Atom Probe Tomography Analysis of Solute Clustering in Al-Mg-Si Alloys: *Gang Sha*¹; Gun Bulent¹; Simon Ringer¹; ¹The University of Sydney

Solute clusters are very important for the formation of precipitates microstructures in Al-Mg-Si alloys during ageing treatment. Most previous investigations employed IDAP or conventional 3DAP to investigate the small solute clusters in the alloys. Those investigations collected only small data sets typically containing <1 millions ions, sometimes suffered

with poor statistics. To date, there is a lack of systematic investigation to reveal the effect of alloy composition on the solute clustering at different temperatures. This contribution carefully investigated the solute clustering in the Al-Mg-Si alloys with Mg/Si ratios in the range of 2:1 to 1:2 aged at different temperatures over different time. A local electrode atom probe has been employed to collect large data sets (containing at least 20 M ions for each analysis) for better statistics in data analysis. The effects of alloy composition and ageing temperature on the clustering behaviours of these Al-Mg-Si alloys have been discussed.

4:25 PM Invited

Origins of Nanocluster Formation with Microalloying Elements Responsible for the Accelerated Precipitation of the Strengthening Phases in Age-Hardenable Aluminum Alloys: *Shoichi Hirose*¹; Tomo Ogura²; Ai Serizawa²; Yoshiki Komiya³; Tatsuo Sato⁴; ¹Yokohama National University; ²Osaka University; ³Meisei University; ⁴Tokyo Institute of Technology

In this paper, microstructural and microchemical analyses of age-hardenable aluminum alloys including Al-Cu-Mg, Al-Zn-Mg and Al-Mg-Si systems with a variety of microalloying elements have been performed by a three-dimensional atom probe (3DAP). It was found that the remarkable difference in mechanical strengths between the alloys with and without a particular microalloying element originates from different kinds of nanoclusters consisting of solute and/or microalloying elements, by which the subsequent strengthening phases are stimulated to precipitate. Such atomistic behavior of microalloying elements has been systematically predicted in terms of the two-body interaction energies based on a first-principles calculation under generalized gradient approximation (GGA) and full-potential Korringa-Kohn-Rostoker (FP-KKR) Green's function method. The established interaction energy map (IE map), in which the estimated interaction energies of microalloying elements are plotted against solute elements, is quite useful in designing high-strength aluminum alloys by means of microalloying additions.

4:50 PM

Chemical-Texture and Nanotopology in Hierarchy-Strengthened Al Alloys: *Peter Liddicoat*¹; Maxim Murashkin²; Xiaozhou Liao¹; Ruslan Valiev²; Simon Ringer¹; ¹The University of Sydney; ²Ufa State Aviation Technical University

Utilising solute structures at multiple length scales, hierarchy-strengthened Al alloys can exhibit yield strengths up to 1 GPa. Such internal alloy architectures are challenging to comprehensively characterise at the atom-scale – transmission-based microscopy (for e.g., TEM, XRD, or SAXS) may regularly encounter spectroscopic beam convolutions, from multiple nanocrystalline grains within a specimen, that can make information retrieval complex or impossible. Atom probe microscopy, a point-projection microscope, is not affected by grain size. Using novel techniques in atom probe to account for the complete activity of solute atoms, we will present the evolution of nanostructure at progressive strain increments imparted by high-pressure torsion in Al-Mg alloys. We will discuss defect-assisted solute clustering and the conceptual developments of chemical-texture and nanotopology to describe the intergranular relationships of misorientation and curvature to provide energetically favourable conditions for solute diffusion and partitioning.

5:05 PM Invited

Catalytic Reactions Investigated by Field Ion Microscopy and Atom-Probe Techniques: *Norbert Kruse*¹; ¹University Libre de Bruxelles

Field ion microscopy (FIM) and atom probe (AP) techniques can be successfully employed to solve fundamental problems related to heterogeneous catalysis. For example, catalyst particles may undergo morphological shape transformation due to adsorption and reaction. In this contribution it will be shown by FIM that a hemispherical Rh nano-

sized particle, conditioned as a tip, is transformed into a truncated half cube-octahedral particle through reaction with oxygen. AP-techniques reveal the outer Rh surface layers transform into RhO₂. Video techniques can be applied to follow “live” the oscillatory reaction of oxygen with hydrogen on the surface of such a reconstructed Rh tip. The question for the identification of local adsorption sites of NO on Pt facets – recently demonstrated by the group of George Smith using the “catalytic AP” – will also be addressed. The reduction of NO with H₂ likewise shows self-sustained oscillations with specific pattern formation on the nanoscale.

5:30 PM

Development and Recent Applications of FIM/APT for Heterogeneous Catalysis: *Paul Bagot*¹; Tong Li¹; Emmanuelle Marquis²; Edman Tsang¹; George Smith¹; ¹University of Oxford; ²University of Michigan

In heterogeneous catalysis, the interaction of gaseous adsorbates with catalytic metal surface atoms is a fundamental area to understand for improving our knowledge and performance of these critically important materials. Over 80% of chemical reactions depend on catalysts, yet there is a great deal of basic science to be explored about the nature of the interactions. These in turn govern important processes including surface reconstruction and diffusion/surface segregation of metal species. FIM/APT studies offer a unique way of studying these processes. Alongside the atomic-scale resolution and chemical identities provided, the hemispherical end-form of the specimens provides a close model for real catalyst particles, exposing multiple crystallographic faces to the environment at the same instant. This presentation will cover experiments characterizing changes to materials following exposures, recent developments in instrumentation and sample preparation, and the latest work using APT to study core-shell particles as used in real catalytic systems.

5:45 PM

Buried Interface Analysis Using Atom Probe Tomography: *Suntharampillai Thevuthasan*¹; Satyanarayana V. N. T. Kuchibhatla¹; Arun Devaraj¹; Fang Liu²; Shutthanandan Vaithiyalingam¹; Manjula Nandasiri¹; Bruce Arey¹; Chongmin Wang¹; Lisa Porter²; Robert Davis²; Ty Prosa³; ¹EMSL, Pacific Northwest National Lab; ²Carnegie Mellon University; ³Cameca Instruments Inc

This presentation examines the feasibility of using atom probe tomography for challenging materials systems that have not been thoroughly examined earlier. We report the first Local Electrode Atom Probe (LEAP®) analysis of bulk oxides which contain ion beam synthesized Au-nanoclusters. The influence of Au on the quality of the mass spectra obtained from the bulk oxides under the laser pulsing mode and the reconstruction results of the Au-clusters in the matrix will be discussed in detail. We will also discuss about the APT, STEM and high-resolution RBS analysis of GaN/InGaN multi-quantum well structures and doped ceria/zirconia multiplayer thin film systems. These results clearly demonstrate the power of APT in conjunction with other capabilities in the characterization of interfaces in layered structures. In all the system we draw the attention towards the significance of parametric space experiments in order to obtain best results from APT analysis.



Energy Nanomaterials: Li-ion Batteries and Beyond

Sponsored by: The Minerals, Metals and Materials Society, TMS Materials Processing and Manufacturing Division, TMS Structural Materials Division, TMS: Advanced Characterization, Testing, and Simulation Committee, TMS: Nanomechanical Materials Behavior Committee

Program Organizers: Reza Shahbazian-Yassar, Michigan Technological University; Ming Au, Savannah River National Laboratory; Meyya Meyyappan, NASA Ames Research Center

Monday PM Room: Swan 3
March 12, 2012 Location: Swan Resort

Session Chairs: Reza Shahbazian Yassar, Michigan Technological University; Ilias Belharouak, Argonne National Laboratory

2:00 PM

Self-Aligned Cu-Si Core-Shell Nanowire Array as a High-Performance Anode for Li-Ion Batteries: Jun Qu¹; Huaqing Li²; John Henry¹; Surendra Martha¹; Miaofang Chi¹; Hanbing Xu¹; Nancy Dudney¹; Michael Lance¹; Shannon Mahurin¹; Theodore Besmann¹; Sheng Dai¹; ¹Oak Ridge National Laboratory; ²University of Tennessee

Silicon nanowires (NWs) have been reported as a high-capacity anode without pulverization during cycling. However, the high-aspect ratio NWs have high electrical resistance and thus inefficient electron transport. The NWs' nano-size interface with the substrate experiences high shear stress during lithiation, potentially causing the wire to separate from the current collector. This study developed a self-aligned Cu-Si core-shell NW array using a low-temperature, catalyst-free process. The amorphous silicon shell accommodates Li-ions without phase transformation, while the copper core functions as a built-in current collector to provide very short (nm) electron transport pathways as well as backbone to improve mechanical strength. Initial electrochemical evaluation has demonstrated good capacity retention and high Coulombic efficiency in a half-cell configuration. No wire fracture or core-shell separation was observed after cycling. However, electrolyte decomposition products largely covered the top surface of the NW array, restricting electrolyte access and causing capacity reduction at high charging rates.

2:20 PM

Investigation of Synthesis of Nano-LiNi_{0.5}Mn_{1.5}O₄ Cathode Material for Lithium-Ion Battery by In-Situ Neutron Diffraction: Lu Cai¹; Zengcai Liu²; Chengdu Liang³; Ke An¹; ¹Spallation Neutron Source, Oak Ridge National Laboratory; ²Center for Nanophase Material Sciences; ³Center for Nanophase Material Sciences

Nano-LiNi_{0.5}Mn_{1.5}O₄ is an attractive cathode material for lithium-ion batteries due to the high voltage plateaus, high discharge capacity, low cost, and non-toxicity. Different synthesis processes result in either disordered LiNi_{0.5}Mn_{1.5}O_{4.6} (where Ni and Mn are randomly distributed at one crystallographic site) or ordered LiNi_{0.5}Mn_{1.5}O₄. Disordered LiNi_{0.5}Mn_{1.5}O_{4.6} exhibit better rate capability and cycling stability than ordered LiNi_{0.5}Mn_{1.5}O₄. Therefore, the performance of the material is strongly dependent on the synthesis process. Neutron diffraction can easily distinguish these two phases because of the different neutron scattering factor of Ni and Mn, thus have the capability to provide direct monitoring of structural evolution during synthesis. In this study, in-situ neutron diffraction is used to study the phase formation and the order-disorder transition during heating and annealing. The correlation of structure to synthesis conditions will be discussed in details. We expect the results will provide guidance on the development of new cathode materials.

2:40 PM

Transmission Electron Microscopy Studies on Lithium Battery Materials II: Characterization of Mesoporous TiO₂ Films: Alpesh Shukla¹; Natacha Krins¹; Guoying Chen¹; Thomas Richardson¹; ¹Lawrence Berkeley National Laboratory

Electrode porosity has significant impact on the performance of energy storage systems such as lithium batteries. However, owing to the complex porous network present in most composite electrodes, the role of pores and that of the active material is difficult to assess. A systematic study to understand the specific role of individual pore types and interconnections is therefore warranted in order to design highly efficient electrodes for lithium batteries. In this study model mesoporous TiO₂ thin films with pore sizes varying from 3 to 40 nm were synthesized by dip-coating of tin-doped indium oxide (ITO) glass substrate using soft-templating methods. STEM tomography was used to characterize the three dimensional porous network and the orientation of pores with respect to the Li-insertion channels in TiO₂. Also, the crystalline nano-domain structure and their orientation with respect to the thin film was studied using aberration-corrected transmission electron microscopy.

3:00 PM Invited

The Facts Influencing Rechargeability of Lithium/Air Batteries: Ming Au¹; Elise Fox¹; Hector Colon-Mercado¹; Thad Adams¹; ¹Savannah River National Laboratory

Li/air batteries attract great attention and interests for their high theoretic energy density and low cost. However, several challenges prevent Li/air batteries from practical application. The oxygen reduction and evolution both take place on the cathode and the effective and long-lasting bifunctional cathodes have not been developed yet. In order to reduce the products of the discharge, effective catalysts have to be developed. To prevent volatile reaction of Li with water, the Li/air batteries have to use non-aqueous electrolyte or use dual electrolyte. The products of discharge, Li₂O₂ and Li₂O are not soluble in the non-aqueous electrolyte currently used by researchers. Focusing on these issues, we have conducted our investigation on cathode architecture, catalyst, electrolyte and anode in regarding of the performance of the Li/air batteries. We will discuss our results and share our vision for the future of this technology.

3:30 PM Break

3:50 PM

Solution Precursor Plasma Synthesized Flexible Manganese Oxide Anodes for Li-Ion Batteries: Ramesh Kumar Guduru¹; Raghavender Tummala¹; Pravansu S. Mohanty¹; ¹Univ of Michigan

The demand for high energy density Li-ion batteries for large scale applications is increasing. But, due to the limited specific capacity of carbon anodes, there has been extensive ongoing search for anode materials with more capacity. Manganese oxide is known for higher capacity than carbon with comparable potential. However, most of the efforts focused on preparation of Manganese oxide anodes employ time intensive techniques to obtain different kinds of nanostructured powders with a requirement of subsequent processing. We have developed a single step, inexpensive and scalable solution precursor plasma deposition route to develop nanostructured flexible manganese oxide electrodes. In this approach, a solution precursor comprising of manganese salts is fed axially into a high temperature plasma plume for accelerated thermochemical conversion prior to depositing a binder less coating onto a current collector. Thus developed electrode films confirmed the desired phase and their detailed microstructural and electrochemical analysis will be reported.

4:10 PM

Transmission Electron Microscopy Studies on Lithium Battery Materials I: Conversion Reactions in Nickel Oxide Nanoplates: *Alpesh Shukla*¹; Jordi Cabana¹; Peter Ercius²; Abhay Raj Singh Gautam²; Ulrich Dahmen²; ¹Lawrence Berkeley National Laboratory; ²National Center of Electron Microscopy, Lawrence Berkeley National Laboratory

Transition metal oxides such as nickel oxide that work via a conversion reaction have emerged as attractive candidates for the negative electrode in lithium batteries because they can store as much as twice the amount of charge per unit of mass than intercalation-based carbon electrodes. In this study, nanoporous nickel oxide plates 100-150 nm in width and 10-15 nm in thickness were synthesized by thermal decomposition of hydrothermally-prepared nickel hydroxide crystals. The pore and domain structures were characterized using STEM tomography and aberration-corrected TEM, respectively. The process of nickel hydroxide decomposition was also observed directly by in-situ TEM experiments. The porosity calculated from the measured decrease in volume upon decomposition and the theoretical volume change obtained from the unit cell volumes of Ni(OH)₂ and NiO were found to be in good agreement with the pore volume measured from the tomograms.

4:30 PM

New Method to Fabricate Nanoporous Silicon for Lithium Ion Batteries: *Xu Jiang*¹; Thomas Balk¹; ¹University of Kentucky

Silicon, because of its high capacity to store lithium, is increasingly becoming an attractive candidate as an anode material for lithium ion batteries (LIB). One significant problem with using Si for the anode is the large strain that accompanies charge-discharge cycling, due to swelling of the Si during Li insertion and desorption. Nanoporous Si (np-Si) offers a large amount of free volume for Li absorption, which allows the anode material to swell without cracking. In this paper we demonstrate a method to fabricate high-purity (100% Si content) np-Si thin films by dealloying precursor materials that had been deposited by magnetron co-sputtering. Microstructural characterization and chemical analysis of np-Si revealed a nanoporous structure with regularly distributed ligaments and pores, with a ligament size approximately 20 nm. Coin-cell battery samples were prepared and subjected to charge-discharge cycling tests. These and other results will be discussed in relation to the suitability of np-Si as a LIB anode material.

4:45 PM

A Novel Type of Carbon Coated Sulfur Nanoparticles for Li/S Batteries: *Yan Yuan*¹; Elton Cairns¹; ¹LBNL

This kind of carbon coated sulfur nanoparticles have been synthesized via a novel liquid-synthesis technique, this reaction in the presence of a surfactant (polyethylene glycol-400) has been developed to get S-C nanoparticles by using sublimed sulfur powders, sodium sulfide, formic acid and carbon black (battery grade) under room temperature. It has been physically characterized by scanning electron microscopy, EDS, and thermo gravimetric analysis instrument. The SEM image shows that the size of carbon coated sulfur nanoparticles is around 30 nm. The TGA result shows that the S-C sample is quite pure, and the ratio of sulfur and carbon is equal to what we set initially. Besides, it can be used as cathode in Li/S batteries, it improved the electrochemical performance of Li/S batteries.

Fatigue and Corrosion Damage in Metallic Materials: Fundamentals, Modeling and Prevention: Fatigue Property-microstructure Relationships and Crack Growth

Sponsored by: The Minerals, Metals and Materials Society, TMS Structural Materials Division, TMS/ASM: Mechanical Behavior of Materials Committee

Program Organizers: Tongguang Zhai, University of Kentucky; Zhengdong Long, Kaiser Aluminum; Peter Liaw, University of Tennessee

Monday PM
March 12, 2012

Room: Oceanic 6
Location: Dolphin Resort

Session Chairs: Youshi Hong, Institute of Mechanics, Chinese Academy of Sciences; Antonios Koutsos, Drexel University

2:00 PM Invited

Identification of Fatigue Crack Initiation from Surface Particles in High Strength Al Alloys: *Xinliang Zang*¹; Wei Wen²; Zhiqiang Xu¹; Alfonso Ngan³; Tongguang Zhai²; ¹Yanshan University; ²University of Kentucky; ³University of Hong Kong

A finite element analysis method was used to analyze the stress and strain fields around the particles in close proximity of the surface in high strength Al alloys, assuming the alloys were linear elastic-plastic continuum homogeneous. It was found that the thickness, position in depth, orientation and clustering of these particles had significant effects on the stress and strain concentration around the particles in the surface region. A focused ion beam was used to investigate the 3-dimensional geometry of the particles where micro-cracks were initiated. The results indicated that the thinner the particles in surface, the easier micro-cracks could be formed from the particles, though these micro-cracks might not necessarily propagate into the matrix of the alloys.

2:20 PM

Influence of the Inclusion Shape on the Rolling Contact Fatigue Life of Carburized Steels: *Yutaka Neishi*¹; Taizo Makino¹; Naoki Matsui¹; Hitoshi Matsumoto²; Masashi Higashida²; Hideki Ambai²; ¹Sumitomo Metal Industries, Ltd.; ²Sumitomo Metals (Kokura), Ltd.

It has been well known that the flaking failure in rolling contact fatigue (RCF) originates from nonmetallic inclusions in steels, and their apparent size is one of the important factors affecting RCF life. However, the influence of inclusion shape on the RCF life has not been fully clarified. In this study, attention was paid to the influence of the inclusion shape on the RCF life. This was evaluated by using carburized JIS-SCM420 (SAE4320) steels which contained two different shapes of MnS-stringer type and spheroidized type-as inclusions. Sectional observations were made to investigate the relation between the occurrence of shear crack in the subsurface and the shape of MnS. It was found that the RCF life was well correlated with the projected length of MnS along the load axis, and the initiation of shear crack in subsurface was accelerated as the length of MnS increased.

2:40 PM

Effects of Size And Position of Al₂O₃ Inclusions On fatigue Crack Initiation in Low Carbon Bainitic Steel: *Tongguang Zhai*¹; Xiucheng Li²; Wei Wen¹; Chengjia Shang³; Linghui Du⁴; ¹University of Kentucky; ²University of Science and Technology Beijing; ³University of Science and Technology Beijing; ⁴CNMC Ningxia Orient Group Co. Ltd

Fatigue tests were conducted on a low carbon micro-alloyed steel produced by thermo-mechanical control processing, using four point bend at room temperature. The results showed that only single crack initiation occurred in each sample and that fatigue cracks were predominantly



initiated from those Al₂O₃ particles. The position of these particles relative to sample surface was considered to be another factor effecting the fatigue crack initiation beside the particle size. A finite element analysis showed that the value of stress intensity factor was dominated by the depth of particle embedment and the real plastic strain at the edge of particle was influenced by the particle size. In addition, the 3-dimensional density of particles with different sizes was also recalculated basing on the 2-dimensional particle cross sectional area statistic result, which can be an explanation of fatigue cracks can initiate from smaller particles in the samples.

3:00 PM

Scale-Bridging Fatigue Monitoring in Magnesium Alloys: *Antonios Kotsos*¹; Kavan Hazeli¹; Prashanth Abraham¹; Jefferson Cuadra¹; Eric Schwartz²; Raghavendra Saralaya¹; Tim Schmidt²; ¹Drexel University; ²Trilion Quality Systems

The objective of this research is to in situ monitor and quantify critical relationships between reversible/irreversible microstructural changes and fatigue loading of Magnesium (Mg)-alloys using an innovative setup combining digital image correlation with acoustic emission monitoring and a conventional load frame. Research on the fatigue behavior of Mg-alloys has been significantly increased in view of the renewed interest on their applications. The limited crystallographic deformation mechanisms in hexagonal close-packed Mg-materials, including a-direction basal, prismatic and pyramidal slip, as well as c-direction pyramidal slip and deformation twinning/detwinning results to a distinct mechanical behavior upon cyclic loading, characterized by asymmetric tension/compression yielding, anisotropic hardening and hysteretic loops. Fatigue testing data of AZ31 specimen that comprise grain scale observations, full-field deformation/strain measurements and acoustic emission activity are presented. The measured strain heterogeneities are associated with pre- and post-damage conditions, while the recorded acoustic emission provides means for continuous fatigue monitoring.

3:20 PM

Effect of Orientation on Fretting Behavior of a Single-Crystal Ni-Base Superalloy: *Nabil Marouf*¹; Siegfried Fouvry¹; Philippe Belaygue²; ¹LTDS; ²TURBOMECA

Single-crystal superalloy turbine blades are designed to improve creep resistance in a radial direction, requiring a radially crystal growth. As a result, cubic orientation in the attachment is constrained by wheel geometry, keeping in mind it is perhaps not the best to stand high multiaxial-cycling stresses and fretting stresses. Fretting experiments were conducted to investigate tribological behavior and cracking response of nickel single-crystal alloy, by means of a cylinder/plane contact (cylinder: Udimet720 plane: MC2). Three configurations were studied, choosing extreme planes orientations (001), (011) and (111). The first step was to determine sliding conditions and coefficients of friction. Then, crack nucleation threshold and growth kinetic were investigated. As expected, relative orientation between octahedral planes and fretting direction has an important effect on crack growth direction and kinetic. On the other hand, nucleation threshold seems to be less influenced by crystal orientation, probably due to plastic strain introduced by shot peening.

3:40 PM Break

3:50 PM

Slip Transfer across Grain Boundaries and Its influence on the Development of Local Strain Heterogeneities in the Plastic Response: *Wael Abuzaid*¹; Michael Sangid²; Jay Carroll³; Huseyin Sehitoglu¹; John Lambros¹; Ravinder Chona⁴; ¹University of Illinois at Urbana-Champaign; ²Purdue University; ³Sandia National Laboratories; ⁴Air Force Research Lab

Heterogeneous plastic flow and strain accumulation at the microstructural level is a precursor for fatigue crack initiation. One of the contributing factors in the development of such strain heterogeneities is the interaction of slip with grain boundaries (GBs), which may block, or transmit

slip across the interface. In this work, our aim is to develop a deeper understanding of strain accumulation in the vicinity of GBs and how it relates to the resistance exhibited by different GBs to slip transmission. Utilizing digital image correlation and electron backscatter diffraction, we establish the most likely dislocation reactions due to slip transmission and use that information to calculate the residual Burgers vector and strain magnitudes across each interface of a plastically deformed polycrystalline aggregate. From our analysis, we quantitatively show an influence of the magnitude of the residual Burgers vector on GB resistance to slip transmission and on plastic strains across GBs.

4:10 PM

Influence of Aluminide Coatings on Fatigue Behavior during Sustained-Peak Low-Cycle Fatigue in a Single-Crystal Ni-Base Superalloy: *Luke Rettberg*¹; Tresa Pollock¹; ¹University of California Santa Barbara

The influence of several different aluminide coatings on fatigue behavior has been examined for single-crystal Ni-base superalloy René N5 during sustained peak low-cycle fatigue (SPLCF). Fatigue specimens, aligned along the (001) direction, were tested in strain-control at 1093°C, with a total strain amplitude of 0.35% and A = -1 (R = -8). The testing cycle consisted of a 120s hold at -0.35% strain and a total unload/reload time of 3.0s. During the 120s hold, creep deformation reduces the compressive stress, causing the specimens to experience a tensile stress upon returning to zero strain. Samples from interrupted tests were examined to measure the depth of crack penetration in the coating, IDZ and substrate. Finite element modeling has been performed to assess the driving forces for extension of the oxide-filled cracks into the substrate. The characteristics of coatings that will extend the fatigue life will be discussed.

4:30 PM

Evolution of Microstructure and Mechanical Properties during Rolling Contact Fatigue in High Strength Case-Hardened and Through-Hardened Steels: *Ghatu Subhash*¹; Nagaraj Arakere¹; Bryan Allyson¹; ¹University of Florida

Through-hardened M50 steel and case hardened M50 NiL and Pyrowear (P675) are commonly used materials in high performance aerospace roller bearing applications. Balls and Rods of above three materials were subjected to a range of rolling contact fatigue (RCF) cycles and the stress affected zones were probed using micro indentation. It was noted that while the increase in hardness of M50 was marginal, both the M50 NiL and P675 revealed an increase in hardness of around 1 GPa. RCF testing of M50 NiL balls (57 mm diameter) revealed a large elliptical shaped transformed region with 1 mm in minor axis and 4 mm size major axis. Stress-strain response of cylindrical specimens extracted from these regions revealed an increase in yield strength of approximately 400 MPa compared to virgin material. The presentation will discuss the associated microstructural modifications and relate them to property changes.

4:50 PM

In Situ Neutron Diffraction Measurements of Stress Fields Around a Fatigue-Crack Tip Under Loading: *Soo Yeol Lee*¹; E-Wen Huang²; *Kuan-Wei Lee*²; Wanchuck Woo³; ¹Department of Materials Science and Engineering, Chungnam National University, Daejeon, 305-764, South Korea; ²Department of Chemical & Materials Engineering and Center for Neutron Beam Applications; ³Neutron Science Division, Korea Atomic Energy Research Institute

Fatigue crack growth mechanisms subjected to three different loading conditions (i.e. fatigued, tensile overloaded, and overloaded-underloaded) were investigated using neutron diffraction. First, the spatially-resolved neutron stress mapping was performed to directly measure the residual stress distribution around a crack tip immediately after applying the various loading conditions. Second, in-situ neutron diffraction was employed on the three compact-tension specimens exhibiting distinct crack-growth rates at the same applied ΔK within the retardation period. The internal strains/stresses evolutions in the vicinity of the crack tip

were carefully examine in situ under loading in order to observe how the stresses near the crack tip are distributed under loading, as the closed crack gradually opens. Finally, the correlation between the measured internal stresses and the fracture mechanics parameters is investigated to account for the transient crack growth behavior, and the mechanisms concerning the overload/underload effects are suggested.

5:10 PM

Influence of Twin-Boundary on the Bauschinger's Effect in Cu Crystal- a Molecular Dynamics Simulation Study: *Di Zhu*¹; Hao Zhang¹; Dongyang Li¹; ¹University of Alberta

Plastic pre-strain may decrease the yield strength of metallic materials when stressed in the opposite direction, known as Bauschinger's effect, which could considerably influence the performance of the materials during cyclic loading processes such as fatigue and fretting. In this study, effects of a twin boundary (TW) as an ordered obstacle on defects' generation, movement and annihilation during cyclic tension-compression loading processes were investigated, in comparison with those occurring in a single crystal (SC) system, using a MD simulation technique. It was observed that the Bauschinger's effect in the TW system was more asymmetrical with higher residual strain energy, compared to the SC system. It was demonstrated that the ductility of the SC system was elevated by the cycling loading but this was less obvious for the TW system. Efforts were made to elucidate mechanisms involved.

From Macro to Nano, Understanding Mechanical Behavior across Length Scales: A Structural Materials Division Symposium in Honor of Robert Ritchie: Fatigue

Sponsored by: The Minerals, Metals and Materials Society, TMS Structural Materials Division, TMS/ASM: Mechanical Behavior of Materials Committee, TMS: Biomaterials Committee
Program Organizers: Jamie Kruzic, Oregon State University; Brad Boyce, Sandia National Labs; Reinhold Dauskardt, Stanford University

Monday PM
March 12, 2012

Room: Mockingbird 1
Location: Swan Resort

Session Chairs: Jamie Kruzic, Oregon State University; Nikhilesh Chawla, Arizona State University

2:00 PM Introductory Comments

2:05 PM

Predicting the Behavior of Short Fatigue Cracks: *Jamie Kruzic*¹; Sarah Gallops¹; Rawley Greene¹; ¹Oregon State University

While extrinsic toughening mechanisms (e.g., crack bridging, transformation toughening, etc.) are effective at providing crack propagation resistance in many materials and composites, these mechanisms result in a crack size dependence (i.e., "short crack effect") for the fatigue properties over crack sizes on the order of the extrinsic toughening zone size. Fatigue threshold R-curves are one route to understand and predict such crack size effects. Experimental results using compact tension and/or beam specimens for several crack bridging materials are presented. It is demonstrated that the fatigue behavior can be predicted by characterizing the bridging zone and quantifying the effects of crack bridging. It is shown how experimentally measured short crack data agrees well with predictions based on quantitative bridging zone characterization. It is expected that this methodology will be extendable to cover a wide range of materials toughened by crack bridging, including ceramics, intermetallics, composites, and biological materials.

2:20 PM

The Continuing Relevance of Small Fatigue Crack Growth Behavior in the Design and Life Management of Structural Aerospace Components: *Michael Caton*¹; Sushant Jha²; M. Burba³; James Larsen¹; Reji John¹; Andrew Rosenberger¹; ¹US Air Force Research Laboratory; ²Universal Technology Corporation; ³University of Dayton

The behavior of small fatigue cracks has represented an area of significant research interest over the past 30 years. Recent fatigue studies of numerous alloys employed in the aerospace industry have demonstrated that incorporation of the behavior of early crack growth remains an essential element to accurately predicting fatigue life limits. For several Ni-base superalloys, Ti alloys, and Al alloys, competing failure modes have been observed to drive the full lifetime distributions, whereby the life-limiting fatigue mechanisms are controlled by early or immediate crack initiation and small crack growth. Since design limits and inspection intervals of fracture-critical components are typically established based upon worst-case lifetimes, a thorough understanding of small crack behavior is required for accurate life predictions. A collection of small crack data will be shown for numerous alloys, examining the influence of loading condition and microstructure, and a framework for probabilistic prediction of life-limits will be presented.

2:35 PM

Relating Fatigue Crack Initiation and Small Crack Propagation to Microstructure in the Polycrystalline Nickel Base Superalloy, Rene 88DT: *Jiashi Miao*¹; Tresa Pollock²; *J. Wayne Jones*¹; ¹University of Michigan; ²University of California Santa Barbara

In the very high cycle fatigue (VHCF) regime crack initiation is generally considered to dominate fatigue life. In this study, small crack propagation behavior and its dependence on the character of microstructural neighborhoods near crack initiation sites in Rene 88DT was examined in the VHCF regime using an ultrasonic fatigue apparatus operating at frequencies close to 20 kHz. Crack initiation resulted from cyclic strain localization on {1 1 1} slip planes near, but not on, S3 twin boundaries in large, favorably oriented grains. The likelihood that these nascent cracks would grow beyond the small crack regime to viable large cracks depended strongly on the local microstructural and particularly on the presence and extent of regions of similarly oriented grains surrounding the crack initiation sites. These findings are discussed in the context of the role of microstructural variability on fatigue life variability.

2:50 PM

Endurance Limits and Non-Propagating Cracks: *Herwig Mayer*¹; Bernd Schönbauer¹; Stefanie Stanzl-Tschegg¹; ¹BOKU University Vienna

S-N curves of several materials show a pronounced change of slope in the high cycle fatigue regime, and failures are rare beyond certain lifetimes. Such behavior is found in mild steel and in several cast aluminium and magnesium alloys. Non-propagating fatigue cracks can be found in some cases analyzing the surface of specimens that did not fail within 109 cycles or more. Such cracks even were found in copper and high strength aluminium alloys at very high numbers of cycles, which are generally attributed to have no endurance limit. Examples of non-propagating cracks will be shown and analyzed with respect to possible minimum load amplitudes that can cause fatigue failure.

3:05 PM

Deformation Mechanisms of Small Crack Growth under Dwell-Fatigue in a Ni-Base Superalloy: *G. B. Viswanathan*¹; Sushant Jha¹; Sam Kuhr²; Jay Tiley¹; Hamish Fraser²; Reji John¹; C. Woodward¹; ¹Air Force Research Laboratory; ²The Ohio State University

The damage mechanisms that affect the small-crack growth behavior in Ni-base superalloys are strongly related to the fine scale microstructural features that surround the crack such as size and scale of second phase γ' precipitates, the grain boundary structures and neighboring grain orientations. A study is undertaken to probe these effects in LSHR, a Ni-base superalloy under high temperature low cycle fatigue (LCF) both under dwell and no-dwell conditions. The small crack growth studies



TMS 2012

141st Annual Meeting & Exhibition

MONDAY PM

were simulated by placing focused ion beam (FIB) notches on the surface of the samples before the tests. The tests were interrupted immediately after a measurable crack growth was observed. The region ahead of the crack was analyzed in detail by EBSD for grain orientations. Thin foils were extracted from grains immediately ahead of the crack for detailed investigation of the deformation substructures in the TEM. The results will be presented and discussed.

3:20 PM

Effects of Local Crystallography and Inclusion Geometry on Nucleation and Propagation of Short Fatigue Cracks in Al 2024-T351: Statistics and Mechanisms: Admir Makas¹; Jaclyn Avallone¹; Ross MacKinnon¹; Ikshwaku Atodaria¹; Dallas Kingsbury¹; Pedro Peralta¹; Aditi Chattopadhyay¹; ¹Arizona State University

Nucleation and growth of short fatigue cracks can represent a significant fraction of the life of a structure. Quantification of these effects and their variability due to microstructural heterogeneity is key to predict residual life. Correlations between short fatigue crack nucleation and growth, crystallography of the local loading axis and inclusion geometry were studied via interrupted testing at stresses close to yielding in notched uniaxial and biaxial (cruciform) samples. Local crystallography was quantified using Electron Backscattering Diffraction. Nucleation sites were characterized using Optical and Electron Microscopy. The crystallographic orientation of grains with broken inclusions was quantified and correlated to the tendency for a matrix crack to propagate from them. Results indicate that local loading axes perpendicular to cracking facets produced by environmental effects favored short crack growth, particularly when combined with elongated Fe-rich inclusions. Damage mechanisms and modeling avenues are discussed. Funding by AFOSR Grant FA95550-06-1-0309, David Stargel program manager.

3:35 PM Break

3:50 PM

Understanding Fatigue Crack Growth by In Situ 3D X-ray Synchrotron Tomography: Nikhilesh Chawla¹; ¹Arizona State University

Prof. Robert Ritchie's contributions in the area of fatigue of materials are seminal. In particular, his work has provided much insight into the fatigue crack growth mechanisms in metallic materials. X-ray synchrotron tomography provides a wonderful means of characterization damage in materials non-destructively. In this talk, I will describe in situ fatigue crack growth experiments in 7075-T6 aluminum alloy, using a three-dimensional (3D) x-ray synchrotron tomography. The approach involves capturing the microstructure during in situ fatigue testing in an x-ray synchrotron, followed by x-ray tomography and image analysis, and 3D reconstruction of the microstructure. Local variations in crack growth rate, investigations of fatigue crack closure, and correlation to local measurements of striation spacing were quantified and will be discussed.

4:05 PM

Leave-in-Place Laser Scanning for Fatigue Damage Monitoring and Prognosis: James Earthman¹; Benjamin Buckner²; Kwai Chan³; Xiaoxi Liu¹; Vladimir Markov²; ¹University of California, Irvine; ²Metrolaser, Inc.; ³Souwest Research Institute

A compact leave-in-place laser-scanning device for the detection and monitoring of fatigue damage precursors has been developed. The current device is shown to be capable of detecting fatigue-related changes in the surface bidirectional reflectance distribution (BRDF) of aluminum test samples, and detectable changes in BRDF are measured at a very early stage of fatigue development, when no cracks larger than about 50 μm in length have yet developed at the monitored location. The system power requirements are compatible with standard sensor mote architectures that are targeted for multiyear lifetimes without battery replacement. Results from our latest in situ fatigue tests will be discussed and compared with mechanistic model predictions of small crack initiation and growth.

4:20 PM

The Effect of Microstructure on Strain Field Inhomogeneities in Fatigue Crack Growth: Jay Carroll¹; Wael Abuzaid²; Mallory Casperson²; John Lambros²; Huseyin Sehitoglu²; Ravinder Chona²; Brad Boyce¹; ¹Sandia National Laboratories; ²University of Illinois at Urbana-Champaign

Variability in fatigue lifetimes can largely be attributed to microstructure, but at this time, most microstructural effects are known only in a qualitative sense. A better quantitative understanding of the relationship between microstructure and inhomogeneous deformation behavior in fatigue could provide more accurate predictions of variability in fatigue crack growth rates and fatigue lifetimes. In this work, multiscale strain measurements from a high-resolution digital image correlation technique were used to study fatigue crack growth in a nickel based superalloy, Hastelloy X. Both sub-grain-level and macroscale strain fields were captured at intervals of fatigue crack growth. Lobes of elevated strain emanating asymmetrically from the crack were observed. The relationship between these inhomogeneities and microstructure was examined by comparing strain fields to full-field microstructural measurements obtained through electron backscatter diffraction. Additionally, the relationship between these strain fields and mode mixity was considered. This work was inspired by Robert Ritchie's compelling multiscale research on fatigue cracks.

4:35 PM

Reducing Uncertainty for Fatigue Life Limits at Notches in Two Structural Alloys: Dennis Buchanan¹; James Larsen²; Andrew Rosenberger²; Reji John²; Sushant Jha³; Alisha Hutson¹; W. John Porter¹; ¹UDRI; ²Air Force Research Laboratory; ³Universal Technology Corporation

Fatigue life variability is modeled as a combination of a mean-lifetime and a dominant life-limiting crack growth mechanism in two materials: a powder metal nickel-base superalloy IN100 and a cold rolled plate of aluminum alloy 7075-T651. Specimens of both materials had a common double-edge notch geometry with a stress concentration factor of $K_t = 1.89$. Fatigue tests were conducted under constant amplitude loading at temperatures of 23°C and 650°C for the 7075-T651 and IN100, respectively. Fatigue failure initiated at sites located either along the notch surface or at the notch corner. Crack growth behavior was predicted for both of these initiation sites using a weight function solution and the cyclic and residual stress profiles from three-dimensional finite element analysis. The predicted fatigue lives for a range of stress levels correlated well with the observed experimental data and the minimum (1 in 1000 probability of failure) lifetime limit for both materials.

4:50 PM

A Comparison of Cast Aluminum Bulkhead Fatigue Resistance: The Effect of Specimen Geometry: Andrea Campbell¹; John Allison²; ¹Ford Motor Company; ²University of Michigan

Automotive cylinder block bulkheads were obtained from two aluminum casting suppliers for a study on the high-cycle fatigue resistance of these materials. The fatigue strengths were measured via a staircase protocol using cylindrical round bars. These values were ~20-30% lower than previously measured data where an hour-glass fatigue sample geometry was used. A model to predict the fatigue life and strength (at a given number of cycles) was developed and revealed that the hour-glass geometry had a predisposition to higher fatigue strengths due to the lower probability of sampling a casting pore local to the region with minimum radius and highest stress. It was concluded that previous fatigue data on the bulkhead materials were inflated due to the choice in fatigue specimen geometry. More conservative values, which better represent the expected material behavior and intrinsic fatigue resistance, were obtained using the cylindrical bar geometry.

5:05 PM

Predicting Fatigue Crack Growth Behavior at Different Crack Size Scales: *Anastasios Gavras*¹; *Diana Lados*¹; ¹Worcester Polytechnic Institute

Along with microstructure, the initial flaw size significantly affects the fatigue crack growth response of a material. In this work, focus was given to the initial flaw size. Long and small fatigue crack growth experiments were performed on various non-ferrous and ferrous structural materials with different microstructures. Long fatigue crack growth tests were conducted at three stress ratios ($R=0.1, 0.5, \text{ and } 0.7$) and small fatigue crack growth tests were run at $R=0.1$. The differences in the response were evaluated, and the controlling crack growth mechanisms were related to microstructural characteristic dimensions specific to each material and microstructure. An original methodology that accounts for the differences between long, short, and microstructurally small crack growth data was also developed and will be presented and discussed from a design perspective.

Integrative Materials Design: Performance and Sustainability: Processing and Properties of Traditional and Novel Materials at Ambient and High Temperatures II and Condition Assessment and Monitoring

Sponsored by: The Minerals, Metals and Materials Society, TMS/ASM: Mechanical Behavior of Materials Committee
Program Organizer: *Diana A. Lados*, Worcester Polytechnic Institute

Monday PM
March 12, 2012

Room: Europe 2
Location: Dolphin Resort

Session Chair: *Diana Lados*, Worcester Polytechnic Institute

2:00 PM Invited

AA362.0 Aluminum Alloy: Utilizing Improved Fatigue Properties of Sustainable Alloys in Design: *Kevin Anderson*¹; *Michael P. Mihelich*²; *William J. Towne*²; *Gregg D. Langenfeld*²; *Raymond J. Donahue*²; ¹Mercury Fellow, Mercury Marine, Product Development & Engineering; ²Mercury Marine, Product Development & Engineering

Traditional secondary (recycled) die-casting alloys have high iron content, lower damage tolerance properties, and a limited ability to be recycled into other alloys. First generation high damage - tolerant die-casting alloys replace iron with manganese, have good damage tolerance properties, and can be easily recycled into other alloys. Unfortunately, they are typically made from 100% virgin aluminum with high embodied energy. Second - generation AA362.0 alloy has good damage tolerance properties, is typically made from 100% recycled aluminum, and is easily recycled into other alloys. Alloy AA362.0 demonstrates that sustainable alloy design and good damage tolerance properties need not be mutually exclusive. The authors will present fatigue data for AA362.0 and show how material properties interact with the design of components to achieve design life goals. Several component examples will be discussed emphasizing where in the design process damage - tolerant material properties can improve performance and reduce development time.

2:25 PM Invited

Reduce Your Burden – Use Magnesium Alloys: *Norbert Hort*¹; ¹Helmholtz-Zentrum Geesthacht

Global warming is an issue for industrialized countries all over the world. Especially in transportation solutions have to be found to reduce the CO₂ emissions drastically. This can be done when the weight of airplanes, cars and trucks is reduced or the payload is increased. The extended use of magnesium alloys may be an appropriate solution to achieve this goal. The specific strength of common magnesium alloys

is superior to widely used aluminium alloys and can even compete with steels. This presentation will give an overview on existing solutions and how an extended use of magnesium alloys can help to reach the climate goals of modern societies and to support a sustainable development.

2:50 PM Invited

Fatigue Crack Growth in Metallic Materials: Mechanisms and Design Methods: *Anastasios Gavras*¹; *Diana Lados*¹; ¹Worcester Polytechnic Institute

Fatigue crack growth experiments were performed on various metallic materials to understand the mechanisms of crack propagation and the responses at different crack size scales. The materials investigated include commonly used alloys, cast and wrought aluminum alloys (A535 and 6061), wrought titanium alloys (Ti-6Al-4V), and gray cast irons, as well as alloys manufactured by novel technologies. The microstructure was altered through chemistry, processing, and heat treatment to shed light on the effects of materials' characteristic features on fatigue crack growth. In addition, initial crack size effects were studied for each material by conducting long and small crack growth tests at various stress ratios ($R=0.1, 0.5, \text{ and } 0.7$). The fatigue crack propagation mechanisms at the microstructure scale were identified and will be discussed. The differences in fatigue crack growth responses between long, short, and small cracks were evaluated, and a new design methodology that accounts for these differences will be presented.

3:15 PM Invited

Production-to-Retirement Condition Assessment and Monitoring for Aircraft CBM+: *David Grundy*¹; *David Jablonski*¹; *Yanko Sheiretov*¹; *Vladimir Zilberstein*¹; *Neil Goldfine*¹; ¹JENTEK Sensors, Inc.

Modern design requirements, including the need to reduce the weight, can result in tighter safety margins in critical components. Effective condition assessment/monitoring is needed to ensure safety, lower life-cycle costs, and improve aircraft availability. Component life management can be improved by baselining component condition at production and mapping the product state and anomalies. This has become practical due to advanced digital nondestructive inspection tools. These tools offer sufficient sensitivity, resolution, and repeatability so that, when combined with digital mapping and tracking methods, they can detect early stages of damage and monitor evolution of the damage. This presentation focuses on the progress in MWM-Array Eddy Current Testing technology and its potential for integration into Condition Based Maintenance Plus Prognosis (CBM+) services. This includes a new failure risk assessment methodology incorporated into Component Adaptive Life Management (CALM™) framework with tools for inspection scheduling, failure risk assessment, and remaining life prediction for CBM+.

3:40 PM Break

4:05 PM Invited

Materials for Aircraft Turbine Engines: *Vasisht Venkatesh*¹; *David Furrer*¹; ¹Pratt & Whitney

Abstract not available.

4:25 PM Invited

Effects of Hot Compressive Dwell Condition on the Fatigue Crack Growth Response of Cast Aluminum Alloys: *Xiang Chen*¹; *Diana Lados*¹; *Richard Pettit*²; ¹Worcester Polytechnic Institute; ²FractureLab, LLC

Fatigue crack growth under Hot Compressive Dwell (HCD) conditions is an important failure mode for many high temperature applications, such as cylinder heads for internal combustion engines. Tensile residual stress build up at the crack root is considered a key factor contributing to crack growth under HCD conditions. To capture this effect, a new model was developed, in which residual stress contributions are added to the elastic response of the material to predict the behavior under HCD condition. Cyclic stress relaxation tests were conducted to model the process of tensile residual stress accumulation. A Blunt Compact Tension (BCT) specimen was designed and analyzed using Franc2D to determine the



TMS 2012

141st Annual Meeting & Exhibition

MONDAY PM

elastic behavior. Finally, crack growth tests on BCT specimens under HCD condition were performed to validate the model. These results will be presented and discussed for a cast 319 aluminum alloy with relevance to engine applications.

4:45 PM Invited

Modeling and Prediction of Elevated Temperature Crack Growth Rates: *Ryan Brodie*¹; ¹Pratt & Whitney Rocketdyne

Crack rate testing was conducted on a Ni-based and an Fe-based superalloy to characterize the interaction between temperature, time and loading waveform, and to better understand the effect on overall crack growth rate. A model and methodology was developed to predict crack growth rate behavior for temperature-time-waveform combinations for which no test data exist.

5:10 PM

Towards an Understanding of the Oxidation Performance of Polycrystalline Nickel Superalloys: *David Crudden*¹; Babak Raeisnia¹; Roger Reed¹; Mark Hardy¹; ¹University of Birmingham

With the ever increasing air traffic, steeper ascents are demanded from aircrafts. This is achieved by operating engines at maximum thrust for longer durations, translating to prolonged exposure of the engine components to high temperatures. Nickel superalloys are the materials of choice for high temperature jet engine components. Operation at these temperatures accelerates material degradation. This problem is examined in the context of five polycrystalline nickel based superalloys that have been isothermally oxidised at 750 °C and 800 °C. The temperature capability of the alloys is characterised in terms of their oxidation behaviour and propensity to formation of undesirable TCP phases. In particular, the role of different alloying elements and grain boundary character is examined. Understanding the performance of these alloys is essential in defining optimum chemistries and microstructures for future alloys that will be engineered for improved oxidation resistance.

5:30 PM Invited

Advancements in Nuclear Materials Research at the Idaho National Laboratory: *John Jackson*¹; Sebastien Teyssyre¹; Richard Wright¹; James Cole¹; Douglas Porter¹; ¹Idaho National Laboratory

Over the past decade, the Idaho National Laboratory (INL) has developed an impressive array of leading edge technology in support of Light Water Reactor Sustainability (LWRS) programs and development of Next Generation Nuclear Power (NGNP) plants. Capabilities in advanced micro-structural analysis of irradiated as well as un-irradiated reactor structural and pressure boundary materials supplement a full suite of mechanical characterization infrastructure. Recent advancements include acquisition of a Local Electrode Atom Probe (LEAP) and Transmission Electron Microscope (TEM) capable of handling irradiated materials as well as highly shielded mechanical test systems intended for characterization of such parameter as Irradiation Assisted Stress Corrosion Cracking (IASCC) resistance, and Fracture Toughness. The INL is currently involved in developing code cases for advanced, NGNP materials and will soon be involved in characterization of irradiated material properties for the LWR life extension effort. This paper covers current and upcoming nuclear materials research programs based at INL.

International Smelting Technology Symposium (Incorporating the 6th Advances in Sulfide Smelting Symposium): Smelter Design, Construction, Commissioning and Operation

Sponsored by: The Minerals, Metals and Materials Society, The Metallurgy and Materials Society of CIM, TMS Extraction and Processing Division, TMS: Pyrometallurgy Committee

Program Organizers: Jerome Downey, Montana Tech of the Univ of Montana; Thomas Battle, Midrex Technologies, Inc.; Jesse White, Elkem Solar Research

Monday PM
March 12, 2012

Room: Northern A3
Location: Dolphin Resort

Session Chair: To Be Announced

2:00 PM

Boliden Rönnskär Smelter: Challenges and Opportunities for Modern Smelting

: Theo Lehner¹; *Jan Stål*¹; ¹Boliden Mineral AB

The Boliden Rönnskär Smelter operates in the European Context of tight environmental, health, and safety limits with ever-increasing regulations and tribulations. In the near future, further burdens may be imposed in the forms of carbon dioxide trading, suppliers' appetite for an increased share of the contained values, changing compositions, and competition for raw materials. In the face of these changes, European smelters, such as Rönnskär and Harjavalta, have demonstrated an astonishing power of survival. This presentation will begin with an up-date on today's operations, list and comment on current challenges, and present opportunities to increase survival power. An example of the latter is the ongoing investment into increased treatment capacity for e-scrap.

2:25 PM

Design and Commissioning of the Ausmelt TSL Lead Smelter at Yunnan Tin Company Limited: Helin Gu¹; Xingcheng Song¹; Xu Lan¹; Ross Baldock²; Ross Andrews²; *Markus Reuter*²; ¹Yunnan Tin Company Ltd; ²Outotec Pty Ltd

A commercial lead smelter using Outotec Ausmelt TSL Technology has been successfully commissioned and put into operation at Yunnan Tin Corporation Ltd operations near Gejiu City, in Yunnan Province, China. The plant was commissioned in July-August 2010 after 3 years of design and construction works. The process uses a 3 stage batch process to produce lead bullion, zinc fume and a discardable slag low in metal values. The paper provides details of this lead smelting project, including the theoretical evaluation of the multi-stage process chemistry, engineering design, plant commissioning and operation. Emphasis has been given in comparison between the design targets and actual performance of the plant highlighting the fast ramp-up to full production of the largest Ausmelt TSL lead furnace built to date.

2:50 PM

Granulation as it Pertains to Electric Furnace Matte, Converter Slag, and Converter Matte in a PGM Smelter: Greg Roset¹; *Dayle Flynn*¹; Jake Bummer¹; ¹Stillwater Mining Company

Stillwater Mining Company operates a Platinum Group Metals smelter located at the base of the Beartooth Mountains in south-central Montana. Commissioned in 1990, the plant processes a copper-nickel sulfide concentrate from two mines, in addition to an intake of spent automobile and petroleum catalyst. Dry concentrates are processed at a rate of approximately 30,000 t/a through a 7.5 MW electric furnace. Stillwater's granulation system is a unique design that allows three different materials to be granulated in one granulator, i.e. Electric Furnace matte, Top Blown

Rotary Converter (TBRC) slag, and TBRC matte. This paper will also discuss process characteristics of Stillwater's granulation system and the improvements made to improve both equipment reliability and material recovery through the circuit

3:15 PM

Design, Development and Early operations of the Konkola Copper Mines Nchanga Smelter Direct Blister Flash Process, Chingola, Zambia: *Enock Mponda*¹; Timothy Smith²; ¹KCM plc; ²SNC Lavalin

Konkola Copper Mines plc owned and operated by the Vedanta group are expanding copper production in their Zambian Copperbelt operations, in particular in relation to the major development of the Konkola Deep Mining Project (KDMP) which will provide high grade long-life copper concentrate supplies. As part of their development plan a decision was made to build a major new greenfield copper smelter in Chingola along with associated acid production facilities. The KDMP mineralogy favoured installation of a direct to blister Flash Smelting furnace and the desire to recover important Cobalt values led to the inclusion of a novel integrated pyro-metallurgical slag treatment circuit with this project. The paper describes the project development, key design features and early operating experience since start-up.

3:40 PM Break

3:55 PM

Waste Heat Recovery from Industrial Smelting Exhaust Gas: *Geir Wedde*¹; Anders Sorhuus¹; ¹Alstom

Vast quantities of energy are released as heat to the environment from industrial operations. Many countries target waste heat recovery to mitigate CO₂ emission. Exhaust gases from industries such as primary aluminium smelting, carry a substantial portion of the waste heat generated. For a cost efficient capture of more valuable heat (higher exergy), heat exchangers should operate on the exhaust gases upstream of the gas treatment plants. Heat exchange surface would be exposed to dust laden gases with risk of fouling. Heat exchangers of innovated design and operation have overcome the potential of excessive fouling rates. Heat exchangers of the "shell and tube" design have been demonstrated for exhaust gases from ferroalloy as well as primary aluminium smelters. In addition to the heat recovery, gas cooling results in smaller gas treatment plants with lower costs and reduced emission. The aluminium experience is exemplified in the paper.

4:20 PM

High Performance Brands for the Nonferrous Metals Industry: *Dean Gregurek*¹; Alfred Spanring¹; Angelika Ressler¹; Sonja Breyner¹; ¹RHI AG

The complexity of metallurgical processes in the non-ferrous metals industry especially changes in the process conditions in combination with diversity of metal processing furnaces requires a precise knowledge of the system for the appropriate refractory product selection. Particular importance is still focused on the specific refractory consumption being as low as possible. The recycling routes in the base metals industry showed also a significant change of slag chemistries, process temperatures etc. which influences the performance of already approved linings. The raw material mix of primary smelters has also changed to a higher amount of secondary raw materials in the smelter feed. This acknowledgement of process-changes with decreased brick life-times was the signal for RHI AG to develop high performance refractory bricks especially for nonferrous metals applications. The internal lab tests with fayalitic slag showed very promising results compared to our approved MgCr – bricks for this highly important industry area.

4:45 PM

Sidewall Design to Improve Lining Life in a Platinum Smelting Furnace: *Isobel Mc Dougall*¹; Jacques Eksteen²; ¹Tenova Pyromet; ²Lonmin South Africa

The matte/slag tidal zone in a platinum smelting furnace is subject to severe process conditions which often lead to premature failure of the lining. The fayalite slag is aggressive to refractory bricks, whilst the Ni-Cu-Fe-S matte is aggressive to water-cooled copper cooling elements. A novel approach to the lining design was taken at Lonmin's new 10MW Furnace 2. An indirectly-cooled graphite ring was applied in this zone, with refractory bricks on the hot face. Thermal FEA modelling was conducted to determine the optimal design of the lining in this region of the furnace. The resistance to damage by slag and matte of two graphite grades was evaluated experimentally. The graphite is not wet by the matte, and is resistant to slag attack at operating temperatures

5:10 PM

SiC Formation in Submerged Arc Furnaces Producing Silicomanganese: *Per Anders Eidem*¹; Jens Davidsen¹; Merete Tangstad²; ¹Eramet Norway AS; ²Norwegian University of Science and Technology

During excavations of submerged arc furnaces producing silicomanganese SiC formations have been found. Contributing to the size of the inactive area of the furnace, the active area of the furnace where reactions happen will decrease thus reducing the potential for pre-reduction in the furnace. This work studies the formation of SiC from the liquid-solid reaction between slag, metal and coke. Slags and metals with different levels of SiO₂ and Si, respectively, has been studied. The slag and metal has been heated together with coke, and the samples investigated in XRD and microprobe. Wettability of slag and metal towards SiC was also done. The results show that SiC is formed on the coke particle through reactions with both slag and metal. For the metal, the carbon probably diffuses through the SiC to react with Si in the alloy. SiC formation with slag probably goes through the reduction of SiO₂ to Si.

IOMMS Global Materials Forum: Materials in a Green Economy: An International Perspective: Session I

Sponsored by: The Minerals, Metals and Materials Society, TMS: Materials and Society Committee, TMS: Public and Governmental Affairs Committee

Program Organizers: Sanak Mishra, Arcelor Mittal India; Jud Ready, Georgia Institute of Technology; Christina Meskers, Umicore

Monday PM
March 12, 2012

Room: Northern A4
Location: Dolphin Resort

Session Chairs: Sanak Mishra, ArcelorMittal India Limited; Diran Apelian, Worcester Polytechnic Institute

2:00 PM Introductory Comments by Dr. Sanak Mishra

2:10 PM Invited

The Role of Materials Recycling in Economic Sustainability: *Brajendra Mishra*¹; Warren Hunt²; ¹Colorado School of Mines; ²Executive Director, The Minerals, Metals & Materials Society

As the enabler of technologies and industrial growth, materials play a pivotal role in global economic sustainability. The current global materials consumption by one estimate is over twelve billion metric tonnes and is expected to reach twenty billion by the middle of this century. This presentation will summarize the findings and recommendations pertaining to resource, recovery and recycling of materials and will focus on optimum engineering solutions to achieve economic, environmental and energy sustainability in manufacturing. These integrated manufacturing solutions to challenges for green economy encompass several interrelated



TMS 2012

141st Annual Meeting & Exhibition

MONDAY PM

areas, such as the transportation, energy, recycling, housing, food, water, and health sectors. Non-renewable materials recovery and recycling are the primary needs to sustain green economy. Specific information will be included on the nucleus of a consensus definition of sustainability as it applies to materials engineering to provide a common basis for deliberation.

2:30 PM Invited

Innovative Developments in Steel Industry to Address Global Environmental Trends: *Debashish Bhattacharjee*¹; ¹Tata Steel Research Development & Technology

The global trends in environment are characterized by scarcity: Scarcity of water, energy and raw materials. As the world population is forecasted to increase enormously, the pressure is put on finding sustainable solutions for energy and clean water for the increasing population. Sustainable energy solutions include exploiting renewable energy sources that will not contribute to the climate change. It also means reducing energy consumption and eliminating wastes. This paper presents examples of innovative development work carried out in Tata Steel to address the global trends in environment. When it comes to renewable energy resources, solar energy is emerging as the most promising source. Work is carried out worldwide to find effective and affordable technologies for harvesting this uninterrupted energy source. Tata Steel is working on advanced technology for harvesting solar energy efficiently.

2:50 PM Invited

Recent Development of Materials for Green Energy in Korea: *Soon Young Hwang*¹; *Jin-Hong Kim*¹; ¹RIST

For the last few years, intensive materials developments for green energy have been made in Korea. In this presentation, recent progresses of developments will be presented including Si, SiC materials and sodium sulfur batteries, and Li-ion battery materials in Korea. For photovoltaics, poly-silicon is the major material, and several new plants have recently been constructed employing the Siemens process. However, a new economical silicone production is being developed such as a metallurgical method. For SiC materials, grand new projects have been initiated to develop semiconducting SiC materials with a number of institutions using various industrial methods. For a energy storage system (ESS), sodium sulfur battery, Li-ion battery, and redox flow battery developments have been also started to reach more than 1 MW generating capacity. Finally, government road maps of green energy materials developments will be shown as a summary.

3:10 PM Invited

Developing High Performance Steels in a Green Economy: *Chengjia Shang*¹; *Yuqing Weng*²; ¹University of Science and Technology Beijing; ²The Chinese Society for Metals

Reduce, reuse and recycle are the principles for eco-material which will be fundamental of green economy in future. Steel has many advantages, but the metallurgical processes generally relates with resource and energy consumption, CO₂ emission, etc. Therefore, how to reduce the consumption of steel would be key issue for green economy, especially in the developing country. In China, with the developing of economy in the past 30 years, steel production is increasing more and more. However, comparing with the developed country, the annual consumption for population is still very low. Therefore, reducing steel requirement by increasing strength and other performance will be the only route for meeting the growing requirement of steel. With the R&D projects aiming to double strength, prolong the life serving time and upgrade safety/durability of steels which funded by government and industries, high performance steels have been developed for fast development of economy in China.

3:30 PM Invited

An Alternative Approach to Sustainable, Low-Carbon Energy: Inertial Fusion Energy and its Materials Challenges: *Tomás Díaz de la Rubia*¹; ¹Lawrence Livermore National Laboratory

Increasing worldwide demand for energy is placing enormous pressure on natural resources, the global ecosystem, and international political stability. Alternative sources of energy are required in order to meet increased energy demand, stabilize the increase of atmospheric carbon dioxide, and mitigate the concomitant climate change. In response to this challenge, governments are urgently trying to develop new economical, sustainable, and environmentally friendly energy technologies. In fact, meeting CO₂ targets and clean energy goals by 2050 requires accelerated development, prototyping, and deployment of new, competitive, low-carbon energy technologies. Business as usual will not do. In this contribution, I will describe how advances and progress at the National Ignition Facility help enable the development and commercial deployment of Inertial Fusion Energy. The NIF is expected to achieve thermonuclear ignition and burn of at DT fuel mixture before the end of 2012.

3:50 PM Break

4:05 PM Invited

Metals, Materials and the Environment: *Bhaskar Roy*¹; ¹M.N. Dastur & Company(P) Ltd

Metals and materials play a dominant role in the overall global socio-economic development. Increasingly exacting demands for newer, high quality materials with special properties and high degree of performance reliability have rapidly impacted the perspective pertaining to engineering and technology, and have, in turn, changed the concept and perception of metallurgy in recent times. Once largely confined to the development of ferrous and non-ferrous metals, stringent application requirement have today encompassed newer fields such as glass, ceramics, polymers and composites. Metal today are a part of the vast spectrum of engineering materials. This has widened the scope and opportunities for new generations of materials scientists and engineers. The role of materials scientists in improving the quality of life of our planet, without significantly impacting its environment, have assumed greater importance, and has become one of the most discussed issues.

4:25 PM Invited

A Strategy of Metal Supply for Sustainable Development and Supporting Technologies for It in Japan: *Takashi Nakamura*¹; *A. Inaba*²; ¹Institute of Multidisciplinary Research for Advanced Materials; ²Major of Applied Chemistry and Chemical Engineering

What are the most serious environmental issues in this century? There are, of course, several answers which depend on personality. "Global Warming, Climate Change" is expected as a most average answer. It is no doubt to be serious. Another answer is also to supply foods and water. These problems are also essential to keep lives. And I would like to add one more to them, which is a stable sustainable supply of mineral resources because most human beings live in the circumstances which are mainly consist of artificial products including many metallic products. So, we are living in natural environment with artificial circumstances. We can't return to old historical lives. How we can success to do harmonious coexistence between keeping environment and economic growth, which is a trade off relation very often.

4:45 PM Invited

Multi-Eye Approach for Clarification of Surface/Interface Phenomena in Environment and Energy Materials: *Kotobu Nagai*¹;

¹National Institute for Materials Science

Key issues of environment and energy materials are multi-phase, nonequilibrium, non-steady processes at surface/interface of functional materials. NIMS-GREEN(Global Research Center for Environment and Energy based on Nanomaterials Science) is a national project of compact size with the mission to explore new methodology for solution of the key issues above-mentioned. The convergence of three research fields of materials process, characterization and computation is a basic structure and they are developing various "Environment Cells" to in-situ simulate the real action of surface/interface with various characterization equipments. The model computation will be applied to recognize the real phenomena using the experimental data.

5:05 PM Invited

Aluminium Production, Manufacturing and Recycling in Australia – Materials Innovation for a Clean Energy Future: *Malcolm Couper*¹;

¹Monash University

According to the Australian Aluminium Council (AAC) Sustainability Report for 2010, bauxite production reached a record 71.5mill tonnes and additional value was added with the production of 20.3mill tonnes of alumina and close to 2mill tonnes of aluminium. CO₂ emissions per ton of aluminium were down 10% from 2009. Around 80% of the alumina and aluminium production is exported and the industry provides direct and indirect employment for around 45,000 people in Australia. The potential rising cost of carbon and possible uncertainty in the allocation of permits and future carbon trading present risks to emission-intensive trade exposed (EITE) industries. Some of the innovative materials developments under way in support of the necessary changes to the aluminium industry in Australia and globally, will be described.

5:25 PM Invited

Natural Fiber Composites – Significant Contribution to a Green Economy: *Sergio Monteiro*¹; Marc-Andre Meyers²; João Carlos Miguez Suarez²;

¹State University of the Northern Rio de Janeiro - UENF; ²Military Institute of Engineering; Brazilian Association for Metallurgy, Materials and Mining

Technological expansion supported by advanced materials, mainly those synthetic and non-renewable, is contributing not only to the global industrial growth, but also to a continuous deterioration in our environmental conditions. All over the world, attention is being focused on the development and application of eco-friendly materials as steps taken toward a green economy. Natural fibers obtained from cellulose-based plants are typical examples of environmentally correct materials. Reinforcement of polymer composites with these lignocellulosic fibers is increasingly regarded as a viable alternative to synthetic fiber reinforcement. Biocomposites found in nature are also being investigated as model for new industrial materials with superior properties. This work presents an overview of the research efforts to develop stronger natural composites as well as their already existing successful industrial applications. In addition to technological advantages, the worldwide economical, social and environmental contribution of these natural composites to a "green" society is assessed.

5:45 PM Concluding Comments by Prof. Diran Apelian

Magnesium Technology 2012: Deformation Mechanisms

Sponsored by: The Minerals, Metals and Materials Society, TMS Light Metals Division, TMS: Magnesium Committee

Program Organizers: Suveen Mathaudhu, U.S. Army Research Office; Wim Sillekens, TNO; Norbert Hort, Helmholtz-Zentrum Geesthacht; Neale Neelameggham, U.S. Magnesium

Monday PM
March 12, 2012

Room: Southern IV
Location: Dolphin Resort

Session Chairs: Bin Li, Mississippi State University; Alok Singh, National Institute of Materials Science

2:00 PM

An Elasto-Plastic Micromechanical Method for Twin Driven Plasticity: *Laurent Capolungo*¹; Pierre Alexandre Juan¹; Stephane Berbenni²; Carlos Tome³; ¹Georgia Institute of Technology; ²Universite Paul Verlaine; ³Los Alamos National Laboratory

Recent measures of the evolution of internal strains within parent and twin domains in hexagonal close packed polycrystals revealed substantial differences in the deformation fields of each domain. It was suggested that these differences arise from back-stresses associated with elastic constant mismatch and plastic incompatibilities between parent and twin domains. A simple elastic study of the grain/twin inclusion problem based on the extension of the Tanaka Mori scheme already delineated the importance of elastic constants mismatches to the development of back-stresses in twin domains. Also, it was found that the effect of twin shape on the stress state within twin domains is particularly pronounced. The proposed work aims at developing a micromechanical based model capable of predicting these phenomena. The approach is to be based on an extension of the Tanaka Mori scheme applied in an Elasto-Plastic framework (EPSC). The model is applied to the case of polycrystalline Mg.

2:20 PM

Anomalous Twin Bands in AZ31 Mg Sheet Bending: James Crawford Baird¹; *Bin Li*¹; Sanaz Yazdan Parast¹; Stephen Horstemeyer¹; Haitham El Kadiri¹; Paul Wang¹; ¹Center for Advanced Vehicular Systems

Micro-texture examination for Mg alloys is usually performed after samples are unloaded. Unloading a deformed sample loses important microstructure and texture information due to detwinning. In fact, we recently reported that detwinning could affect not only stopped twins but residual twins as well. To circumvent this difficulty, a special fixture was designed such that continuous EBSD scan were enabled without unloading. We applied our design to the study of rolled AZ31 Mg sheet bending at room temperature. Through thickness EBSD scan during 3-point bending reveals anomalous {10-12}<10-1-1> twin patterns. In the compressed zone, the {10-12}<10-1-1> extension twins appear in an extremely localized fashion. Alternating twin bands were formed, each band comprising high density twins which allow identification of the originating stress state. In between the twin bands, twins were completely absent.

2:40 PM

Formation of Nano-Scale Twins and Low Angle Grain Boundaries during Fracture of Fine Grained Magnesium Alloys: *Alok Singh*¹; Hidetoshi Somekawa¹; Toshiji Mukai²; ¹National Institute for Materials Science; ²Kobe University

Fine grained magnesium alloys show high fracture toughness, associated with void formation. Detailed microstructural evolution during a fracture toughness test of a fine grained Mg-Zn alloy has been studied here by transmission electron microscopy (TEM). Focused ion beam (FIB) technique was used for obtaining samples near crack. Initially,



TMS 2012

141st Annual Meeting & Exhibition

MONDAY PM

subgrain structures form ahead of the crack tip, after which {10-11} type twins of width of about 400nm form. They further twin by {10-12} twinning. Subsequent twinning occurs at a finer scale near the crack, forming configurations of {10-11}-{10-12} double twins and low angle boundaries. The scale of the twin domains became progressively finer to less than 50nm. It is suggested that in absence of enough dislocations to pile up causing fracture, deformation continues to occur by the twinning.

3:00 PM

Tensile and Creep Deformation Mechanisms in Rolled AZ31: Carl Boehlert¹; Zhe Chen¹; Ivan Gutiérrez-Urrutia²; Jan Bohlen³; Sangbong Yi³; Dietmar Letzig³; Javier Llorca⁴; *Maria Teresa Perez-Prado*⁴; ¹Michigan State University; ²Max Planck Institute for Iron Research; ³Magnesium Innovation Centre MagIC; ⁴IMDEA-Materials

Basal slip and tensile twinning are the prevalent deformation mechanisms in randomly-oriented Mg alloys at low temperatures. At elevated temperatures, non-basal slip systems become active as their CRSS decrease rapidly. In strongly textured rolled or extruded alloys, the choice of slip and twinning systems is highly dependent on the Schmid factor. Here, an extruded Mg-1Mn-1Nd alloy was tensile tested in an SEM at temperatures of 50°C, 150°C, and 250°C in order to analyze the local deformation mechanisms through in-situ observations. EBSD was performed both before and after the deformation. The alloying elements inhibited the <10-10> fiber texture, typical of extruded Mg alloys, leading to the formation of a very weak extrusion texture. The tensile strength decreased with increasing temperature, and no change in the normal anisotropy was apparent. The proportion of the different slip systems activated will be presented and discussed with respect to the temperature, CRSS, and Schmid factor.

3:20 PM

Structural Origin of Reversible Twinning, Non-Schmid Effect, Incoherent Twin Boundaries and Texture of Hexagonal Close-Packed Metals: Bin Li¹; Xiyan Zhang²; Haitham El Kadiri¹; Suveen Mathaudhu³; Quancang Ma¹; ¹Center for Advanced Vehicular Systems; ²Chongqing University; ³Army Research Laboratory

Profuse {10-12}<10-1-1> extension twinning occurs in Magnesium and other HCP metals during plastic deformation. This twinning mode presents abnormal properties such as reversibility, i.e., upon unloading or removal of external load, twins may shrink or disappear, giving rise to the pseudoelasticity. The {10-12}<10-1-1> twinning may also violate the Schmid Law which applies to all dislocation controlled deformations. The twin boundaries of the {10-12}<10-1-1> twinning may significantly deviate from the {10-12} twinning plane, at odds with twinning theory that requires twinning dislocations glide strictly on the twinning plane. HCP metals also present strong propensity of texture during thermomechanical processing such as extrusion, rolling or severe plastic deformation (SPD). We show that these properties of HCP metals can be well understood from the perspective of atomic shuffling that dominates the deformation twinning. EBSD, TEM and HRTEM observations will be presented to support our conclusions.

3:40 PM Break

4:00 PM

Length Changes in Extruded Magnesium Alloy Bars Under Large Strain Free-End Torsion: Huamiao Wang¹; Peidong Wu¹; Ken Neale²; ¹McMaster University; ²University of Sherbrooke

It is well-known that the axial stress development during fixed-end torsion and the axial strain during free-end torsion in polycrystalline metals are mainly due to initial texture and texture evolution. The predictions of these second-order axial effects depend strongly on the constitutive model – in particular on the description of anisotropic hardening. In the present study, large strain free-end torsion of extruded magnesium alloy bars is studied by using the recently developed Elastic Visco-Plastic Self-

Consistent (EVPSC) model with various self-consistent schemes. In these models, both slip and twinning contribute to plastic deformations. It is shown that the predicted second-order length change is very sensitive to the initial texture, texture evolution and the constitutive models employed. Numerical results suggest that the free-end torsion test can provide an effective means for assessing the adequacy of polycrystal plasticity models for magnesium alloys.

4:40 PM

Non-Basal Textures in Magnesium Alloy Strips by Extrusion-Machining: *Dinakar Sagapuram*¹; Mert Efe¹; Wilfredo Moscoso²; Srinivasan Chandrasekar¹; Kevin Trumble¹; ¹Purdue University; ²Pontificia Universidad Catolica Madre y Maestra

The positive effect of fine grain size and non-basal texture on formability of magnesium alloy sheets is well known. In the present work, Large-Strain Extrusion-Machining (LSEM), a low-cost, single-step deformation process was employed to produce commercial Mg-AZ31B alloy strips (0.2 μm thick and 6.4 mm wide). The deformation temperature was varied by preheating the workpiece to different temperatures (up to 375°C). At low deformation temperatures, fine grain structure (~2 μm) with basal poles tilted 30-40° away from the strip normal direction towards the chip-flow direction was observed. At higher deformation temperatures, basal poles were split about the normal direction by 10-20° in the transverse direction, while the grain size was in the 3-6 μm range. The activation of secondary slip systems with increasing deformation temperature is presumed to be the cause for these textural changes.

4:20 PM

Nano-Indentation Studies of Twinned Magnesium Single Crystals: Fumiaki Hiura¹; Raja Mishra²; Michael Lukitsch²; *Marek Niewczas*¹; ¹McMaster University; ²General Motors Research & Development Center

Nano-indentation measurements have been performed on {10-12}<10-11> twin and adjacent matrix regions of deformed magnesium single crystals and the hardness values were analyzed by the Oliver-Pharr method. Although the hardness difference between the twin regions and the adjacent matrix was insignificantly small, the hardness values showed orientation dependence regardless of the twins' size and variants. This observation can be interrupted by texture-softening resulting from the lattice reorientation in the twin regions. In contrast, the experimental evidence for the Basinski hardening mechanism in {10-12}<10-11> twins, which is an increase in strength/hardness as a result of dislocation contributions within twin area, was not obtained from this experiment. This presentation provides framework for the discussion of the hardening/softening effect of {10-12}<10-11> twinning on the plastic flow in single crystalline magnesium and quantitative values for hardening parameters used in the crystal plasticity modeling.

5:00 PM

The Elastic-Plastic Transition in AZ31 Magnesium Alloy: *Kun Yang*¹; Carlos Caceres¹; ¹The University of Queensland

The Kocks-Mecking method of analysis is used to assess the fraction of the polycrystal that remains elastic while full plasticity develops in the aggregate. It is shown that what appears to be a very protracted elastic plastic transition is consistent with hardening by the athermal storage of dislocations around grains with a hard orientation for slip. The microplasticity involved in the process is discussed using data from the literature.

Magnesium Technology 2012: Primary Production

Sponsored by: The Minerals, Metals and Materials Society, TMS Light Metals Division, TMS: Magnesium Committee

Program Organizers: Suveen Mathaudhu, U.S. Army Research Office; Wim Sillekens, TNO; Norbert Hort, Helmholtz-Zentrum Geesthacht; Neale Neelameggham, U.S. Magnesium

Monday PM
March 12, 2012

Room: Southern V
Location: Dolphin Resort

Session Chairs: Neale Neelameggham, IND, Inc; Adam Powell, Metal Oxygen Separation Technologies, Inc.

2:00 PM

Carbothermal Production of Magnesium: CSIRO's MagSonic™

Process: Leon Prentice¹; Michael Nagle¹; Timothy Barton¹; Steven Tassios¹; Benny Kuan²; Peter Witt²; Keri Constanti-Carey¹; ¹CSIRO Process Science and Engineering; ²CSIRO Mathematics Informatics and Statistics

Carbothermal production has been recognized as the simplest and cleanest route to magnesium metal, but has suffered from technical challenges of development and scale-up. Work by CSIRO has now successfully demonstrated the technology using supersonic quenching (the MagSonic™ Process). Key barriers to process development have been overcome: the experimental program has achieved sustained operation, no nozzle blockage, minimal reversion, and safe handling of pyrophoric powders. The laboratory equipment has been operated at industrially-relevant magnesium vapor concentrations (>25% Mg) for multiple runs with no blockage. Novel computational fluid dynamics (CFD) modelling of the shock quenching and metal vapor condensation has informed nozzle design and is supported by experimental data. Reversion below 10% has been demonstrated, and magnesium successfully purified (>99.9%) from the collected powder. Safe operating procedures have been developed and demonstrated, minimizing the risk of powder explosion. The MagSonic™ Process is now progressing to significantly larger scale and continuous operation.

2:20 PM

MagSonic™ Carbothermal Technology Compared with the Electrolytic and Pidgeon Processes: Leon Prentice¹; Nawshad Haque¹; ¹CSIRO Process Science and Engineering

A broad technology comparison of carbothermal magnesium production with present technologies has not been previously presented. In this paper a comparative analysis of CSIRO's MagSonic™ Process is made with the electrolytic and Pidgeon processes. The comparison covers energy intensity (GJ/tonne Mg), labor intensity (person-hours/tonne Mg), capital intensity (USD/tonne Mg per year installed capacity), and Global Warming Potential (GWP, tonnes CO₂-equivalent/tonne Mg). Carbothermal technology is advantageous on all measures except capital intensity (where it is roughly twice the capital cost of a similarly-sized Pidgeon plant). Carbothermal and electrolytic production can be environmentally similar, with typical emissions one-sixth those of the Pidgeon process. Despite recent progress, the Pidgeon process depends upon abundant energy and labor combined with few environmental constraints; pressure is expected to increase on each of those measures over the coming decade. Carbothermal reduction technology is likely to emerge as the optimum choice for future production.

2:40 PM

Scaling-Up Solid Oxide Membrane Electrolysis Technology for Magnesium Production: Soobhankar Pati¹; Adam Powell¹; Steve Tucker¹; Steve Derezinski¹; ¹MOxST Inc.

Metal Oxygen Separation Technologies, Inc. (MOxST) is actively developing Solid Oxide Membrane (SOM) electrolysis technology for

production of magnesium directly from its oxide. The vital component of this technology is the oxygen ion-conducting solid zirconia electrolyte separating the molten flux (a mixture of salts and oxide) and the inert anode. The zirconia not only protects the anode from the flux but also prevents anode gas back-reaction, increasing the efficiency. This makes it possible to produce low-cost high-purity magnesium and high-purity oxygen as a by-product with no direct greenhouse gas emissions. In this paper we discuss the design modifications made to address the scaling-up challenges, particularly for producing magnesium in liquid form. The key accomplishment to date is the successful development of a prototype capable of producing few kilograms of magnesium per day. We will also describe the prerequisite properties of an inert anode and suitable materials for the same.

3:00 PM

Fluid Bed Dehydration of Magnesium Chloride: Kamal Adham¹; ¹Hatch Ltd.

Molten salt electrolysis of MgCl₂ is commonly used for the production of Magnesium metal. However, the electrolysis feed must be completely dry with minimum oxygen content. Therefore, complete dehydration of the MgCl₂ brine or the hydrated salt is a required process, which is very challenging due to the ease of thermal degradation. Fluidized bed dryers are often used, under air and HCl environments. The key features of three different types of fluid bed technologies, which can be applied to MgCl₂ dehydration plants, are described in this paper. In addition, a discussion of chemistry, unit operations and advantages associated with each option, is presented. The background information is provided based on open literature sources, including papers and patents. Most calculations are performed using commercially available metallurgical software, for the thermodynamics and mass/heat balances.

3:20 PM

Demonstration of Solar-Pumped Laser-Induced Magnesium Production from Magnesium Oxide: Yabe Takashi¹; Ohkubo Tomomasa¹; Dinh Thanh Hung¹; Kuboyama Hiroki¹; Nakano Junichi¹; ¹Tokyo Institute of Technology

Studies of storing solar energy into chemical energy of magnesium (Mg) through reduction from magnesium oxide (MgO) by solar-pumped laser were conducted. We succeeded in solar-pumped laser-induced Mg production. Laser system consists of a 4 m² Fresnel lens mounting on a sun tracker platform which focus solar radiation into laser head therefore over 100W (CW) output laser can be irradiated. A single laser beam is focused on a mixture of magnesium oxide and reducing agent silicon. High power density of focused laser leads to high temperature and the reduction reaction resulting in Mg production. The resultant vapor is collected on a copper plate and analyzed in terms of magnesium deposition efficiency. As a result, deposition efficiency of 2.3 mg/kJ was achieved.

3:40 PM Break

4:00 PM

Molten Salt Electrolysis of MgCl₂ in a Cell with Rapid Chlorine Removal Feature: Gökhan Demirel¹; Ishak Karakaya²; ¹Aselsan Inc.; ²Middle East Technical University

An experimental electrolytic magnesium production cell was designed to remove chlorine gas from the electrolyte rapidly and demonstrate the beneficial effects of reduced chlorine dissolution into the molten salt electrolyte. The back reaction that is the main cause of current losses in electrolytic magnesium production was reduced as a result of effective separation of electrode products and decreased contact time of chlorine gas with the electrolyte. Moreover, smaller inter electrode distances employed and lower chlorine gas present on the anode surface made it possible to work at low cell voltages. Electrolytic cell was tested at different current densities and electrolyte compositions. Energy consumption of 7.0 kWh kg⁻¹ Mg that is slightly above the theoretical minimum, 6.2 kWh kg⁻¹ Mg, at 0.68 A cm⁻² anodic current density was achieved for a MgCl₂/NaCl/KCl electrolyte.



TMS 2012

141st Annual Meeting & Exhibition

MONDAY PM

4:20 PM

Preparation of Aluminum-Magnesium Alloy from Magnesium Oxide in RECl₃-LiF-MgF₂ Electrolyte by Molten Salts Electrolysis Method: *Sh Yang*¹; *Fengli Yang*¹; *Xianwei Hu*²; *Zhaowen Wang*²; *Zhongning Shi*²; *Bingliang Gao*²; ¹Jiangxi University of Science and Technology; ²Northeastern University

Aluminum-magnesium alloys were prepared from magnesium oxide by molten salt electrolysis method. 10w%RECl₃-63.5w%KCl-23.5w%MgCl₂-3w%MgO was taken as electrolyte. The results showed that RE could be attained in aluminum-magnesium alloy, and it was proved that the RE was reduced directly by aluminum. Magnesium in the alloy was produced by electrolysis on cathode. The content of RE in the alloy was about 0.8wt %-1.2wt%, and the content of Mg in the alloy was 1wt%~6wt% with electrolytic times. The highest current efficiency was 81.3% with 0.8A/cm² current density. The process of electrolysis was controlled together by electrochemical polarization and concentration polarization.

4:40 PM

Experimental Study on Magnesium Extracted from Ascharite Mineral by Aluminium: *Peng Jianping*¹; *Wu Xiaolei*¹; *Feng Naixiang*¹; *Zhou Shigang*¹; *Di Yuezhong*¹; ¹Northeastern University

In order to effectively utilize the ascharite mineral, in Liaoning province of China, the paper studied to extract magnesium from ascharite mineral with aluminium powder as reductant by vacuum thermal reduction method. And boron of the raw material was saved in residues that could be used to produce non-alkali glass fiber. So environment cannot be polluted during this process, as well as the process can create great economic value. Calcined material and the residues were taken XRD analysis respectively. Based on thermodynamic analysis, the Gibbs free energy and the critical temperature of reduction ascharite with calcium carbide were calculated. Based on some experiments the recovery rate was effected remarkably by the mass of reductant and the making briquettes pressure.

5:00 PM

Electrochemical Investigation on Chlorine and Electrolyte Intercalation into Graphite Anodes during Magnesium Electrolysis Process: *Bing Li*¹; *Jingwei Lou*¹; *Mengfan Yan*¹; ¹East China University of Science and Technology

Cyclic voltammetry(CV) was used to investigate chlorine and electrolyte intercalation into three different graphite anodes from NaCl-KCl-MgCl₂ melts at 700 °C. They were needle-coke (NC), the petroleum-coke (FPC) and common petroleum-coke (CPC), respectively with the same processing technology. Chlorine intercalation amount was characterized by the reduction current (reduction electricity quantity) on the reverse scan during the cyclic voltammograms. And the electrolyte intercalation was presented by the increase in oxidation charge between the forward scan and the reverse scan during the CV measurements. The results show that among the three graphite anodes, NC shows the lowest reduction current and nearly no increase in the charge , while about 5-10 times increase in the charge for the PFC and CPC ,which implied that NC has a better resistance to electrolyte and chlorine intercalation. The results were further confirmed by the electrolysis experiments in NaCl-KCl-MgCl₂ melts at 700 °°.

5:20 PM

Optimization of Preparation for MgO by Calcination from Basic Magnesium Carbonate Using Response Surface Methodology: *Bin Zhang*¹; *Jinhui Peng*¹; *Libo Zhang*¹; *shaohua Ju*¹; ¹Kunming University of Science and Technology

The conditions of technique to prepare MgO by calcination from Basic magnesium carbonate were optimized using a central composite design (CCD) of response surface methodology (RSM). A quadratic equation model for decomposition rate was built and effects of main factors and their corresponding relationships were obtained. The statistical analysis of the results showed that in the range studied the decomposition rate of

Basic magnesium carbonate was significantly affected by the calcination temperature and calcination time. The optimized calcination conditions were as follows: the calcination temperature 435.5°C and the calcination time 121.6 min, respectively. Under these conditions the decomposition rate of cobalt oxalate was 99.17%. The validity of the model was confirmed experimentally and the results were satisfactory. In addition, the sample was characterized by X-ray Diffraction (XRD) and Scanning electron microscopy (SEM), respectively.

Materials and Fuels for the Current and Advanced Nuclear Reactors: Nuclear Fuels - Characterization

Sponsored by: The Minerals, Metals and Materials Society, TMS Structural Materials Division, TMS/ASM: Corrosion and Environmental Effects Committee, TMS/ASM: Nuclear Materials Committee

Program Organizers: Ramprashad Prabhakaran, Idaho National Laboratory; Dennis Keiser, Idaho National Laboratory; Raul Rebak, GE Global Research

Monday PM
March 12, 2012

Room: Swan 2
Location: Swan Resort

Session Chairs: Robert Mariani, Idaho National Laboratory; Ramprashad Prabhakaran, Idaho National Laboratory

2:00 PM

Recent Developments in the Study of the Effects of Irradiation on the Microstructure of U-Mo Nuclear Fuels: *Dennis Keiser*¹; *Jan-Fong Jue*¹; *Jian Gan*¹; *Adam Robinson*¹; *Pavel Medvedev*¹; ¹Idaho National Laboratory

The Reduced Enrichment for Research and Test Reactor (RERTR) program is developing low-enriched U-Mo fuels for use in research and test reactors that currently employ high-enriched uranium fuels. A large part of this development has been in-reactor testing of U-Mo fuels, and the subsequent characterization of the microstructures of the as-irradiated fuel plates. Optical metallography, scanning electron microscopy, and transmission electron microscopy have all been employed for characterizing irradiated fuel plates. This presentation will describe recent results from the different characterization activities and how they can be used to develop better understanding of how the fuel plate microstructures evolve as a function of the time in reactor. The effects of fission density, fission rate, and temperature on fuel plate performance will also be discussed.

2:20 PM

TEM Study on the Phase Development and Microstructure in a U-7 wt.% Mo vs. Al-7 wt.% Ge Diffusion Couple: *E. Perez*¹; *D.D. Keiser*¹; *Y.H. Sohn*²; ¹Idaho National Laboratory; ²University of Central Florida

Fuel development for the Reduced Enrichment for Research and Test Reactors (RERTR) program has demonstrated that U-Mo alloys in contact with Al develop interaction regions with phases that have poor irradiation behavior. The addition of Si to the Al has been considered with positive results. Compositional modification to replace Si with Ge is now under evaluation to further improve irradiation behavior and recycling of spent fuel systems. In this study, the microstructural and phase development of a diffusion couple of U-7 wt.% Mo in contact with Al-7 wt.% Ge was examined by transmission electron microscopy, scanning electron microscopy and energy dispersive spectroscopy. The interdiffusion zone developed a three phase microstructure containing an amorphous phase, the orthorhombic-UGe₂ and the cubic-(U,Mo)(Al,Ge)₃ phase. Results from this study are compared to U-Mo vs. pure Al and U-Mo vs. Al-Si diffusion couples to discuss the differences in the microstructural evolution of the different interdiffusion zones.

2:40 PM

Observations and Analyses of Diffusion Couples, U-10 wt.% Mo vs. Zr: *Ke Huang*¹; *Youngjoo Park*¹; *Dennis Keiser*²; *Yongho Sohn*¹; ¹University of Central Florida; ²Idaho National Laboratory

U-Mo alloys as dispersed and monolithic fuel within Al-alloy matrix are being developed as a low enriched metallic fuel for the Reduced Enrichment for Research Test Reactor program. Interactions due to interdiffusion between the U-Mo fuel and the Al matrix have been observed during fuel processing and irradiation, and are of concern due to potential adverse effects. To explore diffusion barrier materials between U-Mo fuel and Al alloy cladding, U-10 wt.% Mo vs. Zr diffusion study were carried out in the temperature range from 973K to 1273K. The interdiffusion zone and concentration profiles were examined by scanning electron microscopy and electron probe microanalysis, respectively. Mo₂Zr precipitates were observed along the diffusion bonded interface. Concentration-dependence average ternary interdiffusion coefficients on either side of Matano plane were calculated. These coefficients were also carefully examined to estimate respective tracer diffusion coefficients when the concentration of U, Mo or Zr becomes negligible.

3:00 PM

Mechanical Properties of U-Mo Fuels: *Ramprasad Prabhakaran*¹; *Douglas Burkes*²; *Jan-Fong Jue*¹; *Amy DeMint*³; *Jack Gooch*³; *Dennis Keiser*¹; *Daniel Wachs*¹; ¹Idaho National Laboratory; ²Pacific Northwest National Laboratory; ³Y-12 National Security Complex

The Reduced Enrichment for Research and Test Reactors (RERTR) program was initiated to develop new nuclear fuels to enable the research and test reactors to use low-enriched uranium fuels instead of high-enriched uranium fuels, without significant loss in performance. Hence, a new monolithic fuel type that possesses the greatest possible uranium density in the fuel region is being developed, where the fuel region consists of a single foil encased inside an aluminum alloy cladding. Currently, efforts are ongoing to evaluate the mechanical properties and microstructure of fresh U-Mo fuels, as a function of molybdenum content, carbon content and temperature. Small-scale specimen testing techniques, such as sub-size tensile testing, microindentation hardness testing and shear punch testing are being performed. Other materials characterization techniques, such as optical microscopy, XRD and SEM are being used in conjunction with the small-scale mechanical test methods.

3:20 PM

Metallurgical Characterization of the Delta Phase Formation in Uranium-Zirconium Alloy Fuels: *Sandeep Irukuvarghula*¹; *Sean McDeavitt*¹; *Sangjoon Ahn*¹; ¹Texas A&M University

Uranium – 10 wt% zirconium (U-10Zr) alloy nuclear fuels have been used for many decades and new variations are under consideration ranging from U-5Zr to U-50Zr. As a precursor to studying fission gas behavior using ion implantation, a basic study of U-Zr metallurgy was completed. The initial focus was to clarify literature ambiguity regarding the formation of the UZr₂ delta phase. Sample alloys were created containing 0.1, 2, 5, 10, 20, 30, and 50 wt% zirconium. Initial structures were created via “furnace-cooled” and “gamma-quenched” temperature profiles. Samples of each composition and thermal profile were annealed under argon at 600°C for 24, 72, and 168 hours. Quantitative analyses were completed using an electron microprobe. The delta phase formed readily in annealed furnace-cooled samples whereas gamma-quenched samples exhibited sluggish transformations. The rate of cooling U-Zr alloys has a profound impact on the kinetics of delta phase formation.

3:40 PM Break**3:50 PM**

Thermodynamic Assessment of the Uranium-Zirconium Alloy System for Nuclear Energy Applications: *Sangjoon Ahn*¹; *Sandeep Irukuvarghula*¹; *Sean McDeavitt*¹; ¹Texas A&M University

Uranium – 10 wt% zirconium (U-10Zr) alloy nuclear fuels have been used for many decades and new variations are under consideration ranging from U-5Zr to U-50Zr. The thermophysical behavior of the uranium-zirconium system has been revisited using differential scanning calorimetry (DSC) and other methods. Alloys containing 0.1, 2, 5, 10, 20, 30, and 50 wt% zirconium were prepared by melt-casting ~40 g samples in yttrium oxide crucibles. The phase transitions observed using DSC analyses are in general agreement with the established phase diagram with a few notable exceptions that may, in part, be due to impurities. Most notably, the transition from the $\alpha(U)+\gamma$ phase field to the $\beta(U)+\gamma$ phase field at ~662°C was never observed in these experiments. This observation is consistent with earlier experimental assessments of the U-Zr binary phase diagram as compared with the more recent computational assessments.

4:10 PM

Characterization of U-Zr-Ce and U-Mo-Ce Alloy Fuels Doped with In, Sb, and Pd: *Yeon Soo Kim*¹; *Gerard Hofman*¹; *Tom Wienck*¹; *Ed O'Hare*¹; *Jeff Fortner*¹; ¹Argonne National Laboratory

Fast reactor concepts achieving ultra-high burnup (~50%) without requiring refueling using metallic fuel have gained interest. Fission product lanthanide accumulation at high burnup and migration are potential life-limiting phenomena. As a means to prevent this problem, adding an element that forms stable compounds with lanthanides is proposed. The theoretical assessment shows that indium, thalium, and gallium are good candidates. Because these elements are low-melting metal elements, liquid metal embrittlement of cladding is a concern. Some other elements are also proposed that include Sb and Pd. Therefore, how these elements form compounds with the lanthanides is another measure of selection. As a screening test before in-pile tests, alloys of U-10X-2Ce-5Y, where X=Zr, Mo and Y=In, Sb, Pd, are fabricated and characterized by optical metallography and scanning electron micrography to select the best candidate. These metallography results and the theoretical method used to select the candidate elements will be presented.

4:30 PM

Interdiffusion between U - 10wt.% Zr and Fe Diffusion Couples Annealed at 903, 923, 953 and 973K: *Youngjoo Park*¹; *Ke Huang*¹; *Bulent Sencer*²; *Rory Kennedy*²; *Yongho Sohn*¹; ¹University of Central Florida; ²Idaho National Laboratory

Diffusional interaction between 10wt.%Zr metallic fuel and Fe was investigated using solid-to-solid diffusion couples that were annealed at 903K, 923K, 953K and 973K. Development of microstructure and phase constituents within the interaction layer was examined by scanning electron microscopy with X-ray energy dispersive spectroscopy. Multiple layered structures with complex microstructure consisting of various phases such as λ -, ϵ -, and χ -phases were observed. The thicknesses of multi-phase layers were measured at each temperature and employed to calculate the parabolic growth constant and activation energy. The average compositions through the interaction layer were systematically determined, and employed to construct semi-quantitative diffusion path on isothermal ternary diagrams. These diffusion paths are discussed to estimate the diffusional behavior of individual components and their interactions.



TMS 2012

141st Annual Meeting & Exhibition

MONDAY PM

4:50 PM

Microanalysis of Irradiated Coated Particle Fuel from the AGR-1 Irradiation Experiment: *Paul Demkowicz*¹; Isabella van Rooyen¹; Scott Ploger¹; Jessica Riesterer¹; Brandon Miller¹; ¹Idaho National Laboratory

The AGR-1 irradiation of TRISO-coated particle fuel specimens was recently completed and represents the most successful such irradiation in US history, reaching peak burnups of greater than 19% FIMA with zero failures out of 300,000 particles. Extensive post-irradiation examination of the fuel is currently in progress. A critical component of the fuel characterization is microanalysis of the irradiated fuel particles, including ceramography, scanning electron microscopy, wavelength dispersive spectroscopy, and transmission electron microscopy of coatings and fuel kernels. Among the primary objectives of this examination are to determine the effects of irradiation on coating integrity, correlate coating microstructures with the extent of fission product retention, and develop a better understanding of fission product diffusive release. Of particular interest is silver, which has long been known to exhibit relatively high release from coated particle fuel. This paper will highlight some of the microanalytical techniques being utilized and present preliminary results.

5:10 PM

Postirradiation Examination of High Burnup Metallic Fuels: *Heather Chichester*¹; Douglas Porter¹; Steven Hayes¹; ¹Idaho National Laboratory

Within the Fuel Cycle Research & Development program, six metallic fuel alloy compositions were fabricated and irradiated in ATR. Irradiation to 653 effective full power days resulted in fuel burnups ranging from approximately 17-30 at.% HM. These alloys (e.g., U-29Pu-4Am-2Np-30Zr) are being studied in order to understand how fuel incorporating constituents from recycled light water reactor fuel would behave in fast reactors, with particular focus on transmuting actinides. Initial destructive postirradiation examinations of these alloys have been completed, including fission gas release, optical microscopy, and burnup analysis. Select results will be presented and compared to results from lower burnup companion experiments and the historical metallic fuel performance database.

Materials Design Approaches and Experiences III: Material Design Tools

Sponsored by: The Minerals, Metals and Materials Society, TMS Structural Materials Division, TMS: High Temperature Alloys Committee, TMS: Integrated Computational Materials Engineering Committee

Program Organizers: Ji-Cheng Zhao, The Ohio State University; Akane Suzuki, GE Global Research; Deb Whitis, GE Aviation; Michael Fahrman, Haynes International Inc.; Qiang Feng, University of Science and Technology Beijing

Monday PM
March 12, 2012

Room: Europe 11
Location: Dolphin Resort

Session Chairs: Deb Whitis, GE Aviation; Hamish Fraser, The Ohio State University

2:00 PM Invited

Multiscale Modeling of Mechanical Performance from a Perspective of Materials Design: *Dennis Dimiduk*¹; ¹Air Force Research Laboratory

Material and alloy design projects can now access growing set of new materials modeling and simulation tools to guide their efforts. The capabilities of such tools are expanding rapidly for representing mechanisms important to design at disparate length scales. The present talk focuses on the multiscale aspects of mechanical behavior simulation for the purposes of predicting materials performance. Selected tools and techniques are discussed from a viewpoint motivated by two questions:

i) what multiscale tools and methods are able to provide predictive capabilities for materials design problems and, ii) how might the methods be incorporated into an integrated computational materials engineering framework to reduce the need for empirical data. The initial conclusion is that microstructure-level tools are significantly underdeveloped and are likely to remain so for some time; thus, a more structured approach to integrated computational and empirical methods is necessary.

2:30 PM Invited

MaterialsGenome®: Building Blocks of Materials: *Zi-Kui Liu*¹; ¹The Pennsylvania State University

The building blocks of materials are individual phases. The ability of materials design resides on our capability to model the properties of individual phases and their interfaces as a function of materials variables such as temperature, pressure, compositions, and other field variables. In this presentation, we will discuss our activities in developing an infrastructure, named MaterialsGenome® (Trademark of MaterialsGenome, Inc.), for properties of individual phases. MaterialsGenome® is based on ESPEI [1]. ESPEI integrates databases (crystallographic, phase equilibrium, thermochemical, and modeled Gibbs energy data, etc) and database development (automation of thermodynamic modeling). The infrastructure of experimental data storage as well as the automation of database development is uniquely constructed in ESPEI. I. S. Shang, Y. Wang and Z. K. Liu, "ESPEI: Extensible, Self-optimizing Phase Equilibrium Infrastructure for Magnesium Alloys," S. R. Agnew, N. R. Neelameggham, E. A. Nyberg, W. H. Sillekens, Eds., Magnesium Technology 2010, pp. 617-622.

3:00 PM Invited

Experimental Tools for the Materials Genome Initiative: *Ji-Cheng Zhao*¹; ¹The Ohio State University

The Materials Innovation Infrastructure in the Materials Genome Initiative consists of three major components: computational tools, experimental tools and digital data. This talk will discuss experimental tools for high-throughput measurements of several materials properties such as elastic modulus, thermal conductivity, specific heat capacity, and thermal expansion. Application of these tools on composition-varying samples such as diffusion multiples can be used to quickly and efficiently obtain composition-phase-structure-property relationships for materials property database establishment. These tools not only have high spatial resolution, but also high accuracy, thus they can be used to obtain high-quality digital data for various materials properties for accelerated design of new materials. In addition, a diffusion-multiple approach can be used to effectively obtain phase diagram and diffusivity data for establishment of reliable thermodynamic and kinetic databases.

3:30 PM Break

3:50 PM Invited

An Integrated CALPHAD Tool for Modeling Precipitation Kinetics and Accelerating Materials Design: *Qing Chen*¹; Herng-Jeng Jou²; Gustaf Sterner¹; Johan Bratberg¹; Anders Engström¹; Paul Mason³; ¹Thermo-Calc Software AB; ²QuesTek Innovations LLC; ³Thermo-Calc Software, Inc

CALPHAD tools, such as Thermo-Calc and DICTRA, together with related thermodynamic and kinetic databases have now been applied extensively in almost every aspect of materials design, from screening to processing, operating, and recycling. Their success relies on their capability to provide fundamental phase equilibrium and phase transformation information in materials of industrial relevance, which is possible due to the adopted methodology where free energy or atomic mobility of each phase in a multicomponent system is modeled hierarchically from lower-order systems, and model parameters are evaluated by considering both ab-initio and various experimental data. In this presentation, we introduce TC-PRISMA, a new user-friendly

computational tool that extends the Thermo-Calc and DICTRA approach with additional interface property data in order to simulate the kinetics of precipitation process. Nucleation and growth models implemented in the software will be presented. Engineering applications of precipitation modeling and ongoing challenges will also be discussed as well.

4:20 PM Invited

Integrated Computational Materials Engineering for Precipitation Modeling of Multi-Component Alloys: *Fan Zhang*¹; W. S. Cao¹; S. L. Chen¹; Chuan Zhang¹; Y. A. Chang¹; ¹CompuTherm, LLC

Precipitation hardening or age hardening provides one of the most widely used mechanism for strengthening many structural materials. Extensive amount of research has been devoted to simulate the microstructural evolution and the correlated hardening responses during the precipitation of different types of intermetallic phases. However, precipitation is a highly complex process and could involve simultaneous occurrence of nucleation, growth and coarsening. Accurate modeling of the precipitation process requires a synchronous consideration of all these contributions. Moreover, the necessary phase equilibrium information and mobility data must be constantly updated during the simulation. Therefore, such a simulation necessitates a smooth integration of thermodynamic calculation, kinetic simulation and property modeling of the material. In this presentation, we will present a framework for precipitation modeling of multi-component alloys by integrating thermodynamic calculation with multi-level kinetic models. Examples will be given for aluminum alloys and nickel alloys.

4:50 PM Invited

Direct 3-D Materials Characterization and Its Incorporation into Computational Models: John Sosa¹; Daniel Huber¹; Robert Williams¹; Peter Collins²; *Hamish Fraser*¹; ¹The Ohio State University; ²University of North Texas

The successful development of accurate and validated computational tools most often requires an integration with materials characterization. Two functions are served, one being the provision of accurate physically-based descriptions of mechanistic details, and second being the validation of predictions yielded by the models. Hence, the most accurate means of materials characterization are required. In the present work, direct 3-D characterization methods have been developed, covering a wide range of length scales to permit descriptions of features from atomic dimensions to the macroscale. These techniques involve both serial sectioning and tomographical techniques. Considerable effort has been placed on the automation of these techniques, incorporating algorithms for image analysis. The results of these 3-D techniques will be compared with those obtained from stereological procedures using 2-D sections. The use of these new techniques to enable computational models will be described. This work has been supported in part by the ONR D3D program.

5:20 PM Invited

Use of Phase Field Method as a Tool for Alloy Design: Ning Zhou¹; *Yunzhi Wang*¹; ¹Ohio State University

In order to incorporate realistic multi-phase microstructures in property models for microstructure and micro-mechanism based alloy design, we discuss in this presentation the use of phase field method to carry out parametric study of effect of microstructure on deformation mechanisms in multi-phase alloys. Through individual examples we show how to use directly experimental images in phase field modeling at different length scales to explore mechanisms of dislocation-precipitate interactions and how to use computer generated microstructures to study effects of variation in microstructure (such as shape, orientation, and spatial distribution of precipitates) on deformation mechanisms. Such modeling has allowed for the development of (a) criteria and constitutive laws for crystal plasticity modeling and (b) fast-acting models for direct applications in alloy design.

Materials Processing Fundamentals: Physical Metallurgy of Steel

Sponsored by: The Minerals, Metals and Materials Society, TMS Extraction and Processing Division, TMS Light Metals Division, TMS: Process Technology and Modeling Committee
Program Organizers: Lifeng Zhang, Missouri University of Science and Technology; Antoine Allanore, MIT; Cong Wang, Saint-Gobain High Performance Materials

Monday PM
March 12, 2012

Room: Oceanic 8
Location: Dolphin Resort

Session Chairs: Antoine Allanore, MIT; Lifeng Zhang, Missouri S&T

2:00 PM

Estimation of Yield Strength of Linepipe Steel Pipes by Stress-Strain Curves Obtained from Low-Cycle Fatigue Tests: *Seok Su Sohn*¹; Seung Youb Han¹; Sang Yong Shin¹; Jin-ho Bae²; Nack J. Kim¹; Hyoung Seop Kim¹; Sunghak Lee¹; ¹Pohang University of Science and Technology; ²POSCO Corp.

Stress-strain curves obtained from low-cycle fatigue tests which could simulate the spiral piping and flattening processes of an API X80 linepipe steels were analyzed, and the estimation method of yield strength of the outer and inner walls of the pipe was suggested. The low-cycle fatigue test was conducted on the leveled steel sheet, and strain hardening and Bauschinger effects induced from differently subjected strain histories were evaluated and combined by the Swift's equation and Bauschinger stress parameter, respectively. By analyzing stress-strain curves, yield strengths of outer and inner walls were estimated to be 592 MPa and 492 MPa, respectively, which were lower by 20~80 MPa than those of the pipe. This difference was caused by the determining procedure of pre-strain and Bauschinger stress parameter for the simulation, the preposition of same strain hardening behavior depending on strain histories, and the difference between pre-strains depending on thickness location during the piping.

2:25 PM

Evaluation of Phase Transformations in Subcritical Temperature Austenitic Nitriding: *Yingying Wei*¹; Zbigniew Zurecki²; Richard Sisson¹; ¹Worcester Polytechnic Institute; ²Air Products and Chemicals, Inc.

Conventional nitriding of alloy steels is a multi-hour surface hardening process carried out at ferritic temperatures and following a complete heat treatment cycle: austenitizing, transformation quenching and tempering at a temperature exceeding the nitriding temperature used. A novel, subcritical-temperature austenitic nitriding process was developed to accelerate the treatment and optimize the hardness and toughness of the core and nitrided layers while minimizing the distortion of steel parts treated. Due to a transient migration of impurities to the prior austenite grain boundaries, the mechanical properties of parts nitrided by either of these two processes are influenced by tempering conditions selected: time, temperature, and heating/cooling rates. Aiming at elimination of temper embrittlement effects, this paper will present results of research focused on the interplay between the tempering and nitriding conditions and phase transformations in both processes. Kinetics of interstitial diffusion and phase transformation-based dimensional control of nitrided parts will be also discussed.

2:50 PM

Influence of the Hot Rolling Process on the Mechanical Behaviour of Dual Phase Steel: *Mehdi Asadi*¹; Heinz Palkowski²; ¹Benteler Automotive; ²TU Clausthal

In recent years, the increased demand for advanced high-strength steels (AHSS) mainly had been driven by the need of the automotive industry to reduce weight and to improve safety. Beside good ductility and high strength, those steels have a high bake hardening (BH) effect, giving



additional contribution to the strength of structural parts, subjected to the paint baking process. In this paper we concentrate results gained for hot rolled dual phase (DP) steels. For the simulation of changing process conditions within the final hot rolling the specimens were hot deformed using different schedules of temperatures and reductions, selected according to the non-recrystallization temperature (TnRX). It was possible to refine the DP steel structure by controlling the deformation temperature and the amount of strain below TnRX during the thermo-mechanical controlled processing (TMCP). This structure refinement resulted in an improvement of the strength and BH behaviour. A wide spectrum of mechanical properties could be obtained depending on the different hot deformation schedules. The best strength and BH levels were recorded for the deformation below TnRX at the highest amount of strain.

3:15 PM

Molybdenum Effects on the Recrystallization and Austenite Decomposition of a High-Niobium HSLA Steel: *Erik Pavlina*¹; E. Damm²; John Speer³; Chester Van Tyne³; ¹Pohang University of Science and Technology; ²The Timken Company; ³Colorado School of Mines

The effects of molybdenum (0.15 weight percent addition) on the austenite recrystallization and decomposition of nominal Fe-0.05C-0.09Nb steels was investigated. The no-recrystallization temperature was determined from multiple-step hot torsion experiments. The no-recrystallization temperature was reduced by 10 K in the molybdenum-containing alloy compared to the base alloy. The austenite decomposition reaction was examined using no-force dilatometry and dilatometry after deformation ($\epsilon = 1.0$) experiments. Molybdenum expanded the range of cooling rate over which acicular ferrite formed and promoted formation of granular bainite at the fastest cooling rates. Deformation below the no-recrystallization temperature increased the start temperature of austenite decomposition. In addition, deformation expanded the cooling rate regime over which granular bainite forms.

3:40 PM

The Steel Super Strengthening Phenomenon During Intensive Quenching: *Nikolai Kobasko*¹; Michael Aronov²; Joseph Powell²; ¹IQ Technologies, Inc.; ²IQ Technology, Inc.

It is stated that quenching with high cooling rates within the martensite range is equivalent to the low temperature thermo-mechanical treatment (LTMT) process. In this case, the superficial layer acts like a blacksmith: under conditions of high compressive residual stresses the plates of martensite arise explosively, deforming the austenite and creating extremely high dislocation densities, which are frozen during rapid cooling. This process is analogous to LTMT. For intensive quenching of steel parts, different IQ systems were used. They are installed at the Center for Intensive Quenching in Akron, Ohio, and at three commercial heat-treating shops. The paper summarizes the test data, connected with the mechanism of super strengthening phenomenon, obtained during the last several years and presented in numerous papers at different heat-treating conferences and forums.

4:05 PM Break

4:20 PM

Three-Dimensional Characterization of Laser-Welds in 304-L Stainless Steel: *Jonathan Madison*¹; Larry Aagesen²; ¹Sandia National Laboratories; ²University of Michigan

A variety of edge joints utilizing a continuous wave Nd:YAG laser have been produced and examined in a 304-L stainless steel to advance fundamental understanding of the linkage between processing and resultant microstructure in high-rate solidification events. Acquisition of three-dimensional reconstructions via micro-computed tomography and serial-sectioning have allowed for qualitative and quantitative characterization among a matrix of weld joints in a material system of wide use and broad applicability. The presence, variability and distribution

of micro-structural features such as porosity, phase microconstituents, and grain morphology have been examined for average values, spatial distributions and joint integrity. The variability of such measures have also been related to principle processing parameters such as weld speed, power and modulation.

4:45 PM

Continuous Casting Simulation of 2304 Duplex Stainless Steel Via Horizontal Directional Solidification Technique: *Qing Qing Sun*¹; Hong Gang Zhong¹; Xiang Ru Chen¹; Qi Jie Zhai¹; ¹Shanghai University

A horizontal directional solidification equipment, with an in-situ pouring system, was employed to physically simulate the solidification behavior of continuous casting. In this paper, the 2304 duplex stainless steel (DSS 2304) was investigated using this equipment due to its microstructure produced by continuous casting process was usually not satisfied. The grain size combined with the position of columnar to equiaxed transition (CET) of DSS 2304 were observed and the results showed these microstructure characteristics were very close to those of the continuous casting slabs. In addition, the influences of pouring temperatures and cooling conditions on the CET behavior were investigated. The results revealed that the length of the columnar grains decreased with decreasing the pouring temperatures and flow rates of the cooling water. Besides, the content of austenite decreases with increasing the distance from the chilled sidewall.

5:10 PM

Influence Of Cooling Rates On Nitrogen Precipitation Behaviors And The Ferrite Fraction In Cast 2507 Super Duplex Stainless Steel: *Dong Liang*¹; Honggang Zhong¹; Zhenxing Yin¹; Qijie Zhai¹; ¹Shanghai University

2507 super duplex stainless steel (SDSS) has been widely applied in a marine environment, attributing to its excellent pitting corrosion resistance and mechanical properties which are particularly determined by the nitrogen precipitation behaviors and volume fraction of ferrite. In this paper, various cooling rates were obtained by applying four different moulds with the common gating system. By which the influence of cooling rates on nitrogen precipitation behaviors and the ferrite fraction in cast 2507 SDSS was comparatively investigated. The results showed that nitrogen porosity could easily precipitate in cast 2507 SDSS under standard atmospheric pressure. The number of nitrogen holes increased with decreasing the cooling rates, and the holes mainly distributed in three zones, i.e. the interface between the horizontal and vertical columnar grains, top vertical columnar grains and the final solidification region. Additionally, higher ferrite fraction was obtained with lower cooling rates.

5:35 PM

Microstructure and Corrosion Behaviour of TiC Reinforced Duplex Stainless Steels Matrix Composites Synthesized by Laser Melt Injection: *Babatunde Obadele*¹; Peter Olubambi¹; Oluwagbenga Johnson¹; ¹Tshwane University of Technology

The microstructure and corrosion behaviour of titanium carbide (TiC) reinforced duplex stainless steel matrix surface composites synthesized by laser melt injection technique was investigated. The surface melting operation was conducted using a 4.4 kW CW Nd:YAG laser with laser power of 1.5 kW, scanning speed of 0.4 to 1.0 m/min, beam size of 3 mm and argon shield gas flow rate of 4 L/min. The morphologies and microstructures of the coatings examined using SEM revealed homogeneous distribution of fine precipitates of TiC in the matrix, while XRD analysis confirm no phase changes. TiC addition significantly increased hardness values from 236 to 547 Hv0.1 but had decreased the corrosion resistance of the steels in 3.5% NaCl possibly due to the inter-granular carbide coating that prevented chromium from forming continuous passive oxide layers.

Materials Research in Microgravity: Session II

Sponsored by: The Minerals, Metals and Materials Society, TMS Materials Processing and Manufacturing Division, TMS Extraction and Processing Division, TMS: Process Technology and Modeling Committee, TMS: Solidification Committee

Program Organizers: Robert Hyers, University of Massachusetts; Hani Henein, University of Alberta; Valdis Bojarevics, University of Greenwich; James Downey, NASA; Douglas Matson, Tufts University; Achim Seidel, Astrium; Daniela Voss, ESA

Monday PM
March 12, 2012

Room: Asia 3
Location: Dolphin Resort

Session Chair: To Be Announced

2:00 PM

Studies of Thermophysical Properties of Metals and Semiconductors by Containerless Processing under Microgravity: *Achim Seidel*¹; Wolfgang Soellner¹; Christian Stenzel¹; ¹Astrium

Electromagnetic levitation under microgravity provides unique opportunities for the investigation of liquid metals, alloys and semiconductors, both above and below their melting temperatures, with minimized disturbances of the sample under investigation. The opportunity to perform such experiments will soon be available on the ISS with the EML payload which is currently being integrated. With its high-performance diagnostics systems EML allows to measure various physical properties such as heat capacity, enthalpy of fusion, viscosity, surface tension, thermal expansion coefficient, and electrical conductivity. In studies of nucleation and solidification phenomena the nucleation kinetics, phase selection, and solidification velocity can be determined. Advanced measurement capabilities currently being studied include the measurement and control of the residual oxygen content of the process atmosphere and a complementary inductive technique to measure thermophysical properties.

2:25 PM Invited

Advanced Measurement Devices for the Microgravity Electromagnetic Levitation Facility EML: *Juergen Brillo*¹; Holger Fritze²; Georg Lohöfer¹; Michal Schulz²; Christian Stenzel³; ¹DLR; ²TU-Clausthal; ³Astrium

For liquid metals and alloys, the most prominent and ubiquitous surface active element is oxygen. A few ppm can cause a dramatic decrease of the surface tension with a sign-reversal of its temperature coefficient. To obtain reliable surface tension data, measured in electromagnetic levitation on ground or under microgravity, monitoring and control of the oxygen partial pressure in the processing environment is indispensable. For this purpose, an oxygen sensing and control (OSC) system, based on a zirconia oxygen ion pump, has been developed by ESA (contract 19963/07/NL/PM). We report on field tests interfacing the OSC with an electromagnetic levitator. Results of surface tension measurements will be presented for pure liquid metals and alloys as function of temperature, oxygen partial pressure, and alloy composition. These data give insight into the oxygen interaction with liquid metal surfaces. Established thermodynamic models will be critically discussed.

3:00 PM

Electrostatic Levitation Furnace for the ISS: *Keiji Murakami*¹; Naokyo Koshikawa¹; Kohichi Shibasaki¹; Takehiko Ishikawa¹; Junpei Okada¹; Tetsuya Takada²; Tatsuya Arai²; Naoki Fujino²; Yukiko Yamaura²; ¹JAXA; ²IHI Aerospace

JAXA (Japan Aerospace Exploration Agency) has just started the development of Electrostatic Levitation Furnace to be launched in 2014 for the ISS. This furnace can control the sample position with electrostatic

force and heat it above 2000 degree Celsius using semiconductor laser from four different directions. The announcement of Opportunity will be issued soon for this furnace. In this presentation, we will show the specifications of this furnace and also the development schedule.

3:25 PM Break

3:45 PM Invited

Thermophysical Property Measurements Under Reduced Gravity Conditions: Evolution and Status of the ThermoLab Project

: *H-J Fecht*¹; R.K. Wunderlich¹; L. Battezzati²; E. Ricci³; J. Etay⁴; S. Seetharaman⁵; J. Brillo⁶; M. Watanabe⁷; K. Kelton⁸; D.M. Matson⁹; Robert Hyers¹⁰; ¹U. Ulm; ²Universita di Torino; ³CNR-IENI; ⁴CNRS, SIMAP-EPM, PHELMA-Campus; ⁵KTH Royal Institute of Technology; ⁶Deutsches Zentrum für Luft- und Raumfahrt; ⁷Gakushin University; ⁸Washington University; ⁹Tufts University; ¹⁰University of Massachusetts

Thermophysical property values of industrial alloys in the liquid phase provide important input data for the modelling of casting and solidification in industrial metallurgical processes. Owing to the difficulty of handling metallic alloys in the liquid phase there is a considerable need of accurate thermophysical property values in the liquid phase which pertains in particular to high melting point reactive alloys such as Ti-alloys. The ThermoLab project was conceived to alleviate this need by using containerless processing techniques based on electromagnetic levitation in ground based laboratory and under reduced gravity conditions for thermophysical property measurement. In addition, a ground based measurement programme using, where possible, conventional thermoanalytic methods was performed. Properties of interest include calorimetric properties, density, surface tension and viscosity and the electrical conductivity. Alloys of interest are Ti-based alloys, Fe-alloys, Ni-based superalloys and Cu-alloys which are suggested by an industrial project user group. In the course of the project extensive use was made of parabolic flights for the measurement of the surface tension and the viscosity and of TEXUS sounding rocket flights. In addition to the experimental programme ThermoLab is concerned with the modeling of non-contact thermophysical property measurements in an electromagnetic levitation device including the development and verification of non-contact calorimetry and considerations of the influence of fluid flow on viscosity measurements by the oscillating drop method. Another aspect of modelling is concerned with the surface tension in particular the influence of surface active elements on the temperature dependence of the surface tension and with the calculation of phase diagrams. An overview will be given of the current status of the project, recent results and the progress towards implementation of this programme on the International Space Station.

4:20 PM Invited

Electrostatic Levitation: A Tool to Support Materials Research in Microgravity: *Jan Rogers*¹; Michael SanSoucie¹; ¹NASA/MSFC

Containerless processing represents an important topic for materials research in microgravity. Levitated specimens are free from contact with a container, which permits studies of deeply undercooled melts, and high-temperature, highly reactive materials. Containerless processing provides data for studies of thermophysical properties, phase equilibria, metastable state formation, microstructure formation, undercooling, and nucleation. The European Space Agency (ESA) and the German Aerospace Center (DLR) jointly developed an electromagnetic levitator facility (MSL-EML) for containerless materials processing in space. The electrostatic levitator (ESL) facility at the Marshall Space Flight Center provides support for the development of containerless processing studies for the ISS. Apparatus and techniques have been developed to use the ESL to provide data for phase diagram determination, creep resistance, emissivity, specific heat, density/thermal expansion, viscosity, surface tension and triggered nucleation of melts. The capabilities and results from selected ESL-based characterization studies performed at NASA's Marshall Space Flight Center will be presented.



TMS 2012

141st Annual Meeting & Exhibition

MONDAY PM

4:55 PM Invited

Novel Needle-Network Multi-Scale Model for the Solidification of Highly Branched Dendritic Microstructures: Damien Tourret¹; *Alain Karma*¹; ¹Northeastern University

A novel multi-scale modeling approach is proposed to investigate quantitatively the solidification of large dendritic arrays on a scale much larger than the diffusion length. Dendritic branches are represented as a network of “needle crystals” on a scale larger than the tip radius. The tip radius and velocity of each needle is deduced from a standard microscopic solvability condition on the inner tip scale, and a “Flux Intensity Factor” (FIF), measuring the strength of the solutal diffusion gradient at the tip on the scale of the system. The FIF is mathematically isomorphic to the stress intensity factor for pure anti-plane shear and is evaluated using the fracture mechanics J-integral. The method is benchmarked against two-dimensional phase-field simulations on massively parallel Graphic Processing Units. Results demonstrate the power of this approach to simulate complex dendritic microstructures directionally solidified under microgravity conditions and to investigate the growth competition of misoriented columnar grains.

5:30 PM

Status of Viscosity Measurements by the Oscillating Drop Method in an Electromagnetic Levitation Device under Reduced Gravity Conditions: Jacqueline Etay¹; Ivan Egry²; Koulis Pericleous³; *Rainer Wunderlich*⁴; ¹CNRS SIMAP-EPM; ²DLR; ³University of Greenwich; ⁴Universitaet Ulm

The oscillating drop method in an electromagnetic levitation device under reduced gravity conditions has found wide applications for surface tension and viscosity measurements of high temperature reactive metallic alloys. Microgravity conditions are required because under 1-g conditions the strong levitation fields cause turbulent fluid flow which impedes the evaluation of the viscosity from the measured damping time constant of the surface oscillations. Magneto-hydrodynamic modelling predicted a dependence of the damping time constant on the amplitude of the surface oscillations and on the residual positioning field. For a verification of these results a series of experiments on parabolic flights and on a TEXUS sounding were performed. The results indicate an effect of the initial surface oscillation amplitude and an effect of the positioning field on the damping time constant. From these findings limiting values of control parameters for the application of the oscillating drop method in an em-levitation can be set.

Mechanical Behavior at Nanoscale I: Atomistic Modeling on Deformation Mechanisms

Sponsored by: The Minerals, Metals and Materials Society, TMS Materials Processing and Manufacturing Division, TMS: Nanomechanical Materials Behavior Committee, TMS/ASM: Mechanical Behavior of Materials Committee

Program Organizers: Scott Mao, University of Pittsburgh; Julia R Greer, California Institute of Technology; Jianyu Huang, Center for Integrated Nanotechnologies; Marc Legros, CEMES-CNRS; Ting Zhu, Georgia Institute of Technology

Monday PM

March 12, 2012

Room: Asia 1

Location: Dolphin Resort

Session Chairs: Ting Zhu, Georgia Institute of Technology; Christopher Weinberger, Sandia National Laboratory

2:00 PM Invited

Modeling Dislocation Nucleation and Strength in Nanowires and Nanopillars: Andrew Jennings¹; *Christopher Weinberger*²; Julia Greer¹; ¹California Institute of Technology; ²Sandia National Labs

Experiments have shown that plasticity in confined volume single crystals can be controlled either through single arm sources or dislocation nucleation; the transitions of which are size and microstructure dependent.

Here, we develop a simple continuum model that captures the activation energy and activation volume of dislocation nucleation from free surfaces. The nucleation strength dependence on crystal orientation, surface facets and material properties are investigated and compared against traditional single arm source operation. This provides a map for transitions from conventional source limited plasticity controlled by single arm sources to surface nucleation.

2:30 PM Invited

Interface-Facilitated Twinning/De-Twinning: *Jian Wang*¹; Nan Li¹; Irene Beyerlein¹; Nathan Mara¹; Amit Misra¹; ¹Los Alamos National Laboratory

We report recent work on twinning and detwinning in fcc and hcp metals and Cu/Nb multilayers based on the in situ and ex situ TEM observations and molecular dynamics simulations. We found that interfaces (structures and slip systems across interface) play a crucial role in facilitating twinning and de-twinning. Four aspects are discussed. (1) Zeor-strain twinning/detwinning in single-phase fcc metals is achieved in association of incoherent twin boundary; (2) Cu-Ag coherent interface facilitates deformation twinning in Cu via slip transmission; (3) Cu-Nb incoherent {112} interface facilitates twinning in Cu due to the presence of the preferred slip systems across interface; and (4) deformation twinning in hcp metals nucleates at low misorientation angle grain boundaries. The main conclusion is that the atomic structures of interfaces (twin boundaries, two-phase interfaces, and grain boundaries) play a crucial role in nucleating and propagating deformation twins.

3:00 PM

Revealing the Failure Mechanisms in Nanomaterial Electrodes for Lithium Ion Batteries: *Ting Zhu*¹; Shan Huang¹; Xiaohua Liu²; Jianyu Huang²; ¹Georgia Institute of Technology; ²Sandia National Laboratories

Lithium ion batteries (LIBs) are critically important for a wide range of applications, from portable electronics to electric vehicles. We made in situ observations of deformation and fracture in single nanowire/nanoparticle electrodes using a nanobattery cell inside a transmission electron microscope. Novel phenomena were discovered, including the size dependent fracture in silicon nanoparticles, anisotropic swelling and self-splitting in silicon nanowires, reversible nanoporosity formation in germanium nanowires during cycling, and cracking in the coatings of tin oxide nanowires. The multiscale chemomechanics models were developed to reveal the mechanistic origin of failures. The results provide insights into the electrochemically induced microstructural evolution in nanomaterial electrodes, and have implications for designing high capacity electrodes in LIBs.

3:20 PM

Effects of Size and Microstructure in Compression of Nanoscale Metallic Pillars by Molecular Dynamics Simulation: *Frederic Sansoz*¹; ¹University of Vermont

This talk presents some recent advances using a new atomistic simulation technique to quantitatively examine how random dislocation networks evolve during deformation of nanoscale Cu pillars. In particular, this study aims to provide fundamental understanding of differences in finite-temperature plastic deformation between perfectly-crystalline nanocrystals and those containing preexisting dislocations. The technique used enables the simulation of key mechanisms of nanoscale plasticity observed in the past in nanopillars with different methods, such as in-situ nanocompression experiments or DDD simulations. Remarkably, atomistic simulations show that $\langle 111 \rangle$ Cu pillars less than 75 nm in diameter with a high initial dislocation density exhibit the same flow stress scaling in compression, as a function of pillar diameter, than that observed experimentally in Cu crystals with larger diameters and smaller densities. A deformation mechanism map is developed for Cu crystals with different diameters, and used to explain the origin of size-dependent plasticity in nanoscale fcc crystals.

3:40 PM

Emission of Dislocations from Random Grain Boundaries in Nanocrystalline FCC Materials: *Laura Patrick*¹; Diana Farkas¹; ¹Virginia Tech

We report a comparative study of dislocation emission from grain boundaries using model interatomic potentials representing various FCC metals. Molecular dynamics simulation techniques were used to apply virtual tensile tests to simulated samples with random tilt grain boundaries and a 40nm average grain size. The emission of dislocations resulting from tensile straining was analyzed in detail. Emission of leading, trailing and partial dislocations was observed at specific values of the strain that varied depending on the interatomic potential used. In addition to dislocation emission and motion, we analyzed the inhomogeneity of the strain in various regions of the samples. The qualitative pattern of dislocation emission and distribution of the overall strain was remarkably similar for all interatomic potentials analyzed. The results emphasize the critical role of sample geometry and microstructure in determining overall mechanical behavior.

4:00 PM Break**4:10 PM Invited**

Size-Affected Behavior in Pure Compression of Micron-Sized Metallic Crystals – a Theoretical Study: *Satish Rao*¹; Dennis Dimiduk²; Michael Uchic²; Triplicane Parthasarathy¹; Jaafar El-Awady³; Christopher Woodward²; ¹UES Inc.; ²Air Force Research Laboratory; ³Johns Hopkins University

Experimental studies show strong strengthening effects for micrometer-scale FCC as well as two-phase superalloy crystals, even at high initial dislocation densities. This talk shows results from large-scale 3-D discrete dislocation simulations (DDS) used to explicitly model the deformation behavior of FCC Ni as well as superalloy microcrystals under single-slip conditions. The study shows that two size-sensitive athermal hardening processes, beyond forest and precipitation hardening, are sufficient to develop the dimensional scaling of the flow stress, stochastic stress variation, flow intermittency and, high initial strain-hardening rates, similar to experimental observations for various materials. One mechanism, source-truncation hardening, is especially potent in micrometer-scale volumes. A second mechanism, termed exhaustion hardening, results from a break-down of the mean-field conditions for forest hardening in small volumes, thus biasing the statistics of ordinary dislocation processes. Effects of thermally activated cross-slip on the stress-strain behavior of microcrystals of Ni is also discussed.

4:40 PM

Nanoscale Investigation of Twinning and Detwinning during Strain-Path Changes in Magnesium: *Mehul Bhatia*¹; Kiran Solanki²; Amitava Moitra³; ¹CAVS - Center for Advanced Vehicular System; ²Arizona State University; ³Pennsylvania State University

Plastic deformations in hexagonal materials are accommodated through the activation of diverse slip and twinning modes, which are controlled by critical resolve shear stresses and crystallographic orientations. In this work, we investigate the strain-path changes in single crystal and nanocrystalline magnesium to elucidate the load reversal effect on reported $\{10\text{-}12\}$ $\langle 10\text{-}11 \rangle$ twinning and detwinning behavior using molecular dynamics. Simulation results indicate that twinning and detwinning alternates with the reverse loading along $[0001]$ direction, i.e. most of the twins formed during tension, are removed when the load is reversed. The contributions of twinning with strain during deformation were evaluated based on the quantitative statistic of the twin area fraction. Yield asymmetry is more prominent in poly-crystal magnesium compared to single crystal magnesium. The significance of this research is that atomistic simulations of this ilk can help improve continuum strain hardening models for the HCP class of materials.

5:00 PM

Molecular Dynamics Study of Deformation Mechanism Map of Nanostructured Metal: Shigenobu Ogata¹; *Yunjiang Wang*¹; Guo-Jie Gao¹; ¹Osaka University

Deformation mechanism map has been well established for conventional coarse-grained materials by H. J. Frost and M. F. Ashby[1], but there is little knowledge about the creep mechanism of nanocrystalline metals. Here we use classical molecular dynamic to draw a creep-mechanism map for nanoscale copper with grain size down to about 10 nm. We observe a transition from diffusive deformation at high temperature, low stress to displacive deformation at low temperature, high stress. The physical mechanism underlying the interesting mechanism transition will be explained by the competition among different stress-driven thermal activated processes.

5:20 PM

Defect-Free Core/Shell Nanowires Based on New Misfit Strain Relaxation Mechanisms: *Haijian Chu*¹; Jian Wang²; Caizhi Zhou²; Irene Beyerlein²; ¹Yangzhou University; Los Alamos National Laboratory; ²Los Alamos National Laboratory

Combining TEM observation and defect theory, we proposed and demonstrated a relaxation mechanism for misfit strain in core/shell nanowires, in which glide dislocations nucleate from surfaces. To predict the critical shell thickness corresponding to defect-free core/shell nanowires (NWs), we, for the first time, developed an accurate expression in describing the self-energy of a misfit elliptical dislocation loop in an anisotropic crystal that considers the influence of loop circumference, shape, and dislocation core radius on the self-energy. Using the energy formula, we systematically predict the critical shell thickness for defect-free Ge/Si core/shell NWs as a function of growth direction. Significantly the numerical results for the critical shell thickness are consistent with experimental results.

5:40 PM

Core Properties of Mixed Dislocations in BCC Iron: *Emmanuel Clouet*¹; Mathilde Miguras¹; Mathieu Albagna¹; ¹SRMP, CEA Saclay

We used atomic simulations with an empirical potential to study core properties of mixed dislocations in bcc iron. All studied dislocations have a $1/2[111]$ Burgers vector and are gliding on a $\{110\}$ plane. The lowest core energy is obtained for the screw orientation. Variations of the core energy for a character lower than $\sim 30^\circ$ agree with a kinked dislocation description, whereas the core energy is quite constant beyond. The Peierls barriers, under zero stress, have also been calculated. The highest barrier is obtained for a mixed dislocation with a character $\sim 70.5^\circ$. The estimation of the Peierls stress from these different barriers shows that the screw orientation is the hardest to make glide. The $\sim 70.5^\circ$ mixed orientation is also associated with a high Peierls stress. We then use ab initio calculations to look more precisely to the core properties of this $\sim 70.5^\circ$ mixed dislocation.



TMS 2012

141st Annual Meeting & Exhibition

MONDAY PM

Mechanical Behavior Related to Interface Physics: Interface Evolution under Mechanical Loading: Experiment, Characterization, and Theoretical Modeling

Sponsored by: The Minerals, Metals and Materials Society, TMS Structural Materials Division, TMS Materials Processing and Manufacturing Division, TMS/ASM: Mechanical Behavior of Materials Committee, TMS: Nanomechanical Materials Behavior Committee

Program Organizers: Jian Wang, Los Alamos National Laboratory; Nathan Mara, Los Alamos National Laboratory; Izabela Szlufarska, University of Wisconsin-Madison; Zhiwei Shan, Xi'an Jiaotong University

Monday PM Room: Oceanic 1
March 12, 2012 Location: Dolphin Resort

Session Chairs: Irene Beyerlein, Los Alamos National Laboratory; Huiling Duan, Peking University

2:00 PM Keynote

FCC/BCC Interface Evolution in Severe Plastic Deformation: *Irene Beyerlein*¹; Jian Wang¹; Nathan Mara¹; Nathan Mara¹; ¹Los Alamos National Laboratory

The goal of this work is to determine the class of bi-metal interfaces that will create composite materials with extraordinary failure resistance under extreme mechanical strains. The evolution of bi-metal interface properties were studied in Cu-Nb multi-layered composites synthesized using a severe plastic deformation (SPD) technique called accumulative roll bonding (ARB). EBSD and TEM analyses strongly suggest that most interfaces in nanolayered ARB material are $\{112\}_{fcc}/\{112\}_{bcc}$ with a Kurdjumov-Sachs orientation relationship. Atomistic simulation, dislocation theory, and polycrystal plasticity modeling are employed to determine the structural aspects that make this interface stable under SPD and its role in governing slip and twinning activity.

2:30 PM Keynote

Thermo-Mechanical Solution of Film/Substrate Systems under Local Thermal Load and Its Applications: *Huiling Duan*¹; ¹Peking University

Film/substrate structures are widely used in microelectronic and optoelectronic devices for decades and these structures usually undergo a local thermal load in applications. For example, the thermal atomic force microscopy (AFM) or scanning thermal microscopy (SThM) probe is used to heat poly ethylene terephthalate films to induce crystallization of the material, and the SThM is also used in nanoscale lithography on molecular resist films to fabricate various microstructures. A similar situation arises in the Laser Lift-Off technique (LLO) for separating GaN films from substrates. We present the solutions of temperature and stresses in a film/substrate structure under a local thermal load on the film surface. Then, this thermo-mechanical solution is applied to analysis of the temperature distribution, stresses, and damage of a GaN/sapphire system during the LLO process. It is shown that the laser with the Gaussian distribution of energy density can avoid less damage to the GaN films.

3:00 PM

Computational and Experimental Investigation of the Interfacial Dynamic Compressive Behavior of High Strength Aluminum Alloys: William Lee¹; Pratheek Shanthraj¹; Hanadi Salem²; *Mohammed Zikry*¹; ¹North Carolina State University; ²The American University in Cairo

The objective of this study is to identify the dominant microstructural and dislocation mechanisms related to the high strength and ductile behavior of high strength aluminum alloys, and how high strain-rate loading conditions would affect overall behavior on scales ranging from the nano to micro scales. Characterization techniques and specialized microstructurally-

based finite-element (FE) analyses based on a dislocation-density based multiple-slip formulation that accounts for an explicit crystallographic and morphological interfacial representation of Ω and θ' precipitates and their rational orientation relations was conducted. As the microstructural FE predictions have indicated, and consistent with the experimental observations, the combined effects of θ' and Ω precipitates and dispersed Mn particles, acting on different crystallographic orientations, enhance the strength, the ductility, and reduce the susceptibility of high strength aluminum alloys to shear strain localization due to dynamic compressive loads.

3:15 PM

Deformation Mechanisms of Hall-Petch Strengthening in Bimodal Nanocrystalline Materials: *Chandra Pande*¹; ¹Naval Research Laboratory

Recent experimental studies has demonstrated that polycrystals with a bimodal microstructure which consists of a mixture of nanoscale and microscale grains, has significantly higher tensile ductility with only slight reduction in tensile strength when compared to an all-nanocrystalline polycrystal. Bimodal microstructure is also expected to improve the fracture toughness and lower fatigue crack growth rates. We present a theoretical model predicting Hall Petch strengthening for such a system as a function of microstructure variables such as volume fraction of the larger grains and show that the predictions are consistent with experiments.

3:30 PM

Exploring and Exploiting Physical Properties of Molecular Crystals Subjected to Mechanical Milling: *M. Teresa Carvajal*¹; Yuanyuan Jing¹; Andrew Otte¹; John Blendell¹; ¹Purdue University

Mechanical stresses applied to molecule organic solids produce structural changes in the crystal lattice. This often affects key performance properties of pharmaceutical products and compromises their physical stability. There is little information on the structure-property-response of molecular organic crystals to stress. Particularly on microstructural defects such as dislocations and their influence on interfacial phenomena and surface interactions of crystalline particles. The goals of this study are to directly observe, via AFM nano-indentation, the microstructural response to applied mechanical loads and to elucidate their relationship with the bulk and surface properties via DSC and by IGC/XPS, respectively. Of specific interest are the differences in interfacial energies between the native crystals in contact with the defected crystals or the amorphous form. The results show that a systematic characterization of milled materials can be a highly informative tool for a fundamental insight of milling knowing consequences and potentially predict and control bulk behavior.

3:45 PM Break

3:55 PM Keynote

Characterization and Modeling of Heterogeneous Deformation near Grain Boundaries in Titanium and Ti-5Al-2.5Sn: *Thomas Bieler*¹; Darren Mason²; Claudio Zambaldi³; Philip Eisenlohr³; Chen Zhang¹; Hongmei Li¹; Leyun Wang¹; Yiyi Yang¹; Carl Boehlert¹; Martin Crimp¹; Rozaliya Barabash⁴; Wenjun Liu⁵; ¹Michigan State University; ²Albion College; ³Max-Planck-Institut für Eisenforschung; ⁴Oak Ridge National Laboratory; ⁵Argonne National Laboratory

The anisotropic deformation of commercially pure Ti and Ti-5Al-2.5Sn was investigated in tension and bending at 23C using interrupted quasi-static and in-situ creep tests. Initially polished and deformed microstructures were characterized using several electron microscopy, 3-D x-ray microdiffraction, and surface characterization methods. Patches of microstructure that exhibited heterogeneous slip and grain boundary ledge development were computationally deformed using crystal plasticity finite element code to simulate the physical experiments. Phenomenological hardening models were optimized using comparisons with conical indentation experiments. Ledge development was investigated using a

new damage model that accounts for dislocation density mismatch at grain boundaries. By combining a tensorial measure of in-plane grain boundary deformation with localized mode-II shear stresses, a new metric was developed that distinguished between ledge-forming and topographically smooth grain boundaries. Comparisons between measured and simulated slip behavior reveal discrepancies between observed and simulated deformation behavior, and necessary improvements in model assumptions have been identified.

4:25 PM Keynote

Phase Field Modeling for the Effects of Coherency Stress and Vacancy Source/Sinks on the Interface Sharpening and Intermixing Rate in Coherent Nano-Multilayers: Haibo Wan¹; Yao Shen¹; Xuejun Jin¹; ¹Shanghai Jiao Tong University

A phase-field model for vacancy-mediated interdiffusion in coherent multilayers is developed, focusing on the effects of coherency stress and vacancy source/sinks on the interface sharpening and intermixing rate. Two limiting cases are considered: vacancy source/sinks are uniformly and densely distributed, or not present at all. Remarkable interface sharpening is observed (1) at the presence of dense vacancy source/sinks when the two layers differ greatly in vacancy formation energy, or (2) at the absence of source/sinks when they differ greatly in vacancy migration energy. The coherency stress is found to promote the interface sharpening and intermixing rate if the faster component has the smaller lattice constant; otherwise, the stress has the opposite effect. When the difference in vacancy formation energy of the two components is much larger than in migration energies, the intermixing without vacancy source/sinks is faster than with dense source/sink; otherwise, it is slower than with dense source/sinks.

4:55 PM

Electron Backscatter Diffraction (EBSD) Measured Boundary Characteristics of Cu/Nb Nanolamellar Composites Fabricated by Accumulative Roll Bonding (ARB): Rodney McCabe¹; John Carpenter¹; Jonathan Ledonne²; Anthony Rollett²; Nathan Mara¹; ¹Los Alamos National Laboratory; ²Carnegie Mellon University

The interface characteristics of Cu/Nb nanolamellar composites fabricated via ARB are investigated as a function of layer thickness using EBSD. Starting with single, polycrystalline layers of Cu and Nb, repeated ARB steps are used to fabricate multilayers with nominal layer thicknesses (h) ranging from tens of microns to tens of nanometers. Neutron diffraction, performed previously, was used to investigate the evolving texture and found that an atypical rolling texture saturated at h = 128 nm becoming stable with further plastic strain. EBSD is used in this study to examine interface boundary misorientations and plane normal directions within a microstructural reference frame allowing for distinctions to be made between interfacial grains and those associated with the bulk. The EBSD data is used both to study the orientation relationships that occur across hetero-phase interfaces as well as to ascertain whether steady state and/or preferred boundaries are present at the various length scales.

5:10 PM

Chemical Changes Underlying Aging of Silica in Nano-mechanical Contacts: Yun Liu¹; Izabela Szlufarska¹; ¹University of Wisconsin - Madison

Friction and adhesion of silica are important both in naturally occurring phenomena, such as earthquakes, as well as in engineering applications, including wafer bonding. Molecular-level understanding of phenomena that take place in these frictional contacts is currently lacking. Here we focus specifically on aging of silica, a process by which static friction changes with time when two surfaces are held still. The origin of this behavior has been a subject of a decades-long debate. Here we will discuss chemical reactions that can lead to aging of a single-asperity silica contact in aqueous environments. Using calculations based on the Density

Functional Theory and on the ReaxFF reactive force fields, we discovered that the formation of interfacial siloxane bridges can be responsible for the increase of interfacial strength. We demonstrate that the rate of this reaction slows down with time, which explains the experimentally observed logarithmic dependence of aging on hold time.

5:25 PM

Interfacial Response of Friction-Welded 304-Stainless Steel and 6061-Al in Tension: Cheng Liu¹; Manuel Lovato¹; William Blumenthal¹; ¹Los Alamos National Laboratory

An experimental study of the interfacial response of friction-welded 304-stainless steel and 6061-aluminum under uniaxial tension loading was performed using 2-D video digital image correlation (DIC) to obtain full-field deformation mapping of dog-bone specimens perpendicular to the bonded interface. As expected, plastic deformation only occurred in the aluminum portion of the specimen. An unexpected observation was that the mechanical properties of the 6061-aluminum were no longer uniform or representative of the as-received material, but varied significantly within a small distance from the bonded interface due to the welding process. The high spatial resolution of the DIC strain technique (~0.25 mm for this application) allowed accurate evaluation of the mechanical behavior gradient in the aluminum near interface and demonstrated the usefulness of the DIC technique as a tool for improving bonding processes.

Mechanical Performance of Materials for Current and Advanced Nuclear Reactors: Mechanical and Small-Scale Testing of Reactor Materials

Sponsored by: The Minerals, Metals and Materials Society, TMS Structural Materials Division, TMS/ASM: Nuclear Materials Committee

Program Organizers: Nicholas Barbosa, National Institute of Standards & Tech; Greg Oberson, United States Nuclear Regulatory Commission; Matthew Kerr, United States Nuclear Regulatory Commission; Elaine West, Knolls Atomic Power Laboratory; Stuart Maloy, Los Alamos National Laboratory; Osman Anderoglu, LANL

Monday PM
March 12, 2012

Room: Swan 1
Location: Swan Resort

Session Chairs: Greg Oberson, Nuclear Regulatory Commission; Nick Barbosa, NIST

2:00 PM Invited

A Perspective on Current Challenges in Development and Application of Uniaxial Micro-scale Testing Techniques to Characterize the Mechanical Properties of Materials: Paul Shade¹; Michael Uchic¹; Dennis Dimiduk¹; ¹Air Force Research Laboratory

Over the past decade, there has been considerable activity within the materials community to develop and apply mechanical testing methods that operate on micron- and sub-micron scale samples. Potential motivations for testing at small scales include the exploration of fundamental processes that govern plastic deformation and, the ability to probe for variations in properties that are sensitive to local changes in microstructure. Nonetheless, challenges remain in both conducting and interpreting experiments, which must be addressed before these techniques can be widely applied as engineering tools. Experimental challenges include slow and expensive sample fabrication techniques, limited temperature range of testing capabilities and a wide spectrum of device configurations and practices. Interpretation challenges include existence of sample-size effects, as well as a limited understanding of the mechanisms governing the transition from size-dependent to size-independent behavior. The present talk provides a selected perspective of these issues and, identifies areas for future research.



TMS 2012

141st Annual Meeting & Exhibition

MONDAY PM

2:30 PM Invited

Benefits and Challenges of Small Scale Materials Testing for Nuclear

Application: *Peter Hosemann*¹; Daniel Kiener²; Stuart Maloy³; Jenny Martos¹; ¹UC Berkeley; ²Montanuniversitaet leoben; ³LANL

Due to difficult handling of radioactive samples or the use of ion beam irradiated materials and the interest of a specific location on a given component, small scale testing is of great interest to scientists studying radiation damage in materials. While nanoindentation has been used for decades, micro compression and other more complex sample geometries have become available using Focused Ion Beam machining. We show the extent to which small scale mechanical testing on irradiated materials can be used today on structural materials but also on advanced fuel forms in order to gain a better understanding of the changes caused by radiation. However, small scale materials testing on ion beam irradiated materials are not without limitations and therefore it is important to evaluate the importance of size effects and other artifacts.

3:00 PM

Compatibility of MYRRHA Candidate Structural Materials with Lead-Bismuth Eutectic Environment: Effect of Strain Rate and Low Dissolved Oxygen Concentration: *Gunter Coen*¹; Joris Van den Bosch¹; Serguei Gavrilov¹; ¹SCK-CEN

SCK-CEN has taken up the task of designing and building an accelerator driven system (ADS) cooled by lead-bismuth eutectic (LBE), called MYRRHA. To go from the basic design of the reactor towards detailed engineering, building and licensing, there is a need for conservative material data obtained in relevant conditions for the system under design. One of the material degradation effects, which is related to the interaction between the liquid LBE environment and the structural steel is liquid metal embrittlement (LME). It is a reduction of the ductility and fracture toughness of a metal when simultaneously subjected to stress and direct contact with a liquid metal. In order to obtain representative data from mechanical tests performed in LBE environment, one should investigate different factors affecting LME. In this paper, the influence of strain rate and low dissolved oxygen concentration in the LBE on the LME of T91 (modified 9Cr-1Mo) is described.

3:20 PM

Mechanical Testing of Nuclear Materials Using a MEMS Approach: *Nicholas Barbosa*¹; David Read¹; ¹National Institute of Standards & Tech

Miniaturization of specimens used for mechanical testing of nuclear materials is limited by the inability to adequately prepare small specimens; by the inability to test the specimens; and by uncertainty in the interpretation of results. In this presentation, a new approach to performing tests on tensile specimens with sub-millimeter gauge lengths will be discussed. Specimens were prepared through either EDM or chemical etching. A MEMS frame was used to grip the specimens and to link them to the displacement actuators and the load sensor. Displacements were measured through a digital image correlation technique applied to images captured via a microscope. The results of tests performed on 302 stainless steel in the annealed and full-hard conditions will be used to demonstrate the technique and to highlight the challenges and benefits associated with performing bulk measurements at this scale.

3:40 PM

Grain Size Effects in Micro-Scale Tensile Testing of 316L Stainless Steel: *Whitney Poling*¹; Nicholas Barbosa²; Kip Findley¹; David Read²; ¹Colorado School of Mines; ²National Institute of Standards and Technology

A MEMS-based micro-tensile system was developed at NIST and is capable of testing rectangular tensile specimens with gage section dimensions on the order of tens to hundreds of microns. A potential application is in-situ tensile testing in harsh environments, such as a nuclear reactor pressure vessel. The test results can be influenced by microstructure size effects due to the size-scale of the specimens, so these

size effects must be well understood to obtain reliable bulk mechanical property information from the test. Currently, grain size effects are being studied with cold-rolled 316L stainless steel sheet that is annealed to obtain target grain diameters of 5, 10 and 20 microns. With increasing grain size, fewer grains comprise the gage cross-section of the micro-tensile specimens. The effect of the number of grains in the micro-tensile specimen cross-section on measured mechanical properties and their agreement with results from conventional-sized tensile tests is being investigated.

4:00 PM Break

4:20 PM

Small Specimen Testing for Evaluating Radiation-Induced Changes in Mechanical Properties of Structural Reactor Materials at High Irradiation Doses: *Ellen Rabenberg*¹; Kyle Knori¹; Brian Jaques¹; Bulent Sencer²; Darryl Butt¹; F.A. Garner³; ¹Boise State University; ²Idaho National Laboratory; ³Radiation Effects Consulting

During irradiation, the mechanical properties of reactor components progressively change, affecting its structural integrity; namely, ductility. It has previously been observed that hardening from radiation exposure reduces the ductility in metals. However, prior studies involving 12Cr18Ni10Ti austenitic steel report a regained ductility at doses higher than 55 dpa due to a gamma to alpha martensitic transformation, which occurs via the propagation of a deformation wave through the gage section of a tensile specimen. This "deformation wave" is being studied using miniature specimen testing. The shear punch and tensile tests are ideal as they allow post-irradiation examination in lightly shielded environments rather than in a hot cell. Correlations between these non-standard tests have been performed for 304-type stainless and MA957 ODS steels. Different factors affecting correlations between shear punch and tensile experiments and martensite formation, such as surface roughness and applied strain rate, are summarized for both un-irradiated and irradiated metals.

4:40 PM

Study of Size and Irradiation Effects on Mechanical Properties of Silicon Carbide Micropillars: *Chansun Shin*¹; Hyung-Ha Jin¹; Dong-Jin Kim¹; Junhyun Kwon¹; ¹Korea Atomic Energy Research Institute

Silicon carbide (SiC) and SiC/SiC composites have been proposed as a promising candidate material for structural components in fusion reactors due to its good thermal and mechanical properties under high temperature and irradiation. Characterization of the mechanical properties such as fracture strength is important to ensuring the reliability of ceramic structures. In this study, SiC micropillars of various sizes were fabricated by mask and inductively coupled plasma etching technique and compressed by using flat punch nanoindentation. Compressive fracture strength showed a clear specimen size effect. The strength increased from 6.5 GPa up to 18 GPa as the diameter decreased from 5.4 down to 0.7 microns. Brittle-to Ductile transition at room temperature was observed as the specimen size decreases. Ion irradiation was performed with Si ions. The effect of irradiation on the fracture strength of SiC micropillars was evaluated and the potential of this method will be discussed.

5:00 PM

Multi-Axial Mechanical Behavior of Zircaloy-4 and Effect on Initial Texture: *Akawat Siriruk*¹; Matthew Kant¹; *Dayakar Penumadu*¹; Elena Garlea²; ¹University of Tennessee; ²Y-12 National Security Complex

Zircaloy-4 (Zr-4) cylindrical tubes are commonly used in nuclear industry and for many applications requiring mechanical stability in extreme environments. Due to its crystal structure and processing techniques, significant texture and anisotropic mechanical properties are possible. In this study, combined axial-torsional testing is employed to probe macroscopic stress-strain behavior in three dimensions and corresponding yield surface in octahedral plane is obtained. Zr-4 rod samples are evaluated under pure tension and torsion, and Zr-4 tube samples are characterized under pure tension, torsion, and combined

(tension and torsion) loading. 3-D digital image correlation using VIC-3D system was implemented to evaluate surface deformation patterns for evaluating strain localizations. Limited x-ray diffraction based texture analysis is performed to obtain an understanding of the effect of loading path on the material texture. Pole figures for Zr-4 rods and tubes are obtained both in axial and circumferential directions.

Nanocomposites: Processing of Nanocomposites I

Sponsored by: The Minerals, Metals and Materials Society, TMS Structural Materials Division, TMS/ASM: Composite Materials Committee

Program Organizers: Garth Wilks, Air Force Research Laboratory; Jonathan Spowart, Air Force Research Laboratory; Meisha Shofner, Georgia Institute of Technology; John Zhanhu Guo, Lamar University

Monday PM
March 12, 2012

Room: Swan 8
Location: Swan Resort

Session Chairs: Brandon Howe, Air Force Research Laboratory; Garth Wilks, Air Force Research Laboratory

2:00 PM

Development of Al and Co Nanowires by the Method of Phase Separation: *Tanjore Jayaraman*¹; Yuan Tian¹; Jeremy Anderson¹; Jeffrey Shield¹; ¹University of Nebraska

Ability to manipulate nanoscale lengths is important for controlling physical properties in materials including mechanical, electronic, optical, and magnetic properties. Nanocomposites or array of nanowires have wide range of applications in viz. catalysis, solar cells, sensor technology (biological, chemical, photonic, magnetic, and gas). Nanowires with diameters less than 10 nm are known to exhibit many interesting and potentially useful properties. In this work we present the development of sub-10 nm array of nanowires in materials systems (Al-Si, Co-Si and Co-Al), that naturally separate into two distinct phases, and their characterization by x-ray diffraction, scanning electron microscopy, and transmission electron microscopy. By controlling various processing parameters, during physical vapor deposition (magnetron sputtering), including type of substrates, argon flow rate, RF power, substrate temperature, and substrate cooling rate during deposition - the desired two phase fibrous morphology of non-magnetic (Al) and magnetic (Co) nanocomposites were obtained.

2:20 PM

Thermal Modeling of Carbon Nanotube Growth Experiments: Kevin Maxwell¹; Benji Maruyama¹; *Jaimie Tiley*¹; ¹US Air Force Research Laboratory

The use of carbon nanotubes in structural applications requires careful alignment of growth directions. To further refine the processing of these structures, researchers have designed specific heating systems to control growth kinetics and nanotube morphology. In this research, the finite element software Comsol was used to model the laser heating induced thermal behavior of carbon nanotube growth experiments. The analysis consisted of a coupled, multi-scale model governed by the 3D heat equation and a formulation for laser power and intensity. Data for the temperature of the silicon substrate used in the experiments was used to calibrate the model parameters, and the temperature of the nano-scale catalyst particles used to grow carbon nanotubes was predicted from the calibrated model. The results indicate that the temperature of the catalyst particles is similar to the temperature of the silicon substrate and depends on a particle's position with respect to the laser beam.

2:40 PM

Boron Nitride Nanotube Reinforced Aluminum Nanocomposites: *Debrupa Lahiri*¹; Virendra Singh²; Mingdong Bao¹; Luhua Li³; Sudipta Seal²; Ying Chen²; Arvind Agarwal¹; ¹Florida International University; ²University of Central Florida; ³Deakin University

Boron nitride nanotubes (BNNT), with its excellent mechanical properties ($E = 1200$ GPa, tensile strength > 24 GPa) and low density (2.25 g.cm⁻³), is a potential reinforcement for lightweight metal-matrix composites for structural applications. This study reports synthesis and characterization of an aluminum matrix composite reinforced with BNNT. Al-BNNT composite, with 2 and 5 vol.% of reinforcement, is synthesized using two routes - (i) spark plasma sintering; and (ii) cold pressing and sintering in an inert atmosphere. A comparative analysis on densification, microstructural evolution and strengthening of the composite structures, synthesized using the different process routes, is presented.

3:00 PM

Fabrication of Aluminum Matrix Composite Reinforced by Intermetallic Compounds of Various Nano/Micro-Architectures: Can Zhu¹; Yufeng Wu¹; *Gap-Yong Kim*¹; ¹Iowa State University

A novel fabrication technique using spray patterning and pressure-assisted reaction sintering that is capable of synthesizing hierarchically structured metal matrix composites is introduced. The approach uniquely integrates bottom-up and top-down fabrication methods to control nano/microstructures while effectively building large structural components. The spray patterning is utilized to transport Al and/or Ni nanoparticles dispersed in nickel nitrate hexahydrate solution to create nano/micro-architectures that form the reinforcing phase on an aluminum sheet. The patterned sheets are then densified and synthesized into a composite by forming intermetallic compounds of various configurations. Several configurations are fabricated, and bend test results are performed to understand the strengthening contributions from the hierarchical levels.

3:20 PM Break

3:40 PM Invited

From Hard Coatings to Thermoelectrics: Effects of Nanostructure on Fundamental Physical Properties of Hf_{1-x}Al_xN Alloys: *Brandon Howe*¹; Andrey Voevodin¹; Joseph Greene²; Ivan Petrov²; ¹Air Force Research Laboratory; ²University of Illinois

We use the Hf_{1-x}Al_xN alloy as a model system to study the effects of self-assembled and engineered nanostructures on the optical, electronic, thermal transport and elastic properties of Hf_{1-x}Al_xN single crystal layers grown on MgO(001) by reactive unbalanced magnetron cosputter deposition using ellipsometry, temperature-dependent hall effect, picosecond probe thermorefectance and acoustic transport measurements, respectively. I will continue by summarizing a systematic study into the effects of ion bombardment on single crystal reactively-sputtered Hf_{0.7}Al_{0.3}N/HfN superlattice layers and show that I can controllably manipulate the nanostructure in order to study its effects on the physical properties. In all, the physical properties are significantly altered by the nanostructure, leading to independent control of opto-electronic and thermal transport properties and show that by using this growth technique nanostructured transition-metal nitrides can be produced which have great potential for high-temperature energy conversion applications.

4:20 PM

Formation of Nano Dispersed Ceramic-Metallic Composite Coatings: *Ratan Saha*¹; M Farrokhzad¹; T Khan¹; ¹University of Calgary

The use of electrodeposited composite coatings with a nano dispersed ceramic particles have been widely considered for industrial applications in the recent years due to their enhanced hardness and wear resistance properties. In this study, nickel coating reinforced with a dispersion of nano sized Al₂O₃ particles was developed using electrodeposited technique and the coatings were investigated with respect to hardness and wear properties. The effects of post-deposition heat treatment on the morphology of the composite coatings were also studied. The



TMS 2012

141st Annual Meeting & Exhibition

MONDAY PM

microstructural features of the coatings were characterized by scanning electron microscopy and energy dispersive x-ray spectroscopy. Micro-indentation and wear tests were conducted to evaluate the hardness and wear resistance, respectively, of the deposited layer. The results showed that the hardness and the wear properties of the coatings increased with an increase of ceramic particles in the composite coating. The post-deposition heat treatment softens the coated layer.

4:40 PM

Microtruss Cellular Nanocomposites: *Khaled Abu Samk¹; Guojie Huang²; Milan Skocic³; Hatem Zurob²; David Embury²; Olivier Bouaziz⁴; Glenn Hibbard¹; ¹University of Toronto; ²McMaster University; ³Grenoble Institut of Technology; ⁴ArcelorMittal Research*

New types of cellular nanocomposites can be created by carburizing the external surface of low carbon steel microtruss materials. Microtruss architectures are designed to resist externally applied loads through axial deformation and as such can exhibit significantly enhanced strength and stiffness when compared to conventional metal foams. They can also exhibit multifunctional characteristics such as energy absorption and thermal management. This study used the high formability of simple low carbon sheet steels to create an initial microtruss cellular architecture by plastic deformation. Mechanical strength was imparted via a graded composite structure wherein an external skin of ultrafine internal length scale martensite was created by carburizing. The microtruss nanocomposites exhibited up to a five-fold increase in compressive strength when compared to the conventional low carbon steel microtruss reference. The failure mechanisms were investigated in order to determine an optimal composite structure.

5:00 PM

Manufacturing and Characterization of an Auxetic Composite: *Fu-Pen Chiang¹; ¹Stony Brook University*

An auxetic material has a negative Poisson's ratio. As a result, it has some uncommon responses when loaded mechanically. For example, it resists indentation. Thus, the material could be used for platforms for which surface deflection due to load is not desirable. It has a very large shear modulus, thus it could be ideal as a core material for sandwich plates whose prevailing failure mode is core shear failure. Third, it also reduces noise propagation, thus it could be used as a noise insulation material. In this paper, we show how to transform an ordinary PVC foam composite into an auxetic composite by 3-D compression and heat treatment. Tests were performed to show the resulting material's resistance to indentation and low velocity impact. A sandwich plate using fiberglass face sheets was made and loaded in three-point bending. The failure mode was changed to interfacial disbond mode.

5:20 PM

Discarded Ultrafine Particulate Carbonaceous Materials Used as Reinforcers of Rubber Vulcanized Products: *Guillermo Martín-Cortés¹; Fabio Esper¹; Luiz Sálvio Galvão Dantas²; Wildor Hennies³; Francisco Valenzuela-Díaz³; ¹Universidade Estácio de Sá; ²Bentonisa-Bentonita do Nordeste S.A.; ³Polytechnic School-University of São Paulo*

Vulcanized rubber products as tires, auto parts, sport-shoes, and others are widely spread. Raw materials for vulcanized rubber products come from industrial process generating CO₂ emissions. These products commonly use, at least 40phr of carbon-black filler obtained from petroleum in a contaminant process of incomplete burning of the fuel. NAOB® a rubber / organoclay nanocomposite material developed to make vulcanized rubber products without carbon-black is reinforced with only 10phr of organoclay. So to keep the material specific volume, maintaining or increasing its technological characteristics, additional reinforcing materials are used. Between the additional materials, are ultrafine particulate materials discarded from mining of some carbonaceous minerals that can be used directly from the mine or through an organic modification. This paper show some very good technological results obtained in rubber formulations after replacing the carbon-black by these set of materials.

5:40 PM

Properties of Additional Reinforcers Materials Used to Complement NAOB – A Rubber / Organoclay Nanocomposite Material: *Fabio Esper¹; Guillermo Martín-Cortés¹; Luis Sálvio Dantas²; Adriana Cutrim²; Wildor Hennies³; Francisco Valenzuela-Díaz³; ¹Universidade Estácio de Sá; ²Bentonisa - Bentonita do Nordeste S.A.; ³Escola Politécnica da Universidade de São Paulo*

Vulcanized rubber products are widely spread. Auto parts, tires, sport shoes and other products are examples of it. Most of the raw materials used in the formulations of vulcanized rubber products come from industrial process consuming time and energy but also generating CO₂ emissions during the respective transforming processes. The traditional main reinforcing material used in rubber formulations is carbon-black which is a petroleum derivative obtained by the incomplete burning of the fossil fuel. The NAOB – a rubber / organoclay nanocomposite material was developed to make vulcanized rubber products without carbon-black. In NAOB the primary reinforcer is the organoclay, which participates in the formulation of the nanocomposite in much smaller quantities than the carbon-black. So to keep the material specific volume, maintaining or increasing its technological characteristics, additional reinforcing materials are used. This article presents some of the additional reinforcing materials for the NAOB and their technological characteristics.

Neutron and X-Ray Studies of Advanced Materials V: Centennial: In Honor of Dr. Gabrielle Long

Sponsored by: The Minerals, Metals and Materials Society, TMS Structural Materials Division, TMS/ASM: Mechanical Behavior of Materials Committee, TMS: Chemistry and Physics of Materials Committee

Program Organizers: Rozaliya Barabash, Oak Ridge National Laboratory; Xun-Li Wang, Oak Ridge National Laboratory; Gernot Kostorz, ETH Zurich; Lyle Levine, National Institute of Standards and Technology; Peter Liaw, Univ of Tennessee; Yandong Wang, Beijing Institute of Technology; Brent Fultz, California Institute of Technology

Monday PM
March 12, 2012

Room: Southern I
Location: Dolphin Resort

Funding support provided by: Office of Basic Energy Sciences, U.S. Dept. of Energy, Dr. P. Thiyagarajan

Session Chairs: Lyle Levine, NIST; Andrew Allen, NIST

2:00 PM Introductory Comments Lyle Levine

2:05 PM Keynote

Microstructural Changes in Nanotwinned Cu Resulting from Unidirectional and Reversed High Pressure Torsion: *C. Shute¹; Y. Liao¹; K. Tsuchiya²; Y. Zhu³; A. Hodge⁴; T. Barbee⁵; Julia Weertman¹; ¹Northwestern University; ²National Institute of Materials Science; ³North Carolina State University; ⁴University of Southern California; ⁵Lawrence Livermore National Laboratory*

The response of the microstructure of Cu samples containing aligned columns of nanotwins to extreme shear stress produced by high pressure torsion has been studied. The torsion was applied both in one direction only and reversed. It is found that under conditions of unidirectional torsion in which the overall shear strain is about 20, the shear deformation is largely confined to the near surface regions. The twins are destroyed to the depth at which the shear strain drops to about 1. Repeated reversal of the torsion up to the same overall shear strain destroys the twin structure altogether, leading to elongated grains of about 1 micrometer in length. Data will be presented of results of testing over a range of maximum torsions and numbers of reversals.

2:30 PM Invited

The Ultra-Small Angle X-Ray Scattering Instrument (USAXS) Instrument – Delivering Unique Science for More Than 25 Years: *Jan Ilavsky¹; Peter Jemian¹; ¹APS, Argonne National Laboratory*

A prototype USAXS was tested in 1985 at CHESS. In 1987, the instrument began serving users at NSLS X23A3. From 1998, the second-generation USAXS was installed at Advanced Photon Source, first at 33ID-D, then 32ID-B, and now 15ID-D. Since 1986, Gabrielle Long was the scientific lead navigating the instrument to serve a broad scientific community while continuing to develop. New geometries and uses were added: 2D collimated geometry, USAXS imaging, and lately combination with short pinhole SAXS and USAXS-XPCS. USAXS value goes beyond its user community, as it became the producer of standard samples for absolute intensity calibration. To satisfy requirement of future in-situ science investigations, upgrade plans include on-fly (continuous) scanning to reduce the measurement time of a single sample and an increase of operating energies up to 30keV. We will review the USAXS history, user science examples, and Gabrielle Long's influence on this unique and invaluable scientific resource.

2:50 PM Invited

Small-Angle Neutron Scattering Studies of Cement Hydration: *Andrew Allen¹; Jeffrey Thomas²; Hamlin Jennings³; ¹NIST; ²Schlumberger-Doll Research; ³MIT*

Despite much research, basic questions remain regarding the internal structure and role of water in ordinary Portland cement (OPC) concrete, the world's most widely used manufactured material. Most questions concern the primary hydration product and strength-building phase of OPC paste, the calcium silicate hydrate (C-S-H) gel, which precipitates as clusters of near-amorphous, nanoscale particles with an associated water-filled inter-particle pore system. In recent years, neutron scattering experiments, especially SANS, have made significant progress, and provided new insights into the fundamental physics and chemistry of cement hydration. For example, they reveal (for hydration under ambient conditions) that C-S-H has a higher atomic packing density than its mineral analogues, tobermorite and jennite. We can relate this to the chemical shrinkage of concrete during cement hydration, with implications for the design of new concretes incorporating pozzolanic cement additions intended to address environmental concerns and sustainability issues.

3:10 PM

Ultra-Small-Angle X-Ray Scattering—X-Ray Photon Correlation Spectroscopy Studies of Equilibrium and Nonequilibrium Dynamics: *Fan Zhang¹; Andrew Allen¹; Lyle Levine¹; Jan Ilavsky²; Gabrielle Long²; ¹National Institute of Standards and Technology; ²Argonne National Laboratory*

Ultra-small-angle X-ray scattering—X-ray photon correlation spectroscopy (USAXS-XPCS) is a new measurement technique for the study of equilibrium and slow nonequilibrium dynamics in disordered materials. Taking advantage of Bonse-Hart crystal optics, this technique fills a gap between the accessible scattering vector ranges of dynamic light scattering and conventional X-ray photon correlation spectroscopy. It also overcomes the limits of visible light scattering techniques imposed by multiple scattering and is suitable for the study of optically opaque materials containing near-micrometer sized structures. USAXS-XPCS has been applied to study the equilibrium dynamics of micrometer-sized colloidal dispersions and nonequilibrium dynamics of polymer composites and alloy steels. We anticipate that this technique will be important in the understanding of thermally-induced equilibrium dynamics of soft materials and nonequilibrium behavior of both soft and hard materials, and lead to technical payoffs in a wide range of areas such as the manufacture of self-repairing biologically critical materials.

3:25 PM Invited

Probing Materials' Reactivity Using X-Ray Pair Distribution Function Methods: *Karena Chapman¹; ¹Argonne National Laboratory*

Understanding how advanced functional materials react and transform, at an atomic scale, is a characterization challenge with many diverse phenomena possible; components with varying particle size, morphology, and microstructure can evolve from multi-atom clusters to multi-million atom crystals. The pair distribution function (PDF) method shows great promise for providing quantitative insight such reactions. Recent advances in experimental methods, have improved the efficiency of X-ray PDF measurements, to allow time-resolved experiments with sufficient resolution to study reactions in solid materials. The PDF analysis probes the complete reaction from clusters to bulk, amorphous or crystalline, liquid or solid. This is in contrast to Bragg crystallographic analysis which is "blind" to the clusters which nucleate before growing into long-range ordered materials. The structural insights from the PDF data are obtained in parallel with phase concentration to allow different components to be distinguished and a robust quantitative analysis.

3:45 PM Invited

The Many Facets of Guinier-Preston Zones in Al-Rich Al-Ag: *Gernot Kostorz¹; ¹ETH Zurich*

The solubility of silver in aluminum decreases rapidly with decreasing temperature from a maximum of about 25 at.% to less than 0.2 at.% below 200°C. Alloys containing <15 at.% Ag begin to decompose below about 420°C by forming coherent quasi-spherical Guinier-Preston zones followed by a metastable hexagonal phase and the stable Ag₃Al phase. The metastable miscibility gap has been studied by many researchers for over fifty years, but there is still no agreement on the assignment of metastable phases and temperature regimes. In particular, combined results of small-angle scattering and diffuse scattering have shed doubts on the existence of the presumed ϵ phase above about 170°C. These data and results of HAADF electron diffraction suggest that the zones may not always be homogeneous, but have a core-shell structure. The current state of knowledge will be assessed in the light of recent experiments and theoretical calculations published in the literature.

4:05 PM Break**4:10 PM**

The Bonse-Hart Ultra-Small-Angle Scattering Camera Worldwide: Current Status: *Pete Jemian¹; ¹Argonne National Laboratory*

The double-crystal camera design used to measure most ultra-small-angle scattering (USAS) measurements owes its name to two researchers, Ulrich Bonse and Michael Hart, who in 1965 defined the minimum geometry necessary to achieve practical measurements. Since its first incarnation in the 1949 thesis of Paul Kaesberg, the USAS instrument has undergone continual improvement in its design, leading to a wide range of scientific discovery in many fields including bone cement, energy materials, aerospace alloys, reactor steels, automotive tires, colloidal materials, flame pyrolysis, and many others. This talk will describe the development of the Bonse-Hart USAS instrument, noting those who advanced the art, and summarize the current status worldwide of instrumentation for USAS as it expands the base of scientific knowledge. This presentation is in honor of Dr. Gabrielle Long.

4:25 PM Invited

Waveguide-Enhanced Grazing-Incidence X-Ray Scattering: Probing Buried Nanostructures in Thin Films in Three Dimensions: *Jin Wang¹; Zhang Jiang¹; ¹X-ray Science Division, Argonne National Laboratory*

Grazing-incidence x-ray scattering (GIXS) can provide invaluable data to reveal structure of surfaces, interfaces and thin films. Because of their probing q-range (10⁻³-10 nm⁻¹, translating to a real-space length scale ranging from 0.1 nm to 1 μ m) and temporal resolution (10⁻³-1 s), grazing-incidence small-angle and wide-angle x-ray scattering (GI-SAXS and -WAXS) become increasingly important in characterizing nanocomposites and their formation at surfaces and interfaces in real time and real



TMS 2012

141st Annual Meeting & Exhibition

MONDAY PM

conditions. In general, GIXS data yields only the in-plane structure and its correlation in planar samples. X-ray standing waves, generated by the interference of the scattered x rays from parallel surfaces of a thin film, can be used to enhance or reduce the scatterings from certain depths of the film. This work and the use of the Advanced Photon Source were supported by the U.S. Department of Energy, Office of Science, Office of Basic Energy Sciences, under Contract No. DE-AC02-06CH11357

4:45 PM Invited

Interrelation between Grain-Size-Induced and Strain-Induced Broadenings of X-Ray Diffraction Profiles: What We Can Learn from It about Nano-Structured Materials?: *Emil Zolotoyabko*¹; ¹Technion

One of the classical applications of X-ray diffraction to materials science is the measurement of grain size and average parameters of spatial strain distribution, thus characterizing the microstructure of polycrystalline materials. Two average strain parameters are of great importance: the mean strain value (i.e. the first moment of strain distribution), which leads to the shift of the diffraction peak position, and the mean square root value (i.e. the second moment or dispersion of strain distribution), which results in diffraction peak broadening. Usually, the two sources of peak broadening, i.e. due to finite grain size and dispersion of strain distribution, are considered independently. In this paper, we offer a phenomenological equation which relates the dispersion of strain distribution to grain size via the width of grain boundaries and the lattice disorder therein. Worked examples include crystallization processes from the amorphous phase and the order-disorder phase transitions in bio-composites during annealing.

5:05 PM Invited

Studies of the Early Stages of Temperature Induced Glass Devitrification: *Wim Bras*¹; G Neville Greaves²; Simon Clark³; Martin Kunz³; Vladimir Martis⁴; Sabyasachi Sen⁵; ¹Netherlands Organization for Scientific Research; ²University of Wales; ³Lawrence Berkeley Laboratory; ⁴University College London; ⁵UC Davis

The formation of glass ceramics by heat treatments is a mature technological technique. However, the early stages of the process are difficult to study due to the nuclei and nanocrystal size. On-line X-ray scattering methods provide a wealth of information from the earliest stages of the process till larger crystallites have grown. We have studied the devitrification process of different glasses. The crystalline phases in the bulk compared to the surface and the growth kinetics and model of the bulk phase could be quantified. It was possible to determine the stress to which crystallites are subjected due to the mismatch between the specific volumes of the crystallites and the base glass. Surprising was that in some cases the exposure to X-rays induced crystallisation. This was not confined to the area that was directly exposed to the X-ray beam but also in a region of around 300 microns around this.

5:25 PM

Directly Imaging Microstructures Using Ultra-Small-Angle X-Ray Scattering: *Lyle Levine*¹; Gabrielle Long¹; Fan Zhang¹; Jan Ilavsky²; ¹National Institute of Standards and Technology; ²Advanced Photon Source

Ultra-Small-Angle X-ray Scattering (USAXS) imaging has been developed recently to probe directly the morphology and three-dimensional arrangements of small-angle scattering objects. USAXS imaging is an extremely high contrast full-field imaging technique that is size and shape sensitive, where images acquired at different reciprocal scattering vectors can reveal different microstructural features within the same sample volume. Examples will range from model tests on geometrically simple systems to self-assembly of amorphous carbon nanowires embedded in a polymer.

5:40 PM Invited

Measurement of $S(q)$ as $q \rightarrow 0$ in Amorphous Si: *Gabrielle Long*¹; Ruobing Xie¹; Steven Weigand¹; Simon Moss²; Sjoerd Roorda³; Salvatore Torquato⁴; Paul Steinhardt⁴; ¹Argonne National Laboratory; ²University of Houston; ³Université de Montréal; ⁴Princeton University

Amorphous silicon is a continuous random network (CRN) tetrahedrally coordinated glass. Florescu et al. [1] recently conjectured that a tetrahedrally coordinated CRN glass, which also is "hyperuniform" [2], has substantially larger photonic band gaps than CRN glasses that are not. A hyperuniform point pattern is one in which the variance of points scales with surface area rather than with volume, and $S(q \rightarrow 0) = 0$ the same as in crystalline solids, which are the simplest form of hyperuniformity. It has been suggested that the band gap properties of real amorphous materials is related to their degree of hyperuniformity [1]. Our research looks into the nature of a-Si via a highly sensitive measurement of the long wavelength limit of the structure factor $S(q \rightarrow 0)$, which can indicate the presence of hyperuniform ordering. [1] M. Florescu, et al., Proc. Nat. Acad. Sci. USA (2010) 20658 [2] S. Torquato, F.H. Stillinger, Phys. Rev. E 68 (2003) 041113

Pb-Free Solders and Other Materials for Emerging Interconnect and Packaging Technologies: Studies of Mechanical Properties and Effects of Current II

Sponsored by: The Minerals, Metals and Materials Society, TMS Electronic, Magnetic, and Photonic Materials Division, TMS: Electronic Packaging and Interconnection Materials Committee *Program Organizers:* Iver Anderson, Ames Laboratory; Sung Kang, IBM; Albert Wu, National Central Univ; Laura Turbini, Research in Motion; Tae-Kyu Lee, Cisco Systems; Govindarajan Muralidharan, Oak Ridge National Lab; John Elmer, Lawrence Livermore National Lab; Yan Li, Intel

Monday PM
March 12, 2012

Room: Swan 9
Location: Swan Resort

Session Chair: Tae-Kyu Lee, Cisco Systems

2:00 PM Invited

EBSD Investigation of the Relationship between Sn Orientation and IMC Evolution during Electromigration in Idealized SnAgCu Interconnects: *Christopher Kinney*¹; Xioranny Linares¹; Kyu-Oh Lee²; Fay Hua²; J.W. Morris¹; ¹U.C. Berkeley; ²Intel Corporation

In this study, idealized SnAgCu 305 samples, both polycrystalline and single crystalline of varying orientations, were examined initially in the EBSD. It is known that diffusion rates through tin can vary greatly depending on the orientation; and electromigration is also related to diffusion. Samples were subjected to 10,000 A/cm² at 100C for varying amounts of time, and re-examined in the EBSD. When the EBSD results are presented in the typical IPF map, correlations between various samples are not evident. However, when the EBSD results are viewed with respect to current flow, relationships between samples and relationships between the initial tin orientation and the orientation of the IMC Cu₆Sn₅ become clear. It was observed that certain orientations favor rapid IMC growth whereas others do not. Furthermore, some surprising results were found about the difference in IMC growth between single crystalline and polycrystalline samples.

2:25 PM Invited

Effects of Zn Addition on Electromigration Behavior of Sn-1Ag-0.5Cu Solder Interconnect: H. Liu¹; Q. Zhu¹; J. Guo¹; J. Shang²; ¹Institute of Metal Research; ²University of Illinois

Role of Zn addition on the electromigration behavior of SnAgCu alloy was investigated by examining the microstructure and mechanical properties of the Sn-1Ag-0.5Cu and Sn-1Ag-0.5Cu-1Zn solder interconnects. It was found that after electromigration, the polarity effect and strength loss occurred in the Sn-1Ag-0.5Cu solder interconnect but were suppressed in the Sn-1Ag-0.5Cu-1Zn solder interconnect. For the Sn-1Ag-0.5Cu-1Zn solder interconnect, the strong binding of Zn with Cu prevented the dissolution of the IMC at the cathode, and the reverse diffusion of the Zn elements counteracted the increasing vacancy concentration so that the strength loss due to electromigration was successfully inhibited.

2:50 PM

A New Physical Model for Rapid Life Prediction of Pb-Free Flip Chip Solder Joints in Electromigration Tests: Tian Tian¹; Feng Xu²; Jung Kyu Han¹; Daechul Choi¹; Yin Cheng²; Lukas Helfen²; Marco Michiel³; Tilo Baumbach²; King-Ning Tu¹; ¹UCLA; ²Karlsruhe Institute of Technology; ³ESRF

The early stage evolution of voids nucleation and growth induced by electromigration in Pb-free flip chip solder joints has been studied. We have quantitatively measured the growth rate of voids produced during electromigration by 1.0×10^4 A/cm² and 7.5×10^3 A/cm² respectively at 125 °C by synchrotron radiation high resolution x-ray laminography. Johnson-Mehl-Avrami phase transformation theory is proposed to provide a physical model to estimate failure time of the solder joints at early stages. The results were confirmed by statistical model of Weibull distribution function of lifetimes obtained under the same testing conditions. A intrinsic link between the Johnson-Mehl-Avrami model and Weibull distribution was discussed.

3:10 PM

Microstructural Evolution in Nearly Bi-Layered, Two-Phase Alloys from Current Stressing: Andre Lee¹; K.N. Subramanian¹; ¹Michigan State University

Imposition of high current densities causes material migration due to momentum transfer between electrons and atoms/ions. A clear quantitative understanding of the pathway of atoms/ions movement in multi-phase materials is far from complete. Recently, our group has developed a technique to fabricate solder joints with a nearly bi-layer microstructure. Using this type of joint, microstructural evolution in two-phase electronic solder joints were studied using Synchrotron X-rays, Optical, and Scanning Electron Microscopies. These studies have provided unique opportunities to address materials movement, microstructure evolution, as well as solid-state reactions, due solely to the influence of current stressing.

3:30 PM

No Current Crowding to Current Crowding Transition in Pb-free Solder Joint with Extremely Thick Cu: Jung Kyu Han¹; Daechul Choi¹; Masaru Fujiyoshi²; King-Ning Tu¹; ¹UCLA; ²Hitachi Metals, Ltd.

To reduce the current crowding effect, thick Cu Under-Bump-Metallization has been widely adopted in the electronic industry. As a future interconnects technology, Through-Si-Via 3D interconnects or micro-bump structures is believed to have even less current crowding. However, the statistical experiment and 3D finite element simulation indicate that there is a no current crowding to current crowding transition as the void grows. It makes a unique failure mechanism, different from the typical pancake void in flip-chip. Moreover, the study of marker displacement shows two different stages of the drift velocity, which demonstrates the back-stress effect. Since it takes time to build up the compressive stress at the anode, the drift velocity is faster in early stage and slower in later stage. Therefore, the electromigration flux can be likely to be overestimated when the constant velocity is assumed with one measurement or the observation is limited to the early stage only.

3:50 PM Break**4:00 PM**

Effect Of Alloying Elements On Electrification-Fusion Phenomenon Of Sn-based Eutectic Alloys: Gong-An Lan¹; Truan-Sheng Lui¹; Li-Hui Chen¹; ¹Chung-Kung University, Tainan, Taiwan

Microstructural features of Sn-based eutectic alloys (Sn-9Zn and Sn-37Pb) on the electrification-fusion phenomenon are investigated in this study. Experimental results show that the critical fusion current densities (CFCD) of Sn-based alloys are closely related to resistivity of individual phase. The electrical current densities required for triggering microstructural evolution for Sn-9Zn alloy is larger than the CFCD of pure Sn (1399 Amp cm⁻²). Through the in-situ examination of microstructural evolution during electrification-fusion tests, the initial site of electrification-fusion-induced failure significantly emerges from individual Sn-based eutectic phase. The predominant liquidation phase of Sn-9Zn is Sn/Zn eutectic phase; that of Sn-37Pb comprises Sn/Pb eutectic phase, primary Sn phase and Pb-rich phase. According to the fusion distributed density in the liquidation zone, Sn-9Zn alloy has the great potential to replace Sn-37Pb alloy in the future electrification case.

4:20 PM

Irregular Cu Cathode Dissolution in Solder Joints under Electron Current Stressing: Jia-Hong Ke¹; Ting-Jia Huang¹; Ting-Li Yang¹; C. Robert Kao¹; ¹Department of Materials Science & Engineering, National Taiwan University

Metallization dissolution is one of the degradation processes in solder joints under current stressing. This process tends to occur on the cathode side, creating highly irregular interface. The mechanism responsible for such microstructure remains unidentified. In this study, a Cu/Sn/Cu line structure is used to reveal the microstructure evolution of cathode dissolution. We find a pronounced grain boundary grooving of intermetallic compound before the irregular cathode starts to develop. The grooving process is mainly driven by electromigration along grain boundaries or triple junctions. The interdiffusion and reaction in intermetallic phase are more significant at the valley of the grooves, leading to an irregular cathode interface. The result shows that electromigration along the grain boundaries of intermetallic phase has a large influence on the final cathode interface.

4:40 PM

Influence of Cu Column Under-Bump-Metallizations on Current Crowding and Joule Heating Effects of Electromigration in Flip-chip Solder Joints: Yu-Chun Liang¹; W. A. Tsao¹; Chih Chen¹; Da-Jeng Yao²; Yi-Shao Lai³; ¹National Chiao Tung University; ²National Tsing Hua University; ³Central Laboratories, Advanced Semiconductor Engineering, Inc.

Electromigration behavior of SnAg solder bumps with and without Cu column under-bump-metallizations (UBMs) have been investigated under the current density of 2.16×10^4 A/cm² at 150°C. When SnAg solder bumps with Ni UBMs were current stressed, open failure occurred in the bump that has electron flow direction from the chip side to the substrate side. However, for the case with Cu column UBMs, cracks formed along the interface of Cu₆Sn₅ IMCs and the solder on the substrate side in the bump that has electron flow direction from the substrate side to the chip side. A three-dimensional simulation of current density distribution indicated that current crowding effect resulted in the void formation on both the chip and the substrate side for the two kinds of solder bumps. Another important finding is that the alleviation of current crowding by Cu column UBMs also helped decrease Joule heating effect in solder bumps during current stressing.



TMS 2012

141st Annual Meeting & Exhibition

MONDAY PM

5:00 PM

Study of Joule Heating Effects in Eutectic SnPb and SnAg Solder Joints under High Current Density: *Xu Zhang*¹; *Sihan Liu*¹; *Limin Ma*¹; *Guangchen Xu*¹; *Fu Guo*¹; ¹Beijing University of Technology

Basic understanding of heating conduction in electronic solder joints due to the Joule heating effect was carried out by using the infrared microscopy. In order to interpret the corresponding mechanism and provide a better understanding to Electromigration (EM) studies, a newly developed 1D solder joint with same cross-sectional area in solder alloy and Cu electrodes was employed in our thermal imaging analysis. Both eutectic SnPb and SnAg solder alloys were used to fabricate the joints due to their distinct electrical resistivity and thermal conductivity in nature. Joule heating effects under high current density were investigated in this study. Accordingly, the transient and steady-state heat conduction were identified and compared with different experimental conditions. Most important, effects of microstructure evolution of solder joints on temperature redistribution have been investigated as well. The results suggested that the phase segregation induced by EM can alter the temperature distribution of solder joints.

5:20 PM

Comparison of Electromigration Induced Failure between 3D IC and Flip Chip Solder Joints: *Hao Hsu*¹; *Fan-Yi Ouyang*¹; ¹Department of Engineering and System Science, National Tsing Hua University, Taiwan

The reliability issues of 3D IC on electromigration (EM) are being increasingly important since the raising demands on multiple functions and greater performance of consumer electronic products. However, due to the early development of 3D IC packaging technology, the details of reliability challenges in 3D IC packaging are still unclear. Different chips in the 3D IC technology are connected by micro bumps and through Si vias. With the reduction of bump sizes to 20 μ m, EM will be an important issue. In this paper, we have successfully studied the failure mechanism and microstructure change on EM in Pb-free micro-solder bumps. The experimental results of 3D IC were compared to that of flip chip solder joints, suggesting 3D IC exhibited better EM resistance possibly due to larger back stress. Furthermore, 3D simulation and in-situ infrared microscopy were also used to understand the temperature gradient and temperature distribution in the solder joints.

5:40 PM

Study of Electromigration Tests in Ultra-Low-Bump-Height Lead-Free Solder Joints with Nickel UBM Using Kelvin Bump Structure: *Ping Ju Ho*¹; *Yuan-Wei Chang*¹; *Chih Chen*¹; ¹National Chiao Tung University

As electronic products become smaller, three-dimensional integrate circuit (3D-IC) has received more attention recently. In this study, the 5 μ m high Sn2.5Ag solder joint were used to observe the failure mode in the ultra-low bump height case. To precisely monitor the different stages of failure during accelerated EM testing, a specific Kelvin bump structure is designed and fabricated in these samples. While a 8.5 $\times 10^3$ A/cm² current density was applied at 200 °, the microstructures at different stages with the 5 %, 20 %, 100 %, 500 % resistance increase were obtained by scanning electron microscopy (SEM). The resistance curve showed three different stages, which increased rapidly in early stage, then maintained a certain linear slope at middle stage. Finally, the resistance rapidly increases again. With the proper designed Kelvin bump structure and well controlled test conditions, the different stages during EM test can be studied systematically.

Phase Stability, Phase Transformations, and Reactive Phase Formation in Electronic Materials XI: Phase Equilibria and Transformations of the Pb-free Solders and Thermoelectric Materials

Sponsored by: The Minerals, Metals and Materials Society, TMS Electronic, Magnetic, and Photonic Materials Division, TMS: Alloy Phases Committee

Program Organizers: Chih-Ming Chen, National Chung Hsing University; Jae-Ho Lee, Hongik University; Ikuro Ohnuma, Tohoku University; Clemens Schmetterer, TU Bergakademie Freiberg; Yee-Wen Yen, National Taiwan University of Science and Technology; Shih-Kang Lin, University of Wisconsin – Madison

Monday PM
March 12, 2012

Room: Swan 10
Location: Swan Resort

Session Chairs: Ikuro Ohnuma, Tohoku University; Clemens Schmetterer, TU Bergakademie Freiberg

2:00 PM Invited

Directional Solidification and Liquidus Projection of Sn-Co-Cu Alloys: *Kai-Wen Pan*¹; *Sinn-Wen Chen*¹; *Chia-Ming Hsu*¹; *Che-Wei Hsu*¹; ¹National Tsing Hua University

Ternary Sn-Co-Cu alloys are important to the electronic soldering. Liquidus projection is useful for the understanding of alloy solidification. Thirty seven ternary Sn-Co-Cu alloys were prepared from pure constituent elements. Their liquidus temperatures and phase transformation temperatures were determined by differential thermal analysis. The alloys were melted at temperatures higher than their liquidus temperatures and then quenched in air. The primary solidification phases were determined based on the microstructures and compositional analysis results of the as-solidified alloys. Directional solidification experiments of the Sn-5.0at%Co-15.0at%Cu and Sn-3.0at%Co-77.0at%Cu alloys were carried out to facilitate identification of primary solidification phases. The liquidus projection of the Sn-Co-Cu ternary system was constructed based on the experimental results. No ternary intermetallics as the primary solidification phases are found. All of the primary phases are terminal solid solutions and binary intermetallics, and are Sn, CoSn₃, CoSn₂, CoSn, Cu₆Sn₅, Cu₃Sn, Co₃Sn₂, γ , β , Cu and Co phase.

2:20 PM

Early Stages of Solidification in Sn-Cu and Sn-Cu-Ni Solders: *Christopher Gourlay*¹; *Sergey Belyakov*¹; *Adrian Chiang*¹; ¹Imperial College London

Near-eutectic Sn-Cu and Sn-Cu-Ni alloys are widely used as Pb-free solders. For example, Sn-0.7Cu is often sold as a low-cost hobby solder and Sn-0.7Cu-0.05Ni is widely used in microelectronic assembly. This paper investigates the origin of microstructure during solidification of these alloys with a focus on nucleation and the early stages of growth. We examine how the nucleation difficulties of Sn influence the solidification sequence and the competition between coupled eutectic growth and growth of the primary phases in Sn-0.7Cu, Sn-0.9Cu and Sn-0.7Cu-0.05Ni. The paper then discusses the influence of Ni on the nucleation of Sn, the growth morphology of primary (Cu,Ni)₆Sn₅ and the onset of eutectic growth.

2:35 PM

Unidirectional Solidification of Eutectic Alloys in Thermoelectric Pb-Ag-Sb-Te: *Hsin-Jay Wu*¹; *Sinn-Wen Chen*¹; *Teruyuki Ikeda*²; *G. Jeffery Snyder*²; ¹National Tsing Hua university; ²Materials Science, California Institute of Technology

Unidirectional solidification processing of two eutectic alloys with compositions of Ag-40.0at%Sb-36.0at%Te (alloy#1) and Pb-22.0at%Ag-40.0at%Sb-36.0at%Te (alloy #2) were performed using the Bridgman method. In both of the as-solidified alloys, formation of rod or lamellar Ag₂Te phase in a matrix composed by the ternary AgSbTe₂ and d-(Sb₂Te)

phases were investigated. These phases were resulted from a Class I reaction: $L \rightarrow Ag_2Te + AgSbTe_2 + \delta - (Sb_2Te)$. Moreover, the volume fraction of Ag_2Te phase in the alloy #2 changed along the temperature descending direction and caused a rod-eutectic to lamellar-eutectic transition. An electron backscattered diffraction technique (EBSD) was employed to examine the orientation relationship between the Ag_2Te phase and the matrix phases. The Seebeck coefficients at room temperature were measured using a scanning Seebeck coefficient probe, and were $\sim 80 \mu V/K$ of the alloy #1 and $\sim 125 \mu V/K$ of the alloy #2, respectively.

2:50 PM

Phase Equilibria and Solidification of Ternary Sn-In-Cu Alloys: *Shih-Kang Lin*¹; Sinn-Wen Chen²; ¹National Cheng Kung University; ²National Tsing Hua University

Sn-In alloys are promising low-melting-point Pb-free solders. Knowledge of the Sn-In-Cu phase equilibria is important for Sn-In solder applications. The 250 °C isothermal section and liquidus projection of the Sn-In-Cu ternary system are established experimentally. At 250 °C, the $\eta-Cu_6Sn_3$ and $\eta-Cu_2In$ phases form a continuous solid solution and the ternary Cu_3In_2Sn compound is observed. The $\delta_1-Cu_{41}Sn_{11}$ phase is stabilized at 250 °C with the introduction of indium although it transforms into $\alpha-(Cu)$ and $\epsilon-Cu_3Sn$ phases via a eutectoid reaction around 350 °C in the binary Sn-Cu system. Except for the $Cu_{11}In_9$ and Cu_2In_2Sn phases, the other compounds all have significant indium-tin mutual solubilities. In the liquidus projection, a large compositional regime of $\eta-(Cu_6Sn_3, Cu_2In)$ was found as the primary solidification phase and no ternary compound was found in the as-cast alloys. An interesting phenomenon is that the solidification paths of some Sn-In-Cu alloys surpass the liquidus trough after their intersections.

3:05 PM

Microstructure Formation and Phase Stability in Sn-Rich Sn-Ni Alloys: *Sergey Belyakov*¹; Christopher Gourlay¹; ¹Imperial College London

As a result of environmental issues and consequent legislation, lead-free electronics manufacturing has become a global trend. The importance of Ni in lead-free soldering is increasing as nickel is frequently used as a diffusion barrier and solders often contain Ni as an alloying element (e.g. Sn-0.7Cu-0.05Ni). This work investigates microstructure formation during solidification in Sn-Ni alloys containing 0-0.4wt%Ni. Unidirectional and multidirectional solidification experiments have been coupled with analytical electron microscopy to determine the phases that form, the solidification sequence, the crystallography of growth, and the orientation relationships between growing phases. The results are used to discuss the origins of metastability in Sn-rich Sn-Ni alloys.

3:20 PM

Transformation Kinetics and Dimensional Stability of Cu₆Sn₅: *Kazuhiro Nogita*¹; Stuart McDonald¹; Dekui Mu¹; Christopher Gourlay²; Keith Sweatman³; Testuro Nishimura³; ¹The University of Queensland; ²Imperial College London; ³Nihon Superior Co. Ltd.

The use of tin-rich solders on copper substrates typically results in the formation of Cu_6Sn_5 at the soldered-interface. This intermetallic makes important contributions to the mechanical and electrical integrity of the soldered joint. Under equilibrium conditions, Cu_6Sn_5 exists as either a hexagonal or monoclinic allotrope at temperatures above and below approximately 186°C, respectively. In this study the hexagonal-monoclinic transformation is investigated in detail using synchrotron-based, variable temperature X-Ray diffraction. Metastable hexagonal Cu_6Sn_5 was obtained when the cooling rate from the high temperature phase field was sufficiently high. The temperature dependence of the rate of transformation of this metastable phase to the stable monoclinic allotrope was investigated. The significance of the results is discussed with reference to the dimensional stability of Cu_6Sn_5 , which was directly measured in separate dilatometry experiments.

3:35 PM Break

3:50 PM Invited

Materials for HT Lead Free Soldering and Development of the Thermodynamic Database for Relevant Materials: *Ales Kroupa*¹; Alan Dinsdale²; Andrew Watson³; Jan Vrestal⁴; Adela Zemanova¹; Pavel Broz²; ¹Institute of Physics of Materials, ASCR; ²National Physical Laboratory; ³Institute for Materials Research, University of Leeds; ⁴Department of Chemistry, Masaryk University

COST Action MP0602 (Advanced Solder Materials for High Temperature) ran between 2007-2011 and its main objective was to increase the basic knowledge of the crucial properties of alloys that can be used as to current high-temperature Pb-solders. The original aim was to study promising materials and describe their properties, which will allow them to be used successfully in a variety of industrial applications. One of the main outcomes of the Action is a thermodynamic database developed for high temperature lead-free solders (approx. 260-350°C). Currently the database contains 18 elements (Ag, Al, Au, Bi, Co, Cu, Ga, Ge, Mg, Ni, P, Pb, Pd, Sb, Si, Sn, Ti, Zn), but only crucial system assessments are included. The current situation especially in the field of lead free soldering at higher temperatures will be also described here. Examples of existing research projects, mainly oriented towards basic research in this field, will be presented.

4:10 PM

Time-Temperature-Transformation Diagrams of High Purity Powdered Tin: *Kazuhiro Nogita*¹; Stuart McDonald¹; Jonathan Read¹; Shoichi Suenaga²; ¹The University of Queensland; ²Nihon Superior Co. Ltd.

Tin is the main component of contemporary lead-free solders. Under equilibrium conditions, tin exists as either a tetragonal (beta-Sn) or cubic (alpha-Sn) allotrope at temperatures above and below approximately 13°C, respectively. The transformation from beta to alpha, often referred to as 'tin-pest' is poorly understood, despite the phenomena being documented over 100 years ago. With the transition to lead-free solder alloys and the availability of modern analytical techniques there is both an increased need and opportunity to better understand the transformation. This research was conducted to investigate the phase-transformation kinetics of the alpha to beta and beta to alpha transformations in high-purity powdered tin using variable temperature synchrotron XRD analysis. From the results, TTT (time-temperature-transformation) diagrams were developed, with the intention of being used as a baseline for examining the effects of composition in current generation lead-free materials.

4:25 PM

Thermoelectric Materials Design Based on Phase Separation between Half-Heusler MNiSn and Heusler M(Ni,Co)₂Sn (M = Hf, Zr): *Yoshisato Kimura*¹; Naoko Katou¹; Yaw-Wang Chai¹; ¹Tokyo Institute of Technology

Half-Heusler (HH) compounds $MNiSn$ (M = Hf, Zr, Ti) are well-known to show excellent thermoelectric properties at relatively high temperature. Authors found that the n-type properties can be converted to the p-type by the quaternary addition of Co while Co atoms occupy the vacancy site of HH. Further addition of Co results in the formation of a (Full-)Heusler (FH) compound $Zr(Ni,Co)_2Sn$ which exhibits metallic behavior. To understand the phase separation between HH $M(Ni,Co)_xSn$ and FH $M(Ni,Co)_2Sn$ (M = Hf, Zr), microstructure formation according to the phase separation was observed by high-resolution transmission electron microscopy and phase equilibria were investigated in detail. Needle like FH precipitates in the HH matrix at low Co content, and cuboidal HH precipitates in the FH matrix at high Co content. The nano-scaled interfaces formed due to the phase separation could be advantageous for reducing the lattice thermal conductivity through enhancing phonon scattering.



TMS 2012

141st Annual Meeting & Exhibition

MONDAY PM

4:40 PM

Diffusion Mobilities in the Face Centered Phase in the Ag – Cu – In – Sn System: *Wojciech Gierlotka*¹; Md. Azizul Haque¹; ¹YuanZe University

The Ag – Cu – In – Sn system is one of the important lead – free solder alloy. The knowledge about interdiffusion between solder alloys and substrates or UBM layers may help to control the interfacial microstructure evolution and thus to design and optimize suitable soldering and aging process. The optimization of the diffusion parameters and simulation of the atomic mobilities in the face centered phase were done using the DICTRA package. Good agreement between mathematical model and experimental data was obtained.

4:55 PM

Evaluation of Diffusion Barrier between SAC305 and Tellurium: *Chang-Yen Ko*¹; Albert T. Wu¹; Tai-Yin Lin¹; ¹National Central University Dep. Chemical and Materials Engineering

Nickel was selected to be the diffusion barrier by electroless plating between Pb-free Sn3Ag0.5Cu (SAC305) solders and the Tellurium substrates. NiTe intermetallic compound formed at the interfaces between Ni-P and Te while (Cu,Ni)₆Sn₅ and (Ni,Cu)₃Sn₄ formed at the interfaces between solders/Ni-P. SAC305 was reflowed on the Ni-P plated Te substrates and sealed in vacuum. The samples were annealed at 120, 150 and 180°C for different duration of times. The growth kinetics of the IMC layers between SAC305/Ni-P and Ni-P/Te interfaces could be obtained. Nanoindenter was employed to evaluate the mechanical properties of the NiTe layer. EPMA was adopted to analyze the composition.

Processing to Control Morphology and Texture in Magnetic Materials: Processing to Enhance Performance in Rare Earth Permanent Magnets

Sponsored by: The Minerals, Metals and Materials Society, TMS Electronic, Magnetic, and Photonic Materials Division, TMS: Magnetic Materials Committee

Program Organizers: Matthew Kramer, Iowa State University; Mike McHenry, Carnegie Mellon University; David Laughlin, Carnegie Mellon University; Jinfang Liu, Electron Energy Corporation; Bill Soffa, University of Virginia; Ivan Skorvanek, Institute of Experimental Physics

Monday PM

March 12, 2012

Room: Europe 10

Location: Dolphin Resort

Session Chairs: Matthew Williard, Naval Research Laboratory; Oliver Gutfleisch, IFW Dresden

2:00 PM Invited

Advanced Processing and Microstructure of High Performance Permanent Magnets: *Oliver Gutfleisch*¹; Thomas Woodcock¹; Konrad Güth¹; Juliane Thielsch¹; Martina Moore¹; Simon Sawatzki¹; ¹IFW Dresden

In this talk various processing routes yielding highly textured permanent magnets based on rare earth-intermetallics are reviewed. This includes latest progress in sintering NdFeB, thermomechanical processing of melt-spun ribbons and hydrogen-assisted methods (HD and HDDR). Distinct differences in the texture induction in these different types of magnets are elucidated by advanced microstructural characterization down to atomic scale resolution but also using EBSD and magnetic measurements to illustrate meso- and macroscopic texture. Magnetic microstructure is largely affected by texture and this will be shown by in-situ MFM studies. Finally, options for magnetic field processing and bottom-up approaches using nanoparticles or nanoflakes are assessed; this in the context of moving towards textured AND exchanged-coupled systems - the next generation magnets. 1 Gutfleisch et al. *Adv. Mat.* 23 (2011) 821.

2:25 PM Invited

Restructuring of Grain Boundaries of Sintered NdFeB Magnets: *Mi Yan*¹; ¹Zhejiang University

NdFeB sintered magnets are the widest applied RE magnets due to their excellent properties and the high performance/cost ratio. However, since the electrode potentials of the intergranular Nd-rich phases are far lower compared to matrix Nd₂Fe₁₄B, NdFeB magnets are very prone to corrosion. Moreover, the magnetic properties and ductility of NdFeB magnets are sensitive to the morphologies and structure of the grain boundaries. In this paper, through restructuring of grain boundaries, a new approach to substantially improve the corrosion resistance of NdFeB magnets is discussed, together with improvement of magnetic properties and ductility. Some experimental results are presented.

2:50 PM

Investigation of a Unique Texturing Mechanism in Ag-Containing RE₂Fe₁₄B Alloys: Nathaniel Oster¹; Daniel Cavanaugh²; Kevin Dennis²; R. McCallum²; Matthew Kramer²; *Iver Anderson*²; ¹Iowa State University; ²Ames Laboratory

RE₂Fe₁₄B-type permanent magnet alloys display the highest known energy product. Properties can be further increased through the creation of an anisotropic exchange-spring composite. Texture and microstructure control are vital to the creation of an exchange-spring magnet showing desirable properties. One possible method to control these features is through the use of a minor additive. Silver recently has been identified as a promising additive, showing alteration of the solidification microstructure and a unique texture in low wheel speed melt-spun ribbons. In this study the mechanism behind the unique texture in these alloys is investigated through variation of composition and melt-spinning parameters (e.g. wheel speed). Characterization work to be presented includes scanning electron microscopy (SEM), x-ray diffraction (XRD), and orientation imaging microscopy (OIM). The texturing mechanism and its magnetic property implications will be discussed. This work was supported by DOE-EERE, VT Office, PEEM program, through Contract No. DE-AC02-07CH11358 at Ames Laboratory (USDOE).

3:05 PM

Thermodynamics Effect of Magnetic Field on the Solidification of Fe-Nd Eutectic: *Sophie Rivoirard*¹; Eric Beaugnon¹; Thomas¹; ¹CNRS

Magnetic field processing is a new promising tool for the structural and functional control of materials. A high field modifies the Gibbs free energy. As a result, the phase with the highest magnetisation can be stabilised and hence transformation processes are modified. RE-Fe (RE=Pr, Nd) binary alloys have been extensively studied both for their high coercivity and for their important role in the magnetic properties of NdFeB permanent magnets. We used thermomagnetic measurements to evidence the effect of magnetic field on the liquid to solid transition in a Nd-Fe alloy using a Faraday balance. A shift of 1°C/T was observed in the solidification point toward higher temperatures when a magnetic field was applied. A discontinuous rod-like eutectic was observed as well as primary Nd dendrites and a feathered microstructure. A unidirectional solidification of the Nd dendrites parallel to the magnetic field was evidenced, especially for the higher field values.

3:20 PM

Studies of Anisotropic MRE-Fe-B Magnets Fabricated by Hot Deformation in a Vacuum Hot Press (MRE=Nd+Y+Dy): *Wei Tang*¹; Kevin Dennis¹; Nathaniel Oster¹; Matt Kramer¹; Iver Anderson¹; Ralph McCallum¹; ¹Iowa State University

Our mixed rare-earth MRE₂(Fe, Co)₁₄B melt spun ribbons or gas atomized powders in nano-crystalline isotropic microstructures exhibited improved temperature stability at or above 120°C but a relatively lower maximum energy product (BH)_{max} (12 MGOe) compared to about 25 MGOe for (micron-sized) grain-aligned sintered MRE 2-14-1 magnets that were consolidated by traditional high temperature sintering. Unfortunately, these sintered MRE 2-14-1 magnets had a reduced temperature stability due to significant RE segregation within magnetic phase (2-14-1) grains.

In this study, anisotropic magnets induced by grain texture were fabricated by a hot deformation method from over-quenched (substantially amorphous) isotropic MRE 2-14-1 ribbons. The new magnets obtained an improved (BH)max and achieved improved temperature stability. The relationships of magnetic properties and microstructure to compositions and processing parameters of the new sintered magnets were analyzed and discussed. In addition, the effect of extrinsic sintering additives, such as Zn and Al, on magnetic properties was investigated.

3:35 PM Break

3:55 PM Invited

Effect of Particle Size on the Coercivity of R-Fe-B (R=Nd, Pr) Powders Prepared by Surfactant-Assisted Ball Milling: Nilay Gunduz Akdogan¹; Dan Neil¹; Chris Brown¹; Wanfeng Li¹; Dimitris Niarchos²; George Hadjipanayis¹; ¹University of Delaware; ²NCSR "Demokritos"

In this study a two-stage high-energy ball milling (HEBM) was performed to obtain R₂Fe₁₄B (R=Nd, Pr) nanoparticles and nanoflakes; first the coarse powders were made nanocrystalline by milling/melt-spinning, and then they were subjected to surfactant-assisted milling for different times. Different size nanoparticles have been obtained by varying the time of the first stage milling and the speed of the melt-spinning wheel. The coercivity of the nanoparticles was higher than the slurry (nanoflakes) and is increasing with increasing nanoparticle size. The 15 nm Nd₂Fe₁₄B nanoparticles had a coercivity of 9 kOe at 50K and 2.5 kOe at RT. Pr-Fe-B particles made from ribbons precursors had a coercivity above 30 kOe at 50 K. The larger value of coercivity observed in the Pr-Fe-B samples is attributed to the higher magnetocrystalline anisotropy of the Pr-Fe-B compound. Work supported by NSF DMR-1005871, DOE ARPA-E and a Marie Curie Fellowship

4:20 PM Invited

Fabrication of Anisotropic Nanostructured Rare-Earth Bonded Magnets: J.P. Liu¹; ¹University of Texas-Arlington

We report fabrication of anisotropic bonded magnets fabricated using surfactant-assisted ball milling and magnetic-field processing. The fabrication involves preparation of nanocrystalline hard magnetic anisotropic Sm-Co and Nd-Fe-B nanoscale chips by surfactant-assisted ball milling in a magnetic field. The produced nanochips have high aspect ratio with their thickness of tens of nanometers and width and length of several hundred nanometers. It is found that application of magnetic fields during the ball milling strengthens the anisotropy of the nanoflakes and therefore improves the alignment. The aligned hard magnetic nanoflakes can then be processed into anisotropic bonded magnets with high energy product. X-ray diffraction patterns and magnetic characterization show c-axis alignment with strong magnetic anisotropy in the bulk magnets. The high energy product up to 19.1 MGOe has been obtained for anisotropic SmCo₅ bonded magnets compared to 5.4 MGOe for the isotropic bonded magnets.

4:45 PM Invited

Textured Polycrystalline Permanent Magnet Nanoflakes: Jinfang Liu¹; Baozhi Cui¹; ¹Electron Energy Corporation

This paper will review the texture formation, magnetic properties, and microstructure of permanent magnet nanoflakes, which can be formed using ball milling technique for SmCo₅, Sm(Co,Cu,Fe,Zr)_z and Nd₂Fe₁₄B magnets. The magnetic properties of these flakes are very different for these materials. These nanoflakes could potentially be used for the fabrication of permanent magnets with high electrical resistivity, which will reduce eddy current losses and improve motor efficiency.

5:10 PM

Novel Sm-Fe-N Nanoflakes with High Coercivities: Nilay Gunduz Akdogan¹; Wanfeng Li¹; Alexander Gabay¹; George Hadjipanayis¹; ¹University of Delaware

In this work, magnetically hard Sm-Fe-N nanoflakes with coercivity values exceeding 10 kOe have been produced by surfactant-assisted ball milling using two different precursors: Sm₂Fe₁₇ crushed ingot powders

and melt-spun ribbons spun at different speeds. Different techniques were used to prepare the nanoflakes from the crushed powders; in one of the techniques the powders were first nitrogenated and then milled in oleic acid (OA) for different time. In another approach the powders were first milled in oleylamine (OY), and then nitrogenated at 400–450°C. The coercivity was much higher with the former technique, showing values beyond 10kOe. Very promising results were obtained when using melt-spun ribbons as precursors. Nitrogenization of the samples was performed at 400–450 °C and then the nitrogenated powder was milled with OA for 3 h and 4h. The flakes had a thickness below 200nm, an aspect ratio as high as 10²-10³ and H_c>7kOe. Optimization studies are under way and the results will be reported. Work supported by NSF DMR-1005871, DOE ARPA-E and a Marie Curie Fellowship

5:25 PM

Cluster Synthesis, Direct Ordering and Alignment of Rare-Earth Transition-Metal Nanomagnets: Balamurugan Balasubramanian¹; Ralph Skomski¹; Jeffrey Shield¹; George Hadjipanayis²; David Sellmyer¹; ¹University of Nebraska; ²University of Delaware

Rare-earth transition-metal (R-TM) alloys show superior permanent magnetic properties in the bulk, but the synthesis and application of R-TM nanoparticles remains a challenge due to the requirement of high-temperature annealing above about 800 °C for alloy formation and subsequent crystalline ordering. Here we report a single-step method to produce highly ordered R-TM nanoparticles such as YCo₅ and SmCo₅, without high-temperature thermal annealing by employing a cluster-deposition system, and we investigate their structural and magnetic properties. Nanoparticles of size d = 10 nm are monodispersed (s/d ~ 0.15) and have H_c values at T = 300 K of 8.0 and 2.0 kOe for YCo₅ and SmCo₅, respectively. Alignment of the easy axes is performed *via* a field applied to the clusters before deposition. These processing steps are highly desirable to create and assemble R-TM nanoparticle composites for future permanent-magnet and other significant applications.

Randall M. German Honorary Symposium on Sintering and Powder-Based Materials: Current Activated and Conventional Sintering

Sponsored by: The Minerals, Metals and Materials Society, TMS Materials Processing and Manufacturing Division, TMS: Powder Materials Committee

Program Organizers: K. Morsi, San Diego State University; Fernand Marquis, Naval Postgraduate School; John Meyer, Iowa State University; Ahmed El-Desouky, San Diego State University; Eugene Olevsky, San Diego State University

Monday PM

March 12, 2012

Room: Oceanic 2

Location: Dolphin Resort

Session Chair: Javier Garay, University of California-Riverside

2:00 PM Invited

Development of a Simple Empirical Model for Current Activated Pressure Assisted Densification: J. Garay¹; A. Dupuy¹; ¹UC Riverside

The Current Activated Pressure Assisted Densification (CAPAD) technique has been used to effectively densify a wide variety of materials. Various models have been proposed both from the system perspective and the densification perspective. The system models can calculate the important fields of the technique such as current, temperature and stress distribution, while the densification models are helpful in differentiating the effects of experimental parameters on the densification process. While these models are quite useful and are being continuously improved, they are often difficult to implement. Here we present an empirical model that can relate material density to some of the most important experimental parameters: temperature and pressure. The work is based on results from experimental measurement of densification rates on various classes of



TMS 2012

141st Annual Meeting & Exhibition

MONDAY PM

important materials. The model is intended to complement experiments and is particularly useful as a tool for choosing experimental parameters.

2:25 PM Invited

Issues in Transforming SPS (FAST) into a Viable Manufacturing Solution: James Sears¹; ¹South Dakota School of Mines & Technology

Spark Plasma Sintering (SPS) also known as Field Assisted Sintering Technology (FAST) has the potential to revolutionize sintering and densification of various ceramic, metallic and composite materials. The main attributes that make this technology attractive include: short processing times, elimination of binders and sintering aids, minimal grain growth, wide range of materials, ability to handle fine (nano) materials, low cost tooling and near net shape processing. The current systems run in batch mode that limit throughput. This paper examines several scenarios that may lead to improvements in productivity. This paper will also discuss some of the applications currently being commercialized.

2:50 PM

Advances in Current Activated Tip-Based Sintering (CATS): Ahmed El Desouky¹; Kee Moon¹; Sam Kassegne¹; Joanna McKittrick²; Khaled Morsi¹; ¹SDSU; ²UCSD

Current activated tip-based sintering (CATS) is a new process that enables selective sintering of powders under high electric current densities using stationary or moving electrically conducting tips. This unique process has been recently used to produce macro as well as micro-scale sintered features for different systems such as metallic and intermetallic powder compacts. This presentation will discuss recent advancements in research on CATS.

3:05 PM

Low-Thermal Load Consolidation of Sm-Fe-N Flake Powder by Combination of Cyclic Compression and Current Sintering: Kenta Takagi¹; Hiroyuki Nakayama¹; Kimihiro Ozaki¹; ¹National Institute of Advanced Industrial Science and Technology (AIST)

Sm-Fe-N compounds, which possess a high magnet performance, are difficult to sinter due to their thermal decomposability. We tried to fabricate the Sm₂Fe₇N sintered magnets from flake powders by cyclic high-pressure compaction and subsequent current sintering with low temperatures. Under the high pressure compression, the flake particles were densely packed while being broken up and orderly stacked. Thus, bimodal blend of different particle sizes brought disadvantages against densification and the coarser powder provided the denser compact. When the coarse powder of < 355 μm was used, it was densified beyond 85% in relative density only by the cyclic compaction with the pressures above 1.2 GPa. The compacts were rigidly consolidated by the current sintering in the temperature range of 350–400 °C without the decomposition. TEM observation verified interparticle sinter-bonding in the compacts. The developed process finally produced the sintered magnets with the high density up to 93%.

3:20 PM

Fabrication of TiN / Fe-Al Cermet from Mixture of TiN, Fe and Al Powders: Hiroyuki Nakayama¹; Kimihiro Ozaki¹; Keizo Kobayashi¹; ¹National Institute of Advanced Industrial Science and Technology

TiN shows high hardness, good thermal stability. Hence, fabrication of TiN cermet considering an application for cutting tools is desired. Fe-Al intermetallic compounds are one of a candidate for binder of the cermet, because it shows good mechanical property and it is composed of common (low cost) elements. Therefore, in this study, fabrication of TiN / Fe-Al cermets were examined. TiN, Fe and Al powders were mechanically milled using a planetary ball mill under Ar atmosphere. The nominal composition of powder mixture was TiN - 10 mass% Fe₃Al₂. The milled powder was consolidated by current sintering. The sintered compact was composed of TiN and Fe-Al intermetallic compound. The intermetallic compound would be formed by the reaction of molten Al and solid Fe during the sintering process. The bending strength of the cermet showed 1.0 GPa. This value was higher than that of sintered TiN of 0.4 GPa.

3:35 PM Break

3:50 PM Invited

Liquid Phase Sintering of NiTi: David Dunand¹; ¹Northwestern University

Near equiatomic NiTi powders sinter very slowly due to the ordered structure of the intermetallic, resulting in poorly bonded, weak structures even after long sintering times near the melting point. Here, recent research is reviewed on liquid phase bonding of NiTi with small amount of Nb, forming a liquid NiTi/Nb eutectic that wets the powders, and upon solidification, remains ductile and does not affect the shape-memory properties of NiTi. This method is used to create porous NiTi-Nb, where pores with controllable size, shape and volume fraction are created with a space-holder around which the NiTi/Nb powders are fully densified by liquid phase sintering.

4:15 PM

The Effect of Powder Morphology on the Sintering Behavior of Ti and Ti Alloy Powders: Wei Chen¹; Yukinori Yamamoto¹; William Peter¹; Michael Clark¹; Stephen Nunn¹; Jim Kiggans¹; Thomas Muth¹; Ryan Dehoff¹; Craig Blue¹; Brian Fuller²; Kamal Akhtar²; ¹Oak Ridge National Laboratory; ²Cristal US, Inc./ International Titanium Powder

Powder metallurgy offers near-net-shape cost-effective approaches to the fabrication of Ti components. This work compares the sintering behavior of CP-Ti and Ti-6Al-4V powders made by three different processes; gas atomization, the Armstrong Process® and the hydride-dehydride (HDH) process. CP-Ti and Ti-6Al-4V powders were uniaxially die-pressed at designated pressures up to 690 MPa to form cylindrical samples. The powders exhibited different compressibility due to their morphology differences and the morphology differences significantly affected their sinterability. Vacuum sintering below and above the beta-transus were both performed and the effect of sintering temperature was analyzed. Sintering shrinkage was evaluated and an ex-situ technique was used to record the powder morphology change before and after sintering. This research was sponsored by the U.S. DOE, Office of EERE Industrial Technologies Program, under contract DE-AC05-00OR22725 with UT-Battelle, LLC.

4:30 PM

Transparent Polycrystalline Alumina Obtained by SPS: Single and Double Doping Effect: Burcu Apak¹; Halide Esra Kanbur¹; Esra Ozkan Zayim¹; Gultekin Goller¹; Onuralp Yucel¹; Filiz Cinar Sahin¹; ¹Istanbul Technical University

Commercial nanocrystalline alpha alumina powders were used for fabrication of dense and transparent alumina by spark plasma sintering (SPS). High purity dopants such as MgO, Y₂O₃, TiO₂ and CaO with 150 ppm amount were added to alumina and powder mixtures were densified by SPS between 1175 and 1300 °C using 80 MPa pressure for 5 to 20 min durations. The influences of MgO, Y₂O₃, TiO₂ and CaO single and double doping on density, hardness, fracture toughness and microstructures of alumina samples are investigated. The highest hardness value was measured as 24.2 GPa in the sample doped with 150 ppm MgO and 150 ppm CaO sintered at 1175 °C under 80 MPa pressure for 20 min. The fracture toughness values were ranged between 3.3 and 4.9 MPa·m^{1/2}. Alumina ceramic with 150 ppm MgO which was SPSed at 1175 °C for 20 min showed the highest RIT value as 55.5 %.

4:45 PM

Effect of TiC Addition on Sintering Behavior of ZrC: Burak Acicbe¹; Ipek Akin¹; Filiz Sahin¹; Onuralp Yucel¹; Gultekin Goller¹; ¹Istanbul Technical University

Zirconium carbide (ZrC) has many exceptional properties such as high hardness, high melting temperature, chemical inertness, solid state stability, high thermal and electrical conductivity. These properties make it a promising material for ultrahigh temperature applications, wear resistant parts and cutting tools. However, the inherent brittleness, and low fracture toughness limit the applications of ZrC. In this study, ZrC ceramics were

reinforced with TiC particles and composites with different compositions were prepared by using spark plasma sintering (SPS) technique. Samples containing 10 and 20 vol% TiC were sintered at 1900°C for 300 s under a pressure of 40 MPa. Shrinkage of the specimens during SPS process was continuously monitored. Densities of the composites were determined by the Archimedes' method. Fully dense ZrC-TiC composites containing 10 and 20 vol% TiC with a relative density of 99% were obtained. Mechanical properties and microstructural behavior of the composites will also be investigated.

5:00 PM

Sintering of Nanocrystalline Tungsten Powder: *William de Rosset*¹; ¹Army Research Laboratory

Small metal samples have been made from nanocrystalline tungsten powder by sintering with the goal of producing high density parts. The parameters associated with sintering runs have been examined to see if there is an empirical relationship between them and the final part density. A function that depends on the time a sample spends above a critical temperature has been formulated that represents one specific batch of tungsten powder. The function has been applied to other batches of powder with some success.

5:15 PM

Mechanical Properties of Spark Plasma Sintered ZrC-SiC Composites: *Sumbule Sagdic*¹; *Ipek Akin*¹; *Filiz Sahin*¹; *Onuralp Yucel*¹; *Gultekin Goller*¹; ¹Istanbul Technical University

Zirconium carbide (ZrC) is an important structural ceramic due to its high melting temperature, excellent chemical resistance, high electrical conductivity and good mechanical properties. This combination of properties makes it potentially useful in application of cutting tools, high temperature crucibles and thermal protection components. However, the nature of brittleness and lack of damage tolerance is one of the most crucial problems in their applications. In this study, ZrC-SiC composites with different compositions were prepared by using spark plasma sintering (SPS) technique. Samples containing 10 and 20 vol% SiC were sintered at 1900°C for 300 s under a pressure of 40 MPa. Densities of the composites were determined by the Archimedes' method. Fully dense ZrC-SiC composites with a relative density of 99% were obtained. Mechanical properties and microstructural behavior of the composites will also be investigated.

Science and Engineering of Light Metal Matrix Nanocomposites and Composites:

Sponsored by: The Minerals, Metals and Materials Society, TMS Light Metals Division

Program Organizers: Xiaochun Li, University of Wisconsin-Madison; Alan Luo

Monday PM
March 12, 2012

Room: Macaw 2
Location: Swan Resort

Session Chair: Hongseok Choi, University of Wisconsin-Madison

2:00 PM

Uniform Dispersion of Nanoparticles in Metal Matrix Nanocomposites: *Lianyi Chen*¹; *Hongseok Choi*¹; *Axel Fehrenbacher*¹; *Jiaquan Xu*¹; *Chao Ma*¹; *Xiaochun Li*¹; ¹University of Wisconsin Madison

The dispersion of nanoparticles in grains is crucial for the performance of the metal matrix nanocomposites. Uniformly dispersing nanoparticles into the metal matrix is still a great challenge. This paper demonstrates that a uniform dispersion of nanoparticles in metal matrix nanocomposites can be achieved by a combination of liquid state ultrasonic cavitation and solid state stirring. Two examples are presented in this report: (1) uniform dispersion of Al₂O₃ nanoparticles in A206 alloy and (2) uniform

dispersion of graphene nanoplatelets in pure magnesium. The results obtained in this work provide a general methodology to uniformly disperse nanoparticles into metal matrix nanocomposites, paving the way for production of metal matrix nanocomposites with superior properties.

2:20 PM

Effect of Particle Size Distribution on the Response of Particle Reinforced Metal Matrix Composites: *Brandon McWilliams*¹; *KT Ramesh*²; *Chian Yen*¹; ¹US Army Research Laboratory; ²Johns Hopkins University

An enhanced continuum model for the size dependent strengthening of ceramic particle reinforced metal matrix composites (MMCs) is used to explore the effect of particle size distribution on the deformation response of heterogeneous collections of particles. The model incorporates a "punched" zone around the particles that is the result of an increase in dislocation density due to geometrically necessary dislocations generated by the mismatch in coefficients of thermal expansion of the particle and matrix. Geometrically necessary dislocations result in localized hardening of the matrix around the particles, and the strengthening and size of this hardened zone are dependent upon the size of the reinforcing particles. In this work, these zones are explicitly accounted for in mesoscale finite element simulations of representative heterogeneous composite microstructures consisting of randomly distributed particles in a metal matrix. Effects of particle size distribution and strain rate on MMC deformation response is explored using this approach.

2:40 PM

Microstructure and Mechanical Properties of Gas Atomized CP Ti Containing Y₂O₃ and TiB: *Vincent Hammond*¹; *Sesh Tamirisakandala*²; *Brady Butler*¹; *William Hanusiak*²; ¹Army Research Laboratory; ²FMW Composite Systems

Previous results obtained on lab-scale samples of CP Titanium reinforced with yttria (Y₂O₃) nanoparticles have indicated significant improvement in tensile properties. As a result, there is an interest in determining if similar property improvements would be observed in materials produced using large-scale processing methods. Hence, CP Ti powders containing yttria as well as TiB reinforcements were produced through gas atomization. Subsequently, the powders were consolidated into billets and extruded into 12.7 mm bars. The influence of the reinforcements on the performance of CP Ti was evaluated using both microhardness and room temperature tensile tests. Test results indicated that the strength improvements ranged from approximately 25% to more than 60%. The Y₂O₃/TiB reinforced samples showed the highest strengths; however, these samples showed an approximate 50% reduction in elongation whereas the Y₂O₃ only sample showed a negligible reduction. Electron microscopy was used to correlate microstructural features to mechanical properties.

3:00 PM

An Investigation on the Capability of Equal Channel Angular Pressing for Consolidation of Aluminum and Aluminum Composite Powder: *Reza Derakhshandeh Haghi*¹; *Ahmad Jenabali Jahromi*²; ¹Fars Science and Research Branch, Islamic Azad University; ²Shiraz University

In this study equal channel angular pressing (ECAP) was used as a technique for consolidation of attritioned aluminum powder (45µm) with varying concentration of nano alumina powders (35nm) in tube at 200 °C. The effect of ECAP on consolidation behavior of composite powder and mechanical properties of subsequent compacts are presented. It is found that ECAP has the capability of consolidating pure aluminum powder, Al-5vol% Al₂O₃ and Al-10vol% Al₂O₃ to near their theoretical density and also declustering of the agglomerated alumina particles after maximum four passes. However full consolidation of Al-15vol% Al₂O₃ before emanating the cracks on the tube material was not possible and about 7% porosity remains in the compacted composite which degrades the mechanical properties of this composite in comparison to the aluminum composites with 5vol% and 10vol% alumina.



TMS 2012

141st Annual Meeting & Exhibition

MONDAY PM

3:20 PM

Effect of Core-shelled Nanoparticles of Carbon-Coated Nickel on Magnesium: *Yi Sun*¹; Hongseok Choi¹; Hiromi Konishi¹; Vadim Pikhovich²; Robert Hathaway²; Xiaochun Li¹; ¹University of Wisconsin Madison; ²Oshkosh Corporation

Grain refinement is of significance for strengthening Mg alloys. This paper is to study grain refinement effect in cast Mg by carbon-coated Ni nanoparticles. With about 1.0 vol% of C-coated Ni nanoparticles by ultrasonically dispersion in pure Mg, the average grain size of cast magnesium was refined markedly from more than 1000 μ m to 25 μ m. Mechanical property was enhanced significantly. The microstructure was examined by Polarized Light Microscopy, SEM, and TEM. TEM study indicates that a part of carbon-coated Ni nanoparticles remain intact and captured inside grains, while some other nanoparticles dissolved and formed Mg-Ni intermetallic phase near the grain boundary. Moreover, pure Ni was also added to pure magnesium to conduct comparison study. Mg with same amount of Ni can only produce a much larger average grain size, about 140 μ m.

3:40 PM Break

3:55 PM

Microstructural Control during In-Situ Synthesis of (AlN+Mg₂Si)/Mg Matrix Composites: *Xiao Ma*¹; David Johnson¹; Kevin Trumble¹; ¹Purdue University

Fine particulate AlN/Mg composites have successfully been in-situ synthesized using pure bulk Mg and Al and Si₃N₄ powder as raw materials. Reaction under SF₆/CO₂ protective gas atmosphere at 770 to 850°C for an hour was used to produce composites containing 60, 40, 20 or 4.5 vol. % AlN (+residual Mg₂Si) depending on the reaction temperature. The microstructures were characterized using X-ray diffraction, optical microscopy and scanning electron microscope. Fine AlN particles embedded within magnesium matrix in addition to larger size Mg₂Si phase was observed after the in-situ reaction. The AlN particles were found to have formed from the prior Si₃N₄ agglomerates while the morphology of the Mg₂Si phase was dependent upon the composition, temperature, and cooling rate. Thermodynamic calculations including the equilibrium and Scheil solidification paths of the resultant alloy after the in situ reaction were calculated and compared.

4:15 PM

In Situ Composite of (Mg₂Si)/Al-Si-Cu Fabricated by Squeeze Casting: *Huseyin Lus*¹; Gokhan Ozer¹; Kerem Guler¹; ¹Yildiz Technical University

An in situ formed Mg₂Si/Al-Si-Cu reinforced metal matrix composite fabricated by squeeze casting are investigated. It is showed that primary Mg₂Si crystals are formed by adding pure Mg into the hypoeutectic A380 aluminum-silicon-copper alloy. In order to increase castability and to obtain better properties squeeze casting technique is used. The results show that, the average size of primary Mg₂Si particulates decreases from 87 μ m to 21 μ m. Furthermore, the average porosity values of cast samples are decreased from %8.7 to %0.5 with the application of 30 MPa pressure during solidification.

4:35 PM

SiCp/Mg-Zn-Ca-Mn Mg Matrix Composites Fabricated by Stir Casting: *Xiaojun Wang*¹; K.B. Nie²; K Wu²; X.S Hu²; M.Y Zheng²; ¹Harbin Institute of Technology; ²Harbin Institute of Technology

SiCp/Mg-Zn-Ca-Mn magnesium matrix composites were fabricated by stir casting and then extruded. Many particles at grain boundaries were coated by the large second phase, which weakened the bonding between matrix alloy and particles. As the volume fraction of particles increased, the content of the second phase decreased. Chemical reaction was not observed at interface. The Ca₂Mg₆Zn₃ phase was observed at the interfaces. Hot extrusion improved the distribution of particles and refined the grain sizes of the matrix. As extrusion temperatures increased, the particles distribution was improved and the DRX grains grew up.

The content of the second phase decreased with the increase of particle in the extruded composites. Hot extrusion significantly improved the mechanical properties of the composites. But the extrusion temperature differently influenced the mechanical properties in the composites with different volume fractions of particles.

4:55 PM

Ultrasonically Processed AS41 Magnesium Alloy Matrix Composites: Neeraj Srivastava¹; *Gajanan Chaudhari*¹; S.K. Nath¹; ¹IIT Roorkee

TiC-AS41 magnesium alloy matrix composites were fabricated using ultrasound assisted solidification technique. It was observed that application of high intensity ultrasonic vibrations (~ 4.3 kW/cm²) to the melt resulted in uniform dispersion of TiC particles in the AS41 alloy matrix. The creep behavior of AS41 magnesium alloy and ultrasonically processed TiC/AS41 composites (2 % volume fraction of TiC particles) was investigated under conditions of constant compressive stress at temperatures up to 200°C. The results showed that the dispersed TiC particles significantly improved the high-temperature creep property of AS41 magnesium alloy.

5:15 PM

Optimization of Tensile Strength of Friction Stir Welded Al-(10 to14 wt.%) TiB₂ Metal Matrix Composites: *Santhiyagu Joseph Vijay*¹; Natarajan Murugan²; Siva Parameswaran³; ¹Karunya University; ²Coimbatore Institute of Technology; ³Texas Tech University

Metal Matrix Composites (MMCs) play a vital role in replacing many structural materials due to their superior mechanical and metallurgical properties. Processing those composites has always been a major factor influencing their application. Al-TiB₂ MMCs are used as structural members in the marine industry. Friction Stir Welding (FSW) has revolutionized the process of joining those composites. In this paper, an attempt has been made to friction stir weld the Al-TiB₂ MMCs and to develop a regression model for predicting the tensile strength of the weldment. The process parameters considered for FSW are tool rotation speed, tool traverse speed, axial load and weight percentage of TiB₂ in Al matrix. The regression model is used to optimize the process parameter using Desirability Optimization Methodology to improve the tensile strength of the FS welded Al-TiB₂ composites. The effects of process parameters on the tensile strength of the welded composites are analyzed and presented.

Solar Cell Silicon: Silicon Production

Sponsored by: The Minerals, Metals and Materials Society, TMS Extraction and Processing Division, TMS Light Metals Division, TMS: Energy Conversion and Storage Committee, TMS: Recycling and Environmental Technologies Committee
Program Organizers: Arjan Ciftja, SINTEF; Gabriella Tranell, Norwegian University of Science and Technology; Gregory Hildeman, Consultant; Shadia Ikhamyies, Al Isra University

Monday PM
March 12, 2012

Room: Europe 9
Location: Dolphin Resort

Session Chair: Arjan Ciftja, SINTEF Materials and Chemistry

2:00 PM Introductory Comments

2:05 PM

An Investigation into the Electrochemical Production of Si by the FFC Cambridge Process: Emre Ergül¹; Ishak Karakaya²; Metehan Erdogan²; *Fuat Erden*²; ¹Aselsan Inc.; ²Department of Metallurgical and Materials Engineering, Middle East Technical University

The FFC Cambridge process is a promising Si production technique for the expanding solar energy industry. In this study, SiO₂ was successfully reduced to Si in both CaCl₂ salt and CaCl₂-NaCl salt mixture at 2.8 V. In addition, reduction of porous SiO₂ pellets were compared with bulk

SiO₂ plates in terms of reduction rate. The overall reduction potential of SiO₂ pellets against the graphite anode at 750°C in molten CaCl₂-NaCl salt mixture was determined as 2.3 V by cyclic voltammetry which was supported by calculations. SEM examinations, ICP-MS, and XRD analysis were used for characterization. The produced Si powder was brown and found to be contaminated by the Ni and stainless steel plates used as the cathode contacting materials.

2:30 PM

Distribution of Boron and Phosphorus during Alloying and Slag Treatment of Metallurgical Grade Silicon: *Yulia Meteleva-Fischer*¹; Yongxiang Yang²; Rob Boom¹; Bert Kraaijveld³; Henk Kuntzel³; ¹Materials innovation institute/TU Delft; ²Delft University of Technology; ³Solwafer B.V.

Segregation of impurities during refining of metallurgical grade silicon (MG-Si) is an option to produce solar grade silicon (SG-Si). Directional solidification is a last step in production of SG-Si effective for removal of metallic impurities. The possibility is investigated to use metallic impurities originally present in MG-Si for removing boron and phosphorus. MG-Si has been treated using two methods: 1) alloying with calcium and 2) refining with Na₂O-CaO-SiO₂ slag, both by controlled cooling. The microstructure of silicon and the impurities distribution have been studied before and after the treatments. Using EPMA phosphorus and boron have been detected in 1-2 wt% concentration range in several intermetallic compounds in grain boundaries after both treatments. This observation points to a different possible mechanism of silicon refining from boron and phosphorus. Controlled cooling improves migration of phosphorus and boron to the silicide phases in grain boundaries, which can be removed by acid leaching treatment.

2:50 PM

Experimental and Molecular Simulation Studies of Silicon Production in an Microwave Furnace: *Jan-Philipp Mai*¹; Gabriele Raabe²; Juergen Koehler²; ¹JPM Silicon GmbH; ²University of Braunschweig - Institute of Technology

Here we present a new developed microwave furnace capable to produce small amounts of silicon metal. The energy efficient process is capable to produce high quality silicon metal, which can be purified with less complexity to silicon for solar cells. In a special designed microwave furnace a mixture of silicon oxide and carbon is heated up to a maximum temperature of 1,700 °C within a few minutes and silicon is produced. In order to optimize the silicon production it is essential to understand the reaction mechanism. Thus, molecular simulation techniques might provide insight into the complex processes. A new promising approach for MD studies of chemical reactions is the use of the reactive force field ReaxFF [1, 2]. [1] A.C.T. van Duin et al., J. Phys. Chem. A 105, 9396-9409, 2001. [2] A.C.T. van Duin et al., J. Phys. Chem. A 107, 3803-3811, 2003.

3:10 PM Break

3:30 PM

Improved Material Efficiency in the Si Deposition from SiHCl₃ under Mesoplasma Condition: *Makoto Kambara*¹; Toyonobu Yoshida¹; ¹The University of Tokyo

Equilibrium chemistries in the conventional Si deposition from SiHCl₃ confirms that the relative amount of the stable Si solid is as highest ~ 25% at around 1400K because of the formation of more stable Si containing phases such as SiCl₄ and SiCl₂ over a wide temperature range. Under the mesoplasma condition, in contrast, such Si containing species are no longer stable and Si vapor becomes the most stable phase at >2500K instead. One can thus foresee that the deposition efficiency is enhanced if Si vapor is to be rapidly condensed with increased degrees of non-equilibrium. Additionally, the mesoplasma process is characterized by its unique nano-cluster growth precursor which favors fast deposition and

film structure modification. Based on this concept, we have demonstrated Si epitaxial films deposition at the deposition rate of >550 nm/s with the material yield of >50% at an increased RF input power of 24 kW.

3:50 PM

Impurities Distribution between SiO Gas and Reactant Materials in a Silicon Furnace: *Elena Dal Martello*¹; Gabriella Tranell²; Oleg Ostrovski³; Guangqing Zhang³; Ola Raanes⁴; Kai Tang⁴; ¹NTNU ; ²NTNU; ³UNSW; ⁴SINTEF

The control of the impurities inside the silicon furnace is a topic not widely investigated. Impurities in silicon can originate from quartz and carbon materials. In this work we correlate the impurity content in mixture of SiO₂/SiC and SiO₂/Si to the impurities carried out by SiO gas. The experiments represent the operative condition of the middle and bottom part of the furnace. Raw materials both in form of lumps and pellets are heated in graphite crucibles at 1700C and at 1900C. SiO gas is produced and collected as microsilica. Both microsilica and charge materials are analyzed chemically by ICP-MS. The experimental work is supported by thermodynamic simulations. The results give an understanding of the typology of the elements carried out of the furnace by SiO gas. In particular the abundance and typology of these impurities are correlated to the composition, the size and the physical state of the raw materials.

4:10 PM

The Kinetics of Boron Removal during Slag Refining in the Production of Solar-Grade Silicon: *Egil Krystad*¹; Shuang Zhang¹; Gabriella Tranell¹; ¹NTNU

The kinetics of boron removal from liquid silicon during slag refining, as a process step in the production of solar grade silicon, has been investigated by means of small scale mass transfer experimental series at 1600°C, using a graphite crucible. The slags were SiO₂-CaO based, with or without addition of 19 wt% MgO. Experiments were carried out at slag-metal ratios of 1 or 2, where the silicon initially contained approx. 250 ppm boron. The mass transfer coefficients were found to be in the order of 1-3 × 10⁻⁶ m/s and were largely influenced by slag composition. The mass transfer rate was higher for the MgO-containing slag than the slags without MgO. The final equilibrium distribution of boron between metal and slag, L_B, was determined to be in the order of 2.3-3.3.

4:30 PM

Raman Spectroscopic Study of the Structural Modifications Associated with the Addition of Calcium Oxide and Boron Oxide to Silica: *Jeff Kline*¹; Merete Tangstad¹; Gabriella Tranell¹; ¹NTNU

Raman spectroscopy as an instrumental technique for the determination of silicate structure is widely accepted. This method was utilized for analysis of structural modifications associated with the addition of network modifying oxides. Silicate slags are described by the extent of oxygen bridging. Therefore, understanding the structural modification of the silicate melt related to the addition of different oxides will provide important information regarding the removal of boron from silicon. Samples ranging from 45.5-64 wt% SiO₂ in the CaO-SiO₂ binary were evaluated. Boron oxide was added at 10, 5, 1 wt% to two CaO-SiO₂ base slags. Trends associated with the addition of the CaO to silica and structural variations accompanying the presence of boron oxide are presented.

4:50 PM

Structure Silicon Deposits Obtained by Electrolysis SiO₂ in the Chloride-Fluoride Melts: *Oleg Chemezov*¹; Aleksey Apisarov¹; Andrey Isakov¹; Yurii Zaikov¹; ¹Institute of High-Temperature Electrochemistry Russian Academy of Science Ural Division

Silicon deposits containing 99,9 wt.% of main component were obtained by electrolysis SiO₂ from chloride-fluoride melts. The operating temperature was varied from 500 up to 800° °C. The conditions for obtaining crystalline fibrous micro or nanodeposits were determined. The deposits were investigated by ESM method.



Solid-State Interfaces II: Toward an Atomistic-Scale Understanding of Structure, Properties, and Behavior through Theory and Experiment: Morphological Stability

Sponsored by: The Minerals, Metals and Materials Society, TMS Electronic, Magnetic, and Photonic Materials Division, TMS Structural Materials Division, TMS: Chemistry and Physics of Materials Committee, TMS: Nanomechanical Materials Behavior Committee

Program Organizers: Xiang-Yang Liu, Los Alamos National Lab; Douglas Spearot, University of Arkansas; Guido Schmitz, University of Münster; David Seidman, Northwestern University

Monday PM
March 12, 2012

Room: Oceanic 7
Location: Dolphin Resort

Funding support provided by: Los Alamos National Laboratory

Session Chairs: David Seidman, Northwestern University; Emmanuelle Marquis, University of Michigan

2:00 PM Invited

Precipitates in Al-Cu Alloys Revisited: *Donald Siegel*¹; Aniruddha Biswas²; Christopher Wolverton³; David Seidman³; ¹University of Michigan; ²Bhabha Atomic Research Center; ³Northwestern University

Atom-probe tomography, transmission electron microscopy, X-ray diffraction and first-principles calculations are combined to study composition evolution and solute segregation across a range of Al-Cu-based alloy systems, spanning from model alloys to multi-component commercial variants. For model alloys based on Al-Cu(-Si), most GPII zones and theta-prime precipitates are demonstrated to be Cu-deficient at lower aging temperatures. We also find evidence of Si partitioning to GPII zones and theta-prime precipitates, as well as significant Si segregation at the coherent alpha-Al/theta-prime interface. Our results suggest that Si catalyzes the early stages of precipitation in these alloys, consistent with the higher precipitate number densities observed in commercial Al-Cu-Si alloys. For the commercial alloy we report significant qualitative and quantitative differences in solute segregation at coherent and semi-coherent interfaces bounding a single theta-prime precipitate. The role of first-principles calculations will be highlighted as a means to provide "energetic explanations" for the experimental observations.

2:30 PM Invited

Evolution of Hetero-Interfaces in Alloys Forced by Severe Plastic Deformation: *Pascal Bellon*¹; Robert Averback¹; Nhon Vo¹; Yinon Ashkenazy¹; Daniel Schwen¹; Elvan Ekiz¹; Tim Lach¹; Mohsen Pouryazdan²; Horst Hahn²; ¹University of Illinois; ²Karlsruhe Institute of Technology

Plastic deformation can force the mixing of immiscible elements. In multiphase systems, this forced mixing depends significantly on the specifics of interfaces and on the strain path, since the mixing is superdiffusive when the mean free path of dislocations is large, and the mixing is biased by thermodynamics for highly immiscible systems. Atomistic simulations on Cu-X alloy systems (X=Cu, Ag, Ni, Fe, V, Nb) reveal that the rate of forced dissolution of precipitates scales quadratically with precipitate radius for shearable precipitates, but only linearly for unsharable precipitates. In Cu-Nb bilayers, the rate of forced mixing during shearing is a strong function of orientation relationship and interface plane. Special orientations such as Nishiyama-Wassermann, for example, are remarkably stable against mixing. These results are compared to experimental observations on Cu-Ag, Cu-V, and Cu-Nb alloys deformed high-pressure torsion, and characterized by TEM and APT.

3:00 PM

Ab Initio Study of Competitive Coherent Hydride Formation in Zirconium Alloys: Ludovic Thuinet¹; Rémy Besson¹; ¹UMET

We present a detailed atomic-scale investigation of coherent hydrides in Zr alloys. While previous experimental and theoretical studies emphasized the gamma' (ZrH) and zeta (Zr₂H) phases as potential precursors in the hydride precipitation sequence, they led to contradictory conclusions justifying further analysis of the nucleation of these two types of precipitates. To this aim, we take proper account of the three energy contributions (bulk chemical, interfacial and elastic) involved in Classical Nucleation Theory by incorporating original features such as (i) zeta bulk off-stoichiometry, (ii) anisotropic matrix/hydride interfacial energies and (iii) shape factors of platelike nuclei. These effects turn out to be essential to provide a realistic description of the conditions of temperature and H content leading to preferential gamma' or zeta formation. Our work provides a unifying picture of the previous, apparently diverging, works on coherent zirconium hydrides and emphasizes the importance of accurately calculating coherent interfacial energies in such systems.

3:20 PM

Compositional Evolution of Q-Phase Precipitates in an Al-Alloy via 3-D Atom-Probe Tomography: *Aniruddha Biswas*¹; David Seidman²; ¹Bhabha Atomic Research Centre; ²Northwestern University

The results of a 3-D local-electrode atom-probe (LEAP) tomographic study of the compositional evolution of Q-phase precipitates in a commercial age-hardenable aluminum alloy, W319, are presented. Three different aging conditions are investigated: 438 K for 8 h, 463 K for 8 h, and 533 K for 4 h. APT specimens are Ga⁺ milled using a dual-beam focused-ion beam (FIB) microscope and analyzed employing a 3-D LEAP tomograph. After aging at 438 K and 463 K, the Q-phase precipitates exhibit compositions rich in Cu but lean in Mg and Si. They evolve into a Mg-rich phase after aging at 533 K. This research provides the first experimental evidence for partitioning of Zn to the Q-phase precipitates. This effect is detected even though the bulk concentration of Zn is only 0.05 at. %. Furthermore, we observe co-precipitation of the theta-prime and Q-phase precipitates for all three aging conditions.

3:40 PM Break

3:45 PM

Polyhedron Analysis for Structure Identification in Atomistic Simulations: Thomas Schablitzi¹; *Jutta Rogal*¹; Ralf Drautz¹; ¹Ruhr University Bochum

Topologically close-packed (TCP) phases such as the λ 963- λ 956- or Laves phases are of interest for a number of materials, including high-temperature superalloys or high-strength steels. The atomic structure of the different TCP phases is characterized by particular arrangements of Frank-Kasper coordination polyhedra. For the identification of the TCP phases in atomistic simulation data we fingerprint the surrounding of each atom. To this end we first extract the local coordination polyhedron for each atom from the atomistic data. In a second step correlations between the polyhedra are used to identify the structure and sublattices of the TCP phases. We demonstrate our method for a number of crystal structures and for adaptive kinetic Monte Carlo simulations of the interface between TCP phases and the alloy matrix phase.

4:05 PM

Investigation of Interfacial Precipitation and Segregation in Ultra High Strength Steel with TEM and 3D Atom Probe: *Matthew Hartshorne*¹; Paul Novotny²; Michael Schmidt²; David Seidman³; Mitra Taheri¹; ¹Drexel University; ²Carpenter Technology Corporation; ³Northwestern University

Ultra High Strength (UHS) steels used in high performance applications typically require large concentrations of alloying elements to achieve the required strength and toughness. The Carpenter Technology Corporation has developed a new family of UHS steels with comparable mechanical properties to current alloys, yet possessing markedly reduced levels of a wider variety of alloying elements. The strengthening mechanisms of this

system are not well understood, necessitating a detailed investigation of its interfacial precipitation and solid solution hardening. Experiments will be presented detailing precipitate type and location within the microstructure by utilizing high resolution TEM and electron tomography. These experiments are coupled with 3D atom probe studies, which allows for the analysis of solute segregation at grain, lath and precipitate boundaries. The combination of these techniques provides a more comprehensive understanding of the role and interactions of each of the alloying elements in this new alloy.

4:25 PM

Fabrication and Characterization of Oriented Fe-Y₂Ti₂O₇ Interfaces: Implications to the Development and Optimization of Nanostructured Ferritic Alloys: *Tiberiu Stan*¹; Yuan Wu¹; G. Robert Odette¹; Kurt Sickafus²; Hanna Dabkowska³; Bruce Gaulin³; ¹University of California Santa Barbara; ²University of Tennessee; ³McMaster University

Nano-structured ferritic alloys are dispersion strengthened by a high density of nano-features (NF) yielding remarkably high temperature creep strength and radiation damage resistance. The smallest 2-3 nm NF are complex Y₂Ti₂O₇ pyrochlore oxides. The Iron-NF interface is critically important, but is difficult to fully characterize. To complement characterization of the NF, a bulk interface was created by electron beam deposition of a thin Iron (Fe) layer onto a {111} Y₂Ti₂O₇ single crystal surface and characterized using SEM, AFM, XRD and TEM techniques. The polycrystalline Fe layer has two general oxide orientation relationships close to: a) $\{100\}_{Fe} // \{111\}_{ox}$ and $\langle 100 \rangle_{Fe} // \langle 110 \rangle_{ox}$; and, b) $\{110\}_{Fe} // \{111\}_{ox}$ and $\langle 111 \rangle_{Fe} // \langle 110 \rangle_{ox}$. HRTEM shows interfaces that are almost atomically sharp with various defects and more diffuse interface zones that, in some cases, include a thin FeO_x layer. This work will be refined and extended to other orientations and studies of the interface interactions with irradiation induced defects and helium.

4:45 PM

Atomistic Simulations of Cu Growth on ZnO Surfaces Using COMB Potentials: *Yu-Ting Cheng*¹; Tao Liang¹; Bryce Devine¹; Beverly Hinojosa¹; Aravind Asthagiri²; Simon Phillpot¹; Susan Sinnott¹; ¹University of Florida; ²The Ohio State University

Cu/ZnO heterogeneous systems have been shown to catalyze the electrochemical reduction of carbon dioxide into hydrocarbons with high efficiency. Because the electrochemical efficiency and the selectivity of product is highly dependent on the nature of the electrode, the way in which ZnO surfaces support Cu clusters and stabilize their active sites is a key factor for maintaining catalyst activity. In this work, the adsorption of Cu clusters of various sizes on the ZnO surfaces are modeled using atomic-scale molecular dynamics simulations with charge-optimized many-body (COMB) potentials. Further, the adaptive kinetic Monte Carlo (aKMC) will be employed to explore the growth and coalescence of the clusters. The findings are validated against the results of density functional theory calculations and experiments.

5:05 PM

Microscopic Study of Cu-based Dilute Cu-Nb-W Ternary System: *Xuan Zhang*¹; Pascal Bellon¹; Robert Averback¹; ¹UIUC

The dilute Cu-Nb-W thin films with a solid-solution as-grown state have shown some interesting microstructural properties under different treatments. (1) The samples annealed to as high as 830C have a bi-model precipitate size distribution. Smaller precipitates are richer in W. The bcc particle/fcc matrix interfaces are preferably to be K-S type. Particles larger than 5nm have a Nb-rich core and a W-rich shell, which is composed of small W-rich clusters. (2) The samples which are first ion irradiated at room temperature and second annealed at elevated temperatures have shown reversed core/shell structure. The irradiation gives rise to the formation of 1nm-sized W-rich clusters while most Nb atoms are still in solution. The following-up annealing makes the Nb precipitate to cover the W clusters. The variability in structures offers the flexibility in design interfaces optimized for applications, for instance for trapping point defects in irradiated alloys, thus enhancing their radiation resistance.

5:25 PM

Characterization of Reaction Layers in Mn_{1.5}Co_{1.5}O₄ Coated Fuel Cell Interconnects: *Neal Magdefrau*¹; Lei Chen¹; John Yamanis¹; Ellen Sun¹; Mark Aindow²; ¹United Technologies Research Center; ²University of Connecticut

Ceramic coatings on metallic solid oxide fuel cell interconnects are a key component of the SOFC stack. These coatings prevent chromium poisoning of the cathode while also slowing the oxidation kinetics of the underlying alloy. Excessive oxidation of the interconnect alloy can lead to ohmic losses, which in turn limit the life of the stack. However, typical interconnect coating materials such as Mn_{1.5}Co_{1.5}O₄ (MCO) spinels can form complex reaction layers with the underlying alloy. Here we present electron microscopy data obtained from MCO coatings on Crofer 22 and Haynes 230 alloy substrates after static oxidation and area-specific resistance testing. It is shown that both the microstructure of the underlying alloy and the electric current have a profound influence on the morphology/evolution of the chromia subscale and the intermediate reaction layer(s). The significance of these observations for the lifetimes of such coated interconnects is discussed.

Symposium in Memory of Patrick Veyssière: Understanding the Mechanisms Controlling Plastic Flow: Plastic Flow

Sponsored by: The Minerals, Metals and Materials Society, TMS Electronic, Magnetic, and Photonic Materials Division, TMS Structural Materials Division

Program Organizers: Georges Saada, LEM CNRS ONERA; Dennis Dimiduk, Air Force Research Laboratory; Hael Mughrabi, University Erlangen-Nuernberg; Haruyuki Inui, Kyoto University

Monday PM

March 12, 2012

Room: Europe 6

Location: Dolphin Resort

Funding support provided by: National Science Foundation

Session Chairs: D. Caillard, CEMES/CNRS; M. Niewczas, McMaster University

2:00 PM Invited

TEM Deformation Maps : Microstructure & Mechanical Behavior: *Muriel Veron*¹; Edgar Rauch¹; ¹SIMaP

An orientation and phase mapping technique (ASTAR) was recently developed for TEM with good reliability and reasonable acquisition time. Installed on a FEG TEM, orientation and phase maps are obtained with a spatial resolution of 1nm. This technique has many applications such as studying deformation mechanisms in structural materials e.g., steel or magnesium alloys, but also to address new challenges, for instance in-situ deformation of nano-crystalline palladium films. Combined with FIB technology to prepare TEM specimens, ASTAR provides new descriptions of deformation mechanisms in very specific locations. Two examples will be presented: firstly precise deformation mechanisms of Mg single crystals under a nano-indentor tip, followed by a more classical study of steels involving phase transformations.

2:30 PM Invited

Plastic Flow Heterogeneity and Yielding Instabilities: *Georges Saada*¹; Tomas Kruml²; I. Kubena³; ¹LEM CNRS ONERA; ² Institute of Physics of Materials Materials ; ³ Institute of Physics of Materials Materials

The occurrence of sharp yield points associated with band nucleation and propagation in aged and deformed steels (Lüders bands) or Al based alloys (Portevin-Le Châtelier oscillations) has been known for more than one century. The Lüders phenomenon has been shown to disappear by changing the sense of the applied stress. Systematic experiments on Al-Mg alloys, and low carbon steels reported in our communication show the same effect on the Portevin-Le Châtelier oscillations, and confirm



TMS 2012

141st Annual Meeting & Exhibition

MONDAY PM

the disappearance of the Lüders phenomenon in low carbon steels. Using careful measurement of the elastic-plastic transition during reverse straining, we show that this behaviour is a consequence of large scale microstructure heterogeneity, whose general features are analysed, and shown to describe satisfactorily the observed behavior.

2:55 PM Invited

A Dislocation-Based Model for Interpretation of Strain Path Changes in Steel and Magnesium: *Carlos Tome¹; Kohshiroh Kitayama²; Edgar Rauch³; Gabriela Vincze²; Jose Gracio²; Frederic Barlat⁴; ¹Los Alamos National Laboratory; ²University of Aveiro; ³Universite de Grenoble/CNRS Grenoble; ⁴Pohang University of Science and Technology*

Polycrystal aggregates subjected to plastic forming exhibit large changes in the yield stress and extended transients in the flow stress following strain path changes. Since these effects are related to the rearrangement of the dislocation structure induced during previous loading, it is natural to employ a dislocation-based hardening model in order to comprehend such behavior. Here we present such model, implement it in the polycrystal code VPSC, and simulate strain path changes in low carbon steel and Mg AZ31. The path changes consist of tension followed by shear, and forward and reverse simple shear for carbon steel. In the case of Mg AZ31 we do tension followed by tension. In both cases the reloads were performed at different angles with respect to the preload tensile axis. The results are compared to experimental data and highlight the role that directional dislocation structures induced during preload, play during the reload stage.

3:25 PM Break

3:40 PM Invited

Finite Element Implementation of a Self-Consistent Polycrystal Plasticity Model: Application to a-Uranium: *Marko Knezevic¹; Rodney McCabe¹; Ricardo Lebensohn¹; Carlos Tomé¹; Bogdan Mihaila¹; ¹Los Alamos National Laboratory*

In this paper, we adapt a visco-plastic self-consistent polycrystalline model and integrate it in the implicit finite-element framework, to simulate crystallographic texture evolution and mechanical response of wrought a-uranium (orthorhombic structure). The constitutive equations include a multi-scale dislocation-based hardening law for multiple slip and twinning modes. The latter is necessary to model the highly anisotropic response of a-uranium. The predictive capabilities of the model are demonstrated by comparing numerical simulations against experimental measurements in simple compression, simple tension and four-point bending tests. The macroscopic strain hardening, texture evolution and dimensional changes are in good agreement with experiments performed on textured a-uranium.

4:00 PM Invited

Modeling Plasticity and Cracks at the Atomic Scales within a Continuum Framework: *Pierre-Antoine Geslin¹; Benoit Appolaire²; Alphonse Fine²; ¹LEM ONERA / CNRS; ²LEM ONERA / CNRS*

We propose a model for plasticity at the atomic scale relying on continuum fields. It derives from a Lagrangian with a potential periodic in the relevant order parameter based on strain components. It naturally accounts for dislocation motion, but also for dislocation nucleation and annihilation, two features which are usually lacking (or introduced through local phenomenological rules) in other methods, such as discrete dislocation dynamics or continuous approaches based on dislocation densities. This model is thus able to bring qualitative insights on open questions occurring in multiphase materials involving dislocation motion as well as nucleation, such as (i) coherency loss at a precipitate interface and (ii) inheritance of plastic deformation by a growing precipitate. Extension of this model to incorporate damage and cracks will also be presented.

4:30 PM Invited

Spectral Elasto-Viscoplastic Formulation for the Prediction of Micromechanical Fields with Direct Input and Validation from Voxelized Data: *Ricardo Lebensohn¹; Jette Oddershede²; Grethe Winther²; ¹Los Alamos National Laboratory; ²Risoe DTU*

We present the extension to the most general case of elasto-viscoplastic (EVP) polycrystals of a formulation originally developed [1] as an efficient method to compute the micromechanical fields in deformed heterogeneous materials, directly from an image of their microstructure. Under this technique, the input microstructural image is treated using the Fast Fourier Transform (FFT) algorithm to solve the corresponding micromechanical problem. We show an application of the new EVP-FFT method to the prediction of grain-resolved internal stresses measured in situ in a plastically-deformed copper polycrystal using three-dimensional synchrotron X-ray diffraction [2]. References: [1] H. Moulinec and P. Suquet, *Comput. Meth. Appl. Mech. Eng.* 157, 69 (1998). [2] J. Oddershede et al., *Materials Characterization* 62, 651 (2011).

4:50 PM Invited

Binary and Ternary Interaction Coefficients in BCC Metals and Single Crystal Strain Hardening: *Ronan Madec¹; Ladislav Kubin²; ¹CEA, DAM, DIF; ²LEM (CNRS/ONERA)*

Dislocation dynamics simulations have now reached a stage where they are able to tackle such problems as the formation of dislocation microstructures and forest hardening in bulk single crystals. The connection between mesoscopic and continuum approaches of plasticity is based on the knowledge of the interaction matrix between slip systems and of the dislocation mean free paths, from which a hardening matrix can be derived. The objective of the present work is to establish this connection for BCC metals, using a dislocation dynamics simulation that is briefly described. Emphasis is on the determination of the interaction matrix in the high temperature regime, above the so-called "athermal temperature" at which lattice friction vanishes. Results on binary and ternary dislocation reactions will be discussed. Comparison between finite element crystal plasticity calculations using these coefficients and stress vs. strain curves are presented and the orientation dependence of strain hardening is discussed.

Titanium: Advances in Processing, Characterization and Properties: Processing and Process Modeling II

Sponsored by: The Minerals, Metals and Materials Society, TMS Structural Materials Division, TMS: Titanium Committee
Program Organizers: Adam Pilchak, US Air Force Research Laboratory; Christopher Szczepanski, US Air Force Research Laboratory; Vasisht Venkatesh, Pratt & Whitney

Monday PM
March 12, 2012

Room: Oceanic 3
Location: Dolphin Resort

Session Chairs: Michael Glavicic, Rolls-Royce Corporation; Vasisht Venkatesh, Pratt & Whitney

2:00 PM

Effect of Processing on Microstructure and Mechanical Properties of Ti-6Al-4V Fabricated Using Electron Beam Melting (EBM): *Nikolas Hrabe¹; Ryan Kircher²; Timothy Quinn¹; ¹NIST; ²Medical Modeling*

Selective electron beam melting (EBM) is an additive manufacturing technique that shows great promise for fabrication of medical devices and aerospace components. Before its potential can be fully realized, however, a deeper understanding of processing-microstructure-properties relationships is necessary. Titanium alloy (Ti-6Al-4V) samples were built to allow investigation of the following processing parameters: distance from build platform and energy input. There was no discernible difference found in microstructure (prior- β grain size and a needle thickness) or

mechanical properties (UTS, YS, %EL, and Vickers microhardness) as a function of distance from build platform. This is thought to result from the ability of the control software to maintain relatively constant melt pool size. For a wide range of energy input (speed factor 30-40), small but discernible differences in microstructure (20% for a needle thickness) and mechanical properties (3% for UTS, YS, and microhardness) were measured.

2:20 PM

Surface Tension and Viscosity of Industrial Ti-alloys Measured by the Oscillating Drop Method under Reduced Gravity Conditions: *Rainer Wunderlich*¹; Hans -Joerg FECHT¹; ¹Universitaet Ulm

Thermophysical properties of Ti-alloys in the liquid phase are important parameters for modelling of casting and solidification used for improvements of process technology and product quality. Due to the high liquidus temperatures and the high chemical reactivity their measurement is, however, complicated and difficult with conventional techniques. Containerless processing based on electromagnetic levitation offers an alternative. An electromagnetic levitation device was constructed for operation on board parabolic flights and as payload on sounding rocket. Measurements of the surface tension and the viscosity were performed by the oscillating drop method. Microgravity conditions are afforded because under 1-g conditions the large levitation forces induce turbulent fluid flow which renders measurement of the viscosity impossible. An overview is given of the results of surface tension and the viscosity measurements of a variety of Ti-alloys including Ti64 with variants and different \149; -TiAl alloys such obtained.

2:40 PM

Fractographic Characterization of Electron Beam Freeform Fabrication [EBF3] Produced Ti-6Al-4V: *Cynthia Lach*¹; Robert Hafley¹; ¹NASA Langley Research Center

Electron Beam Freeform Fabrication (EBF3) is a layer-additive process that produces net-shaped structural components by feeding wire into a molten pool formed by an electron beam in a high vacuum. Selective aluminum vaporization has been documented due to vapor pressure differences of the alloy constituents. This can lead to variability in the alpha-beta microstructure, mechanical properties and fracture behavior. Ambient temperature tensile and fracture tests were conducted on EBF3-deposited Ti-6Al-4V. Comprehensive fractographic characterization was conducted in two crack growth orientations macroscopically to evaluate overall fracture morphology and microscopically to assess fracture modes. The LT specimens (crack propagating perpendicular to the deposition layers) exhibited slant fracture growth in contrast to the flat fracture observed for the TL specimens (crack propagating parallel to the deposition direction). These results are compared to conventional wrought product to understand the impact of EBF3 processing on the performance of Ti-6Al-4V.

3:00 PM

Microstructure and Mechanical Properties of Ti-6Al-4V Fabricated by Selective Laser Melting: *Marco Simonelli*¹; Yau Yau Tse¹; Chris Tuck¹; ¹Loughborough University

Selective laser melting (SLM) has been used as an alternative manufacturing route to produce Ti-6Al-4V components. This study focuses on the influence of SLM parameters on the microstructure and mechanical properties of resultant Ti-6Al-4V components. Microstructure characterisation was carried out using various microscopy techniques including optical, scanning electron and transmission electron microscopy and electron backscattered diffraction. The SLM produced components shows an apparently lower ductility compared to those manufactured in a conventional ways such as forged or rolled. It is also found that martensitic phase shows different morphology in regions experienced different thermal history in the SLM. The microstructure details observed will be discussed in relation to the SLM parameters.

3:20 PM

Computational Modeling of Aluminum Evaporation and Flow in Electron Beam Button Melting of Ti-6Al-4V: *Zhongkui Zhang*¹; Carl Reilly¹; Daan Maijer¹; Steve Cockcroft¹; ¹The University of British Columbia

The Electron Beam Cold Hearth Remelting (EBCHR) process has emerged as a key process in the production of high quality Ti-6Al-4V ingot and electrode as it is able to effectively consolidate both sponge and scrap material. A comprehensive model of the melt pool produced during electron beam button melting has been developed to serve as an intermediate step in the development of a comprehensive tool for analysis and optimization of the industrial EBCHR process. The thermal-fluid model includes evaporation, compositional and thermally driven buoyancy, compositional and thermally driven Marangoni flow as well as flow attenuation in the mushy regime. Experimental investigations using Ti-6Al-4V and CP Titanium with two different electron beam patterns were conducted to elucidate the role of evaporation of aluminum in driving fluid flow. Surface velocity, temperature, Al concentration, mold heat flux and predicted melt pool profile have been quantified experimentally in order to verify the model.

3:40 PM

Computational Modeling of the Dissolution of Alloying Elements: *Jun Ou*¹; Aniruddha Chatterjee¹; Daan Maijer¹; Steve Cockcroft¹; Carl Reilly¹; ¹The University of British Columbia

The dissolution of alloying elements within the bulk liquid is of utmost importance in alloy production to ensure homogeneity. A mathematical model based on a commercial Computational Fluid Dynamics software package has been developed to describe dissolution of an alloying element in bulk liquid. The model includes the effects of heat transfer, diffusion, buoyancy, Marangoni force and Darcy flow and has been used to assess the contributions of each factor on the dissolution kinetics of alloying elements. The results show that buoyancy and Marangoni forces are significant factors, which influence solute transport. The model has been successfully validated using experimental data from a water-ethanol analogue system, using the quantified temperature at discrete locations, surface velocities and solid/liquid interfacial profiles. The industrial relevance of the model has been demonstrated by modeling the addition of aluminum to titanium. These results show good agreement with experimental results obtained using an electron beam furnace.

4:00 PM Break

4:10 PM

Cost Effective and Eco-Friendly Process for Preparation of Wrought Pure Ti Material via Direct Consolidation of TiH₂ Powders: *Takanori Mimoto*¹; Nozomi Nakanishi¹; Thotsaphon Threrujirapong¹; Junko Umeda¹; Katsuyoshi Kondoh¹; ¹Osaka University

The direct consolidation of titanium hydride (TiH₂) raw powders in solid-state was employed to fabricate pure titanium (Ti) bulk materials by *in-situ* dehydrogenation of TiH₂ powders via powder metallurgy (P/M) route. In general, the production cost of Ti materials is expensive due to using commercially pure (CP) Ti powders after dehydrogenation. On the other hand, the novel process using TiH₂ powders as starting materials is a promising low cost approach for P/M Ti components. Furthermore, this new process is also attractive from a viewpoint of energy saving because the dehydrogenation is integrated into the sintering process. In the present study, TiH₂ raw powders were directly consolidated by conventional press at 600 MPa and the integrated sintering process including dehydrogenation to produce pure Ti billet. The hot-extruded pure Ti material showed excellent tensile strength and elongation, according to the requirement of ASTM Ti Grade 4 and 1, respectively.



4:30 PM

The Effect of Micro-Alloying on the Preform Fabrication of Titanium Alloys and the Forged Mechanical Properties: *Ma Qian*¹; Y. F. Yang¹; X. Wu²; S. D. Luo²; K. Xia²; C. J. Bettles³; G. B. Schaffer²; ¹The University of Queensland; ²The University of Melbourne; ³Monash University

Preform fabrication from powder has the advantages over ingot metallurgy of ensuring excellent chemical homogeneity, fine and uniform grain structures, and flexible compositional changes. The availability of the lower cost quality hydrogenated and dehydrogenated (HDH) titanium powder makes it a practically attractive route to titanium preform fabrication. Micro-alloying is an established simple and cost-effective means of improving the constitutional and microstructural characteristics and mechanical properties of metallic materials. This paper presents a detailed study of the effect of micro-alloying on the preform fabrication of lower cost Ti-Fe and Ti-Cu alloys and the subsequently forged mechanical properties. Micro-alloying with boron (B) and silicon (Si) resulted in noticeable microstructural refinement due to enhanced heterogeneous nucleation and dispersion strengthening in the as-sintered titanium alloy preforms, in addition to the improved densification. The subsequent isothermal forging further substantially modified the microstructure leading to very attractive mechanical properties.

4:50 PM

Linear Friction Welding of Titanium Alloys – Processing, Characterisation and Properties: *Hangyue Li*¹; Simon Bray²; Yina Guo¹; Jiayun Jiang¹; Robin Wilson¹; Paul Bowen¹; ¹The University of Birmingham; ²Rolls-Royce plc

The growing performance requirements for modern engines have motivated the use of integrated blisk constructions, in which separated machined blades and disk are joined to form a solid component, using a linear friction welding technology. The mechanical properties including fatigue, fatigue crack growth resistance, impact toughness and fracture toughness are reviewed for linear friction welded Ti-6Al-4V and Ti-6Al-2Sn-4Zr-6Mo, together with weld integrity assessments and detailed microstructural analysis. An overmatch in hardness has been achieved as results of changes and refinement of microstructure in the welded zone. This gives rise to superior mechanical performance of the welded joints on the smooth and notched testpieces geometries, e.g. high cycle fatigue life and impact toughness, with failure location always identified outside the welded zone. By introducing a fatigue crack into the welded zone, damage tolerance related properties can be measured, which together with other assessments, contribute to the optimisation of welding process.

5:10 PM

Deformation Mechanisms in Near- α Titanium Friction Stir Welds: *Richard Fonda*¹; Keith Knipling¹; Adam Pilchak²; ¹Naval Research Laboratory; ²Air Force Research Laboratory

We have investigated the mechanisms of microstructural evolution that occur during friction stir welding of a fully lamellar near- α titanium alloy. Friction stir welds of α and near- α titanium alloys have a narrow thermomechanically affected zone, often containing alternating bands of acicular α , similar to the base plate microstructure, and refined prior β grains, similar to those observed in the weld nugget. We propose that these bands result from the development of periodic micro-shear bands and support this model through an analysis of 1) the observed microstructure and crystallographic texture and 2) automated reconstruction of the prior β grain structure and orientations that were present during welding. This work represents the first complete analysis of the deformation mechanisms occurring in both the α and β phases in the TMAZ of near- α titanium friction stir welds.

5:30 PM

X-Ray Tomography of CP Titanium Friction Stir Welds Incorporating Fiducial Markers: *Jennifer Wolk*¹; Richard Everett²; Stephen Szpara¹; ¹Naval Surface Warfare Center; ²Naval Research Laboratory

Friction stir welding (FSW) of titanium has the potential to reduce fabrication and life-cycle costs compared to conventional joining techniques. However, commercial-purity (CP) Ti has been found to be rather difficult to FS weld. Voids are frequently present, and control over weld consistency and quality is challenging. Markers have been placed in FS welds to aid flow visualization, process comprehension, and parameter optimization. In this paper, we discuss the initial use of nickel foil markers in 6 mm (0.25 inch) thick CP titanium FS welds. X-ray computed microtomography (XCMT), as well as standard microscopy techniques, has been utilized to study marker location, distribution, and material microstructures in these welds. The presence of the markers affects welding loads, surface finish, and void formation compared to standard welding. The markers clearly show differences in material deposited in the advancing and retreating sides, and are capable of delineating different flows at different depths.

5:50 PM

Effect of Dual-Laser Beam Welding on Microstructure Properties of Thin-Walled 947-TiAl Based Alloy Ti-45Al-5Nb-0.2C-0.2B (TNB): *Jie Liu*¹; Volker Ventzke¹; Peter Staron¹; Heinz-Günter Brokmeier¹; Michael Oehring¹; Nikolai Kashaev¹; Norbert Huber¹; ¹Institute of Materials Research, Helmholtz-Zentrum Geesthacht, Germany

The new generation of TiAl based alloys such as TNB could have a greater potential for industrial applications when suitable joining technologies will be available. Diffusion bonding and friction welding cannot be applied to join thin-walled TiAl structures. This work takes up the economic approach of laser beam welding techniques using two laser beams simultaneously. One laser beam having large spot size is used for pre-heating and the second for keyhole welding. The surrender of furnace equipment to achieve temperatures above brittle-ductile transition region can be realized by the application of this dual-beam process. The laser beam welded TNB is characterized using synchrotron X-ray diffraction, SEM, EDX, EBSD and microhardness testing to describe microstructure, residual stresses as well as microtexture in fusion zone, heat-affected zone and base material. The obtained results are showing that the dual-laser beam can be properly applied for defect-free joining of thin-walled TNB.

T.T. Chen Honorary Symposium on Hydrometallurgy, Electrometallurgy and Materials Characterization: Copper Electrorefining

Sponsored by: The Minerals, Metals and Materials Society, TMS Extraction and Processing Division, TMS: Hydrometallurgy and Electrometallurgy Committee, TMS: Materials Characterization Committee

Program Organizers: Shijie Wang, Rio Tinto Kennecott Utah Copper; J. E. Dutrizac, CANMET; Michael Free, University of Utah; J. Y. Hwang, Michigan Technological University; Daniel Kim, Rio Tinto Kennecott Utah Copper

Monday PM
March 12, 2012

Room: Oceanic 5
Location: Dolphin Resort

Funding support provided by: Rio Tinto Kennecott Utah Copper, ASARCO, and Freeport McMoRan

Session Chair: Michael Moats, The University of Utah

2:00 PM

METTOP-BRX-Technology – Industrial Application: Christine Wenzl¹; Andreas Filzwieser¹; Stefan Konetschnik¹; ¹METTOP GmbH

The METTOP-BRX-Technology is a novel manifold electrolyte inlet, which allows improving productivity and production in new and existing tankhouses by achieving higher current efficiency and cathode quality, as well as using higher current densities higher than 400 A/m². Two installation examples are shown: Montanwerke Brixlegg AG, Brixlegg, Austria (upgrade existing tankhouse) and Xiangguang Copper, Yanggu, China (new tankhouse). Montanwerke Brixlegg AG has been using the METTOP-BRX-Technology since 2005, and converted half of the whole tankhouse to METTOP-BRX in 2011 in order to use a current density of more than 400 A/m². Xiangguang Copper started up their second tankhouse in May 2011. This tankhouse was constructed in the same way as the existing tankhouse, but was designed for 292,000 t/a cathode copper (existing tankhouse: 200,000 t/a) by using the METTOP-BRX-Technology. This production increase is caused by a much higher current density, namely 410 A/m², compared to 280 A/m² in the old tankhouse.

2:20 PM

Implementing Wireless Electrolytic Cell Monitoring System at Kennecott Utah Copper for Improved Operational Efficiency: Ari Rantala¹; Daniel Kim²; ¹Outotec (Finland) Oy, Finland; ²Rio Tinto Kennecott Utah Copper

On-line monitoring of electrolytic cell performance in copper electrorefining requires complex electrical measurement systems and efficient management of enormous volume of data. Based on Kennecott Utah Copper's innovation, Outotec has developed in partnership a novel electrolytic cell monitoring system, CellSense™ System. As the system is based on self-powering from bus bars, wireless communication, on-line adaptive modeling and easy to access information and alarming, traditional obstacles of electrolytic cell monitoring are eliminated. With cell voltage and electrolyte temperature measurements, CellSense™ System enables real-time cell performance discovery and early reaction to critical production or quality disturbances such as short-circuiting, flow blockages, cold cathodes or electrolyte temperature excursions. During past few years the system has been delivered to over 3500 commercial cells. In this paper the largest CellSense™ System recently adapted by Kennecott Utah Copper with 1412 cells monitored on-line for high tankhouse performance, cathode quality and optimized operator work flow is presented.

2:40 PM

Autoclave Pressure Oxygen Leaching Of Anodic Copper Slimes: Tracy Morris¹; Luis Navarro¹; ¹ASARCO LLC

Anodic copper slimes produced during the electrolytic refining of copper are routinely batch leached to remove copper. At the Amarillo Copper Refinery an atmospheric leaching process was converted to an autoclave pressure vessel to improve the removal of copper, reduce the consumption of oxygen, improve leaching time and enhance tellurium recover. The benefits of pressurized versus atmospheric leaching of slimes were soon realized by obtaining the desired level of decopperization with less time and with lesser quantities of reagents. The autoclave was designed and constructed with a unique oxygen injection system that enables good control of the leaching process and with no plug ups. Other features include a mass measuring system that balances the quantity of slimes to be leached to the desired final solution concentration based on initial feed concentrations. The end result was a more efficient and controllable leaching process for removing copper from slimes.

3:00 PM

Mechanism and Thermodynamics of Floating Slimes Formation: Brent Hiskey¹; ¹University of Arizona

The global copper industry faces a technological challenge to develop processing schemes for more complex and impure ores and concentrates. Group 15 elements (As, Sb, and Bi) represent troublesome impurities both in terms of environmental impact and metallurgical processing. These so-call "dirty" copper concentrates are either unacceptable for smelting and refining or incur high penalties. The behavior of Group 15 elements is of critical importance in maintaining product quality and process performance. During copper electrorefining, these impurities are released to the electrolyte by electrochemical dissolution of the anode. Depending mainly on temperature, concentration, and oxidation state these elements can spontaneously co-precipitate from the electrolyte. These precipitates are referred to as floating slimes and their formation can have extremely detrimental effects on cathode purity. In this paper, the mechanism of floating slimes formation will be discussed and the fundamental thermochemistry will be reviewed and analyzed in relation to solubility properties.

3:20 PM Break

3:30 PM

Detellurization Process of Copper Anodic Slimes Leach Liquor by Cementation of Tellurium Using Elemental Copper: Tracy Morris¹; Luis Navarro¹; Weldon Read¹; ¹ASARCO LLC

During the leaching of anodic slimes, tellurium dissolves into the leach liquor together with copper and must be removed before the solution is sent to liberator cells for copper recovery. Prior to the installation of autoclaves tellurium was precipitated using raw slimes that caused a run around of tellurium in the leaching circuit. After autoclaves were installed the old leach tanks were converted into tellurium reactors utilizing copper chips, steam and agitation to form a copper telluride precipitate. Tellurium levels of less than 10 mg/l are achieved in a timely manner.

3:50 PM

New Process of Precipitation of Sb and Bi from Copper Electrolytes with PbO₂: Gerardo Cifuentes¹; Jaime Simpson²; Cristián Vargas¹; ¹USACH; ²ProPipe Ltda.

This paper presents a new process of precipitation of Sb and Bi present in copper refinery electrolytes in the presence of PbO₂ (Chilean Patent No. 45,037). To establish the conditions under which these compounds precipitating are forming, it was necessary to realise testing of PbO₂ consume, antimony extraction efficiency, stability tests, reaction kinetics, diffraction analysis and X-ray fluorescence, separation of size, plus observation of precipitates in the electron microscope. Preliminary tests was carried with synthetic electrolyte similar to copper refinery electrolytes, and then establish final testing with electrolytes from Chilean refineries. This process proves to be a real alternative for the treatment



TMS 2012

141st Annual Meeting & Exhibition

MONDAY PM

of copper refinery electrolytes for control of Sb and Bi in solution, presenting a very simple operation and low cost compared with competing processes. Keywords: Antimony, Bismuth, Precipitation, PbO₂, Copper, Electrorefining.

4:10 PM

Study of Electrolyte Impurity Precipitates at the Kennecott Refinery: *Justin McAllister*¹; Daniel Kim¹; Shijie Wang¹; ¹Rio Tinto

At the Kennecott Utah Copper Refinery, impurities in the electrolyte are being precipitated in the circulation system and form a hard scale on the pipes. This scale must be removed periodically for proper electrolyte flow. Distinct layers of differing composition form as the operating conditions of the tank house changes. Scale samples from the inlet and outlet pipes were analyzed to discover the nature of the precipitate. Each sample was sectioned and examined under optical microscopy and SEM. The composition of the scale was analyzed using ICP, XRD, and SEM/EDX mapping. The rate of deposition was determined through measuring the amount deposited on new pipes after elapsed time intervals. In order to determine how to minimize the formation of the scale the mechanism was studied and the results are presented in this paper.

4:30 PM

Copper Refining Electrolyte Purification by the Use of Molecular Recognition Technology (MRT) for Bismuth Removal: *Luis Navarro*¹; Weldon Read¹; Tracy Morris¹; ¹ASARCO LLC

Bismuth is a renowned contaminant in the electrolytic refining of copper that can render many a cathode to be outside ASTM standards and unsuitable for copper rod and other down stream products if not carefully controlled. This paper portrays the performance of Molecular Recognition Technology (MRT) for Bismuth removal at the Amarillo Copper Refinery and describes how the highly selectivity gel has been successfully used to achieve good bismuth removal and how many pit falls and draw backs have been overcome.

4:50 PM

Optimizing a Cascading Liberator: *Bradford Westrom*¹; Omar Araujo¹; ¹Freeport-McMoRan Copper & Gold

Impurities from electrolytic refinery are typically extracted from the electrolyte utilizing conventional electro winning cells. These cells are arranged in series with cascading solution flow and are commonly referred to as liberator cells. The Freeport McMoRan Copper & Gold El Paso Refinery has optimized the removal of arsenic in cascading liberator cells by utilizing two separate feed solutions. The primary feed solution is recycled liberator electrolyte and the secondary feed solution is "neat" tank-house electrolyte. The secondary feed solution is added based on the voltage response across the individual cells utilizing independent variable frequency drive (VFD) pumps. When the voltage across a cell changes, a signal is sent to the VFD pump to maintain a cell voltage of 1.98 volts. By maintaining this voltage the copper content in each cell exits at 2-4 grams per liter. This safely optimizes the arsenic removal as copper arsenides on the liberator cathodes.

5:10 PM

Copper Electrorefining Impurity Evaluation: *Michael Free*¹; Justin McAllister²; Urian Marshall¹; Megan Marshall¹; Daniel Kim²; Shijie Wang²; ¹University of Utah; ²Kennecott Utah Copper, LLC

Electrorefining copper cathode impurity levels were evaluated based on 1/10th scale laboratory electrorefining tests. Cathodes were evaluated near the top, mid-section, and bottom sections of cathodes on both set and mold sides and strip and scrap cycles. Slime weights were also measured, and slime and electrolyte samples were also evaluated for impurities. Results from these tests have been compiled and compared to evaluate the effects of changes in operating conditions and electrode location on cathode impurities.

Ultrafine Grained Materials VII: Deformation Mechanisms

Sponsored by: The Minerals, Metals and Materials Society, TMS Structural Materials Division, TMS/ASM: Mechanical Behavior of Materials Committee, TMS: Nanomechanical Materials Behavior Committee, TMS: Shaping and Forming Committee

Program Organizers: Suveen Mathaudhu, U.S. Army Research Office; Xiaoxu Huang, Risø National Laboratory for Sustainable Energy, Technical University of Denmark; Hyoung Seop Kim, POSTECH; Terence Langdon, University of Southern California; Terry Lowe, Manhattan Scientifics, Inc.; Ruslan Valiev, Ufa State Aviation Technical University; Xiaolei Wu, Institute of Mechanics, Chinese Academy of Sciences; Michael Zehetbauer, University of Vienna

Monday PM
March 12, 2012

Room: Swan 5
Location: Swan Resort

Session Chairs: Hyoung Seop Kim, POSTECH; Terence Langdon, University of Southern California; Ruslan Valiev, Ufa State Aviation Technical University; Xiaolei Wu, Institute of Mechanics, Chinese Academy of Sciences

2:00 PM Invited

Austenitic Steels Strengthened by Nano-Scale Twins: *K. Lu*¹; Nairong Tao¹; ¹Shenyang National Laboratory for Materials Science, Institute of Metal Research, Chinese Academy of Sciences

Recent studies showed that nano-scale twins are effective in strengthening metals with a superior strength-ductility synergy. By means of dynamic plastic deformation (DPD, i.e., deformation at high strain rates) and subsequent thermal annealing, a mixture structure of micro-sized recrystallized grains embedded with grains with nano-scale twins is formed in austenitic steels with low stacking fault energies. Tensile properties of the single-phased austenitic steels strengthened by nano-scale twins are systematically investigated. Strength and elastic modulus of the nano-twinned grains is determined by means of nano-indentation measurements and calculations in terms of rule-of-mixture, respectively. Strength-ductility combinations of the steel sample are analyzed with regard to the morphologies, volume fraction, and distributions of the nano-twinned grains and recrystallized micro-sized grains.

2:20 PM

Twinning Phenomena in Cryomilled Pure Mg and Mg-Al-Zn Alloy Nanocrystalline Powders: *Baolong Zheng*¹; Ying Li²; Yizhang Zhou¹; Suveen Mathaudhu³; Enrique Lavernia¹; ¹University of California, Davis; ²Los Alamos National Laboratory; ³U.S. Army Research Office,

Twin boundaries in nanocrystalline (NC) metals are of interest due to their potential for strength enhancement with concurrent retention of ductility; their characteristics include: coherent nature, low interface energy, low dynamic recovery, and enabling of dislocation accumulation. Twin formation, however, is rarely observed in NC hexagonal close-packed (HCP) Mg metals when subjected to high levels of grain refinement to the nanoscale. In this study, powders of NC pure Mg and commercial Mg-Al-Zn alloy were synthesized via a cryomilling. The observation of twins with TEM and HRTEM is reported in both cryomilled NC pure Mg and Mg-Al-Zn alloy powders. The formation of twins might be attributed to the presence of a high strain and to the low (cryogenic) temperature during cryomilling. The formation of twins by cryomilling provides a promising approach to improve the mechanical properties of NC Mg and alloys.

2:35 PM

An Elasto-Plastic Dislocation and Disclination Model for Small Scale Plasticity: Application to Grain Boundaries and Triple Junctions: *Laurent Capolungo*¹; Manas Upadhyay¹; Vincent Taupin²; Claude Fressengeas²; ¹Georgia Institute of Technology; ²Universite Paul Verlaine

In a large series of crystalline materials –such as nanostructured materials-, plasticity and thermally activated microstructure evolutions are dominated by the behavior of interfaces (e.g. grain boundaries) and by the interactions between grain boundaries and (1) dislocations and (2) other grain boundaries. In the present work, a general field defect dynamics method –able to model both dislocations and disclinations- is developed such as to address current limitations of constitutive models regarding interface driven plasticity. The work is first applied to a static case where the relationship between triple junction geometry and excess elastic energy is investigated. Second, the dynamics model is applied to the case of grain boundary deformation. In particular, the problems of grain boundary relaxation and of shear couple boundary migration are studied. It is found here that the Field Defect Mechanics model is capable of reproducing some of the key features of grain boundary deformation.

2:50 PM

Effect of Stacking Fault Energy on the Microstructural Evolution of Pure Cu and Cu-Al Alloys during Severe Plastic Deformation: *Xianghai An*¹; Shiding Wu¹; Zhefeng Zhang¹; Roberto Figueiredo²; Nong Gao³; Terence Langdon⁴; ¹Shenyang National Laboratory for Materials Science, Institute of Metal Research, Chinese Academy of Sciences.; ²Department of Metallurgical and Materials Engineering.; ³Materials Research Group, School of Engineering Sciences.; ⁴Departments of Aerospace & Mechanical Engineering and Materials Science, University of Southern California

Pure Cu and Cu-Al alloys with different stacking fault energies (SFEs) were processed by severe plastic deformation (SPD) methods to systematically explore the roles of the SFE in microstructure evolution. With a lowering of the SFE, the deformation mechanisms were gradually transformed from dislocation slip to deformation twins while shear bands were increasingly significant to carry the local plasticity. Concurrently, with decreasing SFE, the grain refinement processes were also transformed from dislocation subdivision to twin fragmentation, while the grain size was refined from the ultrafine region into nanoscale. Furthermore, the homogeneous microstructures are more readily achieved in materials with high or low SFE than in materials with medium SFE due to different mechanisms governing the microstructural evolution. Specifically, recovery processes are dominant in high or medium-SFE materials whereas twin fragmentation is dominant in low-SFE materials.

3:05 PM

Effect of Stacking Faults and Twin Boundaries on Grain Refinement Induced by High-Pressure Torsion: *Yanbo Wang*¹; Xiaozhou Liao¹; Yonghao Zhao²; Enrique J. Lavernia²; Simon P. Ringer¹; Zenji Horita³; Terence G. Langdon⁴; Yuntian Zhu⁵; ¹The University of Sydney; ²University of California; ³Kyushu University; ⁴University of Southern California; ⁵North Carolina State University

A recent model developed to predict the smallest grain sizes obtainable by severe plastic deformation has worked well for materials with medium to high stacking fault energies (SFEs) but not for those with low SFEs. To probe this issue, we selected a Cu–30 wt.% Zn alloy with SFE ~ 7 mJ/m² to investigate the grain refinement mechanism during high-pressure torsion processing. We found that stacking faults and twin boundaries have a significant effect on grain refinement. The density of stacking faults and deformation twins determines the smallest achievable grain size. Our results indicate that the grain refinement mechanisms in materials with low SFEs are fundamentally different from those of materials with medium to high SFEs.

3:20 PM Invited

Effects of Deformation Parameters and Stacking Fault Energy on Grain Refinement in Cu–Al Alloys Subjected to Plastic Deformation: *Nairong Tao*¹; Y. Zhang¹; K. Lu¹; ¹Shenyang National Laboratory for Materials Science Institute of Metal Research, Chinese Academy of Sciences

Plastic deformation is effective in inducing grain refinement in polycrystalline materials, the kinetics of which is determined by deformation parameters and the nature of materials. In this work, effects of stacking fault energy (SFE) and deformation parameters on microstructure characteristics and tensile strength were investigated in Cu–Al alloys. It is shown that plastic deformation is dominated by twinning at the nano-scale in Cu-Al samples with <4.5% Al subjected to dynamic plastic deformation at liquid nitrogen temperature. Hence, the nano-scale grains are achieved via shear banding of nano-twins and interaction between dislocations and twin boundaries. For alloys with SFEs of >50 mJ m⁻², dislocation slip dominates the plastic deformation when deformed by using quasi-static compression at room temperature. A map of deformation modes and corresponding strain-induced grain refinement is drawn in the space of SFE and processing parameters for the Cu–Al alloys.

3:40 PM

The Influence of Dislocation Density on Dislocation-Twin Boundary Interactions in Nanocrystalline Materials: *Song Ni*¹; Yanbo Wang¹; Xiaozhou Liao¹; R.B. Figueiredo²; Hongqi Li³; S.P. Ringer¹; T.G. Langdon⁴; Yuntian Zhu⁵; ¹The University of Sydney; ²Federal University of Minas Gerais; ³Los Alamos National Laboratory; ⁴University of Southern California; ⁵Department of Materials Science & Engineering, North Carolina State University

Dislocation–twin boundary (TB) interactions in nanocrystalline grains with different dislocation densities were investigated. We discovered that, in addition to intrinsic material properties and extrinsic factors reported in the literature including stacking fault energy, energy barriers for dislocation reactions at TBs, twin thickness, and applied stress, the dislocation density also plays a significant role in the dislocation–TB interactions. In a twinned grain with a low dislocation density, a dislocation can fully or partly penetrate or be absorbed by a TB via various dislocation reactions. While in a twinned grain with a high dislocation density, dislocations will be pinned and tangle each other at a TB, making it impossible for dislocations to slip across the TB via dislocation reactions. To release the strain energy caused by dislocation accumulation at the TB, partial dislocations will be emitted from the other side of the TB, resulting in the formation of secondary twins.

3:55 PM Break

4:10 PM Invited

Deformation Mechanism of Columnar-Grained Cu with Preferentially Oriented Nanoscale Twins: *Lei Lu*¹; ¹Institute of Metal Research, CAS

The strengthening mechanism of nanotwinned structure has attracted lots of attention, especially in the equiaxed-grained copper with random edge-on nanoscale twins where enhancements in strength and ductility are achieved simultaneously, and twin boundaries serves as effective barriers for dislocation slip transmission. In this talk, the plastic deformation of columnar grained Cu sample with nanoscale twins, which are preferentially oriented parallel to growth plane, were systematically investigated by tension test. It is interested to find that the effective TB confinement of threading dislocation slip inside the lamellar channels dominates the plastic deformation and strengthening behavior, which is different from the slip transfer process in the equiaxed-grained nt-Cu samples. Detailed microstructure investigation suggests that the columnar-grained Cu samples exhibit inhomogeneous deformation during plastic deformation.



4:30 PM

Deformation Twinning in Commercial Pure Titanium during Severe Plastic Deformation: Yanjun Li¹; Yongjun Chen²; John Walmsley¹; Hans Roven²; ¹SINTEF Materials and Chemistry; ²Department of Materials Science and Engineering, NTNU

Twinning is an important deformation mechanism of hexagonal close packed (HCP) titanium during plastic deformation. However, the twinning behavior of titanium during severe plastic deformation can be much different from that occurred during conventional deformation. In the present work, the twinning behavior of commercial pure (CP)Ti subjected to severe plastic deformation, equal channel angular pressing (ECAP) and high pressure torsion (HPT), at different temperatures has been systematically studied by transmission electron microscopy (TEM) and electron backscattering diffraction (EBSD). The type, size, morphology and the twin boundary structure of different twins have been characterized. The influence of deformation twins on the formation of ultrafine grained microstructures of CP-Ti has been discussed.

4:45 PM

Mechanical Behavior of and Deformation Mechanisms in a Nanocrystalline Alloy: Ruslan Valiev¹; Dmitry Gunderov¹; Aleksander Lukyanov¹; ¹Ufa State Aviation Technical University

To reveal the deformation mechanisms of fully dense metals with less than 30-50 nm grain sizes the tensile straining behavior of a nanocrystalline TiNi alloy has been thoroughly studied in the present work. Formation of the homogeneous ultrafine-grained structure with a grain size of about 30 nm was achieved through application of severe plastic deformation techniques. Microstructure evolution analysis comprised TEM/HREM, SEM, X-ray. Mechanical tests included measurements of strain rate sensitivity of flow stress, strain hardening, activation energy. There were received experimental evidence and provided a model description of dislocation activity, grain boundary sliding and grain rotation in the nanocrystalline material.

5:00 PM

Grain Refinement in Pure Titanium Processed by Severe Plastic Deformation: Y. Chen¹; Y. Li²; X. Xu³; J. Hjelen¹; H. Roven¹; ¹NTNU; ²SINTEF; ³Jiangsu University

Grain refinement of commercial pure (CP) titanium during 1-8 passes of equal channel angular pressing (ECAP) and the effect of temperature on the deformation microstructures of CP Ti after one-pass ECAP are investigated by electron backscattering diffraction (EBSD). The results show that grain refinement mainly takes place in the first pass and the efficiency gradually decreases from 1 to 4 passes, reaching saturation with further increasing strain (6-8 passes). Different types of twins activated during one-pass ECAP at different temperature are analyzed systematically. Misorientation gradients and the driving force of dynamic recrystallization are discussed.

5:15 PM

Grain Boundary Sliding in Ultra-Fine Grained 5083 Al: Ming-Je Sung¹; Jung Hun Han¹; Farghalli Mohame¹; ¹University of California, Irvine

Quantitative measurements and analysis of grain boundary sliding (GBS) in ultrafine-grained (UFG) 5083 Al by AFM was conducted at 573 K. The grain size of as-received cryomilled UFG 5083 Al was characterized by AFM, TEM and EBSD, and the average was found to be about 300 nm. Ion beam polishing/etching technique was used to reveal grain boundaries for AFM characterization. The vertical offset of GBS was measured by comparing predeformation and postdeformation AFM images. By analyzing these measurements, the contribution of GBS to

the total strain was estimated as 22% and 36% at a strain rate of 10^{-4} /sec and 10^{-1} /sec. It was demonstrated that the relatively low value of the contribution of GBS to the total strain is most likely the result of testing under experimental conditions that favor the dominance of region I (low-stress) of the sigmoidal behavior characterizing high strain rate superplasticity, which was previously reported.

5:30 PM

Structural and Mechanical Characterization of Nanostructured Al-1%Si Alloy Produced by Heavy Cold Rolling: Tianlin Huang¹; Qingshan Dong¹; Xu Gong¹; Xiaoxu Huang²; Qing Liu²; ¹Chongqing University; ²Risø National Laboratory for Sustainable Energy, Technical University of Denmark

Recently, recovery annealing induced decrease in tensile elongation has been reported in nanostructured Al samples, which has been attributed to a decrease in the density of mobile dislocations in the annealed samples. This study explores the possibility to prevent this undesired annealing effect by introducing incoherent particles in the microstructure. Nanostructured Al-1% Si alloy (ultra-high pure Al matrix: 99.9996%) samples have been produced by cold rolling to 98% thickness reduction, and then recovery annealed for 1h at temperatures up to 200°C. In all samples micrometer- and nanometer-sized Si particles were present in the microstructure. The cold-rolled sample exhibited a lamellar structure with boundary spacing of 230 nm, which increased to 800 nm after annealing at 200°C. Tensile results showed no decrease in the elongation in annealed samples. TEM observations suggested that an easy generation of dislocations at the particle interfaces may play a role in stabilizing the tensile deformation.

5:45 PM

Processing of Ultrafine-Grained Nickel by Dislocation Activities at Intermediate Dynamic Strain Rate: Microstructure Evolution and Mechanical Properties: Lukasz Farbaniec¹; Guy Dirras¹; Akrum Abdul-Latif²; ¹LSPM - UPR3407 CNRS; ²Laboratoire d'Ingénierie des Systèmes Mécaniques et des Matériaux

Ultrafine-grained Ni microstructures were processed by means of Dynamic Plastic Deformation (DPD) at room temperature (RT) using a falling mass at a velocity of 10.38 m/s. The starting material was a commercially pure texture-free coarse-grained (~9 μm) Ni. The as-processed microstructure and its crystallographic texture were thoroughly investigated. In particular, electron backscattering diffraction and transmission electron microscopy experiments showed that the initial equiaxed grains evolved into a laminar structure of narrow domains of submicron sizes delineated by high angle grain boundaries. The mechanical behavior under quasi-static compression at RT at a strain rate of 2×10^{-3} s⁻¹ was investigated in directions parallel and perpendicular to the DPD compression axis. Stress-strain responses showed an increase of the yield strength (620-750 MPa) compared to the initial state (80 MPa). In addition, the strain hardening behavior was also found to depend strongly on the orientation of the compression axis.

2012 Functional and Structural Nanomaterials: Fabrication, Properties, Applications and Implications: 0-Dimensional Nanomaterials

Sponsored by: The Minerals, Metals and Materials Society, TMS Electronic, Magnetic, and Photonic Materials Division, TMS: Nanomaterials Committee

Program Organizers: Jiyoung Kim, University of Texas; David Stollberg, Georgia Tech Research Institute; Seong Jin Koh, University of Texas at Arlington; Nitin Chopra, The University of Alabama; Terry Xu, UNC Charlotte

Tuesday AM
March 13, 2012

Room: Pelican 1
Location: Swan Resort

Session Chair: Terry Xu, University of North Carolina at Charlotte

8:30 AM Introductory Comments

8:35 AM Invited

Computational Study on Nanoparticles in Catalysis: Da Hye Kim¹; Hyun You Kim¹; Ji Hoon Ryu¹; *Hyuck Mo Lee*¹; ¹KAIST

Recent reports have attributed the remarkable catalytic activity of nanoparticles. We focus on catalysis by nanoparticles to design new catalysts. Computational methods can be used to describe details on surface chemical reactions and to understand and predict variations in catalytic reactivity of nanoparticles. We performed the density functional theory calculations to obtain adsorption properties, reaction pathways, and activation energies for CO oxidation on various nanoparticle systems. Based on calculation results and a modified kinetic model, examples that include how alloying, the structure, charge state of nanoparticles, reaction mechanism, and ligands surrounding nanoparticles affect the electronic configuration and catalytic properties of nanoparticles are reviewed.

9:10 AM

Characterization of Metallic Nano Particles Synthesized by Electrical Wire Explosion Technique for Catalytic Application: *Seung-Yub Lee*¹; Gwang-Yeob Lee²; Hyo-Soo Lee²; Min-Ha Lee²; ¹Columbia University; ²Korea Institute of Industrial Technology (KITECH)

Electrical wire explosion technique, one of the methods for producing metallic nano particles has gained recent interests due to its simple and fast process. In this study, Ni-Fe and Pt-Ni binary nano particles were synthesized from 0.1 mm diameter wires in de-ionized water. Microscopy analysis (TEM & EDX) shows core-shell structure with average particle size of 30 nm. Two metal elements tend to be separated by forming core shells, outer layers of which are oxygen rich compared to the core region. Synchrotron X-ray radiation was utilized to identify precise nano phases as well as their volume fraction. It is also found that the oxygen content in DI water is a critical parameter to control nano oxide layers. Based on these results, the appropriate experimental parameter search is in progress to obtain uniform particle size and desirable phase separation for catalytic application.

9:30 AM

Citrate Mediated Wet Chemical Synthesis of Fe Doped Nanoapatites: A Model for Singly Doped Multifunctional Nanostructures: *Rajendra Kasinath*¹; Michael Klem¹; Robert Usselman²; ¹Montana Tech of the University of Montana; ²NIST-Boulder

The structurally forgiving nature of the apatite lattice can be employed to synthesize functional nano-hydroxyapatite (nHA) particles with calcium site substitution by metal atom doping. In this work we present an effective green synthetic methodology to synthesize equiaxed and highly dispersed Fe(III)-doped multifunctional nHA particles by controlled aging of a calcium phosphate precursor. It was seen that doping in the HA lattice, while employing this wet chemical technique, does not induce a structural change even with 60 atom% Fe-substitution. The Fe(III) doped nanoparticles exhibited both magnetic and luminescent properties.

The magnetic properties were measured employing magnetometry and SQUID. Fe doped nHA particles exhibited green fluorescence under UV excitation as seen from fluorescence spectroscopy. While single property modulation in nHA has been previously shown by doping with metal atoms, herein we show that it is possible to design nHA particles, and perhaps others, with multifunctional properties with only one dopant.

9:50 AM

Selective Electrocatalytic Activity of Ligand Stabilized Copper Oxide Nanoparticles: *Christopher Matranga*¹; Douglas Kauffman¹; Paul Ohodnicki¹; Brian Kail¹; ¹US DOE- NETL

Organic ligands are commonly used as stabilizing agents during the synthesis of nanoparticles (NPs), but very little is known about their effect on NP reactivity. Metal oxide NPs are an interesting platform to study ligand influenced electrocatalysis because their surface composition and oxidation state can influence reactivity and product selectivity. The role of oleic acid ligands on the selective electrocatalytic activity of CuO and Cu₂O NPs has been evaluated and compared to bulk materials, as well as NPs with weakly interacting or no surface ligands present. Oleic acid capped NPs show a significantly enhanced catalytic selectivity and reactivity during methanol oxidation and CO₂ reduction reactions in comparison to the bulk and NP reference systems. In situ Raman, electrocatalytic studies, and ex-situ infrared spectroscopy measurements indicate that the capping ligands sustain surface Cu-O species throughout these reactions which likely play a role in the observed catalytic activity.

10:10 AM Break

10:25 AM

Preparation of Colloidal Quantum Dot Nanocrystals for Analysis by Atom Probe Tomography: *Sonal Padalkar*¹; Bhola Nath Pal²; Jennifer Hollingsworth²; Lincoln Lauhon¹; ¹Northwestern University; ²Los Alamos National Laboratory

Colloidal quantum dots have outstanding luminescent properties, and non-blinking dots have recently been demonstrated through the synthesis of new core-shell structures. Here, giant quantum dots (GQD) consisting of a ~3 – 4 nm luminescent CdSe core and ~12 – 16 nm protective CdS shell were synthesized and prepared for 3D composition analysis by atom probe tomography (APT). Monolayer self-assembly, metal deposition, and lift-out with focused ion beam (FIB) milling were used to prepared GQD samples for atom probe analysis. A wedge shaped lift-out specimen was cut from a monolayer of GQDs sandwiched between two metal layers, and the rotated wedge was mounted on a micropost array to make a vertical specimen. The lift-out was sharpened precisely using annular patterns in the FIB to form a sharp tip with a diameter of ~100 nm. Preliminary APT analysis of the GQD will be presented, along with a discussion of sample preparation procedures.

10:45 AM

Supercapacitive Properties of Hydrothermally Synthesized Co₃O₄ Nanostructures: *David Mitlin*¹; Huatao Wang¹; Li Zhang¹; ¹University of Alberta and NINT NRC

A hydrothermal process was employed to create a variety of Co₃O₄ nanostructures. We demonstrate that nominally minor differences in the synthesis temperature (50, 70 or 90°C) yielded profound variations in the oxide microstructure, with lathe-like, necklace-like and net-like morphologies of different scales resulting. This in turn resulted in significant variations in the supercapacitive performance that ranged from mediocre to superb. Specifically, the mesoporous net-like Co₃O₄ nanostructures that were synthesized at 50°C exhibited very favorable electrochemical properties: The net-like Co₃O₄ had a specific capacitance of 1090 F/g at a mass loading of 1.4 mg/cm². At this high mass loading such performance has not been previously reported. SEM and TEM analysis of these samples revealed an interconnected array of sub-10 nm crystallites interspersed with a high volume fraction of pores that were on the same scale. The poorer performing microstructures were both coarser and much less porous.



TMS 2012

141st Annual Meeting & Exhibition

11:05 AM

Synthesis and Silica Encapsulation of Magnetite Nanoparticles for Biomedical Applications: *Shampa Aich*¹; Pravin Dixit¹; ¹Indian Institute of Technology Kharagpur

Magnetite nanoparticles were prepared by co-precipitation of Fe_3O_4 from a mixture of $FeCl_2$ and $FeCl_3$ upon gradual addition of NH_4OH . Later, to prevent agglomeration and bio-degradation, those nanoparticles were coated with inorganic silica by modified Stöber process using tetraethoxy-ortho-silicate (TEOS) as the silica-shell building material. FE-SEM, DLS, and HR-TEM analyses revealed a successful synthesis of magnetite-core nanoparticles (50-125 nm) with varying shell-thickness. Silica-shell thickness and monodispersity of the core-shell nanoparticles were increased with TEOS addition and mechanical stirring. X-ray diffraction, FT-IR, and zeta (ζ) potential analyses confirm the synthesis of magnetite nanoparticles, silica gel and the silica coated magnetite nanoparticles. Magnetometer (VSM) measurements showed that the original magnetization of magnetite nanoparticle was merely affected by the coating procedure. The results obtained from In-vitro biocompatibility tests using incubated osteoblasts indicate that the silica-coated nanoparticles are promising candidates for further in vivo investigations of applications in medical diagnosis and drug delivering treatments.

2012 Symposium on Surfaces and Heterostructures at Nano- or Micro-Scale and Their Characterization, Properties, and Applications: Surfaces, Deposition, and Coatings

Sponsored by: The Minerals, Metals and Materials Society, TMS Electronic, Magnetic, and Photonic Materials Division, TMS Materials Processing and Manufacturing Division, TMS: Energy Conversion and Storage Committee, TMS: Nanomaterials Committee, TMS: Surface Engineering Committee, TMS: Young Leaders Committee, TMS: EMPMD Council

Program Organizers: Nitin Chopra, The University of Alabama; Ramana Reddy, The University of Alabama; Arvind Agarwal, Florida International University; Sandip Harimkar, Oklahoma State University; Jiyoung Kim, University of Texas at Dallas; Christopher Matranga, National Energy Technology Laboratory

Tuesday AM

March 13, 2012

Room: Pelican 2

Location: Swan Resort

Session Chairs: Sandip Harimkar, Oklahoma State University; Arvind Agarwal, Florida International University

8:30 AM

Microstructures and Performance of Sputter Deposited NiAl-Cr-Hf and NiAl-Cr-Zr Coatings: *Joel Alfano*¹; Mark Weaver¹; ¹Univ of Alabama

Nickel-based superalloy components in the hot sections of commercial gas turbine engines are often protected by aluminide coatings due to their ability to function in oxidative and corrosive environments. However, the microstructures of these coated systems are metastable and change in service due to interactions with the environment and interdiffusion with the underlying substrate. The extent of these changes depends critically upon coating microstructure, chemistry, and the environment that the coated component operates in. This presentation highlights the influences of chemical composition, post-deposition annealing, and isothermal oxidation at 1050°C on the microstructures and properties of NiAl-Cr-Hf and NiAl-Cr-Zr overlay bond coatings. In particular, the results indicated that Hf additions inhibited the Al-depletion resulting in a slower formation of the thermally grown oxide as compared to the Zr containing samples. Hf containing samples also show more resistance to internal oxidation of the coatings. Results are discussed relative to conventional coating systems.

8:50 AM

New Trends in Superhydrophobic Coating Using PS/SiO₂: *Ariosvaldo Sobrinho*¹; Marcos Baracho¹; Rômulo Navarro¹; Felipe Mariz¹; José Nascimento¹; André Rodrigues²; ¹UAEMA / UFCG; ²UFC/DEMA

Superhydrophobic coating materials used in high technology has been shown to be of high relevance in several technological applications such as polymers and composites, anti-corrosion metals, glass and ceramic water repellent, among others. Superhydrophobic surfaces, hydrophobic fabrics, water-repellent materials and superhydrophobicity are among the most widely used terms in the scientific literature. In this work were obtained superhydrophobic nanocomposites based on polystyrene core-shell particles (PS/SiO₂). The angle of contact between the drop of water and surfaces of the materials (polymers, metals and ceramics), were measured by the inclination of the drop, giving an indication of the wettability of surfaces coated with the PS/SiO₂ composites (polymers, metals and ceramics). The influence of the drying temperature and SiO₂ percent on the wettability of nanocomposite coating were investigated. The behavior of the wet surface of the composite PS/SiO₂ obtained depends crucially on the drying temperature and the proportion of SiO₂ nano particles relative to polystyrene.

9:10 AM Invited

Production of SiC Using Thermal Plasma: M. Ramachandran¹; *Ramana Reddy*¹; ¹The University of Alabama

Thermal plasma processing is a high temperature process with high energy content that can tremendously increase the kinetics of a reaction by several orders of magnitude. The production of SiC was carried out using SiO₂ as the feed material and methane as a reducing gas. The process was carried out at different molar ratios of SiO₂:CH₄ = 1:0.8, 1:1; and 1:1.5. The highest product yield of SiC was obtained at a molar ratio of 1:1 (SiO₂:CH₄) at a power of 21.6 kW. The product yield was reduced substantially when the plasma power was reduced to 18.9 kW and resulted in higher amounts of SiO₂ in the product powders. Formation of elemental Si was also observed in some of the experiments. The product powders were characterized using X-Ray Diffraction (XRD), Scanning Electron Microscopy (SEM) and Transmission Electron Microscopy (TEM) to determine the phases formed and their morphology. The presence of nanowires was observed which were characterized using Selective Area Diffraction (SAD) in TEM.

9:45 AM

Surface Nanostructuring of Steel 35 by Electrospark Machining with Electrodes Based on Tungsten Carbide and Added Al₂O₃ Nanopowder: *Sergey Nikolenko*¹; Nikolay Syuy¹; ¹Institute of Materials Science, Khabarovsk Scientific Center, Far Eastern Branch, Russian Academy of Sciences

The study of the process of the AL manufacturing on steel 35 using mechanized ESA by the standard VK8 alloy and the VK8 alloy with an additive of 1–5% Al₂O₃ nanopowder made it possible to determine the reasonable parameters and modes for the model of the developed device. It was shown that the efficiency of the process of rough ESA increases upon an increase of the pulse duration up to the limit appropriate for a certain electrode material. The Al₂O₃ additive in the amount of 1 wt % into VK8 increases, compared to the standard VK8 alloy, the overall mass transfer and efficiency of the process of the AL formation by almost three times. The microhardness of the alloy layers exceeds by three–four times the microhardness of steel 35.

10:05 AM Break

10:10 AM

Synthesis and Characterization of Oxide-Based Core/Shell Nanowires: Lyndon Smith¹; *Nitin Chopra*¹; ¹The University of Alabama

Core/shell nanowire heterostructures are of great importance for energy applications and nanoelectronics. Towards this end, we report a unique hybrid approach to synthesize copper oxide/tantalum oxide core/shell nanowires by coupling bottom-up nucleation and growth processes.

TUESDAY AM

In addition, structure and processing relationships were evaluated for these core/shell nanowires. The structures were characterized using X-ray diffraction (XRD), scanning electron microscopy (SEM), energy dispersive spectroscopy (EDS), transmission electron microscopy (TEM), Raman spectroscopy, X-ray photoelectron spectroscopy (XPS), and UV-vis spectroscopy.

10:25 AM

Triboemission Phenomena: Electronic and Photonic Outputs from Surface Modification, and Its Use as Novel Probes for the Dynamics of Surface Processes: *Gustavo Molina*¹; *Czeslaw Kajdas*²; ¹Georgia Southern University; ²Automotive Industry Institute PIMOT

The authors have obtained extensive data indicating that emission of low energy electrons, called electron triboemission, is produced from mechanical surface work, particularly from surface oxides and semiconductors under contact sliding. Emission of tribo-photons during friction has also been observed, the dynamics of their production being similar to that of electron triboemission. Electron triboemission is often seen as a case of electron exoemission, but such low-energy output may be just a fraction of the total electronic excitation on the surface, the majority of which being internal currents. All these electronic (and concomitant photonic) excitations during mechanical work are known to be important factors in some surface processes, in particular for initiation and control of mechano-chemical reactions and/or during surface interactions. This paper discusses the authors' work on triboemission, and the possible use of the developed measurement techniques as novel probes for the dynamics of surface processes.

10:40 AM Invited

How and Why Do Whiskers Grow from Sn Coatings?: *Eric Chason*¹; *Fei Pei*¹; *Nitin Jadhav*¹; ¹Div of Engineering

Sn whiskers grow spontaneously out of coatings on Cu and have become a critical reliability problem, responsible for numerous system failures. We will describe studies to determine the mechanisms controlling their formation by measuring the relationship between Cu-Sn intermetallic (IMC) formation, stress and whisker density. This (and the work of others) has led to a picture in which stress builds up due to IMC growth and causes whiskers to form at "weak grains", i.e., grains that have a stress relaxation mechanism that becomes active at a lower stress than its neighbors. Real-time SEM/FIB videos illustrate the growth process in detail. These show that whisker-like protrusions grow out of a single grain on the surface with little lateral growth. FEA (finite element analysis) calculations simulate the evolving stress and whisker growth for several different mechanisms that may lead to "weak" grains.

11:10 AM Invited

Flexible, Transparent, Conducting Films of Copper Nanowires: *Benjamin Wiley*¹; ¹Duke University

Copper nanowires with diameters of 60 nm and lengths exceeding 20 μ m have been synthesized in an aqueous solution of NaOH, ethylenediamine, Cu(NO₃)₂ and hydrazine. Meyer rod coating of these nanowires onto plastic substrates produced films with sheet resistances less than 30 ohm/sq, and transmittances greater than 85%. Unlike transparent, conductive oxides, films of copper nanowires remain conductive after severe flexing. The low cost, scalable processing, high electrical and optical performance, and unique mechanical properties of copper nanowire films make them a promising alternative to indium tin oxide for use in flexible displays, organic LEDs, and thin-film photovoltaics.

11:40 AM Invited

Synthesis of Multifunctional Surface Nanocomposites with Tunable Size, Composition, and Properties: *Ritesh Sachan*¹; *Sagar Yadavali*¹; *Nozomi Shirato*¹; *Gerd Duscher*¹; *Hernando Garcia*²; *Stephen Pennycook*³; *Anup Gangopadhyay*⁴; *Ramki Kalyanaraman*¹; ¹University of Tennessee; ²Southern Illinois University in Edwardsville; ³Oak Ridge National Laboratory; ⁴Washington University in St. Louis

Integrating different functionalities in small space is the driving force for present day technological advancement. Multi-functional nanoparticles

is one way to achieve such systems. Here, we discuss a cost-effective synthesis using pulsed laser self-organization of multilayer thin film heterostructures. As a prototypical system, we have chosen immiscible Ag and Co metals and investigated the ensuing ferromagnetism and localized surface plasmon resonances. Such composites have applications in biological sensing and optical communication. We discuss electron microscopy studies of nanostructure of individual particles and correlate this with the observed optical and magnetic behavior. We also established the parameter space for independent control of particle size and composition that leads to predictive tunability in physical properties. These results establish that self-organization of multilayer metal films by nanosecond pulsed laser melting could be a cost-effective method to synthesize nanomaterials with multiple properties.

12:10 PM

Development of Nano-engineered Surfaces and Coating Technologies for Scale Mitigation: *Ghazal Azimi*¹; *Yuehua Cui*¹; *J. David Smith*¹; *Kripa Varanasi*¹; ¹MIT

Scale buildup is among major operational problems facing a wide variety of industrial applications. Despite the pervasiveness of the scaling problem, the fundamentals of scale formation have received relatively little attention, and it is not fully realized how to design scalephobic surfaces by tuning the surface energy attributes. Most state-of-the-art technologies in the field have either focused on developing more effective scale inhibitors, or on improving existing scale removal techniques. These technologies, although promising, are still plagued with environmental and high cost drawbacks. To address these challenges, herein, we adopted a transformational approach by fundamentally altering scale-surface interactions at the interface. Our approach consisted of manipulating both the surface chemistry and surface morphology. Results revealed a significant reduction in scale deposition with reducing the surface energy of the substrates. This work could be considered as an initiative in developing robust scalephobic surfaces by tuning the surface chemistry.

3rd International Symposium on High Temperature Metallurgical Processing: Basic Research of Metallurgical Process

Sponsored by: The Minerals, Metals and Materials Society, TMS Extraction and Processing Division, TMS: Energy Committee, TMS: Pyrometallurgy Committee

Program Organizers: Tao Jiang, Central South University; Jiann-Yang Hwang, Michigan Technological University; Patrick Masset, TU Freiberg; Onuralp Yucel, Istanbul Technical University; Rafael Padilla, University of Concepcion; Guifeng Zhou, Wuhan Iron and Steel

Tuesday AM
March 13, 2012

Room: Southern II
Location: Dolphin Resort

Session Chairs: Onuralp Yucel, Istanbul Technical University; Bing Xie, Chongqing University

8:30 AM

JIM INTERNATIONAL SCHOLAR: Effect of Shear Stress on Crystallization Behavior of Mold Flux for Continuous Casting: *Noritaka Saito*¹; *K. Kusada*¹; *S. Sukenaga*¹; *K. Nakashima*¹; ¹Kyushu University

Ionic liquids, like molten oxides, have a much higher electrical capacitance than solids, which is attributed to the difference in their polarization mechanisms. In the present study, we adopted the difference in the polarization mechanism, and extended it to the detection of crystallization in molten oxides under shear stress. We systematically investigated the effect of shear stress on the crystallization behavior of molten CaO-SiO₂-R₂O (R = Li, Na, or K) slags. As expected, at a particular temperature, the electrical capacitance of the molten silicates abruptly dropped by two or

TUESDAY AM



TMS 2012

141st Annual Meeting & Exhibition

TUESDAY AM

three orders of magnitude, thus clearly indicating crystallization. It was also found that for rotating-rod measurements, the temperatures at which the capacitance abruptly dropped were higher than those without the shear stress.

8:45 AM

Thermal Decomposition and Regeneration of Wüstite: *Zhiwei Peng¹; Jiann-Yang Hwang¹; Zheng Zhang¹; Matthew Andriese¹; Xiaodi Huang¹; ¹Michigan Technological University*

The thermal decomposition and regeneration behaviors of wüstite were investigated by in situ high temperature X-ray diffraction (HT-XRD) under non-isothermal condition at heating rate of 4 K min⁻¹ in vacuum ranging from 294 K to 973 K. Wüstite on heating decomposes to magnetite and iron up to 823 K, above which it exhibits marked tendency to regenerate. Investigation of thermal stability of the reaction system shows that the decomposition proceeds under kinetic reaction control while the regeneration is under thermodynamic control. Kinetics study based on the Coats-Redfern integral approximation method indicates that the decomposition reaction follows a Komatsu-Uemura model-based diffusion-controlled kinetics with activation energy of 32.860 kJ mol⁻¹. The thermodynamics analysis of regeneration reaction demonstrates that wüstite regenerates at lower temperature than stoichiometric ferrous oxide.

9:00 AM

Competitive Precipitation and Growth of Spinel Crystals in Vanadium Slag: *Xie Zhang¹; Bing Xie¹; Jiang Diao¹; Xiaojun Li¹; ¹Chongqing University*

Vanadium is widely utilized as an important element to improve the quality of alloyed steels in iron and steel industry. Moreover, the crystallization process of V-containing spinels plays a significant role due to the aim of achieving a fairly larger size of spinel crystals in vanadium extraction. Thus, a comprehensive exploration and discussion on the competitive precipitation and growth of vanadium, chromium and titanium spinel crystals in vanadium slag during a cooling process were carried out in the present study on the basis of a crystallization kinetic model. To be more specific, the abilities of forming crystal, precipitation order and suitable temperature range for crystallization of the three kinds of spinels were discussed with both theoretical and experimental methods.

9:15 AM

Expert System for Grate-Kiln Pellet Production Based on Mathematical Models of Temperature Field: *Xiaohui Fan¹; Yi Wang¹; Xuling Chen¹; ¹Central South University*

The current control method of grate-kiln iron ore oxide pellet production is lack of accuracy and normalization due to the limited detection conditions. Therefore, mathematical model of grate-kiln temperature field is presented. With calculation of gas-particle heat transfer as well as enthalpy changes of moisture evaporation and magnetite oxidation, the thermal history of pellets throughout grate-kiln process can be acquired and used for estimate of production status. Taking the calculated results as well as detected data in production as inputs, process parameters such as running speed, fan opening and coal injection rate as adjusting objects, expert system for grate-kiln pellet production is outlined. Control rules are described in the form of a decision tree, and an efficient top-down-breadth-first OR tree search strategy is explained. Production application proves that control guidance of this expert system can solve production anomalies effectively and stabilize grate-kiln iron ore oxide pellet production.

9:30 AM

The Influence of Sodium Oxide on the Distribution Behavior of Some Elements at the S-Furnace of the Mitsubishi Process: *Yusuke Kimura¹; Ken-ichi Yamaguchi¹; ¹Mitsubishi Materials Corp.*

Secondary materials have long been processed at the S-furnace of the Mitsubishi continuous copper smelting and converting process at Naoshima Smelter and Refinery. Intensive recycling in the recent years

has caused drastic changes in the chemical properties of the CL-slag, which is separated from matte in the smelting stage. Among various impurities included in secondary materials, the authors have studied the influences of sodium oxides in the CL-slag because the behavior of sodium oxide has scarcely been studied with respect to the copper smelting slag. The examinations have been applied experimentally on the distribution between slag and matte of minor element, especially arsenic whose acidic characteristics suggests strong affinity to sodium-oxide of basic characteristics in silicate melts. The results have been discussed by thermodynamic evaluations and the results of pyro-tests at the commercial furnace.

9:45 AM

Effect of Temperature on the Equilibrium Phase Relations and Liquidus of CaO-SiO₂-FeOx-Al₂O₃ System: *Cuihuan Huang¹; ¹Northeastern University*

CaO-SiO₂-Al₂O₃-FeOx system is not only a primary sub-system of CaO-SiO₂-Al₂O₃-MgO-FeOx-Na₂O oxide system generated during the vitrification of municipal solid waste incineration ash, but also an important slag system for metallurgy process. Thus, its thermodynamic property of CaO-Al₂O₃-SiO₂-FeOx is highly required to provide the essential thermodynamic datas for innocent treatment of the incineration ash and sustainable utilization of the vitrified bottom ash slag, as well as to the production of high quality metal. A comprehensive study involving the combination of high temperature equilibrium experiments with CALPHAD method was conducted to investigate the effect of temperature on the equilibrium phase relations and liquidus of CaO-Al₂O₃-SiO₂-FeOx and its sub-systems. The calculated results with FactSage6.1 showed that the effect of temperature on the equilibrium phase relations and liquidus was appreciable. The liquid regions enlarged with increase of temperature from 1573K to 1873K, while the primary phase fields reduced distinctly. High temperature experimental results showed that the effects of temperature on the phase relations and liquidus location in FeOx-lower area of CaO-Al₂O₃-FeOx system and the mullite primary phase field of SiO₂-Al₂O₃-FeOx system were notable. The liquid zone expanded obviously with the increase of temperature.

10:00 AM

Modelling of Slag Surface Tension from Thermodynamics: *Clemens Schmetterer¹; Patrick Masset¹; ¹TU Bergakademie Freiberg*

Within the efforts of replacing the full water quench in gasification reactors by slag cooling on ceramic particles surface tension of slag is being recognized as an important property. As experimental surface tension measurements under reactor conditions (high temperature and pressure) are a demanding task, surface tension modelling is desirable. The relation between thermodynamics and surface tension is given by Butler's equation. Models based on the activity and the ionic radii of the slag components are available for molten salts and were improved to be used for oxide based systems. Both models were employed to model the surface tension of simple slag systems (e.g. Al₂O₃ - SiO₂). This work was accompanied by experimental determinations of the surface tensions of various mixtures and also of the pure components that are required as an input. In this contribution the modelling results, their background and the experimental results will be discussed and compared.

10:15 AM

Viscosity Determination of the Freeze Slag in Reaction Shaft of Flash Smelting Furnace: *Jinliang Wang¹; Yanxin Wu¹; Liwei Liang¹; Chuanfu Zhang²; ¹Jiangxi University of Science and Technology; ²Central South University*

According to the reaction shaft operation characteristics during the flash smelting process, 15 groups of slag samples containing high Fe₃O₄ were prepared by some chemical reagents, and then the slag viscosities were measured using a RTW-10 type synthetic test instrument for melt physical property by the rotating cylinder method. The effects of Fe/SiO₂, ω_{Fe₃O₄}, ω_{Cu₂O}, ω_{MgO} and ω_{CaO} on the slag viscosity were also studied. Results show that slag viscosity is decreased with the increase

of temperature, Fe/SiO_2 , $\omega_{\text{Cu}_2\text{O}}$, ω_{MgO} and ω_{CaO} , and with the decrease of $\omega_{\text{Fe}_3\text{O}_4}$ under the range of slag contents: Fe/SiO_2 1.36~1.78, $\omega_{\text{Fe}_3\text{O}_4}$ 17.83%~21.18%, $\omega_{\text{Cu}_2\text{O}}$ 3.51%~8.34%, ω_{MgO} 2.21%~6.57%, ω_{CaO} 6.22%~9.87% and temperature range of 1250~1450°C. Only $\omega_{\text{Fe}_3\text{O}_4}$ and ω_{CaO} have great influence on the slag viscosity when temperatures as high as 1400°C or so. To form a freeze slag with higher viscosity inside the reaction shaft, $\omega_{\text{Fe}_3\text{O}_4}$ should be more than 20% and ω_{CaO} should be less than 6%.

10:30 AM Break

10:40 AM

Effect of MgO Content on Melting Features of SiO₂-CaO-MgO-Al₂O₃-FeO Slag in Nickel Laterite Metallurgy: *Xuwei Lv*¹; Cheng Pan¹; ¹Chongqing University, China

Physico-chemical properties of slag at high temperature play an important role in the pyro-metallurgical process of production of ferronickel alloy. It determines the operation efficiency, metal recovery ratio, energy consumption and the distribution of elements like S and P between the slag and metals. In the present work, the effect of MgO content on the melting features of the slag was investigated. The MgO content in the SiO₂-CaO-MgO-Al₂O₃-FeO in the quinary slag system varied from 14.5% to 22.5%. The results show that all the slag samples begin to soften at the same temperature, the softening temperature, melting temperature, flowing temperature decrease with the increase of MgO content when the MgO content is in the range of 14.5 and 20.5 pct mass, and when MgO content up to 22.5 percent, the temperatures increase sharply.

10:55 AM

High Temperature Deformation Behavior Of Nimonic C263 Superalloy: *Maribel De la Garza Garza*¹; Martha Guerrero Mata¹; Alejandro Lara Mendoza¹; Victor Páramo López²; ¹FIME, UANL; ²Frisa Forjados

High temperature operation of superalloys in aerospace and power generation components involve high creep and corrosion resistance. The present work focuses on studying the behavior of a C263 Superalloy, which is a precipitation hardenable nickel-chromium-cobalt alloy with an addition of molybdenum for solid-solution strengthening. Alloy C263 has high strength and corrosion resistance as well as having good formability and high temperature ductility in welded structures. Studying the hardening mechanisms allows the better understanding of its behavior. The hardening phenomenon in most Ni based superalloys is caused by precipitation of second phases, also the grain size evolution and distribution during the whole forging process should be controlled in order to improve mechanical properties. This development could define the parameters of the process route. For this work some samples were wrought varying the forging temperature to study the best flow deformation behavior, then grain size distribution and mechanical properties were analyzed.

11:10 AM

Influence of Silicon Content in Hot Metal on Mineralogical Characterization and Physico-chemical Properties of Vanadium Slag: *Chongyang Zhao*¹; *Bing Xie*¹; *Xiaopeng Zhen*¹; *Qingyun Huang*¹; *Xie Zhang*¹; ¹Chongqing University

Extracting vanadium from vanadium containing hot metal into vanadium slag by BOF is the main vanadium production process in China. In this paper, the influence of Si content in hot metal on the quality of vanadium slag is analyzed. Synthetic vanadium slag with different SiO₂ content were melted at 1673 K and then cooled to 303K at the cooling rate of 3°C/min. Optical microscopy, SEM, EDS and XRD were used to analyze the mineralogical phases and crystallization behavior of vanadium slag. The results show that vanadium slag mainly contains spinel phase and silicate phase; V is enriched in the spinel phases while Si is concentrated in Fe₂SiO₄, CaFeSi₂O₆ and (Fe,Mn)₂SiO₄ as silicate phase. The melting point of slag increases gradually with the addition of SiO₂; whereas viscosity decreases with an addition of 15~19% SiO₂ and increases with an addition of 19~27% SiO₂.

11:25 AM

A Model of Decarburization and Boil of Iron/Carbon Droplets: *Mark Schwarz*¹; ¹CSIRO

A model has been developed for decarburization of iron/carbon droplets in an oxidizing atmosphere containing oxygen and/or carbon dioxide. Mass transfer across the gas-side and liquid-side boundary layers are taken into account as well as decarburization reactions at the interface. A spherically symmetric model was first developed and compared with data from experiments carried out in a tube furnace. This model has been extended to allow for non-uniform mass transfer effects resulting from flow of the oxidizing gas over the droplet. Boil is assumed to occur when the supersaturation partial pressure of CO within the droplet exceeds a critical value for nucleation. Predictions of boil time agree well with the measurements for droplets contained in the tube furnace.

11:40 AM

Analysis of Influence Factors on the Melting Point of the Freeze Slag Inside Flash Smelting Furnace Brickless Reaction Shaft: *Jinliang Wang*¹; *Chuanfu Zhang*²; ¹Jiangxi University of Science and Technology; ²Central South University

Brickless reaction shaft is the latest progress for flash smelting furnace. However, there are many factors influence the melting point of the freeze slag inside brickless reaction shaft, and their variational regularities are not obvious, thus, it's difficult for conventional methods to analyze accurately the complex data. In this research, the experiment data of slag melting point were processed based on optimal discrimination plane. For this method, two orthogonal vectors were firstly built up based on the Fisher's criterion, and then the experiment data were projected onto the two vectors, thus, two-dimensional feature vectors were extracted as criteria to determine the factors effect degree on the slag melting point. Results show that the CaO content is the greatest factor to the melting point of the freeze slag inside brickless reaction shaft, the content of Fe₃O₄, SiO₂, Cu₂O and MgO is the second, and the FeO content is the last.

Advances in Surface Engineering: Alloyed and Composite Coatings: Session III

Sponsored by: The Minerals, Metals and Materials Society, TMS Materials Processing and Manufacturing Division, TMS: Surface Engineering Committee

Program Organizers: Sandip Harimkar, Oklahoma State University; Srinivasa Bakshi, Indian Institute of Technology Madras; Arvind Agarwal, Florida International University

Tuesday AM
March 13, 2012

Room: Macaw 1
Location: Swan Resort

Session Chair: To Be Announced

8:30 AM Introductory Comments

8:35 AM Invited

Chromium Nitride Coatings for Biological Applications: *Aracely Rocha*¹; *Liangxian Chen*²; *Chengming Li*²; *Hong Liang*¹; ¹Texas A&M University; ²University of Science and Technology Beijing

Surface modification through coatings was made in order to improve adhesion between implanting materials and protein. The adhesion of albumen protein to CrN and CrAlN coatings on Ti alloy and Si wafer was studied using a method of rotational shear flow. CrN and CrAlN coatings provide improved wear resistance over pure Cr. These coatings offer a potential alternative to reduce wear in artificial joints. Experimentally, we developed a method to quantitatively evaluate the adhesive strength of proteins to the surface. Subsequently we study the interfacial mechanisms between coating surfaces and protein molecules. Results indicate that the protein adhesion depends on the substrate chemistry. The CrN and CrAlN coatings improve wear resistance with minimum to no influence with the substrate's interaction with the proteins.



TMS 2012

141st Annual Meeting & Exhibition

9:00 AM Invited

Development and Characterization of Aluminum Matrix in-situ Aluminum Di-borides Composites Coatings for Tribological Applications: *Sudeep Ingole*¹; *Rajeshwari Paluri*¹; ¹Texas A&M University

Self-lubricating coatings with better mechanical properties for reduced friction and wear application have everlasting demand. Alumina is one such material which is a good choice for wear resistance applications like pump bearings, seal rings, piston components, etc. We attempt to develop a novel alumina based ceramic composite to further enhance its surface properties and develop composite coatings. This paper focuses on mechanical and surface characterization of borides formation under influence of varying percentages of boron in coating matrix. The results of XRD, FTIR, optical microscopy and E-SEM will be reported. Effect of sintering temperature and percentage of boron on mechanical properties will be discussed. Results showed that increasing percent of boron resulted in grain boundary diffusion and high sintering temperatures resulted in low porosity for lower wt % of boron. XRD results confirmed the formation of aluminum diboride (AlB₂), boron oxide (B₂O₃) and aluminum borate (Al₁₈B₄O₃₃).

9:25 AM

A Nanoindentation Study of Laser Deposited Nickel-Based Carbide Metal Matrix Composite Coating: *Samar Kalita*¹; ¹Advanced Engineered Materials Center - University of North Dakota

The mechanical behavior of direct metal laser deposited (DMLD) carbide metal matrix composite coating is of relevant interest in a variety of applications. Since tensile testing is impractical for this purpose, depth-sensing indentation, which provides wealth of information seems promising. Here, DLMD was used to develop wear and corrosion resistant coating on AISI 1018 steel using a blend of Ni, Cr₃C₂ and WC₁₂Co powders. The coating's integrity, microstructure and composition were analyzed by microscopic and spectroscopic techniques. The coated systems are evaluated in terms of mechanical properties (indentation modulus, M and hardness, H), wear ratio H/Er, and hardness parameters Km and P/S₂, which can discriminate between homogeneous and non-homogeneous systems. The ratio between maximum penetration and contact-depth defined wear characteristics. Properties at different coating-depth were investigated. Hardness and Er at the top and interface vicinity were 8.5 and 201.2 GPa, and 8.4 and 203.5 GPa, respectively; considerably higher than the substrate.

9:45 AM

In-Situ Synthesis of TiC/SiC/Ti₃SiC₂ Composite Coatings by Spark Plasma Sintering: *Ashish Singh*¹; *Sandip Harimkar*¹; *Arvind Agarwal*²; *Srinivasa Bakshi*³; *David Virzi*²; *Anup Keshri*²; ¹Oklahoma State University; ²Florida International University; ³IIT Madras

Composite coatings consisting of TiC/SiC/Ti₃SiC₂ phases have been synthesized on titanium substrate using spark plasma sintering (SPS). SPS technique allows processing of composite coatings in short sintering time and at low temperatures. The processing of composite coatings was achieved at 1300 °C and 1400 °C at 90 MPa. Identification and quantification of the phases have been performed using X-ray diffraction (XRD). Coatings microstructure was evaluated using SEM images. X-ray elemental maps obtained using EDS analysis has been used to study the distribution of different elements in the microstructure and study the phase evolution. A tentative mechanism for phase evolution has been proposed. Microhardness of the coating is found to be 3 times that of the Ti substrate which lead to a ~100 times lower wear weight loss in ball on disc wear tests.

10:05 AM Break

10:20 AM

Microstructure and Wear Properties of Laser In-situ Formation of TiB_x and TiC Titanium Composite Coatings: *J. Liang*¹; *C S Liu*²; *S Y Chen*²; *C X Ren*²; ¹Northeastern University ; ²Northeastern University

Ti-6Al-4V/B₄C mixed powder which are pre-pasted or synchronized fed on Ti-6Al-4V substrates separately were scanned by a 500W pulsed YAG laser to in situ format titanium composite coatings contained TiB_x and TiC ceramic reinforced phases. The influences of processing parameters and powder proportions on the microstructure and properties of the coatings were investigated. Three-layer composite graded coatings were formatted with prepasted B₄C increased 10 wt. % each layer. Microstructures and phases of coatings were analyzed by OM, SEM, TEM and XRD respectively. Results show that the microhardness and the amount of TiB₂ of the layer increased with the increase of B₄C addition. The average micro-hardness of a laser cladding composite graded surface layer is up to 1000HV, which is nearly 3 times of that of the substrate (367HV), and the wear weight loss decreased over 4 times.

10:40 AM

Surface Engineered CVD Diamond Coatings for Dry Machining Applications: *Humberto Gomez*¹; *Delcie Durham*²; *Kevin Chou*³; *Xingcheng Xiao*⁴; *Michael Lukitsch*⁴; *Ashok Kumar*²; ¹Universidad del Norte; ²University of South Florida; ³The University of Alabama; ⁴General Motors R&D Tech. Center

The insufficient adhesion of diamond coating on cutting tool has been the bottleneck in production lines, limiting its application in the dry machining of aluminum and magnesium alloys. In this study, diamond was deposited on WC-Co turning inserts pretreated using chemical etchings and CrN/Cr inter-diffusion barrier interlayer, to overcome the adhesion issues associated with the detrimental effect of cobalt. Rockwell indentations were performed on the diamond surfaces to qualitatively characterize the adhesion. Finally, dry machining processes using these diamond coated turning inserts were performed on a high silicon aluminum alloy. A systematically approach from the initial substrate surface characteristics in terms of the surface texture and surface/subsurface damage produced by the different pretreatments, in addition to the resulting diamond film quality and adhesion, are evaluated in terms of the machining tool life and its consequent wear and failure mechanisms.

11:00 AM

Creep Properties of Y-PSZ Coated 6063 Aluminum Alloy: *Eray Erzi*¹; *Cem Kahraman*¹; *Suat Yilmaz*¹; ¹Istanbul University

Aluminum alloys have been used in industries for years because of light weight. But these materials have some disadvantages like low mechanical properties. For increasing of the mechanical properties of aluminum alloys can be coated with hard ceramics. In this study, T6 heat treated 6063 aluminum alloy were coated with %8 Y-PSZ powders by plasma spraying method. Subsequently, creep properties of the uncoated and coated samples were investigated. Temperature dependent creep tests were carried out at 100, 125, 150°C temperatures and at 170 MPa stress conditions. Stress dependent creep tests were carried out at 120, 145, 170 MPa stresses and at 100°C temperature conditions. The creep results of the uncoated and coated samples were discussed and compared.

11:20 AM

Effect of Pre-Oxidation Treatments on the Mechanical Properties of (Ni,Pt)Al Systems Measured by Nanoindentation: *Juan Alvarado-Orozco*¹; *Alma Mora-García*²; *Haide Ruiz-Luna*; *Haide Ruiz-Luna*²; *Luis Alberto Cáceres-Díaz*²; *John García-Herrera*²; *Juan Muñoz-Saldaña*²; *Jose Ortiz-Merino*²; *Gerardo Trapaga-Martinez*²; *Ricardo Morales-Estrella*²; *Doug Konitzer*²; *Enrique Samaniego-Benitez*²; ¹Centro de Investigación y de Estudios Avanzados del Instituto Politécnico Nacional ; ²Centro de Investigación y de Estudios Avanzados del Instituto Politécnico Nacional

The effect of isothermal oxidation treatments in the range of 900°C to 1200°C for 5h in oxygen controlled atmosphere on the mechanical

properties of (Ni,Pt)Al (BC) + interdiffusion zone (IDZ) + Rene-N5 (SA) systems is presented. The mechanical properties were measured by cross-sectional nanoindentation analysis. The reduced elastic modulus (E_r) and the indentation hardness (H) were estimated based on the Oliver and Pharr method. The results have shown that both, E_r and H of the BC and SA are highly dependent of the oxidation heat treatments as a consequence of the aluminium depletion to form the thermally grown oxide (TGO), the growth of BC+IDZ as a result of a multi-element counter diffusion and the partial dissolution of γ/γ' SA. Trying to correlate the obtained mechanical properties with the structural and chemical properties, XRD and EDX analysis was conducted in the BC.

11:40 AM

Contribution of Ti Addition to the Electronic Structure and Adhesion at the Fe₂Al₅/Fe Interface in 55%Al-Zn Coating: *Guangxin Wu*¹; Yuling Ren¹; Jieyu Zhang¹; Kuochih Chou¹; ¹Shanghai University

We report a density functional theory investigation of the atomic structure, bonding, and ideal work of adhesion of the Ti addition to Fe₂Al₅/Fe interface, in order to explore the potential of Al-Zn-Si-Ti as a protective coating for steel. The results show that the clean interface has an ideal work of adhesion of 0.84 J/m² while the presence of Ti dramatically increase adhesion via rearrangement of electron density and the character of the local density of states upon formation of the interface. Then, the stability and fracture toughness of Ti dopant Fe₂Al₅/Fe interface are discussed with a thermodynamic sense and Griffith fracture theory, respectively. Besides, the chemical bonding properties for the interfacial atoms are also discussed in this paper based on electronic structure and Milliken population. Our results provide theoretical evidence for the excellent adhesion behaviors of Fe₂Al₅/Fe interface.

Alumina and Bauxite: Red Mud Bauxite Residue

Sponsored by: The Minerals, Metals and Materials Society, TMS Light Metals Division, TMS: Aluminum Committee, TMS: Aluminum Processing Committee
Program Organizer: Benny Raahaage, FLSmidth

Tuesday AM
March 13, 2012

Room: Northern E3
Location: Dolphin Resort

Session Chair: Tim Laros, FLSmidth Salt Lake City

8:30 AM

Bauxite Residue Management: *Ken Evans*¹; Eirik Nordheim²; Katy Tsemelis³; ¹Rio Tinto Alcan; ²European Aluminium Association; ³International Aluminium Institute

With some two to four tonnes of Bauxite Residue waste arising for every tonne of aluminium produced, the management of Bauxite Residue (or Red Mud) has always been a significant issue for the aluminium industry. However, the tragic fatal incident in Ajka, Hungary in October 2010 has reinforced the need for safe and effective management of storage areas globally. For the past five years the International Aluminium Institute has been involved in research into the management of bauxite residue and in 2011 created a set of voluntary objectives recommending that best practices are adopted to ensure that the Hungarian incident is never repeated elsewhere. This paper will review the current and best practices of bauxite residue management.

8:50 AM

Tests with New Flocculant for Red Mud Decanting in Alunorte: *Tatiani Santos*¹; Juracy Filho¹; Américo Borges¹; Humberto Lima¹; Juarez Borges¹; Frederico Giust²; Alexandre Rabaça²; ¹Alunorte SA; ²SNF do Brasil

To produce alumina with competitive costs and high efficiency on caustic recover with low flocculant consumption has been a challenge for the filtration area in Alunorte. This area has 7 production lines where

together, handles about 4,4 Mtpy of red mud. Specifically at production lines 6 & 7, the washer chain has only high rate settlers and apart from that, they receive bauxite from Mineração Bauxita de Paragominas. The combination of these two aspects results on lower density in the settler underflows. One of the actions to increase underflow solids content was to replace the conventional polyacrylate flocculant by another one which could be capable to increase the density in the washer underflows. Among other trials were gotten good results from the use of FLOMIN OL 99 polymer in lab tests as well as in the plant. The discussion of these results is the main propose of this paper.

9:10 AM

Red Mud Filtration Test Results using AFP IV™ Automatic Filter Press: *Manfred Bach*¹; ¹FLSmidth

Results of pressure filtration testing demonstrates that a standard design FLS AFP IV filter press can dewater red mud from initial feed concentrations of 30 – 44 wt% and produce final cakes containing 67-70 wt% solids. This paper outlines factors affecting the filtration rate and final cake solids concentration such as feed solids concentration, slurry temperature and feed pump delivery rate/pressure relationship as well as the configuration of the filter plates. The results are presented for different bauxite grades. Additional testing was performed to obtain filter cakes containing 75 wt% cake solids by evaluating high-pressure filtration at 30-60 bar using both recessed plate and membrane plate configurations. The tests demonstrate that high-pressure filtration above 30 bar can produce 75 wt% solids. Additional results from a second test series are presented on Chinese red mud resulting in filter cakes containing cake solids in the range of above 80%.

9:30 AM

Study on Dry –Method Volume Expansion Technology for Wet Red Mud Yard: *Li Mingyang*¹; Xu Shutao¹; Yi Xiaobing²; ¹CHALIECO; ²CHALIECO

The wet red mud yard in Guizhou Branch of CHALCO is closed when it is used up to 1370m high, and it's difficult to construct the new red mud yard within a short term because of the difficulty in land requisition. In order to ensure the continuity of alumina production, it's required to expand the volume of the existing wet red mud yard by dry method. Based on many tests and studies on the basic performances of red mud filtration cake, the author in this article gives introductions of technologies on red mud dewatering, transportation, spreading out & stacking, reinforcing of weak red mud layer, recycle of waste water in red mud yard, and flood control & drainage etc. It's shown by study achievements that good economical and social & environmental benefits can be obtained by using dry-method volume expansion technology for wet red mud yard.

9:50 AM

ETI Aluminum Red Mud Characterization and Processing: *Gokhan Demir*¹; *Sedat Arslan*¹; Bekir Celikel¹; Meral Baygul¹; Carlos Enrique Suarez²; ¹ETI Aluminium; ²Hatch Associates Consultant Inc.

ETI Aluminum has capacity to process 541,000 tons of bauxite, produce 250,000 tons of alumina per year and generate approximately 260,000 tons of red mud. Red mud slurry is disposed at 30 % (w/w) solids and less than 3 g/L Na₂O. ETI is focusing its efforts in maximizing extraction efficiency in digestion and improving decomposers yield. The red mud area is one of the most important topics that require serious study in terms of handling, recovery and environmental impact. A study has been initiated to determine red mud characterization, settling performance and separation strategies. XRF, XRD, TG/DTA, IR, SEM/EDX, BET and PSD analysis have been conducted to define red mud physical and chemical characteristics. Many settling tests have been performed to select the most suitable and economic flocculant that provides the best compaction, overflow clarity with an acceptable settling rate and enhanced rheology. Also ETI might face red mud disposal area problems in the following years. ETI has initiated a fast track program towards the improvement of the dewatering of red mud and increase disposal area life time.



TMS 2012

141st Annual Meeting & Exhibition

10:10 AM

Studies on Metal Flow from Khondalite to Bauxite to Alumina and Rejects from an Alumina Refinery, India: *Birendra Mohapatra*¹; Barada Mishra¹; Chittaranjan Mishra²; ¹Institute of Minerals & Materials Technology(IMMT); ²Other

Alumina is produced from khondalite hosted bauxite of Indian origin in the Alumina refinery employing the time tested Bayer's Process. In the process, about 40% of unwanted elements are rejected as undigested sand and red mud. During the whole cycle; major, minor, trace and RE elements in these litho-units get redistributed, either depleted or enriched. Khondalite, the source rock of bauxite, is rich in silica, moderate in alumina and iron with minor titanium. Bauxite becomes rich in alumina and iron with subordinate titanium and negligible silica. After alumina recovery from bauxite, most of the valuable metals including REE get accumulated in the refinery rejects. The studies, while establishing the extent of various metals dispersed in khondalite, bauxite, undigested sand, red mud and alumina also reveals the state of enrichment of valuable metals in undigested sand and suggests possible means to recover some of them.

10:30 AM

Directions for Large Scale Utilization of Bauxite Residue: *Andrey Panov*¹; Gennady Klimentenok²; Gennadiy Podgorodetskiy³; Vladislav Gorbunov³; ¹RUSAL Vami; ²RUSAL Engineering & Technology Centre; ³National University of Science and Technology "MISIS"

Solving the problem of large-scale utilization of Bayer process bauxite residue (red mud) becomes more and more vital for the increasing number of alumina refineries around the globe. Till now, in spite of the fact that many technically sound process routes have been developed, only a few of them have been implemented, once local economic and market conditions were favorable. Being a complex and poor ore for extraction of iron, alumina and titanium, treated red mud has to compete with other low cost materials; this is often economically unfavourable. In this paper the most promising utilization directions are discussed and focus areas for research by the world scientific community are outlined.

10:50 AM

Production of Pig Iron from NALCO Redmud by Application of Plasma Smelting Technology: *Partha Mukerjee*¹; Bhagyadhar Bhoi¹; Chittaranjan Mishra²; Ramani Dash³; Bijay Satapathy²; Kalidas Jayasankar¹; ¹Institute of Minerals & Materials Technology(IMMT); ²National Aluminium Company Limited; ³Gandhi Institute of Engineering & Technology(GIET)

Red Mud, a by-product generated from the caustic leaching of bauxite to produce alumina in the Bayer Process, causes serious environmental problems & is considered as a hazardous industrial waste. A Novel Process has been developed for production of Pig Iron from NALCO Red Mud by employing Plasma Smelting Technology. Red Mud containing 15-40% Fe₂O₃ was subjected to Thermal Plasma Smelting by use of Extended Arc Plasma Reactor at a temperature of 1600o C for a period of 30 minutes & high quality pig iron was produced. Effect of various process parameters like basicity, amount of reductant, plasmagen gas, input electric power and reduction time for recovery of Pig Iron has been studied and optimised. Basicity of 0.3, reduction time of 25 minutes at 12.5 KW power was found to be optimum for maximum recovery of Pig Iron (70%) from Red Mud in 1 kg scale.

Aluminium Processing: General

Sponsored by: The Minerals, Metals and Materials Society, TMS Light Metals Division, TMS: Aluminium Processing Committee
Program Organizers: Kai Karhausen, Hydro Aluminium Rolled Products GmbH; Edward Williams, Alcoa

Tuesday AM
March 13, 2012

Room: Europe 1
Location: Dolphin Resort

Session Chairs: Kai Karhausen, Hydro Aluminium Rolled Products; Edward Williams, Alcoa

8:30 AM Introductory Comments

8:35 AM

Finite Element Simulation Analysis of the Ultrasonic Vibration Forging of an Aluminum Cylinder Workpiece: *Yanxiang Liu*¹; Qingyou Han¹; ¹Purdue University

The propagation of ultrasonic wave in the solids can greatly affect the material properties. In this paper, the deformation characteristics of the ultrasonic vibration forging for aluminum alloy are investigated. For the ultrasonic vibration forging, during the forging process, the ultrasonic wave propagates in the specimen at the same time. A detailed analysis and understanding of the mechanism of improvement is not possible on the basis of conventional experimental observations because ultrasonic vibration processing phenomenon occurs at a high speed. Hence, in order to study the mechanism of ultrasonic vibration forging, the finite element modeling was performed by using Abaqus/explicit. The metal flow of the ultrasonic vibration forging is totally different from the conventional one, there will have no "drum" effect in the forming process, which is the main characteristic in the conventional forging. Moreover, the stress and equivalent plastic strain distributions after the ultrasonic vibration forging process were explored.

8:55 AM

Refinement of Fe-Intermetallic Compounds by Caliber Rolling Process of Al-Mg-Si-Fe Alloys: *Chakkrist Phongphisutthinan*¹; Hiroyasu Tezuka¹; Tatsuo Sato¹; Susumu Takamori²; Yoshiaki Ohsawa²; ¹Tokyo Institute of Technology; ²National Institute for Materials Science

Fe-intermetallic compounds are well known as harmful to mechanical properties and formability, especially the plate-like β -AlFeSi. Recycling process of aluminum scraps commonly contains high amount of Fe content which results in degraded properties compared with primary aluminum production. In this study, thermo-mechanical process of Al-0.9mass%Mg-(2.0-2.3)mass%Si-(1.0, 1.5 and 2.0)mass%Fe alloys by caliber rolling was performed to investigate the refinement of Fe-intermetallic compounds and mechanical properties. Homogenized ingots were sequentially caliber rolled at 300°C and 450°C to 95% area reduction. The caliber rolling process can effectively refine the harmful Al-Fe-Si compounds into more favorable size and good distribution in the Al matrix. Fine fragmented Fe-intermetallic particles with the size of 200nm were achieved. The caliber rolling can effectively improve mechanical properties with good ultimate strength of 345-360MPa and high elongation of 15-25%.

9:15 AM

Analytical and FEM Modeling of Aluminum Billet Induction Heating with Experimental Verification: *Mark Kennedy*¹; Shahid Akhtar²; Jon Arne Bakken²; Ragnhild Aune²; ¹Norwegian University of Science and Technology; ²Norwegian University of Science and Technology

Induction heating is commonly used in the re-heating of aluminum billets before forging or extrusion. Powerful finite element modeling (FEM) tools are available to assist in the design of such processes; however, such

TUESDAY AM

models should be validated by comparison with analytical solutions or experimental results to ensure accuracy. Induction heating experiments have been performed using a number of different coil designs and work piece dimensions at 50 Hz. Aluminum alloys with different electrical conductivities have been used, i.e. 6060 and A356. Process parameters such as: current, power, magnetic field, electrical conductivity, etc. have been measured with high precision instrumentation. Experimental data are presented and compared with equivalent 1D analytical and 2D axial symmetric FEM modeling results. The effect of frequency on the induction heating process is reviewed using the validated analytical and FEM models. Some recommendations are given with respect to appropriate modeling techniques, boundary conditions and numerical mesh sizes.

9:35 AM Question and Answer Period

9:45 AM Break

10:15 AM

The Evolution of Mechanical Properties and Microstructure in Early Stages of Natural Ageing on 2024 Plates: Gheorghe Dobra¹; Ioan Sava¹; Cristian Stanescu¹; Marin Petre¹; ¹ALRO

The evolution of plasticity of heat treatable alloys in W temper is important for an efficient stress releasing by stretching or compression (Tx51 and Tx52 tempers) but also for some special hardening operations that combine cold working and ageing practices. For the alloys that have a significant natural ageing, the environment temperature has an important influence. In order to evaluate the influence of this temperature, the mechanical properties and the microstructure were investigated at various temperatures between -10 and + 80 °C and ageing time between 0 and 80 h on plates in alloy EN AW 2024, using standard tensile tests, electronic microscopy and X Ray diffraction. The results demonstrate that from many standpoints (mechanical properties, plasticity, electrical conductivity, microstructure etc.) the ageing transformations end before the limit of 96 hours that is considered as standard.

10:35 AM

Formation of Intermetallic Compound on the Interface of Copper/Aluminum Clad Sheet Produced by Asymmetrical Roll Bonding and Annealing: Xiaobing Li¹; Guoyin Zu²; Ping Wang³; Rong Xu⁴; ¹School of Materials and Metallurgy, Northeastern University; ²School of Materials and Metallurgy, Northeastern University; ³Key Laboratory of Electromagnetic Processing of Materials, Ministry of Education, Northeastern University; ⁴The State Key Laboratory of Rolling and Automation, Northeastern University

Copper/aluminum clad sheet produced by asymmetrical roll bonding and annealing possesses good interfacial bonding, but can be damaged by the intermetallic compound (IMC) formed on the interface. The present paper has studied the formation of IMC on the interface of Cu/Al clad sheet with different mismatch speed ratio by scanning electronic microscope equipped with energy dispersive X-ray detector and X-ray diffraction. It is found that the thickness of interfacial layer increases due to the considerable diffusion caused by the shear deformation energy during roll bonding process. The formation of IMC is promoted by the significant element diffusion at high speed ratio. For sample annealed at 400°C for 20 min, the formation of IMC is negligible, but the fracture lies between compounds. The results show that the IMC forms on the interface with annealing, especially for clad sheet roll-bonded with high speed ratio, and the formation destroys the interfacial bonding.

10:40 AM Question and Answer Period

Aluminum Alloys: Fabrication, Characterization and Applications: Thermal Mechanical Processing

Sponsored by: The Minerals, Metals and Materials Society, TMS Light Metals Division, TMS: Aluminum Processing Committee
Program Organizers: Subodh Das, Phinix LLC; Tongguang Zhai, University of Kentucky; Zhengdong Long, Kaiser Aluminum

Tuesday AM
March 13, 2012

Room: Northern E1
Location: Dolphin Resort

Session Chair: Xiyu Wen, University of Kentucky

8:30 AM

Modeling of As-Cast A356 for Coupled Explicit Finite Element Analysis: Matthew Roy¹; Daan Maijer¹; ¹The University of British Columbia

Design tools to simulate the manufacturing processes applied to aluminum components require computationally efficient finite element methods. While static processes such as casting employ implicit techniques, dynamic processes such as forging may only be modeled with explicitly. A commonplace practice to expedite explicit simulations is to employ time or mass scaling, which can lead to unexpected thermal-mechanical behaviour in coupled analyses. In both cases, the development of fully coupled thermo-mechanical simulations necessitates the use of a constitutive model that is capable of defining the flow stress as a function of temperature, strain, and strain rate. In this work, a material model for as-cast A356 is presented and applied in a range of fully coupled deformation models. Implicit and unscaled explicit models will be compared to explicit models with large amounts of scaling. Strategies for applying a material model to minimize error and maximize computational effort are discussed.

8:50 AM

Textures, Particle Structures and Mn Solution in Al Matrix of a Continuous Cast AA3004 Aluminum Alloy after Cold Rolling and Annealing: Xiyu Wen¹; Yansheng Liu²; Jingwu Zhang³; Shridas Ningileri²; Tongguang Zhai¹; ¹University of KY; ²Secat Inc.; ³State Key Laboratory of Metastable Materials Science and Technology

Measurements of textures of an AA3004 aluminum alloy sheets made from twin belt casting after cold rolling and annealing are carried out by use of the orientation distribution function (ODF) method. The particle structures of the sheet samples are observed and analyzed by use of scanning electronic microscopy (SEM) and Transmission electron microscopy (TEM) as well as X-ray diffractionmeter (XRD). In addition, Mn solution in grains with different orientations of Al matrix was evaluated by using Kikuchi pattern from TEM technique. The textures, particle structures and Mn solution in grains with different orientations of Al matrix resulting from the thermo-mechanical processing are studied and presented.

9:10 AM

Observation of Structure Evolution during Annealing of 7xxx Series Al Deformed at High Temperature: Cory Parker¹; David Field¹; ¹Washington State University

Deformation of polycrystalline materials results in a heterogeneous distribution of dislocation structures that are dependent upon the local character of the microstructure. 7xxx series aluminum alloys are particularly complex because of the wide range of particles and solute atoms that are in the material. High temperature deformation results in a microstructure that may be essentially free from dislocation structures at one position but have relatively high dislocation content at another position. Electron backscatter diffraction was used to quantify and map the dislocation density tensor at various positions through the metal.



TMS 2012

141st Annual Meeting & Exhibition

Subsequent annealing resulted in the development of recrystallization nuclei that were also observed by EBSD and related to the measured dislocation structure.

9:30 AM

Study of Homogenization Treatments of DC Cast 5xxx Series Al-Mg-Mn Alloy Modified with Zn: Akram Halep¹; Tamara Radetic¹; Miljana Popovic¹; Endre Romhanji¹; ¹Department of Metallurgical Engineering, Faculty of Technology & Metallurgy, University of Belgrade, Belgrade, Serbia

Microstructural changes of DC-cast 5xxx series Al-Mg-Mn alloy modified with Zn addition during a range of homogenization treatments were studied through the thickness of a rolling ingot. The homogenization treatments included: (i) low temperature annealing at 430°C, (ii) high temperature homogenization at 530-550°C and (iii) low-temperature annealing in the 420-480°C. Microstructure evolution was followed by electrical resistivity measurements, optical microscopy, SEM and TEM characterization and microanalysis. During the homogenization, decomposition of the supersaturated solid solution, present in the as-cast state, occurred. Distribution of the precipitates was dictated by segregations and could be related to the partition coefficients of alloying elements. It was found that during the high temperature homogenization not only dissolution processes occurred, but also precipitation of new phases. This research was supported by the Ministry of Education and Science, Republic of Serbia, and Impol-Seval Aluminum Mill, Sevojno, under contract number TR 34018 and E!4569.

9:50 AM

Microstructure Evolution of 7003 Aluminum Alloy by Equal Channel Angular Extrusion Process: Qingnan Shi¹; Gang Yang¹; Liangwei Chen¹; Xiaoqi Wang¹; Zaohua Liu¹; ¹Kunming University of Science and Technology, School of Materials Science and Engineering

The 7003 Al alloy was prepared by equal channel angular extrusion process (ECAP), which microstructures were characterized by transmission electron microscope (TEM). Results showed that dislocation density increases obviously and the average grain size decreases with increasing passes of ECAP. However, after the fourth pass of ECAP, average grain size fails to decrease remarkably and the microstructure is still inhomogeneous. Some parallel micro-bands and the second phase MgZn₂ are present in the alloy during annealing.

10:10 AM

Steel-Aluminium Composite Castings for High-Performance Die Cooling Applications: Heiner Michels¹; Andreas Bührig-Polaczek¹; David Becker²; ¹RWTH Aachen, Foundry Institute; ²Fraunhofer Institut für Lasertechnik

When processing plastic or metal on die casting machines, controlling the die temperature is a crucial process factor. Optimised cooling can provide short cycle-times and increased productivity, but is hard to realize by common means. Die inserts produced by Selective Laser Melting (SLM) allow a to-the-point layout of shape and cooling conduits. Yet, producing solid SLM volume is time and cost consuming. The relatively low heat conductivity of steel limits the positive effects furthermore. The current study shows results of research directed towards an innovative cost-efficient production of high performance cooling solutions, improving the inserts overall heat conduction, wear and high temperature resistance. An aluminium alloy, procuring high heat conductivity, is poured into a steel SLM shell structure. The formed interbond-phases are analysed, the effect of surface structures to reduce air gap formation and enhance the material interbond is tested as is the deformation and dissolution behaviour of cooling conduits.

10:30 AM Break

10:45 AM

High Strength Al-Mg-Mn Alloy Sheets Fabricated by Twin Roll Casting: Hyoung-Wook Kim¹; Suk-Bong Kang¹; Jae-Hyung Cho¹; ¹Korea Institute of Materials Science

Al-Mg-Mn alloy sheets with different Mg and Mn contents were fabricated by twin roll casting and rolling process and the microstructure of the sheets was investigated. The twin roll cast Al-Mg-Mn alloy sheets had a fine dendrite size and very fine precipitates due to high cooling rate during the casting process. The density of fine Al₆Mn precipitates of the annealed sheets increased with increasing Mn and Mg content, so that large number of fine Al₆Mn precipitates inhibited recrystallization and grain growth in Al-Mg-Mn. The strength of Al-Mg-Mn alloy sheets increased with increasing annealing temperature due to additional precipitation of fine Al₆Mn precipitates at elevated temperature. The maximum tensile strength and yield strength of the samples in this study were 428MPa and 236MPa of the Al-5wt%Mg-1.5wt% alloy sheets annealed at 450°C for 1hour, respectively. The nano-size precipitates and fine grain size improved tensile and yield strength of the Al-Mg-Mn sheets. Al-Mg-Mn sheets fabricated by twin roll casting and rolling have a superior strength to conventional Al-Mg-Mn alloy sheets due to fine Al₆Mn precipitate in Al matrix.

11:05 AM

Increasing Mechanical Properties of AA 6082 by Optimizing Chemical Compositions and processing Parameters during Extrusion: Milan Terce!j¹; Matevz Fazarine¹; Goran Kugler¹; Iztok Perus¹; ¹University of Ljubljana

AA 6082 aluminum alloy is used as constructional material for highly loaded automotive parts thus increasing of yield stress and ductility is of a great importance. Database of mechanical properties of processing parameters and chemical compositions for hot extruded profiles of the alloy was obtained. CAE neural networks individual and spatial analyses was performed to determine the influences of processing parameters and alloying elements, e.g. Mg, Si, Mn, Fe, and Cu, on mechanical properties. The results of the analyses revealed a new understanding of their influences, and the possibility of increasing the mechanical properties if processing parameters and correlations between chemical elements were closer to the optimum values. Optimization was carried out in order to increase yield stress and elongation simultaneously. In practice, the obtained values for mechanical properties have confirmed the optimized values of influential parameters as correct.

11:25 AM

Investigation of the Porosity Evolution during Hot-Compression Tests on an Aluminum Alloy: Agouti Siham¹; Bouchard Pierre-Olivier²; Piellard Mickael³; Le Brun Pierre⁴; Bozzolo Nathalie²; ¹Centre of materials forming; ²Centre of Materials Forming; ³Aubert & Duval; ⁴Constellium CRV

After casting, alloys ingots generally exhibit central voids that must be reduced during the forming process. In this study, a special Aluminum 7050 alloy with a high Hydrogen content is used as a model material. A laboratory hot compression test is used to investigate the voids evolution during hot-deformation. During compression tests, voids may be either completely closed and healed, or closed but un-healed, or un-closed. In order to identify which of these mechanisms do occur, complementary techniques were used: non-destructive ultrasonic control and SEM observations to detect un-closed voids; fracture surface SEM observation to detect closed but un-healed voids. The influence of thermally induced stresses is also assessed by performing heat-treatment and quenching after hot-compression. Comparisons of the ultrasonic control results before and after hot-compression showed that the voids were closed after hot-compression. However, the fracture surface SEM observations on the compressed specimens revealed the existence of un-healed voids.

11:45 AM

Effect of Strain Rate on the Microstructural Development in DC Cast Al-15Si Alloy: Chunxia Wang¹; Fuxiao Yu¹; Dazhi Zhao¹; Xiang Zhao¹; Liang Zuo¹; ¹Northeastern University, China

Hot compression at 573K under different strain rates was conducted on DC cast Al-15%Si alloy. The effect of strain rate on the microstructure development was investigated. Microstructural characteristics and deformation behavior of Al-15% Si alloy were discussed by analyzing of flow curves, optical microscope and EBSD. The results show that the peak and steady-state stresses are influenced by increasing of strain rate. The alpha-Al dendrites are almost disappeared and the morphology and size of Si particles is nearly the same as prior to deformation with less of them cracked after hot deformation under every strain rate. The size of continuous dynamic recrystallized grains (CDRXed) decreases and the volume fraction of these grains increases with the strain rate increases. The fraction of HABs is increased gradually and that of LABs is decreased considerably as strain rate increases. It is realized that deformation under high strain rate help for CDRX to occur.

12:05 PM

Influence of High-Pressure Torsion on Mechanical Properties and Microstructural Evolution in 2197 Al-Li Alloy: Yuan Yuan¹; Huimin Lu¹; Xuguang Li¹; ¹Beihang University

In present work, 2197 Al-Li alloy has been processed by high-pressure torsion (HPT) at applied pressure of 1GPa and different shear strain γ in the range of 77.7 and 259.0. Optical microscope (OM) and transmission electron microscope (TEM) provide the detail information of grain sizes and microstructure of the deforming alloys. Vickers indentation analysis is used to evaluate the microhardness of the deformed samples. Tension test is employed to obtain the tensile strength σ_b and elongation δ at room temperature. The results show that nice microstructure and properties are achieved when the pressure is 1GPa and the shear strain γ is 259.0, for the grain sizes in the range of 0.1~0.4 μ m, microhardness up to 163HV0.2, and σ_b at 500.8 MPa and elongation δ of 10.57%, higher than the peak aging treatment (T8) state of 474.7MPa, with the elongation δ of 9.25%.

Aluminum Reduction Technology: Energy Saving

Sponsored by: The Minerals, Metals and Materials Society, TMS Light Metals Division, TMS: Aluminum Committee, TMS: Aluminum Processing Committee

Program Organizer: Olivier Martin, Rio Tinto Alcan

Tuesday AM
March 13, 2012

Room: Southern III
Location: Dolphin Resort

Session Chair: Martin Segatz, Hydro Aluminium Deutschland

8:30 AM

Research and Application of Energy Saving Technology for Aluminum Reduction in China: Feng Naixiang¹; Peng Jianping¹; Wang Yaowu¹; Di Yuezhong¹; ¹Northeastern University

Aluminum electrolysis is known as more energy consumption and more pollution. The DC power of aluminum electrolysis before the technology of aluminum reduction cells with a new-type of cathodes design being applied in China was about 13000 kWh/t. After 2010, nearly all the aluminum smelters have used the technology of new type of cathode design and 800~1000 kWh/t of aluminum reduction can be achieved easily. The DC power of aluminum electrolysis is nowadays 12100~12300 kWh/t. 18000 kWh DC energy power of an aluminum reduction cell in Chuangyuan Smelter is achieved. In present paper, three different type cathodes design are given and the surface oscillation of liquid metal in the cells are studied by means of hydraulic model and numerical simulation. By using the technology of small size of anode and narrow central channel between the anodes under busbar, the energy power of less 11500 kWh/t of aluminum reduction is expected.

8:50 AM

Low Energy Cell Development on AP Technology™: Olivier Martin¹; Bertrand Allano¹; Etienne Barrioz¹; Aurore Escande¹; Yves Caratini¹; Nolwenn Favel¹; ¹Rio Tinto Alcan

During this decade the energy market is changing rapidly and new smelter projects may face large ranges of energy block size, significantly different energy prices and environmental regulations. To provide more choice in this complex and changing situation, Rio Tinto Alcan announced two years ago a new strategy of developing flexible solutions. On the same platform have been developed cells at very high productivity and cells with low energy consumption. This strategy has been delivered with the APXe and AP60 cells, able to operate with the same framework in the range 500-600 kA with energy efficiency between 12.0 and 13.2 kWh/kg. This new development incorporates an environmental dimension, aiming to reduce dramatically the air emissions of future smelters. The prototype results have confirmed the feasibility of such ambitious targets and shown that innovation is a key factor to develop the cell of 2020's, at low energy consumption and reduced environmental footprint.

9:10 AM

Review on the Energy Saving Technologies Applied in Chinese Aluminum Reduction Industry: Fengqin Liu¹; Songqing Gu¹; ¹Chalco

The energy saving technologies applied in Chinese aluminum reduction are reviewed in this paper. The energy saving technology development in China in the aluminum reduction field could be divided into three stages. The first stage was retrofit of sodburge cells to prebaked anode cells and technology development of large amperage prebaked anode cells, which happened mainly in 1990's. The second stage was wide applications of the large amperage prebaked cell technology and the improvement of such relevant technologies as physical fields simulation, cell control systems and high quality anode and cathode manufacturing etc., which covered the first 6-7 years of this century. The third stage has lasted up to now, which mainly focused on the energy saving in the present prebaked cells by cell cathode and lining structure modifications and high performance operation and control system applications.

9:30 AM

Numerical Simulation on Coupled Multi-field of the Perforated Anode in Aluminium Reduction Cells under Low Carbon Operation: Hesong Li¹; Xi Cao¹; Yingfu Tian²; ¹Central South University, China; ²Chongqing Tiantai Aluminum Industry Co.Ltd

Perforation on the anode block is a new way of thinking. The bubble under the anode block can be eliminated from the holes, and the energy consumption is reduced. The physical and mathematical models of perforated anode and bubble layer were established. The simulation results show that the thickness of the bubble layer is 1.28cm of the perforated anode, reduced by 0.72cm compared to a normal anode, of which corresponding voltage is less than 240mV; the minimum temperature of anode block is 704.3°C, and the temperature distribution in a horizontal plane presents a wave shape due to the holes; the voltage drop of the perforated anode is 379mV and the current density distribution of the perforated anode and ordinary anode are consistent; the maximum of thermal stress is 17.4MPa in the perforated anode, which is far less than the allowable stress. The perforated anode industrial was conducted on three cells. The average cell voltage of perforated anodes decreases 229mV than the traditional reduction cell after long-term operation, which is agreed with the theoretical calculation.

9:50 AM

Improved Energy Management during Anode Setting Activity: Ali Jassim¹; Gregory Meintjes¹; Arvind Kumar¹; Jose Blasques¹; Mohammed Sadiq¹; Maryam Al-Jallaf¹; Ali Al Zarouni¹; ¹Dubai

In prebake aluminium reduction cells, the continuous electrochemical and chemical oxidation of the anodes requires their regular replacement in a predetermined sequence. It's important to maintain cell stability and thermal balance during the anode exchange. The higher amperage operation at Dubai pushed the 'anode current density' towards the anode



TMS 2012

141st Annual Meeting & Exhibition

TUESDAY AM

effect threshold limit. Moreover during anode removal, this threshold limit is challenged causing a higher likelihood of AE. Therefore, the anode setting logic was revamped in order to improve the energy balance whilst operating at an anode current density greater than 1A/cm². An optimum utilization of resistance set point combined with an automated down movement of anodes prior to anode removal was introduced. Thereby it improved the thermal balance resulting in a reduction in anode effect frequency by 29% and cell voltage by 9mV. This paper summarises the methodology of optimising energy balance during anode setting at Dubai.

10:10 AM Break

10:20 AM

The Transition Strategy at Alouette towards Higher Productivity with a Lower Energy Consumption: *Pascal Coursol¹; Jules Coté¹; Francois Laflamme¹; Pascal Thibault²; Alexandre Blais²; Dany Lavoie¹; Serge Gosselin¹; ¹Aluminerie Alouette; ²Rio Tinto Alcan*

The Alouette aluminium smelter at Sept-Iles, Quebec was commissioned in 1992 with a nominal capacity of 215,000 tonnes/year based on AP30 cells operating 264 pots at 300 k Amp. Since that time, the plant has expanded and in 2005 one potline of 312 pots was added plus a test Section of 18 pots. The cells currently operate at nearly 370 k Amp for a capacity of 575,000 tonnes/year. In quest of higher productivity and profitability, Alouette is planning a transition to 400 k Amp based on the new High Performance (HP) AP30 cells, referred to as "400HP". In designing this new cell, lining, rodding procedures and materials of construction were modified. The main performance objectives and the development steps towards putting the 400HP pots online and bringing the production lines to 400kA are described in this paper.

10:40 AM

Experimental Studies of the Impact of Anode Pre-Heating: *Otavio Fortini¹; Srinivas Garimella¹; Edwin Kunn¹; Yimin Ruan¹; Benyam Yacob¹; Jack Sorensen¹; ¹Alcoa*

The adverse impact of anode setting on the current efficiency (CE) is well known in the aluminum industry, although few published studies exist. When a cold anode is lowered into the bath, it immediately quenches a layer of frozen bath, on the bottom surface, that may extend to the metal pad. It takes time, energy, and bath motion to melt this layer. Until then, the anode current distribution is uneven and the bath motion is disrupted around the newly set anodes. These effects are hypothesized to lead to higher noise and lower CE. The paper summarizes experiments, conducted at Alcoa Warrick, during which anodes pre-heated to 480-510 deg C (bottom surface) were set in a few pots over 60 days. The studies suggest potential to double the rate of load up, reduce energy consumption by 40 kWh/mt, and increase CE by 0.5-1%. Approaches to supply hot anodes are discussed.

11:00 AM

Depth Analysis and Potentiality Exploitation on Energy-Saving and Consumption-Reduction of Aluminum Reduction Pot: *Jianfei Zhou¹; Marc Dupuis²; Jun Huang¹; Xiaobing Yi¹; Feiya Yan¹; ¹Guiyang Aluminum Magnesium Design & Research Institute; ²GéniSim Inc*

In view of the existing status with aluminum overcapacity and lower aluminum price in China, many companies adopted various measures to reduce the production cost and the energy consumption, but there has been no normalization theory and method as yet. Aimed at the existing status and the market demand, this paper puts forward the evident effects of energy-saving and consumption-reduction in aluminum reduction pot using new thermal insulation pot lining design, application of optimal cathode structure, reduction of horizontal current device, proper application of new lining materials and proper combination of relevant process parameters based on the finite element software ANSYS and using the thermal field simulation software of international simulation Prof. Mr. Dupuis as calculation method, combining the actual production data. Practice proves that the above-mentioned method combining design, simulation and experiment can become the effective and feasible way to achieve low energy consumption, low cost and high profit.

11:20 AM

Development and Application of SAMI's Low Voltage Energy-Saving Technology: *Dongfang Zhou¹; Xiaodong Yang¹; Wei Liu¹; ¹Shenyang Aluminium & Magnesium Engineering & Research Institute Co. Ltd*

In this paper one low voltage energy-saving technology for aluminum reduction cell is developed by SAMI, this technology can largely reduce horizontal current in the metal pad and improve the MHD stability of the cell. Some industrial testing results of this technology by SAMI and its application on different type cells in Chinese smelter are finally presented to illustrate how their contributions is to make D.C. power consumption close to 12000 kWh/t-Al without current efficiency loss compare to the prior technology.

11:40 AM

Twin Air Compressor for Energy Saving and Backup Capability: *Anne-Gaëlle Hequet¹; Serge Despinasse¹; ¹ECL*

Since the first Pot Tending Machine commissioned by ECL™ 50 years ago, all the new options, tools and technical solutions have been conceived and designed only to meet with smelters' challenges: reduce energy consumption and consequently allow significant cost savings and ensure safe and secure operations. In close collaboration with a world-class air compressor designer and manufacturer, ECL™ has then developed and equipped its Pot Tending Machine with a new standard of air compressor: the twin air compressor. Instead of just one big energy-intensive compressor, two smaller and lighter compressors are in most cases used separately (anode changes), except for tapping operation. By running them alternately at only 90% of their full capacity, there are definite energy savings with the additional benefit of a longer operational life for the compressor. Furthermore, the size and weigh of this new standard greatly ease maintenance operations.

Atomistic Effects in Migrating Interphase Interfaces - Recent Progress and Future Study: Kinetics of Phase Transformations in Ferrous Alloys

Sponsored by: The Minerals, Metals and Materials Society, TMS Materials Processing and Manufacturing Division, TMS/ASM: Phase Transformations Committee

Program Organizers: Tadashi Furuohara, Institute for Materials Research, Tohoku University; Sudarsanam Babu, Ohio State University; Hatem Zurob, McMaster University; Jian-Feng Nie, Monash University; Wen-Zheng Zhang, Tsinghua University; James Howe, University of Virginia

Tuesday AM
March 13, 2012

Room: Europe 3
Location: Dolphin Resort

Session Chairs: Christopher Hutchinson, Monash University; Sudarsanam Babu, Ohio State University

8:30 AM Invited

The Role of Interfaces in the Development of Microstructure in Bainitic Steels: *Gary Purdy¹; R. Hadian¹; G. Botton¹; ¹McMaster University*

The addition of silicon to alloy steels can act to suppress or delay the formation of carbides. In the present work, the formation of ferrite from alloyed austenite with and without Si additions has been used to further elucidate the nature of the bainite transformation. Isothermal transformation products in a Fe-0.5%C-5%Ni (mass %) steel have been compared with a similar alloy with 1.5% Si added and with those in a Fe-0.4%C-3%Mn-1.8%Si alloy. In the Si-containing alloys, ferrite forms initially as groups of Widmanstaetten plates, which thicken with reaction time and adopt increasingly complex morphologies. The orientation relationships, habit planes and defect structures of the resulting ferrite/austenite interfaces are reported. The Si-free steel, isothermally

transformed below Ms, yields a mixture of autotempered martensite and bainitic ferrite. The OR's and habits of the cementite precipitates in the two phases are compared, and consequences for the nature of the bainite reaction are considered.

9:00 AM Invited

A Study on the Kinetics of Bainite in Steel: *Annika Borgenstam*¹; ¹KTH

There have been two conflicting hypotheses about bainite in steel for a long time: the diffusional and the diffusionless hypothesis. The diffusionless hypothesis claims that the growth of bainitic ferrite is rapid and occurs without diffusion of carbon. The diffusional hypothesis on the other hand claims that the growth of bainitic ferrite is controlled by carbon diffusion. It was recently shown that several microstructural observations can be explained by the diffusional hypothesis and it is here shown that several kinetic observations also favor the diffusional hypothesis. The effect of alloying elements on the growth of bainite will also be discussed.

9:30 AM Invited

The Effect of Alloy Composition on the Stagnant Phase during the Austenite-Ferrite Transformation: *Sybrand Van Der Zwaag*¹; Hao Chen¹; ¹Technical University Delft

Recently the concept of cyclic partial transformations has been proposed in order to study the austenite-ferrite interfacial kinetics in the absence of simultaneous nucleation effects. Unlike the case of regular austenite ferrite phase transformations, cyclic partial phase transformations show clear effects of the local interface compositional profile. These effects are most noticeable in the so-called stagnant phase, during which the interface barely moves, even in the presence of a significant driving force. In this paper we will present the result of our simulations on the length of the stagnant phase as a function of the alloy composition.

10:00 AM

A Model for Calculating C-curves for Widmanstätten and Bainitic Ferrite: *Peter Kolmskog*¹; *Annika Borgenstam*¹; ¹Royal Institute of Technology, KTH

A model for calculating C-curves for the transformation of austenite to Widmanstätten and bainitic ferrite is presented. The model is based on the diffusional hypothesis which claims that there is no difference between these two transformation products and that the growth of the two is controlled by carbon diffusion. In this model the start temperature for Widmanstätten and bainitic ferrite, WB_s , is included and needs to be calculated. For calculating the WB_s temperature a model, previously presented by Hillert et al. is improved to get a better predictive capability for Mn, Ni, Cr, Mo, V, Ti and B alloyed steels. The improvement is based on experimental data obtained from both literature and new experiments. Comparisons with other models for calculating C-curves as well as WB_s or B_s are also presented.

10:20 AM Break

10:35 AM

Alloying Element Partitioning and Phase Transformations during Rapid Heating and Cooling: *Tapasvi Lolla*¹; *Brian Hanhold*¹; *Gary Cola*²; *Sudarsanam Babu*¹; ¹Ohio State University; ²Sirius Protection, LLC

An advanced high strength steel (tensile strength > 2000 MPa and elongation > 10%), containing mixed bainite and martensitic microstructure, has been developed through rapid heating (> 400K/s) to austenite phase field and rapid cooling (>500K/s) to room temperature. The mechanism for such microstructure evolution is rationalized based on incomplete dissolution of alloy carbides, originally present the initial microstructure, into the austenite phase. In addition, arguments were made on incomplete carbon homogenization within the austenite phase field. The validity of the above mechanisms was evaluated using computational thermodynamics and kinetic models. Calculations show sensitivity of the dissolution kinetics to composition of alloy carbides (e.g. Chromium concentrations). Some of the challenges of extending local-equilibrium assumption at the carbide/austenite interface (e.g. intermittent formation of Cr enriched ferrite) will be discussed. Impact of these results towards

developing a welding process that minimizes the softening at the heat-affected-zone will be discussed.

10:55 AM Invited

Austenite Stabilization through the Quench and Partition Process: *Amy Clarke*¹; *John Speer*²; *Robert Hackenberg*¹; *Emmanuel De Moor*²; ¹Los Alamos National Laboratory; ²Colorado School of Mines

The quench and partition (Q&P) process has been developed to employ carbon transport from martensite to austenite during a partitioning treatment after initial quenching between Ms and Mf. Quenching within this temperature range produces specific fractions of martensite, while the partitioning treatment promotes stabilization of the remaining austenite through carbon enrichment. The aim of Q&P is to produce substantial amounts of carbon-enriched retained austenite, whereas carbide formation is a more typical means of reducing carbon supersaturation during conventional tempering. In this work, a 0.19C-1.59Mn-1.63Si (wt.%) steel was partitioned at temperatures ranging from 350 to 450°C for times up to 1000s. The kinetics of carbon partitioning and the amount of retained austenite after Q&P processing were examined. The local austenite stability, or the austenite carbon concentration with respect to distance from the austenite/martensite interface, was considered. Bainite formation as a possible mechanism to enrich austenite during partitioning is also addressed.

11:25 AM

Partitioning of Carbon into Austenite Matrix during Bainite Transformation: *Naoki Takayama*¹; *Goro Miyamoto*¹; *Tadashi Furuhashi*¹; ¹Tohoku University

The carbon enrichment to austenite (γ) during bainite transformation is investigated by means of FE-EPMA in an Fe-0.15C-1.5Mn-0.05Si-0.03Nb (mass%) alloy transformed at 873K where bainite transformation stasis was appeared. In the early stage of transformation, carbon is enriched into a large γ region up to the T_0 composition at γ / bainitic ferrite (BF) interface although average carbon concentration in γ is much lower than the T_0 composition. Meanwhile, the carbon concentration within thin γ between parallel BFs is almost uniform and clearly exceeds the T_0 composition. During the stasis, pre-existing inhomogeneous distribution of carbon in γ is diminished by diffusion in BF and γ . And, the average concentration of γ becomes close to the T_0 ' composition. Such carbon enrichment can be understood by the rejection of carbon from BF either a diffusional or diffusionless growth.

Biological Materials Science Symposium: Biological and Bio-Inspired Materials I: Hard Biomaterials

Sponsored by: The Minerals, Metals and Materials Society, TMS Electronic, Magnetic, and Photonic Materials Division, TMS Structural Materials Division, TMS: Biomaterials Committee
Program Organizers: Nima Rahbar, University of Massachusetts Dartmouth; Candan Tamerler, University of Washington; Po-Yu Chen, University of California, San Diego; Molly Gentleman, Texas A&M University

Tuesday AM
March 13, 2012

Room: Swan 7
Location: Swan Resort

Session Chairs: Ryan Roeder, University of Notre Dame; Candan Tamerler, University of Washington

8:30 AM Keynote

Peptide-Tailored Solid Interfaces: From Biocompatibility to Self-assembly and Biomaterialization: *Mehmet Sarikaya*¹; ¹University of Washington

Proteins enable biology to be viable through molecular interactions with <nM specificity to targets. Using biology as a guide at the molecular dimensions, we biocombinatorially select, bioinformatically



TMS 2012

141st Annual Meeting & Exhibition

enhance and genetically tailor solid binding peptides and utilize them as molecular building blocks in carrying out molecular and nanomaterials science and engineering. Genetically engineered peptides for inorganic materials (GEPI) are used as bionanosynthesizers in biomaterialization, heterofunctional linkers to create thermodynamically stable interfaces between dissimilar materials, and as molecular assemblers for the targeted and directed assembly of nanobiomaterials towards addressable ordered architectures with genetically designed functions. Here, we will give an update of the utility of a variety of GEPIs in nano-inorganic formation for hybrid probe design and bionanosensors; biofunctionalization of implants, biomineral formation for tissue regeneration and restoration, and in peptide-enabled nanobioelectronics and -nanobiophotonics to demonstrate the expanding paradigm in nano/bio-technology and nanomedicine. Primary funding is by NSF-MRSEC and BioMat Programs.

9:10 AM

Design of Bone-Mimetic Scaffolds: *Ryan Roeder*¹; Timothy Conrad¹; Robert Kane¹; ¹University of Notre Dame

Metallic scaffolds exhibit excellent mechanical properties but are bioinert and radiopaque, inhibiting radiographic assessment of bone ingrowth. Ceramic and polymer scaffolds are radiolucent and may be bioactive, but are limited to non-load bearing applications due to their brittleness and compliance, respectively. Polyetheretherketone is a high-performance thermoplastic ideal for load-bearing applications, but bioinert. Collagen is a constituent of the extracellular matrix of bone, ideal for synthetic bone graft substitutes, but collagen scaffolds are alone too weak for immediate load-bearing post-implantation. PEEK and collagen scaffolds were reinforced by bioactive calcium-deficient hydroxyapatite whiskers, which are exposed on the surface and embedded within scaffold struts. Hydroxyapatite whisker reinforced PEEK scaffolds were able to mimic the mechanical properties of vertebral trabecular bone. Hydroxyapatite whisker reinforced collagen scaffolds were prepared using novel processing methods and achieved properties up to twenty times greater than any previous collagen scaffold. Scaffold permeability and bioactivity was also investigated in vitro.

9:30 AM

Mechanical Behavior of a Cellulose-Based Scaffold in Vascular Tissue Engineering: *Parisa Pooyan*¹; Rina Tannenbaum¹; Hamid Garmestani¹; ¹Georgia Institute of Technology

As an essential structural component, scaffold plays a significant role in the design of a vascular substitute for small grafts. Stable mechanical properties and appropriate chemical functionalities are the critical parameters in such a design. Cellulose nanowhisker (CNW) with its unique advantages could potentially constitute an acceptable candidate in scaffolding of a tissue-engineered vessel. Inspired by this possibility, we have designed a fully bio-based scaffold reinforced by CNW fibers. Comparable to carbon nanotubes or kevlar, CNWs impart significant strength and directional rigidity at only 0.2 wt%. To verify our experimental results, theoretical mechanical models were also investigated in this study. Based on these comparisons, the formation of a three-dimensional rigid percolating network imparts an excellent mechanical stability at such low fiber concentration. We believe our fibrous porous microstructure with the improved mechanical properties could expand the biomedical applications of cellulose-based materials while provide a potential scaffold in vascular tissue engineering.

9:45 AM

Sheep Hydroxyapatite (SHA)- Commercial Inert Glass (CIG) Composites: *Nermin Demirkol*¹; Faik Oktar²; Eyup Kayali³; ¹Kocaeli University; ²Marmara University; ³Istanbul Technical University

In this study, microstructures and mechanical properties of sheep hydroxyapatite (SHA) - commercial inert glass (CIG) composites were investigated. The production of hydroxyapatite (HA) from natural sources is preferred due to economical and time saving reasons. The goal of development of SHA-CIG composites is to improve mechanical properties of HA. SHA composites were prepared with the addition of

different amounts of CIG and sintered at the temperature range of 1000-1300 °C. The physical and mechanical properties were determined by measuring density, compression strength and Vickers microhardness (HV). Structural characterization was carried out with X-ray diffraction (XRD) and scanning electron microscopy (SEM) studies. The experimental results were discussed to determine optimum amount of CIG addition as a reinforcement material and the effect of sintering temperature on the microstructure and the mechanical properties of SHA composites.

10:00 AM Break

10:10 AM Invited

Mineralization of Dense Collagen Scaffolds Using a Polymer-Induced Liquid-Precursor (PILP) Process: *Yuping Li*¹; Taili Thula²; *Laurie Gower*²; ¹University of Minnesota; ²University of Florida

Bone is a hierarchically-structured composite which imparts it with unique mechanical properties and bioresorptive potential. In our prior studies, we have shown that when using a polymer-induced liquid-precursor (PILP) mineralization process, we can effectively achieve intrafibrillar mineralization of collagen fibrils. While this leads to a nanostructure that emulates that of bone, isolated rigid mineralized fibrils in a porous scaffold will simply crush under an applied load. Therefore, our current efforts are devoted to mineralization of densely packed collagen matrices, which can then provide a means for emulating the microstructure, and therefore mechanical properties, of bone. Here we show that a densified collagen matrix which resembles the extracellular matrix of primary bone can be created with a plastic compression technique. Upon mineralization, these composites can attain a modulus (as determined by nanomechanical analysis) comparable to primary fetal bone.

10:40 AM

Assessing Biocompatibility and Mechanical Properties of Degradable Metallic Biomaterials: *Puneet Gill*¹; Norman Munroe¹; Amit Datye²; Rupak Dua¹; Sharan Ramaswamy¹; ¹Florida International University; ²University of Tennessee Knoxville

Metallic materials continue to play an essential role as biomaterials to assist with the repair or replacement of various diseased or damaged parts of the anatomy. This investigation focuses on the manufacturing of biodegradable metallic stent materials, which degrade at desired rates under body simulated conditions. The alloys are tested for their mechanical integrity, surface energy and biocompatibility. Improved mechanical properties are achieved with the addition of alloying elements. The metallographic characteristics associated with those properties are studied by scanning electron microscopy (SEM), X-ray diffraction (XRD), X-ray photoelectron spectroscopy (XPS) and transmission electron microscopy (TEM).

11:00 AM

Anisotropic Behavior and Phase Transformation in Bone: *Ahmet Ucisik*¹; Mehmet Aksoy²; Isil Kutbay³; Metin Usta³; Cuma Bindal⁴; ¹Bogazici University; ²Ministry of Health Istanbul Division; ³Gezbe Institute of Technology; ⁴Sakarya University

Human bones present extraordinary, exceptional nature as of birth. All of them are always dynamic even while there is no movement. Osteoblast-osteoclast activities, piezoelectricity, flow through Haversian channels, mass transport etc. make bone dynamic. In this study, microstructural differences and variations on the mechanical behavior of bone and phase transformations due to injections of anticoagulants during healing of fractured animal bones are investigated. Several different types of mechanical test, micro-structural analysis, XRD and FTIR studies revealed structural changes caused by injection of anti-coagulants; it is found that same bone may alter its crystallographic nature. Mechanical tests performed on human bones, "femur, tibia, fibula" of the same patient and spongy bone on the hip joint" show differences in "stress-strain" behavior of three bones of the same person that imply each bone has different mechanical behavior and anisotropy in single section of bone respectively.

11:20 AM

Fatigue Behavior of Ti-6Al-4V for Medical Applications after Surface Modification by Anodization: Fernanda Potomati¹; Laís Possato¹; Enrico Giordano¹; *Claudemiro Bolfarini*¹; ¹Universidade Federal de São Carlos

The new developments and studies of surface modifications are generally driven and focused on biological studies. Engineering studies on mechanical properties of the implants with surface modified do not follow the dynamic of the biological studies. As the fatigue life is a determining property in the use of an implant, this work aimed at to study the fatigue behavior of alloy Ti-6Al-4V subjected to a surface modification through a anodization technique. For this, SxN (stress x number of cycles) curves were obtained through methods specified by standards and literature. Scanning electron microscopy and roughness measurements were used for surface characterization. Contrary to previous results obtained by using a surface modified by laser remelting that led to a 30% loss in the fatigue life when compared to Ti-6Al-4V alloy without surface modification, the anodized surface led to a small increase in the fatigue life.

11:40 AM

Morphological Evaluation of Osteoblast-TiO₂ Nanotube Interfaces: *Tolou Shokuhfar*¹; Chang Choi¹; Craig Friedrich¹; ¹Michigan Technological University

The rate and degree of bio-assimilation for an implant is principally governed by the initial cascade of cellular events at the interface. The primary physiological reactions that dictates osteoblast adhesion, and subsequent extracellular bone matrix deposition are now recognized to respond most directly to nanometric topography. Osteoblast interaction and attachment with TiO₂ nanotubes was investigated using focused ion beam milling. The SEM images of the FIB milled cells revealed high attachment and growth of the cell inside the hollow section of the nanotubes. EDS analysis suggested that the bond between the TiO₂ nanotube substrate and the adjacent osteoblast cell layer was composed of Ca and P elements mimicking the bond in the bone tissue itself. These observations revealed a truly direct contact between the osteoblasts and the titania nanotubes followed by calcium and phosphorous deposition on the nanotubes as an indication that TiO₂ nanotubes have regulated osteoblast functionality and differentiation.

Bulk Metallic Glasses IX: Structures and Mechanical Properties I

Sponsored by: The Minerals, Metals and Materials Society, TMS Structural Materials Division, TMS/ASM: Mechanical Behavior of Materials Committee

Program Organizers: Peter Liaw, The University of Tennessee; Hahn Choo, The University of Tennessee; Yanfei Gao, The University of Tennessee; Gongyao Wang, University of Tennessee

Tuesday AM
March 13, 2012

Room: Swan 6
Location: Swan Resort

Session Chairs: Takeshi Egami, University of Tennessee; Katharine Flores, The Ohio State University

8:30 AM Keynote

Atomic Level Flow Dynamics in Metallic Glasses: *Takeshi Egami*¹; Takuya Iwashita¹; ¹University of Tennessee

Traditionally the flow of a liquid is described by continuum fluid dynamics. Atomic dynamics is considered to be irrelevant, because the Brownian motion of an atom is so random. However, such an assumption may not be justified for supercooled liquids, or dynamic flow in glasses, such as those in the shear band. Indeed the molecular dynamics (MD) simulation of steady state flow in metallic glasses shows that the atomic dynamics of flow is highly heterogeneous both in time and space. The MD results were analyzed in terms of the anisotropic pair-density function (PDF). The length-scale of spatial heterogeneity is of the order of 1 nm,

and depends weakly on the strain rate. The atomic level strain in the strained zone is so high that it causes a cascade of atomic level mechanical failure, resulting in dynamic heterogeneity. Work supported by the US Department of Energy, Office of Basic Energy Sciences.

9:00 AM

Nucleation Reactions during Deformation and Crystallization of Metallic Glass: *Seth Imhoff*¹; John Perepezko¹; Mingwei Chen²; Sergio Gonzalez³; Akihisa Inoue²; ¹University of Wisconsin-Madison; ²Tohoku University; ³Universitat Autònoma de Barcelona

Nucleation reactions play a central role in both bulk metallic glasses (BMG) and nanostructured materials. For BMG crystal nucleation must be suppressed. For nanostructured materials it is necessary to promote a high nucleation density. Beyond crystallization reactions nucleation is critical for promoting shear band formation to achieve a homogeneous deformation and useful ductility. The study and analysis of nucleation reactions for these different situations requires a consideration of the stochastic nature of nucleation, the influence of heterogeneous sites, and the controlling transport properties. For shear band nucleation, the stochastic nature can be effectively probed by employing instrumented nanoindentation tests and analyzing a statistically significant number of measurements of the first pop-in shear band nucleation events. In nanostructured composites, the early growth characteristics are linked to the maximum particle density that can be achieved and the coarsening kinetics determine how the population will change during operation at higher temperatures.

9:10 AM Invited

High Energy X-Ray Scattering Studies of Plastic Process Zones around Fatigue Crack Tips in Metallic Glasses: *Todd Hufnagel*¹; Uday Vempati¹; Jon Almer²; ¹Johns Hopkins University; ²Argonne National Laboratory

Metallic glasses can achieve remarkably high fracture toughnesses, given their lack to work hardening or microstructural features usually associated with toughening mechanisms in crystalline materials. To study the fracture process, we have used high-energy x-ray scattering to study the plastic process zone around fatigue crack tips in a metallic glass. Far away from the crack tip, we map the elastic strain as a function of position. Closer to the crack tip, the strain diverges from the expected behavior (from an analytical calculation of the strain around a crack tip), allowing us to determine the extent of the plastic zone. The size of the plastic zone decreases with temperature, correlating with a decrease in the critical stress intensity. Within the process zone, the strain measurement becomes unreliable, because the x-ray scattering pattern is affected by plastic deformation processes.

9:30 AM Invited

Irreversible Lattice Deformation and Enhanced Fragility Under Fatigue in Amorphous Solids: *Despina Louca*¹; Peng Tong¹; Gongyao Wang²; Peter Liaw²; Yoshihiko Yokoyama³; Anna Llobet⁴; Yiming Qiu⁵; Yunfeng Shi⁶; ¹University of Virginia; ²University of Tennessee; ³Tohoku University; ⁴Los Alamos National Laboratory; ⁵NIST Center for Neutron Research; ⁶Rensselaer Polytechnic Institute

Amorphous metals exhibit unique properties that could have a widespread industrial impact. How they mechanically respond and deform under applied stress, which is vital to their functionality, is not yet well understood. Here we show that fragile behavior is enhanced in glasses under fatigue in part due to shrinkage of loosely bonded regions. By combining neutron diffraction, inelastic scattering and specific heat measurements, we observe a drastic local atomic rearrangement that is hysteretic in temperature and scales with the compression frequency. Associated with this is a softening in the dynamics envisaged in the so-called Boson peak where not one but two collective excitations are observed corresponding to two kinds of localized oscillators that may be a signature of strong glass formers. The suppression of the two excitations under fatigue indicates a decrease in the number of soft-like regions of loosely bound atoms that renders the glass more fragile.



TMS 2012

141st Annual Meeting & Exhibition

9:50 AM Break

10:05 AM Invited

Structure and Dynamics of a Metallic Glass during Mechanical Deformation: *Wojciech Dmowski*¹; Takuya Iwashita¹; Konstantin Lokshin¹; Yoshiko Yokoyama¹; Chin-Pi Chuang¹; Matthew Stone¹; Takeshi Egami¹; ¹University of Tennessee

Metallic glasses are inherently disordered, having a distribution of atomic sites, yet it is assumed that deformation is microscopically elastic. We studied changes in the atomic structure and dynamics of metallic glasses in situ during deformation below the elastic limit. We used high energy x-ray diffraction and the anisotropic pair distribution function analysis (PDF). Analysis showed that the anisotropic PDF could be divided into elastic (affine) and anelastic components, and for any applied stress level about 24% of the apparent strain was anelastic. Therefore microscopic deformation is never truly "elastic". The inelastic neutron scattering was performed during compression up to 1.5 GPa. Neutron scattering was analyzed as a function of energy and momentum transfer. The elastic scattering component showed anisotropy typical for compression. However, the inelastic component at Q_p indicated softening under compressive loading. This work was supported by the U.S. DOE under DE-AC05-00OR-22725 and NSF-DMR-0906744.

10:25 AM Invited

Investigation of Microstructure and Property Variations in Metallic Glass Matrix Composites: Nicholas Hutchinson¹; Anupriya Agrawal¹; Wolfgang Windl¹; *Katharine Flores*¹; ¹The Ohio State University

Recent work has demonstrated the effectiveness of adding crystalline phases to a metallic glass matrix in order to improve mechanical performance, such as tensile ductility. This presentation will discuss efforts to quantitatively describe the micro- and atomic-level structure of the glass-crystalline interface, and its effect on damage evolution in the composite. Detailed analysis of three-dimensional microstructure reconstructions of Zr- and Ti-based glasses reinforced by ductile crystalline dendrites reveal changes in the interface curvature with thermal processing which may be linked to shear band multiplication and thus the ductility and toughness of the composite. The influences of the curvature and other microstructural length scales, as well as the properties of the individual phases, on strain distribution are examined via finite element analysis. Molecular dynamics simulations are underway to describe dislocation-shear band interactions at interfaces in simple glass-crystalline composites. Implications for metallic glass matrix composite composition and microstructural design will be discussed.

10:45 AM Invited

Origins of Tensile Ductility and Work-Hardening in TRIP CuZr-Based Bulk Metallic Glass Composites: Y. Wu¹; D. Ma²; A. D. Stoica²; Z. Y. Zhang¹; W. L. Song¹; G. Y. Wang³; G. M. Stoica²; X. L. Wang²; K. An²; *Z. P. Lu*¹; ¹University of Science and Technology Beijing; ²Oak Ridge National Laboratory; ³University of Tennessee

Guided by the concept of "transformation-induced-plasticity" (TRIP) concept, we obtained tensile ductility and work-hardening capability in ZrCu-based bulk metallic glass (BMG) composites which undergo martensitic transformation during tensile deformation. In this talk, we will focus on origins of the observed tensile ductility and work-hardening behavior, including the following aspects: 1). How the composites accommodate the macroscopic plastic deformation, 2). What contributions of the austenitic B2 CuZr phase and the martensitic transformation are, and 3). Why the microalloying elements (such as Co) benefit the mechanical properties of the glassy composites.

11:05 AM

Short and Medium Range Order in Ca-Mg-Cu Amorphous Alloys: *Oleg Senkov*¹; Yongqiang Cheng²; Daniel Miracle¹; Evan Ma²; Emma Barney³; Alex Hannon³; ¹Air Force Research Laboratory; ²John Hopkins University; ³ISIS Facility, Rutherford Appleton Laboratory

The atomic structures of $Ca_xMg_{25}Cu_y$ amorphous alloys were studied as a function of Cu content using the GEM diffractometer at the ISIS high-intensity pulsed neutron source. An increase in the Cu content broadened the first sharp diffraction peak (FSDP) of the structure factor $S(Q)$ and shifted it to higher Q . The shift and broadening of FSDP were interpreted as arising from the shortening of the average interatomic distance and narrowing of the distribution of interatomic distances, respectively. The $S(Q)$ curves contained a medium range order pre-peak at $Q \sim 1 \text{ \AA}^{-1}$. An analysis of the amorphous atomic structures obtained using a combination of quantum molecular dynamics and Reverse Monte Carlo methods allowed identification of specific short range and medium range order features in these Ca-Mg-Cu alloys. In particular, these amorphous structures were interpreted as consisting of closely packed Cu-centered clusters, which resulted in the Cu-Cu medium range order correlation.

11:15 AM Invited

Neutron and X-Ray Diffraction Studies of Crystallization in Bulk Amorphous Alloys: *Dong Ma*¹; Alexandru Stoica¹; X.-L. Wang¹; ¹ORNL

An amorphous alloy has short-to-medium range order and is thermodynamically metastable. Upon heating to near or above its glass transition temperature, crystallization that promotes long range order will take place. In this regard, neutron and x-ray total scattering techniques are useful tools in providing structure/phase information at multiple length scales upon crystallization. Here we report the crystallization behaviors of bulk amorphous alloys investigated using both neutron and x-ray diffraction. The knowledge gained from these measurements, in conjunction with microscopic studies, provides useful insights into the phase transformation kinetics that have important implications on glass-forming abilities.

11:35 AM

Structural Anisotropy of BMGs after Mechanical Deformation: *Yang Tong*¹; Zbigniew Witczak²; Chin-Pin Chuang¹; Takeshi Egami³; Wojciech Dmowski¹; ¹University of Tennessee; ²Inst. High Pressure Phys.; ³ORNL

We performed equal channel angular processing (ECAP) of bulk metallic glasses in Zr and La based systems. The deformation was carried in medium with external hydrostatic pressure of 1.2 GPa. The applied nominal stress during ECAP was about 10% below the elastic limit. The resulting shear strain was 0.2 for Zr and 0.4 for La-based glasses. The as prepared and deformed samples were cut to 0.5 mm thick slices with different orientations with respect to the ECAP channel axis. Structural studies were performed using high energy x-ray diffraction. The data were analyzed to obtain structure and the pair distribution functions. We observed anisotropy in the diffraction pattern implying macroscopic uniform strain. Same diffraction experiment was performed after thermo-mechanical creep. We will discuss origin of the apparent strain without external stress in the ECAP and creep samples. This work was supported by the NSF-DMR-0906744 and U.S. DOE under DE-AC05-00OR-22725.

11:45 AM Invited

In Situ High Temperature X-Ray Diffraction Studies on Bulk Metallic Glasses: *Norbert Mattern*¹; ¹IFW Dresden

The thermal behavior of bulk metallic glasses has been investigated by in situ high energy synchrotron X-ray diffraction. Repeated heating and cooling procedures were performed between glassy and super-cooled liquid state. The observed changes of the structure factor during heating and cooling through the glass transition give evidence for the transition into the super-cooled liquid state at the calorific glass transition temperature. The changes in positions of the first and second diffraction maximum indicate reversible structural changes with temperature differently in the glassy and in the supercooled liquid state. For the glassy phase the shift in position of the first maximum scales approximately with the thermal

linear expansion however not for the super-cooled liquid state. Structural relaxation has only a minor effect on the position of the first maximum. The influence of quenching rate, pre-annealing, and mechanical deformation on the temperature dependence of structural parameters is discussed.

12:05 PM

Mechanical Behavior of Zr/Hf Based Bulk Metallic Glasses under Uniaxial Quasi-Static and Dynamic Compression: *Wei Hua Yin*¹; Laszlo Kecskes²; Qiuming Wei¹; ¹UNC Charlotte; ²WMRD, US ARL

In this work, we have examined the quasi-static (strain rate 10^{-3} s⁻¹) and dynamic (strain rate 10^3 s⁻¹) responses of Zr/Hf based bulk metallic glasses (BMGs) from different casting processes. We find the failure stress of both BMGs increases with decreasing strain rate and weight percentage of Zr. For most of the quasi-static specimens, an amount of 2% plastic strain is observed. However, for dynamic testing, no plastic deformation is detected, and dynamic failure occurred almost immediately after the elastic deformation. Shear-band formation remains the dominant deformation mechanism with light emission during both loading processes. Using SEM to examine the post-loading specimens, a nearly flat fracture surface and a uniform distribution of the vein-like patterns are found in the quasi-static specimens. However, an uneven fracture surface and scattered distribution of vein-like patterns are observed in the dynamic specimens. Multiple shear bands are only found in the quasi-static specimens.

Cast Shop for Aluminum Production: Grain Refinement and Castings

Sponsored by: The Minerals, Metals and Materials Society, TMS Light Metals Division, TMS: Aluminum Committee, TMS: Aluminum Processing Committee
Program Organizer: Trond Furu, Hydro

Tuesday AM
March 13, 2012

Room: Northern A4
Location: Dolphin Resort

Session Chair: Per Arne Tøndel, Alcoa GPP Europe

8:30 AM

Effect of Grain Refiner Amount on the Hot Tearing of 6xxx Alloys During DC Casting: *Muhammad Umar Chandia*¹; Arild Håkonsen²; John Hafssås¹; ¹Hydro Aluminium; ²Hycast AS

The purpose of the grain refiner addition during the Direct Chill (DC) casting of billets is to obtain fine homogeneous grain size and to avoid the hot cracking for a given set of DC casting parameter. However the relation of grain refiner amount to different casting parameters like casting speed and water amount are not very clear. This work was conducted to study the effect of grain refiner amount on the critical casting speed at which hot cracking occurs during DC casting of extrusion billets. Full scale DC casting trials of 6xxx alloy were performed. Four addition rates of grain refiner were used. For each amount of grain refiner the speed of casting was increased step by step after each half meter of casting until hot tears formed in all the billets. In this paper the results of the casting trials will be presented and discussed.

8:50 AM

Grain Refining of Pure Aluminum: *Lucy Han*¹; Corey Vian²; Jie Song²; Zhiwei Liu²; Qingyou Han²; Clause Xu²; Lu Shao³; ¹West Lafayette Jr./Sr. High School; ²Purdue University; ³Hans Tech

Grain refiners are currently used in casting aluminum alloys to reduce the grain size and to produce equiaxed grains during solidification of the alloys. Using inoculants to refine grains makes alloys castable but produces several disadvantages, including particle agglomerates, local defects, and impurities. In contrast, ultrasonic vibrations can be used in the place of grain refiners to refine grains without the disadvantages of using inoculants. In this study, high intensity ultrasonic vibrations

were applied during solidification of pure aluminum. The grains of pure aluminum treated using ultrasonic vibrations were compared to the grains obtained using the TiB₂ grain refiner. It was found that the grain size in the ingots subjected to ultrasonic vibrations was much smaller than those with the addition of grain refiners.

9:10 AM

Study on the Microstructure Changes of Hypereutectic Aluminum Casting Alloy Using Ultrasonic Vibration Process: *Jie Song*¹; Qingyou Han¹; ¹Purdue University

The microstructure changes using the ultrasonic vibration process method and Al-P modifier on permanent mold castings of hypereutectic aluminum alloy (Al-20Si) were studied by using optical and scanning electron microscopy. The Al-P modifier could modify the pro-eutectic silicon phase from a large polyhedral shape to a smaller polyhedral shape but had no effects on the morphology of the eutectic silicon phase. In samples subjected to ultrasonic vibration during its solidification process, however, both hypereutectic and eutectic silicon phases were significantly modified. Furthermore, the aluminum phase was also significantly changed. Small polyhedral silicon particles and globular aluminum grains were formed in the region near the probe (zone one). In the region far away from the probe (zone two), the hypereutectic silicon refined as in zone one, as the partly eutectic phase changed to globular alpha aluminum phase and polyhedral silicon phase.

9:30 AM

A Mathematical Model and Computer Simulations for Predicting the Response of Aluminum Casting Alloys to Heat Treatment: *Chang-Kai Wu*¹; Makhlof Makhlof¹; ¹Worcester Polytechnic Institute

In this publication we report on our efforts to develop a mathematical model and the necessary material database that allow predicting physical and material property changes that occur in aluminum casting alloys in response to precipitation-hardening heat treatment. We use the commercially available finite element software ABAQUS and an extensive database that was developed specifically for the aluminum alloy under consideration – namely, A356.2 alloy. The model produces multiple outputs at each node including the thermal history of the component, the final geometric distortion, the magnitude and type of residual stresses that develop in the component and mechanical properties.

9:50 AM Break

10:10 AM

Understanding and Improving Chemical Capability in the Casthouse: *Kolbjørn Halse*¹; Amanda Bowles¹; *Inge Johansen*¹; ¹Hydro Aluminium

An aluminium casthouse casts aluminium in charges (or drops). These charges are made to particular customers' ordered chemistry specification. The ability for a casthouse to accurately and consistently produce charges inside the customers' specification is crucial for productivity. In addition, it is important that a casthouse can accurately and consistently measure the real composition of each charge. In this paper the sources of uncertainty in the chemistry are classified and discussed. The use of a model to study sensitivities on the predicted process capability (Cpk) from changes in charging accuracy, conditions during analysis, sampling and adjustment is demonstrated. The model can be used as tool to identify improvement potentials.

10:30 AM

Effects of Water Content of Frozen Mold on Fluidity of Aluminum Alloy: *Naoki OMURA*¹; Shuji Tada¹; ¹National Institute of Advanced Industrial Science and Technology(AIST)

A frozen mold which is produced by freezing the mixture of sand and water is expected to improve the poor working environments such as noise, vibration and dust. Actually, the frozen mold is now applied to iron and bronze casting. The fluidity, however, might be the key to spread this technique to light metals because the frozen mold has the possibility to accelerate those solidifications due to its large cooling capacity. In this study, the fluidity of aluminum alloy (AC4CH) cast to the frozen mold



TMS 2012

141st Annual Meeting & Exhibition

was investigated. The flow length of AC4CH aluminum alloy cast into the frozen mold increased with decreasing water content of mold and was much improved by arranging gas vent port to the cavity. It was confirmed that AC4CH aluminum alloy has better fluidity against the frozen mold rather than the conventional green sand mold.

10:50 AM

Simulation Tools to Complement Cast House Design and Daily Operation: *Laszlo Tikasz¹*; Robert McCulloch¹; Scheale Duvah Pentiah¹; Robert Baxter¹; ¹Bechtel Canada Co.

In this paper, cast house operation is considered as a true example of a Flexible Manufacturing System (FMS), whereby a target product mix is reached by adapting both process parameters and production plans, respectively. The examples presented here were initiated by challenging cast house operation situations. The results derived from the simulation scenarios were used to propose mitigating measures and to corroborate suggested solutions. From the components of the simulation tool-set, further models are built. As is often required, models can be configured and applied to, among others, cast house design, production planning, operations decision support and to operator training: In-depth knowledge of cast house operations and dynamic process modeling has been turned to a practical engineering tool. It is regularly used by Bechtel's Mining & Metals "Aluminum Center of Excellence" (ACE) group to deliver recommendations and results to clients in global aluminum smelter projects.

11:10 AM

Formation of Microstructure in Al-Si Alloys under Ultrasonic Melt Treatment: *Liang Zhang¹*; Dmitry Eskin²; Alexis Miroux³; Laurents Katgerman¹; ¹Delft University of Technology; ²Brunel University; ³Materials Innovation Institute

It is well known that ultrasonic melt treatment (UST) provides many benefits to casting processing, especially for the refinement or modification of as-cast structure. There is a lack for systematic studies on Al-Si alloys, although a number of reports are available on hypo-eutectic A356-type and hyper-eutectic (18-24% Si) alloys, showing primary Al or Si refinement. In this paper, the effect of UST on the formation of microstructure was systematically analyzed in hypo-eutectic (6%), eutectic (12.5%) and hyper-eutectic (18%) Al-Si alloys, including commercial piston alloys. The results show that ultrasonic treatment of Al-Si alloys can refine grain structures in all types of Al-Si alloys. Significant refinement of primary Si phase in hyper-eutectic Al-Si alloy can be observed as well. In near-eutectic or eutectic Al-Si alloys, UST, along with its effect on grain refinement, shows some potential in refining primary Si particles in a wide range of melt temperatures.

11:30 AM Break

CFD Modeling and Simulation in Materials Processing: Modeling of Melting and Remelting Processes

Sponsored by: The Minerals, Metals and Materials Society, TMS Extraction and Processing Division, TMS Materials Processing and Manufacturing Division, TMS: Process Technology and Modeling Committee, TMS: Solidification Committee
Program Organizers: Laurentiu Nastac, The University of Alabama; Lifeng Zhang, Missouri University of Science and Technology; Brian Thomas, University of Illinois at Urbana-Champaign; Adrian Sabau, Oak Ridge National Lab; Nagy El-Kaddah, The University of Alabama; Adam Powell, Metal Oxygen Separation Technologies, Inc.; Hervé Combeau, Institut Jean Lamour

Tuesday AM
March 13, 2012

Room: Asia 4
Location: Dolphin Resort

Session Chairs: Alain Jardy, Institut Jean Lamour; Laurentiu Nastac, The University of Alabama

8:30 AM Keynote

A Multiscale Transient Modeling Approach for Predicting the Solidification Structure in VAR Processed Alloy 718 Ingots: *Laurentiu Nastac¹*; ¹The University of Alabama

This paper describes the development and validation of a comprehensive multiscale modeling approach capable of predicting at the mesoscopic scale level the ingot solidification structure and solidification-related defects commonly occurring during the vacuum arc remelting (VAR) process. The approach consists of a coupling between a fully transient macroscopic code and a mesoscopic solidification structure code. The predictions from the multiscale model including grain morphology and size, primary and secondary dendrite arm spacings, Laves and NbC phases, tendency for freckling and columnar-to-equiaxed transition were validated against experimental measurements for a 20-inch diameter VAR alloy 718 ingots. The validated model was then used to investigate the effects of melting rate and ingot diameter on the solidification structure of VAR processed 718 ingots.

9:00 AM Invited

A Multiscale Model for the Simulation of V.A.R. Ingot Solidification: Mathieu Revil-Baudard¹; *Alain Jardy²*; Faustine Leclerc³; Miha Založnik²; Véronique Rebeyrolle³; Hervé Combeau²; ¹Institut Jean Lamour / Areva NP Cezus; ²Institut Jean Lamour; ³Areva NP Cezus

Since the quality of Vacuum Arc Remelted ingots is linked to their chemical homogeneity and metallurgical structure, a modeling study of the solidification during VAR has been undertaken. It is based on the solution of the coupled transient heat, momentum and solute transport equations during the remelting of a cylindrical ingot. Solidification mechanisms implemented in the model include a full coupling between energy and solute transport in the mushy zone, and accounting for nucleation and finite diffusion of solutes at the microscopic scale, in both solid and liquid phases. This modeling can be applied to actual multi-component alloys. In this paper, the macrosegregation in Zircaloy 4 ingots is investigated. To validate the model, one single melt of a homogeneous electrode has been specifically performed. The comparison between the predicted macrosegregation and the experimental results shows the importance of accounting for solutal convection to forecast properly the macrosegregation in remelted ingots.

9:30 AM Invited

The Effect of Slag Cap Thickness on the Pool Depth in Electroslag Remelting: *Jeffrey Yanke*¹; *Rodney Trice*¹; *Matthew Krane*¹; ¹Purdue Center for Metal Casting Research, School of Materials Engineering, Purdue University

In the electroslag remelting process, the slag cap serves as the source of heat to melt the consumable electrode. The slag cap thickness and properties control the solidification time and sump shape of the ingot. Throughout the process, slag freezes to the mold wall forming an electrically and thermally insulating slag skin. This paper uses numerical simulations to investigate the role that slag cap thickness plays on the depth of the liquid metal pool during the ESR process and on the melt rate of the electrode at constant current. To counter the effect of freezing slag, fresh slag is often added during the electroslag remelting process. The effects of the frequency of this addition on the sump shape and melt rate are also studied.

10:00 AM Invited

Mathematical Modeling of Fluid Dynamics and Vessel Vibration in the AOD Process: *Christian Wuppermann*¹; *Antje Rückert*¹; *Herbert Pfeifer*¹; *Hans-Juergen Odenthal*²; *Erich Hovestädt*²; ¹RWTH Aachen University; ²SMS Siemag AG

During the argon oxygen decarburization (AOD) process high-chromium steel melts are de-carburized by oxygen and inert gas injection through sidewall nozzles and a top-lance. Due to the large amount of the injected processing gas, low frequency oscillations of the vessel can be observed. It is suspected that these oscillations can detrimentally influence the converter's structure. The exchange of forces between fluid and the surrounding vessel is the focus of this study. An oscillation model was developed and tested, one objective being to limit the computational effort which is necessary for fully coupled and time resolved CFD and FEM simulations. Experimental results obtained from water-model studies as well as from on-sight measurements are available and were used in order to validate the numerical results. The authors' intention is a contribution towards a more in depth understanding of the factors influencing vessel vibration during the AOD process.

10:30 AM Break**10:50 AM**

Solute Redistribution, Liquid/Solid Interface Instability, and Initial Transient Regions during the Unidirectional Solidification of Ti-6-4 and Ti-17 Alloys: *Laurentiu Nastac*¹; ¹The University of Alabama

The importance of investigating solute redistribution during the unidirectional solidification of multi-component alloys is broadly discussed in the literature. Relevant industrial directional solidification processes for alloy processing include continuous casting, remelting processes (Plasma Arc Melting (PAM), Electroslag Arc Remelting (ESR) and Vacuum Arc Remelting (VAR) processes), Czochralski crystal growth technique, and floating zone techniques. A transient analytical model is used in this article to study the solute redistribution, the liquid/solid interface stability, and the size of the initial transient region during the unidirectional solidification with an axially moving boundary of Ti-6-4 and Ti-17 alloys. The liquid/solid interface stability is based on an extended transient constitutional undercooling criterion. The effective partition coefficients of the alloying elements in these Ti-based alloys were determined based on specially designed experimental measurements. It is shown that both the value of the partition coefficients and the withdrawal velocity magnitude have a significant impact on the directional solidification processing of Ti alloys.

11:10 AM

CFD Modeling of Splash in Molten Materials Processing Operations: *Mark Schwarz*¹; ¹CSIRO

Splash must often be avoided or minimised in many materials processing operations, but in some cases the process can be designed to control splash for heat and or mass transfer. In all cases careful design is required and CFD modelling can play a critical role in this. Unfortunately, splash is a complex process for which CFD modelling has not been widely applied in the design arena. The phenomenon involves multi-scale issues, with surface properties playing an important role. The paper describes the physics of splash mechanisms, particularly as caused by bubbling through molten metals, and summarises some of the CFD techniques that have been used to simulate such splash. Examples of CFD models developed for modelling splash in ferrous and non-ferrous smelting processes are described.

11:30 AM

Numerical Analysis of Electromagnetic Field in an Electroslag Remelting Process with Three -Phases Electrodes: *Baokuan Li*¹; *Fang Wang*¹; *Meilong Shan*¹; *Fumitaka Tsukihashi*¹; ¹Northeastern University

As the advantage of uniform bus loading, the electroslag remelting (ESR) furnaces with three -phase installation by delta or star connection are mainly used to produce the large or super large ingot. The electrical efficiency is significantly improved as the short circuiting through the molten slag. However, little is found about fundamental research on the electromagnetic field of the ESR system with three -phase installation. A three-dimensional (3D) finite element model was developed to simulate the current density, magnetic field, electromagnetic force and Joule heating for a system of electrode, slag and ingot in the ESR system with three -phase installation. Effect of Some parametric such as the applied current, position of electrodes and slag thickness have also been examined.

11:50 AM

Influence of the Electric Current Frequency on the Electroslag Remelting Process: *Abdellah Kharicha*¹; ¹University of Leoben

In the present paper, the droplet formation during melting of a 420 mm diameter flat electrode is simulated with an advanced three dimensional multiphase-Magneto-hydrodynamic numerical model. The momentum, energy and electromagnetic fields are fully coupled. The computational domain includes a layer of slag and a layer of liquid steel. A VOF approach is used for the interface tracking and a potential formulation is used for the electric and the magnetic field. In the present work we present the results for electric current frequency from 1 to 50 Hz. We show that at frequencies lower than 10Hz, the system behaves almost as what was predicted with a DC current. For frequencies higher than 20 Hz, the fluctuations of eddy current start to interact with the liquid dripping frequency. The movement of the slag/metal interface is also affected by the electric skin effect occurring at frequency higher than 30 Hz.



Characterization of Minerals, Metals, and Materials: Characterization of Minerals and Ceramics

Sponsored by: The Minerals, Metals and Materials Society, TMS Extraction and Processing Division, TMS: Materials Characterization Committee

Program Organizers: Jiann-Yang Hwang, Michigan Technological University; Sergio Montero, State University of North Rio De Janeiro; Chenguang Bai, Chongqing University; John Carpenter, US Department of Energy; Donato Firrao, Politecnico di Torino; Byoung-Gon Kim, Korea Institute of Geoscience & Mineral Resources; Mingdong Cai, Schlumberger

Tuesday AM
March 13, 2012

Room: Asia 2
Location: Dolphin Resort

Session Chairs: Doyle Fiona, University of California, Berkeley ; Chen-Guang Bai, Chongqing University

8:30 AM

A Novel Low-Energy Route for the Extraction of Copper And Cobalt Metals/Alloys from the Zambian Sulphide Concentrates: *Yotamu Hara*¹; Animesh Jha¹; ¹Leeds University

Conventional smelting of copper – cobalt – iron sulphide concentrates result in the oxidation of cobalt and iron, which are subsequently lost into the slag. The emission of SO₂ bearing gas from smelting causes serious health and environmental problems. In this research, three different types of copper –cobalt–iron sulphide concentrates, derived from froth flotation were investigated. The concentrates, each containing more than 40 wt % percent gangue material, have been directly reduced in the presence of lime and carbon in the temperature range of 800 °C–1300 °C, for the production of copper, cobalt and iron. We demonstrate the basic principles of process physical chemistry for the recovery of alloy by carrying out a detailed process analysis utilising the predictions from thermodynamic equilibrium and the results from kinetics of reduction reaction. The effects of temperature on the reduction kinetics and alloys formation, have been determined and analysed in detail.

8:45 AM

Structural and Chemical Modification of Sulfide Mineral Surfaces by High-Power Nanosecond Pulses: *Igor Bunin*¹; Valentine Chanturiya¹; Alexey Kovalev¹; Irina Khabarova¹; Elizaveta Koporulina¹; ¹Research Institute of Comprehensive Exploitation of Mineral Resources RAS

This paper presents new theoretical and experimental data on possible mechanisms for the formation of micro- and nanophases on the surfaces of sulfide minerals under the effect of high-power nanosecond electromagnetic pulses (HPEMP). The gas outflow from nanosecond breakdown channels of sulfide minerals under HPEMP is considered, with allowance for the condensation of iron vapors. The condensation of matter in an outflowing jet is shown to be an effective mechanism for structural and chemical transformations of sulfides. It is established, that electrode potential of pyrrhotite is moved together in the negative party owing to formation of iron oxides (hydroxides) and iron sulfates by HPEMP (10(3) pulses), that provides decrease of xanthate sorption and reduction flotation extraction of pyrrhotite, whereas electrode potential of pentlandite gets more positive values at the expense of additional formation of element sulfur, that causes increase of xanthate sorption and, as a consequence, increase of nickel sulfide extraction.

9:00 AM

Characterization of Magnetic and Non-Magnetic Iron Oxide Nanoparticles Synthesized by Different Routes: *Alyssa Maich*¹; E. Yegan Erdem¹; *Fiona Doyle*¹; ¹University of California, Berkeley

There is an expanding interest in synthesizing high quality magnetic nanoparticles, notably for biomedical applications. Different routes have been reported for synthesizing magnetite and maghemite. However, some

ambiguity remains on their precise chemistry, intermediates, and final products, due to the structural similarity of maghemite and magnetite, and the relative ease of redox transitions during synthesis. Here we present TEM, x-ray and electron diffraction, and supplemental studies aimed at characterizing the products from two different reaction systems, thereby clarifying the reaction chemistry. The first hydrolyzed aqueous FeCl₂ and FeCl₃ chlorides with ammonia in a microfluidic reactor; although the product had an even size distribution, it included non-magnetic goethite. The second system thermally decomposed iron(III) acetylacetonate in ether. Although in the second system oleylamine has been reported to serve as both a reducing agent and capping ligand to control particle characteristics, our studies revealed little reduction, with maghemite dominating as a product.

9:15 AM

Characterization of Concentrate, Pellet and DRI Samples for Trace Elements: *Mingming Zhang*¹; ¹ArcelorMittal Global R&D

Three samples received from the EAF shop have been characterized by chemical, X-ray diffraction (XRD), optical microscopy (OM) and scanning electron microscopy (SEM) methods. The objective of this characterization work is to investigate the occurrence of nickel, copper, zinc, sulfur and phosphorus in these samples and identify their origin and associations with iron minerals in the concentrate samples. The samples were identified as Mineral, Pellet, and HRD. The latter is the DRI product. All three samples were received as fine powders. The results indicate that, in the mineral sample, magnetite is the major iron oxide mineral with hematite as a second phase based on the OM and XRD studies. Pyrite [FeS₂], chalcocopyrite [CuFeS₂] and bravoite [(Fe,Ni)S₂] are major sulfide minerals. Trace amounts of apatite [Ca₅(PO₄)₃(F,Cl,OH)], wardite [Na₄CaAl₁₂(PO₄)₈(OH)₈·6H₂O], giniite [Fe₅(PO₄)₄(OH)₃·2H₂O] and vivianite [Fe₃(PO₄)₂·8H₂O] were identified by SEM and XRD. Microscopic studies also indicated that most of the sulfide grains in the mineral sample are present either as liberated fine particles (about 10 microns) or as inclusions within the magnetite and hematite grains. XRD studies revealed magnetite as the major mineral with subordinate amounts of hematite and pyrite confirming the microscopic findings. Copper, nickel, and zinc are mainly present as chalcocopyrite, bravoite, and franklinite [(Zn,Mn,Fe)(Fe,Mn)2O₄] in trace amount in the mineral samples, respectively. Impurities carry over to the Pellet and HRD samples. Chemical analyses of the three iron-bearing samples indicate that sulfur and phosphorus in the Pellet sample exceeded the specification. Since liberated pyrite and chalcocopyrite particles were observed both in mineral and pellet samples, magnetic and flotation processing routes for this ore should be effective for sulfide removal but at the cost of iron losses. The high phosphorus content of all three samples indicates that there are phosphates which are difficult to remove by the current concentrating process (magnetic separation and flotation).

9:30 AM

Dielectric and Temperature-Rising Characteristics of Ore Fines Materials in Microwave Field: *Hongbo Zhu*¹; Linqing Dai¹; Jinhui Peng¹; Wei Liang¹; Zheng Wei¹; Zhenliang Weng¹; Qianxu Ye¹; Jian Chen¹; ¹Kunming University of Science and Technology

The dielectric constant and dielectric loss factor of Dahongshan concentrate, millscale, anthracite and light-burned dolomite were tested in different frequency and temperature. In addition, the temperature-rising characteristics of the materials in the microwave field of 2.45GHz in frequency were studied. The results showed that the Dahongshan concentrate reached 1250°C in 330s, whereas the millscale needed 855s, the anthracite needed 820s, and the microwave absorbing property that sudden changed at about 400°C became stronger with the temperature rising on the condition of the microwave power of 2KW and the mass of 30g. The research provided the foundation of further study on making direct reduced iron by microwave heating.

9:45 AM

Characterization on the Roughness of the Iron Ore Particles: *Xuwei Lv*¹; *Xiaobo Huang*¹; ¹Chongqing University, China

The characterization of the surface roughness of the mineral particles is of vital importance for the studies of the mineral processing. In this study, an evaluation of the roughness of the iron ore particles, with the measurements of size distribution and the measurements of specific surface area with the liquid nitrogen absorption, was developed. The main theory of this method is the fact that the roughness of the particle influences the specific surface area apparently. The specific surface area of the particles can be measured with the laser diffraction method and the liquid nitrogen absorption method. The influence of the surface roughness of the particle can be measured with the nitrogen absorption and cannot be measured with the laser diffraction. Therefore, the roughness can be got by comparing the specific surface area with two measurement methods.

10:00 AM

Synthesis and Characterization of Al, Ag, Ti, Cu, and B Substituted Hydroxylapatite: *Celaletdin Ergun*¹; *Thomas Webster*²; *Gurbuz Gunes*¹; *Abdurrahman Bahadır*³; *Huinan Liu*⁴; *Ibrahim Erden*⁵; ¹Istanbul Technical University; ²Brown University; ³MSTU; ⁴University of California, Riverside; ⁵Yildiz Technical University

Hydroxylapatite, have been used in numerous orthopedic applications. Recently, nano-crystalline HA is used as an adsorbent for removing pathogenic proteins from blood for purification since HA has good blood compatibility as well as a ability for selective protein adsorption. Besides, it has numerous non-medical applications including packing media for column chromatography, gas sensors, catalysis and host materials for lasers and luminescent materials. Its crystal structure permits a wide range of ionic substitutions, which is an effective method to modify its properties. For instance; the substitution of rare-earth ions can lead changes in refractive index and lattice parameters. Ag doping may provide antibacterial resistance, while Ti, Zn, Sr may increase its biological performance. Sb and Mn doping can provide fluorescent performance which is used in fluorescent lamps. The purpose of the current paper is to synthesis B, Ti, Ag, Al, Cu substituted HA and characterize for materials properties and biological performance.

10:15 AM

Electric Resistivity of Fine Chromite Ore: *Cheng Pan*¹; *Xuwei Lv*¹; *Chenguang Bai*¹; *Xuyang Liu*¹; *Donghai Li*¹; ¹Chongqing University

Fine chromite ore is the common raw material to produce ferrochrome alloy through the submerged electric furnace process. The electric resistivity of fine chromite plays an important role in the operation efficiency because it effects the current distribution greatly. The effect of particle size and the contact area between two particles on electric resistivity were investigated at room temperature for various of chromite, and the relationship between the electric resistivity of mixed particles and the volume ratio of lump ore to fine ore was also studied. The results shown that the electric resistivity increases with the increase of particle size, and the electric resistivity of mixture decreases with the increase of volume ratio of fine ore.

10:30 AM

Reduction of Agglomerated Manganese Ores in Ferromanganese Production: *Thomas Brynjulfssen*¹; *Merete Tangstad*¹; ¹Norwegian University of Science and Technology

Manganese ore fines, generated during mining and transportation, can not be added to the submerged arc furnace directly as they will prevent even gas flow through the burden. Low gas permeability in the burden will lower the degree of pre-reduction of ore subsequently increase the carbon and energy consumption of the process. In order to utilize manganese ore fines in the furnace they are agglomerated into sinter, pellet or briquettes. The agglomeration process will however change the reduction properties of the ore. In this work the melting and reduction properties of different agglomerates has been investigated. Agglomerates from different commercial ores have been produced and the melting temperature and

melting mechanisms has been studied. The mineralogy of the raw ores and agglomerated has been found using XRD, and the composition established using EPMA(WDS). The effect of adding fluxes such as dolomite and quartz has also been investigated.

10:45 AM

Making Direct Reduced Iron from Millscale Containing Coal by Microwave Heating: *Linqing Dai*¹; *Hongbo Zhu*¹; *Jinhui Peng*¹; *Jian Chen*¹; *Qianxu Ye*¹; ¹Kunming University of Science and Technology

Recycling of ferro-waste through coal-based direct reduction process not only can eliminate industrial waste pollution, reach clean production, but also improve comprehensive abilities and economic benefits of steel plants. Millscale fines have good microwave heating characteristics, better than anthracite below 720°C. The results showed that on the condition of 60 min at 1100°C, the ratio of coal to material is 22%, the metallization rate increased with the ratio of millscale, and it is up to 98.23%.

11:00 AM

Ceramic Pigments with Spinel Structure Obtained by Low Temperature Methods: *Oscar Restrepo*¹; *Edgar Chavariaga*¹; *Leidy Jaramillo*¹; ¹National University of Colombia

This paper presents the results of the manufacturing ceramic pigments with spinel structure, using methods of synthesis of low temperature. In this work we obtained spinel structures type by the methods of Self-combustion, Coprecipitation, Microemulsion, Gel citrate and Pechini. These methods become an attractive alternative to traditional method (ceramic method), since we can work at a lower temperature, reducing manufacturing costs, lower fuel consumption, less wear on equipment and other environmental and economic implications. Also it is possible to have control over features such as stoichiometry, morphology of the products, reaction times and structures. The products obtained by these routes will be used in the manufacture of ceramic pigments and characterized using different techniques such as X-ray diffraction (XRD), scanning electron microscopy (SEM) and UV-VIS spectrophotometry.

11:15 AM

Synthesis and Characterization of Jarosite-Type Compounds with Arsenic: *Francisco Patiño*¹; *Iván Reyes*¹; *Mizraim Flores*¹; *Miguel Pérez*¹; *Martin Reyes*¹; *Julio Juárez*¹; ¹Universidad Autónoma del Estado de Hidalgo

Jarosites structure type compounds allow the incorporation of several elements of environmental importance such as arsenic during their precipitation. Arsenic integrated into the structure of jarosite can be stabilized in a wide range of environmental conditions (pH, temperature, etc.) that are tolerated by the pure jarosite. Sodium and potassium jarosites with arsenic incorporated were synthesized using the precipitation method in sulfate media and several methods of characterization were used. XRD results showed the products obtained are pure phases. Morphology of both compounds showed spherical particles with majority sizes between 37-54 microns with rhombohedral crystals strongly welded joined together, being more evident in the arsenojarosite. The stoichiometry according to chemical analysis are as follows: for arsenojarosite [K0.75 H3O0.25] Fe1.84 [(SO4) 1.82 (AsO4) 0.18] [(OH) 2.34 (H2O) 3.66] and arsenonatrojarosite [Na0.87 H3O0.13] Fe2.50 [(SO4)1.95 (AsO4)0.05] [(OH)4.45(H2O)1.55], being notorious that the arsenojarosite retains more arsenic in their structure, but is deficient in iron.

11:30 AM

Mechanical Characterization of Cellular Ceramic Materials: *Wilson Acchar*¹; *Fernando Barcelos*¹; *Luis Pereira*²; ¹Federal University of Rio Grande do Norte; ²Federal University of Rio de Janeiro

Porous ceramics have been extensively investigated as structural materials for flow of fluids in many applications, such as filters for molten metals, hot gases, thermal protection systems and heat exchangers. This class of material must have special features: high permeability and mechanical strength. However, these parameters are influenced in different ways by the processing method and the consequent cellular



TMS 2012

141st Annual Meeting & Exhibition

structure. In this work two different types of commercial ceramic filter materials are investigated. Characterization included the evaluation of the strength values as well as the microstructural analyzes of the surface fracture. The results indicate that the strength values are strong dependent on the filament defects.

11:45 AM

Study of Attapulgite for Human Health: *Wilson Acchar*¹; Tulio Moura¹; Antonio Costa¹; Ledjane Barreto²; ¹Federal University of Rio Grande do Norte; ²Federal University of Sergipe

Since the beginning of time, nature has served humanity as a source of various raw materials. Clays are common ingredients in pharmaceutical products both as excipients and active substances. Recently a patented study reports the use of attapulgite as the encapsulating agents both for the protecting the active substance and modulating release into the body. Some clays such as kaolinite, smectites, talc, etc are also used as dermatological protectors. Sepiolite and smectites have the ability to form complexes with organic compounds with absorb ultra-violet radiation, enabling them to be used in sun screens with protection factors. Brazil has a significant reserve of attapulgite located in Teresina, Brazil, making the study of the potential use of this mineral in specs areas very attractive. The objective of this work is to characterize the attapulgite in order to study the potential use of this clay material in the human health.

Computational Thermodynamics and Kinetics: Phase-Field Simulations in Alloys I

Sponsored by: The Minerals, Metals and Materials Society, TMS Electronic, Magnetic, and Photonic Materials Division, TMS Materials Processing and Manufacturing Division, TMS Structural Materials Division, TMS: Alloy Phases Committee, TMS: Chemistry and Physics of Materials Committee, TMS/ASM: Computational Materials Science and Engineering Committee, TMS: Integrated Computational Materials Engineering Committee, TMS/ASM: Phase Transformations Committee, TMS: Process Technology and Modeling Committee

Program Organizers: Zi-Kui Liu, The Pennsylvania State University; Mark Asta, University of California, Berkeley; James Warren, The National Institute of Standards and Technology; Yunzhi Wang, Ohio State University; Raymundo Arroyave, Texas A & M University; Yu Wang, Michigan Tech

Tuesday AM Room: Asia 5
March 13, 2012 Location: Dolphin Resort

Session Chairs: Mikko Haataja, Princeton University; David Wu, IHPC

8:30 AM Invited

Phase-Field Modeling of Evolving Microstructures and Phase Transformations in Solid Oxide Fuel Cells: *Mikko Haataja*¹; ¹Princeton University

Energy conversion processes in solid oxide fuel cell (SOFC) materials are strongly affected by a nonlinear coupling between mass/charge transport, heat transport, and morphology at nanometer and micrometer length scales in a multi-phase/multi-component system. Furthermore, under continuous operation, these complex morphologies and local compositions evolve over time in response to a multitude of physical, chemical, and mechanical cues at elevated temperatures. In order to understand and predict the stability of morphologies and their spatio-temporal evolution, a mesoscale approach, which accurately incorporates both atomic scale information and evolving microstructures, is required. In the first part of my talk, I will present our recent work on quantifying coarsening kinetics of Ni particles in Ni-YSZ anode materials based on "experimentally-informed" phase-field simulations. In the second part of my talk, I will focus on the development of elastic stresses and resulting mechanical failure in SOFC anode materials driven by re-oxidation of Ni particles.

8:55 AM

Inertia Dominated Criticality in Martensites: *Oguz Salman*¹; *Alphonse Finef*²; *Lev Truskinovsky*¹; ¹CNRS - Ecole Polytechnique; ²ONERA-CNRS

When driven slowly, many multiparticle systems with long range interactions evolve through a series of discrete events with power law statistics associated with self-organized criticality. Such dynamics has been experimentally observed through acoustic emission in several shape-memory alloys that undergo martensitic transitions characterized by a strain misfit between the parent and the product phases. We present both an overdamped phase field and a Lagrange-Rayleigh modeling of a prototypical martensitic transition, and show that dynamics exhibits intermittency. If the system is sufficiently underdamped, the discrete events (avalanches) self-organize into a critical state that displays scale invariance. Instead, the overdamped system does not show criticality. To explain the role of inertia, we analyze a simple 1D spring model with a double well potential.

9:10 AM

Continuum-Level Simulation of a Displacement Reaction System Based on Computational Thermodynamics and Kinetics: *Hui-Chia Yu*¹; *Chen Ling*¹; *Jishnu Bhattacharya*¹; *Anton Van der Ven*¹; *Katsuyo Thornton*¹; ¹University of Michigan

Current research and development of Li-ion battery cathode materials have mainly focused on intercalation compounds. However, conversion reaction compounds, an alternative to intercalation compounds, has recently drawn increasing attention from researchers because of the potentially larger energy capacity. In this work we examine spinel Li-Cu_{0.5}-TiS₂, in which Cu is extruded during lithiation, as model system for conversion reaction. The thermodynamic free energy landscape and kinetic transport coefficients are determined by first principles and kinetic Monte Carlo calculations. The calculated phase diagram shows solid solution and two-phase regions exist in different areas of the composition space. We studied the kinetics and accompanying morphological evolution during charge and discharge in the electrode particles in the framework of Fick's diffusion and phase field model. Because of kinetic constraints, the composition evolution follows different paths during discharge and charge processes, which explains the hysteresis, this material system's interesting and important characteristic, during charge-discharge cycles.

9:25 AM

A Phase-Field Model for δ -Zirconium Hydride Formation in Single- and Polycrystalline Zirconium Alloys: *Tae Wook Heo*¹; *Kimberly Colas*¹; *Arthur Motta*¹; *Long-Qing Chen*¹; ¹The Pennsylvania State University

Zirconium alloys are extensively utilized as structural materials in nuclear energy industry for nuclear fuel cladding. The formation of hydrides during reactor operation degrades the mechanical behavior of the cladding. We propose a phase-field model for modeling microstructure evolution during δ -hydride formation in Zr alloys including both structural change and hydrogen diffusion. The stress-free transformation strains of multiple variants for hcp-Zr (α) to fcc-hydride (δ) transformation are derived based on the orientation relationship between α and δ phases. The interface between hydride and Zr matrix is assumed to have mixed coherency: basal planes are coherent and edges are incoherent. The elastic strain energy is calculated using Khachaturyan's microelasticity theory. We discuss the habit plane formation, the effects of grain orientations, and the influences of external loads on the morphological evolution of hydrides and compare the hydride morphologies to experimental observations performed on hydrided Zr, using in situ synchrotron radiation diffraction.

9:40 AM

Phase Field Modeling of Coherent Zirconium Hydrides Reorientation under Applied Load: *Lingfei Zhang*¹; *Ludovic Thuinet*¹; *Alexandre Legris*¹; *Andr e Debacker*¹; *Antoine Ambard*²; ¹UMET; ²EDF R&D

Mechanical properties of hydrided Zircaloy claddings under external load lie in the center of nuclear reactor safety. Numerous experimental

studies revealed hydride reorientation along the radial direction under hoop strength, but until now no sound physical explanations have been proposed. In this work we propose a model based on a micro-mechanical phase field approach under inhomogeneous elasticity assumptions to analyze the influence of an applied stress on the preferential orientation of hydrides either in the basal or prismatic planes. According to a previous experimental work, the fully coherent zeta hydride is considered in this analysis. Our work reveals that under uniaxial stress σ_a parallel to the basal plane, the zeta orientation variants misaligned with σ_a are promoted. Furthermore, beyond a critical stress, orientation outside the basal plane is observed, in agreement with the well known radial reorientation aforementioned.

9:55 AM

Continuum Dislocation Dynamics: Comparison between Models: *Woosong Choi*¹; *Yong Chen*¹; *Stefanos Papanikolaou*¹; *James Sethna*¹; ¹Cornell University

Many continuum theories of dislocation dynamics have been proposed to bridge the gap in between discrete microscopic simulations and macroscale phenomenology. As of yet, however, these theories had limited success in explaining or predicting the physics of microstructure formation and evolution. Recently, we have shown that a simple isotropic continuum model dynamically form walls and exhibit complicated microstructure formation and evolution similar to experiments. Most other continuum theories have not seen such structures emerging, and to what extent this theory explains the physics remains to be answered. We explore several variants of the current theories which have different microscopic physics as to how slip systems, cross-slip, statistically stored dislocations, explicit or effective short range interactions, etc. are treated. Comparisons among simulation results of these models will be presented, and we will discuss the relevant mechanisms and their consequences in the dynamics of microstructures.

10:10 AM Break

10:30 AM

An Accurate Scheme for Resolving Grain Boundaries in a Phase-Field Model of 3D Grain Coarsening: *David Wu*¹; *Zhidong Leong*¹; *Dickson Thian*¹; *Carl Krill III*²; ¹Institute of High Performance Computing; ²Ulm University

Due to the use of diffuse interface, phase-field model is attractive for simulating grain coarsening because it can easily handle complex morphological transitions by avoiding explicit treatment of boundary conditions at grain boundaries. However, the use of diffuse interface presents challenges for resolving grain boundary positions, which is necessary when comparing phase-field results to sharp interface theories such as von Neumann-Mullins law in 2D and MacPherson-Srolovitz law in 3D. In particular, MacPherson-Srolovitz law is formulated with grain volume, edge length, and mean width, the latter of which is extremely sensitive to grain boundary positions. We present an accurate scheme for resolving grain boundaries and calculating geometric properties of grains from phase-field simulation. Compared to known solutions for symmetric grains, we find that calculated geometric properties, including mean width, are accurate even for very small grains.

10:45 AM

Phase Field Approach to Stress-Induced Solid-Solid and Solid-Liquid Phase Transformations: *Valery Levitas*¹; ¹Iowa State University

Recent advances in phase field theory and simulations of stress-induced phase transformations are presented, including: 1. Development of new thermodynamic potentials for multivariant martensitic phase transformations for small and large strains for 3D loading. 2. Introducing an athermal threshold in phase field modeling. 3. Developing thermodynamically consistent expression for interface tension, which is also consistent with the sharp interface limit. 4. Introducing a way to control martensite-martensite surface energy through coupling gradients of different order parameters. 5. Developing thermomechanical theory for

surface-induced transformations. 6. Developing of a model for coherent solid-melt interface with non-spherical transformation strain. Finite element algorithm is developed and numerous problems for martensitic microstructure evolution and pre-melting and melting of nanoparticles are solved and compared to experiments. In particular, our model describes well experimental data on the width of the molten layer versus temperature for the Al plane surface and on melting temperature versus particle radius.

11:00 AM

Topological Effects in Coarsening of Grain-Boundary-Engineered Microstructures: *Ming Tang*¹; *Bryan Reed*¹; *Vasily Bulatov*¹; *James Belak*¹; *Thomas Lagrange*¹; *Joel Bernier*¹; *Mukul Kumar*¹; ¹Lawrence Livermore National Laboratory

In FCC metals such as copper, grain boundary character distributions can be engineered by a technique known as grain boundary engineering. By increasing the special boundary (mainly low S boundaries) content in the network, this method is known to significantly reduce the grain growth rate at elevated temperatures, which makes grain-boundary-engineered materials attractive for potential applications under irradiation conditions. Here we applied phase-field simulations to studying the quantitative relation between grain-boundary-engineered microstructures and their coarsening kinetics. It was found that the special boundary population alone is not sufficient to determine the evolution of the grain boundary network. Microstructures with the same special boundary population but different topologies can exhibit different coarsening behavior, which is influenced by topological features such as triple junction and twin-related-domain size distributions. Such findings underline the importance of capturing the correct topology of grain-boundary-engineered networks in simulations to reliably predict their evolution.

11:15 AM

3D Phase Field Simulation of Phase Coarsening in Binary Two Phase System: *Vishal Yadav*¹; *Nele Moelans*¹; ¹Katholieke Universiteit Leuven

A new phase field model for studying phase coarsening in a binary two phase system is proposed. For this alternative model, the relation with physical input data is more straightforward and accurate. Furthermore, an efficient numerical method for large-scale 2D and 3D simulations of phase coarsening in a binary two phase system is implemented. We performed simulations for realistic systems such as Pb-Sn and Al-Si with a range of system properties. The effect of volume fraction, diffusivities, and the number of order parameters on the coarsening rate and particle size distribution is studied. The findings are compared with experimental studies on Pb-Sn and Al-Si. We also studied the growth behavior in 3D.

11:30 AM

A Phase Field Crystal Study of Rapid Solidification and Solute Trapping in Binary Alloys: *Harith Humadi*¹; *Jeff Hoyt*¹; *Nikolas Provatas*¹; ¹McMaster University

In this study we have incorporated two time scales into the phase field crystal dynamics to explore different solute trapping properties with various interface pulling velocities. With only diffusive dynamics, we demonstrate that the segregation coefficient, k , vs velocity for a binary alloy is consistent with the model of Kaplan and Aziz where k approaches unity in the limit of infinite velocity. However, with the introduction of wave like dynamics in both density and concentration fields the trapping behavior reproduces the prediction of Galenko et al.. In addition, a Floquet linear stability analysis was performed to determine the appropriate time and length scale needed for the wave dynamics to act on the system with the desired physics.

11:45 AM

Enhancement of Field-Induced Strain Responses in Decomposed Two-Phase Nanodispersions: *Wei-Feng Rao*¹; *Armen Khachatryan*¹; ¹Rutgers University

The magnitude and hysteresis of strain responses to externally applied fields are essential to advanced functional materials used in high-performance devices. We took into consideration the field-induced



TMS 2012

141st Annual Meeting & Exhibition

extrinsic reorientations of the domain states within the nanosized precipitates of the low-symmetry phase to increase the strain and reduce the associated hysteresis. The two-phase systems are formed at early stages of a precipitation of the low-symmetry phase from the supersaturated cubic solid solution. The macroscopic strain effect caused by this reorientation through small atomic displacements is a giant value determined by the crystallographic parameters of these phases, which can be regarded as giant quasi-elasticity if the reorientation is driven by a stress or supermagnetostriction if both phases are ferromagnetic and a magnetic field is applied. Using 3D and 2D modeling, we formulated conditions leading to a drastic amplification of hysteresis-reduced strain responses that may reach orders of magnitude.

Computational Thermodynamics and Kinetics: Thermodynamics

Sponsored by: The Minerals, Metals and Materials Society, TMS Electronic, Magnetic, and Photonic Materials Division, TMS Materials Processing and Manufacturing Division, TMS Structural Materials Division, TMS: Alloy Phases Committee, TMS: Chemistry and Physics of Materials Committee, TMS/ASM: Computational Materials Science and Engineering Committee, TMS: Integrated Computational Materials Engineering Committee, TMS/ASM: Phase Transformations Committee, TMS: Process Technology and Modeling Committee

Program Organizers: Zi-Kui Liu, The Pennsylvania State University; Mark Asta, University of California, Berkeley; James Warren, The National Institute of Standards and Technology; Yunzhi Wang, Ohio State University; Raymundo Arroyave, Texas A & M University; Yu Wang, Michigan Tech

Tuesday AM
March 13, 2012

Room: Australia 3
Location: Dolphin Resort

Session Chairs: Vidvuds Ozolins, UCLA; Joerg Neugebauer, MPIE

8:30 AM Invited

Fully Ab Initio Determination of Free Energies: Where Do We Stand?:

Jörg Neugebauer¹; Fritz Körmann¹; Alexey Dick¹; Albert Glensk¹; Blazej Grabowski²; Tilmann Hickel¹; ¹Max-Planck-Institut für Eisenforschung GmbH; ²Lawrence Livermore National Lab

The combination of accurate first principles calculations with mesoscopic/macroscale thermodynamic and/or kinetic concepts has quickly advanced in the past few years and allows now to tackle even the complexity of advanced engineering materials. Key to these studies is the highly accurate determination of free energies. In the talk we will show how efficient sampling strategies together with high convergence density-functional theory calculations allow an unbiased and accurate determination of all relevant temperature dependent free energy contributions. While in the past the focus has been mainly on the quasiharmonic contributions (which are computationally most easily to obtain) new advances in methods and computational power provide now for the first time the opportunity to systematically include anharmonic and magnetic contributions. The flexibility and the predictive power of this approach will be discussed for examples relevant to the design and understanding of modern high strength steels.

8:55 AM

Ab-Initio Discovery of Crystal Structures and Phase Diagrams:

Richard Hennig¹; William Tipton¹; Clive Bealing¹; Kiran Mathew¹; ¹Cornell University

Predictions of structure formation by computational methods have the potential to accelerate materials discovery and design. Here we present an approach based on evolutionary algorithms coupled to ab-initio relaxations that accurately predicts how atoms arrange into crystal

structure and determines the ground state phase diagrams of materials without any prior information about the system. We applied the method to binary Li-Be and elemental Eu under pressure. For Li-Be we discover several stable phases under pressures and observe an unexpected quasi-1D and 2D electronic structure in some of these compounds [1]. For Eu we identify three phase transformations and identify the structure of the superconducting high pressure phase [2]. We currently study the phase behavior of several Li-based systems for battery applications to identify stable and metastable phases and determine the kinetics of Li diffusion in these systems.[1] Nature 451, 445 (2008)[2] Phys. Rev. B 83, 104106 (2011)

9:10 AM

Determinants of Thermal Stability in Nano-sized Binary Alloys: C. C.

Yang¹; Y.-W. Mai¹; ¹The University of Sydney

An extension of the classic thermodynamic theory to nanometer scale has generated a new interdisciplinary theory - nanothermodynamics, which is an indispensable tool for the investigation of size-dependent physicochemical properties in nanocrystals. In this work, a new nanothermodynamic model was established to investigate the size-dependent thermal stability of nanosized binary alloys. It is found that the instability of binary alloys at the nanometer scale is caused by severe bond dangling associated with increased surface/volume ratio. The calculated results are consistent with experimental data and may provide new insights into the fundamental understanding of thermal stability in nanoalloys.

9:25 AM

Fully Ab Initio Determination of Anharmonic Contributions by Efficient Sampling Strategies: Albert Glensk¹; Blazej Grabowski²;

Tilmann Hickel¹; Jörg Neugebauer¹; ¹Max-Planck-Institut, Duesseldorf, Germany; ²Lawrence Livermore National Laboratory

Using ab initio approaches, temperature dependent thermodynamic free energies are nowadays typically calculated within the quasiharmonic approximation. Numerically highly accurate ab initio calculations for Al including anharmonic contributions on the other hand showed a significant change in the heat capacity and a dramatic effect on the entropy of vacancy formation in Al compared to quasiharmonic results [1]. By developing and implementing highly efficient sampling methods, we are now able to routinely determine anharmonic contributions for metals. Using these methods we were able to systematically improve the ab initio based thermodynamic description of Al-Mg-Si-Cu alloys. Particularly, the influence of anharmonicities on the unary subsystems of these alloys, consequences for the phase diagrams and deviations from quasiharmonic results will be discussed.[1] B. Grabowski et al, PRB 79, 134106 (2009)

9:40 AM

High-Throughput Ab-Initio Calculations of Topologically Close-

Packed Phases in Transition-Metal Alloys: Thomas Hammerschmidt¹; Bernhard Seiser²; Ralf Drautz¹; David Pettifor²; ¹ICAMS, Ruhr-University Bochum; ²University of Oxford

Topologically close-packed (TCP) phases play an important role in modern alloys and steels. The formation of TCP phases is attributed to high local concentrations of refractory elements. We present high-throughput ab-initio calculations for a number of binary systems in order to investigate the factors that influence the structural stability of TCP phases in alloys. In particular, we determined the formation energies of the TCP phases A15, σ , ζ , μ , C14, C15 and C36 in the binary systems Ta-V/Nb, Re-V/Cr/Nb/Mo, and Co-V/Cr/Nb/Mo. The observed trends in structural stability are captured and explained by simplified models of the electronic structure. We discuss in particular the role of the number of valence electrons, of the size mismatch between the atoms, of magnetism and of the configurational entropy for the stabilization of TCP phases.

9:55 AM Break

10:20 AM Invited

Thermodynamics of Unstable Structures: *Vidvuds Ozolins*¹; ¹UCLA

Materials scientists often need to know the free energy of a material in a structure that has not been measured experimentally and may even be unstable in the bulk form. This problem acquires great importance in the widely used CALPHAD approach to calculating phase diagrams of metallic alloys. Here, a long-standing discrepancy between the empirically derived and first-principles calculated lattice stabilities has been attributed to the existence of dynamical instabilities in many simple metallic structures (bcc, fcc, and hcp), which invalidate the usual definitions of entropy and free energy. We will review the stability criteria, analyze thermodynamic functions in the vicinity of an instability, and discuss the role of dynamical instabilities in phase diagram calculations. Proposals for treating the thermodynamics of unstable phases will be reviewed and recent attempts to find practical solutions to the problem of defining and calculating entropies of unstable phases will be discussed.

10:45 AM

Ab Initio Thermodynamics of the fcc-bcc Transition in Ca Including All Relevant Finite Temperature Excitation Mechanisms: *Blazej Grabowski*¹; ¹Per Soderlind¹; ²Tilman Hickel²; ³Jorg Neugebauer²;

¹Lawrence Livermore National Laboratory; ²Max-Planck-Institut für Eisenforschung

Phase diagrams are the cornerstone of materials design. Traditional approaches to phase diagrams suffer from fundamental difficulties related to experimental input (e.g., unstable phases). The emerging field of ab initio supported phase diagrams is the unrivaled approach to a true advancement in the field. However, while well approved for the T=0K regime, finite temperature ab initio calculations are still facing enormous challenges. Particularly ambitious is an accurate description of phase transitions often involving additional complications due to instabilities. In this talk, we present methods to accurately and efficiently deal with these issues. In particular, we focus on the fcc-bcc transition in Ca with bcc being unstable at T=0K. We show the correct treatment of the instability to be crucial for the transition and the limits of standard ab initio approximations (xc-functionals).

11:00 AM

Thermodynamic Modeling of Peirce-Smith Converter Slag at the Chagres Smelter, Chile: ¹N Cardona¹; ²P.J. Mackey²; ³P. Coursol³; ⁴R. Parada⁴; ⁵R. Parra⁵;

¹Kingston Process Metallurgy; ²P.J.Mackey Technology Inc.; ³Coursol Consultants; ⁴Chagres Smelter; ⁵University of Concepción

Flash furnace matte at the Chagres smelter in Chile is converted to blister copper in Peirce-Smith converters. The produced slag from each of the two slag blows is transferred to the slag cleaning furnaces (along with flash furnace slag) for cleaning prior to discharge, while the high copper slag from the copper blow is recirculated back to the converter process. The performance of the slag cleaning furnace is dependent in part on the quality of the converter slag. In order to understand the impact of converter slag quality on slag cleaning and to help optimize the slag cleaning operation, thermodynamic modeling of the converter slag, supported by microscopic examination of smelter slag samples, was carried out to characterize the Peirce-Smith converter slag. The results of the investigation are described in this paper.

11:15 AM

Micron-Scale Measurements of Heat Capacity by Time-Domain Thermoreflectance: ¹Xuan Zheng¹; ²Changdong Wei²; ³David Cahill³;

¹Ji-Cheng Zhao²; ¹Seagate Technology; ²The Ohio State University; ³University of Illinois – Urbana-Champaign

A pump-probe optical technique based on time-domain thermoreflectance is developed for localized measurement of specific heat capacity with a spatial resolution on the order of several microns. Benchmark validation of this method is made on several common materials by a

careful comparison between the measured values and the well-accepted literature values. The usefulness of this technique in rapid establishment of composition-phase-property relationships is demonstrated on several diffusion-multiple samples where large amount of solid solution compositions and intermetallic compounds are generated by interdiffusion between the elements. The method together with diffusion multiples provides an efficient way to generate much-needed thermodynamic data for CALPHAD modeling and database construction.

11:30 AM

Quantum Monte Carlo and Statistical Sampling Approach to Reference States for Thermodynamic and Kinetic Models : ¹D. M. Nicholson¹;

²Randolph Hood²; ³P. R. C. Kent¹; ⁴Fernando Reboredo¹; ⁵Markus Eisenbach¹;

¹Oak Ridge National Laboratory; ²Lawrence Livermore National Laboratory

The free energy and diffusivity of reference states form the underpinning of current thermodynamic and kinetic models. As a function of temperature, T, these states may or may not be observable. A uniformly applied ab initio approach holds the greatest potential for a consistent reference state description. We demonstrate the feasibility of using Quantum Monte Carlo for reference state energies at T=0 by presenting energies for: bulk Al as a function of pressure, defects in Al (including transition state energies), and He interstitial formation and binding energies in Al. We further demonstrate the use of Wang-Landau statistical sampling of density functional energies (local approximation) to evaluate magnetic entropy as a function of T in Fe and Fe₃C. Work supported by the CDP, Energy Frontier Research Center of U.S. Department of Energy (DOE), Office of Science, ERKCS99 by the Division of Materials Science (DOE), and Division of Scientific User Facilities (DOE).

11:45 AM

Ab Initio Temperature-Dependent Lattice Dynamics for BCC Uranium: ¹Per Soderlind¹;

²Blazej Grabowski¹; ³Lin Yang¹;

⁴Alexander Landa¹;

¹Lawrence Livermore National Laboratory

The body-centered cubic phase of uranium (or any actinide metal) is stabilized at higher temperatures while first-principle density-functional methods predict it to be unstable at lower or zero temperature. This is a problem when devising models particularly when experimental data are sparse or lacking. Many thermodynamical approaches are available but a recent proposal is a very efficient approach based on a self-consistent procedure to calculate temperature-dependent lattice dynamics from first-principles theory. In this presentation we combine highly accurate all-electron DFT calculations with the self consistent ab initio lattice dynamics (SCAILD) methodology to calculate thermodynamic properties of bcc uranium. This is work performed under the auspices of the U.S. Department of Energy by Lawrence Livermore National Laboratory under Contract DE-AC52-07NA27344.



TMS 2012

141st Annual Meeting & Exhibition

Defects and Properties of Cast Metals: Hot Tearing

Sponsored by: The Minerals, Metals and Materials Society, TMS Materials Processing and Manufacturing Division, TMS: Solidification Committee

Program Organizers: Mark Jolly, University of Birmingham; Brian Thomas, University of Illinois at Urbana-Champaign; Carl Reilly, University of British Columbia

Tuesday AM Room: Oceanic 4
March 13, 2012 Location: Dolphin Resort

Session Chairs: Derya Dispinar, NTNU; Christoph Beckermann, University of Iowa

8:30 AM

Quantitative Characterization of Damage Evolution during the Solidification of Al Alloys Using Fast Synchrotron Tomography:

*Peter D. Lee*¹; Chedtha Puncreobutr²; Thomas Connolly³; Richard W. Hamilton²; ¹The University of Manchester; ²Imperial College London; ³Diamond Light Source Ltd,

Synchrotron sources are now being used relatively routinely to observe the in situ formation of damage in semi-solid metals. Using a number of defects as examples (e.g. porosity and hot tears), methods of quantifying these three-dimensional, time dependent images are discussed. The quantification of the time dependent changes in the morphology of defect structures allows both the relative kinetics, and dominant processes to be determined. Examples are applied to both monolithic and particulate reinforced alloys, illustrating how fast synchrotron tomography can be used to gain significant new insights into the mechanisms controlling defect formation during solidification.

8:55 AM

The Importance of Solidification Structure with Respect to Hot Tearing during Continuous Casting of Steels: *Robert Pierer*¹; Wolfgang Rauter²; Christian Bernhard¹; ¹Chair of Metallurgy, Montanuniversitaet Leoben; ²voestalpine Stahl Donawitz GmbH & Co KG

During the solidification of steels, events such as micro/macro segregation as well as the generation of defects and porosity strongly depends on the solidification grain structure. Until now, the relevant literature generally has dealt with the primary or the secondary dendrite arm spacing to characterize the solidification structure. However, these phenomena and particularly the phenomenon of hot tearing during continuous casting of steels occur mainly between primary grains along primary grain boundaries. In this regard, it is very important to note that the primary grain size increases with increasing distance from the surface of the product. Based on theoretical considerations and investigations into the solidification structure of a continuously cast round bloom in combination with the appearance of hot tears, the present study responds to the following questions: How does the primary grain size and subsequently the number of primary grain boundaries, respectively influence the phenomenon of hot tearing and how does the morphology of the solidification structure (i.e. zone of columnar vs. equiaxed grains) influence the extent of open hot tears and hot tear segregations?

9:20 AM

Hot Tearing Susceptibility in DC-Cast Aluminum Alloys: *Nasim Jamaly*¹; Andre Phillion¹; Steven Cockcroft¹; Jean-Marie Drezet²; ¹University of British Columbia; ²Ecole Polytechnique Federale de Lausanne

Hot tearing and loss of dimensional stability are two key defects related to industrial aluminum alloy casting processes. In order to investigate their occurrence, a new semi-solid constitutive law [1] for AA5182 that takes into account cooling rate, grain size and porosity has been implemented into a Direct Chill casting process model for both round billets and rectangular ingots. The semi-solid stress-strain predictions

and the extent of strain accumulation at high fraction solid resulting from different casting geometries as well as different processing parameters was then used to demonstrate the relationships between defect formation, microstructure, and processing variables. [A.B. Phillion, S.L. Cockcroft, and P.D. Lee, *Model Simul in Mater Sci Eng*, Vol.17:055011, 2009].

9:45 AM Break

10:10 AM

Solidification Phenomena during Casting of Stainless Steel/Cast Iron Composites: *Tim Lucey*¹; Mark Reid²; Michael Cortie¹; Paul Huggett³; Ken Moran⁴; Wing Yeung¹; Richard Wuhrer¹; ¹University of Technology, Sydney; ²University of Wollongong; ³Materials Solutions Pty. Ltd.; ⁴Moran Scientific Pty. Ltd

Vacuum casting has been employed in the past to join dissimilar materials such as mild steel and white cast iron however; the requirement for vacuum conditions makes the process restrictive. The interfacial phenomena occurring when a white iron of low melting point is cast onto a steel substrate in an air atmosphere is considered in this study. It has been found that an interfacial layer of austenite is epitaxially solidified on the steel substrate from the liquid phase, which increases in thickness with soak time. In-situ confocal scanning laser microscopy has been employed to study the solidification of this austenitic rim. Carbon diffuses through this layer into the steel substrate through grain boundaries that lie perpendicular to the steel and act as conduits for accelerated atomic transfer into the substrate and allows for the continued solidification of this austenite rim due to the localised increase in liquidus of the alloy.

10:35 AM

Hot Tear Susceptibility of Al-Mg-Si Alloys with Varying Iron

Contents: *Lisa Sweet*¹; *Mark Easton*¹; John Taylor¹; Cameron Davidson¹; Liming Lu¹; Malcolm Couper²; David StJohn³; ¹CAST crc; ²ARC CoE of Design in Light Metals; ³School of Engineering, The University of Queensland

Hot tear susceptibility in a cast 0.53Si-0.33Mg-xFe 6060 aluminum alloy was investigated using the CAST Hot Tear rig, designed to simulate hot tearing in DC casting. The rig has two cast bars, one that is used to measure the load response and one which is fixed at both ends to restrain thermal contraction so that hot tearing could be observed if it occurred. The iron (Fe) content, ranging from 0.02-0.5wt pct, was seen to have a major influence on the load response during solidification and the crack rating of these alloys. The findings are discussed in terms of the coherency-coalescence model and are related to the influence of Fe content on the morphology, prevalence and precipitation sequence of the β -Al₅FeSi and γ -Al₃FeSi Fe-containing intermetallic phases. Observations made of hot tear fracture surfaces show that these phases may play distinctively different roles within the mechanism of hot tearing in these alloys.

11:00 AM

Rules to Prevent and Mitigate Hot Tearing in Al Based Casting Alloys:

*Shimin Li*¹; Kumar Sadayappan²; Diran Apelian³; ¹Worcester Polytechnic Institute; ²CANMET- Materials Technology Laboratory; ³Worcester Polytechnic Institute

Hot tearing is a common and severe defect encountered in alloy castings. Once it occurs, the casting has to be repaired or scrapped, resulting in significant loss. During the last four years, we have worked to quantitatively measure hot tearing in Al cast alloys. We have developed the equipment with our colleagues at CANMET, have studied the key processing variables and we have developed a basic mechanistic understanding. With this knowledge base we are in a position to present a "rule based controls approach" to mitigate or alleviate hot tearing. The rules to prevent and alleviate hot tearing will be reviewed and discussed.

11:25 AM

The Analytical Model of Microsegregation for Solute Elements in Solidifying Mushy Zone of Steel: *Chao Xiao*¹; Jiongming Zhang¹; Yanzhao Luo¹; ¹University of Science and Technology Beijing

The microsegregation resulting in internal cracks in continuously cast strand is studied by using an analytical model in which the transition of ferrite(δ)/austenite(γ) solidification is considered. The effects of C, Si, Mn, P and S on the interdendritic segregation, zero strength temperature(ZST) and zero ductility temperature(ZDT) are discussed. The results show that C content in steel influences the interdendritic segregation, solidus temperature and solidification front temperature significantly. The segregation of P and S increases greatly when the C content increased from 0.1% to 0.5% while that of the other elements are not obviously changed. The changes of C content have a great impact on ZST and ZDT, while the fluctuations of P and S contents only affect ZDT greatly.

Deformation, Damage, and Fracture of Light Metals and Alloys: Session II

Sponsored by: The Minerals, Metals and Materials Society, TMS Structural Materials Division, TMS Light Metals Division, TMS/ASM: Mechanical Behavior of Materials Committee
Program Organizers: Qizhen Li, University of Nevada, Reno; Fuqian Yang, Univ. of Kentucky; Ke An, Oak Ridge National Laboratory

Tuesday AM
March 13, 2012

Room: Northern A2
Location: Dolphin Resort

Session Chair: Fuqian Yang, Univ. of Kentucky

8:30 AM Invited

Corrosion Damage of Deformed AZ31 Mg Alloy: *Guang-Ling Song*¹; ¹GM Global Research & Development

Hot-rolled AZ31 sheet, a severely deformed Mg alloy, has great potential applications in the automobile industry. Its significantly refined grains resulting from hot-rolling is believed to be beneficial to the enhancement of its overall corrosion resistance. The alloy has crystallographically orientated grains. Its (0001) crystallographic plane dominated rolling surface is more corrosion resistant than its cross-section surface which is mainly composed of crystallographic planes (101 $\bar{0}$) and (112 $\bar{0}$). The microstructures of these two surfaces evolve during heat-treatment, leading to its deteriorated corrosion performance. Surface plastic deformation machining can further improve its corrosion performance due to a combined effect of grain refinement and strong basal texture.

9:00 AM Invited

Relationship of Corrosion Fatigue and Stress Corrosion Cracking Thresholds to Degree of Sensitization in Al-Mg Alloy: *Peter Pao*¹; Ronald Holtz¹; Thomas Longazel¹; Robert Bayles¹; Ramasis Goswami²; ¹Naval Research Laboratory; ²SAIC

Systematic experimental studies of the corrosion-fatigue threshold, ΔK_{TH} and stress-corrosion cracking threshold, K_{ISCC} of Al 5083-H131 heat treated to various degrees of sensitization at temperatures of 70, 100 and 175°C are reported. ΔK_{TH} does not degrade until the ASTM G67 nitric acid mass loss (NAML) exceeds approximately 30 mg/cm². The K_{ISCC} however, degrades continuously with increasing NAML and has dropped by a factor of five when the NAML is 30 mg/cm². The degradations of ΔK_{TH} and K_{ISCC} are associated with the growth of a semi-continuous type of grain boundary coverage by β -Al₃Mg₂. Once the grain boundary is fully covered with β -Al₃Mg₂, typically in the NAML range of 40 to 50 mg/cm², both ΔK_{TH} and K_{ISCC} have already degraded substantially. The aging behaviors of ΔK_{TH} and K_{ISCC} versus NAML are the same, regardless of aging temperature, indicating that only continuity of β is the dominant effect.

9:30 AM

Fatigue and Corrosion Properties of Mg-Al-Mn Alloy by Super Vacuum Die Cast: *Wei Wen*¹; Alan A. Luo²; Tongguang Zhai¹; ¹University of Kentucky; ²General Motors Corporation

AM60(Mg-Al-Mn) alloys fabricated by super vacuum die cast (SVDC) and high pressure die cast (HPDC) were fatigued in four-point bend at room temperature and different humidity. It was found that SVDC alloy had higher fatigue strength than HPDC alloy. Crack initiation was predominantly associated with pore clusters in the surface of SVDC alloy, and with the interfaces between eutectic-phase and the matrix in HPDC alloy. The surface layer that was formed with a low pore density and smaller pores in SVDC alloy accounted for its improved fatigue strength over that of HPDC alloy. Its effects on fatigue properties and corrosion resistance were investigated by comparative experiments using the as-cast sample and the sample with the surface layer being removed. The polarization curves of SVDC sample and HPDC sample were measured in corrosion test to study the effect of SVDC method on corrosion resistance of Mg-alloy.

9:50 AM

Effect of Corrosion on the Strength of Fillet Arc Welded Cu-Lean AA7xxx Joints: *J. Dabrowski*¹; Dr. M. Bruhis¹; Dr. J.R. Kish¹; ¹Centrte for Automotive Materials & Corrosion, McMaster University, Hamilton, ON Canada

Heat-treatable AA6xxx (Al-Mg-Si) and AA7xxx (Al-Zn-Mg) Al alloys, with relatively high strength, toughness, energy absorption, weldability and formability, make it possible to design safe, cost-competitive automotive bumper systems to crush in a controlled fashion. One major technical issue preventing widespread utilization of higher strength AA7xxx extruded beam profiles, in the peak-aged T6 condition, is the susceptibility to intergranular corrosion modes, including exfoliation and stress corrosion cracking. These corrosion modes are of particular concern for arc welded (GMAW) lap joints and fillet T joints, which is a common joining technology used to attach extruded heat-treatable Al alloys. A study was undertaken to document the effect of corrosion on the strength and fracture mode of the arc welded joints. The fracture stress and mode was experimentally determined using tensile shear loading experiments. An ARAMIS strain-mapping system based on digital image correlation (DIC) using a CCD camera was used for strain measurement.

10:10 AM Break

10:20 AM

Micro-Shear Stress and Damage Predictions from Hydrostatic Stress Loading of Aluminum Alloys 7075, 7039, and 7020: *John Chinella*¹; ¹U.S. Army Research Laboratory

Thermodynamics dependent microstructure, phase, and physical model predictions of material characteristics are demonstrated for aluminum alloys 7020 (Al-4.5Zn-1.2Mg), 7039 (Al-4.0Zn-2.8Mg), and 7075 (Al-5.6Zn-2.5Mg-1.6Cu) by direct application of Sente Software's Java Materials Program (JMatPro), mesoscale computation materials engineering software. JMatPro reveals phase constitutions as a function of input composition, temperature, and time and, using material property databases and physical models, calculates temperature-dependent physical and mechanical properties. With secondary application, the elastic bulk moduli for constituent phases and inclusions, derived from Gibbs energy by JMatPro, are used to predict the maximum levels of micro-scale shear stresses under hydrostatic pressure. With comparison to conditions known to cause incipient spall in 7020 alloy, levels of microscale shear stress around inclusions are shown to equal or exceed the level of Von Mises calculated shear yield strength of the alloys, validating that deformation occurs during high-load ballistic spall events, at the initial stages of compression.

TUESDAY AM



TMS 2012

141st Annual Meeting & Exhibition

10:40 AM

Coupling Experimentation and Computation to Investigate Damage Evolution in High Purity Aluminum: *Matthew Tucker*¹; John Bingert¹; Brian Patterson¹; Cheng Liu¹; Ricardo Lebensohn¹; ¹Los Alamos National Lab

Understanding and capturing the intricacies involved in the damage evolution and eventual failure of a component requires a coupling of carefully designed experiments and simulations. In this work, a sample with known initial damage and crystal orientation states is subjected to interrupted tensile testing, while the evolving damage state is characterized *ex situ*. Micro x-ray computed tomography (XCMT) is employed to follow embedded internal tracer particles allowing for the quantification of localized internal strains. The initial damage state is provided by casting porosity, while the size and shape of each pore is measured at global strain intervals. Particles are embedded to serve as tracers for localized internal strains. Localized surface strains are also measured using more traditional digital image correlation (DIC) techniques. Comparing the surface and internal strains shows the result of the evolving damage state and crystal orientations and helps to elucidate the contribution of local strains from each.

11:00 AM

The Effect of Chemistry and Microstructure on the Deformation and Fracture Behavior of (Ti, Zr)Ni-Based Alloys with Aluminum Additions: *Derek Hsen Dai Hsu*¹; B. Chad Hornbuckle²; Gregory Thompson²; Michele Manuel¹; ¹University of Florida; ²The University of Alabama

(Ti, Zr)Ni alloys possess the potential for use in a wide range of industries. Applications can include but are not limited to high-temperature shape memory actuators and bulk metallic glasses. The present work reports the mechanical characterization of $Ti_{31.5-x}Zr_{20}Ni_{48.5}Al_x$ ($X = 0, 1, 2, 3$) alloys. The addition of aluminum to this system changes the microstructure, which subsequently alters the deformation and fracture behavior of these alloys. To determine the relationships connecting microstructure with deformation behavior, advanced characterization techniques including optical microscopy, scanning and transmission electron microscopy, and atom probe tomography are used to examine this quaternary system. This evaluation includes precipitate morphology as a function of chemistry and heat-treatment, and deformation mechanisms such as dislocation, twinning and martensite evolution as a function of strain. The authors would like to acknowledge the support of the NSF under grant number CMMI-0824352 and NASA grant NNX09AO61A from the NASA FAP Supersonics project.

11:20 AM

Investigation of Frequency Effect on Fretting Wear Damage of Titanium Alloy: Qualitative and Quantitative Approaches: *Benjamin van Peteghem*¹; Siegfried Fouvry¹; Patricia De Oliveira Campos Neubauer¹; ¹Laboratoire de Tribologie et Dynamique des Systèmes

In the dovetail blade-disk contact of turbojet engines, the loading cycle is very complex: during startup and shutdown, the normal force and the displacement vary simultaneously. And, during flight, the contact is submitted to small vibrations. In this study, we focused on the largest displacements (i.e. during startup and shutdown), which vary simultaneously with the normal force. In a former study, it has been shown that frequency drives the energy wear rate, and normal force variation drives tribochemical reactions. This new study investigates these two points to define an extended wear law and to formalize the tribochemical behavior of this contact. Frequencies between 0.025 Hz and 5 Hz have been studied, in constant and variable normal force conditions. Two different behaviors were observed, depending on the frequency and the loading. Those behaviors confirm the hypothesis of a major role of oxidation in the wear process induced by fretting.

11:40 AM

Primary Creep in Titanium Alloys: Role of Trace Elements: *Srikant Gollapudi*¹; Tapash Nandy¹; Satyanarayana D¹; Phaniraj C²; ¹Defence Metallurgical Research Laboratory; ²IGCAR

The influence of trace elements viz. Fe and Ni on the primary creep behaviour of Ti-834 alloy was studied. Two Ti-834 alloys, DMR Ti834 and TIMETAL 834 with higher and lower content of (Fe, Ni) respectively were chosen for this study. The creep behaviour of both alloys was studied in the temperature range of 873 – 1023 K at a stress range of 50 - 400 MPa. Subsequent analysis showed that under similar stress and temperature conditions, DMR Ti834 yields a smaller primary creep strain in comparison to TIMETAL 834. The creep activation energy (Q) in the primary creep region was also determined and again found to be smaller in DMR Ti834 ($Q = 284$ kJ/mol) in comparison to TIMETAL 834 ($Q = 399$ kJ/mol). The difference in primary creep strain and Q values was rationalized vis-a-vis the Fe, Ni content.

Electrode Technology for Aluminium Production: Bake Oven Design and Improvement

Sponsored by: The Minerals, Metals and Materials Society, TMS Light Metals Division, TMS: Aluminum Committee, TMS: Aluminum Processing Committee
Program Organizer: Morten Sorlie, Alcoa Norway

Tuesday AM
March 13, 2012

Room: Americas Seminar
Location: Dolphin Resort

Session Chair: André Proulx, Rio Tinto Alcan

8:30 AM

Anode Quality and Bake Furnace Performance of EMAL: *Raja Akhtar*¹; *Markus Meier*²; Peter Sulger²; Werner Fischer²; Ralph Friedrich³; Thomas Janousch³; ¹Emirates Aluminium EMAL; ²R&D Carbon Ltd.; ³Riedhammer GmbH

As part of the worldwide biggest greenfield project, the two open top anode bake furnaces of EMAL were started up in 2010 to reach an annual production capacity of 450'000 tons of baked anodes. Two furnaces are installed with 64 sections each having 9 flues and 8 pits that are equipped with 4 fires each. An unprecedented combination of outstanding anode quality and furnace performance figures could be achieved. This document highlights the distribution of key anode properties, furnace productivity and energy consumption. Furnace design and operational challenges to reach today's standards are discussed.

8:55 AM

Experiences in FTC Design, Operation and Development: *Erik Dupon*¹; Peter Klut²; Edo Engel¹; ¹Danieli Corus Technical Services; ²Danieli Corus BV

Over the past decades, emission control has consistently been a major issue for the developed, aluminium consuming world. Environmental facilities like Fume Treatment Centres have been retrofitted to paste plants and carbon bake furnaces throughout the world. The emerged countries have seen a great increase in aluminium consumption and for all greenfield smelters, the addition of FTC's has been mandatory. Danieli Corus's experience in FTC's extends from retrofit projects in e.g. the EU and Australia up to LSTK projects in developing countries such as India. This article describes how existing FTC's have performed over the past decades in terms of environmental performance and maintenance requirement. For recent projects, specific circumstances of execution in greenfield situations are discussed. In addition, developments in FTC technology and future prospects are presented.

9:20 AM

Boost of Anode Production at Voerdal Aluminium by Advanced and Integrated Control Strategies: Michael Schneider¹; Christian Krupp¹; Detlef Maiwald²; Domenico Di Lisa²; ¹Voerde Aluminium GmbH; ²Innovatherm

Voerde Aluminium GmbH (Voerdal) is operating since more than 40 years a 36 section Kaiser type furnace for the production of anodes. Due to the continuous amperage increase in the potline, the baking furnace capacity had to be increased by 10% in the given boundary conditions of the furnace size and government permission of the maximum flow gas volumes and emissions. Voerdal and the system designer jointly developed new control strategies to ensure the boost of anode production. This was mainly achieved by implementation of new control modules which integrate the FTC feedback values into the overall control strategy. This paper explains the functional principles of these control strategies and describes the phases of implementation. Finally it outlines the actual results achieved.

9:45 AM

New Central Control System Architecture for Anode Baking Furnaces: Nicolas Fiol¹; Xavier Genin¹; Fabienne Virieux²; ¹Solios Carbone; ²Fives Solios

Conventional anode baking firing and control systems are composed of several mobile pieces of equipment with their own local controller to manage the high speed local tasks. Redundant central control units synchronize the actions of each local controller. A fast real time Ethernet network implementation allows simplifying the existing control system architecture: it uses only one real time central controller and remote Inputs/Outputs for each mobile piece of equipment. The robustness and reactivity of the control as well as the required safety loops are preserved. The maintenance and day to day operation are simplified. Furthermore, real time network and accurate time synchronisation between the pieces of equipment open new perspectives to improve the baking process management and to enhance safety.

10:10 AM Break

10:25 AM

Methods to Improve Fuel Utilization for Open Top Anode Baking Furnaces: Rifu Lin¹; Shoulei Gao¹; Lin Tang¹; Yan Li¹; ¹Sunstone

As a baking furnace ages, cracks and openings develop in the furnace which allow outside air to enter. Unless proper corrective actions are implemented, gas consumption can increase, final baking temperatures can decrease, and baked anode properties can deteriorate. In this paper, methods are presented for improving the efficiency of fuel utilization for aging furnaces, and thereby lowering fuel consumption, while maintaining or improving anode finishing temperatures and anode properties.

10:50 AM

Energy Saving Technologies for Anode Manufacturing: Jingli Zhao¹; Qingcai Zhao¹; ¹Jinan Aohai Carbon Products Corporation Ltd.

The energy saving technologies for anode manufacturing are developed and applied in the anode production processes in Jinan Aohai Carbon Products Corporation Ltd. The surplus heat from shaft calciners is recovered for heating coal tar pitch and power generation. The baking furnace structure and the lining materials have been improved so as to get reasonable anode occupation efficiency and less heat loss. The heating curves for anode baking are finely adjusted and controlled for completely burning of the volatiles in the green anodes for less energy input into the baking furnace. Based on the technology application mentioned above a great energy saving and benefit to the plant environment have been achieved in Aohai anode plants.

Electrometallurgy 2012: Session II

Sponsored by: The Minerals, Metals and Materials Society, The Metallurgy and Materials Society of CIM, TMS Extraction and Processing Division, TMS: Hydrometallurgy and Electrometallurgy Committee

Program Organizers: Georges Houlachi, Hydro-Quebec; Antoine Allanore, Massachusetts Institute of Technology; Michael Free, University of Utah; Michael Moats, University of Utah; Edouard Asselin, UBC; Shijie Wang, Rio Tinto Kennecott Utah Copper; James Yurko, Materion Brush Beryllium and Composites

Tuesday AM
March 13, 2012

Room: Europe 5
Location: Dolphin Resort

Session Chairs: Georges Houlachi, Hydro-Quebec; Jim Yurko, Materion Brush Beryllium and Composites

8:30 AM

Molten Carbonates in the Energy Field, as Electrolytes, Composite Materials, Fuel Carriers or Reaction Media: Michel Cassir¹; ¹Chimie ParisTech

The unique properties of molten carbonates offer an open scope of applications in the field of energy. These molten salts are in the center of chemical and electrochemical reactions involving carbon and carbonaceous species, carbon dioxide and carbon monoxide, significant for energy generation. Moreover, such media have also an oxidative character; they can dissolve molecular oxygen and oxygen reduced species which may have an important role in waste treatments and homogeneous catalysis. An overview will be given on the principal physicochemical properties of molten carbonates, before focusing on their main known application, the molten carbonate fuel cell (MCFC). Progress in other new fuel cells applications will also be analyzed, such as direct carbon fuel cell (DCFC), hybrid carbon fuel cell (HDCFC) and composite high-temperature fuel cells combining the features of MCFC and solid oxide fuel cell (SOFC). Afterwards, membranes for the separation and capture of CO₂ will be reviewed.

8:50 AM

The Equilibrium between Titanium Ions and Metal Titanium in Fluoride-Chloride: Qiuyu Wang¹; Hongmin Zhu¹; ¹University of Science and Technology Beijing

The equilibrium between titanium ions and metal titanium was investigated in fluoride-chloride molten salt. The electrochemical properties of titanium ions in fluoride-chloride were studied on a molybdenum electrode by cyclic voltammetry (CV) and square wave voltammetry (SWV). The equilibrium constant of the equilibrium between titanium ions and metal Ti was calculated in KCl-NaCl- 2.5wt %K₂TiF₆ at the temperature of 1073K.

9:10 AM

Surface Area Effects at Liquid-Liquid Interfaces Consisting of a Liquid Metal and an Electrolyte: Paul Burke¹; Brice Chung¹; Brian Oldfield¹; Donald Sadoway¹; ¹MIT

Electrochemical measurements are referenced on the basis of the surface area of the interface between the electrodes and the electrolyte. This area is typically assumed as the apparent geometric area. In the case of liquid electrodes and electrolyte, a perturbation of this interface by vibration or convection can alter the effective surface area. This change in surface area can make the interpretation of electrochemical measurements difficult in systems with liquid electrodes. The current work attempts to quantify this effect by inducing waves at the interface in an electrochemical cell containing liquid electrodes.



TMS 2012

141st Annual Meeting & Exhibition

9:30 AM

Electrochemical Behavior of Calcium-Bismuth Alloys in Molten Salt Electrolytes: *Hojong Kim*¹; Dane Boysen¹; Donald Sadoway¹; ¹MIT

The electrochemical properties of calcium-bismuth alloys were investigated to determine their utility as electrodes in liquid metal batteries. During battery discharge, calcium from the negative electrode is oxidized to form a cation, which is conducted through the molten salt electrolyte to the positive electrode, where it is electrochemically reduced and alloys with molten bismuth metal. Upon charging, calcium from the molten calcium-bismuth alloy positive electrode is oxidized to form a cation, which returns back to the negative electrode through the molten salt electrolyte where it is electrochemically reduced. The cell potential of Ca|Ca-Bi cells was measured as a function of state of charge and temperature over the range of composition spanning $0 < \text{mole fraction, } x_{\text{Ca}} < 0.25$). The electrolyte was a solution of molten $\text{CaCl}_2\text{-NaCl-LiCl-BaCl}_2$. The temperature range was $500^\circ\text{C} - 700^\circ\text{C}$. The composition of the working electrode (Ca-Bi alloys) was varied by coulometric titration.

9:50 AM

Low Temperature Extraction Process for Metals from Metal Oxides Using Ionic Liquids: *Vibha Gill*¹; Ramana Reddy¹; ¹The University of Alabama

A fundamental study on development of a low temperature electrochemical technology for extraction of metals from metal oxides using ionic liquids was undertaken. In this presentation electrochemical extraction of Zn from ZnO dissolved in eutectic solvents Urea ($(\text{NH}_2)_2\text{CO}$) and Choline chloride ($\text{HOC}_2\text{H}_4\text{N}(\text{CH}_3)_3\text{+Cl}^-$) in a 2:1 ratio at 80°C is discussed. FTIR studies of ionic liquids with and without ZnO addition were conducted. Reduction potential of Zn metal in these solvents were determined using CV. Electrochemical experiments using EG&G three electrode cell system with Al as cathode, carbon electrode as anode and Pt as a reference electrode. The deposits were characterized using XRD and SEM-EDS. The results showed that pure Zn was deposited on the Al cathode. The current density of 180A/m^2 with an efficiency of 87.6% was obtained. The process is a low energy consumption and environmental friendly with no GHG emission.

10:10 AM Break

10:25 AM

Towards Sustainable Metals Production by Molten Oxide Electrolysis: *Donald Sadoway*¹; ¹MIT

Molten oxide electrolysis (MOE), the electrolytic decomposition of a metal oxide into molten metal and oxygen gas, is a low-carbon route for metals extraction. MOE avoids consumable carbon anodes and halide electrolytes; this eliminates the need for energy-intensive anode manufacture and guarantees the absence of greenhouse-gas emissions as the by-product of the metal-recovery step. In the author's laboratory a variety of metals have been produced by MOE including iron, nickel, chromium, manganese, silicon, and titanium, each by electrolytic decomposition of the related metal oxide. Promising results for a low-cost, oxygen-evolving anode have been obtained. Beyond sustainable metals production, MOE can serve as the inspiration for scalable electrical energy storage in stationary applications. Liquid-metal/molten-salt cells have been shown to operate as rechargeable batteries that have the potential to handle colossal currents thereby enabling us to store off-peak power from the grid for subsequent delivery on demand during high-usage periods.

10:45 AM

Effect of Electronic Current on the Solid Oxide Membrane (Som) Process for Magnesium Production: *Eric Gratz*¹; Soobhankar Pati²; Jarrod Milshtein¹; Adam Powell²; Uday Pal¹; ¹Boston University; ²Metal Oxygen Separation Technologies

The solid oxide membrane (SOM) process has been used at 1150°C to produce magnesium by direct electrolysis of its oxide. Magnesium oxide is dissolved in a molten $\text{CaF}_2\text{-MgF}_2$ ionic flux. An oxygen-ion-conducting

yttria-stabilized zirconia (YSZ) SOM membrane separates the cathode and the flux from the anode. During electrolysis, magnesium ions are reduced at the cathode and Mg(g) bubbles out of the flux into a separate condenser. The flux has a small solubility for magnesium which imparts electronic conductivity to the flux. The electronic conductivity decreases current efficiency of the process and also degrades the YSZ membrane. This study investigates different methods for reducing the electronic conductivity of the flux due to magnesium solubility. One effective method shown here is inert gas flushing near the magnesium nucleation site. Potentiodynamic and potentiostatic experiments along with AC impedance spectroscopy are used to characterize the effectiveness of the approach.

11:05 AM

Behavior of Silicon Electrodepositing in Fluoride Molten Salts: *Xin Wang*¹; Shuqiang Jiao¹; Hongmin Zhu¹; ¹University of Science and Technology Beijing

The behavior of silicon deposition electrochemically in a molten high-melting-point fluoride electrolyte was studied at temperatures above the melting point of silicon 1412°C . The corresponding structures and morphologies of the product of deposition were characterized by XRD and SEM. A series of tests has been performed on the electrochemical deposition behavior of Si^{4+} ions in $\text{BaF}_2\text{-CaF}_2\text{-Na}_2\text{SiF}_6$ molten salt. The influence of electrochemical parameters of cathode deposition of silicon was also investigated. The results showed that silicon could deposit on the top of fluoride molten salts. The electrochemical deposition of Si^{4+} ions in the molten salts was observed to proceed through two reaction steps.

11:25 AM

VITTORIO DE NORA PRIZE: Development of Electrometallurgical Processes for 21st Century Metal Extraction: *Antoine Allanore*¹; James Yurko¹; ¹Massachusetts Institute of Technology

The late 19th century development of electrometallurgy enabled the discovery of revolutionary metal processing methods, which are at the core of our technology-oriented societies (electrolytic extraction in molten salts for light and rare-earth metals and aqueous electrowinning for copper, zinc, nickel, etc...), or which proved to be necessary to improve metal sustainability (electric arc furnace for recycling). The 21st century challenges related to metal extraction, particularly environmental ones, have led to a reconsideration of electrochemical extraction processes. This presentation will first briefly present some existing extraction methods, in particular electrometallurgical ones, pointing-out the advantages and issues related to the current state-of-the art. The second part of the talk will present how breakthrough electrochemical processes have recently been developed to adapt to environmental and energy constraints, taking the example of low- and high-temperature electrochemical extraction processes scaled-up for transition and light metals. Technical results related to metal production (Fe, Mn, Ti) and oxygen generation by molten oxide electrolysis will be presented in particular, to emphasize the key environmental and metallurgical advantages of electrochemical techniques. The experience gained developing and up-scaling these processes suggest that a paradigm change of commercial production of metals could potentially be achieved with their implementation.

TUESDAY AM

Emeritus Professor George D.W. Smith Honorary Symposium: Steels I

Sponsored by: The Minerals, Metals and Materials Society, TMS Materials Processing and Manufacturing Division, TMS/ASM: Phase Transformations Committee

Program Organizers: Michael Miller, Oak Ridge National Laboratory; Gregory Olson, Northwestern University and QuesTek Innovations LLC; George Krauss, Colorado School of Mines

Tuesday AM
March 13, 2012

Room: Mockingbird 2
Location: Swan Resort

Funding support provided by: Oak Ridge National Laboratory; QuesTek Innovations LLC; AMETEK, Inc

Session Chairs: George Krauss, Colorado School of Mines; Hans-Olof Andren, Chalmers University of Technology

8:30 AM Invited

Some Atoms I Have Known: A Tale of Two Smiths: *Greg Olson*¹; ¹Northwestern University

In the early 1980s, Morris Cohen's dream of establishing the long-sought structural mechanism of early aging phenomena in ferrous martensites was brought to fruition through a collaboration with G.D.W. Smith whose 1D atom-probe microanalysis confirmed the theoretical prediction of a Zener-order-induced spinodal instability of the BCT Fe-C solution, and showed that the composition of the resulting high C modulations is of Fe₈C stoichiometry, now confirmed by DFT calculations. Combining the atomic capability of G. D. W. Smith with the systems vision of C. S. Smith, a Materials Design Initiative was undertaken in 1985. G. D. W. Smith played a leading role in establishing the matrix overlap correction procedures vital to extending the analysis of multicomponent alloys down to the nm scale of efficient strengthening dispersions. Smith's leadership in 3D atom-probe development ultimately enabled full validation of the first commercial alloys to emerge from this design technology, incorporating "carbides by Smith."

8:55 AM Invited

Microstructural Characterisation of Nanometre Scale Irradiation Damage in High-Ni Welds: *Jonathan Hyde*¹; Paul Styman²; Colin English¹; George Smith²; Keith Wilford³; Tim Williams³; Robin Boothby¹; Helen Thompson¹; ¹National Nuclear Laboratory; ²Oxford University; ³Rolls Royce

During service, Reactor Pressure Vessel (RPV) steels harden as a result of the formation of irradiation-induced nanometre-scale microstructural features which act as obstacles to dislocation movement. The hardening may lead to embrittlement and limit the reactor operating life. Microstructural observations of the irradiation-induced features have provided an important contribution to the mechanistic understanding of this degradation phenomenon and to the development of dose-damage relationships. Information from Atom Probe Tomography (APT), which provides information on the spatial distribution of solute atoms within individual grains, and Small Angle Neutron Scattering (SANS), which provides information averaged over many grains, have proved especially informative for characterising well defined solute clusters. In this paper we examine the ability of APT and SANS to characterise the earliest stages of irradiation damage in several neutron-irradiated and thermally-aged RPV steels and discuss the consequences for longer term evolution. The results will be compared with Monte Carlo models.

9:20 AM Invited

Contributions of Atom Probe Tomography to the Understanding of Steels: *Michael Miller*¹; ¹Oak Ridge National Laboratory

Since the introduction of the computer-controlled atom probe field ion microscope in the early 1970s, significant contributions to the understanding of steels have been made primarily due to its near atomic

spatial resolution and the ability to detect carbon and other light elements. Some notable achievements that will be discussed are the solute partitioning between phases in pearlite, the visualization and quantification of carbon segregation to dislocations (Cottrell atmospheres), quantification of the copper-enriched precipitates responsible for the embrittlement of neutron irradiated pressure vessel steels, the low temperature phase separation responsible for the 475° embrittlement of Fe-Cr alloys and the ferrite phase in duplex stainless steels, and the nanoclusters responsible for the remarkable stability of nanostructured ferritic alloys to high dose irradiation. Research supported by ORNL's Shared Research Equipment (SHaRE) User Facility, which is sponsored by the Office of Basic Energy Sciences, U.S. Department of Energy.

9:45 AM

Three Dimensional Characterization of Interfaces in Nanolayered Radiation Tolerant Metallic Thin Films: *Arun Devaraj*¹; Venkata Rama Sessa R Vemuri¹; Tamas Varga¹; Shutthanandan Vaithiyalingam¹; Satyanarayana V. N.T Kuchibhatla¹; Chongmin Wang¹; Thevuthasan Suntharampillai¹; Charles H Henager²; ¹EMSL, Pacific Northwest National Laboratory; ²Pacific Northwest National Lab

Recent research points to the intrinsically high radiation damage resistance of nanolayered materials with interfaces acting as traps and recombination centers for the radiation-induced point defects. This talk will focus on the unique benefits of atom probe tomography (APT) in characterizing the atomic structure of the interfaces in sputtered nanolayered Ti/Al metallic thin films before and after ion beam irradiation. Coupling APT with Rutherford backscattering spectrometry, aberration corrected scanning transmission electron microscopy, and first principle computations helped quantify changes in intermixing as a function of irradiation dose and layer spacing. These insights were used to investigate whether the internal interfaces in metallic multilayers can be manipulated at the nanoscale to enhance dynamic recombination of radiation-produced defects, or self-healing, so as to reduce radiation damage without compromising other properties.

10:00 AM Break

10:30 AM Invited

Ultrahigh Strength Pearlitic Microstructures: Contributions by George D. W. Smith: *George Krauss*¹; Stephanie Miller¹; Emmanuel De Moor¹; David Matlock¹; ¹Colorado School of Mines

Fully pearlitic patented and cold drawn steel wire constitutes a product with ultrahigh ultimate tensile and torsional strengths for demanding applications, including tire reinforcement, springs, and cable for lifts, elevators, suspension bridges and mooring cables. The wire microstructure is a unique composite of very fine aligned and interspersed lamellar ferrite and cementite in eutectoid or near-eutectoid steels consisting only of iron and carbon and small amounts of other elements, including sometimes vanadium as a microalloying element. This presentation reviews some of the major contributions made by Professor Smith in the characterization of these remarkable microstructures and integrates his work with ongoing research designed to further understand and improve ultrahigh strength steel wire.

10:55 AM Invited

Atom Probe Analyses of Advanced Sheet Steels: *Kazuhiro Seto*¹; David Saxey²; George Smith³; ¹JFE Steel Corporation; ²University of West Australia; ³Oxford University

Interstitial atom free (IF) steel and precipitation strengthened steel were analysed using a three-dimensional atom probe. We have confirmed that C and B segregate to grain boundaries in IF steel at very first stage of recrystallisation during annealing although P segregates afterwards. This result is important to control the secondary work brittleness observed in IF steel after press forming. Secondly, very fine precipitates in Ti-V bearing hot rolled formable high strength steel were analysed. Banded microstructure containing nanoscale carbides was clearly observed. The average composition of fine precipitates less than 5nm was rich in Fe



TMS 2012

141st Annual Meeting & Exhibition

whereas the fraction of Fe decreased in large precipitates. The distribution of fine precipitates on a single layer was random, and the mean free distance in three-dimension was estimated as approximately 28nm. The increase of yield strength was weaker than calculation from Orowan mechanism.

11:20 AM Invited

Atom Probe Tomography for Industrial Applications: *Harald Leitner*¹; ¹Montanuniversitaet Leoben

Atom probe field ion microscopy is known as a technique which has the capability of measuring compositional changes on near atomic scale with equal detection efficiency for all elements. Atom probe field ion microscopy has the highest analytical spatial resolution of any microscope, but this technique is still not well-established in industrial research. However, with the development of the three-dimensional atom probe, especially the instruments with large field of view, larger areas can be analyzed and thus the obtained results are more representative for material properties. Furthermore, due to the three-dimensional picture of the analyzed volume, microstructural features are accessible which are not detectable with an one-dimensional atom probe and also other microscopic techniques. In this talk, examples of atom probe investigations on industrial materials such as steels and nickel-base alloys are presented, which gained deeper insight into them by the invention of the three-dimensional atom probe.

11:45 AM

The Application of Atom Probe Tomography to the Identification of Transformation Mechanisms of the Bainite Reaction in Steels: *Francisca Caballero*¹; *Michael Miller*²; *Carlos Garcia-Mateo*¹; *Juan Cornide*¹; ¹CENIM-CSIC; ²ORNL

The bainite transformation of austenite to ferrite between 200–550°C is controversial. The displacive theory states that bainitic ferrite forms by shear, the transformation is essentially martensitic (i.e. the individual atom movements are less than one inter-atomic spacing) and proceeds by the formation of sub-units. The reconstructive theory states that bainite is a product of a reconstructive transformation (i.e., most of the solid state phase transformation occurs by thermally activated atom movements) and grows by the migration of growth ledges on the broad faces of the interface. This atom probe tomography study tracked the atom distributions during the bainite reaction and has provided experimental evidence on the incomplete transformation phenomenon, the carbon supersaturation of ferrite, the plastic accommodation in austenite, and cluster and precipitation formation. Research supported by ORNL's Shared Research Equipment (SHaRE) User Facility, which is sponsored by the Office of Basic Energy Sciences, U.S. Department of Energy.

12:00 PM

Atom Probe Analysis of Nanoscale Austenite Reversion in Steels: *Dirk Ponge*¹; *Dierk Raabe*¹; *Lei Yuan*¹; *Pyuck Choi*¹; *Jim Wittig*¹; ¹Max-Planck-Institut

We design ultra-high strength and ductile martensitic and TRIP steels via nanoscale austenite reversion. The mechanism works via partitioning and kinetic freezing of C or Mn at martensite-austenite interfaces or via Gibbs adsorption isotherm segregation at martensite-martensite grain boundaries. We apply the method to Mn-based maraging steels and Cr-C-based martensitic stainless steels. Nanoscale austenite reversion leads to a variety of GPa steels at a ductility above 15%.

12:15 PM

Control of p-n Heterojunction Abruptness in Vapor-liquid-solid Grown Semiconductor Nanowires: *Daniel Perea*¹; *Jinkyoun Yoo*²; *Daniel Schreiber*¹; *S. Tom Picraux*²; *Theva Thevuthasan*¹; ¹Pacific Northwest National Laboratory; ²Los Alamos National Laboratory

Efforts to continually scale down the size of electronic components is guiding research to explore the use of nanomaterials synthesized from a bottom-up approach – group-IV semiconductor nanowires being one

such material. However, Au-catalyzed synthesis of Si-Ge semiconductor nanowire heterojunctions using the commonly-used vapor-liquid-solid (VLS) growth technique results in diffuse heterojunction interfaces, leading to doubts of producing compositionally-sharp p-n junctions using this approach. However, we have recently reported the ability to increase Si-Ge nanowire heterojunction abruptness by VLS synthesis from a Au(1-x)Ga(x) catalyst alloy. In this work, we have extended the use of a AuGa catalyst alloy to produce more compositionally abrupt p-n junction interfaces compared to using pure Au as directly measured by atom probe tomography. The ability to controllably increase nanowire p-n junction abruptness is important for nanowire applications as tunneling field effect transistors where an increase in device performance is expected from shaper p-n junction interfaces.

Energy Nanomaterials: Photovoltaics I

Sponsored by: The Minerals, Metals and Materials Society, TMS Materials Processing and Manufacturing Division, TMS Structural Materials Division, TMS: Advanced Characterization, Testing, and Simulation Committee, TMS: Nanomechanical Materials Behavior Committee

Program Organizers: Reza Shahbazian-Yassar, Michigan Technological University; Ming Au, Savannah River National Laboratory; Meyya Meyyappan, NASA Ames Research Center

Tuesday AM
March 13, 2012

Room: Swan 3
Location: Swan Resort

Session Chairs: Reza Shahbazian Yassar, Michigan Technological University; Dhandapani Venkataraman, University of Massachusetts Amherst

8:30 AM Invited

Self-Assembly Strategies for Nanoscale Assemblies For Organic Photovoltaic Cells: *Dhandapani Venkataraman*¹; ¹University of Massachusetts Amherst

In this talk, I will focus on the various self-assembly strategies for the assembly of organic semiconductors into nanoscale segregated structures towards efficient organic photovoltaic devices. Specifically, I will focus on two approaches- one focussed on diblock copolymers and the other focused on using semiconducting nanoparticles for obtaining nanoscale structures. Both these strategies are based in our molecular understanding of the evolution of bulk heterojunction structures.

9:00 AM

Atom Probe Contribution to the Characterization of Cigse Grain Boundaries: *Philippe Pareige*¹; *Emmanuel Cadel*¹; *Francois Couzinie-Devy*¹; *Nicolas Barreau*²; *John Kessler*²; ¹Rouen University; ²IMN

Atom Probe Tomography technique is a nano-scale-sensitive analytic tool allowing 3D chemical analysis with atomic scale resolution. In the present study, high efficiency Cu(In,Ga)Se₂ (CIGSe) thin films have been investigated by APT in order to solve interrogations about grain boundaries (GBs) composition. The analyzed CIGSe layers have been grown by co-evaporation on Mo-coated soda-lime glass substrates following the standard 3-stage process. In order to ensure the presence of GB in the analysed volume, location and misorientation of GBs have been determined by electron backscattering scanning diffraction (EBSD). From APT analyses, spatial distribution of CIGSe elements can be imaged at atomic scale; particular attention has been devoted to the composition profiles at the vicinity of the CIGSe GB interface. New results are compared with usual CIGSe GB passivation models.

9:20 AM

Plasma Sprayed Titanium Oxide-Carbon Nanotube Composite Coating for Dye Sensitized Solar Cells: *Cheng Zhang*¹; Ujwal Chaudhary¹; Santanu Das¹; Samarth Thomas¹; Arvind Agarwal¹; ¹Florida International University

TiO₂ is an attractive material for dye sensitized solar cells (DSSC) because it is inexpensive and non-toxic as compared to the Si-based solar cells. Plasma spraying is an ideal method to produce TiO₂ based DSSC due to its high deposition rate and ease of scale-up. In the present study, TiO₂-carbon nanotube (CNT) based composite is explored as DSSC material. It has been shown in the literature that carbon nanotubes improve the conversion efficiency of DSSC in many ways. This study investigates the role of CNT addition in terms of phase transformation from anatase to rutile, microstructural properties and photocatalytic properties. TiO₂ and TiO₂-CNT coatings are prepared by plasma spraying on the stainless steel and FTO glasses. These composite coatings are characterized by X-ray diffraction and scanning electron microscopy. Photocatalytic properties are studied by the MB solution decomposition test.

9:35 AM

Reaction Based Sintering and Applications for Dye Sensitized Solar Cells: *Sukanya Murali*¹; Dunbar Birnie¹; ¹Rutgers University

Dye sensitized solar cells have the potential for low-cost manufacturing, but one key challenge is finding a low temperature sintering process for the titania electrode that can be employed on plastic substrates. To address this need, we have used reactive alkoxide solutions to fuse matrix particles together at low temperature. We discuss our efforts to understand where the reacted material locates itself within final microstructures. A silica-titania model system was employed to identify the reacted titania in the matrix. SEM studies and surface area measurements give insight into the effect of the matrix particle morphology on the properties and connectivity of the titania reaction product. SEM, AFM and TEM studies and image analysis of silica-titania sub-monolayers enable identification and measurement of the titania neck widths for varying titania precursor amounts. Geometrical calculations relate the interparticle neck radius to solution concentration. Implications for design of reactively sintered systems are presented.

9:55 AM Break

10:25 AM Invited

First-Principles-Based Nanomaterials Design for Solar Energy Storage and Conversion: *Alexie Kolpak*¹; Jeffrey Grossman¹; ¹MIT

Large-scale adoption of solar energy storage and conversion technologies requires development of new materials with enhanced efficiency and low cost. With their penchant for exhibiting novel and/or enhanced properties, nanostructured materials offer myriad promising routes toward the development of such materials. In this talk, I will illustrate the potential of this strategy with two examples. First, I will discuss our first-principles-based design of solar thermal fuels composed of chromophore-derivitized carbon nanotubes. These materials can exhibit volumetric energy densities exceeding Li-ion batteries, potentially enabling practical use of this highly renewable, emission-free, and portable solar energy storage and conversion technology. Second, I will discuss our design of photovoltaic (PV) materials that exploit atomic-scale interface properties to drive electron-hole separation and eliminate defect-mediated recombination. Using first-principles computations, I will demonstrate a nanostructured GaAs-based superlattice that could eliminate the need for expensive, high-purity GaAs, potentially enabling replacement of Si with the more efficient GaAs.

10:55 AM

Doped Titanium Oxide Nanotube Arrays with Enhanced Photocatalytic Properties: *Z. Xu*¹; *Q. Li*¹; *S. Gao*¹; *J. Shang*²; ¹Institute of Metal Research; ²University of Illinois

Photocatalytic nanoarrays have attracted much attention because of their potential applications in the low-cost solar cell devices. In this study, self-organized nanotube arrays were made from titanium oxides doped with both anionic and cationic species to improve the photocatalytic properties of titanium oxide nanoarrays. While the cationic additions demonstrated strong influence on the structure of the nanotube arrays, the anionic dopants, such as nitrogen and fluorine, were found to enhance the visible light absorption and the photodegradation efficiency of organic species under the visible light illumination. The enhanced properties were dependent on both the nanotube structural architecture and chemical doping effect.

11:15 AM

New Numerical Method to Calculate the True Optical Absorption of Hydrogenated Nanocrystalline Silicon Thin Films and Solar Cells: *Fatiha Besahraoui*¹; ¹Oran University

The enhanced optical absorption measured by Constant Photocurrent Method (CPM) of hydrogenated nanocrystalline silicon thin films is due mainly to bulk and/or surface light scattering effects. A new numerical method is presented to calculate both true optical absorption and scattering coefficient from CPM absorption spectra of nanotextured nanocrystalline silicon films. Bulk and surface light scattering contributions can be unified through the correlation obtained between the scattering coefficient and surface roughness obtained using our method.

Fatigue and Corrosion Damage in Metallic Materials: Fundamentals, Modeling and Prevention: Fatigue Life Prediction and Enhancement

Sponsored by: The Minerals, Metals and Materials Society, TMS Structural Materials Division, TMS/ASM: Mechanical Behavior of Materials Committee

Program Organizers: Tongguang Zhai, University of Kentucky; Zhengdong Long, Kaiser Aluminum; Peter Liaw, University of Tennessee

Tuesday AM
March 13, 2012

Room: Oceanic 6
Location: Dolphin Resort

Session Chairs: Richard Gangloff, University of Virginia; Nikhilesh Chawla, Arizona State University

8:30 AM Invited

Probabilistic Property-Life Mapping Based P-S-N Experiment Principle of Small Samples: *Liyang Xie*¹; Jianzhong Liu²; ¹Northeastern University, Shenyang, China; ²Beijing Aeronautic Materials Institute

Based on probabilistically mapping from material property to fatigue life, presented is the principle and method of small sample P-S-N experiment programming and statistically data treatment technique. By integrating the life distribution information at different stress levels, P-S-N equation can be acquired satisfactorily from small samples. The principle and method are based on the existence of the relationship between life distribution and stress level. The key to determine P-S-N equation is to obtain the life standard deviation – cyclic stress relationship, and the opinion to determine this relationship is first to determine the mean life – stress level relationship by test data and assume a reasonable std-stress equation. According to the assumed relationships, tested fatigue lives at different stress levels can be converted into the equivalent lives at the first high stress levels. The relationship can be determined when the equivalent life distribution is identical to the tested life distribution.

TUESDAY AM



TMS 2012

141st Annual Meeting & Exhibition

TUESDAY AM

8:50 AM

A Probabilistic Approach to Modeling Fatigue Life Variation: *Julian Raphael*¹; Peter Liaw²; Wei Wu²; ¹J R Technical Services, LLC; ²The University of Tennessee

A method of estimating the fatigue-life variation is presented. The approach consists of introducing finite element results and probabilistic material property simulations into a fatigue or fatigue-crack-growth model and then analyzing the data to develop the cumulative distribution function for life expectancy. The justification for this approach stems from the fact that many empirically-derived material constants, such as the fatigue-ductility exponent and the fatigue-ductility coefficient, are calculated by linear regression of a data set whose correlation coefficient is less than unity. The application of the fatigue-life prediction methodology will be discussed.

9:10 AM

A Non-Linear Damage Accumulation Fatigue Model for Predicting Strain Life at Variable Amplitude Loadings Based on Constant Amplitude Strain Fatigue Data: *Peter Huffman*¹; Scott Beckman¹; ¹Iowa State University

A novel technique for predicting fatigue life from a variable amplitude strain history using constant amplitude loading data is presented. A critical feature of this reversal-by-reversal model is that the damage accumulation is inherently non-linear. The damage from the next reversal in the variable amplitude loading is predicted by approximating the accumulated damage as coming from constant amplitude loading that has the same strain as the next variable amplitude cycle. A key result of this approach is that overloads at the beginning of the strain history have a much more substantial impact on the total lifetime. The predictions made by this model are compared to experimental results, as well as the predictions made by other methods. This technique effectively incorporates the strain history in the damage prediction and has the advantage over other methods in that there are no arbitrary fitting parameters that require substantial experimental data.

9:30 AM

Fatigue Life Prediction of Friction Stir Welded Profiles: *Meysam Mahdavi Shahrri*¹; Torsten Höglund¹; Rolf Sandström¹; ¹Royal Institute of Technology

Friction Stir Welding (FSW) is a low heat input solid state welding technology especially suitable for low melting point metals. FSW technology is seen as providing superior joint integrity compare to those with conventional welding procedures. Euro code 9 is a standard code for fatigue assessment of aluminium structures. However Euro code 9 covers aluminium alloys and welded structures with conventional welding methods but not those with FSW procedure. In the present paper euro code 9 is used to estimate the fatigue life time for different FS welded extruded hollow aluminium profiles. The present study compares fatigue test results from friction stir welded joints with fatigue curves for traditional fusion welded joints in Al 6005 and base material. The result falls in a good agreement with experimental data and FEM predictions. This suggests that Euro code 9 can be used for fatigue assessment of FS welded joints.

9:50 AM

Neural Network Fatigue Life Prediction in Notched Bridge Steel I-Beams from Acoustic Emission Amplitude Data: *Eric Hill*¹; Fady Barsoum¹; Jamil Suleman¹; Andrej Korcak¹; Yi Zhang¹; ¹Embry-Riddle Aeronautical University

Ten notched A572-G50 bridge steel I-beams were transversely loaded in three-point bending, and back propagation neural network (BPNN) fatigue life predictions were performed on the acoustic emission (AE) amplitude histogram data taken during fatigue cycling. BPNN fatigue life predictions based on the AE data from the first (0-25%), second (25-50%), and third (50-75%) quarters of the fatigue life data yielded worst case errors of 18.4%, 16.8% and 5.3%, respectively, for training on five beams and testing (predicting) on the remaining five. The worst case prediction errors decreased to -12.4%, -13.4%, and 4.5% when trained on the AE

data from six beams and tested on four. Thus, it was found that BPNN prediction accuracy was improved both by using more training data (six beams rather than five) and by training on AE data taken later (third quarter) in the fatigue life of the notched I-beams.

10:10 AM Break

10:20 AM

Effect of Laser Shock Peening (LSP) on the Fatigue Behavior of Ti-6Al-4V ELI Alloy: *Sagar Bhamare*¹; Sethuraman Subramanian¹; James Guenes¹; Leonora Felon²; David Kirschman²; Seetha Ramaiah Mannava¹; Dong Qian¹; Vijay K. Vasudevan¹; ¹University of Cincinnati; ²X-Spine Systems Inc.

Based on current bio-medical research that suggest that spinal implants with greater flexibility increase healing rate of spinal fusion, a novel implant rod, made from Ti-6Al-4V ELI was designed to replace current rigid rod, with aim of increasing flexibility and simultaneously enhancing the fatigue strength by applying laser shock peening (LSP) process. Residual stresses generated by LSP were measured using X-Ray diffraction and simulated using finite element method. Residual stress profiles are discussed. Results of four-point bending fatigue tests of both untreated and LSP-treated flexible rods are presented and compared with current design. Additionally, fracture surface of failed samples were characterized by scanning electron microscopy to elucidate the fatigue crack initiation and growth mechanisms. It is found that LSP increases fatigue life of novel design. A strain-life based fatigue life prediction model was developed to simulate fatigue life estimates of LSP treated rods. Effectiveness of life prediction model is discussed.

10:40 AM

Fatigue Behavior of Laser Shock Peened (LSP) Ti6242 Alloy: *Gokulakrishnan Ramakrishnan*¹; Vibhor Chaswal¹; James Guenes¹; Kristina Langer²; Dong Qian¹; S.R. Mannava¹; Vijay.K. Vasudevan¹; ¹University of Cincinnati; ²Air Force Research Laboratory/RBSM, WPAFB

LSP is known to dramatically improve fatigue life by introducing deep residual stresses. Since residual stress is prone to relaxation under thermal and/or mechanical loading, understanding the thermal stability of fatigue life is important. Aerospace alloy Ti6242 was LSP'd using different conditions and the residual stresses were characterized by conventional XRD. Near-surface microstructures and local properties were studied using SEM and nano/micro indentation. The thermal stability of residual stress and microstructure were assessed over a range of temperatures and times. Kinetics of relaxation is modeled using a Zener-Avrami-Wert approach. Static and fatigue tests were conducted at room temperature on the unpeened, LSP-treated and LSP-treated + thermally aged specimens with and without a notch in 3-Point Bend geometry. The fracture surface was subsequently examined by SEM to identify the effect of LSP on crack initiation and growth. The results of the effects of LSP on the fatigue behavior are presented.

11:00 AM

Effect of Grinding Residual Stress on Fatigue Performance of Crankshaft: *Mahesh Dhumal*¹; Ramchandra Prasad²; Suresh Arangi¹; ¹Bharat Forge Limited; ²Department of MEMS, Indian Institute of Technology Bombay

In this study, effect of grinding residual stress on fatigue performance of crankshaft has been investigated. The coolant flow rate during grinding was varied to get different values of surface residual stress. The surface residual stress was measured by using the X-ray diffraction technique. Surface residual stress was further correlated with Barkhausen Noise Analysis (BNA) signal. A consistent increase in surface residual stress and BNA signal was observed with decrease in coolant flow rate. Experimental test results showed that the crankshaft ground with maximum coolant flow rate (52 Lit/min) have compressive residual stress at the surface and enhanced fatigue strength. Micromechanism of fracture surface showed that crankshaft with surface compressive residual stresses (406 MPa)

had crack initiation at the interface of induction hardened layer and core. On the contrary crack had initiated from surface when surface residual stresses (309 MPa) were tensile in nature.

11:20 AM

Effects of Ultrafast Laser Micromachining on Structure and Mechanical Properties of 316 LVM Stainless Steel: *Hossein Lavvafi*¹; John Lewandowski¹; Janet Gbur¹; Dave Dudzinski²; Melissa Young²; David Schwam¹; John J Lewandowski¹; ¹CWRU; ²Cleveland Clinic Foundation

Medical devices, such as guide wires, valves, needles, and stents increasingly demand smaller devices made with difficult to machine materials. Some applications often include fine details that are impossible to achieve with rotary tool machining. As a result, there is greater interest in the use of laser machining. Damage caused to the surface while using laser machining can affect the performance of the components. As devices shrink in size, the greater is the need for athermal manufacturing processes. In this study different type of laser with different pulse width were used to machine AISI 316 LVM biomedical grade wires. The mechanical behavior of these wires were evaluated in uniaxial tension, and in cyclic strain-controlled fatigue with the use of a flex tester operated to provide fully reversed bending fatigue. The effects of laser input energy and pulse width on surface quality and subsequent mechanical response will be reported along with plans for future work.

11:40 AM

Fatigue Response of Aluminium Alloy 7075-T6 Bolted Plates at Flight Environmental Conditions: *Reza Hashemi Oskouei*¹; Raafat Ibrahim¹; John Mikhail¹; ¹Monash University

In this paper, fatigue life of aluminium alloy 7075-T6 bolted plates has been studied at flight temperatures. In order to investigate the effect of the environmental temperature on the fatigue life of both lightly and firmly bolted plates, the specimens were clamped with two different tightening torques and then fatigue tested at ambient (25° C), low (-50° C) and high (60° C) temperatures. Both the lightly and firmly bolted plates experienced more fatigue cycles at -50° C. However, the fatigue behaviour at 60° C was different compared to ambient temperature depending on the amount of applied clamping force.

From Macro to Nano, Understanding Mechanical Behavior across Length Scales: A Structural Materials Division Symposium in Honor of Robert Ritchie: Amorphous and Nanocrystalline Materials

Sponsored by: The Minerals, Metals and Materials Society, TMS Structural Materials Division, TMS/ASM: Mechanical Behavior of Materials Committee, TMS: Biomaterials Committee

Program Organizers: Jamie Kruzic, Oregon State University; Brad Boyce, Sandia National Labs; Reinhold Dauskardt, Stanford University

Tuesday AM
March 13, 2012

Room: Mockingbird 1
Location: Swan Resort

Session Chairs: Brad Boyce, Sandia National Laboratory; Reinhold Dauskardt, Stanford University

8:30 AM Introductory Comments

8:35 AM Keynote

Fracture and Mechanical Behavior of Hybrid Molecular Glass Films: Experiments and Computational Models: *Reinhold Dauskardt*¹; ¹Stanford University

Hybrid organic-inorganic glass films exhibit unique electro-optical and mechanical properties and have application in emerging nanoscience and energy technologies. We describe computational methods to address the

fundamental relationship between their molecular structure and resulting mechanical and fracture properties. Using molecular dynamics and a simulated annealing approach, large distortion-free hybrid glass networks with well-controlled network connectivity can be generated. With this capability along with a novel fracture model and molecular dynamics simulations of elastic deformation, we elucidate the critical effect of network connectivity and nanoporosity on mechanical properties. The accuracy of our computational tools is confirmed through comparison to synthesized hybrid films where the molecular structure, connectivity and nanoporosity is carefully controlled. Having predictive models for how molecular structure affects mechanical properties offers the opportunity for computational design of new hybrids and provides a quantitatively accurate rationale for guiding precursor selection and the molecular design of hybrids with exceptional mechanical properties.

9:15 AM Keynote

Microstructure and Stress State Effects on Fracture of Novel Materials: *John Lewandowski*¹; ¹Case Western Reserve Univ

The presentation will review the effects of changes in microstructure and/or stress state on the fracture mechanisms of a variety of novel materials. Examples will be taken from work at CWRU with former and present students on composites, metallic glasses, and nano-composite materials. Microstructures can be varied from the micro- to nano-scale depending on processing conditions while changes in stress state can be accomplished via notches, superimposed pressure, and other novel test techniques that can help to delineate the micromechanisms of failure in the manner utilized by Prof. Ritchie and students/collaborators over the years.

9:55 AM

Thermography Study on the Temperature Evolution of Bulk Metallic Glasses under Monotonic and Cyclic Loading: *Peter Liaw*¹; Gongyao Wang¹; B. Yang²; Y. Yokoyama³; C. T. Liu⁴; A. Inoue³; ¹University of Tennessee; ²Shell Company; ³Tohoku University; ⁴City University of Hong Kong

In-situ monitoring the mechanical damage of the structural materials is important for controlling the failures. Temperature patterns in the structural materials serve as significant fingerprints during loading. The infrared (IR) camera is an excellent tool to study the failure mechanism of the structural materials. Bulk metallic glasses (BMGs) are good candidates for the structural applications because of their great mechanical behavior. In our lab, a state-of-art IR thermography camera is employed to monitor the temperature evolutions in shear bands and cracks of BMGs under monotonic and cyclic loading. With the understanding of the temperature evolutions during mechanical testing, thermography could provide the direct information and evidence of the stress-strain distribution, shear-band formation and growth, and crack initiation and propagation. In-situ visualizations and qualitative and quantitative analyses have been performed through thermography results. Theoretical models are developed to understand the deformation mechanisms of BMGs under monotonic and cyclic loading.

10:10 AM

R-Curve Behavior of Zr-Ti-Cu-Al Bulk Metallic Glass with Extraordinary Fracture Toughness: *Jian Xu*¹; Qiang He¹; Evan Ma²; ¹Institute of Metal Research, Chinese Academy of Sciences; ²Department of Materials Science and Engineering, Johns Hopkins University

In this work, we demonstrate a $Zr_{61}Ti_2Cu_{25}Al_{12}$ (ZT1) bulk metallic glass (BMG) that simultaneously combines all the desirable properties including the reasonable cost, robust glass-forming ability, high strength ($\sigma_{63} = 1600$ MPa) and high fracture toughness ($K_{JIC} = 133$ MPa \sqrt{m}). In terms of ASTM standard for J-R curve test procedures, R-curve of this BMG was determined, showing K_J as high as ~ 230 MPa \sqrt{m} , comparable to the toughest (Pd-based) BMG recently developed by Caltech. $Zr_{61}Ti_2Cu_{25}Al_{12}$ BMG exhibits a remarkable resistance to crack growth, which results from the crack-tip blunting by multiple-shear events and crack deflection during propagation. As revealed, apparent crack extension



TMS 2012

141st Annual Meeting & Exhibition

under loading for the fatigue pre-crack consists of two contributors, shear-off zone with $\approx 150 \times 181 \mu\text{m}$ in length caused by multiple-shear events and subsequent real sub-critical crack propagation.

10:25 AM Break

10:40 AM

Fatigue-Induced Grain Growth as a Precursor to Crack Nucleation: Brad Boyce¹; Henry Padilla¹; ¹Sandia National Labs

Grain growth is traditionally thought of as a thermally-driven diffusional process. However, even at and below room temperature, nanocrystalline metals can undergo mechanically-induced grain growth. This process is distinct from dynamic recrystallization which is typically thought of as a high-temperature process. The abnormal grain growth process can be induced by monotonic loading at high stresses, or can occur at lower stress under cyclic fatigue loading. In our recent examination of three nanocrystalline nickel alloys, we have consistently observed fatigue-driven grain growth as a precursor to crack initiation, suggesting the possibility of a sequential two-step process. This detrimental fatigue-induced coarsening process may behave athermally, and may not be impeded by traditional metallurgical stabilizers such as solutes or pinning particles. Sandia is a multiprogram laboratory operated by Sandia Corporation, a Lockheed Martin Company, for the United States Department of Energy's National Nuclear Security Administration under contract DE-AC04-94AL85000.

10:55 AM

The Role of Free and Grain Boundary Surfaces in the Fatigue of Nanostructured Metals: Christopher Muhlstein¹; ¹The Pennsylvania State University

Nanostructured, thin, metallic films often exhibit high yield and ultimate strengths (i.e., gigapascals in magnitude) that are accompanied by undesirable strain rate sensitivity, low fracture toughness, and poor resistance to fatigue crack growth. These properties have often been attributed to the most obvious structural features of the materials – their grain boundaries. However, emerging evidence suggests that thin film and grain morphology contributions to fracture and fatigue mechanisms are distinct and can often be described by existing (macroscopic) theories. In this presentation I will review the deformation, fracture, and fatigue behavior of platinum to illustrate how various surfaces control crack growth in face-centered cubic metal films.

11:10 AM

The Mechanical Behavior of Highly Nano-Twinned Cu: Andrea Hodge¹; Timothy Furnish¹; Troy Barbee²; ¹University of Southern California; ²Lawrence Livermore National Laboratory

The ductility and plastic flow behavior of highly aligned nanotwinned copper produced by interrupted magnetron sputtering is presented. Tensile tests were performed at various strain rates at both room and liquid nitrogen temperatures. Higher ductility and strength are reported for all samples tested at 77K. The observed inhomogeneous deformation and shear band propagation are discussed as a function of the testing temperature, decreasing heat capacity at 77K and the low initial dislocation density which leads to a yield peak. Uniformly distributed mobile dislocations introduced by rolling to 20% reduction in thickness eliminated the yield point at both temperatures. The experimental observations clearly demonstrate that the observed yield-point behavior is a direct result of the very low initial dislocation density in these sputtered films as expected for "ideal" nanoscale microstructural materials.

11:25 AM

Mechanical Properties of Nanotwinned and Nanolayered Metal Films: Xinghang Zhang¹; Yue Liu¹; Daniel Bufford¹; Haiyan Wang¹; ¹Texas A&M University

Nanotwinned metals are attractive as twin interfaces enable high strength and ductility, excellent electrical conductivity and thermal stability. Twin interface is identified in a variety of sputtered fcc metals, such as 330 stainless steel, Cu and Ag films. Both coherent {111} and incoherent

{112} twin boundaries are observed. Average twin spacing, on the order of $\sim 10 \text{ nm}$, can be achieved by varying deposition conditions. Twin interfaces are effective barriers to the transmission of dislocations, and thus lead to high strength in monolithic metals. Meanwhile twin interfaces are effective sources and sinks for dislocations during deformation. In situ nanoindentation studies reveal that certain twin interfaces are mobile during deformation due to rapid movement of Shockley partials, and consequently detwinning occurs. Finally strengthening mechanisms in highly textured Cu/Ni multilayers will be discussed, wherein both twin and layer interfaces are proven essential in tailoring the mechanical properties of multilayers.

11:40 AM

A Comparative Study of the Mechanical Properties and Fracture of Nanocrystalline (20 nm), Ultrafine Grained (100 nm) and Coarse Grain Polycrystalline ($> 1 \mu\text{m}$) Ni: Indranil Roy¹; Farghalli Mohamed²; ¹Schlumberger; ²University of California, Irvine

A number of alternatives, often competing, are responsible for the plastic deformation and fracture of crystalline solids. Traversing the length scale of its grain size, from nanocrystalline to microcrystalline we present in this study a comparative analysis of mechanical properties and fracture morphology of nanocrystalline (20 nm), ultrafine-grained (100 nm) and coarse grain polycrystalline ($> 1 \mu\text{m}$) Ni. Salient observations of the low temperature mechanical behavior and deformation mechanism for ED nc-Ni having average grain sizes of 20 and 100 nm were (a) deformation mechanism started as a local ductile fracture manifested by coalescence of nano / micro dimples with a sudden transition to a brittle mode (b) while work hardening had minimal or no response to the increasing test temperature ($T < 0.25 T_m$), it was observed to increase with increasing strain rate, however this was more pronounced for the specimens with smaller average grain size of 20nm.

Integrative Materials Design: Performance and Sustainability: Processing and Properties of Advanced Steels & Sustainable Design, Life-Cycle Analyses, and Recycling

Sponsored by: The Minerals, Metals and Materials Society, TMS/ASM: Mechanical Behavior of Materials Committee
Program Organizer: Diana A. Lados, Worcester Polytechnic Institute

Tuesday AM
March 13, 2012

Room: Europe 2
Location: Dolphin Resort

Session Chair: Diana Lados, Worcester Polytechnic Institute

8:30 AM Invited

Innovation in the Manufacturing of Powder Forged Automotive Connecting Rods: Ian Donaldson¹; ¹GKN Sinter Metals LLC

Powder metallurgy is a proven manufacturing method that owes its market penetration on being a sustainable manufacturing method coupled with the ability to tailor properties through materials and microstructures not achievable via competing technologies. Powder forging (P/F) is a fully dense, well-established method for manufacturing automotive connecting rods. Recent requirements for lighter and higher output engines has led to demands for lighter weight and higher fatigue endurance connecting rods with no degradation in machinability. With the traditional P/F Fe-Cu-C material system, this could be achieved by hardening through phase transformation, but that would result in poor machinability, raising total cost significantly. This study introduces a novel approach for using pre-alloyed Cu to avoid heat treatment or increased processing temperatures while improving chemical homogeneity and mechanical properties over traditional admixed compositions. Aspects of sustainability and integrated design with application of the new alloys will also be presented and discussed.

8:55 AM

New Concepts for Damage Tolerant Steels for High Performance Components:

*Margarita Bambach*¹; Hans Henning Dickert¹; Wolfgang Bleck¹; ¹RWTH Aachen University

Failure within the guarantee terms of high performance components such as gear wheels and bearings leads to high warranty costs. In order to prevent premature failure, fail-safe, damage tolerant steels with a high bearing capacity are necessary. Macroscopic failure is usually caused by effects occurring on a microscopic scale, such as crack initiation at non-metallic inclusions. Much effort has been invested in improving the purity grade of the applied steels. However, purity has already reached its technological-economical limits. This work focuses on the development of damage tolerant steels as an alternative to conventional methods for improving the life time of high performance components. Using a suitable combination of strengthening mechanisms, a high-strength, yet ductile matrix with a high work hardening potential will be developed. Thus, stress concentrations at inclusions can be reduced via plastic deformation. As a result, preliminary failure may be avoided and warranty costs may be kept low.

9:15 AM

Design of Novel Steels with Reduced Density:

*Jonas Schwabe*¹; Wolfgang Bleck¹; Henning Dickert¹; Alexander Zimmermann¹; ¹RWTH Aachen

Steels with reduced density enable considerable weight reductions and therefore enable important economical and ecological savings e.g. in transportation industries. High additions of aluminum provoke a great density reduction and increase the strength of the steels as well. However, the unsatisfactory ductility of the high aluminum steels produced so far does not allow industrial mass applications. The present research describes the design of cold rolled flat steels with density reductions of up to 13% - while maintaining a substantial ductility of minimum 20% fracture strain at strengths up to 600 MPa. The combination of their mechanical and physical properties makes these materials attractive for many applications, especially in the automotive industry. Therefore, tests of the corrosion behavior, the deformation behavior under crash conditions, the deformation behavior at low and at high temperatures, the coating behavior as well as tests concerning the applicability of continuous casting were carried out.

9:35 AM

Effect of Pretreatment on the Strength and Formability of Vehicle Hot-Forming Martensitic Steels:

*Ying Chang*¹; Yipeng Gao²; Ping Hu¹; Liang Ying¹; Zhaohuan Meng¹; Yunzhi Wang²; ¹Dalian University of Technology; ²OSU

The stress-induced martensitic transformation in steel sheet (Fe-1.3wt%Mn-0.003wt%B-0.8wt%RE, 1.6mm thickness) during hot-forming could improve not only its strength and hardness, but also its formability. Based on experimental testing, theoretical analysis and calculation results, optimal properties (including formability) of the high strength steel (HSS) could be achieved by a rapid-cooling pretreatment to the austenite before hot-forming to enhance the stress-induced martensitic transformation during forming. Comparing with the traditional hot-forming HSS, the microstructure obtained in the pretreated samples consists of more uniform, finer lath martensite and retained austenite. The yield strength of the samples is greater than 1000 MPa, the tensile strength is over 1500 MPa, and the hardness is greater than HV435. No fracture bands are formed during forming. As a consequence of the high strength, the sheet thickness can be reduced up to 35% for automobile applications.

9:55 AM

The Contribution of Niobium Bearing Steels and Enhanced Sustainability:

*Steven Jansto*¹; ¹CBMM-Reference Metals Company

With the ever-growing concern for the environment and resource sustainability, the application of advanced high strength Nb-bearing steels for numerous high strength steel applications have been shown to reduce resource usage and improve the carbon footprint. The conservation

and more efficient use of ironmaking and steelmaking raw materials is a global issue for all steel producers. Recent Nb-microalloyed steel applications provide a more efficient product design, reduced steelmaking emissions and less energy consumption per tonne of steel. A sustainability structural steel study presents the positive cost and environmental impact of Nb-microalloyed steel applications. The analysis compares the CO₂ emission reduction and energy savings in the steelmaking process melted via the Basic Oxygen Furnace (BOF) versus the Electric Arc Furnace (EAF) route. The application of Nb-microalloyed structural steels offer the opportunity to reduce the total weight of a given structure, such as a bridge, compared to non-microalloyed steel construction.

10:15 AM Break

10:40 AM Invited

Resource Recovery and Recycling of Materials: Mini-Mills of the Future:

*Diran Apelian*¹; ¹Worcester Polytechnic Institute

Consumption of material goods has created a large supply of scrap that unfortunately is mostly downgraded. The value of scrap is likewise undervalued and sold to various sources, many of them overseas markets. The scenario that exists today is untenable for environmental and economic reasons. The scenario that is sustainable and tenable is to recover and recycle by upgrading our scrap. Mini-Mills that utilizes 100% scrap that are intelligently sorted and processed is the path that we need to follow to produce metallic components. A system analysis for mini mills for light metals will be presented and discussed.

11:05 AM Invited

Engineering Solutions for Sustainability: Materials & Resources:

*Brajendra Mishra*¹; ¹Colorado School of Mines

Integrated engineering solutions to societal challenges in the transportation, energy, recycling, housing, food, water, and health sectors will be discussed. Specific outputs will include: The nucleus of a consensus definition of sustainability as it applies to engineering to provide a common basis for deliberation and action among various disciplines; Delineation of six critical overarching themes for engineering sustainability that provide a unifying framework in formulating strategy and implementing solutions within a diversity of challenges, issues, and stakeholders; Development of a draft Technology and Resources Matrix, designed as a communication tool for guiding research and policy actions within various engineering disciplines. These and other concepts and tools developed through this project lay the foundation for a productive, interdisciplinary dialogue and are intended for use by professional societies, educators, industry leaders, and policy makers to continue building a truly integrated sustainable engineering model.

11:30 AM Invited

Limited Materials Availability: Considering the Importance of Materials Market Dynamics:

*Randolph Kirchain*¹; Elisa Alonso¹; Frank Field¹; ¹Massachusetts Institute of Technology

Discussions about the sustainability of materials consumption have become increasingly prevalent. Popular media has even begun to ask: will we run out of X? Economic theory suggests otherwise, but this does not mean that materials availability does not present a risk to specific industries or technologies. This presentation will discuss how disruptions to materials availability can impact industry; methods for screening for those risks; and strategies for mitigating risk – including the redesign of materials and products. Case studies of materials critical to the future of the automotive and energy supply industries will be discussed. These cases point to the importance of market dynamics, including the price sensitivity of supply and demand, in establishing ultimate economic risk from limited availability. Results of selected dynamic market modeling will be used to demonstrate the value materials and materials process design to mitigating the risk of limited materials availability.



TMS 2012

141st Annual Meeting & Exhibition

TUESDAY AM

11:50 AM Invited

Development of Aluminum Dross Based Material for Engineering Applications: *Chen Dai*¹; *Diran Apelian*; ¹WPI

In order to channel Al dross towards an appropriate engineering application, two different types of dross waste were selected from industrial production streams for characterization. Physical and chemical tests indicated that dross waste may be applied directly but better processed with boiled water to reduce crack-causing gases which form during the hydration reaction. Mechanical property evaluations revealed the possibility for dross waste to be utilized as filler in concrete, resulting in 25% higher flexural strength and a 5% higher compressive strength compared to pure cement. In addition, comparisons were carried out between similar size and fraction of dross powder and sand additions to concrete; the results indicate that fine dross powder had a positive effect on mechanical properties of concrete vs. to additions of sand. The opportunities to utilize a waste material as for engineering applications for construction materials will be reviewed and discussed.

12:10 PM Invited

Increasing Use of Secondary Materials in Production Planning: *Elsa Olivetti*¹; *Randolph Kirchain*¹; *Gabrielle Gaustad*²; ¹MIT; ²Rochester Institute of Technology, Rochester, NY

Increasing the efficient use of secondary (i.e. recycled) resources provides one strategy in moving towards sustainable consumption. Secondary recovery enables energy saving benefits, forestalls depletion of non-renewable resources and avoids the deleterious effects of extraction and beneficiation (recycling does add some impacts of its own). There are several barriers to increased use of secondary materials, particularly in metal systems, that can be addressed through innovative production processing and alloy product design. This presentation will discuss a few of those options including control of incoming compositional variation in secondary materials through explicit incorporation of uncertainty, robust long term batch planning to mitigate compositional accumulation and informed alloy design towards recycling friendly alloys. Research has shown that explicit consideration of operational uncertainties and alloy design that considers the impact of recycling through the use of stochastic programming in production planning can increase the use of secondary materials.

International Smelting Technology Symposium (Incorporating the 6th Advances in Sulfide Smelting Symposium): Current and Emerging Smelting Technologies

Sponsored by: The Minerals, Metals and Materials Society, The Metallurgy and Materials Society of CIM, TMS Extraction and Processing Division, TMS: Pyrometallurgy Committee

Program Organizers: Jerome Downey, Montana Tech of the Univ of Montana; Thomas Battle, Midrex Technologies, Inc.; Jesse White, Elkem Solar Research

Tuesday AM
March 13, 2012

Room: Northern A3
Location: Dolphin Resort

Session Chair: To Be Announced

8:30 AM

The Path to Technology Development, Ralph Baggaley and the Evolution of Copper Smelting Technology: *Larry Southwick*¹; *Ralph Yardley*²; ¹L.M. Southwick & Associates; ²Yardley & Associates

Ralph Baggaley, a Pittsburgh industrialist and associate to George Westinghouse, was instrumental in developing the basic lining and numerous operating features of what became known as the Peirce Smith copper converter. Beginning in the late 1890's Mr. Baggaley conducted

literature, laboratory and larger scale research, acquired and was awarded numerous patents, and visited many operating facilities. A book he wrote responding to examiner comments regarding one of these patents, as well as several other documents provide a unique light into the innovation process as practiced by this uniquely creative man. This paper will review and discuss Baggaley's critique of copper converting technology as it existed and was practiced around the turn of the century, and how he came to form, defend and prove his ideas and concepts. One of the authors, Yardley, is Mr. Baggaley great grandson and provided the information which is the core and genesis of this study.

8:55 AM

Processing of Lead, Zinc, Copper and Nickel Concentrates - The Xstrata Technology Approach: *Gerardo Alvear Flores*¹; ¹Xstrata Technology

Processing of copper, zinc, lead and nickel concentrates is becoming more challenging due increasingly complex mineralogy. Smelters are required to modify their operating flowsheets and strategies to process more complex feed materials economically while meeting stricter environmental regulations. Xstrata operates mines, smelters and refineries around the world. It has developed a number of innovative technologies at various operating sites that provide an economic solution for the production of base metals and silver. These technologies include ISASMELTTM TSL, ISACONVERTTM TSL, IsaKiddTM Tankhouse Technology, BBOCTM and Albion leach technologies. This paper describes process flow sheets that demonstrate how Xstrata's technologies can be combined to treat complex feed materials.

9:20 AM

Ferroalloy Research in Norway – Cooperation between Academia and Industry: *Merete Tangstad*¹; ¹NTNU

In Norway the ferrosilicon/silicon- and ferromanganese- production is strong with a world market of 4 % / 9 % and 4 % respectively. The research and development work in the academia mirrors the national interest, and hence, there has been an extensive research in the academia within these areas. There are some vital drivers and premises for a successful cooperation. The main driver is a win-win situation for both the industry as well as the academia. For the industry this could be cost-, competence- or environmental- benefits and for the academia, building of competence, educate more students as well as possibilities to publish are important drivers. The results from the cooperation in Norway are basic knowledge regarding thermodynamic- and kinetic-data, as well as reaction mechanisms within core processes. Now, the main interests are the challenges within depletion of raw materials as well as environmental issues.

9:45 AM

Status of the Alcoa Carbothermic Aluminum Project: *Christina White*¹; *Øyvind Mikkelsen*¹; *David Roha*²; ¹Alcoa Norway ANS; ²Alcoa Technical Center

Significant resources have throughout the years been spent in the investigation of production of aluminium by carbothermic reduction. Due to the technological challenges involved the efforts have not yet resulted in a commercial process. An initiative to overcome issues that prevented previous attempts to succeed was taken by Alcoa through the Advanced Reactor Process. The research program has resulted in technical developments which have resolved many of the previous issues. Also the knowledge about the process has continuously improved through physical and computer modeling as well as by experimentation at various scales. The technical achievements together with improved process understanding have resulted in a reactor design able to continuously operate the process for several weeks at the time, with hundreds of kilograms of alloy in every tap. This paper gives an overview of the status of the project, the modeling efforts done and the remaining technical challenges.

10:10 AM Break

10:25 AM

Outotec's Smelting Solutions in Non-Ferrous Metals Production: *Asmo Vartiainen*¹; *Outotec Oyj*

Outotec has in its portfolio a wide variety of smelting solutions for non-ferrous metals. These include flash smelting for primary copper and nickel, flash converting for copper, Ausmelt TSL technology for primary and secondary copper, and for Ni, Sn, Pb, Zn residues and waste, Kaldo TBRC technology for secondary copper, lead and precious metals recovery, slag cleaning technology etc. Outotec provides complete tailored process solutions for customers' needs. Decades of experience have resulted in extensive metallurgical know-how that ensures the most profitable process choice and its optimal performance. Outotec's life cycle technology partnership with the customer spans from the early stages of the process solution design all through the supply and commissioning of the entire process chain with integrated process control and holistic service and support concept. Continuous research and development ensure that the customer is provided with the latest advancements in process and equipment solutions.

10:50 AM

Atlantic Copper PS-Converters: A Continuous Commitment to the Future: *Antonio Martin*¹; *Jesús Hurtado*¹; *Francisco Jimenez*¹; *Atlantic Copper SA*

Atlantic Copper is one of the largest copper producers in Europe. Its production facilities, including a primary copper smelter and an electrolytic refinery, are located in Huelva, on the South-West coast of Spain. These installations enable the smelting of over 1 million tpy concentrates to produce up to 260 ktpy of cathodes and 900 ktpy of sulphuric acid. Since the commissioning in 1970 until today, continuous improvements have been made at the PS-Converters such as several improved designs of primary hoods and scrap chargers, blast air control system, operation with OPC online analysers, design of secondary hoods and other environmental projects. All these modifications have been aimed at increasing the capacity of our smelter while keeping a continuous environmental commitment. This paper describes the modifications and improvements carried out over the years at the Converters and the proposals for future developments at Atlantic Copper

11:15 AM

Improvements on Converter Operating Practice at Mufulira Smelter, Zambia: *John Sakala*¹; *Jeyapandian Sasikumar*¹; *Sydney Kwalela*¹; *Mopani*

With the commissioning of the 850,000 tonnes of Concentrate treated per annum capacity Isasmelt in September 2006 the Converter section became a bottleneck to the high throughput. Over 25% of the Isasmelt downtime was attributed to lack of Converter space. Areas that were negatively affecting converter operations were low Tuyere line campaign lives which were averaging 150 blows, high reverts generation, low blister copper conversion rates and high converter cycles time. As a result of the interventions carried out, Converter Campaign lives were increased to over 250 blows, Reverts generation was reduced from 22% to 14% of new concentrate treated, Blister Copper conversion rate was increased from 15tph to 19tph and the blowing time was reduced from 5.7 hours to 4.7 hours.

Magnetic Materials for Energy Applications II: Permanent Magnets for Energy Applications

Sponsored by: The Minerals, Metals and Materials Society, TMS Electronic, Magnetic, and Photonic Materials Division, TMS: Magnetic Materials Committee

Program Organizers: Raju Ramanujan, Nanyang Technological University; Francis Johnson, GE Global Research; S Guruswamy, Univ. of Utah; J Liu, Electron Energy Corporation

Tuesday AM
March 13, 2012

Room: Europe 10
Location: Dolphin Resort

Session Chairs: Raju Ramanujan, Nanyang Technological University; Jinfang Liu, Electron Energy Corporation

8:30 AM Introductory Comments

8:35 AM Invited

Novel Synthesis of Rare Earth Permanent Magnets for Energy Applications: *Raju Ramanujan*¹; *P Deheri*¹; *S Bhame*²; *Nanyang Technological University*; *Univ. of Liege*

Superior high performance permanent magnets are vital in an enormous variety of energy generation and utilization applications, they can reduce energy consumption and increase energy efficiency. There is also a sustainability and strategic need to reduce rare earth content. Hence, novel synthesis techniques were studied, advantages of chemical synthesis include facile elemental substitution and the ease of obtaining nanoparticles. Challenges arise from high reactivity and differences in electrochemical behavior. Chemical synthesis by sol-gel, auto-combustion and microwave based methods were studied. In the sol-gel method, Nd-Fe-B gel was prepared and annealed to produce mixed oxide powders. Hard magnetic Nd₂Fe₁₄B nanoparticles were prepared from these oxides by three step reduction-diffusion. The Henkel plot revealed exchange coupling. The synthesis of exchange coupled 10 nm magnetic nanoparticles by glycine nitrate auto combustion, followed by reduction diffusion, was also carried out. These results and the magnetic properties will be discussed in the presentation.

9:05 AM Invited

High Performance Magnets with Less or No Rare Earth: Challenges and Opportunities: *Jinfang Liu*¹; *Electron Energy Corporation*

China controls over 95% of the rare earth (RE) market, and recently, started to regulate its rare earth industry by introducing environmental protection policies, shutting down small rare earth mining operations, and imposing export quotas. Reduced supply and increased demand have increased the cost of some RE metals by 300 to 500% in the last 12 months, the most unstable being the price of Dy. The RE supply chain risk leads to a strong desire to develop high performance magnets with less or no RE. This paper will discuss the technical challenges and opportunities ahead, including the process challenges to obtain certain microstructure and texture in order to reach theoretical potential of the nanocomposite magnets.

9:35 AM Invited

Synthesis and Characterization (Structural and Magnetic) of Bulk and Nanostructured d-Phase in Mn-Ga System: *Tanjore Jayaraman*¹; *Jeffrey Shield*¹; *University of Nebraska*

Permanent magnets play a vital role in environment-friendly technologies. Currently due to the demand for rare-earth based permanent magnets it is imperative to explore non-rare earth based magnetic systems. In this work we present the synthesis and characterization (structural and magnetic) of bulk and nanostructured d-phase (L10) in Mn-Ga system



TMS 2012

141st Annual Meeting & Exhibition

TUESDAY AM

obtained by conventional melting, rapid solidification (melt-spinning), and mechanical alloying (ball-milling); followed by a sequential heat treatment process that resulted in the formation of d-phase. The mechanical alloying resulted in the formation of a nanostructured powder comprising metastable disordered phase - a suitable precursor for making powders of the d-phase. Both the disordered and the ordered d-phase show ferromagnetic behavior at ambient temperature; the ordered phase exhibit superior magnetic properties. The structure and magnetic properties of the d-phase were found to be sensitive to the composition, heat treatment cycle and processing route.

10:05 AM Invited

Search for New Rare Earth Based Permanent Magnetic Materials: *B. Jensen*¹; K. Dennis¹; R. McCallum¹; ¹Ames Laboratory, US-DOE

There are substantial challenges in researching magnetic materials of the R-TM-X systems (R = rare earth, TM = transition metal) due to synthesis difficulties including high vapor pressure, high reactivity, toxicity, or the refractory nature of the materials. This research focuses on discovering new phases with high anisotropy and high magnetization through closed diffusion couples in which the alloying elements are sealed inside a high purity Fe crucible. Either vapor-solid reactions or powder metallurgy techniques are then employed to isolate a stoichiometric sample based on a potentially magnetic phase found in the diffusion couple. For this research, X = F, Ca, Sr, Se, Zn, Bi, or Cd, TM = Fe, and R = Nd. New ternary phases have been discovered with WDS and EDS, and magnetic transition temperatures have been measured with a SQUID magnetometer and VSM. This work was supported by ARPA-E contract number DE-AR0000046 at Ames Laboratory (USDOE).

10:35 AM Break

10:50 AM Invited

Interfacial Characterisation in Nd-Fe-B Permanent Magnets: *Thomas Woodcock*¹; Gino Hrkac²; Thomas Shreffl³; Oliver Gutfleisch¹; ¹IFW Dresden; ²University of Sheffield; ³St. Pölten University of Applied Sciences

Nd-Fe-B sintered magnets play an important role in energy applications such as hybrid electric vehicles and wind turbines. Production of Dy-free Nd-Fe-B magnets with high coercivity requires greater understanding of the coercivity mechanism. Detailed characterisation of the structure and composition of interfaces is therefore highly important. Aberration-corrected TEM has been used to obtain highest spatial resolution images of interfaces between the Nd₂Fe₁₄B and Nd-rich grains in Nd-Fe-B sintered magnets and the composition of the grain boundary phase has been measured using STEM-EELS. Atomistic simulations based on these results predict the presence of distorted regions of Nd₂Fe₁₄B, leading to local changes in the magnetic anisotropy, which may have a detrimental effect on coercivity. The thickness of the distorted regions was shown to depend on the crystal structure and orientation of the Nd-rich phase. Local orientation changes caused by defects in Nd-rich phases have been observed by HR-TEM and EBSD.

11:20 AM

Effect of Ni Content on the Crystallization Behavior and Magnetic Properties in a Nanocrystalline (Co_{1-x}Ni_x)₈₈Zr₇B₄Cu₁ Soft Magnetic Alloy: *Billy Hornbuckle*¹; Billie Wang¹; Taisuke Sasaki²; Maria Daniil³; Matt Willard⁴; Greg Thompson¹; ¹The University of Alabama; ²National Institute for Materials Science; ³Naval Research Laboratory; ⁴Naval Research Laboratory

Soft magnetic materials with nanocrystalline microstructures have shown the capacity for use in electric motors. These materials could reduce component sizes, provide higher energy conversion, and allow easier thermal management. (Co,Fe)-Zr-B-Cu based alloys have been one of the systems investigated for these reasons. This study branches from that system by creating a series of (Co_{1-x}Ni_x)₈₈Zr₇B₄Cu₁ soft magnetic alloys, where X varied from 0 to 1. These were then melt spun into thin

ribbons to determine the compositional limitations of amorphization. The activation energy for crystallization decreased with increasing Ni content. TEM imaging and atom probe tomography revealed fine nanocrystallite and boron segregation to the grain boundaries with increasing Ni content. Chemical partitioning between species in the as-spun and primary crystallization heat treatments were correlated to the resulting changes in magnetic properties. As expected, reduction in magnetization and Curie temperature accompanied the substitution of Ni for Co in this alloy series.

11:35 AM

The Effect of Substituting Nb and Hf for Zr in Fe-Co-Ni-Zr-B-Cu Nanocrystalline Soft Magnetic Alloys: *Keith Knippling*¹; Maria Daniil¹; Matthew Willard¹; ¹Naval Research Laboratory

Nanocrystalline soft magnetic materials possess a unique combination of large magnetization and permeability with low core loss, achieved by exchange-coupling of nanoscale ferromagnetic grains through a surrounding amorphous matrix. The effectiveness of exchange-coupling is reduced, however, above the Curie temperature of the intergranular amorphous phase, T_c^{am} , thus limiting the alloys' maximum service temperature. We recently showed that small substitutions of Co and Ni for Fe in Nanoperm-type (Fe₈₈Zr₇B₄Cu₁) alloys increases T_c^{am} while maintaining large saturation magnetizations and small hysteretic losses, resulting in improved magnetic properties at elevated temperatures (~250–450 °C). Substituting other early transition metals for Zr is expected to reduce the saturation magnetostriction, λ_s , thereby reducing the hysteretic losses further. In this study, we report on the crystallization behavior and ambient- and elevated-temperature magnetic properties for a series of Fe₇₇Co_{5.5}Ni_{5.5}Zr_xNb_{1-x}B₄Cu₁ and Fe₇₇Co_{5.5}Ni_{5.5}Zr_xHf_{1-x}B₄Cu₁ alloys (x = 0–7), and correlate the measured hysteretic losses to the measured λ_s .

Materials and Fuels for the Current and Advanced Nuclear Reactors: Nuclear Fuels

Sponsored by: The Minerals, Metals and Materials Society, TMS Structural Materials Division, TMS/ASM: Corrosion and Environmental Effects Committee, TMS/ASM: Nuclear Materials Committee

Program Organizers: Ramprashad Prabhakaran, Idaho National Laboratory; Dennis Keiser, Idaho National Laboratory; Raul Rebak, GE Global Research

Tuesday AM
March 13, 2012

Room: Swan 2
Location: Swan Resort

Session Chair: Dennis Keiser, Idaho National Laboratory

8:30 AM Invited

Compatibility of Metallic Transmutation Fuels with Fe-Based Alloys: *James Cole*¹; Thomas O'Holloran¹; Robert Mariani¹; Dennis Keiser¹; J. Kennedy¹; ¹Idaho National Laboratory

Out-of-pile diffusion couple studies have been conducted over the past several years to better understand the complex phase evolution that occurs when U, Pu-based metallic nuclear fuel with and without minor actinides (Am, Np) and rare earth fission products (Ce, La, Pr, Nd) contacts Fe-based cladding alloys at elevated temperature. These studies are being performed to support in-pile tests of similar fuels and bound the expected behavior in terms of formation of brittle or low-melting point phases due to interdiffusion of fuel constituents into the cladding and cladding constituents into the fuel. The complex phase evolution observed will be discussed in terms of available equilibrium phase diagram data and the relation to anticipated in-pile behavior.

9:00 AM

Advanced Fuels with Fission Product Getters to Suppress Fuel-Cladding Chemical Interactions: *T. O'Holleran*¹; R. Mariani¹; Randall Fielding¹; P. Hansen¹; T. Hyde¹; J. Kennedy¹; ¹Idaho National Laboratory

Rare earth fission products in metallic fuels are known to exacerbate undesirable fuel-cladding chemical interactions with steel cladding that can lead to premature failure. Rare earth fission products produced during irradiation migrate to the fuel – cladding interface where they can depress solidus temperatures leading to breach of cladding. Furthermore, recycled fuel for a fast burner reactor used to destroy actinides may contain several percent rare earth fission products prior to reactor insertion, leading to fuel – cladding chemical interactions at the outset. This paper describes the selection of additives to complex rare earth fission products during both fuel production and irradiation. It also describes the fabrication and characterization of experimental fuels to test these concepts. Preliminary results indicate effective gettering of (surrogate) rare earth fission products in as-fabricated fuel doped with rare earths. In fuels fabricated without rare earths, the getter forms intermetallics with other constituents.

9:20 AM

Reducing Fuel Cladding Chemical Interaction by Pinning Lanthanide Fission Products in Metallic Fuel: *Gerald Egeland*¹; Thomas Hartmann¹; Robert Mariani²; Rory Kennedy²; Steve Hayes²; ¹University Nevada Las Vegas; ²Idaho National Lab

Fast reactor metallic fuels produce significant lanthanide fission products which have been shown to diffuse to the fuel periphery and interact with the cladding. With the drive for higher burn-up fuels, this effect increasingly becomes a limiting factor with risk of a cladding breach. To test viability of pinning several lanthanides, palladium was chosen as the pinning dopant based its thermodynamic stability of the lanthanide alloys and its fuel compatibility. Iron was chosen as the base for standard cladding materials. Three lanthanides were tested, neodymium, cerium, and praseodymium, along with their 1:1 palladium alloys, against iron in diffusion couples. These experiments show the effects of palladium alloys versus the pure lanthanides on iron.

9:40 AM

Nanofluid-Based Coatings to Mitigate Fuel Cladding Chemical Interactions (FCCI): *Vahid Firouzidor*¹; Lucas Wilson¹; Kumar Sridharan¹; Brandon Semerau¹; Benjamin Hauch¹; Todd Allen¹; ¹University of Wisconsin-Madison

Diffusion barrier coatings and liners have been proposed for the inner surface of fuel claddings for mitigation of fuel cladding chemical interactions (FCCI) in Advanced Burner Reactors (ABR). We are developing methods to deposit diffusion barrier coatings of Ti, Zr, and V and their respective oxides, and yttria-stabilized zirconia (YSZ) using electrophoretic deposition (EPD) of nanofluid precursors. The coatings have been evaluated using diffusion couple studies using cerium as a surrogate for uranium, as well as by SEM and x-ray diffraction techniques. To obtain the best coating quality, process parameters including, the solution chemistry, nanoparticle concentration, voltage, current, and post-coating sintering are being studied. By using co-axial EPD technique uniform coatings have been successfully deposited on the inside surface of cladding sections up to twelve inches in length. Diffusion couple experiments show excellent reduction in diffusion of cerium into steel using the barrier of YSZ and TiO₂ coatings.

10:00 AM

Microstructural and Chemical Characterization of High Burn-Up Mixed Oxide Fuel: *Melissa Teague*¹; Brian Gorman²; Steven Hayes¹; Jon Carmack¹; ¹Idaho National Laboratory; ²Colorado School of Mines

The increasing demand for cost effective green energy has led to a renewed interest in nuclear energy, including the commercialization of fast breeder reactors (FBR's). For FBRs to become economically competitive with current light water reactors (LWRs) the average burn-up of fuel assemblies in an FBR will need to exceed ~150 GwD/tHM (~15%

FIMA). A secondary reason for interest in FBR is their potential to be used to “burn” or transmute long-lived transuranic isotopes contained in spent nuclear fuel produced by the current fleet of LWR. Currently fast reactor performance is largely defined by the limitations of the materials involved in reactors, especially the metallic or mixed oxide ((U, Pu)O₂) fuel itself. Problems include fission gas generation, changes in thermal conductivity, microstructure changes within the fuel, fuel swelling, and fuel cladding chemical interaction (FCCI). Microstructural and chemical analysis of MOX fuel with burn-ups of 5-24% FIMA will be presented.

10:20 AM Break

10:30 AM

Interdiffusion Kinetics in U-Zr: *Vincenzo Lordi*¹; Mark Wall¹; Luke Hsiung¹; Ron Foreman¹; Patrice Turchi¹; ¹Lawrence Livermore National Lab

The design of reliable advanced nuclear fuels, particularly for high burn-up applications, requires a detailed understanding of degradation mechanisms and kinetics. Phase evolution under operating conditions must be well understood, ideally both experimentally and in simulations. For various advanced U-based fuels, interdiffusion of Zr, both from coatings and also the fuel alloy, is fundamental. In this study, we assess U-Zr interdiffusion data for use in kinetic evolution models and compare to experimental measurements on diffusion couples. The variation of diffusion rates with radiation damage (displacements per atom) is investigated using Zr ion implantation from an ion accelerator to model long-term damage. Damage profiles and dosages from the ion implanter are calibrated with Monte Carlo models of the implantation process. Prepared by LLNL under Contract DE-AC52-07NA27344.

10:50 AM

Forming Process Development for Al-clad U-10Mo Monolithic Fuel Plates: *Kester Clarke*¹; David Alexander¹; Jill Wright²; Pavel Medvedev²; Richard Williamson²; ¹Los Alamos National Laboratory; ²Idaho National Laboratory

A significant goal for the Global Threat Reduction Initiative (GTRI) is converting high performance research reactors from highly enriched (HEU) to low enriched (LEU) uranium, requiring development, qualification, and production of monolithic LEU-10Mo foils. These foils are to be co-rolled with Zr and clad with 6061Al using hot isostatic pressing (HIP). Some reactor designs require a forming/bending operation after HIP processing. The selected method for bending fuel plates is press brake-type forming with solid punches and flexible bottom dies. Small scale trials with multi-layer fuel foils have been performed. Important results include springback evaluation as a function of DU-10Mo and 6061 Al thickness and metallographic examination of the bond zone integrity as a function of bending radius. Plate relaxation as a function of time and temperature was also evaluated, which may be critical to in-reactor performance. Finally, finite element (FE) analysis of forming the multi-layer fuel plate has been performed.

11:10 AM

Characterization of Freeze-Cast Scaffolds as a Novel Fuel Form: *Clarissa Yablinsky*¹; Joan Burger²; Amanda Lang¹; Philipp Hunger²; Thomas Gage¹; Ulrike Wegst²; Todd Allen¹; ¹University of Wisconsin; ²Drexel University

With advanced reactor designs requiring better fuel performance, the search for different fuel forms is essential to increasing the materials possible for fast reactor use. In this study, a novel fuel form, created by a directional solidification process, is being researched because of the ability to load different fuels within a longitudinal pore structure in a controlled fashion. Scaffolds of 316 stainless steel and aluminum oxide with different pore sizes and geometries were created and infiltrated with a fuel surrogate, cerium dioxide. The structure, mechanical, and thermal properties of the scaffolds were characterized in both their porous and filled state. Monte Carlo N-Particle modeling was performed in order to test criticality requirements for the fuel and reactor.



TMS 2012

141st Annual Meeting & Exhibition

11:30 AM

Transport Studies with Porous Metal Fuels: *Robert Mariani*¹; Curtis Clark¹; Thomas O'Holleran¹; Blair Park¹; Randall Fielding¹; J. Kennedy¹; ¹Idaho National Laboratory

Metal nuclear fuels develop significant porosity above approximately 2% burnup (heavy metal basis). Since surfaces can facilitate more rapid transport than the bulk fuel alloy, it is important to characterize the transport of fuel constituents, fission products, and cladding components in porous fuel bodies. Special-effects, out-of-pile tests were therefore designed and are being implemented to assess the significance of porosity on transport, which may be critical to understanding the fuel behavior and to modeling. We describe methods of preparing porous alloy fuels, which included atomizing the alloys into spherical or flake powders. Powders were subsequently sintered and prepared as diffusion couples with reactive counterparts, such as iron. These experiments are a crucial supplement to the traditional bulk diffusion and transport experiments for understanding and modeling fuel properties. We will summarize the rationale and need, experimental plans, recent developments, and future steps.

11:50 AM

Production Scale-Up of Cylindrical Compact Fabrication: *Eric Shaber*¹; Jeffrey Phillips¹; ¹Battelle Energy Alliance/INL

Multiple process approaches have been used historically to manufacture cylindrical nuclear fuel compacts. Scale-up of fuel compacting was required for the NRG Project to achieve an economically viable automated production process capable of providing a minimum of 10 compacts/minute with little or no rejects. In addition, the scale-up effort was required to achieve matrix density equivalent to baseline historical production processes, and allow compacting at fuel packing fractions up to 46 vol%. The scale-up approach of jet milling, fluid-bed overcoating, and hot-press compacting adopted in the U.S. Advanced Gas Reactor (AGR) Fuel Development Program involves significant paradigm shifts to capitalize on distinct advantages in simplicity, yield, and elimination of waste. The scale-up effort is nearing completion with the process installed and operable using nuclear fuel materials. Final process testing is in progress to certify the process for manufacture of qualification test fuel compacts in 2012.

Materials Design Approaches and Experiences III: High Strength High Toughness Steels

Sponsored by: The Minerals, Metals and Materials Society, TMS Structural Materials Division, TMS: High Temperature Alloys Committee, TMS: Integrated Computational Materials Engineering Committee

Program Organizers: Ji-Cheng Zhao, The Ohio State University; Akane Suzuki, GE Global Research; Deb Whitis, GE Aviation; Michael Fahrman, Haynes International Inc.; Qiang Feng, University of Science and Technology Beijing

Tuesday AM
March 13, 2012

Room: Europe 11
Location: Dolphin Resort

Session Chairs: J.-C. Zhao, The Ohio State University; Greg Olson, Northwestern University

8:30 AM Invited

Multi-Scale Modelling to Aid Alloy Design: *Matthias Miltzer*¹; ¹The University of British Columbia

Computational materials science tools have great potential to aid the development of new alloying concepts and processing routes. Industrial process models are currently at least in part based on empirical material parameters to describe microstructure evolution and resulting material properties. Modelling across different length and time scales is a

promising approach in order to develop next generation process models that can rigorously account for the role of alloying elements. Atomistic simulations can be used to gain insight into interfacial properties (e.g. interface mobility) and the interaction of alloying elements with moving interfaces (i.e. solute drag). Phase field models that operate on the length scale of microstructures (the so-called meso-scale) provide an important bridge to link atomistic simulations with the macro-scale of process models. The potential and challenges of this multi-scale modelling approach will be illustrated for phase transformations in advanced low-carbon steels.

9:00 AM Invited

Integrated Computational Materials Design: From Genome to Flight: *Greg Olson*¹; ¹Northwestern University

The historic first flight on December 17, 2010 of the Ferrium S53 Stainless Landing Gear Alloy represents the first fully computationally designed and flight qualified material. This achievement was made possible by the founding of a multidisciplinary research consortium in 1985, which was in turn inspired by the emergence in 1984 of ThermoCalc as a second-generation CALPHAD software and database system offering a new level of accuracy raising the possibility of true materials design. The steady improvement in accuracy of tools and databases has continued to broaden materials design capability, and its integration with the efficient probabilistic framework of the AIM methodology has continued to accelerate the design and qualification cycle. The higher accuracy of new simulation tools has demanded higher fidelity microstructural characterization now enabled by a suite of 3D tomographic tools integrated under the recent ONR/DARPA "D3D" Digital Structure initiative.

9:30 AM Invited

Multi-Scale Microstructure Design of High Performance Structural Steel: *Chengjia Shang*¹; ¹University of Science and Technology Beijing

Steel is key structural material. The mechanical properties of steel generally relate with alloys, phases and other microstructure. Ferrite/pearlite and bainite/martensite are the common phases in steel, with the phase transformation temperature decreasing, strength of steel would increase and the transformation phases are changed from ferrite/pearlite to bainite/martensite. Ferrite is a kind of soft phase that with high uniform elongation, therefore, multi phases (ferrite/bainite or martensite) can play combination roles to modify the strength and ductility. Although, the strength of multi phase steel would be decreased by volume fraction of ferrite, the multi scale precipitates could strengthen either ferrite or bainite/martensite. In this paper, a multi phase and multi scale precipitation controlled steel was designed, the process of how to control the multi phase and multi scale precipitate will be introduced and the excellent properties of such high performance steel will be revealed.

10:00 AM Break

10:20 AM Invited

A Coupled Thermodynamics-Genetic Algorithm Approach For the Design of High Strength Stainless Steels: *Sybrand Van Der Zwaag*¹; Wei Xu¹; ¹Technical University Delft

Up to recently the design of advanced (stainless) steels proceeded via an empirical route. In this work we present an coupled thermodynamic - genetic algorithm approach to the design of precipitation hardened martensitic stainless steels. In this alloy design process not only the formation of a maximum amount of desirable precipitates but also the absence of detrimental phases is taken into account. The model can handle a simultaneous optimisation of alloy composition and heat treatment temperatures. Finally, by adding a cost factor to the various alloying elements the most optimal solution to a low cost high strength stainless steel grade can be determined.

10:50 AM

Material Design and Prediction of Deformation Response of Stainless Twinning Induced Plasticity Steels: *Linda Mosecker*¹; *Alireza Saeed-Akbari*¹; *Wolfgang Bleck*¹; ¹Department of Ferrous Metallurgy RWTH Aachen University

The high-manganese (HM) twinning induced plasticity (TWIP) steels offer excellent mechanical properties applicable to auto industries due to high energy absorption and excellent strain hardening behavior. Nevertheless, the application of conventional austenitic stainless steels in auto industries with similar mechanical properties and deformation mechanisms to HM-TWIP steels is limited mainly due to the higher costs of the alloyed nickel. Therefore, the replacement of nickel by manganese has been found advantageous to achieve an attractive property/cost balance. In the present study, a CALPHAD-based methodology using the sublattice model was employed to develop mechanism maps by which the activation/suppression of deformation induced mechanisms was predicted. In addition, the accuracy of the developed maps was investigated by checking the deformation response of experimental and published results on Fe-Cr-Mn-N-(C) steels. The given strategy supplies critical information for the material design of stainless TWIP steels on the basis of a thermodynamic approach.

11:10 AM

Materials Design Over the Decades, How Far Have We Come?: *Charles Kuehmann*¹; *Heng-Jeng Jou*¹; *Jason Sebastian*¹; *Chris Kern*¹; ¹QuesTek Innovations LLC

Computational materials design methods have been in development since the 80's as computational tools, approaches and systems have emerged. Early examples were established within the Steel Research Group/Northwestern University, focused on steel alloys due to the comparative wealth of data and model development available, focused, in large part, on absolute performance enhancements over incumbent alloys. Through the last two decades of technical maturity, these methods are now being applied to more diverse systems, with designs additionally focused on lower cost, enhanced reliability and minimized process variation. An example of this is the ultra-high-strength, ultra-high toughness Ferrium M54 steel, designed, prototyped, scaled to commercial production and completed an AMS specification, in less than 4 years for the Navy by QuesTek Innovations LLC. Accelerated Insertion of Materials (AIM) techniques forecast probabilistic property minimums expected from manufacturing capabilities. Modeling capability is being applied to accelerate the implementation and qualification of M54 in flight critical components for aircraft.

11:30 AM

Formation and Morphology Control of TCP σ Phase in Austenitic Heat Resistant Steels: *Harumi Inatomi*¹; *Masao Takeyama*¹; ¹Tokyo Institute of Technology

σ phase is considered as detrimental phase in the austenitic heat resistant steels, but it could be a promising strengthener for long-term creep strength if the precipitation kinetics and morphology are appropriately controlled, just like Laves phase. In this study, formation process of σ phase in fcc γ phase in the carbon-free Fe-Cr-Ni alloys has been examined at 1073 K. The σ phase forms through the transformation from non-equilibrium bcc α phase with higher Cr content (α -Cr) precipitated prior at γ grain boundaries, and the precipitation kinetics of the σ phase in the γ matrix is sluggish. The kinetics of the σ phase formation becomes further sluggish when formation of the α -Cr phase is suppressed. The morphology of σ phase, thus, can be controlled through the precipitation kinetics of the prior α phase in γ matrix. Some of the examples of the σ phase morphology will be presented.

11:50 AM

Changes of Work-Hardening-Rate in Advanced High Strength Austenitic Steels by the Applied Deformation and Material Parameters: *Alireza Saeed-Akbari*¹; *Wolfgang Bleck*¹; ¹RWTH Aachen University

The recently developed high-strength austenitic steels within Fe-Mn-C and Fe-Mn-Al-C systems offer superior strain hardening behavior due to the activation of mechanisms like mechanical twinning, deformation-induced martensite formation, and planar dislocation glide. In the present work, variations in the work-hardening-rate diagrams of austenitic high-manganese steels are studied by changing parameters like grain-size-distribution, applied strain rate, temperature, chemical composition, and finally SFE. In addition, different scenarios are reviewed where changing one parameter by keeping others as constant values are shown to make certain alterations in the strain hardening behavior of these materials. The given discussions make it possible to predict the materials response across an extensive range of applied deformation parameters in high-manganese iron-based systems to facilitate the materials design/selection process.

Materials in Clean Power Systems VII: Clean Coal-, Hydrogen Based-Technologies, and Fuel Cells: Fuel Cells

Sponsored by: The Minerals, Metals and Materials Society, TMS Electronic, Magnetic, and Photonic Materials Division, TMS Structural Materials Division, TMS/ASM: Corrosion and Environmental Effects Committee, TMS: Energy Conversion and Storage Committee

Program Organizers: Xingbo Liu, West Virginia University; Teruhisa Horita, National Institute of Advanced Industrial Science and Technology; Jeffrey Hawk, National Energy Technology Lab; Jeffrey Fergus, Auburn University

Tuesday AM
March 13, 2012

Room: Europe 8
Location: Dolphin Resort

Session Chairs: Xingbo Liu, West Virginia University; Teruhisa Horita, National Institute of Advanced Industrial Science and Technology (AIST)

8:30 AM Invited

Fuel Flexibility and Microstructural Change in Anode during Operation of Solid Oxide Fuel Cells: *Koichi Eguchi*¹; *Hiroki Muroyama*¹; *Toshiaki Matsui*¹; ¹Kyoto University

The durability and reliability of solid oxide fuel cells need to be improved before the commercialization. Nickel- yttria-stabilized zirconia (YSZ) cermet is widely used as an anode in SOFCs. The fuel cells are often deteriorated with concentrated hydrocarbon or steam at elevated temperatures. In this study, then, the microstructural change in cell components with an elapsed time was quantified by the FIB-SEM technique to elucidate the degradation of anode. Carbon deposition was sometimes observed with a supply of hydrocarbon fuels to the anode. Morphology and type of carbon were affected by the deposition condition. The degradation behavior was significantly dependent on the fuel humidity and cermet composition. When H₂ fuel with concentrated H₂O was supplied to the anode, the current density decreased gradually soon after the discharge, followed by a sudden drop in current density.



TMS 2012

141st Annual Meeting & Exhibition

TUESDAY AM

9:00 AM

Study of Microstructure and Electrical Conductivity on (Ce_{0.9}Nd_{0.1})_{1-x}MxO_{2-Δ} Electrolytes for Intermediate-Temperature Solid Oxide Fuel Cells: *Fanzhi Meng*¹; N. Trubaki¹; Defeng Zhou²; Yanjie Xia³; Jian Meng³; ¹University of Toyama; ²Changchun Technology of University; ³Changchun Institute of Applied Chemistry, Chinese Academy of Sciences

The Ce_{0.8}Nd_{0.2}O₂ with doped MoO₃ was prepared through modified sol-gel method. The ionic conductivity was studied in air using an impedance spectroscopy. The results showed that the MoO₃ can form a thin amorphous film around particles, which reduces the interparticle friction, and increases the contact area of particles in a compact solid. And this promotes mass diffusivity in the matrix. This leads to the further increase in densification and decrease in the volume fraction of grain boundary. The total and grain boundary conductivity gradually increases due to the decrease of the grain boundary resistance. It shows that the sample Ce_{0.8}Nd_{0.2}O₂ with doped MoO₃ has the higher ionic conductivity ($\sigma_t=4.33 \times 10^{-3}$ S.cm⁻¹, $\sigma_{gb}=5.06 \times 10^{-3}$ S.cm⁻¹) at 600°C. It is obvious that total conductivity enhances one point five times than the sample without MoO₃ doping. The MoO₃ dopants are the perfect sintering promoter for the NDC system.

9:20 AM Invited

Thermal Stability and Structural Evolution of LSM/YSZ Composite Cathode for SOFC by In-Situ Neutron Diffraction: *Ke An*¹; Ling Yang¹; Rebecca Mills¹; Lu Cai¹; ¹Oak Ridge National Laboratory

Lanthanum-strontium-manganese oxides (LSM) and yttria-stabilized zirconia (YSZ) are widely used as cathode and electrolyte for solid oxide fuel cells (SOFCs). Thermal stability and reliability of LSM/YSZ heavily depends on the concentration of Y₂O₃. Therefore, it is obvious to understand the degradation of ionic conductivity by studying LSM/YSZs' structural/phase evolution at elevated temperature. Neutron scattering is superior for this purpose because the large cross-section of all components makes it possible to differentiate different phases and to derive the structural evolution during annealing by Rietveld refinement. On VULCAN instrument at the world most intense pulse based Spallation Neutron Source, a series of LSM/YSZs of 6-10% Y₂O₃ were heated up to 1500°C at 2C/min, meanwhile simultaneous in-situ neutron diffraction and electrochemical impedance spectroscopy were measured to correlate the structural/phase change to electrochemical degradation. The thermal stability and the structural evolution of the LSM/YSZs at elevated temperatures will be presented.

9:50 AM

Relationship between Cathode Performance and Impurity Concentration for Solid Oxide Fuel Cells: *Teruhisa Horita*¹; DoHyung Cho¹; FangFang Wang¹; Taro Shimonosono¹; Haruo Kishimoto¹; Katsuhiko Yamaji¹; Manuel Brito¹; Harumi Yokokawa¹; ¹AIST

Impurities coming from gases can deposit and react with cell components in Solid Oxide Fuel Cells (SOFCs). Especially, chromium and sulfur poisonings are the critical issues for long-term operation. The chromium vapors (CrO₃ etc.) can deposit on the porous cathodes and they are reduced to Cr₂O₃ at the electrochemically active sites. To relational the Cr deposition and electrochemical degradation at cathodes, we have determined the Cr concentration in cathodes by using Secondary Ion Mass Spectrometry (SIMS). From the cathode degradation tests under Cr vapor supply, it was found that the electrochemical active sites were high Cr-concentration, and the degradation trends were different among different cathodes. The sulfur poisoning test was also examined at several candidate cathodes. Cathodes were exposed to dilute SO₂ and the cathode performance was examined for long-term operation. It was found that the poisoning proceeded from the cathode surface and morphological change affected the performance.

10:10 AM Break

10:20 AM

Possibility of Metal Film Supported Electrolyte for Proton-SOFC: *Kenichi Kawamura*¹; Taku Kitahara¹; Shun Kawamura¹; Mitsutoshi Ueda¹; Toshio Maruyama¹; ¹Tokyo Institute of Technology

In operation of proton-type SOFC, the electrolyte conducts not only proton but also oxide ion. When dense metal used as anode, H₂O might be produced at the interface between anode and electrolyte and destroy the electrolyte. In this presentation, I will show the oxygen permeability of Sr(Ce,Y)O₃ and Pd-CeO₂ composite and evaluate the possibility of p-SOFC with metal film anode.

10:40 AM

Advanced Conductive Coating Performance at the Long-Term SOFC Operating Condition: *Jung Pyung Choi*¹; Jeffrey Stevenson¹; Scott Ryan¹; Matt Chou¹; Gordon Xia¹; ¹Pacific Northwest National Laboratory

From the cost and long term performance with safety, metal supported planar SOFC is considering as best design. The ferritic stainless steel interconnects are generally used, due to their low-cost, chromia scale-forming behavior, and good thermal expansion match to other stack components. However, volatile Cr-containing species, which originate from the oxide scale, can poison the cathode material in the cells and subsequently cause power deterioration in the device. MnCo spinel coating has been developed for preventing cathode poisoning. This paper will summarize development of coating method and optimization of the advanced MnCoO spinel material using design of experiment methodology with Taguchi and ANOVA analysis. Then, observed the thickness effect on electrical conductivity with long-term test. The results of this work demonstrate the possibility of automated mass production of dense conductive spinel-coated interconnect materials.

11:00 AM

Transition Metal Doping of Manganese Cobalt Spinel Oxides for Coating SOFC Interconnects: *Jeffrey Fergus*¹; Yingjia Liu¹; Jason Ganley¹; Dileep Chakkathara Janardhanan Nair¹; William Tilson¹; Adam Dekich¹; ¹Auburn University

Manganese cobalt spinel oxide coatings have been shown to be effective for preventing chromium volatilization for interconnect alloys, and the associated cathode poisoning, in solid oxide fuel cells. During high temperature exposure a reaction layer consisting of chromium-containing spinel forms due to reaction with the chromia scale formed on the alloy. The electrical conductivity of this reaction layer is much lower than that of the coating material and thus can increase the overall area specific resistance (ASR) of the system. The approaches to reducing the ASR are to reduce the thickness and/or increase the electrical conductivity of the reaction layer, which includes both the high-chromium spinel phase and the chromia scale. In this paper the effects of transition metal dopants on the amount and properties of reaction products formed during the reaction of spinel oxide coating materials with chromia are presented.

11:20 AM

The Effect of Cerium Oxide Nanoparticle Oxidation State on the Degradation Mitigation of I100 EW Nafion® Composite Membranes: *Benjamin Pearman*¹; Nahid Mohajeri¹; Darlene Slattery¹; Len Bonville¹; Diego Diaz¹; Sudipta Seal²; Michael Hampton²; ¹Florida Solar Energy Center - UCF; ²University of Central Florida

During operation, polymer electrolyte membranes used in hydrogen fuel cells degrade, causing a decline in their long-term performance which can ultimately result in catastrophic membrane failure. The membranes' exposure to radicals, thought to be formed from hydrogen peroxide, is considered the origin of this chemical degradation. To inhibit the destructive effect of these radicals, the addition of chemical mitigators to membranes has been proposed. Cerium oxide, a compound well-known for its ability to easily switch back and forth between its Ce(III) and Ce(IV) oxidation states, shows radical scavenging behavior that is dependent on the initial ratio of those two oxidation states. In this work,

cerium oxide nanoparticles, of various concentrations were added to 1100 EW Nafion® membranes and subjected to degradation experiments, such as liquid Fenton tests, gaseous Fenton tests and accelerated durability runs. The effect of the Ce(III)/Ce(IV) ratio of the nanoparticles on the improved membrane stability was analyzed.

11:40 AM

The Electrochemical Properties of TiAlCrN Coated Stainless Steel with PEMFC Environment: *Min-Seok Moon*¹; Kee-Do Woo²; Myung-Han Yoo³; Shin-Jae Kang⁴; Joon-Hyuk Song³; ¹Chonbuk National University, Jeonju Institute of Machinery Carbon Composites; ²Chonbuk National University; ³Jeonju Institute of Machinery and Carbon composites; ⁴Chonbuk National University, Jeonju Institute of Machinery and Carbon composite

Recently, new energy sources have gained expectation due to hiking oil prices and limits on reserves of fossil fuels. However, increasing global warming and air pollution due to using the fossil fuels have been emerged as social issues. The TiAlCrN coating on STS is not applied to develop the advanced metallic bipolar plate for PEMFC. It will be expected to improve the corrosion resistance on PEMFC environment. The aim of this investigation is to develop the cheap metallic bipolar plate coated with TiAlCrN. The mechanical and electrochemical properties of the TiAlCrN coated specimens were measured. The TiAlCrN coated STS304 has better fuel cell performance such as corrosion resistance, ICP and ICR than other experiment materials, except single cell durability. TiAlCrN coated specimen has been satisfied electrochemical property for DOE target.

Materials Processing Fundamentals: Application of Microwave, Magnet, Laser and Plasma Technology

Sponsored by: The Minerals, Metals and Materials Society, TMS Extraction and Processing Division, TMS Light Metals Division, TMS: Process Technology and Modeling Committee

Program Organizers: Lifeng Zhang, Missouri University of Science and Technology; Antoine Allanore, MIT; Cong Wang, Saint-Gobain High Performance Materials

Tuesday AM
March 13, 2012

Room: Oceanic 8
Location: Dolphin Resort

Session Chairs: Cong Wang, Alcoa Technical Center; Antoine Allanore, MIT

8:30 AM

New Developments in Lorentz Force Velocimetry: *Andre Thess*¹; Yurii Kolesnikov¹; Christian Karcher¹; Rico Klein¹; Michael Gramss¹; Dandan Jian¹; Christiane Heinicke¹; André Wegfrass¹; Christian Resagk¹; Xiaodong Wang¹; Thomas Boeck¹; Thomas Froehlich¹; Falko Hilbrunner¹; Christian Diethold¹; Ilko Rahneberg¹; Michael Werner¹; Bernd Halbedel¹; ¹TU Ilmenau

Lorentz force velocimetry (LFV) a non-contact technique for velocity measurement in electrically conducting fluids. This technique is based on exposing the fluid to a magnetic field and measuring the force acting upon the magnetic-field-generating system. In the present communication we will describe the physical principles of LFV and report results of recent developments aiming both at a better understanding of the fundamental aspects of LFV and the development of new applications. The survey will include results of the application of LFV to local velocity measurement, calibration of Lorentz force flowmeters for application in secondary aluminium industry, time-of-flight LFV as well as the application of LFV to the measurement of velocities in poorly conducting fluids. Acknowledgment: The work is supported by the German Research Foundation (DFG) as a Research Training Group "Lorentz force velocimetry and Lorentz force eddy current testing"

8:55 AM

Non-Contact Measurements in Liquid Metal Free-Surface Flow Using Time-of-Flight Lorentz Force Velocimetry: *Dandan Jian*¹; Christian Karcher¹; ¹TU Ilmenau

Surface velocity measurement is a big challenge in metallurgy. Due to chemical aggressiveness of metal melts at high temperature, only non-contact measurement techniques can be applied. One of such techniques is Lorentz force velocimetry (LFV). It is based on the measurement of the Lorentz force acting on a magnet system. This force is proportional to the flowrate or local velocity and the electrical conductivity of the melt. We present a series of model experiments that demonstrate the feasibility of using an arrangement of two identical measuring devices called Lorentz force flowmeters, termed time-of-flight technique. In this case the free-surface velocity may be purely determined by cross-correlating the two force signals of the two flowmeters. In a first experiment we measure free-surface velocities using GalnSn as a low-melting model melt.

9:20 AM

Microstructure and Mechanical Properties of Friction Stir Welding Zone in SS400(SPHC) Plate: *Kwang-jin Lee*¹; Sang-Hyuk Kim¹; Ik-Hyun Oh¹; Kee-Do Woo²; ¹Korea Institute of Industrial Technology; ²Chonbuk National University

Conventional fusion welding of the most metallic materials produces to defects such as porosity, created metallic compound. However, solid state joining processes as friction stir welding don't form weld pool. Consequently, the defects decrease remarkably and mechanical properties improve in general welding. So, The FSW is a potential candidate for the joining of dissimilar and high melting temperature materials. However, to apply FSW in high melting temperature materials such as steel or Ti alloys etc., the tool with super heat-resisting and abrasion resistance is needed. So, Spark plasma sintering method was selected to fabricate tool material using WC powder. FSW was carried out by 600rpm of tool rotation and 420mm/min of travel speed. Microstructure of the welding zone was precisely investigated by using OM, SEM and TEM. Vickers-hardness, tensile test and impact test were carried out to analyze the mechanical properties of the joint.

9:45 AM

Modeling of Pulsed-Laser Superalloy Powder Deposition Using Moving Distributed Heat Source: *Manas Mahapatra*¹; Leijun Li²; ¹Indian Institute of Technology Roorkee; ²Utah State University

A three-dimensional finite element model with moving heat source was developed for pulsed-laser powder deposition process. Experiments were conducted to study the repairing of superalloy components using the PLPD process. During the experiments, IN 625 powder was deposited on superalloy substrate similar to IN 738. The process was modeled using three-dimensional finite element analysis. Element birth and death technique was used in the finite element model for simulating the deposition of powder layer on the substrate. Moving distributed heat source was used in the thermal model for realistic simulation of the process. Temperature dependent thermal material properties including enthalpy were used for the powder and the substrate in the transient thermal analyses. The fusion zones and peak temperature distributions of the deposits were predicted from the transient thermal analyses.

10:10 AM

Heat Transfer Characteristics of Magnetite under Microwave Irradiation: *Zhiwei Peng*¹; Jiann-Yang Hwang¹; Matthew Andriese¹; Zheng Zhang¹; Xiaodi Huang¹; ¹Michigan Technological University

A simplified finite-difference time-domain (FDTD) algorithm for modeling microwave propagation in magnetic dielectric materials was developed and employed to study the microwave dissipation in magnetite. Heat transfer during microwave heating of magnetite was subsequently investigated by solving heat transfer differential equation using explicit finite-difference (EFD) method. It is observed that temperature of magnetite surface increases rapidly in the first minute due to the rapid strength decays in both electric and magnetic fields within a short distance



TMS 2012

141st Annual Meeting & Exhibition

along the path of microwave dissipation. A temperature peak, initially formed at the surface of the sample slab, migrates inward as heating time extends and microwave power increases.

10:35 AM Break

10:50 AM

Effect of Microwave Curing on GFRP Composites: *T. Srinath*¹; P. Martin Jebaraj¹; Rajaiah K¹; ¹Dr. Ambedkar Institute of Technology

Optimizing matrix for preparation of composites Manufacturing by lay-up and rolling with curing methods namely room temperature, microwave and analysis by Matrix Digestion Test is undertaken in this work. Microwave curing was done on several fluids like water, milk and SAE 90 grade oil. Later resin was tried out at different time intervals. Lay-up specimens were tried for curing in both methods. Except for mat, other specimens showed right response for curing. Rolled specimens cures faster as compared to hand lay-up specimens. This is due to the right compaction which goes into the rolled specimen. Microwave curing initiates at micro level and the results indicate this trend with roving performing better in rolling and electron beam curing than fabric which is denser thereby implying that the wetting of individual strands of glass fiber is a must for proper bonding and thereby faster curing.

11:15 AM

Experimental and Numerical Approach for Surface Finish during Laser Machining of Alumina: *Hitesh Vora*¹; Sameer Paital¹; Sandip Harimkar²; Sandra Boetcher¹; Narendra Dahotre¹; ¹University of North Texas; ²Oklahoma State University

High energy infrared lasers have popularly emerged as a potential tool for bulk material removal of structural ceramics. Despite of having this popularity the actual implementation of this technology is not making inroads into actual application due to the undesirable surface finish generated during laser machining. Addressing this issue via multiphysics modeling and thereby controlling the surface finish by selection of appropriate laser processing parameters is discussed herein. In the current study, the machining of alumina is investigated by using a JK 701 pulsed Nd:YAG laser. The surface roughness of the machined surfaces was characterized using an optical profilometer. A finite element model is developed using COMSOL(TM)multiphysics to understand the influence of physical phenomena such as recoil pressure, Marangoni convection, surface tension, and cooling rates over the surface morphology of alumina and eventually establish the relationship between the surface finish and process parameters of laser machining.

11:40 AM

Refinement Effect of Pulse Magneto-Oscillation on Solidification Structure of Medium Carbon Steel: *Yufeng Cheng*¹; Zhengxin Yin¹; Xin Cao¹; Yongyong Gong¹; Renxing Li¹; Qijie Zhai¹; ¹Shanghai University

This paper investigated the refinement effect of pulse magnet-oscillation (PMO) on the solidification structures of medium carbon steel S45C in metal mould. The induction coil was positioned at the middle of ingot. The results showed that solidification structure of the treated ingot was remarkable modified, forming a large volume of fine globular grains comparing with the untreated ingot. Further experimental investigation and theoretical analysis demonstrated that the reason for grain refinement of solidification structure was that PMO promoted nucleation near mould walls and agitated nuclei into the melt, eventually leading to a transition from columnar crystal to equiaxed crystal.

12:05 PM

Research on Solidification Structure Refinement of SUS430 Ferritic Stainless Steel by Electric Current Pulse: *Xin Cao*¹; Zhenxing Yin¹; Yufeng Cheng¹; Renxing Li¹; Yongyong Gong¹; Qijie Zhai¹; ¹Shanghai University

The influence of electric current pulse (ECP) on the solidification structure of SUS430 ferritic stainless steel (FSS), which is widely used on behalf of the excellent properties and relatively low cost, has been investigated. The parallel electrodes were inserted into the free melt surface to constitute a

current loop. The different influences of three parameters on solidification structure were studied by changing the peak current value, frequency and treating time respectively. The results indicated that the ECP significantly increased the number of equiaxed grains of SUS430 FSS. The as-cast structure without ECP treating was almost wholly columnar, while the number of equiaxed grains of the specimen, which was treated 3min with a peak current of 400kIA, increased to 2698 in the observed surface. To get the best refinement, an optimum range of these three parameters is required and the peak current value plays the most important role.

Materials Research in Microgravity: Session III

Sponsored by: The Minerals, Metals and Materials Society, TMS Materials Processing and Manufacturing Division, TMS Extraction and Processing Division, TMS: Process Technology and Modeling Committee, TMS: Solidification Committee

Program Organizers: Robert Hyers, University of Massachusetts; Hani Henein, University of Alberta; Valdis Bojarevics, University of Greenwich; James Downey, NASA; Douglas Matson, Tufts University; Achim Seidel, Astrium; Daniela Voss, ESA

Tuesday AM

March 13, 2012

Room: Asia 3

Location: Dolphin Resort

Session Chair: To Be Announced

8:30 AM Invited

Ground-Based Studies of the Structure and Properties of High Temperature Liquids for Upcoming ISS Experiments: *Ken Kelton*¹; ¹Washington University

Studies of electrostatically-levitated supercooled liquids have demonstrated strong short- and medium-range ordering in transition metal and alloy liquids, which can influence phase transitions like crystal nucleation and the glass transition. It is also related to the liquid properties. In well ordered liquids, for example, we recently demonstrated local maxima in the expansivity of liquids that form bulk glasses and a specific heat maximum at a temperature above the glass transition temperature in a Zr58.5Nb2.8Cu15.6Ni12.8Al10.3 liquid (Vit 106a). Planned ISS experiments will allow a deeper investigation of these results as well as the first investigations of a new type of coupling in crystal nucleation in primary crystallizing liquids, resulting from a linking of the stochastic processes of diffusion linking with interfacial-attachment. Select ground-based studies and the planned ISS investigations will be discussed. Supported by NASA (NNX07AK27G & NNX10AU19G) and the National Science Foundation (DMR-08-56199).

9:05 AM Invited

Thermophysical Properties Measurement of High-Temperature Liquids under Microgravity Conditions in Controlled Atmospheric Conditions: *Masahito Watanabe*¹; Shumpei Ozawa²; Akitoshi Mizuno¹; Taketoshi Hibiya³; Hiroya Kawauchi¹; Kentaro Murai¹; Suguru Takahashi²; ¹Gakushuin University; ²Tokyo Metropolitan University; ³Keio University

Microgravity conditions have advantages of measurement of surface tension and viscosity of metallic liquids by the oscillating drop method with an electromagnetic levitation (EML) device. We are planning measurements of the surface tension and viscosity in ISS using MSL-EML facilities developed by ESA under the controlled oxygen partial pressure conditions. The measurements will be performed by the international collaboration team including our science team. For the preparation of ISS experiments, we performed the precise observation of surface oscillations of levitated metals liquids by on-board flight experiments under the controlled oxygen partial pressure. These measurements were also performed with the change of currents to coils in order to detect the difference of surface oscillation frequency and dumping time by the electromagnetic force. Base on the present result, we discuss about the improvement of the analysis of surface oscillations to obtain the surface tension and the viscosity for precisely measurements in ISS.

9:40 AM

Microgravity Research on Bulk Metallic Glasses and Composites: *Douglas Hofmann*¹; ¹NASA JPL/Caltech

Bulk metallic glasses (BMGs) are a novel class of amorphous metals which were developed by the Caltech group during microgravity flights on the Space Shuttle and International Space Station under NASA's Microgravity Research Program. The development of these alloys lead to a commercial industry for BMGs including applications such as golf clubs and cell phone cases, among many others. Recent efforts have focused on the development of BMG composites; metal matrix composites reinforced with a ductile phase to improve ductility and fracture toughness. This talk focuses on the study of these alloys under the current NASA ESMD program. A discussion about processing BMG composites in the semi-solid region, along with experimental data obtained using the JPL/Caltech electrostatic levitation platform will be presented. These amorphous materials offer not only a chance to do interesting microgravity science, but also an opportunity to contribute to a wide range of NASA spaceflight hardware.

10:05 AM Break

10:20 AM Invited

Detachment of Tertiary Dendrite Arms during Controlled Directional Solidification in Aluminum – 7 wt% Silicon Alloys: Observations from Ground-based and Microgravity Processed Samples: *Richard Grugel*¹; Robert Erdmann²; James Van Hoose³; Surendra Tewari⁴; David Poirier²; ¹Marshall Space Flight Center; ²University of Arizona; ³Qualis/Jacobs; ⁴Cleveland State University

Electron Back Scattered Diffraction results from cross-sections of directionally solidified aluminum – 7wt% silicon alloys unexpectedly revealed tertiary dendrite arms that were detached and mis-oriented from their parent arm. More surprisingly, the same phenomenon was observed in a sample similarly processed in the quiescent microgravity environment aboard the International Space Station (ISS) in support of the joint US-European MICAST investigation. The work presented here includes a brief introduction to MICAST and the directional solidification facilities, and their capabilities, available aboard the ISS. Results from the ground-based and microgravity processed samples are compared and possible mechanisms for the observed tertiary arm detachment are suggested.

10:55 AM

Microstructure Formations in the Two Phase Region of the Binary Peritectic Organic System TRIS-NPG: *Andreas Ludwig*¹; Johann Mogeritsch¹; ¹University of Leoben, Dep. Metallurgy

In order to prepare for an onboard experiment on ISS on isothermal coupled peritectic growth (PCG), systematic directional solidification experiments were done with TRIS-NPG organic peritectic alloys. It turned out that under specific conditions isothermal PCG were obtained for alloys within the hypo-peritectic region either by (i) reducing the growth velocity from above the critical value for morphological stability of both solid phases to a value below, or by (ii) long-time growing with a constant velocity below the critical value for morphological stability of both solid phases. The later happens via island banding, where nucleation and lateral growth of the peritectic phase compete with growth of the primary phase. Interphase spacings and the widths of alpha and beta lamellae were measured as function of growth velocity for a fixed composition and as function of composition for a fix growth velocity.

11:20 AM

Thermodynamics of Metal-Gas Eutectic Solidification and Potential Effects of Gravity on Microstructural Evolution: *Douglas Swenson*¹; Paul Sanders¹; Amber Lifer¹; Helen Ranck¹; ¹Michigan Technological University

Porous metals may be fabricated by saturating the metal liquid with a soluble gas species, followed by solidification during which the gas comes back out of solution. Under appropriate solidification conditions, cooperative growth of solid metal and aligned, tubular gas pores occurs.

Additionally, it is possible to tailor the microstructure by changing processing conditions, such as by introducing an insoluble gas species that increases the total pressure and affects the volume fraction of pores. In the literature, there is no complete thermodynamic description of such a process. Here, such a description is presented, showing explicitly the effects of both inert and soluble gases on corresponding phase equilibria and porosity of metal-gas systems. The analysis is applied to several common metal-hydrogen systems, based on available literature data. Finally, potential effects of gravity upon microstructural development are discussed.

11:45 AM

Three-Dimensional Phase Field Modeling of Directional Solidification under Microgravity Conditions with Quantitative Experimental Comparison: *Damien Tournet*¹; Alain Karma¹; Rohit Trivedi²; Bernard Billia³; Nathalie Bergeon³; Jean-Marc Debierre³; Rahma Guerin³; ¹Northeastern University; ²Iowa State University; ³Institut Matériaux Microélectronique Nanosciences de Provence, UMR CNRS 6242

We present the first quantitative comparison of three-dimensional phase-field simulations with solid/liquid interface dynamics observed during directional solidification of succinonitrile (SCN)-camphor alloys conducted on the International Space Station. A massively parallel implementation of a quantitative phase-field model on Graphics Processing Units (GPU) is used to simulate large systems of many cells in 3D on experimentally relevant length and time scales. The simulations reproduce an experimentally observed oscillatory mode of cellular hexagonal array structure and show excellent agreement with observed behaviors, such as: (i) the period of the oscillations, (ii) a coordinated motion of three groups of cells of the hexagonal array structure and (iii) tip splitting events, enabling the adjustment of the average cell spacing. Microgravity was crucial in uncovering this oscillatory behavior, normally altered by convection effects under terrestrial conditions. Ongoing work focuses on understanding the mechanism of oscillations and the influence of the array structure and growth parameters.

Mechanical Behavior at Nanoscale I: Deformation Mechanisms at Nanoscale

Sponsored by: The Minerals, Metals and Materials Society, TMS Materials Processing and Manufacturing Division, TMS: Nanomechanical Materials Behavior Committee, TMS/ASM: Mechanical Behavior of Materials Committee

Program Organizers: Scott Mao, University of Pittsburgh; Julia R Greer, California Institute of Technology; Jianyu Huang, Center for Integrated Nanotechnologies; Marc Legros, CEMES-CNRS; Ting Zhu, Georgia Institute of Technology

Tuesday AM
March 13, 2012

Room: Asia 1
Location: Dolphin Resort

Session Chairs: Marc Legros, CEMES-CNRS; Jianyu Huang, Sandia National Lab

8:30 AM Invited

Shear Banding Mechanism in Nano-Twinned Cu–Al Alloy: *C.S. Hong*¹; N.R. Tao¹; X.X. Huang²; *K. Lu*¹; ¹Chinese Academy of Sciences; ²Riso National Lab

Microstructural evolution during shear banding in a nano-twinned Cu–Al alloy processed by means of dynamic plastic deformation was investigated using TEM and high-resolution TEM. The development of a shear band was found to include a nucleation stage followed by thickening. The nucleation consists of initiation of localized deformation, evolution of a dislocation structure, and transformation of the detwinned dislocation structure into a nano-grained structure. Increasing shear strains leads to thickening of shear bands at the expense of the adjoining twin/matrix lamellae, of which the mechanism is carefully characterized. Grain sizes

TUESDAY AM



TMS 2012

141st Annual Meeting & Exhibition

in the well-developed shear bands are found to be obviously larger than the original twin thickness. Experimental observations will be analyzed in comparison with computational simulations.

9:00 AM Invited

Stochastic Effects in Deformation and Fracture of Nanowires: Andreas Sedlmayr¹; Reiner Mönig¹; Steven Boles¹; Gunther Richter²; Oliver Kraft¹; ¹KIT; ²Max-Planck-Institut für Intelligente Systeme

In several studies, nanowires made of different materials with thickness of 100 nm and below were found to have strength of the order of the theoretical strength of the respective material. It has been argued that this relates to a more or less defect free state of the nanowires after fabrication. In this paper, we present tensile tests on nanowires inside a dual beam SEM/FIB. In Au nanowires, significant amounts of plasticity at high stresses in excess of 1 GPa were found. The recorded data show a weak size dependence with a large scatter in the strength values. Different modes of failure were observed which include twinning as confirmed by EBSD indicating activity of partial dislocations. However, the scatter in the strength data suggests that nucleation of partial dislocations occurs at imperfections at the nanowire surface. These observations are discussed considering a weakest-link approach for describing the statistical effects.

9:30 AM

Plasticity in BCC Pillars Observed In-Situ by Laue Diffraction: Helena Van Swygenhoven¹; Julien Zimmermann¹; Cecile Marichal¹; Steven Van Petegem¹; ¹Paul Scherrer Institute

In-situ Laue diffraction is applied on bcc pillars, with the aim to understand the difference in size effect between bcc and fcc single crystals. Mo pillars obtained from a directionally solidified NiAl-Mo eutectic were investigated in the as-grown, in the 11% pre-strained conditions, and after FIB milling. Careful analysis of the diffraction patterns show that the diffraction peaks move initially along a rotation direction corresponding to slip on (1 1 2) plane with streaking along a [1 1 1] direction, the choice of the (112) plane being influenced by pre-existing strain gradients. A similar analysis is performed on W single crystal pillars, a material with a much higher T_c. The Laue diffraction analyses are complemented by SEM slip trace and TEM dislocation analysis. The slip behavior of single bcc pillars is discussed in terms of T_c, the role of FIB damage and the initial presence of dislocations due to pre-straining.

9:50 AM

Discrete Plastic Deformation in Gold Nanowires: Scott Mao¹; He Zheng¹; Christopher R. Weinberger²; Jianyu Huang²; ¹University of Pittsburgh; ²Sandia National Lab

Through in-situ HRTEM observations, we show that the tensile deformation behavior of sub-ten-nanometer Au nanocrystals is drastically different from that of the bulk counterpart. In sharp contrast to the scenario that plasticity is mediated by dislocation emission from Frank-Read sources and multiplication in bulk materials, partial dislocations emitted from free surfaces, which produce fresh surface steps after they annihilate at the free surfaces, dominate the deformation of Au nanocrystals. Stress-relief caused by the surface-mediated plastic deformation is directly visualized. Additionally, these experiments verify that the crystallographic orientation (Schmid factor) is not the only factor in determining the deformation mechanism of nanometer-sized Au. After failure, the Au nanocrystal shows a phase transformation from face-centered-cubic (FCC) to body-centered-tetragonal (BCT) structure. The transformation is facilitated by surface stresses, which are able to drive the <001> crystal along the Bain path from FCC to BCT.

10:10 AM Break

10:20 AM Invited

Deformation Mechanisms in Small Scale Al: An In-Situ TEM Study: Frederic Mompiou¹; ¹CEMES-CNRS

Metals with reduced dimensions demonstrate a clear trend of strengths that scale as a power-law of their size. Because both dislocation nucleation and motion are constrained in these materials, alternate plasticity mechanisms

are expected. In sub-micron monocrystalline Al fibers, where the initial dislocation microstructure is well characterized, we have shown, using in-situ TEM, that the multiplication of dislocations through spiral sources directly causes an increase of the yield stress as the fiber section is reduced. This situation contrast with the brittle behavior of fibers containing no or few initial defects. These observations and measurements bridge the gap between strength of whiskers and the strengthening of micropillars with size. In nanocrystalline and UFG Al, dislocation mechanisms can be shut down in specific conditions. We have found that the coupling of the grain boundary migration with stress can be an efficient deformation process. The strain produced can be measured and tentatively modeled.

10:50 AM Invited

Stochastic Behavior of Dislocation Nucleation in Solids with Defects: David Bahr¹; Yoonkap Kim¹; Christine Joseph¹; Benjamin Revard¹; Iman Salehnia¹; ¹Washington State University

Examining the onset of plasticity in small volumes of materials using nanoindentation requires consideration of two size scales; that of the indenter (and hence stress fields and gradients) and that of the spatial variation in defect location. In this study we examine the effect of vacancies, solid solution impurities, and defects generated by FIB damage on the onset of plasticity in FCC, BCC, and HCP metals. In general the distribution of yield points suggests that multiple defects often control the measured range of incipient plasticity. In most of these systems we are able to also distinguish yield event that correspond to non-uniform deformation processes but are clearly not dislocation nucleation. Using a combination of tip radius and loading rate variation and composition variation it is shown that extremes in yield conditions are likely controlled by defect position relative to the tip size.

11:20 AM

Nanovoid Generation and Growth in Metals: Dislocation Mechanisms: Marc Meyers¹; Yizhe Tang¹; Eduardo Bringa²; Bruce Remington³; ¹University of California, San Diego; ²Univ. Nac.Cuyo; ³Lawrence Livermore National Laboratory

The cooperative emission of shear loops creates the geometrically necessary dislocations responsible for the generation and growth of nanovoids in FCC and BCC metals. The extremities of the dislocation shear loops remain attached to the void surface. In copper, partial dislocation loops generate extended stacking faults that impede cross slip. In tantalum, prismatic loops can form by reaction of multiple shear loops sharing the same <111> slip direction, or by cross slip of the two screw components of a single shear loop in different slip planes. Twinning can also occur. The effect of void-size on the initiation stress was found to be significant. The defect nucleation stress decreases with increasing void size (up to 30 nm radius void in tantalum). This void-size dependent plasticity is also modeled based on dislocation mechanics, and a good agreement is found. In real metals, there is a hierarchy of defects giving rise to voids.

11:40 AM

Deriving Deformation Mechanisms in Nanocrystalline AuCu Thin Films from *in situ* Synchrotron-Based XRD and SEM Tensile Tests: Jochen Lohmiller¹; Patric Gruber¹; Ralph Spolenak²; ¹Karlsruhe Institute of Technology; ²ETH Zurich

A prerequisite to exploit the unique combination of high strength and high ductility of nanocrystalline (nc) materials is a thorough understanding of the underlying deformation mechanisms. *In situ* tensile tests were conducted with a synchrotron-based X-ray diffraction setup and in a SEM on nc gold and gold-copper thin films adherent to polymer substrate. The use of compliant substrate enables macroscopically homogeneous and cyclic deformation of the nc films. Shear banding, film fracture and specific deformation texture formation are identified in the comprehensive study and allocated to different stages of deformation. This allows deriving a series of deformation mechanisms dependent on the applied strain. The results also show composition dependent behavior, in which the proneness to localized deformation and texturing is increasing with enhanced copper

contents, whereas the most ductile films with no or low copper contents did not crack up to maximum strains of 30%.

12:00 PM

Characterization of Deformation Mechanisms during Cold Rolling of Nanocrystalline Nickel: *Jorg Wieszorek*¹; *Andreas Kulovits*¹; ¹University of Pittsburgh

Microstructural evolution of nanocrystalline Nickel in response to cold rolling has been studied by X-ray diffraction (XRD) and transmission electron microscopy (TEM). Glide of individual dislocations emitted and absorbed by grain boundaries (GB) facilitated the necessary orientation and shape changes of grains. Global and local texture changes during cold deformation were determined by combining XRD and TEM measurements. Grain size changes were monitored quantitatively using a novel computer controlled orientation imaging system in the TEM, which is based on precession illumination. Initially during cold rolling the dislocation-GB interactions alter locally the GB character. High angle GB transform into low angle GB and subsequently dissolve, leading to grain coarsening, e.g. by coalescence. At large thickness reductions, coarsened grains facilitate a deformation mechanism change where grain interior dislocation-dislocation interactions instead of dislocation-GB interactions mainly facilitate plastic deformation inclusive of strain hardening.

12:20 PM

Probing the Relation between Indentation Characteristics and Dislocation Substructure: *Lin Li*¹; *Myoung-Gyu Lee*²; *Peter Anderson*¹; ¹The Ohio State University; ²POSTECH

Novel indentation studies [1] show that large (>50%) drops in indentation load correlate with major instabilities in dislocation substructures. We study this phenomenon using a finite element based scheme in which an Al grain is discretized into patches ~dislocation cell size. At a critical resolved stress, a cell can spontaneously shear along any of the 12 $\{111\}/\langle 110 \rangle$ slip systems. This imparts a burst of plastic strain that can trigger large multi-cell avalanches. Large experimental load drops are reproduced when the scale of indentation ~ substructure scale and the magnitude of strain burst ~ critical resolved shear stress/elastic shear modulus. For the Al grain, this corresponds to strain bursts of 4 to 8%, equivalent to 4 to 8 dislocations propagating across ~30 nm cells. This study shows how key features of the dislocation substructure are revealed through nanoindentation traces. [1] Minor, AM, et. al., Nature Mater., (2006) 5, 697.

Mechanical Behavior Related to Interface Physics: Microscopic Characterization of Interface Mechanical Response

Sponsored by: The Minerals, Metals and Materials Society, TMS Structural Materials Division, TMS Materials Processing and Manufacturing Division, TMS/ASM: Mechanical Behavior of Materials Committee, TMS: Nanomechanical Materials Behavior Committee

Program Organizers: Jian Wang, Los Alamos National Laboratory; Nathan Mara, Los Alamos National Laboratory; Izabela Szlufarska, University of Wisconsin-Madison; Zhiwei Shan, Xi'an Jiaotong University

Tuesday AM
March 13, 2012

Room: Oceanic 1
Location: Dolphin Resort

Session Chairs: Andrew Minor, UC Berkeley & LBL; Scott Mao, University of Pittsburgh

8:30 AM Keynote

Understanding Dislocation Interactions with Interfaces: *Josh Kacher*¹; *Ben Eftink*¹; *Ian Robertson*¹; ¹University of Illinois

Interfaces serve both as sources and sinks for dislocations. Despite this important role we are still learning about the relationships between dislocations and grain boundaries as well as with interfaces between

dissimilar metals, and how the relationships scale dimensionally. For example, coarse-grained copper deforms primarily through dislocation slip. However, in copper-silver eutectic alloys it has been observed that the primary deformation mechanism is deformation twinning, with twinning in copper being driven by that in silver. This talk will emphasize how coupling of electron microscopy techniques, including conventional analysis, time resolved and electron tomography, with computational tools is providing new insight as to how dislocations and deformation twins are generated at and interact with interfaces, and how these interactions affect the mechanical response of the material to deformation.

9:00 AM Keynote

Probing the Origin and Evolution of Strength in Small Volumes with In Situ TEM Nanomechanical Testing: *Andrew Minor*¹; ¹UC Berkeley & LBL

Recent progress in both in situ and ex situ small-scale mechanical testing methods has greatly improved our understanding of mechanical size effects in volumes from a few nanometers to a few microns. This talk will describe our recent results from in situ TEM compression and tensile testing of FCC, BCC and HCP metals to illuminate the origin of size-dependent yield strength behavior and fundamental deformation structures in nanoscale samples. In addition, comparing in situ compression and tensile testing has led to some interesting observations regarding the evolution of flow strength in nanoscale samples during testing. Lastly, this talk will comment on recent progress related to in situ TEM nanoscale mechanical testing methods and their relevance to bulk mechanical properties.

9:30 AM

Direct Observation of Dislocation Confined Layer Slip in Multilayers: *Nan Li*¹; *Jian Wang*¹; *Jianyu Huang*²; *Amit Misra*¹; ¹LANL; ²Sandia National Lab

Using in situ nanoindentation in a transmission electron microscope (HRTEM), we have studied the confined layer slipping behavior of threading dislocations in Cu/Nb multilayers with individual layer thickness of ~ 20 nm. The observations indicate that Cu-Nb interface can act both as dislocation source and barriers for slip transmission. These findings provide insights in understanding the plastic deformation mechanisms, the high strength, and work hardening of multilayer systems. This project is supported by the DOE, Office of Science, Basic Energy Sciences, Division of Materials Science and Engineering.

9:45 AM

In Situ Observation of Dislocation Assisted Stress Driven Grain Boundary Migration: *Zhangjie Wang*¹; *Zhiwei Shan*¹; *Ju Li*²; *Jun Sun*¹; *Evan Ma*³; ¹Center for Advancing Materials Performance from the Nanoscale (CAMP-Nano) & Hysitron Applied Research Center in China (HARCC), State Key Laboratory for Mechanical Behavior of Materials, Xi'an Jiaotong University; ²Department of Nuclear Science and Engineering and Department of Materials Science and Engineering, Massachusetts Institute of Technology; ³Department of Materials Science and Engineering, Johns Hopkins University

Grain boundary (GB) hardening has been an efficient way to tailor the mechanical properties of metals and alloys by introducing GBs as the obstacles to dislocation motion. However, with the decreasing of the grain size, the recent published works indicate that the stresses driving GB migration manifested as grain growth in nanocrystalline materials [such as Science, 1686, (2009)]. In our present work, we compressed the Al nanopillar (D~200nm) with one GB inside a TEM. The in situ quantitative testing shows that under 800MPa contact stress, the GB are not mechanically static structures anymore and it migrated out of the pillar finally. Initially, high density dislocations are piled-up against the GB. However, the GB was broken down under high stress state upon the crash of flood-like dislocations. The in situ quantitative examination of a specific and representative GB allows the further understanding of the GB behavior in nanocrystalline materials.



TMS 2012

141st Annual Meeting & Exhibition

10:00 AM

The Influence of Grain Boundary Structure upon Damage Evolution at Grain Boundary Interfaces: *Alejandro Perez-Bergquist*¹; Christian Brandl¹; Juan Escobedo¹; Carl Trujillo¹; Ellen Cerreta¹; George Gray III¹; Timothy Germann¹; ¹Los Alamos National Laboratory

In a prior work, it was found that grain boundary structure strongly influences damage evolution at grain boundaries in copper samples subjected to either shock compression or incipient spall. Here, several grain boundaries with different grain boundary structures, including a S3 (10-1) boundary, are interrogated via conventional transmission electron microscopy (TEM) and high-resolution transmission electron microscopy (HRTEM) to investigate the effects of atomic-scale structural differences on grain boundary strength and mobility. Boundaries are studied both before and after shock compression at a peak shock stress of 10 GPa. Results of the TEM and HRTEM work are used in conjunction with MD modeling to propose a model for shock-induced damage evolution at grain boundary interfaces that is dependent upon coincidence.

10:15 AM Break

10:25 AM Keynote

Surface and Interface Controlled Plasticity and Phase Transition in Nanometer-Sized Au Crystals: *Scott Mao*¹; He Zheng¹; Jianyu Huang²; Christopher R. Weinberger²; ¹University of Pittsburgh; ²Sandia National Lab

We report the in-situ TEM observation on surface and interface controlled deformation and phase transition. In sharp contrast to the scenario that plasticity is mediated by dislocation emission from Frank-Read sources and multiplication in bulk materials, partial dislocations emitted from free surfaces, which produce fresh surface steps after they annihilate at the free surfaces, dominate the deformation of Au nano-crystals. Stress-relief caused by the surface-mediated plastic deformation is directly visualized. After failure, the Au nanocrystal shows a phase transformation from face-centered-cubic (FCC) to body-centered-tetragonal (BCT) structure. The transformation is facilitated by surface stresses, which are able to drive the <001> crystal along the Bain path from FCC to BCT. The central theoretical prediction that plastic deformation in nanometer-sized crystals is dominated by surfaces has been directly verified using in-situ HRTEM.

10:55 AM Keynote

Grain Boundaries and Strength in Nanostructured Metals Produced by Plastic Deformation: *Xiaoxu Huang*¹; Niels Hansen¹; ¹Risø National Laboratory for Sustainable Energy, Technical University of Denmark

Nanostructured metals produced by plastic deformation are characterized by high angle boundaries, low angle dislocation boundaries and interior dislocations and strengthening mechanisms are strongly related to interactions between dislocations and boundaries of various misorientations and structures. In particular, the narrowly spaced high angle boundaries act as sinks of dislocations or as dislocation sources, which will control the strengthening mechanisms. The effect of dislocation structures on the strength and ductility of nanostructured metals processed by plastic deformation to very high strains has been investigated by varying the dislocation structure either by annealing or by additional plastic deformation. It has been found that the yield strength increases after annealing and decreases after additional deformation. These unusual observations are interpreted by introducing dislocation source limited strengthening in the former case and dislocation softening in the latter case.

11:25 AM

Twinning in Bulk Nanolayered AgCu under High Strain Rate: *Ben Eftink*¹; Owen Kingstedt¹; Buyang Cao¹; Doug Safarik²; John Lambros¹; Nathan Mara²; Ian Robertson¹; ¹University of Illinois; ²Los Alamos National Lab

Materials with heterophase interfaces show increased strength and potential for enhanced irradiation resistance. Bulk Ag₆₀Cu₄₀ cast eutectic exhibits a layered structure resulting in a high density of heterophase interfaces. This study investigates the mechanical response of a AgCu cast eutectic after compression at strain rates on the order of 10³ s⁻¹. TEM analysis of the deformed microstructure shows twinning in both silver and copper layers. Twins are observed to run parallel to some interfaces and to extend from both sides of others. This latter result suggests twinning in silver facilitates twinning in copper. The deformation behavior exhibited during high strain rate loading will be discussed in terms of defect interactions with interfaces and dislocation-based deformation mechanisms.

11:40 AM

Interfaces and Mechanical Properties of Highly Textured Cu/Co Multilayers: *Yue Liu*¹; Youxing Chen¹; Haiyan Wang¹; Ji Chen²; Xinghang Zhang¹; ¹Texas A&M University; ²Liaoning Shihua University

Certain metallic multilayers have shown superior properties, including the achievement of close-to-theoretical strength, fatigue resistance, excellent thermal stability and radiation tolerance. In this study, we investigate the interfaces and mechanical properties of sputtered, highly textured FCC(100)Cu / FCC(100)Co and FCC(111)Cu / HCP(0001)Co multilayers with individual layer thickness, h, varying from 1 to 200nm. Coherency along interfaces in the immiscible systems are increases gradually when h decreases to below 10nm, and fully epitaxial films form when h is 2.5nm or less. In FCC(100) Cu/Co multilayers, TEM studies reveal high density of inclined stacking fault in Co, whereas in FCC(111) Cu / HCP(0001)Co multilayers, high density stacking fault and twins are observed. Large discrepancy of size dependent indentation hardnesses in the two systems are observed at all h. The difference in strengthening mechanisms in the systems are discussed and compared to those of highly textured Cu/Ni multilayer systems.

11:55 AM

Deformation and Spallation of Shocked Cu Bicrystals with S3 Coherent and Symmetric Incoherent Twin Boundaries: *Weizhong Han*¹; Sheng-Nian Luo¹; Timothy C Germann¹; Davis L Tonks¹; ¹Los Alamos National Lab

Grain boundaries (GBs) play a critical role in the mechanical performance of metals and alloys. Given the vast number of GB types, it is highly desirable to investigate some elemental processes in order to guide materials design. In this investigation, we perform molecular dynamic (MD) simulations of Cu bicrystals with S3 coherent twin boundaries (CTB) and symmetric incoherent twin boundaries (SITB) under shock wave loading. It is revealed that the shock response of the Cu bicrystals strongly depends on the GB characteristics. At shock compression stage, elastic shock wave can readily trigger GB plasticity at SITB, while not at CTB. The SITB can induce considerable wave attenuation such as elastic precursor decay. At the tension stage, spallation tends to occur at CTB while not at SITB due to the high mobility of SITB. In addition, twinning is a mechanism in inducing surface step during shock.

TUESDAY AM

Mechanical Performance of Materials for Current and Advanced Nuclear Reactors: Characterization and Modeling of Dislocation Structures in Nuclear Materials

Sponsored by: The Minerals, Metals and Materials Society, TMS Structural Materials Division, TMS/ASM: Nuclear Materials Committee

Program Organizers: Nicholas Barbosa, National Institute of Standards & Tech; Greg Oberson, United States Nuclear Regulatory Commission; Matthew Kerr, United States Nuclear Regulatory Commission; Elaine West, Knolls Atomic Power Laboratory; Stuart Maloy, Los Alamos National Laboratory; Osman Anderoglu, LANL

Tuesday AM
March 13, 2012

Room: Swan 1
Location: Swan Resort

Session Chairs: Elaine West, Knolls Atomic Power Laboratory; Osman Anderoglu, Los Alamos National Laboratory

8:30 AM Invited

Understanding the Dislocation Processes and Interactions Responsible for Creating Defect-Free Channels in Deformed Irradiated Metals:

Josh Kacher¹; Grace Liu¹; Ian Robertson¹; ¹University of Illinois

The microstructure of deformed irradiated materials is characterized by cleared channels within a field of irradiation-produced defects. Through a combination of characterization of bulk deformed irradiated stainless steel and in-situ deformation in a transmission electron microscope of irradiated metals, the source of the dislocations responsible for creating the channels, the interaction of dislocations with individual defects and grain boundaries, and channel widening mechanisms have been discovered. This talk will show for stainless steels, the dislocations responsible for creating the channels are generated anew from grain boundaries and stress concentration sites; dislocation progress through the defect field is erratic and intermittent; the channel width reflects the width of the source and complex cross-slip reactions; and dislocation pile-ups form in the grain interior and at dislocation sources as well as at grain boundaries. The complex configuration of dislocations in cleared channels is revealed by using electron tomography.

9:00 AM

Planar Dislocations and Dislocation Channeling in Unirradiated and Irradiated Austenitic Stainless Steels:

Young Suk Kim¹; Sung Soo Kim¹; Dae Whan Kim¹; ¹Korea Atomic Energy Research Institute

Tensile tests were conducted on 316L stainless steel with nitrogen over a temperature range of RT to 750°C at strain rates of 2x10⁻⁴/s. The 316L stainless steel (SS) showed serrated flow in a temperature range of 400 to 600°C where a linear increase of strain hardening was accompanied. Using neutron diffraction, the lattice contraction due to atomic ordering was seen to occur in the 40% cold-worked 316 SS on aging at 400°C. TEM microstructures showed the formation of planar dislocations in 316L SS upon tensile testing at 400°C where SRO and serrated flow appeared. This study demonstrates that SRO is the cause of planar dislocations and serrations in austenitic stainless steels. Given that neutron irradiation produces dislocation channeling and softening after yielding in austenitic stainless steels above some fluences, the cause of dislocation channeling and softening in irradiated 304 stainless steels is discussed with short range ordering.

9:20 AM

Incorporation of Dislocation Climb in Crystal Plasticity Models:

Alankar Alankar¹; Alfredo Caro¹; Ricardo Lebensohn¹; ¹Los Alamos National Laboratory

This work presents an improved plasticity model for single crystals deforming by a combination of dislocation glide and climb. A constitutive framework based on dislocation densities has been implemented in a viscoplastic self-consistent (VPSC) formulation. Accounting for the explicit evolution of edge and screw dislocations densities enables the instantaneous determination of the climb tensor, which depends on the average character of the mobile dislocations. Mobilities of dislocations accommodating deformation by climb and glide, which depend on their interaction with point defects, are determined using kinetic Monte Carlo simulations.

9:40 AM

Polycrystalline Modelling of the Behaviour of Neutron Irradiated Zirconium Alloys and Comparison with TEM Observations:

Fabien Onimus¹; ¹CEA

The deformation mechanisms of recrystallized zirconium alloys are strongly affected by neutron radiation resulting in dramatic change of the macroscopic mechanical behaviour. It is especially observed, using transmission electron microscopy, that the dislocation channelling process in the basal plane is the main deformation mechanism after irradiation. A polycrystalline modelling that takes into account both the specific post-irradiation deformation mechanisms as well as the texture of the material has been developed. This physically based model reproduces the mechanical behaviour of the material for both monotonic and cyclic tests. The slip systems activities have been computed for more than 40 grains that were observed by TEM. The activation of basal slip, observed in many of these grains, is very well predicted by the modelling. Moreover, the activation of (c+a)-pyramidal slip observed only in few grains is also well predicted showing the reliability of the modelling.

10:00 AM

The Interaction Energy between Point and Line Defects in BCC Iron:

Erin Hayward¹; Blas Uberuaga²; Chaitanya Deo¹; Carlos Tome²; ¹Georgia Institute of Technology; ²Los Alamos National Laboratory

The interaction of dislocations with point defects, such as vacancies, interstitials, or impurities, is important for understanding the processes of dislocation climb, creep, and embrittlement. In irradiated materials, the abundance of point defects may enhance these phenomena. The interaction between a dislocation and a given point defect is often described by the interaction energy, a measure of favorability of the positioning of the defect with respect to the dislocation. We calculate the interaction energy between a screw dislocation and various types of point defects in body-centered cubic iron using atomistic methods. These results are compared to energies found using isotropic and anisotropic elastic continuum theory. We find important differences between the results of atomistic and continuum methods, especially near the core, and conclude that anisotropic fields perform significantly better than their isotropic counterparts. Stability of point defects in the presence of a dislocation core will be discussed.

10:20 AM Break

10:35 AM

The Effect of Crowdions on the Dislocation Bias Factor:

Alexander Barashev¹; Stanislav Golubov¹; Bachu Singh²; Roger Stoller¹; ¹Oak Ridge National Laboratory; ²Riso National Laboratory

The observed void swelling rates in metals irradiated with 1 MeV electrons are smaller than the theoretical predictions by an order of magnitude. The attempts to solve this problem all considered three-dimensional (3-D) diffusion of both vacancies and self-interstitial atoms



TMS 2012

141st Annual Meeting & Exhibition

(SIAs) and failed. First principle calculations demonstrated that in metals with the bcc crystal structure the crowdion is more stable than the dumbbell configuration of the SIAs, hence the 1-D migration of SIAs should be realized. Recently we have proposed that this may account for the small dislocation bias factors. In this paper, a quantitative model is developed. It is shown that the crossover between the crowdion- and dumbbell-controlled kinetics occurs when dumbbells are much more stable than crowdions. This explains low swelling levels even in fcc metals and sheds light on the possible reasons for the higher swelling levels observed in fcc as compared to bcc metals.

10:55 AM

Atomic-Scale Study of Strengthening Due to Inclusion-type Obstacles in Iron: *Yury Osetskiy¹; Roger Stoller¹; ¹ORNL*

Voids and He-bubbles, secondary phase and oxide particles in oxide dispersion strengthened (ODS) alloys are common obstacles to dislocation glide in commercial materials for nuclear industry. All these obstacles present a family that can be treated as inclusion-type. In this presentation we discuss results of extensive atomic-scale modeling of moving dislocation interaction with the above spherical obstacles embedded into bcc-iron matrix. We simulated a $\frac{1}{2}\langle 111 \rangle$ edge dislocation gliding in the plane intersecting obstacles of diameter from 1 to 6nm at different distances to their equator. Different interaction mechanisms were observed depending on the dislocation glide plane position and temperature. The strength of different obstacles was compared, the conditions of maximum strength were investigated and the results were discussed in the view of existing experimental data.

11:15 AM

Microstructural Evolution and Dislocation Density Analysis of HT9 Steel Irradiated in the FFTF: *Paula Mosbrucker¹; Donald Brown¹; Levente Balogh¹; Stuart Maloy¹; Thomas Sisneros¹; ¹Los Alamos National Laboratory*

HT9 steel is a ferritic/martensitic alloy being considered for use in fuel cladding in fast reactors in order to achieve high fuel burnup. The microstructural evolution, texture, and dislocation density of an HT9 duct were examined following the six-year irradiation of a fuel assembly in the Fast Flux Test Reactor Facility (FFTF). Material obtained from several positions within the assembly produced samples with a wide range of irradiation dose and irradiation temperature history. Synchrotron x-ray diffraction measurements were performed at beamline 1-ID at the Advanced Photon Source. Using the Convolutional Multiple Whole Profile (CMWP) fitting technique of evaluating dislocation contribution to line broadening, we show that irradiation temperature, rather than dose, most significantly controls dislocation density, with higher temperatures correlating to lower dislocation densities. Further, neutron diffraction texture measurements show larger texture evolution at higher doses. The results of synchrotron XRD deformation experiments and annealing experiments will also be presented.

11:35 AM

A Multiscale Investigation of the Interaction between Edge Dislocations and Voids in BCC Iron: *Sylvain Queyreau¹; Jaime Marian¹; Anasthios Arsenlis¹; Brian D. Wirth²; ¹Lawrence Livermore National Laboratory; ²University of Tennessee*

This work focuses on the strengthening associated to voids –vacancy clusters- which are formed in bcc Iron under irradiation. The dislocation-void interaction is complex and difficult to reproduce in traditional mesoscopic simulations. This is why we propose a new coupling between Dislocation Dynamics and continuum mechanics that accounts for different mechanisms observed in atomic simulations. (i) The dislocation shearing generates a surface step at the void surface synonymous of an increase of potential energy. (ii) A part of the dislocation line energy is recovered inside the empty void. And (iii) a remote interaction stress (image stress) is inherent to the presence of internal free surfaces. This latter is calculated using the non-singular expressions for dislocation stress

fields given in a recent publication. Our simulations suggest that ii and iii lead to larger contributions to the strengthening, although the temperature dependence is controlled by the variation of the surface energy *i*.

11:55 AM

Effects of 3He in ErT2: *Gillian Bond¹; Clark Snow²; James Browning³; Mark Rodriguez²; James Knapp²; Ryan Wixom²; Peter Schultz²; Donald Cowgill²; ¹New Mexico Tech; ²Sandia National Laboratories; ³Oak Ridge National Laboratory*

An overview will be presented of a long-term experimental study of 3He in ErT2 that has been carried out over the last several years. The goal of the study has been to elucidate the evolution of helium bubbles and their impact on the properties of ErT2, including swelling and hardening. The helium bubbles that form in ErT2 have a plate-like morphology and lie on {111} planes. Bubble nucleation is already completed by a He/M ratio of ~ 0.018 , and the plate-like bubbles then grow in size until a He/M ratio of ~ 0.3 after which bubble linkage becomes extensive. As the bubbles begin to link, the lattice swelling decreases along with the hardness. The study includes transmission electron microscopy (TEM), X-ray diffraction (XRD), and nano-indentation (NI), and the data have been used as input for concurrent modeling efforts.

Nanocomposites: Energetic & Catalytic Nanocomposites

Sponsored by: The Minerals, Metals and Materials Society, TMS Structural Materials Division, TMS/ASM: Composite Materials Committee

Program Organizers: Garth Wilks, Air Force Research Laboratory; Jonathan Spowart, Air Force Research Laboratory; Meisha Shofner, Georgia Institute of Technology; John Zhanhu Guo, Lamar University

Tuesday AM
March 13, 2012

Room: Swan 8
Location: Swan Resort

Session Chairs: Christopher Crouse, Air Force Research Laboratory; John Zhanhu Guo, Lamar University

8:30 AM Invited

Synthesis, Reactivity and Mechanical Properties of Aluminized Fluorinated Acrylic (Alfa) Nanocomposites: *Christopher Crouse¹; Christian Pierce¹; Jonathan Spowart¹; ¹Air Force Research Laboratory*

We report the synthesis and characterization of an aluminized fluorinated acrylate (AIFA) reactive composite material as a model system to explore the possibility for improving the mechanical properties of nanoparticle/fluoropolymer composites. Chemical functionalization of nano-Al followed by the in situ polymerization of a fluorinated methacrylate monomer was used to prepare the composites with particle loadings up to 70 wt%. Composites with 60 wt% particle content or less demonstrated thermoplastic behavior and were amenable to extrusion. Direct chemical bonding of the polymer matrix to the embedded particles is anticipated to yield improvements in the strength of these materials. Initial quasi-static compression tests displayed a two-fold increase in the compressive strength for AIFA-50 composite over the neat polymer. A combination of high strain rate (gas gun) experiments and combustion studies were also performed to explore the reactive properties for the new composite materials.

9:10 AM

Silicon-Based Nanocomposites for Energetic Applications: *Paul Redner¹; Neha Mehta¹; Karl Oyler¹; Gartung Cheng¹; Christopher Csernica¹; Jesse Sabatini¹; Jay Poret¹; Zhaohua Luan¹; Russell Broad¹; Deepak Kapoor¹; ¹US Army, RDECOM-ARDEC*

Nanoscale and nanostructured energetic materials are enabling technologies for defense applications. Many current and future requirements cannot be achieved by using more conventional materials

only. By exploiting the “tunable” nature of nanocomposites, one can adjust the energy output, light output, strength of materials, and sensitivity to various stimuli. This is accomplished via altering the constituents, particle or grain size, surface area and surface characteristics of the material. Porous silicon is being explored as a novel fuel to replace a variety of materials in energetic formulations for the above-stated reasons. A matrix of formulations was generated in which magnesium was replaced by silicon and barium chromate was replaced with more environmentally friendly oxidizers in order to improve upon a legacy first fire mixture. The materials were tested for impact, friction, and ESD sensitivity and characterized based on light output and color, burn time, and ignition temperature. Results will be discussed.

9:30 AM Invited

Synthesis and Characterization of Nanoscale & Nanostructured Pyrophoric Nanocomposites: *Chris Haines*¹; Lauren Armstrong¹; Zac Doorenbos²; Kendall Mills¹; Darold Martin¹; Jay Poret¹; Deepak Kapoor¹; ¹US Army ARDEC; ²Innovative Materials & Processes LLC

We have taken both a bottom-up and top-down approach to synthesizing pyrophoric materials for DoD applications. The bottom-up approach utilizes an inductively-coupled plasma (ICP), inert gas condensation process to synthesize nanoscale powders comprised of metals like aluminum, iron, manganese, and alloys thereof which are inherently pyrophoric. The top-down approach employs mechanical alloying (MA) of binary, tertiary, and quaternary alloys comprised of aluminum, iron, manganese, titanium, and magnesium. The high surface area (and resultant nanostructured lamellae) of these MA materials also exhibited pyrophoricity. The influence of processing parameters and chemical composition on the tunability of combustion properties of these materials will be presented. The infrared (IR) spectral performance of select materials will also be discussed.

10:10 AM

The Kinetics of Intermolecular Reactive Composites: *Mathew Cherukara*¹; Karthik Vishnu¹; Alejandro Strachan¹; ¹Purdue University

Intermolecular Reactive Composites have generated significant interest in fields as diverse as defence, reactive joining and medicine. However, the mechanisms that govern the propagation of the reactions are poorly understood, limiting their application. We use molecular dynamics to simulate the exothermic reaction of Ni/Al nano-laminates (both crystalline and amorphous) at different temperatures, periodic lengths and nanostructures. We show that the reaction is diffusion controlled in the bulk phase but the introduction of defects like porosity or a free surface speed up the reaction enormously and lead to ballistic transport. We also study the response of amorphous Ni/Al samples and we find that they exhibit faster and more energetic reactions than their crystalline counterparts.

10:30 AM Break

10:50 AM

Bio-Conjugation of Catalytic Nanoparticles: *Robert Draper*¹; Soumen Das¹; David Reid¹; ¹University of Central Florida

This research explores the possibility of using bio-conjugation to disperse nanoparticles into composite matrices for catalytic purposes. Solid state catalysis is often rate limited by the solid diffusion of catalyst particles to reaction sites, making uniform dispersion of catalysts a desirable trait in solid composite reactions to reduce the overall diffusion distance of the catalyst particles per unit weight. One of the more prevalent methods of nanoparticle conjugation involves DNA based templating, such as Watson-Crick Base Pairing, methods that are not suitable for aggressive solvents, or for conjugating many types of particles. Here we explore a novel method using Protein A and Immunoglobulin affinity for biomolecule based nanoparticle conjugation with application to dispersion of catalytic particles in a solid matrix.

11:10 AM

Comprehensive and Sustainable Recycling of Polymer Nanocomposites: *Jiahua Zhu*¹; John Zhanhu Guo¹; Suying Wei¹; ¹Lamar University

A coupled process to recycle the polystyrene(PS)/Ni@NiO nanocomposites is introduced to synthesize ferromagnetic core@shell Ni@C nanoparticles (NPs) and simultaneously to produce useful chemical radicals or liquid fuels. The PS nanocomposites reinforced with core-shell Ni@NiO NPs are prepared by the solvent extraction method. The Ni@NiO NPs are found to have significant catalytic effects on the pyrolysis of PS. The pyrolysis pathway changes from radical generation and β -scission for PS to radical generation, recombination and hydrogenation for the nanocomposites. GC/MS results confirm the same gas products from pure PS and its Ni@NiO nanocomposites. However, for the liquid products, more saturated products were obtained from the nanocomposites than that of pure PS due to the catalytic hydrogenation of the Ni NPs. A significantly large magnetization (25.0 emu/g) and high specific surface area (236.68 m²/g) were observed in the formed core-shell NPs, and these NPs can be stabilized in acid for a long time.

11:30 AM

Photocatalytic Degradation of TOC by Fe₂O₃/TiO₂ Coated on Light Ceramic: *Ju Hua*¹; ¹Harbin Institute of Technology

Anatase titanium oxide (TiO₂) films were prepared by a conventional sol-gel method on ceramic substrates as an inexpensive photocatalyst for degradation of hydroquinone in water. Investigation of the crystallinity and crack of the Fe₂O₃/TiO₂ Coated on Light Ceramic by XRD and SEM showed that the proper heat-treatment temperature was 400°C, and the as-obtained film displayed best photocatalytic activity among the prepared samples from different calcination temperatures. The prepared inexpensive photocatalyst also displayed good reproducibility, with the photocatalytic activity being maintained at about 54% after 4 cycles. A pseudo-first order reaction model was discovered for the photocatalytic mechanism of the Fe₂O₃/TiO₂ Coated on Light Ceramic.

11:50 AM

Colloidal Ag-Pt/TiO₂ Nanocomposites for Photocatalysis: *Bijith Mankidy*¹; Vinay Gupta¹; Babu Joseph¹; ¹University of South Florida

Novel methods to fabricate nanostructured composites have inspired the design and development of new nanocomposites for advanced applications in catalysis, sensors, and medicine. We will demonstrate a colloidal self-assembly route to synthesize Ag-Pt/TiO₂ nanocomposites for photocatalysis. Here, Ag-Pt bimetallic nanoparticles are surface immobilized on TiO₂ that are prepared using polymeric templates. Pt acts as charge carrier traps and suppresses recombination of photoexcited electron-hole pairs leading to improved quantum efficiency. By alloying Pt and Ag, bimetallic nanoparticle possesses enhanced ability in light harvesting due to the surface plasmon resonance character of Ag, where otherwise photosensitization is achieved by addition of chemical dyes. Another benefit of using AgPt over chemical dyes is that dyes are destroyed during the photoreaction by either photo- or thermal decomposition. In contrast, nanoparticles have higher stability. The nanocomposites are characterized using a combination of several techniques such as dynamic light scattering technique, UV-vis absorption spectroscopy, and TEM.

12:10 PM

Nanodiamond – Polypyrrole Conductive Composite as Working Electrode for Cholesterol Electrochemical Detection: *Pedro Villalba*¹; Purnya Basnayaka¹; Manoj Ram¹; Ashok Kumar¹; ¹University of South Florida

Enhanced properties of nanocomposites material make them a promising candidate for highly sensitive chemical and biological sensors. Under this study, we have electrochemically synthesized nanodiamond (ND) – polypyrrole (PPy) composite as active substrate for cholesterol oxidase (Chx) enzyme functionalization. ND-PPy/Chx structure was used as a working electrode in three electrode for electrochemical cholesterol detection. The ND-PPy films, before and after enzyme immobilization,



TMS 2012

141st Annual Meeting & Exhibition

were thoroughly characterized by using different techniques. The detection mechanism is based on the production of H₂O₂ after the reaction of cholesterol molecule in presence of the Chx attached to the sensor surface. During reaction cholesterol is reduced to 4-Cholesten-3-One. Later, the H₂O₂ molecule is separated into water molecules and free electron that can be amperometrically measured. The calibration curve of cholesterol concentration has been studied using the novel electrode ND-PPy films for different known concentration of the analyte under steady state and dynamic conditions.

Neutron and X-Ray Studies of Advanced Materials V: Centennial: In Honor of Prof. G. Kostorz

Sponsored by: The Minerals, Metals and Materials Society, TMS Structural Materials Division, TMS/ASM: Mechanical Behavior of Materials Committee, TMS: Chemistry and Physics of Materials Committee

Program Organizers: Rozaliya Barabash, Oak Ridge National Laboratory; Xun-Li Wang, Oak Ridge National Laboratory; Gernot Kostorz, ETH Zurich; Lyle Levine, National Institute of Standards and Technology; Peter Liaw, Univ of Tennessee; Yandong Wang, Beijing Institute of Technology; Brent Fultz, California Institute of Technology

Tuesday AM
March 13, 2012

Room: Southern I
Location: Dolphin Resort

Funding support provided by: Office of Basic Energy Sciences, U.S. Dept. of Energy, Dr. P. Thiyagarajan

Session Chairs: Bernd Schoenfeld, ETH; Bennett Larson, ORNL

8:30 AM Introductory Comments Bernd Schoenfeld

8:35 AM Invited

From Diffuse Scattering to Ground State Structures: *Bernd Schoenfeld*¹; ¹ETH Zurich

Local atomic arrangements of alloys are successfully determined quantitatively from diffuse scattering using x-rays and neutrons. Binary alloys are nearly exclusively investigated as the number of pair correlation functions rapidly increases for multicomponent systems. Choosing alloys in states of thermal equilibrium, effective pair interaction (EPI) parameters are determined that allow plausible ground state structures to be discussed. We shall present the situation in some recently investigated binary systems. For Pt-Rh and Au-Pd no ordered structures are experimentally known and a comparison will be done with results from electronic structure calculations. As long-period superstructures are indicated for Au-Pd, small differences in the respective ordering energies are decisive. For Ni-Pt and Fe-Pd ordered structures are well known and order-disorder transition temperatures determined from EPI parameters will be compared with direct experimental findings.

8:55 AM Invited

In Situ Small-Angle X-Ray Scattering Studies of Formation, Aggregation and Dissolution of Nanoparticles in Suspension for Environmental Health and Safety: *Andrew Allen*¹; *Matthew Martin*¹; *Robert MacCuspie*¹; *Vincent Hackley*¹; *Jan Ilavsky*²; ¹NIST; ²Argonne National Laboratory

Solution-mediated nanoparticle formation and interaction processes are of considerable current importance. Not only are solution-mediated reaction routes increasingly exploited for the formation of non-agglomerated and mono-dispersed nanoparticle systems, but the dispersion quality and stability of nanoparticle suspensions under changing solvent conditions are critical for environmental health and safety applications. To gain insights into the relevant processes, small- and ultrasmall-angle X-ray scattering (SAXS and USAXS) measurements, made in situ and in real

time using a remote-controlled, isothermal, circulating fluid flow cell at a 3rd generation synchrotron source, have provided representative, quantitative microstructure characterization over length-scales ranging from less than 1 nm to several micrometers. Results will be presented to illustrate the application of such in situ SAXS and USAXS studies to a nucleating solid phase from solution, to agglomerate formation in the presence of increasing salt concentration, and to the progressive dissolution of nanoparticles under acidic conditions.

9:15 AM Invited

Size-Dependent Transitions in Nanostructured Zirconia-Scandia Solid Solutions. A High Temperature Synchrotron Diffraction Study: *Aldo Craievich*¹; *Paula Abdala*²; *Diego Lamas*³; ¹Institute of Physics - USP; ²ESRF; ³Facultad de Ingenieria - Universidad Nacional del Comahue

The cubic (c) phase of ZrO₂-Sc₂O₃ ceramics exhibits high ionic conductivity, making this material a good candidate as electrolyte for IT-SOFCs. In microcrystalline ZrO₂-Sc₂O₃ ceramics, the cubic phase is stable only above 600°C. Contrarily, rhombohedral phases - stable below 600°C - have a rather low ionic conductivity. Interestingly, rhombohedral phases can be avoided in nanomaterials with average crystallite size, D, below 30 nm. ZrO₂-Sc₂O₃ nanopowders with 10-14 mol% Sc₂O₃, average sizes in the 35-100 nm range, and different fractions of c (or pseudo-cubic t^{''}) and rhombohedral beta and/or gamma phases, were studied by synchrotron X-ray diffraction. Strong size effects were noticed for the beta-c/t^{''} transition while a not so well defined trend was observed for the gamma-c/t^{''} transition. The temperatures of beta-c/t^{''} and c/t^{''}-beta transitions are decreasing linear functions of 1/D. These results indicate that the size dependences of both transition temperatures are well described by the classical Jesser-Couchman equation.

9:35 AM

Depth-Dependent Plastic and Elastic Strain Gradients from Polychromatic Microdiffraction: *Rozaliya Barabash*¹; ¹Oak Ridge National Laboratory

Depth-dependent (3D) measurements of the plastic and elastic strain distributions are now possible with differential-aperture X-ray microscopy (DAXM). This method is ideal for studies of mesoscale evolution of strains and defects. This talk will describe two examples of DAXM applications for 3D studies of plastic/elastic response of the materials under external stress fields: (*) The first example mainly demonstrates formation of rotational (deviatoric) strains in a twinned Ni crystal. Crystal plasticity analysis together with finite element simulations confirm the experimentally observed trends in the plastic response of the matrix and the twin. (**)The 2nd example mainly shows the 3D residual elastic strain distribution in Metal/Matrix composites (MMC). Research supported by the U. S. Department of Energy, Office of Basic Energy Sciences, Materials Sciences and Engineering Division. X-ray microbeam measurements were performed at 34-ID-E at the Advanced Photon Source.

9:50 AM Invited

Kinetics of Nano Quasicrystal Formation from Zr-Based Metallic Glass Ribbons and Its Implication to the Heterogeneous Metallic Glass Structure: *Hiroshi Okuda*¹; *Yusuke Maezawa*¹; *Ryo Arai*¹; *Shojiro Ochiai*¹; *Junji Saida*²; ¹Kyoto University; ²Tohoku University

Structure of stable Zr metallic glasses has been intensively examined using various methods and approaches. In the present work, kinetics of nano-quasicrystallization in Zr-Pt / ZrCuPt glass ribbons has been examined by a combined use of Anomalous Small and Wide Angle X-ray Scattering (ASWAXS) and time-resolved SWAXS methods. Anomalous SAXS analysis is powerful in discussing the compositional and density fluctuation/ partitioning of heterogeneous structure, and time-resolved SWAXS is useful for discussing the relationship between the compositional heterogeneity and (quasi)crystalline domains. By measuring the intensity from a small-angle region up to a diffraction peak continuously, we analyzed them with the same sensitivity and resolution. ASAXS results suggested formation of solute enriched zone

during precipitation in the ternary alloy system. Contrast analysis for as-quenched and annealed samples was made to discuss the heterogeneity in the glass and the precipitated samples.

10:10 AM Invited

In-Situ Diffraction Studies of Microstructural Changes during Deformation and Irradiation: *Ralph Spolenak*¹; ¹ETH Zurich

In-situ diffraction studies offer detailed in deformation studies that may otherwise be missed by interrupted experiments. This paper will illustrate the advantages of this method by three case studies: a. fracture of thin brittle coatings on ductile substrates, b. the deformation behavior of metal thin films at high plastic strains from uniform deformation to shear banding and eventual texture changes and c. the collective rotation of grains in thin metal films under the influence of high energy self-ion irradiation. Results will be presented of both x-ray and electron diffraction.

10:30 AM Invited

Online Microcomputed X-Ray Computer Tomography of the In-Vivo Biodegradation of Mg Implants: Victor Wessels¹; Stefan Fischerauer²; Tanja Kraus²; Annelie-M. Weinberg²; Richard Kickinger³; Anja Hänzli¹; Peter Uggowitzer¹; Jörg Löffler¹; ¹ETH Zurich; ²Medical University Graz; ³University of Applied Sciences Wels

Bioresorbable implants degrade in the body over time and thus do not require surgical removal after they have served their purpose. Mg-alloys show in this context a particularly attractive combination of mechanical, electrochemical and biological properties, but they produce hydrogen during degradation which may cause problems. We will present in this talk the bone and tissue response to degrading Mg pin implants in growing rat skeletons by continuous in-vivo microcomputed x-ray computer tomography (μ CT). With this technique, implant degradation, gas evolution, and bone/tissue response can be monitored simultaneously; it further has the great advantage of being noninvasive, so that no animals need to be sacrificed. The μ CT studies show that bone recovers completely after implant degradation, even in the case of massive gas formation and preceding alterations of the bone. These studies also show that Mg generates enhanced bone neoformation, giving evidence for its good osteoconductivity and osteoinductivity.

10:50 AM Break

10:55 AM Invited

Combined Use of Small-Angle X-Ray and Neutron Scattering: SAS in Color: *Masato Ohnuma*¹; Yojiro OBA¹; Koppoju Suresh¹; Powel Kozikowski¹; ¹National Institute for Materials Science

Thanks to the distribution of glassy carbon for intensity calibration [1], we are now able to get SANS and SAXS data in absolute unit quite easily. Since the scattering contrast between X-ray and neutron shows large difference, we can extract the information about chemical compositions of heterogeneity embedded in matrix from the intensity ratio between SANS and SAXS. We call this method "alloy contrast variation (ACV)". The ACV method is especially powerful to discuss whether the matrix elements are in the nano-size heterogeneity or not. In contrast, the effects from matrix cannot be ignored in other techniques like TEM or atom probe when the size of heterogeneity is below 2-3 nm. In this talk, we'll show some application results of ACV method in different alloys. Ref[1] F. Zhang, J. Ilavsky, G. Long, J. Quintana, A. Allen and P. Jemian : Metall. Mater. Trans. A, 41A(2010), 1151.

11:15 AM Invited

Cascade Dynamics Information Possible from Sub-Picosecond X-Ray Scattering: *Bennett Larson*¹; Jon Tischler¹; Roger Stoller¹; ¹ORNL

The collision of 2-MeV neutrons or 50-keV ions with a lattice atom results in the deposition of 10's of kilovolts of kinetic energy within a few nanometer radius. According to molecular dynamics simulations, the "cascade" of subsequent ion collisions generates several thousand vacancy-interstitial pairs on sub-picosecond time scales. The availability of sub-picosecond 10-keV x-ray pulses from the Linac Coherent Light Source (LCLS) provides the capability to probe cascade dynamics

experimentally. Here we present numerical simulations of time-slice x-ray diffraction patterns based on molecular dynamics calculations for 25-keV primary knock-on cascades in Fe at room temperature. The time dependent diffraction patterns will be correlated with the real-space cascade dynamics from the molecular dynamics simulations. Techniques for interpreting the diffraction patterns in terms of local defects and shock induced pressure waves will be discussed. *Research sponsored by the U.S. DOE, BES, Materials Sciences and Engineering Division, "Center for Defect Physics," an EFRC

11:35 AM Invited

Mechanics of Magnetic Shape Memory Alloys across the Length Scales: *Peter Müllner*¹; ¹Boise State University

Magnetic shape-memory alloys (MSMAs) deform via the motion of twin boundaries, driven by a magnetic field or by a mechanical force. Deformation mechanisms are reviewed with attention to different length scales. At the atomic length scale, twinning dislocations are the agent of deformation. Burgers vector and step height of twinning dislocations were characterized using transmission electron microscopy. At the mesoscopic length scale, groups of twinning dislocations form disclination dipoles. In hierarchically twinned martensite, groups of disclination dipoles control localized deformation at even larger length scale. Grain boundaries suppress twin boundary motion, requiring MSMAs to be prepared as single crystals. Grain boundaries were replaced by porosity in polycrystalline metallic foam. Here, at macroscopic length scale, deformation is governed by the plastic compatibility of architectural elements. At the sample scale, when the interaction of the sample with the surrounding apparatus impacts deformation, all mechanisms contribute to the deformability of the sample.

11:55 AM Invited

Phonons in Martensite and Austenite NiMnGa - Its Relation to Ferromagnetic Shape Memory: *Winfried Petry*¹; Semih Ener¹; Jürgen Neuhaus¹; ¹Technische Universität München (Munich University of Technology)

NiMnGa is the archetype of ferromagnetic shape memory alloys, which have the potential to serve as sensors, actuators or in magnetic refrigeration. Subtle changes in composition of this alloy create drastic changes in the structural and magnetic properties. We present extensive phonon measurements in the austenite as well martensite phase accompanied by structural characterisation, as function of composition, temperature and magnetic field. For example the off-stoichiometric alloy Ni₄₉Mn₃₂Ga₁₉ transforms at 380 K within its ferromagnetic phase from L2₁ (austenite) to five layered martensite and is very well suitable for ferromagnetic shape memory applications. Phonons in the austenite reveal the atomistic mechanism of the transformation. Phonons in the martensite explain the extremely low twinning stress, which is essential for functionality. Calculations of the electronic structure of Ni₂MnGa in both phases (Entel et al. Mater. Sci. Forum 635, (2010), 3) explain the phonon anomalies observed around the structural phase transition.

12:15 PM Invited

Multiple Whole X-Ray Line Profile Analyses for Investigating the Role and Nature of Dislocations in Plastic Deformation of Semicrystalline Polymers

: *Michael Zehetbauer*¹; Florian Spieckermann¹; Gerald Polt¹; Harald Wilhelm²; Michael Kerber¹; Sigrid Bernstorff³; Erhard Schafner¹; ¹University of Vienna; ²Laboratory of Polymer Engineering LKT-TGM; ³Sincrotrone Trieste

Recent publications on semicrystalline polymers show that the method of Multiple whole X-ray line Profile Analysis (MXPA) not only allows for a correct separation of size and strain broadening but also clarifies whether the latter arises from dislocations or not. Thus, these analyses contribute to the long-lasting dispute whether dislocations are present in the crystalline phase and whether their strain-dependent evolution rules the macroscopic deformation. Besides existence, density and arrangement of dislocations, the low symmetry and high anisotropy of the polymer crystals even allow for an identification of the specific dislocation types and populations -



TMS 2012

141st Annual Meeting & Exhibition

provided that the elastic constants are known. Results from several in-situ synchrotron experiments are presented which span semicrystalline polymers like PP, PET, and the biodegradable P3HB. The microstructural data which also comprise the crystal size and the crystallinity provide a good basis to quantitatively describe the macroscopic mechanical properties in terms of microscopic deformation mechanisms.

12:35 PM Invited

Energy-Dispersive Synchrotron Diffraction – a Versatile Method for Advanced Materials Characterization: *Christoph Genzel*¹; ¹Helmholtz-Zentrum Berlin für Materialien und Energie

Energy-dispersive (ED) diffraction experiments performed on polycrystalline materials are characterized by a fixed geometrical setup and the possibility to record complete diffraction patterns simultaneously under well-defined but arbitrary scattering angles and for different measuring directions with respect to the sample reference system. Employing high energy white synchrotron radiation allows for structural analysis with excellent time and/or spatial resolution as well as for the use of complex large and heavy sample environments. With selected examples taken from measurements on the beamline EDDI@BESSY II the broad variety of applications for ED diffraction is demonstrated. With photon energies between about 10 and 120 keV EDDI is particularly dedicated to the analysis of property gradients (residual stress, texture, microstructure and composition) in the highly stressed surface layer of technical components, but also to in-situ monitoring of thin film growth. For data processing single line profile analysis and whole pattern Rietveld refinement can be applied.

Pb-Free Solders and Other Materials for Emerging Interconnect and Packaging Technologies: Effects of Ultrafine Joints and Alloy/microstructure Relationships

Sponsored by: The Minerals, Metals and Materials Society, TMS Electronic, Magnetic, and Photonic Materials Division, TMS: Electronic Packaging and Interconnection Materials Committee
Program Organizers: Iver Anderson, Ames Laboratory; Sung Kang, IBM; Albert Wu, National Central Univ; Laura Turbini, Research in Motion; Tae-Kyu Lee, Cisco Systems; Govindarajan Muralidharan, Oak Ridge National Lab; John Elmer, Lawrence Livermore National Lab; Yan Li, Intel

Tuesday AM
March 13, 2012

Room: Swan 9
Location: Swan Resort

Session Chair: To Be Announced

8:30 AM Invited

Linkages between Microstructure and Mechanical Properties of Ultrafine Interconnections: *Zhiyong Wu*¹; *Zhiheng Huang*¹; *Hua Xiong*¹; *Paul Conway*²; ¹Sun Yat-Sen University; ²Loughborough University

Microstructures within ultrafine interconnections, which change rapidly during manufacturing and evolve continuously in service, have to be taken into account to accurately predict the reliability of electronic packaging, e.g. 3D electronic packaging. This work emphasizes the size and geometry effects on the properties of solder bumps with diameters of about 20 microns by taking into account the microstructures simulated using a phase field method. Irregular boundaries of the solder bumps can be dealt with in the model due to the flexibility in geometries provided by the finite element method. Size and geometry effects on the microstructural evolution and subsequent mechanical property will be discussed by coupling the phase field and mechanical modeling techniques. With the size geometry effects included, the microstructure and properties of solder joints from both experimental and modeling will be compared and the results are expected to highlight the significance of microstructure engineering in ultrafine interconnections.

8:55 AM

Silver Addition Effects on the Ni-Sn Interfacial Reaction for 3D IC Applications: *J. J. Yu*¹; *H. Y. Chuang*¹; *M. S. Kuo*¹; *W. L. Shih*¹; *C. Kao*²; ¹National Taiwan University; ²National Taiwan University

For 3D IC applications, solder volume is extremely small in the chip-to-chip micro joining process. For this reason, solder joints can contain a large portion of intermetallic compounds (IMCs), which results in many peculiar properties. This study aims to uncover effects caused by the miniaturisation of solder volume on the Ni-Sn solid state reactions. When pure Sn is used for, a number of voids were observed at the interface. The void formation is considered as a result of volume shrinkage during the Ni-Sn reactions. Interestingly, an addition of 2.4 wt. % Ag in Sn can effectively avoid the formation of voids. The mechanism will be also discussed.

9:15 AM

Effect of Minor Alloy Additions on the Interfacial Reactions with Low Solder Volume for 3D IC Applications: *Ting-Li Yang*¹; *C. Robert Kao*¹; ¹National Taiwan University

Three dimensional integrated circuits (3D ICs) technology has received a lot of attention due to its high packaging density and better performance. It is well known that minor alloy additions to solders have pronounced effects on the interfacial reactions between solder and substrate. These alloy elements might substantially change the reaction rate and the morphology of the reaction products. Accordingly, it is of interest to investigate the effects of minor additions within the regime of small solder volume. In this study, two extreme types of alloy elements which include inert element, Bi, and a highly reactive element, Zn will be studied. Sandwich structures of Cu/Sn/Cu, Cu/Sn10Bi/Cu, and Cu/Sn0.4Zn/Cu were prepared by chip-to-chip bonding process. The solder thickness between Cu substrate was controlled at 10µm ± 1µm. High temperature storage tests were conducted by isothermal aging at 120 °C. Also, the microstructure evolution was also examined during annealing.

9:35 AM

Preferred Orientation of 30 1956m Fine Pitch Sn2.5Ag Micro-Bumps Studied by Synchrotron Polychromatic X-Ray Laue Microdiffraction: *Tian Tian*¹; *Kai Chen*²; *Martin Kunz*²; *Nobumichi Tamura*²; *Tao-Chih Chang*³; *Chau-Jie Zhan*³; *King-Ning Tu*¹; ¹UCLA; ²Lawrence Berkeley National Laboratory; ³Industrial Technology Research Institute

Synchrotron radiation white beam x-ray microdiffraction was employed to study the grain size and orientation of fine pitch Sn2.5Ag micro-bumps. The indexation results of Laue patterns show that mostly there is one dominated grain orientation in a single micro-bump. Moreover, a statistics study basing on the characterization of 72 micro-bumps, shows that the [001] direction, which is the fast diffusion path for Ni/Cu atoms, is tend to be parallel to the substrate of the test vehicle. This property shows a stability after reflow processes in a statistics view.

9:55 AM

Thermomigration on 3D IC Pb-Free Micro Bump: *Wei-Cheng Jhu*¹; *Fan-Yi Ouyang*¹; ¹National Tsing Hua university

Due to the demands for high performance and miniaturization, packing technology is moving from 2D IC to 3D IC. In 3D IC, joule heating will be serious and heat will accumulate between stacking chips. In order to effectively remove heat, a temperature gradient will be established across the packages. When a difference of 2°C generates across a micro-bump of 20µm in diameter, the temperature gradient will be 1000°C / cm, which has been reported to cause serious thermomigration failure. In this paper, we have successfully designed a novel experiment to establish various temperature gradients across the micro-bump to study the failure mechanism and microstructure change on thermomigration. Furthermore, in-situ infrared microscopy was also used to confirm the temperature gradient and temperature distribution in the solder joints.

10:15 AM

Effects of Small Solder Volume on the Cu/Sn/Cu Interfacial Reactions for 3D IC Applications: *Meng Hsin Chen¹; Hsin Yi Chuang¹; Ting Li Yang¹; C. Robert Kao¹*; ¹National Taiwan University

This study reveals the miniaturized solder volume effect on the interfacial reactions for 3D IC micro jointing. Cu/Sn(10\149;m)/Cu sandwiches were subjected to the solid-liquid and solid state reactions. The results show that the miniaturized solder volume has less impact on types IMC. In solid-liquid reactions at 250°C for 15 min, nearly the entire Sn phase was transformed into IMC. Cu₆Sn₅ grains growing from the opposite interfaces impinged on each other and merged into a single grain. In solid state reaction at 150°C, Sn was consumed after 1008 h of aging. The vertically contacted Cu₆Sn₅ grains remained exhibiting different orientations instead of merging into a single crystal. The detailed microstructure evolution and the IMC growth kinetics are discussed in the present work.

10:35 AM Break**10:45 AM**

Volume Shrinkage Induced by Interfacial Reaction in Micro Ni/Sn/Ni Structure: *C. Li¹; H. Chuang¹; M. Kuo¹; C. Kao¹*; ¹National Taiwan University

In 3D-IC, solder joints of a few microns in size are used to connect Si dies in the third dimension. Theoretically, there is 10.5% shrinkage in volume when Ni reacted with Sn to form Ni₃Sn₄. If it indeed occurs, solder joints would be in a highly stressed state and prone to failure. In this study, alpha-stepper and SEM (scanning electron microscope) analysis were carried out to measure the actual volume shrinkage for Ni/Sn/Ni sandwich structures during an isothermal aging at 180°C for 0-7 days. The results showed there was about 7.3% shrinkage in volume and the remaining 3.2% shrinkage was released by forming voids in Ni₃Sn₄ layer. The internal stress and the forming of voids in small scale Ni/Sn/Ni sandwich structures during solid state aging might induce potential reliability issues.

11:05 AM Invited

The Effect of Doping Nd on the Oxidation Resistance and Wettability of Sn-0.7Cu Solder: *Jian Zhou¹; Yi-Li Fang¹; Xu Chen¹; Yang-Shan Sun¹; Feng Xue¹*; ¹Southeast University

In the present paper, the oxidation behavior of Sn-0.7Cu solders doping with Nd was studied. By checking gain in weight of solders heated at 250°C or 300°C, Sn-0.7Cu-300ppmNd was found less oxidation formed at the surface than that of Sn-0.7Cu and other solders. The oxide surface of solders was investigated by Auger electron spectroscopy (AES). The results showed that the oxide layer thickness at the surface of Sn-0.7Cu-300ppmNd was much thinner than that of Sn-0.7Cu. Neodymium oxide and tin oxide formed on the Sn-Cu-Nd solders. It was indicated that Neodymium oxide layer prevented O atom from diffusion into the solder inner, so the solders doped with Nd shows improved oxidation resistance. Wetting balance method was used to measure wettability of the solders on Cu substrate. The experimental results showed that minute amount of Nd addition to Sn-0.7Cu solder can increase the wetting force and decrease the wetting time.

11:30 AM

Single-Joint Shear Strength of Micro Cu Pillar Bumps with Different Amounts of Intermetallics: *Yu-Jen Chen¹*; C. Robert Kao¹; ¹National Taiwan University

This study investigates the effects of intermetallics on the single-joint shear strength of micro Cu pillar bumps with SAC405 solder caps. The correlation between the shear strength and the intermetallic compound after aging at 180°C for 150, 300, 500, 750 hours is studied. Microstructure characterization reveals that Cu₆Sn₅ was scallop-type after reflow, and Cu₆Sn₅ transforms to planar-type after 150 h of aging. Microvoids are

observed at Cu₃Sn/Cu interface after aging, and the amount of voids increases with aging. According to the shear test results, the shear strength decreased with aging. The formation of a planar Cu₆Sn₅ layer is the major factor leading to a sharp decrease of the joint strength.

11:50 AM

Interfacial Reactions in the Sn-Co-Cu/Ni Couples: *Chih-Ming Chen¹; Chia-Ming Hsu¹; Sinn-Wen Chen¹*; ¹National Tsing Hua University

The Sn-Co-(Cu)/Ni couples reacted at 180°C and 210°C were prepared. In the Sn-0.05wt%Co/Ni and Sn-0.5wt%Co/Ni couples, the reaction products were continuous Ni₃Sn₄ phase layer, and discontinuous (Ni,Co)Sn₄ phase. In the Sn-0.7wt%Cu-0.05wt%Co/Ni and Sn-0.7wt%Cu-0.5wt%Co/Ni couples, the reaction product was the Cu₆Sn₅ phase in the early stage. With longer reaction time up to 100 hours, Ni₃Sn₄ phase was formed between the Cu₆Sn₅ and Ni substrate. Detachment of Cu₆Sn₅ phase in the solder was observed with even longer reaction time to 500 hours, and the results are similar to those in the Sn-0.7wt%Cu/Ni couples. Reaction couples with current stressing were also prepared, and polarity effect was observed. In the Sn-Co/Ni couples, growth enhancement of Ni₃Sn₄ and (Ni,Co)Sn₄ were observed at the interface which electron flow from Sn toward Ni. In the Sn-Co-Cu couple, due to the polarity effect, the different growth rates of Cu₆Sn₅ and Ni₃Sn₄ were found between two different interfaces.

12:10 PM

Microstructural Evolution in SnAgCu Solders and Effect on Constitutive Response During Creep: *Babak Talebanpour¹; Praveen Kumar²; Zhe Huang¹; Chien-Hung Wen¹; Indranath Dutta¹*; ¹Washington State University; ²Indian Institute of Science

Microstructure of a Sn-Ag based solder continuously evolve during storage and service because of its low melting temperature. This necessitates development of a microstructurally adaptive creep model to accurately predict reliability of solder joints. This work presents a systematic study of microstructural evolution in two Sn-Ag-Cu solder alloys, namely Sn-1.0%Ag-0.5%Cu and Sn-3.0%Ag-0.5%, subjected different thermo-mechanical excursions. Quantitative microscopy is utilized to identify the key thermo-mechanical history dependent length parameter associated with the evolving microstructure, including precipitate size, inter-precipitate spacing, proeutectic grain size and eutectic-channel width, of Sn-Ag-Cu solders. A microstructurally adaptive creep model was developed using this length parameter, where in situ changes in the above microstructural features are considered. Contributions of eutectic and proeutectic regions in the total creep response of the solder were incorporated by treating the solder as a composite with two different micro-constituents. Comparisons between modeling and experiments will be presented.



TMS 2012

141st Annual Meeting & Exhibition

Phase Stability, Phase Transformations, and Reactive Phase Formation in Electronic Materials XI: Interfacial Reactions of the Pb-free Solder Joints

Sponsored by: The Minerals, Metals and Materials Society, TMS Electronic, Magnetic, and Photonic Materials Division, TMS: Alloy Phases Committee

Program Organizers: Chih-Ming Chen, National Chung Hsing University; Jae-Ho Lee, Hongik University; Ikuo Ohnuma, Tohoku University; Clemens Schmetterer, TU Bergakademie Freiberg; Yee-Wen Yen, National Taiwan University of Science and Technology; Shih-Kang Lin, University of Wisconsin – Madison

Tuesday AM
March 13, 2012

Room: Swan 10
Location: Swan Resort

Session Chairs: Albert T. Wu, National Central University; Jae-Ho Lee, Hongik University

8:30 AM Invited Kinetics of Solid-State Reactive Diffusion in the Sn/(Ni-X) System: Masanori Kajihara¹; ¹Tokyo Institute of Technology

Tin-base solders are widely used in the electronics industry. If a multilayer Au/Ni/Cu conductor is interconnected with the Sn-base solder, the Au layer quickly dissolves into the molten solder during soldering, and then the Ni layer is directly contacted with the solder. Owing to reactive diffusion at the interconnection between the Ni layer and the solder, Ni-Sn compounds are formed during soldering, and then gradually grow during energization heating at solid-state temperatures. However, the Ni-Sn compounds are brittle and possess high electrical resistivities. Thus, the growth of the compounds deteriorates the electrical and mechanical properties of the interconnection. Addition of alloying element X into Ni may inhibit the compound growth and hence the deterioration of the interconnection. To examine influence of the addition on the compound growth, the kinetics of the solid-state reactive diffusion in the Sn/(Ni-X) system was experimentally observed at temperatures of 433-473 K in the present study.

8:50 AM Invited Properties of Au-Ge Based Alloys for High Temperature Lead Free Solders: Christian Leinenbach¹; Shan Jin¹; Fabrizio Valenza²; Donatella Giuranno²; Rada Novakovic²; Hans-Rudolf Elsener¹; Jiang Wang¹; Simona Delsante³; Gabriella Borzone³; Andrew Watson⁴; ¹Empa-Swiss Federal Laboratories for Materials Science and Technology; ²National Research Council (CNR) – Institute for Energetics and Interphases (IENI); ³University of Genova; ⁴University of Leeds

Low melting Au based alloys offer a combination of high corrosion and creep resistance as well as good electrical and thermal conductivity. Despite their high price, Au alloys are of special interest for high temperature solder applications where these characteristics are essential, e.g. special MEMS devices or in space technology. The alloying system Au-Ge is of particular interests due to a deep eutectic point at 360°C, but information on Au-Ge alloys as solder material is limited. In this work, the feasibility of Au-Ge based alloys as high-temperature lead free solder will be presented. Beside the experimental study and thermodynamic assessment of a number of important alloying systems (Au-Ge-Cu, Au-Ge-Ni, Au-Ge-Sn, Au-Ge-Sb, Au-Ge-Si) wetting and soldering tests using eutectic Au-Ge alloy and relevant substrates were performed. Sound joints with a high strength could be produced. The application of eutectic Au-Ge alloy as solder material for highly loaded components was finally demonstrated.

9:10 AM Study of Intermetallic Compound Growth of Sn-2.3Ag Solder Micro-Bumps during Solid-State Aging: Tao-Chi Liu¹; Yi-Sa Huang¹; Chin-Hsing Tang¹; Chih-Rong Chen²; Chih Chen¹; ¹National Chiao Tung University; ²Integrated Service Technology Inc

We investigate the relationship between the aging duration and microstructure of intermetallic compounds (IMCs) in SnAg microbumps with about ten microns bump height. Three structure, including Cu/solder/Cu, Ni/solder/Cu, and Cu/Ni/solder/Cu were prepared and studied. Contrary to traditional packaging, the growth rate of IMCs is the key concern for electronic reliability of 3D-stacked ICs. In this study, aging tests at 150°C up to 1000 hr were performed on the above three sets of microbumps. The results illustrate that the IMCs on the Cu UBM can be grown above 100 hours at 150°C aging, the thickness of Cu₆Sn₅ is 2.24 microns; and Cu₃Sn is 1.09 microns. Eventually the micro-bump was fully transferred to brittle IMCs within 500 hours aging. Nevertheless, for Cu/Ni/solder/Cu microbumps, The Ni₃Sn₄ IMC on the Ni side was only about 1 micron after aging for 1000 hr. The results will be presented in the conference in details.

9:25 AM Reflow and Solid-State Reactions between SnAgCu-xNi Solder and Au/Pd/Ni Surface Finish: Bo-Mook Chung¹; Yong-Ho Baek¹; Jaeho Choi²; Joo-Youl Huh¹; ¹Korea University; ²Gangneung-Wonju National University

Recently, electroless Ni/electroless Pd/immersion Au (ENEPIG) was introduced as an alternative surface finish to electroless Ni/immersion Au (ENIG) in electronic packaging industry owing to its superior solder joint reliability. However, when the EP layer is relatively thick, Pd atoms resettle as PdSn₄ near the solder/Ni interface during the reflow and aging processes and deteriorate joint reliability. In this study, we have examined the effect of Ni addition to Sn-3.0Ag-0.5Cu solder on Pd resettlement during the reflow and solid-state aging processes. Solder balls (φ 450 μm) of Sn-3.0Ag-0.5Cu-xNi (x=0-0.5 wt.%) were reflowed on ENEPIG finished pads (φ 400 μm) with a 0.3-μm-thick EP layer at 250°C for 120 s. Solid-state aging was carried out at 150°C for pre-determined times. In the presentation, the results for the intermetallic growth and Pd resettlement during the reflow and aging reactions will be discussed with respect to the effects of the Ni contained in solder.

9:40 AM Effect of Interfacial Compound Layer on Pd Resettlement during Reflow and Solid-State Reactions between Sn-rich Solder and Ni Substrate: Yong-Ho Baek¹; Bo-Mook Chung¹; Jaeho Choi²; Joo-Youl Huh¹; ¹Korea University; ²Gangneung-Wonju National University

Electroless Ni/electroless Pd/immersion Au (ENEPIG) surface finish is now becoming a preferable choice in electronic packaging industry to achieve reliable solder joints with SnAgCu (SAC) solders. In this study, we have examined how Pd resettlement depends on the intermetallic compound (IMC) phase, Ni₃Sn₄ or Cu₆Sn₅, formed at solder joints during the reflow and solid-state aging treatments. For Pd resettlement during the reflow process, solder balls (φ 450 μm) of Sn-3.5Ag, SAC302 and SAC305 were reflowed on the ENEPIG finished pads (φ 400 μm). For Pd resettlement during solid-state aging, two kinds of diffusion couples, Pd(1 μm)/Sn-1.0 wt% Cu(60 μm)/Ni and Pd(1 μm)/Sn(60 μm)/Ni, were prepared by electroplating and then aged at 150°C to monitor IMC growth and Pd resettlement at the solder/Ni interface. In the presentation, we will discuss a possible mechanism of how Pd resettlement can be controlled by changing the IMC layer formed initially at the solder/Ni joints.

9:55 AM

Employment of a Bi-Layer of NiP/Cu as a Diffusion Barrier Layer for Cu bump/Sn Bonding Structures for the 3D Integration Applications: *Byunghoon Lee¹; Haseok Jeon¹; Hoo-Jeong Lee¹; ¹Sungkyunkwan University*

Cu bump /Sn layer/Cu bump is a widely-adopted bonding structure for 3D integration; nevertheless, a strong material interaction between Cu and Sn that occurs during manufacturing processes and under actual usage conditions is potentially a serious problem for both thermal and mechanical reliabilities. Here, we propose the introduction of a bi-layer of plated Ni(P) and Cu as a diffusion barrier. The Ni(P) layer with a thickness of 1um serves to prevent Cu diffusion whereas the Cu layer with a thickness of 0.5um is expected to react with Sn and form Cu₆Sn₅, which would subsequently suppress a reaction between Ni and Sn. We deposited the bi-layer barrier using a wet process, electroless-plating for Ni(P) and electroplating for Cu. We examined the effects of the barrier on the thermal stability and bonding morphology using SEM and TEM. Then we carried out lap-shear tests to characterize the mechanical properties.

10:10 AM Break

10:25 AM Invited

The Impacts of Palladium Addition on Phase Formation, Microstructure Evolution and Mechanical Reliability in Sn-Ag-Cu/ENEPIG and Sn-Ag-Cu-Pd/ENIG Solder Joint: *Chien Fu Tseng¹; I-Dai Wang¹; Tae-Kyu Lee²; Kuo-Chuan Liu²; Chih-Yuan Cheng³; Jim Wang³; Jeng-Gong Duh¹; ¹National Tsing Hua Univ; ²Cisco Systems Inc.; ³Shenmao Technology Inc.*

Interfacial reactions of ENIG (electroless nickel and immersion gold) and ENEPIG (electroless nickel, electroless palladium and immersion gold) jointed with Sn-3.0Ag-0.5Cu solder were investigated in this study. It was found that Pd mainly dissolved into Cu₆Sn₅, which further suppressed the growth of intermetallic compound (IMC) in the Sn-3.0Ag-0.5Cu/ENEPIG solder joint. In addition, with slower growth of Cu₆Sn₅, less columnar Kirkendall voids would form in the Ni₃P layer. This study aims to figure out the interfacial variations between ENIG and ENEPIG surface finishes after jointed with lead free solder. Alternatively, a new solder alloy, Sn-3.0Ag-0.5Cu-xPd (x=100, 250, 500 ppm), was developed and jointed with ENIG surface finish in order to explore the effects of Pd on the solder joint. Similar to Sn-3.0Ag-0.5Cu/ENEPIG solder joint, the Pd doing in solder also resulted in slower IMC growth and less columnar voids formation during solid and liquid state reaction. Moreover, the mechanical property showed that the Pd added solder joint was superior to that without Pd addition via the high speed impact tester. The Pd effects on phase formation, microstructure evolution and mechanical testing were investigated and summarized in this study. Finally, the detailed mechanism of Pd addition in interfacial reaction of solder joints will be proposed and discussed.

10:45 AM

The Interfacial Reaction between Diffusion Barrier and Thermoelectric Materials under Current: *Li-Chen Lo¹; Albert T. Wu¹; Tai-Ying Lin¹; ¹National Central University Department of Chemical and Material Engineering*

This paper investigated the interfacial reaction between the diffusion barrier, Ni, and the thermoelectric materials. Ni is a good barrier between Pb-free solder and n-type bismuth telluride (Bi₂Te_{2.5}Se_{0.5}) thermoelectric material to prevent the rapid formation of brittle SnTe intermetallic compound (IMC). Instead of SnTe, Ni₃Sn₄ and NiTe formed at the interfaces. These IMCs would affect the mechanical and electrical properties of the thermoelectric module. Different current densities were applied to the system to investigate the electromigration behavior of the systems at various temperatures. The results suggested that the variation of the thicknesses of the IMCs not only depended on the polarity; it was affected by the localized increase in temperature due to the Peltier effect. The kinetics of the atomic motion will be discussed.

11:00 AM

Interfacial Reactions of the Sn-xZn/Au Couples: *Yee-Wen Yen¹; Hsien-Ming Hsiao¹; Cheng-Kuan Lin¹; ¹National Taiwan Univ of Science & Tech*

The interfacial reactions of the Sn-xZn/Au couples were investigated. When the Zn content was less than 3 wt%, the Au-Sn binary and a few Au-Sn-Zn ternary intermetallic compounds (IMCs) were formed at the interface. Both binary Au-Sn and Au-Zn and Au-Sn-Zn ternary IMCs were formed at the Sn-5Zn/Au interface. When the Zn content was greater than 7 wt%, the Sn-xZn/Au couples were completely transferred to the Au-Zn system. The n value of the Sn-xZn/Au (x < 5 wt%) couples were between 0.25-0.33. The Sn-xZn/Au (x=7 to 15 wt.%) couples also have the similar results when the aging times were less than 144 h. The n value of the Sn-50Zn/Au couple was 0.5, the reaction mechanism was diffusion-controlled. The n value of Sn-90Zn/Au couple was 0.19. The results indicated that the adding the Zn into the Sn-Zn alloys would change the reaction systems from the Au-Sn to Au-Zn systems.

11:15 AM

Asymmetrical Microstructure on the Two Joint Interfaces of Flip-chip Cu/Sn/Cu Solder Joints: *Cheng-Yi Liu¹; Yu Jin Hu¹; ¹National Central University*

In this study, we observed an asymmetrical microstructure between the joint interfaces of Cu/Sn/Cu flip-chip solder joints. A serious Cu-Sn compound phase accumulated near the bottom interface of the Cu/Sn/Cu flip-chip solder joints. On the contrary, no obvious Cu-Sn compound phase can be found near the upper interface of the Cu/Sn/Cu flip-chip solder joints. We believe that this asymmetrical microstructure could be caused by the solidification process after reflowing process. During the solidification process of the flip-chip solder joint, the upper joint interface, i.e., close to the chip side, would be cooling earlier than the bottom interface. So, there is the liquid/solid interface run across the Cu/Sn/Cu solder joint. The liquid/solid line bring the Cu-Sn compounds down to the bottom joint interface. In this talk, the detail microstructure evolution of the solder joint during the cooling process would be discussed.

11:30 AM

Influence of Stress on the Microstructural Development of Sn-Ag-Cu Solder Alloy during Aging: *Choong-Un Kim¹; Huili Xu¹; Tae-Kyu Lee²; Hong-Tao Ma²; Kuo-Chuan Liu²; ¹The University of Texas at Arlington; ²Cisco System Incorporation*

The close linkage between the microstructure of solder and its joint reliability has spurred extensive studies. While many studies have investigated evolution of Sn grain structure with aging, they usually neglect the fact that 1) aging induced change in grain structure is coupled with stress state of joint and 2) stress state can vary significantly depending on the location of joint in the electronic packaging. Our investigation, conducted primarily on Sn-Ag-Cu alloys in PBGA packaging structure, reveals that Sn structure development during aging is indeed affected significantly by stress state (shear, triaxial), and, as a result, Sn structure exhibits strikingly different crystallographic and metallurgical features depending on the joint location in the packaging structure (center, edge and outer corner of package). This paper introduces experimental evidences supporting the unique variation in Sn grain structure with aging and joint location, and the analysis on the stress state leading to such variations.

11:45 AM

Effect of Bump Height on Interfacial Reaction of Cu/SnAg/Ni Structure: *Yi-Sa Huang¹; Chin-Hsing Tang¹; Chih Chen¹; ¹National Chiao Tung University*

Intermetallic compound (IMC) growth of Cu/Sn_{2.3}Ag/Ni solder joint after reflow was observed in this study. The bump height of the solder joints are 10, 20 and 40 μm. In 40 μm-height solder joint, (Cu, Ni)₆Sn₅ as IMC grows rapidly on both sides. In 20 μm-height one, IMC grows slower on Ni side but faster on Cu side. However, the IMC growth information has a different trend when bump height reduces to 10 μm. (Cu, Ni)₆Sn₅ on Ni side stops growing as reflow time increases. Compositional analysis was performed to measure the element concentration in the as-

TUESDAY AM



TMS 2012

141st Annual Meeting & Exhibition

fabricated solder joint. Cu concentration and Ni concentration increase when bump height reduces. In the 10 μm -height solder joint, average Cu concentration is 2.44 at. %, and average Ni concentration is 1.57 at. %. The concentrations are speculated as the main factor which affects the interfacial IMC growth rate on the solder joint.

Phase Transformations and Deformation in Magnesium Alloys: Phase Transformations and Deformation

Sponsored by: The Minerals, Metals and Materials Society, TMS Materials Processing and Manufacturing Division, TMS/ASM: Phase Transformations Committee

Program Organizers: Jian-Feng Nie, Monash University; Sean Agnew, University of Virginia; Suveen Mathaudhu, Army Research Office

Tuesday AM
March 13, 2012

Room: Southern V
Location: Dolphin Resort

Session Chairs: Jian-Feng Nie, Monash University; Tresa Pollock, University of California Santa Barbara

8:30 AM Introductory Comments Jian-Feng Nie, Sean Agnew and Suveen Mathaudhu

8:35 AM Invited

Key Issues in Thermodynamic Mg Alloy Database: *Rainer Schmid-Fetzer*¹; ¹Clausthal University of Technology

Key issues in a large thermodynamic Mg database (20 components, over 450 assessed phases) are consistency, coherency and quality assurance. These issues concern extension, maintenance and updating of the database. For example, merging published assessments of additional binary or ternary subsystems requires scrutinizing the structural modeling especially of pertinent solid phases. First of all it must be checked if a given thermodynamic description is correct in producing the intended stable phase diagram. Also the thermodynamic properties, such as enthalpies of formation and absolute entropies must be checked for realistic values, considering also systematic trends as observed for binary Mg-RE phases. Metastable phases must be assessed with realistic values. These are also the standards for own assessments in combination with key experiments. The second focus of this presentation is on the database application by predicting phase formation during solidification and heat treatment in multicomponent magnesium alloys from thermodynamic calculations.

9:00 AM Invited

Grain Refinement of Magnesium Alloys: Theoretical Developments and Their Application: *David StJohn*¹; Ma Qian¹; Mark Easton²; ¹University of Queensland; ²Monash University

This paper covers developments that have occurred since our Metallurgical and Materials Transactions publication on the Grain Refinement of Magnesium Alloys associated with the previous special symposium on this topic in 2005. Since that time we have developed the Interdependence Theory which provides a new perspective for the study of grain refinement. It is a new model for analyzing grain refinement mechanisms and predicting grain size outcomes. After an introduction to the Interdependence Theory we will revisit the refinement of Mg-Al and Mg-Zr alloys as well as reviewing the broader research on grain refinement of magnesium alloys. Consideration will also be given to reported grain size variations observed in high pressure die cast alloys and ultrasonically treated alloys, both of which exhibit a relationship to the growth restriction factor Q defined by the alloy chemistry. Finally, we discuss the implications of the theory regarding directions for future research.

9:25 AM Invited

Enhancement of Precipitation Hardening of Magnesium Alloys by Microalloying: *Kazuhiro Hono*¹; C. L. Mendis¹; T. T. Sasaki¹; T. Ohkubo¹; T. Bhattacharjee¹; ¹National Institute for Materials Science

The age-hardening responses of rare-earth free magnesium alloys are too low to give extra hardening after wrought processes; however, microalloying to Mg-Zn, Mg-Ca, and Mg-Sn alloys lead to substantial enhancements of age hardening responses. We have systematically worked on the microalloying effect of rare-earth free Mg alloys to investigate the feasibility of developing age hardenable wrought alloys. In this talk, we overview our recent TEM/STEM and 3D atom probe studies on microalloyed Mg-Zn, Mg-Sn and Mg-Ca alloys, and discuss how peak aged microstructure can be refined by microalloying based on TEM/STEM and 3D atom probe studies.

9:50 AM Invited

Modeling Nucleation and Growth during Co-Precipitation in Mg-RE Alloys: Yipeng Gao¹; Hong Liu²; Jianfeng Nie²; Yunzhi Wang¹; ¹The Ohio State University; ²Monash University

Most light alloys are strengthened by precipitation hardening and the size, shape, spatial orientation, coherency state and spatial distribution of precipitates determine the deformation mechanism and mechanical behavior of these alloys. To assist in alloy design, a new modeling framework based on the phase field approach is developed. It is able to use ab initio calculations, CALPHAD database and crystallography of phase transformations from theoretical models and TEM characterizations as direct inputs, and treat nucleation and growth events involving simultaneously displacive and diffusional processes and heterogeneous nucleation near pre-existing lattice defects such as dislocations, grain boundaries and second-phase particles. Using β_1 and β' precipitation in WE54 as an example of the Mg-RE series alloys, we show that the activation energy, critical nucleus configuration and precipitation sequence can be determined using this new approach. These are critically important parameters for alloy design but extremely difficult to determine experimentally.

10:15 AM Break

10:25 AM Invited

Mg-M-RE Alloys Containing LPSO Structures with Synchronization of Stacking and Chemical Modulations: *Yoshihito Kawamura*¹; Michiaki Yamasaki¹; Eiji Abe²; Koji Hagihara³; ¹Kumamoto University; ²The University of Tokyo; ³Osaka University

New heat-resistant wrought Mg-M-RE alloys that are duplexes of a-Mg phase and a novel phase with a long period stacking ordered (LPSO) structure, have been developed in Japan. The M element is Co, Ni, Cu, Zn, or Al, and the RE (rare earth) element is limited to Y, Gd, Tb, Dy, Ho, Er, or Tm. Four kinds of LPSO structures are found in these alloys: 10H, 18R, 14H, and 24R, in which the M and RE elements are enriched in two atomic layers on basal planes at intervals of 5, 6, 7, and 8, respectively. Also, these structures can be called "Synchronized LPSO Structures", because the stacking and chemical modulations are harmonized. These synchronized LPSO phases have more preferable mechanical properties than the a-Mg phase and exhibit kink deformation, which further improves the mechanical properties drastically.

10:50 AM

On the Structure, Transformation and Deformation of Long-Period Ordered Structures in Mg-Y-Zn Alloys: Yuman Zhu¹; Allan Morton²; *Jian-Feng Nie*¹; ¹Monash University; ²CSIRO

Ternary Mg-Y-Zn alloys have attracted increasing attention due to their promising mechanical properties and unique microstructures. The microstructure of the Mg-Y-Zn alloys contains predominantly precipitates of metastable 18R and/or equilibrium 14H long-period ordered structures, depending on the processing conditions of the alloy.

Such 18R and 14H structures are also found in other magnesium alloys such as Mg-Gd-Zn, Mg-Gd-Y-Zn, Mg-Dy-Zn, Mg-Ho-Zn, Mg-Er-Zn and Mg-Y-Cu. This presentation will provide an overview of recent results on the characterisation of the structure, transformation and deformation of the 18R and 14H structures using high-angle annular dark-field scanning transmission electron microscopy and electron diffraction. These recent experimental results will also be discussed in the context of precipitation in other Mg-RE-Zn alloy systems and the design of alloys for higher strength.

11:15 AM Invited

Creep Mechanism in a Mg-6Al-3Ca-0.3Mn Alloy: *Tomoyuki Homma*¹; S. Nakawaki¹; Shigeharu Kamado¹; ¹Nagaoka University of Technology

High temperature resistant Mg-6Al-3Ca-0.3Mn (mass%) alloy has been developed by gravity casting technology. After the solidification, network-shaped compounds form on grain boundaries, suppressing grain boundary sliding. When the Mn-containing alloy is subjected creep deformation, fine and equiaxed Al-Mn type particles distribute in the matrix during the primary creep region. The number density of the fine particles increases as the creep time increases. Due to the presence of the precipitates, threshold stress appears in a strain rate-applied stress diagram. The detailed creep mechanism will be clarified.

11:40 AM Invited

Deformation in Magnesium from First-Principles: *Dallas Trinkle*¹; Joseph Yasi¹; Louis Hector²; ¹University of Illinois, Urbana-Champaign; ²General Motors R&D Center

Predictive modeling of strength from first-principles electronic structure methods offers great promise to inform Mg alloy design. Simulating the mechanical behavior for new alloys requires an understanding of mechanisms for deformation at atomic-length scales, with accurate chemistry, extended to larger length- and time-scales. Modern computational approaches can now investigate dislocations from first-principles, and compute interactions with solutes across the periodic table. We can predict metallurgical trends with changes in size and chemical misfits, and connect those to predictions of mechanical behavior through predictive models. Comparing alkali, alkali earth, and transition metals with rare earth solutes provides new connections between electronic structure and mechanical behavior. Moreover, the computational approach provides a blueprint for attacking new challenges in deformation behavior beyond solute strengthening and softening.

12:05 PM

In-Situ Neutron Diffraction Study of Aging of a Mg-Y-Nd-Zr Alloy (WE43): Effects of Precipitation on Individual Deformation Mechanism Strength and Activity: *Sean Agnew*¹; F. Polesak¹; Bjorn Clausen²; ¹University of Virginia; ²Los Alamos National Laboratory

There is an outstanding question regarding why the age hardening response of Mg alloys is not nearly as good as many competing Al alloys. A recent hypothesis is that it is due to precipitate geometry, since many commercial Mg alloys form either basal plate-shaped precipitates or c-axis aligned rod-shaped precipitates. These are among the least effective shapes to obstruct basal slip. It is further proposed that prismatic plate-shaped precipitates would be most effective for strengthening Mg alloys. The Mg-Y-Nd-Zr alloy, WE43, is an alloy which does form prismatic plate shaped precipitates during aging. In-situ neutron diffraction and crystal plasticity modeling are employed to explore the effect of these precipitates on the strength and hardening responses of basal slip, {10.2} extension twinning, and non-basal slip. The results confirm that basal slip is responsible for yielding in this cast alloy, and that the basal slip mechanism is most affected by the precipitation.

Randall M. German Honorary Symposium on Sintering and Powder-Based Materials: Powder Technology

Sponsored by: The Minerals, Metals and Materials Society, TMS Materials Processing and Manufacturing Division, TMS: Powder Materials Committee

Program Organizers: K. Morsi, San Diego State University; Fernand Marquis, Naval Postgraduate School; John Meyer, Iowa State University; Ahmed El-Desouky, San Diego State University; Eugene Olevsky, San Diego State University

Tuesday AM
March 13, 2012

Room: Oceanic 2
Location: Dolphin Resort

Session Chair: Iver Anderson, Iowa State University

8:30 AM Keynote

Nanostructured Metals: Synthesis and Behavior

from the Nanoscale to the Microscale: *Enrique J. Lavernia*¹; ¹University of California, Davis

Bulk nanostructured materials and composites have matured into a new class of materials that can be synthesized using various methods, including mechanical alloying of powders in liquid nitrogen (cryomilling). Results from various groups around the world reveal considerable improvements in the physical performance of a variety of cryomilled Al alloys, as well as interesting reports of novel deformation mechanisms. Their inherently low plasticity has been addressed via the introduction of additional size scales. In this lecture, recent results are reviewed and discussed with particular emphasis on the following topics: recent findings in the area of cryomilled materials; primary consolidation and secondary processing methods; microstructural evolution from nanostructured powders to bulk materials during consolidation; and mechanical behavior of consolidated materials. The deformation behavior and the underlying mechanisms of cryomilled materials are discussed in an effort to shed light into the fundamental behavior of ultrafine grained and nanostructured materials.

9:00 AM Invited

Effect of Powder Synthesis and Processing on Luminescence Properties: *Joanna McKittrick*¹; Jinkyu Han¹; Jae Ik Choi¹; Jan Talbot¹; ¹University of California, San Diego

Visible light-emitting materials (phosphors) have broad use in a variety of applications, from fluorescent and LED lighting, displays to scintillators. This talk will focus how powder synthesis methods effect the emissive spectral energy distribution, efficiency and color. This work is supported by the US Dept. of Energy, Grant DE-EE-0002003.

9:25 AM Invited

Improved Understanding of Gas and Melt Flow Manipulation for Enhanced Control of Powder Yields from Close-Coupled Gas Atomization Processing: *Iver Anderson*¹; Joel Rieken²; John Meyer²; David Byrd¹; Andrew Heidloff¹; ¹Ames Laboratory; ²Iowa State University

Significant progress in design of discrete-jet close-coupled (DJ-CC) gas atomization nozzles and melt feed tubes has helped achieve powder particle size control and efficient use of gas flow energy for gas atomization of metal and alloy powders. Powder yield characterization and high-speed video observations of atomization trials were performed from Ar atomization of special ferritic stainless steel and other selected metals and alloys. Also, gas atomization flow simulations using surrogate fluids, e.g., water, and schlieren gas flow visualization and aspiration measurements were conducted for Ar and N₂ and a range of parameters for DJ-CC nozzles. Closed wake gas flow patterns were found most effective for enhanced fine powder processing and open wake flow with slotted "trumpet bell" pour tubes were utilized to gain close size control (standard deviation < 1.6) over an order of magnitude of particle diameters (50-500µm). Supported by USDOE-FE and Carpenter Technologies, Inc., through contract no. DE-AC02-07CH11358.



TMS 2012

141st Annual Meeting & Exhibition

TUESDAY AM

9:50 AM Invited

Production, Characterization and Application of Mono-Size Alloy Droplets: *Teiichi Ando*¹; ¹Northeastern University

Mono-size alloy droplets are produced by controlled capillary jet breakup, a droplet generating process, also used in ink-jet printing technology. With Rayleigh instability controlled through the decoupled process parameters of jet diameter, mass flow rate and perturbation frequency, mono-size droplets of desired diameter can be generated at high rates with essentially full yield. The uniform size of droplets assures nearly identical solidification paths for all the droplets generated under fixed process conditions. This permits precise prediction of the motion and thermal and solidification behaviors of the droplets through rigorous process and metallurgical modeling, which is applicable to industrial thermal spray processes as well. Uniform droplets can be in-flight solidified or deposited on a substrate to produce various forms of materials with novel rapid solidification microstructures. Areas of industrial applications are discussed.

10:15 AM Break

10:30 AM Invited

TEM Guided Microstructural Design of MgH₂ Powders and Thin Film Alloys with Room Temperature Volumetric Hydrogen Cycling Ability: *David Mitlin*¹; Peter Kalisvaart¹; Mohsen Danaie¹; Shu Tao²; Ben Zahiri¹; Helmut Fritzsche³; ¹University of Alberta and NINT NRC; ²Eindhoven University of Technology; ³SIMS-CNRC NRC

This presentation is separated into two sections: We will first discuss our recent cryogenic stage transmission electron microscopy (TEM) – based findings on the MgH₂ to Mg (and vice versa) phase transformation in high-energy milled powders. We show that both reactions are nucleation limited, rather than core shell, and identify the dominant metal - hydride orientation relationships. By performing cryo-TEM on ball milled powders we discovered deformation twins in the microstructure. Density functional theory (DFT) analysis demonstrates that the twins significantly affect the kinetics of hydrogen diffusion. In the second portion of the presentation we highlight our recent alloy design efforts for both “bulk” thin films and thin film multilayers. The research culminates in the creation of several classes of catalysts that enable for relatively rapid room temperature volumetric sorption over multiple cycles. The same catalysts allow for ultra-rapid 250+ cycles elevated temperature absorption/desorption at pressures of 1-3 atm.

10:55 AM

Effect of Pre-Consolidation Solidification Structure in Novel Gas Atomization Precursor Powder Approach for Efficient Production of Ni-based Oxide Dispersion Strengthened (ODS) Alloys: *John Meyer*¹; Joel Rieken¹; Iver Anderson²; ¹Iowa State University; ²Ames Laboratory, US DOE

Oxide dispersion strengthened (ODS) Ni-base superalloys have been considered promising candidate materials to combat the challenging operating conditions of future thermal power plants. Traditional processing (i.e. mechanical alloying) of Ni-based ODS materials is very time, energy and cost intensive as well as susceptible to contamination. Gas atomization reaction synthesis with a reactive (Ar/O₂) atomization gas was developed as a simplified route for processing of ODS precursor powders. The pre-consolidation microstructure and amount of solute trapping as a result of rapid solidification were investigated using x-ray diffraction coupled with electron microscopy to determine how it affects the distribution and size of the yttrium-enriched nanometric oxide dispersoids formed during the internal oxygen exchange reactions upon consolidation. The resulting spacing was expectedly similar to the as-atomized solidification structure, a trend observed in similar Fe-based ODS alloys produced via this process. Supported by Carpenter Technology and USDOE-FE-ARM Program through Ames Laboratory contract no. DE-AC02-07CH11358.

11:10 AM

Effect of Rapid Solidification and Heat Treatment on D2 Tool Steel: *Pooya Delshad Khatibi*¹; Hani Henein¹; Douglas Ivey¹; ¹University of Alberta

It is believed that excellent mechanical properties of D2 steels can be achieved from reduced microsegregation and a good distribution of carbides during the solidification. An understanding of the evolution of microsegregation and carbide formation during rapid solidification is necessary to control the microstructure. Impulse Atomization (IA) has been employed to produce rapidly solidified (RS) powders of D2 steel in helium and nitrogen cooling gases. The resulting powders were sieved into different size ranges and the microstructures and phases were examined using SEM, XRD and neutron diffraction. In addition to a substantial refinement of grain size, rapid solidification also suppressed the martensitic transformation and produced supersaturated retained-austenite. Different annealing tests were carried out on the as-atomized powders. SEM images showed a good distribution of precipitated carbides after annealing. The effect of annealing on the RS powders was evaluated using Vickers microhardness measurements and the precipitated carbides were characterized using TEM.

Recycling General Sessions: Metals

Sponsored by: The Minerals, Metals and Materials Society, TMS Extraction and Processing Division, TMS Light Metals Division, TMS: Recycling and Environmental Technologies Committee
Program Organizer: Joseph Pomykala, Alter Trading

Tuesday AM
March 13, 2012

Room: Europe 4
Location: Dolphin Resort

Session Chair: Joseph Pomykala, Alter Trading

8:30 AM

Advantages of Long Term Al Recycling Batch Planning in a Constrained Secondary Material Market: *Tracey Brommer*¹; Britt Elin Gihleengen²; Elsa Olivetti¹; Randolph Kirchain¹; ¹Massachusetts Institute of Technology; ²Norsk Hydro

The sizable energy savings resulting from remelting secondary materials during aluminum production reduce environmental impact and cost. Economic savings result from the lower cost of secondary materials and reducing alloying additions. Strong market demand for secondary materials has restricted material availability for industrial remelters. Optimizing production on a charge by charge basis may lead to non-optimal allocation of secondary materials. Effective use of secondary materials as a means to reduce cost and master alloy consumption is improved by optimization over a longer time horizon. Expanding the optimization time horizon allows the explicit calculation of the optimal allocation of raw materials for each alloy in the production portfolio. In this investigation, the authors evaluate the advantages of optimizing over a longer time horizon using performance metrics of cost, raw material allocation, and out of specification rate.

8:50 AM

Mechanical Dross Processing: The Approach to Zero Waste from Smelter and Secondary Dross: *David Roth*¹; ¹GPS Global Solutions

Mechanical dross treatment was the standard method of dross treatment before the advent of the tilt type rotary furnace. There were four predominant systems used. The first three are no longer used because of maintenance and technical aspects of the equipment and aluminum recovery issues. The classical impact crusher systems are used today for high volume dross processors. The RT Metal/Reclaimer manufactured by DIDION has now allowed small volume dross generators the ability to use this type of technology. This paper will discuss the past systems and how

the RT Metal/Reclaimer System brings dross recycling without the use of salt fluxes to the individual casting and melting facilities, significantly improving the environment and reducing land fill materials.

9:10 AM

Recycling of Aluminium Alloy Scraps by Pressure-Assisted Investment Casting for Aluminium Foam Manufacture: *Seksak Asavavisithchai*¹; Areeya Srichaiyaperk¹; Natthida Jareankieathbovorn¹; ¹Chulalongkorn University

Recycling of ADC12 alloy scraps for fabrication of open-cell aluminium foams has been conducted via pressure infiltration method of replication process. The scrap, up to 50 wt.%, was melted with pure aluminium billet, followed by infiltration in a replicated mold of polyethylene foam structure. Compared with the pure aluminium foam, the compressive strength and hardness are higher for the foams with recycled scraps. The increase in foam mechanical properties is due to the presence of Si hard phase in Al matrix. The strength and hardness of the foams also increase with increasing contents of the scraps.

9:30 AM

In-Process Separation of Mill Scale From Oil at Steel Hot Rolling Mills: *Naiyang Ma*¹; ¹ArcelorMittal

High oil concentration is one of the major barriers for recycling of mill scale of steel hot rolling mills. It is of vital importance to find cost-effective technologies of reducing oil concentration in mill scale in order to recycle the mill scale without causing detrimental effects on production and environment. This paper discusses in-process separation of mill scale from oil at steel hot rolling mills. Formation of mill scale and status of oily wastewater at hot rolling mills are reviewed in the first place. A mathematical model is then formulated to relate oil concentration in mill scale to physical properties of mill scale, chemical and physical properties of wastewater and interacting parameters between mill scale particles and wastewater. From this model, three approaches of in-process separation of mill scale from oil are derived: (1) avoiding contacts between mill scale particles and oily wastewater, and (2) maintaining low oil concentration in wastewater, and (3) collecting mill scale in upper streams of wastewater flows. In-process separation of mill scale from oil might have advantages of lower capital cost, lower operating cost and less additional environmental concerns, compared to other strategies of separating mill scale from oil.

9:50 AM

Recycling of Electric Arc Furnace Dust: *Vicente Sobrinho*¹; Vitor Telles²; Felipe Grillo²; Jose Oliveira¹; Jorge Alberto Tenorio²; Denise Espinosa²; ¹IFES; ²USP

This research aims to study the process of incorporation of the metal iron in electric arc furnace dust (EAFD), from a steel mill producing long steel by liquid iron in addition to the changing temperature of 1400 degree Celsius altering experimental conditions such as how to add the EAFD. Previously, the EAFD will be characterized using the following techniques: chemical analysis, X-ray diffraction, scanning electron microscopy (SEM) and Energy Dispersive Spectroscopy (EDS) microanalysis. After characterization, the EAFD to be added to the bath of liquid iron. The achievement of fusion experiments in laboratory scale, will take place in a vertical tubular furnace with temperature control. The fusion experiments to assess the incorporation of the metal iron will use graphite crucibles. It is expected that the results obtained at the end of the research allow the evaluation of the iron metal incorporation of electric arc furnace dust in pig iron bath.

10:10 AM Break

10:30 AM

Recycling of Electric Arc Furnace Dust in Iron Ore Sintering: *Victor Telles*¹; Denise Espinosa¹; Jorge Tenório¹; ¹University of Sao Paulo - USP

The purpose of this work was to study the reutilization of the steelmaking dust, derived from steel production in the electric arc furnace, in iron ore sintering process aiming zinc elimination. In each sintering process were

collected sintered samples, these materials were analyzed by chemical analysis using atomic absorption spectrophotometry in order to determine the zinc content. Samples of not sintered mixtures were also characterized by chemical analysis aiming to determine the initial amounts of zinc, i.e. in order to check the zinc amounts present in the mixture before the sintering process. The comparison among the zinc contents of samples sintered and not sintered allowed to determine the elimination of zinc during the experiments. Results showed that the zinc elimination in the process is proportional to the ratio reducer/waste. Zinc removal was lower when the reducer/waste ratio was decreased.

10:50 AM

Extraction of Iron Oxide and Concentration of Titanium Compounds in Bauxite Residue: Edilson Magalhães¹; Emanuel Macêdo¹; José Antonio Souza¹; João Nazareno Quaresma¹; Danielly Quaresma¹; *Luis Venancio*¹; ¹Federal University of Pará

The production of alumina from bauxite using the Bayer process generates the residue known by red mud. This material can be used as a source for concentration and recovery of valuable metals such as titanium. The greatest difficulty of concentrating titanium compounds is the large amount of iron oxide present in red mud > 30% by weight. This paper shows the extraction of the iron oxide, increasing the concentration of the titanium compounds. The red mud is leached with H₂SO₄ at 20% and 30% concentration and temperature range of 60°C, 80°C and 90°C. Analysis of the leached and concentrated was made to verify the effectiveness of the iron oxide extracting process and the titanium compounds concentration viability.

11:10 AM

Pyrometallurgical Approaches for Utilization of

Smelting Slag from Cobalt Concentrate: *Jeongsoo Sohn*¹; Kang-In Rhee¹; Soo-Kyung Kim¹; ¹Korea Institute of Geoscience and Mineral Resources

Although a few countries only mine and produce for cobalt, cobalt is used for many applications such as secondary battery, cemented carbide, super alloy, catalyst, magnet, and pigment and so on. There is serious problem that by product (slag) is produced in the course of cobalt ore smelting. That is a major reason to induce the environmental pollution. It is necessary, therefore, to find a utilization of slag as well as to develop eco-friendly efficient smelting technology. For these purposes, reductive smelting of cobalt ore process, eco-friendly leaching process, customized cobalt compound manufacturing process, especially recycling of smelting slag process were proposed. For recycling of smelting slag process, in this study, a novel approach of directly recycling the liquid slag to prepare small drop size ball as can be used for various applications using slag atomizing technology was proposed.

11:30 AM

Heat Treatment of Black Dross for the Production of a Value Added Material - A Preliminary Study: *Reza Beheshti*¹; Shahid Akhtar²; Ragnhild E. Aune³; ¹KTH; ²NTNU; ³NTNU, KTH

The potential use of Black Dross (BD) as a raw material in the production of refractories, fluxing agents and glasses is the main motivation of the present study. Heat treatment experiments were carried out in Ar, and under reduced pressure (20Pa), to evaluate the salt removal efficiency. The chemical composition of the BD after heat treatment was investigated by SEM-EDS and XRD analyses. Based on the present results, it was established that the salt starts to evaporate at 1276 K in Ar, and under reduced pressure. The salt removal efficiency in a 20 g sample was found to increase in both cases as a function of time and temperature. Moreover, in Ar the chloride concentration was lowered to 0.3 wt% after heat treatment at 1573 K for 10 hours. Under reduced pressure, however, 0.2 wt% residual chloride was obtained after 8 hours at 1473 K.



TMS 2012

141st Annual Meeting & Exhibition

11:50 AM

Development of Synthetic Flux for Basic Oxygen Steel Making Using Waste Oxides of Steel Plant: *Jagannath Pal*¹; S. Ghorai¹; P. Venkatesh¹; D. P. Singh¹; M. C. Goswami¹; D. Bandyopadhyay¹; S. Ghosh¹; ¹Council of Scientific and Industrial Research, National Metallurgical Laboratory

In BOF operation, burnt lime as flux often creates problem due to its high melting point (2700°C), poor dissolution, fines generation and hygroscopic nature. Since Fe₂O₃ and 22% CaO form eutectic at 1230°C, in current study, a pre-fused synthetic flux in form of sinter was prepared from LD sludge and lime fines as source of iron oxide and CaO respectively. Mixture of aforesaid fines were pelletized into micropellets (2-6mm) that were strengthened by an innovative treatment using steel plant's waste gas rendering excellent handling properties. The treated micro-pellets were subsequently sintered in a 7-9 kg capacity pot sintering set-up without coke breeze. The produced sinter contains upto 45% CaO and exhibits suitable handling properties, low softening point (1180 °C) and quick dissolution (27-32 sec/g). Being non-hygroscopic it is suitable for storage, handling and charging. Flux prepared through this cokeless sintering has high potential as a flux material in BOF process.

12:10 PM

Addition of Electric Arc Furnace Dusts in Hot Metal: *Felipe Grillo*¹; Denise Espinosa¹; Jose Oliveira²; Jorge Tenório¹; ¹University of Sao Paulo - USP; ²Federal Institute of Espirito Santo

The aim of this work was evaluation of the recovery of Zn and Fe of the EAFD added to the hot metal in the form of a briquette at temperature of 1500°C. the EAFD was agglomerated by cold briquetting and introduced in the hot metal. This study utilized a bench-scale equipment to melt, during this process to kept a flow rate of inert gas above the bath. Were collected periodically metal samples and the samples were analyzed for determination of the content of total silicon and carbon by chemical analysis. Zinc oxide, zinc ferrite and other oxides were reduced and were volatilized and collected by a cleaning system of dust (baghouse) located on top of the oven. More than 98% of iron were recovered from EAFD during the test. It was possible to produce a dust containing about 68% zinc by means of adding of EAFD.

Science and Engineering of Light Metal Matrix Nanocomposites and Composites: Metal Matrix Composites

Sponsored by: The Minerals, Metals and Materials Society, TMS Light Metals Division

Program Organizers: Xiaochun Li, University of Wisconsin-Madison; Alan Luo

Tuesday AM
March 13, 2012

Room: Macaw 2
Location: Swan Resort

Session Chairs: Alan Luo, GM; Xiaochun Li, University of Wisconsin-Madison

8:30 AM

Slow-Shot High Pressure Die-Casting (SS-HPDC) Process for AE44 Magnesium Single-Cylinder Engine Block with Short-Fiber Reinforcement in the Bore: *Bin Hu*¹; Pan Wang¹; Bob Powell²; Xiaoqin Zeng³; ¹Genral Motor China Science Lab; ²General Motors Global R&D Center; ³Shanghai Jiao Tong University

Single-cylinder magnesium engine blocks with short fiber reinforcement in the bore region were prepared by low shot speed, high pressure die casting to infiltrate the fiber preforms and produce sound castings. The magnesium alloy was AE44 and the cylindrical preforms were made with silica-bonded Saffil fibers. The slow shot, high pressure die casting process (SS-HPDC) was intended to simulate squeeze casting. SS-HPDC process

is a promising means for casting the blocks, which were free of porosity could be subjected to T4 and T6 heat treatments without blistering. Processing parameters were identified and optimized. These included the pouring temperature, 760°C; the die temperature, 275°C preform preheat temperature, 750°C and the intensification/infiltration pressure, 90MPa. Their relative contribution to the quality of the cast blocks is discussed and suggestions for further optimization are made.

8:50 AM

Compressive Properties of Al-B4C Composites over the Temperature Range of 25 - 500 °C: *Srinu Gangolu*¹; A Rao²; N Prabhu¹; V Deshmukh²; B Kashyap¹; ¹Indian Institute of Technology Bombay; ²Naval Materials Research Laboratory

Aluminum - Boron carbide (B₄C) composites containing 0, 5, 10, and 15 wt% B₄C were produced by stir casting at 900°C. Compression tests done from room temperature to 600°C and at strain rates of 10⁻⁴ and 10⁻² s⁻¹, exhibit a decrease in flow stress with increasing temperature and decreasing strain rate. The effects of temperature and strain rate on deformation behavior were analyzed to identify the regimes of different operating mechanisms. The role of particulates on strengthening and transition to different mechanisms of deformation were discussed in terms of dislocation activity, diffusion and other high temperature processes. Rolling was done to vary the grain sizes and incorporate the same towards understanding mechanism for deformation in the form of constitutive relationship.

9:10 AM

Mechanical Properties of a Spherical Particle Reinforced Aluminum Composite after Metal Working: *William Harrigan*¹; ¹Gamma Technology

Particle reinforced aluminum composites can be processed by conventional metalworking techniques such as extrusion, forging and rolling. Composites have been made by Gamma Technology with spherical alumina particles. These composites have properties that are similar to composites made with irregular shaped particles. The spherical particles reduce the tool wear during machining operations leading to reduced cost of part manufacture. Composites made with the spherical particles have been extruded, forged and ring rolled. This study looks at the mechanical properties of the composite at several stages of metal working. Tests were conducted after several levels of forging, after several levels of extrusion and after combinations of extrusion, forging and ring rolling. The study documents the development of uniform microstructure and the accompanying uniform mechanical properties.

9:30 AM

Effect of Processing on the Dynamic Response of a Silicon Carbide Reinforced Aluminum Metal Matrix Composite: *Brandon McWilliams*¹; Tomoko Sano¹; Jian Yu¹; Chian Yen¹; ¹US Army Research Laboratory

Microstructure based finite element simulations are conducted to investigate the effects of processing on the dynamic deformation response of ceramic particle reinforced aluminum metal matrix composites (MMC). Samples were obtained from as-cast and hot-rolled MMC plate which had been reduced to various thicknesses. During rolling, ceramic particles fracture leading to a change in particle morphology and particle size distribution in the composite. This combined with a break up of inclusions formed in the casting process leads to dramatically different material response in rolled MMC plate versus the as-cast material. To implement these materials in design applications, a complete understanding of how these microstructures evolve and their effect on properties is required. The modeling approach in this work is used to predict the stress-strain response and explore high rate damage and failure mechanisms of the MMC. In-situ SEM, and macro scale mechanical test results are used to validate the modeling.

TUESDAY AM

9:50 AM

Fabrication and Characterization of Al-SiC Composite Foam: *Geo Harrison*¹; Ganapathy Subramanian¹; Vinoth Kambli¹; Pradeep Kumar¹; ¹College of Engineering Guindy, Anna University

Metal matrix composite foams have very low density, high stiffness and good impact resistance. These properties enable them to be used in various automotive and structural components. Al-SiC composite foams are prepared by dispersion of fine Silicon carbide powder in molten aluminum, followed by blowing of an inert gas and simultaneous stirring. The well dispersed inert gas bubbles form numerous micro-voids during solidification of the composite. A fine Al-SiC composite foam with homogeneous micro-structure is manufactured by this process. The impact resistance, stiffness and the mechanical behavior of the Al-SiC are analyzed subsequently.

10:10 AM Break

10:25 AM

Aluminum Metal Matrix Composite via Direct Metal Laser Deposition: Processing And Mechanical Characterization: *Benjamin Waldera*¹; Samar Kalita¹; ¹Advanced Engineered Materials Center - University of North Dakota

Aluminum metal matrix composites (Al-MMCs) have shown favorable material characteristics for aerospace applications such as airframes, reinforcement materials and joining elements. Similarly, carbide Al-MMC coatings can greatly improve surface performance of aluminum components. In this research, such coatings were developed from a powder blend of pure aluminum, chromium carbide and tungsten carbide nickel alloy, premixed at 2:1:1, on AA 7075 plates through direct metal laser deposition. Microstructure of the carbide Al-MMC was studied by optical and scanning electron microscopy. The hardness and the reduced Young's modulus were assessed through depth-sensing instrumented indentation using a Hysitron-TI950 Nanomechanical Tester. The carbide Al-MMCs demonstrated good interfacial bonding and improved modulus and hardness. A maximum hardness and reduced modulus of 2.47 GPa and 87.43 GPa, respectively, were recorded for the composite. Hardness and reduced modulus of AA 7075 substrate were 1.45 GPa and 70.63 GPa, respectively. This talk will present our recent findings.

10:45 AM

A Microstructure-Sensitive Fatigue Model for SiC Reinforced AA6061 Metal Matrix Composites: *Andrew Brammer*¹; J Jordon¹; ¹The University of Alabama

In this work, a microstructure-sensitive fatigue model is proposed for a SiC reinforced metal matrix composites (MMC's). The fatigue model proposed here was correlated to a discontinuously particulate-reinforced 6061 aluminum alloy tested under stress amplitude controlled fatigue conditions. Experimental results show that the 6061 was strongly influenced by volume fraction of the particulate reinforcement, particularly under high cycle fatigue. The model presented here characterizes the fatigue damage of the MMC into three distinct stages: crack incubation, microstructurally/physically small crack growth, and long crack growth. In this model, the influence of particle volume fraction, nearest neighbor distance and subsequent matrix strength are captured in the three stages of the model. The model showed good results in correlating the fatigue behavior of various percentages of reinforced-particulate. The model illustrated that particle fraction is indeed the controlling factor in fatigue lifetimes and this conclusion was supported by fractography analysis of failed specimens.

11:05 AM

Damage Evolution Model for Hybrid Metal Matrix Composites: *Jessica Dibelka*¹; Scott Case¹; ¹Virginia Polytechnic Institute and State University

In this study, two types of alumina fiber reinforcement, continuous Nextel™ fabric and discontinuous Saffil paper, were used to produce aluminum matrix composites. One of the composites created was a hybrid composite consisting of both reinforcements. This hybrid composite displayed high strength similar to the Nextel™ fabric-reinforced composite while maintaining a reasonable strain to failure typical of the Saffil paper-reinforced composite. Additionally, the hybrid composite exhibited progressive rather than catastrophic tensile failure. When the maximum strength of the composite was reached, the stress dropped 10% and was sustained for a considerable amount of strain before ultimate failure. A modeling framework is presented to describe the progressive damage and ultimate failure of these composites. This framework combines fiber/matrix-scale models for stiffness and strength with layer-level models for stress redistribution. Excellent predictions are obtained for initial failures, with reasonable predictions obtained for subsequent damage events.

11:25 AM

Numerical Simulation of Pressure Infiltration Process for Making Metal Matrix Composites: Effect of Process Parameters: *Bo Wang*¹; *Krishna M. Pillai*¹; ¹University of Wisconsin-Milwaukee

A three-dimensional finite difference model is developed for simulating the pressure infiltration process (PIP) for making metal matrix composites (MMCs) where liquid metal is injected under pressure into a mold packed with reinforcing fibers. The infiltration of liquid (pure) metal into the fibrous preform under a constant applied pressure is modeled using the Darcy's law after assuming fully saturated flow behind the liquid-metal front. The concomitant solidification and heat transfer processes are modeled using a suitable energy equation. The simulation allows one to study the effect of process parameters on the PIP infiltration process through evolution of flow-front during filling, solidification pattern, and pressure and temperature distributions. In this study, the effects of the inlet (applied) pressure and the gate size on the infiltration process are studied. The simulation results for such metal infiltration into porous preforms can be used to optimize the PIP and other related manufacturing processes (such as squeeze casting) for making MMCs.

11:45 AM

A Parametric Study of Hot Rolling of an Aluminum MMC via ANSYS and LS-DYNA: *Charles Mansfield*¹; Nathan Mutter¹; Ali Gordon¹; ¹UCF

Material, geometric, and contact properties all play a role in the consequent mechanical characteristics of hot rolled plates; however, previous numerical parametric simulations have yet to incorporate variability over all of these processing parameters. Hot rolled aluminum metal matrix composites (MMCs) have been identified for high value components of next generation structural applications. Determining the thermo-mechanical processing parameters that optimize the strength and ductility of this class of materials is a means to increase the usability of these materials in practical applications. With the aid of a command line formatted input file for ANSYS and LS-DYNA, this numerical study simulates the effects of plate geometry, roller parameters, and contact parameters on the mechanical response of the plate. Based on the study, models that link processing parameters to (1) the stress-strain response in the plate and (2) accumulation of damage in the plate are developed.

TUESDAY AM



TMS 2012

141st Annual Meeting & Exhibition

Solar Cell Silicon: Refining and Characterization

Sponsored by: The Minerals, Metals and Materials Society, TMS Extraction and Processing Division, TMS Light Metals Division, TMS: Energy Conversion and Storage Committee, TMS: Recycling and Environmental Technologies Committee
Program Organizers: Arjan Ciftja, SINTEF; Gabriella Tranell, Norwegian University of Science and Technology; Gregory Hildeman, Consultant; Shadia Ikhmayies, Al Isra University

Tuesday AM
March 13, 2012

Room: Europe 9
Location: Dolphin Resort

Session Chair: Arjan Ciftja, SINTEF Materials and Chemistry

8:30 AM

High Frequency EM Purification of Silicon: Lucas Damoah¹; Lifeng Zhang¹; ¹Missouri University of Science and Technology

The use of electromagnetic field to remove suspended particles from metals such as aluminum by pushing to the boundary has been well studied. However, the potential of this method is yet to be exploited for the removal of inclusions from silicon. This study investigates and discusses new results on the effect of processing parameters such as composition, coil current, and frequency on the removal of inclusions from silicon under high frequency AC electromagnetic field.

8:55 AM

Mono-Like Ingot/Wafers Made of Solar-Grade Silicon for Solar Cells Application: Sergey Beringov¹; Timur Vlasenko¹; Sergiy Yatsuk¹; Oleksandr Liaskovskiy¹; Iryna Buchovska¹; ¹Pillar Group

Working with solar-grade silicon for solar cells application usually meets some difficulties in comparison to polysilicon produced by Siemens method: higher impurities content leads to lower yield, worse electro-physical parameters and poor performance in solar cells application. However some adjustments in ingot production can show significant improvements in quality of final product: crystalline wafers and cells. Recent investigations have shown that solar-grade silicon is suitable for high effective production process such as mono-like multicrystalline wafer production. Production-scale lots made at Pillar show promising results for solar-grade silicon application: high-quality wafers with significantly big crystalline grains of <100> orientation.

9:15 AM

Preparation and Characterizations of Hydrogenated Microcrystalline Silicon Germanium Thin Films Prepared by RF Magnetron Sputtering: C. H. Chang¹; C. W. Chang²; H. S. Chen¹; J. P. Chu¹; ¹National Taiwan University of Science and Technology; ²Industrial Technology Research Institute

We have investigated the effects of H₂/Ar mixture during deposition and post-annealing temperature on crystal structure, microstructure as well as properties of hydrogenated microcrystalline silicon germanium ($\mu\text{-Si}_0.8\text{Ge}_0.2\text{:H}$) thin films. $\mu\text{-Si}_0.8\text{Ge}_0.2\text{:H}$ thin films were deposited on glass substrates by radio frequency magnetron co-sputtering of Si and Ge in H₂/Ar gas mixture. The electrical and optical properties of $\mu\text{-Si}_0.8\text{Ge}_0.2\text{:H}$ thin films, analyzed with Hall effect measurement and VIS-NIR spectrum, respectively, have been evaluated. The results indicate that the crystallite size, electrical properties and optical properties depend on the annealing temperature. The properties of $\mu\text{-Si}_0.8\text{Ge}_0.2\text{:H}$ thin films will be discussed in light of results obtained.

9:35 AM

Removal of Phosphorus from Silicon Melts by Vacuum Refining: Buhle Xakalash¹; Jafar Safarian²; Merete Tangstad²; ¹Mintek; ²NTNU

Induction vacuum refining testwork has been carried out to study the effect of iron on phosphorus removal from silicon melts. The experiments were carried out through vacuum induction melting of high purity silicon with

additions of phosphorus and iron at temperatures ranging between 1773 K and 1873 K and at a pressure of 0.5 Pa. Holding times varied between 0 s and 7200 s. ICP-MS was the primary analytical technique employed for sample analysis. The experimental results showed that phosphorus can be decreased from 15.5 ppmw to 1.5 ppmw at a temperature of 1873 K and holding time of 7200 s. The removal of phosphorus from silicon via induction vacuum refining seems to be independent of iron concentration for iron concentrations of up to 5000 ppmw. The rate constants for phosphorus removal were determined to be $8.4 \times 10^{-6} \text{m/s}$ and $2.5 \times 10^{-6} \text{m/s}$ at 1873 K and 1773 K, respectively.

9:55 AM

Thermodynamics of Phosphorous Distribution between Si and Fe-Si in Solvent Refining of Silicon: Leili Tafaghodi Khajavi¹; Mansoor Barati¹; ¹University of Toronto

This study involves employing solvent refining as a purification process in which silicon recrystallization takes place from a super-saturated iron-silicon melt. It is believed that iron will act as the impurity "getter" and purified silicon crystals will grow from the alloy melt, while the impurities are segregated to the liquid alloy. Phosphorous is a problematic impurity to remove since its segregation coefficient in pure silicon is relatively large. To assess the feasibility and efficiency of phosphorous removal through solvent refining, it is critical to study its equilibrium distribution between solid Si and the Fe-Si alloy phase. The distribution of phosphorous between solid silicon and iron-silicon melt at 1483-1583 K was measured to evaluate the impurity removal potential of each alloy. Interaction parameter between phosphorous and iron was calculated by varying the concentration of phosphorous in Si.

10:15 AM Break

10:35 AM

Imaging Techniques for the Characterization of Multi-Crystalline Silicon Bricks and Wafers: Steve Johnston¹; Fei Yan¹; Katherine Zaunbrecher²; Mowafak Al-Jassim¹; Omar Sidelkheir³; Alain Blossé³; ¹National Renewable Energy Laboratory; ²Colorado State University; ³Calisolar

Imaging techniques are applied to multi-crystalline silicon wafers and solar cells throughout the production process. Photoluminescence imaging, both band-to-band and defect-band, is used to characterize defects and wafer quality at all process steps. These steps include bricks sawn from ingots, wafer sawing, cleaning and texturing, emitter diffusion, edge isolation and glass removal, anti-reflective coating/passivation, and metallization of finished cells. Bricks, wafers, and cells can be imaged at a rate commensurate with in-line measurement, giving spatial information to characterize quality and defect content. Photoluminescence images on silicon bricks can be correlated to lifetime measured by photoconductive decay and could be used for high-resolution characterization of material before wafers are cut. The defect areas in as-cut wafers are compared to imaging results from electroluminescence and lock-in thermography, and cell parameters of near-neighbor finished cells, showing correlations to efficiency, open-circuit voltage, short-circuit current, and fill factor.

10:55 AM

Silicon PV Wafers: Correlation of Mechanical Properties and Crack Propagation with Defects and Stresses: Khaled Youssef¹; Meirong Shi¹; Prashant Kulshreshtha¹; George Rozgonyi¹; ¹North Carolina State University

The interactions between a propagating crack and crystal growth induced impurities, defects, and residual stresses have been evaluated in thin CZ Si wafers. Nanoindentation was used to evaluate the influence of fast pulling rate and the associated defects and precipitates on the hardness and fracture toughness. Our results showed that defects and stresses associated with fast solidification rates reduce wafer toughness by about 45% and therefore play a major role in thin wafer breakage. In addition, supporting the nanoindentation results, micro-Raman spectroscopy,

FTIR, and AFM profiling were used to investigate phase transformations. A modified brittle-to-ductile fracture mechanism was identified. The phase transformation results indicate that a judicious choice of stress and impurity will facilitate a beneficial change of brittle semiconducting Si to a meta-stable ductile metallic Si phase via deformation. This finding offers the possibility of reducing damage/cracks created during the cutting process by enhancing the ductile mechanisms of cutting.

11:15 AM

Thermodynamics on Boron Rejection during Metallurgical Grade Silicon Oxidation by Silicon Dioxide: *Yaqiong Li¹; Yi Tan¹; Jiayan Li¹; Shenrui Wu¹; Yao Liu¹; ¹Dalian University of Technology*

A metallurgical grade silicon (MG-Si) refining concept process was presented. Under vacuum conditions, silicon was selectively oxidized by high purity silicon dioxide to form gaseous silicon monoxide while impurities with low vapor pressure in MG-Si were rejected in residue; Then high purity silicon was obtained from the disproportionation of condensed silicon monoxide; and by-produced silicon dioxide was recycled for the oxidation step. Thermodynamics on boron rejection during the oxidation were studied in this work. In the temperature range of 1200-1800K, the saturated vapor pressure of boron, and the Gibbs free energy changes, the equilibrium partial pressures of silicon monoxide and boron oxides of potential reactions were calculated. And the effect of boron activity in MG-Si was also discussed. The results indicated that boron in MG-Si can be rejected during the oxidation and it shows the potential for the further development of the new refining process.

11:35 AM

On the Segregation of Impurities in Solar Silicon: *Kader Zaidat¹; Abdallah Nouri¹; Yves Delannoy¹; ¹Grenoble-INSP*

The exponential increase of the photovoltaic market leads to a shortage of high purity Si raw material and the producers are currently using less and less pure Si. However the quality of Si photovoltaic cells depends on the purity of the material and on the grain structure of the ingot from which the wafers are cut. It is necessary to control the segregation of impurities in the grown ingot in order to optimize the cell properties as a function of the raw material purity. We have developed a Bridgman set-up in order to study the solidification of photovoltaic Si under independently controlled solidification parameters: growth rate, thermal gradient, purity and convection. Segregation can be controlled by forced convection which is induced by a travelling magnetic field in order to homogenize or segregate the rejected impurities such as carbon and metallic elements.

11:55 AM

Effect of Solute Hydrogen on Toughness of Feed Stock Polycrystalline Silicon for Solar Cell Applications: *Mohamad Zbib¹; Megan Reynolds¹; Uttara Sahaym¹; Grant Norton¹; David Bahr¹; Wayne Osborne²; ¹Washington State University; ²REC Silicon*

Polycrystalline silicon grown via fluidized bed reactors, mainly used for solar applications, produces mm sized granular beads and 100 nm size powders. Three commercial polysilicon products from different manufacturers were examined. This paper focuses on the relationship between solute hydrogen and mechanical behavior of FBR silicon. Fourier transform infrared spectroscopy was used to identify hydrogen in as grown and annealed samples, and indentation techniques were used to determine mechanical properties. FTIR was able to distinguish between solute H and H impurities accumulated during sample preparation. Annealing decreased solute hydrogen and led to an increase in toughness by 20% in samples with solute H in the as grown condition. The toughness of all samples ranges between 0.74 and 0.97 MPa-m^{0.5}. However, annealing increases the crystallite size between 20% to 50%, which lowers the toughness. Removing solute hydrogen and increasing crystallite size exhibit competing effects on the toughness of FBR silicon.

Solid-State Interfaces II: Toward an Atomistic-Scale Understanding of Structure, Properties, and Behavior through Theory and Experiment: Interface Interaction with Defects

Sponsored by: The Minerals, Metals and Materials Society, TMS Electronic, Magnetic, and Photonic Materials Division, TMS Structural Materials Division, TMS: Chemistry and Physics of Materials Committee, TMS: Nanomechanical Materials Behavior Committee

Program Organizers: Xiang-Yang Liu, Los Alamos National Lab; Douglas Spearot, University of Arkansas; Guido Schmitz, University of Münster; David Seidman, Northwestern University

Tuesday AM
March 13, 2012

Room: Oceanic 7
Location: Dolphin Resort

Funding support provided by: Los Alamos National Laboratory

Session Chairs: Richard Hoagland, Los Alamos National Lab; Alfredo Caro, Los Alamos National Lab

8:30 AM Invited

On the Feasibility of Designing Interfaces Immune to Helium Damage: *Michael Demkowicz¹; Abishek Kashinath¹; Amit Misra²; Nan Li²; ¹Massachusetts Institute of Technology; ²Los Alamos National Laboratory*

Helium implanted into materials operating in fusion reactor environments leads to bubble formation, accelerates void growth, and degrades mechanical properties. Drawing on atomistic modeling and experiments, I will propose a strategy for mitigating these effects by trapping He at interfaces, addressing in particular the relation of interface structure to He trapping and He clustering. I will show that, under some conditions, the effect of He on interface mechanical properties such as tensile strength and shear resistance is tolerable. Finally, I will discuss the potential for designing interfaces immune to He damage by modifying interface structure. This material is based upon work supported by the Los Alamos LDRD program and the Center for Materials at Irradiation and Mechanical Extremes, an Energy Frontier Research Center funded by the U.S. Department of Energy, Office of Science, Office of Basic Energy Sciences under Award Number 2008LANL1026.

9:00 AM Invited

Effect of Nanoparticle-Matrix Interfaces on Cavity Formation in ODS Ferritic Steels under Dual-Beam Irradiation: *Luke Hsiung¹; ¹Lawrence Livermore National Laboratory*

Structures of oxide nanoparticles/clusters and their role in the formation of radiation-induced cavities in ODS ferritic steel have been studied using high-resolution transmission electron microscopy (HRTEM) techniques. The ODS steel contains partially or fully crystallized oxide nanoparticles larger than ~2 nm and amorphous nanoclusters smaller than ~2 nm. The crystal structure of crystalline nanoparticles is mainly Y4Al2O9 (YAM) with a monoclinic structure. Crystalline nanoparticles larger than 20 nm tend to be incoherent with the matrix, and crystalline nanoparticles smaller than 10 nm tend to be coherent/semi-coherent with the matrix. Unimodal distribution of helium-filled cavities (bubbles) was found to form in (Fe + He) dual-beam irradiated ODS steel as a result of the dispersion of high-density nanoparticles/clusters. HRTEM observations of preferred formation of helium bubbles at the particle-matrix interfaces reveal the crucial role of nanoparticles/clusters in the suppression of bubble-to-void conversion (void swelling) in the irradiated ODS steel.



TMS 2012

141st Annual Meeting & Exhibition

9:30 AM

Interface Microstructure Evolution of Heterogeneous Systems under Vacancy Supersaturation: *Enrique Martinez Saez*¹; Jeffery Hetherly¹; Alfredo Caro¹; Michael Nastasi¹; ¹LANL

A new hybrid Molecular Dynamics-kinetic Monte Carlo (MD-KMC) algorithm has been developed in order to study the microstructure evolution of heterogeneous systems in a vacancy-supersaturated environments. The algorithm takes into account both chemical and stress fields. Migration barriers are calculated using a linear approximation in which final and initial energies are obtained from MD. The approximation makes the algorithm fast enough to be able to handle hundreds of vacancies. Therefore, we are able to observe void formation in twist boundaries in Fe and Cu, characterized by different sets of screw dislocations. We have captured as well the jog formation in an edge dislocation dipole in Fe. Incoherent interfaces have been also studied. The de-mixing process after a displacement cascade event for the case of the Cu-Nb system in the presence of a Kurdjumov-Sachs interface is reported. This material is based upon work supported as part of the Center for Materials at Irradiation and Mechanical Extremes, an Energy Frontier Research Center funded by the U.S. Department of Energy, Office of Science, Office of Basic Energy Sciences, and by the LANL LDRD Office.

9:50 AM

Interface Structures, Defects, and Mechanical Properties at fcc-bcc Interfaces from “Tunable” Potentials: *Xiang-Yang Liu*¹; Richard Hoagland¹; Jian Wang¹; Blas Uberuaga¹; Michael Demkowicz²; Michael Nastasi¹; Amit Misra¹; ¹Los Alamos National Lab; ²Massachusetts Institute of Technology

Nanolayered Cu-Nb composites exhibit high strength and enhanced radiation damage tolerance. To understand the relevance of interface structures to interface properties in general fcc-bcc systems, “tunable” potentials offer a fairly simple way to selectively vary parameters independently. In this work, the parameterization of the EAM interatomic potentials in fcc-bcc system is modified to understand the interface structures, defects, and mechanical properties. We change the dilute heats of mixing between Cu and Nb and investigate the effect on interface structures, defect formation energies, and influence on both the interfacial shear strength and the active shear plane at the interface. To understand the interface behavior in different lattice misfit geometries, the relative lattice constants ratio between Cu and the bcc crystal is varied, to examine effects on interface dislocations and defect formation energetics. Defect-interface interactions are studied with MD and other methods, to predict the radiation damage tolerance of these interface systems.

10:10 AM Break

10:20 AM Invited

Defect-Interface Interactions in Oxide Ceramics: *Blas Uberuaga*¹; ¹Los Alamos National Laboratory

It is well established that interfaces and grain boundaries can act as efficient sinks for radiation-induced defects. Recently, we showed that, in Cu, interstitials are preferentially loaded into grain boundaries during collision cascades and that these interstitials, trapped at the boundary, interacted over relatively long distances and short times to help annihilate vacancies remaining in the bulk of the crystal. Here, we explore these phenomena in oxide ceramics. Using a combination of molecular dynamics, molecular statics, and accelerated molecular dynamics, we examine the ability of boundaries in oxides to absorb interstitials during damage production and the subsequent emission of those interstitials to annihilate vacancies. We find similarities but also important differences to the behavior observed in Cu. In particular, strong electrostatic effects present themselves, leading to complex defect-interface interactions.

10:50 AM

On the Solute/Interface-Interaction in the Framework of a Defactant Concept: *Reiner Kirchheim*¹; ¹University of Göttingen

Willard Gibbs Adsorption Isotherm and Carl Wagner’s definition of excess solute at surfaces and grain boundaries were both extended to include other crystalline defects like dislocations and vacancies. Thus solute segregation to dislocations and vacancies and other crystalline defects gives rise to a reduction of their formation energies, too and are called defactants. Under which conditions zero values could be attained, will be discussed. Special emphasis is paid to the segregation of carbon at iron grain boundaries which is experimentally determined by atom probe tomography and which is used to design nanocrystalline steel by ball milling. It will be shown that the excess carbon corresponds to about one monolayer of cementite and that this excess is independent of the character of the large angle grain boundary. Thus solute/solute-interaction plays an important role in grain boundary segregation although often neglected during modelling.

11:10 AM

Interface Facets Identified with Singularity in Interfacial Structures: *Wenzheng Zhang*¹; Xinfu Gu¹; ¹Tsinghua University

Theoretically, candidates of interface facets can be searched according to local minima of interfacial energy in 5D, but this is a nontrivial task. Simple rules in terms of measurable delta g vectors have proved useful for identifying interface facets. In this work, the association of these rules with singularity in the interfacial energy is elucidated with singularity in the interfacial defect structures. While singularity of ledge defects usually leads to rational facets, singularity of dislocation structure is permitted by special interface geometry, usually described with irrational indexes. Interfacial facets defined by singular interfaces usually serve as the terrace planes of growth ledges, so their structures are essential to understanding overall interface migration. Though the description with defect singularity appears lack of atomic details in a relaxed structure, it offers a practical starting point for time-efficient atomic-scale modeling of singular interfaces in real materials.

11:30 AM

On the Factors Governing the Sink Strength of Semicoherent fcc-bcc Interfaces: *Kedarnath Kolluri*¹; Michael Demkowicz²; ¹Massachusetts Institute of Technology

Using atomistic modeling of fcc-bcc interfaces, we investigate the factors that govern the sink strength of interfaces to radiation-induced point defects. The sink strength depends on point defect absorption, emission, and recombination at interfaces. We find that point defects and point-defect clusters are trapped at interface misfit dislocation intersections and misfit dislocation kinks. Trapped defects migrate from trap to trap along misfit dislocations. In addition, migration of untrapped point defects is confined to regions between misfit dislocations. Furthermore, density of defects accommodated by an interface depends on interface misfit dislocation network’s ability to reconstruct. The prospect of predicting sink strength of semicoherent interfaces is discussed. This material is based upon work supported as part of the Center for Materials at Irradiation and Mechanical Extremes, an Energy Frontier Research Center funded by the U.S. Department of Energy, Office of Science, Office of Basic Energy Sciences under Award Number 2008LANL1026.

11:50 AM

Energetics of Point Defect and Impurity Segregation to Grain Boundaries in Fe: *Mark Tschopp*¹; Kiran Solanki²; Nathan Rhodes³; ¹MSU/CAVS; ²Arizona State University; ³University of Florida

Quantifying how point defects and impurities interact with grain boundaries is important for understanding segregation of solute and impurity atoms in metals. The research objective herein is to understand the energetics of the interaction between point defects/impurities and grain boundaries in BCC Fe and quantify the associated uncertainties.

Molecular statics simulations were used to sample a wide array of grain boundary sites and structures. The present results provide detailed information about the interaction energies of vacancies, self-interstitial atoms, and impurities with grain boundaries in iron. Certain grain boundaries have properties different from the remainder of boundaries. Moreover, the formation energies were also found to depend on the local atomic structure and the distance from the center of the boundary. Such studies provide insight into the process of grain boundary segregation and the structure of grain boundaries, which can lead to re-engineering grain boundaries for materials by design applications.

Symposium in Memory of Patrick Veysseyre: Understanding the Mechanisms Controlling Plastic Flow: Screw Dislocations-lattice Friction

Sponsored by: The Minerals, Metals and Materials Society, TMS Electronic, Magnetic, and Photonic Materials Division, TMS Structural Materials Division

Program Organizers: Georges Saada, LEM CNRS ONERA; Dennis Dimiduk, Air Force Research Laboratory; Hael Mughrabi, University Erlangen-Nuernberg; Haruyuki Inui, Kyoto University

Tuesday AM
March 13, 2012

Room: Europe 6
Location: Dolphin Resort

Funding support provided by: National Science Foundation

Session Chairs: H. Inui, Kyoto University; M. Mills, Ohio State University

8:30 AM Invited

The Role of the Initial Dislocation Density in Controlling Size-Affected Flow Response: *Jaafar El-Awady*¹; Michael Uchic²; Dennis Dimiduk²; Satish Rao³; Christopher Woodward²; ¹Johns Hopkins University; ²Air Force Research Laboratory; ³UES Inc.

We report experimental and 3-dimensional discrete dislocation dynamics (DDD) measurements to characterize the effect of starting dislocation density on size-affected flow response. Microcrystals were FIB-milled into a 23% pre-strained bulk Ni single-crystal. The strength-scaling exponent was -0.18, which is considerably lower than that measured for microcrystals with moderate initial dislocation densities. DDD simulations also show a reduction in power-law exponent with increasing initial dislocation density. However, while previous experimental studies suggested that Taylor hardening law fails at micron and submicron length scale, DDD simulations show that the strength-dislocation density response in fact follows a power-law relationship with an exponent equal to -0.2. Also, Taylor hardening is recovered above a size-dependent critical dislocation density. We finally discuss the role of this critical dislocation density in controlling the size-affected flow response, and rationalize the results based on the the stochastics of an existing dislocation network in microcrystals.

9:05 AM Invited

Atomistic Simulations of Intersection Cross-Slip Nucleation in Face-Centered Cubic Materials: *Satish Rao*¹; Dennis Dimiduk²; Michael Uchic²; Triplicane Parthasarathy¹; Jaafar El-Awady³; Christopher Woodward²; ¹UES Inc.; ²Air Force Research Laboratory; ³Johns Hopkins University

Embedded atom potentials and molecular-statics simulations of screw character dislocation intersections with forest dislocations, in FCC Ni and Cu and L12 Ni3Al, illustrate a mechanism for cross-slip nucleation. 3-dimensional dislocation dynamics simulations accounting for Shockley partials qualitatively reproduce the atomistic results for the same dislocation intersections. Investigations using the Nudged Elastic

Band Method and an approximate Escaig-stress technique showed the activation barrier for a screw dislocation to transfer from the glide-plane or the cross-slip-plane to a partially cross-slipped state. The intersections form Glide, Lomer-Cottrell or Hirth locks, having cross-slip activation energies that are a factor of 3- 20 lower than those for the Friedel-Escaig mechanism. The activation barrier for cross-slip is linearly proportional to $(d/b)\ln(v_3*d/b)0.5$, where 'd' is the spacing of the Shockley partial dislocations and 'b' is the screw dislocation Burger's vector. These results suggest a preference for cross-slip at selected screw dislocation intersections in FCC materials.

9:25 AM Invited

Kinetics of Screw Dislocations in Fe and Fe Alloys at Low Temperatures: *Daniel Caillard*¹; ¹CNRS

Pure iron exhibits a discontinuity in the temperature dependence of stress and activation volume, which indicates a possible change of mechanism at around 200-250K. This discontinuity has never been satisfactorily explained, in spite of recent atomistic calculations. In addition, its vanishing upon alloying may help to understand the corresponding softening and hardening effects. To interpret such behaviour, in situ experiments have been carried out first in pure Fe, between 110K and 300K. The videos show two kinds of motion, below and above 200K, which have been related to this change of mechanism. The two behaviours have been compared with results of atomistic calculations and mechanical tests, and modelled. Similar experiments in Fe containing various concentrations of C, P, Si and Cr also show various kinds of screw dislocation motion, which allow us to account for the complex softening/hardening effects of solute atoms.

9:55 AM Invited

A New Type of Dislocation Source in BCC Molybdenum: *Qing-Jie Li*¹; Xiang-Dong Ding¹; Zhi-Wei Shan¹; Ju Li²; Jun Sun¹; Evan Ma³; ¹Center for Advancing Materials Performance from the Nanoscale (CAMP-Nano) & Hysitron Applied Research Center in China (HARCC), State Key Laboratory for Mechanical Behavior of Materials, Xi'an Jiaotong University; ²Department of Nuclear Science and Engineering and Department of Materials Science and Engineering, MIT; ³Department of Materials Science and Engineering, Johns Hopkins University

Due to the lattice symmetry of BCC metals, screw dislocation plays a critical role in their plastic deformation. Usually, the low mobility and self-multiplication of screw dislocations lead to a different mechanical behavior from FCC metals. In the present work, by means of molecular dynamics simulations, we show a new self-multiplication mechanism of screw dislocation in BCC Molybdenum, i.e., double-kinks mechanism. During the motion at a certain stress level, we found screw dislocation can form a dislocation dipole with the thickness of three atomic layers, which can be opened into a dislocation loop at a critical stress. The formation of dislocation dipole is related to the collision and interaction of different kinks which originated from the broken symmetry. This new mechanism may broaden our understanding of the mechanical behavior of BCC metals in both macro- and meso- size scale. Key words: BCC Molybdenum, screw dislocation, self-multiplication

10:15 AM Break

10:30 AM Invited

Elevated Temperature Deformation Mechanisms in Ta2C: *Nicholas De Leon*¹; Billie Wang¹; ¹The University of Alabama

Tantalum carbides, an ultra-high temperature ceramic, exhibit an interesting duality of mechanical responses with temperature; classical ceramic brittle behavior at low temperatures but significant plasticity at elevated temperatures. While the plastic deformation mechanisms of the rock-salt structured TaC phase have been thoroughly defined, the hexagonal like $\sqrt{149}$ -Ta₂C phase, with its CdI antitype structure, has not been extensively investigated and is the scope of this work. Ta₂C specimens were mechanically tested at 1600°C and characterized using



TMS 2012

141st Annual Meeting & Exhibition

dynamical diffraction transmission electron microscopy (TEM) and high resolution transmission electron microscopy (HRTEM) techniques. Density functional theory was also used to compute the stacking fault energies on the basal, prism and pyramidal planes. The two major deformation mechanisms experimentally identified were dislocation slip and stacking faults. Both basal and secondary $a/3\langle 11-23 \rangle\{10-11\}$ non-basal slip were predicted and observed. The basal plane faulting was shown to preferentially occur between the Ta-Ta metallic bonds.

11:00 AM Invited

Screw Dislocations in Zirconium: an ab Initio Study: *Emmanuel Clouet*¹; ¹SRMP, CEA Saclay

Plasticity in zirconium is thought to be controlled by screw dislocations gliding in the prismatic planes of the hexagonal close-packed structure. This prismatic and not basal glide is observed for a given set of transition metals like zirconium and is known to be related to the number of valence electrons in the d band. We used ab initio calculations based on the density functional theory to study the core structure of screw dislocations in zirconium. Dislocations are found to dissociate in two partial dislocations, each with a pure screw character. The dissociation distance observed in the simulations agrees well with the one predicted by elasticity theory using the calculated stacking fault energy. The Peierls barrier have also been calculated for a screw dislocation gliding in a prismatic plane. A low value, $\sim 0.3 \pm 0.1$ meV/Å, has been obtained. The Peierls stress deduced from this barrier is compatible with experimental data.

11:20 AM Invited

Experimental Study and Finite Element Computation of the Single Crystal Behavior of Zirconium: Cyril Lebon¹; *Fabien Onimus*¹; Eva Héripé²; Laurent Dupuy¹; Ludovic Vincent¹; Xavier Feaugas³; ¹CEA; ²Ecole Polytechnique; ³University of La Rochelle

The mechanical behaviour of zirconium alloys, used as cladding of nuclear fuel for water reactor, is well known. However there is yet no single crystal constitutive law for zirconium. In order to determine the single crystal behaviour, a zirconium alloy (containing 100 ppm oxygen) with millimetre grains is used. Tensile specimens are machined to obtain only one grain, well orientated for prismatic slip, in the gauge length. The specimens are covered by a speckled paint. During the tests, the in plane deformation is monitored. Thanks to digital image correlation, the strain field tensor is deduced and resolved along the slip systems giving the shear strain on prismatic planes. The single crystal behaviour for prismatic slip is deduced. Strain rates jumps and relaxation tests are also conducted with the same method to measure the activation volume. Finite elements computations of the full specimens are then performed using the fitted constitutive law.

11:40 AM Invited

Atomistic Simulations of Kinks on $1/2\langle 110 \rangle$ Screw Dislocation in Magnesium Oxide: *Philippe Carrez*¹; Patrick Cordier¹; ¹Lab. UMET CNRS-UMR8207

In lattice friction materials, dislocation move by formation and migration of kink pairs. Plastic deformation of MgO involves a single $1/2\langle 110 \rangle$ Burgers vector associated with two potential slip plane families $\{110\}$ and $\{100\}$. Whereas $1/2\langle 110 \rangle\{110\}$ is characterized by a relatively low lattice friction, $1/2\langle 110 \rangle\{100\}$ shows higher lattice friction and a strong sensitivity of shear stresses to temperature. Here we propose theoretical calculations of structure, geometry and formation energy of kinks on $1/2\langle 110 \rangle$ screw dislocation in MgO for both slip systems. In this study, we used pairwise potentials of Buckingham form which satisfactorily reproduce screw dislocation core structure. Then, isolated kinks are introduced into large simulation cell. Using periodic boundary conditions and fixed surfaces, kink formation energies are extracted from simulations. Preliminary results performed for $1/2\langle 110 \rangle\{110\}$ are consistent with the experimental kink energy of 1.2 eV.

Titanium: Advances in Processing, Characterization and Properties: Microstructure Evolution and Characterization I

Sponsored by: The Minerals, Metals and Materials Society, TMS Structural Materials Division, TMS: Titanium Committee
Program Organizers: Adam Pilchak, US Air Force Research Laboratory; Christopher Szczepanski, US Air Force Research Laboratory; Vasisht Venkatesh, Pratt & Whitney

Tuesday AM
March 13, 2012

Room: Oceanic 3
Location: Dolphin Resort

Session Chairs: Lee Semiatin, US Air Force Research Laboratory; Peter Collins, University of North Texas; Adam Pilchak, US Air Force Research Laboratory

8:30 AM Invited

Formation of Transformation Texture in Supertransus Heat Treated Ti-6Al-4V Sheet: Gordon Sargent¹; Adam Pilchak¹; Kacey Kinsel¹; *Lee Semiatin*¹; ¹US Air Force Research Laboratory

Texture formation in alpha/beta titanium alloys can result from deformation and/or phase transformation. A number of investigations and analyses of deformation-texture formation in such materials have been performed. However, much less effort has been expended to understand or model transformation-texture evolution associated with the non-random selection of alpha variants during the decomposition of the metastable high-temperature beta phase. In this presentation, past research related to variant selection in alloys such as Ti-6Al-4V will be summarized. Subsequently, recent work to establish the effect of process variables on variant selection during the cooling of Ti-6Al-4V sheet following beta annealing will be described. These process variables comprise soak time at peak temperature/beta grain size, cooling rate, stress state during cooling (i.e., unconstrained vs constrained conditions), prestrain prior to cooling, and imposed strain during cooling.

9:00 AM Invited

Variant Selection during Alpha Precipitation in Ti-6Al-4V under the Influence of Local Stress – A Simulation Study: *Rongpei Shi*¹; *Yunzhi Wang*¹; ¹Ohio State University

Variant selection of alpha (HCP) phase during its precipitation from beta (BCC) matrix plays a key role in determining the microstructural state and mechanical properties of alpha+beta titanium alloys. In this work, precipitation of semi-coherent alpha plates from beta matrix in Ti-6Al-4V (wt.%) under the influence of local stress is investigated by using a three-dimensional phase field model. The model is fully quantitative, not only being linked directly to available thermodynamic and mobility databases, but also incorporating the crystallography of BCC to HCP transformation, elastic anisotropy, and defect structure at the alpha/beta interfaces. The volume fraction and spatial distribution of different alpha variants are found to correlate strongly with the stress distribution within a polycrystalline sample. If the grains are highly textured, specific variants may percolate through the entire sample, leading to microtexture.

9:30 AM

Role of Grain-Boundary Characteristics on the Evolution of Allotriomorphic Alpha in Titanium Alloys: *Vikas Dixit*¹; G.B. Viswanathan²; W.A.T. Clark¹; Hamish L. Fraser¹; ¹The Ohio State University; ²Air Force Research Laboratory

Grain-boundary alpha (GBA) has an important role in microstructural evolution and mechanical properties, such as, fatigue and fracture toughness, in alpha/beta titanium alloys. Various grain-boundary parameters, such as, misorientation angle, the orientation of grain-boundary plane and also Burgers orientation relationship (OR) may control the evolution of this phase. In the present work, two methods to determine the orientation of an interfacial plane with respect to one

of adjacent crystals have been developed using FIB, EBSD and TEM and their accuracy has been validated. Subsequently these methods have been utilized to determine the inclination of grain boundary plane relative to neighboring grains in Ti-550 alloy-system. Results indicate a correlation amongst the growth of GBA and various parameters including the misorientation angle, Burgers OR with neighboring prior-beta grains and most notably the inclination of the GB plane. The contribution of these factors on variant selection occurring at grain-boundaries will also be presented.

9:50 AM

Phase Separation and Its Subsequent Influence on Alpha Nucleation in Titanium Alloys: *Soumya Nag*¹; Arun Devaraj¹; Yufeng Zheng²; Robert Williams²; Jaimie Tiley³; Hamish Fraser²; Rajarshi Banerjee¹; ¹University of North Texas; ²The Ohio State University; ³Air Force Research Laboratory

In titanium alloys precipitation of a phase within the β matrix can occur at various heterogeneous nucleation sites that are closely associated with competing instabilities inherent within the β phase. In this study advanced characterization techniques such as synchrotron-based in situ x-ray diffraction, aberration-corrected high-resolution (S)TEM, and atom probe tomography have been coupled to investigate such instabilities and its influence on the early stages of a precipitation in a ternary Ti-5Al-20Mo alloy. During isothermal annealing, the nature of phase separation (compositional partitioning), presumably resulting from a miscibility gap, within the β phase of this ternary alloy, has been investigated in detail. Subsequently, the solute-depleted regions within the matrix nucleate the stable a phase, leading to a homogeneous distribution of highly refined precipitates. These and related results will be presented.

10:10 AM

Morphological, Structural and Compositional Evolution during the Decomposition of Martensite in Ti-2wt%Mo: *Yufeng Zheng*¹; Robert Williams¹; Rongpei Shi¹; Yunzhi Wang¹; Hamish Fraser¹; ¹The Ohio State University

The Binary Ti-Mo system is a good example to study various phase transformations of beta isomorphous (monotectoid) alloys. In this work, Ti-2wt% Mo is used to study decomposition of martensite during tempering. Precipitates were found homogeneously distributed within the parent martensitic plates and to have various morphologies and compositions depending on tempering time and temperature. The effect of tempering on the structure, composition, and morphology of this precipitates was investigated systematically through SEM, TEM and STEM characterization techniques, in conjunction with EDS and EELS for chemical analysis. Phase field simulations were also carried out to study the factors that could influence the morphology of the precipitates.

10:30 AM Break

10:50 AM Invited

Recent Studies on the Evolution of Microstructure in Ti-Based Alloys: *Peter Collins*¹; Peyman Samimi¹; Iman Ghamarian¹; Brian Welk²; Dan Huber²; Rajarshi Banerjee¹; Hamish Fraser²; ¹University of North Texas; ²The Ohio State University

It is well known that the microstructural features of alpha+beta and beta Ti-based alloys have a strong effect on the mechanical properties. As models relating structure to properties continue to mature, it is becoming increasingly important to understand the effect of composition and processing on the evolution of microstructure in Ti-based alloys. Therefore, this paper presents recent advances in assessing the earliest and intermediate stages of microstructural evolution – specifically the effect of composition and processing on these stages. A series of state of the art two-dimensional and three-dimensional characterization techniques have been employed in this study of the evolution of microstructure. Of specific interest are the evolution of grain boundary alpha, equiaxed alpha particles, eutectoid phases, and intragranular alpha precipitates.

11:20 AM

Microstructures in Solid-State Welds of Martensitic and Non-Martensitic Transforming Titanium Alloys: *Thomas Broderick*¹; Adam Pilchak²; Jonathan Orsborn³; Taylor Pratt¹; Andrew Woodfield¹; Hamish Fraser³; ¹General Electric Aviation; ²AFRL Materials and Manufacturing Directorate; ³The Ohio State University

Subscale components made of similar and dissimilar titanium alloys were fabricated using solid-state welding techniques. Process conditions exposed these alloys to very high transients and gradients in temperature and mechanical deformation. The associated graded microstructures ranged from highly metastable, mechanically deformed microstructures at the joined interface, to partially dissolved and lightly worked microstructures from lesser exposures slightly displaced from the joined interface, to unaffected, original microstructures of the parent metals at a distance further from the joined interface. Subsequent residual stress relief and aging heat treatments resulted in subscale components containing quenched and aged, solution and aged and over aged microstructures in one joined structure. These microstructures were examined using optical, SEM/EBSD and TEM imaging techniques. An interpretation of how as-welded and heat treated microstructures formed was developed according to the potential of transients to cause local changes in phase composition, phase stability and activation of transient martensitic transformation paths.

11:40 AM

Microstructure and Mechanical Properties of a Copper Containing Three Phase Titanium Alloy: *Srikant Gollapudi*¹; Tapash Nandy¹; Rajdeep Sarkar¹; Ashok Gogia¹; Sankarasubramanian R¹; Chinta Babu U¹; ¹DMRL

In this study we attempt to improve the strength of titanium alloys by utilizing the precipitation hardening technique, a route that is relatively unexplored in titanium alloy development. It was found that copper satisfies the conditions necessary for precipitation hardening in titanium alloys and hence the following alloy, Ti-6Al-1.5V-2.5Cu (TAVC), was chosen for our studies. It was decided to ascertain the performance of this alloy in comparison to a standard titanium alloy, Ti-6Al-4V (TAV). The higher, albeit limited strengthening, of TAVC vis-a-vis TAV was attributed to the formation of metastable precipitates of Ti-Cu which were revealed by TEM studies. The Mott-Nabarro model was able to rationalize the strengthening provided by the precipitates.

12:00 PM

Recrystallization Behavior in Ti-13Cr-1Fe-3Al Alloy after Severe Plastic Deformation: *Masato Ueda*¹; Hikaru Matsuhira¹; Yuji Takasaki¹; Masahiko Ikeda¹; Yoshikazu Todaka²; ¹Kansai University; ²Toyohashi University of Technology

Ti-13Cr-1Fe-3Al alloy was developed as an affordable priced titanium-based material for general use. Up to now, we've investigated mechanical properties, microstructures and heat treatment behaviors in the alloy. The grain size was refined to around 20 μm by thermo-mechanical treatments, dispersions of titanium boride or yttrium oxide, and so on. This means the grain size reaches the limit of conventional techniques in this alloy. Severe plastic deformation (SPD) has received considerable attention as a useful procedure for significant refinement of microstructures in metallic materials. In this study, recrystallization behavior was investigated in the Ti-13Cr-1Fe-3Al alloy after high-pressure torsion (HPT), which is an SPD procedure. Vickers hardness rapidly increased with the number of turns (N) and saturated around 440 after N= 5. The HPT-processed specimen for N=10 was fully recrystallized at 1023 K for 0.3 ks. Equiaxed crystals could be observed and the size reached 6 μm .



TMS 2012

141st Annual Meeting & Exhibition

T.T. Chen Honorary Symposium on Hydrometallurgy, Electrometallurgy and Materials Characterization: Base Metal Processing

Sponsored by: The Minerals, Metals and Materials Society, TMS Extraction and Processing Division, TMS: Hydrometallurgy and Electrometallurgy Committee, TMS: Materials Characterization Committee

Program Organizers: Shijie Wang, Rio Tinto Kennecott Utah Copper; J. E. Dutrizac, CANMET; Michael Free, University of Utah; J. Y. Hwang, Michigan Technological University; Daniel Kim, Rio Tinto Kennecott Utah Copper

Tuesday AM
March 13, 2012

Room: Oceanic 5
Location: Dolphin Resort

Funding support provided by: Rio Tinto Kennecott Utah Copper, ASARCO, and Freeport McMoRan

Session Chair: Daniel Kim, Rio Tinto Kennecott Utah Copper

8:30 AM

The Development of China's Copper Primary Smelting Technology: Kaixi Jiang¹; Lan Li¹; Yaping Feng¹; Haibei Wang¹; Bang Wei¹; Xiaoping Zou²; ¹Beijing General Research Institute of Mining and Metallurgy; ²Beijing General Research Institute of Mining & Metallurgy

China is currently the world's largest copper producer. In the last five years, 950kt/y smelting capacity was commissioned. Currently, about 1200kt/y smelting capacity is under construction and about 2000kt/y smelting capacity is under feasibility study. Ausmelt/ISA smelting and flash smelting technologies were commonly adopted in China. After the double-flash-smelter was first adopted in 2004, three new double-flash-smelters are scheduled. Recently, two new smelting technologies were developed in China. One is an improved bath side-blown smelting process, and another is SKS bottom-blown process. Both technologies have been in practice for over 3 years and have achieved good technical performance. Approximately 500kt/y new smelting capacity in China and India will adopt these technologies. Both technologies have advantages of low investment cost, low energy consumption and high flexibility for complex raw materials. This paper reviews "green" copper smelting projects in China and introduces the practices of the two new Chinese smelting technologies.

8:50 AM

New Process for Treating SCF Flue Dust at Atlantic Copper: Guillermo Rios¹; Joan Viñals²; Alba Sunyer²; Cristina Arbizu¹; ¹Atlantic Copper; ²University of Barcelona

Atlantic Copper is one of the largest copper producers in Europe. Its production facilities are located in Huelva (Spain) and treat over 1 million tpy concentrates to produce up to 260 ktpy cathodes and 900 ktpy of sulphuric acid. During the copper concentrate smelting the slag coming from the Flash Furnace and the PS converters is treated in an electrical slag cleaning furnace. As a result of the treatment of the off gases from this furnace, approximately 2,000 tpy of a Zn rich filter cake are produced and sent to authorized waste managers. This paper describes the characterization of this material and the preliminary results of a new process to recover zinc as a pure zinc hydroxycarbonate while lead is collected as an indium rich anglesite phase. The behavior of impurities (Cd, As, Tl, Sn, Sb, Bi, Cu, Se, Te) in the leaching, solution purification and precipitation steps are reported

9:10 AM

Direct Leaching Alternatives for Zinc Concentrates: Kurt Svens¹; ¹K. R. Svens Consulting Incorporation

As the zinc consumption is gradually increasing all the time in the world, many zinc plants are looking for possible expansions. As the sulphuric acid market as well as the fertilizer market in many areas is saturated, the costs

for the roasting-acid plant section of the zinc plant will create problems when making the feasibility calculations for the possible expansions. For solving the customers' situation two proven zinc concentrate direct technologies are available. A third one, which is possible, is not having any industrially proven application in the zinc area.

9:30 AM

The Effect of Polytetrafluoroethylene on Pressure Oxidation of Chalcopyrite: Jin Nuo¹; Eduard Guerra¹; ¹Laurentian University

The use of polytetrafluoroethylene, PTFE, as a solid sorbent for elemental sulfur during pressure oxidation of chalcopyrite was investigated. The effect of agitation, PTFE particle size and lignin sulfonate addition were evaluated using leaching conditions that were otherwise similar to those employed in the CESL process. The effects of these factors, and their interactions, on chalcopyrite oxidation are explained in terms of interfacial forces and solid-solid interactions. Using relatively fine PTFE powder with vigorous agitation resulted in ca. 100% copper extraction in less than 90 minutes without the need for grinding of the flotation concentrate.

9:50 AM

The Effect of Complexing Agents and the Anode Material on the Kinetics of Electro-Assisted Reduction of Chalcopyrite: Eliezer Martinez-Jimenez¹; Gretchen Lapidus-Lavine¹; ¹Universidad Autonoma Metropolitana-Iztapalapa

Electro-assisted reduction has shown to be an effective pretreatment to render chalcopyrite less refractory towards oxidative leaching. In this process, chalcopyrite is selectively converted to chalcocite or copper metal in an electrolytic cell at ambient conditions, while ferrous ion is leached into solution. However, the reaction velocity is hampered by the formation of a ferrous sulfide passivating layer on the solid surface, especially at elevated solid to liquid ratios. In the present work, several strategies for overcoming this problem were evaluated. On one hand, specific ligands for the ferrous ion were added in order to increase its solubility and, on the other, an anode material, which promotes the oxidation of the sulfide ion, was chosen. Leaching tests showed citric acid to be an effective ligand for both ferrous and ferric ions and, in combination with a lead-silver anode, significantly increased the kinetics of chalcopyrite reduction.

10:10 AM Break

10:30 AM

Nickel Smelter Slag Microstructure and Its Effect on Slag Leachability: Ilya Perederiy¹; Vladimirov Papangelakis¹; Indje Mihaylov²; ¹University of Toronto; ²Vale Base Metals Technology Development

Nickel slags differ in chemical composition and microstructure. Slow cooling promotes crystallization and growth of crystalline fayalite and magnetite, and vitreous silica. Slag granulation yields either an amorphous solid or highly intergrown crystalline silicate and oxide phases. Smelter slags contain Ni, Co and Cu as dissolved oxides and matte inclusions. Extraction of the entrapped metals by High Pressure Oxidative Acid Leaching (250°C, 70 g/L initial H₂SO₄, up to 90 psi O₂, 45 min) dissolves the metal bearing minerals. The impact of slag microstructure on the accessibility of these minerals to leaching is discussed.

10:50 AM

Characterization of Aluminum Cathode Sheets Used for Zinc Electrowinning: Neil Gao¹; Daniel Liu¹; Maura Malone¹; ¹Teck Metals Ltd.

Corrosion is the primary failure mode for aluminum (Al) cathode sheets used in Teck's Trail Operations zinc electrolytic plant. It was observed that the corrosion performance of Al cathodes from different suppliers varied considerably. This suggests that the material properties of Al cathodes have a strong influence on corrosion resistance. In the current study, various types of Al alloys, including 1050, 1060, 1070, H1S and 1090, were characterized through chemical analysis, corrosion testing, mechanical testing and metallography. The results were discussed with a focus on the effects of impurity elements and second phase particles on corrosion resistance. The findings were used to improve the Al cathode

sheet specification and to develop a standardized screening procedure which details qualification steps for comprehensive evaluation prior to a plant trial.

11:10 AM

Mechanical Pretreatment of Lead Based Alloy Anode for Zinc Electrowinning: Taro Aichi¹; Rie Sato¹; Makoto Muramatsu²; Hideyuki Takahashi²; Kazuyuki Tohji²; ¹Dowa Metals and Mining Co., Ltd.; ²Tohoku University

There have been many ways to condition the lead based alloy anode for zinc electrowinning, namely electrochemical method, chemical treatment and physical treatment. Some of the advantages of physical treatment are its productivity and the variety. In this report, some physical treatments including blasting with silica, alumina, steel grid, and zinc cut-wire were tested. Laboratory tests confirmed there were differences in the formation of anode scale during electrowinning and the suppression of lead dissolution from those anodes.

11:30 AM

Duplex Stainless Steel Corrosion in a Zinc Plant Purification Filter Application: Timothy Moore¹; Michael Heximer¹; Dominic Verhelst¹; ¹Teck Metals Ltd

Teck's Trail Operations recently installed new pressure filters in the cold stage purification step in the zinc leaching plant. Alloy 2205 duplex stainless steel was chosen as the material of construction as it was in use in the hot stage purification stage. Within a year of commissioning, an unacceptably high rate (greater than 1 mm/y) of corrosion was observed on the weld heat affected zone (HAZ). Laboratory and field tests were conducted to establish the conditions under which the corrosion was occurring. The tests isolated the aggressive conditions to a unique combination of materials present during the filter regeneration stage. Further, the change of the duplex grain structure of the alloy during welding resulted in the HAZ being more susceptible to the corrosive environment. A new material of construction was recommended as a result of the investigation.

Ultrafine Grained Materials VII: Mechanical Response

Sponsored by: The Minerals, Metals and Materials Society, TMS Structural Materials Division, TMS/ASM: Mechanical Behavior of Materials Committee, TMS: Nanomechanical Materials Behavior Committee, TMS: Shaping and Forming Committee
Program Organizers: Suveen Mathaudhu, U.S. Army Research Office; Xiaoxu Huang, Risø National Laboratory for Sustainable Energy, Technical University of Denmark; Hyoung Seop Kim, POSTECH; Terence Langdon, University of Southern California; Terry Lowe, Manhattan Scientifics, Inc.; Ruslan Valiev, Ufa State Aviation Technical University; Xiaolei Wu, Institute of Mechanics, Chinese Academy of Sciences; Michael Zehetbauer, University of Vienna

Tuesday AM
March 13, 2012

Room: Swan 4
Location: Swan Resort

Session Chairs: Justin Scott, Institute for Defense Analysis; Joel House, Air Force Research Laboratory; Xiaoxu Huang, Risø National Laboratory for Sustainable Energy, Technical University of Denmark; Pei-Ling Sun, Feng Chia University

8:30 AM Invited

Some Common Features of Ultrafine Grained and Nanocrystalline Bcc Metals Produced by Severe Plastic Deformation: Qiuming Wei¹; Laszlo Kecskes²; Suveen Mathaudhu³; Brian Schuster²; ¹University of North Carolina at Charlotte; ²US ARL; ³US ARO

In this work, we attempt to provide an updated overview on some common features of ultrafine grained (UFG, grain size ranging from 200 nm to 1000 nm) and nanostructured (NS, grain size smaller than 200 nm) metals

with body centered cubic (bcc) structures produced via severe plastic deformation (SPD) such as equal channel angular extrusion (ECAE), ECAE followed by cold rolling, or high pressure torsion. Microstructures were analyzed by TEM of EBSD. Tungsten, tantalum, niobium and iron were studied. Mechanical properties were evaluated both at quasi-static and dynamic loading. Some common features were identified for these UFG/NS bcc metals. For example, all show elastic-nearly perfectly plastic stress strain behavior and much elevated flow stress. It was found that in the UFG regime, they also exhibit reduced strain rate sensitivity, opposing the behavior of fcc metals. Such has rendered most of these metal to show plastic instability under dynamic loading.

8:50 AM

Dynamic Loading of Ultrafine-Grained Aluminum: Matthias Hockauf¹; Lothar Meyer²; Martin Wagner¹; ¹Chemnitz University of Technology; ²Nordmetall Research and Consulting GmbH

The work-hardening behavior of aluminum 99.7 (soft annealed) and of the aluminum alloy AlMgSi (peak-aged) was investigated. Equal-channel angular pressing (ECAP) was used to introduce an ultrafine-grained microstructure that was carefully analyzed by electron microscopy. Compression tests were performed at strain rates between 10^{-4} and 10^3 s⁻¹. Our results show that the ECAP strain path and the resulting dislocation structures affect both the post-ECAP yielding and the hardening response. Furthermore, the precipitates of the alloy have significant influence on strain rate sensitivity. Quasi-static (10^{-4} s⁻¹) and dynamic (10^2 s⁻¹) tensile tests agree well with the compression experiments. The on-set of necking occurs at the end of hardening in stage III. Compared to its influence on flow stress, the influence of strain rate on ductility is rather small. However, uniform elongation and elongation to failure are slightly increased for the ultrafine-grained materials during dynamic tensile loading.

9:05 AM

Quasi-Static and Dynamic Compressive Mechanical Behavior of Friction Stir Processed Ultrafine Grained Al-Mg-Sc Alloy: Nilesh Kumar¹; R. Mishra¹; R. Howell²; K. Cho²; ¹Missouri University of Science & Technology; ²Weapons and Materials Research Directorate

Al-Mg-Sc alloy was subjected to friction stir processing (FSP) to obtain ultrafine grained (UFG) microstructure. Quasi-static and dynamic compression tests were carried out on UFG alloy at strain rates between 10^{-4} to 10^4 s⁻¹. Dynamic compression tests were carried out using split-Hopkinson pressure bar. Strain rate dependence of the flow stress was studied. The evolution of the deformed microstructure has been investigated using electron backscatter diffraction and transmission electron microscope. In general, very limited study exists on high strain rate deformation behavior of UFG face centered cubic materials and in particular, no work exists on the deformation behavior of FSP UFG alloys. This work is an attempt to bridge the gap in the literature.

9:20 AM

Anisotropic Mechanical Properties of Commercially Pure Aluminum Processed by Equal Channel Angular Extrusion: Pei-Ling Sun¹; Sheng-Jie Huang¹; Chung-Yi Yu²; Po-We Kao³; ¹Feng Chia University; ²China Steel Corporation; ³National Sun Yat-Sen University

Commercially pure aluminum AA1050 was subjected to equal channel angular extrusion (ECAE) to a total strain of ~8 at room temperature. Post-ECAE annealing was then conducted on the samples. Compression tests were performed on the ECAEed and annealed samples along different loading directions at room temperature. Both the as-ECAEed and annealed samples show anisotropic mechanical properties, in which the highest compressive stress appears to be along the transverse direction of ECAE. This is attributed to the strain path change effect. Shear bands were observed on the annealed sample surface after compression tests. The presence of shear bands on the annealed sample surface may be attributed to the lower dislocation density after annealing treatment. When the annealed samples were compressively tested, inhomogeneous deformation occurred by the form of shear band deformation.



TMS 2012

141st Annual Meeting & Exhibition

9:35 AM Invited

Tensile Properties and Fracture Mechanisms of Ultrafine Cu Alloys Subjected to Severe Plastic Deformation: *Zhefeng Zhang*¹; P. Zhang¹; X. H. An¹; Y. Z. Tian¹; S. D. Wu¹; T. G. Langdon²; ¹Institute of Metal Research; ²University of Southern California

The mechanical properties and fracture mechanisms of Cu, Cu-Al, Cu-Zn and Cu-Ag alloys subjected to either equal-channel angular pressing (ECAP) or high-pressure torsion (HPT) were investigated. It is found that both the tensile strength and uniform elongation of Cu-Al and Cu-Zn alloys subjected to ECAP increase simultaneously with increasing alloy contents (Al or Zn); whereas there is a peak uniform elongation when the two Cu alloys are processed by HPT. The tensile fracture behaviors of Cu and Cu-Zn alloys changed from necking + shearing then to shear fracture with increasing the number of ECAP passes. Then the macroscopic and microscopic tensile shear fracture mechanisms are analyzed by considering the competitive relationship between the slipping strength and the critical shear strength. As well as the size and density of dimples on the fracture surfaces. Finally the strengthening and toughening mechanisms of ultrafine materials are discussed.

9:55 AM

Microstructure and Tensile Strength of Grade 2 Ti Processed by Equal-Channel Angular Pressing and Cold Rolling: *Vitor Sordi*¹; Megumi Kawasaki²; Maurizio Ferrante¹; Terence Langdon²; ¹Federal University of Sao Carlos; ²University of Southern California

The potential for strengthening of commercially pure titanium using severe plastic deformation constitutes an alternative to the use of complex Ti alloys for many medical or industrial applications. In this work, rods of grade 2 Ti were processed up to six passes by Equal-Channel Angular Pressing (ECAP) at 573K, followed by cold rolling at room (CRRT) or subzero (CRLT) temperatures. After 4 passes of ECAP the grain size was refined down to sub-micron scale, and subsequent CR led to further refinement of structure. Characterization included Vickers microhardness measurements and tensile tests performed at room temperature and in the temperature range 573-773 K. Results show that the tensile strength in this temperature range can be significantly improved using these processing techniques. At room temperature, the ultimate tensile strength of pure Ti after ECAP+CRLT is similar to that of many Ti alloys, while maintaining adequate levels of elongation to failure.

10:10 AM

Strain Rate Sensitivity of Ultrafine Grained and Nanocrystalline Metals via Instrumented Nanoindentation: *Ivan Romero*¹; L. J. Kecskes²; Suveen Mathaudhu³; Qiuming Wei¹; ¹University of North Carolina at Charlotte; ²U.S. Army Research Laboratory; ³Army Research Office

Plastic deformation mechanisms are the object of many studies, especially the thermodynamics and kinetics of the plastic deformation of metals and their changes along grain size. Strain rate sensitivity (SRS) is an indicator that gives information on the plastic deformation that can be obtained by means of the jump test in conventional mechanical testing or by nanoindentation as here presented. Different works have been presented in order to characterize the effects of strain rate in metals since the 1960s; during the last decade works on the ultrafine (UFG) and nanocrystalline (NC) regime has been done with the aim of identifying the trend of metals according to their crystal structure, i.e., FCC, BCC and HCP metals, and the influence of the production methods such as severe plastic deformation or powder metallurgy. In this study, nanostructured bulk metals are probed in order to extract information about their SRS via instrumented nanoindentation.

10:25 AM Break

10:40 AM Invited

Ductility and Strategies for Improving Ductility of Bulk Nanostructured Materials: *Yonghao Zhao*¹; ¹Nanjing University of Science and Technology

The limited ductility of bulk nanostructured materials has emerged as an important obstacle to widespread application of bulk nanostructured materials, despite their other attributes, such as ultra high strength levels, in some cases. This talk will first analyze the intrinsic and extrinsic reasons for the low ductility of the bulk nanostructured materials, and then summarize effective strategies for improving the poor ductility of bulk nanostructured materials. Finally we report on recent successful results by applying some of these strategies in nanostructured NiFe and 7075 Al to obtain both high strength and ductility. Keywords: Nanostructured materials, ductility, microstructures

11:00 AM

True Stress-True Strain Relationships until just before Fracture of Ultrafine-Grained Ferrite-Cementite Steels: *Noriyuki Tsuchida*¹; Tadanobu Inoue²; ¹University of Hyogo; ²National Institute for Materials Science

True stress-true strain relationships until just before fracture were estimated by stepwise tensile test and the Bridgman correction in ultrafine-grained ferrite-cementite steels with average ferrite grain sizes less than 2 μm . The estimated true stress-strain relationships were different from the nominal stress-strain curves including the conventional tensile properties. In the nominal stress-strain curves, strength increased and elongation decreased with decreasing the grain size. However, the balance between true stress and true strain just before fracture became larger with decreasing of the grain size in the true stress-true strain relationships. The estimated true stress-strain relationships for the ultrafine-grained steels suggest that the grain refinement strengthening can improve true stress and true strain until fracture.

11:15 AM

Micromechanical Testing of Nanocrystalline and Ultra Fine Grained bcc Metals: *Jonathan Ligda*¹; Brian Schuster²; Qiuming Wei¹; ¹UNC Charlotte; ²Army Research Laboratory

We report on recent investigations into the mechanical properties of nanocrystalline (NC) and ultra-fine-grained (UFG) body centered cubic metals processed via high pressure torsion (HPT). The microstructures were characterized using synchrotron x-ray diffraction and transmission electron microscopy. The mechanical properties were investigated using site-specific nanoindentation along with micro-tension and compression. These samples have an inherent gradient in microstructure and properties resulting from the HPT processing. Grain sizes vary as a function of radial position on the bulk HPT disk; with increasing distance from the center of the disk, grains transition from UFG to the truly NC regime. W and T_a show a Hall-Petch dependence on hardness well into the NC regime. NC T_a specimens have been shown to retain some significant tensile elongation. Specimens with the smallest grain sizes show a distinct transition to localized plastic deformation.

11:30 AM

The Effect of High Strain Rate on the Mechanical Properties of Nanoporous Metal: *Tanvir Ahmed*¹; Alan Jankowski¹; ¹Texas Tech University

Porous metals are being used in energy absorption devices and renewable-energy system applications. Micro-scratch measurements at high strain rate show that nanoporous metals have an enhanced strain-rate sensitivity in comparison to their dense counterparts. Rate-dependent tribological tests are conducted to measure the sensitivity of porous metal coatings

at the micro- and nano-scale to investigate differences in the operative deformation mechanism at high strain rate. Results for microporous silver indicate the strain-rate sensitivity exponent increases significantly as the strain rate is increased beyond the regime dominated by solution effects and dislocation-based deformation. Similar results are presented for nanoporous gold and aluminum coatings for comparison with dense nanocrystalline counterparts. The morphological effects from porosity are assessed in structural stability and operative deformation mechanisms at high strain rates. The features of length scale are evaluated using electron microscopy, and the mechanical behavior is assessed by the micro- and nano- scratch hardness methods.

11:45 AM

Influence of Cryogenic Processing on the Mechanical Properties of High-Purity Copper: *Joel House*¹; James O'Brien²; Philip Flater¹; Robert De Angelis³; Richard Harris¹; Michael Nixon¹; ¹Air Force Research Laboratory; ²O'Brien and Associates; ³University of Florida

Wang et al (Nature, 2002) demonstrated that cold rolling at cryogenic temperatures could be used to increase the toughness of high-purity copper. Increased material strength was attributed to extremely fine grain structure (grain size 149; 300 nm), in combination with deformation twinning. The current research seeks to extend that characterization by processing copper using Equal Channel Angular Pressing (ECAP) at cryogenic temperatures. After processing, a series of experiments were conducted to characterize the materials response to low temperature annealing (175-275°C) and to characterize the mechanical properties in the as-worked and annealed conditions. The mechanical property characterization included low strain rate and high strain rate loading in both tension and compression. Results of the mechanical property experiments will be discussed in the context of the features of the microstructures that have been characterized using optical microscopy, scanning electron microscopy, and electron-backscattered diffraction.

12:00 PM

Occurrence and Elimination of Yield Point Phenomena in Nanostructured Metals: *Xiaoxu Huang*¹; Jacob Kidmose¹; Tianlin Huang²; Qingshan Dong²; Niels Hansen¹; ¹Risø National Laboratory for Sustainable Energy, Technical University of Denmark; ²Chongqing University

In ultrafine grained aluminum produced by plastic deformation and annealing, the tensile stress-strain curves show an unexpected yield drop, which is detrimental to the formability. The underlying mechanism is related to lack of mobile dislocations in the microstructure. In order to remove the yield drop, two procedures have been explored. One is to introduce extra dislocations by plastic deformation and the other is to add incoherent particles in order to increase the density of potential dislocation sources. Both routes are successful as they can remove the yield drop. This effect is discussed based on detailed strength and structural observations.

Ultrafine Grained Materials VII: Thermal Stability

Sponsored by: The Minerals, Metals and Materials Society, TMS Structural Materials Division, TMS/ASM: Mechanical Behavior of Materials Committee, TMS: Nanomechanical Materials Behavior Committee, TMS: Shaping and Forming Committee
Program Organizers: Suveen Mathaudhu, U.S. Army Research Office; Xiaoxu Huang, Risø National Laboratory for Sustainable Energy, Technical University of Denmark; Hyoung Seop Kim, POSTECH; Terence Langdon, University of Southern California; Terry Lowe, Manhattan Scientifics, Inc. ; Ruslan Valiev, Ufa State Aviation Technical University; Xiaolei Wu, Institute of Mechanics, Chinese Academy of Sciences; Michael Zehetbauer, University of Vienna

Tuesday AM
March 13, 2012

Room: Swan 5
Location: Swan Resort

Session Chairs: Kristopher Darling, U.S. Army Research Laboratory; Radomir Kuzel, Charles University; Christopher Saldana, Pennsylvania State University; Tianbo Yu, Risø National Laboratory for Sustainable Energy, Technical University of Denmark

8:30 AM Invited

Stability and Microstructural Evolution of Grain Boundaries in Severely Deformed Metals: *Gerhard Wilde*¹; Sergiy Divinski¹; Harald Rösner¹; ¹University of Muenster

Severe plastic deformation causes grain refinement due to the creation of large dislocation densities and the subsequent or concurrent socialization into cell- and grain boundaries. Here, detailed grain boundary diffusion studies after different thermomechanical treatment were performed to analyze the rates of atomic transport and the specific excess energy density of such grain boundaries in severely deformed pure metals like Cu, Ni, Ti and Ag. Additionally, the radiotracer analyses are combined with high resolution transmission electron microscopy and local strain field analyses with atomic resolution via geometric phase analysis to examine the stability and the time – and temperature – dependent evolution of grain boundaries in severely deformed metals. The comparison indicates that the theoretical and computational studies can capture important aspects of the properties and the evolution of such grain boundaries even quantitatively, but that they are not in agreement with the entire set of the experimentally observed behavior.

8:50 AM

Thermal Stability in Nanostructured fcc Metals: The Role of Twin Interfaces and Vacancies: *Christopher Saldana*¹; Alexander King²; Srinivasan Chandrasekar³; ¹Pennsylvania State University; ²US Department of Energy, Ames Laboratory; ³Purdue University

In this study we show that nano-scale twinned microstructures produced by low-temperature, severe plastic deformation of pure copper exhibit both strength and thermal stability. Twinned microstructures store less energy in their interfaces than other nanostructured materials, but also appear to exhibit lower vacancy supersaturations, reducing the driving force and mobility for microstructure evolution. While similar combinations of strength and thermal stability are observed in the case of deformed silver, the same behavior is not observed in aluminum and nickel. This suggests that, in applications where thermal stability is critical, the preferred strengthening of certain pure metals may be different from the conventional approach of pushing microstructure refinement to nano-scale equiaxed grain morphologies.



TMS 2012

141st Annual Meeting & Exhibition

9:05 AM

X-Ray Diffraction Study of Thermal Stability of Several Materials Prepared by ECAP and HPT: Radomir Kuzel¹; Zdenek Matej¹; Milos Janecek¹; Ondrej Srba¹; ¹Charles University in Prague, Faculty of Mathematics and Physics

XRD studies of ECAP and HPT materials (mainly Cu, Cu-Zr, Mg) were performed after annealing and by in-situ measurements in high-temperature chamber for samples prepared by different number of passes and number of revolutions, respectively. Strong changes were found for ECAP samples while no dependence was observed in the latter case when differences were found along the radius of disc-shape specimen. In-situ measurements were focused not only on temperature dependence but also on time evolution of the diffraction line widths. The latter were measured at temperatures where significant drop of line widths was observed in isochronal annealing. The widths were decreasing with time but after relatively short time they reached saturated values and for their further reduction an increase of temperature was necessary. Evaluation in terms of dislocation densities, correlation and crystallite size was performed by our own software Mstruct developed for total powder diffraction pattern fitting.

9:20 AM Invited

Stabilization and Mechanical Properties of Nano-Crystalline Copper by Alloying with Tantalum: Kris Darling¹; Laszlo Kecskes¹; David Foley²; Suveen Mathaudhu³; ¹ARL; ²Texas A&M University; ³ARO

The thermal stability of nanocrystalline Cu 10at% Ta prepared through high energy cryogenic mechanical alloying was studied. Nanocrystalline Cu 10at% Ta maintains a mean grain size of 150nm after annealing at 97% of it melting point. Powder samples were consolidated by high temperature equal channel angular extrusion (ECAE). Post processing analysis revealed fully consolidated samples exhibiting high hardness (4-3GPa), low porosity (<1%) without evidence of prior particle boundaries. Samples were tested mechanically under various testing methods. The results are reported here.

9:40 AM

Stability and Grain Growth Mechanisms in Sintered Tungsten: Brady Butler¹; James Paramore¹; Kristopher Darling¹; Micah Gallagher¹; Eric Klier¹; Heidi Maupin¹; ¹U.S. Army Research Laboratory

One common method for achieving ultrafine grained tungsten microstructures is through the addition of particulate phases. These dispersoids operate via a kinetics based pinning mechanism to reduce the mobility of grain boundaries during the final stages of sintering. In recent years an alternative grain refinement mechanism based on increasing the thermodynamic stability of grain boundaries has been proposed for a number of alloy systems. In this paper, the principle of solute segregation as a means of reducing grain boundary energy and thereby reducing the driving force for grain growth is investigated. The application of thermodynamic stabilization techniques for producing ultrafine grained microstructures is demonstrated in a tungsten system and compared to previous results in other alloy systems. In particular, the relationships between thermodynamic stability, densification and grain growth are established.

9:55 AM

Processing and Thermal Stability of Nanocrystalline Tungsten Alloys: Tongjai Chookajorn¹; Christopher Schuh¹; ¹Massachusetts Institute of Technology

Thermal stability is a major practical concern for nanocrystalline metals, as they contain a large volume fraction of interfaces which promote structural coarsening and therefore loss of properties at elevated temperature. In the case of refractory metals, powder-route processing via high energy milling is the processing method of choice to form a high-strength nanocrystalline structure, but the subsequent need to consolidate at elevated temperature introduces a unique requirement for nanostructure stability if bulk nanocrystalline material is to be produced.

Here we describe our work on the processing of nanocrystalline tungsten alloys, with a focus on the problem of nanostructure stabilization through alloying effects such as grain boundary segregation and phase separation. Thermal stability of the nanocrystalline structure is studied as a function of alloying additions, and contact with theoretical models for nanostructure stability is also made.

10:10 AM

The Effect of Deformation Texture on the Thermal Stability of UFG HSLA Steel: Enrico Bruder¹; ¹TU Darmstadt

UFG microstructures produced by SPD are far from the thermodynamic equilibrium thus being prone to undergo coarsening processes at elevated temperatures. Theoretical and experimental investigations revealed that the stability against discontinuous grain growth in UFG metals strongly depends on the fraction of high angle grain boundaries (HAGBs), meaning that discontinuous grain growth does not occur if the fraction of HAGBs exceeds a certain level. The present work focuses on the impact of strong deformation textures on the thermal stability of UFG microstructures in ferritic steels processed by linear flow splitting. It shows that the expected correlation between thermal stability and fraction of HAGBs is valid up to moderate texture intensities, whereas a strong deformation texture promotes discontinuous grain growth in spite of a high fraction of HAGBs. EBSD measurements show that this effect is based on strain induced boundary migration causing a progressive orientation pinning which destabilizes the microstructure.

10:25 AM Break

10:40 AM Invited

GB Segregations in UFG Alloys Processed by SPD: Xavier Sauvage¹; Nariman Enikeev²; Julia Ivanisenko³; Artur Ganeev²; Ruslan Valiev²; ¹University of Rouen, CNRS; ²IPAM-USATU; ³INT - Karlsruhe Institut für Technologie (KIT)

UFG alloys processed by SPD exhibit very specific grain boundaries that are characterized by long range elastic stresses and enhanced free volumes. To minimize the excess energy associated to these specific boundaries, some solute elements may segregate and cover them. Such segregations may significantly affect the mechanical behavior or the thermal stability. Therefore a systematic study was carried out to clarify the mechanisms and especially the role of defects created during SPD. GB segregations were characterized thanks to Atom Probe Tomography in an Al-Mg alloy and in a steel processed by HPT. In the AlMg alloy, heterogeneous distribution of Mg was found along boundaries with local concentrations up to 30at.%, while in the steel, the carbon concentration along the boundary was much lower and more regular. These data will be discussed with a special emphasis on the GB structure and on the mechanisms involved during SPD.

11:00 AM

Low-Temperature Thermal Stability of Cold-Rolled Nanostructured Aluminum: Tianbo Yu¹; Niels Hansen¹; Xiaoxu Huang¹; ¹Risø National Laboratory for Sustainable Energy, Technical University of Denmark

Commercial purity aluminum deformed to high strains was annealed at relatively low temperatures (from room temperature to 220°C), and the evolution of microstructure was characterized using transmission electron microscopy (TEM) and electron backscattered diffraction (EBSD). Triple junctions in a lamellar nanostructure with an average spacing 200~300 nm are classified into three categories based on the structural morphology, and a relationship is formulated between the density of triple junctions and the boundary spacing. Based on TEM and EBSD observations, thermally-activated triple junction motion is identified as the key process during recovery of highly-strained aluminum, leading to removal of thin lamellae and widening of microstructure. A mechanism for recovery by triple junction motion is proposed, which can underpin the general observation that a lamellar structure formed by plastic deformation coarsens into a more equiaxed structure during annealing at low temperatures.

11:15 AM

Conditions for Stabilization of Binary Nanocrystalline Alloys against Grain Growth and Phase Separation: *Heather Murdoch*¹; Chris Schuh¹; ¹MIT

Many nanocrystalline materials are limited in their application by their propensity for grain growth due to the energy associated with their large volume fraction of grain boundaries. Several methods have been proposed to stabilize nanoscale structure; among these grain boundary segregation is appealing as it lowers the thermodynamic driving force for grain growth. This approach to stabilization has been used with some success in various binary metal alloys; however, in many such cases the precipitation of a second phase triggers a rapid loss in stability. Adapting a recent model developed by Trelewicz and Schuh for nanocrystalline stabilization via grain boundary segregation, we examine the conditions under which an alloying element can support a nanoscale grain structure that is thermodynamically stable against second phase formation. We ascertain the materials properties required for stabilization of a nanocrystalline structure, and delineate alloys in which grain boundary segregation is not a viable stabilization strategy.

11:30 AM Invited

Enhancement of Strength and Stability of Nanostructured Ni by Small Amount of Solutes: *Hongwang Zhang*¹; Ke Lu¹; Reinhard Pippan²; Xiaoxu Huang³; Niels Hansen³; ¹Institute of Metal Research; ²Austrian Academy of Science; ³Risoe National Laboratory for Sustainable Energy

Plastic deformation is an effective method to fabricate bulk nanostructured metals and alloys with high strength, however, with limited thermal stability. Foreign elements in solid solution can have a beneficial effect by reducing both dynamic and thermal recovery and thereby increasing the strength at ambient temperature and the thermal stability at elevated temperatures. Here we report exploratory investigation on a comparison of polycrystalline Ni with a purity of 99.7% (with 0.14% Ti) and 99.967wt% deformed by high pressure torsion to a strain of 100. The presence of Ti solute atoms i) decreases the structural scale from 130 to 42 nm, ii) increases the flow stress from 1000 to 1700 MPa, and iii) increases the recrystallization temperature from 150oC to 500oC. The effect of solute on dislocation storage during deformation and on mobility of dislocations and boundaries during annealing are discussed. The strengthening mechanisms and their superposition are also analyzed.

11:50 AM

Processing of Thermally Stable, Ultrahigh-Strength Mg-Alloys: Kristopher Darling¹; Laszlo Kecskes²; *Suveen Mathaudhu*²; ¹U.S. Army Research Laboratory; ²U.S. Army Research Office

Advanced nanocrystalline alloys have shown remarkable property improvements, particularly, order-of-magnitude strength increases, when compared to their coarse-grained counterparts. However, a major obstruction to the widespread application of such materials is the degradation of properties via rapid grain growth at even ambient temperatures. Conventional methods for circumvention of this problem at low temperatures have largely steered toward kinetically pinning the boundaries with disperoids, or through misorientation of grain boundaries, yet even these methods have limited utility at elevated temperatures needed for routine sintering and forming operations. In this work, we will present a synergistic approach to the development of thermally stable nanostructured Mg-alloys which incorporates elements of predictive modeling of suitable alloy systems, fabrication of nanostructured alloy powders by high energy ball milling and consolidation of the powders at elevated temperatures to bulk ultrahigh strength alloys.

12:05 PM

Applying Equilibrium Segregation Theories to Inhibiting Grain Growth: *Brian VanLeeuwen*¹; ¹The Pennsylvania State University

This work reviews the assumptions of the popular Langmuir-McLean segregation isotherm and Guggenheim-Fowler segregation isotherm. It is concluded that these should not be applied to the study of grain

growth inhibition in nanocrystalline alloys because they assume constant interfacial area. An amended isotherm that does not make this assumption is proposed.

12:20 PM

High-Pressure Torsion-Induced Grain Refinement/Growth in Coarse-Grained/Nanocrystalline Cu Powders: *Haiming Wen*¹; Troy Topping¹; Enrique Lavernia¹; Rinat Islamgaliev²; Ruslan Valiev²; ¹University of California, Davis; ²Ufa State Aviation Technical University

Severe plastic deformation (SPD) is widely used to achieve exceptional grain refinement in coarse-grained metals to obtain ultrafine or nanocrystalline (nc) grain size. Deformation-induced grain growth in nc metals has been reported during various plastic deformation processes. However, very few studies have compared or related the two opposite processes (i.e. grain refinement and grain growth). In this study, high pressure torsion (HPT) was used to process coarse-grained or nanocrystalline Cu powders. The results showed that significant grain growth from an average grain size of 46 nm to 90 nm occurred in cryomilled nanocrystalline Cu powders. In comparison, HPT resulted in exceptional grain refinement in coarse-grained Cu powders and also attained an ultimate grain size of ~ 90 nm. The associated mechanisms for the grain refinement/growth were ascertained, and microstructure and mechanical behavior of the samples obtained from the two processing routes were compared and discussed.

2012 Functional and Structural Nanomaterials: Fabrication, Properties, Applications and Implications: 1-Dimensional Nanomaterials and ZnO

Sponsored by: The Minerals, Metals and Materials Society, TMS Electronic, Magnetic, and Photonic Materials Division, TMS: Nanomaterials Committee

Program Organizers: Jiyoung Kim, University of Texas; David Stollberg, Georgia Tech Research Institute; Seong Jin Koh, University of Texas at Arlington; Nitin Chopra, The University of Alabama; Terry Xu, UNC Charlotte

Tuesday PM
March 13, 2012

Room: Pelican 1
Location: Swan Resort

Session Chair: Seung Hyuck Kang, Qualcomm

2:00 PM Invited

Energy Generation and Storage Applications of TiO₂ Nanotubular Arrays by Atomic Layer Deposition and Nanotemplating: *Hyunjung Shin*¹; ¹Kookmin University

Tubular structures of oxides in nanometer have attracted much attention as the most promising 1-D materials for many applications. High crystalline quality of TiO₂ NT arrays templating by atomic layer deposition (ALD) onto anodic aluminum oxides (AAO) and subsequent annealing will be presented. The optimum boosting condition of crystallization has been attained. More than half of micron-meter long anatase single grains resembling the physical properties of the bulk in NTs were obtained, and the most defective form was able to be prepared by pinning the grain growth at the thinnest wall thickness. The former was utilized in high efficient dye-sensitized solar cells, producing photovoltaic cells exceeding conversion efficiency of ~6%, and the high efficiency results were ascribed to the minimization of defect sites. The latter was found to be using in Li-ion battery application, resulting in fast charging up to ~2000 C as well as high charging capacity.

TUESDAY PM



TMS 2012

141st Annual Meeting & Exhibition

TUESDAY PM

2:35 PM

High Performance TiO₂ Nanotubes-Based Biosensors for Streptavidin Detection: *Mingun Lee*¹; Antonio Lucero¹; Taewook Kim¹; Jie Huang¹; Moon Kim¹; Jiyoung Kim¹; ¹University of Texas at Dallas

Biosensors composed of a single titanium dioxide (TiO₂) nanotube were fabricated to detect streptavidin – a popular test vehicle for demonstrating feasibility of a biomolecule-based protein detector. Streptavidin detection is facilitated by functionalizing the nanotubes with biotin or its derivatives via self-assembled alignment in phosphate buffered saline (PBS). The presence of streptavidin is noted by the conductance shift in the nanotubes due to biotin-streptavidin pair bonding occurring on its surface. Our biosensors have achieved detection limit of 10pM, and did not exhibit any change in conductance when exposed to chemicals other than streptavidin, which indicates high sensitivity and selectivity; with further study and modifications, they are likely become highly effective at detecting not only proteins, but other bio-substances as well. This research was supported by a grant (code #:2010K000351) from ‘Center for Nanostructured Materials Technology’ under ‘21st Century Frontier R&D Programs’ of the Ministry of Education, Science and Technology, Korea.

2:55 PM

Nano Boron Carbide in Fabric for Improvement of Ballistic Performance: David Stollberg¹; *Juan Aguilar*¹; ¹Georgia Tech Research Institute

Kevlar fiber is widely used for body armor due to its high strength, tenacity, and energy absorption. Kevlar-based armor systems are often enhanced by adding Boron Carbide (B4C) plates. B4C is used because it is relatively light weight, extremely hard, and has good energy dissipating mechanisms upon impact. One of the main issues with these armor systems is that they are heavy and cumbersome, making it difficult for soldiers to operate while wearing them. Consequently, they are often considered unsuitable for routine wear. The purpose of this study was to improve the ballistic and puncture resistance of protective fabrics (Kevlar and Nomex) by incorporating B4C in a way that does not significantly increase weight or reduce flexibility. This was achieved by depositing nano-thickness films of B4C on the fabrics. The effect of functionalization with carbon nanotubes (CNT) was also explored. The resulting modified fabrics were tested, showing improved puncture resistance.

3:15 PM

Size Dependent Transition of Deformation Mode in Gold Nanowire: A Molecular Dynamics: *Pil Ryung Cha*¹; Na-Young Park¹; Ho-Seok Nam¹; Seung-Cheol Lee²; ¹Kookmin University; ²Computational Science Research Center, Korea Institute of Science and Technology

Inspired by recent experimental results [1] for the deformation behavior of Au nanowire with the diameter of ~100 nm, we have conducted the molecular dynamics (MD) simulations for the deformation of single-crystalline <110>/{111} Au nanowires with various diameters under tensile loading. Our MD results demonstrate size-dependent transition of the deformation mode from fracture by the localization of slip to transformation to <100>/{100} nanowire by twin propagation unlike previous MD researches which have shown the tensile deformation by the localization of slip in Au nanowire. The transition arises from the competition between irreversible slip behavior and pseudo-elasticity represented by twin propagation. Below a critical size, <110>/{111} nanowires showed irreversible behavior by slip localized in the transformed region as soon as a twin region (transformed <100>/{100} wire) formed, which was caused by the yield stress of the transformed <100>/{100} region lower than the flow stress associated with twin propagation.

3:35 PM

Synthesis and Investigation of Growth Mechanisms of Functional Inorganic Oxide Nanomaterials: *Yuanbing Mao*¹; ¹University of Texas-Pan American

One of the remaining challenges in preparing nanomaterials is to develop large scale, controllable, reliable and simplistic synthetic methods. Hence, we present our recent work on the large scale synthesis of luminescent RE doped oxide nanoparticles, including Er:Y2O3 and Er:La2(ZrxHf1-x)2O7, and magnetic double perovskite La2BB'O6 by molten salt synthesis. Their luminescent and magnetic properties have been systematically studied. Moreover, to better control the property and device performance of nanomaterials, growth kinetic and mechanistic information of structure changes should be pursued to provide feedback for the development of new “designer” materials to meet the future challenges. In this presentation, we start with ex situ studies of titanium-based oxide nanomaterials, and then focus on advanced luminescent nanomaterials. Specifically, we present our recent investigation of in-situ time-resolved synchrotron x-ray diffraction (XRD) and absorption spectroscopy (XAS) analyses on the synthesis of rare-earth doped metal oxide nanostructures, including Er:Y2O3 nanotubes and nanoparticles and Er:La2(ZrxHf1-x)2O7 nanoparticles.

3:55 PM Break

4:10 PM

Ultrafine ZnO Nanoparticles Synthesized by Ultraviolet Decomposition Process in Ambient Air: Growth Mechanism and Photoresponsive Activities: *Jyh Ming Wu*¹; Hsin-Hsien Yeh²; Hong-Ching Lin²; ¹Feng Chia University; ²Industrial Technology Research Institute

Zinc oxide nanostructures have been considered as promising materials for applications of sensors, photovoltaic cell, and photocatalysis. In this work, the different solvents such as isopropylalcohol (IPA), acetone, and denatured ethanol were used to prepare a single precursor of Zn(AcAc)₂·H₂O. The single crystalline ZnO nanoparticles were formed as Zn(AcAc)₂·H₂O was irradiated under a ultraviolet lamp (λ~380 nm, 75-150mW/cm²) in ambient air. High-resolution transmission microscopy image and selected-area diffraction pattern revealed that the nanoparticles were single crystalline and belongs to wurtzite-structure ZnO. The particles size of ZnO is ~7-9 nm based on Debye-Scherrer formula and HRTEM investigation. Water molecular was found to be acted as key components during the formation process. As-synthesized ZnO nanoparticles have been investigated using UV lamp (λ~365nm, 2.33mW/cm²). A superior photocurrent to dark current ratio was achieved ~764. As-developed UV-light decomposition process under ambient air is very simple, large-area, and with short process time.

4:30 PM

P-Type Conductive Behaviors of AlN Co-Doped ZnO Films Deposited by the Atomic Layer Deposition: *Yu-Mi Kim*¹; Kwang-Seok Jeong¹; Ho-Jin Yun¹; Seung-Dong Yang¹; Sang-Youl Lee¹; Hi-Deok Lee¹; Ga-Won Lee¹; ¹Chungnam National Univ.

AlN co-doped ZnO (ANZO) films were deposited by the atomic layer deposition (ALD) system on glass substrates at the low temperature of 200 °C. To find out an optimal film condition for the p-type conductive behaviors, the experimental study is carried out by varying N doping concentration (2 at%, 15 at%), 4 kinds of different process sequences and post-annealing temperatures from 300 °C to 700 °C under N₂ ambient. The structural, optical and electrical characteristics of ANZO films with different process sequences are investigated, respectively. The ANZO films with NH₄OH concentration of 2 at% and sequence D (DEZ-NH₄OH-TMA-NH₄OH) show excellent p-type behavior with a high mobility and a hole concentration of 32.41 cm²V⁻¹s⁻¹ and about 2.72×10¹⁶ cm⁻³ at post-annealing temperature of 500 °C, respectively.

4:45 PM

Zinc Oxide Nanorods by the Pulsed Plasma in Liquid and Their Photocatalytic Property: *Emil Omurzak*¹; Kengo Taniguchi²; Tsutomu Mashimo²; ¹Kumamoto University; ²Kumamoto University

Wurtzite-type ZnO (w-ZnO) nanorods were synthesized using the pulsed plasma in liquid method. The pulsed plasma submerged into a liquid enables us to synthesize metastable, high-temperature phase nanocrystalline materials by rapidly quenching from the plasma state. Pulsed plasma generated by electrical discharge between two electrodes made of pure metallic zinc rods submerged into water resulted in production of the w-ZnO nanostructures. Synthesized ZnO nanostructures were of rod shape with a diameter of about 20 nm and length up to 150 nm. UV-Visible absorption spectroscopy analysis of the synthesized ZnO nanorods showed a blue shift (about 0.19 eV) of absorption peak (350 nm) comparing to that of the commercial sample. Photoluminescence spectrum of the sample at the room temperature showed two peaks at 381 nm and 535 nm. Photocatalytic property of the synthesized ZnO nanoparticles was higher than that of the commercial photocatalyst TiO₂ under the visible light. Purer ZnO without metallic Zn could be synthesized by using the SDS and CTAB surfactant materials. In addition, morphologies of the nanorods produced using different surfactants were different from each other.

5:05 PM

ZnO Nanowires Grown on ZnO Thin Film Deposited by Atomic Layer Deposition: *Mikhail Ladanov*¹; Paula Algarin Amaris¹; Pedro Villalba¹; Garrett Matthews¹; Manoj Ram¹; Jing Wang¹; Ashok Kumar¹; ¹University of South Florida

Currently, ZnO nanowires are studied for their applications in a wide variety of devices. Control over the properties of ZnO nanostructures, such as size, shape and density is required. In this work the atomic layer deposition (ALD) technique was used to deposit the seeding layer of ZnO, which was then post-processed using rapid thermal processing. ZnO nanowires were grown using hydrothermal method on the seeding layer. We studied how the annealing of ZnO thin films grown by ALD affect properties of ZnO nanowires grown on this film using the hydrothermal method. ZnO thin films were characterized by means of AFM and grazing incidence XRD, while ZnO nanowires were characterized by means of XRD and SEM. Results suggest strong correlation between properties ALD thin films modified by rapid thermal annealing and resultant ZnO nanowires. Changes in density, size and degree of vertical orientation in ZnO NW are shown.

5:20 PM

Deposition of Organic and Inorganic Hybrid Laminates Using Ozone Based Atomic Layer Deposition: *Sunwoo Lee*¹; Jie Huang¹; Mingun Lee¹; Pil-Ryung Cha¹; Jiyoung Kim¹; ¹The University of Texas at Dallas

Recently, organic materials have been attracting attention due to their low cost and flexibility. However, they have many issues such as electrical instability and short life time. Therefore, a hybrid stack has been developed to compensate for the many issues of organic materials while maintaining their flexibility and functionality. A novel technique for building an organic and inorganic stack has been introduced by M. M. Sung et al. using a modified ALD method.¹ It has the advantage of minimizing the defects during growth of organic and inorganic films because the hybrid films are deposited by an in-situ process through the sequential, self-limiting surface reaction similar to ALD. This research has been partially funded through Korea-US collaboration R/D program by MKE-COSAR-KETI. References [1]. B. H. Lee, et al., J. Am. Chem. Soc., 129, 16034 (2007).

2012 Symposium on Surfaces and Heterostructures at Nano- or Micro-Scale and Their Characterization, Properties, and Applications: Energy and Catalysis

Sponsored by: The Minerals, Metals and Materials Society, TMS Electronic, Magnetic, and Photonic Materials Division, TMS Materials Processing and Manufacturing Division, TMS: Energy Conversion and Storage Committee, TMS: Nanomaterials Committee, TMS: Surface Engineering Committee, TMS: Young Leaders Committee, TMS: EMPMD Council

Program Organizers: Nitin Chopra, The University of Alabama; Ramana Reddy, The University of Alabama; Arvind Agarwal, Florida International University; Sandip Harimkar, Oklahoma State University; Jiyoung Kim, University of Texas at Dallas; Christopher Matranga, National Energy Technology Laboratory

Tuesday PM
March 13, 2012

Room: Pelican 2
Location: Swan Resort

Session Chairs: Christopher Matranga, National Energy Technology Laboratory (NETL); Paul Ohodnicki, National Energy Technology Laboratory (NETL); Nitin Chopra, The University of Alabama

2:00 PM Invited

Characterization and Modeling of 3D Photovoltaics: *Jonathan Guyer*¹; Daniel Josell¹; ¹NIST

First Generation (thick layers of crystalline silicon) and Second Generation (thin films of CdTe, CIGS, etc.) PV devices are both well established, with well defined techniques for fabrication and characterization. Third Generation PV encompasses a wide diversity of materials and nanostructures and commercially viable technologies and means of fabrication are yet to be determined. Many of the proposed structures have considerable microstructural variability that complicate interpretation of macroscopic device measures. We are developing idealized, three-dimensionally patterned templates that can serve as test structures to enable measurement of critical device and materials properties. Initial heterostructures are based around electrodeposited CdTe. To guide and interpret the experimental measurements we are developing open source models of carrier and light transport within arbitrary 2D and 3D device geometries. This talk will compare experimental measurements with simulation results and discuss how the model is used to guide new device geometries.

2:35 PM Invited

More Efficient Polymer Solar Cells by Doping with Ferroelectric Dipoles: Kanwar Nalwa¹; John Carr¹; Rakesh Mahadevapuram¹; Hari Kodali¹; Baskar Ganapathysubramanian¹; *Sumit Chaudhary*¹; ¹Iowa State University

A key requirement for realizing efficient organic photovoltaic (OPV) cells is the dissociation of photogenerated electron-hole pairs (singlet-excitons) in the donor polymer, and charge-transfer-excitons at the donor-acceptor interface. However, in modern OPVs, these excitons are typically not sufficiently harnessed due to their high binding energy. Here, we show that doping the OPV active-layers with a ferroelectric polymer leads to localized enhancements of electric field, which in turn leads to more efficient dissociation of singlet-excitons and charge-transfer-excitons. Bulk-heterojunction OPVs based on poly(3-hexylthiophene):[6,6]-phenyl-C61-butyric acid methyl ester were fabricated. Upon incorporating a ferroelectric polymer as additive in the active-layer, power conversion efficiencies increased by nearly 50%, and internal quantum efficiencies approached 100% – indicating complete exciton dissociation at certain photon energies. Similar enhancements in bilayer-heterojunctions, and direct influence of ferroelectric-poling on device behavior showed that improved dissociation was due to ferroelectric dipoles rather than any morphological change.

TUESDAY PM



TMS 2012

141st Annual Meeting & Exhibition

3:10 PM Break

3:15 PM

Effect of Annealing and Additives on Defects and Recombination in Polymer Photovoltaic Layers: Yuqing Chen¹; Rakesh Mahadevaparam¹; Sumit Chaudhary¹; ¹Iowa State University

Various types of annealing treatments and solvent additives are used in polymer photovoltaics to control nanomorphology and improve device efficiencies. Though their morphological effects are known, it is not clear how they affect the defects and carrier recombination rates/mechanisms. Our experiments reveal some unintuitive results in this regard. Defect densities in the polymer domains are a stronger function of unintentional oxygen dopants rather than the annealing. In fact thermal or solvent annealing enhance oxygen diffusion, which creates even more defects. However, these defects in annealed films do not have much effect on the final device efficiencies and carrier recombination rates. Performance is a stronger function of other structural parameters like domain sizes in the phase separated photovoltaic blends. On a side note, oxygen dopants actually increase the hole concentration, which in turn improves hole mobility and charge transport, and further improves the devices.

3:35 PM Invited

Raman Studies of Hybrid Nanostructures for Solar Energy Applications: Sonal Padalkar¹; KunHo Yoon²; Lincoln Lauhon²; ¹Northwestern University; ²Northwestern University

Raman microspectroscopy was employed to study the optical response of Si nanowires decorated with Au nanoparticles prepared by two different methods. In one approach, Au nanoparticles were drop-cast on Si nanowires, while in the second approach Au nanoparticles were grown directly on Si nanowires from solution. Raman spectra and spatial maps were obtained from both types of nanowires for varying nanowire and nanoparticle geometries. A low particle density was maintained to resolve the single nanoparticle responses. Both enhancement and suppression of the Raman scattering was observed depending on the sizes of the nanowire and nanoparticle. Other features of the Raman spectra showed measurable changes including the line shape, peak position and width. Insights into the trends in the Raman enhancement and suppression were gleaned from finite difference time domain modeling. Raman spectra and modeling provide a sensitive measure of the light harvesting properties of metal-semiconductor hybrid nanostructures.

4:10 PM Invited

Developing Titania/Ferroelectric Heterostructures for Solar Photolysis: Gregory Rohrer¹; Paul Salvador¹; Li Li¹; Andrew Schultz¹; Yiling Zhang¹; ¹Carnegie Mellon University

A series of photochemical reactions have been conducted on thin titania films supported by ferroelectric substrates (BaTiO₃ and BiFeO₃) with a wide range of orientations. For all of the orientations and both phases of titania, the thinnest films have reactivities equal to or greater than the bulk-like films, suggesting that the charge separating characteristics of the substrate have the potential to increase the reactivity of titania. When titania is supported by the narrower bandgap ferroelectric BiFeO₃, photochemical reactions on the titania surface can be stimulated by visible light with an energy smaller than titania's bandgap. Finally, the efficacy of the dipolar field effect is demonstrated by measurements of hydrogen evolution rates from a composite catalyst comprised of BaTiO₃ particles coated with mesoporous titania. The rate of hydrogen evolution from the composite catalyst exceeds the rate of hydrogen evolution from the BaTiO₃ or the mesoporous titania alone.

4:45 PM

Photocatalytic Activity of Heterostructured Powders: Nanostructured TiO₂ Shells Surrounding Microcrystalline (Ba,Sr, Pb)TiO₃ Cores: Li Li¹; Paul Salvador¹; Gregory Rohrer¹; ¹CMU

Heterostructured photocatalysts were prepared to have nanostructured (ns) TiO₂ shells surrounding microcrystalline (mc) (Ba,Sr,Pb)TiO₃ cores. The shells were 50 nm thick and were composed of nanocrystalline, nanoporous, predominantly anatase TiO₂. The mc-(Ba,Sr)TiO₃/ns-TiO₂ core-shell photocatalysts annealed at 600 °C had the highest rates of UV photochemical hydrogen production from water/methanol solutions, rates much greater than those for ns-TiO₂ or mc-(Ba,Sr)TiO₃ alone. The mc-PbTiO₃/ns-TiO₂ core-shell photocatalysts displayed more efficient degradation rate for methylene blue than its components alone under visible light. The improved photocatalytic properties are attributed to the isolation of three processes: light absorption and low scattering in the mc-core, charge separation at the core-shell interfaces, and hydrogen production on the nanostructured TiO₂. The annealing temperature, coating thickness and Pt loading amount are discussed, respectively. Such heterostructured powders represent a new strategy for the design of photocatalysts and the use of nanostructured catalytic coatings.

5:05 PM Invited

Deactivation Mechanism and Hole Scavenging in Heterostructured Visible Light Active CO₂ Photoreduction Catalysts: Christopher Matrangola¹; Congjun Wang¹; Robert Thompson¹; Paul Ohodnicki¹; ¹US DOE- NETL

The design of heterostructured photocatalysts for converting CO₂ into value-added chemicals is an increasingly active area of research in the scientific literature. While many new techniques are being reported for improving the visible light activity of CO₂ reduction catalysts, the hole left in the photocatalyst after electron transfer continues to lead to deactivation, particularly in heterostructures of semiconductor nanocrystals and metal oxides. The fate of the hole in the valence band of semiconductor nanocrystals forming a series of PbS/TiO₂ and CdSe/TiO₂ photocatalysts has been evaluated with X-ray photoelectron spectroscopy and the resulting oxidation of the nanocrystal sensitizer has been characterized. The use of sacrificial hole scavengers based on amine, alcohol, and other chemistries has been evaluated and shown to extend catalyst lifetimes significantly. The mechanism of photocatalytic deactivation and its prevention with hole scavengers will be discussed. Reaction data will also be presented illustrating extended catalyst lifetimes and product distributions.

5:40 PM

Multicomponent Metal-Carbon Junctions in 1-D Geometry: Junchi Wu¹; Paaras Agrawal²; Nitin Chopra¹; ¹The University of Alabama; ²Northridge High School

Vertically aligned and axially heterostructured metal nanowires with uniform diameters (~267-279 nm) and micron-scale lengths were fabricated by combining template process with wet-chemical deposition process. Subsequently, carbon nanotubes (CNTs) were selectively grown on the nanowires resulting in metal-carbon junctions. The length of nanowires and CNT could be controlled by varying the growth duration. The heterostructures were characterized by scanning electron microscopy (SEM), X-ray diffraction (XRD), transmission electron microscopy, Raman spectroscopy and microscopy, and cyclic voltammetry (CV) and ac electrochemical impedance spectroscopy (EIS).

3rd International Symposium on High Temperature Metallurgical Processing: Alloy and Materials Preparation

Sponsored by: The Minerals, Metals and Materials Society, TMS Extraction and Processing Division, TMS: Energy Committee, TMS: Pyrometallurgy Committee

Program Organizers: Tao Jiang, Central South University; Jiann-Yang Hwang, Michigan Technological University; Patrick Masset, TU Freiberg; Onuralp Yucel, Istanbul Technical University; Rafael Padilla, University of Concepcion; Guifeng Zhou, Wuhan Iron and Steel

Tuesday PM
March 13, 2012

Room: Southern II
Location: Dolphin Resort

Session Chairs: Rafael Padilla, University of Concepcion; Jianliang Zhang, University of Science and Technology Beijing

2:00 PM

Future Considerations for Further Processing of Cobalt Alloy at Nchanga Smelter: *Humphrey Chikashi¹*; Credo Ng'uni¹; ¹Konkola Copper Mines

A pyrometallurgical route for producing a sellable, higher value and an easier to treat product from cobalt alloy recovered from the flash smelting slag is introduced and explored in this paper. Theoretical analyses as well as results from actual plant trials of the process are presented. Cobalt content upgrade procedure discussed is done at minimum initial investment and operating cost. The method also offers advantages such as reduced size of downstream hydrometallurgical units to recovery cobalt to metallic form. Results of leaching tests conducted on the cobalt rich slag are also presented and discussed.

2:15 PM

Improving Hot Workability of Ledeburitic Tool Steels: *Matevz Fazarinc¹*; Goran Kugler¹; Iztok Perus¹; *Milan Tercelj¹*; ¹University of Ljubljana

Ledeburitic tool steels are highly alloyed steels, used for specific applications but are characterized by low hot workability. Selecting the right process parameters for these types of steels for improvement of their intrinsic hot workability is thus necessary. Inappropriate selection results in the occurrence of unusual carbides, in terms of type, shape and their distribution. Beside the secondary carbides also other brittle phases precipitated on grain boundary accelerate cracking at lower and medium temperatures of the working range. The main reason for decreased workability at lower temperatures of the working range is appearance of cracks around the carbides. On the other hand, upper limit of temperature range is predominately related to eutectic carbides and phases with low melting point. The aim of this work was to determine the necessary condition for improvement of the intrinsic hot workability.

2:30 PM

Influence of Elements Segregation on Creep Properties of A Single Crystal Nickel-Based Superalloy: *Chao Zhang¹*; Sugui Tian¹; Xingfu Yu¹; Zheng Zeng¹; Chen Liu¹; ¹Shenyang University of Technology

Single crystal nickel-base superalloy is prepared by using the various withdrawing rates. By measuring creep properties and microstructure observation, the influence of the element segregation on creep properties of the superalloys is investigated. Results show that the dendrite spacing and the segregation extent of the elements decrease with the enhancing withdrawing rate. The superalloy with smaller dendrite spacing has lower segregation of the elements and better creep resistance. The dislocations climbing over the rafted γ' phase is thought to be the deformation mechanism of the alloy during steady state creep. In the later stage of creep, the fact that some dislocations shear into the rafted γ' phase may twist the rafted γ' phase. As the creep goes on, the initiation and

propagation of the cracks occur up to occurring creep fracture, which is thought to be the fracture mechanism of the superalloy during creep.

2:45 PM

Preparation of High Titanium Ferrous with Low Oxygen Content Prepared by Enhanced Reduction: *Zhang Ting'an¹*; *Dou Zhihe¹*; Niu Liping¹; Zhang Hanbo¹; Lv Guozhi¹; Liu Yan¹; Li Yan¹; He Jicheng¹; ¹Northeastern University

Rutile, ilmenite and Al-Ca complex reducer were used to prepare high titanium ferrous alloy by enhanced reduction. The effects of the complex reducer compositions and lag types on the reduction process were investigated. The alloys were characterized by XRD, SEM and chemical analysis. The results indicate that the alloys consist mainly of TiFe₂, AlTi₃ and Al₂O₃. The oxide inclusions exist in alloy which results directly in the high oxygen content and micro-structural defects. The titanium and oxygen contents decrease in alloy, but the aluminum content increases while the mass ratio of calcium in the complex reducers increases. When the mass ratio of Al/Ca in the Al-Ca complex reducers varies from 6:1 to 5:1, the titanium, oxygen and aluminum contents vary from 63.75% to 55.00%, from 3.01% to lower than 2.0% and from 10.72% to 14.00% respectively.

3:00 PM

Preparing Aluminum-Scandium Alloys Using Direct Hall Reduction Process: *Chunyang Gruan¹*; Jilai Xue¹; ¹University of Science and Technology Beijing

Al-Sc Alloys have showed many advanced properties for a wide range of industrial application, which is usually produced using thermal reduction process. This work is aimed to develop an electrochemical process to make Al-Sc alloy using industrial Hall aluminum reduction cells. The investigations have been carried out in a lab cell where NaF/AlF₃-Al₂O₃-LiF as electrolyte, Sc₂O₃ as raw material, and liquid aluminum as cathode were used at operating temperature of 950°C. The resulting Al contained 0.2 – 0.6 wt % Sc that is the common range in its content for advanced applications. However, a small fraction of Sc was found from thermal reduction at Al-melts interface. SEM-EDS and ICP-AES analysis showed a uniformed distribution of Sc at varying locations of the Al-Sc alloy sample.

3:15 PM

Production of Fe-Cr-Ni-Ti Alloys by Metallurgical Processes: *Cem Colakoglu¹*; Onuralp Yücel²; ¹Istanbul Technical University; ²Istanbul Technical University

This study consist of Fe-Cr-Ni-Ti alloys production by metallurgical reduction of Fe₂O₃-Cr₂O₃-NiO-TiO₂ powder mixtures. Metallurgical reactions were realized by using a stainless steel SHS reactor. Different ratios of Cr/Ni/Ti were carried out in the metallurgical experiments, and addition of excess stoichiometric amount of metallic Al and Al₂O₃ powders were added to the initial mixture to decrease the adiabatic temperature and specific heat of the system. The raw materials, alloys and slags were characterized by using XRD (X-Ray Diffractometry), and Scanning Electron Microscope (SEM).

3:30 PM Break

3:40 PM

Production of NbAl₃ Powders through Sodium Reduction of Oxides in Molten Salts: *Chao Du¹*; Na Wang¹; Yao Zhang¹; Shuqiang Jiao¹; Hongmin Zhu¹; ¹University of Science & Technology Beijing

Na₂NbAlO₅ was synthesized using Nb₂O₅ and NaAlO₂ as raw materials in molten NaCl-CaCl₂ by a solid reaction. With an addition of sodium into the melts, Na₂NbAlO₅ was subsequently reduced to form NbAl₃ intermetallic compound with a particle size of 50-300nm.

3:55 PM

Recrystallization of L-605 Cobalt Superalloy during Hot-Working



TMS 2012

141st Annual Meeting & Exhibition

Process: *Julien Favre*¹; Yuichiro Koizumi¹; Akihiko Chiba¹; Damien Fabregue²; Eric Maire²; ¹IMR Tohoku University; ²INSA de Lyon

Co-20Cr-15W-10Ni alloy (L-605) is a cobalt-based superalloy combining high strength with keeping high ductility. The aim of this work is to get maximal grain refinement with a homogeneous microstructure after the hot-working process to obtain optimal in life mechanical resistance. Microstructure was observed after high-temperature deformation to determine optimal deformation conditions for obtaining the targeted microstructure. High-temperature deformation behavior is studied by compression tests at temperatures from 1000°C to 1200°C and a strain rate range of 0.001 s⁻¹ to 10 s⁻¹. Microstructure observations revealed the occurrence of dynamic recrystallization for all deformation conditions. For strain rates lower than 0.1 s⁻¹ or higher than 1 s⁻¹, dynamic recrystallization lead to a homogeneous microstructure with a grain size about 10 μm. Deformation at temperatures lower than 1100°C and strain rates about 1 s⁻¹ resulted in a heterogeneous microstructure with grain size lower than 1 μm.

4:10 PM

Research on Inclusions in CuCr Alloy Prepared by Thermit Reduction: *Dou Zhihe*¹; Zhang Ting'an¹; Zhang Zhiqi¹; Niu Liping¹; Lv Guozhi¹; Liu Yan¹; He Jicheng¹; ¹Northeastern University

CuCr alloy can be extensively used as lead frame of electric contact and high strength conductor. We proposed aluminothermy reduction electroslog remelting to prepare the large scale CuCr alloy. But there are pores and oxide in the CuCr alloy prepared by aluminothermy reduction process. This paper analysed the inclusions in CuCr alloy. The ratio of reactant, additive, electromagnetic stirring and the temperature of mold were considered. The slags and CuCr alloy are respectively analyzed by XRD and SEM. The results show that when the additive is Na₃AlF₆, the slag is consist of Al₂O₃ and Cr. when the additive is CaF₂, the slag is consist of Al₂O₃, Cr, CaF₂ and CaAl₄O₇. The inclusions in CuCr alloy are mainly Al₂O₃ and pores which disperse in Cu-rich zone and Cu-Cr phase interface. When 5% CaF₂ and 5% KClO₃ are added , there are less pores and inclusions ,and the microstructure is more better .

4:25 PM

Settling of Inclusions in Top-cut SoG-Si Scraps under Electromagnetic Field: *Lucas Damoah*¹; Lifeng Zhang¹; ¹Missouri University of Science and Technology

Increasing demand for Solar Grade Silicon (SoG-Si) due to rising interest in renewable energy has lead to increased SoG-Si top-cut scraps generated from the multi-crystalline silicon making process. In the current study, experiments under high frequency, high voltage, electromagnetic field were performed and the results showed that SiC inclusions settled within a short time to the bottom of the crucible and the characteristic rod-like morphologies of Si₃N₄ inclusions were not detected.

4:40 PM

Study and Application of the Taphole Clay with High Strength and Friendly Environmental Surroundings in a New Blast Furnace with 3800M3 Volume: *Guotao Xu*¹; Yue Wang¹; Yafei Xiong¹; Huaiyuan Li¹; Shuzhong Li¹; ¹Wuhan Iron and Steel Group Company

The composition, properties and structure of taphole clay with high strength and friendly surrounding used in a new blast furnace with 3800 M3 volume was studied. The developed taphole clay had been applied in the blast furnace for four months, pouring times were 11-13 every day, flowing rate of hot iron was 7.5 t/min and the consumption of taphole clay was 0.49Kg per ton iron, which can make the new blast furnace attach the designed production quickly and decrease the cost of hot iron. The taphole clay is easy to be opened in the channel of hot iron which can be remained in stable shape under the corrosion of slag or hot iron, and it dose not produce poisonous smoke in yellow or dark color in the use process. The development of new taphole clay is useful to improve the work surrounding of the blast furnace.

Advances in Surface Engineering: Alloyed and Composite Coatings: Session IV

Sponsored by: The Minerals, Metals and Materials Society, TMS Materials Processing and Manufacturing Division, TMS: Surface Engineering Committee

Program Organizers: Sandip Harimkar, Oklahoma State University; Srinivasa Bakshi, Indian Institute of Technology Madras; Arvind Agarwal, Florida International University

Tuesday PM
March 13, 2012

Room: Macaw 1
Location: Swan Resort

Session Chair: To Be Announced

2:00 PM

The Roles of Diffusion Factors in Electrochemical Corrosion of TiN and CrN (CrSiCN) Coated Mild Steel and Stainless Steel: *Feng Cai*¹; Qi Yang²; Xiao Huang¹; ¹Carleton University; ²National Research Council Canada

Noble coating on steel components is an effective solution to preventing corrosion attacks. However, through-coating defects, such as pin holes, voids and growth defects play a detrimental role in the degradation of the coating-substrate system. They allow corrosive media to be in contact with the metal substrate, initializing pitting corrosion and eventually resulting in coating failure. This research studies the correlation between coating defects and corrosion behavior of the TiN and CrN (CrSiCN) coated mild steel and stainless steel. Electrochemical impedance technique is used to reveal the corrosion behavior. The results revealed that in a coating-substrate system, two critical factors controlling the corrosion resistance, the effective diffusion coefficient and diffusion layer thickness, which are found to be related to coating microstructure. Denser and thicker coating structures are expected to have lower effective diffusion coefficients and greater effective diffusion layer thicknesses; and showed high electrochemical impedance and resistance to electrochemical corrosion.

2:20 PM

Effect of Electroplating Parameters on "HER" Current Density in Ni-MoS₂ Composite Plating: *Ebru Saraloglu Guler*¹; Ishak Karakaya¹; Erkan Konca²; ¹Middle East Technical University; ²Atilim University

Nickel composites with co-deposited insoluble solid lubricant MoS₂ particles have been reported to reduce friction. The aim of this study was to analyze the influence of the electroplating parameters and interaction effects on the optimum plating current density by factorial and mixture designs for three types of mineral processing surfactants (sodiumlignosulfonate, depriminC, ammoniumlignosulfonate). The parameters and ranges were; MoS₂ (0-30 g/l), temperature (30-50 °C), pH (2-4) and surfactant (0-1 g/l). Electrodeposition was carried out from a typical Watts bath containing leveler, wetting agent and brightener by using a potentiostat. The peak current densities were extended to higher values and the peaks on linear sweep voltammograms became noticeable by increasing the scan rate from 20 to 100mV/s over the range 0 to 2.5 V. Increasing MoS₂, pH decreased whereas temperature increased peak current densities for all three surfactants. Addition of sodiumlignosulfonate and deprimin C decreased, but ammoniumlignosulfonate increased the peak currents.

2:40 PM

Production of Ceramic Layers on Aluminum Alloys by Plasma Electrolytic Oxidation in Alkaline Silicate Electrolytes: *Alex Lugovskoy*¹; Aleksey Kossenko¹; Barbara Kazanski¹; Michael Zinigrad¹; ¹Ariel University Center of Samaria

Plasma electrolytic oxidation (PEO) is a technology allowing obtaining hard wear- and corrosion-resistant in the form of thick and highly-adhesive oxide layer on aluminum surfaces. The process can be performed in several types of electrolyte, of which the alkaline silicate

electrolytes were employed in this study. Silicate electrolytes passivate aluminum alloys, favor micro-arc discharges and contain silicate ions, which modify the technological properties of the coating. The influence of the silicate index of sodium silicates and of their concentration in the electrolyte on the composition, structure and properties of the oxide layer was studied. Electrolyte properties, electrochemical process parameters and the properties of the resulting coating were studied and compared. Optimal electrolyte compositions for the obtaining of hard and corrosion resistant ceramic layer were found. A plausible mechanism of the process was proposed.

3:00 PM Break

3:15 PM

Wear Properties of Plasma Sprayed Y-PSZ Coated 6063 Aluminum Alloy: Eray Erzi¹; Selim Yildirim¹; Suat Yilmaz¹; ¹Istanbul University

Thermal spray methods and especially plasma spray method have an increasing importance and being widely used by industries. This method depends on the purpose of spraying powder based coating materials to a surface. Light alloys like aluminum alloys have some disadvantages like low mechanical strength and wear resistance. Aim of this study is investigating the wear resistance behavior of coated and uncoated T6 heat treated 6063 Aluminum alloys. Coatings were made by plasma spray method and 8 Y-PSZ was used as coating material. Wear tests were done by pin-on-disc method with three different load parameters and results were discussed comparatively.

3:35 PM

Slurry Erosion Behavior of Thermally Sprayed Cr₃C₂-NiCr Coatings: V. N. Shukla¹; R. Jayaganthan¹; B. V. Manoj Kumar¹; V. K. Tewari¹; ¹IIT ROORKEE

High velocity oxy fuel (HVOF) technique was employed to deposit Cr₃C₂-NiCr coating of ~250 μm thickness with average bond strength of ~10000 psi and microhardness of ~8.3 GPa on 310 stainless steel substrate in the present work. The microstructure of the coating consisted of uniformly distributed Cr₃C₂-rich ceramic grains attached with NiCr-rich binder phase. The erosion behavior of the coated samples was studied using 10 and 20 wt% alumina particle concentration in water at normal impact angle for 10 hours. Erosion results indicated a severe loss of material using 20 wt% alumina particle concentration. SEM characterization of the worn coated surface has revealed smearing or cutting of soft binder phase followed by ceramic grain removal, while no change in the phase evolution of surface was observed after erosion. Erosion with 20 wt% of alumina particles in slurry increased crack initiation, and resulted in larger pull-outs and fracture of ceramic grains.

3:55 PM

The Electrochemical Behavior of Surgical Grade 316L SS with and without HA Coatings in Simulated Body Fluid: Tejinder Singh¹; Harjinder Singh²; Hazoor Singh³; Harpreet Saheer⁴; ¹Gulzar Institute of Engineering & Technology, Ludhiana, Punjab, India; ²Govt Medical College; ³Yadvindra College of Engineering, Talwandi Sabo, Bathinda, Punjab, India; ⁴Indian Institute of Technology Ropar

ASTM recommended surgical grade 316L SS stainless steel is one of the most widely used material in orthopedic implants. It has been reported that stainless steel is often susceptible to pitting corrosion. The main aim of this study is to evaluate the corrosion behavior of uncoated and HA coated 316L SS in simulated body fluid conditions. HA coating was produced using thermal spraying technique. The coatings were characterized by XRD, SEM/EDS and electrochemical techniques. The corrosion resistance of 316L SS was found to improve after the deposition of HA coating.

4:15 PM

Modification Research on the Influence on Corrosion Film Properties of Pb-Ca-Sn Alloys of with Addition of Bi, Ag and Zn: Lei Xu¹; Li Jun Liu¹; Pei Xian Zhu¹; ¹Kunming University of Science and Technology

The influences of Bi, Ag and Zn addition on the electrochemical corrosion film properties of Pb-Ca-Sn (Ca=0.08%, Ca=1.2%) alloys were studied in this paper. And the electrochemical properties of corrosion film were investigated respectively by XRD, SEM, Tafel curve test and cyclic voltammetry (CV) test when the Pb-Ca-Sn alloys were in 1.28g/mL H₂SO₄ solution. The results show that: the effects of different elements on the electrochemical corrosion film properties of Pb-Ca-Sn alloys are different and obvious. More specific, the corrosion film becomes thicker and the grain size is big when Bi is added, and besides the corrosion film contains more PbO; However, the corrosion film becomes thinner and grain size is fine when Ag and Zn are added, and the corrosion film contains more PbO₂.

Alumina and Bauxite: Hydrate Precipitation, Calcination and Environment

Sponsored by: The Minerals, Metals and Materials Society, TMS Light Metals Division, TMS: Aluminum Committee, TMS: Aluminum Processing Committee
Program Organizer: Benny Raahauge, FLSmidth

Tuesday PM
March 13, 2012

Room: Northern E3
Location: Dolphin Resort

Session Chair: Hans-Werner Schmidt, Outotech GmbH

2:00 PM

Growth and Agglomeration of Boehmite in Sodium Aluminate Solutions: Wang Zhi¹; Zhang Juan¹; Xu Rongguang¹; Guo Zhancheng¹; ¹Institute of Process Engineering

Boehmite precipitation is a new alternative way from sodium aluminate solutions to alumina, however, the too low particle size becomes one bottleneck for this methods replacing the current production route. Growth and agglomeration of crystals are the main factors influencing product size. The results show that the growth rate of boehmite is in a low range from 0.08 to 2.4 μm/h. Thus, agglomeration of boehmite is a major means to enlarge the particle size of precipitation products from sodium aluminate solutions. By means of laser particle size analyzer and powder attrition index analyzer, the agglomeration efficiency was represented by combining agglomeration degree and attrition index. The influences of seed ratio (SR), temperature, the molar ratio of Na₂O to Al₂O₃ (MR) and organic additives on agglomeration were investigated. The alcohol type additives PPG increases precipitation rate and agglomeration degree, but reduces the strength of products and makes attrition index increase.

2:15 PM

Physical Simulation on Mixing Uniformity in Seed Precipitation Tank: Liu Yan¹; Zhao Hongliang¹; Zhang Ting'an¹; Zhao Qiuyue¹; Wang Shuchan¹; Gu Songqing¹; He Jicheng¹; Zhang Chao¹; ¹Northeastern University

The suspension and dispersion of Al(OH)₃ particles in seed precipitation tank, which may affect the quality and output of alumina besides the deposit on the bottom of the tank, is one of the key steps in Bayer process. In order to solve these problems, the solids concentration profiles of Al(OH)₃ particles were investigated by cold water experiments under simulated industrial conditions. The results showed that, the mixing uniformity in the whole tank was improved with the increase of impeller off-bottom clearance when the impeller of small diameter (D/T = 0.5~0.6) was used, and it deteriorated when the impeller (D/T = 0.65~0.7) was enlarged. The mixing effects can be improved by increasing the impeller diameter and stirring speed, meanwhile the influence of impeller off-



TMS 2012

141st Annual Meeting & Exhibition

bottom clearance was weakened. But the impeller diameter and stirring speed should be controlled in appropriate ranges for the consideration of power consumption and mixing efficiency.

2:30 PM

Kinetics of Boehmite Precipitation from Supersaturated Sodium Aluminates Solutions with Ethanol-Water Solvent: Wang Zhi¹; Xu Rongguang¹; Liu Yang¹; Guo Zhancheng¹; ¹Institute of Process Engineering

Boehmite was prepared from supersaturated sodium aluminates solutions with ethanol-water solvent. The results of thermo-gravimetric analyzer and XRD showed that the product was mixture of boehmite and gibbsite, and the mass ratio of gibbsite and boehmite varied greatly with different process conditions. This work presents the effects of mass ratio of ethanol and temperature on the precipitation rate and phase compositions of alumina hydrate. The ratio of AlOOH in the product increased significantly with the increase of mass ratio of ethanol because the precipitation of gibbsite was restrained. When the solvent was pure ethanol, the ratio of AlOOH in the product reaches the peak of 90%. Ethanol reduces the free caustic concentration and increases initial supersaturation coefficient significantly. The boehmite activation energy of precipitation in ethanol solvent was 13.7 kJ/mol, indicated that ethanol reduces effectively energy barrier of boehmite from sodium aluminate solutions and it was controlled by diffusion process.

2:45 PM

Effect of Crystal Growth Modifier on the Structure of Sodium Aluminate Liquors Analyzed by Raman Spectroscopy: Jianguo Yin¹; Wangxing Li²; Zhanwei Liu²; Zhaohui Su²; Zhonglin Yin²; Wentang Xia¹; ¹Chongqing University of Science and Technology; ²Zhengzhou Research Institute of Chalco

It has been proved that crystal growth modifier (CGM) can improve particle size distribution (PSD) and intensity of the alumina products. Yet few researches have been focused on whether CGM has an effect on the structure of sodium aluminate liquors. Effect of CGM on the structure of synthesized sodium aluminate liquors was studied. It is shown that there is no new characteristic peak and obvious shift in the Raman spectrum of the liquors after adding a certain CGM. By constructing a comparison function and using calculation function of the software of Raman spectrometer, it is found that CGM might have micro effect on the structure of the liquors by changing the concentration of principal ion Al(OH)₄⁻ of the liquors. The results might be helpful for R&D and application of CGM.

3:00 PM

Precipitation Area Upgrade at ETI Aluminum: Murat Kayaci¹; Bekir Çelikel¹; Gokhan Kursat Demir¹; Meral Baygül¹; Carlos Suarez²; ¹ETI Aluminium; ²Hatch

ETI Aluminum is an integrated facility that produces sandy alumina by processing boehmitic bauxite. With the development of aluminum smelting technology and greater attention given to environmental protection, the quality requirements of alumina are much strict. ETI has initiated a study to meet smelter grade alumina specifications of its internal electrolysis customer. The old precipitation circuit at ETI alumina refinery was converted to sandy alumina. The change involved modifications to existing tanks and flows to obtain proper hydrate agglomeration. The challenge has been to improve and control particle size distribution without losing precipitation yield and product quality. ETI has been able to reduce its minus 44 micron particles from approximately 40 % to 6-8 % by means of controlling the precipitation circuit parameters such as, alumina supersaturation, seed charge, temperature and classification. Improvements in hydrate occluded soda and attrition index were obtained.

3:15 PM

Flash -and CFB Calciners, History and Difficulties of Development of Two Calcination Systems: Hans-Werner Schmidt¹; Fred Williams²; ¹Outotec GmbH; ²CMIS Corporation

In the last 40 years, stationary calciners have permanently replaced rotary kilns in existing alumina refineries and are being installed in all new Greenfield alumina refineries. In the 1960's two separate and different approaches to stationary alumina calciners were going through research and development. Alcoa developed a fluid flash system and VAW, together with Lurgi (today Outotec) the Circulating Fluid Bed (CFB) calciner. Both developments had the same targets, but took different approaches to create more efficient calcination systems. Without any joint effort, the industrial stages of both developments were introduced to the industry at the same time. This paper describes the significant steps of the development that both calcination systems went through to reach an industrial stage and the risks and failures that both took. Furthermore the differences and common goals of both approaches are analyzed and described in this paper.

3:30 PM

A Specific Critical Analysis on the Life Time of Alumina Calciners Refractories: Bruno Teider¹; Bruce Graham²; Jorge Gallo¹; Victor Pandolfelli³; ¹Research, Development and Innovation - Alcoa LA&C; ²Alcoa World Alumina, Point Comfort Refinery, USA; ³Materials Microstructural Engineering Group - Federal University of São Carlos - Brazil

In the international literature it is possible to find references of optimized refractory materials for lining circulating fluidized bed alumina calciners. However, unexpected failures of these refractories are still relatively common, impacting in many ways the results of alumina refineries. Due to the importance of this subject, this work addresses the performance analysis of a refractory material which faced harsh operational conditions and resulted in a short life. "Post-mortem" techniques, "in situ" observation and properties evaluation were used to study the materials' behavior. Based on the obtained results, a discussion related to the better performance potential of distinct refractories is presented, highlighting that based on the variety of different features these materials have, significant improvements of calciner refractory life can still be attained.

3:45 PM

The Key Technologies of Energy Efficient Al (OH) 3 Dilute Phase Fluidized Roasting Furnaces: Li Zhaoxia¹; Huang He²; Xue Xin³; Li Xiuju¹; Wang Huan¹; Huang Xingyuan³; ¹Luoyang Luohua Power Engineering and Special Refractory Materials Co., Ltd., Henan, China; ²Luoyang Luohua Ceramic Co., Ltd., Henan, China; ³Henan University of Science and Technology, Henan, China

Research work on new types of castable refractory, pre-casted assembly parts and thermal insulation materials, with resistance to high wear, thermal shock and erosion and low thermal conductivity, were done to solve problems of high system energy consumption, cracking and spalling of partial lining and mismatch of furnace top material and hanging material and so on, caused by unreasonable design of domestic Al(OH)₃ Dilute Phase Fluidized Roasting furnace lining. A full set of techniques including construction, furnace drying, lining maintenance and corresponding standards were developed. Using the ideas of furnace integration and new theory of furnace lining, we have solved the key technologies of high-efficient and energy-saving for furnaces. The achievements have been applied to domestic Al(OH)₃ Dilute Phase Fluidized Roasting furnaces to reduced energy consumption by one thousand MJ per ton of alumina, thus making a furnace lining with higher production, lower energy consumption and less exhaust gas emission.

4:00 PM

Fabric Filter Operating Results with 10 m Long Bags and Low Purging Pressures: *Carl-Vilhelm Rasmussen*¹; ¹FLSmith

Environmental performance of the Gas Suspension Calciners for Alumina installed at QAL and Yarwun in Queensland, Australia, is secured by fabric filters. Gas Suspension Calciners equipped with Fabric Filters represents today's State of the Art of stationary calciners for Alumina. This paper describe the development of the fabric filter technology relevant for this application including selection of filtration medium from an environmental, health and safety aspect as well as cost efficiency point of view. A three year R & D project has confirmed that 10 m long bags can be used for general filter performance within the standard design rules of FLSmith Airtech. FLSmith Airtech has been offering filters with 10 m long bags to customers worldwide in Alumina and Cement market segment since quite some time. Four fabric filter orders or ESP conversions have been received so far with 10 m long bags.

4:15 PM

Optimization of Preparation for α -Alumina by Calcination from Aluminum Hydroxide Using Response Surface Methodology: *Bin Zhang*¹; *Jinhui Peng*¹; *Libo Zhang*¹; *Shaohua Ju*¹; ¹Kunming University of Science and Technology

The conditions of technique to prepare α -Al₂O₃ by calcination from aluminum hydroxide were optimized using response surface methodology (RSM) with a central composite design (CCD). A quadratic equation model for field was built and effects of main factors and their corresponding relationships were obtained. The statistical analysis of the results showed that in the range studied the field of α -Al₂O₃ was significantly affected by the calcination temperature and calcination time. According to results from analysis of variance (ANOVA), the value of the determination coefficient ($R^2=0.9890$) indicates that the model was a good fit that 98.90% of the variation could be explained well by the model. The value of the adjusted determination coefficient ($adj.R^2=0.9811$) was also very high to advocate for a high significance of the model. The optimized calcination conditions were as follows: the calcination temperature 1206.81 °C and the calcination time 2.06 h respectively. Under these conditions the field of α -Al₂O₃ was 95.93%. In addition, the sample was characterized by X-ray Diffraction (XRD).

4:30 PM

Customer Impacts of Na₂O and CaO in SGA: *Stephen Lindsay*¹; ¹Alcoa, Inc.

Two major impurities in SGA directly impact the bath chemistry of smelting customers. Aluminium fluoride is consumed in bulk to neutralize the impact of calcium and sodium that enter the process. Excess consumption solely for the neutralization of excess CaO and Na₂O generates excess bath. The resulting cryolitic material can only be consumed by the primary aluminium industry. In this paper the author discusses points of concern from the perspective of customers with regard to CaO, Na₂O, and the ratio of between CaO and Na₂O. Conclusions include the impact that the growth of excess cryolitic bath will have upon producers of SGA.

4:45 PM

Options for Joint Ventures: *Anthony Kjar*¹; ¹Gibson Crest Pty Ltd

There has been a wide range of joint ventures within resource industries. The author has had direct experience in a number and a keen observer of others. This paper builds on a previous paper that examined the rationale for, history and observations as to the success of longer term joint ventures within the aluminium industry. In this paper options for the structure of joint ventures are discussed.

Aluminium Processing: Casting

Sponsored by: The Minerals, Metals and Materials Society, TMS Light Metals Division, TMS: Aluminum Processing Committee
Program Organizers: Kai Karhausen, Hydro Aluminium Rolled Products GmbH; Edward Williams, Alcoa

Tuesday PM
March 13, 2012

Room: Europe 1
Location: Dolphin Resort

Session Chair: Edward Williams, Alcoa

2:00 PM Introductory Comments

2:05 PM

Fabrication of Porous Aluminum with Directional Pore Aligned in One Direction: *Takuya Ide*¹; *Yutaro Iio*¹; *Hideo Nakajima*¹; ¹Osaka University

Directional pores aligned in one direction provide not only lightweight but also no stress concentration around pores. Therefore porous aluminum with directional pore aligned in one direction (lotus-type porous aluminum) is expected for structural material with lightweight. Lotus metals can be fabricated by pore formation of insoluble gas, when the melt dissolving gas is solidified. However, it is difficult to fabricate lotus aluminum with high porosity because of its low hydrogen solubility. In the present study, fabrication of lotus aluminum was systematically investigated by controlling solidification condition. The effect of solidification conditions on pore formation of lotus aluminum was clarified. Lotus aluminum with higher porosity more than 30% was fabricated at slow solidification velocity. When the solidification velocity becomes slow, insoluble hydrogen rejected into melt near the liquid/solid interface can diffuse into formed pores for longer time in order to promote the growth of the directional pores.

2:25 PM

A New Counter Gravity Sand Process Used for Aluminum Alloy Casting: *Jianmin Zeng*¹; ¹Guangxi University

In order to increase solidification rate of large aluminum casting poured in sand mould, an innovative counter-gravity casting process is invented. The process is based on Bernoulli's principle. The mold and crucible are placed separately in the upper and lower chambers, with the feed tube connected between them. High-speed jet flow of air makes negative pressure in the upper chamber. In this way, pressure differential is created between the two chambers. Thereby the molten metal in the crucible is forced to flow upward smoothly to fill the mold cavity. After that, cold air is introduced into sand mold through aisles that are set within the mold, which results in strong convective heat exchange at the casting/mold interface. So solidification rate of casting is increased dramatically. The microstructures and mechanical properties were investigated and the results indicate great advantage over traditional sand processes.

2:45 PM Question and Answer Period

2:55 PM Break

3:20 PM

The In-Situ Technique for Preparing Al-TiB₂ and Al-Al₃Ti Composites with ESR: *Jun Wang*¹; *Pan Li*¹; *Chong Chen*¹; *Jin Xue*¹; ¹Shanghai Jiaotong University

A novel technique for preparing in situ Al-TiB₂ and Al-Al₃Ti composites by electroslag remelting (ESR) process has been developed in this paper. The microstructure and phases of the composites were investigated by SEM and XRD. The aim of present work was to verify the feasibility of in-situ synthesis of Al-TiB₂ and Al-Al₃Ti composites by ESR process which had unique advantages in promoting fluoride salt-metal reaction



TMS 2012

141st Annual Meeting & Exhibition

efficiency. The reactant concentration and reactant contact area was improved greatly by ESR process and led to a totally complete reaction. The experiment results demonstrate that TiB₂ and Al₃Ti particulates are uniformly distributed in the aluminum matrix and the mean particle size becomes much smaller compared with the conventional casting method. The successful fabrication of in situ Al-TiB₂ and Al-Al₃Ti composites by ESR technique is expected to be significant promotion of the development of in-situ technique for fabricating MMCs.

3:40 PM

Grain Refinement of Al Alloys by Heterogeneous Nucleation of Consumable Ultrasound Horn: Jeong-Il Youn¹; Young-Ki Lee¹; Bong-Jae Choi¹; Young-Jig Kim¹; ¹Sungkyunkwan University

The final quality of castings is broadly dependent upon many factors which will have an effect on the solidification of the metal. Castings with large grains have poor mechanical properties compared to castings with fine equiaxed grain structure. Currently grain refinement in casting alloys is mainly accomplished by the special composition's master alloy as a chemical reagent. However, it has been shown that high intensity ultrasound can change the microstructure, refine the grain size, and improve the uniformity of minor phases and the casting's homogeneity. The main objective of this research is to study the mechanism of the effect on the grain refinement of ultrasound injection before solidification of the A356 and A390 aluminum alloys. Experiments were focused on the effects of uniform dispersion of heterogeneous nuclei in liquid metal on microstructure.

4:00 PM

The Development and Validation of a New Thermodynamic Database for Aluminium Alloys: A Markström¹; Y Du²; S. H. Liu²; L. J. Zhang²; L Kjellqvist¹; J Bratberg¹; Paul Mason³; A Engström¹; Q Chen¹; ¹Thermo-Calc Software AB; ²Central South University; ³Thermo-Calc Software Inc.

Thermodynamic databases developed using the CALPHAD method have been successfully applied to the modeling and simulation of Al based alloys for more than fifteen years. Such databases when combined with suitable software can be used for accelerating alloy design and improving understanding and processing of existing alloys. A new thermodynamic database has been developed for Al-base alloys based on the critical evaluation of all the constituent binary systems across their full range of composition and 59 ternaries, 15 quaternaries and 1 quinary. A hybrid approach of combining experiments, first-principles calculations and CALPHAD modeling was employed to obtain thermodynamic descriptions of the constituent binary and ternary systems over wide composition and temperature ranges. This database contains all the important Al-based alloy phases within a 26-element framework [Al-Cu-Fe-Mg-Mn-Ni-Si-Zn-B-C-Cr-Ge-Sn-Sr-Ti-V-Zr-Ag-Ca-Hf-K-La-Li-Na-Sc] and in total 345 solution and intermetallic phases are included. This presentation will describe development, validation and application of the database.

4:20 PM

Effect of Solid Particles on Fluidity of Semi-Solid Aluminum Alloy Slurry: Yuichiro Murakami¹; Kenji Miwa²; Masayuki Kito³; Takashi Honda³; Keigo Yorioka³; Naoyuki Kanetake⁴; Shuji Tada¹; ¹Advanced Industrial Science and Technology; ²Aichi Science and Technology Foundation; ³Aisan Industry Co., Ltd.; ⁴Nagoya University

The semisolid process is viewed as an attractive and promising manufacturing method for producing near net-shape metal products with reduced porosity and shrinkage. In this study, the fluidity of the Al-Si-Mg alloy slurry was evaluated by injecting into a spiral metallic mold. The solid particles in specimens were analyzed by the image analyzer, and became small and spherical with increasing in shear rate. The fluidity was

increased with increasing in shear rate, and also with decreasing in the size of particles and becoming spherical particles. The fluidity is strongly affected by the roundness than the size of particles.

4:40 PM Question and Answer Period

Aluminum Alloys: Fabrication, Characterization and Applications: Solutioning and Aging Behaviours

Sponsored by: The Minerals, Metals and Materials Society, TMS Light Metals Division, TMS: Aluminum Processing Committee
Program Organizers: Subodh Das, Phinix LLC; Tongguang Zhai, University of Kentucky; Zhengdong Long, Kaiser Aluminum

Tuesday PM
March 13, 2012

Room: Northern E1
Location: Dolphin Resort

Session Chair: Tongguang Zhai, University of Kentucky

2:00 PM

Precipitation Processes in Aged Al-4.0Mg-1.5Cu-(Ge,Si) Alloys: Junhai Xia¹; Zhiguo Chen²; Gang Sha¹; Simon Ringer¹; ¹The University of Sydney; ²Central South University

Microstructure evolutions of Al-4.0Mg-1.5Cu-0.25Ge(Si) (wt.%) alloys have been studied during artificial ageing at 200 °C. Transmission electron microscopy and atom probe field ion microscopy were used to clarify the precipitation processes in those alloys following ageing for 0.1, 1, 10, 25, 120, 336 and 1440 hours. The yield strength increases gradually with the ageing time after a first initial jump, and for both alloys at peak hardness ageing for 25 hours, there are four characteristic features: GPB zones (2-4 nm in diameter), fine S phases (~10 nm in diameter, needle-like) and coarse S phases (~50 nm in diameter, rod-like) in the matrix; and S-phase precipitates (50-100 nm in size) on the grain boundary (GB). Ge elements mainly exist in S phases on GB, while Si addition results in GPB zones and S phases homogeneously dispersed in the matrix with higher aspect ratio (height/diameter) up to a maximal of 30.

2:20 PM

The Role of Co-Clusters in the Artificial Aging of AA6061 and AA6060: Stefan Pogatscher¹; Helmut Antrekowitsch¹; Thomas Ebner²; Peter Uggowitzer³; ¹Montanuniversitaet Leoben; ²AMAG Rolling GmbH; ³ETH Zurich

In this study the role of Mg,Si-co-clusters formed during long-term natural aging on the artificial aging behavior was investigated by hardness measurements for the alloys AA6061 and AA6060. It was found that kinetics and age hardening response of artificial aging at common temperatures (e.g. 170 °C) are lowered by a strong presence of co-clusters, but enhanced at high temperatures (e.g. 250 °C) for AA6061. Co-cluster formation in the alloy AA6060 increases the age hardening response at 170 °C, but barely influences kinetics in both temperature regions. The co-cluster dissolution was analyzed by a model based on temperature dependent reversion of the hardness, which showed similar activation energies for both alloys. It is supposed that the different behavior of the alloys AA6061 and AA6060 can be explained by solute-vacancy interactions.

2:40 PM

Co-Clusters in Al Alloys: Alloy Strengthening and Thermodynamics: Marco Starink¹; ¹University of Southampton

Detailed atom probe studies performed in the last 10 years on heat treatable aluminium alloys such as the Al-Cu-Mg type have revealed that rapid hardening and room temperature hardening is predominantly

due to the formation of co-clusters. In this presentation a theory for the thermodynamics of these co-clusters in metallic alloys is presented. The model incorporates the basic dimer (2 atom) form of co-clusters as well as larger clusters. A model for the strengthening due to co-clusters is also derived. The model encompasses modulus hardening, chemical hardening and (short-) order strengthening. It is shown that in general (short-) order strengthening will be the main strengthening mechanism. The model formulation is tested against an extensive published and new data on the Al-Cu-Mg system and the Al-Zn-Mg system. It is shown that room temperature ageing and rapid ageing at temperature up to about 200°C is due to co-cluster formation.

3:00 PM

The Effects of Aging Treatment and Environment on the Stress Corrosion Cracking Susceptibility of AA6005A Extrusions: *Dan Seguin¹*; Calvin White¹; Richard Dickson²; ¹Michigan Technological University; ²Hydro Aluminum

Stress corrosion cracking (SCC) susceptibility of AA6005A extrusions (0.17% Cu) was found to depend on stress level heat treatment, and pH. Sustained load tests were conducted in an aqueous solutions containing 3.5% NaCl and HCl with pH ranging from 2.00 to 7.00. Stress corrosion cracking was observed in peak aged (T6) specimens within 42 hours when the applied load exceeded the yield strength and the solution pH was 2.00. The severity of SCC decreased when the pH was increased. Specimens tested in a naturally aged (T4) condition were susceptible to SCC at low pH.

3:20 PM

Nature of Grain Boundary Precipitates and Stress Corrosion Cracking in Al-7075: *Ramasis Goswami¹*; Ronald Holtz²; ¹SAIC/Naval Research Laboratory; ²Naval Research Laboratory

It has been observed that stress corrosion cracking (SCC) in Al-7075 is controlled by grain boundary precipitates. The evolution of grain boundary precipitates with aging is not well understood. In particular, the role of Cu in modifying the nature of grain boundary precipitates with aging is unclear. We report here a detailed study of the role of Cu in the evolution of the Mg-Zn-Cu phase at low and high-angle grain boundaries with aging. Transmission electron microscopy (TEM) and fine probe energy dispersive spectroscopy (EDS) were employed to characterize microstructure and composition. In naturally aged alloy, for example, the grain boundaries were observed to be decorated with very fine eta phase, MgZn₂, which is anodic with respect to the matrix, and it becomes susceptible to intergranular corrosion. The details of the microstructure in under aged to over aged condition will be presented, and correlated with the SCC behavior of this alloy.

3:40 PM

Precipitation of the γ' (AlAg₂) Phase on Dislocation Loops in Al-Ag(-Cu) Alloys: *Julian Rosalie¹*; Laure Bourgeois²; Barrington Muddle²; ¹National Institute for Materials Science; ²Monash University

Aluminium-copper-silver has been widely regarded as a “double-binary” precipitation hardening alloy system, in which the γ' (AlAg₂) and θ' (AlCu₂) precipitates nucleate and grow essentially independently. However a more thorough investigation has shown that the precipitation morphology and growth of both phases is actually strongly dependent on the composition. The present study focuses on precipitation of the γ' phase in silver-rich Al-Ag-Cu alloys in which the precipitate nucleates on dislocation loops. Copper plays an important role in this process, as even minor Cu additions alter the nature of the dislocation loops and the precipitation behaviour. The γ' phase was found to form readily on stacking faults associated with the dislocation loops; however, its growth was restricted where the bounding dislocation of the loop was sessile. This study highlights how heterogeneous defects can control not only precipitate nucleation but also growth.

4:00 PM Break

4:15 PM

On Elastic Compressive Stress Aging of an AA7075 Aluminum Alloy: *Jingwu Zhang¹*; Wei Guo¹; Hui Li¹; Men Yang¹; Tiankai Yao¹; Xiyu Wen²; ¹Yanshan University; ²University of Kentucky

Elastic compressive stress aging of an AA7075 aluminum alloy is carried out in aging furnace. The mechanical properties and microstructure after elastic compressive stress aging for the alloy were measured and was observed by using transmission electron microscopy (TEM), respectively. Effect of the elastic compressive stress on the precipitates on the grain boundaries was analyzed and discussed.

4:35 PM

Influence of Mn in Solid Solution in Softening of AA3003 Alloy During Annealing: *Dionisios Spathis¹*; John Tsiros²; ¹Hellenic Aluminium industry (ELVAL SA); ²Hellenic Aluminium Industry (ELVAL SA)

The present paper shows the change in the softening curve of 3003 alloy at final product gauge caused by the variation of Mn in solid solution just prior to the final anneal. The variation was purposely altered using different ingot preheat practices and/or different hot rolling practices. The tight control of Mn in solid solution is necessary to achieve stable mechanical properties in back annealed tempers (-H2X) of 3003 alloy.

4:55 PM

The Influence of Solution-Treatment on the High-Temperature Strength of Al-Si Foundry Alloys with Ni: *Florian Stadler¹*; Helmut Antrekowitsch¹; Werner Fragner²; Helmut Kaufmann³; Peter J. Uggowitzer⁴; ¹University of Leoben; ²AMAG Casting GmbH; ³Austria Metall GmbH (AMAG); ⁴ETH Zurich

Al-Si-Ni alloys can be considered as a coarse two-phase system where a hardening effect is caused by load transfer to an interconnected rigid network of eutectic Si and aluminides. In the course of a solution treatment the contiguity of the eutectic phase is reduced, which leads to a decrease of strength. However, solution treatment is necessary to obtain a high supersaturation of elements in the Al-solid solution, which contribute to high-temperature strength due to precipitation hardening. Despite Ostwald ripening, the distribution of secondary precipitates is still dense enough to act as dislocation obstacles, as was confirmed by TEM-analysis. This work discusses the influence of heat treatments on the elevated-temperature strength of Al-Si foundry alloys with Ni and analyzes the active strengthening mechanisms. In order to investigate the effect of a solution treatment on the high-temperature strength of Ni-containing Al-Si foundry alloys, the tensile properties of various eutectic alloys were determined at 250°C after long-time exposure to test temperature.

5:15 PM

The Effect of Artificial Aging Treatment on Microstructure and Tensile Properties of Al-12.7Si-0.7Mg Alloy: *Fang Liu¹*; Fuxiao Yu¹; Dazhi Zhao¹; Liang Zuo¹; ¹Northeastern University

The microstructure and tensile properties of the extruded Al-12.7Si-0.7Mg alloy aged at 160°C, 180°C and 200°C were investigated. The precipitates in different aging conditions have been characterized by regular and high resolution transmission electron microscopy (TEM and HREM) aiming at understanding the strengthening mechanisms. It was shown that the alloy after T6 treatment exhibits good ductility and much higher proof strength as well as tensile strength compared to 6063 alloy in general. The results have revealed that the strength changes by altering the precipitates size and volume fraction. The strengthening was attributed to be the combining effect of particle, grain boundary and precipitation strengthening.



TMS 2012

141st Annual Meeting & Exhibition

Aluminum Reduction Technology: Anode Effect, Process Control

Sponsored by: The Minerals, Metals and Materials Society, TMS Light Metals Division, TMS: Aluminum Committee, TMS: Aluminum Processing Committee
Program Organizer: Olivier Martin, Rio Tinto Alcan

Tuesday PM
March 13, 2012
Room: Southern III
Location: Dolphin Resort

Session Chair: Claude Ritter, Rio Tinto Alcan

2:00 PM

Latest Results from PFC Investigation in China: Xiping Chen¹; Wangxing Li¹; Jianhong Yang¹; ¹Zhengzhou Research Institute of Chalco

In the first half year of 2011, PFC investigation has been conducted on five potlines whose line currents are at the range of 200~350kA. The total aluminum output is 1.35 million tons per year. Both PFC caused by anode effects and PFC unrelated to anode effects were monitored and calculated. C3F8 was observed during anode effects for the first time and its peaks were at the same location as C2F6 and CF4 at the timetable. The weigh ratio of C3F8/CF4 was 2.66%, and that of C2F6/CF4 was 10.67%. C3F8 was observed only in the monitoring of two potlines and no C3F8 in the other three potlines. Concentration curves of C3F8 were plotted with C2F6. Percentage of continuous PFC from five potlines was calculated. The highest was 92.8%. But the potline has the lowest anode effect frequency (AEF) and its AEF is 0.01 AEs/cell-day.

2:20 PM

Studies of Perfluorocarbon Formation on Anodes in Cryolite Melts: Ole Kjos¹; Thor Anders Aarhaug¹; Egil Skybakmoen¹; Asbjorn Solheim¹; ¹SINTEF

The aluminium industry is today the primary source of perfluorocarbon (PFC) to the atmosphere. These gases have a lifespan of several thousand years, and a greenhouse warming potential (GWP) 6500-10000 times that of CO₂. It is therefore of essential to understand, and reduce, the PFC emissions. Controlled potential electrolysis with gas analysis was utilised to study the PFC production in a laboratory cell during regular electrolysis conditions, and during anode effects. A 3-electrode setup with an Al reference electrode was utilised to monitor the anodic voltage. The combination of Mass Spectrometry (MS) and Fourier Transformed Infrared Spectroscopy (FTIR) was used to characterize the off gas. Traces of CF_x were found in the anode gases at anodic voltages as low as 2.9 V VS the Al reference electrode, confirming that the PFC production can occur unrelated to the anode effect. However C₂F₆ was only detected during anode effects.

2:40 PM

Characteristics of In Situ Alumina PID Ore Feed Control: Michael Schneller¹; ¹Consultant

Point feeders have volumetric chambers that periodically deliver ore to cells through holes pneumatically broken into the crust layer. The period of feeder actuations is controlled by the logic employed to regulate bath alumina concentration. The time evolution of bath alumina is mostly a function of the rates of alumina consumption and feeder mass charge, but is also influenced by other events such as crust seal breaks/leakages and plugged or semi-plugged feeder holes. PID modulated In Situ feed logic addresses variable non-feeder ore related events to control alumina concentrations at targeted levels. Frequent underfeed and overfeed episodes are avoided. The In Situ</> ore feed concept has been successfully tested in the Dyna/Marc cell simulator at a targeted 2.30 % alumina concentration demonstrating both increased current efficiency (CE) and decreased kWh/kg compared to presently employed methodologies. Anode/cathode distances (ACD) can also be accurately measured using In Situ</> alumina predictions.

3:00 PM

Towards On-Line Monitoring of Alumina Properties at a Pot Level: Jayson Tessier¹; Gary Tarcy¹; Eliezer Batista¹; Xiangwen Wang¹; ¹Alcoa

Aluminum reduction cells typically use about 1.9 kg of alumina in order to produce 1 kg of aluminum. Hence, for modern reduction cells operating in the 350 to 400 kA range, 5000 to 6000 kg of alumina is fed to reduction cells on a daily. However, no information is available in an on-line fashion about the alumina properties fed to the pot. Alumina feeding control systems assume that alumina properties are constant for all pots within a potroom and also over time. Therefore, these control systems aim at controlling alumina concentration dissolved in the bath without accounting for the time varying effects of alumina properties and/or pot condition on alumina dissolution. Based on sampling campaigns, this paper presents evidences of time varying alumina properties impacting its dissolution rate and also proposes a novel approach in order to measure on-line, at the pot, parameters that are related to alumina dissolution.

3:20 PM Break

3:40 PM

Controlling the Variability of Pots KPVs : The Variability Matrix: Pierre Baillot¹; Jean-Paul Aussel¹; Armand de Vasselot²; ¹I.P.I.; ²Optimprocess

Over the course of 30 years the Process Control softwares have narrowed the variations of individual reduction cells. The volume of data available for day-to-day management of the potlines have increased considerably while the number of technical personnel per pot and per potline have been considerably reduced. Combining the tools and principles of Continuous Improvement with in-depth knowledge of Reduction Process Control systems allows for a new generation of Potline Process Optimization techniques. These techniques, powered by new generation data integration software, can breathe a new life in the Energy and Environment Performance of all smelters. They can show their owners a new trend for improvement and demonstrate strong care to the local communities without mobilizing expensive capital resources and additional people. How much can we expect? What does it require in terms of Human and System capabilities? Where do we start and how far can we improve?

4:00 PM

Multivariate Statistical Investigation of Carbon Consumption for HSS Reduction Cell: Peter Polyakov¹; Tatyana Piskazhova¹; Nikita Sharypov¹; Alexandr Krasovitskiy²; Sergey Sorokin²; ¹Siberian Federal University; ²RUSAL Nadvoitsy aluminium smelter

In the aluminium reduction technology there is no full awareness concerning the dependence of technical and economical data (TED) including carbon consumption on the changes of raw materials properties and technology parameters. Availability of this information could improve the effectiveness of the reduction technology control. In the paper the multivariate statistical treatment of anode paste consumption depending on the electrolysis parameters is applied. Using principal component analysis the parameters which greatly influence on the anode paste consumption are determined. Statistical models for paste consumption for single pot room and for comparison of the results between rooms are received. Carbon paste consumptions if the parameters changed by three Standard deviations are calculated.

4:20 PM

Experiences with Alstom's New Alfeed System at Emal: Sivert Ose¹; Bjørn Leikvang¹; Sunny John Mathew²; Geir Wedde¹; Anders Sorhuus¹; Odd Edgar Bjarnø¹; ¹Alstom Norway; ²Emirates Aluminium

Alstom's new pot feeding system (Alfeed) was successfully installed and commissioned on Emal's 756 pots during 2009-2010. The Alfeed system consists of 15 km distribution and pot airslides, manufactured in standard sections for maximum ease of installation and use. Alfeed on Emal is connected to 8 enriched alumina silos, each feeding two sections with 48 pots. Each section is 300 m long. The nominal flow rate to each pot is >200kg/h, and to each section >10ton/h. The main issue encountered

during start-up was dusting from the pot's alumina hopper lids. Small puffs of dusty air would leak through a narrow opening, eventually leading to build-ups of alumina on the superstructure. This was resolved through implementation of a clamp to the lid as well as a gasket. As with all new systems, some challenges were encountered and optimisations needed. These are discussed in detail in the paper.

4:40 PM

Computer Algorithm to Predict Anode Effect Events: *Fernando Costa*¹; Leonardo Paulino¹; ¹Alcoa/Alumar

At Alumar the pot voltage is used to detect anode effects every 1 second. Our attempt is to use this fast scan data to distinguish the normal and the pre-anode effect voltage period. An algorithm has been created to detect this behavior, based on the speed of the voltage increase. With simulation we observed that 60-70% of the anode effects are predicted by the new algorithm. The other 40-30% are ignored in order to reduce false detections. Only 2-10% of the predictions are false. The average voltage of prediction is 5.19 where the normal computer detection is 8. The predictor was tested for a month in 102 pots indicating that we can predict the events from 7 to 20 seconds prior to its occurrence. These tests resulted in a reduction of 30% time above 8 volts and 20% reduction in AE/potday.

Aluminum Reduction Technology: Cell Fundamentals, Phenomena and Alternatives I

Sponsored by: The Minerals, Metals and Materials Society, TMS Light Metals Division, TMS: Aluminum Committee, TMS: Aluminum Processing Committee
Program Organizer: Olivier Martin, Rio Tinto Alcan

Tuesday PM
March 13, 2012

Room: Northern E4
Location: Dolphin Resort

Session Chair: Michel Reverdy, Dubai Aluminium

2:00 PM

Effect of Current Density and Phosphorus Impurities on the Current Efficiency for Aluminium Deposition in Cryolite-Alumina Melts in a Laboratory Cell: *Gudrun Saevarsdottir*¹; Geir Haarberg²; Rauan Meirbekove¹; ¹Reykjavik University; ²Norwegian University of Science and Technology

The current efficiency in industrial Hall-Heroult cells for aluminium production may be up to 96%. The back reaction between dissolved metals, such as aluminium and sodium and the anode product play the major part in the loss in current efficiency. Also impurities, such as phosphorous which participates in cyclic red/ox reactions at the electrodes contribute significantly to reduced current efficiency. Phosphorous and other impurities are recycled with secondary alumina. Further potline amperage increase in industrial cells may require higher current densities. Thus the current efficiencies dependence on current density and phosphorous and iron content was studied at current density ranging from 0.85-1.5 A/cm² in a laboratory cell. Current efficiencies from 90 - 97 % were obtained and increased slightly by increasing cathodic current density. The current efficiency decreased by about 0.8 % per 100 ppm of phosphorus in the electrolyte.

2:20 PM

A Thermodynamic Approach to the Corrosion of the Cathode Refractory Lining in Aluminium Electrolysis Cell: Modelling of the Al₂O₃-Na₂O-SiO₂-AlF₃-NaF-SiF₄ System: *Guillaume Lambotte*¹; Patrice Chartrand¹; ¹CRCT, Ecole Polytechnique de Montréal

The corrosion of the cathode refractory lining in electrolysis cells, partly due to the cryolite bath, can shorten the lifespan of the cell. This corrosion is usually studied with laboratory tests and post-mortem analyses of shutdown cells, but the results might not correspond to the reactions

taking place in service. The simplified corrosion problem (Al₂O₃-SiO₂ represents the aluminosilicate refractory, NaF-AlF₃ the cryolite bath) corresponds to the reciprocal system Al₂O₃-Na₂O-SiO₂-AlF₃-NaF-SiF₄. The thermodynamic modelling of this system permits the calculation of complex chemical equilibria occurring at the service temperature. The reciprocal system has been assessed using the Modified Quasichemical Model in the Quadruplet Approximation, which considers both first-nearest- and second-nearest-neighbour short-range order and allows the modelling of the strongly ordered oxyfluoride liquid solution. A unique set of model parameters is used to reproduce the experimental data. The results of the thermodynamic modelling of the Al₂O₃-Na₂O-SiO₂-AlF₃-NaF-SiF₄ system are presented here.

2:40 PM

Influence of the Sulphur Content in the Anode Carbon in Aluminium Electrolysis - a Laboratory Study: *Stanislaw Pietrzyk*¹; Jomar Thonstad²; ¹AGH University of Science and Technology; ² Norwegian University of Science and Technology

The chemistry of sulphur in carbon anodes is not fully understood, especially its influence on the electrolysis parameters. The results of this study are indicative of an important link between the sulphur content in the anode material and the carbon consumption as well as the current efficiency during aluminium electrolysis. By performing a laboratory scale investigation of different carbon anodes with sulphur contents ranging from 1.97 to 3.82 wt% S in addition to graphite anodes with sulphur content close to zero, it was found that increasing sulphur content contributes significantly to a decrease in the current efficiency and a rise in the carbon consumption. When going from 0 to 3.82 wt% S, the current efficiency decreased from 92 to 85% (1.8 % per 1 wt% S), and the carbon consumption rose from 108 to 128% (5.2 % per 1 wt% S).

3:00 PM

Concentration Gradients of Individual Anion Species in the Cathode Boundary Layer of Aluminium Reduction Cells: *Asbjorn Solheim*¹; ¹SINTEF

It is well known that the system NaF-AlF₃, which constitutes the "backbone" of the electrolyte used in primary aluminium manufacture, forms Na⁺, F⁻, and a number of fluoro-aluminate anion complexes in the molten state. Since mainly the Na⁺ ion carries electric current, the aluminium-containing complexes must diffuse towards the cathode, resulting in concentration gradients within the cathode boundary layer. Starting from a structural model for the melt containing five anion species, it was possible to calculate the concentration gradients of the individual ions using the Stefan-Maxwell equation for diffusion in a multi-component system. Generally, AlF₄⁻ and AlF₆³⁻ were transported towards the cathode, while F⁻ and AlF₃²⁻ moved away from the cathode. For NaF/AlF₃ molar ratios higher than 2.0, AlF₅²⁻ moved towards the cathode, while it diffused away from the cathode in more acid melts.

3:20 PM

Electrochemical Behaviour of Carbon Anodes in Na₃AlF₆-K₃AlF₆-Based Low-Melting Electrolytes for Aluminium Electrolysis: *Guihua Wang*¹; Xiaofei Sun¹; Wenyao Zhao¹; Dandan Yang¹; ¹University of Science and Technology Beijing

The anode processes of carbon electrodes in 49wt%Na₃AlF₆-21wt%K₃AlF₆-30wt%AlF₃-Al₂O₃ (saturated or free) melts were studied in a wide range of potentials by cyclic voltammetry. Two peaks were observed on the cyclic voltammograms trace. It is considered that the first peak corresponds to the discharge of oxide ions (or residual oxide ions), and the discharge of fluoride ions occur after the discharge of oxide ions, leading to the anode effect. As the potential increases, PFC gases emission occurs, and the current increases. Compared to the cyclic voltammograms trace obtained from the traditional electrolyte for aluminium industry 84wt%Na₃AlF₆-11wt%AlF₃-5wt%CaF₂-Al₂O₃ (saturated), it can be seen, as the addition of a large amount of AlF₃ and the decrease of electrolysis



TMS 2012

141st Annual Meeting & Exhibition

temperature, the current of the second peak increases obviously. The performance of low temperature aluminium electrolysis increases the risk of a larger emission rate of PFCs.

3:40 PM Break

4:00 PM

Operating Parameters of Aluminum Electrolysis in a KF-AlF₃ Based Electrolyte: Olga Tkacheva¹; John Hryn¹; Jeff Spangenberg¹; Boyd Davis²; Tom Alcorn³; ¹ANL; ²KPM; ³Noranda Aluminum

Sustained operation of the low-temperature, potassium-cryolite-based, aluminum electrolysis process in 20 and 100 Ampere cells fitted with vertical metal anodes and wetted cathodes was performed. The current efficiency, the amount of consumed alumina and the amount of produced aluminum were calculated during electrolysis based on the measured amount of oxygen generated on the anode. The purity of the recovered aluminum was controlled during electrolysis. The cell voltage anomalies caused by the NaF presence in the potassium cryolite were studied using a quasi-reference electrode.

4:20 PM

Effect of KF Additions in NA3ALF6-AL2O3 Electrolytes on Expansion of Cathode Blocks: Zhang Yuehong¹; Feng Naixiang¹; Peng Jianping¹; Wang Yaowu¹; Han Yeyu¹; Zhai Xiujin¹; ¹Northeastern University

Effects of K and Na on expansion of cathode carbon block were studied through an improved instrument measured expansion rate. For a 30% graphitic cathode block, based on the results, in KCl-NaCl electrolysis system K and Na are reacting with graphite and forming graphite intercalation compounds (GICs) during penetration from surface to inside of the cathode block, and K plays more important role in expansion and penetration than Na. The results show that for a NaF-AlF₃-Al₂O₃ system, containing 7% Al₂O₃ and with CR=6.5, during electrolysis at 1000 °C the expansion rate of the 30% graphitic cathode block is increased from 2.3% to 8.7% with 0 to 7% KF addition to the electrolytes. It is also showed that the expansion due to K and Na penetration in cathode become lower with increasing content of graphite in cathode material, and that expansion in the fully-graphitized cathode is very low.

4:40 PM

Preparing Aluminium-Scandium Inter-alloys during Reduction Process in KF-AlF₃-Sc₂O₃ Melts: Qiaochu Liu¹; Jilai Xue¹; Jun Zhu¹; Chunyang Guan¹; ¹University of Science and Technology Beijing

Al-Sc Alloys have attracted much attention in recent years due to their great potential in many advanced applications. In this work, Al-Sc alloys were prepared on liquid Al cathode in KF-AlF₃-Sc₂O₃(CR=1.22) melts during reduction process. Scanning electron microscope (SEM) and Inductively coupled plasma atomic emission spectroscopy (ICP-AES) showed that the primary Al₃Sc were highly faceted and Sc contents were 0.44 and 0.73% mass in the alloys produced at 750 °C with current density of 0.5 and 1.0A/cm², respectively. At 1.0 A/cm², Sc content increased to 0.95% mass at 800 °C and 1.27% mass at 850 °C. But higher mass loss from the melts was found with increased operating temperatures. During reduction process, the decomposition voltage of Sc₂O₃ was 1.7 - 1.8V, closing to its theoretical value (1.72V at 750 °C). Cyclic Voltammetry and Linear Sweep Voltammetry studies demonstrate that the reduction of Sc³⁺ occurs at liquid Al cathode and Al₃Sc formation is electrochemically irreversible.

5:00 PM

Liquidus Temperatures of the System Na₃AlF₆-K₃AlF₆-AlF₃: Lai Yanqing¹; Xin Pengfei¹; Tian Zhongliang¹; Wei Chenjuan¹; Chen Duan¹; Li Jie¹; ¹Central South University

Liquidus temperatures for the primary crystallization of the molten salt system Na₃AlF₆-K₃AlF₆-AlF₃ for aluminum electrolysis were determined by thermal analysis. The data were fitted to an empirical

equation $T=3478-1867 \times [KR]^{0.12}-12.97 \times [AlF_3]^{1.14}+3.538 \times [AlF_3] \times [KR]^{0.98}-0.505 \times [AlF_3]^{1.24} \times [KR]^{1.23}$ Where T is the liquidus temperature in °C and the square brackets denote wt% of components in the system Na₃AlF₆-K₃AlF₆-AlF₃ with $[KR]=K_3AlF_6/(Na_3AlF_6+K_3AlF_6)$. The composition limitations are 20% < AlF₃ < 30%, and 15% < KR < 30%. The isothermal diagram of the molten salt system Na₃AlF₆-K₃AlF₆-AlF₃ was obtained in this composition limitation. Keywords: liquidus temperature, the Na₃AlF₆-K₃AlF₆-AlF₃ system, an empirical equation

Atomistic Effects in Migrating Interphase Interfaces - Recent Progress and Future Study: Interface Migration and Alloy Partitioning

Sponsored by: The Minerals, Metals and Materials Society, TMS Materials Processing and Manufacturing Division, TMS/ASM: Phase Transformations Committee

Program Organizers: Tadashi Furuhashi, Institute for Materials Research, Tohoku University; Sudarsanam Babu, Ohio State University; Hatem Zurob, McMaster University; Jian-Feng Nie, Monash University; Wen-Zheng Zhang, Tsinghua University; James Howe, University of Virginia

Tuesday PM
March 13, 2012

Room: Europe 3
Location: Dolphin Resort

Session Chairs: Hatem Zurob, McMaster University; Amy Clarke, Los Alamos National Laboratory

2:00 PM Invited

Partitioning and Austenite Reversion at Martensite-Austenite Interfaces in Mn-Steels: Dierk Raabe¹; Dirk Ponge¹; Gerhard Inden¹; Julio Millán¹; Pyuck-Pa Choi¹; ¹Max-Planck-Institut

We present atom probe tomography and simulation results of Mn partitioning and segregation effects at martensite-austenite phase boundaries in a precipitation-hardened maraging TRIP steel with 12.2 at.% Mn after a maraging heat treatment (450°C, 48 hours). The system reveals strong compositional changes across the phase boundaries, particularly of Mn. More specific, we observe a change from 5 at.% Mn in martensite to 27 at.% Mn at the martensite-austenite interface. We explain this in terms of partitioning and kinetic freezing. These two effects jointly lead to local austenite reversion. The effects on the mechanical properties are discussed.

2:30 PM

Ferrite-to-Austenite and Austenite-to-Ferrite Phase Transformation in a Fe-2 wt% Mn Alloy Studied In-Situ with 3DXRD Utilizing Synchrotron Radiation: Hemant Sharma¹; Richard Huizenga¹; Jilt Sietsma¹; S. Erik Offerman¹; ¹Delft University of Technology

Analysis of the ferrite-to-austenite transformation data reveals the occurrence of massive transformation from ferrite to austenite. The transformation is characterized by an initial sharp increase in austenite volume fraction above T₀ to about 0.92. Remarkably, this is followed by no change in austenite volume fraction for about 50 K, after which the rest of ferrite transforms to austenite. A similar phenomena is observed during austenite-to-ferrite transformation during cooling. At about 50 K above T₀, a small amount of ferrite (0.15) is formed followed by an arrest in the rate of transformation for 110 K. This is followed by a sharp transformation of the rest of austenite into ferrite (massive). Repetition of the heat treatment on the same sample(s) shows same character, but with increased fractions of 'retained ferrite' during ferrite-to-austenite phase transformation and vice versa. The link between the observations and Mn redistribution during the phase transformations is explored.

3:00 PM

Transitions in Austenite Decomposition Products in a Fe-10%Ni/Fe-5%Ni Diffusion Couple with 0.1%C and 0.3%C: *Eduardo Monlevade*¹; Arthur Nishikawa²; Helio Goldenstein²; ¹Mangels Indústria e Comércio Ltda. - Steel Division; ²Engineering School - University of São Paulo

Two samples extracted from a Fe-5%Ni/Fe-10%Ni diffusion couple were carburized to 0.1%C and 0.3%C. Both samples were austenitized and isothermally transformed at 500°C for 10 minutes in a tin bath. In the 0.1%C sample, allotriomorphic ferrite was present in the low nickel region; with rising nickel content, the decomposition products were upper bainite and pearlite, and finally large blocks of ferrite without carbides. At higher nickel contents, grain boundary allotriomorphs and elongated ferrite particles coexisted at early stages of austenite decomposition. In the 0.3%C sample, upper bainite and degenerate pearlite were seen at the low nickel end of the diffusion couple. With increasing nickel content, the degenerate pearlite disappears substituted by upper bainite, and large formations of parallel ferrite plates are observed at higher nickel regions. Small crystalline misorientations (ca. 7°) were observed between nearby parallel ferrite plates, indicating that its formation occurs by separate nucleation events.

3:20 PM

New Observation of PE Kinetics in Fe-C-X and Fe-N-X Systems: *Mingxing Guo*¹; Catherine Silva¹; Hatem Zurob¹; ¹McMaster University

The effect of interstitial and substitutional solute elements on the kinetics of transformation in steels has been the focus of considerable investigation. In this contribution, the growth kinetics of ferrite was investigated in Fe-0.56wt%C-1wt%Cu and Fe-2wt%N-1.43%Mn by accurately measuring the thickness of the ferrite layer formed during isothermal decarburization/denitriding treatment. In the Fe-C-Cu system the growth kinetics closely follow the prediction of the paraequilibrium (PE) model over the temperature range 755-855°C with no evidence of a transition to local equilibrium kinetics over time. Paraequilibrium is also observed at low-temperatures (<725°C) in the Fe-Mn-N system with evidence of a transition to LENP at longer times. The results are discussed in terms of the recent kinetic transition models in the literature.

3:40 PM Break

4:00 PM Invited

Analysis at the Nanoscale of the Austenite/Ferrite Interface during Ferrite Formation: *Mohamed Gouné*¹; Frederic Danoix²; ¹ArcelorMittal Maizières Research; ²CNRS - Université de Rouen

The need for lightweight automotive structures is a high driving force to develop new steel microstructure concepts for high strength sheets products, including dual phase (DP) steels. The final microstructure of DP steels is partly controlled by the austenite to ferrite transformation, which is dependant on the chemistry of the α/γ interface. 3D Atom Probe Tomography offers great promises to investigate interfacial and near-interface chemistry, and to determine the tie-line governing the a/g transformation. Manganese and carbon profiles obtained by APT are broadly consistent with predictions of a model which includes a transition from Paraequilibrium to Local Equilibrium Non Partitioning contact conditions. Furthermore, the carbon supersaturated martensite will develop, even during holding at RT, carbon fluctuations that will affect the carbon profile resulting from the α/γ transformation. The methods presented show the high promises for future comparisons between predicted and experimental profiles.

4:30 PM

Manganese Partitioning during Pearlite Growth in Fe-C-Mn Medium Carbon Steel: *Maria Martin-Aranda*¹; Juan Cornide¹; *Carlos Capdevila-Montes*¹; Michael Miller²; Francisca Caballero³; Robert Hackenberg³; Esteban Urones-Garrote⁴; ¹CENIM-CSIC; ²ORNL; ³LANL; ⁴Universidad Complutense

The kinetics of the isothermal austenite-to-pearlite transformation in a high purity Fe-C-Mn steel at temperature of 695 °C have been investigated. In this austenite + ferrite + M3C phase field region, it has been reported

that pearlite invariably transforms under non-steady-state conditions with a growth rate which decreases and an interlamellar spacing that increases (divergent) in time. In this work, detailed scanning transmission electron microscopy and atom probe tomography measurements of the manganese concentration profiles across the γ/α and $\gamma/M3C$ growth interfaces were performed as a function of time in order to clarify if local equilibrium (LE) conditions are fulfilled during pearlite growth. Research at the Oak Ridge National Laboratory SHaRE User Facility was sponsored by the Scientific User Facilities Division, Office of Basic Energy Sciences, U.S. Department of Energy

4:50 PM

Formation of Grain Boundary Ferrite in Eutectoid and Hypereutectoid Steels: *Goro Miyamoto*¹; Yosuke Karube¹; Tadashi Furuhashi¹; ¹Tohoku University

Grain boundary ferrite (GB- α) in high carbon pearlitic steels has been considered as one of the reasons for losing ductility of pearlite structure although details have not been well clarified. Thus, effects of transformation temperature and carbon content on the formation of GB- α have been examined in this study. Microstructure of eutectoid and hypereutectoid steels whose nominal compositions are Fe-1%Mn-0.75%C and Fe-1%Mn-1.05%C (mass%), respectively, transformed isothermally at temperatures ranging between 873K and 993K were investigated. GB- α was formed in both eutectoid and hypereutectoid steels from 873K to 948K. The greatest volume fraction of GB- α was obtained in the eutectoid steel transformed at 873K. The fraction decreased by raising transformation temperature or increasing carbon content. In contrast, large amount of GB- α formed in the hypereutectoid steel transformed at 973K, which is just below eutectoid temperature. These facts indicate that there are two different formation mechanism of GB- α depending on transformation temperature.

Biological Materials Science Symposium: Biological and Bio-Inspired Materials II: Hard Biomaterials

Sponsored by: The Minerals, Metals and Materials Society, TMS Electronic, Magnetic, and Photonic Materials Division, TMS Structural Materials Division, TMS: Biomaterials Committee
Program Organizers: Nima Rahbar, University of Massachusetts Dartmouth; Candan Tamerler, University of Washington; Po-Yu Chen, University of California, San Diego; Molly Gentleman, Texas A&M University

Tuesday PM
March 13, 2012

Room: Swan 7
Location: Swan Resort

Session Chairs: Po-Yu Chen, National Tsing Hua University; Dwayne Arola, University of Maryland Baltimore County

2:00 PM Invited

Biomimetic Scaffolds for Regeneration: *Peter Ma*¹; ¹University of Michigan

Regenerative medicine aims to develop biological restorations for lost or diseased tissues. Scaffolding materials provide three-dimensional environments for cells and serve as templates to guide tissue regeneration. Our laboratory develops biomimetic polymer scaffolds that recapitulate certain advantageous features of the natural extracellular-matrices (ECM) and impart engineering design to facilitate tissue regeneration. Novel phase separation techniques have been developed in our laboratory to create biodegradable ECM-mimicking nanofibrous scaffolds. To repair complexly shaped tissue defects, an injectable cell carrier is desirable to achieve accurate fit and to minimize surgical intervention. To incorporate the ECM-mimicking nanofibrous feature into an injectable scaffold format, we have recently developed star-shaped biodegradable polymers that can self-assemble into nanofibrous hollow microspheres as novel



injectable scaffolds. These scaffolds have been shown to advantageously support various stem cells for tissue regeneration, demonstrating the advantages of biomimetic approach in regenerative medicine.

2:30 PM

Hydroxyapatite-Coated Titanium-Based Biomaterials Prepared by RF Magnetron Sputtering: *Guoqing Wang*¹; Liping Niu¹; Sheng Yang¹; TingTing Gao¹; ¹College of Science, Northeastern University

Hydroxyapatite (HAP) coatings are widely used to improve the biocompatibility of the substrate. In this study, titanium-based HAP coatings were prepared by RF magnetron sputtering method, and coating structure and composition were analysed by SEM,EDX and IR spectroscopy. When the sputtering power was 290 W, sedimentary was 120-180min, nano-HAP surface coating has formed on the surface of Ti-based, the average size of grain is 48nm, and elemental composition of the coating is consistent with the HAP coating. coating thickness is 513±15~985±25 nm, Ca/P=1.51±0.03~1.84±0.04, and surface of the coating is smooth, uniform and dense. Adhesion strength of Ti/HAP is more than 25 MPa.

2:50 PM

Estimation of Residual Stresses in Bone Resulting from Surface Treatments: *Jose Viray*¹; Dwayne Arola¹; ¹University of Maryland Baltimore County

Surface treatments are often used to introduce residual stresses within engineering materials for promoting corrosion resistance and extending fatigue life. The objective of this investigation was to identify if residual stresses can be introduced within cortical bone using an airjet treatment and the relationship between the process parameters and the magnitude of residual stress. Sections of cortical bone were treated with an airjet laden with glass or alumina particles. Results distinguished that residual stresses can be introduced within bone using an airjet treatment and that the maximum stresses reach values equivalent to the yield strength of bone. The magnitude of stress was found to be a function of the treatment parameters (treatment intensity, particle size, air pressure) and the bone's microstructure. It was also found that residual stresses in bone have a limited duration due to a viscoelastic recovery process that begins immediately following the treatment. (Supported by NIDCR DE016904).

3:10 PM

Micro-Mechanical Characterization of Bovine Cortical Bone in Bending and Uniaxial Compression: *Kelly Kranjc*¹; Pravin Ramesh¹; Katharine Flores¹; ¹Ohio State University

Mechanical testing of bone at small length-scales offers the possibility of understanding the behavior of individual microstructural building blocks, which can then be used to model the behavior of the aggregate under different conditions, such as age or disease state. In this work, micropillars and microcantilever beams with dimensions on the order of 10 microns are selectively machined within regions of interest, such as osteons, via femtosecond laser machining and focused ion beam milling techniques. The load-displacement response under a variety of test conditions is then obtained using a modified nanoindenter. Elastic modulus measurements of wet and dry bovine cortical bone are in good agreement with bulk measurements. Load relaxation experiments reveal two relaxation time constants which are hypothesized to be associated with processes in the organic and inorganic phases, respectively. Efforts to characterize the cyclic response and microstructural changes associated with damage accumulation will also be discussed.

3:25 PM

The Elastic Modulus of Trabecular Bone: Modeling and Experiments: Elham Hamed¹; Ekaterina Novitskaya²; Jun Li¹; Po-Yu Chen²; *Iwona Jasiuk*¹; Joanna McKittrick²; ¹University of Illinois at Urbana-Champaign; ²University of California, San Diego

Untreated, demineralized, and deproteinized bovine trabecular bones, taken from femoral head, were studied. Their mechanical properties were obtained using compression test. Optical and scanning electron microscopies were used to examine bone microstructural features. Bone porosity for all three groups was estimated by analyzing micro-computed tomography scans, while bone mineral content was estimated using ash content method. These served as inputs and validation for our multiscale model which was employed to theoretically predict elastic moduli of trabecular bone from all three groups. The model assumes trabecular bone to be a porous composite material with a hierarchical structure ranging from nanoscale (collagen-mineral level) to mesoscale (trabecular bone level). The modeling methods accounted for the interpenetrating structure of collagen and mineral phases. Finally, the modeling results were compared with the experimental data obtained by compression testing. Good agreement was obtained between the experimental and modeling results for untreated, demineralized, and deproteinized bones.

3:40 PM Break

3:50 PM Invited

Adhesion in Nanoparticles for Cancer Detection and Treatment: *Winston Soboyejo*¹; ¹Princeton University

This paper explores the role that adhesion can play in the design of interfaces in nanoparticles that are relevant to cancer detection and treatment. These include ligand-conjugated nanoparticles and nanoparticle clusters that are being developed for the early detection and treatment of breast cancer. Dip-coating and atomic force microscopy techniques are used to measure the adhesion between gold or magnetite nanoparticles that are relevant to cancer detection and treatment. These include the adhesive interactions between molecular recognition units (MRUs) that are able to target breast cancer cells, and the interactions between nanoparticle clusters that are relevant to the localized delivery of chemotherapy drugs to breast cancer cells. The implications of the results are discussed for the design of nanoparticle clusters for the early detection and treatment of cancer.

4:20 PM

The Importance of Decussation on the Crack Growth Resistance of Enamel: *Mobin Yahyazadehfar*¹; Dwayne Arola¹; ¹University of Maryland Baltimore County

The most dominant microstructural feature of enamel is a network of highly calcified rods extending between the surface of teeth and the dentin-enamel junction (DEJ). Though oriented parallel to one another near the tooth's surface, the rods are organized into a series of oblique layers approaching the DEJ. In this investigation the importance of this transition in microstructure (i.e. decussation) on the crack growth resistance of enamel was studied. Sections of enamel were obtained from molars of young patients and used in quantifying the incremental crack growth resistance for cracks extending in two orientations. Results showed that decussation is critical to the crack growth toughening of enamel and it causes spatial variations in the degree of anisotropy exhibited by this tissue. The decussation pattern forces cracks to exhaust energy by extending peripherally about the surface of teeth rather than continuing inwards towards the pulp. (Supported by NIDCR DE016904)

4:40 PM

Improved Biocompatible Zirconia and Alumina Based Ceramic Composites: *Koushik Biswas*¹; *Ajoy Pandey*¹; ¹Indian Institute of Technology Kharagpur

Ceria/yttria stabilized zirconia and ceria/yttria stabilized zirconia toughened alumina powders were synthesized by wet chemical method and subsequently consolidated to near full density following an optimized calcination and sintering route. Microstructure and mechanical properties were correlated. Accelerated ageing studied at 134 °C/0.2 MPa shows nucleation of orthorhombic/monoclinic zirconia phase with significantly reduced transformation for CSZ. Surfaces after fretting wear show evidences of microcrack formation, grain pull outs and abrasion. CSZ specimens show better results after ageing. Biocompatibility tests reveal calcium ortho-phosphate and hydroxyapatite like biomineral layers formation on surface of specimens when immersed in simulated body fluid at 37.5 °C. Differential rates of nucleation of minerals for alumina and zirconia based specimens suggest that Zr-OH bond helped accelerated HAp nucleation compared to Al-OH. Incubation and attachment of multi-layered interconnected human osteoblast like cells (MG63) on surfaces; cell proliferation and differentiation were suggesting biocompatibility of the developed materials.

5:00 PM

Effect of Bacteria on Mechanical Properties of Dental Composites: *Dmytro Khvostenko*¹; *Jamie Kruzic*¹; *John Mitchell*²; *Jack Ferracane*²; ¹Oregon State University; ²Oregon Health & Science University

One problem in restorative dentistry is bacterial biofilm development at the tooth-filling interface which can lead to demineralization of tooth tissue and secondary caries. Furthermore, bacterial exposure may also be deleterious to the composite mechanical properties. Bioactive glass (BAG) added as an antimicrobial agent may help mitigate this problem and enhance composite durability. In phase I of this study fatigue crack growth, fracture toughness and 3-point beam bending experiments are being performed on bulk composite samples after two different soaking treatments: 1) 24 hours in distilled water and 2) 60 days in trypticase soy agar broth with streptococcus mutans bacteria. BAG containing composite behavior will be compared to a commercial composite (Heliomolar). In phase II, the issue of demineralization of marginal tooth structure will be examined by in-vivo fatigue testing of tooth samples restored with BAG containing composites to assess the effect of combined mechanical loading and exposure to bacteria.

5:15 PM

Micromechanical Analysis of Strain-Induced Martensitic Transformation in Biomedical Co-Cr-Mo-N Alloy: *Byoung-Soo Lee*¹; *Shou Suzuki*¹; *Hiroaki Matsumoto*²; *Yuichiro Koizumi*²; *Akihiko Chiba*²; ¹Department of Materials Processing, Graduate School of Engineering, Tohoku University; ²Institute for Materials Research, Tohoku University

Biomedical Co-Cr-Mo-N alloys are widely used as implant materials such as hip and knee joints. Strain-induced e-hcp martensitic phase (e-phase) has both beneficial and detrimental characteristics, i.e. enhancement in wear resistance and reduction in deformability. Therefore, it is important to understand the role of e-phase during plastic deformation. Recently, a method proposed by Wilkinson [A.J. Wilkinson, D. Randman, Phil. Mag. A, 90(2010) 1159] has been developed into a powerful tool to determine elastic strain. This study deals with the micromechanical analysis of e-phase in biomedical Co-Cr-Mo-N alloy by means of EBSD-Wilkinson method. Most e-phases nucleated at twin and grain boundaries, and then grew in specific grains, which are oriented to near [101] and [111]. The grains are classified into soft grains ([101] and [111]) and hard grain ([001]). The e-phase nucleates preferentially at the interface between hard and soft grains because of local stress related with heterogeneous stress distribution.

Bulk Metallic Glasses IX: Structures and Mechanical Properties II

Sponsored by: The Minerals, Metals and Materials Society, TMS Structural Materials Division, TMS/ASM: Mechanical Behavior of Materials Committee

Program Organizers: Peter Liaw, The University of Tennessee; Hahn Choo, The University of Tennessee; Yanfei Gao, The University of Tennessee; Gongyao Wang, University of Tennessee

Tuesday PM
March 13, 2012

Room: Swan 6
Location: Swan Resort

Session Chairs: A. Greer, Univ of Cambridge; J. Eckert, IFW Dresden

2:00 PM Keynote

Plastic Deformation and Structure Changes in Metallic Glasses: *A. Greer*¹; ¹Univ of Cambridge

Room temperature (RT) plasticity in metallic glasses is localized on shear bands and associated with dilatation. Elastostatic compression of a metallic glass at RT at less than the yield stress increases the heat of relaxation in the glass, improves its plasticity, and causes dilatation. By deforming homogeneously at RT, relaxation of deformation-induced changes is suppressed, with remarkable effects: the local volume increase associated with each atom in a shear transformation zone is of the order of one atomic volume. The structural effects of deformation and annealing appear to be opposite: “rejuvenation” versus “ageing”. Annealing causes the Poisson’s ratio to decrease. However, elastostatic deformation, despite evident dilatation, also causes Poisson’s ratio to decrease. This paradox is explored through new results on the effects of heavy deformation at liquid-nitrogen temperature. The results may be relevant for interpreting shear banding and the limits to metallic-glass properties.

2:30 PM

Determination of Phase Separation in Amorphous Pd(40+0.5x)Ni(40+0.5x)P(20-x) BMG for x = 0 to 4: *Man Tat Lau*¹; *Si Lan*¹; *Yeuk Lan Yip*¹; *Hin Wing Kui*¹; ¹Chinese University of Hong Kong

Recently, it was found that amorphous Pd_{41.25}Ni_{41.25}P_{17.5} alloys undergo phase separation. On the other hand, the alloy Pd₄₀Ni₄₀P₂₀, which is known to be an easy glass former, is thermally stable even at temperatures about 100 K above its glass transition temperature T_g. In this work, alloy systems of Pd_{40+0.5x}Ni_{40+0.5x}P_{20-x} for x = 0 to 4 were studied for amorphous phase separation by high resolution TEM techniques, which include HREM and high-angle angular dark-field (HAADF) EDX spectrum mapping. It was found that when x = 0, i.e., the alloy system Pd₄₀Ni₄₀P₂₀ falls outside the metastable liquid miscibility gap. On the other hand, for x = 1 to 4, the corresponding alloys are inside the metastable liquid miscibility gap.

2:40 PM Invited

Properties of Shear Transformation Zones in Metallic Glasses: *Michael Atzmon*¹; *JongDoo Ju*¹; *Dongchan Jang*²; ¹University of Michigan; ²Caltech

The concept of shear transformations was coined by Argon, based on observations in bubble-raft models of glasses [1]. Later, 3-D observations in colloidal glasses and molecular dynamics simulations confirmed this picture. Because of the disordered structure of glasses, there is no known contrast mechanism for imaging shear transformation zones (STZs). Diffraction techniques provide macroscopic averages and are unlikely to reveal detailed information about STZs. Using anelastic relaxation experiments, we have recently been able to resolve a hierarchy of STZs that differ from each other by a single atom. In this talk, the results will be contrasted to previous reports, and the implications for the understanding of glass behavior will be discussed. I. A. S. Argon, Acta Metall. 27, 47 (1979).

TUESDAY PM



TMS 2012

141st Annual Meeting & Exhibition

3:00 PM

Mechanical Relaxation in Bulk Metallic Glasses: *Jichao Qiao*¹; J.M. Pelletier¹; W.H. Wang²; ¹INSA-Lyon; ²Institute of Physics, Chinese Academy of Sciences

The primary (or a) relaxation was observed in various bulk metallic glasses (BMGs) forming liquids. At lower temperature (or higher frequency), many BMGs present second relaxation processes (β relaxation). Unfortunately, structural origin of the second structural relaxation in BMGs is not clear. In this investigation, the two multicomponent BMGs, namely, Zr_{41.2}Ti_{13.8}Cu_{12.5}Ni₁₀Be_{22.5} and La₆₀Ni₁₅Al₂₅, were carried out by mechanical spectroscopy (DMA). The correlation between mechanical relaxation and atomic mobility was analyzed. Compared with other non-crystalline solids, such as polymers and amorphous mineral glasses, the second relaxation depends on the chemical nature. Connected with other based BMGs, the present work tries to shed light on the mechanism of the second relaxation in amorphous alloys.

3:10 PM

High Temperature Deformation and Twin Roll Strip Casting Ability of Cu-Zr-based Bulk Metallic Glasses: *Kwang Seok Lee*¹; Young Seon Lee¹; ¹Korea Institute of Materials Science

A study has been made to investigate both high temperature deformation and twin roll strip casting ability of Cu-Zr-based Bulk Metallic Glasses (BMGs). High temperature deformation behavior has first been revealed by conducting a series of compression tests with various initial strain rates at several temperatures within supercooled liquid region. Furthermore, the possibility of continuous roll casting for Cu-Zr-based BMGs was investigated as a form of glassy sheet by means of twin roll strip casting under various process conditions such as roll gaps and wheel rotation speed, which directly related to the cooling rate. Various analyses for strip samples through the rolling and thickness directions were then performed in order to verify the influence of process conditions on the mechanical evolution and subsequent mechanical behaviors. Another application of these BMGs as a joining between dissimilar metals was additionally discussed.

3:20 PM Break

3:35 PM Invited

Formation of B2 CuZr in Metastable CuZr-Based Bulk Glass Forming Alloys: K.K. Song¹; S. Pauly¹; Y. Zhang¹; P. Gargarella¹; N.S. Barekar¹; U. Kühn¹; M. Stoica¹; *J. Eckert*²; ¹IFW Dresden; ²University of Tennessee

Bulk glassy alloys and composites have potential for being used in various fields as advanced high performance materials. However, monolithic amorphous alloys usually lack ductility, and an additional toughening phase is often needed to improve plasticity and to promote local shear events to be distributed more homogeneously in the material. Accordingly, it is important to develop new alloys and composite microstructures by introducing microstructural heterogeneities on different length-scales and combining phases with different elastic constants, hardness and strength, such as to improve the overall mechanical performance of the alloys. As an example, recent results obtained through systematically investigating the formation of the high-temperature B2 CuZr intermetallic phase in a variety of metastable CuZr-based alloys will be presented. The results demonstrate that a B2 CuZr solid phase transformation exists at high temperature. This approach aims to promote the development of metastable CuZr-based glass composites with enhanced deformability.

3:55 PM

Characteristics of Metallic Glass Thin Films Deposited by Using RF, DC and Pulsed DC Sputtering Techniques: *Chia-Lin Li*¹; Jyh-Wei Lee²; Jinn Chu¹; ¹National Taiwan University of Science and Technology; ²Mingchi University of Technology

Zr-based metallic glass thin films were prepared by using different PVD processes, namely RF, DC and pulsed DC sputtering techniques. Microstructures of thin films thus prepared were examined by an

atomic force microscopy (AFM), scanning electron microscopy (SEM) and transmission electron microscopy (TEM). The nanoindenter and differential scanning calorimetry (DSC) were used to evaluate the hardness and thermal behavior, respectively. According to experimental results, various degrees of amorphization and nanocrystallization can be observed in the as-deposited films. A series of comparisons on microstructures, crystallographic and mechanical properties of Zr-based metallic glass thin films will be discussed in the present paper.

4:05 PM Invited

Structural and Mechanical Heterogeneity of Bulk Metallic Glasses: *Mingwei Chen*¹; ¹Tohoku University

Stress-driven mechanical instability of metallic glasses is usually associated with spatially heterogeneous shear transformation zones (STZs) that play a crucial role in the yielding, plastic deformation and failure of metallic glasses. However, the atomic origins and physical nature of STZs have been debated for many years and, particularly, lack experimental insights. Recently, we have developed several experimental approaches to characterize atomic structure and STZs of metallic glasses. Combining with ab initio molecular dynamics simulation, we provide compelling evidence that the STZs arise from atomic-scale structural and chemical heterogeneity of metallic glasses. The size and physical nature of measured STZs are consistent well with a wide-range of MD simulations and coincide with the atomic structure model of metallic glasses.

4:25 PM Invited

Intrinsic Yield Strength and Elastic Strain Limit of Metallic Glasses: *Evan Ma*¹; ¹Johns Hopkins University

We report quantitative in situ tensile tests inside a transmission electron microscope for metallic glasses (MGs). Our experiment employs submicron-sized specimens, high-resolution measurements of the loading forces and accurate strain measurement with deposited markers on the gauge length. The quantitative experiment establishes that the MGs have intrinsic yield strength and yield strain about twice as large as the already-high elastic limit observed in macroscopic samples, in line with model predictions of the intrinsic elastic limit in the absence of heterogeneous shear band nucleation facilitated by extrinsic factors. We also discuss the origin of the apparent "work hardening" seen in the tensile stress-strain curves.

4:45 PM

Critical Temperature for Ductile-to-Brittle Transition for Metallic Glasses: *Golden Kumar*¹; Pascal Neibecker²; Jan Schroers¹; ¹Yale University; ²Universitaet des Saarlandes

A comprehensive analysis of plasticity (and toughness) in bulk metallic glasses (BMGs) is presented. Different effects such as: contribution of shear modulus/bulk modulus ratio, structural relaxation, and cooling rate effect are evaluated for Pt_{57.5}Cu_{14.7}Ni_{5.3}Pt_{22.5} (Pt-BMG), Pd₄₃Cu₂₇Ni₁₀Pt₂₀ (Pd-BMG), and Zr₄₄Ti₁₁Ni₁₀Cu₁₀Be₂₅ (Zr-BMG). We introduce a critical temperature, T_C , which is an intrinsic feature of a BMG former above which the BMG does not embrittle. We demonstrate that T_C/T_g ratio indicates the embrittlement sensitivity of a BMG due to annealing and cooling rate. This ratio is larger than one for Pd-BMG and smaller than one for the Pt-BMG. As a consequence, Pd-BMG is more sensitive to cooling rate and annealing induced embrittlement. In contrast, Pt-BMG does not embrittle during sub- T_g annealing or at practically achievable slow cooling rates. Study of shear modulus/bulk modulus ratio for Pd-BMG and Pt-BMG does not follow the previously proposed critical value for ductile to brittle transition.

4:55 PM Invited

Influence of Shear Band on the Mechanical Behavior of Metallic Glasses: *Yi Li*¹; ¹National University of Singapore

Shear band is the key feature that controls the plastic deformation process of metallic glasses (MGs). However, the investigation directly on the shear band and its influence on the plastic deformation are rarely conducted as it is perceived as extremely narrow. The deformation

and failure of MGs is really an instability process that begins with the formation of shear bands. Here we will show our studies on the formation of shear band, the property of shear band and the influence of shear band formation on the plastic behavior of metallic glasses.

5:15 PM Invited

Review on the Use of Bulk Metallic Glass for Multi-Scale Tooling Applications: *David Browne*¹; Dermot Stratton¹; Michael Gilchrist¹; Cormac Byrne¹; ¹University College Dublin

There is a growing demand for single-use disposable polymer devices with features at sub-micron scales. This requires resilient tooling which can be patterned to scales of the order of hundreds of nm. The requisite topology can be imparted to silicon but it is too brittle to be of use in a die to mold thousands of plastic parts. The polycrystalline nature of tool steel means it cannot be patterned with sub-micron detail. Some bulk amorphous alloys have the requisite mechanical properties to be viable as materials for such dies, and can be patterned – e.g. via embossing as a supercooled liquid into MEMS silicon or using FIB – with sub-micron features which may persevere over many thousands of molding cycles. The composition of the amorphous alloy must be carefully selected to suit the particular molding application (polymer/process). The state-of-the-art of is presented, along with results of our recent experimental investigations.

5:35 PM Invited

Intrinsic and Extrinsic Size Effects in the Deformation of Metallic Glass Nanopillars: *Jeff De Hosson*¹; O. Kuzmin¹; Y.T. Pei¹; ¹Univ of Groningen

Nano-sized pillars with diameters ranging from 90 to 600 nm of four amorphous alloys Cu₄₇Ti₃₃Zr₁₁Ni₆Sn₂Si₁, Zr₅₀Ti_{16.5}Cu₁₅Ni_{18.5}, Zr_{61.8}Cu₁₈Ni_{10.2}Al₁₀ and Al₈₆Ni₉Y₅, were fabricated and tested in-situ in a transmission electron microscope (TEM). Differences among the deformation behavior of tapered (1.5 - 3°) and taper-free systems were also investigated. Upon increasing size all the MGs examined show a transition from ductile-to-brittle behavior under compression, where the transition point, however, depends on the chemical composition of the specific metallic glass investigated. The lower the shear modulus/bulk modulus ratio, the larger pillar diameter above of which more brittle behavior occurs was found. Al₈₆Ni₉Y₅ taper-free metallic glass showed a transition threshold to brittle behavior at the largest diameter of 300 nm pillar. A micromechanical model is presented to explain the various dependencies. [1] Julia R. Greer and Jeff Th.M. De Hosson, Progress in Materials Science (2011) 56: 654–724

Cast Shop for Aluminum Production: Furnace

Sponsored by: The Minerals, Metals and Materials Society, TMS Light Metals Division, TMS: Aluminum Committee, TMS: Aluminum Processing Committee
Program Organizer: Trond Furu, Hydro

Tuesday PM
March 13, 2012

Room: Northern A4
Location: Dolphin Resort

Session Chair: Ragnhild Aune, NTNU

2:00 PM

Automated Measurement of Furnace Liquid Metal Heel and Full Furnace Weights: *John Courtenay*¹; ¹MQP Limited

The benefits of accurate measurement of furnace heel and full furnace weights are well accepted in terms of increasing % right first time batching, increasing productivity and eliminating short casts however the practical realization of a robust system has been problematic. The development of the BatchPilot system, which has overcome these difficulties, is described. To date 47 systems are in operation in 20 casthouses world wide and the

most recent innovations include a fully automated weighing capability and down line integration of the output data into the customer management data network.

2:20 PM

Development of a New Generation Electromagnetic Metal Moving System: *Graham Guest*¹; *Stephen Augustine*¹; *Fabienne Virieux*²; ¹Solios Thermal; ²Fives Solios

For modern aluminium cast house or re-melt facility, Fives Solios have developed an innovative new generation electromagnetic metal moving system called GENIOS that can be incorporated within new installations or retrofitted to existing furnaces. It can be fitted simply and safely to a wide range of furnace types using a patented modular interface and mounting concept. The prototype system is being trialled on a 70 tonne capacity static holding furnace at a large modern re-melting facility in Europe. In this particular case, GENIOS is configured to stir, aid silicon dissolution and transfer to a dedicated casting machine. The trials are in progress and expected to be completed during 2011. This paper will give an overview of the development of the concept and technology. It will also include a brief review of the performance of the prototype and general operational experiences together with comparisons with traditional technology.

2:40 PM

Six Years Experience from Low-Temperature Oxyfuel in Primary and Re-Melting Aluminium Cast Houses: *Henrik Gripenberg*¹; ¹Linde

Low-temperature Oxyfuel technology provides lower peak flame temperatures and a more uniform heat flux and temperature profile in the cast house furnace. The objectives with the technology are to improve melt rates, save energy, reduce dross formation and to reduce NO_x and CO₂ emissions. The paper will discuss operational results, process optimizations and economy from installations in reverberatory melting furnaces, mixing furnaces and tiltable rotary furnaces. The theory behind the technology will be described including reference to CFD simulations and laboratory testing. Low-temperature Oxyfuel is used by a number of aluminium producers including Hydro Aluminium, Sapa Heat Transfer AB, Stena Aluminium and others.

3:00 PM Break

3:20 PM

Energy and Maintenance Cost Savings Review at Several US Aluminum Die Cast Manufacturers Using Unique, Non-Wetting, Micro-Porous Refractory Products: *Robert Cullen*¹; *Kenneth McGowan*¹; ¹Westmoreland Advanced Materials, LLC

Over the past several years, many Aluminum Die Cast Manufacturers in North America have used unique, inherently non-wetting, micro-porous refractory products from Westmoreland Advanced Materials, LLC to line their melting and holding furnaces, as well as their molten metal transport systems. These manufacturers have experienced significant energy and maintenance cost savings through the use of these unique refractory products. A review of the technology behind these unique refractory products, along with specific examples of the energy and maintenance cost savings from several customers will be presented.

3:40 PM

Quality Comparison between Molten Metal from Remelted Sheets; Mill Finish and Coated: *Anne Kvithyld*¹; *Arne Nordmark*¹; *Derya Dispinar*¹; ¹SINTEF

Deterioration of metal quality caused contamination (e.g. coatings) is an issue in remelting of aluminium scrap. The molten metal quality from remelting sheet material with and without coating is compared. In the experiments the crucibles are placed inside a resistance furnace to ensure that the charges are melted under the same conditions at the same time, measuring temperature and hydrogen. The melts was subjected to (i) settling over night (ii) blowing air through a porous plug for 2.5 min to generate oxides and (iii) adding turnings. The bifilm index is used as a measure of metal quality. For mechanical testing 3-point bending was performed. The change in the metal quality was observed.



TMS 2012

141st Annual Meeting & Exhibition

4:00 PM

Numerical Modeling of Oxy-Fuel and Air-fuel Burners for Aluminium Melting: *Jorgen Furu*¹; *Andreas Buchholz*²; *Trond H. Bergström*³; *Knut Marthinsen*¹; ¹NTNU; ²Hydro Aluminium Deutschland GmbH; ³SINTEF Materials and Chemistry

In recent years oxy-fuel combustion has become an increasingly attractive alternative as a heating source when melting aluminium. A recently developed Low Temperature Oxy-fuel burner from Linde Gas was investigated and compared to a conventional cold air-fuel burner in an instrumented pilot scale furnace. Measurements and heating trials of aluminium samples were done for four different case studies. 3-dimensional CFD models using the commercial software package ANSYS Fluent were developed to attain additional knowledge and to demonstrate CFD as a viable tool to model aluminium melting furnaces. Good agreement was found between the numerical models and the measurements where the difference in heat transfer between the two burner technologies was clearly demonstrated.

CFD Modeling and Simulation in Materials Processing: Modeling of Casting and Solidification Processes I

Sponsored by: The Minerals, Metals and Materials Society, TMS Extraction and Processing Division, TMS Materials Processing and Manufacturing Division, TMS: Process Technology and Modeling Committee, TMS: Solidification Committee
Program Organizers: Laurentiu Nastac, The University of Alabama; Lifeng Zhang, Missouri University of Science and Technology; Brian Thomas, University of Illinois at Urbana-Champaign; Adrian Sabau, Oak Ridge National Lab; Nagy El-Kaddah, The University of Alabama; Adam Powell, Metal Oxygen Separation Technologies, Inc.; Hervé Combeau, Institut Jean Lamour

Tuesday PM
March 13, 2012

Room: Asia 4
Location: Dolphin Resort

Session Chairs: Hervé Combeau, Institut Jean Lamour; Charles-André Gandin, Mines ParisTech

2:00 PM Keynote

Multiscale and Multiphysic Models in CFD Modeling and Simulation of Solidification Process: *Hervé Combeau*¹; *Miha Založnik*¹; ¹Institut Jean Lamour

Prediction of solidification defects like macro and mesosegregations and of microstructures constitutes a key issue for industry. The development of models needs to account for several imbricated length scales and different physical phenomena. The goal of this presentation is to introduce the existing models and their principle. The main results of a benchmark on macrosegregation will be presented in order to emphasize the difficulties linked to the resolution of the equations of such models. The more recent applications of these models to solidification process will be presented (steel ingot, aluminum DC casting, VAR). Their ability to help in the understanding of complex phenomena like the competition between nucleation and growth of grains in the presence of convection of the liquid and grain motion will be discussed as well as their predictive capabilities. Finally, the main remaining key issues will be addressed.

2:30 PM Invited

3D CAFE Simulation of a Macrosegregation Benchmark Experiment: *Charles-Andre Gandin*¹; *T. Carozzani*¹; *H. Digonnet*¹; *M. Bellet*¹; ¹MINES ParisTech

Upon heat extraction from a vertical surface of a parallelepipedic domain filled with a metallic melt, thermal buoyancy driven convection of the liquid takes place. In case of a Sn-3wt%Pb alloy, Sn-rich solid forms

close the cooled vertical surface and segregation of Pb occurs. The latter phenomena is named microsegregation when it is only localized in the vicinity of the solid-liquid interface. But in addition to thermal convection, solutal buoyancy driven convection is induced by Pb microsegregation. As a consequence, Pb is redistributed in the entire domain and the so-called macrosegregation develops. This phenomena is simulated using a 3D CAFE model. It is compared with a benchmark experiment.

2:55 PM Invited

Modeling of Multiscale and Multiphase Phenomena in Material Processing: *Andreas Ludwig*¹; *Abdellah Kharicha*¹; *Menghui Wu*¹; ¹University of Leoben, Dep. Metallurgy

In order to demonstrate how CFD can help scientists and engineers to better understand the fundamentals of engineering processes, a number of examples are shown and discussed. The paper will cover (i) special aspects of continuous casting of steel including turbulence, motion and entrapment of non-metallic inclusions, and impact of softreduction; (ii) multiple flow phenomena and multiscale aspects during casting of large ingots including flow induced columnar-to-equiaxed transition and 3D formation of channel segregation; (iii) multiphase magneto hydrodynamics during electro-slag remelting; and (iv) melt flow and solidification of thin but large centrifugal castings.

3:20 PM

Numerical Simulation of Macrosegregation Formation during Solidification Accounting for Inoculants and Equiaxed Grain Transport: *Knut Omdal Tveito*¹; *Marie Bedel*²; *Miha Založnik*³; *Hervé Combeau*³; *Mohammed M'hamdi*⁴; *Arvind Kumar*³; *Pradip Dutta*⁵; ¹Norwegian University of Science and Technology; ²Institut Jean Lamour, Departement SI2M, CNRS – Nancy-Université – UPV-Metz, Ecole des Mines de Nancy; ³Institut Jean Lamour, Departement SI2M, CNRS – Nancy-Université – UPV-Metz, Ecole des Mines de Nancy; ⁴SINTEF Materials and Chemistry; ⁵Department of Mechanical Engineering, Indian Institute of Science, Bangalore

Macrosegregation formation in grain-refined Al-Cu alloys is studied by means of numerical simulations and compared to experimental data. In the modelling, a volume-averaged two-phase multiscale model is employed where macroscopic heat and solute transport, melt convection, and transport of inoculant particles and equiaxed grains are all taken into account. On a microscopic scale, nucleation occurs on inoculant particles, the solid phase is assumed to have globular morphology and the growth kinetics is described by accounting for limited solute diffusion in both liquid and solid phase. The numerical model is applied to horizontal solidification of an Al-22wt.%Cu alloy in a rectangular sand mold. The impact of the inoculant size distribution and the packing fraction on the evolution of the flow pattern, grain transport and macrosegregation formation is discussed. The final macrosegregation and grain size distribution are also compared to experimental data.

3:40 PM Break

4:00 PM

A Numerical Benchmark Exercise on Thermal and Thermosolutal Natural Convection in Liquid Alloys

: *Miha Založnik*¹; *Cédric Le Bot*²; *Stéphane Glockner*²; *Olga Budenkova*³; *Yves Du Terrail*³; *Marius-Vasile Bejinariu*⁴; *Gregor Kosec*⁵; *Dominique Gobin*⁶; *Hervé Combeau*¹; ¹Institut Jean Lamour; ²I2M-TREFLE; ³SIMaP; ⁴Universitatea Tehnica de Constructii Bucuresti; ⁵Institut Jožef Stefan; ⁶EM2C

During casting of alloys, chemical inhomogeneities (macroseggregations) result from solute transport by the flow in the mushy solidification zone. This flow is coupled with the thermosolutal natural convection in the fully liquid zone. Vigorous natural convection occurs either in the initial stage of casting, until the superheat is extracted; or throughout, in processes where thermal gradients are maintained (DC casting, remelting processes). Because of inherent strong nonlinearities, due to the low

Prandtl ($\sim 10^2$) and high Lewis numbers ($\sim 10^4$) of liquid metals, these flows are notoriously difficult to simulate. In the framework of the French project SMACS we present a numerical benchmark exercise comparing the performance of four numerical codes in the prediction of laminar thermal and thermosolutal natural convection related to small castings. We compare predictions on prototypical cases of convection in a square cavity and present the sensitivities of the predictions of global and local heat and mass transfer.

4:20 PM

2D and 3D Numerical Modeling of Solidification Benchmark of Sn-3% Pb Wt. Alloy under Natural Convection: Redouane Boussaa¹; Lakhdar Hachani¹; Bachir Saadi¹; Xiaodong Wang¹; Olga Budenkova¹; Kader Zaidat¹; Hamda Ben Hadid²; Yves Fautrelle¹; ¹Grenoble-INP; ²LMFA-Ecole centrale de Lyon

Numerical modeling of solidification benchmark, with controlled thermal boundary conditions, is proposed. The benchmark experiment consists in solidifying a rectangular ingot of Sn-3% wt. Pb alloys, by using two lateral heat exchangers which allow extracting heat flux from one or two vertical side. An array of fifty thermocouples, placed on the lateral wall, is used to determine the instantaneous temperature distribution. This allows us to evaluate the evolution due to the natural convection, as well as its influence on the initial conditions, the solidification macrostructure and segregation behaviors. After each experiment, the pattern of the segregations have been obtained by X-ray radiograph and confirmed by eutectic fraction measurements. The solute distribution is carried out by ICP analysis. Numerical solidification models are developed to give the distribution of the solute in a solidified sample. The originality of this modeling work is to provide quantitative results comparable with the experimental data.

4:40 PM

Numerical Modeling of the Interaction between a Foreign Particle and a Solidifying Crystalline Interface: Eliana Agaliotis¹; Mario Rosenberger¹; Alicia Ares¹; Carlos Schvezov¹; ¹CONICET - UNaM

The interaction between a solidification front and a spherical particle was modeled and simulated in order to study the phenomenon of "pushing". Finite element methods were employed in axi-symmetric domains. The drag force is calculated from the calculated fluid flow field and the repulsion force is the Lifshitz-Van der Waal force. The thermal field is decoupled from the force field. The model is applied to a metallic matrix containing particles with similar, lower or higher thermal conductivities than the matrix, resulting in planar, convex and concave interface shapes, respectively. The results show that the critical velocities for pushing for concave and convex interfaces are about one order of magnitude larger and one order of magnitude lower than the critical velocity for flat interfaces, respectively. The simulated results were in very good agreement with reported experimental results.

5:00 PM

Simulation of A356 Semi-Solid Die-Casting Using Power-Law Model: Seyed Vahidreza Seyed Vakili¹; Mahmoud Nili-Ahmadaadi¹; ¹University of Tehran

Semi-solid processing (thixoforming) is an innovative metal forming technology bearing a high potential for cost reduction by reducing forming steps, forming forces and improving work piece quality. Mold filling is one of the most important aspects of casting process, which is technically difficult to predict even for expert die designers. In this study, Numerical simulation is the last method which is used in this study. The ProCast software using Cutt-off-Value fluid (Power-Law) model was used to indicate the flow pattern of the fluid in the mold. Some comparisons with experimental tests were also done to prove the simulation results. Also, the effects of some casting parameters were studied to achieve the best casting condition for this process.

5:20 PM

Optimization of Tensile Test Pattern for Aluminum Alloys: Engin Tan¹; Freddy Syvertsen²; Derya Dispinar³; ¹Pamukkale University; ²SINTEF; ³University of Istanbul

It has been shown that the disturbance of the advancing liquid front in the mould cavity may lead to surface entrained defects known as bifilms. These defects can deteriorate the mechanical properties significantly. The developments in the simulation of castings aid many casters. It is quick and economical. Therefore in this work, the aim was targeted to optimise the mould filling of a tensile test pattern design that is used for aluminium alloys. Several different designs, gatings and runner systems were investigated with Vulcan Casting Simulation Software. In addition to the achievement of non-turbulent and quiescent mould filling; other parameters such as temperature profile, porosity and feeding were investigated to optimise the process.

Characterization of Minerals, Metals, and Materials: Characterization Technologies

Sponsored by: The Minerals, Metals and Materials Society, TMS Extraction and Processing Division, TMS: Materials Characterization Committee

Program Organizers: Jiann-Yang Hwang, Michigan Technological University; Sergio Montero, State University of North Rio De Janeiro; Chenguang Bai, Chongqing University; John Carpenter, US Department of Energy; Donato Firrao, Politecnico di Torino; Byoung-Gon Kim, Korea Institute of Geoscience & Mineral Resources; Mingdong Cai, Schlumberger

Tuesday PM
March 13, 2012

Room: Asia 2
Location: Dolphin Resort

Session Chairs: Mingdong Cai, Schlumberger Inc.; John Carpenter, DOE Los Alamos National Laboratory

2:00 PM

3D Characterization of Dendrites in Synthetic and Naturally Occurring Magma: S. Knox¹; A. Shiveley²; G. Viswanathan²; M. Chapman¹; J. Hammer³; J. Tiley²; ¹Southwestern Ohio Council for Higher Education/Air Force Research Laboratory; ²Air Force Research Laboratory; ³Department of Geology and Geophysics, University of Hawai'i

Natural and synthetic lava samples were studied using advanced characterization techniques to determine the crystallographic orientations and growth directions of dendritic structures in the silicate matrix. Focused ion beam SEM, advanced TEM, and EBSD procedures were utilized to evaluate the materials. Specifically, 3 dimensional reconstructions were developed using serial sectioning techniques to elucidate the connectivity of dendritic arm segments. Results indicate the primary growth direction and mechanisms associated with reported rotations that occur during rapid cooling from the melt. Reconstructions and results from TEM analysis will be reported.

2:15 PM

3D Metallography of Multiphase Steels: Martin Fischer¹; Pierre Lutomski¹; Andreas Stieben¹; Wolfgang Bleck¹; ¹RWTH Aachen University

For steel investigation and development, exact knowledge about the microstructural state is required. The information gained from 2-dimensional images often can't properly reflect the real 3D microstructural properties. In order to gain reliable information for meaningful models, simulations and correlations, it is necessary to accompany standard metallography with 3D information, which unfortunately is very difficult to access. This article presents a procedure



TMS 2012

141st Annual Meeting & Exhibition

for serial sectioning in combination with light optical microscopy. Only standard metallographic tools are employed in combination with image manipulation software. 3-dimensional microstructural data were extracted from three multiphase steel grades and in two cases virtual 3D-models of microstructural phases were generated.

2:30 PM

Advantages of Integrating Precession Scanning Transmission Electron Microscopy in the Characterization of Metallic Materials: *Peter Collins*¹; *Hamid Mohseni*¹; *Tom Scharf*²; ¹University of North Texas

The recent advance of precession scanning transmission electron microscopy holds the promise to advance the understanding of structure and properties in various structural metallic materials. Examples obtained from a variety of programs obtained from a recently acquired system will be shown. Results include studies of ultrafine grained materials, tribology structures, crystal refinement of intermetallic phases, and three-dimension diffraction tomography of metastable phases and precipitates.

2:45 PM

Characterization of Microstructure-Property Relations: Applying Complementary 3D Techniques: *John Bingert*¹; *Matthew Tucker*¹; *Robert Suter*²; *Brian Patterson*¹; *Cheng Liu*¹; ¹Los Alamos National Laboratory; ²Carnegie Mellon University

The advancement of non-destructive 3-dimensional (3D) interrogation methods is enabling unprecedented insight into the behavior of polycrystalline materials. For this investigation two complementary techniques were applied to interrogate polycrystals undergoing deformation. First, a novel method of incorporating traditional 2D digital image correlation (DIC), applied to surface and internal planes using micro x-ray computed tomography (XCMT), is combined with electron backscatter diffraction (EBSD) characterization. DIC was used for in situ tracking of local surface strains, while XCMT and EBSD were applied ex situ between interrupted tensile displacements. These combined techniques enabled the measurement of spatially resolved local plasticity and damage evolution on standard-scale test samples. In addition, high-energy diffraction microscopy (HEDM) was used to investigate the effects of shock impact on a sub-size copper polycrystal. Comparisons between the two techniques and their effective application space will be considered.

3:00 PM

Characterization of Open-Pored Metals Using Image Processing: *Bjoern Hinze*¹; *Joachim Roesler*¹; ¹TU Braunschweig

The most important characteristic of open-pored metals are their pores, since they enable all of their functional applications as filters or sound absorbers. Due to the notch effect of the pores, mechanical properties of porous metals are better than the ones of comparable structures made of polymers or ceramics. Consequently, only open-pored metals can be used in aircrafts to reduce flow noise or noise resulting from the core engine by acoustic absorption. Absorption properties depend highly on pore size and porosity of the material, which must be characterized as precisely as possible in order to analyze the correlation between morphology and noise reduction performance. Here, a line segmenting method is explained in order to characterize pore size and porosity of absorber materials using image processing based on two dimensional microscopy images, including sample preparation and specification of the set-up. Then, the influence of the pore structure on the measured absorption behavior is discussed. Demonstrating that the acoustic behavior can be described by pore characteristics and porosity.

3:15 PM

Full-Field Strain Mapping of Woven Structural Composites for Aerospace Applications: *Shahram Amini*¹; *Ellen Sun*¹; ¹United Technologies Research Center

Inadequate understanding of failure mechanisms in woven composite structures obscured by the difficulty of visualizing damage evolution and presence of multiple interacting failure mechanisms has limited their use in critical aerospace applications, such as ceramic-matrix composites for gas turbine engine hot sections. These hindrances are inherently related to the strong influence of the highly heterogeneous and locally anisotropic character of a woven composite material on the distribution of stresses and strains. The technique of surface strain mapping via digital image correlation (DIC) has been recently utilized for resolving the global mechanical behavior and spatial distribution of the strains in complex woven structures. The objective of this research effort is to establish a high fidelity test methodology to perform DIC at various length scales in woven structures targeted for aerospace applications. The results are intended to validate first-principles micromechanics models for systematic approaches to optimal design and tailoring of woven structures.

3:30 PM Break

3:40 PM

Precession Illumination Based Orientation Imaging, Grain Size and Defect Analysis in the Transmission Electron Microscope: *Andreas Kulovits*¹; *Jorg Wiezorek*¹; ¹University of Pittsburgh

We use computer-controlled TEM orientation imaging microscopy (TEM-OIM) to measure grain sizes, orientation distributions, grain-boundary and dislocation character with nanometer resolution. This TEM-OIM involves automated acquisition and indexing of precession illumination diffraction patterns and enables facile analysis of orientation maps akin to those popularized by SEM - EBSD based OIM. The probe size of the TEM instrument determines the lateral resolution of TEM-OIM to ~ 1-2 nm for field emission guns and ~ 15nm for LaB6 guns. Additionally, precession illumination hollow cone dark field imaging has been used for enhanced efficiency grain size measurements even in nanocrystalline aggregates. Finally, precession diffraction based virtual dark field imaging mode introduced for dislocation analysis. Results of orientation and grain size distribution measurements in nanocrystalline Ni and rapidly solidified Al thin films and for Burgers vector analyses in deformed NiAl and TiAl samples will be presented and discussed.

3:55 PM

Micro-Channeled Materials for Acoustic Absorption Applications: *Michael Culler*¹; *Keller Tomassi*¹; *Keri Ledford*²; *Jason Nadler*²; ¹Georgia Institute of Technology; ²Georgia Tech Research Institute

Micro-channeled materials for acoustical absorption have shown promise for noise attenuation in high performance applications, such as aircraft engines, where demanding design constraints include minimal weight, and tolerance of high-temperature, corrosive environments. A technique for creating micro-channeled materials involves electroless nickel deposition onto polyamide fibers, which are subsequently treated at elevated temperatures to both decompose the polymer and sinter the nickel into a coherent matrix. It is of critical importance to identify heating schedules that both facilitate polymer removal and preserve the material structure. To accomplish this, acceptable heating schedules are identified with thermogravimetric, differential thermal analysis, and dilatometric measurements to ensure sufficient removal of the polymer while maintaining the integrity of the nickel matrix. Once the heat treatment schedule is identified, the process can be applied to 30 mm x 50 mm diameter cylindrical samples currently under investigation.

4:10 PM

Surface Characterization of 19th Century and Modern Daguerreotypes Using EBSD & EDS: *Lisa Chan*¹; Patrick Ravines²; Bob Anderhalt¹; Rob McElroy³; Tara Nylese¹; Peter Bush²; ¹EDAX; ²SUNY Buffalo State; ³Archives Studio

Daguerreotype is the first viable imaging process that gave birth to photography and the imaging revolution. Unlike other silver-based black and white photographic processes, daguerreotype is an image that rests on the surface of a silvered copper plate. The gilding step affixes these surface image particles to the plate by coating the surface with a thin gold film. Even though gold is a noble metal, tarnishing readily occurs on the surface of the daguerreotypes. This work presents a study of 19th century and modern contemporary daguerreotypes using EBSD and EDS to examine the metallurgical nature of the silver mercury amalgam image particles and the background surface that was composed of nodules and grains that were tens of nanometers in size. The microstructural, elemental, and crystallographic information observed by EBSD and EDS can potentially explain the occurrence of tarnish as corrosion in the intergranular regions on gilded daguerreotype surfaces.

4:25 PM

Measuring Crystal Elastic Constants Using Ultrafast Laser Generated Surface Acoustic Waves: *Peng Zhao*¹; Changdong Wei¹; Ji-Cheng Zhao¹; ¹Ohio State University

We use a femtosecond pump-probe laser to perform localized measurement of anisotropic elastic constants. A pump laser pulse creates localized surface deformation through laser heating and subsequent thermal expansion. This deformation induces Surface Acoustic Waves (SAW) that propagate on the sample surface. The SAW is then detected by deflection of a probe laser beam several microns away from the pump. By analyzing the group velocity of the SAW propagating in multiple directions, the anisotropic elastic constants were calculated. The pump-probe beam separation can be as small as 7 microns, thus this method can be applicable to samples with a small grain size, e.g. 20 microns. Experimental results on large grain Al and Si and sintered MgB₂ samples will be shown. This measurement makes it possible to measure single-crystal elastic properties from a polycrystalline sample.

4:40 PM

Thermography Assisted Fatigue Testing: Anil Saigal¹; Rongbiao Gu¹; Christopher San Marchi²; *Douglas Matson*¹; ¹Tufts University; ²Sandia National Laboratory

Hydrogen is known to cause early failure of certain structural materials as a result of hydrogen embrittlement. As a result most hydrogen-containing vessels - pipes and valves - subjected to cyclic loading have long-term safety concerns. This work aims to explore the potential use of a thermography-assisted fatigue testing technique to investigate the fatigue properties of materials. 304 stainless steels were found to be strengthened as a result of hydrogen charging and their fatigue life was increased by a factor of 100. The use of thermographic analysis of rotating beam samples as a fatigue test technique is shown to provide repeatable results which are in general independent of test cycle frequency while reducing test times by several orders of magnitude.

Computational Thermodynamics and Kinetics: Diffusion Coefficients

Sponsored by: The Minerals, Metals and Materials Society, TMS Electronic, Magnetic, and Photonic Materials Division, TMS Materials Processing and Manufacturing Division, TMS Structural Materials Division, TMS: Alloy Phases Committee, TMS: Chemistry and Physics of Materials Committee, TMS/ASM: Computational Materials Science and Engineering Committee, TMS: Integrated Computational Materials Engineering Committee, TMS/ASM: Phase Transformations Committee, TMS: Process Technology and Modeling Committee

Program Organizers: Zi-Kui Liu, The Pennsylvania State University; Mark Asta, University of California, Berkeley; James Warren, The National Institute of Standards and Technology; Yunzhi Wang, Ohio State University; Raymundo Arroyave, Texas A & M University; Yu Wang, Michigan Tech

Tuesday PM
March 13, 2012

Room: Australia 3
Location: Dolphin Resort

Session Chairs: Anton van der Ven, U Michigan; Carelyn Campbell, NIST

2:00 PM Invited

Challenges in Constructing Diffusion Mobility Databases for Industrial Alloys: *Carelyn Campbell*¹; ¹National Institute of Standards and Technology

Expanding the use of CALPHAD-based multicomponent diffusion mobility databases to more complex industrial alloys systems is hindered by the lack of a standard reference database for pure elements and limited data for many ordered and complex intermetallic phases. CALPHAD-based multicomponent databases are developed by combining binary and ternary mobility descriptions. However, when the binary descriptions considered do not use the same reference mobilities, the descriptions cannot be combined to assemble a large multicomponent database. Efforts based at NIST to develop a reference diffusion mobility database will be presented, including an initial set of recommendations for many of the commonly used elements. Using these initial recommendations a diffusion mobility database is developed for processing of the α -CuInSe₂ photovoltaic absorber material. The development of this database highlights the challenges of constructing databases with limited data and the importance of understanding the dominate diffusion mechanism when describing the sublattice models for complex phases.

2:25 PM

Computation and Validation of Effective Diffusion Coefficient in a Magnesium Polycrystal: *Bala Radhakrishnan*¹; Nagraj Kulkarni¹; Yongho Sohn¹; Jerry Hunter¹; ¹Oak Ridge National Laboratory

In tracer diffusion measurements in polycrystalline grain structures the measured diffusion profiles are hard to interpret when they result from a combination of diffusion paths in the bulk and along grain boundary surfaces and triple lines. We simulate the diffusivity in the bulk as well as along various grain boundary and triple line types using a molecular dynamics approach based on computing the mean square displacement of atoms. The computed grain boundary and bulk diffusion coefficients are used as inputs to a mesoscale computation of the diffusion profile in the three-dimensional grain structure. The calculated diffusion profiles are compared with those obtained from tracer diffusion measurements for single crystal and polycrystal magnesium specimens. Research sponsored by the U.S. Department of Energy, Assistant Secretary for Energy Efficiency and Renewable Energy, Office of Vehicle Technologies under Contract No. De-AC05-00OR22725 with Ut-Battelle, LLC.



TMS 2012

141st Annual Meeting & Exhibition

2:40 PM

Tracer Diffusion Databases – Benefits and Techniques: *Nagraj Kulkarni¹; Graeme Murch²; Irina Belova²; Yongho Sohn³; Robert Warmack¹; Jerry Hunter⁴; Bala Radhakrishnan¹; ¹Oak Ridge National Laboratory; ²The University of Newcastle; ³University of Central Florida; ⁴Virginia Polytechnic Institute and State University*

Implementation of new initiatives such as the Materials Genome Initiative that seek to accelerate the discovery, development and deployment of advanced materials will require at their foundation robust diffusion databases. The most fundamental descriptor of diffusion is the tracer diffusion coefficient and hence its measurement serves as the basis for the development of tracer diffusion databases. In this presentation, we highlight the wealth of kinetic information provided by tracer diffusion measurements that is applicable to a wide range of materials. We compare and contrast experimental tracer diffusion techniques based on radioactive and stable isotopes. We present some recent results on the use of the stable isotope technique in Mg-alloys that is applicable to the Mg-ICME program. This research was sponsored by the U.S. Department of Energy, Office of Energy Efficiency and Renewable Energy, Vehicle Technologies Program, under contract DE-AC05-00OR22725 with UT-Battelle, LLC.

2:55 PM

Extracting Chemical Diffusion Coefficients from Ternary Diffusion Paths: *Qiaofu Zhang¹; Ji-Cheng Zhao¹; ¹The Ohio State University*

Two intersecting diffusion paths are usually needed to calculate the four interdiffusion coefficients at the crossover composition in a ternary system using classical diffusivity extraction methods such as the Boltzmann-Matano analysis and the extended Saur-Freise analysis. Such analyses are very inefficient since they require data from lots of diffusion couples to construct a diffusivity database for a ternary system. The zero flux method by Dayananda and Sohn and the simulation method by Bouchet allow extraction of diffusion coefficients along one diffusion path, thus, they are more efficient. These diffusivity extraction methods are applied to several ternary systems such as Fe-Ni-Co and Ni-Al-Pt to check their reliability against the classical methods. Built upon Bouchet's analysis, an improved simulation method is developed by combining an optimizing scheme with a finite difference method. A MatLab program is developed to extract diffusion coefficients along a single diffusion path using this method.

3:10 PM

Solute Diffusion in Ordered Bulk Ni₃Al: A First Principles Investigation: *Priya Gopal¹; Srinivasan Srivilliputhur¹; ¹University of North Texas, Denton*

Ni-based superalloys possess desirable high-temperature properties including ductility, fracture toughness as well as resistance to creep and oxidation. The key factor in these properties is due to the precipitation of ordered gamma' precipitated within a gamma Ni matrix. Extensive studies in this area have shown that the mechanical properties can be improved by adding substitutional elements. It is thus very important to understand the electronic structure and diffusion kinetics of the substitutional elements and the role each one has on the overall microstructure. In this talk, we discuss our results on the systematic study of the energetics and migration barriers of solute additions (Cr, Co) in ordered Ni₃Al. Using density functional theory methods and the nudged elastic band method we simulated the migration of vacancy and substitutional elements in a complete set of migration paths and evaluated the barriers in bulk Ni₃Al.

3:25 PM Break

3:50 PM Invited

Interstitial and Substitutional Solid-State Diffusion from First Principles: *Anton Van der Ven¹; ¹University of Michigan*

Solid-state diffusion can become quite complex at the atomic scale in technologically important materials. This is especially true in multi-component solids at non-dilute concentrations where varying degrees of short and long-range order often play a crucial role in determining atomic mobility. First-principles statistical mechanical tools are proving invaluable in elucidating and enabling the prediction of phenomenological transport coefficients for interstitial and substitutional diffusion in metals and alloys for structural applications as well as ceramics for energy storage applications. In this talk I will review the methodology that allows us to link atomic scale kinetic processes to macroscopic transport coefficients and will illustrate its application to a variety of important technological problems including oxidation, interdiffusion in alloys and interstitial Li transport in electrodes for Li batteries.

4:15 PM

Ab Initio Determination of Point Defects and Derived Diffusion Properties in Metals: *Tilmann Hickel¹; ¹Max-Planck-Institut fuer Eisenforschung GmbH*

The accurate simulation of atomistic defects is crucial for various thermodynamic and kinetic effects in materials science. A key quantity for all practical applications is their formation energy. Once known, the equilibrium defect concentration as function of process conditions such as temperature, chemical potentials etc. can be predicted. In particular, the formation energy and concentration of vacancies decisively influences diffusion processes in metals and can also affect the solubility and diffusion of interstitial atoms such as hydrogen. In this contribution, we will therefore apply our highly accurate ab initio methods for free energies to vacancies. We will demonstrate that including all relevant free energy contributions yields an highly non-linear temperature dependence, resulting in substantial deviations between low and high temperature results. Further, we have derived analytic expressions for vacancy concentrations using thermodynamics concepts and taking particularly care of the correct consideration of chemical potentials. These methods will be applied to explain the exceptionally high vacancy concentration in FeAl intermetallic alloys and the exciting effect of superabundant vacancies in steels. Finally, the results will be used to determine the dominating self-diffusion mechanism in the B2 phase of FeAl.

4:30 PM

Diffusion of Silicon in Nickel: The Role of Stress and Its Implications to Microstructural Evolution under Irradiation: *Venkateswara Rao Manga¹; Pascal Bellon¹; Robert Averback¹; Dallas Trinkle¹; ¹University of Illinois at Urbana Champaign*

Understanding the microstructural evolution of irradiated materials requires the knowledge of transportation mechanisms of various types of point defects, their coupling to solute atoms and their interaction with sinks. In this talk we report the ab initio investigation of diffusion in a model system- Si in Ni- at dilute concentrations under the influence of stress by two different mechanisms: 1. Vacancy-mediated and 2. Interstitial. We start by presenting the effect of uniaxial-stress on the migration barriers and energetics of the point-defect complexes of Si in Ni. Migration barriers of 1.1eV and 0.94eV are calculated for vacancy-mediated jumps of host-atom and Si in Ni, respectively, with no stress. Diffusion coefficients are calculated using the Continuous-time random-walk formalism and a multi-frequency model. The anisotropy in the diffusion and the relative contribution of the above mechanisms under stress are computed and the implications of these findings to the microstructural evolution under irradiation are discussed.

TUESDAY PM

4:45 PM

Ab-Initio Calculations of Solute Properties in Magnesium: *Liam Huber*¹; *Ilya Elfimov*¹; *Joerg Rottler*¹; *Matthias Militzer*¹; ¹University of British Columbia

Using density functional theory in the Vienna Ab-initio Simulation Package, we have calculated various properties for Mg-solute interactions on the atomic scale. Using supercells of bulk Mg with site defects we have found solute-vacancy binding energies, migration barriers for site-hopping, and activation energies for vacancy-mediated diffusion. Where experimental data is available we have compared our values and find that our calculations tend to reproduce the same qualitative trends in activation energy. We have also performed solute-grain boundary (GB) binding energy calculations for a variety of solutes using a special near $\sqrt{3} \times \sqrt{3}$ 7 GB. We find that the solutes investigated fall into two families, each sharing the same pattern of binding energies along GB sites. Interestingly, solutes which are known to have a beneficial effect on texture (e.g. Ca, La, Nd) belong to one family while other solutes (e.g. Al, Zn, Ag) belong to the other.

5:00 PM

Accelerated Self-Diffusion in FCC Metals Due to H Induced Superabundant Vacancies: *Roman Nazarov*¹; *Tilmann Hickel*¹; *Jörg Neugebauer*¹; ¹Max Planck Institute for Iron Research

A dramatic increase of the vacancy concentration in an H-rich atmosphere, the so called superabundant vacancy formation, has been experimentally observed in several metals and alloys. In order to study this phenomenon we systematically applied density functional theory to a large set of fcc metals and found that a large amount of H can be trapped by a monovacancy. Based on the defect formation energies from DFT calculations, we have constructed a thermodynamic model and revealed that the vacancy concentration can indeed strongly increase at sufficiently high H concentrations. To understand the phenomenon of accelerated self-diffusion in an H-rich atmosphere we coupled the information on the number of vacancies from the thermodynamic treatment with self-diffusion barriers obtained from DFT calculations. Using this approach we find that the self-diffusion coefficient is reduced not only due to the increased vacancy concentration, but also as a result of an H-induced lubricant effect.

5:15 PM

Oxygen-Solute Interaction in α -Titanium and the Effect on Diffusion: *Henry Wu*¹; *Dallas Trinkle*¹; ¹University of Illinois at Urbana-Champaign

The transport of oxygen in titanium affects the design of high temperature alloys as well as the growth of layered-oxide phases. It has been found that oxygen resides in three distinct interstitial sites in α -titanium: octahedral, hexahedral, and non-basal crowdion. Oxygen diffuses between all three interstitial sites with similar rates such that all transition pathways contribute to diffusion. We compute the interaction energy between oxygen and the alkali, alkaline earth, and transition metals. The octahedral neighbor site is repulsive for almost all solutes and becomes more repulsive with more d-filling. The closer neighbors for the hexahedral and crowdion are correlated for solutes whose interactions form V-shaped curves with dips near half d-filling. The further neighbors for the hexahedral and crowdion are similarly correlated though most solutes at this neighbor site destabilize the crowdion interstitial. We calculate change to oxygen diffusion from solutes, and compare with interaction energy trends.

Computational Thermodynamics and Kinetics: Phase-Field Simulations in Alloys II

Sponsored by: The Minerals, Metals and Materials Society, TMS Electronic, Magnetic, and Photonic Materials Division, TMS Materials Processing and Manufacturing Division, TMS Structural Materials Division, TMS: Alloy Phases Committee, TMS: Chemistry and Physics of Materials Committee, TMS/ASM: Computational Materials Science and Engineering Committee, TMS: Integrated Computational Materials Engineering Committee, TMS/ASM: Phase Transformations Committee, TMS: Process Technology and Modeling Committee

Program Organizers: Zi-Kui Liu, The Pennsylvania State University; Mark Asta, University of California, Berkeley; James Warren, The National Institute of Standards and Technology; Yunzhi Wang, Ohio State University; Raymundo Arroyave, Texas A & M University; Yu Wang, Michigan Tech

Tuesday PM
March 13, 2012

Room: Asia 5
Location: Dolphin Resort

Session Chairs: Long-Qing Chen, Penn State; John Morral, Ohio State University

2:00 PM

A Phase Field Crystal Model of Irradiation Damage in Materials: *Nana Ofori-Opoku*¹; *Jeffrey Hoyt*¹; *Nikolas Provatas*¹; ¹McMaster University

The study of the effects of radiation damage in materials, along with the scientific interest, is also widely of practical relevance as it pertains to the design of future nuclear reactors. Recently, it has been suggested that nanocrystalline materials offer markable resistance to radiation damage. To investigate this claim, we introduce a phase field crystal (PFC) model that includes effects of radiation damage. The ability of the PFC methodology to describe atomistic scale effects on diffusive time scales, makes it an appropriate tool to study the microstructure evolution of nanocrystalline materials under radiation over long length scales. The model is used to study grain growth under radiation damage, and indeed it is found that there is enhanced grain growth of nanocrystalline materials under radiation. This suggests that, although offering some resistance to radiation damage, nanocrystalline materials may not remain nanocrystalline over time.

2:15 PM

Simulating Microstructure Property Relations in Shape Memory Polycrystals: *Rajeev Ahluwalia*¹; *Siu Sin Quek*¹; *Wu David*¹; ¹Institute of High Performance Computing

Materials undergoing diffusion-less martensitic transformations display many unusual mechanical properties such as the shape memory effect. The underlying twinned microstructure critically influences the mechanical behavior. Most technological applications make use of polycrystalline alloys. An important issue is to find the optimal microstructure that will enhance the effective properties of the shape memory alloy. This requires the role of quantities such as the mean grain size, grain size distribution and orientation distribution. To study these issues, we use a Ginzburg-Landau theory for shape memory polycrystals that couples elastic strains with crystallographic orientations. The underlying polycrystal is generated by using nucleation and growth models which allow us to control properties such as the mean grain size and the size distribution. We study how the microstructure and effective stress strain curves depend on the underlying polycrystalline texture and show how such models may be used to design microstructures which give enhanced properties.

TUESDAY PM



2:30 PM

Complex Microstructures Formed in $\bar{a}+B/\bar{a}+\bar{a}'$ Diffusion Couples in Ni-Al-Cr System: Comparison of Phase Field Simulation from a Model System with Experiments: *Xiaoqin Ke*¹; John Morral¹; Yunzhi Wang¹; ¹Ohio State University

Some $\gamma+B/\gamma+\gamma'$ diffusion couples in Ni-Al-Cr system show very complex microstructures such as $\gamma+B<\gamma>\gamma+B>\gamma'>\gamma+\gamma'$ ($>$ and $<$ represent the direction of boundary movement) after interdiffusion at high temperatures. Such microstructure change is difficult to understand or predict by analytical solutions and DICTRA simulations, but is critical for the prediction of coating life. In this work phase field method is used to simulate $\gamma+B/\gamma+\gamma'$ diffusion couples prepared from a model A-B-C system. All kinds of complex microstructures found in experiments have been obtained by the simulations. Moreover, the relationship between the kinds of microstructure formed and the change of initial end alloy compositions identified from the simulations qualitatively matches the experimental observations. An analysis of the diffusion paths based on eigenvectors of effective diffusivities of the initial end alloys will also be provided.

2:45 PM

Phase Field Simulations of Electromigration Driven Failure in SnAgCu Solder Interconnects: *Subramanya Sadasiva*¹; Ganesh Subbarayan-Shastri¹; Lei Jiang²; Daniel Pantuso²; Sandeep Sane²; ¹Purdue University; ²Intel Corporation

The miniaturization of electronics has led to a significant increase in the current densities seen in solder interconnects. This has led to an increase in the importance of electromigration and stress-migration and other diffusion driven mechanisms for failure in solder interconnects. Concurrently, the shift from eutectic PbSn solders to SnAgCu solders, owing to environmental concerns has necessitated dealing with a more complex material system. In this study, we derive a model for the electromigration and stress-migration driven failure in SnAgCu alloys using a multiphase field model. Following the Truesdell-Toupin formalism, governing equations are derived from the conservation of mass and energy. Further, we derive the linear constitutive laws for the system based on the second law of thermodynamics. Finally, we demonstrate a numerical implementation of this model using finite elements. We use the finite element implementation to simulate the void growth and coalescence under forward and reversed current conditions.

3:00 PM

Elastic Effects on Aging in Cu/Sn-Ag-Cu Lead-Free Solder Joints: A Phase-Field Study: *Durga Ananthanarayanan*¹; Patrick Wollants¹; Nele Moelans¹; ¹Department of Metallurgy and Materials Engineering, Katholieke Universiteit Leuven

Sn-Ag-Cu lead-free solders are the most widely studied alternatives to Sn-Pb solder. Despite many desirable properties, the growth of intermetallic compounds Cu_3Sn , Cu_6Sn_5 and Ag_3Sn , leading to crack initiation, remains a major reliability issue. In the present work, the effects of coherency strains on the phase equilibria and aging process in Cu/Sn-Cu and Cu/Sn-Ag-Cu solder joints are simulated using the phase-field technique. The COST 531 thermodynamic database for lead-free solders, developed using the CALPHAD method, is coupled with the phase-field model. Chemical mobilities, elastic constants and lattice parameters for all phases in the system are estimated based on available data in the literature. 2-D simulations at different temperatures and for different distributions of intermetallic phases are performed. The conditions influencing the coarsening of the intermetallic phases and its implications on the stress evolution for both the systems are evaluated.

3:15 PM

Phase-Field Crystal Modeling of Metal-on-Metal Epitaxy: Exploring Routes to Self-Organization: *Srevasan Muralidharan*¹; Raika Khodadad¹; Ethan Sullivan¹; Mikko Haataja¹; ¹Princeton University

Bulk-immiscible binary systems often form stress-induced miscible alloy phases when deposited on a substrate. Both alloying and surface dislocation formation lead to the decrease of the elastic strain energy, and the competition between these two strain-relaxation mechanisms leads to the emergence of compositional nanoscale domains. We develop a quantitative phase-field crystal model for compositional domain formation of binary metallic systems and investigate the cases of partial, single and multi-layer thin film systems deposited on both regular and quasi-crystalline substrates. Our results demonstrate that the presence of misfit stresses and/or dislocations in the underlying layers guides the nucleation and growth of additional layers as well as the controls the spatial organization of compositional domains within layers.

3:30 PM Break

4:00 PM

Numerical Modeling of Dendritic Growth During Solidification of Alloys Using Lattice Boltzmann and Cellular Automaton Methods: *Mohsen Eshraghi*¹; Sergio Felicelli¹; ¹Mississippi State University

A numerical model combining lattice Boltzmann (LB) and cellular automaton (CA) methods is developed to simulate solute-driven dendritic growth in three dimensions. While LB is used to calculate the transport phenomenon, CA is used to capture the solid/liquid interface. The effect of undercooling and degree of anisotropy on kinetics of dendrite growth is studied. Considering the special characteristics of LB and CA methods, the presented model can be considered as an interesting tool for simulation of dendritic solidification in three dimensions.

4:15 PM

Phase-Field Simulation of Segregation to Stacking Fault and Twin Boundaries in Co-Based Alloys

: *Yuichiro Koizumi*¹; Sho Suzuki¹; Takuma Ohtomo¹; Shingo Kurosui¹; Yungping Li¹; Hiroaki Matsumoto¹; Akihiko Chiba¹; ¹Tohoku University

Co-based alloys such as Co-Cr-Mo alloy and Co-Ni-based superalloy are widely used for industrial and biomedical applications. Their mechanical properties are closely related to the stability of HCP-structure and FCC-structure. In Co-Cr-Mo alloys, strain induced epsilon-HCP-phase improves wear resistance [1]. Co-Ni-based superalloys with relatively high FCC-phase stability exhibit high ductility by dislocation slip [2]. Atomistically, local HCP-structures in FCC-matrix, i.e. twin boundaries and stacking faults with ABAB-type stacking embedded in ABCABC-type stacking of FCC-structure, is important for the above-mentioned mechanical properties. The phase-stability at the local-HCP structures can be significantly affected by segregation of solute atoms. In this study, a phase-field simulation of segregation to the local HCP-structures has been developed and applied to a Co-Cr-Mo alloy and a Co-Ni based superalloy. The simulation indicated that segregation behaviors in the two alloys are quite different. [1]Chiba et al. Acta Materialia 2007;55:1309. [2]Chiba et al. Philos Mag A 1999;79:1533.

4:30 PM

A Hybrid Phase-Field / Transmission Electron Microscopy Approach for Quantifying θ' Precipitation Kinetics in Cast Al-Si-Cu Alloys: *Junsheng Wang*¹; Ruijie Zhang²; William Donlon¹; Mei Li¹; Long-Qing Chen³; John Allison⁴; ¹Ford Motor Company; ²University of Science and Technology Beijing; ³Penn State University; ⁴University of Michigan

A hybrid phase-field / transmission electron microscopy (TEM) approach has been developed to quantify the evolution of θ' precipitates in cast 319 aluminum-type alloys. A three dimensional phase-field model was developed to simulate θ' nucleation and growth in ternary Al-Si-Cu alloys. For the nucleation model, we implemented the rate function using classical nucleation theory. The activation energy and number density of

precipitate nuclei were estimated using targeted, quantitative TEM. For the growth kinetics, we modeled the diameter and thickness increase of the anisotropic θ' plates using experimentally validated mobility coefficients, and chemical free energy and diffusion coefficients from ThermoCalc and DICTRA. The model can quantitatively predict θ' particle size distribution as a function of Cu content, aging temperature and time. This model in conjunction with the yield strength model can be used to predict the mechanical properties for cast powertrain components made of A319 aluminum alloys.

4:45 PM

Antiphase Boundaries in Rafted Structures: Experimental Investigation and Phase Field Modeling: *Yann Le Bouar*¹; Adèle Lypreni¹; Alphonse Finel¹; Jean-Sébastien Mérot¹; Loïc Patout¹; François Brisset²; ¹LEM, CNRS/ONERA; ²ICMMO, Université Paris-Sud

During creep loading, the initial microstructure of Ni-base superalloys, made of cuboidal ordered precipitates in a disordered matrix, evolves towards a rafted structure. This evolution is the result of elastic and plastic driving forces, which tend to move precipitates closer to each other along a given direction. When two precipitates meet, they may either coalesce or form an interfacial defect called antiphase boundary (APB). However, plastic activity in the matrix phase is able to remove the APBs, and the question is open whether, under given temperature and stress conditions, APB can still be observed in the rafted structure. We first investigate the existence of APBs in the rafted structure of the CMSX2 superalloy using both scanning and transmission microscopy. Then, a phase field model is developed to account for the large energy difference between the APBs and the precipitate matrix interface.

5:00 PM

Modeling the Kinetics of Diffusive Phase Transformations -Phase Field Method and Thick Interface Model: *Ernst Gamsjäger*¹; Jiri Svoboda²; Franz Dieter Fischer¹; ¹Montanuniversität Leoben; ²Academy of Sciences

In the framework of a recently developed thick interface model the time dependent development of the variables during diffusive phase transformations were calculated by solving the evolution equations. Alternatively, the transformation kinetics can be determined by means of the phase field method (PFM), where an order parameter on a fixed grid indicates the position of the interface as well as the correspondence to the individual phases. Both, the evolution equations for the variables occurring in the thick interface model and the evolution equation of the order parameter can be derived from the thermodynamic extremal principle (TEP). The comparison of the TEP-based thick interface model and the phase field model allows evaluating the PFM results and their relations to the standard thermodynamic parameters. As an example the kinetics of the austenite-to-ferrite transformation in the Fe-Ni system is investigated.

5:15 PM

Morphological Study of Polymer Crystallization by a Phase-Field Model: *Mohsen Asle Zaem*¹; Sasan Nouranian¹; Mark Horstemeyer¹; Paul Wang¹; ¹Mississippi State University

A phase-field model was used to study crystal growth in semicrystalline polymers with various crystal morphologies. The original Kobayashi's phase-field model for solidification of pure metals was adopted to account for polymer crystallization. Evolution of a non-conserved phase-field variable was considered to track the interface between the melt and the crystalline phases. A local free energy density was used to account for the meta-stable states in polymer solidification. The coupled governing evolution equations of the temperature and phase-field variable were solved using a finite element method. The developed model was successfully applied for simulation of two-dimensional polymer single- and polycrystalline morphologies (rectangular, orthorhombic, hexagonal, and spherulitic) in polypropylene and polystyrene. These morphologies were compared based on different supercooling and interface anisotropy.

The unique aspect of this work is that the employed model is capable of simulating multiple arbitrarily-oriented crystals and has no limitations with respect to the crystal morphology.

Defects and Properties of Cast Metals: Solidification Structure and Segregation

Sponsored by: The Minerals, Metals and Materials Society, TMS Materials Processing and Manufacturing Division, TMS: Solidification Committee

Program Organizers: Mark Jolly, University of Birmingham; Brian Thomas, University of Illinois at Urbana-Champaign; Carl Reilly, University of British Columbia

Tuesday PM
March 13, 2012

Room: Oceanic 4
Location: Dolphin Resort

Session Chairs: Matthew Krane, Purdue University; Brian Thomas, University of Illinois

2:00 PM

A Multi-Scale 3D Model of the Vacuum Arc Remelting Process: *Koulis Pericleous*¹; Georgi Djambazov¹; Mark Ward²; Yuan Lang³; Peter Lee⁴; ¹University of Greenwich; ²University of Birmingham; ³Imperial College; ⁴University of Manchester

A multi-scale model of the VAR process was developed to simulate unsteady phenomena within the ingot melt pool due to arc motion and resulting effects on dendritic microstructure. External magnetic field and surface current measurements were used as boundary conditions, to determine the trajectory of the arcs between electrode and ingot and between ingot and sidewalls. The interactions between magnetic field, turbulent metal flow and heat transfer were modelled using CFD techniques and this "macro" model was linked to a micro model, to resolve the evolving dendritic microstructure, and establish a relationship between operational parameters and microstructure defects. Arc-driven solute convection in the mushy zone led to local remelting and changes in local Rayleigh number provided an indicator of when fluid flow channels (freckles) will initiate within the mushy zone. Particle tracking was further used, to characterise the trajectory and dissolution of inclusions entering the melt, causing "white spot" defects.

2:20 PM

Deterministic Origin of Dendritic Side-Branching: *Martin Glicksman*¹; ¹Florida Institute of Technology

Conventional dendritic growth theories are based on stochastic instabilities driven by 'selective amplification' of environmental noise. Quantitative experiments, however, fail to support these theories, verifying only Ivantsov's conduction/diffusion analysis of the normal component of the transport fluxes. The transport field's tangential component along the solid-liquid interface is ignored--save for its limited use as a capillary boundary condition. Treating the Gibbs-Thomson-Herring equilibrium temperature distribution as a real tangential field, with its associated gradients, fluxes, and divergences, then adding negative feedback responses via the LeChatelier-Braun principle, shows that a heretofore unknown dipolar rotation occurs locally on the interface. This rotation 'wrinkles' the interface, and leads to prompt side-branching. Moreover, the interface dipoles interact deterministically with the evolving crystal shape to produce an eigenfrequency that produces the classical dendritic structures in metals and alloys.

2:40 PM

Identification of Defect Prone Peritectic Steel Grades by Analyzing the High Temperature Phase Transformations: *Peter Presoby*¹; Robert Pierer¹; Christian Bernhard¹; ¹Montanuniversitaet Leoben

Continuous casting of peritectic steels is often difficult and critical; bad surface quality, cracks and even breakouts may occur. Particularly, the initial solidification of peritectic steels within the mold leads to formation



TMS 2012

141st Annual Meeting & Exhibition

TUESDAY PM

of surface depressions and uneven shell growth. As commercial steels are always multi-component alloys, it is necessary to take into account also the influence of alloying elements besides carbon on the peritectic phase transition. Especially for new steel grades with high Mn, Si and Al contents, there is a lack of information regarding the solidification sequence and the phase diagrams for initial solidification. Based on a comprehensive method development, the present study shows that high precision Differential Scanning Calorimetry (DSC) measurements allow a clear prediction whether an alloy is peritectic (i.e. critical to cast) or not.

3:00 PM

Effect of Deformation on Microsegregation in Cast Structure of Bearing Steel: *Mitra Basirar*¹; Hasse Fredriksson¹; ¹KTH, Royal Institute of Technology

Microsegregation changes in the cast structure of a five-ton ingot of ball bearing steel were investigated by a series of hot compression tests. Cylindrical specimens were deformed at a temperature range of 800°C to 900°C and strain rates of 0.5 s⁻¹. Samples were quenched after the compression in order to eliminate the homogenization time. Subsequently they were analysed with the aid of Electron Microprobe Analysis (EMPA) in order to investigate the effect of hot compression on microsegregation of Mo, Cr, Mn and Si. It was found that highly segregated regions are regions for formation of deformation bands. It seems that the degree of microsegregation increases by increasing the deformation. An attempt was made to estimate the diffusion coefficients of alloying elements during the deformation process. The increase of microsegregation during deformation is explained by tendency for uphill diffusion.

3:20 PM

Effects of Section Size And Cooling Rate on Microstructure and As-Cast Properties of Investment Cast CO-CR Biomedical Alloy: *Ruth Kaiser*¹; David Browne¹; Kenny Williamson²; Claire O'Brien³; ¹University College Dublin; ²DePuy (Ireland)

ASTM F75, a biomedical grade cobalt alloy, is often used in orthopaedic implants, manufactured using investment casting methods. Quality of the cast medical implants is paramount, defects such as porosity, inclusions or misrun are not tolerated and similarly the mechanical properties have to conform to predetermined standards. It is recognised that casting conditions have an effect on the as-cast properties of materials and that a highly controlled and optimised process can help limit defects and optimise properties. The objective of this work was to determine the effect of casting conditions such as melt and mould preheat temperatures and section size, on the microstructural characteristics and resultant mechanical properties of the alloy investigated. This was done by conducting a series of instrumented control experiments involving solidification of the alloy in typical investment shell moulds, characterisation of the as-cast micro/macro-structure, and a programme of mechanical testing. Any defects observed are also reported.

3:40 PM Break

4:00 PM

The Influence of Cu on Eutectic Nucleation and Morphology in Hypoeutectic Al-Si Alloys: *Anilajaram Darlapudi*¹; ¹University of Queensland

The influence of increasing additions of copper on the aluminium silicon eutectic morphology and nucleation was investigated in Sr-modified and unmodified Al-10wt%Si alloys. In unmodified alloys, increase in copper content resulted in an increase in the number of polyhedral silicon particles and thus nucleation frequency of eutectic cells. In Sr modified alloys, additions of copper resulted in an increase in the nucleation frequency of eutectic cells. Also, at high copper levels in modified alloys, a change in the eutectic interface morphology from near-planar to coral-like was observed. These observations are important as in in-situ observations of eutectic solidification in Al-Si alloys, high amounts of copper is added in order to generate contrast between the solid and the liquid.

4:20 PM

Molecular-Dynamics Simulations of Ni-Based Superalloys: *Christopher Woodward*¹; James Lill²; Dallas Trinkle³; Mark Asta⁴; ¹Air Force Research Laboratory; ²High Performance Technologies Inc.; ³University of Illinois; ⁴University of California

Convective instabilities responsible for misoriented grains (freckle defects) in directionally solidified turbine airfoils are produced by variations in liquid-metal density with composition and temperature across the solidification zone. Accurate prediction of freckle formation is prerequisite for improving production and properties of large scale turbine airfoils used for terrestrial energy production and high-performance aerospace applications. Fundamental properties of molten Ni-based alloys, required for modeling these instabilities, are calculated using ab initio molecular dynamics simulations. Initial calculations of elemental, binary and ternary alloys produce liquid-phase molar volumes ($V(c,T)$) within 0.6-1.8% of available experimental data. Liquid metal densities for a Ni based superalloy, RENE-N4, are calculated at the liquidus and solidus temperatures expected in the solidification zone. Results are compared with recently published parameterizations of $V(c,T)$ developed using binary experimental data from a narrow range of compositions. Predictions for possible liquid metal density inversions, the precursors for freckle defect formation, are presented.

4:40 PM

Microstructure and Microsegregation in Inconel 718 Casting: *Alexis Pautrat*¹; ¹Mines Paristech

The superalloy Inconel 718 is used in parts of the main engine turbopump of the Ariane 5 launcher. The forming process for most of these parts is investment casting. The present study focuses on the conditions for the formation of fragile phases such as Laves. Samples were cast under vacuum at various superheat and cooling rate. Detailed analyses of the microstructures by scanning electron microscopy including automatic indexing of electron back scattered diffraction patterns and energy dispersed spectrometry were used to quantify the volume fraction and composition of primary gamma, NbC, Laves and Delta phases. Besides, a complete numerical simulation of the casting process is developed to identify the solidification and cooling path for each sample. This information will be used for the assessment of a microsegregation model taking into account thermodynamic equilibrium, cooling rate and microstructure parameters.

5:00 PM

Numerical Simulation on Solidification Microstructure of Cast Steel Using Cellular Automaton Method: Bin Su¹; *Zhiqiang Han*¹; Baicheng Liu¹; Yongrang Zhao²; Bingzhen Shen²; Lianzhen Zhang²; ¹Tsinghua University; ²CITIC Heavy Industries Co., Ltd.

A cellular automaton model has been developed to simulate the microstructure evolution of ASTM A216 WCA cast steel during solidification and consequent cooling processes. In the model, the thermodynamics and solute diffusion of the multicomponent system were taken into account by using Thermo-Calc and DICTRA software. The peritectic solidification, α -ferrite/austenite transition and eutectoid transformation as well as the final microstructure can be predicted. To validate the model, a sand mold step-shaped casting was produced and metallographic examination was carried out, in which the percentage and the grain size of proeutectoid ferrite were measured by using optical microscopy, and the mean interlamellar spacing of pearlite was measured by using SEM. It was shown that the simulated results are in good agreement with the experimental results.

5:20 PM

Microstructure Simulation in Pressurized Solidification during Squeeze Casting of Aluminum Alloy A356: Yanda Li¹; *Zhiqiang Han*¹; Alan Luo²; Anil Sachdev²; Baicheng Liu¹; ¹Tsinghua University; ²General Motors Global Research and Development Center

A mathematical model for describing the nucleation and dendrite growth in pressurized solidification during squeeze casting of aluminum alloy

has been developed, where the thermal and mechanical dual effect on the nucleation in pressurized solidification was taken into account. Cellular Automaton method was employed to simulate the dendrite growth during the squeeze casting process, where the solid-liquid interface growth kinetics was determined based on the interfacial equilibrium, i.e. the relationship of temperature, pressure, composition and interfacial tension. Experiments were carried out for an industrial aluminum alloy A356, where direct squeeze casting process was employed and specimens were produced under the atmospheric pressure and the pressures of 27, 82 and 123 MPa. The nucleation and dendrite growth were simulated with the developed model and the effect of pressure on the microstructure evolution of the casting was discussed based on the numerical simulation.

5:40 PM

Modeling of Melt Mixing Phenomena in Cast Iron with Dual Graphite Structure: Simon Lekakh¹; Jingjing Qing¹; Von Richards¹; ¹Missouri University of Science and Technology

Cast iron castings with dual layered structure including flake and spheroidal graphite phases have an interesting combination of high thermal conductivity and strength. Processing for production of controlled dual graphite cast structure in desired casting regions was CFD FLUENT modeled and experimentally investigated. It was shown that the melt mixing phenomena, which includes filling mixing, mixing by post-filling melt momentum and natural convection, prevents the formation of the desired layered microstructure when the mold was sequentially filled by gray and ductile irons. To prevent intensive melt mixing in the mold, different approaches were virtually investigated. The modeling results were validated by pouring experimental castings and different possible processing routes are discussed.

Deformation, Damage, and Fracture of Light Metals and Alloys: Session III

Sponsored by: The Minerals, Metals and Materials Society, TMS Structural Materials Division, TMS Light Metals Division, TMS/ASM: Mechanical Behavior of Materials Committee

Program Organizers: Qizhen Li, University of Nevada, Reno; Fuqian Yang, Univ. of Kentucky; Ke An, Oak Ridge National Laboratory

Tuesday PM
March 13, 2012

Room: Northern A2
Location: Dolphin Resort

Session Chairs: Qizhen Li, University of Nevada, Reno; Wen-Ming Chien, University of Nevada, Reno

2:00 PM Invited

Materials Design in Magnesium Alloy Development: Michele Manuel¹; ¹University of Florida

Magnesium alloys have attracted great interest due to their high specific strength, castability, and machinability. Despite these advantages, this class of alloys has not received the industrial prominence as their main structural counterpart, aluminum. One obstacle that has limited their use is its restricted low temperature deformation behavior. Recently, there has been a significant effort to integrate computational tools to not only provide a fundamental understanding of unit mechanisms but also drive the design of novel alloys that are stronger and more ductile than current alloys. This presentation will provide insight into the status of materials design tools in its application to magnesium alloy development as well as provide forecasts as to the potential of systems-based, predictive design methodologies in accelerating the maturation of this class of materials. The author would like to gratefully acknowledge the support of the National Science Foundation under grant DMR 0845868.

2:30 PM

The Shear Localization Behavior and Mechanisms of Five Light Metals: Al 7039, Al 5083, Al 5059, AZ31B, and AM60: Sara Perez-Bergquist¹; George Gray¹; Ellen Cerreta¹; Carl Trujillo¹; Mike Lopez²; ¹Los Alamos National Laboratory

While a great number of studies have examined the uni-axial stress behavior of light metals under quasi-static loading conditions, less is known about the dynamic response and particularly the shear failure mechanisms, of these same metals. For this reason, the forced shear response of five light metals has been examined as a function of temperature, texture, and strain rate. Specimens of Al 7039, Al 5083, Al 5059, AZ31B, and AM60, have been characterized prior to deformation. Then post mortem characterization of these specimens, using optical microscopy, scanning electron microscopy, electron back scattered diffraction, and transmission electron microscopy, has been utilized to correlate the observed mechanical response to the microstructural evolution during loading that leads to damage and failure of these materials.

2:45 PM

Reducing Forming Time in Warm Forming of Lightweight Metals by Using Variable Forming Speed: Serhat Kaya¹; ¹The Ohio State University

Reducing weight by forming lightweight metals is in the interest of industry. Isothermal warm forming approach has been studied by researchers. In this study, an experimental non-isothermal warm forming setup is used in a servo-drive press. Combined advantages of the non-isothermal approach and the servo press are demonstrated by introducing a critical stroke and a variable forming speed concept (slower at initial stages of drawing and faster afterwards). As a result, total forming time of a round cup has been reduced by 60 % (from 9sec to 3.4sec) with respect to a constant forming speed (9 sec). More importantly, while forming time is reduced significantly, thickness distributions of the cups formed in 3.4 seconds and 9 seconds were very close. It is known that as the forming speed increases the tendency for thinning and fracture also increases. Therefore, this new approach provided a faster process without sacrifice in thickness.

3:00 PM

Influence of Size on Strength of Nickel Nanowires: Ilaksh Adlakha¹; Kiran Solanki²; Amitava Moitra³; Mark Tschopp⁴; ¹SEMTE; ²Arizona State University; ³Pennsylvania State University; ⁴Mississippi State University

Plastic deformation of nanoscale material is highly dependent on the surface-to-volume ratio. In this work, we use molecular dynamics simulations to gain understand the size scale effect under tensile deformation in single crystal and polycrystalline nickel nanowires. Nanowires exhibit an increase in yield strength as the surface to volume ratios, breakdown in this mechanism for samples less than 10nm diameter; due to the rearrangement of surface atoms in smaller samples having high surface-to-volume ratio. In polycrystalline nanowires, the high surface-to-volume ratios the effect of dislocation mediated plasticity to decreases at smaller wire sizes. For smaller grain sizes, plasticity is accommodated through intergranular mechanisms. These results provide insight into the deformation mechanisms in single and polycrystalline nanowires.

3:15 PM

Deformation Twinning Activation of Ti-6Al-4V under Different Loading Conditions: Ming Chu¹; Jeremy Millett²; Yu Chiu¹; Ian Jones¹; ¹University of Birmingham; ²AWE

Ti6Al4V is the most widespread of titanium alloys and finds use in the aerospace industry in the manufacture of fan blades in jet turbine engines. As such, an understanding of its response to impact loading such as bird strike and foreign object damage is of great importance. In this research, Ti6Al4V has been deformed by means of one-dimensional plate impact to stresses of 5 GPa and 10 GPa. The deformation of Ti6Al4V with a large colony size has also been studied using a Charpy impact



TMS 2012

141st Annual Meeting & Exhibition

tester with impact energy varying from 10J to 300J at both liquid nitrogen temperature and room temperature. The deformation microstructure has been observed using transmission electron microscopy in all specimens tested. In addition to the TEM observations, the nature of twinning and dislocation slip and their roles in the deformation will be discussed vis-à-vis the literature on the plastic deformation of the alloy.

3:30 PM Break

3:50 PM Invited

Mechanical Properties of Bulk Nanostructured 7075 Al Alloy Prepared by Severe Plastic Deformation: *Yonghao Zhao*¹; X.Z. Liao²; T.D. Topping³; Y. Li¹; Y.T. Zhu⁴; R. Z. Valiev⁵; E.J. Lavernia¹; ¹University of California Davis; ²University of Sydney, Australia; ³University of California, Davis; ⁴North Carolina State University, Raleigh; ⁵Ufa State Aviation Technical University, Russia

Age-hardened 7000 series Al alloys exhibit the highest strength amongst Al alloys and therefore are of interest in the aerospace, transportation, and sports industries. Grain refinement down to the nanometer region by severe plastic deformation is a promising technique for further enhancing the strength of structural Al alloys. However, precisely how to optimize the mechanical properties (such as strength and ductility) of bulk nanostructured aged hardened Al alloys remains a challenge. In this study, the as-received 7075 Al alloys were first homogenized at 500°C for 5 h to form super saturated solid solution, then processed by equal-channel-angular pressing (ECAP), cryo-rolling and high pressure torsion (HPT) techniques, respectively, to form microstructures with different grain sizes ranging from nanometer to micrometer. Post-deformation aging treatments were then performed to introduce GP zones, metastable /stable yita phases. Precipitation kinetics and responding mechanical properties were finally measured and analyzed.

4:20 PM

1100 Aluminum under Quasi-Static and Dynamic Loading: *Cyril Williams*¹; Guangli Hu²; Changqiang Chen²; Kaliai Ramesh²; Datta Dandekar¹; ¹U.S. Army Research Laboratory; ²The Johns Hopkins University

In this study, as received 1100-O aluminum was cold rolled to 30, 70, and 80 percent reduction. The effects of microstructural evolution due to the cold rolling are studied under quasi-static and dynamic loading conditions using a servo-hydraulic MTS machine and a compression Kolsky bar, respectively. Significant rate sensitivity of the compressive strength was observed for strain rates from 10^3 s⁻¹ to 6×10^3 s⁻¹ for all materials. As the cold work is increased from 1100-O to 70% cold-rolled aluminum, the yield strength and strain hardening rate change significantly. Microscopic studies using Transmission Electron Microscopy were conducted to correlate the microstructural evolution with the macroscopic mechanical response. This study provides material properties that can be used to model and predict the responses of each material under extreme conditions such as spallation following shock loading.

4:35 PM

Study on High Velocity and High Strain Rate Deformation of Aluminum Alloys with Electromagnetic Forming: *Jianhui Shang*¹; Steve Hatkevich¹; Larry Wilkerson¹; ¹American Trim LLC

Aluminum alloys are interested in industries because of their higher strength-to-weight ratio. To fully understand their deformation mechanism, the dynamic behavior of aluminum alloys should be investigated. Electromagnetic forming is a high velocity and high strain rate forming process in which velocities of up to 300 m/s and strain rates of more than 10^3 s⁻¹ can be achieved. In this study, electromagnetic tube expansion was applied to study on high velocity and high strain rate deformation of aluminum alloys. Photon Doppler Velocimetry (PDV) was used to measure the velocity during tube expansion experiments. The numerical simulation was also carried out to study the dynamic behavior of aluminum alloys. The experimental and simulation results will be presented and discussed in this study.

4:50 PM

Dynamic Characterization of Open Cell Aluminium Foam Structures: *Carl Cady*¹; George Gray¹; Etienne Combaz²; Andreas Mortensen²; ¹Los Alamos National Laboratory; ²Ecole Polytechnique Federale de Lausanne

The objective of this presentation is to provide evidence of how open-cell aluminium foam containing an incompressible liquid behaves when it is dynamically loaded. The underlying motivation is the idea that viscous friction in the fluid as it flows through tortuous fine-scale pores in deforming microcellular metal might provide a potent mechanism for the dissipation of mechanical energy. The foam material studied is a high-purity aluminium (99.99%) produced by the replication process, i.e., by pressure infiltration of a cold-pressed salt perform followed by solidification, cool down, machining and leaching. Cylindrical foam samples are tested dry (i.e., with air within the pores) and in the wet condition, i.e., with pores filled by water to evidence the influence of strain rate, temperature, relative density and flow of the fluid on their mechanical behavior.

5:05 PM

Impact Deformation and Dislocation Substructure of Ti-6Al-4V Alloy at Cryogenic Temperatures: *Woei-Shyan Lee*¹; Tao-Hsing Chen¹; Sian-Cing Huang¹; ¹National Cheng Kung University

The aim of this study is to investigate impact response and dislocation substructure of Ti-6Al-4V alloy using a compressive split-Hopkinson pressure bar and transmission electron microscopy technique. Cylindrical specimens are deformed at strain rates ranging from 8×10^2 s⁻¹ to 4.0×10^3 s⁻¹ and temperatures of 0 K and -200 K, respectively. It is shown that the impact properties of Ti-6Al-4V alloy depend strongly on strain rate and temperature. For a constant temperature, the flow stress and strain rate sensitivity increase with increasing strain rate, while the activation volume decreases. Meanwhile, for a constant strain rate, the activation volume increases with increasing temperature, while the flow stress and strain rate sensitivity decrease. The strengthening effect in deformed Ti-6Al-4V alloy is a result primarily of dislocation multiplication. Transmission electron microscopy (TEM) observations show that the dislocation density increases with an increasing strain rate, but decreases with an increasing temperature. The mechanical properties of the impacted specimens are related to the microstructural evolution.

Electrode Technology for Aluminium Production: Carbon Materials for Anode and Cathode

Sponsored by: The Minerals, Metals and Materials Society, TMS Light Metals Division, TMS: Aluminum Committee, TMS: Aluminum Processing Committee
Program Organizer: Morten Sorlie, Alcoa Norway

Tuesday PM
March 13, 2012

Room: Americas Seminar
Location: Dolphin Resort

Session Chair: Carlos Zangiacomi, Alcoa Aluminum Inc.

2:00 PM

Evolution of Anode Grade Calcined Coke: *Les Edwards*¹; Nigel Backhouse²; Hans Darmstadt²; Marie-Josée Dion²; Rain CII Carbon; ²Rio Tinto Alcan

The petroleum refining industry has historically categorized petroleum cokes as either fuel grade, anode grade or needle coke. The term "anode grade coke" has been used as a broad definition to describe delayed coke with a sponge structure containing relatively low levels of trace metals like vanadium and nickel (typically <400ppm) and low to moderate levels of sulfur (0.5-4.0%). However, these historic classifications are less relevant today as a much wider variety of cokes are used in anode blends. This paper will review the growing range of coke qualities used in "anode grade" coke blends. Shortages of traditional quality anode grade coke are driving calciners and anode producers to use cokes with a much

wider range of properties including sulfur and metals levels and structure. Cokes previously regarded as unsuitable for anode production are now being used routinely at varying levels and this trend is likely to continue.

2:20 PM

Studies on Impact of Calcined Petroleum from Different Sources on Anode Quality: *Binuta Patra*¹; Rabindra Barik¹; ¹National Aluminium Company Ltd

Calcined petroleum coke is a major raw material for manufacturing of carbon anodes for any Aluminium Smelter operation. Productivity & profitability of a smelter is influenced to a large extent by the performance of anodes in electrolytic pots. National Aluminium Company Ltd. has been using C.P.Coke from different sources since its inception. Quality of c.p.coke varies in different supplies depending on the raw material used by the calciner and the process parameters maintained during operation. This paper presents the quality of C.P. Coke from different sources and their influence on anode quality. Anode bench scale studies have also been carried out by blending c.p.coke from different sources and assessment of the anode quality.

2:40 PM

Prebaked Anode from Coal (3) - Carbonization Properties of Hypercoal Blended with Coal-Tar Pitch: *Maki Hamaguchi*¹; Niriuyuki Okuyama¹; Nobuyuki Komatsu¹; Naoki Kikuchi¹; Jiro Koide²; Hideki Kasahara²; ¹Kobe Steel, Ltd.; ²Sumitomo Corporation

Hypercoal is our propriety solvent extraction technology of coal which produces fusible carbonaceous feedstock of extremely low ash content. In the recent papers, we have reported that prebaked anode can be successfully prepared from hypercoal coke. Hypercoal coke has an advantages of low sulfur, vanadium, and nickel content and superior thermal stability compared to conventional petroleum coke. In this report, we will describe the carbonization properties of hypercoal blended with coal-tar pitch in an attempt to utilize the hypercoal as an alternative for binder pitch of prebaked anode production. It is also reported that self-sintering Hypercoal carbon was fabricated by thermal treatment of Hypercoal.

3:00 PM

Importance of Primary Quinoline Insoluble in Binder Pitch for Anode: *Minoru Sakai*¹; Yulong Wang¹; Takashi Fukuoka¹; Hitomi Hatano¹; ¹JFE Chemical Corporation

Laboratory scale anodes were made of a fixed coke and six binder pitches having different primary QI in the range between 9 and 22%. Binder matrices were also made for oxidation test against air and CO₂. Three of them were commercial products and the others were made experimentally, and none of them contained secondary QI. Softening point of these pitches was around 110 °C. Pitches containing larger amount of primary QI showed higher coking value, which resulted in higher bulk density of baked anodes. The increase in bulk density improved compressive strength. The electrical resistivity, which decreased with increasing bulk density, was not deteriorated by the larger amount of primary QI in pitch. No acceleration of oxidation in air and CO₂ was observed in the binder matrix test. These results showed that pitches with high primary QI are more favorable as binder pitches for anodes.

3:20 PM

Investigation on Air Reactivity and Electrolysis Consumption of Anode Carbons with Anthracite Additions: *Jilai Xue*¹; Meizhi Han¹; Jun Zhu¹; ¹University of Science and Technology Beijing

The increasing price of coke and shortage in local supply for anode manufacture has presented challenge for smelters with added cost into the metal product. This paper is to show an effort in searching alternative carbons to replace part of traditional coke for the prebaked anodes. Some calcined anthracite was selected as starting materials and pre-treated in a chemical process. Then it was added into the carbon mixtures, formed and baked into the anode samples (F25X45mm) that tested for air-reactivity with ISO standard. The results showed that the ash content of the pretreated anthracite was lowered than that without the pretreatment,

and varied with the anthracite additions of 20 - 40wt%. Kinetics of the air-reaction process with anthracite addition was also investigated. So far the anode samples with the anthracite additions around 20 wt% is promising for potential industrial application.

3:40 PM

Experiences on Anode Reconstruction Process in Soderberg Technology: *Carlos Zangiacomi*¹; Jose Luis Garcia Garcia²; Andre De Abreu¹; Ciro Kato¹; ¹Alcoa Aluminum Latin America; ²Alcoa INESPAL, S.A.

Anode construction is a challenging process for Soderberg Cells. In order to reestablish the full Plant capacity at Alcoa Pocos de Caldas, southern of Brazil, it was necessary to develop a new process to bake anodes within the Potrooms environment. Using line load as baking element and controlling the current passing through each stubs, it was possible to assembly new anodes with quality and proper condition for optimum cell operations. This paper describes the sequence of activities applied for assembling new Soderberg anodes, the techniques implemented to monitor and control the baking process and finally the outcome after pot start-up.

4:00 PM Break

4:10 PM

Cathode Performance Evaluation at Votorantim Metais - CBA: *Jean Pardo*¹; ¹Votorantim Metais - CBA

The cathode is a set of items with a high cost in the primary aluminum production, this set is usually composed of carbon materials, refractory and insulating materials, which have their basic raw materials extracted from nature. There is great concern about cathode performance, this with respect to life and electric power consumption, several works have been performed in order to maximize the life cathode thereby avoiding costs and waste, more commonly known as SPL (spent pot life) as well as an hazardous waste to the environment and has a high cost for recycling. In this paper, we present the results summarized in a series of autopsies to determine the main reasons of cathode failures and present the results of actions developed to maximize the life cathodic CBA.

4:30 PM

Green, Safe and Clean Carbon Products for the Aluminium Electrolysis Pot: *Bénédicte Allard*¹; Régis Paulus¹; ¹Carbone Savoie

Carbon products used in aluminium electrolysis pots are generally based on coal-tar pitch or resin binders. Coal tar pitch is considered by REACH as very high concern product, and it is carcinogenic classified. Phenol, a typical component of resin binders used in carbon products, is also carcinogenic classified. In face of these hazards, solutions that guarantee a clean and safe environment for the workers have to be brought. Last year a 100% clean ramming paste NeO² has been introduced, based on a new binder type containing no CMR product and no hazardous substance. This paste was fully anthracitic. Since then, Carbone Savoie made developments to complete its Green range with a 100% clean semi-graphitic grade of ramming paste, using the same type of binder and with a 100 % clean glue, which could be used at different locations in the pot. Characteristics of these new products will be presented.

4:50 PM

A New Material for Collector Bar Sealing – LRM2: *Thiago Simoes*¹; Marcio Guimaraes¹; Marcelo Assuncao¹; ¹Novelis

The collector bar sealing is an important procedure during the cathode construction. The material selection and the installation techniques have to be very well managed in order to obtain a high performance pot with low cathode voltage drop and long lifetime. A new material has been developed to be used for this purpose providing easy installation, good electrical resistance and stability for the pot. The formulation proposed, called LRM2, has been applied on Ouro Preto Smelter in place of old sealing material since 2008 and has shown lower electrical resistance than the old carbon glue and very easy installation when compared with the cast iron alternative. The present paper explores a discussion among the types of bar/block sealants and the Novelis efforts to make improvements



TMS 2012

141st Annual Meeting & Exhibition

in this field. Our results are discussed here highlighting the benefits using iron powder pastes when compared with other techniques.

5:10 PM

Dry Barrier Mix in Reduction Cell Cathodes: *Richard Jeltsch*¹; Chen Cairong²; ¹Jeltsch Consulting; ²Chalieco/Gami

Dry barrier mix (DBM) has been successfully tested as a replacement for barrier bricks in several reduction cell technology types and has been adopted as standard practice in all three of the Chinese cell technologies. DBM reacts with cathodic bath in-situ to form a glass-like barrier which retards the further penetration of bath components, protecting the lighter insulation from contact with the bath. Laboratory "cup tests" show that silicate based DBM formulations are more effective than anorthite formulations or conventional refractory aggregates in formation of the glassy barriers. Cell bottom temperatures remain stable over the lifetime of the cell, indicating the barrier formation protects the insulating value. Cell autopsies show partial penetration of the DBM with barrier formation and preservation of the bottom portion of the DBM. Cell lining life is at least equivalent to that of brick barrier cells.

Electrometallurgy 2012: Session III

Sponsored by: The Minerals, Metals and Materials Society, The Metallurgy and Materials Society of CIM, TMS Extraction and Processing Division, TMS: Hydrometallurgy and Electrometallurgy Committee

Program Organizers: Georges Houlachi, Hydro-Quebec; Antoine Allanore, Massachusetts Institute of Technology; Michael Free, University of Utah; Michael Moats, University of Utah; Edouard Asselin, UBC; Shijie Wang, Rio Tinto Kennecott Utah Copper; James Yurko, Materion Brush Beryllium and Composites

Tuesday PM
March 13, 2012

Room: Europe 5
Location: Dolphin Resort

Session Chairs: Michael Moats, University of Utah; Edouard Asselin, University of British Columbia

2:00 PM

Capacities of Molten Slags and Their Practical Use: *Kazuki Morita*¹; ¹The University of Tokyo

Molten slags have been generated in various metallurgical processes. Furthermore, their role as refining fluxes is also significant. Chemical composition of molten slags often becomes the key in the optimization of each refining process. Among others, basicity is known to be a major factor in the red-ox reactions in the metal refining processes. Since Carl Wagner proposed several capacities as semi-quantitative measures of the basicity of slags, several capacities, such as sulfide capacity and phosphate capacity, have been brought into practical use in optimizing steel refining processes for the last several decades. Present author also defined some capacities, such as chloride, ruthenate and rhodate capacities of slags, in the investigation of the recycling processes of plastics and PGMs. In the present paper, the concept of the capacities will be reviewed and the newly defined capacities will be introduced together with the practical use in the high temperature recycling processes.

2:20 PM

Investigation of Nucleation and Plating Overpotentials during Copper Electrowinning using the Galvanostatic Staircase Method: *Michael Moats*¹; Alexander Derrick¹; ¹University of Utah

The Winand Diagram was developed and has been used for decades to illustrate the interaction between polarization, mass transport and inhibition on the resulting structure of a metal electrodeposit. Recently,

Adcock et al. criticized the Winand Diagram and developed their own structural diagram based on nucleation and plating overpotentials. Their work was based on zinc electrodeposition using a galvanostatic staircase method. This work explores the nucleation and plating overpotentials for copper electrodeposition using conditions typical for primary electrowinning using the galvanostatic staircase experimental technique. Additionally, the effect of organic additives and plating substrate on these overpotentials are reported.

2:40 PM

Nucleation and Growth of Copper on Stainless Steel Cathode Blanks in Electrorefining: *Jari Aromaa*¹; *Olof Forsén*¹; *Antti Kekki*¹; ¹Aalto University

The deposition of copper on inert substrate depends on the number of active sites that will react at certain overpotential. The critical overpotential depends on surface morphology, surface film resistance and additives on cathode surface. The surface properties and copper nucleation and growth rates were studied for used stainless steel blanks from several tankhouses. The surfaces of the blanks were characterized with electrochemical and mechanical methods. Electrochemical deposition tests were done at current density 300 A/m² for 10, 30 and 60 seconds. The nucleation density and copper coverage were estimated using image analysis. The surface film resistance did not correlate with copper growth. Increasing surface roughness correlated with lower copper growth.

3:00 PM

An Overview of the Design of the New Nickel Tankhouse at Anglo American Platinum's Base Metal Refinery: *Deborah Erasmus*¹; *Nicko Prinsloo*¹; ¹Anglo American Platinum

Anglo American Platinum has recently commissioned a new nickel electrowinning tankhouse as part of their strategic Base Metal Refinery expansion project. The tankhouse design includes permanent cathode technology, automated stripping, semi-automated harvesting, anode skirts and cell hoods to reduce worker exposure to aerosols and solutions that contain nickel sulfate and acid. The development and testing of the technology has been performed in-house to attain an average ambient nickel aerosol concentration of <0.05mg/m³ in the new tankhouse building, which is well below the current MHSA OEL of 0.1mg/m³. This paper provides a process description of the new tankhouse and highlights some of the challenges and successes experienced during the initial commissioning phase.

3:20 PM

Developments in Base Metal Electrowinning Cellhouse Design: *Tim Robinson*¹; *Kathryn Sole*²; *Michael Moats*³; *Frank Crundwell*⁴; *Masatsugu Morimitsu*⁵; *Lauri Palmu*⁶; ¹Republic Alternative Technologies; ²Independent Consultant; ³University of Utah; ⁴CM Solutions (Pty) Ltd; ⁵Doshisha University; ⁶Talvivaara

Zinc and Nickel and Copper electrowinning cellhouse process technology and design trends include focus on energy reduction, productivity and acid mist abatement. Larger electrodes, longer cells, automation and higher current densities are leading to more capital effective designs. Latest cellhouse designs include further installation of automated electrode handling systems, thereby removing more operators from the cellhouse. In summary these technology and design trends have further resulted in lower electrowinning operating costs and improved electrowon cathode purity.

3:40 PM Break

3:55 PM

The Recovery of Manganese from the Boleo Project Using Leach, Precipitation and Electrolytic Manganese Metal Production: *Thomas Gluck*¹; David Dreisinger²; Jianming Lu²; ¹Baja Mining Corp.; ²Univ of B.C.

The recovery of manganese from the Boleo project of Baja Mining is via an acid oxidation and acid reduction process in seawater. Manganese as manganese dioxide is leached into solution as manganese sulphate with the addition of sulphur dioxide gas as a reductant and then precipitated as manganese carbonate. The use of the manganese carbonate intermediate to produce electrolytic manganese metal (EMM) has been extensively studied. The manganese carbonate can be used in place of natural (MnCO₃) or reduced ores (MnO) of manganese as a feed to the EMM plant. Manganese carbonate can be dissolved in spent electrolyte from manganese plating, followed by purification using ammonium sulphide precipitation of minor elements and then electrowinning in the selenium free process. The results of small cell and full height cell testing of manganese electrowinning will be reported.

4:15 PM

Underpotential Dissolution of Precious Metals from Intermetallic Compounds with Zn: *Hideaki Sasaki*¹; Takashi Nagai¹; Masafumi Maeda¹; ¹Institute of Industrial Science, The University of Tokyo

The dissolution of precious metals (PMs) can be enhanced by alloying with other metals such as Zn. During the dissolution of PM-Zn alloys or intermetallic compounds, Zn dissolves preferentially and precious metals form transient small particles. Because small particles have higher activity than the bulk state, the PM particles may dissolve at low potentials where PM dissolution usually does not occur. This "underpotential dissolution" can be utilized in the hydrometallurgical recovery process for PMs. If the alloying pretreatment with Zn vapor enables dissolution of PM by weak and inexpensive chemical agents, the cost and environmental load for the recovery can be reduced. This study examined dissolution of PM-Zn compounds by electrochemical measurement to propose an appropriate condition for enhancing dissolution of PMs.

4:35 PM

The Recovery of Cobalt from the Boleo Deposit Using Leach, SX and EW: *David Dreisinger*¹; Thomas Gluck²; Jianming Lu¹; ¹Univ of B.C.; ²Baja Mining Corp.

The Boleo project of Baja Mining (Vancouver) will process a mixed oxide-sulfide ore using an acid oxidation and reduction process in seawater to extract copper, zinc, cobalt and manganese. Copper will be extracted via SX-EW as copper cathode, zinc will be recovered as a zinc sulphate monohydrate crystal and cobalt will be produced as a cobalt cathode product after phosphinic acid extraction. Manganese may be recovered from the final solvent extraction raffinate by precipitation as manganese carbonate. The development of the cobalt recovery process (solvent extraction and electrowinning) will be discussed. The pilot plant solvent extraction circuit and subsequent bench and small pilot testing of cobalt electrowinning will be discussed. The Boleo project will produce nearly 2,000 tonnes per annum of cobalt metal when fully commissioned.

Emeritus Professor George D.W. Smith Honorary Symposium: Steels II and Superalloys

Sponsored by: The Minerals, Metals and Materials Society, TMS Materials Processing and Manufacturing Division, TMS/ASM: Phase Transformations Committee

Program Organizers: Michael Miller, Oak Ridge National Laboratory; Gregory Olson, Northwestern University and QuesTek Innovations LLC; George Krauss, Colorado School of Mines

Tuesday PM
March 13, 2012

Room: Mockingbird 2
Location: Swan Resort

Funding support provided by: Oak Ridge National Laboratory; QuesTek Innovations LLC; AMETEK, Inc

Session Chairs: Gregory Olson, Northwestern University; Frédéric Danoix, Université de Rouen

2:00 PM Invited

Ordering Processes in Ni₂(Cr,Mo) Alloy Investigated by TEM and 3D-AP: *Nelia Wanderka*¹; Amit Verma¹; Nikolai Lazarev²; M Sundararaman³; J Singh⁴; ¹Helmholtz Zentrum Berlin für Materialien und Energie GmbH; ²NSC Kharkov Institute of Physics and Technology, Kharkov, Ukraine; ³Hyderabad Central University, India; ⁴Bhabha Atomic Research Centre, Structural Metallurgy Section, Mumbai, India

The study of short range ordered state and the evolution of long range ordered state from it in metallic alloy systems is always a field of interest for theoreticians and experimentalists. In the present study an attempt has been made to rationalize the short range ordered state in stoichiometric alloys of Ni₂(Cr,Mo) composition based upon the experimental evidence obtained from transmission electron microscopy and 3-dimensional atom probe investigations. Experiments were carried out on specimens with the same alloy composition but prepared by two different routes namely: by splat quenching and by casting, homogenising treatments. Aging treatments over a wide temperature range were used to follow the ordering. Three-dimensional atom probe data were evaluated by several statistical methods such as cluster searching and density spectrum analysis. Monte Carlo simulation was performed for interpretation of the observed ordering processes. The analyzed data are correlated with TEM results and calorimetric data.

2:25 PM Invited

The Effect of Creep on the Rhenium Distribution Close to the $\bar{a}\bar{a}$ Interfaces in a Nickel-Based Superalloy: *Alessandro Mottura*¹; Michael Miller²; Roger Reed³; ¹University of California, Santa Barbara; ²Oak Ridge National Laboratory; ³The University of Birmingham

Atom probe tomography was used to estimate the rhenium distribution in uncrept and crept (550h to 1170h at 1223K and 185MPa) specimens of a commercial single-crystal CMSX-4 nickel-based superalloy. Rhenium proximity histograms both transverse and longitudinal to the loading axis were obtained across the γ/γ' interfaces. As expected, rhenium strongly partitioned to the γ -phase, and a rhenium enriched area was observed close to most primary γ' interfaces on the γ -phase side. The rhenium concentration profile appeared unaffected by the duration of creep tests and by the orientation of interfaces relative to the loading direction. Conversely, the rhenium concentration profile was strongly affected by phase morphology ahead of the interfaces. These findings indicate that the rhenium enrichment forms upon cooling from service temperature and has little effect on the creep properties of CMSX-4. Research sponsored by the U.S. DOE-Office of Basic Energy Sciences SHaRE user program [APT and MKM].



TMS 2012

141st Annual Meeting & Exhibition

TUESDAY PM

2:50 PM Invited

Spinodal Decomposition in Fe-Cr and Fe-C Systems: *Frederic Danoux*¹; ¹CNRS - Université de Rouen

Spinodal decomposition proceeds from unstable solid solutions, resulting, by contrast to classical nucleation and growth, in the absence of any incubation period. The initial stages are characterised by low amplitude – small extend composition fluctuations, which develop towards a mixture of the equilibrium phases. In Fe-based alloys, G.D.W. Smith was involved in the study of two different systems: Fe-Cr and Fe-C. In the first case, interfacial energy is limited, which leads to the development of ‘isotropic’ spinodal decomposition, where Fe rich and Cr rich regions form two interconnected networks. The evolution of this specific microstructure was characterised in details in 3D in his group. Concerning the Fe-C system, G.D.W. Smith and his co workers proposed in the early 80’, based their atom probe data, that C supersaturated martensite could experience spinodal decomposition. Recent investigations confirmed this hypothesis, and a previously developed by Khachaturyan model is adapted to account for it.

3:15 PM

High Strength Conductors for High Field Magnets: *Ke Han*¹; Jun Lu¹; ¹National High Magnetic Field Laboratory

A study led by Smith demonstrated a considerable difference in the tensile deformation behavior between fine and coarse pearlite. The concepts are widely accepted and used for material designs, including ones for high field magnets (HFM). The mechanical strength and deformation behavior of the conductors in HFMs are two of the important factors to determine the maximum magnetic field strength and life in magnets. When a magnet operates at very high field, a complex stress status occurs, and other material properties have to be taken into account to ensure the integrity of a magnet. Typical mechanical properties are fatigue endurance, fracture toughness and elongation. All those are related to the deformation behavior of the high strength conductors that have similar microstructure to pearlite. This paper will address the material characterization issues in high strength conductors and the importance to relate the material properties to operation and manufacture conditions.

3:30 PM

Applications of Atom Probe Tomography in Computational Materials Design: *Jason Sebastian*¹; Gregory Olson¹; Jim Wright¹; Abhijeet Misra¹; Eric Hamann¹; ¹QuesTek Innovations LLC

As part of a symposium honoring Prof. George D.W. Smith of Oxford University, QuesTek will provide an overview of its use of atom probe tomography (APT) in computational materials design. Within the framework of QuesTek’s system-based approach to materials design, APT is an essential tool that allows for the confirmation of an alloy’s designed nanostructure. The composition, morphology, and size distribution of nanoscale strengthening precipitates can be measured directly. Nanoscale interfacial phenomena (segregation, film formation, etc.) can also be directly observed. Specific results from a variety of QuesTek APT analyses on prototype and commercial alloys will be summarized, including carbide strengthened steels, intermetallic strengthened Ni- and Fe-based alloys, aluminum alloys, and others.

3:45 PM Break

4:10 PM

Examination of Carbon Redistribution in Quench and Tempered 4340 Steel: *Amy Clarke*¹; Michael Miller²; David Alexander¹; Robert Field¹; Kester Clarke¹; ¹Los Alamos National Laboratory; ²Oak Ridge National Laboratory

Quenching and tempering of martensitic steels significantly influences the resulting mechanical properties. During quenching (autotempering) and/or subsequent tempering of martensite, several carbon redistribution processes are possible, including carbon segregation to dislocations or lath boundaries, carbon clustering, carbon partitioning to austenite, transition carbide and/or cementite formation, and retained austenite decomposition.

In this work, a 4340 steel was oil or water quenched and tempered at temperatures ranging from 325 to 575°C. Tensile, compression, and Charpy V-notch testing was performed on the oil quenched and oil quenched and tempered conditions to determine the influence of thermal processing on mechanical behavior. The complex, ultrafine scale microstructures and the location of carbon within the martensite were examined with atom probe tomography†. Transmission electron microscopy was also performed. †Research at the Oak Ridge National Laboratory SHaRE User Facility was sponsored by the Scientific User Facilities Division, Office of Basic Energy Sciences, U.S. Department of Energy.

4:25 PM

Microstructural Evolution of Second Phases in Austempered High-Al TRIP Steels Examined by Atom Probe Tomography: *Hyoung Seok Park*¹; Jae Bok Seol¹; Jai Hyun Kwak²; Chan Gyung Park¹; ¹Pohang University of Science and Technology (POSTECH); ²POSCO

Recently, light-weight transformation-induced-plasticity (TRIP) steel has been developed for automotive parts. In order to reduce the specific weight without degrading mechanical properties of TRIP steels, about 6 wt.% aluminum is added. Their mechanical properties significantly depended on the morphology and composition of constituent phases formed: M₃C-type κ-carbides in nm size coexisting with γ-Fe or α-Fe. In the present study, therefore, microstructural evolution of 2nd phases, depending on austempering treatment, has been examined by using the combined analyses of APT, TEM and EBSD. As austempering temperature increased, the fraction of retained γ decreased with increased second phases, which were identified as (Fe,Mn)₄x(AI,C)_x carbides and/or retained austenite decomposed. Both phases revealed quite similar morphology of thin lenticular platelets or laths. Based on our results, the correlation between the mechanical properties, the role of alloying elements, especially Al, and the structure and chemistry of the constituent phase evolved will be discussed.

4:40 PM

Insight into Cluster Strengthening in a Nb-Microalloyed High Strength Low Alloyed Steel Using Atom Probe Tomography: *Kelvin Xie*¹; Andrew Breen¹; Michael Moody¹; Julie Cairney¹; Simon Ringer¹; ¹The University of Sydney

The yield strength of a UCS (ultra thin cast strip) steel strip produced by the CASTRIP process, microalloyed with 0.084 wt% Nb can be further improved substantially without compromising ductility. Additional 165 MPa yield strength was gained by performing simple heat treatment at 700 °C for 4 min. The optimal strengthening can be attributed to dispersion of Nb-rich monoatomic layer clusters mostly aligned along dislocations, which were precursors of Nb(C,N) nanoprecipitates. Cluster dispersion was observed to be a more effective strengthening method. Application of Orowan-Ashby equation showed that cluster strengthening used much less Nb atoms than conventional Nb(C,N) nanoprecipitates but can still achieve the same strengthening effect. A method that directly correlates atom probe results and TEM observations of those Nb-rich clusters was also proposed, which expanded the spatial resolution limit of atom probe in the study of clusters in HSLA steels. The presenter would like to have an oral presentation and would like to participate in the Young Scientist Award competition.

4:55 PM

Cluster Strengthening of Microalloyed Castrip® Steels: *Sachin Shrestha*¹; Kelvin Xie¹; Chen Zhu¹; Julie Cairney¹; Simon Ringer¹; Chris Killmore²; Kristin Carpenter²; Frank Barbaro²; James Williams²; ¹The University of Sydney, Australian Key Centre for Microscopy and Microanalysis; ²BlueScope Steel, Metallurgical Technology

This study investigates the microstructure and mechanical properties of Nb-microalloyed Castrip® steels aged at temperatures below and above the Ac1 temperature (525-800°C). Ageing provides both rapid strength enhancements and improvements in ductility, where normally one of these properties would be lost at the expense of the other. Atom probe tomography (APT) reveals that the strengthening is due to heterogeneous

formation of Nb rich clusters and precipitates within the microstructures that are thought to retard the movement of dislocations during deformation. APT data mining is used to characterize the size and distribution of these clusters and precipitates. The strengthening kinetics are compared across a range of different temperatures using an Arrhenius model. The model allows us to understand the temperature dependence of peak ageing times and evaluate the strengthening mechanisms at various temperatures based on the activation energy of precipitation strengthening.

5:10 PM

The Application of Atom Probe Tomography to Oxide-Dispersion-Strengthened Steels: *Ceri Williams*¹; Emmanuelle Marquis²; Paul Bagot¹; George Smith¹; ¹University of Oxford; ²University of Michigan

Oxide-dispersion-strengthened ferritic steels are candidate structural materials for fusion reactors. Very high densities of Y-Ti-O nanoclusters (~2nm diameter) provide strength at temperatures up to ~650°C and improve radiation tolerance. In this work, an Fe-14%Cr-2%W ODS alloy with 0.1-0.4%Ti and 0.3%Y₂O₃ is analysed by Atom Probe Tomography (APT). APT is unique in the chemical resolution attainable at the nanometre level, and substantial improvements in the field of view afforded by the current generation of instruments means that thousands of nanoclusters can be analysed per specimen. With this, we can therefore quantify changes in the nanocluster dispersion. Such changes, and the validity of various data analysis techniques used to analyse composition and size distribution of the nanoclusters will be addressed. Significant changes to the chemistry of nanoclusters are observed depending on the initial composition of the alloy. The resulting impact on the high temperature stability of the nanoclusters will also be discussed.

5:25 PM

APT Characterization of Nanometer Scale Features in RPV Steels and Nanostructured Ferritic Alloys: Insight, Challenges and Opportunities: *Peter Wells*¹; Nick Cunningham¹; Eric Stergar¹; Yuan Wu¹; G. Robert Odette¹; ¹UC Santa Barbara

APT tools and techniques, many pioneered by Professor Smith and his Oxford group, have been used for more than 20 years to study nm scale Cu-Mn-Ni-Si precipitates in irradiated RPV steels, and more recently to characterize Y-Ti-O nanofeatures in nanostructured ferritic alloys. While enormously valuable, the APT results have sometimes not been fully consistent with those found by other characterization techniques. We show specific examples of well-known phenomena that standard reconstruction treatments do not treat. Perhaps the most important is the local evolution of the tip morphology due to evaporation field differences leading to variations in the magnification factor and associated trajectory aberrations. For lower evaporation field the topology changes increase the number of atoms nominally in the feature volume. We focus on quantifying the tip morphology evolution, and suggest approaches to improved reconstructions. We also discuss low evaporation field features affects on increase in multiple hits.

5:40 PM

Initial Age Hardening and Nanostructural Evolution in a Cu-Ni-P Alloy: *Yasuhiro Aruga*¹; ¹Kobe Steel, Ltd.

Initial age hardening and clustering behavior during ageing at various temperatures for up to 10000s after solution treatment in a Cu-0.41Ni-0.11P (mass%) alloy have been investigated. The evolution of an atomistic-level nanostructure has been characterized by a three-dimensional atom probe (3DAP). The experimental results have showed that no difference in hardness between non-aged material and that aged at 523K for 100s, whereas increasing the ageing time beyond 100s at 523K causes an obvious increase in hardness. It can be seen that the hardness increases gradually throughout ageing at 623K. It is shown that the initial age hardening is caused by Ni-P clusters in the alloys. The clustering and precipitation behavior related to the change in the hardness is discussed in terms of diffusion and driving force for nucleation.

5:45 PM

Quantitative Three Dimensional Atom Probe Analysis of In-Situ Tic Reinforced Ni Composite: *Junyeon Hwang*¹; Sundeep Gopagoni¹; Kristopher Mahdak¹; Jaimie Tiley²; Rajarshi Banerjee¹; ¹University of North Texas; ²AFRL

Nickel-titanium carbide (Ni-TiC) composites were prepared by the laser engineered net shaping (LENS) process. The as-deposited microstructure consists of primary TiC and eutectic TiC precipitates distributed within a nickel matrix. The resulting microstructures were characterized by coupling electron backscatter diffraction (EBSD), energy dispersive X-ray (EDX) analysis, and detailed transmission electron microscopy (TEM) studies. Site-specific laser-pulsed atom probe tomography tomography (APT) studies have been performed on the carbide in the Ni matrix. The experimentally measured carbon concentration within the primary TiC appears to be changing from the carbide/nickel interface towards the core of the carbide while the eutectic TiC precipitates appear to exhibit a more uniform carbon concentration. Additionally, the structure of the TiC/Ni interface and the orientation relationship between carbides and matrix will also be discussed in this study.

Energy Nanomaterials: Photovoltaics II

Sponsored by: The Minerals, Metals and Materials Society, TMS Materials Processing and Manufacturing Division, TMS Structural Materials Division, TMS: Advanced Characterization, Testing, and Simulation Committee, TMS: Nanomechanical Materials Behavior Committee

Program Organizers: Reza Shahbazian-Yassar, Michigan Technological University; Ming Au, Savannah River National Laboratory; Meyya Meyyappan, NASA Ames Research Center

Tuesday PM
March 13, 2012

Room: Swan 3
Location: Swan Resort

Session Chairs: Reza Shahbazian Yassar, Michigan Technological University; Zohreh Razavi, Georgia Institute of Technology

2:00 PM Invited

Morphology Engineering of 1D, 2D and 3D TiO₂ Nanostructures and Their Application in Dye-Sensitized Solar Cells: *Ziqi Sun*¹; Jung Ho Kim¹; Yue Zhao¹; Shixue Dou¹; ¹University of Wollongong

Titanium dioxide is one of the most important wide-gap semiconductors and is widely studied for use in the areas ranging from photovoltaic/ photocatalysis to photo-/electrochromics and sensors. Synthesis of TiO₂ nanostructure with controlled size and shape is of considerable interest, owing to that the performance of TiO₂-based devices is largely influenced by the size and shape of TiO₂ building units, especially in nanometer scale. In this presentation, the recent progress on the synthesis of 1D, 2D and 3D TiO₂ nanostructures and their application in dye-sensitized solar cells will be summarized at first. Then our latest results on the tunable growth of diverse morphology of TiO₂ 1D, 2D and 3D nanostructures will be presented. Based on the understanding on the crystal growth mechanism, the morphology and size of TiO₂ nanostructures were easily controlled. As an example application of these controllable nanostructures, the morphology effect on the performance dye-sensitized solar cells was studied.

2:30 PM

Microstructural Evolution of SnS Thin Films Grown by Electrodeposition: *Ho Seong Lee*¹; H. Hennayaka¹; ¹Kyungpook National University

Among the IV-VI semiconductor materials, tin monosulphide (SnS) has attracted considerable attraction during last two decades due to its possibility of applications in the field of photoelectronics. SnS, with orthorhombic structure, a direct band gap around 1.3 eV and a high optical absorption coefficient (>10⁴ cm⁻¹), has been reported to exhibit



TMS 2012

141st Annual Meeting & Exhibition

p-type conductivity. These properties confirm that SnS has appropriate electrical and optical features suitable for an absorber layer in solar cells. In this work we have deposited SnS on indium-tin-oxide (ITO) glass and gold-coated Si substrates by a low temperature electrochemical deposition (ECD) method. The morphology and composition of the SnS films were analyzed by scanning electron microscopy (SEM) and an energy dispersive spectroscopy (EDS). The crystal structure of the films was characterized by XRD patterns. The microstructural properties of the deposited SnS films were investigated by transmission electron microscopy (TEM) analysis.

2:45 PM Break

3:05 PM Invited

Synthesis of Nanostructured TiO₂ /Carbon Nanotube Heterojunction Electrodes for Solar Energy-Driven Applications: *Zohreh Razavihesabi¹; Paul Szymanski²; Hamid Garmetani²; Mostafa Elsayed²; ¹Georgia Institut of Technology; ²Georgia Institute of Technology*

Highly ordered anodically grown TiO₂ nanotubes as well as TiO₂ nanoparticles were integrated with one-dimensional carbon nanotubes (CNTs). CNT/TiO₂ heterojunctions were prepared by grafting functionalized CNTs to TiO₂ nanoparticles/nanotubes. The synthesized hybrid nanostructures were used as photoanodes to split water photoelectrochemically and compared to the widely-used photoanodes, pure TiO₂ nanotubes. The effect of CNTs as well as TiO₂ morphology on the efficiency of hybrid nanostructures and possible enhancement mechanisms are discussed in detail.

3:35 PM

Phase-Field Simulations of Patterned Quantum Dot Growth: *Larry Aagesen¹; Pei-Cheng Ku¹; Leung Lee¹; Katsuyo Thornton¹; ¹University of Michigan*

Quantum dots have potential applications in high-efficiency photovoltaic-cell designs such as intermediate-band cells and hot-carrier cells. To maximize cell efficiency, the quantum dots must be grown with a high degree of regularity in shape, size, and ordering. To meet this need, techniques such as selective area epitaxy and focused-ion beam substrate patterning have been developed. However, the morphology of the dots, which depends on the pattern size and geometry as well as deposition parameters, remains difficult to control. Phase-field simulations have been used to simulate epitaxial growth of patterned arrays of quantum dots. For selective area epitaxy simulations, the phase-field model is coupled with the smoothed boundary method, which is used to specify the contact angle between the quantum dots and mask. Phase-field simulations have also been applied to understand and predict the morphological evolution of quantum dots that form during multi-layer growth on focused-ion beam patterned substrates.

3:55 PM

Electrophoretic Co-Deposition of TiO₂ and ZnO Photoelectrodes for Flexible Dye-Sensitized Solar Cells: *Sheng-Jye Cherng¹; Chih-Ming Chen¹; ¹National Chung Hsing University*

A procedure for composite photoanode made of TiO₂ and ZnO particles is developed based on electrophoretic co-deposition (EPD) which deposits two kinds of nanocrystallized semiconductors on a flexible ITO/PEN substrate. EPD is a low-cost processing technique and can fabricate a homogenous layer of controllable thickness with simple equipment. Microstructure of this composite layer is examined by scanning electron microscope (SEM), transmission electron microscope (TEM), and X-ray diffractometer (XRD). A flexible ITO/PEN substrate with sputtered platinum (Pt) is used for counterelectrode. The performance of the dye-sensitized solar cells (DSSCs) employing the composite photoanode and platinized counterelectrode is measured by Keithley model 2400 digital source meter under AM 1.5G(100 mW/cm²) irradiation. The charge transfer resistance at the ZnO-TiO₂/dye/electrolyte (R₂) and the electron lifetime (τ_n) are examined by electrochemical impedance spectroscopy (EIS).

Fatigue and Corrosion Damage in Metallic Materials: Fundamentals, Modeling and Prevention: Fatigue Behaviors at Elevated Temperature

Sponsored by: The Minerals, Metals and Materials Society, TMS Structural Materials Division, TMS/ASM: Mechanical Behavior of Materials Committee

Program Organizers: Tongguang Zhai, University of Kentucky; Zhengdong Long, Kaiser Aluminum; Peter Liaw, University of Tennessee

Tuesday PM
March 13, 2012

Room: Oceanic 6
Location: Dolphin Resort

Session Chairs: E-Wen Huang, National Central University; Peter Liaw, The University of Tennessee

2:00 PM

Thermal Relaxation of Residual Stresses in Laser Shock Peened IN718 SPF and Ti-6Al-4V Alloys: Experiments and Finite Element Modeling: *Amrinder Gill¹; Vijay Vasudevan¹; Dong Qian¹; Zhong Zhou¹; S.R. Mannava¹; Kristina Langer²; ¹University of Cincinnati; ²Air Force Research Laboratory*

Thermal relaxation of the compressive residual stresses induced by laser shock peened (LSP) in titanium and nickel-base aero engine alloys can significantly affect their fatigue life. In the present study, LSP induced residual stresses in IN718 SPF and Ti-6Al-4V alloys, and their thermal relaxation due to exposure at elevated temperatures are investigated through a series of controlled experiments and a coupled thermal-structural analysis using LS-DYNA finite element method (FEM). The Johnson-Cook (JC) material model was employed to represent the nonlinear constitutive behavior under LSP, and model parameters for IN718 SPF and Ti-6Al-4V alloys were calibrated by comparing the prediction of LSP residual stress with experimental data obtained using the conventional x-ray diffraction method. Good agreement between the thermal relaxation simulation and experimental results was obtained in LSP-treated coupons. The Zener-Wert-Avrami analytical model was applied to model the kinetics of relaxation, and activation enthalpy of thermal relaxation process was obtained.

2:20 PM

Effects of Intermediate Temperature Long Term Exposure on Mechanical Behavior of 5083-H116 and 5456-H116: *Mohsen Seifi¹; Justin Brosi¹; John Lewandowski¹; ¹Case Western Reserve University*

Al-Mg 5xxx alloys are desirable in a wide array of structural applications and provide an excellent balance of Mg solid-solution strengthening, as well as appreciable ductility after cold working. However, mechanical property changes may result from intermediate temperature exposures. Commercially available 5083-H116 and 5456-H116 alloy plates have been thermally treated up to 10,000 hrs. at temperatures of 80°C - 175°C. Room temperature tension, fracture toughness, fatigue crack growth and hardness tests have been completed to determine changes in mechanical properties in the LT orientation. Longitudinal splitting in the short-transverse (ST) direction has been observed during fatigue after sufficient time and temperature exposure combinations. Fracture and fatigue testing has revealed reductions in ST properties for long-time sensitized material in the ST orientation. The evolution of properties with thermal exposure at these (and lower) temperatures has significant practical implications for various structural applications.

2:40 PM

Measuring Effects of Holding Time and Oxidation on Thermo-Mechanical Fatigue Properties of Compacted Graphite Iron Using Notched Specimens: *Sepideh Ghodrat*¹; Michael Janssen²; Roumen (R.H) Petrov³; Leo (L.A.I.) Kestens³; Jilt Sietsma²; ¹Materials Innovation Institute (M2i), TUDelft; ²TUDelft; ³Ghent University, TUDelft

In cast iron cylinder heads heating and cooling cycles can lead to localized cracking due to Thermo-Mechanical Fatigue (TMF). Traditionally TMF behaviour is studied by cyclically loading smooth specimens until failure. The number of cycles to failure constitutes a single parameter that can be used to predict actual service failures. Nevertheless, some drawbacks also exist: long testing times and a huge scatter of results. A possible solution to deal with these drawbacks is the use of notched specimens. Tests on circumferentially notched specimens showed that TMF lifetime decreases monotonically with increasing notch depth. Furthermore, the lifetime for a specific notch depth could well be predicted using Paris' fatigue crack growth law. This allowed the prediction of the TMF lifetime of smooth specimens. Using this procedure, notched specimens were used to evaluate the effects of holding time during the load cycle and of the environment on the TMF properties.

3:00 PM

Thermal Fatigue Properties Evaluation of 18% Cr Ferritic Stainless Steel Weld HAZ: *Kyutae Han*¹; Seunggab Hong²; Changhee Lee¹; ¹Hanyang University / Division of Materials Science & Engineering; ²POSCO / Technical Research Laboratory

The microstructural changes and precipitation behavior during thermal fatigue of 18% Cr ferritic stainless steel weld heat affected zone were investigated. The simulation of weld HAZ and thermal fatigue test were carried out using a metal thermal cycle simulator under complete constraint force in the static jig. Thermal fatigue properties of the weld HAZ deteriorated during cyclic heating and cooling in the temperature range of 200°C to 900°C due to the decrease of Nb content in solid solution and coarsening of MC type precipitates, laves phase, M6C with coarsening of grain and softening of matrix. Crack initiated from the notch of the specimen at around 60% of life cycles due to the coarsened particles and grain boundary oxidation. As fatigue cycle increases, transgranular crack propagated toward the center of the specimen and finally fracture finished by merging with the spontaneously formed and coarsened cavities in the specimen during thermal cycle.

3:20 PM

Fatigue Deformation Behavior of Dispersion Hardened New Heat Resistant Aluminum Alloy at Elevated Temperature: *Kee-Ahn Lee*¹; Kyu-Sik Kim¹; Si-Young Sung²; Jung-Chul Park³; Bum-Suk Han²; ¹Andong National University; ²Korea Automotive Technology Institute; ³RIST

Tensile and high cycle fatigue behaviors of new heat resistant Al alloy at elevated temperature were studied. This alloy consists of Al matrix, small amount of Mg₂Si and (Co, Ni)₃Al₄ particles. Tensile tests showed that yield and tensile strengths of this alloy somewhat decreased and elongations increased slightly from R.T. to 350°C. HCF tests were conducted with stress ratio= 0.1, frequency= 30 Hz at 130°C. Fatigue limit was 120 MPa at 10⁷ cycles which is a superior value than that of A319. And also, regardless of conditions of maximum stresses, new heat resistant Al alloy has outstanding fatigue life. Results of fractographical observation showed that particles, especially (Co, Ni)₃Al₄, affected effectively to resistance of fatigue crack propagation. This study also attempted to clarify the micro-mechanism of fatigue behavior at elevated temperature related with its microstructure. [Supported by the Fundamental R&D program for Core technology, Korea]

3:40 PM Break

3:50 PM

Effect of Almen Intensities on High Cycling Fatigue of Al 2024-T4: *Yasser Ahmed*¹; Mostafa El Metwally¹; ¹German University in Cairo

The present work was aimed to evaluating the effects of shot peening on the high cycle fatigue performance of the age hardening aircraft alloy Al 2024 at different almen intensities. Shot peening to full coverage (100%) was performed using spherically conditioned cut wire (SCCW 14) with an average shot size of 0.36 mm and at almen intensities of 0.1 mmA, 0.2 mmA and 0.3 mmA. After applying the various mechanical surface treatments, the changes in the surface and near surface layer properties such as micro-hardness, residual stress-depth profiles and surface roughness were determined. The microhardness, surface roughness and the residual stresses increased proportionally with the almen intensity. Electropolitically polished conditions were used as reference in the mechanically surface treated specimens. A significant improvement was seen in the fatigue performance of the 0.1 mmA.

4:10 PM

The Effects of Microstructure upon Remaining Life of Carburized Ethylene Pyrolysis Tubes: *Amy McLeod*¹; Kevin Stevens²; Milo Kral¹; ¹University of Canterbury; ²Quest Integrity NZL Limited

Carburization in ethylene pyrolysis tubes is one of the contributing causes of failure of these tubes, but the timing of tube failures in ethylene pyrolysis furnaces is problematic as there is no reliable indicator that the tubes are near to their end-of-life. Remaining life assessments of carburized ethylene pyrolysis tubes based on microstructure and operating history are of interest to plant operators. The present work studies the effect of carburization on tube performance and remaining life. Laboratory carburized samples have been created, and ex-service and laboratory carburized tube material with differing levels of carburization has been studied. The samples have been characterized using a combination of elemental composition analysis, and optical and electron microscopy.

4:30 PM

Fatigue Crack Growth Analysis from Acoustic Emission Data on the Navy H-60 Seahawk Helicopter Tail Gearbox: Eric Hill; *Fady Barsoum*¹; Jun Shishino¹; Ning Leung¹; Prathikshen Salvadorai¹; Alan Timmons¹; William Hardman¹; ¹Embry-Riddle Aeronautical University

There have been multiple incidents of H-60 and H-60 variant helicopters that experienced fatigue cracks in the tail rotor gearbox assembly, specifically in the bevel gear splines. This paper discusses how acoustic emission (AE) data gathered from a crack growth test on a Sikorsky H-60 helicopter tail rotor gear box was processed and classified using a Kohonen self-organizing map (SOM) neural network. The tail rotor gearbox bevel gear had a seeded fault in one spline that grew to a crack 110 degrees around the shaft before the test was ended. The SOM was able to sort out the AE data into five mechanisms including two types of fatigue crack growths - plane strain and plane stress. Further AE testing is recommended in order to determine the fatigue life and the critical crack length for ultimate structural failure.

4:50 PM

Exploratory Research in Erosion Effects of Nanofluids on Metallic Materials: *Gustavo Molina*¹; Mosfequr Rahman¹; Mario Hulett¹; Valentin Soloiu¹; ¹Georgia Southern University

Nanofluids are fluids containing engineered colloidal suspensions of nanoparticles in ordinary base fluids, that are of interest for cooling systems because of their enhanced transport properties, especially thermal ones, as compared to those of the base fluids. However, the interactions (i.e., erosion, corrosion and possible nanoparticle deposition) of such nanofluids with metallic materials are largely unknown. The authors have designed, built and instrumented an erosion-test instrument for nanofluids, which allows accelerated testing of the effects of a nanofluid jet on metal targets. Exploratory work is presented on the wear and erosion effects on copper and aluminum targets when impacted with suspensions

TUESDAY PM



TMS 2012

141st Annual Meeting & Exhibition

of alumina and of silicon oxide nanoparticles in coolant fluids (i.e., for weight concentrations of up to 2% nanopowders in distilled water and in solutions of ethylene glycol in water). The observed erosion and corrosion effects, and material surface changes are discussed as baseline for further investigation.

From Macro to Nano, Understanding Mechanical Behavior across Length Scales: A Structural Materials Division Symposium in Honor of Robert Ritchie: Small Scale Mechanical Behavior and Theory

Sponsored by: The Minerals, Metals and Materials Society - , TMS Structural Materials Division, TMS/ASM: Mechanical Behavior of Materials Committee, TMS: Biomaterials Committee
Program Organizers: Jamie Kruzic, Oregon State University; Brad Boyce, Sandia National Labs; Reinhold Dauskardt, Stanford University

Tuesday PM Room: Mockingbird 1
March 13, 2012 Location: Swan Resort

Session Chairs: James Foulk, Sandia National Laboratory; Andrew Minor, University of California, Berkeley

2:00 PM Introductory Comments

2:05 PM Keynote

Elastic-Plastic Analysis of Nanoscale

Fracture Toughness: *William Gerberich*¹; Natalia Tymiak¹; Eric Hintsala¹; ¹University of Minnesota

Extracting fracture toughness from nanospheres and nanopillars using routine programs for elastic-plastic analysis can involve various assumptions. This is partially due to the inherent non-dimensional nature of finite element analysis. Experimentally, it is known from high temperature measure of the brittle-to-ductile transition in silicon and 4H-SiC that at the transition there is a sharp breakdown in the usefulness of elasticity calculations. The present approach uses matching load-displacement curves and a length scaling procedure to estimate the K_{Ic} , fracture toughness, for small Si and MgO spheres and pillars. Substantial increases in toughness from converted J-integral values compared to elasticity solutions are discussed.

2:45 PM Keynote

Mechanical Behavior at the Limit of Strength: *John Morris*¹; ¹University of California Berkeley

The one problem in mechanical behavior that can be solved from first principles is the limit of strength, the upper limit of stress at which a solid becomes elastically unstable and can no longer support mechanical load. While we are (quite properly) taught to focus on crystal defects as the keys to the mechanical behavior of most solids, research on behavior at the limit of strength has shown that a variety of important mechanical phenomena are, in fact, inherent in the limit of strength. These particularly include the differences in patterns of deformation and fracture between bcc and fcc metals, and the fact that the former have an inherent ductile-brittle transition while the latter ordinarily do not. Experimentally, ultimate strength governs the limit of hardness observed in nanoindentation, limits the achievable toughness in high strength steels, and governs the attainable strength of a very interesting class of new alloys.

3:25 PM

Connecting Nanoscale Mechanical Testing with Bulk Properties: *Andrew Minor*¹; ¹UC Berkeley & LBL

The concept that the strength of a material changes with sample size is a well established but not a well understood concept in small-scale plasticity. While the general notion of increasing strength with reduced dimension has been observed in a wide variety of materials, we have

yet to find a governing equation that can accurately link mechanical properties at the nanoscale to important bulk values related to concepts such as toughness, fracture & fatigue. Perhaps we will never be at the point of substituting a nanopillar compression test for a bulk toughness measurement . . . but our ability to connect nanoscale tests with bulk properties becomes increasingly relevant as nanoscale mechanical testing methods improve. This talk will focus on recent progress related to nanoscale mechanical testing methods in light of this view, and include a few in situ TEM nanopillar compression movies for the enjoyment of Professor Robert Ritchie.

3:40 PM

Mechanical Behavior in Metallic Nanowires: *Scott Mao*¹; Jianyu Huang²; ¹University of Pittsburgh; ²Sandia National Lab

This talk is based on the publication of H. Zheng, A. Cao, C. R. Weinberger, J. Huang, D. Du, Y. Ma, Y. Xia, S. X. Mao, Discrete plasticity in sub-ten-nanometer-sized Au crystals, *Nature Communication* (2010). The mechanical behavior of bulk metals is usually characterized as smooth continuous plastic flow following by yielding. Here we show, by using in-situ TEM and molecular dynamics simulations, that the mechanical deformation behaviors of single-crystalline Au nanowires are quite different from their bulk counterparts. Correlation between the obtained stress-strain curves and the visualized defect evolution during deformation processes clearly demonstrates that a sequence of complex dislocation slip processes results in dislocation starvation, involving dislocation nucleation, propagation and finally escaping from the wire system, so that the wires deformed elastically until new dislocation generated. This alternating starvation of dislocations is unique in small-scale structures.

3:55 PM Break

4:10 PM

The Impact of Sidewall Roughness on the Macroscopic Tensile Strength of Polycrystalline Silicon: *James Foulk*¹; Brad Boyce¹; Earl Reedy¹; James Ohlhausen¹; ¹Sandia National Laboratories

In order to design efficient, reliable microelectromechanical systems (MEMS), one must understand the statistics of failure. For brittle systems, we can better understand strength distributions through flaw distributions. Specifically, we seek to investigate the role of sidewall flaw depth and curvature on the macroscopic tensile strength of polycrystalline silicon through targeted atomic force microscopy (AFM) and finite element (FE) simulations. The coupled AFM/FE approach hinges on accurate surface representations and predictive analysis methods. Crack initiation and propagation are modeled through a cohesive zone approach and the predicted strengths are parameterized to determine that grain boundary grooves, both deep and sharp, are the dominant sidewall defects. Sandia National Laboratories is a multi-program laboratory managed and operated by Sandia Corporation, a wholly owned subsidiary of Lockheed Martin Corporation, for the U.S. Department of Energy's National Nuclear Security Administration under contract DE-AC04-94AL85000.

4:25 PM

Forward and Reversed Loading of Thin Copper Wires at Ambient and Elevated Temperatures: *Andy Bushby*¹; Julian Feuvrier¹; David Dunstan¹; ¹Queen Mary, University of London

The deformation behaviour of metals at very small strains is critical to fatigue behaviour but difficult to study in conventional tests. Here we describe experiments on long thin copper wires that achieve micro-strain resolution using a load-unload method. A high ratio of gauge length to wire diameter provides the extraordinary strain sensitivity. Reversal of the loading direction was possible through rotation of the wire in the opposite direction. Passing an electric current through the wire allowed experiments to be conducted at elevated temperatures. The elastic limit could be clearly identified and the early stages of plastic deformation studied at plastic strains far below the recognisable macroscopic yield strength. The reversibility of the dislocation structures formed under load

could be observed by annealing experiments at high temperature. The observed increase in the elastic limit for wires of smaller diameter implies that size effects could be used to control fatigue behaviour.

4:40 PM

A Combined Experimental and Computational Investigation of Work Hardening in Micron and Submicron Dimensions: *Daniel Kiener*¹; Andrew Minor²; Padubiri Guruprasad³; S. Keralavarma³; Gerhard Dehm¹; Amine Benzerga³; ¹University of Leoben; ²University of California; ³Texas A&M University

Size-effects affecting strength in finite volumes have attracted considerable interest recently. However, less attention was devoted to the size-dependence of hardening in the micron and sub-micron regime. We combined in-situ SEM and in-situ TEM compression testing with 2.5D discrete dislocation computations to address the yield and, more importantly, the hardening behavior at small scales. Cu samples were prepared by FIB milling with dimensions from sub-100 nm to ~10 μm . Physics based constitutive rules and careful parameters determination entering the simulations from experiments were key for good quantitative agreement. Smaller samples are stronger and show higher hardening. This is not governed by Taylor hardening or loss of mobile dislocations, rather the size-dependent evolution of local geometrically necessary dislocation structures describes the observations in the micron regime best. In the deep sub-micron range the hardening processes are dislocation source controlled, in accordance with in-situ TEM observations and 2.5D/3D DDD simulations.

4:55 PM

Dislocation Dynamics Simulation of Indentation of FCC Crystals: *Mamdouh Mohamed*¹; Ben Larson²; Giacomo Po³; Nasr Ghoniem³; Anter El-Azab¹; ¹Florida State University; ²Oak Ridge National Laboratory; ³University of California, Los Angeles

We present a methodology of dislocation dynamics simulation of mesoscale deformation of FCC crystals under indentation. In addition to revealing the details of plastic deformation evolution under indentation loading, this work aims to compare induced local elastic strain and lattice rotation fields with the X-ray measurements of the same fields in 3D. The simulation framework consists in coupling a dislocation dynamics code with the finite element method, with the latter serving to update the crystal geometry during deformation. Nucleation of dislocations is introduced based on local elastic stability criterion that is guided by related molecular dynamics studies. The comparison between simulations and experiments involves computational coarsening of the elastic strain and lattice rotation fields of the dislocation system to match the pixel size of the X-ray data. Preliminary simulation results are presented along with X-ray data.

5:10 PM

The Elastic Anisotropy of Steel Investigated by Nanoindentation: *Ude Hangen*¹; David Vodnick¹; ¹Hysitron, INC.

A nanoindentation experiment results in a single indentation modulus that shows a value close to the Hills average of moduli. This is different for small - fully elastic indentations. The values of reduced modulus of elastically anisotropic steels are determined at sub-10nm, several-10nm and several-100nm indentation depths, by use of a calibrated Hertzian and Oliver and Pharr's methods. The values of reduced moduli determined at sub-10nm indentations are similar to the theoretical uni-directional reduced moduli values. On the other hand, with increasing penetration depth to several-10nm, the reduced moduli gradually deviate from the uni-directional values to the averaged values calculated from materials stiffness matrix. This evolution in the reduced modulus values is related to the evolution of stress state beneath the indentation and the indentation induced phenomena. These findings are of large importance as the anisotropic modulus can be determined on very small volumes of material.

Integrative Materials Design: Performance and Sustainability: Advances in Integrated Computational Materials Engineering (ICME) & Residual Stress Considerations in Design

Sponsored by: The Minerals, Metals and Materials Society, TMS/ASM: Mechanical Behavior of Materials Committee
Program Organizer: Diana A. Lados, Worcester Polytechnic Institute

Tuesday PM
March 13, 2012

Room: Europe 2
Location: Dolphin Resort

Session Chair: Diana Lados, Worcester Polytechnic Institute

2:00 PM Invited

An ICME Approach to Predict Performance Margins Caused by Microstructural Variability: *Elizabeth Holm*¹; Corbett C. Battaile¹; Thomas E. Buchheit¹; Christopher R. Weinberger¹; ¹Sandia National Laboratories

There is no question that variations in microstructure cause variability in materials properties; however, engineering analysis models rarely include this source of uncertainty, often necessitating substantial overdesign. An integrated computational materials engineering (ICME) approach has been initiated to create the capability to determine uncertainty reliably and efficiently. As a proof-of-principle, we examine the performance of weldments in austenitic steels and in BCC tantalum. Our approach integrates mechanistic understanding from the atomic scale into single crystal models that inform individual grain response at the polycrystalline scale. Polycrystalline results are homogenized to deliver a continuum model that can be used in full-systems models by the design engineer. At each length scale, experimental discovery and validation are critical to developing dependable models. This ICME approach represents a paradigm shift from the idealistic view that all parts are created equal to the realistic view that structure, properties, and performance are probabilistic.

2:25 PM Invited

Predicting the Properties of Magnesium Sheets by Means of a Multiscale Approach – from the Atomistic to the Macroscopic Scale: *Joern Mosler*¹; Malek Homayonifar¹; Mintesnot Nebebe¹; ¹Technische Universität Dortmund and Helmholtz-Zentrum Geesthacht, Germany

The macroscopic behavior of magnesium sheets is strongly influenced by the underlying manufacturing processes. A realistic physical model of those processes would thus allow to design sheets with application-dependent optimized properties. As a first step toward this goal, a rolling process is considered within the present contribution. For modeling the texture evolution of magnesium during that process, a multiscale approach is discussed. Starting at the atomistic scale, the interactions between dislocations and deformation induced twins are analyzed using MD simulations. The results of such simulations enter a micro-mechanical model (crystal plasticity theory) which acts in turn as the lower scale for a connection to a phenomenological macroscopic description. Based on the final macroscopic approach, all important mechanical properties for technically relevant large-scale engineering applications are consistently defined. Within the present talk, focus is on the formability of magnesium sheets.

2:50 PM Invited

Simulation-Based Strategies to Support Alloy Design for Fatigue Resistance: *David McDowell*¹; ¹Georgia Institute of Technology

Concepts are introduced concerning microstructure-sensitive modeling of fatigue of advanced materials, particularly with regard to modeling variability of fatigue response as a function of microstructure. We consider sensitivity of fatigue crack formation and early growth at the scale of the grains in polycrystalline and polyphase microstructures to facilitate



TMS 2012

141st Annual Meeting & Exhibition

TUESDAY PM

preliminary parametric design exploration aimed at comparing a range of microstructure morphologies for nominally the same composition. A general methodology for stages of small crack formation and growth is introduced, including fatigue crack nucleation and early growth at the scale of grains (incubation), microstructurally small crack growth, physically small and long crack growth. Scatter in HCF and VHCF is computationally assessed using multiple statistical volume elements and the distribution of computable mesoscopic Fatigue Indicator Parameters (FIPs). Future challenges and desirable advances are briefly discussed.

3:15 PM Invited

Managing Uncertainty in Fracture: *Brad Boyce*¹; Corbett Battaile¹; James Foulk¹; E. David Reedy¹; ¹Sandia National Labs

Most current design methods treat material properties such as fracture strength as a deterministic value. Yet fracture is a stochastic process dictated by the complexities of the microstructure and native flaw population. Poorly understood statistical representations of material properties cause engineers to overdesign components. In this overview, we will illustrate fracture variability in two extremely different material systems: perfectly brittle silicon microsystems and ductile austenitic stainless steel weldments. In both material systems, a detailed examination of the statistics of fracture provides insight into the true design thresholds and the features that govern reliability. As materials scientists, we must strive to better understand the origins of stochastic material response and find pathways to convey statistical representations of material response in engineering design. Sandia is a multiprogram laboratory operated by Sandia Corporation, a Lockheed Martin Company, for the United States Department of Energy's National Nuclear Security Administration under contract DE-AC04-94AL85000.

3:40 PM Invited

An Integrated Framework for Reducing Uncertainty in Fatigue Life Limits of Turbine Engine Alloys: *James Larsen*¹; Sushant Jha²; Michael Caton¹; Reji John¹; Andrew Rosenberger¹; Christopher Szczepanski¹; Patrick Golden¹; Dennis Buchanan³; Jay Jira¹; ¹Air Force Research Laboratory; ²Universal Technology Corporation; ³University of Dayton Research Institute

Design and life-cycle sustainment of Ti and Ni alloys used in fracture-critical rotor components in advanced turbine engines require a delicate balance of performance, safety, and affordability. Traditional approaches have involved large experimental programs from which statistically based life limits are derived by extrapolation from mean fatigue behavior. However, we have recently found that the fatigue lifetime under a given test condition often exhibits a bimodal form, and the trends in mean vs. minimum fatigue lifetime typically respond differently to loading and microstructural variables. The underlying life-limiting mechanisms appear to follow a probabilistic microstructural hierarchy that is controlled by susceptibility to early damage and growth of small cracks. This presentation reviews the strategy for reducing uncertainty in prediction of lifetimes and highlights the integration between experiments and simulations of representative Ti and Ni turbine engine alloys, as part of the Air Force initiative on Integrated Computational Materials Science and Engineering.

4:05 PM Break

4:30 PM Invited

Probabilistic Prediction of Minimum Fatigue Life of a Shot Peened Titanium Alloy: *Reji John*¹; Sushant Jha²; James Larsen¹; ¹Air Force Research Laboratory; ²Universal Technology Corporation

The benefits of shot-peen induced compressive residual stresses in improving fatigue life and retardation of crack growth have been extensively demonstrated. Incorporating surface-treatment induced residual stresses (RS) in life prediction has been hampered by the variability in the RS profile and relaxation, and a lack of physics-based

measure of the benefit of RS on the lifetime. Hence, the fatigue variability behavior of the alpha+beta titanium alloy, Ti-6Al-2Sn-4Zr-6Mo, was studied at 260°C under RS-free, low stress ground and shot-peen surface conditions. The variability in the RS profile for the low stress ground and shot-peen conditions was determined. The influence of the surface treatment effects on the variability in the location and size of the failure initiation sites was characterized. This distribution of initiation sizes was coupled with the variability in micro-scale small crack growth and RS depth profiles to probabilistically predict the observed fatigue lifetime limit in Ti-6Al-2Sn-4Zr-6Mo.

4:55 PM Invited

Effects of Residual Stress on the Behavior of Metallic Materials: *Michael Hill*¹; ¹University of California, Davis

In recent years, advances in residual stress engineering methods have improved our ability to quantify the effects of residual stresses on structural performance. Residual stresses are locked into structural materials during manufacture, or subsequent processing of components, and are known to significantly affect mechanical performance. Typically, they affect subcritical cracking due to fluctuating stress (fatigue) and environmental exposure (environmentally assisted cracking) and may increase or decrease the time required for cracks to nucleate and then the rate of crack growth. Structural engineering practice has largely avoided explicitly accounting for residual stresses, and instead handled their consequences through empirical approaches. Those empirical approaches are specific to a given application of material and process, and, in the case of residual stresses, part geometry. Recent and continuing research is developing more fundamental, and less empirical, approaches for residual stress engineering, particularly in metallic materials, and some of this research will be described.

5:20 PM Invited

An Evaluation of the Crack-Compliance Method for Determining the Stress Intensity Resulting from Residual Stress: *Keith Donald*¹; ¹Fracture Technology Associates

Residual stress contributions can be a significant source of variability in life prediction methodology. As such, excess weight penalties may result due to uncertainty in the fatigue crack growth response. The crack-compliance method offers the ability to determine $K_{residual}$ by measuring the change in displacement at zero force during a crack growth rate experiment. This method gives the same result as Schindler's cut-compliance method but does not require influence functions. The practical application of this methodology requires sufficient signal stability and linearity to determine $K_{residual}$. Examples will include residual stresses resulting from extrusions, forgings, quenching and friction stir welding processes. Test coupon types will include compact tension and middle crack tension samples. Sources of measurement error will be presented. Once the $K_{residual}$ profile has been determined, normalization methods will be presented to establish a fatigue crack growth rate response that is independent of the effect of residual stress.

5:40 PM Invited

The Relative Importance of Various Mechanical Properties on Structural Performance: *Ted Anderson*¹; ¹Quest Integrity Group

While it is an obvious platitude that good mechanical properties are preferable to poor properties, economic considerations usually dictate that a "suitable" material be chosen over the "best possible" material for a given application. There are often trade-offs in mechanical properties, such as strength versus toughness in structural metals. Achieving both high strength and high toughness typically requires alloying additions and advanced processing, both of which add to material cost. This paper presents a series of parametric analyses and case studies that explore the relative importance of strength, toughness, and fatigue crack growth constants on material selection.

International Smelting Technology Symposium (Incorporating the 6th Advances in Sulfide Smelting Symposium): Pretreatment and Recycling Processes

Sponsored by: The Minerals, Metals and Materials Society, The Metallurgy and Materials Society of CIM, TMS Extraction and Processing Division, TMS: Pyrometallurgy Committee
Program Organizers: Jerome Downey, Montana Tech of the Univ of Montana; Thomas Battle, Midrex Technologies, Inc.; Jesse White, Elkem Solar Research

Tuesday PM
March 13, 2012

Room: Northern A3
Location: Dolphin Resort

Session Chair: To Be Announced

2:00 PM

Integrated Recycling at Boliden's Rönnskär Smelter; Formation of Slag Products: Sina Mostaghel¹; Hannes Holmgren²; Taishi Matsushita³; *Caisa Samuelsson*¹; ¹Luleå University of Technology; ²Rönnskär Smelter, Boliden Mineral AB; ³Royal Institute of Technology (KTH)

Rönnskär Smelter of Boliden Mineral AB, Sweden, is a large end-processor of secondary raw materials and waste, including electronic scrap. E-scrap may introduce various impurities to the smelter's flow-sheet, among which alumina is one of the most common and significant ones. Current article summarizes the results of an ongoing research at Luleå University of Technology, Sweden, to study the influences of alumina on different properties of slag from the zinc fuming process at Rönnskär smelter. A combination of different experimental techniques and thermodynamic calculations has been used to investigate properties such as density, surface tension, effective thermal diffusivity, viscosity, melting and leaching behaviors. Results show that addition of alumina to this slag increases the degree of polymerization of the melt, and the properties vary correspondingly. Mineralogy of the semi-rapidly solidified samples is also changed due to alumina addition. A correlation between mineralogy and leaching behavior can be observed.

2:25 PM

Promotion of Recycling Business by Combination of a Pre-Treatment Plant and the Mitsubishi Process at Naoshima Smelter & Refinery: *Yuji Mizuta*¹; Nobuhiro Oguma¹; Shigehiko Iwahori¹; Hideya Sato¹; ¹Mitsubishi Materials Corporation

Recyclable materials containing copper and precious metals have been treated at the Mitsubishi Process in Naoshima. In 2003, a new incinerating and melting plant (pre-treatment plant) for waste materials, such as shredder residue of automobile and scrapped appliance, was constructed. All of produced slag/metal mixture is treated at the Mitsubishi Process, and which results in the significant increase of recyclable materials' treatment. The combination of two processes has realized a highly efficient and environmentally friendly system for recycling valuable metals in the waste which used to be sent to a landfill. Naoshima continues to make efforts to achieve the highly efficient operations of the two processes, and plans to increase the treatment of recyclable materials further. This paper summarizes the recent operations and the various improvements implemented in the pre-treatment plant.

2:50 PM

Optimum Feed Preparation for Sulfide Smelting: *Jyri Talja*¹; Shaolong Shen¹; Hannu Mansikkaviita¹; ¹Kumera Corporation

For optimum smelting result proper treatment of the feed is needed to ensure favourable conditions for ignition characteristics, heat balance, mass balance with tolerable impurity levels, and overall process economics. This consists of physical treatments before drying (blending), chemical treatments before drying, (roasting, if required), drying itself and physical treatments after drying (fractioning, if required). Effects of

fluctuation on mineralogy and moisture should be minimized by blending the concentrates in a bedding plant prior to drying. Alternatively to drying, any additional treatments, like roasting for impurity removal, may be needed for part of the concentrate. Sustainability, energy efficiency, utilization of waste energy, low gas and dust emissions, product quality, availability and occupational exposure reduction are decisive criteria in drying today. These criteria are best met by the Kumera steam dryer with best energy efficiency, zero CO₂ emission, lowest operational and maintenance expenses, superior availability and fine product quality.

3:15 PM

Partially Reduced Feedstocks and Blast Furnace Ironmaking Carbon Intensity: *Petrus Pistorius*¹; ¹Carnegie Mellon University

Use of coke in blast furnace ironmaking is the main origin of carbon dioxide emissions from integrated steelmaking. Using pre-reduced iron feedstocks would reduce the coke rate and, if pre-reduction were carried out with natural gas, would decrease the overall carbon intensity of ironmaking. Blast furnace productivity would also increase, because the blast volume per unit of hot metal would decrease. It will be shown that these trends can be predicted quantitatively, by using a conceptually simple Rist-style blast furnace mass and energy balance, assuming furnace productivity to be limited by the tuyere gas flow rate. Such predictions would assist in optimizing the choice of the degree of reduction and relative amount of pre-reduced blast furnace feed.

3:40 PM Break

4:00 PM

Injection of Alternative Carbon Containing Materials in the BF: *Lena Sundqvist Ökvist*¹; Gunilla Hyllander²; Michael Hensmann³; Erik Olsson⁴; Olavi Antila⁴; Stefan Schuster⁵; Maria Lundgren¹; ¹Swerea MEFOS AB; ²LKAB; ³VDEh-Betriebsforschungsinstitut; ⁴SSAB EMEA; ⁵voestalpine Stahl GmbH

Residual materials from the integrated plant itself or other sources often contain valuable compounds as e.g. iron and carbon. Dust and sludge have to be agglomerated to be able to recycle to the BF via top-charging. By injection of the materials preparation methods in terms e.g. drying and/or screening only, can be used. BF dust and sludge have been successfully injected up to levels of 60 kg/tHM in the LKAB experimental BF (LKAB EBF\149;). Efficiency in recovery of valuable compounds as well as the behaviour of undesired elements have been evaluated and are discussed.

4:25 PM

Experiences of Using Various Metallurgical Reactors for Reduction of V-Bearing Steel Slags and Other Wastes: *Mikael Lindvall*¹; Guozhu Ye¹; ¹Swerea MEFOS AB

The Swedish iron ore contains about 0.1%V. The vanadium is reduced to the hot metal in a blast furnace and ends up in the slag in the converter. The high V-content, up to 5%V, leads to a very limited external application of the slag in Sweden. Since 2004, MISTRA - the Swedish Foundation for Strategic Environmental Research has together with the steel and mining industry in Sweden and Finland initiated and supported a long term project aiming at efficient recovery of vanadium in the slag and at the same time a useful slag product with low V-content. The aimed concept consists of a reduction step and a phosphorus removal step. This paper will highlight some of the results with focus on the various metallurgical reactors used for slag reduction, including results from recently performed pilot trials using a DC furnace for co-treatment of metallurgical slags and other wastes.

4:50 PM

Phase Change and Morphology in the Oxidation of Zinc Sulfide Powder: *Okano Satoshi*¹; Hiromichi Takebe¹; Takahiko Okura²; ¹Hime University; ²Tokyo University

There is a problem of calcine accretion in a fluidized bed roaster for finer zinc concentrates. In order to avoid the calcine accretion, the oxidation behavior of zns powder was basically studied in terms of phase change and particle morphology. a commercial high-purity zns powder was



analyzed by thermo gravimetry(tg). from tg results, the zns powder was heat-treated at 400–1000°C for 1h in air. samples were characterized by various analyzer. zns phase was directly oxidized to zno phase at 700°C with reducing the size of powder form. the sintering of zno powder products occurred at higher temperatures of >700°C. The reaction process is supposedly affected by the state of roasting gas flow at zns particle surface. Sulfate phases such as $\text{zno} \cdot 2\text{zns}_4$ was formed and decomposed by so_2 gas around the particle surface, depending on the flow rate of atmospheric gases for tg and heat-treatments.

5:15 PM

Using of Fluidized Roasting Technology in Comprehensive Utilization of Magnetized Gold Smelting Waste: *Xiaoyin Liu¹; Yongfu Yu¹; Wen Chen¹; Xiaosu Lu¹; Zeyou Peng¹; Jialin Li¹; ¹Changsha Research Institute Of Mining And Metallurgy*

This paper introduces the principle and techniques of magnetized fluidized roasting technology, using of this technique in comprehensive utilization of gold smelting waste. Through this technology iron concentrates with grade of 60%, iron yield 85% can be obtained from the gold smelting waste which contains 35% iron. Based on the 50 Kt/a industrial test which verifies the bench-scale experiment results, the comprehensive utilization of magnetized gold smelting waste is realized, which enters a new stage for the using of gold smelting waste.

Materials and Fuels for the Current and Advanced Nuclear Reactors: Structural Materials I

Sponsored by: The Minerals, Metals and Materials Society, TMS Structural Materials Division, TMS/ASM: Corrosion and Environmental Effects Committee, TMS/ASM: Nuclear Materials Committee

Program Organizers: Ramprashad Prabhakaran, Idaho National Laboratory; Dennis Keiser, Idaho National Laboratory; Raul Rebak, GE Global Research

Tuesday PM
March 13, 2012

Room: Swan 2
Location: Swan Resort

Session Chair: Kumar Sridharan, University of Wisconsin - Madison

2:00 PM Invited

Light Water Reactor Materials for Commercial Nuclear Power Applications: *Brian Burgos¹; ¹Westinghouse Electric / Research and Technology*

A nuclear vendor perspective will be presented describing light water reactor materials issues facing the nuclear industry. A historical perspective will capture issues that the commercial nuclear industry faced along with a look into the future of materials related issues challenging future plant builds.

2:30 PM

Cold Spray Technology: A Potential Approach to Address Materials Aging Issues in Nuclear Reactor Systems: *Kumar Sridharan¹; Benjamin Maier¹; Benjamin Hauch¹; Youngki Yang¹; Todd Allen¹; ¹University of Wisconsin*

Cold spray process is a materials deposition technology that is being investigated for a number of engineering applications. In the cold spray process, powder particles are propelled at supersonic velocities on to the surface of a part to form a coating with superior properties. Because of the high deposition rates, the process has the potential to repair cracks and restore dimensions in recessed regions caused by stress corrosion, corrosion, and erosion. In the cold spray process the powders are not melted, and deposition occurs at low temperatures. Therefore, the process can deposit dense coatings and filler materials that are well-bonded to

the substrate, relatively free of oxidation and porosity, and with no heat affected zone in the base material. Potential applications of this technology for nuclear reactor systems will be discussed.

2:50 PM

Stress Corrosion Crack Initiation Testing of Cold Worked 316 Stainless Steel in Simulated PWR Primary Water under the Spring Loaded Condition: *Yuichi Miyahara¹; Toshio Yonezawa¹; Atsushi Hashimoto²; ¹Tohoku University; ²Kobe Material Testing Laboratory Co., LTD.*

Recently, several papers on the inter-granular stress corrosion cracking (IGSCC) growth rate for the highly cold worked 316 stainless steels in simulated PWR primary water. However, the IGSCC initiation test in simulated PWR primary water environment was scarcely reported except slow strain rate testing (SSRT). In this study, various SCC initiation tests under the spring loaded conditions were conducted on cold worked 316 stainless steel in simulated PWR primary water. That is, spring loaded type U-bend specimens with or without hump forming, reverse U-bend specimens etc., were studied to decrease an effect of stress relaxation during the SCC tests, in this study. From these test results, IGSCC initiation was found on humped U-bend specimens. The effect of prior cold work on IGSCC susceptibility was contrary to the reported results obtained by SSRTs. In this paper, IGSCC initiation characteristics of the cold worked 316 stainless steel was discussed.

3:10 PM

Creep-Fatigue Behavior of an Advanced Austenitic Alloy Strengthened by Nano-Scale MC Precipitates: *Laura Carroll¹; Mark Carroll¹; Richard Wright¹; ¹Idaho National Laboratory*

An advanced austenitic alloy, HT-UPS (high temperature - ultrafine precipitate strengthened), is a potential candidate material for structural components of fast reactors and energy-conversion systems. The HT-UPS alloy, with a composition based largely on modifications to 316 stainless steel (SS), demonstrates improved creep resistance through additions of Ti and Nb that form nano-scale MC precipitates. The cycles to failure at 650°C of HT-UPS and 316 SS are similar in fatigue and creep-fatigue despite differences in peak stress profiles and the deformed microstructures. Internal grain boundary damage resulting from the tensile hold is present in the form of fine cracks for longer hold times, and substantially more of these internal cracks are visible in 316 SS than HT-UPS. The cycled dislocation substructure in 316 SS has regions with an equiaxed cellular structure and regions with a lath structure, whereas tangles of dislocations are pinned at the nanoscale MC precipitates in HT-UPS.

3:30 PM

Impact of Hydrogen Absorption on the Thermophysical Properties of Zircaloy Cladding: *J. B. Henderson¹; A. T. Nelson²; K. J. McClellan²; ¹Netzsch Instruments NA; ²Los Alamos National Laboratory*

Under normal operating conditions, chemical reactions occur between the fuel/coolant and the cladding. This results in the formation of a ZrO_2 layer as well as hydrogen and oxygen absorption produced by the $\text{H}_2\text{O} + \text{Zr}$ reaction. During loss of coolant accidents, these reactions are accelerated because of the higher temperatures. The end result is embrittlement of a portion of the cladding and reduction of the thickness of the load-bearing material. In addition, the thermophysical properties are significantly impacted. For example, the thermal conductivity is reduced, resulting in poor heat transfer and higher fuel/cladding temperatures. The purpose of this work was to measure the thermal diffusivity (\Rightarrow thermal conductivity) as a function of temperature and H/Zr ratio. The H/Zr ratio was fixed by varying the partial pressure of hydrogen and verified by mass measurements. Identical test conditions were then applied for the thermal diffusivity measurements. The results of this work will be presented.

3:50 PM Break

4:00 PM

A Novel Fe-Based ODS Fabrication Process: *Joel Rieken*¹; Iver Anderson²; Matthew Kramer²; ¹Iowa State University; ²Ames Laboratory

Oxide dispersion forming ferritic stainless steel (i.e., Fe-Cr-(Ti,Hf)-Y-O) powders were generated using a novel gas atomization reaction synthesis technique. During this process an ultra-thin metastable Cr-enriched surface oxide layer formed and encapsulated the rapidly solidified powders. This oxide layer was used as a vehicle to transport a prescribed amount of solid-state O into the consolidated microstructure. Elevated temperature heat treatment was then used to facilitate thermodynamically driven internal O exchange between trapped films of Cr-enriched oxide and Y-containing intermetallic precipitates, resulting in highly stable mixed oxide dispersoids (i.e., Y-(Ti,Hf)-O) that were identified using high-energy XRD and TEM. Following dispersoid formation, thermal-mechanical processing was used to fabricate a fine scale dislocation sub-structure for ultimate strengthening of the ODS alloy. Preliminary mechanical properties were examined using elevated temperature tensile testing. Support from the Department of Energy, Office of Fossil Energy (ARM program) through Ames Laboratory contract no. DE-AC02-07CH11358 is gratefully acknowledged.

4:20 PM

Evaluation of Silicon Carbide Joining for Nuclear and Fusion Applications: *Yutai Katoh*¹; Monica Ferraris²; Tatsuya Hinoki³; Charles Henager⁴; ¹Oak Ridge National Laboratory; ²Politecnico di Torino; ³Kyoto University; ⁴Pacific Northwest National Laboratory

Based on the recent development of highly radiation-resistant silicon carbide-based ceramic matrix composites, applications of these materials to nuclear and fusion energy are presently proposed and being researched. However, development of joining for these materials for use in the harsh radiation environment remains as a significant challenge. Moreover, additional requirements such as gas impermeability and corrosion resistance have to be considered for specific application environments. In the recent collaborative project among the U.S. Fusion Materials Program, Politecnico di Torino, and Kyoto University, development and evaluation of joining technologies for silicon carbide ceramics and composites for use in fusion and nuclear reactors were attempted. This paper will discuss the recent progress including 1) identifying promising joining techniques for radiation services, 2) development of small specimen test technique adequate to evaluate the shear strength of ceramic joints, 3) baseline characterization of the joint mechanical properties, and 4) progress in neutron irradiation program.

4:40 PM

Precipitation of Sigma Phase in Cast Duplex Stainless Steel Z3CN20.09M for Primary Coolant Pipe of Nuclear Power Plants and Its Influence on Localized Corrosion: *Yongqiang Wang*¹; *Bin Yang*¹; Jun Han¹; ¹University of Science and Technology Beijing

Work was undertaken to establish reliable time-temperature-precipitation (TTP) diagram for sigma phase formation in cast duplex stainless steel Z3CN20.09M for primary coolant pipe of nuclear power plants and the mechanism of sigma phase formation was determined too. It was found that the formation of sigma phase occurred in the temperature range 600-950°C by nucleation and growth at the ferrite/austenite phase boundaries and higher kinetics of sigma phase precipitation was obtained at 850°C. The influence of sigma phase on intergranular corrosion (IGC) and pitting corrosion of Z3CN20.09M has been investigated by chemical and electrochemical methods and related to the microstructure as observed using light optical microscopy, scanning electron microscopy, and transmission electron microscopy. The results showed that IGC and pitting corrosion resistance of Z3CN20.09M has decreased markedly with increase of sigma phase. The more sigma phase the lower pitting potential (Eb) and critical pitting temperature (CPT) and the higher ratio Ir/Ia.

5:00 PM

Effect of Tellurium on Intergranular Cracking in Nickel-based Alloy: *Yanyan Jia*¹; Wenguan Liu¹; Yang Zou¹; Zhijun Li¹; Yanling Lu¹; Min Liu¹; Xingtai Zhou¹; Hongjie Xu¹; ¹Shanghai Institute of Applied Physics, Chinese Academy of Sciences

Embrittlement problem of alloy induced by fission-product, for example tellurium, affects the safety of molten-salt reactors (MSRs) seriously. Previous research has suggested that tellurium was responsible for intergranular cracking that occurred in Hastelloy-N alloy, while chromium might prevent the dynamics process of embrittlement induced by tellurium attacking. In order to understand the mechanism that tellurium induces grain boundary cracking, a series of experiments were designed to get morphology, distribution and number of the cracks in Nickel-based alloy with different Cr contents. These experiments indicate that the depth of intergranular cracks caused by Te in the alloys with various contents of Cr is different in the same conditions. With the increase of the content of Cr, the tendency to form cracks in Nickel-based alloy is reduced. In addition, the penetration mechanism of Te in Nickel-based alloy with different Cr contents is also discussed in detail.

5:20 PM

Oxide Dispersion Strengthened Steels via Mechanical Alloying and Spark Plasma Sintering: *Somayeh Pasebani*¹; Indrajit Charit¹; Kerry Allahaar²; James Cole³; Darryl Butt²; ¹University of Idaho; ²Boise State University; ³Idaho National Laboratory

Oxide dispersion strengthened (ODS) alloys are a promising class of materials for advanced reactor applications because of their high creep and tensile strength, and excellent radiation damage resistance. Copious nano-precipitates formed during hot consolidation act as obstacles against dislocation motion, serve as point defect sinks, and promote helium trapping. Unlike the traditional ODS alloys using yttria as dispersoids, in this study ~0.4 wt.% lanthana is added to the elemental metallic powders (Fe-14Cr-1Ti-0.3Mo, wt.%), followed by high energy ball milling and subsequent consolidation via spark plasma sintering (SPS). Ball milling was conducted for 10 and 20 hours in a high energy shaker mill. SPS is performed at different temperatures, pressures, heating ramp rates and dwell times. The density and hardness of SPSed samples are measured. Transmission electron microscopy is used to study the morphology of the oxide nano-features formed during SPS.

5:40 PM

Wollastonite Based-Chemically Bonded Phosphate Ceramics with Boron Contents as a Potential Material for Nuclear Shielding Applications: *H. A. Colorado*¹; J Pleitt²; J-M Yang¹; C. H. Castano²; ¹University of California, Los Angeles; ²Missouri University of Science and Technology

The shielding properties to neutrons as well as the mechanical effects of boron incorporation into wollastonite based chemically bonded phosphate ceramics (Wo-CBPC) composites are presented. The Wollastonite-based CBPC was fabricated by mixing a patented aqueous phosphoric acid formulation with Wollastonite powder. CBPC has been proved to be good structural material, with excellent thermal resistant properties, and research already showed their potential for gamma radiation shielding applications. Wo-CBPC is a composite material with several crystalline and amorphous phases. Irradiation experiments were conducted on different Wollastonite-based CBPCs with Boron contents. Radiation shielding potential, attenuation coefficients in a broad range of energies pertinent to engineering applications and density experiments showing the effect of the boron content are also presented. Microstructure was identified by using scanning electron microscopy and X-ray diffraction. Compressive strength and setting time were also evaluated.



Materials Design Approaches and Experiences III: Non-ferrous Alloys and Processes

Sponsored by: The Minerals, Metals and Materials Society, TMS Structural Materials Division, TMS: High Temperature Alloys Committee, TMS: Integrated Computational Materials Engineering Committee

Program Organizers: Ji-Cheng Zhao, The Ohio State University; Akane Suzuki, GE Global Research; Deb Whitis, GE Aviation; Michael Fahrman, Haynes International Inc.; Qiang Feng, University of Science and Technology Beijing

Tuesday PM Room: Europe 11
March 13, 2012 Location: Dolphin Resort

Session Chairs: Michael Fahrman, Haynes International, Inc.; Christopher Hutchinson, Monash University

2:00 PM Invited

Design, Microstructure Evolution, Properties, and Applications of Advanced Intermetallic TiAl Alloys: *Helmut Clemens*¹; *Svea Mayer*¹; ¹Montanuniversität Leoben

After almost three decades of intensive fundamental research and development activities intermetallic titanium aluminides based on the γ -TiAl phase have found applications in automotive and aircraft engine industries. The advantages of this class of innovative high-temperature materials are their low density, their good strength and creep properties up to 750°C. A drawback, however, is their limited ductility at room temperature, which is expressed in a low plastic fracture strain. Advanced TiAl alloys are complex multi-phase alloys which can be processed by ingot or powder metallurgy as well as precision casting methods. Each process leads to specific microstructures which can be altered and optimized by thermo-mechanical processing and/or subsequent heat-treatments. This presentation gives a comprehensive summary regarding our current research activities.

2:30 PM Invited

Tools for Manipulating Precipitation Processes: Alloy and Process Design: *Christopher Hutchinson*¹; ¹Monash University

Controlling the particle distribution in precipitate hardenable alloys is the primary means of modifying the mechanical properties of such alloys. However, the nucleation, growth and coarsening processes that govern the evolution of precipitate structures are complex, competing and overlapping processes and controlling these is non-trivial. Three approaches to manipulating aspects of the precipitation process are outlined in this presentation. The first is a thermo-kinetic criterion for choosing microalloying elements that catalyze the nucleation of hardening precipitates and can give rise to large refinements in the scale of the precipitate structure with significant increases in strength. The second approach attempts to modify the shape of precipitates at approximately constant scale and allows for improvements in the thermal stability of alloys. The third approach uses temperature as a processing variable to control the overlap and competition between nucleation, growth and coarsening processes. Large efficiencies in processing and properties can be realized.

3:00 PM Invited

Magnesium Alloy Development Using Computational and Experimental Tools: *Alan Luo*¹; *Raja Mishra*¹; *Bob Powell*¹; *Anil Sachdev*¹; ¹General Motors Global Research and Development

This talk summarizes the development of new cast and wrought magnesium alloys using computational thermodynamics and experimental methods. The work illustrates the role of calculated phase diagrams, solidification paths and phases in predicting and interpreting the final microstructure of Mg-Al-Ca and Mg-Al-Sn cast alloy systems and Mg-Al-Mn and Mg-Zn-Ce wrought alloy systems. The Mg-Al-Ca alloys show excellent creep resistance due to the formation of high-temperature (Mg,Al)₂Ca

phase. The Mg-Al-Sn alloys are designed for mechanical properties and corrosion resistance by optimizing the Mg₁₇Al₁₂ and Mg₂Sn phases in the microstructure. AM30 (Mg-3Al-0.3Mn) alloy was developed to have significantly improved extrudability and slightly improved mechanical properties compared to AZ31 alloy, due to the absence of low eutectic-point Mg-Al-Zn ternary phases existing in the AM30 alloy. In the Mg-Zn-Ce system, Zn provides strength through solid solution strengthening, while Ce increases the ductility by creating a favorable texture.

3:30 PM Break

3:50 PM Invited

Design of a Nanocrystalline Alloy Coating for Electrical Connector Applications: *Christopher Schuh*¹; *Alan Lund*²; ¹MIT; ²Xtalic Corporation

Electrical connectors require a unique set of physical and mechanical properties, including low bulk and interfacial resistivities that remain stable even after significant exposure to atmospheric corrosion, temperature, and multiple cycles of sliding wear. This talk will provide an overview of a new Ni-W alloy nanocrystalline coating material designed as the functional barrier layer in electrical connectors. The coating is electrodeposited as an interlayer between Cu-based substrate materials and an outer finish of precious metal, and is delivered with a finely-tuned nanocrystalline structure that is stabilized by a solid solution alloying addition that decorates grain boundaries. The nanostructure of the coating has been optimized to deliver a substantial improvement in the key property set for this application. The design process for this coating will be described from the laboratory to the industrial scale, comprising elements of theory and simulation, advanced characterization, property measurements, and engineering qualification testing.

4:20 PM Invited

Develop ICME Tool for High Ductility Cast Aluminum Alloys for Automotive Body Applications: *Mei Li*¹; *J. Forsmark*¹; *J. Zindel*¹; *L. Godlewski*¹; *Xuming Su*¹; ¹Ford Motor Company

One heat treatable high ductility Al-Si-Mg alloy was investigated in this study. To achieve the full potential of strength and ductility of this alloy, super vacuum die casting (SVDC) process was used to produce the high integrity Al cast components free of air entrapment. A semi-empirical model based on Shercliff and Ashby's process model for age hardened Al alloys and experimental data were developed. The model can predict the effect of solidification time, aging temperature and time on yield strength. A quality mapping approach was adopted to predict the local ductility based on criteria functions from commercial casting simulation program MAGMASoft and experimental data. A new materials card was then built for crash performance analysis in LS-DYNA which includes the impact of local yield strength and ductility. Finally this ICME tool was validated on component level three-point and four-point bending testings.

4:50 PM

Systems Engineering Framework for the Integrated Computational Design of Advanced Aluminum Alloys: *Abhijeet Misra*¹; *James Wright*¹; *Heng-Jeng Jou*¹; *William Counts*¹; *Charles Kuehmann*¹; ¹QuesTek Innovations LLC

Computational materials design integrates targeted materials process-structure-property models within a systems framework to meet specific engineering needs. A key component to materials design models is a basis on fundamental thermodynamics, phase equilibria, and diffusion, implemented in a multicomponent framework. The application of ICME tools towards the computational design of advanced aerospace and marine aluminum alloys is discussed. Key process-structure design tools for aluminum alloys include solidification and homogenization modeling, simulation of the hot working process (for wrought alloys), inoculation modeling (for cast alloys) and the simulations of precipitation behavior during thermal treatment. Key structure property models include mechanistic quench sensitivity models, strength models, hot-tearing resistance models (for castings) and toughness, SCC and corrosion resistance models. The modeling effort and application in the design of

advanced wrought and cast aerospace and marine Al alloys demonstrates the utility of ICME to accelerate and reduce risk during development of complex materials.

5:10 PM

The Use of In-Situ Characterization Techniques for the Development of Intermetallic Titanium Aluminides: Svea Mayer¹; Thomas Schmoelzer¹; Helmut Clemens¹; ¹Montanuniversitaet Leoben

Urgent topics concerning energy efficiency and environmental politics require novel approaches to materials design. One recent example is thereby the implementation of lightweight intermetallic TiAl alloys as structural materials in aerospace applications as well as in the next generation of automotive engines. Their low density and exceptional high-temperature strength make them the first choice to gradually replace the dense Ni-base superalloys and high-alloyed steels particular for operating temperatures up to 750°C. To develop stable and sustainable processing routes, knowledge on solidification processes and phase transformation sequences in advanced TiAl alloys are fundamental. Therefore, in-situ diffraction techniques employing synchrotron radiation and neutrons were used for establishing phase diagrams, investigating advanced heat-treatments and for optimizing thermo-mechanical processing. Additionally, the evolution of the materials microstructure was subject of our investigations.

Materials in Clean Power Systems VII: Clean Coal-, Hydrogen Based-Technologies, and Fuel Cells: Materials for Hydrogen Production, Separation, and Storage

Sponsored by: The Minerals, Metals and Materials Society, TMS Electronic, Magnetic, and Photonic Materials Division, TMS Structural Materials Division, TMS/ASM: Corrosion and Environmental Effects Committee, TMS: Energy Conversion and Storage Committee

Program Organizers: Xingbo Liu, West Virginia University; Teruhisa Horita, National Institute of Advanced Industrial Science and Technology; Jeffrey Hawk, National Energy Technology Lab; Jeffrey Fergus, Auburn University

Tuesday PM
March 13, 2012

Room: Europe 8
Location: Dolphin Resort

Session Chairs: Ya Xu, National Institute for Materials Science; Omer Dogan, National Energy Technology Laboratory

2:00 PM

Catalytic Properties of Ni-Al Intermetallic Nanoparticle Catalysts for Hydrogen Production from Methanol and Methane: Ya Xu¹; Junyong Yang²; Masahiko Demura¹; Toshiyuki Hirano¹; ¹National Institute for Materials Science; ²Huazhong University of Science and Technology

Recently, we found that Ni₃Al intermetallic compound, in the form of both powder and foil, shows catalytic activity and selectivity for methanol decomposition and methane steam reforming, indicating a possibility to develop Ni-Al intermetallic compounds as catalysts for hydrogen production. In order to pursue high catalytic performance of Ni-Al intermetallic compounds for hydrogen production, we synthesized Ni-Al intermetallic nanoparticles from Ni-Al alloy ingots by vacuum arc plasma evaporation technique for the first time. The characterization of the synthesized nanoparticles was carried out using X-ray diffraction, scanning electron microscopy, transmission electron microscopy, energy dispersive X-ray spectroscopy. The catalytic properties of the Ni-Al nanoparticles for methanol decomposition were evaluated. It is found that the nanoparticles had a large surface area above 70 m²/g, and showed very high catalytic activity for methanol decomposition and methane steam reforming.

2:20 PM

Ca, Li and Mg Based Lightweight Intermetallics for Hydrogen Storage: Beau Biller¹; Ji-Cheng Zhao¹; ¹Ohio State University

Intermetallics with Laves structures have the potential to be hydrided to a maximum of AB₂H₆ due to the impeding H-H interactions where A and B are metallic elements. Ca, Li, and Mg-based Laves phases are among the lightest intermetallic compounds that can potentially serve as the highest capacity reversible interstitial metal hydrides for hydrogen storage. Possible multi-component compositions based on these elements will be discussed to optimize the structures of Laves phases to store hydrogen amongst the B₄, AB₃ and A₂B₂ sites. This talk will present our experimental exploration in these lightweight systems for hydrogen storage applications

2:40 PM

Effects of Long Term Aging on Creep Properties of HP Alloy Hydrogen Reformer Tubes: Milo Kral¹; Karl Buchanan¹; ¹University of Canterbury

The centrifugally cast HP series has become the dominant hydrogen reformer tube material for the petrochemical industry. HP alloys with small additions of Nb and Ti are reported to have superior creep properties over standard HP alloys in accelerated testing. However, accelerated testing of ex-service material typically indicates these tubes have lower remaining life in comparison to that predicted from the as-cast data. This discrepancy is largely due to microstructural evolution during service. The present work studies the effects of long-term laboratory aging on the creep performance of HP-Niobium and HP-Micro alloys, un-stressed at 1000-1100°C for 500-10,000 hours. Samples were also subjected to accelerated creep testing. Detailed characterization of as-cast, aged and creep samples was carried out using high resolution SEM and TEM, with particular attention paid to the size and distribution of the intragranular and intergranular precipitate networks.

3:00 PM

Free Form Fabrication of Catalytic Substrates: Tyler Salisbury¹; Jerome Downey¹; William Gleason¹; Stacy Davis¹; G. Pinson²; R. Christianson¹; M. Berlin²; R. James¹; E. Rosenberg²; K. Gleason³; R. Hiebert³; J. McCloskey³; ¹Montana Tech of the Univ of Montana; ²University of Montana; ³Center for Advanced Mineral and Metallurgical Processing

Direct digital manufacturing techniques offer promise for fabricating complex support structures for applications such as hydrogen purification membranes for fuel cells. Free form fabrication enables composite structures to be formed from design drawings. In subsequent sintering operations, parameters are controlled to adjust density, pore structure, pore pathways, and strength in constructs to be used as catalytic substrates. Through research being conducted under the auspices of the Center for Advanced Mineral and Metallurgical Processing, efforts are currently underway to define the effects of key process variables on the chemical and mechanical properties of the substrate.

3:20 PM

Microstructure and Hydrogen Transport Property of a Mg-Doped Cu-Pd Alloy: Omer Dogan¹; Rongxiang Hu²; Michael Gao²; Xueyan Song³; ¹DOE National Energy Technology Laboratory; ²URS; ³West Virginia University

To produce high purity hydrogen fuel from coal, hydrogen gas has to be extracted from syngas, a product of coal gasification. Gas separation membranes can be utilized to achieve this goal. Although a variety of hydrogen separation membrane materials exist today, none of them is shown to be suitable to be employed in contaminant laden syngas at elevated temperatures. Cu-Pd alloys with ordered bcc (B₂) phase have demonstrated some promise for being resistant against surface poisoning and corrosion. In these alloys, the superior hydrogen flux increases up to temperatures at which the alloy transforms primarily into fcc structure where a sharp drop in flux occurs. First principles DFT calculations and



TMS 2012

141st Annual Meeting & Exhibition

experiments (XRD, SEM, TEM) have shown that magnesium additions to the Cu-Pd alloy extend the stability of the B2 phase field, potentially improving the hydrogen permeability at higher temperatures.

3:40 PM Break

3:50 PM

Improved Palladium Coatings for Hydrogen Purification Applications: Stacy Davis¹; Jerome Downey¹; William Gleason¹; Tyler Salisbury¹; G. Pinson²; R. Christianson¹; M. Berlin²; R. James¹; E. Rosenberg²; K. Gleason³; R. Hiebert³; J. McCloskey³; ¹Montana Tech of the Univ of Montana; ²University of Montana; ³Center for Advanced Mineral and Metallurgical Processing

Surface membranes and catalytic structures are critical components in applications that range from petroleum refining to hydrogen purification membranes. Autocatalytic reduction processes that are capable of producing stable surface-layered structures in a cost effective manner are especially attractive for manufacturing palladium alloy purification membranes used in hydrogen production. Although interactions between hydrogen and palladium alloys have been extensively studied, the fundamental membrane formation mechanisms are not well understood. The Center for Advanced Mineral and Metallurgical Processing is currently developing a membrane production technology that is based on autocatalytic reduction of palladium from an aqueous solution onto a unique porous substrate. The research identified three distinct deposition mechanisms and results suggest that the mechanisms can be manipulated to provide substantial control over the resulting membrane. This paper details the preliminary findings of work currently in progress.

4:10 PM

Thermodynamic and Transport Properties of Abundant-Vacancy Pd_{1-x}In_x: Douglas Safarik¹; Paul Tobash¹; Anna Llobet¹; Sven Rudin¹; ¹Los Alamos National Laboratory

Vacancies in metals are stabilized by hydrogen. As a result, vacancy concentrations can be orders of magnitude larger in a H-containing material than the H-free analog. Furthermore, because each vacancy is coordinated by several H atoms, the H-storage capacity of "abundant-vacancy" materials can be many times larger than for the vacancy-free analog. This may present an interesting route to development of new hydrogen storage materials. On the other hand, it may have negative consequences for phase and structural stability, particularly for materials experiencing radiation damage in the presence of hydrogen. We have investigated the thermodynamic and transport properties of abundant-vacancy Pd_{1-x}In_x (-0.02 < x < 0.08) alloys, both with and without hydrogen. These alloys are convenient prototypes because (i) they can be prepared with a large and controlled concentration of thermally stable constitutional vacancies, and (ii) they absorb hydrogen. We discuss our results in terms of the electronic and phononic properties of the alloys.

4:30 PM

Phase Transitions of Ammonia Borane Investigated Using Raman Spectroscopy at Low Temperature and High Pressure: Shah Najiba¹; Jiuhua Chen¹; Vadym Drozd¹; Andiry Durygin¹; Yongzhou Sun¹; ¹Florida International University

The phase transition of ammonia borane complex (NH₃BH₃) was investigated by Raman spectroscopy in diamond anvil cell from 3 to 15 GPa with the temperature down to 90K. Ammonia borane undergoes several phase transitions within this temperature and pressure range. Three new low temperature phases were discovered through changes in characteristic Raman spectra. The room temperature high pressure Cmc21 phase (Phase I) transforms to a new phase (Phase IV) at 150K. Room temperature high pressure phase (Phase II) which is stable in the range of 5.5 GPa to 8.5 GPa, transforms to another new phase (Phase V) at 140K. Room temperature high pressure phase (Phase III) that appears at ~ 8.5 GPa, exhibits transition to another new phase (Phase VI) at 130K. These

results provide information about the stability and bonding characteristics of this potential hydrogen storage material at low temperature and high pressure region.

4:50 PM

Mixed Conducting Molten Salt Electrolyte for Na/NiCl₂ Cell: Tannaz Javadi¹; Anthony Petric¹; ¹McMaster University

Na/NiCl₂ battery contains two types of electrolytes, one liquid (NaAlCl₄) and one solid (Na-β"-alumina). During cycling (300°C), NaCl or NiCl₂ phases are formed alternately in the cathode. Electrons are distributed within the cathode by a matrix of excess Ni metal powder. SEM micrographs show that during charging, the NiCl₂ phase forms on Ni particles. Moreover, during discharge, isolated Ni particles can form, surrounded by liquid electrolyte. In this regard, the electronic conductivity of Ni particles is impeded by both the NiCl₂ phase and the liquid electrolyte. Therefore, the capacity of the cell decreases as the number of available active sites for reaction is reduced. Having a mixed conducting electrolyte can facilitate both ionic and electronic transfer inside the cathode. Therefore, different dopants were added to promote electronic conductivity in the ionically conductive NaAlCl₄. The conductivity of the electrolyte was measured by using EIS. The dopant type and concentration were optimized.

5:10 PM

Effect of Al-Substitution and Melt-Spining Process on Microstructural and Hydrogen Storage Properties of LaNi₅ Intermetallic Compounds: O. Uzun¹; F. Yilmaz²; M.F. Kilicaslan³; G.Y. ÖZALP⁴; Soon-Jik Hong⁵; ¹Gaziosmanpasa University; ²Gaziosmanpa University; ³Kastamonu University; ⁴International Centre for Hydrogen Energy Technologies; ⁵Kongju National University

Hydrogen storage alloys have been investigated as environmental-friendly materials for hydrogen gas storage as a fuel source and negative electrode of a rechargeable battery. Researchers have shown great interest in intermetallic compound LaNi₅ because of its high hydrogen capacity, easy activation and fast reaction kinetics, etc. In order to improve the overall properties of LaNi₅, the substitutions of B site element (Ni) with other metals have been studied by many researchers. In this study, LaNi_{4.7}Al_{0.3} alloy was prepared by arc-melting followed by a melt-spinning treatment, the influence of the either alloy preparation methods or Al addition on the microstructure and hydrogen absorption/desorption properties of the alloys was investigated by means of SEM, XRD and Sievert's type apparatus. The results showed that substituting Ni with Al led to desirable decrease in absorption/desorption plateau pressure as well as hysteresis; whereas melt-spinning process only reduced absorption pressure without reduction in its hydrogen capacity.

5:15 PM

Phase Transitions of Nano-scaffold Confined Ammonia Borane Dependent on Pressure: Yongzhou Sun¹; Jiuhua Chen¹; Vadym Drozd¹; Shah Najiba¹; ¹Florida International University

Nanoconfinement has attracted more and more interests based on its excellent thermal dynamic and kinetic property for decomposing ammonia borane. We have conducted in situ Raman spectroscopy study to investigate phase stability of nano-scaled ammonia borane in SBA-15 (mixed with 1:1 ratio) at high pressures up to 11 GPa (with an interval of 0.35 GPa) using diamond anvil cell (DAC). Similar work has been conducted to neat ammonia borane up at different temperature from 20 °C to 80 °C as a comparison. At room temperature, we found the two pressure-induced phase transitions were shifted to ~0.5GPa, ~9.7GPa for nanoscaled ammonia borane from ~0.9 GPa, ~10.2 GPa for neat ammonia borane, respectively.

Materials Processing Fundamentals: Metallurgy of Non-Ferrous Metals

Sponsored by: The Minerals, Metals and Materials Society, TMS Extraction and Processing Division, TMS Light Metals Division, TMS: Process Technology and Modeling Committee

Program Organizers: Lifeng Zhang, Missouri University of Science and Technology; Antoine Allanore, MIT; Cong Wang, Saint-Gobain High Performance Materials

Tuesday PM
March 13, 2012

Room: Oceanic 8
Location: Dolphin Resort

Session Chairs: Cong Wang, Alcoa Research Center; Lifeng Zhang, Missouri S&T

2:00 PM

Annealing Effect and Tensile Interface Fracture Mechanism of Pure Silver Bonding Wires: *Hao-Wen Hsueh*¹; *Fei-Yi Hung*¹; *Truan-Sheng Lui*¹; *Li-Hui Chen*¹; ¹Department of Materials Science and Engineering, National Cheng Kung University, Tainan, Taiwan

Since Ag wires have similar hardness and bonding properties to Au wires, they can be applied in some pads. In the present study, the annealing effect (at 225°C~275°C for 30min) on the tensile mechanical properties of silver wires with $\phi 149$; $\approx 23\mu\text{m}$ was investigated. In addition, the microstructural characteristics and the mechanical properties before and after an electric flame-off (EFO) process were also studied. Experimental results indicate that with annealing temperatures of more than 250°C, the silver wires possessed a fully annealed structure, the tensile strength and the hardness decreased, and the elongation was raised significantly. Under the thermal effect of EFO, the necks of the Ag balls underwent recrystallization and grain growth was induced, and the annealed Ag wires had a shorter zone of HAZ (220 μm). The bonding strength and the neck-strength of the Ag wires were more than 7gf and possessed excellent bonding properties.

2:25 PM

Directional Solidification of Zn-Sn Alloys: *Marco Zurco*¹; *Carlos M. Rodriguez*²; *Carlos E. Schvezov*²; *Claudia M. Mendez*¹; *Alicia Ares*²; ¹Faculty of Sciences, University of Misiones; ²CONICET/FCEQyN-UNaM

Zinc-Tin alloys were directionally solidified in an horizontal device. During solidification the distribution of temperatures were measured by using thermocouples located strategically. From the measured temperatures the following parameters were calculated; the local temperature gradient, the cooling rate and the velocities of the liquidus and solidus fronts. Comparing the structure of the samples and the values of these parameters it was found that the temperature gradient at the instant of the columnar-to-equiaxed transition (CET) reaches minimum values of as low as - 1.5 °C/cm, and the velocities of the fronts were around 0.1 cm/s. In addition, the grain size and secondary dendrite arm spacing were measured along the length of the samples and correlated with thermal parameters and compared with the predictions from available models. The results are presented and discussed in the frame of the available theories and the results obtained before in our group for other alloy systems.

2:50 PM

Dynamic Recovery during Low Temperature Deformation in an Al-0.1Mg Alloy: *Yan Huang*¹; *Philip Prangnell*²; ¹Brunel University; ²The University of Manchester

An Al-0.1Mg alloy was firstly deformed at room temperature by ECAE to a true strain of 10, where a steady state deformation was established and further processing had little effect on grain refinement. The ECAE samples, with an average grain size of $\sim 0.55\mu\text{m}$, were then compressed in a channel die at 77K- 473K to various reductions. Microstructures were characterized by electron backscatter imaging and EBSD in a FEGSEM.

Grain refinement to the ECAE submicron structure occurred during deformation at cryogenic temperatures of 77 – 213K, whereas coarsening took place during deformation at elevated temperatures of 373-473K. A steady state deformation was observed at all temperatures where a constant grain structure was developed and maintained upon further straining due to dynamic recovery. The analysis of thermal activation behaviour in relation to the dynamic recovery suggested that quantum effect should be considered in order to understand the kinetics of the dynamic recovery.

3:15 PM

Applications of Thermo-Chemical and Thermo-Physical Models in the Copper and Lead Pyrometallurgical Industries: *Pengfu Tan*¹; ¹Xstrata Copper

The thermodynamic models for copper smelting and converting, lead smelting and refining, the slag chemistry model and the slag viscosity model have been developed. Those models have been applied successfully in several copper and lead smelters in Australia, the Philippines, Zambia, Kazakhstan and Italy. Those models have been applied to optimize the process parameters and to solve the industrial technical issues, such as high copper loss in slag and converter foamover etc. Several examples for the industrial applications have been presented in this paper.

3:40 PM Break

3:55 PM

Challenges in Compound Forging of Steel-Aluminum Parts: *Klaus-Georg Kersch*¹; *Bernd-Arno Behrens*¹; ¹Institute of Metal Forming and Metal-Forming Machines, Leibniz Universität Hannover

In times of increasing energy costs automotive lightweight construction is gaining more importance. This paper deals with the production of hybrid steel-aluminum compounds by forging. The compound forging process is a promising method to successfully manufacture functional parts by applying resource-saving process steps. Nevertheless, challenges resulting from the different material properties must be solved. The heating of hybrid material work pieces made of steel and aluminum is a great challenge. Steel is forged at a temperature of at least 900°C, while aluminum should not exceed a temperature of 500°C. For the realization of the required temperature gradient extensive experimental investigations have been carried out. Intermetallic phases form during the manufacturing process and influence the bonding and the global part quality. In addition methods for the characterization of the joining zone between the materials steel and aluminum are analyzed and the factors influencing the formation of intermetallic phases are determined experimentally.

4:20 PM

Study of Supercritical CO2 Emulsion in Ni Electroplating and Application in Fabrication of Defect-Free Micromechanical Component with High Aspect Ratio: *Tso-Fu Mark Chang*¹; *Chiemi Ishiyama*¹; *Masato Sone*¹; ¹Tokyo Institute of Technology

Application of supercritical fluid (SCF) in integrated circuit industry and micro-electro-mechanical-systems is believed to be one of the solutions for problems encountered in miniaturization of the devices. Critical point of CO2 is relatively low compared to other solvents, which makes supercritical CO2 (Sc-CO2) as one of the commonly used and studied solvent. However, Sc-CO2 is non-polar, which limits its application in electrochemistry. The limitation is overcome by usage of a surfactant to create an emulsified phase composed of the aqueous electrolyte and Sc-CO2. Film smoothening and grain refinement effects have been reported for Ni film electroplated by Sc-CO2 emulsion (Sc-CO2-E). In this study, effects of Sc-CO2-E, such as pressure, volume fraction of CO2 and the surfactant in electroplating of Ni are studied. Defect is often found in electroplating of micromechanical components using high current density. By application of Sc-CO2-E, defect-free Ni micro-pillars can be fabricated using high current density.



TMS 2012

141st Annual Meeting & Exhibition

4:45 PM

Investigation of the Mechanical Properties and Microstructure of Friction Stir Welded Aluminum Alloy 6061 Sheets: Daniel Colby¹; Benjamin Goodman¹; Travis Spealman¹; Shabbir Choudhuri¹; Prince Anyalebechi¹; ¹Grand Valley State University

The evolution of microstructure and associated tensile properties along the length of friction stir butt welded 4.6 mm thick AA 6061-T6511 sheets have been investigated. The Friction Stir Welding (FSW) was performed on a vertical milling machine with a profiled cylindrical H-13 tool steel probe. A 2 x 2 factorial design was used to select the FSW process parameters. Consistent with published results, preliminary hardness profiles suggest that softening of the alloy occurred in the stir, thermo-mechanically affected, and heat affected zones. The extent of the softening appeared to be different along the length of the welded sheets, being greatest towards the end of the weld. This is tentatively attributed to the expected increase in friction-induced heat ahead of the welded joint and the attendant dissolution of the precipitates in the age hardened alloy. These results are compared to those observed on gas tungsten-arc welded sheets of the same alloy.

Materials Research in Microgravity: Session IV

Sponsored by: The Minerals, Metals and Materials Society, TMS Materials Processing and Manufacturing Division, TMS Extraction and Processing Division, TMS: Process Technology and Modeling Committee, TMS: Solidification Committee

Program Organizers: Robert Hyers, University of Massachusetts; Hani Henein, University of Alberta; Valdis Bojarevics, University of Greenwich; James Downey, NASA; Douglas Matson, Tufts University; Achim Seidel, Astrium; Daniela Voss, ESA

Tuesday PM
March 13, 2012

Room: Asia 3
Location: Dolphin Resort

Session Chair: To Be Announced

2:00 PM Invited

ISS-Experiments and Modeling of Columnar-to-Equiaxed Transition in Solidification Processing: Laszlo Sturz¹; Gerhard Zimmermann¹; Charles-Andre Gandin²; Bernard Billia³; Nathalie Mangelinck³; Henry Nguyen-Thi³; David John Browne⁴; Wajira U. Mirihanage⁴; Daniela Voss⁵; Christoph Beckermann⁶; Alain Karma⁷; ¹Access e.V.; ²MINES ParisTech CEMEF; ³Université P. Cézanne, Marseille; ⁴University College Dublin; ⁵European Space Agency - ESA/ESTEC; ⁶University of Iowa, USA; ⁷Northeastern University, USA

The main topic of the research project CETSOL in the framework of the Microgravity Application Promotion (MAP) programme of the European Space Agency (ESA) is the investigation of the transition from columnar to equiaxed grain growth during solidification. Microgravity environment allows for suppression of buoyancy-driven melt flow and for growth of equiaxed grains free of sedimentation and buoyancy effects. This contribution will present first experimental results obtained in microgravity using hypo-eutectic AlSi alloys in the Materials Science Laboratory (MSL) on-board the International Space Station (ISS). The analysis of the experiments confirms the existence of a columnar to equiaxed transition, especially in the refined alloy. Temperature evolution and grain structure analysis provide critical values for the position, the temperature gradient and the solidification velocity at the columnar to equiaxed transition. These data will be used to improve modeling of solidification microstructures and grain structure on different lengths scales.

2:35 PM Invited

Dendrite Growth into Undercooled Melts: Investigated on Earth and in Reduced Gravity: Dieter Herlach¹; ¹Deutsches Zentrum für Luft- und Raumfahrt

Methods of containerless undercooling and solidification are applied to study the dendrite growth velocity as a function of undercooling. On Earth electromagnetic and electrostatic levitation are used. For equivalent experiments in reduced gravity the German facility TEMPUS (German acronym for Containerless Electro-Magnetic Processing Under Weightlessness) is utilized in reduced gravity during parabolic flight and TEXUS sounding rocket missions offered by DLR and ESA. A high-speed camera allows to measure the rapid advancement of the solidification front with a picture frame rate of 50000 pictures per second. Al-Ni and Cu-Zr alloys are investigated. Al-rich Al-Ni alloys show an anomalous dendrite growth dynamics in such that the dendrite growth velocity decreases with increasing undercooling under terrestrial conditions. These measurements are compared with results obtained in reduced gravity. Measurements on Cu-Zr alloys show a maximum in the growth velocity-undercooling relation. The results will be discussed within the frame of models of dendrite growth

3:10 PM

Coupled Growth in Ternary Systems under Directional Solidification Conditions: Ralph Napolitano¹; Irmak Sargin¹; ¹Iowa State Univ

Exhibiting multiphase composite structures as well as nonplanar growth modes associated with solutal instability, eutectic solidification in ternary and higher-order systems may give rise to a broad scope of solidification morphologies, where microstructural evolution depends on the interplay between local eutectic phase topology, crystallographic orientation/misorientation, eutectic fault configuration, faulted domain and grain structure, and segregation phenomena, all relative to geometric constraints and applied thermal fields. In the study reported here, directional solidification methods are used to investigate the mechanisms of grain boundary migration and grain selection, the origin and configuration of eutectic faults, interface destabilization, and both two- and three-phase couple growth structures in Al-Cu-Ag alloys. Specific attention is given to three-dimensional morphology, transient evolution of solidification structures, and implications for microgravity research. This work is sponsored by the National Aeronautics and Space Administration, under contract NASA-CGA NNX10AT61G, in collaboration with the European Space Agency SETA Project.

3:35 PM Break

3:55 PM Invited

Influence of Convection on Dendrite Growth and Microstructure Evolution by Using AC + DC Electromagnetic Levitator: Hideyuki Yasuda¹; Yuki Kanzawa¹; Takashi Fukuda¹; Tomoya Nagira¹; Masato Yoshiya¹; ¹Osaka University

Electromagnetic levitator has been widely used for examining solidification in undercooled melt and for measuring physical properties. The electromagnetic force causes not only the lift force but also the stirring force. As a result, oscillation and convection are induced in a levitated droplet. Simultaneous imposition of static magnetic field with a sufficient intensity can suppress oscillation and convection and a droplet rotates like a hard sphere. Thus, the levitator using alternating and static magnetic fields allows to study solidification in a undercooled droplet without convection. This paper presents dynamics of a levitated droplet and effect of magnetic field on dendrite growth and microstructure evolution. Based on the results, effect of convection on solidification will be also discussed.

4:30 PM

Liquid Droplet Dynamics in Gravity Compensating High Magnetic Field: *Valdis Bojarevics*¹; Stuart Easter¹; Koulis Pericleous¹; ¹University of Greenwich

Numerical models are used to investigate behaviour of liquid droplets suspended in magnetic fields of various configurations providing microgravity-like conditions. Using a combination of DC and AC fields it is possible to create conditions with laminar viscosity and heat transfer to measure viscosity, surface tension, electrical and thermal conductivities, and heat capacity of a liquid sample. Even a purely DC magnetic levitation can be used for advanced material research. The oscillations in a high DC magnetic field are quite different for an electrically conducting droplet, like liquid metal. The transition of the droplet behaviour from the low to high magnetic field is the subject of investigation in this paper. At the high values of magnetic field some oscillation modes are damped quickly, while others are modified with a considerable shift of the oscillating droplet frequencies and the damping constants from the non-magnetic case.

4:55 PM Invited

Measurements of Dendritic Growth Velocities in Undercooled Melts of Pure Nickel Under Static Magnetic Fields: *Jianrong Gao*¹; Zongning Zhang¹; Yingjie Zhang¹; ¹Northeastern University

Dendritic growth velocities in undercooled melts of pure Ni have been intensively studied over the past fifty years. However, the experimental data are at marked variance with the prediction of the LKT model both at low and at large undercoolings. In the present work, bulk melts of pure Ni samples of different impurities were undercooled by glass fluxing treatment under a static magnetic field. The recalescence processes of the samples at different undercoolings were recorded using a high-speed camera, and were modeled using a software to determine the dendritic growth velocities. The present data confirmed the effect of melt flow on dendritic growth velocities at undercoolings below 100 K. On the other hand, the present data suggested the effect of impurities on dendritic growth velocities at undercoolings larger than 200 K.

5:30 PM

Diamagnetic Levitation by a Superconducting Magnet: A Method for Non-Contact Measurement of the Surface Tension of Aqueous, and other, Diamagnetic Liquids: *Richard Hill*¹; Laurence Eaves¹; ¹University of Nottingham

We use diamagnetic levitation by a superconducting magnet to study the shapes and dynamics of aqueous droplets in a pseudo-weightless environment. The diamagnetic force balances the force of gravity at the molecular level throughout the body of the liquid, and may be compared with the centrifugal force on an orbiting body. Precise measurements of a liquid's surface tension can be obtained from the oscillations of a droplet in zero gravity. Our experiments show close agreement between the oscillation frequencies of a levitated water droplet and those in zero-g. There is a small effect on the resonant frequencies of the droplet owing to the cohesive force of the magnetic 'trap'. We have obtained an analytic expression for the perturbation, enabling high precision measurements of the surface tension to be obtained by this technique. *RJA Hill and L Eaves, Phys. Rev. Lett.* 101, 2340501 (2008); *Phys. Rev. E* 81, 056312 (2010).

Mechanical Behavior at Nanoscale I: Nanowires, Pillar, Multilayers and Nanocrystalline

Sponsored by: The Minerals, Metals and Materials Society, TMS Materials Processing and Manufacturing Division, TMS: Nanomechanical Materials Behavior Committee, TMS/ASM: Mechanical Behavior of Materials Committee

Program Organizers: Scott Mao, University of Pittsburgh; Julia R Greer, California Institute of Technology; Jianyu Huang, Center for Integrated Nanotechnologies; Marc Legros, CEMES-CNRS; Ting Zhu, Georgia Institute of Technology

Tuesday PM
March 13, 2012

Room: Asia 1
Location: Dolphin Resort

Session Chairs: Gerhard Dehm, Erich Schmid Institut für Materialwissenschaft; Xiaodong Li, University of South Carolina

2:00 PM Invited

Deformation Mechanisms in Cu-Nb Nanolamellar Composites Produced via Severe Plastic Deformation: *Nathan Mara*¹; John Carpenter¹; Weizhong Han¹; Jon LeDonne²; Jian Wang¹; Irene Beyerlein¹; ¹Los Alamos National Laboratory; ²Carnegie Mellon University

In this presentation, we report on the plastic deformation mechanisms in Cu-Nb lamellar nanocomposites processed via Severe Plastic Deformation as a function of decreasing layer thickness. We utilize Accumulative Roll-Bonding (ARB) to process bulk Cu-Nb nanolamellar composites from 1 mm thick high-purity polycrystalline sheet down to layer thicknesses of 10 nm. This processing technique has the advantage of producing bulk quantities of nanocomposite material, and also exposes the interface and bulk constituents to large strains (1000's of percent). These extreme strains result in rolling textures, interfacial defect structures, and deformation mechanisms very different from those seen in nanolamellar composites grown via Physical Vapor Deposition methods. Results will be discussed in terms of the effects of interfacial content on deformation processes at diminishing length scales, and defect/interface interactions at the atomic scale.

2:30 PM

Characterization of Defects Generated during the Martensitic Transformation in Pseudoelastically-Deformed NiTi Microcrystals: *Matthew Bowers*¹; Michael Mills¹; Sivom Manchiraju¹; Peter Anderson¹; ¹The Ohio State University

The present study investigates the effects of orientation and specimen size on the pseudoelastic response of NiTi shape memory alloy. The primary goal in this investigation is to determine the means by which the matrix accommodates the large strain associated with the martensitic transformation. This information is critical for extending the working life of components under cyclic loading/heating. It is theorized that the accommodation may take place by matrix plasticity and/or by inducing additional transformation variants, however no experimental verification exists. We demonstrate that micron-scale pillar testing can isolate individual martensite plates, allowing for the investigation of the microstructural evolution related to particular variants in the absence of interactions between competing plates. FIB-machined, micropillars of various crystal orientations have been tested in compression and analyzed via mechanical response measurements and post-mortem TEM observations. Crystallographic theory of martensite and micromechanics-based stress field calculations are used to explain the results.

TUESDAY PM



TMS 2012

141st Annual Meeting & Exhibition

2:50 PM

Deformation Behavior of a Dual-Phase Sheet Steel: *Hassan Ghassemi Armaki*¹; Robert Maaß²; Julia Greer²; Shrikant Bhat³; Sriram Sadagopan³; Sharvan Kumar¹; ¹Brown University; ²California Institute of Technology; ³ArcelorMittal

The deformation behavior of a dual-phase sheet steel consisting of ferrite and martensite was examined in uniaxial tension. Specimens tested to various strains were evaluated by nanoindentation of the coexisting phases to understand the behavior of the individual phases as a function of global deformation. The hardness of ferrite increases gradually with increased global plastic deformation. In contrast, the ferrite close to the ferrite/martensite interface is initially harder than in the interior but softens with increasing deformation. Martensite exhibits a larger scatter in nanoindentation hardness and only a modest change with global straining. A few micropillars were FIB machined in the ferrite and martensite in the as-rolled condition and after 7 percent global plastic strain and were deformed using a flat-punch nanoindenter to generate compression stress-strain curves. The microscopic deformation behavior of the individual phases and their relation to the macroscopic deformation response of the dual-phase steel will be discussed.

3:10 PM

Deforming Nanoporous Gold: Non-Size Effects: *Hai-Jun Jin*¹; Xing-Long Ye¹; Jörg Weissmüller²; ¹Institute of Metal Research, Chinese Academy of Sciences; ²Institut für Werkstoffphysik und -Technologie, Technische Universität Hamburg-Harburg

Nanoporous metals exhibit a strong "size dependence" as other nanostructured materials: the strength increases with decreasing ligament size. Here we demonstrate that some non-size parameters have also great impact on the deformation behavior of nanoporous metals. Compression tests have been performed on crack-free, millimeter-sized nanoporous gold (npg) samples prepared by dealloying, with ligament size at nanometer scale. We found that the strength and brittleness of npg can be altered by changing the surface state (e.g., surface oxygen adsorption) via controlling the electrode potential while doing the compression in situ with potentiostatic controls (Jin and Weissmüller, Science 2011). We also found that the roles of initial lattice dislocation in deformation of npg are very different from that in massive Au. These observations have implications on the understanding of crystal deformation at nm scale, and may also lead to new strategies for making tougher (or less brittle) nanoporous metals.

3:30 PM Break

3:40 PM

Effects of Alloying, Temperature and Strain-Rate on the Mechanical Behavior of Nanocrystalline Palladium Alloys: *Thomas Neithardt*¹; Oliver Kraft¹; Ruth Schwaiger¹; ¹Karlsruhe Institute of Technology, Institute for Applied Materials

It is now well accepted that for grain sizes up to about 50nm the dislocation activity is significantly reduced. Other deformation mechanisms were shown to gain importance, which is corroborated by the small activation volumes and increased strain rate sensitivity typical of nanocrystalline materials. We investigated nanocrystalline Pd and PdAu-alloys using indentation and microcompression tests. An increase of the hardness as well as the strain rate sensitivity for these nanocrystalline materials compared with coarse-grained Pd is typically observed. The alloying content has no significant effect on the strain rate sensitivity and the activation volume for grain sizes well below 100nm. To better understand the deformation mechanisms and their thermal activation, a heating stage was designed. The deformation behavior was studied in the temperature regime up to 90°C, for which no significant grain growth is expected to occur. First indentation and microcompression results as a function of temperature will be presented.

4:00 PM

Mechanical Behaviors of Nanostructures of Low Melting Temperature Metals as Revealed by Synchrotron Laue X-Ray Microdiffraction: *Arief Budiman*¹; M. J. Burek²; G. Lee²; D.-C. Jang³; N. Tamura⁴; M. Kunz⁴; T. Tsui²; ¹Los Alamos National Laboratory (LANL); ²University of Waterloo; ³California Institute of Technology; ⁴Advanced Light Source (ALS), Berkeley Lab

Mechanical behaviors at the nanoscales of low melting temperature metals, such as indium and tin, have not been much studied. Both indium and tin are key materials in advanced microelectronics and nanotechnology industry, and understanding their mechanical behaviors at nanoscales becomes increasingly important to ensure lifetime reliability of their nanoscale devices. Synchrotron X-ray microdiffraction has been utilized to examine defect structures of nanoscale materials. For indium and tin especially, this technique offers unique advantage as conventional methods such as TEM and EBSD will expose the structure to high energy electron beams that may significantly alter the microstructure and defect structure during analysis. Using this approach, we found interesting differences in term of X-ray peak broadening after deformation which indicates differences in plasticity mechanisms in the nanostructures of indium and tin. Understanding these differences could lead to better control of mechanical properties of low melting temperature metals at the nanoscales.

4:20 PM

Tensile Properties of Nano-Twinned Cu Nano-Pillars through Nano-Mechanical Testing, Electron Microscopy, and Atomistic Simulations: *Dongchan Jang*¹; Xiaoyan Li²; Huajian Gao²; Julia Greer¹; ¹California Institute of Technology; ²Brown University

Nano-twinned materials have attracted great scientific interest because of their simultaneous attainment of high strength and ductility. While most reports on nano-twinned metals to date are polycrystalline, where randomly oriented nano-twins are embedded within grains, we developed a fabrication technique producing arrays of thousands of free-standing vertically-aligned Cu nano-pillars. Here, entire specimen consists of uniformly aligned nano-twins with {111} orientations at different inclinations and no grain-boundaries. Through in-situ uniaxial tensile testing, we are able to define the parameter space for dominant deformation mechanism and ultimate tensile strength. Microstructural changes due to plastic deformation were investigated via transmission electron microscopy. Results indicate that while nano-pillars containing orthogonally-oriented twin boundaries (TB) show intensive inter-TB dislocation activities, de-twinning was observed with TBs inclined by 20\176. Through molecular dynamics simulation, these findings are discussed in the framework of dislocation nucleation at the surfaces and subsequent glide along or across TBs.

4:40 PM

Dislocation Multiplication and Nucleation in Small Metallic Fibers under Stress: The Input of In Situ Transmission Electron Microscopy: *Marc Legros*¹; Frédéric Mompou¹; Daniel Gianola²; Andreas Sedlmayr³; Oliver Kraft⁴; Daniel Caillard¹; ¹CEMES-CNRS; ²University of Pennsylvania; ³Karlsruhe Institute for Technology; ⁴Karlsruhe Institute for Technology

Whiskers, thin films, and micro pillars display an increase of their strength as an inverse power law of their size. For sub-micrometre single crystalline pillars and fibers, where no external boundaries or interfaces are confining the dislocations, this trend has to root in the initial microstructure and its ability or not to nest dislocation sources. Despite a lack of detailed experimental investigations, dislocation multiplication is now widely recognized as the key parameter to explain the unusual mechanical behavior of these small objects. Here, we will show that determining a dislocation density may not be sufficient to fully predict the response of Al fibers fabricated by selective chemical etching of an eutectic lamellar Al/Al₂Cu alloy. Combining in situ TEM and SEM tensile

tests allowed us to relate yield stresses to intermittent spiral sources. As they operate closer to the surface, increasing stress values are needed, giving rise to the size effect.

5:00 PM

Deformation of Gold Nanowires: How Impurities Change the Game: *Francesca Tavazza*¹; *Lyle Levine*¹; *Anne Chaka*¹; ¹National Institute of Standards and Technology

The role of impurities in Au nanowire deformation and quantum conductance has been heavily debated. We have used extensive density functional theory simulations to investigate the deformation of [110]-gold nanowires in the presence of light atomic or molecular impurities for several different tensile axes and effective strain rates. Substantial differences in both the wire evolution and the calculated conductance traces are found, with respect to the uncontaminated case. Different contamination mechanisms are investigated by changing the stage of deformation at which the impurity is added to the system. Lastly, the likelihood of an impurity being incorporated into a single-atom-chain is also examined.

5:20 PM

Deformation and Fracture of Color-patterned Pulsed Laser Oxides on Stainless Steel: *Samantha Lawrence*¹; *Douglas Stauffer*²; *Ryan Major*²; *David Adams*³; *William Gerberich*⁴; *David Bahr*¹; *Neville Moody*³; ¹Washington State University; ²Hysitron Inc.; ³Sandia National Laboratories; ⁴University of Minnesota

Localized heating from a focused laser beam produces dielectric phases, creating unique metastable colored layers. Little research has focused on pulsed laser colorized films and none studied mechanical behavior. We have, therefore, begun to investigate the mechanical behavior of color-patterned oxides on polished 304L stainless steel where film and substrate properties control macroscopic wear and fracture processes. Quasi-static and dynamic nanoindentation probed oxide deformation and fracture, resulting in modulus and hardness values of approximately 160GPa and 12GPa, respectively. Conductive nanoindentation measured electrical contact resistance (ECR) for colored oxides indicating a correlation between laser exposure, current, conductance, and indentation response. In this presentation we will show that combining indentation and microscopy techniques provides a unique approach for defining mechanical behavior and processes. This work was supported by DTRA Basic Research Award #IACRO 10-4257, NSF Grant NSF/DMR-0946337, and Sandia National Laboratories, a Lockheed Martin Company for USDOE NNSA under contract DE-AC04-94AL85000.

5:40 PM

Strain Heterogeneities within a Sub-Micron Grain in a Polycrystalline Thin Film as Probed by X-Ray Coherent Diffraction during a Thermal Cycle: *Nicolas Vaxelaire*¹; *Stephane Labat*¹; *Henry Proudhon*²; *Christoph Krichlechner*³; *Olivier Perroud*¹; *Marie-Ingrid Richard*¹; *Thomas Cornelius*⁴; *Jozef Keckes*³; *Samuel Forest*²; *Olivier Thomas*¹; ¹CNRS - Aix-Marseille University; ²MINES ParisTech - CNRS; ³Erich Schmid Institute of Materials Science; ⁴ESRF

Strain heterogeneities in polycrystalline thin films are of great interest in technology because many fabrication and reliability problems are stress related. Nevertheless measuring local strains in sub-micron grains remains a real experimental challenge. This work is focused on the use of X-ray Coherent Diffraction Imaging. A 3D mapping of 111 Bragg reflection from a Au sub-micron grain was measured during a thermal cycle. Because of the difference in thermal expansion between the glass substrate and the film, the film undergoes a biaxial compression test. Coherent properties of the beam have been used to retrieve a component of the displacement field in 3D from a single grain with a resolution around $17 \times 17 \times 22$ nm via phase retrieval procedures. Besides, it has been possible to compute realistic FEM simulations and compare the displacement fields. These results pave the way to non destructive strain mapping at the nanoscale.

Mechanical Behavior Related to Interface Physics: Structure and Mechanical Behavior of Amorphous and Crystalline Nanocomposites

Sponsored by: The Minerals, Metals and Materials Society, TMS Structural Materials Division, TMS Materials Processing and Manufacturing Division, TMS/ASM: Mechanical Behavior of Materials Committee, TMS: Nanomechanical Materials Behavior Committee

Program Organizers: Jian Wang, Los Alamos National Laboratory; Nathan Mara, Los Alamos National Laboratory; Izabela Szlufarska, University of Wisconsin-Madison; Zhiwei Shan, Xi'an Jiaotong University

Tuesday PM
March 13, 2012

Room: Oceanic 1
Location: Dolphin Resort

Session Chairs: Rozaliya Barabash, Oak Ridge National Laboratory; Alla Sergueeva, NanoSteel Company

2:00 PM Keynote

Crystal-Glass Interfaces: *Ju Li*¹; ¹Massachusetts Institute of Technology

Unlike grain boundaries (GB) which have 3 mis-orientations and 2 inclinations degrees of freedom, crystal-glass interfaces (CGI) have only 2 inclinations degrees of freedom and constitute a different class of internal interfaces. Due to this essential difference in structure, the manners of inelastic deformation transduction at CGIs differ a great deal from those near GBs, which significantly impact the plasticity and fracture behaviour of nanoscale crystalline-amorphous aggregates. Recent experimental work have highlighted the importance of CGIs on the ductility of crystalline-amorphous multilayers (PNAS 104 (2007) 11155), and the cyclability and efficiency of Li-ion batteries (Science 330 (2010) 1515).

2:30 PM Keynote

Interface-Dominated Mechanical Properties of Layered/Fibrous Composites: *Rozaliya Barabash*¹; ¹Oak Ridge National Laboratory

Interfaces play a crucial role in materials properties, in part because interfaces themselves possess unique physical properties distinct from the bulk constituent phases. In layered/fibrous composites, the overall interface area is very large. Interfaces between the phases are the key elements responsible for the unique micro-mechanisms of plasticity in composites. A predictive understanding of the interface interactions between the matrix and the lamellae/fibers under external fields would allow interface engineering to create the best combination of the materials properties. In this study the depth-dependent strain distributed in the layered/fibrous composite and partitioned across the interfaces is directly measured at submicron length-scales using X-ray microdiffraction and compared to a detailed micromechanical stress analysis. Interface strength is estimated from the near-surface depth-dependent strain gradients. Several examples for directionally solidified composites are presented. Research supported by the Materials Sciences and Engineering Division, Office of Basic Energy Sciences, U.S. Department of Energy.

3:00 PM

Dislocation-Interface Interaction in Crystalline-Amorphous Metallic Multilayers: *Christian Brandl*¹; *Timothy Germann*¹; *Amit Misra*¹; ¹Los Alamos National Laboratory

The combination of amorphous nanoscale layers with crystalline nanoscale layers has exhibited extraordinarily high toughness, i.e. ultra-high strength in conjunction with high elongation-to-failure. The plastic deformation is confined by the crystalline-amorphous interface, which additionally has to maintain deformation compatibility to mediate homogeneous plastic flow. Contrary to crystalline-crystalline interfaces, where crystalline phases exhibit long range order, the amorphous structure is characterized by a lack of long-range order. Using molecular dynamics (MD) methods, the compensation mechanism of this reduced long-range order at the interface is studied for the Cu (FCC) / CuxZr(1-x)



TMS 2012

141st Annual Meeting & Exhibition

(amorphous) system. The ordering decreases with increasing distance from the amorphous-crystalline interface. The implication of the interface ordering on dislocations impinging upon the interface is studied via MD. The interface response is discussed in terms of (1) rearrangement of interface order, and (2) co-deformability of the amorphous and crystalline layers, and the resulting implications on layer size effects.

3:15 PM

Mechanical Characterization of Nanolayered Al/SiC Composites by High Temperature Nanoindentation: S. Lotfian¹; J. Molina-Aldareguia¹; K. Yazzie²; J. LLorca¹; A. Misra³; *Nikhilesh Chawla*²; ¹IMDEA Materials Institute, 28040-Madrid, Spain; ²Arizona State University; ³Los Alamos National Laboratory, Los Alamos, NM

Multilayered Al/SiC composites exhibit extremely high strength and toughness. In this paper we discuss the high temperature nanoindentation behavior of these materials. The nanolaminates were processed by physical vapor deposition (PVD) using magnetron sputtering. Layer thickness and morphology was studied using a dual beam focused ion beam (FIB). The mechanical properties were characterized by high temperature nanoindentation at 100, 200, and 300°C. Finally, post-deformation microstructural analysis was carried by FIB and atomic force microscopy (AFM) to provide insight into the deformation mechanisms.

3:30 PM

The Interfacial Mechanics of the Thin Oxide Skin on Liquid Gallium Alloy: Ju-Hee So¹; Rashed Khan¹; *Michael Dickey*¹; ¹NC State University

We describe the mechanics of the thin oxide skin that forms on a liquid metal. The alloy, eutectic gallium indium, is useful for moldable microelectrodes, stretchable antennas, and flexible solar cells. The ability to micromold the metal for these applications is enabled by the mechanical properties of a thin oxide skin that forms spontaneously on its surface; the material is therefore effectively a composite. The oxide skin is elastic and yields under a critical stress, at which point the metal flows. The ability to flow the metal is important for shaping (and re-shaping) it into useful geometries. We studied the mechanical properties of the oxide skin under different environments using a rheometer with a parallel-plate geometry. The rheological properties of the low viscosity liquid are dominated by the interfacial skin. These studies provide new tools to study thin films and engineer the forces under which the metal will flow.

3:45 PM Break

3:55 PM Keynote

Tensile Ductility and Necking in Small-Volume Metallic Glasses: In the Limit of Suppressed Shear Banding: *Evan Ma*¹; ¹Johns Hopkins University

In bulk samples of amorphous metals, shear banding is the norm upon room temperature plastic deformation. Almost all the plastic strains are localized in the quasi-2D shear band. When the sample size is on submicron- and nano- scale, however, such severe shear localization can be suppressed. Here we show new tensile testing schemes inside TEM that allowed quantitative evaluation of the intrinsic properties and deformation mode of ~100 nm diameter samples. We observe that the formation of the thin shear band, with “interfaces” that are energy-costing, gives way to distributed deformation followed by gradual necking. The resulting high strength (2.5 to 4 GPa), elasticity (up to 5%), and appreciable tensile elongation (~10%) make small-volume metallic glasses appealing for MEMS applications. This work is a collaboration with Lin Tian, Zhiwei Shan, Ju Li, Qingsong Deng and Xiaodong Han.

4:25 PM Keynote

Ductility Mechanisms in Glass Matrix Nanomaterials: *Alla Sergueeva*¹; Sheng Cheng¹; Brian Meacham¹; Daniel Branagan¹; ¹The NanoSteel Company

Metallic glasses and nanomaterials have shown great commercial promise due to their unique combination of properties which include very high strength (up to 50% of theoretical) and hardness. However, achieving usable ductility in these materials has been a compelling unsolved issue for several decades. Furthermore, operational theories on how this can be achieved, including the structure type and enabling mechanism of deformation, have not been clearly defined in theory or proven by experimentation. In this presentation, the ability to obtain usable ductility is shown in materials which combined features of both classes of the materials. Enabling metallurgical structure, mechanisms of ductility at room temperature as well as a role of glass/crystal interfaces in glass matrix nanomaterials are analyzed.

4:55 PM

Analysis of Heterogeneous Deformation along Grain Boundaries in Tensile Tests of Pure Tantalum: *Ian Jarvis*¹; Thomas Bieler¹; Martin Crimp¹; Darren Mason²; Brad Boyce³; ¹Michigan State University; ²Albion College; ³Sandia National Laboratory

Deformation and failure of polycrystals results from heterogeneous deformation that accelerates after the ultimate tensile stress is reached. During the failure process, the difference in strain of hard and soft grains leads to formation of voids. In-situ deformation of pure tantalum polycrystals was monitored in SEM and EBSP maps were obtained at several stages of strain. Direct observation clearly shows how some grains deformed more than others, and distinct orientation gradients became evident along some boundaries. The sequential orientation maps were analyzed to identify locations where large gradients in deformation developed using grain boundary slip transfer concepts and a new modeling approach where the origin of grain boundary ledges arising from heterogeneous deformation was effectively predicted in titanium polycrystals. Simulation of this microstructure patch with crystal plasticity finite element models was used to obtain estimates of the local stress tensors. Agreement between model and experiment is assessed and discussed.

5:10 PM

Novel Design of Functional Nanoporous Metal Architectures: *Eric Detsi*¹; Sergey Punzhin¹; Patrick R. Onck¹; Jeff T.M. De Hosson¹; ¹University of Groningen

Nanoporous metals synthesized by dealloying have attracted considerable attention in recent years due to their potential for various applications including catalysts, sensors, actuators and drug delivery platforms. Downscaling the size of ligaments and pores to smaller dimensions is particularly interesting because this enhances the specific surface area as well as the material properties. Obviously, the size of microstructural elements cannot be scaled down indefinitely and in our work we address this limitation by searching for alternative nanoporous metal architectures. By exploiting grain boundaries misorientation in the alloy precursor, we have designed nanoporous metals with multilayer architectures during dealloying. The novel porous layers architecture displays intriguing functional properties. In particular giant charge-induced strains are measured, roughly two order of magnitude larger than in conventional nanoporous metals.

Mechanical Performance of Materials for Current and Advanced Nuclear Reactors: Characterization and Modeling of Microstructural Evolution in Nuclear Materials

Sponsored by: The Minerals, Metals and Materials Society, TMS Structural Materials Division, TMS/ASM: Nuclear Materials Committee

Program Organizers: Nicholas Barbosa, National Institute of Standards & Tech; Greg Oberson, United States Nuclear Regulatory Commission; Matthew Kerr, United States Nuclear Regulatory Commission; Elaine West, Knolls Atomic Power Laboratory; Stuart Maloy, Los Alamos National Laboratory; Osman Anderoglu, LANL

Tuesday PM
March 13, 2012

Room: Swan 1
Location: Swan Resort

Session Chairs: Elaine West, Knolls Atomic Power Laboratory; Paula Mosbrucker, Los Alamos National Laboratory

2:00 PM Invited

Microstructures and Mechanical Properties in Carbide and Nitride Ceramics for Advanced Nuclear Systems: *Todd Allen*¹; *Yong Yang*²; *Clayton Dickerson*³; ¹University of Wisconsin-Madison; ²University of Florida; ³Argonne National Laboratory

Many advanced nuclear systems aim to operate such that structures are exposed to higher irradiation dose, operate at higher temperatures, and use cooling media other than water. Interest in advanced ceramics comes from many areas including high-temperature gas-cooled reactors, fusion systems, and advanced water-cooled reactors. The radiation response and micromechanical response of two carbides, ZrC and TiC, and two nitrides, ZrN and TiN have been studied using controlled temperature high-energy proton irradiation. Following radiation microstructures have been characterized using x-ray diffraction and transmission electron microscopy while changes in mechanical properties have been estimated using deflection of micro-pillars machined from irradiated samples using a focused ion beam technique. In general, some lattice expansion is noted due to the accumulation of radiation-produced defects, a series of irradiation-induced dislocation loops is formed, and the fracture toughness increases relative to the unirradiated material.

2:30 PM

In-Situ Studies and Modeling of the Deformation and Fracture Mechanism for Wrought Zircaloy-4 and Zircaloy-2 as a Function of Stress-State: *Brian Cockeram*¹; *Kwai Chan*²; ¹Bechtel-Bettis; ²Southwest Research Institute

In-situ deformation and fracture studies were performed on wrought Zircaloy-4 and Zircaloy-2 over a range of stress-states using Compact Tension (CT) and smooth and notched tensile specimens to evaluate the mechanism for fracture initiation and propagation. Both annealed and beta-treated conditions were tested to understand both the role of microstructure and orientation. Unstable crack extension is shown to occur under plastic constraint by a process of void nucleation, growth, and coalescence under all stress-states. A constant value of critical local strain is shown to initiate void nucleation for all stress-states. The strain for failure is shown to be controlled by the process of void growth and coalescence that is strongly dependent on stress-state. A micromechanical model is developed for the mechanism of ductile tearing by void growth and coalescence. Excellent agreement between the model and experimental measurements of the critical strain for failure initiation and strain for fracture is observed.

2:50 PM

Mechanical Properties of Nanocrystalline Zr from Atomistic Simulation: *Zizhe Lu*¹; *Dong-Hyun Kim*¹; *Mark Noordhoek*¹; *Michele Manuel*¹; *Susan Sinnott*¹; *Simon Phillpot*¹; ¹University of Florida

Zirconium alloys are used as fuel clad because of their mechanical properties, and high resistance to corrosion and irradiation. Using molecular-dynamics simulation, we characterize the slip and twinning processes governing mechanical phenomena in fine-grained Zr. Two different descriptions of the interatomic interactions are employed: an embedded-atom method (EAM) potential [1], and a charge-optimized many body (COMB) potential recently developed by the authors. The modes of slip and twinning obtained using the different potentials are compared with those in experiments. Grain boundaries are found to act as heterogeneous nucleation sites of dislocations and twins. This work was supported by the Consortium for Advanced Simulation of Light Water Reactors (www.casl.gov), an Energy Innovation Hub (<http://www.energy.gov/hubs>) for Modeling and Simulation of Nuclear Reactors under U.S. Department of Energy Contract No. DE-AC05-00OR22725.[1] Mendelev MI, Ackland GJ. Philosophical Magazine Letters 2007;87:349

3:10 PM

Plastic Accommodation of Zirconium Hydrides: *Cindy Smith*¹; *Ian Robertson*¹; *Mohsen Dadfarnia*¹; *Petros Sofronis*¹; ¹University of Illinois

The formation of a field of dislocations around a gamma-hydride in a zirconium alloy is revisited by using electron tomography to determine the three-dimensional spatial distribution of the dislocation structure associated with the hydride. Electron tomography as applied to the studies of defects is a relatively new and challenging technique but the additional insight gain from moving from a projected to fully three-dimensional image is proving invaluable. Here this technique is coupled with conventional TEM analysis methods to explore the distribution of dislocations surrounding a gamma-hydride in a zirconium alloy. It will be shown that the dislocations associated with the hydride have the same Burgers vector, are coplanar, and originate from a common source on the hydride. These results will be considered in terms of proposed mechanisms for accommodating the misfit strain by generation of shear loops or reducing the interfacial energy through formation of emissary dislocations.

3:30 PM

Microstructural Evolution and Fracture Toughness Recovery by Thermal Annealing in HT9 Steel Irradiated to High Doses: *Osman Anderoglu*¹; *Thak Sang Byun*²; *Stuart Maloy*¹; ¹Los Alamos National Laboratory; ²Oak Ridge National Laboratory

An HT-9 duct, ACO-3, was irradiated in a fast reactor to a maximum dose of 155 dpa at 380-505°C. Significant hardening and reduction of toughness at lower irradiation temperatures were observed. In an effort to recover the original mechanical properties, thermal annealing was performed at 550 and 650°C for up to 2 hours. Fracture toughness was measured at 22-600°C after annealing using the TPB specimens. The results indicate that fracture toughness is completely recovered when annealed at 650°C after low temperature irradiation, while it is partially recovered in other cases. TEM shows a high density of second phase precipitates at low temperature irradiations. It is thought that these precipitates are partly responsible for degradation of mechanical properties. We performed in-situ TEM annealing experiments to observe evolution of microstructure up to 500°C. In this talk we will report the results of microscopic changes and discuss the effects on the macroscopic properties.



TMS 2012

141st Annual Meeting & Exhibition

3:50 PM Break

4:05 PM

Molecular Dynamics Simulations of Cascade Evolution near Trapped Interstitial Clusters: *Nathan Capps*¹; Aaron Kohnert²; Karl Hammond¹; Donghua Xu¹; Brian Wirth¹; ¹University of Tennessee; ²University of California

The overlap of displacement cascade is believed important in the development of visual defect clusters in thin film, in-situ ion irradiation studies. Here, we report molecular dynamics simulation results to investigate how impurities and damage induced by displacement cascades affect the mobility of pre-existing, interstitial-type dislocation loops in BCC iron. It is well known that impurities, such as oxygen, carbon, and nitrogen affect the ability of interstitial dislocation loops, and are likely responsible for differences in loop diffusivities between simulations and experiment. Molecular dynamics simulations with varying energy and direction of the primary knock on atom (PKA) reveal that cascades from PKAs with energy > 10 keV can cause the loop to detrapp from impurities, but the loop may rapidly become trapped in the cascade debris. Furthermore, on several occasions, the cascade has induced a change in orientation or Burgers vector of the dislocation loop.

4:25 PM

Atomistic Modelling of Helium Trapping by Nanoscale Precipitates: *Niraj Gupta*¹; Alfredo Caro²; Enrique Martinez²; Srinivasan Srivilliputhur¹; ¹University of North Texas; ²Los Alamos National Lab

Irradiation damage and helium generation pose a major challenge to the development of advanced materials for proposed fusion reactor designs. Recent experimental efforts have shown that nanostructured ferritic alloys exhibit exceptional helium tolerance due to defect recombination and helium trapping in small gas bubbles due to an ultrahigh density of oxide "nanofeatures." The trapping mechanism is believed to be geometric in nature, and is modeled in our work using a prototype Cu-Nb system. Helium addition to FCC Cu precipitates in a BCC Nb matrix and vice versa were simulated using MD and Monte Carlo simulations. Both these simulations yield preferential interfacial helium trapping, illustrating that this behavior is general to any stable high-interface density material systems irrespective of chemistry. The role of coherency of the interface is also explored by contrasting with helium behavior in the Fe-Cr system wherein both Fe and Cr have body-centered-cubic structure and similar lattice constants.

4:45 PM

Influence of the Coherency of Nano-Oxides in ODS Materials on the Coarsening Kinetics: *Joel Ribis*¹; Yann De Carlan¹; ¹CEA

Ferritic/martensitic ODS alloys are candidates as structural materials for components subjected to very high irradiation doses at high temperature. They are reinforced by a homogeneous dispersion of nano-oxides within the matrix. Nano-oxides exhibit an amazing thermal stability. In the new Fe-14Cr1W CEA ODS alloy, after hot extrusion and annealing 1 hour at 1400°C there size remain close to 10 nm. Thanks to high resolution TEM observations, the coherency of the nano-phases has been shown. The interfacial and elastic energy have been determined. It explains the great thermal stability of the oxides but a recrystallization of the material breaks the coherency between the nano-phases and the matrix and increases the coarsening kinetics.

5:05 PM

Spinodal Decomposition in Duplex Stainless Steel: *Julie Tucker*¹; George Young¹; Michael Miller²; ¹Knolls Atomic Power Laboratory; ²Oak Ridge National Laboratory

Duplex stainless steels are desirable for use in power generation systems due to their attractive combination of strength, corrosion resistance, and cost. However, thermal embrittlement at ~475°C limits upper service temperatures for many applications. New lean grade duplex alloys have improved thermal stability over standard grades and potentially increase their upper service temperature. The thermal stability of lean grade, alloy

2003 is compared to standard grade, alloy 2205, through isothermal aging between 280°C and 815°C for 1 to 10,000 hrs. Samples were characterized by microhardness, Charpy-impact toughness and atom probe tomography (APT). APT results indicated that α - α' phase separation occurred via spinodal decomposition for both alloys and identified a complex Cu-Ni-Si-Mn-P second phase in alloy 2205 that may contribute to the embrittlement rate. Research supported by ORNL's Shared Research Equipment (SHaRE) User Facility, which is sponsored by the Office of Basic Energy Sciences, the U.S. Department of Energy.

5:25 PM

Elemental Solubility Tendency for the Phases of Uranium by Classical Models Used to Predict Alloy Behavior: *Van Blackwood*¹; Travis Koenig¹; Saleem Drera¹; David Olson¹; Brajendra Mishra¹; Doug Porter²; Robert Mariani²; ¹Colorado School of Mines; ²Idaho National Lab

Traditional alloy theory models, specifically Darken-Gurry and Miedema's analyses, have been used to assist in predicting alloy behavior. These models will be applied relative to the three solid phases of uranium: alpha, beta, and gamma. These phases have different solubilities for specific alloy additions as a function of temperature. The Darken-Gurry and Miedema models, with modifications based on concepts of Waber, Schneider, and Brewer will be used to predict the behavior of four types of solutes: 1) Transition metals that are associated with the containment as alloy additions in the uranium fuel 2) Transuranic elements in uranium 3) Rare earth fission products 4) Transition metals and other fission products. Using these solute map criteria, elemental behavior will be predicted and used to compare solute effects during uranium phase transformations. The solute map overlap is a convenient first approximation tools for predicting alloy behavior.

Nanocomposites: Nanocomposite Interfaces and Characterization

Sponsored by: The Minerals, Metals and Materials Society, TMS Structural Materials Division, TMS/ASM: Composite Materials Committee

Program Organizers: Garth Wilks, Air Force Research Laboratory; Jonathan Spowart, Air Force Research Laboratory; Meisha Shofner, Georgia Institute of Technology; John Zhanhu Guo, Lamar University

Tuesday PM

March 13, 2012

Room: Swan 8

Location: Swan Resort

Session Chairs: Meisha Shofner, Georgia Institute of Technology; Javier Garay, University of California, Riverside

2:00 PM

Positron Lifetime Analysis of Polyurea-Nanoclay Composites: *Naidu Seetala*¹; Danny Hubbard¹; Gabriel Burks¹; Alex Trochez¹; Valery Khabashesku²; ¹Grambling State University; ²University of Houston

Positron lifetime spectroscopy (PLS) is used to study 1-5 wt% nanoclay incorporated aliphatic polyurea films prepared by two different methods. Set-1 used aliphatic polyaspartate polyurea system consists of aliphatic diisocyanate resin, while set-2 used pre-made aliphatic-polyurea granules. PLS was used to study pore structure in polyurea samples. The third lifetime component, related to positronium formation in free spaces, provided the information on pore size and concentration of pores. The third lifetime component showed ~ 2 ns for set-1 and ~ 1.8 ns for set-2 with relative intensities of 16% and 19%, respectively; indicating that set-1 polyurea has larger pores with lesser concentration compared to set-2 polyurea. There is good correlation between positronium lifetime parameters (both lifetime and intensity) and % nanoclay in set-1 polyurea, but no correlation is observed for set-2 polyurea. The set-2 films showed bad quality and the polymer curing is not as good as set-1 films.

2:20 PM

Effect of Interfacial Reaction on Mechanical and Corrosion Properties of Oxide Nano-Particle Reinforced Aluminum Matrix Composites: *Jaehyuck Shin*¹; Jiyeon Suh¹; Donghyun Bae¹; ¹Yonsei University

Interface characteristics, with their mechanical and corrosion properties, have been investigated for aluminum based composites reinforced with oxide nano-particles (TiO₂, SiO₂). The composites are produced by hot rolling the ball-milled mixture of Al powders and nano-particles. During a milling process, nano-particles are gradually dispersed and embedded within the Al powders. After the annealing process, interface of the composite is modified to be amorphous structure by inducing the formation of nanoscale diffusion layer between the nano-particle and the matrix. With increasing the annealing time, the composites show enhanced yield strength and ductility. Furthermore, interfacial reaction has beneficial effect on corrosion resistance of the composites due to the dispersion of oxide atoms into the matrix. Mechanical properties with increasing annealing time and their corrosion properties will be presented.

2:40 PM Invited

Interfaces in Functional Nanocomposites: *J. Garay*¹; ¹UC Riverside

The influence of nano-scale defects (grain/phase boundaries, pores, etc) can be significantly different from micro-scale features. We will discuss how interfaces in nanocrystalline materials interact with light, electric and magnetic fields and how precise control of these defects can be used to tune materials properties. In particular we will concentrate on light transparency in the visible range, magnetic exchange coupling and magneto transport. We will also briefly discuss our main processing technique, current activated pressure assisted densification has proven effective in overcoming the grain growth challenge. The materials produced have applications as magneto-optical diodes, magnetic sensors and permanent magnets.

3:20 PM Break

3:40 PM

Nano-Scale Characterization on the Metal/Carbon Nanotube Interface: Tushar Borkar¹; *Junyeon Hwang*¹; Sandip Harimkar²; Jaimie Tiley³; Soon-Hyung Hong⁴; Rajarshi Banerjee¹; ¹University of North Texas; ²Oklahoma State University; ³Air Force Research Laboratory; ⁴Korea Advanced Institute of Science and Technology

The properties of metal/carbon nanotube hybrid structures are critically dependent on the structure and chemistry of the metal-carbon nanotube interface. Therefore, the characterization of the interface at the highest possible resolution is of prime importance but rather challenging. In this study, interfaces of Ni/CNT nanocomposites fabricated by laser process and spark plasma sintering technique are characterized and compared with their mechanical properties. In addition, the interface deposited by vacuum process technique has been analyzed by analytical transmission electron microscope combined with three-dimensional atom probe tomography. The structural stability of the metal/CNT interface will also be discussed and related to potential implications on properties of these hybrid structures.

4:00 PM

Extended X-Ray Absorption Fine Structure (EXAFS) Studies of Radiation Damage-Tolerant Nanocomposites: *Simerjeet Gill*¹; Avishai Ofan¹; Lynne Ecker¹; Amit Misra¹; ¹Brookhaven National Lab

Nanocomposites such as Oxide Dispersion Strengthened (ODS) are promising fuel cladding materials for future reactors. One important challenge in ODS steels is that the atomic environment of the metal-oxide interface in a ferritic matrix is difficult to access due to the geometric complexity of the internal interfaces. In order to understand fundamental mechanisms of radiation-induced defect evolution and annihilation at interfaces of ODS steels with complex structure, model nanocomposite systems with regularly spaced interfaces in a multilayer geometry were studied. Nanocomposite layered systems with both metal-oxide/metal (Y₂O₃/Fe) and metal-metal (Cu/Nb) interfaces are reported. Nanocomposite systems have demonstrated high strength and good thermal stability, but local molecular structure at the interface is not clearly understood. In present studies, EXAFS is used to investigate changes in molecular structure and lattice distortions induced at interface in nanocomposite layered systems. The effect of annealing and irradiation conditions on the local molecular structure is reported.

4:20 PM

Structure and Transport Properties of Zeolite-Polymer Composite Membranes for Energy-Efficient Separations: Role of Interactions and Geometry: *Carson Meredith*¹; Jung-Hyun Lee¹; ¹Georgia Tech

We present measurements made with atomic force microscopy of the interfacial adhesion between key membrane-forming polymers and a model zeolite. These are used to determine the primary intermolecular interactions governing adhesion and are compared to transport and mechanical properties of polyamide- and poly(vinylacetate) (PVAc)-based composite membranes. Zeolite (all-silica MFI) adhesion to polyamides is governed primarily by acid-base interactions in which carbonyl groups on the polymer, as well as adsorbed surface water, play a key role. Models for these adhesion mechanisms are presented and compared as well. In particular, we find that adhesion can be correlated strongly with known surface tension values if measurements with a variety of solvents (protic and aprotic, polar and non-polar) are available. In addition, we present evidence of the beneficial effect of nanostructured roughening of the zeolite surface on adhesion, transport, and mechanical properties.

4:40 PM

Diffusion of Atmospheric Penetrants in Crosslinked and Uncrosslinked Polydimethylsiloxane Based Nanocomposites: Varun Ullal¹; *Douglas Spearot*¹; ¹University of Arkansas

Molecular dynamics (MD) simulations are used to compute diffusion coefficients for N₂ and O₂ penetrants in polydimethylsiloxane (PDMS) based nanocomposite models with metallic inclusions. PDMS is modeled using a hybrid coarse-grained interatomic potential which retains atomic distinction along the siloxane backbone but models the methyl side groups as united atoms. To validate the simulation methodology, diffusion data is computed for pure PDMS with different chains lengths over a range of temperatures and compared with experimental data. For nanocomposite simulations, both crosslinked and uncrosslinked PDMS models are constructed. Crosslinked PDMS networks are formed by mixing silanol-terminated PDMS chains with the molecule tetra(dimethylsiloxy)silane and employing a numerical algorithm to dynamically create crosslinks at the ends of the PDMS chains. Simulations show that nanoparticle volume fraction plays a primary role on the diffusion coefficient and that the interface between the PDMS and the metallic inclusions can influence the behavior of the diffusing species.



Neutron and X-Ray Studies of Advanced Materials V: Centennial: Dislocations, Strains, Deformation I

Sponsored by: The Minerals, Metals and Materials Society, TMS Structural Materials Division, TMS/ASM: Mechanical Behavior of Materials Committee, TMS: Chemistry and Physics of Materials Committee

Program Organizers: Rozaliya Barabash, Oak Ridge National Laboratory; Xun-Li Wang, Oak Ridge National Laboratory; Gernot Kostorz, ETH Zurich; Lyle Levine, National Institute of Standards and Technology; Peter Liaw, Univ of Tennessee; Yandong Wang, Beijing Institute of Technology; Brent Fultz, California Institute of Technology

Tuesday PM
March 13, 2012

Room: Southern I
Location: Dolphin Resort

Funding support provided by: Office of Basic Energy Sciences, U.S. Dept. of Energy, Dr. P. Thyagarajan

Session Chairs: Matteo Leoni, University of Trento; Davor Balzar, University of Denver

2:00 PM Keynote

In-Situ Laue Diffraction during Mechanical Testing: *Helena Van Swygenhoven*¹; Julien Zimmermann¹; Cecile Marichal¹; Steven Van Petegem¹; ¹Paul Scherrer Institute

In-situ Laue diffraction during microcompression has been developed at the MicroXAS beamline of the Swiss Light Source. Diffraction patterns are obtained in transmission with a 4-24 keV X-ray beam, FWHM of 0.5 -1 μm . Pillars with diameters up to a few microns can be deformed in-situ and Laue scans allow mapping of spatially distribution of strain gradients in the deformed pillars. The evolution of position and shape of the Laue reflections provides information on local crystallographic orientation and activated dislocation slip systems. Microcompression is a small testing device that is now widely used. The advantage of performing microcompression in-situ during Laue diffraction is demonstrated, emphasizing the boundary constraints of the test, the influence of sample shape and preparation on slip systems in single crystal fcc and bcc pillars. The first efforts towards the development of a computational bottom-up approach for the calculation of Laue patterns will be discussed.

2:25 PM Invited

Deformation Twinning in Mg Probed with Diffraction at Multiple Length Scales: *Donald Brown*¹; Levente Balogh¹; Bjorn Clausen¹; Carlos Tome¹; ¹Los Alamos National Lab

Diffraction is well suited to the study of microstructural evolution during plasticity. The length scale probed by diffraction is most strongly a function of the probe particle utilized. Electron diffraction provides information on a very short length scale, but also penetrates only a short distance into materials. Neutrons penetrate into the depth of most materials, providing a statistical sampling of the bulk of the material. The advent of high energy synchrotron x-ray diffraction over the last decade has bridged the gap between these two extremes. As part of a larger program to understand and model the deformation of hexagonal metals, we have utilized each of these probe particles to characterize deformation microstructures as the length scale has dictated. This talk will describe how the results obtained with distinct diffraction probes with length scales from sub-micron to cm's have been integrated to direct development of plasticity models in hexagonal metals.

2:45 PM Invited

Structure/Microstructure Analysis of Faulted and Modular Materials from Powder Diffraction Data: Beyond the Deterministic Approach: *Matteo Leoni*¹; ¹University of Trento

Lattice parameters, asymmetric unit, symmetry elements and modulation vectors are usually employed for the description of a crystalline material. However, not always such information is sufficient to reconstruct the X-ray powder diffraction pattern (XRPD) of a real specimen, even if instrument and specimen-related broadening effects are properly taken into account. Odd profile shapes, deeply anisotropic broadening, extra features can in fact be present e.g. as the result of local breaking of the 3D periodicity of the lattice. The modular approach should be invoked in this case to move from a deterministic (regular) to a probabilistic (quasi-regular or irregular) description of the material. When single crystals are available, diffuse scattering and the Reverse Monte-Carlo approach are the ideal tools to analyse the extra intensity appearing in between Bragg peaks. It will be here shown how faulted structures and modular systems built with 2D symmetric modules can be analysed from XRPD data.

3:05 PM

Scientific Opportunities at the High Flux Isotope Reactor Neutron Powder Diffractometer: *Ovidiu Garlea*¹; ¹Oak Ridge National Laboratory

The neutron powder diffractometer HB2a at the High Flux Isotope Reactor was designed to achieve an optimum balance between high neutron flux and high resolution. It is equipped with a vertically focused Ge monochromator that provides one of three wavelengths: 2.41Å, 1.54Å, and 1.12Å. Due to its versatility, the instrument can be employed for a large variety of experiments, but it is particularly adapted for determining structures with large interplanar spacing, as well as complex magnetic structures. Furthermore, studies of phase transitions, thermal expansion, quantitative analysis, and ab-initio structure solution from powder data can be undertaken. A full range of ancillary environments can be used to provide a complete control of thermodynamic variables, which are essential to unravel the complex relationship between structure and materials properties. This presentation will give an overview of the HB2a diffractometer focusing on recent parametric diffraction studies on several new materials.

3:20 PM

Characterization of Superelasticity in a New Fe-Based Shape Memory Alloy Using Neutron and Synchrotron Radiation: *Saurabh Kabra*¹; Klaus-Dieter Liss¹; Kun Yan¹; David Carr¹; Yuuki Tanaka²; Toshihiro Omori²; Ryosuke Kainuma²; ¹ANSTO; ²Tohoku University

A novel Fe-based shape memory alloy was recently discovered by Tanaka et al. [1]. This material has shown one of the highest recoverable superelastic strains ever reported. In addition, it shows a very high strength of ~1.0 GPa and very large damping capacity. In this study, we have characterized both the parent austenite and the reversible martensite phase responsible for the superelasticity. The texture of the parent material was characterized using neutron diffraction while in situ tension experiments were conducted in a synchrotron, high energy x-ray beam to characterize the crystallography of the martensite phase and to quantify the amount of martensite phase. Furthermore, processing of these alloys was investigated by rolling the polycrystalline samples to varying amounts and measuring diffraction patterns at several orientations. [1] Y. Tanaka, Y. Himuro, R. Kainuma, Y. Sutou, T. Omori, and K. Ishida. Ferrous Polycrystalline Shape-Memory Alloy Showing Huge Superelasticity. *Science* 327, 1488 (2010)

3:35 PM Invited

Line Profile Analysis of Plastically Deformed Single Crystals: *Andras Borbely*¹; ¹Ecole des Mines de Saint-Etienne

X-ray line profile analysis (XLP) is an inverse method for quantitative microstructure determination. As all methods of this type it requires microstructural input obtained with imaging or other techniques. We present the momentum method of XLP based on the asymptotic behavior

of different order restricted moments of the intensity distribution, for which the extra required information is supplied by mathematics. The particularity of the method is related to the very simple analytical form of the moments when small crystallite size and dislocations are sources of line broadening. We apply the method to plastically deformed Cu and Al single crystals. The microstructure is evaluated not only in terms of usual parameters like: coherent domain size, average dislocation density and dislocation arrangement parameter, but also in terms of second order quantities like dislocation density fluctuation and dislocation polarization, pointing beyond the popular Wilkens approximation.

3:55 PM Invited

Structural Study of Textured Nanocrystalline ZnO Thin Films Prepared by Pulsed Laser Deposition: Radomir Kuzel¹; Jakub Cizek¹; Michal Novotny¹; ¹Charles University in Prague, Faculty of Mathematics and Physics

Thin nanocrystalline ZnO films of thickness 40-80 nm were grown on sapphire (0001), MgO (100) and fused silica (FS) substrates. A combination of different XRD scans on the Eulerian cradle was required for revealing of main structural features. The film deposited on FS showed fiber texture but ZnO film grown on MgO was highly textured and exhibited local epitaxy in a form of domains with two different orientations. Surprisingly, 40nm thick film on sapphire didn't show expected (0001) texture but more complicated orientation of several domains epitaxially grown on the substrate. Extremely high compressive in-plane stress in the film on MgO was detected by mapping of diffraction spots. The films on sapphire and FS were stress-free and in tensile stress, respectively. Crystallite size and microstrain were estimated from the Williamson-Hall plots constructed for different asymmetric reflections. Positron annihilation revealed high density of open-volume defects in films on MgO and sapphire.

4:15 PM Break

4:25 PM Invited

Residual Strain Tensor Determination from the Refinement of Multiple Diffraction Patterns: Davor Balzar¹; Nicolae Popa²; Sven Vogel³; Donald Brown³; ¹University of Denver; ²National Institute for Materials Physics; ³Los Alamos National Laboratory

The determination of residual strain/stress and texture is a common but still challenging problem. One of the newer approaches is expanding strain and stress tensor components in series of spherical harmonics, which allows for accurate determination of strain and stress for arbitrary crystal and sample symmetries without making Voigt or Reuss approximations. The method yields the texture-weighted strain orientation distribution function (WSODF) and average strain and stress tensors that are usually of engineering interest. This approach requires the measurements of interplanar spacing of the several Bragg reflections or Rietveld refinement of the diffraction patterns at multiple sample orientations. Thus, energy-dispersive measurements and multiple detectors are very useful. We will present new results of the neutron time-of-flight (TOF) measurements carried out at the LANSCE SMARTS station on several samples.

4:45 PM Invited

Utilizing In-Situ Neutron Diffraction for Mesoscale Simulation of Recrystallization Texture in Polycrystalline Aluminum: Bala Radhakrishnan¹; Sarma Gorti¹; Grigoreta Stoica¹; Alexandru Stoica¹; Govindarajan Muralidharan¹; Muth Thomas¹; Xun-Li Wang¹; ¹Oak Ridge National Laboratory

Direct modeling of nucleation during recrystallization is difficult because of our inability to capture the details of the complex deformation substructure and their rearrangement. Currently available nucleation models are largely empirically based. We illustrate an approach to model nucleation based on in-situ neutron diffraction to monitor the peak profile changes associated with recovery. Neutron diffraction data are obtained for straight rolled as well as cross-rolled Al-Mg alloy with or without an externally applied stress during annealing. The nucleation model is used in a mesoscale simulation of recrystallization of deformed

microstructures calculated by a crystal plasticity based model in order to predict the dependence of the deformation path and the external stress on the recrystallization texture development in the alloy. Research sponsored by the Laboratory Directed Research and Development Program of Oak Ridge National Laboratory (ORNL), managed by UT-Battelle, LLC for the U. S. Department of Energy under Contract No. De-AC05-00OR22725.

5:05 PM Invited

Application of In-Situ Neutron and X-Ray Measurements at High Temperatures in the Development of Co-Re-Based Alloys for Gas Turbines: Debashis Mukherji¹; Juri Wehrs¹; Joachim Rösler¹; Pavel Strunz²; Ralph Gilles³; Michael Hofmann³; Markus Hölzel³; Helmut Eckerlebe⁴; ¹Technische Universität Braunschweig; ²Nuclear Physics Institute ASCR; ³Technische Universität München; ⁴Helmholtz-Zentrum Geesthacht

There is a primary need to develop new alloys with very high melting point for future gas turbines. Presently, Ni-based superalloys are extensively used in the hot section of turbines but they are now reaching limits posed by their melting temperatures. High melting Co-Re-Cr based alloys introduced by the TU Braunschweig in 2007 [1] show promise as a new material class for high temperature application. In the Co-Re alloy development two main concepts of strengthening, namely precipitation hardening with MC carbides and composite hardening by Cr₇Re₃-type σ phase are explored separately. In-situ measurements at high temperatures by synchrotron and neutron scattering are used to study high temperature phase evolution and transformation. These new tools are providing vital information and guiding the alloy development. Selected results of microstructural characterizations by neutron and X-ray measurements are presented here. References:[1] J. Rösler, D. Mukherji, T. Baranski: Adv. Eng. Mater. 9 (2007) 876-881.

5:25 PM

Evolution of Residual Strains in Nanocrystalline Metals Studied by Diffraction: Steven Van Petegem¹; Lin Li²; Julien Zimmermann¹; Peter M. Anderson²; Helena Van Swyngenhoven¹; ¹Paul Scherrer Institute; ²The Ohio State University

For nanocrystalline f.c.c. metals the evolution of lattice strain as a function of applied stress is highly debated. In literature various trends are reported, which are seemingly inconsistent. However, the results are all different from what is expected for the coarse-grained counterparts. This often led to the conclusion that at the nanoscale intragranular slip is suppressed and grain boundary sliding mechanisms are responsible for the observed mechanical properties. In this work we present recent results obtained from in-situ mechanical testing during x-ray diffraction of several nanocrystalline metals. In particular we focus on electrodeposited Ni, Ni-20%Fe and Ni-50%Fe. The results are discussed in view of insights obtained from molecular dynamics and quantized crystal plasticity simulations. It is found that, due to the specific nature of plasticity mechanisms at the nanoscale, intragranular slip does not exhibit the same diffraction footprints compared to those observed at the microscale.

5:40 PM

Through-Thickness Distribution of Residual Stresses in One-Pass and Multi-Pass 70-mm Thick Welds: Wanchuck Woo¹; Vyacheslav EM¹; Ji Hyun Yoon¹; Jeong-Ung Park²; Gyu-Baek An³; ¹KAERI (Korea Atomic Energy Research Institute); ²Chosun University; ³POSCO Steel

Two extra thick welds were prepared with the dimension of 300-mm wide, 230-mm long and 70-mm thick ferritic steel plates. One was joined using 1-pass electro-gas welding and the other was 60-pass flux-cored arc welding methods. Residual stresses were determined through the thickness of each plate along the weld centerline, heat-affected zone, and base material using neutron diffraction. Such a deep penetration capability was achieved by using the 211 and 110 reflections with the wavelengths of 1.55 and 2.39 Å, respectively. The wavelengths are located near the minimum total cross sections but off the Bragg edges. The gauge volumes were 4x4x8 mm³ (longitudinal) and 4x4x20 mm³ (transverse/normal), and 'stress-free' do were also considered. Significant amounts of tensile



TMS 2012

141st Annual Meeting & Exhibition

longitudinal stresses were developed along the heat-affected zone of the one-pass weld, while those were observed along the weld centerline of the multi-pass weld approaching the yielding strength (570 MPa).

5:55 PM

Strain-Induced Dimensionality Crossover in the Modulated Structure of Ferromagnetic Shape Memory Alloy Ni₂MnGa: *Zhihua Nie*¹; Yandong Wang¹; Yang Ren²; Dongmei Liu³; Zhenwei Huang³; ¹Beijing Institute of Technology; ²Argonne National Laboratory; ³Northeastern University

Structural modulations have been observed in a large variety of materials, including superconductors, ferroelectrics, and shape memory alloys, and their underlying physics is still not clear. A strain-induced dimensionality crossover of atomic modulation has been studied in a Ni₂MnGa single crystal by high-energy X-ray diffraction technique, showing that the 3D modulated structure of pre-martensite first transform to a 2D modulated phase before finally convert to the martensite with a quasi-1D modulation. First-principles electronic calculations show that the electronic states of the pre-martensitic phase have been significantly altered by the uniaxial stress field, showing an enhanced nesting feature of a single band before the martensite appears. The observation of the stress-induced dimensionality crossover of atomic modulation has broad impacts in understanding not only the mechanical properties of advanced shape memory alloys, but also the physical properties of condensed matter with heterogeneous structures.

Pb-Free Solders and Other Materials for Emerging Interconnect and Packaging Technologies: Alternative Interconnects and Harsh Environmental Influences

Sponsored by: The Minerals, Metals and Materials Society, TMS Electronic, Magnetic, and Photonic Materials Division, TMS: Electronic Packaging and Interconnection Materials Committee
Program Organizers: Iver Anderson, Ames Laboratory; Sung Kang, IBM; Albert Wu, National Central Univ; Laura Turbini, Research in Motion; Tae-Kyu Lee, Cisco Systems; Govindarajan Muralidharan, Oak Ridge National Lab; John Elmer, Lawrence Livermore National Lab; Yan Li, Intel

Tuesday PM
March 13, 2012

Room: Swan 9
Location: Swan Resort

Session Chair: To Be Announced

2:00 PM Invited

Aligned Nanowires for Packaging and Circuit Interconnects: *Sungho Jin*¹; ¹UC San Diego

Conductive nanowires offer interesting possibilities for new approaches of circuit interconnection and electronic packaging. Vertically aligned carbon nanotubes as well as metallic or conductive oxide nanowires can be considered for such interconnect applications. Control of the nanowire structure and geometry is essential for their successful electronic packaging applications including advanced solder connections, solderless connections, or thermal interfacing. In this talk, novel fabrication approaches to create vertically aligned nanowire configurations will be discussed, some of which exhibit solderability, enhanced electronic transport characteristics, and improved thermal conduction. Well controlled and processed vertically aligned semiconductor nanowire arrays can also be useful for solar cells and vertical nanotransistor arrays. Planarization of such periodically-arranged nanowire structures will be discussed in relation to circuit interconnection and construction of three-dimensional multilayer device configurations.

2:25 PM

Compliant Structures as Off-Chip Interconnects: *Suresh Sitaraman*¹; ¹Georgia Institute of Technology

The high coefficient of thermal expansion (CTE) mismatch between an organic substrate and a silicon die creates thermo-mechanical stresses in flip-chip assemblies. These thermo-mechanical stresses could crack or delaminate on-chip low-k dielectric material and also result in early fatigue failure of off-chip interconnects. Epoxy-based underfill materials, although helpful for solder bump reliability, create additional die stresses and pose processing challenges for fine-pitch assemblies. To address these challenges, compliant structures can be used as off-chip interconnects that will decouple the die from the substrate, and thus, can reduce the thermo-mechanical stresses. In this presentation, we will discuss the status of several off-chip compliant interconnect technologies that are being pursued in academia and industry. The topics will include, but not limited to, electrical and thermo-mechanical performance of compliant interconnects, cost-effective wafer-scale fabrication process, uniformity in interconnect geometry, ease of assembly, operational reliability, scalability, and integration into existing infrastructure.

2:50 PM

Mechanical Stress Measurements in Cu Through-Silicon Via (TSV) Using Synchrotron X-Ray Microdiffraction for 3-D Integration: *Arief Budiman*¹; H.-A.-S. Shin²; B.-J. Kim²; S.-H. Hwang²; H.-Y. Son³; M.-S. Suh³; Q.-H. Chung³; K.-Y. Byun³; Y.-C. Joo²; R. Caramto⁴; L. Smith⁴; M. Kunz⁴; N. Tamura²; ¹Los Alamos National Laboratory (LANL); ²Seoul National University (SNU); ³Hynix, Inc.; ⁴SEMATECH; ⁵Advanced Light Source (ALS), Berkeley Lab

One key to enable the successful implementation of 3-D interconnects using Through-Silicon Via (TSV) is the control of the mechanical stresses. The synchrotron-sourced X-ray microdiffraction technique has been recognized to allow some important advantages compared to other techniques, namely stress measurement of individual Cu TSV as well as the silicon substrate surrounding it simultaneously at the submicron resolution, stress measurement in situ during annealing and while Cu TSV is still buried under the silicon substrate (mimicking the conditions of real device). Using this approach, we have studied Cu TSV samples from Hynix, Inc. as well as from SEMATECH and found interesting differences in the stress states of the Cu TSV. We studied the stress evolution throughout its thermal history, and proposed an explanation of the observed differences. This understanding could lead to improved stress control in Cu TSV as well as to reduce the impact to the silicon electron mobility.

3:10 PM

Conductive Anodic Filament Formation in Fine Pitch Halogen-Free Organic Substrates: *Koushik Ramachandran*¹; Fuhan Liu¹; Nitesh Kumbhat¹; Raj Pulugurtha¹; Venky Sundaram¹; Rao Tummala¹; ¹Georgia Institute of Technology

This study is aimed at investigating Conductive Anodic Filament (CAF) formation in laser-drilled through-vias at pitch sizes (< 200 \956m) in halogen-free glass reinforced package substrates. The need for high I/O density in 3D IC packages and multi-functional packages is driving the continuous reduction in through-via diameters and pitches. This fine-pitch requirement can potentially lead to reliability failures due to CAF that involves electrochemical migration of copper; this type of failure has been previously reported in brominated epoxy-glass composites (FR4) in printed wiring boards. However CAF reliability in "green" package substrates that incorporate halogen-free flame retardants such as inorganic fillers and phosphorus-based compounds has not yet been thoroughly investigated. In this study, accelerated testing method was used to investigate CAF formation in newly developed halogen-free package substrates. The test coupons were characterized using SEM and EDX to determine the nature and chemical composition of CAF in these advanced substrates.

3:30 PM

Investigations of Interfacial Features in Thick Al Wire Bonds: *Golta Khatibi*¹; Brigitte Weiss¹; Johannes Bernardi²; ¹University of Vienna; ²Vienna University of Technology

This investigation includes detailed microstructural characterization of ultrasonic thick Al wire bonds as used in power semiconductor devices. The objective of the study is to understand the relationship between the bonding quality and microstructure of Al wire bonds. SEM-EBSD techniques are employed to characterize the size, distribution and orientation of the grains in the bonded region and to investigate the global substructure of the grains of the deformed Al wire bonds. TEM investigations highlight the microstructural features of the interface between the wire and metallization layer. The bonding interface shows an inhomogeneous structure consisting of highly deformed grains with dislocation cell structures, nanostructured grains, voids, amorphous particles and oxides. These results indicate that the reliability of the wire bonds is not affected by the strong inhomogeneity of the interface so far a sufficient bonded area has been formed.

3:50 PM

Effects of Combined Harsh Conditions on Wire Bond Reliability: *Maria Mirgizoudi*¹; Changqing Liu¹; Paul Conway¹; Steve Riches²; ¹Loughborough University; ²GE Aviation Systems - Newmarket

The work focuses on the failure modes identification for wire-bonds under the combined conditions of thermal and vibration loadings. 48-pin DIL HTCC packages with Au/Ni plated surfaces were wire-bonded using Au and Al wires. Pull tests have been performed to evaluate the interfacial bonding strength and bonding adhesion of the wire-bonds. Electrical characterization has also been performed. The test packages have been subjected to sinusoidal and random vibration tests with the frequency ranging from 10Hz to 2000Hz, while keeping the temperature stable at 250°C. The analysis focused on the mechanical behaviour of the wires and microstructural characterization of the wire-bonds. Particularly, optical microscopy and SEM analysis have been performed to determine the mechanical deformation of the wires and, thermal and high speed cameras have been employed as well as laser interferometry for in-situ analysis. The results have contributed to further improve our understanding on interconnect failure under combined extreme loadings.

4:10 PM

Advances in Pressure-Less Sintering for High Temperature Electronic Applications: *Jiong (Jenny) England*¹; Srinivas Chada¹; Richard Kuder¹; Julissa Eckenrode¹; Javier Gutierrez¹; Paul Gleeson¹; ¹Henkel

During the past decade green initiatives have spearheaded implementation of lead-free solutions and recycling efforts in electronics packaging and interconnect industry. Although several lead-free alloys have successfully implemented for second level interconnects, there still is a need for a robust solution at first level. The current paper presents a lead-free first level interconnect material based on principle of low-temperature pressure-less silver sintering technology. This novel formulation enables achieving low bond-line porosity comparable to pressure-assisted sintering process. Also, compared to most pressure-less nano-silver technologies, the use of micro-scaled silver particles in this formulation offers a competitive balance among cost, performance, and processing capability. The proposed silver sintering paste can be sintered at a temperature as low as 200°C in a standard box oven without need for any specialized capital intensive equipment. Thermal and electrical properties as well as reliability tests that detail process-property-microstructure relationships will be explored in this paper.

4:35 PM Invited

Novel Sinter Paste Concept - A Lead Free Die Attach Alternative: Wolfgang Schmitt¹; Thomas Krebs¹; *Yvonne Loewer*²; ¹W.C. Heraeus; ²Heraeus Materials Singapore Pte Ltd

Especially power electronic packaging industry has a need for new lead free interface materials which do not re-melt at the 2nd level packaging. In ideal case these materials can be processed at temperatures below

260°C. Additionally they have to provide highest reliability beside perfect thermal and electrical conductivity. Silver sinter materials do provide most properties mentioned before. But commercial available Silver Sinter Materials do have the need for very special processes or they are based on nano silver, which is expensive and problematic in handling. Heraeus has developed a novel concept for silver sinter pastes. The new concept uses micro scale silver particles combined with sinter additives. The novel pastes can be used in pressure free or low pressure bonding processes. Physical properties like shear strength at 260°C, electrical and thermal conductivity are outstanding. The paper describes the material properties and results in reliability testing.

5:00 PM

Effect of Solder Properties on Microstructural and Damage Evolution in Au-Sn Solder Joints: *Govindarajan Muralidharan*¹; Kanth Kurumaddali¹; Andrew Kercher¹; Scott Leslie²; ¹Oak Ridge National Laboratory; ²Powerex Inc

There is a significant need for next-generation, high-performance power electronic packages and systems with wide band gap devices that operate at high temperatures in automotive and electric grid applications. Au-Sn solder is a candidate for use in such packages with potential operating temperatures up to 200oC and higher. The results of a study on the damage evolution occurring in large area Au-Sn solder joints between silicon carbide dies and Direct Bonded Copper (DBC) substrates subject to thermal cycling between 200°C and 5°C is presented in this paper. Differences in the damage accumulation as a function of thermal cycling characterized using high resolution x-ray radiography in Au-Sn solder will be compared to that in Sn-3.5Ag solder. Effect of geometry and solder properties on observed damage will be presented. *Work sponsored by the U.S. Department of Energy, Office of Electricity Delivery and Energy Reliability.

5:20 PM

Microstructure and Sn Crystal Orientation Evolution in Sn-3.5Ag Lead-Free Solders in High Temperature Packaging Applications: *Bite Zhou*¹; Govindarajan Muralidharan²; Kanth Kurumadalli²; Andrew Kercher²; Chad Parish²; Scott Leslie³; Thomas Bieler¹; ¹Michigan State University; ²Oak Ridge National Laboratory; ³Powerex Inc

Understanding the reliability of Sn-3.5Ag and other lead-free solders in high temperature packaging applications is of significant interest in power electronics for electric vehicles, and the next generation electric grid. Large area (2mm×2mm) Sn-3.5Ag solder joints between silicon dies and direct bonded copper (DBC) substrates were thermally cycled between 5°C and 200°C. Initial microstructure including Sn crystal orientations, and its evolution due to thermal cycling were characterized using scanning electron microscopy (SEM) and electron backscatter diffraction (EBSD). Effects of the geometry of the solder joint, and stresses induced by differential thermal expansion on the evolution of microstructure and texture following thermal cycling will be discussed. Influence of the microstructural evolution on reliability of the solder joint will be evaluated. Work sponsored by the U.S. Department of Energy, Office of Electricity Delivery, and by the SHaRE User Facility supported by the Scientific User Facilities Division of the Office of Science.

5:40 PM

Comparison of Thermal Measurement Methodologies Used in Electronics Industry: *Dan Maslyk*¹; Srinivas Chada¹; Scott Allen¹; Julissa Eckenrode¹; ¹Henkel

The constant push for smaller and smaller footprints with faster and larger computing power has put thermal management into the forefront. Thermal management is fast becoming a necessity, requirement, and an integral factor needed to achieve the desired electrical performance and reliability. It is not uncommon for many an application engineer to use a material reported to have “good” thermal values, only to be disappointed by the poor performance during application at device level. This obvious gap between design and application values of many commercially available thermal materials can be attributed to the methods used in the gathering



TMS 2012

141st Annual Meeting & Exhibition

of data. Thus, it is imperative to understand the different methods used to gather thermal properties as well as the pertinent details that the data represents. In this paper we will compare and contrast the most popular measurement methods used in the electronic industry to evaluate thermal materials.

Phase Stability, Phase Transformations, and Reactive Phase Formation in Electronic Materials XI: General Issues in Microelectronics

Sponsored by: The Minerals, Metals and Materials Society, TMS Electronic, Magnetic, and Photonic Materials Division, TMS: Alloy Phases Committee

Program Organizers: Chih-Ming Chen, National Chung Hsing University; Jae-Ho Lee, Hongik University; Ikuo Ohnuma, Tohoku University; Clemens Schmetterer, TU Bergakademie Freiberg; Yee-Wen Yen, National Taiwan University of Science and Technology; Shih-Kang Lin, University of Wisconsin – Madison

Tuesday PM

March 13, 2012

Room: Swan 10

Location: Swan Resort

Session Chairs: Yee-Wen Yen, National Taiwan University of Science and Technology; Shih-Kang Lin, National Cheng Kung University

2:00 PM Invited

Synthesis and Characterization of Low Temperature Sn-Cu and Sn Nanoparticles for the Fabrication of Highly Conductive Ink: Yun Hwan Jo¹; Inyu Jung¹; *Hyuck Mo Lee*¹; ¹KAIST

A various size of Sn-Cu nanoparticles were synthesized by using a modified polyol process for low temperature electronic devices. Monodisperse Sn-Cu nanoparticles with diameters of 21 nm, 18 nm and 14 nm were synthesized. The eutectic composition shift was also observed in nano-sized particles as compared with bulk alloys. By controlling the size and eutectic composition, a significant melting temperature depression of 30.3C was achieved. These approaches will reduce adverse thermal effects in electronic devices. Additionally, we synthesized a gram scale of uniformly sized Sn nanoparticles and observed a significant size-dependent melting temperature depression. To improve the electrical property, we applied the surface treatments of hydrogen reduction and plasma ashing. The two treatments had the effect of diminishing the sheet resistance. In addition, conductive patterns (1 cm x 1 cm) were successfully drawn on the Si wafer using an inkjet printing instrument with conductive Sn ink.

2:20 PM Invited

Electrochemical Study on the Silica Particles Dispersed Permalloy Composite Coating: So-Yeon Park¹; Myung-Won Chung¹; *Jae-Ho Lee*¹; ¹Hongik University

The composite electroplating is accomplished by adding inert materials during the electroplating. The surface wear resistance of a permalloy can be enhanced by incorporation of silica nanoparticles in its electroplated layer. In this study, the permalloy composite coating was obtained by electroplating. The dispersion of silica nanoparticles in the permalloy electroplated layer was reported with variation of current density, additives, sonication time, rotating speed and bath conditions. At high current density (40mA/cm²), the surface of coating has many cracks during electrodeposition. Additives change the surface morphologies of the electroplated layer as well as the silica nanopowder contents. In alkaline bath, smooth surface morphology and relatively high contents of silica nanopowder codeposition were obtained with addition of sodium lauryl sulfate. From zeta potential analysis, silica nanopowder has a negatively charged surface in an alkaline bath. Using a horn type sonicator promoted excellent silica dispersion in permalloy coating.

2:40 PM

Thermodynamic Stability and Diffusion Barrier Properties of Amorphous Ta-Rh Alloys for Cu Metallization: *Neda Dalili*¹; Qi Liu¹; Douglas Ivey¹; ¹University of Alberta

Implementation of copper as interconnect/metal lines in electronic devices has created the problem of Cu reaction with and/or diffusion in Si/SiO₂. Application of a barrier layer between the active region and Cu layer is, therefore, crucial. Refractory metal-transition metal alloys are a promising group of materials, as they offer a combination of good conductivity and high thermal stability together with high glass-forming ability. Thermodynamic calculations for possible supersaturated solid solutions and glassy phases were performed to find the glass-forming composition of the Ta-Rh binary system. Various compositions of the alloy were deposited by co-sputtering and the model was confirmed by structural characterization using XRD, TEM and XPS analysis. Thin layers of Ta-rich, Ta-Rh glassy alloys were then deposited on Si substrates followed by deposition of Cu. Barrier performance was studied after annealing in N₂/H₂ gas by employing resistivity measurements, XRD analysis, elemental depth profiling and electron microscopy.

2:55 PM

Application of High-Performance, Advanced Barrierless Cu Alloy Film in Cu Metallization: *Chon-Hsin Lin*¹; ¹Asia-Pacific Institute of Creativity/Environmental Engineering

We developed a high-performance Cu alloy film for using it as an advanced barrierless interconnect. Cu diffuses rapidly into the Si layer and deteriorates device properties. Therefore, a diffusion barrier must be inserted between Cu and Si to prevent device failure. However, the challenge lies in reducing the size of these barriers, which make device miniaturization difficult. Herein, we propose a novel alloy-seeding technique for barrier-free Cu metallization. The Cu seed layer, which acts as a barrier to Cu/Si interdiffusion, was alloyed with small amounts of insoluble substances, e.g., VN, SnN, and HoN. The seed layer was characterized using X-ray diffraction, focused ion beam microscopy, secondary-ion mass spectroscopy, and transmission electron microscopy, and by film resistivity and current-voltage measurements. We assessed the reliability of the seed layer in copper interconnects by studying the time-dependent dielectric breakdown of MOS structures. The results show that the Cu film has enhanced thermal stability.

3:10 PM

Effects of Levelers on Copper Electroplating in Patterned Substrate: Myung-Won Jung¹; In-Seok Kang¹; Ki-Tae Kim¹; *Jae-Ho Lee*¹; ¹Hongik University

In recent days, the wire width of IC was narrowed and the degree of integration of IC was increased to obtain the higher capacity of the devices in semiconductor industry. However, the defects such as scratch or dent on FCCL (Flexible Copper Clad Laminate) and void in via filling process cause low reliability of the products. In this study, the behaviors of additives especially levelers in electroplating were investigated since the leveling action is very important to improve the properties of electrodeposits. The defectless and flat copper surface was obtained after optimizing concentrations of all additives such as accelerator, suppressor and leveler. The behaviors of five levelers in copper electroplating were investigated. Prior to copper electroplating on patterned substrate, the nucleation and growth behavior of copper with variation of additives were also studied. The electrochemical methods such as polarization plots, galvanostatic and potentiostatic plots were employed to analyze copper deposits.

3:25 PM

The Electrical Characteristics and Interfacial Interaction of Ti/Ni/Ag/Au Multilayers under Thermal Cycling Test: *Fu-Jung Yeh*¹; Tsung-Chieh Chiu¹; Kwang-Lung Lin¹; ¹National Cheng Kung University

The Ti/Ni/Ag/Au multilayers combination was chosen for the metallization of AlN submount of flip chip high power LED. The interfacial interactions and electrical characteristics of the Ti/Ni/Ag/Au multilayers, under various periods of thermal cycling between -40°C and 125°C, were investigated by depositing on Si substrates. The electrical properties of the multilayer thin films were determined by two-probe nano-electronics measurement. The electrical resistance of Ti/Ni/(Ag,Au) and Ni/(Ag,Au) multilayer was founded to be 9MO and 8.5MO respectively, which shows that the Ni/(Ag,Au) determines the overall resistance of the multilayer combination. The results of XPS depth profile analysis indicate that Ag atoms diffused passing through the pure Au layer to the surface after thermal cycling. The outward diffusion of Ag atoms expands the mixed region of Ni, Ag and Au, resulting in higher resistance of the Ni/(Ag,Au) layer.

3:40 PM Break

3:50 PM Invited

New Solution Method for SiC Crystal Growth: *Shigeto Nishitani*¹; Yosuke Yamamoto¹; Tadaaki Kaneko¹; ¹Kwansei Gakuin University

Professor W. Shockley, a Nobel prize winner and the 'father' of the transistor, predicted in the 1950s that SiC would soon replace Si in devices because of its superior material properties. His prediction, however, has not yet come true because of the high cost of manufacturing SiC wafers. Very recently, the present authors reported a novel process for fabricating epitaxial SiC. This process has the potential to cost less and to provide SiC wafers with high crystalline quality. Here we present a new synthesis process for manufacturing SiC. In this process, the driving force for crystal growth is elucidated by considering a similarity -- the coexistence of the stable and metastable phases -- with the diamond synthesis process reported by Bonenkirk et al. of General Electric.

4:10 PM Invited

Method of Selective Electroplating having Strong Adhesion and Exceptional Uniformity by Nanoparticle Immobilization: *Shien Ping Feng*¹; Bo Yu²; Shuo Chen²; Zhifeng Ren²; Gang Chen³; ¹The University of Hong Kong; ²Boston College; ³Massachusetts Institute of Technology

This research relates to a new method of selectively electroplating an electrically conducting material onto a substrate having strong adhesion and exceptional uniformity, with particular emphasis on transparent conductive oxide (TCO) substrates. A thin nanoparticle layer is initially deposited onto a TCO substrate by wet process. Cyclic voltammetry was used to define an optimum voltage range of selectively electroplating various metals on TCO with and without nanoparticles. AFM, SEM and puff-off test were used to evaluate surface topography and adhesion. Nanosphere lithography which is one of the cheap lithography methods was chosen to define a submicron pattern. A desired metal is then selectively electroplated onto the predetermined nanoparticle area by operating within an optimum voltage range during the exposure process of TCO substrate to an electrolytic solution.

4:30 PM

A Study on the Formation Mechanism of Ytterbium Germanide for Schottky Contact Applications: *Sekwon Na*¹; Byunghoon Lee¹; Hwayoul Choi¹; Haseok Jeon¹; Juyun Choi¹; Yujin Seo²; Hyoungsub Kim¹; Seok-Hee Lee²; Hoo-Jeong Lee¹; ¹Sungkyunkwan university; ²Korea Advanced Institute of Science and Technology

As the conventional method of improving the device performance of CMOSFETs by scaling-down the device size faces limitations, Ge-

based FETs have gained attention. The development of Ge-based FETs requires challenging research endeavor in several fronts. Among them, a scheme to form a contact with low source/drain series/contact resistances is a critical issue. Here, we explored the possibility of using ytterbium germanide as a contact material. The ytterbium films were annealed for formation of germanide using RTA. Combination of HRTEM and EDS helped us to unravel several interesting aspects of the germanidation process. Interdiffusion between Ge and Yb was extensive even at low temperatures and led to the formation of an amorphous layer, followed by the nucleation of crystalline YbGe_{2-x}. Upon annealing at a higher temperature, the germanide layer grew thicker as a flat layer of a uniform thickness with epitaxial relation with the underlying Ge lattice.

4:45 PM

Electrochemical Behavior of CIGS Electrodeposition for the Application of Photovoltaic Cell: *Hyunju Lee*¹; Jae-Ho Lee²; Yangdo Kim¹; ¹Pusan National University; ²Hongik University

Cu(In_{1-x}Ga_x)Se₂ (CIGS) have become attractive candidates for economic polycrystalline solar cells, due to their high absorptivity (>105cm⁻¹) and stability against photo-degradation. In this study the electrochemical behavior of CIGS electrodepositions were investigated and the electrochemical conditions to prepare stoichiometric CIGS thin films were suggested. In acidic solutions containing Cu²⁺, In³⁺, Ga³⁺ and Se⁴⁺ ions, the CIGS films of different Cu/In/Ga/Se chemical compositions were electrodeposited on Mo/Glass substrate. The films were analyzed by XRD, SEM, and EDS. The results show that annealed films have pure CIGS phase with good crystallization and the morphology of the films are very uniform and dense.

5:00 PM

Intermetallic Compound Formation and Morphology Evolution in the Bi-xSn Solder Joint with Cu Substrate: *JinYi Wang*¹; Chih-Ming Chen¹; ¹National Chung Hsing University

Although lead (Pb)-free solders have been widely used in the electronic packaging industries, high-Pb solders are still used in some specific applications because high temperature Pb-free solders are still under investigation. In this study, high-Bi solders (Bi-10Sn, Bi-5Sn, and Bi-2Sn, in wt.%) were prepared as the high temperature Pb-free solders. The reactions between high-Bi solders and Cu substrate were investigated. The different composition of Sn in high-Bi solders influences the intermetallic compound formation at the interface during the soldering reaction. With increasing the reflow time, massive spalling of Cu-Sn intermetallic compounds between high-Bi solder and Cu substrates was also observed.

5:15 PM

Study of EM-Induced ENEPIG Bond-Pad Consumption at Sn(Cu)/ENEPIG Joint Interface: *Shih Han Wu*¹; Cheng Yi Liu¹; ¹National Central University

In this study, we investigated the EM effect on the joint interfaces of the Pb-free Sn(Cu) solder/ENEPIG solder joints at different annealing temperatures. The applied current density is 104 A/cm². The compositions of Sn(Cu) solders joined with ENEPIG pad are Sn_xCu (x=0.2,0.7,1). According to the preliminary result, a serious EM-induced Ni(P) consumption. With increasing of the Cu content in the Sn(Cu) solders, the resistance to the EM-induced Ni(P) consumption would be enhanced. In other words, the more Cu content in the Sn(Cu) solders, the less consumption of the ENEPIG pad. Also, we study the EM effect on the ENIG bond-pads joined with the same Sn(Cu) solder bumps at the same EM conditions. We found that, as compared to the previous Sn(Cu) ENEPIG results, the degree of the Ni(P) consumption is much serious and it also depends on the Cu content in the Sn(Cu) solder bumps.



Phase Transformations and Deformation in Magnesium Alloys: Deformation Twinning and Texture

Sponsored by: The Minerals, Metals and Materials Society, TMS Materials Processing and Manufacturing Division, TMS/ASM: Phase Transformations Committee
Program Organizers: Jian-Feng Nie, Monash University; Sean Agnew, University of Virginia; Suveen Mathaudhu, Army Research Office

Tuesday PM
March 13, 2012

Room: Southern V
Location: Dolphin Resort

Session Chairs: Sean Agnew, University of Virginia; Suveen Mathaudhu, Army Research Office

2:00 PM Invited Generalized Approach for Analyzing Strengthening Effects of Twins in Polycrystalline Metals and Alloys: *Subhash Mahajan*¹; ¹University of California

When a polycrystalline material deforms simultaneously by slip and twinning, stress concentrations can develop when a twin terminates within a crystal and during slip-twin, twin-twin, and twin-grain boundary interactions. We have developed a generalized approach to understand the relaxation of these stresses. We will present its salient features, and the supporting experimental observations from BCC, FCC and HCP metals and alloys. We will argue that the presence of twins will always strengthen a solid and the magnitude of strengthening will depend on the number of coherent twin boundaries per unit volume; the higher the number, the greater the strengthening. The author is grateful to Professors J.P. Hirth and Ke Lu for fruitful discussions.

2:25 PM Interaction between Dislocation and Tensile Twin in Magnesium Single Crystals: *Ming Zhe Bian*¹; *Kwang Seon Shin*¹; ¹Magnesium Technology Innovation Center, Seoul National University

The objective of this study is to identify the effects of the tensile twin on the slip and twinning behavior of magnesium single crystals with various orientations by using multi-step compression (MSC) tests. Single crystal specimens with loading directions between [0001] and [10-10] were prepared and compressed along the <11-20> direction to activate the tensile twins. Then these compressed specimens were then rotated 90 degrees and compressed along the loading direction to generate slip dislocations and twins. It was found that tensile twin boundaries acted as barriers to dislocation motion and increased the flow stress of all specimens. A transmission electron microscopy (TEM) study also showed stacking faults within the tensile twin bands. The interaction process of the slip dislocation with the twin boundary was systematically examined with TEM.

2:50 PM Deformation Twinning in Nanocrystalline Mg-Alloys: *Suveen Mathaudhu*¹; *Baolong Zheng*²; *Khaled Youssef*³; *Marta Pozuelo*⁴; *Laszlo Kecskes*⁵; *Yizhang Zhou*²; *Wei Kao*⁴; *Sungho Kim*⁶; *Bin Li*⁶; *Xiaolei Wu*⁷; *Carl Koch*³; *Jenn-Ming Yang*⁴; *Enrique Lavernia*²; *Yuntian Zhu*³; ¹U.S. Army Research Office; ²University of California - Davis; ³North Carolina State University; ⁴University of California - Los Angeles; ⁵U.S. Army Research Laboratory; ⁶Mississippi State University; ⁷Chinese Academy of Sciences

Contrary to what is observed in nanocrystalline face-centered cubic metals, nanocrystalline hexagonal close-packed (hcp) metals are rarely observed to deform by twinning, although twinning is a major deformation mechanism in their coarse-grained counterparts. Here we report the use of novel, high-energy powder processing and consolidation

strategies which produce bulk nanostructured Mg-alloys that remarkably show evidence of deformation twinning. Experimental results, including HRTEM observations of activated deformation twinning systems, and computational molecular dynamics simulations will be used to illustrate the thermomechanical processing environments and deformation mechanisms by which twinning may be activated in nanocrystalline Mg-alloys. These results point to a promising approach for the design of nanocrystalline hcp alloys with superior strength and concurrent ductility.

3:15 PM Invited A Physically Based Phenomenological Model for Deformation Twinning in Magnesium Alloys: *Matthew Barnett*¹; ¹Deakin University

A partial differential equation is developed that captures the evolution of key characteristics of tensile twinning in magnesium base alloys. The objective is to provide a framework for ascertaining the effects of hardening – due to grain refinement, precipitation and dislocation substructure – on twin volume fraction, thickness and length. The model is developed with the help of observations made on alloy AZ31. It is shown that it is necessary to consider the nucleation of twins at locations where neighbouring twins impinge on the grain boundary. The model provides a reasonable approximation for the role of grain size on twinning. It predicts a period of low apparent work hardening following yielding and shows that this should be more extensive for finer grain sizes, in agreement with experiment. Finally, some predictions are made on the effect of changing the resistance to twinning.

3:40 PM Invited Effect of Particle Shape and Habit on Twinning in Magnesium Alloys: *Joseph Robson*¹; *Nicole Stanford*²; *Matthew Barnett*²; ¹University of Manchester; ²Deakin University

Precipitates in magnesium alloys typically take the form of plates or rods aligned on well-defined crystallographic planes. Such precipitates are known to have highly anisotropic behavior with respect to slip inhibition. This paper demonstrates that the same is also true for twinning. In particular, it is shown that basal plates of the type formed in Mg-Al-Zn alloys are highly effective inhibitors of {10-12} twin growth, and this can be understood by the large back-stress induced if the material surrounding such precipitates twins. Whilst twin growth is suppressed in precipitate containing alloys, nucleation may be promoted. This phenomenon is attributed to the additional stress driving twinning when precipitates suppress slip. The differences in the anisotropy of the slip and twinning modes in magnesium due to particle shape and habit suggest mechanical asymmetry can be manipulated by controlling these parameters. Experimental evidence confirming these predictions is presented for two precipitate forming alloys.

4:05 PM Break

4:20 PM Invited Structure Evolution in AZ61L along a Fine-Grain Sheet Processing Path: *Tracy Berman*¹; *William Donlon*¹; *Victoria Miller*¹; *Jack Huang*²; *Ray Decker*²; *Wayne Jones*¹; *Tresa Pollock*³; ¹University of Michigan; ²nanoMag; ³University of California Santa Barbara

Mg alloys, with the lowest density among all structural metallics, have substantial promise for lightweighting of structural systems. A significant challenge remains in defining alloys and processing paths that give sufficient combinations of strength and ductility. Structure evolution in AZ61L has been studied at each stage of a process which consists of (a) Thixomolding to establish an initially fine-grained structure, (b) partial solutioning and sheet rolling at ~0.5Tm and (c) post-deformation annealing. Average grain size is refined from 4.1 μm to as low as 2.6 μm following final annealing. EBSD studies indicate only a weak development of texture along the processing path, resulting in tensile elongations of up to 22%. The evolution of the β phase and its role in the process will be discussed.

4:45 PM Invited

Effect of Ca Addition on Texture Evolution and Deformation Behavior of Mg-Zn Alloy Sheets: D.-W. Kim¹; J. H. Bae¹; B. C. Suh¹; M. S. Shim¹; D. H. Kim²; *Nack J. Kim*¹; ¹POSTECH; ²Yonsei University

Wrought Mg alloy sheets typically exhibit strong basal textures, which have an adverse effect on ductility and formability at room temperature. It has been recently reported that the additions of rare earth elements or Y (RE/Y) can weaken the basal texture of Mg alloy sheets. However a rather strategic nature of these elements might prevent their widespread utilization as alloying elements for wrought Mg alloys. In the present study, the effect of an alternative element, Ca, on texture evolution and its concurrent effects on deformation behavior and mechanical properties of Mg-Zn base alloys have been investigated. It shows that Mg-Zn-Ca (ZX) alloys have much weaker basal textures than the other Mg alloys. These alloys also show not only higher yield strength but also better formability than Al 5052 alloy, showing their potential as highly formable wrought Mg alloys. The mechanisms responsible for such improvements will be discussed.

5:10 PM Invited

Effect of Deformation Structure on Static Recovery and Recrystallization of AZ31 Magnesium Alloy: *Qing Liu*¹; Zhen Zeng¹; Yunchang Xin¹; ¹Chongqing University

In the present work, AZ31 Mg alloy sheets with initial texture of c-axis parallel to the normal direction (ND) and the transverse direction (TD) were rolled respectively at 150°C to different reductions followed by a static annealing at 250°C. It was found that both contraction and double twins dominated in the TD-sheet sample of 9% reduction and grains were preferred to nucleate near these twin boundaries. For the TD-sheet, {10-12} extension twins dominated in the sample of 9% reduction and new grains were preferred to nucleate at original grain boundaries instead of the twin boundaries. For both the ND and TD-sheets, large amount of shear bands were formed with increasing strain and acted as the new grains nucleates sites during annealing. Based on the experimental results, a static recovery and recrystallization mechanism was discussed by comparing the annealing behavior of the two types of rolling sheets with different deformation microstructures.

5:35 PM Invited

Work Hardening Behavior of the Magnesium Alloy AZ80 under Multi-Axial Loading: Philip Tomlinson¹; Chad Sinclair¹; Michael Gharghour²; *Warren Poole*¹; ¹University of British Columbia; ²National Research Council Canada

The widespread application of magnesium alloys requires an understanding of their behaviour under complex loading paths. This work examines the deformation of alloy AZ80 under a variety of biaxial loading conditions. Multiaxial tests were conducted on thin-walled tubes using combinations of internal pressure and axial loading to produce a range of ratios of tensile stress to hoop stress. The effect of initial microstructure on mechanical response was examined using as cast material exhibiting a with weak initial texture and extruded and recrystallized material having a strong texture. The evolution of crystallographic texture was determined from neutron diffraction measurements. From the stress-strain response, the yield surface and its evolution with strain have been determined for the tension/tension quadrant of biaxial stress space. The results show that the kinetics of twinning are affected by the stress state and this has been interpreted using crystal plasticity simulations.

Processing to Control Morphology and Texture in Magnetic Materials: Role of Magnetic Fields and Texturing to Improved Magnetic Materials

Sponsored by: The Minerals, Metals and Materials Society, TMS Electronic, Magnetic, and Photonic Materials Division, TMS: Magnetic Materials Committee

Program Organizers: Matthew Kramer, Iowa State University; Mike McHenry, Carnegie Mellon University; David Laughlin, Carnegie Mellon University; Jinfang Liu, Electron Energy Corporation; Bill Soffa, University of Virginia; Ivan Skorvanek, Institute of Experimental Physics

Tuesday PM
March 13, 2012

Room: Europe 10
Location: Dolphin Resort

Session Chairs: David Laughlin, Carnegie Mellon; Sophie Rivoirard, CNRS

2:00 PM Invited

The Role of Magnetic Energy in the Remnant State of Spinodally Decomposed Titanomagnetite-Magnetite Minerals: *Michael McHenry*¹; Nicholas Jones¹; Huseyin Ucar¹; Amanda Velázquez¹; Catherine Groschner¹; Marina Diaz-Michelena²; David Laughlin¹; ¹Carnegie Mellon University; ²Instituto Nacional de Técnica Aeroespacial

Paleomagnetic minerals, like the magnetotitanates, are crucial in explaining the Martian crustal magnetization. A remnant magnetization comparable to magnetite could explain field anomalies as large as 200 nT. The magnetite must be monodomain with a mechanism for pinning the magnetization to prevent thermal switching. The pseudo-binary system between magnetite (Fe₃O₄) and antiferromagnetic Ulvöspinel (TiFe₂O₄) undergoes spinodal decomposition of a solid solution into lamellae of two monodomain phases. The lamellar width ensures monodomain behavior and the antiferromagnet pins the magnetization. We discuss the role of magnetic energy in determining the asymmetric miscibility gap and other changes in the phase diagram, which give rise to the decomposition, and its effect on the wavelength of composition fluctuations. We also discuss how the remnant state is set during the decomposition process and the micromagnetics of switching in this naturally occurring spring exchange ferromagnetic system.

2:25 PM Invited

Effect of Magnetic Field Annealing on the Random Magnetocrystalline Anisotropies in Nanocrystalline Soft Magnetic Alloys: *Kiyonori Suzuki*¹; ¹Monash University

The effective magnetic anisotropy in nanocrystalline alloys is suppressed by the exchange softening effect. This softening effect is promoted dramatically by reducing the mean grain size and thus, the primary focus in the alloy development has been homogeneous fine-grained microstructures. However, there is a growing awareness that the exchange softening process in magnetic nanostructures is affected by macroscopic induced anisotropies (K_u). Our analytical solution to an extended random anisotropy model with K_u predicts that the grain size (D) dependence of the coercivity changes from D^6 to D^3 when the ratio of the random magnetocrystalline anisotropy $\langle K_1 \rangle$ and K_u is approximately 1 to 2. This suggests that the magnetic softness in nanocrystalline alloys could be improved dramatically by controlling K_u . This paper presents an overview of the effectiveness of magnetic field annealing on controlling the induced uniaxial and random magnetocrystalline anisotropies in nanocrystalline soft magnetic alloys.



TMS 2012

141st Annual Meeting & Exhibition

2:50 PM

Neutron Scattering Analysis of Magnetostructural Phase Transformations of High Magnetic Field Textured Shape Memory Alloys: *Ben Shassere*¹; Orlando Rios¹; Khorgolkhuu Odbadrakh¹; Jason Hodges¹; Saad Elorfi¹; Alex Melin¹; Gerry Ludtka¹; Boyd Evans¹; ¹Oak Ridge National Laboratory

Magnetic shape memory alloys are important for both their shape memory properties and as magnetic refrigeration materials due to their coupled structural and magnetic phase transformations. Experiments to observe the structural and magnetic phase transformations were performed at the Spallation Neutron Source (SNS) at Oak Ridge National Laboratory (ORNL) on two magnetic shape memory materials, alloys of Ni-Mn-Ga and Fe-Ni-Co-Al-Ta. Both alloys are a first-order magnetocaloric material in which the structural and magnetic phase transformations are coupled and contribute to the giant magnetocaloric effect (MCE). The FeNiCoAlTa alloy that was solidification processed under high magnetic fields (20 Tesla) at the National High Magnetic Field Lab using a unique high temperature apparatus developed at ORNL's magnetic processing facility are characterized up to 16 Tesla using a split core magnet at the SNS. Data of the observations will be further presented and discussed.

3:05 PM

High Magnetic Field Effect on the Solid State Phase Transformation in Fe-Co Alloys: *Bianca Frinco*¹; Sophie Rivoirard¹; Olivier Geoffroy²; Thierry Waeckerle³; ¹CNRS/CRETA Grenoble; ²Grenoble Electrical Engineering laboratory; ³ArcelorMittal Research Center

Thermo-magnetic processing can be considered as a new technology for modifying phase equilibria and phase transformation kinetics, with the goal of developing novel microstructures and properties unattainable through conventional thermo mechanical processing. We investigated the high magnetic field influence on the α/γ phase transformation of Fe-Co alloys. An increase of the phase transformation temperature with magnetic field was experimentally observed using dilatation measurements. In order to quantify the effect of a high magnetic field on the α/γ transformation in Fe-Co alloys, a thermodynamics analysis was conducted. The magnetic contributions to the respective Gibbs free energies as a function of the applied magnetic field were calculated using magnetization measurements. These magnetic energy terms were found to account for the modification of the α/γ transformation temperature, which amounts to approximately 2 K/T. Thus, thermo-magnetic processing has proved to be interesting to tailor microstructure of Fe-Co alloy in view of their magnetic properties.

3:20 PM

Effects of FeCo Magnetic Nanoparticles on Microstructure and Mechanical Properties of Sn-Ag-Cu Alloy: *Siyang Xu*¹; Ashfaque Habib¹; *Michael McHenry*¹; ¹Carnegie Mellon University

Sn-Ag-Cu (SAC) alloys are regarded as the most promising candidates for Pb-free solders in the electronic packaging industry. We have synthesized SAC solder-FeCo magnetic nanoparticles (MNP) composite paste with different MNP weight percentages and used AC magnetic fields to cause their localized heating for reflow. XRD patterns and optical micrographs indicate a decrease in the amount of primary Ag₃Sn and γ -Sn dendrites, and an increase in the amount of eutectic microconstituents with increasing weight percentage of MNPs. These microstructural feature impact the modulus and hardness data measured by nanoindentation. These show a parabolic and a linear increasing trend as a function of MNP weight percentage, respectively. The addition of FeCo MNPs is argued to promote the solidification of γ -Sn by providing more heterogeneous nucleation sites, at relatively low undercoolings, which results in the change of phase amount and enhanced mechanical behavior in the as-prepared solder joints.

3:35 PM Break

3:55 PM Invited

Classical Nucleation Theory Description of Phase Selection and Compositional Partitioning in Co-Rich (Co,Fe)ZrB-based Nanocrystalline / Amorphous Nanocomposites: *Paul Ohodnicki*¹; Michael Widom²; Samuel Kernion²; David Laughlin²; Michael McHenry²; ¹National Energy Technology Laboratory; ²Carnegie Mellon University

(Fe,Co)-based nanocrystalline / amorphous nanocomposite alloys produced through rapid solidification processing and subsequent thermal processing will play an important role as advanced inductor materials in the next generation of high frequency power electronics. Co-rich alloys are of interest for these applications due to a large field induced magnetic anisotropy that can be developed through crystallization in the presence of a magnetic field. Similar free energies for BCC, FCC, and HCP phases in Co-rich Fe,Co-alloys results in the formation of multiple nanocrystalline phases during the crystallization process over a range of Fe,Co-ratios with a preferential tendency for BCC phase formation as compared to expectations based solely on the binary phase diagram of the Fe,Co system. Various factors governing phase selection and compositional partitioning between phases will be presented using classical nucleation theory supplemented with thermodynamic parameters obtained through ab-initio modeling. Recent and relevant experimental results will be discussed within this framework.

4:20 PM Invited

Nanostructuring and Texturing for Improved Magnetic Materials: *David Sellmyer*¹; Y. Liu¹; T.A. George¹; Ralph Skomski¹; ¹University of Nebraska

The concept of achieving a useful high-energy-product magnet through appropriate nanostructuring of known hard and soft phases has been tantalizing researchers since the idea was first proposed. The fabrication of exchange-coupled nanocomposite magnets faces several challenges including aligning the easy anisotropy axes of the hard-phase grains. Here we investigate experimentally and by model calculations two-phase nanostructures of hard $L1_0$ -ordered FePt and soft iron-rich fcc Fe-Pt. The Fe-Pt thin films were produced by epitaxial co-sputtering onto MgO (001) which leads to a strong (001) texture. The experimental and theoretical hysteresis loops indicate nearly ideal exchange coupling, and excellent magnetic properties are obtained, including high values of coercivity (51k Oe), saturation magnetization (1287 emu/cc, $J_s = 16.2$ kG), and nominal energy product (54 MGOe). Extension to $L1_0$ (Fe, Co) Pt and fcc (Fe, Co)-Pt shows high values of J_s and H_c , and this and other systems will be discussed.

4:45 PM Invited

Roles of Texture Formation and Grain Refinement on Nanocomposite Magnetic Alloys: *Matthew Willard*¹; Lamar Minter²; Matt Brandes³; Maria Daniil⁴; ¹Naval Research Laboratory; ²Tennessee State University; ³The Ohio State University; ⁴George Washington University

Development of new magnetic materials capable of providing higher energy products for permanent magnets and lower core losses for soft magnets enable smaller, lighter, and more efficient devices. Over the past two decades, a major focus of research has been microstructure refinement to the nanoscale, which has advantages for each class of magnetic material – allowing permanent magnets to store more energy and allowing soft magnets to dissipate less energy than alternative materials. Texture development plays an important role in each of these areas, providing improvements in nanostructured permanent magnets and deteriorated properties in nanostructured soft magnets. This presentation will highlight recent work on nanocomposite magnetic materials produced by rapid solidification processing. The effect of nanostructure and the role of texture on the magnetic material performance will be shown experimentally with theoretical discussion.

TUESDAY PM

5:10 PM Invited

High Pressure Crystallization of FeCo Based Alloys: *Matthew Lucas*¹;

¹Air Force Research Laboratory

In crystalline materials the application of pressure alters the relative stability of alloy phases. For example, at ~13 GPa pure iron transforms from the body-centered-cubic (bcc) phase to the hexagonal-closed-packed (hcp) phase. Crystallization of amorphous metals may be significantly altered by application of pressure prior to heating. Diffusion is typically lowered, resulting in smaller average grain sizes. For Finemet, it was experimentally shown by Zhang et al. [J. of App. Phys. 84 (1998) 1918] that crystallizing at pressures up to 2 GPa results in both an increase in the volume fraction of crystallites and a decrease in the average grain size from ~12 nm to ~8 nm. According to Herzer [IEEE Transactions on Magnetics 26 (1990) 1397], the reduction in grain size should significantly lower the coercivity. Here we report results of high pressure crystallization on FeCo based magnetic materials. Initial results of in-situ neutron diffraction measurements are also presented.

Radiation Effects in Ceramic Oxide and Novel LWR Fuels: Experimental Characterization of Radiation Damage in Uranium Fuel and Surrogate Materials

Sponsored by: The Minerals, Metals and Materials Society, TMS Structural Materials Division, TMS/ASM: Nuclear Materials Committee

Program Organizers: Peng Xu, University of Wisconsin; Jian Gan, Idaho National Laboratory; Ram Devanathan, Pacific Northwest National Laboratory; Edward Lahoda, Westinghouse Electric Company; Michele Manuel, University of Florida; Ramprashad Prabhakaran, Idaho National Laboratory; Todd Allen, University of Wisconsin-Madison

Tuesday PM
March 13, 2012

Room: Macaw 2
Location: Swan Resort

Funding support provided by: The Center for Materials Science of Nuclear Fuel, an Energy Frontier Research Center led by the Idaho National Laboratory

Session Chairs: Todd Allen, University of Wisconsin - Madison; Jian Gan, Idaho National Laboratory

2:00 PM Introductory Comments

2:05 PM Invited

Irradiation-Induced Defects in Oxide Nuclear Fuels: *William Weber*¹;

¹University of Tennessee

Fundamental aspects of irradiation-induced defect production and migration in UO₂, PuO₂, and ThO₂ will be reviewed, along with similar behavior in the widely used surrogate material, CeO₂. Defect production and recovery from self-radiation (alpha decay), ion irradiation, and neutron irradiation (fission product damage) have been widely investigated over the years. Under irradiation at cryogenic and room temperature conditions, the measured defect concentrations increase with dose to saturation values. At least four distinct defect recovery stages are observed at temperatures from 77 to 1300 K. While the behavior of defects on the oxygen sublattice is reasonably understood, inconsistencies in interpretation remain for cation defects. In the case of fission, the electronic stopping power of fission products is below the threshold for track formation in UO₂; however, thermal spike simulations indicate the formation of isolated defects. This work was supported by the Materials Science of Actinides, an EFRC funded by U.S. DOE-BES.

2:35 PM

XPS Measurements of Radiation Damage in Thin Film Single Crystal UO₂ and U₂O₃: *Brent Heuser*¹; *Melissa Strehle*¹; ¹University of Illinois

We present x-ray photo-electron spectroscopy (XPS) measurements of the valence state of uranium in thin film single crystal UO₂ and U₂O₃ grown via reactive-gas magnetron sputtering. XPS is sensitive to the cation valence state via the photo-electron binding energy; we observed changes photo-electron binding energy as a function of growth conditions, sputtering, impurity concentration, and heavy-ion bombardment. Discussion of our results will focus on the generation of point defects under Frenkel and Schottky equilibrium.

2:50 PM

Irradiation Damage of CeO₂ with Xe and Kr Implantation: *Lingfeng He*¹; *Clarissa Yablinsky*¹; *Mahima Gupta*¹; *Todd Allen*¹; *Jian Gan*²; ¹University of Wisconsin-Madison; ²Idaho National Laboratory

Microstructure, fission products, and lattice defects have great influence on the thermal transport in nuclear fuel and the mechanical integrity of both the fuel and cladding. CeO₂ has a fluorite-type structure and serves as a surrogate material for UO₂ and PuO₂. This study is to investigate defect production and microstructural evolution of CeO₂ under irradiation. To simulate fission fragments damage, 150 keV Xe and Kr ions were used to irradiate CeO₂ to various doses. Thermal recovery of defects in irradiated CeO₂ was studied by annealing the samples at 800°C and 1200°C for 1 hr. TEM was used to characterize the irradiation-induced microstructural features in CeO₂, such as dislocations and gas bubbles. The stoichiometry change of CeO₂ versus dose was determined by XRD, XPS and WDS. This research was supported as part of the CMSNF, an Energy Frontier Research Center funded by the U.S. Department of Energy, Office of Science.

3:05 PM

Stoichiometry Dependence of the Evolution of Irradiation-Induced Defect Clusters in Ce_xLa_{1-x}O₂: *Weiyang Chen*¹; *Bei Ye*¹; *Aaron Oaks*¹; *Yinbin Miao*¹; *Brian Kleinfeldt*¹; *Mark Kirk*²; *James Stubbins*¹; ¹U of Illinois at Champaign-Urbana; ²Argonne National Laboratory

To study the stoichiometry dependence of irradiation effects in fluorite-type oxide nuclear fuel (UO₂), the technique of ion implantation in La doped ceria (Ce_xLa_{1-x}O₂) is used. Kr ions with energy 0.15-1 MeV were implanted into CeO₂ single crystals with 0%, 5% and 25% La concentration at 800°C. In-situ TEM was utilized to observe the damage process and the defects created by the ion beam irradiation. A substantial difference in the evolution of dislocation loops and bubbles for CeO₂ with different La concentration was observed at the same dose. For example, the dislocation loop growth rate in 25% La doped CeO₂ is about three times than that in 5% La doped CeO₂ during the low dose stage up to 8×10¹⁴ ions/cm². MD and KMC calculations were performed to study the diffusivity of each element. Calculation results show the diffusivity dependence on La concentration, which compliments the experiment results.

3:20 PM Break

3:45 PM Invited

Microstructure Characterization and Thermal Annealing of Irradiated Oxide Fuels: Understanding Gas Behavior and Restructuring at High Burnups: *Thierry Wiss*¹; *Arne Janssen*¹; *Bert Cremer*¹; *Hatmut Thiele*¹; *Ondrej Benes*¹; *Jean-Yves Colle*¹; *Dragos Staicu*¹; *Vincenzo Rondinella*¹; *Rudy Konings*¹; ¹EC - JRC - Institute for Transuranium Elements

The safe operation of a nuclear fuel imposes to understand its behaviour in normal operation but also in ab-normal operating conditions (temperature transient for example). The analysis of the release behaviour of fission products during laboratory thermal anneals of irradiated fuels is a convenient way to study migration and segregation of fission products in oxide fuels. Microstructure characterization by electron microscopy on irradiated fuels helps to understand their evolution after exposure to severe radiation damaging sources especially at high burnups.



TMS 2012

141st Annual Meeting & Exhibition

The combined analysis of the microstructure, of the fission products behaviour and of other properties (e.g. thermo-physical) enables a good understanding and prediction on the nuclear fuel performance and safety. This work schematically discusses experimental results from Knudsen Cell mass spectrometry measurements of thermal release of fission gases and volatile fission products from irradiated fuels, coupled with electron microscopy (SEM and TEM) examinations.

4:15 PM Invited

TEM Characterization of Irradiated RERTR Dispersion Fuels: *Jian Gan*¹; Dennis Keiser¹; Brandon Miller¹; Adam Robinson¹; Jan-Fong Jue¹; Pavel Medvedev¹; Daniel Wachs¹; ¹Idaho National Laboratory

The USA fuels program on Reduced Enrichment Research and Test Reactors (RERTR) is to develop low enrichment fuels to be used in the research and test reactors. Dispersion type plate fuels are popular for many research and test reactors, a special class of LWRs. A typical dispersion fuel plate in a test reactor consists of three layers with the outer layers of aluminum cladding and the middle layer of aluminum alloy dispersed with U-xMo ($x=7-10$ in wt%) or U₃Si₂ fuel particles. Fuel-Matrix Interaction (FMI) layer can develop as a result of fuel fabrication and reactor irradiation. The microstructural stability of the fuel under irradiation could strongly affect the fuel performance. This work reports the microstructure characterization using TEM on the irradiated RERTR dispersion fuels. The detailed microstructural features will be analyzed and compared with the results in literature. The impact of the observed microstructure on fuel performance will be discussed.

4:45 PM

3D Microstructural Characterization of Oxide Nuclear Fuel Surrogates: Effect of the Processing Conditions on Grain Boundary Distributions: *Karin Rudman*¹; Darrin Byler²; Harn Lim¹; Robert McDonald¹; Pedro Peralta¹; Chris Stanek²; Kenneth McClellan²; ¹Arizona State University; ²Los Alamos National Laboratory

The initial microstructure of an oxide fuel can play a key role in its performance. At low burn ups, the diffusion of fission products has a strong dependence on the grain size distribution and grain boundary (GB) characteristics (crystallography, geometry and topology), which in turn depend on processing conditions. Microstructural data are then needed as inputs for microstructurally explicit mesoscale simulations and atomistic models. Serial sectioning techniques were developed to obtain Electron Backscatter Diffraction (EBSD) data for depleted UO₂ pellets. Samples were manufactured under different conditions, including oxygen stoichiometry variations. The EBSD data were used to create 3D reconstructions of the microstructure and GBs. These models were then used to gather statistical information on the grain crystallography, determine five GB macroscopic degrees of freedom, and to study the GB character (twist, tilt, mixed). The results were compared for the different samples to understand how processing conditions can affect microstructure evolution.

5:00 PM

Ion Irradiations in La Doped CeO₂: the Effects of Impurity and Excessive Oxygen Vacancy Environment: *Di Yun*¹; Aaron Oaks²; Jeffrey Rest¹; Abdellatif Yacout¹; Marquis Kirk¹; Wei-ying Chen²; James Stubbins²; ¹Argonne National Laboratory; ²University of Illinois at Urbana-Champaign

To evaluate impurity effects in nuclear fuels, systematic experiments have been conducted. CeO₂ was selected as surrogate material for UO₂ due to its many similar properties. Lanthanum (La) was doped in CeO₂ to investigate the effect of impurities. The presence of La introduces a controlled concentration of oxygen vacancies, making it possible to investigate irradiation behaviors in a vacancy excessive environment. The influence of two La concentrations, 5% and 25%, were examined. Both in situ and ex situ TEM (Transmission Electron Microscopy) experiments were performed to study the evolution of defect clusters under irradiation

with two common fission products: Xe and Kr. Irradiation damage caused formation of dislocation loops, segments and networks, cavities and bubbles. Quantitative results were obtained to characterize the fluence and temperature effects. The higher La concentration was found to induce both significant trapping reducing bubble swelling and higher sink strengths leading to slower defect kinetics.

5:15 PM

Analysis and Modeling of Swift Heavy Ion Irradiation Defects in CeO₂: *Clarissa Yablinsky*¹; Anthony Schulte¹; Peng Xu²; Jianguo Yu³; Jian Gan³; Todd Allen¹; ¹University of Wisconsin; ²Westinghouse Electric Company; ³Idaho National Laboratory

The investigation of damage caused by fission fragments is often studied in the realm of nuclear stopping and cascade damage. However, damage created within the electronic stopping regime is studied to a lesser extent, and further insight into these mechanisms is important in studying fuel performance. In this study, cerium oxide was irradiated with gold ions at energies of 300MeV, 1GeV, and 2.1GeV to fluences above 1×10^{10} ions/cm². As-received and irradiated specimens were characterized using scanning electron microscopy, transmission electron microscopy (TEM), and high resolution TEM. Additionally, atomic ordering was investigated using high energy x-ray scattering at the Advanced Photon Source. Also a thermal-spike model will be applied to characterize and interpret the observed damage structure of the latent tracks generated by electron excitation mechanisms. This work is funded by the U.S. Department of Energy, Office of Basic Energy Sciences, as part of an Energy Frontier Research Center.

Randall M. German Honorary Symposium on Sintering and Powder-Based Materials: Powder Processing and Consolidation I

Sponsored by: The Minerals, Metals and Materials Society, TMS Materials Processing and Manufacturing Division, TMS: Powder Materials Committee

Program Organizers: K. Morsi, San Diego State University; Fernand Marquis, Naval Postgraduate School; John Meyer, Iowa State University; Ahmed El-Desouky, San Diego State University; Eugene Olevsky, San Diego State University

Tuesday PM
March 13, 2012

Room: Oceanic 2
Location: Dolphin Resort

Session Chair: Z. Zak Fang, University of Utah

2:00 PM Keynote

A Tribute to the Breadth and Depth of the Influence of Randall M. German on Particulate Materials Processing: *John Smugeresky*¹; ¹Sandia National Laboratories, Livermore, CA 94551

This paper traces the early work in the career of Randall M. German with examples of collaborations representing his insight into the then current as well as the then evolving rise in the interest and importance of powder metallurgy in the world of materials processing. It focuses on the pioneering expansion of his interests and that of the powder metallurgy community for fully dense and near-net shape metal processing. It starts with conventional press and sinter processing for fabricating controlled porosity stainless steel, expanding to use of hot isostatic pressing, atomization, and rapid solidification for creating new alloys and microstructures that have impacted one of his colleagues. Materials include 300 series stainless steels, maraging steels, iron base superalloys, titanium, and copper cermets. This progression summarizes ways to improve strength, compositional uniformity, grain refinement, and unique metastable microstructures all taking advantage of the rapid solidification capability of metal powder atomization.

2:30 PM Invited

Application of Metal Injection Molding to Soft Magnetic Materials: *Hideshi Miura*¹; ¹Kyushu University

Soft magnetic materials need several characteristics to realize high performance. Powder metallurgy is an effective way to produce the complex shaped parts, and also decrease the eddy current loss in high frequency by subdividing the eddy current area due to the small grains. Especially, metal injection molding (MIM) process allows nearly full dense and net shaping of a variety of engineering materials. The application of MIM process to hard and brittle materials such as ferromagnetic materials demonstrates the potential of this novel process. This study considers the processing of three types of soft magnetic materials such as Fe-6.5Si, Fe-9.5Si-5.5Al and Fe-50Ni alloy compacts through the MIM techniques using different types of powders to obtain high performance of soft magnetic properties.

2:55 PM Invited

Novel Approaches to Powder Processing: Structure and Mechanical Properties: *Marc Meyers*¹; *C Wei*¹; *E Olevisky*¹; *Naresh Thadhani*¹; ¹UCSD

We present an overview of the contributions of our group to the production of compacts through quasistatic, dynamic, and shock compaction, reaction synthesis, and their combination. This work, carried out since 1980, has focused on the development of explosive consolidation methods, on combustion synthesis followed by quasistatic and dynamic densification, and on the combined densification-reaction of powders geared at producing defect-free compacts with unique compositions and structures. The mechanical properties and microstructures obtained are presented with emphasis on mechanistic aspects. A wide variety of ceramics, ceramic-based composites, and metals were investigated. We present the advantages and limitations of the techniques developed: hot explosive consolidation, double-tube explosive consolidation, SHS + QIP, SHS + dynamic densification, laser-induced reactions.

3:20 PM Invited

Dynamic Shock-Compression of Particulate Materials: Current Understanding and Possibilities: *Naresh Thadhani*¹; ¹Georgia Institute of Technology

The response of powders or particulate materials to dynamic loading is dominated by the intrinsic and extrinsic properties of constituent materials which influence not only their densification behavior, but also the nature of interactions of particles with shock waves. The highly heterogeneous nature of particulate materials makes realistic predictions of their crush-up strength, compressibility, and overall consolidation response difficult. Preferential flow of particles into voids and variations in localized deformation, due to varying extents in which the void-collapse energy is dissipated at particle surfaces or in the interiors of particles, can lead to inter-particle bonding of inert powders, or alloying and release of energy. Current state of the understanding of the mechanisms of shock densification, shock-induced reaction, and particulate material interactions, will be described based on our recent work employing time-resolved gas-gun experiments and meso-scale particle-level simulations performed on imported micrographs of powders (and powder mixtures) using CTH multi-material hydrocode.

3:45 PM

Pressureless Sintering of Si₃N₄/SiC Nanopowders Prepared by High Energy Reaction Milling of Silica Fume: *Jyothi Suri*¹; *Leon Shaw*¹; ¹University of Connecticut

Due to their good mechanical and thermal properties at both room and elevated temperatures, Silicon nitride-silicon carbide nanocomposites are the promising materials for high temperature structural applications. The current work deals with fabrication of these nanocomposites using mechanically activated silica fume and graphite mixtures, for the first time. The obtained powder mixtures were subjected to carbothermal reduction and nitridation (CRN) at 1465°C to produce nano-Si₃N₄/SiC powders having particle sizes of 15-30 nm. These nano-Si₃N₄/SiC powders

are thereby pressureless sintered using liquid-forming compositions in the Y₂O₃-Al₂O₃ system as additives, at 1700-1950°C in nitrogen atmosphere and their microstructure, phase composition, hardness, and fracture toughness were investigated. The effects of Y₂O₃ and Al₂O₃ as sintering additives on degree of densification, sample shrinkage and phase transformation of these nanocomposites were studied. The key emphasis is laid on the production of low cost Si₃N₄/SiC nanocomposites, in addition to producing a nanoceramic with superior mechanical properties.

4:00 PM Break

4:15 PM

Development of Solid Freeform Fabrication for Metallic Parts Using Selective Inhibition of Sintering: *Mahdi Yoozbashizadeh*¹; *Behrokh Khoshnevis*¹; ¹University of Southern California

The SIS-Metal process based on microscopic mechanical inhibition is a layer-based rapid prototyping process. In the process, salt solution is printed in the selected area of each metal powder layer; the salt re-crystallizes when water evaporates; salt crystals decompose and grow rapidly during sintering; the decomposed salt particles spread between metal powder particles and prevent the fusing of these particles together, hence inhibiting the sintering process in the affected regions. In this paper titanium and stainless steel powder in addition to bronze metal powder will be used in the SIS process. The reason behind inhibition of sintering will be presented followed by introducing sucrose as a new inhibitor. The factors affecting the SIS-Metal process based on microscopic mechanical inhibition will be identified. By the aid of response surface methodology the effective factors will be evaluated to improve the part strength, surface quality and dimensional accuracy produced by the SIS-Metal process.

4:30 PM

Numerical Simulation of Cold Pressing of Armstrong CP-Ti Powders: *Adrian Sabau*¹; *Sarma Gorti*¹; *William Peter*¹; *Wei Chen*¹; *Yukinori Yamamoto*¹; ¹Oak Ridge National Laboratory

Numerical simulation results for the cold pressing of Armstrong CP-Ti Powders are presented. The computational model was implemented in the commercial finite element program ABAQUS. Several simulation cases were conducted for cylindrical samples with different aspect ratios and different compaction pressures. Numerical simulation results for the density distribution are compared against experimental data in order to validate the computational model.

4:45 PM

The Effect of Coke Particle Size on the Thermal Profile of the Sintering Process Product: *Nader Tahanpesarandezfuly*¹; *Ali Heidary Moghadam*¹; ¹Azad University

In this research, the effect of coke particle size on thermal profile in the production process is investigated in the laboratory environment. Baking process and sinter production was performed for different ranges of coke particle size while other parameter like, iron ore, lime and sintering mixture particle sizes, suction conditions and so on were kept constant. Thermal profile was achieved by measuring the temperature in different places of sintering bed. Investigating the thermal profile in different tests confirmed that coke grain size has a significant effect on thermal profile. The effect of coke particle size on coke combustion velocity, maximum temperature, the amount of produced melting phase as well as the flame front speed was understood by analyzing the achieved profiles and consequently the optimal grain size was known. The coke suitable particles size could have a great effect on quality of the produced sinter.

5:00 PM

Issues and Trends in Powder Injection Molding in Korea; Research and Applications: *Seong Jin Park*¹; ¹POSTECH

Powder injection molding (PIM) is one of the most important manufacturing process. PIM is a net-shape fabrication technology that combines the complex shape-forming ability of plastic injection molding, the precision of die-casting, and the material selection flexibility of powder metallurgy. This paper discusses about many ongoing issues and trends of



increasing attentions and interests on PIM research and applications in Korea. Furthermore, future research directions on simulation, optimization and informatics are discussed.

5:15 PM

Consolidation of Ferritic Oxide Dispersion Strengthened Alloys by Spark Plasma Sintering: *Kerry Allahar*¹; *Jatuporn Burns*¹; *Brian Jaques*¹; *Indrajit Charit*²; *Darryl Butt*¹; *James Cole*³; ¹Boise State University; ²University of Idaho; ³Idaho National Laboratory

The application of spark plasma sintering (SPS) for the production of oxide dispersion strengthened (ODS) ferritic alloys is presented. These alloys have improved resistance to radiation, thermally induced creep and swelling; properties that make them excellent candidates for cladding material in advanced nuclear reactors. Ferritic ODS alloys processed through conventional hot extrusion and hot isostatic pressing do not provide the advantages of SPS, which include faster heating rates, lower sintering temperatures and shorter dwell times. SPS samples were consolidated from a pre-alloyed Fe/Cr/Mo powder that was mechanically alloyed with Y₂O₃ (0 - 0.5 wt.%) in a high energy ball mill. SPS conditions included sintering temperatures from 900 oC to 1100 oC, dwell times from 0 to 60 minutes, heating rates from 50 oC/min to 200 oC/min and sintering pressures of 40 MPa and 80 MPa for process optimization. Microstructural characterization was performed using electron backscatter diffraction and transmission electron microscopy.

Recycling General Sessions: Electronics

Sponsored by: The Minerals, Metals and Materials Society, TMS Extraction and Processing Division, TMS Light Metals Division, TMS: Recycling and Environmental Technologies Committee
Program Organizer: Joseph Pomykala, Alter Trading

Tuesday PM
March 13, 2012

Room: Europe 4
Location: Dolphin Resort

Session Chair: Joseph Pomykala, Alter Trading

2:00 PM

Control of Gas Emission during Pyrolysis of Waste Printed Wiring Boards: *Alex Luyima*¹; *Honglan Shi*¹; *Lifeng Zhang*¹; *Jaan Kers*²; ¹Missouri University of Science and Technology; ²Tallinn University of Technology

The rapid technological development has led to a substantial increase in the volume of waste Printed Wiring Boards (PWBs). Pyrolysis process has been suggested as one of the best methods for recycling PWBs. However, pyrolysis process generates a lot of toxic gases like HBr and CO. In current study, the pyrolysis of PWBs was investigated by a 50 gram-scale tube furnace at 300–1173 K. The kinetics and the control of emitted gas using different chemical additives for the pyrolysis of PWB powders were studied under various heating rates and gas flow rates. Moreover, the possibility of controlling toxic exhaust gases and recovering beneficial gaseous fuels like CH₄ and H₂ from pyrolysis process is discussed.

2:20 PM

Leaching Studies for Metals Recovery from Waste Printed Wiring Boards (PWBs): *Alex Luyima*¹; *Honglan Shi*¹; *Lifeng Zhang*¹; ¹Missouri University of Science and Technology

Printed wiring Boards (PWBs) is a critical part of almost all electronic waste and accounts for ~3% of all e-waste by weight. Leaching process has been suggested to recover precious metals from waste PWBs. In this study, the leaching behavior of most metals present in waste printed wiring boards (PWBs) is evaluated. Different leaching acid reagents (hydrochloric acid, nitric acid and aqua regia) are compared. The effects of acid concentration, particle size of sample, leaching time and temperature are examined. Preliminary results revealed that most metals are present in

small particle size and sequential leaching of PWBs with a combination of both nitric acid and aqua regia are capable of dissolving most of the metals content of PWBs.

2:40 PM

Effects of Inoculums Volume on Metals Extraction from Printed Circuit Boards of Computers by Bacterial Leaching: *Luciana Yamane*¹; *Denise Espinosa*¹; *Jorge Tenório*¹; ¹Polytechnic School of São Paulo University

The present work investigated the effect of inoculums volume on bioleaching of metals from printed circuit boards of computers using *Acidithiobacillus ferrooxidans*-LR. Printed circuit boards from obsolete computers were mechanically processed by comminution followed by magnetic separation. In the non-magnetic fraction were concentrated base metals such as copper, lead, tin, zinc and aluminum. A shake-flask study was carried out on the non-magnetic fraction samples using a rotary shaker at 30°C, 170rpm and different volumes of oxidized solution culture as inoculum (%v/v): 5, 10, 20, 30, 40, 50 e 60. Leaching in acidic ferric sulphate media was also performed. The analyzed parameters were pH, ferrous iron concentration and metals analysis (AAS). The results showed that using 10%v/v of inoculums were extracted 99.2% of copper and 60% of aluminum by bioleaching. Zinc, lead and tin extraction were not influenced by bacterial leaching and extractions rate were obtained by chemical leaching promoted by acid medium. Ferric iron leaching extracted less copper (35%) than bioleaching. SEM analysis shown difference on surface after bioleaching showing corrosion pits formed by the bacteria contact.

3:00 PM Break

3:20 PM

Removal of Copper Cyanide Complexes from Solutions Formed in Silver/Gold –Cyanation Recovery Process: *Jose Parga*¹; *Jesus L. Valenzuela*²; *Luciano Ramirez*¹; ¹Institute Technology of Saltillo; ²University Hermosillo

An innovative process for removing copper cyanide complexes including silver and zinc from cyanidation circuits has been developed. The technology was based on the inducing the nucleated precipitation of copper and silver in a tube serpentine reactor, using sodium sulfide as the precipitate and sulfuric acid as pH control. The results showed that pH had a great effect on copper cyanide removal efficiency and the optimum pH was about 3 to 3.5. At this pH value copper cyanide removal efficiency could be achieved above 97 and 99 % , when influent copper concentration ions were 650 and 900 ppm respectively. In this process (sulphidation-acidification-recycle-thickening), the cyanide associated with the copper cyanide complexes is released as HCN gas under weakly acidic conditions, allowing it to be recycled back to the cyanidation process as free cyanide. This system was successfully commercial applied at Minera William in Mexico.

3:40 PM

Dissolution of Mixed Zinc-Carbon and Alkaline Battery Powders in Sulphuric Acid Using Ascorbic/Oxalic Acid as a Reductant: *Muammer Kaya*¹; ¹ESOGÜ

The objective of this study is to investigate the effectiveness of H₂SO₄ and ascorbic/oxalic acids as a reducing agent for the simultaneous recovery of Zn and Mn from used AA and AAA sizes Zn-C and alkaline battery powder mixtures. Reductive acid leaching tests were conducted to evaluate the leaching behavior of Zn and Mn metals under different S/L ratio, temperature, H₂SO₄ concentration, mixing rate and leaching times. The effects of H₂SO₄, ascorbic/oxalic acid, temperature and time on metal dissolutions were investigated according to 2K full factorial design. Without a reductant, 99.42% Zn and 40.94 % Mn were dissolved; whereas, 74.88% Zn and 96.79% Mn were extracted using 30g/l oxalic acid. The optimum reductive acid leaching conditions were determined as 3h, 70°C, 0.5M H₂SO₄, 13 g/L ascorbic acid, 1/20 g/mL S/L ratio and 200 rpm. Under these conditions, the dissolution efficiencies were 99.99% for Zn and 99.25% for Mn.

4:00 PM

Selective Recovery of Precious Metals by Selective Adsorption on Garlic Peel Gel: *Kai Huang*¹; Shuqiang Jiao¹; Hongmin Zhu¹; ¹University of Science and Technology Beijing

An adsorption gel was prepared by using garlic peel as the raw material, which is rich in amino- and thiol-groups, exhibiting a high affinity for Au(III). It was prepared by cross-linking garlic peel with concentrated sulfuric acid. Adsorption tests for different metal ions such as Au(III), Pd(II), Pt(IV), Fe(III), Cu(II), Ni(II) and Zn(II) from hydrochloric acid media found Au(III) to be selectively adsorbed on the cross-linked garlic peel gel over the other metal ions investigated. From the adsorption isotherms, this adsorbent was found to exhibit remarkably high adsorption capacity. The thermodynamic parameters indicated that the adsorption was governed by an endothermic reaction.

4:20 PM

Separation of Si/SiC Wiresaw Cutting Powder through Sedimentation by Adjusting the Solution pHs: *Kai Huang*¹; Hao Deng¹; Jichao Li¹; Hongmin Zhu¹; ¹University of Science and Technology Beijing

Silicon and silicon carbide mixing micropowders obtained from the saw cutting industry of polycrystalline silicon ingot is separated by a simple sequential sedimentation. The Zeta potentials of the powders in the aqueous suspension are adjusted by varying the pHs with dilute acid or alkaline reagents. The dispersion and aggregation content of the microparticles is significantly influenced by pHs, and so their settlement velocity in the same hydraulic conditions are quite different, and silicon powders tend to suspend in the upper section of the suspension for its finer size and smaller density under the stronger Zeta potential repulsion force. The original content of the cutting powders with 30%wt silicon are separated into the Si-rich and SiC-rich powder respectively, and 62%wt Si-rich powder can be obtained after 4 times of sedimentation under pH = 8.0, showing the great potential for Si and SiC powder separation and recovery in a cost-effective way.

Solid-State Interfaces II: Toward an Atomistic-Scale Understanding of Structure, Properties, and Behavior through Theory and Experiment: Mechanical Properties

Sponsored by: The Minerals, Metals and Materials Society, TMS Electronic, Magnetic, and Photonic Materials Division, TMS Structural Materials Division, TMS: Chemistry and Physics of Materials Committee, TMS: Nanomechanical Materials Behavior Committee

Program Organizers: Xiang-Yang Liu, Los Alamos National Lab; Douglas Spearot, University of Arkansas; Guido Schmitz, University of Münster; David Seidman, Northwestern University

Tuesday PM
March 13, 2012

Room: Oceanic 7
Location: Dolphin Resort

Funding support provided by: Los Alamos National Laboratory

Session Chairs: Amit Misra, Los Alamos National Lab; Pascal Bellon, University of Illinois

2:00 PM Invited

Creep Deformation in Ion Irradiated Nanocrystalline Cu Alloys: *Robert Averback*¹; Pascal Bellon¹; Yinon Ashkenazy²; Kaiping Tai¹; Jonathan Schäfer³; Karsten Albe³; ¹University of Illinois; ²Hebrew University of Jerusalem; ³Technische Universität Darmstadt

A straight forward strategy for designing materials with good radiation resistance is simply to include a large density of neutral sinks and traps for point defects. One means to achieve this microstructure is through the synthesis of ultra-fine grained materials, which can now be stabilized to temperatures approaching their melting points. Since materials

with small grain sizes are susceptible to creep damage, a fundamental question that must be addressed concerns the dimensional stability of irradiated nanocrystalline materials at elevated temperatures. In this work in situ creep measurements on ion-irradiated nanocrystalline Cu alloys are presented which show that a random flux of point defects to grain boundaries can result in creep deformation. We also present MD simulations illustrating how defect relaxations in the grain boundaries make this possible. The simulations also show how thermal creep might be suppressed in these alloys.

2:30 PM Invited

Resolving the Contribution of Interfaces in the Deformation of Nanocrystalline Copper with Atomistic Simulations: *Garritt Tucker*¹; Shreevart Tiwari¹; Jonathan Zimmerman²; David McDowell¹; ¹Georgia Institute of Technology; ²Sandia National Laboratories

The deformation of nanocrystalline FCC metals involves activating various distinct deformation mechanisms. The interfaces between grains, or grain boundaries, in addition to dislocation nucleation/migration, fundamentally govern material plasticity in nanocrystalline metals. In this work, atomistic simulations employing volume-averaged kinematic metrics from continuum mechanics are utilized to elucidate the influence of grain size on the role of interfacial deformation during uniaxial tension. We show that the metrics offer insight into each deformation mechanism through reference configuration neighbor lists. In addition, lattice distortion due to atomic shear shuffling and rearrangement is captured using the microrotation metric. As average grain size is reduced, the influence of grain boundary deformation increases, and its contribution to the overall strain of the material is quantitatively computed using the Green strain metric. The ability of the metrics to capture fundamental mechanisms is illustrated, and we discuss the potential to translate nanoscale interface behavior into larger-scaled models.

3:00 PM

Heterophase Interface Character Distributions (HICDS) in Accumulative Roll-Bonded (ARB) CU-NB Multilayered Composites at Multi-Scale: *Sukbin Lee*¹; Jonathan LeDonne¹; Irene Beyerlein²; Nathan Mara²; Anthony Rollett¹; ¹Carnegie Mellon University; ²Los Alamos National Lab

Multilayered Cu-Nb composites are known to have exceptional strength, conductivity, and radiation damage resistance with decreasing layer thickness into the nano-scale and, hence, increasing heterophase interface area. Therefore, it is of great interest to characterize the types of heterophase interfaces and investigate their relationship to the desired properties. In the light of that, the full five-parameter heterophase interface character distributions (HICDs) in accumulative roll-bonded (ARB) pure Cu-Nb multilayer composites are presented as functions of layer thickness and annealing. The heterophase interfaces are segmented and smoothed on two-dimensional electron back-scatter diffraction (EBSD) maps or orientation maps from ASTAR techniques in the TEM, depending on the layer thickness (50 μm to 20 nm). Supports from the Center for Materials at Irradiation and Mechanical Extremes, an Energy Frontier Research Center funded by the U.S. Department of Energy, Office of Basic Energy Sciences, the BES-supported CMIME and the NSF-supported MRSEC at CMU are acknowledged.

3:20 PM

Lithium Segregation at Matrix/Precipitate Interfaces in Al-Li-Sc and Al-Li-Sc-Yb Alloys: Thermodynamic Treatment, and Effects on Aging Microhardness: *Matthew Krug*¹; David Dunand²; *David Seidman*²; ¹General Electric Aviation; ²Northwestern University

Al-2.9 Li-0.11 Sc (at.%), and Al-5.53 Li-0.048 Sc-0.009 Yb (at.%) were isothermally-aged to peak-strength at 325 °C, followed by isochronal aging to 450 °C. This resulted in precipitation of nanometer L12 alpha-prime-Al3(Li,Sc) and Al3(Li,Sc,Yb) precipitates, which exhibit significant excesses of Li at alpha-Al matrix/alpha-prime-Al3(Li,Sc,Yb) interfaces. As the aging temperature increases, the Li- and Yb-concentrations of the alpha-prime-Al3(Li,Sc,Yb) precipitates decrease, while the relative



TMS 2012

141st Annual Meeting & Exhibition

TUESDAY PM

interfacial Li excesses increase. This result indicates that the alloys are not in thermodynamic equilibrium. The large interfacial excesses of Li at the aging temperature of 450°C, lead to interfacial free energy decreases of -81 ± 3 and -160 ± 8 mJ m⁻² for Al-Li-Sc and Al-Li-Sc-Yb, respectively. These decreases influence the nucleation and coarsening of the strengthening precipitates. The effects on the evolution of mechanical properties is suggested by comparing atom-probe tomographic analysis of precipitates, to aging hardness data to a study on similar Al-Sc(-Yb) alloys with and without a Li addition.

3:40 PM Break

3:45 PM

Intergranular Fracture Behavior in UO₂: Molecular Dynamics Simulations: *Yongfeng Zhang*¹; *Xiangyang Liu*²; *Bulent Biner*¹; *Paul Millett*¹; *Michael Tonks*¹; *David Andersson*²; ¹Idaho National Lab; ²Los Alamos National Lab,

The intergranular fracture behavior in UO₂ is studied using molecular dynamics simulations with the Basak potential. A bi-crystal simulation cell is used with the <100> symmetrical tilt S5 grain boundaries (GBs). Uniaxial tension is applied normal to the GB plane to model the mode-I crack. In the absence of an initial crack, the deformation proceeds by phase transformations from the Fluorite to the Scrutinyite or the Rutile structures, with coherent boundaries in between them. The evolution of such metastable phases is also confirmed by separate density-functional-theory calculations. With an initial crack created at the GBs, these metastable phase transformations shield the crack at the onset of plastic deformation. At higher strain, cleavage crack propagation takes place preferably along the GBs, with rare exceptions along the newly formed phase boundaries. In addition, results with random GBs will also be presented to elucidate the effects of GB structure.

4:05 PM

On the Fracture Toughness of Polycrystalline LiCoO₂: *Meng Qu*¹; *William Woodford*¹; *John Maloney*¹; *W. Craig Carter*¹; *Yet-Ming Chiang*¹; *Krystyn Van Vliet*¹; ¹Massachusetts Institute of Technology

LiCoO₂ is a widely used cathode material in rechargeable lithium-ion batteries. The stress induced by reversible lithium-ion intercalation during electrochemical cycling is related directly to crack initiation and growth. In this study, we employed instrumented nanoindentation to probe the fracture toughness within individual grains of polycrystalline LiCoO₂. We compared the crack length extrapolated from instrumented indentation load-displacement responses to those measured using direct imaging of surface cracks, and confirmed that these two approaches provide comparable crack length values. We found that the average fracture toughness varies among different grains in LiCoO₂ over one order of magnitude. We also considered possible correlations between fracture toughness and grain misorientation, and found no conclusive correlation for the present sampling. This work demonstrates an efficient method to study the fracture toughness of lithium-ion battery materials. It can also be further applied to explore the fracture toughness of LiCoO₂ particles in lithium ion battery electrodes.

4:25 PM

Rate Dependence Dissipation in Dynamic AFM: *Gabriela Venturini*¹; *Alejandro Strachan*¹; ¹Purdue University

Despite the growing importance of Atomic Force Microscopy (AFM) in material research, the link between the actual experimental observables and the underlying material properties remains tenuous. This talk will present a molecular dynamics (MD) approach to simulate the dynamics of tip-substrate interaction under conditions relevant to tapping mode AFM. We simulate a semi-spherical silica tip contacting an amorphous poly(methyl methacrylate) (PMMA) sample and study how deformation rate, indentation depth, and surface topology affect the effective tip-sample interaction. We find that interaction force curves depend strongly on local surface topology for small tip penetrations into the sample and these dependency decreases as the depth of the indentation increases.

Interestingly, we find the total energy dissipated during the interaction to be rather independent of deformation rate when the interaction time varies from 0.040 to 4 ns.

4:45 PM

Mechanisms for the Nucleation of Lattice Dislocations from fcc/bcc Incoherent Interfaces: *Ruifeng Zhang*¹; *Jian Wang*¹; *Irene Beyerlein*¹; *Timothy Germann*¹; ¹LANL

Dislocation nucleation from fcc/bcc incoherent interfaces under mechanical deformation is studied using atomistic simulations. Two broad classes of interfaces are studied: ones containing intrinsic interface dislocations (i) with their Burgers vectors lying within the interface plane or (ii) with their Burgers vectors lying normal to the interface plane. We find that for the former type of interface, nucleation results from localized interface shear. The interfacial shear strain field that develops under stress is governed by the spatially non-uniform shear resistance of interface. For the latter class of interface, nucleation is attributed to the dissociation of preexisting interface dislocations. Using our single loop isolation method, the activation barrier for nucleation from these interfaces are found to be much lower than that for homogeneous nucleation in perfect fcc lattice, indicating that an incoherent interface, by virtue of its intrinsic defect structure, can act as a viable source of lattice dislocations.

5:05 PM

Molecular Dynamics Simulation of the Mechanical Behavior of Metallic Glass/Crystalline Composites: *Anupriya Agrawal*¹; *Logan Ward*¹; *Katharine Flores*¹; *Wolfgang Windl*¹; ¹The Ohio State University

Bulk Metallic Glasses (BMGs) represent a new class of metallic alloys with a wide range of potential applications. However, a major disadvantage of BMGs is the potential for rapid shear localization leading to catastrophic failure, particularly under tensile load conditions. Among the investigated solutions to this problem is the introduction of crystalline phases to control the propagation of shear bands in the glassy matrix. In this work, we have studied the mechanical behavior of a model crystalline metal-metallic glass composite system using Molecular Dynamics, with a focus on the c-Cu - a-(Cu-Zr-Ti) interface. The interface was studied under different applied stress states and with pre-formed dislocations on the crystalline side. We will present the effects of the system size, glass phase composition, annealing temperature and dislocation type and density on the dislocation motion and interaction with the interface, as well as the resulting mechanical properties of the composite.

Stochastic Methods in Materials Research: Session I

Sponsored by: The Minerals, Metals and Materials Society, TMS Materials Processing and Manufacturing Division, TMS/ASM: Computational Materials Science and Engineering Committee, TMS: Integrated Computational Materials Engineering Committee
Program Organizers: Dallas Trinkle, University of Illinois, Urbana-Champaign; Richard Hennig, Cornell University

Tuesday PM
March 13, 2012

Room: Europe 9
Location: Dolphin Resort

Session Chairs: Richard Hennig, Cornell University; Dallas Trinkle, University of Illinois at Urbana-Champaign

2:00 PM Invited

Automated Materials Design of Metallic Glasses Using Genetic Algorithms: *Logan Ward*¹; *Katharine Flores*¹; *Wolfgang Windl*¹; ¹The Ohio State University

Metallic glasses are a unique class of engineered materials with excellent properties for a wide array of applications ranging from hard-tissue implants to high-performance transformer cores. Before becoming a widely-used class of material, however, more alloy compositions need to be identified that are optimized for specific applications, which is

experimentally a slow and expensive process. In this work, we propose a computation-only approach to designing optimized metallic glass alloys. Methods for predicting material properties using molecular dynamics were integrated with optimization using genetic algorithms to select the best alloy from millions of candidates. In our first test of this method, we were able to predict a low-density, fracture resistant metallic glass from first-principles that matched closely with an alloy experimentally known to have those properties. This versatile tool is in the process of being used to design glasses with more-complex properties and can easily be applied to different materials.

2:30 PM

Data-Driven Models Evolved through Multi-Objective Genetic Algorithms and Their Materials Applications: Nirupam Chakraborti¹; ¹Indian Institute of Technology

This paper presents two recent Evolutionary Computational strategies for Data-driven modeling, developed in author's research group, and some of their materials applications. The first strategy is called Evolutionary Neural Net, where a flexible network architecture evolves as a Pareto tradeoff between the complexity of the model and its accuracy. A bi-objective Predator-prey type Genetic Algorithm locates an optimized Pareto frontier consisting of many such models, out of which one is selected by applying the Corrected Akaike Information Criteria. The second approach involves a similar strategy for Genetic Programming, where a tree encoding is used to evolve a suitable mathematical expression for the data in hand. Models developed this way tend to avoid overfitting and underfitting problems, and prune the insignificant inputs in a systematic manner. Coupled with established modeling strategies like Molecular Dynamics, these techniques lead to powerful meta-models for the materials systems, as will be demonstrated in this paper.

2:50 PM

Optimum Approximation for Three-Point Correlation Function: Majid Baniassadi¹; Hamid Garmestani²; ¹Georgia Institute of Technology Materials Science and Engineering ; ²Georgia Institute of Technology Materials Science and Engineering

Microstructural two-point correlation functions are among a well-known class of statistical descriptors that can be used for the characterization of microstructural heterogeneous systems. The main advantage of the statistical continuum approach is the direct link to statistical information of microstructure. Two-point correlation functions are the lowest order of correlation functions that can describe the morphology and the microstructure-properties relationship. In this study, a new optimized approximation has been developed based on Two-point correlation functions to predict Three-point probability functions. The optimum approximation for Three-point correlation functions is found and compared to the real probability functions. This comparison proves that our new developed approximation is capable of describing three-point correlation functions with the needed accuracy for materials with a wide variety of micro-structure. The ramification of the new procedure is investigated for the homogenization of the three-phase composite microstructure of Solid Oxide Fuel Cells for the prediction of the relevant transport properties ins.

3:10 PM Break

3:20 PM Invited

Stochastic Geometry and Transformation Kinetics Theories: Basics and Results: Paulo Rios¹; Elena Villa²; ¹UFF-EEIMVR; ²University of Milan

Aim of this talk is to show the important role played by Stochastic Geometry in Transformation Kinetics Theories. We generalize the early Kolmogorov, Johnson, Mehl and Avrami theory, to more general nucleation-and-growth processes. In particular the notion of point process will be introduced to model various kinds of nucleation processes, for

instance inhomogeneous nucleation, cluster nucleation and nucleation on lower dimensional sets. Volume fraction, mean volume and surface densities of the transformed phase are studied by methods of Stochastic Geometry making use of the notion of causal cone.

3:50 PM

Forward and Inverse Analysis of Engineering Neutron Diffraction Data with Neural Networks: Seung-Yub Lee¹; Hyuntae Na²; Ersan Ustundag²; ¹Columbia University; ²Iowa State University

Integration of engineering neutron diffraction data analysis and solid mechanics modeling offers a powerful approach to deduce in-situ constitutive behavior of materials. Since diffraction data originates from spatially discrete subsets of the material volume, extrapolation of the data to the behavior of the overall sample is non-trivial. The finite element model (FEM) and self-consistent model (SCM) have been widely used for interpreting diffraction data by optimizing model parameters via iterative processes. In order to maximize the rigor of such analysis and to increase fitting efficiency and accuracy, we have developed an optimization algorithm based on the neural network architecture. In this presentation, I will discuss the programming concepts utilized in the development of this tool and show examples of analysis for actual samples.

4:10 PM Break

4:20 PM

Probabilistic Modeling of Microstructure Evolution Using Finite Element Representation of Statistical Correlation Functions: Veera Sundararaghavan¹; ¹University of Michigan

A probabilistic finite element scheme is presented for simulating evolution of polycrystalline microstructures during deformation. The microstructure is described using conditional orientation correlation function (COCF), defined as the probability density of occurrence of a crystal orientation g' at a distance r from a given orientation g . The COCF is represented using three interconnected layers of finite element meshes in the g' , r and g spaces. As the microstructure evolves, the reoriented neighborhood and strain field close to an orientation (g) is captured by updating probability fields in these finite element meshes. For this purpose, a novel total Lagrangian approach has been developed that allows evolution of probability densities while satisfying normalization constraints, probability interdependencies and symmetries. The improvement in prediction of texture and strains achieved by the COCF approach over ODF-based methods is quantified through deformation analysis of a planar polycrystalline microstructure.

4:40 PM

Unsupervised Learning Algorithm for the Estimation of Crystallographic Texture from Discrete Orientation Measurements: Stephen Niezgod¹; Jared Glover²; Carlos Tome¹; Rodney McCabe¹; ¹Los Alamos National Laboratory; ²Massachusetts Institute of Technology

Traditional methods for estimating the orientation distribution function (ODF) in polycrystalline materials, were developed as solutions to inferring the complete crystallographic texture from incompletely measured lower-order distributions (pole figures) obtained by diffraction. For discrete orientation data, produced using electron backscatter diffraction (EBSD) or used in polycrystal modeling, application of these methods relies on the, ad hoc, choice of filtering, smoothing and bandwidth. Here we present an unsupervised learning algorithm for ODF estimation from discrete orientations as a mixture of Bingham distributions over the rotation group. We formulate the fitting as an expectation-maximization algorithm which seeks to find the ODF that maximizes the probability of collecting the sampled data while minimizing the number of distributions needed to accurately represent the data. The framework eliminates the necessity of the ad hoc assumptions and is demonstrated to accurately capture a wide range of ODFs from sharp near single crystal to near uniform random.



TMS 2012

141st Annual Meeting & Exhibition

5:00 PM

A Calibrated Monte Carlo Approach to Quantify the Impacts of Misorientation and Different Driving Forces on Texture Development:

Liangzhe Zhang¹; Anthony Rollett²; Timothy Bartel³; Di Wu⁴; Mark Lusk¹; ¹Colorado School of Mines; ²Carnegie Mellon University; ³Sandia National Laboratories; ⁴Northeastern University

A calibrated Monte Carlo (cMC) approach, which quantifies grain boundary kinetics within a generic setting, is presented here. The influence of misorientation is captured by adding a scaling coefficient in the flipping probability equation, while the contribution of different driving forces is weighted using a partition function. The calibration process relies on the established parametric links between Monte Carlo (MC) and Sharp-Interface (SI) models. The cMC algorithm quantifies microstructural evolution under complex thermomechanical environment and remedies some of the difficulties associated with conventional MC models. After validation, the cMC approach is applied to quantify the texture development of polycrystalline aluminum with influences of misorientation and inhomogeneous bulk energy across grain boundaries. The results are in good agreement with theory and experiments.

Symposium in Memory of Patrick Veysseyre: Understanding the Mechanisms Controlling Plastic Flow: Intermetallic Alloys

Sponsored by: The Minerals, Metals and Materials Society, TMS Electronic, Magnetic, and Photonic Materials Division, TMS Structural Materials Division

Program Organizers: Georges Saada, LEM CNRS ONERA; Dennis Dimiduk, Air Force Research Laboratory; Hael Mughrabi, University Erlangen-Nuernberg; Haruyuki Inui, Kyoto University

Tuesday PM
March 13, 2012

Room: Europe 6
Location: Dolphin Resort

Funding support provided by: National Science Foundation

Session Chairs: Helena Van Swygenhoven-Moens, Paul Scherrer Institute; T. Pollock, MSE/Michigan University

2:00 PM Invited

Plasticity and Dislocation Structures in L12-Ordered Intermetallic Compounds and Transition-Metal Silicides: Haruyuki Inui¹; Kyosuke Kishida¹; Norihiko Okamoto¹; ¹Kyoto University

Our recent results of investigations on plasticity and dislocation structures in L12-ordered intermetallic compounds and transition-metal silicides will be presented. The classification of L12 compounds in terms of the temperature dependence of yield stress is discussed in relation to the observed dislocation dissociation modes. The key issue is that although the rapidly decreasing yield stress at low temperatures observed for some L12 compounds is usually attributed to non-planar core structures either for 1/2[110] dislocations separated by APB on {001} or for 1/3[121] dislocations separated by SISF on {111}, the same yield behavior is observed for many L12 compounds even with dislocations dissociated into two 1/2[110] partials separated by APB on {111}. Some new strategies to improve the thermal stability of microstructures in two-phase MoSi₂-based alloys will also be reviewed. The key issue is how the energy of interphase boundaries can be controlled with segregation of alloying elements on the boundary.

2:30 PM Invited

Some Long-Period Superstructures and the Related Motion of Dislocations in Al-Rich TiAl Single Crystals: Takayoshi Nakano¹; Yukichi Umakoshi¹; ¹Osaka University

Various long-period superstructures appeared in Al-rich TiAl are composed of three pairs of primitive cells, Ti₂Al, Ti₃Al and Ti₄Al with periodic atomic arrangements of unique shapes of lean rhombi, fat rhombi

and squares, respectively, on the (002)Ti layers. These long-period superstructures play important roles on the operative deformation mode, configuration of dislocations and the related plastic deformation behavior in Al-rich TiAl, depending on the Al concentration. Fourfold ordinary dislocations, for example, often move as a group in Al₅Ti₃ superstructure based on the lean rhombi and squares embedded in the L1₀ matrix. In this paper, relationship between the periodic long period superstructures and dislocation motion will be discussed from the viewpoint of APBs formed in each superstructure. This work was partially performed with our unforgettable old excellent friend, Dr. Patrick Veysseyre, ONERA-CNRS, France.

3:00 PM Invited

Determination of Fundamental Characteristics of Dislocations in Intermetallic Compounds Using γ -Surfaces: Vasek Vitek¹; ¹University of Pennsylvania

Dissociated dislocations are planar while if a splitting cannot occur their cores may be non-planar and deformation characteristics may strongly differ in these two cases. In structures like FCC the stacking faults are determined by the symmetry and it is usually assumed that the symmetry also determines APBs in compounds. However, it will be shown here that that this is not the case. A powerful tool that can identify planar faults is the γ -surface. It needs to be evaluated using the DFT in the case of compounds involving transition metals. Such calculations are relatively easy while studies of dislocations employing DFT are much more difficult. As examples we shall discuss stacking faults in a number of B2 intermetallics and demonstrate that metastable planar faults cannot be determined using simple models. Different faults are found in different B2 compounds and consequences for the plastic properties of B2 compounds will be discussed.

3:30 PM Invited

STEM Imaging and Analysis of the Fine Structure of Dislocations in Ni-Based Superalloys: Patrick Phillips¹; Hallee Deutchman¹; Yi Yun Li¹; Ning Zhou¹; Yunzhi Wang¹; Michael Mills¹; ¹The Ohio State University

Diffraction contrast scanning transmission electron microscopy and high angle annular dark field imaging have provided significant new insights into the rich variety of deformation processes that control deformation in Ni-based superalloys. At intermediate temperatures, the deformation mechanisms involve shearing by <112> type partials, and include microtwinning, a[112] dislocation ribbons, and superlattice intrinsic and superlattice extrinsic stacking faults. On the basis of high resolution imaging and ab initio calculations, these processes are thought to be mediated by reordering at the faults created in the precipitates. At higher stresses, shearing of precipitates by 1/2<110> dislocations on both {111} and {001} planes occurs. The importance of cube slip in superalloys and the relationship to the behavior of L₁ single crystals will also be discussed in light of Patrick Veysseyre's seminal contributions. Examples will be provided where novel STEM imaging techniques have been instrumental in developing this fundamental understanding in these commercially important alloys.

4:00 PM Break

4:15 PM Invited

Influence of Dislocation Activity in the Alpha 2 Phase on the Plastic Deformation of Titanium Aluminides: Jörg Wiezorek¹; Michael Loretto²; Hamish Fraser³; ¹University of Pittsburg; ²University of Birmingham; ³The Ohio State University

Two-phase titanium aluminides (γ TiAl and α_2 Ti₃Al phases) exhibit some interesting mechanical properties, but with usually somewhat low values of ductility. Detailed investigations, involving transmission electron microscopy (in concert with much of Patrick's experimental research!) reveal that while deformation in the γ phase occurs readily, dislocation activity in the α_2 phase is somewhat restricted.

The present study has been aimed at understanding the influence of the deformation behavior of the alpha 2 phase on the limited ductility often observed in these two phase alloys. Three aspects have been considered: firstly, the intrinsic deformation behavior of the alpha 2 phase; secondly, the role of alloying elements on the dislocation activity in this phase; and, thirdly, the mechanisms and role of slip transfer through lamellae of the alpha 2 phase. This presentation will include French protests that Patrick would have made regarding some of the claims we make!

4:20 PM Invited

A Dislocation Dynamics Simulation of the Temperature Dependence of the Flow Stress of L12 Alloys. *Ronan Madec*¹; Patrick Veyssi re²; Georges Saada²; ¹CEA, DAM, DIF; ²LEM (CNRS/ONERA)

The part played by the thermally-activated formation of Kear-Wiltsdorf locks in the positive temperature dependence of the L12 alloys flow stress is well established. KW locks are formed by cross-slip of dislocations from {111} slip planes to {001} planes in which slip motion is severely hindered. Several models based on this mechanism have been published which can be classified into two classes. In one, deformation is achieved by formation and destruction of the locks, the alloy strength is controlled by the lock stability. In the other, plastic flow proceeds from the kinks connecting the locks, the alloy strength is determined by the frequency of immobilization. These models exhibit varied agreement with the L12 flow stress anomaly set of mechanical properties. The present simulation investigation will explore the contribution of the lock formation frequency and of the lock stability to the mechanical properties of a model Ni3Al alloy.

4:40 PM Invited

A First Principles Study of the Effect of Ti and Ta on the SFE of the γ' Phase of Co-based Superalloys. *Alessandro Mottura*¹; Anderson Janotti¹; Tresa Pollock¹; ¹University of California, Santa Barbara

Co-based superalloys are a potential candidate for use in the hottest parts of gas turbines. The presence of the $\gamma+\gamma'$ phase field in the Co-Al-W ternary system allows for the casting of single-crystals which can be heat-treated to form the typical $\gamma+\gamma'$ microstructure observed in traditional single-crystal Ni-based superalloys. The addition of Ta results in anomalously high yield strengths at high temperatures. This effect has been observed in conjunction with high densities of intrinsic stacking faults within the γ' precipitates. In this work, the Axial Ising Model is used in conjunction with Special Quasi-random Structures to study the effect of Ti and Ta additions on the intrinsic stacking fault energy from first principles. Results show that the strengthening effect observed at high temperatures may be due to Ta raising the γ' solvus, rather than Ta decreasing the SFE of the γ' phase of Co-based superalloys.

5:00 PM Invited

Cyclic Behavior of a Ni-Based Superalloy Characterized by Electron Microscopy. *Patrick Phillips*¹; David Mourer²; Dan Wei²; Michael Mills¹; ¹Ohio State University; ²GE Aviation

The deformation behavior of the polycrystalline superalloy R104 has been characterized via scanning transmission electron microscopy (STEM). Specimens seeing either pure low cycle fatigue (LCF) or sustained-peak low cycle fatigue (SPCLF) were examined based on testing temperature, total strain range, and/or cycle number. In order to sufficiently characterize various damage mechanisms, both diffraction-contrast and high-resolution STEM imaging were performed, with the latter necessary given the fine-scale defects frequently present. The introduction of a dwell at maximum stress indeed influences the deformation modes, which are observed to vary from those observed in pure LCF – an effect which is likely a direct result of the dramatic cyclic softening the SPCLF specimens experience.

Titanium: Advances in Processing, Characterization and Properties: Microstructure Evolution and Characterization II

Sponsored by: The Minerals, Metals and Materials Society, TMS Structural Materials Division, TMS: Titanium Committee
Program Organizers: Adam Pilchak, US Air Force Research Laboratory; Christopher Szczepanski, US Air Force Research Laboratory; Vasisht Venkatesh, Pratt & Whitney

Tuesday PM
March 13, 2012

Room: Oceanic 3
Location: Dolphin Resort

Session Chairs: Ayman Salem, Materials Resources, LLC; Henry Rack, Clemson University; Adam Pilchak, US Air Force Research Laboratory

2:00 PM Invited

Characterization of Elongated Microtextures in Ti Alloys by Ultrasonic Backscattering. *Stan Rokhlin*¹; Jia Li¹; Oleg Lobkis¹; Adam Pilchak²; ¹The Ohio State University; ²US Air Force Research Laboratory

Theoretical and experimental analysis of a spectral representation of ultrasonic backscattering in polycrystalline materials with elongated grains is applied to inverse characterization of microstructure/microtexture in Ti alloys. It is shown that the dominant effect on the backscattering is the averaged ellipsoidal radius in the direction of wave propagation, instead of the ellipsoidal cross-section. The theory was applied to a simplified model of Ti alloy duplex microstructure and was compared with experiment. It is demonstrated that the grain size and grain morphology can be determined from directional measurements (morphological information is more accurate and easily obtainable). Also a new nondimensional parameter was introduced and measured. This parameter provides the relative contribution of the second phase (crystallites) to the backscattering signal, the effect of which is measurable and important. Comparison of the model with experiment shows there is significant advantage in using the directional ratios of backscattering coefficients for data analysis.

2:30 PM Invited

Quantifying Ti-6Al-4V Bimodal Microstructure Using Microstructure Informatics. *Ayman Salem*¹; David Turner²; Dan Satko²; Joshua Shaffer²; Stephen Niezgod a³; Surya Kalidindi²; ¹Materials Resources LLC; ²Drexel University; ³Los Alamos National Laboratory

Microstructure Informatics tools, based on 2-point statistics, have been developed and applied successfully to quantify a broad range of Ti-6Al-4V microstructures. The applicability of the tools has been demonstrated on datasets captured by Electron Backscatter diffraction patterns (EBSD) and Backscatter Electron (BSE) images. Multiple filters and image processing techniques have been utilized to automatically segment various features of interest in the microstructure. Primary alpha grains, secondary alpha colonies, and secondary alpha laths have been quantified individually. The spatial correlations between various features have been captured in addition to morphologies and micro-texture attributes. Procedures have also been developed to extract legacy metrics from datasets. Comparisons between measured metrics using legacy standards and the ones computed by our novel methods revealed tremendous cost savings with the later.

3:00 PM

An Experimental Study on the Effect of Microstructure on Oxygen Ingress in Ti-6242S Alloy. S. Knox¹; G. Viswanathan²; M. Chapman¹; A. Shiveley²; J. Tiley²; ¹Southwestern Ohio Council for Higher Education/Air Force Research Laboratory; ²Air Force Research Laboratory

Excessive oxygen ingress at high temperature has been known to adversely affect the mechanical properties of α/β Ti alloys. Although studies in the past have investigated oxygen ingress in Ti alloys, the impact of microstructure on the diffusion of oxygen and the formation of alpha case is only beginning to emerge. This study focuses on the roles of alpha orientation and morphology. Samples of Ti-6242S α/β



TMS 2012

141st Annual Meeting & Exhibition

TUESDAY PM

alloy were solutionized in a vacuum furnace and held at temperature to produce large beta grains. Slow cooling was used to produce large colony microstructures. The samples were subsequently oxidized at 650C for 100 hours. The material was sectioned and analyzed using optical microscopy, SEM and EBSD techniques to investigate the effect of morphological orientation of (α + β) colony microstructure on oxidation. Additionally, the oxidized samples were examined for nucleation of surface cracks under tensile loads to determine effects of microstructure on mechanical performance.

3:20 PM

Characterizing and Exploring the Broad Utility of Kinetic Metallization, a Novel Subsonic Cold Spray Metal Deposition Technique: *John Sosa*¹; Peter Collins²; Hamish Fraser¹; ¹The Ohio State University; ²University of North Texas

Kinetic Metallization (KM), a subsonic cold-spray metal deposition technique, avoids elevated temperatures and offers a promising way to produce unique titanium-based coatings and bulk material. However, there has been limited work to characterize the mechanisms of powder deformation and particle/particle interactions in the final product form. DualBeam™ (FIB/SEM) 3D characterization, incorporating EBSD, of single particles and particle-clusters has permitted a robust investigation of such mechanisms and interactions. Additionally, KM deposits have been subjected to both hot isostatic pressing and laser heat-treatments to probe the degree of recrystallization given their presumably high stored strain-energy. SEM, TEM, and FIB-3D have been used to characterize the phase transformations within binary metal composites and explore the influence of particle/particle interface character on such transformations. Finally, unique Ti/Mg metal-matrix composites have been fabricated using KM and their microstructure evaluated using multiple characterization techniques.

3:40 PM

Determining the Variance and Distribution of Quantified Microstructure in a + β Processed Ti-6Al-4V and Their Contribution to the Accuracy of Property-Predictive Neural Network Models: *Meg Noble*¹; Daniel Huber¹; John Sosa¹; Travis Presley¹; Hamish Fraser¹; ¹Ohio State University

The use of quantified microstructures as inputs to neural network models for property prediction has been pioneered by Center for the Accelerated Maturation of Materials at The Ohio State University to provide predictive tools for mechanical properties in titanium alloys while phenomenological models are developed. The work presented focuses on testing the neural network models, their predictive capability, and developing additional robust models. A generation of new automated tools developed by CAMM has permitted quantification of the variance and distribution of a + β processed Ti-6Al-4V, which will provide inputs for testing the neural networks. The output accuracy of these models will be compared to the quantified variance and distribution to better understand the source of any model inaccuracy. The observed variations in quantified microstructures revealed variation in a host of Ti-6Al-4V microstructures, thus providing more precise prediction models.

4:00 PM

Calculation of Kearns Number Plots (KNP) and Kearns Number Maps (KNM) from EBSD Data: Application to Ti-6Al-4V with Bimodal Microstructure: *Ayman Salem*¹; Adam Pilchak²; Surya Kalidindi³; ¹Materials Resources LLC; ²Air Force Research Laboratory; ³Drexel University

A method for calculating and presenting Kearns' texture factor from discrete orientations obtained by electron backscatter diffraction data was developed for titanium alloys. This form of quantitative texture analysis was visualized via new plots that display the Kearns numbers for all possible directions in the sample reference frame. In addition, new maps were generated to visualize the spatial distribution of Kearns number throughout the sample. The method is general and applicable to any

material exhibiting hexagonal symmetry. The methods have been applied individually to the primary alpha grains and secondary alpha colonies in a hot rolled Ti-6Al-4V plate.

4:20 PM

The Study of Phase Transformation in Beta Titanium Alloys Using Electrical Resistivity Measurement, Image Processing Technique and Electron Microscopy: *Yufeng Zheng*¹; Robert Williams¹; Hamish Fraser¹; ¹The Ohio State University

Due to the combination of high strength and great ductility, beta titanium becomes a promising candidate for the future use in the biomedical implants field as well as the aerospace application. Understanding the microstructural evolution in beta titanium alloys is essential to manipulating its properties. Using state of the art equipment, the phase transformation sequence of the beta titanium in the heating process and the kinetics of alpha precipitation in the isothermal treatment was studied by electrical resistivity measurement in the Electro-Thermal-Mechanical Tester (ETMT). With the high resolution transmission electron microscopy, the onset of the alpha precipitate formation in the material could be studied in details and with image processing technique, the TTT diagram of isothermal treatment could be plotted conveniently. The microstructure evolution in Ti-Mo binary alloy and Ti-5Al-5Mo-5V-3Cr will be introduced to illustrate the power of the method above.

4:40 PM

Phase Transformations and Mechanical Properties of Alpha-Beta Solution Treated Ti-6.8Mo-4.5Fe-1.5Al: *Jana Smilauerova*¹; Petr Harcuba¹; Miloš Janeček¹; Josef Stráský¹; Radomír Kužel¹; Henry Rack²; Herbert Boeckels²; ¹Charles University; ²Clemson University

Formation and growth of omega and alpha phase particles in TIMETAL LCB (Ti-6.8Mo-4.5Fe-1.5Al, wt. %) were examined by electrical resistivity and DSC measurements during linear heating. The influence of alpha-beta solution treatment between 700 and 745°C used to control the volume fraction, size and contiguity of grain boundary alpha and subsequent ageing at 450 and 500°C for times at 8 and 16 hours on mechanical and fatigue properties was studied. Related microstructure evolution – omega and alpha phase particle size and spatial distribution – was examined by transmission and scanning electron microscopy and by means of X-ray diffraction.

5:00 PM

Effect of Titanium Borides on the Formation of Equiaxed Alpha in Titanium Alloys: *Peeyush Nandwana*¹; Soumya Nag¹; Jaimie Tiley²; Hamish Fraser³; Rajarshi Banerjee¹; ¹University of North Texas; ²Air Force Research Laboratory; ³The Ohio State University

Titanium boride (TiB) is a promising reinforcement phase in Ti alloy matrices that may lead to enhanced stiffness, strength, and wear resistance. Furthermore, during the solid-state precipitation of α in a matrix of β titanium, the presence of TiB precipitates act as additional nucleation sites for a phase. Interestingly, the α that is nucleated on the TiB precipitates exhibit an equiaxed or globular morphology in contrast to the α precipitated on other nucleation sites such as grain boundaries, which exhibit a more lath-like morphology. The current study uses Electron Backscattered Diffraction (EBSD) and Transmission Electron Microscopy (TEM) techniques to investigate the effect of borides on subsequent nucleation and growth of a precipitates. For this, various cases were considered where the α phase was in close proximity to boride particles and different orientation relationships existing between a Ti, TiB and β matrix were identified.

5:20 PM

Effect of Heating Rate on the Short Time Aging Kinetics of Ti-6.8Mo-4.5Fe-1.5Al: *Herbert Boeckels*¹; Henry Rack¹; ¹Clemson University

This investigation has examined the influence of heating rate on the short time, less than 4 h, kinetics of ω and α phase precipitation in beta solution-treated Ti-6.8Mo-4.5Fe-1.5Al utilizing measurements of the time dependent calorimetric response observed during aging in the temperature

range 200-550°C. While transformations were observed at all aging temperatures for the lower rate, 5°C/ min., heating at 50°C/min. tended to suppress the observed transformations to higher aging temperatures. For example, single reactions, associated with the evolution of the ω phase, were found at aging temperatures = 400°C and = 450°C for 5°C and 50°C heating rate respectively. Above these temperatures duplex reactions involving both ω and α phase were observed. This behavior has been examined using the JMAK analysis methodology and will be discussed in terms of ω stability and a precipitation during isothermal aging as influenced by heating rate, aging temperature and aging time in Ti-6.8Mo-4.5Fe-1.5Al.

5:40 PM

Phase Evolution as a Function of Heat Treatment in

Ti-48Al-16Nb Alloys: Narayana Garimella¹; A. K. Singh²; N.K. Mukhopadhyay³; G.V.S. Sastry³; ¹University of Maryland School of Medicine; ²Defence Metallurgical Research Laboratory Hyderabad India; ³Department of Metallurgical Engineering Banaras Hindu University India

Several research works have focused on phase transformation in Ti-48Al based alloys with the aim of improving their formability characteristics. Precipitation, growth and distribution of B2 phase within the matrices of either 'Gamma' or lamellae of 'Gamma-Alpha2' or both Gamma and 'Gamma-Alpha2' phases is found to be the important factor of contribution to enhance the room temperature formability of Ti-48Al-16Nb Alloys. In this work, phase evolution in Ti-48Al-16Nb alloys was evaluated as a function of aging time and temperature. The alloys were solution treated at 1400°C, and were aged at several lower temperatures ranging from 400°C to 1300°C for the descending durations of aging respectively. Relatively increased amount of B2 phase was resulted for the aging condition of 1200°C for 4 hrs sample with the subsequent decrease in vicker's hardness. Physical and mechanical metallurgy aspects of the results are discussed with the aids of phase transformation and mechanical strength.

T.T. Chen Honorary Symposium on Hydrometallurgy, Electrometallurgy and Materials Characterization: Transition Metal Processing

Sponsored by: The Minerals, Metals and Materials Society, TMS Extraction and Processing Division, TMS: Hydrometallurgy and Electrometallurgy Committee, TMS: Materials Characterization Committee

Program Organizers: Shijie Wang, Rio Tinto Kennecott Utah Copper; J. E. Dutrizac, CANMET; Michael Free, University of Utah; J. Y. Hwang, Michigan Technological University; Daniel Kim, Rio Tinto Kennecott Utah Copper

Tuesday PM
March 13, 2012

Room: Oceanic 5
Location: Dolphin Resort

Funding support provided by: Rio Tinto Kennecott Utah Copper, ASARCO, and Freeport McMoRan

Session Chair: Michael Free, University of Utah

2:00 PM

FeTi Alloy Production by Electrolytic Reduction of (Fe, Ti) Oxide Electrode in Molten Calcium Chloride: Panigrahi Mrutyunjay¹; Atsushi Iizuka¹; Etsuro Shibata¹; Takashi Nakamura¹; ¹IMRAM, Tohoku University

In this work, TiO₂ and Fe₂O₃ powder were mixed in proper molar ratio followed by preparing pellets and heat treated at (1000°C-1300°C) to increase the conductivity and strength. For electrolysis, the CaCl₂ was dehydrated to remove the moisture followed by pre-electrolysis at 2.6

V for the remaining amount of moisture and other volatile impurities. The heat treated (1000°C for 2 hrs.) pellet was electrolyzed by constant voltage electrolysis process (3 volt for 20 hrs) at 950°C. The conductivity of the electrolyzed pellet was measured and characterized by XRD, SEM and EDX. From these analyses, it is confirmed that the surface of the product contains FeTi, H₂FeTi and amorphous carbon and the cross section contains FeTi, TiO_{1.04}, amorphous carbon and TiO₂. However, more experiments should do with a longer electrolysis time to avoid the unwanted phases.

2:20 PM

A New Method for Production of Titanium Dioxide Pigment – Eliminating CO2 Emissions: Scott Middlemas¹; Z. Zak Fang¹; Peng Fan¹; ¹University of Utah

Titanium dioxide (TiO₂) has been widely used as pigment in paints, paper and cosmetic products, as well as high-tech applications such as PV Cells, semiconductors, biomedical devices and air purification. TiO₂ pigment is primarily produced by the high temperature chloride process, resulting in considerable CO₂ emissions. A novel hydrometallurgical process for making TiO₂ pigment without CO₂ emission is investigated. The new method promises to eliminate direct CO₂ emissions, consume significantly less energy, and produce minimal environmental waste. The novel process involves molten salt roasting of titania slag, with subsequent washing, leaching, hydrolysis, bleaching, calcination and post-treatment stages, resulting in high-purity anatase or rutile pigments while realizing significantly reduced environmental impacts. Pigment whiteness is critically sensitive to trace amounts of discoloring impurities such as iron and chromium. Several methods for reducing the levels of these impurities are investigated. Energy consumption and emission models are also developed.

2:40 PM

Extraction of Titanium and Vanadium by Chloride Leach Processes: Lucky V.I. Lakshmanan¹; R. Sridhar¹; T. Sheikhzainoddin¹; Md. Halim¹; R. Roy¹; ¹Process Research Ortech Inc.

Chloride metallurgy is emerging as an alternative process for the production of base metals. Process Research ORTECH Inc. (PRO) has been at the forefront of technological development of chloride metallurgy. PRO has developed an innovative technology for the production of high purity titanium dioxide from ilmenite ores and concentrates. PRO is also developing its proprietary mixed chloride technology for the extraction of vanadium from different sources such as ilmenite and oil shales. In this paper, the developments in chloride metallurgy for the extraction of Ti and V will be reviewed and some results from the test work conducted at PRO will be presented.

3:00 PM

Formation of Titanium Liquid Alloy by Mechanical Mixing and Electrochemical Method: Sho Maruyama¹; Shohei Hayashi¹; Yuya Kado¹; Tetsuya Uda¹; Yoshitaro Nose¹; ¹Kyoto university

We are trying to establish a new smelting process of titanium. The new process consists of two consecutive cells, Reduction cell and Refining cell. In the Reduction cell, titanium raw material is reduced to liquid alloy and in the Refining cell pure titanium is obtained by electrolytic refining. As the basic study, we made titanium liquid alloys by melting some metals or their alloys in titanium crucibles at 1173 K. But the titanium compositions in some liquid alloys (ex. Sn, Pb, Sn-Cu) were very smaller than those in reported phase diagrams. We found intermetallics is formed on the surface of the crucible with uniform thickness and it prevents titanium from dissolving into liquid alloy. Only antimony alloys contained approximately 10 at.% titanium which coincided with the value in the phase diagram. Some results of electrochemical reduction of titanium raw materials to the liquid alloy will be introduced.



TMS 2012

141st Annual Meeting & Exhibition

3:20 PM Break

3:40 PM

Anion-Exchange Separation of Zr from Hf using Multi-Column

Method: Masahito Uchikoshi¹; Kouji Mimura¹; Minoru Isshiki¹; ¹Tohoku University

HfO₂ is expected to be a gate dielectric used in ULSI alternative to SiO₂. Although the materials used in ULSI are required to be sufficiently purified, commercial Hf contains > 2 mass% Zr. It is important to establish process of removing Zr from Hf. In the present study, anion-exchange separation using multi-column method was employed. The separation tests were carried out in variety of temperatures and flow rates. The decrease in the flow rate of the mobile phase made the elution curves of both Hf(IV) and Zr(IV) broadened contrary to the case of Co(II), Cu(II), or Fe(III). This is caused by the difference in adsorption rate on anion-exchange resin. In addition, more than one column were connected in series in order to enhance the separation ability. As a result, the content of Zr(IV) was successfully reduced down to 1/100 relative to the raw material.

4:00 PM

Recovery of Metals from Molybdenite Concentrate by Hydrometallurgical Technologies:

*Yufang Wang*¹; Kaixi Jiang¹; Xiaoping Zou¹; Lei Zhang¹; Sanping Liu¹; ¹Beijing General Research Institute of Mining and Metallurgy

Molybdenite concentrates are usually treated by roasting; but low concentration SO₂ pollution is a problem. Extraction of Molybdenum and rhenium from molybdenite concentrates with pressure oxidative leaching and solvent extraction (SX) process was studied. A series of POX-SX lab and pilot tests were carried out on the molybdenum concentrate. In POX stage, more than 95% rhenium and 15-20% molybdenum were leached into solution. Solvent extraction extracted rhenium and molybdenum from POX solution. The extraction rate of Re and Mo reached above 98%. The loaded organic reagent is stripped with ammonia. The stripping ratio of Mo is more than 98%. Comparison with roasting process the total recovery of Mo can increase from 93% to 97%, and Re from 50% to 80%. In the coming five years POX-SX technology is competitive in China.

4:20 PM

The Effect of Phosphate Additions on the Microstructure and Performance of Cr₂O₃ Gasifier Refractories:

*Kyei-Sing Kwong*¹; James Bennett¹; Jinichiro Nakano²; John Sears²; Xueyan Song³; ¹NETL, US DOE; ²URS Corp.; ³West Virginia University

Gasification is an efficient, environmentally clean, technology capable of processing coal, petroleum coke, or biomass into syngas used in the production of electric power or chemicals. However, the short service life of the Cr₂O₃ refractory used to protect the outer steel containment shell from coal slag attack and insulate it from the high temperature process is one of the factors limiting gasification technology. Post mortem analysis of Cr₂O₃ refractories has been conducted by XRD, ICP, SEM, and TEM to find failure mechanisms and to study the reaction between gasifier slags and refractories. Structure spalling caused by slag penetration has been identified as one of the major failure mechanisms. New improved phosphates containing Cr₂O₃ refractories were developed and successfully proven in gasifier field tests. The effect of phosphates has been characterized using TEM and SEM and its mechanism in decreasing slag penetration will be discussed.

4:40 PM

Extraction Impurities such as Fe, Ca and Mg from a Titanium Material in Chloride Acid System with Microwave Eenergy Leaching:

*Shaohua Ju*¹; Jin-Hui Peng¹; Sheng-Hui Guo¹; Wang Xin¹; Lie-Xing Zhou¹; Meng-Yang Huang¹; ¹Kunming University of Science and Technology

This work intends to leach the impurities such as Fe, Ca and Mg out from a low grade Titanium mineral, to increase the grade. The original material contains 65% TiO₂, 16.12% Fe, 9.4% CaO + MgO, 4.2% SiO₂, 1.25% Al₂O₃, and the particle size is between 0.053-0.045mm. The microwave energy was used to enhance the leaching effect. The result showed that

when normal heating method was used to leaching the mineral, the extraction of impurities Fe, Ca and Mg are very low. However, when microwave energy is introduced to this system, the extraction of Fe, Ca and Mg increased dramatically. The optimized conditions are: relative power equals to 5W/g, the concentrate of HCl equals to 15%, leaching at 160°C for 20 min with a ratio of liquid to solid 12:1, and the material obtained contains 92.73% Ti, 0.207% Ca + Mg, and 0.8% Fe.

5:00 PM

Study on Sodium Roasting and Chromium Extracting of Fe-Cr Spinels:

*Hai-Xing Fang*¹; *Hong-Yi Li*¹; Bing Xie¹; ¹Chongqing University

In duplex melting process of converter, chromium forms chromium spinels, the study of which will help to explore Hongge ores (rich in chromium) in Panzhihua-Xichang area in China. Mimicked chromium slag was synthesized in experimental conditions. The oxidation and decomposition mechanism of Fe-Cr spinels was studied in sodium roasting process. Effects of temperature, roasting time and amount of soda addition on the conversion rate were investigated. The leaching-reduction-precipitation-calcination process to extract Cr₂O₃ was also optimized. Results showed that the optimized roasting temperature was about 1000°C with Na₂CO₃ addition in stoichiometric amount. Roasted materials were leached by distilled water and filtered to obtain chromium-containing solution, which was adjusted to pH 1.60~1.80. Reducing reagent NaHSO₃ was added in stoichiometric ratio and the solution was then adjusted to pH 7.25~8.25. Maximum Cr(OH)₃ precipitation was obtained and calcined at 1050°C for 2h to obtain Cr₂O₃ with recovery rate over 96%.

Ultrafine Grained Materials VII: Processing-Microstructure-Property Relationships: Al-, Mg- and Ti-Alloys

Sponsored by: The Minerals, Metals and Materials Society, TMS Structural Materials Division, TMS/ASM: Mechanical Behavior of Materials Committee, TMS: Nanomechanical Materials Behavior Committee, TMS: Shaping and Forming Committee

Program Organizers: Suveen Mathaudhu, U.S. Army Research Office; Xiaoxu Huang, Risø National Laboratory for Sustainable Energy, Technical University of Denmark; Hyoung Seop Kim, POSTECH; Terence Langdon, University of Southern California; Terry Lowe, Manhattan Scientifics, Inc.; Ruslan Valiev, Ufa State Aviation Technical University; Xiaolei Wu, Institute of Mechanics, Chinese Academy of Sciences; Michael Zehetbauer, University of Vienna

Tuesday PM
March 13, 2012

Room: Swan 5
Location: Swan Resort

Session Chairs: David Morris, CENIM, CSIC; Edgar Garcia-Sanchez, Universidad Autónoma de Nuevo León; Jung Bahadur Singh, Bhabha Atomic Research Centre; Jozef Zrník, Comtes FHT, Inc.

2:00 PM Invited

Development of Ultra-High Strength Al-Mg Alloys Processed by Severe Plastic Deformation:

*Hans Roven*¹; Manping Liu²; Maxim Murashkin³; Ruslan Valiev³; Tamas Ungár⁴; Levente Balogh⁴; ¹Norwegian University of Science and Technology (NTNU); ²Jiangsu University; ³Ufa State Aviation Technical University; ⁴Eötvös University

One of the recent interests applying severe plastic deformation to light alloys is the possibility to achieve ultra-high strength. The present work focuses on the strength potentials of the solid solution strength system Al-xMg applying high pressure torsion. The binary Al-Mg alloy system has been studied systematically in the range from commercial purity aluminium up to Al-10wt%Mg. Different post deformation characterization methods such as high-resolution transmission electron microscopy, X-ray diffraction and mechanical testing have been applied to reveal the embedded nanostructures and strengthening mechanisms. A remarkably high tensile yield strength of 830 MPa is obtained in an Al-

8.0wt%Mg alloy. This significant improvement in strength is attributed to the cooperative interactions of solute atoms, high dislocation densities, grain boundaries and planar interfaces.

2:20 PM

Dynamic Precipitation in AA6060 during HPT Processing at Different Temperatures: *Gang Sha*¹; Xiaozhou Liao¹; Kaan Tugcu¹; Maxim Murashkin¹; Ruslan Valiev¹; Simon Ringer¹; ¹The University of Sydney

Severe plastic deformation (SPD) is well known to be effective in modification of materials microstructures and achieving significant refinement on grain size. The SPD processing is able to have a significant influence on the formation of precipitate microstructures. In this contribution, AA6060 alloy quenched after a solution treatment has been processed using high-pressure torsion (HPT) at room temperature, 100 °C and 180 °C up to 10 revolutions under a pressure of 6 GPa. The precipitates microstructures of the alloy have been characterised systematically using both transmission electron microscopy and atom probe tomography (APT). In addition to the amount of strain applied by HPT processing, processing temperature has been found to have a significant influence on the formation of precipitate microstructures of the alloy. With the quantitative structural and chemical information of precipitates revealed by APT characterisation, this contribution will comprehensively address the kinetic and thermodynamic effects of the dynamic precipitation in AA6060 during HPT processing.

2:35 PM

ECAP Processing of Al5052 Alloys at Room and Cryogenic Temperatures: *Jung Singh*¹; Garima Sharma¹; Apu Sarkar¹; V Basavaraj²; Jayanta Chakravarty¹; ¹Bhabha Atomic Research Centre; ²IIT Bombay

ECAP processing of Al5052 alloys has been carried out by deforming it at room and cryogenic temperatures. Samples were deformed using the Be route up to 14 passes in a 120° angle die. Development of microstructure with number of ECAP passes has been monitored at intermediate intervals using transmission electron microscopy (TEM) and Electron backscatter diffraction (EBSD) techniques. Deformation temperature was found to have a strong effect on the substructure of the microstructure developed and consequently on the room temperature strength.

2:50 PM

Effects on Hardening and Ductility of Severe Plastic Deformation of Al-Cu-Li and Cu-Cr-Zr Precipitation Hardening Alloys: *David Morris*¹; Kesman Valdes Leon¹; Maria Muñoz-Morris¹; ¹CENIM, CSIC

Severe plastic deformation of precipitation hardening alloys offers the possibility of processing the solutionised material at room or high temperature, with ageing before or after deformation. Different strengths and ductilities arise because of complex interactions between precipitates and dislocations. Such interactions have been examined by ECAP of two precipitation hardening alloys. ECAP of Al-Cu-Li at room temperature leads to moderate strength with poor ductility, with subsequent ageing improving both. ECAP at elevated temperatures gives good strength with moderate-to-good ductility, depending on processing conditions. Detailed microstructural analysis shows that precipitates play a major role in determining both strength and ductility. ECAP of solutionised and/or aged Cr-Cr-Zr leads to hardening but low ductility, while subsequent ageing increases substantially both strength and ductility. The role of ECAP temperature is complicated, determining the microstructural state. The balance of substructural refinement and dislocation and precipitate hardening is analysed here to explain the mechanical properties.

3:05 PM

Structural Evolution in Aluminium Alloy AA6082 during HPT Deformation at Increased Temperature: *Jozef Zrnik*¹; Libor Kraus¹; Reinhard Pippan²; Martin Fujda³; Karel Sperlink⁴; ¹Comtes FHT, Inc.; ²Austrian Academy of Science; ³Technical University in Kosice; ⁴CSNMT

Aluminium alloy AA6082 of different initial structure was deformed by HPT at increased temperature of 150°C. The impact of various effective strain rate and temperature on fine grain structure evolution and mechanical

properties was investigated. The refinement of coarse initial alloy structure, modified by thermal treatment performed prior deformation, was investigated using TEM of thin foils respecting the effect of different shear strain across the disc. The tensile tests and microhardness were performed with aim to evaluate mechanical properties changes as effect of straining. The torque versus number of turns was measured as well. The microstructure results showed that ultrafine grained structure was formed across the disc applying the first turn. Effectively homogenized ultrafine grained structure across the disc was attained. Tensile test results showed that effect of deformation strengthening was increasing as effective stress increased. The hardness results pointed out to the reverse dependence of strength across the disc.

3:20 PM

Effect of Short Annealing and Ageing on Microstructure and Mechanical Properties of Ultrafinegrained Al-Mg-Si Alloy: *Nageswararao Palukuri*¹; Jayaganthan R¹; ¹IIT Roorkee

In the present investigation, ultrafine grained Al 6061 alloy was developed through cryorolling (CR) by giving 90% reduction and further short-annealed (SA) for 10 min at 200°C followed by low temperature ageing. Micro structural and Mechanical properties were characterized through (TEM), EBSD technique, Vickers hardness testing and Tensile testing unit. This has been compared with Al 6061 developed through cryorolling for 80% and hot rolling from 80 % to 90 % reduction at 200°C with soaking time of 10 min followed by ageing. Cryorolling followed by hot rolling has shown improved Vickers hardness and UTS (115HV, 360MPa) compared to (96HV, 285MPa) of the samples subjected to CR+ SA. The post-CR hotrolling (200°C) followed by ageing treatment (120°C.) of the Al 6061 alloy has shown an improved strength and well defined ultrafine grain structure as compared to the samples subjected to post-CR short annealing (200°C, 10 min) followed by ageing treatment.

3:35 PM Break

3:50 PM Invited

Nanostructure Evolution in Pure Aluminum Heavily Deformed by Torsion: *Nobuhiro Tsuji*¹; Sunisa Khamsuk¹; Hiroki Adachi²; Daisuke Terada¹; ¹Kyoto Univ; ²University of Hyogo

Continuous torsion straining was applied to a commercial purity aluminum (JIS-1100) at various strain rates and temperatures. Elongated ultrafine grains having microstructural parameters comparable to those formed in other severe plastic deformation like ARB were found in the specimens deformed by torsion to high equivalent strains at room temperature. The effects of simple shear deformation, temperature and strain rate on the nanostructure evolution are experimentally shown and discussed.

4:10 PM

Effect of the Severe Plastic Deformation on the Wear Behavior of an Al-Mg-Si Alloy: *Edgar Ortiz-Cuellar*¹; M. A. L Hernandez-Rodriguez¹; *E. Garcia-Sanchez*²; ¹Universidad Autónoma de Nuevo León -Facultad de Ingeniería Mecánica y Eléctrica

With the aim to study the effect of the severe plastic deformation on the wear properties, grain refinement and mechanical properties in an aluminum alloy in this work a commercial Al-Mg-Si alloy under two initial microstructural conditions has been deformed at room temperature by multi-pass 90° equal channel angular pressing (ECAP). After the processing each sample was evaluated by means of microhardness tests and the microstructural condition was determined by electron microscopy. Subsequently sliding wear test was undertaken in a ball on disk configuration under lubricated and unlubricated conditions using a steel ball. It was found a wear resistance increasing with the rise in the deformation promoted by the number of extrusion passes; the effect of the initial microstructure on the wear decreases with the level of strain in the material. The lubrication condition promotes changes in the response of the material. The dominant wear mechanisms were identified and correlated.



TMS 2012

141st Annual Meeting & Exhibition

4:25 PM

Effect of Multi Directional Forging at Liquid Nitrogen Temperature on Microstructure and Mechanical Properties of Al-Mg-Si Alloy: Jayaganthan R¹; Nageswararao P¹; IIT Roorkee

Multi directional forging was conducted on solution treated Al-Mg-Si alloy at liquid nitrogen temperature (-193°C) with total number of cycles 6 and to the cumulative strain of 3.6. After every two cycles, the deformed microstructure was examined by EBSD and transmission electron microscopy (TEM). The results have shown that at lower strains in liquid nitrogen temperature, the microstructure exhibits higher dislocation density. Significant grain refinement was observed in multidirectionally forged sample at cryogenic temperature. Grain refinement occurs due to effective suppression of dynamic recovery upon submerging the sample in liquid nitrogen during forging. The mechanical properties were studied through Vickers hardness testing machine and Tensile testing unit. Vickers hardness has been taken across the cross-section and it was observed that the hardness value of cryoforged alloy has increased from 45 HV to 110 HV by imparting 3.6 accumulated strains. Tensile strength of cryoforged sample was observed to be 340 MPa.

4:40 PM

Effect of Nano-Structural Modification on the Mechanical Behavior of Lamellar Gamma TiAl Alloy: Yu Sun¹; Anil Sachdev²; Enrique Lavernia¹; ¹University of California, Davis; ²Chemical Sciences and Materials Systems Lab, GM Global R&D Center, Warren, MI

Lamellar gamma TiAl alloys exhibit high stiffness, specific strength and creep resistance for temperatures up to 1000°C, and have emerged as promising materials for high-temperature structural applications. The lamellar microstructure can be substantially varied by the modification of the length scale between γ -TiAl/ α 2-Ti3Al and the effect on mechanical properties. This paper describes the nanoscale modification of the lamellar phase microstructure on the mechanical behavior of these alloys. Cryomilling is utilized to generate nano-grained gamma powders, and the fully lamellar TiAl alloy, with the ultrafine colony size, is consolidated by spark plasma sintering. A careful design of the cooling route after sintering allows a manipulation of the lamellar γ -TiAl/ α 2-Ti3Al spacing, distribution and orientation, all of which are determined with TEM and EBSD. The size-effect of the lamellar colony, and the spacing, orientation and distribution of the lamellar γ -TiAl/ α 2-Ti3Al are investigated in terms of the macroscopic mechanical response and microscopic fracture mechanism.

4:55 PM

Development of Ultrafine Grained Mg-Y-RE Alloy by Multi Pass Friction Stir Processing: S. K. Panigrahi¹; R.S. Mishra¹; R. DeLorme²; B. Davis²; R. A. Howell³; K. Cho³; ¹Centre for Friction Stir Welding and Material science and Engineering; ²Magnesium Elektron North America Inc.; ³Weapons and Materials Research Directorate

Rare earth containing magnesium alloys have received significant attention in aerospace and automotive industries due to their high strength to weight ratio, high damping performance and better creep resistance. The strength, ductility and superplasticity of these alloys can be enhanced further by refining the grain structure to the ultrafine regime. Friction stir processing (FSP) is emerging as an attractive technique for producing fine grained microstructure in Mg based alloys. Although a number of researchers have achieved ultrafine grained (UFG) microstructure on different Mg-Al-Zn alloy system by FSP, the development of UFG microstructure in Mg-Y-RE alloy has not been reported. In the present study, a multi pass FSP approach was used to develop UFG Mg-Y-RE alloy. The microstructure was refined to 240 nm after successful implementation of a three pass FSP. The influence of precipitates and heat input during FSP on microstructural refinement and texture modification were addressed in detail.

5:10 PM

Microstructure and Defect Structure Evolution in Commercial Magnesium Alloys Processed by Severe Plastic Deformation: Miloš Janeček¹; Jakub Cízek¹; Jitka Vrátná¹; Julia Mueller¹; Jenő Gubiza¹; ¹Charles University

MgAlZn and MgZnZr were processed by hot extrusion and equal channel angular pressing (ECAP) known as EX-ECAP. Microstructure and defect structure evolution with strain due to ECAP was investigated by TEM, positron annihilation spectroscopy (PAS), and X-ray diffraction. Significant grain refinement was obtained in all alloys by EX-ECAP. The dislocation density evolution with strain as determined by PAS followed the same scheme in all three alloys. In the ex-extruded condition a very low density of dislocations was observed. Sharp increase of dislocation density occurred during the first two passes of ECAP, followed by saturation and even a decline manifesting the dynamic recovery at higher strains. XRD line-profile analysis confirmed the results of PAS with slightly higher values of dislocation densities in individual conditions. Detail analysis of contrast factors allows to determine the type of dislocations and to draw conclusions about slip activation and its variations with strain in individual alloys.

5:25 PM

Effect of HPT Processing Temperature on the Evolution of Strength in a Magnesium Alloy: Yi Huang¹; Roberto Figueiredo²; Terence Langdon³; ¹University of Southampton; ²Federal University of Minas Gerais; ³University of Southern California

It is now well known that processing by severe plastic deformation can significantly increase the strength of metallic materials by refining the grain structure and increasing the density of defects. The rapid increase in strength observed in the early stage of deformation is expected to slow down and saturate at large strains due to an increase in recovery of the material. Therefore, a saturation of strength is expected to depend on the processing temperature. The present paper analyses this parameter by determining the evolution of hardness of a magnesium alloy processed by high-pressure torsion at different temperatures. Keywords: high-pressure torsion, magnesium alloys, microhardness test

5:40 PM

Some Studies on the Microstructural Changes in a Mg-Based AE42 Alloy Subjected to Friction Stir Processing: Brij Dhindaw¹; Harpreet Singh¹; Harpreet Singh Arora¹; I.I.T. Ropar

The study report microstructural changes taking place in a Mg-based alloy (AE42) subjected to FSP under different cooling conditions. FSP process was carried out with single as well as multipass options. It was observed that FSP tends to fragment the elongated precipitates and produces near homogeneous distribution of fine particles. The smallest particle size was observed to be produced by double pass FSP supplemented by rapid cooling, thereby generating in-situ nano-composites. Nearly two times increase in the micro-hardness of AE42 was observed in case of double pass FSPed AE42 with cooling at temperature of about -20°C. To further confirm these observations, another magnesium alloy AM50 was also FSPed under similar conditions. Fine submicron grain structure produced in FSPed AE42 alloy, immensely contributed towards grain boundary strengthening and Orowan strengthening had only marginal influence. Sub grain boundary pinning by in-situ nano-particles has contributed significantly in the strengthening process.

TUESDAY PM

Ultrafine Grained Materials VII: Processing-Microstructure-Property Relationships: Fe-, Cu- and High-Entropy Alloys

Sponsored by: The Minerals, Metals and Materials Society, TMS Structural Materials Division, TMS/ASM: Mechanical Behavior of Materials Committee, TMS: Nanomechanical Materials Behavior Committee, TMS: Shaping and Forming Committee
Program Organizers: Suveen Mathaudhu, U.S. Army Research Office; Xiaoxu Huang, Risø National Laboratory for Sustainable Energy, Technical University of Denmark; Hyoung Seop Kim, POSTECH; Terence Langdon, University of Southern California; Terry Lowe, Manhattan Scientifics, Inc.; Ruslan Valiev, Ufa State Aviation Technical University; Xiaolei Wu, Institute of Mechanics, Chinese Academy of Sciences; Michael Zehetbauer, University of Vienna

Tuesday PM
March 13, 2012

Room: Swan 4
Location: Swan Resort

Session Chairs: Tadahiko Furuta, Toyota Central R & D Labs., Inc.; Rainer Hebert, University of Connecticut; Rimma Lapovok, Monash University; Z.B. Wang, Institute of Metal Research, Chinese Academy of Sciences

2:00 PM Invited

Structure and Properties of the Stainless Cr-Ni-Ti Steel after High Pressure Torsion at T= 300-500°C: *Sergey Dobatkin*¹; Ruslan Valiev²; Olga Rybalchenko¹; Maksim Murashkin²; ¹A.A. Baikov Institute of Metallurgy and Materials Science of RAS; ²Ufa State Aviation Technical University

The regularities of the structure formation in the stainless Cr-Ni-Ti austenitic steel (0.07% C, 17.3% Cr, 9.2% Ni, 0.7% Ti) upon high pressure torsion (HPT) under 6 GPa at 300 and 500°C have been studied. The HPT at room temperature leads to martensitic transformation. However, the martensitic structure deteriorates the corrosion resistance. The aim is to obtain fully austenitic structure after deformation. The electron-microscopic examination of the Cr-Ni-Ti steel after HPT at 300 and 500°C revealed the formation of nano- and submicrocrystalline structures with average sizes of structure elements of 87 and 123 nm, respectively. X-ray diffraction analysis revealed the presence of only austenitic phase. The HPT substantially increases the strength characteristics of the Cr-Ni-Ti steel: the YS and UTS increase almost by a factor of 6 and 3, respectively. The maximum yield strength (1740 MPa) is observed after HPT at T = 300°C. The work was supported by RFBR (project no. 10-03-00996).

2:20 PM

Effect of Alloy Composition on Mechanical Properties of Bulk Nanostructured Fe-Ni-Co-Ti Alloys Produced by High-Pressure Torsion: *Tadahiko Furuta*¹; Shigeru Kuramoto¹; Kaveh Edalati²; Zenji Horita²; ¹Toyota Central R & D Labs., Inc.; ²Kyushu University

Microstructural evolution and mechanical properties were studied in Fe-(18.1-24.2)%Ni-(32.3-35.8)%Co-(3.9-9.3)%Ti (in at%) alloys after processing by high-pressure torsion (HPT) at room temperature with a rotation speed of 1 rpm under a pressure of 6 GPa. The HPT-processed alloys were composed of ultrafine grains having the sizes of less than 20 nm in diameter, regardless of the alloy compositions and of occurrences of phase transformation during HPT. However, the alloy compositions affect mechanical properties of these bulk nanostructured Fe-Ni-Co-Ti alloys: ultimate tensile strength (UTS) increases with decreasing Ni and increasing Ti contents and the highest strength is attained in the Fe-18.1%Ni-34.9%Co-9.3%Ti alloy with UTS of about 2.7 GPa. This result suggests that UTS of the present Fe-Ni-Co-Ti alloys is not determined wholly by the grain size after HPT. In this paper, possible strengthening mechanism in the Fe-Ni-Co-Ti alloys will be discussed.

2:35 PM

Synthesis and Characterization of Nanocrystalline High Entropy Alloys: *Koteswararao Rajulapati*¹; P Chandrashekar¹; M Sundararaman¹; K Bhanu Sankara Rao¹; ¹University of Hyderabad

High entropy alloys are a new class of alloys whose thermodynamic stability is achieved mainly by maximizing their configurational entropy and this can be maximized by making alloys of equi-atomic composition with large number of constituent elements. These materials have been reported to form as simple solid solutions than intermetallic compounds and have exhibited high thermal stability even at elevated temperatures. The present study reports the results of investigations carried out on the stability of two equi-atomic alloys of Al-Ti-V-Cu-Zn-Nb and Al-Cu-Co-Cr-V-Zn compositions processed by mechanical alloying. The milled as well as the aged powders are characterized by XRD, SEM, TEM and DSC to determine their crystal structure, microstructural and morphological changes occurring in them, their thermal stability and the grain growth kinetics. The influence of different synthesis routes on the nature and stability of these alloy powders has also been investigated in this work.

2:50 PM Invited

Influence of Strain Path on the Fracture Behavior of Severely Plastically Deformed Iron: *Anton Hohenwarter*¹; Reinhard Pippan¹; ¹Erich Schmid Institute of Materials Science, Austrian Academy of Sciences

The fracture behavior of pure iron, deformed by equal channel angular processing was under investigation. The fracture toughness was determined for different crack plane orientations and additionally with respect to two different deformation routes, route A and route Bc, respectively. The results demonstrate that for route A the crack plane orientation has a tremendous influence on to the fracture toughness. For route Bc the crack plane influence is less pronounced, however, in comparison to route A a strong increase of fracture toughness was found. The relation between the microstructure depending on the deformation route leading to the same strength but to enormous differences in the fracture toughness will be in focus of this paper.

3:10 PM

Microstructure Evolution and of a F138 Austenitic Stainless Steel after Severe Plastic Deformation: *Andrea Klikauga*¹; Sergey Dobatkin²; ¹Universidade Federal de São Carlos - UFSCar; ²Baikov Institute of Metallurgy and Materials Science RAS

A F138 austenitic stainless steel was solution heat treated, deformed by equal channel angular extrusion (ECAE) at room temperature up to 2 passes and at 300°C up to 4 passes and deformed by high pressure torsion at 300 and 480°C, applying 6GPa pressure and 5 turns. Microstructure evolution was observed by transmission electron microscopy (TEM), electron back-scattered diffraction (EBSD) and X-ray diffraction. The ECAE processed material had a uniform distribution of deformation whereas the deformation of the HTP samples was much more intense at the outside diameter. At room temperature deformation twinning was the predominant deformation mechanism. Further deformation led to grain subdivision inside deformation bands and the onset of new grains formation after 2 ECAE passes. The deformation at 300 and 480°C lead to the formation of recrystallized grains of the order of 100 nm size. No martensite formation was observed by selected area and x-ray diffraction.

3:25 PM

Grain Size Effect on High Speed Deformation of Hadfield Steel: *Rintaro Uejji*¹; Daisuke Kondo¹; Yoshinori Takagi¹; Takashi Mizuguchi¹; Yasuhiro Tanaka¹; Kazunari Shinagawa¹; ¹Kagawa University

Hadfield steel with chemical composition of 12mass%Mn-1% C-bal.%Fe were rolled and subsequently annealed at various temperature to obtain the samples with various mean grain sizes ranging from 1.3 micron to a few 10 micron. Tensile test were conducted at wide range of constant strain rate from 0.001/sec (quasi-static) to 1000/sec (high speed). At the quasi-static test, the fractures of all samples took places without necking



TMS 2012

141st Annual Meeting & Exhibition

and the fracture surfaces indicates brittle like manners. When the strain rate changed to the high speed state, both the strength and the elongation improved largely in all the samples. The fracture at high speed in the samples with conventional grain size happens in ductile manner with necking, whereas that in the fine grained samples was similar to the brittle fracture at quasi-static state. These tendencies were discussed especially focused on twinning behaviors.

3:40 PM

Austenitization Process in a Nanostructured Ferritic Steel Produced by Means of Surface Mechanical Attrition Treatment: *Z.B. Wang¹, L.M. Wang¹, K. Lu¹*; ¹Institute of Metal Research, Chinese Academy of Sciences

A nanostructured surface layer was produced on a ferritic steel (Fe-9Cr) by means of surface mechanical attrition treatment (SMAT). The mean grain sizes of ferrite and carbides in the top surface layer are ~ 8 and 4 nm, respectively. And they increase gradually with increasing depth. In-situ X-ray diffraction and differential scanning calorimetry were used to investigate the austenitization process in the nanostructured surface layer during heating. It was shown that the austenitization temperature decreases gradually with decreasing depth and is ~ 120 K lower in the top SMAT surface layer than in the original sample. In addition, the two-step austenitization process in the original sample becomes a one-step process in the SMAT surface layer. Further microstructural observations of the SMAT sample after annealing showed that an obvious reduction of ferrite grain size occurs after the austenitization during heating and the reversed decomposition of austenite during cooling.

3:55 PM Break

4:10 PM Invited

Recent Progress in High-Entropy Alloys: *Ming-Hung Tsai¹, Jien-Wei Yeh²*; ¹North Carolina State University; ²National Tsing Hua University

It has been considered that alloys consisting of a greater number of principal elements will form complicated and brittle microstructures. Hence research regarding such alloys has received little attention. To overcome this misunderstanding high-entropy alloys (HEAs) have been proposed and explored since 1995. With the high mixing entropy HEAs tend to have simplified microstructures with solid-solution phases. This new alloy concept generates numerous alloys and activates a new research area beyond traditional alloys. In addition to high entropy effect, sluggish diffusion, severe lattice distortion, and cocktail effects are significant in affecting the structures and properties of HEAs. HEAs have been found to possess a wide spectrum of microstructures and properties, and hence provide a number of promising applications. This presentation reviews the recent progress in HEAs and also forecasts the future trend.

4:30 PM

Refinement of Second Phase Particles in Creep-Resistant Iron Aluminides using High-Temperature Severe Plastic Deformation: *David Morris¹, Maria Muñoz-Morris¹*; ¹CENIM, CSIC

Severe plastic deformation (typically by Equal Channel Angular Pressing or High Pressure Torsion) is useful for processing ductile materials to obtain fine grain sizes. This study uses multidirectional high strain forging at high temperatures in order to refine coarse second-phase particle dispersions. The materials examined are cast iron aluminide alloys containing different borides or Laves phase. Following forging to strains of about 4-6, materials have relatively coarse grain sizes with greatly refined second phase particles. It is easy to refine particles by fracture from elongated to equiaxed morphology, but further refinement requires strain levels well beyond the capability of the forging technique. The choice of alloy composition and casting conditions, as well as morphology and intrinsic mechanical behaviour of the second phase, are important for determining the evolution of particle size. Excellent creep resistance has been demonstrated after severe plastic deformation has led to extensive second phase particle refinement.

4:45 PM

Thickness Effect in Micro Drawing of Ultrafine and Coarse Grained Copper: *Andrey Molotnikov¹, Rimma Lapovok¹, Chengfan Gu¹, Chris Davies¹, Yuri Estrin¹*; ¹Monash University

The effect of the blank thickness in deep drawing operation was investigated by modelling and experiment. The thickness of a copper blank was varied and deep drawing was done for coarse grained and ultrafine grained material, leading to a change in the thickness-to-grain diameter ratio. For the coarse grained copper a decrease in maximum load was detected, which cannot be predicted by classical continuum plasticity models. The drawing force drops with decreasing thickness when the sheet thickness falls below a critical level (a fifteen-fold of grain diameter in our case). The proposed dislocation density based model, which accounts for the effects of specimen dimensions and grain size, was used to calculate the Limiting Drawing Ratio. It was found that in deep drawing process biaxial ductility does not suffer to the same extent as uniaxial tensile ductility after grain refinement to sub-micron levels, while strength of the material is improved significantly.

5:00 PM

Accumulative Roll Bonding of Cu-Mo Multilayers: Mechanical Property-Microstructure Relations: *Girija Marathe¹, Rainer Hebert¹*; ¹University of Connecticut

The repeated rolling and folding of arrays of metallic foils produces bulk samples with nanoscale laminate- or particulate composite microstructures. Among the most interesting and challenging aspects is the mutual interaction between microstructures, deformation modes, and mechanical properties. Using Cu-Mo multilayers as an example of the technologically important class of Cu-bcc composites, the role will be highlighted of the initial temper condition of the starting foils and the difference in the mechanical properties of the starting foils on the microstructure- and hardness evolution. The formation of shear bands during the initial ARB stage is affected by the initial temper condition. By contrast, the hardness ratio between the component layers approaches a range between about 1.2 and 2.5 over an intermediate strain range irrespective of the initial hardness ratio. The results provide guidelines for the synthesis of nanolaminate or nanoparticulate composites with ARB processing.

5:15 PM

Combination of DRECE Process and Heat Treatment to Achieve Refining Structure of Brass: *Stanislav Rusz¹, Karel Malanik², Jan Kedron¹, Jan Dutkiewicz³, Lubomir Cizek¹, Stanislav Tylsar¹, Michal Salajka¹*; ¹VSB - Technical University of Ostrava; ²VUHZ a.s.; ³Institute of Metallurgy and Materials Science of Polish Academy of Sciences

Contribution concerned the whole production of UFG materials, using forming process DRECE (Dual Roll Equal Channel Extrusion) in brass. This research concerned the whole production of UFG materials, using Severe Plastic Deformation (SPD). Use of these materials is very versatile – either directly as semi-products for subsequent further processing with lower number of operations (created structure is preserved in final products), or for production of final products from semi-products. The heat treatment of part of sheet was applied after DRECE processing. Preliminary metallographic analysis was performed for indicative information, so as to find whether grains were really refined. Mechanical properties of studied samples were tested by Vickers hardness method. Keywords: DRECE machinery, hardness, structure

5:30 PM

Microstructural Evolution and Mechanical Behaviour of Warm Multi-Axially Forged HSLA Steel: *Aditya Padap¹, G Chaudhari², V Pancholi², S Nath²*; ¹Bundelkhand Institute of Engineering and Technology Jhansi, UP India 284128; ²Indian Institute of Technology Roorkee, India

In the present work, detailed studies are conducted on the microstructural evolution and mechanical behavior of a high strength low alloy (HSLA) steel processed by warm multi-axial forging (MAF). After nine MAF

strain steps, the initial ferrite grains of average 13 μm size reduced to submicron sized grains with over 0.7 fraction of high angle grain boundaries. Pearlitic cementite is fragmented and refined to about 50-100 nm size particles. The microstructure evolution with respect to fraction of HAGB with increase in number of strain steps is more sluggish in HSLA steel as compared to plain carbon steel of comparable carbon content. This is ascribed to the Zener pinning effect of (Ti, Nb) carbide particles. Tensile strength and hardness values of MAFed steel increased by more than 45% and 58 % respectively after nine warm MAF strain steps, whereas the fracture strain was reduced from 21 to 12%.

2012 Functional and Structural Nanomaterials: Fabrication, Properties, Applications and Implications: Nanomaterials for Energy Technology

Sponsored by: The Minerals, Metals and Materials Society, TMS Electronic, Magnetic, and Photonic Materials Division, TMS: Nanomaterials Committee

Program Organizers: Jiyoung Kim, University of Texas; David Stollberg, Georgia Tech Research Institute; Seong Jin Koh, University of Texas at Arlington; Nitin Chopra, The University of Alabama; Terry Xu, UNC Charlotte

Wednesday AM
March 14, 2012

Room: Pelican 1
Location: Swan Resort

Session Chairs: Terry Xu, Univ. North Carolina at Charlotte; Deyu Li, Vanderbilt University

8:30 AM Introductory Comments

8:35 AM Invited

Selected Synthesis Techniques of Thermoelectric Nanomaterials and Their Role in Higher Performance Thermoelectric Materials: *Terry Tritt*¹; Jennifer Graff²; Wenjie Xie²; Xinfeng Tang³; ¹Clemson University; ²Wuhan University of Technology; ³Wuhan University of Technology

This talk will give a brief introduction to thermoelectric (TE) phenomena with an overview of several former and current applications. Several methods will be discussed pertaining to the synthesis of nanomaterials that can be incorporated into a bulk matrix as well as methods that yield in-situ growth of nanodots. Both of these methods yield what is termed as a nanocomposite; nanomaterials incorporated into a bulk TE matrix. The compaction techniques, specifically spark plasma sintering allow these materials to be densified into a bulk pellet, that is typically very close to the theoretical density of the matrix. The ability to decouple the electron and phonon scattering mechanisms is very important in the development of higher efficiency thermoelectric (TE) materials, wherein the figure of merit, ZT, can be greater than unity. Recent results in TE nanomaterials as well as TE nanocomposites from several research groups, including my own, will be presented.

9:10 AM Invited

Thermal Transport Through Individual Nanowires/Nanotubes and Their Contacts: *Deyu Li*¹; ¹Vanderbilt University

Nanoscale thermal transport attracts much attention over the past decade because of its important applications in thermoelectric energy conversion and thermal management of microelectronic and optoelectronic devices. Thermal transport through individual nanowires and nanotubes and their contacts is of particular interest because of the intriguing underlying physics involved. In this talk, I will present experimental measurements of thermal conductivities of individual nanowires and nanotubes and thermal boundary resistance between these nanowires and nanotubes. The effects of various factors, such as nanowire surface, alloying, and van der Waals interactions, on phonon transport through these nanostructures and

interfaces will be discussed. Better understanding of these mechanisms will help to engineering thermal properties of nanostructured materials for different applications.

9:45 AM

Structure and Thermomechanical Behavior of Nanoporous Nickel Thin Films: *Lei Wang*¹; Jiang Xu¹; ¹University of Kentucky

High-purity nanoporous nickel (np-Ni) thin films with fine ligaments were successfully produced from NiMg precursor films using the dealloying method. The dealloyed films exhibit a microstructural length scale comparable to Raney nickel, with an average ligament width less than 7nm, and are thus potential candidates for catalytic applications. High-resolution scanning and transmission electron imaging was performed to characterize the structure and morphology of np-Ni films. Thermomechanical behavior was investigated with thermal cycling and stress relaxation experiments performed in a wafer curvature system. np-Ni films exhibited linear, thermoelastic stress-temperature curves between room temperature and 250°C. Elastic modulus was calculated from these tests and combined with measurements of the films' relative density to investigate the scaling relationships for porous material mechanical behavior. Finally, activation energies for the stress relaxation mechanisms in films of various thickness were determined and will be discussed.

10:00 AM Break

10:15 AM Invited

All Inorganic "Sensitized" Solar Cells Based on Large Bandgap Semiconductors: *Yong Zhang*¹; ¹UNC Charlotte

Wide bandgap semiconductors are typically used as transparent conductive electrodes, passivation layers, and carrier transporters in optoelectronic devices. For a single junction solar cell, conventional wisdom would suggest to find a semiconductor with a bandgap in the range of 1.0 – 1.6 eV to serve as the absorber layer, based on the Shockley-Queisser detailed balance theory. However, it has been recently predicted that when two large bandgap semiconductors form a type II heterojunction, it can absorb a much broader spectrum of light than they are alone, due to the type II interfacial transition, as though the heterojunction has a much lower bandgap than any of the components. One could view this approach as two large bandgap components mutually sensitizing each other. The feasibility of this idea has recently been demonstrated using a ZnO/ZnSe core/shell nanowire array solar cell with a photoresponse threshold of ~1.6 eV.

10:50 AM

Catalytic Properties of AgCu Bimetallic Nanoparticles for PEMFC Cathode: DFT Study: *Kihyun Shin*¹; Da Hye Kim¹; Sang Chul Yeo¹; *Hyuck Mo Lee*¹; ¹KAIST

Noble metals such as Pt have been widely used for catalysts such as in fuel cells. However, due to the high price of Pt, there have been many efforts to reduce the Pt amount or substitute it. We considered AgCu bimetallic nanoparticles as an ORR catalyst. We studied firstly the structural stability of Ag, Cu, and AgCu bimetallic nanoparticles with different sizes and configurations by using DFT calculations. To evaluate the catalytic properties, we determined the oxygen adsorption site and the adsorption energy for each nanoparticle and obtained the energy barrier for oxygen dissociation. Oxygen dissociation is the rate determining step in ORR. As a result, we found the effect of size, configuration, and alloying effect on the oxygen adsorption energy and the energy barrier for oxygen dissociation. Through the comparison of the catalytic properties of each nanoparticle, we propose a new available catalyst for ORR.



TMS 2012

141st Annual Meeting & Exhibition

11:05 AM

High-Performance Electrochemical Capacitors Based on Nanocomposites of Transition Metal Oxide Aero-Gel / Vertically Aligned Carbon Nanotubes: *Minsub Oh*¹; *Younghak Song*¹; *Sangmin Kim*²; *Haseok Jeon*¹; *Ju Hee Kim*³; *Haekyoung Kim*³; *Seungmin Hyun*²; *Hoo-jeong Lee*¹; ¹Sungkyunkwan University; ²Korea Institute of Machinery & Materials; ³Yeungnam University

Electrochemical capacitors have received much attention as a candidate for a next-generation battery. Nevertheless, the development has been hampered by their inherently-low energy density. Recent several studies have proposed nanostructured materials or hybrid materials that combine conductive carbon-based materials with nanostructured metal oxide to improve the energy density by utilizing the high surface areas of nanostructured materials. Here, we combined vertically-aligned carbon nanotubes grown using thermal CVD and aero-gel transition metal oxide (NiCo₂O₄) including several nanometer-sized pores. The hybrid structure was designed to enhance the electrical conductivity of the electrode while increasing the surface area. A careful characterization of the hybrid structure using various characterization tools such as XRD, SEM and TEM helped us elucidate the details of the morphology and microstructure of the aero-gel oxide coated on the VACNTs. The results underscore that the morphology and microstructure of the electrode critically determined the electrochemical properties of the electrode.

11:20 AM

3D Multiwall Carbon Nanotubes (MWCNTs) for Li-Ion Battery Anode: *Chiwon Kang*¹; *Indranil Lahiri*¹; *Rangasamy Baskaran*²; *Mansoo Choi*²; *Won Gi Kim*²; *Yang-Kook Sun*²; *Wonbong Choi*¹; ¹Nanomaterials and Device Laboratory, Department of Mechanical and Materials Engineering, Florida International University, USA; ²Department of Energy Engineering, Hanyang University, Seoul, Korea

Carbon nanotubes have attracted great attention as promising electrode materials for Li-ion batteries due to major advantages including large surface area and low resistance path. We developed novel multiwall carbon nanotubes (MWCNTs) based 3-dimensional anode for high-efficiency Li-ion batteries. The MWCNTs were synthesized through catalytic thermal chemical vapor deposition (CVD) on 3-dimensional Cu electrode. The 3D Cu electrode played a crucial role in accommodating much larger number of MWCNTs, leading to more amount of Li⁺ ion intake. Results from electrochemical characterization of Li-ion battery with 3D anode indicate better properties as compared to those with MWCNTs on 2D Cu foil anode. In addition, MWCNTs with sputtered amorphous Si (a-Si) layer on them (a-Si/MWCNTs core-shell structure) were also used as anode using a 3D geometry and improved electrochemical properties of these modified MWCNT anode were observed. Moreover, relation between electrochemical performance and structural properties of the MWCNTs and hybrid a-Si/MWCNTs composite on 3D Cu electrode is discussed.

2012 Symposium on Surfaces and Heterostructures at Nano- or Micro-Scale and Their Characterization, Properties, and Applications: I-Energy II-Magnetic Materials III-Chemical Sensing and Surfaces

Sponsored by: The Minerals, Metals and Materials Society, TMS Electronic, Magnetic, and Photonic Materials Division, TMS Materials Processing and Manufacturing Division, TMS: Energy Conversion and Storage Committee, TMS: Nanomaterials Committee, TMS: Surface Engineering Committee, TMS: Young Leaders Committee, TMS: EMPMD Council

Program Organizers: Nitin Chopra, The University of Alabama; Ramana Reddy, The University of Alabama; Arvind Agarwal, Florida International University; Sandip Harimkar, Oklahoma State University; Jiyoung Kim, University of Texas at Dallas; Christopher Matranga, National Energy Technology Laboratory

Wednesday AM
March 14, 2012

Room: Pelican 2
Location: Swan Resort

Session Chairs: Sumit Chaudhary, Iowa State University; Nitin Chopra, The University of Alabama; Jiyoung Kim, University of Texas at Dallas

8:30 AM

Transport and Electrical Properties of Two Dimensional Hole Gas in δ -MIGFET in GaAs: *Outmane Oubram*¹; *Oracio Navarro Chávez*²; *Luis Manuel Gaggero-Sager*³; ¹Instituto de Investigaciones en Materiales, Universidad Nacional Autónoma de México; ²Instituto de Investigaciones en Materiales, Universidad Nacional Autónoma de México; ³Facultad de Ciencias, Universidad Autónoma del Estado de Morelos

Rapid and predictable scaling of planar CMOS devices is becoming difficult. As it is well known to conserve the MOORE's law within the conventional microelectronics technology is very hard, so searching for new alternative is critical. We study hole transport and electrical properties in a new alternative device δ -MIGFET (Delta-Multiple Independent Gate Field Effect Transistor) in GaAs. In this work we will analyze hole transport phenomena, due to ionized impurity scattering in a δ -MIGFET. We report theoretical results for hole transport in a δ -MIGFET using the hole structure of the device. The differential capacitance and resistivity are analyzed as well as the regions where the device is operating in digital or analog mode. The width of the Ohmic region and the Negative Differential Resistance (NDR) properties of the system are also characterized.

8:45 AM

Electrochemical Behavior of Nanoceria in Different pH Solution: *Shashank Saraf*¹; *Naveen Chandrasekaran*¹; *Sudipta Seal*¹; ¹University of Central Florida

Cerium oxide has found its uses in many applications because it catalytic converter in automobiles, radiation protective coatings, solid oxide fuel cells, biosensors etc. All of these require cerium oxide molecule to be electrochemically active which should have redox potential associated. In literature there are reports of redox potential of cerium ions in different pH and those plots are termed as Pourbaix diagram. So it's imperative to measure redox potential of cerium oxide molecules as well. In this report we propose to find redox potential of cerium oxide in different pH by

using ceria coating on platinum substrate by using cyclic voltammetry experiments. The redox potential of bulk will then be compared with nano cerium oxide molecules having different morphologies, chemical state and shape. Obtained ceria coatings will be first characterized by SEM, XPS and XRD to know their morphology and measure chemical state and crystallite size respectively.

9:00 AM

Facile Preparation and Advanced Characterization of ZnO Nanoparticles: *Hulya Kafelen*¹; Kasim Ocakoglu¹; Emre Erdem²; ¹Mersin University; ²Institut für Physikalische Chemie I, Albert-Ludwigs-Universität Freiburg

Zinc oxide (ZnO) nanoparticles have a great attention in recent years due to their potential and promising technological applications in gas sensors, light-emitting materials, nonlinear optics and field-effect transistors. In this study, elemental ZnO powders (Merck, 99.9%, particle size 7.4 μm) were milled for 0, 10, 20, 30 min in a FreezerTM Magneto/Mill. A significant broadening of X-ray diffraction peaks and decrease of their intensities with milling time were observed as a result of grain refinement and build up strain during milling. Crystallite size of nanoparticles after 30 min of milling was measured as ~ 35 nm by using TOPAS 3 (BrukerTM AXS) software whereas from scanning electron microscope analysis we obtained 45 nm mean particle size for the spherical ZnO particles for the same milling time. Electron paramagnetic resonance (EPR) results revealed strong surface effects by going to nanosize ZnO indicating the increase of concentration of defect centers at the surface.

9:15 AM Invited

Spherical Barium Ferrite (S-BaFe) Nanoparticles for Ultra High-Density Information Data Storage: *Yang-Ki Hong*¹; Jeevan Jalli¹; Sung-Hoon Gee²; ¹The University of Alabama; ²Seagate Technologies

Recently, using ultra-fine hexagonal barium ferrite platelets (H-BaFe) tape media, a recording aerial density of 29.5 Gb/in² was demonstrated [1]. H-BaFe platelets form poker-chip-like stacks, thereby, degrading the media recording capability, i.e. poor signal-to-noise ratio (SNR) [2]. To achieve better media recording performance, S-BaFe particle was proposed [3]. We converted spherical magnetite [4] and spinel barium-iron oxide [5] to 24 - 30 nm and 25 - 45 nm S-BaFe particles, respectively. Saturation magnetization (ss) and coercivity (Hc) of S-BaFe particles were higher than 40 emu/g and 4 kOe. To estimate the thermal stability factor (KuV/kBT) of the S-BaFe particles, dynamic coercivity measurement was performed. The thermal stability factor was measured to be greater than 80. This study suggests that S-BaFe nanoparticles are thermally stable and suitable for higher recording density media application than 29.5 Gb/in² if other recording factors are optimized. *Supported by Information Storage Industry Consortium (INSIC).

9:50 AM Invited

Perpendicular Magnetic Tunnel Junctions for Spin-Torque Transfer Random Access Memory (STT-RAM): *Subhadra Gupta*¹; Anusha Natarajarathinam¹; Amritpal Singh¹; ¹The University of Alabama

Fully perpendicular magnetic tunnel junctions have a clear advantage for non-volatile spin-torque transfer random access memory (STT-RAM). However, such perpendicular MTJ's have been seen to have limited tunneling magnetoresistance (TMR) compared to MgO-based in-plane tunnel junctions. We will present an overview of the science and technology of the fabrication and growth of perpendicular MTJ's, including an analysis of what limits the TMR. We will detail exciting new developments in this field that result in much higher TMR of about 40% and improved switching times that may make this technology a competitive and viable one for the future. Micromagnetic simulations that closely match the experimental results will be shown. Transmission electron microscopy (TEM) and local electron atom probe (LEAP) characterization were carried out on these MTJ's to understand better the correlation between structural and magnetic properties of these devices.

10:25 AM Break

10:30 AM Invited

Nanocomposite Soft Magnetic Materials: Role of Composition on Properties(Invited): *Matthew Willard*¹; Maria Daniil²; Keith Knipling¹; ¹Naval Research Laboratory; ²George Washington University

Over the past two decades, a major focus of research has been microstructure refinement to the nanoscale, which has enabled reduction in coercivity. These advantages originate in the exchange correlation length – a fundamental magnetic length scale determined by the strength of coupling between magnetic moments causing them to align – which has typical values with nanoscale dimensions. This presentation will highlight recent work on nanocomposite soft magnetic materials produced by rapid solidification processing over a broad composition range. The effect of nanostructure and the role of composition on the magnetic material performance will be shown experimentally with theoretical discussion.

11:05 AM Invited

Optical Thin Films for Gas Sensing in Advanced Coal Fired Power Plants: *Paul Ohodnicki*¹; Thomas Brown¹; John Baltrus¹; Sittichai Natesakhawat²; Congjun Wang³; ¹National Energy Technology Laboratory; ²National Energy Technology Laboratory and University of Pittsburgh; ³National Energy Technology Laboratory and URS Corporation

The National Energy Technology Laboratory (NETL) is developing technologies for the next generation of higher-efficiency, lower emission fossil-fueled power plants, including oxy-fuel combustion processes for carbon capture and sequestration, and coal gasification to produce H₂-rich synthetic gas which can be converted to electrical power using solid-oxide fuel cells or gas turbines. Improved sensor technologies that can operate under extreme conditions (high temperature, high pressure, corrosive gases) are needed for process monitoring and control. Optical sensors based on metal oxide thin films are important candidates, and an improved understanding of the fundamental link between structural/chemical changes in thin films and measured optical properties in the presence of various gas species under relevant conditions is needed to aid in sensor development efforts. Results of synthesis and characterization of metal oxide-based films will be presented, and future work plans that fully leverage unique expertise and facilities available at NETL will be discussed.

11:40 AM

Hierarchical Metallic and Ceramic Nanostructures via a Hybrid Approach Combining Laser Interference Ablation and Block Copolymer Phase Separation: *Taiwo Alabi*¹; Dajun Yuan¹; Suman Das¹; ¹Georgia Institute of Technology

We report on a novel approach that combines pulsed laser interference ablation and block co-polymer phase separation to enable the formation of periodic metallic and ceramic nanostructures having a primary ordering (30-100 nm range) conforming with the domain spacing in a phase separated PS-P4VP polymer, and a secondary ordering (0.2 to 2 microns range) conforming with the periodicity of interfering laser beams. The primary domain spacing of the nano-structures was varied by tuning the loading time of the block copolymer thin films and changing the length of the P4VP chain of the block copolymer. The secondary ordering was varied by changing either the intensity of Nd:YAG nanosecond light source, angle of interfering beams, or number of interfering beams. The nanostructures were characterized with AFM, SEM, XPS and XRD characterization techniques. Data obtained indicates the formation of PtO₂, PdO₂, Au and Fe₂O₃ hierarchical features with some degree of crystallinity.



TMS 2012

141st Annual Meeting & Exhibition

11:55 AM

Rapid Fabrication of Diverse Two-Dimensional and Three-Dimensional Gold Nanostructures Through Laser Interference Patterning: *Dajun Yuan*¹; Suman Das¹; ¹Georgia Institute of Technology

Gold nanostructures have been extensively studied. Here, we report on the development of a simple, one-step method for the fabrication of diverse 2D and 3D nanostructures through laser interference patterning on gold films over areas spanning 1 cm². Various periodic 2D and 3D nanostructures can be patterned on gold films of thickness 10-500 nm. The variety of possible structures including grooves and gratings with feature sizes ranging from 100 nm to 2 μm, hexagonal close-packed arrays of cavities and holes with feature sizes ranging from 100 nm to 2.5 μm, nanodomes, nanomushrooms, and nanoneedles with feature sizes ranging from 10 nm to 2 μm can be created through careful adjustment of the laser intensity and the interference period. Characterization of the fabricated nanostructures through AFM and SEM reveals the probable mechanisms of their formation through pulsed laser induced melting and resolidification, in combination with surface tension driven effects.

12:15 PM Invited

Development of Superhydrophobic Nano-structured Ceramics to Promote Dropwise Condensation: *Ghazal Azimi*¹; Kripa Varanasi¹; ¹MIT

Developing robust hydrophobic surfaces with improved water repellency and dropwise shedding condensation has been a subject of intense research over the past decades. Conventional approach of fabricating such surfaces include first, creating a rough or textured surface, and then modifying the surface with materials of low surface energy. Most cutting edge research in the field, however, have only focused on designing more complex structures, while overlooking the material aspect, which is equally, if not more important. Such developments, although promising, face major material-related hurdles that limit their scale up and industrial implications. To address these challenges, herein, we developed a novel hydrophobic ceramic that surpasses other ceramics in its ability to repel water droplets, while offering other unique properties, including thermal stability and chemical inactivity. The material developed in this work promoted dropwise condensation with remarkably improved heat transfer coefficient, when tested in a condensation chamber under simulated industrial conditions.

3rd International Symposium on High Temperature Metallurgical Processing: Sintering and Synthesis

Sponsored by: The Minerals, Metals and Materials Society, TMS Extraction and Processing Division, TMS: Energy Committee, TMS: Pyrometallurgy Committee

Program Organizers: Tao Jiang, Central South University; Jiann-Yang Hwang, Michigan Technological University; Patrick Masset, TU Freiberg; Onuralp Yucel, Istanbul Technical University; Rafael Padilla, University of Concepcion; Guifeng Zhou, Wuhan Iron and Steel

Wednesday AM
March 14, 2012

Room: Southern II
Location: Dolphin Resort

Session Chairs: Mark Schwarz, CSIRO; Xiaohui Fan, Central South University

8:30 AM

A Study of Co-V-Al Alloys by Self Propagating High Temperature Synthesis: *Murat Alkan*¹; Ozlem Altinordu¹; Seref Sönmez¹; Onuralp Yücel¹; Bora Derin¹; Vladimir Sanin²; Vladimir Yukhvid²; ¹Istanbul Technical University; ²Institute of Structural Macrokinetics and Materials Sciences

Self-propagating high temperature Synthesis (SHS) process is one of the highly productive and economically reasonable methods for the metallurgical industry. This study covers information about a process

based on self propagating high temperature synthesis to produce Co-V-Al alloys using a mixture of Co₃O₄-V₂O₅-Al powders. Different Co/V ratios are carried out in the SHS experiments; also addition of excess stoichiometric amount of Al₂O₃ between % 0 and % 20 is added to the mixture to decrease the adiabatic temperature of the system. The thermodynamic simulations and the calculations of adiabatic temperature were examined with FactSage program. The samples were characterized by the X-Ray Diffraction method (XRD) and Scanning Electron Microscope (SEM) techniques.

8:45 AM

Strengthening the Sintering of Iron Concentrate Fines by High Pressure Roller Grinding Pretreatment: *Yufeng Guo*¹; Kelang Mu¹; Jiang Tao¹; Dao Su¹; Jinghua Zeng¹; ¹Central South University

The improvement in sintering of fine hematite-limonite concentrate by high pressure roller grinding (HPRG) were investigated in this paper. The results of sinter pot test show that, when HPRG is adopted to pretreat hematite-limonite concentrate, productivity is increased from 1.16t/(m²•h) to 1.53 t/(m²•h) dramatically, and tumbler index of sinter is able to be improved from 64.67% to 67.20%. It is found that ballability of hematite-limonite concentrate is dramatically improved and the ratio of fine particles increases greatly after being pretreated by HPRG, which contributes to better granulation property and higher reactivity in solid phase reaction of hematite-limonite concentrate in sinter process. Thus, the yield and quality of sinter increase accordingly.

9:00 AM

A Study of Ni-Cr-Al Alloys by Self-Propagating High Temperature Synthesis: *Bora Derin*¹; Ozlem Altinordu¹; Murat Alkan¹; Seref Sonmez¹; Onuralp Yucel¹; Vladimir Sanin²; Vladimir Yukhvid²; ¹Istanbul Technical University; ²Institute of Structural Macrokinetics and Materials Sciences, ISMAN

Self Propagating High Temperature Synthesis (SHS) has many advantages such as very short processing time, simple operation, low initiation energy requirement and low cost. After ignition of an SHS initial mixture, the combustion front is formed and propagates throughout the reactant mixture yielding the desired product. The present work proposed a process based on self-propagating high temperature synthesis to produce Ni-Cr-Al alloys using a mixture of NiO and Cr₂O₃, Al and Al₂O₃ powders. The addition of excess stoichiometric amount of Al₂O₃ is added to the mixture to decrease the adiabatic temperature of the system. The thermodynamic simulations and the calculations of adiabatic temperature were examined with FactSage program. The samples were characterized by the X-Ray Diffraction method (XRD) and Scanning Electron Microscope (SEM).

9:15 AM

Research on Sintering Properties of Vanadium-Titanium Magnetite Concentrate: *Xiaohui Fan*¹; Qiang Wang¹; Xuling Chen¹; Min Gan¹; Lishun Yuan¹; Shan He¹; ¹Central South University

The sintering properties of vanadium-titanium magnetite concentrate(VTC) was studied in this paper. Through the optimizing the sintering process of VTC, the suitable granulation moisture and coke proportion were determined. The sintering velocity decreased from 23.05 mm/min to 18.22 mm/min. With the increase of VTC proportion from 0 to 46%, the specific productivity and tumbler index were respectively decreased from 1.55 t/(m²•h) to 1.21 t/(m²•h), and 62.93% to 57.73%. The temperature of liquid phase formations of mixtures increased, the amount of liquid lowered, and the content and sharp of sintering mineral gradually changed with the increase of VTC, these lead that sinter quality became worse.

9:30 AM

Influence of Limonite Proportion on Sinter Quantity and Quality: Xiaohui Fan¹; Dao Su¹; Ganghua Fu¹; Xuling Chen¹; Min Gan¹; Tao Jiang¹; Yufeng Guo¹; ¹Central South University

Sintering properties and performances of typical limonite such as FMG and YD in the sintering of ore fine system and concentrate system are studied. The results show: limonite has big size, in the sintering of limonite and fine, content of small size of mixture reduces, relative basicity of small size of mixture increases, the fluidity of liquid phase is so good that the strength of sinters is bad especially proportion of limonite exceeds 55%. In the sintering of limonite and concentrate which has small size, the size of mixture is more reasonable that suitable fluidity of liquid phase can be produced, besides exothermic reaction of concentrate oxidation can make up heat loss by the remove of crystal water in limonite, data show that the sintering index is good when proportion of concentrate is about 35%~45%, and the coke rate is low.

9:45 AM

In Situ Observation of High Temperature Properties of Iron Ore during Sintering Process: Pei Dong¹; ¹Shougana China

Confocal scanning laser microscope (CSLM) has been applied to carry out the in-situ observation of melting and solidifying characteristics during iron ore sintering process, accompanied with TG-DSC test. It can be found that apparent Liquid phase forming temperature(LFT) and ending solidifying temperature(EST) is about 1190°C and 1160°C, respectively. Forming liquid phase during sintering process go through four courses, that is shrinking, expanding, shrinking and expanding coexisting and expanding totally. For Yandi fine, the corresponding temperature of this four courses is about 1120-1160°C, 1190-1196°C, 1218-1220°C and 1233-1270°C, respectively. Although CAJ fine has more difficulty in forming initial liquid phase, but when liquid phase expands, it may have better fluidity and easier liquid phase formation. Adding enough CaO, CAJ fine takes on high fluidity like Yandi fine, because liquid phase during sintering process is formed mainly by reaction between CaO and Fe₂O₃.

10:00 AM Break

10:10 AM

The Influence of m(V₂O₅)/m(TiO₂) on Compositions and Structures of V-Ti-Fe Alloys: Bin Wang¹; Kuiren Liu¹; Jianshe Chen¹; Jilin He²; ¹Northwestern University; ²Northwest Rose Metal Materials Research Institute

The preparation of V-Ti-Fe master alloys with metallothermic reduction method was studied. The influences of m(V₂O₅)/m(TiO₂) on structures and compositions of the alloys obtained were investigated systematically. The results show that the compositions can be changed flexibly by variations of m(V₂O₅)/m(TiO₂). With reducing m(V₂O₅)/m(TiO₂) ratio, the recovery rate of Ti and V decreases along with an increase in contents of Al and Si impurity. Besides the V-based solid solution phase and the C14-type Laves phase, some impurity phases also exist in the V-Ti-Fe alloys. The results of energy spectrum analysis show that the elements of vanadium and iron distributed uniformly in the alloys. Segregation for titanium, i.e. the titanium-rich phase forms, was detected. It is mainly caused by the rapid cooling process. An appropriate heat treatment and refining process should be adopted to improve the quality of the alloys.

10:25 AM

Air Leakage Online Monitoring and Diagnosis Model for Sintering: Fan Xiaohui¹; Jiang Lijuan¹; Chen Xuling¹; ¹Central South University

In order to solve air leakage of sintering testing cumbersome, inaccurate results, and other issues, the sinter machine air leakage characteristics were studied, and combining the mathematical modeling and the field detection. The temperature before air leakage was calculated by mathematical model, energy balance equation was established according to sintering process, using Adams prediction correction method which has strong stability and high precision, to solve hyperbolic partial differential equation with astringency problem. The temperature after air leakage is

detected by instruments, according to energy conservation calculation the sintering air leakage rate. According to the sintering continuity and periodicity, sintering air leakage location diagnosis expert system was established to judge specific air leakage locations.

10:40 AM

Investigation on the Interfaces of M42/45 Steel Bimetal Composites Sintered by Spark Plasma Sintering: Xu Jinfu¹; You Hang¹; ¹Institute of Materials Engineering, Ningbo University of Technology

The sintering of M42 P/M high speed steel and its jointed to 45 steel had been realized at the same time using Spark Plasma Sintering (SPS) technology, its contact surface's microstructure appearance, element density distribution, microhardness and interphase forming process have been tested and analysed. The analyzing results are as follows: The morphology and micro-hardness of M42/45 steel joints exist as a gradient distribution. The joint hasn't distortion and microcracks, the thickness of transition layer up to 10 ~ 20um. The interface connection of M42/45 steel is comprehensive synergy between fusion connection and diffusion connection, and fusion connection takes a priority at early sintering, while diffusion connection gradually becomes dominant at later sintering.

10:55 AM

Influence of MgO on the Strength of High Basicity Sinter: Xiaohui Fan¹; Wenqi Li¹; Min Gan¹; Guohua Bai¹; Tao Jiang¹; Zhiyun Ji¹; Zhiyuan Yu¹; Xiaoxian Huang¹; ¹Central South University

The influence of MgO on the tumbler index (TI) of high basicity sinter is studied. The result shows that TI of sinter decreases from 71.33% to 61.13% when MgO content increases from 1.15% to 3.5%. The mechanism research shows that the temperature of liquid formation of sintering mix increases and the content of liquid phase decreases with the increase of MgO content. And Mg²⁺ mostly dissolves in magnetite which diffuses into crystal lattice of magnetite and makes the magnetite more stable. So the content of magnetite in sinter increases and needle-like calcium ferrite decreases due to the retarding of magnetite oxidation, which is the main reason of MgO deteriorating TI of sinter. Experiments also indicate that the mineralization ability of dolomite is weaker than that of limestone. TI of sinter can be improved by optimizing the size distribution of dolomite which can facilitate the mineralization of dolomite.

Advances in Surface Engineering: Alloyed and Composite Coatings: Session V

Sponsored by: The Minerals, Metals and Materials Society, TMS Materials Processing and Manufacturing Division, TMS: Surface Engineering Committee

Program Organizers: Sandip Harimkar, Oklahoma State University; Srinivasa Bakshi, Indian Institute of Technology Madras; Arvind Agarwal, Florida International University

Wednesday AM
March 14, 2012

Room: Macaw 1
Location: Swan Resort

Session Chair: To Be Announced

8:30 AM

Tribological Behavior of Plasma Sprayed Al-Si Composite Coatings Reinforced with Different Carbon Allotropes: Mingdong Bao¹; Cheng Zhang¹; Debrupa Lahiri¹; Arvind Agarwal¹; ¹Florida International University

Al-Si composite coatings reinforced with nanodiamond, grapheme nanoplatelet, carbon nanotube and graphite were synthesized by plasma spraying. Effect of addition of carbon in different allotropic forms on the microstructure, hardness, and elastic modulus of the composite coatings is investigated. Tribological performance of different composite coatings and the wear mechanism in the presence of nanodiamond, graphene and graphite are also studied.



TMS 2012

141st Annual Meeting & Exhibition

8:50 AM

Evaluation of Brittle Layers Obtained on Boronized Cr-Mo Based Steels: *Noe Lopez Perrusquia*¹; Marco Doñu Ruiz¹; ¹Instituto Politécnico Nacional

In the present study, identify the fracture toughness and strength adhesion of borided layers on Cr-Mo based Steels by Boronizing, two commonly used steel AISI 4140 and AISI 9840 are considered, the steels contain 1.0, 0.8 wt% Cr and 0.20, 0.25 wt% Mo, respectively. The formation of the borided layers was carried out by the powder pack boriding process at a temperature range of 1123 -1273 K for 4, 6 and 8 h. X-ray diffraction analysis revealed peak of FeB, Fe₂B and CrB, the Fracture toughness of the layers is estimated at 15 and 30 um from surface using four different Vickers indentation loads, using Palmqvist crack model, the adherence of the layer/substrate was evaluate in qualitative form though the Rockwell C. The fracture toughness of the borides depends strongly on temperature and time boronizing. Also, good adhesion is obtained around the Rockwell C indentation prints on the borided layer-substrate-interface.

9:10 AM

Evaluation of Residual Stress in Fe₂B Coating on Ductile Cast Iron: *Marco Doñu Ruiz*¹; Noe Lopez Perrusquia¹; Victor Jorge Cortez Suarez²; David Leoncio Rosado Cruz³; ¹IPN; ²UAM; ³UPVM

The boriding thermochemical treatment enhances mechanical properties, depending on the condition under which it is produced the thin boride layer formed during a pack boriding process may be either Fe₂B or FeB/Fe₂B coatings that influences by the presence of residual stresses. The present study employ the finite element method for evaluate of thermal residual stress across Fe₂B coatings produced on surface Ductile Cast Iron ASTM class 80-55-06, taking into account the power-pack boriding condition, the results of simulation was carried out in ANSYS environment were compared whit the experimental results determinate by means of X-ray Diffraction (XRD) shows that there is very good agreement. It was found that the residual stress varied regular with the heat treatment, globular graphites and the thickness of the coating, the distributions of residual stress determined in the Fe₂B coatings are compressive with magnitudes ranging from -370 to -1537 MPa.

9:30 AM Break

9:45 AM

Regression Model of Oxidation Behavior of 6061 Al/SiC Composite: *Priyamvada Bhaskar*¹; ¹National Institute of Technology, Surathkal

This paper analyses variation of weight gain, Δm , of 6061 Al/SiC composite due to oxidation with time, t , using regression model. Using curve fitting technique, mathematical equations for oxidation behavior of the composite are formulated. The generated data are analyzed and compared with the experimental data. More specifically, regression analysis helps in understanding how the typical value of the mass gain (dependent variable) changes when the time of oxidation (independent variable) is varied, while the other independent variable (Temperature) held fixed. The effect of aging treatment and protective coatings like Aluminium and AlCrN on the oxidation behavior of the 6061 Al/SiC composite was studied. It was observed that coatings increase the oxidation behavior of the composite. The regression analysis carried out shows a two-fold linear variation of weight gain (Dependent variable) with respect to time and temperature of oxidation (Independent variables).

10:05 AM

An Alternative Solution for Aluminium Extrusion Die Surfaces: The Qualified Hard Coatings (AlCrN and AlTiN): *Behiye Yuksel*¹; Yucel Birol¹; ¹TUBITAK MAM Materials Institute

Extrusion is an important method frequently used in forming of aluminum products. The die materials used for the aluminum extrusion process should have a high level of hardness, yield strength and creep resistance as well as chemical resistance at elevated temperature. However the bearing surface of die during extrusion process is exposed to high temperature,

chemical and tribological loads. Wear of the die bearing causes important technological and economic problems. Nowadays, scientists have studied on different applications to further improve the performance of the die. One of them is able to make the bearing surface more wear resistant by different surface treatments. The main aim of this study is the investigation of the wear behavior of AlCrN and AlTiN coatings which is coated by physical vapor deposition (PVD) on AISI H13 hot work tool steel as used almost on extrusion die material.

10:25 AM

On the Production of Mo-MoSi₂ FGM by Diffusion Technology: *Ma Ruixin*¹; Li Shina¹; Zhang Juping¹; ¹USTB

Mo-MoSi₂ functionally graded material, FGM, was fabricated by diffusion the silicon into a molybdenum matrix under high temperature. The effects of temperature and the duration time on the Mo- Mo₃Si₅-MoSi₂ gradient layer characteristics, such as thickness, components, phase and morphology are studied by means of metallographic microscope, XRD and SEM. The experimental results show that when heated at 1350°C and duration time is 300 minutes, a FGM layer was fabricated with a thickness of over 200 μ m. The composition of FGM layer, from surface to molybdenum base, was MoSi₂, Mo₃Si₅, Mo₅Si₃ and Mo. A transition layer of about 5-10 μ m exist between different layer.

Alumina and Bauxite: Energy and Processing Alternative Rawmaterials

Sponsored by: The Minerals, Metals and Materials Society, TMS Light Metals Division, TMS: Aluminum Committee, TMS: Aluminum Processing Committee
Program Organizer: Benny Raahauge, FLSmidth

Wednesday AM
March 14, 2012

Room: Northern E3
Location: Dolphin Resort

Session Chair: Tony Kjar, Gibson Crest Pty Ltd

8:30 AM

Decrease of Heat Consumption at Nepheline Processing to Alumina and By-Products: *Vladimir Kazakov*¹; *Vadim Lipin*²; ¹St. Petersburg State Technologic University of Vegetable Polymers; ²Saint Petersburg State Polytechnical University

It is resulted technological and heat engineering substantiation of the new original hardware-technological scheme of nepheline processing by sintering method. In this scheme the autoclave desilication of aluminate liquor and evaporation of a soda solution are united in one technological process. As a result the degree of thermodynamic perfection (exergic efficiency) raises from 70 up to 90 %, the charge of a steam from thermal power station decreases in 1,6 times, improve of ecological safety and operational reliability of equipment.

8:50 AM

Influence of Na₂O on the Phase Compositions and the Alumina Leaching Properties of Calcium Aluminate Slag: *Yingjie Li*¹; Z. F. Tong²; Lixiu Lian¹; ¹Jiangxi University of Science and Technology; ²Jiangxi University of Science and Technology

The influences of Na₂O on phase composition, self-disintegrating and alumina leaching property of calcium aluminate slag were investigated by XRD, laser particle size analyzer and chemistry analysis, and the measures of eliminating the adverse impacts of Na₂O on calcium aluminate slag were proposed. The results show that when the content of Na₂O is 3% and less than 3%, the main phase are Ca₁₂Al₁₄O₃₃ and γ -Ca₂SiO₄, the self-disintegrating rate of slag is above 90%, the alumina leaching rate is above 80%. The leaching rate is evidently decreased when Na₂O is 4%, which is 75.56%. Decreasing the ratio of n(CaO) and n(Al₂O₃) of slag containing 4% of Na₂O, the leaching rate is 83.5% when the ratio of

$n(\text{CaO})$ and $n(\text{Al}_2\text{O}_3)$ is 1.53, the adverse effects of Na_2O on the slag is basically eliminated, the slag meets alumina leaching requirements.

9:10 AM

Influence of Titania on the Phase Compositions and the Alumina Leaching Properties of Calcium Aluminate Slag: Z. F. Tong¹; Yingjie Li²; Lixiu Lian²; ¹ Jiangxi University of Science and Technology; ² Jiangxi University of Science and Technology

The influences of TiO_2 on phase composition, self-disintegrating and alumina leaching property of calcium aluminate slag were investigated by XRD, laser particle size analyzer and chemistry analysis, and the measures of eliminating the adverse impacts of TiO_2 on calcium aluminate slag were proposed. The results show that when the content of TiO_2 is 2% and less than 2%, the main phases are $\text{Ca}_{12}\text{Al}_{14}\text{O}_{33}$ and $\gamma\text{-Ca}_2\text{SiO}_4$, the self-disintegrating rate of slag is above 95%, the alumina leaching rate is above 85%. The leaching rate is evidently decreased with the content of TiO_2 increasing when TiO_2 is greater than 2%, the leaching rate was only 73.4% with 5% of TiO_2 . To add CaO into 5% of TiO_2 of slag, the leaching rate is 84.1% when the ratio of $n(\text{CaO})$ added and $n(\text{TiO}_2)$ is 1.25, the adverse effects of TiO_2 on the slag is basically eliminated, the slag meets alumina leaching requirements.

9:30 AM

Research of Al and Si Occurrence States on Acid Leaching Performance of High-Alumina Fly Ash: Zhang Ting'an¹; Lv Guozhi¹; Dou Zhihe¹; Nan Xiangli; Song Dan¹; Li Yan¹; He Jicheng¹; ¹Northeastern University

High-alumina fly ash is a kind of important materials for future alumina production. This paper researched the acid leaching performances of fly ash from Western Inner Mongolia, Chongqing and Shanxi of China. Effects of leaching temperature, acid concentration, leaching time and liquid-solid ratio on the leaching performance were investigated as well. Leaching experiments indicate that: the leaching rates of alumina in fly ash from Western Inner Mongolia, Chongqing and Shanxi provinces are 97.41%, 68.94% and 23.61% respectively, under the conditions of leaching temperature 150°C, liquid-solid ratio 20:1, stirring rotary speed 500rpm, leaching time 120min, sulfate concentration 20% and particle sizes $< 74\mu\text{m}$. The effects of existing forms, crystallinity and coating situation of Al-Si phase on leaching performance of high-alumina fly ash were discussed by SEM and XRD. The results show that the crystallinity of fly ash from Western Inner Mongolia is about 75% which is worse than the others.

9:50 AM

Study on the Effect of Si and Silicide on Leaching Al_2O_3 from Magnesium Smelting Reduction Slag: You Jing¹; Wang Yaowu¹; Feng Naixiang¹; Peng Jianping¹; Di Yuezhong¹; ¹Northeastern University

The main phases of the reduction slag from magnesium production by vacuum aluminothermic reduction using dolomite and magnesite as materials and using Al-Si alloy as reductant are $\text{CaO}\cdot\text{Al}_2\text{O}_3$ and $2\text{CaO}\cdot\text{SiO}_2$. It also has amount of unreacted Si. The Al_2O_3 content of reduction slag is about 60% and SiO_2 is about 10%. When leaching Al_2O_3 with a mixture solution of sodium hydroxide and sodium carbonate, Si and SiO_2 would enter into leaching solution and has a negative effect on Al_2O_3 leaching. The effect of Si and silicide on leaching Al_2O_3 from magnesium smelting reduction slag was studied in laboratory. The results show that total Si and partial SiO_2 would enter into leaching solution and react with $\text{NaAl}(\text{OH})_4$ to form $(\text{Na}_2\text{O}\cdot\text{Al}_2\text{O}_3\cdot\text{SiO}_2)_6\cdot 27\text{H}_2\text{O}$ which is present in leaching residue and makes a loss of Al_2O_3 .

10:10 AM

Extracting Alumina from Coal Fly Ash Using Acid Sintering-Leaching Process: Kang Liu¹; Jilai Xue¹; ¹University of Science and Technology Beijing

Local shortages of bauxite in recent years present a challenge to develop a sustainable aluminum industry in China. Coal fly-ash from coal-fired power plants is rich in Al_2O_3 content with potential use as a resource for alumina refinery. This paper will describe our recent investigation on extracting Al_2O_3 from coal fly-ash using an acid sintering-leaching process. Thermal weight loss testing against temperature were first carried out to find an appropriate sintering temperature for avoiding heavy volatilization of the coal fly ash - H_2SO_4 (98%) mixture. Then, the mixture was subjected to sintering at 220°C, dissolving in water at 85°C, adjusting alkaline level in solution by CaCO_3 addition, removing iron by KMnO_4 and MnSO_4 , precipitating $\text{Al}_2(\text{SO}_4)_3\cdot 17\text{H}_2\text{O}$ particles, and heating-treated at 850°C to produce Al_2O_3 powders. The rate of recycling Al_2O_3 can reach 70 – 90 % with relative lower processing temperature and fewer amounts of solid residues.

10:30 AM

Study on Secondary Reaction Mechanism during Alumina Leaching Process of Calcium Aluminate Slag: Wang Bo¹; Sun Hui-Lan²; Yu Hai-Yan¹; Pan Xiao-Lin¹; Tu Gan-Feng¹; ¹Northeastern University; ²Hebei University of Science and Technology

SiO_2 of calcium aluminate slag exists in the form of $\gamma\text{-}2\text{CaO}\cdot\text{SiO}_2$ which is more stable than $\beta\text{-}2\text{CaO}\cdot\text{SiO}_2$. But it will also be decomposed by sodium carbonate solution during alumina leaching process, and this will cause the occurrence of secondary reaction. The occurrence degree of secondary reaction of calcium aluminate slag is studied in this paper, and its effect mechanism is discussed by the methods of XRD and SEM. The results show that the decomposition ratio of $\gamma\text{-}2\text{CaO}\cdot\text{SiO}_2$ increases as leaching time and sodium carbonate concentration go up, and the main product of secondary reaction is hydrate garnet. SiO_2 concentration of solution rises at first then dropped with the increase of leaching temperature. XRD results indicate that the stable product of secondary reaction is hydrate garnet at lower temperature, but under higher temperature, hydrate garnet transforms into sodium hydrate alumina-silicate.

10:50 AM

Production of Novel Zeolite of Type Na-P from Sodium Aluminate Liquor/Spent Liquor/Alumina Tri-Hydrate of Nalco's Alumina Refinery, Damanjodi, Orissa, India: A Unique Builder Material for Detergent Formulation: Chitta Mishra¹; ¹National Aluminium Company Limited

A process for production of novel synthetic crystalline porous aluminosilicate Zeolite Na-P consisting of the oxides of silicon and aluminium represented by the formula $a\text{Na}_2\text{O}:\text{Al}_2\text{O}_3:b\text{SiO}_2$, wherein $a = 0.1 - 1.0$ and $b = 2.2 - 5.0$ has been developed from three different raw materials viz. Sodium Aluminate Liquor/ Spent Liquor /Alumina Tri-hydrate of NALCO's Alumina Refinery, Damanjodi, Orissa. Zeolite Na-P was produced by preparing a gel by mixing Sodium Silicate, Sodium Aluminate Liquor/Spent Liquor/Alumina Tri-hydrate, autoclaving the gel at 80-150°C for a period of 2hrs to 4 days under static or stirred condition, quenching the resultant crystalline material in cold water, separating the catalyst formed, washing with water, drying the solid catalyst at a temperature of 80-120°C for a period of 3-12 hrs to obtain the product which can be used as a builder material for detergent formulation.



TMS 2012

141st Annual Meeting & Exhibition

Aluminum Alloys: Fabrication, Characterization and Applications: Material Characterization

Sponsored by: The Minerals, Metals and Materials Society, TMS Light Metals Division, TMS: Aluminum Processing Committee
Program Organizers: Subodh Das, Phinix LLC; Tongguang Zhai, University of Kentucky; Zhengdong Long, Kaiser Aluminum

Wednesday AM Room: Northern E1
March 14, 2012 Location: Dolphin Resort

Session Chair: William Golumbfskie, Naval Surface Warfare Center

8:30 AM

Characterization of High Strength Wrought and Rapidly Solidified Al Alloys for Aero Engine Applications: *Eric Ott*¹; ¹GE Aviation

Potential aero engine applications of aluminum are expected to be subjected to combinations of high static and cyclic stress, thermal cycles where aging effects may become a consideration, and the presence of salt-containing corrosive environments. Assessment of the properties, stability and corrosion resistance of several alloys including 7075, 7055, 2099, and selected dispersion and precipitation-strengthened, rapid-solidification processed alloys will be presented. Sensitivity to thermal exposure was assessed at times up to 2000 hours and temperatures up to 300°F. Environmental testing involved salt spray testing via ASTM B117 for times up to 168 hours followed by tensile testing and comparison to unexposed samples. Processing of rapidly solidified alloys was performed by several techniques and materials were subjected to extrusion prior to testing. Results and key considerations for aero engine applications of Al will be presented.

8:50 AM

Metallographic Identification of Phases in 5xxx Series Aluminum Alloys: *Young-Ki Yang*¹; Todd Allen¹; ¹University of Wisconsin

Nine different phases in 5083 aluminum alloys in H131 and H116 tempers were metallographically identified in a clear and consistent manner using scanning electron microscopy (SEM). Four Fe-rich, two Mn-rich, one Si-rich, one Cu-rich, and β phase (Al_3Mg_2) were found in as-received material. Cu-rich phase, in particular, was commonly observed in materials annealed at around 290 °C. β phase was found not only in material artificially sensitized, for example, at 100 °C but also in as-received material. Many of these phases were identified with SEM for the first time which sheds light on the overall characteristics of the microstructure. These accomplishments were made possible by the development of a new etching solution, dissolved ammonium persulfate in water. This solution can increase data gathering statistics of in-depth microstructure analysis in 5xxx series aluminum alloys significantly by allowing the use of SEM rather than transmission electron microscopy (TEM).

9:10 AM

Studies on Flow Characteristics at High-Pressure Die-Casting: *Christian Chimani*¹; Richard Kretz¹; Simon Schneiderbauer²; Stefan Puttinger²; Stefan Pirker²; ¹LKR Leichtmetallkompetenzzentrum Ranshofen GmbH; ²JKU Johannes Kepler Universität

The flow and filling characteristics influence product quality of high pressure die castings. A planar jet of liquid aluminum is formed at the ingate due to its high inlet velocity. The ingate design triggers the flow characteristics of the jet. Analytical investigations show that the process of drop formation at the liquid planar free jet is dominated by atomization at the ingate. Numerically, high-pressure die casting is attacked by a Volume of Fluid approach. Drop formation at the phase interphase cannot be captured by the numerical model since drops are much smaller than feasible grid spacings. Global spreading of the free jet in the casting mold is well pictured by this first numerical simulation. Experimentally the

process is studied by water modelling validating the numerical results. The observed flow characteristics are discussed in comparison to product quality results observed in Al pressure die casting parts of the similar design.

9:30 AM

Electrohydraulic Sheet Metal Forming of Aluminum Panels: *John Bonnen*¹; Sergey Golovoshchenko¹; Scott Dawson¹; Alexander Mamutov²; Alan Gillard¹; ¹Ford Motor Company; ²Oakland University

In this paper, we present results of testing from sheet metal forming trials using pulsed electrohydraulic technology. Pulsed electrohydraulic forming is an electrodynamic process, based upon high-voltage discharge of capacitors between two electrodes positioned in a fluid-filled chamber. Electrohydraulic forming (EHF) combines the advantages of both high-rate deformation and conventional hydroforming, and electrohydraulic forming allows more uniform distribution of strains, widens the formability window, and reduces elastic springback in the final part when compared to traditional sheet metal stamping. This extended formability allows the fabrication of aluminum panels that are difficult to make by conventional stamping of EDDG steel, and it thereby vastly improves the number automotive weight reduction opportunities. The paper presents discoveries regarding die and chamber design, electrode erosion, forming, and results of finite element multiphysics simulations of system performance.

9:50 AM

Forming of AA7075 under Cryogenic Conditions: *Sebastian Fritsch*¹; Stephanie Hunger¹; Matthias Hockauf¹; Martin F.-X. Wagner¹; ¹Chemnitz University of Technology

As high strength aluminum alloys are generally hard to deform, the application of conventional severe plastic deformation methods, which in principle allow the generation of ultra fine grained microstructures and increasing strength, is limited. In this study, we explore cryogenic deformation as an alternative approach to deform a 7075 alloy, considering two different processing routes: (i) cryogenic rolling and (ii) cryogenic ECAP. Rolling is performed different low temperatures (minimum temperature: -196 °C) and different degrees of deformation. The cryogenic ECAP procedure uses a tool with an internal angle of 90°. We demonstrate that cryogenic rolling (followed by suitable heat treatments) results in increases of the degree of deformation, strength and ductility. Moreover, we present first results on the effect of cryogenic ECAP on microstructural evolution and mechanical properties of the same alloy that demonstrate the potential of cryogenic forming to produce improved properties of high-strength aluminum alloys.

10:10 AM Break

10:25 AM

Metallurgical Characterization of Aluminum Alloys by Matrix Dissolution: *Marcelo Paes*¹; Francisco Pinheiro¹; Miguel Borodiak¹; ¹Votorantim Metais - CBA

Aluminum foils produced by cold rolling are able to show defects caused by primary particles that are formed along center line segregation. These particles are formed during casting process where some parameters are critical. In the same way, aluminum extruded parts are also able to show defects caused by intermetallic phases. They were used billets of AA6351 alloy (Al-Mg-Si) produced by "Direct Chill" and also sheets of AA8011 alloy (Al-Fe-Si) produced by "Twin Roll Casting". Samples were submitted to a chemical etching based on methanol and iode whose target is corrodes only aluminum matrix. Thus, intermetallic phases were analyzed using optical microscopy and SEM and EDS. On AA8011 alloy, they were identified the phases β -FeSiAl5 and α -Fe₂SiAl8 in as-cast samples, that are hazardous to final foil because they do not dissolve during homogenization treatment. On AA6351 alloy, they were identified the phases Mg₂Si, α -(Fe, Mn)₃Si₂Al₁₅.

10:45 AM

Effect of Silicon Particles on the Tensile Properties of Heat Resistant Al-Si-Cu-Ni-Mg Alloy Pertaining to Different Tensile Temperature: *Chuang Hsu-Chi¹; Lui Truan-Sheng¹; Chen Li-Hui¹; ¹National Cheng Kung University*

The deformation behavior of Al-11Si and Al-11Si aluminum alloy in hot tensile procedure from 200 oC to 450 oC was investigated in this study. The results indicated that the flow stress was strongly dependent on second phase particles of d (Al₃CuNi), Q (Al₅Cu₂Mg₈Si₆), t1 (Al₉FeNi) and Si particles. At 200 oC to 300 oC, the yield and ultimate tensile strength of Al-11Si were higher than Al-1Si. It can be found that the amount of intermetallic d particles increasing will increase the deformation resistance whereas Si particle is detrimental. However, at elevated temperatures, Al-1Si would exhibit a higher elongation at 450oC but Al-11Si was higher than Al-1Si after 400oC. Microstructural observations showed Si particles would restrain the failure of matrix and increase the ductility.

11:05 AM

Work-Hardening and Flow Behavior of AA7055 Alloy Extrusions: *Geo Harrison¹; Rama Krishna²; Tejaswini²; Chandan Monadal³; ¹College of Engineering Guindy, Anna University; ²JNTU College of Engineering; ³Defence Metallurgical Research Laboratory, Hyderabad.*

AA7055 is a high strength precipitation hardenable aluminium alloy and is widely used in compression dominated air-craft structures. In particular, extrudates of AA7055 alloy exhibits very high strength with reasonable ductility in the stress corrosion resistant RRA tempers. In the present work, mechanical properties of the AA7055 alloy extrudates having varying processing parameters (viz. initial billet temperature, extrusion ratio). Tensile properties of the extrudates have been characterized at room temperature for different heat treatment tempers. From the experimental data, plastic flow curves have been calculated and fitted to several semi-empirical flow curve models. It has been shown that a modified voce equation fits the data well for all the variants. The variations of the fit parameters with respect to the processing conditions and the heat treatment tempers are further discussed in collaboration with the microstructural features.

11:25 AM

Factors Influencing Tensile Mechanical Properties of Al-7Si-Mg Casting Alloys A356/7: *Heinrich Moller¹; Waldo Stumpf²; Gonasagren Govender¹; ¹CSIR; ²University of Pretoria*

Conventional casting alloys Al-7Si-Mg A356/7 contain between 6.5 and 7.5% Si, together with 0.25-0.7% Mg and are used for critical castings in the automotive and aerospace industries. The tensile mechanical properties of these alloys are influenced by factors such as casting method, chemical composition variations and heat treatment. The casting method employed has an influence on the primary alpha-Al structure, which is dendritic using conventional liquid casting techniques and globular using semi-solid metal processing. The most important elements that influence mechanical properties are magnesium and iron. Temper condition dictates the degree of spheroidisation of eutectic Si-particles, as well as the strengthening precipitates formed. An equation to convert Vickers hardness to 0.2% proof stress in different temper conditions using the strain hardening exponent is proposed. Linear correlations between hardness, strength and (at% Mg-content available for precipitation hardening)^{1/2} are found. It is shown that ASTM Standard B969-10 needs to be revised.

Aluminum Reduction Technology: Cell Technology and Operation

Sponsored by: The Minerals, Metals and Materials Society, TMS Light Metals Division, TMS: Aluminum Committee, TMS: Aluminum Processing Committee
Program Organizer: Olivier Martin, Rio Tinto Alcan

Wednesday AM
March 14, 2012

Room: Southern III
Location: Dolphin Resort

Session Chair: Bjørn Moxnes, Hydro Aluminium

8:30 AM

DX+, An Optimized Version of DX Technology: *Abdalla Al Zarouni¹; Ali Al Zarouni¹; Michel Reverdy¹; Sergey Akmetov¹; Lalit Mishra¹; Nadia Ahli¹; Ibrahim Baggash¹; ¹DUBAL*

DUBAL has engaged in self-development of proprietary reduction technology since the 1990s. DX and DX+ Technologies in-house designed, modelled, tested and optimized are the products of this development process. In view of decreasing capital cost per tonne, DUBAL designed DX+ Pot Technology and started up five demonstration cells from June to August 2010. This paper summarizes the achieved targeted performance of the DX+ demonstration pots during their first year of operation at 420 kA. DX+ pots are similar to DX pots but larger in size: the productivity per square meter of potroom is increased by more than 17%. This paper describes the DX+ pot design evolution from DX Technology. The DX+ Technology has been selected for EMAL Phase-2 project. The FEED study completed in June 2011 is based on one potline of 444 DX+ pots. The design allows for operating amperage up to 460 kA.

8:50 AM

AP40 : The Latest of the AP Technology™ Solutions: *Laurent Fioi¹; Benedicte Champel¹; Sylvain Fardeau¹; Pierre Bon¹; David Munoz¹; Olivier Martin¹; ¹Rio Tinto Alcan*

Another significant step in the AP30 development has been successfully demonstrated; one that further enhances productivity. After AP30 technology validation, an enhanced operating point has allowed cells to operate above 400 kA without decrease in energy efficiency. Since July 2010, these cells, now referred to as AP40, operate at St Jean de Maurienne in the range of 400-405 kA with specific energy consumption below 13,150 kWh/t. To achieve this performance required an extensive review of operational aspects including busbar capability, operational quality, and process control. Also essential was the use of an "operating window" approach to determine the optimal operating point. By following a cell development methodology over two years, results have demonstrated a high level of process performance (anode effect frequency, current efficiency and energy consumption). Measurement campaigns have confirmed the excellent level of pot robustness.

9:10 AM

A Techno-Economic Optimization Model For Aluminum Electrolysis Production: *Yanfang Zhang¹; Wangxing Li¹; Jianhong Yang¹; Dengpeng Chai¹; Shilin Qiu¹; Jingyi Li²; ¹Zhengzhou Research Institute of Chalco; ²Graduate School of Business and Law, RMIT*

The major factors affecting the profit of an enterprise are the price of the product, the price of raw materials and energy consumed, depreciation of fixed assets, labor cost, output and process consumptions, etc. In this paper, based on a cost-volume-profit (CVP) analysis method and the process techniques of aluminium production, a series of techno-economic analysis and optimization models for the production of the aluminium smelter enterprises are built. The models can be used for the aluminium smelters in various market situations to get the optimum technical



TMS 2012

141st Annual Meeting & Exhibition

parameters of production, which are necessary for obtaining the greatest economic benefit. Thus, it will guide the aluminium smelters in different market environment, according to their own conditions, to adopt different technical parameters of production to maximize the gains and to minimize the losses. We also have studied the optimization of potline current of a 300 kA aluminium smelter by the models as an example

9:30 AM

The Successful Implementation of DUBAL DX Technology at EMAL: *Michel Reverdy*¹; B. Kakkar²; David Spencer²; Walid Al Sayed²; Ali Al Zarouni¹; Kamel Al Aswad¹; Abdalla Al Zarouni¹; ¹DUBAL; ²EMAL

756 DX pots have been successfully commissioned at EMAL smelter in Abu Dhabi between 2nd December 2009 and 2nd January 2011. DUBAL DX Technology has gone through a fast track development from prototyping to large scale industrialization, with the design and engineering phase in 2004, followed by commissioning of five prototype pots in 2005, a demonstration line of 40 pots in 2008 and finally the commissioning of the giant smelter at EMAL in 2009/2010. The commissioning and normalization of the pots was very smooth without single lining incident. This has been achieved by the excellent team work and coordination between the various teams at all stages (pot preparation, preheat, start-up and normalization). It has also shown the robustness of the DX Technology. The potlines are operating at 353 kA with excellent performances exceeding 96.0% current efficiency and achieving 13.0 kWh/kgAl for more than 18 months since start-up.

9:50 AM

Commissioning of Emirates Aluminium Smelter Potlines: *B.K. Kakkar*¹; Spencer¹; Walid Al Sayed¹; Salman Abdulla¹; ¹Emirates Aluminium company

Abstract On the 2nd of December 2009 Emirates Aluminium (Emal) commenced its journey of starting 756 Dubai DX technology reduction cells. This undertaking was successfully completed on the 2nd of January 2011, thirteen months later, resulting in an average start-up rate of 13.3 pots per week. This sets a new benchmark for Greenfield Smelters. This remarkable achievement was possible due to an efficient work-organization, with committed and experienced employees. The pot start-up rate and pot technical results give measures of the success by which the task was accomplished. This article provides insights into the experiences gained and systems used by the Reduction Operations Team, in managing the organizational complexities of commissioning the largest Greenfield Smelter start-up to-date.

10:10 AM Break

10:30 AM

Update on the Development of D18 Cell Technology at Dubal: *Daniel Whitfield*¹; Tariq Majeed¹; Sergey Akhmetov¹; Maryam Mohamed Al-Jallaf¹; Kamel Al-Aswad¹; Ibrahim Baggash¹; Ali Al-Zarouni¹; ¹Dubai Aluminium

Dubai Aluminium commenced operation in 1979 with 3 potlines, each with 120 P69 technology cells. After further refinement by Dubal (and renamed D18), a fourth potline of 144 cells was added in 1990. While more advanced cell technologies have since been developed and implemented at Dubal, the original cell technology has continued to be updated and improved so that it remains a vital contribution of the overall smelter production. The four D18 potlines have been combined into two potline circuits, and additional busbar added to all cells to reduce the specific energy consumption. Other changes such as improved noise control logic, resistance control, review of the anode set adder, and various changes to the alumina feed logic have enabled the D18 technology to reach the target amperage of 200kA and its subsequent stabilisation and optimisation at this milestone.

10:50 AM

Prebake Potline Restart after Power Supply Interruption: *Mikhail Lukin*¹; John Johnson²; ¹Kubikenberg Aluminium AB; ²RUSAL ETC

In early January 2011 the decision was taken to perform an emergency shutdown of the newly converted prebake potlines of Kubikenberg Aluminium AB (Kubal). This was due to power interruptions that resulted in bath shrinkage, which was followed by the onset of random anode failures in numerous cells when attempts were made to re-energize the potline. The present paper covers the methods for restarting the potline. These methods were first considered and tested on one or two pots to evaluate the individual method, taking into consideration the availability of trained personnel; cell limitations and logistics; metal purity for existing customer supply commitments; environmental regulations; and speed of restart. In addition, the paper will provide the criteria used to select the appropriate re-start procedure for different cell conditions and the results obtained by each of the methods used.

11:10 AM

The Restart of Two Idled Pot Lines at Ormet Primary Aluminum: *Cecil Smith*¹; Mark Christman¹; ¹Ormet Primary Aluminum

In November of 2010, Ormet Primary Aluminum Corporation announced an aggressive plan of restarting 2 potlines before the end of the 1st quarter of 2011. In order to accomplish this goal several key factors were utilized including the experience of the plant personnel, management of anodes and bath generation at start-up, initial power and chemistry control of the cells, and the fact that the shutdown of the lines was efficient and controlled. The total time from the restart announcement until all 344 cells were brought on took only 92 days, and the time from when the first line was energized until the final cell was cut in on the second line took only 71 days. This paper will discuss the key factors and obstacles that had to be overcome to allow Ormet to achieve this goal while also striving for safety as no recordable accidents occurred during the restart.

11:30 AM

Vertical Stud Soderberg Technology Development by UC RUSAL in 2004 -2010: *V.Yu. Buzunov*¹; Victor Mann²; Evgeniy Chichuk¹; Nikolay Pitertsev²; Igor Cherskikh¹; Vladimir Frizorger¹; ¹RUSAL ETC; ²UC RUSAL

Due to considerable amount of VSS cells (more than 70 % of total capacity), RUSAL continues to develop the Soderberg process successfully. Alumina point feeding systems, dry gas scrubbers were introduced and anode paste production was modernized in Krasnoyarsk smelter. The amperage was increased in all RUSAL VSS potlines. Cell design has been permanently improved. These actions have increased an aluminium production efficiency and environmental sustainability. Besides, RUSAL Engineering and Technological Centre has successfully fulfilled the R@D program creating the new modification of VSS technology (so-called "colloid anode") with the reaching the new environmental standards. The results of these and other activities of the Company from 2004 to 2010 are shown in the article.

11:50 AM

Uniform Cathode Current Collection / Distribution Effect on Cell Stability (Nine Months of Continuous Treatment of a Sick Cell): *Hadi Fanisalek*¹; ¹Hormozal

This paper describes a useful experience, which was conducted during last year's start-up and potroom operation regarding a sick cell treatment in an aluminium smelter in Iran, which we will call smelter X in this paper. Different parameters in the potroom have influence on cell stability, which need to be considered all together. Metal pad stability is the main concern for a smooth operation in an aluminum smelter to reach a low noise level and a high current efficiency. One of smelter X's aluminum reduction cells,

which was started with good and smooth operating parameters, turned into a sick cell with a very high noise level two months after its start up. A special team started to monitor, test, analyze and try different strategies to bring the cell back to normal condition. This paper is a summary of the aforementioned challenge, team endeavor, possible solutions and final results to overcome this problematic issue.

Atomistic Effects in Migrating Interphase Interfaces - Recent Progress and Future Study: Modelling and Mechanisms of Interface Migration

Sponsored by: The Minerals, Metals and Materials Society, TMS Materials Processing and Manufacturing Division, TMS/ASM: Phase Transformations Committee

Program Organizers: Tadashi Furuhashi, Institute for Materials Research, Tohoku University; Sudarsanam Babu, Ohio State University; Hatem Zurob, McMaster University; Jian-Feng Nie, Monash University; Wen-Zheng Zhang, Tsinghua University; James Howe, University of Virginia

Wednesday AM
March 14, 2012

Room: Europe 3
Location: Dolphin Resort

Session Chairs: Sybrand van der Zwaag, Technical University Delft; Mohamed Gouné, ArcelorMittal Maizières Research SA

8:30 AM Invited

Effects of Alloying Elements on the Growth of Ferrite from Austenite in Multi-Component Fe-C Base Alloys: Masato Enomoto¹; Ran Wei¹; Guohong Zhang²; Dongwoo Suh²; ¹Ibaraki University; ²Pohang University of Science and Technology

The nucleation and growth rates of ferrite in Fe-C alloys containing more than one alloying element are often different from the averages in component ternary alloys. For example the parabolic growth rate constant of ferrite in Fe-C-Mn-Si alloys was closer to that in Fe-C-Mn alloys than the average with Fe-C-Si alloys, whereas a similar tendency was observed with nucleation rate to a lesser extent. The deviation from the averages of ternary alloys can be produced by co-segregation (accumulation) of alloying elements at ferrite/austenite phase boundaries, diffusional interaction and change in partitioning of individual elements due to the change of transformation temperature. Experimental data on alloying element partitioning and parabolic growth rate constants recently obtained in Fe-C base quaternary and quinary alloys are compared with calculation and the possible mechanisms for synergistic effects are discussed.

9:00 AM Invited

Modeling of the Austenite to Ferrite Transformation in Fe-C-X Alloys: Joakim Odqvist¹; Annika Borgenstam¹; Henrik Larsson²; Lars Höglund¹; John Ågren¹; Mats Hillert¹; ¹KTH (Royal Institute of Technology); ²Thermo-Calc Software AB

The surprising results from experiments on Fe-C-Mn from Zurob et al. of a transition from LENP (local equilibrium-negligible partitioning) to PE (paraequilibrium) conditions during growth of ferrite at high temperatures have spurred new modeling attempts. In this work the dissipation of Gibbs energy approach is used to model the austenite to ferrite transformation in Fe-C-X alloys and the results are compared with experiments. Such calculations were performed by some of the present authors already 2002 but were based on very high ferrite/austenite interface mobility and indicated Ni segregation to the phase interface. Such segregation has not been confirmed experimentally and it has been found that the interface mobility may be many orders of magnitude lower than previously thought and thus the calculations will now be repeated. The simulations will also be compared with a more recent model by Larsson et al.

9:30 AM

New Model for Kinetics of the “ γ ” to “ α ” Transformation in Fe-C-X Systems: Damon Panahi¹; Hatem Zurob¹; Gary Purdy¹; Christopher Hutchinson²; Yves Brechet³; ¹McMaster University; ²Monash University; ³Grenoble Institute of Technology

A newly developed model for growth of the proeutectoid ferrite has been employed to study the evolution of contact conditions at the ferrite/austenite interface during ferrite growth in Fe-C-X systems (X= Mo, Mn, Ni, Cr, Cu). The present model uses discrete atomic jumps to describe the diffusion of the substitutional elements across the interface. The free energy dissipation associated with these jumps is evaluated and its effect on contact conditions and interface velocity is taken into account. In line with this, recently obtained experimental observations and modeling results for the growth kinetics of the ferrite layer during decarburization of Fe-C-Mo and Fe-C-Mn systems will be presented. At the end, the compatibility of these experimental observations with the theoretical calculations will be discussed.

9:50 AM Break

10:05 AM Invited

Precise Measurements of Phase Transformation Kinetics: What Can It Tell Us about the Atomic Mechanisms of Interface Migration?: Christopher Hutchinson¹; Hatem Zurob²; ¹Monash University; ²McMaster University

This symposium brings together two communities interested in phase transformations in solids. One community is interested in the local structure of phase interfaces. The other is interested in the transformation kinetics. The latter community acknowledges the key role of the interface structure but hides this in the interface mobility parameter. The former community similarly acknowledges that the structure and atomic mechanisms of interface migration may depend on the local chemistry and driving force acting on the interface but it is not clear how to include the effects. This presentation summarizes experiments that allow high precision measurements of the interface migration kinetics. The kinetics is interpreted using growth models and we discuss what conclusions regarding the atomic mechanisms of migration might be drawn. We attempt to highlight questions that would benefit from collaboration between the two communities to develop a description that couples thermodynamic, kinetic and structural aspects of interface migration.

10:35 AM Invited

Direct Computation of the Solute Drag on a Moving Interface using Atomistic Simulations: H. Humadi¹; Y. Yang²; D. Buta³; B. B. Laird²; D.Y. Sun⁴; Jeffrey Hoyt¹; M. Asta⁵; ¹McMaster University; ²University of Kansas; ³University of California, Davis; ⁴East China Normal University; ⁵University of California, Berkeley

Solute drag, or the dissipation of free energy arising from diffusional processes within the interfacial region of a moving interphase boundary, is an important phenomenon when describing microstructural evolution processes in alloys. In this work we show how atomistic simulations can be used to obtain quantitative values of the solute drag contribution of a moving crystal-melt interface for an embedded atom description of Cu-Ni. Molecular dynamics simulations have been used to extract both the interface velocity and the concentration profile for various driving forces. In addition, Monte Carlo simulations are utilized to determine the free energy of the system as a function of composition and temperature. From the free energy and velocity relationship the solute drag component is extracted and the results are compared with various theoretical treatments.

11:05 AM

Atomistic Simulations of Solute-Interface Interactions in Iron: Hao Jin¹; Ilya Elfimov¹; Matthias Militzer¹; ¹The University of British Columbia

The kinetics of austenite-ferrite phase transformation is markedly affected by substitutional alloying elements. Therefore, it is of fundamental importance to quantify the interactions of solutes with interfaces in Fe



alloys. In this study, the effects of common alloying elements (e.g. Nb, Ti, Mo, Cu, Mn, Si, Co, Cr, V, Ni) on structure, segregation and magnetic properties of Fe interfaces are systematically investigated using first-principles density functional theory (DFT). Minimum energy pathways for diffusion and associated saddle point structures were determined with the climbing image nudged elastic band method. Using the activation energies obtained with DFT self- and solute diffusivities along and across interfaces have been determined with atomistic Kinetic Monte Carlo (KMC) simulations. Calculated results confirm the strong interaction of Nb, Ti, and Mo with interfaces, and show that interface diffusion is faster than bulk diffusion.

11:25 AM

Atomistic Modelling of Interstitial Solute Interacting with Moving Interface: *Aulia Wicaksono*¹; Matthias Militzer¹; Chad Sinclair¹; ¹UBC

A parametric study of the interactions between a moving solid-solid interface and mobile interstitial solutes has been performed using kinetic Monte Carlo (kMC) simulations. A new kink migration approach for the motion of an interface has been introduced and used to study the interaction with mobile interstitial solute. Above a critical temperature a roughening transition for the interface is observed that modifies the migration mechanisms, i.e. initiation-propagation for $T < T_c$ and stochastic fluctuation for $T = T_c$. It is found that the interaction between the interface and the solute depends on the simulation temperature relative to T_c . More generally, the velocity of the moving interface decreases with solute segregation to the interface, the level of segregation depending on the interface morphology, the binding energy between solute and the interface and the solute diffusivity. These observations are compared and contrasted with the classical mean field theory for solute drag.

**Biological Materials Science Symposium:
Biological and Bio-Inspired Materials III: Soft Biomaterials**

Sponsored by: The Minerals, Metals and Materials Society, TMS Electronic, Magnetic, and Photonic Materials Division, TMS Structural Materials Division, TMS: Biomaterials Committee
Program Organizers: Nima Rahbar, University of Massachusetts Dartmouth; Candan Tamerler, University of Washington; Po-Yu Chen, University of California, San Diego; Molly Gentleman, Texas A&M University

Wednesday AM
March 14, 2012

Room: Swan 7
Location: Swan Resort

Session Chairs: Molly Kennedy, Clemson University; Molly Gentleman, Texas A&M University

8:30 AM Invited

A Detailed Physicochemical Study of Peptide-Mineral Interactions; Importance of Peptide Composition, Particle Size, Surface Chemistry, pH and Buffer Identity: *Carole Perry*¹; Valeria Puddu¹; David Belton¹; ¹Nottingham Trent University

The study of interactions occurring at the mineral- biomolecule interface is a subject of longstanding interest having implications in fields from biomimetic materials synthesis through to the development of drug delivery vehicles and nanodevices. Although extensive studies have been performed on a colloidal level to describe the interaction between organic species and inorganic materials, to date, a clear understanding of the processes occurring at a molecular level are still far from been achieved. A great challenge is the formulation of guidelines for the prediction of the functional groups that will preferentially interact with the surface, which forces will contribute to the interaction and to which extent. In this respect, we believe that to gain insights into the mechanistic aspects of

the interaction, a comprehensive knowledge of the biomolecule and the inorganic material is of fundamental importance. In this contribution we show the results of studies on silica and titania.

9:00 AM

Specific Targeting Molecular Probes: From Materials to Cells: Hilal Yazici¹; Marketa Hnilova¹; Hanson Fong¹; Hai Zhang¹; *Candan Tamerler*¹; ¹University of Washington

Molecular immobilization on inorganic surfaces has become an engineering consideration in a wide arrange of areas from sensing to biomaterials engineering. Requirements vary in each applications depending on the immobilization density, chemical and biological stability, material specific assembly, directionality. The characteristics of recognition, self assembly and ease of genetic manipulation make inorganic binding peptides an ideal molecular tool for addressable assembly of biomolecules. We therefore build upon the modularity of peptide domains and produce multifunctional peptides that can controllably bind to a given solid material, in particular to those relevant for nanomedicine. Here we will show specific examples on the flexible and modular use of peptides for biological surface functionalization and, demonstrate enhanced bioactivity as well as controlled antimicrobial property in the presence of different cells on a variety of biomaterials, i.e. implants and imaging agents. Research is supported the NSF-MRSEC at UW, NSF-BIOMAT, NSF IRES Projects.

9:20 AM

Possible Key Property of Nanoparticles that Can Maximize Its Cancer Killing Capacity: *Vanessa Moosavifazel*¹; Soumen Das²; Sudipta Seal²; ¹University Central Florida ; ²University Central Florida

Previously, we have reported the ability of dextran-coated nanoceria (Dex-CNP) to kill cancer cell (IC50 150µM). It is well known that physicochemical properties of a nanoparticle are crucial to the interaction of the particle with the cell. Therefore, to maximize the efficacy of the nanoparticles to kill the cancer cell we need to figure out which chemical or physical property is the key. In this study we have synthesized similar shape and size Dex-CNP with varying surface oxidation (Ce3+/Ce4+) state ratio, by exposing Dex-CNP to light initiating a color change from dark yellow to pale yellow which is an indication of Ce4+ to Ce3+ conversion. Nanoceria has been characterized by using uv-vis and x-ray photon spectroscopy. Interestingly, we have found that light exposed nanoceria coated with dextran loss it's cytotoxicity towards squamous cell carcinoma cell line (CCL30). Summarizing, lower surface Ce3+/Ce4+ may be efficient for cancer killing.

9:40 AM

Response of Mice 7F2 Osteoblast and Porcine Dental Pulp Stem Cells to Substrate Topography: *Marian Kennedy*¹; Xue Chen¹; Terri Bruce¹; Delphine Dean¹; Julia Sharp¹; ¹Clemson University

Currently, there are no restorative dental techniques capable of dentin fabrication. For this to become a reality, researchers must understand external influences to dental pulp stem cells (DPSCs). This work aims to identify the influence of substrate topography on DPSCs. Forty-eight unique micropatterns were produced with a range of feature heights (100-1000nm), widths (5-50µm) and shapes (lines, dots, holes and hexagons). Two types of cells were utilized- mice 7F2 osteoblasts and porcine DPSCs. The osteoblasts were plated as a control and confirmed earlier findings. The DPSCs did not show any cell alignment or proliferation (as indicated by cell density) with isotropic or anisotropic micropatterns. Significance of the osteoblast and DPSCs normalized densities were analyzed with statistical software (SAS, 2010). This analysis showed that there were no significant geometry effects. However, variation existed between each cell plating repetition and when repetition is taken into account, the feature height influenced average density.

10:00 AM

Determination of Mechanical Properties in Escherichia Coli by Nanoindentation: *Cody Wright*¹; *Abdelmageed Elmustafa*¹; *Claretta Sullivan*²; ¹Old Dominion University; ²Eastern Virginia Medical School

The cytoplasmic membrane of *Escherichia coli*, a gram-negative bacteria, is shielded from the harsh environment by a cell wall which is comprised of a peptidoglycan and outer membrane. In hypoosmotic conditions, the peptidoglycan together with cellular proteins mitigate the osmotic stress which would otherwise cause lysis. Mechanical properties of *E. coli* and its individual layers have been investigated using atomic force microscopy (AFM). For precise measurements of elastic modulus and hardness, contact area and load should be well defined. The AFM cantilever spring constant can accurately describe the load however the contact area can only be estimated. This uncertainty in contact area can lead to propagating uncertainties in results. We propose a methodology for determining the nanomechanical properties of *E. coli* using nanoindentation. The mechanical properties of live bacteria will be determined in liquid in order to simulate biologically relevant conditions.

10:15 AM Break

10:25 AM Invited

Measurement of the Cell Adhesion Strength of Patterned Fibroblasts Using Hydrodynamically-Confined Microfluidics: *Kevin Turner*¹; *Kevin Christ*²; ¹University of Pennsylvania; ²University of Wisconsin-Madison

Cell adhesion to the extracellular matrix (ECM) is a critical process that affects cell growth, differentiation, and fate. Here we present a new cell adhesion strength measurement technique using hydrodynamically-confined microflows that enables rapid analysis of the adhesion of single cells in open fluidic environments. Hydrodynamically-confined microflows (HCMs) are microfluidic flows that are confined on the top and bottom by solid walls, and on the sides by a surrounding liquid; hence, they can easily be created in common open cell culture environments, such as Petri dishes. Here we use HCMs to apply uniform mechanical stresses to detach adherent cells from protein-functionalized surfaces. We have designed and used an HCM device optimized for shear stress application to characterize the adhesion strength of patterned NIH3T3 fibroblasts as a function of shape. Details of the device design and fabrication as well as results from the experiments will be presented.

10:55 AM

The Role of Surface Free Energy of Cell Adhesion in TiO₂ Systems: *Eileen Gentleman*¹; *Kyle Krzywosinski*²; *Matthew Scorsone*²; *Molly Gentleman*²; ¹King's College London; ²Texas A&M University

Titanium implants have gained popular use in orthopedic implants, specifically hip implantation. As a result, effort is being made to increase the osseointegration between these load bearing artificial implants and native bone. In previous studies the observed wettability of a surface has been shown to be a good indicator of the quality and rate of osseointegration. In this study, the role of surface energy on cell adhesion density and the quality of bone nodule growth are explored for a range of titanium dioxide samples. Modifications made to the acid and base surface energies of these oxides will be discussed with respect to the efficiency of cell maturation as measured by staining and Raman spectroscopic techniques.

11:15 AM

Mechanical Response of Brain Tissue Surrogate Material under Impact Loading: *Marius Ellingsen*¹; *Deepthi Saini*¹; *Karim Muciküchler*¹; *Brandon Hinz*¹; ¹South Dakota School of Mines and Technology

Brain tissue surrogate materials are necessary to study injuries related to head impacts which can occur during sports or accidents. Brain tissues are soft and weak materials with complex nonlinear mechanical behaviors, including hysteresis and strain softening. Acceptable surrogate materials must have similar dynamic properties to that of brain tissues. The primary objective of this study is to investigate the dynamic response of candidate brain tissue surrogate materials during high strain rate

loading. Shear rheological characterizations of Perma-Gel and Agarose gel were conducted using a computer-controlled rheometer. The results showed that the Agarose gel had mechanical behavior similar to the porcine brain tissue as reported in the literature. Impact experiments were then conducted on Agarose gel to study its mechanical behavior at a high loading rate aimed at representing the scenario encountered in crash loading conditions. The results from the rheological and impact tests are compared and examined in detail.

11:30 AM

Photocatalytic Responses of Bacterial Cells: *J. Zhang*¹; *X. Wang*¹; *P. Wu*²; *Q. Li*¹; *J. Shang*³; ¹Institute of Metal Research; ²Superior Graphite Co.; ³University of Illinois

Antimicrobial materials based on TiON visible-light photocatalysis have shown great potential in inactivating a wide range of microbiological species. However, there is a serious lack of basic understanding of the antimicrobial behavior of these materials. In this study, the photocatalytic responses of bacterial cells were examined, in "live" and post-mortem conditions, by a series of microscopic and microbiological techniques to investigate the mechanisms of bacterial inactivation by TiON photocatalysts. Significant alterations in the structure and morphology were observed in the bacterial cells. These changes are related to the antimicrobial properties of the photocatalysts.

11:45 AM

Polydimethylsiloxane Mechanical Properties and Their Effects on Cell Growth: *Zhixin Wang*¹; *Kranthi Elineni*¹; *Nathan Gallant*¹; *Alex Volinsky*¹; ¹University of South Florida

In this work, Polydimethylsiloxane (PDMS) network is used as a substrate to grow live cells. A series of PDMS network samples with different crosslink density were tested to obtain the relationship between their biological behaviors and mechanical properties. A macroscopic compression test instrument was designed for PDMS mechanical properties testing. The relationship between PDMS network elastic modulus and its base/agent ratio was established, where the PDMS network elastic modulus is linear with its percent of crosslinker. The same PDMS network samples were also tested with the Hysitron TriboIndenter to verify the elastic modulus and other mechanical properties. The ongoing work is to study the effect of substrate elasticity on the cell adhesion strength independently of the bio-chemical cues. This work would establish the relevance of PDMS as a biomaterial and more significantly in designing biomaterials by incorporating gradients of mechanical and bio-chemical cues.

Bulk Metallic Glasses IX: Fatigue and Corrosion

Sponsored by: The Minerals, Metals and Materials Society, TMS Structural Materials Division, TMS/ASM: Mechanical Behavior of Materials Committee

Program Organizers: Peter Liaw, The University of Tennessee; Hahn Choo, The University of Tennessee; Yanfei Gao, The University of Tennessee; Gongyao Wang, University of Tennessee

Wednesday AM
March 14, 2012

Room: Swan 6
Location: Swan Resort

Session Chairs: Yoshikazu Nakai, Kobe University; Despina Louca, University of Virginia

8:30 AM Invited

On the Fatigue Strength of Monolithic and Composite Bulk-Metallic Glasses: *Bernd Gludovatz*¹; *Marios Demetriou*²; *Maximilien Launey*³; *Douglas Hofmann*²; *William Johnson*²; *Robert Ritchie*¹; ¹Lawrence Berkeley National Laboratory; ²California Institute of Technology; ³NDC

High strength and ease of processing make bulk-metallic glasses (BMGs) promising candidates for many structural/functional applications. However, poor fatigue strengths in the form of low fatigue limits have



TMS 2012

141st Annual Meeting & Exhibition

been reported (in some alloys approaching 0.04 UTS), which clearly limits their utility as structural materials. This follows because the absence of microstructure provides no local arrest features for pre-existing cracks. Recently developed glass-matrix composite BMGs with crystalline second-phase dendrites, however, have displayed fatigue limits of ~0.3 UTS. Here, provided the inter-dendritic spacing does not exceed the critical crack size, the second phase can arrest incipient cracks leading to significantly higher fatigue strengths. The question that we now pose is whether such fatigue properties can be achieved in monolithic BMGs. In a 1.5 GPa strength Pd-Ag-based monolithic BMG we can achieve a fatigue limit comparable with that in composite BMGs, although the mechanisms underlying such high fatigue resistance are quite different.

8:50 AM

Surface Coating of Zr-Based Metallic Glass Film for the Fatigue Property Improvements of Ti-6Al-4V Alloy: *Cheng-Min Lee*¹; J. P. Chu¹; ¹National Taiwan University of Science and Technology

In this study, we propose the use of the Zr-based glass-forming material as a promising coating film for enhancing four-point bending fatigue property of Ti-6Al-4V alloy. A 200nm-thick $Zr_{30}Cu_{27}Al_{10}Ni_3$ thin film was prepared by sputtering deposition system on Ti-6Al-4V substrate. The fatigue life is improved from 3.1×10^5 cycles for the uncoated sample by ~17.3 times to 5.3×10^6 cycles at a stress level of 1.3 GPa. Our Zr-based film is much thinner than traditional hard coatings but has a remarkable performance on the fatigue properties enhancement of the substrate. The excellent mechanical properties of the metallic glass thin film play a critical role. The mechanisms for the substrate fatigue property improvements have been studied and the results will be discussed.

9:00 AM Invited

Environment Assisted Cracking of Zr-Based Bulk Metallic Glass in the Region near Threshold: *Yoshikazu Nakai*¹; Toyohiko Koyama¹; ¹Kobe University

Crack propagation tests on a bulk metallic glass, Zr₅₅Cu₃₀Ni₅Al₁₀, were conducted in aqueous sodium chloride (NaCl) solutions under constant crack opening displacement tests where value of stress intensity factor decreased with crack extension. Tests were also conducted under cyclic loading of $\square K$ decreasing test, and the effect of stress ratio was examined. Comparisons of the time based crack growth rate under cyclic loading and static loading will be conducted. The effect of environment on fatigue crack growth in the region near threshold (Region A) was also examined.

9:20 AM Invited

Statistical Modeling of Fatigue for Zr₅₅Cu₃₀Ni₅Al₁₀ Bulk-Metallic Glass: *D Gary Harlow*¹; Yoshihiko Yokoyama²; ¹Lehigh University; ²Tohoku University

Fatigue lives of bulk-metallic glasses (BMGs) exhibit large scatter in excess of four orders of magnitude especially for longer lifetimes. In order to be able to make meaningful lifetime predictions, sufficient data must be available to develop accurate probability and statistics models. The statistical properties of Zr₅₅Cu₃₀Ni₅Al₁₀ BMG are examined in the context of standard stress and fatigue-life cycles (S-N) response. The experimental data include stress amplitudes ranging from 500 to 1000 MPa for the as-prepared (no annealing) BMG. Subsequent comparisons to the BMG after annealing are made to evaluate its impact. For all these cases, the majority of the fractures were caused by fatigue damage initiation from the surface. Limited microstructural evidence will also be presented.

9:40 AM Break

9:55 AM Invited

Understanding Fatigue Resistance in Bulk Metallic Glasses: *Jamie Kruczic*¹; ¹Oregon State University

Fatigue crack growth rates were measured for $Zr_{44}Ti_{11}Ni_{10}Cu_{10}Be_{25}$, $Zr_{38.5}Nb_{2.8}Cu_{13.6}Ni_{12.8}Al_{10.3}$, and $Zr_{32.5}Cu_{17.9}Ni_{14.6}Al_{10}Ti_5$ bulk metallic glasses (BMGs). The Zr-Ti-Ni-Cu-Be BMG was tested in different initial

free volume states, different residual stress states, and in both ambient air and dry nitrogen environments. Fatigue crack growth rates were relatively unaffected by the initial free volume state. This was attributed to the formation of a fatigue transformation zone of increased local free volume at the fatigue crack tip. When casting residual stresses were annealed out it was found that the fatigue threshold and fracture toughness decreased. Finally, it was observed that testing in a dry nitrogen environment significantly increased the fatigue threshold, suggesting a corrosion fatigue mechanism in ambient air. A similar environmental effect was observed for the Zr-Nb-Cu-Ni-Al BMG while the Zr-Cu-Ni-Al-Ti BMG was immune to ambient air environmental effects and exhibited fatigue crack growth resistance comparable to crystalline metals.

10:15 AM

The Study of Fatigue-Induced Damage in Zr-Based Bulk Metallic Glasses: *Chih-Pin Chuang*¹; Wojciech Dmowski¹; Wei Guo¹; Gongyao Wang¹; Peter Liaw¹; Takeshi Egami¹; Yoshihiko Yokoyama²; Ran Li³; Tao Zhang³; ¹University of Tennessee; ²Tohoku University; ³Beihang University

It's well known that bulk metallic glasses (BMGs) will fatigue even when the applied cyclic-loading is far below its yielding stress, where the stress-strain curve indicated that the deformation should be macroscopically elastic. Yet, the mechanisms responsible for the fatigue-induced damage are varied and inconclusive. In the present work, we investigate the effect of "fatigue" on the fatigue behavior and atomic structure of Zr-based BMG. The compression-compression fatigue tests were conducted on the as-cast and the pre-fatigue-to-failure samples. The results indicated that pre-fatigued samples had similar or longer life (cycles-to-failure). The pair-distribution function (PDF) analysis of the as-cast, and post-fatigue samples using high energy synchrotron X-ray scattering showed no, or very small changes of local atomic structure. The results suggest that the fatigue life of these Zr-based BMG is dominated by the localized damage accumulated around crack tip. The sample will fail before globalized atomic structure changes were observed.

10:25 AM

The Atomic Structure Changes of a Metallic Glass under Creep and Fatigue Loadings: *Wei Guo*¹; Wojciech Dmowski¹; Andrew Chuang¹; Gongyao Wang¹; Yoshihiko Yokoyama²; Yang Ren³; Peter Liaw¹; Akihisa Inoue²; Takeshi Egami¹; ¹University of Tennessee, Knoxville; ²Tohoku University; ³Argonne National Lab

We studied the atomic structure evolutions in a Zr₅₀Cu₄₀Al₁₀ metallic glass under room temperature creep and cyclic loadings below yielding point. The creep loading was held for 24hrs. and 72 hrs. at 60% and 80% of the yield stress (YS). The fatigue experiments were conducted for 105 and 106 cycles at mean stresses of 40% and 60%YS. The structure function S(Q) and the pair distribution functions (PDFs) were determined from high energy X-ray diffraction experiments. Results show that creep samples undergo greater changes than the fatigue samples indicated by the PDF peak sharpening and shifting. Significant difference was neither observed among samples loaded at different stress levels in creep experiments, nor in fatigue samples at different cycles. Loading direction influences the structure changes in the creep samples: The PDFs observed in the direction parallel to the loading have greater changes than in the normal direction.

10:35 AM Invited

Characterization of Shear Bands and Cracks Induced by Three-Point Bending Fatigue Test in Zr-Cu-Al Bulk Metallic Glass: *Pei-Ling Sun*¹; Gongyao Wang²; Peter Liaw²; ¹Feng Chia University; ²University of Tennessee, Knoxville

Zr₅₀Cu₄₀Al₁₀ bulk metallic glass was deformed by three-point bending fatigue test in the air. Inhomogeneous shear bands/cracks were observed on the tensile and compressive regions after deformation. Characterization of shear bands by scanning electron microscopy reveals

the presence of different fracture modes: river pattern and smooth fracture path on the tensile region. However, only a fracture path appears on the compressive surface. Cross sections of the shear bands/cracks were cut by focused ion beam for transmission electron microscopy (TEM) observation. Examinations of the shear band/crack microstructures reveal that nanocrystallites only appear on the crack fracture surface. Additionally, the compositions of matrix, shear band and nanocrystallite were found to be different. Shear bands contain more oxygen content but nanocrystallites have more copper content. These results are related to diffusion and thermally activated processes. The same sample tested in vacuum will be examined by TEM and the deformation mechanism will be discussed.

10:55 AM Invited

Static and Cyclic Deformation Effects on the Thermomechanical Behavior of Bulk Metallic Glass: *Rainer Hebert*¹; Arif Mubarak¹; Gongyao Wang²; Peter Liaw²; Yoshihiko Yokoyama³; Akihisa Inoue³; ¹University of Connecticut; ²University of Tennessee at Knoxville; ³Tohoku University

Static and cyclic elastic loading of bulk metallic glasses yields unusual results. Static compression at about 70 % of the yield/fracture strength induces permanent length changes in a structurally-relaxed Cu₅₀Hf_{41.5}Al_{8.5} BMG at room temperature but only after about 25 hours of compression. Irreversible length changes during heating after static compression depend on the direction relative to the applied static load. Following cyclic tension-tension tests, i.e., fatigue tests, a Zr₅₀Cu₄₀Al₁₀ BMG revealed a slight shift in the glass-transition temperature to lower temperatures, compared to the as-cast sample. Zr₅₀Cu₄₀Al₁₀ BMG was conducted with a tension-tension cyclic loading at an R-ratio of 0.1 and a frequency of 10 Hz. The fatigue lifetime is 7049 cycles with a maximum stress of 978 MPa. The thermal expansion data of the statically-elastically loaded Cu-based BMG is analyzed with an activation-energy spectrum approach. The results are coherent with a re-orientation of atomic bonds during deformation.

11:15 AM Invited

Fatigue Behavior of Zr-Based Metallic Glass at Micro- and Nano-Scales: *Dongchan Jang*¹; Peter Liaw²; Gongyao Wang²; Julia Greer¹; ¹California Institute of Technology; ²University of Tennessee

Recent reports indicate that crystalline strength significantly increases when extrinsic sample dimensions are reduced to nano-scale. In some cases, metallic glasses have also been shown to attain increased tensile strength and ductility under quasi-static monotonic loading for sample sizes below ~100 nm. Size effects under cyclical loading have rarely been addressed. Here we present mechanical behavior and morphology evolution in Zr-based metallic-glass micro-/nano-pillars subjected to compression-compression fatigue. Cylindrical micro-/nano-pillars with diameters between several microns and ~200nm were fabricated via Focused Ion Beam (FIB) and tested in both G200 (Agilent) nanoindenter equipped with a flat punch tip and in the in-situ Scanning-Electron-Microscopy-based nano-mechanical instrument, SEMentor. The stress versus fatigue-life cycles (S-N) plots exhibit significantly enhanced lifetime and endurance limit compared with bulk, suggesting high fatigue damage tolerance in small-scale metallic glasses. These findings are discussed in the framework of unique microstructural deformation mechanisms occurring in micro-/nano-sized metallic glasses.

11:35 AM

Thermography Study of Fatigue on Different Amorphous Alloy Systems: *Gongyao Wang*¹; Q. M. Feng¹; M. D. Demetriou²; Y. Yokoyama³; P. Liaw¹; W. L. Johnson²; A. Inoue³; ¹University of Tennessee; ²California Institute of Technology; ³Tohoku University

Zr-based bulk metallic glasses (BMGs) generally show shear failure during cyclic loading, while Fe-based BMGs demonstrate splitting failure during cyclic loading. This fact suggests that the fatigue mechanisms

could be different between the relative “ductile” (Zr-based) BMGs and the relative “brittle” (Fe-based) BMGs. A state-of-art infrared (IR) thermography camera is employed to monitor the temperature evolutions of both Zr- and Fe-based BMGs during fatigue experiments. With the understanding of the temperature evolutions during fatigue, thermography could provide the direct information and evidence of the stress-strain distribution, shear-band formation and growth, and crack initiation and propagation. In-situ visualizations as well as qualitative and quantitative analyses of fatigue-damage processes have been performed using thermography results. Theoretical models combining thermodynamics and heat-conduction theory are developed to understand the fatigue behavior of BMGs. A mechanistic understanding of the fatigue behavior of Zr-based and Fe-based BMGs is suggested. The fatigue mechanisms of BMGs are discussed.

11:45 AM Invited

A Study of Corrosion Behavior of Zr-Based Metallic Glass Thin Films Deposited by Pulsed DC Magnetron Sputtering Technique: *Yi-Chia Liao*¹; *Jyh-Wei Lee*²; Ching-Yen Chung²; Chia-Lin Li³; Jenq-Gong Duh⁴; Jinn P. Chu³; ¹Tungnan University; ²Ming Chi University of Technology; ³National Taiwan University of Science and Technology; ⁴National Tsing Hua University

The Zr-based metallic glass thin films were fabricated on Si and SUS420 substrates by pulsed DC magnetron sputtering technique. Microstructures of thin films before and after corrosion tests were investigated by an atomic force microscopy (AFM), field emission electron probe microanalyzer (FE-EPMA) and transmission electron microscopy (TEM). The potentiodynamic polarization technique was carried out to study the corrosion resistance of thin films in HCl and H₂SO₄ aqueous solutions, respectively. Further analysis on the chemical compositions of corrosion products were explored using FE-EPMA. The pitting corrosion, crevice corrosion and filiform corrosion behaviors were observed. The possible corrosion mechanisms of Zr-based metallic glass thin films was discussed in the present paper.

12:05 PM

Utilization of Electrochemical Dissolution Processes for Micro-Machining of Bulk Metallic Glasses: *Annett Gebert*¹; *Jakub Koza*¹; *Ralph Suetz*¹; *Margitta Uhlemann*¹; *Jürgen Eckert*¹; *Ludwig Schultz*¹; ¹IFW Dresden

A recent trend in BMG research is the development of suitable techniques for production of micro-parts and micro-patterned surfaces. Thermo-mechanical processing is very promising but has also some limitations [1]. Here another approach operating at r.t. is introduced which utilizes the transpassive dissolution of metallic glasses. Electrochemical micro-machining (ECMM) with a micro-tool electrode is for the first time employed to generate micro-patterns on BMG surfaces by strict control of the local electrochemical process. The principal method is described and first experiments using a Zr-based BMG are presented for discussing the advantages and challenges of this advanced technique. Micro-hole structures were machined with significant aspect ratios at depths of ~40 μm. The effect of process parameters such as electrolyte, pulse voltage and pulse length was investigated and their influence on the machined structure morphology is established. [1] J. Schroers, *Adv. Mater.* 21, (2009) 1.



TMS 2012

141st Annual Meeting & Exhibition

Cast Shop for Aluminum Production: Dross and Melt Quality Control

Sponsored by: The Minerals, Metals and Materials Society, TMS Light Metals Division, TMS: Aluminum Committee, TMS: Aluminum Processing Committee
Program Organizer: Trond Furu, Hydro

Wednesday AM
March 14, 2012

Room: Northern A4
Location: Dolphin Resort

Session Chair: Gerd-Ulrich Gruen, Hydro

8:30 AM

A New Approach to Identify Aluminum Dross Reduction Opportunities Using an Integrated Weighing System: *Simon L'Heureux*¹; Vincent Goutière¹; Joseph Langlais¹; David-Alexandre Tremblay¹; Peter Waite¹; ¹Rio Tinto Alcan

Cast house operations involving molten aluminum processing and furnace charging result in dross generation. This undesirable residue is composed mainly of metallic aluminum and oxides, and engenders costs exceeding 1000 US\$ per MT of dross. Considering that no batch-to-batch measurements of dross weight are generally performed in the cast house, the task of dross reduction has always been complicated since the key process parameters and batch preparation practices affecting dross are not well known. As such, a new integrated weighing device was developed to continuously measure dross generation. The data generated will be used not only to follow-up on long-term furnace performance, with respect to dross generation, but also to complete a statistical analysis aimed at identifying key dross contributors. This paper describes the industrial dross weighing strategy that was developed, as well as the equipment that was installed in a RTA cast house.

8:50 AM

Statistical Analysis of Dross Data for Hydro Aluminium Casthouses: Christian Rosenkilde¹; Inge Johansen¹; Amanda Bowles¹; ¹Hydro Aluminium

Reducing the formation of dross is important for a sound economic result in aluminium casthouses. In order to reduce the amount of dross the main drivers affecting the dross creation need to be identified. The first step towards identifying these drivers is to measure the dross amount on a charge basis. With a sufficiently large dataset it is possible to apply statistical methods to look for correlations between different parameters and the dross formation. It is also possible to rank the different parameters and identify those that are the most import for dross formation. In this paper multivariate statistical analysis is used to correlate the various input parameters and dross formation on a charge basis and to identify the most important driver/s for dross formation. Examples from a remelt extrusion ingot casthouse and a primary extrusion ingot casthouse are given and discussed.

9:10 AM

Wettability of Aluminium with Aluminium Carbide (Graphite) in Aluminium Filtration: *Sarina Bao*¹; Kai Tang²; Anne Kvithyld²; Thorvald Engh¹; Merete Tangstad¹; ¹NTNU; ²SINTEF

Graphite filters have previously been employed based on petrol coke. Wetting between molten aluminium and graphite is studied. Al₃C₄ is formed at the interface between aluminium and graphite. In filtration of aluminium inclusions such as Al₃C₄ formed in the hall electrolysis are removed. Wetting between aluminium and Al₃C₄ (graphite) is determined in kinetic studies in the higher temperature range 1000-1300°C. The results are extrapolated down to temperatures employed in the industry around 700°C. The contact angle between aluminium and graphite decreases with time. It may be divided into three steps: removal of an oxide layer on aluminium, formation of Al₃C₄ at the interface, finally giving an equilibrium value for the contact angle of Al-Al₃C₄. This value is found to be around 92.5° at 700°C.

9:30 AM

A New Fused Magnesium Chloride Containing Refining Flux Based on a Ternary System: *John Courtenay*¹; ¹MQP Limited

The major cost factor in the production of fused refining fluxes is raw materials and in particular the cost of potassium chloride, which because of its role in fertilizer production has been subject to large price increases in the period 2008 – 2009, having risen by more than 350%. As demand for potash for world food production and bio-fuels is increasing again with the recovery in the global economy further price rises are expected, with the price having risen already by 43% from November 2010 to July 2011. A program of work has been undertaken to develop an alternative flux based on a ternary system comprising magnesium chloride and potassium chloride; where the potassium chloride is partially replaced with sodium chloride. The results of a study of the thermodynamics together with laboratory measurement of viscosity, interfacial tension and differential thermal analysis are presented.

9:50 AM Break

10:10 AM

High Frequency Electromagnetic Separation of Inclusions from Aluminum: *Lucas Damoah*¹; Lifeng Zhang¹; ¹Missouri University of Science and Technology

Electromagnetic purification method for the removal of inclusions has been proposed to complement the existing methods, and many researchers have devoted a lot of effort to studying the electromagnetic inclusion removal process. It has been widely published that high frequency electromagnetic field is limited in the depth of penetration into the molten metal thereby rendering the separation method ineffective. The contribution of the high circulatory fluid flow associated with such high frequencies has also been reported to be negative. The effect of wall temperature to the electromagnetic inclusion removal process has also not been clearly established. This study presents new results that show that, fluid flow contributes greatly in the presence of lower wall temperature to remove particles during high frequency (63 kHz) EM purification of aluminum, contributing to overcoming skin depth effect in small and large crucibles.

10:30 AM

Measurement of Non-Metallic Inclusions in the Size Range of 10-20µm by LiMCA: *Mark Badowski*¹; Stephen Instone¹; ¹Hydro Aluminium

Regular monitoring of the melt quality is employed in Aluminum cast houses production where optimized processes and high quality are required. A well established method for the quantitative measurement of non-metallic inclusions is the LiMCA system. In this method, inclusions flowing together with the liquid Aluminium through a 300µm orifice of a submerged glass tube are detected due to their high electrical resistance. The LiMCA system can identify the size, typically in the range between 20µm and 300µm and number of particles in the liquid Aluminium. Increasing product quality standards have resulted in demands to monitor particles even smaller than 20µm. This paper reports results of a parametric study to assess the capability of the LiMCA system to monitor non-metallic inclusions in the particle size range of 10-20µm through changing the orifice hole size and by adjustment of the basic measurement parameters.

10:50 AM

Relationship between the Permeability of the Porous Disk Filter and the Filtrate Weight-Time Curves Generated with the PoDFA / Prefil® Footprinter Method: *Stephen Instone*¹; Daniel Krings¹; Gerd-Ulrich Gruen¹; Roland Schmoll¹; Mark Badowski¹; ¹Hydro Aluminium Rolled Products GmbH

Current methods to quantify metal quality suffer from disadvantages in complexity, expense or response time. One method suggested to provide a real-time quantitative assessment of metal quality is the use of filtrate weight-time curves produced by filtering the metal through a porous disk

filter. The slope and overall shape of this curve should indicate the level of inclusions present in the metal. Hydro Aluminium increasingly employs such methods to assess the quality of both Aluminium and Magnesium alloys. Several different types of crucible and porous disk filter are used. Due to the increasing importance of this assessment method a better understanding of the importance of variations in the permeability of the filter was considered necessary. This paper describes a device to measure the permeability of the filter discs and gives details of trials conducted to quantify the effect of variations in filter permeability on the filtrate weight time curves.

11:10 AM

Study of Ni-Impurity Removal from Al Melt: *Muhammad Akbar Rhamdhani*¹; Mohammad Dewan¹; Jason Mitchell¹; Cameron Davidson¹; Geoffrey Brooks¹; Mark Easton¹; John Grandfield¹; ¹CAST CRC

Impurity control in the production of Al alloys is very important for achieving the desired properties of the products. There has been an increasing impurity concentration (particularly nickel and vanadium) in the coke used in the primary Al production which will end up in the Al. Vanadium can be removed in the casthouse through boron treatment. Nickel, however, is a non-reactive element and difficult to be removed. There is currently no technique available in the casthouse to remove nickel impurity. The current paper focuses on the study of nickel impurity removal from Al melt. A literature review on the available techniques for the removal of nickel and other elemental impurities from Al melt was carried out; followed by a systematic thermodynamic analysis of various Al-Ni-X systems for possible formation of Ni-containing phases in Al melt. Laboratory experiments were carried out to test the possible systems identified from the thermodynamic analysis.

11:30 AM Break

CFD Modeling and Simulation in Materials Processing: Modeling of Casting and Solidification Processes II

Sponsored by: The Minerals, Metals and Materials Society, TMS Extraction and Processing Division, TMS Materials Processing and Manufacturing Division, TMS: Process Technology and Modeling Committee, TMS: Solidification Committee
Program Organizers: Laurentiu Nastac, The University of Alabama; Lifeng Zhang, Missouri University of Science and Technology; Brian Thomas, University of Illinois at Urbana-Champaign; Adrian Sabau, Oak Ridge National Lab; Nagy El-Kaddah, The University of Alabama; Adam Powell, Metal Oxygen Separation Technologies, Inc.; Hervé Combeau, Institut Jean Lamour

Wednesday AM
March 14, 2012

Room: Asia 4
Location: Dolphin Resort

Session Chairs: Laurentiu Nastac, The University of Alabama; Nagy El-Kaddah, The University of Alabama

8:30 AM

Modeling of Centrifugal Casting Processes with Complex Geometries: *Nicholas Humphreys*¹; Diane McBride²; Nick Croft²; Dimitri Shevchenko¹; Nick Green¹; Mark Cross²; ¹University of Birmingham; ²Swansea University

Centrifugal casting offers a route to high quality products in difficult to cast high temperature low superheat alloys and thin section molds. Under centrifugal forces metal is forced into thin sections and can fill thicknesses of less than a millimetre. However, due to the high liquid metal velocities there is a high risk of surface turbulent flow and air entrainment within the liquid metal. The combination of interacting flow-thermal-solidification phenomena and associated defects is a challenging modeling task which

the authors have previously described and validated. Capturing the metal-air interface, on what are inevitably complex three dimensional geometries, results in highly computationally expensive simulations and simulating a single cast can take weeks on a single processor. This contribution reports on modeling a complex centrifugal cast, gas entrainment, bubble transport and solidification, employing meshes of up to a million elements and investigates the scalability of the model on high performance clusters.

8:55 AM Invited

Influence of Feeding Flow and Shrinkage Pipe Formation on Macrosegregation of Investment Cast -TiAl Alloys: *Sailei Zhang*¹; Jeff Yanke¹; David Johnson¹; Matthew Krane¹; ¹Purdue Center for Metal Casting Research, School of Materials Engineering, Purdue University

A single-domain multi-phase model is developed to predict macrosegregation of investment tilt cast γ -TiAl, considering the effect of both buoyancy and shrinkage induced flow. The model combines the volume of fluid method for tracking the gas/liquid and gas/solid interfaces during the formation of shrinkage pipe with continuum transport equations for velocity, temperature and composition. This model is used to investigate the influence of riser shapes and volume on the composition distribution and the shrinkage pipe shape in the final cast part. The influence of cooling conditions on fluid flow and shrinkage pipe formation during solidification is also studied.

9:20 AM

CFD Modeling of Macro-Shrinkage and Shrinkage Porosities in A356 Castings: *Laurentiu Nastac*¹; ¹The University of Alabama

An advanced casting simulation approach was applied in this study to assist in the improvement of the mold design of aerospace components made of A356 alloy. By using this approach, mold filling and solidification related defects (including macro-shrinkage and shrinkage porosity) were significantly minimized and hence it helped in cost reduction, performance enhancement and quality assurance of complex A356 cast parts. An experimental validation and detailed calibration procedures of the models for prediction of macro-shrinkage and shrinkage porosities were performed using A356 plates cast in furan-silica sand molds using the Prometal Rapid Casting Technology (RCT) mold printing technology. Correlations between Niyama values and the pore percentage were also developed. Thus, the severity level of shrinkage porosity can be determined via the Niyama criterion. Predictions were then compared with the macro-shrinkage and porosity measurements in plates of various plate thicknesses and in other commercial A356 casting components.

9:40 AM

CFD Modeling of Microstructural Development in the Scanning Laser Epitaxy Process: *Ranadip Acharya*¹; Rohan Bansal¹; Justin Gambone¹; Suman Das¹; ¹Georgia Institute of Technology

This paper focuses on modeling of the scanning laser epitaxy (SLE) process that is currently being investigated and developed at the Georgia Institute of Technology. SLE is a laser-based manufacturing process for the creation of equiaxed, directionally solidified and single-crystal deposits of nickel superalloys onto superalloy substrates through melting and resolidification of alloy powders using a scanning laser beam. The thermal modeling of the system, done in a commercial CFD software package, simulates a heat source moving over a powder bed and dynamically adjusts the property values for consolidating CMSX-4 nickel superalloy powder. The associated melting and re-solidification process is modeled using an immediate consolidation approach, and the predicted melt depth is compared with the experimental data obtained. For a given position of the beam, geometrical parameters of the melt pool are used to estimate the resulting microstructure. The influence of the processing parameters on the microstructural evolution is also discussed. This work is sponsored by the Office of Naval Research through grants N00173-07-1-G031, N00014-10-1-0526 and N00014-11-1-0670.



TMS 2012

141st Annual Meeting & Exhibition

10:00 AM Invited

CFD Modeling and Analysis of Casting of Energetic Materials in Cylindrical Ingots Controlled by the ACH Solidification Technology: *Laurentiu Nastac*¹; Ruslan Mudryy²; ¹The University of Alabama; ²U.S. ARMY

This paper investigates the solidification shrinkage problem in casting of energetic materials in cylindrical molds. An active cooling and heating (ACH) control solidification technology is applied to achieve unidirectional solidification during casting. The design parameters of the ACH technology are developed via Computational Fluid Dynamics (CFD) modeling. In particular, the media heating and cooling temperatures as well as the number of cooling/heating sections and their time sequences are optimized based on the mold diameter, thermo-physical properties of the energetic material, and mold thickness and type. It is demonstrated that the ACH technology can successfully be applied to significantly minimize the solidification related defects (including macro-shrinkage and shrinkage porosities) in cast energetic materials.

10:25 AM Break

10:45 AM

Defect Analysis by Casting Simulation Software in Rolling Roll Manufactured by GGG70: *Engin Tan*¹; Ali Taraki¹; Derya Dispinar²; ¹Pamukkale University; ²University of Istanbul

Nowadays, the casting industry is developing parallel with the information technologies (IT). Particularly the casting simulation software is being frequently used in foundry floors for casting quality control and optimisation. In this study, the filling and solidification analysis of a rolling roll manufactured by spherical graphite cast iron were carried out by Vulcan casting simulation software. The appropriate defect relieving suggestions were presented by anticipation of defects that may form during the casting process.

11:05 AM

SPH Model Approach Used to Predict Skin Inclusions into Semisolid Metal Castings: *Frédéric Pineau*¹; Guillaume D'Amours¹; ¹National Research Council Canada

Semisolid metal processing of metallic alloys takes advantage of the thixotropic behavior of material with non-dendritic microstructure to produce near-net-shape parts with improved mechanical properties. The much higher apparent viscosity of the semisolid billet limits the risk of oxide formed on the free surfaces to become incorporated into the casting during the process. But, the external-skin on the periphery of the billet, which is often partially solidified and contaminated with lubricants, should not be included into the casting, as this can be a cause of reject for most structural parts. In this paper, a preliminary model is set-up using the LS-DYNA SPH formulation to follow the paths of the skin. Calculations carried out show that this approach appears to be very promising to predict the paths of contaminated skins into semisolid castings. It can then be utilized to design suitable molds and gating systems.

11:25 AM

Influence of Mould Vibrations on the Solidification during a Horizontal Spin Casting: *Abdellah Kharicha*¹; ¹University of Leoben

The aim of the present study is to investigate the influence of the vibrations on the flow and on the solidification during a centrifugal spin casting. A 2D shallow water model was built in order to simulate the dynamics of a liquid metal film under the influence of the centrifugal and coriolis forces. The mass transfer due to solidification was calculated using Stefan condition. The average dynamics of liquid metal film in a horizontal axially vibrating cylinder is studied. The different vibration and rotation frequencies are considered. The generation of toroidal vortices periodic along the rotation axis and the formation of quasi-steady interface relief are predicted. It is shown that quasi-steady wave shapes are induced by the tangential vibrations. These waves have considerable effects on the quality of the solidified layer.

11:45 AM

Inverse Modeling for Determination of Thermal Properties of the Investment Casting Ceramic Mold: *Mingzhi Xu*¹; Simon Lekakh¹; Von Richards¹; Shelly Dutler²; ¹Missouri University of Science and Technology; ²MAGMA Foundry Technologies, Inc

This study presents determination on the thermal properties of investment casting shell molds used in casting process modeling. Superheat and latent heat from solidification and cooling of a casting can either be accumulated by ceramic shell for thin-walled casting or transfer to environment for massive casting. Heat capacity and thermal conductivity both play important roles in casting solidification. Thermal properties of ceramic shell depend on shell composition and fabrication techniques as well as thermal history during shell preparation process due to multiple phase transformations. Inverse modeling was combined with corrected Laser Flash method to determine the applicable thermal properties of the shell during casting solidification. Pure nickel was poured into ceramic shells containing two thermocouples and experimental cooling curves were obtained. These curves were then fitted to the model by adjusting temperature dependent heat capacity and thermal conductivity.

Characterization of Minerals, Metals, and Materials: Characterization of Environmental and Construction Materials

Sponsored by: The Minerals, Metals and Materials Society, TMS Extraction and Processing Division, TMS: Materials Characterization Committee

Program Organizers: Jiann-Yang Hwang, Michigan Technological University; Sergio Montero, State University of North Rio De Janeiro; Chenguang Bai, Chongqing University; John Carpenter, US Department of Energy; Donato Firrao, Politecnico di Torino; Byoung-Gon Kim, Korea Institute of Geoscience & Mineral Resources; Mingdong Cai, Schlumberger

Wednesday AM
March 14, 2012

Room: Asia 2
Location: Dolphin Resort

Session Chairs: Naiyang Ma, ArcelorMittal; Gaifeng Xue, Wuhan Iron and Steel Corp.

8:30 AM

Tile Production Using Wastes from Mining Industry of the Mining District Pachuca and Real Del Monte: Juan Hernandez¹; Eleazar Salinas¹; Francisco Patiño¹; Isauro Rivera¹; J. Flores¹; Norma Trápala¹; Miguel Pérez¹; Mizraim Flores¹; Iván Reyes¹; ¹Universidad Autónoma del Estado de Hidalgo

This work is related with the production of tiles using wastes from mining and metallurgical industry of Hidalgo State, as raw material. These wastes present a majority particle size (60 %), minor than 53 m (mesh 270, in Tyler Series) with the following composition; 70.01 % wt. of SiO₂, 12.82 % wt. of Al₂O₃, 3.80 % wt. of Fe, 0.70 % wt. of Mn, 3.98 % wt. of K₂O, 3.34 % wt. of CaO, 2.50 % wt. of Na₂O, 0.04 % wt. of Zn, 0.026 % wt. of Pb, 56 grams per ton of Ag and 0.6 grams per ton of Au. In this work, the partial results and experimental conditions for the preparation of some composites to produce tiles are shown. The composite that offers the best results in productions of tiles was that with 66.67 % wt. of mining waste, 26.67 % wt. of red mud and 6.67 % wt. of black mud.

8:50 AM

Concrete Using the Composite of Steel Slag and Granulated BF Slag Powders as Cementitious Material: *Honghui Fang*¹; Jiannyang Hwang¹; Gaifeng Xue¹; Lijun Lu¹; ¹Wuhan Iron and Steel Group Company R&D Center

Steel slag has been stockpiled in many steel mills due to its poor performance in various construction related applications. Free lime in steel slag has been considered as a major barrier for its utilization. Composite

of steel slag and powders of granulated blast furnace slag have been found an excellent cementitious material for concrete. Portland cement is not required in this kind of concrete. Concretes with various amounts of steel slag and powders of granulated blast furnace slag additions have been investigated. Physical and chemical properties of the products were determined. High performance concrete can be obtained. Field testing of the concrete products was conducted for various applications, including buildings and pavements, and the results demonstrated the soundness of the concrete. Drill cores of field tested concrete, with ages up to 26 years, were examined for the microstructures under SEM.

9:10 AM

Setting Time of Concrete Material; Laboratory Measurements Versus Field Applications: Mourad Riad¹; Samir Shoukry¹; Gergis William¹; ¹West Virginia University

Setting of concrete material is defined as the transitional period between states of true fluidity and true rigidity. Initial and final setting times are measured in the laboratory on the mortar sieved from the mix in a controlled environment where temperature and moisture values are constant. On the other hand, field applications are held in outdoor environments where environmental variations have direct impact on setting time values. In this study, initial setting time of class K concrete, usually used for bridge decks and concrete pavements, are investigated highlighting discrepancies between laboratory and field measurements. 72 mixes have been cast in variable environments and collected data from concrete mixes and the ambient conditions are reported. In light of the collected data, the effects of variable setting times on early age cracking of concrete material are studied and means to minimize such cracks are presented.

9:30 AM

Experimental Research to Improve the Soundness of Cementitious Material Blended with Cycled Fluidized Bed Ash: Zhu Shu Jing¹; He Xinghua¹; ¹Department of Water Supply in South Company of China Metallurgical Group

Cycled fluidized bed ash, a significant portion of fly ash produced from coal-fired power plants and rejected from the ash classifying process, has remained unused due to its high free CaO and SO₃ content. It is necessary to extend research on the method to reduce the expansion and improve the compressive strength by some effective chemical activator. This paper presents experimental results on the expansion by Le chatelier tester and the compressive strength. Hydraulic ash-zeolite(HAZ) cementitious material was blended as the chemical activator to study the effects of the activator on the expansion and the compressive strength. The results show that HAZ can not only reduce the expansion, but also increase the prisms compressive strength. Scanning electron microscope observation and X-ray diffraction analysis indicate that the main hydrated products of the sample are calcium hydroxide, ettringite, zeolite and calcite, which can explain the results of the expansion and the strength tests.

9:50 AM

Characterization of Dust Generated in the BOF Converter: Eduardo Junca¹; José Oliveira²; Denise Espinosa¹; Jorge Tenório¹; ¹University of São Paulo; ²Instituto Federal do Espírito Santo

Steel industry has been expanding every year, consequently there has been an increase in waste generation in this area. Thus, companies in this sector are finding it difficult to give a correct destination of waste. For example, only in a blast oxygen furnace (BOF) converter are generated about 18kg of dust per ton of steel. The aim of this work was the characterization of dust generated in the BOF converter. The characterization was performed by chemical analysis (titration for iron and its oxides and Inductively Coupled Plasma Atomic Emission Spectroscopy for other elements), scanning electron microscopy, size analysis using Mastersizer 2000 equipment and X-ray diffraction. It was observed that dust is composed mainly iron in form of magnetite, metallic iron and wustite with approximately 99% of the particle size below 100µm.

10:10 AM Break

10:20 AM

Production of Apatitic Material Using Turkish Colemanite Mineral: Cagatay Moral¹; Gulhayat Nasun-Saygili¹; ¹Istanbul Technical University

The aim of this study is to prepare the apatitic material using colemantite mineral (2CaO.3B₂O₃.5H₂O) which was obtained from Eastern Anatolia, Turkey. For this purpose, colemantite mineral was reacted with different phosphate sources, namely, dipotassiumhydrogen phosphate, ammoniumhydrogen phosphate and orthophosphoric acid at various temperatures and time periods. Experiments were run in batch system. The apatitic material was prepared by a wet method and followed by heat treatment at various temperatures. Structure of the samples were analyzed by XRD, FTIR, XRF and SEM. The particle size analysis was also made for the result product. The experiments showed that reaction temperature, contact time and heating temperature are important parameters to transform the colemantite into apatitic structure. Reaction of colemantite with dipotassiumhydrogen phosphate and ammoniumhydrogen phosphate results in amorphous, non-stoichiometric hydroxyapatite type structure, while acid based phosphate source gives brushite and monetite type product before and after heat treatment, respectively.

10:40 AM

Mercury Oxidation and Capture over SCR Catalysts in Simulated Coal Combustion Flue Gas: Wei Gao¹; Qingcai Liu¹; Jian Yang¹; Wenchang Xi¹; ¹University of Chongqing

The process of the reaction among elemental mercury and reactive flue gas components across the selective catalytic reduction (SCR) catalyst was studied in a laboratory-scale reactor. The SCR catalysts were tested for oxidation and capture of elemental mercury and its capture in simulated coal combustion flue gas representing those from combustion of low-rank coals. Experiments were conducted in a fixed-bed reactor at temperatures ranging from 100 to 350°C. The reaction mechanisms over the catalysts at SCR operating temperatures were investigated using individual flue gas components (HCl, NO) with O₂ balanced in N₂. The monomeric vanadyl sites on the catalyst surface were found to be responsible for the adsorption of both Hg⁰ and HCl, which means they are active for mercury oxidation. NO promoted Hg⁰ oxidation and capture in the presence of O₂, but their promotional effects were insignificant in the absence of O₂.

11:00 AM

Gas Emission and Structural Changes in the Firing of Red Clay Ceramics with Addition of Sanitary Ware Mass Wastes: Roberto Faria¹; Vanessa Souza¹; Shirley Cosin²; Rosane Toledo¹; Helion Vargas¹; ¹North Fluminense State University; ²Federal University of São Carlos

With the purpose of decrease environmental impact, caused by industrial residues (just discarded in the environment) and clay extraction in the ceramic industry, sanitary ware wastes were incorporated into clay. In contrast, it is important to evaluate not only the technological essays but also gases emissions in the ceramic firing process. The pollutant gases emitted in ceramic with residues can be in much larger concentrations than that in a pure clay ceramic firing or, on the other hand, can decrease the pollutant gas concentrations. With the aid of thermal analyses and photoacoustical techniques it was observed that sanitary ware waste can reduce the CO₂ emission. The gas emissions were shown as in function of firing temperature from 300 °C to 1100 °C. In order to analyse phase transformations during the firing process, clay samples and wastes were both analysed by x-rays fluorescent chemical analysis and x-rays diffraction mineralogical analysis.



TMS 2012

141st Annual Meeting & Exhibition

Computational Thermodynamics and Kinetics: Molecular Dynamics: Potentials and Simulations

Sponsored by: The Minerals, Metals and Materials Society, TMS Electronic, Magnetic, and Photonic Materials Division, TMS Materials Processing and Manufacturing Division, TMS Structural Materials Division, TMS: Alloy Phases Committee, TMS: Chemistry and Physics of Materials Committee, TMS/ASM: Computational Materials Science and Engineering Committee, TMS: Integrated Computational Materials Engineering Committee, TMS/ASM: Phase Transformations Committee, TMS: Process Technology and Modeling Committee

Program Organizers: Zi-Kui Liu, The Pennsylvania State University; Mark Asta, University of California, Berkeley; James Warren, The National Institute of Standards and Technology; Yunzhi Wang, Ohio State University; Raymundo Arroyave, Texas A & M University; Yu Wang, Michigan Tech

Wednesday AM
March 14, 2012

Room: Australia 3
Location: Dolphin Resort

Session Chairs: Graeme Murch, The University of Newcastle; Byeong-Joo Lee, POSTECH

8:30 AM Invited

Recent Progress in Atomistic Computational Thermodynamics: *Byeong-Joo Lee*¹; ¹Pohang University of Science and Technology

Computational thermodynamics, often associated with the CALPHAD technique, provides a thermodynamic basis to the phase field method simulation technique and contributes to predict phase transformations and microstructure evolution. For more accurate prediction, the phase field method needs wider range of fundamental materials properties as input data than provided by the CALPHAD technique. Typical examples of those properties are the grain boundary, interface and surface energy which are known to have a decisive effect on the microstructure evolution. In the present talk, recent progress in an empirical atomistic approach to provide such thermodynamic information will be outlined. This atomistic approach is based on the 2NN MEAM interatomic potential model which is highly applicable to multi-component alloy systems. A scheme to couple this atomistic computational thermodynamics with the phase field method and to extend the approach to multi-component systems and dynamic interfacial properties (diffusion and mobility) will also be discussed.

8:55 AM

A New Many-Body Potential Based on the Second-Moment Approximation of Tight-Binding Scheme for Alpha Hafnium: *Xidong Hui*¹; *Deye Lin*¹; *Yi Wang*²; *Shunli Shang*²; *Zi-kui Liu*²; ¹University of Science and Technology Beijing; ²The Pennsylvania State University

In this work, we have proposed a new analytic function of the many-body potential based on the second moment approximation of the tight-binding scheme (TB-SMA) by introducing two polynomial factor functions into the original Finnis and Sinclair's (F-S) model for alpha-Hafnium. All the parameters of the new many-body potential have been systematically evaluated by fitting to ground-state properties including cohesive energy, lattice constants, elastic constants and vacancy formation energy. By using the present model, we also performed molecular dynamics simulations to predicate the melt point, thermal expansion coefficients, point defects and surface energy of α -Hf. It is shown that these properties can be reproduced well by the present model. Compared with previous works, some results calculated by present model are more closed to experimental data, indicating that this work has made substantial progress in development of TB-SMA for hexagonal close packed metals.

9:10 AM

Development of Concentration Dependent Interatomic Potential and Study of Deformation Mechanisms for Light-Weight Mg-Li Alloys: *Shivraj Karewar*¹; *Niraj Gupta*¹; *Alfredo Caro*²; *Srinivasan Srivilliputhur*¹; *Enrique Martinez*²; ¹University of North Texas; ²Los Alamos National Lab

The Mg-Li alloys are light weight-high strength candidate alloys for many automotive and aerospace applications. However, magnesium has low ductility and lithium additions increase its ductility as well as corrosion behavior. To study such effects, we need a reliable atomistic model for the Mg-Li system. Here, we present our newly developed, thermodynamically and mechanically reliable Mg-Li potential based on a concentration dependent method. We verify and validate our potential using alloy properties such as heat of mixing, elastic constants, and defect energetics available in the literature. Furthermore, we use this potential to create phase diagram for the Mg-Li system. This potential will be used to study clustering processes in the bulk, special grain boundaries and free surfaces of hexagonal-close-packed Mg-Li alloys using a Monte Carlo method.

9:25 AM

Charge-Optimized Many Body (COMB) Potential for Uranium: *Yangzhong Li*¹; *Tzu-Ray Shan*¹; *Tao Liang*¹; *Simon Phillpot*¹; *Susan Sinnott*¹; ¹University of Florida

The prevalent phases of most metals have very symmetric ground state structures such as fcc or hcp. The low-temperature phase of uranium (α -U) has a low symmetry orthorhombic structure, a result of the strong correlations of the f electrons. As a result, it has proven very difficult to construct a classical empirical potential suitable for molecular-dynamics (MD) simulations. Here, a Charge-Optimized Many Body (COMB) potential for α -U is developed. The lattice parameters, elastic constants, defect formation energies and thermal expansion coefficients are compared to experimental values where available, and to the results of Density Functional Theory (DFT) calculations. This work was supported by the Center for the Materials Science of Nuclear Fuel, a DOE-BES Energy Frontiers Research Center.

9:40 AM

Structure of Martensite Phase in Free Standing Nano-Particles: *Zhen Zhang*¹; *Xiaobing Ren*²; ¹Frontier Institute of Science and Technology, Xi'an Jiaotong University; ²National Institute for Materials Science, Japan

The structure and morphology of martensite phase are important parameters in understanding the physical properties of shape memory alloys (SMA). For bulk SMA, the role of transformation strain and point defect have been revealed by observing the structure of self-accommodated martensite phase, adaptive phase, and strain glass state. For nanoscale SMA, however, the information on structure of martensite phase is still lacking. Therefore, the origin of size-dependent martensitic transition is still under controversial. We have studied the martensitic transformation in free standing nano-particles by molecular dynamics simulation method. This atomic approach enabled us to map the structure of martensite phase directly. It is found that the martensite phase in nano-particles is not homogeneous but tends to go back to parent phase when approaching surface. Moreover, a simple analytical model is established based on our direct observation and successfully reproduces the size dependent property of martensitic transition.

9:55 AM

Nano Phase Diagram, Structural Change and Catalytic Application of Ag-Au Bimetallic Nanoparticles: *Sang Chul Yeo*¹; *Da Hye Kim*¹; *Kihyun Shin*¹; *Hyuck Mo Lee*¹; ¹KAIST

Bimetallic nanoparticles (NPs) have attracted considerable interest due to their unique properties. One unique trait is that their physical and chemical properties can be modulated when their size is changed. This capability enables bimetallic NPs to have a wide application in areas such as catalysts. We study the structural evolution of 270 atom (2nm) Ag-

Au NPs with composition and temperature. The solid-to-liquid transition region and the solid-state structure were investigated using molecular dynamics simulations together with the caloric curve, mean square displacement and structural deviation. As a result, we constructed a phase diagram of the 2nm-scale AgAu nanoparticle. Additionally, we performed the density functional theory calculations to explore the CO oxidation, O₂ adsorption and dissociation on the Ag-Au bimetallic NPs. In this way, we investigated their effect on the catalytic properties.

10:10 AM Break

10:30 AM

Molecular Dynamics Determination of the TTT Diagram For Crystallization of an Undercooled Liquid NiAl Alloy: Elena Levchenko¹; Irina Belova¹; Alexander Evteev¹; *Graeme Murch*¹; ¹The University of Newcastle

MD with an embedded-atom method potential is used to explore amorphous NiAl. First our recent MD results are summarized of the transient formation of amorphous NiAl that can form on reactive interdiffusion at the nano-level. Next, new MD results are described for the determination of the TTT diagram for crystallization of stoichiometric intermetallic NiAl. This diagram shows a typical nose-like shape. Analysis demonstrates that the critical cooling rate of liquid NiAl alloy to produce an amorphous state is very high, about $10^{11} - 10^{12}$ K/s and is comparable with similar estimations for pure metals. These findings reveal a low glass-forming ability of undercooled liquid NiAl and suggest why there is a lack of experimental data on synthesising of amorphous and nanocrystalline structures of this intermetallic by rapid solidification.

10:45 AM

Hybrid Deterministic and Stochastic Approach for Long Time Scale Atomistic Simulations: *Pratyush Tiwary*¹; Axel van de Walle²; ¹Caltech; ²Brown University

We propose a hybrid deterministic and stochastic approach to achieve extended time scales in atomistic simulations that combines the strengths of molecular dynamics (MD) and Monte Carlo (MC) simulations in an easy-to-implement way. The method exploits the rare event nature of the dynamics similar to most current accelerated MD approaches but goes beyond them by providing, without any further computational overhead, (a) rapid thermalization between infrequent events, thereby minimizing spurious correlations, and (b) control over accuracy of time-scale correction, while still providing similar or higher boosts in computational efficiency. We present two applications of the method: (a) Vacancy-mediated diffusion in Fe yields correct diffusivities over a wide range of temperatures and (b) source-controlled plasticity and deformation behavior in Au nanopillars at realistic strain rates ($10^3/s$ and lower), with excellent agreement with previous theoretical predictions and in situ high-resolution transmission electron microscopy observations. In (b), we also calculate detailed temperature and stress dependence of activation free energy for surface nucleation of dislocations in pristine nanowires. The method gives several orders-of-magnitude improvements in computational efficiency relative to standard MD and good scalability with the size of the system.

11:00 AM

Spatially-Dependent Cluster Dynamics Modeling of Microstructure Evolution in Low Energy Helium Irradiated Tungsten: *Thibault Faney*¹; Brian Wirth²; Niklas Juslin²; ¹UC Berkeley; ²University of Tennessee

In fusion reactors, one key plasma facing component, the divertor, will face high fluxes of low energy (~100 eV) helium and hydrogen. The behaviour of Tungsten (the leading material candidate for the divertor) under high dose irradiation with coupled helium/hydrogen exposure remains to be determined. This study's aim is to understand and predict primary defect production and defect diffusion, clustering and interaction close to the inner surface of the divertor due to low energy helium irradiation. These defects can be interstitial and vacancy clusters, helium

interstitials and helium-vacancy clusters. Molecular dynamics simulations have been performed in order to calculate mobilities and binding energies of the different types of defects. These results are then input into a spatially-dependent cluster dynamics model based on reaction-diffusion rate theory to describe the evolution in space and time of all of these defects. Modelling predictions are then compared with experimental data available in the literature.

11:15 AM

Reciprocal-Space Approach for Atomic Interactions and Configuration Correlations in Inhomogeneous Systems: *Mariya Rasshchupkyna*¹; Volodymyr Bugaev¹; Alexander Udyansky²; Miguel Castro-Colin¹; Peter Wochner¹; ¹Max Planck Institute for Intelligent Systems; ²Max Planck Institute for Iron Research GmbH

Reciprocal space configurational thermodynamics of disordered systems [1,2] deals with cooperative concentration modes that take into account statistical coupling, which is essential for studies of highly inhomogeneous (liquid, amorphous) states. The main parameter of this theory is a Fourier component of the inter-particle potential function. The form of this function determines the structural and thermodynamic behavior of a system. Therefore, the right choice of the potential in statistical-thermodynamic modeling is of crucial importance. Coherent scattering data enables the extraction of parameters to construct an interaction potential, which is used to calculate two-body and, especially, many-body correlation functions. By this token, orientational pair-pair correlations are of particular interest in the present study since they describe bond-angle distributions as well as mid-range correlations[3].[1] V.N.Bugaev, A.Udyansky, O.Shchyglo, H.Reichert, H.Dosch, Phys.Rev. B74, 024202-1 (2006).[2]R.V.Chepulskaa, Phys.Rev. B69, 134431 (2004).[3]P.Wochner, C.Gutt, T.Autenrieth, T.Demmer, V.N.Bugaev, A.D.Ortiz, A.Duri, F.Zontone, G.Grübel, H.Dosch, PNAS 106, 11511 (2009).

11:30 AM

Atomistic Simulation of Nucleation during Crystallization: *Ramanarayan Hariharaputran*¹; Pavlo Rutkevych¹; David Wu¹; ¹Institute of High Performance Computing, Singapore

Crystallization from melt is a widely adopted materials processing route for various technological applications. Nucleation, an important step in the crystallization process, is altered by varying the thermodynamics and kinetics of transformation, to achieve varied microstructural outcomes with distinct material properties such as single crystal, fine grained polycrystal and glass. To gain insight into nucleation process, we present our studies of nucleation during crystallization using molecular dynamics (MD) simulation. Due to limitation in time and length scales accessible, MD simulations of nucleation are normally performed at high driving forces, which may introduce artifacts in the simulation. We propose non-equilibrium modifications of the boundary conditions to avoid artifacts arising from high driving forces. Our simulation results for a unary system are interpreted within the classical nucleation theory framework to yield parameters such as critical size, free energy barrier, and interfacial energy, to be used as inputs for mesoscale simulations of crystallization.

11:45 AM

Screening High-Performance Liquid Metal Anode for SOFC: Combining Ab Initio Molecular Dynamics Simulations and Experiments: *Michael Gao*¹; Harry Abernathy¹; Mike Widom²; Yves Mantz¹; Kirk Gerdes¹; ¹National Energy Technology Lab; ²Carnegie Mellon University

The performance of liquid metal anode SOFC critically depends on oxygen transport through the anode, from the anode/electrolyte interface to the fuel/anode interface(s). The aim of this study is to efficiently and reliably screen alloy compositions that have the potential to outperform the benchmark alloy (pure liquid tin) with respect to enhanced oxygen diffusivity and solubility. We combine ab initio molecular dynamics simulations based on density functional theory and experiments that measure the density, solubility, diffusivity and current. NVT molecular dynamics simulations are performed for a series of Sn-based (binary,



TMS 2012

141st Annual Meeting & Exhibition

ternary and quaternary) liquid alloys at $T=1073\text{K}$. The phase stability of various hypothetical $\text{Sn}_{16}\text{-xR}_x\text{O}_{32}$ alloys (prototype rutile titania) are also predicted. Down selected alloy compositions are recommended for experimental verification, and the predicted density, structure, and diffusivity are compared with available experimental values.

Computational Thermodynamics and Kinetics: Oxides, Steels, and Nuclear Materials

Sponsored by: The Minerals, Metals and Materials Society, TMS Electronic, Magnetic, and Photonic Materials Division, TMS Materials Processing and Manufacturing Division, TMS Structural Materials Division, TMS: Alloy Phases Committee, TMS: Chemistry and Physics of Materials Committee, TMS/ASM: Computational Materials Science and Engineering Committee, TMS: Integrated Computational Materials Engineering Committee, TMS/ASM: Phase Transformations Committee, TMS: Process Technology and Modeling Committee

Program Organizers: Zi-Kui Liu, The Pennsylvania State University; Mark Asta, University of California, Berkeley; James Warren, The National Institute of Standards and Technology; Yunzhi Wang, Ohio State University; Raymundo Arroyave, Texas A & M University; Yu Wang, Michigan Tech

Wednesday AM
March 14, 2012

Room: Asia 5
Location: Dolphin Resort

Session Chairs: Raymundo Arroyave, Texas A & M; Bengt Hallstedt, RWTH-Aachen

8:30 AM Invited

Thermodynamic Modeling of Oxide Systems – From Slags to Advanced Functional Materials: *Bengt Hallstedt*¹; RWTH Aachen University

Oxide materials are used in a huge number of applications. In many of them phase equilibria and phase transformations play an important role. It is clear that thermodynamic modeling will then be useful in order to design new materials, to develop process routes etc. The level of sophistication needed can be very different; sometimes just a rough idea under which conditions a phase is stable is needed and sometimes detailed knowledge about defect chemistry is needed. In this talk currently used models for liquid and solid phases will be discussed. For liquids associate, quasi-chemical and ionic sublattice models are in use. For solids the compound energy formalism (CEF) has become dominating. CEF can be used to model also defect chemistry, but it has some fundamental differences compared to traditional defect chemistry. This discussion will be illustrated with examples from solid oxide fuel cells, lithium ion batteries and high-temperature superconductors.

8:55 AM

Thermodynamic and Kinetic Calculations Supporting the Development of Tool Steels: *Karin Frisk*¹; Greta Lindwall¹; Swerea KIMAB

Application of thermodynamic and kinetic calculations in the development of high nitrogen tool steels, and for understanding the secondary carbide precipitation in hot work tool steels is presented. New types of tool steel with high nitrogen contents (up to over 4%) have recently been developed. The substitution of C for N in these steels has a strong effect on the precipitate type, size, and on the compatibility with other steels, and these effects are described using thermodynamic and diffusion calculations combined with model alloy verifications. Modelling of the precipitation of secondary carbides based on a thermodynamic description coupled with kinetic parameters, through multi-component nucleation and growth models show that the effect of composition on precipitation can be described by the simulations. The most critical input to the calculations, for both applications, is the thermodynamic description of the individual phases.

9:10 AM

Thermodynamic and Elastic Properties of β -Fe from First-Principles Calculations: *Martin Friak*¹; Fritz Koermann¹; Alexey Dick¹; Alexander Udyansky¹; Tilmann Hickel¹; David Holec²; Joerg Neugebauer¹; ¹Max Planck Institute for Iron Research; ²Montanuniversitaet Leoben

Understanding and tailoring the thermodynamic and elastic properties of paramagnetic body-centered cubic iron (β -Fe) is fundamental for developing Fe-based materials operating at elevated temperatures. We have therefore studied β -Fe, modeled by an antiferromagnetic supercell, with the internal distribution of local magnetic moments having the special quasirandom structure (SQS). In contrast to previously suggested antiferromagnetic models that were found to be mechanically unstable with respect to tetragonal deformations, the proposed SQS supercell is stable. Using this approach the thermodynamic stability of beta-Fe with respect to tetragonal and trigonal deformations has been studied. The corresponding total energies have been determined for a broad range of deformations and are compared with those calculated for ferromagnetic (FM), non-magnetic (NM), and antiferromagnetic single-layer (AFM-1) magnetic states. The calculated single-crystalline elastic constants are found to closely reproduce experimental data detected within the temperature range of β -Fe.

9:25 AM

Thermodynamic Properties of Cementite Including Magnetic, Vibrionic, and Electronic Excitations from Ab Initio: Alexey Dick¹; Fritz Körmann¹; Tilmann Hickel¹; Jörg Neugebauer¹; ¹Max-Planck-Institut für Eisenforschung GmbH

A profound knowledge of the thermodynamic properties of binary phases is critical for the construction of phase diagrams for steels. The experimental investigations for cementite, the most frequent carbide in steels, are, however, rather infrequent and difficult due to the presence of other phases. We have, therefore, performed a first-principles study of cementite employing density functional theory (DFT). Thermodynamic effects due to phonons and electrons are described within the quasiharmonic approximation and finite-temperature DFT. To account for magnetic excitations we have developed an effective model based on a numerically exact solution of a quantum spin Hamiltonian. Consistent with findings for nonmagnetic materials, the accuracy of the calculated free energies is mainly limited by the DFT $T=0\text{K}$ potential energy surface. Our approach reliably describes the temperature dependence of the heat capacity of cementite, and clearly demonstrates the importance of ab initio calculations to advance the calculation of Fe-based phase diagrams.

9:40 AM

Ab-Initio Calculation of High-Temperature Rare Earth Phases Using Large-Displacement Phonon Methods: *Nikolas Antolin*¹; Oscar Restrepo¹; Wolfgang Windl¹; ¹Ohio State University

With recent developments in green technology, research into the previously under-utilized lanthanide series elements has become increasingly relevant. Ab-initio calculations have been hugely successful in the past in providing the necessary free energies to predict phase transformations and phase stability for elemental and alloyed materials. The application of ab-initio methods, however, is problematic when it comes to model metals and their alloys with mechanically unstable high-temperature phases, such as the bcc high-temperature phases of Ti, Hf, and rare earths. Using a novel large-displacement phonon method, the free energies and elastic constants of high-temperature phases of a model transition metal (hafnium) and several unexplored rare earth metals were calculated. We suggest a method to approximate the necessary displacement from the appropriate first principles calculation and demonstrate agreement with experimental data for several systems before extending the method to previously unmeasured high-temperature rare earth materials.

9:50 AM Break

10:20 AM

A Genetic Algorithm Approach to Maximize Austenite Volume Fraction in TRIP Steels: *Shengyen Li¹; Ruixian Zhu¹; Ibrahim Karaman¹; Raymundo Arroyave¹; ¹Texas A&M University*

The purpose of this work is to predict the optimum temperatures for two-step heat treatment to maximize the retained austenite in TRIP steel by employing a thermodynamic approach. TRIP steel consists of ferrite, bainite, martensite and retained austenite. Austenite contributes directly to the TRIP effect as its transformation to martensite during deformation provides additional plasticity. Under normal conditions austenite is metastable at room temperature but can be stabilized by saturation with carbon. Enrichment of austenite can be achieved through a two-step heat treatment. During intercritical annealing (IA) a dual phase structure (ferrite+austenite) is achieved. A further bainite isothermal treatment (BIT) leads to carbon enrichment of IA austenite through the formation of carbon-free ferrite. In this work, a thermodynamic approach is coupled to a Genetic Algorithm-based optimization procedure to design the treatment temperatures to maximize the volume fraction of retained austenite in a Fe-0.32C-1.42Mn-1.56Si alloy. The results are compared with experiments

10:35 AM

CarbonitridingTool© - Modeling the Carbonitriding Process: *Yuan Xu¹; Liang He¹; Guannan Guo¹; Huaxia Yu¹; Laura Patricia Rivera¹; Richard D. Sisson¹; ¹Wooster Polytechnic Institute*

Computational models have been developed to simulate the surface hardening of steel. The CarbonitridingTool© has been developed to model the carbonitriding heat treating process in the paper. The finite difference method is used to simulate the absorption and diffusion of carbon and nitrogen into several steels during carbonitriding processes. The diffusional interactions between carbon and nitrogen have been experimentally and theoretically determined and are included in the model. Carbon concentration, nitrogen concentration and microhardness in the carbonitrided layer can be predicted with the software. The experimental results will be presented along with the beta version of the validated model. The effects of carbon potential and ammonia addition in the endogas atmosphere will also be presented and discussed.

10:50 AM

Modeling of Low Alloy Steel Gaseous Nitriding Process: *Mei Yang¹; Richard Sisson¹; ¹WPI*

The microstructural development during the nitriding of quenched and tempered low alloy steels has been theoretically and experimentally investigated. The result is compared with the calculations from Thermo-Calc, which use thermodynamic data to predict multi-component phase behavior during nitriding. Customized Lehrer diagrams are developed to predict the relationship between the nitriding potential and the phase development at different temperatures. In addition, a computational model is developed to predict the nitriding kinetics. The methodology and preliminary results for this model will be presented and compared with experimental results.

11:05 AM

Advanced Stochastic Cluster Dynamics for Studying of Defect Evolution in Materials under Multi-beam Irradiation Conditions: *Tuan Hoang¹; Jaime Marian¹; Vasily Bulatov¹; Daryl Chrzan²; ¹Lawrence Livermore National Laboratory; ²University of California, Berkeley*

Stochastic Cluster Dynamics (SCD), a new modeling approach has been developed to study defect evolution and property degradation in materials subjected to particle irradiation in fission and fusion nuclear reactors and in various material testing facilities. More specifically, we seek to understand synergistic effects caused by the simultaneous bombardment of the material by energetic particle beams of different types, emulating the conditions in real nuclear reactors and multi-beam facilities. SCD is

proposed as an alternative to the traditional rate theory (RT) approach which becomes computationally expensive when dealing with complex species comprised of more than two components as those present in the ODS steel and, still more expensive, kinetic Monte Carlo (kMC) method. Furthermore, to improve fidelity of our computational predictions we have enabled more consistent treatments of defect sinks, specifically, dislocations and grain boundaries, as opposed to drastic simplifications in the treatment of sinks presented in standard RT approach.

11:20 AM

Computational Modeling of Dislocation Loop Coarsening: *Andrew Boyne¹; Ximiao Pan²; Yunzhi Wang²; ¹University of North Texas; ²The Ohio State University*

Frank-type dislocation loops are common defects, for example as irradiation damage in nuclear reactor materials or “End of Range” defects in Silicon wafers. We have constructed a computational model of vacancy mediated climb in dislocation loops, and employed it to investigate the coarsening behavior of these defects. The model extends the previously developed microscopic phase field model of dislocations to consider coarsening and vacancy supersaturation driven climb in arbitrary configurations of vacancy loops. We compare the predictions of the model to previously developed analytical and line-tracking models of loop climb. The coarsening kinetics of populations of loops are simulated, including in the presence of vacancy sources (i.e. continuous irradiation). Straight-forward extensions of the model are possible, which would enable it to simulate multiple climb systems and the coupled evolution of both vacancy and interstitial point defects.

11:35 AM

Simultaneous and Sequential Transformations: Computational Simulation, Analytical Methods and Experimental Results: *Paulo Rios¹; Wesley Assis¹; Tatiana Salazar¹; Andre Alves¹; Simone Oliveira¹; ¹UFF-EEIMVR*

In a recent work, Rios and Villa presented an analytical methodology suitable for the situation in which transformations take place simultaneously or sequentially. In this work, simultaneous and sequential reactions are simulated using cellular automata. The simulations are compared with published data on the recrystallization kinetics of IF steels and with the analytical methodology. It is shown how kinetic models reactions in isolation may be combined to predict the behavior of these transformations when they take place simultaneously or sequentially. It is also shown how one may extract theoretical information from the experimentally measured or computer simulated quantities.

11:50 AM

Identifying the Energetics of He-Point Defect Interactions in Fe: *Xunxiang Hu¹; Donghua Xu²; Brian Wirth²; ¹UC Berkeley; ²University of Tennessee, Knoxville*

Helium effects on the microstructural evolution and mechanical properties of structural materials are among the most challenging issues facing fusion materials research. In this work, we combine thermal helium desorption spectroscopy (THDS) with positron annihilation spectroscopy and a spatially-dependent cluster dynamics model to investigate the kinetics of helium-point defect interactions of helium implanted single-crystalline iron. This combination allows identification of possible mechanisms responsible for the He releasing peaks. Furthermore, the model predicts the depth dependence of the Helium and Helium – defect clusters as a function of time and temperature during the desorption measurement which can be identified by positron annihilation spectroscopy measurements at a variety of material conditions. This will provide an overview of the self-consistency of the model predictions based on the assumptions made in terms of the He-point defect binding and interaction energies, and diffusivities.



Defects and Properties of Cast Metals: Ductility, Creep, Stress and Cracks

Sponsored by: The Minerals, Metals and Materials Society, TMS Materials Processing and Manufacturing Division, TMS: Solidification Committee

Program Organizers: Mark Jolly, University of Birmingham; Brian Thomas, University of Illinois at Urbana-Champaign; Carl Reilly, University of British Columbia

Wednesday AM
March 14, 2012

Room: Oceanic 4
Location: Dolphin Resort

Session Chairs: Dai Xiaojun, The University of Birmingham; Mei Li, Ford Motor Company

8:30 AM

Thermal-Mechanical Model Calibration with Breakout Shell Measurements in Continuous Steel Slab Casting: Junya Iwasaki¹; Brian Thomas²; ¹Nippon Steel Corp.; ²University of Illinois at Urbana-Champaign

A thermal-stress model of continuous steel slab casting is calibrated with detailed measurements of a breakout and applied to simulate longitudinal off-corner cracks. First, a fluid mass balance is applied together with the measured slide-gate position, mold level, casting speed histories to reconstruct the transient events that occurred during the breakout, including the flow-rate and solidification time histories. A three-dimensional heat transfer model of the mold is calibrated to match the measured mold heat flux and thermocouple temperatures, with the help of an efficient 1D model, CONID. Using these results, a 3D finite-element thermal-stress model of the solidifying shell and mold matched the measured shell thickness profiles, and was applied to reveal insights into the interfacial gap condition and the formation of off-corner longitudinal cracks.

8:55 AM

Transverse Creep Behavior of Superalloy Bicrystals: Kaitlin Gallup¹; Tresa Pollock¹; ¹University of California, Santa Barbara

Creep properties of bicrystals loaded normal to the boundary have been studied in the nickel-based superalloy René N4 and GTD444. Creep specimens were taken from directionally solidified bicrystals containing low and high angle boundaries (<10° misorientation, 20°, >30°). Alloy variants with and without additions of boron and carbon, and those cast using the liquid metal cooled or Bridgman method were studied. Creep mechanisms are compared between single crystal bars and the bars containing a singular grain boundary at two testing conditions of 982°C/206MPa and 760°C/690MPa. Damage occurring along interdendritic regions at the grain boundary is quantified by use EBSD and correlated with shape parameters to measure the local degree of rafting. Light optical profilometry is also used to characterize boundary and fracture surface roughness. Additionally, instances where the orientation to the tensile axis has a larger effect on creep life the presence of the boundary are discussed.

9:20 AM

Effect of Cooling Structure on Stress Distribution of Copper Plates of Slab Continuous Casting Mold: Xiang-Ning Meng¹; ¹Northeastern University

A three-dimensional finite-element thermal-stress model of slab continuous casting mold is conducted to predict stress distribution on copper plates of mold. The results show that specific stress distribution of hot surface and cross-sections of copper plates of mold is determined by materials properties and casting conditions. It is recommended to select metal material that thermal properties close to copper to replace nickel as wear-resistant coating or to design copper-nickel transition region in mold waist to avoid abrupt stress. It is reasonable to design deep water slot in narrow face corner as slope, and a fillet or chamfer should be designed

in upper part of slope slot. Also, design of slope deep slot in corner of narrow face is appropriate, while deepening slot is not helpful to control heat fatigue and avoid permanent creep of copper plates and original slot depth is suitable.

9:45 AM

An Integrated Methodology for Optimizing Al-Si Diecastings in Automotive Applications Part2 – Model Validation in Structural Components: Nicola Gramegna¹; Franco Bonollo²; Giulio Timelli²; Stefano Ferraro²; Gianluca Quaglia¹; ¹ENGINSOFT S.p.A.; ²University Of Padova

An automotive safety component is studied in order to optimize the casting process and the mechanical characteristics. The design of the component follows the path that a good project manager would usually adopt, but at the virtual level before undergoing the final physical tests. A process simulation of original and optimized geometry of a structural component was made, in order to enhance the quality of the casting. The local mechanical properties and residual stresses were identified and transferred to FEA code for impact analysis, both in the initial version design and after the optimization cycle that was implemented using the new approach. Sampling of two different optimized geometries was made. The produced diecastings were analyzed (X-Ray, tomography, microstructure, etc.), in order to identify the distribution and amount of defects. Mechanical tests were also carried out and the experimental data were used to validate the results given by numerical simulations.

10:10 AM Break

10:35 AM

Embrittlement in Superaustenitic Stainless Steels: Sermin Turhan¹; Barry King²; Eren Kalay³; Scott Chumbley²; ¹Cankaya University; ²Iowa State University; ³METU

Attributed to its extreme toughness and corrosion resistance, cast superaustenitic steels are widely used in extreme environments such as off-shore oil wells, seawater systems. However, according to recent time-temperature transformation diagram results, if the alloy is incorrectly heat-treated as little as 15 mins., it embrittles and the toughness is decreased by 50%. In this study we've investigated possible reasons for this embrittlement by using a superaustenitic stainless steel CN3MN at relatively short annealing times. Specimens were heat treated at 927 for various annealing times and their impact strengths were tested. The fracture surfaces were investigated with using scanning electron microscope. A ductile to brittle failure transition was observed for a relatively short annealing. The corresponding microstructures for ductile and brittle specimens were investigated with using transmission electron microscope and electron back-scattered diffraction. The change in microstructure with respect to annealing and its effect on embrittlement for CN3MN will be discussed.

11:00 AM

Deformation Prediction of a Heavy Hydro Turbine Blade During Casting Process with Consideration of Martensitic Transformation: Jinwu Kang¹; Tianjiao Wang¹; ¹Tsinghua University

Heavy hydro turbine castings are made of martensitic stainless steel, which undergoes martensitic transformation during casting process. Therefore, the residual stress and deformation are affected not only by uneven cooling but also by martensitic deformation. However, only thermal stress is processed during the usual numerical simulation of casting process. In this paper, the coupled thermo-martensitic phase transformation-stress model is established and it is implemented by secondary development in ABAQUS, which also incorporates the thermal and mechanical boundaries, the contact pair between casting and mold. The system is applied into the stress analysis of a heavy hydro blade castings. The stress, displacement and phase percentage are obtained. It is found that martensitic phase transformation has significant effect on the stress and deformation results. The simulated results are compared with measured results, and their agreement is improved with the consideration of martensitic phase transformation.

11:25 AM

Reasonable Temperature Schedules for Cold or Hot Charging of Continuously Cast Slabs: *Yang Li¹; Peng Lan¹; Ke Liu¹; Haibo Sun¹; Hongzhi Chen¹; Jiaquan Zhang¹;* ¹State Key Laboratory of Advanced Metallurgy, University of Science and Technology Beijing

There are occasionally transversely fracture problems for some continuously cast slabs during transportation or handling away from their storage state. There are also steel slabs being very sensitive to the formation of surface cracks during hot charging or following rolling process. It is revealed that steels with higher contents of pearlite delayed transformation elements have higher crack-sensitivity with room cooling condition, which should be slowly cooled down after cut to length from hot strand or charged to reheating furnace directly. Steels with higher contents of carbonitride forming elements, however, are even crack sensitive to hot charging temperatures due to the precipitation induced ductility tough. Based on thermodynamic theory for carbonitride precipitation in austenite and a solid-state phase transformation model, the CCT diagrams and the hot charging brittleness temperature range of related steels have been presented for the reasonable determination of their cold or hot charging temperature schedules.

11:50 AM

Affection of Charging Temperature on the Hot Ductility of Nb-Containing Steel: *Yongjian Lu¹; Qian Wang¹;* ¹College of Materials Science and Engineering, Chongqing University

The hot charging process for HSLA steel slabs was hindered by the formation of surface cracks in HSLA steel plate produced by hot charging rolling process. The hot ductility of a Nb-containing steel has been investigated by means of hot tensile tests simulating the charging process. It is indicated that the hot ductility of the steel is affected obviously by the charging temperature while there is less affection on the hot tensile strength. If the charging temperature is between Ar₃ and Ar₁, ductility as measured by reduction of area was generally low for all charging temperatures. This ductility loss can be explained in terms of finely precipitation of carbonitride at grain boundaries and the formation of duplex austenite grains during reheating process. The charging temperature controlled to be above Ar₃ is favorable for avoiding plate surface cracking in Nb bearing steel with hot charging process.

Deformation, Damage, and Fracture of Light Metals and Alloys: Session IV

Sponsored by: The Minerals, Metals and Materials Society, TMS Structural Materials Division, TMS Light Metals Division, TMS/ASM: Mechanical Behavior of Materials Committee

Program Organizers: Qizhen Li, University of Nevada, Reno; Fuqian Yang, Univ. of Kentucky; Ke An, Oak Ridge National Laboratory

Wednesday AM
March 14, 2012

Room: Northern A2
Location: Dolphin Resort

Session Chair: Ke An, Oak ridge national lab

8:30 AM Invited

Influence of Deformation Path and Heating Rate on Recrystallization Kinetics in Al-2%Mg Alloy: *Grigoreta Stoica¹; G. Muralidharan²; B. Radhakrishnan²; S. B. Gorti²; A. D. Stoica²; S. Vogel³; H. M. Reiche³; K. An²; D.E. Fielden⁴; H. Cao²; H.D. Skorpenske²; R.A. Mills²; T. Ungar⁵; B.C. Chakoumakos²; X-L. Wang²;* ¹ORAU/ORNL; ²ORNL; ³LANL; ⁴UTK; ⁵Eötvös University of Budapest

The effect of a tensile load on the recrystallization kinetics of a highly deformed Al-2%Mg alloy was investigated by in-situ time-of-flight [TOF] neutron diffraction at VULCAN [SNS]. The samples were annealed at temperatures of up to 350°C and at stresses ranging from 2 to 20 MPa. Peak profiles analyses were used to monitor: [1] the evolution

of the energy stored in the dislocation substructure, and [2] the growth kinetics of recrystallizing grains. The results demonstrate that the heating rate and the presence of stress significantly affect the recovery rate, as well as, the grain growth. Texture measurements at HB-3A [HFIR] and HIPPO [LANSCE] showed enhanced or diminished texture components depending on the initial texture and the deformation path. Research was sponsored by the Laboratory Directed Research and Development Program of Oak Ridge National Laboratory (ORNL), managed by UT-Battelle, LLC for the U. S. Department of Energy under Contract No. De-AC05-00OR22725.

9:00 AM Invited

Deformation and Fracture Behavior of Magnesium Alloy WE43 at Temperatures and Strain Rates Relevant to Deformation Processing:

Sean Agnew¹; F Polesak¹; ¹University of Virginia

Magnesium alloy, WE43, containing 4 wt% yttrium and 3 wt% rare earth elements (mainly neodymium), has superior ballistic behavior compared on an equal areal density to traditional Al alloy 5083 armor. In order to be implemented, it is necessary to optimize plate production. Hot torsion testing was used to simulate the rolling process. In the range of T = 150–250°C, dynamic strain aging and deformation twinning are observed. At the highest temperatures (T ≥ 400°C), power law behavior typical of dislocation climb and glide is observed. The material undergoes power law breakdown at stresses above ~120 MPa. From 150–425°C, plate-shaped precipitates appear within the grain interiors during the deformation. Sparsely, round precipitates are observed at temperatures above 425°C, the temperature above which uniform dynamic recrystallization is observed. In order to achieve the desired refined microstructure and have sufficient ductility, deformation should be performed at a minimum of 450°C.

9:30 AM

An Investigation of Plastic-Deformation Dynamics on a Wrought AZ31B Magnesium Alloy Using Real-Time In-Situ Neutron-Diffraction Measurements: *Wei Wu¹; Ke An²; Peter Liaw¹;* ¹The University of Tennessee; ²Oak Ridge National Laboratory

Investigations of plastic deformation are worth scientific efforts for structure applications of magnesium alloys, which exhibit the integrated properties of light weight, high strength-to-weight ratio, and high specific stiffness. In the present research, the plastic-deformation dynamics of a wrought AZ31B magnesium alloy has been studied, using real-time in-situ neutron-diffraction measurements at room temperature. We took advantage of the state-of-art VULCAN engineering diffractometer of the Spallation Neutron Source (SNS), Oak Ridge, Tennessee, to achieve the real-time in-situ neutron-diffraction measurement. Instead of using the “traditional” step-loading method, the neutron-diffraction measurements were performed under a continuous loading condition, while the neutron-diffraction data were collected, and then the data were sliced to small time bins. The lattice-strain and diffraction peak-intensity evolution of interested hkl's were examined under the monotonic-loading condition. The new approach provides the detailed information related to the plastic-deformation dynamics, such as the twinning and detwinning behavior of the wrought magnesium alloy.

9:50 AM Break

10:00 AM

In-Situ Neutron Diffraction Study of Plastic Deformation in Solid-Solution-Strengthened Mg-Al and Mg-Zn Binary Alloys: *Soo Yeol Lee¹; Michael A. Gharghouri²; Huamiao Wang³; Ghazal Nayyeri⁴; Peidong Wu³; Warren J. Poole⁴; Wei Wu⁵; Ling Yang⁶; Ke An⁶;* ¹Chungnam National University; ²National Research Council Canada; ³McMaster University; ⁴The University of British Columbia; ⁵The University of Tennessee; ⁶Oak Ridge National Laboratory

Neutron diffraction has been employed to measure lattice strains and bulk texture evolution during tension and compression in a series of solid-solution-strengthened extruded binary Mg-Al and Mg-Zn alloys with composition ranges typical of common commercial alloys (Mg-1,



TMS 2012

141st Annual Meeting & Exhibition

5, 9 wt.%Al and Mg-1, 2 wt.%Zn). Two starting textures were used: 1) the as-extruded texture, T1, in which the basal poles are preferentially oriented normal to the extrusion axis, and 2) a reoriented texture, T2, in which the basal poles were preferentially oriented parallel to the extrusion direction. The results provide insights into the effects of texture, load direction, and composition on the plastic deformation of the magnesium alloys investigated. The data are used to validate elastic-viscoplastic self-consistent models of polycrystal plasticity, from which the critical resolved shear stresses and hardening behaviour of the available slip and twinning modes can be determined.

10:20 AM

In-Situ Microstructure Evolution of Pure Aluminum Single Crystal under Plane Strain Tension: *Yong Seok Choi*¹; Do Hyun Kim¹; Hyun-Sik Choi¹; Suk Hoon Kang²; Jun-Hyun Han³; Heung Nam Han¹; Kyu Hwan Oh¹; ¹Seoul National University; ²Korea Atomic Energy Research Institute; ³Chungnam National University

A novel micro deformation system to analyze plane strain tension behavior was designed, which can measure directly the plastic deformation behavior of sheet metals. Microstructural evolution of single crystal during deformation significantly depends on its crystal structure and potential slip systems related to the tensile direction. In this study, the microstructure and texture evolutions of pure aluminum single crystal during in-situ plane strain tension were investigated by high-resolution EBSD. The formation of slip bands and the orientation rotation behaviors of local areas were traced and analyzed during the deformation. The measured results were compared with the calculated ones based on a crystal plasticity theory. Furthermore, intersection behavior of subdivided slip bands inside of a single crystal was observed using a TEM. This result can be used for the study on the deformation behavior of sheet metals based on a FCC structure and the construction of FLD of aluminum single crystal.

10:40 AM

Low Temperature Superplastic Deformation of Mg-Bi-Si Alloys: Sergei Remennik¹; *Alexander Katsman*¹; Dan Shechtman¹; ¹Technion - Israel Institute of Technology

Magnesium alloys with high room temperature ductility may find applications as biodegradable implant materials. A BS50 alloy with the composition of Mg-5%Bi-0.5%Si (wt%) and ~1.2 μm average grain size was prepared by rapid solidification and extrusion. Tensile tests were conducted at different strain rates in the range 10^{-4} - 10^{-2} s^{-1} and at various temperatures in the range 20-150°C. Superplastic-like behavior, with up to ~200% elongation-to-failure and stress exponent values close to 2 at 150°C, was observed. The activation energy of the process, $Q=91.9$ kJ/mol, was related to a grain boundary sliding mechanism. The stress exponent increases with decreasing temperature and reaches the value $n=3.6$ at 20°C. This was addressed to the contribution of dislocation climbing which controls accommodation processes at grain boundary triple junctions. The threshold stress increases with decreasing temperature. A corresponding energy term, $E=11.4$ kJ/mol, was associated with the binding energy between solute atoms and grain-boundary dislocations.

Electrode Technology for Aluminium Production: Characterization of Anode Materials

Sponsored by: The Minerals, Metals and Materials Society, TMS Light Metals Division, TMS: Aluminum Committee, TMS: Aluminum Processing Committee
Program Organizer: Morten Sorlie, Alcoa Norway

Wednesday AM
March 14, 2012

Room: Americas Seminar
Location: Dolphin Resort

Session Chair: Victor Buzunov, UC RUSAL

8:30 AM

Improving the Precision and Productivity of Green Coke VCM Analysis: Les Edwards¹; *Kevin Hon*¹; James Marino¹; Marvin Lubin¹; ¹Rain CII Carbon

Volatile and Combustible Matter (VCM) analysis of green petroleum coke is an important measurement for determining the calcination behavior and properties of calcined coke. Green cokes with high VCM (>12%) are more difficult to calcine and result in a higher porosity and lower bulk density in calcined coke. The paper will review current methods for measuring the VCM of green coke based on ASTM Quartz and Platinum crucible methods and Macro TGA methods. Detailed experimental results comparing the Quartz crucible and macro TGA methods are presented in the paper. When used in combination with a high speed knife mill, automated TGA equipment offers significantly improved speed and precision and the capability for simultaneous measurement of ash and moisture contents. As the range of green coke qualities used for calcination increases, the need for a more rapid and more precise measurement of VCM increases.

8:50 AM

Discrete Element Method Applied to the Vibration Process of Coke Particles: *Behzad Majidi*¹; Kamran Azari¹; Houshang Alamdari¹; Mario Fafard¹; Donald Ziegler²; ¹Laval University; ²Alcoa Canada

Physical properties of coke particles including particle shape and size distribution have direct effects on their packing density. In the present work, effects of particle shape and size distribution on vibrated bulk density (VBD) of dry coke samples have been investigated. Discrete Element Method (DEM) has also been used to simulate the vibration process. Results showed that the shape and size distribution of particles influence the bulk density of coke and these parameters can be used to describe the packing density of coke particles. In general, mixed samples provide higher VBD than mono-size samples and as the fraction of coarse particles increases vibrated bulk density increases. However, existence of 10 wt.% of fine particles to fill the pores between coarse particles is essential. Simulation results were also reasonably consistent with experimental data. Finally, it is noteworthy that a well-tailored DEM model is capable of predicting the particle rearrangement and density evolution during the vibration process.

9:10 AM

Vibrated Bulk Density using Semi-automated Device: Simplifying Sample Preparation while Improving Accuracy and Precision: *Jignesh Panchal*¹; Jeffrey Rolle¹; ¹A.J.Edmond Company

Vibrated Bulk Density (VBD) of calcined petroleum coke is widely utilized as one measure of quality and is useful for quantifying binder demand in the anode production process of the aluminum reduction industry. ASTM D 4292-10 is one of the methods used widely by the carbon and aluminum reduction industries to measure VBD. Recently the carbon producer and consumer industries have jointly worked together to increase the competence and benefit of this method. Geopyc is a semi-

automated device that potentially yields better precision compared to traditional vibrator device specified in D 4292. This paper presents an innovative use of the Geopyc instrument in measuring VBD, the results of which correlate well with D 4292; especially to the 28x48 Tyler Mesh size fraction. This novel sample preparation does not involve complicated roll crushing steps as specified in the ASTM method(s) and thus simplifies the method while improving the accuracy and precision.

9:30 AM

Characterization of Pre-Baked Carbon Anode Samples Using X-Ray Computerized Tomography and Porosity Estimation: *Donald Picard¹*; Houshang Alamdari¹; Donald Ziegler²; Bastien Dumas¹; Mario Fafard¹; ¹Aluminium Research Centre-REGAL, Laval University; ²Alcoa Canada Primary Metals

Computed tomography has been used in the last years to gather information on carbon anodes which can be used to calibrate numerical models dedicated to simulating the anode forming process. To this end, samples with diameters varying from 50 mm up to 300 mm and cored from an industrial anode have been scanned in a Somatom Sensation 64. A correlation could be established between the CT scan results and the apparent density. To validate the correlation, an extended campaign was performed on 50 mm diameter samples cored in 20 different anodes, thus with possibly varying raw materials. In addition to the CT scan results, the apparent and real densities have been experimentally measured to estimate the porosity level. Similarly to the apparent density, a correlation between the CT scans results and the porosity has been proposed.

9:50 AM

Diagnosing Anode Quality Problems Using Optical Macroscopy: *Barry Sadler¹*; ¹Net Carbon Consulting Pty Ltd

Anode quality assessment has become largely focussed on laboratory tests undertaken on anode core samples. This is important, giving valuable insight to many anode quality problems and their potential causes. Anode "structural integrity" is, however, a critical anode property that is not directly assessed by these traditional anode core tests. Structural integrity is best described as how well an anode has been made, as evidenced by the visual appearance of the anode structure. Several methods have been used previously to visually examine anode structures, including optical image analysis. While these methods can highlight individual structural features, they are not well suited to assessing overall anode structural integrity. This paper will outline a simple method for assessing baked anode structural integrity that uses USB microscopy to evaluate anode quality and diagnose problems.

10:10 AM Break

10:25 AM

Properties and Production Conditions Affecting Crack Formation and Propagation in Carbon Anodes: *Odd Einar Frosta¹*; Arne Petter Ratvik²; Harald A. Øye²; ¹Norsk Hydro ASA; ²Norwegian University of Science and Technology

The objective of the present work is to achieve a better understanding of anode thermal shock fracture in the early stage after an anode change in the electrolysis cell. In order to better show the mechanisms leading to anode fracture and crack propagation, a thermo-mechanical model of the thermal shock experienced by an anode when it is positioned in the pot was developed. The model allows calculation of stresses and strains within the anode, as function of time. The time interval of the modelling lasts for 1 hour after the anode change. Baked anodes are inhomogeneous and anisotropic due to the raw materials and production process. Core samples from industrial scale anodes were analysed and the results provided gradient plots of physical and mechanical properties. The results were used as input to the model and together with a set of boundary conditions, the thermal shock resistance was calculated.

10:45 AM

New Method for Representative Measurement of Anode Electrical Resistance: *Marie-Josée Chollier-Brym¹*; Denis Laroche¹; Alain Alexandre¹; Michel Landry¹; Claude Simard¹; Lucien Simard¹; Danny Ringuette¹; ¹RioTinto Alcan

Electrical anode resistance is more and more recognized as a key parameter for pot operation as the carbon material itself contributes to close to 50% of the anode assembly voltage drop. Factors such as raw materials, forming and baking conditions are sources of significant variation in anode properties, including anode resistance. Anode resistance will vary within an anode and between anode batches reaching voltage differences up to several tens of millivolts. The current method for resistivity measurement is based on core sampling on limited locations of a small population of anodes and may not be representative of the anode resistance. The current study proposes a non destructive method reproducing the current distribution in service and providing immediate results. Such results could be used to improve anode resistance and help potrooms cope with the anode batches variability.

11:05 AM

Increasing Coke Impurities – Is this Really a Problem for Metal Quality?: *Gyan Jha¹*; Frank Cannova²; Barry Sadler³; ¹Tri-Arrows Aluminum; ²BP Coke; ³Net Carbon Consulting

Increases in the Vanadium and Nickel content of anode grade coke in recent years have predictably affected smelter metal quality. This has now reached the point where some smelters struggle to meet traditional metal purity specifications. New metallurgical studies have shown that metal specifications for impurities such as Vanadium and Nickel may be unnecessarily restrictive. Increasing the levels of these impurities higher than the current specifications may provide opportunities to create new alloys in downstream processing. Given this, and the reality that any potential impact of these impurities on anode performance can be mitigated by maintaining adequate anode cover, there is a strong case to revise current metal and coke specifications

11:25 AM

Aluminum Electrolysis Anti-Oxidation Coating Carbon Anode: *Sh Yang¹*; Fengli Yang¹; Zhaowen Wang²; Zhongning Shi²; Bingliang Gao²; ¹Jiangxi University of Science and Technology; ²Northeastern University

Anti-oxidation coating for carbon anode in aluminum electrolysis was studied in this paper. Different compounds of the anti-oxidation coating had different effects on carbon anode. The results showed that hot weight loss rate of coated anode was lower 10-30% than that of uncovered anode. The compounds of the anti-oxidation coating were optimized by SEM and tests of hot weight loss. It was proved that the anti-oxidation coating had great inoxidizable effects on carbon anode, and it was no influence on normal aluminum electrolysis.



TMS 2012

141st Annual Meeting & Exhibition

Electrometallurgy 2012: Session IV

Sponsored by: The Minerals, Metals and Materials Society, The Metallurgy and Materials Society of CIM, TMS Extraction and Processing Division, TMS: Hydrometallurgy and Electrometallurgy Committee

Program Organizers: Georges Houlachi, Hydro-Quebec; Antoine Allanore, Massachusetts Institute of Technology; Michael Free, University of Utah; Michael Moats, University of Utah; Edouard Asselin, UBC; Shijie Wang, Rio Tinto Kennecott Utah Copper; James Yurko, Materion Brush Beryllium and Composites

Wednesday AM
March 14, 2012

Room: Europe 5
Location: Dolphin Resort

Session Chairs: Antoine Allanore, Mass. Inst. Techn.; Michael Free, University of Utah

8:30 AM

Electrochemical Study of the Kinetics of Copper Metal Leaching with Ferric Iron: *Tomas Vargas*¹; Rolando Espinoza¹; ¹University of Chile

The kinetics of the oxidative leaching of copper metal with ferric iron at 60 °C was studied using electrochemical techniques. Studies were conducted in a three-electrode cell using rotating disk electrodes made either of copper or platinum as working electrodes. The kinetics of anodic dissolution of copper was determined from i-E measurements conducted on copper disk electrodes in iron-free solutions containing 160 g/l sulphuric acid. The kinetics of ferric reduction was determined from i-E measurements conducted on platinum disk electrodes and mixed potential determinations conducted on copper disk electrodes in 160 g/l sulphuric acid solutions containing iron in the range 1-3 g/l and Fe³⁺/Fe²⁺ concentration ratios in the range 1-0.3. Experimental measurements were conducted at 60, 300 and 1000 rpm. A kinetic expression for the rate of copper leaching was obtained from the experimental data applying the mixed potential theory.

8:50 AM

Fundamental Reduction Kinetics of Fe(III) on Chalcopyrite Surface: *Guikuan Yue*¹; Edouard Asselin¹; ¹The University of British Columbia

Most of the chemical or electrochemical research on chalcopyrite leaching has focused on understanding the kinetics and mechanisms of the oxidative processes or the reduction reactions of chalcopyrite itself. However, the cathodic reduction of ferric ions on CuFeS₂ is also of great significance because they can affect the overall leaching rate of the process, as predicted by mixed potential theory. In the present study, electrochemical measurements, especially cathodic potentiodynamic polarization and cyclic potentiodynamic polarization, have been employed to study the kinetics of ferric reduction in H₂SO₄ solution. Our work aims to explore the possibility of obtaining fundamental electrochemical kinetic parameters, such as exchange current density and transfer coefficients, thereby obtaining more detailed information about the electrochemical processes involved.

9:10 AM

Influence of Anodic and Cathodic Sub-Processes on the Rate of Copper Dissolution during Ferric Leaching of Chalcopyrite at 70 °C: Hector Jordan¹; *Tomas Vargas*¹; ¹University of Chile

The influence of anodic and cathodic sub-processes on the rate of chalcopyrite dissolution during ferric leaching of chalcopyrite at 70 °C was characterized using electrochemical techniques. Experiments were conducted in a three-electrode electrochemical cell using a working electrode made of chalcopyrite particles. Anodic dissolution of chalcopyrite was characterized from chronopotentiometric experiments conducted in deoxygenated iron-free sulfuric acid solutions at pH 1.7 at

potential values of 0.55, 0.6, 0.7, 0.8 and 0.9 V/SHE. Reduction of ferric ion on chalcopyrite was characterized from linear sweep voltammograms conducted in deoxygenated sulfuric acid solution at pH 1.7 containing total iron concentrations in the range 0.005 – 0.3 M. The Fe³⁺/Fe²⁺ ratio was also varied in these experiments so that solution Eh ranged between 0.55 – 0.9 V/SHE. The obtained experimental results provided a better insight to explain the dependence of chalcopyrite dissolution rate on solution Eh and total iron concentration.

9:30 AM

Cathodic Reactions on Oxidized Chalcopyrite Electrode: *Ahmad Ghahremaninezhad*¹; Edouard Asselin¹; David Dixon¹; ¹The University of British Columbia

In this study pertaining to the electrochemical dissolution of chalcopyrite, the active/passive behavior of a chalcopyrite in sulfuric acid solution was investigated. OCP measurements, potentiostatic and cyclic potentiodynamic polarization, and electrochemical impedance spectroscopy methods were conducted to analyze the electrochemical parameters of the electrode. XPS experiments were used to study the composition of the passive film on the surface. The passive film was an n-type semiconductor with donor density of ~10²³ m⁻³. The results of electrochemical experiments have proved that the surface layer (passive film) of chalcopyrite is a good electron conductor but a poor ionic conductor. Using electrochemical methods, the kinetics of the Fe³⁺/Fe²⁺ couple reaction on the surface of passive chalcopyrite was investigated. A kinetic model of the passivation process for chalcopyrite is proposed. The model was found to be in quantitative agreement with the results of the electrochemical impedance spectroscopy and steady state current vs. potential experiments.

9:50 AM

Investigation of Charge Transfer Resistance at Pyrite Electrodes Modified by Gold and Silver Nanoparticles: *Maziar Eghbalnia*¹; David Dixon¹; ¹University of British Columbia

Gold and silver nanoparticles (NPs) were deposited on pyrite at ambient temperature from colloidal solutions prepared by reduction of hydrogen tetrachloroaurate or silver nitrate by sodium sulfide or sodium tetrahydridoborate. The nanoparticles were characterized using Ultraviolet-Visible (UV-Vis) spectroscopy and the experimental spectra were fitted using Mie - Gans modeling. The modified pyrite was investigated using Electrochemical Impedance Spectroscopy (EIS). Electrodes were prepared from both natural and modified pyrite samples and were modeled using an equivalent circuit (EC) based on the EIS data. The comparison of the results revealed a decrease in charge transfer resistance for the ferric ferrous redox couple associated with the modified pyrite. From this behavior it is concluded that the electronic transport between the nanoparticles and the electrode surface over distances in nanometer scale is enhanced. Nanoparticles below a certain size act as quantum dots due to electronic confinement. Decreased charged transfer resistance at the nanometer scale may be caused by electron transport through tunneling mechanism via quantum dots.

10:10 AM Break

10:25 AM

Electrochemistry of Enargite: Reactivity in Alkaline Solutions: *Robert Gow*¹; Courtney Young¹; Hsin Huang¹; Greg Hope²; Yasushi Takasaki³; ¹Montana Tech of the University of Montana; ²Griffith University; ³Akita University

The presence of enargite (Cu₃AsS₄) is problematic in gold processing as it is refractory, increasing cyanide and oxygen consumption, and environmentally hazardous. Selective leaching and treatment of the arsenic would prove advantageous to conventional gold leaching methods. The reactivity of enargite samples from Montana, US and Quiruvilca,

Peru were studied under alkaline conditions, pH range of 8-13, using a cyclic voltammetry corrosion cell setup. Raman spectra of the surface were taken during and after cycling to compare surface species against theoretical predominance diagrams. Under slightly oxidizing conditions, covellite (CuS) peaks were found on the surface in a short matter of time, above ~0 V vs SHE for pH 9-13, suggesting arsenic leaching, but for longer conditioning times, elemental sulfur peaks were also found, which created a passivating surface layer. By operating above pH 12, under reducing conditions, ~-0.500 V vs SHE, arsenic can be leached as a thioarsenate ($\text{AsS}_{(4-x)}\text{O}_x^{3-}$), without sulfur formation.

10:45 AM

Electrochemical Evaluation of Petzite Leaching: *Laurence Dyer*¹; Maziar Eghbalnia¹; David Dixon¹; John Rumball²; Edouard Asselin¹; ¹University of British Columbia; ²Barrick Gold Corporation

Gold and silver tellurides, such as calaverite (AuTe₂), hessite (Ag₂Te) and petzite (Ag₃AuTe₂), are commonly in many precious metal deposits. While gold and silver are easily leached via several processes (cyanidation, thiosulfate leaching, etc.), their telluride minerals prove far more difficult to treat. Petzite samples synthesized in the laboratory were examined using cyclic voltammetry to elucidate the reactions occurring during leaching in order to determine the factor(s) that inhibits precious metal dissolution.

11:05 AM

Effect of pH And Temperature on Meso-2,3-Dimercaptosuccinic Acid Mediated Dissolution of Polycrystalline Au Electrodes: Scott Smith¹; *Eduard Guerra*¹; Jeffrey Shepherd¹; ¹Laurentian University

Electrochemical and spectroscopic evidence of alkylthiol-mediated Au dissolution is presented. Initial studies were performed on Au electrodes modified with a monolayer of meso-2,3-dimercaptosuccinic acid (DMSA), which was determined to be stable over a narrow range of potentials using cyclic voltammetry. However, at more positive polarizations, DMSA undergoes oxidative desorption. Electrochemical impedance spectroscopy suggested that part of the charge transfer reaction may be associated with Au oxidation. Gold dissolution was confirmed after holding the electrode at 0.8 V vs. Ag/AgCl for 12 hours in LiClO₄ containing 10mM DMSA. This routine resulted in a small, but detectable quantity of Au in the electrolyte. Acidification of the electrolyte coupled with an increase in temperature to 50°C improved Au leaching kinetics, yielding an average rate of extraction 40.1 μg cm⁻² hr⁻¹. The implications of this process in the industrial leaching of Au will be discussed.

11:25 AM

Design and Commissioning of a Laboratory Scale Electrocoagulation Reactor: *Eduard Guerra*¹; *Padmavathy Mahadevan*²; Samir Chefai²; ¹Laurentian University; ²Barrick Gold Corporation

Electrocoagulation is a technique for treating wastewater streams from metallurgical plants whereby electrodes are corroded to generate gases (most notably oxygen at the anode and hydrogen at the cathode) and solid particulates which acts as substrates for coprecipitation of impurities. The performance of electrocoagulation reactors in terms their efficiency for removing a particular impurity is highly dependent on several factors, most notably: the nature of the electrodes, the spacing between electrodes, the current density, the height of the electrodes, the solution flow rate, and application of periodic current reversal. Because these variables have complex interactions, in order to ensure reliable scale-up of laboratory results, experiments should be conducted under conditions that closely match those that would be employed at an industrial scale. To that end, this article describes the design and commissioning of a versatile laboratory scale electrocoagulation reactor that allows for the control of all the aforementioned variables along with the ability to measure the instantaneous spatial distribution of current within the reactor.

Energy Nanomaterials: Supercapacitors

Sponsored by: The Minerals, Metals and Materials Society, TMS Materials Processing and Manufacturing Division, TMS Structural Materials Division, TMS: Advanced Characterization, Testing, and Simulation Committee, TMS: Nanomechanical Materials Behavior Committee

Program Organizers: Reza Shahbazian-Yassar, Michigan Technological University; Ming Au, Savannah River National Laboratory; Meyya Meyyappan, NASA Ames Research Center

Wednesday AM

March 14, 2012

Room: Swan 3

Location: Swan Resort

Session Chairs: Reza Shahbazian Yassar, Michigan Technological University; Ming Au, Savannah River National Laboratory

8:30 AM

Electrochemical Synthesis of Nanostructured Vanadium Oxides for Use as Supercapacitor Electrodes: Allison Engstrom¹; *Fiona Doyle*¹; ¹University of California, Berkeley

Nanostructured vanadium (V) oxide, V₂O₅, was deposited on planar platinum electrodes by potentiostatic anodic electrochemical deposition from an aqueous salt solution. Vanadium (IV) oxide, V₂O₄, and vanadium (III) oxide, V₂O₃, were then prepared by potentiostatically reducing the deposited V₂O₅ at appropriate potentials and pH. An agar gel layer, containing either water or 1.0 M KCl, was used to control dissolution and morphological change upon reduction. Cyclic voltammetry and galvanostatic charge/discharge cycling revealed that the deposited oxides initially exhibited pseudocapacitive behavior ideal for supercapacitor electrodes. The capacitance degraded markedly with cycling when tested in a standard three-electrode cell allowing transport of vanadium species into the bulk electrolyte. Degradation was significantly suppressed when the electrodes were tested in a two-electrode configuration acting as a symmetric supercapacitor device that confined the vanadium species in the gap between the electrodes. The electrochemical performance is correlated with the deposit morphology and mass transport during operation.

8:50 AM

Flexible Zn₂SnO₄/MnO₂ Core/Shell Nanocable-Carbon Microfiber Hybrid Composites for High-Performance Supercapacitor Electrodes: Lihong Bao¹; Jianfeng Zang¹; *Xiaodong Li*¹; ¹University of South Carolina

We demonstrate the design and fabrication of a novel flexible nanoarchitecture by facile coating ultrathin (several nanometers thick) films of MnO₂ to highly electrical conductive Zn₂SnO₄ (ZTO) nanowires grown radially on carbon microfibers (CMFs) to achieve high specific capacitance, high-energy density, high-power density, and long-term life for supercapacitor electrode applications. The crystalline ZTO nanowires grown on CMFs were uniquely served as highly conductive cores to support a highly electrolytic accessible surface area of redox active MnO₂ shells and also provide reliable electrical connections to the MnO₂ shells. These results suggest that such MnO₂/ZTO/CF hybrid composite architecture is very promising for next generation high-performance supercapacitors.

9:10 AM Invited

Dealloyed Nanoporous Metals for Energy Storage: *Mingwei Chen*¹; ¹Tohoku University

Growing demands for energy storage devices with outstanding sustainability and environmental friendliness have stimulated intensive research on electrochemical supercapacitors which can store and deliver energy at fast charging/discharging rates for high-power applications. Pseudocapacitive materials, such as metal oxides, offer higher levels of



TMS 2012

141st Annual Meeting & Exhibition

specific capacitance and energy storage via Faradic surface redox reactions, circumventing the key limitation of conventional electrochemical double-layer capacitors with low energy density. However, the limited cycle life and low power density, as the compromise of increased energy density, intrinsically restrict the applications of pseudo-capacitors in practical devices. In this talk, we will introduce nanoporous metal based nanocomposites, fabricated by dealloying and electroless plating, as robust electrodes for high-performance supercapacitors. The novel nanoarchitecture provides high electrochemical and mechanical stability and excellent electronic/ionic conductivity, giving rise to ultrahigh energy density and power density along with excellent cycling stability and ultrafast rate capability.

9:40 AM

Supercapacitive Properties of Hydrothermally Synthesized Co₃O₄ Nanostructures: *David Mitlin*¹; Huatao Wang¹; Li Zhang¹; ¹University of Alberta and NINT NRC

A hydrothermal process was employed to create a variety of Co₃O₄ nanostructures. We demonstrate that nominally minor differences in the synthesis temperature (50, 70 or 90°C) yielded profound variations in the oxide microstructure, with lathe-like, necklace-like and net-like morphologies of different scales resulting. This in turn resulted in significant variations in the supercapacitive performance that ranged from mediocre to superb. Specifically, the mesoporous net-like Co₃O₄ nanostructures that were synthesized at 50°C exhibited very favorable electrochemical properties: The net-like Co₃O₄ had a specific capacitance of 1090 F/g at a mass loading of 1.4 mg/cm². At this high mass loading such performance has not been previously reported. SEM and TEM analysis of these samples revealed an interconnected array of sub-10 nm crystallites interspersed with a high volume fraction of pores that were on the same scale. The poorer performing microstructures were both coarser and much less porous.

10:00 AM Break

10:30 AM

Graphene/Polyaniline Hybrids-Based Supercapacitor: Li Li¹; *Shiren Wang*¹; ¹Texas Tech University

Polyaniline demonstrates low cost, environmental stability, and unique doping/de-doping characteristics. Graphene also exhibits many exceptional properties, including exceptional mechanical, electrical, and thermal properties, as well as large specific surface area. Synergistic integration of them in a novel structure is anticipated to create high-performance supercapacitors for electrical energy storage. In this paper, polyaniline nanowires were synthesized in the presence of graphene sheets. The resultant hybrids were tuned into various morphologies and the morphology-effect on the electrical conductivity and surface area were investigated. The hierarchical hybrids were also utilized as an electrode of supercapacitor, and the galvanostatic charge-discharge tests were carried out. With optimized hybrid morphology, the specific capacitance is as high as 1100 F/g and it is stable for more than 1000 times. This research suggests that graphene/polyaniline hybrid has great potential for energy storage applications.

10:50 AM

Three-Dimensional Nanoporous Bulk Composite Electrodes Utilized in Battery-Like Electrochemical Capacitors: *Weifeng Wei*¹; Xinwei Cui²; Weixing Chen²; Douglas Ivey²; ¹Central South University; ²University of Alberta

Electrochemical capacitors (ECs), with rapid charge/discharge rates and higher energy density than conventional capacitors, have become a potential solution to various emerging energy applications. The

commercialization of ECs, however, is restricted to much lower energy density than batteries, owing to the low utilization efficiency of active materials in ECs. A battery-like EC that combines the energy density of batteries with the rate capability of capacitors would considerably advance electrical storage technology. Nanostructured electrodes with desirable three-dimensional (3D) architectures are generally believed to enhance active material utilization through facilitating ionic/electronic kinetics and reducing inactive electrode components (e.g., current collectors, electrode binders, conductive additives, etc), although their realization is still challenging. Here we demonstrate a facile solution combustion synthesis process to prepare bulk 3D nanoporous composite sheets used as EC electrodes. Employing such composite electrodes, significant improvement in energy density over traditional bulk electrodes is demonstrated while maintaining the same charge/discharge rates.

11:10 AM

Interdigital Hybrid Graphene/CNT Micro-Electrodes for Supercapacitor Application: *Majid Beidaghi*¹; Chunlei Wang¹; ¹Florida International University

Recently, graphene has been introduced as an excellent material for Electrochemical Double-Layer Capacitors (EDLC). Theoretically, graphene is able to deliver a specific capacitance of 550 Fg⁻¹ if its surface area is fully utilized. However, in practice agglomeration and restacking of single layer graphene sheets during electrode preparation limits their accessible surface area. Moreover, the conventional 2D stacking of the electrodes also limits the penetration of electrolyte ions between the graphene planes. In this work, we have tackled these problems by developing a process to fabricate interdigital micro-electrodes of hybrid graphene/CNT electrodes. The addition of CNTs between the graphene layers minimizes the restacking of graphene sheets, thus providing a higher accessible surface area. Moreover, the interdigital in-plane design of the micro-electrodes provides a better pathway for penetration of ions between the graphene layers. The micro-device also has high surface to volume ratio. The electrochemical performance of the micro-device will be presented.

11:25 AM

Nanostructured Manganese Oxide Supercapacitor Electrodes via Solution Precursor Plasma Synthesis: *Raghavender Tummala*¹; Ramesh Kumar Guduru¹; Pravansu S Mohanty¹; ¹Univ of Michigan

Supercapacitors require high power densities with longer cycle life. Particularly, the metal oxide electrodes exhibit higher specific capacitance than carbon and conducting polymers. Manganese oxides (Mn₂O₃/Mn₃O₄) are one such inexpensive electrode materials with superior electrochemical characteristics. But, most of the conventional approaches involve powder synthesis with subsequent coating steps on the charge collectors, and thereby result in multi-step procedures. We present a single step and inexpensive synthesis technique for manganese oxide electrodes using solution precursor plasma deposition process. A solution precursor comprising manganese salt and deionized water was atomized into fine droplets for rapid thermo-chemical conversion in the plasma plume prior to deposition on the current collector. X-ray diffraction studies confirmed the desired phase and microstructures revealed rough morphology with porosity. Electrochemical characterization of these electrodes in aqueous KOH electrolyte will be reported.

Fatigue and Corrosion Damage in Metallic Materials: Fundamentals, Modeling and Prevention: Fatigue and Corrosion Interaction and Materials Corrosion

Sponsored by: The Minerals, Metals and Materials Society, TMS Structural Materials Division, TMS/ASM: Mechanical Behavior of Materials Committee

Program Organizers: Tongguang Zhai, University of Kentucky; Zhengdong Long, Kaiser Aluminum; Peter Liaw, University of Tennessee

Wednesday AM
March 14, 2012

Room: Oceanic 6
Location: Dolphin Resort

Session Chairs: Jeffrey Evans, University of Alabama in Huntsville; Ronald Holtz, Naval Research Laboratory

8:30 AM

Microstructural and Environmental Effects on Corrosion and Fatigue Crack Growth in 7075 Aluminum Alloy: Amir Bonakdar¹; Jason Williams¹; Nikhilesh Chawla¹; ¹Arizona State University

The corrosion and fatigue behavior of aluminum alloys is greatly influenced by environment and precipitate structure. The driving force at the crack tip is clearly a combination of chemical and mechanical processes operating together. We have been conducting experiments in ultra high vacuum (UHV) and shown that the “intrinsic” material behavior can be extracted in a UHV environment. In this talk, the role of moisture on fatigue crack growth behavior of 7075 Al alloy will be presented. Rolled 7075 Al alloy was heat-treated to underaged, peak-aged, and overaged conditions. Fatigue crack growth rates were measured under various partial pressures of water vapor. Standard compact tension specimens were used, and testing was performed under load ratios of $R = 0.1$ and $R = 0.8$. The microstructure and morphology of the fracture surfaces were examined by scanning electron microscopy (SEM) and correlated with the crack growth behavior.

8:50 AM

Model for the Superimposed Effects of Stress-Corrosion Cracking and Environmentally Enhanced Fatigue in Aluminum-Magnesium Alloy 5083: Ronald Holtz¹; Peter Pao¹; ¹Naval Research Laboratory

Comprehensive studies have been completed of the fatigue crack growth behavior of aluminum-magnesium alloy 5083 in vacuum, air, and NaCl solution, for both unsensitized and sensitized conditions. At low load ratio, R , sensitization has no effect on the fatigue thresholds in vacuum, air or NaCl, and only small effect on crack growth rates. At high R , fatigue in air and vacuum does not depend on sensitization at all. However, in NaCl solution, the high R fatigue behavior depends very strongly on sensitization. To reconcile all observations, we consider a model of two superimposed environment effects: an environmentally enhanced cyclic mode acting in both air and NaCl solution, and a stress-corrosion cracking mode acting at high stress intensity in NaCl. The model details of the two modes are described. The two modes are combined within the “small-time-scale” approach of Lu & Liu [Int. J. Fatigue, 2010].

9:10 AM

Governing Factors for the Corrosion-to-Fatigue Transition in 7075-T651: James Burns¹; Richard Gangloff¹; ¹University of Virginia

Factors governing the drastic fatigue life reduction due to corrosion damage are poorly separated and understood. Crack surface markerbands quantify formation cycles (N_f) from a pit to a 10-20 micron crack in 7075-T651. N_f increases dramatically from 23°C to -90°C, and involves a complex interaction of macro-pit induced elastic stress concentration coupled with local micro-topographic plastic strain concentration, further enhanced by microstructure (sub-surface constituents). Such interactions

leads to high variability in N_f . At high-applied stress N_f can be assumed to be nil, at low stress N_f is a significant portion of life as predicted by coupling macro-pit and micro-feature elastic-plastic stress-strain concentrations from finite element analysis with empirical fatigue life models. SEM-EBSD and stereology within 20 microns of pristine-specimen initiation sites shows no cracking on {111} slip planes, suggesting that slip-based crack initiation models are inadequate for environmental fatigue in Al alloys. A hydrogen embrittlement model perspective is proposed.

9:30 AM

Enhanced Corrosion Fatigue Resistance of AISI304 Bellows Expansion by Modifying the Bellows Shape: Takafumi Ono¹; Hiroyuki Miyamoto¹; Toshiyuki Uenoya¹; Tomomi Fujikawa¹; ¹Doshisha University

Bellows are widely used as the element of expansion joint in various piping systems. The U-shaped bellows is known as one of popular expansion joints which are widely used. Mostly, these bellows are made from austenitic stainless steel such as AISI304. Metastable austenitic SS such as AISI304 transforms to deformation-induced martensite (DIM) if it is subjected to the cyclic plastic strain range larger than 0.3wt%, and lose its corrosion resistance. In order to avoid the transformation, new μ -shaped bellows are proposed to extend the corrosion fatigue life by modifying the shape to have smaller plastic strain range than the critical value. It was demonstrated that μ -shaped bellows have 6 times higher fatigue life than conventional U-shaped counterpart. The austenitic stainless steels lose the resistance to localized corrosion when they are exposed to chloride solutions. The relations between the formation of cracks and DIM have been focused.

9:50 AM

Corrosion Fatigue and Crack Propagation of Different Austenitic Stainless Steels in High Chloride Solutions at Elevated Temperatures: Clemens Vichytil¹; Gregor Mori¹; Michael Panzenböck²; Reinhard Pippan³; Rainer Fluch⁴; ¹CD-Laboratory of Localized Corrosion; ²Montanuniversität Leoben; ³Austrian Academy of Science; ⁴Bohler Special Steels

Different CrMnN stabilized austenitic stainless steels and CrNiMo austenites have been investigated in this research. Corrosion fatigue and crack propagation behaviour has been studied to determine damage and failure mechanisms in high chloride containing environments under cyclic loading. S/N curves and crack propagation rate curves have been recorded in 43 wt.-% CaCl_2 solution and in inert glycerine at 120 °C. Additionally electrochemical behaviour of all materials has been studied under testing conditions. CrNiMo steels are very chemically stable in high chloride environments and exhibit a minor reduction in fatigue strength compared to inert glycerine. Surprisingly crack propagation is significantly reduced in corrosive environment compared to inert glycerine. CrMnN steels have superior mechanical properties, but are very susceptible to stress corrosion cracking in test solution, resulting in a pronounced reduction in fatigue strength and increased crack propagation in this corrosive environment. Possible explanations of the different behaviours are critically discussed.

10:10 AM Break

10:20 AM

Creep-Fatigue-Environment Crack Growth Kinetics: Jeffrey Evans¹; ¹University of Alabama in Huntsville

Several time-dependent damage mechanisms can operate during creep-fatigue loading. In the crack tip region creep deformation, stress relaxation, oxygen diffusion along grain boundaries, grain boundary oxidation, and surface oxidation are all occurring during the dwell period of a creep-fatigue cycle, and are influenced by temperature and microstructure. Each of these processes can be described in terms of kinetics. A comparison of kinetics can determine which mechanisms are operational and which mechanism is the rate limiting step in the time-dependent damage process during creep-fatigue crack growth. This paper will evaluate approaches to determining the kinetics of creep-fatigue-environment crack growth and



TMS 2012

141st Annual Meeting & Exhibition

discuss a graphical method that can be used for comparing the kinetics of various time-dependent crack tip processes operating during the dwell period of a trapezoidal creep-fatigue loading cycle. A comparison is shown that evaluates the kinetics for the superalloy 718.

10:40 AM

Effect of Corrosive Environment on High Cycle Fatigue of Friction Stir Welded Al-Mg Alloy: *Gaurav Argade*¹; Nilesh Kumar¹; Rajiv Mishra¹; ¹Missouri University of Science and Technology

AA5083 plates were welded using friction stir welding and gas metal arc welding techniques. Microstructural characterization was carried out using electron backscattered diffraction technique. The influence of microstructure on fatigue life was studied in 3.5 wt% NaCl solution. For comparison the fatigue properties were also characterized in air. Fractography of tested samples was carried out using scanning electron microscope.

11:00 AM

Galvanic Corrosion Behavior of Ni-C Filled Conductive Silicon Rubber Coupled to Magnesium Alloys: *Hu Zhou*¹; Zhidong Xia¹; Zhe Li¹; Fu Guo¹; ¹Beijing University of Technology

The galvanic corrosion behavior of conductive silicon rubber (CSR) having a different resistivity couples of magnesium alloys were investigated in 3.5% sodium chloride solutions at different temperatures. Such investigation was carried out by means of mechanical measurement, electrochemical measurement, weight-loss determination, and surface characterization. The results showed that the lower the resistivity, the higher the potential of conductive silicon rubber, and then the larger the corrosion current density and the corrosion rate of magnesium alloys. The corrosion morphology from SEM suggested that the corrosion of magnesium alloys took place mostly along the grain boundaries and became increasingly severe as a function of corrosion time. However, the CSR coupled magnesium alloys were not corroded due to its zero corrosion rate. After corrosion, the resistivity of CRS was drastically increased, while the mechanical property change was not significant. XRD analysis also indicated that the major corrosion product of magnesium alloy was Mg(OH)₂.

11:20 AM

Interfacial Reaction between Co-Based Alloy and Molten Al: *Ning Tang*¹; Yunping Li²; Shingo Kurosu²; Hiroaki Matsumoto²; Yuichiro Koizumi²; Akihiko Chiba²; ¹Graduate School of Engineering, Tohoku University, Japan; ²Institute for Materials Research, Tohoku University, Japan

In Al die-casting industry, the dies, which are currently made of hot-work tool steels, always suffer from the premature failure caused by corrosion of molten Al alloys and/or thermal fatigue during producing cycles. Therefore, Co-based alloys, whose corrosion resistance to molten Al and thermal fatigue resistance were reported to be higher than that of hot-work tool steels [1,2], are promising die materials. In this study, the Co-29Cr-6Mo (wt%) alloy was reacted with molten Al, and the interfacial reaction was investigated with the combination of interface structure and reaction kinetics. The results showed that two intermediate layers formed on the solid-liquid interface and thickness loss of the Co-based alloy followed a linear relationship with immersion time. These results may be applicable for enhancing the corrosion resistance of Co-based alloys to molten Al. [1] M. Yan, *J Mater Sci* 2001; 36: 285, [2] Y. Birol, *Mater Sci Eng A* 2010; 527: 1938.

11:40 AM

The Preparation Technics of a Alloy Coating with Special Properties: *Li Naijun*¹; ¹Science College of Shenyang University

The treatment technics for substrate was researched and improved though out experimentations, the research of plating technics and additive for forming ornamental and functional multicomponents alloy was carried out completely, the optimum technics of plating three-components alloy was been found. The coatings made by optimum technics were excellent

in corrosion-resistance, wear-resistance and oxidation-resistance, and also has a smooth, fine, shining surface. It was proved that phosphorus content in the coating is 8.4% by determinations, the coating is amorphous crystal. The properties of coating were test, the result shown that the combination force between the substrate and the coating was very good, the properties of coating to resist corrosion and abrasion were much better than that of others alloy by the tests. And the coating was finery in ornamentally also.

From Macro to Nano, Understanding Mechanical Behavior across Length Scales: A Structural Materials Division Symposium in Honor of Robert Ritchie: Environmental Effects and Hydrogen Embrittlement

Sponsored by: The Minerals, Metals and Materials Society, TMS Structural Materials Division, TMS/ASM: Mechanical Behavior of Materials Committee, TMS: Biomaterials Committee

Program Organizers: Jamie Kruzic, Oregon State University; Brad Boyce, Sandia National Labs; Reinhold Dauskardt, Stanford University

Wednesday AM
March 14, 2012

Room: Mockingbird 1
Location: Swan Resort

Session Chairs: Brian Somerday, Sandia National Laboratories; Richard Gangloff, University of Virginia

8:30 AM Introductory Comments

8:35 AM Keynote

Models for Fracture in Lithium-Ion Battery Storage Particles: *Robert McMeeking*¹; ¹UCSB

Models are developed for the transport of Li ions in the electrolyte, their diffusion through storage particles, and their kinetics at the interface between the electrolyte and the particles. As a consequence of Li intercalating in the storage particles, their lattice swells, leading to elastic stress when the concentration of Li ions in the particles is not uniform. The resulting model is used to compute stress in the storage particles, and to deduce the likelihood of fracture. The objective is to assess designs of porous electrode microstructures that permit rapid charging and discharging, but obviate the likelihood of fracture that limits the performance and reliability of the battery. The swelling associated with lithium storage, and the resulting stresses have interesting consequences for lithium transport and the crack tip stress intensity factor, analogous to other situations where transformation strain is a significant crack tip phenomenon.

9:15 AM Keynote

Understanding and Modeling Environment Effects on Intrinsic Fatigue Crack Propagation: *Richard Gangloff*¹; ¹University of Virginia

Rob Ritchie has long championed similitude-based modeling of crack growth built on understanding mechanisms of crack tip and wake processes; this perspective is central to next-generation prognosis of fatigue in airframe aluminum alloys. Environment-produced hydrogen dominates intrinsic cracking rates and damage accumulation mechanisms, particularly in the low growth rate regime. In this regard, recent research results are highlighted: (1) prediction of the environmental exposure dependence of fatigue crack growth rate based on mass transport/reaction-rate modeling leading to better life assessment and alloy development, (2) high resolution characterization of fatigue crack path crystallography (SEM/EBSD) and crack tip dislocation structure (FIB/TEM) leading to a damage physics model which includes cyclic plasticity (916K) and maximum tensile stress (K_{max}), (3) measurement of crack formation and

growth from corrosion damage necessary for a validated microstructure-scale model of small-crack fatigue, and (4) ionic inhibition of H uptake leading to vacuum-like fatigue behavior and reduced prognosis complexity.

9:55 AM Keynote

Mechanism of Hydrogen Embrittlement in Fatigue: *Yukitaka Murakami*¹; ¹Kyushu University/ International Institute for Carbon-Neutral Energy Research

The effect of hydrogen on fatigue crack growth rate was strongly dependent on load frequency both in BCC and FCC metals. Even very small amount of hydrogen of level of 2-3 ppm initially contained in commercial austenitic stainless steels accelerates fatigue crack growth rate under frequency of 0.0015Hz. The well known term 'hydrogen embrittlement' expresses undesirable effects due to hydrogen such as loss of ductility, decreased fracture toughness, and degradation of fatigue properties of metals. However, the experimental results on austenitic stainless steels show, surprisingly, that hydrogen can have an effect against HE. A dramatic phenomenon was found in which charging a supersaturated level of hydrogen into specimens of austenitic stainless steels drastically improved the fatigue crack growth resistance. The acceleration of crack growth rate due to hydrogen in a high strength steel was caused by nucleation of secondary cracks along grain boundaries and carbide boundaries ahead of main crack.

10:35 AM Break

10:50 AM

Micromechanics of Hydrogen-Induced Fracture: From Experiments and Modeling to Prognosis: *Petros Sofronis*¹; *Mohsen Dadfarnia*¹; *Brian Somerday*²; *Philip Schembri*³; *Dorian Balch*²; ¹University of Illinois; ²Sandia National Laboratories; ³Los Alamos National Laboratory

Development and validation of a lifetime prediction methodology for failure of materials used for hydrogen containment components is of paramount importance for a hydrogen-powered society. In this presentation, we summarize recent developments on fracture prognosis for various materials by accounting for the deformation mechanisms at the microscale. Arguably the most devastating mode of hydrogen-induced degradation is the hydrogen embrittlement of high-strength steels. We present an approach to quantify the effect of hydrogen on the fracture strength and toughness of a martensitic steel through the use of a statistically-based micromechanical model for the critical local fracture event. To understand the mechanics of subcritical cracking in a gaseous hydrogen environment, we investigate crack propagation in the Fe-Ni-Co superalloy IN903. We identify the microstructural characteristic length that controls ductile fracture initiation in low pressures and make an effort to predict the threshold stress intensity for intergranular cracking at high pressures.

11:05 AM

Connecting Hydrogen Enhanced Plasticity to Fracture—A New Multi-Scale Approach: *May Martin*¹; *Akihide Nagao*¹; *Mohsen Dadfarnia*¹; *Petros Sofronis*¹; *Ian Robertson*¹; ¹University of Illinois

Several different metallic systems have been subjected to various loading conditions, including fatigue loading, either in the presence of hydrogen or in the hydrogen charged state. The mechanical properties are as expected in that hydrogen reduces the ductility and in some systems causes a change in fracture mode. Focused Ion Beam machining has allowed samples for subsequent examination in the TEM to be extracted from site specific locations on the fracture surface. This approach has provided an unprecedented view of the dislocation substructure immediately beneath the fracture surface, which provides the missing connection between hydrogen enhanced plasticity and hydrogen-induced failure. Collectively the results from the different systems demonstrate the deformation structure accelerated by hydrogen provides the conditions to establish locally the fracture mechanism and fracture path. This claim will be supported by examples subjected to different loading conditions.

11:20 AM

The Effect of Trace Oxygen on Gaseous Hydrogen-Accelerated Fatigue Crack Growth in a Low-Strength Pipeline Steel: *Brian Somerday*¹; *Chris San Marchi*¹; *Kevin Nibur*²; ¹Sandia National Laboratories; ²Hy-Performance Testing

Low-strength ferritic steels are commonly considered to be resistant to hydrogen-induced subcritical cracking; however, this resistance depends on material, environmental, and mechanical loading variables. For example, Suresh and Ritchie (e.g., *Metal Science*, vol. 16, 1982, p. 529) demonstrated that the threshold for gaseous hydrogen-induced subcritical cracking is dramatically lower under cyclic (fatigue) loading compared to static loading in low-strength steels. The onset of accelerated fatigue crack growth was associated with the maximum stress-intensity factor (K_{max}^I). Extending this foundation, the present study examines the effect of mixed hydrogen/oxygen gas (21 MPa H₂ with 10 to 1000 vppm O₂) on fatigue crack growth in the low-strength X52 pipeline steel. Results show that K_{max}^I systematically increases as the oxygen content increases but the absolute value depends on load-cycle frequency. These results are interpreted based on the competition between rates of bare-metal exposure associated with mechanical crack extension and rates of oxygen adsorption.

11:35 AM

Next-Generation Microelectronic Solder Joints and Their Mechanical Properties: *Hyeilim Choi*¹; *Heeman Choe*¹; ¹Kookmin University

In recent years, the demand for special semiconductors packages used in harsh operating environment is substantially increasing in various industries. Being as equally important as electrical properties in microelectronic packages, the reliability and stability issue of solder joints therefore has attracted considerable attention. Furthermore, rapidly diminishing ball pitch and size of a solder joint has been regarded as a potential reliability concern for its mechanical and physical properties. Nevertheless, few systematic studies have been devoted to the microelectronic package used under harsh environment such as in automobile, aerospace industries. This study suggests potential solutions for a solder joint of the next-generation semiconductor package under extreme operating conditions. A trace amount of B or Y is added to lead-free Sn-1.0Ag-0.5Cu solder to significantly improve its mechanical properties. The pull test result indicates that B, Y-doped solder joints can retain high fracture strengths, regardless of the aging time and reflow frequency.

11:50 AM

Microstructure and Mechanical Properties of Electroplated Nickel-Cobalt Alloys with Cobalt Content Less Than 3wt. %: *Rong Yuan*¹; *Christopher Panichas*¹; *Yi He*¹; *Mitul Modi*¹; ¹Intel Corporation

This paper presents a comprehensive study of electroplated nickel-cobalt alloys on microstructure, mechanical strength and creep. Two types of alloys are investigated: high strength alloy (2 wt.% Co), and high hardness alloy (0.8 wt.% Co). Both alloys start with similar grain size at nano-scale. Following annealing at 200°C, 350°C, 500°C, and 700°C show that grain growth occurs from 200°C to 350°C based on FIB images although DSC curves do not show signal. Correspondingly, YS and UTS of the two alloys decrease with annealing temperatures, with high hardness alloy being stronger than high strength alloy. Tension test at elevated temperatures at 100°C, 150°C, 200°C, and 250°C show the same trend. However, high hardness alloy is subject to hydrogen embrittlement after annealing at 700°C whereas the high strength alloy seems not affected. Creep tests at 150°C and 200°C show that high hardness alloy has larger creep resistance than high strength alloy.



TMS 2012

141st Annual Meeting & Exhibition

Integrating and Leveraging Collaborative Efforts for ICME Education: Session I

Sponsored by: The Minerals, Metals and Materials Society, TMS Materials Processing and Manufacturing Division, TMS: Education Committee, TMS: Integrated Computational Materials Engineering Committee

Program Organizers: Laura Bartolo, Kent State University; James McGuffin-Cawley, Case Western Reserve University

Wednesday AM
March 14, 2012

Room: Europe 2
Location: Dolphin Resort

Session Chairs: Laura Bartolo, Kent State University; James McGuffin-Cawley, Case Western Reserve University

8:30 AM Invited

Advances in ICME Education: *Greg Olson*¹; ¹Northwestern University

Multiyear design education initiated in the materials curriculum at Northwestern employs an integrated research/education system in which funded graduate research in technical design provides the infrastructure for graduate student coaching of undergraduate design teams. A Materials Design Studio serves as a central teaching facility where software tools introduced throughout core courses are integrated in a required junior-level Materials Design course centering on computational design. Under a new Design Institute, cross-disciplinary concurrent computational engineering of materials and structures in multiyear engineering schoolwide "Institute Projects" now involve multidisciplinary undergraduate teams spanning freshman to senior level. At the graduate level, skills of multidisciplinary collaboration are fostered by a new cross-departmental doctoral "cluster program" in Predictive Science and Engineering Design, and an affiliated one-year MS program in ICME has been initiated.

9:15 AM

Computational Training in Design of Hot Strip Rolling: *Matthias Miltzer*¹; ¹The University of British Columbia

A state-of-the-art hot strip mill model (HSMM) is introduced to 4th year materials engineering students as an example to illustrate the power of integrated computational materials engineering tools. The students use the HSMM to design hot strip rolling process routes that will lead to a hot-rolled steel product with specified properties, e.g. for automotive applications. The design study includes the selection of a suitable steel grade, the identification of microstructure phenomena that markedly affect properties, the determination of critical processing steps and a sensitivity analysis to evaluate the robustness of potential processing paths. In preparation of using the HSMM, the students develop their own spreadsheet type models for individual microstructure phenomena, e.g. recrystallization and precipitation, and associated properties, e.g. yield stress.

9:40 AM

Centralized Computing Resources for Large or Dispersed Audiences: *David Gutschick*¹; *Peter Anderson*¹; ¹Ohio State University

A thorough understanding of many macroscopic phenomena requires familiarity with the underlying (3D) atomic-level phenomena. The wide variation in spatial and temporal intuition among students means that 2D, static illustrations are insufficient. They are effective primarily for those already familiar with the concept. Even 3D illustrations/animations are deficient if the student is unable to comprehend the 3D nature from a 2D display. An obvious solution is interactive applications. Consider, for example, a deformation mechanism map which associates a given stress and temperature with 3D, interactive animations of the macro and atomic-level processes. This tends to be computationally expensive, but technologies like server virtualization or application multiserving on a platform such as NanoHUB allows all members of an audience to individually interact with an application through the internet while the computational load is dealt with remotely.

10:05 AM

ICME in Transport Phenomena for Materials Processing: *James McGuffin-Cawley*¹; ¹Case Western Reserve University

In teaching transport phenomena in materials processing a combination of approaches are used. These include: standard analytical approaches of the textbooks, numerical methods using computer programming, and a commercial multiphysics software package. The relative advantages of each is discussed. In particular, the relative benefits of programming versus the use of a commercial package in the teaching environment is considered. The conclusion that is reached is that a mixed approach has advantages for the students.

10:30 AM Break

10:45 AM Invited

The 2011 Summer School for Integrated Computational Materials Education: *Katsuyo Thornton*¹; *Larry Aagesen*¹; *Mark Asta*²; *Edwin Garcia*³; *John Allison*¹; *Laura Bartolo*⁴; *Jon Guyer*⁵; *Paul Mason*⁶; *Anton Van der Ven*¹; *Gregory Olson*⁷; ¹University Of Michigan; ²UC Berkeley; ³Purdue University; ⁴Kent State University; ⁵NIST; ⁶Thermo-Calc Software Inc.; ⁷Northwestern University

The primary purpose of the NSF supported Summer School for Integrated Computational Materials Education was to "educate the educators" in order to enable rapid implementation of computational tools into undergraduate materials science and engineering curriculum around the world. This program allowed participants to return to their home institutions with the knowledge, skills, and materials to incorporate computational materials science and engineering (CMSE) in thermodynamics and kinetics courses. The Summer School curriculum also included an overview of CSME applications, the fundamental theory and advanced topics, as well as training for teaching the modules to undergraduate students. Twenty five faculty, postgraduate researchers, and graduate students from MSE departments and programs in the U.S. participated in this innovative program held at the University of Michigan in Ann Arbor, MI.

11:30 AM

Interactive Two-Dimensional Simulations as an Introduction to Core ICME Concepts: *Colin Ashe*¹; *David Yaron*¹; *Laura Bartolo*²; *John Portman*²; *W. Craig Carter*³; *Donald Sadoway*³; ¹Carnegie Mellon University; ²Kent State University; ³Massachusetts Institute of Technology

The 2008 NRC report on ICME exhorts universities to incorporate "ICME modules into a broad spectrum of materials science and engineering courses". While research- and industry-grade simulations are appropriate for upper-level courses, students in introductory courses would benefit from simulations of simpler systems that clearly convey central concepts. Combining efforts in MSE, chemistry, physics, and digital libraries, we have developed a web-based computational engine for simplified two-dimensional simulations of atoms and molecules that allows students to visualize and interact with simulations as they run. These capabilities provide a means to introduce students to both the underlying materials science concepts as well as to key concepts from computational science, such as choosing a suitable simulation time-step. In this talk, we will highlight the capabilities of our system, provide examples of its use with students, and discuss how educators interested in partnering with us might use it in their own ICME modules.

11:55 AM

Cyber-Enabled Materials Simulations via NanoHUB.org: *Alejandro Strachan*¹; *Bejamin Haley*¹; *Ravi Pramod Vedula*¹; ¹Purdue University

Multi-resolution materials modeling and simulation have the potential to revolutionize the design of new materials and their certification. The materialization of this potential would be enormously accelerated by making advanced simulation tools and training material widely and easily available to researchers, educators and students. nanoHUB.org is a science web-portal created by NSF's Network for Computational Nanotechnology (NCN); it provides its users access to simulation tools and computational

resources free of charge and simply using a web-browser, with no need to download and install any software. Such a drastic reduction of the barriers to simulation opens significant opportunities in the education of a next generation of engineers and scientists and provides an efficient avenue to transfer advanced simulation tools from developers to materials scientists and engineers interested in design, optimization and certification. nanoHUB.org serves over 170,000 users annually and I will describe the key elements that contributed to its success.

International Smelting Technology Symposium (Incorporating the 6th Advances in Sulfide Smelting Symposium): Fundamentals: Thermodynamics, Phase Equilibria, and Kinetics

Sponsored by: The Minerals, Metals and Materials Society, The Metallurgy and Materials Society of CIM, TMS Extraction and Processing Division, TMS: Pyrometallurgy Committee
Program Organizers: Jerome Downey, Montana Tech of the Univ of Montana; Thomas Battle, Midrex Technologies, Inc.; Jesse White, Elkem Solar Research

Wednesday AM
March 14, 2012

Room: Northern A3
Location: Dolphin Resort

Session Chair: To Be Announced

8:30 AM

Departure from Equilibria in Ilmenite Smelting: *Petrus Pistorius*¹; ¹Carnegie Mellon University

Ilmenite smelting involves partial reduction of iron oxide from a slag consisting mainly of TiO_2 , Ti_2O_3 and FeO, yielding as products iron (with approximately 2% carbon) and titanium slag. Slag purity requirements preclude any fluxing additions, and the aggressive nature of the slag necessitates a furnace freeze lining. Large departures from thermal and chemical equilibrium hold in the smelter, with implications for process stability. The slag is approximately 150K hotter than the metal, which means that the metal temperature is below the slag melting point; this has been shown to lead to formation of a solidified Ti_3O_5 -rich layer between the slag and metal. Recent equilibrium measurements have confirmed that the slag and metal are not in chemical equilibrium either, with significantly more reducing conditions in the metal than in the slag. After solidification, the pseudobrookite slag structure is metastable below approximately 1400K, and may transform upon slight oxidation.

8:55 AM

Distribution of Boron and Calcium between Silicon and Calcium Silicate Slags: *Lars Klemet Jakobsson*¹; Merete Tangstad¹; ¹NTNU

Removal of boron from silicon by slag refining is one of the possible refining steps on a metallurgical route for production of silicon for crystalline silicon solar cells. The level of boron in silicon has to be brought down to 0.3 mg/kg or less if the silicon is to be used for solar cells, and boron is one of the hardest elements to remove from silicon. Slag refining is a promising method for boron removal, and in this work the distribution coefficient of boron, L_B , between slag and silicon was measured at 1600 °C for calcium silicate slags with a CaO/SiO₂ mass ratio between 0.6 and 1.3. The measured distribution coefficient can be approximated by the formula; $L_B = 0.437V + 1.93$, where V is the CaO/SiO₂ mass ratio within the range of the experiments.

9:20 AM

High Temperature Experimental Investigations and Thermodynamic Modelling in the FeTiO₃-Ti₂O₃-TiO₂ Ternary Slag System: *Stian Seim*¹; Leiv Kolbeinsen²; In-Ho Jung³; ¹Eramet Titanium & Iron; ²Norwegian University of Science and Technology; ³McGill University

The current work presents new experimental data in the iron-unsaturated region of the FeTiO₃-Ti₂O₃-TiO₂ slag system. The samples are prepared by melting pure reactants in a high frequency induction furnace which

employ a cold crucible. Such an experimental set-up have previously been described in literature and proven to suitable to investigate high titania slags. The FeO content of the samples range from 3.7 to 21.8 wt% and the Ti₂O₃ content range from 3.6 to 30.1 wt%. The liquidus temperature of the samples is measured in-situ by a spectropyrrometer and range from 1450 to 1645 °C. In addition an improved thermodynamic database for the FeO-Ti₂O₃-TiO₂ system has been developed. Ternary parameters have been included and optimized to fit previously published experimental data. This optimization minimizes the discrepancy between experimental data and thermodynamic calculations as previously discussed in literature. New liquidus projection plots are proposed for the FeO-Ti₂O₃-TiO₂ and the FeTiO₃-Ti₂O₃-TiO₂ systems.

9:45 AM

Reaction Mechanisms in Carbothermic Production of Silicon, Study of Selected Reactions: *Eli Ringdalen*¹; Merete Tangstad²; ¹SINTEF; ²NTNU

The paper presents an overview over results from SINTEF/NTNU regarding new and ongoing Research in Silicon production. The main studies are related to condensation of SiO gas and cavity formation. Experimental work has shown formation of different types of condensates under different conditions, where temperature is the most important parameter. Development of cavity under industrial conditions has also been simulated. Physical appearance of zones in industrial furnaces and selected reactions in these will be discussed based on results from excavation of industrial furnace and results from laboratory experiments. This will be combined with some results from ongoing modelling work.

10:10 AM Break

10:30 AM

High Temperature Phases in Chromium Containing Cu-Fe-Ni-S Mattes: *Rauf Eric*¹; Sanele Nkosi²; ¹University of the Witwatersrand; ²Council for Mineral Technology

Experiments were conducted to determine the phases that develop when smelting and converter mattes of the Cu-Fe-Ni-S system containing chromium were solidified. These mattes are employed in the PGM smelting industry of South Africa. It is important to determine the phases that form and act as collectors for PGMs. Synthetic mattes representing were prepared from pure chemicals. They were sealed in evacuated quartz capsules and heated up to 1300°C. After equilibration they were quenched and examined using optical microscopy, SEM-EDX and X-ray diffraction. The effects of iron, sulfur and chromium contents were systematically examined on phase assemblages that developed during equilibration. One of the most noteworthy observations in mattes containing 1 to 5% Cr was the formation of (Fe, Cr) 1-XS phase, in addition to the metallic FeNi, bornite and the liquid phases at temperatures 1150°C and lower. Chromium did not dissolve in the FeNi and Cu sulfide phases.

10:55 AM

Stabilities of Phases in the Cu₂S-FeS-PbS System: Hannu Johto¹; Pekka Taskinen¹; ¹Aalto University School of Chemical Technology

Copper sulfide concentrates contain often impurities such as lead and iron. The phase stabilities of the sulfide impurity systems in metallurgical process conditions are in many cases unsatisfactorily known. Thermodynamic information of a system gives better understanding of its behavior of metal making processes, but has also effects on the economic and environmental factors of the production process. In this study, isothermal equilibrium and quenching experiments of about the stable phases of the system Cu₂S-FeS-PbS at 700 and 900 °C were carried out and based on the experimental results, Gibbs triangle of equilibrium phases of the system was outlined.



11:20 AM

Experimental Thermodynamic Study of the Equilibrium Phase Assemblage AgBi_3S_5 - Bi_2S_3 -S: Fiseha Tesfaye¹; Pekka Taskinen¹; ¹Aalto University School of Chemical Technology

A thermodynamic study of the equilibrium phase assemblage AgBi_3S_5 - Bi_2S_3 -S was made by an EMF-technique, using the RbAg_4I_5 solid electrolyte. The ternary phase was synthesized from the pure Ag_2S and Bi_2S_3 in an evacuated silica ampoule and grinded in to powder and mixed with appropriate compositions of Bi and S, in a series of experiments, for pressing in to pellets. The pellets were assembled in a unique fashion to form the galvanic cells $\text{Pt}(-) | \text{Ag} | \text{RbAg}_4\text{I}_5 | \text{AgBi}_3\text{S}_5 + \text{Bi}_2\text{S}_3 + \text{S} + (\text{C}) | \text{Pt}(+)$. The EMF-measurements were made in the temperature range 304 – 451 K. The EMF values for each equilibrium phase assembly were expressed as a function of temperature, in the different temperature regions of phase stabilities. In this article, thermodynamic functions of AgBi_3S_5 (pavonite) coexisting with Bi_2S_3 and S have been determined. The agreement between the obtained results and the literature values were established.

11:45 AM

Vacuum Distillation Refining of Crude Tin - Thermodynamics Analysis and Experiments on the Removal of Arsenic from the Crude Tin: Yifu Li¹; Bin Yang¹; Dachun Liu¹; Baoqiang Xu¹; Yongnian Dai¹; ¹Kunming University of Science and Technology

The removal of impurity arsenic from crude tin is one of the major problems in the process of tin refining. Through the thermodynamics analysis on vacuum refining process of crude tin, the vapour pressure of impurity arsenic under different temperatures can be obtained, which demonstrates that it is possible to separate tin and arsenic by the vacuum refining process. This paper attempts to verify the behaviors of impurity arsenic. The experiment result shows that through vacuum distillation, crude tin with 0.16% arsenic can be refined from crude tin with 0.96% arsenic, and about 50% impurity arsenic can be collected in the form of metallic arsenic.

12:10 PM

Investigation of Removing Cadmium and Thallium from Crude Indium by Vacuum Distillation: Jiang Wenlong¹; ¹National Engineering Laboratory of Vacuum Metallurgy, Kunming University of Science and Technology,

In usual, glycerin-KI and glycerin- NH_4Cl were used to remove Cd and Tl in electrolysis method which products were In99.995%. Lots of polluted industrial wastewater cloud easily polluted environment was come into being. By calculated results the saturated vapor pressure of Cd and Tl between 1~200Pa were much larger than In, so study of removing Cd and Tl were carried out at the temperature range between 700~950°C and pressure between 1~15Pa. In results, after vacuum distillation the content of Cd and Tl in crude indium cloud sharply fall blow 0.5ppm at least.

Magnesium Technology 2012: Alloy and Microstructural Design

Sponsored by: The Minerals, Metals and Materials Society, TMS Light Metals Division, TMS: Magnesium Committee
Program Organizers: Suveen Mathaudhu, U.S. Army Research Office; Wim Sillekens, TNO; Norbert Hort, Helmholtz-Zentrum Geesthacht; Neale Neelameggham, U.S. Magnesium

Wednesday AM
March 14, 2012

Room: Southern V
Location: Dolphin Resort

Session Chairs: Jian-Feng Nie, Monash University; Nack J. Kim, POSTECH

8:30 AM

Age Hardening Behavior of Mg-1.2Sn-1.7Zn Alloy Containing Al: Taisuke Sasaki¹; Tadakatsu Ohkubo¹; Kazuhiro Hono¹; ¹National Institute for Materials Science

Mg-Sn is a promising heat resistant precipitation hardenable system because of the higher melting temperature of the Mg₂Sn phase. Recent investigations also reported excellent extrudability of the alloy. However, previously studied Mg-Sn alloys require high solution treatment temperature above 500°C because of the high solidus temperature for the Mg-2.2Sn base composition. In this work, we have investigated the age hardening behavior of Mg-1.2at.%Sn based alloys to reduce the solution treatment temperature. To enhance the age hardening response with the reduced Sn content, Zn and Al were alloyed. Mg-1.7Zn-1.2Sn-2.0Al alloy showed the peak hardness of 79 VHN at 200°C. The peak aged Mg-1.2Sn-1.7Zn-2.0Al alloy consisted of cuboidal β_1' precipitates with the size of less than 50 nm, and fine lath shaped Mg₂Sn phase while Mg-1.2Sn-1.7Zn alloy was mainly strengthened by coarse rod shaped β_1' phase with over 500 nm in length.

8:50 AM

Evaluating the Effect of Pre-Ageing Deformation on β' Precipitate Size and Distribution in Mg-Zn-(Y) Alloys: Julian Rosalie¹; Hidetoshi Somekawa¹; Alok Singh¹; Toshiji Mukai²; ¹National Institute for Materials Science; ²Kobe University

The effect of pre-ageing deformation on the precipitate diameter and length distribution in Mg-Zn-(Y) alloys was examined. Extrusion and pre-ageing deformation were used to introduce dislocations while precluding twin formation. Dislocations provided nucleation sites for rod-like β' precipitates, resulting in a refinement of the precipitate size distribution. 5% strain reduced the average precipitate length from 450nm to 60nm, and average diameter from 14 to 9 nm. The average interparticle spacing of the rod-like precipitates was measured by Delaunay triangulation. The precipitate distribution was found to be significantly inhomogeneous, with measured interparticle spacings approximately 32% greater than predicted. For 5% pre-ageing deformation the yield strength approached 95% of the ultimate tensile strength.

9:10 AM

Effect of Zinc Content on the Microstructure and Mechanical Properties of Extruded Mg-Zn-Y-La Alloys with LPSO Phase: Jonghyun Kim¹; Yoshihito Kawamura²; ¹Kumamoto Technology & Industrial Foundation; ²Kumamoto University

Several wrought magnesium alloys such as AM- and AZ-series are structural materials which are suitable for use in the computers, mobile phone and automobile industries mainly because of their low densities. However, the number of commercially available Mg alloys is still limited especially for application at room and elevated temperatures.

For example, the above-mentioned alloys of AM- and AZ-series could not be applied to power train parts operating at temperatures higher than 130°C due to their poor elevated temperature mechanical properties. The investigation reported here focused on the influence of Zinc, which was also effective in strengthening Mg-Zn-Y alloys at elevated temperature, on the microstructure and mechanical properties of the Mg-Zn-Y-La alloys.

9:30 AM

Effect of Ca Addition on the Microstructural and Mechanical Properties of AZ51/1.5 Al₂O₃ Magnesium Nanocomposite: *Md Ershadul Alam*¹; *Rowshan Rima*¹; *Nguyen Bau*²; *Albedmagid Hamouda*¹; *Manoj Gupta*²; ¹Qatar University; ²National University of Singapore

In the present study, new AZ51/1.5Al₂O₃-1Ca magnesium nanocomposite was successfully synthesized by simultaneously adding 2 wt. % aluminum, 1 wt.% Ca and 1.5 vol.% nano-sized Al₂O₃ (50 nm) into AZ31 matrix using an innovative disintegrated melt deposition technique. AZ51/1.5Al₂O₃ nanocomposite was developed following the same processing route except adding Ca. All nanocomposite samples were then subsequently hot extruded at 400 °C and characterized. Microstructural characterization studies revealed uniaxial grain size, reasonably uniform distribution of intermetallics and minimal porosity. Results also showed that the Ca addition into AZ51/Al₂O₃ nanocomposite helped to reduce the average grain size. Physical properties characterization revealed that addition of Ca reduced the coefficient of thermal expansion when compared to Ca free nanocomposite. The presence of Ca also assisted in improving overall mechanical properties including microhardness, 0.2% yield strength and ultimate tensile strength while the ductility was compromised.

9:50 AM Break

10:10 AM

Effect of Zn Concentration and Grain Size on Prismatic Slip in Mg-Zn Binary Alloys: *Nicole Stanford*¹; *Matthew Barnett*¹; ¹Deakin University

Mg-Zn binary alloys with concentrations between 0 and 2.8wt% Zn have been prepared and processed via hot rolling and annealing to produce specimens with a strong basal texture and a range of grain sizes. These have been deformed in tension, a condition in which the deformation is dominated by prismatic slip. This data has been used to assess the Hall-Petch parameter as a function of Zn concentration for deformation dominated by prismatic slip. Pure magnesium showed non-linear Hall-Petch behaviour at large grain sizes, and this is compared to the values for prismatic slip measured on single crystals. The differences between critical resolved shear stress measurements made through single crystal, polycrystal and mathematical modelling techniques are also discussed.

10:30 AM

Microstructural Characterization of Homogenised and Aged Mg-Gd-Nd Alloys Containing Zn, Y and Zr: *Suzan Khawaled*¹; *Menachem Bamberger*¹; *Alexander Katsman*¹; ¹Technion - Israel Institute of Technology

Magnesium alloys containing heavy rare earth metals are very attractive candidates for the automotive industry including racing cars and aerospace applications, due to their high strength properties combined with low density. The microstructure of the Mg-6%Gd-3.7%Nd-0.3%Zn-0.18%Y-0.15%Zr (%wt) alloy has been investigated after solution treatment at 540°C for 24hr followed by isothermal aging at 175°C up to 32 days by X-ray diffraction and by SEM with EDS. It was observed that the homogenized alloy contained primary α -Mg solid solution, eutectic structures, cuboid shaped phases and Zr-rich clusters. The eutectic structures were the products of a 'quasibinary eutectic reaction' α -Mg+ β -Mg₂RE. The eutectic phase was characterized to be of Mg₂Gd prototype with stoichiometry near Mg₂(Gd_{1-x}Nd_x), $x \approx 0.2$). The cuboid shaped phases, with the composition Gd₂(Nd_xY_{1-x}), $x \approx 0.6$, grew during aging and reached $\sim 3\mu\text{m}$ average size. The maximum microhardness was achieved after 16 days of aging.

10:50 AM

Mechanical Properties and High-temperature Oxidation Behavior of Mg-Al-Zn-Ca-Y Magnesium Alloys: *Young-Min Kim*¹; *Bong Sun You*¹; *Myeong-Shik Shim*²; *Nack Joon Kim*²; ¹Korea Institute of Materials Science; ²Pohang University of Science Technology

Simultaneous improvement in ignition resistance and mechanical properties of magnesium alloys can be achieved by the formation of protective oxide layer on the melt and the change in the morphology and volume fraction of secondary phases by alloying. In this study, the effects of alloying elements on the ignition resistance and mechanical properties of magnesium alloys were investigated. The results of this study show that the combined addition of calcium and yttrium can lead to significant increase in both ignition temperature and tensile properties, comparing to only Ca-added magnesium alloys with lamella-shaped eutectic phases. This is because the reduction of calcium content and the addition of a small amount of yttrium bring about a reduced amount Ca-containing phases and the formation of multi-layered protective oxides consisting of CaO, Y₂O₃, MgAl₂O₄, and MgO that effectively prevent oxygen penetration into the melt.

11:10 AM

Effects of Ca on Microstructure and Mechanical Properties of ZA62 Alloys: *Zhang Gang*¹; ¹Shenyang University of Technology

Effects of Ca element on microstructure and mechanical properties of ZA62 alloys were investigated by using zeiss microscope, scanning electron microscope equipped with an energy dispersive spectrometer, X-ray diffractometer, and electronic universal testing machine. The results show that Ca can significantly refine microstructure and cause the precipitation of Mg₂Ca and Al₂Ca phases on grain boundary of ZA62 alloys. The addition of Ca can improve the tensile properties of alloys at room temperature. When the content of Ca is 2%, good properties are obtained, the tensile strength and yield strength of Mg-6Zn-2Al-2Ca alloy reaches 240.79MPa and 82.78MPa respectively.

11:30 AM

Effects of Si on Microstructure and Mechanical Properties of Mg-5Sn-2Sr Alloy: *Hao Shuai*¹; ¹Shenyang University of Technology.

Phase constitution and microstructure of the Mg-5Sn-xSi-2Sr (x=0, 1, 2) alloys were analyzed by X-ray diffractometer, optical microscope and scanning electron microscope with an energy dispersive spectrometer. The tensile properties of the alloys were tested by electronic universal testing machine, and the fracture surfaces of the alloys were observed with scanning electron microscope. The results show that the microstructure of the Mg-5Sn-2Sr alloy consists of α -Mg, MgSnSr, Mg₂Sn phases. The addition of Si element can promote the formation of Mg₂Si phase on the grain boundary, and the content of Mg₂Si phase increases with increasing the Si element. Mg₂Si is a strengthening phase, it can effectively prevent grain boundary sliding and dislocation motion, and thus, the mechanical properties of the alloys were obviously enhanced. The mechanical properties of Mg-5Sn-2Si-2Sr alloy are better than other alloys, the tensile strength, yield strength, elongation and hardness are 147MPa, 110MPa, 5.0% and 47HB respectively.



Magnesium Technology 2012: Casting and Solidification

Sponsored by: The Minerals, Metals and Materials Society, TMS Light Metals Division, TMS: Magnesium Committee
Program Organizers: Suveen Mathaudhu, U.S. Army Research Office; Wim Sillekens, TNO; Norbert Hort, Helmholtz-Zentrum Geesthacht; Neale Neelamegham, U.S. Magnesium

Wednesday AM
March 14, 2012

Room: Southern IV
Location: Dolphin Resort

Session Chairs: Norbert Hort, Helmholtz-Zentrum Geesthacht; Yongho Sohn, University of Central Florida

8:30 AM

Twin Roll Casting of Thin AZ31 Magnesium Alloy Strip with Uniform Microstructure and Chemistry: Iman Bayandorian¹; Ian Stone¹; Yan Huang¹; Zhongyun Fan¹; ¹Brunel University

Magnesium alloys produced by the existing twin roll casting (TRC) technique have coarse and non-uniform microstructures and severe centre-line segregation. Consequently, TRC strip is cast typically no thinner than 5-9 mm, relying on costly subsequent downstream processing to produce thin strip with an improved microstructure. In the research described herein melt conditioning by intensive melt shearing was used prior to TRC to promote heterogeneous nucleation and provide a refined and uniform microstructure without severe macrosegregation. Additionally, a TRC machine with small diameter rolls was used to cast AZ31 strip of less than 2 mm in thickness suitable for direct component manufacturing such as stamping, without the necessity of hot rolling. The effects of process parameters, such as casting speed and melt superheat, on as-cast microstructure were studied. Experimental results show that the melt conditioning process provided considerable reduction in as-cast grain size and elimination of centre-line segregation. The texture and mechanical properties of melt conditioned strips were much improved over conventional TRC strips, offering the potential for higher quality final components.

8:50 AM

Mathematical Modeling of the Twin Roll Casting Process for AZ31 Magnesium Alloy – Effect of Set-Back Distance: Amir Hadadzadeh¹; Mary Wells¹; Elhachmi Essadiqi²; ¹University of Waterloo; ²CANMET Materials Technology Laboratory

A 2-D coupled thermal-fluid-stress model was developed and used to simulate the twin roll casting (TRC) of an AZ31 magnesium alloy using the commercial software package, ALSIM. The model was used to predict the fluid flow, temperature distribution and mechanical behavior of the AZ31 strip in the roll bite. An important parameter in controlling the TRC process is the set-back; distance between the nozzle entry to the kissing point of the rolls. There are two approaches to increase the set-back: 1) increasing the entry thickness and 2) decreasing the final strip thickness. In this study different set-back distances have been studied for different casting speeds to assess their effect, particularly the thermo-mechanical behavior of the strip during the process. The thermo-mechanical behavior of the strip has a significant effect on the final quality as defect formation depends on such behavior.

9:10 AM

Interdiffusion and Phase Formation in the Mg-Y System: Katrina Bermudez¹; Sarah Brennan¹; Yongho Sohn¹; ¹University of Central Florida

Rare earths have been added to magnesium alloys in order to improve the creep resistance, corrosion resistance and strength. Solid-to-solid diffusion couples were assembled between Mg (99.9%) and Y (99.9%) to investigate the parabolic growth of intermetallic phases and interdiffusion in the Mg-Y system. The diffusion anneals were performed at 450, 500 and 550°C for 360, 240 and 120 hours, respectively. The intermetallic

layers that developed were the d-Mg₂Y and e-Mg₂₄Y₅ phases, however the MgY phase did not form. A substantial penetration of Y in Mg was observed, however along with Kirkendall porosity that indicates faster diffusion of Mg than Y in Mg solid solution. The activation energies for growth, assumed parabolic, in e-Mg₂₄Y₅ and d-Mg₂Y were determined to be 89 and 77 kJ/mol, respectively. Relevant interdiffusion coefficients including activation energies in Mg-Y system were calculated for the e-Mg₂₄Y₅, d-Mg₂Y, and Mg solid solution wherein reliable concentration gradients were observed.

9:30 AM

Microstructure and Mechanical Properties of High Pressure Die Cast AM50 Magnesium Alloy Containing Ce: Faruk Mert¹; Ahmet Özdemir¹; Karl Ulrich Kainer²; Norbert Hort²; ¹Gazi University; ²Helmholtz-Zentrum Geesthacht (HZG)

Over the past decades, the necessity to decrease the weight of automobile parts has created a considerable interest in magnesium alloy. The need to develop magnesium die casting alloys for car components motivates R&D in high temperature magnesium alloy development. In order to improve magnesium alloys with low cost, high strength and with notable elevated temperature properties, the effect of Ce addition (0.5/1.0 wt.-%) on microstructure and mechanical properties of AM50 was studied. Results show that addition of Ce to AM50 resulted in grain refinement and the formation of the secondary phase Al₁₁Ce₃. Mechanical properties of investigated alloys at both room and elevated temperature were remarkably increased. AM50 containing 1%wt. Ce showed relatively better refinement and mechanical properties compared to AM50 with 0.5%wt. Ce.

9:50 AM

Effect of Intensive Melt Shearing on DC Cast Ingots of Magnesium Alloys: Yubo Zuo¹; Zhongyun Fan¹; Bo Jiang¹; Yijie Zhang¹; ¹Brunel University

Direct Chill (DC) casting process is still one of the major methods to produce magnesium alloy ingots. A new melt conditioned DC (MC-DC) process, has been developed for producing high quality ingots of magnesium alloys by application of intensive melt shearing through a rotor-stator high shear device during the conventional DC casting process. The rotor-stator high shear unit can provide not only macro flow of liquid metal in the DC casting mould but also intensive melt shearing within the high shear device, which can enhance the heterogeneous nucleation and result in a uniform temperature field and a compositional filed. Experimental results have demonstrated that the MC-DC casting process can produce magnesium alloy billets with significantly refined microstructure and reduced cast defects. In this paper, we introduce this new MC-DC casting process, report the effect of intensive melt shearing on the DC casting process and discuss the grain refining mechanism.

10:10 AM Break

10:30 AM

Effect of the Solidification Rate on Microstructure of Cast Mg Alloys at Low Superheat: Gregory Poole¹; Nathan Rimkus²; Aerial Murphy¹; Paige Boehmcke¹; Nagy El-Kaddah¹; ¹The University of Alabama; ²Los Alamos National Laboratory

This paper investigates the effect of cooling rate on the grain size and microstructure of Mg AZ31B alloy cast at a superheat of 8°C using the Magnetic Suspension Melting (MSM) process, which is capable of melting and casting at superheats less than 5°C. In this study, the Mg alloy was unidirectionally solidified in a bottom-chill mold with stainless steel and copper chill blocks. The solidification parameters, namely growth velocity (V) and temperature gradient (G), were determined from numerical simulation of the cooling curves, which was found to be in good agreement with measurements. For the investigated solidification rates,

metallographic examination showed globular solidification morphology, and the grain size was inversely proportional to the square root of the cooling rate. Microprobe analysis of the cast ingots also showed that Al segregation occurs primarily at the grain boundaries, and the solidification rate affects the size and distribution of both the secondary phase and the intermetallic Mg₁₇Al₁₂ phase

10:50 AM

Impact and Energy Dissipation Characteristics of Squeeze and Die Cast Magnesium Alloy AM60: *Sante DiCecco*¹; Henry Hu¹; William Altenhof¹; ¹University of Windsor

High-pressure die cast (HPDC) magnesium alloy AM60 is recognized for its versatility in the manufacturing of weight sensitive components of relatively thin cross section. To further expand practical applications of the alloy, squeeze casting has been proposed to allow for thicker castings. In this study, AM60 alloy specimens of 10mm thickness were squeeze cast using a hydraulic press with an applied pressure of 60 MPa. Fracture energies, following a Charpy Impact Testing protocol, of the squeeze cast specimens were characterized in comparison with the HPDC counterparts using both experimental and numerical techniques. The experimental results show the squeeze cast alloy absorbing approximately 46.2% more energy during impact than its HPDC counterpart. Scanning electron microscopy fractography reveals the favourable quasi-cleavage fracture mode of the squeeze cast alloy AM60, relative to the decohesive rupture fracture mode present in the die cast alloy.

11:10 AM

Sliding Wear Behavior of Squeeze Cast Magnesium Composite AM60-9% (Al₂O₃): *Anindya Banerji*¹; Henry Hu¹; Ahmet Alpas¹; ¹University Of Windsor

Increasingly stringent demands of improved fuel economy and emissions prompted the study of Mg and its composites as they provide and combination of properties of high strength and low density. In the present paper development of magnesium composites and their subsequent wear behavior is studied. Magnesium matrix composites were synthesized by reinforcing AM60 alloy with Al₂O₃ fibres using squeeze casting method with varying alumina fibre volume percentage. Lubricated wear tests were conducted on these composites under 1.0-5.0 N load at a constant sliding velocity against AISI 52100 steel balls. Mainly two mechanisms of wear were identified-ultramild wear and mild wear. The transition from ultramild wear regime to the mild wear regime was increasingly delayed as the applied load was decreased. The effect of Al₂O₃ fibre content on the wear resistance of AM60 composites was also investigated.

11:30 AM

Solidification Studies of Mg-Al Binary Alloys: *Manas Paliwal*¹; Youn-Bae Kang²; Elhachmi Essadiqi³; In-Ho Jung¹; ¹McGill University; ²GIFT, POSTECH; ³CANMET-MTL

This study emphasizes on the evolution of as cast microstructure of Mg-3, 6 and 9 wt. % Al alloys solidified in the cooling rate range of 0.05 K/sec to 940 K/sec. The alloys have been solidified using different techniques like directional solidification (classical Bridgmann technique), sand mould casting, graphite mould casting, wedge casting, copper and steel mould casting and injection mould casting to obtain different cooling rates. The as-cast microstructures are characterized to reveal secondary dendrite arm spacing (SDAS), Primary dendrite arm spacing (PDAS) and second phase volume fraction as a function of cooling rate and composition. The microstructural features and different growth morphologies of Mg alloys have been systematically studied as a function of Al composition and it is found that increasing solute content can have a remarkable effect on the evolution of as cast microstructure.

Magnetic Materials for Energy Applications II: Magnetocaloric and Magnetostrictive Materials

Sponsored by: The Minerals, Metals and Materials Society, TMS Electronic, Magnetic, and Photonic Materials Division, TMS: Magnetic Materials Committee

Program Organizers: Raju Ramanujan, Nanyang Technological University; Francis Johnson, GE Global Research; S Guruswamy, Univ. of Utah; J Liu, Electron Energy Corporation

Wednesday AM
March 14, 2012

Room: Europe 10
Location: Dolphin Resort

Session Chairs: R. Mahendiran, National University of Singapore; Ivan Skorvanek, Slovak Academy of Sciences

8:30 AM Invited

Magnetocaloric Effect in Pr-Doped La_{0.7}Ca_{0.3}MnO₃: Magnetic and Calorimetric Studies: *Ramanathan Mahendiran*¹; ¹National University of Singapore

Magnetic refrigeration using solid state magnetic refrigerants is currently attracting much attention because of its higher energy efficiency and environmental cleanliness. Pervoskite manganites are one of the candidates considered for magnetic refrigeration. Here, we report magnetocaloric effect in Pr-doped La_{0.7}Ca_{0.3}MnO₃ samples. The magnetic entropy change (ΔS_m) was measured using a differential scanning calorimeter (DSC) working in a magnetic field environment. Temperature change in the sample during the magnetic field sweep was measured using a differential thermal analyser. The paramagnetic state of these compounds was found to be unstable with respect to magnetic field. The applied magnetic field induces a low to high moment transition (metamagnetic transition) over a wide temperature range compared to other well known magnetocaloric systems such as Gd-Si-Ge, Mn-Fe-P-As and La-Fe-Si. As a result, these doped oxides show a large magnetic entropy and a refrigeration capacity.

9:00 AM Invited

Magnetocaloric Effect in GdFeCo-Based Melt-Spun Ribbons: *Jozef Marcini*¹; *Zbigniew Sniadecki*²; *Jozef Kovac*¹; *Bogdan Idzikowski*²; *Ivan Skorvanek*¹; ¹Institute of Experimental Physics; ²Institute of Molecular Physics

The magnetocaloric effect (MCE) is attracting a great deal of interest because it is a basis of the new environmentally friendly magnetic refrigeration technology. In this work, we report on a beneficial effect of partial Co substitution for Fe on the magnetocaloric behaviour in the melt-spun Gd(65)Fe(20-X)Co(X)Al(10)(Si,B)(5) (x=5,10 and 15) ribbons. The highest values of the maximal magnetic entropy change, ΔS_m , and the refrigeration capacity, RC, for the Gd₆₅Fe₁₀Co₁₀Al₁₀B₅ ribbon under 50 kOe reached 7.02 J/kg K and 766 J/kg, respectively. The markedly enhanced values ΔS_m as compared to the Co-free compositions extended over a wide temperature range together with the good magnetic softness leading to the low hysteresis losses make the partially Co-substituted GdFeCoAl(Si,B) amorphous ribbons promising magnetic refrigerants in the temperature range from 80 to 220 K.

9:30 AM Invited

Novel La(Fe,Si)₁₃-Based Composites for Magnetic Refrigeration: *Julia Lyubina*¹; *Ullrich Hannemann*²; *Mary Ryan*²; *Lesley Cohen*²; ¹Imperial College London; ²Imperial College London

Materials with a giant magnetocaloric effect (MCE) arising as a consequence of a first-order magnetic phase transition and in particular La(Fe,Si)₁₃-based alloys are attractive candidates for magnetic cooling application. It has recently been shown that introducing porosity in LaFe_{13-x}Si_x alloys provides long-term mechanical stability and results in the desired reduction of the hysteresis [1]. However, the thermal



TMS 2012

141st Annual Meeting & Exhibition

conductivity of porous $\text{LaFe}_{13-x}\text{Si}_x$ decreases significantly. Here, we report the preparation and magnetocaloric effect of novel composite materials consisting of the active magnetic phase $\text{La}(\text{Fe},\text{Si})_{13}$ and a ductile, high thermal conductivity material, such as Cu or Ag. In the composites, giant MCE is successfully retained and at the same time the thermal conductivity is improved. The magnetic and thermal properties of the composites will be discussed. *This research was supported by a Marie Curie Intra European Fellowship within the 7th European Community Framework Programme.* [1] J. Lyubina, J. Appl. Phys. 109 (2011) 07A902.

10:00 AM

Optimizing the Magnetic Field Response of Magnetocaloric Materials by Nanostructuring: *Victorino Franco¹; Rafael Caballero-Flores¹; Alejandro Conde¹; Laszlo Kiss²; Laszlo Péter²; Imre Bakonyi²; ¹Sevilla University; ²Hungarian Academy of Sciences*

In order to be of practical use in magnetic refrigerators, magnetocaloric materials should have a large refrigerant capacity at moderate magnetic fields. In order to achieve this, two alternative approaches exist: a) the design of new alloys and compounds with such properties and b) the use of materials engineering techniques for the optimization of already existing materials. Although the first one is a highly desirable line of research, the expectations of success are limited due to additional restrictions on the materials' composition, operating temperature, etc. The materials engineering approach is a complementary line of research with larger certainty of its success due to the deep knowledge of the constituent phases that has been already achieved. We will overview how nanostructuring is a good strategy for obtaining magnetocaloric responses qualitatively different from the bulk materials and for controlling the field responsiveness in the magnetic field range appropriate for technological applications.

10:15 AM Break

10:30 AM

Comprehensive Study on Microstructure and the Magnetocaloric Properties in Mn-Substituted $\text{La}(\text{Fe},\text{Si})_{13}$: *Maria Krutz¹; Cristiano Teixeira¹; Konstantin Skokov¹; Jian Liu¹; James Moore¹; Paulo Wendhausen²; Ludwig Schultz¹; Oliver Gutfleisch¹; ¹IFW Dresden; ²Federal University of Santa Catarina*

$\text{La}(\text{Fe},\text{Si})_{13}$ intermetallic compounds are relevant materials for magnetic refrigeration, showing a large magnetocaloric effect (MCE) in the vicinity of T_C and consisting of abundant 3d-metal in contrast to other magnetocaloric materials, like Gd and Gd-based alloys. For application, T_C should coincide with the working temperature demanded in the refrigeration device. In $\text{La}(\text{Fe},\text{Si})_{13}$ T_C is about 200K and it is known that T_C can be raised above room temperature by hydrogenation. However, precise control of a partial H-content, to cover a range of $T_{C,S}$, is challenging. Fully hydrogenated $\text{La}(\text{Fe},\text{Si},\text{Mn})_{13}$ -compounds present a possible solution, since $T_{C,S}$ significantly decreases with increasing Mn content. Here, we present a comprehensive study on $\text{LaFe}_{13-x}\text{Mn}_x\text{Si}_{12}$ and $\text{LaFe}_{13-x}\text{Mn}_x\text{Si}_{1.4}$ ($x = 0.0, 0.1, 0.2, 0.3$ and 0.4) compounds and their hydrides. Results on magnetocaloric properties were obtained by magnetometry and direct ΔT_{ad} measurements. Finally, we assess the synthesis parameters to obtain near single-phase material in an economical manner.

10:45 AM

The Maximum Possible Cooling Power of $\text{La}(\text{FeSi})_{13}$ and Gd Based Magnetic Refrigerators: *Konstantin Skokov¹; Alexey Karpenkov¹; Oliver Gutfleisch¹; ¹Leibniz Institute for Solid State and Materials Research*

To comprehensively characterize magnetocaloric properties of potential magnetic refrigerant materials, adiabatic temperature change (ΔT_{ad}), the heat capacity (c_p), the thermal conductivity and the magnetic entropy change need to be known. Yet, these parameters do not completely characterize the efficiency of the magnetic refrigerator which can be built on the basis of alloys such as $\text{La}(\text{FeSi})_{13}$ and Gd. The magnetic refrigerator

itself must simultaneously meet two basic criteria: large temperature span and large cooling power. The thermal span is strongly related to ΔT_{ad} . But the cooling power depends on c_p and ΔT_{ad} in complex fashion and cannot be written analytically. In this work, by numerical simulation based on our ΔT_{ad} and c_p data we determined the temperature span and the maximum possible cooling power for reversible refrigeration cycles with $\text{La}(\text{FeSi})_{13}$ alloys and Gd-metal as a working substances. The results clearly demonstrate the functional ranges of these refrigerators.

11:00 AM

Effect of W Substitution on the Magnetostrictive Behavior of [001] Fe-Ga Alloy Single Crystal: *Chai Ren¹; Biswadeep Saha¹; Meenakshisundaram Ramanathan¹; Sivaraman Guruswamy¹; ¹University of Utah*

Fe-Ga alloys have a large low-field magnetostriction and these alloys are attractive candidates in energy conversion and harvesting applications. Small additions of W also increase the magnetostriction of Fe. In this paper changes in magnetostriction by W substitution for Ga in various Fe-x at.% Ga alloys are presented. Fe-Ga-W single crystals were grown using vertical Bridgman Growth technique. [001]-orientated single crystal samples were prepared with faces within 1 degree off $\langle 100 \rangle$ orientation. The samples were annealed at 1150 degree C in the alpha-phase region and water quenched. The magnetostriction coefficient $(3/2)\lambda_{100}$ measurements were made on these Fe-Ga-W single crystals. The result on the effects of W substitution and annealing on the magnetostrictive behavior of these alloys are discussed. *Support of this work by NSF-DMR under the award DMR-0854166 is gratefully acknowledged.

11:15 AM

Influence of Deformation and Ga Content on Magnetostriction in Fe-Ga Alloys: *Biswadeep Saha¹; Meenakshisundaram Ramanathan¹; Chai Ren¹; Sivaraman Guruswamy¹; ¹University of Utah*

Influence of plastic deformation and gallium content is examined in Fe-Ga alloys. Fe-Ga single crystals were prepared using the vertical Bridgman technique. Parallelepiped shaped samples were prepared with faces oriented within 0.5 degree off from the desired crystallographic orientation. Samples were annealed in alpha phase region and quenched in water. Annealed samples were plastically deformed to a predetermined strain level. Magnetostriction was measured in as grown, after annealing and after deformation. A decrease in magnetostriction is observed after deformation as compared to annealed sample at all Ga content examined. *Support of this work by NSF-DMR under the award DMR-0854166 is gratefully acknowledged.

11:30 AM

Modeling Magnetic and Structural Phase Transformations in Co-Ni-Al Ferromagnetic Shape Memory Alloys FSMA's: *Hassan Thawabi¹; Navdeep Singh¹; ¹Texas A&M University*

Ferromagnetic shape memory alloys FSMA's have shown promising features as high precision self-actuating materials with environmentally friendly energy conversion in diverse applications, specifically in the Aerospace and Bio-medical industries. In this study, we examine the effect of configurational ordering on the magnetic properties of Co-Ni-Al ordered (L2₁) and disordered (B2) austenite and martensite structures. The magnetic properties are analysed by means of employing Monte-Carlo simulations to get the magnetization, magnetic susceptibility, specific heat and entropy in response to temperature variation to obtain the Curie temperature and therefore alloy predicted operational temperatures. Magnetic exchange parameters are obtained using Ab-Initio self-consistent field calculations and the results are used in the Monte-Carlo simulations. All the results are compared with experimental literature, and their overall effect on the martensitic structural transformation are elucidated.

WEDNESDAY AM

Materials and Fuels for the Current and Advanced Nuclear Reactors: Structural Materials II

Sponsored by: The Minerals, Metals and Materials Society, TMS Structural Materials Division, TMS/ASM: Corrosion and Environmental Effects Committee, TMS/ASM: Nuclear Materials Committee

Program Organizers: Ramprashad Prabhakaran, Idaho National Laboratory; Dennis Keiser, Idaho National Laboratory; Raul Rebak, GE Global Research

Wednesday AM
March 14, 2012

Room: Swan 2
Location: Swan Resort

Session Chair: Kumar Sridharan, University of Wisconsin - Madison

8:30 AM Invited

Materials Development for the Traveling Wave Reactor: *Micah Hackett*¹; Gary Povirk¹; James Vollmer¹; ¹TerraPower

The TerraPower Traveling Wave Reactor (TWR) concept envisions a fast reactor breed-and-burn core that initially starts on a combination of low-enriched uranium and depleted uranium, and then operates with additions of depleted uranium by in-situ breeding of its own fuel. TWRs can utilize depleted uranium stockpiles for fuel and produce significantly less spent-fuel waste than LWRs without reprocessing and with reduced enrichment. Perhaps the most significant constraint in TWR development, however, is the dose limit for the core materials and burnup limits for the fuel and clad. This talk will focus on present efforts toward TWR development, which includes: data analysis to support development of a creep and swelling model for HT9 ferritic/martensitic steel; an ion irradiation program for cladding and duct development, of both HT9 and, in the future, advanced materials; and a neutron irradiation test program to qualify materials to high doses.

9:00 AM

Materials Corrosion in Liquid Fluoride Salt for NRG Applications: *Kumar Sridharan*¹; Luke Olson¹; Robert Sellers¹; Brian Kelleher¹; Wei-Jen Cheng²; James Ambrosek¹; Mark Anderson¹; Todd Allen¹; ¹University of Wisconsin; ²National Taiwan University of Science and Technology

Liquid fluoride salt FLiNaK (LiF-NaF-KF: 46.5-11.5-42 mol %) is being considered as the secondary coolant for fluoride salt-cooled high temperature reactor (FHR) and also as fluid for the transport of high temperature process heat from VHTR for the operation of chemical plants. Materials corrosion will be an important issue in high temperature liquid FLiNaK salt because of the inherent in reactivity of fluoride ion and the relative instability of the protective oxide layer on alloys in liquid fluoride salt environment. Corrosion performance of several high temperature alloys in liquid FLiNaK will be discussed. Chromium in the alloys is particularly prone to dissolution and electrochemical techniques have been developed for the quantitative detection of chromium in the liquid salt. Ni-plating was found to be remarkably effective in mitigating materials corrosion in liquid FLiNaK. Addition of zirconium to liquid FLiNaK alters its redox potential and can be used to control materials corrosion.

9:20 AM

Corrosion Behavior of a F91/Fe-12Cr-2Si Composite in Liquid Lead-Bismuth-Eutectic as a Function of Oxygen Potential in the Temperature Range 600-715°C: *Michael Short*¹; Ronald Ballinger¹; ¹MIT

The corrosion characteristics of the ferritic/martensitic alloys F91 and Fe-12Cr-2Si in liquid lead and Lead-Bismuth-Eutectic (LBE) have been investigated at low (600-615°C) and high (700-715°C) temperatures.

Tests were performed at oxygen potentials above and below the potential for formation of iron oxides. Fe-12Cr-2Si alloys develop a multi-layered oxide film with a Si-rich oxide layer formed beneath a Cr-rich oxide layer. Fe-12Cr-2Si quickly forms a protective layer system of chromium, silicon and iron oxides. A thin inner layer of silica forms beneath the chromium oxide layer that acts as a powerful diffusion barrier to further corrosion. Extrapolated corrosion rates for Fe-12Cr-2Si are less than 1 μm/yr at 700°C. A composite system using F91 clad with the new Fe-12Cr-2Si alloy is shown to be highly resistant to corrosion in liquid lead or LBE at temperatures up to 700°C which represents enabling technology for the lead-cooled fast reactor or accelerator driven target system.

9:40 AM

Effects of Ordering Reaction on Lattice Variation in Alloy 690: *SungSoo Kim*¹; Young Suk Kim¹; ¹Korea Atomic Energy Research Institute

Alloy 690 is a standard steam generator tubing material in pressurized water reactor at present. It is known that the ordering reaction causes lattice variation during the reactor operation. In order to investigate the effect of thermo-mechanical treatment on dimensional stability in alloy 690, cooling rate variation and cold work are applied, and those are aged at 400°C up to 15,000 hours. The results showed that the lattice contraction is anisotropic; it is increased to be three times by cold work; however, the effect of cooling rate appeared little. The maximum lattice contraction appeared to be 0.05~0.07% according to lattice planes. The activation energy for the ordering reaction determined by differential scanning calorimeter was 240kJ/mol.

10:00 AM Break

10:10 AM

Effect of Coatings on the Corrosion-resistance of Fe, 9-14% Cr Steels in Supercritical Water: *Selçuk Kuyucak*¹; Jian Li¹; Wenye Zheng¹; ¹Dept. of Natural Resources Canada

Oxide dispersion strengthened ferritic steels having 9-14% Cr have been considered for in-core structural applications in the "next generation" nuclear reactor designs. These steels have high irradiation resistance because of their ferritic matrix and absence of nickel, high creep resistance, but moderate to low corrosion resistance. Higher chromium levels for greater corrosion resistance are not feasible as the steel becomes brittle in the absence of nickel. Application of coatings is one option to improve the corrosion resistance of such steels. The performance of a Fe-25Cr metallic coating applied by the cold-bonding process to various Fe, 9-14% Cr steels has been investigated with particular reference to the supercritical water-cooled nuclear reactor (SCWR) design.

10:30 AM

Studies on Stacking Fault Energy of Low Carbon Austenitic Stainless Steels: *Toshio Yonezawa*¹; Ken Suzuki¹; Suguru Ooki²; Hideshi Tezuka²; Shunichi Suzuki²; ¹Tohoku University; ²Tokyo Electric Power Company

The stacking fault energy (SFE) for austenitic stainless steels has been studied by many researchers. The calculation equations of SFE value based upon chemical compositions have been also reported by some researchers. But, these equations are not so well coincident with each other. Especially, the consensus is still not obtained about the effects of interstitial elements on SFE value. Recently, the calculation equation of SFE value based upon chemical compositions is attracted attention from the view point of decreasing of intergranular stress corrosion cracking susceptibility or radiation induced segregation for austenitic stainless steels in nuclear industrial field. SFE values for 56 heats of austenitic stainless steels were measured on width of isolated extended dislocations by dark field image of TEM, and the factors of main elements were verified by thermodynamics theoretical calculation. From these analyses, more reliable calculation equation of SFE value for austenitic stainless steels was discussed and proposed.



TMS 2012

141st Annual Meeting & Exhibition

10:50 AM

Formation and Thermal Stability of Nanosized Oxide Precipitates in NiAl-(Y2O3,Ti) Alloys: *Yongdeog Kim*¹; Hyon-Jee Lee¹; Zuhair A. Munir²; Lizhen Tan³; Jeremy T. Busby³; Brian D. Wirth⁴; ¹UC BERKELEY; ²UC Davis; ³Oak Ridge National Laboratory; ⁴University of Tennessee, Knoxville

NiAl oxide dispersion strengthened alloys were produced by mechanical alloying of NiAl with Y2O3 and Ti alloying powders, followed by spark plasma sintering, with the objective of improving the high temperature strength and creep resistance. These target properties are expected due to a presence of high number density of thermally stable nano-meter scale clusters, akin to those recently observed to improve creep strength and radiation resistance in nano-structured ferritic alloys. In this presentation, the alloy production process and characterization of the NiAl ODS alloys will be summarized. The improved mechanical properties will be explained in connection with the size, structure, and number density of the precipitated oxide particles, which are obtained using transmission electron microscopy, Atom Probe Tomography, and Small Neutron Scattering. Finally, the thermal stability of oxide precipitate will be discussed using the mechanical properties and microstructural characterization results of NiAl ODS alloys as a function of thermal annealing.

11:10 AM

Finite Element Creep Behavior Analysis in Welded Joints of Modified 9Cr-1Mo Steel: *Mehdi Basirat*¹; Triratna Shrestha¹; Gabriel Potirniche¹; Indrajit Charit¹; Karl Rink¹; ¹University of Idaho

Modified 9Cr-1Mo steel is one of the first candidates for very high temperature reactor (VHTR) pressure vessels. Although modified 9Cr-1Mo steel has a good creep resistance, the material microstructure will degrade during welding process, hence material creep resistance investigation at the welded zone is essentially curtail. In this research, a microstructural creep model combined with a continuum damage mechanics model is developed. The numerical model has been implemented into Abaqus commercial finite element software by writing a User MATerial Subroutine (UMat). The creep behavior of the material was simulated at heat affected zone (HAZ) and the weld material. Furthermore, tensile creep behavior of the welded specimens at temperature range of 550-700 °C and stress level of 80-200 MPa was studied. Finally, the simulation results have been compared to the experiments and there is a good consistency.

11:30 AM

Study on Microstructural Changes and Corrosion Resistance of Ti-5Ta-2Nb/304L SS Explosive Clads in Concentrated Nitric Acid: *Sudha Cheruvathur*¹; Ravishankar A¹; Prasanthi T.N¹; Kamachi Mudali U¹; Saroja S¹; ¹Indira Gandhi Centre for Atomic Research

Dissimilar joints of Ti-5Ta-2Nb and 304L stainless steel are fabricated using explosive cladding process. Detailed characterization of explosive clads confirmed (1) absence of intermetallic phases at clad interface and (2) deformation induced phase transformation in both 304LSS and Ti-Ta-Nb. Corrosion resistance of the clads was assessed in liquid (LP), vapour and condensate phases of 11.5M nitric acid. Except in LP, corrosion rate was <1mpy in other two phases. High corrosion rate in LP was explained based on intergranular corrosion of 304LSS. Nature of passive films forming on both alloys after exposure to nitric acid were identified using XPS. In LP, in the Ti alloy, more stable and protective oxides like TiO₂, Ta₂O₅, Nb₂O₅ and NbO were detected whereas in 304LSS, Cr existed both in +3 and +6 oxidation states. This observation is in line with the conclusion drawn from corrosion experiments. Further details will be discussed in the paper.

Materials Design Approaches and Experiences III: Superalloys

Sponsored by: The Minerals, Metals and Materials Society, TMS Structural Materials Division, TMS: High Temperature Alloys Committee, TMS: Integrated Computational Materials Engineering Committee

Program Organizers: Ji-Cheng Zhao, The Ohio State University; Akane Suzuki, GE Global Research; Deb Whitis, GE Aviation; Michael Fahrman, Haynes International Inc.; Qiang Feng, University of Science and Technology Beijing

Wednesday AM
March 14, 2012

Room: Europe 11
Location: Dolphin Resort

Session Chairs: Akane Suzuki, GE Global Research; Deb Whitis, GE Aviation

8:30 AM Invited

The Alloys by Design Approach in Superalloy Development: *Nils Warnken*¹; ¹University of Birmingham

The development of Ni-based Superalloys has reached a remarkable level of complexity. Current alloys consist of 10 and more major alloying elements, which have to be carefully balanced in order to achieve the desired alloy properties. This complexity makes it necessary to explore and utilize new approaches in alloy design. Newly designed alloys are not necessarily aiming at improving overall alloy performance, but also at finding the right balance of properties for a given task. In order to achieve these goals without the conduction of lengthy and costly experimental trials, a computational approach is presented which allows for the comparison of a large number of candidate alloy compositions; Merit-indices for characteristic properties such as for example creep and oxidation resistance, manufacturability, microstructure and density are used to identify promising alloys. Further virtual testing is illustrated by using computationally more intense techniques such as the phase-field method.

9:00 AM Invited

Development of Superalloy GTD262 at GE: Liang Jiang¹; *Ganjiang Feng*²; Ji-Cheng Zhao¹; ¹GE Global Research; ²GE Energy

A project was initiated in 2002 and executed by GE Global Research and GE Energy to replace Ta in superalloy GTD222 which was widely used as nozzles in GE power generation gas turbines. By integrating computational thermodynamic predictions of phase equilibria with GE's property models and databases, we designed four alloys with Nb replacing Ta and with modifications to the concentrations of other elements to optimize key properties. Laboratory-scale tests were performed for mechanical properties, oxidation resistance, weldability and castability. The best of the four alloys doubled creep-resistance performance while maintained comparable other properties than the Ta-bearing GTD222; and it was subjected to a production trial and successfully passed the qualifications without any technical hurdles. The new alloy was named GTD262, was successfully introduced in GE gas turbines starting in 2006, and is experiencing much widened adoption today. The alloy development process and the lessons learned will be presented.

9:30 AM Invited

New Co-Base Superalloys Strengthened by γ' Phase - Alloy Design and Applications: *Kiyohito Ishida*¹; ¹Tohoku University

Phase stability of intermetallic compounds in Co-base alloys are briefly reviewed and compared with those in Ni-base alloys focusing on the GCP (geometrically closed-packed) phase. Although only Co₃Ti is known to be a stable γ' (L12) compounds, there are some metastable γ' phase in the Co-X binary system such as Co₃Al, Co₃W, Co₃Ta, etc. Recently, we

discovered ternary compounds of Co₃(Al, W), Co₃(Ge, W) and Co₃(Ga, W) with L1₂ structure. The $\gamma + \gamma'$ Co₃(Al, W) two-phase alloys show the positive temperature dependence on flow stress. Therefore, the Co-Al-W base alloys have potential for new-type of superalloys strengthened by γ' phase. In this paper, the phase equilibria, alloy design and some properties of Co-Al-W base alloys will be shown. The applications of this new wrought and cast Co-base superalloys will also be presented.

10:00 AM Break

10:20 AM

High Temperature Microstructure and Properties of New L1₂-Containing Co-Al-W Alloys: *Michael Titus*¹; Jun Zhu²; Alessandro Mottura¹; Akane Suzuki³; Tresa Pollock¹; ¹University of California, Santa Barbara; ²University of Michigan; ³GE Global Research

New cobalt-based alloys containing ordered L1₂ precipitates have been investigated. Alloying approaches for enhancing the two-phase $\gamma-\gamma'$ microstructure have been indentified. Predictions of a new thermodynamic database on transformation temperatures and phases present will be compared to experimental observations. Single crystal tensile creep tests have been performed under vacuum at 900°C with stresses between 200 and 350 MPa. Based on minimum creep rates, the high temperature creep properties of the Co-base alloys are comparable to first-generation commercially available superalloy single crystals. The implications for design of new cobalt-base alloys will be discussed using the new thermodynamic database.

10:40 AM

Effect of Alloying Elements on Microstructure and Mechanical Property of Co-Al-W-Base Superalloys: Fei Xue¹; Meiling Wang¹; Qiang Feng¹; ¹University of Science and Technology Beijing

The newly developed Co-Al-W-base superalloys with γ' -strengthening exhibit promising properties as candidates for aircraft engines and industrial gas turbines, but the knowledge of principal alloying effects has not been fully understood yet. In this study, the influence of Ti, Nb, Ta, V, Mo, Hf and Cr on microstructure and mechanical property of Co-9Al-10W-base alloys were investigated after heat treatment at 900°C. The results revealed that the morphology, size, volume fraction and solvus temperature of γ' precipitates were influenced by different alloying additions in different ways. The partition ratios of alloying elements were also examined to better understand the lattice misfit and γ' morphology, which were correlated with microstructural stability. The relationship of microstructure and mechanical property by the influence of alloy elements were analyzed based on the above experimental results. The present work will offer fundamental information to modify the compositional design for Co-Al-W-base alloys.

11:00 AM Invited

Accelerating Insertion of Materials at GE Aviation: *Deborah Whitis*¹; Arturo Acosta¹; Daniel Wei¹; Liang Jiang¹; ¹General Electric Company

Material and process development for aircraft engines has, in the past, required long and costly experimental programs, imposing a significant barrier to the insertion and exploitation of new materials and manufacturing processes. With the advent of computer modeling and simulation of materials processing, and the accelerated insertion of materials (AIM) approach, we have begun to provide the tools to industrial materials designers that they need to increase productivity and reduce cost of alloy and process development. This presentation will provide an overview of the implementation of the AIM approach at GE Aviation. The integration of materials models, historical databases, and analysis tools have allowed us to more rapidly downselect new alloys and manufacturing processes, responding quickly to the design requirements of a particular component and engine environment. Current progress in applying these techniques to nickel-based superalloys will be reviewed.

11:30 AM Invited

Development of High Temperature Capability P/M Disk Superalloys: Eric Huron¹; Kenneth Bain¹; David Mourer¹; ¹General Electric Company

A study was conducted to optimize the major element chemistry of powder metallurgy (PM) alloys for the challenging goals of a High Speed Civil Transport (HSCT) application. Two iterations were performed. Subscale heats of experimental powders were atomized, consolidated by extrusion, isothermally forged, and supersolvus heat treated. Key relationships were identified between alloying elements resulting in the identification of an optimized alloy composition. The final alloy showed significant improvements in creep and in hold time crack growth compared to state-of-the-art commercial alloys.

12:00 PM

Computational Development of Polycrystalline Alloys Using Automated Importance Sampling: *Bryce Conduit*¹; Gareth Conduit¹; Paul Mignaneli¹; Howard Stone¹; Mark Hardy²; ¹University of Cambridge; ²Rolls-Royce plc

Increasingly stringent demands are being placed on alloys used for high temperature structural applications. For such applications, the successful development of new alloys requires them to exceed numerous property targets. Combinatorial alloy design tools to achieve this are now available. However, efficient selection of optimal alloy compositions requires automated optimisation algorithms. In this work, an approach utilising importance sampling has been used to design a new Ni-based polycrystalline alloy. Neural network models have been built to describe various mechanical and thermodynamic properties for Ni-based superalloys. Minimum acceptable values for these properties were then specified, according to design criteria. The boundary of those compositions which satisfy these minimum requirements was then established by the automated importance sampling technique. On a standard desktop computer this technique can output up to ~100000 sets of compositions and design variables per second, which satisfy the design specifications.

Materials in Clean Power Systems VII: Clean Coal-, Hydrogen Based-Technologies, and Fuel Cells: Materials for Clean Coal Technologies, Turbines

Sponsored by: The Minerals, Metals and Materials Society, TMS Electronic, Magnetic, and Photonic Materials Division, TMS Structural Materials Division, TMS/ASM: Corrosion and Environmental Effects Committee, TMS: Energy Conversion and Storage Committee

Program Organizers: Xingbo Liu, West Virginia University; Teruhisa Horita, National Institute of Advanced Industrial Science and Technology; Jeffrey Hawk, National Energy Technology Lab; Jeffrey Fergus, Auburn University

Wednesday AM
March 14, 2012

Room: Europe 8
Location: Dolphin Resort

Session Chairs: Junpin Lin, University of Science and Technology Beijing; Axel Kranzmann, Federal Institute of Materials

8:30 AM Invited

Corrosion and Materials Degradation in Microturbines: *Wendy Mathews*¹; Karren More²; ¹Independant Consultant; ²Oak Ridge National Laboratory

Microturbines operate on a number of different gaseous and liquid fuels. Some of the fuels are standard fuels (natural gas, diesel, kerosene), while others are alternative/renewable fuels (sour gas, landfill gas, digester gas, bio-diesel). Variations in alternative/renewable fuel composition and the normal operating conditions of the microturbine, even with standard fuels, present many materials challenges. Hot corrosion/sulfidation has been found in microturbine components exposed to fuels containing high



TMS 2012

141st Annual Meeting & Exhibition

Sodium and/or Potassium (such as bio-diesel). Accelerated oxidation of components may also occur, most notably in thin foil Primary Surface Recuperators (PSR), as a result of the presence of water vapor in the products of combustion. Microstructural and compositional analyses of these types of materials degradation will be presented and various possible solutions will be discussed.

9:00 AM

Development of Cast Alumina-Forming Austenitic Stainless Steel Alloys: Govindarajan Muralidharan¹; Yukinori Yamamoto¹; Michael Brady¹; Larry Walker¹; ¹Oak Ridge National Laboratory

There is significant interest in the development of alumina forming creep resistant alloys for use in various industrial process environments. Earlier studies have outlined the development of wrought Alumina Forming Austenitic (AFA) alloys. These alloys achieve good high-temperature oxidation resistance due to the formation of protective Al₂O₃ scales while multiple second-phase precipitation strengthening contributes to excellent creep resistance. This work will summarize the results on the development of cast AFA alloys. Oxidation resistance and creep properties have been evaluated in the as-solidified condition and compared with that achieved in the wrought alloys over the temperature range of 650°C to 800°C. This talk will summarize the effect of alloying element additions on the oxidation and creep properties of cast AFA alloys. Research sponsored by the U.S. Department Of Energy, Office of EERE Industrial Technologies Program, under contract DE-AC05-00OR22725 with UT-Battelle, LLC.

9:20 AM

Impact of Casting Superheat on the Mechanical Properties of Traditionally Wrought Ni-Based Superalloys for USC Steam Turbines: Paul Jablonski¹; Jeffery Hawk¹; Daniel Purdy²; Philip Maziasz³; ¹US Department of Energy; ²GE; ³ORNL

The high temperature components within conventional coal fired power plants are manufactured from ferritic/martensitic steels. In order to reduce greenhouse gas emissions the efficiency of pulverized coal steam power plants must be increased. The proposed steam temperature in the Advanced Ultra Supercritical (A-USC) power plant is high enough (760°C) that ferritic/martensitic steels will not work due to temperature limitations of this class of materials; thus Ni-based superalloys are being considered. The full size castings are quite substantial: ~4in thick, several feet in diameter and weigh 5-10,000lb each half. Small scale castings of alloys 263 and 282 with comparable section size and controlled cooling rate were cast with three levels of superheat. A multi-step homogenization heat treatment was developed in order to better deploy the alloy constituents. The mechanical properties of the alloys (tensile and fatigue) as well as the microstructure are reported here.

9:40 AM

Mechanical Behavior of Tempered Martensitic Steels for Ultrasupercritical Steam Applications: Jeffrey Hawk¹; Paul Jablonski¹; Christopher Cowen²; ¹U.S. Department of Energy, National Energy Technology Laboratory; ²United States Department of the Treasury

Advanced 9-12% Cr tempered martensitic steels form the majority of tonnage of components used in coal fired power plants that operate in the temperature range of 570-620°C. Computational and experimental alloy development efforts at NETL have focused on raising the use temperature of this steel class to 650°C. An improvement in alloy high temperature capability would increase power plant efficiency while decreasing the carbon footprint. This presentation focuses on microstructure feature design considerations for typical high temperature martensitic steels, primary microstructural stability concerns, the preservation of strengthening mechanisms and their high temperature mechanical behavior. Tensile and creep properties for these alloys relative to commercially available 9% Cr steels will be discussed. Microstructure development during processing and post processing microstructural changes due to creep will be discussed for newly developed NETL alloys as well as for COST E, B2, and FB2 alloys.

10:00 AM Break

10:10 AM

Influence of SO₂ and Water on the Corrosion in Oxyfuel Coal Power Plant: Axel Kranzmann¹; Alexander Findeisen²; ¹Federal Institute for Materials Research and Testing; ²BTU Cottbus

The flue gas of coal fired Oxyfuel Power Plants is characterised by the high partial pressure of CO₂, water and SO₂/SO₃. Experimental simulations of the gas corrosion in the temperature between 490 °C and 620 °C including the mechanical stress under working conditions and ash were performed. Tubular specimen and plates from power plant steels were prepared from industrial parts. The tubes were loaded with an inner pressure of about 270 bar was applied by steam. The comparison between these different experiments indicate that the main influence of the ash is due the reaction between ash and oxide layer and and higher sulphur oxide fugacity within the ash layer. A simple heuristic model to describe the role of water supporting the diffusion of SO₂ and CO₂ through the oxide layer is included in the discussion of the corrosion effects.

10:30 AM

Microstructure Characterization of Crept Ni-Base Alloys for High Temperature Use: Jeffrey Hawk¹; John Sears²; Paul Jablonski¹; ¹U.S. Department of Energy, National Energy Technology Laboratory; ²URS, NETL

High temperature alloys typically use a combination of matrix strengthening precipitates, carbides and high dislocation density to impart strength. In Ni-base superalloys for use at high temperatures the main strengthening phase is gamma prime. Volume fraction and precipitate morphology are two important factors in alloy strength and influence matrix strength and deformation behavior in the alloy. The character of the grain boundaries as well as phase found there are also important in generating high temperature creep strength and long-term microstructure stability. This presentation will examine two alloys, Haynes 282 and Nimonic 105 as potential candidate alloys for steam turbine components. The microstructure of each alloy will be discussed from the point of view of the unstressed versus the stressed state (creep deformation), with important high temperature strengthening mechanisms highlighted. These features will be related to the creep behavior of the alloy.

10:50 AM

Strengthening Concepts & Mechanical Behavior of Ni-Base Alloys in A-USC Steam Turbines: Jeffrey Hawk¹; Paul Jablonski¹; ¹U.S. Department of Energy, National Energy Technology Laboratory

Experience with nickel-base alloys for use at 1400°F has shown that commercial, "off-the-shelf" nickel superalloys exist for these applications, and while promising, the alloy in the off-the-shelf condition may not provide for all long-term mechanical needs in steam. One alloy, Haynes 282, has shown robust capability in terms of starting microstructure (gamma prime size & volume fraction). Another alloy, Nimonic 105, has exhibited the potential for improved creep behavior in the peak aged condition as well as when aged. These alloys are among several that offer the best potential for building steam turbine components for a power plant operating at =1400°F. Design strategy, strengthening concepts and creep behavior will be discussed for each alloy, highlighting differences in each alloy and their respective strengths relative to use as steam turbine components. Suggestions for improving alloy performance will also be discussed.

11:10 AM

The Effect of Temperature on Equilibrium of Coal-Petcoke Slag Mixtures under Gasification Conditions: Jinichiro Nakano¹; Sudhir Ranjan²; Kye-Sing Kwong¹; James Bennett¹; Xueyan Song³; Seetharaman Sridhar²; ¹NETL; ²Carnegie Mellon University; ³West Virginia University

In gasifiers, molten slags forming from non-volatile impurities from carbon feedstock are known to cause wear of the protective liner materials. A recent industrial trend of increased use of petcoke to coal feedstock

has drastically modified slag chemistry due to the high vanadium content, and caused new chemical equilibria in the slag system. In this work, synthetic slags corresponding to coal-petcoke fuel mixtures were studied for phases present under gasification conditions. Equilibration of samples ($\text{SiO}_2\text{-Al}_2\text{O}_3\text{-Fe}_2\text{O}_3\text{-CaO-V}_2\text{O}_5$) exposed at 1425, 1500, and 1575°C in $\text{Po}_2=10\text{-}8\text{atm}$ for 72 hours, samples containing up to 9 wt% V_2O_5 was investigated by XRD, SEM-WDX, ICP, and TEM. Mullite, karelianite, and anorthite were found in equilibrium with slag at 1425°C, while mullite and karelianite were predominant at higher temperatures. The slag homogeneity expanded with increasing temperature. The presence of the solid phases is discussed in terms of its impacts on slag fluidity and refractory degradation.

11:30 AM

Nano-Scale Carbide Characterization in a Tempered Martensitic 9Cr Steel Used for Ultrasupercritical Steam Power Plants: *Niven Monsegue*¹; Mitsuhiro Murayama¹; William Reynolds¹; ¹Virginia Tech

The 9Cr steel designated COST B2 is currently used in various USC coal power plant applications; however, microstructural stability under various service conditions such as evolution of strengthening factors has not been fully understood. In this study, three samples of COST B2 consisting of as-cast and two creep tested COST B2 were examined by transmission electron microscopy. The creep test parameters were: (1) 650°C for 655 hrs with 172 MPa stress and (2) 650°C for 2039 hrs with 138 MPa. Particular focus was placed on nano-size carbides, one of the major creep resistance factors in COST B2, and their correlating characteristics with varying stress and temperature.

Materials Research in Microgravity: Session V

Sponsored by: The Minerals, Metals and Materials Society, TMS Materials Processing and Manufacturing Division, TMS Extraction and Processing Division, TMS: Process Technology and Modeling Committee, TMS: Solidification Committee

Program Organizers: Robert Hyers, University of Massachusetts; Hani Henein, University of Alberta; Valdis Bojarevics, University of Greenwich; James Downey, NASA; Douglas Matson, Tufts University; Achim Seidel, Astrium; Daniela Voss, ESA

Wednesday AM
March 14, 2012

Room: Asia 3
Location: Dolphin Resort

Session Chair: To Be Announced

8:30 AM Invited

Solidification Modeling: from Electromagnetic Levitation to Atomization Processing: *Charles-Andre Gandin*¹; D. Tourret²; T. Volkman²; D. Herlach²; A. Ilbagi³; H. Henein³; ¹MINES ParisTech; ²DLR; ³University of Alberta

A segregation model for multiple phase transformations is presented together with solidification experiments using electromagnetic levitation. Comparison is made between predictions and measurements. Thanks to coupling with thermodynamic equilibrium calculations, as well as the treatment of dendritic, peritectic and eutectic reactions, quantitative agreement is found for the cooling curves and the fraction of microstructures measured, thus providing a validation of the kinetics of phase transformations. Application is then possible for the impulse atomization process. It reveals the importance of the competition between the various microstructures formed from the melt and the role of the nucleation and growth kinetics. Simulation for samples processed by electromagnetic levitation in the ISS in 2013 will be performed.

9:05 AM Invited

X-Ray Radiographic Observation of Directional Solidification under Microgravity: XRMON-GF Experiments on MASER12 Sounding Rocket Mission: *Guillaume Reinhart*¹; Henri Nguyen-Thi¹; Aboul-Aziz Bogno¹; Bernard Billia¹; Ragnvald Mathiesen²; Gerhard Zimmermann³; Ylva Houltz⁴; Kenneth Löth⁴; Daniela Voss⁵; Antonio Verga⁵; Fabio De Pascale⁵; ¹IM2NP - Université Paul Cézanne; ²NTNU; ³ACCESS e.V.; ⁴Swedish Space Corporation; ⁵European Space Agency

The European Space Agency (ESA) - Microgravity Application Promotion (MAP) programme entitled XRMON (In situ X-Ray MONitoring of advanced metallurgical processes under microgravity and terrestrial conditions) aims to develop and perform in situ X-ray radiography observations of metallurgical processes in microgravity and terrestrial environments. The use of X-ray imaging methods makes it possible to study alloy growth processes with spatio-temporal resolutions at the scales of relevance for microstructure formation. XRMON has been selected for MASER 12 sounding rocket experiment, scheduled in autumn 2011. Although the microgravity duration is typically six minutes, this short time is sufficient to investigate a solidification experiment with X-ray radiography. This communication will report on the preliminary results obtained with the experimental set-up developed by SSC (Swedish Space Corporation). Results deal with the directional solidification of Al-Cu and they confirm the great interest to perform in situ characterization to analyse dynamical phenomena during solidification processes.

9:40 AM

Innovative Video Diagnostic Equipment for Material Science Experiments in Space

: *Giuseppe Capuano*¹; Daniele Titomanlio¹; Wolfgang Soellner²; Achim Seidel²; ¹Techno System Developments; ²Astrium

Materials science experiments under microgravity increasingly rely on advanced optical systems to determine the physical properties of the samples under investigation. This includes video systems with high spatial and temporal resolution. The acquisition, handling, storage and transmission to ground of the resulting video data are very challenging. Since the available downlink data rate is limited, the capability to compress the video data significantly without compromising the data quality is essential. We report on the development of a Digital Video System for EML which provides real-time video acquisition, high compression using advanced Wavelet algorithms, storage and transmission of a continuous flow of video with different characteristics in terms of image dimensions and frame rates. The DVS is able to operate with the last generation of high-performance cameras acquiring high resolution video images up to 4Mpixels at 15 fps or high frame rate video images up to 1000 fps at 256x256pixels.

10:05 AM Break

10:25 AM Invited

Three-Dimensional Interface Pattern Evolution in Directional Solidification under Microgravity Conditions: *Nathalie Bergeon*¹; Anthony Ramirez¹; L Chen¹; Bernard Billia¹; Alain Karma²; Jiho Gu³; Min Xu³; *Rohit Trivedi*³; ¹Université Paul Cézanne; ²Northeastern University; ³Iowa State University

Experiments under low gravity conditions have been carried out on the International Space Station using the Directional Solidification Insert in the DECLIC facility to investigate the dynamic of spatially extended three-dimensional array of cells and dendrites under diffusive growth conditions. Experiments were conducted in a transparent system of succinonitrile-0.24 wt% camphor alloy, and the dynamics of three-dimensional interface pattern evolution under different growth conditions were visualized in situ through two cameras (bright field) and a laser interference technique. Several important results on the dynamics of three-dimensional pattern evolution will be presented with a detailed analysis of the time-evolution of their spatial arrangement. New observations on the formation of multiplets in three-dimensions will be described and novel



TMS 2012

141st Annual Meeting & Exhibition

oscillating modes were observed during the cellular growth at low velocity in which the hexagonal array split into three groups of cells showing oscillations in time with a phase difference of 1/3 with each other.

11:00 AM

Containerless Measurements of Density and Viscosity of Fe-Co Alloys: *Jonghyun Lee*¹; Douglas Matson²; Robert Hyers³; ¹Tufts University and UMass Amherst; ²Tufts University; ³University of Massachusetts

During the past years, extensive collaborative research has been done to understand phase selection in undercooled metals using novel containerless processing techniques such as electrostatic and electromagnetic levitation. Of major interest is controlling a two-step solidification process, double recalescence, in which the metastable phase forms first and then transforms to the stable phase after a certain delay time. The previous research has shown that the delay time is greatly influenced by the internal convection velocity. In the prediction of internal flow, the fidelity of the results depends on the accuracy of the material properties. This research focuses on the measurements of density and viscosity of Fe-Co alloys which will be used for the fluid simulations whose results will support upcoming International Space Station flight experiments.

11:25 AM

TEMHD Effects On Solidification under Microgravity Conditions: Andrew Kao¹; *Koulis Pericleous*¹; ¹University of Greenwich

An unexplored potential exists to control microstructure evolution through the use of external DC fields. Thermoelectric currents form during solidification and interact with this external field to drive microscopic fluid dynamics within the inter-dendritic region. The convective heat and mass transport can have profound changes on the dendritic structure. Levitation/confinement and control of the macroscopic fluid dynamics is often achieved through the combined use of both AC and DC magnetic fields. In the absence of gravity the effect of the AC field can be used purely for positioning, while the DC field can be chosen to be significantly large to interact with the thermoelectric currents. In this paper the effect of high magnetic fields on a solidifying droplet is demonstrated through the use of both 3-dimensional and 2-dimensional models. The results show that the application of a magnetic field causes significant disruption to the dendritic morphology.

Mechanical Behavior at Nanoscale I: Deformation/strength at Nanoscale and Li- induced Deformation

Sponsored by: The Minerals, Metals and Materials Society, TMS Materials Processing and Manufacturing Division, TMS: Nanomechanical Materials Behavior Committee, TMS/ASM: Mechanical Behavior of Materials Committee

Program Organizers: Scott Mao, University of Pittsburgh; Julia R Greer, California Institute of Technology; Jianyu Huang, Center for Integrated Nanotechnologies; Marc Legros, CEMES-CNRS; Ting Zhu, Georgia Institute of Technology

Wednesday AM
March 14, 2012

Room: Asia 1
Location: Dolphin Resort

Session Chairs: David Bahr, Washington State University; Nathan Mara, Los Alamos National Laboratories

8:30 AM Invited

Unveiling the Strengthening and Toughening Mechanisms of Nacre – Lessons from Nature: *Xiaodong Li*¹; ¹University of South Carolina

Nacre is a natural nanocomposite with superior mechanical strength and eminent toughness. What is the secret recipe that Mother Nature uses to fabricate nacre? What roles do the nanoscale structures play in the strengthening and toughening of nacre? Can we learn from this to produce nacre-inspired nanocomposites? The recent discovery of

nanoparticles in nacre is summarized, and the roles these nanoparticles play in nacre's strength and toughness are elucidated. It was found that rotation and deformation of aragonite nanoparticles are the two prominent mechanisms contributing to energy dissipation in nacre. The biopolymer spacing between nanoparticles facilitates the particle rotation process. Individual aragonite nanoparticles are deformable. Dislocation formation and deformation twinning were found to play important roles in the plastic deformation of individual nanoparticles, contributing remarkably to the strength and toughness of nacre upon dynamic loading. This talk also presents future challenges in the study of nacre and nacre-inspired materials.

9:00 AM

Size Effect on the Mechanical Behaviour of GaAs Nanowires: *Yanbo Wang*¹; Qiang Gao²; Xiaozhou Liao¹; Yiu-Wing Mai¹; Chennupati Jagadish²; ¹The University of Sydney; ²The Australian National University

The mechanical properties of semiconductor nanowires (NWs) are of great importance for NW applications because they affect the reliability and functionality of NW-based devices. Recent investigations showed that mechanical strain in NWs can significantly change the optical, electrical and magnetic properties of the NWs. Here, we applied an in-situ transmission electron microscopy (TEM) nano-compression technique and finite-element analysis (FEA) to investigate the mechanical behaviour of GaAs NWs. Our results demonstrate significant size effect on the mechanical behaviour of the NWs: (1) the elastic strain limit of NWs with diameters of 50–150 nm is ~ 11%, which is 100 times higher than that of conventional bulk ceramics; (2) obvious plastic deformation occurs in NWs with diameters smaller than 25 nm; and (3) a repeatable self-healing process takes place in partially fractured NWs with diameters smaller than 15 nm that restores their original structure after the external compressive force is removed.

9:20 AM

Plasticity of Metal Nanoparticles in Nanoextrusion: *Antti Tolvanen*¹; Karsten Albe¹; ¹TU-Darmstadt

Recent transmission electron microscopy experiments have shown how nanoparticles can be encapsulated inside carbon onions and electron irradiation induced contraction of these onions can be used to apply pressure of tens of GPa to the encapsulated particle. If an orifice is opened to the carbon onion, this system can be used to study the extrusion of the encapsulated material and thus the plasticity of individual crystallites at the nanoscale. In this study, the results of molecular dynamics simulation of the extrusion of Cu, Pd and Al nanoparticles pressurised in spherical force field mimicking the behaviour of contracting carbon onion are presented. We compare the plastic behavior single-crystalline nanoparticles of Cu, Pd and Al with multiply-twinned nanoparticles. The effects of the different stacking fault energies of Cu and Pd, and the effect of twins on the dislocation nucleation and propagation is reported and a pressure driven athermal amorphisation process is presented.

9:40 AM

Anisotropic Swelling of Si Nanowires and Size-Dependent Fracture of Si Nanoparticles during Lithiation: *Xiaohua Liu*¹; He Zheng²; Li Zhong²; Shan Huang³; Khim Karki⁴; Li Qiang Zhang²; Yang Liu⁴; Akihiro Kushima⁵; Wen Tao Liang⁶; Jiang Wei Wang²; Jeong-Hyun Cho⁷; Eric Epstein⁴; Shadi Dayeh⁷; Tom Picraux⁷; Ting Zhu³; Ju Li⁵; John Sullivan¹; John Cumings⁴; Chunsheng Wang⁴; Scott Mao²; Zhi Zhen Ye⁸; Sulin Zhang⁶; Jian Yu Huang¹; ¹Sandia National Laboratories; ²University of Pittsburgh; ³Georgia Institute of Technology; ⁴University of Maryland; ⁵University of Pennsylvania; ⁶Pennsylvania State University; ⁷Los Alamos National Laboratory; ⁸Zhejiang University

We report direct observations of an unexpected anisotropic swelling of Si nanowires and a size-dependent fracture of Si nanoparticles during lithiation with advanced in situ transmission electron microscopy (TEM). Lithiation of the <112>-oriented Si nanowires resulted in anisotropic expansion (larger swelling along <110> than along <111>)

and a dumbbell-shaped cross-section, due to plastic flow and an ensuing necking instability that was induced by the tensile hoop stress buildup in the lithiated shell. A strong size-dependent fracture behavior of Si nanoparticles was discovered, i.e., there exists a critical particle diameter of ~ 150 nm, below which the particles did not crack, above which the particles first formed surface cracks and then fractured, due to lithiation-induced swelling and the buildup of large tensile hoop stress in the surface layer. These results provide direct evidence of the mechanical robustness of small silicon nanoparticles for their applications in lithium ion batteries.

10:00 AM Break

10:10 AM Invited

Physical Origin of Large Strain Bursts in Submicron Al Pillars: Zhangjie Wang¹; Yuan Gao²; Qingjie Li¹; Zhiwei Shan¹; Ju Li³; Zhuo Zhuang²; Jun Sun¹; Evan Ma⁴; ¹Center for Advancing Materials Performance from the Nanoscale (CAMP-Nano) & Hysitron Applied Research Center in China (HARCC), State Key Laboratory for Mechanical Behavior of Materials, Xi'an Jiaotong University; ²Applied Mechanics Laboratory, School of Aerospace, Tsinghua University, Beijing; ³Department of Nuclear Science and Engineering and Department of Materials Science and Engineering, Massachusetts Institute of Technology; ⁴Department of Materials Science and Engineering, Johns Hopkins University

Compression testing of micro- and nano- sized Al pillars indicate two sample size regimes with contrasting mechanisms underlying the large strain bursts. For small pillars the bursts originate from the inability to store dislocation network inside, characterized by ultrahigh collapse stresses and nearly pristine postmortem microstructure. For larger pillars the bursts result from the destruction of jammed dislocation configurations, featuring relative low stress level and retention of dislocation networks after bursts. Computer simulations reveal a critical pillar size required to form "junction-chain" structures for robust dislocation jamming.

10:30 AM

In-Situ Transmission Electron Microscopy Observation of Discrete Hopping Lithiation in ZnO Nanowire: Akihiro Kushima¹; Xiao Liu²; Guang Zhu³; Ju Li⁴; Zhong Wang³; Jian Huang²; ¹Department of Materials Science and Engineering, University of Pennsylvania; ²Center for Integrated Nanotechnologies, Sandia National Laboratories; ³School of Materials Science and Engineering, Georgia Institute of Technology; ⁴Department of Nuclear Science and Engineering and Department of Materials Science and Engineering, Massachusetts Institute of Technology

The charging processes of individual ZnO nanowire (NW) electrode in Li-ion battery configuration were observed by in situ transmission electron microscopy. A unique reaction front morphology and dynamics, causing the single-crystalline NW to become a nanoglass (H. Gleiter, MRS Bulletin 34 (2009) 456), was discovered. First, partial lithiation of crystalline NW induces large stress and nanocracking ~ 70 nm in front of the main lithiation front. This is followed by rapid surface diffusion of Li⁺ and solid-state amorphization along the open crack surfaces. Finally the crack surfaces merge, leaving behind an amorphous-amorphous interface and possibly residual voids. Such reaction front instability also repeats in the interior, further subdividing the NW into different nanoglass domains (nanoamorphization). Our observations lead to important insight for developing battery with better performance and cyclability. Furthermore, the results highlight the importance of lithium embrittlement in battery behavior.

10:50 AM

Multiple-Stripe Lithiation Mechanism of Individual SnO₂ Nanowires in a Flooding Geometry: Jianyu Huang¹; Scott Mao²; Li Zhong²; Xiaohua Liu¹; Guofeng Wang²; ¹Center for Integrated Nanotechnologies, Sandia National Laboratories; ²Department of Mechanical Engineering and Materials Science, Univ. of Pittsburgh

The atomic scale lithiation mechanism of individual SnO₂ nanowires in a flooding geometry was revealed by in situ transmission electron microscopy. The lithiation was initiated by the formation of multiple

stripes with a width of a few nanometers parallel to the (020) plane traversing the entire wires, serving as multiple reaction fronts for later stages of lithiation. Inside the stripes, we identified a high density of dislocations and enlarged interplanar spacing, which provided an effective path for lithium ion transport. The density of the stripes increased with further lithiation, and eventually they merged with one another, causing a large elongation, volume expansion, and the crystalline-to-amorphous phase transformation. This lithiation mechanism characterized by multiple stripes and multiple reaction fronts was unexpected and differed completely from the expected core-shell lithiation mechanism.

11:10 AM

Thickness Dependent Deformation Behaviour of Multilayer Metallic Nanopillars: Mark Hoffman¹; Pranesh Dayal¹; Nick Savvides¹; ¹The University of New South Wales

The creation of metallic nanolayered structures leads to a significant increase in hardness with decreasing layer thickness. The exact mechanism of this nanohardening remains however contentious. In this study we have created Al/Pd nanolayered structures, based upon the theory of Koehler, with equal layer thickness of each material ranging from 1 to 20 nm thickness. A profound increase in hardness measured by nanoindentation is observed as layer thickness falls below 10 nm. We have then created nanopillars of 1, 10 and 20 nm thickness. It is found that the deformation changes from brittle cross-pillar shearing with high flow stress, to extrusion of the Al phase with increasing layer thickness at lower stress. TEM cross-sections of the compressed pillars reveals the presence of grain rotation within the layers of some thickness providing elucidation of the deformation mechanism and the nanohardening process.

11:30 AM

In Situ TEM Electrical Contact Indentation Observations in Doped Si Nanopillars: Douglas Stauffer¹; Sanjit Bhowmick¹; Sergei Krylyuk²; Albert Davydov²; Ryan Major¹; ¹Hysitron, Inc.; ²Metallurgy Division, Material Measurement Laboratory (MML)

Shrinking dimensions of microelectronic devices and rapid development of nanostructured materials require novel techniques to measure electrical and mechanical properties of materials at the nanoscale. However, typical electrical measurements are done with very large probe radii or toxic materials such as mercury. Here, a depth sensing indenter is used to simultaneously probe the electrical and mechanical responses of silicon nanostructures. VLS-grown silicon pillars, with diameters from 120 nm to 160 nm and up to 800 nm in length are contacted in situ using both TEM and SEM to aid in positioning. Moduli values less than bulk Si, 121 ± 16 GPa, are found. Absolute conductance measurements show increases in contact area as the probe meets the indenter followed by changes depending on the amount and type of plasticity caused by compression. From these measurements, true conductivity can be found knowing contact resistance and dimensions of the nanostructure.

11:50 AM

Multiscale Modeling of Anisotropic Growth in Lithiated Silicon Nanowires: Sulin Zhang¹; Hui Yang¹; Xu Huang¹; Shan Huang²; Ting Zhu²; ¹The Pennsylvania State University; ²Georgia Tech

We formulated a multiscale model to account for the anisotropic growth of lithiated silicon nanowires. On the atomic level, molecular dynamics simulations coupled with pathway sampling schemes were employed to compute the migration barriers of lithium ions in stressed silicon nanowires. The derived lithium diffusivity was then passed into a continuum-level diffusion equation, which is further coupled to the stress field calculations based on finite element analysis. The multiscale model provides atomistic mechanisms of lithiation of silicon nanowires, and explains well the anisotropic growth of lithiated silicon nanowires.



TMS 2012

141st Annual Meeting & Exhibition

12:10 PM

Study of Dislocation Climb at Nanovoids in BCC Metal: *Mishreyee Bhattacharya*¹; A. Dutta²; A. Giri¹; N. Gayathri¹; P. Barat¹; ¹Variable Energy Cyclotron Centre; ²Jadavpur University

Defects of the order of nanometer size, often created by radiation damage in metals in nuclear reactors form obstacles to dislocation glide and eventually affect the mechanical properties. Depending on the material and irradiation conditions, point defects agglomerate to form nanovoids and in-silico methods are most fruitful in providing detailed information about this dislocation-nanovoid interaction to model material properties. Here, we employ techniques of atomistic simulation to investigate the dislocation-nanovoid interaction in bcc Molybdenum, where the phenomenon of climb has occurred. Though void-mediated dislocation climb has been reported in recent molecular statics and dynamics simulations, the underlying mechanism is not yet revealed. We have performed simulations by varying depinning load and nanovoid size as well. These results suggest the possibility of a mechanism of dislocation climb, which can be fundamentally different from the conventional diffusion based process. In this work, the distinctive features of this void-mediated dislocation climb are highlighted.

Mechanical Behavior Related to Interface Physics: Interface Structures: Characterization, Theory, and Modeling

Sponsored by: The Minerals, Metals and Materials Society, TMS Structural Materials Division, TMS Materials Processing and Manufacturing Division, TMS/ASM: Mechanical Behavior of Materials Committee, TMS: Nanomechanical Materials Behavior Committee

Program Organizers: Jian Wang, Los Alamos National Laboratory; Nathan Mara, Los Alamos National Laboratory; Izabela Szufarska, University of Wisconsin-Madison; Zhiwei Shan, Xi'an Jiaotong University

Wednesday AM
March 14, 2012

Room: Oceanic 1
Location: Dolphin Resort

Session Chairs: Nathan Mara, Los Alamos National Laboratory; Sreeramamurthy Ankem, University of Maryland

8:30 AM Keynote

Disconnection Mechanisms in Twin Growth: *Robert Pond*¹; ¹University of Exeter

The basic mechanism of twin growth is the motion of dislocations along the twin plane. The Burgers vectors and step heights of admissible disconnections can be predicted using topological theory. However, for a fuller understanding, atomic-scale simulations are necessary, and recent progress is illustrated and discussed. The intrinsic mobility of a glissile disconnection is generally enhanced by a wide core structure, small step height, and minimal shuffling. Glissile disconnections are not necessarily blocked on encountering a sessile disconnection: modest applied stresses enable such obstacles to be overcome in a mechanism that is conservative overall. In a similar mechanism, a sessile disconnection under stress can act as a source for glissile disconnections, leading to irregular boundaries, as seen experimentally in Ti for example. Growth of deformation twins is suppressed by twin blunting: observations and simulations of this process in Al are presented, and contrasted with the low stacking-fault energy material Ni₂MnGa.

9:00 AM Keynote

Exploiting the Atomic Structure of Interfaces in Crystalline Solids: *Richard Hoagland*¹; Jian Wang¹; Michael Demkowicz²; Amit Misra¹; ¹Los Alamos National Laboratory; ²MIT

The atomic structure of interfaces defines their properties and thereby the properties they impart to polycrystalline and polyphasic materials. This talk focuses primarily on the atomic structures of a few types of

interfaces that have been observed in fcc/bcc composites. In spite of the relative simple crystallographic orientations, the differences in lattice parameter of the constituents leads to rather complex structures that are nearly periodic. Misfit dislocations in these structures are discussed and are shown to account for high strength by impeding slip, and to act as potent sinks for Frankel defects. The structure of interfaces is shown to depend on orientation and misfit strain, variables that may be adjusted to alter both mechanical strength and sink strength in controllable ways. This work was supported by Los Alamos National Laboratory Directed Research and Development project ER20110573 and the US Department of Energy, Office of Science, Office of Basic Sciences.

9:30 AM

Atomic Cu/Nb Interface Structures Characterized by Transmission Electron Microscopy: *Shijian Zheng*¹; Weizhong Han¹; Robert Dickerson¹; Nathan Mara¹; ¹Los Alamos National Laboratory

Cu/Nb nanosize multilayered composites have shown high strength and high ductility which are due to their high density of interfaces. In this work, Cu/Nb nanolayered composites were prepared by accumulative roll bonding (ARB). To understand the interface effect on mechanical behavior, atomic Cu/Nb interface structures were studied by (scanning) transmission electron microscopy (TEM). It was found that Cu and Nb often have {112} KS orientation relationship, and their interfaces are faceted. The faceted interfaces are closely linked to twinning in Cu. Also, composition gradients at the interfaces were characterized by scanning transmission electron microscopy (STEM), energy dispersive X-ray spectroscopy (EDS) and electron energy loss spectroscopy (EELS). The effect of deformation on intermixture of Cu and Nb, as well as O segregation at the interfaces will be discussed.

9:45 AM

Evaluation of Twin Boundary Interfaces to Strain Hardening by Electron Channeling Contrast Imaging: *Ivan Gutierrez-Urrutia*¹; Dierk Raabe¹; ¹Max-Planck-Institut for Iron Research

The formation of twin interfaces during deformation of FeMn alloys leads to an outstanding strain-hardening behavior, the so-called twinning induced plasticity (TWIP) effect. Because of the nanoscale size of the twins, the quantitative characterization of these interfaces and accordingly, their influence on strain hardening is still a challenging task. Conventional electron microscopy techniques, such as electron backscatter diffraction (EBSD) and transmission electron microscopy (TEM) are limited due to the low angular resolution and small field of view, respectively. We present a quantitative characterization of twin substructure by electron channeling contrast imaging (ECCI) in a FeMn alloy. A novel ECCI set-up is used which makes use of EBSD to obtain twin and dislocations images at optimum contrast. The influence of initial grain size and crystal orientation on twin substructure is analyzed. The role of twin interfaces on strain hardening mechanisms and their interaction with the underlying dislocation substructure will be discussed.

10:00 AM

Ultra Fast Grain Boundary Segregation In Hot Deformed Nickel: *Marion Allart*¹; Frédéric Christien¹; René Le Gall¹; ¹Université de Nantes

Hot deformation of nickel alloys (500-800°C) can lead to a dramatic loss of mechanical properties due to sulfur grain boundary segregation. In this work, both equilibrium and non-equilibrium sulfur grain boundary segregation in nickel were studied at 550°C. They were obtained respectively by simple annealing and by hot-compression. Segregation was quantified by Wavelength Dispersive X-ray Spectroscopy and was found to be thousands of times as fast during hot-compression as during annealing at the same temperature: it takes about 20 minutes at 550°C to saturate the grain boundaries with sulfur during compression at 3.10⁻⁵ s⁻¹, whereas three months are needed by simple annealing at the same temperature. Cross-section observations show that subgrains form during hot compression. A model based on sulfur diffusion along the subgrain boundaries (dislocation walls) enables to account for the observed ultra-fast segregation during hot-compression.

10:15 AM Break

10:25 AM Keynote

The Role of Interfacial Interaction Stresses and Crystallography on Deformation Mechanisms of Two-Phase Titanium Alloys: William Joost¹; Zane Wyatt¹; Sreeramamurthy Ankem¹; ¹University of Maryland

The deformation mechanisms and mechanical properties of two-phase titanium alloys strongly depend upon the crystallographic relationship between phases. The crystallographic relationships, in turn, determine the nature of the interaction stresses that are needed to maintain compatibility at the interfaces. In this study, the interaction stresses at the alpha-beta interfaces were determined by the finite element method. It is shown that interaction stresses combined with the applied stress will influence the deformation mechanisms in two-phase titanium alloys. It was found that the deformation mechanisms in two-phase titanium alloys can be different than those found in the respective single-phase alloys. For example, during low-temperature creep a single-phase beta titanium alloy deforms by twinning, but the same beta phase in the presence of an alpha phase deforms by stress induced martensite. Details of the investigation will be presented. This work is being supported by the National Science Foundation under grant number DMR-0906994.

10:55 AM

Quantitative NanoSIMS Analysis of Grain Boundary Segregation in Bulk Samples: Frederic Christien¹; Katie Moore²; Clive Downing²; Chris Grovenor²; ¹University of Nantes; ²University of Oxford

Solute grain boundary (GB) segregation is an important metallurgical phenomenon that has been extensively studied, especially by Auger spectroscopy of fractured surfaces. More recently, it has been demonstrated that High Resolution SIMS (NanoSIMS) analysis can detect solute GB segregation on a simple polished cross-section. The aim of this work is to demonstrate the ability of NanoSIMS to achieve quantitative analysis of GB segregation. The material used in this study is high purity nickel containing 5 wt ppm of sulfur. Samples were annealed at different temperatures to get different equilibrium sulfur GB concentrations, ranging from about 1% to 50% of a monolayer. For each sample, about 20 GBs were analyzed by NanoSIMS. The measured GB sulfur concentrations range from ~0.02 to 0.5 monolayer and are in very good agreement with the data from literature. The potential advantages of this new technique with respect to Auger spectroscopy are discussed.

11:10 AM

Increased Adhesion of Cr-PI Interface at High Temperatures: Megan Cordill¹; Aidan Taylor¹; Gerhard Dehm²; ¹Erich Schmid Institute of Materials Science; ²Dept. Material Physics

Metal films on polymer substrates are used in flexible electronics and gas barrier applications and the adhesion between films and substrates is essential. Chromium adhesion layers are used to enhance film adhesion for Cu and Au conduction lines. The use of conduction lines involves elevated temperatures making it important to understand how adhesion is affected by temperature. The adhesion energy of Cr-polyimide interfaces has been quantified using tensile straining and the resulting compression-induced buckles. This analysis has been made for films strained at 25C, at 350C and annealed at 350C and strained at 25C. Tensile straining at 350C caused an increase in the buckling strain and in the adhesion. TEM examination of the Cr/PI interface revealed a 3-4 nm interlayer prior to heating and after annealing indicates a change in the interface structure and chemistry. These changes in the interfacial microstructure and chemistry directly correlate to the measured adhesion values.

11:25 AM

Atomistically Informed Dislocation Dynamics Simulations on Dislocation-Interface Interactions: Caizhi Zhou¹; Jian Wang²; Irene Beyerlein²; Curt Bronkhorst²; ¹ Los Alamos National Laboratory; ²Los Alamos National Laboratory

Atomic-scale modeling of unit processes suggests that the mechanical properties of nanoscale composites under deformation are dominated by defect-interface interactions. Discrete dislocation dynamics (DD)

simulations, in which dislocations are the simulated entities, offer a way to extend length and time scales beyond those of atomistic simulations. In this study, we develop a DD simulation model based on experiment observation and atomic scale simulations to study the dislocation-interface interactions at micro- and nanoscales and provide a generic bi-metal interface model that represents the key characteristics of the structure and properties of the interface. In order to capture the fundamental physics of dislocation-interface interactions, dislocation annihilation, nucleation and emission from the interface are all considered in our simulations, which is different from traditional DD simulations on single-phase materials. Our DD-interface model can improve current knowledge of macroscopic mechanical properties of nanoscale composites with the knowledge gained from simulation results.

11:40 AM

The Periodic Unit of Doubly-diffracted Reflections from Periodic Grain Boundaries in Cubic Crystals and Its Relationship with Coincident Site Lattice: Mohammad Shamsuzzoha¹; ¹University of Alabama

A geometrical formulation is provided of how double diffraction from a periodic grain boundary in a cubic crystal yields doubly diffracted reflection unit within the space of a coincident site of reciprocal lattice (CSRL). The doubly diffracted reflection unit is a primitive zero layer displacement shift complete (ZLDC) unit of the coincident site of reciprocal lattice. Its reciprocal transformation yields a real space unit of coincident site lattices that includes the real zero layer coincident site lattice(CSL)of the periodic boundary. The formulation is applied in a case study on the determination of the CSL from the double diffraction patterns of a S3 [110]/ (111) grain boundary of Al.

Mechanical Performance of Materials for Current and Advanced Nuclear Reactors: Irradiation and Testing of Fuels and Cladding Materials

Sponsored by: The Minerals, Metals and Materials Society, TMS Structural Materials Division, TMS/ASM: Nuclear Materials Committee

Program Organizers: Nicholas Barbosa, National Institute of Standards & Tech; Greg Oberson, United States Nuclear Regulatory Commission; Matthew Kerr, United States Nuclear Regulatory Commission; Elaine West, Knolls Atomic Power Laboratory; Stuart Maloy, Los Alamos National Laboratory; Osman Anderoglu, LANL

Wednesday AM
March 14, 2012

Room: Swan 1
Location: Swan Resort

Session Chairs: Stuart Maloy, Los Alamos National Laboratory; Osman Anderoglu, Los Alamos National Laboratory

8:30 AM Invited

In-Situ and Post Irradiation Mechanical Testing of Ion Irradiated Materials: Gary Was¹; Anne Campbell¹; Vani Shankar²; Cheng Xu¹; ¹University of Michigan; ²IGCAR

Ion irradiation offers the capability to conduct well controlled, in-situ mechanical property experiments as well as ex-situ tests of the response of materials to irradiation and stress. In-situ irradiation creep provides a unique opportunity to track creep rate continuously in real time in the low dose regime. We have developed the capability to conduct irradiation creep on both metallic and non-metallic materials to study their behavior in their respective realms of application. Creep in ferritic-martensitic steels is measured in the 1-3 dpa range at dose rates up to 10-5 dpa/s and temperatures from 400-600°C relevant to fast reactor core structural materials, while creep in graphite, pyrolytic carbon and SiC are being studied in the temperature range 900-1200°C, appropriate to TRISO fuel particles in the VHTR. In addition, irradiation hardening, the evolution of



TMS 2012

141st Annual Meeting & Exhibition

localized deformation and stress corrosion cracking of irradiated austenitic alloys have provided important insights to their microstructural origins.

9:00 AM

Ion Implantation as a Neutron Analogue in Tungsten Alloys: Measuring Mechanical Properties: *David Armstrong*¹; Steve Roberts¹; Angus Wilkinson¹; ¹University of Oxford

Tungsten and tungsten alloys are promising materials for plasma facing components, especially the divertor, for nuclear fusion power plants. The effects of neutron irradiation on mechanical properties are of great importance. Specimens of pure tungsten, and W-5%Ta and W-5%Re were irradiated using 2 MeV W ions, at 350°C, producing damage levels of 0.07dpa to 33dpa in a layer of depth ~300nm. Nanoindentation showed a significant increase in hardness in the implanted layer. The hardness increases are greatest in the W-5Ta alloy and smallest in the pure W. The hardness increases most rapidly in the low dose range, and appears to saturate by 13dpa. Atomic-force-microscopy was used to study plastic flow patterns around the nano-indenters in W-5wt%Ta. Significant pile-up is seen in the unirradiated samples, however even damage levels of 0.07dpa causes pile up to be almost totally suppressed. This may indicate a change in work-hardening behaviour after irradiation.

9:20 AM

In-Situ Proton Irradiation Creep of Ferritic-Martensitic Steel T91: *Cheng Xu*¹; Gary Was¹; ¹University of Michigan

In-situ proton irradiation creep of F-M steel T91 exhibits linear dose rate and stress dependence at 500°C. Microstructure analyses of irradiation creep samples were conducted to relate microstructure evolution to macroscopic behavior to achieve full understanding of irradiation creep. Hardness measurements were made on the T91 sample to quantify hardening during irradiation creep. TEM investigation of irradiation creep T91 samples at different stresses and temperatures were made on the <100> and <111> zone axes using a JOEL 2010 TEM. Irradiation hardening occurred after irradiation creep up to 1dpa, and the amount of hardening decreased with increasing applied stress. Analysis of the microstructure of crept samples irradiated to 1 dpa revealed mainly a_0 -<100> dislocation loops dispersed homogeneously within the sample. The dislocation loop sizes at 1dpa are comparable to those found for unstressed irradiations at 3dpa. This talk will focus on the correlation of irradiation creep behavior and the irradiated microstructure.

9:40 AM

In-Situ Ion Irradiation TEM and Nanoindentation Studies of 316L and HT9: *Khalid Hattar*¹; Alexander McGinnis²; Thomas Buchheit¹; Luke²; ¹Sandia National Laboratories; ²Naval Postgraduate School

To validate new cladding materials or predict the properties of existing reactors under extended life conditions, techniques are needed that permit insight into the microstructural and mechanical property evolution that occurs under these extreme environments. This presentation will highlight the recent improvements made to the in-situ ion irradiation TEM at Sandia and the resulting additional capabilities. To highlight these capabilities, in-situ ion irradiation of both 316L and HT9 samples prepared by FIB lift-out will be presented. In addition, the nanoindentation results from 316L stainless steel and HT9 irradiated under various conditions, as well as diffusion coupled with various refractory metals, will be presented. To relate the microstructural evolution to the nanoindentation results, a FEM incorporating a SRIM-based vacancy distribution profile will be provided. The combination of in-situ ion irradiation TEM and small scale mechanical property testing of ion irradiated materials provides a rapid method for characterizing microstructural evolution.

10:00 AM

On the Radiation Growth in HCP Metals: *Stanislav Golubov*¹; Alexander Barashev¹; Roger Stoller¹; ¹ORNL

Many models of radiation growth proposed to date are based on the assumption that the primary damage produced by neutron irradiation is in the form of single point defects. These models do not account for the

most important features of the primary damage under neutron irradiation, namely, intra-cascade clustering of self interstitial atoms and their one dimensional diffusion. During the last twenty years 'Production Bias Model' has been developed, which takes into account the cascade properties. Since the cascades in HCP metals, e.g. Zirconium, are found to be similar to those in cubic crystals, the PBM should provide realistic framework for the HCP metals as well. The main objective of the present work is to describe this model and demonstrate that all the usual growth stages are explained. The conditions leading to particular observations, such as the so-called "negative growth" and coexistence of vacancy and interstitial a-type loops are revealed.

10:20 AM Break

10:40 AM

Grain Size Effect on Radiation Induced Defect Morphology in Nanocrystalline Iron: *Greg Vetterick*¹; Chris Barr¹; John Baldwin²; Khalid Hattar³; Mark Kirk⁴; Pete Baldo⁴; Amit Misra²; Mitra Taheri¹; ¹Drexel University; ²Los Alamos National Laboratory; ³Sandia National Laboratories; ⁴Argonne National Laboratory

Interfacial regions constitute up to 40 vol.% of a nanocrystalline material, providing a high number of annihilation sites for point defects during cascade events and subsequent diffusion. MD simulations in nanocrystalline Ni and Fe have shown reduced interstitial survival and excess vacancy production immediately following the cascade event. In Pd, Au, and Ni alloys, an absence of defect clusters has been found below a critical grain size proportional to their respective self-diffusion lengths. This work presents the study of point defect cluster formation in free standing nanocrystalline Fe films. Films were irradiated *in-situ* to approximately 5dpa at 300°C using 1MeV Kr²⁺ ions at Argonne and *ex-situ* using 20MeV Si⁴⁺ ions at Sandia National Laboratories. Dislocation loops displayed strong size dependence with grain size, and an approximate minimum grain size for cluster formation prevention was determined. This work is supported by DOE, Office of Science, Office of Basic Energy Sciences.

11:00 AM

Development of W-UO₂/CeO₂ CERMET Fuels for Ultra High Temperature Reactor Applications: *Jonathan Webb*¹; James Werner¹; Robert Hickman²; ¹Idaho National Laboratory; ²NASA Marshall Space Flight Center

Historical and contemporary space reactor designs require the use of refractory materials to withstand steady state operational temperatures that range from 1000 K to 3000 K. This paper outlines the initial steps of a fuels program to recapture the technology required to fabricate W-UO₂ fuel forms for hydrogen cooled nuclear rocket applications. The results and lessons learned from a robust literature search of the ANL CERMET fuels program and the General Electric 710 programs are detailed in this study. This paper also describes an initial effort to spheroidize particles of CeO₂ which are also coated with tungsten to a 40 vol.% ratio. The particles are consolidated into fuel specimens and prototypic fuel element segments via Pulsed Electric Current Sintering (PECS) and Hot Isostatic Pressing (HIPing) techniques. Comparisons are made between the microstructure and basic properties of the specimens fabricated by PECS and HIP techniques.

11:20 AM

Structure and Property Relationship in Spark Plasma Sintered UO₂ Pellets: *Ghatu Subhash*¹; James Tulenko¹; Ronald Baney¹; Ge Lihao¹; Andrew Cartas¹; ¹University of Florida

UO₂ powder has been sintered at a range of temperatures using spark plasma sintering technique. The sintered material density varied between 85-97% theoretical density. Ultrasonic measurements (both shear and longitudinal wave measurements) were conducted on sintered disks to determine their modulus and Poisson's ratio. The evolved microstructure was investigated using SEM and optical microscopy. Hardness measurements were conducted using a Vickers indentation tester. In

addition, thermal conductivity measurements were also conducted. These measurements and their relationship to the evolved microstructure as well as a comparison to UO₂ produced by other methods will be discussed in detail during the presentation.

11:40 AM

Non-Destructive Analysis of Microstructural Evolution after Irradiation of Zr-2.5Nb Pressure Tubes Using Neutron Diffraction Line Profile Analysis:

*Levente Balogh*¹; Donald Brown¹; Mark Daymond²; ¹Los Alamos National Laboratory; ²Queen's University

Zr-2.5Nb samples removed from a CANDU reactor are investigated using the high resolution Neutron Powder Diffractometer at Los Alamos National Laboratory, to determine the microstructural changes induced by neutron irradiation. It is shown that Diffraction Line Profile Analysis (DLPA), performed here using the extended Convolutional Multiple Whole Profile (eCMWP) software, combined with time-of-flight neutron diffraction is a valuable tool for the characterization of irradiated materials. The dislocation density is observed to increase from 6×10^{14} to 24×10^{14} m⁻² after 7 years of service. It is shown that this increase is due to < a > Burgers vector type dislocations created by the neutron irradiation. DLPA also reveals a fundamental change in the arrangement of the dislocation structure induced by the irradiation compared to the cold worked, pre-irradiated state. Tensile tests indicate the activation of new deformation mechanisms in irradiated Zr-2.5Nb, the microstructural background of this effect is being explored by DLPA.

Nanocomposites: Nanocomposites for Magnetic and Dielectric Applications

Sponsored by: The Minerals, Metals and Materials Society, TMS Structural Materials Division, TMS/ASM: Composite Materials Committee

Program Organizers: Garth Wilks, Air Force Research Laboratory; Jonathan Spowart, Air Force Research Laboratory; Meisha Shofner, Georgia Institute of Technology; John Zhanhu Guo, Lamar University

Wednesday AM
March 14, 2012

Room: Swan 8
Location: Swan Resort

Session Chairs: John Zhanhu Guo, Lamar University; Matthew Lucas, Air Force Research Laboratory

8:30 AM

Removal of As(III) from Water and Decolorization of Methylene Blue by Mn₃O₄-Coated Magnetite Nanoparticles:

*Gabriela Silva*¹; Fabiana S. Almeida²; Nathália C. Pissolati²; Maria Sylvania S. Dantas¹; Ângela M. Ferreira²; Virginia S.T. Ciminelli¹; ¹UFMG; ²CEFET-MG

Mn₃O₄ magnetic composites were successfully synthesized by precipitating Mn₃O₄ in presence of previously obtained magnetite nanoparticles. Powder X-ray diffraction, Raman spectroscopy, Fourier transform infrared spectroscopy, Mössbauer spectroscopy, superconducting quantum interference device (SQUID) and nitrogen physical adsorption were used to characterize the composites. The composites are superparamagnetic at room temperature and can be separated by an external magnetic field. The capacity of the composites to remove As(III) and methylene blue (MB) from aquatic systems was investigated. Oxidative decolorization of methylene blue (MB) by the synthetic materials was investigated by using UV-Vis absorption spectroscopy. The hybrids show a high binding capacity for As(III) probably due to the increased adsorption sites which occurs by oxidation of As(III) to As(V). Results show near complete (over 99.8%) arsenic removal within 10 ppm and near complete decolorization of MB from its aqueous solution on treating the dye in acidic media.

8:50 AM

Synthesis and Electrical Analysis of Nano-Crystalline Barium Titanate and PLZT Nanocomposites for Use in High-Energy Density Applications:

*Christopher DiAntonio*¹; Todd Monson¹; Tom Chavez²; ¹Sandia National Laboratories

Ceramic based nanocomposites have recently demonstrated the ability to provide enhanced permittivity, increased dielectric breakdown strength, and reduced electromechanical strain making them potential materials systems for high energy density applications. A systematic characterization and optimization of barium titanate and PLZT based nanoparticle composites employing a glass or polymer matrix to yield a high energy density component will be presented. This work will present the systematic characterization and optimization of barium titanate and lead lanthanum zirconate titanate nanoparticle based ceramics. The nanoparticles have been synthesized using solution and pH-based synthesis processing routes and employed to fabricate polycrystalline ceramic and nanocomposite based components. The dielectric/ferroelectric properties of these various components have been gauged by impedance analysis and electromechanical response and will be discussed. Sandia is a multiprogram laboratory operated by Sandia Corporation, a Lockheed Martin company, for the United States Department of Energy's National Nuclear Security Administration under contract DE-AC04-94AL85000.

9:10 AM

Conductive Polyaniline-Magnetite Nanocomposites:

*Hongbo Gu*¹; Yudong Huang¹; Xi Zhang¹; Jiahua Zhu¹; Suying Wei¹; John Zhanhu Guo¹; ¹Lamar University

Polyaniline (PANI) nanocomposites filled with magnetite (Fe₃O₄) nanoparticles (NPs) are fabricated by using surface-initiated-polymerization (SIP) method. The structures of PANI/ Fe₃O₄ nanocomposites are characterized by Fourier transform infrared spectroscopy (FT-IR). The thermal properties of the PANI/Fe₃O₄ nanocomposites are performed by thermogravimetric analysis (TGA) and differential scanning calorimetry (DSC). Both transmission electron microscopy (TEM) and Scanning electron microscope (SEM) are used to characterize the dispersion of Fe₃O₄ NPs and the morphology of PANI/ Fe₃O₄ nanocomposites. The effect of the Fe₃O₄ NPs on the crystallization behavior of the PANI during polymerization is studied. The electrical conductivity, dielectric permittivity and magnetic properties of these nanocomposites are investigated in detail.

9:30 AM

Synthesis of Tailored Core-Shell Magnetic Microparticles for Intravascular Embolization:

*Gabriella Ferreira*¹; Alexandre Umpierre¹; *Fabricio Machado*¹; ¹Universidade de Brasília

Spherical core-shell microparticles of magnetic poly(vinyl acetate) / poly(vinyl alcohol) polymers intended for medical applications such as intravascular embolization procedures and hyperthermia treatment of injured areas were synthesized by in situ incorporation of surface modified magnetite nanoparticles through suspension polymerization process. The proposed experimental methodology showed to be very efficient for the synthesis of micro-sized magnetic particles with controlled morphology. Partially hydrolyzed magneto-polymeric nanocomposites exhibited good thermal stability that observed for the pure poly(vinyl acetate). It was also noted that the morphology of the precursor polymer is preserved when mild reaction conditions are applied during the hydrolysis reaction. Micro-sized polymeric particles showing good magnetic properties were obtained, which indicates that core-shell poly(vinyl acetate) / poly(vinyl alcohol) polymers can be successfully used as embolic agents.



TMS 2012

141st Annual Meeting & Exhibition

9:50 AM Break

10:10 AM Invited

Electromagnetic Field Shielding Polyurethane Nanocomposites Reinforced with Core-Shell Fe-Silica Nanoparticles: Jiahua Zhu¹; Suying Wei¹; John Zhanhu Guo¹; Lamar University

A modified Stöber method is introduced to synthesize Fe@SiO₂ nanoparticles (NPs) using 3-aminopropyltriethoxysilane (APTES) as a primer to render the metal particle surface compatible with silica. High resolution transmission electron microscopy and selected area electron diffraction results indicate a highly crystalline iron core coated with a uniform layer of silica. Polyurethane (PU) nanocomposites are fabricated via a surface initiated polymerization (SIP) method. Both Fe@SiO₂ NPs and Fe@SiO₂/PU nanocomposites exhibit better thermal stability and antioxidation capability than Fe@FeO and Fe@FeO/PU, respectively owing to the barrier effect of the silica shell, revealed by the thermalgravimetric analysis. Meanwhile, the silica shell greatly reduces the eddy current loss and increases the anisotropy energy. The Fe@SiO₂/PU nanocomposites show good electromagnetic wave absorption performance (reflection loss, RL < -20 dB) at high frequencies (11.3 GHz), while the best RL of Fe@FeO/PU is still larger than -20 dB even with a larger absorber thickness.

10:50 AM

Hysteretic Magneto-Photoluminescence in Mn Ion Implanted Silicon Rich Oxide Thin Films: Wei Pan¹; Sandia National Labs

Spintronics, with combined magnetism and solid state electronics via spin-dependent transport processes, has generated much recent excitement. Such devices are expected lead to new electronic functionalities that will enhance the speed of information processing and storage density. The challenge lying ahead is to control magnetic phenomena at quantum length scales in reduced dimensions. Here we wish to report a hysteretic behavior in magneto-photoluminescence in Mn ion implanted silicon rich oxide (SRO) thin films. When the photoluminescence peak intensity is plotted against applied magnetic (B) field, surprisingly, a hysteretic behavior is observed for B sweeping up and down. This hysteretic behavior disappears when the temperature ~ 60 K. Similar measurements in the SRO sample without Mn-ion implantation was also carried out and no hysteresis is observable down to 1.3K. We propose that the origin of this hysteresis is probably due to a ferromagnetic order in Mn ion implanted thin films.

11:10 AM

Structure-Property Relationships Nanostructured Dielectric Materials: Lawrence Drummy¹; Scott Fillery¹; Hilmar Koerner¹; Richard Vaia¹; Air Force Research Laboratory

The unprecedented control over organic-inorganic hybrid nanomaterial structure afforded by polymer synthesis and functionalization techniques provides a toolbox for materials property design. For applications such as high energy density dielectrics, a high volume fraction of inorganic material is desired while maintaining an appropriate interparticle separation distance, thus avoiding percolation which leads to dielectric breakdown. We have functionalized the surface of oxide (BaTiO₃, TiO₂, SiO₂) nanoparticles with polymers (PS, PMMA) of controlled molecular weight and purified the resulting hybrid nanoparticles so that no unbound polymer remained. The resulting nanoparticles were assembled into films which showed increased dielectric constant with increasing volume fraction of inorganic, while maintaining their dielectric breakdown strength. Finally, 3D electron tomography and small angle X-ray scattering were used to develop structure-property relationships which showed that control of both the nano-structure (interparticle separation distance) and the meso-structure (void size) are critical to achieving the desired material properties.

11:30 AM

Effects of Thermal Processing on Crystallinity and Dielectric Properties of P(VDF-HFP) Nanocomposites: Hongxu Liu¹; Fiona Doyle¹; University of California, Berkeley

Adding nanoparticulate fillers to polymers has been recently investigated as a way to enhance energy density for use in capacitors. This paper discusses the relationships between the thermal processing of polymer nanocomposites and the resulting crystal structures and dielectric properties. The polymer of interest is poly(vinylidene fluoride-co-hexafluoropropylene) (P(VDF-HFP)), a relaxor ferroelectric with high energy density and low ferroelectric hysteresis. Consistent with the literature, we have shown that the temperature at which the polymer solution is cast impacts the crystal phase of the polymer, and can greatly affect its breakdown strength. In addition, we have found that post-casting thermal treatments change crystallinity and can increase breakdown strength by five-fold. The addition of nanoparticulate fillers such as barium titanate and montmorillonite clays can increase the permittivity of the polymer film but also disrupts the crystallinity of the films.

11:50 AM

Soft Magnetic Nanocomposite for High Frequency Applications: Matthew Lucas¹; Air Force Research Laboratory

FeCo based nanocrystalline materials have excellent soft magnetic properties, but are limited to low frequency applications due to their relatively low electrical resistivity, which results in high eddy current losses. The alloy (Fe₈₁Co₁₉)₈₄Ta₉B₇ was identified as having a high resistivity of 140 μΩ-cm after annealing at the crystallization temperature of 552°C for 45 minutes. Results from in-situ x-ray diffraction as a function of temperature reveal that crystallization begins at 500°C, with the crystallite sizes determined from the Scherrer analysis growing from 13±4 nm at 525°C to 31±3 nm at 600°C. Resistivity measurements performed as a function of temperature clearly show a reduction of the resistivity with annealing temperature, as expected. These results indicate that the annealing temperature may be used to tune the electrical resistivity and grain size, which may be used to optimize the high frequency magnetic properties for specific applications.

12:10 PM

Dramatic Expansion of Luminescence Region in GaP/Polymer Nanocomposites: Sergei Pyshkin¹; John Ballato²; Academy of Sciences of Moldova; ²Clemson University

GaP nanoparticles were prepared using mild aqueous or colloidal syntheses at decreased temperature followed by ultrasonication and stored as dried powder or suspension in water-ethanol mixture or toluene. Selected mixtures of GaP nanoparticles, based on dimensions, exhibit at room temperature bright broad band luminescence from UV until yellow-red region with controlled band-width and spectral position of maximum. Poly (2-vinylpyridine) (P2VP), biphenyl vinyl ether (BPVE) and tetrahydrofuran (THF) polymers were used to prepare GaP based nanocomposites. The resulting nanocomposites showed pronounced quantum confinement effects and other discussed in this work important for application interesting phenomena leading to dramatic 1 eV expansion of GaP luminescence to the UV spectral region. These GaP nanoparticles and GaP/polymer nanocomposites provide significant enhancement of blue-shifted luminescence from which novel light emissive device structures may be fashioned.

Neutron and X-Ray Studies of Advanced Materials V: Centennial: Alloys, Correlations, Phase Transitions

Sponsored by: The Minerals, Metals and Materials Society, TMS Structural Materials Division, TMS/ASM: Mechanical Behavior of Materials Committee, TMS: Chemistry and Physics of Materials Committee

Program Organizers: Rozaliya Barabash, Oak Ridge National Laboratory; Xun-Li Wang, Oak Ridge National Laboratory; Gernot Kostorz, ETH Zurich; Lyle Levine, National Institute of Standards and Technology; Peter Liaw, Univ of Tennessee; Yandong Wang, Beijing Institute of Technology; Brent Fultz, California Institute of Technology

Wednesday AM
March 14, 2012

Room: Southern I
Location: Dolphin Resort

Funding support provided by: Office of Basic Energy Sciences, U.S. Dept. of Energy, Dr. P. Thyagarajan

Session Chairs: Brent Fultz, California Institute of Technology; Miguel Castro-Colin, Max Planck Institut Fuer Intelligente Systeme

8:30 AM Keynote

Structural Characterization of Complex Materials Using Total Scattering: *Thomas Proffen*¹; ¹Oak Ridge National Laboratory

In this presentation an overview of experimental advances in neutron and x-ray total scattering measurements as well as the current state-of-the-art in modeling of disordered materials will be presented. Examples include local disorder in exotic oxides, hydrogen storage materials, nano-particles and their ligand structure as well as complex systems such as 'green' geopolymer concrete. Experiments were performed at the Advanced Photon Source at Argonne National Laboratory and at the Lujan Neutron Scattering Center at Los Alamos National Laboratory. New opportunities for total scattering experiments at the Spallation Neutron Source at Oak Ridge National Laboratory will also be discussed.

8:55 AM

Inelastic Scattering Studies of Iron Alloys: *Matthew Lucas*¹; ¹Air Force Research Laboratory

Inelastic scattering provides quantitative information on the vibrations of atoms in materials, which is useful for understanding the relative stability of alloy phases. Using both neutrons and x-rays it has become a common practice to measure the phonon density of states of materials. Of particular usefulness is a combination of techniques which tells us information on the vibrations of particular elements in an alloy. Nuclear resonant inelastic x-ray scattering, a synchrotron Mossbauer technique, may be used to determine the vibrations of only the 57-Fe atoms. Combined with results from inelastic neutron scattering this information may be used to determine the vibrations of the other elemental species in binary alloys. The results of recent inelastic experiments of Fe alloyed with Ti, V, Cr, Co, Ni, Al, Pd, Pt, and Au are discussed along with general trends of alloying. Application of these techniques to more complex systems are presented.

9:10 AM Invited

Local Structure and Diffuse Scattering in Modern Ferroelectric Materials: *Marek Paszciak*¹; *Ross Whitfield*¹; *Darren Goossens*¹; *Richard Welberry*¹; ¹Australian National University

Modern ferroelectric materials are characterized by a complex structure frequently comprising occupational disorder and displacement correlations (polar fluctuations) on different length scales. Therefore, local structure probes are necessary for understanding structure-property relationship and facilitating the design of new materials. Diffuse scattering has become a main source of information on nanoscale phenomena in ferroelectrics, e.g. polar nanoregions. Yet its interpretation is often troublesome and advanced modelling techniques are necessary to explain observed patterns

which usually host contributions from both dynamic effects and static disorder. We concentrate on the examples of $\text{Pb}(\text{Mg}_{1/3}\text{Nb}_{2/3})\text{O}_3$ - PbTiO_3 and $\text{Pb}(\text{Zn}_{1/3}\text{Nb}_{2/3})\text{O}_3$ - PbTiO_3 compounds. We show how, by using different modelling approaches, the pieces of information can be retrieved from the diffuse scattering, aiding the understanding of the excellent electro-mechanical properties of these materials.

9:30 AM

The PDF of Glassy Solids - Pitfalls and Traps of Experiment and Interpretation: *Wojciech Dmowski*¹; *Takeshi Egami*²; ¹University of Tennessee; ²ORNL

Structural characterization of glasses, liquids and disordered solids is challenging. The standard approach is to obtain the pair distribution function (PDF). PDF is obtained by a Fourier transformation of the structure function $S(Q)$. The $S(Q)$ has to be extracted from the diffracted intensity and normalized to absolute units to obtain a meaningful PDF. Frequently PDFs obtained for the same sample are different. Therefore it is important to establish procedures that put $S(Q)$ on the absolute scale and allow obtaining reproducible PDF using different detectors and beamlines. We will discuss common traps and pitfalls of using high energy x-ray diffraction, area detectors and mouse and click GUIs and present some simple procedures to minimize normalization errors. We also will show x-ray and neutron data sets to illustrate our points. This work was supported by the U.S. DOE under DE-AC05-00OR-22725 and NSF-DMR-0906744.

9:45 AM Invited

X-Ray Cross-Correlation Analysis and Sample Ensemble Averaging Effect: *Miguel Castro-Colin*¹; *Peter Wochner*¹; *Mariya Rasschchupkyna*¹; *Volodymyr Bugaev*¹; *Christian Gutt*²; *Gerhard Gruebel*²; ¹Max-Planck-Institut fuer IS; ²DESY

Disordered matter has been traditionally described using the pair-distribution function, which can, through modeling, extract coordination shell information about the sample and indirectly exhibit cluster symmetry existent within the sample. The cross-correlation technique is an alternative to study disordered matter, and can directly extract, cluster symmetry information by taking into consideration speckle intensity cross-correlations. These correlations are obtained from appropriate evaluation of the speckle intensity at constant momentum transfer Q , but variable azimuthal position ϕ , i.e. taking into account intensity diffraction rings. Such correlations can be Fourier decomposed and their individual coefficients analyzed. We seek to show the effect that ensemble averaging has in the value of those Fourier coefficients and contrast such results with the variance of the Fourier amplitudes of the intensities. For that purpose a disordered tri-dimensional sample was simulated via molecular dynamics and different subsets extracted and treated in the fashion indicated above.

10:05 AM Invited

Characterization of Complex Precipitation Pathways Using Small Angle X-Ray Scattering: *Alexis Deschamps*¹; *Frédéric de Geuser*²; ¹Grenoble Institute of Technology; ²CNRS

In realistic situations, precipitation processes in metals leading to useful mechanical properties usually show a high degree of complexity: precipitate systems are usually multi-component, with a compositional indetermination of the forming phases; precipitation occurs through a sequence of metastable phases with a variety of nucleation conditions; thermal paths are often non-isothermal, and may involve plastic deformation; in processes that involve welding, the precipitate microstructures may be spatially heterogeneous. This contribution will review recent advances in synchrotron small-angle X-ray scattering that address some of this complexity. Examples will be given in Aluminum alloys, with in-situ studies along non-isothermal paths, evaluation of precipitate compositions using anomalous X-ray scattering and precipitate mapping of heterogeneous microstructures. Emphasis will be made of the usefulness of combining these small-angle scattering approaches with complementary techniques (such as Atom Probe Tomography) to obtain a full quantification of the precipitation phenomena.



10:25 AM

Characterization of Nanostructures in Co-Pd-Si-O Soft Magnetic Nanogranular Film Using Compact type Small-Angle Neutron Scattering Spectrometer: *Yojiro Oba*¹; Masato Ohnuma¹; Shigehiro Ohnuma²; Michihiro Furusaka³; ¹National Institute for Materials Science; ²Research Institute for Electromagnetic Materials; ³Hokkaido University

Quantitative values of microstructure obtained from small-angle X-ray (SAXS) and neutron scattering (SANS) are useful to understand the origin of the materials' properties. Combined use of SAXS and SANS provides further information about the chemical compositions of nanostructures. Recently, owing to development of compact type SANS, which is called mini-focusing SANS (mf-SANS) spectrometer, the SANS of the nanostructures with a few nm has been able to be easily measured. In this study, the analysis of the morphologies and chemical compositions of the Co-Pd nanoparticles in a Co-Pd-Si-O soft magnetic nanogranular film using SAXS and mf-SANS is reported. The magnetic structures of the nanogranular is also investigated using the magnetic scattering contribution of SANS.

10:40 AM Break

10:50 AM

Synchrotron SAXS of Reverted Al-4wt.%Cu during In Situ Artificial Ageing: *Brad Diak*¹; Marsha Singh¹; Shig Saimoto¹; Luke Westfall¹; Lixia Rong²; ¹Queen's University; ²Stony Brook University

Stimulated by early developments in x-ray diffraction of metals, Guinier and Preston were the first "materials scientists" to successfully apply new x-ray tools to interpret diffuse scattering from decomposing Al-4wt.%Cu solid solutions as nano-sized clusters. Afterwards Al-Cu alloys became the model system to study GP zones [cf. Baur and Gerold, 1966]. Osamura, Otsuka and Murakami [1982] used laboratory SAXS to quantify the volume fraction and zone size of Al-4wt.%Cu single crystals after quenching and ageing. The rapid diffusivity of Cu in Al makes it experimentally difficult to study the as-quenched and early stages of ageing. More recent studies of GP zones have applied time resolved synchrotron SAXS [Okuda et al., 1997]. In the present study, reverted Al-4wt.%Cu, which is a more stable than the as-quenched condition, was artificially aged in situ while probing with SAXS configured at beam-line X27C at NSLS. Results of the phase decomposition will be presented.

11:05 AM Invited

Local Structure Models of Diffuse Scattering in Relaxor Ferroelectrics: *Branton Campbell*¹; Benjamin Frandsen¹; Va-Yee Vue¹; Matthew Gardner¹; Kevin Seppi¹; ¹Brigham Young University

The lead-based relaxor ferroelectrics like $\text{Pb}(\text{Zn}_{1/3}\text{Nb}_{2/3})\text{O}_3$ - PbTiO_3 (PZN-PT) have exceptional piezoelectric properties. X-ray scattering techniques have recently been applied to investigate the local structures of these materials, in which marked changes have been observed upon the application of a strong electric field. We have reconstructed high-resolution reciprocal-space volumes of PZN-PT using single-crystal x-ray diffuse scattering images, which provide an excellent three-dimensional probe of this phenomenon. We will discuss quantitative fits of local structure models to this scattering.

11:25 AM

The Structural Relationship between Negative Thermal Expansion and Quartic Anharmonicity of Cubic ScF_3 : *Chen Li*¹; Xiaoli Tang¹; Jorge Munoz¹; Douglas Abernathy²; Brent Fultz¹; ¹Caltech; ²ORNL

Cubic scandium tri-fluoride ScF_3 has a large negative thermal expansion over a wide range of temperature. Inelastic neutron scattering experiments were performed to study the temperature dependence of the lattice dynamics of ScF_3 from 7 to 750 K. The measured phonon densities of states (DOS) show a large anharmonic contribution with a thermal stiffening of modes around 25 meV. Phonon calculations with first-principles methods identified the individual modes in the DOS, and

frozen phonon calculations showed that some of the modes with motions of F atoms transverse to their bond direction behave as quantum quartic oscillators. The quartic potential originates from harmonic interatomic forces in the DO_9 structure of ScF_3 , and accounts for phonon stiffening with temperature and a significant part of the negative thermal expansion.

11:40 AM

In-Situ Measurement of Crystalline Lattice and Amorphous Strains in Fluoropolymers by Neutron Diffraction: *Eric Brown*¹; Bruce Orlor¹; Cynthia Welch¹; Dana Dattelbaum¹; Rex Hjelm¹; Arthur Scholz²; Don Brown¹; ¹Los Alamos National Laboratory; ²UC Santa Barbara

Strain measurements by neutron diffraction are employed as an in situ technique to obtain insight into the deformation modes of crystalline and amorphous domains in a deformed semi-crystalline polymer. The SMARTS (Spectrometer for Materials Research at Temperature and Stress) diffractometer has been used to measure the crystalline lattice displacements in polytetrafluoroethylene (PTFE). The chemical structure of PTFE makes it ideally suited for investigation by neutron methods as it is free of hydrogen that results in limited penetration depths and poor diffraction acquisition in most polymers. The LQD (Low-Q Diffractometer) has been used to measure the amorphous response in PTFE and a (3:1) copolymer of PCTFE (polychlorotrifluoroethylene) and PVDF (polyvinylidene fluoride). Perturbations of the chain are determined by deviations of the scattering from the static result ($I-Q-2$), measurement of the radius of gyration, and a distorted form factor that is likely to be anisotropic.

11:55 AM

Lattice Defects Diffuse Scattering from Thin Films of Si-Ge System with Low Energy Ar+ and Xe+ Bombardments during MBE Growth: *Paul Rozenak*¹; ¹Hydrogen Energy Batteries LTD

Growth of Si, Ge and SiGe layers using molecular beam epitaxy (MBE) was carried out with the Si and Ge (001) substrates, in the order to studied effects of ion bombardment on the crystalline strains of grown materials. Although, ion energies and ion/atom fluxes used in the experiments results to significant lattice distortions along the growth direction. High resolution X-ray diffraction (HRXRD) and transmission electron microscopy (TEM) characterizations of lattice distortion forms, caused by low energy Ar+ and Xe+ bombardment of grown thin epitaxial films on (001) substrates were investigated. The intensity distribution consists of two maxima, one from the distorted layer and the other from original un-effected lattice. The significant changes in the 2θ location, peak broadening and integrated intensity from the (004)* reflections were obtained as the function of aging temperatures. The effects to the ion bombardment induced formation and injection of different types of pointlike defects and defects clusters which modified new optical and electrical properties of grown layer.

12:10 PM

Vibrational Entropy of Amorphous Copper Zirconium: *Hillary Smith*¹; Chen Li¹; Glenn Garrett¹; Matthew Lucas²; Matthew Stone³; Douglas Abernathy³; Brent Fultz¹; ¹California Institute of Technology; ²Air Force Research Lab; ³Oak Ridge National Lab

Inelastic neutron scattering spectra were measured from 300 to 1020 K on equiatomic CuZr, initially quenched to form a bulk metallic glass at 300 K. The role of vibrational entropy in stabilizing or destabilizing the amorphous phase was determined by comparing the amorphous material above and below the glass transition temperature, in its equilibrium two-phase crystalline state at low temperatures, and at high temperatures in the B2 phase. Phonon density of states curves showed considerable softening of high-energy modes in the crystallized material in comparison with the amorphous state, indicating that the equilibrium two-phase mixture has a larger vibrational entropy than the glass. The vibrational entropy of the high-temperature B2 phase will also be reported.

Neutron and X-Ray Studies of Advanced Materials V: Centennial: Local Structure from Diffraction

Sponsored by: The Minerals, Metals and Materials Society, TMS Structural Materials Division, TMS/ASM: Mechanical Behavior of Materials Committee, TMS: Chemistry and Physics of Materials Committee

Program Organizers: Rozaliya Barabash, Oak Ridge National Laboratory; Xun-Li Wang, Oak Ridge National Laboratory; Gernot Kostorz, ETH Zurich; Lyle Levine, National Institute of Standards and Technology; Peter Liaw, Univ of Tennessee; Yandong Wang, Beijing Institute of Technology; Brent Fultz, California Institute of Technology

Wednesday AM
March 14, 2012

Room: Northern E4
Location: Dolphin Resort

Funding support provided by: Office of Basic Energy Sciences, U.S. Dept. of Energy, Dr. P. Thyagarajan

Session Chairs: Emil Bozin, Brookhaven National Laboratory; Nidia Gallego, Oak Ridge National Laboratory

8:30 AM Keynote

Toward an Atomistic Interpretation of Diffraction Line Profile Broadening: Paolo Scardi¹; ¹University of Trento

Even the most advanced methods of diffraction Line Profile Analysis (LPA) still rely on a theoretical background firmly established more than forty years ago, and mostly unchanged to this day. The traditional LPA approach deals with ideal continuous solids, in most cases simple geometrical shapes like spheres, cubes, cylinders, tetrahedra or octahedra, treated as perfect edifices made of a periodic arrangement of unit cells. Microstructural effects most notably those given by lattice defects are introduced as a perturbation to the coherency of such idealized perfect crystals, with more or less simplified assumptions whose reliability cannot be easily assessed on a general basis. An atomistic modelling can provide a realistic description of materials: nano-polycrystalline microstructures built from space tessellation algorithms, followed by atom filling and equilibration procedures provide test systems in which the role of each feature in determining the diffraction line profile can be clearly understood.

8:55 AM Invited

Local Structural Aspects of the Metal-Insulator Transition in Cu(Ir_{1-x}Crx)₂S₄ from Total Scattering X-Ray Study: Emil Bozin¹; ¹Brookhaven National Laboratory

CuIr₂S₄ cubic Pauli paramagnetic metallic spinel with mixed-valence Ir³⁺/Ir⁴⁺ state, undergoes at ~230K on cooling a metal-insulator transition, with simultaneous charge and orbital ordering and Ir⁴⁺ spin-dimerization, yielding temperature-independent diamagnetism, all within triclinic structure. Spin-dimerized Ir⁴⁺-Ir⁴⁺ distance is ~0.5 Angstroms shorter than for nondimerized Ir-Ir pairs. From insulating state, metallic state can be invoked by temperature, Cr-doping and X-ray irradiation. Atomic PDF study using 100 keV synchrotron X-rays [1] indicates that short-range ordered spin-dimers survive in the metallic state induced by X-ray irradiation, but are completely removed in the metallic state achieved by Cr-doping and temperature, emphasizing fundamental difference between the two metallic states. I will also discuss novel surprising local structural observations made in the high-T metallic state from the PDF. [1] E.S. Bozin et al., Phys. Rev. Lett. v.106, 045501 (2011).

9:15 AM Invited

Industrial Applications at Small Angle Neutron Scattering and Neutron Diffraction of HANARO Reactor: Baek Seok Seong¹; Eunjoo Shin¹; Young-Soo Han¹; Chuck Woo¹; ¹KAERI

Small angle neutron scattering (SANS) technique is used to characterize nano-sized (1 ~ 100 nm) fluctuations in the density and composition of the material. This is an excellent tool for obtaining the structural information about macromolecules and heterogeneities like precipitates, micro voids and magnetic inhomogeneities in the material. A new 40M SANS and a recently upgrade 18M SANS were installed in cold neutron facility building of HANARO and are under operational from last year. In this presentation, I would like to present the status and future plan of HANARO neutron scattering facilities and some scientific results carried out on HANARO neutron scattering facilities will be presented.

9:35 AM

Internal Stresses and Microstructure Studied by Neutron Diffraction Profile Analysis: Comparison with Other Techniques: Vadim Davydov¹; Petr Lukáš²; Martin Petrenc³; Helena Van Swygenhoven¹; Ondrej Man⁴; Pavel Strunz²; Radomír Kužel²; ¹Paul Scherrer Institut; ²Nuclear Physics Institute; ³Institute of Physics of Materials; ⁴Brno University of Technology; ⁵Charles University

The neutron and X-ray diffraction techniques combined with electron microscopy methods has been used to study the internal microstresses and microstructure in low carbon steel. Since the real structure features affect the width and shape of the neutron or X-ray diffraction pattern, and, as these real structure aspects are very numerous and mutually superposed, diffraction effects in terms of real structure characteristics are not simple to interpret. Using the recently modified single-line profile analysis method, the dislocation content was addressed and compared in terms of dislocation density parameter with the results obtained by other microscopy methods. The single-line neutron diffraction profile analysis performed at NPI was extended using full diffraction patterns collected in time-of-flight mode at POLDI materials science diffractometer at PSI.

9:50 AM Invited

Microstructural Mapping Using High-Energy X-Ray Scattering: Jonathan Almer¹; ¹Argonne National Laboratory

Advanced characterization methods at the APS permit unique in-situ studies of energy-relevant materials and processes. In this talk, use of high-energy x-rays at the 1-ID beamline for strain, phase and microstructural mapping will be presented. The combination of an undulator source, brilliance preserving optics and focusing lenses provides high-energy x-rays (E~50-120 keV) with transverse beamsizes down to the micron-level. Reconstruction of scattering data, together with sample translation/rotations, can be used to provide 3D information in select cases. Studies presented will include combined small- and wide-angle scattering measurements of strain partitioning under in situ loading, and strain and phase mapping of layered systems including batteries and fuel cells. Finally, recent advances will be discussed, including a new area detector configuration to permit simultaneous interrogation of materials under different measurement modes, and planned beamline upgrades to improve data fidelity and user access.

10:10 AM

New Approach to Measure Lattice Strains under Torsional Shear Using In Situ Neutron Diffraction for Polycrystalline Materials: Robin Woracek¹; Jeffrey Bunn²; Dayakar Penumadu²; Camden Hubbard³; ¹University of Tennessee & Helmholtz Zentrum Berlin; ²University of Tennessee; ³Oak Ridge National Laboratory

Torsion provides a unique opportunity to study the mechanical behavior of materials subjected to a state of pure shear stress and is of significance as most engineering components fail under the influence of shear, or combination of shear and axial stress. However, measurement of shear



TMS 2012

141st Annual Meeting & Exhibition

strain is limited to (near) surface measurements with most techniques. The authors introduce an experimental approach applying the concept of a “strain rosette” for the measurement of shear strain based on lattice spacing changes under in-situ torsional loading, using recent data obtained at ORNL-NRSF2 in conjunction with a custom developed axial-torsional loading-system. Aspects of the technique, such as required gauge volume size (=1mm³) and precise alignment using a Laser Tracker system are addressed. The lattice specific shear moduli for Fe(211), Fe(200) and Fe(110), which were experimentally determined while elastically loading a circular steel rod (d=6mm), are presented and compared to Young’s moduli of the same sample.

10:20 AM Break

10:25 AM

Effect of Different Loading Condition on the Accumulation of Internal Strain in a Creep Resistant Bainitic Steel: *Michael A. Weisser*¹; Steven Van Petegem¹; Stuart R. Holdsworth²; Helena Van Swyghoven¹; Paul Scherrer Institute; ²EMPA

The strengthening mechanisms at both ambient and elevated temperatures in a creep resistant 1%CrMoV steel are governed by the interplay between the ductile ferrite matrix, cementite particles and a fine dispersion of carbides. These individual components have different mechanical properties and as a consequence, load-sharing between cementite/carbide and the plastifying matrix can yield large interphase stresses. Synchrotron and neutron diffraction measurements have been carried out in-situ during tensile deformation and ex-situ after deformation. Samples have been deformed under tensile load at room temperature and elevated temperature (565°C) and under creep conditions (565°C). The residual interphase strains are strongly reduced in the samples deformed at elevated temperature and this for both loading conditions. The character of the internal strain accumulation is discussed as function of the deformation strain, temperature and loading condition, shedding light on the role played by the different type of precipitates in the load-sharing. (Acta Mat 59 2011)

10:40 AM Invited

Verification of Site Occupancies in a Nickel Base Superalloy Using Synchrotron and Neutron Diffraction Techniques Coupled with Atomistic Modeling and High Resolution TEM: *J. Tiley*¹; G. Viswanathan¹; S. Knox²; A. Shiveley¹; S. Nag³; R. Banerjee³; H. Fraser⁴; ¹Air Force Research Laboratory; ²Southwestern Ohio Council for Higher Education/Air Force Research Laboratory; ³Department of Materials Science, University of North Texas; ⁴Department of Materials Science and Engineering, The Ohio State University

Creep behavior in nickel alloys is a critical property that impacts their use in propulsion systems. Previous research has shown that tertiary and secondary gamma prime precipitates dramatically influence the mechanical response for these alloys, and that chemical composition and location of elements within the gamma prime phases influence the lattice parameters and phase formation energies. Researchers in this investigation studied specific site occupancies of elements within Rene88DT using synchrotron and neutron diffraction techniques coupled with atomistic modeling, atom probe tomography, and hi-resolution EELS. Chemical compositions were experimentally measured and used in Rietveld analysis to determine site occupancies for major alloying elements within Rene88. Specifically, the models were validated using experimental techniques to determine changing structures within gamma prime precipitates and estimate phase volume fractions.

11:00 AM

Plastic Deformation of Nanocluster-Strengthened Ferritic Steel Studied by In-Situ Neutron Diffraction: *Alexandru Stoica*¹; Grigoreta Stoica¹; Zhongwu Zhang²; Xun-Li Wang¹; ¹ORNL; ²Auburn University

In-situ neutron diffraction data were recorded on nanocluster-strengthened ferritic steel specimens under uniaxial tensile loading. The tensile experiments were performed at RT and 800°C in displacement-controlled mode. The RT measurements reveal the evolution of lattice strains and intragranular accumulation of microstrains due to the plastic deformation. Both, the development of intergranular stresses and the increase of residual dislocation densities with the level of stress, prove that RT plasticity in nanocluster-strengthened ferritic steel is mediated by dislocation slip, and the material undergoes a strain hardening by dislocation pinning on nanoclusters. At high temperatures, the deformation process seems to be different. The absence of plasticity-induced intergranular strains, as well as, a modest intragranular broadening, suggest a diffusion-controlled grain-boundary sliding as the main plastic deformation mode at high temperatures. An unusually low creep rate was observed in constant load experiments and diffraction data confirm the outstanding stability of microstructure at high temperature.

11:15 AM

In-Situ Neutron Study of Phase Transformation Kinetics under Far-From Equilibrium Conditions in Advanced High-Strength Steels: *Zhenzhen Yu*¹; Zhili Feng¹; Wei Zhang¹; Ke An¹; Rebecca Mills¹; Eliot Specht¹; Xun-Li Wang¹; ¹Oak Ridge National Laboratory

Advanced high-strength steels (AHSS) used in automotive industry rely on highly engineered microstructures to balance the strength and ductility for lightweight and crash-resistant structures. The characteristic microstructures are obtained through alloying and advanced thermomechanical processing, which typically involves phase transformations under far-from-equilibrium conditions. Subsequent vehicle assembly processes such as welding involve fast heating and cooling conditions, which can further alter the microstructures and cause unexpected property degradation. We designed and performed a novel in-situ real-time neutron diffraction measurement in two different AHSS (DP980 and DR210 steels), in order to understand the non-equilibrium phase transformation kinetics under various thermal cycles. The effects of heating rates ranging from 1C/s to 30C/s on phase transformation were clearly observed. The governing kinetics for such behavior are presented and compared with the phase transformation kinetic models. The roles of non-equilibrium phase transformation in developing the next generation AHSS and overcoming welding-induced property degradation are discussed.

11:30 AM Invited

SANS and QENS Studies of Phase Behavior and Dynamics of Hydrogen Confined in Nanopores: *Nidia Gallego*¹; Cristian Cotescu¹; Dipendu Saha¹; Lilin He¹; Eugene Mamontov¹; Alexander Kolesnikov¹; Yuri Melnichenko¹; ¹Oak Ridge National Laboratory

Room-temperature in-situ small angle neutron scattering (SANS) of hydrogen adsorbed in nanoporous carbon have provided for the first time information on extreme densification of hydrogen confined in carbon pores (0.9 – 3.5 nm) in equilibrium with the gas phase (up to 200 bar). The density of adsorbed hydrogen varies with pore size and pressure and approaches liquid hydrogen density in 0.9 nm pores at 200 bar, where internal pressure is many times higher than external gas pressure. In parallel, the dynamics of confined hydrogen was studied using quasi elastic

neutron scattering spectroscopy (QENS) at cross-critical temperatures (10 – 35 K). The results showed an 8-10 K elevation of “melting” temperature for hydrogen extremely confined in 0.7 nm pores. Mobility increases on the increase of temperature, but remained lower than that of bulk liquid hydrogen. Sponsored by the Materials Science and Engineering Division, Office of Basic Energy Sciences, U. S. DOE.

11:50 AM

Strain-Rate-Effect on the Lattice-Strain Evolution of a Generation-IV-Reactor-Power-Plant Alloy: E-Wen Huang¹; Shan-Yu Wu¹; Wei Wu²; Ke An³; Yang Ling³; Chung-Hao Chen⁴; Peter K. Liaw²; ¹Department of Chemical & Materials Engineering and Center for Neutron Beam Applications, National Central University; ²Department of Materials Science and Engineering University of Tennessee; ³Neutron Scattering Sciences Division Oak Ridge National Laboratory; ⁴Department of Mathematics and Computer Science North Carolina Central University

Inconel 617 is a structural-material candidate for the intermediate heat exchanger used in the Generation IV Reactor Power Plant. It is important to investigate its thermomechanical behavior. One of the key parameters is the strain rate. In this work, we use both the high-flux neutrons at the Spallation Neutron Source and the novel data acquisition and reduction technique at the VULCAN Engineering Diffractometer, Oak Ridge, Tennessee, to create an in-situ experimental environment. The dynamics of the structural evolution of the Inconel 617 subjected to three different strain rates of 4×10^{-4} , 1×10^{-3} , and 1×10^{-2} s⁻¹ during the continuous monotonic tensile deformation at room temperature are recorded. The lattice-strain evolution is compared with the bulk-deformation behavior, such as the applied stresses and the thermal responses as a function of the elongation. The thermomechanical phenomena are analyzed by following the classic Zener-Hollomon concept. The refined neutron-diffraction results are used to modify strain-rate-dependent equations.

12:05 PM

In-Situ High-Energy X-Ray Study of Effect of High Magnetic Field on the Phase Transition of Antiferromagnetic CoO Crystal: Gang Wang¹; ¹Northeastern University

The magnetic-field-driven preferential rearrangements of martensite multivariants in antiferromagnetic CoO crystal has been successfully observed in the previous experiments by the synchrotron high-energy x-ray diffraction measurement. A selection principle on martensite variants different from that found in the ferromagnetic shape memory alloys was deduced. In the present work, the effect of high magnetic field (6T) on the phase transformation of CoO crystal was studied by the synchrotron high-energy x-ray diffraction measurement at temperature between 180K-320K at Beamline 11-ID-C, Advanced Photon Source, Argonne National Laboratory. The results provided important information for understanding the magnetic-field-driven strain observed in the antiferromagnetic alloys.

Pb-Free Solders and Other Materials for Emerging Interconnect and Packaging Technologies: Solder Alloy Design for Challenging Applications

Sponsored by: The Minerals, Metals and Materials Society, TMS Electronic, Magnetic, and Photonic Materials Division, TMS: Electronic Packaging and Interconnection Materials Committee
Program Organizers: Iver Anderson, Ames Laboratory; Sung Kang, IBM; Albert Wu, National Central Univ ; Laura Turbini, Research in Motion; Tae-Kyu Lee, Cisco Systems; Govindarajan Muralidharan, Oak Ridge National Lab; John Elmer, Lawrence Livermore National Lab; Yan Li, Intel

Wednesday AM
March 14, 2012

Room: Swan 9
Location: Swan Resort

Session Chair: To Be Announced

8:30 AM Invited

Influence of Composition on the Morphology of Primary Cu₆Sn₅ in Sn-4Cu Alloys: Kazuhiro Nogita¹; Stuart McDonald¹; Jonathan Read¹; Tina Ventura¹; Motonori Miyaoka²; Keith Sweatman²; Testuro Nishimura²; ¹The University of Queensland; ²Nihon Superior Co. Ltd.

Alloys from the composition range Sn-0.7 to 7.6wt%Cu consist of primary Cu₆Sn₅ surrounded by a eutectic Sn-Cu₆Sn₅ mixture and find applications as high temperature solder alloys (typically up to 400°C). The primary Cu₆Sn₅ intermetallics commonly adopt an elongated needle-like morphology, which is not optimal for the mechanical properties of the soldered joint. This report presents the results of an investigation into the effect of trace elemental additions on the size and morphology of the primary Cu₆Sn₅ in a Sn-4wt%Cu alloy with and without Ni additions. Elements investigated include ppm additions of Al, Ag, Ge and Pb. It is shown that Al has a marked effect on the solder microstructure and refines the size of the primary Cu₆Sn₅, even at very low addition levels. The effect of this refinement on mechanical properties is discussed with reference to the alloy microstructure.

8:55 AM

Relating the Microstructure to the Shear Strength of Fluxless AuSn Solder Bonds: Jeffrey Florando¹; Ilya Golosker¹; Barry Olsen¹; ¹Lawrence Livermore National Laboratory

Solder joints consisting of 80Au20Sn solder are being developed to fluxlessly join Ni/Au metalized alumina substrates to flexible ENIG Cu cables using a heater bar. In optimizing the attachment process, the reflow time, temperature, and pressure were changed, which affected the ensuing solder microstructure. After attachment, the samples were shear tested and the cross-section of the bonds were examined in the SEM to compare and correlate the solder microstructure to the shear strengths observed. In addition, samples were aged at 90C and tested to understand the effects of aging on the microstructure and shear strength. The hardness of the phases that formed during the solder process was also measured using nanoindentation and correlated with the measured global shear strengths.



TMS 2012

141st Annual Meeting & Exhibition

9:15 AM

The Initial Reflow Interaction between Sn_{3.0}Ag_{0.5}Cu Solder and Ni Metallization: *Yu-Wei Lin*¹; Kwang-Lung Lin¹; ¹National Cheng Kung University

The early stage interaction between Sn_{3.0}Ag_{0.5}Cu solder and Ni metallization was investigated at soldering temperature of 250 °C for 5 seconds followed by rapid quench in liquid nitrogen. The interfacial HRTEM (High Resolution Transmission Electron microscope) image reveals that Ni lattice distortion, a few atom layers, took place immediately adjacent to the Ni metallization. An amorphous Ni-Cu-Sn diffusion zone was formed next to the distorted Ni layer. Nano-crystalline Cu₆Sn₅ and metastable NiSn compounds exist within the amorphous diffusion zone. Meanwhile, a little NiSn also exists immediately adjacent to the distorted Ni layer. Homogeneous nucleation was proposed for the nanocrystals in the amorphous region while heterogeneous nucleation for the NiSn adjacent to the distorted Ni layer. The TEM inverse FFT (Fast Fourier Transform) image further shows the formation of many short-range-order structures within the amorphous diffusion region, showing the preliminary stage for the nucleation of the interfacial IMC.

9:35 AM

Intermetallic Compound Formation and Growth at the Lead-Free Solder/Cu Interface during Laser Reflow Soldering and during Isothermal Aging: *Hiroshi Nishikawa*¹; Noriya Iwata¹; Tadashi Takemoto¹; ¹Osaka University

With the miniaturization of electronic productions and the use of heat sensitive electronic components, the laser soldering process brings several advantages in terms of localized heating, and rapid rise and fall in temperature. In this study, the formation and growth of an intermetallic compound (IMC) at the Sn-Ag-Cu solder/Cu interface during laser reflow soldering and during isothermal aging were investigated to clarify the characteristics of the laser reflow soldering. The results show that the rapid rise and fall in temperature strongly affected the IMC formation at the interface and the IMC thickness for the laser soldering was thinner than that for the traditional reflow soldering. During isothermal aging, the growth rate of IMC layer at the interface for the laser soldering was much faster than that for the traditional soldering. Then, after isothermal aging for 504 h, many voids at the Cu₃Sn/Cu interface were formed.

9:55 AM

The Effect of Microstructure on the Reliability of Lead Free Solder Joints: *Babak Arfaei*¹; Liang Yin²; Eric Cotts¹; Peter Borgesen¹; ¹Binghamton University; ²Universal Instruments Corporation

We have shown the final solidification temperature after lead free solder joint assembly to vary systematically with the combination of joint size, shape, and contact pad metallurgies. This has consequences for the initial distribution of secondary precipitates, and Sn grain morphology. Overall, ball grid array (BGA) scale SnAgCu joints usually consist of either a single Sn grain or a 'beach ball' twinning structure, while smaller solder balls tend to undercool more, and may show an interlaced twinning structure. Systematic thermal cycling testing of specially designed model assemblies showed the smallest SAC305 joints to have a clearly superior fatigue resistance for a given cyclic strain range, a trend which was not observed for SnPb joints. The evolution of the microstructure during thermal cycling test was carefully characterized. The effects of the precipitate distributions and the Sn grain morphology on the eventual recrystallization and failure were reported.

10:15 AM

The Effect of Composition on the Thickness Morphology and Growth of Interfacial Intermetallic in Pb-Free Solders: *Keith Sweatman*¹; Jonathan Read²; Tetsuro Nishimura¹; Kazuhiro Nogita²; ¹Nihon Superior Co., Ltd.; ²University of Queensland

Since the interfacial intermetallic compound is commonly identified as a factor in the reliability of solder joints the variation in its initial thickness and subsequent growth rate with solder composition could be a consideration in the formulation and selection of lead-free solder alloy. In work reported in this paper the thickness of the interfacial intermetallic layer in 8 alloys that are representative of solder formulations currently commercially available or under consideration was measured in the as-soldered condition and after 1000 hours ageing at 130°C, 140°C and 150°C. To deal with irregular morphology the average thickness was estimated by dividing the cross-sectional area by the length of interface. The alloys are based around the Sn-Cu and Sn-Ag-Cu eutectic with additions of Ni, Bi, Ce and Ge. While some additions have the greatest affect the thickness and morphology of the joint as-soldered others affect mainly the rate of growth during subsequent ageing.

10:35 AM Break

10:45 AM Invited

The Development and Validation of a New CALPHAD Thermodynamic Database for Lead Free Solders

: *Paul Mason*¹; Pingfang Shi²; Andreas Markström²; Johan Bratberg²; Anders Engstrom²; Qing Chen²; Huashan Liu³; Zhanpeng Jin³; ¹Thermo-Calc Software Inc.; ²Thermo-Calc Software AB; ³Central-South University

This presentation describes the development of a new thermodynamic database for Pb free solders using the CALPHAD methodology based on various types of available experimental data and theoretical information. This new database contains all the important Au-/Ag-/Cu-/Sn-based solder alloy phases within a 16-element framework [Ag-Al-Au-Bi-Co-Cu-Ge-In-Ni-Pb-Pd-Pt-Sb-Si-Sn-Zn] and in total 150 phases (most of them as multicomponent alloy solutions and/or intermediate compound solutions, and the rest as intermediate stoichiometric compounds) are included. The database can be used with Thermo-Calc for predicting various thermodynamic properties, stable/metastable phase equilibria and phase transformations of Au-/Ag-/Cu-/Sn-based solder systems (Pb-containing/Pb-free), and for simulating the effects of non-equilibrium solidification and micro-segregation of various soldering/brazing processes. Such predictions can be used to screen candidate solder alloys and identify unsuitable freezing temperature ranges or the presence of undesirable precipitate phases and are a useful compliment to experimental studies.

11:10 AM

Investigation of Ti-Alloyed Sn-Ag and Sn-Cu Solders for Their Microstructure, Solidification, Mechanical Properties and Interfacial Reactions: *W. Chris Chen*¹; Sung K. Kang²; C. Robert Kao³; ¹National Taiwan University; ²IBM T.J. Watson Research Center; ³National Taiwan University

To improve the integrity and reliability of Pb-free solder joints, minor alloying elements have been commonly added to Sn-base solders. In this study, Ti-added Sn-Cu and Sn-Ag solders were investigated for their microstructure, solidification, mechanical properties, high temperature aging, and interfacial reactions. Different cooling rates were employed to evaluate the effect of cooling rates on their microstructure and mechanical properties. DSC analysis was used to study their melting and solidification behaviors, confirming Ti addition being very effective in reducing their undercooling. The intermetallic compounds formed in Sn-Cu-Ti and Sn-Ag-Ti were identified by SEM/EDX analysis. The microstructure of Ti-added solders was found to be very stable in an extreme aging condition, such as 200°C, 100 h. This was also confirmed by the microhardness measurements of the aged vs as-reflowed solders. The interfacial reactions of Ti-added solders with Au/Ni and Cu were also investigated in comparison to the solders without Ti additions.

11:30 AM

Lead Free Solder Joint Void Growth during Multiple High Temperature Reflows: Yan Li¹; John Moore¹; Rajen Dias¹; Deepak Goyal¹; ¹Intel

Voids in lead free solder joints are formed by entrapped volatiles during the reflow process and they have a negative impact on product performance, mechanically and electrically. Post-SMT (Surface Mount Technology) cumulative voiding criteria in lead free solder joints is less than 25% according to IPC-J-STD-001E and IPC-A-610E specifications. For the solder joints that experience multiple high-temperature reflows process prior to SMT, it is important to understand and predict how any voids will interact during subsequent high temperature exposures. Both in-situ 2D X-ray and 3D X-ray were used to study the growth kinetics of the solder joint voids during multiple reflow cycles. The results suggest that the voids start to grow when solder get melted in each reflow cycle. The growth kinetics have been modeled and shown to follow a diffusion controlled law of out-gassing bubble growth in a supersaturated molten solder liquid.

11:50 AM

Effect of Temperature on the Mechanical Properties of Cu₆Sn₅ and (Cu,Ni)₆Sn₅: Dekui Mu¹; Han Huang¹; Kazuhiro Nogita¹; ¹The University of Queensland

Sn-based alloys are important lead-free soldering materials for the modern electrical industry. During the interface reaction between Sn-based alloys and Cu substrates, a layer of Cu₆Sn₅ intermetallic is formed. This Cu₆Sn₅ has different mechanical and thermal properties compared to the adjacent Cu and Sn-rich alloys. When operating temperatures change, thermal stresses will be generated due to mismatches in thermal expansion coefficients. Thus a comprehensive knowledge of the mechanical properties of Cu₆Sn₅, especially at elevated temperatures, would be useful in the predictive modeling of solder joint behaviour. The effects of temperature and Ni content on the mechanical properties of Cu₆Sn₅ were investigated using nanoindentation at elevated temperatures, in combination with SEM and EDS. The elastic modulus and hardness of Cu₆Sn₅ were found to decrease with the increased temperature from room temperature to 175°C. The combined effects of temperature and Ni content on the mechanical properties of Cu₆Sn₅ were discussed.

12:10 PM

Effects of Minor Pd Doping on Microstructural Evolution and Interfacial Reactions in Sn-3.0Ag-0.5Cu-xPd/Cu during Isothermal Aging: Hsiu-Chuan Chuang¹; Jenq Gong Duh¹; Chih-Yuan Cheng²; Jim Wang²; ¹Tsing Hua University; ²Shenmao Technology Inc. Micro Material Institute

Cu-based under bump metallurgy (UBM) has been widely used in flip-chip technology. The major disadvantages of Cu UBM are fast consumption of copper, rapid growth of intermetallic compounds and the formation of Kirkendall voids. In this study, the effects of minor Pd addition into Sn-3.0Ag-0.5Cu-xPd/Cu solder joints on the growth of IMCs during thermal aging were investigated. For minor Pd doped solder joints, the growth rate of Cu₃Sn and Kirkendall voids was significantly suppressed during thermal aging. Elemental distribution and quantitative analysis demonstrated that Pd atoms would dissolve into Cu₆Sn₅ IMC. The Cu₆Sn₅ with Pd addition is regarded as a barrier to suppress the growth of Cu₃Sn and the formation of Kirkendall voids. Furthermore, the high speed impact test was introduced to evaluate mechanical reliability. This study demonstrated that a novel Sn-3.0Ag-0.5Cu-xPd solder alloy is beneficial for retarding consumption of Cu UBM and improving the reliability of solder joints.

Radiation Effects in Ceramic Oxide and Novel LWR Fuels: Computational Modeling of Defect Evolution under Irradiation

Sponsored by: The Minerals, Metals and Materials Society, TMS Structural Materials Division, TMS/ASM: Nuclear Materials Committee

Program Organizers: Peng Xu, University of Wisconsin; Jian Gan, Idaho National Laboratory; Ram Devanathan, Pacific Northwest National Laboratory; Edward Lahoda, Westinghouse Electric Company; Michele Manuel, University of Florida; Ramprasad Prabhakaran, Idaho National Laboratory; Todd Allen, University of Wisconsin-Madison

Wednesday AM

March 14, 2012

Room: Macaw 2

Location: Swan Resort

Funding support provided by: The Center for Materials Science of Nuclear Fuel, an Energy Frontier Research Center led by the Idaho National Laboratory

Session Chairs: Ram Devanathan, Pacific Northwest National Laboratory; Michele Manuel, University of Florida

8:30 AM Invited

On the Problem of Void Growth in Irradiated Materials: Anter El-Azab¹; ¹Florida State University

We present a continuum physics framework for the problem of void nucleation and growth in irradiated materials. This framework is based on the principles of non-equilibrium thermodynamics of heterogeneous materials with defects. From this general framework, the equations governing the evolution of voids will be extracted in both sharp and diffuse interface senses and the consistency of the sharp and diffuse interface models will be demonstrated. Numerical results will be presented for void nucleation and growth under irradiation and the results will be compared with experimental data for single- and multi-component materials. This research was supported as a part of the Energy Frontier Research Center on Materials Science of Nuclear Fuel funded by the U.S. Department of Energy, Office of Basic Energy Sciences under subcontract # 00091538 at Florida State University.

9:00 AM

Interactions of Voids and Grain Boundaries in UO₂ by Molecular Dynamics Simulation: Tsu-Wu Chiang¹; Aleksandr Chernatynskiy¹; Bowen Deng¹; Susan Sinnott¹; Simon Phillpot¹; ¹University of Florida

Uranium dioxide (UO₂) is the most important fuel material for light water reactors. Its thermal transport properties are strongly influenced by defects and microstructure, which evolve considerably during burn-up. The large thermal gradient in the pellet and the high thermal stresses result in defect migration and interaction. Here we analyze the interactions between voids and grain boundaries using molecular-dynamics simulation. Specifically, we construct a UO₂ bicrystal structure and place a void some distance away from it. Thermal and/or stress are used to drive the migration of each such that they interact. The nature of the interaction – including possible effects such as pinning, void dissolution, and GB microcracking are characterized. The effects of different void sizes and different types of grain boundaries are explored. This work was supported by DOE Office of Nuclear Energy's Nuclear Energy University Programs.

9:15 AM

Computational Studies of the Formation and Migration of Atomic Defect Clusters in UO₂ under Irradiation: Xian-Ming Bai¹; Anter El-Azab²; Todd Allen³; Idaho National Laboratory; ²Florida State University; ³University of Wisconsin-Madison

The production and migration of point defects and defect clusters in uranium dioxide (UO₂) under irradiation are two important mechanisms of radiation damage and microstructure changes in this material.

WEDNESDAY AM



Investigating the atomistic details of these two processes is critical for understanding the microstructural evolution of UO₂ under irradiation. Here we first use molecular dynamics simulations to investigate collision cascade induced defect production at the picosecond timescale at both 300 K and 1000 K. The energy of the primary knock-on atom is 2 keV. Based on 200+ cascade simulations, we obtain the distributions of defect clusters in terms of their compositions and sizes at both temperatures. We then use temperature accelerated dynamics to investigate the migration barriers of these interstitial and vacancy clusters and determine their mobility. Finally we examine the interaction between different types of defect clusters and discuss their opportunities of forming larger clusters at long timescales.

9:30 AM

Atomistic Simulation of Radiation Effects in Nano-Grained Cerium Oxide: Amit Kumar¹; Ram Devanathan²; Vaithiyalingam Shutthanandan²; Satyanarayana Kuchibhatla²; Suntharampillai Thevuthasan²; Sudipta Seal¹; ¹University of Central Florida; ²Pacific Northwest National Laboratory

We have used classical molecular dynamics simulations to study defect production in bulk and nanograined cerium oxide (CeO₂) under irradiation conditions chosen to represent nuclear stopping and electronic stopping separately. Our results show the formation of isolated point defects with a greater abundance of defects on the oxygen sublattice. In ceria, Ce can exist in Ce³⁺ and Ce⁴⁺ charge states. We augmented our MD simulations with Monte Carlo simulations of Ce³⁺ distribution in nano-grained ceria containing 10% Ce³⁺. Simulations were performed in conjunction with irradiation experiments on single and poly crystalline CeO₂ thin films prepared using molecular beam epitaxy on 10 mol % yttria stabilized zirconia and sapphire substrates, respectively. We irradiated the ceria thin films with 2 MeV He⁺ ions and characterized the Ce oxidation state change by in-situ x-ray photoelectron spectroscopy. We will discuss the findings of this integrated study in the context of radiation tolerance of ceramics.

9:45 AM

Electrochemistry of Defects in Irradiated UO₂: Abdel-Rahman Hassan¹; Thomas Hochrainer¹; Jianguo Yu²; Xianming Bai²; Todd Allen³; Anter El-Azab¹; ¹Florida State University; ²Idaho National Laboratory; ³University of Wisconsin

Stoichiometric changes play a critical role in the dynamics of defects and microstructure evolution in oxides under irradiation. We investigate the electrochemistry of defects in UO₂ under irradiation, where both the atomic displacements by energetic collision cascades and the exchange of oxygen with the ambient drive stoichiometric changes in the material. The problem is cast in the form of balance laws of lattice and electronic defects under defect generation and diffusion, with boundary conditions dictated by the oxygen partial pressure at the free surface. Inherent to this problem is the electrostatic field resulting from the segregation of charged lattice and electronic defects. Thus, the scenario of dynamic stoichiometric changes in a UO₂ film under ion irradiation will be illustrated in detail. This research was supported as a part of the EFRC on Materials Science of Nuclear Fuel funded by the U.S. DOE, BES under subcontract #00091538 from INL to FSU.

10:00 AM Break

10:15 AM Invited

Multi-Scale Modeling of Fission Gas Evolution in UO₂: Blas Uberuaga¹; David Andersson¹; Xiang-Yang Liu¹; Pankaj Nerikar¹; Christopher Stanek¹; ¹Los Alamos National Laboratory

Fission gases in uranium dioxide (UO₂) nuclear fuels, of which Xe is one of the most prominent, influence fuel performance during reactor operation and have implications for accident scenarios. Their behavior, including the nucleation and growth of fission gas bubbles, is a multiscale problem. We use a multiscale modeling approach to understand the behavior of Xe in UO₂ as a function of microstructure by considering the effect of different types of grain boundaries on the evolution of Xe. Using

density functional theory we calculate the activation energies for Xe diffusion in UO_{2+x} and we determine the interaction of Xe with different types of grain boundaries in UO₂ using molecular statics. These results are then input into atomistic model that predicts the evolution of Xe as a function of microstructure containing different distributions of grain boundaries. We find that the evolution of Xe depends significantly on the microstructure.

10:45 AM

Mesoscale Modeling of Intergranular Bubble Growth and Percolation: Paul Millett¹; Michael Tonks¹; ¹Idaho National Laboratory

The production of fission gas products, namely xenon and krypton, in irradiated nuclear fuel elements leads to a variety of phenomena that directly influence fuel performance. Central to the retention and release of fission gases is the evolution of bubbles existing on grain boundaries and grain triple junctions. Here, three-dimensional phase-field simulations of the growth and coalescence of intergranular Xe bubbles in UO₂ bicrystal grain geometries will be presented. We investigate the dependency of bubble percolation on three factors: the initial bubble density, the Xe grain boundary diffusivity, and the bubble shape, which is governed by the ratio of the grain boundary energy over the surface energy. The simulations show that variations of each of these factors can lead to large discrepancies in the bubble coalescence rate, and eventual percolation, which may partially explain this observed occurrence in experimental investigations. This research was supported by the NEAMS program within DOE-NE.

11:00 AM

Self-Healing Response of Oxides to Irradiation: Dilpunet Aidhy¹; Dieter Wolf¹; ¹Argonne National Laboratory

Molecular dynamics simulations of irradiated CeO₂ (often considered a surrogate for UO₂, the most widely used nuclear fuel) reveal the formation of charge-neutral interstitial dislocation loops identical to ones observed recently in experiments. Focusing on the kinetic phase that follows the initial damage cascade, our simulations of the cluster-formation mechanism reveal a self-healing response of the perfect crystal to the radiation-induced defects. Remarkably, the lattice responds to point defects created during irradiation with the spontaneous creation of new point defects. We demonstrate that these new 'structural defects', with a negative energy of formation, neutralize the cluster by screening its long-range Coulomb potential, thereby lowering the overall energy and localizing the damage. A similar lattice response was recently identified also in simulations of MgO and UO₂, although very different types of clusters were formed, suggesting that this self-healing screening response may be an intrinsic reaction of all ionic crystals to irradiation.

11:15 AM

Computer Simulation of Dislocation Loop Evolution in Irradiated Cerium Oxide with Lanthanum Dopant: Yinbin Miao¹; Aaron Oaks¹; Wei-Ying Chen¹; Bei Ye¹; Brian Kleinfeld¹; James Stubbins¹; ¹University of Illinois at Urbana-Champaign

Recent transmission electron microscope (TEM) experiments of irradiated ceria doped with lanthanum, which acts as a surrogate for the fluorite type mixed oxide of nuclear fuel, indicate the dislocation loops formed in {111} planes. Also, there exists prominent variation of loop growth rate in specimens of different lanthanum dopant concentrations. Static calculation is utilized to explore the energetic preference of defect configurations. Frenkel pairs (FP's) are introduced into ceria systems with various doping conditions to simulate defect evolution under irradiation via molecular dynamics. The dislocation loops observed are proved to be stoichiometric planar interstitial clusters. The loop formation and growth are dominated by cation FP's due to their resistance to recombination and assisted by anion FP's which neutralize local charge. Anion FP recombination is faster in higher dopant concentration cases whereas lanthanum FP's are energetically favored compared to cerium FP's, explaining the growth rate difference. Coalescence of close loops, observed in in-situ TEM, is also simulated.

11:30 AM

Segregation of Ru to Edge Dislocations in Uranium Dioxide: *Anuj Goyal*¹; Bowen Deng¹; Minki Hong¹; Aleksandr Chernatynskiy¹; Susan Sinnott¹; Simon Phillpot¹; ¹University of Florida

Mechanical behavior of nuclear fuel during irradiation depends on a great number of individual phenomena, but only a few of which are adequately understood. Dislocation behavior is therefore significant in understanding the formation and clustering of defects on atomic scale. We used atomistic simulation methods to investigate the interaction of Ru fission products with the core of an edge dislocation in UO₂. Molecular static simulations are employed to study the {110}<110> and {100}<110> slips systems in stoichiometric UO₂. Segregation behavior of Ru with various charge states at various cationic substitution site is examined and characterized in terms of the charge state, ionic radius and local stress state. This research is being performed using funding received from the DOE Office of Nuclear Energy's Nuclear Energy University Programs.

Randall M. German Honorary Symposium on Sintering and Powder-Based Materials: Powder Processing and Consolidation II

Sponsored by: The Minerals, Metals and Materials Society, TMS Materials Processing and Manufacturing Division, TMS: Powder Materials Committee

Program Organizers: K. Morsi, San Diego State University; Fernand Marquis, Naval Postgraduate School; John Meyer, Iowa State University; Ahmed El-Desouky, San Diego State University; Eugene Olevsky, San Diego State University

Wednesday AM
March 14, 2012

Room: Oceanic 2
Location: Dolphin Resort

Session Chair: K Morsi, San Diego State University

8:30 AM Invited

Powder Material Principles Applied to Additive Manufacturing: *David Bourell*¹; ¹University of Texas

Laser Sintering (LS) is an additive manufacturing process in which a part is constructed from powders without the use of part-specific tooling. Production of metallic, ceramic and composite parts in some cases requires some form of pre-processing or post-process sintering to achieve full density. Powder Densification Maps are a tool for optimizing the pre- and post-processing parameters. Such maps are computational representations of part density as affected by time, temperature, pressure and materials properties. This paper summarizes LS developments with emphasis on the utility of powder densification mapping of powder pre-processing and part post-processing. Specific emphasis includes developments in Powder Densification Map production for zirconia, Ti 6Al 4V, nickel-based Alloy 625 and copper. A comparison of theoretically predicted and experimentally determined densities for a variety of processing conditions is presented.

8:55 AM Invited

Optimizing Ductility and Strength of Ultrafine Grained Nickel via Cryo-Milling and Ceracon Forging: *Yonghao Zhao*¹; T.D. Topping¹; J.F. Bingert²; E.J. Lavernia¹; ¹University of California Davis; ²Los Alamos National Laboratory

When bulk nanostructured (NS) materials are prepared via consolidation of individual particles, agglomerates or clusters, extraneous defects, such as porosity, insufficient bonding, and impurities are sometimes introduced leading to the degradation of ductility. In this study we prepared bulk ultrafine grained Ni with high density and purity via optimizing cryomilling, degassing and Ceracon forging processes. As a result, the consolidated fine-grained Ni have good combinations of a yield strength of 470 MPa and a ductility of 42%, and a yield strength of 310 MPa and a ductility of 49%. The combination of strength and ductility of our Ni

is superior to those of the nanocrystalline/ultrafine-grained Ni prepared by electrodeposition, cryo-rolling, and equal-channel angular pressing methods. The microstructural origins for such combinations of good strength and high ductility will be discussed (Advanced Materials 20, 3028).

9:20 AM Invited

Powder Metallurgy and Terabytes: *Pavan Suri*¹; ¹Heraeus Materials Technology

Powder metallurgy processing is typically associated with Fe-based, refractory metal based and super alloy based near net shaped products. Precious metal based products are typically not well known. This presentation gives an introduction to the materials and fabrication methods of Platinum based products made via powder metallurgy and used in the magnetic data storage industry to make hard disk drives.

9:45 AM Invited

Controlling Performance of PM Consolidation in Extrusion: *Wojciech Misiolek*¹; ¹Lehigh University

Extrusion gives flexibility in consolidation of metal powders while applying hydrostatic compressive stresses in the deformation zone. The extrusion parameters can be adjusted to obtain the desired process performance. The selection of the extrusion process and its parameters depends on powder and material characteristics. Ductile metal powders like Aluminum and Copper can be cold consolidated to theoretical density under specific conditions of powder extrusion without the need for sintering when plastic deformation follows the consolidation stage. This leads to the retention of initial microstructure of the powders and at the same time achieving the desired density and mechanical properties. A review of studies performed on different grades of Aluminum and Copper powders is presented. The consolidation behavior of each grade of powder was analyzed and determined from the density / porosity 2D and 3D contour maps of billets and extrudates as well as from the extrudates' hardness measurements.

10:10 AM Break

10:25 AM Invited

Advances in Synthesis and Densification of Heterogeneous Materials: *Fernand Marquis*¹; ¹Naval Postgraduate School

Because the strength, toughness and other engineering properties of heterogeneous materials are strongly dependent on their grain size and density, the quest to achieve simultaneously dense and fine/ultrafine grain size materials has been one of the most important in materials science and engineering. In this work we explore novel approaches for producing dense and fine/ultrafine heterogeneous materials. Typical approaches consist of reaction synthesis, combustion synthesis and shock synthesis followed by dynamic and static consolidation and densification pre and post reaction synthesis. Typical heterogeneous materials covered in this paper consist of tungsten heavy alloys, coated graphite powders, metal silicides and multiphase, multi microstructural constituent ceramic armor materials. The synthesized and densified materials were fully characterized by OM, SEM, TEM, EDX analysis, quantitative image analysis, X-Ray diffraction and mechanical testing. This paper presents and discusses the effect of reaction and processing parameters on the microstructure, densification and strength and toughness of typical heterogeneous materials.

10:50 AM

Processing Challenges of Dual-Matrix Carbon Nanotube Aluminum Composites: *Amal Esawi*¹; Khaled Morsi²; Ihab Salama¹; Hany Saleeb¹; ¹The American University in Cairo; ²San Diego State University

The interest in nanostructured materials has grown considerably in recent years. Significant enhancements in strength have been reported. A common problem, however, is the associated reduction in the materials ductility. Efforts to overcome this ductility challenge by designing multi-modal or hierarchical microstructures have recently been reported. In this work, we report on the processing of dual matrix carbon nanotubes composites in which composite particles of aluminum reinforced with



TMS 2012

141st Annual Meeting & Exhibition

carbon nanotubes are embedded within a soft aluminum matrix. Such approach aims at combining the high strength of the CNT-reinforced region with the ductility of the soft aluminum matrix. Preliminary results, however, show that the interface quality is pivotal in promoting bonding between the two dissimilar particles since a poor interfacial bond is found to lead to deterioration in the composite properties; thus making it impossible to achieve the desired paradox of strength and ductility. Processing-related challenges in this regard are discussed.

11:15 AM

The Versatility of Combustion Synthesis Processing: *K. Morsi¹*; ¹San Diego State University

Over the past few decades the process of combustion synthesis (CS) has been combined with other processes and effects. This has led to level-1, level-2 and higher new CS-based hybrid processes with the potential to improve on conventionally produced CS products and eliminate some of inherent disadvantages of CS. This presentation discusses fundamental aspects of CS in light of new research, and provides an overview of single and multi-level hybrid processes exemplifying the versatility of combustion synthesis processing. Research work by the author in this context is also discussed.

Recent Developments in Biological, Electronic, Functional and Structural Thin Films and Coatings: Process-Properties-Performance Correlations I

Sponsored by: The Minerals, Metals and Materials Society, TMS Electronic, Magnetic, and Photonic Materials Division, TMS: Thin Films and Interfaces Committee

Program Organizers: Nuggehalli Ravindra, New Jersey Institute of Technology; Jian Luo, Clemson University; Xing Yang (Mark) Liu, National Research Council Canada; Nancy Michael, University of Texas at Arlington; Roger Narayan, University of North Carolina and North Carolina State University; Choong-un Kim

Wednesday AM
March 14, 2012

Room: Swan 10
Location: Swan Resort

Session Chairs: Nancy Michael, University of Texas at Arlington; Xing Yang (Mark) Liu, National Research Council

8:30 AM Introductory Comments

8:35 AM

Atomic Scale Characterization of the Nanoscaled Structure of Sputtered Fe-C Thin Films: *Xavier Sauvage¹*; Amélie Fillon¹; Jean Marie Le Breton¹; Ben Lawrence²; Michel Perez³; Colin Scott⁴; Arnaud Weck⁵; Chad Sinclair²; ¹University of Rouen, CNRS; ²Department of Materials Engineering, The University of British Columbia; ³Université de Lyon - INSA de Lyon, MATEIS; ⁴ArcelorMittal Research Maizières; ⁵Mechanical Engineering Department, University of Ottawa

Sputtered Fe-C thin films were deposited on Si and Fe substrates with various carbon contents, from 10 to 40at.%. Depending on the carbon concentration, the as-deposited films exhibit an amorphous (high C content) or nanoscaled structure (low C content). Films were characterized by conventional Mössbauer spectroscopy, conventional and High Resolution TEM. The spatial distribution of carbon atoms was measured thanks to Atom Probe Tomography. During isothermal annealing, the super saturated solid solution of the nanoscaled thin films decomposes giving rise to the nucleation and growth of carbides and carbon free ferrite nanoscaled grains. Thin films with a higher C content and that are amorphous, do crystallize and also decompose into ferrite and carbides nanoscaled grains. A special emphasis was given on the influence of the carbon concentration on the decomposition kinetics.

9:05 AM

Dependence of Tribology of Carbide Derived Carbon Films on Humidity: *Marcin Thustochowicz¹*; ¹CTLGroup

Tribologically advantageous films of carbide derived carbon (CDC) have been successfully synthesized on binderless tungsten carbide by reacting it with chlorine at 1000°C. Some of the treated samples were later dechlorinated by an 800°C hydrogenation treatment. The results of detailed characterizations of the CDC films and sliding contact surfaces were correlated with the friction and wear behavior of the CDC films in various tribosystems, including CDC-steel, CDC-WC, and CDC-CDC and in two specific environments: moderately humid air and dry nitrogen, as well as in an environment of changing water vapor pressure. Friction coefficient values as low as 0.11 in moderately humid air and 0.03 in dry nitrogen were obtained. A model of tribological behavior of CDC has been proposed that takes into consideration the tribo-oxidation of counterface material, the capillary forces from adsorbed water vapor, the carbon-based tribofilm formation, and the lubrication effect of both chlorine and hydrogen.

9:35 AM

Structural and Optical Properties of Silicon Carbonitride Thin Films Deposited by Reactive DC Magnetron Sputtering: *Okan Agirseven¹*; Tolga Tavsanoglu¹; Esra Ozkan Zayim¹; Onuralp Yucel¹; ¹Istanbul Technical University

In this study, silicon carbonitride thin films of variable compositions were deposited on glass and AISI M2 high-speed steel substrates by reactive DC magnetron sputtering of high purity silicon target using CH₄ and N₂ as reactive gases. The composition of the coatings has been modified by the change in the reactive gas flow ratios. Microstructural properties were investigated by cross-sectional SEM analyses. Spectrophotometer has been used to measure the optical transmittance and reflectance of silicon carbonitride thin films over the spectral range from 280 to 1000 nm. The optical constants and band gap values of the films are further evaluated with respect to the gas flow rate. The results of analyses and calculations provided the information about the relationship between the reactive gas flow rates, microstructure, optical constants and band gap values of silicon carbonitride films.

9:55 AM

Influence of TIG Re-Melting and RE (La₂O₃) Addition on Microstructure, Hardness and Wear of Ni-WC Composite Coating: Bal Mukund Dhakar¹; *Dheerendra Dwivedi¹*; Satpal Sharma²; ¹Indian Institute of Technology Roorkee; ²Gautam Buddha University

Influence of re-melting and lanthanum oxide (La₂O₃) addition on microstructure, hardness and abrasive wear behavior of Ni-WC composite coating developed by flame spraying has been presented in this paper. The Ni-WC coating was modified with the addition of La₂O₃. Unmodified and modified coatings were subjected to re-melting by gas tungsten arc welding. EDS and XRD analysis were carried for elemental and phase analysis of the unmodified and modified coatings. Vickers microhardness of various coatings was carried out to study influence of the La₂O₃ addition and re-melting on hardness of the coatings. Abrasive wear was carried out at different normal loads against two abrasive grit sizes 120 and 600. SEM analysis of worn out surfaces was carried out to understand operating wear mechanism. The La₂O₃ addition and re-melting result in finer grain structure, increase in hardness, improvement in abrasive wear resistance of the coating as compared to that of unmodified coating.

10:25 AM Break

10:40 AM

Evaluation of Mechanical Properties of Ni-Ti Bi-Layer Thin Film: Maryam Mohri¹; *Mahmud Nili-Ahmadabadi¹*; ¹University of Tehran

Shape memory thin films are attractive candidates for micro-electro-mechanical-system because of their large deformation and strong recovery force. In the present study Ni-Ti thin films have been deposited on glass substrates by dc magnetron sputtering source fitted with an alloy target, which prepared in vacuum arc remelting (VAR). In this study, three types

of thin films have been deposited; Ni₄₅Ti₅₀Cu₅ and Ni_{50.7}Ti_{49.3} thin films were separately deposited on glass substrate and also a composite bi-layer of Ni_{50.7}Ti_{49.3} and Ni₄₅Ti₅₀Cu₅. The as deposited Ni-Ti thin films were crystallized to change the amorphous to a nano-structured material to characterize shape memory and superelastic behaviors. The composition of targets and films were determined by energy dispersive X-ray spectroscopy. The crystallization, surface morphology and structural features were studied using X-ray diffraction (XRD), atomic force microscope (AFM). Mechanical properties were characterized by nanoindentation analysis and compared to each other.

11:00 AM

Anodic TiO₂ Nanotubular Arrays with Pre-Synthesized Hydroxyapatite - A Promising Approach to Enhance the Biocompatibility of Titanium: *Luning Wang*¹; ¹University of Alberta

Hydroxyapatite (HA) coating is widely applied on metallic implant substrate to enhance the bioactivity for orthopaedic and orthodontic application. Highly ordered titanium dioxide (TiO₂) nanotubular arrays on titanium obtained via electrochemical anodization has been shown a certain bioactivity for biomedical application. In the present work, an alternative immersion method (AIM) is applied on the TiO₂ nanotubular to rapidly preload synthetic HA. The AIM treatment promised to dramatically enhance the HA coating formation on TiO₂ nanotubular. To study the effect of AIM treatment, the different of geometrical and crystal structure of the TiO₂ nanotubular was carried out. The as-treated specimen and as-formed HA coating was evaluated for HA formation and cell culture test to evaluate its biocompatibility. Results showed that AIM is a promised treatment to highly enhance the biocompatibility of TiO₂ nanotubular arrays in comparison with non-treated TiO₂ nanotubular arrays.

11:30 AM

Preparation and Properties of Cu₂ZnSnS₄ Thin Films by Electrodeposition and Sulfurization: *Chao An*¹; Huimin Lu²; Xi Chen¹; ¹Beihang University

The environmental-friendly Cu₂ZnSnS₄(CZTS) thin film is a promising alternative to semiconductors based on Ga or In as solar absorber material for its beneficial properties like good optical properties, high absorption coefficient and an ideal band gap for photovoltaic applications, not to speak of abundant and cheap raw materials. In this paper, Cu₂ZnSn precursor films were electrochemically deposited on Mo-coated glass substrate at room temperature from the air- and water-stable ionic liquid based on chloride/urea eutectic mixture. Then the precursor films were sulfuretted in a tube furnace at a series of sulfurization temperatures using argon as the carrier gas to successfully form CZTS thin films. The films prepared were characterized by X-ray diffraction (XRD), scanning electron microscope (SEM) and energy dispersive spectroscopy (EDS). The CZTS thin films having good tin pyrite-type phase structure with the preferential grain orientation along (112) were obtained as revealed in XRD analysis.

12:00 PM

HR-STEM Characterization of Sr₂FeMoO₆ Thin Films Possessing Both High Saturation Magnetization Values and T_c: *Manisha Dixit*¹; Robert Williams¹; Adam Hauser²; Fengyuan Yang²; Hamish Fraser¹; ¹Materials Science and Engineering Department, The Ohio State University; ²Department of Physics, The Ohio State University

Thin films of double perovskite Sr₂FeMoO₆ (SFMO) were grown along <001> and <111> on SrTiO₃ substrates by magnetron sputtering. Initial characterization using Rutherford back-scattering spectrometry showed the presence of stoichiometric SFMO while X-ray diffraction data indicated pure phase SFMO. These films also exhibited the unusual characteristic of both a high T_c of ~850K and a high saturation magnetization value close to 4μB per formula unit. To further characterize the structure of these thin films, TEM samples were prepared using a FEI Helios™ Nanolab FIB and characterized using a FEI-Titan™ 80-300 aberration-corrected scanning transmission electron microscopy

(STEM) using high-angle annular dark-field mode. STEM imaging was complemented with electron energy loss spectroscopy, energy filtered TEM and energy dispersive x-ray spectroscopy. The films were found to have regions of iron lean and iron rich phases with variable oxidation states that adapt to the double perovskite crystal structure and lead to enhanced magnetic properties.

Recycling General Sessions: Building Materials

Sponsored by: The Minerals, Metals and Materials Society, TMS Extraction and Processing Division, TMS Light Metals Division, TMS: Recycling and Environmental Technologies Committee
Program Organizer: Joseph Pomykala, Alter Trading

Wednesday AM
March 14, 2012

Room: Europe 4
Location: Dolphin Resort

Session Chair: Jeffrey Spangenberg, Argonne National Laboratory

8:30 AM

Ecological Recovery Process for Textile Waste: *Eftalea Carpus*¹; Emilia Visileanu¹; Michaela Dina Stanescu¹; ¹The Research-Development National Institute for Textile and Leather

Humanity must learn from the global financial and economic crisis experience - is the conclusion of the policy makers who should develop a strategy designed to reinvigorate the economy and make possible an "intelligent, sustainable and favourable to inclusion" growth, by a better coordination of national and European policies. The recovery and reintroduction into the economic circuit of the textile material resources must be considered as component parts of the strategies of harmonizing the relationships between the economic growth, consumption of natural resources and environmental protection. It is obvious that at the origin of pollution there are the technological processes of textile processing with impact on air, water, soil, as well as the storage processes. Ecological methods were tested on the basis of separating the respective components of polymers-cellulose blends, for example the removal of cellulose fibers with enzymatic products for isolating the polyester component for subsequent processing.

8:50 AM

Technical Tools for Increasing the Eco-Efficiency of Textile Products: *Emilia Visileanu*¹; Eftalea Carpus¹; ¹The Research-Development National Institute for Textile and Leather

Textile industry is one of the most important sectors of the global economy, both in terms of exports and in terms of employment. It is an active and innovative sector, consisting of a large number of sub-sectors, covering the entire production cycle, from the production of raw materials as semi-finished products (fibers, yarns, woven fabrics, knitted fabrics, nonwovens) to multifunctional, interactive, intelligent textile products and systems. Adapting infrastructure and logistics that encourages the marketing of "sustainable", "fairly traded" and "green" products will facilitate the transition towards dematerialization and eco-efficiency among producers. The ecological recovery of textile waste requires the use of new management tools (life cycle analysis, clean production, environmental cost management, etc.), as well as new methods of training and ecological education (the development of ecological consciousness, sense of responsibility, ability to make decisions).

9:10 AM

Characterization of the Chemical Changes and Surface Properties of Carbonated Waste Cement: *Kwangsook Yoo*¹; Seong-Ho Lee¹; Sun-Ho Hwang¹; Ji-Whan Ahn¹; ¹Korea Institute of Geoscience and Mineral Resources

This study investigated changes in the chemical properties of carbonated waste cement, including the phase transformation, gel polymerization, and specific surface area, as well as cation exchange capacity (CEC) and the



TMS 2012

141st Annual Meeting & Exhibition

adsorption ability of heavy metal ions (Cr⁶⁺ and Cu²⁺). Highly crystalline calcite and highly polymerized silica gel with a three-dimensional network were found to form in carbonated waste cement. The specific surface area and the CEC of waste cement increased with an increase in the carbonation percentage. In addition was a linear relationship between the specific surface area and the carbonation percentage of the waste cement. When the carbonation percentage of waste cement was 35%, the CEC of the carbonated waste cement reached approximately 22 meq/100g. The increase of the CEC confirmed that carbonated waste cement could adsorb heavy metals.

9:30 AM

Recycling of Flat Glass Waste into Clayey Ceramic: Thais da Costa Caldas¹; Alline Cordeiro Morais¹; Sergio Neves Monteiro¹; Carlos Fontes Vieira¹; ¹State University of the North Fluminense Darcy Ribeiro

This work has as its objective to evaluate the firing behavior of a kaolinitic clayey body from Campos dos Goytacazes-RJ incorporated with flat glass waste (FGW) from civil construction. Incorporations of the waste, with a particle size less than 74 μm (200 mesh), were performed in the red ceramic in the following amounts: 0%, 2.5%, 5% and 10wt%. Specimens were prepared by uniaxial press-molding and then fired at 850 and 1050°C. The characterization of FGW was done by X-ray Fluorescence. The physical and mechanical properties evaluated were: linear shrinkage, water absorption and flexural rupture strength. The microstructure of the fired ceramics was evaluated by optical microscopy (OM). The obtained results showed that the flat glass waste can be used as a component of ceramic bodies once it was noticed tolerable modifications of technological behavior.

9:50 AM Break

10:10 AM

A Study on Waste Packaging Containers Generated by Household in Taiwan: Esher Hsu¹; Chen-Ming Kuo²; ¹National Taipei University; ²I-Shou University

This study aims to estimate the amount of waste packaging containers generated by household in Taiwan and also explore its spread based upon the estimation of recycled and un-recycled amount. A sampling survey with ratio estimation is conducted for estimating the recycled amount and the refuse sampling method for municipal solid waste composition is employed to estimate the un-recycled amount. Total amount of waste packaging containers in 2009 generated by household in Taiwan is estimated to be 708,532 m.t. which is much larger than the amount declared by importers and producers. It implies that the amount of waste packaging containers is underestimated around 1/3. In which, 70.3% of the waste packaging containers are recycled and 29.7% are landfilled or incinerated. 94% of the recycled waste packaging containers are recycled through official certified recycling system. The declaration mechanism for products with packaging containers in Taiwan has to be improved.

10:30 AM

Manufacture of Calcium Sulfoaluminate with Alumina Waste: Ji-Whan Ahn¹; Sun-Ho Hwang¹; Seong-Ho Lee¹; Kwangsuk Yoo¹; ¹Korea Institute of Geoscience and Mineral Resources

The high functional cements have been focused on, with increase on the need for multistoried building, complex constructions and so on. The calcium sulfoaluminate is a representative cement with high functions. The aluminate resource, such like bauxite, is used as main raw material to manufacture calcium sulfoaluminate. Unfortunately, the aluminate minerals are almost not buried in south Korea. Therefore, This study proposes a method to manufacture a calcium sulfoaluminate with industrial by-products, which are containing a large amount of aluminate. This study proposes the modified calcium modulus quantitatively to deduce the optimum mixing condition of raw materials before sintering process. This calcium modulus represents the relative proportion of

calcium oxide, iron oxide, sulfate, alumina oxide, and silica on the form of the calcium oxide. When the modified calcium modulus was applied to synthesis CSA with alumina waste, CSA with high quality was formed with dicalcium silicate phase.

10:50 AM

Recycling of Styrene-Divinylbenzene Copolymer through Sequential Mass-Suspension Polymerization Process: Nathália Campelo¹; Alexandre Umpierre²; Fabricio Machado²; ¹Universidade Católica de Brasília; ²Universidade de Brasília

The present work illustrates the reuse of macroporous anion exchange resins (employed for decolorization of solutions of organic substances such as sugar syrup and fruit juice concentrates in the soft-drink and beverages industries), based on crosslinked styrene-divinyl benzene copolymer (Sty-DVB) to the production of polymeric materials. Micro-sized particles of polystyrene and poly(styrene-ethyl acrylate) were obtained by mass-suspension sequential polymerization process. The proposed experimental technique was able to perform proper dispersion of the Sty-DVB in the thermoplastic matrix of polystyrene. The final material showed good thermal stability, showing degradation profile similar to that observed for the pure polystyrene. It was also noticed that polymer particles with spherical morphology can be obtained. In addition, the incorporation of ethyl acrylate monomer into the polystyrene chains minimizes the undesirable effect of fracture in polymeric particles, improving the mechanical and end-use properties of the final polymeric composite.

11:10 AM

Modeling of Heavy Metals Ions Adsorption by Polyamidoamine Dendrimers: Mohamed Barakat¹; J Kuhn²; ¹KAU University; ²USF

Polyamidoamine (PAMAM) dendrimers have potential for many environmental, applications including separations. This study presents a kinetic model of metal ions by generation 4 PAMAM-OH with ethylenediamine core based on data obtained from ultraviolet-visible (UV-Vis) spectroscopy. This work will discuss aspects related to characterization of the dendrimer before and after adsorption using nuclear magnetic resonance (NMR) spectroscopy, gas chromatography/mass spectrometry (GC/MS) characterization of the metal structures, molecular simulations using quantum mechanics/molecular mechanics (QM/MM), and immobilization onto titanium (IV) dioxide (titania). The results of this study will be used in the development of separation processes that employ PAMAM dendrimers for adsorption of heavy metals from wastewater. The produced samples will be evaluated by adsorption of heavy metals such as Cu(II), Ni(II), and Cr(III) from electroplating wastewater (in a separate article).

11:30 AM

Mullites Bodies Produced From the Kaolin Residue Using Microwave Energy: Maria Brasileiro¹; Romualdo Menezes²; André Rodrigues¹; Gelmires Neves³; Lisiane Santana³; ¹Universidade Federal do Ceará; ²Universidade Federal da Paraíba; ³Universidade Federal de Campina Grande

Mullitization behavior of a mixture of kaolin residue and alumina as the starting materials was examined by microwave heating. X-ray diffraction results showed that in times of 15 minutes was possible to obtain mullite. Microstructure of samples heated in a microwave oven and conventional electric furnace were compared. Results showed that the grain growth of mullite was sharper by microwave heating. It was observed that with the increase of the processing variables of the peak intensity of mullite phase increased.

Refractory Metals 2012: W and Mo Alloys | Structure, Microstructure and Properties

Sponsored by: The Minerals, Metals and Materials Society, TMS Structural Materials Division, TMS: Refractory Metals Committee
Program Organizers: Eric Taleff, The University of Texas at Austin; Todd Leonhardt, Rhenium Alloys Inc; Rachel DeLucas, H.C. Starck; Gary Rozak, HC Starck Inc

Wednesday AM
March 14, 2012

Room: Mockingbird 2
Location: Swan Resort

Session Chairs: Todd Leonhardt, Rhenium Alloys Inc.; Gary Rozak, HC Starck Inc

8:30 AM

Brittle to Ductile Transition in Forged Tungsten and Tungsten-Tantalum Alloys: *David Armstrong*¹; J Gibson¹; J Lachanary¹; Angus Wilkinson¹; Steve Roberts¹; Michael Rieth²; ¹University of Oxford; ²Karlsruhe Institute of Technology

Tungsten alloys are considered the most likely materials for the divertor of a fusion power plant due to tungsten's high melting point, low sputtering yield and low activity. There is a critical need to understand their fracture properties. Four point bend tests have been performed on millimetre-scale specimens of forged W5wt%Ta, W1wt%Ta and UHP tungsten at temperatures from 290K to 1273K. These alloys have highly anisotropic microstructures, with "pancake" grains following the forging direction. In the L-T direction (parallel to the "pancakes") failure is by brittle, intergranular fracture at all temperatures. In the L-S direction (normal to the "pancakes") below 600K, brittle fracture occurs, but with the fracture path predominantly along the long axis of the bar. EBSD shows that the fracture follows specific grain boundaries. Above 600K mixed mode failure occurs by delamination of the specimen along these weaker boundaries.

8:50 AM

The Re Effect on Fracture Toughness of Mo- and W-Based Alloys for Nuclear Applications: *Mikhail Sokolov*¹; Evan Ohriher¹; Roger Stoller¹; ¹ORNL

The refractory alloys are always considered as attractive structural materials for high-temperature nuclear applications due to high melting point, good thermal conductivity and excellent high temperature strength. Unfortunately, these advantages are coupled with very low fracture toughness and serious difficulties associated with fabrication. In this study, the alloy compositions of Mo-15% Re and Mo-25% Re (by weight) were produced by vacuum arc remelting. The melt stock consisted of commercial molybdenum rods from powder metallurgy processing and electron beam melted Mo-Re master alloy. The ingots were canned in Mo and hot extruded to rectangular sheet bar. The purpose is to investigate whether intermediate Re content could still result in good fracture toughness compared to diluted alloys and in improved radiation resistance compared to concentrated Mo-Re alloys at the same. The "Re-effect" was also studied on W-5Re and W-25Re alloys. Fracture toughness of these alloys are compared to pure W properties.

9:10 AM

Room Temperature Fracture Toughness of Mo-41%Re and Mo-47.5%Re Alloys: Dylan Liebl¹; *Jennifer Gaies*²; Mark Opeka²; ¹University of Wisconsin-Madison; ²NSWC Carderock Division

The room temperature fracture toughness of Mo-41%Re and Mo-47.5%Re was measured for alloys produced by three processes: hot isostatic pressing, swaging, and hot rolling. Fracture toughness testing and analysis was performed per the ASTM E1820 standard. The various fabrication processes yielded microstructures that differed in grain size, porosity, and texture, and the fracture toughness values are compared.

9:30 AM

Stress-Controlled Cyclic Deformation Response of Mo, Mo-Re and Mo-Si Solid Solutions: *Xiaojiao Yu*¹; Sharvan Kumar¹; ¹Brown University

The addition of solute atoms such as Rhenium and Silicon to Molybdenum appears to alter its response to cyclic loading significantly. In this study, stress-controlled cyclic deformation behavior has been evaluated as a function of temperature on two solid solution alloys, one which is a concentrated solid solution, Mo-41 wt.% Re and the other is a dilute solid solution, Mo-0.3 wt.% Si. Fatigue life and ratcheting strain evolution are compared to pure Mo to understand the effect of alloying. The resulting dislocation substructure evolution has been characterized by electron microscopy to understand differences in observed behavior. Further, the imposition of a dwell time during cyclic loading, both at the maximum and minimum stresses, enables the examination of the influence of creep on these parameters. The results of these experiments will be presented and their implications for the behavior of multiphase alloys will be discussed.

9:50 AM

Fabrication of Tungsten and Tungsten-Rhenium Alloys via Pulsed Electric Current Sintering: *Jonathan Webb*¹; Cory Sparks²; Mary O'Brien¹; Indrajit Charit¹; Darryl Butt²; Megan Frary²; Mark Carroll³; ¹University of Idaho; ²Boise State University; ³Idaho National Laboratory

This study describes some microstructural characteristics and macroscopic properties of highly dense tungsten and tungsten-rhenium specimens manufactured by the consolidation of submicron tungsten powder via Pulsed Electric Current Sintering (PECS). Tungsten powder batches with an average particle size of ~0.425 micrometer were consolidated at temperatures ranging from 1373 K to 1973 K and isothermal hold times from 2 to 30 minutes at applied stresses of 20 to 80 MPa via PECS. The relative densities of the consolidated specimens ranged from 80% to 97% (with respect to the theoretical density of tungsten). Alloyed powders of tungsten and rhenium were also sintered under similar conditions. The sintering mechanisms were studied by dynamic kinetics analysis based on the specimen time-temperature dependent displacement. Tensile properties of the fabricated samples were characterized using a micro-tensile testing apparatus. This research is supported by the NEUP contract # 42246-57.

10:10 AM Break

10:20 AM

Stress-Strain Behavior of Nb Single Crystal Tensile Specimens with Different Grain Orientations: *Di Kang*¹; Derek Baars¹; Aboozar Mapar¹; Payam Darbandi¹; Thomas Bieler¹; Farhang Pourboghra¹; Chris Compton²; ¹Michigan State University; ²Nat'l Superconducting Cyclotron Lab

Nine Nb single crystal tensile specimens with different grain orientations were extracted from a Ningxia ingot slice. All specimens were deformed to 40% engineering strain, and the stress-strain curves are presented. OIM scans were done at the center of the gauge length of each specimen before and after deformation to investigate the effect of strain on grain orientations. As a reference, OIM scans were also done on undeformed specimens that were cut adjacent to the deformed specimens. Some of the undeformed specimens show a noticeable orientation gradient along the gauge length. The effect of this gradient on the deformation behavior is examined. SEM images on the top and transverse surfaces of the deformed specimens were taken in order to identify slip systems. The results are compared with crystal plasticity finite element simulations of the same experiments to examine how well models can predict observed slip activity.



TMS 2012

141st Annual Meeting & Exhibition

10:40 AM

Synthetic 3D Tantalum Microstructures: *Veronica Livescu*¹; John Bingert¹; Davis Tonks¹; Joseph Tucker²; Gregory Rohrer²; ¹Los Alamos National Laboratory; ²Carnegie Mellon University

Physics-based damage models must account for the microstructural complexity of materials to enable accurate prediction of ductile failure. Microstructural variables must be captured in a statistical framework to enable mean-field modeling of meaningful volumes. This work is concerned with the characterization in 3D of high-purity tantalum using planar Electron Backscatter Diffraction data, toward the development of statistical descriptions of real polycrystalline microstructures. Distributions of grain size and orientation were analyzed from the tantalum. Representative statistics were implemented into MBuilder, virtual microstructure-generating software developed at Carnegie Mellon University. Boundary segments extracted from EBSD data were used to describe the distribution of grain boundary misorientations and orientations of grain boundary planes. Observations are discussed in the context of understanding the contribution of microstructural features to damage nucleation under shock loading. Virtual microstructures offer a starting point for damage models to screen for microstructural instantiations of tantalum based on actual structural distributions.

11:00 AM

Coherent Precipitates in Cr Colid Solution: *Omer Dogan*¹; Xueyan Song²; Michael Gao³; ¹DOE National Energy Technology Laboratory; ²West Virginia University; ³URS

Lack of structural materials that can be used in aggressive environments is a major barrier for development of more efficient fossil energy conversion technologies. Refractory metals present a potential for development of high-temperature materials due to their high melting point and good high-temperature strength. Solid solution refractory metal based alloys can mimic Ni-based superalloys in that they can precipitate phases coherent with the matrix and stable at high temperatures to give them superior creep strength. Ab initio calculations predicted Ni, Al, and Ti containing phases with a B2 crystal structure to be coherent with the bcc solid solution Cr. A series of Cr- Ni-Al-Ti alloys was produced by arc melting and solidification. Microstructural characterization was performed using XRD, SEM, and TEM. Along with major phases (Cr solid solution and Ni₂AlTi), a fine distribution of TiNi precipitates with ordered B2 crystal structure was identified in the Cr solid solution phase.

11:20 AM

Strengthening Mechanisms of the Molybdenum-Base Alloy MHC: *Christopher Poehl*¹; Juergen Schatte²; Harald Leitner¹; ¹Montanuniversität Leoben; ²Plansee SE

The particle strengthened molybdenum-base alloy MHC (molybdenum hafnium carbon) is known for its high temperature strength, which is caused by hafnium carbides. The strengthening mechanism of the carbides is known to be twofold, either by interacting direct with dislocations or indirect by stabilizing the substructure. The aim of the present work is to quantify the contribution of these two hardening mechanisms. For this reason molybdenum - hafnium and the molybdenum-base alloy MHC are compared. The alloys are produced via powder metallurgical route and after a thermomechanical treatment the alloys are recrystallized. To determine the mechanical properties, compressive tests and Vickers hardness are performed. The microstructure is characterized by scanning electron microscopy and transmission electron microscopy. Furthermore, the orientation relationship and the phase boundary conditions between matrix and carbides are investigated with high resolution transmission electron microscopy.

11:40 AM

Nature and Results of Dynamic Abnormal Grain Growth in Tantalum: *Nicholas Pedrazas*¹; Elizabeth Holm²; Eric Taleff¹; ¹The University of Texas at Austin; ²Sandia National Labs

Dynamic abnormal grain growth (DAGG) is an abnormal grain growth phenomenon that is initiated and propagated by plastic straining at

elevated temperature. Large single crystals have been produced in two different refractory metals, Mo and Ta, through DAGG, which occurs at much lower temperatures than typical of historically observed static abnormal grain growth phenomena. The largest abnormal grains produced in Ta through DAGG, approximately one centimeter in diameter, are smaller than those produced in Mo, which can be many centimeters in length. The factors which affect this difference in abnormal grain size will be discussed. These include microstructure stability and initial grain size. The character of abnormal grains produced in Ta through DAGG will be discussed. A simple model will be proposed to explain the mechanism of DAGG.

12:00 PM

Influence of the Heating Rate on the Recrystallization Behavior of Molybdenum: *Sophie Primig*¹; Harald Leitner¹; Wolfram Knabl²; Alexander Lorich²; Helmut Clemens¹; Roland Stickler³; ¹Montanuniversität Leoben; ²Plansee SE; ³Universität Wien

Due to its high stacking fault energy, the recrystallization behavior of molybdenum is strongly dominated by concurrent recovery processes. Therefore, the extent of pre-recovery is believed to influence any subsequent recrystallization. In the present investigation, this influence was studied by isochronal heating experiments of cold compressed specimens with heating rates in the range of 1 to 1000 K/min to target temperatures in between 800 and 1300°C. The subsequent microstructural characterization was carried out by SEM, hardness tests and EBSD. This revealed that pre-recovery seemed to promote subsequent recrystallization at lower heating rates (1-100 K/min) which resulted in increased volume fractions of recrystallized grains with decreasing heating rate. In contrast to that, upon fast heating (1000 K/min), low temperature pre-recovery seemed not to occur. Consequently, there was enough stored energy for ultra-fast recrystallization at higher temperatures. The effects of the heating rate on the recrystallization behavior of molybdenum are discussed.

Solid-State Interfaces II: Toward an Atomistic-Scale Understanding of Structure, Properties, and Behavior through Theory and Experiment: Non-metallic Interfaces, Electronic Structures

Sponsored by: The Minerals, Metals and Materials Society, TMS Electronic, Magnetic, and Photonic Materials Division, TMS Structural Materials Division, TMS: Chemistry and Physics of Materials Committee, TMS: Nanomechanical Materials Behavior Committee

Program Organizers: Xiang-Yang Liu, Los Alamos National Lab; Douglas Spearot, University of Arkansas; Guido Schmitz, University of Münster; David Seidman, Northwestern University

Wednesday AM
March 14, 2012

Room: Oceanic 7
Location: Dolphin Resort

Funding support provided by: Los Alamos National Laboratory

Session Chairs: Blas Uberuaga, Los Alamos National Lab; Steven Valone, Los Alamos National Lab

8:30 AM Invited

Semiconductor Interfaces – Structure, Properties, and Dopant Segregation: *Wolfgang Windl*¹; ¹Ohio State Univ.

The thin-film design of modern semiconductor devices causes their interfaces to have crucial influence on their properties. Important questions include the effect of interfaces on dopant distribution; intermixing vs. sharp interfaces; and polarization effects in heterostructures that offer additional design choices (2DEG). In this talk, we will discuss atomic-resolution investigations of Si/SiO₂ and III-V heterostructure interfaces through a combination of density-functional theory and several

WEDNESDAY AM

experimental techniques with focus on electron microscopy. We will first discuss combined theoretical/experimental methods to resolve the atomic structure of interfaces, with focus on amorphous SiO₂ on Si. Next, we will examine segregation of dopant atoms to this interface and the difficulties in resolving their detailed configuration, while concentrations can be determined with very high resolution. Finally, we will look at polar interfaces and discuss on the example of AlN/GaN heterostructures novel ways to determine fields and interface charges with very high precision.

9:00 AM Invited

A First Principles Thermodynamic Study of Si-HfO₂ and Pt-HfO₂ Interfaces: *Rampi Ramprasad*¹; Hong Zhu¹; ¹University of Connecticut

Si-HfO₂ and Pt-HfO₂ interfaces are found in the emerging technologically important “high-k” MOSFETs. The phase diagrams of these interfaces as a function of temperature and oxygen pressure have been determined using first principles thermodynamics (FPT), i.e., by combining density functional theory results with statistical thermodynamics. The vibrational and configurational entropic contributions to the free energies of the condensed phases are explicitly included. We demonstrate that the predictions of the FPT approach are in quantitative agreement with experiments. In particular, under UHV conditions, the correct Si-HfO₂ silica-like interface and an interfacial oxygen coverage of 0.5-1.0 monolayer at the Pt-HfO₂ interface are predicted. These results have important implications both for the applicability of FPT methods for the considered classes of interfaces as well as for high-k dielectrics-based electronic devices in which such interfaces are expected.

9:30 AM

Interfacial Reconstruction of Au/TiO₂ from ab Initio: Min Yu¹; *Dallas Trinkle*²; ¹Lawrence Berkeley National Laboratory; ²University of Illinois, Urbana-Champaign

We determine the stability and properties of interfaces of low-index Au surfaces adhered to TiO₂(110), using density functional theory energy density calculations. We consider Au(100) and Au(111) epitaxies on rutile TiO₂/TiO₂(110) surface, as observed in experiments. For each epitaxy, we consider several different interfaces: Au(111)/TiO₂(110) and Au(100)/TiO₂(110), with and without bridging oxygen, Au(111) on 1×2 added-row TiO₂(110) reconstruction, and Au(111) on a new 1×2 TiO reconstruction. The density functional theory energy density method computes the energy changes on each of the atoms while forming the interface, and evaluates the work of adhesion to determine the equilibrium interfacial structure. The new results showcase an unusual change in chemistry that is possible in an interface: additional reduction of the TiO₂(110) surface combined with mixing in the layer.

9:50 AM

Structure and Properties of the Y₂O₃/Fe Interface from First Principles Calculations: *Samrat Choudhury*¹; Christopher Stanek¹; Blas Uberuaga¹; ¹Los Alamos National Laboratory

Nanostructured ferritic alloys are considered excellent candidate materials for structural applications in nuclear reactors as they exhibit exceptionally high creep strength due to the presence of highly stable nanometer sized Y-Ti-O precipitates. It is believed that these properties result from the characteristics of the particle and ferritic matrix interface. Y₂O₃ has also been shown to form nanoprecipitates in Fe and is a simpler surrogate for the Y-Ti-O precipitates. In this work, we will present the behavior of the interface between the ferritic matrix and Y₂O₃ using density functional theory. In particular, the role of alloying elements and orientation relationship on the atomic structure of the particle-matrix interface, segregation energies of the alloying elements, electronic structure at the interface, and calculated interfacial energy will be discussed. These results form the basis of a phase-field model that will examine the nucleation and growth of Y₂O₃ precipitates in Fe.

10:10 AM Break

10:20 AM Invited

The Structure of Interfaces in GaSb/InAs Superlattices: *Emil Zolotoyabko*¹; ¹Technion

Short-period superlattices, based on semiconductor or oxide layers, have wide range of applications from infrared imaging to giant magneto-resistance devices. Some applications require deposition of sub-layers with thicknesses below one monolayer. Under such constraints, the interface quality becomes crucial for device functioning. Most common imperfections are related to atomic intermixing during growth, which is difficult to characterize on this length scale. We use for this purpose a set of advanced techniques, which include high-resolution transmission electron microscopy (HR-TEM) for lattice imaging and, especially, high-angle annular dark field (HAADF) HR-STEM for Z-contrast imaging, scanning tunneling microscopy (STM) for direct defect counting, atom-probe tomography (APT) for chemical analysis with a nm-resolution, and high-resolution X-ray diffraction (HR-XRD) for spatial profiling of d-spacings. All this is applied in order to examine the atomic intermixing and interface roughness in GaSb/InSb/InAs/InSb superlattices. We discuss the suitability, limits, complementarity, and uniqueness of the above mentioned characterization techniques.

10:50 AM

In Situ TEM Investigations of Wetting-Dewetting Transitions of Ultra-Thin Nickel Films on (100) Silicon Substrates: Andrew Thron¹; *Klaus van Benthem*¹; ¹University of California, Davis

For solid/solid interfaces changes in temperature alter the wetting behavior of thin films on substrates by unbalancing the current equilibrium of surface and interface energies. This can lead to dispersion of the thin film, the so-called wetting-dewetting transition. For this study, thin nickel films were deposited at room temperature onto the (100) surface of silicon. Cross-sectional high-resolution transmission electron microscopy characterization of the as-deposited films revealed a complex interface structure consisting of up to four distinct layers with varying structure and composition. Electron energy-loss spectroscopy combined with aberration-corrected scanning transmission electron microscopy identified the formation of reaction layers with gradually changing nickel silicide composition, followed by a silicon oxide layer that acts as a diffusion barrier for the remaining ultrathin nickel film. In-situ annealing of the interface structure leads to a wetting-dewetting transition of the remaining nickel film and hence the formation of faceted, nanometric nickel islands.

11:10 AM

Hybrid Monte Carlo–Molecular Dynamics Simulations of Nanometer-Scale Y–Ti–O Precipitation in BCC Iron: *Karl Hammond*¹; Lauren Marus²; Hyon-Jee Lee Voigt²; Brian Wirth¹; ¹University of Tennessee, Knoxville; ²University of California, Berkeley

Nanometer-scale clusters containing yttrium, titanium and oxygen have been observed experimentally to precipitate from supersaturated solid solutions of mechanically alloyed Fe–Cr–Ti–Y–O powders. Our simulation work to date has used on-lattice Monte Carlo simulations that aim to understand so-called “nanocluster” nucleation, growth, and stability. Such simulations require a rigid lattice, which imposes artificial stresses and strains on atoms in the clusters, particularly the large (relative to iron) titanium and yttrium atoms. Here, we report hybrid Monte Carlo–molecular dynamics simulation results to study off-lattice relaxations of yttria/titania clusters in BCC iron. These simulations use relatively simple, computationally inexpensive pairwise potential energy models that allow for off-lattice relaxation, which enables the preferred size and spatial arrangement of the nanoclusters to evolve naturally through strain partitioning processes. The hybrid approach provides insight into plausible pathways of titania/yttria cluster formation in ferritic alloys.



TMS 2012

141st Annual Meeting & Exhibition

11:30 AM

Phase-Field Simulation of Segregation to Lamellar Interface in Refractory NbSi₂/MoSi₂ Duplex Silicide: Yuichiro Koizumi¹; *Toshihiro Yamazaki*¹; Akihiko Chiba¹; Koji Hagihara²; Takayoshi Nakano²; Koretaka Yuge³; Haruyuki Inui³; ¹Tohoku University; ²Osaka University; ³Kyoto University

NbSi₂/MoSi₂ duplex silicide is one of the most promising candidates for ultra-high-temperature structural materials for a new high efficiency gas turbine power generation systems. Recently, a C40/C11b lamellar structure of (Nb,Mo)Si₂ system was found to improve its high-temperature strength, and it was demonstrated that Cr-addition stabilize the lamellae by Cr-segregation [K. Hagihara, T. Nakano, S. Hata, O. Zhu, Y. Umakoshi, Scripta Mater. 2010;62:613.] Theoretical understanding is important for further improvement. In this study, a phase-field model of segregation to C40/C11b lamellar boundary has been developed, and the segregation behavior was examined focusing on the effect of elastic strain energy. In the absence of elasticity, solute-distribution simply agreed with the equilibrium phase diagram; the concentrations monotonically varied. In the presence of elasticity, Nb-atoms are depleted at the C11b-side and segregated at the C40-side of the interface. Namely, the interfacial segregation occurred so as to reduce the interfacial misfit.

11:50 AM

Solute Segregation at Cu/Alumina Interface and Its Influence on Alumina Growth Kinetics in Alumina Dispersion-Strengthened Copper: Jian Wu¹; Jianmin Huang²; Zhuohui Xu²; Xuanhui Qu³; *Shaojun Liu*⁴; ¹Graduate School at Shenzhen, Tsinghua University; ²Shenzhen Zhongjin Lingnan Nonfermet Co., Ltd., Shenzhen; ³University of Science and Technology Beijing; ⁴Central South University

Alumina dispersion-strengthened copper (ADSC) that has been used commonly in automobile and electronics industry possesses high strength at elevated temperatures combined with high electrical and thermal conductivity. The effectiveness of the dispersion strengthening of alumina is closely related to the particle size, interparticle spacing, and bonding strength at alumina/Cu interface. In the present work, we focus on the silver segregation kinetics at alumina/Cu interface and alumina growth kinetics under various thermal and stress conditions in a silver-doped ADSC. Additionally, the influence of silver segregation at heterogeneous alumina/Cu interface on the structure and chemistry of the interface is investigated. These results show that the silver segregation kinetics and the alumina growth kinetics are interacted with each other. Based on the experimental results, a model is proposed to simulate these two interacted kinetics. This model can be an important progress in optimizing the processing and improving the properties of ADSC.

Stochastic Methods in Materials Research: Session II

Sponsored by: The Minerals, Metals and Materials Society, TMS Materials Processing and Manufacturing Division, TMS/ASM: Computational Materials Science and Engineering Committee, TMS: Integrated Computational Materials Engineering Committee
Program Organizers: Dallas Trinkle, University of Illinois, Urbana-Champaign; Richard Hennig, Cornell University

Wednesday AM
March 14, 2012

Room: Europe 9
Location: Dolphin Resort

Session Chairs: Dallas Trinkle, University of Illinois at Urbana-Champaign; Richard Hennig, Cornell University

8:30 AM Invited

Statistics of Fracture: Weibull, Gumbel and Other Questions...: *Ashvini Shekhawat*¹; Claudio Manzano²; Phani Nukala³; Mikko Alava⁴; Stefano Zapperi⁵; James Sethna¹; ¹Cornell University; ²Universita di Modena e Reggio Emilia; ³Oak Ridge National Laboratory; ⁴Aalto University; ⁵CNR - Consiglio Nazionale delle Ricerche

A common problem in engineering studies of fracture is the lack of large experimental datasets of fracture strength distributions. Should the available data be fit to a Weibull distribution or a Gumbel distribution? How far should such fits be extrapolated? We address these questions by using a combination of critical droplet theory and extreme value statistics. We find that for a class of disordered brittle systems the Gumbel distribution is the correct form of fracture strength distribution, however, the convergence to the Gumbel form is extremely slow. We explore the question of extrapolating fracture data in to the 'low reliability tail' and find that while extrapolating the Gumbel distribution is perilous, the Weibull distribution can be extrapolated on a case-by-case basis. We present numerical results based on studies of disordered fuse network models.

9:00 AM

Development of a Novel Support Vector Machine (SVM) Model to Predict the Process-Structure-Property Relations in Materials Informatics: *Osama Abuomar*¹; Hongjoo Rhee²; Roger King¹; ¹Department of Electrical and Computer Engineering, Center for Advanced Vehicular Systems (CAVS), Mississippi State University, Mississippi State, MS 39762; ²Center for Advanced Vehicular Systems (CAVS), Mississippi State University, Mississippi State, MS 39762

The main objective of this study is to develop a novel stochastic-based model to predict process-structure-property relations by analyzing intrinsic materials properties and output mechanical responses. Output mechanical properties of the laser-deposited material were modeled using Support Vector Machine (SVM) and other unsupervised learning methodologies after imposing different modes of straining onto the specimen. Three distinctive types of specimens with different porosity levels (e.g., solid state, isolated pores, and connected pores) were fabricated by laser engineered net shaping (LENS) process. Given the various material input data (e.g., morphology, density, total length, and the nearest neighbor distance of pores) and by applying loads to the specimen, the relationship between the intrinsic materials properties due to process parameters and the output mechanical properties such as strength, ductility, total elongation, etc. were achieved. The SVM was then optimized by proper regression, classification and other data mining techniques.

9:20 AM

Bootstrap Analysis of Experimental Uncertainties Affecting the Accuracy of a Flow Stress Model for Metal Forming: Thomas Henke¹; Markus Bambach¹; Gerhard Hirt¹; ¹RWTH Aachen University

Numerical simulations are widely used in metal forming to design and optimize processes and products. The accuracy of process simulations in metal forming strongly depends on the prediction of flow stress, which is determined in mechanical tests. Due to scatter in material properties, variations in testing conditions and measurement errors, tests conducted multiple times under the same conditions do not show identical results. With few exceptions, the uncertainty that results from experimental scatter is not taken into account in metal forming simulations, although it affects the reliability of the model predictions. This paper investigates the potential of two Bootstrap resampling methods to statistically analyze and capture stochastic effects in flow stress modeling. Confidence intervals for the parameters and predictions of a microstructure-based flow stress model are derived and compared for both methods. It is shown that resampling the model residuals is a more efficient method than resampling individual flow curves.

9:40 AM Break

9:50 AM Invited

Uncertainty Quantification Of Yield Stress Predictions In Nanocrystalline Nickel: Lei Cao¹; Marisol Koslowski¹; ¹Purdue University

Recent experimental and theoretical studies on nanocrystalline (nc) plasticity reveal that the mechanical behavior of nc materials cannot be characterized only by the average grain size, without considering the effect of the grain distribution. To quantify uncertainties in the prediction of the inelastic response, including yield and creep, we carry out dislocation dynamics simulations with a Phase Field Dislocation Dynamics model. The dependence of the yield stress on the grain size and initial dislocation density is characterized and compared to the Hall-Petch relation. The comparison between the predicted yield stress on uniform and non-uniform grained nc Nickel indicates that grain size distribution has a more significant influence on the yield stress for smaller grains. Finally, we show predictions of the yield stress distribution of the Nickel membranes in a RF-MEMS device.

10:20 AM

Continuum Theory of Dislocation Cellular Structures: Fractals, Scaling Theories, and X-Ray Diffraction: Yong Chen¹; Woosong Choi¹; Stefanos Papanikolaou¹; James Sethna¹; ¹Cornell University

We present a minimal continuum dislocation dynamics model[1] to explain the emergent mesoscale self-similar cellular dislocation structures observed in plastically-deformed crystals. In three dimensions, we evolve the geometrically necessary dislocations to minimize the elastic free energy in a single crystal within an isotropic approximation, starting from a smooth initial deformation. Whether or not climb is forbidden, GNDs always evolve into self-similar structures. This striking self-similar morphology is measured in terms of correlation functions of physical observables, like geometrically necessary dislocation density, plastic distortion, and crystalline orientation. We provide a generic scaling theory to show that all these correlation functions, exhibiting spatial power-law behaviors, share a single underlying universal critical exponent[2]. We also develop experimental observers (simulating X-ray diffraction experiments) to visualize the underlying dynamics of sub-grain cell structures under loadings. [1] Yong S. Chen et al. , *Phys. Rev. Lett.* 105,105501, 2010. [2] Yong S. Chen et al. , arXiv:1106.0195.

10:40 AM

Stochastic Modeling and Simulation of Fiber Evolution during Melt-Blowing Slag Fiberization: Dimitrios Gerogiorgis¹; Dimitrios Panias¹; Ioannis Paspaliaris¹; ¹National Technical University of Athens (N.T.U.A.)

Red mud fiberization is a process with remarkable potential, alleviating environmental pressure by transforming an aluminum by-product into marketable products. A promising mineral wool process is molten slag fiberization via an free-falling vertical jet which meets an impinging air jet, inducing intensive droplet generation and subsequent fiber elongation. The fibers follow independent trajectories towards a collection chamber, often breaking up to form shots (off-spec product). Fiber as well as shot size and geometry distributions are pivotal in order to predict and ensure mineral wool product quality. This paper focuses on stochastic modeling and simulation of molten slag fiber generation and evolution: the model encompasses published, validated correlations of dimensionless numbers within the well-defined cone of fiber dispersion. Fiber elongation and breakup along trajectories are explicitly studied, considering temperature-dependent slag transport properties and explicit variability of both flight trajectory and operating conditions, towards achieving process optimization.

11:00 AM Break

11:10 AM

Thermal Conductivity Prediction of Nano Fluid Using ANN/GA - A Hybrid Approach for a Radiator Design: Payodhar Padhi¹; France Behera¹; Debashish paNDA¹; ¹Konark Institute of Science & Technology

Thermal conductivities of nano fluid in a two-phase having different compositions of both base fluid as well as nano particles in a closed thermosyphon system that is thermally enhanced by a radiator has been predicted by a proposed hybrid model i.e. Artificial Neural Network (ANN) & Genetic Algorithm (GA) that predicts the thermo syphon behaviour correctly within the given range of the training data. In this study, a new approach for the radiator design of neural networks, based on a genetic algorithm, has been used to predict collection output of a closed thermo syphon system. Here the cooling fan is replaced by the use of nano fluid circulation under an ultrasonic field thus saving the energy and weight of radiator. The ultrasonic field strength, particle size, volume fraction of nano fluid in base fluid were used as input parameters and the thermal conductivity was used as output parameters.

11:30 AM

Effect of Discrete Particle Size Distribution of Iron Ore on the Porosity in Fluidization Process: Guoliang Yin¹; Liangying Wen¹; ¹Chongqing University

As for fluidized bed as pre-reduction reactor in iron-making process, cold test is used to study the change of bed porosity under the condition of different iron particle size distribution. Particles are divided according to Binomial and Poisson distribution in the process of experiment. There are three types of experiment: from fine particles to coarse ones, from coarse particles to fine ones, mixing up. Conclusion is to be drawn: when particles are put in the fluidized bed from fine to coarse, the bed porosity have nothing to do with particle size distribution; when particles are put in from coarse to fine, particles are fluidized layer by layer and the required flow of granule fluidization in each layer is changed with particle size distribution. When particles are mixed up thoroughly, the rate of bed porosity will increase with the increasing of Fa values.



TMS 2012

141st Annual Meeting & Exhibition

11:50 AM

Research on Prediction of the Stability of Partially Stabilized Zirconia Prepared by Microwave Heating Using Levenberg Marquardt-Back Propagation Neural Network: Lijun Liu¹; Shenghui Guo¹; Dongbo Li¹; Jinhui Peng¹; Guo Chen¹; Lei Xu¹; ¹Faculty of Metallurgical and Energy Engineering, Kunming University of Science and Technology; Key Laboratory of Unconventional Metallurgy, Ministry of Education; Engineering Laboratory of Microwave Application and Equipment Technology, Yunnan Province

In the present study, Levenberg Marquardt-Back Propagation (LM-BP) neural network model was proposed for the prediction of the stability of partially stabilized zirconia (PSZ) prepared by microwave (MW) heating. The inputs of the LM-BP neural network model are the holding temperature, rising rate of temperature, holding time, decreasing rate of temperature and hardening temperature. And the stability of PSZ is the only output. Typical data collected from 58 experiments were used for training and testing. The predicted results agreed with the actual value within reasonable experimental error, which indicates that the model is reasonable. Besides, multiple influence factors can be comprehensively considered in the LM-BP neural network model. And a new highly effective method for predicting the stability of PSZ prepared by MW heating is provided for prospective application.

Symposium in Memory of Patrick Veysseyre: Understanding the Mechanisms Controlling Plastic Flow: Nanograined Materials

Sponsored by: The Minerals, Metals and Materials Society, TMS Electronic, Magnetic, and Photonic Materials Division, TMS Structural Materials Division

Program Organizers: Georges Saada, LEM CNRS ONERA; Dennis Dimiduk, Air Force Research Laboratory; Hael Mughrabi, University Erlangen-Nuernberg; Haruyuki Inui, Kyoto University

Wednesday AM
March 14, 2012

Room: Europe 6
Location: Dolphin Resort

Funding support provided by: National Science Foundation

Session Chairs: D. Dimiduk, AFRL/RXLM; E. Georges, Ohio State University

8:30 AM Invited

Fabrication Routes and the Effect of Microstructure on the Mechanical Behavior of Ni-Base Superalloy Thin Films and MEMS Structures: Devin Burns¹; Yong Zhang¹; Timothy Weihs¹; Kevin Hemker¹; ¹Johns Hopkins University

Commercial Ni-base superalloys possess remarkable elevated temperature properties owing primarily to their highly developed multi-phase microstructures. Macro-scale components of Ni-base superalloys are produced by casting, forging and machining, but these processes cannot be employed to fabricate and shape thin films or micro-scale structures. Here we report on the optimization of deposition parameters to sputter deposit relatively thick films of a first generation superalloy, Haynes 718. Following deposition as a solid solution subsequent heat treatments evoke unique kinetic pathways to nucleation of intermetallic phases and lead to novel, nanoscale microstructures. The resultant ultra-fine microstructures impart very beneficial strength and ductility and enjoy impressive high-temperature microstructural stability. Applications as thin film sensors and coatings and MEMS or NEMS devices are envisioned. This work supported by the NSF Materials World Network under grant No. 0806753.

8:55 AM Invited

Following Deformation Mechanisms in Nanocrystalline Ni Using In Situ Synchrotron Techniques and Orientation Imaging: *Patric Gruber*¹; Jochen Lohmiller¹; Oliver Kraft¹; Christian Braun²; Manuel Grewer²; Rainer Birringer²; Aaron Weis³; Christian Kuebel⁴; Veijo Honkimäki⁵; ¹Karlsruhe Institute of Technology, Institute for Applied Materials, P.O. Box 3640, 76021 Karlsruhe, Germany; ²Universität des Saarlandes, Lehrstuhl für Experimentalphysik, Campus D2 2, 66041 Saarbrücken, Germany; ³Karlsruhe Institute of Technology, Institute of Nanotechnology, P.O. Box 3640, 76021 Karlsruhe, Germany; ⁴Karlsruhe Institute of Technology, Institute of Nanotechnology, P.O. Box 3640, 76021 Karlsruhe, Germany and Karlsruhe Institute of Technology, Karlsruhe Nano Micro Facility, Herrmann-von-Helmholtz-Platz 1, 76344 Eggenstein-Leopoldshafen, Germany; ⁵European Synchrotron Radiation Facility, Materials Science Group, BP 220, 38043 Grenoble Cedex, France

The contribution and activation of specific deformation mechanisms which have been proposed for nanocrystalline (nc) materials is still under heavy debate. In situ characterization is necessary in order to (i) detect reversible mechanisms and (ii) separate and ascribe the active mechanism to the respective strain regime. Therefore in situ compression tests are conducted on nc Ni specimens using high energy synchrotron X-ray diffraction (XRD). A fast area detector allows for continuous recording of complete Debye-Scherrer rings. Based on this unique setup the deformation behavior of nc Ni can be unraveled and is determined to be a distinct sequence of elastic grain interaction, grain boundary sliding, grain rotation, dislocation activity and grain growth. The succession of the different deformation mechanisms leads to a specific in-plane texture which could be determined for the first time and could also be verified by Orientation Imaging in a transmission electron microscope.

9:15 AM Invited

Studying the Micromechanical Behavior of fcc/bcc Metals by Quantitative In-Situ TEM and μ -Laue: *Daniel Kiener*¹; Andreas Schneider²; Nobumichi Tamura³; Martin Kunz³; Andrew Minor⁴; Patric Gruber⁵; ¹University of Leoben; ²INM - Leibnitz Institute for New Materials; ³Lawrence Berkeley National Laboratory; ⁴University of California; ⁵KIT - Karlsruhe Institute of Technology

Mechanical properties of miniaturized single-crystals, being stronger when smaller, have drawn considerable attention. While in-situ studies yielded understanding of the deformation mechanisms in fcc metals, the situation is less clear for bcc materials. We investigated vanadium and copper samples prepared by FIB from melt-grown single-crystals. Sample testing was performed by in-situ TEM, allowing direct observation of plastic deformation. Additionally, μ -Laue investigations were performed before and after loading. Complementary to TEM, μ -Laue depicts the global strain field and its evolution in the cause of deformation. The different size-effect for bcc materials compared to fcc is not related to increased dislocation-dislocation interaction, but governed by activation of individual dislocation sources. The deformation behavior is similar to fcc, but the stress level is different due to the limited mobility of screw dislocations in bcc materials. Overall, combining in-situ TEM and μ -Laue allows a better understanding of the deformation of micron- and submicron-sized samples.

9:45 AM Break

10:00 AM Invited

Understanding the Small-Scale Plasticity of Pillars in Compression and Fibers in Tension: *E. P. George*¹; P. Sudharshan Phani²; K. E. Johanns²; G. M. Pharr²; ¹Oak Ridge National Laboratory; ²University of Tennessee

We review here the small-scale plasticity of Mo-alloy pillars and fibers. A transition in strength from theoretical to bulk is observed as the specimen size and/or the dislocation density is increased. At intermediate sizes and densities, the strengths tend to be highly stochastic whereas at the two extremes (theoretical and bulk) the strengths show very little scatter. Transmission electron microscopy showed that the

high (theoretical) strengths correspond to specimens containing no dislocations whereas the low (bulk) strengths correspond to specimens containing many dislocations. Stochastic strengths in the intermediate regime are observed when the dislocation distribution is itself stochastic. These observations are explained with the help of a statistical model and Monte Carlo simulations based on a random distribution and orientation of dislocations. In addition to predicting the average yield strengths, the model correctly predicts the scatter in the yield strengths and the different behaviors observed in compression and tension.

10:25 AM Invited

Deformation Mechanisms in Nanocrystalline Alloys: *Steven Van Petegem*¹; *Julien Zimmermann*¹; *Helena Van Swygenhoven*¹; ¹Paul Scherrer Institute

It is well known that nanocrystalline metals exhibit increased hardness and strength compared to their coarse-grained counterparts. The mechanisms responsible for these enhanced properties are still under debate, especially for the smallest grain sizes. This is even more the case for nanocrystalline alloys due to the additional complexity of segregation, change of elastic constants, etc. Recently the presence of upper and lower yield points upon strain rate change was found for nanocrystalline Ni-Fe. In this work we study the temperature dependence of this phenomenon by in- and ex-situ mechanical testing during x-ray diffraction. The results are discussed in view of results obtained from transient testing and insights from molecular dynamics and quantized crystal plasticity simulations.

11:00 AM Invited

Two Strain Hardening Mechanisms in Nanocrystalline Austenitic Fe-Cr-Ni-W Steel: *Michael A. Weisser*¹; *Helena Van Swygenhoven*¹; *Heinrich Schloth*¹; *Steven Van Petegem*¹; *V. Subramanya Sarma*²; *Martin Heilmaier*³; ¹Paul Scherrer Institute; ²Indian Institute of Technology Madras; ³TU Darmstadt

The mechanical behaviour of nanostructured austenitic steels with nominal composition [wt%] of Fe-18Cr-8Ni-2W, one without and the other with 0.5% Y₂O₃ [wt%] particles were investigated using in-situ synchrotron diffraction during tensile deformation. The experiments were carried out at the MS beamline of the Swiss Light Source. The observations demonstrate the concurrent occurrence of two strain hardening mechanisms in both types of austenitic nc steel. The first one is predominantly connected to the austenite-martensite phase transformation, which saturates after 80% of the austenite is transformed. The second hardening mechanism can be related mainly to deformation twinning in the fragmented retained austenite. The kinetics of martensitic phase transformation is remarkably enhanced in the nanocrystalline structure compared to ultrafined and coarse grained metals. The effect of the ODS particles lies predominantly in the enhancement of the yield stress.

11:30 AM Invited

Deformation, Strengthening and Intermittency Behavior of Ni3Al Alloy Microcrystals: *Dennis Dimiduk*¹; *Michael Uchic*¹; *Satish Rao*²; *Paul Shade*¹; *Chris Woodward*¹; *Ed Nadgorny*³; ¹Air Force Research Laboratory; ²UES, Inc.; ³Michigan Technological University

Ni₃Al alloys exhibit selected unique deformation characteristics at small scales when compared with other materials for similar loading conditions. The present work examines the microcrystal deformation of Ni₃Al with respect to deformation phenomenology, strengthening and flow intermittency and, evaluates these responses relative to sample size or deformation conditions for this material. The findings are analyzed with respect to current understanding and models for each aspect of plastic response. This will include analysis of the relevance of flow-stress anomaly mechanisms, dislocation nucleation, the single-arm source model, exhaustion hardening, and the mean-field avalanche model for describing the response of Ni₃Al alloy microcrystals. While aspects of the flow stress anomaly mechanisms and, a form of the single-arm source model work remarkably well, other limitations exist for understanding Ni₃Al behavior from current data and models.

Titanium: Advances in Processing, Characterization and Properties: Fatigue of Titanium Alloys

Sponsored by: The Minerals, Metals and Materials Society, TMS Structural Materials Division, TMS: Titanium Committee
Program Organizers: Adam Pilchak, US Air Force Research Laboratory; Christopher Szczepanski, US Air Force Research Laboratory; Vasisht Venkatesh, Pratt & Whitney

Wednesday AM
March 14, 2012

Room: Oceanic 3
Location: Dolphin Resort

Session Chairs: Sushant Jha, UTC/US Air Force Research Laboratory; Matt Brandes, The Ohio State University; Chris Szczepanski, US Air Force Research Laboratory

8:30 AM Invited

Understanding Fatigue of Ti Alloys: *James Williams*¹; ¹The Ohio State University

The phenomenology of the fatigue behavior of Ti alloys is reasonably well understood. However, the basic causes for some particular fatigue failures and the details of actual failure modes are less well understood. One consequence of this lack of understanding is the need to design very conservatively in many failure critical situations. Another is the potential for “misdiagnosing” the cause of a failure. A key example in failure analysis of alpha + beta Ti alloys is reaching an understanding of the formation of planar facets on the fracture surface and the implications these have for determining the root cause of failure. This talk will discuss several of these situations and suggest approaches to improve our understanding.

9:00 AM Invited

3D Observations of Short Fatigue Crack Interaction with Lamellar and Duplex Microstructures in a Two-Phase Titanium Alloy: *Soran Biroscá*¹; ¹University of Cambridge

EBSD and Synchrotron X-ray microtomography were used to investigate crack tip interaction with microstructure. Three samples with different microstructures were tested; lamellar, duplex and a heterogeneous microstructure. The three microstructures showed significantly different short crack propagation rates. It was found that a columnar lamellar microstructure creates a relatively smooth crack front while a basket weave type microstructure forces the crack tip to undulate at the lath width scale. Crack bridging of the fine lamellar region of the duplex microstructure was observed, which seems to hinder significant crack bifurcation to occur, but still provides improved crack growth resistance. In the third microstructure the crack tended to grow slightly asymmetrically due to the heterogeneous nature of the microstructure, which resulted in the intermediate growth rate. EBSD grain orientation and Schmid factor analysis revealed that the crack path is strongly influenced by the crystallographic orientation of the grains.

9:30 AM

Experimental Correlation Between a Microscopic Non-Local Strain Parameter and Macroscopic Fatigue Crack Growth in Beta-Annealed Ti-6Al-4V: *Pedro Peralta*¹; *Thomas Villarreal*¹; *Ikshwaku Atodaria*¹; *Aditi Chattopadhyay*¹; ¹Arizona State University

Correlations between crack tip strain, applied loads and fatigue crack growth kinetics are studied in beta-annealed Ti-6Al-4V. Tension-tension fatigue testing was performed using Compact-Tension specimens at R=0.1 and constant ΔK , (10 to 20 MPa.m^{0.5}). In-situ loading and Digital Image Correlation (DIC) were used to obtain the area integral of the opening strain field ahead of the crack tips over the cyclic plastic zone and found to be a power-law of ΔK , with an exponent approximately equal to the Paris exponent describing crack growth kinetics. Results are interpreted in terms of the dependence of strain fields on applied load and hardening exponent



TMS 2012

141st Annual Meeting & Exhibition

and a length scale parameter is deduced that predicts the measured Paris exponent for the material based on plasticity arguments. This length scale is shown to be proportional to the accumulated plastic displacement ahead of the crack tip, and discussed in terms of plastic blunting and cumulative damage models.

9:50 AM

Microstructural Crack Initiation and Growth during the High Cycle Fatigue Damage of a Ti-6Al-4V Alloy: *Edward Chen*¹; ¹Transition45 Technologies, Inc.

The development of a methodology for predicting high cycle fatigue (HCF) lifetimes in titanium-base alloys will provide design engineers with a tool to more accurately predict failure in gas turbine engine components, optimize designs to fully utilize a material's mechanical properties, and extend the maintenance-free life of the engines. Potential payoffs include decreased failure rates, improved system safety, reduced maintenance and spare parts cost, and reduced system weight. This study looked at advancing a mechanistic understanding of fatigue crack initiation and early crack growth under HCF conditions in an $\alpha + \beta$ Ti alloy in an initially undamaged state. Effort focused on identifying the initiation and growth mechanisms of the critical cracks that govern the useful material life under HCF. An improved understanding of HCF crack initiation provides a foundation for developing physics-based mechanistic models necessary to predict HCF life of Ti-base materials under a wide range of operational/environmental conditions.

10:10 AM

Monitoring of Small Fatigue Crack Initiation and Evolution in Ti Alloys: *Stan Rokhlin*¹; *George Connolly*¹; *Jia Li*¹; *Bahman Zoofan*¹; ¹The Ohio State University

The development and integration of several nondestructive evaluation methods for monitoring and sizing microcracks in titanium fatigue samples are described. For in-situ monitoring of crack initiation and evolution ultrasonic Lamb wave is excited and acquired continuously during fatigue tests at different levels of fatigue load using a high-speed acquisition system. The data are collected for a range of applied fatigue and modulation load levels and for a range of spatial propagation positions with each fatigue cycle. These samples are characterized by strong microstructure-induced ultrasonic scattering. To enhance crack identification a post-processing subtraction technique is introduced to improve the signal-to-noise ratio. Microradiography and scanning ultrasonic techniques have been also performed to confirm the localization and sizing of the detected cracks with other ultrasonic NDE techniques. The fusion of data from different NDE techniques provides useful information on the initiation, location, shape, size and growth history of fatigue cracks.

10:30 AM Break

10:40 AM Invited

Deformation and Fracture in Titanium Alloys: Microscale Characterization: *M Brandes*¹; ¹The Ohio State University

It is widely known that the creep, fatigue, and fracture properties of titanium alloys of alpha, near-alpha, and alpha/beta titanium alloys are greatly affected by material structure, particularly those related to the elastic and plastic anisotropies of the alpha-phase. Although macroscale properties are intimately linked to plastic behaviors at the microscale, understandings of these relationships have yet to be fully developed.

Recent advancements in materials characterization technologies and techniques have provided new capabilities to investigate Ti alloys at length scales relevant to the factors that control their properties. This paper discusses the microscale phenomena that dictate the performance of titanium alloys, and the techniques that may be utilized to investigate them.

11:10 AM

Dislocation Level Mechanisms of Dwell Fatigue Crack Initiation and Propagation in Near-Alpha Titanium: *Matt Brandes*¹; *Adam Pilchak*²; *Robert Williams*¹; *Michael Mills*¹; *Hamish Fraser*¹; *James Williams*¹; ¹The Ohio State University; ²Air Force Research Laboratory

Facet formation during dwell fatigue loading has invariably been associated with marked decreases in lifetime. Despite their importance to explaining the dwell debit, the mechanisms of facet formation have not been thoroughly investigated. In this work, we have analyzed crack initiation and propagation sites in the near-alpha Ti-8Al-1Mo-1V alloy. The dislocation activity and degree of lattice rotation in cracked and uncracked grains of the same orientation were investigated by way of TEM and EBSD analysis, respectively, of site-specific foils extracted from the fracture surface and from bulk material. The results show that $\langle c+a \rangle$ slip bands intersect planar basal $\langle a \rangle$ slip bands to form extended pileup structures at grain and phase boundaries. These pileups, and the accompanying large lattice rotations, appear to play an important role in the crack initiation process. Crack propagation through hard-oriented grains, on the other hand, is accommodated by $\langle c + a \rangle$ slip that is extremely localized near the fracture surface to accommodate crack tip opening and the formation of sub-micron sized tear ridges on the facet surfaces.

11:30 AM

Micromechanisms of Fatigue in Ti-5Al-5Mo-5V-3Cr: *Nicholas Jones*¹; *David Dye*¹; *Trevor Lindley*¹; ¹Imperial College London

High strength metastable beta titanium Ti-5Al-5Mo-5V-3Cr (Ti-5-5-5-3) is increasingly being used in large sections, such as aircraft landing gear truck beams. The wide two phase region enables a range of microstructures to be produced allowing property optimisation. A recently developed heat treatment schedule has produced a lower strength yet more damage tolerant microstructure, leading to interest in using this material in unconventional areas of the airframe. The high cycle fatigue performance of this material has been reported to be significantly better than that of Ti-6Al-4V, with a $\sim 50\%$ higher $1e7$ cycle endurance stress. However, relatively little is known about the micromechanisms of fatigue crack initiation and propagation in these alloys, and the influence of microstructure. In the present study, the high cycle fatigue performance of different Ti-5-5-5-3 microstructures is considered. The micromechanisms of fatigue cracking will be discussed in terms of the influence of the underlying microstructural features.

T.T. Chen Honorary Symposium on Hydrometallurgy, Electrometallurgy and Materials Characterization: Precious Metals, Recycling and the Environment

Sponsored by: The Minerals, Metals and Materials Society, TMS Extraction and Processing Division, TMS: Hydrometallurgy and Electrometallurgy Committee, TMS: Materials Characterization Committee

Program Organizers: Shijie Wang, Rio Tinto Kennecott Utah Copper; J. E. Dutrizac, CANMET; Michael Free, University of Utah; J. Y. Hwang, Michigan Technological University; Daniel Kim, Rio Tinto Kennecott Utah Copper

Wednesday AM
March 14, 2012

Room: Oceanic 5
Location: Dolphin Resort

Funding support provided by: Rio Tinto Kennecott Utah Copper, ASARCO, and Freeport McMoRan

Session Chair: Bradford Westrom, Freeport-McMoRan El Paso Refinery

8:30 AM

Simulating the Blanking of Preg Robbers in Gold Ores by Treating Activated Carbon with Hard Paraffin Wax: *Gus Van Weert*¹; John Jiang²; Olivia Wang³; Yeonuk Choi²; ¹ORETOME Limited; ²Barrick Gold Corporation; ³Process Research ORTECH

As part of a general review of processing double refractory ores through Barrick Gold's autoclaves / CIL facility at Goldstrike, NV, blanking the gold cyanide adsorbing native carbon in the ore with hard (m.p. >55 C) paraffin wax was proposed. To avoid interference from other ore constituents in the exploratory testwork, commercial activated carbon was substituted for native carbon to establish the best conditions for de-activation of carbon with molten wax.

8:50 AM

Dissolution of Platinum, Palladium and Rhodium in 250g/l NaCl Solution: *Kristian Lillkung*¹; Jari Aromaa¹; Olof Forsén¹; ¹Aalto University, School of Chemical Technology

The dissolution rates of Pt, Pd and Rh in 250 g/l NaCl solution were calculated from the current densities determined by polarization curves and potentiostatic measurements measured with wire electrodes under atmospheric pressure. The results achieved with the two methods were similar. The dissolution rates at open corrosion potential were in the order of few nanometers per hour. The polarization curves indicated that to achieve dissolution rates required for economical operation in industrial scale, the samples need to be polarized to higher potentials. When polarized to higher potentials, the metal dissolution rates were in the order of micrometers per hour. As the Tafel slopes of the metal dissolution region are fairly steep, the potential affects the dissolution rate greatly. Based on the activation energies, the dissolution reactions were controlled by charge transfer step.

9:10 AM

Silver Recovery from Complex Concentrates- A Mineralogical Approach: *Joe Ferron*¹; ¹Hydropro

This paper presents results of non-conventional techniques to recover silver from complex concentrates. The Platsol process was developed to recover in one step base metals and precious metals from sulphide concentrates too low grade to enter the mainstream extraction processes. Due to solubility limits, silver is only partially recovered in solution. However, the silver minerals are transformed into silver chloride that can then be recovered from the Platsol residue using traditional techniques. Some South American silver concentrates contain impurities (mostly arsenic) such that the smelter penalties incurred significantly affect the process economics. Metallurgical results have shown that a low

temperature calcinations pre-treatment transform the concentrate into a calcine well suited to traditional recovery processes. Metallurgical details are provided as well as the results of mineralogical studies that helped clarify the process mechanisms.

9:30 AM

Development of New Recycling Process of PGMs: *Toru Okabe*¹; Jumpei Mitsui¹; Katsuhiko Nose¹; ¹The University of Tokyo

In order to develop a new process for recovering platinum group metals (PGMs) directly from scrap, fundamental studies on enrichment/extraction processes of platinum (Pt) metal and its compounds were conducted. Both chemical dissolution technique and physical separation technique are studied to enrich and extract the Pt. Various types of recycling processes that are presently under development, are introduced, and their features and differences are discussed. The advantages and disadvantages of the new recycling processes are evaluated, and the possibility of establishing new recycling processes in the future is discussed from a multilateral perspective.

9:50 AM

Molybdenum Recovery and Impurity Removal from Smelter Dusts: Troy Bednarski¹; *Violina Cocalia*¹; Tyler McCallum¹; Matthew Soderstrom¹; Alexis Soto²; ¹Cytec Industries Inc., USA; ²Cytec Chile Ltda

Solvent extraction (SX) is a well established separation technology that can be extremely selective toward a specific target metal. Smelter dusts have been identified to contain significant concentrations of molybdenum, which can be leached and economically recovered from the solution. Other impurities such as As, Bi, and Sb will also be leached and removed from the dust recycle, which can improve anode quality. This paper will describe a method of selectively recovering molybdenum from leach solutions using a phosphinic acid-based reagent developed by Cytec Ind. Molybdenum stripping is achieved by using ammonia/ammonium carbonate mixtures to achieve a high concentration of molybdenum in the rich liquor. Piloting results confirm the ability to purify and concentrate Mo from acidic solutions. Molybdenum is then precipitated to produce a mixture of Mo salts, which can be further purified into ammonium molydates.

10:10 AM Break

10:30 AM

Acid Separation for Impurity Control and Acid Recycle using Short Bed Ion Exchange: *Michael Sheedy*¹; Paul Pajunen¹; ¹Eco-Tec Inc.

Short bed ion exchange is now well established technology in copper refinery tankhouses. Liberator bleeds are treated by short-bed-systems to produce an acid free byproduct stream containing the bleed metals and valuable nickel. Removing acid eliminates the need for black acid evaporators and reduces the sodium carbonate required to selectively precipitate nickel. Recovered sulfuric acid can be recycled to the tankhouse. The technology also treats hydrochloric, nitric, and hydrofluoric acid. For hydrochloric the process can selectively separate Zn, Pb, and Cu chloro-anionic complexes, which are then eluted with water. The technology can be coupled with ion exchange processes to minimize regenerant acid consumption. Resin regeneration often requires an acid dosage multiple times the stoichiometric minimum. Coupling an acid recovery bed with the IX column allows recovery and recycle of the free acid in the spent regenerant, thus reducing the overall acid consumption to just slightly more than stoichiometric.

10:50 AM

Various Arsenic Treatments in Non-Ferrous Metallurgy and Other Potential Applications: *Tetsuo Fujita*¹; Shun Fujieda²; Kozo Shinoda²; Shigeru Suzuki²; ¹Dowa Metals & Mining company limited; ²Tohoku University

Dowa Metals & Mining Co. Ltd. has developed and plant-practiced a unique scorodite synthesis technology (DMSP®) for arsenic immobilization by oxidizing Fe(II) ions in the presence of As(V) ions. Dowa has improved the DMSP® technology and has developed the



TMS 2012

141st Annual Meeting & Exhibition

process extensively for other applications. This paper focuses on the applicability of the DMSP® for various cases of copper smelting, and introduces other technologies for fixing arsenic and recycling gallium from GaAs, simultaneously processing (fixing) arsenic and thallium, and fixing and recovering arsenic from dilute arsenic solutions. The DMSP® was found to be applicable not only for various processes in nonferrous smelting, but also for other applications with a high potential for reducing environmental problems.

11:10 AM

New Vermiculite-Copper Nanoparticle Product with Antibacterial Properties: Jaroslaw Drelich¹; Bowen Li¹; Jiann-Yang Hwang¹; ¹Michigan Technological University

Vermiculite covered with copper nanoparticles is a new antimicrobial material that was prepared in this study through ion-exchange process and hydrogen reduction. Copper ions were introduced to an interlayer structure of vermiculite from concentrated copper sulfate solutions and then reduced to a metallic copper at 400-600°C in hydrogen atmosphere. During the reduction process copper diffused to surfaces of vermiculite and formed copper nanoparticles. Strong adhesion of copper nanoparticles to the vermiculite carrier makes this hybrid material very stable and durable. The vermiculite-metallic copper hybrid shows strong antibacterial activity against *Staphylococcus aureus* at 37°C. Vermiculite is an inexpensive mineral that is very stable under a wide range of industrial and environmental conditions, and extensively used as filler in fireproof materials, plastics, paints and lightweight concrete. The addition of metallic copper as an antimicrobial agent opens new avenues for the application of vermiculite in consumer products and other areas.

11:30 AM

Scorodite Solubility and Storage Management Systems for Arsenic-Bearing Compounds: Tetsuo Fujita¹; Shun Fujieda²; Kozo Shinoda²; Shigeru Suzuki²; ¹Dowa Metals & Mining Company Limited; ²Tohoku University

Dowa's scorodite, synthesized by oxidation of Fe(II) ions in the presence of As(V) ions at atmospheric pressure, was characterized. The scorodite was well crystallized and had a very low solubility. To examine the conditions for stable storage of the scorodite for long periods, experiments with various synthesis and leaching conditions were done. The scorodite had a very low arsenic solubility in sea water. It was estimated in consecutive leaching tests that the arsenic concentration would eventually converge to zero. The prevention of arsenic leaching by adding goethite or ferrihydrite was limited in some cases. Very low toxicity was confirmed by toxicity tests. The investigation results suggest that disposal at a specifically designed well-controlled storage place is preferable for the scorodite whose toxicity had been made sufficiently low. Disposal to an isolated final disposal site with more stringent prevention for the outflow of toxic substances was thought another option.

Ultrafine Grained Materials VII: Advanced Analysis Methods

Sponsored by: The Minerals, Metals and Materials Society, TMS Structural Materials Division, TMS/ASM: Mechanical Behavior of Materials Committee, TMS: Nanomechanical Materials Behavior Committee, TMS: Shaping and Forming Committee

Program Organizers: Suveen Mathaudhu, U.S. Army Research Office; Xiaoxu Huang, Risø National Laboratory for Sustainable Energy, Technical University of Denmark; Hyoung Seop Kim, POSTECH; Terence Langdon, University of Southern California; Terry Lowe, Manhattan Scientifics, Inc.; Ruslan Valiev, Ufa State Aviation Technical University; Xiaolei Wu, Institute of Mechanics, Chinese Academy of Sciences; Michael Zehetbauer, University of Vienna

Wednesday AM
March 14, 2012

Room: Swan 4
Location: Swan Resort

Session Chairs: Malgorzata Lewandowska, Warsaw University of Technology; Peter Liddicoat, The University of Sydney; M. Ravi Shankar, University of Pittsburgh; Marco Starink, University of Southampton

8:30 AM Invited

Neutron Scattering Studies on the Stability of Texture in Cu/Nb Nanolamellar Composites Fabricated via Accumulative Roll Bonding: John Carpenter¹; Sven Vogel¹; Irene Beyerlein¹; Nathan Mara¹; ¹Los Alamos National Laboratory

Current work has shown that the texture of Cu/Nb nanolamellar composites fabricated via physical vapor deposition remain stable under mechanical and irradiation extremes. In this work, the stability of texture in bimetallic composites fabricated via accumulative roll bonding (ARB) will be explored. Prior work on ARB Cu/Nb multilayers found an atypical rolling texture saturated at a layer thickness (h) of 128 nm and was stable with increasing plastic strain (ε). Through the use of high temperature in-situ neutron diffraction, the stability of the saturated texture will be investigated. The hypothesis is that a texture that is stable at one extreme (ε) will also be stable at another extreme (temperature). Also, neutron scattering will be used to investigate the effects of ε and h on the saturation of texture in ARB Cu/Nb multilayers. The hypothesis is that texture saturates as a function of ε rather than as a function of h.

8:50 AM

Homogeneity of SPD Processed Ultrafine Grained Aluminium: Malgorzata Lewandowska¹; Michal Przybysz¹; Mariusz Kulczyk²; Wacław Pachla²; ¹Warsaw University of Technology; ²Institute of High Pressure Physics PAS

Homogeneity of technical purity aluminium (1050) produced by hydrostatic extrusion with a total true strain of ~3 or via the combination of equal channel angular pressing (ECAP) technique and hydrostatic extrusion – total true strain of ~11 has been investigated. Microstructure of the samples has been investigated by focus ion beam (FIB) and transmission electron microscopy. The scatter of the properties has been determined by microhardness mapping on the cross and longitudinal section and by tensile testing using microsamples. The results show that 1050 aluminium processed by SPD techniques are to some extent non-homogeneous. It exhibits hard and strong core surrounded with a softer surface regions. In addition, it has been found that samples obtained by the combination of ECAP and HE methods are more homogeneous than the ones produced by HE alone. The gradient of variability of mechanical properties observed on the cross section is related to microstructure inhomogeneity.

9:05 AM

In Situ Measurements of Deformation Strain and Strain-Rate in Equal Channel Angular Pressing: *Saradhi Koneru*¹; Saurabh Basu¹; M. Ravi Shankar¹; ¹University of Pittsburgh

Equal Channel Angular Pressing (ECAP) offers a viable route for the manufacture of bulk nanostructured metals of large cross-sections. In ECAP, strain and strain-rate are central variables of plasticity that determine microstructural refinement and process outcomes. Here, we observed the deformation of soft metals in an optically transparent ECAP die using high-speed CCD cameras. From resulting time-sequence images of metal-flow in the deformation zone, we present results of digital image correlation algorithms that were used to measure the strain and strain-rate fields in ECAP as a function of the scale, deformation speed and die geometry. Implications of these observations for optimizing process parameters in ECAP to achieve desired thermomechanical conditions and controlled microstructural outcomes are presented.

9:20 AM Invited

Influence of Alloying on a Strain Induced Grain Growth in Nanocrystalline Pd: *Lilita Kurmanaeva*¹; Yulia Ivanisenko¹; ¹Institute of Nanotechnology, KIT

An investigation of nanocrystalline (nc) materials is one of the key topics of modern material science. These materials demonstrate superior hardness, strength and fatigue properties as compared with their coarse grained counterparts. One of the intriguing aspects in a deformation behavior nc materials is the deformation-induced grain growth, which has no analogy in coarse grained materials. Even in the absence of deformation, nanocrystalline materials can undergo significant grain growth at ambient conditions. Plastic deformation significantly accelerates the growth rate. Therefore the search for strategies to improve the stability of nc microstructure is an important issue for further developments in this area. Here, we present investigation of the microstructure evolution of nanocrystalline Pd and Pd-alloys at severe plastic deformation by high pressure torsion. The obtained results on microstructure development at HPT and related mechanical properties of Pd and Pd alloys are discussed.

9:40 AM

Nanostructural Evolution in Hierarchy-Strengthened Al-Mg Alloys: *Peter Liddicoat*¹; Maxim Murashkin²; Xiaozhou Liao¹; Ruslan Valiev²; Simon Ringer¹; ¹The University of Sydney; ²Ufa State Aviation Technical University

Reducing the average grain-size in a polycrystalline material necessarily increases the density of grain interfaces and heightens grain-boundary influence over material properties. The magnitude and mode of grain-boundary influence is not easily predicted by extensions of conventional boundary dispersion and misorientation relationships - nanostructured Al alloys, for example, possess yield strengths up to 1 GPa and contain a hierarchy of intergranular and intragranular solute structures. Beam convolutions, from multiple nanocrystalline grains within a specimen, make retrieval of the required 3D atomic-level chemical and spatial information complex or impossible using transmission-based microscopes (e.g., TEM, XRD, or SAXS). Using novel techniques in atom probe microscopy, a point-projection microscope, we will present the evolution of solute structuring, chemical-texture and nanotopology at progressive strain increments imparted by high-pressure torsion in Al-Mg alloys and discuss the intergranular relationships of misorientation and curvature to provide energetically favourable conditions for solute diffusion and partitioning.

9:55 AM

Validation and Analysis of a Model for Grain Refinement by Cold Severe Plastic Deformation: *Marco Starink*¹; Xiaoguang Qiao¹; Nong Gao¹; ¹University of Southampton

We present a model to predict grain refinement and strength/hardness of Al alloys after very high levels of cold deformation through techniques including cold rolling, equal channel angular pressing (ECAP), high

pressure torsion (HPT), accumulative rolling bonding (ARB) and embossing. At the beginning of deformation, the generated dislocations are stored in grains and contribute to overall strength. With increase in strain, excess dislocations form and/or move to new cell walls/grain boundaries and grains are refined. The model is tested against data on a range of SPD processed Al based alloys. It is shown that grain size and strength/hardness are correctly predicted to a good accuracy. It is also shown that general trends in strengthening in all fcc pure metals are consistent with the model.

10:10 AM Break

10:25 AM Invited

Spatial Distribution of the Dislocation Density and the Strength of Nb and Ta Deformed by High-Pressure-Torsion Determined by X-Ray Peak Profile Analysis: Bertalan Jóni¹; Erhard Schafner²; *Tamás Ungár*¹; Michael Zehetbauer²; ¹Eötvös University Budapest, Hungary; ²University of Vienna, Austria

Niobium and Tantalum are two bcc metals with very different elastic anisotropy. The $Az=2 \times c44/(c11-c12)$ constants for Nb and Ta are 0.51 and 1.58, respectively. Submicron grain-size state of the two refractory metals is produced by the method of high-pressure-torsion (HPT) with different pressures 2 and 4 GPa, and two different deformations of 0.25 and 1.5 rotations, respectively. The grain size, the dislocation density and the screw or edge type of dislocation character are investigated by high resolution diffraction peak-profile analysis. The beam size on the specimen surface is 0.2×1 mm allowing to characterize the sub-structure along the radius of the specimen. The strength of the samples is determined by microhardness testing. The sub-structure parameters are correlated with the strength data. The deformation mechanisms of the two different metals are discussed in terms of the different deformation modes, the elastic anisotropy and the dislocation structure.

10:45 AM

Mapping Microstructures Resulting from Severe Simple Shear Deformation: Sepideh Abolghasem¹; Saurabh Basu¹; Shashank Shekhar¹; Jiazhao Cai¹; *M. Ravi Shankar*¹; ¹University of Pittsburgh

Grain refinement from interactive effects of severe shear strains, strain-rates and temperatures often follow complex trajectories. Microstructure control under these conditions can be simplified by delineating a map-space for projecting characteristics of deformed microstructures when it is parameterized as functions of the variables of deformation, while remaining cognizant of the underlying mechanisms of refinement. Using Large Strain Machining (LSM) as a test of material response in simple-shear, quantitative microstructure analysis is performed across broad deformation conditions, while simultaneously measuring the thermomechanics of the process using high-speed digital image correlation and infrared thermography. The implications of the microstructure maps generated from the emerging data-sets for predicting and custom-designing grain-refined materials are presented.

11:00 AM

A Crystal Plasticity FEM Study about Influence of Crystal Orientation on the Texture Evolution and Heterogeneity of ECAPed Copper Single Crystals: *Guanyu Deng*¹; Cheng Lu¹; Lihong Su¹; Kiet Tieu¹; Xianghua Liu²; ¹University of Wollongong; ²Northeastern University

Equal channel angular pressing (ECAP) has been widely used to produce ultra-fined grains (UFG) in bulk materials over the last two decades. The present work investigates texture evolution and deformation heterogeneity of copper single crystals subjected to one-pass ECAP at room temperature using a crystal plasticity finite element method (CPFEM) model. Two special orientations are designed to examine the effect of initial crystallographic orientation on texture evolution and heterogeneity. The first orientation (Crystal I) meets the macroscopic shear deformation of ECAP and the second orientation (Crystal II) is rotated around the transverse axis (TD) by 20° in a counter-clockwise direction from Crystal I. It has been found that the initial orientation has a great influence on the



TMS 2012

141st Annual Meeting & Exhibition

plastic deformation zone (PDZ) and texture developments during ECAP. The crystal rotation during deformation is quantitatively estimated. These simulation results agree well with the experimental observations.

11:15 AM Invited

Using Deformation Mechanism Map to Depict Flow Processes in Superplastic Ultrafine-Grained Materials: *Megumi Kawasaki*¹; Terence Langdon¹; ¹University of Southern California

The introduction of significant grain refinement is very attractive because small grains lead to excellent creep properties especially superplastic ductility at elevated temperatures. Since the strain rate in superplastic flow varies inversely with the grain size raised to a power of two, a reduction in grain size to the submicrometer level will bring about the occurrence of superplasticity at higher strain rates of $> 10^{-2}$ s⁻¹. In the present report, an analysis was conducted to examine the flow behavior of several different ultrafine-grained metals processed by severe plastic deformation process in equal-channel angular pressing and high-pressure torsion. The analysis shows the superplastic flow of the UFG materials may be represented using a flow mechanism developed earlier for coarse grains and the flow process of high strain rate superplasticity is depicted using deformation mechanism maps.

11:35 AM

Modeling Temperature-Dependent Mechanical Response of UFG Al-1100 at High Strain Rates: *Emily Huskins*¹; K.T. Ramesh¹; ¹Johns Hopkins University

Recent improvements in the strength of aluminum alloys have been obtained through the development of complex microstructures containing reduced grain sizes. Under dynamic compression, failure in these materials often initiates as localization of plastic deformation. Localized plastic work results in a local temperature rise, and thus softening of the material. To understand bulk failure it is necessary to understand the thermal softening of the material under these high strain rate and high temperature conditions. In this work, a modified Kocks-Mecking model is developed to predict the thermal softening observed for UFG commercially pure aluminum. This is a mechanism-based constitutive model which accounts for temperature, strain rate, and grain size effects through the evolution of dislocation density during deformation. The model predictions are compared to experimental results on UFG Al-1100 tested at high temperatures (298-573K) and high strain rates on a modified Kolsky bar system.

Ultrafine Grained Materials VII: Powder Processing

Sponsored by: The Minerals, Metals and Materials Society, TMS Structural Materials Division, TMS/ASM: Mechanical Behavior of Materials Committee, TMS: Nanomechanical Materials Behavior Committee, TMS: Shaping and Forming Committee

Program Organizers: Suveen Mathaudhu, U.S. Army Research Office; Xiaoxu Huang, Risø National Laboratory for Sustainable Energy, Technical University of Denmark; Hyoung Seop Kim, POSTECH; Terence Langdon, University of Southern California; Terry Lowe, Manhattan Scientifics, Inc.; Ruslan Valiev, Ufa State Aviation Technical University; Xiaolei Wu, Institute of Mechanics, Chinese Academy of Sciences; Michael Zehetbauer, University of Vienna

Wednesday AM
March 14, 2012

Room: Swan 5
Location: Swan Resort

Session Chairs: Mikheil Chikhradze, Georgian Technical University/; David Tingaud, Université Paris 13- Institut Galilée; Hyoung Seop Kim, POSTECH; Troy Topping, University of California, Davis

8:30 AM Invited

Stress-Induced Grain Growth in Ultra-Fine Grained 5083 Al during Hot Extrusion: Yaojun Lin¹; Ying Li¹; *Enrique Lavernia*¹; ¹University of California, Davis

Due to the potential for high tonnage manufacturing, the approach to produce ultrafine grained (UFG) materials via mechanical milling has received particular attention. Minimization of grain growth during consolidation of mechanically milled powders, including primary consolidation, such as hot isostatic pressing (HIPing), and secondary consolidation, such as extrusion, rolling and forging, is critical for retention of UFG structure in the resultant materials. Stress-induced grain growth during secondary consolidation heretofore remains poorly understood. Consequently, this presentation reports on a study of the influence of second-phase particles and solute/impurity segregation at grain boundaries (GBs) on stress-induced grain growth during hot extrusion of 5083 Al consolidated by HIPing mechanically milled powders. Based on TEM and HRTEM observations, the contributions of GB migration and grain rotation to grain growth are analyzed and discussed. On the basis of the analysis, we propose that grain rotation is the predominant mechanism responsible for stress-induced grain growth.

8:50 AM

Large Scale Powder Processing of High Strength Copper Alloys: *Joseph Paras*¹; Kris Darling²; Laszlo Kecskes²; Suveen Mathaudhu³; Deepak Kapoor¹; ¹U.S. Army ARDEC; ²U.S. Army Research Laboratory; ³U.S. Army Research Office

Research is currently being conducted on the stabilization of grains in nanocrystalline materials. Recent progress has shown nanocrystalline alloys with high temperature stability because of the interfacial energy reduction associated with solute segregation. These materials are typically synthesized through powder processing in non equilibrium conditions, such as high energy milling, and carefully consolidated to preserve the engineered microstructure. The intent of this work was to scale up the processing of such nanocrystalline alloys beyond the laboratory scale. Previous work on the thermally stabilized nanocrystalline Cu-10at%Nb was applied to a Cu-10at%Ta system and the powders produced were initially consolidated into 40mm diameter discs with 5mm thickness via field assisted sintering and 25mm diameter billets via instrumented hot isostatic pressing. Preliminary results have shown 75% retention of the microhardness going from the powder to bulk form. This work will provide appropriate processing and consolidation parameters for large scale fabrication of these materials.

9:05 AM

Mechanical Properties of Nanocrystalline Cu-, Mg-, and Fe-Base Alloys from In-Situ and HPT Consolidated Ball-Milled Powders: *Khaled Youssef*¹; Daria Setman²; Michael Zehetbauer²; Suhrit Mula³; Pengchao Kang⁴; Ronald Scattergood¹; Carl Koch¹; ¹North Carolina State University; ²University of Vienna; ³National Institute of Technology; ⁴Harbin Institute of Technology

Since ultra-high strength nanocrystalline metals often suffer from poor ductility, it has been a challenge for researchers for years to improve it. Another challenge has been to produce nanocrystalline materials with a fine grain size in bulk form without processing artifacts. Recent progress in processing – e.g. in ball milling involving in-situ consolidation – allowed to come about both problems. While related works so far mostly concerned pure nanocrystalline metals, this work was devoted to ball milled nanocrystalline alloys including fcc (Cu-Zn-Al, Cu-Nb), hcp (Mg-Zn-Y), and bcc (Fe-Y, Fe-Zr) crystal structures, not at least due to their potential for enhancing the thermal stability. This is attributed to kinetic mechanisms impeding grain boundary migration, and/or thermodynamic mechanisms reducing the grain boundary energy, as a result of solute segregation. Experiments are reported which focused on the variation of processing parameters, also attempting High Pressure Torsion (HPT) for consolidation, and on tensile tests providing the mechanical properties.

9:20 AM Invited

Microstructure Features, Strengthening Mechanisms and Hot Deformation Behavior of Oxide-Dispersion Strengthened Al6063 Alloy with Ultrafine-Grained Structure: *A. Simchi*¹; H. Asgharzadeh¹; H.S. Kim²; ¹Sharif University of Technology; ²Pohang University of Science and Technology

Ultrafine-grained (UFG) Al6063/Al₂O₃ (0.8 vol%, 25 nm) nanocomposite was prepared via powder metallurgy route. The grain structure of the nanocomposite composed of nano-size grains (< 0.1 μm), ultrafine grains (0.1-1 μm) and micron-size grains (>1 μm) with random orientations. It was found that the yield strength of the UFG nanocomposite is mainly controlled by the Orowan mechanism rather than the grain boundaries. The deformation activation energy at temperature ranges of T < 300 °C and 300 °C ≤ T < 450 °C was determined to be 74 and 264 kJ mol⁻¹, respectively. At the higher temperatures, significant deformation softening was observed due to dynamic recrystallization of non-equilibrium grain boundaries. A duplex microstructure consisting of large substructured grains and fine grains separated by high-angle grain boundaries was formed after hot deformation. The deformation behavior is described based on the formation of nonequilibrium grain boundaries with high internal stress and dislocation-based models.

9:40 AM

Microstructure and Mechanical Properties of Polycrystalline Nickel with Controlled Micro/Nano Grain Volume Fractions: *Guy-Daniel Kollo*¹; *David Tingaud*¹; *Guy Dirras*¹; ¹Université Paris 13- Institut Galilée

Nickel powder blends were prepared by mixing nano and micron-sized powder. Bulk polycrystalline Ni samples with controlled volume fractions of 100%, 60%, 30% and 0% of micro-sized (mc) grains embedded in an ultrafine-grained matrix (ufg) were processed by spark plasma sintering. The relative mass density was higher than 96%, reaching 100% for the sample containing 60% of mc grains for which the number average grain sizes within the matrix and the mc inclusions were about 300nm and 1.60μm, respectively. EBSD investigations showed the presence of a high amount of high angle boundaries (>30%) in both the ufg matrix and the mc inclusions. Quasi-static compression tests performed at room temperature and at a strain rate of 10⁻³ s⁻¹ indicates a decrease of the yield strength from 1450 to 500 MPa while the strain to failure starts to 6% and exceeds 40% for the fully ufg and mc samples, respectively.

9:55 AM

Nickel with Multimodal Grain Size Distribution Achieved by SPS: Microstructure and Mechanical Properties: *Guy-Daniel Kollo*¹; *David Tingaud*¹; *Guy Dirras*¹; ¹Université Paris 13- Institut Galilée

Bulk nickel ultrafine-grained (ufg) Ni samples were processed by spark plasma sintering of high purity Ni nanopowders. Microstructural investigations showed that the powder was heterogeneous, comprising ultrafine (0.05-1μm) as well as coarse particles (1-5μm). Sintering resulted in bulk Ni samples having a relative mass density of ~97%. Thorough microstructural investigation was carried out by EBSD and revealed composite-like microstructure consisting of ~10 vol. % of large multi-crystalline agglomerates of 10μm in diameter embedded the ufg (200-300 nm) matrix. The mechanical behavior was investigated by compression tests conducted at room temperature at strain rates of 2x10⁻⁴ s⁻¹ and 2x10⁻² s⁻¹. After the onset of yielding, a softening behavior was observed for the sample deformed at 2x10⁻⁴ s⁻¹ while at 2x10⁻² s⁻¹ a large strain hardening behavior was observed. As a consequence the measured strain to failure was two times higher than the one measured for the lower strain rate.

10:10 AM

Quantifying Strengthening Mechanisms in Cryomilled Al Alloys and Their Composites: *Troy Topping*¹; *Zhihui Zhang*¹; *Ying Li*¹; *Enrique Lavernia*¹; ¹University of California, Davis

Aluminum alloys with nanocrystalline (NC) and ultra-fine grain (UFG) size are of interest because of their high strength – typically more than 30% stronger than conventionally processed alloys. By generating NC powders via cryomilling in liquid nitrogen, a thermally stable UFG microstructure evolves during thermomechanical processing (TMP). The constituents that stabilize the microstructure – dispersed oxides and nitrides – also contribute to the strength of the system. By examining microstructures and stress-strain data generated for cryomilled pure Al and Al-Mg alloys, with various milling times and media, the strengthening mechanisms can be dissected to improve understanding of cryomilled Al alloys. Hall-Petch, Orowan, solid solution and dislocation hardening mechanisms are quantified based on experimentally developed UFG Al alloys crossing multiple investigations. Additionally, the intentional addition of ceramic particulates, such as Al₂O₃ and B₄C, provides the basis for analyzing systems using basic composite models.

10:25 AM Break

10:40 AM

Mechanics of Powder Equal Channel Angular Pressing: *Hyounng Seop Kim*¹; ¹POSTECH

Manufacturing bulk nanostructured materials with least grain growth from initial powders is challenging because of the bottle neck of bottom-up methods using the conventional powder metallurgy of compaction and sintering. In this study, bottom-up type powder metallurgy processing and top-down type SPD approaches were combined in order to achieve both real density and grain refinement of metallic powders. ECAP, one of the most promising processes in SPD, was used for the powder consolidation method. For understanding the ECAP process, investigating the powder density as well as internal stress, strain distribution is crucial. We investigated the consolidation and plastic deformation of the metallic powders during ECAP using the finite element simulations. This work was supported by the National Research Foundation of Korea (NRF) grant funded by the Korea government (MEST) (No.2010-0026981).

10:55 AM

Microstructure Evolution and Mechanical Behavior of Ultrafine Grain Structured Al 7075 Developed by Cryomilling: *Kaka Ma*¹; *Troy Topping*¹; *Enrique Lavernia*¹; *Julie Schoenung*¹; ¹University of California, Davis

Al 7075 alloys are used extensively in aircraft and aerospace structures due to their high strength-to-density ratio as well as moderate toughness and corrosion resistance. It has been commonly accepted that a sequence



TMS 2012

141st Annual Meeting & Exhibition

of precipitation reactions occur in conventional Al 7075 with increasing temperature: solid solution \rightarrow Guinier-Preston (G-P) zones \rightarrow η' \rightarrow η . The formation and dissolution of the precipitates have a significant influence on the mechanical behavior of the materials. In this paper, gas atomized Al 7075 powder was modified by using the cryomilling technique to develop an ultrafine grain microstructure. The cryomilled material is compared to conventional material by investigating the morphology and microstructure of the powders, the precipitation reactions, and the mechanical behavior and microstructure evolution in bulk consolidated materials.

11:10 AM

Explosive Fabrication of Bulk Ultrafine Grained Al-Ni-Ti Composite Materials: Nikoloz Chikhradze¹; Akaki Gigineishvili¹; Mikheil Chikhradze¹; ¹Mining Institute/Georgian Technical University

The properties of Al-Ni-Al composite materials significantly improved if they are prepared in nanostructured/ultrafine grained form. Same time the industrial fabrication of Al-Ni-Ti ultrafine grained bulk materials is reduced. The preparation of the precursors and compaction technique of Al-Ti-Ni- blend for obtaining bulk samples is discussed in the paper. For homogenization, mechanical alloying and transformation in amorphous and ultrafine grained structure of the Al-Ni-Ti blend the high energy planetary ball mill was used. The explosive generated shock wave compaction technique is selected and investigated for obtaining ultrafine grained bulk materials. Structural investigations and micro-hardness measurements were used to characterize the phase composition and mechanical properties of the materials. The results of analysis revealing the effects of the compacting conditions and precursor particles sizes, affecting the consolidation and the properties of this new ultra high performance alloys are discussed.

11:25 AM

Mechanical Properties of Nanostructured Al-Bi Alloys: Koteswararao Rajulapati¹; Sreedevi Varam¹; K Bhanu Sankara Rao¹; ¹University of Hyderabad

The size and volume fraction of the second-phase particles greatly influence the mechanical properties of the matrix in composite materials. Al and Bi are mutually insoluble both in the liquid state as well as solid state. Nanostructured Al-Bi alloy powders were synthesized using high energy ball milling and are characterized using X-Ray Diffraction (XRD), Transmission Electron Microscopy (TEM) and Differential Scanning Calorimetry (DSC). XRD data of Al-Bi alloy samples milled for 50 hours showed both Al and Bi peaks with no considerable change in lattice parameter values of Al, indicating a two-phase structure. Further analysis of the synthesized powders is in progress. The mechanically alloyed powder samples will be Consolidated using uniaxial compression and/or Spark Plasma Sintering (SPS) and the mechanical properties of these bulk samples are evaluated by micro indentation and nanoindentation. The wear properties of the bulk samples are determined and correlated with the nanostructure.

11:40 AM

Effect of Grain Size Distribution and Zr Addition on Mechanical Properties and Oxidation Resistance of Fe-Cr-Ni Alloys: Mahesh Venkataraman¹; Raman Singh¹; Carl Koch²; ¹Monash University; ²North Carolina State University

The effects of nanocrystalline and bimodal grain size distributions as well as alloying additions of Cr and Zr on the oxidation resistance of nanocrystalline (nc) Fe-based alloys has been investigated. Fe-Cr-Ni-Zr alloys having nc and bimodal grain size distributions were prepared using mechanical alloying followed by a novel multi-step hot-compaction route. The ductility of bimodal alloys, determined by shear punch test, was found to be significantly superior to the nc alloys owing to the presence of the microcrystalline grains in the matrix of the bimodal alloys. The oxidation resistance of these alloys, in a temperature range 500-700 °C, has been compared with conventional micro-crystalline stainless steel.

The remarkably superior oxidation resistance of these alloys as compared to stainless steel is attributed to the enhanced diffusivity of Cr in nc and bimodal alloys, which results in the enrichment of Cr at the metal oxide interface even at lower bulk Cr contents.

11:55 AM

Comparison of Structure and Properties of Nanomaterials Processed by Ball Milling and High Pressure Torsion: Jelena Horky¹; Daria Setman¹; Michael Kerber¹; Hamed Bahmanpour²; Carl Koch²; Ron Scattergood²; Michael Zehetbauer¹; ¹University of Vienna; ²North Carolina State University

Cu nanomaterials processed by Ball Milling (BM) and High Pressure Torsion (HPT) were investigated by microhardness, multiple whole X-ray profile analysis, and differential scanning calorimetry (DSC). The strength of BM samples and its dependence on milling time (equivalent to strain) is much higher than that of HPT samples, which can be related to the huge difference between coherent domain sizes (CSD) after BM and HPT, respectively. Therefore, very high values of fatigue strength in BM samples can be expected. The stored energy of BM samples derived from DSC again is much higher than those of HPT, but strongly decreases with increasing milling time finally reaching the level of HPT. Since neither dislocation density nor CSD can account for this behaviour, the extra high energy stored in BM samples is attributed to a very high concentration of deformation induced vacancy type defects which appear to gradually anneal with increasing milling time.

12:10 PM

Synthesis and Characterization of Binary Al-Mn Alloys for Structural Applications: Lauren Armstrong¹; Rajendra Sadangi¹; Kris Darling²; Chris Haines¹; Deepak Kapoor¹; ¹US Army, ARDEC; ²US Army, ARL

Nanocrystalline and amorphous Al-Mn alloys, produced by electrodeposition, have demonstrated exceptionally high hardness (>5GPa). Powder metallurgy is being examined as a viable route to produce pilot scale quantities of Al-Mn alloys. Binary Al-15 wt. % Mn alloys were synthesized via high energy mechanical alloying (MA) of elemental, gas atomized, and rapidly solidified powders. These alloys were characterized with an array of techniques, including x-ray diffraction, electron microscopy, calorimetry, and mechanical indentation. Influence of synthesis route and processing parameters on structure and properties will be presented. Formation and thermal stability of the ultra-fine grained phases will also be discussed in reference to hot consolidation of the powders. I. Ruan S, Schuh CA; "Electrodeposited Al-Mn alloys with microcrystalline, nanocrystalline, amorphous and nano-quasicrystalline structures"; *ACTA MATERIALIA* 57, 3810, 2009.

12:25 PM

Grain Size Dependence of Deformation Microstructure Formation in Compressed Aluminum: Guomin Le¹; Andy Godfrey¹; Xiaoxu Huang²; Niels Hansen²; Grethe Winther²; ¹Tsinghua University; ²Risø National Laboratory for Sustainable Energy, Technical University of Denmark

The effects of grain size on the extent and patterning of the dislocation storage during plastic deformation has been examined in samples of aluminum with average grain sizes ranging from 30 μ m to 0.7 μ m deformed by compression. Initial fine grain samples were produced using spark plasma sintering to obtain fully recrystallized grains with a low dislocation density. In the coarsest grain samples the deformation microstructure follows the pattern previously reported during tensile deformation, with cells formed in grains with a compression axis near [100] and extended planar boundaries formed in other grains showing an orientation dependence in their crystallographic alignment. With decreasing average grain size the crystallographic alignment of the planar boundaries becomes less well defined and the fraction of grains showing cell structures increases. In the finest grains examined only loose dislocations are found. These observations are discussed with respect to the differences seen in the work-hardening of the samples.

Ultrasonic Fatigue of Advanced Materials and Systems:

Ultrasonic Fatigue of Metals and Alloys I

Sponsored by: The Minerals, Metals and Materials Society, State Research Center for Mathematical and Computational Modelling, University of Kaiserslautern, Germany, State Research Focus "Advanced Materials Engineering", University of Kaiserslautern, Germany, TMS Light Metals Division, TMS Structural Materials Division, TMS: Advanced Characterization, Testing, and Simulation Committee, TMS/ASM: Computational Materials Science and Engineering Committee, TMS: Materials Characterization Committee, TMS/ASM: Mechanical Behavior of Materials Committee, TMS: Young Leaders Committee
Program Organizers: Frank Balle, University of Kaiserslautern; Dietmar Eifler, University of Kaiserslautern; Guntram Wagner, University of Kaiserslautern

Wednesday AM
March 14, 2012

Room: Europe 1
Location: Dolphin Resort

Session Chairs: Frank Balle, University of Kaiserslautern (Germany); Dietmar Eifler, University of Kaiserslautern (Germany); Guntram Wagner, University of Kaiserslautern (Germany)

8:30 AM Introductory Comments: Frank Balle, Symposium organizer-in-chief

8:35 AM

A Method for In Situ Capture of Cyclic Strain Accumulation during Ultrasonic Fatigue of Structural Alloys: *Jason Geathers*¹; *Samantha Daly*¹; *J. Wayne Jones*¹; ¹University of Michigan

A novel experimental capability that combines ultrasonic fatigue instrumentation and Digital Image Correlation (DIC) to has been developed to enable the quantification of cyclic damage accumulation at the microstructural length scale during Very High Cycle Fatigue (VHCF). Both macro-DIC and micro-DIC, the latter using calibrated stereomicroscopes for image capture, are employed to examine the evolution of small-scale strain fields in local microstructural neighborhoods that favor crack initiation. Damage evolution and cyclic strain localization leading to crack formation is examined for a range of polycrystalline metals will be described, as will the characterization of small crack propagation in both bulk ultrasonic specimens and in thin foils ($t \sim 150 \mu\text{m}$) cycled at 20 kHz. The unique advantages of these combined techniques, as well as the experimental challenges encountered, will be discussed.

8:55 AM

Influence of Grain Size and Precipitates on the Fatigue Lives and Deformation Mechanisms in the VHCF-Regime: *Heinz Werner Höppel*¹; ¹University Erlangen-Nürnberg

Research in the field of very high cycle fatigue (VHCF) strongly increased during the last decade. It is meanwhile established that when investigating the deformation mechanisms in the VHCF-regime it has to be separated between inclusion free type I materials and materials with inclusions (type II). Despite all the attempts made so far, a basic understanding on the dominating deformation mechanisms in the VHCF-regime is still missing. Hence, in this study the deformation mechanisms of the aluminium alloy AA6082 (type II material) were investigated. The material was investigated in the as-received condition and after different heat treatments. The heat treatment changes the deformation mechanism from internal crack initiation to initiation from the surface. In the as-received condition a non-defect crack initiation site was detected. Based on thorough investigations using EBSD, FIB-techniques and nanoindentation mechanisms for featureless crack initiation are discussed and compared to other data in literature.

9:15 AM Invited

Ultrasonic Fatigue Testing at Different Load Ratios under Constant and Variable Amplitude: *Herwig Mayer*¹; *Michael Fitzka*¹; *Reinhard Schuller*¹; *Stefanie Stanzl-Tschegg*¹; ¹BOKU, Institute of Physics and Material Science, Vienna

Ultrasonic resonance fatigue testing is a powerful tool to investigate the High Cycle Fatigue (HCF) and Very High Cycle Fatigue (VHCF) properties of materials in short testing times. Closed loop control of load amplitude and resonance frequency to obtain high accuracy, and pulsed loading to prevent heating of specimens, for example, allow endurance and fatigue crack growth experiments with high precision. New technique performing ultrasonic tests with Variable Amplitude (VA) at constant load ratio R is presented and used to investigate 2024-T351 aluminium alloy. VA lifetimes at $R=-1$, $R=0.1$ and $R=0.5$, respectively, are presented and compared with Constant Amplitude (CA) tests. Non-propagating cracks are detected in specimens surviving more than 10×10^7 CA cycles that formed at fractured iron-containing constituent particles. VA tests and damage accumulation calculations show that VHCF lifetimes can hardly be predicted from HCF data, which indicates the technical importance of the presented technique.

9:35 AM Break

10:05 AM Keynote

Damage Mechanisms in the VHCF Regime in Quasi Defect-Free Metals Regarding Different Levels of Microstructural Inhomogeneity: *Martina Zimmermann*¹; *Hans-Juergen Christ*¹; ¹Universitaet Siegen

Numerous experimental studies of metal failure in the very high cycle fatigue (VHCF) range have proven that fatigue life is dominated by the crack initiation phase rather than the crack growth period. Microstructural discontinuities play a major role in the VHCF behavior of quasi-defect free metals, acting as local stress raisers or decreasing the resistance to slip transmission across or along grain boundaries. The crack initiation sites are manifold, reaching from crack initiation at slip bands at the surface, triple junctions of Sigma3 twin boundaries, clusters of similarly oriented grains to second phases or large particles. An overview of the diversity of damage mechanisms will be given for a wide range of non-ferrous metals with focus on an increasing level of microstructural inhomogeneity. Results on the VHCF behavior of pure metals such as copper, aluminum and nickel and their alloys will be presented based on latest methods in metallography.

10:35 AM

Local Cyclic Plastic Deformation and Damage during Ultrasonic Fatigue: *Guocai Chai*¹; ¹Sandvik Materials Technology

During ultrasonic or very high cycle fatigue (VHCF), the applied stresses or strains are sometime well below the bulk yield strength or in the elastic regime of the material. How can a cyclic plastic deformation or damage occur in such a case? Fatigue behaviors of three metals with respectively one phase, dual phase and multiphase have been studied by ultrasonic fatigue testing and then evaluated using SEM, EBSD and TEM. It was found that the strains in the specimens were highly localised where the local maximum strain can be eight times higher than the average strain value in the specimen. This can cause a local plasticity exhaustion that leads to fatigue damage and finally crack initiation. The results in this study show that fatigue damage and crack initiation mechanisms in the VHCF regime can be different in different metals, but mainly due to local plasticity exhaustion.

10:55 AM

Comparison of Fatigue Property of Metallic Materials under Conventional and Ultrasonic Testing Methods: *Benjamin Guennec*¹; *Yuki Nakamura*²; *Tatsuo Sakai*¹; *Akira Ueno*¹; *Isamu Nonaka*³; ¹Ritsumeikan University; ²Toyota National College of Technology; ³Tohoku University

Ultrasonic testing method, due to its very high frequency of stress solicitations, is a very convenient response of the new challenges of which fatigue researches have to cope with. To reach 10^9 or 10^{10} cycles is



TMS 2012

141st Annual Meeting & Exhibition

really faster with this type of machines, compared to conventional servo-hydraulic machines. In addition, for many researchers, it is possible to obtain S-N properties of materials by using ultrasonic devices even for high cycle fatigue domain, which is extended from 10^4 to 10^7 cycles. This paper deals with a comparison of results from conventional and ultrasonic tests, taken from literature, in the high cycle fatigue domain. A direct comparison and a statistical study have been carried out. Both indicate some divergences between these two methods.

11:15 AM

Basic Need of Standardization for Ultrasonic Fatigue Testing: *Claude Bathias*¹; ¹University Paris Pouest

The ultrasonic fatigue testing is a new approach in perfect agreement with the real fatigue life of modern machines, structures, engines, according to the policy of sustainable economy. As the main international standards do not take account the very high cycle fatigue, it is of interest to sum up the research results published in the literature, concerning the gigacycle fatigue carried out at 20kHz, facing the conventional fatigue data, in push pull or rotating bending. The remaining questions are always the same: what about the frequency effect-what about the size effect-influence of the shape of the specimen-temperature rising at 20kHz-influence of the pulse control-fatigue corrosion in ultrasonic fatigue-environmental effect at 20kHz. The topic of this paper is to give a tentative answer in order to prepare a scientific approach for standardization of ultrasonic fatigue.

2012 Functional and Structural Nanomaterials: Fabrication, Properties, Applications and Implications: Structural Nanomaterials

Sponsored by: The Minerals, Metals and Materials Society, TMS Electronic, Magnetic, and Photonic Materials Division, TMS: Nanomaterials Committee

Program Organizers: Jiyoung Kim, University of Texas; David Stollberg, Georgia Tech Research Institute; Seong Jin Koh, University of Texas at Arlington; Nitin Chopra, The University of Alabama; Terry Xu, UNC Charlotte

Wednesday PM
March 14, 2012

Room: Pelican 1
Location: Swan Resort

Session Chair: Yonghao Zhao, Nanjing University of Science and Technology

2:00 PM Invited

Mechanical Properties and Deformation in Multi-scale Nanostructured Cu and Ti: *Yonghao Zhao*¹; Y. Li²; T. Topping²; Y.T. Zhu³; R.Z. Valiev⁴; E.J. Lavernia²; ¹University of California Davis; Nanjing University of Science and Technology; ²University of California Davis; ³North Carolina State University; ⁴Ufa State Aviation Technical University

Multi-scale nanostructured materials containing bi-/multi-modal grain size distributions can be engineered to display unusual balance of properties, such as strength and ductility. Despite well documented reports of enhanced ductility in multi-scale nanostructured materials, systematic identification of the quantitative relationship between mechanical properties and microstructures as well as underlying deformation mechanisms has not been accomplished. In this work, we selected high-purity Cu and commercial pure Ti as a model material system in an effort to elucidate the underlying mechanisms. The bi-/multi-modal Cu and Ti were prepared by equal-channel-angular pressing (ECAP) and subsequent annealing. Transmission electron microscopy (TEM) in combination with tensile testing are used to characterize the deformation mechanisms and mechanical behavior.

2:35 PM

Mechanical Behavior of Bulk Diamantane Stabilized Aluminum Matrix Nanocomposites: *Khinlay Maung*¹; *Colin Arnold*¹; *Ali Yousefiani*²; *Farghalli Mohamed*¹; *James Earthman*¹; ¹University of California, Irvine; ²Boeing Research & Technology

A bulk aluminum matrix nanocomposite has been produced by cryomilling with the addition of 0.5 and 1 wt.% diamantane diamondoid molecules. The milled powders were consolidated to at least 99% density by hot isostatic pressing at 421°C and 521°C and subsequent extrusion at room temperature. The average grain diameter of each diamantane-stabilized nanocomposite sample was found to be consistently smaller (58 to 95 nm) than those achieved in previous studies of the commercially pure counterpart. Furthermore, the mechanical properties were assessed after full consolidation and after additional post-consolidation heat treatment at 575°C. As expected, Hall-Petch associated strengths were measured after cryomilling, and further strengthening was evident after post-consolidation heat treatment steps. Evidence of pore formation and Al-organic precipitation was also revealed following the 521°C HIP and post-consolidation heat treatment. Pore formation and precipitation were not observed in the samples that were consolidated at 421°C.

2:55 PM

Mechanical Characterization of Alumina In-Situ Aluminum Diborides Nano Composites: *Sudeep Ingole*¹; *Zulfikar Khan*²; *Rajeshwari Paluri*¹; *Fevzi Ozaydin*¹; ¹Texas A&M University; ²Bournemouth University

High strength with in-situ lubricious phases can potentially enhance the service life of sliding interfaces. Nano composites are developed with in-situ lubricious phases using alumina and boron. The mechanical characterization of Al₂O₃ matrix nano composites using 2 wt. %B will be reported. The mechanical properties such as Vicker's hardness, fracture strength will be discussed. The effect of milling time and sintering temperature on mechanical properties will be evaluated. It is hypothesized that the reduced grain size will enhance the mechanical properties of composites. This will be a significant contribution towards specific industrial applications. Additionally, formation of borate (Al₁₈B₄O₃₃) will also contribute to the enhancement of mechanical properties as well. The scanning electron micrographs showed the grain refinement as compared to as-received materials (i.e. alumina and boron).

3:15 PM

Phase Transformations during Mechanical Alloying of Ni-Al-Cr Powders Mixture to Produce Nanocrystalline Intermetallic Compounds: *M.H. Enayati*¹; A. R. Shirani²; A. Shokohfar³; ¹Isfahan University of Technology; ²Azad University; ³Khaje Nasir Toosi Technical University

Phase transformation of the Ni₅₀Al₅₀, Ni₂₅Cr₂₅Al₅₀ and Ni₅₀Cr₂₅Al₂₅ system by mechanical alloying (MA) was investigated. The structural changes of powder particles during MA were studied by XRD, SEM and TEM. The results showed that for all three compositions a gradual interdiffusion of elements was occurred during MA leading to the development of different phases. The final product obtained by MA for Ni₅₀Al₅₀ and Ni₂₅Cr₂₅Al₅₀ had nanocrystalline structure while MA of Ni₅₀Cr₂₅Al₂₅ led to the formation of a partially amorphous structure. The details of structural evolution of powder during MA and after subsequent heat treatment are being investigated.

3:35 PM Break

3:50 PM

Synthesis of Gold, Manganese and Nickel Alloy Films Possessing Nano and Various Microstructures: *Bassey Udofo*¹; ¹Aerospace

Alloy films of Au, Ni, Fe-Mn, Fe-MnP, Ni, Fe-Ni nano or microcrystalline structures can be thermally or electrochemically deposited or joint from vacuum or solvent systems that are aqueous onto a conductor, semiconductors, insulators or glass substrate. The films produced by electrochemical means can be produced by thermal means but such process is expensive usually requiring the use of high temperature and high energy conditions. These films have nano, microstructures ranging from single ordered crystalline to polycrystalline disordered structures. The hysteresis loop of Fe-Mn, Fe-Ni alloy films characterized under a vibratory sample magnetometer and cyclic voltammetry shows the films to have soft magnetic properties and codeposited at a single potential. Codeposition of Mn with Fe occurred at a potential nearer that of Mn resulting in less Mn deposition but in the Fe-Ni systems the deposition was nearer the potential of the Fe resulting in less Ni deposition, presenting anomalous condition.

4:10 PM

Formation of Aluminum Di-Borides in Alumina Matrix Through Mechanical Mixing for Tribological Applications: *Sudeep Ingole*¹; *Fevzi Ozaydin*¹; *Rajeshwari Paluri*¹; ¹Texas A&M University

The synthesis and characterization of borides in an Al₂O₃ matrix using 2 wt. %B via mechanical alloying will be reported. These phases can be used as in-situ reinforcement to develop nano composite materials for reduced friction, and wear applications. The evolution of the reaction products with milling time and sintering temperature and the microstructure analysis is carried out using microprobe analysis and X-ray diffraction techniques. Preliminary results showed the reduced grain size as compared to as received powders used in this study. In addition to aluminum diboride (AlB₂), other phases such as aluminum borate (Al₁₈B₄O₃₃) and boron oxide (B₂O₃) were formed as reaction products. The SEM analysis indicated a duplex or bimodal grain size distribution of the microstructure at low milling time however, as the milling time increased more uniform grain size distribution was observed.

4:30 PM

Fabrication and Characterization of Porous Zinc via Selective Dealloying of Al-Zn Alloys: *Elvin Estremera*¹; *Rafael Soler*¹; *Amarilis Decler*¹; *Ulises Barajas-Valdes*¹; *O. Marcelo Suarez*¹; ¹University of Puerto Rico

Porous zinc was fabricated via chemical dealloying of various Al-Zn alloys. These alloys were quenched to promote finer microstructure. The alloy specimens were cut and polished prior to the selective corrosion to favor a uniform dealloying process. Sodium hydroxide solutions were used to selectively remove the aluminum atoms. Concentration and cooling rate were varied to observe their effect on the attained pore size. The microstructure of the resulting porous sponge was characterized using X-ray diffraction (XRD) and scanning electron microscopy (SEM). Nanoindentation measurements were used in the characterization of the materials mechanical properties. Our results revealed that porosity depends highly on the Zn concentration of the alloy, the cooling rate upon alloy fabrication while the mechanical properties were affected by that cooling rate and the corrosion levels.

4:45 PM

Refinement of Ligaments of Nanoporous Ag Ribbons by Controlling the Surface Diffusion of Ag: *Tingting Song*¹; *Yulai Gao*¹; *Zhonghua Zhang*²; *Qijie Zhai*¹; ¹Shanghai University; ²Shandong University

Nanoporous silver (NPS) with different nanoporosity was manufactured by chemical dealloying of rapid solidified Al-Ag ribbons consisting of two distinct phases of a-Al(Ag) and Ag₂Al. The as-dealloyed samples were

characterized by X-ray diffraction (XRD), scanning electron microscopy (SEM), and energy dispersive X-ray (EDX) analysis. It has been found that the width of the average ligaments can be dramatically decreased and be more homogeneous when surfactants were added to the H₂SO₄ solution, which would definitely increase the specific area of NPS and is pretty desirable for certain applications, such as catalyst, absorption, etc. The finer ligaments were attributed to the hindered surface diffusion of Ag atoms by surfactants, and the surface diffusion coefficient (Ds) of Ag was decreased from the order of 10⁻¹⁴ to 10⁻¹⁶ m²/s as a result of surfactants. This simple method to reduce the ligament width of NPS is also anticipated to prepare the other related nanoporous metals.

5:00 PM

Synthesis and Morphology of Nanoporous Cu and Cu Oxide Foams: *I-Chung Cheng*¹; *Andrea Hodge*¹; ¹University of Southern California

Nanoporous copper foams (65-80% porous) were synthesized by dealloying different copper alloys, including Cu₂₀Zn₈₀, Cu₃₅Zn₆₅ and Cu₃₀Al₇₀. Ligament sizes, porosities, and oxide content of the nanoporous copper foams were examined to determine the structure and thermal stability of the foams. The pore and ligament size of nanoporous copper foam can be controlled by either the dealloying process or a subsequent heat treatment. Pore and ligament sizes of 35 to 220 nm were observed. Heat treated samples were analyzed using Raman spectroscopy and XRD. The data showed no copper oxide peaks for the as-prepared samples; however, copper oxide peaks appeared after any heat treatment above 200 °C. These foams were shown to retain their structural integrity even after oxidation. A novel method was thus determined for synthesizing nanoporous Cu oxide foams by heat treating nanoporous copper.

5:15 PM

Pulsed Laser Melting and Solidification of Metallic Nanoparticles: *Ritesh Sachan*¹; *S. Yadavali*¹; *N. Shirato*¹; *A. Gangopadhyay*²; *G. Duscher*¹; *R. Kalyanaraman*¹; ¹University of Tennessee-Knoxville; ²Washington University

Metallic nanoparticles subjected to thermal cycling, such as in medical therapeutic applications, can undergo changes to their nanostructure, which in turn influences their physical properties. Here, we present studies of nanosecond (ns) pulsed laser melting and the ensuing granular structure of Ag and Co metallic nanoparticles which have applications as plasmonic and ferromagnetic systems. Thermal modeling of the ns pulsed laser melting and solidification established that significant but transient temperature gradients exist in the nanoparticles. Transmission electron microscopy studies were performed to investigate the size and arrangement of the grains within these nanoparticles. By utilizing classical nucleation theory, we established that the thermal gradients play a critical role in controlling the nanostructure of the particles. Therefore, modifying the thermal behavior, such as by choice of laser and substrate parameters appears to be a potential route to manipulate the granular nature of nanoparticles.



2012 Symposium on Surfaces and Heterostructures at Nano- or Micro-Scale and Their Characterization, Properties, and Applications: I-Chemical Sensing and Devices II-Biomaterials and Applications

Sponsored by: The Minerals, Metals and Materials Society, TMS Electronic, Magnetic, and Photonic Materials Division, TMS Materials Processing and Manufacturing Division, TMS: Energy Conversion and Storage Committee, TMS: Nanomaterials Committee, TMS: Surface Engineering Committee, TMS: Young Leaders Committee, TMS: EMPMD Council

Program Organizers: Nitin Chopra, The University of Alabama; Ramana Reddy, The University of Alabama; Arvind Agarwal, Florida International University; Sandip Harimkar, Oklahoma State University; Jiyoung Kim, University of Texas at Dallas; Christopher Matranga, National Energy Technology Laboratory

Wednesday PM
March 14, 2012

Room: Pelican 2
Location: Swan Resort

Session Chairs: Nitin Chopra, The University of Alabama; Ramana Reddy, The University of Alabama

2:00 PM Invited

Nanometal-on-Semiconductor Substrates for Single-Molecule Spectroscopy: *Kaan Kalkan*¹; ¹Oklahoma State University

The present work has developed a single-molecule surface-enhanced Raman scattering (SERS) technique, based upon monolayers of Ag nanoparticles chemically reduced on semiconductor thin films. The acquisition starts with spotting of an aqueous aliquot on the SERS substrate. Subsequently, SERS from the water-Ag interface is collected that captures temporal appearance of discernable Raman peaks over a weak background. On the average, these spectral jumps sustain about a second which are associated with single molecules diffusing in and out of SERS hotspots. Typically, ~50 spectra can be recorded during a 1-s-long jump that serve like the "molecule's logbook", which records the structural steps taken by the molecule in the "1-s-long visit". Over the past five years, the technique enabled capturing the light-driven conformational changes in various photoactive molecules at the single molecule level, such as photoactive yellow protein, green fluorescent protein, and azobenzene.

2:30 PM Invited

Plasmonics Based Harsh Environment Compatible Chemical Sensors: *Michael Carpenter*¹; ¹University at Albany-SUNY

The surface plasmon resonance band of gold nanoparticles embedded in metal oxide heterostructure films is used as an optical beacon for the detection of emission gases, CO, NO₂ and H₂, at temperatures ranging between 500 and 800°C. A summary of previous experiments detailing the sensing characteristics will be provided. A challenge for the detection of emission gases is not only high levels of sensitivity but the selective detection of the gas of interest. Recent work will be detailed which shows the implementation of sensing arrays for the detection of emission gases. Multiple sensing elements within the array are probed simultaneously and principal components analysis (PCA) is used to characterize the selective detection characteristics of the array. Variations in gold particle size and shape as well as the chemistry of the metal oxide matrix are being varied to produce sensing arrays with enhanced selective sensing properties.

3:00 PM

2012 Shri Ram Arora Award: Novel Sensor Structure of SnO₂ Thin Film Integrated with Catalytic Micro-Discs for the Detection of Trace Level NO₂ Gas: *Anjali Sharma*¹; *Monika Tomar*¹; *Vinay Gupta*¹; ¹University of Delhi

Rf sputtered SnO₂ nano-thin film based sensor structures integrated with various metal oxide catalysts (WO₃, TeO₂, NiO and Al₂O₃) have been exploited for trace level detection of NO₂ gas at lower operating temperature. Metal oxide catalysts were dispersed in the form of nano-thin micro-discs (8 nm thickness and 600 micrometer diameter) over SnO₂ and gas sensing characteristics have been studied towards NO₂ gas as a function of temperature. SnO₂ sensor structure with WO₃ micro-discs showed a drastic increase in sensor response (~5.4x10⁴) as compared to other catalysts at a relatively low operating temperature (100 °C) with a fast response time of ~62 sec and recovery time of ~15 min towards 10 ppm of NO₂ gas. Such an improvement in the sensing response, response time and recovery time could be attributed to the spill-over of sensing gas molecules over the uncovered surface of SnO₂ thin films by WO₃ micro-discs catalyst.

3:35 PM Invited

Sub-Nanometer Scale Nanostructures: Ultrathin Nanowires and Nanoclusters: *Yuping Bao*¹; *Yaolin Xu*¹; *Soubantika Palchoudhury*¹; ¹The University of Alabama

The extremely small sizes of ultrathin nanowires (d, ~ 2 nm) and nanoclusters (tens of atoms) place them at the transition from super molecules to typical nanocrystals, resulting in new chemical and physical phenomena. These novel properties are highly promising for applications in emerging technologies such as gas sensing, photocatalysis, spintronics devices, batteries, and bioimaging. In this presentation, we will discuss the importance of the surface to the synthesis of ultrathin nanowires, their structural characterization, and potential applications. Au/Ag nanoclusters (< 2 nm) consist of several to tens of atoms and exhibit size-dependent fluorescent emissions, similar to the semiconductor quantum dots, which are of great fundamental and technical importance. Here, using small capping molecules, we will discuss the synthesis and coupled behaviors of these nanoclusters. Finally, the integration of magnetic and fluorescent nanostructures has led interesting properties.

4:05 PM

Magnetic Particles Accumulated in Acidithiobacillus Ferrooxidans Cells under Static Magnetic Field Affection: *Hongxu Li*¹; *Chao Li*¹; *Zhi Qian Zhang*¹; *Lin Wang*¹; ¹University of Science and Technology

It has studied the rule of Acidithiobacillus ferrooxidans cell growth and magnetic particles accumulated under static magnetic. The processed results under 15, 20, 25, 30, 35, 40, 45, 50mT show that more intensify static magnetic field (>10mT) might restrain the cell density increasing, especially when magnetic field high than 25mT, it could led to severe leakage of nucleic acid from cell. SEM, TEM, VSM were used for characteristic analyzing of cell and nano particle. It observed that one part of nano-particles in the cell was compact spheroidal configuration, the size is about 50nm, the other parts were loose anomalous shape, and the smallest particle size was below 10nm with fixed and distributed around the cytoderm.

4:20 PM

Nanotechnology For Drug Formulation: Improving Solubility of Insoluble Drugs: *Ariel Murphy*¹; *Dennis Leung*²; ¹University of Alabama; ²Merck Sharp & Dohme Corporation Inc.

Many of the marketed drugs we use today are practically insoluble. Nanomaterials science is being studied to improve the solubility of these drugs. Nanosize particles are ideal because they cover more surface area which improves exposure and bioavailability and they have faster dissolution rates in the body. Nanoparticle stability is a major issue because Van der Waals forces cause the particles to aggregate and clump together and Ostwald Ripening causes the particles to increase in size

over time. Because of the stability issues polymer/surfactant stabilizers are being studied to help prevent aggregation and recrystallization. In this experiment, drug nanosuspension formulations were created using three model compounds and five different stabilizers. Each drug/stabilizer combination was tested for particle size, zeta potential, solubility, and chemical stability. The purpose of this experiment is to understand why certain drug/stabilizer combinations are more efficient than others by analyzing what properties make each combination unique.

4:35 PM

Tunable and Functional Silica Cross-Linked Micellar Core-Shell Nanoparticles: *Fangli Chi*¹; Bin Yang¹; Qisheng Huo²; Jiu-hua Chen¹; ¹Florida International University; ²Jilin University

Size-tunable silica cross-linked micellar core-shell nanoparticles (SCMCSNs) were successfully synthesized from a Pluronic nonionic surfactant (F127) template system with organic swelling agents such as 1,3,5-trimethylbenzene (TMB) and octanoic acid at room temperature. The size and morphology of SCMCSNs were directly evidenced by TEM imaging and DLS measurements (up to ~90 nm). Pyrene and coumarin 153 (C153) were used as fluorescent probe molecules to investigate the effect and location of swelling agent molecules. Papaverine as a model drug was used to measure the loading capacity and release property of nanoparticles. The swelling agents can enlarge the nanoparticle size and improve the drug loading capacity of nanoparticles. Moreover, the carboxylic acid group of fatty acid can adjust the release behavior of the nanoparticles.

4:50 PM

Vertically Aligned and Axially Heterostructured Metal Nanowires and Their Soft Composites: *Junchi Wu*¹; Nitin Chopra¹; ¹The University of Alabama

Here we report an efficient approach to fabricate vertically aligned and axially heterostructured metal nanowires by coupling template method and wet-chemical deposition process. In order to prepare a smart and multi-functional material utilizing these nanowires, they were incorporated into a smart polymer that could be stimulated by chemical and magnetic triggers. The hybrid materials showed strong potential for drug delivery devices. Also, the hybrid materials were processed further to result in a carbon shell/membrane on the metal surface. X-ray diffraction (XRD), scanning electron microscopy (SEM), transmission electron microscopy (TEM), and Raman spectroscopy were used to completely characterize these axially heterostructured architectures.

5:05 PM

Superhydrophobic Properties of Polymethylmethacrylate (PMMA) Nano Modified: *Ariosvaldo Sobrinho*¹; Marcos Baracho²; Edjânio Araújo³; Luiz Pontes³; Analigia Araújo¹; Geilza Porto¹; Daniel Campos⁴; ¹UAEMA / UFCG; ²UAEC / UFCG; ³DTM / UFPPB; ⁴UAEQ / UFCG

Recent works has shown that natural phenomena seen in some animals and plants through the well-known phenomenon called the "Lotus Effect" have served increasingly as a source of inspiration for the rise of new materials for coating various substrates (metals, polymers, ceramics and biomaterials). A relatively simple method of obtaining superhydrophobic surface was presented in this paper and can be used on metal surfaces, polymeric, ceramic and biomaterials interface. The aim of this work was to obtain polymethylmethacrylate(PMMA)nano modified with superhydrophobic properties in presence of SiO₂, organophilic clays and trimethylsiloxysilicate.

5:20 PM

The Bioadsorption Behavior of Rhodococcus Opacus on the Surface of Calcium and Magnesium Minerals: *Hongxu Li*¹; An Li¹; Binbin Liu¹; ¹University of Science and Technology

The paper focused on the Rhodococcus opacus adsorption behavior on surface of calcite, serpentine and dolomite by bio adhesive test, contact angle measurements, Zeta potential, FTIR spectra and TEM

images. The results show that the cell of Rhodococcus opacus adsorption was dependent on the pH value and temperature. The minerals contact angle decreased after Rhodococcus opacus attached on the surface. Zeta potential measurements elucidated that the cell with charge was opposite to the minerals on the broad pH value scope. The TEM images revealed that R. opacus combined tightly with mineral, and a large number of small mineral particles gathered around the cell and FTIR spectra showed the active group of the cell wall gave a net charge on the surface.

5:35 PM

The Formation of an Eutectic Mixture for Predicting the Ideal Solubility of Thermally Stable and Unstable Compounds: *Rodolfo Pinal*¹; Ryan McCain¹; ¹Purdue University

The melting properties of organic compounds are critical to the solubility behavior of APIs (active pharmaceutical ingredients). Solubility of poorly water soluble APIs is one of the largest challenges in formulation development. Estimating solubility by means of the melting temperature and heat of fusion is a widely established practice. However, a common problem in drug development is that some APIs are thermolabile and undergo chemical decomposition before melting. This situation makes the essential melting parameters experimentally inaccessible. Eutectic microcrystalline mixtures offer the potential advantage of increased dissolution rates at lower temperatures without changing the selected crystalline form of the API. Eutectic mixtures also offer a means to overcome the hurdles imposed by thermal limitation. The purpose of this work was to develop and test a thermodynamic model for estimating the enthalpy of fusion of thermolabile compounds, based on the entropy of fusion, thus enabling further prediction of their ideal solubility.

5:50 PM Invited

Microstructure and Mechanical Properties of Multistructured Peacock Feathers: *Neelima Mahato*¹; Debrupa Lahiri²; Arvind Agarwal²; *Kantesh Balani*¹; ¹Indian Institute of Technology Kanpur; ²Florida International University

Brilliant iridescence of a peacock's feather has been explored using electron and fluorescence microscopy. The morphology and anatomy of an Indian peacock reveals high level of complexity in the structural patterns of barbules. The complicated diffraction and interference patterns of colors and different levels of iridescence are attributed to the difference in the complex arrangement of structures on the barbules of differently colored regions of the peacock's feather. Such a response has been compared with that of white peacock's feather to isolate the coloration behavior. Further, the nanomechanical properties (elastic modulus and hardness) have also been correlated corresponding to the equivalent regions of a coloured and white peacock feather. Such a correlation of mechanical properties with coloration of peacock feather can allow engineering of artificial structures to show iridescence.

6:20 PM

Production of Various Silicates from Rice Hull Ash: *Ozgul Taspinar*¹; Evre Sadic¹; Onur Ozcan¹; ¹Istanbul Technical Univ.

This study covers the laboratory scale production method of magnesium, calcium, barium, zinc and aluminum silicates from rice hull ash (RHA). Sodium silicate solution was obtained firstly by extraction of SiO₂ content of RHA with boiling 1 N NaOH solution. This solution was then treated with magnesium, calcium, barium, zinc and aluminum salts individually to precipitate the silicates of these reagents. Silicate products were then analyzed using TGA, X-ray and BET analysis techniques. Chemical compositions of the silicate products for calcium, magnesium and zinc were as 45-49% SiO₂ and 13-14 % MO by weight. The compositions of barium and aluminum silicates however were different as 44.7% SiO₂, 23.3% BaO for barium silicate and 30.3% SiO₂, 7.0% Al for aluminum silicate. All the silicates have an amorphous structure. Surface areas of Mg, Al, Ca, Ba and Zn silicates were also obtained as 625, 309, 141, 84 and 60 m²/g, respectively.



3rd International Symposium on High Temperature Metallurgical Processing: Energy and Environment

Sponsored by: The Minerals, Metals and Materials Society, TMS Extraction and Processing Division, TMS: Energy Committee, TMS: Pyrometallurgy Committee

Program Organizers: Tao Jiang, Central South University; Jiann-Yang Hwang, Michigan Technological University; Patrick Masset, TU Freiberg; Onuralp Yucel, Istanbul Technical University; Rafael Padilla, University of Concepcion; Guifeng Zhou, Wuhan Iron and Steel

Wednesday PM
March 14, 2012

Room: Southern II
Location: Dolphin Resort

Session Chairs: Mansoor Barati, University of Toronto; Hongmin Zhu, University of Science & Technology Beijing

2:00 PM

Current Status of Heat Recovery from Granulated Slag: *Shaghayegh Esfahani*¹; Mansoor Barati¹; ¹University of Toronto

The produced slag both in the ferrous and non-ferrous industry is a high potential heat source which if treated properly can contribute to recovery of a significant amount of energy and more importantly avoid the harm to the environment. The idea behind all the approaches is to granulate slag and use it as a material which is energy intensive to produce such as cement. In this article, the development, application and advantages of various granulation techniques currently in use and the subsequent energy recovery processes are described. The discussed heat recovery processes include thermal energy recovery and chemical heat recovery. Based on the discussed processes, possible solutions will be introduced and evaluated.

2:15 PM

Contribution to the Energy Optimization in the Pyrometallurgical Treatment of Greek Nickeliferous Laterites: Konstantinos Karalis¹; Charalabos Zografidis²; *Anthimos Xenidis*¹; Stelios Tabouris²; Eamonn Devlin³; ¹National Technical University of Athens; ²General Mining and Metallurgical Company S.A. LARCO; ³NCSR Demokritos

The main parameters that affect the energy consumption in smelting reduction of the Greek nickeliferous laterites in submerged arc electric furnaces (E/F) were investigated. Within this framework, operational data of the E/Fs, such as energy consumption indicators, electrode consumption indicators and chemical characteristics of Fe-Ni and slag, were correlated with the physicochemical characteristics of the calcine produced by the roasting reduction of laterite in rotary kilns (R/Ks), such as reduction degree, temperature, chemical composition and granulometry. The obtained results provide serious input for further research on the modelling of the roasting reduction – smelting reduction process, which is a critical tool for energy optimization.

2:30 PM

Strengthening Sintering of Refractory Iron Ore with Biomass Fuel: *Xiaohui Fan*¹; Zhiyun Ji¹; Min Gan¹; Xuling Chen¹; Wenqi Li¹; ¹Central South University

Abstract: Specularite and vanadium-titanomagnetite are difficult to granulate, and with the increase of their proportions, the permeability of sintering bed is deteriorated, so is the combustion velocity of fuel for the shortage of air through the sintering bed, which can lower sintering speed and specific production capacity significantly. The biomass charcoal utilized in this research has a higher combustion velocity than coke breeze, therefore, the productivity of specularite and vanadium-titanomagnetite ore can be improved remarkably by replacing coke breeze partly with biomass charcoal. The results showed that the sintering speed and specific production capacity of 35% specularite were improved from 19.06mm/min, 1.33 t/(m²·h) to 21.45mm/min, 1.47 t/(m²·h) when the proportion of biomass fuel replacing coke is 40%, and that of 55%

vanadium-titanomagnetite were improved from 17.23mm/min, 1.11 t/(m²·h) to 22.80mm/min, 1.44 t/(m²·h). As a conclusion, biomass fuel is effective to strengthen sintering of refractory iron ore.

2:45 PM

Combustion Behavior of Pulverized Coal Injection in Corex Melter Gasifier: *Zhang Shengfu*¹; Zhu Feng¹; Bai Chenguang¹; Wen Liangying¹; Qiu Guibao¹; Hu Meilong¹; Qin Yuelin¹; ¹College of Materials Science & Engineering, Chongqing University

The COREX process is the first reduction ironmaking technology with coal and pure oxygen to get high quality hot metal, which consumes a lot of high quality lump coal and some coke. In order to increase the utilization of fine coal, reduce coke consumption and enhance the competitiveness of the technology, the combustion behavior of pulverized coal injection (PCI) in melter gasifier is studied experimentally. The results show that the combustion rate of PCI is increased with the increase of temperature. And the combustion rate is increased with the decrease of coal granularity. Compared bituminous coal with anthracite, the former's burning ratio is higher than the latter in the same granularity. The combustion effect is remarkable when the smaller sized mixed coal with bituminous coal and anthracite is pulverized in COREX process.

3:00 PM

Improved Short Coil Correction Factor for Induction Heating of Billets: *Mark Kennedy*¹; Shahid Akhtar²; Jon Arne Bakken²; Raghild Aune²; ¹Norwegian University of Science and Technology; ²Norwegian University of Science and Technology

To determine the heating rate of billets using 'short coils', an appropriate correction factor must be applied to the theoretical relationship. In 1945, Vaughan and Williamson published a semi-empirically modified Nagaoka coefficient applicable for moderate frequency induction heating processes (10 kHz). Recently it was demonstrated that the method of Vaughan and Williamson gives <10% error in the estimated power when heating aluminum billets at 50 Hz. In the present study, experiments have been conducted on aluminum billets in order to verify an empirical frequency corrected 'short coil' equation. Measurements of electrical conductivity ($\pm 0.5\%$), current ($\pm 1\%$), heat ($\pm 1-3\%$), and magnetic flux density ($\pm 1-2\%$) have been performed. The results are compared with 1D analytical calculations, and 2D axial symmetric FEM modeling using COMSOL 4.2®. The frequency corrected equation has proven to provide accurate predictions of power (<math><4\%</math> error) within the frequency range 50 Hz to 500 kHz.

3:15 PM

Liberation of Metallic-Bearing Minerals from Host Rock Using Microwave Energy: *Matthew Andriese*¹; Jiann-Yang Hwang¹; Zhiwei Peng¹; ¹Michigan Technological University

It has been demonstrated that metallic-bearing minerals are physically liberated from host rock when exposed to microwave (MW) energy. The metallic minerals are iron sulfides and spinel oxide minerals contained in peridotite rock. Experimental evidence has shown ore particles readily couple with MW energy at 2.45 GHz, 1000 W resulting in rapid heating. Thermal stresses are generated by highly absorbing metallic-bearing minerals resulting in cracking and embrittlement of ore particles that assists in crushing and grinding processes. The liberated metallic-bearing minerals are shown to report to coarser size fractions as a result of MW exposure.

3:30 PM Break

3:40 PM

Effects of Binders Additives on Compressive Strength of Hematite Pellets in Firing Process: *Yanfang Huang*¹; Guihong Han¹; Tao Jiang¹; Guanghui Li¹; Yuanbo Zhang¹; Dan Wang¹; ¹Central South University

Hematite concentrates are characterized by bad high-temperature reactivity and poor balling index, which restrict their large-scale application in the production of oxidized pellets. An organic additive, namely MHA, was authorized and used as binder recently in China.

Compared with bentonite, the effects of MHA on compressive strength of hematite pellets at various firing conditions were investigated in this study. Experimental results showed the compressive strengths of preheated pellets with different binders were increased with increasing the preheating temperature and time. The compressive strength of preheated pellets with MHA binder was lower than that of pellets with bentonite, which can be ascribed to the high porosity of pellets with MHA binder. However, the compressive strength of roasted pellets with MHA binder was higher than that of pellets with bentonite. The compressive strength of finished pellets balled with MHA binder 1.0 wt% could meet the operation requirements of grate-kiln process.

3:55 PM

Mechanisms of NO Formation during SiO Combustion: *Nils Eivind Kamfjord*¹; Halvard Tveit¹; Edin Myrhaug²; Mari Næss¹; ¹NTNU; ²ELKEM

As a part of the FUME research programme being done by the Norwegian Ferroalloy Research Association (FFF), the SINTEF Group and NTNU several measurements towards quantifying the gaseous and solid emissions from the draining of the silicon furnaces for metal have been carried out. Based on the measured size distribution of the formed fume particles and known particle growth theory an estimate of the growth time for the given particles has been calculated. The formation time for the measured NO amount has also been calculated based on the fume measurements and a thermodynamic model of the furnace gases combusting with air. The two "formation" times is in the same order of magnitude and they are therefore used as parameters in a CFD model, modelling that the formed fume particles heating up the surrounding air and thereby form NO according to the Zeldovich mechanism.

4:10 PM

New Technologies of Energy Saving and Low CO2 Emission for Iron Making: *Xiuwei An*¹; Jingsong Wang¹; Qingguo Xue¹; ¹University of Science and Technology Beijing

Energy saving has drawn more and more attention of the world due to the pressure of the environment and society. Metallurgy is one of the biggest energy consumption industries, accounting for about 16% of the total industry, basically the same ratio as the emission of CO2 and other pollutants. About 70% of total energy for steel production is consumed in iron-making process with the same ratio of CO2 discharged, so it has a great significance to achieve energy saving and low CO2 emission in iron-making process. The new iron-making technologies with energy saving and low CO2 emission such as oxygen blast furnace, ITmk3, application of waste plastics and biomass in iron-making, were introduced in the present work. Particularly, the latest research progress, merit and demerit were compared, and the contribution of the different technologies to low CO2 emission and the energy saving were analyzed.

4:25 PM

Pilot Scale Measurements of NOx Emissions from the Silicon Process: *Nils Eivind Kamfjord*¹; Ingeborg Solheim²; Halvard Tveit¹; ¹NTNU; ²SINTEF

The NOx emissions has an increased focus as an environmental problem. The production of high silicon alloys is carried out in open reduction furnaces that give NOx in the off-gas. Earlier and new industrial measurements towards FeSi- and Si-metal furnaces reveal substantial NOx-emission. The NOx is believed to be produced in the combustion zone above the furnace surface, mainly as thermal NOx. In order to expand the knowledge on NOx-formation in silicon metal production, a pilot scale experiment in a 440 kVA silicon furnace has been carried out. The experimental set-up was especially designed to investigate the formation mechanisms for NOx by controlling the flow of false air into the off-gas system. The resulting NOx-values showed significantly variation between the different air inlet geometries.

4:40 PM

The Effect of Thermal State of Raw Pellets on the Strength of Reduced Pellets: *Zhu-Cheng Huang*¹; Daoguang Yang¹; Ling-Yun Yi¹; ¹Central South University

In the traditional gas-based direct reduction process, the burden of reduction furnace are roasted pellets which had experience cooling process. In this work, hotroasted pellets without cooling process used as the burden of the reduction furnace has been studied. The strength of reduced pellets could be increased by using hotroasted pellets in place of coldroasted pellets as the burden. Nucleation and growth mechanism of iron crystal grain in gas-based direct reduction process of hotroasted pellets were investigated by optical microscope. The iron crystal nucleus is formed firstly on the interface of grains and the edge of wustite, then gradually grow from surface layer to inner core as reduction carries on. Using the hotroasted pellets in gas-based reduction can promote the accumulation, transportation and growth rate of iron crystal grain eventually.

Aluminum Alloys: Fabrication, Characterization and Applications: Emerging Technologies

Sponsored by: The Minerals, Metals and Materials Society, TMS Light Metals Division, TMS: Aluminum Processing Committee
Program Organizers: Subodh Das, Phinix LLC; Tongguang Zhai, University of Kentucky; Zhengdong Long, Kaiser Aluminum

Wednesday PM
March 14, 2012

Room: Northern E1
Location: Dolphin Resort

Session Chair: Subodh Das, Phinix

2:00 PM

Effect of Tool Rotational Speed on the Microstructures and Tensile Properties of 7075 Aluminum Alloy Via Friction Stir Process (FSP): *Ming-Hsiang Ku*¹; Fei-Yi Hung¹; Truan-Sheng Lui¹; Li-Hui Chen¹; ¹National Cheng Kung University

7075-T6 aluminum alloy plates were subject to FSP with various tool rotational speeds (1230, 1450 and 1670 rpm) followed by different heat treatments (natural aging and T4T6 treatments). The influences of tool rotational speeds and aging treatments on the microstructures and tensile properties were discussed. The experimental results showed that the tensile strength of FSPed specimens with various tool rotational speeds were close. After aging treatments, higher tool rotational speeds (1670 rpm) had an embrittlement phenomenon on the SZ due to the contribution of low element bands (LEBs) and precipitates. EPMA analysis showed that the LEBs are low element distributions, such as Zn, Mg, Cu. Decreasing the tool rotational speeds, the LEBs were not obvious and restrained the brittle behavior to improve the ductility. Compared with natural aging, after T4T6 treatments, the tensile strength of FSP specimens with all tool rotational speeds was improved obviously.

2:20 PM

Improving Microstructure of AISI H13 Extruding Dies Using Ion Nitriding: *Francisco Montalvo*¹; *Eulogio Velasco*²; *Adrian Canales*¹; ¹CUPRUM; ²Texas State University

A varied range of aluminum profile shapes are produced by hot extrusion and the typically used die is steel AISI H13. The quality and dimensions of the extruded piece are determined by tribological and surface conditions of the die bearing surface. Dies for hot extrusion require good metallurgical characteristics and chemical stability against hot aluminum. Experiments were conducted to evaluate the performance of specimens treated with conventional nitriding, and the ion nitriding process. Microstructural characterization, X-ray diffraction profiles, and wearing tests were carried out on the surface of H13 specimens. The ion nitriding process showed advantages over the conventional nitriding process, including productivity and tooling life.



TMS 2012

141st Annual Meeting & Exhibition

2:40 PM

Linear Friction Welding of a 2024 Al Alloy: Microstructural, Tensile and Fatigue Properties: Alessandro Morri¹; Lorella Ceschini¹; Fabio Rotundo¹; ¹University of Bologna

The aim of this work was to evaluate the possibility of using linear friction welding (LFW) to produce high quality joints on a aerospace grade aluminium alloy (AA2024). In this solid state joining process the bonding of two flat edged components is achieved through frictional heating induced by their relative reciprocating motion, under an axial compressive force. The Al joints were subjected to microstructural and mechanical characterization, including hardness and tensile test at different welding conditions. S-N probability curves were also computed after axial fatigue tests. No post-weld heat treatment was performed. The microstructural analyses showed substantially defect-free joints, with a relevant plastic flow in the thermo-mechanically altered zone. Maximum hardness decrease in the joint zone was approximately 10% in respect to the base material. The joint efficiency was about 90%, although with a slight reduction in the elongation to failure. Good fatigue performances were detected.

3:00 PM

The Effect of Friction Stir Welding on the Microstructure and Tensile Properties of Al 2139-T8 Alloys: Tomoko Sano¹; Jian Yu¹; Chian-Fong Yen¹; Kevin Doherty¹; ¹US Army Research Laboratory

In this research, two plates of Al 2139-T8 alloys were welded together by friction stir welding (FSW). An evaluation of the crystallographic texture, grain size, and morphology of the grains in the FSW region, in comparison to those of the grains outside of the weld region, was made by scanning electron microscopy (SEM) and electron backscattered diffraction. In addition, the quasi-static tensile behavior of samples from the FSW region and those from outside of the FSW zone was characterized by in-situ tensile experiments in the SEM with digital image correlation. It was found that the ultimate tensile strength and elongation were greater in the samples from the FSW region except in the through thickness, parallel to the FSW direction. The full results of the effect of the FSW on the Al2139 microstructure and tensile behavior will be discussed.

3:20 PM Break

3:35 PM

Friction Stir Welding of Al-Zn-Mg Alloy AA7039: Chaitanya Sharma¹; Dheerendra Dwivedi¹; Pradeep Kumar¹; ¹Indian Institute of Technology Roorkee

In this present investigation Al-Zn-Mg alloy AA7039 was friction stir welded (FSW) successfully employing a rotary speed of 635 rpm and welding speed of 75 mm/min, in order to elucidate the effect of FSW on mechanical and corrosion properties. Three points face and root bend tests were conducted to reveal welding defects. The yield and ultimate tensile strength of the joint was found lower (33.75 and 14.41 %) than the base material while ductility was higher (41.45 %) than the base material. The joint efficiency of friction stir welded joint was 85.59 %. The microstructure and other unique features associated with different weld zones of FSW were studied by optical and scanning electron microscopy. Failure initiates from the breaking of secondary strengthening precipitates MgZn₂. Immersion corrosion tests on friction stir welded joints are to be performed to investigate the effect of corrosive environment on the performance of welded joints.

3:55 PM

Fabrication and Particle Pushing of TiB₂ Particle Reinforced Aluminum Composites: Meng Wang¹; Qingyou Han¹; ¹Purdue University

In this article TiB₂/Al composites with different particle sizes ranging from 0.5-20µm were fabricated by casting method with the aid of ultrasonic casting. The observation by optical and scanning electron microscopy (SEM) showed good interface bonding between matrix and particle. By controlling different casting temperatures, cooling rates and

particle sizes, the particle distribution situation was observed and analysis with qualitative and quantitative methods and the results were compared with the ones got from the composites fabricated without ultrasonic vibration. It showed that with the aid of ultrasonic, particles were more prone to be distributed inside grains, while most of them stayed at grain boundary because of the effect of particle pushing during the solidification process. Higher casting temperature and cooling rates facilitated particle pushing, and smaller particles might be engulfed. The experimental results were compared with theoretical explanation, and the reason of discrepancy between them was analyzed.

4:15 PM

Post Weld Heat Treatment of Friction Stir Welded AA2017: Mohamed Ahmed¹; Bradley Wynne²; ¹Suez Canal University; ²The University of Sheffield

In this study a friction stir welded AA2017 is post weld heat treated at 500°C for 20, 40 and 60 min holding time and then quenched in water and naturally aged. The effect of post weld heat treatment on the microstructure and hardness is investigated across the transverse cross section of the weld. Experimental results show that the PWHT causes abnormal grain growth of the grain structure mainly near to the advancing side of the weld. The grain size increases with the increase of the holding time however the region near to the retreating side of the weld retained its fine grain structure. EBSD has been used to examine the microstructure and texture before and after PWHT. EBSD investigation showed that the grain growth is texture dependent as grain growth occurs in some grains of (B+C) texture components while in the adjacent grains of texture components B- does not occur.

Aluminum Reduction Technology: Cell Fundamentals, Phenomena and Alternatives II

Sponsored by: The Minerals, Metals and Materials Society, TMS Light Metals Division, TMS: Aluminum Committee, TMS: Aluminum Processing Committee
Program Organizer: Olivier Martin, Rio Tinto Alcan

Wednesday PM
March 14, 2012

Room: Northern E4
Location: Dolphin Resort

Session Chair: Patrice Chartrand, Ecole Polytechnique Montreal

2:00 PM

Cryoscopic Data for Hall-Héroult Bath Containing Magnesium Fluoride, Calcium Fluoride, Potassium Cryolite, and Sodium Chloride: Ashjorn Solheim¹; Lisbet Stoen¹; Jannicke Kvellø¹; ¹SINTEF

The well-known cryoscopy equation for a binary system was extended to the ternary system NaF-AlF₃-B, where B is a substance present in small amounts. It was derived that the depression in the liquidus temperature for a given molar fraction of B depends on how B influences the activity of NaF, as well as on the NaF/AlF₃ molar ratio. This implies that it is difficult to estimate the effect on the liquidus temperature of contaminants in the Hall-Héroult bath, and the three-component cryoscopy equation can be regarded as a theoretical justification of the cross-terms used in most empirical equations for calculating the liquidus temperature. New cryoscopic data are given for the system Na₃AlF₆-CaF₂ as well as for some substances that are normally present in only small amounts, and empirical equations containing cross-terms between these substances and aluminium fluoride are suggested.

2:20 PM

Potentiometric Fluoride Analysis with Improved Analytical Performance: Thor Anders Aarhaug¹; Kalman Nagy¹; ¹SINTEF

Since the 1960s SINTEF has in collaboration with the Nordic aluminium smelters developed methods for sampling and analysis of fluoride. Unlike conventional potentiometric analysis, this methodology involves

detection of fluoride in acidic media. At low pH, the electrode kinetics is improved, resulting in faster analysis. Reduced leak of fluoride from the ion-selective electrode improves the sensitivity of the method. Standard addition methodology is applied for improved analytical performance. The acidic media makes it possible to perform a direct analysis of fluoride in biological samples. In this way, fluoride is extracted from the biological matrix by the acid. The high sensitivity requires low sample masses to be used and thus does not interfere with the fluoride detection at the ion-selective electrode. This is far more efficient than the conventional approach of ashing the sample at elevated temperatures. Acid extraction can also be applied to filter dust samples.

2:40 PM

Investigation of the Mechanism of Mass Transport between the Anode-Bath Interface and the Active Bubble Generating Sites in the Hall-Héroult Cells: Sandor Poncsak¹; Laszlo Kiss¹; ¹Univeristy of Quebec at Chicoutimi

During the last decades, lots of efforts were spent to investigate different aspects of the Hall-Héroult cells. However, many questions remain unanswered due to the complexity of the process and the hostile environment. For example, the mechanism of the transport of the carbon-oxide gas between the active electrolysis sites and the bubble evolving anode pores is still non-clarified. Generally, during electrolysis in aqueous systems, the generated gas is dissolved and transported through the electrolyte. However, the solubility of CO₂ in the molten cryolite is poor and the anodes are highly porous. In this paper, different mechanisms of the carbon-oxide transport between the CO₂ generating anode - bath interface and the bubble releasing sites are examined. The majority of the anode gas seems to be transported through a thin superficial layer of the porous anodes, while transport via the molten bath and gas adsorption by the anodes plays a secondary role.

3:00 PM

Depolarized Gas Anodes for Electrowinning of Aluminium from Cryolite-Alumina Melts in a Laboratory Cell: Geir Martin Haarberg¹; Saijun Xiao¹; Arne Petter Ratvik¹; Tommy Mokkalbost²; ¹Norwegian University of Science and Technology; ²SINTEF

Consumable carbon anodes are used in the electrowinning of aluminium by the Hall-Heroult process and in other proposed processes for electrowinning in molten salts. Emissions of CO₂ may be eliminated by introducing an inert oxygen evolving anode, which however will require a higher anode potential. By introducing natural gas or hydrogen to the anode the CO₂ emissions can be reduced and the anode potential can be lowered. Laboratory experiments were carried out in a modified Hall-Heroult electrolyte with excess AlF₃ at 850 °C. Porous anodes of platinum, tin oxide and graphite were tested during electrolysis at constant current, with the supply of argon, methane and hydrogen through the anodes. Laboratory studies showed that by introducing both hydrogen and methane separately through a SnO₂ anode in molten Na₃AlF₆-AlF₃-Al₂O₃ (4.5 wt%) at 850 °C the anode potential was lowered by several hundred millivolts for a limited time during electrolysis.

3:20 PM Break

3:40 PM

Reduction of the Operating Temperature of Aluminium Electrolysis: Low-Temperature Electrolyte: Alexey Apisarov¹; Juan Barreiro²; Alexander Dedyukhin¹; Leopoldo Galán²; Alexander Redkin¹; Olga Tkacheva¹; Yuri Zaikov¹; ¹Institute of High Temperature Electrochemistry; ²Aleatur

Aluminium Potassium Fluoride obtained as a byproduct in the production of Aluminium grain refiners and master alloys may be used as an additive to the existing aluminum reduction process. The component leads to a considerable reduction in the melting temperature, and maintains other important parameters such as conductivity and solubility of alumina. Both, laboratory tests and semi industrial trials in a 100A cell have

been conducted in order to test the suitability of this new additive to the electrolytic process, with positive results. Aluminium Potassium Fluoride can be also used as a basic component of the low-temperature electrolyte for aluminum electrolysis.

4:00 PM

Specific Molecular Features of Potassium-Containing Cryolite Melts: Evgeny Antipov¹; Dmitri Glukhov²; Alexander Gusev³; Veronika Laurinavichute¹; Renat Nazmutdinov²; Dmitri Simakov³; Sergey Vassiliev¹; Tamara Zinkicheva²; Galina Tsirlina¹; ¹Moscow University; ²Kazan State Technological University; ³RUSAL ETC

Experimental in situ Raman spectra are presented for potassium, sodium and mixed fluoroaluminate melts. More acidic melts with cryolite ratio (CR) below 2 are accentuated. The cation-dependent ratio of integral band intensities is assigned to specific interactions of potassium cations with low coordinated fluoroaluminates. For alumina containing melts, the effect of potassium on the stoichiometry of predominating oxofluoroaluminate anion is observed indirectly. Density functional theory and classical molecular dynamics are employed to investigate behavior of different fluoroaluminates (including dimers) and their associates formed by alkali metal cations. The results are discussed in the context of CR-dependent thermodynamic data.

4:20 PM

Aluminium Fluoride Purity Test by Different Techniques: Hussain Al Halwachi¹; ¹Aluminium Bahrain (Alba)

The purity test is one of the key parameter for Aluminium fluoride material used in Aluminium smelting process. Aluminium Fluoride is added to the reduction cell to react with Alumina impurities such as Cao and Na₂O and to generate more Alumina (Al₂O₃) and cryolite to the reduction cell. Good quality AlF₃ usually having purity between 89 to 93%, purity has to be measured accurately, through quick and safe method. This study provides several solutions for measuring AlF₃ Purity by instrumental methods such as NMR, XRF dilution, SEM and XRF standard less qualitative method as an alternative for the wet chemical methods known for this test. This approach is applicable also for Al₂O₃/AlF₃ mixed sample, due to the close physical shape of both material, the differentiation between Al₂O₃ and AlF₃ is required by reduction staff in case of any cell disturbance.

4:40 PM

Micro-Raman Spectra Research on NaF-AlF₃-NaCl Melts: Xianwei Hu¹; Jingjing Liu¹; Huan Li¹; Bingliang Gao¹; Zhongning Shi¹; Yaxin Yu¹; Zhaowen Wang¹; ¹Northeastern University

Raman spectra of NaF-AlF₃-NaCl melts with the compositions in aluminum electrolysis practice are recorded by using the ultraviolet laser source. A kind of sealed sample cell was used to improve the measuring precision. Ionic structure of the melts with different cryolite ratio (molar ratio between NaF and AlF₃) and NaCl contents was studied. The effect of the composition and temperature was analyzed. The results have shown that with the addition of the NaCl to the acid NaF-AlF₃ melts, the relative amount of the Al-F entities have been changed, obviously. It is thought that the relative amount of the complex ions is also greatly influenced by the temperature.



TMS 2012

141st Annual Meeting & Exhibition

Aluminum Reduction Technology: Environment II

Sponsored by: The Minerals, Metals and Materials Society, TMS Light Metals Division, TMS: Aluminum Committee, TMS: Aluminum Processing Committee
Program Organizer: Olivier Martin, Rio Tinto Alcan

Wednesday PM Room: Southern III
March 14, 2012 Location: Dolphin Resort

Session Chair: Anders Sørhuus, Alstom Norway AS

2:00 PM

GHG Measurement and Inventory for Aluminum Production: *Jerry Marks*¹; Chris Bayliss²; ¹J Marks & Associates; ²International Aluminium Institute

The primary aluminum industry has achieved good progress over the past decade in reducing GHG emissions associated with metal production. The reductions have been measured through well documented protocols for the measurement of GHGs associated with production processes as well as established inventory methodology vetted with stakeholders from within and outside the industry. These protocols and inventory methodologies are currently in the process of being updated to reflect new findings and changes in the industry over the past decade to further enhance the accuracy and robustness of GHG accounting for the aluminum industry. This paper discusses the revisions being considered and the factors driving the changes.

2:20 PM

Optimization and CFD Simulation in the Ventilation of AP60 Reduction Cell Buildings: Edmund Baltuch¹; *Siegmar Baltuch*¹; ¹Air-Therm Inc.

Ventilation of the reduction buildings of the state of the art Rio Tinto Alcan AP60 Technology is critical to proper process function. Correctly engineered systems evacuate the surplus of thermal energy from the process area and allow an optimized air change rate. Computational fluid dynamic simulations combined with 4 dimensional CAD modeling and 365 day, 24 hour environmental conditions were used to demonstrate to sophisticated end users and assist engineers, coupled with traditional calculations and physical modeling as predictive tools that the optimal solution was being put forward for smelter ventilation. Due to the highly confidential nature of the technology and project, some empirical data will not be included in the report. Results from modeling and calculations are currently in place on Phase 1 and we continue to study, optimize and innovate as new tools become available to provide the best possible engineered solutions for particular applications.

2:40 PM

HEX Retrofit Enables Smelter Capacity Expansion: *Hussain Qassab*¹; Sayed Salah Aqeel Ali Mohd¹; Geir Wedde²; Anders Sorhuus²; ¹Aluminium Bahrain; ²Alstom

Aluminium Bahrain is one of the largest producers of primary high quality aluminium in the world, and continues to consider further expansions such as the planned new line 6. In parallel the amperage on existing pot lines will be increased further. A bottleneck in the amperage creep projects is limitations on gas flow and temperature to the existing gas treatment centers (GTCs). Cooling can be provided by adding dilution air, or water injection, but in both cases additional scaling, HF emissions and operation costs are expected, as well as reduced lifetime of filter bags due to increased hydrolysis. Another option is to install heat exchangers integrated into each compartment in the existing GTCs (IHEXs) to cool the potgas. Stable heat transfer and pressure drop, and successful avoidance of scaling are demonstrated. The performance is compared to the HEX data collected for close to 3 years at Alcoa Mosjoen.

3:00 PM

Experimental and Theoretical Study on the Fluidization of Alumina Fluoride Used in the Aluminum Smelter Processes: *Paulo Douglas Vasconcelos*¹; André Luiz Mesquita²; ¹Albras Alumínio Brasileiro S.A.; ²Federal University of Pará

Fluidization is an engineering unit operation that occurs when a fluid (liquid or gas) ascends through a bed of particles, and these particles get a velocity of minimum fluidization enough to stay in suspension, but without carrying them in the ascending flow. As from this moment the powder behaves as liquid at boiling point, therefore the term “fluidization”. This operation is broadly used in the aluminum smelter processes, for gas dry scrubbing (mass transfer) and in the modern plant for continuous alumina pot feeding (particles’ momentum transfer). The understanding of the alumina fluoride rheology is of capital importance in the design of fluidized beds for gas treatment and fluidized pipelines for pot feeding. This paper demonstrates the results of the experimental and theoretical values of the minimum and full fluidization velocities for the alumina fluoride used to project the state of the art round non-metallic air-fluidized conveyor of multiples outlets.

3:20 PM Break

3:40 PM

A Method for Comparing the HF Formation Potential of Aluminas with Different Water Contents: *Camilla Sommerseth*¹; Karen Osen²; Christian Rosenkilde³; Astrid Meyer⁴; Linda Kristiansen³; Thor Aarhaug²; ¹Norwegian University of Science and Technology, NTNU; ²SINTEF; ³Hydro Aluminium; ⁴Norsk Hydro

In the aluminium industry today, smelters often have to rely on more than one alumina supplier. This creates diversity in the properties of smelter grade alumina (SGA). A method has been developed to compare the HF formation from aluminas containing different amounts of water. The water content of the different aluminas was determined by loss on ignition tests (LOI) and thermal gravimetric analysis (TGA). Further, the aluminas were added to a cryolitic melt kept in a gas tight furnace with a constant nitrogen flow rate. The HF concentration in the off gas during the alumina additions was measured in-situ using a tunable diode laser. A correlation between the quantity of water found from LOI characterisation and the amount of HF formed has been found. It was also found that in this laboratory setup, all types of water contribute to HF formation; structural hydroxyl, physisorbed and chemisorbed water.

4:00 PM

Visualising the Sources of Potroom Dust in Aluminium Smelters: *David Wong*¹; Nursiani Tjahyono¹; Margaret Hyland¹; ¹University of Auckland

‘Potroom dust’ comprises one of the major sources of particulate emissions from a smelter to the environment. With regulatory emission limits for particulates continually tightening, there is a need for smelters to understand the sources and pathways by which dust is generated in a potroom. Only armed with this understanding can smelters develop targeted strategies to counter these emissions. Methodologies to sample and analyse the composition of potroom dust (both settled on surfaces and airborne) have been applied in four smelters. By taking samples across a range of potroom locations and elevations, an overall compositional picture of dust can be built and visualised for any potroom. In general, settled dust is dominated by cover material and alumina – the role of each, however, is influenced by the granulometry of cover and how alumina is delivered to the pot. In contrast, airborne dust in a potroom is typically dominated by bath-related compounds.

4:20 PM

Impurity Elements in Raw Gas Ultra-Fines from Aluminum Electrolysis Cells: *Heiko Gaertner*¹; Arne Petter Ratvik¹; Thor Anders Aarhaug²; ¹NTNU; ²SINTEF

In the present work the effect of cell operation on the amount and composition of dust in raw gases was investigated. Particle size distribution of ultra-fines ($D_i < 10 \mu\text{m}$) were measured in real time and the chemical composition of particle size groups were analyzed. Mass concentrations from cells under different operational condition are computed based on the density estimates calculated from measured number concentrations and fraction weights. EDS analysis and HD ICP-MS revealed a significant increase in contaminant level for particle with a $D_i > 0,75 \mu\text{m}$. The findings indicate that particles with $D_i < 1,2 \mu\text{m}$ consist mainly of quenched bath fume basically NaAlF_4 , $\text{Na}_5\text{Al}_3\text{F}_{14}$ partly hydrolyzed to Na_3AlF_6 and Al_2O_3 with a low level of contaminants, while particles with $D_i > 1,2 \mu\text{m}$ exhibit significant levels of contaminants presumably entrained particles from the combustion of anode carbon and alumina feed.

Atomistic Effects in Migrating Interphase Interfaces - Recent Progress and Future Study: Roles of Interface on Microstructure Development

Sponsored by: The Minerals, Metals and Materials Society, TMS Materials Processing and Manufacturing Division, TMS/ASM: Phase Transformations Committee

Program Organizers: Tadashi Furuhashi, Institute for Materials Research, Tohoku University; Sudarsanam Babu, Ohio State University; Hatem Zurob, McMaster University; Jian-Feng Nie, Monash University; Wen-Zheng Zhang, Tsinghua University; James Howe, University of Virginia

Wednesday PM
March 14, 2012

Room: Europe 3
Location: Dolphin Resort

Session Chairs: Masato Enomoto, Ibaraki University; Annika Borgenstam, Royal Institute of Technology

2:00 PM Invited

Structural Transformations in Binary Alloys with Phase Field Crystals: Michael Greenwood¹; Nana Ofori-Opoku²; Nikolas Provatas²; Joerg Rottler¹; *Chad Sinclair*¹; Mathias Millitzer¹; ¹University of British Columbia; ²McMaster University

The phase field crystal model for structural transformations is extended to include two-component alloys via two-particle correlation functions. These free energy kernels result in broad density modulations that can be treated with high numerical efficiency. A simplified binary alloy model is shown to describe the equilibrium properties of eutectic and peritectic binary alloys in two and three dimensions. Using the simplified binary model, the drag effects of composition on the interfacial motion under applied driving pressures is examined.

2:30 PM Invited

Application of the Diffusion-Multiple Approach in Alloy Development: *Ji-Cheng Zhao*¹; ¹The Ohio State University

Diffusion multiples are assemblies of many diffusion couple and triples that are diffusion annealed at elevated temperatures for extended periods of time to promote interdiffusion between/among the elements. Local equilibrium at phase interfaces evaluated from microprobe analysis allow rapid establishment of phase diagrams that are essential input for CALPHAD modeling. Diffusion profiles obtained from the diffusion multiples allow extraction of diffusion coefficients for kinetic databases and kinetic simulations. Micron-scale resolution tools were recently developed to measure thermal conductivity, elastic modulus, and coefficients of thermal expansion (CTE). A combination of compositional gradients in diffusion multiples and localized property measurements/

mapping allows fast establishment of composition-structure-property relationships and databases for accelerated materials development. Precipitation kinetics can also be very effectively evaluated from diffusion multiples for alloy development. This talk will show examples to demonstrate the effectiveness of the diffusion-multiple approach in alloy design.

3:00 PM

Modelling Growth and Dissolution Kinetics of Grain-Boundary Cementite in Cyclic Carburizing: *Kouji Tanaka*¹; Hideaki Ikehata¹; Hiroyuki Takamiya¹; Hiroyuki Mizuno²; Takeyuki Shimada²; ¹Toyota Central R&D Labs., Inc.; ²Aichi Steel corp.

Vacuum carburizing is a rapid and energy-saving industrial heat treatment. However, filmy cementite ($\theta_{g,b}$) precipitates on γ grain boundary and short-time cyclic carburizing is followed by diffusion periods to eliminate it. In order for an accurate prediction of C profiles, kinetic models have been required for the growth and dissolution of $\theta_{g,b}$, both of which highly depend on steel chemistry. Based on the analysis on AISI 5120 carburized steel, they have been formulated with the parabolic rate constants for partitioning process of a single element. And a multicomponent diffusion simulation have validated the constants as a function of fixed C activity. The kinetic models were incorporated in solving C diffusion in γ which was supersaturated while carburizing and undersaturated in later diffusion period. Calculations on C profiles and $\theta_{g,b}$ fractions represented experimental observations quite well. We will discuss how the Si(Cr) diffusion in $\gamma(\theta)$ controls the growth (dissolution) rate.

3:20 PM Break

3:40 PM Invited

Mechanisms for Negative Creep in Nickel Base Superalloys: *J. Tiley*¹; S. Knox²; S. Nag³; G. Viswanathan¹; R. Banerjee³; H. Fraser⁴; ¹Air Force Research Laboratory; ²Southwestern Ohio Council for Higher Education/Air Force Research Laboratory; ³Department of Materials Science, University of North Texas; ⁴Department of Materials Science and Engineering, The Ohio State University

Advanced characterization techniques and atomistic models were used to investigate negative creep in Rene88DT. Specifically, researchers analyzed the site occupancy of alloying elements and their role in changing lattice parameters associated with the early stages of heat treatment. Samples were aged at 760 degree C and evaluated using advanced TEM, atom probe tomography, and diffraction using both neutron and x-ray approaches. Atomistic modeling of element interactions and their mechanisms were compared with high resolution EELS and APT techniques. Results indicate the major mechanisms associated with negative creep.

4:10 PM Invited

Transient High Temperature Oxidation of a Ni Base Superalloy: *Emmanuelle Marquis*¹; Roger Reed²; ¹University of Michigan; ²University of Birmingham

The empirical knowledge about oxidation behavior has often been sufficient for the development of current alloys. However, further development and efficient design of new alloys requires the detailed mechanistic understanding of the early stages of oxide formation and development. In particular, controlling the roles of solute and alloying elements in modifying the oxidation resistance of alloys can be complex. It is often speculated that interfacial segregation, preferential oxidation are responsible for the observed behaviors. In the case of a novel single crystal nickel-based superalloy of high Cr content, the addition of Si has been associated with superior oxidation resistance exhibited by this alloy as compared to those used currently for aeroengines. Atom probe tomography and electron microscopy observations of the oxide scale provides unique and new insights into the mass transport mechanisms occurring at the metal/oxide interface, oxide grain boundaries and into the exact role of alloying elements.



TMS 2012

141st Annual Meeting & Exhibition

4:40 PM

Interphase Precipitation of Vanadium Carbide in Low Alloy Steels: *Tadashi Furuhashi*¹; *Toshio Murakami*²; *Goro Miyamoto*¹; *Naoya Kamikawa*¹; ¹Institute for Materials Research, Tohoku University; ²Kobe Steel Ltd.

Recently, fine dispersion of alloy carbide formed by interphase precipitation during ferrite transformation attracts lots of attentions as a promising microstructure for high strength and high ductility. In this study, the microstructures obtained by interphase precipitation of vanadium carbide in low alloy steels are examined. 0.3mass% of vanadium was added to carbon steels containing 0.1 and 0.45mass% carbon. Specimens are isothermally transformed to ferrite after austenitization. TEM observation was made to analyze the carbide dispersion quantitatively. As transformation temperature is lowered, the carbide sheet spacing becomes narrower. Finer and denser particle distribution is obtained at lower ferrite transformation temperature. Interestingly, the carbide sheet spacing is decreased as approaching toward the growth front of ferrite in the 0.45C steel which suggests a slower growth rate results in more frequent nucleation of carbide. Some discussions will be made based upon a new interphase precipitation model taking a time-dependent segregation of vanadium into account.

5:00 PM

The Effect of Molybdenum on Niobium, Titanium Carbonitride Precipitate Stability and Grain Refinement in a High-Temperature Vacuum Carburizing Steel: *Charles Enloe*¹; *J.G. Speer*¹; *K.O. Findley*¹; ¹Colorado School of Mines, Advanced Steel Processing and Products Research Center

Coarsening and compositional evolution of mixed Nb,Ti(C,N) carbonitride precipitates have been investigated in molybdenum-bearing microalloyed SAE 4120 steel. The effects of molybdenum on niobium-bearing carbonitride interfacial energy and niobium diffusion during reheat to carburizing temperatures were of special focus. Characterization of precipitate evolution is fundamental to process design for the retardation of abnormal grain growth at increasingly high processing temperatures. The experimental characterization techniques include analytical scanning transmission electron microscopy (STEM) and three dimensional atom probe tomography (APT). A reduction in the ripening rate of carbonitrides was observed in molybdenum-bearing alloys containing 0.05 wt pct and 0.10 wt pct niobium. Molybdenum incorporation was observed in spheroidal carbonitrides less than 30 nm in diameter, but APT and STEM investigations revealed no appreciable molybdenum segregation to the particle/matrix interface.

5:20 PM Concluding Comments **Hatem Zurob**

Biological Materials Science Symposium: Biological and Bio-Inspired Materials IV: Soft Biomaterials

Sponsored by: The Minerals, Metals and Materials Society, TMS Electronic, Magnetic, and Photonic Materials Division, TMS Structural Materials Division, TMS: Biomaterials Committee
Program Organizers: Nima Rahbar, University of Massachusetts Dartmouth; Candan Tamerler, University of Washington; Po-Yu Chen, University of California, San Diego; Molly Gentleman, Texas A&M University

Wednesday PM
March 14, 2012

Room: Swan 7
Location: Swan Resort

Session Chairs: Paul Calvert, University of Massachusetts Dartmouth; Molly Gentleman, Texas A&M University

2:00 PM Invited

Bionic Hydrogel Sensors and Actuators: *Paul Calvert*¹; ¹University of Massachusetts

There is a need for devices that can allow a dialog between electronics and soft, wet biocompatible sensors and actuators. We have used inkjet printing and extrusion methods to form gels based on epoxy-amine chemistry that can be coupled to electronic systems. These gels may be used to sense strain or biochemicals, they can be induced to contract under electrical stimulation and may be used to deliver small or large molecules to cells or the surrounding tissue. The mechanical, transport and response properties of these gels will be discussed in the context of forming a bionic devices with flexible electrodes embedded in an active gel.

2:30 PM

The Effect of Polyvinyl Alcohol (PVA) Weight Ratio on Apatite-PVA Composites: *Tugba Basargan*¹; *Gulhayat Nasun-Saygili*¹; ¹Istanbul Technical University

It is known that natural bone is an organic-inorganic composite in which inorganic apatite crystals are accumulated on organic collagen fibers. Thus, inorganic apatite-organic polymer composites have been gained interest for their possible usage in biomedical area. In this work, apatite-PVA composites were prepared in two steps. In the first step, apatite was produced using dipotassium hydrogen phosphate and colemanite (2CaO.3B2O3.5H2O). Wet method was used to obtain the apatite. In the second step, apatite and PVA were physically mixed with different weight ratios to investigate the effect of PVA content on the composite structure. During the experiments, apatite-PVA slurries were dried using a laboratory scale spray dryer. Samples in each step were structurally analyzed by XRD and FTIR. Also boron analysis was made volumetrically. It was showed that apatite-PVA composites were successfully synthesized. The intensity of characteristic peaks of PVA changed according to the PVA content of the composite.

2:50 PM

Silver Base Nano-Particle Preparation by Ion Bioadsorption of Bacillus Megaterium: *Hongxu Li*¹; *Yunchi Guo*¹; *Chuanqi Jiao*¹; ¹University of Science and Technology

The paper aims at the silver base nano-particle prepared during Bacillus megaterium culture and growth. The biosorption properties of Ag⁺ and surface bioreduction reaction of [Ag(NH₃)₂]⁺ by Bacillus megaterium were evaluated and the particles were almost globular and the average particle size was 14.5nm. The influence factors experiments results show that the adsorption efficiency was affected greatly by initial biomass concentration and initial Ag⁺ concentration and the determined best adsorption pH value was 6. The surface mechanism of silver biosorption by Bacillus megaterium included electrostatic adsorption and complexation. FTIR studies demonstrated that amino and carboxyl groups were confirmed to be the main active groups. The silver sol was well-distributed by the mean of TEM.

3:10 PM

A Comprehensive Study of Hydrogel Material Mechanical and Tribological Properties at Small Scales: *Bo Zhou*¹; Nicholas Randall¹; Drew Griffin¹; Rahul Nair¹; ¹CSM Instruments

The unique properties of soft hydrogels have caused them to be widely adopted in various fields, such as for biomedical applications and contact lenses. In this study, a series of up-to-date methodologies were employed to investigate hydrogel properties, such as stiffness, elastic recovery, viscoelasticity, adhesion, and friction properties. An Ultra Nanoindentation Tester was employed for mechanical measurements. Long load-holding tests were performed in order to accurately monitor the evolution of creep. Nanoindentation was also used for surface adhesion force evaluation. The dehydration effect on the gel stiffness was investigated by performing a series of indentations over a period of dehydration time. A Nano Scratch Tester was used to quantify the elastic/viscoelastic properties of hydrogels. Moreover, the surface coefficient of friction was evaluated with a Nano Tribometer. The tests yielded distinctive results compared to bulk data, which could play an important role in the fundamental study of small scale hydrogel materials.

3:30 PM

Biomechanics Studies at the Advanced Photon Source Using High-Energy X-rays: *Jonathan Almer*¹; Stuart Stock²; ¹Argonne National Laboratory; ²Northwestern University

The fracture propensity of bone and teeth has been linked to both fracture strength and loading spectra, so it is important to quantify mechanical input and identify “weak-link” microstructures or changes in global parameters characterizing microarchitecture. Here we present recent efforts to reveal this information with wide- and small-angle x-ray scattering under in situ loading. High-energy x-rays ($E > 60$ keV) and a transmission geometry are used at the Advanced Photon Source to provide true bulk sampling across several mm² cross-sections of animal tissue. Wide-angle scattering is used to quantify texture, particle size and internal strains in the apatite mineral phase. Small angle x-ray scattering reveals the average mineral platelet spacing, mediated by collagen, which is used to infer the load transfer between the constituent phases. The ability to create small (micron-level) x-ray beams reveals gradient information, as will be illustrated in the vicinity of the dento-enamel junction in teeth.

3:50 PM Break

4:00 PM Invited

Adhesion of Shells: Applications in Bacteria Aggregation and Transportation in a Porous Medium: *Jiayi Shi*¹; Sinan Muftu¹; April Gu¹; *Kai-Tak Wan*¹; ¹Northeastern University

Spherical and cylindrical shells adhere to a rigid substrate in the presence of electrical double layers (EDL). The adhesion-detachment mechanics is governed by the DLVO surface potential with two energy minima. If a shell interacts weakly with the substrate and only the outer secondary energy minimum is involved, the JKR-type “pull-off” predicted conforming to the classical colloidal filtration theory (CFT) are predicted. Should the shell acquire sufficient energy to overcome the energy barrier and reach the deep primary minimum, the adhesion mechanics and CFT must be substantially modified. The new model has significant impacts on bacteria adhesion-aggregation-transportation behavior in porous medium and is consistent with experimental measurements using conventional column test. We will also report new methods to characterize the mechanical and viscoelastic properties of convex shells of hydrogels and bacteria glycoprotein shells of single cells. These results have strong implications in waste water treatment and transportation of pollutants.

4:30 PM

Nanoindentation: Potential Diagnostic Method for Cancerous Transformation of Melanocyte: *Ana Paula Benaduce*¹; *Debrupa Lahiri*¹; Lidia Kos¹; Arvind Agarwal¹; ¹Florida International University

Nanoindentation could be a valuable tool to analyze the differences in mechanical properties of normal and cancerous cells and act as a potential marker of cellular transformation. In this study, we evaluated the changes in nano-mechanical properties to distinguish between normal and transformed melanocytes. We adapted nanoindentation technique to compare the elastic modulus and membrane rupture load of human primary melanocytes and human melanoma cells in-vitro. We found that primary melanocytes are 2.5 times stiffer and 3.5 times harder than melanoma cells. This difference in elasticity may facilitate the migration and invasion of cancerous cells during metastasis. Previous studies have suggested the activation of Endothelin receptor b by Endothelin 3 (Edn3) may be involved in melanoma progression. Our results demonstrate that primary melanocytes and melanoma cells modulate their biomechanical properties differentially upon Edn3 exposure.

4:45 PM

Antimicrobial Efficacy and Degradation Route of Silver-Based Coated Endotracheal Tubes: *Minoo Arzpeima*¹; Gunilla Björling²; Sigbritt Karlsson¹; Ragnhild. E Aune³; ¹Royal Institute of Technology; ²Karolinska Institute; ³Norwegian University of Science and Technology (NTNU)

At present silver-based coatings are being increasingly developed. Several studies have questioned the antimicrobial efficacy of silver, which might be obscured due to inactivation of the coating by biological fluids. Poor adhesion between the coating and the substrate can, however, also inhibit long-term efficacy of the coating. In the present work, a novel silver-based coating applied to Endotracheal Tubes (ETT) was studied. The efficacy of the coating in preventing bacterial colonisation was evaluated in-vitro, both before and after exposure to relevant Synthetic Biological Fluids (SBF) for 10 days. The surface properties of the coating and its degradation after exposure to SBF and bacteria were studied by Scanning Electron Microscopy (SEM), Atomic Force Microscopy (AFM) and X-ray Photoelectron Spectroscopy (XPS). According to the results obtained by Inductive Coupled Plasma Mass Spectrometry (ICP-MS) the release rate of silver was clearly more significant in the initiating hours of the exposure to SBF.

5:00 PM

Nano-Scale Mechanical Response of the Organic Constituent in Abalone Nacre: *Maria Lopez*¹; Yu-Chen Chan²; Hsien-Wei Chen²; Pao-Sheng Chen²; Po-Yu Chen²; Jenq-Gong Duh²; Joanna McKittrick¹; Marc Meyers¹; ¹UCSD; ²National Tsing Hua University

Abalone nacre is a natural multilayered composite structure that exhibits excellent mechanical properties due to the hierarchical organization of CaCO₃ tiles and organic interlayers. In this study, the contribution of the organic interlayer on the overall mechanical properties of the abalone nacre is investigated. Nanoindentation and nanoscratch tests are employed on untreated and deproteinized abalone nacre. Contrast in the mechanical behavior of these materials demonstrates the impact of the organic matrix to the toughness of the entire structure. Nanoindentation and AFM experiments are performed on the organic interlayer. These results can quantitatively assess the relationship between the overall strain and expansion undergone by the organic membrane. Specimens are characterized by SEM to verify the toughening and deformation mechanisms. This approach generates a comprehensive picture of the mechanical response of the organic layer and its effect on the mechanical properties of the abalone nacre. EAPSI-Grant1108531; NSF-Grant1006931; Ford Foundation Fellowship.



5:15 PM

Cell Toxicity of Go/Rgo: Function of Size and Oxygenated Functional Group Density: *Soumen Das*¹; Sanjay Singh¹; Virendra Singh¹; Daeha Joung¹; Janet Dowding¹; Rameech McCormack¹; Lei Zhai¹; Saiful I. Khondaker¹; William Self¹; Sudipta Seal¹; ¹University of Central Florida

Herein, we report in-vitro toxicological effect of graphene oxide (GO). We have synthesized different size and differentially reduced GO, and characterized using atomic force microscopy (AFM) and x-ray photoelectron spectroscopy (XPS). GO and RGO were found to be toxic to cells, with smaller GO/RGO materials exhibiting more significant toxicity. We also observed GO is more toxic when compared to RGO using both MTT and LDH release to assess toxicity. To explore the cause of GO/RGO toxicity, we have quantified the heme oxygenase 1 and thioredoxin reductase mRNA expression levels, known to be expressed during oxidative stress. Significant decreases in both mRNA levels were observed with more reduced GO, and this supports the hypothesis that oxidative stress mediated cellular toxicity. Therefore, it can be concluded that though size of the GO sheet plays a role, the functional group density on the GO sheet is also a key component mediating cell cytotoxicity.

Bulk Metallic Glasses IX: Simulation and Modeling

Sponsored by: The Minerals, Metals and Materials Society, TMS Structural Materials Division, TMS/ASM: Mechanical Behavior of Materials Committee

Program Organizers: Peter Liaw, The University of Tennessee; Hahn Choo, The University of Tennessee; Yanfei Gao, The University of Tennessee; Gongyao Wang, University of Tennessee

Wednesday PM
March 14, 2012

Room: Swan 6
Location: Swan Resort

Session Chairs: Mo Li, Georgia Institute of Tech; Yunfeng Shi, Rensselaer Polytechnic Institute

2:00 PM Invited

Packing, Cluster Formation and Their Roles in Physical and Mechanical Property of Metallic Glasses: *Mo Li*¹; Qikai Li²; ¹Georgia Institute of Tech; ²Tsinghua University

Ordered packing, either short- or medium-ranged, and the clusters formed by such ordered packing has been investigated as "structural unit" in metallic glasses. Their roles range from affecting crystal nucleation, diffusivity and viscosity in undercooled liquids, to mechanical properties. In this work, we re-examine the packing and cluster formation and their roles with the physical and mechanical properties. We show that the seemingly ordered structure has little bearing on being the structural unit in thermodynamic sense. Rather, we show that those local patterns exert large kinetic effect on liquid as well as solid behaviors.

2:20 PM Invited

First-Principles Tensile and Compression Experiments on a Model Metallic Glass: *Wai-Yim Ching*¹; Yungfeng Shi²; Despina Louca³; Gongyao Wang⁴; Peter Liaw⁴; ¹University of Missouri-Kansas City; ²Rensselaer Polytechnic Institute; ³University of Virginia; ⁴University of Tennessee

An Ab initio method has been applied to investigate the mechanical behavior of a metallic glass (MG). A periodic supercell model of a-Cu_{0.5}Zr_{0.5} with 256 atoms is constructed using classical molecular dynamics and then fully relaxed using VASP to near zero stress. Tensile and compressive experiments are performed by successively applying tensile/compressive loads in small steps until the stress reaches a maximum and beyond. At each step, the structure is fully relaxed, and the r.m.s. value of $|s|$ of the stress (s_{xx} , s_{yy} , and s_{zz}) and the corresponding strain $|e|$ in a given direction are extracted. The stress vs. strain data are compared with that of crystals. The calculated bulk, Shear, Young's modulus and Poisson

ratio for this MG model are 117, 24, 67 GPa and 0.40 respectively. The electronic structure and bonding of the BMG are also evaluated. On average, Zr loses 0.61 electrons to Cu per atom.

2:40 PM Invited

Simple Analytic Models for Plastic Deformation and Slip Avalanches: From Crystals to Amorphous Materials to Granular Materials: *Karin Dahmen*¹; Yehuda Ben-Zion²; Jonathan Uhl¹; Georgios Tsekenis¹; ¹University of Illinois at Urbana Champaign; ²University of Southern California

Slowly sheared crystalline materials are known to deform in an intermittent way with slip avalanches. In many materials power laws govern the statistics of the avalanches. A basic micromechanical model for deformation of solids with only one tuning parameter (weakening e) is introduced [1]. The model can reproduce observed stress-strain curves, acoustic emissions and related power spectra, statistics of slip avalanches, and geometrical properties of slip, with a continuous phase transition from brittle to ductile behavior. Exact universal predictions for the power law exponents and scaling functions are extracted using mean field theory and renormalization group tools. The results agree with recent experimental observations and simulations of dislocation dynamics, sheared amorphous materials, and granular materials [2],[1] K.A. Dahmen, Y. Ben-Zion, J.T. Uhl, Phys. Rev. Lett. 102, 175501 (2009)[2] K.A. Dahmen, Y. Ben-Zion, J.T. Uhl, Nature Physics 7, 554-557 (2011)

3:00 PM

Phase-Field Simulation Study of Nucleation and Propagation of Shear Bands in Bulk Metallic Glasses with Stress-Induced Precipitation of Martensitic Nanocrystals: *Alireza Zakeri*¹; Fadi Abdeljawad¹; Mikko Haataja¹; ¹Princeton University

Bulk Metallic Glasses (BMGs) exhibit a unique combination of mechanical properties, such as high strength and large elasticity limit. On the other hand, plastic strain localization via the nucleation and propagation of shear bands limits the overall ductility of such systems. Recent experimental findings have demonstrated that BMG systems, in which stress-induced precipitation of martensitic shape memory alloy nanocrystals occurs, display enhanced mechanical properties. In this work, a continuum phase-field modeling framework is employed to investigate the nonlinear interaction between stress-induced precipitation of martensitic nanocrystals and shear band formation in two spatial dimensions. In agreement with experimental observations, simulation results show that the presence of martensitic nanocrystals enhances the overall ductility relative to monolithic BMGs. Finally, we quantify the roles of the area fraction of the martensitic particles and their intrinsic hardening behavior on the overall ductility of the system.

3:10 PM Invited

Correlations during Plastic Flow in Model Metallic Glasses: *Craig Maloney*¹; ¹Carnegie Mellon University / Civil & Environmental Engineering

Computer simulations of sheared glasses exhibit profound spatio-temporal correlations in the local strain. These correlations directly impact the macroscopic viscoplastic response and may have important consequences for macroscopic shear localization. We will review recent developments in this area and discuss how observations from computer simulation relate to experimental studies such as those on the distribution of serration sizes in stress-strain curves during mechanical tests and acoustic emission measurements.

3:30 PM Invited

Computer Simulation of the Structure of Zr-Based Amorphous Alloys: *Mikhail Mendeleev*¹; Ames Laboratory

A new interatomic potential for the Ni-Zr system will be presented. This potential was developed specifically to match with scattering data from Ni, Zr and NiZr₂ liquids. This potential and similarly developed potential for the Cu-Zr alloys have the C11b being more stable than C16 in the CuZr₂ alloy while C16 is the more stable than C11b in the NiZr₂

alloy, consistent with experiments. It was found that in contrast to the crystalline alloys, the Ni-Ni, Cu-Cu and Zr-Zr separations are almost the same in both disordered alloys. On the other hand, Cu-Zr separations are considerably larger than the Ni-Zr separations. The differences in the structures of the disordered alloys will be discussed and it will be shown that most features can be explained by the smaller Ni-Zr separation driven by the higher heat of mixing. Work at the Ames Laboratory was supported by DOE BES under Contract No. DE-AC02-07CH1135.

3:50 PM Break

4:05 PM Invited

Simulating the Effect of Poisson Ratio on Metallic Glasses: *James Morris*¹; ¹Oak Ridge National Laboratory

The Poisson ratio of a glass has been correlated with the fragility of the liquid phase and with the fracture energy of a glass. There has been little theoretical work supporting this, due to a lack of a direct method of incorporating this. We have developed an interatomic potential that allows the Poisson ratio to be tuned. Simulations of the liquid show that increasing the Poisson ratio stabilizes the liquid phase, and increases the liquid fragility. Structural and dynamic properties in the liquid phase all show changes on undercooling that indicate a change in the liquid behavior above the glass transition. Research supported by the US Department of Energy, Basic Energy Sciences, Materials Sciences and Engineering Division.

4:25 PM

Analysis of Glass-Forming Ability through Atomistic Modeling: *Logan Ward*¹; Katharine Flores¹; Wolfgang Windl¹; ¹The Ohio State University

Recently-developed techniques for measuring glass-forming ability using molecular dynamics have enabled the validation of many structural and dynamic properties as traits of glass-forming ability. In this work, we will present a computational tool for identifying glass-forming alloys using molecular dynamics. This method approximates the kinetics and driving force for nucleation in a liquid by studying its fragility and the relative amount of energetically-favorable short-range order. With this technique complete, it was possible to investigate how other properties correspond with glass formation in several systems for which interatomic potentials are available. It was also possible to alter the nature of bonding between species to study their effects on those key properties and glass-forming. The combination of these efforts yields not only a useful tool for identifying candidates for amorphous alloys, but a means of improving existing intuition for what properties are contributing factors in the stability of bulk metallic glasses.

4:35 PM Invited

Bauschinger Effect in Metallic Glass Nanowires under Cyclic Loading: *Yunfeng Shi*¹; Jian Luo¹; Louca Despina²; Gongyao Wang³; Peter Liaw³; ¹Rensselaer Polytechnic Institute; ²University of Virginia; ³The University of Tennessee

We present a molecular dynamics simulations on fatigue behaviors of model metallic glass nanowires. We found asymmetric hardening in fatigued metallic glass nanowires, which is analogous to the Bauschinger effect commonly observed in metals and polymers. Here both compression-compression and tension-tension cyclic loading are imposed using strain-controlled loading scheme up to 100 cycles, with the maximum strain of 4 %. It was found that, upon compression-compression fatigue tests, the metallic-glass nanowire hardens in compression tests, while softens in tensile tests. However, upon tension-tension cyclic loading, it was found that the metallic-glass nanowire softens in compression tests, while hardens in tensile tests. The observed Bauschinger effect cannot be explained by population variations of preferred short-range orders such as icosahedral clusters, as it was shown to be almost a constant. Instead, such asymmetric hardening behavior is related to the anisotropic distribution of icosahedral pairs, which evolves during cyclic loading.

4:55 PM

Modeling the Intrinsic Shear Strength of Metallic Glass: *Yongqiang Cheng*¹; Evan Ma¹; ¹Johns Hopkins University

The intrinsic (ideal) strength has been extensively studied for crystalline alloys, but remains largely unsettled for metallic glasses. This study, by combining computer simulations and the cooperative shear model (CSM, Johnson and Samwer, Phys. Rev. Lett. 95, 195501, 2005), found that, at the athermal limit, the yield strain of metallic glass can be as high as ~10% in pure shear, and the corresponding ideal shear strength is $\sim G/10$ (where G is the shear modulus), at which shear bands nucleate homogeneously in the metallic glass. The athermal extrapolation of the measured strength in conventional loading tests is much lower, owing to the unavoidable imperfections in realistic samples, where shear band nucleation is always heterogeneous and facilitated by stress concentrators. The two scenarios have different temperature dependence and merge at elevated temperatures, when the yielding mode eventually changes from strain localization to homogeneous flow.

5:05 PM Invited

Atomistic Anisotropy in Deformed Metallic Glasses Studied via Molecular Dynamics Simulations: *Yunche Wang*¹; Chun-Yi Wu¹; Peter Liaw²; ¹National Cheng Kung University; ²University of Tennessee

Recent studies on the deformation mechanisms in metallic glasses led to the atomically anisotropic behavior of the materials under loading. It has been shown that if the anisotropy is not included in the data analysis, synchrotron experiments may overestimate the modulus values of the materials. In this study, two metallic glasses are adopted. The Cu-Zr-Al glasses and Zr₇₀Ni₁₆Cu₆Al₈ are studied. The simulated, as-deposited films were amorphous. After the deposition, the samples were subject to uniaxial loading/unloading MD simulations, and results were compared with experimental data from in-situ synchrotron experiments. Calculated elastic constants are in agreement with experimental data. Diffraction pattern calculations are performed to compare with experimental ones to disclose the anisotropic deformation, through change of coordination numbers, at atomic scales in metallic glasses under loading. The effects of the anisotropy alter the short range order of amorphous alloys, and hence need to be incorporated to correctly interpret experimental data.

5:25 PM Invited

Structures, Phase Transformations and Elastic Properties of High-Entropy Al_xCoCrCuFeNi Alloys: Ab Initio Molecular Dynamics Simulation: *Michael Gao*¹; Louis Santodonato²; Peter Liaw²; ¹National Energy Technology Lab; ²University of Tennessee

The high-entropy Al_xCoCrCuFeNi alloys are known for their high strength and good wear resistance at elevated temperatures. The mechanical properties critically depend on especially aluminum contents and annealing temperatures, both of which dictate the microstructures and subsequent phase transformations involving A1, A2, and B2 phases. In the present study, ab initio molecular dynamics simulations are performed to reveal the atomic structures as a function of Al contents and temperatures. A comprehensive analysis on the atomic pair correlation function, structure factors, electronic charge density distribution, and atomic diffusion constants are performed in the liquid, as-quenched state, and annealed state in comparison to the crystalline A1, A2, and B2 structures. Elemental partitions among these phases are predicted and compared with experimental findings. The elastic properties are also calculated using density function theory (DFT) methods and compared with experimental measurements.

5:45 PM

Quasi-Phase-Transition Model of Shear Bands in Metallic Glasses: *Zengqian Liu*¹; Ran Li¹; Gang Wang²; Sujun Wu¹; Xuyang Lu¹; Tao Zhang¹; ¹Beihang University; ²Shanghai University

A quasi-phase-transition model of shear bands in metallic glasses (MGs) is presented from the thermodynamic viewpoint. Energy changes of shear banding in the sample-machine system are analyzed following the fundamental energy theorems. Three characteristic parameters, i.e.



TMS 2012

141st Annual Meeting & Exhibition

the critical initiation energy ΔG_c , shear-band stability index k_0 , and the critical shear-band length l_c , are derived for elucidating the initiation and propagation of shear bands. The criteria for good plasticity in MGs with predominant thermodynamic arrestment of shear bands are proposed as low ΔG_c , large k_0 , and small l_c . The model combining with experimental results was used to analyze some controversial phenomena about deformation behaviors in MGs, like the size effect, the effect of testing machine stiffness and the relationship between elastic modulus and plasticity. This study has important implications for the fundamental understanding of shear banding as well as deformation mechanisms in MGs and provides theoretical basis for improving the ductility of MGs.

Cast Shop for Aluminum Production: Direct-Chill Casting and Microstructures

Sponsored by: The Minerals, Metals and Materials Society, TMS Light Metals Division, TMS: Aluminum Committee, TMS: Aluminum Processing Committee
Program Organizer: Trond Furu, Hydro

Wednesday PM Room: Northern A4
March 14, 2012 Location: Dolphin Resort

Session Chairs: Pierre Le Brun, Constellium CRV; Trond Furu, Hydro

2:00 PM

Improving Strip Surface Quality Using Different Casting Atmospheres for the Horizontal Single Belt Strip Casting (HSBC) Process

: Donghui Li¹; Mihaiela Isac¹; Roderick Guthrie¹; ¹McGill Metals Processing Centre

The surface quality of as-cast strip is a key factor in the production of strips produced by Horizontal Single Belt Strip Casting process (HSBC). Aluminum alloys were cast on an HSBC simulator, using different casting atmospheres at meniscus region, including preheated air and pure oxygen. The strip's bottom surface was analyzed in order to evaluate the effect of casting atmosphere on strip surface quality. The preheated air or oxygen was injected into the hollowed backwall refractory and was released through the orifices on the bottom of the refractory, close to the back-wall meniscus region. The purpose was to flush out the ambient air entrained above the moving substrate. The possibility of eliminating surface defects caused by air pockets' on the strip's bottom surface and improving surface quality by controlling the casting atmosphere in the meniscus region were confirmed. The surface profiles of the sand-blasted substrates and those of the related strips were analyzed using 3D Profilometry. The interfacial heat fluxes through using an oxygen atmosphere at the upstream meniscus were also enhanced greatly, as compared to the casting process using a graphite coating on the substrate. A novel way for improving strip surface quality with high attendant interfacial heat fluxes is now proposed for the HSBC process.

2:20 PM

Influence of Casting Direct Chill Casting Process Variables on Surface Quality of Aluminum Alloy Sheet Ingots: Mostafa El-Bealy¹; ¹Ain Shams University, (CC)

The effect of surface defects formation on surface quality of aluminum direct-chill cast ingots has been investigated by metallographic examinations and mathematical modeling. The influence of process variables such as alloy composition, casting speed and lubricant on the surface defects has been determined. The metallographic study for collected samples of plant trials involved visual surface, macro, microstructure examinations and macrosegregation analysis. A 2-D mathematical model has been developed to characterize the thermal, solidification, interdendritic strain and macro-segregation distributions. The model predictions were compared to measurements from collected

samples to verify the model, where good agreements were obtained. The model predications illustrate that all the process variables tested in this study have observed effect on the surface quality by different levels. The mathematical analysis of thermal fields as well as metallographic study has been used to explain and discuss the effects of different process variables on the surface quality.

2:40 PM

Square Rolling Slabs from Start of Casting - the Elimination of Butt Swell: Arild Hakonsen¹; Harald Næss²; Idar Steen¹; Terje Iveland³; ¹Hycast AS; ²Hydro Aluminium; ³Hydro Aluminium

The thickening of the bottom part of DC cast rolling slabs, butt-swell, is a well known problem in the aluminium business. The slabs are scalped, normally in the rolling plant, prior to rolling to a absolute rectangular shape. The rolling mill therefore prefers rolling slabs with geometry close to rectangular from the casthouse. Due to geometry specifications from the rolling mills the supplier casthouse has to cut off the bottom part of the slab before shipping. The bottom cut length is typically 0.3-0.6m (1-2') depending on the thickness and casting speed. This paper describes the basic principles behind the development of the flexible mould technology, and the operational experience so far from close to 15 years of operation. For 600mm thick ingots flexible moulds typically reduce the total scrap rate in the casthouse with more than 5% compared to conventional moulds with fixed geometry.

3:00 PM

Residual Stresses in As-Cast Billets: Neutron Diffraction Measurement and Thermomechanical Modeling: Jean-Marie Drezet¹; Thilo Pirling²; Christophe Jaquero³; ¹Ecole Polytechnique Federale Lausanne; ²Institut Laue Langevin; ³Constellium Valais SA

Stress relief treatment is often required prior to sawing aluminium DC cast products in order to prevent crack formation and significant safety concerns due to the presence of high residual stresses generated during casting. Numerical models have been developed to compute these residual stresses and yet have only been validated against measured surface distortions. In the present contribution, the variation in residual strains and stresses have been measured using neutron diffraction in two AA6063 grain-refined cylindrical billet sections cast at two casting speeds. The measured residual stresses compare favorably with the numerical model, in particular the depth at which the axial and hoop stresses change sign. Such results provide insight into the development of residual stresses within castings and show that the stored elastic energy varies linearly with the casting speed, at least within the range of speeds that correspond to production conditions.

3:20 PM Break

3:40 PM

The Deepwater Horizon Explosion and Correlations to the Aluminium Casthouse: Alex Lowery¹; Terry Bateman²; Joe Roberts³; ¹Wise Chem LLC; ²Pyrotek Pyt Ltd.; ³Pyrotek Inc

On April 20, 2010, an explosion rocked the Deepwater Horizon in the Gulf of Mexico. Resulting the 11 deaths. Tens of thousands of documents were released during the investigation for the root cause of the explosion. "What emerges is stark and singular fact: crew members died, suffered terrible injuries because every one of the Horizon's defenses failed on April 20. Some were deployed but did not work. Some were activated too late, after they had almost certainly been damaged by fire or explosions. Some were never deployed at all. Parallels with the aluminium industry stand out when comparing the Deepwater Horizon disaster (violent explosions, damaged equipment, worker deaths, worker injuries). Aluminium plants, just as deepwater oil rigs, value training and safety measures to prevent accidents from occurring. On April 20, 2010 every safety measure employed failed, could safety measures employed in a casthouse to prevent a molten metal steam explosion fail too?

4:00 PM

Deformation Behaviors of Pure Al and Al-4.5 Mass%Cu Alloy in Semi Solid State: *Nobuhito Sakaguchi*¹; ¹Sumitomo Light Metal Industries, LTD.

To clarify the hot tearing mechanism in DC casting ingot, the mechanical properties and the deformation behaviors of pure Al and Al-4.5mass%Cu alloy in semi solid state were investigated by the new tensile test method. In Al-4.5mass%Cu alloy, the tensile strength and the elongation decreased remarkably above the solidus. The healing phenomenon the liquid flowed into the crack was observed at high temperature range in semi solid state by in situ observation. Pure Al had a very high ductility until near the liquidus. The deformation behaviors of both alloys in semi solid state were classified into four stages according to these mechanical properties, fracture surface morphologies and in situ observations of the tensile tests. The brittle temperature range in which the hot tearing occurs was determined in both alloys. These data obtained by the tensile test in semi solid state were able to apply to several simulations.

4:20 PM

Chemical Additions to Reduce Hot Tearing in the Cast House: Lisa Sweet¹; John Taylor¹; *Mark Easton*¹; Malcolm Couper²; Nick Parson³; ¹CAST Co-operative Research Centre; ²ARC Centre of Excellence of Design in Light Metals; ³Rio Tinto Alcan

Hot tear susceptibility in VDC casting is strongly affected by the chemical additions of alloys, hardeners and grain refiners. This paper assesses a few different approaches to reducing hot tearing in the casthouse. Grain refinement is commonly used in the casthouse, including dosing at cast start. Another approach is to control the alloy content, through the additions of Si, Mg, Mn or Fe which can influence the type and amount of intermetallics present during the final stages of solidification when hot tearing occurs. This paper summarizes experimental findings which assess the influence of additions on the hot tear rating in 6xxx series alloys. Strategies which could be used in the cast house are discussed. While changes to the bulk metal can have consequences for alloy specification and quality control, additions at cast start could be used to reduce scrap from hot tearing without changing the composition of the saleable product.

4:40 PM Break

CFD Modeling and Simulation in Materials Processing: Electromagnetic and Ultrasonic Processing of Materials

Sponsored by: The Minerals, Metals and Materials Society, TMS Extraction and Processing Division, TMS Materials Processing and Manufacturing Division, TMS: Process Technology and Modeling Committee, TMS: Solidification Committee

Program Organizers: Laurentiu Nastac, The University of Alabama; Lifeng Zhang, Missouri University of Science and Technology; Brian Thomas, University of Illinois at Urbana-Champaign; Adrian Sabau, Oak Ridge National Lab; Nagy El-Kaddah, The University of Alabama; Adam Powell, Metal Oxygen Separation Technologies, Inc.; Hervé Combeau, Institut Jean Lamour

Wednesday PM
March 14, 2012

Room: Asia 4
Location: Dolphin Resort

Session Chairs: Andre Thess, TU Ilmenau; Valdis Bojarevics, University of Greenwich

2:00 PM Keynote

Modeling Magnetically Excited and Magnetically Damped Liquid Metal Flow: *Valdis Bojarevics*¹; Koulis Pericleous¹; ¹University of Greenwich

A number of different methods have been developed for noncontact electromagnetic treatment of liquid metal and to investigate the melting/

solidification processes. Applying AC magnetic field in terrestrial conditions, along with the buoyancy and thermo-capillary forces, results in turbulent flow. The use of a homogenous DC magnetic field allows damping both of the turbulence and the large scale flow at different rates leading to surprising results at some stages. The dynamic interaction of the turbulent flow with the oscillating interface needs to be accounted if it is required to levitate liquid metal of up to few kilograms without the contact to container walls. At the high values of magnetic field some oscillation modes are damped quickly, while others are modified with a considerable shift of the oscillating droplet frequencies and the damping constants from the non-magnetic case. Even a purely DC magnetic levitation can be used for advanced material research.

2:30 PM Invited

Numerical Simulation of Liquid Metal Flows under the Influence of Magnetic Fields: *Andre Thess*¹; Thomas Boeck¹; Christian Karcher¹; Joerg Schumacher¹; Dmitry Krasnov¹; Gautam Pulugundla¹; Saskia Tympel¹; Vitaly Minchenya¹; Shuai Dong¹; ¹TU Ilmenau

We report a wide range of high-resolution numerical simulations of liquid metal flows interacting with DC magnetic fields ranging from fundamental studies of magnetohydrodynamic turbulence to applications like simulation of electromagnetic flow measurement devices for metallurgical applications.

2:55 PM Invited

Numerical Analysis of the Influence of Melting and Application of Electromagnetic Stirring Prior to Solidification on Macrosegregation Formation during Casting of a Binary Alloy: *Knut Omdal Tveito*¹; Mohammed M'Hamdi²; Hervé Combeau³; Miha Založnik⁴; Xiaodong Wang⁵; Bachir Saadi⁵; Yves Fautrelle⁵; ¹Norwegian University of Science and Technology; ²SINTEF Materials and Chemistry; ³Institut Jean Lamour, Département SI2M, CNRS – Nancy-Université – UPV-Metz, Ecole des Mines de Nancy; ⁴Institut Jean Lamour, Département SI2M, CNRS – Nancy-Université – UPV-Metz, Ecole des Mines de Nancy; ⁵SIMAP – CNRS – INPG - Université Joseph Fourier

Numerical simulations of macrosegregation formation during horizontal solidification of a hypoeutectic Sn-Pb alloy in a rectangular cavity is presented and compared to experimental results. The experiment involves a melting phase, a holding stage at constant temperature with or without application of electromagnetic stirring, and finally solidification. We simulate all stages of the experiment and study the segregation of Pb throughout the experiment. A two-phase volume-averaged model is used for the numerical simulations, accounting for thermo-solutal convection and assuming perfect microscopic mixing (lever rule). The influence of the melting phase and of the electromagnetic stirring is studied with different cases to illustrate the consequences on the flow pattern and on Pb segregation during melting and during solidification. The numerical simulations are compared to the experimental data and the impact of chemical inhomogeneities prior to solidification on macrosegregation formation is discussed.

3:20 PM Invited

Multiscale Modeling of Ingot Solidification Structure Controlled by Electromagnetic and Ultrasonic Stirring Technologies: *Laurentiu Nastac*¹; ¹The University of Alabama

Two advanced control solidification technologies were studied in this article to improve the quality of the cast ingots as well as to control the solidification structure evolution during the plasma arc melting [PAM] processing of Ti-6-4 ingots: (i) electromagnetic stirring (EMS), and (ii) ultrasonic treatment (UST). The developed EMS modeling approach is based on the numerical solution of Maxwell's equations, fluid flow, and heat transfer equations, and mesoscopic modeling of the grain structure. The UST analysis tool is capable to model acoustic streaming and cavitation. Predictions of the macrostructure, CET formation and primary dendrite arm spacing for PAM Ti-6-4 ingots processed with and without EMS or UST were discussed.



TMS 2012

141st Annual Meeting & Exhibition

3:45 PM Break

4:05 PM

Evolution of the Velocity Field during Solidification in an Electromagnetically Stirred Melt: Gregory Poole¹; Nagy El-Kaddah¹; ¹The University of Alabama

This paper describes the evolution of electromagnetically driven flows during unidirectional solidification in a bottom chill mould. The electromagnetic field in the metal and chill blocks was computed using the mutual inductance technique, while the temperature and flow field equations were solved using the control volume method. The k-ε model was used to determine the turbulent viscosity in the melt. The computed results showed that the flow field at the beginning of solidification is characterized by four recirculating loops typically found for stationary magnetic fields and changes to two loops at the end of solidification. The velocity was also found to vary along the solid-liquid interface. The magnitude of the velocity was not found to be constant, but increases as solidification progresses. The significance of these findings on grain refinement in electromagnetically-stirred melts will be discussed.

4:30 PM

Modeling the Case Hardening of Crankshafts: Tiruttani Kamal¹; Suresh Sundarraj¹; ¹General Motors

A 3-D numerical model of the induction hardening process of steel cranks has been developed and the predicted results of temperature, stresses, and phase distribution during this solid state phase transformation process are verified with experimental data from the literature. This heat treatment process involves heating the crank to the austenitic temperature range using an induction coil followed by rapid quenching in water to harden the surface of the crank. The model has been developed using ABAQUS, a commercial FEA software. The formation of martensite, pearlite, and retained austenite phases are modeled and implemented through a user defined function in ABAQUS. A sensitivity study on the various process parameters affecting the amount of phase distribution has been carried out. Based on this study, some recommendations are arrived at in selecting optimum crank rotation speed and quenching temperature and time during the induction hardening process.

4:50 PM

Study of De-Agglomerations Ceramic Nano Particles in the Aluminium Melt under Cavitation Phenomenon for Processing of Metal Matrix Nanocomposites: Payodhar Padhi¹; Pragyan Mohanty²; ¹Konark Institute of Science & Technology; ²ITER

The present study models the dispersion of ceramic nano particles in the liquid aluminum melt during the cavitation process. Cavitation produces when high-intensity ultrasound wave passes in the liquid which is used for de-agglomeration, dispersing and mixing of the fine particles in the liquids. When sound wave propagates into the liquid alternating high pressure (compression) and low-pressure (rarefaction) cycles depending upon frequencies are generated. When the bubble reaches a critical size at which it can no longer absorb energy, they collapse violently during high-pressure cycle. During the collapse of bubbles, high-pressure shock waves are generated and propagate through the liquid at velocities above the speed of sound, which creates high velocity collisions among solid particles suspended in such liquids. Here we have applied eulerian granular flow model using ANSYS R12 to study the particle de-agglomeration and dispersion during cavitation process which helps to process nanocomposites

5:10 PM

Fundamental Study on Behavior of Inclusion in Electromagnetic Swirling Flow in Immersion Nozzle in Continuous Casting Process: Su Zhijian¹; Li Dewei¹; Yang Ying²; Nakajima Keiji²; Jönsson Pär²; Marukawa Katsukiyo³; He Jicheng¹; ¹Northeastern University; ²Royal Institute of Technology (KTH); ³Sumitomo Metal Industries, Ltd.

Swirling flow in an immersion nozzle is effective on improving quality of casting block and casting speed in continuous casting process of steel. A refractory swirl blade installed in the nozzle is liable to cause

clogging, which limit the application of the process. A new process of electromagnetic swirling flow in immersion nozzle has been developed by EPM lab, China. That is a rotating electromagnetic field is set up around an immersion nozzle to induce swirling flow in it. The magnetic, flow and temperature field have researched. However the behavior of inclusion in this process is essential for the product quality. In this study, the inclusion trajectory in the immersion nozzle and square mold in the process is given, together with the magnetic, flow and temperature field. Results show that the swirling flow can achieve the same effects generated by the swirling blade process without the clogging in the nozzle.

Characterization of Minerals, Metals, and Materials: Characterization of Energy, Electronic and Optical Materials

Sponsored by: The Minerals, Metals and Materials Society, TMS Extraction and Processing Division, TMS: Materials Characterization Committee

Program Organizers: Jiann-Yang Hwang, Michigan Technological University; Sergio Montero, State University of North Rio De Janeiro; Chenguang Bai, Chongqing University; John Carpenter, US Department of Energy; Donato Firrao, Politecnico di Torino; Byoung-Gon Kim, Korea Institute of Geoscience & Mineral Resources; Mingdong Cai, Schlumberger

Wednesday PM

March 14, 2012

Room: Asia 2

Location: Dolphin Resort

Session Chairs: Sergio Monteiro, State University of North Rio de Janeiro; Zheng Zhang, Michigan Technological University

2:00 PM

Influence of La2O3 Additive Content on the Phase Stability, Sintering and Microstructure of 8 MOL% Y2O3 Stabilized Zirconia (8YSZ) Ceramic Used for Solid Oxide Fuel Cell Applications: Suleyman Tekeli¹; Bulent Aktas²; Serdar Salman³; ¹Gazi University; ²Harran University; ³Marmara University

The effect of La2O3 content up to 15 wt% on phase stability, sintering and microstructure of cubic zirconia (8YSZ) was investigated. XRD results showed that specimens containing up to 15 wt% La2O3 were composed of only cubic structure. Also, the specimens doped up to 5 wt% La2O3 revealed no La2O3 peaks, indicating that La2O3 was completely solubilised in cubic structure. However, when > 5 wt% La2O3 was added, the peak of La2Zr2O7 compound emerged, showing that overdoped La2O3 was not solubilized in the 8YSZ matrix. The lattice parameter of 8YSZ slightly decreased with increasing La2O3 content up to 1 wt% but further increase in La2O3 amount resulted in an increased lattice parameter. The comparison of grain size of 8YSZ specimens with various La2O3 content showed that grain size slightly increased with increasing La2O3 content up to 1 wt% but further increase in La2O3 amount resulted in a decreased grain size.

2:15 PM

Development and Characterization of Carbonaceous Materials Incorporated with Metal (Ti, V and Zn)-Organic Compounds for Hydrogen Storage: Mala Nath¹; Asheesh Kumar¹; Arjit Mallick¹; ¹Indian Institute of Technology Roorkee

Activated charcoal incorporated either with titanium n-butoxide, titanium diisopropoxide bis(2,4-pentanedionate), vanadium bis(2,4-pentanedionate) or zinc bis(2,4-pentanedionate) having 2–8 wt% of the metal were prepared using ethanol as solvent at 40–50 °C followed by calcinations at 100, 150 and 200°C, except the samples with titanium diisopropoxide bis(2,4-pentanedionate) calcinated at 80 °C. AAS and FESEM revealed that the maximum incorporation of metals (Zn, V and Ti) in activated charcoal was observed with 4 wt% of zinc bis(2,4-pentanedionate) calcinated at 150 °C, 4 wt% of vanadium bis(2,4-

pentanedionate) at 100 °C, 2 wt% of titanium n-butoxide at 100 °C and 2 wt% of titanium diisopropoxide bis(2,4-pentanedionate) at 80 °C, using equilibration time of 20-24 h. Hydrogen sorption behavior at 77.4 K and 1 bar indicated that the highest hydrogen uptake was obtained 1.45 wt% (164.5 cm³ (STP)/g at P/P₀ = 1.0) for activated charcoal incorporated with 4 wt% of zinc 2,4-pentanedionate calcinated at 150 °C.

2:30 PM

Characterization of Nickel Oxide Nanoparticles for Hydrogen Adsorption with External Electric Field: Zheng Zhang¹; Xiang Sun¹; Zhiwei Peng¹; Jiann-Yang Hwang¹; ¹MTU

Nickel oxide nanoparticles were synthesized using sodium dodecyl sulfate as the surfactant and urea as the hydrolyzing agent and different calcination temperatures and time were selected for preparation. Nitrogen adsorption (BET), X-ray diffraction (XRD) and scanning electron microscope (SEM) were subsequently used to characterize the prepared samples. The effect of an external electric field on hydrogen adsorption over a prepared nickel oxide was carried out. The electric field was introduced by a piezoelectric element, which is capable of autogenously generating charges under hydrogen pressure. Increased hydrogen adsorption was obtained from this study, which indicated a stronger interaction between the adsorbent surface and hydrogen.

2:45 PM

Ag /Diamond Composite Shims for High-Performance Thermal Management: Jason Nadler¹; Lee Bannister¹; ¹GTRI

A silver-diamond (Ag-Di) composite thermal shim has been developed in efforts to meet the thermal management challenges and dimensional constraints of next generation high-power wide-bandgap semiconductor devices. Some of these devices can generate heat fluxes exceeding 8kW/cm² at temperatures over 225°C, and consistently dissipating this heat requires thermal expansion (CTE) matched, high thermal conductivity, small form factor shims. Composite shims consisting of a high volume fraction of diamond (50-75%) serving as both a high-conductivity phase and CTE-modifier distributed in a silver matrix integrate and tailor these key requirements. Shim microstructures are designed to have multi-modal diamond particle size and spatial distributions based on a primary diamond monolayer. Initial performance has been characterized through thermal expansion and effective thermal resistance measurements up to 250°C as well as quantitative microstructural analyses to evaluate suitability for high power device integration.

3:00 PM

Nanocrystalline CdS Thin Films Prepared by Vacuum Evaporation: Shadia Ikhmayies¹; ¹Al Isra University

Nanocrystalline CdS thin films were prepared by vacuum evaporation on glass substrates at ambient temperature. The films were characterized by recording and analyzing their transmittance, X-ray diffraction (XRD) patterns, scanning electron microscope (SEM) images and Energy dispersive X-ray spectra. X-ray diffractograms revealed that the material is nanocrystalline with cubic crystal structure and preferential orientation along (111) plane. SEM micrographs confirmed the nanostructure of the material and showed uniform and well covered surfaces. EDX reports revealed that the films are cadmium rich and contain oxygen. The first derivative of the absorbance was used to estimate the effective bandgap energies of the nanocrystallites and the hyperbolic band model was used to estimate their radii. The results were compared with those obtained by XRD and SEM measurements.

3:15 PM

Structure-Property Correlation of Pb(Ni_{0.33}Nb_{0.67})O₃-(1-x)Pb(Zr_{0.31}Ti_{0.69})O₃ Based Relaxor-Ferroelectric Ceramics Synthesized Via Columbite Precursor Method: Bandi Malleshham¹; T. V. Jayaraman²; A. R. James³; Dibakar Das¹; ¹University of Hyderabad; ²University of Nebraska; ³Defence Metallurgical Research Laboratory

Lead based relaxor-ferroelectric material, with nominal compositions xPb(Ni_{0.33}Nb_{0.67})O₃-(1-x)Pb(Zr_{0.31}Ti_{0.69})O₃ (PNN-PZT) (0.2 ≤ x ≤ 0.6), have been synthesized by columbite precursor method. Homogeneous mixture

of the oxide powders was calcined at 850°C for 4 h to obtain phase pure perovskite followed by sintering of the pellets of PNN-PZT at 1100°C for 4 h. The presence of phase pure perovskite structure was confirmed by the X-ray diffraction (XRD) analysis; it also revealed structural transitions from rhombohedral to tetragonal phase with increasing PZT content. A morphotropic phase boundary (MPB) is observed at x = 0.5. Electrical polarization measurements showed high remnant polarization (19.12 μC/cm²) and low coercive field (6.89 kV/cm) at MPB as compared to other compositions. The electromechanical planar coupling coefficient (k_p) was estimated to be ~33% at MPB. A high piezoelectric strain coefficient (d₃₃ = 398 pC/N) was obtained at the MPB.

3:30 PM

Evolution of High-Energy Electron Beam Irradiation Effects on Zeolite Supported Catalyst: Metal Nanoprecipitation: Kai Song¹; Jinsong Wu¹; Dana Sauter¹; Vinayak Dravid¹; Peter Stair¹; ¹Northwestern University

The high-energy electron irradiation effects on Fe-loaded, zeolite-supported catalyst were examined by transmission electron microscopy. Metal nanoparticles were found to precipitate quickly under beam illumination with electron dose of 2.4 × 10⁷ nm⁻² or above at room temperature. Since electron microscopy was widely applied in characterization of all sorts of catalyst supported on zeolites, the current observations could be treated as a model system to distinguish the metal nanoparticles existing in original catalyst from those precipitated by electron beam irradiation. It was the electron radiation, other than temperature, that played an important role in the formation and growth of metal precipitates. In the current system, the induced nanoprecipitations were identified as pure Fe metal with a FCC structure by electron energy loss spectroscopy (EELS), high-resolution transmission electron microscopy (HRTEM) and electron diffraction.

3:45 PM

The Characteristics of Optical Recording Media Affected by The Accelerating Aging Test: Der-Ray Huang¹; ¹NDHU

In this paper, some DVD-R discs have been selected for long time light exposure test and high temperature and humidity test. Generally, recordable media under long time light exposure maybe be defected seriously. If we use Jitter value 8% as a reference to determine the life time of DVD-R samples, some discs defect after 5 hours of light exposure while some discs can endure over 25 hours. Also if we use reflectivity 45% to determine the life time, some discs defect after 20 hours light exposure while some discs can endure over 50 hours. From our results, the good samples show good characteristics of PI error. The absorption spectrum of recordable media is a good reference to justify the quality of dye media. These results can be used to estimate the life time of recordable discs. Also, these data provide good references for the research of long lifetime recordable media.

4:00 PM

A Comparison between the Properties of Spray-Pyrolyzed SnO₂:F/CdS:In Structures Prepared by Using NH₄F and HF as a Source of Fluorine: Shadia Ikhmayies¹; Riyad Ahmad-Bitar²; ¹Al Isra University; ²University of Jordan

SnO₂:F/CdS:In structures were prepared by the spray pyrolysis technique on glass substrates at a substrate temperature T_s = 450 °C. NH₄F and HF were both tried as the sources of fluorine in the precursor solution of SnO₂:F. A comparison between the properties of structures obtained by using the two doping compounds was performed. X-ray diffraction (XRD), scanning electron microscopy (SEM) and transmittance measurements were used to characterize the films. The structures prepared by using HF as a fluorine source were found to have more ordered crystal growth, larger grain size and sharper absorption edge. From the inspection of the first derivative of the absorbance it is expected that more interdiffusion on the SnO₂:F/CdS:In interface takes place in the structures made by using HF. These results confirm that these films are better as forecontacts for CdS/CdTe solar cells.



TMS 2012

141st Annual Meeting & Exhibition

4:15 PM

Transmission Electron Microscopy Study on Interfaces in Cu/CuZr Multi-layer Thin Films: *Ying Li*¹; Robert Dickerson¹; Amit Misra¹; ¹Los Alamos National Laboratory

Cu/CuZr multi-layer thin films with different layer thickness were synthesized by magnetron sputtering. The interface structures in these films were investigated by transmission electron microscopy (TEM), scanning TEM (STEM), high resolution TEM (HRTEM), energy dispersive X-ray spectroscopy (EDX), electron energy loss spectroscopy (EELS) and energy filtered TEM (EFTEM) method. The bonding between the two phases, atomic structure around the interface, the crystallization phenomena of CuZr phase at the interface and other microstructural features were studied in detail. Based on the comparison of microstructure characterization in the Cu/CuZr multi-layer thin films with different thickness, the microstructure evolution at the interfaces induced by layer thickness was also investigated.

4:30 PM

Characterization and Preparation of Anti-Reflection Coatings in the RANGE of 3-5 μm for Si Optical Window: *Khurram Iqbal*¹; Asghari Maqsood¹; ¹National University of Sciences and Technology

It is suitable for application in the infrared array camera (IRAC)

4:45 PM

Investigation of Room Temperature Dislocation Mobility in Metal Diborides (ZrB₂) Using Nano and Micro Indentation: *Ghatu Subhash*¹; Dipankar Ghosh¹; ¹University of Florida

Unlike structural ceramics that exhibit brittle behavior, transitional metal diborides (ZrB₂ and HfB₂) which are potential candidates for ultra high temperature applications, exhibit ductile deformation features and high electrical conductivity similar to metals. To further investigate this behavior, we have conducted nano- and micro-indentations and noted extensive slip-line patterns akin to those observed in metals. TEM analysis revealed multiple sets of dislocations and dominance of pyramidal slip. Nano indentation experiments on individual grains before and after macroindentation-induced deformation revealed that these slip regions are harder than the virgin material. The dislocation plasticity and hardening behaviors are argued on the basis of its chemical bonding and non-localized dislocation core structure.

Computational Thermodynamics and Kinetics: Cluster Expansion, Kinetic Monte Carlo, and First-principles

Sponsored by: The Minerals, Metals and Materials Society, TMS Electronic, Magnetic, and Photonic Materials Division, TMS Materials Processing and Manufacturing Division, TMS Structural Materials Division, TMS: Alloy Phases Committee, TMS: Chemistry and Physics of Materials Committee, TMS/ASM: Computational Materials Science and Engineering Committee, TMS: Integrated Computational Materials Engineering Committee, TMS/ASM: Phase Transformations Committee, TMS: Process Technology and Modeling Committee

Program Organizers: Zi-Kui Liu, The Pennsylvania State University; Mark Asta, University of California, Berkeley; James Warren, The National Institute of Standards and Technology; Yunzhi Wang, Ohio State University; Raymundo Arroyave, Texas A & M University; Yu Wang, Michigan Tech

Wednesday PM
March 14, 2012

Room: Australia 3
Location: Dolphin Resort

Session Chairs: Brent Fultz, Caltech; Axel van de Walle, Brown University

2:00 PM Invited

Cluster Expansion Methods - Progress and Outlook: *Axel van de Walle*¹; ¹Brown University

Although ab initio methods excel at calculating physical properties for any given atomic arrangements, proper modeling of the thermodynamic properties of solid-state alloys demands the exploration of the large number of states visited in thermal equilibrium, a task that is computationally intractable via a brute-force approach. This talk will overview the field research devoted to overcoming this problem, through a combination of computational techniques that are able to efficiently model electronic excitations, lattice vibrations and configurational disorder within a unified framework. This framework is the so-called cluster expansion formalism in conjunction with a suitable coarse-graining of the partition function. Various approaches that have been proposed to construct an optimal cluster expansion will be contrasted and examples of application will help illustrate the methods discussed and their capabilities.

2:25 PM

Kinetic Monte Carlo Simulations of Diffusion-Limited Nucleation: *Yang Hao Lau*¹; Ramanarayan Hariharaputran¹; David Wu¹; ¹Institute of High Performance Computing

Nucleation, the stochastic formation of clusters of a stable phase from a metastable phase, is the first step in many phase transformations. Due to its simplicity, classical nucleation theory (CNT) is often used to estimate nucleation rates, but since its derivation depends on the growth rate's being collision (or interface) limited, Kelton has recently modified CNT for diffusion-limited growth, which involves long-range diffusion and applies, e.g., to oxygen precipitation in silicon and, more generally, to crystallization in alloys [Kelton, K. F., *Acta mater.*, 2000, 48, 1967]. Unfortunately, critical tests of either CNT or Kelton's theory have been prevented by the lack of key input parameters, which are notoriously difficult to obtain experimentally. We therefore perform kinetic Monte Carlo simulations of diffusion-limited crystallization in 2D to obtain theoretical input parameters, nucleation rates, and size distributions of clusters. The predictions of CNT and Kelton's theory are compared to simulation results.

WEDNESDAY PM

2:40 PM

Kinetics of Tellurium Precipitation in CdTe-Based Materials: Vincenzo Lordi¹; ¹Lawrence Livermore National Lab

CdTe and related alloys, such as CdZnTe, are important materials for solar photovoltaic application as well as for high-resolution room-temperature gamma radiation detectors. However, the performance of devices, particularly in high-energy applications, is limited by various material defects. Among the most important defects are Te precipitates caused by non-stoichiometric growth conditions. In this work, we study the kinetics of Te aggregation and precipitation at the atomic scale, using a multi-scale modeling approach informed by first-principles calculations. Density functional theory is used to compute the energetics, migration rates, and binding energies of point defects involved in Te aggregation, which include various interstitials, vacancies, and anti-site defects. Kinetic Monte Carlo is then used to simulate the aggregation process leading to precipitation nuclei. The mechanism and kinetics of formation, and the resultant structures, of these Te-rich regions are compared for various conditions of stoichiometry and temperature. Prepared by LLNL under Contract DE-AC52-07NA27344.

2:55 PM

Influence of Misfit Stresses on Sputter-Induced Patterns on Alloy Thin Films: Bharathi Srinivasan¹; Ramanarayan Hariharaputran²; Yong-Wei Zhang¹; ¹Institute of High Performance Computing, Singapore; ²Institute of High Performance Computing

Understanding self assembly of nanoscale patterns like quantum dots, ripples and nanowires have gained significant importance recently for their role in devices for optoelectronic applications. Sputtering using low energy ion beams is one of the emerging techniques to grow these self-organized nanostructures. In single phase materials, these patterns are formed as a result of competition between sputtering and surface diffusion. In alloys, the component dependent diffusivity results in coupling between composition and surface modulation patterns. In alloy films epitaxially grown on substrate, the mismatch strains enrich these patterns by additional path of morphological evolution due to Asaro-Tiller instability. We present the results of kinetic Monte Carlo simulations of the formation and evolution of patterns on binary alloy surfaces under the influence of the non-uniform misfit stresses. Our talk would focus on the influence of parameters such as sputter yield, composition and misfit stress on the composition and height patterns.

3:10 PM Break

3:40 PM

Continuous Displacement Cluster Variation Method and Its Applications: Tetsuo Mohri¹; ¹Hokkaido University

Continuous Displacement Cluster Variation Method (CDCVM) is a revised version of conventional Cluster Variation Method and local lattice distortion effects are efficiently incorporated into the free energy formula. By employing CDCVM, the calculations of a phase diagram and diffuse intensity spectra originating from the local distortion are attempted for fcc based alloys. As compared with the transition temperature obtained by conventional CVM for an ordering system, the result of the CDCVM yields lower transition temperature, indicating the stabilization of a disordered phase. Diffuse intensity spectra are obtained in a systematic way in terms of concentration and temperature. The intensity distribution in the k-space is discussed in view of the atomic potentials of a given system.

3:55 PM

Positive Vibrational Entropy of Chemical Ordering in FeV and Its Electronic Origin: Brent Fultz¹; Jorge Munoz¹; Lisa Mauger¹; Chen Li¹; Matthew Lucas²; Olivier Delaire³; Douglas Abernathy³; Matthew Stone³; ¹California Institute of Technology; ²Wright-Patterson AFB; ³Oak Ridge National Laboratory

Inelastic neutron scattering and nuclear resonant inelastic x-ray scattering were used to measure phonon spectra of FeV as a B2 ordered compound and as a bcc solid solution. The two data sets were combined to

give an accurate phonon density of states, and the phonon partial densities of states for V and Fe atoms. Contrary to the behavior of ordering alloys studied to date, the phonons in the B2 ordered phase are softer than in the solid solution. Ordering increases the vibrational entropy by $+0.22 \pm 0.03 k_B/\text{atom}$, stabilizing the B2 ordered phase to higher temperatures. First-principles calculations showed that the electronic generalized susceptibility was isotropic and well behaved, and the number of electronic states at the Fermi level increased upon ordering. During ordering, the increased screening between ions reduced the interatomic force constants. The effect of screening was larger at the V atoms than at Fe atoms.

4:10 PM

Ab Initio Study of Advanced Metallic Nuclear Fuels for Fast Breeder Reactors: Alexander Landa¹; Per Söderlind¹; Patrice Turchi¹; Andrei Ruban²; Levente Vitos²; ¹Lawrence Livermore National Laboratory; ²Royal Institute of Technology

The U-Zr and U-Mo alloys proved to be very promising fuels for fast breeder reactors. In this work we perform *ab initio* study of the ground state properties of bcc U-Zr and U-Mo alloys and compare their heats of formation with CALPHAD assessments. We discuss how the heat of formation in both alloys correlates with the charge transfer between the alloy components, and how the specific behavior of the density of states in the vicinity of the Fermi level promotes stabilization of the U₂Mo compound. Our calculations suggest that bcc U-Mo alloys should have much lower constituent redistribution than U-Zr alloys. We also explore the idea of stabilization of the UZr₂ compound against the α -Zr due to increase of Zr d-band occupancy by the addition of U to Zr. This work was performed under the auspices of the US Department of Energy by Lawrence Livermore National Laboratory under Contract DE-AC52-07NA27344.

4:25 PM

Ordering of Oxygen and Vacancies in Hexagonal Closest Packed Zr and Hf: ZrO_x; and HfO_x (0 ≤ X ≤ 1/2): Benjamin Burton¹; Axel van de Walle²; ¹NIST; ²California Institute of Technology

First principles phase diagram (FPPD) calculations were performed for the hcp-based systems: ZrO_x; and HfO_x (0 ≤ X ≤ 1/2). The Vienna Ab Initio Simulation Package (VASP) was used to calculate formation energies which became input for Alloy Theoretic Automated Toolkit (ATAT) fits of cluster-expansion (CE) Hamiltonians, and these were used in Monte-Carlo phase diagram calculations. Very similar CE-Hamiltonians were obtained for both systems, but significantly different phase diagrams were calculated. In both CEs nearest-neighbor (nn) interactions parallel- and perpendicular to c_{hex} were strongly repulsive for O-O nn-pairs, but farther nn pair-terms were significantly larger in HfO_x. In ZrO_x, Long Period Superstructures (LPSS) were reported in samples with bulk compositions near Zr₃O, but they were not reproduced by the FPPD calculation. In HfO_x, no such phases have been observed experimentally, but Devil's Staircases of ordered phases were predicted in (metastable) Hf₃O and Hf₂O.

4:40 PM

DFT Study of Initial Oxidation State on TiN Step Surfaces: Minki Hong¹; Simon Phillpot¹; Susan Sinnott¹; ¹University of Florida

Titanium nitride (TiN) film has extreme hardness, high chemical reactivity and high electrical conductivity and thus is widely used for wear and corrosion resistant coatings as well as diffusion barriers and gate electrodes in microelectronic devices. They are thus routinely subjected to extreme conditions such as high pressure and temperature, corrosive environments, and consequently undergo oxidation. Here, density functional theory calculations are used to determine the mechanisms associated with step-related oxidation process and the formation of nitrogen exit channels induced by Ti surface diffusion. The energy barrier associated with Ti diffusion on (210) step surface is ~3 eV while the energy barrier for oxygen dissociation is almost zero.



TMS 2012

141st Annual Meeting & Exhibition

4:55 PM

Generalized Cluster Expansion of III-V Semiconductor Alloys: *Gregory Pomrehn*¹; Axel van de Walle²; ¹California Institute of Technology; ²Brown University

The III-V system of semiconducting alloys (Al, Ga, In cations and N, P, As anions) is investigated through the use of a generalized cluster expansion. This method provides a general expression relating the state of atomic order of an alloy to various tensor-valued properties, such as static strain, elastic constants, carrier masses and dielectric properties. The unknown coefficients in this general expansion are determined via first-principles calculations. The resulting structure-property relationships can provide helpful guidance in the design of optoelectronic devices.

Defects and Properties of Cast Metals: Novel Processes and Applications

Sponsored by: The Minerals, Metals and Materials Society, TMS Materials Processing and Manufacturing Division, TMS: Solidification Committee

Program Organizers: Mark Jolly, University of Birmingham; Brian Thomas, University of Illinois at Urbana-Champaign; Carl Reilly, University of British Columbia

Wednesday PM
March 14, 2012

Room: Oceanic 4
Location: Dolphin Resort

Session Chairs: Peter Lee, University of Manchester; Mark Jolly, University of Birmingham

2:00 PM

Flux Entrapment Defects in Electroslag Remelting of High Ti, Low Al Nickel Based Superalloys: *Jonathan Busch*¹; Jack deBarbadillo²; Matthew Krane¹; ¹Purdue University; ²Special Metals Corporation

High Ti, low Al nickel based alloys, such as INCOLOY alloy 800 and 825, are particularly prone to macroscale slag inclusions and microscale cleanliness issues. These issues can result in significant yield losses (~10%) due to surface grinding. Slag inclusion samples from near the outer radius of the toe end of alloy 800 and 825 ingots were found to have a multiphase microstructure consisting of CaF₂, CaTiO₃, Ca₁₂Al₁₄O₃₃, MgAl₂O₄ and MgO. These inclusions were often surrounded by a field of smaller TiN cuboidal particles 1 to 10 microns in size. Several process changes have been enacted at the Special Metals facility in Burnaugh, KY to reduce the exposure of liquid metal to atmospheric nitrogen in an attempt to mitigate these issues. However, the slag inclusion and microscale cleanliness problems persist and the exact mechanism by which they form is still under investigation.

2:25 PM

Defect Control on Al Castings for Excellent Quality and Improved Performances through Novel Rheocasting Processes: *Mario Rosso*¹; Ildiko Peter¹; ¹Politecnico di Torino

Commonly, components of complex shapes are prepared by casting or by forging processes, the choice is based on economical, as well as performance basis. Casting technologies versus forging are decidedly more competitive from the economical point of view, while forging is able to guarantee the best performances, thanks to the highest soundness. Castings can be affected by defects like voids or cavities, inclusions and oxides. Semi-solid processes are able to better control the defect level and can reduce the existing gap between casting and forging. In this paper the attention will be focused on some very promising rheocasting processes, which have been recently developed. Particular emphasis will be devoted to the study and discussion of the possible causes of defects, of their origins and mechanisms, in order to realize their full control and to attain the production of high performance and reliable complex shape components at competitive costs.

2:50 PM

Defect Elimination in Cast Al Components via Friction Stir Processing: *Ning Sun*¹; Diran Apelian¹; ¹Worcester Polytechnic Institute

Friction stir processing (FSP) is an outgrowth of Friction stir welding (FSW) that locally manipulates the microstructure by imparting a high level of energy in the solid state resulting in improved mechanical properties. Our work to date has shown that FSP can be implemented as a post-casting method to locally eliminate casting defects, such as porosity due to gas evolution during casting. Coarse second phase are broken into fine nearly equiaxed particles and distributed uniformly in the matrix; grain refinement is also attained by dynamic recrystallization during FSP. This results in improved tensile properties and fatigue behavior of the cast Al A206 alloy. Such improvements have important implications for manufactured components for a variety of automotive and other industrial applications. The convenience of FSP as a post-processing step that can easily be adapted during machining operation makes it quite attractive for adoption. These results will be reviewed and discussed.

3:15 PM Break

3:40 PM

Quality Improvement of Aluminium Alloy Castings by application of a New Casting Facility instead of a Conventional Investment Casting Process: *Xiaojun Dai*¹; Mark Jolly¹; Bin Xu Zeng¹; ¹University of Birmingham

The production of aluminium alloy castings in traditional investment casting process usually uses chunky runner system and top filling method. The large runner system has a low yield and generates lots of wastes. The top filling method (gravity filling method) makes the liquid flow in the runner system in turbulent behaviour. In this way the oxide films on the liquid metal will fold, break up and trap into the liquid. When the liquid metal is solidified, the trapped oxide films will form the porosities and cracks which will damage the mechanical properties of the castings. By using a new facility, called CRIMSON, the weight of the runner system and defects are drastically reduced. The experimental outcomes can validate the simulation results. It was verified that the castings produced by the new facility have better mechanical properties in comparison with the castings produced by traditional method.

4:05 PM

Ribbon-Substrate Adhesion and Catastrophic Sticking in the Planar-Flow Melt Spinning of Metals: *Anthony Altieri*¹; Eric Theisen²; Paul Steen¹; ¹Cornell University; ²Metglas, Inc

In the planar-flow melt spinning process, liquid metal is brought into contact with a cold, rotating wheel and a thin, solid ribbon is spun off. The ribbon adheres to the wheel until it detaches naturally or is mechanically removed. In the absence of a mechanical removal system, the natural detachment mechanism is thermo-elastic contraction of the solidified ribbon as it cools. Under certain conditions, the ribbon does not contract sufficiently to detach in the time of a wheel revolution. This event is called catastrophic sticking. In this situation, the ribbon reenters the liquid-wheel contact region which typically ruins the integrity of the ribbon and can damage the casting equipment. The transition between successful detachment and catastrophic sticking happens rapidly and depends primarily on the wheel surface-temperature. A model of ribbon cooling which successfully predicts the point of ribbon detachment and the sudden transition to catastrophic sticking will be presented.

4:30 PM Concluding Comments

Deformation, Damage, and Fracture of Light Metals and Alloys: Session V

Sponsored by: The Minerals, Metals and Materials Society, TMS Structural Materials Division, TMS Light Metals Division, TMS/ASM: Mechanical Behavior of Materials Committee
Program Organizers: Qizhen Li, University of Nevada, Reno; Fuqian Yang, Univ. of Kentucky; Ke An, Oak Ridge National Laboratory

Wednesday PM
March 14, 2012

Room: Northern A2
Location: Dolphin Resort

Session Chairs: Qizhen Li, University of Nevada, Reno; Wen-Ming Chien, University of Nevada, Reno

2:00 PM Invited

Study of the High-Performance Super-Light Mg-Li Alloys and Heat-Resistant Mg-RE Alloys: Milin Zhang¹; Ruizhi Wu¹; Jinghui Zhang¹; Fengchun Jiang¹; ¹Harbin Engineering University

The research results about Mg-Li alloys and heat-resistant Mg alloys in Harbin Engineering University are summarized. As for the super-light Mg-Li alloys, we mainly investigated the alloying effect, the ageing reaction and the superplasticity. As for the high strength and heat-resistant Mg-RE alloy, we investigated a new Mg-Gd-Dy-Zn alloy. The results showed that the as-cast sample with 14H long period stacking ordered (LPSO) structure exhibits acceptable strength and high ductility, and the peak-aged sample with basal plane stacking faults (SF) shows high strength and adequate elongation.

2:30 PM

Effect of Stacking Fault Energy and Solute Size on the Rare Earth Texture Evolution and Deformation Behavior of Magnesium Alloys: Zachary Bryan¹; Ryan Hooper¹; Michele Manuel¹; ¹University of Florida

It has recently been shown that rare earth solutes in magnesium modify the conventional basal-dominated texture during recrystallization and lead to increased formability. It is thought that the unique texture component arises from shear band nucleation and solute drag effects due to the solute's large atomic radius. The effect of variable stacking fault energy, which is important in deformation and thus annealing, has not been studied concurrently with atomic size. This study systematically varied solute misfit strain and stacking fault energy through alloy selection to determine their individual and combined effects on the mechanical properties and annealed texture. Mechanical tests were performed at temperatures from 25 to 300°C and strain rates from 10⁻⁴ to 10⁻¹ s⁻¹ to elucidate the effect of dynamic strain aging on texture evolution. This work is supported by the National Science Foundation (Award#: DMR-0845868) and the Department of Energy Office of Science Graduate Fellowship (Contract#: DE-AC05-06OR23100).

2:45 PM

Strengthening Mechanisms in Solution-Annealed Ni-rich NiTi Alloys: Billy Hornbuckle¹; Taisuke Sasaki²; Ron Noebe³; Glen Bigelow³; Mark Weaver¹; Greg Thompson¹; ¹The University of Alabama; ²National Institute for Materials Science; ³NASA Glenn Research Center

The two properties generally associated with NiTi alloys are shape memory and superelasticity. As such, most NiTi research has concentrated on near equiatomic compositions. In the present study, we have investigated the Ni-rich 60NiTi (Ni55Ti45 at.%) composition. This composition still possesses superelasticity, but also exhibits elevated Vickers micro-hardness values. In the hot-rolled condition, the alloy contained the NiTi (B2), Ni4Ti3, and Ni3Ti phases with a Vickers micro-hardness value of 375 Hv. This alloy was then solution annealed at 1050 deg. C for 10 hours and water quenched. This resulted in a significant increase in Vicker's microhardness to 645 Hv. Similar solution aging for a 57NiTi (Ni52Ti48 at.%) alloy only resulted in a Vicker's microhardness of 450 Hv. The retained phases, post-solution annealing, for both compositions

was B2 and Ni4Ti3. Through TEM and Atom Probe analysis, the increase in hardness is discussed in terms of nanoscale precipitates and local chemical modulations.

3:00 PM Break

3:20 PM

Twinning Mechanisms in Hexagonal Close-Packed Metals: Bin Li¹; Xiyan Zhang²; ¹Center for Advanced Vehicular Systems; ²Chongqing University

We present atomistic simulations on configurations of twinning dislocations and transmission electron microscopy observations on interfacial structures of twin boundaries of major twinning modes in HCP metals (Mg, Ti, Zr, Co etc.), i.e., {10-11}<10-1-2>, {10-12}<10-1-1>, {11-21}<11-2-6> and {11-22}<11-2-3>. Our results show excellent agreement with the classical theory in terms of the magnitudes of the Burgers vectors of the twinning dislocations, but the structure of the twinning dislocation differs drastically from one mode to another because of the diversity in shear and shuffle. The most commonly observed {10-12}<10-1-1> twinning is an extreme case in which shear is negligible and shuffle is dominant. The {11-21}<11-2-6> twinning is an extreme case in which no shuffle is involved and shear dominant. The {10-11}<10-1-2> twinning is shear dominant with minor off-plane shuffles; and the {11-22}<11-2-3> twinning is in the middle where shear and shuffle are nearly equal but the shuffles are in-plane.

3:35 PM

Alloy Development and High Temperature Deformation of TiAlNbCrMo Alloys: Glenn Bean¹; Michele Manuel¹; ¹University of Florida

Titanium aluminides have been of great interest due to their high specific strength and good mechanical properties below 700°C. Limited research has been conducted towards increasing strength and operating temperatures of these alloys, by developing a γ (TiAl)+ σ (Nb₂Al) microstructure. Alloys with over 50% σ -phase have shown excellent high temperature properties up to 1000°C, but are brittle at room temperature. Recently, alloys with less than 30% σ -phase have been investigated with regards to alloy development, characterization, and deformation behavior at elevated temperature, while exploring relationships between chemistry and microstructure, and the resulting mechanical properties. Alloys in the TiAlNb(Cr,Mo) system with varying Nb content have been produced and characterized at high temperature ($\geq 700^\circ\text{C}$) under compression at strain rates ranging from 10⁻² to 10⁻⁵ s⁻¹. Microstructural analysis was conducted to determine the deformation and damage characteristics of the alloys. This work has been supported by the National Science Foundation under award number DMR-0856622.

3:50 PM

Role of Substitution Elements on Twinning Nucleation Mechanism in Magnesium: Mehul Bhatia¹; Kiran Solanki¹; Amitava Moitra²; Mark Tschopp³; ¹SEMTE; ²Department of Chemical Engineering and Materials Science and Engineering; ³CAVS - Center for Advanced Vehicular System

Within hcp materials, plastic deformation along the <c> axis, is primarily accommodated through twinning due to the limited number of slip modes imposed by c/a ratio. Moreover deformation twinning is greatly influenced by the alloying contents. In this work, we investigate the role of substituting elements (Al) on homogenous nucleation of twins and its profound effect in the strain hardening behavior of defect-free pure magnesium using molecular dynamics. Simulation results reveal multiple {101 $\bar{2}$ }<101 $\bar{1}$ > twin nucleation under uniaxial tensile loading along [0001] direction. With an increase in Al content, the deformation mechanism changes and the twin nucleation was no longer observed with Al substitution contents greater than 8%. Consistent with the advanced fracture theory of Sleswyk (1969), nanovoids nucleated in pure Mg due to twin-twin interactions. Finally, these results reveal complex mechanisms associated with solute-twin and twin-twin interactions and also provide a basis for new alloy design.



4:05 PM

Effect of Aging Treatment on Fatigue Behavior of an Al-Cu-Mg-Ag Alloy: *Michael Burba*¹; Michael Caton²; Sushant Jha³; Christopher Szczepanski²; ¹University of Dayton; ²US Air Force Research Laboratory; ³Universal Technology Corporation

An investigation of the fatigue properties of an Al-Cu-Mg-Ag alloy with two different heat treatments, underaged and peak-aged, was conducted. Particular focus was on the effect of these treatments on the lifetime distribution and the role played by crack initiation versus the small-crack growth regime. Tests were performed to characterize the distribution in fatigue lifetimes at a given stress level and the small-crack growth behavior under the two aging treatments. Results showed that there was almost no difference in mean lifetimes for either heat treatment but a significant difference in the minimum lifetimes, where the peak-aged condition had a higher propensity for life-limiting failure mechanisms. Further, the small-crack growth rates at room temperature were largely unaffected by the aging treatments. Based on this study, it is suggested that the under-aging treatment primarily influences the crack-initiation regime in terms of reducing the likelihood of developing a life-limiting deformation condition.

Electrode Technology for Aluminium Production: Characterization of Cathode Materials

Sponsored by: The Minerals, Metals and Materials Society, TMS Light Metals Division, TMS: Aluminum Committee, TMS: Aluminum Processing Committee
Program Organizer: Morten Sorlie, Alcoa Norway

Wednesday PM
March 14, 2012

Room: Americas Seminar
Location: Dolphin Resort

Session Chair: Egil Skybakmoen, SINTEF

2:00 PM

Spent Potlining: an Update: *Rudolf Pawlek*¹; ¹TS+C

This paper continues a review given in 1999 and resumes practices to treat the waste of worn cathodes of the primary aluminium industry. The waste cathode lining consists of a carbon part and a refractory part. Spent potlining contains water-soluble fluorides and small amounts of leachable cyanides, and is therefore classified as hazardous. Besides inertization such as treatment at high temperatures, by vitrification, or by leaching and flotation the refractory component can also be used for instance in the manufacture of cement, concrete and brick, or as a road pavement additive, or as a potline electrolyte additive for the production of Al-Si pre-alloys. The carbon component can be used as a fuel additive in cement kilns but also as an additive in the pig iron and steel industry. Various ways to treat and use spent potlining have been published in the meantime and will be reviewed.

2:25 PM

Analysis of Porous Structures of Graphitic Cathode Materials and the Correlation to Penetrated Sodium: *Xiang Li*¹; Jilai Xue¹; Jun Zhu¹; Qingcheng Zhang¹; ¹University of Science and Technology Beijing

Cathode materials used in aluminum reduction cell today are of porous structure. This work is aimed to have better control of the cathode quality through quantitatively analyzing the pore structure and its correlation to the penetrated sodium (metallic Na and NaF). The cathode samples were made of graphite aggregate and pitch, and formed with various pressures (12 - 36Mp). Image analysis was applied to characterize their porous structures. XRD and SEM-EDS were used to analyze the penetrated sodium. When the forming pressure was at 20Mp, the cathode density got to its maximum value (1.58 g/cm³) with the minimum total porosity (21.96%) and the least pore number (549). When the pore connectivity was from 9.81% up to 37.95%, the depth of sodium penetration was from 11mm to 39mm. The other porous structure parameters, such as

total porosity, pore number and shape factor, showed little correlation to penetrated sodium.

2:50 PM

Characterization of Carbon Cathode Materials by X-Ray Microtomography: *Martin Brassard*¹; Martin Lebeuf¹; Alexandre Blais²; Loig Rivoaland²; Martin Désilets¹; Gervais Soucy¹; ¹Université de Sherbrooke; ²Rio Tinto Alcan

The carbon cathode is the main component of the aluminium reduction cell. As it is the container for molten electrolytic bath and aluminum, it provides the electrical contact that is essential for electrolysis. Its properties are thus crucial. X-ray microtomography was used to compare different virgin cathode materials, as well as cathode materials that had been used in laboratory-scale aluminium reduction cells. Results demonstrated significant differences in terms of bath penetration, pore distribution and metallic inclusions. X-ray microtomography was shown to be a powerful tool for 3-D characterization of cathode materials.

3:15 PM

New Observations in Creep Behavior of Ramming Paste in Aluminium Electrolysis Cell: *Sakineh Orangi*¹; Donald Picard¹; Houshang Alamdari¹; Donald Ziegler²; Mario Fafard¹; ¹NSERC/Alcoa Industrial Research Chair MACE3 and Aluminium Research Centre-REGAL, Laval University; ²Alcoa Canada

Creep of ramming paste was studied from ambient to operational temperature in order to characterize its mechanical behavior as used in the peripheral joint of aluminium electrolysis cells. Two types of uniaxial creep test over a specified stress level were performed on two inch samples: tests at room temperature for samples baked at different temperatures and test at temperatures close to the sample baking temperature. It is concluded that at certain baking temperatures and given stress level, three types of creep, called primary, secondary and tertiary, take place successively. In addition, at lower baking temperatures (200 °C), the creep level is larger in comparison with creep at higher baking temperatures. Also, for specified baking temperature, creep strain obtained by high temperature testing is larger than creep strain obtained by room temperature testing. These results give new insights on the ramming paste behaviour in aluminium electrolysis cell.

3:40 PM Break

3:55 PM

Wetting of KF-AIF₃-Based Melts on Graphite Cathode Materials for Aluminium Electrolysis: *Yanan Zhang*¹; Jilai Xue¹; Jun Zhu¹; Xiang Li¹; ¹University of Science and Technology Beijing

Graphite cathode materials are nowadays used in aluminum reduction process where KF-AIF₃-based melts may serve as an alternative electrolyte. In this work, wetting angles of KF-AIF₃-based melts on graphite cathode materials were measured using a modified sessile drop method. A fresh drop of the melt was injected through a BN tube on to the samples surface, and then the wetting angles were photographed against time elapsed. It was found that the wetting angles on the full graphitic and graphitized cathode samples were larger than those on the semi-graphitic at 750 °C, and their values changed with alumina content (3 - 5 wt%), cryolite ratio (1.2 - 1.5) and time elapsed (0 - 20 min). The melt penetration profiles on the cross-sections of the melt-graphite interface after wetting tests were also inspected using SEM-EDS technique. The results obtained can be useful for optimizing the properties and compositions of graphite cathode materials.

4:20 PM

Fundamentals of Aluminum Carbide Formation: *Bronislav Novak*¹; Kati Tschöpe¹; Arne Petter Ratvik¹; Tor Grande¹; ¹Norwegian University of Science and Technology

The fundamentals of formation of aluminum carbide were studied by aluminum-carbon diffusion couple experiment. The diffusion couples consisted of pure liquid aluminum and graphitized carbon, and the diffusion couple experiments were performed at temperatures 1000-

1200°C in stagnant argon atmosphere. In some experiments the diffusion couple interface was coated with small amount of cryolite. The formation of aluminum carbide layer at the solid-liquid interface was confirmed by X-ray diffraction and electron and optical microscopy. The kinetics of the formation of the carbide layer was investigated in detail and the influence of molten cryolite and possible gas phase transport will be discussed.

4:45 PM

Investigation of the Cathode Wear Mechanism in a Laboratory Test Cell: *Kati Tschöpe*¹; Anne Store²; Stein Rørvik²; Egil Skybakmoen²; Tor Grande¹; Arne Ratvik¹; ¹NTNU; ²SINTEF Materials and Chemistry

Cathode wear has become one of the major challenges for the life time of high amperage aluminium reduction cells due to the use of graphitized cathodes. The fundamentals of the cathode wear are still a matter of debate, and a laboratory procedure for testing of cathode materials is desired. Here, we present a laboratory electrolysis cell designed to investigate the cathode wear of industrial cathode materials. The formation and transport of aluminum carbide is considered to be an important factor for the cathode wear, and the laboratory test cell is designed in such a way that the cathode is exposed directly against the electrolyte, and aluminum carbide formed at the cathode can then be more easily dissolved in the electrolyte. Here we present a study of cathode wear of selected cathode materials where the influence of the cathode surface morphology, diffusion and hydrodynamics in the electrolyte have been in focus.

5:10 PM

Study on Graphitization of Cathode Carbon Blocks for Aluminum Electrolysis: *Gao Feng*¹; ¹Northeastern University

High quality graphite cathode carbon blocks require low resistivity, strong resistant erosion to melt salt and liquid aluminum in the aluminum electrolytic cells. It not only can decrease cathode voltage drop and reduce the powder consumption, and but also can improve service life of the cell. Applying hot mould technology under 40 MPa pressure, different amount petroleum coke in anthracite mixtures is graphitized in graphitized furnace. By the X-ray diffraction parameters, density, compressive strength and resistivity drop measured, the experimental results show that compressive strength and volume density of graphitized containing 30% of petroleum coke block respectively are 1.366 g/cm³ and 4.8 MPa, resistivity drop from 114μO · m to 13μO · m, most confirms to the production requirements.

Energy Nanomaterials: Thermoelectrics and Thermal Transport

Sponsored by: The Minerals, Metals and Materials Society, TMS Materials Processing and Manufacturing Division, TMS Structural Materials Division, TMS: Advanced Characterization, Testing, and Simulation Committee, TMS: Nanomechanical Materials Behavior Committee

Program Organizers: Reza Shahbazian-Yassar, Michigan Technological University; Ming Au, Savannah River National Laboratory; Meyya Meyyappan, NASA Ames Research Center

Wednesday PM
March 14, 2012

Room: Swan 3
Location: Swan Resort

Session Chairs: Meyya Meyyappan, NASA Ames Research Center; Reza Shahbazian Yassar, Michigan Technological University

2:00 PM

Ab-Initio Thermal Conductivity for Thermoelectric Nanostructured Materials: *Derek Stewart*¹; Anupam Kundu²; Natalio Mingo²; Alistair Ward³; David Broido³; ¹Cornell University; ²CEA-Grenoble; ³Boston College

Manipulating the thermal properties of materials by embedding nanoparticles is a successful route to improve thermoelectric materials. The development of a first principles approach to predict thermal transport can

help this effort by identifying potential material candidates and providing insight into nanoscale heat transfer. We present a new ab-initio approach for predicting thermal conductivity in bulk and nanoscale materials. Harmonic and anharmonic interatomic force constants are calculated from density functional perturbation theory and used to solve the phonon Boltzmann transport equation exactly. We find excellent agreement with experiments for technological materials (Si, Ge, and diamond). We can also examine thermal transport in materials with nano-inclusions, such as nanoparticle embedded in alloy thermoelectrics (NEAT) materials. I will discuss how nanoparticle composition and size can significantly affect thermal conductivity in SiGe alloys. Linking these force constants with a Green's function approach, we can also manipulate thermal transport in nanotubes and graphene.

2:25 PM

Characterization of Nanostructured Thermoelectric Materials Using Electron Backscattered Diffraction: *Matt Nowell*¹; ¹EDAX-TSL

Recent trends in thermoelectric materials development are directed towards using nanostructural engineering to reduce thermal conductivity and improve material performance. Understanding how to optimize this engineering requires structural characterization on a nanometer scale. In this work, Electron Backscatter Diffraction (EBSD) has been used to characterize nanostructured Bi₂Te₃ precursor powders and consolidated bulk samples. A variety of consolidation processes have been used and the resulting structures characterized and compared. The effects of the spatial resolution limits of EBSD as a function of both sample and analytical data acquisition conditions will also be addressed. For this work, grains as small as 20nm have been resolved. Comparisons with other characterization techniques will also be discussed.

2:50 PM

Study to Bi₂Te₃-Based Thermoelectric Nanocomposite Added Silver Nanoparticles by Metal-Organic Decomposition: *Hsin-Hsien Yeh*¹; Chiung-Hsiung Chen²; Hong-Ching Lin²; Ming-Wei Lai²; Chien-Neng Liao¹; ¹National Tsing Hua University; ²ITRI

Bulk nanostructure is one of methods to enhance the figure of merit of thermoelectric materials. In this study, nano-silver particles were dispersed well at the grain boundary by metal organic decomposition (MOD) to improve the characteristics of bulk nanocomposite of bismuth telluride. The Bi₂Te₃ powders were milled with the solution of silver salts and dehydrated alcohol by the planetary miller then formed the bulk by spark plasma sintering (SPS) process. The bulk materials were cut into rectangular bars (3x2x6 mm³) for measuring electrical conductivity and Seebeck coefficient by commercial equipment of ULVAC model ZEM-3. The microstructure of the modified powders and the bulk materials were examined using field emission scanning electron microscopy and high-resolution transmission electron microscopy. The compositions were analyzed by energy-dispersive x-ray spectroscopy.

3:15 PM

Enhanced Performances of Micro-Thermoelectric Devices Integrating Layered A₂Te₃ (A= Sb, Bi) Films: *Tanming Tan*¹; ¹Beihang University

Herein, an approach for the fabrication of devices integrating the layered Sb₂Te₃ and Bi₂Te₃ thin films with ordered structures was reported by radio-frequency (RF) magnetron sputtering method. The composition and microstructure of the films were studied by X-ray diffraction (XRD), scanning electron microscopy (SEM), and energy dispersive X-ray spectrum (EDS), presenting a well preferential crystal growth along the planes perpendicular to the c-axis. The thermoelectric properties of the layered thin films were characterized. The power generation and the cooling of the two types of micro devices with n and p elements in series or parallel circuit, respectively, have been tested. The results have proved that high-performance micro devices could be realized by introducing the layered Sb₂Te₃ and Bi₂Te₃ thin films with ordered structure.



TMS 2012

141st Annual Meeting & Exhibition

3:30 PM Break

4:00 PM Invited

Thermal Transport in Nanomaterials for Energy Applications: *Xinwei Wang*¹; ¹Iowa State University

Nanomaterials have attracted significant attention for their great applications related to energies. Examples include nanostructured thermoelectric materials for significant efficiency improvement, and nanofibers/wires for photo-voltaic applications. Thermal transport capability of nanomaterials plays a critical role for energy conversion efficiency and sustained device functionality. In this talk, I will give a review on the experimental and theoretical work we have done/are doing about the thermal transport in nanoscale/structured energy materials. For experimental investigations, our research focuses on development of advanced technologies to characterize thermophysical properties of nanomaterials. Examples will be given about the study on anatase TiO₂ nanofibers and their secondary porosity, thermal contact resistance between TiO₂ nanotubes, and the thermal transport in carbon related nanomaterials. The theoretical work will be focused on the structure and localized thermal transport in coherent thermoelectric materials, ballistic and non-Fourier thermal transport in graphene nano-ribbon, and coherent phonon dynamics in materials.

4:30 PM

Effects of Surface Faceting and Twinning on Thermal Transport Characteristics of Silicon Nanowires: *Frederic Sansoz*¹; ¹University of Vermont

Precise control over phonon transport in nanowires is critical to the development of next-generation thermoelectric devices in semiconductors. This talk particularly examines the impact of surface morphology and twinning on thermal conductivity in crystalline Si nanowires, with particular emphasis on circular, hexagonal and sawtooth-faceted shapes, by using non-equilibrium molecular dynamics simulations. From this study, 47% reduction of thermal conductivity is found in sawtooth-faceted {111}/100 Si nanowires compared to nanowires of equivalent diameter with smooth sidewalls. This effect is shown to result from a strong dispersion of surface phonons in {100}-type facets. However, the simulations reveal that phonon dispersion is less pronounced with {113}-type facets and absent with {111}-type facets, which suggests a new means to control phonon dynamics at the nanoscale. Also I show that some anomalous thermal transport characteristics exist in periodically-twinned Si nanowires due to this unique faceting dependence on phonon modes.

4:55 PM

Mechanical and Thermal Energy Transport in Biological and Biologically Inspired Nanostructures: *Markus Buehler*¹; ¹Massachusetts Institute of Technology

We present molecular-based computational studies of mechanical and thermal energy transport in biological and biologically inspired nanostructures. A series of studies will be presented, including energy transport in carbon nanotubes and interfaces of graphite, graphene and carbon nanotubes with other materials (e.g. metals), protein materials (e.g. beta-sheet nanocrystals and amyloids), as well as polymers. The concept of thermomutability will be introduced, a mechanism by which the energy transport of materials is controlled by external cues such as mechanical strain. We present a case study that demonstrates how hierarchical structures of carbon nanotubes, based on biological designs of mass and energy transport in cells and tissues, can be used to achieve a superior level of material performance for applications in thermal management and energy harvesting.

Energy Technologies and Carbon Dioxide Management: CO₂ Management and Utilization

Sponsored by: The Minerals, Metals and Materials Society, TMS Extraction and Processing Division, TMS Light Metals Division, TMS: Energy Committee

Program Organizers: Maria Salazar-Villalpando, DOE/National Energy Technology Laboratory; Neale Neelameggham, IND LLC* ; Donna Guillen, Idaho National Laboratory; Subodh Das, Phinix, LLC; Ramana Reddy, Univ of Alabama; Animesh Jha , Univ of Leeds; Soobhankar "Sib" Pati, Metal Oxygen Separation Technologies (MOxST); Mark Jolly, Univ of Birmingham; Lakshmanan Vaikuntam, Process Research ORTECH Inc

Wednesday PM
March 14, 2012

Room: Europe 8
Location: Dolphin Resort

Session Chairs: Maria Salazar-Villalpando, DOE/National Energy Technology Laboratory; Neale Neelameggham, IND LLC; Mahesh Jha, DOE; Jung-Kun Lee, University of Pittsburgh

2:00 PM Introductory Comments

2:05 PM Keynote

Meeting the Materials Challenges to Enable Clean Coal Technologies: *Bryan Morreale*¹; *Cynthia Powell*¹; ¹US DOE National Energy Technology Laboratory

Realization that the environmental impact of energy production must be reduced on a global scale, combined with an increased national desire to reduce dependence on foreign energy, is driving significant change in the energy outlook of the United States. While renewable energy resources will continue to grow in importance, environmentally responsible fossil energy production will be necessary to provide a bridge to the next energy revolution. This drive to increase process efficiencies and reduce the environmental impact in fossil-based energy production will require processes with increased operating temperatures and pressures, and increasingly aggressive operating environments. The practical result is a requirement for affordable and reliable high-performance materials and materials systems to enable these next-generation fossil energy systems. This talk will focus on the research being performed within the National Energy Technology Laboratory's Office of Research & Development to meet this requirement for high performance yet affordable materials.

2:25 PM Keynote

Liquid Fuels from CO₂, Water, and Solar Energy: *Aldo Steinfeld*¹; ¹ETH Zurich

Solar thermochemical processes for the production of synthetic liquid fuels make use of concentrated solar radiation as the energy source of high-temperature process heat. Considered are H₂O/CO₂-splitting thermochemical cycles via metal oxide redox reactions, encompassing two steps: 1st step) a solar-driven endothermic reduction of the metal oxide into a metal or reduced-valence metal oxide and O₂ evolution, and; 2nd step) an exothermic reaction of the reduced metal/metal oxide with H₂O/CO₂ which yields H₂/CO, together with the initial form of the metal oxide; the latter is recycled to the first step. The syngas mixture H₂/CO can be further processed via Fischer-Tropsch and other catalytic processes to liquid hydrocarbon fuels. ZnO and CeO₂ based redox pairs have emerged as highly attractive because of their rapid fuel production kinetics, cyclability, and high selectivity. The solar tower technology is presented.

2:45 PM

Solar Activated Photocatalytic Conversion of CO₂ and Water to Fuels by TiO₂-Based Nanocomposites: *Qianyi Zhang*¹; *Lianjun Liu*¹; *Ying Li*¹; ¹University of Wisconsin-Milwaukee

Photocatalytic conversion of CO₂ and water to value-added products (CO, methane, and/or methanol) by sunlight is potentially a promising sustainable energy technology that not only reduces greenhouse gas

emissions but also produces renewable fuels. However, the low CO₂-to-fuel conversion efficiency has impeded the development of this technology. TiO₂ has been widely used as a photocatalyst due to its low cost, high stability, and environmental benignness. In this work, material innovations have been made to TiO₂ nanostructures to improve the CO₂ conversion efficiency by increasing the surface area, inhibiting photoinduced electron-hole recombination, and enhancing visible light utilization. The catalysts are well characterized by UV-vis, XRD, SEM, TEM, XPS, and BET analysis. The experiments of photocatalytic CO₂ reduction with water vapor are conducted under visible light, UV-visible, and simulated sunlight, respectively. The product yield and selectivity are correlated with the nanostructures and the reaction mechanisms are proposed.

3:00 PM

Photocatalytic Efficacy of 1-Dimensional Nanocomposite Electrode:

*Bo Ding*¹; *Jung-Kun Lee*¹; ¹University of Pittsburgh

The photocatalytic splitting of water into H₂ and O₂ by oxide nanoparticles has received much attention. However, the full potential of photo-catalysts for efficient hydrogen generation out of water has not been fully realized yet due to unresolved limitations including the low electrical conductivity and ineffective carrier extraction. In this presentation, we report composite oxide materials consisting of 1-dimensional (1-D) transparent conducting oxide (TCO) core and TiO₂ shell. The TCO core is first synthesized by vapor-liquid-solid growth technique and the TiO₂ layer is subsequently deposited through atomic layer deposition. The photoelectrodes consisting of these 1-D nanocomposites have increased carrier mobility due to the TCO core, while the TiO₂ shell provides the photocatalytic functionalities. In addition, the built-in-potential at the interface between TCO core and the TiO₂ shell improves the collection of charge carriers from TiO₂ to TCO. These factors altogether contribute to increasing the photocurrent of the device under light.

3:15 PM

Electro-Catalytic Conversion of Carbon Dioxide into Hydrocarbon Fuels: A Theoretical Study of Selectivity and Efficiency of Copper Catalysis: *Tao Liang*¹; *Yu-Ting Cheng*¹; *Simon Phillpot*¹; *Susan Sinnott*¹; ¹University of Florida

Electrocatalytic reduction of carbon dioxide into fuels would provide an ideal storage medium for intermittent renewable energy sources. Copper electrocatalysts have been found to be capable of producing significant quantities of hydrocarbons such as methane and ethylene from CO₂. Despite extensive studies on electro-reduction of CO₂ at metal electrodes, the mechanisms associated with catalytic reactions on Cu electrodes have remained elusive. Here, we use third-generation charge optimized many body (COMB3) potentials to determine the reaction free energy and atomic scale mechanisms associated with electrocatalytic reactions on Cu surfaces and clusters supported on metal oxide surfaces. The influence of system conditions on the results is quantified.

3:30 PM Break

3:35 PM

Reduction of Energy Consumption and GHGs Emission in Investment Casting Process by Application of a New Casting Method: *Xiaojuan Dai*¹; *Mark Jolly*¹; *Binxu Zeng*¹; ¹University of Birmingham

In traditional investment casting process of aluminium alloys for the application of the aerospace industry, to assure the quality of the final casting, usually the foundry uses bulky runner system which results in low yield, high energy consumption and high GHGs emission. In one case of this investigation, the yield is between 5 ~ 10% which means that the current casting process wastes large amount of energy and generates lots of scraps. By applying a new casting method, the bulky runner system and the melting/holding time are greatly reduced, the quality of the casting is improved, and in the meantime the related energy consumption and emission of CO₂ are significantly decreased. In the investigation, the energy efficiencies and emission of CO₂ of between the current and traditional processes are calculated and compared.

3:50 PM

Bauxite Residue Neutralization and Carbon Sequestration from Flue Gas: *Luis Venancio*¹; *Emanuel Macedo*²; *José Antonio Souza*²; *Fernando Botelho*²; *Otacílio Dias*²; ¹Federal University of Para ; ²Federal University of Para

The production of alumina from bauxite using the Bayer process generates 0.7 to 2.0 ton of the residue known as red mud and about 800 kg of CO₂ per ton of alumina. The direct use of exhaust gases to react and neutralize the bauxite residue may allow a double gain: open a wide range of new applications for bauxite residue reducing its reactivity and sequester from 38 to 107 kg of CO₂ per ton of alumina. This paper shows a pilot scale reaction of a suspension of bauxite residue-water with flue gas produced from direct burning oil, similar to the exhaust gases of a refinery. Two different types of reactors are used, a spray tower and a packed column. The inlet and exhaust gases are analyzed using electrochemical cells and non-dispersive infrared sensors. The pH of the suspension is monitored during the reaction and after to evaluate the buffer effect.

4:05 PM

50% Reduction of Energy and CO2 Emission in Metallurgical Furnaces by Burners: *Michael Potesser*¹; *Davor Spoljarić*¹; *Burkhardt Holleis*¹; *Martin Demuth*¹; ¹Messer Group

The efficiency of industrial combustion processes can be raised in two ways, either by preheating the fuel and combustion air or by oxyfuel. The most important issue of the usage of oxygen burners is the substantially increasing melting rate by lowering the specific production costs because of the higher combustion efficiency. The flameless combustion (internal offgas recirculation) and the external offgas recirculation solves the problem with the high flame temperature and leads to cold combustion and lower dross formation or alloying elements combustion. The Oxipyr®-Air combines the technology of diluted combustion during air and oxygen usage decreasing the emission of pollutants. Constitutive of the Oxipyr®-Air development a fuel-oxygen-burner, Oxipyr®-Flex, was designed for a maximum of flexibility for the customer. The Oxipyr®-Air and Oxipyr®-Flex have been developed for the specific needs of melting and recycling companies for all non ferrous metals. The paper shows the theory, practical installations and economical outlook

4:20 PM

CO2 Removal from Industrial Off-Gas Streams by Fluidized Bed Carbonation: *Koullis Pericleous*¹; *Mazaher Molaei*²; *Mayur Patel*²; ¹University of Greenwich; ²University of Greenwich

The future trading of carbon credits and increased financial cost necessitates substantial cuts in incidental CO₂ emissions in the production of metals (iron, steel, aluminum, zinc, lead). Although greener methods of production are being developed, in the short term the use of point-source CO₂ extraction using existing technology remains attractive. Accelerated natural carbonation, in a fluidized bed is a feasible technological route investigated in this research. CFD modelling has been used to study the efficiency of CO₂ capture in a fluidized bed reactor containing a CaO solid sorbent. A Lagrangian/Eulerian scheme describes describe CaO particle trajectories and exchange of mass, momentum and energy with the carrier gas, with a typical off-gas composition. Different reactor geometries are considered (with uniform, stepped and gradually expanding cross-section), to maximize conversion for a given particle loading and size distribution (100-200 microns). Removal efficiencies of up to 80% are demonstrated, making this a viable process.

4:35 PM

A Hydro-Mechanical Model and Analytical Solutions for Geomechanical Modeling of Carbon Dioxide Geological Sequestration: *Zhijie Xu*¹; *Yilin Fang*¹; *Timothy Scheibe*¹; *Alain Bonneville*¹; ¹Pacific Northwest National Laboratory (PNNL)

We present a hydro-mechanical model and deformation analysis for geological sequestration of carbon dioxide. The model considers the poroelastic effects by taking into account the two-way coupling between the geomechanical response and the fluid flow process in greater detail.



In order for analytical solutions, the simplified hydro-mechanical model includes the geomechanical part that relies on the theory of linear elasticity, while the fluid flow is based on the single-phase Darcy's law. The model was derived through coupling the two parts using the standard linear poroelasticity theory. Analytical solutions for fluid pressure field were obtained for a typical geological sequestration scenario and the solutions for ground deformation were obtained using the method of Green's function. Solutions predict the temporal and spatial variation of fluid pressure, the effect of permeability and elastic modulus on the fluid pressure, the ground surface uplift, and the radial deformation during the entire injection period.

Fatigue and Corrosion Damage in Metallic Materials: Fundamentals, Modeling and Prevention: Materials Corrosion and Prevention

Sponsored by: The Minerals, Metals and Materials Society, TMS Structural Materials Division, TMS/ASM: Mechanical Behavior of Materials Committee

Program Organizers: Tongguang Zhai, University of Kentucky; Zhengdong Long, Kaiser Aluminum; Peter Liaw, University of Tennessee

Wednesday PM
March 14, 2012

Room: Oceanic 6
Location: Dolphin Resort

Session Chairs: Gary Harlow, Lehigh University; Richard Ricker, NIST

2:00 PM Invited Characterization of Constituent Particles in 7075-T6 Aluminum Alloy: D Gary Harlow¹; ¹Lehigh University

Corrosion in aluminum alloys results from local galvanic coupling between constituent particles and the metal matrix. Since pitting is caused by particles, proper statistical characterization of the geometrical aspects of the particles is critical to the modeling. One of the more important statistics is the particle size distribution. Extensive optical microscopic observations on common 7075-T6 aluminum alloy have resulted in rather large sets of data for particle geometry. Thus, accurate statistical modeling is possible. Furthermore, similar data have also been collected from teardown specimens taken from seven different outer wing panels constructed from 7075-T6 aluminum alloy. The purpose of this effort is to use advanced multimodal statistical modeling methods to appropriately characterize the geometrical properties of constituent particles in these specimens. Comparisons between the teardown specimens and the common alloy are made. Suggestions for use in corrosion modeling are also presented.

2:20 PM Invited Effect of Hydrogen on the Localized Corrosion of Stainless Steels: Lijie Qiao¹; ¹University of Science and Technology Beijing

Hydrogen enhances nucleation of micro-cracks, increases propagation rates of stress-corrosion cracks, and reduces the threshold stress in stainless steel. Hydrogen decreases corrosion and pitting potentials, and increases passivation current of 2507 duplex stainless steels in 0.5mol/LH₂SO₄+3%NaCl solution. Both hydrogen and Cl⁻ decrease linearly corrosion and pitting potentials, and increase the passivation current of carbon steel in boric acid buffer solution. Study of Scanning Kelvin probe force microscopy shows that many lower potential regions appear in the ferrite and the interface of ferrite and austenite after hydrogen charging. The region means the hydrogen clusters pitting location.

2:40 PM Invited Water-Induced Damage of Subsurface Layer in AA 2037 Al Alloy Probed by a Slow Positron Beam: Yichu Wu¹; Peihai Li¹; Tongguang Zhai²; Paul Coleman³; ¹Wuhan University; ²University of Kentucky; ³University of Bath

Water-induced damage in AA2037 Al-Cu alloys processed by two different thermomechanical conditions was measured with positron beam-based Doppler broadening spectroscopy, in combination with XRD, AFM and TEM. Defect profiles in depth in the alloys were analyzed by measuring the S parameter as a function of incident positron energy up to 30 keV. It was found that, when the samples with more T (Al₂₀Cu₂Mn₃) phases were immersed in the deionized water up to 20 days, a small decrease in the S parameter near the surface was observed, which did not change with immersion time. However, a significant decrease in S parameter, depending on immersion time, was observed in the samples with less T phase. This indicated that the AA2037 Al alloy with more T phase presented more stable surface oxide film and better resistance to water damage than the alloy with less T phase.

3:00 PM Investigation on Corrosion Behavior of Ni-Based Alloys in Molten Fluoride Salt Using Synchrotron Radiation Technique: Min Liu¹; Yanling Lu¹; Yanyan Jia¹; Junyi Zheng¹; Zhijun Li¹; Yang Zou¹; Xiaohan Yu¹; Xingtai Zhou¹; ¹Shanghai Institute of Applied Physics, Chinese Academy of Sciences

Due to perfect corrosion resistance and excellent mechanical properties, Ni-based high temperature alloys are widely used in nuclear reactor. In this paper, corrosion processes of Ni-based superalloys including Inconel 600, Hastelloy X and Hastelloy C-276 were investigated in molten fluoride salts (LiNaKF) at 750°C. Then the samples were analyzed using scanning electron microscope (SEM), X-ray fluorescence analysis (μ-XRF) and X-ray diffraction (XRD). μ-XRF results have shown that the Ni-based alloy corrosion behavior in molten fluoride salt is mainly due to the erosion of element Cr. XRD results indicate that the alloying element Mo of Hastelloy c-276 have formed the Mo₂C structure, which can enhance anti-corrosive performance of Ni-based alloy in molten fluoride salt. Among the three Ni-based alloys mentioned in this paper, Hastelloy C-276 has the best corrosion resistance in molten fluoride salts at 750°C.

3:20 PM Electrochemical Measurement Methods for Evaluation of the Effects of Hydrogen on the Mechanical Properties of Metals: Richard Ricker¹; ¹NIST

Electrochemistry makes available to investigators a number of promising tools and measurement methods for investigating the influence of hydrogen on the mechanical properties of metals and alloys. Experiments ranging from simple cathodic charging experiments to the measurement of the response to transients, periodic waveforms, and noise can be used to investigate the interactions that can lead to the absorption, diffusion, and embrittlement of metals and alloys. Experiments can be designed to answer fundamental questions about the effects of cyclic loading and metallurgical variables. This paper will review work at NIST investigating and comparing different electrochemical techniques for investigating hydrogen embrittlement including electrochemical permeation, absorption, repassivation transients, and optimization of cathodic charging conditions.

3:40 PM Break

3:45 PM

Evaluation of Residual Stresses by Sen ² θ Method and Its Relationship with the Corrosion Resistance of ER NiCrMo-4 Weld Overlays on C-Mn Steel Pipelines: Raphael Henrique de Melo¹; *Theophilo Maciel*¹; Marcos da Silva¹; Valmir Batista¹; Marcos Antonio dos Santos¹; ¹Federal University of Campina Grande)

The aim of this study was to evaluate the influence of nozzle-to-plate distance (stickout) on the dilution and geometric characteristics (penetration, reinforcement, and width) of the overlays, as well to verify the influence of the Fe content and level of residual stresses by X-ray diffraction, on its corrosion resistance. The increase of the stickout promoted a reduction of approximately 9% in the dilution of the overlays, thus reducing the Fe content in the surface. The residual stresses presented predominantly compressive and it had been noted that for same levels of residual stress the corrosion resistance is directly influenced by the Fe content, however, when the level of residual stresses becomes sufficiently dissimilar, the Fe content starts to be less meaningful. In addition, it was found that the less the level of the compressive residual stresses, lower will be the corrosion resistance.

4:05 PM

Influence of Non-Metallic Inclusions on Pitting Corrosion Resistance of Cr-Ni-Mn Austenitic Stainless Steel: Alexander Ramirez²; *Adriana Murcia Santanilla*¹; Neusa Alonso-Falleiros¹; ¹University of São Paulo

The aim of this work is to evaluate the influence of non-metallic inclusions on the pitting corrosion resistance of the Cr-Ni-Mn austenitic stainless steel in presence of chloride and bromide ions. The pitting potential (E_p) was determined by potentiodynamic polarization method in electrolytes containing 0.6M NaCl, 0.45M NaCl+0.15M NaBr, 0.3M NaCl+0.3M NaBr and 0.6M NaBr. The results showed that when this steel was tested using the 0.6M NaBr and 0.3M NaCl+0.3M NaBr, the pitting potential was almost constant, but, when it was tested in the electrolytes containing, 0.45M NaCl+0.15M NaBr and 0.6M NaCl the pitting potential decreased with increasing of chloride content into electrolyte. In this work was evaluated the influence of non-metallic inclusions as pit nucleation sites. There were found some non-metallic inclusions attacked by aggressive ions, such as: aluminum oxide and both silicon and aluminum oxide.

4:25 PM

A Study on the Effect of Applied Potentials on Tress Corrosion Cracking of X70 Pipeline Steel in High pH CarbonateBicarbonate by EIS: *Ayda Shahriari*¹; Taghi Shahrabi¹; Aliakbar Oskuie¹; ¹Tarbiat Modares University

Stress corrosion cracking (SCC) behavior of X70 pipeline steel in high pH carbonatebicarbonate solution at different applied potentials was investigated using slow strain rate testing (SSRT). Electrochemical impedance spectroscopy (EIS) has been used to detect stress corrosion cracking in X70 pipeline steel sample exposed to high pH carbonatebicarbonate solution at different applied potentials. Morphology of X70 pipeline steel fracture surfaces at different applied potentials were also observed by scanning electron microscope (SEM). The results suggest that X70 pipeline steel is susceptible to SCC in a narrow window of potential. EIS measurements showed that a phase shift of impedance at particular frequencies is related to the length of a stress corrosion crack.

4:45 PM

Comparative Study of the Influence of Welding Parameters on the Characteristics of Stainless Steel Weld Overlays Applied by FCAW and SAW Process: Raphael Henrique de Melo¹; *Theophilo Maciel*¹; ¹Federal University of Campina Grande)

Welding is the main manufacturing process used not only in the assembly and repair of pipes, but for application of coatings for corrosion protection. The geometric shape of the weld overlays is directly affected

by the process parameters being an indicative of the quality of the coatings. In this paper the modeling, analysis and optimization of the characteristics of stainless steel weld overlays deposited by SAW and FCAW welding processes were made. The experiments were conducted based on the technique of design of experiments with three factors at two levels of control and mathematical models were developed through multiple regression. Response parameters and the influence of welding parameters was discussed, the models provide parameters to optimize economically the process through the optimal geometry and deposition efficiency. The results showed that less voltage values and greater feed rate less will be the dilution with significative reflection on corrosion resistance

5:05 PM

Effect of Conversion Coatings on SCC Behavior of Pipeline Steels: *Aliakbar Oskuie*¹; Taghi Shahrabi¹; ¹Tarbiat Modares University

In this study the effect of application of conversion coatings on SCC behavior of API X70 pipeline steels in high pH carbonate-bicarbonate solution was investigated. Zinc phosphating and chromating were two conversion coatings were used to modify the surface of pipeline steels. The mechanical properties of the samples coated by these two methods were determined by slow strain rate tests (SSRT). These results were compared with mechanical properties of the sample tested in air. Tensile tests were conducted at 50°C. To monitor crack growth, electrochemical impedance tests were carried out at fixed durations along the tests. Stereo and scanning electron microscopy were used for fractography as well.

Federal Funding Workshop: Panel Discussion

Sponsored by: The Minerals, Metals and Materials Society, TMS: Public and Governmental Affairs Committee

Program Organizers: Robert Shull, National Institute of Standards and Technology; Jud Ready, Georgia Institute of Technology

Wednesday PM

March 14, 2012

Room: Northern C

Location: Dolphin Resort

4:00 PM Panel Discussion with Panelists:

Looking for Transformative Approaches for the Materials Genome Initiative: *Diana Farkas*, Program Director, Condensed Matter and Materials Theory, Division of Materials Research, National Science Foundation

Basic Research Challenge in Materials; *Julie Christodoulou*, Director, Naval Materials Division, Office of Naval Research

New Efforts on Computational Materials: *Diana Bauer*, Director of the Office of Economic Analysis, U.S. Department of Energy

Advancing Superalloys: Michael Caton, Senior Materials Research Engineer, Materials & Manufacturing Directorate, Air Force Research Laboratory

5:15-6:00 PM: Networking Reception with the Panelists

Sponsored by the Georgia Institute of Technology



TMS 2012

141st Annual Meeting & Exhibition

From Macro to Nano, Understanding Mechanical Behavior across Length Scales: A Structural Materials Division Symposium in Honor of Robert Ritchie: Deformation and Fracture

Sponsored by: The Minerals, Metals and Materials Society, TMS Structural Materials Division, TMS/ASM: Mechanical Behavior of Materials Committee, TMS: Biomaterials Committee
Program Organizers: Jamie Kruzic, Oregon State University; Brad Boyce, Sandia National Labs; Reinhold Dauskardt, Stanford University

Wednesday PM Room: Mockingbird 1
March 14, 2012 Location: Swan Resort

Session Chairs: Philip Withers, The University of Manchester; Brad Boyce, Sandia National Laboratories

2:00 PM Introductory Comments

2:05 PM Keynote

Fracture Mechanics by 3D Crack-Tip Microscopy: *Philip Withers*¹;
¹University of Manchester

Prof. Ritchie has made a major contribution clarifying the crack-tip driving force in terms of intrinsic damage occurring ahead of a growing crack, and the extrinsic shielding mechanisms behind it. Increasingly, materials are designed at the microscale, or even the nanoscale, for improved resistance to sub-critical crack growth. Traditional global macroscopic approaches are insufficient. To progress, we need a means of extracting quantitative information about the local crack-tip environment. This paper will describe the concept of a 3D 'crack-tip x-ray microscope', by combining diffraction and imaging modes, as in an electron microscope. Critically, unlike an electron microscope we can follow the crack-tip deep in engineering samples under realistic conditions. Synchrotron x-ray diffraction is used to map crack-tip stresses, hence the operative stress shielding micromechanisms that slow cracks and 3D x-ray tomography to image the damage accumulation that contribute to crack growth and crack closure and deflection that impede it.

2:45 PM

Fracture Behavior of Tungsten: *Bernd Gludovatz*¹; Stefan Wurster²; Andreas Hoffmann³; Reinhard Pippan²; ¹Lawrence Berkeley National Laboratory; ²Erich Schmid Institute of Materials Science, Austrian Academy of Sciences; ³Plansee SE

Tungsten shows the typical change in fracture behavior from brittle at low temperature to ductile at high temperatures, however, the brittle fracture behavior of the material is not well understood yet. Crack propagation occurs either intergranularly or transgranularly and parameters like grain size and shape as well as texture, chemical composition and grain boundary impurities are amongst the main influences controlling the crack path. In order to analyze some of these parameters different microstructures were produced by high pressure torsion (HPT) and analyzed using techniques like Auger electron spectroscopy (AES) or electron backscatter diffraction (EBSD). AES revealed a limited influence of impurities on the crack path below a certain impurity concentration. Investigations on the crack propagation resistance showed an increasing fracture resistance with crack extension, so-called R-curve behavior. EBSD analyses revealed that this is mainly caused by crack bridging and increasing plasticity around the propagating crack with increasing temperature.

3:00 PM

Grain Boundary Cracking in Sn-Rich Pb-free Solders: *J. Shang*¹;
¹University of Illinois

Health and environmental concerns over Pb have prompted the recent transition from Pb-bearing to Pb-free solders in microelectronic industry. Among many Pb-free solder alloys, the Sn-rich alloys have emerged as

the primary replacement alloys. Our recent work has shown that Sn and Sn-rich alloys are very susceptible to grain boundary cracking under mechanical and electrical loading. While the classical grain boundary fracture mechanisms prevailed under mechanical loading, the divergence of vacancy concentration at the grain boundary induced grain tilting, rotation, sliding, and finally grain boundary cracking. Under cyclic loading, an intergranular cracking model was developed for cycle-dependent softening of Pb-free solders. The model was applied to explain the dependence of cyclic response to grain size, strain amplitude, and temperature in Sn-rich solder alloys.

3:15 PM

Tensile Deformation of Quenched and Partitioned Steel - A Third Generation High Strength Steel: Jason Coryell¹; *Josh Campbell*²; Vesna Savic¹; John Bradley²; Sushil Mishra¹; Shashank Tiwari¹; Louis Hector Jr²; ¹General Motors; ²GM R&D Center

Quenching and partitioning (Q&P) is a steel heat treatment process that promotes carbon enrichment of retained austenite thereby enhancing ductility without substantially compromising strength. Deformation and fracture of Q&P steel, a new third generation advanced high strength steel, was investigated in quasi-static tensile tests ranging from -100 °C to 200°C. Strain fields of specimens tested at 25°C were measured with digital image correlation (DIC) using a stereo system, while standard tests with an extensometer were conducted at the other temperatures. The data were used to determine how the measured strength and ductility of Q&P steel compare with other advanced high strength steels such as TRIP (transformation induced plasticity) and TWIP (twinning induced plasticity). The temperature effect on the yield stress, ultimate tensile strength, and strain at uniform elongation was explored in detail. This provided insight into the austenite to martensite phase transformation at higher temperatures.

3:30 PM

The Influence of Microstructure and Texture on Strain Localization in Thin Stainless Steel Sheet: Eric Buchovecky¹; *Louis Hector Jr*²; Siguang Xu²; John Bradley²; Sushil Mishra²; Allan Bower¹; ¹Brown University; ²General Motors

Crystal plasticity finite element (CPFE) simulations are used to identify controllable material properties (e.g. distributions of grain size, grain shape, crystal orientation) that inhibit or enhance thinning instabilities in 75-90 µm thick ferritic stainless steel sheet. The CPFE material model is calibrated against a suite of oriented uniaxial tensile tests. Statistical measures of grain morphology and orientation from electron backscattered diffraction (EBSD) analyses are used to generate multiple FE meshes with grain morphologies and crystal textures that are statistically-equivalent to those of the actual material. Necking and failure in CPFE simulations of uniaxial tension and a simple plane strain forming process are correlated with statistical measures of texture and microstructure from EBSD.

3:45 PM Break

4:00 PM

Microscale Testing of Fracture Toughness in Graded Pt-Ni-Al Bond Coats on Superalloys: Jaya Nagamani¹; *Vikram Jayaram*¹; Sanjay Biswas¹; ¹Indian Institute of Science

Diffusion bond coats that confer oxidation resistance to superalloys in aeroengines are typically produced by pack aluminising. The failure of the resultant graded microstructure is driven by a combination of stresses from thermal gradients, oxidation, centrifugal loading and particle impact. In order to understand failure modes and to develop design criteria, it is critical to understand the fracture process in different regions of the coating. We use FIB to machine beams from different positions across the coating and subjecting them to fracture in a depth sensing indenter. Because the ends of the beam are not free to move as in conventional 3-point bending, finite element analysis is used to validate the experimentally observed load-displacement response. The toughness, averaged from several

beams at each of four locations reveals variations from as low as 5 to 20 MPa root m which can be correlated to microchemistry from SEM-EDS.

4:15 PM

Deformation Response of Cold-Drawn and Annealed MP35N Wire: *M.J.N.V. Prasad¹; Sharvan Kumar¹; ¹Brown University*

The alloy, MP35N (35%Co-35%Ni-20%Cr-10%Mo) is used in implants, especially as lead wires in pacemakers, because of its ultra-high strength and excellent corrosion resistance. In this study, low-Ti, MP35N alloy wire, 100 μm in diameter, was characterized both in the as-drawn and annealed conditions. In the as-drawn condition, numerous cold-drawing-induced nanotwins were observed; when deformed in this condition in uniaxial tension at room temperature, high strengths up to 2 GPa, limited ductility of 3 percent and strain rate sensitivity were noted. In contrast, the recrystallized wire (annealed) displayed improved ductility (~30%) and reduced strength (~0.6 GPa). The deformed microstructure is being characterized by bright field and dark field transmission electron microscopy as well as HRTEM. In the as-drawn condition, plastic deformation is enabled by both slip and twinning/de-twinning. Characterization of the annealed material is in progress. These results will be presented and the underlying deformation mechanisms will be discussed.

4:30 PM

Mechanical Behavior of Copper Single Crystal in the Presence of Point Defects: *Iman Salehina¹; David Bahr¹; ¹WSU*

Structural defects affect both the nucleation and propagation of dislocations. Atomistic simulations of nanoindentation tests were used to explore the stochastic response of dislocation nucleation in copper in the presence of vacancies, solute atoms and self-interstitial atoms. Because of non-uniform and highly concentrated stress filed under the indenter, a spatial variation in defects varies the mechanical response even in a small simulation box, allowing stochastic behavior to be examined. The simulations exhibited maximum yield stress reductions of 8% and 20% in the presence of a vacancy and a self-interstitial atom, respectively. The distribution of Al solute atoms was used to demonstrate both concentration and distribution play role on altering the measured yield stress during nanoindentation. Since the shear stresses around a crack tip and an indenter are similarly high, the effect of these defects when positioned near a crack tip was also explored using tensile tests.

4:45 PM

Effect of Grain Boundary Character on Strain Localization and Grain Boundary Sliding during Creep Deformation of Nickel-Bases Superalloys: *Jennifer Carter¹; Michael Uchic²; Michael Mills¹; ¹The Ohio State University; ²Air Force Research Laboratory, Materials & Manufacturing Directorate*

This work details how deformation localizes at grain boundaries in nickel-based superalloys using a novel in-situ digital image correlation technique to create full-field deformation maps. In-situ experiments at 700°C were conducted while periodically acquiring SEM images. Full-field deformation maps of localized behavior (including grain boundary sliding events) are correlated with microstructural features, such as grain boundary character and grain orientation as determined from EBSD mapping. Subsequent analysis of the displacement fields from image correlation with the EBSD maps allows for assessment of the direct relationship between strain localization and microstructural features. Site specific extraction of TEM foils and serial sections using the FIB are conducted at grain boundaries exhibiting large strain localization due to accumulation or grain boundary sliding. This allows for additional correlations between micro-scale 2-D strain data with underlying dislocation activity and 3-D nano-scale microstructural features, such as boundary topology; including nano-scale serrations and grain boundary borides.

5:00 PM

Comparison of Deformation Mechanisms for Constant Strain Rate and Creep Testing of a Ni-Based Superalloy: *Hallee Deutchman¹; Michael Mills¹; ¹The Ohio State University*

The effect of strain rate on deformation mechanisms was investigated under creep and constant strain rate conditions on an advanced, polycrystalline Ni-based disk superalloy. A detailed microstructure characterization aimed at measuring the gamma-prime precipitate size, morphology, and distribution was performed prior to mechanical testing experiments so that the effects of microstructure can be correlated with the deformation response. Constant load creep tests and constant strain rate tests were performed at the same temperature so that the influence of strain rate on deformation substructure can be assessed. Following mechanical testing, a thorough TEM characterization study was done to determine the operative deformation mechanisms. Significant differences have been observed with dislocation-mediated mechanisms at higher strain rates and microtwinning and faulting of precipitates at low strain rates. Funding for this work has been provided by AFRL through the Metals Affordability Initiative (MAI) program.

International Smelting Technology Symposium (Incorporating the 6th Advances in Sulfide Smelting Symposium): Pyrometallurgical Process Modeling, Control & Instrumentation

Sponsored by: The Minerals, Metals and Materials Society, The Metallurgy and Materials Society of CIM, TMS Extraction and Processing Division, TMS: Pyrometallurgy Committee
Program Organizers: Jerome Downey, Montana Tech of the Univ of Montana; Thomas Battle, Midrex Technologies, Inc.; Jesse White, Elkem Solar Research

Wednesday PM
March 14, 2012

Room: Northern A3
Location: Dolphin Resort

Session Chair: To Be Announced

2:00 PM

Comparison of Classical Tools and Modern Finite Element Modeling in the Electrical Design of Slag Resistance Furnaces: *Mark Kennedy¹; Melina Garcia²; Finn Olesen³; ¹Norwegian University of Science and Technology; ²Elkem AS; ³Elkem Bjølvefossen AS*

Furnace resistance is a function of the complex interrelationship between many factors including: operating practice, slag conductivity, temperature, power intensity, and geometry (electrode shape, diameter, spacing, immersion, slag depth, etc.). Accurate prediction of resistance is critical for success of the overall furnace design. The sizing of electrodes, columns, bus-bars, and transformers are all impacted. Estimation of minimum and maximum resistance or maximum operational current, as well as the maximum operating voltage are of fundamental importance. Various mathematical tools have been developed to assist designers with the selection of furnace dimensions and the prediction of resistance. Elkem found the methods of Downing et al. 1965 and Westly 1975 to be particularly useful. In the current paper, comparisons are drawn between data from spent aluminium pot lining (SPL) demonstration testing at Elkem Bjølvefossen and predictions based on these classical tools and 3D finite element modeling (FEM) with COMSOL®.

2:25 PM

CFD Modelling of Combustion Behaviour in Slag Fuming Furnaces: *Md Huda¹; Jamal Naser¹; Geoffrey Brooks¹; M. Reuter²; Robert Matuszewicz²; ¹Swinburne University of Technology; ²Outotec Limited*

A thin slice CFD model of a conventional tuyere blown slag fuming furnace has been developed in Eulerian multiphase flow approach. The model was developed by coupling CFD with kinetics equations developed



TMS 2012

141st Annual Meeting & Exhibition

by Richards et al. for a zinc fuming furnace. The model integrates submerged coal combustion and chemical reactions with the heat, mass and momentum interfacial interaction between the phases in the system. The model predicts the velocity, temperature field of the molten slag bath, generated turbulence, vortex and coal utilization behaviour from the slag bath. Highest coal penetration distance was found to be at $l/L = 0.2$, where l distance from the tuyere tip and L is the total length (2.44m) of the modelled furnace. The model also predicts that 10% of the injected coal bypasses the tuyere gas stream un-combusted and carried to the free surface, which contributes to ZnO reduction near the free surface.

2:50 PM

Modeling as a Tool for Scale-Up of an Iron Smelt-Reduction Process: Mark Schwarz¹; Mark Davis²; ¹CSIRO; ²Hismelt Corp

The Hismelt Process is a smelt-reduction process involving the injection of iron ore and coal into a molten iron bath, and post-combustion of CO and H₂ above the bath by means of a top jet of air to increase energy efficiency. Substantial fluid dynamic related challenges are involved in developing such a process: these include ensuring that the solids are injected down into the metal bath and that post-combustion heat is effectively transferred back to the bath while minimising oxidation back reaction. Reactive multi-phase Computational Fluid Dynamics (CFD) modelling can be used in conjunction with experimental modelling and plant trials to achieve reliable scale-up. The application of these modelling tools will be described.

3:15 PM

Validating Temperature Measurements in Pyrometallurgical Applications – A Case Study: Håvard Molnås¹; Joalet Steenkamp²; Merete Tangstad¹; ¹NTNU; ²University of Pretoria

Temperature affects several aspects of pyrometallurgical systems, including thermodynamics and reaction kinetics. Reliability of temperature measurements in laboratory and plant applications is thus important from process, safety and financial perspectives. This case study briefly introduces different techniques used for temperature validation, and demonstrates temperature validation on laboratory scale utilizing the wire-bridge method. Pt/Pt13Rh thermocouple hot junctions were constructed by mechanically connecting thermocouple wires through a pure metal bridge consisting of copper, gold, nickel or palladium wire. When heating the wire-bridge thermocouple alongside a regular Pt/Pt13Rh thermocouple, temperature offsets were quantified as the wire-bridge thermocouple short-circuited at the melting points of the pure metals. At the melting points of gold (1064°C) and palladium (1555°C), average measured temperature offsets were $-2.1^\circ\text{C} \pm 2.3^\circ\text{C}$ and $0.2^\circ\text{C} \pm 0.4^\circ\text{C}$, respectively. Results from the copper and nickel wire-bridges were inconclusive. The paper concludes with a discussion on the potential industrial applications of the technique.

3:40 PM Break

4:00 PM

Electric Slag Furnace Dimensioning: Mark Kennedy¹; ¹Norwegian University of Science and Technology

Electric furnaces containing high quantities of slag are applied in many areas of pyrometallurgy, often for smelting or slag cleaning. A variety of ratios or rules of thumb have been employed in the industry for the dimensioning of these vessels, in most cases with no clear technical basis. In this paper, several design guidelines are presented (electrode size, spacing, vessel dimensions, energy intensity, etc.) as an attempt to provide some technical basis for optimal dimensioning. Furnace heat generation is related to side wall copper cooler heat losses, in an attempt to establish a methodical design strategy particularly for minimum electrode to wall spacing for modern furnaces with cooled linings. Issues regarding the true nature of heat production in a slag furnace are discussed with regards to the possible impact on accurate modeling and design.

4:25 PM

Physical Modeling Study on Mixing Phenomena in a C-H₂ Smelting Reduction Furnace Bath with Asymmetric Side Blowing Process: Jinyin Xie¹; Jieyu Zhang¹; Kongfang Feng¹; Jixu Wang¹; Fei Ruan¹; Zhiyu Liu¹; Shaobo Zheng¹; Xin Hong¹; ¹Shanghai University

The mixing phenomena in smelting reduction furnace with asymmetric side blowing process was studied in this paper. Mixing phenomena in smelting reduction furnace was represented as the mixing time by electrical conductivity measurements. Experiment was performed in a water modeling under various operating conditions to determine the effects of the upper/lower side nozzle horizontal angle, radial angle, inserting depth, flow rate and the included angle between the upper-side nozzle and the lower side nozzle on mixing phenomena in smelting reduction furnace. Comparing mixing time and mixing phenomena, the optimal conditions obtained through asymmetric side blowing process were listed as follow: the upper side nozzle horizontal angle at -15° , radial angle at 15° , inserting depth at 100mm, flow rate at 1.5m³/h; the lower side nozzle horizontal angle at 40° , radial angle at 15° , inserting depth at 0mm, flow rate at 1.5m³/h; the included angle between the upper-side nozzle and the lower-side nozzle at 60° .

4:50 PM

Successful Application of Model Based Predictive Control for Production and Thermal Efficiency Optimization of High Temperature Melters: Erik Muijsenberg¹; ¹Elkem Technology

In the past decade, advanced multiple input/multiple output (MIMO) process control systems have found their way into the high temperature melting processes. Today a growing number of high temperature melters have been equipped with a supervisory control system. Daily regulation of fossil fuel firing and electric energy supply to stabilize temperatures is no longer in the hands of the operator, but fully taken over automatically by the ES IITM MPC controller, which provides consistent process control, 24 hours per day, focused to operate the entire glass production process in the most efficient way. The presentation will show practical results and benefits achieved in the high temperature glass and cement industry.

Magnesium Technology 2012: Corrosion and Coating

Sponsored by: The Minerals, Metals and Materials Society, TMS Light Metals Division, TMS: Magnesium Committee
Program Organizers: Suveen Mathaudhu, U.S. Army Research Office; Wim Sillekens, TNO; Norbert Hort, Helmholtz-Zentrum Geesthacht; Neale Neelameggham, U.S. Magnesium

Wednesday PM
March 14, 2012

Room: Southern IV
Location: Dolphin Resort

Session Chairs: Guang-Ling Song, GM Global Research & Development; Michelle Manuel, University of Florida

2:00 PM

“Electroless” E-Coating for Mg Alloys: Guang-Ling Song¹; ¹GM Global Research & Development

By utilizing the unique electrochemistry of Mg, a thin organic film can rapidly be deposited on the surface of a Mg alloy through simply dipping the Mg alloy in an E-coating bath solution without applying a current or potential. This “electroless” E-coating pre-film can offer sufficient corrosion protection for Mg alloys in a chloride-containing environment. The stability of the film can be further significantly improved after curing. The coating performance is influenced by the substrate Mg alloy and the surface treatment process. Several differently pre-treated Mg alloy surfaces by means of dry-polishing, wet-polishing and chemical etching are compared for their suitability for the “electroless” E-coating on process. It is found that a pretreatment including a wet process and a heat-

treatment of the substrate could be a cost-effective surface preparation/treatment process for the “electroless” E-coating. The dipping coating can also act as a base for further powder-coating or E-coating.

2:20 PM

The Influence of Galvanic Current on Cerium-Based Conversion Coatings on Mg, Al, and Galvanized Steel Couples: *Surender Maddela*¹; Matthew O’Keefe¹; Yar-Ming Wang²; ¹Missouri University of Science and Technology; ²GM Research and Development

The influence of galvanic current on cerium-based conversion coatings (CeCCs) for magnesium (AZ91, AZ31), aluminum (6016), and electro-galvanized steel (EGS) couples has been studied using zero resistance ammeter (ZRA) measurements in prohesion solution. The galvanic current measured between magnesium-aluminum, magnesium-galvanized steel, and aluminum-galvanized steel couples correlated with significant changes in coating morphology and deposition rate. The ZRA galvanic currents (mA) were 0.02 for 6016-EGS, 0.38 for AZ91-EGS, 0.72 for AZ91-6016, 1.08 for AZ31-EGS, and 1.08 for AZ31-6016 couples. The corrosion performance of the coated couples was evaluated by ASTM B117 neutral salt spray testing and electrochemical polarization measurements. Cerium conversion coated couples performed better in salt spray testing compared to uncoated couples. The correlation of galvanic current, cerium deposition, and corrosion performance will be discussed.

2:40 PM

Effect of Sn⁴⁺ Additives on the Microstructure and Corrosion Resistance of Anodic Coating Formed on AZ31 Magnesium Alloy in Alkaline Solution: *S. Salman*¹; K. Kuroda²; N. Saito²; M. Okido²; ¹Graduate School of Engineering, Al-Azhar University, Nasr City, Cairo 11371, Egypt; ²Nagoya University

Magnesium is the lightest structural metal with high specific strength and good mechanical properties. However, poor corrosion resistance limits its widespread use in many applications. Magnesium is usually treated with chromate conversion coatings. However, due to changing environmental regulations and pollution prevention requirements, a significant push exists to find new, alternative for poisonous Cr⁶⁺. Therefore, we aim to improve corrosion resistance of anodic coatings on AZ31 alloys using low cost non-chromate electrolyte. Anodizing was carried out in alkaline solutions with tin additives. The effect of tin additives on the coating film was characterized by SEM and XRD. The corrosion resistance was evaluated using anodic and cathodic polarizations and electrochemical impedance spectroscopy (EIS). Corrosion resistance property was improved with tin additives and the best anti-corrosion property was obtained with addition of 0.03 M Na₂SnO₃ · 3H₂O to anodizing solution.

3:00 PM

Effect of Thickness on the Morphology and Corrosion Behavior of Cerium-Based Conversion Coatings on AZ31B Magnesium Alloy: *Carlos Castano*¹; Surender Maddela¹; Matthew O’Keefe¹; Yar-Ming Wang²; ¹Missouri University of Science and Technology; ²GM R&D Center

Cerium-based conversion coatings (CeCC) were deposited onto AZ31B magnesium alloy substrates using a spontaneous reaction of CeCl₃, H₂O₂ and gelatin in a water-based solution. The coating thickness was adjusted by controlling the immersion time in the deposition solution. Prior to deposition, the surface of the AZ31B substrates were treated using an acid pickling in nitric acid and then an alkaline cleaning in sodium metasilicate pentahydrate. After deposition, the coated samples were immersed in a phosphate bath that converted cerium oxide/hydroxide into cerium phosphate. Electrochemical impedance spectroscopy, potentiodynamic polarization, and neutral salt spray testing studies indicated that ~100 nm thick CeCC had better corrosion performance than ~400 nm coatings. The morphology of cerium-based conversion coatings was characterized by transmission electron microscopy (TEM) which revealed a structure consisting of three layers with different compositions.

3:20 PM

Mechanical and Corrosion Properties of As-Cast and Extruded MG10GD Alloy for Biomedical Application: *Petra Maier*¹; Sören Müller²; Hajo Dieringa³; Norbert Hort³; ¹University of Applied Sciences Stralsund; ²Extrusion Research and Development Center TU Berlin; ³Helmholtz-Zentrum Geesthacht

Due to the good specific strength and the moderate corrosion rate Mg-RE alloys have found growing interest for medical applications as implant material. In this study extruded Mg10Gd has been investigated, once by voltametric measurements and again under cyclic load. Corrosion exposure is known to reduce the fatigue strength strongly. The data are compared to Mg10Gd cast alloys and show an increase in fatigue properties and similar corrosive behaviour. The form of corrosion and the influence of the temperature during voltametric tests are discussed. A temperature increase from room to body temperature accelerates the corrosion processes. Due to stress peaks under load pitting corrosion is not preferred. The influence of the microstructure on the corrosion form is discussed. Casted Mg10Gd reveals large dendrites, which change into a globular microstructure during extrusion resulting in improved mechanical properties, mostly the elongation to fracture up to 20%.

3:40 PM Break

4:00 PM

Corrosion Behavior of Various Steels by AZ31 Magnesium Melt: *Cheuk Kin Tang*¹; Marie-Aline Van Ende¹; In-Ho Jung¹; ¹McGill University

During the production of Mg and its alloys, the melt is in contact with steel at various stages of the process. Steel can be eroded and corroded through chemical reactions with molten Mg and the protective gases such as SF₆ or SO₂. The dissolution rate and corrosion mechanism of steels in molten Mg were investigated by the rotating cylinder method. The effects of temperature (650 to 700 °C) and rotation time (1 to 10 h) on the rate of dissolution of four steel grades, i.e. high carbon and low carbon steel, stainless steel 316 and 400, were examined for AZ31 melt under N₂-SF₆ gas atmosphere. The corrosion rates were found to be different depending on steel grades. It is found that the corrosion mechanism of steels in Mg melts involves a two-stage process consisting of oxidation of Fe and its reduction by Mg melt.

4:20 PM

Corrosion of Ultrasonic Spot Welded Joints of Magnesium to Steel: *Tsung-Yu Pan*¹; Michael Santella¹; ¹Oak Ridge National Laboratory

Mixed-metal joining, especially between magnesium and steel, is one of the critical technologies in achieving light-weighting vehicle body construction. However, galvanic corrosion between mixed metal joints is inevitable but not well quantified. In this study, 1.6 mm thick Mg AZ31B-H24 is joined to 0.8 mm thick galvanized mild steel by ultrasonic spot welding in lap-shear configuration. Corrosion test is conducted with Ford Arizona Proving Ground Equivalent Corrosion Cycle (APGE) test procedure which includes cycles of dipping in the salt bath, air drying, then subject to constant humidity environment. Lap shear tensile strength, X-ray diffraction, cross-section micrographs, and fractographs are obtained and are presented in the paper.

4:40 PM

Effects of Orientation on Corrosion Behavior of Magnesium Single Crystals: *Nguyen Dang Nam*¹; Ming Zhe Bian¹; Kwang Seon Shin¹; *Hwa Chul Jung*¹; ¹Magnesium Technology Innovation Center, Seoul National University

Magnesium alloys have distinct advantages such as low density and high specific strength, but limited corrosion resistance restricts their widespread use in industrial applications. Therefore, it is important to examine the critical factors that could affect the corrosion behavior of magnesium alloys in order to develop new corrosion resistant alloys. It has been reported that the corrosion resistance of magnesium alloys could be influenced by texture. However, there has been little study on the effects of the surface orientation on the corrosion behavior of magnesium



TMS 2012

141st Annual Meeting & Exhibition

single crystals. In this study, magnesium single crystals with various crystallographic orientations were prepared for corrosion tests in order to identify the effects of surface orientation on the corrosion behavior in a systematic manner. Corrosion tests were carried out using electrochemical techniques such as potentiodynamic polarization and electrochemical impedance spectroscopy in a 3.5 wt.% NaCl solution. The specimen surfaces were analyzed using SEM and XRD.

5:00 PM

Effect of Some Microstructural Parameters on the Corrosion Resistance of Magnesium Alloys: Yaning Hu¹; Joseph Kish¹; *Joseph McDermid*¹; Wenyue Zheng²; ¹McMaster University; ²CANMET-MTL

The influence of the β -Mg₁₇Al₁₂ phase and the solute composition of the α -Mg matrix on Mg-alloy passive film stability were investigated by cyclic polarization and anodic potentiostatic polarization tests on AM60B, AM30 and AZ31B Mg alloys in a mildly aggressive neutral environment. Results showed that the alloys corroded in a passive state at the corrosion potential in this environment. It was also determined that the alloys studied showed similar breakdown and repassivation potentials. This indicates that the solute matrix composition and β -phase distribution did not thermodynamically affect the alloy passivation and repassivation behavior. It was further determined that a semi-continuous grain boundary network of γ -phase improved the overall AM60 alloy corrosion resistance and that the presence of β phase did not have a significant effect on the α -Mg matrix dissolution rate. This paper presents the results of this investigation and discusses implications for use of these alloys in automotive structures.

5:20 PM

Influence of Aluminum Content on Corrosion Resistance of Mg-Al Alloys Containing Copper and Zinc: *Hiroyuki Kawabata*¹; Naohisa Nishino¹; Yoshikazu Genma²; Tsuyoshi Seguchi²; ¹Toyota Central R&D labs., inc.; ²Toyota Motor Corporation

Corrosion resistance of Mg-Al alloys gets worse significantly with increasing copper content, because copper-based intermetallic compounds are formed in alloys. Therefore, the tolerance limit of copper is commonly fixed at less than 300ppm for keeping the corrosion resistance. It is necessary to expand the tolerance limit for reduction of the cost of magnesium alloys and products. So, it is very important to prevent the corrosion resistance from getting worse by copper containing. In this study, the corrosion resistance of Mg-Al alloys containing copper and zinc was investigated. We revealed the optimum content of zinc and aluminum for high corrosion resistance.

Magnesium Technology 2012: High Temperature Processing and Properties

Sponsored by: The Minerals, Metals and Materials Society, TMS Light Metals Division, TMS: Magnesium Committee

Program Organizers: Suveen Mathaudhu, U.S. Army Research Office; Wim Sillekens, TNO; Norbert Hort, Helmholtz-Zentrum Geesthacht; Neale Neelameggham, U.S. Magnesium

Wednesday PM
March 14, 2012

Room: Southern V
Location: Dolphin Resort

Session Chairs: Paul Krajewski, General Motors; Warren Poole, University of British Columbia

2:00 PM

Effect of Rolling Temperature on the AZ31B Magnesium Alloy Microstructure: *Litzy Lina Catorceno*¹; Angelo Fernando Padilha¹; ¹USP

The influence of rolling temperature and the effect of strain rate on the microstructure of AZ31B Mg alloy were determined in order to improve its formability. A plate of AZ31 alloy was found to be sensitive to strain rate at high temperature and anisotropy was adversely impacted in cold

rolling sheets. Thus, AZ31B has better workability within the temperature range of 200 to 250 oC, due to the grain refinement, caused by the dynamic recovery and dynamic recrystallization. The effect of rolling temperature was studied on recrystallized sheets (2 mm in thickness) which were deformed by rolling at different temperatures (25, 100, 200 and 250 oC) and the effect of strain rates was evaluated on two different rolling speed (10 and 20 rpm). The microstructural characterization was achieved using several complementary techniques of microstructural analysis, such as optical microscopy, scanning electron microscopy, X-ray analysis by energy dispersive, X-ray diffraction and microhardness.

2:20 PM

Hot Formability Curves for Four Mg AZ31B Sheets Obtained by the Pneumatic Stretching Test: *Fadi Abu-Farha*¹; Ravi Verma²; Louis Hector²; ¹Penn State Erie; ²General Motors

The formability of four Mg AZ31B sheets produced by either direct chill or twin roll casting, and having different initial grain sizes, was investigated at 400 °C and 5x10⁻³ s⁻¹ using pneumatic stretching. Blanks were pneumatically bulged through four elliptical die inserts, with aspect ratios ranging between 1.0 and 0.4, producing ellipsoidal domes with different biaxial strain combinations. The major strains were aligned either along or across the rolling direction of the material. Strain combinations were measured in the deformed material and mapped onto a formability diagram. Three zones were distinguished in constructing the formability curves for each of the four sheets: safe (no necking), marginal (some necking), and failure (extreme necking and/or rupture). Formability comparisons as a function of sheet rolling direction were quantified with "composite FLDs." Results obtained for the four sheets are indicative of differences in grain structure and material inhomogeneities.

2:40 PM

Texture Evolution during Hot Deformation Processing of Mg-3Sn-2Ca-0.4Al Alloy: Dharmendra Chalasani¹; *Pitcheswara Kamini*¹; Y.V.R.K. Prasad²; Norbert Hort³; Karl Kainer³; ¹City University of Hong Kong; ²Independent Consultant; ³Helmholtz-Zentrum Geesthacht

An experimental investigation of texture evolution during high temperature compression of Mg-3Sn-2Ca (TX32) alloy containing 0.4%Al using electron backscatter diffraction (EBSD) technique is reported. Isothermal uniaxial compression tests were performed at different combinations of temperatures and strain rates in the ranges 300-500 °C and 0.0003-10 s⁻¹ to examine the influence of processing conditions on the dynamic recrystallization (DRX) behavior and texture evolution. The onset of DRX during compression at low temperatures (300 and 350 °C) and low strain rates (0.003 and 0.001 s⁻¹) gave rise to a fine, partially recrystallized and necklaced grain microstructure, with the basal planes aligned at about 15-30° to the compressive direction although they were split. Certain deformation conditions at high temperatures resulted in a fully recrystallized microstructure and an almost random crystallographic texture. It is clear from Schmid factor analysis that the contribution of pyramidal slip system is significant for deformation at temperatures above 400 °C.

3:00 PM

The Effects of Strain and Stress State in Hot Forming of Mg AZ31 Sheet: *Alex Carpenter*¹; Paul Sherek²; Louis Hector³; Paul Krajewski³; Jon Carter³; Eric Taleff³; ¹The University of Texas at Austin; ²Mercer; ³General Motors

Wrought magnesium alloys, such as AZ31 sheet, are of considerable interest for light-weighting of vehicle structural components. The poor room-temperature ductility of AZ31 sheet has been a hindrance to forming the complex part shapes necessary for practical applications. However, the outstanding formability of AZ31 sheet at elevated temperature provides an opportunity to overcome that problem. Complex demonstration components have already been produced at 450°C using gas-pressure forming. Accurate simulations of such hot, gas-pressure forming will be required for the design and optimization exercises necessary if this

technology is to be implemented commercially. We report on experiments and simulations used to construct the accurate material constitutive models necessary for finite-element-method simulations. In particular, the effects of strain and stress state on plastic deformation of AZ31 sheet at 450°C are considered in material constitutive model development. Material models are validated against data from simple forming experiments.

3:20 PM

Effect of Strain Rate on Dynamic Recrystallization in Magnesium under Compression at High Temperature: *Q. Ma¹; B. Li¹; A.L. Oppedal¹; W. Whittington¹; S.J. Horstemeyer¹; E.B. Marin¹; H. El Kadiri¹; P.T. Wang¹; M.F. Horstemeyer¹;* ¹Mississippi State University

Interrupted uniaxial compression tests were performed on an extruded Mg-Al-Mn magnesium alloy (AM30) at 450°C and various strain rates of 0.001 s⁻¹, 0.1 s⁻¹, 0.5 s⁻¹ and 0.8 s⁻¹. Texture and microstructure evolution were examined using the electron back-scatter diffraction (EBSD) and the X-ray diffraction (XRD) techniques. The results show that the microstructure strongly depends on the strain rate, with twinning activated at high strain rates. The extension twinning and the non-basal slips play crucial roles in dynamic recrystallization of the magnesium alloy. The Schmid factors of the slip modes and the twinning mode were calculated, and slip trace analysis was conducted to clarify the dynamic recrystallization (DRX) mechanisms.

3:40 PM Break

4:00 PM

Effect of Strain Rate on the Kinetics of Hot Deformation of AZ31 with Different Initial Texture: *Mehdi Sanjari¹; Amir Farzadfar²; Atefeh Nabavi²; Elhachmi Essadiqi³; In-Ho Jung²; Steve Yue²; ¹McGill; ²McGill; ³CANMET*

In this work, the effects of strain rate and initial texture on the flow behaviour and microstructure evolution on AZ31 Mg alloy were studied by compression tests. Cast plates were, homogenized and hot rolled and then compression tests were performed on samples with longitudinal axes either parallel to the rolling direction (RD) or the normal direction (ND). Compression tests were performed to various strains and samples were quenched to investigate the effect of dynamic recrystallization on the texture and microstructural evolution. Results show that for the samples machined in both rolling and normal direction, the rate of texture evolution is increased by increasing strain rate. The deformation mechanism was changed by increasing the strain rate for ND samples and at strain rate of 1s⁻¹ from slip dominated flow to twin dominated flow. By using EBSD, the deformation mechanism and twinning types were investigated and double and tension twins were detected.

4:20 PM

Precipitation Behaviour of Micro-Alloyed Mg-Al-Ca Alloys during Heat Treatment and Hot Compression: *Jing Su¹; Shirin Kaboli¹; Abu Syed Humaun Kabir¹; Phuong Vo¹; In-Ho Jung¹; Steve Yue¹;* ¹McGill

Based on thermodynamic calculations, two micro-alloyed Mg-Al-Ca alloys, Mg-0.3Al-0.2Ca and Mg-0.1Al-0.5Ca, were selected in terms of the equilibrium precipitation temperatures of Al₂Ca and Mg₂Ca, respectively. The basic idea is to form precipitates during hot compression to examine their effect on hot deformation. Both alloys, cast by copper mould, were solution treated at 500°C for 8 hours to dissolve eutectic precipitates which formed in the as-cast microstructure, and then isothermally heat treated at 350°C for different times. SEM analysis of the heat treated alloys generally agreed with thermodynamic calculations. Hot compression tests were also conducted on solution treated alloys at 350°C with a strain rate of 0.01 s⁻¹ and different strains (from 10% to 90%). The precipitation behaviour and microstructural evolution which was characterized by optical microscopy and SEM with EDS and EBSD of two alloys during isothermal heat treatment and hot compression were compared.

4:40 PM

Diffusion Couple Investigation of the Mg-Zn System: *Sarah Brennan¹; Katrina Bermudez¹; Nagraj Kulkarni²; Yongho Sohn¹;* ¹University of Central Florida; ²Oak Ridge National Laboratory

Phase layer growth and interdiffusion in the binary Mg-Zn system was investigated utilizing solid-to-solid diffusion couples annealed at 295°, 315° and 325°C for 21, 7 and 5 days, respectively. The diffusion microstructure was examined by scanning electron microscopy and concentration profiles were determined using X-ray energy dispersive spectroscopy and electron microprobe analysis. The Mg solid solution, Mg₂Zn₁₁, MgZn₂ and Mg₂Zn₃ in all three couples were observed in addition to the high temperature, Mg₅₁Zn₂₀ phase at 325°C. The MgZn₂ phase was observed to grow the thickest layer, followed by the Mg₂Zn₃ and the Mg₂Zn₁₁ phases. Activation energies for the parabolic growth were calculated to be 105 kJ/mol and 207 kJ/mol for the Mg₂Zn₃ and MgZn₂, respectively. Relevant interdiffusion coefficients were calculated for the phases present by analyses of concentration profiles. This study was sponsored by the US Department of Energy, Office of Energy Efficiency and Renewable Energy, Vehicle Technologies Program (DE-AC05-00OR22725).

5:00 PM

Biaxial Deformation Behavior of AZ31 Magnesium Alloy at High Temperature: *Yamashita Daisuke¹; Masafumi Noda¹; Kunio Funami¹;* ¹Chiba Institute of Technology

Plastic deformation of metals is typically characterised with the uniaxial tensile test. However, multiaxial loading in sheet metal plastic forming requires more complex tests, such as the controlled biaxial test with cruciform specimens. Then, AZ31 magnesium alloy investigated relation between biaxial deformation behavior and microstructure for initial strain rate of 3.0×10⁻³ s⁻¹ and 2.8×10⁻⁴ s⁻¹ at 573 K and 623 K by cruciform specimens. As a result, the flow stress increased with decrease the sheet thickness and tensile twin is formed of during biaxial tensile deformation at 623 K for 2.8×10⁻⁴ s⁻¹ in cross section. It's deformation behavior and evolution of microstructure peculiar to biaxial tensile test, and this deformation behavior was not recognized in uniaxial tensile test. In other words transition point of microstructure is biaxial tensile tested condition at 623 K for 2.8×10⁻⁴ s⁻¹.

Materials and Fuels for the Current and Advanced Nuclear Reactors: Modeling I

Sponsored by: The Minerals, Metals and Materials Society, TMS Structural Materials Division, TMS/ASM: Corrosion and Environmental Effects Committee, TMS/ASM: Nuclear Materials Committee

Program Organizers: Ramprashad Prabhakaran, Idaho National Laboratory; Dennis Keiser, Idaho National Laboratory; Raul Rebak, GE Global Research

Wednesday PM
March 14, 2012

Room: Swan 4
Location: Swan Resort

Session Chair: Paul Millett, Idaho National Laboratory

2:00 PM

Cluster Dynamics and Kinetic Monte Carlo Simulations of Atomistic to Nanoscale Defect Dynamics in In-Situ TEM Irradiation on Thin Molybdenum Foils: *Donghua Xu¹; Brian Wirth¹; Meimei Li²; Mark Kirk²;* ¹University of Tennessee-Knoxville; ²Argonne National Laboratory

In-situ TEM experiments and computer simulations are closely combined to investigate the detailed defect dynamics during irradiation of Molybdenum thin foils with 1 MeV Kr⁺. Specifically, the number density and size distribution of interstitial and/or vacancy clusters are obtained as a function of dose (time), dose rate, foil thickness and irradiation temperature. A spatially-dependent cluster dynamics (CD) model has been



designed and parameterized to directly compare with the experiments. The CD model incorporates 1D spatial dependence to account for free surface sinks. A kinetic Monte Carlo model is used to directly capture the full 3D spatial dependence of the defect evolution. The effects of interstitial/vacancy cluster mobility and intra-cascade cluster production are examined, in addition to other material and irradiation parameters. Detailed comparisons provide the opportunity to validate understanding of defect diffusion and interaction kinetics, including key mechanisms controlling defect cluster evolution, and the assumptions of the cluster dynamics model.

2:20 PM

Kinetic Monte Carlo Simulation of He Bubble Nucleation at Different Types of Grain Boundaries in Mo: *Liangzhe Zhang*¹; Paul Millett¹; Michael Tonks¹; Yongfeng Zhang¹; Bulent Biner¹; ¹Idaho National Laboratory

The kinetic Monte Carlo (KMC) algorithm, which offers a relatively long time description of microstructural evolution at atomistic level, is adopted to investigate the Helium bubble nucleation process at grain boundaries (GBs) in Mo. To make KMC simulations robust, corresponding molecular dynamics simulations are consulted, which provide the nucleation mechanisms in detail within various settings. In the current work, the He bubble nucleation process at three types (twin, tilt and twist) of GBs is studied with randomly distributed He atoms as the initial condition. It is found that He bubbles nucleate at GBs with different rates and more He bubbles appear at tilt and twist boundaries. This is because the He binding energy of tilt and twist GBs is superior over the counterpart of twin GBs. Furthermore, inhomogeneous nucleation occurs with the impact of dislocations.

2:40 PM

He Bubble Nucleation at Grain Boundaries (GBs) in BCC Mo: Molecular Dynamics Simulations: *Yongfeng Zhang*¹; Paul Millett¹; Michael Tonks¹; Liangzhe Zhang¹; Bulent Biner¹; ¹Idaho National Lab

The He bubble nucleation at three different GBs, the (100) twist S29, the <110> symmetrical tilt (10.1°), and the twin, are simulated at 2000K. The results are quantified in terms of He binding energy, effective He diffusivity, and GB structure. He interstitials of 1000 appm are inserted into the grain interior initially, and the microstructural evolution is monitored for 2 ns. The He binding energy is about 0.5, 2.5 and 2.9 eV for the twin, the tilt, and the twist GBs respectively. Correspondingly, He atoms diffuse 3D and much faster in the cell with twins, 2D in the twist GBs, and 1D in the tilt GBs along the dislocation cores. As a result, less He bubbles form at twins than at the other two GBs, with a larger average size. The He clusters forms randomly in the twins and twist GBs, and along the dislocation cores in the tilt GBs.

3:00 PM

Strip-Yield Modeling of Creep Crack Incubation and Growth in Cr-Mo Steels for Nuclear Reactor Applications: *Gabriel Potirniche*¹; Mehdi Basirat¹; ¹University of Idaho

Cr-Mo heat-resistant steels are considered as possible materials of choice for reactor pressure vessels and reactor internals for nuclear power plants, thus modeling the creep damage in these materials becomes essential. In this work, a numerical strip-yield model was developed to simulate creep crack incubation and growth in Cr-Mo steels. Simulations of crack incubation and growth, evolution of the crack-tip plastic zone and damage evolution in the near crack-tip regions are performed. The strip-yield model is coupled with a dislocation-based model of creep deformation to compute the extent of each creep stage (primary, secondary and tertiary) in the near crack-tip region and calculate crack advance rates. The model assumes a pre-existing crack in a specimen, and models the behavior of the material prior to the onset and during the crack advance stage. Comparison with experimental data is performed, and good correlation is obtained.

3:20 PM

Peculiarities of Creep Temperature Dependence in Irradiated Materials: *Pavlo Selyshchev*¹; Volodimir Sugakov²; ¹University of Pretoria; ²Institute for Nuclear Research

In the framework of a dislocation climb-glide model a theoretical approach is developed to explain the appearance of a break (local minimum and maximum) on a curve of creep rate dependence on temperature in irradiated materials. The peculiarities of creep temperature dependence were explained by competition of radiation and thermal defect fluxes. At some temperature the both radiation and thermal fluxes become equal and compensate each other, which causes the creep to decrease. It was shown that the presence of sinks with different preference coefficients is important for explanation of appearance of the break. Theoretical and experimental results are in good agreement.

3:40 PM Break

3:50 PM

Ab Initio Study of Radiation Induced Amorphization in ZrC: *Ming-Jie Zheng*¹; Dane Morgan¹; Izabela Szlufarska¹; ¹University of Wisconsin - Madison

ZrC is of interest for application in nuclear reactors due to its high melting temperature and possible effectiveness as a barrier layer to fission products. However, the response of ZrC to irradiation is poorly understood. We study the radiation induced amorphization in ZrC by using an ab initio based rate theory framework. The kinetics of the dominating Frenkel pairs in ZrC is investigated through the density functional theory calculation. It is demonstrated that the dose to amorphization vs. temperature curve and the critical temperature to amorphization T_c are sensitive to both migration barriers and recombination barriers. By using an approximate amorphization energy for ZrC, T_c is found to be much lower than the room temperature. This result may explain why it is hard to observe amorphization in experiments on ZrC conducted at room temperature or higher temperatures, even under high dose of radiation.

4:10 PM

Phase-Field Simulation and Experimental Studies of Oxidation of Zirconium: *Mohsen Asle Zaeem*¹; Haitham El Kadiri¹; Mark Horstemeyer¹; ¹Mississippi State University

We study the oxidation kinetics of zirconium by both simulations and experiments. A phase-field model is presented for oxidation of pure metals in which the diffusion-controlled phase transformation is the mode of oxide growth. The metal is zirconium which produces zirconia in the oxidation process. A conserved phase-field variable is considered which represents the oxygen concentration and another non-conserved phase-field variable is used as the marker of different phases. The governing evolution equations of phase-field variables are coupled to mechanical equilibrium equations to investigate the evolution of stresses in the oxide and the zirconium substrate. The governing equations are solved using a finite element model. This model captures the composition depth profile of the oxygen in the oxide layer and in the metallic substrate and stresses induced by compositional changes close to the metal-oxide and oxide-fluid interfaces. The oxidation kinetics of zirconium achieved by phase-field simulations is validated by experiments.

4:30 PM

Characterization and Modeling of Creep Mechanisms in Zircaloy-4: *Benjamin Morrow*¹; Robert Kozar²; Ken Anderson²; Michael Mills¹; ¹The Ohio State University; ²Bechtel Marine Propulsion Corp.

Zirconium alloys are used primarily as a structural material in nuclear reactors. Accurately predicting creep deformation throughout their lifecycle depends on reliable deformation models. The Modified Joggled-Screw (MJS) model asserts that the motion of tall jogs on screw

dislocations act as the rate-controlling mechanism during creep in certain stress-temperature regimes. Previous studies have demonstrated the applicability of the MJS model to the thermal creep behavior of hcp metals, but many aspects of the model have never been fully explored. TEM was used to directly observe and characterize the dislocation substructure of creep-tested Zircaloy-4 over a range of conditions, and quantify pertinent model parameters. Effects of accumulated strain were examined through interrupted testing. Thorough characterization can provide a better understanding of material behavior in both primary and secondary creep regimes, resulting in more robust creep deformation predictions. Results of substructural observations and improvements to the MJS model are discussed.

4:50 PM

High-Temperature Creep and Superplasticity in Zirconium Alloys: Applications to LOCA Conditions: *Ali Massih*¹; ¹Quantum Technologies

Understanding the high-temperature deformation property of zirconium alloys used as fuel cladding tubes is essential for analysis of fuel rod behavior during a postulated loss-of-coolant accident (LOCA) in water cooled reactors. Here, the high-temperature (900-1400 K) steady-state creep test data on as-received zirconium alloys, Zr-1wt%Nb and Zircaloy-4, are evaluated by employing two sets of models. In one modeling approach, the constitutive relations for the two single phase regions (alpha and beta) are combined through a phase transition model and a phase mixing rule; in another, a superplasticity model is used to calculate the creep deformation rate as a function of stress and temperature in the (alpha+beta)-domain. The results show that the former approach is inadequate in capturing the experimental data, while the latter provides a fair agreement with experiments. The two models are also used and compared in a computer code to assess fuel cladding rupture under LOCA conditions.

5:10 PM

Charge Optimized Many Body (COMB) Potential for the Zr-ZrO₂ system: *Mark Noordhoek*¹; *Tao Liang*¹; *Tzu-Ray Shan*¹; *Susan Sinnott*¹; *Simon Phillpot*¹; ¹University of Florida

Fuel clad for Light Water Reactors is made from zircaloy, a zirconium alloy. Oxidation and hydridation of zircaloy are important degradation processes. Here, a Charge Optimized Many Body (COMB) potential for the Zr-ZrO₂ system is developed and fitted to the structure and properties of Zr and ZrO₂, obtained from experiment and from density functional theory calculations. The hcp structure of Zr is found to be the most stable, with a non-ideal c/a ratio in good agreement with experiment. For Zr, satisfactory values are obtained for the stacking fault, surface and defect formation energies. Corresponding analyses are performed for ZrO₂. This work was funded by the Consortium for Advanced Simulation of Light Water Reactors (www.casl.gov), an Energy Innovation Hub (<http://www.energy.gov/hubs>) for Modeling and Simulation of Nuclear Reactors under U.S. Department of Energy Contract No. DE-AC05-00OR22725.

Materials and Fuels for the Current and Advanced Nuclear Reactors: Structural Materials - Characterization

Sponsored by: The Minerals, Metals and Materials Society, TMS Structural Materials Division, TMS/ASM: Corrosion and Environmental Effects Committee, TMS/ASM: Nuclear Materials Committee

Program Organizers: Ramprashad Prabhakaran, Idaho National Laboratory; Dennis Keiser, Idaho National Laboratory; Raul Rebak, GE Global Research

Wednesday PM

March 14, 2012

Room: Swan 2

Location: Swan Resort

Session Chair: Micah Hackett, Terra Power

2:00 PM

Long-Term High-Temperature Microstructure Stability and Mechanical Properties of Advanced Ferritic-Martensitic Steels: *Lizhen Tan*¹; *Jeremy Busby*¹; ¹Oak Ridge National Laboratory

Ferritic-martensitic (FM) steels, e.g., 9-12 wt.%Cr, are important structural materials for use in advanced nuclear reactors due to their greater void-swelling resistant, higher thermal conductivity, and lower thermal expansion compared to austenitic stainless steels. Their high-temperature performance stability during long-term services is critical for reactor safety and design. High-strength FM steels are being developed at ORNL by means of optimizing alloy composition and thermomechanical treatment. Long-term thermal annealing at 650°C for times up to 10000 hours are being performed on the samples of the steels. Microhardness measurement and tensile testing showed that the mechanical properties are deteriorated by the long-term high-temperature annealing. Transmission electron microscopy characterization, together with electron backscatter diffraction, indicates that the annealing-induced microstructural evolution, including subgrains, dislocations, and precipitates, can reasonably explain the degraded mechanical properties. The understanding of the degradation mechanism is essential for further development of advanced FM steels with superior high-temperature performance.

2:20 PM

Characterization of Surface Modifications of 316L Stainless Steel: *Giovanni Facco*¹; *Andreas Kulovits*¹; *Jorg Wieszorek*¹; ¹University of Pittsburgh

Linear raking, a novel severe surface plastic deformation process, and heat treatments are used to surface modify 316L stainless steel. This processing combination holds promise for grain boundary engineering of surface and near-surface regions to improve the degradation resistance of machined components utilized in pressurized water reactor. The influence of the rake angle on deformation processing related microstructural responses and the heat treatment related evolution of grain boundary character, grain orientation distribution and grain size have been studied quantitatively using transmission and scanning electron microscopy (TEM and SEM) and X-ray diffraction. TEM based orientation imaging microscopy enabled nanoscale measurements for even heavily deformed and grain refined states. Grain size and grain boundary character changes were effectively monitored. Stored strain and orientation-spread evolution were determined by conventional TEM diffraction. Dramatic differences in the rake-angle dependent responses of the 316L microstructure have been identified.



TMS 2012

141st Annual Meeting & Exhibition

2:40 PM

Investigation of Effect of Zr Allotropic Transformation on Interdiffusion between Mo and Zr: *Ashley Ewh*¹; Judith Dickson¹; Yongho Sohn¹; ¹University of Central Florida

Interdiffusion between molybdenum and zirconium was studied via solid-to-solid diffusion couples. The couples were assembled with disks of 99.95% pure Mo and 99.2 % pure Zr and were isothermally annealed at temperatures between 700 and 950°C for various times. Based on the binary phase diagram, Zr undergoes an allotropic phase transformation from α -(hcp) to β -(bcc)Zr at approximately 860°C and only one intermetallic phase (Mo₂Zr) exists. Microstructural observations were made via scanning electron microscopy and phase constituents were identified using a combination of energy dispersive spectroscopy and x-ray diffraction. Concentration profiles were determined by electron probe microanalysis and were used to determine effective interdiffusion coefficients. The effect of the allotropic transformation on both the rate of diffusion and the absence of the Mo₂Zr intermetallic phase will be presented and discussed.

3:00 PM

Characterization of Oxide Dispersion-Strengthened (ODS) Alloy Powders Processed by Mechano Chemical Bonding (MCB) and Ball Milling: *Longzhou Ma*¹; Bruce Kang²; C.C Huang³; ¹University of Nevada Las Vegas; ²West Virginia University; ³Hosokawa Micron Powder Systems

Oxide dispersion-strengthened (ODS) nickel-based alloying powders were processed by two approaches, MCB (mechano chemical bonding) and MCB plus conventional ball milling. The processed powders were characterized using XRD, SEM, and TEM to examine the microstructure of alloying powders. The results showed that compared to the commercial ODS MA 956 alloying powders subjected to ball milling for 72 hours, MCB plus ball-milling process allowed the alloying powders to receive remarkable deformation and to be mixed homogeneously, forming the dispersion effects similar to MA 956 powders. Powders subjected to only high speed MCB processing could form the composite structure consisting of Ni or Cr as hosting particles and deformed other starting particles including nano-sized yttria. Two approaches, MCB plus ball milling and MCB, are expected to act as alternatives to prepare the ODS alloying powders to fabricate ODS alloy with reduction of milling time.

3:20 PM

Laser Welding of Alloy 690 for Nuclear Power Systems: *Julie Tucker*¹; Terry Nolan¹; George Young¹; ¹Knolls Atomic Power Laboratory

Advances in laser welding technology are increasing the applicability of this joining technique to nuclear power systems. Advantages of laser welding include fiber optic delivery, high power density, small heat affected zones, minimal distortion, and limited susceptibility to cracking. These advantages are of special interest to next generation nuclear power systems where new alloys and dissimilar metal welds are likely. This work focuses on nuclear structural material Alloy 690 to illustrate the effects of shield gas, travel speed and beam focus on the defect density in autogenous welds. Alloy 690 welds are shown to be especially prone to porosity and these defects have been characterized by light optical microscopy and x-ray computed tomography to quantify their number, size and distribution. This work provides a process map that describes the trade off between weld penetration and defect density.

3:40 PM Break

3:50 PM

Pulsed Magnetic Welding for Advanced Core and Cladding Steels: *Yong Yang*¹; Sindo Kou²; Todd Allen²; ¹University of Florida; ²University of Wisconsin-Madison

Advanced alloys including NF616, ODS Steel variants, and High Temperature-Ultra-fine Precipitate Strengthened Steel (HT-UPS) with specially tailored microstructures, have improved high temperature strength and exceptional radiation resistance, and they are being

considered for the next generation of reactor. A potential issue that directly affects the application of them is the change in properties associated with welding. Since the superior properties depend on the uniform tempered martensitic microstructure or the evenly distributed nano-sized dispersed oxides and ultrafine precipitates for ODS steels and HT-UPS, respectively, any changes induced by conventional fusion formed welding may be deleterious. A solid-state joining method, pulsed magnetic welding, for welding the advanced core and cladding steels was studied in this paper. The flat coupon lap joints and pin/tube welding were tried, and the strength of welding was examined using a tensile shear test. The microstructures of welding were studied using electron back-scatter diffraction and transmission electron microscopy.

4:10 PM

Effects of Laser Shock Peening on Residual Stress, Microstructure and Corrosion Behavior of Alloy 600: *Abhishek Telang*¹; Amrinder Gill¹; James Guenes¹; S Mannava¹; Dong Qian¹; Vijay Vasudevan¹; ¹University of Cincinnati

Nuclear steam generator tubing materials like austenitic stainless steels, Ni-based alloys like alloy 600 and their weldments are susceptible to stress corrosion cracking (SCC) in different environments. The present work was undertaken to evaluate the effects of laser shock peening (LSP) on the SCC resistance of alloy 600. As-received and heat-treated coupons of alloy 600 were LSP-treated and residual stresses, near-surface microstructure were characterized. Single loop and double loop Electrochemical Potentiokinetic Reactivation (EPR) tests were used to quantify the degree of sensitization (DOS) and characterize the effect of LSP on the corrosion resistance and hence on the susceptibility of Alloy 600 to Intergranular SCC. Modified Huey tests and bend tests in thiosulfate environment were used to investigate the effect of LSP on SCC behaviour. Results show that LSP introduces deep compressive residual stresses and EPR tests indicate lower DOS, decreased extent and width of grain boundary attack after LSP.

4:30 PM

Nanoindentation and the Micromechanics of Zry-4: *Christabel Evans*¹; Trevor Lindley¹; David Dye¹; ¹Imperial College London

Zircaloy-4 is widely used to contain fuel in light water reactors. During service at around 330C, corrosion occurs at the cladding/water interface producing hydrogen, which diffuses into the zirconium alloy. As hydrogen content increases beyond the room temperature solubility, hydrides precipitate on cooling leading to brittleness in the material. In addition, if a stressed crack is present hydrogen can migrate to the crack tip, promoting crack propagation. This delayed hydride cracking phenomenon is of concern for dry storage of present generation irradiated fuel. Little is known about the micromechanics of hydrides at the individual plate level and therefore in the present study nanoindentation is used to characterise the mechanical properties of individual hydride plates in a sheaf and how they interact with the surrounding matrix. Post-indentation TEM has been used to investigate dislocation arrays across the hydride and at each indent.

4:50 PM

Characterization of Zirconium Excel Alloy for Generation IV CANDU SCW Reactors: *Mohammad Sattari*¹; Richard Holt¹; Mark Daymond¹; ¹Queen's University

Zirconium Excel alloy (Zr-3.5 Sn-0.8Nb-0.8 Mo) is the candidate material for pressure tube in Generation-IV CANDU® Super Critical Water-cooled Reactor (SCWR) design. It is a dual phase material, hcp α -Zr and bcc β -Zr; and it has better creep resistance compared to the current pressure tube material, Zr-2.5Nb, mainly due to solid solution strengthening effect of Sn as well as potential age hardening. In order to understand the metallurgy of this alloy and improve its mechanical properties, it is important to know the transformation temperatures, i.e. $\alpha \rightarrow \alpha + \beta$ and $\alpha + \beta \rightarrow \beta$. Metallography techniques as well as Differential Scanning Calorimetry (DSC) and resistivity measurement has been employed to study the transformation temperatures. Thorough

microstructural characterization has been done using optical and electron microscopy techniques. Different heat treatment has been developed to study the aging response of this alloy and to improve its mechanical properties, particularly creep resistance which is investigated using accelerated stress-rupture experiments.

5:10 PM

Order-Disorder Transformation in a Ni-Cr-Mo Alloy: Amit Verma¹; Jung Singh¹; M Sundararaman²; Nelia Wanderka³; ¹Bhabha Atomic Research Centre; ²University of Hyderabad; ³Helmholtz-Zentrum Berlin für Materialien und Energie GmbH

Ni-Cr-Mo alloys are potential candidates for structural materials application for high temperature reactors. These alloys form a long-range order (LRO) Ni₂(Cr,Mo) (Pt₂Mo type structure) phase, in the intermediate temperature range. Evolution of this phase has been studied using resistivity and transmission electron microscopy (TEM). The relative change in resistance as a function of temperature could be divided into 5 regimes, which could be attributed to different microstructural states. TEM investigations revealed the presence of a {1 ½ 0} type of short-range order (SRO) and subunit cells of Pt₂Mo structure in solution treated and quenched state. Formation of the LRO could be identified to initiate at {1 ½ 0} SRO state. The progress of the SRO and LRO states has been correlated to the resistance change profile during continuous heating. The SRO state has also been found to have a strong influence on the kinetics of the transformation.

Materials Design Approaches and Experiences III: High Strength Steels

Sponsored by: The Minerals, Metals and Materials Society, TMS Structural Materials Division, TMS: High Temperature Alloys Committee, TMS: Integrated Computational Materials Engineering Committee

Program Organizers: Ji-Cheng Zhao, The Ohio State University; Akane Suzuki, GE Global Research; Deb Whitis, GE Aviation; Michael Fahrman, Haynes International Inc.; Qiang Feng, University of Science and Technology Beijing

Wednesday PM
March 14, 2012

Room: Europe 11
Location: Dolphin Resort

Session Chairs: Qiang (Charles) Feng, University of Science and Technology Beijing; Michael Fahrman, Haynes International, Inc.

2:00 PM Invited

Alloy Design of 9% Cr Steel for High Efficiency Ultra-Supercritical Power Plants: Fujio Abe¹; ¹National Institute for Materials Science

Boundary and sub-boundary hardening is shown to be the most important strengthening mechanism in creep of tempered martensitic 9% Cr steel base metal and welded joints at 650°C. The addition of boron reduces the coarsening rate of M₂₃C₆ carbides along boundaries near prior austenite grain boundaries during creep, enhancing the boundary and sub-boundary hardening at long times. Excess addition of nitrogen to the 9Cr-boron steel promotes the formation of boron nitrides during normalizing heat treatment, which consumes most of soluble boron and degrades the creep strength. Newly alloy-designed 9Cr steel with 100-150 ppm boron and 70-85 ppm nitrogen exhibits much higher creep strength of base metal than conventional steel P92 and also no degradation in welded joints at 650°C. The protective Cr₂O₃-rich scale forms on the surface of 9Cr steel by pre-oxidation treatment in Ar gas, which significantly improves the oxidation resistance in steam at 650°C.

2:30 PM Invited

Advanced Heat Resistant Austenitic Stainless Steel for A-USC Power Plant: Guocai Chai¹; ¹Sandvik Materials Technology

Energy requirement, security and environmental concerns have promoted a worldwide develop in clean coal fired power technologies. Austenitic

stainless steel grade UNS S31035 or Sanicro 25 has been developed for this purpose and will be used in the next generation of A-USC power plant at material temperatures up to 700°C. This new grade shows very good resistance to steam oxidation and hot corrosion, and higher creep rupture strength than other austenitic stainless steels available today. This presentation will provide a review on the development and application of this material. The structural stability, creep strength and resistances to oxidation and hot corrosion and the relations between microstructure and properties will be focused. The creep and fracture mechanisms at different conditions studied using TEM and SEM will be discussed. In order to predict the long term creep properties, different models have been used to evaluate the long-term creep behavior of the grade.

3:00 PM Invited

In Situ Inclusion Behavior in Ultra-High Strength Steels: Jon Groh¹; Mark Rhoads¹; ¹General Electric Company

The mechanical properties, especially low cycle fatigue behavior (LCF), of ultra-high strength steel materials are significantly impacted by the existence of non-metallic inclusions. To better understand the behavior of precipitates and inclusions on the behavior of Marage 250 and GE1014, specially designed SEM in-situ tensile and fatigue tests were conducted. The entire process of crack initiation and propagation to fracture in these ultra-high strength steels was accomplished at room temperature. Micro-mechanical behavior, such as crack initiation and propagation at tensile and fatigue tests, of inclusions in ultra-high strength steels GE1014 were investigated in detail.

3:30 PM Break

3:50 PM Invited

Development of High-Performance Structural Alloys for Nuclear Energy Systems: Steven Zinkle¹; Michael Brady¹; Yuki Yamamoto¹; Michael Santella¹; Phillip Maziasz²; David Hoelzer¹; Jeremy Busby¹; Lizhen Tan¹; Govindarajan Muralidharan¹; ¹Oak Ridge National Laboratory

Numerous structural materials are required for the operation of fission and proposed fusion energy systems. A series of high performance pressure vessel steels, austenitic alloys, and tempered ferritic/martensitic steels have recently been designed and fabricated for aggressive operating environments such as fossil and nuclear energy systems. The alloy design utilized a variety of tools such as computational thermodynamics to rapidly converge on an optimized alloy composition. Several examples of these high-performance alloys that are tailored for specific extreme operating environments will be given, based on traditional ingot-based steel metallurgy methods and alternative techniques such as powder metallurgy production of oxide dispersion strengthened steels. Recent work to design a series of creep-resistant steels that form a self-healing alumina surface film at high temperatures will be summarized.

4:20 PM Invited

Design Approaches and Performance of Novel Austenitic Heat Resistant Steels Strengthened by TCP/GCP Intermetallics for A-USC Power Plants: Masao Takeyama¹; Imanuel Tarigan²; ¹Tokyo Institute of Technology, Consortium of the Japan Research and Development Center for Materials (JRCM); ²Tokyo Institute of Technology

For sustainable and reliable energy supply sources, advanced thermal power plants (A-USC) is receiving more attention since shutdown of nuclear power plants by an unprecedented devastating earthquake in Japan. For A-USC in reality, new materials with superior long-term creep rupture strength longer than 10⁵ hours under 100 MPa at 973 K are desired. Besides some Ni base alloys, none of the conventional austenitic heat resistant steels meet this requirement. Why? This is due to microstructure instability of major strengthening species/metallic carbides during high temperature exposure. We have developed novel austenitic steels strengthened by two intermetallic phases of GCP (geometrically close-packed) and TCP (topologically close-packed), and revealed excellent creep performance. In this talk, the design approaches based



TMS 2012

141st Annual Meeting & Exhibition

on phase diagram calculation and new strengthening mechanism called "Grain-boundary precipitation strengthening" by TCP Laves phase is presented. Part of this study was carried under the research activities of the Consortium, financially supported by NEDO.

4:50 PM

Effect of Grain Boundary Laves Phase on Mechanical Properties of Fe-20Cr-30Ni-2Nb Steels: Naoya Kanno¹; Naoki Takata²; Masao Takeyama²; ¹Tokyo Institute of Technology; ²Tokyo Institute of Technology, Consortium of the Japan Research and Development Center for Materials (JRCM)

We have developed novel austenitic heat resistant steels Fe-20Cr-30Ni-2Nb (at.%) strengthened by Fe₂Nb-Laves phase for A-USC power plant. The steels show superior long-term creep strength due to "grain boundary precipitation strengthening" by Laves phase. Question is whether the grain boundary Laves phase embrittles the steels. In this study, thus, we intentionally prepared the steels with the area fraction of Laves phase (ρ) in the range of 0 to 90 %, and examined the tensile and Charpy impact properties at room temperature. The tensile elongation reduces from 50 % to 30 % with increasing the ρ from 0 to 80 %. The impact absorption energy decreases from 200 J/cm² to 30 J/cm² with increase in the ρ from 0 to 90 %. In any samples, however, there is no indication of intergranular fracture, indicating that grain boundary Laves phase is not a factor to deteriorate the properties.

5:10 PM

Microstructural Studies on Thermomechanically Processed Plain Carbon Dual Phase Steel: Abhishek Singh¹; G Chaudhari¹; Mukesh Bharadawaj¹; S Nath¹; I. I. T. Roorkee

Dual phase steel, whose microstructure consists of primarily ferrite plus martensite, is categorized under advanced high strength steel (AHSS). This is due to its high UTS, adequate ductility, high work hardening rate and absence of yield point phenomenon. A lot of effort is being put to improve its strength along with its ductility. This steel is primarily aimed for automotive industries. In the present work, plain low carbon steel is thermomechanically worked in the intercritical temperature range by using thermomechanical simulator Gleeble 3800. Intercritical temperature, strain and strain rate have been varied to process the dual phase steel. It has been found that the steel thermomechanically worked in the intercritical region shows decrease in ferrite grain size, increase in volume fraction of ferrite and refinement of martensite island size as compared to dual phase steel with no thermomechanical treatment

Materials Research in Microgravity: Session VI

Sponsored by: The Minerals, Metals and Materials Society, TMS Materials Processing and Manufacturing Division, TMS Extraction and Processing Division, TMS: Process Technology and Modeling Committee, TMS: Solidification Committee

Program Organizers: Robert Hyers, University of Massachusetts; Hani Henein, University of Alberta; Valdis Bojarevics, University of Greenwich; James Downey, NASA; Douglas Matson, Tufts University; Achim Seidel, Astrium; Daniela Voss, ESA

Wednesday PM
March 14, 2012

Room: Asia 3
Location: Dolphin Resort

Session Chair: To Be Announced

2:00 PM Invited

Coarsening of Two-Phase Mixtures: Experiments on the International Space Station: J. Thompson¹; E. Gulsoy¹; Peter Voorhees¹; ¹Northwestern University

In any two-phase mixture that contains particles of different sizes, the large particles tend to grow while the small particles shrink. Solid-liquid mixtures are ideal systems to study this coarsening process and compare the results to theory. Using the microgravity environment of the

International Space Station it is possible to study the coarsening process in solid-liquid mixtures with reduced interference from the sedimentation that occurs on Earth. Specifically we have studied the coarsening process in systems consisting of particles of tin suspended in a liquid tin-lead alloy. A series of experiments were performed in the Microgravity Glove Box. The analysis of the experiments employs three-dimensional reconstructions of the microstructures. We have analyzed samples with a range of volume fraction of solid, and have compared the coarsening rates, particle size distributions, and interparticle spatial correlation functions with those predicted by theory. The implications of this test of theory will be discussed.

2:35 PM Invited

Multi-Scale Modeling on Liquid Phase Sintering Affected by Gravity: Preliminary Analysis: Eugene Olevsky¹; Randall M. German¹; ¹San Diego State University

Results of the multi-scale simulations of the gravitational role on liquid phase sintering are reported in terms of densification, distortion, and microstructure development. The gravity influence is taken into account at both the micro- and macro-scales. At the micro-scale, the diffusion mass-transport is directionally modified in the framework of kinetic Monte-Carlo simulations to include the impact of gravity. The micro-scale simulations provide the values of the constitutive parameters for macroscopic sintering simulations. At the macro-scale, we are attempting to embed a continuum model of sintering into a finite-element framework that includes the gravity forces and substrate friction. If successful, the finite elements analysis will enable predictions relevant to space-based processing, including size and shape and property predictions. Model experiments are underway to support the models via extraction of viscosity moduli versus composition, particle size, heating rate, temperature, time and these reflect bonding, dihedral angle, and liquid and solid phases.

3:10 PM

Self-assembly of Ni-nanoparticles in Aerosols Produced Thermally On-ground and under Microgravity Conditions: Stefan Lösch¹; Bernd Günther¹; Daniela Nolle²; Eberhard Göring²; ¹Fraunhofer; ²Max-Planck-Institut

The self-assembly behavior in Ni-aerosols was studied on-ground and under microgravity conditions by using the European sounding rocket MAXUS 8 and the parabolic flight aircraft A300 Zero-G. In microgravity, convection within the thermally produced aerosols could be effectively suppressed. It is shown that due to magnetic dipole interaction the Ni-particles agglomerate in a chain-like morphology both on-ground and in parabolic flights. It is shown that the chain length increases with increasing agglomeration time. This time scale could be extended in the range of minutes by using the sounding rocket microgravity platform. In general, under microgravity condition the intrachain size distribution of the Ni-particles is narrower than gets narrower. This is reduced to the ideal flow condition in microgravity. Surprisingly the sounding rocket platform did not result in chain-like Ni-agglomerates. Instead irregular morphology of fluffy agglomerates resulted similar to those observed for non-magnetic nanoparticles. These results are explained by considering the thermal history during particle synthesis in this process.

3:35 PM Break

3:55 PM Invited

Crystallographic Stability of Metastable Phase Formed by Containerless Processing in REFeO₃ (RE: Rare-Earth Element): Kazuhiko Kuribayashi¹; M.S. Vijaya Kumar²; ¹Shibaura Institute of Technology; ²Institute of Space and Astronautical Science, JAXA

Undercooling a melt often facilitates a metastable phase to preferentially nucleate. In case of REFeO₃ (RE: Rare-earth element), although the equilibrium phase is perovskite, the space group of which is Pbnm, metastable hexagonal phases of P6₃cm or P6₃/mmc are formed from the deeply undercooled melt. The stability of perovskite structure can be well described by the tolerance factor TF. That is, TF=1: ideal, 0.8<TF<

WEDNESDAY PM

1: stable, and $TF < 0.8$: unstable. For the metastable hexagonal phase of $REFeO_3$, however, there has been no criterion for the crystallographic stability. In the present investigation, based on the geometrical consideration on the ionic radii of constituent ions, RE^{3+} , Fe^{3+} and O_2 , the criterion for metastable hexagonal phase to be formed is also expressed by tolerance factor, as $TF = 0.87$: ideal. $TF < 0.87$: stable, and $TF > 0.87$: unstable, respectively. Experimental result using aerodynamic levitator (ADL) well agreed with this prediction under reduced oxygen partial pressure, P_{O_2} , as well as in ambient one.

4:30 PM

On-Line Real Time Diagnostics of a Single Fluid Atomization System: *Pooya Delshad Khatibi*¹; *Arash Ilbagi*¹; *Hani Henein*¹; ¹University of Alberta

A drop tube-impulse atomization technique was used to produce copper powders. In this method, by a plunger movement, energy is transferred to a liquid resulting in spherical droplets emanating from orifices. A mathematical model of the evolution of droplet velocity and temperature at various heights for different sized droplets was developed. To measure the velocity (Shadowgraph) and radiant energy (DPV-2000), a 3-D translation stage was designed, constructed and installed in the drop tube. Using experimental and model results, it was found that the falling droplets do not reach their terminal velocity at their melting point, and the acceleration of falling droplets is close to gravitational acceleration. The results of in-situ measurements showed that at each height, radiant energy of larger droplets is larger than that of the smaller ones. Correlation between experimentally measured radiant energy and predicted temperature of falling droplets at different heights will be discussed in this paper.

4:55 PM

Electrodeposition of Metals in Microgravity Conditions: *Yasuhiro Fukunaka*¹; ¹JAXA/Waseda University

Metal electrodeposition may introduce various morphological variations depending on the electrolytic conditions including cell configurations. For liquid electrolytes, a precise study of these deposits may be complicated by convective motion due to buoyancy. Zero-gravity (0-G) condition provided by drop shaft or parabolic flight gives a straightforward mean to avoid this effect: we present here 0-G electrodeposition experiments, which we compare to ground experiments (1-G). Two electrochemical systems were studied by laser interferometry, allowing to measure the concentration variations in the electrolyte: copper deposition from copper sulfate aqueous solution and lithium deposition from an ionic liquid containing LiTFSI. For copper, concentration variations were in good agreement with theory. For lithium, an apparent induction time was observed for the concentration evolution at 1-G: due to this induction time and to the low diffusion coefficient in ionic liquid, the concentration variations were hardly measurable in the parabolic flight 0-G periods of 20 seconds.

5:20 PM

Propagation Regime of Iron Dust Flames: *Francois Tang*¹; *Samuel Goroshin*²; *Andrew Higgins*²; ¹European Space Agency; ²McGill

A flame propagating through an iron-dust mixture can propagate in two asymptotic regimes. When the characteristic time of heat transfer between particles is much smaller than the characteristic time of combustion, the flame propagates in the continuum regime where the heat release by reacting particles can be modelled as a space-averaged function. In contrast, when the characteristic time of heat transfer is much larger than the combustion time, the flame can no longer be treated as a continuum due to dominating effects associated with the discrete nature of the particle reaction. The discrete regime is characterized by a weaker dependence of the flame speed on the oxygen concentration compared to the continuum regime. The discrete regime is observed in flames propagating in a mixture of iron dust in a gas mixture containing xenon, while the continuum regime is obtained when xenon is substituted with helium.

Mechanical Behavior at Nanoscale I: Nanomechanical Experiment and Modeling

Sponsored by: The Minerals, Metals and Materials Society, TMS Materials Processing and Manufacturing Division, TMS; Nanomechanical Materials Behavior Committee, TMS/ASM; Mechanical Behavior of Materials Committee

Program Organizers: Scott Mao, University of Pittsburgh; Julia R Greer, California Institute of Technology; Jianyu Huang, Center for Integrated Nanotechnologies; Marc Legros, CEMES-CNRS; Ting Zhu, Georgia Institute of Technology

Wednesday PM
March 14, 2012

Room: Asia 1
Location: Dolphin Resort

Session Chairs: Daniel Gianola, University of Pennsylvania; Julia Greer, California Institute of Technology (Caltech)

2:00 PM Invited

Effect of Electric Current on Nanoindentation of Copper: *Fuqian Yang*¹; ¹University of Kentucky

The electromechanical behavior of electronic interconnects plays an important role in determining the reliability and lifetime of microelectromechanical devices and structures. Using the nanoindentation technique, the effect of electric current on the indentation deformation of copper wires was studied under the indentation load of 0.05 mN to 1 mN at room temperature. During the indentation, a constant direct electric current of the current density in a range of 6.4 to 31.8 kA/cm² was passed through the copper wires, which introduced electromechanical interaction. The indentation results showed that the apparent contact modulus decreased with increasing electric current density and the apparent indentation hardness increased slightly with increasing electric current density. The decrease of the apparent contact modulus with increasing electric current density was likely due to the momentum exchange among high-speed electrons and atoms.

2:20 PM

Structure Effects on the Bending Strength of Si Nanowires: *Gheorghie Stan*¹; *Sergiy Krylyuk*¹; *Albert Davydov*¹; *Igor Levin*¹; *Robert Cook*¹; ¹National Institute of Standards and Technology

Nanoscale mechanical tests for elasticity, plastic deformation, fracture, toughness, creep, and fatigue provide key information in selecting materials and structures for reliable and high performance functionality of emerging nanoscale devices. In this work, a new and direct method for testing the fracture strength of substrate-supported nanowires is introduced. The ultimate fracture strengths of Si nanowires with radii in the 20 nm to 60 nm range were measured through a sequential atomic force microscopy manipulation-scanning protocol. Using crystallographic structure analysis provided by transmission electron microscopy, the fracture strength of the measured Si nanowires was assessed in terms of microstructure and surface effects. On one hand, the internal twin-structure of the nanowires can account to some extent for the large average values of the measured fracture strengths. On the other hand, the radius dependence of the fracture strength can be rationalized as a surface effect determining the number of stress-concentrating surface flaws.

2:40 PM

Extended Structure of Point Defects in Graphene: *Mark Jhon*¹; *David Srolovitz*¹; ¹Institute of High Performance Computing

Nanoscale materials are often flexible, and can bend easily relative to bulk systems. If a flexible nanostructure has internal stresses due to, for instance, crystallographic defects, it can bend to accommodate them. The mechanical deformations associated with point defects can potentially cause large changes to the shape of the nanostructure. Considering graphene flakes as a model flexible nanostructure, we analyze the extended shape of point defects using continuum elasticity. We find conditions under which graphene will buckle due to a point inclusion.



TMS 2012

141st Annual Meeting & Exhibition

The continuum analysis is validated by comparison to molecular statics calculations using empirical potentials.

3:00 PM

Estimation of Dislocation Nucleation Stresses from Nanoindentation by Combined Modeling and Experiment: *Li Ma*¹; Dylan Morris²; Stephanni Jennerjohn³; David Bahr³; Lyle Levine¹; ¹NIST; ²Michelin North America; ³Washington State University

The dislocation nucleation stress of crystalline materials is frequently estimated from the maximum shear stress assuming Hertzian contact up to the first “pop-in” event, which is a sudden displacement burst during load-controlled nanoindentation. However, real Berkovich indenter tips may have irregular shapes. Here, we assess possible errors and pitfalls of the Hertzian estimation of initial plastic yield at the nanoscale. The near-apex shape of two Berkovich indenters, one sharp and one worn, were measured by atomic force microscopy and directly input into finite element approach (FEA) models for “virtual” nanoindentation experiments on single-crystal tungsten. Experiments were also carried out with those indenters. Excellent agreement is found between experimental and FEA force-displacement relationships, but the discrepancies between Hertzian and FEA estimates of the shear stresses are over 30%. This indicates that small irregularities in the shape of indenter tips may cause significant deviations from the Hertzian estimation of dislocation nucleation stress.

3:20 PM

Interaction of the Microstructure and Test Geometry on the Size Dependence of Plasticity: *Andy Bushby*¹; David Dunstan¹; ¹Queen Mary, University of London

Nanoscale plasticity is often studied within single crystals of material, for instance in nanoindentation, micro-pillar compression and micro-tensile experiments, and the size effects considered separately from those associated with microstructure. Theoretical models of size dependant plasticity also do not consider the mutual effect of microstructure. Here we present experimental data that explore the combined influence of different size effects in the flexure of thin foils, the torsion and tension of thin wires and nanoindentation, in which the grain size is varied in relation to the structure or stressed volume. This approach allows for cross-correlation between structure size and grain size. By carefully choosing different test geometries and grain sizes, the destination of dislocations can be manipulated and the interaction of the different length scales studied. The results are used to rigorously test the ability of theoretical models to describe the yield and flow in metals at the nanoscale.

3:40 PM

Quantifying Polysilicon Strength Size Effects Using an In-Situ on-Chip Tensile Test Platform: Mohamed Saleh¹; Siddharth Hazra¹; *Jack Beuth*¹; Maarten de Boer¹; ¹Carnegie Mellon University

Freestanding polycrystalline silicon (polysilicon) is a brittle material, necessitating a statistical representation of strength data supported by a large number of tests. In this research, size effects in the strength of polysilicon are studied using a compact micro/nanoscale testing platform using an on-chip thermal actuator to apply stresses to a self-aligned tensile specimen. The testing platform allows the testing of hundreds or more specimens on the same wafer, and results are presented for test trials of 200-300 specimens. Size effects in polysilicon strength are caused by a distribution of crack-like flaws that form at grain boundaries during processing. With results from large testing trials, Weibull statistics are used to predict the size-dependent strength of unnotched and notched tensile specimens over the full range of practical component sizes. Experimental results are presented yielding insights into the accuracy of such predictions and how they can be used effectively in designing MEMS devices.

4:00 PM Break

4:10 PM

Humidified Nanoindentation: Grant Klafehn¹; *Corinne Packard*¹; ¹Colorado School of Mines

The relative humidity of the testing atmosphere can have a marked influence on mechanical behavior—from fracture in ceramics to creep in hydrated polymers and biomaterials. The fundamentals of deformation in processes like these can be elucidated using the high-resolution measurement capabilities of nanoindentation. However, testing in humidified environments presents several challenges, including atmospheric control and monitoring, condensation management, sensitivities of equipment to corrosion, and mitigation of thermal drift for elevated temperature experiments. Historically, approaches to humidified indentation have ranged from the placement of saturated salt solutions close to the sample to custom apparatuses and commercial systems. In this talk, previous applications of indentation in humidified environments are reviewed and the development of a recently designed custom system for performing nanoindentation in a humidified environment with temperature control is presented. System design features and performance are described in detail and compared to the existing state of the art.

4:30 PM

A Nanoscale Investigation on Effect of Hydrogen in Confined Volumes: *Ilaksh Adlakha*¹; Kiran Solanki¹; Amitava Moitra²; Mark Tschoopp³; ¹SEMTE; ²Pennsylvania State University; ³Mississippi State University

The detrimental effects of hydrogen on mechanical behavior of metals are well known. There are several proposed mechanisms to explain this behavior, but no general consensus has been reached. In this work, we use molecular dynamic simulations to gain a better understanding of the effect of hydrogen in confined volumes. Single crystal nanowires of different diameters are doped with various hydrogen percentages. Doping hydrogen severely decreases the yield strength across the studied size spectrum. It is hypothesized that studying the hydrogen diffusivity under changing stress state can shed light on its effect on mechanical properties. As hydrogen concentration is increased, the yield asymmetry increases; these findings are correlated with the diffusivity of hydrogen. These results help us gain a better understanding of the effect of hydrogen at nanoscale.

4:50 PM

Automated Analysis of Crystal Defects in Large-Scale Atomistic Computer Simulations: *Alexander Stukowski*¹; Tom Arsenlis¹; ¹Lawrence Livermore National Laboratory

Large-scale atomistic simulation methods such as molecular dynamics (MD) are routinely used to study the deformation of crystalline materials at the atomic scale. We present a set of sophisticated computational analysis methods to extract and characterize structural defects in such simulations in a fully automated way. The newly developed techniques cover defects such as stacking faults, grain boundaries, interfaces, dislocations, point defects, and defect clusters in a wide range of crystal lattices. To exemplify the range of applications of our approach, we discuss the identification of grain boundary dislocations in MD simulations, allowing us to directly visualize their interaction and/or reaction with lattice dislocations. We also show how atomic trajectories obtained from MD can be used to calculate the strain tensor field, and how it can be decomposed into elastic and plastic components to quantify the contribution of dislocations to total strain.

5:10 PM

Nanoindentation of Nanoporous Polycrystalline Platinum: Ran Liu¹; Yuan Li¹; *Antonia Antoniou*¹; ¹Georgia Institute of Technology

Nanoporous Pt (np-Pt) is synthesized by electrochemical dealloying of co-sputtered Ptx-Si1-x amorphous films. The initial alloy deposition conditions and dealloying conditions were varied and their effect on the assembled NP Pt was examined. We find that the spatial arrangement of

nano-sized ligaments can be tailored. Nanoindentation tests reveal that the hardness of isotropic NP Pt is ~1 GPa but it can increase by as much as 3-4 times due to the geometrical arrangement of NP metal ligaments.

5:30 PM

Deformation Mechanism of Nanocrystalline Copper during Relaxation Test: Junya Inoue¹; Saethavuth Krasienapibal¹; Toshihiko Koseki¹; ¹The University of Tokyo

Void and twin formations in nanocrystalline Cu during relaxation experiments were quantitatively studied to clarify the effect of grain size distribution on the deformation behavior in nanocrystalline Cu at room temperature. Cu films with various thicknesses were deposited on Si/SiO₂/TaN and polyimide substrates by magnetron sputtering deposition method. On the top and bottom surfaces of the Cu layer, Ta layers were deposited to suppress the surface diffusion of Cu during the relaxation test. The Cu films were annealed after the deposition to stabilize grain structure in a vacuum. Microstructural evolution as well as void formation was studied after relaxation experiment. Voids were found at the grain boundary triple points in the films subjected to the relaxation experiment. A clear grain-size dependencies of the number of void and the twin density was demonstrated. The competition between the accommodation processes will be further discussed.

Mechanical Behavior Related to Interface Physics: Deformation Mechanisms in Nanoscale Materials

Sponsored by: The Minerals, Metals and Materials Society, TMS Structural Materials Division, TMS Materials Processing and Manufacturing Division, TMS/ASM: Mechanical Behavior of Materials Committee, TMS: Nanomechanical Materials Behavior Committee

Program Organizers: Jian Wang, Los Alamos National Laboratory; Nathan Mara, Los Alamos National Laboratory; Izabela Szlufarska, University of Wisconsin-Madison; Zhiwei Shan, Xi'an Jiaotong University

Wednesday PM
March 14, 2012

Room: Oceanic 1
Location: Dolphin Resort

Session Chairs: Julia Greer, California Institute of Technology; Jianyu Huang, Sandia National Laboratories

2:00 PM Keynote

Deformation Mechanisms in Single Boundary-Containing Metallic Nano-Pillars: Grain, Phase, and Crystal Boundaries: Julia Greer¹; Robert Maass¹; Xun Gu¹; Qiang Guo¹; Siddhartha Pathak¹; ¹California Institute of Technology

When microstructural (intrinsic) or external material dimensions of materials are reduced to nano-scale, they exhibit size-dependent strengths. To date, most studies on "size effects" have focused on single crystalline metals. While these studies provide powerful foundation for fundamental deformation processes at small scale, they are a far reach from representing real materials, whose microstructure is often complex. To elucidate specific role a particular boundary plays on material deformation and mechanical properties, we fabricate nanopillars containing a single known boundary with diameters from 50nm to 1micron by E-beam lithography/electroplating and via FIB. Their mechanical response in uniaxial compression and tension is subsequently measured in in-situ mechanical deformation instrument, SEMentor. We present nano-mechanical behavior in four distinct metallic systems containing single well-characterized boundary: bi-crystalline Al, Cu/Fe (fcc/bcc), Cu/Ni (fcc/fcc), and Ni₃Al precipitates in Ni-rich matrix. We discuss their deformation in context of dislocation activity when free surfaces and interfaces are present concurrently.

2:30 PM Keynote

Lithiation Induced Stress and Failure of Anode Materials in Lithium Ion Batteries: Jianyu Huang¹; ¹Sandia National Laboratories

Lithiation induced stress and failure in anode materials were observed by in-situ electron microscopy. The stress and failure were strongly materials, size, and orientation dependent. Upon charging of SnO₂ nanowires, we observed high density of dislocations in the reaction front, while in charging of ZnO nanowires, we observed discrete cracks in the reaction front. In charging Si nanowires, we found the volume expansion was highly anisotropic, resulting in a dumbbell-shaped cross-section and cracking, eventually splitting the single nanowire into sub-wires. Carbon coating not only increases rate performance but also alters the lithiation-induced strain of SnO₂ nanowires. The radial expansion of the coated nanowires was completely suppressed. The lithiation process of individual Si nanoparticles was strongly size-dependent, i.e., there exists a critical particle size with a diameter of ~150 nm, below which the particles neither cracked nor fractured upon lithiation, above which the particles first formed cracks and then fractured.

3:00 PM

Effect of Contact Interface on the Mechanical Behavior of Submicro Sized Au Particles: Zhangjie Wang¹; Zhiwei Shan¹; Ju Li²; Jun Sun¹; Evan Ma³; ¹Center for Advancing Materials Performance from the Nanoscale (CAMP-Nano) & Hysitron Applied Research Center in China (HARCC), State Key Laboratory for Mechanical Behavior of Materials, Xi'an Jiaotong University; ²Department of Nuclear Science and Engineering and Department of Materials Science and Engineering, Massachusetts Institute of Technology; ³Department of Materials Science and Engineering, Johns Hopkins University

Pristine single crystalline gold particles with sizes ranging from 300~700 nm have been fabricated through high-temperature (1150°C) liquid dewetting of gold thin films, and fixed atop a specially designed SiO₂/Si substrate for in situ TEM testing. Quantitative compression tests indicated that these particles display structural collapse upon high stresses (over 1GPa) in the early stage. The initial structural collapse results in a nearly pristine postmortem microstructure. When the contact interface diameter *d* is small enough, spatially and temporally correlated load shedding is proposed to explain the pristine to pristine structural collapse. Upon further compression, once the *d* increases above a critical value (~250 nm), continuous plastic deformation begins to set in under relatively low flow stress with the postmortem microstructure containing a high density of tangled dislocations, indicating a critical *d* for dislocation interaction volume for multiple slip is needed for the dislocation storage and normal dislocation plasticity.

3:15 PM

Exhaustion Hardening in Mo-alloy Nanofibers: Claire Chisholm¹; Hongbin Bei²; Matthew Lowry¹; Jason Oh²; S.A. Syed Asif²; Oden Warren³; Zhiwei Shan⁴; Easo George⁵; Andrew Minor¹; ¹University of California, Berkeley and National Center for Electron Microscopy; ²Materials Science and Technology Division, Oak Ridge National Laboratory; ³Hysitron Incorporated; ⁴Center for Advancing Materials Performance from the Nanoscale (CAMP-Nano), State Key Laboratory for Mechanical Behavior of Materials, Xi'an University and Hysitron Incorporated; ⁵Materials Science and Technology Division, Oak Ridge National Laboratory and Department of Materials Science and Engineering, University of Tennessee, Knoxville

The evolution of defects in Mo alloy nanofibers with dislocation densities ranging from 0 to ~1 x 10¹⁴ m⁻² were studied using an in situ "push-to-pull" (PTP) device in conjunction with a quantitative nano-indenter in a transmission electron microscope (TEM). By augmenting the in situ testing method with Digital Image Correlation (DIC), we can determine the true stress and strain in local areas of deformation. With no initial dislocations, the Mo-alloy nanofibers suffered sudden catastrophic elongation and softening at ultrahigh stresses. On the other extreme, fibers with a high dislocation density operated with sustained homogeneous



TMS 2012

141st Annual Meeting & Exhibition

deformation, but failed at lower stresses. Between these two extremes nanofibers with intermediate dislocation densities demonstrated clear exhaustion hardening behavior, where the progressive exhaustion of dislocations increases the stress required to drive plasticity.

3:30 PM

Fracture Toughness of Nanocrystalline Cu and Cu-Cr pillars Thin Film Composites: *Sharvan Kumar*¹; Seong-Woong Kim²; Jin-Woo Yi¹; Hyun-Gyu Kim³; Kyung-Suk Kim¹; ¹Brown University; ²Korea Institute of Materials Science; ³Seoul National University of Technology

A hybrid method of experiments and finite element analyses is developed to measure in-plane elastic modulus and fracture toughness of free-standing, uniform-thickness, electron-transparent nanocrystalline thin films and thin film composites. Electron beam evaporation coupled with lithography and patterning is used to produce these films of nanocrystalline Cu and Cu-Cr “pillar” composites with uniform diameter and spacing of Cr pillars. The in-plane modulus of such films is measured non-destructively by using a modified bead-tip AFM in conjunction with a newly developed diamagnetic normal force calibrator capable of measuring forces from 0.1 nN to 1.0 μN with three digit accuracy. The films are then in-situ tested by loading in the TEM to advance a crack tip; the crack opening profile is used to obtain the fracture toughness employing an iterative finite element inverse analysis; the crack kinking angle at the Cu-Cr interface is then used to evaluate the interface fracture toughness.

3:45 PM Break

3:55 PM Keynote

Friction and Mechanics of Lamellar and Nanostructured MoS₂: Eric Bucholz¹; Simon Phillpot¹; *Susan Sinnott*¹; ¹University of Florida

Classical molecular dynamics (MD) simulations are used to investigate the influence of structural changes on tribological and mechanical properties of MoS₂ with lamellar, fullerene-like, and nanotubes structures. The simulations probe the effect of edges on the friction behavior of the lamellar structures by considering two-dimensional periodic sheets, one-dimensional periodic ribbons, and non-periodic flakes across a range of temperatures as a function of applied load. In the case of fullerene-like nanoparticles, two specific configurations with three nested layers each are considered: a curved, ellipsoidal particle and a faceted nanooctahedron. This allows for the characterization of the role of curved and faceted morphologies as well as grain boundaries on the rolling and sliding behavior as well as any lamellar exfoliation of individual nanoparticles. In the case of nanotubes, the simulations investigate compression, tension, torsion, and bending to explore the effect of aspect ratio on their mechanical properties.

4:25 PM Keynote

Dislocation-Twin Interactions in Nanocrystalline fcc Metals: *Yuntian Zhu*¹; ¹North Carolina State University

Dislocation interaction with and accumulation at twin boundaries have been reported to significantly improve the strength and ductility of nanostructured face-centered cubic (fcc) metals and alloys. Here I describe plausible dislocation interactions at twin boundaries. Depending on the characteristics of the dislocations and the driving stress, possible dislocation reactions at twin boundaries include cross-slip into the twinning plane to cause twin growth or detwinning, formation of a sessile stair-rod dislocation at the twin boundary, and transmission across the twin boundary.

4:55 PM

Investigating the Role of Grain Boundaries during the Plastic Deformation of Bicrystalline Nanowires Using Molecular Dynamics: *Garritt Tucker*¹; Zachary Aitken²; Julia Greer²; Christopher Weinberger¹; ¹Sandia National Laboratories; ²California Institute of Technology

The competition between free surfaces and grain boundaries to act as preferred sites for dislocation nucleation in aluminum nanowires is investigated using molecular dynamics simulations at room temperature. A number of bicrystalline nanowires containing various minimum energy boundaries are studied under uniaxial compression, providing a broad, inclusive look on the competition between the two types of sources. The simulation results provide insight into recent micro-compression experiments on bicrystals, suggesting the role of the vertical grain boundaries as sinks rather than sources for dislocations. Furthermore, this work compares the behavior of nanowires containing both low and high-angle symmetric tilt boundaries with those containing random high-angle boundaries.

5:10 PM

Interpreting Hardness Data in Multilayer Thin Films: *Michael Gram*¹; John Carpenter²; George Pharr³; Peter Anderson¹; ¹Ohio State University; ²Los Alamos National Laboratory; ³University of Tennessee

Metallic multilayer thin films are often characterized by hardness obtained from nanoindentation and more recently by compressing micron-scale pillars. However, the Tabor factor relating hardness and flow strength is unexplored for such high strength, nanoscale composite systems. Here, we show that the hardness to flow strength ratio can dip below 2, substantially less than ~3 used for conventional metals. This is demonstrated through finite element simulations of Cu/Ni multilayer thin films employing a variety of bilayer periods, Cu:Ni volume fraction ratio, and residual stress states. The largest reductions in the Tabor factor occur when there is a large disparity in flow strength between Cu and Ni layers and/or a large residual tension on the film. Nanoscale films are particularly sensitive to these effects because the flow strength is extraordinarily large, often reaching several percent of the composite elastic modulus. These findings are applied to experimental data for the Cu/Ni system.

5:25 PM

Interaction between Lattice Dislocation and Weak Interface in Anisotropic Bi-Crystal Composites: *Haijian Chu*¹; Jian Wang²; Caizhi Zhou²; Irene Beyerlein²; ¹Yangzhou University; ²Los Alamos National Laboratory; ²Los Alamos National Laboratory

“Weak interface strengthening mechanisms” have been proposed based on atomistic simulations and demonstrated by experiments on nanolayered composites. Related theoretical models in meso/macro scales remain, however, absent. We studied the interaction between lattice dislocations and weak interfaces in anisotropic bi-layer composites by using the Green’s function method. The influence of interface strength on dislocation transmission is investigated. Also, the nucleation and growth of interface dislocations are considered as a lattice dislocation approaches the interface. The core collapse of interface dislocations that accompanies the emission of lattice dislocation from interfaces is taken into account. The numerical results show that 1) in contrast to elastic isotropy, elastic anisotropy has a strong influence on both the image force on the dislocations and stress distribution along the interface plane; 2) dislocation transmission across the interface is much easier for a strong interface (no interface dislocations are activated) than weak one.

Mechanical Performance of Materials for Current and Advanced Nuclear Reactors: Irradiation Performance of Advanced and Model Alloys

Sponsored by: The Minerals, Metals and Materials Society, TMS Structural Materials Division, TMS/ASM: Nuclear Materials Committee

Program Organizers: Nicholas Barbosa, National Institute of Standards & Tech; Greg Oberson, United States Nuclear Regulatory Commission; Matthew Kerr, United States Nuclear Regulatory Commission; Elaine West, Knolls Atomic Power Laboratory; Stuart Maloy, Los Alamos National Laboratory; Osman Anderoglu, LANL

Wednesday PM
March 14, 2012

Room: Swan 1
Location: Swan Resort

Session Chairs: Osman Anderoglu, Los Alamos National Laboratory; Stuart Maloy, Los Alamos National Laboratory

2:00 PM Invited

Effect of Irradiation on the Tensile and Impact Properties of Structural and Cladding Materials: Jean Henry¹; Xavier Averty¹; Philippe Dubuisson¹; ¹CEA

The performance of structural and cladding materials is a key issue for the safe and reliable operation of nuclear reactors. In this presentation, we will illustrate the effect of irradiation up to high doses on the mechanical behaviour of structural and cladding materials, such as austenitic stainless steels and 9-12Cr ferritic-martensitic steels, with emphasis on tensile and impact properties. Microstructural evolution and the related degradation of mechanical properties depend strongly on the irradiation temperature but also on the radiation environment. For instance, high quantities of helium produced by transmutation in a fusion environment may induce drastic embrittlement of ferritic-martensitic steels. Advanced materials, such as nanodispersed ODS alloys are being developed in the hope that they will provide, in addition to good high temperature strength, excellent resistance to radiation and helium embrittlement. As a conclusion, we will discuss the irradiation behaviour of ODS alloys, based on fission and spallation data.

2:30 PM

Rate Sensitivity in Irradiated HT-9 for Reactor Applications: Stuart Maloy¹; Tarik Saleh¹; Tobias Romero¹; Sara Perez-Bergquist¹; Mychailo Toloczko¹; ¹Los Alamos National Laboratory

The Fuel Cycle Research and Development program is investigating methods of burning minor actinides in a transmutation fuel through various fuel cycle options. To achieve this goal, the fast reactor core materials (cladding and duct) must be able to withstand very high doses (>200 dpa) while in contact with the coolant and the fuel. In order to develop physics-based models of cladding materials for fast reactor applications, more specific testing is required in addition to typical tensile testing. Analysis of a duct made of HT-9 after irradiation to a total dose of 155 dpa at temperatures from 370 to 510°C is almost complete including tensile, Charpy impact and fracture toughness testing. Specific rate jump tests are underway to investigate rate sensitivity before and after irradiation. Detailed microstructural analysis has also been performed with TEM. A summary of rate sensitivity will be presented in connection with detailed analysis of controlling defects.

2:50 PM

High Temperature Mechanical Properties of Nanostructured Ferritic Alloys and Advanced Ferritic-Martensitic Steels: Thak Sang Byun¹; David Hoelzer¹; Lizhen Tan¹; Stuart Maloy²; ¹Oak Ridge National Laboratory; ²Los Alamos National Laboratory

Both the nanostructured ferritic alloys (NFAs) and the advanced ferritic-martensitic (FM) steels have been developed as primary candidate materials for the fission and fusion applications. High temperature tensile

and fracture tests have been performed at RT-700°C for various NFAs and FM steels including 14YWT, PM2000, Fe-9Cr NFAs, NF616, and advanced 9Cr steels. The discussion aims at comparing the mechanical behaviors to elucidate strengths and weaknesses of these advanced materials in high temperature applications. The newly produced data as well as published data are integrated and compared in terms of the temperature dependences of their strength, ductility, plastic instability stress, fracture toughness, etc. Although the ductility and fracture toughness of NFAs are significantly lower than those of the advanced 9Cr FM steels, their high temperature strengths are generally higher. Comparing the strain hardening parameters, however, it is shown that the characteristic difference between NFAs and FM steels is not significant.

3:10 PM

Radiation Damage in ODS Ferritic Steel under Multi-Ion-Beam

Irradiation: Luke Hsiung¹; Michael Fluss¹; Scott Tumey¹; Bill Choi¹; ¹Lawrence Livermore National Laboratory

A major challenge in designing fusion reactors is to develop high performance materials for first wall and breeding-blanket components that will be exposed to high fluxes of high-energy neutrons and helium and hydrogen gases. Although ferritic and martensitic steels and ODS steels are promising candidate materials, it remains to be understood the role of helium and hydrogen in the dimensional stability of the steels under fusion environment. One technique used to study the damage structure utilizes TEM examinations of specimens simultaneously bombarded by heavy ions and helium and/or hydrogen ions through "multi-beam" experiments. The heavy ions generate atomic displacements; the gas ions generate helium and hydrogen gases. HRTEM studies were conducted to compare radiation damage in Fe-14Cr alloy and Fe-16Cr ODS steel through (He + Fe) dual-beam and (H + He + Fe) triple-beam experiments. Results are presented to reveal the role of nanoparticles/clusters in the suppression of void swelling.

3:30 PM

Radiation Tolerant Metallic Multilayers: Xinghang Zhang¹; L. Shao¹; H. Wang¹; E.G. Fu²; Nan Li²; A. Misra²; Y-Q Wang²; ¹Texas A&M University; ²Los Alamos National Laboratory

Metallic materials in nuclear reactors are subjected to harsh radiation environment. Severe damage such as void swelling and embrittlement accompanied by hardening is frequently observed in structural steels. Strategies that can alleviate radiation damage may assist the design of radiation tolerant materials. We will summarize our recent studies on radiation damage in sputtered metallic multilayers with individual layer thickness of 1 - 200 nm, subjected to Helium ion irradiations up to 18 displacements-per-atom at room temperature. Swelling, Helium bubble density, lattice expansion and radiation hardening all decrease significantly with decreasing layer thickness. Pressurized He bubbles appear to play an important role on lattice distortion and radiation hardening. The study demonstrates that certain type of interfaces can significantly reduce radiation induced defect density, and consequently leads to radiation tolerant metallic nanocomposites.

3:50 PM Break

4:10 PM

Irradiation Response of Nanostructured Austenitic Model Alloy: Yong Yang¹; Cheng Sun²; Xinghang Zhang²; Todd Allen³; ¹University of Florida; ²Texas A&M University; ³University of Wisconsin-Madison

A model austenitic alloy was processed using the equal channel angular pressing (ECAP) method to obtain the average grain size of 360 and 250 nm at two different processing temperatures, respectively. The irradiation response regarding to different grain size and grain boundary character was examined on the specimens after Fe⁺⁺ and H⁺ irradiations. The irradiation effect on the grain size and grain boundary character distribution was evaluated using NanoMEGAS, an advanced electron diffraction tool in a transmission electron microscopy (TEM). And the irradiated microstructures included defect cluster and dislocations were



TMS 2012

141st Annual Meeting & Exhibition

examined using TEM at systematically tilted diffraction conditions, and irradiation induced hardening was studied using a nano-indenter.

4:30 PM

Microstructure and Mechanical Properties of Proton Irradiated Titanium Aluminides: *Ming Tang*¹; *Yong-won Kim*²; *Yongqiang Wang*¹; *Stuart Maloy*¹; ¹Los Alamos National Laboratory; ²UES-Materials & Processes

Titanium aluminide is being considered as innovative structural materials for its potential application in advanced nuclear energy system. Ensuring adequate mechanical properties and dimensional stability under radiation is a key part in practical application. However, there is very limited radiation response data for titanium aluminides available. In the present study, we report on microstructure and mechanical properties of titanium aluminides, following irradiation with 1.3 MeV proton at room temperature to a dose of 1.5 dpa. The materials of interest in this presentation are Ti-48Al-2Nb-2Cr and Ti-43.5Al-4Nb-3Mn, both of them in the duplex and fully lamellar microstructures. The radiation induced damage microstructure is examined using transmission electron microscopy (TEM). The mechanical properties (Young's modulus and hardness) of these irradiated samples are determined by cross-sectional nano-indentation measurements as a function of ion penetration depth. Related to their different microstructure and composition, the different radiation response of these materials will also be discussed.

4:50 PM

Mechanical Properties and Radiation Response of Ultrafine Grained Fe-Cr-Ni Alloy: *C. Sun*¹; *J. Ma*¹; *K.Y. Yu*¹; *K. T Hartwig*¹; *L. Shao*¹; *S.A. Maloy*²; *X Zhang*¹; ¹Texas A&M University; ²Los Alamos National Lab

Austenitic stainless steels are widely used as structural materials in nuclear industry. However, their further application is hindered by the relatively low mechanical strength, limited resistance to significant void swelling, radiation hardening and embrittlement. In this study, we present detailed investigations of mechanical properties and radiation response of ultrafine grained Fe-Cr-Ni alloy, which was synthesized by equal channel angular pressing. The deformation mechanisms, including strain hardening and strain rate sensitivity of the alloy, were investigated through a combination of uniaxial tensile tests and various microscopy experiments. Helium ion irradiation was performed to probe its radiation tolerance. Radiation-induced defects and hardening mechanisms will be discussed.

5:10 PM

In Situ Study of Radiation Damage in Pure Zr and Zircaloy-2: *Yasir Idrees*¹; *Zhongwen Yao*¹; *Mark Daymond*¹; ¹Queens University

In situ real-time dynamic observations of the radiation damage evolution in pure Zr and Zircaloy-2 under heavy-ion irradiation have been carried out using Intermediate Voltage Electron Microscopy (IVEM)-Tandem facility at Argonne National Lab. Thin foils were irradiated with 1 MeV Kr²⁺ ions. Materials have been irradiated to different damage levels ranging from 0.01 dpa to 3.3 dpa and different temperatures ranging from 573 K to 773 K. Direct formation of nano defects from individual displacement cascades at the early stages of damage development at very low dose (0.01 dpa) has been observed by TEM. In situ observations of growth and evolution of these small defects into complex defect structures at high dose (3.3 dpa) have been recorded. Furthermore, irradiation of materials at different temperatures provided an opportunity to investigate the temperature dependence of defect accumulation, damage structures, defect densities, and their dynamic growth.

Minerals, Metals and Materials under Pressure: Damage and Microstructure

Sponsored by: The Minerals, Metals and Materials Society, TMS Electronic, Magnetic, and Photonic Materials Division, TMS Materials Processing and Manufacturing Division, TMS Structural Materials Division, TMS: Chemistry and Physics of Materials Committee, TMS/ASM: Phase Transformations Committee
Program Organizers: Ellen Cerreta, Los Alamos National Laboratory; Richard Hennig, Cornell University; Dallas Trinkle, University of Illinois, Urbana-Champaign; Vijay Vasudevan, Univ. Cincinnati

Wednesday PM
March 14, 2012

Room: Europe 9
Location: Dolphin Resort

Session Chair: Ellen Cerreta, Los Alamos National Laboratory

2:00 PM Invited

Isolating the Influence of Kinetic and Spatial Effects on Dynamic Damage Evolution in OFHC Cu: *Darcie Dennis-Koller*¹; *Pablo Escobedo-Diaz*¹; *Ellen Cerreta*¹; ¹Los Alamos National Laboratory

The need to control material performance in extreme environments is the motivation for this study to examine the separate effects of kinetics (in the form of high strain rate dynamic loading rate) from that of spatial effects (in the form of microstructural defect distributions). Plate impact experiments are design and executed to produce a state of insipient spall in OFHC Cu samples of well-characterized microstructures. Post experiment soft recovery and metallurgical analysis correlates loading conditions, microstructure, and resultant damage effects. This provides a link between in situ mesoscale effects and continuum level measurements for process aware material models. Experimental results will be presented as well as a description of length scale and kinetic processes as a function of loading condition.

2:30 PM

Effect of Release Rate on the Dynamic Tensile Response of Polycrystalline Copper: *Juan Escobedo*¹; *Ellen Cerreta*¹; *Darcie Dennis-Koller*¹; *Carl Trujillo*¹; *Curt Bronkhorst*¹; ¹Los Alamos National Laboratory

Plate-impact experiments were conducted to examine the effect of release or de-compression rate on the dynamic tensile response of high purity copper samples. Samples with similar grain size and other microstructural features were subjected to a variety of shock-loading conditions. The compressive stresses were in the 1.5 – 2.5 GPa range and the release rates were modified by using copper, z-quartz and aluminum impactors. The free-surface velocity histories showed increasing values of strength with increasing release rate. Accordingly, the volume fraction of damage (voids) was observed to decrease as the release rates were increase. In addition, an accompanying large plastic dissipation, in the form of grain misorientation measured by means of electron backscatter diffraction, was present in the samples deformed at higher release rates, suggesting a time dependent behavior of the process that converts plastic dissipation into void growth.

2:50 PM

Continuum Scale Material Modeling under Large Strain, Strain Rates and Pressure Incorporating Microstructure Effect: *Nicola Bonora*¹; *Andrew Ruggiero*¹; *Gianluca Iannitti*²; *Simone Dichiario*¹; ¹University of Cassino; ²Techdyn Engineering

Microstructure effect on the macroscopic material response becomes more evident under high strain rate deformation. Continuum scale constitutive models requires appropriate modification for representing microstructural features. In this paper two experimental tests, the dynamic extrusion test (DTE, high strain rate) and ECAP (low strain rate), in which

the material is subjected to severe plastic deformation and pressure, have been investigated using an advanced constitutive modeling. The average grain size and normalized dislocation density are used as microstructure evolution descriptors and two levels of coupling accounts for the microstructure evolution on the material strength. Numerical simulations have been validated with experimental data for high purity copper with different grain size

3:10 PM

Mechanical Properties and Constitutive Modeling of Metals under Shock Deformation: *Shuh Rong Chen*¹; *Geroge Gray*¹; ¹Los Alamos National Laboratory

Metals under shock loading conditions exhibit enhanced hardening in some cases, no apparent enhanced hardening in others, and with softening for those undergo phase transformation. In this talk examples will be presented to illustrate the shock effect on mechanical properties. Advanced constitutive model will be modified to include the shock effect. *Work support by the US Department of Energy

3:30 PM

3-D Modeling of Incipient Spall Damage in Shocked FCC Multicrystals Using Crystal Plasticity: *Kapil Krishnan*¹; *Leda Wayne*¹; *Andrew Brown*¹; *Pedro Peralta*¹; *Shengnian Luo*²; *Darrin Byler*²; *Aaron Koskelo*²; ¹Arizona State University; ²Los Alamos National Laboratory

3-D finite element (FE) simulations were used to study effects of microstructure, e.g., grain boundaries (GBs), on spall damage in copper multicrystals. Laser-driven plate impact experiments were conducted at low pressures (2-6 GPa) to induce incipient spall damage. The 3-D model was created using serial sectioning and analysis was performed with ABAQUS/EXPLICIT. Post-impact characterization revealed a need to distinguish damage due to either interfacial strength or stress concentrations at the interfaces. Crystal plasticity was used to account for material anisotropy, whereas damage evolution was modeled using two approaches – (1) Damage mechanics via a modified Gurson-Tvergaard-Needleman (GTN) model and (2) a cohesive zone model for GBs. The GTN model predicts the global damage characteristics relatively well whereas the cohesive zone model helps in predicting damage relative to the GB characteristics. The FE simulations show how local microstructure plays a role in void nucleation and growth, particularly in its incipient stage.

3:50 PM Break

4:00 PM Invited

Low Temperature Twinning in Tantalum: *Mukul Kumar*¹; ¹Lawrence Livermore National Laboratory

Twinning is considered an alternative to slip as a deformation mechanism under high strain rate or synonymously low temperature loading. This holds true particularly for BCC and HCP metals. The extent of twinning under such conditions will be explored for the case of polycrystalline Ta, which has been deformed in compression at liquid nitrogen temperatures under strain rates ranging from quasi-static rates (10^{-4} /s) to dynamic conditions without pressure (10^4 /s). Samples have also been tested at high rates (up to 10^8 /s) using laser-based shock compression drives. Post-mortem analysis using EBSD and TEM has revealed the influence of the prior deformation substructure on the onset of twinning. The implication of these observations on a critical stress based criterion for the onset of twinning will be examined. This work was performed under the auspices of the U.S. Department of Energy by Lawrence Livermore National Laboratory under Contract DE-AC52-07NA27344.

4:30 PM

Review of Pressure Effects on Flow and Fracture of Materials: *John Lewandowski*¹; ¹Case Western Reserve Univ

The presentation will review the effects of pressure on flow and fracture of polycrystalline metals using a recent review article (1) as background. The effects of superimposed pressure on the flow stress will be reviewed, followed by effects on fracture. While the flow stress of most cubic crystalline metals are not very pressure dependent, some exceptions from the literature will be reviewed. The pressure dependence of the ductility and fracture behavior is very dependent on the mechanism(s) of failure. The presentation will conclude with more recent work on novel materials such as composites, bulk metallic glasses, and nano-composite materials. (1) *International Materials Reviews*, 43(4), pp. 145-188 (1998)

4:50 PM

The Effects of Microstructural Evolution on the Spall Response of 1100 Aluminum: *Cyril Williams*¹; *Changqiang Chen*²; *Kaliat Ramesh*²; *Datta Dandekar*¹; ¹U.S. Army Research Laboratory; ²The Johns Hopkins University

As received 1100-O aluminum was cold rolled (CR) to 30 and 70 percent reduction respectively to study the effects of microstructural evolution on the spall response using plate impact experiments. The results show a sharp increase in pullback velocity for 1100-O aluminum with increase in peak shock stress between 4.0 and 8.5 GPa, followed by a decrease for peak shock stresses up to 11.5 GPa. This maximum was not observed for the 30% CR, which showed only an increase in pullback velocity over the shock stress range of 4 - 12 GPa. As the rolling increased with the 70% CR, no change was observed in the pullback velocity over the range tested. EBSD and TEM were used to probe the deformation mechanisms in all cases to validate the hypotheses that shock hardening and recovery can explain these macroscopic observations.

5:10 PM

The Role of Crystallite Orientation & Grain Boundary Character on the Uniaxial Dynamic Tensile Response in Commercially Pure 1050 Aluminum: *Nathaniel Sanchez*¹; *Darcie Dennis-Koller*²; *David Field*³; ¹Los Alamos National Laboratory/Washington State University; ²Los Alamos National Laboratory; ³Washington State University

A series of plate impact experiments were performed on well characterized samples of commercially pure 1050 aluminum with grain sizes of 28 μ m, 43 μ m, 55 μ m, and 200 μ m. These experiments were designed to soft capture incipient spall damage in shock loaded samples which could be correlated to microstructural features through metallographic analysis with electron back scatter diffraction (EBSD). An optical velocimetry (VISAR) trace from the free surface was utilized to correlate the effects of damage growth rate observed through EBSD to changes in free surface velocity pull back rate. The influence of defect distribution (spatial effects) was isolated by varying the grain size while controlling shock loading conditions, which controls the total grain boundary area loaded in dynamic tension during the experiment. The shock wave shape and pulse duration were held constant. The role of crystallite orientation and grain boundary character on the nucleation and growth of voids will be discussed.



TMS 2012

141st Annual Meeting & Exhibition

Nanocomposites: Nanocomposites for Energy Transport, Harvesting and Storage

Sponsored by: The Minerals, Metals and Materials Society, TMS Structural Materials Division, TMS/ASM: Composite Materials Committee

Program Organizers: Garth Wilks, Air Force Research Laboratory; Jonathan Spowart, Air Force Research Laboratory; Meisha Shofner, Georgia Institute of Technology; John Zhanhu Guo, Lamar University

Wednesday PM
March 14, 2012

Room: Swan 8
Location: Swan Resort

Session Chairs: Garth Wilks, Air Force Research Laboratory; Jaime Grunlan, Texas A & M University

2:00 PM Invited

Thermoelectric Nanocomposites:

Effect of Nanostructures on Lattice Thermal Conductivity

: Terry Tritt¹; Wenjie Xie²; Xinfeng Tang²; ¹Clemson University; ²Wuhan University of Technology

This talk will give a brief introduction to thermoelectric phenomena and challenges that these materials present to the researcher along with an overview of several former and current applications. Recently there has been an ever-increasing research effort on thermoelectric nanocomposite material; a mixture of bulk thermoelectric materials with nanoparticles incorporated within the bulk matrix in some manner. However, we have found that the growth of “in-situ nanodots” exhibit a significant impact on the lattice thermal conductivity. The ability to decouple the electron and phonon scattering mechanisms is very important in the development of higher efficiency thermoelectric (TE) materials, wherein the figure of merit, ZT, can be greater than unity. The role of phonons in these nanocomposites may be one of the most important parameters to understand in these novel materials. A discussion of recent results in nanocomposite TE materials from several research groups, including my own, will be presented.

2:40 PM

Stabilization of Graphene-Polyaniline Based Nanocomposite Electrodes Using Barium Strontium Titanate for Supercapacitor Application: Supriya Ketkar¹; Manoj Ram¹; Ashok Kumar¹; Thomas Weller¹; Andrew Hoff¹; ¹University of South Florida

Supercapacitors provide the high power and long durability needed for several new energy devices in electric vehicles, backup sources for various electrical devices and uninterrupted power supplies. Graphene (G)-polyaniline (PANI) has successfully incorporated graphene's and aniline monomer's superior properties to produce highly conductive nanocomposite material. A leakage current due to Faradic reactions at electrode-surface hinders the application of supercapacitors in many low power battery-like electronic applications. Coating the surface of the electrodes with a thin film of a dielectric material generates a potential barrier which reduces the reaction rate, with a slight drop in specific capacitance but increases the relative dielectric constant by increasing the capacitance of the supercapacitor. For this report we have deposited nm-thickness of high dielectric constant, Barium Strontium Titanate (BST), material on GPANI using electrophoretic technique. This will enhance the energy storage capability of the capacitor making it desirable for application in hybrid vehicle batteries.

3:00 PM Invited

Thermoelectric Study of InGaN-Based Materials for Thermal Energy Harvesting: Liqing Su¹; Bahadir Kucukgok¹; Elisa Hurwitz¹; Ian Ferguson; Na Lu²; ¹University of North Carolina at Charlotte; ²University of North Carolina at Charlotte

InGaN-based materials have recently been demonstrated to have promising thermoelectric (TE) properties, providing a potential solution to the thermal energy harvesting of nitride-based high power devices. In addition, these materials have outstanding features that are environmentally friendly for TE applications include the ability for high power and high temperature operation, high mechanical strength and stability, and radiation hardness. However, the experimental data available on InGaN with respect to the indium concentration is very limited and does not clearly reflect the expected theoretical trends. In this work, the Seebeck coefficient and the electrical conductivity of MOCVD grown InGaN alloys at various indium concentrations are investigated, and the power factors are calculated. The results reveal that InGaN-based materials could be potentially applied in thermal energy harvesting.

3:40 PM

Nanocomposites for Electrochemical Energy Storage: Yuanbing Mao¹; Elizabeth Martinez¹; ¹University of Texas-Pan American

Nanocomposite materials have great potentials for applications in the field of energy store. To achieve high energy densities at high rate capabilities, it is necessary to use innovative electrode materials with architecturally tailored nanostructures for these devices, such as batteries and supercapacitors. Heterogeneous nanostructured materials with multi-components can be tailored to address different demands for these types of novel electrodes, which are expected to exhibit synergic properties. In this presentation, the design and synthesis of hierarchical carbon material/conductive polymer/metal oxide ternary nanocomposites for high performance electrochemical energy storage will be reported. The performance, i.e. specific capacitance, of the fabricated supercapacitors will be shown based on cyclic voltammetry and charge-discharge measurements and compared with literature results.

4:00 PM Break

4:20 PM Invited

Thick and Thin Film Polymer – Carbon Nanotube Composites for Thermoelectric Energy Conversion and Transparent Electrodes: Jaime Grunlan¹; Yeon Seok Kim¹; Choongho Yu¹; Yong Tae Park¹; Gregory Moriarty¹; ¹Texas A&M University

Segregated network (latex-based) composites containing carbon nanotubes were used to produce electricity from a thermal gradient. Thermoelectric materials harvest electricity from waste heat or any temperature gradient in the environment. The present work demonstrates that nanotube-filled polymer composites can be viable for energy conversion. By combining double-walled carbon nanotubes (DWNT), stabilized with poly(3,4-ethylenedioxythiophene): poly(styrene sulfonate) in water, an electrical conductivity (μ) near 2000 S/cm is achieved in a poly(vinyl acetate) latex-based matrix. When combined with a Seebeck coefficient (S) above 40 μ V/K, a power factor ($S^2\sigma$) above 370 μ W/m²K² is achieved at room temperature. Additionally, highly transparent and electrically conductive thin films as a potential indium tin oxide (ITO) replacement using layer-by-layer assembly of DWNT. A 23 nm film has ~ 100 Ω /sq sheet resistance following nitric acid doping. These unique thin films are potentially useful as flexible transparent electrodes for a variety of applications (e.g., touch screens).

5:00 PM

Epoxy Resin Nanocomposites Reinforced with Conductive Polyaniline Nanostructures: Xi Zhang¹; Jiahua Zhu¹; Suying Wei¹; John Zhanhu Guo¹; ¹Lamar University

Epoxy resin nanocomposites prepared by two different polyaniline nanoparticles (NP) are studied and compared. The effect of the structure on the properties was investigated. Polyaniline nanoparticles in spherical

shape offers better thermal stability, however, epoxy nanocomposites prepared with polyaniline nanofibers have higher conductivity and better rheological behaviors. The rheology result shows that compare with pure epoxy, viscosity of epoxy nanocomposites prepared with both kinds of PANI nanostructures decreases with the addition of NP at 1 wt%, however, when reach certain loading amount, the viscosity of nanocomposites becomes higher than that of pure epoxy, and the transition loading of fiber shape NPs is higher than that of the spherical shape ones. DMA is also run for these nanocomposites. Liquid sample test indicates the percolation threshold is also associated with NP's structure, the threshold occurs at lower loading percent of fiber shape NPs than spherical shape one.

5:20 PM

Synthesis, Characterization & Applications of Nanodiamond – Conductive Polymer Nanocomposites Films: *Humberto Gomez*¹; Manoj Ram²; Ashok Kumar²; ¹Universidad del Norte; ²University of South Florida

Nanocomposites of nanodiamond particles (NDs) with conductive polymers (i.e. polyaniline (PANI) and regioregular polyhexylthiophene (RRPHTh)) displayed novel properties resulting from the molecular interaction level of diamond with polymer molecules. We have synthesized the NDs-Polymer nanocomposites by oxidative polymerization under controlled conditions. The ND-Polymer nanocomposite films were characterized by UV-Vis, FTIR, electrochemistry, impedance, Scanning Electron Microscope (SEM), Transmission Electron Microscope (TEM) and electrical conductivity techniques, respectively. The electrochemical investigation on ND-PANI revealed the wider potential values with independent redox characteristics of polyaniline and nanodiamond. The ND-PANI film shows excellent corrosion inhibitor characteristics for metals (steel and aluminum) due to its chain conformation and electronic properties, as demonstrated in this work. The photoelectrochemical study has revealed photoinduced electron transfer in nanohybrid regioregular polyhexylthiophene (RRPHTh) with donor and ND as acceptor providing a molecular approach to high-efficiency photoelectrochemical conversion properties. The ND-RRPHTh has shown promising morphological and photoelectrochemical properties than RRPHTh films.

5:40 PM

Evaluation of Electrochemical Performance of a graphene-poly(o-toluidine) Nanocomposite for Supercapacitor Applications: *Punya Basnayaka*¹; Farah Alvi¹; Manoj Ram¹; Ashok Kumar¹; ¹University of South Florida

Supercapacitors are unique energy storage devices, where the selection of electrode material is one of the most vital factors in developing high energy density and longer cycle life devices. A novel graphene (G) – poly(o – toluidine) (POT) nanocomposite material has been synthesized using oxidative polymerization method. The physical characterization of the electrode material was performed by scanning electron microscopy (SEM), transmission electron microscope (TEM), UV-vis spectroscopy, Raman spectroscopy and x-ray diffraction spectroscopy (XRD) techniques. The observed change in the morphology and electrical conductivity of G-POT are due to the incorporation of graphene in polymer matrix. The electrochemical and capacitive properties of supercapacitor were studied using cyclic voltammetry (CV), impedance spectroscopy and charging-discharging measurement methods. The G-POT nanocomposite based supercapacitor showed enhanced capacitive property with highest specific capacitance of 424 F/g in 2M H2SO4 acidic electrolytic solution, revealing that G-POT could be a promising material for the supercapacitor applications.

Neutron and X-Ray Studies of Advanced Materials V: Centennial: Three Dimensional Studies

Sponsored by: The Minerals, Metals and Materials Society, TMS Structural Materials Division, TMS/ASM: Mechanical Behavior of Materials Committee, TMS: Chemistry and Physics of Materials Committee

Program Organizers: Rozaliya Barabash, Oak Ridge National Laboratory; Xun-Li Wang, Oak Ridge National Laboratory; Gernot Kostorz, ETH Zurich; Lyle Levine, National Institute of Standards and Technology; Peter Liaw, Univ of Tennessee; Yandong Wang, Beijing Institute of Technology; Brent Fultz, California Institute of Technology

Wednesday PM
March 14, 2012

Room: Southern I
Location: Dolphin Resort

Funding support provided by: Office of Basic Energy Sciences, U.S. Dept. of Energy, Dr. P. Thyagarajan

Session Chairs: John Budai, Oak Ridge National Laboratory; Leyun Wang, MSU

2:00 PM Keynote

Next Generation 3DXRD: *Henning Poulsen*¹; Søren Schmidt¹; Erik Lauridsen¹; Andrew King²; Gavin Vaughan²; Jonathan Wright²; Wolfgang Ludwig²; Jette Oddershede¹; Xiaoxu Huang¹; Wolfgang Pantleon¹; Dorte Juul Jensen¹; ¹Risoe DTU; ²ESRF

3DXRD has become a mature methodology for generation of 3D maps of the morphology, orientation and type-II stress of poly-crystals with a thousand grains and with a spatial resolution of order 1 μm . We present exploratory work on generalising the concept in several directions: 1) Improved spatial resolution: Work on microscopy approaches for achieving 100 nm resolution is outlined. The connection to recent work on 3D orientation mapping with 1 nm resolution using TEM is discussed. 2) Orientation Imaging Microscopy: A non-destructive and 3D equivalent of the familiar EBSD technique has been established. 3) Mapping of phases: Work on the coupling of 3D imaging and multigrain crystallography is outlined. 4) Plastic strain tomography: The strain field of an Al alloy was mapped in 3D to 10% strain and compared to the 3D grain structure and local rotations. Finally, the coupling to 3D materials simulations will be discussed.

2:25 PM Invited

X-Ray Topography Studies of Synthetic Diamonds for Use as Optical Elements at Synchrotron X-Ray Sources: *Albert Macrander*¹; Xianrong Huang¹; Ali Khounsary¹; Josef Maj¹; Lahsen Assoufid¹; ¹Argonne National Laboratory

Diamonds have a number of uses on beamlines such as monochromator crystals, phase plates to manipulate the x-ray polarization, and beam splitters, among others. Strain due to mounting as well as fabrication induced surface strain can severely degrade the performance of these crystals. In addition, grown-in lattice defects such as stacking faults are also deleterious to the performance. Studies involving both measurements and simulations that have been made over the last several years will be summarized, and more recent white beam topography results for bonded samples will be presented. This work supported by U.S. Dept. of Energy, Office of Science. Office of Basic energy Sciences under contracts DE-AC02-06CH11357.



TMS 2012

141st Annual Meeting & Exhibition

2:45 PM Invited

Microstructure inside Nanocrystals Using Laue X-Ray Micro/Nanodiffraction: *John Budai*¹; Jonathan Tischler¹; Zhengwei Pan²; Alexander Tselev¹; Andrei Kolmakov³; ¹Oak Ridge National Laboratory; ²University of Georgia; ³Southern Illinois University

High-brightness x-ray sources and focusing optics have enabled the transformation of white-spectrum Laue diffraction from a single-crystal tool to a spatially-resolved microscopy technique for imaging microstructures inside polycrystals. At the APS, we have developed a polychromatic, scanning microbeam facility currently with ~300 nm spatial resolution. In this talk, I will emphasize the ability to investigate microstructures in individual nanostructures using two examples. First, we have studied the lattice structures of strongly-photoluminescent EuAlO nanorods with different chemical compositions, different optical emission spectra, and with crystal structures not reported for bulk materials. In a second example, I will describe in-situ studies of local phase separation and microstrains observed inside individual microcrystals of vanadium dioxide as it cycles through a metal-insulator phase transition. Finally, I will discuss planned extensions of diffraction techniques to include x-ray beams focused to diameters below ~100 nm. Research supported by Materials Sciences and Engineering Division, U.S. DOE-BES.

3:05 PM Invited

In-Situ Micro-Beam X-Ray Diffraction Studies on Advanced High-Strength Steels: *Niels van Dijk*¹; ¹Delft University of Technology

In novel high-strength steels deformation often leads a significant strengthening of the complex multiphase microstructure. In Transformation Induced Plasticity (TRIP) steels the combined high strength and good formability originates from a martensitic transformation of the metastable austenite phase, while for TWinning Induced Plasticity (TWIP) steels it is achieved by twin formation. Recent advances at synchrotron sources make it possible to perform in-situ X-ray diffraction experiments using micro-beams of high-energy X-rays. The combination of a high penetrating power and a good spatial resolution allows us to quantify the local structure evolution within the multiphase material at the level of single grains during tensile deformation at variable temperatures. By simultaneously monitoring the thermo-mechanical behavior of a collection of individual grains in combination with a powder analysis of the overall phase response new insight is obtained in the mechanism responsible for the improved mechanical behavior of high strength steels.

3:25 PM

3D Visualization and Modeling of Deformation in Pb-Free Solders Using X-Ray Tomography: *Eric Padilla*¹; Vaidehi Jakkal¹; Mario Pacheco²; Nikhilesh Chawla¹; ¹Arizona State University; ²Intel Corporation

3D X-Ray Tomography was used to visualize and reconstruct the pore microstructure of Sn-3.9Ag-0.7Cu/Cu solder joints. The incremental changes to the joint microstructure caused by progressive straining were imaged in 3D using X-Ray Tomography. The evolution of individual pore deformation and strain localization in the joint was tracked using the shape parameters of the pores as a function of strain. The experimental results were compared to a Finite Element Model, which incorporated the reconstruction of the as-processed joint and used the Ductile Damage Model to simulate shear deformation and eventual failure of the joint. The Finite Element Model correctly predicted the location of crack nucleation and broad features of deformation. The effectiveness of this technique in understanding the effect of size, shape, and distribution of pores on local and global plasticity of solder joints will be discussed.

3:35 PM

Nondestructive Determination of Residual Stress Using Strain Pole Figure Measurements and a Multiscale Workpiece Discretization: *Jun-Sang Park*¹; Matthew Miller¹; Eralp Demir¹; Paul Dawson¹; Ulrich Lienert²; ¹Cornell University; ²Argonne National Laboratory

Quantifying the internal residual stress field in a processed polycrystalline component is important for predicting its mechanical properties and its behavior. In this work, a new method for measuring residual stresses is described. We focus on the experimental setup that combines monochromatic high energy synchrotron x-rays and a set of conical slits that allow the non-destructive measurement of strain pole figures (SPFs) for diffraction volumes located inside a polycrystalline aggregate. We also describe a novel optimization method that proposes a residual stress field that is consistent with the SPF measurements at the microscopic scale and enforces the macroscopic boundary conditions and equilibrium. To demonstrate the new method, a polycrystalline shrink-fit sample with a 3D stress gradient was manufactured from a low solvus high refractory (LSHR) Ni-based superalloy. The internal stress field determined using the new method compares favorably with an analytic approximation of the stresses within the shrink-fit sample.

3:50 PM

Annealing Study of Grain Boundary Engineered Copper Using High Energy X-Ray Diffraction Microscopy: *S. F. Li*¹; R. Suter¹; C. Hefferan¹; J. Lind¹; U. Lienert²; J. Bernier³; M. Kumar³; B. Reed³; ¹Carnegie Mellon University; ²Argonne National Lab; ³Lawrence Livermore National Lab

High Energy X-ray Diffraction Microscopy (HEDM) is a non-destructive orientation imaging technique housed at the high energy and brilliance x-ray source at the Advanced Photon Source. HEDM is applicable to bulk polycrystalline material characterization because of its robustness against grain size distribution and orientation moaiscity. Recent advances in reconstruction and data collection methods have led to availability of volumetric orientation maps with sub-degree and micron angular and spatial resolutions for millimeter sized samples. The result is an unprecedented nondestructive access into the microstructure and grain boundary networks under the influence of external stimuli. Using HEDM, microstructural evolution of grain boundary engineered (GBE) copper was observed before and after annealing. The resulting grain boundary character distribution (GBCD) was compared against that of a high purity copper specimen without GBE processing; three-dimensional grain boundary networks were also examined. GBCD evolution suggests that special boundaries (CSL) play an interesting role in Copper annealing.

4:05 PM Break

4:15 PM Invited

Study of Geometrically Necessary Dislocations by Depth-Resolved 3D X-Ray Microdiffraction and Crystal Plasticity Modeling: *Leyun Wang*¹; Hongmei Li²; Rozaliya Barabash³; Martin Crimp²; Carl Boehlert²; Philip Eisenlohr⁴; Thomas Bieler²; Wenjun Liu¹; ¹Argonne National Laboratory; ²Michigan State University; ³Oak Ridge National Laboratory; ⁴Max-Planck-Institut für Eisenforschung

In polycrystalline metals, gradients in slip of individual grains is often observed, which gives rise to geometrically necessary dislocations (GNDs). An effective method to characterize GNDs is by analyzing streaked diffraction patterns from depth-resolved 3D X-ray microdiffraction experiment. Using polycrystalline alpha-Ti and a near-alpha Ti alloy as sample materials, it has been found that GNDs tend to pile up near grain boundaries and twin boundaries, especially when the slip transfer to the neighboring grain is difficult. Accumulation of GNDs eventually leads to the development of ledges or cracks at grain boundaries and twin boundaries. A crystal plasticity finite element model (CPFEM) was also used to simulate slip gradient in the same regions, and the simulations were compared with the experimental results. This work was supported by grants from DOE/BES and NSF/DMR.

4:35 PM

The Plastic Behavior of Micron Sized Single Crystals under Compression and Tension Analyzed by X-Ray μ Laue dDiffraction: *Christoph Kirchlechner*¹; Marlene Kapp²; Wolfgang Grosinger¹; Peter Imrich²; Christian Motz²; Jozef Keckes¹; Jean-Sebastien Micha³; Olivier Ulrich³; Gerhard Dehm¹; ¹University of Leoben; ²Austrian Academy of Sciences; ³ESRF

The influence of the samplesize on different aspects of plastic deformation is of paramount concern for the development and use of MEMS-devices. However, the plastic behavior at the micron scale is still under debate. For a thorough understanding of the mechanisms governing plastic deformation it is essential to characterize the initial and evolving defect-structure in these dimensions. We have performed in situ μ Laue tensile and compression tests on micron sized, single crystalline copper specimens at BM32 at ESRF. Microstructural changes were analyzed using position and shape of Laue spots as described by Ice and Barabash. Besides the expected activation of the primary slip system the tensile experiments show – in some cases – an early activation of a lower-ranked slip system. Dislocations on these slip systems are stored at low strains, but continuously escape at the sample surface at higher strains leading to a sample-center free of geometrical necessary dislocations.

4:50 PM

Plasticity Evolution in the Nanoscale Cu/Nb Multilayers as Revealed by Synchrotron X-Ray Microdiffraction: *Arief Budiman*¹; N. Li¹; L. A. Berla²; N. Tamura³; M. Kunz³; W. D. Nix²; J. Wang¹; A. Misra¹; ¹Los Alamos National Laboratory (LANL); ²Stanford University; ³Advanced Light Source (ALS), Berkeley Lab

There is much interest in the recent years in the nanoscale metallic multilayered materials due to their unusual mechanical properties such as very high flow strength and stable plastic flow to large strains. In an effort to shed light on these topics, successive uniaxial compression experiments (total strains = 1%, 2%, 10% and 20%) on nanoscale Cu/Nb multilayer pillars using ex situ synchrotron-based X-ray microdiffraction technique were conducted. We found significant X-ray peak broadening in both Cu and Nb layers initially (up to strains of about 4%) which was then followed by the saturation of the X-ray ring width broadening (up to large strains of 20%). This observation indicates that the interfaces in the nanolayered Cu/Nb are very stable and effective in trapping and annihilating dislocation content during mechanical deformation, and explains why the Cu/Nb nanolayers can be deformed to large plastic strains without any onset of plastic instabilities.

5:05 PM

Grain Growth of High Purity Nickel with High Energy X-Ray Diffraction Microscopy (HEDM): *C.M. Hefferan*¹; S.F. Li²; J. Lind¹; U. Lienert³; A.D. Rollett¹; R.M. Suter¹; ¹Carnegie Mellon University; ²Lawrence Livermore National Laboratory; ³Argonne National Laboratory

The ability to non-destructively interrogate polycrystalline systems has been aided by the emergence of synchrotron based, high energy x-ray diffraction (HEDM). Specifically, an enhanced capability in monitoring the evolution of microstructures as they respond to thermo-mechanical stimuli has been realized. We present results from a high purity nickel specimen subject to incremental anneals resulting in differential grain growth. Repetitive probing of the same 0.25 cubic millimeter volume of microstructure, containing on the order of 2500 grains yields an experimental picture of the grain growth process. The progression of the microstructure is interpreted in the context of the five parameter grain boundary character distribution, with emphasis on special grain boundary types. This work is supported by the NSF Metals and Nanostructures program under grant DMR-0805100; SFL and JL are supported by DOE/BES contract number DESC0002001. Use of the Advanced Photon Source is supported by DOE/BES under Contract No. DE-AC02-06CH11357.

5:20 PM Invited

X-Ray Laue Diffraction 3D Microscopy - Upgrade and New Opportunities: *Wenjun Liu*¹; Ruqing Xu¹; Paul Zschack¹; John Budai²; Jon Tischler²; ¹Argonne National Laboratory; ²Oak Ridge National Laboratory

Significant progress has been made at the Advanced Photon Source over the past ten years in developing and applying focused x-ray diffraction techniques in spatially-resolved structural studies for material science. Laue diffraction 3D microscopy is applicable to a wide range of exciting problems in many diverse fields, including materials engineering, condensed matter physics, high-pressure geophysics, mineralogy, and environmental science. In this report, we will present the upgrade plan of pushing microdiffraction techniques with significant improvements in smaller beam sizes, beam and sample stability, detector performance, scanning speeds, and increased beamtime availability. This will enable new scientific progress towards a fundamental, predictive understanding of materials processing. A few examples will be highlighted.

5:40 PM

Investigation of Twin Inception and Growth in Three Dimensions: *Hamid Abdolvand*¹; *Marta Majkut*¹; Jette Oddershede²; Ulrich Lienert³; Bradley Diak¹; Mark Daymond¹; ¹Department of Mechanical and Materials Engineering, Queen's University; ²Risø National Laboratory for Sustainable Energy, Technical University of Denmark; ³Advanced Photon Source, Argonne National Laboratory

Tensile samples cut from rolled Mg-AZ31B were used to study twin inception and growth. In-situ three-dimensional synchrotron X-ray diffraction was used to determine the center of mass and volume of each grain, as well as elastic strain and stress inside each grain during straining along the plate normal direction. The tensile sample was strained up to a plastic strain 1.6 % by which many of the grains were twinned. Using Laguerre tessellation from the measurement center of mass and volume of each grain, grains were mapped into a crystal plasticity finite element code. Experiment and model were compared in terms of twin inception and propagation. Results demonstrate that newly formed twins are generally found at stresses different from those of the parent grain. The simulation results demonstrate that the CPFE code is able to predict inception sites very well on a statistical basis but not perfectly at a local level.

5:50 PM

X-Ray Micro-Diffraction Study of Crystallographic Orientation and Strain Distribution inside Microscopic Shear Bands Consisting of Martensite Plates: *Nan Li*¹; Yandong Wang¹; Wenjun Liu²; Dongping Wang¹; Guilin Wu¹; Peter Liaw³; ¹Beijing Institute of Technology; ²Argonne National Laboratory; ³The University of Tennessee

The traditional phenomenological crystallographic theory (PCT) of martensitic transformation can only explain the shape deformation and crystallography of a martensite plate in a single crystal. While martensitic transformation occurs in polycrystals, the microscopic shear bands (MSBs) are usually formed due to the fact that a martensite plate is blocked by grain boundaries. However, the stress evaluation to trigger the formation of deformation-induced martensite plates cannot be predicted by PCT. Here we used the synchrotron X-ray micro-diffraction technique to trace in-situ local strain/orientation distribution inside individual martensite plates and their parent grains in a polycrystalline 304 stainless steel during uniaxial tensile loading. It was found that there is a large gradient in strain of martensite plates inside MSBs. The crystallographic orientation of martensite plates strongly depends on orientation of the parent grains. Based on the above experimental findings, a modified PCT suitable for a polycrystal will be proposed in this presentation.



TMS 2012

141st Annual Meeting & Exhibition

Pb-Free Solders and Other Materials for Emerging Interconnect and Packaging Technologies: Whisker Growth in Tin and Related Solder Alloys

Sponsored by: The Minerals, Metals and Materials Society, TMS Electronic, Magnetic, and Photonic Materials Division, TMS: Electronic Packaging and Interconnection Materials Committee
Program Organizers: Iver Anderson, Ames Laboratory; Sung Kang, IBM; Albert Wu, National Central Univ; Laura Turbini, Research in Motion; Tae-Kyu Lee, Cisco Systems; Govindarajan Muralidharan, Oak Ridge National Lab; John Elmer, Lawrence Livermore National Lab; Yan Li, Intel

Wednesday PM Room: Swan 9
March 14, 2012 Location: Swan Resort

Session Chair: Laura Turbini, Research in Motion

2:00 PM Invited

Effects of Grain Misorientation & Strain Distribution on Whisker Formation on Electroplated Sn-Cu films: *Carol Handwerker¹*; Pylon Sarobol¹; Wei-Hsun Chen¹; Peng Su²; John Blendell¹; ¹Purdue University; ²Cisco

Tin whiskers spontaneously grow from electrodeposited Sn-containing films and can form short circuits in microelectronics. In order to better understand the nucleation and growth mechanisms, the local properties—grain misorientations and strain distribution—around whiskers and hillocks on electroplated SnCu films were examined via synchrotron x-ray micro-diffraction. High misorientation angles are observed between whisker/hillock grains and their surrounding grains, whereas low misorientation angles are associated with other grains in the film away from the defects. Out-of-plane strain distributions in regions around whiskers and hillocks from OOF2 simulation and micro-diffraction measurements were compared. Due to local grain misorientations, high strain is predicted by simulation at whisker/hillock locations. After growth, the strain is relaxed and is measured to be near zero. We are planning to use these results to construct a whisker growth model to predict whisker propensity and nucleation sites for Sn films with specific textures.

2:30 PM Invited

Probing Mechanisms for Sn Whisker Growth by In Situ Nanoindentation in a Scanning Electron Microscope: Nicholas Chapman¹; Jason Williams¹; *Nikhilesh Chawla¹*; ¹Arizona State University

The presence of a protective oxide has been postulated to control the formation of Sn whiskers from Sn thin films. In this investigation, the effects of oxygen on the degree of whisker formation was studied. Sn films were fabricated by electrodeposition. Nanoindentation was used to introduce local compressive stresses to drive whisker growth on the surface of the Sn thin film. The experiments were conducted under ultra-high vacuum, inert atmosphere, and air, and observed in situ in a scanning electron microscope. The propensity, location of the whiskers relative to the indentation, and the morphology of the whiskers were controlled by environment and indentation stress. The relationship between stress, oxide on the surface, and whiskering mechanisms will be discussed.

3:00 PM

Understanding the Variation in Mechanical Properties of Sn Films with Alloying and Modification of Microstructure: *Nitin Jadhav¹*; Maureen Williams²; Fei Pei¹; Gery Stafford²; Eric Chason¹; ¹Brown University; ²National Institute of Standards and Technology

Though it is well understood that compressive-stress due to IMC formation is the main driving force for whisker formation in SnCu System, the underlying mechanisms that control the stress-distribution

and cause whiskering are not clear. In order to understand the propensity of whiskering in Sn-films it is essential to study their response to stress buildup. To avoid the complexity in the SnCu-system, we studied the evolution of stress due to the difference in thermal-expansion between Sn and the Si-substrate. We present the results of studies done to understand how modification of the Sn-layer (alloying and microstructure) affects its response to stress buildup. We found that alloying with Pb changes Sn's microstructure from columnar to equiaxial-grains and greatly enhances its stress-relaxation. An equiaxial-microstructure was also fabricated by pulse-plating Sn-Bi alloy, which do not relax stress as much as alloying with Pb does but nonetheless having equiaxial-grains significantly does enhance Sn-films relaxation.

3:20 PM

Mitigation and Verification Method of Sn Whisker Growth for Pb-free Automotive Electronics: *Won Sik Hong¹*; Cul Min Oh¹; Do Seop Kim²; ¹Korea Electronics Technology Institute(KETI); ²Hyundai Motor Company

Mitigation method of Sn whisker growth in Pb-free car electronics is a key issue. The verification of whiskering failure is essentially demanded because of long service life of automotives. Though JEDEC, IPC, iNEMI and industries have already recommended whisker evaluation method, but those have a disadvantage to take very long time for evaluating whisker formation and growth. Also, effective and economical verification method for use environment of automotives is demanded. Therefore, this research suggested the optimized test conditions based on conducting high temperature and high humidity test, thermal cycling test and ambient test and then analyzed whisker growth mechanism. To find out efficient mitigation effects of whisker growth, we have verified a validity of annealing, surface finish and conformal coating. Surface finish of component was Ni/Sn and Ni/Pd. Finally, mitigation effects of acryl, silicone and rubber coating were compared with non-coating components under various whisker test conditions.

3:40 PM Break

3:50 PM

Crystallographic Characterization of an Electroplated Zinc Coating: *Philippe Pareige¹*; Auriane Etienne¹; Agnès LINA²; Laurent Crétonin²; ¹Rouen University; ²EDF

Whiskers grow spontaneously from cadmium, zinc or tin coatings at room temperature. Although whiskers have been studied for several decades, mechanisms of whisker growth are still not well understood. While a large number of studies have been focused on tin whiskers and the minimization of their formation, only a limited numbers of researches were interested on zinc whiskers. The risk of electronic failures caused by Zn whiskers in automotive, aerospace or energy industry but also in computer data centre is significant. In order to avoid failures, whisker formation needs to be mitigated and so, mechanisms of whisker growth need to be clarified. At first, the understanding of whisker growth mechanism needs microstructural characterization of Zn whiskers and their coatings. In the present work, Zn coating has been investigated using SEM/FIB, EBSD and EDS. The observed samples were prepared and extracted from the root of the whisker.

4:10 PM

Real-Time Study of Whisker Formation in Tin/Copper Systems by EBSD Characterization: *Fei Pei¹*; Nitin Jadhav¹; Eric Chason¹; ¹Brown University

We performed a systematic real-time study of whisker formation using electron back-scattering (EBSD) to simultaneously monitor surface morphology and grain orientation changes. A unique procedure for making samples with smooth surfaces was developed to enable the EBSD to index a large fraction of the grains over repeated scans. According to the experiment results, most whiskers or hillocks initiated from grains that

had already been formed during sample preparation. The orientation of these grains did not change much after the surface morphology changed, suggesting whiskers can grow without undergoing recrystallization or nucleation of new grains. After the real-time study, the tin films were chemically stripped to expose the IMC (intermetallic compound) growing at the Sn-Cu interface. The IMC at the interface was measured over the same region as the surface morphology to correlate the surface evolution with the interface. No apparent accumulation of IMC was observed underneath the whisker sites.

4:30 PM

Tin Whisker and Hillock Formation on Thermally Cycled, Large Grained Pb-Free Solder Alloy Films: *John Koppes*¹; *Pylin Sarobol*¹; *Wei-Hsun Chen*¹; *Peng Su*²; *John Blendell*¹; *Carol Handwerker*¹; ¹Purdue University; ²Cisco Systems

Tin whiskers can grow long enough to contact adjacent leads and cause short circuits in electronic devices. For many years, Sn whiskers were only a concern on fine grained electroplated films. Furthermore, it was believed that if the film was melted and solidified (reflowed), the Pb-free Sn-film would be immune to whisker formation. Recently, surface defects (whiskers and hillocks) have been observed forming on large grain (~ 2 mm) Pb-free solder alloy films formed by solidification. The large grain size of the solidified solder alloys allowed for surface defects (whiskers and hillocks) to be readily studied relative to the local microstructure. It is observed that the formation of the surface defects occurs primarily along grain boundaries; and the linear defect density, along the grain boundary, is related to the local orientations of the adjacent grains and the corresponding anisotropic physical properties, including thermal expansion coefficient.

4:50 PM

Precipitation of Large Ag₃Sn Intermetallic Compounds in SnAg_{2.5} Microbumps after Multiple Reflows in 3D-IC Packaging: *Ming-Yung Guo*¹; *Wei-Chi Sung*¹; *Chih Chen*¹; ¹National Chiao Tung University

Microbumps have been adopted as interconnects between Si chips in 3D integrated-circuit packaging. The solder volume of a microbump decreases dramatically due to fine-pitch requirement and it is approximately two orders smaller in magnitude than that of a traditional flip-chip solder joint. The metallurgical reactions in the microbumps may behave quite differently to those in flip-ship bumps. Liquid-state metallurgical reactions were examined in SnAg_{2.5} microbumps with Ni metallization. The results indicate that large particles of Ag₃Sn intermetallic compounds (IMCs) precipitate after a 1-min reflow on microbumps with 2.0- μ m-thick solder, which does not occur with flip-chip solder bumps. It is proposed that the Ag concentration in the remaining solder may increase as Sn reacts with Ni. The increase in the Ag concentration is mainly responsible for the occurrence of the large Ag₃Sn precipitates. The formation of these Ag₃Sn IMCs would be detrimental to the mechanical properties of the microbumps.

Processing to Control Morphology and Texture in Magnetic Materials: Thin Films and Applications

Sponsored by: The Minerals, Metals and Materials Society, TMS Electronic, Magnetic, and Photonic Materials Division, TMS: Magnetic Materials Committee

Program Organizers: Matthew Kramer, Iowa State University; Mike McHenry, Carnegie Mellon University; David Laughlin, Carnegie Mellon University; Jinfang Liu, Electron Energy Corporation; Bill Soffa, University of Virginia; Ivan Skorvanek, Institute of Experimental Physics

Wednesday PM
March 14, 2012

Room: Europe 10
Location: Dolphin Resort

Session Chairs: William Soffa, University of Virginia; Ichiro Takeuchi, University of Maryland

2:00 PM Invited

Nanostructure Optimization of FePt Thin Films for Magnetic Recording: *Kazuhiro Hono*¹; *Yukiko K Takahashi*¹; ¹National Institute for Materials Science

The L10 ordered FePt granular thin film is considered as the most promising candidate for next generation ultrahigh density magnetic recording media, because of the high magnetocrystalline anisotropy. For the application of FePt films as recording media, the c-axis of magnetically isolated L10-FePt particles of less than 5 nm must be strongly [001] textured. We recently reported well separated perpendicular anisotropic granular films with a narrow size distribution by cosputtering FePt and C on MgO interlayer. Polycrystalline MgO layer grows with a strong (001) texture on amorphous substrates, which works as effective seedlayer for the epitaxial growth of (001) FePt particles. Ag addition to FePt-C film enhances the L10 ordering to attain a very high coercivity exceeding 38 kOe. In this talk, we review how the microstructures of FePt thin films has been optimized and discuss how they must be optimized further for thermally-assisted magnetic recording.

2:25 PM Invited

Control of Texture and Morphology of Thin Films for Magnetic Recording Applications: *David Laughlin*¹; *En Yang*¹; *Hoan Ho*¹; *Vincent Sokalski*¹; *Jimmy Zhu*¹; ¹Carnegie Mellon

Thin films used as magnetic recording media need to have a granular microstructure, with the magnetic grains (which are on the order of 5-8 nm) isolated from each other by a non-magnetic material. In this paper we review various methods used to produce such media in current and future applications. How the texture, morphology, crystal structure and magnetic exchange of Co alloys and FePt media is controlled during sputtering will be discussed.

2:50 PM

Combinatorial Search of Rare-Earth-Free Permanent Magnets: Magnetic and Microstructural Properties of Fe-Co-W Thin Films: *Tieren Gao*¹; *Ichiro Takeuchi*¹; *Yaqiao Wu*¹; *Matthew Kramer*¹; *Iver Anderson*¹; *Bill McCallum*¹; *Kevin Dennis*¹; ¹University of Maryland

We are using the thin film composition spreads to search for rare-earth free permanent magnetic materials by ternary co-sputtering. As one of the initial systems, the structural properties of W doped Fe-Co films with different heat treatment are mapped by synchrotron diffraction. We find that there is a phase transition from a crystalline to an amorphous state at about 10% atomic W composition in the as deposited state. The W concentration in phase transition area increases with increasing annealing temperature. By using SEM and TEM, we found that the grains of low W content Fe-Co films which show enhanced coercive fields vertically standing platelet-like structures. The angular dependence of the switching field of Fe-Co-W films indicates that the magnetic reversal process evolves from domain wall displacement to coexistence of domain wall displacement and coherent rotation with increasing W content.



3:05 PM

Effect of Rapid Annealing on the Microstructure of FeSiNbBCu Alloys: Pradeep Konda Gokuldoss¹; Pyuck-pa Choi¹; Dierk Raabe¹; Giselher Herzer²; ¹Max Planck Institute for Iron Research GmbH; ²Vacuumschmelze GmbH & Co. KG

Fe-Si-Nb-B-Cu model alloys have been studied for years because of their excellent soft magnetic properties. Upon annealing the melt-spun amorphous Fe-Si-Nb-B-Cu ribbons undergo nanocrystallization, where soft magnetic Fe-Si nanocrystals are formed. The process of Fe-Si nucleation is reported to be heterogeneous, wherein the nucleation sites are clusters of Cu atoms. In the present work an optimised composition of Fe_{73.5}Si_{15.5}Nb₃B₇Cu₁ melt spun alloy was annealed under a small tensile stress for a short duration of about 4s at temperatures ranging from 500 – 700 °C, about 100 °C higher than the conventional prolonged heat treatments. Such a difference in heat treatment has an effect on the size and number density of Cu clusters, the expected nucleation sites for Fe-Si nanocrystals. The samples were studied by atom probe tomography, transmission electron microscopy and x-ray diffraction. Surprisingly, the crystallite sizes of the Fe-Si nanocrystals remain well below 15 nm.

3:20 PM Break

3:40 PM Invited

Large Abnormal Grain Growth Behavior in Galfenol Rolled Sheets: Qingfeng Xing¹; Adam Boesenberg²; Eric Summers²; Thomas Lograsso¹; ¹Ames Laboratory; ²ETREMA Products, Inc.

Galfenol alloys (Fe-Ga alloys) exhibit large magnetostrictions along the <100> magnetic easy axis directions. One requirement for practical applications is to cost-effectively produce thin sheets with strong <100> texture components. Rolling followed by recrystallization and heat treat processes produce large Goss grains {110}<001> in excess of 125 cm² in the sheet plane with magnetostrictions > 250 ppm. Niobium carbide additions are critical in obtaining this large abnormal grain growth response. In the present work, thin sheets are sliced from non-rolled drop cast ingots with a range of carbon concentrations and annealed to investigate the effect of carbon concentration on abnormal grain growth. Normal grain growth is observed in a carbon free alloy and an alloy with high carbon concentration. An alloy with medium carbon concentration displays abnormal grain growth from the edges. This suggests carbon concentration is a key factor in achieving an abnormal grain growth response.

4:05 PM Invited

The Role of Crystallographic Texture in Microwave and Millimet: Yajie Chen¹; Anton Geiler²; Trifon Fitchorov¹; Andrew Daigle²; Carmine Vittoria¹; Vincent Harris¹; ¹Northeastern University; ²Metamagnetics Inc.

Crystallographic texture in the hexaferrites is closely related to magnetocrystalline anisotropy energy and fields. The magnetic anisotropy in turn is valuable in defining both the ferromagnetic resonance frequency and the frequency dependence of permeability. The setting of the FMR frequency determines among other things the operational frequency and frequency agile device performance. Here, we review the role of crystal texture in determining the magnetic anisotropy fields of a series of hexaferrite materials including the M, Y and Z type structures. Furthermore, the ability to strongly texture materials as powder compacts, and thick and thin films is explored in detail. Strategies to realize crystal texture include lattice matching of substrates and buffer structures as well as the use of magnetic fields during processing. The application of hexaferrites in microwave circulators, phase shifters, and in the design and processing of low profile antennas are demonstrated.

4:30 PM

Role of Alloying Elements in Improvement of Alnico Permanent Magnet Alloys: Scott Long¹; R.W. McCallum¹; M.J. Kramer¹; Kevin Dennis¹; D.T. Cavanaugh¹; Y.Q. Wu¹; I.E. Anderson¹; ¹Ames Laboratory

The historical development of Alnico permanent magnets was mainly empirical. A variety of transition metals were identified that improve Alnico performance, but the reasons are not well understood. We focused

on identifying the role of these previous additions and other promising elements in formation of the initial aligned solidification microstructure (e.g. Nb, and Ta) and on controlling the spinodal decomposition process (e.g. Cu and Ag) that forms the anisotropic Fe-Co precipitates. Initial microprobe results of directionally solidified structures show fluctuations in composition within the grains indicating possible dendritic growth. Further castings will be studied which are produced from more closely controlled solidification, with and without additional alloying elements. Typical spinodal spacing in Alnico is ~50 nm, adjustments in this spacing by alloying additions and various heat treatments will be studied. Characterization methods include TEM, SEM, electron microprobe, and VSM. Funding provided by DOE-EERE-FCVT Office through Ames lab contract DE-AC02-07CH11358.

4:45 PM

Structure and Chemistry of the Alnico Spinodal: Matthew Kramer¹; YaQiao Wu²; V. Antropov²; S. Long²; K. Dennis²; R. McCallum²; I. Anderson²; S. Constantinides³; ¹Iowa State University; ²Ames Laboratory; ³Arnold Magnetic Technologies

Modeling of the magnetic structure reveals that the size and shape of the FeCo cells and chemical gradient between the FeCo and AlNi phases are critical to their magnetic properties. A high resolution and analytical TEM study of an Alnico 5-7 alloy along the transverse and longitudinal orientations were performed. The spinodal's separation in the transverse orientation is ~ 50 nm while the individual cells are in excess 100 nm. The FeCo bcc lattice aligns with the primitive cubic lattice of the AlNi ({001} || {001} and <100> || <100>). The HRTEM of the alloy reveals the nearly perfectly coherent interface between the FeCo and the AlNi phases. While structurally sharp, concentration profiles obtained indicate that the chemical gradient is ~ 10 nm and the AlNi phase contains a significant amount of Co and Fe. Implications of the chemical gradient and its effect on the magnetic properties will be discussed.

Radiation Effects in Ceramic Oxide and Novel LWR Fuels: Effects of Radiation on Thermal Transport and Fuel Performance

Sponsored by: The Minerals, Metals and Materials Society, TMS Structural Materials Division, TMS/ASM: Nuclear Materials Committee

Program Organizers: Peng Xu, University of Wisconsin; Jian Gan, Idaho National Laboratory; Ram Devanathan, Pacific Northwest National Laboratory; Edward Lahoda, Westinghouse Electric Company; Michele Manuel, University of Florida; Ramprashad Prabhakaran, Idaho National Laboratory; Todd Allen, University of Wisconsin-Madison

Wednesday PM
March 14, 2012

Room: Macaw 2
Location: Swan Resort

Funding support provided by: The Center for Materials Science of Nuclear Fuel, an Energy Frontier Research Center led by the Idaho National Laboratory

Session Chairs: Edward Lahoda, Westinghouse Electric Company; Peng Xu, Westinghouse Electric Company

2:00 PM Invited

Effects of Radiation on Thermophysical Properties

of Ceramic Oxide Fuels: Dragos Staicu¹; ¹European Commission, Joint Research Centre, Institute for Transuranium Elements

Knowledge of the thermophysical properties of the fuel of a nuclear reactor is required for the prediction of fuel performance, in particular for the determination of the temperature distribution and of the fission gas release. The principal objectives of this presentation are to give elements useful to understand the phenomena causing the evolution

of the thermophysical properties during irradiation, in particular the degradation of the thermal conductivity, and to provide guidance for the interpretation and comparison of in-pile or out-of-pile measurements, especially as a function of burn-up and for samples having different irradiation temperatures, in-pile histories and microstructures. The importance of such studies is renewed when the discharge burn-up of the fuel is increased and with the formation of the high burn-up structure. The impact of the introduction of plutonium or additives (Gd, Cr, etc.) in standard UO₂ is also reviewed. Various approaches, from correlations to atomistic modelling, are presented.

2:30 PM

Effect of Dislocations on Thermal Conductivity of UO₂: *Bowen Deng*¹; Aleksandr Chernatynskiy¹; Priyank Shukla²; Susan Sinnott¹; Simon Phillpot¹; ¹University of Florida; ²Georgia Institute of Technology

The microstructure of a UO₂ fuel pellet evolves considerably during burn-up. Such microstructural evolution has considerable effects on the thermal transport properties. In a highly burn-up fuel, dislocations have a density as high as about $5 \times 10^{14} \text{m}^{-2}$, which can affect the thermal conductivity through phonon-dislocation scattering. Here we use molecular-dynamics simulations to explore the decrease in thermal conductivity caused by incorporating a dipole of straight dislocations into perfect single crystal UO₂. Comparisons are made between different dislocation densities and different types of dislocations. These results are compared with Klemen's classic calculations, and the differences explained. This work was supported by the Center for the Materials Science of Nuclear Fuel, a DOE-BES Energy Frontiers Research Center.

2:45 PM

Radiation-Enhanced Diffusivity Measurements of Nd in Single Crystal Thin Film UO₂: *Xiaochun Han*¹; Brent Heuser¹; ¹University of Illinois

We present measurements of the radiation-enhanced diffusion (RED) of Nd, a +3 impurity and high-yield fission product, in single crystal thin film UO₂ as a function of temperature, heavy-ion bombardment fluence and fluence rate. We use SIMS to characterize the broadening of a discrete Nd layer in our UO₂ thin films up to 1100K and burnup to 2% FIMA. The use of thin films allows us to simulate uniform fission product damage with heavy-ion bombardment and to apply microanalytical techniques such as SIMS. We present diffusivities as a function of temperature, fluence, and fluence rate in the single crystal matrix. The application of kinetic rate theory yields the cation impurity migration energy under recombination-limited kinetics without the convolution of grain boundary diffusion. We have performed similar measurements of La RED in single crystal ceria; discussion of our results will focus on important differences in mass transport in the two systems.

3:00 PM

Thermal Properties of ThO₂-Based Fuel Using Atomic Level Simulations: *Rakesh Behera*¹; Aleksandr Chernatynskiy²; Simon Phillpot²; Chaitanya Deo¹; ¹Georgia Institute of Technology; ²University of Florida

Thorium-based nuclear fuel cycles are promising for their intrinsic proliferation resistance and greater thorium abundance. In this presentation we will focus on the thermal properties of ThO₂ using atomic level simulations. We have developed several empirical interactions to describe the properties of bulk ThO₂. Molecular dynamics is used to evaluate the effect of temperature using these developed interatomic potentials. We will present the thermal expansion and thermal conductivities of ThO₂ and compare the predicted values with available experimental results. Phonon dispersion curves and phase stability of ThO₂ will be discussed along with implications for the properties of mixed ThO₂-UO₂ oxide fuels. This research is being performed using funding received from the DOE Office of Nuclear Energy's Nuclear Energy University Programs.

3:15 PM

Thermal Transport in Uranium Dioxide from First Principles: *Aleksandr Chernatynskiy*¹; Simon Phillpot¹; ¹University of Florida

Thermal transport is one of the most important performance metrics of nuclear fuel. Uranium dioxide is by far the most widely used fuel material. Yet, detailed understanding of the thermal conductivity in uranium dioxide, UO₂, is missing: the only first principles calculations in the literature estimate thermal conductivity from Gruneisen parameters; moreover the calculated thermal transport properties differ sharply from measurements. To date, calculations based on lattice dynamics and Boltzmann Transport Equation currently have been performed only for classical interatomic potentials and they also disagree with the experimental data for the phonon properties, such as lifetimes. We present the results of thermal conductivity calculations within the lattice dynamics framework in UO₂ using DFT calculations. Comparison of the phonon lifetimes with the recently measured lifetimes is provided. This work was funded by the Center for the Materials Science of Nuclear Fuel, a DOE-funded Energy Frontiers Research Center.

3:30 PM Break

3:40 PM Invited

Simulation of the Pellet Cladding Interaction Phenomenon with the PLEIADES Fuel Performance Software Environment: *Bruno Michel*¹; Chrystelle Nonon¹; Jerome Sercombe¹; Frederic Michel¹; Vincent Marelle¹; Isabelle Ramiere¹; ¹CEA

This paper is focused on the simulation of Pellet Cladding Interaction (PCI) in Pressurized Water Reactor (PWR) under nominal, transient and accidental loading conditions. Scientific results presented are based on a cooperative program, between EDF, AREVA and the Atomic Energy Commission CEA, devoted to PCI modelling and the development of a unified fuel performance software environment called PLEIADES. First, the PLEIADES multi-concept fuel software environment is described. Attention is focused on the multi-dimensional PCI simulation with the fuel performance code ALCYONE of the PLEIADES platform. Improvements brought by the use of a multi-dimensional PCI modelling are detailed, in particular concerning the simulation of the coupling between gaseous swelling and mechanical behaviour of the fuel pellet. In the second part, 3D single pellet fragment simulation results are illustrated through the validation and sensitivity analyses of the PCI loading to material behaviour. To conclude, new functionalities of ALCYONE are presented.

4:10 PM Invited

Mechanistic Modeling of Fuel Microstructure Evolution and Fission Product Release under Irradiation: *Mikhail Veshchunov*¹; ¹Nuclear Safety Institute (IBRAE) of Russian Academy of Sciences

The mechanistic code MFPR was developed for analysis of fission products (FP) release from irradiated UO₂ fuel in collaboration between IBRAE and IRSN (Cadarache, France). The main outputs of the code are fuel microstructure, chemical speciation of solid-phase FPs, fuel oxygen potential evolution with burnup, densification, swelling and FP release. The code models self-consistently describes evolution of fuel microstructure (point defects, such as vacancies and interstitials, and extended defects, such as gas bubbles, sintering pores and dislocations), which strongly influences intra- and intergranular diffusion transport of gas atoms in irradiated UO₂, as well as fuel thermo-physical and mechanical properties. New microscopic parameters characterizing the crystal defect structure naturally arise, however, being physically grounded, these can be fixed from the analysis of available experimental data and/or from atomic scale investigations, and then used without any artificial tuning in further calculations.



TMS 2012

141st Annual Meeting & Exhibition

4:40 PM

Theoretical Investigation on Interplay of Defect Clusters and Fission Gas in Uranium Dioxide: *Ying Chen*¹; Hua Y Geng²; Yasunori Kaneta³; Motoyasu Kinoshita⁴; Shuichi Iwata⁴; ¹Tohoku University; ²Institute of Fluid Physics; ³The University of Tokyo; ⁴Central Research Institute of Electric Power Industry

Interaction between the nuclear fuel and the fission gases product in nuclear reactor influences the performance of fuels remarkably. First-principles LSDA+U calculations have been performed taking Xe in UO₂ as a prototype to investigate the interplay of the defect clusters and gases in the fuel. A prominent effect of the self-defect clusters in bulk matrix on the thermodynamic behavior of fission gases is found, a thermodynamic competition between the uranium vacancy and tri-vacancy sites to incorporate xenon in hyper-stoichiometric regime at high temperatures is revealed. The observation that gas atoms are ionized to a charge state of Xe⁺ at a uranium vacancy site implies the possibility to control temperature to tune the preferred site of gas atoms and then the bubble growth rate. The quasi-annealing procedure, as a solution to the meta-stable states difficulty frequently encountered in DFT+U applications, is proposed and discussed over the example of UO₂-Xe system.

4:55 PM

Microstructurally Explicit Multi-Physics Simulation of Intergranular Mass Transport in Oxide Nuclear Fuels: *Harn Chyi Lim*¹; Karin Rudman¹; Kapil Krishna¹; Robert McDonald¹; Pedro Peralta¹; Chris Stanek²; Kenneth McClellan²; ¹Arizona State University; ²Los Alamos National Lab

Diffusion of fission products and the presence of large temperature gradients can affect the performance of oxide nuclear fuels. In particular, mass diffusion can be influenced by grain boundary (GB) characteristics, which suggests that microstructure could be manipulated to enhance fuel behavior. This research looks into the microstructure of depleted UO₂ and simulates the effects of GB characteristics on mass transfer, as affected by large temperature gradients. The percolation behavior of mass transport is studied, along with the differences between dual (heat and mass) and single (mass) physics models. A 3D finite element model with microstructure information is created by serial sectioning of a depleted uranium oxide sample using Electron Backscattered Diffraction. The model contains information about the GB network, which is characterized based on misorientation angles and the Coincident Site Lattice model. Simulations reveal the development of percolating paths controlled by the contrast of local GB properties.

5:10 PM

Potential Performance Improvements of New Fuels: Ed Lahoda¹; *Peng Xu*¹; Sumit Ray¹; Lars Hallstadius¹; ¹Westinghouse Electric Company

Uranium dioxide fuel was picked as the fuel of choice in the late 1950's because its properties and performance in reactor were well known and because the performance expectations were quite low. In the last 50 years, issues such as minimization of spent fuel, increased cycle lengths by achieving higher burnups, and increased power density have become the major goals of the nuclear power industry. A preliminary screening was carried out of multiple fuel types that are currently being researched and several fuels that have the potential to out perform UO₂ were identified. They do have issues, but their potential performance benefits will likely outweigh the costs. This paper presents this evaluation, notes the issues, and lists the cladding requirements that if the goals of higher burnup and linear power are to be met.

5:25 PM Concluding Comments

Randall M. German Honorary Symposium on Sintering and Powder-Based Materials: Powder Processing and Consolidation III

Sponsored by: The Minerals, Metals and Materials Society, TMS Materials Processing and Manufacturing Division, TMS: Powder Materials Committee

Program Organizers: K. Morsi, San Diego State University; Fernand Marquis, Naval Postgraduate School; John Meyer, Iowa State University; Ahmed El-Desouky, San Diego State University; Eugene Olevsky, San Diego State University

Wednesday PM
March 14, 2012

Room: Oceanic 2
Location: Dolphin Resort

Session Chair: J. Sears, South Dakota School of Mines & Technology

2:00 PM

LASER Powder Deposition of AlMgB14-TiB2 Ultra-Hard Coatings on Titanium, Steel, and Cast Iron Substrates: *Jacob Fuerst*¹; Michael Carter¹; James Sears¹; ¹South Dakota School of Mines and Technology

BAM is an ultra-hard ceramic compound created, at Ames Laboratory in 1999, by combining Aluminum Magnesium Boride (AlMgB14) and Titanium Diboride (TiB2). The high hardness, low coefficient of friction, and relative high temperature chemical inertness of BAM make it an ideal material for wear resistant coatings. Current BAM coatings are produced by Physical Vapor Deposition (PVD) or magnetron sputtering and are capable of only thin films. Using LASER Powder Deposition (LPD), high hardness (1300 HV) BAM coatings of 1 mm thickness, with increased fracture toughness were produced on Ti-6Al-4V, mild steel, and cast iron substrates. Initial tests demonstrate LASER Powder Deposition to be a capable means of manufacturing large, highly wear resistant surfaces.

2:15 PM

Pre-Sintered Preforms - Applications for Gas Turbine Components:

*Jeremy Boyle*¹; ¹AIM MRO

Advanced materials development in aero and industrial gas turbine components has been driven by increasing firing temperatures. These high performance superalloy articles must be repaired and refurbished to meet the expected life cycles and to assure the original equipment manufacturer's performance criteria. To meet these demands, preform brazing is becoming a vital process for airlines, utilities, and OEMs. This paper addresses the evolution and application of such processes.

2:30 PM

Modeling of Compaction Behavior Al6061 and SiC Powder by Semi-Solid Powder Forming: *Yufeng Wu*¹; *Gap-Yong Kim*¹; ¹Iowa State University

Semi-solid powder forming (S2PF) involves compaction of metallic alloy powders in temperature ranges where both solid and liquid phases coexist. In this work, compaction behavior of Al6061 and Al6061+SiC powders were modeled and compared with experimental results for liquid fractions up to 30%. A modified Shima-Oyane model was developed to predict the densification behavior of Al6061 powder. The model showed a good agreement with the experimental results below the liquid phase content of 20%. In this range, all the normalized pressure vs. relative density curves merged into one, which could be expressed in a simple exponential form for Al6061 powder. When the liquid phase content was above 20%, non-uniform distribution of the liquid phase was observed resulting in the deviation of the model from the experiments. Furthermore, a work in progress on modeling of the compaction behavior of Al6061+SiC powder is presented.

2:45 PM

Novel Amalgams for In-Space Fabrication of Replacement Parts:

Calvin Cochran¹; James Van Hoose²; Richard Grugel³; ¹Hendrix College; ²Qualis/Jacobs; ³Marshall Space Flight Center

Being able to fabricate replacement parts during extended space flight missions precludes the weight, storage volume, and speculation necessary to accommodate spares. Amalgams, widely used in dentistry, are potential candidates for fabricating parts in microgravity environments as they are moldable, do not require energy for melting, and do not pose fluid handling problems. Unfortunately, amalgams have poor tensile strength and the room temperature liquid component is mercury. To possibly resolve these issues a gallium-indium alloy was substituted for mercury and small steel fibers were mixed in with the commercial alloy powder. Subsequent microscopic examination of the novel amalgam revealed complete bonding of the components, and mechanical testing of comparable samples showed those containing steel fibers to have a significant improvement in strength. Experimental procedures, microstructures, and test results are presented and discussed in view of a simple model and further improving properties.

3:00 PM

Role of Al-Si Eutectic Powder on Sintering Aspects of Aluminum Alloy:

Gaurav Gupta¹; Anish Upadhaya²; O.P. Modi¹; ¹AMPRI bhopal; ²IIT Kanpur

The Al-Cu-Si alloy has been prepared from elemental powder of Aluminum and copper blended with Al-Si eutectic powder instead of using pre-alloyed atomized powder as the matrix material. The present investigation looked into the effect of sintering temperature and Al-Si powder content on the sintering behaviour of the alloy. Compaction was done at 200 and 500 MPa. Sintering was carried out in Nitrogen atmosphere. Further the Densification parameter and hardness were measured of the sintered sample and microstructures were examined. Densification parameter increased with sintering temperature at both the compaction pressures due to enhanced diffusion. Densification parameter increased with Al-Si content at lower compaction pressure but trend reversed at higher compaction pressure. Higher liquid content with low level of porosity leads to swelling of the sample. Higher Hardness was obtained in all condition at higher compaction pressures due to low porosity and Hardness also increased with Al-Si content.

3:15 PM Break

3:35 PM

Characterization of Surface Oxides on Steel Powders – Experiments and Modelling:

Karin Frisk¹; Sophie Caddeo Johansson¹; Alexander Angré¹; ¹Swerea KIMAB

Surface oxides on steel powders originating from the atomization and/or from powder handling, constitute an important source of oxygen in powder-based steel. The properties are detrimentally affected by oxygen and the content should be minimised, and it is thus of interest to characterise oxides, and the conditions where they are formed or reduced. In the present work different methods to investigate surface oxides on steel powder, and oxides in HIP-compacted steel, are presented. Experimental investigations, using Photo Acoustic Spectroscopy (PAS); analysis of oxygen contents in powder and in compacted samples produced in a lab-scale atomizer (10kg) equipped with an oxysensor; and by microstructure investigations using SEM / TEM with FIB (Focussed Ion Beam); are coupled with calculations of the stability of complex oxides to characterise the type of oxides.

3:50 PM

Corrosion Resistant Austenitic (316L) Stainless Steel through Sintering and Surface Modification by Electrostatic Spray Coating:

Kandala Ramakrishna¹; Kantesh Balani¹; Anish Upadhaya¹; ¹Indian Institute of Technology

Powder metallurgical stainless steels are finding increased demand in automotive, marine, structural, biomedical and food industries applications due to their unique characteristics of low processing temperature, near net

shape product with greater material utilization (>95 %) and more refined or homogeneous microstructure. However, the application of powder metallurgical stainless steel is limited by their inferior corrosion resistance and tribological properties. In the present study, an attempt has been made to enhance the corrosion resistance and tribological properties of sintered 316L stainless steel through surface modification. This study compares the electrochemical and wear behavior of electrostatically coated ultra high molecular weight polyethylene on conventional and microwave sintered 316 L (at supersolidus 1400°C for 1 h in reducing atmosphere). The corrosion behavior was investigated in 3.5% NaCl and 0.1N H2SO4 solutions by potentiodynamic polarization, electro chemical impedance spectroscopy (EIS) and surface characterization. The microstructure, processing and corrosion and wear behavior were correlated.

4:05 PM

Intense Pulsed Light Sintering Technique for Nanomaterials:

H. A. Colorado¹; S. R. Dhage²; J. M. ¹; H. T. ¹; ¹University of California, Los Angeles; ²International Advanced Research Center for Powder Metallurgy & New Materials (ARCI)

The Intense Pulsed Light (IPL) from a xenon flash lamp can sinter nanoparticles in few milliseconds. Such a short reaction time prevents oxidation of the elements and second phase generation. Another valuable benefit of IPL sintering is that the materials can be sintered without damaging the glass or temperature-sensitive flexible polymer substrate materials. The solid state diffusion of nanoparticles in a very short reaction time of few milliseconds is great benefit of Intense pulsed light system over the conventional sintering methods. It is believed that if the particles have very high surface area-to-mass ratio, very little light is needed to activate and diffuse the particles. Melting and recrystallization of particles to larger grains without structural deformation and phase transformation are possible because of very short reaction time. Thus, IPL can be a very promissory technique for ultra rapid processing of nanomaterials and thin films. Several study cases are presented.

4:20 PM

Reactive Spark Plasma Sintering of AlON Ceramics:

Halide Esra Kanbur¹; Burcu Apak¹; Gultekin Goller¹; Onuralp Yucel¹; Filiz Cinar Sahin¹; ¹Istanbul Technical University

In this study, aluminum oxynitride ceramics (AlON) with using AlN and Al2O3 starting powders were prepared by Spark Plasma Sintering (SPS) under nitrogen atmosphere. AlN and Al2O3 mixtures with sintering additives (Mg, La) were prepared. Several mixtures of Al2O3 and AlN were ball milled with alumina balls for 24 h. The obtained powder mixtures were sintered at several temperatures and periods at 40 MPa under nitrogen atmosphere by SPS system. The phase compositions of the samples were examined by X-ray diffraction (XRD) and microstructures were observed by SEM technique. The hardness and fracture toughness of the sintered samples were measured. The effects of SPS temperature, heating rate, soaking time and sintering additives on phase transformation, microstructure, mechanical properties, density and transparency of AlON were investigated.

4:35 PM

Spark Plasma Sintering of Silicon Carbide Ceramics:

Mehtap Unlu¹; Gultekin Goller¹; Onuralp Yucel¹; Filiz Sahin¹; ¹Istanbul Technical University

SiC ceramics were fabricated by spark plasma sintering (SPS) technique with the use of sintering additives. The sintering process was carried out at four different temperatures in the range of 1800-1950°C applying two different pressures 40MPa and 80MPa under vacuum atmosphere. The effect of additives, different temperatures and pressures on density, vickers hardness, fracture toughness, and microstructure were examined. The hardness and fracture toughness of the samples were evaluated by the vickers indentation technique. Microstructure of spark plasma sintered SiC samples were characterized by using SEM technique.



TMS 2012

141st Annual Meeting & Exhibition

4:50 PM Invited

Progress in Additive Manufacturing as a Powder Based Solution:

*James Sears*¹; ¹South Dakota School of Mines & Technology

Additive Manufacturing (AM) has matured in the last 20 years to a point it has become a viable powder-base solution for part manufacturing or enhancement. The application space that AM encompasses range from Aerospace and Defense to Bio-Medical. Additive Manufacturing comprises technologies that add material to existing structures for form and/or function. AM is a CAD/CAM solid freeform fabrication technology that uses metal powder and fusion for manufacturing or repairing of components without the use of hard tooling. Fusion can be invoked through laser, electron beam, and arc-based energy sources. AM is also achieved through solid state techniques that utilize friction and ultrasonic energy. Inherent to AM is the ability to add material for repair or manufacture of critical components with minimal heat affect to the under lying material. An overview of AM developments will be provided along with details of manufacturing and repair for several applications.

Reaching New Heights: Materials Innovation in the Aerospace Industry: Session I

Sponsored by:

Program Organizers: Robert Shull, National Institute of Standards and Technology; Jud Ready, Georgia Institute of Technology; George Gray, Los Alamos National Laboratory; Thomas Battle, Midrex Technologies

Wednesday PM
March 14, 2012

Room: Northern E2
Location: Dolphin Resort

Session Chair: Chuck Ward, US Air Force

2:00 PM Introductory Comments

2:05 PM

Materials Genome Initiative: *James Warren*¹; ¹NIST

The Materials Genome Initiative is a new, multi-stakeholder effort to develop an infrastructure to accelerate advanced materials discovery and deployment in the United States. Over the last several decades there has been significant Federal investment in new experimental processes and techniques for designing advanced materials. This new focused initiative will better leverage existing Federal investments through the use of computational capabilities, data management, and an integrated approach to materials science and engineering. The development of advanced materials can be accelerated through advances in computational techniques, more effective use of standards, and enhanced data management. This talk will provide a brief introduction to the initiative, and set the stage for the case studies discussed in this session.

2:15 PM

ICME: Promise and Future Directions: *Robert Schafrik*¹; ¹GE Aviation

At GE Aviation, we have demonstrated success of this strategy with a 2-year development time (from project start to full engine qualification) for two low rhenium single crystal airfoils alloys that entered production in 2009, and a 4-year development time for a new cast-and-wrought turbine disk alloy that will enter full scale production in 2012. In both these cases, a typical development cycle would have been 3 times as long. As we look to the future, we see several key ICME areas that need to be further developed to make ICME the standard development approach: i) cyber infrastructure that facilitates collaboration between various stakeholders; ii) federated heterogeneous databases; iii) further development of key M&P models across all material systems, including standard interfaces; and iv) standardized Terms & Conditions for licensed software.

2:45 PM

Lessons Learned from the Trenches and Implications on ICME and the MGI: *Charles Kuehmann*¹; ¹QuesTek Innovations LLC

The President's Material's Genome Initiative (MGI) challenges us to innovate materials modeling and engineering methods, enabling new materials to reach commercial application in half the time of current capabilities. QuesTek's more than a decade of experience in applying Materials by Design technology and Accelerated Insertion of Materials (AIM) methods has taken four alloys to commercial production and flight qualification with many more in process. This unique experience provides key insights into a Materials Genome infrastructure and related Integrated Computational Materials Engineering (ICME) methods enabling the grand MGI vision. Important conclusions from recent materials commercialization successes can be made. First, a specific engineering problem must dictate the priorities for developing MGI and ICME related modeling, tools and data, not the other way around. And secondly, while challenging, the overall goal of the MGI is certainly achievable. A review of recent successes and implications of the MGI will be presented.

3:15 PM

Enabling the Era of Hybrid Materials - A Tipping Point of Change: *Michael Dudzik*¹; Rick Barto¹; ¹Lockheed Martin Corporation

The ongoing state of the art transition in the field of materials science from metal alloys to composites to hybrid materials offers the aerospace market unique design solutions to meet ever demanding requirements in product manufacturing cost reduction, system performance enhancement and total lifecycle sustainability. The rapidly growing interest in hybrid materials - those with multiple functionalities - has opened a new era in materials usage for advanced aerospace products beyond mono-functional materials. Since 2008, Lockheed Martin has been actively engaged in blending hybrid materials with ICME practices to create new solutions to complex design and manufacturing needs. The benefits of the Materials Genome Initiative will expand and accelerate the transition of hybrid materials across greater product applications. A review of recent successes achieved through better utilization of computational physics, material data management, certification, and the manufacturing supply chain will be presented.

Recent Developments in Biological, Electronic, Functional and Structural Thin Films and Coatings: Process-Properties-Performance Correlations II

Sponsored by: The Minerals, Metals and Materials Society, TMS Electronic, Magnetic, and Photonic Materials Division, TMS: Thin Films and Interfaces Committee

Program Organizers: Nuggeshalli Ravindra, New Jersey Institute of Technology; Jian Luo, Clemson University ; Xing Yang (Mark) Liu, National Research Council Canada; Nancy Michael, University of Texas at Arlington; Roger Narayan , University of North Carolina and North Carolina State University; Choong-un Kim

Wednesday PM
March 14, 2012

Room: Swan 10
Location: Swan Resort

Session Chairs: Jian Luo, Clemson University ; Choong-un Kim, University of Texas at Arlington

2:00 PM Introductory Comments

2:05 PM

Near-Surface Residual Stress-Profiling by Incremental Micro-Slot Cutting Method: Assessment of Stress-Calculation Errors: *Bartlomiej Winiarski*¹; Philip Withers¹; ¹University of Manchester

This paper quantifies residual-stress (RS) calculation errors of the incremental micro-slot cutting method (μ SC) for the investigation of residual stress profile in near-surface layer on a submicron scale. We

WEDNESDAY PM

analyse five main sources of RS calculation errors: (a) displacement-measurement errors; (b) slot-depth-measurement errors; (c) slot-width-measurement errors; (d) incorrect material constants; and (e) unit pulses method (UPM) uncertainty. Within the scope of μ SC method the residual-stresses are inferred using Finite-Element Analysis (FEA) of the surface relaxation, as measured by Digital Image Correlation (DIC) from Field-Emission-Gun Scanning Electron Microscope (FEGSEM) images, which occur when a micro-slot is step-wise micro-machined by Focused Ion Beam (FIB). The calculation algorithm, which solves this inverse problem of residual-stress estimation, is based on UPM and is stabilised by Tikhonov Regularisation (TR). We demonstrate the influence of particular sources of errors on RS estimates in homogeneous materials and coatings, and we present a guidelines to minimise the uncertainties.

2:35 PM

Properties of Coatings Formed by Plasma Electrolytic Oxidation of AM60B Magnesium Alloy in Electrolytes Containing Al₂O₃ Suspension: Xijin Li¹; Mark Liu¹; Ben Luan¹; ¹National Research Council Canada

Magnesium alloys are attractive lightweight materials for many industrial applications, but their relatively low resistance to corrosion and wear is a key drawback of the materials. To improve the wear and corrosion resistance of an AM60B magnesium alloy, ceramic coatings were formed by plasma electrolytic oxidation (PEO) in aluminate electrolytes with and without Al₂O₃ particle suspensions. Pin-on-disc wear tests showed that the addition of Al₂O₃ suspensions in the electrolytes can significantly improve the wear resistance of the coatings. The mechanisms of coating performance improvements were investigated through examining microstructures, coating compositions and phase constituents of the coatings.

3:05 PM

Adhesion between Polymer/Metal interfaces: Sina Youssefian¹; Nima Rahbar¹; ¹Umass Dartmouth

Polymer-Metal interactions in majority of engineering polymers are experimentally difficult to measure. Molecular Dynamics (MD) simulation for quantifying the adhesion between PMDA-ODA polyimide and Aluminum (Al) and Aluminum Oxide (Al₂O₃) is used to have better understanding of the metal-polyimide interfacial properties. A model composed of a small molecular fragment of the polymer repeating units and a block of metal and metal oxide is used for the simulation. COMPASS force field methodology was used in MD simulations to calculate the energy of adhesion between the polymer and the surfaces. Results are shown that introduction of oxygen atoms to metallic surface significantly increases the adhesion energy. The energy of adhesion between PMDA-ODA and Al₂O₃ is more than that of with Al. Keywords: Adhesion, Polymers, Contact mechanics

3:25 PM

Hyperthermal Hydrocarbon Modification of PMMA: Leah Hill¹; Travis Kemper¹; Susan Sinnott¹; ¹University of Florida

Ion beams and plasma can be used to functionalize or modify the surface of a polymer, which affects properties such as adhesion, biocompatibility and chemical resistance. Hydrocarbon molecules are used in plasma modification of surfaces. Here, molecular dynamics simulations are performed to examine the mechanisms by which hyperthermal hydrocarbon polyatomics, which are present in low-energy plasmas, modify polymer surfaces. The forces on the atoms are determined using the second generation Reactive Empirical Many-Body (REBO) potential. In particular, H, C₂H, CH₃, and C₃H₃ are deposited on a poly(methyl methacrylate) (PMMA) substrate at kinetic energies of 25, 50, and 100 eV. The effects of deposition on crosslinking are explored, and functionalization of the polymer substrate is evaluated to better understand the effects of ion beam depositions on plasma polymerization. This work is supported by the NSF (CHE-0809376).

3:45 PM Break

4:00 PM

Mechanism of Creep Deformation in Porous Organosilicate Thin Films: Emil Zin¹; Tingqin Zhao¹; Nancy Michael¹; Choong-Un Kim¹; Huili Xu¹; ¹The University of Texas at Arlington

Silicate based porous thin films are extensively used in many engineering structures and devices, including high efficiency catalyst and low-k for microelectronics devices. One of the presumption in the related field is that the film would maintain its structural integrity as long as load is kept below the yield point. However, our studies find that the prevailing belief is false as the films are found to exhibit creep. Detailed investigation on the mechanism, conducted at various temperature, loading condition, and film condition, indicates that the creep occurs by viscous flow due to chemical reaction. When the film is exposed to -OH, the hydration reaction results in the weakening of the local bond, which leads to body translation of the entire film. This paper presents 1) characterization methodology for creep deformation of porous silicate thin films, 2) kinetic mechanisms of creep and 3) chemical and mechanical mechanism leading to the creep.

4:20 PM

Characterization of Ceramic Layers on Al Alloy by Plasma Electrolytic Oxidation in Two Different Electrolytes Including Sodium Tungstate: In Jun Hwang¹; Ki Ryong Shin¹; Sang il Yoon¹; Young Gun Ko²; Dong Hyuk Shin¹; ¹Hanyang University; ²Yeungnam University

This study demonstrated tribological properties of ceramic layers on Al alloy by plasma electrolytic oxidation (PEO) in two kinds of electrolytes, namely phosphate and silicate, including sodium tungstate. X-ray diffraction patterns revealed two crucial facts: Firstly, when PEO coating was carried out in phosphate electrolyte, the ceramic layer possessed a large quantity of WO₃ compound since the electric potential of electro-migration for tungstate ions was abruptly reduced by phosphate ions which could be complexing agent. On the other hand, the mullite and α -Al₂O₃ compound was formed with ease in the ceramic layer with rapid growth rate during PEO treatment in the silicate electrolyte due to the intrinsic characteristics of silicate ions. Overall, predominant WO₃ compound in the ceramic layer from phosphate electrolyte disclosed better tribological properties after short PEO-process time while silicate electrolyte was favorable to fabricate tribologically hard ceramic layer beyond relatively long process time.

4:40 PM

Characterization of High Temperature Mechanical Properties of Two Unique Experimental Coatings: Amit Pandey¹; Vladimir Tolpygo²; Kevin Hemker³; ¹ORNL; ²Honeywell; ³JHU

Two coatings discussed here are coating "a" which is a typical NiCoCrAlY and was deposited by plasma spray and the coating "B" is a modified Ni-base superalloy (i.e. two-phase gamma / gamma-prime Ni alloy) and was deposited by laser cladding. Results on thermal expansion experiments reveal that both coatings possess wide range of coefficient of thermal expansion (CTE) and the CTE curves follow distinct path dependency with temperature. It is found that the CTE mismatch between coating and substrate is significantly lower for the coating "B". Microtensile experiments at room temperature show that the coating "a" has slightly higher YS and a very low value of failure strain (ϵ_f) as compared to the coating "B" and is very different at higher temperature. Results from this study indicate that coating "B" could be a better choice for a thermal barrier system.

5:00 PM

Effect of Temperature on the Structure and Properties of Nano-Twined Cu Thin Film Deposited by Unbalanced Magnetron (UBM) Sputtering: Kai Hung Yang¹; Fan-Yi Ouyang¹; ¹National Tsing Hua University

Nano-twined Cu thin films were successfully deposited on Si (100) substrate using unbalanced magnetron sputtering (UBMS) system. The objective of this study was to investigate the effect of temperature on



TMS 2012

141st Annual Meeting & Exhibition

the structures and mechanical properties of Cu thin films. The electro-resistance was measured by four-point probe and the hardness was measure by nano-indentation. Transmission Electron Microscopy (TEM) was used to examine microstructure and preferred orientation of the nano twin. The residual stresses of all Cu films were also measured. The results show that (111) was the dominant preferred orientation in the Cu films. The effects of the temperature were strongly varied on the hardness, nano-twin spacing, and grain size. Furthermore, the results suggested nano-twin structure tended to form at lower temperature with high deposition rate. A possible mechanism of nano twin formation was also discussed in this paper.

5:30 PM

Formation of Crystalline and Amorphous Phases During Deposition of Ni_xTi_{1-x} Thin Film on Si Substrate – Interpretation of Experimental Results Using Molecular Dynamics Simulations: *Shampa Aich*¹; Geetha Priyadarshini B¹; M. Gupta¹; Sudipto Ghosh¹; Madhusudan Chakraborty²; ¹Indian Institute of Technology Kharagpur; ²Indian Institue of Technology Bhubaneswar

This research was undertaken to study the crystallization and amorphization of magnetron-sputtered Ni_xTi_{1-x} thin films using composition variations and various substrate bias voltages. Variation of deposition efficiency with composition and bias voltage suggests that Ni resists re-sputtering. In case of Ti thin film, increase in negative bias voltage caused decrease in crystallinity due to re-sputtering. But, the bias voltage did not affect significantly the crystallinity of Ni thin film. On the other hand, high bias voltage induced crystallinity in otherwise amorphous Ni_xTi_{1-x} thin film. In order to explain some of the observed trends molecular dynamics simulations based on embedded atomic method (EAM) potential for Ni-Ti system were carried out. Simulations could explain the partial amorphization of crystalline film and partial crystallization of amorphous film which occurred due to re-sputtering.

Recycling General Sessions: Waste Utilization

Sponsored by: The Minerals, Metals and Materials Society, TMS Extraction and Processing Division, TMS Light Metals Division, TMS: Recycling and Environmental Technologies Committee
Program Organizer: Joseph Pomykala, Alter Trading

Wednesday PM
March 14, 2012

Room: Europe 4
Location: Dolphin Resort

Session Chair: Jeffrey S. Spangenberg, Argonne National Laboratory

2:00 PM

Experimental Research on Acid Magenta Dye Decolor Dynamics: *Ding Lichao*¹; Chen Yunnen¹; ¹Jiangxi University of Science and Technology

In this paper the simulated acid magenta dye discoloring the reaction process was researched. The results showed that it attained highest decolorization efficiency for acidic magenta simulation dye wastewater when pH 9 and reaction time 10 min. With the initial dye wastewater concentration increased, the decolor rate decreased. The decolor rate in general kept a tendency to increased with the temperature increased. Kinetics researches showed that when pH 9, reaction temperature 20 and 35 °C, the decoloring reaction process for the dyes accorded with the first-order dynamic equation. The decoloring reaction rate constant was influenced by initial concentration of dye wastewater and temperature.

2:20 PM

Study on a River Containing Fluorine and the Pollution Control Method: *Luo Jianzhong*¹; Zhang Zheng¹; ¹Guangdong University of Technology

No matter the contents of fluorine in river is too high or too low ,they will have a bad effect on human health and habitats, and thus the study on fluoride pollutants in river is related to people's lives and health safety.

The article studies the fluoride content in a stream of the Pearl River of China. The fluoride concentration is excessive all the time in this stream, fluoride content in water is up to 1.65mg/L, exceeding 65%. Through the investigation of the key sources of pollution, there are 58 aluminum processing plants, 55 glass factories, 161 iron and steel factories, 199 ceramics factories, 30 brick factories and 38 cement factories in this near areas. These plants emitted high fluoride wastewater, and need to strengthen the fluoride pollution control, or close the factories which cannot reach the environmental standard.

2:40 PM

Study on a Stream Contained Fluorine Excessively and the Industry Pollution Control of Fluorine in the Stream: *Luo Jianzhong*¹; Zhang Zheng¹; Zhang Minyi¹; Zhang Qian¹; Luo Shuai¹; ¹Guangdong University of Technology

No matter the content of fluorine is too high or too low in water, they will have a bad effect on human health and habitats, and thus the study on water fluoride pollutants is important to people's lives and health safety. The fluoride content in a stream water of the Pearl River in China is up to 1.65mg/L, exceeding standard 65%. Through the investigation of the key sources of pollution near this stream, there are 58 aluminum processing plants, 55 glass factories, 161 iron and steel factories, 199 ceramics factories, 30 brick factories, 38 cement factories. These factories emitted high fluoride wastewater, need to strengthen the pollution control, or close the factories which cannot reach the environmental standard.

3:00 PM

Investigation of Mo Extraction from a Spent Hydro-Cracking Catalyst by Fungi at Optimal Conditions: *Farnaz Amiri*¹; ¹Sharif University of Technology

Spent hydro-processing catalysts have been identified as hazardous wastes by USEPA since 1999; so, recovery of the contained heavy metals in the spent catalyst is critical in view of environmental and economic benefits. Bioleaching has been considered as a possible alternative to polluting and costly traditional extraction methods such as hydro-metallurgy and pyro-metallurgy for the recovery of metal values from spent catalysts. Statistically based experimental designs, Plackett–Burman factorial design and central composite design, were applied respectively to screen and optimize the bioleaching of spent catalyst by *Aspergillus niger* and *Penicillium simplicissimum*. The production of organic acids as the main agent in fungal leaching and changes of the fungi dry weight with time were also investigated. The maximum Mo recoveries corresponding to optimal conditions were (98.8 ± 0.9) % and (99.5 ± 0.4) % achieved by *Penicillium simplicissimum* and *Aspergillus niger*, respectively, which were comparable to the conventional approaches results.

3:20 PM

Leaching Thermodynamics and Kinetics of Preparation of Synthetic Rutile: *Wu Zhang*¹; Li Zhangli¹; Xiang Feng¹; ¹Northeastern University

Leaching thermodynamics and kinetics of preparation of synthetic rutile were discussed. Leaching Gibbs free energy change of reactions were calculated. The metal and water E-pH formula were obtained at different temperatures. Potential-pH formulas of reactions and Potential-pH diagram of MeO-H₂O systems were drawn at the temperature of 298K and 313K when the ionic activity is 1.0. Kinetic experiments and calculations show that the leaching process can be modeled with the shrinking core model which indicates that the control factor of the leaching process is chemistry reactions. The apparent activation energy of alkali leaching process is 43.52kJ/mol.

3:40 PM Break

4:00 PM

Phase Equilibria and Liquidus in CaO-SiO₂-FeOx-Al₂O₃ System in the Temperature Range 1673K to 1873K: *Cuthuan Huang*¹;

¹Northeastern University

To provide essential data for efficient utilization of vitrified bottom ash slag, the thermodynamic properties of CaO-Al₂O₃-SiO₂-FeOx-MgO-Na₂O oxide system are highly required. In this work, the equilibrium phases and liquidus of CaO-SiO₂-FeOx-Al₂O₃ system, one sub-system of the multi-component oxide systems, were investigated in the temperature range from 1673K to 1873K. The liquid phase regions enlarged with increase of temperature, while the primary phase fields reduced distinctly. The equilibrium phases of CaO-SiO₂-FeOx-Al₂O₃ system systems were identified between 1673K to 1873K.

4:20 PM

Precipitation Selectivity of Perovskite Phase from Ti-Bearing Blast Furnace Slag under Reducing Conditions, Argon Atmosphere and Dynamic Oxidation Conditions: *Li Zhang*¹; *Wu Zhang*¹; ¹Northeastern University

The precipitation selectivity of perovskite phase from Ti-bearing blast furnace slag under reducing condition, an argon atmosphere and dynamic oxidation were investigated, respectively. The aim of this work was to investigate the effect of different modified conditions on the selective enrichment of Ti components into perovskite phase and precipitation of perovskite phase. The results under reducing conditions show that the higher melting temperature and slag basicity had little effect on the precipitation selectively of perovskite phase, and Ti components remained the dispersed distribution in various fine grained, almost same as un-modified slag; the results under an argon atmosphere show that the higher melting temperature and slag basicity promoted the precipitation of perovskite phase, but had little effect on the selective enrichment of Ti components into perovskite phase; the result under dynamic oxidation show that the dispersed Ti components were enriched into perovskite phase, and perovskite phase could be selectively precipitate.

4:40 PM

Recovery of Magnesium from Waste Effluent in Nickel Laterite Hydrometallurgy Process: *Ninglei Sun*¹; *Jinshan Liu*¹; *Kuiting Wang*¹; *Aiguo Dong*¹; *Yeda Lu*¹; ¹China ENFI Engineering Co. Ltd.

Eliminating the environmental threat caused by waste effluent containing magnesium sulfate discharged from the process of nickel laterite sulfuric acid leaching and subsequent nickel precipitation is always a focus in the metallurgy field. A new flowsheet whose procedures include vaporization, crystallization, precipitation of magnesium by ammonia, secondary precipitation, causticizing treatment of filtrate and ammonia recycle was investigated. Both the details of the flowsheet and its application are described in this article. It is confirmed to be an effective and economical method to prevent the pollution by the waste effluent, in addition, a series of magnesium products recovered during the process own good economic returns.

5:00 PM

Recycling of Reverted IN738LC with Reference to Mechanical Properties and Control of Chemical Composition: *Reza Rahimi*¹; *Mahmood Nili Ahmadabadi*¹; ¹University of Tehran

Because of high cost and shortage of primary resources of Ni-base superalloys, researchers are looking for new methods to reach origin ingot without using pure metals or master alloys alone and one of the attractive resources that are suitable for gaining this goal is reverted alloy. The current study is based on recycling of IN738LC, a Ni-base superalloy, using 30% reverted alloy and 70% virgin raw materials. Therefore, it has been attempted to cast an alloy with references to standard chemical composition and mechanical properties. After charging and casting in vacuum melting furnaces, chemical composition verification and non-

destructive tests (i.e. PT and RT), quality of samples were evaluated by various mechanical experiments such as stress-rupture as well as room and elevated temperature tension tests. Results acquired from chemical composition and mechanical tests indicate that cast ingots using 30% reverted alloy is reliable and consistent with the quality control requirements.

5:20 PM

A Kinetics Study on the Hydrometallurgical Recovery of Vanadium from LD Converter Slag in Alkaline Media: *Amirhossein Shahnazi*¹; *Fereshteh Rashchi*¹; *Ehsan Vahidi*²; ¹University of Tehran; ²University of South Florida

During the oxidation process of the molten pig iron, contains high concentration vanadium bearing materials, vanadium transfers to the slag. In this research, recovery of vanadium from LD converter slag of steelmaking plant was investigated. The leaching residue was characterized by XRD, XRF and SEM/EDX techniques. The maximum vanadium recovery was achieved at 70°C, S/L:1/15, NaOH concentration:3M and leaching time:150min. It was determined that the dissolution rate increased with increasing NaOH concentration and decreasing particle size. The experimental data were treated graphically to explain the kinetics of the vanadium recovery process using shrinking core model (SCM). As a result, the controlling regimes in the SCM were analyzed separately using liquid-film diffusion control, solid-product diffusion control and reaction control mechanisms. Kinetic findings were in consistent with the activation energy and also a linear relationship between the rate constant and the inverse square of the initial particle diameter was observed.

Refractory Metals 2012: Alloy Predictions and Synthesis | Oxidation and Corrosion

Sponsored by: The Minerals, Metals and Materials Society, TMS Structural Materials Division, TMS: Refractory Metals Committee
Program Organizers: Eric Taleff, The University of Texas at Austin; Todd Leonhardt, Rhenium Alloys Inc; Rachel DeLucas, H.C. Starck; Gary Rozak, HC Starck Inc

Wednesday PM
March 14, 2012

Room: Mockingbird 2
Location: Swan Resort

Session Chairs: Eric Taleff, The University of Texas at Austin; Rachel DeLucas, H.C. Starck Inc.

2:00 PM

Ab Initio Phase Diagrams of Bcc-Based Transition Metal Alloys – Consequences on Properties: *Patrice Turchi*¹; *Vaclav Drchal*²; *Josef Kudrnovsky*²; ¹Lawrence Livermore National Laboratory; ²Institute of Physics, Czech Academy of Science

The unique properties of refractory metals and their alloys require a fundamental understanding of alloy phase stability and ordering based on a proper description of the scattering properties of the electrons. Phase stability properties of substitutional alloys of the fifteen combinations among the six bcc-based transition metals with prediction of equilibrium properties and coherent phase diagrams are discussed in the framework of the first-principles fully relativistic tight-binding linear muffin-tin orbital (TB-LMTO) method, within the coherent potential approximation (CPA) and the local density approximation of density functional theory. The statistical mechanics part of the problem is solved with a generalized mean-field approach with effective pair interactions obtained from the ab initio generalized perturbation method. We show that electron-driven tendencies toward order exist for some of these bcc-based alloys although the assessed phase diagrams indicate complete miscibility. Work performed under the auspices of the U.S. DOE by LLNL under contract DE-AC52-07NA27344.



2:20 PM

Bond-Order Potentials for bcc Refractory Metals: *Miroslav Cakl¹; Thomas Hammerschmidt¹; Ralf Drautz¹; ICAMS, Ruhr University Bochum*

Refractory metals play an important role in many materials for high-temperature applications. These elements are involved in a variety of microstructural peculiarities ranging from the formation of topologically close-packed (TCP) phases to transitions between symmetric and asymmetric dislocation cores. An atomistic understanding of refractory metals requires a reliable and computationally efficient representation of the interatomic interaction. To this end we developed tight-binding based analytic bond-order potentials (BOPs) for the bcc refractory metals Tungsten, Molybdenum, Niobium and Tantalum. The potentials parameters were optimised for the equilibrium bcc structure and extensively tested for atomic environments far from equilibrium that were not included in the optimisation: structural energy differences; tetragonal, trigonal, hexagonal and orthorhombic deformation paths; formation energies of point defects and phonon spectra. A comparison with density-functional and tight-binding calculations shows very good transferability of our analytic BOPs. We show the application of the BOPs to the simulation of grain boundary properties.

2:40 PM

Effect of Alloying on Phase Stability and Deformation Behavior of Niobium Silicides: *Oleg Kontsevoi¹; Arthur Freeman¹; Northwestern University*

Niobium silicide-based alloys are promising materials for ultra-high temperature applications with a potential to replace traditional Ni based superalloys. One of drawbacks is poor fracture toughness at room and intermediate temperatures. In order to develop a fundamental basis for a further enhancement of performance of these materials through alloying, we apply theoretical density-functional theory calculations to investigate the effect of Al, transitional metals (Ti, V, Cr, Fe) and refractory metals (Mo, Ta, W) on phase stability and deformation behavior of the multiphase Nb - Nb₅Si - Nb₂Si₃ system. We determine site preference, phase partitioning of alloying elements, and their effect on shear behavior and preferred deformation modes. The results are discussed in connection with possible ways of enhancement of deformation properties of niobium silicide alloys.

3:00 PM

Microstructure and Properties of New Refractory High Entropy Alloys: *Oleg Senkov¹; Svetlana Senkova¹; Daniel Miracle¹; Christopher Woodward¹; Air Force Research Laboratory*

Results on the development of several new refractory high entropy alloys containing Nb, Mo, Ta, Hf, Cr, V, Ti, Zr and Al as principal alloying elements will be presented. Some of these multi-component alloys have a single-phase, disordered BCC crystal structure, while other alloys contain several crystal phases among which a disordered BCC phase dominates. The crystal types and chemical compositions of the phases, the alloy density, hardness, compression properties in a temperature range from 295 to 1473 K, and microstructures will be reported. Finally, the relationships between the composition, microstructure and properties will be outlined for these new alloys. This work was conducted under the U.S. Air Force contract FA8650-10-D-5226.

3:20 PM

Facile Synthesis and Characterization of Inexpensive Superhard Refractory Metals: *Richard Kaner¹; Reza Mohammadi¹; Andrew Lech¹; Miao Xie¹; Christopher Turner¹; Beth Weaver¹; Michael Yeung¹; Sarah Tolbert¹; UCLA*

With the shortcomings of traditional cutting tool materials such as diamond (expensive) and tungsten carbide (low hardness), the search for new high-performance superhard materials has recently led to the exploration of dense transition metal borides. For example, we have synthesized rhenium diboride (ReB₂) using arc melting at ambient pressure. This superhard material possesses excellent electrical

conductivity and mechanical properties. Under an applied load of 0.49 N, we have measured a Vickers microindentation hardness of 48.0 GPa for ReB₂. To further increase the hardness and lower the materials costs, we have begun exploring higher boron content metal borides including tungsten tetraboride (WB₄). We have synthesized WB₄ by arc melting and measured a Vickers microindentation hardness of 43.3 GPa under a load of 0.49 N. Solid solutions of this material with Re have resulted in a hardness of ~50 GPa when 1 at.% of W is substituted with Re.

3:40 PM Break

3:50 PM

Microstructural Characterization of Multicomponent Nb-Ti-Si-Cr-Al-X Alloys: *Raghvendra Tewari¹; Hyo-Jin Song²; Amit Chatterjee³; Vijay Vasudevan²; Bhabha Atomic Resrach Centre; ²Department of Chemical and Materials Engineering, University of Cincinnati, OH, 45221-0012; ³Rolls Royce Corporation*

In the present work, microstructures of multicomponent Nb-Ti-Si-Cr-Al-X alloys were studied and effect of temperature and time on phase evolution was examined. Microstructures of the alloys comprised the matrix- β , silicides and Laves phase. The silicides in these alloys were generally stable during heat treatment, whereas the Laves phase was observed to dissolve or precipitate out depending upon temperature of aging. In addition, the β -matrix showed phase separation tendency. The volume percentage and chemical composition of each phase has been determined and the changes in microstructure have been rationalized in terms of the distribution of elements in various phases. The role of alloying elements on the formation of these phases has also been critically examined.

4:10 PM

Cobalt-Base Alloys for High Temperature Applications: *Rabindra Mahapatra¹; M. Ashraf Imam²; Charles Lei¹; Jerry Feng²; Naval Air Systems Command; ²Naval Research Lab*

The isothermal oxidation behavior and thermal stability of a cobalt base (Co-Al-Si-Cr-W-Ni-Ce-Hf) alloy were investigated up to a period of 312 hr in air from 1000 to 12000C. A comparison of oxidation behavior of this alloy with a conventional nickel-base superalloy (Inconel 713C) has been conducted in detail. The cobalt base alloy oxidizes by forming layers of Al₂O₃, Cr₂O₃, HfO, CoO and traces of SiO₂ with WO₂ oxides on the surface of the specimen in contact with air. Optical and scanning electron microscopy (SEM) were used to study the microstructure, morphology and compositions of oxides formed after the exposure. Thermal stability of the alloy after extended periods of exposures to air at 1000, 1100 and 12000C was studied using transmission electron microscopy (TEM).

4:30 PM

Oxidation Behavior of Nb-Ti-Si-Cr-Al-X Based Multi-Component Based Alloys: *Raghvendra Tewari¹; Amit Chatterjee²; F. J. Boerio³; Vijay Vasudevan³; Bhabha Atomic Resrach Centre; ²Rolls Royce Corporation; ³University of Cincinnati*

Several Nb-Ti-Si-Cr-Al-X alloys have been exposed in air for various temperature and time and nature and sequence of reactions that occur upon oxidizing in these alloys have been systematically studied. The morphology of oxide layer, formation of various oxides and ingress of oxygen into the base materials have been studied as a function of time and temperature. Complementary techniques like scanning electron microscope and x-ray photon spectroscopy have been used to understand the nature and sequences of the oxidation. The role of different alloying elements in the formation of the oxide layer has been examined and a possible mechanism of the oxidation has been proposed.

4:50 PM

Oxidation Behavior of the Nb-10Si-20Cr and Nb-10Si-20Cr-5Al Systems: *Victoria Rangel*¹; S.K. Varma²; ¹The University of Texas at El Paso; ²The University of Texas at El Paso

The oxidation behavior of Nb-10Si-20Cr and Nb-10Si-20Cr-5Al has been studied in a range of temperature from 700 to 1400C in static air. Isothermal oxidation experiments indicate that addition of 5 atomic percent Al is beneficial in reducing the weight gain per unit area. The phases present include Nb solid solution, NbCr₂, Nb₅Si₃ and Nb₉Si₂Cr₃. However, low temperature peeling appears to be a problem especially at 800C. High temperature oxidation is characterized mainly by spalling. However, internal oxidation has been observed by the formation of Al₂O₃ along inter-phase interfaces. The characterization techniques include SEM and XRD including BSE, EDS and x-ray mapping modes in SEM.

5:10 PM

The Effects of Silicon on the Nb-Cr-Si Alloy System: *Daniel Voglewede*¹; S. Varma¹; ¹University of Texas at El Paso

The effect of Si on the oxidation resistance of the Nb-20Cr-(10-40) Si alloys have been studied. The major contribution of Si is to produce Nb₅Si₃ phase which helps for enhancing the oxidation resistance and the high temperature strength. A range of Si from 10 to 40 atomic percent allows to determine the microstructural stability especially for the silicides and Laves phase (NbCr₂). It has been observed that the weight gain per unit area is lower with increased Si concentration. There may be other silicides besides Nb₃Si₃ which may be contributing to the results. Characterization has been performed using XRD and EDS, BSE and x-ray mapping modes in SEM. A comparison between the theoretically expected and experimentally observed microconstituents has been made.

Solid-State Interfaces II: Toward an Atomistic-Scale Understanding of Structure, Properties, and Behavior through Theory and Experiment: Grain-boundaries and Triple Junctions

Sponsored by: The Minerals, Metals and Materials Society, TMS Electronic, Magnetic, and Photonic Materials Division, TMS Structural Materials Division, TMS: Chemistry and Physics of Materials Committee, TMS: Nanomechanical Materials Behavior Committee

Program Organizers: Xiang-Yang Liu, Los Alamos National Lab; Douglas Spearot, University of Arkansas; Guido Schmitz, University of Münster; David Seidman, Northwestern University

Wednesday PM
March 14, 2012

Room: Oceanic 7
Location: Dolphin Resort

Funding support provided by: Los Alamos National Laboratory

Session Chairs: Guido Schmitz, University of Münster, Germany; Reiner Kirchheim, University of Göttingen, Germany

2:00 PM Invited

Thermodynamics and Kinetics of Grain Boundary Junctions: *Günter Gottstein*¹; Lasar Shvindlerman¹; Luis Barrales-Mora¹; Bingbing Zhao¹; ¹RWTH Aachen University

Grain Boundaries in polycrystals are connected by grain boundary junctions, which coordinate the kinetic behavior of connected grain boundary systems, like migration or segregation. Therefore, grain boundary networks are likely to behave differently from solitary grain boundaries. We show that grain boundary junctions are crystal defects on their own with specific thermodynamic and kinetic properties and that these properties affect microstructural evolution during grain growth. Novel experimental methods will be introduced on how to determine the thermodynamic and kinetic properties of junctions, and theoretical approaches will be proposed how to modify existing theories of polycrystal

kinetics to account for junction effects. Finally, computer simulations of grain boundary motion and grain growth will be presented to demonstrate the effect of junctions on kinetics, grain size, and texture.

2:30 PM Invited

Interfaces, Grain Boundaries and Triple Junctions in Metallic Multilayers: *Zoltán Balogh*¹; Patrick Stender¹; Mohammed Chellali¹; Guido Schmitz¹; ¹Westfälische Wilhelms Universität, Münster

Triple junctions (TJs), the topological substructures where three grain boundaries (GBs) merge can have significant volume fraction, when the grain size decreases to about 10 nm. Yet, because of the difficulties in characterizing a thin, pipe-like tilted/curved structure, experimental results about these defects are rare. By using a tomographic atom probe one can reconstruct a 3D virtual representation of a specimen with subnanometer resolution in every directions. With this method identifying TJs and investigating their atomic transport properties is possible. We measured interdiffusion profiles in the Ni/Cu system along the TJs and the GBs as well as measured directly the GB width after different annealing treatments. Our results indicate that TJs are two-three orders of magnitude faster diffusion paths than standard high angle GBs. These experiments were part of a broader project, where other materials as well as the properties of the interfaces separating the layers were evaluated.

3:00 PM

Grain Boundary Junction Transitions during Annealing of a Model Columnar Microstructure: *James Belak*¹; Bryan Reed¹; Vasily Bulatov¹; Ming Tang¹; Tom Lagrange¹; Joel Bernier¹; Mukul Kumar¹; ¹Lawrence Livermore National Laboratory

Grain boundary junctions play an important role during microstructure evolution [1]. A model columnar microstructure with [011] texture for MD simulations is used. The Finnis-Sinclair potential is used to represent copper during thermal coarsening. Our choice of GB misorientation leads to a microstructure consisting entirely of S₃, S₉ and S₂₇. Depending on the orientation of nearby (111) planes to the junction, we observe the junction to transform into one with [111] symmetric tilt boundaries (STGB). These STGBs join with the original S₃s at an unstable grain boundary kink. Further evolution occurs by dislocation emission from the asymmetric tilt boundaries, forming long twin segments. Results will be compared to experimental observations. [1] G. Gottstein, L.S. Shvindlerman, and B. Zhao, Scripta Materiala 62 (2010) 914-917. Work was performed under the auspices of the U.S. DOE by LLNL under Contract DE-AC52-07NA27344 and supported by the DOE Office of Basic Energy Sciences.

3:20 PM

Effect of Three-Dimensional Grain Boundary Structure, Crystallography and Chemistry on Sensitization in Al-Mg Alloys: *Alexis Lewis*¹; Keith Knipling¹; ¹Naval Research Laboratory

Aluminum-magnesium (5xxx series) alloys are widely used in Naval applications requiring lightweight, high-strength, formable, corrosion-resistant structural materials. These alloys, however, become susceptible to intergranular corrosion and stress corrosion cracking when exposed to elevated temperatures (70–200 °C). This “sensitization” of the grain boundaries has been attributed to elemental segregation and grain boundary precipitation of the β phase, Al₃Mg₂. To date, most research has focused on the effects of bulk alloy composition and annealing treatment on grain-boundary β precipitation. However, the nucleation and growth of grain-boundary β is also strongly influenced by the grain-boundary character, with both misorientation and inclination influencing the precipitate nucleation rate and precipitate morphology. This study seeks to quantify the relationship between the complex polycrystalline grain boundary character and β precipitate formation in AA5083, using 3D characterization techniques to understand and quantify the complex relationship of grain-boundary microstructure, crystallography, and chemistry to the resulting sensitization behavior.



TMS 2012

141st Annual Meeting & Exhibition

3:40 PM Break

3:50 PM Invited

The Disconnection Mechanism of Coupled Migration and Shear at Grain Boundaries: *Robert Pond*¹; Hassan Khater²; Anna Serra²; John Hirth³; ¹University of Exeter; ²Universitat Politecnica de Catalunya; ³Private individual

Disconnections are line-defects with dislocation and step character, so their motion along an interface produces concomitant migration and shear, or coupling. Extensive experimental evidence shows that disconnection motion is an active mechanism of coupling in high-angle grain boundaries, but less is known about low-angle cases. Here, we simulate the atomic structures of a series of [0001] tilt boundaries in an hcp metal. For each tilt angle, the perfect boundary is created, as well as one containing a disconnection capable of conservative motion. Both types of boundary are subjected to a simple shear strain parallel to the boundary. In all cases, coupled motion occurs at significantly lower applied stresses for boundaries containing a disconnection. The Peierls stress for disconnection motion increases monotonically in the low-angle regime, reaching a maximum of about 17MPa. However, this stress decreases precipitately in the high-angle regime, remaining around 2MPa. The reasons underlying this behaviour are discussed.

4:20 PM

Geometrical construction of $90^\circ \sqrt{2}$ (hk0) Quasi-periodic Grain Boundaries in Cubic Crystals: *Mohammad Shamsuzzoha*¹; ¹University of Alabama

A special category of quasi-periodic boundaries in cubic crystals termed as $90^\circ \sqrt{2}$ (hk0) quasi-periodic boundaries is geometrically constructed on the basis of the vector representation of lattice sites in participating grains. The construction process involves a 90° mutual rotation of a unique position vector, termed as the sigma generating vector (SGV), present in the common [hk0] projected zero-layer lattices of two grains. The mutual rotation allows the SGV of one grain to superimpose on the position vector that is coplanar normal to the SGV belonging to the other grain. The plane normal to the thus superimposed SGV of one grain and the coplanar normal vector of SGV become the boundary plane of such quasi-periodic boundaries. In these quasi-periodic boundaries, the stacking ratio of the lattices of opposing crystals that are aligned normal to the boundary plane assumes a value that is close to an irrational number, such as $\sqrt{2}$. Such a quasi-periodic boundary has been found to exist in the thin film of bcc $Fe_{81}Ga_{19}$ crystals.

4:40 PM

Observations and Trends of Shear-Coupled Grain Boundary Motion: *Eric Homer*¹; Stephen Foiles²; Elizabeth Holm²; David Olmsted³; ¹Brigham Young University; ²Sandia National Laboratories; ³University of California, Berkeley

Analysis of grain boundary (GB) migration in a catalogue of 388 GBs has resulted in new observations of shear-coupled GB motion using the synthetic driving force method. This analysis includes observations of shear coupling in [100]-symmetrical tilt GBs that match previous results of Cahn, Mishin, et al. even though the driving force for the motion is different. In addition, we demonstrate observations of shear coupling in [110]- and [111]-symmetrical tilt GBs that, in general, match theoretical predictions of shear coupling obtained through the Frank-Bilby equation. Finally, we present temperature-dependent trends of shear coupling behavior where we see one of three trends in a single boundary as a function of temperature: (1) perfect shear coupling, which is independent of temperature; (2) decayed shear coupling, where coupling decreases in magnitude with increasing temperature; and (3) temperature-dependent shear coupling mechanisms, where the mechanism (and direction) of the shear coupling change with increasing temperature.

5:00 PM

Surface Effects and Resolving Apparent Inconsistencies in Grain Migration Rate Measurements in Aluminum: *Arkady Vilenkin*¹; ¹The Hebrew University of Jerusalem

In experiments by Rath & Hu [Trans Am Inst Min Eng 1969;245:1577], in a wedge shaped bicrystal of aluminum, the grain boundary velocity was seen to be proportional to the power $n=4$, of the driving force, which was taken as the reciprocal of the radius of the cylindrically shaped grain boundary, and while according to well established theories the exponent n should be equal one. We show analytically that such kinetic effects could be caused by interaction of the grain boundary with the external surface, if velocity of the surface triple junction is taken to be proportional to the power n of the lateral force that the grain boundary applies to the junction because of a layer of alumina on the exterior surface. We discuss the possible influence of the layer on surface diffusion problem and on the mobility of the triple junction.

5:20 PM

Stress Induced Migration of Symmetric Tilt Grain Boundaries in Zinc: *Askar Sheikh-Ali*¹; ¹Kazakh-British Technical University

Stress-induced behavior of high-angle coincidence, near coincidence and general boundaries has been examined in bicrystalline specimens of zinc. Symmetric tilt boundaries are characterized with $\langle 1010 \rangle$ axis of rotation and the following misorientations: 89 ± 0.5 , 123.6 ± 0.5 , 125.8 ± 0.5 and 129.1 ± 0.5 degrees. These boundaries were tilted at 45 deg with respect to the tensile axis. For different types of the boundaries, two different mechanisms of boundary migration have been identified: capillary driven boundary migration enhanced by grain boundary sliding (GBS) - for general boundaries, and the motion of extrinsic grain boundary dislocations - for coincidence and near-coincidence boundaries. The stimulation of migration of general boundary by GBS is explained by the increase in the reduced boundary mobility due to continuous change in grain boundary atomic structure during GBS. Different coupling factors in the case of coincidence and near-coincidence boundaries are explained by sensitivity of parameters of extrinsic secondary GBDs to boundary misorientation.

Symposium in Memory of Patrick Veyssi re: Understanding the Mechanisms Controlling Plastic Flow: Deformation Mechanisms

Sponsored by: The Minerals, Metals and Materials Society, TMS Electronic, Magnetic, and Photonic Materials Division, TMS Structural Materials Division

Program Organizers: Georges Saada, LEM CNRS ONERA; Dennis Dimiduk, Air Force Research Laboratory; Hael Mughrabi, University Erlangen-Nuernberg; Haruyuki Inui, Kyoto University

Wednesday PM
March 14, 2012

Room: Europe 6
Location: Dolphin Resort

Funding support provided by: National Science Foundation

Session Chairs: M. V ron, Phelma; K. Hemker, John Hopkins University

2:00 PM Invited

Deformation Mechanisms in B2 Intermetallic CoTi: *Rupalee Mulay*¹; Sean Agnew¹; ¹University of Virginia

Many B2 compounds, like NiAl, exhibit slip primarily on the $\langle 001 \rangle \{110\}$ slip systems, which provide only 3 independent slip systems and, hence, fail to satisfy von Mises criterion for polycrystalline ductility. Recent in-situ neutron diffraction measurements on CoTi coupled with elasto-plastic self consistent modeling have reinforced that the primary slip systems in this alloy are $\langle 001 \rangle \{110\}$, but also exposed a transition in strain hardening beyond which a secondary deformation mechanism is activated. The present study examines the dislocation types present in B2

CoTi beyond this transition using $g \cdot b$ analysis in a transmission electron microscope (TEM) and in-grain misorientation axes (IGMA) obtained from electron backscattered diffraction. TEM and IGMA analysis shows the presence of $\langle 110 \rangle$ and $\langle 111 \rangle$ dislocations. Even a limited number of $\langle 110 \rangle$ or $\langle 111 \rangle$ dislocations can reduce stress concentrations that could otherwise lead to premature fracture. Source and mobility issues related to the activity of these dislocations are discussed.

2:30 PM Invited

Development of a Crystal Model for Twinning in Tantalum: *Jeffrey Florando*¹; Nathan Barton¹; James McNaney¹; Luke Hsiung¹; Mukul Kumar¹; ¹Lawrence Livermore National Laboratory

A crystal level twinning model has been developed in an effort to examine the competition between dislocation slip and twinning in tantalum. A sensitivity study has been performed to assess the effect of the parameters on the overall twinning behavior. The model has been compared to single crystal plate impact experiments that were recovered and examined using EBSD and Transmission Electron Microscopy (TEM). The experimental results suggest a strong orientation dependence on the amount of twinning observed, and a change in the dependence at higher shock pressures. Utilizing the crystal model, simulations of the experiment suggest that the observed orientation dependence for twinning is strongly coupled to the initial dislocation density and its evolution.

3:00 PM Invited

Nucleation Versus Propagation of Deformation Twins in Tantalum Driven by High Shear Strain Rate at Low Temperature: *Changqiang Chen*¹; Kalia Ramesh¹; Kevin Hemker¹; Mukul Kumar²; Jeff Florando²; ¹Johns Hopkins University; ²Lawrence Livermore National Laboratory

The competition between deformation twinning and dislocation slip, as well as the process of twin nucleation vs propagation in bcc metals, such as tantalum, has been a long standing issue. In this work, we use both laser shock and low temperature dynamic shear to drive the formation of deformation twins in polycrystalline tantalum. Transmission electron microscopy (TEM) and atomic scale TEM (HREM) have successfully captured the early stage of the formation of deformation twins. Consequently, the competition between nucleation, propagation, and coalescence of deformation twins are found to be responsible for several unique characteristics of deformation twins that are observed for the first time in tantalum, as well as for the formation of a unique twin network. A relationship between slip and twinning nucleation is also established in terms of the coalescence of twinning dislocations and dissociation of emissary dislocations.

3:30 PM Invited

Laser Shock Induced Changes in Microstructure, Residual Stress, Plasticity and Properties of Aero Engine and Other Alloys: Amrinder Gill¹; Yixiang Zhao¹; Abhishek Telang¹; Zhong Zhou¹; Seetha Mannava¹; Dong Qian¹; *Vijay Vasudevan*¹; ¹University of Cincinnati

Laser shock peening (LSP) generates deep compressive residual stresses and near-surface microstructural changes through shockwaves, thereby leading to dramatic improvements in fatigue and crack propagation resistance of alloys. We report results of LSP effects on the behavior of IN718, IN718+, Ti64, Ti6242 alloys and alloy 600. Residual strains and stresses were characterized using high-energy synchrotron x-ray diffraction and conventional XRD. The near/sub-surface microstructure changes were studied using EBSD/OIM and TEM. Local properties were determined using nanoindentation, microhardness and micropillar compression tests. Fatigue tests were conducted and the thermal stability of LSP-induced microstructural changes and residual stress was also assessed. Finally, controlled experiments and analytical and finite element modeling and simulation were utilized to predict the laser shock induced residual stress and thermal relaxation thereof. The results showing the relationship between shock parameters, microstructure, residual stress, thermal stability, and mechanical properties, including hardening and fatigue, will be presented and discussed.

3:50 PM Break

4:05 PM Invited

A Comparison of Dislocation Microstructures Formed during Severe Plastic Deformation of an Al-2.5 Mg Alloy at Room and Cryogenic Temperatures and Their Effect on Alloy's Room-Temperature Strength: *Jung Singh*¹; Apu Sarkar¹; Garima Sharma¹; Jayanta Chakravarty¹; ¹Bhabha Atomic Research Centre

This work reports a comparison of dislocation microstructures that formed in ultra-fine grains of a commercial Al-2.5 Mg alloy produced by equal channel angle pressing at room and cryogenic temperatures. Though the room- and cryogenic-temperatures pressing of the alloy produced ultra-fine grains of similar grain sizes for the same amount of equivalent strain, there was a significant difference in their respective room-temperature compression strengths. This observed difference in the room-temperature strengths corresponding to two microstructures has been attributed to differences in their dislocation substructures.

4:25 PM Invited

Relationship between Plasticity Mechanism and "Multiple-Slip" Volume in FCC Metals at Nanoscale: *Qing-Jie Li*¹; Zhang-Jie Wang¹; Zhi-Wei Shan¹; Ju Li²; Jun Sun¹; Evan Ma³; ¹Center for Advancing Materials Performance from the Nanoscale (CAMP-Nano) & Hysitron Applied Research Center in China (HARCC), State Key Laboratory for Mechanical Behavior of Materials, Xi'an Jiaotong University; ²Department of Nuclear Science and Engineering and Department of Materials Science and Engineering, MIT; ³Department of Materials Science and Engineering, Johns Hopkins University

Plasticity mechanism for FCC metals at nanoscale is a fundamental scientific question. Two widely accepted and debated mechanisms are surface dislocation nucleation and single-arm dislocation operation. In the present work, we performed molecular dynamics (MD) simulations on compression of pristine gold particles and Aluminum pillars with multiple-slip orientation and found that a quite large volume of the samples is deformed by single-arm dislocations which is produced by the robust dislocation jamming (internal dislocation source) formed within a small volume directly beneath the indenter due to simultaneous multiple-slip. However, when sample size is sufficiently small, surface dislocation nucleation dominates the plasticity due to the lack of "multiple-slip" volume. This result indicates that "multiple-slip" volume which could be influenced by both sample size and preparation methods plays an important role in plasticity mechanism of nanoscale FCC metals. Key words: nanoscale FCC metals, plasticity mechanism, multiple-slip volume

4:45 PM Invited

Direct and Derived Dislocation Density Vectors: *Craig Hartley*¹; ¹El Arroyo Enterprises LLC

Dislocation dynamics simulations produce detailed, 3-D pictures of the dislocation structure of deformed crystals. The development of these structures with increasing strain can be followed by constructing the Dislocation Density Vectors (DDV) formed from the projections of edge and screw components of dislocations on each active slip plane. Each of the vectors on an active slip system is composed of a Geometrically Necessary component and a Statistically Stored component which add up to the Total Dislocation Density Vector for the slip system. A composite DDV containing weighted contributions from all active slip systems in a computational volume can be constructed at each step of the simulation process and used to follow the evolution of dislocation structure resulting from deformation. Examples of the application of this method of representing dislocation structures for several simulations are presented and the relationship of the DDV to the kinematics of deformation is discussed.

5:05 PM Concluding Comments



Titanium: Advances in Processing, Characterization and Properties: Mechanical Properties

Sponsored by: The Minerals, Metals and Materials Society, TMS Structural Materials Division, TMS: Titanium Committee
Program Organizers: Adam Pilchak, US Air Force Research Laboratory; Christopher Szczepanski, US Air Force Research Laboratory; Vasisht Venkatesh, Pratt & Whitney

Wednesday PM
 March 14, 2012

Room: Oceanic 3
 Location: Dolphin Resort

Session Chairs: Soran Biroscas, University of Cambridge; Chris Szczepanski, US Air Force Research Laboratory

2:00 PM Invited

Crack Initiation and Microstructurally Short Crack Growth of Ti-6Al-4V: *Hans-Juergen Christ¹; Helge Knobbe¹; Philipp Koester¹; Claus-Peter Fritzen¹; Martin Riedler²; ¹University of Siegen; ²Böhler Schriedetechnik GmbH & Co KG*

Ti-6Al-4V was investigated in two different forged conditions with respect to fatigue crack initiation and short crack growth characteristics. The experimental findings based on interrupted fatigue tests, thorough SEM examination in combination with orientation imaging and 3-D information from FIB-cuts were implemented into a mechanism-based short-crack model, which describes crack propagation as a partially irreversible dislocation glide on a crystallographic slip plane. The numerical model is based on dislocation dipole boundary elements. The non-uniform propagation kinetics of short cracks is considered by defining grain boundaries as obstacles to plastic slip and crack propagation. The described model was used to simulate crack propagation behavior for the purpose of life assessment. By means of virtual microstructures, microstructural parameters such as grain size and volume fractions can be varied in order to identify the optimum fatigue-resistant material condition.

2:30 PM Invited

Computational Indicators for Structure-Fatigue Property Relations in Ti Alloys: *Craig Przybyla¹; David McDowell²; ¹AFRL; ²Georgia Institute of Technology*

This paper discusses a methodology to estimate the microstructure dependence of the extreme value probabilities of fatigue crack formation at the scale of the grains in polycrystalline and polyphase alpha-beta Ti microstructures to facilitate preliminary parametric design exploration and property assessment. A simulation-based methodology is introduced for computing correlation functions of microstructure attributes marked by the extreme value microstructure-scale fatigue indicator parameters. Multiple statistical volume elements of microstructure are simulated using a crystal plasticity constitutive model via finite element analysis to characterize these extreme value marked correlation functions. By comparing marked correlation functions to traditional correlation functions sampled from the bulk material, the interacting microstructure attributes relevant to extreme value response(s) are identified. Effects of the a free surface are considered in terms of any effects on modification or amplification of fatigue indicator parameters relative to bulk regions.

3:00 PM Invited

Hierarchy of Fatigue Deformation Heterogeneities in a Titanium Alloy: A Pathway for Predicting Life-Limiting Failures: *Sushant Jha¹; Robert Brockman²; Christopher Szczepanski³; Craig Przybyla³; James Larsen³; ¹Air Force Research Laboratory/Universal Technology Corporation; ²University of Dayton Research Institute; ³US Air Force Research Laboratory*

Fatigue damage can initiate by multiple mechanisms, even under a given microstructure and loading condition. Each mechanism is found to be associated with a microstructural arrangement, which can range

from single microstructural unit to various combinations of many units. In terms of fatigue lifetime, this plurality of mechanisms produces increased variability. However, lifetimes often group into two divergent populations, which are termed as life-limiting and mean-dominating distributions. Furthermore, fatigue crack initiation appears to occur within the first few cycles in life-limiting failures. This presentation will discuss possible physical origins and probabilistic predictions of life-limiting events in the alpha+beta titanium alloy, Ti-6Al-2Sn-4Zr-6Mo. A crystal plasticity model was employed to calculate the distribution in cyclic strain based deformation parameters in an alpha+beta titanium alloy with duplex microstructure. The results were employed in a probabilistic fatigue model to quantify the propensity for life-limiting failures in Ti-6Al-2Sn-4Zr-6Mo.

3:30 PM

In-Situ Microscale Testing to Evaluate Fatigue Behavior: *Christopher Szczepanski¹; Sushant Jha²; Paul Shade¹; Robert Wheeler³; James Larsen¹; ¹US Air Force Research Laboratory; ²AFRL/UTC; ³UES*

A recent study of fatigue crack-initiation mechanisms and their relationship to lifetime variability in bulk samples of Ti-6Al-2Sn-4Zr-6Mo has revealed that crack initiation can occur in a variety of characteristic microstructural neighborhoods. In many cases, specimens with similar crack initiation sites exhibit significantly different fatigue lifetimes and this scatter was shown to result from variability in crack initiation behavior. To characterize these mechanisms under controlled conditions, an in-situ micro-scale tensile testing technique has been adapted to complete fatigue tests in an SEM on micro-specimens extracted from representative fatigue-critical microstructural neighborhoods. EBSD has been completed and FIB markers were machined in micro-specimens to enable displacement mapping. Additionally, the use of micro-scale samples enables 3D microstructural characterization of the full specimen gage volume. The mechanical behavior and microstructural characterization of these experiments will be presented, with an emphasis on identifying microstructurally driven cyclic damage accumulation processes leading to fatigue crack initiation.

3:50 PM Break

4:00 PM

Analysis of Dislocation Structures Underneath Nanoindentations in an α -Ti Alloy: *J. Kwon¹; P.Sudharshan Phani²; M.C. Brandes¹; A. Pilchak³; E.P. George⁴; G.M. Pharr²; M.J. Mills¹; ¹The Ohio State University; ²The University of Tennessee; ³WPAFB; ⁴Oak Ridge National Laboratory*

The mechanical responses of alpha titanium alloys are well known to be both elastically and plastically anisotropic. Plastic anisotropy can be attributed to the large differences in the critical resolved shear stresses necessary to activate slip on <c> component slip systems. In this study, the plastic anisotropies of a polycrystalline, single-phase alpha Ti-7Al alloy are investigated via nanoindentation techniques where it has been found that the onset of plasticity depends on numerous factors. Observations of pop-in events were observed to be sensitive to crystal orientation, surface condition, and initial dislocation content. The dislocation structures under indents were characterized by post-mortem SEM, EBSD, and STEM imaging. Results show that dislocation configurations and slip system activity is dependent on grain orientation.

4:20 PM

Three-dimensional Investigation of the Microtexture near Tensile Crack Tip in Ti-6Al-4V: *Xu Xu¹; Yau Yau Tse¹; Geoff West¹; ¹Loughborough University*

Ti-6Al-4V alloy with bimodal microstructure often contains microtextured regions which were reported to have a significant effect on the crack growth in fatigue experiments. An implicit quantitative relationship between the crystallographic orientation and crack growth remains to be established. It is found in this study that the microtextured regions in a hot rolled Ti-6Al-4V alloy are of about 30 μ m wide and contain elongated grains with the c-axis parallel to transverse direction.

The crack produced in an interrupted tensile test was characterized using electron back-scattered diffraction (EBSD). Particularly, 3D EBSD study was carried out at the crack tip to elucidate the relationship between crack growth and grain orientation. It has been found that trans-granular cracking occurs in grains with (0001) basal plane parallel to the transverse direction while most cracking paths are along grain or alpha-beta interphase boundaries. The implication of crystallographic orientations on the cracking will be discussed.

4:40 PM

The Effect of Temperature and Stress on the Creep Deformation Modes of Ti-5Al-2.5Sn (wt.%): Hongmei Li¹; Carl Boehlert¹; Thomas Bieler¹; Martin Crimp¹; ¹Michigan State University

Creep deformation modes of a forged Ti-5Al-2.5Sn (wt.%) alloy were analyzed at elevated temperature using *in-situ* scanning electron microscopy. Creep tests were performed at temperatures between 455-500\176C and stresses between 200-300MPa, and electron backscatter diffraction was performed on the samples prior to testing. Grain boundary sliding was an active deformation mode for all the conditions examined. At 250MPa and 455\176C, about 10% of the grains observed *in-situ* exhibited basal slip and very few grains showed prism slip. At higher stresses, both basal and prismatic slip systems were active, suggesting basal slip operated at lower stress than prism slip and the activity of prism slip was increased by increased stress. Compared to the 455\176C and 250MPa condition, the 490\176C and 250MPa condition exhibited more slip activity and correspondingly, the prism slip activity was also increased. The evolution of slip and grain boundary sliding will be discussed.

5:00 PM

Comparison of CPFE and Experimental Results for the Study of Interaction between Grain Boundary and Dislocation Slip in Ti-5Al-2.5Sn: Chen Zhang¹; Hongmei Li¹; James Seal¹; Martin Crimp¹; Carl Boehlert¹; Thomas Bieler¹; ¹Michigan State University

The interaction between grain boundaries and dislocation slip plays an important role in anisotropic plastic deformation of polycrystalline materials like Ti-5Al-2.5Sn, yet its mechanism has not been fully understood. Crystal Plasticity Finite Element (CPFE) method is a dislocation slip based computation model. Unlike other commonly used computational models, it is developed to study the deformation process of polycrystalline materials at grain and sub-grain level, which makes it a suitable tool to study dislocation slip dominated deformation process. A CPFE mesh was generated based upon heavily characterized microstructure patch from a room temperature deformed Ti-5Al-2.5Sn sample. By comparing the CPFE simulation and experimental results, the interaction between grain boundary and dislocation slip can be studied to assess simulated vs. measured slip activity, which will bring new understanding of the grain boundaries role in the deformation process.

5:20 PM

Machining of Coarse Grained and Ultra Fine Grained Titanium: Rimma Lapovok¹; Andrey Molotnikov¹; Ashan Bandaranayake¹; Yuri Estrin¹; ¹Monash University

Machining of titanium is quite difficult and expensive. Heat generated in the process of cutting does not dissipate quickly, which affects tool life. In the last decade the ultra fine grained (UFG) titanium became an option for substitution of more expensive titanium alloys. Extreme grain refinement can be readily performed by so-called severe plastic

deformation techniques. This grain refinement was shown to change both mechanical and physical properties of materials. A study of the microstructure and shear bands formation in chips in coarse grained and UFG titanium machined with three different depths and three different speeds has been conducted. A change in thermal characteristics of CP Ti with grain refinement has been studied through comparing heating / cooling measurements with an analytical solution of the heat transfer boundary problem. It is demonstrated that an improvement in overall wear of the machining tool can be expected for UFG titanium.

5:40 PM

Machinability of β -Titanium Alloy Ti-10V-2Fe-3Al with Different Microstructures: Hendrik Abrahams¹; Christian Machai¹; Dirk Biermann¹; ¹Technische Universität Dortmund

The aerospace sector uses titanium-based materials to manufacture lightweight safety parts such as structural components, turbine disks and blades or landing gears. By heat treatment, β -enriched titanium alloys offer low, as well as the highest strength-to-weight ratio among all titanium alloys. Machining processes are strongly affected by the changes within the microstructure and the emerging mechanical properties of the material. Low cutting data and rapid development of tool wear lead to challenges in machining operations. Therefore the fundamental characteristics of machining differently microstructured β -titanium Ti-10V-2Fe-3Al rods and hollow shafts are presented. The experimental results identify varying static and dynamic process forces, tool wear mechanisms and process limitations depending on the microstructure. A presented adopted machining process by cooling with carbon dioxide snow can delay the development of tool wear and offers an increasing tool life and higher stock removal rates.

6:00 PM

Residual Stress Relaxation Effects on the Cracking and Wear Processes of Shot Peened Ti-6Al-4V Titanium Alloy under Fretting-Fatigue Loading: Romain Ferre¹; Siegfried Fouvry²; Bruno Berthel²; Rémi Amargier¹; Antoine Ferre²; ¹SNECMA; ²Laboratoire de tribologie et Dynamique des Systèmes (LTDS)

This study focuses on shot-peened residual stress relaxation of Ti-6Al-4V titanium alloy under fretting-fatigue loading. This study highlights the fretting-fatigue life time increase due to residual stresses. Wöhler curves are plotted for Ti64 and Ti64 shot-peened of a cylinder/plane contact. Next part shows the competition between wear and cracks with "bell curves". Same surface treatments are performed for an industrial flat rounded contact. Shot-peening slow down crack initiation and increase the fatigue life time. For the second part, the used methodology sweeps a large range of fretting displacements and reveals several wear/cracks competition zones on "bell curves". Shot-peening rise is observed on the cracking domain without wear. The second zone presents a life time decrease and relaxation of residual stresses. With larger displacements, wear appears and leads to a life time increase of Ti64 specimens. This effect is not observed with shot-peened tests. The residual tensile zone explains this phenomenon.



T.T. Chen Honorary Symposium on Hydrometallurgy, Electrometallurgy and Materials Characterization: Processing and Properties I

Sponsored by: The Minerals, Metals and Materials Society, TMS Extraction and Processing Division, TMS: Hydrometallurgy and Electrometallurgy Committee, TMS: Materials Characterization Committee

Program Organizers: Shijie Wang, Rio Tinto Kennecott Utah Copper; J. E. Dutrizac, CANMET; Michael Free, University of Utah; J. Y. Hwang, Michigan Technological University; Daniel Kim, Rio Tinto Kennecott Utah Copper

Wednesday PM
March 14, 2012

Room: Oceanic 5
Location: Dolphin Resort

Funding support provided by: Rio Tinto Kennecott Utah Copper, ASARCO, and Freeport McMoRan

Session Chair: Shijie Wang, Rio Tinto Kennecott Utah Copper

2:00 PM

Selecting the Right Filter Media for the Application: William Wilkie¹; Robert Boller¹; ¹Sefar Inc.

There is a wide variety of different types of woven filter media to choose from for hundreds of different filtration applications. Factors such as type of fiber, synthetic polymers used, weave style, fabric finishes and fabrication techniques all play an important part in selecting what is best for a specific type of filter and process application. The purpose of this paper is offer some basic knowledge of these factors and how they can impact the performance of a filter, the life of the media and the overall cost of operation though case studies of actual plant filtration applications.

2:20 PM

Thermodynamic Study for Removal of Phosphorus from Molten Silicon: Takashi Nagai¹; Hideaki Sasaki¹; Masafumi Maeda¹; ¹The University of Tokyo

The production of solar cells is increasing dramatically and the shortage of polycrystalline silicon for these cells has become a serious problem, making development of a low-cost production process for solar grade silicon essential. An electron beam melting technique is known to be effective for the removal of phosphorus from molten silicon. Although the phosphorus is removed by preferential evaporation in this process, the rate of removal is not sufficient, and its improvement requires thermodynamic information on phosphorus in the molten silicon. In this research, the vapor pressure of phosphorus in equilibrium with a silicon-phosphorus alloy was measured by double Knudsen cell mass spectrometry with a system blowing gas into the Knudsen cell. Activity of phosphorus in silicon, Gibbs energy change of dissolution reaction of phosphorus to silicon, and other factors were estimated from the results. Using these data, we provided guidelines on how this process can be improved.

2:40 PM

Fatigue and Fracture Mechanics Characterization of Advanced Automotive Steels: Paolo Matteis¹; Giorgio Scavino¹; Donato Firrao¹; ¹Politecnico di Torino

Advanced, high-strength steel sheets are increasingly used to make lighter cars. These sheets are manufactured by hot rolling, cold rolling and continuous heat-treating, and are cold drawn and welded to fabricate car bodies. This work aims to characterize their fatigue crack growth behavior and their fracture toughness, and to correlate them with microstructures, tensile properties and stress-endurance fatigue properties. Due to the small thickness, the fracture toughness is studied by resistance curve tests. Fracture mechanics properties are not presently considered in car-body design and verification, however, they are prominent in aeronautic design, in which weight is even more important; hence these fracture mechanics

materials data are expected to be required by the car-building industry in future, in pursuit of further weight reduction. For example, knowledge of the steel fatigue crack growth behavior and fracture toughness would allow to evaluate the cracks which could arise from welding defects.

3:00 PM

Kinetic and Thermochemical Analysis of Rubidium Jarosite Decomposition in Alkaline Media: Miguel Perez-Labra¹; Antonio Romero-Serrano²; Eleazar Salinas-Rodriguez³; Erika Avila-Davila³; Guillermo Juarez-Lopez⁴; Juan Hernandez-Avila¹; ¹AACTYM UAEH; ²IPN MEXICO; ³Instituto Tecnológico de Pachuca; ⁴Centro de Investigaciones en Nuevos Materiales Universidad Tecnológica de la Mixteca

Rubidium jarosite was synthesized as a single phase by precipitation from aqueous solution. X ray diffraction and SEM-EDS analysis showed that the synthetic product is a solid rubidium jarosite phase formed in spherical particles with an average particle size of about 35 μm . The chemical analysis showed an approximate formula $\text{Rb}_0.9432\text{Fe}_3(\text{SO}_4)_2.1245(\text{OH})_6$. The decomposition of jarosite in terms of solution pH was thermodynamically modeled using FACTSage by constructing the potential-pH diagram at 298.15 K. The E-pH diagram showed that the decomposition of jarosite leads to a goethite compound ($\text{FeO}\cdot\text{OH}$) together with Rb^+ and SO_4^{2-} ions. The experimental Rb-jarosite decomposition was carried out in alkaline solutions with five different $\text{Ca}(\text{OH})_2$ concentrations. The decomposition process showed a so called "induction period" followed by a progressive conversion period where Rb^+ and SO_4^{2-} ions formed in the aqueous solutions, whereas calcium was incorporated in the solid residue and iron gave place to goethite. The kinetic analysis showed that this process can be represented by the shrinking core chemically controlled model with a reaction order with respect to $\text{Ca}(\text{OH})_2$ equal to 0.4342 and a calculated activation energy of 98.70 kJ mol⁻¹.

3:20 PM Break

3:40 PM

Phase Equilibrium and Characterization Studies of Binary Organic Thermal Energy Storage Materials: Wen-Ming Chien¹; Ivan Gantan¹; Amrita Mishra¹; Dhanesh Chandra¹; Vamsi Kamisetty¹; Prathyusha Mekala¹; ¹University of Nevada, Reno

The binary organic thermal energy storage materials have been performed the phase equilibrium and characterization studies by using high temperature X-ray diffraction (XRD) and differential scanning calorimetric (DSC) methods. The organic thermal energy storage materials undergo a solid-solid state phase transition before melting which will store large amounts of thermal energy. Three materials [tris(hydroxymethyl) aminomethane (TRIS), 2-Amino-2-methyl-1, 3-propanediol (AMPL) and Pentaglycerine (PG)] were used for this study. The binary samples of AMPL-TRIS and AMPL-PG were prepared to perform high temperature XRD characterization and DSC studies. The binary AMPL-TRIS and AMPL-PG phase diagrams were developed. The high temperature solid-state phases of AMPL and TRIS were characterized as a disordered BCC structure, and PG was characterized as FCC. Calculation of Phase Diagrams (CALPHAD) modeling technique is used to calculate the AMPL-TRIS and AMPL-PG binary phase diagrams by using the Thermal-Calc software.

4:00 PM

Laboratory Test Works and Plant Trials for Milling and Flotation of Slow Cooled Copper Slag: Pengfu Tan¹; ¹Xstrata Copper

Laboratory flotation tests of the slow cooled converter slag have showed that 92.5% copper recovery at the copper cut-off grade of 24 – 25 % can be achieved using the 50:50 ratio of DSP330 and SIBX at the natural pH of 7 and grinding time of 18.5 minutes. 70 μm is the P80 achieved at this grinding time. MIBC is the frother and 46% was the solid content in the flotation feed. In the plant trials, 2 types of collectors at 2 different feed particle sizes for both the normal and slow cooled slag were operated. The

particle size was controlled by the feed rate. The P80 of 75 μm at the feed rate between 32 – 36 t/h were tested. The plant trials have demonstrated that the copper recovery in the milling and flotation process of the slow cooled slags have been improved by 3%.

4:20 PM

An Experimental Study of Chemical Oxygen Demand Removal from the Coking Wastewater Using Three-Dimensional Electrode Reactor:

Lei Zhang¹; Gai-Feng Xue¹; J.Y Hwang¹; ¹WISCO

The removal of chemical oxygen demand (COD) from coking wastewater was experimentally investigated using a three-dimensional electrode reactor. The experimental results showed that the refractory organics in coking wastewater can be effectively removed by this process, and COD removal efficiency was affected by the operating parameters, such as electrolytic time, particle electrode dosage, initial pH, current density, aeration amount and electrical conductivity, etc. Experimental results shows that the three-dimensional electrode could have a COD removal efficiency of more than 60% and running cost is no more 6YUAN/t(RMB), which revealed great potential of three-dimensional electrode reactor in engineering application as an advanced treatment of coking wastewater.

4:40 PM

Behavior of Various Impurities during the Precipitation of Hematite from Ferric Sulphate Media at 225°C:

John Dutrizac¹; Tzong Chen¹; ¹CANMET-MMSL

Zinc, cadmium, copper, cobalt and thallium are not significantly incorporated in the hematite precipitates. The nickel contents increase to 0.22% as the Ni concentration increases to 60 g/L. However, part of the Ni may be present as tiny particles of NiSO₄.H₂O. Increasing germanium concentrations to 2,000 mg/L result in products containing up to 0.59% Ge. The Ge occurs either in solid solution in the hematite or is adsorbed on the nanometer-size hematite crystallites. Increasing As(V) concentrations to 10 g/L increase the AsO₄ contents of the products up to 16%. The products consist of hematite together with AsO₄-containing Fe(SO₄)(OH) and an Fe-AsO₄ species. Increasing Se(VI) concentrations to 2.0 g/L cause the SeO₄ content of the products to increase to ~0.5%. All the hematite products contain ~1% SO₄ which appears to be adsorbed on the hematite nanocrystallites composing the micron size hematite products.

5:00 PM

New Process for Granulation of Red Mud and Its Physical Property Assessment:

Shuai-Dan Lu¹; Shaohua Ju¹; Jin-Hui Peng¹; Sheng-Hui Guo¹; Ya-Jian Wang¹; Lei Guo¹; ¹Kunming University of Science and Technology

The granulation of a red mud is of great importance for recycling the waste as adsorption material for waste water or gas. A new granulating process was proposed and its effect is evaluated. To reduce the cost of granulating process, the wet filter cake (containing 25% water) was directly mixed up with different cement content (4%, 6%, 8% and 10% based on wet material). And the mixtures were placed in a moist environment for 4 days, and then were washed with deionized water until the pH value is lower than 9.0. The mudding ratio, surface area and particle size of the aged mixture was detected respectively by bottle shaking experiments, N₂ adsorption equipment and screening. The results showed that the best addition of cement is 8%, with a particle size of lower than 1 mm, mudding ratio of 9.5%, and with an adsorption surface area of about 30 m²/g.

Ultrafine Grained Materials VII: Young Scientist

Sponsored by: The Minerals, Metals and Materials Society, TMS Structural Materials Division, TMS/ASM: Mechanical Behavior of Materials Committee, TMS: Nanomechanical Materials Behavior Committee, TMS: Shaping and Forming Committee
Program Organizers: Suveen Mathaudhu, U.S. Army Research Office; Xiaoxu Huang, Risø National Laboratory for Sustainable Energy, Technical University of Denmark; Hyoung Seop Kim, POSTECH; Terence Langdon, University of Southern California; Terry Lowe, Manhattan Scientifics, Inc.; Ruslan Valiev, Ufa State Aviation Technical University; Xiaolei Wu, Institute of Mechanics, Chinese Academy of Sciences; Michael Zehetbauer, University of Vienna

Wednesday PM

March 14, 2012

Room: Swan 5

Location: Swan Resort

Session Chairs: Justin Scott, Institute for Defense Analysis; Matthias Hockauf, Chemnitz University of Technology; Suveen Mathaudhu, U.S. Army Research Office; Yuntian Zhu, North Carolina State University

2:00 PM

3D-Architecturing Aluminium Sheets by ARB Processing with Graded Copper Particle Reinforcement:

Christian W. Schmidt¹; Mathis Ruppert¹; Patrick Knödler¹; Heinz Werner Höppel¹; Mathias Göken¹; ¹Friedrich-Alexander-Universität Erlangen-Nürnberg

In this work copper particles ($d \sim 1 \mu\text{m}$) are introduced in a highly controlled manner by airgun spraying from aqueous suspension into aluminium AA1050A during ARB. A 3D-architecture by controlling spatial distribution of particles is demonstrated. In sheet plane, spraying distance and feed rate of the air spray gun are used to control the particle content. In sheet height certain distributions including homogeneous and stepwise graded distributions are generated by a smart stacking sequence during ARB processing. In the system Al-Cu continuous and stepwise gradation of particle distribution are proven by solutionizing and subsequent mechanical testing as well as through visualisation by micro-computer-tomography. With this freedom of design concerning particle distribution, the material properties of ultrafine-grained sheets can be adjusted within one tailored sheet in a certain range with a desired 3D-profile. In the case of Al-Cu a combination of high strength with high electrical conductivity is exemplarily demonstrated.

2:15 PM

Advantageous Anisotropy: Designed Performance in Mg Alloy:

David Foley¹; Sonia Modarres-Razavi¹; Suveen Mathaudhu²; Laszlo Kecskes³; Ibrahim Karaman¹; K. Hartwig¹; Vince Hammond³; ¹Texas A&M University; ²US Army Research Office; ³US Army Research Laboratory

One general characteristic of wrought Mg alloys is a strong texture developed during forming. These strong textures, combined with high critical resolved shear stress ratios between deformation mechanisms, result in large mechanical anisotropy. While some alloying elements and processing conditions can weaken this texture and encourage more isotropic deformation, this is not always desirable. For example, if component failure is only expected under only one loading direction, enhanced performance in that deformation condition may be advantageous even at the expense of others. This talk will cover SPD and post-SPD thermomechanical processing methods to engineer mechanical response in AZ31B. Strain path and temperature control result in high strength UFG materials with twice the strength of the starting wrought material.



TMS 2012

141st Annual Meeting & Exhibition

2:30 PM

Analysis of Microstructure and Microhardness of Zr-2,5%Nb Processed by High Pressure Torsion (HPT): *Mychelle Comphanoni¹; Jose Matheus¹; Andre Pinto²; ¹Military Institute of Engineering (IME); ²Brazilian Center for Physics Research (CBPF)*

Nanostructured materials have been widely studied due the improvement of their mechanical properties comparing to coarse grain materials. The present work intended to analyze the microstructure and microhardness of Zr-2,5%Nb processed by high-pressure torsion (HPT), one of the severe plastic deformation (SPD) techniques. The deformations were carried out at room temperature using a pressure of 5 GPa and five anvil turns. Vickers indentation was used to evaluate the microhardness of the samples. Transmission electron microscope (TEM) and X-ray diffraction were used to analyze the microstructure. The results showed a significant refinement from the initial microstructure achieving nanometric grain size lower than 50 nm and phase transformation $\alpha \rightarrow \omega$ induced by shear. The Vickers microhardness values of material submitted to HPT technique were significantly higher than non-deformed material. Also, HPT procedure resulted in a huge grain refinement of the material and phase transformation.

2:45 PM

Combining Extrusion and ECAP – an Efficient Processing Route for Large Scale UFG Materials: *Philipp Frint¹; Matthias Hockauf¹; Thorsten Halle¹; Gernot Strehl²; Martin F.-X. Wagner¹; Thomas Lampke¹; ¹Chemnitz University of Technology; ²S+C Extrusion Tooling GmbH*

The use of ultrafine-grained materials processed by equal-channel angular pressing (ECAP) in industrial applications is limited because of the small volumes of the billets and difficulties in integrating them into conventional extrusion processes. Here, we propose a combination of extrusion and large scale ECAP (cross section: 50mm x 50mm) performed at room temperature as an efficient two-step process followed by a suitable heat treatment. We demonstrate that, for the aluminum alloy 6060, an improvement of yield and tensile strengths by up to 20% can be achieved – without a further reduction of ductility – compared to “conventionally” ECAPed material. Microstructural analysis shows that this excellent combination of strength and ductility can be related to the beneficial effects of fine precipitates, ultrafine grains and a recovered microstructure. These results highlight the potential of our combined ECAP/extrusion process for the production of homogenous, high performance aluminum materials on an industrial scale.

3:00 PM

Consolidation of Nanostructured Copper and Copper Based Alloys via High Pressure Torsion: *Hamed Bahmanpour¹; Daria Setman²; Jelena Horky²; Michael Kerber²; Susi Kahofer²; Suhrit Mula¹; Michael Zehetbauer²; Ronald Scattergood¹; Carl Koch¹; ¹North Carolina State University; ²Faculty of Physics, University of Vienna*

Samples of pure Cu, and Cu alloyed with Zn and Nb were processed by high energy ball milling. Small flakes with homogeneous nanostructures revealing grain sizes below 40nm were produced after milling at 77K. The milled flakes were used as a precursor for consolidation with high pressure torsion (HPT). The resulting samples were analyzed by means of XRD, TEM and mechanical tests not only comprising microhardness but also tensile tests. HPT processing yielded entirely flaw-free samples with only slightly increased grain sizes provided more than 50 revolutions and hydrostatic pressures of about 8 GPa were carried out. For example, those samples exhibited values of UTS up to 892 MPa (Cu) and 1240 MPa (Cu-10%Zn), and values of tensile strain up to 5.8% (Cu) and 10% (Cu-10%Zn), which all seem to be outstanding compared to data published so far in literature on SPD consolidated powder materials.

3:15 PM

Effects of Post Process Treatments on the Mechanical Stability of Rolled Nanostructured Aluminum: *Jacob Kidmose¹; Lei Lu²; Grethe Winther¹; Niels Hansen¹; Xiaoxu Huang¹; ¹Risø DTU; ²Institute of Metal Research*

Nanostructured aluminum produced by cold rolling to high strains shows an early onset of localized necking causing a low ductility during straining in tension. In order to improve the properties, post-process treatments such as annealing and cold deformation have been applied to aluminum sheets produced by accumulative roll bonding. The treatments have been followed by tensile testing where in-situ high resolution maps of the strain distribution over the tensile sample gauge length and thickness have been obtained by using a commercial ARAMIS system. These maps allow localized and diffuse necking to be characterized and to obtain correlation between the mechanical behavior and the structural changes being a result of the post-process treatments.

3:30 PM

Nanoindentation Analysis for Local Properties of Ultrafine Grained Copper Processed by High Pressure Torsion: *Hyeok Jae Jeong¹; Eun Yoo Yoon¹; Nack Joon Kim²; Hyeong Seop Kim¹; ¹Department of Materials Science and Engineering, POSTECH, Korea; ²Graduate Institute of Ferrous Technology, POSTECH, Korea*

Recently, severe plastic deformation (SPD) techniques have been available for producing bulk UFG metallic materials. High pressure torsion (HPT) leads to smaller microstructures than those achieved using the other SPD processes because of its higher strain. It is known that HPT processed metals show highly heterogeneous not only along radius due to the nature of torsional deformation but also through the thickness. Since the sample size for the HPT is small, the local properties of the HPT processed samples have not been investigated yet. Recently we propose a method converting the nanoindenting curve to stress-strain curve combining the finite element method and the recursion method. In this presentation, we employ the nanoindentation technique in order to elucidate the local mechanical properties especially stress-strain curves. This work was supported by the National Research Foundation of Korea (NRF) grant funded by the Korea government (MEST) (No. 2010-0026981).

3:45 PM Break

4:00 PM

Strengthening of Al through Addition of Fe and by Processing with High-Pressure Torsion: *Jorge Cubero-Sesin¹; Zenji Horita¹; ¹Kyushu University*

Iron (Fe) is a common impurity element in aluminum (Al) and is expected to be used in a controlled manner. In this work, High-Pressure Torsion (HPT) was applied to 10 mm in diameter bulk disk-type samples of Al-Fe alloys with different Fe weight fractions: 0.5%, 1%, 2% and 4%, and initial states: as-cast, extruded, and annealed at 500°C for 1 hour. Powder samples were also consolidated in the HPT facility with similar Fe contents including an additional 10% Fe. HPT was carried out at room temperature under a pressure of 6 GPa for several numbers of revolutions: 1, 10, 20, 50 and 75. Vickers microhardness and tensile tests were performed on specimens extracted from the disks. Microstructural analyses by transmission electron microscopy and x-ray diffraction revealed significant potential to improve mechanical properties via microstructure refinement, supersaturation of Fe and dispersion of intermetallic phases throughout the Al matrix.

4:15 PM

Structural Parameters and Strengthening Mechanisms in Cold-Drawn Pearlitic Steel Wires: *Xiaodan Zhang¹; Andy Godfrey²; Xiaoxu Huang³; Niels Hansen³; ¹Tsinghua University, Risø DTU; ²Tsinghua University; ³Risø DTU*

Pearlitic steel wires have a nanoscale structure and a strength which can reach 5 GPa. In order to investigate strengthening mechanisms, structural parameters including interlamellar spacing, dislocation density and

cementite decomposition, have been analyzed by transmission electron microscopy and high resolution electron microscopy in wires cold drawn up to a strain of 3.7. Three strengthening mechanisms, namely boundary strengthening, dislocation strengthening and solid solution hardening have been analyzed and good agreement has been found between the measured flow stress and the value estimated based on an assumption of linear additivity of the three contributions.

4:30 PM

Study of Grain Boundary Weakening using In-Situ Synchrotron X-Ray Diffraction of Ultrafine Grained Materials: *Jennifer Girard*¹; Jiuhua Chen¹; Helen Couvy²; Xiaoyang Liu³; ¹Florida International University; ²University of Michigan; ³Jilin University

When size of crystal grain decreases down to nanometers, volume fraction of near surface atoms becomes significant. Comparative in situ synchrotron x-ray diffraction at high pressures on micron and nano crystalline powder samples has been conducted to determine the effective bulk modulus of grain boundary. The volume vs. pressure data of the micron and nano specimens obtain from the x-ray diffraction are used to determine their bulk moduli through equation of state. Using a shell/core grain model, the bulk modulus of grain boundary is derived from the moduli of micron-size sample and nano-size sample (representing significant contribution from the shell). The result indicates that the bulk modulus of grain boundary is remarkably smaller than that of the core, by 37% in magnesium silicate, Mg₂SiO₄, and by near 50% in metal(Ni). While strengthening by smaller grain size is expected by Hall-Petch law, these results reveal an inverse Hall-Petch relation.

4:45 PM

Understanding the Ultrafine Grain Formation and Recrystallization Mechanisms in Magnesium through Extrusion-Machining: *Mert Efe*¹; Dinakar Sagapuram¹; Wilfredo Moscoso²; Srinivasan Chandrasekar¹; Kevin Trumble¹; ¹Purdue University; ²Pontificia Universidad Catolica Madre y Maestra

Large Strain Extrusion Machining (LSEM), a constrained chip formation SPD process, is demonstrated as a method for producing ultrafine grained sheet/foil of magnesium AZ31. Temperature is varied locally in the deformation zone through adiabatic heating due to the high strain rate nature of the process. Ultrafine grain formation and recrystallization mechanisms responsible for various microstructures are explained as a function of temperature and strain rate. Continuous dynamic recrystallization (CDRX) is shown to operate at low temperatures (below 170°C) and results in ultrafine grain sizes (100-200 nm), high hardness values (120 HV) and non-basal textures. At high temperatures (above 170°C), the recrystallization mechanism switches to discontinuous dynamic recrystallization (DDRX), which results in fine grain sizes (2-3 µm), low hardness (50 HV) and basal-type textures. Implications for formability and mechanical properties will be discussed.

5:00 PM

Reinforcement Phase Size Effects on a Cryomilled Al - B₄C Nanocomposite: *Henry Yang*¹; Troy Topping¹; Zhihui Zhang¹; Enrique Lavernia¹; Julie Schoenung¹; ¹University of California Davis

Cryomilled Al 5083 - boron carbide (Al-B₄C) metal matrix composites (MMCs) are of interest due to their light weight and high strength. Cryomilling is a mechanical milling process during which the powder is ball milled in a liquid nitrogen slurry at cryogenic temperatures. In

addition to generating nanocrystalline powder, cryomilling breaks up the nascent oxide layer on the as-received Al powder and introduces nitrides into the microstructure. The dispersed nano-metric inclusions enhance the thermal stability of the powder for subsequent consolidation and thermomechanical processing, ensuring the MMC retains an ultra-fine grained (UFG) microstructure. In this study, the effect of milling time, B₄C particle size, and consolidation variables on the microstructure and mechanical properties of consolidated bulk nanocomposites was investigated. Specific attention was placed on the differences resulting from the incorporation of 0.5 µm and 6 µm B₄C particulates. The relationship between microstructure and mechanical properties of the nanocomposites are discussed.

5:15 PM

Homogenizing Process and Strain Hardening Behavior of a Two-Phase Cu-Ag Alloy Processed by High-Pressure Torsion (HPT): *YZ. Tian*¹; Z.F. Zhang¹; R.B. Figueiredo²; N. Gao³; T.G. Langdon⁴; ¹Institute of Metal Research, Chinese Academy of Sciences; ²Federal University of Minas Gerais; ³University of Southampton; ⁴University of Southern California

Disks of a two-phase Cu-28 wt.% Ag alloy were processed by high-pressure torsion (HPT) from 1 to 20 revolutions to reveal the microstructural evolution and the mechanical properties. It is shown that the deformation starts at the outer region of the disks in the form of local vortices and then spreads inwards with increasing the number of revolutions. Deformation patterns were also observed near the center of the disk after HPT for 20 revolutions. It is found that the Cu-Ag alloy displays a much stronger strain hardening capability than Cu due to a continuous refinement of the microstructure. A two-stage Hall-Petch relationship was obtained for the Cu-Ag alloy which is attributed to the development of multiple strengthening mechanisms.

5:30 PM

Microhardness and Microstructural Evolution in Cu-Zr Alloy after High-Pressure Torsion Processing: *Jitraporn Wongsan-Ngam*¹; Megumi Kawasaki¹; Terence Langdon¹; ¹University of Southern California

A copper alloy, Cu-0.1% Zr, was subjected to severe plastic deformation at room temperature using the procedure of high-pressure torsion. Disks were strained through different numbers of revolutions up to 10 turns with an applied pressure of 6.0 GPa in order to examine the evolution of hardness and microstructure. Microhardness results reveal lower values in the center regions in the early stages and there is a high degree of hardness homogeneity after 5 and 10 turns. For these conditions, the average grain sizes and the distributions of grain boundary misorientations are similar in the center and at the periphery of the samples. It is shown that there is a gradual evolution in both hardness and microstructure with increasing numbers of turns.



Ultrasonic Fatigue of Advanced Materials and Systems: Ultrasonic Fatigue of Metals and Alloys II; Very High Cycle Fatigue of Composites and MEMS

Sponsored by: The Minerals, Metals and Materials Society, State Research Center for Mathematical and Computational Modelling, University of Kaiserslautern, Germany, State Research Focus "Advanced Materials Engineering", University of Kaiserslautern, Germany, TMS Light Metals Division, TMS Structural Materials Division, TMS: Advanced Characterization, Testing, and Simulation Committee, TMS/ASM: Computational Materials Science and Engineering Committee, TMS: Materials Characterization Committee, TMS/ASM: Mechanical Behavior of Materials Committee, TMS: Young Leaders Committee

Program Organizers: Frank Balle, University of Kaiserslautern; Dietmar Eifler, University of Kaiserslautern; Guntram Wagner, University of Kaiserslautern

Wednesday PM
March 14, 2012

Room: Europe 1
Location: Dolphin Resort

Session Chairs: J. Wayne Jones, University of Michigan (USA); Hans-Juergen Christ, University of Siegen (Germany)

2:00 PM

Very High Cycle Fatigue (VHCF) Behavior of Sn-Rich (Pb-Free) Solder Joints: *Martina Zimmermann*¹; Kyle Yazzie²; Martin Cremer¹; Hans-Juergen Christ¹; Nikhilesh Chawla²; ¹Universitaet Siegen; ²Arizona State University

Solders are an integral part of electronic packaging. Recently, there has been a significant drive to replace Pb-Sn solders with Pb-free, environmentally-benign solders. Given the widespread use of Pb-Sn solder in the manufacture and assembly of circuit boards, a fundamental understanding of microstructure evolution and deformation behavior of Pb-free solders is crucial for the successful substitution of these materials in the electronics industry. Reliability of electronic devices is controlled by fatigue behavior at very high frequencies due to mechanically induced vibrations during application. However, damage evolution during cyclic deformation in the VHCF range has not yet been investigated. In this study soldered Sn-rich alloys/Cu samples were tested by means of ultrasonic fatigue testing. This technique enabled a peak stress amplitude to be applied solely in the center region of the specimen allowing a systematic evaluation of the effect of the microstructural features on fatigue life beyond $N > 10E7$ cycles.

2:20 PM

Ultrasonic Fatigue of Ti6Al4V in the Very High Cycle Fatigue Regime: Stefan Heinz¹; Guntram Wagner¹; Frank Balle¹; *Dietmar Eifler*¹; ¹University of Kaiserslautern

At the Institute of Materials Science and Engineering of the University Kaiserslautern an ultrasonic testing facility (UTF) was developed to perform experiments in the VHCF regime. The individual design of the testing facility allows to control the process parameters and to measure the relevant fatigue data in detail. Furthermore for the first time high resolution 3D-laser measurements were carried out to describe the oscillation behavior of ultrasonic fatigue specimens under load. To investigate the fatigue behavior in the VHCF-regime load increase tests were performed with the titanium alloy Ti6Al4V. Based on the high-frequency measurements of the displacement of the specimen at their free end a correlation between the frequency and the actual fatigue state was realized. In constant amplitude tests cyclic deformation curves as well as damping curves of Ti6Al4V in the range 10^{10} were determined.

2:40 PM Invited

Combining Ultrasonic Fatigue with Synchrotron X-radiography and in situ Nonlinear Ultrasonic Measurements to Detect Crack Initiation: *Naji Hussein*¹; Clinique Brundige¹; Anish Kumar¹; Tresa M. Pollock¹; J. Wayne Jones¹; ¹University of Michigan

Ultrasonic fatigue testing provides an excellent method to examine the unique nature of crack initiation and early crack propagation in the very high cycle fatigue regime. This presentation reviews two recently developed in situ techniques for examining fatigue crack initiation and early crack propagation during ultrasonic fatigue in a wide range of structural alloys. In the first case, a technique has been developed to allow in situ imaging of propagating fatigue cracks by synchrotron x-ray imaging. The technique involves employing a "carrier specimen" cycling in resonance at 20kHz to which is attached a foil specimen ranging in thickness from 100-300µm. Examples from crack propagation nickel base superalloys, aluminum and magnesium alloys will be described. In the second case, a technique for in-situ characterization of fatigue damage accumulation and the crack initiation lifetime using nonlinear ultrasonic measurements via analysis of the feedback signal of a closed-loop ultrasonic fatigue system is described.

3:00 PM

In-Situ Characterization of the Damage Evolution of Welded Aluminum Alloy Joints during Very High Cycle Fatigue (VHCF) with Nonlinear Ultrasonic Technique: *Martin Cremer*¹; Martina Zimmermann¹; Hans-Jürgen Christ¹; ¹University Siegen

Fatigue behaviour in the very high cycle range is dominated by local plastic deformation caused predominantly by microstructural defects. In case of welded joints process-related imperfections such as pores, hot cracks or incomplete fusions act as local stress raisers, leading to a pronounced scattering of fatigue results. Depending on the severity of the defect-related notch effect, VHCF life is dominated by the stress concentration factor, the remaining cross section and the corresponding crack growth behaviour. With crack propagation emanating from the specimen's interior, a characterization of crack growth behaviour with conventional optical methods is impossible. In the given study welded samples from the aluminium alloy EN AW 6082 are tested by means of ultrasonic fatigue testing, thus reaching number of load cycles $N > 10E8$. Damage evolution, i.e. crack growth, is characterized in-situ by the change in higher harmonics registered by the non-linear feedback signal of the ultrasonic system.

3:20 PM Break

3:40 PM

Ultrasonic Fatigue of Aluminum Matrix Composites (AMC) in the VHCF-Regime: *Guntram Wagner*¹; Matthias Wolf¹; Dietmar Eifler¹; ¹University of Kaiserslautern

At the Institute of Materials Science and Engineering of the University of Kaiserslautern ultrasonic testing facilities (UTF) are used to perform fatigue experiments in the VHCF-regime. With the UTF it is possible to characterize the actual fatigue state by changes of different process parameters such as the generator power, the dissipated energy or the oscillation amplitude. Furthermore the experiments can be interrupted to investigate the formation of intrusions or extrusions as well as changes of the electrical resistance. With the UTF load increase as well as constant amplitude tests can be realized. The microstructure of the investigated AMC was characterized by EDX- and EBSD-analysis and consists of an AlCu4Mg1 (AA2124) matrix reinforced with 25 vol. % SiC particles. The appropriate geometry for the ultrasonic fatigue specimens was determined by FE-simulations based on ABAQUS CAE.

4:00 PM

Ultrasonic Fatigue Testing System Combined with Nondestructive Online Testing for Carbon Fiber Reinforced Composites: *Frank Balle¹; Daniel Backe¹; Thomas Helfen²; Ute Rabe²; Sigrun Hirsekorn³; Dietmar Eifler¹; Christian Boller³; ¹University of Kaiserslautern; ²Saarland University; ³Fraunhofer Institute for Nondestructive Testing, Saarbrücken, Germany*

The fatigue properties of carbon fiber reinforced polymers (CFRP), especially in the Very High Cycle Fatigue (VHCF) regime, are rarely investigated. To analyze the VHCF properties and the specific failure mechanisms of CFRP a new ultrasonic testing system for 3 and 4-point cyclic bending in combination with nondestructive online testing was developed. The oscillation to realize cyclic bending is generated by an ultrasonic resonance system with a frequency of 20 kHz at a stress ratio of $R > 0.1$. As a representative material a carbon fiber reinforced polyphenylsulfide (CF-PPS) has been chosen. The fatigue process is split up in pulse and pause sequences to hold the specimen in a temperature range well below the glass transition temperature. The current fatigue status of the specimen during ultrasonic testing will be detected via thermography, laser vibrometry, microwave analysis and non-linear ultrasound techniques.

4:20 PM

Small-Scale Multiaxial Fatigue Experiments in the Very High Cycle Regime: *Thomas Straub¹; Tobias Kennerknecht¹; Paulin Robin²; Morgan Tort²; Geoffroy Kieffer²; Yuri Lapusta²; Christoph Eberl¹; ¹Karlsruhe Institute of Technology (KIT); ²French Institute of Advanced Mechanics (IFMA)*

Small-scale fatigue takes place in many applications such as micro-electro-mechanical-systems, surface acoustic wave devices and microelectronics, in which cyclic loading leads to failure. Multiaxial fatigue experiments with micro samples at kHz frequencies require novel experimental setups. Therefore, resonant micro fatigue systems for uniaxial and multiaxial cyclic loading have been developed. Finite Element simulations have shown that dimensions of the samples can be chosen in a way that the resonant frequencies of bending and torsional modes are very close, which is a requirement for multiaxial cyclic loading. For the initial tests, samples made from copper, aluminium, or nickel with a rectangular cross section of 500 μm by 200 μm have been used. Hence, scaling and size effects are expected to dominate reliability of such components. The recent experiments show that the resolution of the resonant system allows to observe and study the initiation of slip bands and short cracks.

4:40 PM

High and Very High Cycle Fatigue in Al and Cu Thin Films on Si Substrate: *Sofie Burger¹; Christoph Eberl¹; Alexander Siegel²; Alfred Ludwig²; Oliver Kraft¹; ¹Karlsruhe Institute of Technology; ²Ruhr-Universität Bochum*

In technical applications like MEMS devices thin films undergo cyclic loading and will fail eventually due to fatigue. The mechanisms in the high cycle and very high cycle fatigue regime are still not well understood, although the mechanical properties of thin films have been studied extensively in the past years. To better understand these mechanisms we investigate the fatigue processes by a novel resonant bending fatigue setup for thin films on Si cantilever substrates after up to 10^9 cycles. The cyclic bending of the Si substrate induces a strain amplitude gradient in the thin film. The maximum can be found at the fixed end and the in situ observation of the damage front allows to derive one lifetime diagram per cantilever. We investigated the microstructural evolution in pure Al and Cu during fatigue. All films show extrusion and pore formation but differ in shape and number, which will be discussed.

5:00 PM

Environmental Effects on Fatigue Crack Initiation in the HCF and VHCF Regimes for LIGA Ni Thin Films: *Eva Baumert¹; Olivier Pierron¹; ¹Georgia Tech*

The present study investigates the fatigue degradation properties of 20-micron-thick, electrodeposited Ni films (columnar microstructure) in a mild (30° C, 50% RH) and humid (80° C, 90%RH) environment, using Ni MEMS micro-resonators. The specimens are tested under bending and subjected to fully-reversed loading at resonance (~8 kHz) for a large range of strain amplitudes encompassing the HCF and VHCF regimes. The change in resonant frequency resulting from a change in compliance of the structure is monitored throughout the fatigue tests. In addition, the fatigued sidewalls of the Ni thin films are periodically observed using SEM to detect the onset of fatigue crack initiation. It is found that the resonant frequency provides an accurate metric for detecting the degree and rate of fatigue crack initiation in the Ni thin films. The influence of the environment on the fatigue properties and the implications on reliability of Ni MEMS devices will be discussed.

5:20 PM Concluding Comments Dietmar Eifler, Symposium organizer

Wettability and Interfacial Phenomena between Metals and Ceramic/Refractory Materials: Session I

Sponsored by: The Minerals, Metals and Materials Society, TMS Materials Processing and Manufacturing Division, Not Applicable
Program Organizers: Martin Pech-Canul, Centro de Investigacion y de Estudios Avanzados del Instituto Politecnico Nacional; Golam Newaz, Wayne State University; Tapas Laha, Indian Institute of Technology Kharagpur; Zariff Chaudhury, Materion Corporation

Wednesday PM
March 14, 2012

Room: Macaw 1
Location: Swan Resort

Session Chairs: Martin Pech-Canul, Cinvestav Saltillo; Zariff Chaudhury, Materion Corporation; Tapas Laha, Indian Institute of Technology Kharagpur

2:00 PM

Chemical Wear of Basic Brick Linings in the Non-Ferrous Industry: *Dean Gregurek¹; Alfred Spanring¹; Marcus Kirschen; Christian Majcenovic¹; ¹RHI AG*

In the non ferrous metals industry particularly in the copper and lead smelting furnaces the working lining made of magnesia-chromite bricks is exposed to several stresses. These can be classified as chemical, thermal and mechanical stresses occurring as a single wear factor or in combination. The chemical factors include corrosion caused by slag and/or gaseous SO₂ diffusion, redox effects and hydration. In most of the non-ferrous metallurgical processes the chemothermal load by Fe-silicatic slags of fayalitic type is a common wear mechanism of the magnesia-chromite bricks. Nevertheless the extraordinary massive SiO₂-supply caused by changes in the processing and the uncontrolled addition of silica sand results in a severe formation of forsterite respectively in a volume expansion due to "forsterite bursting". Such a wear phenomenon is experienced seldom in the non-ferrous applications but quite typical for the regenerator chamber in the glass industry in case of extreme SiO₂ supply ("carry over").

2:20 PM

Diffusion Bonding between Ti₃SiC₂ and NiTi Shape Memory Alloy: *Ankush Kothalkar¹; Patrick Mahaffey¹; Sandip Basu¹; Miladin Radovic¹; Ibrahim Karaman¹; ¹Texas A&M University*

Diffusion kinetics and bonding between Ti₃SiC₂ and NiTi is studied in the range of 800 to 1200°C. The microstructure of the interfacial layer, formed at different temperatures and after different bonding times, has



TMS 2012

141st Annual Meeting & Exhibition

been characterized using scanning electron microscopy and microprobe elemental analysis to determine its phase composition and mechanism of diffusion bonding. At 1200°C, the bonding mechanism observed is liquid phase whereas solid state diffusion bonding was observed at lower temperatures. The interfacial layers form by diffusion of Si from Ti_3SiC_2 into the interface and its subsequent reaction with NiTi to form Ni-Ti-Si ternary phases. Elastic modulus and hardness of different phases present in the interfacial layer are determined using nanoindentation. Vickers hardness data shows considerably higher hardness at the interface layer compared to both Ti_3SiC_2 and NiTi. However, the absence of any significant cracking near the indents confirms a high fracture toughness of the interfacial bonding phase.

2:40 PM

Effect of Surface Modification of Al₂O₃ Particles on the Microstructure and Mechanical Properties of Al-Al₂O₃ Nanocomposites: *Hossein Beygi¹; Seyyed Abdalkarim Sajjadi¹; Seyyed Mojtaba Zebarjad¹; ¹Ferdowsi University of Mashhad*

Aluminum matrix composites containing dispersed Al₂O₃ nanoparticles are widely prepared through stir casting method; however in this method wettability of reinforcement particles within the matrix melt is really poor. In this study in order to improve wettability of Al₂O₃ particles in Al matrix, surface of Al₂O₃ particles (50nm diameter) were modified with metallic Cu layer (20nm thickness) by using two step electroless coating techniques. Subsequently Cu coated Al₂O₃ particles were annealed at temperature of 450 °C and then injected into the molten Aluminum. Nanocomposite samples containing different weight percentage of Al₂O₃ particles were prepared by stir casting. Products were characterized using SEM, TEM and EDX. The results show when copper coated particles are applied, reinforcement wetting by molten matrix significantly improves, strong interfacial bonding appeared due to the formation of CuAl₂ intermetallics in matrix/reinforcement interface, reinforcement's segregation limited and uniform distribution of Al₂O₃ nano particles within Al matrix observed.

3:00 PM

Study on Wettability of Cu and 85Cu-15Ni Alloy on 18NiO-NiFe₂O₄ Composite Ceramics: *Jinjing Du¹; Yihan Liu¹; Guangchun Yao¹; Zhigang Zhang¹; Guoyin Zu¹; ¹Northeastern University*

The wetting wettability of Cu, 85Cu-15Ni alloys on 18NiO-NiFe₂O₄ composite ceramics was investigated by a sessile drop method. The contact angles of the two metal systems on the ceramic matrix were measured in various temperatures with time. The results show that 85Cu-15Ni alloy exhibits a better wetting ability on 18NiO-NiFe₂O₄ composite ceramics than that of Cu. With introducing 1wt% MnO₂ into the 18NiO-NiFe₂O₄ composite ceramic substrates, the wettability between Cu, 85Cu-15Ni alloy(s) and substrate is improved. In addition, the morphology of metal/ceramic interface is observed by means of scanning electron microscopy (SEM), X-ray diffraction (XRD), and energy dispersive spectroscopy (EDS). Observation of 85Cu-15Ni alloy /ceramic interface shows a good solubility between Cu and Ni in the droplet, and partial Cu diffused into the NiFe₂O₄ substrates.

3:20 PM

Wetting and Wicking Behavior of Refractory Coatings Used in Lost Foam Casting: *Robin Woracek¹; Indraneel Sen¹; Dayakar Penumadu¹; ¹University of Tennessee*

The wetting and wicking behavior of polymer melts with refractory coatings (Mica and Silica based), as used in the Lost Foam Casting (LFC) process for obtaining near net shape aluminum castings, are characterized in this study. Refractory coating applied on the Expanded Polystyrene (EPS) foam pattern surface plays a key role in controlling the metal flow and overall success of the LFC process, as the EPS foam pyrolysis takes place while the casting mold is being filled. An experimental system, incorporating a modified Wilhelmy plate technique, was custom developed for investigating the dynamic advancing and receding force between PS melt and coated probe and the related hysteresis loop. Results associated with polymer surface tension and advancing/receding contact angles for PS melts at temperatures between 220-300°C, where they show pronounced viscoelastic behavior, are included. The experimental system is well suited to study nearly any liquid-solid interface for temperatures between 0-800°C.

3:40 PM

Interfacial Reactions in the Liquid/Solid and Liquid/Vapor Interfaces of Al-Si-Mg Alloys and B12 (Bc2) Substrates: *Oziel Herrera-Romero¹; Martin Pech-Canul¹; Zariff Chaudhury²; Golam Newaz³; ¹Centro de Investigacion y de Estudios Avanzados del Instituto Politecnico Nacional; ²Arkansas State University; ³Wayne State University*

Interfacial reactions between the Al-6 Si-14 Mg alloy and B12 (BC2) substrates were studied in wettability tests by the sessile drop technique using an L8 Taguchi experimental design. Specimens of the alloy in the form of cubes were placed on boron carbide substrates prepared by the uniaxial compaction of B12 (BC2) powders. Sessile drop tests were conducted varying the following parameters: temperature (1000 and 1200 °C), time (90 and 120 min), atmosphere (N₂ and Ar \149; N₂), and substrates prepared with uncoated and coated powders with colloidal SiO₂. The contact angles were measured from photographs, the interfaces were characterized by XRD and SEM, and the thermodynamic feasibility of possible reactions in the system was determined using the HSCTM software and data bases. The nonwetting contact angles observed and the detachment of the metal drop from the substrate can be attributed to the formation of MgO and Al₂O₃ on the meniscus surface.

WEDNESDAY PM

2012 Functional and Structural Nanomaterials: Fabrication, Properties, Applications and Implications: Joint Session with "2012 Surface and Heterostructures"

Sponsored by: The Minerals, Metals and Materials Society, TMS Electronic, Magnetic, and Photonic Materials Division, TMS: Nanomaterials Committee

Program Organizers: Jiyoung Kim, University of Texas; David Stollberg, Georgia Tech Research Institute; Seong Jin Koh, University of Texas at Arlington; Nitin Chopra, The University of Alabama; Terry Xu, UNC Charlotte

Thursday AM
March 15, 2012

Room: Pelican 1
Location: Swan Resort

Session Chair: Nitin Chopra, University of Alabama

8:30 AM Invited

Modification of Micro-Stereolithography-Fabricated Microneedles Using Pulsed Laser Deposition: Shaun Gittard¹; Philip Miller¹; Chunming Jin¹; Timothy Martin¹; Ryan Boehm¹; Bret Chisholm²; Shane Stafslie²; Justin Daniels²; Nicholas Cilz²; Nancy Monteiro-Riviere³; Adnan Nasir⁴; *Roger Narayan*¹; ¹Univ of North Carolina & North Carolina State Univ; ²North Dakota State University; ³North Carolina State University; ⁴University of North Carolina

Hollow microneedles are small-scale hypodermic needle-like structures, which may be used for transdermal delivery of nucleic acid-containing agents, protein-containing agents, and other pharmacologic agents. Translation of microneedles to clinical use would benefit from the development of cost-effective microneedle fabrication techniques. A rapid prototyping technique known as visible light dynamic mask micro-stereolithography was used to create solid microneedle arrays; this technique uses digital light projection to selectively polymerize a liquid resin. Pulsed laser deposition was then used to deposit silver and zinc oxide thin films on the surfaces of the visible light dynamic mask micro-stereolithography-fabricated acrylate-based polymer microneedle arrays. In vitro studies were used to demonstrate the antimicrobial activity of the silver- and zinc oxide-coated microneedle array structures. This work shows that visible light dynamic mask micro-stereolithography and pulsed laser deposition may be used to create antimicrobial microneedles for treating local skin infections.

9:05 AM

Nanosphere Lithography of Co/Pd Multilayer Film for Advanced Media: *Suzanne Kornegay*¹; Shraeyansh Thakur¹; Erica Barnes¹; Anondo Bannerjee¹; Marelly Villanueva¹; Hao Su¹; Zhenzhong Sun¹; Dawen Li¹; Subhadra Gupta¹; ¹The University of Alabama

We reported for the first time nanosphere lithography (NSL) of perpendicular anisotropy Co/Pd multilayer film for advanced media application. NSL is an inexpensive patterning technique that includes the formation of a monolayer of polystyrene spheres, shrinking of the nanospheres, and then ion milling of the film into nanopillars with reduced nanospheres acting as a mask. Polystyrene nanospheres were shrunk under different conditions of oxygen plasma ashing. Field emission scanning electronic microscopy (FESEM) and X-ray diffraction (XRD) were employed to observe the morphology and the crystal structure respectively of magnetic nanocolumn arrays. Alternating gradient magnetometer (AGM) was used to characterize the magnetic properties, such as Mst, Mrt and squareness of patterned films and correlated structural properties. We have developed a hard mask technique compared with NSL to further decrease the nanopillar size to ~10nm for improved recording density.

9:20 AM

Optimization of CoPt-AIN Granular Media for High Density Applications: *Hao Su*¹; Anusha Natarajarathinam¹; Elizabeth Philip¹; Kristy Tippey¹; Subhadra Gupta¹; ¹The University of Alabama

The effects of AIN volume and thermal annealing on CoPt-AIN granular media have been studied. CoPt/AIN multilayers were first deposited, and then thermally annealed to fabricate the granular media. AIN layers were deposited by reactive sputtering from an Al target while CoPt was co-sputtered using cobalt and platinum targets. Various ratios of Co and Pt, ranging from Co80Pt20 to Co50 Pt50, were used to deposit CoPt-AIN multilayers with different thicknesses of AIN layers, after which they were post-deposition annealed in vacuum from 300 to 600 °C. X-ray diffraction (XRD), transmission electron microscopy (TEM), local electrode atom probe (LEAP), and alternating gradient magnetometer (AGM) were employed to characterize the structural vs. magnetic properties. The Co-Pt phase diagram was used to predict the magnetic vs. structural ordering temperatures for each CoPt alloy, and compared with the experimental results.

9:35 AM

Reproducible Resistive Switching Behavior in Sputtered TiOx Films: *R. J. Jeng*¹; W. Z. Chang¹; J. P. Chu¹; ¹National Taiwan University of Science and Technology

The electronic industries have been attempting to improve the cache memory and flash device performance to be fast, small, and less energy consuming. Although the studies on RRAM have shown some results recently with the transition metal oxide, titination, more detailed microstructure and crystallographic analysis titanium oxide (TiOx), there still needs more stable and better memory properties. This study is thus directed toward improving RRAM properties of TiOx. In the two conditions of the sputtering atmosphere, which were 75% and 100% of the oxygen, the as-deposited TiOx had the good switching effects. The switching voltages from set to reset were 1.9 V and 2.0V for 75% and 100% oxygen sputtering atmospheres, respectively, whereas from reset to set the voltages were 0.87 V and 0.77 V. In this preseesults are revealed and discussed.

9:55 AM

Improving Resistance Switching Behavior of HoScO3 Film for the RRAM Application: Effects of Annealing: *W. Z. Chang*¹; S. F. Wang²; J. P. Chu³; ¹Graduate Institute of Engineering, National Taiwan University of Science and Technology; ²Department of Materials and Minerals Resources Engineering, National Taipei University of Technology; ³Graduate Institute of Engineering and Department of Materials Science and Engineering, National Taiwan University of Science and Technology,

A 35nm-thick of HoScO3 (HSO) thin films were deposited by r.f. magnetron sputtering, followed by annealing at 200 °C and 400 °C. The effects of annealing atmospheres as well as annealing temperatures on the resistance switching behavior of the HSO films were investigated in this study. As-deposited HSO film did not show the resistance switching behavior with high resistance, while it had unipolar switching behavior after annealing in high vacuum or in N2 atmosphere. The reliability improved with increasing annealing temperature. The formation and redistribution of defects such as metal ion and oxygen vacancy during thermal annealing are considered to be responsible for those variations in resistance switching properties.



TMS 2012

141st Annual Meeting & Exhibition

THURSDAY AM

10:10 AM Break

10:25 AM

Environmental Cracking Susceptibility of a Surface Nanocrystallized Stainless Steel in Contrast to its Coarse Grained Counterpart: *Indranil Roy*¹; Jian Lu²; Yuntian Zhu³; Colin Longfield¹; Rashmi Bhavsar¹; Enrique Lavernia⁴; Farghalli Mohamed⁵; ¹Schlumberger; ²City University of Hong Kong; ³North Carolina State University; ⁴University of California, Davis; ⁵University of California, Irvine

Stressed C rings of a surface nanocrystallized precipitation hardened stainless steel were exposed to high pressure high temperature (HPHT) hostile environments (acid gas and corrosive high density zinc based uninhibited completions brine) per NACE TM0177 – Method C. Susceptibility to environmental cracking (EC) of the surface nanocrystallized alloy was assessed in contrast to its untreated coarse grained counterpart. It is evident from the experimental results that surface nanocrystallized steel performed better in (a) HPHT sour hostile environments (b) high density low pH (~ 3.5) tri-salt brine and (c) acidizing environments in comparison to untreated counterparts without any indication of EC. Microstructural data and a comparative analysis of pits are discussed. Moreover, the results show that the compressive stress induced on the surface due to the ultrasonic shot peening in conjunction with the effect of grain boundary orientation due to grain refinement abets EC resistance of the treated alloy.

10:45 AM

Investigation of Al₂O₃ Nanostructures Using Charge Optimized Many Body Potentials: *Dundar Yilmaz*¹; Bryce Divine²; Simon Phillpot¹; Susan Sinnott¹; ¹University of Florida; ²U.S. Army Engineer Research and Development Center

Aluminum oxide nanostructures have drawn attention due to their interesting physical and optical properties. In particular, Photoluminescence peaks for these systems are attributed to oxygen vacancies. Here, we develop third-generation Charge Optimized Many Body (COMB) potentials for the Al-Al₂O₃ system. These potentials are used to investigate the properties of Al₂O₃ nanostructures. COMB potential not only simulates chemistry of the system but also handle realistic sized systems with an accuracy close to the first principles methods which are limited to small sized systems. In particular, the elastic properties and local atomistic strain distribution are calculated. The vibrational spectra are determine from the velocity auto correlation function. The effect of oxygen vacancies on the local strain and vibrational spectra are also characterized and analyzed. This work is supported by NSF/DMR under Grant No. 1005779.

11:05 AM

Microstructure, Interfaces, Intermixing and Magnetic Properties of FePd/MgO/FePt/Pt/CrRu Films Deposited on SiN/Si Substrate: *Ramasis Goswami*¹; Shu Cheng²; Konrad bussmann²; ¹SAIC/Naval Research Laboratory; ²Naval Research Laboratory

We have investigated the microstructure, interfaces and intermixing in sputter-deposited FePd/MgO/FePt/Pt/Cr₉₀Ru₁₀/Si₃N₄/Si magnetic tunnel junctions by high-resolution transmission electron microscopy (HRTEM) and correlated these results to the magnetic properties. Cr₉₀Ru₁₀ is used as a texturing layer for the growth of perpendicular magnetic anisotropy (PMA) films. HRTEM confirmed the formation of the desired (001) texture in cubic Cr₉₀Ru₁₀ as well as in the L1₀-FePt layer using our growth methods. A 2.5 nm layer of MgO was deposited as a tunnel barrier. The HRTEM observations show that the MgO layer was crystalline but randomly oriented. The FePd layer was also found to grow as discrete islands having a width of 5 to 10 nm with random orientations. The magnetic properties show out of plane coercivity larger than that of the in-plane values but with a loss of squareness in concert with the loss of (001) texture in the top magnetic layer.

11:25 AM

Fluorescence from Polymers in Uniaxially Stretched Electrospun Nanofiber Mats: *Stephen Young*¹; Indraneel Sen¹; Rohit Uppal¹; Dayakar Penumadu¹; ¹University of Tennessee, Knoxville

Electrospun polymer nanofibers are attractive due to their volume-to-space, electrical, chemical, and unique optical properties. Uniaxially stretched polymer thin films have shown a change in optical properties with increasing applied tensile strain. High molecular weight polyvinylcarbazole (PVK) and polystyrene (PS) blends of various concentrations were electrospun and aligned by traditional electrospinning methods. Fiber mats were characterized using scanning electron microscopy (SEM) for morphology, fourier transform infrared spectroscopy (FTIR) and x-ray diffraction (XRD) to obtain polymer chain orientation, and fluorospectroscopy for optical properties. The fiber mats were then mounted onto a custom tensile stage where steady-state fluorescence properties of electrospun nanofiber mats were studied under tensile loadings at room temperature.

11:40 AM

Synthesis and Characterization of Core-Shell TaN_x Nanocomposites: *Lianyun Liu*¹; *Kai Huang*¹; Zheng Wang¹; Jungang Hou¹; Hongmin Zhu¹; ¹University of Science and Technology Beijing

Core-shell TaN_x nanocomposites were prepared through the in-situ coating process on the basis of synthesis of TaN_{0.5} nanoparticles. The X-ray diffraction results showed the nanocomposites consisted of TaN and TaN_{0.5} crystalline phase. TEM and SEM images demonstrated that TaN nanopowders as a coating layer grew on the surface of TaN_{0.5} nanoparticles, producing TaN_x nanocomposites with core-shell structure. The specific surface area of nanocomposite powders was as large as 4.87m²g⁻¹-6.13m²g⁻¹, indicating that such TaN_x nanocomposites exhibited great potential of application to the capacitor with ultra high specific capacitance.

11:55 AM Concluding Comments

3rd International Symposium on High Temperature Metallurgical Processing: Treatment and Recycling of Solid Slag/Wastes

Sponsored by: The Minerals, Metals and Materials Society, TMS Extraction and Processing Division, TMS: Energy Committee, TMS: Pyrometallurgy Committee

Program Organizers: Tao Jiang, Central South University; Jiann-Yang Hwang, Michigan Technological University; Patrick Masset, TU Freiberg; Onuralp Yucel, Istanbul Technical University; Rafael Padilla, University of Concepcion; Guifeng Zhou, Wuhan Iron and Steel

Thursday AM
March 15, 2012

Room: Southern II
Location: Dolphin Resort

Session Chairs: Xiangxin Xue, Northeastern University; Zhiwei Peng, Michigan Technological University

8:30 AM

An Integrated Strategy for Whole Ecological Utilization of Typical Industrial Solid Wastes in China: *Xiangxin Xue*¹; He Yang¹; Tao Jiang¹; Yong Li¹; ¹Northeastern University

In this paper, we describe the current status and research progress on the utilization of typical industrial solid wastes in China. We propose a creative method called “eco-utilizing wastes” with an aim of both integration and increment but without second-time waste and pollution, in terms of the characteristics of typical industrial solid wastes, such as titanium-bearing blast furnace slag, high-silicon iron tailing and boron-enriched slag as well as oil shale.

8:45 AM

Chlorination Behaviors of Copper Phases by Calcium Chloride in High Temperature Oxidizing-Chloridizing Roasting: *De Qing Zhu*¹; Dong Chen¹; Jian Pan¹; Tie Jun Chun¹; Guo Lin Zheng¹; Xian Lin Zhou¹; ¹Central South University

The high temperature oxidizing-chloridizing roasting is one of useful methods to separate nonferrous metals from pyrite cinder and metallurgy slag. However, as one kind of main nonferrous metals in pyrite cinder and metallurgy slag, copper's chlorination behavior is not demonstrated. In the present study, chlorination behaviors of CuO, Cu₂O and CuS at the temperature range of 1025-1175°C in air by simulating the chloridizing roasting process of pyrite cinder and metallurgy slag have been investigated. It is shown that Cu₂O and CuS is much easier to remove, CuO is refractory to remove. In addition, the presence of SiO₂ and CaO increases the Cu removal rate from CuO while the presence of SiO₂, Al₂O₃, CaO and MgO decreases the Cu removal rate from Cu₂O. Fe₃O₄ influences the Cu removal rate from CuO and Cu₂O positively.

9:00 AM

Decomposition of Zinc Ferrite in Zinc Leaching Residue by Reduction Roasting with Carbon: *Mi Li*¹; Bing Peng¹; Liyuan Chai¹; Jiming Wang¹; Ning Peng¹; ¹Central South University

Abstract: Decomposition of zinc ferrite in zinc leaching residue (ZLR) into zinc oxide and magnetite by reduction roasting with carbon as reducing agent was conducted in a muffle furnace under nitrogen atmosphere. The effects of roasting temperature, roasting time and the mass ratio of reducing agent to ZLR on the decomposition rate of zinc ferrite were investigated. The results showed that roasting temperature and usage amount of reducing agent were significant on the decomposition rate of zinc ferrite. More than 90% of zinc ferrite was decomposed after roasted at temperature over 850°C for 2h under carbon to ZLR mass ratio of 10%. The phase changes during reduction roasting process were detected by using XRD and SEM-EDS for the roasted and unroasted ZLR. A new flow sheet of ZLR treatment for the recovery of zinc and iron was proposed.

9:15 AM

Effect of Iron Containing Metallurgical Byproducts on Pulverized Coal Combustion Efficiency: *Zou Chong*¹; Wen Liangying¹; Zhang Shengfu¹; Bai Chenguang¹; Tan Xiuqin¹; ¹Chongqing University

Eight typical metallurgical byproducts containing iron were selected based on the effect of the chemical composition, particle size, additives on the burnout degree of pulverized coal. Effect of three typical byproducts including fine iron ore, BOF dust and BOF sludge on combustion reactivity and combustion efficiency were investigated using TG-DSC method. The results indicated that the three additives have obvious catalytic effects on pulverized coal. By comparison, the relative active sequence of byproducts to the catalytic combustion can be described as follows: BOF dust>BOF sludge>fine iron ore. Moreover, adding BOF dust as component of additives also shows significant catalytic effects on combustion efficiency during rapid heating process.

9:30 AM

Effect of SiO₂ Addition on Production of Fe-Si-Mn Alloy from Adjusted Converter Slag: *Cuthuan Huang*¹; Min Chen¹; ¹Northeastern University

Production of Fe-Si-Mn alloy from adjusted converter slag was investigated by thermodynamic analysis. The calculated results showed that the solubility of SiO₂ in slag increased with increment of temperature, and the solubility was about 80% at 1800°C. With increment of SiO₂ content, MnO activity and CaO activity decreased, while FeO activity increased to the maximum when SiO₂ content was about 30%. As a result, Fe was reduced from the adjusted converter slag firstly, followed by the reduction of Mn, P and Si. The reduction order was Fe→P→Mn→Si when SiO₂ content in the slag was from 46.4% to 54.2%, and changed to the order of Fe→Si→P→Mn when SiO₂ content exceeded 54.2%. The

mass fraction of Si in the alloy phase increased with increasing of SiO₂ content in the slag, and the mass fraction of Si in the alloy reached to 62.2% at 1800°C.

9:45 AM

Experimental Research on Recovery of Heavy Metals from EAF Stainless Steel Dust: *Canguo Wang*¹; Fei Jin¹; Guodong Sun¹; Mei Zhang¹; Min Guo¹; ¹University of Science and Technology Beijing

EAF stainless steel dust contains some valuable metals such as Fe, Cr, Zn, and Ni. To recycle these heavy metals, it is quite important to know the reactivity and metallurgical behavior of these heavy metals contained in EAF stainless steel dust. According to thermodynamic analysis, the reduction temperature of ZnFe₂O₄, Fe₂O₃, NiO, ZnO and Cr₂O₃ by carbon was 848K, 978K, 708K, 1218K and 1534K, respectively. The heavy metals can be recycled from EAF stainless steel dust by selective reduction with carbon. In the present study, the effects of temperature and time on the reduction ratio of the metals were investigated with 200ml/min N₂ and (mass%_{dust})/(mass%_C)=4 at 1773K, 1823K and 1873K. It was found that the reduction ratio of metals (Fe, Ni and Cr) increased with the increase of the reaction time and the temperature. In 20 minutes, the reduction ratio of metals reached 90% or so at 1873K.

10:00 AM

Research on the Control Model of Vanadium Recovery by BOF Process Based on Neural Network: *Qingyun Huang*¹; Bing Xie¹; Yugang Li¹; Chongyang Zhao¹; ¹Chongqing University

Manual operation dependent on experience and feeling of operators is applied in Pan Steel for vanadium recovery from low V-bearing hot metal by BOF process, which would lead to unstable quality of vanadium slag and semi-steel. On the basis of analyzing extraction vanadium in BOF characteristics, a control model based on neural network with ability of self-adaptive and self-learning is established. The model includes coolant sub-model, oxygen-blown volume sub-model and prediction sub-model. Added coolant and oxygen-blown volume were calculated, and the quality of semi-steel and vanadium slag was taken as control target. Industrial experiment in Pan Steel shows that the calculation is satisfying and the control strategy is effective, which could afford good guidance to the production of vanadium extraction.

10:15 AM Break

10:25 AM

Solidification of EAF Stainless Steel Dust: Bing Peng¹; Ji Peng¹; Liyuan Chai¹; Di Yu¹; ¹Central South University

Electric arc furnace (EAF) stainless steel dust has been classified as a hazardous waste by various government regulatory agencies as it releases heavy metals to environment. The solidification of EAF dust is to stabilize the hazardous components to the amorphous silica-alumina-based clays. The process of solidification is investigated and the softening temperatures of dust and additive clay mixtures are measured for economical thermal treatment. The results indicate that the mixture of dust and local clay with the ratio of 1:1 has the lowest softening temperature 1100°C and it could pass the toxicity characteristics leaching procedure (TCLP) test for the environmental regulatory limits after thermally treated at softening temperature for 15 min. Major phases of thermal solidification product clinker are CaAl₂Si₂O₈, (Fe, Cr)₂O₃, (Fe, Mg)(Cr, Al)₂O₄ and Al₆Si₂O₁₃.

10:40 AM

Study on Cementing Material Making with Electrolytic Manganese Residue: Wang Jia¹; Peng Bing¹; Chai Li-Yuan¹; Zhang Qiang¹; Liu Qin¹; ¹Central South University

Electrolytic Manganese Residue (EMR) was used as the main material to prepare cementing material activator for the utilization of the residue from electrolytic manganese dioxide (EMD) or electrolytic metallic manganese (EMM) production. The effects of chemical activation, thermal activation and mechanical activation on retarding activity and excitation activity of EMR were investigated according to the setting time and activity index



of EMR-slag cementing material. The results showed that the EMR exhibited good activating performance after being ball-milled for 18 min and then treated for 1-2 hours at temperature range of 350-450°C. The optimal properties of cementing material activator were achieved at the weight percent ratio 30 : 3 : 5 of EMR/Ca(OH)₂/cement clinker.

10:55 AM

Utilization of BF Ash and BOF Sludge to Produce Burden of Blast Furnace: Xiulan Deng¹; Tiejun Chun¹; Jian Pan¹; ¹Central South University

BF (Blast furnace) ash and BOF (basic oxygen furnace) sludge are solid waste containing ferrous in iron and steel company, and they are not utilized due to the high zinc content. In this paper, the utilization of BF ash containing 26.40%Fe and 5.77%Zn, and BOF sludge containing 56.30%Fe and 2.27%Zn was conducted. The pellets were made by blends of BF ash, BOF sludge and pyrite cinder. The final product pellets, assaying Fe total 64.23% and 0.016% Zn and compressive strength of 1440N per pellet was obtained under the conditions of reduction temperature at 1300°C for 15min and C/Fe (mass ratio) of 0.5, which can be used the burden for blast furnace.

11:10 AM

Study on the Desulfuration of Pyrite Cinder Pellets: Zhiyong Ruan¹; Deqing Zhu¹; Tiejun Chun¹; Jian Pan¹; Zhao Qiang; ¹Central South University

In this paper, the desulfuration of pyrite cinder pellets was carried out. Phase analysis shows that most sulfur of pyrite cinder exists in the form of elementary sulfur. Compared to roasting stage, most sulfur was removed in preheating stage. 81.25% sulfur was removed and the average SO₂ concentration of exhaust gas was 1365ppm when the pellets was preheating at 950°C for 9 min. The final product, assaying 62.42wt%Fe and 0.02wt% S content at 96.88% desulfuration was achieved under the conditions of preheating at 950°C for 9 min and roasting at 1200°C for 15 min, which can be used the burden for blast furnace.

Aluminum Reduction Technology: Equipment

Sponsored by: The Minerals, Metals and Materials Society, TMS Light Metals Division, TMS: Aluminum Committee, TMS: Aluminum Processing Committee
Program Organizer: Olivier Martin, Rio Tinto Alcan

Thursday AM
March 15, 2012

Room: Europe 1
Location: Dolphin Resort

Session Chair: René von Kaenel, KAN-NAK SA

8:30 AM

Integrated Desalination and Primary Aluminium Production: Anders Sorhuus¹; Geir Wedde¹; Dario Breschi¹; Guillaume Girault²; Nolwenn Favel²; ¹Alstom; ²Rio Tinto Alcan

Primary aluminium is produced increasingly in regions where there is a scarce supply of clean and fresh water. A self sustainable, secure supply of fresh water is of strategic importance for aluminum smelters. Desalination plants can be installed in combination with gas-fired power plants, and it is shown that part of the natural gas consumed for production of water in the desalination process can be replaced with waste heat from the aluminium smelter pot gas. Besides, installation of heat exchangers allows a significant downsizing of Gas Treatment Centers as well as improved control of stack fluoride emissions. It is shown that a compact, robust double-effect desalination plant can provide the water required during predicted variations in water consumption and profitably use wasted heat for a typical AP40 smelter. The corresponding calculated cost of water is comparable to the cost of water available commercially.

8:50 AM

Busbar Displacement Study of Aluminum Reduction Cell: Xiquan Qi¹; ¹Northeastern University Engineering and Research Institute, Co., Ltd

With the increasing of cell capacity, busbar length, current load in each branch and the magnetic field intensity around the cell all are increasing consequently, so are the electro-magnetic forces on each busbar and the thermoelectric stress inside the busbar. As a result, big displacement occurs on busbars and even worse, the insulation bricks are crushed by busbar movement. Displacement of busbars leads to deformation of flexes, which will also be detrimental to cell life. With the longest and highest-current branch as an example, busbar displacement and stress status are studied systematically for a large reduction cell.

9:10 AM

Impact of Amperage Creep on Potroom Busbars: Thermal-Mechanical Aspects: Andre Felipe Schneider¹; Daniel Richard¹; Olivier charette¹; ¹HATCH Ltd.

The mechanical performance of pot-to-pot busbars is intimately linked to the temperature and thermal expansion of conductors. With amperage creep, busbars are typically running hotter than they were at start-up, so that adequate temperature fields for both standard and bypass conditions must be considered to accurately represent the thermal stresses acting over the system. To assist smelters to evaluate the performances of busbars systems under realistic operating conditions, a methodology was developed using ANSYSTM-based numerical simulation, where the temperature field obtained from a thermal-electrical model is applied as a load to a thermal-mechanical model. The bolted connections at the shunting-clamping stations, the weld plates and the contact mechanics between bars are taken into account explicitly. A test case based on a demonstration busbar system is presented and the typical impact of line current and selected operational procedures on thermal-mechanical performance and reliability of specific design features is discussed.

9:30 AM

Effective Insulation Control Monitoring System: The CANDITM Solution for a Safer Production: Anne-Gaëlle Hequet¹; Serge Despinasse¹; ¹ECL

The key to the chemical reaction necessary to convert alumina to metallic aluminium is the running of an electrical current through the cryolite/alumina mixture. The process requires the use of direct current. In the meantime, various interventions performed by the PTM, electrically connected to the ground, are required on the electrolysis cells to complete the smelting process. Thus, contact with electricity while performing on the potlines may result in hazardous situation and serious injuries for the operator (electrocution due to overvoltage up to 2 000 volts). Hence the importance of insulating electrically the driver's cabin, the tool trolley and the tools themselves to avoid often irreparable situations. To prevent such risks and above all to make the work environment safer, ECLTM designed an efficient device capable of monitoring the insulation level to earth and giving an audible and visual indication of abnormally low insulation values: the CANDI solution.

9:50 AM Break

10:10 AM

Potline Open Circuit Protection: Laurent Troubat¹; Roland Mathevon¹; Pierre Marcellin¹; Didier Lamant¹; Michel Jacon¹; Dominique Duvall¹; Andy Johnston¹; ¹Rio Tinto Alcan

A potline open circuit event is a catastrophic danger. It results in a high power arc, which feeds oneself as the DC current is not cut. It can escalate into an explosion, destroying not only the equipment in question but potentially anything within proximity. The consequences can include loss of the potline. To reduce the risk, the potline and the substation must be protected against the danger of open circuit. The protection system settings must be optimised according to the operating conditions (potline current, potline restart after shutdown, pot stopped, anode effects, etc.). It must be well engineered to achieve effective protection so that quick

tripping of the rectifying groups occurs when the open circuit is detected, while avoiding an inappropriate potline shutdown. The theoretical aspects of potline opening circuit and the behaviour of rectifying groups are presented. An overview of the protection systems deployed in RTA smelters is shown.

10:30 AM

Maximize Efficiency and Safety of Smelters through Advanced Multipurpose Simulator Solution: Anne-Gaëlle Hequet¹; Denis Chapdelaine¹; ¹ECL

Modern smelters have made the reduction process efficiency and safety a key issue: produce more, faster in a safer environment. By designing and developing highly technical automated machines, equipment suppliers greatly help and support smelters in their objective. However it must be acknowledged that despite such innovation, human remains at the very heart of any reduction process operation and has a significant impact on it. To avoid production losses, reduce maintenance cost and increase safety reflexes of the crane operators in case of emergency, ECL™ has recently endowed its PTM simulator with some new revolutionary functions. The operator, facing a double screen on which a 3D virtual potroom is generated, will be now equipped with some 3D glasses putting him in a total virtual reality. (Cabin rotation, cranes translations). Well trained, the operator will fully contribute to improve production and increase safety of the smelter.

10:50 AM

Challenges in Using Discrete Logistics as a Management Decision Tool for Aluminium Production: Maarten Meijer¹; Rienk Bijlsma²; Martijn Riesenkamp²; ¹Hencon; ²Systems Navigator

Discrete event simulation software has been used in multiple ways for various logistics projects in the Aluminium Industry; as a strategic decision support tool during major investments and upgrades of Aluminium smelters. Although it can predict and simulate operational behaviour of the system before and after the investment, it very often is not considered to be a management tool for operational and or tactical decisions. Since 2007 we used simulation software to make a realistic discrete models of many events involved with Aluminium production and introduced these models to various operational teams to support them in making decisions. In this paper we will describe our experiences and how these models have been used to support both capital investment decisions as well as day to day operational decisions.

Aluminum Reduction Technology: Modelling I

Sponsored by: The Minerals, Metals and Materials Society, TMS Light Metals Division, TMS: Aluminum Committee, TMS: Aluminum Processing Committee

Program Organizer: Olivier Martin, Rio Tinto Alcan

Thursday AM
March 15, 2012

Room: Southern III
Location: Dolphin Resort

Session Chair: Donald Ziegler, Alcoa Canada Primary Metals

8:30 AM

Current Distribution and Lorentz Field Modelling Using Cathode Designs: A Parametric Approach: Subrat Das¹; ¹Deakin University

A mathematical model of magnetohydrodynamic (MHD) effects in an aluminium cell using numerical approximation of a finite element method is presented. The model predicts the current distribution in the cell and calculates Lorentz force from the external magnetic field in molten metal for different size and shape of cathode blocks. The electrical conductivity of the cathode-block and the collector bar is so poor relative to the molten metal that the outer third of the collector bar and cathode, nearest the sidewall of the cell, carries the most of the current load, creating a very

uneven current distribution within the cathode. Such distribution has not only an impact on cathode-surface phenomena but also influence the current distribution in metal. The predicted results show that the cathode shapes have significant impact on current distribution in the metal and thereby would have a great relevance to cell stability and energy savings.

8:50 AM

Electromagnetic and MHD Study to Improve Cell Performance of an End-to-End 86 kA Potline: Amit Gupta¹; Manoj Chulliparambil¹; Sankar Namboothiri¹; Satheesh Mani¹; Biswajit Basu¹; Jinil Janardhanan²; ¹Aditya Birla Science & Technology Company Ltd.; ²Hindalco Industries Ltd.

Electromagnetic forces in the electrolyte and metal pad region of aluminum reduction cells affect the metal/electrolyte flow pattern and hence the cell performance, indicated by current efficiency and specific energy consumption. Numerical simulation has become an effective tool for analyzing such complex physics. In this paper, an electromagnetic and MHD study conducted for an 86 kA end-to-end potline is described. A detailed three-dimensional electromagnetic model was built in commercial ANSYS software package and steady state MHD (velocities and metal heave) in the cell were computed using CFX software. Magnetic field from the model was validated with the plant measurements. Various busbar configurations were analyzed using the developed model. The results show that new magnetic compensation designs effectively improve the magnetic field, the metal flow profile and the metal heave, thereby providing conditions for improving cell performance.

9:10 AM

Study on the Influences of Potline Status on the Magnetic Fields of Aluminum Reduction Cells: Xiquan Qi¹; ¹Northeastern University Engineering and Research Institute, Co., Ltd

The principle of busbar current balance and its criteria are presented. A coupled modeling algorithm of electro-magnetic field of reduction cells has been systematically introduced. With this algorithm, magnetic fields of cells at different location in the potline and under different potline status are computed. It is found that Bx pattern in the cells is generally identical for cells at different locations, while their By and Bz vary both in distribution and in values. With adjacent cell being bypassed cells, US-bypassed cell has bigger adverse influence on the operating cell than that of the DS-bypassed cell. Feed-in-end cells are more stable than those feed-out-end cells. If one cell is bypassed, its influence on non-adjacent operating cells decreases drastically with operating cells standing between. Of all factors on cells stability, Bz pattern and |Bz|ave values play the biggest role.

9:30 AM

Modeling of Interface Wave of Electrolyte/Aluminum Melt in Aluminum Reduction Cell with Novel Cathode Structure: Baokuan Li¹; Fang Wang¹; Xiaobo Zhang¹; Naixiang Feng¹; ¹Northeastern University

A finite element model has been developed is used to examine the electromagnetic field and interface wave of electrolyte/aluminum melt in aluminum reduction cell with the novel cathode structure. Magnetic vector method and edge-based method are used to solve the Maxwell equations. The result shows that the current density distribution in the novel cathode structure aluminum reduction cell becomes more uniform than the traditional cells, weak horizontal current appears on the convex surface, and weakened the longitudinal waves of molten aluminum. The voltage drop of the entirely novel aluminum reduction cell has reduced. Simulated flow field shows that the movement of molten aluminum affected by the electromagnetic force dominates and two reverse eddies in horizontal plane arise in aluminum reduction cell. The velocity and amplitude of molten aluminum wave reduce in the novel cathode structure aluminum reduction cell.



TMS 2012

141st Annual Meeting & Exhibition

THURSDAY AM

9:50 AM Break

10:10 AM

The Use of Vortex Method in the Analysis of Multiphase Flow in Aluminum Reduction Cells: Zhang Hehui¹; Zhang Hongliang¹; Li Jie¹; Xu Yujie¹; Yang Shuai¹; Lai Yanqing¹; ¹School of Metallurgical Science and Engineering, Central South University

As the principal character of flow pattern, the vortex distribution plays a dominant role in the flow behavior of aluminum reduction cells, thereby affecting the cell performance. Based on the commercial CFD software CFX12, the methods of vorticity and swirling strength were introduced to analyze vortex structures of the bath and metal phases quantitatively in a 300 kA cell, in which both the influences of electromagnetic forces (EMFs) and gas bubbles were included. Research results prove that, compared with velocity vector distribution and streamline picture, it can provide more flow field information with the above method, which may help to the optimization of alumina feeding points configuration. Vortexes usually occur as reverse symmetrical pairs. The single factor comparative study shows that the EMFs tend to trigger large vortexes near the upstream side, while gas bubbles mainly stir the bath and generate small ones around anodes.

10:30 AM

Anodic Bubble Behavior in Hall-Héroult Cells: Kristian Etienne Einarsrud¹; Stein Tore Johansen²; Ingo Eick³; ¹Norwegian University of Science and Technology; ²SINTEF Materials and Chemistry; ³Hydro Aluminium Deutschland GmbH

A phenomenological model for the creation and transport of anodic gas bubbles in Hall-Héroult cells is presented. Due to the large variation in bubble topology and length scales, a multiscale approach is introduced in which molecular gas is assumed to be formed as supersaturated CO₂ in the electrolyte. This paper describes models and constitutive relations that are intended for the simulation of anodic gas bubbles, ranging from the generation of molecular gas species through Faraday's law and subsequent bubble nucleation, to the evolution of macroscopic bubbles by means of a volume of fluid model. The coupling between macro- and micro scales is performed by means of a population balance. The model is applied to a 2D-cross section of a lab scale electrolysis cell, showing that essential properties are well represented by the proposed approach. Finally, the influence of Lorentz forces on the global bubble behaviour is investigated.

10:50 AM

Numerical Investigation of Bubble Dynamics in Aluminium Electrolytic Cells: Kaiyu Zhang¹; Yuqing Feng²; Phil Schwarz²; Mark Cooksey²; Zhaowen Wang³; ¹Northeastern University & CSIRO; ²CSIRO; ³Northeastern University

Gas generated beneath anodes in aluminium electrolytic cells play an important role for the circulation of the bath, alumina mixing, and heat balance. Those bubbles cause an extra voltage drop, which is largely affected by the amount and shape of the bubbles beneath anodes. Therefore, understanding the dynamic behaviour of bubbles in aluminium electrolytic cells has been a major research focus worldwide in recent decades. This paper presents a numerical investigation of the motion of single bubble beneath an anode and its escaping from the anode edge. Using 2 dimensional geometry of part of a real cell, the motion of different sized bubbles has been simulated. It was found that the bubble size affects bubbling dynamics significantly as is measured by bubble shapes, sliding velocity beneath anodes and bubble induced turbulence. Simulations have been also conducted using an air-water system to check its relevance to the CO₂-Cryolite system.

Battery Recycling: Session I

Sponsored by: The Minerals, Metals and Materials Society, TMS Electronic, Magnetic, and Photonic Materials Division, TMS Extraction and Processing Division, TMS: Energy Conversion and Storage Committee, TMS: Recycling and Environmental Technologies Committee

Program Organizers: Gregory Krumdick, Argonne National Laboratory; Linda Gaines, Argonne National Laboratory

Thursday AM
March 15, 2012

Room: Europe 4
Location: Dolphin Resort

Session Chairs: Gregory Krumdick, Argonne National Laboratory; John Sullivan, Argonne National Laboratory

8:30 AM Introductory Comments

8:35 AM

Economic and Environmental Trade-Offs for Li-Based Battery Recycling: Gabrielle Gaustad¹; Matthew Ganter¹; Xue Wang¹; Chelsea Bailey¹; Callie Babbitt¹; Brian Landi¹; ¹Rochester Institute of Technology

Current trends, motivated by fossil fuel dependence and unprecedented GHG emissions, show lithium-ion batteries (LIBs) emerging as a competitive energy storage technology due to higher power and energy densities compared to Pb-acid and Ni-metal hydride chemistries. These trends may be of concern, however, as environmental impacts are not well understood for either the LIB itself, or for the nanoparticles consumed or released during the battery's production, use, or end-of-life. This study combines economic modeling, dynamic material flow analysis, and fundamental material characterization methods in order to quantify some of the economic and environmental trade-offs for LIBs at their end-of-life. As expected, results show that as chemistries transition from Li-Co based cathodes to Li based Fe, Mn, and S cathodes, LIB recovery value decreases dramatically. These initial results aim to inform collection policies being proposed currently as well as enable future deployment of novel recycling techniques.

9:00 AM

Impacts of the Manufacturing and Recycling Stages on Battery Life Cycles: John Sullivan¹; Jennifer Dunn¹; Michael Barnes¹; Linda Gaines¹; ¹Argonne National Laboratory

The life cycle of batteries includes four stages: 1) material production, 2) component manufacture and battery assembly, 3) battery application, and 4) battery end of life. The first two of these stages represent the cradle-to-gate (CTG) components of the battery life cycle. This work provides new information on the battery materials production stage. Further, a detailed analysis is presented on the battery manufacturing stage, where anodes and cathodes are made and assembled with other components into batteries. This new battery production information (energy, carbon dioxide and other emissions) has been derived from suppliers and Argonne's research production line. As recycling doesn't necessarily reduce stage 2 impacts, reliable manufacturing data is especially important, as previous work suggests its magnitude is comparable to material production from virgin materials. The significance of this stage and battery material production will be compared to the overall life cycle of batteries.

9:25 AM

Battery Recycling by Hydrometallurgy: Evaluation of Simultaneous Treatment of Several Cell Systems: Carlos Nogueira¹; Fernanda Margarido²; ¹LNEG; ²IST - Instituto Superior Técnico (TULisbon)

A research work has been carried out aiming at evaluating the possibility of treating several electrochemical systems of spent batteries using the same process, in order to overcome the high costs and difficulties of selective collection and sorting. Zn-MnO₂ systems, representing more than 75% of portable battery market, shall be treated in dedicated processes. The treatment assessment of the other major systems (NiCd, NiMH and Li-ion), having Ni and Co as main metals, by a single hydrometallurgical

process, was the aim of the research work here reported. The leaching with sulphuric acid was demonstrated to be adequate for dissolving more than 90% of the metals of interest contained in batteries. The subsequent separation of metals by solvent extraction, using organophosphorous extractants like DEHPA and Cyanex 272, allowed the production of pure solutions of rare earths, cadmium/manganese, cobalt, nickel and lithium, allowing their further recovering.

9:50 AM

Hydrometallurgical Process for Manufacturing of Cathode Active Materials from Spent Lithium Ion Battery Packs in Used Hybrid Electric Vehicle: *Soo-Kyung Kim*¹; Jeongsoo Sohn¹; Kang-In Rhee¹; ¹Korea Institute of Geoscience and Mineral Resources

The physical treatment/chemical treatment for recycling of cathodic active materials from the batteries were performed. The result by physical treatment showed that over 95% ternary cathodic active material was concentrated in -65mesh with 88% Al elimination from the batteries. Through reductive leaching with H₂O₂ and H₂SO₄, leaching efficiency of valuable metals with -65mesh powder was over 99% Co, Mn, Ni and Li under the condition of 2M H₂SO₄, 5 Vol% H₂O₂, 60°C, 300rpm, 50g/500ml, and 2h. After removing some impurities such as Cu, Al, and Fe the leaching solutions containing Co, Mn, Ni, and Li could be utilized for manufacturing precursor of cathodic active material of Li ion battery. The precursor was manufactured by co-precipitation from the filtrate under the condition over pH11, 60°C, 300rpm, 5h. The filtrate after co-precipitation was used for Li recovery as a Li₂CO₃ by addition of Na₂CO₃ solution under the condition of 60°C, 300rpm, 5h.

10:15 AM Break

10:25 AM

Recycling Yearly Up to 7,000 Tons of Rechargeable Batteries: *Mark Caffarey*¹; ¹Umicore USA

Umicore started its UHT battery recycling facility May 2011 at its Hoboken, Belgium facility. The Ultra High Temperature process is the only recycling process that combines superior recycling efficiency, low energy usage and low environmental impact with less than 3% of material destined for landfill. Any Li ion and Ni metal hydride battery chemistries can be processed. Recoveries of high value materials are ongoing while recovery of lower value metals (Li,...) and difficult to recover materials (rare earths,...) are being studied. Materials recovered are used in battery or added value concrete applications. A detailed overview of this industrial recycling process will be given.

10:50 AM

The Use of Liquid-Liquid Extraction and Electroplating to Metals Recovery from Spent Batteries: *Kellie Provazi*¹; Denise Espinosa¹; Jorge Tenório¹; ¹University of São Paulo

The purpose of this paper is to study metal separation and recovery from a sample composed of a mixture of the main types of spent household batteries, using liquid-liquid extraction and metals electroplating. The preparation of the solution consisted of: grinding the waste of mixed batteries, reduction and volatile metals elimination using electric furnace and acid leaching. From this solution were studied the liquid-liquid extraction using Cyanex 272 [bis(2,4,4-trimethylpentyl) phosphoric acid] with tributyl phosphate as extracting agent. After study of solvent extraction and stripping has been recover and separate the metallic ions and with electroplating was recovered the manganese, copper, nickel and cobalt in their metallic forms.

11:15 AM

Distribution Logistics and Proper Disposal of Batteries for Downhole Oilfield Operations: *Amit Mohan*¹; Indranil Roy¹; David Wang¹; Ryan Davies¹; Jack Booker¹; ¹Schlumberger

Schlumberger is the Oil&Gas Industry leader in introducing new tools & technology to enable oilfield operations through cutting-edge research. Most of the downhole tools used in field operations need some kind of power source to operate. While most of the wireline tools have a power

and telemetry cable linking downhole tools to surface control for power, communications and conveyance, almost all other electronically operated downhole tools use batteries as a power source (for example - production logging tools, downhole testing, completions, drilling, slickline, coil tubing etc.). These are qualified for various operating environments including high temperatures and pressures. As Schlumberger operates across 160 countries in thousands of field locations, handling very large volumes of batteries is a mammoth task. This paper will deal with the processes in place within Schlumberger to handle distribution logistics and proper disposal of batteries for downhole oilfield operations in large quantities in a global setup.

11:40 AM Concluding Comments

Biological Materials Science Symposium: Bio-Inspired Materials: Implants and Devices

Sponsored by: The Minerals, Metals and Materials Society, TMS Electronic, Magnetic, and Photonic Materials Division, TMS Structural Materials Division, TMS: Biomaterials Committee
Program Organizers: Nima Rahbar, University of Massachusetts Dartmouth; Candan Tamerler, University of Washington; Po-Yu Chen, University of California, San Diego; Molly Gentleman, Texas A&M University

Thursday AM

March 15, 2012

Room: Swan 7

Location: Swan Resort

Session Chairs: Nima Rahbar, University of Massachusetts Dartmouth; James Guest, John Hopkins University

8:30 AM Keynote

Structural Testing at the Micro and Nano Scales: Breaking Invisible Specimens with Zero Force: *Roberto Ballarini*¹; ¹University of Minnesota

I will describe the use of microelectromechanical systems (MEMS) platforms to measure the mechanical response of materials and structures at the micro and nano scales. Selected examples include measurements of strength, toughness, high cycle and static fatigue of brittle MEMS materials, the strength, ultimate strain capacity and viscoelasticity of individual collagen fibrils, and the fracture energy of the carbon nanotube-epoxy matrix interface. A brief description of several the theoretical and computational models that were inspired by the experimental observations will also be presented.

9:10 AM

Nanoengineering of Implant Surfaces for Enhanced Biointegration: *Fereydoon Namavar*¹; Renat Sabirianov²; Alexander Rubinstein¹; Geoffrey Thiele¹; Laura Koepsell¹; John Sharp¹; Roxanna Namavar¹; Hani Haider¹; Kevin Garvin¹; ¹University of Nebraska Medical Center; ²University of Nebraska - Omaha

By mimicking the nanostructure of the lotus leaf and applying ion beam assisted deposition, we have demonstrated the fabrication of pure cubic ZrO₂ coating with 2-25 nm grain size which is comparable to the protein dimensions. Adhesion and proliferation experiments were performed with a bona fide mesenchymal stromal cells cell line (OMA-AD) on the nanostructured coatings and compared to CoCr, Ti, and HA. Our experimental results indicated that nanoengineered coatings are superior in supporting growth, adhesion, and proliferation. Absorption experiments with fibronectin from human plasma using an ELISA-based technique resulted in higher fibronectin adsorption on nanoengineered surfaces as compared to other conventional orthopaedic materials. These experiments indicated a clear correlation between cell adhesion and fibronectin adhesion. We examined possible mechanisms of the enhanced protein absorption using quantum mechanical force field parameterization of protein-surface interactions and Monte Carlo simulations of the fibronectin fragment (13FN3-14FN3) absorption on designed nanostructured ZrO₂ surfaces.



9:30 AM

New In Vitro and In Vivo Approaches in Evaluating Bioabsorbable Metal Candidates for Stents: Jeremy Goldman¹; Patrick Bowen¹; Jesse Gelbaugh¹; Jessica Rhadigan¹; Jon Stinson²; Heather Getty²; *Jaroslav Drellich*¹; ¹Michigan Technological University; ²Boston Scientific Corporation

A series of unconventional approaches are under development at Michigan Technological University which aim to screen candidate materials for use in bioabsorbable stents and reduce the scale of necessary animal studies. Using a novel in vivo approach, metal wires are implanted into the wall of the coronary artery of rodents for several weeks to gauge the host response, measure the severity of in vivo degradation, and characterize the resulting products. An in vitro method is being developed to identify bioabsorbable candidate materials, reproduce the corrosion products formed in vivo, and predict the degradation rate of stents. To accomplish this goal, wires encapsulated in an extracellular matrix are corroded in a cell culture medium. Encapsulation of the wires is necessary to slow down the material degradation process and mimic in vivo conditions. After in vivo and in vitro tests, wires undergo tensile testing to quantify the rate of material degradation.

9:50 AM

Investigation of Structure-Mechanical Property Relationship of Porous Titanium and Titanium Alloys: *Ziya Esen*¹; Sakir Bor²; ¹Cankaya University; ²Middle East Technical University

In this paper attention has been focused on the deformation characteristics of biomedical titanium and Ti6Al4V alloy foams under compression loading together with their energy absorption capabilities under quasi static conditions. Porous titanium and Ti6Al4V alloy foams were manufactured using powder metallurgy in which magnesium powders were utilized to create porosities via their evaporation. The cold compacted Ti/Ti6Al4V-Mg powder mixtures were slowly heated under high purity argon gas to sintering temperature of 1200°C where all the samples were sintered and the magnesium was eliminated completely by leaving the porosity in the structure. Then, the manufactured titanium and Ti6Al4V alloy foams containing porosities in the range 42-82 vol.% were characterized mechanically under quasi static conditions using compression loads and energy absorption characteristics of foams were characterized using energy efficiency approach. Microscopy studies have been carried out on the cross-sections of the samples using optical and scanning electron microscopes.

10:10 AM Break

10:15 AM Invited

Design of Biomaterials – Achieving Targeted Properties and Manufacturability with Topology Optimization: *James Guest*¹; ¹Johns Hopkins University

This paper will present recent advances in topology optimization for the computational design of material structures, or architectures, that achieve targeted homogenized properties and prescribed constitutive symmetries. While useful in a wide-range of settings, we focus on the application of topology optimization to the design of bone scaffolds. Various surrogates have been proposed in literature for use in the design process to enhance delivery of biologics and enable regeneration, including (for example) thermal conductivity, fluid permeability, and diffusion. Optimal material architectures found considering these objectives will be discussed, as will extensions to including manufacturability and uncertainty into the multi-physics scaffold design formulation.

10:40 AM

Investigation of Sr and Ca Containing Mg Alloys for Biodegradable Implant Applications: Harpreet Brar¹; *Ida Berglund*¹; Benjamin Keselowsky¹; Malisa Sarntinoranont¹; Michele Manuel¹; ¹University of Florida

Biocompatibility, mechanical strength and controlled degradation are essential requirements for a material to be used as a biodegradable implant for orthopedic applications. Magnesium (Mg), with its non-toxicity, high

specific strength and elastic modulus comparable to bone, is an ideal candidate for such applications. However, the low corrosion resistance and yield strength of pure Mg hinder its possible use as an implant material. In the present study, strontium (Sr) and calcium (Ca) were investigated as prospective alloying elements due to their biocompatibility, strengthening potential, and grain refining properties. The degradation behavior of binary Mg-Sr and ternary Mg-Ca-Sr alloys in simulated body fluid was investigated and an in-vitro cytotoxicity evaluation of the alloys was conducted on osteoblastic cells using the LDH cytotoxicity assay. Furthermore, the effect of alloying additions on the microstructure and mechanical properties was analyzed.

11:00 AM

The Effect of Sr and Ca on Corrosion Behavior of Magnesium as Biodegradable Implant: *Mandana Bornapour*¹; Mihriban Pekguleryuz¹; ¹McGill University

Having specific properties such as light weight, similar mechanical properties to that of human bone and non-toxicity, Mg is known as a potential element to serve as biodegradable metallic implant. In this study, we developed particular Mg alloy with controlled degradation rate. The microstructure, surface characteristics and corrosion behavior of Mg with addition of Sr and Ca was investigated by using SEM, X-ray diffraction, XPS, immersion tests and electrochemical experiments. The results of invitro corrosion tests in simulated body fluid (SBF) indicated that the degradation rate of Mg alloys can be adjusted by addition of 0.5-0.7wt% of Sr and Ca. The microstructural observation revealed that the grain boundaries are the prone regions to be degraded in SBF. The formation of hydroxyapatite was demonstrated on the surface of Mg after in-vitro corrosion test. The indirect cytotoxicity test revealed that Mg content 0.5-0.7wt% Sr or Ca did not show any toxicity effect.

11:15 AM

Chemotherapy-Induced Surface Degradation and Thrombogenicity of Intravascular Catheters: A Preliminary In-Vitro Study with Focus on Breast Cancer: Minoo Arzpeima¹; Annika Rosén¹; Emma Strömberg¹; Javier Sanchez²; Gunilla Björling²; Sigbritt Karlsson¹; *Ragnhild. E Aune*³; Samuel Rotstein²; ¹Royal Institute of Technology; ²Karolinska Institute; ³Norwegian University of Science and Technology (NTNU)

Vascular Access Devices (VADs) are commonly used for administration of chemotherapeutic drugs in treatment of patients with breast cancer, and are associated with an increased risk for complications i.e. nosocomial infections and thrombosis. In turn, this may subsequently lead to prolonged care, increased patient suffering and health care costs. In order to investigate the degradative effect of the chemotherapeutic drugs on Peripherally Inserted Central Catheter (PICC), chemotherapeutic treatment was step by step simulated in detail during 18 weeks (6 treatments). The inner surface of the catheters was studied after each treatment using different characterisation techniques; Scanning Electron Microscopy (SEM), Atomic Force Microscopy (AFM), and Fourier Transform Infrared Spectroscopy (FT-IR). Moreover, the thrombogenicity of both uncoated and coated catheters was analysed both before and after exposure to the drugs. The results clearly indicate an association, as a function of time, between the observed surface changes and an increased thrombogenicity.

11:30 AM

LASER Powder Deposition of Titanium - Tantalum Alloys Surfaces for Use in Biomedical and Corrosion Resistant Applications: *Jacob Fuerst*¹; Michael Carter¹; Dana Medlin¹; James Sears¹; ¹South Dakota School of Mines and Technology

Tantalum is commonly used in industry as a cladding in highly corrosive environments. It has also garnered interest in the biomedical community for increased biocompatible and osseointegrative properties compared to other metals. The high cost of tantalum makes it prohibitively expensive to use in bulk. Cladding a tantalum surface to a titanium substrate is inherently difficult because of the small difference between the melting temperature of tantalum, 3017°C, and the boiling point of titanium, 3287°C. LASER Powder Deposition (LPD) is a fusion operation using

a Nd:YAG LASER to melt a small volume of substrate into which metal powder is sprayed. This produces a surface layer of tantalum or a tantalum/ titanium alloy depending on the desired properties and the powder deposited. Cell culturing to test the biomedical applications of LPD tantalum alloy surfaces has shown this material to have increased osseointegrative properties compared to other orthopedic titanium alloys.

11:45 AM

In Vivo Osseointegration of Nano-Designed Composite Coatings on Titanium Implants: *Sybille Facca*¹; Debrupa Lahiri²; Florence Fioretti³; Nadia Messadeq⁴; Didier Mainard⁵; Nadia Benkirane-Jessel⁶; Arvind Agarwal²; ¹FIU; ²FIU; ³INSERM U977; ⁴IGBMC; ⁵CNRS UMR 7561

This is the first in vivo study of carbon nanotube (CNT) reinforced hydroxyapatite (HA) coating on titanium implants embedded in rodents' bone. Three types of titanium pieces were implanted: uncoated, and with HA and HA-CNT coatings. After one month, implants were retrieved and bone around coated implants was compared using TEM and histological observations. Elastic modulus of new bone was compared with the modulus of HA-CNT/bone interface to understand the mechanical integrity of the implant. No adverse effect or cytotoxicity of CNT addition on bone tissues, and cells was observed. Normal bone growth was observed around HA-CNT coated implants. CNT addition induces higher osseointegration as compared to HA. Our study proved CNTs could be used as reinforcement to plasma sprayed HA coatings for orthopedic applications.

Bulk Metallic Glasses IX: Mechanical and Other Properties

Sponsored by: The Minerals, Metals and Materials Society, TMS Structural Materials Division, TMS/ASM: Mechanical Behavior of Materials Committee

Program Organizers: Peter Liaw, The University of Tennessee; Hahn Choo, The University of Tennessee; Yanfei Gao, The University of Tennessee; Gongyao Wang, University of Tennessee

Thursday AM
March 15, 2012

Room: Swan 6
Location: Swan Resort

Session Chairs: Paul Voyles, University of Wisconsin, Madison; Jian Xu, Institute of Metal Research, Chinese Academy of Sciences

8:30 AM Invited

Structure and Relaxation of Zr-Cu-Al Bulk Metallic Glass from Hybrid Reverse Monte Carlo Modeling of Fluctuation Electron Microscopy Data: *Paul Voyles*¹; Jinwoo Hwang¹; Zenon Melgarejo¹; Don Stone¹; Ilkay Kalay²; Matt Kramer²; ¹University of Wisconsin, Madison; ²Iowa State University

We have used hybrid reverse Monte Carlo modeling based on fluctuation electron microscopy (FEM) experimental data and an empirical interatomic potential to determine the structure of $Zr_{30}Cu_{45}Al_5$ bulk metallic glass. In addition to quasi-icosahedral Voronoi polyhedra (VP), we find a significant density of more crystal-like VPs with rectangular and hexagonal faces. Our models also have strong medium-range order, consisting of groups of like VPs. The crystal-like VPs form a three-dimensional structure, while the icosahedral-like VPs form chains. A model refined against only the potential shows primarily quasi-icosahedral VPs, but it shows no agreement with the FEM data. Models refined against data from samples relaxed below the glass transition show a trajectory with increasing annealing from crystal-like VPs, through mixed VPs with some crystal-like and some icosahedral-like character, ending in icosahedral-like VPs. This is the first experimental result showing significant structural evolution with relaxation in a glass.

8:50 AM

Evaluation of Microstructure and Mechanical Behavior of Cu Based Bulk Metallic Glass-Carbon Nanotube Composites: *Jonathan Nguyen*¹; Troy Topping¹; Hidemi Kato²; Yizhang Zhou¹; Enrique Lavernia¹; ¹University of California, Davis; ²Tohoku University

Cu-Zr and Cu-Zr-Al bulk metallic glasses (BMG) have become a subject of recent interest due to their high strength and enhanced ductility. In this study, wet process dispersion of multi-wall CNT using a zwitterionic surfactant has been used to synthesize CNT reinforced BMG. A fundamental criterion is that the surfactant used must functionalize the CNTs thereby enabling it to attach to metallic powder surfaces. Spark plasma sintering was used to consolidate the BMG composite powders with 0.1 wt% CNT. The microstructural evolution and the interface between the CNT and the BMG matrix were characterized using electron microscopy, DSC and Zeta potential measurement. Compression tests were carried out to evaluate the mechanical behavior of consolidated bulk samples. Particular emphasis has been placed on establishing the structural and mechanical interaction at the interface between CNT and the BMG matrix.

9:00 AM Invited

Oxidation Resistance of Zr- and Ti- Based Bulk Metallic Glasses in the Supercooled Liquid Region: Ka Ram Lim¹; Sung Hyun Park¹; Min Young Na¹; Se Yun Kim²; Sang Soo Jee²; Eun-Sung Lee²; Won Tae Kim³; *Do Hyang Kim*¹; ¹Yonsei University; ²Samsung Advanced Institute of Technology; ³Cheongju University

Recently, it has been shown that the bulk metallic glasses (BMGs) can be successfully applied for fuel cell catalyst or Ag paste binder for screen printing Si solar cell due to high thermo-plasticity and good wetting characteristics in the supercooled liquid (SCL) state. Therefore, it is highly required that the BMGs should have a good oxidation resistance particularly in the SCL state. In the present study oxidation resistance of Zr-, and Ti-based BMGs in the supercooled liquid region has been investigated. The results show that the oxidation resistance of SCL state widely varies with alloy chemistry of BMGs. For example, the oxidation resistance of Cu₄₅Zr₄₅Al₈Be₂ in the SCL state is much higher than that of Cu₄₆Zr₄₆Al₈, although the oxidation rates in the crystallized Cu₄₆Zr₄₆Al₈ and Cu₄₅Zr₄₅Al₈Be₂ are almost same. Detailed oxidation mechanism has been unveiled by analyzing oxide layer cross section prepared by FIB technique.

9:20 AM

Study of Plastic Deformation in Structural Modified Zr-Cu-Al Metallic Glasses by Broadband Nanoindentation Creep: *Zenon Melgarejo*¹; Jinwoo Hwang¹; Chuan Zhang¹; Joseph Jakes²; Eren Kalay³; Matt Kramer³; Paul Voyles¹; Donald Stone¹; ¹University of Wisconsin-Madison; ²Performance Enhanced Biopolymers, United States Forest Service, Forest Products Laboratory; ³Iowa State University

Plastic deformation models in metallic glasses (MGs) theorize shear transformation zones (STZs) as the elementary units of plastic deformation. Activation energy for shear of an STZ depends on stress. Activation parameters should vary systematically with atomic structure including short and medium range order and should be sensitive to composition, quenching rate, and annealing. In this study we employ broadband nanoindentation creep (BNC), to measure hardness across 5-6 decades of deformation rate and characterize activation volume as a function of the stress in Zr-based MGs. Additionally, BNC enables to assess the form of the activation energy function and estimate STZ size. Bulk and ribbon Zr₅₄Cu₃₈Al₈ (T_g = 676K) and Zr₅₀Cu₄₅Al₅ (T_g = 667K) are studied. Annealing treatments are performed in a differential scanning calorimeter (DSC) at 573°K and at slightly above the glass transition temperature. Effects of annealing treatments on hardness, activation parameters and STZ sizes for these alloys are reported.



TMS 2012

141st Annual Meeting & Exhibition

THURSDAY AM

9:30 AM Invited

Potential Energy Landscape of Glasses: Distributions of Activation Energies, Volumes and Attempt Frequencies: *David Rodney*¹; Pawel Koziatek¹; Peter Derlet²; Jean-Louis Barrat³; ¹INP Grenoble; ²Paul Scherrer Institut; ³Université Joseph Fourier

Molecular dynamics is a powerful tool to simulate the atomic-scale processes that occur in bulk metallic glasses either at rest during aging or under plastic deformation. This technique is however limited to short-time dynamics and does not give access to the slow thermally-activated events that progressively dominate the glass dynamics when the temperature and/or the strain rate are decreased. We report here results obtained with a saddle-point search method, the Activation-Relaxation Technique, used to determine thermally-activated paths in glasses. From the paths, we determined the distributions of activation energies, activation volumes and attempt frequencies, the three parameters that characterize thermally-activated processes. We studied in particular the influence by the history and level of relaxation of the glass on the above distributions, with a special attention paid to the effect of a plastic deformation.

9:50 AM Break

10:05 AM Invited

Weibull Analysis of Fracture Strength for $Zr_{55}Ti_2Co_{28}Al_{15}$ Bulk Metallic Glass: Tension-Compression Asymmetry and Porosity Effect: *Jian Xu*¹; Hui-li Gao¹; Yong Shen¹; ¹Institute of Metal Research, Chinese Academy of Sciences

In this work, two- and three-parameter Weibull statistics were used for analyzing the variability of fracture strength for $Zr_{55}Ti_2Co_{28}Al_{15}$ bulk metallic glass (BMG), both in compression and tension testing. In contrast to the compression in which the specimens fail via the massive shear-off, however, failure mode in tension for the as-cast BMG is flaw-controlled crack opening due to the presence of cast defects. For the BMG rods of 6 mm in diameter, three-parameter Weibull modulus m_{sp} and threshold stress is 3.4 and 1780 MPa, respectively. However, tensile fracture strength of the BMGs manifests a large variability. The specimen failure at different stress is associated with two types of defects: large pores on/near the surface of specimens and small internal pores. Using bimodal and three-parameter Weibull analysis, Weibull modulus m , and threshold stress σ_{at} at lower stress level is 1.8 and 250 MPa, respectively.

10:25 AM

Quantitative Microstructural Characterization of Metallic Glass/Crystalline Composites: *Nicholas Hutchinson*¹; Katharine Flores¹; ¹The Ohio State University

Bulk metallic glasses are limited in application by their propensity for highly localized deformation with little ductility when loaded in tension. In order to control this localization, a number of Ti-Zr metallic glass/crystalline composites with highly interconnected microstructures have been created. The effectiveness of the crystalline reinforcement phase on improving toughness and ductility depends upon the transfer of deformation across the glass-crystalline interface, which depends on both composition and the local microstructure. In the present work, we characterize two composite systems with vastly different mechanical properties. Three-dimensional microstructural features are characterized using serial sectioning techniques. In addition to critical average length scales, such as reinforcement size and spacing, this technique enables local, quantitative descriptions of the interface, such as its principal curvatures. Finite element analyses of models based on the 3D microstructure are used to measure the strain distribution in the microstructure under tensile loading for comparison with experimental measurements.

10:35 AM Invited

Micromechanisms of a Dendrite/Zr-Based Bulk-Metallic-Glass Composite Subjected to Plastic Deformation: E-Wen Huang¹; Junwei Qiao²; Bartłomiej Winiarski³; Richard Moat³; Andrew Chuang⁴; Mario Scheel⁵; Marco Michiel⁵; Philip Withers³; *Yu-Lih Huang*¹; Yong Zhang⁶; Peter Liaw⁴; ¹National Central University, Taiwan; ²Taiyuan University of Technology, Taiyuan, China; ³University of Manchester, Manchester, United Kingdom; ⁴The University of Tennessee; ⁵European Synchrotron Radiation Facility Beamline ID15; ⁶University of Science and Technology Beijing

In the current study, a Zr-based BMG that contains a dendritic crystalline phase performs remarkably with a large plastic strain. The plastic-deformation micromechanisms of the dendrite/Zr-based bulk-metallic-glass-matrix composite (BMGMC) are revealed. A three-dimensional (3-D) tomography experiment was carried out using the European Synchrotron Radiation Facility (ESRF). The correlating successive images qualitatively indicate the load-sharing micromechanisms. Meanwhile, we simultaneously measured the Bragg peaks with in-situ synchrotron x-ray. During loading-unloading cycles, there is asymmetric Bragg-peak evolution subjected to different levels of deformation. The in-situ peak profile analyses suggest that there is asymmetric load sharing between the amorphous matrix and the crystalline dendrites. The relationship between the microstructures and mechanical properties of the BMGMC materials is summarized. PKL and AC appreciate the support of NSF in the Division of CMMI under CMMI-0900271 and CMMI-1100080, and the Materials World Network Program, under DMR-0909037. EWH and YLH is grateful for the support by NSC-100-2221-E-008-041 Program.

10:55 AM

Load Relaxation Behavior Of Fe-Based Metallic Glass Supercooled Liquid: *Rui Yamada*¹; Noriharu Yodoshi¹; Akira Kawasaki¹; ¹Tohoku University

The load relaxation behavior within the supercooled liquid region of Fe-based metallic glass [(Fe_{0.5}Co_{0.5})_{0.75}Si_{0.05}B_{0.2}]₉₆Nb₄ was investigated. A spherical particle of the metallic glass with a diameter of about 500 μ m was uniaxially compressed. A crosshead was kept constant at a certain strain level and the load relaxation was then recorded as a function of time. The relaxation time was determined as the normalized load f/f_0 reaching $1/e$. A micro-compressive test was conducted at various crosshead speeds for various temperatures in the supercooled liquid region. Our study has revealed that the relaxation behavior can be well fitted by the Kohlrausch-Williams-Watts (KWW) relation. The temperature dependence of the relaxation time was described by an Arrhenius relation and the corresponding apparent activation energy was found to be anomaly high. The high value of activation energy might suggest the presence of a co-operative movement of a large number of atoms during the relaxation.

11:05 AM Invited

Tensile Micromechanism Crossover for Bulk-Metallic-Glass-Matrix Composites: From Working Hardening to Softening: *Junwei Qiao*¹; A.C. Sun²; E.W. Huang³; Y. Zhang⁴; P.K. Liaw⁵; C.P. Chuang⁵; ¹Taiyuan University of Technology; ²Yuan Ze University; ³National Central University; ⁴University of Science and Technology Beijing; ⁵The University of Tennessee

A Ti-based bulk-metallic-glass-matrix composite (BMGMC) with a homogeneous distribution of dendrites and with a composition of Ti₄₆Zr₂₀V₁₂Cu₅Be₇ is characterized by a high tensile strength of ~1,640 MPa and a large tensile strain of ~15.5% at room temperature. After tension, the fragmentation of dendrites is responsible for the distinguished tensile ductility. The subdivisions within the interior of dendrites are separated by the shear bands and dense dislocation walls, and the local separation among dendrites under modes I and II prevails. Theoretical analyses reveal that the constitutive relations: the elastic-elastic, elastic-plastic, and plastic-plastic stages of the dual-phase BMGMCs, generally correspond to deformation stages: (1) elastic, (2) working hardening, and

(3) softening, respectively. The capacity of the work-hardening behavior is highly dependent on the large plastic deformation of dendrites and high yielding strength of glass matrix. The present study provides a fundamental basis for designing work-hardening dual-phase BMGMCs exhibiting remarkably homogeneous deformation.

11:25 AM

Evaluations of Physical and Optical Properties of Metallic Glass Patterns Formed in Micro/Nano Scales: *Y. C. Chen*¹; *S. Song*²; *T.R. Tsai*²; *J. S. C. Jang*³; *Y. M. Chen*¹; *S. E. Lee*¹; *Jinn P. Chu*¹; ¹National Taiwan University of Science and Technology; ²National Taiwan Ocean University; ³National Central University

Metallic glasses (MGs) exhibit viscous flow at high temperatures in the supercooled liquid region; thus they can be used to produce devices via micro-/nano-imprinting and a candidate for molding material because of its high strength, hardness and elastic limit. The simplified fabrication process of imprinting mold prepared with BMG is achievable when comparing to the conventional lithography and patterning technique. In this study, we demonstrate that micro-/nano-patterns of Pd-based BMG can be imprinted from a mold in air. We further used the patterned BMG as a mold to replica patterns on PDMS, a commonly used polymer for precision patterns. The physical and optical properties of the BMGs and PDMS parts formed in micro/nano scales are evaluated and the evaluation results are discussed. The obtained results suggest that the BMG is a suitable material for micro-/nano imprinting, and is also a good mold material for imprinting.

Bulk Metallic Glasses IX: Structures and Other Properties I

Sponsored by: The Minerals, Metals and Materials Society, TMS Structural Materials Division, TMS/ASM: Mechanical Behavior of Materials Committee

Program Organizers: Peter Liaw, The University of Tennessee; Hahn Choo, The University of Tennessee; Yanfei Gao, The University of Tennessee; Gongyao Wang, University of Tennessee

Thursday AM
March 15, 2012

Room: Swan 1
Location: Swan Resort

Session Chairs: Jörg Löffler, ETH Zurich; Maria Baró, Universitat Autònoma de Barcelona

8:30 AM Invited

Effect of Structure on the Devitrification Pathways in Al-Tb System: *Matthew Kramer*¹; *Y. Kalay*²; *Paul Voyles*³; *Hwang Jinwoo*³; *Ryan Ott*⁴; *Matt Besser*⁴; *Ying Zhang*⁴; *YaQiao Wu*⁴; ¹Iowa State University; ²Middle East Technical University; ³University of Wisconsin, Madison; ⁴Ames Laboratory

We compare the glassy state of a rapidly solidified Al90Tb10 alloy to that of a magnetron sputtered film. To study the as-deposited state, a 70 nm thick film deposited simultaneously on a thin carbon substrate and an array of thin Si tip for TEM and atom probe tomography (APT). Electron and X-ray diffraction of the vapor deposited films are very similar to the melt spun alloys with thickness of 25-30 μm . The thermal analysis shows a very different devitrification pathways between the melt spun and sputtered films. High resolution TEM and APT results show Al-rich and Al-depleted regions within the melt spun alloys. A network structure of Tb-rich regions divides the matrix into \sim 1-2 nm isolated Al-rich clusters. Preliminary TEM and APT of the thin films suggest that the high cooling rate of sputtered films suppress the formation of the nm clustering resulting in a different pathway for devitrification.

8:50 AM

Thermomechanical Joining of Bulk Metallic Glass Composites: *Scott Roberts*¹; *Douglas Hofmann*²; *William Johnson*¹; ¹California Institute of Technology; ²NASA - JPL

Bulk metallic glasses (BMG) and bulk metallic glass matrix composites (BMGMC) are cutting edge materials with the potential for high performance structural applications. Crystallization and embrittlement of these materials when heated limits their ability to be welded effectively. Thus, other joining techniques that preserve the high strength and amorphous nature of BMGs and BMGMCs are required. This presentation introduces an improved thermomechanical joining strategy for assembling and welding BMGMC components. Tension test results demonstrating that the strength of the parent glass can be obtained in the weld region and samples of several monolithic cellular structures assembled through this process will be exhibited.

9:00 AM Invited

Dynamics of Shear Banding in Bulk Metallic Glasses: *Jörg Löffler*¹; *David Klaumünzer*¹; *Robert Maass*¹; ¹ETH Zurich

New insights into the mechanism of shear banding in bulk metallic glasses can be gained by combining time-resolved compression tests with in-situ acoustic emission monitoring. The load and displacement data using high acquisition rates allow for a characterization of the shear-band propagation, which is found to be thermally activated and in the mm/s range at room temperature. In addition the propagation follows an intermittent, stick-slip process, which is also known across macroscopic underlying length scales ranging from granular systems to tectonic faults. We are able to attribute the acoustic emission signal, which reflects the moment of shear-band initiation, to a mechanism of structural dilatation by inferring a model picture from stick-slip in granular media. The critical volume change associated with this shear-band initiation is evaluated to be a few percent only, which is the typical excess free volume found in the undercooled liquid region near the glass transition temperature.

9:20 AM

Thermodynamics of Isolated Bi-Atomic Clusters: *Garth Wilks*¹; *Jose Reveles*²; *Daniel Miracle*¹; *Shiv Khanna*²; ¹Air Force Research Laboratory; ²Virginia Commonwealth University

Recent efforts have confirmed that atomic clusters with specific coordination and mixed occupancy of species are the fundamental structural units of nearly all metallic glasses. In this work, a quasi-chemical approach is used to determine the total energy of each possible bi-atomic configuration in a 12-fold coordinated (icosahedral) cluster containing Cu and Zr. This defines a configurational density of states from which the enthalpy, entropy, and free energy of Cu-Zr and other such isolated clusters can be determined via a statistical-mechanics-type analysis. Results of this analysis are contrasted with a parallel approach based on ab initio techniques to determine the total energy of each Cu-Zr cluster in the same ensemble configuration space. These results are then compared with known data to assess the efficacy of using such an analysis of bi-atomic clusters as a proxy for the thermodynamic properties of Cu-Zr-based metallic glasses.

9:30 AM Invited

Primary Transformation Kinetics and Mechanical Properties of Zr-Al-Ni-Cu-Based Metallic Glass in Various Relaxation States: *Junji Saida*¹; *Albertus Setyawan*¹; ¹Tohoku University

It is well known that the relaxation state of glassy structure correlates to the structure, transformation behavior, mechanical and magnetic properties of metallic glasses. The authors can prepare the primary quasicrystal (QC)-forming Zr₆₅Al_{7.5}Ni₁₀Cu_{12.5}Pd₅ bulk metallic glasses (BMGs) in various relaxation states under different cooling rates. The grain growth rate of QC at the crystallization temperature is approximately 1×10^{-9} m/s in less relaxed (i.e. higher cooling rate) BMGs and it increases approximately twice as large in relaxed (i.e. lower cooling rate) BMGs. The homogeneous nucleation rate of the less relaxed samples is $5 \times 10^{19} - 1 \times 10^{20}$ /m³s, which is five to ten times higher than those



in the relaxed BMGs. The compressive plasticity is also lost with the relaxation. We conclude that the relaxation state has a marked effect on properties of glassy alloys. The results also provide useful information on the application as well as structural control of BMGs.

9:50 AM

Ion Irradiation Induced Nanocrystallization of Metallic Glasses: *Lin Shao*¹; ¹Texas A&M University

The effect of gas implantation in metallic glass was investigated for its application in radiation environments. We have shown that upon high fluence helium ion irradiation, metallic glass Cu₅₀Zr₄₅Ti₅ becomes highly porous at the depth of helium projected range, featured by the formation of a tunnel like structure and self-linkage of nanometer size gas bubbles. Furthermore, the irradiation leads to randomly distributed nanometer size Cu_xZr_y crystals. The finding evidences that He-filled bubbles have attractive interactions and expose considerable mobility. The bubble movement was believed to be assisted by ballistic collisions. A multiscale modeling by combining Monte Carlo simulation and finite element analysis has been carried out to simulate thermal spike quenching upon ion irradiation. We have found that the nanocrystal formation is not induced by localized phase transition upon ion hitting, since the heating quenching is faster than the critical cooling rate required for metallic glass formation.

10:00 AM Break

10:15 AM Invited

Pressure-Induced Phase Transitions in Metallic Glasses: *Jianzhong Jiang*¹; ¹University of Tennessee

The nature of amorphous-to-amorphous transition induced by pressure has been a topic of considerable research activities in several directional substances, e.g., ice, silicon, silica, and carbon. These structural polyamorphic transitions from a low-density amorphous (LDA) state to high-density amorphous (HDA) state often result from an increase in atomic coordination. Metallic glasses have many unique properties which have put these materials at the cutting edge of materials research. However, their disordered structure and electronic behavior are far less understood than other disordered amorphous materials such as network-forming glasses. Such coordination increase, and thus polyamorphism, was thought to be impossible in nondirectional, densely-packed metallic glasses that already have the maximum coordination number (12-14) of random nearest neighbors. In this talk, we review recent progress of phase transitions in Ce-containing metallic glasses. The origin for the transitions will be addressed.

10:35 AM

Crystallization Kinetics of Ca-Based Bulk Metallic Glasses: *Lei Hu*¹; *Feng Ye*¹; ¹University of Science and Technology Beijing

Several Ca-based bulk metallic glasses (BMGs) with diameter of 7 mm were fabricated by unidirectional quenching into water-cooled Ga-In-Sn liquid alloy. Thermal stability and crystallization kinetics have been investigated by differential scanning calorimeter (DSC). For Ca₆₅Mg₁₅Zn₂₀, the kinetics studies show that glass transition as well as crystallization behaves in a typically kinetic nature with Kauzmann temperature T_k about 267K and activation energies of $E_g=126$ kJ/mol and $E_x=116$ kJ/mol for glass transition and crystallization, respectively. The unusual phenomenon that E_g is close to E_x was discussed in this paper. The liquid fragility of Ca-based BMGs was studied by Vogel-Fulcher-Tammann (VFT) equation. The large fragility parameter D^* comparable to SiO₂ suggests the strong liquid behavior, which is one of the reasons for their excellent glass-forming ability (GFA). Furthermore, the glass transition temperature, crystallization temperature and their apparent activation energy are markedly affected by preannealing induced relaxation.

10:45 AM Invited

Effects of Alloying On the Glass Forming Ability and Mechanical Properties of Ti-Based Bulk Metallic Glasses: *Ke-Fu Yao*¹; *Pan Gong*¹; ¹Tsinghua University

Ti-based bulk metallic glasses are very attractive due to their low density, high strength, good anti-corrosion properties, low cost, and so on. However, compared with other alloy systems, the glass-forming ability (GFA) of Ti-based BMGs is relatively small. According to the reported results, the critical size of most Ti-based BMGs is smaller than 5 mm. Then improving the GFA of Ti-based BMGs, together with enhancing their mechanical properties, is necessary and important for their application. In present work, the effects of alloying elements on the glass-forming ability and mechanical properties of Ti-Zr-Be glassy alloys have been studied. It has been found that the glass forming-ability and mechanical property of the Ti-Zr-Be alloys could be significantly improved by alloying methods. Some of them exhibit large supercooled liquid temperature range ΔT , large critical size, and good mechanical properties. The related mechanism has been discussed.

11:05 AM

Study on Fracture Strength Reliability of Mg-Zn-Ca Bulk Metallic Glasses: *Junhua You*¹; ¹Shenyang University of Technology

Mg_{70-x}Zn_{25+x}Ca₅(x =1,2,3,4) amorphous alloys with a diameter of 2 mm were fabricated by cooper mold casting method. The microstructures, phase constituents, thermal and mechanical properties were investigated using scanning electron microscopy (SEM), x-ray diffractometer (XRD), differential scanning calorimetry (DSC) and universal electronic material testing machine, respectively. The results show that the crystallization processes consist of 3 to 4 steps for these bulk metallic glasses. The first onset crystallization temperature increases with Mg content. Meanwhile, the high strength and certain plastic strain can be attained for these amorphous alloys. Weibull statistic analysis shows that there exists different fracture strength reliability for the investigated alloys. The alloys with vein pattern fracture surfaces have higher Weibull modulus, which is corresponding to better fracture strength reliability.

11:15 AM Invited

Tensile Fracture Criterion of Metallic Glasses: *Zhefeng Zhang*¹; *R. T. Qu*¹; ¹Institute of Metal Research

We find that the classical failure criteria, i.e. maximum normal stress criterion, Tresca criterion, Mohr-Coulomb criterion and von Mises criterion, cannot satisfactorily explain the tensile fracture behavior of the bulk metallic glass (BMG) materials. For a better description, we propose an ellipse criterion as a new failure criterion to unify the four classical criteria above. In order to distinguish the normal stress effect, the Mohr-Coulomb criterion (M-C) and the Ellipse criterion are further compared and the normal stresses acting on the tensile fracture planes were controlled and varied in a wide range by introducing inclined notches with different inclination angles to a series of Zr-based MG specimens. The experimental results reveal that the Ellipse criterion gives a better prediction than the M-C criterion for the tensile fracture behaviors of the investigated Zr-based MG in a wide normal stress range.

11:35 AM

The Deformation Modes and Universal Scaling Properties in Metallic Glasses: *Pengyang Zhao*¹; *Ju Li*²; *Yunzhi Wang*¹; ¹The Ohio State University; ²Massachusetts Institute of Technology

Using a mesoscale model we study the deformation modes of metallic glasses. The effect of strain-induced softening on promoting the shear band is demonstrated in both 2D and 3D computer simulations. The role of free surface is also investigated to compare simulation results with experiments on deformation of nanopillars. In particular, the mechanical and structural heterogeneities near the free surface are introduced to study their effects on the initiation of shear bands. Furthermore, statistical analysis is performed and a universal scaling relationship is found in the distribution of local plastic avalanches. By reversing the softening

sign, i.e. designing a “work-hardening” metallic glass, the same scaling relationship persists, but with a different scaling exponent. These distinct exponents could be employed to distinguish different deformation modes.

11:45 AM Invited

Evolution of the Mechanical, Magnetic and Anti-Corrosion Behavior of Fe-Co-B-Si-Nb Bulk Metallic Glass during Thermally-Induced Devitrification: Jordina Fornell¹; Sergio González¹; Emma Rossinyol¹; Eva Pellicer¹; Santiago Suriñach¹; Dimitri Louzguine¹; Akihisa Inoue¹; Jordi Sort¹; Josep Nogués¹; *Maria D Baró*¹; ¹Universitat Autònoma de Barcelona

Fe₃₆Co₃₆B_{19.2}Si_{4.8}Nb₄ bulk glassy rods with 2 mm in diameter were manufactured by copper mould casting. The effects of annealing treatments on the microstructure, mechanical, magnetic and anticorrosion properties of this alloy are investigated. Annealing below the glass transition temperature causes the formation of small atomic clusters showing a pseudo-tenfold symmetry quasicrystal-like structure with close relationship to the Fe₂₃B₆ phase. This phase is actually the first to crystallize upon annealing, although two further crystallization events occur at higher temperatures. The as-cast alloy exhibits ultra-high hardness (> 14 GPa), high Young’s modulus (> 200 GPa) and good wear resistance. These properties are further enhanced after thermal treatments. In turn, the coercivity of the as-cast alloy also increases after thermally-induced devitrification. Electrochemical measurements show that both the as-cast and annealed specimens exhibit good corrosion resistance. The possible mechanisms responsible for these annealing-induced changes in the behavior of the Fe-based metallic glass are discussed.

12:05 PM

Fabrication and Mechanical Properties of Melt-Extracted Fe-Based Amorphous Wires: *Weibing Liao*¹; Yong Zhang¹; ¹University of Science and Technology Beijing

Metallic glasses often show good mechanical and physical properties as a consequence of their random atomic packing. However, as a new kind of potential engineering material, metallic glasses have proposed new requirements to traditional processing methods. In current study, the Fe74.5Cr3.5Si10B12 amorphous wires at micro scales with a smooth surface and negligible fluctuation in diameter were prepared by the melt-extraction method. The mechanical properties were evaluated by carrying out tensile and bending tests, and their reliability was estimated using Weibull analysis. High bending ductility implies the ability of the wire to bend through 180° without fracture.

CFD Modeling and Simulation in Materials Processing: Modeling of Steelmaking Processes

Sponsored by: The Minerals, Metals and Materials Society, TMS Extraction and Processing Division, TMS Materials Processing and Manufacturing Division, TMS: Process Technology and Modeling Committee, TMS: Solidification Committee
Program Organizers: Laurentiu Nastac, The University of Alabama; Lifeng Zhang, Missouri University of Science and Technology; Brian Thomas, University of Illinois at Urbana-Champaign; Adrian Sabau, Oak Ridge National Lab ; Nagy El-Kaddah, The University of Alabama; Adam Powell, Metal Oxygen Separation Technologies, Inc.; Hervé Combeau, Institut Jean Lamour

Thursday AM
March 15, 2012

Room: Oceanic 6
Location: Dolphin Resort

Session Chairs: Brian Thomas, University of Illinois at Urbana-Champaign; Koulis Pericleous, University of Greenwich

8:30 AM Keynote

Transport and Entrapment of Particles in Steel Continuous Casting: *Brian Thomas*¹; Quan Yuan²; Rui Liu¹; Sana Mahmood¹; Rajneesh Chaudhary¹; ¹University of Illinois at Urbana-Champaign; ²Dow Chemical Company

A particle-entrapment model based on local force balances has been developed, implemented into computational models of turbulent fluid flow, and applied to simulate the entrapment of slag inclusions and bubbles during the continuous casting of steel slabs. Turbulent flow of molten steel is computed in the nozzle and mold using transient CFD models. Next, the transport and capture of over 30,000 particles are simulated using a Lagrangian approach. Particles touching the dendritic interface may be pushed away, dragged away by the transverse flow, or captured into the solidifying shell according to the results of a local balance of ten different forces. This criterion was validated by reproducing experimental results in two different systems. Finally, the model is applied to predict the entrapment distributions of different sized particles in a typical slab caster. Although more large particles are safely removed than small ones, the capture rate as defects is still high.

9:00 AM Invited

Mathematical Modeling of a Compressible Oxygen Jet Interacting with a Free Surface in a Basic Oxygen Furnace for Steel Production: *Koulis Pericleous*¹; Bruno Lebon²; Georgi Djambazov²; Mayur Patel²; ¹University of Greenwich; ²University of Greenwich

High speed compressible jets are used in a number of steel-making applications. In the case of the BOF, a compressible oxygen jet reacts with a carbon-rich iron bath to reduce carbon levels and produce steel. The intensity of the process is governed by the speed of the jet and depression created in the metal and slag free surface. This is a difficult CFD problem, since there are compressible and incompressible regions in the flow domain, which need to be handled differently in a FV pressure-correction scheme. Also, standard turbulence models do not account for compressibility, or the large difference in density between the cold oxygen jet and the hot reacting surround. Corrections are introduced to the k-γ turbulence model to remedy this deficiency and the results validated against experimental data. The compressible/incompressible boundary is handled through a transition region at the free surface, based on Mach number.



TMS 2012

141st Annual Meeting & Exhibition

THURSDAY AM

9:25 AM

CFD Model for Prediction of Liquid Steel Temperature in Ladle during Steel Making and Casting: *Anurag Tripathi*¹; J.K. Saha¹; J.B. Singh¹; S.K. Ajmani¹; ¹Tata Steel Ltd

The quality of steel is a major concern in the metallurgical industry. The control of liquid steel temperature can enhance the level of cleanliness in steel. Ladle is one of the major vessels used to transfer liquid steel between different stations. The heat transfer phenomenon taking place in this vessel needs to be monitored for controlling the liquid steel temperature. A CFD model was developed for prediction of liquid steel temperature during complete process cycle of ladles in direct heats. The model was validated with liquid steel temperature measured at on-line purging station and tundish during teeming from one of the actual steel plant. The accuracy of model was 96 %. The results obtained show insignificant effect of slag thickness, tapping temperature and ladle life on liquid steel temperature in the ladle. However, the importance of initial refractory temperature was noticed. The CFD model developed in present work can generate the thermal history of liquid steel and refractory walls of any ladle at any stage.

9:45 AM

Multiphase Flow in a Steelmaking Converter Using an Unconventional Lance: *Miguel Barron*¹; Isaias Hilerio¹; Antonio de Ita¹; ¹Universidad Autonoma Metropolitana Azcapotzalco

The influence of an unconventional lance on the multiphase fluid flow in a steelmaking converter is studied in this work by means of CFD simulations. The lance has four peripheral supersonic nozzles and a vertical central nozzle. The oxygen flow in the central nozzle is considered independent from the main oxygen supply. Transient two-dimensional numerical simulations were carried out considering just molten steel and gaseous oxygen as the existing phases. Numerical results show that bath agitation and droplet generation are enhanced as a result of the central nozzle. However, the performance of the unconventional lance strongly depends on the distance of the lance tip to the molten steel surface and the velocity of the oxygen jet.

10:05 AM Break

10:25 AM

Fluid Flow and Inclusion Removal in Multi-Strand Tundish with Nozzle Blockage: *Pradeep Jha*¹; Sabin Mishra¹; Satish Sharma¹; Satish Ajmani²; Manas Mahapatra¹; ¹IIT Roorkee; ²Tata Steel

Due to mechanical/ electrical failure in the C.C. line or inadequate availability of molten steel from coming ladle, sometimes one/two outlets of a multi-strand tundish in continuous casting unit is closed. Closing any of the outlets affects the flow distribution inside the tundish which in turn governs the quality of steel coming out. Hence it is important to study which of the outlets should be closed to have proper results in terms of flow behavior and inclusion removal inside the tundish. Present study aims at finding the effect of closing one or two outlets on flow behavior and inclusion removal in a multi strand tundish. It was found that closing the near outlet (outlet near to the inlet) increases the inclusion removal tendency than closing the other two outlets in a six-strand billet caster tundish (only three outlets are considered because of symmetry).

10:45 AM

CFD Modeling of Fluid Flow Behavior and Bath Surface Deformation in LD Converter: *Tarun Kundu*¹; ¹IIT Kharagpur

Concrete understanding of fluid dynamics properties inside basic oxygen furnace (LD converter) and hot-metal surface deformation by impinging oxygen jet is important for optimization of reaction kinetics and maximization of productivity and refractory lining life. In this study various k- γ turbulence models and volume of fluid (VOF) method have been used to model fluid flow and interaction of impinging oxygen jet with hot metal for an industrial scale top blown LD converter. RNG, standard and realizable k- γ turbulence models are used to study velocity magnitude, stream function, turbulence intensity profiles. Turbulence kinetic energy, turbulence eddy dissipation, velocity magnitude and probable mixing time have been calculated in three locations inside the converter. The average rate of oxygen jet penetration, location of vortex formation, centre line and superficial velocity of impinging oxygen jet, probability of emulsification are studied by VOF method. These studies provide better understanding of phenomena occurring inside LD converter.

11:05 AM

Effect of Thermal Buoyancy Force on the Flow, Temperature Distribution and Residence Time Distribution of Molten Steel in the Slab Casting Tundish: *Haibo Sun*¹; Bo Yan¹; Jiaquan Zhang¹; ¹State Key Laboratory of Advanced Metallurgy, University of Science and Technology Beijing

Based on the validation of steady-state isothermal mathematical model by a 0.4-scale water model for the single-strand slab casting tundish, the effect of varying pouring temperature on the flow, temperature field, and residence time distribution (RTD) of the liquid steel was studied by a transient hydrodynamic model. Due to the decreasing temperature of ladle stream over a casting period of 50 min, the direction of vortex flow at the downstream side of dam changes to clockwise from the anticlockwise at 4 min after the new teeming, and reverts to anticlockwise direction again at 43 min. Meanwhile, the melt flow state in the hole of the dam is also varying with time. For conventional isothermal water modeling, the RTD parameters obtained are much different as compared with the non-isothermal ones. For the flow control devices (FCD) design, however, the same optimal scheme can be concluded from the point of view of isothermal modeling.

11:25 AM

Time Zone Analysis of F-Curve for Intermixing during Ladle Change-Over: *Pradeep Jha*¹; *Suman Kant*¹; Pradeep Kumar¹; Anand Kumar¹; ¹IIT Roorkee

It has been a major challenge to reduce the intermixed grade formation during ladle change-over operation in continuous casting process of tundish steelmaking. The F-curve generated by step input of the tracer (new grade steel) tells about the intermixed grade amount for different grade specifications. While use of flow modifiers is beneficial in reducing the intermixed grade because of the change in slope (in different time zones) and position of the F-curve due to their placement at tundish bottom. Present study aims at investigating the role of dam placed before the outlet in a multi-strand tundish with reference to the slope behavior of F-curve in different time zones during the teeming operation plays an important role in determining the intermixed amount.

Characterization of Minerals, Metals, and Materials: Characterization of Carbon and Soft Materials

Sponsored by: The Minerals, Metals and Materials Society, TMS Extraction and Processing Division, TMS: Materials Characterization Committee

Program Organizers: Jiann-Yang Hwang, Michigan Technological University; Sergio Montero, State University of North Rio De Janeiro; Chenguang Bai, Chongqing University; John Carpenter, US Department of Energy; Donato Firrao, Politecnico di Torino; Byoung-Gon Kim, Korea Institute of Geoscience & Mineral Resources; Mingdong Cai, Schlumberger

Thursday AM
March 15, 2012

Room: Asia 2
Location: Dolphin Resort

Session Chairs: Shadia Ikhmayies, Al Isra University; Jinhui Peng, Kunming University of Science and Technology

8:30 AM

Thermal Properties of Polyester Composites Incorporated with Coir Fiber: *Helvio Santafé Júnior*¹; Noan Simonassi¹; Sérgio Monteiro¹; ¹Universidade Estadual do Norte Fluminense-Darcy Ribeiro

The fiber extracted from the husk of coconut fruit, known as coir fiber, has been extensively investigated as a second phase incorporation into polymer composites. However limited attention has been given to the effect of the temperature on the thermal stability of coir fiber reinforced composites. This work investigated the thermal properties of polyester matrix composites incorporated with coir fiber. Specimens with up to 30% wt% of continuous and aligned coir fibers were thermogravimetric evaluated by TGA/DTG technique and analyzed by differential scanning calorimetry, DSC. It was found a marked loss of mass from 150 to 500°C due mainly to the degradation of the polyester matrix. The DTG peaks also revealed evidence of lignin and cellulose degradation in the coir fiber. DSC peaks could be associated with the release of formation water in both the polyester and coir fibers.

8:45 AM

High Temperature Plastic Crystal Structure Characterization Studies of Orientationally Order/disordered Organic Compounds - Pentaglycerine and 2-Amino-2-methyl-1, 3-propanediol Binary System: *Wen-Ming Chien*¹; Ivan Gantan¹; Amrita Mishra¹; Dhanesh Chandra¹; ¹University of Nevada, Reno

The binary orientationally order/disordered organic compounds, Pentaglycerine (PG) and 2-Amino-2-methyl-1, 3-propanediol (AMPL), have been performed the phase equilibrium and characterization studies by using high temperature X-ray diffraction (XRD) and differential scanning calorimetric (DSC) methods. The organic compounds (also called as thermal energy storage materials) undergo a solid-solid state phase transition before melting which will store large amounts of thermal energy. The binary samples of PG-AMPL were prepared to perform high temperature XRD characterization and DSC studies. The XRD results show that low temperature order solid state phase of PG was characterized as the tetragonal structure, and AMPL was the monoclinic structure. The high temperature orientationally disordered (plastic) phases of PG and AMPL were characterized as the FCC and BCC, respectively. Experimental binary PG-AMPL phase diagram were also developed, and the calculated PG-AMPL phase diagram was obtained by using the Calculation of Phase Diagrams (CALPHAD) modeling technique and Thermal-Calc software.

9:00 AM

Investigating the Rheology of LCPs through Different Die Geometries: *Arash Ahmadzadegan*¹; *Michael Zimmerman*¹; *Anil Saigal*¹; ¹Tufts University

The rheology of liquid crystalline polymer melts through different die geometries is simulated using Polyflow™. The main goal here is to develop the necessary rheological model to simulate the orientation effects due to flow. Rheological properties of the LCPs are close to long chain polymers and their directionality is close to those of small molecule liquid crystals. As a result, different rheological models (both viscoelastic and generalized Newtonian) for long chain polymers were chosen based on the available capillary rheometer data. Using different parameters it is possible to model shear viscosity, normal stress differences and relaxations times. The free surface of the extrudate coming out of the die is simulated and the amount of die swell is compared. This study allows us to determine which of the available rheological models best apply to main-chain thermotropic LCP materials and to predict the orientation of crystallines inside and outside the die.

9:15 AM

Characterization of Graphite from PAN Aerogels: *Shruti Mahadik*¹; *Clarissa Wisner*¹; *Anand Sadekar*¹; *Abhishek Bang*¹; *Massimo Bertino*²; *Chariklia Sotiriou-Leventis*¹; *Nicholas Leventis*¹; ¹MS&T; ²Virginia Commonwealth University

Bundles of carbon microrods similar to those observed in some natural graphites were "grown" by pyrolysis of polyacrylonitrile (PAN) aerogels. The latter were synthesized in toluene by free radical co-polymerization of acrylonitrile with two variable-length bi-functional acrylates, ethylene glycol dimethylacrylate (EGDMA) and hexamethylene diacrylate (HDDA). PAN aerogels were aromatized oxidatively at 240°C and further treated pyrolytically to graphite under helium atmosphere at 2300°C for 24 hours. Properties of each graphitized form as well as of intermediates after pyrolysis at 800°C and 1600°C were characterized by scanning electron microscopy (SEM), high resolution transmission electron microscopy (HRTEM), X-ray powder diffraction (XRD), and Raman spectroscopy studies. Although the two crosslinkers, EGDMA and HDDA, are decomposed completely by 800°C, their original signature remains through to the crystalline order of each graphitized form.

9:30 AM

Effect of the Fiber Equivalent Diameter on the Elastic Modulus and Density of Sisal Fibers: *Artur Camposo Pereira*¹; *Sergio Monteiro*¹; *Wellington Inácio*¹; ¹Universidade Estadual do Norte Fluminense

Natural fibers are currently gaining attention as reinforcement of polymer composites for uses in engineering parts for automobile and building construction. In spite of environmental, economical and societal advantages, the natural lignocellulosic fibers are not as uniform in their dimension and properties as compared to synthetic. In recent works it was found that the variation in strength could be correlate to the equivalent diameters for several lignocellulosic fibers including the sisal fibers. In the present work an investigation on a possible correlation of the equivalent diameter with changes in density and elastic modulus was carried out. Precise measurements of the equivalent diameter, conducted in a profile projector, were correlated with the density and the elastic modulus by means of the Weibull statistic analysis. The results showed that an inverse correlation with the diameter also applies for both the density and the elastic modulus with a high degree of prevision.

9:45 AM

Tensile Fracture Analysis of Polymer Matrix Composites: *Jeongguk Kim*¹; *Sung-Cheol Yoon*¹; *Jung-Seok Kim*¹; *Hyuk-Jin Yoon*¹; *Sung-Tae Kwon*¹; ¹Korea Railroad Research Institute

The tensile failure behavior of glass fiber reinforced epoxy polymer matrix composites (PMCs) was investigated during tensile testing. The PMCs have been used for railway bogie materials application for the purpose of lightweight in bogie. Through tensile testing, the fracture



initiated at the epoxy matrix, and the brittle failure mode was observed. In order to monitor tensile damage evolution of PMC sample, a high-speed infrared camera was used to measure surface temperature changes during tensile testing. Through the thermographic image analysis, crack initiation and propagation were qualitatively monitored. Moreover, the microstructural characterization using scanning electron microscope (SEM) was performed to correlate the mechanical failure mode with thermographic results. In this investigation, an IR camera and SEM investigation were used to facilitate a better understanding of damage evolution and failure mode of PMC materials during tensile testing.

10:00 AM

Correlation between the Density and the Diameter of Buriti Fibers: *Anderson Barbosa*¹; *Michel Oliveira*¹; *Alex Almeida*¹; *Núbia Santos*²; *Frederico Margem*¹; *Sergio Monteiro*¹; ¹State University of the Northern Rio de Janeiro, UENF; ²State University of Pará

Environmental considerations in addition to technical, economical and societal benefits are increasingly promoting the substitution of natural fibers for glass fiber in polymer matrix composites. However, natural fibers are heterogeneous in their dimensions, specially the cross section, which plays an important role in their mechanical strength. The fibers extracted from the petiole of the buriti palm tree is a promising stiff natural fiber for composite reinforcement. In this work, a statistical analysis of the density of buriti fibers using the Weibull methodology was performed. An attempt to correlate the fiber density with the diameter, precisely measured by means of a profile projector, was carried out. The results revealed an inverse dependence between the buriti fiber diameter and corresponding density. Fracture tip observation by SEM suggested a possible mechanism that could justify this inverse correlation.

10:15 AM

Thermal and Morphological Behavior of EVOH/Piassava Fiber Composites: *Beatriz Nogueira*¹; *Anne Chinellato*²; *Angel Ortiz*¹; *Arifa Parveen*³; *Vijaya Rangari*³; *Esperidiana Moura*¹; ¹Instituto de Pesquisas Energéticas e Nucleares - Ipen-Cnen/Sp; ²Universidade Federal do ABC - UFABC; ³Tuskegee University

Composite consisting of ethylene vinyl alcohol (EVOH) with short piassava fibers were prepared by extrusion process and their thermal and morphological behavior were investigated. The EVOH reinforced with 5 and 10 % of piassava fiber particle, based on the percentage weight ratio (wt %), untreated and treated with a commercial silane coupling agent, were prepared and the influence of fiber loading and the effect of chemical treatment on their thermal and morphological behavior were evaluated by SEM, DSC and TG analyses. Melt flow index (MFI) of the composites have been determined to evaluate the effects of fiber reinforcement on dynamic viscoelastic melt of the EVOH. In addition, piassava fibers characterization by SEM, FTIR, and organic and inorganic composition have also been carried out. The SEM results of the composites showed surface micrographs without microvoids and a good distribution, dispersion and compatibility between the fillers and the EVOH matrix.

10:30 AM

Characterization of Thermal Behavior of Epoxy Composites Reinforced with Banana Fibers by TGA/DTG and DSC: *Nathalia Rosa*¹; *Lucas Martins*¹; *Sergio Monteiro*¹; *Ruben Rodriguez*¹; *Tereza Castillo*¹; ¹UENF

The fibers extracted from the pseudostem of the banana plant have been studied as possible reinforcement in polymer composites due to their environmental and technical advantages. Some possible uses above room temperature require information on the thermal behavior of composites reinforced with banana fibers. Therefore, the objective of the present work was to investigate the thermal behavior of epoxy matrix composites incorporated with up to 30% in volume of banana fibers. Thermogravimetric analysis TGA/DTG and differential scanning calorimetry were used in this investigation. It was found that thermal degradation associated with weight loss occurred in two stages. Changes

were also observed from 150 to 400°C in the DTG peaks. Moreover, the DSC results showed endothermic events associated with water release and possible molecular chain degradation. Comparison with similar composites permitted to propose mechanisms that explain this DSC thermal behavior.

10:45 AM

Comparative Studies OF Crushing Behavior of Various Fiber Reinforced Skin Polyurethane Foam Cored Composite Sandwich Structures: *Krishna Sharma*¹; *Sripathy Mallaiah*¹; ¹Bangalore University

The conventional fiber reinforced plastic does not participate in the plastic deformation or enter the large plastic deformation state during collision. The objective of this study is focused on investigating the crushing of sandwich structure made of sisal / coir / bamboo / glass fabrics acting as the reinforcement materials and with polyester resin to form the composites skin with polyurethane foam as core. Experiments showed that the underlying crushing mechanism of sandwich structures is very different from that of solid-section thin-walled structures. When a sandwich structure is subjected to crushing, the core deforms in the shear mode whereas the face undergoes bending independently. The damage is through the width zone of crushed foam core accompanied by a residual dent in the skin. It is shown that such damage causes a significant reduction of compressive strength.

11:00 AM

Elastic Modulus Variation with Diameter for Ramie Fibers: *Alice Bevitoni*¹; *Isabela da Silva*¹; *Renan Carreiro*¹; *Sergio Monteiro*¹; ¹UENF

The ramie fiber is one of the strongest lignocellulosic fibers with applications ranging from simple items such as fabrics and ropes to engineering composites for automobile parts and building panels. Characterization of the ramie fiber has recently been conducted for physical and mechanical properties. In principle, thinner ramie fiber could be comparatively stronger and consequently more effective as a composite reinforcement. In this work an attempt to correlate the ramie fiber elastic modulus obtained in tensile test with its corresponding diameter, precisely measured by means of a profile projector, was carried out. Tensile results analyzed by the Weibull statistic showed a significant increase in elastic modulus with decreasing the diameter of ramie fiber. Scanning electron microscopy observation of the fracture of selected ruptured fiber revealed possible mechanisms that could justify the elastic modulus/diameter inverse dependence.

11:15 AM

Comparative Study of the Sugarcane Bagasse Fiber/HDPE Composite Properties Using Electron-Beam and Gamma Radiation Treatments: *Amanda Pereira*¹; *Alejandra Soria*²; *Anibal Abreu*²; *Anne Chinellato*³; *Nélida del Mastro*¹; *Esperidiana Moura*⁴; ¹Instituto De Pesquisas Energéticas E Nucleares - IPEN-CNEN/SP; ²Laboratório Tecnológico del Uruguay; ³Universidade Federal do ABC - UFABC; ⁴Instituto De Pesquisas Energéticas E Nucleares - IPEN-CNEN/SP

This work presents a comparative study of the thermo-mechanical and morphological properties of sugarcane bagasse fiber/HDPE composite treated with electron-beam and gamma radiation. The composite samples obtained by extrusion and injection molding processes were irradiated at 50 and 90 kGy using either a 1.5 MeV electron beam accelerator or gamma irradiator EMI-9, at room temperature in presence of air. The irradiated and non-irradiated samples were submitted to thermo-mechanical tests, differential scanning calorimetry (DSC), thermogravimetric analysis (TGA), scanning electron microscopy (SEM) X-ray diffraction (XRD) and sol-gel analyses and the correlation between their properties was discussed. In addition, the MFI tests were done to evaluate the effects of bagasse fiber on dynamic viscoelastic melt of the HDPE. It was found that by using electron-beam or gamma radiation treatment, the properties of the bagasse fiber/HDPE composite were improved.

11:30 AM

Effect of Diameter on the Density and Tensile Elastic Modulus of Curaua Fibers: *Felipe Lopes*¹; Renan Carreiro²; Noan Simonassi²; Ailton Ferreira³; Sergio Monteiro²; ¹IME; ²UENF; ³UFF

The fibers extracted from the leaves of curaua plant (*Annanas erectifolius*) are among the strongest lignocellulosic and being already applied as reinforcement of polymer composites in engineering applications. It was recently found that the tensile strength of the curaua fiber is markedly depend on its diameter. For very thin fibers strength above 1200 MPa were reported. In the present work the density and tensile elastic modulus of curaua fibers were evaluated as a function of the equivalent diameter measured by profile projector. Using the Weibull statistic analysis it was verified that both the density and elastic modulus follow inverse correlation with the diameter. An additional investigation on the microstructure of the fiber and its tensile fracture, by means of scanning electron microscopy, revealed that the distribution of defects and participation of microfibrils play a relevant role on the variation of the curaua fiber properties with the diameter.

Characterization of Minerals, Metals, and Materials: Characterization of Light Metals

Sponsored by: The Minerals, Metals and Materials Society, TMS Extraction and Processing Division, TMS: Materials Characterization Committee

Program Organizers: Jiann-Yang Hwang, Michigan Technological University; Sergio Montero, State University of North Rio De Janeiro; Chenguang Bai, Chongqing University; John Carpenter, US Department of Energy; Donato Firrao, Politecnico di Torino; Byoung-Gon Kim, Korea Institute of Geoscience & Mineral Resources; Mingdong Cai, Schlumberger

Thursday AM
March 15, 2012

Room: Europe 6
Location: Dolphin Resort

Session Chairs: Xuewei Lv, Chongqing University; Gulhayat SAYGILI, Istanbul Technical University

8:30 AM

Influence of Deformation on the Properties of carbon-Fiber Reinforced 2024 Alloy Matrix Composites: *Wu Linli*¹; ¹Northeastern University

The influence of deformation on the properties of short-carbon-fiber reinforced 2024 alloy matrix composites was investigated in this study. It was found that the distribution of carbon fibers changed from the random state before deformation to the ordered state that carbon fibers arranged along the direction of rolling and extruding after deformation. Under the temperature range in control, the increase of rolling and extruding temperature would benefit to improve strength and elongation of composites, but was not conducive to enhance the hardness of composites. With the increment of total deformation, all the strength and hardness of composites became greater, nevertheless the elongation decreased. Moreover, after being rolled and extruded, the strength and hardness of composites are improved. Strength of extruded 2024 alloy matrix composites was higher than that of rolled 2024 alloy matrix composites under the same heat treatment conditions.

8:45 AM

Microstructure and Deformation Behavior of Mg-Zn-Al-Re Magnesium Alloy: *Jing Zhang*¹; Fusheng Pan¹; Chenguang Bai¹; ¹Chongqing university

The microstructure and hot deformation behaviour of an Er-modified Mg-Zn-Al alloy were evaluated. The results showed that the addition of rare-earth Er changed the morphology of the quasi-continuous grain boundary networked eutectic compound to globular particles. Moreover, a self-strengthening effect was identified for the alloy, which determined

its deformation behavior. After hot extrusion, the yield strength and elongation to failure of the Mg-Zn-Al-Re alloy at 200°C were increased by 105% and 120%, respectively, due to an emerged dynamic precipitation strengthening mechanism.

9:00 AM

Microstructures and Properties of Solid and Open-Cellular γ -TiAl Fabricated by Electron Beam Melting (EBM): *J. Hernandez*¹; L. E. Murr¹; S. M. Gaytan¹; S. J. Li²; X. Y. Cheng²; Y. X. Tian²; F. Medina¹; R. B. Wicker¹; ¹University of Texas at El Paso; ²Shenyang National Laboratory for Materials Science

Gamma TiAl has been considered to be an ideal replacement for Ni-base superalloy aerospace applications, particularly weight-critical applications. While bulk, fully dense gamma-TiAl is 50% less dense than Ni-base superalloys, it also has excellent mechanical properties at high temperature (up to ~800°C). In this study we have fabricated solid and open-cellular prototypes of gamma-TiAl by electron beam melting (EBM) from pre-alloyed Ti-48Al-2Cr-2Nb precursor powder. The solid prototype density (ρ_s) was ~4.0 g/cm³ while mesh and foam prototypes were fabricated with relative densities as low as $\rho/\rho_s = 0.12$. Corresponding dynamic stiffness (or elastic modulus) measurements indicated an ideal foam behavior. The solid and open-cellular component microstructures were observed by optical metallography and TEM, and supported by XRD analysis. The exhibited duplex microstructure composed of relatively equiaxed γ grains and interspersed lamellar colonies characterized by thin a_2 plates having an orientation relationship: $(111)_\gamma || (0001)_{a_2}$.

9:15 AM

Microstructures and Tensile Mechanical Properties of Mg-9Zn-0.6Zr-2Er Magnesium Alloy Processed by Hot Rolling and Heat Treatment: *Jing Zhang*¹; *Baoxiang Zhang*¹; ¹Chongqing University

As extruded Mg-9Zn-0.6Zr-2Er magnesium alloys were hot-rolled at 400°C, followed by solution treatment at 400°C for 1.5h and artificial aging at 200°C for 10h. Microstructures and tensile mechanical properties of the alloys after hot rolling, solution and aging treatment were examined respectively. Optical micrographs of the as-rolled and as-solution alloys showed fine grain structures, due to the formation of Er- and Zn-bearing compounds at grain boundaries which obviously improved the thermal stability of the alloy. Yield strength as high as about 335 MPa was obtained for the as-rolled alloy, showing that the mechanical properties of the alloy was greatly benefit from the grain refinement and dynamic precipitation of fine MgZn₂ during hot rolling. Due to solution heat treatment, vast majority of the Mg-Zn phases dissolved into the matrix, and precipitated out again as fine dispersoid during the subsequent aging, resulting in an enhanced aging-hardening effect.

9:30 AM

Nanobond - The Perfect Refractory Choice for Quick Lining and Repairing of Aluminium Melting Furnaces: *Thomas Schemmel*¹; Helge Jansen¹; Bertram Kesselheim¹; Uwe Kremer²; ¹Refratechnik Steel GmbH; ²TRIMET Aluminium GmbH

During the last decades the refractory life time of the different aggregates of the secondary aluminium production was improved significantly. Anyhow, each repair and installation of refractory material affects the operating schedule and can cause costs in the million range. The downtime of only one melting furnace generate costs of 100.000 to 400.000 \$ per day. Besides cooling down of the kiln and its repair, the heating-up procedure takes the longest time of the shutdown. Usually, heating-up of low cement or ultra low cement castables takes 120 to 150 hours. In order to reduce such expensive downtimes Refratechnik developed a unique and novel product series: Nanobond. These materials can be heated up in only a third of the usual time. This paper talks about the theoretical aspects as well as the mechanical and physical properties and especially practical experience.



TMS 2012

141st Annual Meeting & Exhibition

THURSDAY AM

9:45 AM Break

9:55 AM

Study on Graphitization of Cathode Carbon Blocks for Aluminum Electrolysis: *Gao Feng*¹; *FengNai Xiang*²; *Yang Jian Zhuang*²; *Niu Qing Ren*³; *He Hua*³; *Han Li Guo*³; ¹Northeastern University; ²Northeastern University; ³Qingtongxia Aluminum Limited Corporation, Qingtongxia

High quality graphite cathode carbon blocks require low resistivity, strong resistant erosion to melt salt and liquid aluminum in the aluminum electrolytic cells. It not only can decrease cathode voltage drop and reduce the powder consumption, and but also can improve service life of the cell. Applying hot mould technology under 40 MPa pressure, different amount petroleum coke in anthracite mixtures is graphitized in graphitized furnace. By the X-ray diffraction parameters, density, compressive strength and resistivity drop measured, the experimental results show that compressive strength and volume density of graphite containing 30% of petroleum coke block respectively are 1.366 g/cm³ and 4.8 MPa, resistivity drop from 114μO • m to 13μO • m, most confirms to the production requirements.

10:10 AM

Wear Resistance of Graphite /Aluminum Compound Material that Prepared by Stirring Casting: *Wu Linli*¹; *Yao Guangchun*¹; ¹Northeastern University

The graphite reinforced aluminium matrix composites were prepared by stir-casting, reinforcement of graphite particles coated with oxide, and the friction behavior was investigated perfectly. The results indicated that, the aluminium matrix composites reinforced with 6 wt.% graphite particles coated with oxide have a good property of self-lubrication under the condition of dry friction with a pressure of 40 N, a relative rate of 2.62 m/s of frictional backing gear, a wear time of 60 min, in addition, the friction factor and wear capacity of the graphite / aluminium matrix composites were less than those of bulk alloy. Moreover, the friction factor and wear capacity of the graphite / aluminium matrix composites decreased with an increase in mass fraction of the graphite coated with oxide, and the friction factor of composites became bigger while the fraction of the graphite particles was over 6wt.%.

10:25 AM

Characterization of Grit Blasted Metallic Biomaterials by Thermoelectric Power Measurements: *Hector Carreon*¹; *Sandra Barriuso*²; *Jose Luis González-Carrasco*²; *Francisca Garcia-Caballero*²; *Marcela Lieblich*²; ¹UMSNH; ²Centro Nacional de Investigaciones Metalúrgicas (CENIM-CSIC)

The grit blasting, a surface improvement treatment is used to enhance mechanical fixation of the implants through increasing their roughness. As a result of the severe plastic surface deformation, it produces additional effects such as grain refinement, hardening and compressive residual stresses which are generally evaluated with destructive techniques. In this research work, we present preliminary results of the non-contacting and contacting thermoelectric power measurements in blasted Ti-6Al-4V and 316LVM specimens using Al₂O₃ and ZrO₂ particles respectively. This study correlates the microstructural changes induced by the grit blasting treatment and the limitations and advantages of each of the nondestructive thermoelectric techniques based on Seebeck effect used to evaluate these biomaterials.

10:40 AM

Exploring Microstructure-Corrosion Property Correlations in 5000-Series Alloys Using Higher-Order Statistical Metrics: *Daniel Satko*¹; *Jonathan Kaufman*¹; *Joshua Shaffer*¹; *Roger Doherty*¹; *Surya Kalidindi*¹; ¹Drexel University

The non heat-treatable aluminum alloys of the 5000 series are known to be susceptible to intergranular corrosion and stress corrosion cracking upon exposure to slightly elevated temperatures for Mg content in excess of about 3 wt%. Sensitization of these alloys is due to precipitation of a continuous film of anodic Al₃Mg₂ intermetallic η phase along grain

boundaries. It has been shown that 1-point metrics, based on volume fractions, are inadequate to describe the salient microstructural features. In this paper, we specifically explore correlations between higher-order spatial statistical metrics obtained from datasets combining EBSD orientation information with η phase distributions and susceptibility to intergranular corrosion of selected high-Mg alloys from this series.

10:55 AM

Modeling the Mechanical Response of Aluminum A359-SiCp-30%: *James DeMarco*¹; *Justin Karl*¹; *Yongho Sohn*¹; *Ali Gordon*¹; ¹UCF MMAE Dept.

Various aluminum metal-matrix composites (Al-MMCs) are currently under consideration for use in structural components of next-generation heavy ground vehicles. However, processing remains costly, due in part to material loss through edge cracking. In recent work, the authors have investigated the dependence of mechanical properties of as-cast A359-SiCp-30% on strain rate and temperature. The observed trends in material behavior were used to calibrate and test a multiaxial temperature- and strain rate-dependent constitutive model which allows numerical simulation of hot rolling. A damage model which is also temperature- and strain-rate dependent is used to predict failure.

Computational Thermodynamics and Kinetics: Interfaces

Sponsored by: The Minerals, Metals and Materials Society, TMS Electronic, Magnetic, and Photonic Materials Division, TMS Materials Processing and Manufacturing Division, TMS Structural Materials Division, TMS: Alloy Phases Committee, TMS: Chemistry and Physics of Materials Committee, TMS/ASM: Computational Materials Science and Engineering Committee, TMS: Integrated Computational Materials Engineering Committee, TMS/ASM: Phase Transformations Committee, TMS: Process Technology and Modeling Committee

Program Organizers: Zi-Kui Liu, The Pennsylvania State University; Mark Asta, University of California, Berkeley; James Warren, The National Institute of Standards and Technology; Yunzhi Wang, Ohio State University; Raymundo Arroyave, Texas A & M University; Yu Wang, Michigan Tech

Thursday AM
March 15, 2012

Room: Australia 3
Location: Dolphin Resort

Session Chairs: Jeff Hoyt, McMaster University; Christopher Woodward, US Air Force

8:30 AM Invited

First Principles Modeling of Solid-Solid Interfaces: *Christopher Woodward*¹; ¹Air Force Research Laboratory

Over the last decade there have been significant advances in our ability to predict the spatial and chemical morphology of solid interfaces. Simultaneously, characterization methods based on electron microscopy (i.e. High Angle Annular Dark Field Scanning Transmission Electron Microscopy) and Local-Electrode Atom-Probe tomography have advanced to the level of chemical resolution at the atomic-scale. The combination of emerging modeling and characterization methods provides a potent tool for exploring boundary properties and validating computational methods. Progress in modeling of interfacial boundaries will be illustrated using examples in (Ni and Al) engineering alloys, with the focus primarily on first principles methods that include entropic contributions to the free energy. While these methods are typically limited to coherent interfacial boundaries, there are examples of first principles calculations of incoherent metal-oxide boundaries without entropic contributions. Time permitting, examples on how such results inform meso and macro scale models will also be presented.

8:55 AM Invited

Grain Boundary Energy Function for FCC Metals: *Vasily Bulatov*¹; ¹LLNL

To quantify the driving forces acting on the GB networks under thermal coarsening and/or irradiation conditions, it is desirable to express the GB energy as a function of five macroscopic degrees of freedom. The very existence of such a function has been controversial but recent computer simulations suggest that such a function should exist. In this development we focus on the global topology of the functional 5-space of the GB energy function and examine positions and connectivity of its singular points – cusps. The resulting energy function reflects all relevant symmetries of the bi-crystal, its functional form is universal for FCC crystallography but contains material-specific parameters that can be fit to energies measured or computed for just a handful of special boundaries. The resulting function provides a high quality fit to the extensive data sets of GB energies computed by Olmsted et al.

9:20 AM

Topological Evolution of Grains in 3D Monte Carlo Modeled Grain Growth: *Burton Patterson*¹; Robert DeHoff¹; Veena Tikare²; David Rule¹; Amy Adams¹; ¹University of Florida; ²Sandia National Laboratories

Grains traverse a complex path of topological states during 3D grain growth. Their numbers of faces increase and decrease through the three fundamental topological events of grain encounter, grain separation and contact with disappearing tetrahedra. These topological changes control their individual growth and shrinkage rates, which are tied to their integral mean curvature, in turn related to their number of faces. 3D Monte Carlo simulation has enabled monitoring the traversal of individual grains up and down the Schlegel tree of topological states. This previously inaccessible information provides a valuable first look at these fundamental processes of grain growth.

9:35 AM

Modeling the Asymptotic Grain Face Distribution in Terms of Topological Event Rates: *Robert DeHoff*¹; Burton Patterson¹; Veena Tikare²; David Rule¹; Amy Adams¹; ¹University of Florida; ²Sandia National Laboratories

The steady-state grain face frequency distribution during grain growth has been modeled in term of kinetic topological parameters obtained from 3D Monte Carlo (3DMC) simulations. Each face class experiences six fluxes of grains into and out of it due to the different fundamental topological events occurring in it and the adjacent face classes. Equations for the net gain and loss of grains from each face class were constructed in terms of the relative rates of these events in the system and the participation probabilities of each face class for those events. Simultaneous solution of the set of equations for all face classes provided the asymptotic distributions for those event rate ratios. Event ratios were obtained from 3DMC simulations with different initial volume distribution widths, producing different asymptotic volume and face distributions and event rates. Solutions based on these event ratios successfully modeled the asymptotic 3DMC distributions from which they came.

9:50 AM

4D Grain Growth Kinetics in High-Purity Aluminum: *Anthony Johnson*¹; Stefan Poulsen²; Andrew King³; Wolfgang Ludwig³; David Rule⁴; Burton Patterson⁴; Peter Voorhees¹; Erik Lauridsen²; ¹Northwestern University; ²Risø National Laboratory for Sustainable Energy; ³European Synchrotron Radiation Facility; ⁴University of Florida

We have employed Diffraction Contrast Tomography (DCT) and a multi-order parameter phase-field model to study 4D grain growth kinetics in aluminum. DCT was used at the European Synchrotron Radiation Facility to produce 3D grain maps of a high-purity aluminium sample at nine time steps during an anneal. The annealing temperature was chosen such that grain boundary movement was small but finite, in order to accurately measure grain boundary velocities. These velocities, along with the grain boundary and triple line curvatures, are compared with the MacPherson-

Srolovitz equation for the evolution of individual grains. The data set is also used as initial conditions for a multi-order parameter phase field simulation, to test the validity of the model, measure the degree of grain boundary mobility and energy anisotropy, and to determine the role of triple line energy and mobility in the grain growth process observed in the experiments.

10:05 AM Break**10:35 AM Invited**

Grain Boundary Migration and Grain Growth: What I Do & Do Not Understand: *David Srolovitz*¹; ¹Institute for High Performance Computing, Agency for Science, Technology and Research, Singapore

In this presentation, I will examine several topics in grain boundary migration and grain growth. The topics are heavily biased towards my own interests and hence the coverage is idiosyncratic. I will first discuss grain boundary migration mechanisms. What have we learned from molecular dynamics simulations and dislocation dynamics models? What happens as we change bicrystallography, temperature, the form of the driving force,... Next, I will discuss several fundamental issues in normal grain growth: recent extensions of the Mullins-von Neumann description to all integer dimensions (>1), differences between 2 and 3 dimensions, correlations in geometry and topology in normal grain growth microstructures,... I will conclude with a “shopping list” of open questions in both areas that I believe require more attention and opportunities presented by recent advances in the 3d characterization of microstructure.

11:00 AM Invited

The Mobility of Interfaces and Grain Boundaries from Molecular Dynamics Simulations: H. Song¹; M. J. Rahman¹; *Jeffrey Hoyt*¹; ¹McMaster University

Molecular dynamics (MD) simulations have proven to be quite useful in extracting thermodynamic and kinetic properties of crystalline interfaces. In this work we will review various techniques that have been developed recently to compute grain boundary mobilities in pure metals. The techniques include: curvature driven growth, the random walk method, equilibrium boundary fluctuations, stress driven migration and the artificial driving force method. MD derived mobility vs. misorientation data will be summarized for several systems and new results will be reported for the temperature dependent mobility of a low angle 112 tilt boundary in Al. In addition, the application of MD to the case of an FCC-BCC interphase boundary in pure Fe will be discussed and the atomistic growth mechanisms as well as the temperature dependence of the mobility will be presented.

11:25 AM

Lattice Monte Carlo Determination of Harrison Kinetics Regimes for Grain Boundary Diffusion in Materials with Inhomogeneous Grain Structures: *Irina Belova*¹; Graeme Murch¹; Thomas Fiedler¹; ¹The University of Newcastle

Identification of the Harrison kinetics regimes (Types A, B and C) has been investigated by the authors for the case of grain boundary self-diffusion in materials with grains of the same size. Real materials of course generally have much more complicated grain size distributions. For the first time, we analyse the grain boundary diffusion problem with an inhomogeneous grain structure by means of the Lattice Monte Carlo (LMC) method that has been extensively developed by the authors to address phenomenological diffusion problems. The LMC method is used here for to determine the transitions that occur between the Harrison grain boundary kinetics regimes. Importantly, it is shown that the distributions of grain sizes can contribute significantly into the resulting concentration profiles with possible consequent overestimation of both lattice and grain boundary diffusion coefficients. It is shown that a new approach for calculating the diffusion parameters for Harrison classification purposes is needed.



11:40 AM

Molecular Dynamics Study of Solid-Liquid Interface Migration in Ni-Zr Alloys: *Mikhail Mendeleev*¹; ¹Ames Laboratory

While several dozens of molecular dynamics (MD) simulation works reporting the solid-liquid interface (SLI) velocities in pure metals have been published the number of works where the SLI migration was studied in alloys is very limited. I will present the results of the MD simulations of the SLI migration in the Ni₅₀Zr₅₀ and NiZr₂ alloys. The crystal phases in these alloys are congruently melting stoichiometric compounds and a potential development procedure which allows fitting the melting temperatures for these compounds will be discussed. The developed semi-empirical potential allows in the case of the Ni₅₀Zr₅₀ alloy the simulation of the SLI migration for both B2 and B33 phases. The temperature dependence and anisotropy of the SLI velocity and point defect formation during solidification will be discussed. Work at the Ames Laboratory was supported by the Department of Energy, Office of Basic Energy Sciences, under Contract No. DE-AC02-07CH1135.

Electrode Technology for Aluminium Production: Inert Anode and Wetttable Cathode Materials

Sponsored by: The Minerals, Metals and Materials Society, TMS Light Metals Division, TMS: Aluminum Committee, TMS: Aluminum Processing Committee
Program Organizer: Morten Sorlie, Alcoa Norway

Thursday AM
 March 15, 2012

Room: Americas Seminar
 Location: Dolphin Resort

Session Chair: Jilai Xue, University of Science and Technology Beijing

8:30 AM

Electrolysis Expansion Performance of Modified Pitch Based TiB₂-C Composite Cathode in [K₂AlF₆/Na₃AlF₆]-AlF₃-Al₂O₃ Melts: Fang Zhao¹; Xu Jian²; Hou Jin-Long²; Li Lin-Bo¹; *Zhu Jun*¹; ¹School of Metallurgical Engineering, Xi'an University of Architecture and Technology; ²School of Metallurgical Science and Engineering, Central South University

Electrolysis expansion of pitch, modified by furan, phenolic-aldehyde and epoxy, based TiB₂-C composite cathodes in [K₂AlF₆/Na₃AlF₆]-AlF₃-Al₂O₃ melts were investigated, and EDS as well as TGA were respectively used to conduct elemental micro-analysis and study dynamics relate to pyrolytic process. The results show that compared with the electrolysis expansion of unmodified pitch based composite cathode, pitch modified by furan, phenolic-aldehyde and epoxy based composite cathodes all exhibit lower electrolysis expansion which are 1.61%, 1.62% and 1.68% respectively. The maximum depressed amplitude can reach 13.77%. Apparent activation energy(AAE) concerning pyrolysis process of pitch is related to electrolysis expansion of composite cathodes. The higher the AAE, the lower the electrolysis expansion. The AAE of unmodified pitch is 47.21kJ/mol, while the AAE of pitch modified by furan, phenolic-aldehyde, and epoxy are 66.25kJ/mol, 57.07kJ/mol and 63.24kJ/mol. The values of them can account for test result of electrolysis expansion mentioned above.

8:55 AM

Pulse Electrodeposition of TiB₂ onto Graphite from TiO₂-B₂O₃-KF-LiF Melts: *Bing Li*¹; Lushan Jiang¹; Heng Wang¹; ¹East China University of Science and Technology

TiB₂ has attracted much attention for being the most suitable cathode material in the aluminum electrolysis process. Electrodeposition of TiB₂ coating provides a convenient and low-cost way. In this paper, TiO₂ and B₂O₃ were selected as the active components, KF-LiF as the supporting electrolyte. Ti⁴⁺ ions and B³⁺ ions reduction processes in TiO₂-B₂O₃-LiF-KF melts were investigated by cyclic voltammograms, square-wave voltammograms and chronopotentiograms, respectively.

And electrodeposition of TiB₂ on graphite substrate was carried out from TiO₂-B₂O₃-LiF-KF melts at 800°C by using CCP (continuous current plating) and PCP (pulsed current plating). The effects of cathodic current density, pulse current on and off ratio and B/Ti molar ratio on the coatings were examined by SEM (electron scanning microscope). The coatings prepared by PCP exhibit better qualities compared with those obtained by CCP, they were uniform, dense, adherent and fewer cracks with metallic brightness.

9:20 AM

Ball-Milled Cu-Ni-Fe-X Materials as Inert Anodes for Al Production in KF-AlF₃ Low-Temperature Electrolyte: *Sébastien Helle*¹; Valery Ouyarov-Bancalero¹; Boyd Davis²; Daniel Guay¹; Lionel Roué¹; ¹INRS-Énergie, Matériaux et Télécommunication; ²Kingston Process Metallurgy Inc

In our previous works, we have identified the mechanically alloyed Cu₆₅Ni₂₀Fe₁₅ compound as a promising inert anode material for Al production. However, the purity of the produced Al is still insufficient (99.3%) and thus, further works are required for improving its corrosion resistance. In this context, Cu-Ni-Fe-X materials are prepared by ball milling, consolidated to form dense electrodes and then evaluated as inert anodes for aluminum production in low-temperature (700°C) KF-AlF₃ electrolyte. Their morphological, structural and chemical characteristics are studied at different stages of their preparation and after 20 h of electrolysis. The key role played by the element X on the electrode corrosion resistance is highlighted. Some of these Cu-Ni-Fe-X materials are identified as promising inert anodes for producing aluminum with a good purity (= 99.7%).

9:45 AM Break

10:00 AM

Effect of Nanopowder Content on Properties of NiFe₂O₄ Matrix Inert Anode for Aluminum Electrolysis: *Zhigang Zhang*¹; Yihan Liu¹; Guangchun Yao¹; Di Wu¹; Junfei Ma¹; ¹Northeastern University

Two-step sintering process was adopted to prepare NiFe₂O₄ matrix inert anode for aluminum electrolysis in this research. In the process of synthesizing NiFe₂O₄ spinel, Fe₂O₃ and NiO powders as raw materials added additives were synthesized at 1000°C for 6h. Through crushing and screening, adding NiFe₂O₄ nanopowder, particle gradation and compression molding, the nickel ferrite matrix ceramic inert anode was sintered secondarily at 1300°C for 6h. The effect of NiFe₂O₄ nanopowder content on the density and porosity, bending strength and impact toughness was investigated in details. The results showed the addition of NiFe₂O₄ nanopowder had considerable influence on the properties of NiFe₂O₄ matrix ceramic inert anode. Inert anodes had the best comprehensive properties while adding 30wt% nanopowder. The values of density and porosity were 4.86g/cm³ and 3.5% respectively, the value of bending strength was 42.47MPa and the value of impact toughness was 3.31J/cm².

10:25 AM

Effect of MnO₂ Addition on Early-Stage Sintering Behavior and Properties of NiFe₂O₄ Ceramics: *Jinjing Du*¹; Yihan Liu¹; Guangchun Yao¹; Xiuli Long¹; Xiao Zhang¹; ¹Northeastern University

The samples with small amounts of MnO₂ (0, 0.5, 1.0, 1.5, 2.0, 2.5 wt%, respectively) were prepared via ball-milling process and two-step sintering process from commercial powders (i.e. Fe₂O₃, NiO and MnO₂). Micro-structural features, phase transformation, the early-stage sintering behavior and mechanical properties of Mn-doped NiFe₂O₄ composite ceramics have been investigated. Results indicate that the reduction of MnO₂ into Mn₂O₃ and following the reduction of Mn₂O₃ into MnO existed during sintering process. No new phases are detected in the ceramic matrix, the crystalline structures of the ceramic matrix are still NiFe₂O₄ spinel structure. MnO₂ addition can promote the sintering process. The temperature for 1wt% MnO₂-doped samples to reach the maximum shrinkage rate is 59°C lower than that of un-doped samples.

10:50 AM

Study on the Inert Anode for Al Electrolysis Based on the NiFe₂O₄ Spinel Ceramics: *Yihan Liu*¹; Ming Zhao¹; Jing Li¹; ¹Northeastern University

A kind of cermet inert anode for Al electrolysis based on NiFe₂O₄ had been studied in this paper. Firstly, the effect of NiFe₂O₄ pre-sintering temperature on properties of inert anodes was researched, and then the appropriate technological conditions were determined by the orthogonal test. The properties such as density, conductivity, corrosion rate, mechanical property and thermal shock resistance have been used as controlling parameter to obtain the optimum technological condition. The inert anode sized F50mm×15mm is prepared and tested as anode for 10h Al electrolysis in laboratory. This anode behaves good corrosion resistance to cryolite molten salt. The result gives that the corrosion rate of the anode was 1.5×10⁻⁴g·cm⁻²·h⁻¹ after the 10h electrolysis, and the purity of the aluminum gained from Al electrolysis test was 92%–93%. The analysis shows the main contaminations in the raw aluminum are Fe, Ni and Ag.

Energy Nanomaterials: Fuel Cells, Hydrogen Storage, Ferroelectrics, Wind Energy

Sponsored by: The Minerals, Metals and Materials Society, TMS Materials Processing and Manufacturing Division, TMS Structural Materials Division, TMS: Advanced Characterization, Testing, and Simulation Committee, TMS: Nanomechanical Materials Behavior Committee

Program Organizers: Reza Shahbazian-Yassar, Michigan Technological University; Ming Au, Savannah River National Laboratory; Meyya Meyyappan, NASA Ames Research Center

Thursday AM
March 15, 2012

Room: Swan 3
Location: Swan Resort

Session Chairs: Hamid Garmestani, Georgia Institute of Technology; Reza Shahbazian Yassar, Michigan Technological University

8:30 AM Invited

Multi-Physics Functional Design of HeteroFoAM Nanomaterials for Energy Systems: *Ken Reifsnider*¹; Fazle Rabbi¹; Rassel Raihan¹; ¹University of South Carolina

In 2007 a group of scientists introduced the concept of HeteroFoAMs, a contraction of Heterogeneous Functional Materials. The functional focus of these materials is typically energy conversion and storage devices, such as solid oxide fuel cells (SOFCs). The multiphysics of HeteroFoAMs typically involves balance of mass, momentum, energy and charge, reflecting the fact that mass (fuel, electrons, and ions) are usually transported in such devices, electrochemistry occurs, and the devices are electrical circuits during operation. The functional design of these materials requires the coupled balance of mass, momentum, energy and charge, to embrace chemical, electrochemical, thermal, mechanical, and electrical functionality. The present paper will discuss some examples of such energy nanomaterial design, with a special focus on design for conductivity and dielectric charge management.

8:55 AM

Electrochemical Properties of Hydride Reduced LaSrCoO_{4-0.948} as IT-SOFC Cathode Material Based on Ba(Zr_{0.1}Ce_{0.7}Y_{0.2})O₃ Electrolyte: *Bo Peng*¹; Gang Chen¹; Tao Wang¹; Jun Zhou¹; Jiaojiao Guo¹; Yonghong Cheng¹; Kai Wu¹; ¹Xi'an Jiaotong University

Efficient intermediate temperature (600°C–800°C) solid oxide fuel cells (IT-SOFCs) demand catalytically active cathodes and highly conductive electrolytes. In the present study, we utilize solid state reduction, with CaH₂ as the reducing agent, to introduce abundant oxygen vacancies to the K₂NiF₄-type LaSrCoO_{4-0.948} phase. Electrochemical properties

of the composite cathode, which include both the hydride reduced phase (H-LaSrCoO_{4-0.948}) and a high performance proton conductor Ba(Zr_{0.1}Ce_{0.7}Y_{0.2})O₃ (BZCY), are investigated by means of ac impedance spectroscopy and dc polarization measurements. At 750°C, the cathode shows a polarization resistance of 0.229Ω·cm². And a cathodic overpotential of 25mV is also detected at a current density of 150mA·cm⁻² at 750°C. These good properties can be attributed to the high oxygen vacancy concentration of the H-LaSrCoO_{4-0.948} phase which enhances some key steps of the cathodic oxygen reduction reaction (ORR).

9:10 AM

Crystallization and Electrochemical Performance of LSCF-CGO Thin Film Cathodes Processed by Single Solution Spray Pyrolysis: *Elliott Slamovich*¹; Bainye Angoua¹; Patrick Cantwell²; Eric Stach³; ¹Purdue University; ²Lehigh University; ³Brookhaven National Laboratory

La_{0.6}Sr_{0.4}Co_{0.2}Fe_{0.8}O_{3-d}-Ce_{0.8}Gd_{0.2}O_{1.9} (LSCF-CGO) thin films obtained by spray pyrolysis of a single precursor solution were investigated by XRD, TEM and impedance spectroscopy at annealing temperatures ranging from 500–900°C. Films annealed at 600°C contained a mixture of amorphous regions and crystalline regions composed of fine crystallites (< 5 nm). Annealing above 600°C increased the ratio of crystalline to amorphous material and led to film segregation into distinct LSCF and CGO phases. At testing temperatures of 400°C and below, the polarization resistance of films with lower annealing temperatures was larger than the polarization resistance of films with higher annealing temperatures. However, at testing temperatures of 500°C and above this trend was reversed. The varying electrical behavior may be related to microstructural changes that made bulk diffusion the rate-limiting step in films with lower annealing temperatures and oxygen dissociation the rate-limiting step in films with higher annealing temperatures.

9:25 AM Invited

Oxides as Energy Materials: *Shriram Ramanathan*¹; ¹Harvard Univ

I will discuss some examples concerning phase transitions in functional oxides and their applications in solid state devices for energy conversion and electronics. The talk will center on problems concerning ionic-electronic transport, point defect thermodynamics in low-dimensional oxides and experimental methods to study these rigorously. Thin film solid oxide fuel cells as portable power sources will be used an example to illustrate broader relevance. Experimental routes to fabricate high performance electrodes for low temperature oxide-based fuel cells will be considered. Finally, I will point out the inevitable convergence of electrochemistry and solid state physics towards solving pressing societal problems.

9:45 AM Invited

A Quantitative Understanding of Interface Dynamics in Complex Oxides with In Situ TEM: *Mitra Taheri*¹; ¹Drexel University- Department of Materials Science & Engineering

Understanding atomic scale mechanisms in oxides is a crucial step toward the realization of these materials in a multitude of applications, ranging from solid oxide fuel cells to magneto-electric devices. Magneto-electric coupling in BiFeO₃ (BFO), for example, allows control of the ferroelectric and magnetic domain structures via applied electric fields. Because of these unique properties, BFO and other magneto-electric multiferroic oxides constitute a promising class of materials for incorporation into high-density ferroelectric and magnetoresistive devices. However, the magneto-electric coupling in BFO is mediated by volatile ferroelastically switched domains that make it difficult to incorporate this material into devices. To facilitate device integration, an understanding of the microstructural factors that affect ferroelastic relaxation and ferroelectric domain switching is needed. In this study, domain switching behavior was examined using in situ biasing in TEM. Specifically, the evolution of ferroelastically switched ferroelectric domains in BFO thin films during many switching cycles was investigated.



TMS 2012

141st Annual Meeting & Exhibition

THURSDAY AM

10:05 AM Break

10:25 AM

Design of Light Weight Structure for Wind Turbine Tower by Using Nano-Materials: *Ying Li¹; Jian Lu¹; ¹City University of Hong Kong*

Wind power develops very fast nowadays. The engineering base and computational tools have to be developed to match machine size and volume. This paper reports a new design scheme of light weight structure for wind turbine tower. This design scheme is based on the integration of the nano-structured materials produced by the Surface Mechanical Attrition Treatment (SMAT) process. This process creates a nano-crystallized layer on the metal surface which can effectively improve the yield strength of the original metal material while keep the material's ductile at certain level. The objective of this study is to accomplish the weight reduction by optimizing the wall thickness of the tower while combining the appropriate material properties into optimization. Two main kinds of static loads on the tower are bending and buckling. The individual as well as the combined influence of loads are studied. The eccentric compression on the tapered tube will be discussed.

10:40 AM

Improved Design of Metal-Organic Framework Family for Efficient Hydrogen Storage: *Sang Soo Han¹; William Goddard²; ¹Korea Research Institute of Standards and Science; ²California Institute of Technology*

Recently, Yaghi and co-workers pioneered the metal-organic frameworks (MOFs), covalent-organic frameworks (COFs), and zeolitic imidazolate frameworks (ZIFs), new class of ordered, three-dimensional extended solids composed of metal ions and organic linkers that comprise promising material for H₂ storage. Therefore we investigated the materials as practical hydrogen storage media with ab-initio based grand canonical Monte-Carlo (GCMC) simulations, providing a good agreement with experimental H₂ adsorption isotherms of the MOF, COF, and ZIF. And we discussed several strategies for the improvement of hydrogen storage in the porous materials. The strategies include appropriate pore size, impregnation, substitution of metal oxide with lighter metals, functionalized organic linkers, open metal sites with transition metals and alkali metals. Among them, the Li-doped MOF can store H₂ of more than 6wt% near room temperature, indicating that it could be a promising candidate for practical hydrogen storage.

10:55 AM

Magnesium-Based Hydrogen Storage Nanomaterials: *Hongmin Kan¹; Ning Zhang¹; Xiao-Yang Wang¹; Hong Sun¹; ¹Shenyang University*

An overview of recent advances in the application of Magnesium-based nanostructured materials in hydrogen storage is presented in this review. The main focus is on Magnesium NC/polymer composites, Magnesium alanate, Al-Mg Alloy powders and other Magnesium-based metal hydrides. Recent advances in the area of Magnesium NC/polymer composites show they broke through the basic thermodynamic and kinetic barriers and made a good combination material in the design of nanocomposite material. The polymer in new composite materials and nano-metal particles can be effectively balance; Nanocrystallinity of the Magnesium alanate material is synthesized. Due to its high hydrogen content of 9.3 wt. %, a maximum reversible content of 7 wt. % may be expected if reaction can be made reversible; The hydrogen storage properties of magnesium can be effectively modified by alloying with aluminum. The thermodynamical properties (lower desorption temperature), and kinetics of hydrogenation/dehydrogenation are improved.

11:10 AM

TEM Guided Microstructural Design of MgH₂ Powders and Thin Film Alloys with Room Temperature Volumetric Hydrogen Cycling Ability: *David Mitlin¹; Peter Kalisvaart¹; Mohsen Danaie¹; Shu Tao²; Ben Zahiri¹; Helmut Fritzsche³; ¹University of Alberta and NINT NRC; ²Eindhoven University of Technology; ³SIMS-CNRC*

This presentation is separated into two sections: We will first discuss our recent cryogenic stage transmission electron microscopy (TEM) – based findings on the MgH₂ to Mg (and vice versa) phase transformation in high-energy milled powders. We show that both reactions are nucleation limited, rather than core shell, and identify the dominant metal - hydride orientation relationships. By performing cryo-TEM on ball milled powders we discovered deformation twins in the microstructure. Density functional theory (DFT) analysis demonstrates that the twins significantly affect the kinetics of hydrogen diffusion. In the second portion of the presentation we highlight our recent alloy design efforts for both “bulk” thin films and thin film multilayers. The research culminates in the creation of several classes of catalysts that enable for relatively rapid room temperature volumetric sorption over multiple cycles. The same catalysts allow for ultra-rapid 250+ cycles elevated temperature absorption/desorption at pressures of 1-3 atm.

11:25 AM

Development of Novel Nanostructured Electrolytes for Low Temperature Solid Oxide Fuel Cells Applications: *Hoda Amani Hamedani¹; ¹Georgia Institute of Technology*

High performance low-temperature solid oxide fuel cells (SOFCs) require design of new electrolyte architectures with enhanced ionic transport properties at low temperatures. In this work, fabrication and characterization of one-dimensional composite nanostructures of yttria-stabilized zirconia (YSZ) and Sr-doped TiO₂ as potential material system with high ionic conductivity at low temperatures is reported. The morphological and structural characteristics of the composite nano-architectures were studied using scanning electron microscopy coupled with scanning transmission electron microscopy, X-ray diffraction and atomic force microscopy. Preliminary studies of ion transport properties by electrochemical impedance spectroscopy were performed to investigate oxygen-vacancy formation and revealed enhanced oxygen exchange at the YSZ/Sr-doped TiO₂ interface of these nano-architectures.

11:40 AM Invited

Development of Superhydrophobic Nano-structured Surfaces for High Efficiency Power Generation: *Ghazal Azimi¹; Kripa Varanasi¹; ¹MIT*

Developing robust nanoengineered surfaces and coating technologies for the efficiency improvement of phase change processes has been a subject of intense research over the past decades. Although it has been known since the 1930s that heat transfer coefficients for dropwise condensation are significantly higher than those of filmwise condensation, there has not yet been any successful method commercialized for promoting dropwise condensation due to the lack of suitable material candidates. To address these challenges, herein, we developed novel hydrophobic materials that surpass their counterparts in ability to repel water droplets, while offering other unique properties, including thermal stability and chemical inactivity. Nanoengineered embodiments of these new materials possessed dropwise condensation with remarkably improved heat transfer coefficient, when tested in a condensation chamber under simulated industrial conditions. Such designs are envisioned to enhance the overall performance of various industrial applications.

Energy Technologies and Carbon Dioxide Management: Energy Technologies

Sponsored by: The Minerals, Metals and Materials Society, TMS Extraction and Processing Division, TMS Light Metals Division, TMS: Energy Committee

Program Organizers: Maria Salazar-Villalpando, DOE/National Energy Technology Laboratory; Neale Neelameggham, IND LLC*; Donna Guillen, Idaho National Laboratory; Subodh Das, Phinix, LLC; Ramana Reddy, Univ of Alabama; Animesh Jha, Univ of Leeds; Soobhankar "Sib" Pati, Metal Oxygen Separation Technologies (MOxST); Mark Jolly, Univ of Birmingham; Lakshmanan Vaikuntam, Process Research ORTECH Inc

Thursday AM
March 15, 2012

Room: Europe 8
Location: Dolphin Resort

Session Chairs: Mahesh Jha, US Dept of Energy; Maria Salazar-Villalpando, DOE/NETL; Animesh Jha, University of Leeds; Soobhankar Pati, Metal Oxygen Separation Technologies

8:30 AM Introductory Comments

8:35 AM

Energy Opportunities in the Aluminum Processing Industry: *Cynthia Belt¹*; ¹Consultant

Energy management is critical to aluminum processing given the high energy requirements of melting and processing aluminum. Energy costs have always been high percentage of the total production costs within this industry. Energy management at many plants relied on better technology that many times required high capital. As carbon management has grown in importance and project payback becomes more critical, a larger view of a plant's process is required. This paper looks at the energy requirement due to current typical practices in overall product recovery, metal loss, utilization, and technology to understand potential methods of reducing overall energy within a plant and within the aluminum processing industry.

8:55 AM

An Overview of Energy Consumption and Waste Generation in the Recovery of Cobalt from Copper Sulphide Smelting and Converting Slag and the Proposed Solution: *Animesh Jha¹, Yotamu Hara¹*; ¹University of Leeds

High Curie temperature and large magnetic anisotropy make cobalt an important magnetic material for power engineering applications of magnets operating above ambient. It is also an essential constituent of modern lithium-cobalt oxide batteries, without which modern electronic gadgets will be functionless. Both these applications of cobalt save energy and reduce CO₂ emission. Ironically, however the production of cobalt from copper and nickel smelting in the world remains one of the least energy efficient process. The paper analyzes the energy balance, material and process chemistry of overall cobalt recovery and the waste generated, which entail the process limitations. We discuss a novel approach of mineral reduction with CaSO₄, permitting better separation of metals from slag and generating higher concentrations of SO₂ seems to be an alternative energy efficient option for processing and further purifying cobalt. The results are discussed in the context of process thermodynamics and reaction kinetics for Co-alloy production.

9:15 AM

High Thermal Energy Storage Density LiNO₃-NaNO₃-KNO₃-KNO₂ Quaternary Molten Salts for Parabolic Trough Solar Power Generation: *Tao Wang¹*; Divakar Mantha¹; Ramana Reddy¹; ¹The University of Alabama

A new eutectic LiNO₃-NaNO₃-KNO₃-KNO₂ quaternary molten salt system was calculated using thermodynamic modeling. The eutectic temperature was predicted to be 100°C. The melting point and heat capacity of the salt eutectic composition were determined using DSC.

The experimentally determined melting point is an excellent agreement with the predicted value. The melting point is 122°C lower than that of the KNO₃-NaNO₃ solar salt. The density of the molten salt was experimentally determined as function of temperature. Using the density, heat capacity and the melting point, thermal energy storage density and gravimetric storage density of the quaternary molten salt were calculated and compared with that of solar salt. The larger storage density value of this molten salt indicates that this salt has a better energy storage capacity for solar power generation systems.

9:30 AM

Global Primary Aluminium Industry 2010 Life Cycle Inventory: *Chris Bayliss¹*; Marlen Bertram¹; Kurt Buxmann¹; Bernard de Gelas¹; Samantha Jones¹; Linlin Wu¹; ¹International Aluminium Institute

Environmental management is one of the industry cornerstones of sustainable development. In order to understand fully the environmental aspects associated with the raw material acquisition, production, use, and end-of-life operations of aluminium products, the Aluminium Industry has developed an approach based on Life Cycle Analysis (LCA) methodology. Within this framework, the Primary Aluminium Industry has established a global Life Cycle Inventory (LCI) data set. Inventory flows include inputs of raw materials, energy and water, emissions to air and water, and solid waste. This paper presents the latest LCI data update by the International Aluminium Institute for the year 2010, based on a survey of aluminium plants globally, including bauxite mining, alumina refining, anode production, electrolysis and casting. This update also includes some performance tracking based on the last LCI data collection in 2005, reflecting progress in efficiency and technology, as well as changes in the geographical location of the industry.

9:45 AM Break

9:55 AM

Analysis of Combustion Efficiency Using Laser-Induced Fluorescence Measurements of OH-Radicals: *Matthias Schnitzler¹*; Ralf Bölling¹; Herbert Pfeifer¹; ¹IOB RWTH Aachen

To transform metals high temperatures are usually needed. A fast and efficient heating can reduce the CO₂ emitted. The fastest way to heat metals is called direct flame impingement (DFI). The flame impinges upon the item being heated. For this method it is important to know the shape and length of the flame. Laser-induced fluorescence (LIF) technology allows measurements of a two-dimensional field without influencing the reaction or the flow. Commonly used is the measurement of OH-radicals, an indicator of the reaction zone. In the presented study measurements of a turbulent diffusion flame are shown. The position of the reaction zone and the influence of the distance between the item being heated and the burner are investigated. Conventional measurements and LIF-measurements are compared and the potential of DFI to increase the efficiency of heating metals is discussed.

10:10 AM

A Solid State Thermoelectric Power Generator Prototype Designed to Recover Radiant Waste Heat: *Marit Takla¹*; Odne Burheim¹; Leiv Kolbeinsen¹; Signe Kjelstrup¹; ¹Norwegian University of Science and Technology

This paper presents a Seebeck-type solid state thermoelectric power generator unit, designed to investigate the possible recovery of radiant waste heat at a silicon plant in Norway where roughly 70 % of the total input energy leaves the process as waste heat. The unit is 0.5 m x 0.5 m and is built of 36 commercially available thermoelectric devices based on bismuth telluride p - and n - type semiconductors. Thermoelectric devices directly convert fractions of a heat flux into an electric current (and vice versa) and may therefore be convenient for recovery of waste heat when the heat source is discontinuously available. The purpose of the thermoelectric unit is to give a proof of principle of direct thermoelectric energy conversion on a large scale. We present the initial test results for the generator. At an average temperature difference between the heat reservoir

and the heat sink of 98 °C, we measured an open circuit potential of 23.44 ±0.06 V and the matched load power output was 39.4 W. At a temperature difference of 220°C, we predict the generator open circuit potential to be 40.8 V, which corresponds to an efficient Seebeck coefficient of 242 μV/K per pair of semiconductor, and matched load power output to be 120 W.

10:25 AM

Study on Smelting Reduction of Coal-Containing Pellets of V-Ti Bearing Beach Placers by Combined Rotary Hearth Furnace and Direct Current Arc Furnace: *Huimin Lu¹; Jingbo Xu¹; Qiang Li¹; ¹Beihang University*

The smelting reduction of vanadic-titanomagnetite sand by combined rotary hearth furnace and direct current arc furnace was studied in laboratory. It takes the aid of back propagation (BP) neural network theory to build the nonlinear mapping relations between the crucial process variables such as content of carbon, temperature and time and the degree of reduction and separation of iron and slag. Then by the integrating BP neural network and genetic algorithm (GA), the optimized process parameters for the high degree of reduction and separation of iron and slag were searched. The comparisons between experiment results and neural network simulation results show that GA-based on BP method can predict the degree of reduction and separation of iron and slag with higher prediction accuracy. Calculations show that the integrated energy consumption of new technology is 580kgce/tHM, less than the current existing blast furnace.

10:40 AM

A Novel Method Combined Ionothermal Synthesis and Microwave Energies for Rapid Production of ZIFs: *Lisha Yang¹; Huimin Lu¹; Shi Zhou¹; ¹Beihang University*

The Zeolitic imidazolate frameworks (ZIFs) were successfully rapid synthesized by applying a combination of ionothermal synthesis and microwave energies. The synthesis was proceeded under various conditions including different raw materials, reaction temperature as well as microwave irradiation time. Zeolitic imidazolate frameworks (ZIFs), also known as coordination polymers, are new type of porous materials formed by inerratic polyhedral in three-dimensional. They are the ideal crystalline substances for gas separation and storage. The as-synthesized samples were characterized by X-ray diffraction (XRD), scanning electron microscopy (SEM), thermal gravimetric analysis (TGA) and CO₂ adsorption test. Results illustrated that the synthesized samples had stable structure, high thermal stability (up to 530°C) and CO₂ adsorption capacity (1.63 cm³/g at 273 Kelvin under ambient pressure). This novel method also showed great advantage with high energy efficiency, safe synthesis conditions, and rapid crystallization time (about 60 minutes).

10:55 AM

The Relationship between Energy Consumption and CO₂ Emissions in Iron and Steel Making: *Hao Bai¹; Xin Lu¹; Hongxu Li¹; Lihua Zhao¹; Xueting Liu¹; Ning Li¹; Wei Wei¹; Daqiang Cang¹; ¹University of Science and Technology Beijing*

Based on the principle of carbon balance, a model was built to calculate CO₂ emissions of each process and correspondingly the total course of production in iron and steel making. The data from a typical integrated steelworks in China was applied in the model. The results show that the BF and coking process account for the most emissions. Generally, CO₂ emissions in integrated steelworks depend on three factors, resources utilization efficiency, energy utilization efficiency and energy consumption structure, which were considered in an equation in this paper. Especially, General Emission Factor (GEF) was proposed to assess the relationship between CO₂ emissions and energy consumption. The results show that, higher GEF will result in more CO₂ emissions with the same energy consumption and in iron and steel making, the optimization of energy structure and development of eco-industrial park both have significant benefit on the carbon reduction.

11:10 AM

Development and Application of Shaft Kiln in China: *Zhen Guo Li¹; Dong Li²; Guang Zhen He³; ¹Shanghai Cadre Environment Energy Science and Technology Co., Ltd; ²Shanghai Cadre Environment Energy Science and Technology Co., Ltd; ³Shenyang He Carbon Furnace Design Institute*

The new type shaft kiln is developed and designed by CADRE itself on the basis of the conventional shaft kiln. The actual application in a number of calcination plants have proven that they are of very good effect. Calcined coke heated by the shaft kiln have high quality, lower lost by fire. The shaft kiln need no additional fuel when it is working. Anode Carbon Plant and calcined coke Plant commonly used the shaft kiln in domestic. The waste heat from the shaft kiln can be recuperated to generate electricity and to make the steam or power for produce. This paper introduces the working principle and characteristics of the shaft kiln. It also demonstrates measured process parameters of the new type shaft kiln. The shaft kiln proves its own technical characteristics and advantages: higher capacity, high quality products, provides more energy for power generation, Equipment operation and maintenance costs lower.

11:25 AM

Preparation of Biodiesel by Transesterification of Canola Oil Using Solid Base Catalyst KOH / γ -Al₂O₃: *Seyed Mojtaba Sadrameli¹; Mohamad Omraei¹; ¹TMU*

The aim of this research work was to produce biodiesel (fatty acid methyl esters, FAME) from canola oil using KOH loaded on γ -Al₂O₃ support as a heterogeneous catalyst. Different parameters such as effects of the molar ratio of methanol to oil, catalyst amount and reaction time on the yield were investigated. Scan electron microscope (SEM) and X-ray diffraction (XRD) were used for characterization of the catalysts. A biodiesel yield of 86.67% was obtained under catalyst preparation and transesterification conditions of calcinations temperature of 773 K, 4 h of reaction time at 338 K, and using 3.5 wt% catalysts and molar ratio of methanol/oil of 15:1. The leaching of potassium species in the spent catalyst was observed.

From Macro to Nano, Understanding Mechanical Behavior across Length Scales: A Structural Materials Division Symposium in Honor of Robert Ritchie: Mechanical Behavior of Novel Materials

Sponsored by: The Minerals, Metals and Materials Society, TMS Structural Materials Division, TMS/ASM: Mechanical Behavior of Materials Committee, TMS: Biomaterials Committee
Program Organizers: Jamie Kruzic, Oregon State University; Brad Boyce, Sandia National Labs; Reinhold Dauskardt, Stanford University

Thursday AM
March 15, 2012

Room: Mockingbird 1
Location: Swan Resort

Session Chairs: Jamie Kruzic, Oregon State University; Mark Hoffman, The University of New South Wales

8:30 AM Introductory Comments

8:35 AM Keynote

Crack-Tip Process Zones in Piezoelectric Ceramics under Mechanical and Electrical Quasistatic and Fatigue Loading: *Mark Hoffman¹; ¹The University of New South Wales*

Crack growth in piezoelectric ceramic is dependent upon the extent of domain re-orientation that occurs at the crack tip. This is known to depend upon both the magnitude of the load and whether it is mechanical or electrical. Under cyclic load, there is frequency dependence. The process is also influenced by pre-poling conditions. In this work, domain orientations around a mechanically and electrically-loaded crack in poled

and unpoled PZT have been resolved using high-energy synchrotron x-rays, at both the crack tip and in the crack wake. This elucidates the size of the process and wake zones and the strains which are expected in these zones and may be used to explain observed crack-growth resistance behaviour. It is shown that when the crack is cyclically loaded the extent of ferroelastic domain movement at the crack tip is cycling frequency dependent with the size of residual zones decreasing with increasing frequency.

9:15 AM

In Situ Ultrahigh Temperature X-Ray Microtomography Facility for New Generation Structural Material: *Hrishikesh Bale*¹; Abdel Haboub²; James Nasiatka²; Alastair MacDowell²; Brian Cox³; David Marshall³; Robert Ritchie¹; ¹University of California, Berkeley; ²Lawrence Berkeley National Lab.; ³Teledyne Scientific LLC

Textile composites comprising of Carbon-Carbon and Carbon-SiC systems are excellent candidates for high temperature applications in the field of hypersonics and other ultra high temperature (>1200°C) applications. The material properties and performance of these materials is however intricately linked on several features that exist on a hierarchy of length scales. Due to the hierarchical structure of these materials, failures are generally complex and often occur/initiate at multiple length scales, in the form of fiber breaks, matrix cracking, multiple fiber bundle fractures etc. X-ray computed micro-tomography is an invaluable tool for providing the 3D structural information non-destructively at a relevant length scale ranging from a few micrometers to several millimeters. In the present work, we present first-time results obtained using our newly developed in-situ ultra-high temperature X-ray micro-tomography facility, wherein micro-structural features and their associated structure-property relationships that control the ultimate performance of these materials are being studied in three dimensions.

9:30 AM

Investigation of the Mechanical Properties of Ti_2SC & Ti_3SiC_2 via In-Situ Neutron Diffraction and Elasto-Plastic Self-Consistent Modeling: *Mohamed Shamma*¹; Volker Presser¹; Bjorn Clausen²; Don Brown²; Michel Barsoum¹; ¹Drexel University; ²Los Alamos National Laboratory

Herein we report on the results of in-situ neutron diffraction experiments on fine-grained polycrystalline Ti_2SC and Ti_3SiC_2 with two different grain sizes. The macroscopic and individual planes' strains are modeled via elasto-plastic self-consistent (EPSC) model. We not only show that the response of Ti_2SC to stress is linear elastic up to 700 MPa but that the ab initio derived elastic constants can accurately model this response. In the case of Ti_3SiC_2 , the response was typical of kinking nonlinear elastic, KNE, solids. The in situ results confirm that neither slip nor twinning is responsible for the KNE response. The response, however, is consistent with the formation of incipient kink bands, the micromechanism proposed to explain KNE behavior.

9:45 AM

Multi-Scale Energy Absorption Mechanisms in Micro-Architected Materials: *Lorenzo Valdevit*¹; Alan Jacobsen²; Tobias Schaedler²; William Carter²; ¹University of California, Irvine; ²HRL Laboratories

Recent progress in advanced manufacturing enables fabrication of macro-scale metallic lattices with unit cells in the millimeter range and sub-unit cell features at the nano-scale, thus yielding a topologically architected cellular material with structural hierarchy spanning seven orders of magnitude in length scale. When appropriately designed, these materials exhibit unique damping characteristics, unprecedented for a metallic system. The energy dissipation involves mechanisms occurring at three different length scales. We present an experimental protocol, which enables characterization of such mechanisms, allowing identification of the most relevant phenomena and the dominant length scale. By combining the experimental investigation with numerical modeling, clear guidelines for the optimal design of cellular materials for maximum energy absorption are extracted. The same design tools

can be applied to the simultaneous optimization of damping and strength (typically antagonistic objectives), revealing the unique benefits of micro-architected materials.

10:00 AM Break

10:15 AM

Effect of Grain Neighborhood on Pseudoelastic Performance of Polycrystalline Shape Memory Alloys: Harshad Paranjape¹; *Peter Anderson*¹; ¹The Ohio State University

Simulations of polycrystalline NiTi shape memory alloys show a grain-to-grain variation in pseudoelastic strain of 2% to 6%. Moreover, the strain varies by 2% among grains with a similar orientation. This grain "neighborhood" effect is assessed by studying trends in local stress-strain response and the types of martensite habit plane variants (plates) formed. Stress redistribution tends to suppress the performance of favorably-oriented grains and enhance that of unfavorably-oriented grains. The net effect, however, is to reduce polycrystalline performance, relative to a collection of single crystal counterparts. A primary culprit is that neighboring constraint induces less favorable habit plane variants, particularly in less-favorably-oriented grains. Despite these drawbacks, predictions are shown where stress redistribution and constraint enable dramatic, sometimes beneficial manipulation of polycrystalline shape memory alloy response.

10:30 AM

Novel Characterization of the Martensitic Transformation Temperature of NiTi Shape Memory Alloys via Micro-Indentation: *Bin Gan*¹; Sara Cantonwine¹; Mathilde Gatepin¹; Sammy Tin¹; ¹Illinois Institute of Technology

Nickel-Titanium (NiTi) shape memory alloys possess an extraordinary capability to recover plastic strain and return to its original shape when heated above the martensite transformation temperature. Using a high temperature instrumented micro-indentation system, we have demonstrated the ability to perform in-situ measurements of the martensitic transformation temperature of NiTi alloys. Following indentation of the material at room temperature, the system was heated while the indenter remained in contact with the surface while maintaining a constant load. The onset of martensitic transformation was determined by plotting the resulting displacement of the indenter as a function of temperature. Results from the depth sensing experiments were compared and found to be consistent with Differential Scanning Calorimeter (DSC) measurements and conventional mechanical tests followed by heating. Results from the study will be presented and the implications of the novel characterization technique will be discussed.

10:45 AM

Fatigue Life-Prediction of Nitinol under Multiaxial Loading: *David Xu*¹; Robert Ritchie¹; ¹UC Berkeley

Modern measurements of medical implants are providing new information on the magnitude of complex in vivo loads. Thin-walled tubes of Nitinol were tested in tension and torsion to investigate the fatigue behavior and develop a life-prediction model for multiaxial loads based on uniaxial behavior. The strain-life torsional e-N curve for superelastic Nitinol at zero mean strain and positive mean strain results appear to collapse reasonably well. However some high mean strain tensile data fails to merge under such technique. An alternative approach using transformation strain is found to collapse all data reasonably. This holds promise for normalizing cyclic fatigue data with a strain-based methodology. The improved approach can be expressed in terms of a Coffin-Manson type formulation where the alternating equivalent transformation strain is related to the -1/2 power of cycles to failure. It allows a satisfactory normalization for all testing modes studied over the entire range of strain ratios.



11:00 AM

Adhesion of Nickel-Titanium Shape Memory Alloy Wires to Polymeric Materials: Theory and Experiment: *Louis Hector Jr¹; Federico Antico²; Pablo Zavattieri²; ¹GM R&D Center; ²Purdue University*

A combined experimental/theoretical study of adhesion between a Nickel-Titanium (NiTi) shape memory alloy wire embedded in a Thermoplastic Polyolefin (TPO) matrix is presented. NiTi wire surfaces were modified to improve adhesion by functionalizing with an acid etch or chemical coupling agent or application of a surface microgeometry. Wire surface features from each treatment were examined with atomic force microscopy. Pull-out tests were conducted and the extent to which each treatment increased the pull-out force was quantified. Results from a nonlinear finite element analysis wherein the NiTi/TPO matrix interface is modeled with a cohesive zone model suggest that the interface behavior strongly depends on the cohesive energy during pull-out, and less on the cohesive strength. Additionally, a parametric analysis is performed to take into account how the residual stresses from manufacturing process affect the local mode mixity during debonding.

11:15 AM

Toughening in Bio-Inspired Shape Memory Alloy Embedded Composites: *Fatmata Barrie¹; Michele Manuel¹; ¹University of Florida*

Shape memory alloy (SMA) reinforced composites are being investigated due to their enhanced mechanical properties over monolithic materials, namely increased strength, dampening abilities, and toughness. The focus of this study is to characterize the effect of the SMA reinforcement phase transformation properties on the composite toughening behavior. These composites are inspired by biological systems like mollusks whose increased toughness can be attributed to the presence of a ductile reinforcement in a brittle matrix. The results of a systematic investigation of SMA embedded composites using the J-integral fracture toughness testing method will be presented to reveal underlying structure-property relationships. In addition to extrinsic toughening mechanisms, the R-curve behavior is quantified and correlated to the underlying martensitic transformations in the SMA reinforcement. The results will lead to a deeper understanding of fracture and deformation mechanics driving toughening behaviors in composites with ductile-like, phase transforming reinforcements. The authors would like to gratefully acknowledge the support of the National Science Foundation under grant number CMMI-0824352.

11:30 AM

The Effect of Morphology on the Mechanical Behavior of Cu(Ni)-C Nanocomposites: *Alan Jankowski¹; Tanvir Ahmed¹; ¹Texas Tech University*

Nanostructures synthesized with a composition fluctuation along the growth direction are metastable engineered nanolaminates with physical properties that can range far from equilibrium. Common to each nanolaminate is the interface structure and the periodic or random distribution of interfaces. The ability to form a well-defined layered structure is affected by both the chemical solubility of constituent elements as well as superlattice distortions. Both of these attributes are present in the copper(Cu)-nickel(Ni)-carbon(C) alloy system. Transition from a 3-D to 2-D nanostructure occurs as the morphology changes from dispersed Cu(Ni) nanoparticles in a C-based matrix, to distinct a nanolaminate structure as the Ni concentration is increased within the Cu layer. Results are presented on the effects that strain and chemical solubility have on the morphology and the mechanical properties of nanocrystalline Cu(Ni)-C as assessed using high resolution electron microscopy, and dynamic nanoindentation test methods in the scratch and tapping mode.

Magnesium Technology 2012: Advanced Processing and Joining

Sponsored by: The Minerals, Metals and Materials Society, TMS Light Metals Division, TMS: Magnesium Committee
Program Organizers: Suveen Mathaudhu, U.S. Army Research Office; Wim Sillekens, TNO; Norbert Hort, Helmholtz-Zentrum Geesthacht; Neale Neelameggham, U.S. Magnesium

Thursday AM
March 15, 2012

Room: Southern V
Location: Dolphin Resort

Session Chairs: Suveen Mathaudhu, U.S. Army Research Office; Brian Jordan, University of Alabama

8:30 AM

Microstructure and Creep Properties of MEZ Magnesium Alloy Processed by Thixocasting: *Emma Deyanira Morales Garza¹; Hajo Dieringa¹; Norbert Hort¹; ¹Helmholtz-Zentrum Geesthacht*

Whereas in most magnesium applications die casting is the dominant manufacturing process, thixocasting recently came into focus of producers. This is mainly due to the improved microstructure, reduced porosity and better mechanical properties. An important issue for the introduction and use of magnesium alloys in automotive industry is their creep resistance. Aluminium free magnesium alloys are known to show improved creep strength compared to conventional aluminium containing alloys due to the absence of beta phase (Mg₁₇Al₁₂). In this paper, the mechanical and creep properties from thixocast MEZ alloy are evaluated from creep tensile tests at temperatures of 135°C, 150°C and 175°C and at stresses between 60 and 100 MPa. The creep activation energy and the stress exponent are calculated and discussed. Optical and scanning electron microscopy of the microstructural features developed after the mechanical tests helps to understand the deformation mechanisms occurring during creep and to explain the improved creep properties after thixocasting.

8:50 AM

The Effect of Friction Stir Processing on Microstructure and Tensile Behavior of Thixomolded AZ91 Magnesium Alloy: *Bilal Mansoor¹; Raymond Decker²; Sanjay Kulkarni²; Steve LeBeau²; Marwan Khraisheh¹; ¹Masdar Institute of Science and Technology, Abu Dhabi, UAE; ²Thixomat Inc.*

Friction Stir Processing (FSP) to partial sheet thickness can be utilized to engineer unique microstructures in metallic alloys. These composite microstructures consist of three distinct layers associated with stirred, transition and core microstructural regions. The stirred region is of particular interest where severe plastic deformation imparted by the rotating and translating FSP tool under frictional heat leads to grain refinement down to ~1 μm grain size. In this work, partial depth penetration into thixomolded AZ91 Mg plate from the top and bottom surfaces by friction stir processing is explored. Furthermore, low temperature aging treatments are applied to the processed material. The present results with AZ91 Mg show that FSP processed material exhibits higher strength (> 300 MPa), and improvement in ductility (> 7 % tensile elongation). It is found that in addition to Hall-Petch strengthening produced by ~1 μm grain size in the stirred region, the enhanced strength levels and ductility are strongly influenced by dispersoids of the intermetallic precipitates found in this alloy.

9:10 AM

Effect of Weld Structure on Fatigue Life of Friction Stir Spot Welding in Magnesium AZ31 Alloy: *Harish Rao¹; J Jordan¹; ¹The University of Alabama*

In this paper the fatigue behavior in friction stir spot welded coupons of magnesium AZ31 alloy manufactured under different welding conditions are investigated. Two sets of lap-shear coupons were welded based on varying the plunge depth and tool geometry. Metallographic analysis

of the untested lap-welds revealed differences in microstructural and geometrical features. Results from the load controlled cyclic tests showed that one set of welds exhibited better fatigue performance compared to the other set. Optical fractography of the failed fatigue coupons revealed that fatigue cracks initiated at the weld interface in both sets of coupons. However, the fracture mode showed variability between the two sets of coupons. As such, the main conclusion of this study is that the effective top sheet thickness, which is largely determined by the shoulder plunge depth, plays a significant role in the fatigue behavior of the friction stir spot welds in magnesium alloys.

9:30 AM

Effect of Corrosion on the Tensile Properties of Friction-Stir Welded AZ31B Sheet: *Jennifer Thuss*¹; *Joseph Kish*¹; *Joseph McDermid*¹; ¹Centre for Automotive Materials and Corrosion, McMaster University

To facilitate the use of magnesium and its alloys within automotive structures, it is necessary to characterize their corrosion and possible mechanical property degradation in typical application environments. This work examines the effect of exposure to NaCl-based corrosive environments on the mechanical properties of friction stir welded (FSW) AZ31B magnesium alloy sheet. A complete microstructural, electrochemical, residual stress and mechanical property characterization of the as-received FSW panels was performed. Samples were subsequently exposed to 0.01M and 0.1M NaCl solutions for a variety of times and any changes in mechanical properties as a function of exposure to the corrosive environment monitored. This paper will present the relationship between the changes in mechanical properties of the FSW joints resulting from exposure to the corrosive environment as a function of the FSW microstructure, localized electrochemical potentials arising from the FSW microstructure and residual stress in the welded joints.

9:50 AM

High Speed Rolling of AZ31 and Mg-Zn-Ce Alloys: *Mehdi Sanjari*¹; *Amir Farzadfar*²; *In-Ho Jung*²; *Steve Yue*²; *Masahiro Hattori*³; *T Sakai*³; *Hiroshi Utsunomiya*³; *Elhachmi Essadique*⁴; ¹McGill; ²McGill; ³Osaka University; ⁴CANMET

One of the benefits of using high speed rolling for Mg alloys is for improving the hot rollability. In this study AZ31 and four Mg-Zn-Ce alloys were investigated under number of different rolling schedules. At a rolling temperature of 450 °C and rolling speed of 1000 m/min, the peak intensity of the (0001) pole figure tilted 10-15° towards the RD direction to form a double peak texture for both AZ31 and Mg-Zn-Ce alloys. A texture variation through thickness was observed. From the surface to the center of thickness, the direction of the (0001) peak TD-split rotated 90°. After annealing, the basal texture component of the Mg-1Zn-1Ce magnesium alloy sheets was weakened, and replaced by a new component rotated 45° towards the transverse direction. The hot tensile tests results confirm that the Mg-1Zn-1Ce alloy sheets with this non-basal texture component exhibit a higher ductility than the alloys with basal texture.

10:10 AM Break

10:30 AM

On the Effect of Ti₂AlC on the Formation of Thermally Stable Mg Nano Grains: *Babak Anasori*¹; *Michel Barsoum*¹; ¹Drexel University

When Mg and Mg-alloys are reinforced with Ti₂AlC, - using a simple pressureless melt infiltration method - the result is nanocrystalline, nc, Mg-matrix composites with outstanding mechanical properties. As an added bonus, the nc Mg-matrix is extraordinarily thermally stable up to above the melting point of Mg. When Mg-alloy, AZ61, is used to infiltrate the Ti₂AlC preform, ultimate tensile stresses of 800 MPa are achieved. The reasons that lead to the formation of the nc-Mg are as of yet not understood. In this study, the different composite's microstructures are investigated by X-ray diffraction, scanning electron and transmission electron microscopy. The results shed light on why the Mg forms as nano-grains and why they are as stable as they are.

10:50 AM

Experimental Investigations on the Deformation Behavior of Thixo-Molded Mg Sheet Alloy: *Muammer Koc*¹; *Omer Cora*²; *Ryan Snell*³; *Ray Dekker*⁴; *Jack Huang*⁴; ¹Istanbul Sehir University; ²Karadeniz Tech Univ; ³VCU; ⁴Thixomat

Deformation behavior and formability limits of thixo-mold Mg alloy sheets at elevated temperature conditions were investigated experimentally. Uniaxial tensile, hydraulic bulge tests as well as closed-die hydroforming tests were conducted to understand the material behavior at temperatures ranging from 25°C to 300°C and strain rates at 0.0013, 0.013, and 0.13 s⁻¹. As a result of the experimental findings, it was found that flow stress and the maximum plastic strain increased with increasing temperature and decreasing strain rate. Closed-die warm hydroforming tests were also performed to determine the process window for the alloy. Die cavity filling ratios and thinning of the sheet blanks were measured with non-contact optical photogrammetry. Results indicated that slower strain rates and higher temperatures increase formability, particularly after a temperature level of 200°C.

11:10 AM

Effects of High Temperature Shot Peening on Surface Characteristics and Fatigue Properties of Forged AZ31 Magnesium Alloys: *Ichihara Yuki*¹; *Masahumi Noda*¹; *Kunio Funami*¹; ¹Chiba Institute of Technology

In this present study, the effect of high-temperature shot peening (HSP) on surface characteristics and fatigue properties of forged AZ31 magnesium alloy were investigated. HSP process were performed by peening pressure 0.2 MPa and time 6 s at peening temperature 523 K with the low-carbon steel ball. As the result, graded microstructures formed at the near surface region about 150 μm from surface edge. It was composed by ultra fine-grained region, residual working strain region and twin region. HSP processed material was increased fatigue strength compared with non-HSP processed material. From measurement of crack propagation rate, it was found that the improvement of fatigue properties was lead of the delay of crack propagation rate in the ultra fine-grained region and the residual working strain region.

11:30 AM

Solid Solution Hardening Effect of Aluminum on the Creep Deformation of AZ91 Magnesium Alloy: *Farhoud Kabirian*¹; *Reza Mahmoudi*²; ¹University of Maryland, Baltimore County; ²University of Tehran

It has been previously shown that separate additions of 2% rare earth elements (RE) and 0.6% Zr to the AZ91 base alloy improve creep properties. However, in this investigation using impression creep method, it is shown that simultaneous addition of these elements not only cannot improve creep properties but also leads to its deterioration. According to the creep deformation mechanism of the base alloy and microstructural evidences, it is believed that this drop in creep resistance mainly stems from depletion of grain interiors and the areas adjacent to grain boundaries from aluminum solute atoms. Reduction of aluminum content as solute atoms is due to the great affinity of RE and Zr atoms for aluminum. This leads to the weakening of Al solute atoms role as obstacles against dislocation movement, even though the volume fraction of the thermally stable particles tends to be high.



Magnesium Technology 2012: Processing-Microstructure-Property Relationships I

Sponsored by: The Minerals, Metals and Materials Society, TMS Light Metals Division, TMS: Magnesium Committee
Program Organizers: Suveen Mathaudhu, U.S. Army Research Office; Wim Sillekens, TNO; Norbert Hort, Helmholtz-Zentrum Geesthacht; Neale Neelamegham, U.S. Magnesium

Thursday AM
 March 15, 2012

Room: Southern IV
 Location: Dolphin Resort

Session Chairs: Hidetoshi Somekawa, National Institute of Materials Science; Kyu Cho, U.S. Army Research Laboratory

8:30 AM

Microstructure Modeling of Magnesium Alloys for Engineering Property Prediction: *Erin Barker*¹; Dongsheng Li¹; Xin Sun¹; Mohammad Khaleel¹; ¹Pacific Northwest National Lab

Magnesium alloys have found increasing application in the transportation industry due to their low weight and high strength. However, wider application is hindered by limited ductility. Microstructural features, such as porosity, brittle eutectics, and grain size, can significantly influence the macroscopic response of a component. These features can vary widely throughout a component. Our approach to studying the microstructures influence on bulk properties begins with measuring microstructural features in different regions of a component. These measurements are used to create statistically equivalent, 3D synthetic samples of the microstructure. The synthetic microstructures are meshed using finite elements and used to simulate the response and investigate the influence of specific features. We will demonstrate how the digital microstructure samples are generated, how variations in microstructural features influence the bulk properties, and how this methodology can be used to predict component performance and optimize processing.

8:50 AM

Microstructure Modification and Deformation Behavior of Fine-Grained AZ61 Sheet Produced by Thixomolding and Thermomechanical Processing (TTMP): *Tracy Berman*¹; William Donlon¹; Victoria Miller²; Jack Huang³; Raymond Decker³; Tresa Pollock²; J. Wayne Jones¹; ¹University of Michigan; ²University of California Santa Barbara; ³nanoMAG, LLC

X-ray diffraction and hardness measurements are used to study recrystallization in fine-grained AZ61L sheet produced by warm-rolling of Thixomolded\174 material. The as-rolled sheet is partially dynamically-recrystallized, with a strong basal texture and a sub-micron grain size. Significant increases in ductility with moderate reductions in tensile strength were produced by annealing at temperatures greater than 250\176C. A weakening in basal texture was observed in samples annealed at over 250\176C. Static recrystallization was determined to be responsible for the reduction in texture and associated increase in elongation.

9:10 AM

Development of High Strength and Toughness Magnesium Alloy by Grain Boundary Control: *Hidetoshi Somekawa*¹; Alok Singh¹; Tadanobu Inoue¹; Toshiji Mukai²; ¹National Institute for Materials Science; ²Kobe University

The fracture toughness is one of the important mechanical properties to identify the safety and reliability for the structural parts; however, magnesium alloys is reported to be lower fracture toughness compared to that in aluminum alloys. Recent studies show that the grain boundary control, i.e., formation of sub-grain structure, is one of the effective methods to improve the fracture toughness with remaining high strength and ductility properties in magnesium alloy. This is resulted that the sub-grain boundaries are not the site for the micro-void formation; sub-grain

boundaries can prevent or reduce the stress concentration by the free movement of dislocations. In this study, using AZ61 alloy, the fine grain structures, which were surrounded by sub-grain boundaries and dispersed with fine precipitate particles, were produced by the severe plastic deformation, i.e., caliber rolling. This alloy showed the high strength and fracture toughness balances corresponding to the conventional high strength aluminum alloys.

9:30 AM

Effects of Direct Extrusion Process on Microstructure, Texture Evolution and Yield Strength of Magnesium Alloy AZ31: Shiyao Huang¹; *Mei Li*¹; John Allison²; Shaorui Zhang³; Dayong Li³; Yinghong Peng³; ¹Ford Motor Company; ²University of Michigan; ³Shanghai Jiao Tong University

Direct extrusions of commercial as-cast AZ31 alloy were carried out at elevated temperatures with different extrusion velocities. Microstructure and texture distribution of extruded rods were investigated with optical microscopy (OM) and electron backscattered diffraction (EBSD). Tensile tests were conducted at room temperature using samples from both casting billets and extruded rods. The experimental yield strength can not be solely described by average grain size. In this paper, the grain size and orientation in the extruded samples were characterized by EBSD, and Hall-Petch equation was applied to each individual grain with the input from EBSD results (individual grain size and orientation). The yield strength of tensile sample (polycrystalline aggregate) and individual grain was related by Taylor assumption. The predicted yield strength showed the same trend as experiment results.

10:10 AM Break

9:50 AM

Comparison of Tensile Properties and Crystallographic Texture of Three Magnesium Alloy Sheets: *Junyong Min*¹; Ying Cao¹; Jon Carter²; Ravi Verma²; ¹Tongji University; ²GM R&D

The most common commercially available rolled magnesium sheet alloy is AZ31B (typ. 3% Al, 1% Zn, 0.4% Mn, balance Mg). One of the often-cited shortcomings of this sheet is its limited formability at room temperature, which is attributed in part to a strong crystallographic texture. Attempts have been made to avoid this rolling-induced texture by changing either (a) the alloy composition or (b) the rolling process. Specifically, sheet has been made using the conventional rolling practice, but changing the alloy to ZEK100 (typ. 1% Zn, 0.2% Nd, 0.2% Zr, balance Mg), or by keeping the AZ31B composition but rolling at 100°C higher than conventional practice dictates. In this report, both types of sheet are compared with conventionally rolled AZ31B sheet. Both show reduced texture and attractive tensile properties, and therefore both are expected to show greater room-temperature formability than conventionally rolled AZ31B.

10:30 AM

Strain Hardening of ZK60 Magnesium Alloys: *Jaehyung Cho*¹; Suk Bong Kang¹; ¹Korea Institute of Materials Science

ZK60 alloys (Mg-Zn-Zr) had improved mechanical properties of high strength and high elongation, comparing other wrought magnesium alloys. In general, Mg-Zn system possessed precipitate hardening behaviors during aging. Rod- and disc-shaped precipitates were usually found, and microhardness and strength of the alloys changed with aging. The ZK60 alloys have finer grains and improved mechanical properties than the usual Mg-Zn system by addition of Zr element. In this research, we investigated precipitate variation with aging process. Two types of specimens, solution-heat treated (T4) and aged (T6) samples, were prepared to examine precipitates and mechanical properties. Casted ZK60 ingot was cut, and then solution-heat treatment was carried out 10 hrs at 400°C. Aging process was intended to have peak hardening and thus heat treatment was carried out 12 hr at 175°C. Deformation behavior of ZK60 alloys were also investigated by uni-axial compression. Precipitates and microstructure were investigated using TEM, and EBSD.

10:50 AM

Strain-Rate Effects of Sand-Cast and Die-Cast Magnesium Alloys under Compressive Loading: *J.P. Weiler*¹; J.T. Wood¹; ¹University of Western Ontario

The strain-rate effects of cast magnesium alloys were investigated with uniaxial compression and compressive impact testing. The compressive material response of specimens cut from sand cast AZ91, AE44, and AM60, and high-pressure die-cast AM60 was determined for strain-rates ranging from quasi-static levels to typical rates experienced during crash situations. Several different constitutive material models (Johnson-Cook, Cowper-Symonds, etc.) were used in an attempt to characterize the experimental results. These material models are typically available in commercial finite-element packages and can be used to model the resulting material response of die-cast automotive components produced with these alloys to more complex loading conditions. The resulting deformed microstructures and fracture surfaces of each alloy at different strain-rates were also analyzed.

11:10 AM

Mechanical Properties of Newly Developed Mg-Alloys AMX602 AND ZAXE1711 under Quasi-Static and Dynamic Loading: *Jianghua Shen*¹; Weihua Yin¹; Katsuyoshi Kondoh²; Tyrone L. Jones³; Suveen N. Mathaudhu⁴; Zhiliang Pan¹; Laszlo Kecskes³; Qiuming Wei¹; ¹UNC Charlotte; ²Osaka University; ³US Army Research Laboratory; ⁴U.S. Army Research Office

We present some experimental results on two newly developed Mg-alloys, AMX602 and ZAXE1711. We have evaluated the dependence of the mechanical properties of these alloys on the extrusion temperatures under both quasi-static (strain rate $\sim 1 \times 10^{-3}$ s⁻¹) and dynamic (strain rate $\sim 4 \times 10^3$ s⁻¹) uniaxial compressive loadings. We have observed that the quasi-static yield strength of AMX602 exhibits slight dependence on the extrusion temperature, whereas the ultimate strength and the deformation-to-failure are absent of such dependence. On the other hand, the dependence of the mechanical properties of ZAXE1711 is much more complicated. We have also found that the deformation-to-failure of both alloys increases at increased strain rate. For comparison, we have tested two conventional Mg-alloys, WE43 and AZ91C under the very similar conditions. We have found that AMX602 and ZAXE1711 show significantly improved mechanical properties compared with WE43 and AZ91C under either quasi-static or dynamic loading.

11:30 AM

Phase Field Modeling of β_1 Precipitation in WE54 Alloy: *Yipeng Gao*¹; Hong Liu²; Rongpei Shi¹; Zhou Xu²; Jianfeng Nie²; Yunzhi Wang¹; ¹The Ohio State University; ²Monash University

WE54(Mg-5wt%Y-2wt%Nd-2wt%RE), which has high strength and light weight at elevated temperatures, has been identified as one of the most successful magnesium alloys. The strength of WE54 can be achieved via precipitation strengthening by aging at 150~250°C during which precipitations of intermediate phases β_1 and β' and equilibrium phase β take place. In order to understand the microstructure evolution of β_1 phase and its effects on β' and β precipitation, a phase field model of β_1 precipitation has been developed. Model inputs, including lattice parameters, precipitate-matrix orientation relationship, elastic constants and free energy data, are obtained from experimental characterization, ab initio calculations and thermodynamic databases. Through computer simulations, the equilibrium shape and spatial distribution of and stress field around the β_1 precipitates are quantitatively determined. The effect of elastic interactions among different precipitates on the multi-variant morphology is investigated and the corresponding effect on the strength of the alloy is discussed.

Magnetic Materials for Energy Applications II: Power Conversion and Microstructural Effects

Sponsored by: The Minerals, Metals and Materials Society, TMS Electronic, Magnetic, and Photonic Materials Division, TMS: Magnetic Materials Committee

Program Organizers: Raju Ramanujan, Nanyang Technological University; Francis Johnson, GE Global Research; S Guruswamy, Univ. of Utah; J Liu, Electron Energy Corporation

Thursday AM
March 15, 2012

Room: Europe 10
Location: Dolphin Resort

Session Chairs: Michael McHenry, Carnegie Mellon Univ.; Jun Ding, National University of Singapore

8:30 AM Invited

Nanocomposite Alloy Design for High Frequency Power Conversion Applications: Shen Shen¹; Paul Ohodnicki²; Samuel Kernion¹; Alex Leary¹; Vladimir Keylin³; Joseph Huth³; *Michael McHenry*¹; ¹Carnegie Mellon University; ²National Energy Technology Laboratory; ³Division of Spang & Company

Recent DOE workshops highlight the need for advanced soft magnetic materials leveraged in novel designs of power electronic components and systems for power conditioning and grid integration. Dramatic weight and size reductions are possible in these applications through operating at increased frequencies. This manuscript discusses processing and composition design approaches for optimizing FeCo-based nanocomposites for higher frequency operation at 100 kHz and above. The proposed strategy involves starting with prior compositions known to exhibit high inductions, optimal field crystallization induced anisotropy, and excellent mechanical and high temperature magnetic properties. Proposed alloy modifications for the applications of interest would include increased amorphous phase resistance, optimum induced anisotropy, and minimized or carefully engineered magnetostriction. Relevant process developments would target reduction of ribbon thickness by optimizing the casting process or post-processing treatments such as chemical thinning or rolling. Three archetypes FeCo-based nanocomposites are described including near equiatomic FeCo-based, Fe-rich and Co-rich alloys.

9:00 AM Invited

Economic and Low-Temperature Fabrication of Highly-Textured Ferrite Films and Their Potential in Power-On-Chip Application: Y Yang¹; Jun Ding²; ¹Natl. Univ. of Singapore; ²National University of Singapore

Recently, magnetic films have been investigated for components in power supplier on chip, for example DC-DC converter. These devices can make IT products to be more energy-efficient. MnZn- and NiZn-spinel ferrites are microwave magnets used in inductors and other devices. Sol-gel has been widely used in the fabrication of spinel ferrite films. However, the formation of the spinel phase often requires a post-annealing at a high temperature. Components of power supplier on chip must be CMOS technology compatible. Therefore, temperature during fabrication should never exceed 400 °C. Most recently, our research work has achieved highly texture spinel ferrite films via a chemical route – thermal decomposition at a temperature below 300 °C. High values of magnetization with excellent soft magnetic properties have been obtained in MnZn- and NiZn-ferrite films. In this presentation, we will report synthesis, structure and magnetic properties of these spinel ferrite films and their potential applications.



9:30 AM

Magnetic Properties of Strontium Ferrite Prepared Using Submicron-Sized SrFe_{12-x}Al_xO₁₉ Powders: *Vladimir Menushenkov*¹; Vladimir Shubakov²; Sergey Ketov²; ¹National University of Science and Technology; ²National University of Science and Technology,

The glass samples were obtained by melting of the oxides mixture SrO-Fe₂O₃-B₂O₃-(Al₂O₃) at 1250-1300°C with subsequent quenching of the melt on quickly rotating steel roller. Submicron-sized SrFe_{12-x}Al_xO₁₉ particles were formed in glass-ceramic matrix during the crystallization aging of glass. The aging temperature Tag varied in the range 600–950°C. The submicron-sized hexaferrite powder was obtained by removing of the matrix phases using etching. The samples were characterized by X-ray diffraction, scanning electron microscopy and magnetization measurements. The glass-ceramic material exhibits very high coercivity value up to 10 kOe. The samples of magnets were obtained by pressing of the hexaferrite powder at RT and subsequent aging in the range 900–1200°C. The aged samples exhibit high coercivity value up to 8 kOe.

9:45 AM Break

10:00 AM

Effects of Magnetic Field on Microstructure Evolution in Decomposition Process: *Yongmei Jin*¹; Stephen Hackney¹; ¹Michigan Technological University

Decomposition processes in spinodal-type magnetic alloys under external magnetic field are investigated by phase field modeling and simulations. The model explicitly treats structural and magnetic domains and takes into account multiple thermodynamic driving forces, including chemical, interfacial, magnetostatic, elastostatic, magnetocrystalline, exchange, and external magnetic and mechanical loading. Various spinodal-type magnetic systems of different magnetic properties and misfit strains are considered. The simulations show the influences of magnitude and direction of applied magnetic field to the microstructure evolution in diffusional phase separation, and reveal the underlying mechanisms of magnetic domain formation and internal magnetic field development responsible for the two-phase morphology. The simulation results provide insights into the effective microstructure control in various spinodal-type magnetic alloys by magnetic annealing.

10:15 AM

Electrical and Structural Characteristics of Ba₂DyNbO₆: *Suharto Chjatterjee*¹; Koushik Biswas²; Mukul Pastor²; ¹Ace Calderys Ltd; ²Indian Institute of Technology, Karagpur, India

The electro ceramic material Ba₂DyNbO₆ has been prepared by a standard solid-state reaction technique. Structural analysis was performed with XRD in which dominant (98%) cubic perovskite phase was found. The tolerance factor of the sample was found to be 0.891 suggesting that the sample is stable. The FTIR analysis showed good bond strength in the sample. The experimental results of impedance spectrum indicate that the material exhibits (i) electrical resistance due to bulk material up to 575°C (ii) negative temperature coefficient of resistance (NTCR)-type behaviour and (iii) temperature-dependent relaxation phenomena up to 500°C. The behaviour of the modulus spectrum is suggestive of temperature-dependent ion hopping mechanism for electrical conduction (charge transport) in the system. The AC conductivity spectrum was found to obey Jonscher's universal power law. Conductivity phenomenon has been explained with respect to thermal activation resulting in mobile charges.

10:30 AM

Impact of Magnetic Fields on the Corrosion Degradation of Ferromagnetic Materials in Aqueous Electrolytes: *Ralph Sueptitz*¹; Kristina Tschulik¹; Margitta Uhlemann¹; Ludwig Schultz¹; Annett Gebert¹; ¹IFW Dresden

Beside their magnetic properties, the corrosion resistance of magnetic materials is crucial for ensuring a low loss of efficiency during the life time of electromagnetic devices. While the corrosion behaviour of many magnetic materials is well known, the effect of superimposed magnetic field on the corrosion process is scarcely investigated. The impact of applied magnetic fields on the free corrosion and anodic dissolution of iron and NdFeB permanent magnetic materials was investigated. Low concentration electrolytes, relevant to current applications were also studied. After electrochemical tests the surface profiles of the electrodes were analyzed. The effects of magnetic field on the corrosion rate of these materials and the localization of the corrosion reaction is summarized. Depending on the magnetic field to electrode configuration, magnetically enhanced or reduced corrosion rates and localized material loss is reported. A mechanism of magnetic field action on electrochemical reactions in low concentrated electrolytes is described.

10:45 AM

Influence of Magnetization on the Hydrogen Embrittlement Behavior in AISI 4340 Steel: *Meenakshisundaram Ramanathan*¹; Biswadeep Saha¹; Chai Ren¹; Sivaraman Guruswamy¹; Micheal McCarter¹; ¹University of Utah

Three-point bend test was used to study the effect of electrochemically charged hydrogen and magnetic field on the embrittlement behavior of AISI 4340 steel in this work. Acoustic emission signals were collected during the test and analyzed to gain an understanding of the crack growth process. Cathodic hydrogen charging in AISI 4340 steel resulted in drastic reduction of ductility and strength. Hydrogen embrittlement was characterized by a change in fracture surface from dimpled ductile surface to quasi cleavage type fracture. No significant effect was observed in the presence of magnetic field. The acoustic emission signals collected during the test provided an indication of the extent of energy released during the crack growth process.*Support of this work by NSF through the award DMR-0854166 is gratefully acknowledged

11:00 AM

The Effect of Dynamic Electropulsing on Mechanical and Microstructural Properties of Cold Rolled Fe-6.5%Si Alloy Sheet: *Yongfeng Liang*¹; Feng Ye¹; Hongchan Zhou¹; Fuming Wang¹; Guoyi Tang²; Junpin Lin¹; ¹University of Science and Technology Beijing; ²Tsinghua University

Fe-6.5%Si alloy is a very excellent soft magnetic material compared with conventional Si steel, especially in high frequencies with reduced iron losses and noises. But it is hard to be fabricated due to its brittleness at room temperature. Mechanical and microstructural properties are investigated with different electropulsing and strain rate. The dynamic electropulsing is applied to the cold rolled Fe-6.5%Si sheet during tensile deformation. It is found that the yield stress decreases and the elongation increases with application of dynamic electropulsing. It is indicated that the work hardening could be reduced with the dynamic electropulsing during deformation, which provides a promising way to fabricate this alloy sheet much easier.

Materials and Fuels for the Current and Advanced Nuclear Reactors: Modeling II

Sponsored by: The Minerals, Metals and Materials Society, TMS Structural Materials Division, TMS/ASM: Corrosion and Environmental Effects Committee, TMS/ASM: Nuclear Materials Committee

Program Organizers: Ramprasad Prabhakaran, Idaho National Laboratory; Dennis Keiser, Idaho National Laboratory; Raul Rebak, GE Global Research

Thursday AM
March 15, 2012

Room: Swan 4
Location: Swan Resort

Session Chairs: Patrice Turchi, Lawrence Livermore National Laboratory; Michael Tonks, Idaho National Laboratory

8:30 AM

Pressure Effects in Iron-Uranium Diffusion Couples: *Daniel Koury*¹; Gerald Egeland¹; Abu Iqbal¹; Thomas Hartmann¹; ¹Harry Reid Center, University of Nevada - Las Vegas

The interdiffusion of different metals has been widely studied. The properties of different couplings depend on such extrinsic variables as annealing time, annealing temperature, and intrinsic properties such as solubilities of each material in the other and surface morphology. The focus of this work is on pressure between two pure materials in a diffusion couple. Results of diffusion experiments, conducted to model the interaction of fast reactor fuel products and fuel cladding materials, have suggested that pressure affects the diffusion rate of one metal into another. This work consists of iron-uranium diffusion couples in a three-point flexural apparatus. The iron and uranium system has been studied and is well-suited to study pressure effects. The three-point flexural system provides pressure and tension zones that are modeled by finite element analysis to calculate stress gradients throughout the materials. The results of the simulations will be compared to the results of the diffusion.

8:50 AM

Thermodynamic Properties of Complex Actinide Alloys: *Patrice Turchi*¹; Alexander Landa¹; Per Söderlind¹; ¹Lawrence Livermore National Laboratory

Nuclear fuels for fast spectrum nuclear reactors raise challenging questions on the role of minor actinides and fission products and gases on properties and performance. Hence, prediction of phase stability trends and phase diagrams of complex actinide-based alloys is undoubtedly required to be able to predict materials performance. CALPHAD, combined with first-principles electronic structure results, is a powerful tool to predict the thermodynamic properties of actinide-based multi-component alloys. After a brief review of the available knowledge on {Am,Np,Pu,U,Zr} that are the basis for candidate metallic fuels, we focus on two examples, Am-Pu and Mo-U, for which ab initio input provides useful guidance for well-chosen experiments that can lead to full validation and verification of the thermodynamic driving force that is critically needed for subsequent work on materials evolution and performance. Work performed under the auspices of the U.S. DOE by LLNL under contract DE-AC52-07NA27344.

9:10 AM

Effects of Stress on Void Formation under Irradiation: *Srujan Rokkam*¹; Karim Ahmed¹; Anter El-Azab¹; ¹Florida State University

We investigate the effects of stress on the nucleation and growth of voids in irradiated materials with a phase-field approach. The formulation couples point defect dynamics and void evolution with elastic effects due to the non-uniform lattice relaxation defects and inhomogeneity effects introduced by voids. The coupled problem requires the solution of two Cahn-Hilliard equations for evolution of vacancy and interstitial

concentration fields, an Allen-Cahn equation for void phase dynamics, and a subsidiary stress equilibrium problem. Analysis of the coupled model recovers the corresponding sharp interface formalism for point defects diffusion and void growth under applied stress, with zero traction boundary condition over the void surfaces. We present the formalism and discuss results showing the effect of applied stress on the defect migration, void growth, void-void interactions and void self-organization. This research was supported by the EFRC on Materials Science of Nuclear Fuel under subcontract 00091538 from INL to FSU.

9:30 AM

KMC Modeling of Helium-Vacancy Clustering in Iron: *Aaron Oaks*¹; James Stubbins¹; ¹University of Illinois, Urbana-Champaign

Ferritic alloys are considered candidate materials for advanced nuclear power systems as a result of their excellent resistance to void swelling, superior thermal conductivity, lower thermal expansion and acceptable high temperature mechanical strength compared to austenitic stainless steels. The FeCr-based alloy system is considered the lead alloy system for a variety of advanced reactor components and applications. In this modeling study, we will use kinetic Monte Carlo (kMC) to look at the effect of helium on the accumulation of defects and defect clusters in the iron system. Formation, migration, and binding energies from ab initio and molecular statics studies will be used as input to the kinetic Monte Carlo model to simulate defect diffusion and clustering over the relevant time scales. These results will help to provide a fundamental understanding of the interactions between vacancy defects and helium introduced as a result of irradiation.

9:50 AM

Radiation-Induced Compositional Patterning and Segregation in Concentrated Binary Alloys: *Santosh Dubey*¹; Anter El Azab¹; ¹Florida State University

A reaction-diffusion model to capture material redistribution in a concentrated binary alloy under irradiation will be presented. In addition to vacancies, three interstitial configurations are considered: AA, BB and AB dumbbells. The overall model tracks the space and time evolution of three species on the lattice (A, B atoms and vacancies) and three interstitial types. Atomic displacement cascades are modeled as stochastic events in space and time, with each cascade event introducing a source of point defects that is localized over a finite region. With this model we have quantified the formation of self-organized compositional patterns as a function of irradiation-specific control parameters. Using free boundary conditions, segregation of alloying elements and its effect on morphological changes at the free surfaces has also been studied. This work has been extended further to study the effect of segregation on phase stability and evolution of defect microstructures (voids) under phase field formulation.

10:10 AM

Interaction of Self-Interstitial Clusters with Carbon Atoms and Carbon-Vacancy Complexes in Fe-C Alloys: *Anna Serra*¹; Napoleon Anento¹; ¹Universitat Politècnica de Catalunya

The mobility of $\frac{1}{2}\langle 111 \rangle$ and $\langle 100 \rangle$ self-interstitial (SIA) clusters and glissile dislocation loops created in irradiated Fe-C alloys is affected by their interaction with interstitial carbon atoms (C) and carbon-vacancy complexes (Cn-Vm). The interaction energy maps of $\frac{1}{2}\langle 111 \rangle$ clusters of 7 and 61SIAs with a single C and {C-V, C2 -V, C-V2} complexes have been studied by molecular statics and molecular dynamics simulations using a metallic-covalent bonding interatomic model for the Fe-C system derived by Hepburn and Ackland (2008). The interaction energy of C with a $\frac{1}{2}\langle 111 \rangle$ {110} edge dislocation is presented as limiting case. C acts as a weak trap for clusters whereas C-V complexes are stronger traps. The stability of the cluster-(C-V) group is studied as a function of temperature. The interaction energy of C with $\langle 100 \rangle$ clusters from 9 to 361 SIAs is presented: C is a stronger trap for $\langle 100 \rangle$ clusters.



10:30 AM Break

10:40 AM

Interaction of $\frac{1}{2}\langle 111 \rangle\{110\}$ Edge Dislocation With Interstitial Carbon Atoms in α -Iron: *Hassan Khater*¹; *Anna Serra*¹; *Ghiath Monnet*²; ¹Universitat Politecnica de Catalunya (UPC); ²EDF – R&D

The atomic scale behaviour of a $\frac{1}{2}\langle 111 \rangle\{110\}$ edge dislocation near a single and 400ppm carbon interstitial atoms (C) in α -iron has been simulated at $T \geq 0K$. The behavior is correlated with the stress tensor due to single C which can be high but effectively short ranged. The sites where C interacts significantly with the dislocation have been investigated as well as the critical stress for the dislocation to overcome a row of C. C close to the dislocation glide plane provides the strongest barrier to slip. The dislocation unpinning stress decreases at high temperatures and saturates to a constant value above 400K. C jumps in the core of the dislocation occur before dislocation unpinning at relatively low temperatures and was found to be sensitive to strain rate. Dislocations in a distribution of 400ppm C glide at stresses less than that of a dislocation in pure iron for long dislocation lines.

11:00 AM

Structure of Overlapping Ions Tracks in Solids: *Andrii Demchyshyn*¹; *Pavel Selyshchev*²; ¹Taras Shevchenko National University of Kyiv; ²University of Pretoria

Formation of extensive structures from separate tracks depending on the characteristics of the projectile beam and on parameters of the swift heavy ions induced tracks were theoretically modelled. We examined tracks like a chain of deal spherical regions. The dependence of the sample surface area after exposure and removal of the modified substance from the irradiation dose and the swift heavy ions incidence beam angle were search out. Angular dependence of the sample surface area has maximum value at certain "critical" ions incidence angle. Based on the scaling hypothesis large-scale curve were constructed, critical exponents for this percolation model were established. Calculated values of critical exponents were compared with known values for the continuous percolation model. Correlation of individual track regions results in higher ratio of the critical exponents than in a continuous percolation model, that talks about the higher connectivity of track regions structure in this model.

11:20 AM

A New Model for Predicting the Oxidation/Gasification of Nuclear Graphite: *Ryan Paul*¹; *John Morral*¹; ¹The Ohio State University

A persistent concern for nuclear graphite is loss of graphite due to thermal oxidation in air or steam. This presentation will discuss a new analytical model for the oxidation/gasification of graphite that applies when reactions have a constant rate and only occur at the walls of pores that are open to the graphite free surface. Also, the model assumes there is an internal oxidation front that moves into the sample from the surface at a constant rate, thereby connecting closed pores in the graphite interior to the free surface. Pores are modeled either as a single sphere or as a cluster of spheres in order to imitate the pore structure of real graphitic materials. Both phase field simulations and TGA experiments on graphite in air have been performed to validate the analytical model.

11:40 AM

Cluster Dynamics Modeling of Microstructural Evolution in Ferritic/Martensitic Iron Chrome: *Aaron Kohnert*¹; *Brian Wirth*²; *Donghua Xu*²; *Djamel Kaoumi*³; *Arthur Motta*⁴; *Cem Topbas*⁴; ¹University of California; ²University of Tennessee; ³University of South Carolina; ⁴Pennsylvania State University

The primary goal of this modeling is to investigate the development of defect clusters during exposure to heavy ion irradiation at a wide range of temperatures as observed at the IVEM facility at Argonne National Lab. The cluster dynamics model used in this study is an expansion of simpler rate theory models with added consideration of the possibility of defect reactions to form arbitrarily large clusters and to explicitly include spatially dependent defect sinks. Primary damage production is implemented with

a multiscale approach using a database of molecular dynamics simulations of displacement cascades to implant damage in the form of defect clusters in addition to Frenkel pairs. Particular attention is given to determining the appropriate diffusivity for clusters of various sizes in light of the differences between experimental and computational studies of interstitial cluster mobility. The role of cascade-defect interactions in determining the ultimate mobility of defects is also considered.

12:00 PM

2D/3D Simulation of δ -Hydride Re-Orientation under External Load by Phase Field Approach in Zircaloy Matrix: *Lingfei Zhang*¹; *Ludovic Thuinet*²; ¹Electricité de France (EDF) R&D MMC; ²University of Lille 1

The mechanical property of hydrided-Zircaloy cladding under external load lies in the center of nuclear reactor safety. Numerous experimental studies revealed that hydride re-orient from circumferential to the radial direction under the hoop strength. However the true mechanism and kinetics of re-orientation is very complicated and still under investigation. Advanced in numerical simulation by phase field approach is made with newly developed 3D code by large scale parallel computing that enables us to investigate the hydride re-orientation from particular crystallographic plane in 2D to the whole space in 3D. The result showed that the hydride precipitation is more complex than thought to the external load assuming constant magnitude. The simulation also reveals that classical inhomogeneous solid theory has limitation in prediction of habit plane when hydride was considered as isolated particle in an infinite plane and modification has to be done. Phase field modeling provides proof to support such modification.

Materials and Fuels for the Current and Advanced Nuclear Reactors: Structural Materials - Irradiation Studies I

Sponsored by: The Minerals, Metals and Materials Society, TMS Structural Materials Division, TMS/ASM: Corrosion and Environmental Effects Committee, TMS/ASM: Nuclear Materials Committee

Program Organizers: Ramprashad Prabhakaran, Idaho National Laboratory; Dennis Keiser, Idaho National Laboratory; Raul Rebak, GE Global Research

Thursday AM
March 15, 2012

Room: Swan 2
Location: Swan Resort

Session Chairs: Todd Allen, University of Wisconsin - Madison; Ramprashad Prabhakaran, Idaho National Laboratory

8:30 AM Invited

Microstructures of Ferritic-Martensitic Alloys Irradiated to High Dose at High Dose Rates: *Gary Was*¹; *Zhijie Jiao*¹; ¹University of Michigan

Ferritic-martensitic (F-M) alloys are attractive candidates for structural components in sodium-cooled fast reactors. To reach the high doses expected in this application, high dose rate self-ion irradiation is used. In this study, F-M alloys HT9, HCM12A, T91 and a model 9Cr alloy were irradiated at 400 or 500°C to doses of 30 to 500 dpa using 5 MeV Fe⁺⁺ ions at 10-3 dpa/s. Samples were prepared using FIB for TEM to characterize dislocation microstructure, voids, and RIS, and for APT to characterize RIP. Results show that Cr enriches at the grain boundary and Ni/Si/Mn-rich and Cu-rich precipitates nucleate following Fe⁺⁺ irradiations. At a very high dose of 500 dpa, a high density of radiation-induced Cr-rich carbides was observed in HCM12A. The evolution of RIS and precipitation at high dose and high temperature and their potential effect on the alloy mechanical properties will be presented and discussed.

9:00 AM

Irradiation Studies on Friction Stir Welded MA956 and MA754: *Ramprashad Prabhakaran*¹; J Wang²; B Miller¹; J Cole¹; I Charit³; R Mishra²; K Murty⁴; ¹Idaho National Laboratory; ²Missouri University of Science and Technology; ³University of Idaho; ⁴North Carolina State University

Efforts are ongoing to examine the feasibility of using oxide dispersion strengthened (ODS) alloys in the advanced nuclear reactors. Conventional fusion welding of ODS alloys could cause various undesirable effects such as coalescence of oxide dispersoids and significant porosity. Efforts are ongoing to optimize the friction stir welding technique with regard to joining ODS alloys, MA956 and MA754. In this study, MA956 and MA754 alloys were friction stir welded in a bead-on-plate configuration. Higher weld efficiencies have been achieved in both the alloys. Microhardness and shear punch testing of the fresh and irradiated (1 and 2 dpa) parent and processed materials were carried out to evaluate the mechanical properties. Optical microscopy, SEM, TEM and APT were used to study the microstructures of fresh and irradiated parent and processed materials. The study has been partially supported by an ATR National Scientific User Facility grant.

9:20 AM

The Use of a Local Electrode Atom Probe Method to examine the Microstructure of Zircaloy: *Brian Cockeram*¹; Lance Snead²; M. Miller²; ¹Bechtel-Bettis; ²Oak Ridge National Laboratory

Literature data has shown that the irradiation of Zircaloy at very low fluencies on the order of 7×10^{22} n/m² (E<1MeV) or lower results in measurable irradiation hardening, but the defect clusters responsible for such hardening are below the resolution limit of electron microscopy. Efforts to analyze Zr-based alloys using conventional atom probe that could be applied to resolve defect clusters have been largely unsuccessful due to the poor electrical conductivity of zirconium at cryogenic temperatures that generally results in premature fracture of specimens prior to obtaining a viable dataset. In this work the parameters for a LEAP are optimized using non-irradiated material, and the applied to wrought Zircaloy-2 and Zircaloy-4 following neutron irradiation at nominally 358°C to a fluence of 2.9×10^{25} n/m² in the High Flux Isotope Reactor (HFIR). These results are used to determine if solute clustering at <a> loops or fine defect clusters are formed during irradiation.

9:40 AM

Phase Stability and Elemental Redistribution under High-Dose Ion Irradiation in 14YWT Nanostructured Ferritic Alloy: *Yanwen Zhang*¹; Zihua Zhu²; Chad Parish¹; Philip Edmondson¹; Michael Miller¹; ¹Oak Ridge National Laboratory; ²Pacific Northwest National Laboratory

Structural materials for advanced nuclear reactors require long-term stability and radiation tolerance at elevated temperatures over extended lifetimes. Ion irradiation can be used to simulate knock-on damage and evaluate radiation-induced microstructural instabilities that may occur as a result of accumulation of radiation damage during neutron irradiation. A 14YWT nanostructured ferritic alloy was irradiated with 10 MeV Au/Pt to a penetration depth of ~1.5 μm and doses up to ~500 dpa between -100 and 750°C. Heavy ions are used to maximize the deposited energy and minimize the implanted ion content for a given displacement damage level. The irradiation-induced redistribution of Cr, W, C, N, O, Ti and Y and the response of the microstructure to high doses were characterized by complementary techniques of electron microscopy, atom probe tomography, X-ray diffraction, and secondary ion mass spectrometry. This research was sponsored by the U.S. DOE-BES-MSED and SUFD (SHaRE [APT and TEM])

10:00 AM

Influence of Cr Content on Radiation Induced and Enhanced Precipitation in Neutron Irradiated Fe-Cr Model Alloys of Low Purity: Comparison with Ion Irradiation: *Philippe Pareige*¹; Slava Kuskonko¹; Cristelle Pareige¹; ¹Rouen University

Fe-Cr model alloys of high-Cr ferritic-martensitic (FM) steels, which are candidates for structural materials in Generation IV reactors, are investigated in the framework of the GETMAT European project. 3D atom probe experiments have been performed in neutron irradiated Fe-Cr model alloys with different chromium content: 12at%Cr, 9%Cr, 5% and 2.5%Cr. These model alloys of low purity were neutron irradiated at 300°C up to 0.6 dpa. Two families of clusters have been revealed: alpha' clusters and NiSiPCr-enriched clusters. Depending on the Cr content, only one of the two families of clusters can be observed. Results obtained on the neutron irradiated Fe-9%Cr alloy are compared to data collected on the same alloy, irradiated at the same temperature, with Fe⁺ ions having three different energies (0.5, 2 and 5 MeV) in order to obtain a constant damage up to 1.4 μm, the radiation dose being equal to 1 dpa.

10:20 AM Break**10:30 AM**

Study of Ion Irradiation Effects on Microstructure of ODS Ferritic Steels by Atom Probe Tomography: *Bertrand Radigue*¹; Yves Serruys²; Olena Kalokhtina¹; Mathieu Couvrat³; Laurent Chaffron³; Fabrice Legendre²; Philippe Pareige¹; ¹GPM UMR CNRS 6634 - Université et INSA du Rouen; ²CEA Saclay - DEN - DMN - SRMP; ³CEA Saclay - DEN - DMN - SRMA - LTME

Oxide dispersion-strengthened (ODS) ferritic steels are promising candidates as structural materials for fusion and Generation IV nuclear reactors. They exhibit a limited swelling under irradiation, characteristic of ferritic/martensitic (F/M) matrix, and excellent creep and tensile properties at high temperatures compared to standard F/M steels, thanks to reinforcement by dense nano-oxides dispersion. Because of the interest in ODS steels for nuclear applications, it is important to determine if the nano-oxides remain stable when exposed to irradiation up to high doses in terms of displacement per atoms (dpa). In this work, 5 MeV Fe ion irradiations were performed at 500°C (in JANNUS facility) on a Fe-18Cr-1W-0,3Ti-0,3Y₂O₃ ODS ferritic steel. Its microstructure was characterised at the atomic scale by atom probe tomography in order to study the stability of nano-oxides and the matrix under irradiation up to 50 dpa.

10:50 AM

Influence of Grain Boundary Character and Grain Orientation on Radiation Damage by Ion Irradiation and Implantation: *Dhriti Bhattacharyya*¹; Yongqiang Wong²; Pranesh Dayal¹; David Carr¹; Amit Misra²; Robert Harrison¹; Lyndon Edwards¹; ¹Australian Nuclear Science and Technology Organization; ²Los Alamos National Laboratory

In a metallic system the damage caused by ion implantation, in the form of point-defect clusters, voids, bubbles, and chemical segregation is influenced by the presence of grain boundaries. The nature of the grain boundaries in terms of their misorientation and crystallographic plane can control these effects significantly. In this study these grain boundary effects are studied in ion-irradiated metals by using electron backscatter detection (EBSD) to obtain grain misorientation information, followed by focused ion beam (FIB) extraction of transmission electron microscopy (TEM) samples from specific types of grain boundaries, and subsequent examination of the samples in the TEM. Diffraction contrast was used to image defect clusters, Fresnel contrast for imaging voids and bubbles, and energy dispersive spectroscopy (EDS) and energy filtered TEM (EFTEM) for studying chemical segregation. The preliminary results of these investigations are presented here.



11:10 AM

Corrosion of HT-9 in Contact with Molten Lead Bismuth Eutectic with and without Simultaneous 6 MeV Proton Irradiation: Staffan Qvist¹; Magdalena Serrano de Caro²; Alan Bolind¹; *Yongqiang Wang*²; Mark Bourke²; Peter Hosemann¹; ¹University of California Berkeley; ²Los Alamos National Laboratory

A major unknown in the development of materials for advanced nuclear systems is related to the question of corrosive materials degradation under “in-service” operating conditions. In this work, we describe the irradiation/corrosion experiment, namely ICE*, performed at LANL within the Los Alamos National Laboratory – University of California Berkeley (LANL-UCB) collaboration. The purpose of this work is to study synergistic effects of irradiation on steel corrosion, and investigate if and how a steady state concentration of defects continuously created by displacement cascades affects surface chemistry such as oxidation or dissolution. ICE* builds-up on the experience gained in a previous ICE-I experiment, where HT-9 steel was exposed to proton irradiation in the presence of Lead Bismuth Eutectic (LBE) at high temperature. ICE* constitutes a natural continuation with improved capabilities, i.e. monitoring Oxygen content in LBE, ability to reach higher temperatures and dose values.

11:30 AM

On the Stability of Nanostructured 18-Chromium ODS Steels under High Dose Ion-Irradiation: *Marie-Laure Lescoat*¹; Joël Ribis¹; Emmanuelle MARQUIS²; Yimeng CHEN²; Aurélie Gentils³; Odile Kaïtasov³; Yves SERRUYS¹; Patrick ROCCELLIER¹; Arthur Motta⁴; Yann de Carlan¹; Alexandre Legris⁵; ¹CEA Saclay; ²University of Michigan; ³CNSM, CNRS/IN2P3; ⁴Pennsylvania State University; ⁵Université de Lille 1

Ferritic-Martensitic Oxide Dispersion Strengthened (ODS) steels are promising candidates for fuel cladding of high burn-up fast neutron reactors. To meet requirements, the stability of reinforcing nano-oxides has to be settled in the irradiation and temperature service conditions. In this work, ion irradiations are performed on 18-Chromium ODS steels and the induced microstructural modifications are investigated by the Transmission Electron Microscopy and Atom Probe Tomography complementary techniques. In-situ irradiations (CNSM-JANNuS Orsay) of Fe18Cr1W0.4Ti+O.6Y2O3 showed that Y-Ti-O nanoclusters are apparently stable up to 45 dpa at 500°C. However, at 235 dpa (SRMP-JANNuS Saclay), radiation-induced modifications of sizes and compositions were suspected. Furthermore, inert gas irradiations (IVEM-Argonne) performed on a Fe18Cr1W0.8Ti+0.3MgO model ODS alloy showed that the coherency of oxide/matrix interfaces plays a key role on the nucleation of Kr-stabilized cavities at room temperature.

11:50 AM

Temperature Effects on the High Dose Radiation Resistance of Nano-Sized Clusters in Nanostructured Ferritic Alloys: *Alicia Certain*¹; Satyanarayana Kuchibhatla²; Vaithiyalingam Shutthanandan²; Chad Parish³; Todd Allen¹; David Hoelzer³; ¹University of Wisconsin-Madison; ²Pacific Northwest National Laboratory; ³Oak Ridge National Laboratory

Nanostructured ferritic alloys (NFAs) have been developed to operate at higher temperatures than traditional ferritic-martensitic steels, and are expected to play an important role as cladding for fission reactor fuels or fusion blanket structural components operating in the temperature range of 350–700°C and to doses up to 200 displacements per atom (dpa). These steels contain nanometer-sized Y–Ti–O clusters for additional strengthening. Nickel ion irradiations have been performed on the NFA 14YWT up to 100 dpa at a range of temperatures (-75°C to 600 °C.) Energy-filtered transmission electron microscopy (EFTEM) and atom probe tomography (APT) have been used to analyze the evolution of the nanoclusters post-irradiation. Preliminary interpretation of results indicates that clusters are not stable for the low temperature-high dose condition studied, but appear to be stable for the higher temperature irradiations. FIB supported by DOE-BES-SUFD (SHaRE).

12:10 PM

Planar Dislocations and Dislocation Channeling in Unirradiated and Irradiated Austenitic Stainless Steels: *Young Suk Kim*¹; Young Suk Kim¹; Dae Whan Kim¹; ¹Korea Atomic Energy Research Institute

Tensile tests were conducted on 316L stainless steel with nitrogen over a temperature range of RT to 750°C at strain rates of 2x10⁻⁴/s. The 316L stainless steel (SS) showed serrated flow in a temperature range of 400 to 600°C where a linear increase of strain hardening was accompanied. Using neutron diffraction, the lattice contraction due to atomic ordering was seen to occur in the 40% cold-worked 316 SS on aging at 400°C. TEM microstructures showed the formation of planar dislocations in 316L SS upon tensile testing at 400°C where SRO and serrated flow appeared. This study demonstrates that SRO is the cause of planar dislocations and serrations in austenitic stainless steels. Given that neutron irradiation produces dislocation channeling and softening after yielding in austenitic stainless steels above some fluences, the cause of dislocation channeling and softening in irradiated 304 stainless steels is discussed with short range ordering.

Materials Design Approaches and Experiences III: Joining and Microstructure-Property Relationships

Sponsored by: The Minerals, Metals and Materials Society, TMS Structural Materials Division, TMS: High Temperature Alloys Committee, TMS: Integrated Computational Materials Engineering Committee

Program Organizers: Ji-Cheng Zhao, The Ohio State University; Akane Suzuki, GE Global Research; Deb Whitis, GE Aviation; Michael Fahrman, Haynes International Inc.; Qiang Feng, University of Science and Technology Beijing

Thursday AM
March 15, 2012

Room: Europe 11
Location: Dolphin Resort

Session Chairs: J.-C. Zhao, The Ohio State University; Warren Poole, The University of British Columbia

8:30 AM Invited

Application of Microstructure Engineering to the Heat Affected Zone of Welds: *Warren Poole*¹; Matthias Militzer¹; Mehran Maalekian¹; ¹UBC

There is currently a significant interest in understanding the development of microstructure in the heat affected zone (HAZ) of gas metal arc welded linepipe steels, particularly for applications in Arctic environments. In this work, we have developed an integrated model for microstructure development in HAZ which includes sub-models for i) austenite grain growth including dissolution of microalloying precipitates and ii) the subsequent decomposition of austenite. The sub-model for austenite grain growth has been developed using a novel laser ultrasonic measurement technique. The integrated model is applied into experimentally determined thermal cycles for actual weld trials to predict the spatial distribution of microstructure in the heat affected zone.

9:00 AM Invited

Weldable Materials System Design - Application of Computational Thermodynamics and Kinetics: *Sudarsanam Babu*¹; ¹Ohio State University

With rapid progress in integrated computational materials science and engineering (ICME) models, it is quite possible to design new generation of steels with targeted high- and low-temperature mechanical properties. For example, advanced steels (e.g. BA160 and Hard bainite) with high strength, good toughness, and ballistic performance had been developed using ICME models, without experimental trial and error optimization. In contrast, welding system design, i.e., optimization of heat-affected-zone (HAZ) and weld metal (WM) properties, requires experimental trial and error optimization. The talk will provide highlights of the research

on microstructure development in HAZ and WM towards developing a modeling framework to reduce this trial and error optimization. The methodology includes description of physical processes that occur during liquid-gas-slag metal reactions, solidification and solidification. Some of the challenges associated with non-unique solutions, scatter in properties and sensitivity to welder practice will be discussed.

9:30 AM

Effect of Pre-Weld Heat Treatment Environment on the Microstructure and Crack Behaviors in the Laser Repair Welded René 77 Nickel-Based Superalloy: Huei-Sen Wang¹; Sian-Jih Deng¹; Chen Ming Kuo¹; ¹I-Shou University

To study the effects of pre-weld heat treatment vacuum levels on the microstructure and crack behaviors of repair welded René 77 nickel-based superalloy, the preselected heat treatment conditions were operated under three selected vacuum levels i.e. under 1 atmospheric pressure shielding with pure argon, vacuum levels of 1×10^{-2} torrs and 1×10^{-4} torrs. After heat treated, the samples were welded using a pulsed Nd:YAG laser process with various welding parameters coupling with René 41 filler wire. The microstructure, cracking behaviors, mechanical properties in the weld metal (WM), heat affected zone (HAZ) and parent material (PM) were evaluated using a optical microscope (OM), scanning electron microscope (SEM) equipped with energy dispersive spectrometer (EDS) and microhardness. The experimental results showed that, the higher vacuum levels, the less volume of MC-type carbides and γ - γ' eutectic was observed and the liquation crack in the HAZ or around WFZ is significantly reduced.

9:50 AM Invited

An ICME Approach to Solder Joint Lifetime Prediction: Michael Neilsen¹; Paul Vianco¹; Elizabeth Holm¹; ¹Sandia National Laboratories

Because solders operate at high homologous temperatures, microstructural evolution, cracking, and failure can occur during service. Since circuit boards must function reliably for thousands of thermal cycles in applications such as aircraft and satellites, lifetime prediction is critical for product design and maintenance. We have developed a combined experimental and computational approach to predict both aging (crack initiation) and failure (open circuit) during thermomechanical cycling of lead-tin and lead-free solder joints. By including microstructural evolution and damage parameters in a unified creep plasticity model, we accurately predict crack initiation, location and growth morphology during thermomechanical fatigue for a variety of solder joint geometries. At each step, experiments inform and validate from model predictions. The resulting ICME model for solder joint lifetime is used in materials selection, engineering design, and stewardship programs at Sandia and elsewhere.

10:20 AM Break

10:40 AM

Characterization of the Performance at High Temperature of an Incoloy 718 for Improving the Ring Production: Martha Guerrero¹; Maribel de la Garza¹; Patricia Zambrano¹; Pedro Paramo¹; ¹Universidad Autonoma de Nuevo Leon

Aeronautical, petrochemical and energy industries use the Incoloy 718, which exhibits good mechanical properties at high temperature thanks to the solid solution and precipitation phenomena taking place during the heat treatment. The aim of the present work is to improve the thermomechanical route for the production of rings. Cylindrical samples of the as received alloy of 150 mm x 125 mm height and diameter were forged in an industrial press at 980, 1000, 1020 and 1040°C, using 1 pass or 2 passes to achieve a reduction of 73% or 85%. Samples from the different reductions were obtained to undergo various heat treatments and mechanical testing at high temperature. After forging, heat treatment and mechanical testing samples were cut for advanced microstructural analysis, a microhardness and grain size measurements. Results were analyzed to determine the influence of the different thermomechanical parameters on the final microstructure and mechanical properties.

11:00 AM

Heat Treatment Effects on Creep Behavior of Directionally Solidified CM247LC Superalloy: Ken-Tu Hsu¹; Huei-Sen Wang¹; Wei Bin He¹; Chen-Ming Kuo¹; Hui-Yun Bor²; Chao-Nan Wei²; ¹ISU University; ²Chun-Shan Institute of Science and Technology

This study investigates how the heat treatments affect the creep behavior of directionally solidified CM247LC superalloy. Use two different heat treatment: (HT1) solution treatment at 1260°C for 2 h, then first aging at 1079°C for 4 h and followed by second aging at 871°C for 20 h; (HT2) solution treatment at 1230°C for 10 h, then the same aging procedure. The microstructural observations and quantitative statistical analyses indicate that heat treatments change the γ' characteristics: HT1 resulting in more regularly cuboid morphology of γ' particle and reduction of γ - γ' eutectic phase. Furthermore, the modification of γ' morphology in HT1 specimens enhances better creep rupture life under 760°C /724MPa creep test. The HT1 grains, dislocation motions are restricted because of more regularly cuboid morphology of γ' particle, which is conducive to against high temperature creep deformation. Nevertheless, the γ - γ' eutectic phase is the main cause of creep rupture of DS CM247LC superalloy.

11:20 AM

Influence of Processing Conditions on the Mechanical Properties of High-Nitrogen 18Cr-18Mn Austenitic Steels for Generator Retaining Ring: Byoungchul Hwang¹; Jong-Ho Shin²; Tae-Ho Lee¹; Heon-Young Ha¹; Jong-Wook Lee²; Sung-Joon Kim¹; ¹Korea Institute of Materials Science; ²Doosan Heavy Industries & Construction Co., Ltd.

Retaining rings are used on the shaft ends of power generators and required to have non-magnetic, high strength, high ductility and good corrosion resistance. High-nitrogen 18Cr-18Mn austenitic steels with high yield strength have been recently developed and used for retaining ring material. In the present study, several high-nitrogen 18Cr-18Mn austenitic steels with different N content were fabricated and then tensile and Charpy V-notch impact tests were conducted on them in order to investigate the effect of processing conditions on the mechanical properties. The yield and tensile strengths usually increased with N content, but an increase in strength by cold working was varied depending on N content. Although both the yield and tensile strengths was rather increased after stress relieving, a variation in the strengths was largely affected by the amount of cold working. The cold working and stress relieving treatment also exerted a significant influence on the impact toughness.

11:40 AM

γ (Ni)/ γ' (Ni3Al)-d(Ni3Nb) Eutectic Ni-Base Superalloys: The Relationship between Composition, Solidification Characteristics and Microstructure: Mengtao Xie¹; ¹Illinois Institute of Technology

Polycrystalline γ (Ni)/ γ' (Ni3Al)-d(Ni3Nb) eutectic alloys have been recently demonstrated to possess promising high-temperature properties for structural applications at temperatures below 800°C. Many of their unique attributes could be potentially harnessed to extend the temperature and pressure limits associated with the advanced turbine engine designs. However, studies regarding this class of materials are limited and qualitative in nature. To better understand this novel class of materials, a systematic study of the influence of various elemental additions on the solidification behavior and microstructural characteristics of this Ni-Al-Nb based γ / γ' -d eutectic system is necessary. The effects of Cr, Ta, W, and Mo additions on the solidification microstructure, phase volume fraction and phase transformation temperatures of this novel class of alloys were assessed. Results from this study will be presented and implications of these finding with respect to alloy design will be discussed.



Mechanical Behavior at Nanoscale I: Thin Film and Multilayers

Sponsored by: The Minerals, Metals and Materials Society, TMS Materials Processing and Manufacturing Division, TMS: Nanomechanical Materials Behavior Committee, TMS/ASM: Mechanical Behavior of Materials Committee

Program Organizers: Scott Mao, University of Pittsburgh; Julia R Greer, California Institute of Technology; Jianyu Huang, Center for Integrated Nanotechnologies; Marc Legros, CEMES-CNRS; Ting Zhu, Georgia Institute of Technology

Thursday AM Room: Asia 1
March 15, 2012 Location: Dolphin Resort

Session Chairs: Jianyu Huang, Sandia National Laboratories; Fuqiang Yang, University of Kentucky

8:30 AM Invited

Mechanics of Low Dimensional Material for Energy Harvesting and Storage: *Reza Shahbazian-Yassar*¹; Hessem Ghassemi¹; Kasra Momeni¹; Anjana Asthana¹; Yoke Yap¹; Gregory Odegard¹; ¹Michigan Technological University

Low dimensional materials have received considerable attention for their unique properties in energy storage (batteried) and energy harvesting (nanogenerators) devices. In this presentation, we cover the mechanics of Boron Nitride nanotubes (BNNTs), Zinc Oxide nanowires (ZnO NWs), and Silicon nanorods (Si NRs). Size scale effect on electromechanical properties of ZnO nanobelts (NBs) was studied using molecular dynamics (MD) simulations on graphical processing units (GPUs). The piezoelectric coefficient of ZnO nanobelts increases when the lateral dimensions are reduced. Size scale effects were observed in ZnO nanowires and were explained by the modification of atomic structure at the nanowire surface. In addition, the rippling and bifurcation of multiwalled BNNTs were observed upon buckling and were quantified in terms of number of walls and nanotube's diameter. We also studied the mechanics of lithiated Si NRs to understand the effect of lithium intercalation into the structure of NRs.

8:50 AM

Micro-Scale Grain Boundary Fracture in Copper and Nickel Alloys: *David Armstrong*¹; Helen Dugdale¹; Angus Wilkinson¹; Sergio Lozano-Perez¹; Steve Roberts¹; ¹University of Oxford

Brittle fracture is often controlled by grain boundary behaviour. Until now measuring the fracture properties of single grain boundaries has required macroscopic bi-crystals. We have developed techniques to measure the fracture toughness of selected grain boundaries using micro-cantilevers (typically $\sim 5\mu\text{m}$ wide and $25\mu\text{m}$ long), made by focussed ion-beam machining, loading them using a nanoindenter. In bismuth-embrittled copper, grain boundary fracture toughness values were found to be between 1 and 7 MPa^m^{0.5}, with no strong correlation between crystallography and toughness. All brittle boundaries contained Bi; non-fracturing boundaries did not. In Ni alloy 600 embrittled in simulated reactor primary water at 340°C for 2000hrs, TEM analysis showed many surface-intersecting boundaries to be oxidised. In micro-cantilever tests, such boundaries fail by brittle fracture, with fracture toughness of ~ 7 MPa^m^{0.5}, while non-oxidised boundaries deform in a ductile manner.

9:10 AM

Plastic Strain Recovery in Nanocrystalline Nickel: *Marisol Koslowski*¹; Yuesong Xie¹; ¹Purdue University

Grain refinement in crystalline materials leads to an enhancement of several materials properties including yield and fracture strength and superior wear resistance. This reduction in grain size is also responsible for new deformation mechanisms like plastic strain recovery. Even though, plastic deformation is not recoverable in coarse grained crystalline materials, recent experiments in nanocrystalline aluminum, nickel and

gold thin films and bulk nanocrystalline aluminum recovered more than 50% of plastic strain after unloading. We will present dislocation dynamics simulations of nanocrystalline Nickel that show that plastic strain recovery is observed only if the sample has a large scatter in the grain size distribution. These findings reveal that the average grain size itself is not enough for a complete characterization of the microstructure in nanocrystalline materials but variations in the grain size distribution should also be considered.

9:30 AM

Study on the Nanomechanical Properties of High Quality ZnO Microwires by Nanoindentation: *Zhi Lin*¹; JianPing He²; ZhiWei Liu²; ¹State Key Laboratory for Advanced Metal Materials; ²University of Science & Technology Beijing

Nanomechanical properties of high quality ZnO microwires that were synthesized by a simple chemical vapor deposition method were studied by nanoindentation. The hardness and elastic modulus of microwires were obtained and compared with the values of ZnO bulk and nanowire/nanobelt. It was found that the two values of microwires are between those of the bulk and the nanowire/nanobelt. An interesting phenomenon of the shape self-healing was found and discussed. Moreover, the conductivity change of the ZnO microwires caused by indentation was also investigated. Based on the piezoresistive effect theory, the electromechanical phenomenon was explained. This work is believed to provide the initial information for safe working condition of devices that uses ZnO microwires as building blocks in MEMS engineering.

9:50 AM Invited

Defect and Interface Engineering in Semiconductor Nanowires: *Shadi Dayeh*¹; Jian Wang¹; Jian Yu Huang²; Samuel Thomas Picraux¹; ¹Los Alamos National Laboratory; ²Sandia National Laboratories

Semiconductor nanowires have emerged as building blocks for applications in sensing, (opto)-electronics, thermoelectrics, energy harvesting and storage. The purpose of this talk is to address the underlying science behind some of the challenges in controlling structure and morphology in semiconductor nanowires and show how this understanding establishes the structure-electronic property correlations in Ge/Si and InAs semiconductor nanowires. We distinguish between two defect types and discuss techniques to eliminate them. Stacking defects result in the pinning or rotating of nucleation sites along the vapor-liquid-solid interface in elemental (Ge, Si) as well as create spontaneous polarization charges in polymorph III-V nanowires (InAs). We then discuss the first experimental measure of critical thicknesses in core/shell Ge/Si nanowires, the type of dislocations by which they relax misfit strain, and the resulting corrections for current models on coherency limits.

10:10 AM

Deformation Hardening under Friction of Cu Samples with Different Virgin Grain Size in the Lubrication Conditions: *Alex Laikhtman*¹; Lev Rapoport¹; Alexey Moshkovich¹; Vladislav Perflyev¹; Louisa Meshi²; Shmuel Samuha²; Sidney Cohen³; ¹Holon Institute of Technology (HIT); ²Ben-Gurion University of the Negev; ³The Weizmann Institute of Science

Friction and wear of copper rubbed with lubrication in wide range of loads and sliding velocities were studied. The results of friction and wear experiments are presented as the Stribeck curve: the boundary lubrication (BL), mixed, and elastohydrodynamic lubrication (EHL) regions are considered. The structural state of subsurface layers in different lubricant regions was studied by different spectroscopic and microscopic techniques. Dislocation density and nanohardness at thin surface layers in EHL and BL regimes was determined and compared. The dominant friction and wear mechanisms in different lubrications regions are discussed. Severe plastic deformation (SPD) of subsurface layers under friction is correlated with nanocrystalline structure obtained by different methods of grain refinement. It was found that SPD of thin surface layers under friction is accompanied by formation of shear bands in sublayers of contact spots. The main difference between the friction conditions is different gradients of strain, hardness and temperature.

10:30 AM Break**10:40 AM**

Effect of Indentation Depth and Displacement Rate on spherical Nanoindentation of NiTi Shape Memory Alloys: *Indrani Sen*¹; Martin Wagner¹; ¹Technische Universität Chemnitz

NiTi based shape memory alloys, owing to their superior recoverability, are finding applications in a wide variety of technologies and especially in miniaturized devices. Nanoindentations with spherical tip have been performed on this alloy to appreciate its small length scale pseudoelastic characteristics. From the typical load-displacement data, accurate estimation of zero-point and extraction of nano-scale stress-strain curves have been performed, which is otherwise difficult to obtain from conventional experiments. Effects of indentation depth varying between 100 to 1000 nm and displacement rate between 1 to 50 nm per second have been studied on the mechanical behavior of the alloy. With increasing indentation depth, a loss in pseudoelasticity with decrease in recoverable strain (by ~20%) has been observed. However, an isothermal stress state prevails at the applied strain rate range with no significant effect observed in the critical transformation stress of the alloy.

11:00 AM

A Versatile Microelectromechanical System for Monotonic and Fatigue Testing of Nanostructures: Ehsan Hosseinian¹; Brian Allen¹; Bhaskar Pant¹; *Olivier Pierron*¹; ¹Georgia Tech

Microelectromechanical systems (MEMS) were recently described as superior mechanical testing systems for nanomaterials. Currently, the most advanced MEMS setups are best suited for *in-situ* SEM or TEM studies, since they require high magnification images to measure strain. Here we present a MEMS material testing setup that relies on electronic measurements of nanospecimen elongation. Compared to previously demonstrated MEMS devices that rely on high magnification images to measure elongation, this MEMS is more versatile, allowing both *in situ* TEM testing and *ex situ* (e.g., in an environmental chamber) testing of nanomaterials with high accuracy and precision (sub nm). The MEMS device comprises two identical capacitive sensors on each side of the nanospecimen that are used to electronically measure the specimen gap change. The mode of operation of the MEMS setup is illustrated with *ex-situ* uniaxial tensile tests and fatigue tests of nanocrystalline nickel nanobeams.

11:20 AM

Tribological Properties of Nanocrystalline Metallic Contacts: *Michael Chandross*¹; Shengfeng Cheng¹; ¹Sandia National Laboratories

Gold is a desirable material for use in high performance electrical contacts because it offers low contact resistance, does not corrode or oxidize, and can be easily made into thin sheets. However, gold contacts generally suffer from high adhesion and friction. The tribological issues are mitigated in nanocrystalline gold alloys (with, for example, Ni or Co), which can exhibit both low friction and low contact resistance. The atomic scale mechanisms responsible for the change in frictional response are poorly understood. We will present the results of large scale molecular dynamics (MD) simulations which study the tribological response of nanocrystalline films of pure gold and alloys under a variety of sliding conditions. Our results indicate that cold welding and microstructural reorientation can lead to high friction in pure metals, while suppression of this behavior lowers the friction considerably.

11:40 AM

Nanoscale Investigation of Segregation and Embrittlement in λ 149; -Fe due to Hydrogen and Grain Boundary Character: *Kiran Solanki*¹; Mark Tschopp²; Nathan Rhodes²; ¹Arizona State University; ²Mississippi State University

Material strengthening and embrittlement are often controlled by interactions between dislocations and hydrogen-induced defect structures that can adversely affect deformation mechanisms. The objective of this research is to explore the role of grain boundary morphology on H segregation and embrittlement process in λ 149; -Fe. Molecular statics simulations were used to calculate the segregation energies H and subsequent fracture behavior for a wide range of grain boundary structures. Simulation results show that grain boundary morphology plays a significant role in the segregation and embrittlement process in λ 149; -Fe. The significance of this work is that a better fundamental understanding of the role of grain boundary character in segregation and embrittlement may provide insight into how the ductility of polycrystalline materials can be improved. By engineering microstructure to change the hydrogen segregation and embrittlement process, the local deformation mechanisms can be tailored to improve ductility.

12:00 PM

Small Scale Mechanical Behavior of Silicon as a Function of Electronic Doping: *Jacques Rabier*¹; Rudy Ghisleni²; Jean Luc Demenet¹; Johann Michler²; ¹CNRS; ²EMPA

The effect of electronic doping on the mechanical properties of silicon at temperatures larger than 650°C are well documented. However it has been demonstrated by experiments under pressure and by atomistic simulations that at high stress and low temperature a different type of dislocations controls the plasticity of silicon: perfect shuffle dislocations. In this context deformation of nanopillars of silicon with different doping has been performed in order to check for the effect of doping on plastic deformation at high stresses. The mechanical tests are conducted on $\langle 111 \rangle$ oriented single crystal nanopillars with diameters ranging from 500 nm to 2 μ m obtained by focused ion beam machining. Wafers with different electronic doping are tested: intrinsic ($N_n \leq 10^{14}$ cm⁻³); n type ($N_n = 6 \times 10^{18}$ cm⁻³), and p type ($N_p = 1 \times 10^{18}$ cm⁻³). The results of *in situ* SEM deformation experiments at room temperature and up to 200°C will be discussed.

12:20 PM

Three-Dimensional Dislocation Dynamic Simulations in BCC Metal Micro-Pillars: *Ill Ryu*¹; Wei Cai¹; William Nix¹; Christopher Weinberger²; ¹Stanford University; ²Sandia National Laboratories

Recent micro-pillar experiments have shown strong size effects at small pillar diameters. This 'Smaller is stronger' phenomenon is widely believed to involve dislocation motion, which can be studied using dislocation dynamics (DD) simulations. In the present study, we make a 3-D DD model to study the collective dislocation behavior in BCC micro-pillars under compression. Following the work of Weinberger and Cai [1], we consider a surface-controlled cross-slip process, involving image forces and non-planar core structures, that leads to multiplication without the presence of artificial pinning points. We follow both the evolution of the dislocation structure and the corresponding stress-strain relation. In an effort to make the model conform to *in-situ* TEM experiments that seem to show persistent plastic flow even for very small pillars and low dislocation densities, the effects of point defects on dislocation dynamics are being explored. [1] Weinberger CR, Cai W., *Proc. Natl. Acad. Sci.* (2008)



TMS 2012

141st Annual Meeting & Exhibition

THURSDAY AM

Mechanical Behavior Related to Interface Physics: Dynamic Response of Interfaces: Experiment and Modeling

Sponsored by: The Minerals, Metals and Materials Society, TMS Structural Materials Division, TMS Materials Processing and Manufacturing Division, TMS/ASM: Mechanical Behavior of Materials Committee, TMS: Nanomechanical Materials Behavior Committee

Program Organizers: Jian Wang, Los Alamos National Laboratory; Nathan Mara, Los Alamos National Laboratory; Izabela Szlufarska, University of Wisconsin-Madison; Zhiwei Shan, Xi'an Jiaotong University

Thursday AM
March 15, 2012

Room: Oceanic 1
Location: Dolphin Resort

Session Chairs: Timothy Germann, Los Alamos National Laboratory; Xuejun Jin, Shanghai Jiao Tong University

8:30 AM Keynote

Interface Role in the Shock Response of Cu/Nb Metallic Multilayers: Timothy Germann¹; Ruifeng Zhang¹; Weizhong Han¹; Jian Wang¹; Shengnian Luo¹; Irene Beyerlein¹; Amit Misra¹; ¹Los Alamos National Laboratory

Molecular dynamics (MD) simulations and post-mortem transmission electron microscopy (TEM) analysis of shock-recovered samples are used to study the role of interface structure and layer thickness on the mechanical response of Cu/Nb nanolayered composites to shock compression. Post-mortem TEM analysis indicates that deformation twinning in Cu layers is preferentially nucleated from Cu(112)/Nb(112) interface habit planes, as opposed to the more common Cu(111)/Nb(110) interfaces (with a Kurdjumov-Sachs orientation relationship in both cases). Non-equilibrium MD simulations of the shock loading of Cu/Nb multilayers containing exclusively one interface structure or the other confirm the key role which interface structure plays in this preference, and provide insight into the role of atomic Cu-Nb interface structures on the nucleation, transmission, absorption, and storage of dislocations during shock loading of Cu/Nb nanolayered composites.

9:00 AM

Dynamic Thermo-Mechanical Properties of Ferroelastic Reinforced Metal Matrix Composites: Jack Tilka¹; Zachary Bryan¹; Jacob Jones¹; Michele Manuel¹; ¹University of Florida

Previous research has shown that the presence of ferroelastic particles in a metal matrix could yield a composite with an anomalous dynamic elastic modulus. It is believed that the origin of this anomalous mechanical behavior is due to the thermo-mechanical coupling at the interface between the frequency-dependent ferroelectric particles and dampening metal matrix. A systematic study is presented that focuses on the interaction between barium titanate particles and a damping metal matrix in composites prepared using powder metallurgical techniques. Composites were characterized with microscopy, dynamic mechanical analysis, differential scanning calorimetry, and x-ray diffraction to determine the frequency and temperature dependence of the barium titanate phase transitions and their resulting effect on the mechanical behavior of the composite. These studies provide insight into the unique inter-relationship at the interface between phase transforming particles constrained in a non-transforming, dampening matrix. The authors would like to gratefully acknowledge the support of the National Science Foundation under grant number CMMI-0824352.

9:15 AM

Effect of Film Thickness on Mechanical Properties of Free-Standing Thermoset Nanofilms by Molecular Dynamics Simulations: Chunyu Li¹; Alejandro Strachan¹; ¹Purdue University

Free-standing polymer nanofilms have two solid/air interfaces. The potential applications of polymer nanofilms are in numerous areas. To fully realize the potential applications of polymer nanofilms, an in-depth understanding of their mechanical properties is critically necessary. Experimental efforts are very few because of the difficulties in nanoscale measurements. No modeling work at the molecular-level has been done on the mechanical properties of free-standing thermosetting polymer films. In this presentation, we will describe our recent molecular dynamics simulations free-standing nanofilms of thermosets (EPON825/33DDS) and the predictions of their mechanical properties. The effect of film thickness on the stiffness and yield stress is investigated. The conclusion is that Young's modulus and yield stress of nanofilms are lower relative to the bulk values but both increase with increasing film thickness and approach to the bulk values at about 100nm. Interestingly, the yield strains are all within 10-14% regardless of film thickness or bulk.

9:30 AM

Meso-Scale Simulations of Interface Configuration on Shock Wave Propagation in Multilayered Ni-Al Composites: Paul Specht¹; Naresh Thadhani¹; Timothy Weihs²; ¹Georgia Institute of Technology; ²The Johns Hopkins University

The response of shock-wave propagation through multi-layered Ni-Al cold-rolled composites is investigated using meso-scale simulations performed employing real microstructures. The orientation of the layers is varied at 0°, 45°, and 90° to the direction of shock-front propagation, to determine the differences in the bulk shock-compression response and the effects of strain localization due to the mismatch in elastic and plastic properties across the interface. The results reveal noticeable differences in the pressure, temperature, and strain response. Geometric dispersion is seen to alter the shape of the resulting pressure pulse and inhibit the development of a steady-state shock wave in the laminated geometry. Strain-localization at the interfaces causes shock-wave dissipation through interfacial heating and shearing, resulting in high levels of viscosity and attenuation. The dissipative effects also alter the dependence of shock velocity on particle velocity, making it a major contributor to the bulk response of multilayered composites under shock compression.

9:45 AM Break

9:55 AM Keynote

High Temperature Twinning Correlated with Grain Growth in a Nano-Grained Co Based Alloys: Xuejun Jin¹; Jiayao Li¹; Yao Shen¹; ¹Shanghai Jiao Tong University

Twinning is one of structural changes of metals and ceramics in response to mechanical stresses with other changes being slip (by dislocation motion), phase transformations and fracture. Mechanical twinning observed at relatively low temperature can have two effects on plastic deformation: subdivision of grains; contribution to the amount of plastic deformation due to twinning shear. Here a high temperature twinning triggered by a grain growth was observed around 300°C in a nano-grained Co based alloys produced by electro-deposition, while the slip mechanism usually dominates in coarse-grained alloys with identical chemical composition at the same temperature range. A grain growth correlated competition mechanism of slip and twinning is proposed and discussed in association with temperature, nucleation parameters, phase transformation kinetics, grain sizes and stacking-fault energy. The introduction of twinning at high temperature is of significance to explore the optimal mechanical properties in various engineering alloys.

10:25 AM Keynote

Grain Boundary Mediated Deformation Mechanisms of Nanocrystalline NiFe Alloy under Cyclic and Dynamic Loading: *Yonghao Zhao*¹; S. Cheng²; Y.Z. Guo³; Y.M. Wang⁴; Y. Li¹; Q.M. Wei³; X.-L. Wang⁵; P.K. Liaw²; E.J. Lavernia¹; ¹University of California Davis; ²University of Tennessee, Knoxville, USA; ³University of North Carolina, Charlotte; ⁴Lawrence Livermore National Laboratory, Livermore; ⁵Oak Ridge National Laboratory, Oak Ridge

Deformation mechanisms of nanocrystalline NiFe alloy with an average grain size of about 18 nm under dynamic and cyclic loading were investigated by employing post-mortem electron transmission microscopy. Upon dynamic loading, highly improved plasticity (from 8% deformation strain under quasi-static deformation to a maximum strain of ~22%) was achieved. Significant grain coarsening and de-twinning occurred due to grain rotation and grain boundary sliding (Adv. Mater. 21, 2009, 5001). Under compressive cyclic loading, a high fatigue life is obtained at high applied stress. Significant grain size coarsening was associated with the path of crack propagation and was realized mainly through the grain lattice rotation and coalescence under the high stress concentration at the crack tip. Away from the crack path, no apparent grain coarsening was observed. At the same time, loss of the growth twins was observed in the coarsened grains (Phys. Rev. Lett. 104, 2010, 255501).

10:55 AM

Fracture Toughness Testing of Sub-Micron Sized Bi-Embrittled Cu Bicrystals: *Mark McLean*¹; Austin Wade¹; Masashi Watanabe¹; Rick Vinci¹; ¹Lehigh University

It has long been known that impurity elements segregated to grain boundaries can cause significant reduction in the ductility of metals. However, despite the significant work done on the subject, the true mechanism responsible for boundary segregation-induced embrittlement is still unclear. We have developed a notched-tensile beam test technique for measuring the fracture toughness of individual grain boundaries at the sub-micron scale using a new SEM-compatible nanoindentation device. Using this technique, we have measured the fracture toughness of Bi-doped Cu bicrystals. Tests have been conducted on several different grain boundaries in order to determine the effect of boundary character on fracture behavior. In addition to fracture testing, samples have been prepared from the same boundaries for atomic-resolution STEM imaging in order to locate and quantify the segregant atoms contained in each boundary. Combining the results will provide vital information to include in atomistic simulations of grain boundaries.

11:10 AM

Molecular Dynamics Simulations of Plastic Deformation of Nanocrystalline FCC and BCC Metals in Tension and Compression: *Marc Meyers*¹; Yizhe Tang¹; Eduardo Bringa²; ¹UCSD; ²U Nacional de Cuyo

In FCC metals the principal deformation mechanism in tension and compression is the emission of partial dislocations from GBs and their annihilation at an opposing GB. The conventional H-P relation breaks down at $d \sim 15\text{-}20$ nm for Cu. Tensile failure starts at the GBs through void initiation associated with profuse dislocation emission. For BCC metals, the scenario is different. In tension, decohesion of GBs normal to loading direction occurs before emission of dislocations, due to the high resistance of the lattice to plastic deformation which exceeds the GB cohesive strength at that strain rate. In compression, plasticity occurs, but the defects are different. Perfect dislocations emitted from GBs dominate process at $d > 10$ nm, while grain-boundary sliding dominates when $d < 10$ nm. Grain rotation is found when $d \sim 5$ nm. The Hall-Petch transition ($d > 40$ nm) is larger than for FCC metals. Few twins were found in samples with larger grain sizes. Funding: UCRL Program.

11:25 AM

Effects of H Impurities on Grain Boundary Cracking and Plasticity: *Diana Farkas*¹; Martin Gamarra¹; Laura Patrick¹; ¹Virginia Tech

The effect of H impurities segregated to grain boundaries in FCC metals is studied. The deformation behavior under tension is modeled using molecular dynamics and embedded atom interatomic potentials developed for dilute interstitial H impurities. The digital samples have a polycrystalline thin-film configuration with randomly oriented grain boundaries. The results show that the samples containing the H impurities show decreased overall ductility, due to increased crack nucleation at the boundaries and triple junctions. The H impurities also had significant effects on the emission of dislocations from the grain boundaries and in the possibilities of grain boundary sliding and migration.

11:40 AM

Insights into Basal Slip Dominated Plasticity of Mg from In Situ TEM Tensile Testing: *Qian Yu*¹; Raj Mishra²; Andrew Minor¹; ¹UC Berkeley; ²General Motors Research and Development Center

Magnesium is a lightweight metal that would be much more useful for structural applications than it currently is if not for its complicated and anisotropic plastic deformation behavior. Basal slip is the most important slip system for the plastic deformation of Mg because its CRSS is much lower than that of prismatic and pyramidal slip. Recently we have run a systematic series of in situ TEM tensile tests on pure Mg with different size crystals where we have quantitatively measured and characterized the basal slip behavior. Strong crystal size effects on basal slip were found. More interestingly, basal slip based on surface nucleation of dislocations is significant in samples with extremely small size, which can directly lead to the high strength and ductility of the nanoscale material.

Minerals, Metals and Materials under Pressure: Phase Transformations and Microstructure

Sponsored by: The Minerals, Metals and Materials Society, TMS Electronic, Magnetic, and Photonic Materials Division, TMS Materials Processing and Manufacturing Division, TMS Structural Materials Division, TMS: Chemistry and Physics of Materials Committee, TMS/ASM: Phase Transformations Committee
Program Organizers: Ellen Cerreta, Los Alamos National Laboratory; Richard Hennig, Cornell University; Dallas Trinkle, University of Illinois, Urbana-Champaign; Vijay Vasudevan, Univ. Cincinnati

Thursday AM

March 15, 2012

Room: Europe 9

Location: Dolphin Resort

Session Chair: Dallas Trinkle, Univ. Illinois, Urbana-Champaign
8:30 AM Invited

Influence of Interstitial Content and Stress State of the Shock-Induced Phase Transitions in Zr, Ti, and Fe: *George Gray*¹; Ellen Cerreta¹; Larry Hull¹; Paulo Rigg¹; ¹Los Alamos National Laboratory

Dynamic and shock loading of materials is well known to induce a range of defects in metals and alloys, including dislocations, deformation twins, point defects, as well as shock-induced phase transitions in many select metals and alloys. In this paper, examples of the role of chemistry and stress state on transitions in Zr, Ti, and Fe will be discussed. Observations of the influence of interstitial content on the kinetics of the alpha-omega transition in Zr will be detailed including the results of diamond cell, gas gun, and Z-machine shock data. The alpha-omega transition in Zr is shown to strongly depend on interstitial oxygen content as well as differ significantly between diamond cell, shock loading, and ramp loading. Recent results of the effect of 1-D versus sweeping-detonation wave loading on the alpha-epsilon transition and substructure evolution in Fe will be presented.



TMS 2012

141st Annual Meeting & Exhibition

THURSDAY AM

9:00 AM

Probing the Role of Temperature on Texture Evolution in Tantalum during Dynamic-Tensile-Extrusion: *Carl Trujillo*¹; Juan Escobedo¹; Ellen Cerreta¹; George Gray III¹; Daniel Martinez¹; ¹Los Alamos National Laboratory

The effect of high strain-rate and high strains on the mechanical behavior in Tantalum has been previously explored at room temperature. To incorporate and investigate the effect of temperature, a cross section of a gun barrel was converted into a furnace to allow specimens to be heated up to 600°C before acceleration. Specimens were machined in two directions from the as-received plate: In-plane(IP), parallel to the rolling direction, and through thickness(TT) of the plate. Using the dynamic tensile extrusion technique developed at LANL, Ta bullets were heated up to 600°C and accelerated up to velocities of 600m/s. Specimens were extruded through a high strength steel die. A combination of in-situ and post-mortem characterization techniques has been used, including Photonic Doppler Velocimetry to capture the time and extrusion velocity of the deforming specimen through the die. Quantitative examination of the influence of temperature, texture, and extrusion velocity will be presented.

9:20 AM

The Role of Interfaces on Shock-Induced Damage in Two Phase Metals: *Saryu Fensin*¹; Ellen Cerreta¹; Steven Valone¹; Steven Valone¹; George Gray¹; Adam Farrow¹; Carl Trujillo¹; ¹Los Alamos National Laboratory

For ductile metals, the process of dynamic fracture during shock loading is thought to occur through nucleation of voids, void growth, and then coalescence that leads to material failure. Particularly for high purity metals, it has been observed by numerous investigators that voids appear to heterogeneously nucleate at grain boundaries. However, for materials of engineering significance, those with inclusions, second phase particles, or chemical banding it is less clear what the role of grain boundaries versus other types of interfaces in the metal will be on nucleation of damage. To approach this problem four materials have been systematically investigated: (1) high purity copper, (2) copper with 1% lead, (3) 260 brass, and (4) leaded 360 brass. The role of lead at grain boundaries and its behavior during shock loading will be discussed in conjunction with the results from experiments and Molecular Dynamics simulations.

9:40 AM

3-D Study of Microstructural Weak Links in Shock Loaded Copper Polycrystals with Incipient Spall Damage: *Andrew Brown*¹; Quan Pham¹; Kapil Krishnan¹; Pedro Peralta¹; Shengnian Luo²; Brian Patterson²; Scott Greenfield²; Darrin Byler²; Kenneth McClellan²; Aaron Koskelo²; ¹Arizona State University; ²Los Alamos National Laboratory

Correlations between incipient spall damage and global and local microstructures were investigated in polycrystalline copper plates of varying microstructures. The samples were impacted by laser-driven flyer plates at low pressures (2-6 GPa) to encourage incipient spall damage. Serial sectioning and Electron Backscattering Diffraction (EBSD), along with through thickness optical microscopy and X-ray tomography, were used to create 3-D renditions of the voids and surrounding microstructure and compare local and global geometrical and crystallographic characteristics. The damage distribution along the spall plane in 3-D was correlated to grain boundary (GB) misorientations, GB inclination to the shock, and grain size. Preferred damage nucleation and localization sites were identified via statistical sampling from serial sectioning. Results indicate that pre-existing plastic deformation biases damage to the GBs, which have a misorientation dependent strength. When plastic deformation is removed via heat treatments, the grains become weaker, causing a mix of intergranular and transgranular damage modes.

10:00 AM

Characterization of Near-Surface Microstructures in IN718 Alloy Laser Shock Peened with and without an Ablative Overlay: *Amrinder Gill*¹; *Vijay Vasudevan*¹; S.R. Mannava¹; Dong Qian¹; ¹University of Cincinnati

Laser shock peening without a protective overlay has become of increasing interest because of the ability to reduce the process time. Peening without an overlay results in both mechanical and thermal loading of the material. Surface layers of the material experience melting and re-solidification along with deformation due to the shock wave. The recast layer hence formed was characterized. Coupons of the alloy were laser peened with and without a protective coating and the surface layers were characterized using various techniques including X-ray Diffraction, Nanoindentation, Transmission Electron Microscopy, Scanning Electron Microscopy, Electron Back scattered Diffraction and Energy Dispersive X-Ray Spectroscopy. The results show tensile residual stress state in near-surface regions to a depth of about 50 microns, followed by a compressive residual stress state. The presence of a non-uniform recast layer with increased surface roughness was observed, as well as areas with modified chemistry and the presence of nano particles.

10:20 AM Break

10:30 AM Invited

Melting Line of Alkali Metals: *Shanti Deemyad*¹; ¹Cornell University

Melting line of alkali metals have been of great interest for a long time. These elements generally exhibit very low melting temperatures and it has been shown in few cases that at very high pressures the melting line exhibits a maximum. Temperature determination between 400K and 700K is difficult in diamond anvil cell and the determination of onset of melting is another problem that makes these measurements very tedious. There has been inconsistency in several reports in past. Here I present a new experimental approach in measuring the melting at high pressure which can increase our accuracy in determination of the melting lines.

11:00 AM

Investigating the Effects of High Pressure Shock Loading on Ni-Al Mixtures Using a Laser-Accelerated Flyer Setup: *Sean Kelly*¹; Naresh Thadhani¹; ¹Georgia Institute of Technology

The effects of high-pressure dynamic loading on Ni-Al mixtures in various configurations and any subsequent phase transformations were investigated. Ni-Al mixtures represent an example of a Structural Energetic Material (SEM) that combines strength and stiffness with the energy-release capabilities of a molecular explosive. High-pressure shock-loading can cause intimate constituent mixing, leading to chemical reactions, forming an intermetallic, and releasing energy. Experiments were performed on different forms of nickel-aluminum mixtures (i.e. powder compacts, vapor-deposited foils, single layers) over a range of shock pressures using a laser-accelerated flyer system in attempt to characterize the processes leading to complete reaction. VISAR and PDV interferometry were used to infer the occurrence of any shock-induced chemical reactions. Post-mortem microstructural characterization was performed to identify the reaction products and isolate the processes that lead to reaction initiation. In this presentation, the influence of flyer momentum and Ni-Al reactant configuration on the reaction response will be discussed.

11:20 AM

Phase-Field Reaction-Pathway Method Coupled with Plasticity Theory of the Shock Induced Alpha-Epsilon Martensitic Transition in Iron: *Aurélien Vattré*¹; Christophe Denoual¹; ¹CEA

Pressure induced alpha-epsilon martensitic transition in iron is known to be very complex due to the interplay of transformation strains and long range stresses induced by the emerging microstructure. We propose a predictive modeling of this martensitic transition during shock loading by using a phase-field technique with reaction pathway (PFRP) coupled with plasticity theory. The hybrid method allows to define precisely both stored

elastic energy and crystalline energy along the martensitic reaction path in iron. After a short introduction to PFRP, the microstructures obtained during shock and after reversion to alpha phase (just after shock release) with and without plasticity will be discussed.

11:40 AM

High Pressure Phase Transitions in Layered Tin Monoselenide Crystals: Ajay Agarwal¹; Paras Trivedi²; Prakash Naik²; Dipesh Patel³; ¹Shree J P Arts & Science College; ²Shree J P Arts & Science College; ³V S Patel College of Arts & Science

Tin monoselenide crystals belong to IV–VI layered binary semiconducting compound category. These semiconducting materials are useful because of their applications in holographic-recording systems, optoelectronics and memory switching. Several investigators have utilized Mossbauer Spectroscopy and Hydrostatic Pressure techniques to examine the bonding of the Sn atoms in SnS and SnSe. It is therefore thought worthwhile to study the effect of pressure on the thermoelectric power and the electrical resistance of SnSe crystals synthesized by a modified direct vapour transport technique. The electrical resistance has been found to be pressure dependent. The transition in electrical resistance behaviour, observed at 65 Kbar, has been explained on the basis of transition from a predominantly two-dimensional material to a more three-dimensional one. Similar to the resistance behaviour, the thermoelectric power is also found to be pressure dependent. The increase in thermoelectric power with pressure at the transition pressure of 65 Kbar has been explained.

Nanocomposites: Processing of Nanocomposites II

Sponsored by: The Minerals, Metals and Materials Society, TMS Structural Materials Division, TMS/ASM: Composite Materials Committee

Program Organizers: Garth Wilks, Air Force Research Laboratory; Jonathan Spowart, Air Force Research Laboratory; Meisha Shofner, Georgia Institute of Technology; John Zhanhu Guo, Lamar University

Thursday AM
March 15, 2012

Room: Swan 8
Location: Swan Resort

Session Chairs: Meisha Shofner, Georgia Institute of Technology; Frank Fisher, Stevens Institute of Technology

8:30 AM Break

8:50 AM

Structural and Thermal Stability Properties of Cellulose Nanocomposites with Polylactic Acid Matrix: Na Lu¹; ¹University of North Carolina at Charlotte

The use of cellulose nanowhiskers as reinforcement has captured great interests in nanocomposite community owing to their superior mechanical properties, large surface area and biodegradability. In this work, nanocomposite based on cellulose nanowhiskers (CNW) and polyactic acid (PLA) were prepared in various compositions ranging from 5 to 20% CNW volume fraction. The surface morphology of various nanocomposites were examined by scanning electron microscope (SEM). The optical transparency properties were studied by Fourier Transform Infrared Spectroscopy (FTIR). The results from the thermo gravimetric analysis (TGA) have showed great improvement in thermal stability with the higher CNW volume fraction. The dynamic mechanical thermal analysis (DMA) results indicated higher CNW volume fraction resulting in an improvement in storage modulus together with a shift in the Tan Delta.

9:10 AM

Synthetic Process Engineered Polyaniline Nanostructures: Xi Zhang¹; Jiahua Zhu¹; Suying Wei¹; John Zhanhu Guo¹; ¹Lamar University

In this talk, three methods are used to synthesize polyaniline at different synthetic conditions, which affect the quality of polyaniline nanostructures. Polyaniline nanofibers obtained by interfacial polymerization is studied and compared with polyaniline prepared by ultrasonic stirring and polymer acid methods. For polyaniline nanofibers, the effects of reaction time, interfacial area size, scale and concentration of the reactant on the crystalline structure, thermal stability, morphology, conductivity and dielectrical property are systematically studied and will be reported.

9:30 AM Invited

Nanoparticle-Enhanced Crystallization of Semicrystalline Polymer Nanocomposites: Frank Fisher¹; ¹Stevens Institute of Technology

The introduction of nanoparticles into semicrystalline polymers can alter the development and influence of crystallization present within a semicrystalline polymer nanocomposite. For example, nanoparticles may act as heterogeneous nucleation sites, leading to an increase in nucleation rate, a decrease in crystallite sizes, changes in crystalline structure, and a change in the overall degree of crystallinity. Such differences are often observed and reported under quiescent loading conditions; however, we have found that such changes in crystallization behavior can be drastically accelerated and more pronounced if the crystallization occurs under an external applied loading. Such findings require further study as realistic industry-processed nanocomposites are typically manufactured via techniques that subject the polymer nanocomposite to a complex thermomechanical history. Our results indicate how nanoparticles, even at very small loadings, can significantly alter the processing-induced crystallization of semicrystalline polymer nanocomposites, and suggest pathways for leveraging this crystallization behavior in semicrystalline polymer nanocomposites.

10:10 AM

Processing-Structure-Property Relationships in Hydroxyapatite Nanocomposites with a Copolymer-Compatibilized Interface: Meisha Shofner¹; Ji Hoon Lee¹; ¹Georgia Institute of Technology

To date, much of the research concerning polymer nanocomposites has focused on creating randomly dispersed systems where individual nanoparticles are surrounded by and interacting with the polymer matrix. Beyond the fully dispersed morphology, research concerning directed assembly systems and purposefully inhomogeneously dispersed nanocomposites has shown that there are advantages to designing different nanocomposite morphologies. In this research, the substantial specific surface area available from nanoparticles and prescribed processing operations are used to direct nanocomposite component orientation and arrangement. Specifically, hydroxyapatite nanoparticles of two different shapes are synthesized using micelles formed from a poly(ethylene oxide)-b-poly(methacrylic acid) block copolymer in aqueous solution and subsequently dispersed in a poly(ethylene oxide) matrix. Experimental results concerning the effects of particle shape and loading on polymer crystallinity, thermal transitions and mechanical properties are presented to understand processing-structure-property relationships in these materials.

10:30 AM

Self-Healing, High Molar Mass Polymer Nanocomposites: Julie Harmon¹; Roger Bass²; ¹University of South Florida; ²Air Force

This research focuses on the development of high molar mass, self-healing polycarbonate-containing polyurethane (PCU) nanotube composites. Healing in these materials is: Autonomous- no intervention is needed to induce healing such as heat, light, continuous pressure or electrical stimulus. However, healing is accelerated by heat. Intrinsic- no sequestered healing agents are added to the matrix. Reversible- the composites and neat polymer are capable of multiple healing events. Processing, characterization and structure-property relations demonstrate that these PCUs and PCU composites are part of a new direction in



TMS 2012

141st Annual Meeting & Exhibition

THURSDAY AM

materials development. Unlike most autonomous, intrinsic healing systems that use lower molar mass matrices held together by non-covalent interactions, this research demonstrates that a special class of high molar mass (covalently bonded) thermoplastic polyurethanes exhibit self-healing properties.

10:50 AM

Tacticity Effect Studies of PMMA and PMMA-QDs Composites: *Suying Wei*¹; Narendhar Anumandla¹; Jaishri Sharma¹; ¹Lamar University

Polymer based composites have found wide applications in various fields including electronic, optical and biomedical; effects of filler choice, filler loading levels, and the interaction between the polymer matrix and the filler on the properties of polymer composites have attracted attention and been explored extensively. However, effects of stereochemistry of polymers on their physicochemical and biological properties have less been studied. In this paper, PMMA is chosen as a model polymer to study tacticity effect on its corresponding physicochemical properties. CdSe-ZnS core-shell quantum dots (QDs) are incorporated into different tactic PMMA polymers to form different PMMA-QDs nanocomposites in either film or fiber forms. The effects of tacticity on the fluorescence emission will be explored and rationalized. Chemical interaction between the polymer and QDs will be probed by attenuated total reflectance Fourier transform infrared spectroscopy (ATR-FTIR). Thermal stability and glass transition temperature will also be investigated.

11:10 AM

Thermal Properties of Hemp-High Density Polyethylene Composites: Effect of Two Different Chemical Treatments: *Na Lu*¹; Shubhashini Oza²; ¹University of North Carolina at Charlotte; ²University of North Carolina at Charlotte

The drive towards environmentally sustainable materials has resulted in use of natural fibers as an alternative to glass fibers for reinforcement in composites. Hemp has a greatest potential of being used as a reinforcing fiber since it is one of the strongest and stiffest natural fibers along with being biodegradable, low cost and fast growth. However, the incompatibility of hemp fiber with thermoplastic matrix results in poor interface adhesion and lower thermal and mechanical properties. In this study, we have systematically investigated the effects of two chemical treatments of hemp fibers on the thermal stability of hemp-HDPE composites. Composites of various volume fractions were synthesized with sodium hydroxide and silane treated hemp fibers. Thermogravimetric analysis was used for thermal stability characterization. The results indicate that chemical treatment of hemp fibers with silane treated yield composites with better thermal stability compared to that of composites treated with NaOH or untreated hemp-HDPE.

11:30 AM Invited

Multifunctional Nanostructures through Functional Polymers: *Yuping Bao*¹; Soubantika Palchoudhury¹; Yaolin Xu¹; ¹The University of Alabama

Functional polymers play an important role in many nanostructured materials. In this presentation, we will specifically discuss the roles of polymers in the formation of multifunctional nanoparticles, such as polyacrylic acids and polyethyleneimines. These polymers can be effectively attached onto iron oxide nanoparticle surfaces to increase the solubility of nanoparticles in water. The thickness of the polymers led to different magnetic properties and subsequent magnetic relaxivity. Further, using these polymers as linkers, we successfully attached sub-nanometer scale nanostructures onto the surface, such as Ag/Au nanoclusters and 2 nm Pt nanoparticles. The Ag/Au nanocluster attached iron oxide nanoparticles have both magnetic and fluorescent properties, offering a bifunctional imaging probe for bioimaging. The small Pt-attached iron oxide nanoparticles have potential in both catalytic and therapeutic research.

12:10 PM

Organic to Inorganic Conversion Process of PDMS: *Jihoon Lee*¹; Hyun Ae Lee²; Umesh Singh³; Cheol-Woong Yang²; Hyoung Jin Cho³; Hyoungsub Kim²; ¹Sungkyunkwan University; ²Sungkyunkwan University; ³University of Central Florida

Polydimethylsiloxane (PDMS) resin has been widely used for replicating nano- to micro-scale features with high precision due to its low viscosity and no shrinkage during casting process. PDMS has been crucial to soft lithography and microfluidic applications. However, features of elastomeric PDMS that are subjected to high stress can be easily distorted. In addition, permeable PDMS can be swollen when exposed to organic solvents. In this work, we studied the conversion process of PDMS into inorganic silicon compound by annealing at high temperature in reducing gas ambient, by which rigid and chemically inert structures could be formed. Micro-scale features were predesigned and analyzed before and after the conversion process. The mechanical and chemical characteristics of the PDMS as a function of annealing temperature will be presented, which were obtained using micro-indentation, DTA, FTIR, SEM, AFM, and XPS analyses. The proposed method could make the PDMS-based components suitable for demanding environments.

Neutron and X-Ray Studies of Advanced Materials V: Centennial: Dislocations, Strains, Deformation II

Sponsored by: The Minerals, Metals and Materials Society, TMS Structural Materials Division, TMS/ASM: Mechanical Behavior of Materials Committee, TMS: Chemistry and Physics of Materials Committee

Program Organizers: Rozaliya Barabash, Oak Ridge National Laboratory; Xun-Li Wang, Oak Ridge National Laboratory; Gernot Kostorz, ETH Zurich; Lyle Levine, National Institute of Standards and Technology; Peter Liaw, Univ of Tennessee; Yandong Wang, Beijing Institute of Technology; Brent Fultz, California Institute of Technology

Thursday AM
March 15, 2012

Room: Southern I
Location: Dolphin Resort

Funding support provided by: Office of Basic Energy Sciences, U.S. Dept. of Energy, Dr. P. Thyagarajan

Session Chairs: Peter Liaw, University of Tennessee; Klaus-Dieter Liss, Australian Nuclear Science and Technology Organisation

8:30 AM Keynote

In-Situ, Time-Resolved Diffraction Studies in Thermo-Mechanic Processing: *Klaus-Dieter Liss*¹; ¹Australian Nuclear Science and Technology Organisation

Neutron and synchrotron radiation have been employed and analysis methods developed to follow materials undergoing plastic deformation, giving direct insight into the crystalline arrangements of the bulk of the materials, in-situ, in real time and in multiple dimensions. Neutron white beam Laue diffraction on very grained, quasi single-crystalline copper and magnesium probes the entire orientation sphere during ongoing plastic compression and delivers mosaic broadening, subgrain formation or twinning. In contrast, the fine size of a high-energy X-ray beam, penetrating through a bulk specimen, probes a small but representative number of embedded grains. The discontinuous illumination of the diffraction rings allows to conclude on the behavior of the microstructure, such as phase composition, grain size, orientations, grain rotation, subgrain formation, dynamic recovery and recrystallization, strain and texture. Those primary results allow to conclude on the deformation mechanisms, the kinetics and the phase transformations. Examples are presented on selected high-temperature deformation processes.

8:50 AM Invited**Dislocation Densities, Burgers Vector Populations and Slip System Activity in Different Texture Components Determined by Diffraction Peak-Profile Analysis:** *Tamás Ungár*¹; ¹Eötvös University Budapest

The deformation of polycrystalline materials is heterogeneous on all different scales. Heterogeneity on the grain scale is strongly coupled to texture. In different texture components the dislocation density, the Burgers vector population and slip activity is usually very different. The method of diffraction peak-profile analysis can be applied to obtain the sub-structure in different texture components. Parallel beam high resolution diffractometry is used with systematically varying the angle between the incident-beam and specimen normal. Complementary texture data along with relative peak intensity evaluation are used to select the peaks corresponding to specific texture components. The method is used to characterize the sub-structure in different texture components in polycrystalline austenite and Mg, in Cu-Nb multilayers and in thin films.

9:10 AM**In-Situ Study of Fatigue Damage in a Ni-Based Superalloy by Synchrotron X-Ray Diffraction:** *Michael Hemphill*¹; *Andrew Chuang*¹; *Yan Gao*²; *Jon Almer*³; *Tim Hanlon*²; *Liang Jiang*²; *Peter Liaaw*¹; ¹University of Tennessee; ²General Electric Global Research; ³Argonne National Lab

Nickel-based superalloys are ideal for use in various components under complex thermo-mechanical stresses at elevated temperatures due to their high strengths, phase stability, and corrosion resistance. An important consideration in component design is the fatigue behavior under these complex conditions. The microscopic deformation behavior of a fine-grained, fatigued superalloy was studied by high-energy synchrotron x-ray diffraction (XRD). Specimens were fatigued to 0.5%, 10%, 50%, and 75% of the expected life with a virgin sample used as a reference. They were further subjected to a tensile force at elevated temperature. Under these conditions, in-situ strain and microstructure maps of the specimens were obtained through transmission-based XRD measurements. The damaged zones were identified, and the deformation behaviors at different fatigue lifetime periods were revealed.

9:25 AM**Investigation of Hydride Phase Transformations at Dislocations in Deformed Pd Using Neutron Scattering and Advanced Computational Techniques:** *Brent Heuser*¹; *Hyunsu Ju*¹; *Dallas Trinkle*¹; *Douglas Abernathy*²; *Terrence Udovic*³; ¹University of Illinois; ²ORNL; ³NIST

While Pd is not an advanced material, our use of small-angle neutron scattering (SANS) and incoherent inelastic neutron scattering (IINS) to study the phase behavior of hydrogen trapped at dislocations represents a body of experimental work that is unique to date. Our ability to resolve the specific behavior of only hydrogen trapped at dislocations is due to the use of the strongest neutron sources (HFIR, SNS, and NIST) available in the US. Our interpretation of these results is dependent on the development of advanced computational results within the DFT framework. Discussion of our results will focus 1) the observation of a phase transformation of trapped hydrogen versus temperature, 2) the loss of degeneracy due to the local strain of the dislocation core and near-core trapping sites, and 3) the prediction of the phase transformation and loss of degeneracy of hydrogen trapped at dislocations with DFT and continuum elasticity theory.

9:40 AM**In-Situ Neutron Diffraction Study of Nanobainitic Steels in Conjunction with Transmission Electron Microscopy:** *Khushboo Rakha*¹; *Hossein Beladi*¹; *Saurabh Kabra*²; *Sean McTrustry*²; *Stewart Pullen*²; *Ilana Timokhina*¹; *Peter Hodgson*¹; *Klaus-Dieter Liss*²; ¹Centre for Material and Fibre Innovation, Deakin University, Victoria 3216, Australia; ²Bragg Institute, Australian Nuclear Science and Technology Organisation, Lucas Heights, NSW 2232, Australia

In-situ neutron diffraction, together with a new thermal quench environment was employed to monitor the evolution of nano-structured bainitic ferrite during low temperature isothermal heat treatment of

austenite. This was undertaken to study the widely debated transformation mechanism for the formation of nanostructured bainite at low temperatures. The neutron peak characteristics were quantified and linked to changes in lattice parameter, volume fraction and carbon content and provided evidence of carbon partitioning during transformation. The results were compared with previous studies using different characterization techniques. The lath characteristics (i.e. size, size distribution) were determined from changes in Full Width Half Maximum (FWHM) of the diffraction peaks. The same characteristics were also studied via transmission electron microscopy and were found to differ from the neutron diffraction results. These differences were attributed to the presence of dislocation build up during low temperature isothermal transformation.

9:50 AM**In-Situ Neutron-Diffraction Study of a Ferritic Superalloy during Tensile Deformation at Room and Elevated Temperatures:** *Shenyang Huang*¹; *Yanfei Gao*¹; *Ke An*²; *Wei Wu*¹; *Lili Zheng*¹; *Michael Rawlings*³; *David Dunand*³; *Peter Liaw*¹; ¹University of Tennessee; ²Oak Ridge National Laboratory; ³Northwestern University

The ferritic superalloy, Fe-10Ni-6.5Al-10Cr-3.4Mo strengthened by coherent coplanar ordered (Ni,Fe)Al B2-type precipitates, is a candidate material for ultra supercritical steam-turbine applications above 923 K. However, the creep resistance of this material at high temperatures needs to be further improved, which requires a fundamental understanding of the deformation micromechanisms at the local phase and grain levels. In-situ neutron diffraction has been utilized to investigate the lattice strain evolution during tensile deformation at room and elevated temperatures. The neutron diffraction experiments were conducted at VULCAN diffractometer, Spallation Neutron Source, ORNL, with the state-of-art thermomechanical loading capabilities. Evolution of internal stresses and load-sharing mechanisms are revealed in both elastic and plastic deformation regimes. Finite-element simulations based on crystal plasticity are employed to compare with the experimental results, qualitatively and quantitatively. Insights into the microscopic deformation mechanisms and their dependence on temperature are discussed from the interphase and intergranular levels.

10:00 AM**Exploring Dislocation Source Strengths in Nanocrystalline Ni Using X-Ray Diffraction Footprints:** *Lin Li*¹; *Steven Van Petegem*²; *Helena Van Swygenhoven*²; *Peter Anderson*¹; ¹The Ohio State University; ²Paul Scherrer Institut

X-ray diffraction measurements show that NC metals display trends in intergranular stress vs. uniaxial deformation that are different from coarse-grained counterparts. The NC trends are also inconsistent, with tensile vs. compressive vs. negligible shifts observed among different samples. This peculiarity is investigated using Quantized Crystal Plasticity (QCP) simulations [1], which model the intergranular stress redistribution when dislocations propagate unstably across individual NC grains. These finite element-based simulations are interrogated to produce diffraction spectra for specific $\langle hkl \rangle$ peaks. A principal conclusion is that the grain-to-grain distribution of dislocation source strengths for electrodeposited NC Ni has a different, truncated form compared to coarse-grained counterparts. The seemingly inconsistent experimental trends are attributed, in part, to different prior deformation histories. This experiment-simulation approach is also applicable to study deformation physics in ultra-fine grain metals and dislocation cell structures. [1] L. Li et al., Acta Mater. 57, 812 (2009).

10:10 AM**Time-Resolved X-Ray Tomography of Semi-Solid Alloy Deformation:** *Kristina Maria Karez*¹; *Peter Lee*²; *Christopher Gourlay*¹; ¹Imperial College London; ²The University of Manchester

During the casting of aluminium alloys, regions of the casting are commonly a mixture of numerous equiaxed crystals and liquid. This two-phase mixture is deformed by phenomena such as shrinkage, and defects including segregation and cracking can result. In this work, Al-



TMS 2012

141st Annual Meeting & Exhibition

THURSDAY AM

15 wt.% Cu with a solid fraction of approximately 0.7 and with globular morphology has been deformed during time-resolved x-ray synchrotron tomography to understand the dynamic crystal-scale response to load. The rotation, translation and deformation of individual globules has been quantified during macroscopic deformation. A particular focus is given to the behaviour of agglomerates under load, allowing globule-scale deformation mechanisms to be compared with those suggested from past post-mortem studies on semi-solid deformation.

10:20 AM Break

10:25 AM Invited

Investigation of Residual Stress in Key-Hole Laser Formed Weldments Measured by Neutron and Synchrotron Diffraction: *Anna Paradowska*¹; Wojciech Suder²; Stewart Williams³; T. Connolley⁴; U. Lienert⁵; ¹ISIS, Rutherford Appleton Laboratory; ²Cranfield University; ³Cranfield University; ⁴Diamond Light Source; ⁵Advanced Photon Source,

There is a new generation of lasers available for materials processing. The new lasers include fibre and disc laser are characterized by very high beam quality at very high power levels providing extremely high energy density. In general laser welding is selected over other welding processes because of the minimisation of the heat input, residual stresses and distortion, for this reason they are increasingly popular over a wide range of industries. The narrowness of the welds makes it challenging to resolve the details of the residual stresses produced by the welding process. Residual strain/stress measurements in weldments produced using the fibre laser were performed on Engin-X, at ISIS and on I-ID at Advanced Photon Source. Across the weld and through thickness line distributions as well as maps are reported in this paper.

10:45 AM

Study of Embryos and Nanoscale Precipitates in a Ferritic Steel by Small Angle Neutron Scattering and Atom Probe Tomography: *Z. W. Zhang*¹; C. T. Liu²; X.-L. Wang¹; K. C. Littrell¹; M. K. Miller¹; K. An¹; B. A. Chin³; ¹Oak Ridge National Labs; ²City University of Hong Kong; ³Auburn University

State-of-the-art microstructural characterization techniques of small angle neutron scattering and atom probe tomography have been applied to characterize the evolution of solute-enriched embryos into nanoscale precipitates. Both techniques are able to detect number densities of sub-nanometer sized embryos that were higher than randomly expected within the solid solution in an as-quenched multicomponent ferritic steel. The results indicated that the nanoscale precipitates nucleate from the embryos and that the growth of the precipitates is dictated by volumetric diffusion. This type of mechanistic understanding of the nucleation and growth behavior of nanoscale nanoclusters is essential for the design of new classes of precipitation-strengthened materials. Research supported by Auburn University, City University of Hong Kong, NJUST Research Funding (No. 2010GIPY031), National Natural Sciences Foundation of China (No. 50871054), MSED (MKM, XLW, ZWZ) and SUFD (ORNL SHaRE User Facility (APT), HFIR, and Spallation Neutron Source) BES, U.S. DOE.

11:00 AM

Effect of Oxygen Content and Processing on Deformation Modes in a Zirconium Alloy: *Christopher Cochran*¹; Song Cai¹; Mark Daymond¹; ¹Queen's University

In situ neutron diffraction tests were performed during compression on samples of the two-phase alloy, Zr-2.5wt%Nb, used in pressure tubes in CANDU nuclear reactors. Three alloys with different oxygen concentrations were each prepared with three different heat treatments. The different heat treatments resulted in changes to crystallographic texture and microstructure. Oxygen is an interstitial solid solution element in zirconium alloys that results in a significant strengthening. Macroscopic stress-strain analysis showed the expected contribution to strengthening, while analysis of the neutron diffraction patterns reveals the role of oxygen on specific deformation modes. Changes in the onset

of twinning and the load sharing between alpha and beta phases was identified. Combining the experimental results with an elastic-plastic self-consistent (EPSC) model allows for the quantitative determination of the role of oxygen interstitials on specific slip / twinning systems. These studies highlight the role of neutron diffraction in potential alloy optimization.

11:10 AM

Study the Hydrogen Induced Volume Expansion and the Embrittlement of Zr-Based Bulk Metallic Glasses: *Chih-Pin Chuang*¹; Wojciech Dmowski¹; Yun Liu²; Terrence Udovic²; Peter Liaw¹; Lu Huang³; ¹University of Tennessee; ²National Institute of Standards and Technology; ³Beihang University

We report the hydrogen-induced structural change of Zr-based bulk metallic glasses. The hardness of hydrogen-charged sample was increased, but was accompanied by the significant reduction in the toughness and strength. The featureless, smooth fracture surface after hydrogenation suggests the embrittlement of the sample. The changes of the local atomic structures of amorphous alloys were investigated by the radial-distribution-function (RDF) analysis using high-energy X-ray, and the hydrogen occupation sites were determined by neutron vibrational spectroscopy (NVS). The results indicate that hydrogen expands the whole amorphous matrix by selectively occupying the 4-Zr tetrahedral sites. Locally, hydrogen only increase the Zr-Zr inter-atomic distance, but, globally, create a long range stress field in the amorphous matrix. The comparison of RDF of the hydrogenated sample with the as-cast sample under a tensile stress suggest that the hydrogen induced structural changes is equivalent to the changes produced by the tensile stress of 1.2 GPa.

11:20 AM

Characterization of Residual Stress in Laser Shock Peened IN718 SPF Alloy with X-Rays of Different Wavelengths: *Amrinder Gill*¹; S.R. Mannava¹; *Vijay Vasudevan*¹; Dong Qian¹; Gokul Ramakrishnan¹; Mohammed Belassel²; ¹University of Cincinnati; ²Proto Manufacturing Limited

X-ray diffraction is widely used to determine residual stresses in variety of materials. In the current study, coupons of IN718 SPF alloy were laser shock peened and through thickness residual stresses were determined by measuring strain in different sets of lattice planes: (331), (220) and (311) using Cu-Kalpha, Cr-Kalpha and Cr-Kbeta/Mn-Kalpha radiations, respectively. X-ray Elastic constants were also measured using a four-point bend fixture. The results showed large variations in the residual stress values, with those measured in the near-surface regions using Cu-Kalpha x-rays being much lower than those measured using Mn-Kalpha and Cr-Kbeta. The values were more or less similar in regions far below the surface. It is believed that this difference is due to plastic anisotropy, which can result in widely different strain responses in different lattice planes. Samples were also characterized using Synchrotron with conical slits for high spatial resolution and results compared with conventional XRD.

11:30 AM

In Situ Time-of-Flight Neutron Diffraction Study of the Phase Transformation in a TC18 Titanium Alloy: *Xiaopeng Liu*¹; Ru Lin Peng²; Yandong Wang³; Shuyan Zhang⁴; Sten Johansson²; ¹Northeastern University; ²Linköping University; ³Beijing Institute of Technology; ⁴Rutherford Appleton Laboratory

The high strength TC18 titanium alloy is of particular interest to the aerospace industry for its applications as bogie frames of aircraft landing gears. The mechanical properties of the alloy depend on its microstructure consisting of an hcp (α) and a bcc (β) phase, which can be influenced by thermal or thermomechanical process. For a better understanding of the development of phase-to-phase strain/stress and phase transformation behaviour, in-situ neutron diffraction experiments under cyclic heating and cooling between 20 and 900°C were performed on a TC18 rod material using ENGIN-X diffractometer at the ISIS Facility in UK. The evolution of diffraction spectra with temperature was monitored, based

on which detailed information such as changes of the relative volume fraction and lattice parameters for both α - and β -phases was analysed. The present study provides material parameters required for establishing further a FEM-based micromechanical model of titanium alloys with phase transformation.

11:45 AM

Non-Destructive Evaluation of Strain-Stress and Texture in Cold Drawn Tubes by Neutrons and Hard X-Rays: Adele Carradó¹; Thilo Pirling²; Robert Wimpory³; Heinz-Guenther Brokmeier⁴; Heinz Palkowski⁴; ¹IPCMS, UMR 7504 UDS-CNRS; ²Institut Laue-Langevin; ³Helmholtz Zentrum Berlin; ⁴Clausthal University of Technology

Seamless tubes are used for applications where strength, resistance to corrosion, microstructure and extended product life can be important design parameters. Cold drawing is widely applied in the industrial production of seamless tubes, employed for various mechanical applications. During pre-processing, deviations in tools and their adjustment lead to geometrical inhomogeneities – e.g. eccentricity - of the tubes as well as in the flow behaviour and cause a gradient in residuals and texture. In this paper the residual stress state and the texture in SF-copper tubes, drawn under controlled laboratory conditions, are presented. The residual stresses were evaluated by neutron diffraction on SALSA at the Institute Laue Langevin (France) and on E3 at Helmholtz-Zentrum Berlin (Germany), the texture by synchrotron radiation on the high energy beam line BW5 at DESY HASYLAB (Hamburg, Germany). The aim is to use the results for defining the process parameters for an optimized production process.

New Advances in Synthesis, Characterization, and Application of Layered Double Hydroxides: Session I

Sponsored by: The Minerals, Metals and Materials Society, TMS Electronic, Magnetic, and Photonic Materials Division, TMS Structural Materials Division, TMS: Chemistry and Physics of Materials Committee

Program Organizer: Jewel Gomes, Lamar University

Thursday AM
March 15, 2012

Room: Oceanic 2
Location: Dolphin Resort

Session Chairs: Hylton McWhinney, Prairie View A&M University; Jeanne Hossenlopp, Marquette University; Jewel Gomes, Lamar University

8:30 AM Introductory Comments Hylton McWhinney, Prairie View A&M University

8:35 AM Invited

Advances and Biochemistry of Using Layered Double Hydroxides in Treatment, Health and Wellness: *David Cocks*¹; Gary Beall; ¹Lamar University

Layered double hydroxides (LDHs) are being explored as vehicles for organic anions that can help diagnose and treat disease, promote health through prevention and enhance wellness. Synthetic LDH systems with positively charged brucite type layers of mixed metal hydroxides and positive charge located in interlayer spaces provide adjustable confinement for biochemically active anions. Selected advances in synthesis, exchange technology and associated biochemistry will be highlighted and discussed in terms of future applications for important human conditions where survivability, designed structure and controlled release of these materials are advantageous.

9:00 AM

Designing Layered Double Hydroxides for Targeted Applications: *Jeanne Hossenlopp*¹; ¹Marquette University

Layered double hydroxides (LDHs), and other similar nanodimensional layered metal hydroxides, offer promise for a number of applications ranging from controlled release of bio-active compounds to polymer fire retardant additives. Tailoring LDHs for controlled release or adsorbant applications requires an understanding of the kinetics and thermodynamics of anion release or analyte uptake. Recent work in our laboratory on the effects of systematic alteration of the metal hydroxide layer and/or anion structure will be discussed. The composition of the metal hydroxide layer provides wide tunability in reactivity for controlled release or anion exchange reactions. Anion polarity and hydrogen bonding capability can be utilized to vary the extent and rates of exchange reactions. Similar approaches to LDH structural alterations are applied to the design of potential polymer fire retardant additives. The effect of metal hydroxide layer composition and anion structure and packing influences the morphology of LDH-polymer (nanocomposites) and their thermal/fire properties.

9:20 AM

Electrochemical Synthesis of Layer Double Hydroxides, Its Characterization, and Performance Study for Removal of Nitrate and Arsenic: Md Haider¹; *Jewel Gomes*¹; Kevin Urbanczyk²; David Cocks¹; Hylton McWhinney³; George Irwin¹; Paul Bernazzani¹; ¹Lamar University; ²Sul Ross State University; ³Prairie View A&M University

Green rust (GR) is an important intermediate Layered Double Hydroxides (LDHs) which exist in oxidative transformation of iron(II) phase. Anionic and cationic species can replace their corresponding parts in the layered structure, and different species can also be accumulated in between the layers. GR can play an important role in wastewater remediation, such as reduction and removal of toxic compounds. An effort was made to synthesize LDH electrochemically, and to characterize it by Mössbauer, x-ray diffraction, scanning electron microscopy/energy dispersive x-ray analysis, x-ray photoelectron spectroscopy, and Fourier transform infrared spectroscopic techniques. GR was used to remove nitrate and arsenic from wastewater. The optimized conditions for removal of these water pollutants were also investigated. The resistance against oxidation of GR was increased using dopants, such as magnesium and aluminum, so that it can be used for water treatment in remote areas.

9:40 AM

Enhanced Removal of Various Phosphates over Ca Based Fe-Layered Double Hydroxide (LDH): *Guangren Qian*¹; Ji Zhi Zhou¹; Zhi Ping Xu²; Yunfeng Xu¹; Jianyong Liu¹; ¹Shanghai University; ²The University of Queensland

Ca-Al-layered double hydroxide (LDH) has exhibited its efficient removal capacity to aqueous anions such as SeO₄²⁻, AsO₄²⁻ though corresponding Ca-precipitate formation. Despite the similar structure to Ca-Al-LDH, Ca-Fe-LDH is barely investigated for anionic pollutants removal. In current work, the removal of various phosphates such as PO₄³⁻, pyrophosphate (P₂O₇⁴⁻, PP) and triphosphate (P₃O₁₀⁵⁻, TPP) was performed on Ca-Fe-LDH. Our research indicates that the dissolution-precipitation played an important role on the phosphates removal due to the Ca-P precipitate formed. In particular, the PO₄³⁻ and P₂O₇⁴⁻ removal was enhanced as the adsorption of phosphate on Ca_xFe(OH)(3+2x) which was the hydrolyzed Ca-Fe-LDH. Such enhancement was not observed in the case of P₃O₁₀⁵⁻ as the formation of highly soluble Ca-TPP complex. Moreover, the introduction of Mg into Ca-Fe-LDH enabled a Mg_{0.5}Ca_{1.5}Fe-LDH to take up higher amount of TPP than that on Ca-Fe-LDH. It is due to the combination of adsorption/intercalation and dissolution-precipitation.



TMS 2012

141st Annual Meeting & Exhibition

THURSDAY AM

10:00 AM

Removal of Direct Red and Orange II Azo Dye from Synthetic Textile Water Using Electrochemically Produced Fe-LDH: *Sadia Jame¹*; Jewel Gomes¹; David Cocke¹; ¹Lamar University

Layered double hydroxides are produced as an intermediate phase during in-situ electrochemical coagulation technique using iron sacrificial electrode. Its structure consists of cationic layers, $\text{Fe}(\text{OH})_2\text{n}^+$, alternating with anionic layers stacked in a six-layer repeating sequence, giving rise to a hexagonal or pseudo-hexagonal symmetry. This Fe-LDH has also the ability to trap organic impurities in the interlayers when it is mixed with wastewater. This hypothesis was verified using dye molecules, such as Direct Red and Orange II. Generally, textile industries use various kinds of chemicals including dyestuffs and pigments during dyeing and finishing processes. Their effluent is extremely toxic and environmentally hazardous. Fe-LDH was found to remove dye molecules with satisfactory efficiency. Optimum conditions were explored by changing current density, dye concentration, conductivity and pH during the LDH generation process. The floc was characterized using SEM/EDS, XRD and FTIR.

10:15 AM Break

10:30 AM Invited

Charge Density and Counter ion Effects on Synthesis and Thermal Decomposition Character of Hydrotalcites: *Gary Beall¹*; David Cocke²; Sergio Crosby¹; Andrew Gomes²; Doanh Tran²; ¹Texas State University; ²Lamar University

A series of hydrotalcites have been synthesized with exchange capacities ranging from 100 to 500 meq/100 g at temperatures ranging from room temperature up to 180 °C. These hydrotalcite have been characterized by x-ray diffraction, scanning electron microscopy, and by thermal decomposition techniques. The temperature of synthesis has the largest effect upon crystallinity and the unit cell parameters are sensitive to charge density. The thermal decomposition of the hydrotalcites has been followed by thermal gravimetric analysis coupled with off gas analysis of the decomposition products. The off gas analysis yields very distinct decomposition profiles that are very dependant upon both charge density and counter anion. The mechanisms of decomposition will be discussed in detail.

10:55 AM

Microwave Synthesis and Vibrational Spectroscopy of Chemically Substituted Layered Double Hydroxides with Carbonate, Chloride and Sulfate Ions: *Anderson Dias¹*; Andiara Vieira¹; Lumena Cunha¹; ¹UFOP

A hybrid material based on the intercalation of carbonate, chloride, and sulphate anions has been synthesized at mild temperatures through microwave-assisted hydrothermal synthesis. Chemically substituted layered double hydroxides were produced by changing both bivalent (Ni, Zn, Mn, Co, Mg) and trivalent cations (Al, Fe) into the structure. Powder X-ray diffraction patterns showed pure layered double hydroxide phases having crystallite size around 50 nm. Raman scattering measurements exhibit shifting of bands with changing of both divalent or trivalent metal ion type for all samples with carbonate, chloride or sulphate anions. Differential scanning calorimetry and thermogravimetry analysis exhibit the three stages of thermal degradation, which is characteristic behavior of hydrotalcites. Investigations carried out through transmission electron microscope showed a characteristic platelet morphology with the platelets stacked one above the other. Detailed discussion on the processing conditions and the final morphology and vibrational features is presented.

11:15 AM

Removal of Arsenic Using Green Rust and Other Electrochemically Generated Floc: *Md Rahman¹*; Jewel Gomes¹; Kevin Urbanczyk; David Cocke¹; ¹Lamar University

Arsenic contamination from groundwater is a worldwide problem. It is considered as one of the toxic materials being controlled by Environmental Protection Agencies in several developed and developing countries. The most common form of inorganic arsenic in natural water system is arsenate and arsenite. Arsenite (As(III)) is more toxic than Arsenate (As(V)) and it is more abundant in anaerobic condition such as in groundwater. Removal of arsenic from synthetic wastewater was carried out by using green rust floc which belongs to the layered double hydroxide (LDH) family and it was produced in-situ during electrocoagulation procedure using iron sacrificial electrode. Other electrochemically generated flocs using copper and aluminum electrodes were also used for the removal of arsenic from synthetic wastewater. The maximum arsenic removal efficiency was recorded as 99.9%. The sludge produced during electrocoagulation was assessed for semi conductive property with diffuse reflectance UV-Vis spectroscopy.

11:30 AM

Formation of Layered Double Hydroxides in Self-Purification of Polynary Metal Electroplating Wastewaters for Effective Removal of Anionic Dye: *Jizhi Zhou¹*; Guangren Qian¹; Zhi Ping Xu²; Yueying Wu¹; ¹Shanghai University; ²The University of Queensland

The synchronous formation of layered double hydroxide (LDH) precipitates was performed for the self purification of wastewaters containing Ni^{2+} , Zn^{2+} , and Cr^{3+} . With ~99% of metal ions removed, a pure Ni-Zn-Cr-bearing LDH was formed by accelerated carbonation process. The obtained LDH were characterized by XRD, FT-IR, SEM and BET surface area techniques. Moreover, the removal of a dye, Acid Scarlet GR (GR), from aqueous solution on the LDH was studied under varying conditions of pH, adsorbent dose and contact time. It is observed that Ni-Zn-Cr-LDH could effectively remove GR from aqueous solutions and the removal capacity increased with rising temperature. The final solution after dye removal exhibited rare heavy metal was dissolved. These results suggest a strategy to treat heavy metal wastewater efficiently and propose Ni-Zn-Cr-LDHs as an environmental friendly adsorbent for anionic dye removal.

11:45 AM

Characterization and Chemical Modification of Electrochemically Produced Layered Double Hydroxides as Nanomaterials: *Md Islam¹*; Jewel Gomes¹; Paul Bernazzani¹; ¹Lamar University

Electrocoagulation (EC) is one of the most effective electrochemical techniques for the removal of trace amount of metal contaminants from waste water. The intermediate step of this process using sacrificial iron electrode is generation of layered double hydroxides generally known as green rust. When trace copper is removed using EC, the produced EC floc contains mostly iron and lesser proportion of copper incorporated in it. Instead of disposing the EC-floc as waste, it was further treated to produce important nanomaterials. The EC floc was chemically treated to convert nanowire of iron. The different proportion of copper was incorporated into iron floc to see the effect of the change of the ratio of iron to copper in the structure, size, and shape of the nanowires. Copper was recaptured both chemically and electrochemically, and converted to nanorods. These nanomaterials were characterized using SEM, EDX, XRD, FTIR and TG-DSC.

Pb-Free Solders and Other Materials for Emerging Interconnect and Packaging Technologies: Physical Property Effects and Responses to Current

Sponsored by: The Minerals, Metals and Materials Society, TMS Electronic, Magnetic, and Photonic Materials Division, TMS: Electronic Packaging and Interconnection Materials Committee
Program Organizers: Iver Anderson, Ames Laboratory; Sung Kang, IBM; Albert Wu, National Central Univ.; Laura Turbini, Research in Motion; Tae-Kyu Lee, Cisco Systems; Govindarajan Muralidharan, Oak Ridge National Lab; John Elmer, Lawrence Livermore National Lab; Yan Li, Intel

Thursday AM
 March 15, 2012

Room: Swan 9
 Location: Swan Resort

Session Chair: To Be Announced

8:30 AM Invited

Critical Studies to Evaluate the Events Controlling TMF Reliability of Sn-Ag Solder Joints: Stephanie Bergman¹; Andre Lee¹; K.N. Subramanian¹; ¹Michigan State University

In order to gain a better understanding of the events controlling the solder joint reliability under thermomechanical fatigue thermal excursions with varying temperature differences in different temperature ranges were imposed on the joints. Such studies were focused on the very early stages of thermal excursions. Specimens were first subjected to limited number cycles of a chosen thermal profile were subsequently subjected to additional number of cycles of different thermal profile. Residual shear strength of the joints subjected to various combinations of these thermal profiles is used to evaluate the roles of critical microstructural events that control the thermomechanical fatigue reliability of solder joints.

8:55 AM

In-Situ Mechanical Assessment of Thermomechanically Fatigued POSS-Added Pb-Free Nanocomposite Solder Joints: Stephanie Bergman¹; Andre Lee¹; K.N. Subramanian¹; ¹Michigan State University

Silanol of polyhedral oligomeric silsesquioxane (POSS-silanol) when incorporated in Pb-free, electronic solders increase the residual shear strength and reliability of thermomechanically fatigued (TMF) solder joints. Such enhanced TMF reliability has been attributed to the strongly bonded inert POSS-silanol at the boundaries of various microstructural entities in solder joints. Depending on the service temperature, presence of POSS-silanol can either increase the stress needed to cause decohesion or reduce the sliding motion between different entities. Recently a dynamic mechanical method has been used for TMF induced damage assessment in Pb-free solder joints by imposing temperature and frequency sweeps. The small shear strain amplitudes used in such evaluation does not cause additional damage. Hence, it is an ideal in-situ assessment method for monitoring the progression of TMF induced damages in the same solder joint. This presentation compares the findings on joints made with various Pb-free solder alloys, with and without POSS additions.

9:15 AM

Experimental and CPFEM Investigation of Stress Distribution in Shear Tests and Thermal Cycling in Lead-Free Solder Joints: Payam Darbandi¹; Bite Zhou¹; Farhang Pourboghra¹; Thomas Bieler¹; Tae Kyu Lee¹; Kuo Chuan Liu¹; ¹MSU

A set of crystal plasticity analyses was used to evaluate stress, strain and shape change resulting from shear experiments on single lap shear specimens with different known crystal orientations. Phenomenological flow models for ten systems were estimated based upon semi-quantitative information available the literature and new experiments, along with known anisotropic elastic information. Optimization of material parameters is done to match prior experimental results where

slip systems activity has been quantified. This is also used to assist analysis of elastic strains measured in single crystal joints identified using synchrotron X-ray diffraction patterns during in-situ solidification studies and subsequent thermal cycling between 0°C-100°C strains from CPFE simulations are used to compute changes in d-spacings to be compared with measured d-spacings in order to provide comparisons between model and simulation that will assist in improving the model and gaining quantitative understanding of strain evolution.

9:35 AM

Thermal and Mechanical Characterization of Cu/ Cu-In Solder Joints for Thermal Interface and Interconnect Applications: Effects of Interfacial Layers: Jia Liu¹; Praveen Kumar¹; Indranath Dutta¹; Rajen Sidhu²; ¹Washington State University; ²Intel Corporation

Cu-In composites, for thermal interface and interconnect applications, were prepared using liquid phase sintering. Two Cu pieces were joined using optimized Cu-In composite solder, having ~2.5 times higher thermal and electrical conductivities, and ~30% lower yield strength than commercial (Sn, Ag, Cu)-based solders. Mechanical properties in shear, and thermal and electrical resistance of these joints were measured as functions of inter-layer between solder and Cu, joint thickness and thermo-mechanical history. The joints showed higher shear compliance as compared to similar joints prepared using Sn-3.0%Ag-0.5%Cu and higher thermal and electrical conductivity as compared to those prepared using In and Sn-3.0%Ag-0.5%Cu. Minimizing interfacial contact-resistance is desired, especially for small joint thicknesses, and hence interfacial engineering is conducted based on the role of different interfacial layers. A nanometer thick Au layer coating on Cu-substrate reduces the contact-resistance by an order of magnitude. Structure-property relationship will be discussed in detail.

9:55 AM Break

10:05 AM

Wetting Behavior and Interfacial Reaction between New Electrolytic Ni-Pd Surface Finish/Sn-3.0Ag-0.5Cu Solder Joints: Cheng Ying Ho¹; Jenq Gong Duh¹; ¹National Tsing Hua University

ENEPIG, a new substrate surface finish in electronic package, was expected to take place of traditional ENIG substrate because of its low consumption, good reliability, and free "black-pad". However, the popularity of ENEPIG was restricted by complicated process and ultra-high cost. In this study, single Ni-2wt%Pd alloy electroplating process without gold layer was designed to be a replacement. Wetting behavior with molten Sn-3.0Ag-0.5Cu (SAC305) solder and the formation of metallic oxide under 150°C aging were analyzed. The Pd dopant tends to enhance the surface wettability, and the possible mechanism will be discussed. Furthermore, interfacial reaction between substrate and SAC305 under various aging time is studied. Growth mechanism of IMC and influence of Pd dopant in solder joints will be also evaluated.

10:25 AM

Analytical Modeling of Diffusion and Growth Processes in Sn-Ag Alloy Systems: Sri Chaitra Chavali¹; Ganesh Subbarayan¹; Mysore Dayananda¹; ¹Purdue University

SnAg and SnAgCu solder alloys are common in microelectronic assemblies. These evolve in their mechanical behavior and microstructure due to environmental conditions. The dispersed Ag₃Sn microscopic precipitates are an example of interface mediated shape evolution that evolve into needle-like structures during the course of static aging. In this paper, we develop an analytical model based on Zener's diffusion model to describe the kinetics of particles during the aging process. The ultimate goal is to develop a refined kinetics and thermodynamics based sidewise growth model for Ag₃Sn precipitates in beta-Sn matrix. Aging experiments were carried out (ranging 298-398K for 1, 5, 15, 30 and 90 days) to induce microstructural evolution and quantitative metallographic characterization of the evolving microstructure. From the microstructural information obtained on growth of the particles, we derive



TMS 2012

141st Annual Meeting & Exhibition

THURSDAY AM

the interdiffusion parameters at homologous temperatures of 0.5-0.7T_m (that are usually experienced in Microelectronic industry for SnAgCu systems).

10:45 AM

Effect of Solder Thickness on Electromigration in Sn_{2.5}Ag Solder Joints: *Woei haw Khew*¹; Chih Chen¹; ¹Department of Materials Science and Engineering, National Chiao Tung University, Hsinchu, Taiwan 30010, Republic of China

As the solder bump size becoming smaller, electromigration failure is a critical reliability issue. As 3D-IC will become an important packaging technology for high performance devices, the bump height will decrease to 10 to 20 micron. In this research, the effect of different solder thickness of electromigration is investigated. The solder joint consists 10 μm Sn_{2.5}Ag solder joint with 3 μm electrical Ni on the chip side and 5 μm electroless Ni on the substrate side. The current density was about 5×10³ A/cm² and the testing temperature at 150°C controlled by using micro-thermal sensor. The result indicates that void and intermetallic compound formation was easily observed at higher solder thickness. Back stress may play an important role in electromigration of solder joints with a smaller bump height. We will investigate whether there is a critical thickness, below which there is no electromigration damage due to the back stress effect.

11:05 AM

Relationship between Reliability and Effect of Solid Solution Hardening at Solder Joints: *Minoru Ueshima*¹; ¹Senju Metal Industry

The change of the microstructure causes the decrease in the fracture strength. On the other hands, the strength of Sn-Ag-Cu system alloys contained Sb and Bi, doesn't decrease very much after annealing at 125°C. The reliabilities of the solder joints at the alloys contained Sb and Bi are investigated by measuring the shear strength of solder joints at the big chip resister (6.4 × 3.2 mm) and the small one (3.2×1.6 mm) after every 1000 cycles between -55 and 125°C. The lives of solder joints at the new alloys become twice more than at Sn-3Ag-0.5Cu alloy. Furthermore, addition of Bi is effective on improving the reliability at thermal fatigue tests between -55 and 150°C. The effect of solid solution hardening of Bi never disappears at 200°C.

11:25 AM

Current-Induced Phase Transformation Study of Ni-Sn Intermetallic Compounds in 18 \149; m Microbumps in Three-Dimensional Integrated-Circuit Packaging Using Kelvin Bump Structure: *Yuan-Wei Chang*¹; Chih Chen¹; ¹National Chiao Tung University

The electromigration behavior is investigated in 20 μm SnAg microbumps with Cu/Ni under-bump-metallization (UBM) at 150 °C. A Kelvin bump structure was designed and fabricated in these samples to measure the bump resistance of only one bump, and the different stages (initial stage, 5% resistance increase, and 20% resistance increase) were in-situ monitored. The monitored bump resistance increased abruptly right after the current stressing by 4.6 × 10⁴ A/cm², but the resistance rose much slower after a certain period of time. Microstructural analysis indicates that the formation of the high-resistivity Ni₃Sn₄ intermetallic compounds (IMCs) is responsible for the abrupt resistance increase in the beginning of current stressing. The whole solder joint can be transformed into IMC joint in a short time, which has a higher electromigration resistance than the original SnAg solder and results in a much slow increase in resistance afterwards. The electromigration failure mechanism is also examined.

Recent Developments in Biological, Electronic, Functional and Structural Thin Films and Coatings: Applications to Bio, Energy and Electronic Systems

Sponsored by: The Minerals, Metals and Materials Society, TMS Electronic, Magnetic, and Photonic Materials Division, TMS: Thin Films and Interfaces Committee

Program Organizers: Nuggehalli Ravindra, New Jersey Institute of Technology; Jian Luo, Clemson University; Xing Yang (Mark) Liu, National Research Council Canada; Nancy Michael, University of Texas at Arlington; Roger Narayan, University of North Carolina and North Carolina State University; Choong-un Kim

Thursday AM
March 15, 2012

Room: Swan 10
Location: Swan Resort

Session Chairs: Roger Narayan, University of North Carolina and North Carolina State University; Sufian Abedrabbo, University of Jordan

8:30 AM Introductory Comments

8:35 AM

Multilayer Roll Bonded Sandwich: Processing, Mechanical Performance and Bioactive Behavior: *Adele Carradò*¹; Heinz Palkowski²; ¹IPCMS, UMR 7504 UDS-CNRS; ²Clausthal University of Technology

Multi functionality of the materials makes it necessary to use hybrid systems such as combination of metals with polymers. Their applications can be found in all areas where light weight and improved mechanical properties as well as high functionality are necessary. Moreover adapted types of hybrids can be interesting for biomedical applications as under specific condition they show for e.g. good strength combined with high elasticity. The present study shows preliminary tests on the biomimetic behaviour of 316L/polypropylene copolymer/316L sandwich. The autocatalytic and biomimetic coating routes were applied to induce calcium phosphate layer in a way similar to the process of natural bone formation. Knowledge of the formability of three-layered sandwich sheets and their biomedical application are presented.

9:05 AM

Effect of Multiple Quaternary Ammonium Ion Salts on the Performance of Heparin Ionic Complex Coating: *Narayana Garimella*¹; Bartley Griffith¹; Zhongjun Wu¹; ¹University of Maryland School of Medicine

Dissolved quaternary ammonium salts are excellent surfactants and can effectively coat numerous substrate materials and also form ionic complexes with negatively charged enzymes. Chemical constitution and dissolution of the salts in polar and non-polar solvents governs the substrate binding and retaining characteristics, whereas forming a precipitate of ionic complex along with heparin enzyme governs the applicability of bioactive coating. In this current study, effect of multiple quaternary ammonium salts on the performance of heparin ionic complex coating is studied from the view point of surface modification to polymeric hollow fiber membranes of artificial lung. Pre and post coating characteristics of the surfaces are evaluated in contact with normal saline, ringer's lactate and 1 mol/L NaCl solutions to determine stability of coating. Immobilized enzyme activity was confirmed using biochemical and chemical assay methods. In-vitro blood compatibility experiments proved coating's ability to prevent platelet adhesion.

9:35 AM

Bio-Inspired Organic/Inorganic Multi-Layer Coating Synthesized by RF-Magnetron Sputtering and Pulse Laser Deposition: Yu-Chen Chan¹; Hsien-Wei Chen¹; Li-Wei Ho¹; Jyh-Wei Lee¹; Po-Yu Chen¹; Jenq-Gong Duh¹; ¹National Tsing Hua University

Abalone shell is a natural composite of 95 wt% stacked CaCO₃ tiles and 5 wt% organic layers of chitin and protein hierarchically organized into a “brick-and-mortar” microstructure, which leads to exceptional mechanical properties. In this study, abalone-inspired organic/inorganic multilayer coatings were synthesized by combining RF-magnetron sputtering (inorganic) and pulse laser deposition (organic) in a single chamber. Selected inorganic nitrides and organic polymers were used. SEM and TEM images showed uniform polymeric layers (10-50 nm) sandwiched between ceramic layers (~0.5 μm). The microstructure and organic/inorganic thickness ratio were fine controlled to be the same as those in abalone shell. Additionally, organic/inorganic multilayers with increasing interfacial roughness were made to mimic the nano-sized asperities and mineral bridges observed in abalone. Nano-indentation and nano-scratch tests were performed on the synthetic multilayer coatings and abalone shell followed by SEM and AFM characterization. Mechanical properties and toughening mechanisms were discussed and comparisons were made.

10:05 AM

Nanomechanical Properties of Polyethylene Glycol Coatings on Flat Gold Substrates: Frank DelRio¹; Gheorghe Stan¹; Robert MacCuspie¹; Robert Cook¹; ¹National Institute of Standards and Technology

Medical devices have long utilized both gold and polyethylene glycol (PEG) as inert, biocompatible, and safe surfaces. A necessary step in advancing the use of PEG coatings is to provide direct and reliable nanoscale property characterization. In this work, atomic force microscopy (AFM) and atomic force spectroscopy (AFS) were used to study the morphology and mechanical properties of thiol-functionalized PEG coatings on flat gold substrates in solution and in air. AFM was used to investigate the morphology of PEG coatings as a function of concentration and molecular weight; the commonly-observed coverage was in the form of sparse brush-like islands. AFS was used to study the mechanical properties of PEG coatings in compression and tension as a function of molecular weight. Together, the various models were used to map a number of mechanical properties over individual PEG islands, which enabled a statistical approach for assessing the heterogeneity of PEG properties.

10:35 AM Break

10:50 AM

Doping and Co-Doping of Bandgap-Engineered ZnO Films for Solar Driven Hydrogen Production: Sudhakar Sher¹; Nuggehalli Ravindra²; Yanfa Yan¹; Mowafak Al-Jassim¹; ¹National Renewable Energy Laboratory; ²New Jersey Institute of Technology

The co-doped ZnO:(Al,N) and ZnO:(Ga,N) films were deposited by co-sputtering using radio-frequency magnetron sputtering on F-doped tin-oxide-coated glass. We found that the ZnO:(Al,N) and ZnO:(Ga,N) films exhibited greatly enhanced crystallinity compared to ZnO:N films doped by pure N and grown at the same conditions. Furthermore, the ZnO:(Al,N) and ZnO:(Ga,N) films showed much higher N-incorporation than ZnO:N films grown with pure N doping. As a result, the ZnO:(Ga,N) films showed significantly higher photocurrents than ZnO:N doped only by N. The ZnO:(Cu,Ga) films were synthesized by RF magnetron sputtering in O₂ gas ambient at room temperature and then annealed at 500°C in air for 2 hours. We found that the carrier concentration tuning does not significantly change the bandgap and crystallinity of the ZnO:Cu films. However, it can optimize the carrier concentration and thus dramatically enhance PEC response for the bandgap-reduced p-type ZnO thin films.

11:20 AM

Characterization of Thin Film Photovoltaic Microstructure and Correlation with Conversion Efficiency: Matt Nowell¹; ¹EDAX-TSL

Thin film photovoltaic devices have become an increasingly viable option for solar power generation. The conversion efficiencies of CdTe and CIGS polycrystalline thin film devices are higher than their single crystal equivalents. This indicates that the microstructural features present in the polycrystalline films play a beneficial role in device performance. In this work, Electron Backscatter Diffraction (EBSD) has been used to characterize CdTe photovoltaic thin films deposited by magnetron sputtering. These films were examined in the as-deposited state, and after annealing. This annealing, with a CdCl₂ solution, is a standard treatment used to produce high performance films. Investigation of the as-deposited films provides information on the growth mechanisms of the films while investigation of the annealed films allows for correlation of microstructure with final device performance. In these films, significant twinning occurs during annealing, and these twins provide beneficial properties to the final microstructure.

11:50 AM

Magnetic Field Assisted Heterogeneous Device Assembly: Vijay Kasisomayajula¹; Michael Booty¹; Anthony Fiory¹; Nuggehalli Ravindra¹; ¹New Jersey Institute of Technology

Heterogeneous device assembly using magnetic fields is analyzed. Small cylindrical solenoids are used as sources for a controlled magnetic field. This paper investigates the theoretical and experimental lower limit using technology in extant on the dimension of the solenoids and the devices that can be assembled using magnetic field assisted assembly.

12:10 PM

Study on Organic Thermal Mode Photo-Resist for the Application of Nano-Lithography: Der-Ray Huang¹; ¹NDHU

A new technology call thermal mode lithography which developing a new photoresist with temperature sensitive characteristic that can breakthrough optical diffraction limit[1]. There have the photo UV absorption and thermal properties are the important characteristics of thermal mode photoresists[2]. It can be control the submicron pattern size and resolution. The decomposition and gasification mechanism of the thermal photoresists are analyzed by the thermal properties such as melting temperature(T_m) and cracking temperature (T_d). The surface morphology of nano pattern can be controlled by using different laser power exposure on thermal photoresists.



Solid-State Interfaces II: Toward an Atomistic-Scale Understanding of Structure, Properties, and Behavior through Theory and Experiment: Interface Dynamics, Oxidation

Sponsored by: The Minerals, Metals and Materials Society, TMS Electronic, Magnetic, and Photonic Materials Division, TMS Structural Materials Division, TMS: Chemistry and Physics of Materials Committee, TMS: Nanomechanical Materials Behavior Committee

Program Organizers: Xiang-Yang Liu, Los Alamos National Lab; Douglas Spearot, University of Arkansas; Guido Schmitz, University of Münster; David Seidman, Northwestern University

Thursday AM
March 15, 2012

Room: Oceanic 7
Location: Dolphin Resort

Funding support provided by: Los Alamos National Laboratory

Session Chairs: Douglas Spearot, University of Arkansas; Douglas Medlin, Sandia National Labs

8:30 AM Invited

Shrinking Island Grains: Mobilities and Driving Forces: David Olmsted¹; *Mark Asta*¹; Colin Ophus²; Tamara Radetic³; Ulrich Dahmen²; ¹University of California, Berkeley; ²Lawrence Berkeley National Laboratory; ³University of Belgrade

In this talk we will describe the results of molecular-dynamics simulations examining processes related to the shrinking of island grains in Authin films. The island grains investigated in this work are bounded by $\langle 110 \rangle$ tilt grain boundaries with 90 degree misorientations, but varying grain-boundary inclinations. Our interest in this system is motivated by parallel experimental investigations of the dynamics of the same type of island grains in mazed-bicrystal thin films, using in-situ electron-microscopy. We focus in this talk on analyses of the simulation results designed to probe the magnitudes of the grain-boundary interface stiffnesses and mobilities underlying the rate of grain shrinkage derived in the simulations. In addition, we analyze the variations in these properties with grain-boundary inclination, and discuss the relationship between these anisotropies and the dynamic shape of the island grains. Comparison with experimental observations obtained by in-situ microscopy will also be presented.

9:00 AM

The Dynamics of Shrinking Grains: Molecular-Dynamics Simulations and In-Situ Electron Microscopy Studies of Shrinkage, Shape, Rotation and Dislocation Production: *David Olmsted*¹; Tamara Radetic²; Colin Ophus³; Ulrich Dahmen³; Mark Asta⁴; ¹University of California, Berkeley; ²University of Belgrade; Lawrence Berkeley National Laboratory; ³Lawrence Berkeley National Laboratory; ⁴Lawrence Berkeley National Laboratory; University of California, Berkeley

Theoretical models and computer simulations of grain growth have shown that island grains may rotate as they shrink. This can result from shear-coupled boundary motion, or attraction to low-energy cusps. Here we study the dynamics of shrinking island grains for $\langle 110 \rangle$ 90 degree tilt boundaries in Au, which feature higher disorientations than have been studied previously. The experimental study is based on in-situ electron-microscopy of mazed bicrystal samples. Molecular-dynamics simulations of island grains with identical crystallography have been undertaken. The combination of experiment and simulation leads to detailed comparison of the rate of shrinkage, grain shape and rotation. In both experiment and simulation, dislocations may remain after the island grain is consumed. Possible sources of these dislocations are considered. This research is supported by the Director, Office of Science, Office of Basic Energy Sciences, Materials Science and Engineering Division, of the US Department of Energy, under contract no. DE-AC02-05CH11231.

9:20 AM

Coupled Motion of Interstitial-loaded Grain Boundaries in Bcc Tungsten as a Possible Radiation Damage Healing Mechanism under Fusion Reactor Conditions: *Valery Borovikov*¹; Xian-Zhu Tang¹; Danny Perez¹; Xian-Ming Bai²; Blas Uberuaga¹; Arthur Voter¹; ¹LANL; ²INL

As a potential first-wall fusion reactor material, tungsten will be subjected to high radiation flux and extreme mechanical stress. We propose that under these conditions, coupled grain boundary motion, and enhanced mobility of interstitial-loaded grain boundaries, can lead to a radiation-damage self-healing mechanism, in which a grain boundary absorbs interstitials produced in collision cascades, activating motion of the grain boundary, which sweeps up the less-mobile vacancies. We examine the stress-induced mobility characteristics of a number of grain boundaries in W to investigate the likelihood of this scenario.

9:40 AM

Calculation of Grain Boundary Mobility in Slow-Moving Nickel Bicrystals: *Shawn Coleman*¹; Stephen Foiles²; Douglas Spearot¹; ¹University of Arkansas; ²Sandia National Laboratories

Different computational methods to determine grain boundary mobility are compared using synthetic driving force molecular dynamics simulations of nickel bicrystals. Grain boundaries with a wide range of mobility are selected in this study. Particular focus is placed on grain boundaries demonstrating mobility at the lower measurable limit within the timescale of molecular dynamics simulations. Slow moving grain boundaries are of interest because they play a limiting role in microstructure evolution, e.g., the kinetics of recrystallization or grain growth in polycrystalline materials. It is found that the level of consistency between different methods is dependent on the simulation temperature and synthetic driving force energy.

10:00 AM

The Mobility and Grain Boundaries Study of Austenite-Ferrite Interface in Pure Fe from Molecular Dynamics Simulations: *Huajing Song*¹; Jeff Hoyt¹; ¹McMaster University

A molecular dynamics (MD) method has been developed to simulate the austenite – ferrite transformation in pure iron. For low index FCC/BCC crystallographic orientations no interface motion is observed, but for slight misorientations steps are introduced at the interface and sufficient mobility is observed over MD time scales. The misorientation geometry generates a primary and secondary disconnection structure on the FCC/BCC interphase boundary and both defect arrays are necessary to activate interface motion. The effect of misorientation, dislocation and disconnection density on the interface mobility and activation energy will be discussed. In addition, a multi crystal simulation to observe the net effect of different FCC/BCC grain boundaries during the transformation is presented.

10:20 AM Break

10:25 AM

Thermally Activated Avalanches: Jamming and the Progression of Needle Domains: *Xiangdong Ding*¹; E.K.H. Salje²; Turab Lookman³; Avadh Saxena³; ¹Xi'an Jiaotong University; ²University of Cambridge; ³Los Alamos National Laboratory

Interface pinning, depinning, doping, the formation of global interfacial patterns and 'glassy' states are important phenomena in metallurgy. Typical examples are the twin boundaries in ferroelectric/martensitic materials, conducting interfaces in an insulating matrix, and magnetic interfaces in ferromagnetic materials. The interfaces remain a coherent part of the crystal and can be moved under appropriate forcing (stress, thermal, electric or magnetic fields). The kinetic process of the wall movement can be smooth, jerky, or combine both aspects. It can also be athermal or thermally activated. However, it is not clear whether all jerks are defect-generated avalanches and whether athermal behavior is required to generate such avalanches. In this presentation, by means of atomistic simulations, we demonstrate that this is not necessarily the case.

At moderate temperatures we find jerky behavior which displays classic power-law exponents without any extrinsic defects, while jerks can be thermally activated at high temperatures.

10:45 AM

Atomic-Scale Modeling of the Mobility of Boundaries of Deformation Twins in Alpha-Iron: *Jinbo Yang*¹; Yuri Osetsky¹; Roger Stoller¹; ¹ORNL

Twinning plays an important role in plastic deformation of alpha-iron at low temperatures, and it also occurs in association with martensitic transformation in steels. Twinning in bcc metals is a simple shear process which takes place by moving successive planes of {112} by a displacement $\langle 111 \rangle / 6$. The underlying mechanism can be attributed to the glide of partial dislocations $\langle 111 \rangle / 6$ or $\langle 111 \rangle / 3$. These partial dislocations will form non-coherent boundaries of twin embryos. However, the mobility of these non-coherent boundaries has not been systematically studied. The atomic-scale modeling has been performed here to simulate various non-coherent twinning boundaries in alpha-iron. The results provide a satisfactory rationale of many unexplained experimental observations, e.g. why the formed twin boundaries lose their mobility when the applied stress is reversed during twinning in alpha-iron.

11:05 AM

First Principles Study of Ti (10-12) Twin Boundary: Interactions with Oxygen Interstitials and Screw Dislocations: *Maryam Ghazisaeidi*¹; Dallas Trinkle¹; ¹University of Illinois at Urbana-Champaign

Interaction of twin boundaries with dislocations and oxygen interstitials influences the plastic deformation of titanium. We investigate the interactions of (10-12) twin boundary with oxygen from first principles. The energetics of four interstitial sites in the twin geometry is compared with the bulk octahedral site. We show that the sites located at the boundary are attractive while the others are repulsive compared to bulk. Also, we model a [1-210] screw dislocation in the twin boundary using interfacial flexible boundary conditions. The dislocation is placed at narrow and wide spacing sites at the boundary. In both cases, the cores are compact and trapped in the boundary without dissociation. Electronic density of states plots show the change in directional bonding of the Ti d electrons in the dislocation core region at the presence of the twin boundary. The results provide a better understanding of how twin boundaries change mechanical properties of Ti.

11:25 AM Invited

Insights into the Oxidation Behavior of Alloys: Oxide/Metal Interfaces at the Atomic Scale: *Emmanuelle Marquis*¹; ¹University of Michigan

The roles of solute and alloying elements in modifying the oxidation resistance of alloys can be complex. It is often speculated that interfacial segregation, preferential oxidation are responsible for the observed behavior. However, the lack of detailed chemical information on metal/oxide interfaces and the oxide microstructure is lacking to confirm the existing models. Such information would allow the efficient design of novel oxidation resistant alloys required for high temperature and power generation applications. It will be shown how the systematic use of high resolution microscopy and atom probe tomography in particular can provide unique insights into the mechanisms taking place during alloy oxidation both at the surface and along grain boundaries.

11:55 AM

HR-STEM Investigation of Cu/SnO₂ Interfaces in the Internal Oxidation Zone of a CuSn9 Alloy: *Xavier Sauvage*¹; Megha Dubey¹; Samuel Jouen¹; Béatrice Hannoyer¹; ¹University of Rouen, CNRS

A CuSn9 alloy was oxidized in air laboratory at 580°C during several hours leading to some surface oxidation but also to some internal oxidation of Sn. The internal oxidation layer is about 10 micrometers thick and contains a large density of elongated SnO₂ particles. The crystallographic structure and the orientation relationship with the matrix and the growth direction were determined by conventional and high resolution TEM. SnO₂ particles were also analyzed by STEM-EDS and EELS. Then, a special emphasis was given on Cu/SnO₂ interfaces thanks to HAADF

atomic scale STEM. These experimental data seem to indicate that the interface is covered by an oxygen rich layer. It is assumed that this layer could be a fast diffusion path for oxygen atoms coming from the surface, leading to the peculiar growth of SnO₂ particles.

Titanium: Advances in Processing, Characterization and Properties: General Abstracts

Sponsored by: The Minerals, Metals and Materials Society, TMS Structural Materials Division, TMS: Titanium Committee
Program Organizers: Adam Pilchak, US Air Force Research Laboratory; Christopher Szczepanski, US Air Force Research Laboratory; Vasisht Venkatesh, Pratt & Whitney

Thursday AM

March 15, 2012

Room: Oceanic 3

Location: Dolphin Resort

Session Chair: Alexander Donchev, Dechema

8:30 AM

Efficient Oxidation Protection of Ti- and TiAl-alloys by Fluorine Treatments: *Alexander Donchev*¹; Michael Schütze¹; Rossen Yankov²; Andreas Kolitsch²; ¹DECHEMA; ²HZDR

Ti-alloys suffer from high oxidation rates and oxygen uptake during exposure in oxidizing environments at elevated temperatures above approximately 600°C. TiAl-alloys have the same problem due to the insufficient oxidation resistance at temperatures above 850°C. The use of these alloys is hence limited. The fluorine effect is a very promising way to improve the oxidation resistance of TiAl-alloys. Defined amounts of fluorine in the surface zone of TiAl-components change the oxidation mechanism. A protective alumina layer is formed which prevents further oxidation and subsequently allows the use of this new alloy family in several high temperature applications. The Al-content of standard Ti-alloys is not enough to get the fluorine effect to operate but after Al-enrichment of the surface zone a subsequent fluorination leads to the same results. In this paper results of oxidation tests of untreated and treated Ti- and TiAl-alloys will be presented and their behavior compared.

8:50 AM

Characteristics and Wear Performance of Nitrided Ti6Al7Nb: *Farid Syahjani*¹; ¹Istanbul Technical University

Samples of a Ti6Al7Nb were treated by gas nitriding for 3,5,7 and 12 h at 1120 °C. Gas nitriding provided formation of TiN layer whose hardness and thickness changed with respect to nitriding time. The titanium nitride layer exhibited excellent wear resistance along with a lower coefficient of friction against alumina ball under dry sliding conditions when compared to the as-received state.

9:10 AM

Characterization of Texture Development in Multi-Layered Ti-Al-Nb Sheets Processed by Accumulative Roll Bonding at Different Rolling Speeds: *Liming Zhou*¹; Viola Acoff¹; ¹The University of Alabama

The influence of rolling speed on texture development in multilayered Ti-Al-Nb processed by accumulative roll bonding (ARB) was studied in this paper. The process of ARB followed by annealing has proven to be a high efficiency method to manufacture gamma-based titanium aluminide sheet materials. Unlike thermal activities and kinetics associated with this process, heterogeneous distribution of the anisotropic texture characteristics is still unclear. In this investigation, the Ti layers in the as-cold rolled sheets were characterized using a layer by layer approach. Both bulk and microtexture analyses using X-ray diffraction, electron backscattered diffraction (EBSD) and TEM were employed to characterize the development of texture as a function of rolling speed. Results indicate that texture intensity variation not only exists for variation of rolling speed and deformation ratio but also suggests different dominant texture compared with conventional rolling results of Ti slab.



TMS 2012

141st Annual Meeting & Exhibition

THURSDAY AM

9:30 AM

Ti-TiAl₃ Metallic-Intermetallic Laminate Composites Processed Using Accumulative Roll Bonding: *Derrick Stokes¹; Xiu-Ren Bu²; Jennifer Conway¹; Stan Jones¹; Viola Acoff³; ¹The University of Alabama; ²Clark Atlanta University*

Metallic-Intermetallic Laminate Composites (MLCs) perform well in structural applications because they can withstand high tensile stresses when load is applied in the laminate direction. MLCs are commonly produced in industry, but there are issues with the current manufacturing process. In this study, MLCs are processed using accumulative roll bonding (ARB) of alternating layers of pure titanium and aluminum foils. After stacking, the foils are subjected to annealing. During annealing, the desired MLC is processed from the transformation that occurs from diffusion which promotes the transformation for pure titanium and aluminum to alternating layers of Ti and TiAl₃. Since the Ti-TiAl₃ MLCs made by this process are prime candidates for use in military applications, especially in the area of ballistics, they will be subjected to perforation testing using a method developed by researchers at The University of Alabama. This study will provide information that relates MLC structure to mechanical properties.

9:50 AM

Composition Analysis of Diffusion Bonded γ -TiAl Intermetallic:TiAlV Alloy Interface by Using STEM: *Sivagnanapalani P¹; Gouthama .¹; M Sujata²; ¹IIT Kanpur; ²National Aerospace Laboratories*

Diffusion bonding occurs when two similar or dissimilar materials are brought together under the application of pressure and temperature for sufficient time. In the present study, diffusion bonding of γ -TiAl intermetallic with Ti-6Al-4V alloy is carried out in high vacuum. The diffusion bonding is performed at temperatures of 800°C and 850°C under the constant pressure of 40MPa and at varying time. The diffusion bonded region is analysed by Scanning transmission electron microscope (STEM). From the results obtained, the diffusion bonded region is found to be a fairly extended junction zone of few micrometers width. From EDS results obtained, some regions were rich in aluminium and some regions are rich in vanadium. The compositional variation across the interface is not gradual but rather abrupt. The observations are discussed in the light of the solid solubility of variation element in different phases, phase equilibria and phase transformation characteristics of the materials involved.

10:10 AM

Effect of Erbium Addition on Microstructure of As-Cast Ti-22Al-25Nb Alloy: *Jingru Dai¹; Huimin Lu¹; Zhijin Cai¹; ¹Beihang University*

The rare earth metal erbium was added to ternary Ti-22Al-25Nb(at.%) alloys. This work investigated effects of erbium on the microstructure of Ti₂AlNb based alloy and the morphologies of rare earth-rich phases by XRD, OM, SEM, TEM and EDS. It was found that the grain size of this orthorhombic intermetallic alloy can be greatly refined by Er additive; the grain size of Ti-22Al-25Nb was in the range of 250-1200 μ m, while the materials containing erbium consisted of grain size of as fine as approximately 40 μ m, and the grain size was more uniform; Adding Er to the Ti-22Al-25Nb alloy yields precipitates of rare earth-rich phases, which mainly distributed in grain boundaries in the shape of net, and some ellipsoids and clavate precipitates were also observed within the grains.

10:30 AM Break

10:40 AM

Titanium Coatings Using Cold Spray: *Phillip Leyman¹; Rob Hrabec²; Brian James³; Christian Widener⁴; ¹Army Research Laboratory; ²H.F. Webster Inc.; ³GS-12, Supervisor AF Engineering Technical Services; ⁴South Dakota School of Mines and Technology*

Department of Defense (DOD) aircraft have been experiencing a significant chaffing problem of titanium hydraulic tubing resulting in significant cost in maintenance man-hours and reduction in operational readiness rates. The U.S. Army Research Laboratory has developed a

cold spray process that deposits a fully dense adherent titanium coating on titanium hydraulic tubing to either repair the already chaffed area or provide additional wear surface on new titanium tubing to extend the lifetime of the tubing. The deposition characteristics of titanium coatings deposited by cold spray process using helium gas were evaluated. The microstructure of the feedstock powders and deposited coatings were examined using optical and scanning electron microscopy. The characteristics of the cold spray titanium coatings were evaluated using density, hardness and bond strength measurements. Due to work hardening via plastic deformation induced by cold spraying, the titanium coatings have twice the hardness of wrought titanium.

11:00 AM

Novel Surface Coating Techniques for Titanium Alloys: *Mingxing Zhang¹; Shoumou Miao¹; ¹The University of Queensland*

Two novel surface coating techniques for titanium alloys have been developed aiming at effective improvement of the surface durability of Ti alloys. One is the refined packed powder diffusion coating (PPDC) approach, which is simple, reliable and low cost. The PPDC treatment leads to formation of composite coating with thickness varying from 100 μ m to 1500 μ m depending on the process. Compared with the substrate, the PPDC coating offers high wear resistance, high corrosion resistance and extremely high oxidation resistance at temperature up to 1000°C, which is comparable with Ni-based superalloys. Thus, the PPDC treatment makes it possible to partially replace the very expensive superalloys with coated Ti alloys in aeronautical industry. Another is a low coat nitriding process that produces up to 100 μ m thick TiN layer on Ti alloy substrate, which significantly increases the wear resistance of the components by 3 to 4 order magnitude.

11:20 AM

Fracture Behaviors of TiN and TiN/Ti Multilayer Coatings on Ti Substrate during Nanoindentation

: Yong Sun¹; Cheng Lu¹; Anh Kiet Tieu¹; Yue Zhao¹; Hongtao Zhu¹; Kuiyu Cheng¹; Charlie Kong²; ¹University of Wollongong; ²University of New South Wales

TiN monolayer and TiN/Ti multilayer thin films were deposited on commercially pure Ti substrates using a filtered arc deposition system (FADS). Surface topography and chemical composition have been characterized by atomic force microscopy (AFM) and X-ray diffraction (XRD), respectively. Fracture properties of coatings induced by nanoindentation have been investigated. Focused ion beam (FIB) and transmission electron microscopy (TEM) were used to identify the fracture modes. It was found that the TiN/Ti multilayer coating exhibited a higher pop-in force, which indicated good film ductility. Transmission electron microscope (TEM) observation showed that the small bending crack was the dominant crack in the TiN/Ti multilayer coating. The Ti layer shows that it could efficiently suppress the crack propagation, which was responsible for the improved ductility of the TiN/Ti multilayer coating.

11:40 AM

Deformation Mechanism in Nanoindentation of Ti63.375Fe34.125Sn2.5 Alloy: *Kuiyu Cheng¹; Cheng Lu¹; Kiet Tieu¹; Laichang Zhang²; Yong Sun¹; ¹University of Wollongong; ²The University of Western Australia*

Ti63.375Fe34.125Sn2.5 alloy was fabricated by arc melting. In this study nanoindentation technology has been used to investigate the mechanical properties of the main component phases (TiFe and β -Ti). It has been found that the β -Ti and the TiFe phases have close values of Young modulus and hardness. The cross section beneath the indent was cut out by focus ion beam (FIB) and analysed by transmission electron microscopy (TEM). It was found that the high strength and limited plasticity of Ti63.375Fe34.125Sn2.5 alloy are related to the interaction between dislocation and phase boundary. Phase boundaries stop the dislocation movement in most simulations. Dislocation only can pass through phase interfaces when the conjoint β -Ti and the TiFe phase are in particular orientation relationships.

T.T. Chen Honorary Symposium on Hydrometallurgy, Electrometallurgy and Materials Characterization: Characterization

Sponsored by: The Minerals, Metals and Materials Society, TMS Extraction and Processing Division, TMS: Hydrometallurgy and Electrometallurgy Committee, TMS: Materials Characterization Committee

Program Organizers: Shijie Wang, Rio Tinto Kennecott Utah Copper; J. E. Dutrizac, CANMET; Michael Free, University of Utah; J. Y. Hwang, Michigan Technological University; Daniel Kim, Rio Tinto Kennecott Utah Copper

Thursday AM
March 15, 2012

Room: Oceanic 5
Location: Dolphin Resort

Funding support provided by: Rio Tinto Kennecott Utah Copper, ASARCO, and Freeport McMoRan

Session Chair: Jaroslaw Drellich, Michigan Technological University

8:30 AM

Characterization of Nanocrystalline SnO₂:F Thin Films Prepared by the Spray Pyrolysis Technique: Shadia Ikhmayies¹; ¹Al Isra University

Nanocrystalline fluorine-doped tin oxide SnO₂:F thin films were prepared by the spray pyrolysis (SP) technique on glass substrates. The films were characterized by using X-ray diffraction (XRD), scanning electron microscope (SEM) observations, X-ray dispersive spectroscopy EDX and transmittance measurements. X-ray diffraction patterns revealed the nanocrystalline nature of the films where the grain size was estimated from Sherrer formula. SEM micrographs showed that the films are uniform and totally covered with the material and they confirmed the nanocrystalline nature of the films. The absorbance was deduced from the transmittance measurements and its first derivative was used to estimate the optical bandgap energy. Bandgaps larger than the bandgap of the bulk SnO₂:F were obtained which is evidence on the presence of quantum dots. The hyperbolic band model was used to estimate the radii of the nanocrystallites. A comparison between the results from the different methods was performed.

8:50 AM

Characterization of the Orthotropic Elastic Constants of a Micronic Woven Wire Mesh through Experiments and Modeling: Steven Kraft¹; Ali Gordon¹; ¹University of Central Florida

Woven structures are steadily emerging as excellent reinforcing components in composite materials. Metallic woven wire mesh materials in particular display good ductility and relatively high strength and resilience. While use of this class of materials is rapidly expanding, a significant gap in property characterization still remains. Through the use of uniaxial tensile experiments, and 3D meso-scale finite element modeling, this research classifies the orthotropic material properties of a representative twill-dutch woven wire mesh. Digital Image Correlation (DIC) methods, along with the meso-scale model, are employed to investigate the relationship between local and global elastic strain accumulation, and evidence of significant elastic damage in this material is displayed.

9:10 AM

Complex Impedance Plots of CdS:In Thin Films Prepared by the Spray Pyrolysis Technique: Shadia Ikhmayies¹; Riyad Ahmad-Bitar²; ¹Al Isra University; ²University of Jordan

Cadmium sulfide thin films were prepared on glass substrates by the spray pyrolysis technique at a substrate temperature of $T_s = 490$ °C. Some of the films were etched by HCl in distilled water, others were heat treated in nitrogen atmosphere, and another set of films were first etched by HCl thin annealed. Room temperature impedance spectroscopy measurements on the films were performed using coplanar geometry in the dark and room

light in the frequency range 20 Hz to 1 MHz. The experimental data was represented by the complex plane diagrams and showed one well-defined semicircle in the high frequency region. Hence the equivalent circuit that models the CdS:In thin films was found to be a single RC circuit, which indicates the bulk conduction through the grains. The influence of treatments on the electrical properties was investigated.

9:30 AM

Characterization of Mexico Magnetic Concentrate Samples for Trace Elements Ni, Cu, Zn, S and P: Mingming Zhang¹; ¹ArcelorMittal Global R&D

Magnetic concentrate samples from Mexico were characterized by chemical, X-ray diffraction (XRD), optical microscopy (OM) and scanning electron microscopy (SEM) methods. The objective of this work is to investigate the occurrence of nickel, copper, zinc, sulfur and phosphorus in these samples and identify their origin and associations with iron minerals. The results indicated that magnetite is the major iron oxide mineral with hematite as a second phase based on the OM and XRD studies. Pyrite, chalcopyrite and bravoite are major sulfide minerals. Trace amounts of apatite, wardite, giniite and vivianite were identified by SEM and XRD. Microscopic studies also indicated that most of the sulfide grains in the mineral sample are present either as liberated fine particles (<10 microns) or as inclusions within the magnetite and hematite grains. XRD studies confirmed the microscopic findings. Copper, nickel, and zinc are mainly present as chalcopyrite, bravoite, and franklinite in trace amount, respectively.

9:50 AM Break

10:10 AM

Preparation and Characterization of High-Magnetization Microspheres of Fe₃O₄ Encapsulated with SiO₂ and TiO₂ Layers: Nan Zhang¹; Gaifeng Zue¹; Shangchao Liu¹; Benquan Fu¹; ¹Research and Development Center of Wuhan Iron & Steel Group Corp.

The high-magnetization Fe₃O₄@SiO₂@TiO₂ microspheres were prepared. They were characterized by FTIR spectroscopy, transmission electron microscopy and scanning electron microscopy. These high-magnetization microspheres could be readily dispersed by shaking while they could be fast separated from the aqueous solution simply by applying an external magnetic field. The two shells of SiO₂ and TiO₂ protected the iron oxide core well and the microspheres were stable in acid and base solution. Therefore, they have a good potential in applications such as phosphopeptides enrichment and photocatalytic activity.

10:30 AM

Characterization of Amorphous Vacuum-Evaporated SnO₂ Thin Films: Shadia Ikhmayies¹; ¹Al Isra University

Tin oxide (SnO₂) thin films of thickness in the range 100-700 nm were prepared on glass substrates by vacuum evaporation at ambient temperature. The films were characterized by transmittance measurements, X-ray diffraction (XRD), scanning electron microscope (SEM) observations and energy dispersion X-ray analysis (EDX). It is found that the films have high transmittance and non sharp absorption edge. XRD diffractograms showed that the films are amorphous and the SEM micrographs showed that the surfaces are smooth, uniform and well covered with the material. The EDX analysis showed that the films are rich in oxygen. Indirect optical bandgap energy and Urbach tailing in the bandgap was observed and the width of the tail which is related with disorder and localized states was estimated.

10:50 AM

Preparation of β -Diketone Modified Silica Gel and its Application to the Removal of Heavy Metal Ions from Industrial Wastewater: Nan Zhang¹; Gaifeng Xue¹; Lei Zhang¹; Pu Liu¹; Lina Wang¹; ¹Research and Development Center of Wuhan Iron & Steel Group Corp.

A novel β -diketone modified silica gel was synthesized. The prepared material was characterized by diffuse reflectance FTIR spectroscopy and it was used for the adsorption of heavy metal ions in industrial wastewater.



The main parameters affecting the sorption of heavy metal ions, including pH, water flow rate and temperature, have been investigated in detail. Under the optimized operating conditions, most of the heavy metal ions could be removed. The material could be simply regenerated by acid. The method is rapid, selective, economical and applicable to the removal of heavy metal ions in industrial wastewater.

11:10 AM

Elastic Modulus and Density Dependence on the Diameter of Piassava Fibers: *Felipe Lopes*¹; Alice Bevitori²; Isabela Silva²; Renan Carreiro²; Denise Nascimento²; Sergio Monteiro²; ¹IME; ²UENF

Natural fibers obtained from plants have increasingly been used as reinforcement of polymeric composites in engineering applications. This is the case of the fiber extracted from the piassava palm tree, a native of the southeast region of South America and since long time used in simple items like brooms and brushes. Recently it was reported that the tensile strength of the piassava fiber varied inversely with the equivalent diameter. Following that previous work, it was investigated the elastic modulus and the density dependence on the diameter of stiffer piassava fibers of the *Attalea funifera* specie. Precise measurements with profile projector and Weibull analysis of the experimental results indicated that both the elastic modulus and the density of piassava fibers also follow an inverse correlation with the diameter. Scanning electron microscopy observation, of the microstructure and fracture surface showed that defects and participation of microfibrils are responsible for this correlation.

T.T. Chen Honorary Symposium on Hydrometallurgy, Electrometallurgy and Materials Characterization: Processing and Properties II

Sponsored by: The Minerals, Metals and Materials Society, TMS Extraction and Processing Division, TMS: Hydrometallurgy and Electrometallurgy Committee, TMS: Materials Characterization Committee

Program Organizers: Shijie Wang, Rio Tinto Kennecott Utah Copper; J. E. Dutrizac, CANMET; Michael Free, University of Utah; J. Y. Hwang, Michigan Technological University; Daniel Kim, Rio Tinto Kennecott Utah Copper

Thursday AM
March 15, 2012

Room: Oceanic 4
Location: Dolphin Resort

Funding support provided by: Rio Tinto Kennecott Utah Copper, ASARCO, and Freeport McMoRan

Session Chair: JY James Hwang, Michigan Technological University

8:30 AM

Leaching of Lithium Cobalt Dioxide Using Citric-Thiosulfate Solutions: *Alejandro Alonso*¹; Gretchen Lapidus-Lavine¹; Lizeth Alvarado¹; ¹Universidad Autonoma Metropolitana

Cobalt and lithium recovery from spent Li-ion secondary batteries is of great interest due to the high value of both metals and the low proven reserves for lithium. Up until now, the standard method uses first the deactivation and crushing of batteries; the spinel (CoLiO₂) from the battery cathode is then leached using a highly acid solution, such as 1.5 to 2.0M HCl or H₂SO₄, in a temperature range from 120°C to 250°C. Once the cobalt is separated by electrodeposition and lithium by precipitation, large amounts of carbonate are needed in order to precipitate lithium carbonate at alkaline pH values. In the present work, citric-thiosulfate solutions are used to leach the spinel at room temperature, by reducing the cobalt-lithium dioxide and stabilizing cobalt (II) as cobalt citrate and lithium (I) as Li⁺ at pH 5, with recoveries of about 99% for both metals.

8:50 AM

Hydrometallurgical Purification from Leach Liquor of Printed Circuit Board with Cyanex 272: *Adriana Santanilla*¹; Viviane Tavares de Moraes¹; Jorge Alberto Soares Tenorio¹; Denise Crocce Romano Espinosa¹; ¹Polytechnic School of University of São Paulo

Increasing volumes of solid waste are generated worldwide, due to the continuous technological advances, the electronic scrap is part of these waste, requiring the study of recycling processes to stimulate this activity or the reuse of its components. The separation of nickel from sulphate leach solution, which also containing iron, zinc and aluminium was carried out using bis-(2,4,4-trimethylpentyl) phosphinic acid (Cyanex 272) as extractant, in order to determinate the effects of pH and temperature. The number of stages required for extraction was also assessed; the results showed that the ions metals extraction increased with the pH increasing, on the other hand, with the increasing temperature was found a behavior no favorable for all metals, however, under conditions used in this paper the purification of solution containing nickel was possible.

9:10 AM

Leaching of Chalcopyrite Concentrate with Organic Ligand Compounds: *Oscar Solis-Marcial*¹; Gretchen Lapidus-Lavine¹; ¹Universidad Autonoma Metropolitana-Iztapalapa

Oxidative dissolution of copper from refractory phases, such as chalcopyrite, represents a technological challenge that has occupied hydrometallurgists for more than half a century. Innumerable processes have been suggested, but the majority operates at high temperatures or employ corrosive media. Recent studies have revealed that the origin of this refractory nature is the formation of passivating phases of iron(III) or copper. One option is to add non-corrosive ligands that complex these metal ions, facilitating their dissolution. In the present work, the effect of acetone in sulfuric acid solutions was studied, first on chalcopyrite carbon paste electrodes using cyclic voltammetry, where greater reactivity was observed in its presence. Later, leaching tests with hydrogen peroxide, cupric sulfate, ozone and mixtures of these, as oxidants, were performed. High levels of extractions were achieved in three hours at 50°C. Solid residues contained the iron in the form of oxides (Fe₂O₃ and FeOOH).

9:30 AM

The Electrochemical Behavior of Electro-Deoxidation Process of Ilmenite Concentrate in Molten Salt: *Xuyang Liu*¹; Meilong Hu¹; Chenguang Bai¹; Xuewei Lv¹; ¹Chongqing University

The electro-deoxidation process of titanium concentrate in molten salt was studied by cycle voltammetry and AC impedance spectrum. The result of cycle voltammetry is consistent with AC impedance spectrum. The result showed that the electro-deoxidation process of titanium concentrate consists of two processes. One step is that Fe is firstly reduced from titanium concentrate. The second reaction is the decomposition of TiO₂. Intermediate product is CaTiO₃. In the low voltage, the electrochemical reaction is the main step. With the potential increasing, the diffusion of ion is the main rate control step of the electro-deoxidation of FeTiO₃.

9:50 AM Break

10:10 AM

Vanadium Extraction from High Calcium-Content Vanadium Slag by Calcification Roasting: *Hong-Yi Li*¹; Ning Wang¹; Bing Xie¹; ¹Chongqing University

Compared to traditional sodium roasting, calcified roast inhibits chlorine pollution. Especially, vanadium extracting technique based on calcified roast is suitable to high silicon low vanadium slag. In this report, V₂O₅ was extracted from vanadium slag by calcified roast followed by acid leaching and hydrolysis precipitation. In optimized conditions, the high silicon low vanadium slag was roasted at 850°C for 2 hours without CaO addition. The roasted materials was leached with 35 % H₂SO₄ in solid-liquid ratio of 1:5 (g/mL) at 95°C for 4 hours. The leaching rate of vanadium was up to 97.66%. These results are instructive to V₂O₅ production in industry.

10:30 AM

The Kinetic Investigation of the Dissolution Of Powellite in Oxalic Acid Solutions: *Sedat Ilhan*¹; Ahmet Kalpakli¹; Cem Kahruman¹; Ibrahim Yusufoglu¹; ¹Istanbul University

In this study, the effects of oxalic acid concentration, temperature, stirring rate and particle size on the dissolution rate of synthetically prepared calcium molybdate and concentrated scheelite ore which includes powellite as contamination were investigated. Calcium molybdate dissolves in oxalic acid solutions as series – parallel type reaction. In the first reaction step, calcium aqua oxalato molybdate is formed as complex chelate intermediate product. In the second reaction step, molybdic acid formed during the slow hydrolysis of calcium aqua oxalato molybdate reacts rapidly with oxalic acid by forming the polymeric hydrogen oxalate dimolybdate complex chelate as end product. The activation energies and frequency factors for both steps were calculated.

10:50 AM

Metallurgical Characterization of Waspaloy Presenting Variations on Chemical Composition, Grain Size, and Hardness: *Miguel Neri*¹; Alberto Martinez -Villafañe¹; Caleb Carreño¹; Octavio Covarrubias-Alvarado²; Alma Gonzalez-Escarcega¹; ¹CIMAV, S.C.; ²FRISA AEROSPACE S.A. DE C.V.

Waspaloy is a super alloy used to manufacture some aeronautical parts subjected to high temperatures and stresses, during it thermo-mechanical processing cracks are generated, causing that some parts will be rejected during their processing. In order to determine the causes of these cracks, this alloy was characterized using techniques such as Chemical Analysis, Optical Microscopy, Scanning Electron Microscopy, and EDX analysis. Heterogeneous grain size on the microstructure causes a non-uniform strain distribution on these parts, and may originate cracks on zones with different grain sizes.

11:10 AM

Recent Trends in the Processing of Complex Sulphide Ores: *Sarveswara Rao Katragadda*¹; ¹(Retd.) IMMT (CSIR)

In view of increasing importance to process lean grade ores as potential future resources, efforts are made worldwide to develop suitable technologies for recovery of both nonferrous, base and precious metals. There are various types of lean grade ores and present in many countries. Gradually, the mineral reserves for production of the metals have undergone complex changes with regards to their grades and particularly the physical and chemical properties of minerals to be separated from each other. So, there is a need for upgrading the existing technologies to recover metal values from the ores that are otherwise unutilized. Accordingly, an overview of different existing types of mineral resources and economical processes based on ore horizons, consumption of energy and reagents and environmental concerns is made in this paper, along with a summary of metallurgical and engineering challenges to be overcome when implementing alternate technologies.

11:30 AM

Biosorption Characteristics of Pb(II) from Aqueous Solution onto Poplar Cotton: *Kai Huang*¹; Shuanglong Du¹; Ting Luo¹; Tao Gui¹; Yifan Xiu¹; Hongmin Zhu¹; ¹University of Science and Technology Beijing

Poplar cotton, a cellulosic material, was found to adsorb the metals ions effectively. In present study, the biosorption characteristics of Pb(II) onto poplar cotton, were evaluated as a function of pH, contact time, biomass dosage, initial concentration and temperature. Within the pH range investigated (1.0-6.0), the optimal pH value suitable for the uptake of Pb(II) was determined. The maximum adsorption capacity obtained from the Langmuir model is around 0.52 mol kg⁻¹ for the poplar cotton sorbent. Equilibrium time is 60 min for the studied concentrations. Above results suggest that the poplar cotton can be directly used as an effective and low-cost biosorbent for removal of Pb(II) from aqueous solution.

Ultrafine Grained Materials VII: Applications and Transitions

Sponsored by: The Minerals, Metals and Materials Society, TMS Structural Materials Division, TMS/ASM: Mechanical Behavior of Materials Committee, TMS: Nanomechanical Materials Behavior Committee, TMS: Shaping and Forming Committee

Program Organizers: Suveen Mathaudhu, U.S. Army Research Office; Xiaoxu Huang, Risø National Laboratory for Sustainable Energy, Technical University of Denmark; Hyoung Seop Kim, POSTECH; Terence Langdon, University of Southern California; Terry Lowe, Manhattan Scientifics, Inc.; Ruslan Valiev, Ufa State Aviation Technical University; Xiaolei Wu, Institute of Mechanics, Chinese Academy of Sciences; Michael Zehetbauer, University of Vienna

Thursday AM

March 15, 2012

Room: Swan 5

Location: Swan Resort

Session Chairs: Terence Langdon, University of Southern California; Aibin Ma, North Carolina State University; Suveen Mathaudhu, U.S. Army Research Office; Indranil Roy, Schlumberger

8:30 AM Introductory Comments Young Scientist Award Presentation**8:35 AM Invited**

Exceptional Mechanical and Functional Properties of Ultrafine-Grained NbZr Biomedical Alloys: *Ibrahim Karaman*¹; Hans Maier²; Gencaga Purcek³; Felix Rubitschek²; Thomas Niendorf²; ¹Texas A&M University; ²University of Paderborn; ³Karadeniz Technical University

Niobium–1.3 wt.% zirconium (NbZr) alloys demonstrate exceptional mechanical properties in UFG condition. In this talk, we will summarize the unconventional mechanical and functional properties of UFG NbZr samples that were processed using ECAP at room temperature. Monotonic tensile and low-cycle fatigue responses and the corrosion fatigue behavior in simulated body fluid (SBF) will be reported. The room temperature processing resulted in UFG microstructure, high density of high angle grain boundaries, a favorable combination of high strength and ductility with superior biocompatibility and excellent corrosion resistance. The corrosion resistance of UFG NbZr was similar to that of Ti-6Al-4V. High-cycle fatigue tests showed no alteration in the crack initiation behavior due to the SBF environment, and absence of pitting and corrosion products. Internal oxidation of UFG NbZr formed nano-ZrO₂ precipitates on the surface, significantly intensified the surface hardness without deterioration of the surface quality, and thus remarkably improved the fatigue performance.

8:55 AM

Electrochemical Corrosion of Bulk Cryomilled UFG Al5083 in Contrast to its Coarse Grained Counterpart in Aerated 3.5wt% NaCl Solution: *Indranil Roy*¹; John Meng²; Enrique Lavernia³; Farghalli Mohamed⁴; ¹Schlumberger; ²Honeywell Corrosion Solutions; ³University of California, Davis; ⁴University of California, Irvine

In this study bulk cryomilled ultrafine-grain (UFG) Al5083 and its coarse grain polycrystalline (CGP) commercial counterpart were exposed to aerated 3.5-wt% NaCl solution at 120F for various holding times. To compare their electrochemical corrosion behavior(s) linear polarization resistance and cyclic potentiodynamic polarization experiments were also carried out in the same aerated solution. Deep pits were observed on the commercial Al5083 alloy in contrast to numerous microscopic pits manifested in the UFG-material. Uniaxial tensile tests performed on specimens of UFG-Al5083 exposed to the same neutral halide solution for various holding times exhibited far better performance in contrast to catastrophic failures of CGP Al5083. In line with recent publications [1,2] that nano-materials perform better than their CGP counterparts, our results affirm that grain refinement abets the corrosion performance in contrast to their CGP counterparts. 1. Mishra et al., Corros. Sci. 46, 3019-3029 (2004). 2. Qiu J., Mater. Sci. Forum, 437-438, 211-214 (2003).



TMS 2012

141st Annual Meeting & Exhibition

THURSDAY AM

9:10 AM

Microstructural Aspects of Enhancing Strength and Ductility of Ultra-Fine Grained Ti Rods Processed by ECAP-Conform: *Irina Semenova*¹; *Georgy Raab*¹; *Alexander Polyakov*¹; *Ruslan Valiev*¹; *Terry Lowe*²; ¹Ufa State Aviation Technical University; ²Manhattan Scientifics

This work is focused on understanding the strength and ductility of the UFG titanium processed by ECAP-Conform with further drawing. UFG materials can have decreased ductility due to low strain hardening rate and strain localization. This resulted from the low dislocation storage efficiency associated with small grains and very high dislocation densities. By examining specific combinations of ECAP-Conform and drawing we have determined that size and shape of grains, substructure formation, and grain boundary state are the main microstructural parameters that determine the strength and ductility in UFG Ti. For example, for the UFG Ti Grade 4 the contribution to increase of uniform tensile elongation is made by equiaxed shape of grains with low density of lattice dislocations, high-angle misorientation of boundaries and grain-boundary segregations. The correlations of microstructure with high strength and ductility further allowed us to define the main requirements to increase the fatigue resistance of UFG titanium.

9:25 AM Invited

Potential of UFG Materials as High Performance Penetrator Materials: *Kyung-Tae Park*¹; *Lee Ju Park*²; *Hyung Won Kim*²; *Chong Soo Lee*³; ¹Hanbat National University; ²Agency for Defense Development; ³POSTECH

UFG materials possess high potential as high performance penetrator materials. Shear localization, one of the main deformation characteristics of UFG materials at room temperature, enhances the self-sharpening effect which is essential to kinetic energy penetrators. High strain rate superplasticity of UFG materials is to be highly possible to improve metal jet formability of chemical energy penetrators. In this study, the effects of UFG morphology on shear formability of a 4130 steel were examined. A lamellar UFG structure exhibited better shear formability than the equiaxed UFG one. In addition, the metal jet formability of UFG OFHC Cu will be compared to that of coarse grained counterpart. The enhanced shear formability and metal jet formability of UFG materials are to be discussed in view of their microstructural characteristics. The present preliminary study may provide an informative guidance for early industrial application of bulk UFG materials.

9:45 AM

Study of a New SPD technique: High Pressure Tube Twisting (HPTT): *Roxane Arruffat*¹; *Mandana Arazaghi*²; *Arnaud Pougis*¹; *Jean Jacques Fundenberger*¹; *Laszlo Toth*¹; ¹University Paul Verlaine; ²Institut PPRIME, UMR 6617 CNRS,

The new Severe Plastic Deformation (SPD) technique was invented in 2008. This process designated as High Pressure Tube Twisting (HPTT), is a continuous process for grain refinement in bulk metallic materials with tubular geometry. It consists of placing a mandrel into the tube before applying an axial compression directly on the tube confined on both sides to produce high hydrostatic pressure. The tube is then twisted by an external torque with the help of the friction force generated by the hydrostatic pressure. In the present study, experiments were conducted on Copper, Aluminium (commercially pure and AA6061) and IF Steel to the different amounts of shear deformation. The ultra-fine grained structures produced with HPTT are confirmed using transmission electron microscopy and their microstructure and mechanical properties were evaluated. Microstructural evolution is studied by electron backscattered diffraction and texture measurements were carried out using both X-ray and the EBSD technique.

10:00 AM

SPD Procedure and High Performance of Ultrafine-Grained Cu-Mg Alloy for Electrical Railway: *Ai-Bin Ma*¹; *Chengcheng Zhu*¹; *Jinghua Jiang*¹; *Dan Song*¹; *Wenyong Xu*¹; ¹Hohai University

Continuous Con-form plus equal-channel angular pressing (EACP) was applied to produce ultrafine-grained Cu-Mg contact wire materials with high strength and good conductivity, aim to push back the catenary barrier of high-speed trains by maximizing the tension and improving the power delivery. Microstructure change and mechanical properties of Cu-Mg alloys after various severe-plastic-deformation (SPD) routes were investigated by microscopic analysis and tensile tests. The results show that the Cu-0.2wt% Mg samples after multi-pass ECAP at 473K obtain ultrafine grains with homogeneously distributed secondary phases, having obviously improved strength. The more passes of ECAP make the finer grains and the higher strength of Cu - 0.2 Mg alloy, but the strength increment of ECAPed alloys is appreciably lower with increasing ECAP temperature up to 673K. Grain refinement via continuous SPD procedures can endow Cu-Mg contact wire materials superior strength, high conductivity and anti-softening characteristics, which are advantageous to high-frequency electrification railway systems.

10:15 AM Break

10:30 AM

Twenty-five Years of Severe Plastic Deformation: Recent Developments in Evaluating the Degree of Homogeneity through the Thickness of Disks Processed by High-Pressure Torsion: *Megumi Kawasaki*¹; *Roberto Figueiredo*²; *Terence Langdon*¹; ¹Univ of Southern California; ²Federal Univ of Minas Gerais

The processing of disks by high-pressure torsion (HPT) leads to an inhomogeneous distribution in strain with a high strain around the perimeter of the disk and a zero strain in the center. Despite this apparent inhomogeneity, there are now many experiments showing that the hardness values on the surfaces of disks gradually evolve with increasing strain to give a high level of homogeneity. This report examines whether this high level of homogeneity extends also through the thickness of the disks or whether there are inhomogeneities within the vertical cross-sections. Results are presented for high-purity aluminum and a magnesium alloy as two representative materials showing different hardness characteristics.

10:45 AM

Anti-Corrosion Behavior of Ultrafine-Grained Al-26wt% Si Alloy Fabricated by ECAP: *Jinghua Jiang*¹; *Aibin Ma*²; *Dan Song*²; *Jun Shi*²; *Kaile Wang*²; *Donghui Yang*²; *Jianqing Chen*²; ¹hohai university; ²Hohai University

Grain refinement of hypereutectic Al-Si alloys, through severe plastic deformation (SPD), can endow its improved physicochemical properties and wider application in the automotive, aerospace and construction industries. Herein, Ultrafine-grained (UFG) Al-26wt.%Si alloy was achieved through multi-pass equal-channel angular pressing (EACP) procedure and subsequent tested in 3.5wt.%NaCl solution for electrochemical corrosion evaluation. The results show that the ECAPed alloy with more pressing passes obtains lower mass-loss ratios, nobler Ecorr and Epit, lower Icorr values and higher anode polarization. The increased corrosion resistance of the ECAPed alloy results from the homogeneous UFG structure with the breakage of brittle large primary silicon crystals, which is contributed to a higher pitting resistance. The oxidation product with improved adhesion force and protection efficacy can be formed more easily on UFG alloys, making UFG Al alloy from SPD more corrosion resistant.

11:00 AM

Ultrafine-Grained Thermoelectrics Processed by HPT Featuring Enhanced ZT Values: *Michael Zehetbauer*¹; Gerda Rogl¹; Peter Rogl¹; Ernst Bauer²; Daria Setman¹; Jelena Horky¹; Erhard Schafner¹; ¹University of Vienna; ²Vienna University of Technology

This lecture reports on processing of nanocrystalline thermoelectric p- and n-type skutterudites by High Pressure Torsion (HPT). Ultrafine grained materials were achieved by introducing many defects like interfaces, dislocations or point defects, making use of HPT advantages such as sustaining the samples' dimensions during processing, and providing an enhanced hydrostatic pressure preventing cracks. Both p- and n-type skutterudites were deformed by HPT at pressures 2-4 GPa and temperatures till 500°C resulting in an oriented lamellar nano-grained structure with crystallites of 30 nm in size, amorphous aggregates and an enhanced dislocation density. In comparison with ball milled / hot pressed skutterudites, the HPT samples exhibited a 3x smaller grain size and an 100x larger dislocation density, resulting in an 40%-decrease of thermal conductivity. Although the electrical resistivity is markedly higher in parallel with an only slightly higher Seebeck coefficient, HPT proved to enhance ZT values up to 30%.

11:15 AM Invited

Application of High-Pressure Sliding for Bismuth-Telluride Thermoelectric Materials: Kiyonari Tazoe¹; Kanako Mitarai¹; Takahiro Hayashi²; Shinji Munetoh¹; *Zenji Horita*¹; ¹Kyushu University; ²Yamaha Corporation

High-pressure sliding (HPS) is a newly developed process of severe plastic deformation. This process is similar to high-pressure torsion (HPT) as it is operated under high pressure but the difference is that HPS uses samples having a rectangular sheet shape while HPT uses with a disk or ring shape. In this study, HPS is applied to bismuth-telluride thermoelectric materials. Samples with dimensions of 1.3×2.95×64 mm³ were subjected to HPS under a pressure of 1 GPa at 773 K for sliding distances of 5, 10 and 15 mm with a sliding speed of 0.2 mm/s. Measurements of Vickers microhardness, electrical resistivity, Seebeck coefficient and thermal conductivity were carried out including microstructural observation and X-ray diffraction analysis. It is shown that the HPS processing leads to an improvement of thermoelectric performance of the materials.

11:35 AM

Application of High-Pressure Torsion to Ceramic-Based Materials: *Kaveh Edalati*¹; *Zenji Horita*¹; ¹Kyushu University

Ceramics are generally brittle materials at room temperature because of strong ionic or covalent bonding which makes the dislocations motion very difficult through the crystalline structure. This study shows that intense plastic deformation is feasible in ceramic-based materials such as alumina, zirconia and tungsten carbide at room temperature using high-pressure torsion (HPT). Several interesting phenomena were observed following the HPT processing of ceramics: dislocations generation, nanograins formation, allotropic phase transformations and decreasing the sintering time and temperature even when compared to those for hot isostatic pressing (HIP).

11:50 AM

Microstructure and Mechanical Properties of Thixomolded Mg Alloys After Thermomechanical Processing: *Bilal Mansoor*¹; Raymond Decker²; Sanjay Kulkarni²; Steve LeBeau²; Marwan Khraisheh¹; ¹Masdar Institute of Science and Technology, Abu Dhabi, UAE; ²Thixomat Inc.

Thixomolded Mg alloy sheets with fine grain size offer a favorable starting point to produce wrought Mg alloys with superior mechanical properties by severe deformation processing [1-2]. Following a similar approach a novel processing technique was developed by Thixomat Inc. to Thixomold then Thermomechanically Process (TTMP) to produce

wrought Mg alloy sheets with ultrafine grain size, improved creep resistance and higher specific stiffness and strength [2]. In this work, a detailed characterization of microstructure is carried out by optical and electron microscopy. Additionally, mechanical properties of TTMP processed AZ Mg alloys are studied by hardness and tensile tests. The microstructure and mechanical properties of TTMP material is also compared with commercial Mg alloys. The significant improvement in mechanical properties achieved after thermomechanical processing opens several avenues of research related to these materials.

12:05 PM Invited

Development of Nanostructured Coating via Electro-Chemical Method: *Young Gun Ko*¹; Dong Hyuk Shin²; ¹Yeungnam University; ²Hanyang University

The application of nanocrystalline solids has long been facilitated by the wide range of cutting edge techniques such as sol-gel, vapor condensation, mechanical milling, and chemical anodizing. At present, the nanostructured coating utilizing high energy plasma has been shown to possess unique and often enhanced materials properties in comparison to the cermet coatings via current technology. Now, the behavior of nanostructured materials subjected to plasma electrochemical coating was rendered complex by the choice of factors such as electrolyte, electric parameters, and cell atmosphere. Thus, it is essential to optimize the processing design which could lead to the achievement of excellent materials performance heretofore unattainable via conventional coatings. The present paper is to offer a general overview of recent progress in the area of high performance nanostructured coatings, paying much attention to underlying fundamental issues.

12:25 PM

Equal Channel Angular Extrusion of GLIDCOP for use in High-Field Pulsed Magnet Applications: Ryan Need¹; *David Mutnick*¹; Adriana Tudela¹; Weston Lee¹; David Alexander¹; Robert Field¹; Charles Swenson¹; ¹Los Alamos National Laboratory

High-field pulsed magnets are capable of producing fields of up to 96T. However, these fields create large mechanical and thermal stresses on the conducting wires. In this study, equal channel angular extrusion (ECAE) is evaluated as a potential processing route to create high strength, high conductivity materials for use in pulsed magnets. Alumina dispersion-strengthened copper alloys (tradename GLIDCOP) were subjected to 1 to 4 passes of ECAE by route BC. Mechanical properties were measured by means of quasi-static, uniaxial tensile testing. Electrical conductivity was quantified via the four point probe method. Microstructural evolution was evaluated by scanning electron microscopy (SEM) and electron backscatter diffraction (EBSD). Grain size refinement is posited as the primary mechanism for the observed changes in material properties. The performance of these materials is compared with other existing and proposed magnet conductors.

12:40 PM Concluding Comments

3rd International Symposium on High Temperature Metallurgical Processing: Pelletizing and Raw Materials Processing

Sponsored by: The Minerals, Metals and Materials Society, TMS Extraction and Processing Division, TMS: Energy Committee, TMS: Pyrometallurgy Committee

Program Organizers: Tao Jiang, Central South University; Jiann-Yang Hwang, Michigan Technological University; Patrick Masset, TU Freiberg; Onuralp Yucel, Istanbul Technical University; Rafael Padilla, University of Concepcion; Guifeng Zhou, Wuhan Iron and Steel

Thursday PM

March 15, 2012

Room: Southern II

Location: Dolphin Resort

Session Chairs: Ender Keskinilic, Atilim University; Guanghui Li, Central South University

2:00 PM

Developing Cost-Effective Air Separation Plants for the Mining and Mineral Processing Industry: *Goutam Shahani*¹; ¹Linde Engineering

Today, the mining and mineral processing sectors are being impacted by highly fluctuating supply – demand, extreme price volatility and tremendous market uncertainty on a world-wide basis. The market for many non-ferrous metals such as gold, nickel and copper has become very robust. This pattern is expected to continue for the foreseeable future. Mineral processing by smelting and various hydrometallurgical operations requires oxygen and oxygen enriched air. This provides greater thermal efficiency and improved emissions. While these processes can be based on air, the use of pure oxygen results in smaller equipment and more complete mineral recovery. Consumers of industrial gases (oxygen, nitrogen) in tonnage quantities have to make informed investment decisions in these uncertain economic times. Plant owners – operators need to carefully examine their current and future industrial gas needs in order to develop the most cost-effective industrial gas plant configuration.

2:15 PM

Effects of Sodium Salts-Modified Paigeite on Dephosphorization of High-Phosphorus Oolitic Hematite during Reduction Hematite during Reduction: *Guanghui Li*¹; Ting Lei¹; Tao Jiang¹; Mingjun Rao¹; ¹School of Minerals Processing and Bioengineering, Central South University

With the rapid development of the iron and steel industry, the iron ore supply can not meet the current demand for iron and steel industry in China, although large reserves of oolitic hematite have been discovered but with low iron grade (30% ~ 45%) and high phosphorus content (0.4% ~ 1.8%). Traditional processes for utilization of this ore are characterized as either high production cost or inefficient dephosphorization. In this study, the sodium salts-burdened paigeite was prereduced as an additive firstly, and then the intensified reduction roasting of oolitic with addition of the previous additive followed by magnetic separation was carried out. The type of sodium salts, the amount of sodium salt, and the effects of the reduction time and reduction temperature were investigated. A magnetic concentrate with iron grade of 91.37% and phosphorus content of 0.084% was obtained under the optimal condition.

2:30 PM

Study of Certain Parameters in Laboratory-Scale Smelting of Sivrihisar Laterite Ores of Turkey: *Ender Keskinilic*¹; Saed Pournaderi²; Ahmet Geveci²; Yavuz A. Topkaya²; ¹Atilim University; ²Middle East Technical University

Conventional ferronickel smelting has five main steps: Drying, calcination, prereduction, smelting and refining. In the scope of the current work, smelting experiments were conducted using Sivrihisar laterite ores (1.26% Ni) of Turkey. The ore samples previously subjected to drying, calcination and prereduction stages were smelted in alumina crucibles in a laboratory-scale horizontal tube furnace under argon atmosphere.

Smelting experiments were performed at 1500, 1550 and 1600 °C. The amount of excess coal used in prereduction step was another variable. Sivrihisar laterite ore is a limonitic one with low MgO composition. Therefore, MgO was added to the smelting charge as a flux. The effects of experimental variables on metal Ni content and slag composition were investigated.

2:45 PM

Dephosphorization Technology of High Phosphorus Oolitic Hematite in Rotary Hearth Furnace Direct Reducing Process: *Hongliang Han*¹; *Dongping Duan*¹; *Jiwei Zhao*¹; ¹Institute of Process Engineering, Chinese Academy of Sciences

In this study, physical, chemical and microscopic characteristics of high phosphorus oolitic hematite were investigated firstly. Based on which, the reduction mechanism of apatite in high phosphorus hematite was discussed. And the experiments of high phosphorus hematite used in the ‘solid state reduction by rotary hearth furnace + high-intensity magnetic separation’ and iron bead by rotary hearth furnace direct reduction processes were studied. The experiment results showed that high temperature, low basicity and high carbon content is conducive for the apatite in iron ore to reduce into molten iron, but not conducive to the removal of phosphorus. Through optimization of process parameters, dephosphorization rate of high phosphorus hematite is more than 60% by ‘Solid State Reduction Roasting+ High-intensity magnetic separation’ process while that is up to 80% by iron bead process. This study can provide theoretical and technical basis on economical and rational use of high phosphorus oolitic hematite.

3:00 PM

Effect of Basicity and MgO on the Pelletizing of Specularite Concentrate: *De Qing Zhu*¹; *Jinliang Zhang*¹; *Jian Pan*¹; *Zhao Qiang*; ¹Central South University

Burned-Magnesite and limestone were added to vary MgO contents and Basicity (CaO/SiO₂ ratio) of pellets for investigating their influences on the specular hematite pellets quality. At fixed MgO content, the addition of limestone don't effect on the quality of green pellets significantly. Burded-Magnesite addition plays a very important role on the quality of green pellets, especially on the cracking temperature, without burned-magnesite addition the cracking temperatures are about 400°C, but when adding burned-magnesite, the cracking temperature will be increased obviously. For preheated pellets, when the magnesite is added, the compressive strength will be decreased. For roasted pellets, without burned-magnesite, the calcium additives can form binding phase of calcium-ferrite, and suitable liquid phase will improve recrystallization of hematite, but excessive liquid will destroy the structure of pellets, so the compressive strength of pellet increases firstly and then decreases, when adding burned-magnesite, the strength will increase as the Basicity increases.

3:15 PM

Effects of MHA Binder on Roasting Behaviors of Oxidized Pellets from Specularite Concentrate: *Youlian Zhou*¹; *Yuanbo Zhang*¹; *Tao Jiang*¹; *Guanghui Li*¹; *Daoyuan Zhang*¹; ¹Central South University

Modified humic acid (MHA) has been developed by Central South University and authorized in China. It has reported that MHA is an effective binder for oxidized pellets prepared from specularite concentrates with poor hydrophilicity and ballability as well as bad high-temperature reactivity. In this study, effects of MHA binder on roasting behaviors of the specularite pellets are studied by chemical analysis, optical microscopy, XRD, etc. MHA is an organic binder, containing much carbon, hydrogen, oxygen, etc. During the roasting, MHA can provide heat because of combustion or decomposition, which is beneficial for the recrystallization form of Fe₂O₃ in the specularite oxidized pellets at high temperature. The original hematite is first reduced to magnetite, then, magnetite is oxidized into secondary hematite, which obviously improves the roasting performance of specularite pellets.

3:30 PM Break**3:40 PM****A Study of Carbon-Burdened and Cold-Bonded Pelletizing-Electrosmelting Process Disposing Low-Grade Manganese Ore:** Zhao Qiang¹; ¹Changsha Research Institute of Mining and Metallurgy

The carbon-burdened and cold-bonded pellets-electrosmelting process is used to dispose low-grade manganese, and the qualified rich-manganese slag is obtained. On the condition that reduction roasting temperature was 1000°C, reduction time was 45min, particle-size was -1mm, reductant dosage was 1.6%, basicity was 0.3, smelting temperature was 1410°C, smelting time was 60min, it had a good effect on the melting between slag and metallographic phase, the manganese content was 32.58%, manganese recovery was 92.16% in the slag; while the iron content was 94.40%, iron recovery was 95.32% in the metallographic phase. It was proved by the demonstration tests.

3:55 PM**The Characteristics of Roasting of Magnesium Pellets and Roasting Strengthening:** Xiaohui Fan¹; Luben Xie¹; Min Gan¹; Xuling Chen¹; Lishun Yuan¹; ¹Central South University

The effect of magnesium additives on roasting quality of iron ore oxidized pellets was studied. The result shows that no matter the major components of the pellets is magnetite concentrate or hematite concentrate, the mechanical strength of roasted pellets decreases as the contents of MgO increased by adding magnesite, serpentine and MgO powder. The main reasons are that MgO dissolves in magnetite, and MgO promote hematite decomposing into magnetite. Adding calcium-containing or boron-containing materials to promote low melting point material generating can increase the strength of magnesium pellets. The results of microstructure test indicate that the generation of low melting point materials which contain calcium or boron can bring in suitable amount of liquid accelerating the diffusion of Fe³⁺ and Mg²⁺, promoting the recrystallization of Fe₂O₃ which results in good pellets strength.

4:10 PM**Research on Dephosphorization of Complex and Refractory Oolite Hematite Ore:** Chaoying Qi¹; Tiejun Chun¹; ¹Central South University

With the rapid development of iron and steel industry in China, a significant increase in the demand for iron ores has been occurring in the past few years, resulting in a high dependence on imported iron ores, which enhanced the developing of low grade and complicated iron ore resources, especially the oolite hematite ore in China. The mineralogical results demonstrate that the phosphorus of ROM (Run of mine) iron ore mainly occurs in the form of colophonite. The apatite aggregates are composed mainly of colophonite as phosphatic mineral with some kaolinite, illite, quartz, gypsum as gangue minerals. Some different ways of magnetic separation, flotation, roasting, acid leaching and microbiological leaching were used to treat the oolite hematite ore. The results show that the process of roasting-magnetic separation-reverse flotation is an effective way to treat the oolite and the phosphorus reduces from 0.85% to 0.18%.

4:25 PM**Separation of Iron from Zinc Calcine by Magnetic Roasting and Dressing:** Ning Peng¹; Bing Peng¹; Liyuan Chai¹; Mi Li¹; Jiming Wang¹; ¹Central South University

A novel technological routine for iron separation from high iron-bearing zinc calcine was proposed. The zinc ferrite (ZnFe₂O₄) in zinc calcine was decomposed to zinc oxide and magnetite under reduction atmosphere at temperature over 800°C. The magnetic dressing was carried out to separate magnetite from reduction roasting products. The effects of roasting temperature, roasting time and magnetic intensity on grade and recovery of iron were investigated and the results showed that roasting temperature had a significant impact on iron recovery. In addition, ultrasonic dispersion and mechanical milling were performed to break the structure of the magnetic phases and non magnetic phases before magnetic dressing. The results indicated that ultrasonic dispersion

could improve the iron recovery while mechanical milling could increase the grade of iron in concentrates. More than 80% of iron was recovered by using the optimal magnetic roasting and dressing.

4:40 PM**Study on Mechanism of Limonite Granulation Gas-Based Roasting-Magnetic Separation Techniques:** Zhucheng Huang¹; Shiyu Tian¹; Tao Jiang¹; ¹Central South University

In connection with the refractory low-grade limonite, the granulation Gas-based Roasting-magnetic separation technological is used for experimental study. Optical microscope, XRD, and SEM detection is used to detect production's porosity changing, phase transformation and microstructure characteristics before and after roasting. Study results show that: on condition that the weak reducing atmosphere CO:CO₂:N₂ is 1:2:2 and the temperature is 650-750°C, roasting time is 10 minutes, and magnetic separation iron concentrate grade is 61.26% after ball milling and magnetic separation, at the same time recovery rate is 86.27%. Most of limonite phase are transformed into artificial magnetite; microscopic performance shows that after roasting iron minerals are uniformly reduced, iron phase uniform distributed. On the different test conditions artificial magnetite's micro-topography and features are differences.

4:50 PM Concluding Comments**Aluminum Reduction Technology: Modelling II and Measurement**

Sponsored by: The Minerals, Metals and Materials Society, TMS Light Metals Division, TMS: Aluminum Committee, TMS: Aluminum Processing Committee
Program Organizer: Olivier Martin, Rio Tinto Alcan

Thursday PM
March 15, 2012

Room: Southern III
Location: Dolphin Resort

Session Chair: Jianhong Yang, Chalco

2:00 PM**Modeling Cathode Cooling Due to Power Interruption:** Marc Dupuis¹; Alton Tabereaux²; ¹GeniSim; ²Consultant

Extended electrical power interruptions often result in the shutdown and cooling of cells which causes the formation of numerous cooling cracks on the surface of cathode blocks. New ANSYS® based thermal cooling models (2D+ full cell slice model, 3D full side slice model and a 3D full cell quarter) were developed to determine the cathode cooling rates, the differences in the temperature gradients and the resultant stress from cooling cathodes for 24 to 48 hours. The results indicate significant temperature gradients and corresponding stress develop during cooling to cause cracking of the cathode blocks. Reducing the aluminum metal level in cells during cooling was found to reduce the level of stress and thus reduce, if not eliminate the cathode surface cracks. Having no metal at all creates a completely new pattern of stresses that may produce cracks in the block edge instead of the block surface.

2:20 PM**Modeling the Mass and Energy Balance of Different Aluminium Smelting Cell Technologies:** Vanderlei Gusberti¹; Dagoberto Severo¹; Barry Welch²; Maria Skyllas-Kazacos²; ¹CAETE Engenharia - Brazil; ²School of Chemical Engineering - UNSW - Australia

The modern primary aluminium industry is continuously aiming to reduce the cell energy consumption and the harmful cell emission rates. In order to optimize both aspects, a comprehensive understanding and prediction of the electrolysis cell mass and energy balance must be obtained. Traditionally, many cell heat balance models have presented limited considerations on the mass balance, reactions above the cavity crust and cell duct flow. The thermal balance model presented in this paper is entirely based on the first law of thermodynamics. The extended



TMS 2012

141st Annual Meeting & Exhibition

THURSDAY PM

cell control volume that includes the hooded cell space is adopted. This new approach allows automatic accounting for important exothermic reactions and the study of the impact of duct gas flow rate on the energy balance. A user-friendly software tool for studying the cell energy balance was developed. The new modeling tool is applied to assess the mass and energy consumption rates of different cell technologies.

2:40 PM

Current Efficiency Predictive Model and Its Calibration and Validation: *Zhiming Liu*¹; Wangxing Li²; Qingjie Zhao²; Jiemin Zhou¹; Yueyong Wang²; ¹School of Energy Science and Engineering Central South University; ²Zhengzhou Research Institute CHALCO Ltd.

Current efficiency is one of the most important technical and economic parameters. Current efficiency loss is due to dissolved aluminum reacting with the anode bubbles by the back reaction, which is assumed to be responsible for the largest part of current efficiency loss in Hall-Héroult aluminum reduction cells. The magnetohydrodynamics flow in cells can be seen as a gas-liquid-liquid flow by neglecting the mima effect of alumina particles. An current efficiency predictive model (CEPM) was developed based on multiphase multicomponent flow. The model takes the flow in cells as a three-phase (the bath, the metal, and the anode bubbles) and multicomponent problem (the bath phase: bath species and dissolved Al species; the anode-bubble phase: CO₂ and CO), which is able to incorporate the mechanism of current efficiency loss in cells. The model was calibrated by a 160kA cell and validated by a 300kA cell. This study provides a new approach for predicting current efficiency of aluminum reduction cells.

3:00 PM

Wireless and Non-Contacting Measurement of Individual Anode Currents in Hall-Héroult Pots; Experience and Benefits: *James Evans*¹; Nobuo Urata²; ¹University of California, Berkeley & Wireless Industrial Technologies; ²Alumilab and Wireless Industrial Technologies

Continuous measurement of individual anode currents in Hall-Héroult cells is now becoming practical. It has the advantage of early warning of anode effects and possibly improvements in current efficiency and operation (e.g. warning of anode burn-off). The paper describes the approach of Wireless Industrial Technologies which entails a "master-slave" arrangement with a slave measuring the magnetic field produced by the current in each anode rod each second and the masters wirelessly communicating the data to a computer. With this system there is no direct contact with the anode rods and thereby no interference with normal pot operations such as changing anodes. Such a system has been under test at a smelter in the USA since December, 2010. A second smelter will be conducting tests of the system by the time of the Orlando conference. Experience with this system is described and projections made concerning potential economic benefit.

3:20 PM Break

3:40 PM

Impacts of Anode Set on the Energy Re-distribution of PB Aluminum Smelting Cells: *Cheuk-Yi Cheung*¹; Chris Menictas¹; Jie Bao¹; Maria Skyllas Kazacos¹; Barry Welch¹; ¹The University Of New South Wales

The routine work practice of anode setting has become a more critical operation as the anode sizes have increased at the expense of liquid bath volume, especially for low superheat operation. The spatial operating disturbances as each anode is changed in different parts of the cell alter the control envelope and decision making limits. This paper presents a dynamic thermal model that can simulate the impacts of anode setting on the local thermal balance and hence the overall operating condition, by incorporating individual anode current signals acquired from an operating prebaked reduction cell. By incorporating real plant data, the model can predict the local thermal conditions during the increase of current pick

up of a newly replaced anode and the change in current distribution. This model can also be employed in an online fault diagnostic system to help isolating other disturbances, hence improve early detection of impending abnormal conditions.

4:00 PM

Dimensional Analysis in Cold Water Model Experiments of New Cathode Structure Aluminum Cell: *Liu Yan*¹; Zhang Ting'an¹; Li Chong¹; Zhao Qiuyue¹; Wang Shuchan¹; Feng Naixiang¹; He Jicheng¹; ¹Northeastern University

Compared with the traditional cathode structure cell, the new cathode structure cell can restrain the level fluctuations of aluminum liquid, effectively reduce polar distance and decrease cell voltage, it makes greatly electricity saving into reality. In this paper, using cold water model experiment basing on principle of similitude to study the level fluctuations by anode gas disturbance, and investigate the rules of level fluctuations in new cathode structure electrolytic cell. Numerical simulation of the anode structure with Fluent was also carried out. Simulation results are basically consistent with experimental results, which can verify possibilities of using Fluent to study fluctuations in the interface of cell. According to the analysis of experimental data, the empirical formula of amplitude are obtained by using dimensional analysis, which are associated to a variety of material factors, operating factors, equipment factors. After the theoretical analysis, Dimensionless equation is in good agreement with experimental results.

4:20 PM

Flow Field Comparison between Traditional Cell and New Structure Cell by Chaclo by CFD Method: *Zhiming Liu*¹; *Fengqin Liu*¹; Yueyong Wang¹; ¹Zhengzhou Research Institute of Chalco

Energy saving receives more and more attention because of high energy price and environment requirement. The flow field and interface wave of new structure cell by Chaclo were studied by ANSYS and CFX combination. The results show that the maximum velocity of traditional cells is 26.74 cm/s and the maximum velocity of new structure cell is 21.22cm/s. The maximum velocity is reduced. The interface wave of traditional cells is between -2.19cm and 3.41cm and that of new structure cell is between -1.15cm and 2.50cm. The interface wave is weakened by 34.82%. The industrial practice shows that the anode-cathode distance of new structure cell can be reduced without current efficiency loss in comparison with traditional cells.

Bulk Metallic Glasses IX: Other Related Alloys and Properties

Sponsored by: The Minerals, Metals and Materials Society, TMS Structural Materials Division, TMS/ASM: Mechanical Behavior of Materials Committee

Program Organizers: Peter Liaw, The University of Tennessee; Hahn Choo, The University of Tennessee; Yanfei Gao, The University of Tennessee; Gongyao Wang, University of Tennessee

Thursday PM
March 15, 2012

Room: Swan 6
Location: Swan Resort

Session Chairs: Oleg Senkov, UES, Inc.; Yuri Petrusenko, National Science Center - Kharkov Institute of Physics & Technology

2:00 PM Invited

New Refractory High Entropy Alloys: *Oleg Senkov*¹; Svetlana Senkova¹; Daniel Miracle¹; Christopher Woodward¹; ¹Air Force Research Laboratory

Several new refractory high entropy alloys containing Cr, Hf, Mo, Nb, Ta, Ti, V, Zr and Al as principal alloying elements have recently been produced by vacuum arc melting. The as-solidified alloy samples

have been hot isostatically pressed (HIPd) and homogenized prior to the microstructure/properties analysis. Some alloys have a single-phase, disordered BCC crystal structure, while other alloys contain several crystal phases among which a disordered BCC phase prevails (more than 50% by volume). The chemical composition of the phases has been identified using EDS and WDS analyses. The microstructure of these alloys has been studied using SEM and EBSD techniques. These results, together with the alloy properties such as density, microhardness, compression modulus, yield strength and ductility, will be reported and the relationships between the composition, microstructure and properties will be outlined for these new alloys. This work was conducted under the U.S. Air Force contract FA8650-10-D-5226.

2:20 PM

Disordered and Weakly-Ordered Solid-Solution Phases in the High-Entropy Alloy System of Al-Co-Cr-Cu-Fe-Ni: *Louis Santodonato*¹; Zhi Tang²; Andrew Chuang²; Peter Liaw²; ¹ORNL and UT; ²University of Tennessee

The high-entropy alloy system Al_xCoCrCuFeNi is known to form solid-solutions with a face-centered-cubic phase (A1), dominating at low aluminum contents, and a body-centered-cubic phase (A2), dominating at higher aluminum contents. The A2 phase, however, separates into a modulated structure with ordered (B2) and disordered (A2') regions, possibly indicating the formation of intermetallic compounds. The present study examines the structural evolution of these phases, using neutron and X-ray diffraction at elevated temperatures up to 800 °C, and applies a semi-empirical model to interpret the results. It is shown that the A2 phase separates into the A2' (Al-Ni depleted solid-solution) and the B2 (Al-Ni rich, partially ordered solid-solution), which lowers the total free energy. It is also shown that the A1, A2' and B2 phases coexist in significant fractions throughout the wide temperature range of room temperature to at least 800 °C.

2:30 PM Invited

Properties Optimization of High-Entropy and Amorphous Alloys by Alloying and Multiple Processing: *Yong Zhang*¹; ¹University of Science and Technology Beijing

A criterion for the solid-solution phase formation in the high-entropy alloys was proposed based on two parameters $\Omega > 1.1$ and $\Delta < 6.6\%$. The properties of several high-entropy alloys were optimized by alloying, and multiple processing, e.g., Bridgman solidification, cold rolling, annealing, water quenching. The low temperature properties of the high-entropy and amorphous alloys were studied, and an equation for predicting the low temperature strength of the amorphous alloys was proposed. The strengthening mechanism of the dendrite/amorphous alloy composite were analysed by using a two phase model.

2:50 PM Invited

High-Entropy Carbides Based on High-Entropy Alloys: Yu-An Yeh¹; Ming-Hung Tsai²; Jien-Wei Yeh¹; ¹National Tsing Hua University; ²North Carolina State University

Based on the concept of high-entropy alloys, first high-entropy bulk carbide (Cr, Nb, Ti, V, W)50C50 with equal-mole transition metals has been synthesized through mechanical alloying and solid-state sintering. The sintered carbide is a thermally-stable NaCl-type FCC solid solution of five binary carbides. This simple FCC phase formation demonstrates that high entropy effect in enhancing solid solution in high-entropy alloys also works in this five-component carbide. Nano-powder prepared by ball milling is the key factor to realize the successful pressureless sintering at a low temperature around 0.56 of the melting point. The average nanohardness value is 32 ± 3 GPa which is higher than the mixture-rule hardness, 23 GPa, by around 40 %. This suggests that high-entropy carbides also exhibit large solution hardening effect.

3:10 PM Invited

Accumulation and Recovery Processes in a High-Entropy Alloy Irradiated with 2.5 MeV Electrons: *Yuri Petrusenko*¹; Alexander Bakai¹; Valeriy Borysenko¹; Eduard Mayevsky¹; Peter K. Liaw²; Gongyao Wang²; Jien-Wei Yeh³; ¹National Science Center - Kharkov Institute of Physics & Technology; ²Department of Materials Science and Engineering, The University of Tennessee; ³Department of Materials Science and Engineering, National Tsing Hua University

The accumulation and annealing characteristics of irradiation-induced defects in an Al-Co-Cr-Cu-Fe-Ni high-entropy alloy have been studied during low-temperature (80 K) irradiation with 2.5 MeV electrons and subsequent isochronous annealing. The data obtained are compared with the literature results on the point-defect generation and annealing behavior in crystalline Fe-Cr-Ni alloys and steels under electron irradiation. Qualitatively irradiation dose dependences of the electrical resistivity of both families of alloys are rather similar and can be interpreted using the basic parameter of a resistivity increase per Frenkel pair. The isochronous annealing behavior for the high-entropy alloy is also similar to that of the Fe-Cr-Ni system. The characteristic activation energy of the vacancy-annealing stage is estimated. It is concluded that the increase of the resistivity during electron irradiation is induced by the Frenkel pair generation. The observed resistivity changes during annealing are caused by vacancies and compositional ordering and disordering.

3:30 PM

Spark Plasma Sintering of Fe-Based Bulk Metallic Glasses: *Sandip Harimkar*¹; Ashish Singh¹; ¹Oklahoma State University

Amorphous alloys or bulk metallic glasses represent a new class of advanced materials exhibiting attractive combinations of properties such as high strength/hardness and excellent wear/corrosion resistance. While bulk processing of amorphous alloys using conventional casting processes is often difficult, micrometer-sized powders of the amorphous can be readily processed using gas atomization processes. The novel spark plasma sintering (SPS) presents tremendous potential for the bulk processing of these exciting alloys using starting atomized amorphous powder. In this presentation, our recent results on microstructure and properties of SPS processed Fe-based bulk amorphous alloys will be discussed.

3:40 PM Break

3:55 PM Invited

Formation of HfW₂ in Mechanically Alloyed W-Based Alloy Systems: *Laszlo Kecskes*¹; Anthony Roberts¹; Kristopher Darling¹; ¹US Army Research Laboratory

The lethality of depleted uranium (DU) as a kinetic energy penetrator (KEP) is ascribed to its high density 18.95 g/cm³ and its ability to undergo adiabatic shearing. An alternative replacement, a tungsten (W)-based bulk metallic glass would inherently incorporate the necessary physical attributes for an ideal KEP. Several W-based binary systems may form the basis for a refractory, high-density glass composition. Phase diagrams for the binary systems W-Hafnium (Hf) and W-Zirconium (Zr) are similar, but equilibrium melting studies preclude the use of Hf, due to the formation of the HfW₂ intermetallic. However, Hf remains advantageous as it has a relative density of 2 compared to Zr and thus will result in a higher density glass. The current investigation utilizes the non equilibrium method of high energy mechanical alloying, to investigate if the suppression of HfW₂ formation could be accomplished in both the binary and higher-order amorphous alloy systems.



4:15 PM

Manifestation of Short-Range Order, Medium-Range Order, and Structure Defects in Bulk Metallic Glasses: *Yuri Petrusenko*¹; Alexander Bakai¹; Ivan Neklyudov¹; Igor Mikhailovskij¹; Sergij Bakai¹; Peter K. Liaw²; Gongyao Wang²; Qingming Feng²; Tao Zhang³; Lu Huang Huang³; Zengqian Liu³; ¹National Science Center - Kharkov Institute of Physics & Technology; ²Department of Materials Science and Engineering, The University of Tennessee; ³School of Materials Science and Engineering, Beijing University of Aeronautics and Astronautics

The idea that bulk metallic glass (BMG) structures can be regarded as an ensemble of clusters is confirmed by direct and indirect observations. There is a finite set of the structure units, "perfect" (locally preferred) coordination polyhedra, specified by compositional and topological order. The clusters of poor order form structural defects. Field emission and transmission electron microscopy reveal regions of ~10 nm in size, which can be identified as locally ordered clusters separated by diffuse poorly ordered boundaries. In the defectless regions, the point defects, vacancies, and interstitials are stable. The most important extended defects of BMGs are intercluster boundaries. The revealed size dependence of the BMG strength, Kaiser Effect, and feature of the low- and high-frequency compression-compression fatigue are presented in this report. They are considered as manifestation of the shear transformation, sliding and creep in boundary layers. As result, shear bands and crack initiation and propagation takes place.

4:25 PM

Structural Relaxation in Zr-based BMGs Viewed from Potential Energy Landscape: *Osami Haruyama*¹; Hiroyuki Sawada¹; Yoshihiko Yokoyama²; Kohichi Tsuchiya³; Kazumasa Sugiyama²; ¹Tokyo University of Science; ²Institute of Materials Research, Tohoku University; ³National Institute of Materials Research

The structural relaxation in amorphous alloys has been classified into two categories. One is called the topological short range ordering (TSRO) process, which is manifested in accompanying with annihilation of quenched-in free volume under T_g . Another is the chemical short range ordering (CSRO) process whose characteristic is the reversible variation in physical properties during relaxation. The kinetics of both processes conforms to a stretched exponential relaxation function with an index β less than 1. The β of TSRO process is largely temperature-dependent, while the CSRO process has a constant value of β . Following the potential energy landscape, the structural relaxation in BMGs is regarded as a transition between local potential energy minimum locations on a multidimensional potential energy hyper-surface. In the present study, we examine the structural relaxation of BMGs in both high-temperature region (roughly $T_g - 60 \text{ K} \leq T \leq T_g + 10 \text{ K}$), and low-temperature region ($T_g - 250 \text{ K} \leq T \leq T_g - 150 \text{ K}$) based upon this model.

4:35 PM

Investigation of Porous Zr-Based Bulk Metallic Glass: *Junhua You*¹; ¹Shenyang University of Technology

The Zr₅₇Cu_{15.4}Ni_{12.6}Al₁₀Nb₅ porous bulk metallic glass with a diameter of 6mm was fabricated by melt infiltrating casting method. The porous cell morphology, structure, fracture surface and phase constituent of the porous material were investigated by scanning electron microscopy (SEM) and X-ray diffractometry (XRD), respectively. And the mechanical properties and cell structure were also discussed. The results show that a uniform distribution of porous cells with size of 0.2-0.8 mm forms by introducing CaC₂ particles as space holders. The density and porosity of the porous bulk metallic glass are 3.57 g/cm³ and 47%, respectively. The largest yield strength of this porous material is 384 MPa and it gradually declines accompanied by serrated flow under compression. The final failure occurs at a strain of 18.6%, well in excess of monolithic amorphous alloys.

Bulk Metallic Glasses IX: Structures and Other Properties II

Sponsored by: The Minerals, Metals and Materials Society, TMS Structural Materials Division, TMS/ASM: Mechanical Behavior of Materials Committee

Program Organizers: Peter Liaw, The University of Tennessee; Hahn Choo, The University of Tennessee; Yanfei Gao, The University of Tennessee; Gongyao Wang, University of Tennessee

Thursday PM
March 15, 2012

Room: Swan 1
Location: Swan Resort

Session Chairs: Jeff De Hosson, Univ of Groningen; Hongbin Bei, Oak Ridge National laboratory

2:00 PM Invited

Controlled Nanocrystallization of a Bulk Metallic Glass in the Zr-Al-Cu-Ni-Co System – Structure, Properties and Ways to New Materials Design: *Rainer Wunderlich*¹; Arnaud Caron¹; Hans-Joerg Fecht¹; ¹Universitaet Ulm

A controlled two-phase mixture of nanocrystalline and amorphous phases offers the possibility of tailoring the ductility and mechanical strength of BMG forming complex alloys. This has been investigated in the Zr-Al-CuNiCo alloy system as a function of the Al-concentration varied between 7 and 20 at% and of the Co-concentration between 2 and 8 at%. At the composition limit of glass formation different amorphous to crystalline phase ratios have been obtained by casting and investigated by XRD, SEM, atomic resolution TEM. Detailed recent AFAM measurements point to a phase separation in the initially amorphous and fully relaxed states. The phase contrast originates from the difference in elastic properties on the scale of a few hundred nanometers. Minor compositional variations result excellent glass forming ability and two widely separated crystallization. Controlled crystallization allows a wide variation of nanocrystalline / glassy microstructures and related properties and, thus, a new way of materials design.

2:20 PM

Magnetocaloric Effect of Fe-Based Amorphous Metals: *Anja Waske*¹; Björn Schwarz¹; Norbert Mattern¹; Konstantin Skokov¹; Jürgen Eckert¹; ¹IFW Dresden

Magnetocaloric materials could one day be the basis of a new magnetic cooling concept for consumer use, replacing conventional refrigeration technology. However, currently known materials with high magnetic entropy changes are challenging to implement into devices for actual consumer use, since they contain either very expensive or toxic components or exhibit large magnetoelastic effects, which question their long-term stability. Here, we report on the magneto-caloric effect in Fe-based metallic glasses. Although exhibiting only moderate magnetic entropy changes, metallic glasses offer a range of qualities very well suited for application in a cooling device. Also, Fe-based alloys are among the cheapest compounds showing the magnetocaloric effect. We show tuning of Curie temperature upon doping Fe-based amorphous alloys with Nb. Furthermore, the influence of selected rare earth addition will be discussed. Differences between using bulk metallic glasses and amorphous ribbons for application in a test cooling device will be commented on.

2:30 PM Invited

Work Hardening of High Strength Nanocrystalline Ni-W Alloys: *Tohru Yamasaki*¹; Kazutaka Fujita²; ¹University of Hyogo; ²Ube National College of Technology

It is well known that nanocrystalline alloys exhibit very low ductility under tensile testing conditions. This may be due to the formation of highly localized shear bands because of their low work hardening ability. We have developed the nanocrystalline Ni-16.9 at. W alloy having grain size of about 5 nm by electrodeposition. This alloy exhibited high tensile

strength of 2,900 MPa with large plastic strain of about 1.0 %. In this case, large work hardening was observed during plastic deformation. Many ductile dimples with a size of about 100 nm were observed at the fractured surface. By using the high-resolution SEM, local grain growth up to about 20 nm in diameter were observed near the fractured surface. It is suggested that the local grain growth near the fractured surface may be occurred by rapid heating during plastic deformation, resulting the hardening according to the inverse Hall-Petch strengthening law.

2:50 PM

Medium Range Order Correlations in Liquid and As-Quenched Al-Tb System: *Eren Kalay*¹; Matthew Kramer²; Tuba Demirtas¹; Merve Genc¹; Jinwoo Hwang³; Paul Voyles⁴; ¹METU; ²Ames Laboratory US DOE; ³University of California, Santa Barbara; ⁴University of Wisconsin, Madison

We've investigated the glassy and the liquid states of Al-Tb alloys by a combined study of HEXRD, APT, FEM, molecular dynamics and RMC simulations. The experimental HEXRD indicated a pre-peak and side-peak in the total structure factor function in liquid and amorphous Al-Tb which is also confirmed by MD simulations at the corresponding temperatures. We believe that these extra reflections are resulted due to clustering of RE atoms at relatively longer length scales as compared to short-range ordering in liquid state. The APT and RMC clearly shows the compositional fluctuations in the amorphous states resulted in formation of a network structure of Al-depleted regions between which ~1 nm of isolated clusters of pure Al exist. Fluctuation electron microscopy results demonstrate that these Al rich and depleted regions tend to order themselves into MRO structure. The chemical and topological order in question will be discussed and presented during the talk.

3:00 PM Invited

Plasticity of BMG with Shear Bands-Sized Sample: *Scott Mao*¹; ¹University of Pittsburgh

This talk will be based on publication of J. H. Luo, F. F. Wu, J. Y. Huang, J. Q. Wang, and S. X. Mao*, "Superelongation and Atomic Chain Formation in Nanosized Metallic Glass", PRL 104, 215503 (2010). Bulk metallic glasses are brittle and fail with no plastic strain at room temperature once shear bands propagate. How do metallic glasses deform when the size is less than that of shear bands? Here we show that Al90Fe5Ce5 metallic glass with a size <20 nm can be extremely elongated. Remarkably, even an atomic chain was formed after sample necking, which was never observed in metallic glasses. The unexpected ductility may originate from the fast surface diffusion and the absence of shear band formation, and may guide the development of ductile metallic glasses for engineering applications.

3:20 PM

Hydrogen Solubility and Permeability of Ni-Nb-Zr Amorphous Alloy: *Narendra Pal*¹; Steve Paglieri²; Dhanesh Chandra¹; Sang-Mun Kim¹; Wen-Ming Chien¹; Anjali Talekar¹; Ted Flanagan³; Michael Dolan⁴; ¹University of Nevada, Reno; ²TDA Research Inc.; ³University of Vermont; ⁴Commonwealth Scientific and Industrial Research Organisation

Hydrogen from coal gasification is one of the cheaper routes considered for hydrogen production on sustainable basis. Conventionally, Pd alloys have been used as filtration membranes for hydrogen permeation. The prospective alternative could be Ni-Nb-Zr amorphous alloys which can reduce the membrane cost drastically. The Ni42Nb28Zr30 amorphous alloy membrane was fabricated using melt-spinning and was coated with thin Pd layer (500nm) by sputtering. The P-C-T isotherms were obtained from solubility test in Sievert's apparatus at different temperatures (200-400°C). The solubility of Pd at 200°C was found to be 0.63, which matches with previous published data. The permeability of Ni42Nb28Zr30 was measured to be 1.2×10^{-8} mol m⁻¹ s⁻¹ Pa^{-0.5} at 400°C which is close to the permeability of Pd at this temperature. As Ni42Nb28Zr30 amorphous alloy shows permeability close to Pd, the solubility data of Pd at different temperatures would be compared with Ni42Nb28Zr30 in details.

3:30 PM Break

3:45 PM Invited

Understanding Mechanical Properties of Bulk Metallic Glasses Using Nanoindentation Pop-In Experiment: *Hongbin Bei*¹; Yanfei Gao²; ¹Oak Ridge National laboratory; ²University of Tennessee/Oak Ridge National Laboratory

Pop-in events during nanoindentation have been used extensively to probe dislocation plasticity in crystalline metals. In amorphous metals (metallic glasses), dislocation-mediated plasticity is not possible because those materials lack long-range order. However, Pop-ins are also observed in bulk metallic glasses (BMGs) during spherical nanoindentation. The first pop-in marks the transition from perfectly elastic to plastic deformation, i.e., the onset of plastic flow (incipient plasticity) in BMGs. The dependence of pop-in on materials and loading conditions provides the unique information for the development of constitutive models for BMGs. We conduct many indentation experiments on the as-cast (in different cooling rate), annealed, deformed metallic glass samples to investigate effects of cooling rate, relaxation, pre-existing shear band on the onset of yielding of BMGs. Based on the experiment observation, a statistic model was used to explain the strength distribution and how they are affected by the processing.

4:05 PM

Sliding Wear Behavior of Cu50Hf41.5-xAl8.5Yx (x = 0, 2, 5, 8, 10 at. %) Bulk Metallic Glass: *Dharma Maddala*¹; Rainer Hebert¹; ¹University of Connecticut

The sliding wear behavior was investigated of Cu50Hf41.5-xAl8.5Yx (x = 0, 2, 5, 8, 10 at. %) bulk metallic glasses (BMG). Alloying with yttrium resulted in a gradual increase in hardness, but the notch toughness decreased. The wear resistance increased up to 5 at. % of Y addition, but deteriorated with further increase in the Y content. The results suggest that the hardness controls the wear behavior at small Y levels. At higher Y concentrations the toughness decrease outweighs the hardness in its effect on the wear behavior. The comparison with the wear behavior of a Cu50Hf41.5Al8.5 BMG shows the same trend in the wear behavior with changes in hardness and toughness for partially devitrified samples. While the processing conditions for optimal wear can be predicted approximately from the hardness and toughness data, a refined wear prediction has to consider the wear mechanisms and their changes with alloying or precipitation.

4:15 PM

Ultra-High Fracture Strength and Elongation to Failure of Submicron-Sized Metallic Glasses: *Lin Tian*¹; Yong-Qiang Cheng²; Cheng-Cai Wang¹; Zhi-Wei Shan¹; Ju Li³; Xiao-Dong Han⁴; Jun Sun¹; Evan Ma²; ¹CAMP-Nano, Xi'an Jiaotong University; ²Department of Materials Science and Engineering, Johns Hopkins University; ³Department of Nuclear Science and Engineering and Department of Materials Science and Engineering, MIT; ⁴Institute of Microstructure and Property of Advanced Materials, Beijing University of Technology

For the first time, the mechanical properties of submicron-sized metallic glasses (MGs) were studied through quantitative in situ tensile test inside a transmission electron microscope, which employs high-resolution measurements of the loading forces and accurate strain measurement with deposited markers on the gauge length. The quantitative experiment establishes that the small-volume MGs have fracture strength and elongation to failure reaching record high values of about 4 GPa and 6%, respectively. At the same time, the yield stress and elastic strain limit are found to be about twice as large as the already-high elastic limit observed in macroscopic samples, in line with model predictions of the intrinsic limit in the absence of heterogeneous shear band nucleation facilitated by extrinsic factors. The origin of the apparent "work hardening" seen in the tensile stress-strain curves will be also discussed in this talk.



4:25 PM

Smaller is Stronger in Amorphous Metals: *Chengcai Wang*¹; Zhiwei Shan¹; Jun Sun¹; Ju Li²; Evan Ma³; ¹Xi'an Jiaotong University; ²Massachusetts Institute of Technology; ³Johns Hopkins University

The mechanical properties and deformation mechanisms of metallic glasses at the micro- and nano-scale are receiving much attention recently. However, in comparison with the well-accepted "smaller is stronger" trend in their crystalline counterparts, the size-dependent yield strength and deformation mode in metallic glasses is still under intense debate. Here we demonstrate the "smaller is stronger" trend in submicron-sized aluminum-based metallic glasses through quantitative in situ tension tests inside a TEM. In a 100-nm thick beam, the elastic strain could reach 3.8% and fracture strength is about 1.75 GPa, almost twice that of bulk samples of the same composition. Meanwhile, a tendency towards "homogeneous-like" distributed deformation is observed in compression studies of nanopillars, which is in line with earlier findings.

4:35 PM

The Correlation between Glass Formation and Hardness of the Amorphous Phase: *Zhitao Wang*¹; Kaiyang Zeng¹; Yi Li¹; ¹National University of Singapore

We report a non-monotonous behavior of the hardness of amorphous Cu-Zr films as a function of composition, via applying a combinatorial deposition and nanoindentation method with unparalleled compositional resolution. Distinct peaks in hardness were found at particular compositions to match well with the previously reported density peaks. Our results not only provide a shortcut to search for new glass-formers, but also raise the possibility to develop bulk metallic glasses with enhanced plasticity and/or ductility for engineering applications.

4:45 PM

Atomic Packing and Its Correlation with Glass Transition in Metallic Glasses: *Xiong-Jun Liu*¹; Zhao-Ping Lu¹; Xidong Hui¹; C. T. Liu²; ¹University of Science and Technology Beijing; ²City University of Hong Kong

Deciphering the atomic structure of metallic glasses (MGs) is a longstanding scientific challenge. Despite considerable effort has been devoted to resolving this issue over the years, a general description of atomic packing for various MGs is still lacking at present. Moreover, the structural origin of the glass transition remains a great puzzle. In this paper, we will present a global feature to describe the atomic packing in MGs, and then correlate the structural parameter with the glass transition. By statistically analyzing the rule of peak positions in the pair distribution functions for a variety of MGs, we have revealed that the complex atomic configuration in MGs can be virtually characterized by a combination of the spherical-periodic order and local translational symmetry (LTS). By quantitatively exploring the evolution of LTS-order atoms during glass transition, we have identified the correlation of the glass transition event with the extent of the LTS order.

4:55 PM

Amorphous Phase Separation in a Bulk Metallic Glass of Negative Heat of Mixing: *Si Lan*¹; Yeuk Lan Yip¹; Man Tat Lau¹; Hin Wing Kui¹; ¹Chinese University of Hong Kong

Amorphous phase separation has been a controversial issue for many years in the field of metallic glass (including bulk metallic glass). For example, there are reports saying that amorphous phase separation occurs in Pd-Ni-P, which has a negative heat of mixing. On the other hand, there are as many reports claiming that phase separation is absent in amorphous Pd-Ni-P alloys. The difficulty is mainly due to a lack of direct experimental evidences. In this work, high resolution TEM techniques, including HREM and high-angle angular dark-field (HAADF) EDX spectrum mapping were employed for the purpose. It was found that amorphous Pd₄₁Ni₄₁P_{17.5} will undergo phase separation after an intermediate thermally annealing.

Characterization of Minerals, Metals, and Materials: Characterization of Ferrous Metals II

Sponsored by: The Minerals, Metals and Materials Society, TMS Extraction and Processing Division, TMS: Materials Characterization Committee

Program Organizers: Jiann-Yang Hwang, Michigan Technological University; Sergio Montero, State University of North Rio De Janeiro; Chenguang Bai, Chongqing University; John Carpenter, US Department of Energy; Donato Firrao, Politecnico di Torino; Byoung-Gon Kim, Korea Institute of Geoscience & Mineral Resources; Mingdong Cai, Schlumberger

Thursday PM
March 15, 2012

Room: Europe 6
Location: Dolphin Resort

Session Chairs: Mingming Zhang, ArcelorMittal Global R&D; Zhiwei Peng, Michigan Technological University

2:00 PM

Comparison of Creep Life Assessment between Tin-Based Lead-Free Solders and Lead Solders: *Kenji Monden*¹; ¹Denki Kagaku Kogyo K.K.

The creep properties of tin-based lead-free solders, Sn₃Ag_{0.5}Cu and Sn_{0.7}Cu_{0.1}Ni, and lead solders, 10Sn-90Pb and 50Sn-50Pb, were investigated at temperatures between 298K and 398K. The creep rupture time decreases with increasing the initial stress and the temperature. The analysis of creep curves of those solders apply the Omega method. The creep rate $d\epsilon/dt$ is expressed by following formula: $\ln(d\epsilon/dt) = \ln(d\epsilon_0/dt) + \Omega\epsilon$, where $d\epsilon_0/dt$ and Ω are experimentally determined. The parameter $d\epsilon_0/dt$ increases with increasing the initial stress and the temperature. The activation energy for $d\epsilon_0/dt$ is 108 kJ/mol at Sn₃Ag_{0.5}Cu and 85 kJ/mol at Sn_{0.7}Cu_{0.1}Ni. The energies suggest that the lattice diffusion of tin is dominant. The energy of 10Sn-90Pb is 37 kJ/mol and that of 50Sn-50Pb is 67 kJ/mol. The creep rupture time is calculated using the parameters, $d\epsilon_0/dt$ and Ω . The calculated creep rupture time is good agreement with the measured creep rupture time.

2:15 PM

Correlation between JIC and Equivalent Fracture Strain Determined by Small-Punch Test in JN1, JJ1 and JK2 Austenitic Stainless Steels: *Victor Lopez-Hirata*¹; Maribel Saucedo-Muñoz²; Toshiyuki Hashida²; ¹Instituto Politecnico Nacional (ESIQIE); ²Tohoku University

Small-punch tests and determination of fracture toughness JIC were conducted at 4 and 77 K on new cryogenic JN1, JJ1 and JK2 austenitic stainless steels, after isothermal aging. Equivalent fracture strain was determined by measuring the reduction of thickness in the small-punch test specimen. A linear dependence of JIC on equivalent fracture strain was found in these new materials. Regression analysis of experimental data produced the following linear relation $JIC = 1304.1$ equivalent fracture strain + 8.09 [kJm⁻²]. An analysis of present work relation was pursued on the basis of material properties and evaluation method of JIC. Results showed that the slope value has a strong dependence on material yield strength and JIC evaluation method. This linear relation is useful for the evaluation of fracture toughness JIC, measuring the equivalent fracture strain by means of small-punch test.

2:30 PM

Effect of Heat Treatment on the Surface Characteristics of AISI D2 Steel Machined by Wire EDM: *Milind Dhobe*¹; I Chopde²; Chandrashekhar Gogte³; ¹P.E.S. College of Engineering, Aurangabad; ²Visvesvarya National Institute of Technology; ³Marathwada Institute of Technology

The quality of machined surface is becoming more and more important to satisfy the increasing demand of components performance and its reliability. While machining any component, it is necessary to satisfy

the surface integrity requirements. Heat treatment plays an important role in improving the characteristics of the material. In this research work it has been tried to investigate the effect of heat treatment on the surface characteristics of AISI D2 tool steel after Wire Electro Discharge Machining. The test specimens were prepared by hardening and tempering and then machined with Wire –Electro Discharge Machining (W-EDM) process. Optical and scanning electron microscopy, surface roughness and micro hardness tests were used to study the surface characteristics of the machined specimens. After analyzing the microstructure and test results, it is observed that the recast layer droplets are of smaller size with reduced white layer thickness resulting in higher hardness and lower surface roughness.

2:45 PM

Formability of Multilayered Steel Composites with Improved Strength-Ductility Combination: *Shoichi Nambu*¹; *Junya Inoue*¹; *Toshihiko Koseki*¹; ¹The University of Tokyo

Authors developed a multilayered steel composites consisting of high-strength steel and ductile steel with improved strength-ductility combination (ultimate tensile strength above 1.3GPa and fracture elongation above 25%). In this study, the formability of the multilayered steel composites such as a forming limit diagram (FLD), a crash test, and an impact bending test was investigated. From the FLD result, the fracture elongation in plane strain is about 20%, and the good formability was demonstrated in spite of ultra-high strength. For the crash test and the impact bending test, 590DP steels were also prepared for comparison. The profiles of buckling after crash test were almost identical, while the amount of buckling of multilayered steel composites was smaller than that of 590DP steel. The similar phenomenon was also observed for the impact bending test. These results demonstrate that the multilayered steels composite has a good impact resistance in spite of ultra-high strength.

3:00 PM

Wear And Nanoindentation Study Of Hardfacing Dual Layer Clad Of Austenitic Stainless Steel And Tungsten Carbide-Cobalt Alloy: *Samar Kalita*¹; ¹Advanced Engineered Materials Center - University of North Dakota

Many engineering applications demand surfaces with high wear and corrosion resistance for dynamic operating environments. Carbide metal matrix composites (MMC) are preferred choice for such critical applications. Here, tungsten carbide–cobalt (WC-Co) thick MMC coatings were developed through direct metal laser deposition. As WC laser clads often has cracks and pores, an intermediate austenitic stainless steel clad was applied for corrosion protection. The clad integrity was examined by optical microscopy, while the microstructure and composition were analyzed by SEM and EDS techniques. The mechanical properties were evaluated in terms of hardness and reduced elastic modulus using Vickers hardness testing, and depth-sensing instrumented indentation using a Hysitron-TI950 Nanomechanical Tester. Wear resistance was evaluated according to ASTM F1978-00e1 using a Taber abrader. SEM and LSM analyzed worn surface morphologies. Hardness of WC-Co, austenitic stainless steel and AISI 1018 steel substrate were found to be 1100, 252 and 172 HV, respectively.

3:15 PM

Hot Deformation Study by Processing Maps of N Containing Microalloyed Steel: *Martina Dikovits*¹; *Cecilia Poletti*¹; *Fernando Warchomicka*²; *Gajanan P. Chaudhari*³; *Vivek Pancholi*³; ¹IWS, TU Graz; ²IMST, TU Vienna; ³IITR, Roorkee

The hot formability of a microalloyed steel with 0.16wt%C modified with N is studied by using processing maps. Compression tests of cylindrical samples are carried out using a Gleeble®3800 simulator in the range of temperature between 750-1000°C and strain rates between 0.01-

100 s⁻¹. For this alloy, an Ar3-temperature about 740°C is determined by means of dilatometry. Processing maps are calculated using the modified dynamic material model developed by Murty and Rao for different logarithmic strains. For the instability map, the parameter k_j developed by the authors in previous works is used and compared with other instability values. Softening in the flow curves provoked by induced ferrite during deformation at low temperatures and low strain rates is reflected in the α -value. Light optical microscopy (LOM) and electron back scattered diffraction (EBSD) measurements are used to study the microstructure of the hot deformed samples to determine the deformation mechanisms active and to verify the processing maps.

3:30 PM

Influence of Annealing Treatment on Microstructure and Mechanical Properties of Cold-Rolled Sheet of Fe-36Ni Invar Alloy: *Xiang Jiang*¹; *Lijuan Li*¹; *Xin Xia*¹; *Junjun Huang*¹; *Qijie Zhai*¹; ¹Shanghai University

Some experiments with different annealing temperatures (1173, 1223, and 1273K) and different holding times (3, 4, 5, 6min) were carried out on cold-rolled plate of Fe-36Ni invar alloy. The microstructure and the mechanical properties were observed and tested respectively, and the fracture morphology was observed by SEM. The results show that with increasing of the temperature and the annealing time, the austenite grains gradually grow up accompanied by a small amount of annealing twin crystals, meanwhile, its plasticity and toughness are improved, and it is typical ductile fracture under the condition of tensile failure. After annealed at 1223K, the invar alloy has better comprehensive properties than that at the other annealing temperatures, and the grains size is more uniform. Furthermore, when the annealing time is 4min, the invar alloy has the best comprehensive properties.

3:45 PM

Mechanical Properties of Friction Stir Welded Inconel 600/SS 400 Lap Joints: *Kuk Hyun Song*¹; *Won Yong Kim*¹; *Kazuhiro Nakata*²; ¹Korea Institute of Industrial Technology; ²Joining and Welding Research Institute

The present study was carried out to evaluate the mechanical properties of friction stir welded Inconel 600/SS 400 lap joints. In this process, friction stir welding (FSW) was performed at a tool rotation speed of 200 rpm and welding speed of 100 mm/min, and argon gas was utilized to prevent surface oxidation during the welding. Application of FSW notably decreases the grain size of Inconel 600 alloy from 20 μ m in the base material to 8 μ m in the stir zone. However, the grain size of SS 400 in the weld zone was slightly coarsened, when compared to the base material. Also, the hooking in the advancing side and the intermetallic compounds (M7C3) in the weld interface between Inconel 600 and SS 400 were well formed. These intermetallic compounds and hooking were effective to increase in mechanical properties such as tensile and peel strengths.

4:00 PM

Thermodynamic Analysis and Observation on Precipitation of Inclusions in RE-253MA Heat Resistance Steel: *Zhou Cai*¹; ¹Chongqing University of Science and Technology

The effect of Ce on modifying inclusions of 253MA Heat Resistance stainless steel was studied by metallographic examination, SEM and electron spectroscopy. Thermodynamic calculation was used to analyze the formation and transformation of RE inclusions in 253MA Heat Resistance stainless steel. The result shows that Al₂O₃ and MnS can be entirely replaced by Ce₂O₂S and CeS that are spherical.

Energy Nanomaterials: Catalysts and Photocatalysts

Sponsored by: The Minerals, Metals and Materials Society, TMS Materials Processing and Manufacturing Division, TMS Structural Materials Division, TMS: Advanced Characterization, Testing, and Simulation Committee, TMS: Nanomechanical Materials Behavior Committee

Program Organizers: Reza Shahbazian-Yassar, Michigan Technological University; Ming Au, Savannah River National Laboratory; Meyya Meyyappan, NASA Ames Research Center

Thursday PM Room: Swan 3
March 15, 2012 Location: Swan Resort

Session Chairs: Reza Shahbazian Yassar, Michigan Technological University; Masashi Watanabe, Lehigh University

2:00 PM Invited

Computational Studies of Graphene-Supported Metal Nanoparticle Catalysts

Catalysts: Ashwin Ramasubramaniam¹; Ioanna Fampiou¹; ¹University of Massachusetts Amherst

The synthesis of well-dispersed, size-controlled metal nanoclusters on carbon supports is highly desirable in order to enhance catalytic activity and selectivity in a variety of chemical reactions. However, metal clusters interact rather weakly with defect-free carbon supports and coarsen over time leading to loss of surface area and thence catalytic activity. Defects in carbon supports play an important role in enhancing metal-carbon bonding, thereby reducing the propensity for cluster coalescence. Using a combination of density functional theory and empirical potential simulations, we examine the interaction of Pt clusters with point and line defects in graphene. We compare and contrast the binding energies and diffusivities of clusters bound at defects and on pristine graphene. We examine the influence of support-metal interactions on the morphology, electronic structure, and CO-tolerance of bound nanoparticles. Our results suggest possible avenues for controlling the dispersion and activity of catalyst nanoclusters on carbon supports via defect engineering.

2:30 PM

Oxygen Reduction Reaction (ORR) Activity and Electrochemical Stability of Thin-Film Bilayer Systems of Platinum on Niobium Oxide

David Mulin¹; Li Zhang¹; Liya Wang²; Chris Holt¹; Titichai Navessin³; Kourosh Malek³; Michael Eikerling²; ¹University of Alberta and NINT NRC; ²Department of Chemistry, Simon Fraser University; ³NRC Institute for Fuel Cell Innovation

We used electrochemical testing and theoretical calculations based on density functional theory to examine the oxygen reduction reaction (ORR) activity of platinum electrocatalyst supported on several forms of niobium oxide. Bi-layer electrocatalysts were synthesized in the form of 5 nm thick Pt layers (ca. 0.01 mg/cm²), deposited on 5 or 10 nm thick niobium oxide and backed by glassy carbon (GC) electrodes. The NbO and NbO₂ supports enhance the specific electrochemical activity of Pt relative to the identically synthesized baseline system of Pt on GC, but have no positive effect on the mass activity. The electrochemical stability of the Pt/NbO₂ bi-layer system was investigated by potential cycling with up to 2500 CV cycles. After 2500 cycles, data indicates minimal electrochemical area loss. Using DFT calculations, we have evaluated effects of oxygen incorporation on stability, electronic structure, and electrochemical activity of Pt/Nb_xO_y systems.

2:50 PM

Development of Highly Active Titania-Based Nanoparticles for Composite Propellant Combustion: *David Reid¹; Kevin Kreitz²; Matthew Stephens²; Jessica King¹; Ponnusamy Nachimuthu³; Eric Petersen²; Sudipta Seal¹; ¹University of Central Florida; ²Texas A&M University; ³Pacific Northwest National Laboratory*

Recent research in the field of energetic materials has focused on the development of nanostructured fuels and oxidizers to enhance performance and energy release rates. However, these nanoparticulates present serious challenges due to their safety hazards, instability, and difficulty of manufacture. Our research focuses on an alternate route, the use of nanoscale metal-oxides to catalyze reactions between micrometer-scale energetic constituents. By tuning the physical and chemical properties of nano-TiO₂ suspensions in polymer-matrix energetic composites, we have achieved an 81% increase in the combustion rate of HTPB-AP based composite solid propellants with a nanoparticle loading of 1 wt %. These findings make nano-TiO₂ a viable material for advanced propulsion while avoiding the safety hazards and manufacturing difficulties of competing technologies.

3:05 PM Invited

Hierarchical Microporous Materials: Rational and Designable Heterogeneous Catalysts for Renewable Energy: *Wei Fan¹; ¹University of Massachusetts Amherst*

One of the challenges for utilization of renewable biomass resources by biorefinery is the discovery and investigation of novel and efficient catalysts for the conversion of biomass into fuels and chemicals. It has been recognized that biorefinery require multi-step conversion from biomass to desired chemicals and biofuels. Cascade reactions achieved through integration of different active sites in the same catalyst could enable new one-pot processes. There is, thus, a persistent need for the synthesis of hybrid multi-functional microporous catalysts which are capable of performing multiple "primary" functions simultaneously or sequentially in time. In this talk, we will show how a wide range of the combination of different functions of microporous catalysts (zeolites) and/or with other functional materials can be realized by controlling the architecture of microporous catalysts at a nanoscale level with using a confined growth method.

3:35 PM Break

3:55 PM Invited

Characterization of Chemistry of Nanomaterials by (Scanning) Transmission Electron Microscopy: *Masashi Watanabe¹; ¹Lehigh University*

Nanoscale composition variations within particles can be an important factor in controlling their physical functionality. The chemistry of individual nanoparticles can in principle be analyzed by (scanning) transmission electron microscopy ((S)TEM) with X-ray energy dispersive spectrometry (XEDS) and electron energy-loss spectrometry (EELS). However, there are still several problems to overcome for characterization of nanomaterials: useful signals from individual nanoparticles are extremely weak because of the limited volume and the analysis is further complicated when the particles are in close proximity to other supported materials. In addition, if the elemental distribution fluctuates locally within a single particle, individual point analyses could miss such variations. Therefore, an elemental mapping approach is essential to characterize nanomaterials. The limited signals can be offset by applying spectrum imaging combined with multivariate statistical analysis (MSA). In this talk, several examples for characterization of the local chemistry variations in nanomaterials in combination with MSA will be presented.

4:25 PM

TiO₂ Nanotube Arrays Grown in Ionic Liquids: High-Performance in Photocatalysis and Energy Storage: Huaqing Li¹; Jun Qu²; Surendra Martha²; Qingzhou Cui²; Hanbing Xu²; Huimin Luo²; Miaofang Chi²; Roberta Meisner¹; Nancy Dudney²; Wei Wang²; Sheng Dai²; ¹University of Tennessee; ²Oak Ridge National Laboratory

This study overcomes the previously reported limitations in anodization potential (<10 V) and tube dimension (<600 nm) for synthesizing TiO₂ nanotubes in ionic liquids (ILs). Several micrometers long, debris-free NTs were obtained under anodization voltages of 10-50 V in 1-butyl-3-methylimidazolium tetrafluoroborate with an optimized water content of ~2wt.%. IL electrolytes decompose at a lower rate and thus induce fewer contaminants to the TiO₂ matrix due to their higher electrical conductivity compared to conventional organic electrolytes. As a result, NTs grown in ILs (IL-NTs) have no nano-cracks or tube wall separations, which are commonly observed in NTs fabricated in ethylene glycol-based electrolytes (EG-NTs) and are believed to cause deterioration in the NTs' photoelectrical properties. The ILs-NTs have demonstrated great potential in both photocatalysis and energy storage applications with much higher photocurrent in water splitting and substantially better capacity retention as the anode in a half-cell Li-ion battery cycling compared with EG-NTs.

4:45 PM

Solid State Reactions in TEA Precipitated Cr-ZnO Nanoparticles and Their Use in Photochemical Splitting of Water: Octavio Dominguez¹; Luisa Flores¹; Adriana Gaona¹; Guadalupe Sanchez¹; Roel Cruz¹; ¹San Luis Potosi University

This work reports the preliminary results about solid state reactions of nanometric Cr-ZnO solid solutions and ZnCr₂O₄ particles obtained with triethanolamine (TEA). Different compositions were prepared: 0.65, 2.7, 8, 16 and 33.3 at% chromium, the last one corresponding to ZnCr₂O₄ spinel. Infrared Spectroscopy (FTIR) together with X-ray diffraction (XRD) peaks of the powders with Cr³⁺ between 0.65 and 16.0 at% were assigned to Cr-ZnO solid solution after treatment at 400 °C due to the only presence of ZnO structure. FTIR spectra indicating that Cr-O bonding exists even if there was no presence of ZnCr₂O₄. From Williamson-Hall and Rietveld methods the lattice dimensions were assigned to chromium incorporation in ZnO structure and the lattice contraction by particle size refinement. Cr-ZnO nanoparticles were tested for photoelectrochemical splitting of water under UV irradiation, showing some improvement as Cr³⁺ content was increased.

Energy Technologies and Carbon Dioxide Management: Waste Heat Recovery

Sponsored by: The Minerals, Metals and Materials Society, TMS Extraction and Processing Division, TMS Light Metals Division, TMS: Energy Committee

Program Organizers: Maria Salazar-Villalpando, DOE/National Energy Technology Laboratory; Neale Neelameggham, IND LLC* ; Donna Guillen, Idaho National Laboratory; Subodh Das, Phinix, LLC; Ramana Reddy, Univ of Alabama; Animesh Jha , Univ of Leeds; Soobhankar "Sib" Pati, Metal Oxygen Separation Technologies (MOxST); Mark Jolly, Univ of Birmingham; Lakshmanan Vaikuntam, Process Research ORTECH Inc

Thursday PM
March 15, 2012

Room: Europe 8
Location: Dolphin Resort

Session Chairs: Animesh Jha, Univ. of Leeds; Maria D. Salazar-Villalpando, DOE/NETL; Soobhankar Pati, Metal Oxygen Separation Technologies

2:00 PM Introductory Comments**2:05 PM**

Effect of Materials on the Autoignition of Cyclopentane: Donna Guillen¹; ¹Idaho National Laboratory

Cyclopentane, a flammable hydrocarbon, is being considered as a working fluid for waste heat recovery applications. Experiments were conducted to determine the ignition delay time (IDT) of cyclopentane using an Ignition Quality Test (IQT) device. Two sets of experiments were conducted per ASTM D6890 (with exception to charge pressure and temperature) to determine ignition delay of the fuel at atmospheric pressure for normal air (~21% oxygen) and vitiated air (13.3% oxygen) at a temperature of 530oC. Operation of the IQT device at a much lower pressure (1 bar) than normal operation (21.1 bar) led to very rich conditions and wetting of the stainless steel chamber walls. Catalytic effects produced small IDTs. Experiments were repeated with a modified injector to prevent wall wetting, resulting in average IDTs that are substantially longer.

2:25 PM

Low Grade Waste Heat Driven Desalination and SO₂ Scrubbing: Srinivas Garimella¹; Donald Ziegler¹; James Klausner²; ¹Alcoa; ²University of Florida

By 2015, nearly half the world's population will live in "water stressed" areas. Production of fresh water utilizing waste heat from industrial processes has been identified globally as a research priority. About 15% of the electricity required to produce aluminum is lost as waste heat in the off-gas. However, the heat's low grade limits reuse. The off-gases contain 50-150 ppm SO₂; tightening regulations coupled with increasing coke sulfur levels are motivating SO₂ control, for which seawater scrubbing is attractive for smelters with suitable access. We describe a process that produces fresh water, utilizing the waste heat while scrubbing SO₂. It uses direct contact between seawater and off-gas to humidify the off-gas. The vapor is subsequently condensed. In smelter trials, a unit treating a slip stream produced high quality water at anticipated levels, attaining over 95% SO₂ scrubbing. Future work involves scaling the process to be economically attractive.

2:45 PM

Waste Heat Integration Potential Assessment through Exergy Analysis in an Aluminum Production Facility: Cassandre Nowicki¹; Louis Gosselin¹; Carl Duchesne¹; ¹Aluminium Research Centre - REGAL, Laval University

Quebec's primary aluminium production industry consumes roughly 39 TWh of electricity per year and is accountable for roughly 7 million tons of CO₂ equivalent. By tapping only a small portion of waste heat and integrating it inside the production facility itself, we can significantly



reduce GHG emissions and energy consumption. Although the amount of thermal waste can be adequately estimated by applying an energy balance to production processes, this provides very little information on the quality of waste heat and its potential for integration. A measure of exergy is required. Waste heat streams characterized by high exergy content may generally offer valuable incentives for recovery and integration. More generally, exergy values constrain integration possibilities. An exergy analysis is provided for the aluminium electrolytic reduction process. This is meant to guide future heat recovery initiatives and energy efficiency measures.

3:00 PM Break

3:05 PM

Study on Drying Characteristics of Australian Brown Coal Using Superheated Steam: *Tsuyoshi Kiriya*¹; Shozo Kaneko¹; Akira Hashimoto¹; Masafumi Maeda¹; ¹The University of Tokyo

Coal produces about 40% of the CO₂ emission in the world, and it is essential that it to be used more efficiently to prevent global warming. Victorian brown coal in Australia has over 60wt% moisture content and, when dried, it becomes highly reactive. Due to the difficulty in transporting it, brown coal is used as fuel for the thermal power stations near the mines. If a highly efficient drying system were developed, a dramatic increase in efficiency would be possible for these brown coal fired power stations. Moreover, brown coal can be easily gasified and converted to synthetic gaseous and liquid fuels or used in IGCC (Integrated coal Gasification Combined Cycle). This research focused on superheated steam drying, where the weight and temperature of variously sized single particles of brown coal were measured by this process, and the basic drying characteristics were investigated.

3:20 PM

Sustainability, Energy Efficiency and CO₂ Elimination in Concentrate Drying: *Jyri Talja*¹; Shaolong Chen¹; Hannu Mansikkaviita¹; ¹Kumera Corporation

Drying (water removal) prior to smelting is always economically feasible. Unnecessary heating of vapour can thus be eliminated resulting in savings of 5-15 MUSD every year. Thermodynamically removal of one ton of water out of copper concentrate at 100 °C requires some 3300 MJ/tH₂O. This consists of water heating (377 MJ), concentrate heating (509 MJ) and water evaporation (2260 MJ). More heat is needed as higher temperature is practiced to enhance the drying performance and reduce the equipment size. However, major nominator in drying energy efficiency is amount of gases. Drying technologies based on direct heating with fossil fuels (high gas flow rate), require additional energy of 1400-1600 MJ/tH₂O, compared to indirect modern drying at 250-400 MJ/tH₂O. Significant energy benefits (900-1300 MJ/tH₂O) with additional bonus profit of 2-4 MUSD/y year and full elimination of 40 000 tpy CO₂ / smelter are available by selecting sustainable, energy efficient steam drying.

3:35 PM

COURSE50 Development of Heat Recovery System from Steelmaking Slag: *Yasutaka Ta*¹; Hiroyuki Tobo¹; Yuuki Hagio¹; Michihiro Kuwayama¹; ¹JFE Steel Corporation

The steel industry in Japan has been working on the projects of "Environmentally Harmonized Steelmaking Process Technology Development (COURSE50)". COURSE50 aims at developing technologies to reduce CO₂ emissions by approximately 30%. As one of the projects, JFE Steel Corporation has been developing sensible heat recovery process from steelmaking slag. Molten slag, which is also generated in steel plants, has high temperature, but its energy has not been harnessed. To recover the thermal energy from the slag and to apply to separation of CO₂ are economical and environmental conscious ways because CO₂ separation technology requires an enormous amount of energy. In our process, molten slag is solidified continuously on water-cooled roll and the solidified slag plates are charged into counter-current

heat recovery equipment. In laboratory scale experiments, more than 30% heat recovery ratio was optimizing by controlling the thickness of slag. This research was carried out as NEDO project.

3:50 PM

Dry Granulation of Molten Blast Furnace Slag and Heat Recovery from Obtained Particles: *Qin Yuelin*¹; Lv Xuewei¹; Bai Chenguang¹; Qiu Guibao¹; ¹College of Materials Science & Engineering, Chongqing University

Blast furnace slag (BFS), is the main by-product in the ironmaking process, which contains large amounts of sensible heat. To recover the sensible heat, this paper described the hot experiments which were carried out in a rotary multi-holes cup atomizer, where the molten BFS was transformed into granules without water impingement; subsequently, a new method—pyrolysis the printed circuited board (PCB) with the hot BFS particle, was proposed for recovering the sensible heat in this study. The gaseous products were analyzed by gas analyzer. The residual of the PCB was analyzed by FT-IR and XRD respectively, and the obtained slag particles were analyzed by XRD. The results showed that it is a feasible process of pyrolyzing PCB powder with the hot BFS particle. The sensible heat of hot BF slag could be converted to chemical heat and a large amount of combustible gas could also be generated during the process.

4:05 PM

The Environment Load Assessment of Iron and Steel Producing BF-BOF and EAF Route Process: *Hongxu Li*¹; Shengli Tao¹; Hao Bai¹; Daqiang Cang¹; ¹University of Science and Technology

The life cycle inventory was compiled and assessment model based on Gabi software was established. Environmental impact of two different routes of BF-BOF and the EAF were analyzed respectively and intercompared. The results show that the EAF route is superior to the traditional BF-BOF route on almost all the environmental impact indexes, which including acidification potential, eutrophication potential, global warming potential, ozone depletion potential, etc. In the whole life cycle of BF-BOF route in China, the transporting process ranks the biggest contribution to the overall global warming potential, which caused by fossil fuel burning of transporting vehicles during the long distance from Australia to China. Apart from transporting process, Coking, blast furnace and iron mining processes could induce great environmental problems, while for the EAF route, the electricity consumption is considerable, which causing large amount of CO₂ emission indirectly. Based on the analysis, several further countermeasures were proposed.

4:20 PM

Aluminum Smelter Waste Heat Recovery Plant (Heat Exchangers Fouling and Corrosion-A Detailed Investigation): *Hadi Fanisalek*¹; Mohsen Bashiri¹; Reza Kamali¹; ¹Hormozal

The main bottleneck for primary aluminum production industry is dealing with a huge amount of input energy. The fact is that part of provided energy to aluminum production smelters will be lost as waste heat and it never used for aluminum production. One part of waste heat is escaping from the potroom exhaust gases, which was studied for possible recovery in a desalination plant to produce distilled water and the paper was presented in 2011 TMS Annual Meeting. However, it was shown that waste heat recovery plant to produce distilled water is highly profitable but the main fact is that the exhaust gases from potroom are highly corrosive, abrasive and dusty. The main challenge for desalination plant construction, which is using aluminum smelter exhaust gases as the main heat source, is the highly corrosive environment that makes the situation difficult and complicated for equipments design and plant construction. In this paper, we are trying to study a detailed investigation regarding the heat exchangers fouling, corrosion in heat exchangers including heat exchangers' material, how often we need to shut down the plant for maintenance or cleaning, and plant thermal efficiency with considering fouling.

Magnesium Technology 2012: Energy and Biomedical / Primary Production

Sponsored by: The Minerals, Metals and Materials Society, TMS Light Metals Division, TMS: Magnesium Committee
 Program Organizers: Suveen Mathaudhu, U.S. Army Research Office; Wim Sillekens, TNO; Norbert Hort, Helmholtz-Zentrum Geesthacht; Neale Neelameggham, U.S. Magnesium

Thursday PM
 March 15, 2012

Room: Southern V
 Location: Dolphin Resort

Session Chairs: Wim Sillekens, TNO; Neale Neelameggham, IND LLC

2:00 PM

In-Vitro Corrosion Studies of Bioabsorbable Magnesium Alloys: Puneet Gill¹; Norman Munroe¹; ¹Florida International University

In this investigation, the electrochemical degradation of various cast manufactured binary, ternary and quaternary magnesium alloys were studied in accordance with (ASTM G 102-89) and by immersion test (ASTM G 31-72) in simulated body fluid (SBF) and SBF with amino acids at 37°C. Hydrogen evolution from each alloy was measured under simulated body conditions and the concentration of metal ions in the medium after each corrosion test was determined by inductive coupled plasma mass spectroscopy (ICP-MS). The change in surface morphologies, composition and the microstructure of the alloys were observed before and after corrosion tests by scanning electron microscopy (SEM), X ray diffraction (XRD) and transmission electron microscopy (TEM).

2:20 PM

High-Capacity Hydrogen-Based Green-Energy Storage Solutions for the Grid Balancing: Fabrizio D'Errico¹; Adamo Scirenci²; ¹Politecnico di Milano; ²Mc Phy Energy SA

One of the current main challenges in green-power storage and smart grids is the lack of effective solutions for accommodating the unbalance between renewable energy sources, that offer intermittent electricity supply, and a variable electricity demand. Energy management systems have to be foreseen for the near future, while they still represent a major challenge. Integrating intermittent renewable energy sources, by safe and cost-effective energy storage systems based on solid state hydrogen is today achievable thanks to recently some technology breakthroughs. Optimized solid storage method made of magnesium-based hydrides guarantees a very rapid absorption and desorption kinetics. Coupled with electrolyzer technology, high-capacity storage of green-hydrogen is therefore paracticable. Besides these aspects, magnesium has been emerging as environmentally friend energy storage method to sustain integration, monitoring and control of large quantity of GWh from high capacity renewable generation in the EU.

2:40 PM

Reaction Sintering of Mg₂Si Thermoelectric Materials by Microwave Irradiation

Zhou Cai¹; Bai Guang²; ¹Chongqing University of Science and Technology; ²Chongqing University

In order to reduce the oxidizing and volatilizing caused by Mg element in the traditional methods for synthesizing Mg₂Si compounds, solid state phase reaction at low temperature was introduced by microwave field. XRD was used to characterize the powders. At the same time, the influences of parameters during the synthesis processing were discussed. The results suggest that the heating profile is also dependent on the initial green density and higher green density provides lower heating rate while power setting are fixed and the oxidation of Mg can be rest rained by changing microwave heating programs. It was found that high purity Mg₂Si intermetallic compound can be obtained with excessive content of 8at% Mg from the stoichiometric Mg₂Si, 853K and 30 min.

3:00 PM

Charge-Discharge Mechanism of MgC Powders and Mg-Li Alloy Thin Film Materials: Yen-Ting Chen¹; Fei-Yi Hung²; Truan-Sheng Lui²; Ren-Syuan Xiao¹; Yi-Wei Tseng¹; Chih-Hsien Wang²; ¹Institute of Nanotechnology and Microsystems Engineering, Center for Micro/Nano Science and Technology, National Cheng Kung University, Tainan, TAIWAN 701.; ²Department of Materials Science and Engineering, National Cheng Kung University, Tainan, TAIWAN 701.

Magnesium-carbon powders and Magnesium-lithium powders were used as the anode materials for lithium ion batteries to investigate the structure and electrochemical behavior in room temperature. The composition of Mg-C powders contained 1:1 and 9:1. The powders and the thermal evaporated films of Mg-10Li were compared with Mg-C systems. In addition, Mg-10Li thermal evaporated film was used as the experimental materials to process the annealing treatment. The results show that Mg-C powders system had the interface effect of a Cu foil to reduce the electrochemical reaction. With increasing the carbon powder content, the charge-discharge characteristics of Mg-C powders was raised. Notably, the Mg-10Li specimen had better cycling properties than that of Mg-50C (1:1). After annealing at 200°C for 1hr, Mg-10Li alloy film not only increased the capacity, but also improved the charge-discharge cyclability.

3:20 PM Break

3:40 PM

Control of Yttrium Diffusion Out of Yttria Stabilized Zirconia During SOM Electrolysis for Magnesium Production: Eric Gratz¹; Soobhankar Pati²; Jarrod Milshtein¹; Adam Powell²; Uday Pal¹; ¹Boston University; ²Metal Oxygen Separation Technologies

The solid oxide membrane (SOM) process has been used to produce magnesium by direct electrolysis of its oxide. In this process MgO is dissolved in a molten CaF₂-MgF₂ flux and an yttria-stabilized zirconia (YSZ) SOM membrane separates the cathode and the flux from the anode. YSZ membrane stability limits the operating life of the SOM electrolyzer. The YSZ membrane is known to degrade due to diffusion of yttrium into the flux. Yttrium diffusion can however be decreased by adding YF₃ to the flux. This study investigates the long-term stability of the YSZ membrane. Yttrium composition profiles in the YSZ membrane were determined using WDS as a function of immersion time and YF₃ content in the flux. An analytic solution to the diffusion equation was used to model the diffusion process. This study allows the determination of the optimum YF₃ content needed in the flux to minimize yttrium diffusion and increase membrane stability to be determined.

4:00 PM

Study on the Thermodynamic and Experimental Carbothermic Reduction of Garnierite: Tao Qu¹; Yang Tian¹; Bin Yang¹; Bao-Qiang Xu¹; Da-Chun Liu¹; Yong-Nian Dai¹; ¹National Engineering Laboratory for Vacuum Metallurgy, Kunming University of Science and Technology

The overall utilization of magnesium and other metals should be systematically considered during the exploration of deficient garnierite. In this paper the thermodynamic analysis of the carbothermic reduction process for extracting metal magnesium from garnierite in vacuum was carried out to investigate its feasibility. The calculation results indicate that it is feasible technically that the carbothermic reduction process for extracting metal magnesium from garnierite in vacuum. Under the temperature of 1500°C and vacuum degree is less than 300Pa, metal magnesium was obtained. The Nickel content in residue is more than twice as garnierite ore.

4:20 PM

Mechanism of Carbothermic Reduction of Magnesia and Reverse Reaction: Yang Tian¹; Tao Qu¹; Bin Yang¹; Hong-Xiang Liu¹; Cheng-Bo Yang¹; Yong-Nian Dai¹; ¹Kunming University of Science and Technology

Abstract: In this paper, the mechanism of the carbothermic reduction process to extract magnesium from magnesia and the reversion reaction in vacuum were investigated. The carbon monoxide (CO) content of the gas,



phases of the condensing product, surface morphology of the reduction slag and phase of the distillation product were measured by means of gas chromatography (GC), XRD, and SEM. The experimental results indicated that Mg is generated by magnesia and carbon at 1623K and 30~100Pa in the carbothermic reduction process. The main gas in carbothermic reduction process is carbon monoxide, no carbon dioxide occurred at any reaction time, the reduction reaction is $MgO(s)+C(s)=Mg(g)+CO(g)$. The gas-phase reversion will commence as soon as a saturated gas mixture is cooled. The reversion reactions are favored below 1373K. The distillation product by vacuum distillation process produced a high purity metal magnesium product, it can be deduced that reversion reaction occurred at low temperature and 30~100Pa during carbothermic reduction. Through the calculation of reversion reaction, the peak value of γ is less than 9%.

Magnesium Technology 2012: Processing-Microstructure-Property Relationships II

Sponsored by: The Minerals, Metals and Materials Society, TMS Light Metals Division, TMS: Magnesium Committee
Program Organizers: Suveen Mathaudhu, U.S. Army Research Office; Wim Sillekens, TNO; Norbert Hort, Helmholtz-Zentrum Geesthacht; Neale Neelameggham, U.S. Magnesium

Thursday PM
 March 15, 2012

Room: Southern IV
 Location: Dolphin Resort

Session Chairs: Alan Luo, GM Global Research and Development; Fabrizio D'Errico, Politecnico di Milano

2:00 PM

Enhancement of Strength and Ductility of Mg₉₆Zn₂Y₂ Rolled Sheet by Controlling Structure and Plastic Deformation: *Masafumi Noda*¹; Yoshihito Kawamura²; Hiroshi Sakurai²; Kunio Funami³; ¹Chiba Institute of Technology; ²Department of Materials Science, Kumamoto University; ³Department of Mechanical Science and Engineering, Chiba Institute of Technology

Mg-Zn-Y alloys are well known that dramatically enhanced strength during plastic deformation because the kink bands formed in the LPSO phase. On the other hands, high strength Mg-Zn-RE alloy is achieved by an extrusion process it was difficult to know a development of LPSO and Alpha Mg Phases during processing. In this present study, the effect of fine dispersed LPSO and alpha Mg phase on development of high strength Mg-Zn-Y rolled sheet a few pass schedules and its mechanical properties and the thermal stability were investigated. The tensile yield strength and elongation of Mg-Zn-Y rolled sheets achieved to 360 MPa and 5 % at 673 K and 4 pass used by thermo-mechanical controlled processing, respectively. On the other hands, tensile yield strength decreases while elongation improves in 623K or more so that alpha Mg phase grain growth and kink bands induced LPSO phase recovere.

2:20 PM

Microstructural Characteristics of High Rate Plastic Deformation in Elektron WE43 Magnesium Alloys: *Joseph Hamilton*¹; Sarah Brennan¹; Yongho Sohn¹; Bruce Davis²; Rick DeLorme²; Kyu Cho³; ¹University of Central Florida; ²Magnesium Elektron North America; ³US Army Research Laboratory

High strain rate deformation of WE43 magnesium alloy was carried out by high velocity impacts, and the characteristics and mechanisms of microstructural damage were examined. Six samples were subjected to a variety of high velocity impact loadings that resulted in both partial and full damage. Optical, scanning and transmission electron microscopy analyses were performed in order to identify regions of shear localization. These regions were used to map, both quantitatively and qualitatively, the effects of deformation on the microstructure. Shear localization was observed in every sample, and its depth was measured. Evidence of shear

localization was observed to a greater extent in samples with partial damage while fracturing was observed more frequently in samples with full damage.

2:40 PM

Microstructure and Mechanical Properties of As-Extruded Mg-Sn-Al-Zn Alloys: *Sung Hyuk Park*¹; Young Min Kim¹; Chang Dong Yim¹; Ha-Sik Kim¹; Bong Sun You¹; ¹Korea Institute of Materials Science

Mg-xSn-yAl-1Zn (x=5, 6, 7 and 8 wt.%, x+y=9 wt.%) alloys were subjected to indirect extrusion and the extruded bar was examined by scanning electron microscopy, transmission electron microscopy, electron backscatter diffraction (EBSD) and X-ray diffraction. Tensile and compressive tests at room temperature were performed parallel to extrusion direction to assess the tension-compression asymmetries in yield behavior. The results showed that the basal texture are basically similar, however, the grain size decreases and the amount of fine particles such as Mg₂Sn phase increase with increasing the Sn content. Mg-8Sn-1Al-Zn alloy, which has a higher number of particles and smaller grain size, showed the highest yield strength due to the combined effects of grain boundary hardening and precipitation hardening. While, Mg-5Sn-4Al-1Zn alloy exhibited a lower degree of yield asymmetry because twinning was retarded during compression by fine particles of Mg₁₇Al₁₂ phases formed on the non-basal plane.

3:00 PM

Tensile Properties of Three Preform-Annealed Magnesium Alloy Sheets: *Junyong Min*¹; Jon Carter²; Ravi Verma²; ¹Tongji University; ²GM R&D

Automotive structural application of magnesium alloy sheet has been hindered by the low room-temperature formability of typical sheets. One approach to effectively increase formability is to change the forming process from one which involves a single stamping hit to one which utilizes two hits plus an intermediate anneal (i.e., "preform anneal process"). In this paper, the preform annealing behavior of three rolled sheets was studied using uniaxial tensile tests. The sheets studied were: conventionally rolled (CR) AZ31B, CR ZEK100, and specially rolled (SPR) AZ31B. The preform annealing process was found to increase the total elongation of all three sheets compared to the elongation in the annealed O-temper. The CR ZEK100 with a thickness of 1.5 mm showed more attractive tensile properties than the 1.6 mm CR AZ31B. Although the SPR AZ31B has a thickness of only 0.7 mm, it still has elongation comparable to the 1.6 mm CR AZ31B.

3:20 PM

The Role of Intermetallics on Creep Behaviour of Extruded Magnesium Alloys: *Michelle Fletcher*¹; Lukas Bichler¹; *Dimitry Sediako*²; ¹UBC Okanagan; ²NRC - CNRC

This study analyzed six extruded high performance magnesium alloys (AE33, AE42, AJ32, AX30, EZ33 and ZE10) developed for elevated temperature applications. In-Situ Neutron diffraction was used to determine alloy tensile and compressive creep behavior at 150 and 175°C in the radial as well as transverse directions to determine the effect of texture on creep performance. The aluminum containing alloys exhibited larger creep strains than the EZ and ZE alloys; the highest strain was seen by AE33 of 9.9% compared to 0.2% exhibited by ZE10. Microstructure analysis has shown that the distribution and composition of secondary phases is critical for creep resistance. The aluminum containing alloys have acicular and globular intermetallics, whereas the EZ and ZE alloys contain fine and irregular intermetallics which effectively pinned grains under high temperature stresses. Significant recrystallization was also apparent in the aluminum containing alloys but was not observed in the EZ and ZE alloys.

3:40 PM Break**4:00 PM****High Performance Mg-System Alloys for Weight Saving Applications: First Year Results from the GREEN METALLURGY EU Project:**

*Fabrizio D'Errico*¹; Gerardo Garces Plaza²; Markus Hofer³; Shae Kim⁴; ¹Politecnico di Milano; ²Centro Nacional de Investigaciones Metalúrgicas; ³Buhler AG; ⁴Korea Institute of Industrial Technology

The GREEN METALLURGY Project, a LIFE+ project co-financed by the EU Commission, has just concluded its first year. The Project seeks to set manufacturing processes at a pre-industrial scale for nanostructured-based high-performance Mg-Zn(Y) magnesium alloys. The Project's goal is the reduction of specific energy consumed and the overall carbon-footprint produced in the cradle-to-exit gate phases. Preliminary results addressed potentialities of the upstream manufacturing process pathway. Two Mg-Zn(Y) system alloys with rapid solidifying powders have been produced and directly extruded for 100% densification. Examination of the mechanical properties showed that such materials exhibit strength and elongation comparable to several high performing aluminum alloys; 390 MPa and 440 MPa for the average UTS for two different system alloys, and 10% and 15% elongations for two system alloys. These results, together with the low-environmental impact targeted, make these novel Mg alloys competitive as lightweight high-performance materials for automotive components.

4:20 PM**Effect of Extrusion Conditions on Microstructure and Texture of Mg-1% Mn and Mg-1% Mn-1.6% Sr Alloys:** *Hemant Borkar*¹; Mihriban Pekguleryuz¹; ¹McGill University

Mg-1% Mn (M1) and Mg-1% Mn-1.6% Sr alloys have been subjected to hot extrusion and the effect of extrusion conditions on the microstructure and texture has been investigated. Addition of Sr to M1 alloy refines the extruded microstructure. Two different ram speeds of 4 mm/s and 8 mm/s and two different temperatures of 300°C and 350°C have been used in the study. The extent of recrystallization increases with increasing ram speed. The texture of extruded M1 weakens with Sr addition. The mechanism of texture weakening is suggested to be PSN with formation of new grains having orientations different than that of parent grains.

4:40 PM**On the Deformed Microstructure of Rolled Mg-2.9Y:** *Amir Farzadfar*¹; Mehdi Sanjari¹; In-Ho Jung¹; Elhachmi Essadiqi²; Stephen Yue¹; ¹McGill University; ²CANMET

The hot and cold rolled microstructures of a Mg-2.9Y alloy were examined by means of metallography, X-ray texture measurement and EBSD technique. It is found that Y in solid solution suppresses dynamic recrystallization even at 450 °C. After rolling, a heterogeneous microstructure containing twins and bands is obtained. The bands were found to originate from double and compression twins, and are locations of high stored energy. The bulk texture of the rolled material consists of the typical basal component, and also a component from the ND towards the TD. The latter component results from the presence of parent grains with c-axis along the TD. The strain is accommodated in such parent grains by extension twinning and possibly prismatic slip. At all rolling temperatures, internal strain exhibits a relatively uniform distribution, indicating that all grains contributed to the deformation.

Materials and Fuels for the Current and Advanced Nuclear Reactors: Nuclear Fuels and Materials

Sponsored by: The Minerals, Metals and Materials Society, TMS Structural Materials Division, TMS/ASM: Corrosion and Environmental Effects Committee, TMS/ASM: Nuclear Materials Committee

Program Organizers: Ramprashad Prabhakaran, Idaho National Laboratory; Dennis Keiser, Idaho National Laboratory; Raul Rebak, GE Global Research

Thursday PM
March 15, 2012

Room: Swan 4
Location: Swan Resort

Session Chair: Leah Squires, Idaho National Laboratory

2:00 PM**Neptunium Oxide Reduction Technique:** *Leah Squires*¹; Paul Lessing¹; James Stuart¹; Bryan Forsmann²; ¹Idaho National Laboratory; ²Boise State University

A process to reduce neptunium oxide (NpO₂) to neptunium metal was developed. NpO₂ is combined with calcium and heated to temperatures between 650°C and 850°C under argon. Three successful trials were conducted to yield a total of approximately 20 g of neptunium with purity estimated greater than 97%. The metal is needed to determine important thermal and phase properties of binary neptunium systems as well as fresh metallic fuels that simulate the compositions of recycled fuel. The process development was necessary since most of the neptunium available is present as the oxide. Future efforts are planned for understanding the process parameters in relation to neptunium purity, and for purifying the metal produced.

2:20 PM**Enthalpy of gamma-delta Transition in Ternary U-Pu-Zr Fuel Alloys:** *Cynthia Papesch*¹; Thomas O'Holleran¹; Robert Mariani¹; Matthew Cromwell²; ¹Idaho National Laboratory; ²University of Idaho

Several ternary nuclear fuel alloys were investigated using differential scanning calorimetry. The results were evaluated using a curve-fitting routine, and the enthalpies of individual phase transitions were determined. Individual transitions were assigned with reference to published ternary phase diagrams, and a compositional analysis for the partial transformations of each alloy allowed the first determination of the gamma-delta transition enthalpy for the ternary fuel alloys. These results agree with prior research for binary fuel alloys that found the enthalpy to be approximately 5 kJ per mole with some variation depending on the exact composition within the broad delta-UZr₂ phase range. The comparable results suggest that the heat of solution for the zirconium in the ternary delta-phase is similar to that for zirconium in the binary delta-phase, which might be expected; however it is possible that the activities of Pu and Zr in the delta phase may be self-compensating.

2:40 PM**Microstructural Analysis of Ion-Implanted PyC/B-SiC:** *Rob Coward*¹; Shyam Dwarknath²; Mitra Taheri¹; ¹Drexel University; ²University of Michigan

Common metallic fission products, such as Ag, diffuse through PyC/SiC to create precipitates in the SiC zinc blende structure. In this work, the effect of ion implantation of Ag on pyrolytic carbon (PyC) coated CVD β-silicon carbide (SiC) was studied using X-ray photoelectron spectroscopy (XPS), electron backscatter detection (EBSD), Auger electron spectroscopy (AES), and transmission electron microscopy (TEM). The PyC coated β-SiC samples were implanted with 400 keV

Ag at 22°C to a fluence of 1×10^{16} atoms/cm², which corresponds to a peak of 1.25 atom % at a depth of approximately 170 nm into the PyC. The samples were then annealed at temperatures of 1600°C, 1300°C, 1100°C and examined using XPS, EBSD, AES, and TEM to verify the microstructural evolution and also to examine preferential segregation of the implanted Ag along specific grain boundaries.

3:00 PM

Role of Microstructure on Ag and Cs Diffusion in SiC: *Tyler Gerczak¹; Todd Allen¹*; ¹University of Wisconsin-Madison

TRIStructural-ISOTropic fuel has been identified as the fuel of choice for the very high temperature gas cooled reactor. In the fuel design the SiC layer is the main fission product barrier, however Ag and Cs fission products have been observed to release from intact particles resulting in safety and operational issues. The release has been suggested to be dictated by the SiC microstructure. To understand Ag and Cs diffusion in TRISO, we simulated diffusion via ion implantation diffusion couples exposed to elevated temperature. The effect of microstructure is understood by investigating diffusion in various SiC substrates, single crystal and polycrystalline SiC. Depth profiles measured by SIMS suggest grain boundary diffusion to be a fast diffusion pathway. The role of individual grain boundaries will be investigated by atom probe tomography to understand the contribution of grain boundary character on diffusion.

3:20 PM

Grain Size Dependence of Radiation Response in Silicon Carbide: *Laura Jamison¹; Peng Xu¹; Kumar Sridharan¹; Todd Allen¹*; ¹University of Wisconsin-Madison

Silicon carbide is of interest in nuclear systems as a structural material or as a diffusion barrier coating material in TRISO fuel particles because of its stability at high temperatures. Nanocrystalline silicon carbide (ncSiC) is of particular interest because the increased concentration of grain boundaries may cause the material to be more radiation resistant. The goal of this research is to compare the behavior of ncSiC and micron-scale grain size SiC under ion irradiation. To accomplish this, nanopowder SiC samples and bulk CVD SiC samples were irradiated with Kr⁺ ions in an in-situ irradiation experiment. Additionally, the synthesis of bulk ncSiC by spark plasma sintering SiC nanoparticles is being investigated. Results of experiments to achieve satisfactorily high bulk densities while maintaining nanometer-scale grains will be presented. This work is supported under a DOE-NEUP Graduate Fellowship, DOE-BES grant DE-FG02-08ER46493, and utilized NSF-supported shared facilities at the University of Wisconsin-Madison.

3:40 PM Break

3:50 PM

Silver Diffusion in PyC Coated β -SiC: *Shyam Dwaraknath¹; Gary Was¹*; ¹University of Michigan

Understanding the mechanism and quantifying the rate by which silver diffuses through CVD β -silicon carbide (SiC) is crucial to the success of the TRISO fuel design. The diffusion of Ag was studied using Rutherford backscattering spectrometry (RBS) on a novel specimen design. Thin (~300 nm) films of highly anisotropic pyrolytic carbon (PyC) were deposited on CVD β -SiC specimen. The PyC films were subsequently implanted with 400 keV Ag at 22°C to a dose of 1×10^{16} cm⁻², which corresponds to a peak of 1.25 atom % at a depth of approximately 170 nm into the PyC layer. A 10 nm Mo cap was then deposited by electron beam evaporation to retain the implanted Ag in post-deposition annealing treatments. RBS was used to determine the Ag composition profiles as a function of annealing temperature: 1600°C, 1300°C, 1100°C, from which diffusion coefficients were calculated.

4:10 PM

Mechanism of Proton Irradiation-Induced Creep of Pyrolytic Carbon: *Anne Campbell¹; Gary Was¹*; ¹University of Michigan

Determining the mechanism of irradiation-induced creep of pyrolytic carbon is critical to predicting the integrity of the TRISO fuel particles for the Generation-IV Very High Temperature Reactor. Proton irradiation-induced creep experiments have been performed on graphite samples to provide a baseline for comparison of the pyrolytic carbon behavior. The experiments performed on graphite show a linear dependence on both applied stress and dose rate. The irradiation-induced creep behavior of the pyrolytic carbon will be presented and compared with the graphite behavior at similar stress, dose rate, and temperature ranges. Finally a mechanism will be proposed that describes the proton irradiation-induced behavior of pyrolytic carbon. The mechanism will be supported with analysis of the effect of irradiation-induced creep on the sample anisotropy, density, and Young's modulus.

4:30 PM

Gas Evolution from Lithium Hydride During X-Irradiation: *Carol Haertling¹; Joseph Tesmer¹; Yongqiang Wang¹; William McAlexander¹*; ¹Los Alamos National Laboratory

Lithium hydride (LiH) is a highly reactive solid that may be used in radiation environments, where ionizing radiation is present that can disrupt the structure of a material. This disruption creates defects and can produce gases, most obviously H₂ gas; irradiation of LiH corrosion products may produce further gases. We have performed introductory experiments to determine the effects of radiolysis on LiH and its ubiquitous hydrolysis product, LiOH. Our experiments focus on x-ray irradiations. We have used a particle accelerator in the Ion Beam Materials Laboratory to produce characteristic x-rays at desired energies from metal targets. During irradiation, evolved gases were measured, particularly H₂, and quantified. Our data allows prediction of concentrations that could be released over time.

4:50 PM

Study of MnO₂/Ag₂O Mixture for an Efficient Trapping of Hydrogen: *Kevin Galliez¹; Philippe Deniard²; David Lambertin¹; Stephane Jobic²; Florence Bart¹*; ¹CEA; ²CNRS

Management of explosion risk from hydrogen produced by radiolysis of organic compounds in waste packages is a major problem for the safety of radioactive wastes transportation. This risk can be minimized through the use of a hydrogen getter. Different getters exist to trap hydrogen: organic materials, recombiners, hydrides and mineral oxides. Among different mineral oxides MnO₂/Ag₂O mixture forming the so called getter has been selected. MnO₂ plays the role of a trap whereas Ag₂O that of the promoter. In the MnO₂ family the nsutite variety leads to the best efficiency when it is added to 13wt% of Ag₂O, tested under hydrogen/nitrogen atmosphere. Parameters, such as specific area and defects have been studied as well as the role of the promoter. From magnetism measurements the reduction of manganese IV⁺ to III⁺ has been clearly evidenced, highlighting a chemisorption process of hydrogen trapping.

5:10 PM

Novel Methods of Hydrogen Isotope Sequestration using Proton Conducting Ceramic Separation Membranes in Next Generation Nuclear Energy Systems: *Kyle Brinkman¹*; ¹Savannah River National Laboratory (SRNL)

A technical hurdle to the use of high temperature heat from the exhaust produced in the next generation nuclear processes in commercial applications such as nuclear hydrogen production is the trace level of tritium present in the exhaust gas streams. Successful tritium sequestration in situ will make it possible to maximize the heat values available for hydrogen production and other commercial applications in NGNP systems. In addition, tritium collection and confinement is required from next generation fusion machines where a highly tritiated water (HTW) stream could be generated in such processes like vacuum vessel wall conditioning, and cryopump regeneration. This presentation outlines

the synthesis and characterization of perovskite based (ABO₃) proton conducting ceramic materials for use as hydrogen isotope gas separation membranes and high temperature solid oxide electrolysis cells.

Materials and Fuels for the Current and Advanced Nuclear Reactors: Structural Materials - Irradiation Studies II

Sponsored by: The Minerals, Metals and Materials Society, TMS Structural Materials Division, TMS/ASM: Corrosion and Environmental Effects Committee, TMS/ASM: Nuclear Materials Committee

Program Organizers: Ramprasad Prabhakaran, Idaho National Laboratory; Dennis Keiser, Idaho National Laboratory; Raul Rebak, GE Global Research

Thursday PM Room: Swan 2
March 15, 2012 Location: Swan Resort

Session Chair: James Cole, Idaho National Laboratory

2:00 PM Invited

Microstructural Characterization of Activated Materials with Neutron Diffraction: *Donald Brown*¹; Thomas Sisneros¹; Paula Mosbrucker¹; Levente Balogh¹; ¹Los Alamos National Lab

Diffraction is well suited to the characterization of microstructures. Neutron diffraction, in particular, has some undeniable advantages for studying activated samples. Neutrons penetrate millimeters into most materials, providing a statistically relevant probe of the microstructure in the bulk of the material. Moreover, little or no hazardous and costly sample preparation is necessary, which enables repeat tests on the same sample or even in-situ measurements under simulated operating conditions. Finally, neutron detectors are often insensitive to background gamma radiation emitted from activated samples. The SMARTS diffractometer at the Lujan Center was designed to study engineering materials under their operating conditions and, as such, has sophisticated sample environments enabling in-situ ND studies during deformation and at non-ambient temperatures. This talk will use the example of in-situ diffraction measurements during annealing and deformation of irradiated HT-9 steel to highlight the capabilities of the instrument, in particular, related to the study of activated materials.

2:30 PM

On the Influence of Proton and He Irradiation on Mechanical Properties and Microstructure of Intermetallic Strengthened Steels: *E. Stergar*¹; Christina Hofer²; S. A. Maloy³; P. Hosemann¹; ¹University of California-Berkeley; ²University of Leoben; ³Los Alamos National Laboratory

Proper heat treatment of specialized tool-steels (maraging-steels) leads to formation of coherent, nanometer-sized, fine dispersed intermetallic precipitates with a number density of 10^{23} - 10^{24} m⁻³. These number densities are comparable to those of nanostructured alloys which gain their radiation resistance from nanometer sized (oxides) precipitates. In contrast to nanostructured alloys where elaborate and complicated manufacturing processes (powder milling, HIPping) are necessary intermetallic precipitates are formed by solution annealing and subsequent heat treatment. Although not suitable for very high temperature applications, recent investigations show promising mechanical properties and thermal stability in radiation environment up to 480/176C. In this work the concept of intermetallic precipitates acting as defect sinks and their evolution under irradiation is explored. For this study Ion beam irradiations were performed to cause radiation damage up to 2 dpa. High resolution post irradiation examination (nanoindentation, TEM, atom-probe) was used to link changes in materials properties and microstructure of different maraging-steels.

2:50 PM

Characterization of Ion Irradiation Effects on the Microstructure of 316 Austenitic Stainless Steel: *Alexandre Volgin*¹; Bertrand Radiguet²; Philippe Pareige²; Marie-France Barthe³; Pierre Desgardin³; Brigitte Décamps⁴; Aurélie Gentils⁴; Cédric Pokor⁵; ¹EDF R&D MMC / GPM UMR CNRS 6634 - Université et INSA de Rouen; ²GPM UMR CNRS 6634 - Université et INSA de Rouen; ³CEMHTI CNRS UPR 3079; ⁴CSNSM, CNRS-IN2P3, Université Paris-Sud; ⁵EDF R&D MMC

Internal structures of Pressure Water Reactors (PWR) are maintained by bolts made of 316 austenitic stainless steel (SS). They are subjected to neutron irradiation, which can lead to the cracking of bolts by the complex phenomenon of Irradiation Assisted Stress Corrosion Cracking (IASCC). One of the origins of IASCC is the evolution of the steel microstructure during irradiation. In order to get a better understanding of irradiation effects on the microstructure of austenitic SS, model alloys (FeCrNi, FeCrNiSi) and 316 austenitic SS were ion irradiated at 200°C and 450°C, up to 5 displacements per atom (dpa). Complementary techniques were used to characterize the steel: Atom Probe Tomography to quantify local chemical changes, Transmission Electron Microscopy to get information about defects clusters (loops and cavities) and Positron Annihilation Spectroscopy to characterize vacancy type defects. The experimental results, obtained in the PERFORM60 European project, will be detailed and discussed in this talk.

3:10 PM

Irradiation Induced Phase Change and Microstructures in X-750 CANDU Spacer Materials: *Ken Zhang*¹; Colin Judge²; Zhongwen Yao¹; ¹Queen's University; ²AECL – Chalk River Laboratories

Work on X-750 spacers removed from CANDU reactors has shown the development of many small cavities within the metal matrix and along grain boundaries. To simulate the neutron irradiation induced phase and microstructural changes, in-situ heavy ion irradiations under observation of an intermediate voltage electron microscope (IVEM) are carried out at various temperatures. Apart from dislocation loops, the irradiation damage consists mostly of stacking fault tetrahedra (SFTs), the remaining being unidentified defects. The size and fraction of SFTs appears to be independent of dose. The γ' precipitates were apparently disordered at very low dose (<0.2 dpa) when irradiated at temperature up to 400°C, but stable up to high doses (>6 dpa) at 500°C. Contrary to the evidence collected for ex-service spacers, no voids were observed at all doses and temperatures, indicating that the radiation damage rate and Helium production may influence the formation of cavities.

3:30 PM

Pair Distribution Function Analysis of Irradiated Cladding and Duct Reactor Materials: *Avishai Ofan*¹; Simerjeet Gill¹; Stuart Maloy²; Lars Ehm¹; Lynne Ecker¹; ¹BNL; ²LANL

Ferritic-martensitic (F/M) steels have properties such as low swelling, low activation, resistance to embrittlement and hardening, and good corrosion resistance thus making them good candidates' materials for Generation IV reactors. To qualify candidate materials for nuclear structural materials for Generation IV reactors their response to long term irradiation to high doses at high temperatures should be investigated. Total scattering and pair distribution function (PDF) analysis are useful for atomic structure analysis of materials with high degree of disorder, thus making them promising techniques for studying phase transition and defects in irradiated steels. In this presentation we will discuss the microstructure of the F/M HT9 steel duct taken from representative locations of the ACO-3 duct of Fast Flux Test Facility (FFTF) after long term irradiation up to a dose of 147 dpa and temperatures from 416 to 504°C based on XRD and PDF analysis results.



TMS 2012

141st Annual Meeting & Exhibition

THURSDAY PM

3:50 PM Break

4:00 PM

Toward a Better Understanding of the Hydrogen Impact on the Radiation Induced Growth of Zirconium Alloys: *Lea Tournadre*¹;

Fabien Onimus¹; Jean-Luc Bechade¹; Didier Gilbon¹; Jean-Marc Cloue²; Jean-Paul Mardon²; Xavier Feaugas³; Ovidiu Toader⁴; ¹CEA; ²AREVA; ³Laboratoire d'Etude des Matériaux en Milieux Agressifs (LEMMA); ⁴Michigan Ion Beam Laboratory (MIBL)

Under neutron irradiation, recrystallized zirconium alloys, used as structural materials for Pressurized Water Reactor fuel assemblies, undergo stress-free growth which accelerates for high irradiation doses. This acceleration is correlated to the formation of c-component vacancy dislocation loops. Some feedbacks from neutron irradiations show that the in service hydrogen pick-up could influence the fuel assembly radiation-induced elongation. 2 MeV proton irradiations were performed on as received and pre-hydrided materials in M5® and recrystallized Zircaloy-4. The irradiations were conducted on a Tandem Accelerator (MIBL/University of Michigan) at 623K up to three doses. Observations by Transmission Electron Microscopy show, in some cases, a significant impact of the hydrogen content on densities and distributions of the c-component loop microstructures. For both grades, the c-component loops evolution with dose will be examined and compared to the neutron irradiated microstructures. Then, the role played by hydrogen in solid solution and as precipitated hydrides will be discussed.

4:20 PM

Influence of Copper Level on Neutron Irradiation Effects in Low Copper Pressurized Water Reactor Vessel Steels: *Hefei Huang*¹; Bertrand Radiguet¹; Patrick Todeschini²; François Clémendot³; Philippe Pareige¹; ¹GPM UMR CNRS 6634 - Université et INSA du Rouen; ²EDF R&D MMC; ³EDF-CEIDRE

Neutron irradiation results in hardening and embrittlement of Reactor Pressure Vessel (RPV) steels. To guarantee safe operation of reactors, this embrittlement has to be conservatively evaluated. Since it is linked with the microstructure evolution of the steel (formation of solute clusters, point defects clusters ...), microstructural data on irradiated steels bring information on the validity of the models used for embrittlement prediction. So different base metals from French RPV surveillance program (neutron irradiation in production reactor conditions) were characterised at atomic scale, by Atom Probe Tomography. The evolution of solute cluster characteristics as a function of neutron fluence (up to doses corresponding to 40 years of operation) were characterised. The comparison between results obtained on several French fleet RPV steels provides information about the effect of small variation of nominal copper level. Experimental results are compared with the latest correlation used for the embrittlement assessment of French RPV fleet.

4:40 PM

A Synchrotron X-ray Diffraction and Transmission Electron Microscopy Study of Ion-Implantation Induced Microstructure Evolution on the Nuclear-Grade Graphite: *E-Wen Huang*¹; *Chang Chung-Kai*²; Shuo-Cheng Tsai³; Ji-Jung Kai³; ¹Department of Chemical & Materials Engineering and Center for Neutron Beam Applications, National Central University; ²Central University; ³Department of Engineering and System Science, National Tsing-Hua University

We simulate the neutron-irradiation damage on nuclear-grade graphite by C²⁺ ion-implantation. The graphite was artificially irradiated with 3 MeV C²⁺ ion to mimic the fast neutron-radiation damage of the High Temperature Gas-cooled Reactor (HTGR) core environment. The irradiation temperature were controlled at 600°C and 900°C in a high vacuum environment of 10⁻⁷ torr, respectively. The irradiation effect induced the graphite damage and caused the undesirable change in internal energy, microstructure and physical property – called Wigner effect. We quantify the structural integrity of the graphite with/without irradiation via synchrotron x-ray diffraction experiments and High-Resolution Transmission Electron Microscopy (HRTEM). The results

reveal the microstructure development subjected to the combination of the irradiation and high temperature effects. We described the standard deviation of d-spacing changing from irradiation effect at different temperature as disorder coefficient of d-spacing to discuss the mechanism of deformation by synchrotron x-ray diffraction and High-Resolution Transmission Electron Microscopy.

5:00 PM

Investigating the Dissolution of Oxide Particles in ODS Steels under

Irradiation: *Ceri Williams*¹; Emmanuelle Marquis²; Paul Bagot¹; George Smith¹; ¹University of Oxford; ²University of Michigan

Oxide-dispersion-strengthened ferritic steels are candidate materials for structural applications in fusion power plants. A dispersion of ~2nm oxide nanoclusters maintains strength at high temperatures (~650°C), and stabilises the microstructure under irradiation. The majority of research reports no significant change to the nanoclusters after irradiation however, Allen et. al. have shown a reduction in particle size after ion irradiation up to doses of 150 dpa at 500–700°C (Journal of Nuclear Materials 2008, vol.375 p.26-37). To clarify the effect of temperature on the stability of the oxide dispersion, we use Atom Probe Tomography (APT) and TEM to characterise a 14Cr-2W-0.3Ti ODS alloy after Fe²⁺ ion implantation (5dpa up to 500°C). A significant reduction in mean particle size is observed at low temperatures. The mechanisms of particle dissolution will be discussed, together with the validity of using ion implantation as an analogue for fusion reactor conditions.

5:20 PM

Effects of Neutron Irradiation on Select MAX Phases: *Darin Tallman*¹;

Elizabeth Hoffman²; Dennis Vinson²; Robert Sindelar²; Gordon Kohse³; Michel Barsoum¹; ¹Drexel University; ²Savannah River National Lab; ³Massachusetts Institute of Technology

Gen IV nuclear reactors need materials that can withstand harsher environments than in current reactors. The Mn+1AX_n (MAX) phases are a group of layered machinable ternary compounds, where M is an early transition metal, A is a group 13 to 16 element, and X is C and/or N. These compounds possess mechanical properties atypical for ceramics, notably thermal conductivity and plasticity at high temperatures. Data about their irradiated properties are required to fully realize their potential. Research is thus ongoing to characterize their irradiated properties. The post-irradiated characterization of samples irradiated to 0.1 dpa will be presented, including TEM analysis of microstructure, and electrical resistivity.

5:40 PM

TEM Analysis of the Microstructure Evolution in Ion Irradiated Austenitic Stainless Steels: *Alexandre Volgin*¹; Cedric Pokor¹; Brigitte Decamps²; Aurelie Gentils²; Bertrand Radiguet³; Philippe Pareige³;

Abderrahim Al-Mazouzi¹; ¹EDF R&D; ²Centre de Spectrométrie Nucléaire et de Spectrométrie de Masse CNRS-IN2P3; ³Groupe de Physique des Matériaux UMR CNRS 6634

Austenitic stainless steels are widely used in nuclear power plants as internal structures of PWR. These steels are subjected to severe irradiation and temperature conditions. Understanding of microstructural changes of austenitic steels due to these conditions is an important task for safety and life-extension reasons. Ni ion irradiation on thin foils and in bulk is done in CSNSM-Orsay on commercial purity 316L and model FeNiCr alloy to a dose of 5 dpa at 450°C. These conditions are representative of several operational years. A detailed defect analysis (dislocation loops, cavities, induced phases) is performed by TEM techniques combination and discussed in the two alloys. TEM studies are associated with APT, detailed in an other paper. A special attention is ported on the differences in defects accumulation between both type of irradiated samples (thin and bulk). This work is done as a part of the FP7 European Collaborative project Perform60.

Minerals, Metals and Materials under Pressure: New Materials and Properties

Sponsored by: The Minerals, Metals and Materials Society, TMS Electronic, Magnetic, and Photonic Materials Division, TMS Materials Processing and Manufacturing Division, TMS Structural Materials Division, TMS: Chemistry and Physics of Materials Committee, TMS/ASM: Phase Transformations Committee
Program Organizers: Ellen Cerreta, Los Alamos National Laboratory; Richard Hennig, Cornell University; Dallas Trinkle, University of Illinois, Urbana-Champaign; Vijay Vasudevan, Univ. Cincinnati

Thursday PM
 March 15, 2012

Room: Europe 9
 Location: Dolphin Resort

Session Chair: Richard Hennig, Cornell University

2:00 PM Invited

Pressure Stabilized Alkali Metal Polyhydrides: *Eva Zurek*¹; ¹University at Buffalo, SUNY

Stabilization of solid phases with unusual stoichiometries and unexpected electronic structures may be achieved by applying external pressure. Theoretical work has predicted that LiH_6 and LiH_2 become particularly stable phases at about 100 GPa. NaH_9 is predicted to be the most stable combination of Na and H by 25 GPa. These hydrogen-rich materials with nontraditional stoichiometries are computed to undergo an insulator to metal transition at a pressure lower than that necessary to metalize hydrogen. The evolutionary algorithm XtalOpt has been employed to search for the most stable stoichiometries of the heavier alkali polyhydrides as well confirming that under pressure there is an increased tendency to form multicenter bonds.

2:30 PM

Polaron Hopping in LiFePO_4 at Elevated Pressures and Temperatures: *Lisa Mauger*¹; *Sally Tracy*¹; *Jorge Munoz*¹; *Hongjin Tan*¹; *Hillary Smith*¹; *Brent Fultz*¹; ¹California Institute of Technology

LiFePO_4 has high technological potential as a Li-ion battery cathode material but it suffers from low electrical conductivity resulting from a large electronic band gap. Electron conduction in LiFePO_4 occurs via small polaron hopping between Fe sites. Synchrotron Mossbauer Spectroscopy (SMS) was used to measure the hyperfine fields of $\text{Li}_{x=0.6}\text{FePO}_4$ at elevated temperatures and pressures in an externally heated diamond anvil cell. The polaron hopping frequency was studied by analyzing the lifetime effects evident in the quadrupole splitting signal of the various Fe valence states. The observed polaron hopping rate increases with temperature, but applied pressure suppresses the onset of this behavior. The polaron activation energy and activation volume are extracted by examining the temperature evolution of the SMS patterns at different pressures. The positive polaron activation volume in LiFePO_4 will be discussed along with its implications for improving the electrical conductivity of this material.

2:50 PM

Effect of Pressure on the Critical Resolved Shear Stress of MgO Single Crystal: Insights from Numerical Modeling: *Philippe Carrez*¹; *Jonathan Amodeo*¹; *Patrick Cordier*¹; ¹Lab. UMET CNRS-8207

The study of plastic properties of minerals is of primary importance to model the Earth's mantle rheology, responsible for plate tectonics. Numerical modeling provides an alternative to deformation experiments to address the behaviour of materials under extreme (P,T) conditions. In this study, we use a hierarchical multi-scale model to study the effect of high pressures (up to 100 GPa) on the critical resolved shear stresses (CRSS) of MgO (one of the main constituents of the Earth's mantle). Using a generalised Peierls-Nabarro model, we show that core structure

of $1/2\langle 110 \rangle$ screw dislocation is strongly sensitive to pressure, with an inversion of the easiest slip plane from $\{110\}$ to $\{100\}$ around 60 GPa. By applying kink pairs theory, we find that pressure increases CRSS and shifts athermal temperatures towards higher temperatures. Under high pressure, MgO is thus characterized by a significant lattice friction on both slip systems.

3:10 PM

High Pressure Study of the Effects of Vacancies on the Lattice Dynamics of B2 FeAl: *Matthew Lucas*¹; ¹Air Force Research Laboratory

Ordered intermetallic B2 FeAl alloys are of technological interest as high-temperature structural materials due to their high resistance to corrosion, low density, and high strength. The usefulness of these alloys are hindered by their brittleness, which is due to a propensity to develop an abnormally high equilibrium vacancy concentration at high temperature. A combination of ambient pressure inelastic neutron scattering and high pressure elastic and inelastic scattering in a diamond anvil cell were used to probe the effect of vacancies on the lattice dynamics of B2 FeAl. It was observed that the effects of vacancies on the phonon spectrum were largely due to changes in volume and were generally consistent with the quasiharmonic approximation. Vacancies on the Fe site alter phonons by their effect on the specific volume of the crystal, where the decrease in volume leads to an increase in the phonon energies.

3:30 PM

Amorphization and Nanocrystallization in Boron Carbide and Silicon Carbide Impacted at High-Velocity: *Jerry LaSalvia*¹; *Eugene Shanholtz*¹; ¹U.S. Army Research Laboratory

Boron carbide and silicon carbide are common hard-face components in lightweight ballistic protection technologies. Ballistic impact involves the generation of transient, large amplitude, spatially and temporally varying stresses and deformations. Material responses can be complex, involving phenomena which span atomistic-to-macroscopic length-scales driven by hydrostatic, deviatoric, and principal stresses. In this investigation, a hot-pressed boron carbide and modified-CVD silicon carbide were ballistically impacted with cemented carbide spheres at high velocity. Recovered ceramics were sectioned through the impact site and polished to reveal sub-surface features. Beyond multi-scale cracking and fragmentation, evidence for solid-state amorphization and nanocrystallization was observed in both compressive and tensile stress regions. The discreteness of these features reflects the importance of shear stress and deformation on these phenomena. These features were subjected to SEM, EDS, micro-XRD, and micro-Raman spectroscopy in an effort to characterize them. Atomistic modeling results and thermodynamic-based considerations are presented which aid in explaining these findings.

3:50 PM Break

4:00 PM Invited

Random Search - A Tool for Discovery at High Pressure: *Chris Pickard*¹; ¹University College London

Much progress has been made in the prediction of structure from first principles. My approach - ab initio random structure searching (AIRSS) [1,2] is simple and powerful. Its lack of bias makes it particularly suitable for theoretical explorations leading to new and unexpected phenomena. I have uncovered ionic phases of ammonia[3], and structural richness at terapascal pressures in aluminium[4], iron[5] and carbon. In this talk I will focus on the hunt for novel physics, illustrated by the discovery of a new route to bulk magnetism in the elements[6]. [1] C.J. Pickard and R.J. Needs, *PRL*, 2006, 97, 45504 [2] C.J. Pickard and R.J. Needs, *JPCM*, 2011, 23, 053201 [3] C.J. Pickard and R.J. Needs, *Nature Materials*, 2008, 7, 775-779 [4] C.J. Pickard and R.J. Needs, *Nature Materials*, 2010, 9, 624-627 [5] C.J. Pickard and R.J. Needs, *JPCM*, 2009, 21, 452205 [6] C.J. Pickard and R.J. Needs, *PRL*, 2011 (in press)



TMS 2012

141st Annual Meeting & Exhibition

THURSDAY PM

4:30 PM

Equation of State of Solid Solution $Mg_{2.4}Fe_{0.6}Al_2Si_3O_{12}$ Measured in Diamond Anvil Cell: *Shu Huang*¹; *Jiuhua Chen*¹; *Bin Yang*¹; *Vadym Drozd*¹; *Andriy Durygin*¹; ¹Florida International University

The Pressure-Volume relation of synthetic pyrope-almandine garnet ($Mg_{2.4}Fe_{0.6}Al_2Si_3O_{12}$) was measured at ambient temperature and pressure up to 9.3 GPa in diamond anvil cell with synchrotron X-ray diffraction. The p-v data were fitted to a third order Birch-Murnaghan equation of state. With fixed values for the ambient cell volume ($V_0 = 1511.4(4) \text{ \AA}^3$) and the pressure derivative of the isothermal bulk modulus ($K'_{T0} = 5.45$), an isothermal bulk modulus of $K_{T0} = 178(3) \text{ GPa}$ was obtained. This data agrees well with previous measurements on almandine-pyrope garnets and fits in between the bulk modulus range of pyrope and almandine. This result shows that the bulk modulus of garnet along py-alm join is proportional to the almandine percentage in this binary solid solution.

4:50 PM

HPHT Synthesis of Phosphorus Doped Diamond from Triphenylphosphine and Graphite: *Bin Yang*¹; *Fangli Chi*¹; *Ernesto Vallejo*¹; *Jiuhua Chen*¹; ¹Florida International University

Phosphorus doped diamonds have attracted great attentions in recent decades because of their n-type semiconductor properties. Most of them can be successfully produced by chemical vapor deposition (CVD) method. However, at high pressure high temperature (HPHT) conditions, the P-doped diamonds only obtained from carbon solution in phosphorus melt. We explored a new route to synthesize P-doped diamond. The diamond has been synthesized at 19 GPa and 1800 °C for 1 min in a multi-anvil apparatus by using triphenylphosphine [$P(C_6H_5)_3$] and graphite as starting materials. The molar ratio of P to C was 1:100. The X-ray diffraction confirmed the existence of the diamond. The diamond crystallite size was determined to be about 14 nm. The Raman spectroscopy revealed a large shift in the diamond peak position between the sample (1326.9 cm^{-1}) and the pure diamond (1332 cm^{-1}). It may be caused by the phosphorus doping. The further studies are in progress.

5:10 PM

High Pressure X-ray Diffraction Studies for Piezoelectric Materials: *Lingping Kong*¹; *Zhenhai Yu*²; *Luhong Wang*²; *Haozhe Liu*³; *Wenge Yang*¹; *Ho-kwang Mao*¹; ¹Carnegie Institution of Washington; ²Argonne National Laboratory; ³Harbin Institute of Technology

The structural stability of several piezoelectric materials under high pressure has been investigated through in situ high pressure angle dispersive X-ray diffraction experiments at room temperature. For the $Pb(Yb_{1/2}, Nb_{1/2})O_3-PbTiO_3$ (PYNT) case, the crystal structure evolution up to 24.5 GPa was measured, which revealed a ferroelectric-paraelectric phase transition at about 8.0 GPa. The bulk moduli of ferroelectric and paraelectric phases were estimated as $B_0 = 99(3)$ and $204(4)$ GPa, respectively. The structural stability of other piezoelectric materials, including $Ca_3TaGa_3Si_2O_{14}$ and $La_3Ga_5SiO_{14}$, were studied as well. These experimental results will give us insight into the origins of piezoelectric properties, and provide input for the better design of this kind of materials with optimized structure-property relationship.

Production, Recovery and Recycling of Rare Earth Metals: Session I

Sponsored by: The Minerals, Metals and Materials Society, TMS Electronic, Magnetic, and Photonic Materials Division, TMS Extraction and Processing Division, TMS Light Metals Division, TMS: Magnetic Materials Committee, TMS: Recycling and Environmental Technologies Committee

Program Organizers: Lifeng Zhang, Missouri University of Science and Technology; Joseph Pomykala, Alter Trading; Oliver Gutfleisch, IFW Dresden

Thursday PM
March 15, 2012

Room: Europe 4
Location: Dolphin Resort

Session Chairs: Lifeng Zhang, Missouri S&T; Joseph Pomykala, Alter Trading; Oliver Gutfleisch, Institute of Metallic Materials

2:00 PM Introductory Comments

2:05 PM

Recycling of Rare Earth Metals: A Review: *Lifeng Zhang*¹; ¹Missouri University of Science and Technology

Over 100 literature papers on the recycling of rare earth metals are reviewed. The benefits and the main technologies for the recycling of rare earth metals were summarized.

2:35 PM

Hydrogen Processing – a Novel Route for the Recycling of Sintered Nd-Fe-B Magnets: *Oliver Gutfleisch*¹; *Konrad Güth*¹; ¹IFW Dresden

There is an increasing demand for permanent magnets based on Nd-Fe-B in HEV and wind turbine applications. These magnets contain a significant amount of rare earth elements, generally for excellent magnetic performance (light RE) and then to ensure appropriate thermal stability in these specific applications (heavy RE) [1]. Some of them, Dy and Tb are indeed rare; all of them have seen drastic price increases. Sustainable usage of such resources is pivotal and the recycling of advanced magnets will become increasingly important. We investigate the feasibility of recycling scrap sintered Nd-Fe-B by hydrogen processing. A combination of HD and HDDR is used to recover magnetically anisotropic powder, suitable for the subsequent production of polymer bonded highly textured magnets. Microstructure and magnetic properties were studied by SEM/EBSD and magnetometry. Comparable properties to those of non-recycled polymer bonded magnets were obtained. [1] Gutfleisch et al. Adv. Mat. 23 (2011) 821.

3:05 PM

Electrochemical Behaviour of Neodymium in Aqueous Electrolytes: *Ralph Sueptitz*¹; *Kristina Tschulik*¹; *Margitta Uhlemann*¹; *Ludwig Schultz*¹; *Annett Gebert*¹; ¹IFW Dresden

The rare earth metals are essential for highly energy-efficient technologies with many applications. The electrochemical behaviour, especially the material degradation by corrosion, is crucial for a long lifetime of electromagnetic devices. While the corrosion properties of some compounds containing these metals (e.g. NdFeB permanent magnets) has been characterized, the electrochemical behaviour of the pure metals is scarcely investigated. However, to understand the electrochemical behaviour of the alloys and compounds it is necessary to know the electrochemical behaviour of the pure elements. This will then allow developing corrosion protection strategies to ensure a low loss of efficiency during the lifetime of an electromagnetic device. Here, an electrochemical characterization of Neodymium in various aqueous electrolytes is presented. The corrosion properties and passive film formation are summarized and the local breakdown of passivity due to aggressive anions in the solution is shown. Furthermore, an abnormal hydrogen evolution under anodic polarization conditions is discussed.

3:35 PM

Recovery of Rare Earth Metals via Liquid Metal Extraction: *Ryan Ott¹*; Dan Cavanaugh²; Warren Straszheim²; Matthew Kramer²; Larry Jones²; ¹Ames Laboratory (USDOE); ²Ames Laboratory (USDOE)

With the increased demand for rare earth (RE) metals in critical technologies coupled with supply concerns, recycling of RE metals has become increasingly more important. Here we describe utilizing liquid Mg to extract RE metals from magnetic scrap material. By utilizing induction melting of liquid Mg followed by vacuum distillation, we were able to recover >98% pure RE metal. From the recovered RE metals, we synthesized RE₂Fe₁₄B₁-type magnetic alloys for comparison with alloys synthesized from pure RE metals. The magnetic properties and the microstructure of the alloys prepared from the two different starting materials are discussed. Lastly, we discuss the extraction of RE metals from oxidized samples.

4:05 PM Break**4:15 PM**

Rapid Separation of Rare Earth Elements with Interstitial Polymer Network Ion Exchange Columns: *Richard Hammen¹*; John Hammen¹; Anupam Goyal¹; ¹IntelliMet LLC

Rare earth element (REE) production is essential for much of 21st Century technology. Current methods of producing purified REE metals require multi-stage solvent extractions that are expensive due to high capital, operational, and environmental costs. We describe a new generation of ion exchange columns that are effective for REE separation. The columns are manufactured with beds of silica particles that have thinly cross-linked polymer networks crossing the interstitial spaces between the particles. These interstitial polymer networks (Spiderwebs) suspended between silica particles have enhanced rates of equilibration with solutions flowing through the Spiderweb. When the Spiderweb-like polymer networks are modified with REE-selective chelating agents, the columns are able to rapidly separate RE ions from mixtures. We report the separation of cerium and lanthanum from RE mixtures to give highly purified metal salts. In addition, we describe the separation of praseodymium and neodymium in one pass through a Spiderweb column.

4:45 PM

Selective Extraction of Neodymium from Nd-Fe-B alloys Using Magnesium: *Taek-Soo Kim¹*; Hongjun Chae¹; Ryan Ott¹; ¹Korea Institute of Industrial Technology (KITECH)

This study is to investigate a selective diffusivity of Nd to Mg from Nd-Fe-B, a typical permanent magnet composition. The process will be an environmental friendly recycling process, compared with the conventional chemical method. The effects of the holding time on the reactivity in the high frequency vacuum induction melting (VIM) were analyzed using Scanning-electron microscopy (SEM), X-ray diffraction (XRD) and Energy-dispersive spectrum (EDS). Microstructural and compositional change happened during the reaction was also examined. The experimental results showed that the Nd initiated to diffuse into Mg as the Nd-Fe-B specimen contacted with Mg melt, and form a dendritic Mg-Nd eutectic phases. Diffusivity was found to vary with holding time.

5:15 PM

Effect of Tellurium Reduction and Thermoelectric Properties on Thermoelectric Materials Produced by Rapid Solidification Processes and Hot Extrusion.: *Hyo-Seob Kim¹*; Taek-Soo Kim²; *Soon-Jik Hong¹*; ¹Kongju National University; ²Korea Institute of Industrial Technology(KITECH)

Due to their potential application in power generation and cooling devices along with their advantages, Tellurium-based thermoelectric(TE) materials have attracted much interest and attention. However, a severe issue that ought to be faced is the low reserves of the scarce element tellurium and its rapidly increasing usage in industries. New tellurium-free or low-tellurium bearing materials to replace traditional commercial Tellurium-based TE materials need to be explored. Recently, it has been

reported that the TE properties can be increased with low-tellurium bearing TE materials, using rapid solidification process. In this study, we investigated the effect of Tellurium reduction on the TE properties of TE materials by introducing a new rapid solidification (Gas-Atomization) method, followed by hot extrusion under different conditions(ratio: 10:1~25:1, temperature: 350~500°C). The structure, morphology, mechanical and TE properties of these materials are investigated by means of different techniques including electron microscopy(SEM), X-ray diffraction(XRD), micro Vickers hardness and TE measurements.

5:45 PM

Study on the Cerium Oxide Prepared by Pyrolysis of Cerium Chloride Solution: *Bian Xue¹*; Wu Wenyuan¹; ¹Northeastern University

This paper aims to explore a kind of process for the preparation of cerium oxide (CeO₂) which is CeO₂ prepared by CeCl₃ solution direct pyrolysis. The optimal condition of Roasting temperature for 950°C. Material liquid concentration for 270g/L and feeding speed for 0.23ml/s is obtain by orthogonal regression equation. In the optimal condition, conversion rate of CeO₂ is 99.9%, and the grain size is about 500nm.

Recent Developments in Biological, Electronic, Functional and Structural Thin Films and Coatings: Process-Properties-Performance Correlations III

Sponsored by: The Minerals, Metals and Materials Society, TMS Electronic, Magnetic, and Photonic Materials Division, TMS: Thin Films and Interfaces Committee

Program Organizers: Nuggehalli Ravindra, New Jersey Institute of Technology; Jian Luo, Clemson University; Xing Yang (Mark) Liu, National Research Council Canada; Nancy Michael, University of Texas at Arlington; Roger Narayan, University of North Carolina and North Carolina State University; Choong-un Kim

Thursday PM
March 15, 2012

Room: Swan 10
Location: Swan Resort

Session Chairs: Nuggehalli Ravindra, New Jersey Institute of Technology; Sudhakar Shet, NREL & NJIT

2:00 PM Introductory Comments**2:05 PM**

Morphologies in Polycrystalline Film Growth: *Ramanathan Krishnamurthy¹*; Mikko Haataja²; ¹Purdue University; ²Princeton University

Polycrystalline films are commonly used in materials applications; however, growth models rarely include time-dependent lateral grain size effects. We employ a thermodynamics-based method to effectively handle grain grooving / lateral grain growth and film growth. Previously, we exercised the model to successfully predict experimental features related to polydisperse-sized film annealing (zero deposition flux) including ghost lines, groove asymmetry and their relation to annealing kinetics, and the non-monotonous time-variation of film roughness. Here we examine film growth (non-zero deposition flux). For large, spatially uniform deposition fluxes, the accompanying greater chemical potential driving grooving produces enhanced grooving / impeded grain growth. When deposition fluxes vary spatially as in diffusion limited processes (e.g. electrodeposition), the ratio of the length scale characteristic of the deposition process and grain size critically affects growth morphologies, and different features such as impeded grain growth, and characteristic non-equilibrium grain surface morphologies are found for different values of this ratio.



2:35 PM

Nitrogen Doped ZnO (ZnO:N) Thin Films Deposited by Reactive RF Magnetron Sputtering for PEC Application: *Sudhakar Shet¹*; Kwang-Soon Ahn²; Nuggehalli Ravindra³; Yanfa Yan¹; Mowafak Al-Jassim¹; ¹National Renewable Energy Laboratory; ²School of Display and Chemical Engineering; ³New Jersey Institute of Technology

ZnO:N films were deposited by reactive RF magnetron sputtering on F-doped tin oxide coated glass in mixed N₂ and O₂ gas ambient. Their PEC properties were measured and compared with those of as-grown and annealed ZnO films. The ZnO:N films exhibit photoresponse in the visible-light region, yielding higher total photocurrents than ZnO thin films. With combined ultraviolet/infrared and color filtering, our data indicate that the main contribution to the high photocurrent is from the absorption of light in long-wavelength regions.

3:05 PM

Hydrothermal Synthesis of Zinc Oxide Thin Film for Printed Electronics: *Ruihong Zhang¹*; Carol Handwerker¹; ¹Purdue University

Hydrothermally synthesized zinc oxide is a promising semiconductor for printed electronics due to its higher mobility than the organic semiconductors and its simple and environmentally benign processing route for thin film formation. In this study, the rapid, low-temperature synthesis of dense and continuous ZnO thin films from 70 nm nanoparticle seed layers was examined using aqueous solutions with the initial pH ~5 at 90°C for times ranging from 0.25 h to 2 h. The effects of counter ions, complexing agents, pH, and solution concentration on film growth, morphology and texture were characterized using SEM and x-ray diffraction. The mobilities of the ZnO thin films measured by the Hall Effect are correlated to the thin film microstructures observed by high resolution transmission electron microscopy (HR-TEM), thereby establishing the relationship between the morphology and the mobility of the films.

3:25 PM

Spin-Coated Erbium-Doped Silica Sol-Gel Films on Silicon: *Sufian Abedrabbo¹*; Bashar Lahlouh¹; Sudhakar Shet²; Anthony Fiory³; Nuggehalli Ravindra³; ¹University of Jordan; ²National Renewable Energy Laboratory; ³New Jersey Institute of Technology

This work reports optical functionality contained in, as well as and produced by, thin film coatings. A sol-gel process, formulated with precursor active ingredients of erbium oxide and tetraethylorthosilicate (TEOS), was used to produce by spin-coating thin (~130 nm) erbium-doped (~6 at. %) silica films on single-crystal silicon. Annealed films produce infrared emission in the 1.5-micron band from erbium ions in the film, as well as greatly enhancing (> 100X) band-gap emission from the underlying silicon. The distinctly different mechanisms for the two modes of optical activity are interpreted in terms of optical emission theory and modeling; prospects for opto-electronic applications are discussed.

3:55 PM Break

4:10 PM

Influence of Annealing on the Martensitic Transformation and Magnetocaloric Effect in Ni₄₉Mn₃₉Sn₁₂ Ribbons: *Dianzhen Wu¹*; Sichuang Xue¹; Hongxing Zheng¹; Qijie Zhai¹; ¹Shanghai University

Magnetocaloric effect associated with martensitic transformation (MT) can be induced in Ni₄₉Mn₃₉Sn₁₂ alloy. The influence of annealing on the martensitic transition and magnetocaloric effect in metamagnetic polycrystalline Ni₄₉Mn₃₉Sn₁₂ ribbons produced using melt spinning

technique was investigated systemically based on the results of vibrating specimen magnetometer (VSM) measurements. Ribbons were annealed at 1273K for 4h, followed by water quenching or furnace cooling to room temperature. Magnetic-field induced reverse MT from paramagnetic martensite phase to ferromagnetic austenite phase together with large magnetization change is evident in thermal-magnetic curves, thus entropy change appears. The magnetic entropy change enhances strikingly for all annealed ribbons in comparison of melt-spun ribbons. The magnetic refrigerant parameters for ribbon water quenched exhibits optimum values, of potential extensive application in practical refrigerant cycles.

4:30 PM

Metal Diaphragm Based Magnetic Field Sensor: *Asahel Banobre¹*; Ivan Padron¹; Anthony T. Fiory¹; Nuggehalli M. Ravindra¹; ¹NJIT

A diaphragm based magnetic field sensor is designed and fabricated. A thin metal diaphragm is used as a sensing element and it responds to an external magnetic field. Deformation of the diaphragm due to the pressure produced from the interaction between the magnetic field and the metal surface can be detected electronically through a Wheatstone bridge placed over the diaphragm. Analytical and experimental analyses are used to study the precision and accuracy of devices for sensing magnetic field flux.

4:50 PM

Optical and Electronic Properties of III-V Nitrides: *Chiranjivi Lamsal¹*; Nuggehalli Ravindra¹; ¹New Jersey Institute of Technology

The optical properties of III-V binary and ternary nitrides have been analyzed in this study. The analysis takes into account the optical properties such as the reflectance and transmittance of these nitrides. The related optical properties such as the energy dependent dielectric function, refractive index, extinction coefficient and absorption coefficient are evaluated utilizing Kramers-Kronig relation. Model calculations based on those of Penn and Wemple-Didomineco are deployed to interpret the peaks in the reflectivity spectra. Temperature and pressure dependence of the energy gap and the refractive index and their nature have been analyzed. Influence of substrates on the optical properties of these nitrides is discussed.

5:10 PM

Application of Expanding Thermal Plasma for Deposition of Hydrogenated Diamond like Carbon Thin Films on Rubber Seals: *Ali Reza Eivani¹*; Yutao Pei¹; Jeff Th.M. De Hosson²; Teodor Zaharia¹; Richard M.C.M. Van de Sanden³; ¹Materials Innovation Institute (M2i); ²University of Groningen; ³Eindhoven University of Technology

Hydrogenated diamond-like carbon (DLC) thin films were deposited on nitrile butadiene rubber (NBR) using expanding thermal plasma (ETP) apparatus in a C₂H₂ / Ar plasma. Effect of arc current on the tribological behavior of the coated rubber is investigated with ball-on-disc tribology test under dry sliding condition against 100Cr6 ball. Coefficient of friction (CoF) of the coated rubber decreases significantly by reducing arc current due to the changes occurred in the plasma chemistry and consequently deposition of a softer film. High resolution scanning electron microscopy (SEM) is used for characterization of the surface morphology of coated rubbers to correlate microstructure to CoF. Wear scar of the counterpart, i.e., 100Cr6 steel ball, has also been investigated and its wear morphology is discussed in correlation with SEM micrographs and CoF measurements.

2012 Functional and Structural Nanomaterials: Fabrication, Properties, Applications and Implications: Poster Session

Sponsored by: The Minerals, Metals and Materials Society, TMS Electronic, Magnetic, and Photonic Materials Division, TMS: Nanomaterials Committee

Program Organizers: Jiyoung Kim, University of Texas; David Stollberg, Georgia Tech Research Institute; Seong Jin Koh, University of Texas at Arlington; Nitin Chopra, The University of Alabama; Terry Xu, UNC Charlotte

Monday PM
March 12, 2012

Room: Atlantic Hall
Location: Dolphin Resort

U-1: A Facile, One Pot and Completely 'Green' Synthesis of Sugar-Reduced Silver Nanoparticles: Lucwaba Yolisa¹; Vulyewa Ncapayi¹; Odey Akpa¹; Sandile Songca¹; *Oluwafemi Oluwatobi¹*; ¹Walter Sisulu University

We herein report the synthesis of highly monodispersed water soluble silver nanoparticles (Ag-NPs), via an eco-friendly, completely green method in a natural polymeric media. The method involves the use of silver nitrate, gelatine and maltose as the silver precursor, stabilising agent and reducing agent respectively in aqueous solution. By varying the reaction time, we monitored the optical and structural properties of the colloidal Ag-NPs. The nanoparticles were characterised using UV-vis absorption spectroscopy, Fourier transform infrared spectroscopy (FTIR), x-ray diffraction (XRD), transmission electron spectroscopy (TEM), high resolution electron transmission microscopy (HRTEM) and energy dispersive spectroscopy (EDS). The absorption maxima of the as-synthesised materials were blue-shifted as the reaction time increases indicating decrease in particle size. The TEM images showed well-defined monodispersed, spherical particles with average particle diameter of less than 4 nm at higher reaction time and are in agreement with the absorption analysis.

U-2: Analysis of RTS Noise Characteristics in Fin-Type Silicon-Oxide-High-k-Oxide-Silicon (SOHOS) Flash Memory: *Seung Dong Yang¹*; Sang Youl Lee²; Ho Jin Yun²; Kwang Seok Jeong²; Yu Mi Kim²; Jae Sub Oh²; Hi-Deok Lee²; Ga Won Lee²; ¹Chungnam University; ²Chungnam university; ³National Nanofab Center

This paper discusses the Random Telegraph Signal (RTS) noise in Fin-type Silicon-Oxide-High-k-Oxide-Silicon (SOHOS) flash memory. As the device dimensions continue to shrink with each new generation of flash memory, the so called RTS noise, characterized by discrete switching events of the channel current, have often been observed and attributed to the trapping and de-trapping of conduction carriers by individual interfacial defects. In flash memory, RTS noise is one of major reason for problem of threshold voltage shift which causes performance errors. Fin-type SOHOS device using HfO₂ trapping layer shows superior Program/Erase speed. However, the data retention properties are degraded. To find out the causes, we carried out the RTS noise analysis in fabricated a SOHOS flash memory and distribution of traps is looking for the cause of poor data retention characteristics.

U-3: Atmospheric-Pressure Plasma Sintering of Silver Nanopaste Screen-Printed on PI: *Kwang-Seok Kim¹*; Woo-Ram Myung¹; Seung-Boo Jung¹; ¹Sungkyunkwan University

Recently, the field of printed electronics has gradually matured. Numerous researches have proposed feasible applications such as interconnections for micro-circuitry on a printed circuit board, and electrodes for thin film transistor circuits. Heat treatment is inevitably required because direct printing technology is based on an additive manufacturing method. However, conventional heating is not compatible

with common polymer substrates that have a relatively low glass transition temperature. Therefore, we suggest atmospheric-pressure plasma (APP) sintering. The microstructure and electrical resistivity were investigated with a FE-SEM and a 4-point probe station, respectively. Argon and helium were used for APP sintering. As experimental results, the selective sintering of Ag nanopaste was achievable by APP without affecting a polyimide substrate. Also, the electrical resistivity was achieved less than one order of magnitude higher than that of bulk Ag. The mechanism of these phenomena will be deeply discussed in the conference site and full manuscript.

U-4: Effects of Calcination Conditions on Particle Size and Morphology of NiFe₂O₄ Nanoparticles Synthesized by Solid-State Reaction: *Zhigang Zhang¹*; Yihan Liu¹; Guangchun Yao¹; Di Wu¹; Junfei Ma¹; ¹Northeastern University

Nickel ferrite (NiFe₂O₄) nanoparticles were synthesized via low temperature solid-state reaction. The precursors prepared by grinding the mixture of FeSO₄·7H₂O, NiSO₄·6H₂O, NaOH and dispersant (NaCl) sufficiently at room temperature were calcined under various calcination conditions to obtain NiFe₂O₄ spinel nanoparticles. The effects of the calcination conditions, namely calcination temperature and heat preservation time, on particle size and morphology have been investigated in detail. X-ray diffraction (XRD) and transmission electron microscopy (TEM) were employed to characterize the as-synthesized particles. The results indicate that particle size and morphology can be controlled by calcination conditions. The low temperature solid-state reaction technique is a convenient, inexpensive and effective preparation method of NiFe₂O₄ in high yield.

U-5: Electrical Characterization in Pillar Type Silicon-Oxide-Nitride-Oxide-Silicon Flash Memory Using Bandgap Engineering Method: *Sang Youl Lee¹*; Seung Dong Yang¹; Jae Sub Oh²; Ho Jin Yun¹; Kwang Seok Jeong¹; Yu Mi Kim¹; Hi Deok Lee¹; Ga Won Lee¹; ¹ChungNam University; ²National Nanofab Center

Continued scaling down of flash memory device causes reliability problems such as increasing leakage current and changing a operate voltage due to thinner tunnel oxide. Thinner tunnel oxide is easily degraded when a lot of program and erase process are repeated. To solve these problems, many researchers have studied new memory structures such as Nano Floating Gate Memory (NFGM), 3D structures and Silicon-Oxide-Nitride-Oxide-Silicon (SONOS). However, the SONOS structure is recently focusing as the next generation memory device due to a better scale down characteristics than previous flash memory devices. Band Engineering (BE) method that is adding a thin layer in a tunneling oxide is also well known as a process to improve data retention and charge writing/erasing characteristics. Therefore, we fabricated the conventional pillar type SONOS and BE-SONOS flash memory devices. Through these devices, it is found out that the BE device has better reliability characteristics.

U-6: Electrical Characterization of TiO₂ Thin Films Prepared by Atomic Layer Deposition: *Antonio Lucero¹*; Mingun Lee¹; Jiyoung Kim¹; ¹University of Texas at Dallas

Titanium dioxide has received considerable interest in the study of nanomaterials. The material has been proposed for use in a variety of applications ranging from chemical sensors to dye sensitized solar cells. Titanium dioxide nanotubes, nanoparticles and porous films are frequently tested in these roles. This work attempts to characterize the properties of nanoscale TiO₂ by looking at thin films deposited by atomic layer deposition (ALD). Thin films can be patterned with traditional lithography techniques. Their reproducibility is one advantage over materials such as nanotubes, which are often produced with a random distribution of sizes. Electrical characteristics are studied as a function of both film thickness and length, and the effects of temperature and gas environment are observed.



U-7: Electrospinning of the Dendritic Polymer (Acrylonitrile /Acrylic Acid) and the Properties of Fibers: *Elahe Helmi*¹; ¹Engineering Faculty

To produce a dendritic structure, CA has been used as a generation by divergent synthetic route for the synthesis of a dendritic polymer on the surface of (Acrylonitrile /Acrylic acid) base copolymer. Nanofiber mats of the synthesized dendritic structure were fabricated by electrospinning method. The effects of the dendritic structure generation on the nanofiber formation and their diameter were studied. Morphology and diameter of the nanofibers were studied using optical and scanning electron microscope. The results showed that increase in dendritic generation increases the average of nanofiber diameter. Results were discussed on the base of the change in solution shear viscosity and dendrimer structure.

U-8: Fabrication of Bulk Al-Fe-V-Si Nanocrystalline Alloy by Mechanical Alloying and Hot Pressing: *M.H. Enayati*¹; H. Ashrafi¹; R. Emadi¹; ¹Isfahan University of Technology

In this study, bulk nanocrystalline Al-Fe-V-Si alloy was produced by mechanical alloying and hot pressing. The elemental powders of Al, Fe, V and Si were milled in a planetary ball mill for 60 h to obtain a nanocrystalline Al solid solution. The milled powders were hot pressed in a uniaxial die at 550°C under pressure of 300 MPa for 0.5 h to acquire a bulk nanostructured alloy. The microstructure of consolidated sample consisted of Al₁₂(Fe,V)₃Si in nanocrystalline Al matrix with a grain size of 55nm. The consolidated sample had a hardness value of about 280 HV.

U-9: Implementation of Parylene as a Low-κ Gate Dielectric Material for Graphene Field Effect Transistors (GFETs): *Greg Mordt*¹; Srikar Jandhyala¹; Jiyoung Kim¹; ¹University of Texas at Dallas

Graphene, a two-dimensional (2D) hexagonal carbon lattice has been used as the conducting channel for field effect transistors because of its exceptional electrical properties. For a top gated FET, the graphene-dielectric interface play an important role in the FET behavior and mobility degradation mainly due to carrier scattering after the dielectric deposition process has been reported. In this work, we report on the fabrication and characterization of top gated graphene field effect transistors using a thin layer of parylene-C as gate dielectric. Parylene C excellent bulk properties such as its moisture barrier, high mechanical strength, thermal stability, phenyl structure and electrical insulation make it an ideal candidate as a top gate dielectric material for graphene devices. The thickness of the parylene and surface morphology was characterized by ellipsometry and AFM techniques. Electrical measurements reveal excellent characteristics with room temperature mobility in excess of 4000cm²/Vs.

U-10: Mechanical Properties of WC-10wt.%Co Hard Materials Prepared by SPS Process for FSW Tool Application: *Hyun-Kuk Park*¹; *Hee-Jun Youn*¹; *Ik-Hyun Oh*¹; ¹KITECH / Automotive Components Center

Using the spark plasma sintering method, WC-10wt.%Co hard materials were densified using an ultra fine WC-Co powder. The WC-Co was almost completely dense with a relative density of up to 100 % after the simultaneous application of a pressure of 60 MPa and an electric current for 12 minutes without any significant change in the grain size. The average grain size of WC that was produced through SPS was about 730 nm. Also, it was found that the Vickers hardness and fracture toughness of WC-Co sintered body were 2068.38 kg/mm² and 10.21 MPa.m^{1/2}, respectively.

U-11: Nanotechnology Coating of Buildings with Sol-Gel Method: *Aref Sadeghi Nik*¹; *Ali Bahari*²; *MohammadH. Khalilpasha*³; *Adel Sadeghi Nik*¹; ¹Young Researchers Club, Jouybar Branch, Islamic Azad University, Jouybar, Iran; ²Department of Physics, University of Mazandaran, Babolsar, Iran; ³Dept. of Civil Engineering, Islamic Azad University, Jouybar branch, Jouybar, Iran

The hydrophilic nature of the coating causes water that comes into contact with it to form an exterior building layer, thereby allowing the dust and dirt that have accumulated on the surface to be washed away.

In fact, hydrophilic property can also allow stains to cover the exterior surfaces. This point of the coating in the present work has been done with using different percent of Zycosil (1:20, 1:15, 1:10 and 1:5 and noting to ASTM C642 standard procedure. With this coating technology, the surface building maintenance, especially for skyscrapers, since they reduce the need for costly surface cleaning. Moreover, the obtained results which have been obtained with sol – gel method and AFM (Atomic Force Microscopy) indicate that it reduces the frequency of washes and correspondingly, drive down the coast of building maintenance.

U-12: PHB Nanocomposite Microcapsules with Brazilian Smectitic Clays: *Francisco Valenzuela-Diaz*¹; *Maria da Silva-Valenzuela*¹; *Wang Shu Hui*¹; *Helio Wiebeck*¹; ¹Universidade de Sao Paulo

The search for better materials has placed the polymer/clay nanocomposites in the centre of attention. Biopolymer-based nanocomposites as polyhydroxybutyrate (PHB), due to the current concern over environmental problems and biomedical use, can be a good alternative to produce microcapsules with application in drug delivery systems. In this work, we describe for the first time, from our knowledge, the preparation of microcapsules from two PHB nanocomposite systems: a) PHB/OMMT (Cloisite 20A), (PHB1) and b) PHB/montmorillonite (MMT), natural Brazilian green polycationic clay, (PHB2). The microcapsules PHB/OMMT and PHB/MMT nanocomposite were prepared by solvent evaporation technique. The XRD of films and microcapsules do not show d(001) peak, evidencing an exfoliated structure in the nanocomposites. The films have shown by SEM a homogeneous distribution of the clay mineral particles spread uniformly in the PHB film matrix. By SEM the microcapsules revealed spherical particles with a porous surface structure very similar to a “hydrangea”.

U-13: Raman Spectroscopy of Graphene and Plasma Treated Graphene under High Pressure: *Ali Hadjikhani*¹; *Jiuhua Chen*¹; *Santanu Das*¹; *Won-bong Choi*¹; ¹FIU

Due to its exceptional mechanical and electrical properties, graphene (one layer sheet of carbon atoms) has attracted a lot of attention since its discovery in 2004. The purpose of this research is to compare the Raman spectra of graphene with plasma treated graphene sheets which have been treated by changing the different parameters affecting the plasma treatment like gas flow, power, pressure and treatment time. We report a Raman spectroscopy study of graphene on copper substrate at high pressures. A diamond anvil cell (DAC) was used to generate pressure. In situ Raman spectra were collected at pressures up to 10 GPa. The result indicates that the G band of graphene shifts with pressure significantly (about 5 cm-1/GPa) whereas the 2D band changes very little.

U-14: Research on Preparation of Anisotropic Sm2Co17 Nano-flakes by Ball Milling under Magnetic Field: *Ying Chang*¹; *Jian Zhao*¹; *Xiaodong Li*; *Zhiyong Wei*¹; *Minggang Zhu*²; *Zhaohui Guo*²; *Wei Li*²; ¹Dalian University of Technology; ²China Iron & Steel Research Institute Group

High anisotropy magnetic nanoparticle materials have drawn great attention for their potential applications in anisotropic nanocomposite magnets. Surfactant assisted ball milling has already been proven to be an effective way to prepare high anisotropy magnetic nanoparticle materials such as Nd₂Fe₁₄B, SmCo₅ flakes. In this study, a new preparation method of Sm₂Co₁₇ flakes was investigated. Nanocrystalline hard magnetic Sm₂Co₁₇ flakes with 20-100nm thickness were obtained by milling in heptanes and oleic acid under 1T magnetic field for 3-6 hours. It was shown that the magnetic anisotropy of the prepared Sm₂Co₁₇ flakes after aligned at 1.5 T magnetic field could be further enhanced. The best (BH)_m of 16MGOe was obtained for the magnetic anisotropic Sm₂Co₁₇ nano-flakes.

U-15: Room-Temperature Synthesis of Spherical and Flowerlike Ag Nanostructures in Different Solvent: *Guoliang Li¹; Bing Peng²; Liyuan Chai²; Lei Jiang²; Liyuan Zhang²;* ¹Central South University; ²Central South University

Nano Ag particles with different morphologies are synthesized by mixing silver nitrate and para-phenylenediamine (PPD) in different solvent at room temperature. The characterizations of the as-synthesized Ag particles are performed using SEM, EDS, UV-Vis spectra and XRD. It is found that the type of solvent has a significant effect on the formation and growth of these novel nanostructures. The possible formation mechanism of Ag nanostructure is also discussed.

U-16: Scaling Down High-k Gate Dielectrics for Graphene-Based Device Applications: *Srikar Jandhyala¹; Greg Mord¹; Jiyoung Kim¹;* ¹University of Texas at Dallas

In order to realize graphene-based field-effect-devices, one of the foremost requirements is the ability to deposit high-quality, high- κ dielectrics on graphene for effectively modulating the gate potential. But, being just one atom thick and having an inert surface, it poses a challenge to develop a top-gate dielectric process for graphene which preserves its pristine properties. Here, we will present our approach based on atomic layer deposition through ozone functionalization to deposit high- κ dielectrics (such as Al₂O₃) with physical thicknesses in sub (\approx) 5nm regime. In this study we have investigated the effect of ozone dose on Al₂O₃ coverage using HOPG (Highly Oriented Pyrolytic Graphite) and single-layer graphene. Electrical characteristics of dual-gated graphene field-effect transistors (GFETs) fabricated with single-layer graphene and Al₂O₃ as top-gate dielectric will be discussed.

U-17: Selective Area Atomic Layer Deposition (ALD) with E-Beam Lithography (EBL) on Self-Assembled Monolayers (SAM): *Jie Huang¹; Mingun Lee¹; Jiyoung Kim¹;* ¹University of Texas at Dallas

In this study, nano-line patterns are defined by electron beam lithography (EBL) on octadecyltrichlorosilane (OTS) SAMs modified Si/SiO₂ substrates. During the EBL process, SAMs on solid substrates can be damaged or removed to generate discernible patterns. A thin film of titanium oxide (TiO₂) is deposited by atomic layer deposition (ALD), of which deposition mechanism is a self-limiting surface reaction, selectively on the e-beam patterned nano-lines. To control the width of the metal oxide patterns, we have optimized the conditions of both EBL and ALD. As characterized by scanning electron microscope (SEM), atomic force microscope (AFM) and high resolution transmission electron microscope (HRTEM), selectively deposited TiO₂ line patterns with sub-30 nm in width and 50 nm in pitch were achieved with e-beam voltage of 2 kV and line dose of 10 nC/cm. Proximity effect prevent dense line to be patterned closer than 50 nm in pitch.

U-18: Sensitive Colorimetric Detection of Cysteine in the Presence of Glutathione Using Gold Nanoparticles Aggregation: *Ensieh Seyedhosseini¹; M.Reza Hormozi-Nezhad²;* ¹Chemistry Department, Sharif University of Technology; ²Institute for Nanoscience and Nanotechnology(INST), Sharif University of Technology

Low-molecular-mass amino thiols such as cysteine (Cys), homocysteine (Hcy) and glutathione (GSH) play a critical role in many biochemical pathways. Their level in biological fluids such as human plasma and urine are important for clinical diagnostics of a variety of diseases. A fast, easy and very sensitive way to monitor plasma amino thiols is needed to constantly monitor levels as a diagnostic tool for biological concern. We report here in the development of a highly sensitive colorimetric method for detection of cysteine using citrate capped gold nanoparticles (Au-NPs). This assay relies upon the distance-dependent of gold nanoparticles surface plasmonic resonance band of gold nanoparticles. By controlling ionic strength, pH and Au-NPs concentration, the ratio intensities of absorbance at longer wavelength (640 nm) to original wavelength (521 nm) allow us to develop a simple colorimetric method for determination of cysteine in the presence large amounts of glutathione in biological samples.

U-19: Study on Liquid Sodium with Suspended Nanoparticles-(1) Fabrication and Dispersion of Nanoparticles: *Koichi Fukunaga¹; Masahiko Nagai²; Kuniaki Ara³; Jun-ichi Saito³;* ¹Mitsubishi Heavy Industries, Ltd.; ²Mitsubishi Heavy Industries, Ltd.; ³Japan Atomic Energy Agency

Although liquid sodium has an excellent thermal property as a coolant of the fast breeder reactor, it has disadvantage due to the high chemical reactivity with water and oxygen. The purpose of this study is the development of the technology to suppress the chemical activity of sodium by the dispersion of the nanoparticle in liquid sodium. In this paper, fabrication technology and dispersion technology of nanoparticles are reported. The conditions to suspend the nanoparticle into sodium stably are approximately 10nm in diameter and non-oxidation surface. So the evaporation method was used to produce nanoparticles. It became clear that the cooling rate of metallic vapor was a key factor to control the diameter of nanoparticle. The morphology of nanoparticles in sodium was observed by TEM. The diameter of nanoparticles did not grow in liquid sodium at elevated temperature. These results mean that nanoparticles were suspended stably in liquid sodium.

U-20: Study on Liquid Sodium with Suspended Nanoparticles-(2) Atomic Interaction and Characteristics of Liquid Sodium with Suspended Nanoparticles-: *Jun-ichi Saito¹; Keiichi Nagai¹; Kuniaki Ara¹;* ¹Japan Atomic Energy Agency

Liquid sodium has superior thermal properties as a coolant of the fast reactor. However it has high chemical reactivity with water and oxygen. The purpose of this study is to suppress the high chemical reactivity by dispersing nanoparticles into liquid sodium. An idea of this study is to use an atomic interaction between the nanoparticle and sodium to suppress the chemical reactivity. The theoretical calculation showed the atomic bonding between nanoparticle and sodium was stronger than that between sodium atoms. It is expected that the fundamental and reaction properties change by the atomic interaction. Evaporation rate and surface tension of sodium with suspended nanoparticles changed. It is caused by the atomic interaction. Also the reaction behavior with water or oxygen of sodium with suspended nanoparticles was suppressed. It means that there is the possibility of suppression of reactivity of liquid sodium by the atomic interaction.

U-21: Study on Microstructure Control and Atmospheric Corrosion of Micro-alloying Heavy Rail Steel: *Wang Xiao Li¹;* ¹University of Science and Technology Beijing

Atmospheric corrosion of steel is a universal and serious problem that caused great damage every year. There are advantages in mechanical properties for micro-alloying heavy rail steel. If improved the steel corrosion resistance, it can be obtained good mechanical properties and corrosion resistance. In this paper, the effects of alloying elements on atmospheric corrosion of Micro-alloying heavy rail steel were studied by accelerated corrosion in laboratory. This provides a feasible technical route for development of a corrosion resistant high strength heavy rail steel.

U-23: The Post-Annealing Effects of N-Doped ZnO Films Deposited by the Atomic Layer Deposition: *Kwang Seok Jeong¹; Yu Mi Kim¹; Ho Jin Yun¹; Seung Dong Yang¹; Sang Youl Lee¹; Young Su Kim²; Hi Deok Lee¹; Ga Won Lee¹;* ¹Chungnam National University; ²Nanofab Center

ZnO-based optical devices are expected to be efficient and practical due to wide band gap (~3.4 eV) and the large exciton binding energy (~60 meV). However, the ZnO film suffers from the difficulty with p-type film formation due to the drawbacks of the ZnO film itself. N doped ZnO films of 15 at% are deposited to form the p-type film on Si₃N₄/Si substrate of 150 °C by the atomic layer deposition process and then the post-annealing process is carried out from 300 °C to 700 °C under N₂ ambient. From XRD analysis, as-grown and post-annealed N-doped ZnO films show larger FWHM values of the (002) peaks, compared with those of as-grown ZnO films, which means that N atoms and/or N-H complexes are



TMS 2012

141st Annual Meeting & Exhibition

incorporated on O sites or in the ZnO lattice. Afterwards, through Hall effect measurement, it is found out that P-type ZnO films is successfully formed at 500 °C.

U-24: Thermo-mechanical properties investigation of PMMA nanocomposites using functionalized zirconia nanoparticles: Muhammad Sajjad¹; ¹Vienna University of Technology

PMMA-ZrO₂ nano-composites were prepared by in-situ polymerization of zirconia dispersions in methyl methacrylate (MMA). Zirconia nanoparticles in two different size ranges, one in the low nanometer range (about 10 nm) and other in the high nanometer range (about 50 nm) were modified with two types of organo-phosphorus coupling agents, one with short alkyl chain (C2) and other with long alkyl chain spacer (C10). SAXS (small angle x-ray spectroscopy) and TEM (transmission electron microscopy) investigations revealed homogeneous dispersion of the modified zirconia nanoparticles in PMMA. Thermo-mechanical characterization of the prepared nano-composites films showed significant positive effect on the properties of PMMA with both types of modified nano-particles. PMMA nano-composites exhibited improvements in glass transition temperature, storage modulus, micro-hardness and thermal stability. Positive effects on properties are attributed to coupling agents responsible for creating strong interaction between the organic polymer phase and modified interface of nano-particles.

Alumina and Bauxite: Poster Session

Sponsored by: The Minerals, Metals and Materials Society, TMS Light Metals Division, TMS: Aluminum Committee, TMS: Aluminum Processing Committee
Program Organizer: Benny Raahauge, FLSmidth

Monday PM
March 12, 2012

Room: Atlantic Hall
Location: Dolphin Resort

M-1: Acid Cleaning of Titanium Based Scales Formed on Preheaters in the Bayer Process: Ibrahim Akpınar¹; Yasemin Guldogan²; Oktay Uysal²; Gökhan Demir³; Meral Baygul³; Yücel Sahin⁴; ¹Entekno industrial, technological and nano materials ltd.; ²Entekno Industrial, Technological and Nano Materials Ltd.; ³Eti Alüminyum A.S.; ⁴Anadolu University

The titanium impurity in the bauxite leads to titanium based scale formation on the preheater units at the Bayer process. Scale formation leads to decreased heat transfer coefficient, increased energy consumption and higher maintenance costs. For these reasons, periodical cleaning of the scale is essential for alumina plants. Acid cleaning is used whenever other methods of cleaning are not effective. For different kinds of scale the effect of acid types differs considerably. While H₂SO₄ and HCl acids are affective for cleaning sodium aluminosilicate type scales they are not affective for cleaning titanium containing scales. In this work, effects of types of acids on the cleaning performance of titanium based scales in the Bayer process were investigated with respect to time and thickness of the scale by using dynamic and static conditions at room temperature. This paper reports an acid formulation which is best suited for titanium based scales.

M-2: Extracting Alumina from Coal Fly Ash with Ammonium Sulfate Sintering Process: Laishi Li¹; Xinqin Liao¹; Yusheng Wu²; Yingying Liu¹; ¹Shenyang Aluminum & Magnesium Engineering & Research Institute Co., Ltd.; ²School of Materials Science and Engineering, Shenyang University of Technology

The whole process of extracting alumina from coal fly ash was gotten by experiments. Alumina was prepared with sintering, leaching, separating, precipitation with ammonia water and calcination units. The effects of the sintering temperature and the sintering time, molar ratio of ammonium sulfate and alumina in fly ash and the size of fly ash on the extracting efficiency of alumina in fly ash were studied. The extracting efficiency of alumina can reach 95% under the optimum conditions.

M-3: Study on Absorption of Low-Concentration SO₂ with Basic Slag Intensified by Ultrasonic Wave: Nan Xiangli¹; Zhang Ting'an¹; Zhang Lu¹; Liu Yan¹; Lv Guozhi¹; Zhao Qiuyue¹; ¹Northeastern University

In this paper, it focuses on the absorption of low-concentration SO₂ with red mud to eliminate the harm of both the low-concentration SO₂ and Bayer red mud to the environment. It studies on the absorption experiments intensified by ultrasonic wave of 20 kHz at different ultrasonic power. It also investigates the effects of experimental conditions on desulfurization and dealkalization processes, which are different liquid-solid ratio, stirring speed of impeller, gas flow, temperature and ultrasonic power. Through the single factor experiment and orthogonal test, the results were analyzed by the chemical and XRD analysis technology. The conclusion shows that the desulfurization and dealkalization processes can be intensified by ultrasonic wave. The optimal conditions are: liquid-solid ratio is 9:1; stirring speed of impeller is 250 rpm; gas flow is 0.1 m³/h; the ultrasonic power is 550 W. The amount of desulfurization reaches 36.7 ml/g at 25°C.

Aluminum Alloys: Fabrication, Characterization and Applications: Poster Session

Sponsored by: The Minerals, Metals and Materials Society, TMS Light Metals Division, TMS: Aluminum Processing Committee
Program Organizers: Subodh Das, Phinix LLC; Tongguang Zhai, University of Kentucky; Zhengdong Long, Kaiser Aluminum

Monday PM
March 12, 2012

Room: Atlantic Hall
Location: Dolphin Resort

L-1: A Study of Microstructural Stability of Friction Stir Welded Joints of Al-Mg Alloys during Subsequent Thermal Exposure: Chun-Yi Lin¹; Truan-Sheng Lui¹; Li-Hui Chen¹; ¹National Cheng Kung University

Al-Mg wrought alloys such as Al-2.6Mg, Al-4.6Mg and Al-4.6Mg-1Si were friction stir welded and a subsequent thermal exposure was carried out in this study. The effects of elements addition and exposure temperature on the microstructural stability of welded zone were investigated. A grain refinement was found in the weld zone of each alloy and the average grain size of friction stir welded Al-2.6Mg, Al-4.6Mg and Al-4.6Mg-1Si was 10.1, 7.4 and 4.7µm, respectively. Thermal exposure caused drastic coarsening of grains in the stirred zone and abnormal grain growth initiated at some preferred sites such as upper surface and bottom. The volume fraction of coarsening grains increased with increasing exposure temperature; however an unexpected decrease in grain size was found at 550°C in compare to 500°C. Besides, the addition of Mg and Si deteriorated the thermal stability of grain structure in stirred zone.

L-2: Characterization of the Compressive Behaviour of an Al Foam by X-Ray Computerized Tomography: Girolamo Costanza¹; F. Mantino²; Severino Missori¹; Maria Elisa Tata¹; Andrea Sili²; ¹University of Rome "Tor vergata"; ²Università di Messina

Al metal foams manufactured by the powder-method have been investigated. Compression tests were performed on the same sample at increasing deformation steps: at each stage the sample was observed by X-ray computerized tomography. A geometric evaluation of porosity on many sections was performed by calculating, for each pore, its area, equivalent diameter, perimeter and circularity. During compression tests at first deformation occurs in the weakest zones of the samples, leading to cells collapse and densification that progressively propagates in a wide region until final densification. Going on compression, cells reduce progressively their dimensions: at each compression step it can be observed the disappearance of cells with the greatest equivalent diameter and the increasing of the number of cells with the smallest diameter. In particular at the last step the reduction of the total cells number occurs.

L-3: Computer Aided Cooling Curve Thermal Analysis of Al-Si-Cu-Mg Alloys: First and Second Derivative Curves: *Saeed Farahany*¹; Ali Ourdjini¹; Mohd Hasbullah Idris¹; ¹Universiti Teknologi Malaysia

Since industrial alloys behave far from ideality and equilibrium, computer aided cooling curve thermal analysis (CA-CCTA) is more practical compare to DTA, DSC and TGA. Determining critical characteristic parameters is crucial to control the quality of melt in terms of level of grain refinement, Si modification and impurity. Due to the small amount of heat evolved of some phase transformation, first derivative curve is used to reveal characteristic temperatures. However, there are contradicting views about the application of second derivative curve. The intention of this study is to establish a relationship between those curves. Two slope-tangents cross technique was used to measure TN based on the first derivative curve. However, in this research, a turning point at the second derivative curve was considered the precise moment when the dT/dt shifts upwards. Moreover, second derivative curve was introduced as a criterion for determining dendrite coherency point (DCP) based on one thermocouple technique.

L-4: Effect of Co on the Microstructure of Al-20Si-5Fe Alloys: O. Uzun¹; M.F. Kılıçaslan²; F. Yilmaz³; *Soon-Jik Hong*⁴; ¹Gaziosmanpaşa University; ²Kastamonu University; ³Gaziosmanpaşa University; ⁴Kongju National University

Al-20Si-5Fe-XCo (X=0, 3) alloys were produced by both conventional sand casting and melt-spinning at 20m/s disc velocity. The microstructures of the alloys were investigated using XRD, OM, and SEM. Vickers microhardness tester was used to see changing tendency of hardness with the effect of Co. Results of measurements showed that the microstructure of cast alloys consisted of α -Al, coarse intermetallic compounds and Si particles, and fine lamellar ternary eutectic microstructure. Co had little effect on both primary and eutectic Si in cast alloys. With addition the Co, the morphology of δ -intermetallic compound was changed from acicular to rod-like. In the case of the melt-spun ribbons, the addition of Co brought about changing of the microstructure drastically. The melt-spun ribbons had finer microstructure compared to the cast alloys. There was an increase in hardness values of both the cast and the melt-spun alloys parallel to the addition of Co.

L-5: Effect of Pin Tool Pass on the Quality of Friction Stir Weldment: An Experimental Evaluation: *Abdelrahman Shuaib*¹; Fadi Al Bedour¹; Nesar Merah¹; Abdulaziz Bazoune¹; ¹King Fahd University of Petroleum & Minerals

Most of the current applications of friction stir welding of aluminum parts involve the conventional butt, corner, edge, lap, and tee joints in which the pin-tool travels along a straight line. There are increasing efforts in introducing friction stir welding in relatively more complex contoured welding applications such as end joining of small diameter pipes and joining tubes to tubesheets in heat exchangers. This paper presents the results of an experimental investigation on the effect of the tool path on the weld quality of a 600 aluminum grade. A fully instrumented experimental RM-1 Friction Stir Welding machine manufactured by Manufacturing Technologies, Inc. (MTI) with a CNC controller is used to produce two types of weldments: a straight butt weld, and a contoured weld simulating the pass of tube-tubesheet joint. The results of the tests are used to identify the process parameters that are influenced by the changes in weld geometry.

L-6: Energy Absorption of Aluminum Foam-Filled Tubes under Quasi-Static Axial Loading: *Huan Liu*¹; Guangchun Yao²; Zhuokun Cao²; ¹Northeastern University; ²Northeastern University

Closed aluminum foams fitted thin-walled circular tubes was investigated for its energy absorption characteristics. Compression test was carried out to obtain the representative quasi-static stress-strain curves. The deformation characteristic (foam, tube and their combination) was analysed. The results indicated that the plateau region of the stress-strain curve exhibited a marked fluctuant serration which was related to the formation of folds and cracks. The foam-tube configuration absorbed more energy than the sum of foam and tube due to the interaction between

tube and filler which contains friction, extrusion, crack formation and growth. In addition, the energy absorption of foam-tube configuration was 4.5 times of aluminum foams. The experiment results reflected that the foam-tube configuration was a potential energy absorber candidate for car industry and transportation cask.

L-7: Fabrication and Characterization Al-SiC Composite Foam: *Geo Harrison*¹; Ganapathy Subramanian²; Vinoth Kambli²; Pradeep Kumar²; ¹COLLEGE OF ENGINEERING GUINDY, ANNA UNIVERSITY; ²College of Engineering Guindy, Anna University

Metal matrix composite foams have very low density, high stiffness and good impact resistance. These properties enable them to be used in various automotive and structural components. Al-SiC composite foams are prepared by dispersion of fine Silicon carbide powder in molten aluminum, followed by blowing of an inert gas and simultaneous stirring. The well dispersed inert gas bubbles form numerous micro-voids during solidification of the composite. A fine Al-SiC composite foam with homogeneous micro-structure is manufactured by this process. The impact resistance, stiffness and the mechanical behavior of the Al-SiC are analyzed subsequently.

L-8: Friction Stir Welding of Aluminum Alloys: *Jaehyung Cho*¹; Chang Gil Lee¹; ¹Korea Institute of Materials Science

Microstructure and mechanical properties of friction stirred aluminum alloys, AA5xxx (solid solution alloys), and AA6xxx (aging alloys) were investigated. Microstructural feature and texturing according to various welding conditions were examined. AA5xxx alloys had comparatively narrower welding zone than AA6xxx. Strength of the welded zone of AA5xxx was almost similar to that of the base materials. While, AA6xxx had lowered strength near the weld and HAZ, comparing with the base materials. The weld zone is wider than the diameter of the tool probe. In both alloys, fined and recrystallized grains were mainly observed near the weld zone. Elongated and curved grains from the base to the weld zone clearly disclosed the typical metal flow during welding. Various shear texturing was also observed with position and the equi-axed grain shapes reflected that they were fully-recrystallized due to high heat generation during welding process.

L-9: Mechanical and Microstructural Characterization of a 2618 Aluminum Alloy under Compression Tests: *Adriana Salas Zamarripa*¹; Edgar Fragoso¹; Ana Macias¹; Martha Guerrero Mata¹; ¹Universidad Autonoma de Nuevo Leon

Identification and quantification of microstructural heterogeneities in a 2618 aluminum alloy under three different heat treatment routes, such as second phase particles, inter- and trans- granular quenched precipitates and precipitate free zones, were done during this investigation. The relationship between these heterogeneities, specially the second phase particles (FeNiAl9), and the mechanical performance under compression was evaluated. Scanning Electron Microscopy (SEM) and image analysis were employed to identify and quantify the FeNiAl9 particles. This analysis was done before and after the compression tests. The compression tests were done under three different rates and under high temperature to emulate forging conditions. The results showed differences in amount, size, and shape factor of the FeNiAl9 particles and these characteristics had an effect in the compression behavior of this material.

L-10: Optimization of Process Parameters of Preparing Foamed Al-Si Alloy Based on Ga-Based Bp Neural Network: *Jingbo Xu*¹; Huimin Lu¹; Qiang Li¹; ¹Beihang University

This paper analyses the dependence of the structures of foamed Al-Si alloy on the process parameters. It takes the aid of back propagation (BP) neural network theory to build the nonlinear mapping relations between the crucial process variables and the quality of pores. Then by the integrating BP neural network and genetic algorithm (GA), the optimized process parameters for high porosity of foamed Al-Si alloy can be searched. The comparisons between experiment results and neural network simulation results show that GA-based on BP method can predict the porosity with



TMS 2012

141st Annual Meeting & Exhibition

higher prediction accuracy. The effects of viscosity and cooling conditions on the foamability are also important. The mechanism of thickening agent has been analyzed theoretically. The suitable solidification method of the melt is good for promoting uniformity of the pore structure of the alloy foams.

Biological Materials Science Symposium: Poster Session

Sponsored by: The Minerals, Metals and Materials Society, TMS Electronic, Magnetic, and Photonic Materials Division, TMS Structural Materials Division, TMS: Biomaterials Committee
Program Organizers: Nima Rahbar, University of Massachusetts Dartmouth; Candan Tamerler, University of Washington; Po-Yu Chen, University of California, San Diego; Molly Gentleman, Texas A&M University

Monday PM Room: Atlantic Hall
March 12, 2012 Location: Dolphin Resort

G-1: Aging Heat Treatment and Phase Transformations in Ti-Nb-Sn Alloys: Eder Lopes¹; Alessandra Cremasco¹; Rodrigo Contieri¹; Rubens Caram¹; ¹University of Campinas

Application of titanium in the orthopedic biomaterials field is ever growing. Research has recently focused on the β Ti alloys, that can be produced from non toxic elements and depending on composition and processing routes applied, can present low elastic modulus, enhanced biocompatibility, high corrosion resistance and high strength-to-weight ratio. Mechanical behavior of β titanium alloys depends on microstructural features and it can be improved by tailoring the microstructure through the control of their phase transformations. The objective of this investigation is to discuss phase transformations during aging heat treatment of β Ti-Nb-Sn alloys and to correlate microstructure and mechanical behavior. The results obtained from high temperature XRD experiments showed decomposition of orthorhombic α'' phase, which is followed by β and α phases precipitations. The mechanical behavior of Ti-Nb-Sn alloys was found to be very sensitive to the microstructural changes caused by addition of Sn and heat treatments.

G-2: Corrosion Behavior under Biological Environment of $Zr_{61}Ti_2Cu_{25}Al_{12}$ Amorphous Alloy: Ling Shi¹; Xu Zhao¹; Qiang He¹; Jian Xu¹; ¹Institute of Metal Research, Chinese Academy of Sciences

Electrochemical behavior of $Zr_{61}Ti_2Cu_{25}Al_{12}$ (ZT1) amorphous alloy in PBS and artificial saliva with NaF addition simulating the fluoride contents in commercial toothpastes was investigated. The corrosion resistant i.e. a decrease in the corrosion rate and anodic current density and an increase in the pitting potential decreased with increasing NaF concentration. The equivalent circuits from EIS test were proposed. Mott-Schottky analysis showed the passive film is n-type semiconductor and the donor density increased sharply with 0.5% NaF addition. A change from a high field-controlled layer growth to a diffusion-controlled oxide layer formation with increasing NaF was observed. XPS analysis indicated the outmost surface was predominantly composed of Zr^{4+} and Al^{3+} species. Compared with Ti-6Al-4V, ZT1 exhibits a lower penetration rate (CPR) with NaF=0.01% and then a higher CPR with NaF=0.1%. This indicates the presence of fluoride ions was detrimental to the protective ability of the ZrO_2 -based film on ZT1.

G-3: Effect of Heat Treatment on Oxidation Behavior and Brightness of Oxide Film Formed on Ti-Nb-Ta-Zr Alloy: Eri Miura-Fujiwara¹; Soichiro Yamada²; Yoshimi Watanabe²; Toshihiro Kasuga²; Mitsuo Niinomi³; Tohru Yamasaki¹; ¹University of Hyogo; ²Nagoya Institute of Technology; ³Tohoku University

Metallic materials for dentistry have excellent mechanical properties as a load bearing material, however, they are inferior in point of esthetic. "White metal", which has excellent mechanical properties like

metal with white color top has been long awaited. Now, we have found oxide film on Ti-29Nb-13Ta-4.6Zr alloy formed at high temperature has a white color and high exfoliation strength. In this study, the oxide film formation behavior and effect of heat treatment condition on brightness of oxidized surface were investigated. Dense white-colored oxide film was formed by heat treatment in air, and it was found by a x-ray diffraction and a x-ray photoemission spectroscopy that oxidation film was consisted of rutile and Ti(Nb, Ta)2O7. Brightness of the oxidized surface increased with increasing oxidation time, since thickness of the oxide layer increased with increasing. Optimum oxidized condition without exfoliation was determined.

G-4: Effects of Nitrogen Addition on Mechanical Properties of Hot-Forged Biomedical Co-Cr-Mo Alloys with Ultrafine-Grained Microstructures: Kenta Yamanaka¹; Manami Mori²; Akihiko Chiba¹; ¹Tohoku University; ²NISSAN ARC, LTD.

The ultrafine-grained (UFG) microstructures of Ni-free Co-29Cr-6Mo (wt.%) alloys, which are designed for biomedical applications, have been successively fabricated by conventional hot forging process. The mean grain size of 0.8 μ m was obtained by hot forging reduction of 83% (true strain of 1.8), which is much smaller than those in so-called severe plastic deformation. Significant grain refinement drastically enhanced tensile strength, while the elongation was limited to a few percent in Co-Cr-Mo ternary alloys. We have revealed that the addition of nitrogen, as is known to be one of the non-toxic \square phase (fcc) stabilizer, improves the elongation remarkably. The excellent ductility of the UFG alloys with N doping should be involved in constituent phase and strain-induced martensitic transformation. The present method characterized by ultragrain refinement with nitrogen addition to stabilize the \square phase can provide a potent strategy to obtain superior mechanical properties.

G-5: Evaluation of Properties of TiO₂ Ceramic Dental Block Fabricated by Magnetic Pulsed Compaction (MPC): Hyo-Young Park¹; Jin-Sung Choi¹; Hyo-Seob Kim¹; Uk-Hyon Joo²; Jar-Myung Koo¹; Soon-Jik Hong¹; ¹Kongju National University; ²BioMaterials Korea Inc

TiO₂ is well known for its excellent properties and dental application, such as biocompatibility, good fracture resistance, high fracture toughness and hardness. However, commercially available bulks still lack good mechanical properties. In this study, to improve the mechanical properties, TiO₂ bulk was fabricated using TiO₂ powders with addition of Ti and P-25 (Degussa) by magnetic pulsed compaction (MPC). In order to evaluate the effect of Ti and P25, MPC pressure (0.5~2GPa) and sintering temperature (800~1450°C, 2h) on TiO₂ bulk, various mixing conditions has been investigated (Ti: 2wt%, P-25: 0~8wt%). Results suggest that all of the samples' density and mechanical properties are improved with increased MPC pressure and sintering temperature. In addition, density and hardness of bulks decrease with addition of P-25 powder whereas fracture toughness and hardness increase with addition of Ti on the sintered bulks.

G-6: In Vivo Osteogenic Capability of Rat-Derived Mesenchymal Cells Cultured on Biomimetic Hydroxyapatite: Mina Khorami¹; Saeed Hesaraki¹; Sajad Farhangdoust¹; Ali Zamanian¹; Hamid Nazarian¹; ¹materials and energy research center

Nanostructured-carbonated hydroxyapatite (n-CHA) was prepared utilizing hydraulic conversion of calcium phosphates and characterized using TEM/SEM, XRD and FTIR. Rat-derived Mesenchymal stem cells (MSCs) were seeded on n-CHA in osteogenic agent-free medium. The MSCs/scaffold constructs were cultured up to 14 days and proliferation, alkaline phosphatase activity and morphology of MSCs were determined. Osteogenic differentiation of seeded MSCs was assayed by alizarin Red staining as well as ALP, Osteopontin and osteocalcin expression which was further confirmed by Real-time PCR analysis as osteogenic differentiation markers. The results confirmed that n-CHA comprised needlelike crystals of carbonated-apatite with thick diameter ranging 20-30 nm. It was observed that MSCs attached and spread well on n-CHA scaffold with enhanced proliferation and ALP activity. Interestingly, the

osteogenic differentiation of MSCs was confirmed by the expression of bone specific proteins including osteocalcin, osteopontin and alkaline phosphatase. Overall, the osteoconductive bone-like n-CHA apatite may also serve as an osteoinductive materials.

G-7: Mechanical Behavior and Corrosion Resistance of Nanostructured $Ti_{67.79}Fe_{28.36}Sn_{3.85}$ and $Ti_{53}Nb_{35}Zr_7Ta_5$ Alloys for Biomedical Applications: Anna Hynowska¹; Jordina Fornell¹; Eva Pellicer¹; Sergio González¹; Nele Van Steenberge¹; Santiago Suriñach¹; Maria Dolors Baró¹; Jürgen Eckert¹; Jordi Sort¹; ¹Universitat Autònoma de Barcelona

The mechanical behavior and corrosion resistance, in simulated body fluid, of nanostructured $Ti_{67.79}Fe_{28.36}Sn_{3.85}$ and $Ti_{53}Nb_{35}Zr_7Ta_5$ alloys are compared to those of commercial Ti-Al6-V4. The as-cast $Ti_{67.79}Fe_{28.36}Sn_{3.85}$ rods consist of few β -Ti (Im3m) dendrites embedded in a β -Ti/FeTi (Pm3m) nanoeutectic matrix. The $Ti_{53}Nb_{35}Zr_7Ta_5$ alloy shows a composite-like microstructure consisting of several β -Ti phases with different amounts of Nb, Zr and Ta. Nanoindentation experiments reveal that the $Ti_{67.79}Fe_{28.36}Sn_{3.85}$ rods exhibit very large hardness (~8 GPa) and high Young's modulus. In turn, the $Ti_{53}Nb_{35}Zr_7Ta_5$ alloy shows rather low Young's modulus (~88 GPa), which is advantageous in terms of biomechanical compatibility with bone. All the samples show a rather similar corrosion potential, E_{corr} around -20 mV vs Ag/AgCl, but differ in the corrosion current density values, j_{corr} . The $Ti_{53}Nb_{35}Zr_7Ta_5$ system has low j_{corr} , very close to that of commercial Ti-Al6-V4, whilst the $Ti_{67.79}Fe_{28.36}Sn_{3.85}$ shows a much larger value.

G-8: Nature's Inspiration: How Do Quills Protect Porcupines?: Wen Yang¹; Ekaterina Novitskaya¹; Sara Bodde¹; Zherrina Manilay²; Christy Chao³; Joanna Mckittrick¹; ¹Materials Science and Engineering Program, University of California, San Diego; ²Department of Mechanical and Aerospace Engineering, University of California, San Diego; ³Brown University

African and American porcupine quills were examined using microscopic methods and tested in compression and flexure. Quills are light-weight, composed of alpha-keratin and protect the animal from predators. The African porcupine quills are larger than the American ones and have longitudinal stiffeners (ribs) that extend from the cortex to the center, with foam that fills the remaining volume. This is in contrast to the American quills, which are only filled with foam. The cortex of quill has similar compressive strength to that of the whole quill whereas the foam has a much lower strength but a larger strain to failure, indicating that the cortex functions to resist deformation while the foam functions as a buffer that absorbs energy. Deformation mechanisms and structure-mechanical property relationships are evaluated and discussed. This research is supported by the NSF, DMR, Ceramics Program Grant 1006931.

G-9: Nitinol Commercialization Accelerator – Ohio Third Frontier: Janet Gbur¹; JR Lewandowski¹; H Lavvafi¹; M Young²; D Schwam¹; JD McGuffin-Cawley¹; MV Nathal³; S Padula³; JJ Lewandowski¹; ¹Case Western Reserve University; ²Cleveland Clinic; ³NASA Glenn Research Center

The Ohio Third Frontier Wright Projects Program recently funded a collaborative effort between the Cleveland Clinic, CWRU, University of Toledo, NASA Glenn Research Center, and Norman Noble, Inc. in order to develop a better understanding of the metallurgical processing and mechanical characterization of nitinol for use in biomedical and aerospace applications. Biomedical applications range from orthodontia to implantable devices while higher temperature shape memory alloys are of interest for aerospace. The collaboration is designed to create synergy amongst collaborators in the research and development of nitinol products. CWRU is developing a facility wherein the effects of composition changes on mechanical performance can be determined. The CWRU facility includes a vacuum arc melter and heat treatment system, high temperature DSC, laboratory extrusion press, and various fatigue testers. Capabilities and preliminary fatigue data will be provided.

G-10: Parametric Study of Fibroblast Attachment Kinetics on Fibronectin-Coated Polystyrene Tissue Culture Plates: Shawn Regis¹; Sina Youssefian¹; Nima Rahbar¹; Sankha Bhowmick¹; ¹UMass Dartmouth

Cell adhesion is mediated by specific interaction between receptors and ligands. This research presents the results of a numerical and experimental study on cellular attachment to fibronectin-coated 24-well polystyrene plates. This process relies on the interaction between the $\alpha 5 \beta 1$ integrin and fibronectin ligands. This project focuses on the generation of insightful models to accurately represent fibroblast ability to attach to fibronectin. Based on existing literature and experimental parameters, a dynamical model of fibroblast attachment kinetics on fibronectin coated tissue culture plates was developed. This was accomplished using a phase plane analysis of a system of nonlinear ordinary differential equations, which govern the changes in free receptor density and bond density within the contact area with time. Furthermore, experimental data of receptor-ligand bond density was used to analyze the accuracy of the devised model.

G-11: Peptide-Enabled Control of Metal Nanoparticle Biomaterialization: Marketa Hnilova¹; Dmitriy Khatayevitch¹; Hanson Fong¹; Candan Tamerler¹; Mehmet Sarikaya¹; ¹University of Washington

Peptide mediated synthesis of metallic nanostructures is biocompatible and non-toxic alternative to conventional chemical methods. Here we examine formation mechanism, kinetics and morphology of nanoparticles (NPs) produced by combinatorially selected Au binding peptides (AuBP). We produced AuBPs in linear and cyclic forms to determine effect of molecular constraints on peptides' catalytic activities. Both AuBPs catalyze gold formation in aqueous solution under ambient conditions resulting in stable peptide-capped AuNPs. By varying reaction conditions, we tailor NP morphology by controlling the nucleation and growth rates during the biomaterialization process. The synthesis is controlled such that NPs in the size range of 2 nm to >100 nm can be produced with fairly uniform distribution. Peptide-based biomimetic syntheses have implications in a wide range of applications including nanobiophotonic and biosensing platforms. Research is supported by NSF-IRES, -BioMat (DMR 0706655) and -MRSEC Programs through the University of Washington GEMSEC (DMR 0520567).

G-12: Processing and In Vivo Evaluation of Spark Plasma Sintered Al₂O₃-YSZ-TiO₂ Composites: Ipek Akin¹; Viorica Simon²; Simona Cavalu³; Gultekin Goller¹; ¹Istanbul Technical University; ²Babes-Bolyai University; ³University of Oradea

In this study, Al₂O₃ and Al₂O₃/YSZ composites with 3 and 5 wt% TiO₂ were prepared by spark plasma sintering at 1400°C for 300 s under 40 MPa. Adult rats from the Wistar-Furth lineage were used for in vivo evaluations. They were kept in a proper environment under natural lighting and temperature. A 0.75cm x 1.5cm bone defect was created on the body of each mandible in animals using a low RPM Sorensen 7.5 spherical burr. The defects were filled with granular Al₂O₃-based composites containing YSZ and TiO₂, and blood plasma harvested from each animal prior to surgery. A collagen film was placed on the top of the filled defect in order to improve the biocompatibility of the implanted material. The histopathological tests of the surrounding tissue and specimens containing the junction between the implanted material and natural bone were characterized by using a scanning electron microscope.

G-13: Strong Fiber Reinforced Hydrogel Composite: Animesh Agrawal¹; Sina Youssefian¹; Nima Rahbar¹; Paul Calvert¹; ¹University of Massachusetts Dartmouth

This work is focused on designing a new class of hydrogels, based on fiber reinforced composites technique with a cartilage-like structure. In analogy to the spinning of a spider web, a pultrusion system is developed to spin micron-diameter fibers from polymer solution in order to build three dimensional patterned fibrous structures. Impregnating the fibrous construct with epoxy-amine hydrogel forms fiber-reinforced hydrogel composites. The fibrous construct improves the strength, modulus and toughness of the hydrogel and also constrains the swelling. By altering the construct geometry and studying the effect on mechanical properties



TMS 2012

141st Annual Meeting & Exhibition

we will develop the understanding needed to design strong hydrogels for biomedical devices and soft machines. Also experimental results were compared with hyper-elastic and poro-elastic theories in order to predict the mechanical behavior of composite hydrogels.

G-14: Strontium Releasing And Physicochemical Properties of Novel Calcium Sulfate Bone Substitute Materials: Saeed Hesaraki¹; *Sajad Farhangdoust*²; Hadis Bandegani²; Mina Khorami²; Ali Zamanian²; ¹materials and energy research center; ²Materials and Energy Research Center

This paper describes strontium-releasing, physicochemical and cellular properties of gypsum bioceramics doped with 0.19 – 2.23 wt. % of strontium ions. Strontium-doped gypsum (gypsum: Sr) was obtained by mixing calcium sulfate hemi-hydrate powder and solutions of strontium nitrate. Gypsum was the only phase found in the composition of both pure and gypsum: Sr, with slight right-shift in XRD peaks of latter. The compressive strength of pure gypsum was ~ 28 MPa which was reached to ~ 42 MPa by incorporating 2.23 wt% of Sr. Microstructure of all specimens consisted of rod-like crystals entangled to each other with more elongation and higher thickness in the case of gypsum: Sr. Continuous release of strontium ions was observed from gypsum: Sr during soaking in simulated body fluid. Compared to pure gypsum, gypsum: Sr showed better proliferation rate and higher alkaline phosphatase activity of osteoblasts. The results predict better in vitro performance of strontium-doped gypsum compared to pure one.

G-15: Sulfate- Reducing Bacteria Biofilm Corrosion Behavior of High Strength Steel (API-5L X80) Weldment: *Faisal Al-Abbas*¹; Tony Kakpovbia¹; David Olson²; Brajendra Mishra²; John Spear²; ¹Saudi Aramco; ²Colorado school of Mines

The utilization of high strength carbon steels in the oil and gas transporting systems has been increased recently. This work investigates microbiologically influenced corrosion (MIC) of API 5L X80 linepipe steel weldment by Sulfate Reducing Bacteria (SRB), *Desulfovibrio africanus* sp. The biofilm and pit morphology that developed with time were characterized by using scanning field emission scanning electron microscopy (FESEM). Electrochemical Impedance Spectroscopy (EIS), linear polarization resistance (Rp) and open circuit potential (OCP) were used to analyze the corrosion behavior. Through circuit modeling, EIS results were used to interpret the physicoelectric interactions between the electrode, biofilm and solution interfaces. These results confirmed that corrosion activity of *Desulfovibrio africanus* sp is due to the formed biofilm and a porous iron sulfide layers on the metal surface developed over time. Corrosion products were characterized by X-ray diffraction (XRD) which identified the presence of different sulfide and oxide constituents.

G-16: Weibull Analysis of the Behavior on Tensile Strength of Bamboo Fiber of the Specimen *Dendrocalmus Giganteu*: *Lucas Martins*¹; Nathalia Rosa¹; Sergio Monteiro¹; ¹UENF

The fibers extracted from the stem of the bamboo plant have been investigated as possible reinforcement composites due to their relatively high tensile strength. However no work was conducted to dimensional characterize the distribution and the effect of diameter on the mechanical resistance of bamboo fiber of the specimen *dendrocalmus giganteus*. The aim of the present work was to statistically characterize the distribution of the diameter of a lot of bamboo fibers of that specimen. Based on this characterization, diameter intervals were set and the dependence of the tensile strength of these fibers with a corresponding diameter was analyzed by the Weibull Method. The results indicated an inverse dependence between the diameter and the resistance of that fiber that was adjusted with a hyperbolic equation. An analysis of the microstructure by means of scanning electron microscope revealed possible mechanism for this correlation.

G-17: Wet Chemical Synthesis of Hydroxyapatite from Egg Shells:

*Muhammad Aftab Akram*¹; Razaqat Hussain²; Mohammad Islam¹; ¹National University of Sciences and Technology Pakistan; ²University Teknologi Malaysia, 81310 UTM Skudai, Johor Darul Ta'zim, Malaysia.

Hydroxyapatite is well known bioceramic that possess excellent in-vivo and in-vitro properties due its chemical and structural similarity with mineral part of bone and is widely used as bone graft material in orthopedic surgery and dental implants. In this research a simple green chemistry and environment friendly wet precipitation route was adopted for synthesis of micro crystalline hydroxyapatite from egg shells by using phosphoric acid as phosphorus precursor. Resulting powder was characterized using TGA/DTA for thermal stability, XRD for structural analysis which proved phase purity and SEM for morphological evaluation which showed spherical particles. FTIR and particle size analysis was also performed. Dielectric studies were also performed at varying temperatures to evaluate trends of relative permittivity, dielectric loss and AC conductivity for its potential sintering in microwave furnace.

Computational Thermodynamics and Kinetics: Poster Session

Sponsored by: The Minerals, Metals and Materials Society, TMS Electronic, Magnetic, and Photonic Materials Division, TMS Materials Processing and Manufacturing Division, TMS Structural Materials Division, TMS: Alloy Phases Committee, TMS: Chemistry and Physics of Materials Committee, TMS/ASM: Computational Materials Science and Engineering Committee, TMS: Integrated Computational Materials Engineering Committee, TMS/ASM: Phase Transformations Committee, TMS: Process Technology and Modeling Committee

Program Organizers: Zi-Kui Liu, The Pennsylvania State University; Mark Asta, University of California, Berkeley; James Warren, The National Institute of Standards and Technology; Yunzhi Wang, Ohio State University; Raymundo Arroyave, Texas A & M University; Yu Wang, Michigan Tech

Monday PM
March 12, 2012

Room: Atlantic Hall
Location: Dolphin Resort

C-1: A Kinetic Study of the Leaching of Germanium Dust and Fume by Sulfuric Acid: *Wankun Wang*¹; Jinhui Peng¹; Zebiao Zhang¹; Lijuan Chu¹; Guodong Lai¹; ¹Kunming University of Science and Technology

A kinetic study of the leaching of germanium dust and fume by sulphuric acid has been investigated. The effects of (a) acid concentration ranging from 3.15 to 9.45 mol/L and (b) temperature ranging from 60 to 80°C on germanium dissolution are reported. The dissolution rates are significantly influenced by the temperature and concentration of the sulphuric acid solutions. The experimental data for the dissolution rates of germanium have been analyzed with the shrinking-core model for reaction control. The observed effects of the relevant operating variables on the dissolution rates are consistent with a kinetic model for diffusion control. The apparent activation energy for the dissolution of germanium has been evaluated using the Arrhenius expression. Moreover, the apparent reaction order and the kinetic equation for the dissolution of germanium were obtained.

C-2: Continuous Modeling of Microstructure Evolution Coupled with Plastic Activity: *Maeva Cottura*¹; Yann Le Bouar¹; Alphonse Finel¹; Benoît Appolaire¹; Samuel Forest²; ¹Laboratoire d'Etude des Microstructures, CNRS/ONERA; ²Mines ParisTech, Centre des Materiaux CNRS UMR 7633

Plastic activity is often involved during microstructure evolution. The Phase Field Method (PFM) is the most powerful technic to understand microstructure evolution during phase transformations at mesoscale. In this work, a model able to describe both microstructure evolution and

plastic activity is derived by coupling a phase field model with a continuous viscoplasticity model. In a heterogeneous material, it is well known that, when the domains are small enough (below typically 1 micron), the plastic behavior of each domain depends on its size. In a continuous modeling, this effect can only be accounted for using a scale dependent plasticity model. Our approach follows a second gradient theory from generalized continuum mechanics. We will present this model and apply it to the study of microstructural evolutions in Ni-based superalloys under creep loading.

C-3: Convex Projection to Estimate Heat Content of Cold Charges in Peirce-Smith Converting: *Alessandro Navarra*¹; Anna-Maria Pubill Melsió²; Joël Kapusta³; ¹Universidad Católica del Norte; ²Air Liquide; ³BBA Inc.

Peirce-Smith converting (PSC) is applied in over half of the primary production of copper and nickel. PSC generally follows a continuous smelting process, leads a sequence of batch operations, and can thus be a natural bottleneck in copper and nickel production. The main feed for a Peirce-Smith converter is molten matte. Additionally, there are several cold streams that are fed into the converter, which can be mixtures of matte, recycled slag or flue dust. The current work focuses on a technique to estimate the heat content of these cold streams. The heat balance between the hot matte and the cold charges is a major operational constraint that has implications throughout the metal production process. The heat estimation technique is based on geometrical projections in the chemical phase space, and has been conveniently implemented as a function within Microsoft Excel.

C-4: Effects of Sub-Surface He Bubbles on Tungsten Surface Evolution: *Faiza Sefta*¹; Karl Hammond²; Niklas Juslin²; Brian Wirth²; ¹UC Berkeley; ²University of Tennessee

Tungsten is a leading candidate material for the divertor in ITER and other future nuclear fusion reactors. However, helium plasma bombardment experiments have demonstrated that surface defects and bubbles form even at modest ion energies, and in some cases “fuzz” and “coral” like surface features exist after a few hours of exposure. We investigate the formation mechanisms behind these surface features using atomistic molecular dynamics. Sub-surface helium bubbles, in particular, are found to leave behind relatively stable surface defects after they burst. Assuming sub-surface bubbles are in an equilibrium helium density state, we investigate how surface evolutions leading to a thinning of the tungsten layer above the sub surface bubble can lead to bubble bursting and subsequent surface deformation. Under these conditions, we quantify the conditions in which equilibrium and above equilibrium helium bubbles burst as a function of temperature, surface crystallography, bubble depth and tungsten surface deformations.

C-5: Establishment and Analysis of the Composite Key Stratum Model Layer on the Winkler Foundation: *HongYu Pan*¹; Shu-Gang Li¹; Peng-Xiang Zhao¹; ¹Xi'an University of Science and Technology

With the depth and intensity of exploitation increase, some proximal hard rock appeared composite effect, the resulting of rock press appearance poses new challenges to safety in coal seam. The Composite Key Stratum Model Layer on the Winkler Foundation was established by using composite material structural mechanics theory and Key Stratum theory, which was used to analyze Composite Key Stratum's force theoretically and detruide Winkler foundation Composite Key Stratum's interval. Composite Key Stratum flexure formed advance pressure on the near under stratum. Making use of its transfer, spreading and attenuation, the advance pressure and the width of limit equilibrium zone under the Composite Key Stratum were analyzed. Provided theoretical basis for determining working face's cross-off pace and support lectotype in the condition of Composite Key Stratum.

C-6: First-Principles-Based Phase Diagram for (Mo_xNb_{1-x})Si₂ Pseudobinary Alloys: *Koretaka Yuge*¹; Yuichiro Koizumi²; Koji Hagihara³; Takayoshi Nakano⁴; Kyosuke Kishida¹; Haruyuki Inui¹; ¹Department of Materials Science and Engineering, Kyoto Univ.; ²Institute for Materials Research, Tohoku University; ³Department of Adaptive Machine Systems, Graduate School of Engineering, Osaka University; ⁴Division of Materials & Manufacturing Science, Graduate School of Engineering, Osaka University

MoSi₂/NbSi₂ duplex silicide is one of the most promising structural materials at ultra-high temperature for improving gas turbine engine performance in power generation systems. It was confirmed [T. Nakano et al., *Intermetallics* 6 (1998) 715.] that fine lamellae composed of C11_b and C40 phases are formed at (Mo_{0.85}Nb_{0.15})Si₂, improving high-temperature strength. However, its phase stability is assessed for limited portion by experiment or is not fundamentally well-understood by theory, which should be significant information for understanding and controlling formation of the lamellae. In this study, we employ first-principles calculation with cluster expansion to quantitatively investigate the phase stability in (Mo_xNb_{1-x})Si₂ pseudobinary alloys. We find that (i) there is no stable intermediate structure between MoSi₂ and NbSi₂, (ii) complete miscibility cannot be achieved below melting temperatures, (iii) C40 phase exhibit around ten times larger solubility than C11_b, and (iv) temperature-dependence of solubility in C40 is much stronger than that in C11_b.

C-7: Gaseous Nitriding Process Control: Application of Customized Lehrer Diagrams: *Mei Yang*¹; Richard Sisson¹; ¹WPI

The experimental Lehrer diagram for pure iron is widely used in industry to specify the nitriding potential for nitriding process. However, applying the pure iron Lehrer diagram for alloy steels can lead to incorrect results because of phase stabilities in alloy steels. A customized Lehrer diagram for AISI4140 has been developed by using CALPHAD approach to predict the relationship between the nitriding potential and the phase development as a function of temperature. The prediction is in excellent agreement with the experimental investigation and this proves the utility of using thermodynamic database to calculate the customized Lehrer diagrams for alloy steels. In the present work, series of Lehrer diagrams are developed to analyze the effects of elements such as carbon and manganese for the nitriding process. These diagrams can not only provide the nitriding process parameters for specified alloys but also pave a way for computational materials design to nitriding alloys.

C-8: Intelligent Heat Treating: Simulation of Carburization Process: *Lai Zhang*¹; Yingying Wei¹; Liang He¹; Richard D Sisson¹; ¹WPI

An effective simulation software CarbTool is developed to predict the carburization performance of a variety of steels. The software is needed not only to predict the carbon profile but also to optimize the process in terms of the cycle time and the cost. It can meet these needs for both gas and vacuum carburization. In this paper, CarbTool predictions were used to provide recipes for the carburization of four types of steels, heat treated by both gas and vacuum carburizing processes. With the industrial experimental results, the simulation parameters are verified. Based on the excellent agreement of model predictions and experimental results, CarbTool may be used to predict the carbon concentration profile for a variety of alloys in both gas and vacuum carburizing processes.

C-9: Molecular Dynamics Simulation Study of the Alloying Reactions of Nanostructured Al/Ni Clad Particles System under Thermal Loading: *Shijin Zhao*¹; ¹Shanghai University

We present molecular dynamics simulations of the alloying reaction process of nanostructured Al/Ni clad particles under thermal loading. The calculations indicate that the properties of nanostructured Al/Ni clad particles depend strongly on their nanostructures and combustion parameters such as particle size and mass density. With the particle size increasing, both the adiabatic temperature and pressure of system rise but the propagation velocity of reaction front decreases. However, when either mass density or ignition temperature increases, the adiabatic combustion temperature, the pressure of the system, and the propagation velocity of



the reaction front increase. The cracking of nickel layer, governing the contact surface and mass diffusion of aluminums and nickels, plays a key role in the propagation process of Al/Ni clad particles.

C-10: Numerical Simulation of Directionally Solidified Structure of Ti-47Al-2Cr-2Nb Alloy Based on CA Method: Jixiang Xu¹; Qingyan Xu¹; Jin Cheng¹; Hu Zhang²; Baicheng Liu¹; ¹Tsinghua University; ²Beihang University

Physical and mathematical models for microstructure evolution of Ti-47Al-2Cr-2Nb (atomic fraction, %) alloy during directional solidification process were developed based on CA method, considering peritectic reaction. Growth of peritectic phase during directional solidification was simulated. Simulated results show that a phase nucleates on the interface of liquid and β below the peritectic temperature and grows into the β phase and the liquid. Competitive growth of columnar grains was simulated to investigate the influence of different preferred growth orientations on the morphologies of columnar dendrites. Microstructure was simulated at the withdrawal rates of 1.2mm/min, 5mm/min and 10mm/min, which shows that directional growth zone is composed mainly of columnar grains of primary β phase and a small volume fraction of peritectic α phase can be observed in the interdendritic regions of β phase. Primary dendrite arm spacing of columnar grains decreases with the increasing withdrawal rate, which agrees well with experimental results.

C-11: Phase Diagram Determination for Several Fe-Based and Ni-Based Ternary Systems: Siwei Cao¹; Ji-Cheng Zhao¹; ¹The Ohio State University

A diffusion multiple was made by assembling finely-polished Ni, Fe, Co, Cr, and Mo metal pieces, followed by a hot-isostatic-pressing (HIP) treatment. Long-term heat treatment was performed at both 1200 °C and 1000 °C. Electron probe microanalysis (EPMA) are performed to obtain local equilibrium information at the phase interfaces to construct isothermal sections for some of the following ternary systems: Fe-Co-Ni, Fe-Mo-Ni, Fe-Cr-Ni, Mo-Cr-Ni, Mo-Co-Ni, Mo-Cr-Fe, Mo-Cr-Co, and Co-Cr-Fe. These phase diagrams will be important input data for thermodynamic modeling of these systems, especially related to the topologically close packed (TCP) phases. Lower temperature heat treatment is also planned to assess the stability of the R-phase in some of these ternary systems.

C-12: Reactivity of the Faying Surface in Al-Mg₂Si Metal Matrix Composite/Magnesium Alloy Bonds: Mehdi Mazar Atabaki¹; Andrew Mullis¹; ¹University of Leeds

A model of dissolution and isothermal solidification during low temperature-partial transient liquid phase bonding process of Al/Mg₂Si metal matrix composite to AZ91D joints using Al interlayer is presented. It was found that the lower temperature gradient resulted in increase of isothermal solidification. It is showed that kinetics of the bonding process significantly accelerated in presence of reinforcement (Mg₂Si). This acceleration is attributed to the increased solute diffusivity through grain boundaries of the metal matrix composite. The numerical model estimates the fraction of wafer layer, formed at the surface of the substrates. Results suggest that Si and Mg contained in the interlayer favours the partial disruption of the aluminium oxide film, making easier the bonding process. However, the diffusion of Mg and its component to the grain boundary of the Al metal matrix composite was the main controlling factor in the bonding process.

C-13: Study on Blowing Nitrogen Alloying of Stainless Steel AISI410 with LF Refining: Zhou Cai¹; ¹Chongqing University of Science and Technology

The effect of nitrogen blowing time, nitrogen rate and liquid temperature in normal atmosphere condition on nitrogen content has been tested and studied by using 40tLF for refining stainless steel AISI410 and the control model of nitrogen alloying during LF refining has been established. The

experimental results show that with increasing nitrogen blowing time and nitrogen rate the nitrogen content in steel increases, the nitrogen content in liquid is more than 0.05% as nitrogen blowing for 10 min in normal atmosphere, with increasing nitrogen rate the time that come to saturated nitrogen in liquid decreases and with decreasing temperature of liquid the solubility of nitrogen increase. The analysis on nitrogen absorption is carried out by thermodynamic model and the calculated nitrogen content is in good agreement with the measured one, which provides reference for controlling nitrogen content by blowing nitrogen gas in LF refining stainless steel

C-14: Understanding H Induced Failure Mechanisms in Metallic Alloys: The Role of Attractive H-H Interactions in Nano-Precipitate Formation: Johann von Pezold¹; Alexander Udyansky¹; Ugur Aydin¹; Tilmann Hickel¹; Joerg Neugebauer¹; ¹Max-Planck-Institut für Eisenforschung GmbH

Attractive H-H interactions have recently been shown to induce the formation of local hydride precipitates even in non-hydride forming matrices, such as Ni [1]. The formation of these nano-hydrides in the strain field of extended lattice defects has been correlated to the long-standing problem of hydrogen embrittlement in these metals. In this study we systematically investigate H-H interactions in a range of fcc matrices, including Ca, Mn, Fe, Co, Ni, Al and Pd, using density functional theory. While the interaction between H atoms in nearest neighbour interstitial sites is generally attractive, the nature of this interaction is strongly system and site dependent. Hence, the interaction between octahedral sites is predominantly of elastic nature, while interactions between tetrahedral sites exhibit a significant chemical contribution. Based on our results we discuss the possibility of nano-hydride formation in fcc metals. [1] J. von Pezold et al., Acta Mat. 59, 2969 (2011).

Deformation, Damage, and Fracture of Light Metals and Alloys: Poster Session

Sponsored by: The Minerals, Metals and Materials Society, TMS Structural Materials Division, TMS Light Metals Division, TMS/ASM: Mechanical Behavior of Materials Committee
Program Organizers: Qizhen Li, University of Nevada, Reno; Fuqian Yang, Univ. of Kentucky; Ke An, Oak Ridge National Laboratory

Monday PM
March 12, 2012

Room: Atlantic Hall
Location: Dolphin Resort

N-1: Correlation between Melt Quality and Fatigue Properties of 2024, 6063 and 7075: Engin Tan¹; Ali Tarakcilar¹; Derya Dispinar²; ¹Pamukkale University; ²University of Istanbul

Extruded 2024, 6065 and 7075 alloys were subjected to Strain Induced Melt Activated (SIMA) process and average of 80 μ m spherical grains were obtained. T6 solution heat treatment was carried out to all alloys. In addition to the typical water quenching at 20°C, temperature controlled bath was used where the water was set to 80°C and some samples were quenched in that water. High mean stress values were selected (0.9, 0.8 and 0.7 μ m) and load stress ratio (R) was selected to be 0.1. The fatigue test results were analyzed by Weibull and the distributions were compared with metal quality. SEM analysis was carried out on the fracture surface. A good correlation was found between bifilm index and the fatigue properties; as the quality was lowered, the scatter of the test results was increased.

Magnesium Technology 2012: Poster Session

Sponsored by: The Minerals, Metals and Materials Society, TMS Light Metals Division, TMS: Magnesium Committee
Program Organizers: Suveen Mathaudhu, U.S. Army Research Office; Wim Sillekens, TNO; Norbert Hort, Helmholtz-Zentrum Geesthacht; Neale Neelameggham, U.S. Magnesium

Monday PM
March 12, 2012

Room: Atlantic Hall
Location: Dolphin Resort

K-1: Characteristics of β' Phase in an Aged Mg-10Gd-3Y-0.5Zr Alloy: *Dejiang Li*¹; ¹Shanghai Jiao Tong University

The precipitation behavior at 225°C of Mg-10Gd-3Y-0.5Zr (GW103K) alloy was studied by transmission electron microscope. Particular attention was paid on the characteristics of meta-stable phase β' . The crystal structure, chemical composition and habit precipitation plane of β' were identified by TEM and EDS, which are as same as that studied by others in GW series alloys. However, the shape of β' at early stages during precipitation was significantly different with that reported by previous studies. Plate-shaped rather than globular-shaped β' phase was recognized with the plate diameter of about 10nm and thickness of several atomic layers along c-axes of Mg in the alloy after aged for 2h. With time prolonged to peak aging condition of 16h, β' phase gradually changed to convex lens-shaped though simultaneously growing along [10-10] and [0001] direction. Based on the microstructure observation, the coarsening mechanism of β' phase during isothermal aging treatment was discussed.

K-2: Coherency Strain and Interfacial Energy of Mg₃-Rare Earth D019 Precipitates from First-Principles: *Ahmed Issa*¹; James Saal¹; Chris Wolverton¹; ¹Northwestern University

The potential to greatly strengthen magnesium alloys has driven current research, with a recent focus on strengthening precipitates, particularly involving rare earth (RE) dopants. The morphology of these precipitates dictates their effect on the strength of the alloy, and quantifying the coherency strain and interfacial energies between the precipitates and the Mg matrix is key to determining the morphology of the precipitate. We apply density functional theory (DFT) to systematically predict the formation energies as well as interfacial energies and coherency strain energies of D019 precipitates in Mg-RE systems along several crystallographic directions. In particular, we look for D019 precipitates that will favorably form plate-shaped morphologies along non-basal planes, as this morphology should be effective obstacles to plastic deformation. These Mg-RE systems also provide an interesting testing ground for the accuracy of DFT methods for intermetallic compounds containing f- electrons.

K-3: Combination of Cooling Curve and Micro-Chemical Phase Analysis of Rapidly Quenched Magnesium AM60 Alloy: *Paul Marchwica*¹; Jerry Sokolowski¹; Adam Gesing²; John Jekl³; Carsten Blawert⁴; Richard Berkmortel³; ¹University of Windsor; ²Gesing Consultants Inc.; ³Meridian Technologies Inc.; ⁴GKSS Forschungszentrum Geesthacht GmbH

Universal Metallurgical Simulator and Analyzer (UMSA) Technology Platform macro test samples of magnesium alloys AM60 and AE44 were melted and quenched at maximum instantaneous cooling rates ranging from 5°C/s to 250°C/s and the resultant cooling curves were analyzed. Characteristic reactions on these curves corresponding to the nucleated phases were identified with the aid of known data as well as metallographic analysis. The results indicate that the relative proportion of fraction solid of phases in the alloys shift with relation to the cooling rate. These higher cooling rates are typical of real industrial solidification processes such as die-casting. These findings can be used to improve future computer models of magnesium (and other alloys) casting solidification processes.

K-4: Corrosion Behavior of Pure Mg Extrudate: *Chang Dong Yim*¹; Young Min Kim¹; Sung Hyuk Park¹; Ha-Sik Kim¹; Byoung-Gi Moon¹; Bong Sun You¹; ¹Korea Institute of Materials Science

The effect of grain size on corrosion behavior of pure Mg extrudate was evaluated via various method. The pure Mg extrudates with different grain size were prepared by indirect extrusion followed by heat treatment. With increase of average grain size, current density was slightly increased. No obvious feature was not observed on the surface of specimen during cathodic polarization. In the case of specimen with small and homogeneous grain size, corrosion occurred uniformly on the surface of specimen. But in the case of specimen with large and inhomogeneous grain size, corrosion occurred locally. It was concluded that the corrosion behavior of pure Mg extrudate was strongly dependent on grain size and smaller and more homogeneous grain size was more favorable to higher corrosion resistance of pure Mg.

K-5: Critical Grain Size for Change in Tensile Deformation Behavior and Transition in Tension- Compression Asymmetry in a Magnesium Alloy: *S. K. Panigrahi*¹; K. Kandasamy¹; N. Kumar¹; R. S. Mishra¹; R. DeLorme¹; B Davis¹; R.A. Howell¹; K Cho¹; ¹Centre for Friction Stir Welding and Material science and Engineering

In polycrystalline materials, tensile deformation behavior is dependent on grain size. The influence of grain size on deformation behavior of fcc and bcc metals and alloys in the grain size range from nano to micrometer has been widely studied. However, similar work on hcp materials such as on magnesium alloys, has not been systematically investigated. Magnesium alloys often develop deformation texture during processing which results in tension-compression yield asymmetry. The tension-compression yield asymmetry in magnesium alloys restricts its use for structural applications. In the present work, the effect of grain size and texture on mechanical properties and yield asymmetry in a Mg-Y-RE alloy was studied. A critical grain size for transition in deformation behavior from strain hardening to strain softening during tensile testing has been identified. Below the critical grain size, no yield asymmetry was observed.

K-6: Doping Effect on the Formation Energy of the Basal-Plane Stacking Faults in Binary Mg-X Alloys: First-Principles Calculations: *William Yi Wang*¹; Shun Li Shang¹; Zhi Gang Mei¹; Yi Wang¹; Suveen Nigel Mathaudhu²; Xi Dong Hui³; Zi-Kui Liu¹; ¹Pennsylvania State University; ²US Army Research Office; ³University of Science and Technology Beijing

Three kinds of low-energy intrinsic and extrinsic basal-plane stacking faults in the Mg, such as growing fault, deformation fault and external fault, are investigated via the first-principles calculations. Additionally, the doping effect of the favorable and unfavorable elements in the binary Mg-X alloys on the formation energy of these structures are reported, the variation tendency of which has the potential application to design the advanced Mg alloys with good mechanical properties, especially the ductility and creep resistance.

K-7: Ductility Improvement in Equal Channel Angular Processed AZ31 Magnesium Alloy: *Sonia Modarres-Razavi*¹; David Foley¹; Ibrahim Karaman¹; Karl T. Hartwig¹; Laszlo Kecskes²; Suveen Mathaudhu²; Vincent Hammond²; ¹Texas A&M University; ²U.S. Army Research Laboratory

A commercial AZ31 magnesium alloy has been processed using a multiple-temperature equal channel angular processing (ECAP) to enhance its mechanical properties by introducing ultra-fine grained structure with grain size of about 400 nm. A total of six to eight passes were applied starting at 200 °C for the first four passes to get advantage of softening through dynamic recrystallization (DRX) and then conducting additional passes at lower temperatures down to 125 °C following a combination of routes A and C, to suppress DRX and grain growth. Tension experiments in the flow direction of the processed sample demonstrated high strength levels up to 385 MPa in yield and 460 MPa in ultimate strength with elongation-to-failure of 14%. In order to improve



the ductility, the samples were annealed shortly followed by ECAE. This promising technique enhanced the ductility appreciably without much sacrifice in strength.

K-8: Effect of CaO on Creep Behavior of Magnesium Alloys: *Hyun Kyu Lim*¹; Shae K. Kim¹; ¹KITECH

Magnesium alloys offer the opportunity for significant weight reductions in automotive components due to their low density. Nevertheless, there are strong needs for magnesium alloys with improved high temperature mechanical properties to apply to power train parts in vehicles. In this study, two magnesium alloys were investigated; one is modified MRI153 alloy, where Ca and Sr were replaced with CaO and the other is 1.5 wt.% CaO added AM60 alloy. Test specimens of three alloys (modified MRI153, CaO added AM60, and conventional MRI153 (for comparison) alloys) were prepared by re-melting and casting into steel mold with ingots and machining. The mechanical properties and the creep behavior of these specimens were determined and their microstructures were characterized using OM and SEM. In addition, fluidity test were carried out with spiral mold. It is proposed that replacement of CaO or adding CaO is beneficial to the creep resistance at elevated temperature.

K-9: Effect of Gadolinium and Yttrium Content on Microstructure and Strength of Mg-Li Alloys: *Min Li*¹; Guangchun Yao¹; Guoyin Zu¹; Mengxiao Chen¹; Jun Cheng¹; Qingyan Zhu¹; ¹Northeastern University

Effect of gadolinium and yttrium addition on strength of Mg-Li alloy was investigated using the metallographic observation, scanning electron microscope (SEM) and X-ray diffraction (XRD). The results indicate that the strengths were greatly improved with gadolinium and yttrium additions, in which the tensile strength was 209 MPa and the elongation was 18.4%, respectively. Through comparing with the Mg-Li alloy, the increments of tensile strength was 57 MPa, respectively. The improved strength was mainly correlated to the grain refining effect, the strengthening effect of the Mg₅Gd phases and also the hardening effect of the solutioned gadolinium and yttrium atoms.

K-10: Effect of Grain Refinement and Texture Changes Induced by Burnishing on Corrosion Resistance of Magnesium Alloy for Biomedical Applications: Z. Pu¹; S. Yang¹; G.-L. Song²; O.W. Dillon, Jr.¹; D. A. Puleo¹; I.S. Jawahir¹; ¹University of Kentucky; ²General Motors

Magnesium alloys are emerging as an attractive candidate material for biodegradable implants including orthopedic implants and vascular stents. However, premature failure may occur due to their low corrosion resistance in physiological environments. In this study, the surface of AZ31B was burnished with a custom made tool under dry and liquid nitrogen spraying conditions. It was found that significant grain refinement occurred near the surface when using both burnishing conditions due to dynamic recrystallization induced by severe plastic deformation. In addition, a strong crystallographic basal texture was generated on the burnished surface. While the burnished surface was reported to have improved corrosion resistance in a corrosive NaCl solution by using hydrogen evolution method and electrochemical methods, contradictory results on corrosion performance were found in a simulated body fluid by the two methods. The possible causes of the disagreement are briefly discussed.

K-11: Effect of Heat Input on Microstructure and Mechanical Properties of Pulsed TIG Welded AZ31 Magnesium Alloys: *Alireza Amirkhani*¹; Alireza Ebrahimi¹; Rasool Azari Khosroshahi¹; ¹Sahand University of Technology

The process of pulsed TIG welding was used for joining Magnesium Alloy AZ31 using alternating current and the effect of heat input was investigated over the microstructure and mechanical properties of the welded joint. For this reason, the heat input was manually increased from 80.2 J/mm to 157J/mm and, simultaneously, the heat input was measured using a wet calorimeter. Results of microstructure observations showed that by approaching the fusion zone, grains gradually changed in to equiaxed form and in the center of fusion zone fine equiaxed grains

together with lots of brittle precipitated particles of β -Mg₁₇Al₁₂ were formed. In addition, ultimate tensile strength (UTS) of the welded joint increased by increasing the heat input, but too much increasing of the heat input led to decrease in UTS. In this case, decrease in microhardness due to increasing of the heat input, slowed down while too much heat input was applied.

K-12: Effect of Zn Concentration on the Microstructures and Mechanical Properties of Extruded Mg-Y-Gd-Zr Alloys: *Jian Meng*¹; Ke Liu¹; Xin Qiu¹; Deping Zhang¹; Yangde Li²; ¹Changchun Institute of Applied Chemistry, Chinese Academy of Sciences; ²Dongguan e-ande Co. Ltd

In this article, Microstructures and mechanical properties of the Mg-7Y-4Gd-xZn-0.4Zr (x = 0.5, 1.5, 3, and 5 wt.%) alloys in the as-cast, as-extruded, and peak-aged conditions have been investigated by using optical microscopy, scanning electron microscope, X-ray diffraction, and transmission electron microscopy. It is found that the peak-aged Mg-7Y-4Gd-1.5Zn-0.4Zr alloys have the highest strength after aging at 220°C. The highest ultimate tensile strength and yield tensile strength are 418 and 320 MPa, respectively. The addition of 1.5 wt.% Zn to the based alloys results in a greater aging effect and better mechanical properties at both room and elevated temperatures. The improved mechanical properties are mainly ascribed to both a fine β' phase and a long periodic stacking-ordered structure, which coexist together in the peak-aged alloys.

K-13: Effects of Friction Stir Process on the Tensile Properties of AZ61 Magnesium Alloy at Room Temperature to 200°C: *Hsiang-Ching Chen*¹; Truan-Sheng Lui¹; Li-Hui Chen¹; Fei-Yi Hung¹; ¹National Cheng Kung University

Effect of friction stir process (FSP) on the microstructural evolution and tensile mechanical properties of AZ61-O magnesium alloy was investigated in this study. The tensile test was carried out from room temperature to 200°C. Experimental results show the metal flow microstructure, which includes both fine and coarse grains, was observed in the stir zone. The AZ61-FSP specimen possesses higher total elongation than AZ61-O at room temperature and 50°C. However, the AZ61-FSP specimen possesses lower total elongation than AZ61-O at 100 and 200 °C. The ultimate tensile strength and yield strength performance of the AZ61-O and AZ61-FSP specimens were decreased with increasing deformation temperature. In comparison, the strength of the AZ61-FSP specimen was all inferior to the AZ61-O specimen.

K-14: Enhanced Corrosion Resistance of AE42 Magnesium Alloy Achieved by SPD: *Peter Minárik*¹; Robert Král¹; Miloš Janeček¹; ¹Charles University in Prague

The effect of refinement of microstructure on corrosion of AE42 magnesium alloy was investigated. Electrochemical impedance spectroscopy in normal salinity solution (0.1 M NaCl) showed a substantially higher charge transfer resistance in the fine-grained samples processed by equal channel angular pressing (ECAP) as compared to as-extruded material. The corrosion layers developed on the samples were investigated by SEM and differences between samples were found. The layer created on the ECAPed sample was more stable and physical processes behind this were investigated.

K-15: Eutectic Formation in Binary Alloys: *Morteza Amoorezaei*¹; Rameez Ashraf¹; David Montiel¹; Nikolas Provatas¹; ¹McMaster University

We experimentally and computationally explore the formation and distribution of eutectic phases in binary alloys of magnesium. The criterion for the eutectic nucleation is obtained based on local solute concentration and undercooling within the melt, as determined from the complex solid-liquid topology determined from phase field simulations. The resulting morphology will be compared to experiments in organic metal analogues as well as experiments on magnesium alloys.

K-16: Finite Element Analysis of the Evolution of Damage during Equal Channel Angular Pressing of a Mg-3Al-1Zn Alloy: *Feng Kang*¹; Jing Tao Wang²; Chao Hong Zhang¹; Ping Cheng¹; Hai Ying Wu¹; ¹Jinxi Axle Co., LTD; ²Nanjing University of Science and Technology

Finite element analysis was used to simulate the evolution of damage in an Mg-3Al-1Zn alloy processed by equal channel angular pressing (ECAP). Oyane criterion for damage was selected to evaluate the fracture characteristic. Finite element modeling was used with experimental data obtained from tension and compression testing. The results show that initial crack may form in severe flow localization (i.e. in the inner corner) and these cracks may propagate leading to billet segmentation. The flow grid in simulation result is similar with previously experimental result.

K-17: High Strength Magnesium Alloys as Light Weight Advanced Structural Materials for Automotive and Aerospace Applications: *Ankit Gupta*¹; ¹Assistant Manager, Materials Department, Tata Motors Limited, Pantnagar Works, INDIA

Vehicle weight reduction is one of the major means available to improve automotive fuel efficiency. Magnesium is a promising material for automotive use, primarily because of its light weight, ease of fabrication and the highest strength-to-weight ratio of all structural metals when alloyed. Conventional magnesium alloys are strength-competitive, not only with aluminum alloys, but also with steels and titanium alloys. Magnesium alloys with aluminum characterizes good mechanical properties, corrosion resistance and castability after sand and die casting. Magnesium Matrix Composites reinforced with ceramics and graphite fibers or particles present a new class of ultralightweight structural materials joined by brazing. The use of magnesium alloys in car design is expanding, and now includes ultralightweight matrix composites. The objective of this study is to review the classification of magnesium alloys and evaluate their applications in automotive and aerospace industry that can significantly contribute to greater fuel economy and environmental conservation.

K-18: Hot and Cold Deformation of Twin Roll Cast AZ31 Magnesium Alloy: Modeling and Experiments: *Hesamaldin Askari*¹; John Young¹; Hussein Zbib¹; David Field²; Ghassan Kridli²; Mohammed Khaleel³; ¹Washington State University; ²Texas A&M University at Qatar; ³Pacific Northwest National Laboratory

Among all the manufacturing processing techniques, the twin roll casting process is of particular importance since it yields a microstructure with enhanced superplastic properties. However, superplastic deformation could be a relatively slow process, but the process can be accelerated by controlling certain microstructural features, such as grain size, and forming parameters, such as strain rate path. The objective of this study is to establish a physically-based constitutive model that integrates the effects of the underlying microstructure (grain boundaries, twinning, and dislocations) with other continuum properties. The modeling approach is by use of a self-consistent viscoplastic model based on crystal plasticity to study hot and cold deformation behavior and microstructure evolution in AZ31 magnesium alloy at different strain rates. The material response and evolving microstructure obtained by the model are then compared to experiments and EBSD analyses.

K-19: Improved Sintering of Mg Powder Metallurgy Compacts by Thermal Pretreatment: *Paul Burke*¹; Florian Saint-Lebes²; Georges Kipouros³; ¹Massachusetts Institute of Technology; ²ICAM; ³Dalhousie University

Magnesium and its alloys are attractive materials for use in automotive and aerospace applications because of the low density and good mechanical properties. Powder metallurgy (P/M) can be used to alleviate the formability problem through near-net-shape processing and also allows unique chemical compositions that can lead to new alloys with novel properties. However, the surface layer formed on the Mg powders during processing acts as a barrier to diffusion and sintering is problematic. The

layer contains oxides, hydroxides, and carbonates of magnesium formed by reactions with the atmosphere. Magnesium hydroxide and carbonate are both unstable at temperatures well below the sintering temperature and can be decomposed, creating cracks in the remaining oxide layer. These cracks are pathways for unimpeded diffusion and interparticle bonding. To take advantage of this phenomenon a thermal pretreatment under vacuum prior to compaction was tested to assess the effect on sintered density, apparent hardness and microstructure.

K-20: Influence of Section Thickness on Microstructure and Mechanical Properties of Squeeze Cast Magnesium Alloy AM60: *Xuezhi Zhang*¹; Meng Wang¹; Zhizhong Sun¹; Henry Hu¹; ¹University of Windsor

Squeeze cast light alloys has been approved for advanced engineering design of light integrity automotive applications. An understanding of the effect of section thicknesses on mechanical properties of squeeze cast magnesium alloys is essential for proper design of different applications. The present work studied the tensile properties of magnesium alloy AM60 with different section thickness of 6, 10 and 20mm squeeze cast under an applied pressure of 30MPa. The results of tensile testing indicate that the yield strength (YS), ultimate tensile strength (UTS) and elongation (Ef) increase with a decreasing in section thicknesses of squeeze cast AM60. The microstructure analysis shows that the improvement in the tensile properties of squeeze cast AM60 is mainly attributed to the low level of gas porosity and the high content of eutectic phases and fine grain structure which resulted from high solidification rates taking place in the thin section.

K-21: Influence of Zinc-Yttrium Ratio and Cerium on the Mechanical Properties of Hot Rolled and Friction Stir Processed Mg-Zn-Y Alloys: *Arun Mohan*¹; Rajiv Mishra¹; Ravi Verma¹; ¹Missouri University of Science and Technology

Four different alloys with Zn-Y weight % ratio ranging from 0.2 to 0.71 with a total alloying content similar to AZ31 alloy were hot rolled. Two different levels of Cerium were used. Cerium has been reported to increase ductility and decrease anisotropy. In order to maximize the impact of alloying addition, aging studies were conducted at 160°C, 190°C and 220°C for duration up to 8 days. An optimum aging condition was chosen based on peak hardness values. In the current work, microstructure and tensile properties of the as rolled, rolled+aged, friction stir processed (FSP) and FSP+aged sheets were evaluated and correlated with texture and alloy chemistry. Finally, mechanical properties of Mg-Zn-Y sheets were compared with direct chill cast and twin roll cast AZ31 sheets to establish the levels of reduction in anisotropy and improvements in strength and ductility.

K-22: Insights into the Nucleation of Extension Twins in Mg Alloys: *Ali Khosravani*¹; Raja Mishra²; Brent Adams¹; David Fullwood¹; ¹Brigham Young University; ²General Motors

This work presents an investigation of the correlation between extension twin nucleation and dislocation densities in AZ31 magnesium alloys using high resolution electron backscatter diffraction (HR-EBSD). Strongly textured fine grain size sheet samples and randomly oriented large grain billet samples are deformed to small strains in tension and compression and examined by HR-EBSD to determine local dislocation densities from lattice curvature measurements. To activate different twin variants in the textured sample, tensile and compression tests along both RD and TD direction of the sheet are performed. Together with the data obtained from Mg-Ce alloy samples, it is shown that twin nucleation not only happens at the grain boundaries but also at the highly mis-oriented areas inside the grain where local dislocation pile-ups are detected by HR-EBSD. Quantitative measurement of dislocation density required for activation of different twin variants in different microstructures will be discussed.



K-23: In Situ Quantitative Tension and Compression Study on Twinning and Detwinning in Submicron-Sized Mg Crystals inside a Transmission Electron Microscopy: *Boyu Liu*¹; *Zhiwei Shan*¹; *Xiyan Zhang*²; *Jun Sun*¹; *Evan Ma*³; ¹Xi'an Jiaotong University; ²Chongqing University; ³The Johns Hopkins University

Quantitative testing on submicron-sized Mg single crystals have been conducted both in tension and compression mode inside a transmission electron microscope (TEM), for tensile loading along the c-axis and subsequent compressive loading perpendicular to the (new) c-axis. Comparing to conventional testing approaches on bulk scale samples, in which initial grown-in twins might exist, this in-situ TEM quantitative testing conducted on a submicron-sized single crystal is more advanced and visualized. This work directly observes the {10-12} twinning which instantly reorients the crystal by nearly 90° and detwinning which gradually recovers the twinned sample. The {10-12} twinning deformation remains predominant at a certain loading direction when sample size is reduced to ~200 nm, with the twinning stress far exceed that known for bulk Mg. The twinning stress is lower than the stress that is required to drive detwinning propagation during compressive loading perpendicular to the (new) c-direction.

K-24: Investigation of Mechanical Properties of AZ31 Mg Alloys Coated by Plasma Electrolytic Oxidation: *Ahmet Ucisik*¹; *Salih Durdu*; ¹Bogazici University

In this study, AZ31 Mg alloy produced by twin roll casting was coated by a plasma electrolytic oxidation (PEO) in solution, consisting of Na₂SiO₃·5H₂O + KOH electrolyte at 0,085 A/cm² current density for 15, 30, 45 and 60 minutes. Thickness of the coated layer, surface morphology, phase structure, hardness and adhesion strength of the layer were analyzed by an eddy current, SEM, XRD, Vickers hardness and micro scratch tester, respectively. The average coating thickness ranged from 17 to 56 μm. A number of pores were formed on the coated layer. XRD revealed that Mg₂SiO₄ (Forsterite) and MgO (Periclase) phases were formed on the surface of the magnesium alloy. Average coating hardness was measured as 660 HV, while the hardness of the magnesium alloy was 72 HV. Adhesion strength of coatings was increased by increasing duration time.

K-25: Investigation of the Corrosion for Mg-Li-xGd-yY (x=7, 8, 9, 10, 11 wt%; y=1, 2, 3, 4, 5 wt%) Alloys: *Min Li*¹; *Guangchun Yao*¹; *Guoyin Zu*¹; *Jun Cheng*¹; *Qingyun Liu*¹; *Liping Zhou*¹; ¹Northeastern University

The corrosion behaviors of Mg-Li-xGd-yY (x=7, 8, 9, 10, 11 wt%; y=1, 2, 3, 4, 5 wt%) alloys in 3.5 wt.% NaCl aqueous solutions have been investigated by immersion test and polarization curve method. The corrosion products and their morphologies formed in the solution have been analyzed by SEM and XRD. It was found that the morphologies of the film of corrosion products varied with different elements. The results shows that the denser corrosion film of Mg-Li alloy was formatted due to the addition of gadolinium and yttrium, which can increase the corrosion potential alloy.

K-26: Magnesium Recycling of Partially Oxidized, Mixed Magnesium-Aluminum Scrap through Combined Electrorefining and Solid Oxide Membrane (SOM) Electrolysis Processes: *Xiaofei Guan*¹; *Peter Zink*¹; *Uday Pal*¹; ¹Boston University

Pure magnesium (Mg) is recycled from 19g of partially oxidized 50.5wt.%Mg-Aluminum (Al) alloy. During the refining process, potentiodynamic scans (PDS) were performed to determine the electrorefining potential for magnesium. The PDS show that the electrorefining potential increases over time as the Mg content inside the Mg-Al scrap decreases. Up to 100% percent of magnesium is refined from the Mg-Al scrap by a novel refining process of dissolving magnesium and its oxide into a flux followed by vapor phase removal of dissolved magnesium and subsequently condensing the magnesium vapors in a separate condenser. The solid oxide membrane (SOM) electrolysis process is employed in the refining system to enable additional recycling of magnesium from magnesium oxide (MgO) in the partially oxidized Mg-Al scrap. The combination of the refining and SOM processes yields

7.4g of pure magnesium; could not collect and weigh all of the magnesium recovered.

K-27: Measuring Heat Transfer during Twin Roll Casting of Metals: *Pedram Mehraram*¹; *Mary Wells*¹; ¹University of Waterloo

Accurate knowledge of the heat transfer coefficient during casting (between a molten material and the mold) is critical to develop representative mathematical models for casting process such as Twin Roll Casting. In this project, an experimental apparatus was developed to enable to measurement of the interfacial heat transfer coefficient at the interface between a liquid metal and a chill. The experimental apparatus consists of a cylinder surrounded by a heater to melt the metal samples and a number of sensors to monitor temperature in both the molten metal and chill part. The interfacial heat transfer was calculated using an inverse heat conduction method in conjunction with the known thermo-physical properties of the chill and solidifying metal. The apparatus was tested successfully by using AZ31 and Sn-7.5%Sb-3.5%Cu alloy as the casting metal solidifying against H13 chill block. The effect of chill surface texture was investigated on the heat transfer coefficient.

K-28: Mg-Rich Region of the Mg-Gd-Al and Mg-Gd-Sn Ternary Phase Diagrams: *John Kuper*¹; *J.-C. Zhao*¹; ¹The Ohio State University

Mg alloys containing Gd are currently being explored for potential automotive applications to reduce the weight of vehicles. The strength of Mg-Gd alloys is a result of precipitation strengthening from interlocking, plate-shape precipitates of Mg₅Gd (Mg₄₆Gd₉). To further increase the strength and balance the properties of these alloys, Al and Sn are considered as additional alloying elements for solid solution strengthening. To help understand the phase stability and alloying behavior of these alloys, diffusion multiples of Mg, Mg-25at%Gd, Mg-33%Sn and Al were made to map the Mg-rich corner of both the Mg-Gd-Al and Mg-Gd-Sn ternary systems at 400 °C and 300 °C. The phase stability results will be presented in this talk.

K-29: Microstructure and Mechanical Properties of Mg-5Sn-5Zn-xCa Alloys: *Liu Bin*¹; ¹Shenyang University of Technology

Mg-5Sn-5Zn-xCa (x=0.5, 1, 2) alloys were melted by the vacuum melting furnace. The microstructures and phase compositions were analyzed by the scanning electron microscope (SEM) and X-ray diffraction (XRD). The mechanical properties were tested by the electronic universal test machine. The fracture surface were observed by scanning electron microscope (SEM). The results indicate that the microstructures of Mg-5Zn-5Sn-xCa alloys are composed of CaMgSn phases, layer MgZn₂ phases and Mg₂Sn phases. Matrix precipitates onset Mg₂Ca phase, when the content of Ca is 2 wt%. With the increasing of the Ca content, the needle CaMgSn phases gradually become rods, the layer MgZn₂ phases and plate Mg₂Sn phases become continuous, ultimate tensile strength decrease. Mg-5Zn-5Sn-0.5Ca alloy obtains the ultimate tensile strength 184Mpa.

K-30: Microstructure and Mechanical Properties of Nanocrystalline Pure Mg via Cryomilling, Spark Plasma Sintering and Extrusion: *Baolong Zheng*¹; *Troy Topping*¹; *Yuhong Xiong*¹; *Yizhang Zhou*¹; *Suveen Mathaudhu*²; *Enrique Lavernia*³; ¹University of California, Davis; ²U.S. Army Research Office

Nanocrystalline (NC) Mg alloys are of interest due to their high specific strength, but most show a marked ductility decrease with grain refinement. In order to explore the mechanical response of Mg with grain refinement to the nanoscale, pure Mg powder with an average grain size of 67 nm was synthesized via a cryomilling (mechanical milling under cryogenic temperature) in liquid argon for 8 hours, and subsequently consolidated using spark plasma sintering (SPS) and extrusion. The microstructure evolution after each processing step was characterized with XRD, SEM and TEM/HRTEM. The mechanical properties and micro-hardness of consolidated bulk NC pure Mg were evaluated at room temperature. The influence of materials processing on microstructure evolution and

resultant mechanical response are discussed in an effort to provide insight into understanding of fundamental deformation phenomena in NC pure Mg.

K-31: Microstructures and Mechanical Properties of Rapidly Solidified Mg-RE Base Alloy Powder Produced by Using LME Method: *Hong Jun Chae*¹; Sun Woo Nam¹; Tae Bum Kim¹; Taek-Soo Kim¹; ¹Korea Institute of Industrial Technology

Recently, the effect of addition of rare-earth elements (REE) on the mechanical properties and corrosion resistance of Mg alloys have been investigated by many researchers, and small addition of REE could improve the properties of Mg alloys effectively. However, systematic studies on the relationships between crystal structures and macroscopic properties in this Mg-RE alloy system are still necessary. Addition of Nd element to Mg alloy can increase high-temperature strengths and corrosion resistance of Mg alloy. However, the applications of Mg-Nd alloy are very limited due to expensive cost. In this study, the master alloys of Mg-Nd were produced by liquid metal extraction (LME) method from waste Nd-Fe-B scrap by using molten Mg. Also, The Mg-Nd base alloy powders were fabricated by gas atomization, and consolidated by the severe plastic deformation (SPD) method. The effects of process parameters on the homogeneity and the property of specimens were presented and discussed.

K-32: Microstructure and Texture Effects on the Deformation Behaviors of the Statically Recrystallized Mg-Zn-MM Alloy Sheets: *Heon Kang*¹; SeEun Shin¹; DongHyun Bae¹; ¹Yonsei University

The Mg-Zn-MM alloy sheets produced by warm rolling processes were annealed at two different temperatures and mechanical properties and texture effect were evaluated. Few grains were observed in as-rolled sheets and the different grains size and orientations were analyzed in annealed sheets at 220°C, 380°C for 5min by electron back scattering diffraction. The heat treated sheet at 220°C showed the grain size of 4 μm. The heat treated sheets at 220°C exhibited superior elongations to failure at room temperatures and the values of elongation to failure in the range of 100°C up to 350°C were found to around 2 times higher than those of commercially used AZ31 alloy sheet without the loss of tensile strength. The enhanced ductility was mainly stemming from the statistically recrystallized small grains which were initially developed and low recrystallized temperature. The details of deformation behavior of the alloy will be also presented.

K-33: Modeling of Deformation Behavior of Multiphase Wrought Magnesium: *Dongsheng Li*¹; Curt Lavender¹; Eric Lavender¹; Xin Sun¹; Mohammed Khaleel¹; ¹Pacific Northwest National Laboratory

Synthetic microstructure of multiphase wrought magnesium was reconstructed from experimental data from OM, SEM and XRD. The synthetic microstructure is statistically stable with high resolution and enough components to represent the local and global structure. Simulated behavior from this synthetic microstructure is stable and accurate, comparing with simulation using microstructure information obtained by discrete chemical imaging modality. Correlation function and other statistical representation functions are used in microstructure reconstruction. Efficiency and accuracy in microstructure representation and property prediction were investigated.

K-34: Nanostructure Formation in a Quenched Mg Alloy: *Wanqiang Xu*¹; Michael Ferry¹; ¹University of New South Wales

Mg alloy has superior stiffness-to-weight ratio, generates potential application in aerospace and aircraft structures as well as structural components in ultra-light weight communication systems, but is low in strength. In this paper, the quenched microstructure of a bulk Mg alloy was investigated by TEM, atom probe and high resolution XRD. Results show a large amount of nano sized grains (~20-40nm) are formed by the decomposition of its high temperature phase during quenching process. These nano grains keep coherent with the remained high temperature phase in room temperature, resulting in a significant increase in hardness and strength.

K-35: One-Step Approach to Enhance Corrosion Resistance of Coating Layer on AZ91 Mg Alloy via Plasma Electrolytic Oxidation in Electrolyte Containing Ammonium Vanadate: You Chan Jung¹; *Kang Min Lee*¹; Sang Il Yoon¹; Young Gun Ko²; Dong Hyuk Shin¹; ¹Hanyang University; ²Yeungnam University

The main purpose of this work is made to investigate the formation of anti-corrosive coating layer on AZ91 Mg alloy produced via plasma electrolytic oxidation (PEO) in the electrolyte containing ammonium vanadate. The PEO coatings were carried out as a function of ammonium vanadate under AC condition with current density of 100 mA/cm² for 150 sec. In terms of the microstructure, the average pore size on the surface was decreased and the coating layer with vanadium oxide was much denser, followed by the addition of the ammonium vanadate due to complicated electrochemical process i.e., electrochemical reactions, diffusion and ion exchange. According to X-ray photoelectron spectroscopy analysis, the vanadium compound was here existed to be V₂O₃ and V₂O₅ compounds in the coating layer. Overall, it is obviously demonstrated that those vanadium oxides enhanced the corrosion resistance properties of the coating layer, confirmed by electrochemical corrosion tests.

K-36: Phase Dissolution of γ -Mg₁₇Al₁₂ during Homogenization of As-Cast AZ80 Magnesium Alloy and Its Effect on Room Temperature Mechanical Properties: *Rahul Kulkarni*¹; Nityanand Prabhu¹; Peter Hodgson²; Bhagwati Kashyap¹; ¹Indian Institute of Technology Bombay; ²Deakin University, Australia

The phase proportions and their sizes in as-cast AZ80 magnesium alloy were studied by using optical microscopy, X-ray diffraction, scanning electron microscopy. Differential scanning calorimetry reveals endothermic peaks at 439° and 453°C. Microstructure evolution during homogenization was investigated as a function of time for 0.5 to 100 h and over the temperature range of 400°- 453°C. This alloy contains α -Mg; partially and fully divorced eutectic of α and γ (Mg₁₇Al₁₂), and lamellar eutectic of α and γ phases. With increasing homogenization time, dissolution of lamellar eutectic occurs first which is sequentially followed by dissolution of fully divorced eutectic and partially divorced eutectic. The kinetics and mechanisms of dissolution of γ phase was analyzed. Micro-hardness of individual phases, macro-hardness and tensile properties were measured at room temperature as a function of homogenization time and temperature, and their contributions were evaluated to bring out the effect of progress in phase changes.

K-37: Precipitation Formation and Grain Refinement of Mg-Al-Sn Alloy during Hot Deformation: *Abu Syed Humaun Kabir*¹; Jing Su¹; Phuong Vo¹; In-Ho Jung¹; Stephen Yue¹; ¹McGill University

Magnesium alloys are very popular in the automobile industry due to its high strength to weight ratio. However, the use of commercial magnesium alloys as sheet is limited by room temperature ductility. One way to improve the ductility may be to form precipitates during hot rolling. These may delay dynamic recrystallization, possibly leading to grain refinement, which is known to improve ductility. Equilibrium diagrams obtained from thermodynamic modeling software FactSage were used to design Mg-3Al-2Sn alloy, which should form Mg₂Sn precipitates during hot rolling temperatures around 300 °C. To investigate this prediction, the alloy was cast in a copper mould and precipitates formation characteristics were studied by using optical microscope (OM), scanning electron microscope (SEM) equipped with an energy-dispersive X-ray spectroscopy (EDS).

K-38: Production of Mg-Ni Alloy by Consumable Cathode Molten Salt Electrolysis: *Bian Xue*¹; Wu Wenyuan¹; ¹Northeastern University

In producing process of Mg-Ni alloy, the low melting point and density caused the loss of Mg. In order to solve this problem, the production of Mg-Ni was studied by consumable Molten Salt Electrolysis in this paper. Using MgO as starting material, 60%cryolite-40%NaCl as electrolyte, Ni bar as cathode, graphite as anode, Mg-Ni alloy was produced, when temperature was 950°C. The current efficiency increased with increasing of temperature and primary current density. When temperature was 1000, primary current density of cathode and anode was 5 A·cm² and 1



$\text{A}\cdot\text{cm}^2$ respectively, the current efficiency is 79.4%. The testing results of SEM, EDS and XRD were shown that MgO and Al_2O_3 of cryolite were reduced at the surface of Ni bar, and the fusion alloy produced. The phases composition were MgNi_2 , Al_3Ni_2 and Al_3Ni .

K-39: Quasi-Static and Dynamic Compressive Mechanical Behavior of Coarse Grained and Ultrafine Grained Mg-Y-RE Alloy: *Nilesh Kumar*¹; S. Panigrahi¹; R. Mishra¹; R. DeLorme²; B. Davis²; R. Howell³; K. Cho³; ¹Missouri University of Science & Technology; ²Magnesium Elektron North America Inc.; ³Weapons and Materials Research Directorate

Quasi-static and dynamic compression tests were carried out to study the deformation behavior of wrought Mg-Y-RE alloy at strain rates between 10^{-4} to 10^4 s^{-1} . The alloy was tested in two different microstructural states – (a) coarse grained (20 μm), and (b) ultrafine grained (0.5 μm) – selected on the basis of their strength-ductility combination. In both the cases the alloy was tested in peak aged condition. The high strain rate (HSR) compression tests were carried out using split-Hopkinson pressure bar. Microstructural evolution during HSR deformation and dependence of deformation behavior were investigated. The deformed microstructure was characterized using electron backscatter diffraction and transmission electron microscope.

K-40: Secondary Ion Mass Spectrometry for Mg Tracer Diffusion: Issues and Solutions: *Jay Tuggle*¹; Jerry Hunter¹; Nagraj Kulkarni²; Yongho Sohn³; ¹VT; ²Oak Ridge National Laboratory; ³University of Central Florida

Historically, tracer diffusion studies have been performed using radioactive isotopes as tracers. Handling these radioactive isotopes demands a significant increase in safety requirements over non-radioactive isotopes resulting in increased cost and effort. In this study we have used Secondary Ion Mass Spectrometry (SIMS) to measure tracer diffusion of stable Mg isotopes avoiding the need for radio tracers. SIMS analysis of magnesium is subject to a number of artifacts that will lead to a significant loss of depth resolution resulting in a significant error in the measured diffusion coefficient. Methods to minimize these errors will be discussed. Additionally, a method to measure long (>20 μm) diffusions will be presented and compared to the more traditional top-down profiling methods. Research sponsored by the U. S. Department of Energy, Office of Energy Efficiency and Renewable Energy, Vehicle Technologies Program, under contract DE-AC05-00OR22725 with UT-Battelle, LLC.

K-41: Semisolid Joining of Magnesium AZ91 Alloy by Partial Remelting and Mechanical Stirring: *Hossein Aashuri*¹; Vahid Hosseini¹; ¹Sharif University

A technique to achieve the globular weld structure of magnesium AZ91 alloy using stirring a localized semisolid zone during butt-joining is developed. A gas heating system was used for heating the joint up to the required temperature. A dried and free oxygen gas was prepared when a stream of gas could pass closely around a hot element. Hot and pure gas flow through a precise ceramic nozzle was used to create a localized semisolid pool. At this stage a fine stirrer was introduced into the weld seam in order to mix the two sides into a single uniform joint. Substrates were moved in direction of joint line by a small trolley to avoid the deviation of nozzle from the joint line and its distance and angle from the substrate. A fixture system was used to hold two substrates together on the trolley.

K-42: Severe Plastic Deformation of Magnesium Alloys by Machining: *Saurabh Basu*¹; M. Ravi Shankar¹; ¹University of Pittsburgh

The microstructural consequences of severe plastic deformation of a prototypical Mg alloy –AZ31, during chip formation in machining are presented. Here, a plane-strain machining setup was utilized to examine the strain, strain-rate and temperatures in the deformation zone using high-speed imaging and infrared thermography. Subsequently, the microstructural consequences were elucidated in the chip and on the machined surface using X-ray and electron backscattered

diffraction analysis. It is shown that chip formation in machining leads to a refinement of the microstructure in the chip and on the surface and that the shear deformation also offers a more favorable modulation of the crystallographic texture. The implications of these observations for enhancing the mechanical and functional properties of Mg alloys are discussed.

K-43: Slip and Twin Behavior of Magnesium Single Crystals: *Ming Zhe Bian*¹; Kwang Seon Shin¹; ¹Magnesium Technology Innovation Center, Seoul National University

The deformation behavior of magnesium single crystals was investigated using compression tests parallel to the c-axis at room temperature to 623K. The {10-12} tensile twin and the {10-11} compression twin, as well as the {10-11}-{10-12} double twin, were observed in compression tests. In the case of the {10-11} twin, new fine grains were formed due to dynamic recrystallization (DRX), indicating that sufficient energy was accumulated in the compressive twin region for recrystallization. The {10-13} twin and the {10-13}-{10-12} double twin were found to form at a compressive strain of only 2% at 473K. The dislocation and twin structures were systematically examined by TEM under various diffraction conditions.

K-44: Stress Corrosion Cracking Susceptibility of Ultrafine Grained AZ31: *Gaurav Argade*¹; Wei Yuan¹; Kumar Kandasamy¹; Rajiv Mishra¹; ¹Missouri University of Science and Technology

Stress corrosion cracking (SCC) behavior of AZ31 was studied using slow strain rate testing (SSRT) technique in 3.5 wt% NaCl solution. Friction stir processing was employed to obtain grain size in micron and sub-micron range. The samples for SSRT were extracted from processed region and were tested in air and solution at an initial strain rate of 10-6 s-1. Lower time to failure was observed for processed samples. Parent material as well as processed samples showed susceptibility towards SCC, with processed samples showing higher susceptibility as compared to parent material.

K-45: The Effect of Precipitation on the Mechanical Properties of Extruded AZ80: *Ran Liu*¹; Jing Wang¹; De Yin¹; ¹Nanjing University of Sci & Tech

The effect of aging temperature and time on precipitates in AZ80 magnesium alloy was studied by optical microscope to investigate the change on mechanical properties. The results show that precipitation distributed as band along the extruded direction with no twinning. After aging, precipitation dispersed. When ageing at 150°C, discontinues precipitated phase could increase the yield and tensile strength but not good to the ductility of the material. Ageing at 300°C, with the increase the aging time, static ductility increase first and then decrease. That means recrystallization induced by continuous precipitation is benefit to the strength and ductility. However, the effect of ageing hardening under 300°C is not better than 150°C. And twinning also activated in compression much more than in tensile samples, that's the same as in AZ31 alloy.

K-46: The Investigation of Twin Interface Structure in AZ31 Magnesium Alloys: *Daisuke Ando*¹; Yuji Sutou¹; Junichi Koike¹; ¹Tohoku University

Deformation twinning is an important factor for deformation and fracture mechanisms in magnesium. We reported that {10-11}-{10-12} double twins are crack initiation sites and {10-12} twins tend to be crack propagation sites. However, it is not clear why only {10-12} twin interfaces tend to be crack initiation sites among other twin types. In the past studies, the twin interface structure has been reported only in the {10-12} type in pure Mg, but not in other twin types. So in this work, the twin interface structure of AZ31 was investigated by HRTEM. Results indicated that the twin interface structure of {10-12} in AZ31 is the same as in pure Mg. The (10-12) twin interface is composed of a (10-12) plane and a zigzagged step structure formed by (0001)twin/(1-100)matrix planes. Based on the obtained results, that the step structure of the (0001) twin/(1-100)matrix planes is the most likely sites for crack propagation.

Materials Processing Fundamentals: Poster Session

Sponsored by: The Minerals, Metals and Materials Society, TMS Extraction and Processing Division, TMS Light Metals Division, TMS: Process Technology and Modeling Committee
Program Organizers: Lifeng Zhang, Missouri University of Science and Technology; Antoine Allanore, MIT; Cong Wang, Saint-Gobain High Performance Materials

Monday PM
 March 12, 2012

Room: Atlantic Hall
 Location: Dolphin Resort

Q-1: A Physical Model for Growth of Graphene Layers from Metallic Melts: *Shaahin Amini*¹; Haamun Kalaantari²; Reza Abbaschian²; ¹University of California Riverside; ²University of California Riverside

Recently growth of graphene nanocrystals from metal-carbon melts was introduced by present authors. In this process, dissolved carbon in metallic melts consisting of Ni or Cu was found to grow as graphene or graphite layers on the surface of the melt along with graphite growing in the interior of the melt with morphologies including thick flakes or spheres. A comprehensive model is presented here to examine the effect of processing parameters on graphite growth morphologies. The model relates the solid-liquid interfacial kinetics in basal and prism directions to melt supercooling and cooling rates. It is found that at low supercoolings, the faceted basal plane lags behind the prismatic face, resulting in the formation of flakes. At increased supercoolings, however, basal plane becomes kinetically roughened with growth rate comparable to that of prismatic face, thus altering the morphology into bulky spheres. The analytical results are finally compared to experimental observations.

Q-2: A Way to Control Distortion of Metal Parts during Heat Treatment Process: *Yuan Lu*¹; *Jin-wu Kang*¹; ¹Tsinghua Univ

The distortion of metal parts during heat treatment process is one of the main obstacles in industry to ensure high-quality work and less or no machining allowance, especially for large but thin steel castings such as heavy turbine blades. In the paper, a method is proposed to control the distortion by adjusting heat transfer coefficient of metal parts during heat treatment process. Required heat transfer coefficients can be realized by getting the metal parts into contact with various media such as water spray, insulation felt or materials with different heat conductivity. The control method based on this idea is set up and achieved. By using insulation felt and water spray to change the heat transfer coefficient during the stages of heat treatment process, the results indicate that the proper control time and vary with materials.

Q-3: Analysis of Open Forging of Cylindrical Blanks between Two Flat Die Surfaces: *Ahmed Elkholy*¹; Dhari Almutairi¹; ¹Kuwait University

The successful and efficient execution of a forging process is dependent upon the correct analysis of loading and metal flow of blanks. This paper investigates the Upper Bound Technique (UBT) and its application in the analysis of open forging process when a possibility of blank bulging exists. In this regards, the kinematically admissible velocity field is obtained by minimizing the total forging energy rate. The significant advantages of this method is the speed of execution while maintaining a fairly high degree of accuracy. The information from this analysis is useful for the design of forging processes and dies. Results for the prediction of forging loads and stresses, metal flow and surface profiles with the assured benefits in terms of press selection and blank preform design are outlined in some detail. The predictions compared well with results obtained experimentally with a maximum error of no more than 14%.

Q-4: Effects of Tempering on the Microstructure and Hardness of a Spray-Formed Hot Work Tool Steel: *Wang Cunlong*¹; ¹Guangdong University of Technology

Spray forming is a new way to produce high property materials. This paper was based on spray-formed hot working tool steel; a non-conventional heat treatment of the material was carried out, by doing so, the hardness of the material reached more higher than conventional. And OM, SEM, EDS and XRD were used to study the microstructure of the steels and different phase formation in the heat treatment process.

Q-5: Hot Deformation Behavior of Nb Microalloyed Coiled Tubing Steel: *Zhendong Zhang*¹; Haitao Zhou²; Xianghua Liu¹; Sijun Li³; Guofei Si¹; Bingyu Zhang¹; ¹Northeastern University; ²Central South University; ³Laiwu Iron and Steel Corp

Hot compression test of Nb microalloyed coiled tubing steel is performed on Gleeble3500 at 1123K—1373K and strain rate from 0.001 to 5s⁻¹. It is found that flow softening occurs and the flow curves exhibit a peak with a characteristic of dynamic recrystallization (DRX) and change with temperature and strain rate significantly. The peak stress and peak strain are dependent on Zener-Hollomon relationship with activation energy of 390 KJ/mol. On the basis of Avrami equation and the Zener-Hollomon parameter, it is obtained that the dynamic recrystallization kinetics equation with which the calculated and measured recrystallization fraction is very close. On the results of hot compression test, the Nb microalloyed coiled tubing steel is rolled by Thermo-Mechanical-Control-Processing (TMCP), and it is obtained that the yield strength and tensile strength of Nb microalloyed coiled tubing steel are 565MPa and 685MPa respectively, and the elongation percentage is 30.1%.

Q-6: Investigation of the Relationship of the Melt Structures and Solidification Behaviors of Cu-Sb70 Alloy Explored by Electrical Resistivity Method: *Yun Xi*¹; *Jin Yu*¹; *Li-Na Mao*¹; *Fang-Qiu Zu*¹; ¹Hefei University of Technology

According to the behaviors of resistivity-temperature of Cu-Sb70 melt, which suggests a partly reversible temperature induced liquid structure transitions (LST) could occur in this alloy, in this paper, we investigated the dependence of solidification on the liquid state. Both resistivity and temperature were measured to track solidification process. The results show that the nucleating undercooling of the melt which experienced the LST increased and the solidified time decreased. Meanwhile, the solidified microstructures refined evidently, with the microscopic pattern of primary phase changes from disordered pillarlike dendrites into homotaxial ones. Moreover, it is verified that the microstructures would be different if the reversible part of the LST was restrained. The new phenomena and results reflected in this paper suggest that grasping the rules of melt structure change with temperature before material processing will give help for controlling the solidification more effectively and finally resulting in more ideal microstructures.

Q-7: Microstructure of Al₂O₃/YAG/ZrO₂ Eutectic In Situ Composite Prepared by Laser Floating Zone Melting: *Kan Song*¹; *Jun Zhang*²; *Xiaojiao Jia*²; *Haijun Su*²; *Lin Liu*²; *Hengzhi Fu*²; ¹Northwestern Polytechnical university; ²Northwestern Polytechnical university

Al₂O₃/YAG/ZrO₂ eutectic in situ composite has now been regarded as new generation of high temperature structural material due to its excellent performance even close to its melting point. The directionally solidified Al₂O₃/YAG/ZrO₂ eutectic ceramics are prepared by recently developed Laser Floating Zone Melting (LFZM) apparatus in which a splitter mirror is used to obtain two beams with the same quality from one CO₂ laser. With the two laser beams irradiate the sample from opposite directions, the sample is zone melted. The apparatus configuration and the solidification processing are described in detail. The solid/liquid interface morphology is studied and the mechanism of microstructure formation especially the characteristic of eutectic cellular is discussed. It is shown that YAG and ZrO₂ phases play a leading role during the ternary eutectic growth. Meanwhile, the relationship between the solidification microstructure and the processing parameters are investigated.



TMS 2012

141st Annual Meeting & Exhibition

Q-8: Net Shape Manufacturing of a Novel Cermet Using Self-Propagating High Temperature Synthesis: *Atefeh Nabavi*¹; Alexander Capozzi¹; Sam Goroshin¹; David Frost¹; Francois Barthelat¹; ¹McGill University

In this study, a novel chromium–chromium sulfide cermet was produced by self-propagating high-temperature synthesis (SHS). Conventional techniques for manufacturing metal sulfides are complex, environmentally harmful, and not suitable for producing complex-shape articles. To overcome these disadvantages, a new method for the preparation of the precursor charge in metal-sulfur by SHS is proposed which can be described as reactive casting. Cermet samples that are synthesized at atmospheric pressure have a porous structure which leads to low mechanical strength. The possible sources of porosity were investigated. The porosity was reduced from 40% to 12% by applying a vacuum during melting of the precursor mixture, varying the mixture stoichiometry, and carrying out the synthesis under high ambient pressure of an inert gas. Finally, the mechanism of flame propagation was studied by determining the influence of mixture properties on the critical flame quenching distance.

Q-9: Response Surface Methodology for the Optimization of the Dehydration Curve of Scheelite Concentrate by Microwave Heating: Lei Guo¹; Libo Zhang¹; Jinhui Peng¹; Xinhui Duan¹; Xin Wang¹; ¹Key Laboratory of Unconventional Metallurgy, Kunming University of Science and Technology

Response surface methodology is applied for the process optimization of microwave drying scheelite concentrate, influences of process conditions such as drying temperature, drying time and material weight on the relative dehydration rates are investigated. Each predictor variable was tested at three levels with conditions of material temperature for 80°C, 95°C, 110°C, drying time for 70s, 125s, 180 s and material quality for 80g, 190g, 300g. The results indicated that with the increase of material temperature and drying time, the relative dehydration rates also increased, and the increasing of material weight, the relative dehydration rate decreased.

Q-10: Study on Inclusions in 65Mn Thin Slabs Produced by a CSP Process: Yi Tan¹; Huigai Li¹; ¹Shanghai University, Shanghai, China.

Abstract: The influence of superheat degree on the distribution and volume content of inclusions were studied in 65Mn thin slab produced by CSP. The results showed that the diameters of inclusions are mainly less than 5µm. Most of the inclusions gathered at the 1/4 thickness direction for the thin slab of 27°C superheat degree, compared with the center position for that of 37°C. There are more inclusions larger than 50µm in the low superheat samples, which is caused by the short floating time. In addition, the inclusions were observed and analyzed by metallurgical microscope, SEM and EDS in order to ensure their composition, type and further find their source. It was found that the types of these inclusions mainly are Al₂O₃, SiO₂, CaO and their composites, a few of them are TiN and MnS.

Q-11: The Optimization of Copper Utilization during Decoppering of Technical Lead: *Ahmet Haxhijaj*¹; Izet Zeqiri¹; Bajram Haxhijaj¹; Mursel Rama¹; ¹University of Pristina

In order to have increased utilization of copper during the decoppering process of technical lead in lead refinery in Trepça two samples have been analyzed with the same chemical composition. Furthermore, identical parameters have been used for both samples which are: the quantity of technical lead, the process temperature, the quantity of brimstone loaded, the mixing time and the time of removal of schlicker, and the dismantle of rings formed in the walls of caldron for refinery. After the removal of brimstone schlicker and chemical analyses one calculates the balance of melting phases and decoppering and the scale of copper utilization. The majority of copper is removed from technical lead with the oxide schlicker, one part with the liquation and remaining part by decoppering

with brimstone. The paper reflects on increasing utilization of copper in the decoppering of technical lead which is achieved with effective engagement of human factor.

Materials Research in Microgravity: Poster Session

Sponsored by: The Minerals, Metals and Materials Society, TMS Materials Processing and Manufacturing Division, TMS Extraction and Processing Division, TMS: Process Technology and Modeling Committee, TMS: Solidification Committee

Program Organizers: Robert Hyers, University of Massachusetts; Hani Henein, University of Alberta; Valdis Bojarevics, University of Greenwich; James Downey, NASA; Douglas Matson, Tufts University; Achim Seidel, Astrium; Daniela Voss, ESA

Monday PM
March 12, 2012

Room: Atlantic Hall
Location: Dolphin Resort

B-1: Advanced Optical Systems for Materials Science Experiments under Microgravity: *Martin Naegle*¹; Michael Baumgarten¹; Wolfgang Soellner²; Achim Seidel²; ¹OptoPrecision GmbH; ²Astrium

Since materials science experiments under microgravity are often performed with highly reactive metals and alloys which are processed above and below their melting temperatures the use of non-contact diagnostics techniques is essential. This applies in particular to temperature and dimensional measurements of the samples under investigation. Dedicated optical systems are therefore employed in various experimental set-ups. While their specific design is tailored to the intended application they all have to comply with stringent optical, mechanical and environmental requirements. Solutions range from systems made up of sapphire and tungsten components for observations close to heated zones within a vacuum furnace (FMF) to combined camera/pyrometer systems for monitoring of Electromagnetic Levitator (EML) samples, which involve features like beam splitting into visual and near-infrared wavelength ranges, high spatial resolution using telecentric lenses, and objectives that are switchable into distinct measurement modes.

B-2: Containerless Processing on ISS: Ground Support Program for EML: Stefan Schneider¹; Rainer Willnecker¹; Angelika Diefenbach¹; ¹DLR MUSC

EML is an electromagnetic levitation facility planned for the ISS aiming at processing liquid metals or conductive semiconductors by using electromagnetic levitation technique under microgravity and reduced electromagnetic field and convection conditions. Its diagnostics and processing methods allow to measure thermophysical properties and to investigate solidification phenomena. The EML project is a common effort of ESA and the German Space Agency DLR. The Microgravity User Support Center MUSC at Cologne, Germany, has been assigned the responsibility for EML operations. For the EML experiment preparation a ground support program is established at MUSC, providing scientific and technical services in the preparation, performance and evaluation of the experiments. Its final output is the transcription of the scientific goals and requirements into validated facility control parameters. The presentation will outline the extensive scientific support programme and provide insights into the results obtained so far.

B-3: Directional Solidification Experiments on Board the ISS Using MSL: *Daniela Voss*¹; ¹ESA
TBA

B-4: EML - A Multi-User Electromagnetic Levitation Facility for Containerless Processing Experiments Onboard the ISS: *Achim Seidel*¹; Wolfgang Soellner¹; Christian Stenzel¹; ¹Astrium

Electromagnetic levitation under microgravity is a powerful technique for containerless processing of electrically conducting samples such as metals and semiconductors. Based on the long and successfully heritage of

the TEMPUS program which included parabolic flights, sounding rocket flights, and Spacelab missions a multi-user facility for electromagnetic levitation experiments onboard the International Space Station is currently being developed by EADS Astrium under contracts to ESA and DLR. During its 5 year operation the EML payload can process up to 180 samples in 10 batches, accommodating a wide range of experiments of nucleation phenomena or phase formation as well as the measurement of a range of thermophysical properties both above the melting temperature and in the undercooled regime. Upgrades of the basic configuration are under development, in particular instruments to precisely determine the electrical conductivity of the samples and to measure and control the residual oxygen content of the process atmosphere.

B-5: EML Experiments on Board the ISS: *Daniela Voss*¹; ¹ESA
TBA

B-6: Fluid Flow in Phase Selection Experiments Using Electromagnetic and Electrostatic Levitation: *Briana Tomboulia*¹; Robert Hyers¹; Douglas Matson²; ¹University of Massachusetts; ²Tufts University

Understanding and predicting internal flow in levitated samples is critical to designing the experiments and processing the samples successfully. Previous work demonstrated that the solidification path of some alloys is strongly affected by the flow velocity of the molten phase during solidification, yet many ranges in velocity have not been explored due to experimental limitations. We have developed simulations of spherical samples in electromagnetic levitation (EML) and electrostatic levitation (ESL). Flow is induced during EML by electromagnetic field body forces, while in ESL it is driven by a temperature gradient. Both models have been validated using cases with known analytical solutions and previous results from the literature. These simulations predict the flow velocities within a liquid drop, from which it may be possible to determine the solidification path, and provide an explanation for the microstructure. Estimates of the flow velocity within a sample can also be used to design experiments.

B-7: FMF: An MSL Furnace Insert for Float-zone Crystal Growth on the ISS: Adam Hess¹; *Arne Cröll*¹; Jan Zähringer¹; Christian Stenzel²; Dirk Bräuer³; Harald Sauermann³; Volker Uhlig³; ¹Albert-Ludwigs University Freiburg; ²Astrium; ³Technische Bergakademie Freiberg

A laboratory model of a Floating Zone Furnace with Rotating Magnetic Field (FMF) for float-zone crystal growth experiments of Germanium-Silicon with process temperatures of up to 1500°C has been realised and tested. A flight version of this furnace is intended to be implemented as a further insert to the Materials Science Laboratory on the ISS. Under microgravity convection phenomena and their impact on segregation effects can be examined apart from the buoyancy driven ones. The FMF is a precisely temperature controlled 7 zone resistance furnace that provides thermal stability (± 0.05 K) and a variable temperature gradient (5-50 K/cm) at the phase boundary. In addition it allows visual observation in order to control the zone height and the interface, which until now was only possible in mirror furnaces. A rotating magnetic field was introduced to influence and control the melt flow during crystal growth.

B-8: High-Precision Temperature Control of a Crystal Growth Furnace at 1500°C: *Christian Stenzel*¹; Arne Croell²; Adam Hess²; Dirk Bräuer³; Hartmut Sauermann³; ¹Astrium; ²University of Freiburg; ³Technical University Freiberg

For crystal growth of semiconductor materials a short-term temperature stability of 0.1°C at 1500°C is one of the essential parameters to be addressed for achieving high-quality crystals. Hence, for temperature monitoring and control with high precision in a floating zone furnace two sets of thermo-sensors, type S thermocouples and optical fibre thermometers, have been implemented and successfully operated in the furnace for more than 2000 h. The optical fibre thermometers consist of an optical system made of sapphire (two fibres plus a prism for deflection) and transmit the infra-red radiation of the heater to the outside of the hot core of the furnace for pyrometric temperature measurement. A dedicated

control algorithm has been set up which controlled the power settings to the individual heaters. But sensor types showed no degradation after this period and yielded a short-term stability at 1200°C of 0.05°C (optical fibre thermometers), respectively 0.08°C (thermocouples).

B-9: Inductive Measurement Device for Microgravity Electromagnetic Levitator: Georg Lohoefer¹; *Juergen Brillo*¹; ¹German Aerospace Center, DLR

For the containerless processing of high temperature metallic melts the electromagnetic levitation technique, which utilizes high frequency alternating magnetic fields for the contactless, inductive positioning and heating of electrically conducting samples, is well established. The existence of alternating magnetic fields in electromagnetic levitation facilities suggests to use inductive methods also for the non-contact detection of liquid metal properties. Not only the electrical resistivity but also the shape change during the damped oscillation of an electromagnetically levitated liquid metal droplet, which is determined by its surface tension and viscosity, can be detected inductively. This contribution presents a measurement device designed and constructed by DLR, which utilizes the high frequency magnetic dipole fields of the microgravity electromagnetic levitation facilities TEMPUS, applied for parabolic flights, and EML, applied on board of the space station ISS, simultaneously also for an inductive determination of thermophysical properties of levitated metallic melts.

B-10: In-Situ Observation of Directional Solidification Processes in Transparent Materials on the ISS: *Daniela Voss*¹; ¹ESA
TBA

B-11: Investigation of Thermocapillary Convection of High Prandtl Number Fluid under Microgravity: *Ruquan Liang*¹; ¹Northeastern University

The flow and thermal fields of the thermocapillary flows in floating zone crystal growth configurations under microgravity has been investigated numerically. The Navier-Stokes equations coupled with the energy conservation equation are solved on a staggered grid. The new mass conserving level set approach is used to capture the free surface deformation of the liquid bridge, while the existing numerical simulations for liquid bridges adopted simplified models without considering the dynamic free surface deformation. The numerical results show that two vortices are generated due to the thermocapillary convection in the liquid bridge initially, and then the vortex centers move toward the free surface. The recirculating flow generates a radial convection, which tends to make the bulk fluid temperature distribution rather uniform near the free surface. Therefore, the temperature gradient in the hot corner decreases, while the temperature gradient in the cold corner increases.

B-12: Modeling for ISS Experiments on Transient Nucleation in Glass- and Quasicrystal-Forming Melts: *Xiao Ye*¹; Kenneth Kelton²; Robert Hyers¹; ¹University of Massachusetts; ²Washington University

Testing the theory of coupled nucleation in glass- and quasicrystal-forming metals requires that the diffusion fields around nuclei be left to grow unaffected by convection. Because the nuclei are so small, they follow the flow exactly and are not affected by the magnitude of the velocity. However, the gradient in velocity, which is the shear rate, can cause the diffusion fields to overlap. Magnetohydrodynamic calculations show the range of parameters that will permit the experiment to proceed without convective contamination.

B-13: Real Time In-Situ Observations of Equiaxed Dendrite Coherency in Al-Cu Alloys Using High Brilliance 3rd Generation Synchrotron Sources: *Andrew Murphy*¹; David Browne¹; Wajira Mirihanage²; Ragnvald Mathiesen²; ¹University College Dublin; ²Norwegian University of Science and Technology

In the last decade synchrotron X-ray sources have fast become the tool of choice for performing high resolution imaging in materials science, particularly in alloy solidification. This paper presents the results of an experimental campaign carried out at the European Synchrotron



TMS 2012

141st Annual Meeting & Exhibition

Radiation Facility, using a Bridgman furnace, to monitor phenomena during solidification of Al-Cu alloys - specifically the onset of equiaxed dendrite coherency. Conventional experimental methods for determining coherency involve measuring the change in viscosity or measuring the change in thermal conductivity across the solidifying melt. Conflicts arise when comparing the results of these experimental techniques to find a relationship between cooling rate and coherency fraction. It has been shown that the ratio of average velocity to the average grain diameter has an inversely proportional relationship to coherency fraction. In-situ observation therefore makes it possible to measure these values directly from acquired images sequences and make comparisons with published results.

B-14: Surface Tension and Viscosity of Ni-Al Catalytic Precursor Alloys Measured by the Oscillating Drop Method on Different Microgravity Platforms: *Rainer Wunderlich*¹; *Hans-Joerg Fecht*¹; ¹Universitaet Ulm

The surface tension and the viscosity of a variety of catalytic precursor Ni-Al alloys including Raney-NiAl have been measured by the oscillating drop method in an electromagnetic levitation device under reduced gravity conditions on board parabolic and in a TEXUS sounding rocket flight. Surface tension values such obtained agree very well with values obtained in ground based em-levitation providing a verification of the Cummings and Blackburn correction of the shift of the surface oscillation frequency due to the magnetic pressure of the levitation field with a confidence level better \149; 2%. The good agreement of viscosity values obtained in the microgravity experiments with values obtained from the oscillating cup method under 1-g gives support to the application of the oscillating drop method in an electromagnetic levitation device with a confidence level of \149; 20%. Experimental results obtained are compared with the predictions of several semiempirical thermodynamic models.

B-15: Truncated Dual Cap Nucleation Site Development: *Douglas Matson*¹; *Paul Sander*¹; ¹Tufts University

During heterogeneous nucleation within a metastable mushy-zone, several geometries for nucleation site development must be considered. Traditional spherical cap and dual cap models are compared to a truncated dual cap to determine the activation energy and critical cluster growth kinetics in ternary Fe-Cr-Ni steel and Fe-Co magnetic alloys.

B-16: XRMON Modules on Sounding Rockets: *Daniela Voss*¹; ¹ESA
TBA

Mechanical Behavior at Nanoscale I: Poster Session

Sponsored by: The Minerals, Metals and Materials Society, TMS Materials Processing and Manufacturing Division, TMS: Nanomechanical Materials Behavior Committee, TMS/ASM: Mechanical Behavior of Materials Committee

Program Organizers: Scott Mao, University of Pittsburgh; Julia R Greer, California Institute of Technology; Jianyu Huang, Center for Integrated Nanotechnologies; Marc Legros, CEMES-CNRS; Ting Zhu, Georgia Institute of Technology

Monday PM
March 12, 2012

Room: Atlantic Hall
Location: Dolphin Resort

A-1: Atomistic Prediction of Precipitate Strengthening in Nanoscale Metallic Multilayers: *Niaz Abdolrahim*¹; *Ioannis Mastorakos*¹; *Hussein Zbib*¹; ¹Washington State University

Nanoscale metallic multilayer's (NMM) can play a leading role in the future micromechanical devices due to their high structural stability, mechanical strength, high ductility, toughness and resistance to fracture and fatigue. The design of better NMMs can be achieved by properly tailoring the nanostructure using appropriate materials-by-design

algorithms. However, before those materials are put into service in any significant applications, many important fundamental issues remain to be understood. Among them, the role of the second phase particles on the strengthening properties of the nanocomposite materials. The purpose of this work is to address the question if the second phase particles can strengthen the nanoscale materials in the same manner as in bulk crystalline solids. In this view, Cu/Nb thinfilms with spherical Nb particles inside the Cu layer were examined using molecular dynamics simulations and show to exhibit a significant improvement on their mechanical behavior, compared to similar structures without particles.

A-2: Atomistic Simulations of the Adhesion of Alumina/epoxy Interfaces Using ReaxFF: *Fidel Valega Mackenzie*¹; *Barend Thijssse*¹; ¹Delft University of Technology

Alumina/epoxy interfaces are of great importance in many engineering environments. Not only due to aging but also because of temperature, moisture, shearing and mechanical loading they are subjected to failure. In order to understand how it occurs, reliable inter-atomic potentials need to be developed. Here we introduce the Reactive Force Field (ReaxFF) for alumina/epoxy interfaces, which describes the possible interactions between both of this surfaces. By making use of ReaxFF the polymer and the metal oxide were built and different interfaces were then created varying the roughness of the alumina surface by introducing the presence of defect-islands. The work of adhesion between this rough metal oxide surfaces and the epoxy is calculated, as well as its dependence with temperature. The effect of shearing parallel to the interface is also examined and discussed, presenting possible ways in which this interfaces may undergo failure.

A-3: Characterization of Coherency Limits in Si/Ge Core-Shell Nanowires Using Molecular Dynamics: *Yumi Park*¹; *Alejandro Strachan*¹; ¹Purdue University

We use molecular dynamics simulation with Stillinger-Weber potential to characterize how surface roughness and core diameter affect strain relaxation and coherency limit of Si/Ge core-shell nanowires. To this end, we vary core diameter and surface roughness, but keep the shell thickness and the wavelength of the roughness as constants proportional to the core diameter for all cases. After the coherency is lost, a significant strain relaxation is observed especially in the core. Interestingly, defect nucleation does not affect the axial strain for the wires with small roughness; only wires with significant roughness exhibit axial strain relaxation. Surface roughness also affects the coherency limits of the wires. For 20 nm diameter wires the instability limit decreases with increasing roughness; however, for smaller diameter wires (10 nm) we observe little dependence of the coherency limit with roughness. We also identify and quantify the defects responsible for the strain relaxation in the nanowires.

A-4: Controlling the Lithiation Induced Strain and Charging Rate in Nanowire Electrodes by Coating: *Liqiang Zhang*¹; *Xiaohua Liu*²; *Yang Liu*²; *Shan Huang*³; *Ting Zhu*³; *Lianguin Gui*⁴; *Scott X. Mao*¹; *Zhizhen Ye*⁵; *Chongmin Wang*⁶; *John P. Sullivan*²; *Jianyu Huang*²; ¹University of Pittsburgh; ²Sandia National Laboratories; ³Georgia Institute of Technology; ⁴Tsinghua University; ⁵Zhejiang University; ⁶Pacific Northwest National Laboratory

Lithium ion batteries (LIBs) are presently the best advanced battery system, but they cannot meet requirements for more demanding applications due to limitations in capacity, charging rate and cyclability. One leading cause of those limitations is the lithiation-induced-strain (LIS) in electrodes that can result in high stress, fracture and capacity loss. Here we report that by utilizing the coating strategy, both the charging rate and LIS of SnO₂ nanowire electrodes can be altered dramatically. The SnO₂ nanowires coated with carbon, aluminum, or copper can be charged about 10 times faster than the non-coated ones. Intriguingly, the radial expansion of the coated nanowires was completely suppressed, resulting in enormously reduced tensile stress at the reaction front, as evidenced by the lack of formation of dislocations. Our work demonstrates that

nanoengineering the coating enables the simultaneous control of electrical and mechanical behaviors of electrodes, pointing to a promising route for building better LIBs.

A-5: Dislocation-Interface Interaction Mechanisms in Nanoscale Laminates with Enhanced Interface Models: *Firas Akasheh*¹; S. M. Yead Jewel¹; ¹Tuskegee University

Nanoscale metallic laminates consist of alternating layers of two metals with individual layer thickness is on the order of nanometers. Recently, these structures have been receiving a great deal of attention due to their exceptional properties, including ultrahigh strength beyond the prediction of the rule-of-mixtures, and high ductility. Although such properties are attributed to the nature of dislocation interactions in confined nanoscale regions and, more so, to dislocation-interface interactions, a detailed understanding is still missing. In this work, we follow up on our previous studies on dislocation mechanisms in (001) epitaxial nanolaminates by including a new model of interface resistance in coherent systems and incoherent systems. We also include cross slip and the effect of Koehler image forces. We show the mechanism by which intersecting dislocations interactions lead to the breakdown on the interface as a barrier along with the corresponding hardening effect over the basic obstacle-free yield strength.

A-6: Effect of Hydrogen on Subsurface Deformation during Indentation of Pipeline Steel: *Moo Young Seok*¹; In-Chul Choi¹; Yong-Jae Kim¹; Dong-Woo Suh²; Jae-il Jang¹; ¹Hanyang university; ²GIFT, POSTECH

To prepare the up-coming era of so-called ‘hydrogen economy’, many researches focused on the related topics are actively conducted all round the world. With a viewpoint of industrial field applications, one of the important topics being studied is hydrogen transmission (more specifically, ‘hydrogen pipeline’). So, the development of advanced high-pressure hydrogen pipelines is highly desirable. As a good starting point for the purpose, one might wonder whether conventional pipeline steels (designed for oil and natural gas transmission) can be used as the hydrogen pipeline materials or not. To answer the question, we attempted to systematically analyze the influence of hydrogen on the mechanical performance of API linepipe steels. As a first step, here we examined the subsurface deformation produced during macroscopic indentation of the API X70 steel samples (before and after hydrogen charging) prepared by interface-bonding technique.

A-7: Effects of Focused-Ion-Beam Irradiation and Prestraining on the Mechanical Properties of FCC Au Microparticles on a Sapphire Substrate: *Seok-Woo Lee*¹; Dan Mordehai²; Eugen Rabkin²; William Nix¹; ¹Stanford University; ²Technion-Israel Institute of Technology

We have studied the effects of focused-ion-beam (FIB) irradiation and prestraining on the mechanical properties of nearly defect-free Au microparticles on a sapphire substrate. The Au microparticles, which were produced by a solid-state diffusion dewetting technique, were FIB-irradiated and/or prestrained, the latter using a nanoindenter with a flat ended punch operating under a nanohammering mode. Also, the prestrained Au microparticles were exposed to FIB to examine the effects of ion-beam damage on the properties of crystals containing mobile dislocations. We found that both FIB irradiation and prestraining reduced the yield strength of pristine Au microparticles significantly and made the stress-strain curves jerky. However, FIB irradiation does not affect the mechanical properties of prestrained Au microparticles very significantly. Once a microparticle contains mobile dislocations, its mechanical properties are not influenced much by the defects generated by FIB irradiation, even at the submicrometer scale.

A-8: Effects of Ti on Electronic Structure and Mechanical Property of Uranium: a First-Principles Study: *Jianbo Qi*¹; Jieyu Zhang¹; ¹Shanghai University

In order to improve the tensile strength and elastic modulus properties of a-U, first principles plane wave pseudopotential method based on density functional theory (DFT) was utilized to calculate electronic structure, ground state energy and elastic constant of uranium-0.75 wt.%

titanium alloy. Optimization structures of equilibrium phase (a-U) and metastable phase (martensite a'-U) are firstly calculated. Then calculation of the tensile test is preformed to predict mechanical properties and chemical bonding nature from density of state (DOS) and Mulliken population analysis are used to illuminate the calculation results. Finally, the macroscopic stiffness properties of a-U and a'-U, such as Young's, shear and bulk modulus, are determined by the elastic constants. Our results show that after Ti addition, tensile strengths of a-U and a'-U increase from 464MPa to 1162MPa while elastic moduli are 175GPa and 190GPa, respectively. These conclusions are in good agreement with our experimental results.

A-9: Investigation of the Crystal Structure on the Nanomechanical Properties of Pulsed Laser Deposited NbN Thin Films: *Cody Wright*¹; M Mamun¹; A Farha¹; Y Ufuktepe²; H Elsayed-Ali¹; A. Elmustafa¹; ¹Old Dominion University; ²Cukurova University

The nanomechanical properties of NbN/Nb deposited by pulsed laser deposition (PLD) were investigated as a function of the film/substrate crystal structure. In addition to the β -Nb₂N phase, the X-ray diffraction shows peaks correspond to d-NbN cubic and d'-NbN hexagonal phases. Several samples were tested of varied crystal structure between dominant cubic to dominant hexagonal. X-ray diffraction analysis, scanning electron microscopy, atomic force microscopy were employed to characterize their phases, microstructure, and surface morphology. Nanoindentation was used to investigate the nanomechanical properties of the films. A Nanoindenter XP equipped with a DCM II head was used in conjunction with the continuous stiffness method (CSM) in depth and load control modes to evaluate the hardness and modulus of the NbN thin films as a function of the crystal structure. The results show that there are clear effects of the crystal structure on the elastic modulus of the PLD-grown NbN films.

A-10: Investigation of the Indentation Size Effect in FCC Metals Using Activation Volume Analysis: *David Stegall*¹; A Elmustafa¹; ¹Old Dominion University

The activation volumes for plastic deformation for different FCC pure metals and alloys were measured using nanoindentation. The indentation size effect in FCC metals is examined using the rate effects characterized by the sensitivity of the hardness and the effective strain gradient beneath the indenter. The hardness was measured using a XP nanoindenter with a high load attachment capable of producing loads up to 10 N using a single Berkovich tip. The materials included pure polycrystalline aluminum, nickel, silver, and alloys; 70/30 copper zinc (alpha-brass), 7075 aluminum (aluminum zinc), 70/30 nickel copper, and 90/10 platinum rhodium. The activation volume, $(9KbT/\square H/\square \dot{\epsilon})$ is referred to as a measure of the Burger's vector (b) times the area swept out by dislocations during the process of thermal activation, the so-called ‘activation area’ or $\cdot H$ is the hardness and $\dot{\epsilon}$ is the effective strain rate beneath the indenter.

A-11: Laser Compression of Nanocrystalline Tantalum: *Chia-Hui Lu*¹; Brian Maddox²; Bruce Remington²; Eduardo Bringa³; Megumi Kawasaki⁴; Terence Langdon⁴; Hye-Sook Park²; Bimal Kad¹; Marc Meyers¹; ¹University of California, San Diego; ²LLNL; ³Conicet & ICB, U. N. Cuyo; ⁴University of Southern California

Nanocrystalline tantalum was prepared by HPT (High Pressure Torsion) from monocrystalline [100] stock yielding a grain size of 70 nm. It was subjected to laser driven compression at energy levels of ~ 350 J to ~ 850 J in the Omega facility (LLE, U. of Rochester) yielding pressures as high as ~ 180 GPa. The laser beam created a crater of significant depth (~ 100 μ m). Transmission electron microscopy (TEM) revealed dislocations in the grains but no twins in contrast with monocrystalline tantalum. Hardness measurements were conducted and show the same trend as monocrystalline tantalum. The grain size was found to increase close to the energy deposition surface. The experimentally measured dislocation densities are compared with predictions using an analysis based on the constitutive response and the similarities and differences are discussed in terms of the mechanisms of defect generation.



A-12: Lithiation Induced Embrittlement of Multi-Walled Carbon Nanotubes: *Yang Liu*¹; He Zheng²; Xiaohua Liu¹; Shan Huang³; Ting Zhu³; Jiang Wei Wang²; Akihiro Kushima⁴; Nicholas Hudak¹; Xu Huang⁵; Sulin Zhang⁵; Scott Mao²; Xiao Feng Qian⁶; Ju Li⁴; Jian Yu Huang¹; ¹Sandia National Laboratories; ²University of Pittsburgh; ³Georgia Institute of Technology; ⁴University of Pennsylvania; ⁵Pennsylvania State University; ⁶Massachusetts Institute of Technology

Lithiation of individual multi-walled carbon nanotubes (MWCNTs) was conducted in-situ inside a transmission electron microscope. Upon lithiation, the intertube spacing increased from 3.4 to 3.6 Å, corresponding to about 5.9% radial and circumferential expansions and ~50 GPa tensile hoop stress on the outermost tube wall. In-situ compression and tension tests show that the lithiated MWCNTs were brittle with sharp fracture edges. The lithiation-induced embrittlement is attributed to the mechanical effect of a “point-force” action posed by the intertubular lithium that induces the stretch of carbon-carbon bonds additional to that by applied strain, as well as the chemical effect of electron transfer from lithium to the antibonding p orbital that weakens the carbon-carbon bond. The combined mechanical and chemical weakening leads to a considerable decrease of fracture strain in MWCNTs. Our results provide direct evidence and understanding of the degradation mechanism of carbonaceous anodes in lithium ion batteries.

A-13: Mechanical Anisotropy and Texture in Caliber Rolled Twinning-Induced Plasticity Steels: *Young Soo Chun*¹; Junmo Lee²; You-Hwan Lee²; Kyung-Tae Park³; Chong Soo Lee¹; ¹POSTECH; ²POSCO; ³Hanbat Nat'l Univ.

A study was made to investigate the yield anisotropy in caliber rolled 18Mn-0.6C-1.5Al twinning-induced plasticity (TWIP) steel with the variation of reduction area (RA). As-received hot-rolled sheets with 10 μm grain size were cold rolled by use of caliber rolling machine from 31 to 82% RA. Electron back scattered diffraction and transmission electron microscopy were conducted to analyze the microstructure. In order to investigate anisotropic deformation behavior, compression test was conducted on the specimens of which loading axes were aligned to have L and C axis of a caliber rolled rod, respectively. The results showed that with the increase of RA, the {111} and {100} textures were progressively developed parallel to L axis, resulting in the greater yield anisotropy in the L and C axis. Detailed mechanisms responsible for such anisotropy were discussed based on the texture analysis and microstructural evolution during the deformation.

A-14: Mechanical Behavior and Thermal Stability of Differently Oriented Nanotwinned Ag Films: *Daniel Bufford*¹; Xinghang Zhang¹; Haiyan Wang¹; ¹Texas A&M University

Epitaxial nanotwinned Ag films with (111) and (110) orientation were deposited by magnetron sputtering. The twin boundary spacing in the as-deposited films is 9 nm in Ag (111) and 42 nm in Ag (110), with the twin boundaries normal to the growth direction in the (111) films and at an angle in the (110) films. Size dependent strengthening is observed in Ag films and related mechanisms are discussed. Thermal stability of films was investigated via isothermal annealing in argon up to 800°C. The evolution of microstructure and mechanical behavior of films will be presented.

A-15: Mechanical Behavior for Different Cutting Directions on Copper and Rhodium Single Crystals: *Seisuke Kano*¹; Atsushi Korenaga¹; ¹National Institute of Science and Technology (AIST)

Mechanical behavior on the metal surface is strongly related on the surface fracture by a mechanical cutting especially shaper type cutting to apply ultra-fine optics manufacturing and several nan-technologies. To realize the ultra-fine cutting, the crystallographic interface physics is quite important to control the surface fracture behavior. In this study, the surface fracture behavior evaluated using copper and rhodium single crystals cut on the (100) plane for several directions. As results of the cutting, the shapes of the cutting groves were different with the cutting direction between [010] direction and the others. The reason of this result was considered that the cutting tool moved along the slip plane belongs

to [111] direction or not. In the case of shallow cutting under 1 \149; m, the spring back behavior was observed for the cutting directions. The mechanisms would be connected to the interface among the slip plane fracture by the cutting tool.

A-16: Mechanical Properties and Deformation Mechanism of Nanostructured Two-Phase Fe₃₀Ni₂₀Mn₂₀Al₃₀ Alloy: *Xiaolan Wu*¹; I. Baker¹; ¹Dartmouth College

This presentation will discuss the deformation mechanisms that control the strength of nanostructured, two-phase Fe₃₀Ni₂₀Mn₂₀Al₃₀. Two different microstructures of Fe₃₀Ni₂₀Mn₂₀Al₃₀ were studied: the ultrafine (wavelength of ~ 8 nm), as-cast modulated B2/L2, microstructure, possibly formed by spinodal decomposition; and the <100>-aligned two-phase (phase width of ~ 25 nm) B2/L2, microstructure, produced by a 72 h anneal at 823K. The alloy was mechanically tested over a range of temperatures and strain rates. The annealed alloy showed a lower brittle-to-ductile transition temperature (~ 573 K) than the as-cast material (~ 673 K). Dislocation analyses, based both on post-mortem and in-situ straining TEM, were performed in order to understand the deformation mechanisms of this alloy

A-17: Mechanical Properties of Nanostructured TiAlN Based Coatings: Sai Pramod Pemmasani¹; *Koteswararao Rajulapati*¹; Ramakrishna M²; Krishna Valleti²; Ravi Chandra Gundakaram²; Shrikant V Joshi²; ¹University of Hyderabad; ²International Advanced Research Centre for Powder Metallurgy and New Materials

Transition metal nitrides are being used in novel configurations such as multilayers, nanolayers, superlattices and nanocomposites. In the present study, nitride coatings were deposited on tool steel substrates by cathodic arc evaporation under varied processing conditions. As-deposited coatings were characterized by XRD, SEM, FIB milling, TEM, nanoindentation, nano-scratch and wear testing. Nanoindentation was performed on both the surface and cross-section of the coatings followed by imaging of the indents and a qualitative determination of toughness. Post-scratch and post-wear imaging was used to determine the scratch and wear depths. The effect of processing induced microstructural changes on the coating hardness, modulus and adhesion was studied. The effect of multilayering and composition on the coating properties was also explored. A combination of electron microscopy along with nanoindentation and scratch testing was used to arrive at correlations between the coating microstructure and properties and these will be presented.

A-18: Mechanics of Individual Amorphous Carbon Nanoparticles from Experiment and Simulation: *Eric Bucholz*¹; Susan Sinnott¹; ¹University of Florida

In situ transmission electron microscopy experiments can be used to visualize and manipulate individual amorphous carbon (aC) nanoparticles which facilitate determination of their mechanical responses to external forces, which is critical for optimizing their use as lubricating additives to base oils in tribological applications. Complementary molecular dynamics simulations are used to characterize the behavior of aC nanoparticles at an interface during compression. In particular, their response as a function of particle diameter and normal load are quantified based, in part, on the ratio of sp²:sp³ carbon atoms. The simulations predict that the transition from elastic to plastic deformation is triggered by an increase in the percentage of sp³ carbon atoms with the mechanical response being independent of nanoparticle size over the range of diameters considered (2 – 5 nm). This work is supported by the Office of Naval Research.

A-19: Micromechanical Testing of Nanocrystalline BCC Metals: *Jonathan Ligda*¹; Brian Schuster²; Qiuming Wei¹; ¹UNC Charlotte; ²Army Research Laboratory

High pressure torsion (HPT) processing has been utilized to refine the grain size of body centered cubic metals into the ultra-fine-grained and nanocrystalline regime. Because of the limited bulk specimen dimensions and the gradient in structure and properties in a single HPT disk, site-specific nanoindentation and focused ion beam based mechanical testing

has been applied to systematically examine the effect of grain size on the strength and deformation mode. In-situ tensile testing within a scanning electron microscope employs a customer built test stage consisting of piezoelectric positioners, a high resolution linear actuator for load application and a strain gage based load cell. The system is controlled with a data acquisition program and strains are calculated using digital image correlation. Application of the above to nanocrystalline tantalum has shown a distinct transition in deformation mode from homogeneous to localized plastic deformation across the HPT disk.

A-20: Microstructural Changes Across Shear Bands in Nanotwinned Cu Foils Deformed at Room Temperature and 77K: *Timothy Furnish*¹; *Andrea Hodge*¹; ¹University of Southern California

Copper samples containing highly aligned nanotwins (mean spacing approx. 40nm) were tested in tension at both room temperature and 77K. The initial Cu samples present 500-800 nm grain width, medium twin density ($3.0 \times 10^6 \text{ m}^2/\text{m}^3$), high strength (540 to 690 MPa), low initial dislocation density and little to almost no strain hardening. The formation of shear bands appeared to be a dominant deformation mechanism and an increase in ductility at 77K compared to room temperature was observed. A higher number of shear bands formed in the samples tested at 77K, which is thought to be a contributing factor to the enhanced localized ductility. In this presentation, the microstructure of the as-prepared and tested samples will be discussed with emphasis on the changes within and across the shear bands in each of the samples.

A-21: Nano-Compression Testing of Freestanding Tetragonal Ni₃Al Particles: *Bin Gan*¹; *Robert Maaß*²; *Julia R. Greer*²; *Sammy Tin*¹; ¹Illinois Institute of Technology; ²California Institute of Technology

Recent advances in nano-compression testing techniques have enabled the development of powerful characterization tools that enable quantification of location specific mechanical properties within the microstructure of various classes of engineering materials. Tetragonal Ni₃Al precipitates with edge lengths varying from 200 to 600 nm were electro-chemically extracted from a Ni-based single crystal superalloy. The freestanding, tetragonal particles possess plane normals that are oriented along the <100> directions and an aspect ratio bigger than 1.5. By carefully selecting and manipulating individual tetragonal precipitates, the response of individual freestanding Ni₃Al particles to uniaxial compression was measured. Results from in-situ observations that detail the dynamic deformation response of these precipitates in both a Transmission Electron Microscope and a Scanning Electron Microscope will be presented and discussed.

A-22: Nanoindentation Investigation of VO₂ Films Synthesized by Reactive Bias Target Ion Beam Deposition (RBTIBD): *Cody Wright*¹; *M. A. Mamun*¹; *D. Nminibapie*¹; *Wei Cao*¹; *D. Gu*¹; *H. Baumgart*¹; *Jiwei Lu*¹; *H. Elsayed-Ali*¹; ¹Old Dominion University

Vanadium dioxide has a metal-semiconductor transition at 340 K, just above ambient temperature. For this reason the material has attracted a lot of attention as a potential candidate for novel phase transition switching and sensor applications based on electrically driven transitions. The low-temperature semiconducting phase has a monoclinic crystal structure, while the metallic phase has a rutile structure above the transition temperature. The objective of this study is to investigate and to understand the nanomechanical properties of the VO₂ films. To this end we have performed nanoindentation experiments using a Nanoindenter XP with a DCM II head. The VO₂ films were synthesized by both Pulsed Laser Deposition and Reactive Bias Target Ion Beam Deposition. The PLD experimental settings and the influence of the oxygen partial pressure on the stoichiometry is described. Physical analysis by X-ray diffraction and SEM and TEM was applied in order to characterize the PLD VO₂ films.

A-23: Nanomechanical Behavior of Teflon-MWCNT Bilayer Films: *Rachel Schoepner*¹; *Anqi Qiu*¹; *Douglas Stauffer*²; *Ryan Major*²; *Jack Skinner*³; *Thomas Zifer*³; *Greg O'Bryan*³; *Andrew Vance*³; *William Gerberich*⁴; *David Bahr*¹; *Neville Moody*³; ¹Washington State University;

²Hysitron Inc.; ³Sandia National Laboratories; ⁴University of Minnesota

Teflon MWCNT suspensions have the potential for creating conductive coatings on insulating films for static dissipation. However, there are few studies on polymer MWCNT suspension properties and even fewer that use Teflon. To define mechanical and electrical property relationships in this film system, we created bilayer Teflon AF MWCNT films with differing concentrations of functionalized and nonfunctionalized MWCNTs. Nanoindentation revealed that addition of MWCNTs increased modulus while hardness remained constant. Conducting indentation showed that films with 8 w/o MWCNT exhibited uniform stable conductance once indentation depth exceeded several hundred nanometers. Films with lower concentrations of MWCNTs were insulating. In this presentation, the results will be used to show that the two techniques provide a unique description of structure property relationships in this suspension film system. This work was supported by Sandia National Laboratories, a Lockheed Martin Company for the USDOE NNSA under contract DE-AC04 94AL85000.

A-24: Nanomechanical Properties of Atomic Layer Deposition Sb₂Te₃ Thin Films: *Cody Wright*¹; *M Mamun*¹; *D Gu*¹; *D Nminibapie*¹; *H Baumgart*¹; *H Robinson*²; *V Kocherger*³; *A. Elmustafa*¹; ¹Old Dominion University; ²Virginia Tech University; ³MicroXact

The nanomechanical and structural properties of Antimony Telluride (Sb₂Te₃) thin films deposited by atomic layer deposition were investigated and reported. X-ray diffraction analysis, scanning electron microscopy (SEM) with energy dispersive x-ray spectroscopy analysis (EDS), atomic force microscopy (AFM), spectroscopic ellipsometry and high resolution transmission electron microscopy (HRTEM) were employed to characterize the Sb₂Te₃ single film composition and layered nanocomposites. Nanoindentation was used to investigate the nanomechanical properties of the films. A Nanoindenter XP equipped with a DCM II head was used in conjunction with the continuous stiffness method (CSM) in depth and load control modes to evaluate the hardness and modulus of the Sb₂Te₃ thin films. In addition the influence of the ALD fabrication parameters and post deposition anneal processes on the mechanical and structural properties are reported. The stoichiometry of the ALD synthesized Sb₂Te₃ thin films were investigated by secondary ion mass spectroscopy (SIMS) and Rutherford Backscattering (RBS).

A-25: NanoMechanical Properties of Hydrogen Implanted AlN for Layer Transfer by Ion-Induced Splitting: *Cody Wright*¹; *M Mamun*¹; *K Tapily*¹; *O Moutanabbir*²; *D Gu*¹; *H Baumgart*¹; *A. Elmustafa*¹; ¹Old Dominion University; ²Max-Planck Institute

The nanomechanical and structural properties of epitaxially grown AlN were investigated as a function of different H-fluences and thermal evolution by nanoindentation, x-ray diffraction, atomic force microscopy, and high resolution transmission electron microscopy. A 2µm thick AlN layer was epitaxially grown on sapphire. The nanomechanical properties were measured using nanoindentation. The AlN samples were implanted with hydrogen ions at 50 keV with various fluences ranging from $0.5 \times 10^{17} \text{ cm}^{-2}$ to $3 \times 10^{17} \text{ cm}^{-2}$. The modulus and hardness were carefully determined for each sample. A virgin non-implanted AlN sample was also used as benchmarking. The samples were then annealed in air at temperatures ranging from 300°C to 600°C for 5 min to study the influence of pre-layer splitting treatments on the nanomechanical properties. Once the H implantation was introduced, the hardness increased from 18 GPa for the virgin sample to ~25 GPa for the highest fluence of $3 \times 10^{17} \text{ H cm}^{-2}$.

A-26: Phase Field Dislocation Dynamics in Confined Volumes: *Lei Lei*¹; *Marisol Koslowski*¹; ¹Purdue University

When the material characteristic size or certain characteristic length, such as grain size or sample dimensions, approaches the nanometer range, metals display a strong size dependency given by an increase in the yield stress as the characteristic size decreases. The change in yield stress due to the interaction of dislocations with stress free surfaces has implications not only in micron and submicron size single crystals but also in void growth



in solids undergoing plastic straining and is potentially important to the understanding of ductile fracture. We will present a phase field dislocation dynamics model that includes the interaction of dislocations with stress free surfaces in single crystals. Stress free surfaces are modeled using Eshelby's eigenstrain approach, which enables the simulation of arbitrary geometries. The effect of stress free surfaces, crystal size and geometry, and the initial dislocation density on the strength of Nickel in small dimensions is examined.

A-27: Processing of ta-C Protective Films on Mold for Glass Lens: Seungkeun Oh¹; *Youngman Kim*¹; ¹Chonnam National University

Recently aspheric lenses are widely used for superprecision optical instruments, such as cellular phone camera modules, digital cameras and optical communication modules. The aspherical lenses are processed using mold core under high temperature compressive forming pressure. It is imperative to develop superhard protective films for the life extension of lens forming mold core. Especially ta-C films with higher sp³ fractions receive attentions for the life extension of lens forming mold and, in turn, the cost reduction of lenses due to their superior high temperature stability, high hardness and smooth surfaces. In this study ta-C films were processed on WC mold as a function of substrate bias voltage using FVA (Filtered Vacuum Arc) method. The processed films were characterized by Raman spectroscopy and nano-indentation to investigate bonding nature and hardness, respectively. The film with maximum 87% of sp³ fraction was obtained at the substrate bias voltage of -60V, which was closest to ta-C film. ta-C films showed better high temperature stability by sustaining relatively high fraction of sp³ bonding even after 2,000 glass lens forming applications.

A-28: Size and Asperity Height Effect on the Contact Hardness in Nanoscale Metallic Asperities Contact : Molecular Dynamics Study: *Hojin Kim*¹; Alejandro Strachan¹; ¹Purdue University

The macroscopic mechanical response of contacts between surfaces of interest in microsystems is dominated by the geometry and local properties of nanoscale asperities present in them. If the local stress experienced a given asperity is greater than its hardness, plastic deformation will permanently change its shape and increase the effective contact area between the two surfaces. We use large-scale molecular dynamics to study the hardness of nanoscale metal-metal contacts as a function of their size and shape. Two platinum slabs with different-sized asperities are compressed at a rate of 20MPa/20ps closing rate. We find the hardness of the asperities shows to increase with decreasing contact size. However, asperities with low aspect ratios (thin and tall) exhibit a strongest size and their hardness decreases for sizes below this critical value. We provide an atomic picture of the mechanisms responsible for these complex size effects.

A-29: Size Dependence of Mechanical Properties of Refractory Carbides: *Sara Kiani*¹; Suneel Kodambaka¹; Jenn-Ming Yang¹; ¹UCLA

Ultra-high temperature ceramics (UHTC), such as refractory transition-metal and Si-based carbides, are promising class of materials for applications in aerospace industry owing to their excellent high-temperature oxidation-, ablation-, and erosion- resistance, and high-strength as well as toughness. Improvement in their thermal, chemical, and mechanical properties is desirable for the construction of next generation space vehicles and hypersonic flights. This requires a thorough understanding of the factors influencing the thermochemical and thermomechanical properties of UHTCs. As a first step, we focused on understanding the role of size on the mechanical properties of single-crystalline SiC(0001) and ZrC(100). We carried out compression tests on one-dimensional cylindrical pillars (about 20 μm long and 6-3 μm in diameter), prepared via focused ion beam milling. From the load-displacement measurements, we found that the ultimate compression strengths at 10% strain of both SiC and ZrC increased with decreasing pillar diameter and are higher than their bulk counterparts.

A-30: Size Effects of Single-Crystal Magnesium: Microcompression Experiments and Modeling: *Cynthia Byer*¹; KT Ramesh¹; ¹Johns Hopkins University

The increasing amount of literature on microcompression experiments suggests that for some materials, decreasing the diameters of these micro-scale pillars increases their yield stresses and amount of strain hardening. However, we still lack a complete understanding of size effects, especially for hexagonal close packed (hcp) materials, which have lower crystallographic symmetry than their more common face centered cubic (fcc) and body centered cubic (bcc) counterparts. In this study, we focus on the dependence of orientation and initial dislocation density on the deformation mechanisms, mechanical response, and size effects of single-crystal magnesium. We conduct microcompression experiments on micropillars that range from approximately 600 nanometers to 10 micrometers in diameter, and we use these experimental results, along with an adapted stochastic-based model that considers the available dislocations in the specimen, to obtain a better understanding of size effects in magnesium.

A-31: Strong Sample-Dimension Dependence of Submicro-Sized Single Crystal Mo Pillars: *Ling Huang*¹; Qingjie Li¹; Zhiwei Shan¹; Ju Li²; Jun Sun¹; Evan Ma³; ¹Xi'an Jiaotong University; ²Massachusetts Institute of Technology; ³Johns Hopkins University

In situ TEM compression tests were carried out to investigate the mechanical behavior of single crystal molybdenum pillars with diameters ranged from 75 nm to 1200 nm. There exists a critical size (~ 200 nm for Mo at room-temperature) below which the strengthening exponent in Hall-Petch like regression increases dramatically, from ~ 0.3 to ~ 1 . Thus, a new regime for size effects in BCC is discovered that converges to that of FCC, revealing deep connection in the dislocation dynamics of the two systems. In addition, we demonstrate that with the pillar diameter decreasing to hundreds of nanometers, significant mechanical annealing (significant drop in stored dislocation density in response to applied stress) does occur in BCC Mo like previous observation in FCC metals. We attribute the observed phenomena to the diminishing mobility difference between screw and edge dislocations at high stresses.

A-32: Temperature Effect on Displacement Burst of Iron Nano-Particles: *Qing-Jie Li*¹; Ling Huang¹; Christopher R. Weinberger²; Zhi-Wei Shan¹; Ju Li³; Jun Sun¹; Evan Ma⁴; ¹Center for Advancing Materials Performance from the Nanoscale (CAMP-Nano) & Hysitron Applied Research Center in China (HARCC), State Key Laboratory for Mechanical Behavior of Materials, Xi'an Jiaotong University; ²Sandia National Laboratories; ³Department of Nuclear Science and Engineering and Department of Materials Science and Engineering, MIT; ⁴Department of Materials Science and Engineering, Johns Hopkins University

Recent experiments conducted at CAMP-Nano showed dramatic displacement burst of iron nano-particles during in situ compression test. Based on the experimental observations, molecular dynamics(MD) simulations on compression of iron nano-particles were performed to study the temperature effect on displacement burst. Simulations under isothermal condition with different temperature showed different yield load and different initial burst displacement but similar displacement burst size, while simulations under adiabatic condition revealed a significant temperature rise during the collapse/burst process. This indicates that temperature field during the burst process is crucially important. The temperature shock would have different spatial-temporal characteristics from the incipient dislocation plasticity shock. This indicates that there could be a critical length scale above/below which temperature field variation is important/unimportant.

A-33: The Role of Stacking Fault Energy and Deformation Twinning on the Indentation Size Effect of FCC Pure Metals and Alloys: *David Stegall*¹; A Elmustafa¹; ¹Old Dominion University

The effect of inter-facial phenomena including the stacking fault energy (SFE) and twinnability, on the magnitude of indentation size effect of several FCC metals was investigated using nanoindentation

and electron backscattered diffraction (EBSD). The hardness was measured using a XP nanoindenter with a high load attachment capable of producing loads up to 1 N using a single Berkovich tip. The materials included pure polycrystalline aluminum, nickel, silver, and alloys; 70/30 copper zinc (alpha-brass), 7075 aluminum (aluminum zinc), 70/30 nickel copper, and 90/10 platinum rhodium. The plastic deformation of FCC metals is influenced by two competing mechanisms, dislocation slip and deformation twinning. The SFE is an important inter-facial characteristic and affects the deformation of FCC metals due to its influence on dislocation cross slip and dynamic recovery. The influence of deformation twinning is thought to affect the ISE given a twin boundary can disrupt the movement of dislocations.

A-34: Time-Dependent Mechanical Behavior of Indium Nanopillars: *In-Chul Choi*¹; Yong-Jae Kim¹; Moo-Young Seok¹; Ting Y. Tsui²; Jae-Il Jang¹; ¹Hanyang University; ²University of Waterloo

To apply novel nanoelectronic devices, it is necessary to predict lifetime and reliability of nano-scale materials (especially, low-melting-temperature materials that can creep even at room temperature) that have many important applications. In this regard, here we performed compression test for indium nanopillars fabricated by electron beam lithography and electroplating, and attempted to analyze the time-dependent mechanical behavior of the materials and its size dependence.

Mechanical Behavior Related to Interface Physics: Poster Session

Sponsored by: The Minerals, Metals and Materials Society, TMS Structural Materials Division, TMS Materials Processing and Manufacturing Division, TMS/ASM: Mechanical Behavior of Materials Committee, TMS: Nanomechanical Materials Behavior Committee

Program Organizers: Jian Wang, Los Alamos National Laboratory; Nathan Mara, Los Alamos National Laboratory; Izabela Szlufarska, University of Wisconsin-Madison; Zhiwei Shan, Xi'an Jiaotong University

Monday PM
March 12, 2012

Room: Atlantic Hall
Location: Dolphin Resort

E-1: Delamination Characterization of Bonded Interface Using Surface Based Cohesive Model: Manivannan Ramamurthi¹; *Young Suk Kim*¹; ¹Kyungpook National University, Daegu, South Korea.

Element based Cohesive zone model (ECZM) is employed widely in studying delamination (or) decohesion of interface surface in adhesively bonded materials using finite element method (FEM). This paper uses surface based cohesive model (SCZM) available in commercial finite element Analysis (FEA) code in the place of ECZM by considering similarities between both models when interface thickness is zero for the advantages of less input parameters, easy modeling, reduced computational time. Mode I fracture study with 90 degree peel test experiment and simulation are done in polymer coated steel for this analysis. Results are compared with ECZM. Surface based cohesive model predicts delamination well and results are closer to ECZM. Cohesive model requires fine meshing in FEM to predict delamination closely. To verify the feasibility of using it in coarse meshes, same simulations are done with Coarse meshes. The results reveal that coarse mesh simulations also predicts delamination closer to fine meshes with reasonable accuracy.

E-2: First-Principles Investigation of Grain Boundary Cohesion by Magnesium in Aluminum: *Shengjun Zhang*¹; Oleg Kontsevoi¹; Arthur Freeman¹; Gregory Olson¹; ¹Northwestern University

Despite extensive experimental and theoretical investigations, whether magnesium segregation into the aluminum grain boundaries (GBs) leads to stress corrosion cracking (SCC) is still controversial. To understand the mechanism of magnesium-induced SCC at the electronic level, we provides a comprehensive investigation of magnesium on GB cohesion

in aluminum by means of first-principles calculations with the highly-precise full-potential linearized augmented plane-wave method. We found: (i) Mg has a large driving force to segregate from Al bulk to the symmetrical GB core site; (ii) The calculated embrittling potency indicates that magnesium is a cohesion enhancer; (iii) Both atomic size effect and charge transfer effect have influence on the GB cohesion. A net result of these two competing effects combined increases the strength of the GB, which indicates that charge transfer effect plays a dominant role. This work establishes that Mg segregation does not contribute to SCC in Al alloys.

E-3: In-Situ Fracture Toughness Studies in Magnesium Aluminate Spinel: *Wanjun Cao*¹; Animesh Kundu¹; Mark McLean¹; Martin Harmer¹; Richard Vinci¹; ¹Lehigh University

Micro-size Focused Ion Beam (FIB) machined pre-notched cantilevers were fabricated in magnesium aluminate (MgAl₂O₄) spinel specimens. They were tested to failure using a SEM based nano-mechanical testing system. Young's modulus, fracture stress and fracture toughness values were determined by the micro-cantilever deflection technique. It was verified that the Young's modulus and fracture toughness results of single crystal spinel obtained from the micro-scale beam deflection tests are in good agreement with values obtained from conventional mechanical tests. The in-situ cantilever deflection testing technique was successfully employed to obtain fracture toughness values of bicrystal interface. Fracture toughness results of both doped and undoped magnesium aluminate spinel bi-crystal interfaces are compared and discussed.

E-4: Plasticity in Al/Nb Nanoscale Multilayered Materials: Effects of Interface Shear Strength: *Arief Budiman*¹; Youbin Kim²; Kevin Baldwin¹; Nathan Mara¹; Amit Misra¹; Seungmin Han²; ¹Los Alamos National Laboratory (LANL); ²KAIST

Microcompression tests were performed on the nanoscale Al-Nb multilayers with bi-layer thicknesses of 5nm and 50nm. The Al-Nb multilayers showed increase in strength as the bi-layer thickness was reduced; the average 5% flow stress of the 5nm and 50nm specimens were determined to be 2.1GPa and 1.4GPa, respectively. Comparison with the previous report on nanoscale Cu-Nb multilayers indicates that Al-Nb nanolayers have lower flow stress. Al-Nb with negative heat of mixing has higher degree of intermixing and thus would likely have a "stronger interface in shear" that would result in lower barrier to slip transmission as compared to Cu-Nb which interface is weak in shear and thus is a strong trap for glide dislocations via core spreading in the interface plane. This could lead to easier transmission of dislocations across the interface and therefore lower flow stresses for Al-Nb when compared to the case for the Cu-Nb multilayers.

E-5: Slip Transfer Across a Cu Bicrystal Interface: *Alankar Alankar*¹; Niraj Gupta²; Shivraj Karewar²; Ricardo Lebensohn¹; Alfredo Caro¹; ¹Los Alamos National Laboratory; ²University of North Texas

The current work examines the slip transfer across grain boundary in a Cu bicrystal. The experimental observations from the literature are compared with predictions of dislocation density based crystal plasticity model and a molecular dynamics simulation. The orientation images acquired from EBSD during interrupted channel die deformations of a Cu bicrystal show crystallite fragmentation near the grain boundary. The grain reorientation measurement also shows a strong influence of non-local slip activity and grain boundary character. The microstructure sensitive crystal plasticity model is able to show, to some degree of success, reorientation of crystallites and correct slip system activity. However, due to local nature of the constitutive behavior employed in the CPFEM model, it is not able to account for the non-local effect via grain boundary. The molecular dynamics simulation shows the occurrence of slip transmissivity and cooperative slip activity. These results are used for setting up a slip transfer criterion.



TMS 2012

141st Annual Meeting & Exhibition

E-6: The Effects of Aspect Ratios in Liquid Bridge on Surface Driven Flow under Microgravity JEMISS: *Shinichi Yoda*¹; Satoshi Matsumoto¹; Atsushi Komiya²; ¹JAXA; ²Touhoku University

The surface tension driven flow (Marangoni) experiments were carried out by using liquid bridge of Silicones oil with 50mm diam. under microgravity condition on Japanese Experiment Module on International Space Station. The parameters in these experiments were liquid bridge length being corresponded to aspect ratio, which is defined as liquid length/liquid diam., and temperature difference between hot and cold disks, which sustains the liquid bridge. Observing the movement of the particles by three CCD cameras, we can determine the flow behavior of Marangoni with different temperature as 3 dimension flow. The critical Marangoni numbers that the transition from laminar to oscillatory flow was dependent on aspect ratios. The smaller aspect ratio around showed smaller critical Marangoni numbers, whereas the larger those were larger the numbers. This relationships are good agreement with numerical simulation results.

E-7: The In-situ Intrinsic Stress Measurements of Cu and Al Thin Films: Jun Young Yu¹; *Youngman Kim*¹; ¹Chonnam National University

We observed the in-situ stress evolution of Cu and Al thin films during deposition on (111) Si wafers using a thermal evaporation method in terms of deposition rates. Cu and Al films were deposited at rates ranging from 0.5 to 1.5Å for Cu and for Al. In-situ stress values in the growing films were obtained using multi-beam curvature measurement system installed in the chamber of thermal evaporator. For the copper films the in-situ intrinsic stress showed a typical three step behavior of initial compressive, tensile and gradual compressive stresses. For the aluminum films the in-situ intrinsic stress showed rather unstable behavior without highly reliable repeatability.

Nanocomposites: Poster Session

Sponsored by: The Minerals, Metals and Materials Society, TMS Structural Materials Division, TMS/ASM: Composite Materials Committee

Program Organizers: Garth Wilks, Air Force Research Laboratory; Jonathan Spowart, Air Force Research Laboratory; Meisha Shofner, Georgia Institute of Technology; John Zhanhu Guo, Lamar University

Monday PM
March 12, 2012

Room: Atlantic Hall
Location: Dolphin Resort

V-1: Formation of Carbides in the Aluminum Matrix Composites Reinforced by Multi-Walled Carbon Nanotubes: *Seun Shin*¹; Heon Kang¹; Donghyun Bae¹; ¹Yonsei University

Enormous work has been conducted on the strengthening behavior of aluminum- multi-walled carbon nanotubes(MWCNTs) composites by powder metallurgy. Generally, MWCNTs are individually dispersed and mechanically interlocked in the aluminum matrix of Al/MWCNT composites and they thermally diffuse to form aluminum carbides from aluminum matrix during hot process. However, the process of the formation of carbides has not well attended. This study clearly explores the formation of carbides during heat treatment for the samples which damaged MWCNTs which thermally diffused more actively using argon containing 3% hydrogen atmosphere. While Al/MWCNT composite annealed at 500°C, the aluminum atoms decomposed from aluminum matrix and they diffused to individually dispersed MWCNTs to form aluminum carbides, then they occupied the interstitial sites of MWCNTs as a sphere. The hardness decreases when the composites are annealed for up to 3 h, and it gradually increases up to 24 h, significantly decreases as annealing time up to 72 h.

V-2: Impact Resistance of Nanostructured Partially Stabilized Zirconia Reinforced Porcelains: *Emmi Ngo*¹; Harry Yang¹; Ricardo Castro¹; ¹University of California, Davis

Partially stabilized zirconia(PSZ) is a heavily studied ceramic due to its unique properties. Most notable is PSZ's ability to undergo a phase transformation when placed under an applied stress. This transformation toughening relies on the relative stability of each of the polymorphs, which is dependent on the particle size. This creates the possibility of further improving the transformation toughening by exploiting nanostructured phases. In this study, we analyzed the mechanical properties of PSZ and fully stabilized zirconia(FSZ) reinforced porcelains. We focused on the effect of the particle sizes by systematically evaluating the improvement of mechanical properties when replacing kaolin in the porcelain composition by nano or microsized particles. In addition to the expected improved mechanical properties caused by the introduced nanoparticles, the phase transition in the PSZ is observed to provide improved features when compared to FSZ nanoparticles. The results are discussed based on the interface energetics and microstructure analysis.

V-3: Influence of the Type of Clay on the Morphology of Nanocomposites: *André Rodrigues*¹; Maria Brasileiro¹; Tomas Melo²; Edcleide Araujo²; Ariosvaldo Sobrinho²; Mucio Nobrega¹; ¹UFC; ²UFCG

In this work, polypropylene/bentonite and polypropylene/compatibilizer/bentonite nanocomposites were prepared by melt intercalation method using a modular co-rotational twin screw extruder and a counter rotating twin screw extruder. Initially, bentonitic clays were organophilized with ionic and non-ionic surfactants with the aim of obtaining organophilic clays. The XRD results showed that the ionic and non-ionic surfactants were incorporated into the clay, confirming the organophilization. Subsequently, the organophilic bentonitic clays were incorporated into PP and PP/PP-g-MA. From the results obtained through XRD, OM, SEM, TEM analyses, the method used and the processing conditions, it may be concluded that it is possible to develop nanocomposites with mixed structure (agglomerates, tactoids and exfoliated particles) with predominance of an intercalated structure. The processing conditions (screw type, feeding rate and screw speed), matrix viscosity, concentration and type of the bentonite clay and PP-g-MA concentration had little effect on the nanocomposite obtention and on its properties, in general.

V-4: Mechanical Properties of Fe-Based Nanocomposites with Dispersed Multi-Walled Carbon Nanotubes: *Ji-Yeon Suh*¹; Jaehyuck Shin¹; Donghyun Bae¹; ¹Department of Materials Science and Engineering, Yonsei University

Multi-walled carbon nanotubes (MWCNTs) are favorable reinforcement with outstanding mechanical properties. However, it has been difficult to reveal the remarkable properties of MWCNTs in metal matrix composites (MMCs) due to poor interfacial bonding with metals. The present study deliberates to disperse MWCNTs uniformly in the Fe matrix in which cohesive energy between them is relatively high. High-energy ball milling under an argon atmosphere is carried out for homogeneous dispersion of MWCNTs in Fe powders. MWCNTs are dispersed through deformation of the powders to transform from flake-like shape to sphere during milling process. The ball-milled powders are consolidated during the hot-pressing. Yield stress increases with increasing the volume fraction of MWCNTs, and the composites containing 4 vol. % MWCNTs exhibits superior yield stress of 2.3 GPa under compression by interfacial bonding between MWCNTs and Fe matrix. The detailed fabrication process and mechanical properties will be presented.

V-5: Modeling Elastic Behaviors of Peptide Reinforced Hydrogel Nanocomposites: *Jingjing Qiu*¹; ¹Texas Tech University

A novel mathematical model based on Eshelby equivalent tensor is developed to analyze the elastic properties of peptide reinforced hydrogel nanocomposites. The model takes into account the effect of small size

of reinforcement phase and stochastic distribution of peptide into the formulation. The overall effective elastic modulus is predicted using micromechanics. The effect of interfacial bonding on the overall effective elastic modulus is also investigated.

V-6: Modification of the Temperatures of Phase Transformations of Alumina by the Insertion of MgO and ZrO₂: *Deise Cristina Rosário¹; Douglas Gouvêa¹; ¹University of São Paulo*

Due to the stability and diversity of different polymorphs of alumina, this becomes a very interesting material for the study of stability in accordance with changes in surface energy. This study aims at understanding the phenomena that change transformation amorphous-gamma phase temperature by inserting additives, MgO and ZrO₂, taking into account the effects of Thermodynamic. Powders synthesized by Pechini's method were characterized by DSC, XRD, BET and FTIR. The results showed an increase in the stability for the amorphous phase for the doped samples, which showed the formation of solid solution and surface segregation independently of the doping concentrations. Although a second phase formation was not observed, it noted a change in the chemistry surface to samples.

V-7: Role of Nano-Silica on Alkali-Silica Reactivity of Concrete: *Mohammad Islam¹; ¹UBC*

Past research investigations revealed that the ASR-induced expansion decreased with an increase in the silica content of the cementitious materials. The main objective of this study was to suppress the excessive expansion of concrete caused by alkali-silica reactivity with the use of nano-silica having 99.99% SiO₂ by weight. The experimental program consisted of four highly reactive aggregates, nano-silica and superplasticizer. The mortar bar specimens were prepared with each trial aggregate and three dosages of nano-silica, 3, 6, and 9% by weight of cement replacement. The required dosages of superplasticizer, a percentage of the weight of the cementitious materials, which produced a uniform flow with no bleeding or segregation, were also adjusted depending on the amount of nano-silica. Mortar bars without nano-silica were also used as control specimens. The ASR-induced expansions of the test mortar bars were also evaluated based on the failure criteria of the mortar bars at the immersion ages of 14, 28, 56 days. The study showed that the expansion of the test mortar bars decreased with an increase in the nano-silica content. The results of the study concluded that, for the most trial aggregates, the mortar bars containing 9% nano-silica was not capable of reducing the ASR-induced expansions below the expansion limits of ASTM C 1260 at the above-mentioned three immersion ages.

V-8: Thermal Properties of Mg-Nanocomposites Reinforced by CNT in Relation to Pure-Mg: *Sardar Iqbal¹; ¹Southern Illinois Univ, Carbondale*

Thermal properties, of Mg-nanocomposites were measured from 25-500°C to determine thermal diffusivity, thermal expansion coefficient and specific heat capacity. The Mg and Mg-CNT nanocomposites (0.5, 1, 2 and 5 %) were prepared with powder metallurgy method by cold press followed by sintering at 620°C. Density of pure Mg decreased with increasing CNTs whereas porosity increased. Thermal diffusivity and heat capacity of 1%CNT-Mg nanocomposites showed the highest value. The thermal conductivity calculated for Mg nanocomposites (1%CNT) was the highest with temperature. The results show that thermal properties of Mg improved significantly with the addition of CNTs. The microstructure was characterized by polarized light microscopy and SEM, and structure by TEM and X-ray diffraction patterns.

Neutron and X-Ray Studies of Advanced Materials V: Centennial: Poster Session

Sponsored by: The Minerals, Metals and Materials Society, TMS Structural Materials Division, TMS/ASM: Mechanical Behavior of Materials Committee, TMS: Chemistry and Physics of Materials Committee

Program Organizers: Rozaliya Barabash, Oak Ridge National Laboratory; Xun-Li Wang, Oak Ridge National Laboratory; Gernot Kostorz, ETH Zurich; Lyle Levine, National Institute of Standards and Technology; Peter Liaw, Univ of Tennessee; Yandong Wang, Beijing Institute of Technology; Brent Fultz, California Institute of Technology

Monday PM
March 12, 2012

Room: Atlantic Hall
Location: Dolphin Resort

Funding support provided by: Office of Basic Energy Sciences, U.S. Dept. of Energy, Dr. P. Thyagarajan

F-1: An Investigation of the Tempering Kinetics and Residual Stress States of a Cryogenically Treated and High Magnetic Field Processed Steel via Neutron Scattering Experiments: *Orlando Rios¹; Tom Watkins¹; Ling Yang¹; Alexandru Stocia¹; Ben Shassere¹; Don Nicholson¹; Gerry Ludtka¹; Gail Ludtka¹; ¹Oak Ridge National Laboratory*

Commercial steel and heat-treating operations have been plagued with costly conventional processing steps (e.g., cryogenic treatments, long double-temper cycles) to reduce the amount of retained austenite (RA). Research at ORNL is investigating the application of high magnet fields to destabilize retained austenite and reduce residual stresses. Neutron scattering experiments were performed at the Spallation Neutron Source on the VULCAN instrument to investigate the residual stress state and tempering kinetics in a steel sample processed under extreme conditions (9 Tesla) alongside cryogenically processed materials. The neutron scattering experiments revealed a structural rearrangement in the tetragonal phase at temperatures below 100C and indicated that the massive transformation was complete at much lower temperatures than expected. First principles calculations help identify alternative arrangements of interstitial carbon and their relationship to residual strain. Additionally, the residual stress state was examined and correlated to the structural relaxation of the metastable phases. Study funded by DOE-ITP-EERE.

F-2: The Study of Structural Stability for TiSi₂ under High Pressure: *Chunyu Li¹; Zhenhai Yu²; Jingeng Zhao¹; Luhong Wang²; Tianquan Liu³; Haozhe Liu²; ¹Brookhaven National Laboratory; ²Argonne National Laboratory; ³Harbin Institute of Technology*

Over the past decades, metallic silicides have attracted considerable interest because of their special properties for engineering uses in hostile environment of extreme temperature and pressure. In this paper, the in situ high-pressure angle dispersive X-ray diffraction experiment on TiSi₂ (for C54 phase, space group:Fddd) has been performed using a diamond anvil cell with synchrotron radiation at room temperature. The diffraction patterns of C54 phase TiSi₂ were gathered and its high-pressure structural stability was systematically analyzed. The lattice constants were refined using Rietveld method. With fixed B₀² as 4, isothermal bulk modulus at ambient pressure was estimated as 169(2) GPa, according to a second-order Birch-Murnaghan equation of state.



Pb-Free Solders and Other Materials for Emerging Interconnect and Packaging Technologies: Poster Session

Sponsored by: The Minerals, Metals and Materials Society, TMS Electronic, Magnetic, and Photonic Materials Division, TMS: Electronic Packaging and Interconnection Materials Committee
Program Organizers: Iver Anderson, Ames Laboratory; Sung Kang, IBM; Albert Wu, National Central Univ.; Laura Turbini, Research in Motion; Tae-Kyu Lee, Cisco Systems; Govindarajan Muralidharan, Oak Ridge National Lab; John Elmer, Lawrence Livermore National Lab; Yan Li, Intel

Monday PM
 March 12, 2012

Room: Atlantic Hall
 Location: Dolphin Resort

H-1: Effect of Multiple Reflows on Interfacial Reaction and Tensile Property of Sn-xAg-0.5Cu Solder Joints with Cu Substrate: *Long-Tai Chen¹*; ¹National Cheng Kung University

The interfacial reactions and tensile properties of SAC105 and SAC305 solder joints were investigated during multiple reflows. A continuous needle-type Cu₆Sn₅ IMC layer was formed at the solder/Cu interface. With the increasing number of reflows, the thickness of IMC on all reaction samples increased gradually and the IMC grain coarsened. The needle-type spalling of the Cu₆Sn₅ IMC was observed in the liquid-state reaction for the solder alloys. It was found that the bonding strength of the 1Ag and 3Ag solder joints tended to increase slightly with an increase in the number of reflow cycles. The 3Ag solder joints provided the excellent mechanical properties before five cycles of reflow. The fracture of all 1Ag and 3Ag solder joints mainly occurred in the bulk solder. The ductile fracture indicated that the bonding strength of solder joints could significantly influenced by the thickness and morphology of the interfacial IMC.

H-2: Microstructure Change of Au Stud Bumps Joined with Sn-3.5Ag Solder with Flip Chip Bonding Parameters: *Young-Kyu Lee¹*; *Won-Myoung Ki¹*; *Jeong-Han Kim²*; *Sehoon Yoo²*; *Chang-Woo Lee²*; ¹University of Science & Technology; ²Korea Institute of Industrial Technology

In this study, effect of flip chip bonding parameters on the formation of intermetallic compounds (IMCs) between Au stud bumps and Sn-3.5Ag solder was investigated. Flip chip bonding was performed at 260°C and 300°C with bonding time of 5, 10, and 20 sec. AuSn, AuSn₂, and AuSn₄ IMCs were found at the interface of the joint, and (Au, Cu)₆Sn₃ IMC was observed near Cu pad in the joint. At bonding temperature of 260°C, AuSn₄ IMC obviously grew more than other Au-Sn IMCs as bonding time increased. At bonding temperature of 300°C, AuSn₂ IMC clusters, which were surrounded by AuSn₄ IMC, were observed in the solder joint due to fast diffusivity of Au to molten solder with increased bonding temperature. Bond strength of Au stud bump joined with Sn-3.5Ag solder was approximately 23 gf/bump and fracture mode of the joint was intergranular cleavage between AuSn₂ and AuSn₄ IMCs.

H-3: Physicochemical Properties of Sb, Sn, Zn and Sb-Sn, SAC and SAC+Bi Alloys: *Tomasz Gancarz¹*; *Janusz Pstrus¹*; *Wladyslaw Gasior¹*; *Hani Henein²*; ¹Institute of Metallurgy and Material Science PAS; ²Department of Chemical and Materials Engineering, University of Alberta, Edmonton, AB, Canada

The aimed of this work is comparing several methods for the measurement of physical properties for molten SAC, SAC+Bi and SbSn alloys. The method used for viscosity in this work is the modified capillary and free flow method[1]. For surface tension and density, using the maximum bubble pressure method and the dilatometer technique compared with free flow method, respectively, for SAC and SAC+Bi

alloys at 550K to 1200K temperature. Investigation were undertaken on the new equipment for five SbSn alloys at 550K to 850K temperature. The results show that all the physicochemical properties decrease with temperature and with increasing Sb content in the SbSn alloy. The method was confirmed on pure metals Sb, Sn, Zn and compared with the literature data. Keywords: viscosity, density, surface tension, Sb, Sn, Zn, SAC, SbSn. I. T. Gancarz, Z. Moser, W. Gasior, J. Pstrus, H. Henein, Int. J. Thermophys. 32, 1210 (2011)

H-4: The Different Failure Mechanism of the Ni UBM in the Lead-Free Solder Joints under Constant Current Stressing at Various Temperatures: *Chung Kuang Lin¹*; *Wei An Tsao¹*; *Chih Chen¹*; ¹National Chiao Tung University

The Ni under bump metallization (UBM) is one of the most common reaction layer used for flip-chip solder joints. Under the current-stressing test, observe two different failure mechanisms at various-temperatures. Above the 150 °C, the void-formation is the major mechanism under the electromigration-test. In the other hand, the major mechanism changed to the intermetallic compound (IMC) formation below the 150 °C. However, according to the results, the thickness of IMC between the Ni and Sn affects significantly the dominant failure mechanism. At higher temperature, the more electromigration flux of Ni atom penetrates the IMC layer to react with Sn and forms thicker IMCs. By contrast, the IMC layer inhibits the electromigration flux of Ni atom at lower temperature. Therefore, the Sn atom in the cathode-side migrates to the anode side during current-stressing test. The void-formation under the IMC layer in the cathode-side becomes the major failure mechanism at lower testing-temperatures.

H-5: The Electromigration Behavior of Ni₃Sn₄ in Sn2.5Ag Solder Joints: *Chun-Yi Wu¹*; *Chih Chen¹*; ¹National Chiao Tung University

Microbumps have been adopted for interconnects in 3D-IC packaging. The bump height decreases to 10-20 μm. Due to the small volume of solder and high current-density, intermetallic compounds (IMCs) forms rapidly in the solder joints during electromigration. So the electromigration performance of IMC become a critical issue. In this study, 5 μm Sn₂.5Ag solder joint with 50 μm copper column and 3 μm electrical nickel in the chip-side and 5 μm electroless nickel in the substrate-side. After aging for 500 hours at 200°C, all the solder joints transform into the IMCs. Electromigration tests were performed at a current-density of 10⁴ A/cm² at 200°C. The bump resistance was measured by using Kelvin structure, and defined the bump resistance to increase 20%, 50%, 100%, 500% initial bump resistance as failure stages. There was longer incubation time than SnAg solder bump. Failure mechanisms of the Ni₃Sn₄ will be discussed in the meeting.

H-6: Thermal Cycling Test on Sn2.3Ag Microbump with Different UBM Structure after Heat Treatment: *Chun-Chieh Mo¹*; *Yon-Chun Liang²*; *Chih Chen²*; ¹National Chiao Tung University; ²National Chiao Tung University

Metallurgy interaction in microbump with different under-bump-metallization (UBM) structures after thermal cycling test (TCT) was examined in this study. The microbump specimens were fabricated by a solder reflow process using a lead-free Sn-2.3Ag solder. The UBM structures are classified as Cu/Sn₂.3Ag/Cu, Cu/Sn₂.3Ag/Ni, and Ni/Sn₂.3Ag/Ni with different bump heights. After different reflow times at 260°C, the microbumps were tested under cycling from -55°C to 125°C each cycle, and the cycle time is 1 hour. The fatigue crack was observed at IMC/solder interface in Cu/Cu UBM structure after reflow at 260°C for 6 minutes. As increased with the reflow time, the Cu₆Sn₅ IMC bridged and blocked the crack propagation. The crack propagation phenomenon of Cu/Ni and Ni/Ni UBM structure are also discussed.

H-7: Real Time Monitoring of Whisker Growth Failure Using by 3-D Geometry Comb Pattern: *Won Sik Hong*¹; Chul Min Oh¹; Do Seop Kim²; ¹Korea Electronics Technology Institute(KETI); ²Hyundai Motor Company

Most international specifications of whisker growth evaluation have recommended long term test duration and periodical monitoring of whisker length. But it is impossible to know exact failure time as these test method. Thus, to solve the problem, this study proposed the feasibility of in situ monitoring method related to whisker formation and growth with specimen gap. To measure the whisker growth failure occurrence time, we prepared 1 μ m thickness pure Sn electroplated Cu plate($t=192\mu$ m, 30X0.7mm) for real time monitoring of whisker growth. After conformal coating on the Cu plate specimen, two Cu plates which maintain 150 μ m gap was fixed with insulator and we applied DC voltage for measuring insulation resistance. If whisker growth occurs, we made test cell to detect the insulation resistance drop, continuously. The whisker failure criteria was $10^{-6} \Omega$. Through this experiment, we confirmed the feasibility of in situ monitoring for whisker growth.

H-8: Recrystallization-Induced Void Migration in Electroplated Cu Films: *Sunghwan Kim*¹; Jin Yu¹; ¹KAIST

An analysis based on cross-sectional micrographs is presented that addresses the recrystallization-induced void migration in 20 μ m thick electroplated Cu films. Specimens were isothermally aged at T (T = 573, 623, 673 K) for varying time. For morphological investigation, scanning electron microscopy, transmission electron microscopy, and focused ion beam microscopy were used. In addition, studies of preferred orientation of Cu films by thin film x-ray diffractometer were performed before and after isothermal aging. It was shown that voids were formed at the interface between non-recrystallized grains and recrystallized grains. Formation of voids in the Cu films was highly affected by aging temperature, and radius of voids was increased and voids migrated to the surface of Cu films with increasing aging time. Results indicate that recrystallization by isothermal aging of Cu films induced migration of voids and formed voids relieved the stress of Cu films during morphological transformation of Cu grains.

H-9: Vibration Test at Elevated Temperature for Pb-Free Solders: *Yong-Ho Ko*¹; Young-Kyu Lee²; Jeong-Han Kim¹; Sehoon Yoo¹; Chang-Woo Lee¹; ¹Micro-Joining Center, Korea Institute of Industrial Technology, Incheon, 406-840, Korea; ²Dept. of Electronic Packaging Engineering, University of Science & Technology, Daejeon, 305-333, Korea

The vibration reliability at elevated temperature was evaluated for Pb-free solders (Sn3.5Ag, Sn0.7Cu and Sn5.0Sb). The electrical resistance increased and shear strength decreased during the vibration test at elevated temperature. The resistance increment and the shear strength degradation of Sn3.5Ag solder joints were the highest among three solders, while those of Sn0.7Cu were the smallest. For the Sn3.5Ag samples, crack propagation occurred within Cu6Sn5 IMC during the vibration test at the elevated temperature. On the other hand, no crack formation and propagation was observed for the Sn0.7Cu and Sn5.0Sb solder joints. The fracture mode of Sn0.5Cu after the shear test was ductile. On the other hand, the fracture mode of the Sn3.5Ag solder joints showed ductile to brittle transition as the test time increases. Among three solders, Sn0.7Cu was the most stable under the vibration at elevated temperature.

H-10: Wettability and Interfacial Microstructure of Pb-Free Sn3.5Ag Alloy Powders on Cu Substrate: *Jin Zhao*¹; Weipeng Zhang¹; Tingting Song¹; Yulai Gao¹; Qijie Zhai¹; ¹Shanghai university

Sn3.5Ag powders in different sizes were prepared by arc technique. Powders in different sizes mixed with Rosin Mildly Activated (RMA) fluxes were soldered on pure Cu substrate. The contact angle is a critical parameter to affect the quality of solder joints. Presently the Pb-free Sn3.5Ag solder has been widely applied in industry. However, its wettability on Cu substrate is not good enough, and the contact angle of commercial Sn3.5Ag solder paste is about 26°. In contrast, the contact angles of the Sn3.5Ag solder paste prepared in the present study are 16.1°, 13.9°, and 21.4° respectively, depending on the specific characteristics of the powders. So good wettability was obtained attributing to the novel technique to prepare Sn3.5Ag powders. In addition, the intermetallic compounds (IMCs) were observed by optical microscope and scanning electron microscope, and the results showed that continuous intermetallic compounds layer formed, confirming the validity of the packaging.

Radiation Effects in Ceramic Oxide and Novel LWR Fuels: Poster Session

Sponsored by: The Minerals, Metals and Materials Society, TMS Structural Materials Division, TMS/ASM: Nuclear Materials Committee

Program Organizers: Peng Xu, University of Wisconsin; Jian Gan, Idaho National Laboratory; Ram Devanathan, Pacific Northwest National Laboratory; Edward Lahoda, Westinghouse Electric Company; Michele Manuel, University of Florida; Ramprasad Prabhakaran, Idaho National Laboratory; Todd Allen, University of Wisconsin-Madison

Monday PM
March 12, 2012

Room: Atlantic Hall
Location: Dolphin Resort

Funding support provided by: The Center for Materials Science of Nuclear Fuel, an Energy Frontier Research Center led by the Idaho National Laboratory

O-1: Microstructural Investigations of Ion (Kr, Xe) Irradiated CeO₂ and UO₂ With and Without Impurities: *Brian Kleinfeldt*¹; Weiyang Chen¹; Bei Ye¹; Yinbin Miao¹; Aaron Oaks¹; James Stubbins¹; ¹University of Illinois at Urbana-Champaign

The importance of understanding microstructural damage processes in nuclear fuel as a result of radiation is becoming increasingly important in developing and modeling new fuels. Irradiation damage processes are studied in UO₂ and CeO₂ through simulated fission product damage using Kr and Xe ion beams at temperatures from 0-800C. Primarily ex situ irradiations are performed on thin films that are then characterized through transmission electron microscopy. 150 keV Xe ions are used for bubble implantation while higher energy (1MeV) Kr atoms are used for defect creation. The role of impurities (La) is investigated by comparing Kr and Xe bubble growth and formation for the different materials as a function of dose. The impurity concentration varies from 0-25% molar. The comparison of these two materials is important as CeO₂ is often used as a surrogate material for UO₂ due to their common fluorite structure and similar properties.



TMS 2012

141st Annual Meeting & Exhibition

Randall M. German Honorary Symposium on Sintering and Powder-Based Materials: Poster Session

Sponsored by: The Minerals, Metals and Materials Society, TMS Materials Processing and Manufacturing Division, TMS: Powder Materials Committee

Program Organizers: K. Morsi, San Diego State University; Fernand Marquis, Naval Postgraduate School; John Meyer, Iowa State University; Ahmed El-Desouky, San Diego State University; Eugene Olevsky, San Diego State University

Monday PM
March 12, 2012

Room: Atlantic Hall
Location: Dolphin Resort

S-1: Effect of Nanosized Cobalt Amounts on WC-Co Sintered Bulks Fabricated by Spark Plasma Sintering (SPS): Joon-Woo Song¹; Sol Lee¹; Rumman Md. Raihanuzzaman¹; Hyoun-Seon Hong²; Soon-Jik Hong¹; ¹Kongju National University; ²Institute for Advanced Engineering (IAE)

In this research, different compositions of WC-7.5wt%Co, WC-7wt%Co, WC-6wt%Co, WC-5wt%Co have been used, where ball milling and subsequent sintering were applied on the mixed powders. Since cobalt is becoming more expensive these days, one of the primary intention was to reduce the amount of cobalt or replace it with nano-sized cobalt, in order to improve the mechanical properties. Low energy ball milling for 1 hour at a speed of 100 rpm was used, while spark plasma sintering was applied on the ball milled powders at 1300°C with a holding time of 10 minute. FE-SEM and HR-TEM were used for each compositions, after sintering, and micrographs were analysed to observe the difference in microstructure, crack formation, densification behaviour and hardness. In addition, other mechanical properties, including fracture toughness, of the sintered bodies were attempted to analyse as well.

Recycling General Sessions: Poster Session

Sponsored by: The Minerals, Metals and Materials Society, TMS Extraction and Processing Division, TMS Light Metals Division, TMS: Recycling and Environmental Technologies Committee
Program Organizer: Joseph Pomykala, Alter Trading

Monday PM
March 12, 2012

Room: Atlantic Hall
Location: Dolphin Resort

R-1: AMD Treatment Using Rice Husk as Biosorbent: Flávia Silvas¹; Bianca Medeiros²; Daniella Buzzi³; José Oliveira²; Ivo Schneider⁴; Denise Espinosa³; Jorge Tenório³; ¹Polytechnic School of São Paulo University; ²Instituto Federal de Educação, Ciência e Tecnologia do Espírito Santo; ³Polytechnic School of São Paulo University; ⁴Universidade Federal do Rio Grande do Sul

AMD is one of the main problems associated with mining activities and the techniques used in their treatment may be the biosorption. The aim of this work was to study the rice husk as a biosorbent for the AMD treatment keeping constant: pH (2.6), biomass concentration (1g/L), temperature (25°C) and agitation (175rpm). And varying the contact time of 5, 20, 60 and 240 minutes. Rice husk samples will be characterized before and after the biosorptives tests through analysis of SEM and IR.

The micrographs indicate the occurrence of micro-precipitation and changes in biomass physical structure. Since the infrared spectra indicate changes in functional groups present in the biomass before and after the biosorptives tests. AMD synthetic solutions will be analyzed by ICP in order to quantify the metals concentration captured by biomass.

R-2: Incorporation of Building Rejects in Portland Cement: Shirley Cosin¹; Francisco Valenzuela Diaz¹; ¹University of São Paulo

A procedure for incorporating building rejects in Portland cement was studied. Cylindrical test bodies with 2,5cm of diameter and 5,0cm of height were done using 50 parts of water for each 100 part of cement. The test bodies were incorporated with 1, 5, 10 and 20 parts of rejects for each hundred parts of cement. After 28 days of aging in humid chamber they were tested for compression strength, porosity and density. The best performing composition was used in a new batch of test bodies with 5,0cm of diameter and 10,0cm of height. After 28 days of aging, they were tested for compression strength, porosity and density. The incorporation of 10 parts showed the best results and this composition was used in pilot production blocks which were tested for compression strength and lixiviation showing mechanical properties in accordance with the technical standards, making this incorporation procedure suitable for industrial application.

Refractory Metals 2012: Poster Session

Sponsored by: The Minerals, Metals and Materials Society, TMS Structural Materials Division, TMS: Refractory Metals Committee
Program Organizers: Eric Taleff, The University of Texas at Austin; Todd Leonhardt, Rhenium Alloys Inc; Rachel DeLucas, H.C. Starck; Gary Rozak, HC Starck Inc

Monday PM
March 12, 2012

Room: Atlantic Hall
Location: Dolphin Resort

J-1: Effect of Al on the Oxidation Behavior of Alloys from Nb-Cr-Si System: Amanda Gutierrez¹; Nydia Esparza¹; Brenda Arellano¹; Shailendra Varma¹; ¹UTEP

Oxidation behavior of Nb-30Cr-10Si and Nb-30Cr-10Si-(5,10) Al alloys has been investigated in a range of temperatures from 700 to 1400°C. Alloys were subjected to 24 hour exposure to air at the oxidation temperature and then furnace cooled to room temperature. Weight gain per unit area (W) has been used to follow the oxidation behavior as a function of temperature. Characterization was performed using XRD and EDS and x-ray mapping modes in SEM. The Al addition to the alloy has been found to be beneficial for enhancing oxidation resistance. Samples with no Al suffered from 100% peeling at 1000°C even though oxidation at higher temperatures was much better. Al addition, however, demonstrates internal oxidation by the formation of Al₂O₃ at the interface between the solid solution and silicides. High temperature oxidation, particularly, is superior with Al addition.

Solid-State Interfaces II: Toward an Atomistic-Scale Understanding of Structure, Properties, and Behavior through Theory and Experiment: Poster Session

Sponsored by: The Minerals, Metals and Materials Society, TMS Electronic, Magnetic, and Photonic Materials Division, TMS Structural Materials Division, TMS: Chemistry and Physics of Materials Committee, TMS: Nanomechanical Materials Behavior Committee

Program Organizers: Xiang-Yang Liu, Los Alamos National Lab; Douglas Spearot, University of Arkansas; Guido Schmitz, University of Münster; David Seidman, Northwestern University

Monday PM
March 12, 2012

Room: Atlantic Hall
Location: Dolphin Resort

Funding support provided by: Los Alamos National Laboratory

D-1: Adhesion Strength at Cu(111)/ α -Alumina(0001) Interfaces with Metal Dopants in Alumina Dispersion-Strengthened Copper: Kelun Zhao¹; Xuanhui Qu²; *Shaojun Liu*³; ¹Materials Science and Engineering Division, Shenzhen Graduate School, Harbin Institute of Technology; ²State Key Laboratory for Advanced Metals and Materials, University of Science and Technology Beijing; ³State Key Laboratory for Powder Metallurgy, Central South University

The local bonding and adhesion strength at the heterogeneous metal/oxide interface are strongly influenced by the presence of impurities and dopants. In the present work, the atomistic structure and the energetics of Cu(111)/ α -alumina (0001) interfaces with a various of metal dopants are investigated by using the first-principles methods and density functional theory. Based on the analysis of the electronic structure of interfaces and the segregation energies of dopants at Cu(111)/ α -alumina(0001) interfaces, it is found the stability of interfaces is dependent on the structure and chemistry of Cu(111)/ α -alumina(0001) interfaces. The adhesion strength of Cu(111)/ α -alumina(0001) interfaces is significantly enhanced by Ag doping, while it is slightly reduced by Ni doping. In contrast, metal dopants (Ti, Zr, Hf, and Zn) could result in the crack of Cu(111)/ α -alumina(0001) interfaces and subsequently the decrease of adhesion strength. These are in a good consistent with the observed experimental results in alumina dispersion-strengthened copper.

D-2: Atomistic Simulation of Doped (La,Y,Mg) α -Alumina Interfaces for Transparent Ceramic Applications: *Abhishek Tewari*¹; Sandra Galmarini¹; Paul Bowen¹; ¹Ecole Polytechnique Federale de Lausanne

To achieve high Real Inline Transmittance (RIT) for transparent applications with alumina, fully dense ultrafine crystalline alumina is desired. Doping of alumina with transition elements (e.g. Y, Mg, La) has been an effective tool for controlling the grain size during the sintering step, moreover codoping being even more effective. This may be attributed to the segregation of dopants at the grain boundaries, producing the grain or solute drag effect. However, the atomistic mechanisms behind these observations, especially codoping effect, are still not clear. The current goal is to understand the atomistic mechanisms behind doping and codoping using atomistic modeling methods. Studies on 9 surfaces and 9 grain boundaries showed segregation of dopants to be energetically favorable in all the cases and a coordinative arrangement was observed in case of codoping. When linked to Monte Carlo simulations and a microstructural model, nominal solubilities and second phase precipitate diagrams can be predicted.

D-3: Atomistic Simulations of Nanoindentation and Nanoscratching of Thin Films: *Xuan Sun*¹; Tzu-Ray Shan¹; Simon Phillpot¹; Susan Sinnott¹; ¹University of Florida

Molecular dynamics (MD) simulations are used to investigate the atomic scale responses of semiconductor/gate oxide interfaces to nanoindentation and nanoscratching. The simulations utilize the variable charge, empirical

charge optimized many-body (COMB) potential to simulate the mechanical response of the interfacial systems to a rigid semispherical indenter. The particular interfaces investigated are between Si and SiO₂ or HfO₂ of different film thicknesses. The nanoscratch tests are conducted at various normal loads. Phenomena such as plastic deformation, pile-ups, and wear are also observed. The predicted hardness, reduced modulus, fracture mechanism, and friction coefficient are determined, as well as the effect of dynamic charge transfer to the overall results.

D-4: Grain Boundary - Dislocation Interaction: Linking Molecular Dynamics and Dislocation Dynamics: *Sebastian Echeverri Restrepo*¹; Barend Thijssse¹; Lucia Nicola¹; Xiaoming Liu²; Erik van der Giessen²; ¹TU Delft; ²University of Groningen

Molecular dynamics (MD) is a powerful tool that can be used to describe the behavior of dislocations and interfaces at the nano scale. Nevertheless, due to current computational limitations, as the size of the simulated sample increases, alternative methods have to be considered, like 2D dislocation dynamics (2D-DD). An effort to link MD with 2D-DD is presented. Since 2D-DD works under the assumption of an isotropic medium, a bicrystal with a misorientation that minimizes the effects of anisotropy is generated. Then a dislocation is inserted into one of the crystals and a stress is applied to the sample in such a way that the dislocation is made to interact with the grain boundary. This is done for various stress values. Qualitative and quantitative analyses of the interaction are presented.

D-5: In Situ TEM investigation of Electrical Current Effect on Aluminum Interconnect: *Degang Xie*¹; Zhiwei Shan¹; ¹Center for Advancing Materials Performance from the Nanoscale (CAMP Nano)

Electro-migration is the phenomenon that metallic atoms are transported by electron wind due to high electrical current density in the metal line. Factors like interconnect length, crystallographic texture, grain size and its distribution, and grain boundary structures have been extensively documented to have a major impact on electron-migration induced plasticity. Consequently, understanding the exact mechanism and evolution of electrical current effect on interconnect has become critical for designing reliable devices. In situ TEM will become the best tool for studying the microstructure evolution of nanoscale interconnects under the effect of electrical current. In this work, we developed a novel method for preparing samples that can be studied in situ inside a TEM under the effect of electrical current. By employing a Hysitron PI95 ECR type holder, we found that the defects density inside the Al grains can be reduced dramatically by the applied current which we termed as electrical annealing.

D-6: Phase Field Crystal Simulation of Curvature Driven Grain Boundary Migration: *Vishal Yadav*¹; Nele Moelans¹; ¹Katholieke Universiteit Leuven

A systematic study of grain boundary migration on the atomistic scale is carried out using the Phase Field Crystal (PFC) method. Since the PFC model is atomistic in space and diffusive in time, it can depict realistic grain boundary structures during grain boundary movement. In this study, the effect of misorientation between grains, grain geometry, grain size and temperature on the structure, energy and mobility of the grain boundaries is analyzed. At certain temperatures and misorientation angles, faceting is observed which slows down the grain boundary migration. It is also observed that in some cases, triple junctions slow down the grain boundary migration by pinning grain boundaries.

D-7: Quantification of Compositional Effects on Transformation Kinetics in High Strength Low Alloy Steels Using In Situ TEM: *Asher Leff*¹; Michael Grimes²; Nerea Isasti³; Christopher Winkler¹; Pello Uranga³; Mitra Taheri¹; ¹Drexel University; ²Lehigh University; ³University of Navarra

High strength low alloy steels (HSLAS) contain a small fraction of various alloying elements to produce increased thermal and mechanical stability. Although the individual effects of these additives are known, the



TMS 2012

141st Annual Meeting & Exhibition

interactions between them are not well understood and are critical to the behavior and kinetics of grain boundaries, dislocations and precipitates. Two HSLAS containing Niobium (Nb) and either Molybdenum (Mo) or Vanadium (V) were compared. HSLAS containing both Nb and Mo are known to retain their strength at higher temperatures than comparable alloys, while the combination of Nb and V yields similar but less drastic effects. In situ TEM tempering experiments have been carried out in order to compare the effects of the alloy components on precipitation, grain growth, and phase transformation kinetics. By achieving a greater understanding of these mechanisms, the composition and processing procedure of HSLAS can be optimized to predictively improve their thermal and mechanical properties.

D-8: Segregation-Induced Phase Transformation on Grain Boundaries in Fe-Mn: *Michael Herbig¹; Pyuck-Pa Choi¹; Dirk Pongel¹; Dierk Raabe¹; ¹Max-Planck-Institut für Eisenforschung GmbH*

In order to deepen our understanding of the nucleation of new phases on defects, in particular grain boundaries, it would be desirable to know the phase distribution, orientation and elemental composition around the defects on the nanometer scale. Our approach to gather this information is the combination of transmission electron microscopy (TEM) and atom probe tomography (APT). Investigations have been done on the binary Fe-Mn system. After quenching from the austenite regime the material is composed of 100% martensite. During tempering Mn segregates to the grain boundaries where new austenite is formed. APT samples containing the grain boundaries of interest were prepared using focused ion beam milling and then investigated by TEM and APT.

D-9: Study of Shear Behavior of Al, TiN, and Their Interface Using *ab initio* Method: *Satyesh Yadav¹; Xiang-Yang (Ben) Liu¹; Rampi Ramprasad²; Amit Misra¹; ¹Los Alamos National Laboratory; ²Institute of Materials Science, CMBE*

Recently 2 nm Al-TiN multilayer nanocomposites measured high flow strength, high deformability and unusually high work hardening rate. Due to high proportion of interfaces in such system it is important to understand their role in achieving such exceptional mechanical properties. In this *ab initio* work we use density functional theory to study shear behavior of Al, TiN, and coherent Al/TiN interface under uniaxial stresses. We find that the ultimate shear strength of the interface is of the order of ultimate shear strength of Al or TiN depending on the Ti or N termination at the interface, respectively. As a first step, we establish the slip system in Al and TiN by considering both the ultimate shear strength and volume relaxation. We then develop a methodology to calculate the shear strength of interfaces, so that the shear strength does not depend on number of layers in the supercell.

D-10: The Effect of Molybdenum on Nb,Ti(C,N) Precipitate Evolution and Grain Refinement in a High-Temperature Carburizing Steel: *Charles Enloe¹; John Speer¹; Kip Findley¹; ¹Colorado School of Mines, Advanced Steel Processing and Products Research Center*

Coarsening and compositional evolution of mixed Nb,Ti(C,N) carbonitride precipitates have been investigated in molybdenum-bearing microalloyed SAE 4120 steel. The effects of molybdenum on niobium-bearing carbonitride interfacial energy and niobium diffusion during reheat to carburizing temperatures were of special focus. Characterization of precipitate evolution is fundamental to process design for the retardation of abnormal grain growth at increasingly high processing temperatures. The experimental characterization techniques include analytical scanning transmission electron microscopy (STEM) and three dimensional atom probe tomography (APT). A reduction in the ripening rate of carbonitrides was observed in molybdenum-bearing alloys containing 0.05 wt pct and 0.10 wt pct niobium. Molybdenum incorporation was observed in spheroidal carbonitrides less than 30 nm in diameter, but APT and STEM investigations revealed no appreciable molybdenum segregation to the particle/matrix interface.

T.T. Chen Honorary Symposium on Hydrometallurgy, Electrometallurgy and Materials Characterization: Poster Session

Sponsored by: The Minerals, Metals and Materials Society, TMS Extraction and Processing Division, TMS: Hydrometallurgy and Electrometallurgy Committee, TMS: Materials Characterization Committee

Program Organizers: Shijie Wang, Rio Tinto Kennecott Utah Copper; J. E. Dutrizac, CANMET; Michael Free, University of Utah; J. Y. Hwang, Michigan Technological University; Daniel Kim, Rio Tinto Kennecott Utah Copper

Monday PM
March 12, 2012

Room: Atlantic Hall
Location: Dolphin Resort

Funding support provided by: Rio Tinto Kennecott Utah Copper, ASARCO, and Freeport McMoRan

P-1: A Kinetics Study on the Hydrometallurgical Recovery of Vanadium from LD Converter Slag in Alkaline Media: *Fereshteh Rashchi¹; ¹University of Tehran*

TBA

P-2: Annealing Effects in Martensitic Transformation Temperature of the Ni-Ti Shape Memory Alloy Rapidly Solidified: *Walman Castro¹; Carlos de Araújo¹; George Anselmo¹; ¹Universidade Federal de Campina Grande*

One important challenge of microsystems design is the implementation of miniaturized actuation principles efficient at the micro-scale. Shape memory alloys (SMAs) have early on been considered as a potential solution to this problem as these materials offer attractive properties like a high-power to weight ratio, large deformation and the capability to be processed at the micro-scale. Ti45Ni55 shape memory alloy was prepared by melt spinning technique at different wheel speed. The effect of annealing at different temperatures on a rapidly solidified/melt-spun Ni-Ti alloy has been investigated in depth. The analysis of these treatments was made by means of DSC. Changes on martensitic transformation temperatures in Ti44,8Ni55,2 melt spun ribbons were observed with the increase if the wheel speed and variation of annealing temperature.

P-3: As(III) Oxidation with Bacteria and AP: *Qian Li¹; Qiong Deng¹; Hong-Jing Yuan¹; Yong-Bin Yang¹; Tao Jiang¹; ¹Central South University*

Bio-pretreatment is a hot research subject to refractory arsenic-bearing gold ores. However, the product of As(III) is poisonous to the bacteria, so the technical application is limited. Bio-oxidation action of As(III) with or without bacteria or AP is investigated. The results indicated that it is an effective method of using AP as oxidant to enhance As(III) to As(V) without bacteria. In the condition with bacteria, the Fe²⁺ will be oxidized by the AP and the energy for bacteria will be reduced. Moreover, there is great influence between the different ways to add AP. When the AP is added into the solution after the bacteria being survived, the bacterial activity will be stronger than it is added at the beginning. The AP can reduce arsenic level of the solution to make the bacteria alive, which makes the bio-oxidation more effective.

P-4: Comprehensive Utilization of Waste Printed Circuit Boards: *Yu Xia¹; Long-Sheng Yi¹; Qi-Ming Feng¹; Qian Li¹; ¹Central South University*

The comprehensive utilization of valuable metals from the waste printed circuit boards is investigated. The waste printed circuit boards are crushed and separated into two parts of 26.20% metal and 73.80% nonmetal materials by crushing machine. The metal materials, which contained copper, zinc, tin, lead, gold, silver et.al, were leached by sulfuric acid and hydrogen peroxide. After two-stage leaching, the leaching rates of Cu, Zn, Sn, Pb was 99.99%, 100.00%, 100.00%, 2.47%. The leaching

residue contained 74.31%Pb, 15.39%Ag and 8.29% Au. The study result has guiding significance for the recycle and reuse of waste printed circuit boards.

P-5: Dephosphorization of Yunnan Refractory High- Phosphorus Low-Manganese Ore by Shaking Table and Hydrometallurgical Processing: Guodong Lai¹; Zebiao Zhang¹; Jinhui Peng¹; Lijuan Chu¹; Shixing Wang²; ¹Faculty of Metallurgy and Energy Engineering; ²Yunnan Institute of Product Quality Supervision and Inspection

The beneficiation of poor manganese ore containing phosphate gangue is very difficult by conventional processes, due to the similarities in physico-chemical properties of constituent minerals in the system. The shaking table gravity concentration process and mixing concentrated strong acid selective intensified leaching process were used for dephosphorisation of Yunnan manganese ore. The leaching process was effective. The effects of intensified leaching time, solid-liquid ratio and particle size were investigated. The relevant leaching factors were optimized as -0.125+0.088 mm particle size ore with 68% nitric acid for 24 h when using a solid-liquid ratio of 1:1 at room temperature and pressure atmosphere. Under these conditions, the P/Mn ratio was reduced from 0.0107 to 0.0056, and the grade of manganese was increased from 12.32% to 42.76%. The dissolution of manganese during leaching was negligible.

P-6: Dissolution Behavior of Impurities in Scheelite Mineral in Oxalic Acid Solutions: Ahmet Kalpaklı¹; Sedat İlhan¹; Cem Kahruman¹; İbrahim Yusufoglu¹; ¹Istanbul University

Scheelite mineral is the main raw material in tungsten production. In hydrometallurgical processes, extraction of tungstate ions is very important. During the leaching of scheelite mineral in oxalic acid solutions, tungsten completely dissolves as chelate complex. Scheelite mineral includes impurities along with calcium tungstate. Determination of dissolution of these impurities is important for further tungsten production stages. In this study, scheelite mineral was dissolved in oxalic acid solutions and the dissolution of impurities were investigated. The quantities of dissolved impurities were determined by ICP – OES and characterization of undissolved impurities in leach residues were carried out by SEM – EDS analysis.

P-7: Effect of Different Parameters on Synergistic Separation of Nickel and Cadmium from Sulphate Solutions using D2EHPA and Cyanex 302: Ataollah Babakhani¹; Fereshteh Rashchi¹; Ehsan Vahidi¹; Alireza Zakeri²; ¹University of Tehran; ²Iran University of Science & Technology

Synergistic effect of Cyanex 302 on the solvent extraction of nickel and cadmium from sulphate solution with D2EHPA diluted in kerosene was investigated with the aim of increasing the separation efficiency. Experiments were carried out in the pH range of 0.1–5.0 using sole D2EHPA and D2EHPA-Cyanex 302 mixtures in different ratios. Increasing Cyanex 302 to D2EHPA ratios in the organic phase caused a left shifting of the extraction isotherm of cadmium and a right shifting of the extraction isotherm of nickel. As a result, optimum separation was found with a Cyanex 302 to D2EHPA ratio of 0.1: 0.5. In the present system, effect of a modifying reagent such as TBP was studied. Influence of various diluents including kerosene and carbon tetrachloride was also investigated.

P-8: Electrochemical Reduction of TiO₂-Rich Slag to High-Titanium Ferroalloy in the CaCl₂-NaCl Melt: Qian Xu¹; ¹Northeastern University

The high-titanium ferroalloy was electrochemically prepared in the CaCl₂-NaCl melt from the titania-rich slag with 70% mass percent TiO₂, which was provided by the Titanium Plant of Panzhihua Iron and Steel Group Corporation, Sichuan, China. The product mainly contained TiFe and Ti with impurities of Si, Al and Mg. When the titania-rich slag was upgraded by the joint process of alkali-activation and acid leaching, the effective removal of the impurities was achieved, and metallic Ti with minor amount of TiFe alloy can be produced by electro-deoxidation. An

investigation into the reaction pathway of the electrochemical reduction was performed in order to better understand the reaction mechanism of the process for preparation of high-titanium ferroalloy.

P-9: Evaluation of Banana Fibers Density with Different Diameters: Nathalia Rosa¹; Lucas Martins¹; Sergio Monteiro¹; ¹UENF

Polymer composites reinforced with natural fibers are gaining interest of several engineering sectors due to specific advantages such as lower cost and lower density as well as environmental benefits associated with the fact that natural fibers are renewable, biodegradable, recyclable and neutral with respect to CO₂ emissions. Among these natural fibers, the banana fiber has been studied as possible reinforcement in polymer composites. In spite of works conducted on the diameter dependence of the tensile strength, no investigation has been conducted so far to evaluate the relation between the density and different diameters. Then, the objective of this work is to evaluate the banana fibers density to the different diameters. It was found an inverse correlation between the diameter and the fiber density. This correlation could be explained in terms of defects and microstructural characteristics by means of SEM observation.

P-10: Interdiffusion Studies between Ti-5Ta-2Nb Alloy and 304L Austenitic Stainless Steel Joined by Explosive Cladding Process: Sudha Cheruvathur¹; Prasanthi T.N¹; Saroja S¹; Vijayalakshmi M¹; ¹Indira Gandhi Centre for Atomic Research

In this study, evolution of the interface microstructure in explosively clad joints of Ti-5Ta-2Nb and 304L austenitic stainless steel due to heat treatment is elaborated. Heat treatment in the temperature range of 823 to 1273K resulted in considerable microstructural and microchemical changes at clad interface. Diffusion path followed at each temperature was identified based on electron microprobe analysis. From elemental concentration profiles, diffusion coefficient of the alloying elements was calculated using Den Broeders and Hall's method. Diffusion of Fe in ⁹⁴⁵Ti (10⁻¹⁶m²/sec) was found to be faster (10⁻¹⁵m²/sec) than diffusion of Ti in ⁹⁴⁷-Fe (10⁻¹⁸m²/sec). Diffusion of Fe in bcc ⁹⁴⁶-Ti phase was found to be faster than the self diffusion of Ti (10⁻¹⁷m²/sec). Apparent activation energy for the formation of zones containing ⁹⁴⁶-Ti and intermetallic phases was obtained as 183 and 32kJ/mol respectively. Concentration dependence of interdiffusion coefficients was calculated which will be discussed in the paper.

P-11: Leaching S from Pressure Acid Leaching Residue of Zinc Concentrate: Parameters Optimization Using Response Surface Methodology: Lijuan Chu¹; Zebiao Zhang¹; Peng Peng²; Guodong Lai¹; Guo Cheng¹; ¹Kunming University of Science and Technology; ²University of Minnesota

The pressure acid leaching residue of zinc concentrate contains large quantity of sulfur. The present study attempts to leach sulfur using a mixture of ammonium sulfide and water solution at 25°C. Effects of three leaching variables: ammonium sulfide concentration, leaching time, liquid to solid ratio on the sulfur leaching rate were investigated. The process conditions were optimized using response surface methodology based on the central composite design. From the analysis of variance (ANOVA), the significant factors on response were identified. The optimum conditions for leaching elemental sulfur from pressure acid leaching residue of zinc concentrate were obtained by using ammonium sulfide concentration of 2.5mol/L, leaching liquid-solid ratio of 6.5:1 and leaching time of 7 min. Under the optimum experimental conditions, a maximum of 98.50% of sulfur was extracted. The experimental results obtained agreed satisfactorily with the model predictions, with a correlation coefficient (R²) of 0.99.

P-12: Measurement of Contact Angle for Iron Ore Particles: Xiaobo Huang¹; Xuewei Lv¹; Chenguang Bai¹; Rende zhang¹; Maojun Zhou²; ¹College of Materials Science and Engineering, Chongqing University; ²Ironmaking plant, Baoshan Iron & Steel Co., Ltd.

Wettability of the iron ore plays a great role during iron ore granulation process. As a characterization of wettability, the contact angle of iron ore particles was measured via Washburn Osmotic pressure method, which is



a deformation of capillary penetration method. Correctness and accuracy of the experiment are always affected by some factors, which are the main topics of this study. It was found that the compaction status in the packed beds, the size distribution of the particles, temperature and humidity all affect the testing process. The optimal measurement conditions are suggested as follow:(a) sample with size distribution of 240-400 mesh (61 μ m -38 μ m);(b) Consistency and stability of temperature and humidity. The advancing contact angles of five ores varied from 20 to 85°, and have a notable correlation with chemical and physical properties.

P-13: Mixture Design Applied to the Electrochemical Reduction Of CaWO₄ to W: *Metehan Erdogan*¹; *Ishak Karakaya*¹; *Orhan Gökçe Göksu*²; ¹Department of Metallurgical and Materials Engineering, Middle East Technical University; ²Other

An experiment (mixture) design was created to study the process parameters of the electrochemical reduction of CaWO₄ to W in molten CaCl₂-NaCl eutectic mixture. Temperature, applied voltage and Kanthal wire winding of the CaWO₄ pellets were selected as the process parameters and allowed to vary between the predetermined minimum and maximum values. The rates of the electrochemical reductions were interpreted from the variations of current and total charge vs. time graphs under different conditions. The analysis pointed out 640°C and 2.81 V from the created mixture design for the fastest reduction and it was seen that the effect of Kanthal wire winding on the output current was less pronounced when compared to the other two parameters.

P-14: Preparation and Characterization of PBT/Clay Nanocomposite: *Mariana Sartori*¹; *Rene Oliveira*¹; *Francisco Diaz*²; *Vijaya Rangari*³; *Angel Ortiz*⁴; *Esperidiana Moura*⁴; ¹Instituto de Pesquisas Energéticas e Nucleares - IPEN-CNEN/SP; ²Universidade de São Paulo - USP; ³Tuskegee University; ⁴Instituto de Pesquisas Energéticas e Nucleares - IPEN-CNEN/SP

This work presents the preparation and characterization of a nanocomposite based on PBT and Brazilian smectitic clay (bentonite chocolate clay). Before being incorporated as clay nanoparticles in PBT resin, the clay was organically modified by the addition of a quaternary salt and sodium carbonate. PBT/Clay nanocomposite (96.3:3.70 wt %) was obtained by using a twin-screw extruder machine. After extrusion process, the nanocomposite was characterized by tensile, flexural and impact tests, SEM, Vicat, HDT, DSC, TGA and XRD tests. The results showed that the properties of the nanocomposite obtained were superior to those of neat PBT. Concerning the temperature of thermal distortion (HDT) an expressive gain of around 45 % was presented to PBT/Clay nanocomposite compared to PBT evidencing the interaction of nanofiller with the polymeric matrix.

P-15: Removal of Pb(II) by Modified Watermelon Peel Adsorbent: *Kai Huang*¹; *Lianyun Liu*¹; *Bo Jiang*¹; *Hongmin Zhu*¹; ¹University of Science and Technology Beijing

Watermelon peel is selected as a novel adsorbent to remove Pb(II) from aqueous solution. A simple saponification process is proposed to modify the peel and the adsorbent is characterized by SEM and FTIR. The effects of pH, contact time, initial concentration of Pb(II), biosorbent dosage and temperature on adsorption of Pb(II) are investigated. Different models are used to fit experimental data and indicating that the adsorption process follows Langmuir model and pseudo-second-order model. The maximum adsorption capacity obtained from Langmuir model is 1.05mol kg⁻¹ for the prepared sorbent. Equilibrium time is attained at 5-10min for the studied concentrations. Thermodynamic parameters indicate that the adsorption process is endothermic and spontaneous. So the watermelon peel can be used as an effective and low-cost biosorbent for removal of Pb(II) from aqueous solution.

P-16: Sulphuric Acid Leaching Germanium from Germanium Dust and Fume: Process Optimization Using Response Surface Methodology: *Wankun Wang*¹; *Jinhui Peng*¹; *Zebiao Zhang*¹; *Shixing Wang*¹; ¹Kunming University of Science and Technology

Germanium leaching from germanium dust and fume was carried out using sulphuric acid. Response surface methodology, based on a five level, four variable central composite designs, was employed to obtain the best possible combination of liquid/solid ratio, leaching time, sulphuric acid concentration and leaching temperature for germanium leaching. The experimental data obtained were fitted to a one-order polynomial equation using multiple regression analysis and also were analyzed by analysis of variance. The 3-D response surface plot and the contour plot derived from the mathematical models were applied to determine the optimal conditions. The conditions were: liquid/solid ratio of 10, leaching time of 1 h, sulphuric acid concentration of 15.75 mol/L, and leaching temperature of 87.8 °C. Under these conditions, the germanium leaching rate was 65.14%, which is well in close agreement with the value predicted by the model. The samples were characterized before and after leaching using X-ray diffraction.

P-17: Surfaces Improvement by Mecano-Chemicals Processes: *Isaias Hilerio*¹; *Miguel A. Barrón*¹; *Roberto T. Hernández*¹; *Alejandro Altamirano*¹; ¹UAM Azcapotzalco

The principal objective of finishing surfaces is protect and/or decorate them. This can obtain by adding or removing material of the work surface.. In this work we'll be interested in develop the improvement of surfaces by remotion of material. The Barreling or Polishing by Friction Method is utilized. The process is based in the rubbing or friction by abrasives. The pieces are arranged in the barrel with a natural or synthetic abrasive and an additive. The machine produces a rotating movement on the pieces. The rubbing action is developed when the superior layer of the charge is sledged to the inferior extreme when the barrel rotates, which can be hexagonal or octagonal to facilitate the skidding of the charge. To rotate the barrels is used an impulsion with wheel spindle or rolling pins, that the can be ride horizontally or tilted to produce an additional movement of the charge.

P-18: The Effect of Temperature on Complex Permittivity and Microwave Absorption Properties of an Ilmenite Concentrate at 2450MHZ: *Chenhui Liu*¹; *Libo Zhang*¹; *Jinhui Peng*¹; *Bingguo Liu*¹; *Hongying Xia*¹; *Wei Li*¹; ¹Key Laboratory of Unconventional Metallurgy, Kunming University of Science and Technology

Dielectric property is an important limiting factor in the development of microwave processing minerals and ores. In this study, we used an open-ended coaxial sensor method to measure the complex permittivity of an ilmenite concentrate (41%TiO₂) and microwave absorption properties from room temperature to 100 °C. The results show that both the dielectric constant and loss factor increase with temperature rising at 2.45GHz, the loss tangent have a linear relationship with temperature at 2.45GHz. Microwave absorption properties of this ore are highly dependent on temperature and frequency. The research will be helpful in explaining the thermal running of microwave dielectric heating the ilmenite concentrate.

P-19: Thermal Characterization of Jute Fibers by TGA/DTG and DSC: *Isabela Silva*¹; *Victor Silva*¹; *Alice Bevitori*¹; *Sergio Monteiro*¹; ¹UENF

Several natural fibers are increasingly being considered as viable alternatives to substitute glass fiber in polymer composites reinforcement. In practice, lignocellulosic fibers extracted from plants have shown a real potential for this substitution. Their comparative advantages are lower density an cost as well as renewability, biodegradability, recyclability and neutrality with respect to CO₂ emission, which is responsible for global warming. By contrast, the thermal resistance of the lignocellulosic fibers is restricted and may affect their application in engineering composites.

Jute fibers is worldwide used in many single items and is now considered for composite reinforcement. The mechanical proprieties of the jute fiber has been extensively investigated but only limited works have been devoted to its thermal characterization. The present work investigated these characterization in terms of thermo-gravimetric analysis TGA/DTG and differential calorimetry, DSC. It was found that the jute fiber starts deteriorating around 150°C and undergoes total degradation at 500°C.

P-20: Thermal Decomposition Kinetics of the Thermal Decomposition Products of Ammonium Heptamolybdate Tetrahydrate in Air and Inert Gas Atmospheres: *Hande Çavusoglu*¹; Cem Kahruman¹; Ibrahim Yusufoglu¹; ¹Istanbul University

In this study, decomposition intermediate solid products of ammonium heptamolybdate tetrahydrate were obtained and thermal decomposition reaction kinetics were investigated under air and inert gas atmosphere, using nonisothermal thermogravimetric analysis, differential thermal analysis and mass spectrometry and isothermal thermogravimetric analytical techniques and activation energies, frequency factors were calculated and appropriate kinetic models were proposed. The characterization of the intermediate solid products obtained in each decomposition step was carried out by X-ray Powder Diffraction and Fourier Transform - Infrared analytical techniques.

Ultrafine Grained Materials VII: Poster Session

Sponsored by: The Minerals, Metals and Materials Society, TMS Structural Materials Division, TMS/ASM: Mechanical Behavior of Materials Committee, TMS: Nanomechanical Materials Behavior Committee, TMS: Shaping and Forming Committee
Program Organizers: Suveen Mathaudhu, U.S. Army Research Office; Xiaoxu Huang, Risø National Laboratory for Sustainable Energy, Technical University of Denmark; Hyoung Seop Kim, POSTECH; Terence Langdon, University of Southern California; Terry Lowe, Manhattan Scientifics, Inc.; Ruslan Valiev, Ufa State Aviation Technical University; Xiaolei Wu, Institute of Mechanics, Chinese Academy of Sciences; Michael Zehetbauer, University of Vienna

Monday PM
March 12, 2012

Room: Atlantic Hall
Location: Dolphin Resort

T-1: Application of High-Pressure Torsion for Thick Samples: *Hideaki Iwaoka*¹; Zenji Horita¹; ¹Kyushu University

High-Pressure Torsion (HPT) is a powerful method to make ultrafine grains in materials. Although HPT is applicable to hard and less ductile materials, there is a practical limitation that it can be used only with samples typically less than 1 mm thick. Thus far, we have processed by HPT a high-purity Al with 4 mm thickness. It was shown that the strain was introduced more intensely in the center of thickness on the cross section. This area expands with increasing number of revolutions and expansion saturates before covering entirely. However, it is probable that this can be due to characteristic behavior of high-purity Al because its hardness decreases by intense strain. In this study, thick Cu or Al alloys samples are used, whose hardness does not decrease by intense strain for HPT processes. Microstructural observation across the thickness is carried out using transmission electron microscopy to correlate with hardness variation.

T-2: Bulk Ultra-fine Grained Materials from Reprocessed Machined Chips: *S Giribaskar*¹; Gouthama¹; ¹Indian Institute of Technology Kanpur

Focus of the present investigation is on the development of bulk ultra-fine grained materials by rotary swaging of plane-strain machined Al-Li alloy chips having ultra-fine grains. The premise is that machined chips are severely deformed during plane-strain machining process to have ultra-fine grains and it should be possible to obtain bulk ultra-

fine grained material by bottom-up approach. Hence efforts are made to develop bulk ultra-fine grained material by cold swaging process and optimal thermomechanical treatments. SEM is used to study the flow characteristics of material due to the shearing action during the plain-strain machining process. TEM used to investigate the microstructural characteristics of as-machined chips and as-swaged chip compacts. It has been shown that the chips formed are having grains in the size range from sub-micron meter to nanometer range. Microstructural evolution in as-machined chips and swaged compacts before and after optimal annealing treatments are also presented and discussed. Present study suggests that machining might be an attractive processing route for producing bulk materials with ultra-fine structures.

T-3: Carbide Free Bainitic Steel: *Xiaoxu Zhang*¹; ¹McMaster University

Carbide-free bainitic steels exhibit excellent combination of strength and ductility. The microstructure and mechanical properties are investigated in a steel containing 0.4%C-2.8%Mn-1.8%Si. The microstructure was characterized using optical and transmission electron microscopy. It consisted of bainitic ferrite, martensite and retained austenite, which are all in nano-scale. These microstructures exhibited a long elasto-plastic transition with very high initial work hardening rates and delay the onset of necking. Strain path reversals to measure the Bauschinger effect showed that this high hardening rate results from kinematic hardening due to the mechanical contrast of the microstructural constituents. The fracture properties were also investigated to reveal the importance of the prior austenite grain boundaries on the fracture process. The former austenite grain boundaries are believed to initiate fracture in the present materials. The fracture strength is improved by refining the prior austenite grain.

T-4: Characterization of Al-Al Laminates Processed by ECAP: *Sapthagireesh Subbarayan*¹; Hans Jorgen Roven¹; ¹NTNU

ECAP has been widely used to process Al alloys to produce ultra fine grained structures; however, the application of ECAP for the processing of laminates and bimetallics at room temperature has not been reported so far. The present work demonstrates the ability of ECAP for processing laminates using ECAP at room temperature. Al-Al laminates processed by ECAP at room temperature found to have bonded very well. Samples evolved with no interface and complete bonding was possible even after one pass. EBSD studies have been carried out to characterize the microstructure evolution to determine the grain size, grain shape structure and misorientation relationship. The effect of stacking, effect of strain, effect of back pressure and oxidation on the microstructure evolution has been studied. Microhardness was also investigated and correlated to the microstructure evolution.

T-5: Concurrent Structural Evolution of the FCC and BCC Phases in Duplex Stainless Steel Induced by High-Pressure Torsion: *Yang Cao*¹; Yanbo Wang¹; Xiaozhou Liao¹; Roberto Figueiredo²; Simon Ringer¹; Terence Langdon³; Yuntian Zhu⁴; ¹The University of Sydney; ²Federal University of Minas Gerais; ³University of Southern California; ⁴North Carolina State University

High-pressure torsion (HPT) has been the most effective severe plastic deformation technique for grain refinement to produce bulk nanostructured materials. Previous investigations of HPT processing concentrated mostly on single-phase materials or multi-phase alloys with only a small amount of secondary phases. However, many practical materials are of two phases with comparable volume fractions of each phase. Understanding how HPT processing will affect the structure and the mechanical properties of dual-phase materials is therefore very important. Here we apply transmission electron microscopy and scanning electron microscopy to investigate the microstructural evolution of a duplex stainless steel processed by HPT. The material comprises roughly the same volume fractions of the face-centered cubic austenite (the gamma phase) and the body-centered cubic ferrite (the alpha phase). The relative deformation of the two phases at different deformation stages will be presented in detail.



T-6: Dynamic Torsion Deformation of Ultrafine Grained Ferrite-Martensite Steel Fabricated by ECAP: *Hyunmin Kim*¹; Young Gun Ko²; Dong Hyuk Shin³; Sunghak Lee¹; ¹POSTECH; ²Yeungnam University; ³Hanyang University

The paper dealt with the dynamic deformation behavior of ultrafine grained (UFG) ferrite-martensite steel fabricated by equal channel angular pressing (ECAP) together with subsequent heat treatment. A martensite structure used as a perform microstructure was deformed by 4-pass ECAP and, then, heat-treated in an intercritical regime for 10 minutes, which would lead to the resultant microstructure consisting of ferrite and martensite grains of ~ 0.8 μm with their homogeneous mixtures. Dynamic torsion assessment utilizing Kolsky bar exhibited that the total strain of the UFG ferrite-martensite sample was approximately twice as large as that of the deformed martensite sample whilst the shear stress became lower with the introduction of multi-phase. In addition, observation of the localized area beneath the fractured surface revealed that adiabatic shear bands of ~ 20 μm appeared in the deformed martensite sample, which minimized the total strain, whereas they were barely formed in the UFG ferrite-martensite sample.

T-7: Effect of Preheating on Microstructure and Mechanical Properties of Ultrafine Grained AA1050 Deformed by Accumulative Roll Bonding (ARB) Method: *Kuiyu Cheng*¹; Cheng Lu¹; Lihong Su¹; Kiet Tieu¹; ¹University of Wollongong

Ultrafine-grained AA1050 sheets have been produced by accumulative roll bonding (ARB). Two ARB processes with and without preheating have been compared in this study. The preheated ARB process heated the specimens at 250°C for 3 mins prior to rolling. The microstructures of the ARB specimens at different positions along the thickness have been investigated by transmission-electron-microscope (TEM). It has been found that all ARBed specimens present strong rolling texture with elongated grains in the middle part of the sheet and roughly equiaxed grains near the surface regardless of the preheating. However, less grain refinement and more in-grain dislocations have been found in the preheated specimens. The bond strength test, tensile test and superplasticity test have been conducted in an Instron-type machine. The results showed that the preheating improved significantly bonding strength and slightly increased ductility at room temperature. However, the superplasticity behaviour seemed to be independent of the preheating.

T-8: Effects of Ageing after Cryogenic and Warm Rolling on Mechanical Properties of Al 6061 Alloy: *Nageswararao Palukuri*¹; Jayaganthan R¹; ¹IIT Roorkee

Cryogenic rolling conjunction with static ageing was used to develop high strength ultrafine grained precipitation hardenable Al 6061 alloy in the present work. Cryogenic (93K) and warm rolling (418 K) followed by the static ageing treatment (393 K for 60 hrs) were used for the simultaneous improvement of strength as well as ductility of Al 6061 alloy. It was found that micro hardness and tensile strength (119 HV, 365 MPa) of combined cryogenic and warm rolled specimens are more than cryorolled specimens (101HV, 295 MPa) alone. Based on XRD, DSC and TEM observations, it may be concluded that the improved mechanical properties are attributed to faster dynamic ageing than dynamic recovery during warm rolling, which leads to slight decrease in dislocation density. Post deformation ageing treatment was given for precipitation of the retained second phase in solid solution in order to increase the strength and ductility by static recovery.

T-9: Effects of Ball Milling and High-Pressure Torsion for Improving Mechanical Properties of Al-Al₂O₃ Nanocomposites: *Maki Ashida*¹; Zenji Horita¹; ¹Kyushu University

Powder consolidation is feasible using HPT and thus makes it possible to produce a bulk form of metal-ceramic nanocomposites at lower temperature. In the present study, effects of Ball Milling and HPT process on the mechanical properties and microstructure of Al-Al₂O₃ nanocomposites were investigated. Powder mixture of Al-30vol%Al₂O₃ was processed by BM for 100-200 min at a rotation speed of 200-400 rpm.

The mixture was then consolidated by HPT at room temperature under a pressure of 3.0 GPa for 10 revolutions. For comparison, the Al-Al₂O₃ composites were prepared by HPT without BM. Microstructures were characterized by optical microscopy and transmission electron microscopy including X-ray diffraction analysis. Density, Vickers microhardness were also measured. By applying BM at 300 rpm, the HPT-processed ring sample showed a uniform dispersion of nano-sized Al₂O₃ particles in the Al matrix. Hardness was enhanced by BM and HPT in comparison to that processed by HPT without BM.

T-10: Effects of High-Pressure Torsion Parameters on the Microstructure and Mechanical Properties of Bulk Metallic Glasses: *Bal Bashyal*¹; Yanbo Wang¹; Dongdong Qu²; Megumi Kawasaki³; Xiaozhou Liao¹; Simon Ringer¹; Terence Langdon³; Jun Shen²; ¹The University of Sydney; ²Harbin Institute of Technology; ³University of Southern California

Although bulk metallic glasses (BMGs) have superior mechanical properties including high strength, high hardness and large elastic limit, their practical structural applications have been severely limited by their poor ductility due to shear localization and strain softening leading to catastrophic failure. Substantial efforts have been made to explore methods which improve the ductility of BMGs. In this presentation, we apply the quasi-constrained high-pressure torsion (HPT) technique with varying values of processing parameters (pressure and strain) to manipulate the structure of Zr-based BMGs and to explore the effect of structural change on the mechanical behaviour of the materials. X-ray diffraction, differential scanning calorimetry, scanning electron microscopy, focussed ion beam lithography, microindentation, and in-situ deformation transmission electron microscopy are used in this investigation.

T-11: Engineering Surface Microstructures Using Severe Plastic Deformation in Machining: *M. Ravi Shankar*¹; *Saurabh Basu*¹; Sepideh Abolghasem¹; ¹University of Pittsburgh

Machining processes are widely utilized in the manufacture of engineering components. Surface generation by material removal during chip formation in this process involves severe plastic deformation over a broad range of strains (1-10), strain-rates (10⁻¹⁰ to 10⁵) and thermomechanically-coupled temperature rises (ambient to ~melting temperature). Here, we present opportunities for endowing bulk metals with ultra-fine grained microstructures through combinatorial choices of strains, strain-rates and temperatures across this spectrum of thermomechanical conditions using machining. These include controlling grain and subgrain scale, distribution, grain-boundary structure, dislocation-densities etc. Opportunities for engineering novel multifunctional property combinations inherited from grain-refined surfaces, directly using machining are also discussed.

T-12: Enhanced Mechanical Properties of Ultrafine Grained Titanium Deposits Fabricated via High-Velocity Impacts of Micron-Sized Particles: *Gyuyeol Bae*¹; Jae-Il Jang¹; Changhee Lee¹; ¹Hanyang University

Kinetic spraying (or cold spraying) has emerged as a new and innovative particle deposition technique because the process operates at low temperature and high pressure compared with conventional thermal spraying processes. Micron-sized particles impacted subsequently at high velocities (i.e., subjected to severe plastic deformation) undergo strain-induced adiabatic heating, accompanied by shear instability. These thermomechanical characteristics of metallic particles upon impact at high strain rates enable both metallurgical bonds formation and microstructural refinement of the deformed particles. Especially, due to the low processing temperature and high deposition rate, this process is suitable for rapid production of oxidation sensitive materials, such as titanium. Here, we report randomly orientated equiaxed ultrafine- and nanocrystalline grains formed homogeneously over wide areas inside the kinetic-sprayed pure titanium deposits. Also, these features are analyzed through finite element simulations considering conductive heat transfer, and directly correlated to improved mechanical properties that were evaluated by microindentation and nanoindentation experiments.

T-13: Estimation of Friction under High Pressure – Application to High Pressure Tube Twisting (HPTT): *Arnaud Pougis*¹; Jean-Jacques Fundenberger¹; Laurent Faure¹; Sylvain Philippon¹; Roxane Arruffat¹; Laszlo Toth¹; ¹University Paul Verlaine

Severe Plastic Deformation (SPD) processes are used to obtain ultra-fine grain materials by achieving very high strain under hydrostatic pressure. The friction has to be very low in some process (ECAP) but very large for other (HPT, HPTT). Most of numerical analyses do not take into account the friction into the simulations. The contact is assumed to be stuck for HPTT processes. An experimental setup is presented to evaluate the coefficient of friction under high pressure. Numerical simulations are carried out to simulate the SPD process High Pressure Tube Twisting, the effect of the friction during the deformation and load requirement.

T-14: Evaluation of Hardness Homogeneity and Mechanical Properties in an Aluminum Alloy Processed by High-Pressure Torsion: *Shima Sabbaghiannrad*¹; Megumi Kawasaki¹; Terence Langdon¹; ¹University of Southern California

Processing by high-pressure torsion (HPT) was performed on Al-7075 alloy samples at room temperature. The alloy was annealed at 480°C and processed by HPT under a pressure of 6.0 GPa up to 10 turns. Vicker's hardness values obtained from the samples show that the hardness value is lower at the center of all the samples and higher as it moves farther from the center, moreover an increase in the hardness is observed by increasing the number of turns in HPT. Mechanical testing and microstructural analysis support the results obtained from the hardness testing.

T-15: Fatigue Behavior of Friction Stir Processed Ultrafine Grained 8242 Al Alloy: *Mageshwari Komarasamy*¹; Nilesh Kumar¹; Rajiv S. Mishra¹; ¹Missouri University of Science and Technology

The ultrafine grained (UFG) microstructure in 8242 Al alloy was produced by friction stir processing. The cyclic properties of UFG materials were evaluated using fully reversible bending fatigue and compared with the coarse grained microstructure. The microstructure of UFG material before and after cyclic deformation was characterized using orientation imaging microscopy. Particular emphasis was given to the role of microstructure on evolution of deformation structure. Transmission electron microscope was used to determine the dislocation structure in the tested samples. The influence of grain size on transition of fatigue mechanism from persistent slip band to persistent shear band is discussed. The fractured samples were inspected under scanning electron microscope to understand the failure mechanism in UFG material.

T-16: High Strength Al 6061 Alloy by the Application of Cryogenic and Warm Rolling: *Ui Gu Kang*¹; HoJin Lee¹; WonJong Nam¹; ¹Kookmin Univ.

The ultrafine-grained Al 6061 alloy which was fabricated by the combination of cryogenic rolling with warm rolling, exhibited high strength, ultimate tensile strength, 420MPa. The strengthening effect was compared with the results by other severe plastic deformation methods. This notable increase of tensile strength was achieved by the formation of fine precipitates during warm rolling. The presence fine precipitates of diameter below 100nm, in ultrafine-grained matrix, were confirmed with TEM and STEM. Estimated precipitation-strengthening by the fine precipitates was approximately 150 MPa. Based on the results, it was found that the cryogenic rolling combined with warm rolling would be effective in increasing strength and expanding application area in industries.

T-17: Influence of Deformation Route on Microstructure Evolution of Ferrite Steels via Shear Rolling with Differential Speeds: *Jae Sik Lee*¹; Jordan Suharto¹; Young Gun Ko¹; ¹Yeungnam University

The effect of deformation routes on microstructure evolution of ferrite steels fabricated by differential speed rolling (DSR) was investigated in this study. Under the DSR condition giving an effective strain of ~0.4 per each passage through the rolls whose speed ratio was 1:4 for

lower and upper rolls, respectively, samples were rotated using three different routes such as no rotation, vertical 180° rotation, and vertical-horizontal 180° rotation, which were designated as routes A, B, and C. Microstructural observation using electron back-scattered diffraction and transmission electron microscope showed that the role of shear deformation on microstructure change in ferrite steel was pronounced. In addition, mechanical assessment was analyzed in terms of micro-hardness and tension tests at room temperature and discussed in relation to shear characteristics determined by DSR routes.

T-18: Influence of Texture on the Strength and Fracture Behavior of Severe Plastically Deformed Nickel: *Georg Rathmayr*¹; Reinhard Pippan¹; ¹Erich Schmid Institute of Materials Science

Severe plastic deformed (SPD) materials are of particular interest due to their interesting mechanical and physical properties. For example, SPD materials exhibit high yield stresses by simultaneously keeping a high elongation to failure which is clearly contrary to conventional cold worked materials. During SPD deformation, a shear texture develops in the final microstructure. In the current work we focused on the texture influence on the strength and fracture behavior of high purity SPD deformed nickel which was investigated by using different oriented macro tensile samples. We used nickel because it is a "model material" in the SPD community. Beside the results of the orientation dependency of the mechanical properties, the limiting factor of inclusion on the ductility is outlined. Furthermore, a detailed discussion about the influence of deformation temperature and the beneficial influence of carbon on the mechanical properties will be presented.

T-19: Influence of Ultrafine Grained Microstructure on the Superplastic Deformation Mechanism of 7075 Al Alloy: *Arum Mohan*¹; Partha De¹; Rajiv Mishra¹; ¹Missouri University of Science and Technology

Commercially available rolled 7075 Al plates were friction stir processed (FSP) to obtain ultrafine grained (UFG) material with average grain size of ~0.6 μm. Thermal stability of UFG microstructure was investigated to decide on the optimum temperature range for superplasticity. Tensile tests were done in the temperature range of 300-450°C in the strain rate range of 10⁻³s⁻¹ to 10⁻¹s⁻¹. The UFG test results were compared with fine grained FSP 7075 Al alloy with grain sizes ranging from 3 to 8 μm. In UFG 7075 Al, superplastic strain rate was higher and superplastic temperatures were significantly reduced compared to fine grained 7075 Al. Normalized stress versus normalized strain rate plot was used to compare the kinetics of superplastic flow in UFG and fine grained 7075 Al. Analysis of grain size dependence, stress exponent and activation energy revealed the role of grain boundary sliding in the superplastic deformation of UFG 7075 Al.

T-20: Microstructure and Mechanical Properties of 5005/6061 Laminated Composite Processed by Accumulative Roll Bonding: *Lihong Su*¹; Cheng Lu¹; Guanyu Deng¹; Kuiyu Cheng¹; Kiet Tieu¹; Xudong Sun¹; ¹University of Wollongong

The 5005/6061 laminated composite has been fabricated by the accumulative roll bonding (ARB) using commercial 5005 and 6061 aluminium alloy. In the ARB process. The materials were heated at 250 °C for 5 min before each rolling process and were deformed up to four cycles to an equivalent strain of 3.2 and form a 5005/6061 laminated composite. Mechanical properties and microstructure of the laminated composites were tested. The hardness and tensile strength increases and the grain size decreases with ARB cycles. Ultrafine grains elongated along the rolling direction are developed during the ARB process. The thickness of the grains of both the 5005 and 6061 layer are less than 200 nm after the fourth cycle. The uniform elongation decreases after the first and second cycle and increases slightly after the third and fourth cycle ARB. The hardness of the 5005 layer is slightly lower than that of the 6061 layer.



T-21: Microstructure Evolution in an UFG Al-7Mg Alloy Processed by ECAP during Subsequent Annealing: *Min Zha*¹; Yanjun Li²; Ragnvald Mathiesen²; Hans Roven¹; ¹Department of Materials Science & Engineering Norwegian University of Science & Technology (NTNU); ²Sintef, Materials and chemistry; ³Department of Physics, Norwegian University of Science & Technology (NTNU)

A binary Al-7Mg alloy has been processed by equal channel angular pressing (ECAP) via route Bc. After 5 passes ECAP, an ultrafine grained (UFG) material with an average grain size of $\sim 0.2 \mu\text{m}$ and a Vickers hardness value of ~ 205 is obtained. In order to study the thermal stability of the UFG alloy, a series of annealing treatments have been carried out. The microstructure evolution of the alloy during annealing has been characterized by transmission electron microscopy (TEM) and electron backscattered diffraction (EBSD). The recovery and recrystallization behavior of the alloy is discussed and also compared with the coarse grained Al-7Mg alloy processed by 3 passes ECAP.

T-22: Novel C-Extrusion towards Ultra-Fine Grained Aluminum: *Terje Hals*¹; Hans Roven¹; ¹Norwegian University of Science and Technology

The present highly novel approach explores the potentials for producing UFG commercial purity aluminium extrusions. The primary goal is to demonstrate grain refinement towards the sub-micrometer range. Variations in granular feedstock characteristics, deformation temperature, extrusion speed and accumulated strain are investigated. The produced materials are subjected to characterization methods such as FEG-SEM, high resolution EBSD, nano-indentations and mechanical testing. The obtained results are compared to similar material produced by conventional extrusion and standard ECAP performed at room temperature. It should be noted that the applied deformation processing method has the potential to be combined with ECAP, producing UFG materials in a continuous manner.

T-23: Plasmanitriding of HSLA Steels with Ultrafine Grained (UFG) Surface Layers: *Jennifer Schuster*¹; Enrico Bruder¹; Clemens Mueller¹; ¹TU Darmstadt

Linear flow splitting (LFS) is an innovative process to produce bifurcated profiles in integral style. Due to severe plastic deformation, an UFG-microstructure evolves. Because of their geometry, LFS-profiles are qualified for wear loaded applications as linear guides, which makes plasmanitriding of the profiles reasonable to increase their hardness and wear resistance. Up to now it is uncertain, to which extend the hardness of UFG-microstructures can be enhanced by nitriding and if the UFG-microstructure with its outstanding mechanical properties can be preserved during the nitriding process. The experimental results on different linear flow split HSLA steels clearly reveal that nitriding leads to a considerable increase in hardness, which is significantly more pronounced in UFG-microstructures than in classically cold formed microstructures. Furthermore it will be shown on the base of EBSD and HREM measurements that nitriding leads to a stabilization of the UFG-microstructure, so that nitriding becomes feasible even at 500 °C.

T-24: Production of High-Strength Ultra-Fine Grained Joints in AA2014 by Multiple Pass Friction Stir Welding: *Geo Harrison*¹; Preetam Anbukarasu¹; Ganapathy Subramanian¹; ¹College of Engineering Guindy, Anna University

AA2014 is one of the high strength and low density aluminum alloys having various industrial applications. Conventional welding processes yield unsatisfactory results in AA2014. Friction stir welding is an advanced joining process which can produce welds with appreciable mechanical properties. This process not only produces sound welds but also helps in reduction of grain size along the weld zone. When AA2014 T6 plates were subjected to multiple pass friction stir welding, joints with very high grain refinement and low grain size were obtained. The specimens also exhibited good tensile properties and micro-hardness values. Multiple-pass friction stir welding is a possible method for producing ultra-fine grained joints in AA2014 alloy.

T-25: Recrystallization Microstructure and Microtexture in an Ultrafine-Grained AlMgSi Alloy: *Aicha Loucif*¹; Thierry Baudin²; François Brisset²; Roberto Figueiredo³; Rafik Chemam¹; Terence Langdon⁴; ¹University Annaba; ²University Paris-Sud France; ³Federal University of Minas Gerais; ⁴Departments of Aerospace & Mechanical Engineering

Microstructure and microtexture evolution were experimentally studied using EBSD measurements during an isothermal annealing treatment at 250°C of an AlMgSi alloy. The alloy had an initial grain size of 150 μm and was subjected to high-pressure torsion (HPT) up to 5 turns under an applied pressure of 6.0 GPa. The processing by HPT refined the microstructure to a mean grain size of approximately 500 nm. The annealing treatment gave grain growth so that the grain size reached about 2.5 μm after 15 minutes. The results show the strength directly correlates to the grain size and decreases when the grain size increases. An orientation distribution function (ODF) calculation revealed an isotropic texture for the initial state. After deformation, the ideal torsion texture components, in particular the C {001}<110> component, tended to develop. The texture sharpness increased during the annealing temperature.

T-26: Repetitive Corrugation and Straightening Rolling as a State of the Art Bulk Deformation Procedure: *Arya Mirsepasi*¹; *Mahmoud Nili-Ahmadabadi*¹; Mohammad Habibi-Parsa¹; Hadi Ghasemi-Nanesa¹; ¹University of Tehran

Much attention has been directed recently to ultra-grain refining of metallic materials, where the grain size is reduced to less than 1 μm . It has been reported that ultrafine grains can be obtained by different methods of severe plastic deformation (SPD) such as equal channel angular pressing (ECAP), high pressure torsion (HPT), and accumulative roll bonding (ARB) as the most renowned ones. A recently developed SPD procedure called repetitive corrugation and straightening rolling (RCSR), has shown promising results in fabrication of UFG metallic materials to induce high strains after repetitive cycles. RCSR consists of corrugated rolls accompanying the capability of changing the position of the samples during different routes. Samples of Fe-Ni-Mn martensitic steel sheets were intensively deformed to a large accumulated strain by RCSR procedure. Microstructural and mechanical properties of the samples were studied by the aid of optical and scanning electron microscopy as well as mechanical testing.

T-27: Scaling up Equal-Channel Angular Pressing and its Effect on Billet Homogeneity: *Stephanie Hunger*¹; Martin F.-X. Wagner¹; Matthias Hockauf¹; ¹Chemnitz University of Technology

Equal-channel angular pressing (ECAP) is a well known method for the processing of ultrafine-grained materials. Recently, several attempts have been made to upscale this process from laboratory scale to industrially relevant dimensions. In the present study, we investigate the influence of upscaling ECAP on billet homogeneity for oxygen-free high conductivity copper. The material was processed up to 8 passes at room temperature in two similar tools with cross sections of 15 x 15 mm² and 50 x 50 mm², respectively. Post-ECAP hardness area plots from the longitudinal planes of the billets indicate the presence of similar gradients (in terms of the degree of plastic deformation) after both small and large scale ECAP. These findings are also supported by microstructural characterization using electron backscatter diffraction. Our study reveals an excellent reproducibility of microstructural features and mechanical properties after ECAP processing in laboratory and industrial scale.

T-28: Severe Plastic Deformation on Surfaces by Exploiting Transitions in Material Removal by Machining: *Yang Guo*¹; Narayan Sundaram¹; Srinivasan Chandrasekar¹; ¹Purdue University

It is shown using direct image correlation measurements that large strains can be imposed over regions extending hundreds of micrometers in depth by "machining" with highly negative rake angle tools. The key to this method of severe plastic deformation (SPD) on surfaces is suppression of chip formation and transitions to various forms of flow, wherein material displaced by the tool forms various types of stationary

“waves” ahead of the tool, as distinct from dead metal zones and chips. The conditions for establishing these waves, and the deformation imposed as the material traverses them are characterized by measurement and simulation. By compounding the deformations using appropriate tool designs, very large strains are imposed on the surface and into the depth. Ultrafine grained (UFG) microstructures consistent with the large deformation are observed.

T-29: Synthesis and Mechanical Properties of Cnt Reinforced Copper Based Nanocomposites: *Koteswararao Rajulapati¹; K Sreelatha¹; V V S Srikanth¹; K Bhanu Sankara Rao¹; ¹University of Hyderabad*

Copper and copper based alloys have widely been used for electrical and thermal applications due to their high electrical and thermal conductivity. However when copper was strengthened by grain refinement, electrical conductivity has come down due to grain boundary scattering. Therefore, in order to have materials with high electrical conductivity as well as high strength, efforts are made to reinforce nanostructured copper matrix with carbon nano tubes (CNTs). Owing to their high electrical and thermal conductivity, CNTs reinforcement into the copper matrix could improve the performance of composites. In the present work, CNT reinforced copper based nanocomposites are synthesized by ball milling and structural details are investigated by XRD, TEM and Raman analysis. This nanostructured Cu-CNT composite is sintered using uniaxial compression and/or Spark Plasma Sintering to achieve full density and mechanical properties are evaluated micro/nanoindentation. The salient features pertaining to the microstructure, electrical and mechanical properties will be presented.

T-30: Synthesis ,Microstructure and Mechanical Behavior of Bulk Nanostructured Cu-30%Zn Alloy by Spark Plasma Sintering of Cryomilled Powders: *Haiming Wen¹; Troy Topping¹; Enrique Lavernia¹; ¹University of California, Davis*

Powder metallurgy is widely used to synthesize bulk nanostructured metals. Cryomilling is one of the commonly used approaches to producing nanostructured metal powders. Spark plasma sintering (SPS) is an efficient consolidation technique. In this study we report on the synthesis of bulk nanostructured Cu-30%Zn alloy by cryomilling and subsequent consolidation of cryomilled powders by SPS, and microstructure and mechanical behavior of the consolidated bulk material. The results showed that cryomilling resulted in an average grain size of ~ 30 nm, and high density of deformation twins. Nearly full density was achieved after SPS. The sintered sample had a bimodal structure, with majority of grain sizes in the range of ~ 100 nm. A relatively high density of twins was retained after SPS. Mechanical tests showed that the sintered bulk sample had high strength and good ductility. The associated mechanisms were ascertained and discussed.

T-31: The Effect of Alloying with Hafnium on the Thermal Stability of Chromium Bronze after Severe Plastic Deformation: *Daria Shangina¹; Natalia Bochvar¹; Sergey Dobatkin¹; ¹A.A.Baikov Institute of Metallurgy and Materials Science, Russian Academy of Sciences*

The structure, microhardness, and electrical resistivity of the Cu-0.75%Cr and Cu-0.66% Cr-0.89%Hf alloys after high pressure torsion (HPT) have been studied. The alloys were deformed in two initial states: in the as-quenched state (T=900°C) and after annealing (T=600°C). The initial heat treatment of the Cu-Cr alloy affects the properties of the material after following heating: quenching compared to the annealing significantly increases the thermal stability of the alloy (up to 250°C and 150°C, respectively). It is shown that alloying with hafnium improves the properties of low-alloy chromium bronze, and the strengthening of the Cu-Cr-Hf alloy upon HPT is substantially higher than that of the Cu-Cr alloy, both for the “quenching + HPT” and “annealing + HPT” regimes. In the alloy with hafnium, the softening begins at substantially higher temperature (450°C), which is the same for both treatments. The work was supported by RFBR (project no. 10-08-00594).

T-32: The Effects of Deformation Strain and Temperature on Microstructures and Tensile Properties in a Commercial Purity Aluminium: *ShinWoong Jeong¹; Ho Jin Lee¹; Won Jong Nam¹; ¹Kookmin University*

The microstructures of a commercial purity aluminium (Al 1050) deformed at cryogenic temperature was investigated, compared with that deformed at room temperature. The microstructural evolution with increasing the deformation strain was investigated using transmission electron microscope for sample deformed at both temperatures. The results showed that the deformation at cryogenic temperature produced a higher work hardening rate than the deformation at room temperature at low strain. The difference of hardness might be attributed to the difference of the rate in accumulating dislocations during deformation. However, at high strain the difference of hardness between two deformation temperatures becomes negligible. This would come from the occurrence of dynamic recovery. In addition, the kinetic of softening behavior during post-deformation annealing was discussed with the data from differential scanning calorimeter.

T-33: Transmission Electron Microscopy and Synchrotron X-ray Texture Analysis of BCC Metals Processed by High Pressure Torsion: *Jonathan Ligda¹; Brian Schuster²; Yang Ren³; Qiuming Wei¹; ¹UNC Charlotte; ²Army Research Laboratory; ³Argonne National Laboratory*

Grain refinement by severe plastic deformation, specifically high pressure torsion (HPT), is capable of introducing large amounts of strain into disks with only millimeter dimensions, resulting in nanometer level grain sizes. However, this is an inhomogeneous process, creating a strain gradient between the center and edge of the disk. Differing amounts of total strain could lead to a change in the deformation texture and microstructure with position. Texture analysis of six body center cubic metals processed by HPT is done by collecting transmission Debye-Scherrer patterns at multiple locations across the sample disk. Studies are performed at the Advanced Photon Source in Argonne National Lab, using beamline 11-ID-C. Using a focused ion beam microscope, transmission electron microscope lamellas are also created at multiple locations to record any microstructure changes. The combination of methods allows for an accurate record of any microstructure changes, which could influence the mechanical properties of the material.

T-34: UFG-Surface Layer on DD11 Mild Steel Profiles Produced by Linear Bend Splitting (LBS): *Vanessa Kaune¹; Clemens Müller¹; ¹Technische Universität Darmstadt*

An approach to improve global properties of a component is the generation of an ultrafine grained (UFG) surface layer induced by surface severe plastic deformation (SSPD). Linear Bend Splitting (LBS) is a new continuous process, which generates bifurcated profiles in integral style from plain metal sheet. Due to the high deformation in the splitting zone, an UFG microstructure develops on the surface of the produced flanges up to a depth of several hundred microns. In the present paper, the linear bend splitting process will be presented with special regard to the SSPD aspects, leading to UFG micro structural gradients in the flanges. On the low alloyed mild steel DD11, the microstructure and the mechanical properties of the linear bend split profiles are investigated, using EBSD measurements, hardness indentations and tensile tests. From the results, some interesting technical applications of LBS will be derived.

T-35: Ultrafine Grain Refinement of Biomedical Co-Cr-Mo Alloy from Cryogenic Burnishing for Enhanced Wear Resistance: *S. Yang¹; Z. Pu¹; O.W. Dillon¹; D.A. Puleo¹; J.C. Outerio²; I.S. Jawahir¹; ¹University of Kentucky; ²Catholic University of Portugal*

Co-Cr-Mo alloy was subjected to a novel mechanical processing method-cryogenic burnishing; the surface of Co-Cr-Mo pins was burnished with a custom tool under a liquid nitrogen spraying condition. The processing led to a more than 100 μm thick surface layer with remarkably refined microstructures formed on the surface. From an initial grain size of 80 μm, an ultrafine-grained microstructure with a grain size of approximately 500 nm was obtained within this surface layer due to



severe plastic deformation (SPD) induced dynamic recrystallization (DRX) and effective cooling by liquid nitrogen. The grain refinement due to DRX was identified by means of scanning electron microscopy (SEM) observations. Large compressive residual stresses and deep compressive residual stress field (more than 200 μm) were identified on the surface and within subsurface layers by X-ray diffraction measurements. The wear performance of the cryogenically burnished pins was evaluated by pin-on-disc wear tests.

T-36: Unusual Martensite Decomposition in a UFG Cu-Al Alloy: *Guofan Zhang*¹; Xavier Sauvage²; Jing Tao Wang¹; Nong Gao³; Terence G. Langdon⁴; ¹NUST; ²University of Rouen; ³University of Southampton; ⁴University of Southern California

The phase decompositions of both coarse-grained and as-processed ultrafine martensite were investigated in Cu-11.8wt.%Al alloys. High Pressure Torsion (HPT) was used to process the alloy. The microstructures were characterized by optical microscopy (OM), X-ray diffraction (XRD), scanning electron microscopy (SEM) and transmission electron microscopy (TEM) and the microhardness of all states was measured. The results show that, before the $\beta' \rightarrow (\gamma_1 + \alpha)$ decomposition reaction, some transition phases appear firstly in the coarse martensite, while the ultrafine martensite skips the transition phase and the $\beta' \rightarrow (\gamma_1 + \alpha)$ decomposition reaction occurs directly in the early stage of annealing. It was also found that the decomposition of the ultrafine martensite is much faster than in the coarse-grained state although there are similar phases after annealing.

T-37: Wear Resistance of Nanocrystalline Cu-Diamond Composites Processed by High Pressure Torsion: *Eun Yoo Yoon*¹; Dong Jun Lee¹; Taek-Soo Kim²; Ha-Guk Jeong²; Chong Soo Lee¹; Hyoung Seop Kim¹; ¹POSTECH; ²Korea Institute of Industrial Technology (KITECH)

In this work, superior mechanical properties of nanocrystalline metal matrices embedded with diamonds were obtained by HPT. Neither heating nor sintering was required with the HPT process so that an in situ consolidation was successfully achieved at ambient temperature. Significant nanocrystalline structures by increasing diamond volume fractions were observed by EBSD. Hardness and wear resistance of the Cu-diamond nanocomposites are enhanced, compared to those of Cu matrix. The enhancement of the hardness is due to good bonding in Cu-diamond interfaces and high relative density of the nanocomposites. The diamonds Cu-matrix nanocomposite gives significantly enhanced wear resistance by retarding the peeling of Cu grains during sliding wear process. This study was supported by a grant from the Fundamental R&D Program for Core Technology of Materials (10037206) funded by the Ministry of Knowledge Economy, Korea.

General Poster Session: Session I

Sponsored by: The Minerals, Metals and Materials Society, TMS Electronic, Magnetic, and Photonic Materials Division, TMS Extraction and Processing Division, TMS Light Metals Division, TMS Materials Processing and Manufacturing Division, TMS Structural Materials Division

Monday PM
March 12, 2012

Room: Atlantic Hall
Location: Dolphin Resort

Session Chair: To Be Announced

W-1: A Novel Simultaneous Thermal Analysis (STA) Furnace with Tungsten Heating Element for Measurements under High-Purity Inert Gas Atmospheres and High Vacuum: *Ekkehard Post*¹; Bob Fidler²; ¹NETZSCH Geraetebau GmbH; ²NETZSCH Instruments North America, LLC

Many high-melting metals form metal carbides or also eutectic systems with carbon. By trying to determine the melting point of such metals by means of the differential thermal analysis (DTA) technique in a furnace with carbon heating elements, this value is often false or too low. This

is generally due to the carbon-containing atmosphere in these furnaces which can be explained by the considerable vapor pressure of the carbon at such high temperatures. This can also cause problems during melting of high-melting oxides. Here, premature decomposition can occur. A tungsten furnace, however, allows for an oxygen- and carbon-free atmosphere during DTA measurements and therefore yields the true values for the melting point and melting enthalpy. This poster illustrates the design of the furnace and STA instrument, respectively. With the example of measurement results on metals/ceramics, the differences in the results obtained with a graphite furnace and a tungsten furnace are presented.

W-2: A Study on Fatigue Strength of Railroad Truck: *Sung Cheol Yoon*¹; Jeongguk Kim¹; Sung Hyuk Park¹; Dong Hoe Koo¹; Kang Youn Choe¹; ¹Korea Railroad Research Institute

This paper describes the results of structural analysis and loading test of a truck frame. The purpose of the analysis and test is to evaluate the safety and functionality of the truck frame under maximum load. The truck system consists of the truck frame, suspensions, wheel-sets, a brake system and a transmission system. Among these components, the truck frame is the major component subjected to the vehicle and passenger loads. The truck frame, which is a running system for railway rolling stock, is a key structural part that supports the car body's load. And it significantly influences the safety of the passengers and the railway vehicle, running performance, and riding comfort. The performance test was conducted by installing the strain gauge where high stress is expected under each load condition, based on the result of the structural analysis.

W-3: A Study on Production of Fe-Cr-Ni-Ti Alloys by Metallothermic Processes: *Cem Colakoglu*¹; Murat Alkan¹; Onuralp Yücel¹; ¹Istanbul Technical University

This study covers information about Fe-Cr-Ni-Ti alloys production by metallothermic reduction of $\text{Fe}_2\text{O}_3\text{-Cr}_2\text{O}_3\text{-NiO-TiO}_2$ powder mixtures. Metallothermic reactions were realized by using a stainless steel SHS reactor. Different ratios of Cr/Ni/Ti were carried out in the metallothermic experiments, and addition of excess stoichiometric amount of Al_2O_3 powders were added to the initial mixture. The raw materials, alloys and slags were characterized by using XRD (X-Ray Diffractometry), and Scanning Electron Microscope (SEM).

W-4: Ab Initio Optical Properties of Orthorhombic CdGeO₃: *Eudencilon Albuquerque*¹; Umberto Fulco¹; ¹Universidade Federal do Rio Grande do Norte

The structural and optoelectronic properties of orthorhombic perovskite cadmium germanate CdGeO₃ was studied using quantum first principles calculations based on the density-functional theory (DFT) formalism, considering both the local density and generalized gradient approximations, LDA and GGA, respectively. Our results suggest that it has some features of a wide band gap semiconductor and that it is potentially useful for optoelectronic applications. The electronic part of the GGA dielectric constant for CdGeO₃ as a polycrystalline sample is 6.29, and the optical absorption presents its first pronounced peak due to electronic transitions from valence bands to conduction bands originated mostly from Ge 4s orbitals. A comparison with the corresponding results for CaGeO₃ orthorhombic is also performed, showing how the replacement of Ca (Pauling ionic radius 0.99 Å) with Cd (Pauling ionic radius 0.97 Å) modifies the electronic band structures and partial densities of states, as well as their optical properties.

W-5: An Investigation of the Electrochemical Properties of TiAlCrN PVD Coated in STS316: *Min-Seok Moon*¹; Kee-Do Woo²; Min-Goo Lee²; Je-Ha Oh³; Shin-Jae Kang⁴; Dae-Up KIM⁵; ¹Chonbuk National University, Jeonju Institute of Machinery Carbon Composites; ²Chonbuk National University; ³Jeonju Institute of Machinery and Carbon Composites; ⁴Chonbuk National University, Jeonju Institute of Machinery and Carbon Composites; ⁵Korea Institute of Industrial Technology

Bipolar plate is a key component of PEMFC and other Fuel Cell system, and it has a big portion of the weight and total cost of a fuel cell stack. Nowadays, many investigators consider replacement bipolar plate materials from non-porous graphite to the metallic bipolar plate. In this study, try to TiAlCrN nitride coating process on an austenitic stainless steel (STS316) by PVD technology (plasma enhanced reactive evaporation) to increase the corrosion resistance of the STS316. STS316 has good corrosion resistance in the atmosphere. This study is the focus on this coated material could potentially be used in PEMFCs as a bipolar plate material provided. It is also satisfying the physical and mechanical property such as the interfacial contact resistance, light weight, high mechanical strength and manufacturing ability.

W-6: Atomistic Simulations of Oxygen Diffusion in Alumina: Ulrich Aschauer¹; *Abhishhek Tewari*²; Paul Bowen²; ¹Eidgenössische Technische Hochschule Zurich; ²Ecole Polytechnique Federale de Lausanne

Understanding diffusion is a cornerstone in materials science. Nevertheless, solid state diffusion mechanisms are poorly understood even for well-studied systems, such as alumina. Previous simulation studies have failed to capture experimental observations, calculated activation energies being smaller than experiment. We developed a new approach based on the combination of Metadynamics and kinetic Monte Carlo simulations, to simulate oxygen vacancy diffusion in alumina. A set of highly correlated low energy transitions forms closed triangular loops, which do not contribute to macroscopic diffusion. Vacancy diffusion is governed by jumps with relatively higher activation energy, but still lower than that reported experimentally. The method was further developed for a fully periodic environment enabling the study of the atomic diffusion of oxygen in alumina, which allows us to compare simulation results with experimental Oxygen atomic diffusion plots. Effect of dopant/defect association is the focus of current study to explain the high experimental activation energies.

W-7: Bonding between Al and Cu by both Vacuum Hot Pressing and Solid-Liquid Hybrid Sheet Fabrication Process: *Kwang Seok Lee*¹; Yong-Nam Kwon¹; ¹Korea Institute of Materials Science

Cladding between dissimilar metals has attracted great attention indebted to their unique advantage for the viewpoint of multi-functionality. For example, Al/Cu bimetallic joint materials have advantages due to their excellent properties combining aluminum's lightweight, low density, corrosion resistance, with copper's high conductivity. However, aluminum surface is easily oxidized which hinders Al-Cu joint in metallurgical bonding. From bad to worse, various intermetallic compound (IMC) layers are usually generated on the Al-Cu interface at elevated temperatures, which causes detrimental effect on both mechanical properties and electrical conductivity of the entire hybrid composite. In order to overcome aforementioned drawback, we systematically investigated the possibility to bond between the dissimilar metals like Cu and Al using both the solid-based vacuum hot pressing and hybrid sheet fabrication technique by utilizing solid Cu-liquid Al. The influence of process conditions upon the interface microstructure and subsequent physical/mechanical properties for the entire composites was then discussed.

W-8: Characterization and Performance of Novel Amorphous Oxide Anodes for Chlorine Evolution in Industrial Electrolysis Using Chloride-Based Solutions: *Akari Miwa*¹; Masatsugu Morimitsu¹; ¹Doshisha University

This paper presents a novel amorphous oxide anode for chlorine evolution from chloride-based solutions used in industrial electrolysis such as chloro-alkali electrolysis, electrowinning, and electroplating. The amorphous oxide was produced by thermal decomposition of a precursor solution. The characterization of the oxide was carried out with XRD, SEM, and XPS. The performance of the anode was also investigated using aqueous solutions containing chloride ions, in which chlorine evolution is the main reaction on the anode. The results indicated that the developed anode showed a low chlorine overpotential comparable to commercially available dimensionally stable anodes with ruthenium and titanium composite oxides.

W-9: Characterization of an Aged Ti49Ni26Au25 Shape Memory Alloy: *Todd Butler*¹; Mohamed Abdalla²; B. Hornbuckle¹; Ronald Noebe³; Glen Bigelow³; Gregory Thompson¹; Mark Weaver¹; ¹Univ of Alabama; ²Tuskegee University; ³NASA Glenn Research Center

Ternary NiTi-X based alloys, where X = Pt, Pd, Hf, Au or Zr, show promise as high temperature shape memory alloys (HTSMAs). In comparison to binary NiTi alloys, some hypostoichiometric versions of these ternary compositions exhibit higher transformation temperatures and better mechanical stability due to the formation of nano-scale precipitates. In this study, Ti49Ni26Au25 (at.%) was solution annealed at 1050 °C for 3 hours and aged at 400 °C. Peak hardness was achieved after aging for 48 hours, which was slow in comparison to similar alloys with Pt and Pd additions. The structure and chemistry of the phases formed in this alloy were characterized by x-ray diffraction, transmission electron microscopy, scanning electron microscopy, energy-dispersive x ray spectroscopy, and three-dimensional atom probe tomography. The results will be discussed relative to other potential precipitate-reinforced HTSMAs.

W-10: Characterization of Oxide Bifilm Inclusion Defects in Vacuum Cast Ni-Base Superalloy: *Max Kaplan*¹; Gerhard Fuchs¹; ¹University of Florida

Oxide bifilms are reported to form during turbulent pouring of castings via furling of a thin skin of oxide that forms on the surface of the melt by reacting with residual environmental oxygen. This oxide is said to entrain into the bulk of the material, reside in the interdendritic region of the alloy, and unfurl and inflate by ingress of dissolved gasses to create casting porosity. It has also been reported that EDS is a viable technique for characterizing bifilms found in vacuum cast Ni-base superalloys. B1900 was used to investigate casting porosity and dendritic structures within casting porosity appearing to be coated by bifilms. Examination by SEM imaging and characterization by EDS were utilized. The results of this work did not indicate the presence of bifilms, and instead led to explanation of casting porosity with more conventional concepts.

W-11: Combined Cavitation and Particle Erosion of Brass: Amarendra H.J.¹; *Gajanan Chaudhari*¹; S.K. Nath¹; ¹IIT Roorkee

The material removal in hydraulic components may occur either by particle erosion or cavitation erosion or by the combined action of both. A novel method is employed that combines the effect of particle erosion and cavitation erosion, in order to test brass under laboratory conditions. Triangular prismatic bluff bodies are used as cavitation inducers in the conventional slurry pot tester. In the slurry pot the brass test specimens are exposed to water/slurry, with and without cavitation inducers. Analysis of the wear results reveals significant variations in material loss confirming synergistic erosion damage. Effects of the apex angles and positioning of the cavitation inducer with respect to the test specimen are systematically investigated.



W-12: Determination of Interfacial Heat Transfer and Air-gap Formation during ingot Casting into Permanent Metal Moulds: *Jason Swan*¹; ¹University of Birmingham

The formation of an air gap at the casting-mould interface during solidification significantly affects local cooling rates and the magnitude of heat transfer mechanisms. The thickness of the air-gap was investigated experimentally by optically measuring displacements of the mould and the casting surface during solidification of Aluminium and Nickel-based alloys cast into cylindrical grey cast iron moulds. Temperature measurements of the mould and casting allowed Interfacial Heat Transfer Coefficients (IHTC) to be calculated. The measured IHTC values were used to validate a numerical model of heat transfer and shrinkage during casting. It is predicted for the Nickel-based alloy when the air-gap is below 0.3mm heat conduction is the dominant heat transfer process; above 0.3mm radiation is the dominating factor. Due to the lower temperatures in Aluminium the transition from conduction being dominant to radiation is predicted to occur at 2.3mm; above the expected air-gap magnitude in these experiments.

W-13: Development of 3D Porous Nickel Electrodes for Hydrogen Production: *Valentín Pérez-Herranz*¹; *Isaac Herráiz-Cardona*¹; *Emma Ortega*¹; *José García-Antón*¹; ¹Universidad Politécnica de Valencia

The production of hydrogen is of particular interest because hydrogen is considered as a clean fuel. Hydrogen production via electrolysis of water from alkaline aqueous electrolytes is a well-established conventional technology. However, the high energy consumption retracts its large-scale application at present. This work focusses on the development of nickel electrodes with excessive surface areas. The construction of 3D porous structures was achieved by means of a hydrogen bubble dynamic template, prepared from electrochemical deposition processes. Cu was electrodeposited and grew within the interstitial spaces between the hydrogen bubbles to form a macroporous film of Cu nanoparticles on the substrate. Subsequently, a Ni layer was electrodeposited on the Cu template. The hydrogen evolution reaction was evaluated in alkaline media by means of steady-state polarization curves and electrochemical impedance spectroscopy. The developed electrodes exhibited a significantly reduced overpotential for the HER when comparing to the commercial smooth Ni electrode

W-14: Development of Fretting Fatigue Parameter: *Hyukjae Lee*¹; ¹Andong National University

New multi-axial, critical plane based, fretting fatigue crack initiation parameter is developed by the addition of a new term into the Modified Shear Stress Range (MSSR) parameter. The newly developed parameter (MSSR²) is then used to evaluate fretting fatigue life of titanium alloy, Ti-6Al-4V with various contact conditions. Finite element analysis is also used in order to obtain stress distribution on the contact surface during fretting fatigue test, which is then used for the calculation of fretting fatigue parameter. The MSSR² parameter shows better performance in predicting fretting fatigue lives from the conventional fatigue data, and less scattering within fretting fatigue data with different contact geometries.

W-15: Development of Ru_xTi_{1-x}O₂/Ti Anodes by Low Temperature Thermal Decomposition for Nickel Electrowinning: *Masaru Matsuda*¹; *Masatsugu Morimitsu*¹; ¹Doshisha University

Smart anodes, MSATM, consisting of a composite oxide, Ru_xTi_{1-x}O₂, formed on a titanium substrate for nickel electrowinning were developed by thermal decomposition of a precursor solution containing ruthenium and titanium compounds. Low temperature thermal decomposition produced less crystalline or amorphous composite oxides on the substrate, and such oxides showed a high catalytic activity for chlorine evolution and reduced the cell voltage of nickel electrowinning from chloride-based solutions. The effects of the thermal decomposition temperature on the crystallographic structure, the surface morphology, and the performance of the anode will be shown.

W-16: Effect of Al₂Ca Addition and Mg Content on Microstructure and Tensile Properties of Diecast Al-9Si-2Cu-Mg Alloys: *Jung Ho Seo*¹; *Nam-Seok Kim*¹; *Young-Ok Yoon*¹; *Shae K. Kim*¹; ¹Korea Institute of Industrial Technology

Al-Si-Cu-Mg casting alloys are widely used in the automotive components because of high fluidity and high corrosion resistance. Although it is well known that the strength of Al alloys increases with increasing Mg content, the Mg content is kept under 0.3 wt% in most current Al-Si-Cu-Mg casting alloys. That is because Mg-based oxides and hard inclusions which decrease melt fluidity and mechanical properties are formed more largely during alloying and casting due to the high oxygen affinity of Mg especially in mass production on-site. In this study, the effect of Al₂Ca addition and Mg content on microstructure and tensile properties of diecast Al-9Si-2Cu-Mg alloys were investigated. The ingots for high pressure diecasting were prepared from Al-9Si-2Cu with Mg master alloys containing Al₂Ca for the addition of Al₂Ca and high Mg in Al-9Si-2Cu. Microstructure and tensile properties of these diecast alloys were examined in comparison with those of conventional Al-9Si-2Cu-Mg alloys.

W-17: Effect of Be and CaO on the Ignition Resistance of Mg Melts: *Lee Jin-Kyu*¹; *Yang Won-Seok*¹; *Kim Shae K.*¹; ¹Korea Institute of Industrial Technology

Molten Mg and Mg alloys are easily oxidized and ignited without melt protective gases during melting and casting processes due to their high reactivity. There have been 3 approaches to overcome this problem. The molten Mg should be protected from oxidation by blanketing the surface with flux or protective gases. Beryllium is added into almost Mg alloys. It has been revealed to be very useful in terms of suppressed ignition of Mg melts, related melt cleanliness and ensuring safety during manufacturing and application. However, beryllium addition should be carefully handled due to its toxicity. CaO added Mg alloys (Eco-Mg alloys) can improve ignition resistance of Mg melts and melt quality. This paper will discuss the effect of beryllium addition on ignition resistance of Mg melts under protective gas atmosphere. The ignition resistance results were evaluated in comparison with those of CaO added Mg alloys.

W-18: Effect of Ca Addition on Creep and Mechanical Properties in Mg-4Zn Alloys: *Gun Young Oh*¹; *Hyun Kyu Lim*¹; *Shae K Kim*¹; ¹KITECH

Mg alloys exhibit a promising combination of properties including low density, high specific strength, stiffness, good process-ability, and adequate ductility. Because of these attractive properties, Mg alloys are considered to have a strong potential for weight saving in automotive and aerospace components. The researches on Mg alloys so far mainly concentrated on the improvement of strength and ductility of the conventional alloy systems such as AZ91 alloys. But Mg-Al alloy system is unstable for use at temperatures above 120°C because of its poor creep resistance and strength at elevated temperature. In the present study, the effect of Ca addition on creep and mechanical properties in Mg-4Zn alloys has been investigated. Creep properties of Mg-4Zn based alloys measured at 150°C under applied stresses of 80 MPa were improved with increasing Ca content. This result comes from the existence of thermally stable phases such as Mg₂Ca and Ca₂Mg₆Zn₃ phases.

W-19: Effect of Carbon on Structural Changes in Ni₃Al Phase: *Andrzej Janas*¹; *Ewa Olejnik*¹; *Beata Grabowska*¹; *Jacek Nawrocki*²; ¹AGH University of Science and Technology; ²WSK Rzeszow S.A.

The paper presents the X-ray diffraction and metallographic studies of carbon influence on structural changes in Ni₃Al phase. The base alloys were prepared maintaining the nominal atomic ratio of Ni/Al = 3:1. Next, carbon was instilled into the liquid alloy at a rate of 0.2, 0.25, 0.5, 0.75, 1 and 1.25 wt.% by weight for individual alloys, respectively. Final castings were cut into pieces and specimens were prepared for X-ray diffraction and microscopic studies. Their phase composition was analyzed together with structural changes occurring within the Ni₃Al phase. Some changes in the lattice constants of Ni₃Al phase were noticed, and they amounted to

0.3580 nm and 0.3589 nm for 0.2 wt.% C and 1.25 wt.% C, respectively. In the alloy containing 1.25 wt.% C, a graphite (001) atomic plane was noticed. This result was also confirmed by researches with SEM imaging, in which numerous graphite precipitates of lamellar and nodular shape were observed.

W-20: Effect of Carbon on Wear Resistance in Self-Lubricating Fe-Cr-C-Mn-Cu Alloys: Ki Nam Kim¹; Myung Chul Park¹; Gyeong Su Shin¹; Min Ho Shin¹; Seon Jin Kim¹; ¹Hanyang Univ.

Recently, because of safety and environmental concerns, there has been a tendency to use solid self-lubricating composites for bearing materials. In this study, we developed a Fe-Cr-C-Mn-Cu cast composite alloy as a self-lubricating composite and investigated the effect of carbon on the formation of protective tribofilms during sliding. The wear resistance of these materials is mainly affected by carbon concentrations because wear transitions from delamination to tribo-oxidation, reducing wear rate. The improved wear resistance likely results from protective tribofilms that form on the surface during sliding.

W-21: Effect of Dispersed SiC and Y2O3 Particles on the High-Temperature Oxidation of AZ91D Magnesium Alloys: Min Jung Kim¹; Chenguang Zhao¹; Seulki Kim¹; Dong Bok Lee¹; ¹Sungkyunkwan University

AZ91D magnesium composites containing SiC and Y2O3 dispersoids were cast, and their high-temperature oxidation was investigated in air. In case of Y2O3-containing composites, oxidation rates increased linearly, with an increase in the temperature and time. SiC particles did not oxidize during oxidation, and increased the oxidation resistance through diminishing the exposed surface area. With the increase in the amount of SiC particles from 5 to 10, and to 20 wt.%, the oxidation resistance increased. In case of SiC-containing composites, Al and Mg diffused into Y2O3 particles to form (Al,Y)O and to supersaturate within Y2O3. Although Y2O3 increased the oxidation resistance, the composite experienced rapid oxidation and burning, because non-protective MgO was the main oxide. Acknowledgement. This work is the outcome of "Environment-friendly and Energy-efficient Manufacturing Technology of Eco-Mg" program (No. 10035292-2010-01) funded by the Korea government Ministry of Knowledge Economy (MKE).

W-22: Effect of Hydrothermal Process on the Relative Surface Area of Porous Ni-Based BMG Foam: Ji Su Kim¹; Do-Hyang Kim²; Min-Ha Lee¹; ¹Kitech; ²Yonsei University

Metallic foams are under consideration as highly functional material, such as energy absorbers or ultra-lightweight, due to their porous structure combined with desirable strengths at relatively low densities. In current study, Ni-based metallic glass foams were fabricated by extruding powder mixtures comprised of metallic glasses blended with various kinds of fugitive phases followed by dissolution of the fugitive phases in an aqueous chemical solution to yield the final porous structure. The effect of surface treatment by hydrothermal process on the specific surface area in porous Ni₅₉Zr₂₀Ti₁₆Si₂Sn₃ metallic glass was investigated. As a result of hydrothermal reaction, intermetallic phases was growth on the surface of warm extruded porous Ni₅₉Zr₂₀Ti₁₆Si₂Sn₃ metallic glass under high pressure and temperature autoclave conditions during 12 hr, 24 hr and 48 hr, respectively. The characterization of hydrothermal processed Ni-based metallic glass foam was evaluated by SEM, XRD, DSC and BET method.

W-23: Effect of Porosity on Room Temperature Thermal Conductivity and Mechanical Properties of Porous Ti2AlC: Liangfa Hu¹; Sandip Basu²; Rogelio Benitez²; Ibrahim Karaman¹; Miladin Radovic¹; ¹Materials Science and Engineering Program, Texas A&M University; ²Department of Mechanical Engineering, Texas A&M University

The ternary compound Ti2AlC - one of the best studied materials from the MAX phase family - is a potential material for high temperature structures due to its high oxidation resistance and damage tolerance. Whereas, the properties of fully dense Ti2AlC have been well characterized, little is known about processing and properties of porous

Ti2AlC. In this work, we demonstrate a simple and inexpensive way to process porous Ti2AlC with controlled porosity and pore-sizes, using NaCl as the pore former. Porous Ti2AlC with porosity levels ranging from 5 to 75 vol.% and different pore-sizes, i.e 45-90 um, 180-250 um and 355-500 um, were successfully fabricated and characterized. The effects of porosity on the room temperature thermal conductivity, elastic moduli and compressive strength of porous Ti2AlC are determined. It follows that porosity becomes a useful microstructural parameter that can be used to tune thermal and mechanical properties of Ti2AlC.

W-24: Effect of Powder Morphology, Powder Preheating,

Nozzle Geometry on the Properties and Deposition Behavior of Titanium Coating in Cold Spray: Kee-Ahn Lee¹; Jae-Nam Hwang¹; Ji-Sang Yu¹; Hyung-Jun Kim²; ¹Andong National University; ²RIST

Cold spray deposition using Ti powder was carried out to investigate the effects of powder morphology (spherical and irregular), powder preheating (30°C and 500°C) and nozzle geometry (round and plate) on the coating properties such as deposition efficiency, porosity, hardness, and microstructure. The in-flight particle velocity of powder in cold spray process was directly measured using PIV equipment. The correlations of in-flight particle velocity with the coating properties were tried. Coating layer by using irregular morphology powder represents lower porosity, and higher deposition efficiency & hardness. Porosity also decreases and deposition efficiency and hardness increase with increasing pre-heating temperature. The particles using round nozzle shows higher in-flight particle velocity, thus results in better coating properties. The deposition mechanism of particles in cold spraying process was also discussed. [supported by "the program for the Industrial Strategic Technology Development" and "the program for the Training of Graduate Students in Regional Innovation", Korea]

W-25: Effect of Processing Parameters on Morphology of Electrodeposited CZTS Thin Films: Marilene Serna¹; Eguiberto Galego¹; Lalgudi Ramanathan¹; ¹CNEN-IPEN/SP

CZTS (Cu₂ZnSnS₄) thin films are viable materials for low-cost thin film type solar cells. The effect of electrolyte pH and temperature as well as deposition sequence on the morphology of electrodeposited CZTS films was studied. Control of CZT film morphology is essential to avoid loss of tin and to allow diffusion of sulfur during annealing. The three elements were electrodeposited on Mo foil, in stages from corresponding unstirred baths. In each bath, the pH was controlled by addition of sodium hydroxide and choline chloride. In-between baths with distinct pH, the substrate was dipped in dilute sulfidric acid. Comparison of micrographs suggests that sodium hydroxide and choline chloride helped smooth the surface of each layer in the stack.

W-26: Effect of Reactive Extrusion on the Mechanical Properties of PLA Blends: Gustavo Brito¹; Shirley Cavalcanti¹; Pankaj Agrawal¹; Edeleide Araujo¹; Tomás Mélo¹; ¹Federal University of Campina Grande - UFCG

Biodegradable polymers has attracted great attention in the latest years. Due to its characteristics, the poly(lactic acid) presents potencial to replace some petroleum-based polymers. Unfortunately, the inherent brittleness of PLA prevent it from practical applications. Blending PLA with other polymers presents a measure to obtain toughened polymers. However, most of the systems are immiscible, so they need to be compatibilized. An in situ reaction between the components during melt-blending, forming copolymers at the interface, is one manner to obtain a good compatibilization. In this study, attention was focused on the improvement of the mechanical properties of PLA, especially, impact strength. The PLA was blended with two flexible polymers, one with reactive groups and the other one without reactive groups. Mechanical tests and morphological analysis were carried out. The flexible polymers with reactive groups presented a better interaction between the components of the blend and greater impact strength.



W-27: Effect of the Seed Layer on the Growth of ZnO Nanorod Arrays: *Kyung-Bong Park*¹; Jun-Ho Shin¹; Hyukjae Lee¹; ¹Andong National University

ZnO nanorod arrays on the ZnO seed layer are synthesized for Dye Sensitive Solar Cell (DSSC). ZnO thin film as a seed layer is prepared by spin-coating, and the grain size and preferred orientation of the seed layer are strongly depend on the post annealing condition. These grain size and preferred orientation of the seed layer also affect the growth characteristics of the ZnO nanorod arrays, which grow on the seed layer using chemical bath deposition. Finally, the current-voltage characteristics of the DSSC using ZnO nanorods are measured with a solar cell test system.

W-28: Effect of Thiodiglycolamide Addition to Di-n-hexyl Sulfide on the Pd(II) Extraction Rate: *Hirokazu Narita*¹; Mikiya Tanaka¹; Shinji Ueno²; ¹National Institute of Advanced Industrial Science and Technology; ²N. E. CHEMCAT

For the palladium extraction, di-n-hexyl sulfide (DHS) has been widely introduced for practical use. Although they can selectively extract Pd(II) from acidic chloride solution, the Pd(II) extraction is very slow. Therefore, in this study, we investigated the effect of thiodiglycolamide (TDGA) addition to DHS on the extraction rate of Pd(II) from hydrochloric acid solutions. In the 0.1 M DHS (diluent: 80 vol% n-dodecane and 20 vol % 2-ethylhexanol)-5 g/L of Pd(II) in 1 M HCl system, it takes more than 240 min to attain the extraction equilibrium. In contrast, the Pd(II) extraction is accelerated by adding a small amount of N,N'-dimethyl-N,N'-di-n-octyl-thiodiglycolamide (MOTDGA): the extraction percentage of Pd(II) with 0.01 M MOTDGA-0.09 M DHS reaches almost 100% in the very short extraction time (= 5 min).

W-29: Effect of TiO₂ Composite Photoelectrode on the Photovoltaic Efficiency of Dye-Sensitized Solar Cells: *Kyung-Bong Park*¹; Jin-Il Park¹; Hyukjae Lee¹; ¹Andong National University

One-dimensional nanomaterials in dye-sensitized solar cells are expected to improve the electron transfer and light scattering, which can enhance the light-to-electricity conversion efficiency of dye-sensitized solar cell (DSSC). However, the reduced surface area of one-dimensional nanomaterials as compared to the nanoparticulates can be detrimental. Thus, TiO₂ nanoparticles/nanowire composite electrode was prepared by hydrothermal method in this study in order to improve the electron transfer without costing the high surface area. The experimental results showed that the DSSC made of TiO₂ nanoparticles/nanowire composite photoelectrode had better photovoltaic performance than those with TiO₂ nanoparticulate or nanowire photoelectrodes.

W-30: Effects of Different Gas Additions in Hydrogen for Hydrogen Storage Capacity on Li-Based Hydrides after Pressure Cycling: *Wen-Ming Chien*¹; Joshua Lamb¹; Dhanesh Chandra¹; ¹University of Nevada, Reno

Lithium imide/amide hydriding/de-hydriding pressure equilibrium isotherms were obtained at 255°C after cycling with different gas additions in hydrogen between Li₂NH and LiNH₂. The results showed that the nitrogen addition both improved the hydrogen capacity as well as improved the stability of the hydrides after cycling. Other results by using different gas additions in hydrogen showed the loss of the hydrogen storage capacity after cycling. After 560 pressure cycles, 100 ppm O₂ in hydrogen were most detrimental (0.4 wt%H₂ capacity remaining out of ~5.6 wt.%) as compared to 100 ppm H₂O in hydrogen gas (2 wt%H₂). It was found that 1.65 wt.% hydrogen remained after 500 cycles by using industrial hydrogen. The 100 ppmN₂ addition in H₂ improved the hydrogen storage capacity to 7.0 wt.% after 853 cycles, and for 20%N₂ in H₂, the capacity was improved to 9.0 wt.% after 516 cycles.

W-31: Effects of Heat Treatment on the Anisotropic Fatigue Behavior of Rolled Aluminum 2024: *Jaclyn Avallone*¹; ¹ASU

Fatigue crack nucleation and initial propagation in Al 2024-T351 exhibits anisotropic behavior, due to preferential alignment of inclusions and crystallographic orientations parallel to the rolling direction. However,

studying these effects individually is complicated experimentally. In this work, 2024-T351 samples were heat treated to the O condition to eliminate the effects of the initial temper, while keeping the alignment of the inclusions unchanged. Materials were first characterized using EDS and EBSD, followed by tensile and cyclic plasticity experiments performed in smooth samples to evaluate the plastic behavior of the two tempers. Finally, tests were performed in notched samples to study crack nucleation and short crack growth and their correlation to size and chemistry of broken inclusions, and crystal orientation of the grains containing the nucleation sites. The results are compared and discussed, with emphasis on the individual roles of inclusions and matrix plasticity on anisotropic fatigue behavior of rolled Al 2024.

W-32: Effects of Modified Sintering on Mechanical Properties of Nd-Fe-B Sintered Magnets: *Jin Woo Kim*¹; Se Hoon Kim¹; Sun Yong Song¹; Young Do Kim¹; ¹Hanyang University

Sintered Nd-Fe-B magnets have attracted considerable attention in recent decades for application in the motors of hybrid or electric vehicles due to their excellent magnetic properties. However, Nd-Fe-B permanent magnets have very low bending strength and fracture toughness, strictly limiting their use in such application areas. Many researchers have shown that the Nd-rich phase was essentially important for high mechanical properties. This study applied a modified sintering process to improve mechanical properties by controlling the Nd-rich microstructure in the production of Nd-Fe-B sintered magnets. Further, it examined the effect of change in the microstructure in accordance with sintering behaviors and process conditions on mechanical properties, thereby attempting to present optimal conditions of the sintering process.

W-33: Effects of Mo, W, Si on the Solid Particle Erosion Resistance of Austenitic Fe-12Cr-0.4C-5Mn-xMo/W/Si Alloys: *Ki Nam Kim*¹; Hye Won Kim¹; Jae Yong Yun¹; Jun Ki Kim²; Seon Jin Kim¹; ¹Hanyang Univ.; ²Korea Institute of Industrial Technology

Solid particle erosion (SPE), which implies the removal of material from component surfaces due to successive impacts of hard particles, has been recognized as a serious in various engineering applications such as hydrotransport lines, power plants and gas turbine blades. Recently, present authors confirmed that a strain-induced martensitic transformation (SIMT) improved abrasive, adhesive wear and cavitation erosion resistance in Fe-based alloys. While the mechanism of SPE is different from that of abrasive, adhesive wear and cavitation erosion, it was considered that the SIMT may have a significant effect on improving the solid particle erosion resistance by absorbing the impact energy of particles. The present study is a part of a project in which SPE resistance improves by applying a SIMT; the effect of Mo, W, Si on the SPE resistance of austenitic Fe-12Cr-0.4C-5Mn-xMo/W/Si alloys was investigated in terms of the SIMT.

W-34: Effects of Pulsed Magnetic Annealing on the Grain Boundary of Primary Recrystallized Microstructure in the Grain-Oriented Silicon Steel: *Junjun Huang*¹; Lihua Liu¹; Xin Xia¹; Xiang Jiang¹; Lijuan Li¹; Qijie Zhai¹; ¹Shanghai University

In this work, the effects of pulsed magnetic field applied during the annealing of grain-oriented silicon steel on the grain boundaries in the primary recrystallized microstructure were investigated. Samples of cold rolled grain-oriented silicon steel were annealed under pulsed magnetic field with the maximum strength 1T from three different directions-rolling direction, transverse direction and normal direction at the temperature of 700°C for 16 minutes. Electron Backscattering Scanning Diffraction (EBSD) technology was used to measure grains for texture determination, and software called Channel 5 was used to calculate the messages of boundaries. Results show that pulsed magnetic field can influence the development of grain boundaries. It is found that the frequency of the low angle boundaries increases when pulsed magnetic field is applied, especially from the rolling direction. Compared to the ordinarily annealed sample, the frequencies of CSL boundaries vary in samples annealed with pulsed magnetic field in different directions.

W-35: Elastic Properties of Ti-Nb-Ta-Zr-O Alloys: Masakazu Tane¹; Takayoshi Nakano²; Shigeru Kuramoto³; Masashi Hara³; Mitsuo Niinomi⁴; Naohisa Takesue⁵; Takeshi Yano⁵; Hideo Nakajima¹; ¹The Institute of Scientific and Industrial Research, Osaka University; ²Graduate School of Engineering, Osaka University; ³Toyota Central Research and Development Laboratories Incorporated; ⁴Institute for Materials Research, Tohoku University; ⁵Graduate School of Science, Fukuoka University

Elastic properties of cold-worked Ti-Nb-Ta-Zr-O alloys, referred to as Gum metal, were investigated with a focus on the effects of the oxygen concentration, electron-atom (e/a) ratio, and cold working process. The temperature dependence of the microstructures and elastic properties of single crystals and cold-worked polycrystals with different oxygen concentrations was analyzed, which revealed that Young's modulus increases upon 90% cold working due to formation of the ω (orthorhombic) martensite or ω (hexagonal) phase with high elastic modulus in the β (bcc) phase matrix. However, the Young's modulus after the cold working decreases with increasing oxygen concentration, because oxygen addition decreases the amount of the formed α'' and ω phases while retaining the low-stability phase. Therefore, cold working and oxygen addition achieve a low Young's modulus and high strength at the same time.

W-36: Electrochemical Capacitance of Polyaniline, Evaluated in Acid and Neutral Systems: Omar Martínez Alvarez¹; Ma. Concepcion Arenas Arrocena²; Héctor Hugo Rodríguez Santoyo¹; José Ulises Cruz Perez¹; ¹Universidad Politécnica de Guanajuato; ²Universidad Nacional Autónoma de México

Electrochemical capacitors (EC) are novel energy storage devices that possess high power density, exhibit excellent pulse charge/discharge property and very long life. The Polyaniline (PANI) is considered the most promising material in the supercapacitors due to its high capacitive characteristics, low cost and ease of synthesis. In this work we present a comparative study of charge storage in acid and neutral electrolytic systems 1M H₂SO₄ and 1M NaNO₃. The electrodes were prepared by electropolymerization of polyaniline (PANI) on the vitreous carbon. The surface morphology of electrodes was characterized by scanning electron microscopy (SEM) and atomic force morphology (AFM). The electrochemical properties of electrodes and the capacitive behavior of the electrodes were systematically studied using cyclic voltammetry (CV) and constant current charge/discharge tests. It is important to mention that the specific capacitance of PANI electrodes is strongly influenced by the electrolytic system used and is manifested in the responses obtained.

W-37: Electrochemical Recovery of Zinc Present in the Spent Pickling Baths Coming from Hot Dip Galvanizing Processes: Valentín Pérez-Herranz¹; Jordi Carrillo-Abad¹; Montserrat García-Gabaldón¹; Emma Ortega¹; ¹Universidad Politécnnica de Valencia

Hot dip galvanizing processes offer a simple and effective method for corrosion protection of steel. In this process, during the pickling step, HCl reacts with iron and iron oxides. Spent pickling baths contain hydrochloric acid, ZnCl₂ and FeCl₂ as principal compounds. Due to the inadequate existing techniques to treat the spent pickling solutions, the decrease of natural reserves of non-ferrous metals and the requirement of environmental protection, in the present work, the cathodic electrodeposition of zinc present in the spent pickling baths coming from hot dip galvanizing industries is studied. As the electrode potential was shifted towards more negative values, the fractional conversion increased. Simultaneously, the specific energy consumption decreased initially due to the increase in the zinc conversion rate but decreased for the most cathodic potential value due to hydrogen evolution reaction. Even though iron deposition does not take place for any experimental condition under study.

W-38: Electronic Transport in Quasiperiodic Graphene p-n-p Junctions: Manoel Vasconcelos¹; Luciano da Silva¹; ¹Universidade Federal do Rio Grande do Norte

Graphene is a promising candidate material for future microelectronic devices. It is a sheet of crystal carbon that behaves as a ballistic conductor with a long mean free path, that can be locally gated, whose interaction of carriers with electrostatic barriers is influenced by Klein tunneling. This effect has been studied for periodic potentials and the effect of disorder on the charge transport through multiple barriers has been considered. Here we investigate the interaction of charge carriers in graphene with a series of p-n-p junctions arranged according to a deterministic quasiperiodic Fibonacci sequence. Spectra of quasi-confined states are calculated for several generations of the sequence. Our results show that, as the Fibonacci generation is increased, the dispersion relation form energy bands distributed as a Cantor-like set. Besides, the electronic tunneling probability as a function of energy shows a large transmission peak for small incidence angles.

W-39: Estimating Stress Exponent of Advanced Materials through Spherical Indentation Creep Test: In-Chul Choi¹; Byung-Gil Yoo¹; Yong-Jae Kim¹; Moo-Young Seok¹; Jae-il Jang¹; ¹Hanyang University

Among various nanoindentation creep tests, the constant-load method using a sharp tip may be the most popular one. However, here it was found that there can be some difficulties in applying the method to estimate creep exponent, and thus we proposed a modified way to use a spherical tip. Both sharp and spherical indentation creep experiments were performed on nanocrystalline materials and metallic glasses that are known to show creep-like behavior at room temperature. The results suggest that spherical indentation creep may produce more reliable data than sharp indentation creep.

W-40: Evaluation of Mechanical Properties of Polymer Matrix with Bionanocomposites Poly (Lactid Acid) - PLA: Shirley Cavalcanti¹; Gustavo Brito¹; Pankaj Agrawal¹; Edcleide Araújo¹; Tomás Mélo¹; ¹UFMG

In the last 50 years from oil polymers have been widely used due to its versatility and relatively low cost. But oil is an exhaustible raw materials and polluting nature. In this context, Biodegradable polymers have attracted considerable attention. Poly (lactic acid) - PLA is a biodegradable polymer that has high fragility preventing its use in practical applications. For this reason, we used copolymers, methyl acrylate and glycidylmethacrylate in an attempt to improve some mechanical properties. Therefore mechanical tests and morphological analysis were performed. In general, we observed the formation of different morphologies directly interfered in the performance of mechanical properties.

W-41: Evaluation of Structural Strength in Tank Car: Sung Cheol Yoon¹; Jeongguk Kim¹; ¹Korea Railroad Research Institute

To check the structural strength of the body in the Tank car, load was added to the underframe of the Tank car. The objective of this study is to evaluate whether or not the underframe of a Tank car under the maximal strength is safe. The carbody of rolling stock is a principal structure that supports major equipment of the underframe and the tank freight. Therefore, the strength evaluation of this structure is important. Both structural analysis and loading test were performed under the loading condition. Prior to the evaluation of structural strength, finite element method was used for structural analyses on stress distribution in a carbody of a Tank car. The strain gauges were attached on the car based on FEM results. The test results showed that the carbody is safe under the condition of the designed load.

W-42: Evolution of Internal Strain and Microstructure in Depleted Uranium in the Presence of Hydrides: Elena Garlea¹; T. A. Sisneros²; D. W. Brown²; S. C. Vogel²; J. S. Morrell¹; ¹Y-12 National Security Complex; ²Los Alamos National Laboratory

The aging effects on mechanical behavior of depleted uranium in the presence of hydrides have been investigated by in-situ neutron diffraction. Cylindrical compression specimens of rolled depleted uranium were



charged with three different amounts of hydrogen, specifically 0 wppm, 0.3 wppm, and 1.8 wppm hydrogen, and tested at room temperature. The as-rolled condition was kept as reference. The strain measurements were carried out by in-situ uniaxial compressive loading, to 10% macroscopic strain, to monitor the evolution of lattice strain. Neutron diffraction strain results were coupled with bulk texture studies to understand the effects of hydrides on deformation modes responsible for the observed behavior. The investigation of microstructures developed during the hydrogen charging and loading process showed grain growth and enhanced twinning activity.

W-43: Existence of Niobium in Ductile Iron and Its Effect on the Morphology of Graphite Ball: *Sun Xiaoliang*¹; ¹ShangHai University

Niobium is a powerful carbide forming element, and its partial solid solution in austenite which improves the stability and quench-hardening ability of supercooled austenite. Niobium can refine grain and improve the mechanical properties in the role of the grey cast iron. However, published work on the effect of niobium on ductile is very few. This paper mainly studies the existence of niobium in ductile iron and its effect on graphite ball which was quantitatively analysed by the image analysis software. The results showed that, with the increasing amount of niobium, micro hardness of matrix increased obviously and the size and number of Nb-rich phase increased and enrichment of Nb-rich phase appeared. When addition of niobium was below 0.55 wt%, number and spheroidization rate of graphite ball was similar, but too much addition of niobium will decrease the number and spheroidization rate.

W-44: Experimental Indicators of Materials Processing Progress in Mechanical Alloying: *Priya Radhi Santhanam*¹; Edward Dreizin¹; ¹New Jersey Institute of Technology

Mechanical milling is widely explored to prepare advanced alloyed and composite materials. However, transfer of production from lab-scale to large scale manufacture is often ambiguous. Recently, a simplified approach was proposed, in which the rates of energy transfer to the material from milling tools were calculated for three different mills using discrete element modeling (DEM). These rates, taken as a function of the milling time, were correlated with the averaged rates of increase in the yield strength of an oxide reinforced composite. The results were encouraging and required additional validation. In the present study, correlations between the power consumption, torque, and rpm of an attritor mill and the powder refinement are examined. Such real-time indicators of milling progress do not require recovery of the powder samples and offer a convenient option for materials, for which measurements of yield strength are impractical.

W-45: Experimental Study on the Behavior of Slag Entrapment and Inclusion Removal in 44 ton Ladle with Argon Blowing: *Shu-Guo Zheng*¹; ¹Northwestern University

The powder entrapment and inclusion behavior in 44 ton ladle with argon blowing was studied in a water model. The effect of gas flowrate on powder entrapment in the ladle was investigated by choosing the mixture of kerosene and vacuum pump oil simulated as slag, and the effects of time and gas flowrate on inclusion removal were investigated by choosing emulsion drops simulated as inclusions. The results show that the critical gas flowrate for powder entrapment was 0.66 Nl/min, and the powder entrapment occurred continuously with those gas flowrates larger than 3.31 Nl/min. Most of the inclusions can be removed in eight minutes, and all the inclusions which can be removed almost disappeared from the system in twenty-eight minutes. The inclusion removal rate decreased first and then increased with the increase of gas flowrate. Furthermore, it had been found that the inclusion removal was in exponential relationship with gas blowing time.

W-46: Fabrication and Property Evaluation of Titanium Sputtering Target by Spark Plasma Sintering: *Hyun-Kuk Park*¹; Ik-Hyun Oh¹; Hee-Jun Youn¹; Jung-Han Ryu¹; ¹KITECH / Automotive Components Center

Spark Plasma Sintering is utilized to consolidate Titanium for sputtering target. Densification to near theoretical density in a relatively short time can be accomplished using this process. Sintered-body of Ti (Diameter

150, Thickness 6mm) with a relative density of up to 99.5% and average grain sizes of about 30 micro-meter without purity could be obtained by sintering temperature at 1000 for 5 min under a pressure of 50 MPa pressure. The sintered-body had specific resistance of $8.63 \times 10^{-6} \Omega \cdot \text{cm}$.

W-47: Fabrication of Lotus-Type Porous Copper by Centrifugal Casting Technique: *Yun-Soo Lee*¹; Hyeong-Tae Kim¹; Myoung-Gyun Kim²; Soong-Keun Hyun¹; ¹Inha University; ²Research Institute of Industrial Science & Technology (RIST)

A centrifugal casting technique was developed to fabricate, under low hydrogen pressure similar to atmospheric pressure level, lotus-type porous copper with long cylindrical pores aligned parallel to the solidification direction. The molten copper under a hydrogen gas pressure of 0.1MPa was poured into the mold using a rotational velocity of 200-1000RPM. The effects of rotational velocity on the porosity and the pore morphology were investigated. The porosity of each specimen fabricated by rotational velocity of 200-1000RPM was 55.4%-43.4% and the average pore diameter of each specimen was 338.3 μm -150.2 μm respectively. These results show smaller pore diameter than those of conventional fabricating process under 0.1MPa[1]. It is concluded that the centrifugal casting technique is a promising method for the manufacturing cost reduction and safety production of lotus-type porous metals. Reference [1] H. Nakajima, Prog. Mater. Sci. 52 (2007) 1091-1173.

W-48: Fabrication of Porous Cu by Freezing CuO/Camphor-Naphthalene Slurry: *Myung-Jin Suk*¹; Sung-Tag Oh²; Si-Young Chang³; ¹Kangwon National University; ²Seoul National University of Science and Technology; ³Korea Aerospace University

Porous Cu with macroscopically aligned channels was synthesized using a freeze-drying process. CuO powder and camphor-naphthalene alloy are used as the source material of Cu and sublimable vehicles, respectively. The slurry of camphor-40wt% naphthalene alloy mixed with CuO powders was prepared by milling at 60°C with a small amount of dispersant. Freezing of a slurry was performed in Teflon cylinder attached to a copper bottom plate cooled at -40°C while unidirectionally controlling the growth direction of the camphor-naphthalene vehicle. Pores were generated subsequently by sublimation of the camphor-naphthalene vehicle during drying. The green body was hydrogen-reduced at 200°C for 30 min, and sintered at 500°C for various time under a hydrogen atmosphere. Microstructural characteristics were analyzed by XRD and SEM. All of the samples showed porous structure after sintering, and composed of only Cu phase. Microstructural evolution depending on processing was discussed.

W-49: Fabrication of Sintered-Body Ti from Hydride Dehydride Ti Powder for Machine Tool and Its Mechanical Properties: *Ik-Hyun Oh*¹; Hyun-Kuk Park¹; ¹KITECH / Automotive Components Center

Spark Plasma Sintering method is utilized to consolidate Titanium from Hydride dehydride Ti powder. Densification to near theoretical density in a relatively short time can be accomplished using this process. Sintered-body of Ti (Diameter 100, Thickness 2mm) with a relative density of up to 99.8% and average grain sizes of about 60 micro-meter could be obtained by sintering temperature at 1000 for 5 min under a pressure of 60 MPa pressure. The average micro vickers hardness and tensile strength were about 350 kg/mm² and 350 MPa, respectively.

W-50: Finite Element Simulation of the Roll Forming Process of HSLA Steel Profiles: *Guadalupe Maribel Hernández Muñoz*¹; Patricia del C. Zambrano Robledo¹; Martha Patricia Guerrero Mata¹; Luis Leduc Lezama¹; ¹Universidad Autonoma de Nuevo Leon

A key part of the global economy is the automotive industry, which involves designing of automotive parts, optimizing processes and materials, among other things. The most important automotive parts are cold formed, manufactured mainly through the process of roll forming which is also considered highly productive for the manufacturing of profiles. The characteristics and properties for High Strength Low Alloy Steel makes it a widely used in the manufacture of various automobile

parts, such as rails, beams, braces, suspension arms and other parts. This paper presents the results of a numerical simulation using the element finite method with ABAQUS™, modeling of a symmetrical rectangular profile section from HSLA 50 steel, carried out by a cold forming process through rollers, also known as roll forming process. The parameters selected for this study are the roll forming line velocity and the inter-distance between roll stations. Results will allow optimization of the process.

W-51: First-Principles Coupled Calphad Modeling of BaO-TiO₂ and La₂O₃-TiO₂ Pseudo-Binary Systems: *Lei Zhang*¹; Chad Althouse¹; James Saal²; Dongwon Shin³; Shunli Shang¹; Yi Wang¹; Zi-Kui Liu¹; ¹Pennsylvania State University; ²Northwestern University; ³Oak Ridge National Laboratory

Compounds from BaO-TiO₂ and La₂O₃-TiO₂ have excellent dielectric, piezoelectric and electro-optic properties, making them competitive candidate materials for relevant applications. However, their thermodynamic properties have not been generated and made into database, though they are crucial for manufacturing those materials. In this research project, I searched all the experimental data and then modified the two pseudo-binary systems with assisting from First-principles calculation. Every compound from these systems has been defined with a reasonable thermodynamic description and phase diagrams are obtained. For BaTiO₃, a new sub-lattice model is used based on the latest defect reactions. The results can be readily used by industry as a reference for future manufacturing and other simulations such as phase field method.

W-52: Friction and Wear of AZ31B Magnesium Alloy during Sliding against Tool Steel: *Yong-Suk Kim*¹; Hyuk Woo Kwon¹; ¹Kookmin University

Galling is the most frequently observed surface damage during hot forming of magnesium alloys. This study was undertaken to examine tribological phenomena during sliding of tool steel against AZ31B Mg alloy and to find out formation mechanism of the galling. Reciprocating sliding of tool steel (AISI D2 and H13) against the Mg-alloy plate was carried out at various temperatures and normal loads. Surface roughness of the tool steel was also varied to see the effect of the roughness on the galling. Friction coefficient was measured during the sliding to monitor the interaction between the surfaces. To investigate the galling, surface of the tested Mg-alloy plate was examined by SEM and the friction-coefficient variation was analyzed. It was found that magnesium particles were transferred from the plate to the tool steel by asperity rupture and aggregation; they were oxidized to become hard oxide particles, which resulted in the galling.

W-53: Friction Stir Welding of High Melting Temperature Material Plate: *Sang-Hyuk Kim*¹; Kwang-Jin Lee¹; Ik-Hyun Oh¹; Kee-Do Woo²; ¹Korea Institute of Industrial Technology; ²Chonbuk National University

The friction stir welding (FSW) is a potential candidate for the joining of dissimilar and high melting temperature. However, to apply FSW in high melting temperature materials such as steel or Ti alloys etc., the tool with super heat-resisting and abrasion resistance are needed. And suitable parameters such as rotation speed of tool, travel speed are must considered. The tool material was manufactured by Spark plasma sintering method using WC-X%Co. Because WC have High melting point(2900°C), high hardness(1780Hv) and high elastic modulus(72,000kg/mm²). Diameter of shoulder and probe of the tool is 15 ϕ and 4.5 ϕ , respectively. The process parameters were : rotation speed, 500~700rpm ; travel speed, 60~180mm/min. the rotating probe travelled along the butt line between the two base materials. Optical microscope, Scanning electron microscope were applied to investigate the microstructure of weld region. Vickers-hardness, tensile test were carried out to analyze the mechanical properties of the joint.

W-54: Grain Refining Effect of Al₂Ca in A383.0 Al Alloy: *Nam-Seok Kim*¹; Jung-Ho Seo¹; Young-Ok Yoon¹; Shae K. Kim¹; ¹Korea Institute of Industrial Technology

Die casting, one of casting processes, has many advantages such as high productivity, excellent casting surface and possibility of making thin parts. Therefore, this process has widely been used from transportation equipment to electrical components. Especially, many Al alloy parts are manufactured by this method because they have good castability. In the A383.0 Al alloy, the strength increases with increasing Mg content. On the other hand, the Mg addition is limited under 0.1wt% since it accelerates the formation of Mg-based oxides and hard inclusions during alloying and casting due to its high oxygen affinity, causing the drop in the mechanical properties of alloys and melt fluidity. In this study, the results of Al₂Ca added A383.0 Al alloy about grain refining effect and mechanical properties were compared with those of conventional A383.0 Al alloy. Microstructure observation was carried out using OM and SEM. Mechanical properties were evaluated by tensile and hardness tests.

W-55: Heat and Moisture Transfer and Shrinkage during Drying of Ceramic Materials: *José Nascimento*¹; Ariosvaldo Sobrinho¹; Antonio Lima¹; Luiz Pontes²; Mirtes Carvalho³; Karla Campos⁴; ¹UFCEG; ²LMPC/UFPE; ³UAEC/UFCEG; ⁴UFCEG/LMI

This work reports a transient three-dimensional mathematical model to describe the simultaneous heat and mass transport and shrinkage. The model assumes to be constant thermo-physical properties and convective boundary condition at the surface of the solid. The governing equations were solved using finite-volume method and implicit fully formulation. The mathematical formulation was used to describe the drying of ceramic bricks, in the following air drying conditions: temperatures T=60, 80 and 110°C and relative humidity's RH=10.07, 4.66, 4.96, 2.30 and 1%, respectively. The experimental tests were made using two clay materials for production of red ceramic and white ceramic (ball-clay). Several results of the mean moisture content and temperature along the process are shown and analyzed. Numerical results were compared with experimental data and the transport coefficients were determined.

W-56: Hidrotalcite with Gentamicine, of the Type Mg_{0.68}Al_{0.32}(OH)₂(NO₃)_{0.32}•0.1H₂O, Formed by Chemical Coprecipitation in Controlled Atmosphere: *Hector Hugo Rodriguez-Santoyo*¹; Omar Martínez-Alvarez¹; ¹Universidad Politécnica de Guanajuato

This work consisted in the development for coprecipitation and characterization for X-ray diffraction of a hidrotalcite of the type Mg_{0.68}Al_{0.32}(OH)₂(NO₃)_{0.32}•0.1H₂O, capable of liberate in vitro gentamicin. The objective of this project was to generate a new material capable of remedy infections for the bacteria Staphylococcus Aureus, when this bacterium is introduced fortuitously in the body of a patient through of implants o prosthesis. A new method at the vacuum for condensation of vapor was developed of the hidrotalcite synthesis. Gentamicin was introduced in ionic clay, for a process of ionic interchange. The sensibility to the new product was tested in Staphylococcus aureus antibiograms. The results suggest a high sensibility of this kind of bacteria to the new product.

W-57: High Temperature Compressive Deformation Behavior of Ni-Fe-Cr-Al Based Porous Metal: *Sung-Whan Choi*¹; Jung-Yeol Yun²; Young-Min Kong³; Byung-Kee Kim³; *Kee-Ahn Lee*¹; ¹Andong National University; ²Korea Institute of Materials Science; ³University of Ulsan

This study investigated the high temperature compressive deformation (25°C~800°C) behavior of Ni-Fe-Cr-Al porous metal manufactured via powder process. Two different porous metals – 30 PPI (Pores Per Inch) and 40 PPI – were used. The densities were 0.49 g/cm³ for the 30PPI and 0.68 g/cm³ for the 40PPI material. Those materials were to consist of γ phase and Ni₃Al. The compression results, regardless of temperature, revealed typical three stages of deformation behavior (elastic, plateau, and densification region). At all temperatures, 40 PPI (a higher density) showed higher strengths than those of 30 PPI. However, the difference of strength continuously decreased with increasing temperature. Fractography



TMS 2012

141st Annual Meeting & Exhibition

revealed that the fine cracks easily propagated along interphase boundary in the strut regardless of deformation temperature and porosity condition. Based on these results, the mechanism of high temperature deformation of porous metal was also discussed. [Supported by the Fundamental R&D program for Core technology, Korea]

W-58: High Temperature Mechanical Behavior Fe-12Cr ODS Containing Nb: *SungSoo Kim*¹; Dae Whan KIM¹; Jin Sung Jang¹; ¹Korea Atomic Energy Research Institute

In order to increase operating temperature in next generation nuclear reactors, the oxide dispersion strengthened (ODS) alloy is promising for this purpose. The ferritic martensitic steel based on Fe-Cr ODS alloy is a candidate material due to the excellent resistance to neutron damage during service. Two kinds of Fe-12Cr-0.3%Y₂O₃ ODS with and without niobium were prepared by same process. The elemental powders were mechanical alloyed, and the ODS alloys were prepared by spark plasma sintering (SPS), HIP, and hot rolling. The high temperature tensile behaviors were investigated up to 800°C and compared. The effect of niobium addition on the mechanical behavior is pronounced at above 600°C. The 2% Nb addition improves the yield strength at 700°C by 50%. This seems to be due to the formation of fine intermetallic compound of Cr₂Nb and Fe₂Nb during high temperature deformation.

W-59: Hydrogen Absorption in CexGd1-x Alloys: *Joseph Bloch*¹; ¹NRCN

The effect of alloying on the thermodynamics of hydrogen absorption was studied for CexGd1-x alloys (0=x=0.5) at temperatures between 600°C and 800°C and for a pressure range 10-2 - 102 Pa. The terminal solubility of hydrogen in Gd is approximately four times higher than in Ce in the temperature range between 800 and 1000 K. At a given temperature, the hydrogen solubility and the terminal solubility were found to decrease with increasing x. This behavior is different than for substitutional solutions of the vanadium and the titanium groups for which the hydrogen terminal solubility increases with increasing solute concentrations. The heat of formation of the dihydride exhibits a pronounced maximum around x=0.3. This observation correlates with the presence of intermediate Sm-type (delta) phase around this composition. It is concluded that the hydride associated with the delta phase is considerably more stable than both cerium and gadolinium dihydrides.

W-60: Impact of the Sequence of Strain Hardening and Precipitation Hardening on Mechanical Properties of Grade 6201 AlMgSi Alloy Wire: *Beata Smyrak*¹; ¹AGH - University of Science and Technology

Precipitation-hardenable AlMgSi alloys grade 6101 of 0.5% Mg and 0.5% Si contents, are used for the construction of homogenous wires in overhead power lines. The suitability of these alloys lies in the characteristics of their electrical and mechanical properties within a wide range of heat treatment. Development of AlMgSi wires technology resulted in producers' competitive attempts to obtain more and more sublimated mechanical and electrical properties. The dominating group of alloys with increased electrical conductivity is the AlMgSi alloy group, these are HC, EHC and EEHC type materials with tensile strength at approximately 300 MPa and electrical conductivity lower than conventional wires (30nOm-31.2nOm). This paper is a comprehensive analysis of the technologies for the manufacturing of wires from AlMgSi alloys. It shows the possibility of shaping the mechanical and electrical properties of rods and wires.

W-61: Improved Room-Temperature Hydrogen Sensing Characteristics of Nanocrystalline Tin Oxide Through Fabrication of Nanowire Arrays: *Rameech McCormack*¹; Nozomi Shirato²; Amit Kumar¹; Umesh Singh¹; Hyoung Cho¹; Ramki Kalyanaraman²; Sudipta Seal¹; ¹Univeristy of Central Florida - MMAE; ²University of Tennessee Knoxville - MMAE

Tin Oxide (SnO₂) nanowire arrays were prepared on oxidized Si substrates by nanosecond pulse laser irradiation. Characterization of device using Atomic Force Microscopy showed the SnO₂ nanowires were of 20 nm in diameter and tens of microns in length. The SnO₂ nanowire

and precursor thin film were tested for sensing hydrogen gas from 6000-300 ppm. It was observed that the electrical response of nanowire was drastically improved compared to that of the thin films. The intrinsic properties due the SnO₂ nanowire structure correlates to simultaneous increases in the unbounded surface atoms and surface to volume ratios. Consequently, manipulation of the depletion layer and chemical reactions involved in sensing hydrogen gas are more pronounced. Thus, improved detecting capabilities towards hydrogen were observed. The fabricated SnO₂ nanowire arrays reveal potential for producing devices that have ultra-low detection limits for hydrogen gas also fast response and recovery time for real-life hydrogen sensing applications.

W-62: Industrial Use of a New Ultrasound Spray for Cooling and Wet Gas Treatment in the Pyrometallurgical Processes: *Milorad Cirkovic*¹; Vlastimir TRUJIC¹; Željko KAMBEROVIC¹; ¹Mining and Metallurgy Institute Bor

This paper presents the results of a new industrial use the ultrasonic spray for gas cooling from sulphide copper concentrate roasting in the fluo solid reactor and the results of wet gas treatment (washing) in the scrubber plant during treatment the secondary copper bearing raw materials in RTB Bor (Serbia). The use of a new ultrasonic nozzle for gas cooling from the fluo solid reactor resulted as a necessity because the efficiency of existing installed spray of foreign manufacture was very bad. The possibility of its dismantling (disassembly) has allowed a complete cleaning and reliable operation and the nozzles, currently used, are in a continuous operation over a decade. The new design of ultrasonic spray and its successful use for cooling and cleaning the metallurgical gases will be applied in modernization the Copper Smelter in RTB Bor.

W-63: Influence of Heat Treatment on the Corrosion of Steels in CCS Environment: *Anja Pfennig*¹; Sabrina Schulz¹; *Axel Kranzmann*²; Thomas Werlitz¹; Stephan Wetzlich¹; Enrico Bülow¹; Jan Tietböhl¹; Christian Frieslich¹; ¹HTW Berlin; ²BAM

With CO₂ being one reason for climate change carbon capture and storage (CCS) is discussed to mitigate climate change. When emission gases are compressed into deep geological layers CO₂-corrosion can easily cause failure of injection pipes. Differently heat treated steels used as injection pipe (X46Cr13, X20Cr13 and X5CrNiCuNb16-4) were tested in in-situ laboratory corrosion experiments where synthetic aquifer water was saturated with technical CO₂ at a flow rate of 3 l/h. After 1000 h of exposure time pits are found on all 3 with maximum pit heights around 20 µm. Corrosion rates obtained via mass loss vary in a wide range (0,005 to 2.5 mm/year). The least amount of pits is found on hardened steels with martensitic microstructure where X5CrNiCuNb16-4 shows less pits than X46Cr13 followed by X20Cr13. The complicated multiphase corrosion scale reveals FeCO₃, alpha-FeOOH, gamma-FeOOH, FeS and Fe₈O₈(OH)₈Cl_{11.34} as well as spinelphases of various compositions.

W-64: Influence of Hf on Inhibiting Precipitation in Ni-rich NiTiPdHf Shape Memory Alloys: *Anne Coppa*¹; Ron Noebe²; Glen Bigelow²; Mark Weaver¹; Greg Thompson¹; ¹The University of Alabama; ²NASA Glenn Research Center

The transformation characteristics of Ni-rich NiTiPd and NiTiHf alloys can be significantly improved through the formation of nanoscale precipitates. In the Ni-rich NiTiPd alloys, cuboidal precipitates denoted as the P-phase, have been observed. This phase has a monoclinic unit cell with laminate variant stacking. The precipitates observed in Ni-rich NiTiHf alloys are plate-like in morphology but specifics of the crystal structure have yet to be defined, though effort is continuing. In the present work, a Ni-47Ti-23Pd-2Hf was studied. In this quaternary alloy, precipitation of either phase or any other precipitate phase typically observed in Ni-rich NiTi alloys (i.e., Ni₄Ti₃, Ni₃Ti₂ or Ni₃Ti) was inhibited. Even after 300 hours of aging at 400°C, the matrix crystal structure remained B2. Although the alloy does not exhibit precipitation, an increase in hardness was observed with aging time. The results will be discussed in terms of atom probe tomography and transmission electron microscopy.

W-65: Influence of Process and Thermo-physical Parameters on the Heat Transfer at Electron Beam Melting of Cu and Ta: *Katia Vutova*¹; Veliko Donchev¹; Vania Vassileva¹; Georgi Mladenov¹; ¹Institute of electronics, Bulgarian Academy of Sciences

Electron beam melting and refining (EBMR) in vacuum is an ecological friendly method for metal purification, scrap regeneration and reuse of expensive metals and special alloys needed for all areas of human activity. The thermal transfer processes are important for production of metal blocks with good quality and the mathematical modeling is a tool for studying and control of these processes. The temperature variations of the thermal conductivity and the heat capacity for Ta and Cu are estimated and are taken into account in the presented heat model. Some results on the influence of the casting velocity, beam power and ingot dimensions on the heat streams through different boundaries and on the crystallization front shape for EBMR of Cu and Ta are presented and discussed. Calculated and experimentally obtained crystallization front forms are compared and a good correspondence is observed. Electron beam casting conditions for obtaining of good quality copper ingot are optimized.

W-66: Infrared Thermographic Characterization of Tensile Fracture in Railway Steels: *Jeongguk Kim*¹; ¹Korea Railroad Research Institute

The tensile fracture behavior of railway steels, which are used for railway vehicle components such as wheel, axle, bolster, etc., was characterized using the infrared (IR) thermographic method with a high-speed infrared camera. The tensile specimens were prepared from the actual railway vehicle parts, which were used for over 20 years. An infrared camera was used to monitor damage evolution during tensile testing in terms of surface temperature measurements. A qualitative image analysis was conducted to explain failure mode and mechanisms in different railway steel samples based on infrared thermographic images obtained during tensile testing. Moreover, the microstructural characterization using scanning electron microscope (SEM) was performed to correlate the mechanical failure mode with thermographic results. In this investigation, an IR camera and SEM characterization method were used to facilitate a better understanding of fracture behavior of different types of railway steels during tensile testing.

W-67: Investigating Strain-Induced Martensitic Transformation in Steel through In-Situ TEM Test: *Yong-Jae Kim*¹; *In-Chul Choi*¹; *Byung-Gil Yoo*¹; *Takahito Ohmura*²; *Jae-Il Jang*¹; ¹Hanyang University; ²National Institute for Materials Science

Strain-induced phase transformation from metastable austenite to martensite in steels has attracted lots of scientific and engineering interests due to a resultant mechanical improvement, i.e. the combination of high strength and good ductility. Although it is well known that the size of materials can affect their mechanical properties (such as strength and elastic modulus), there have been little efforts to investigate the strain-induced transformation behavior of steels in nano-scale. In this regard, we investigated the strain-induced martensitic transformation of steel in nano-scale with ex-situ and in-situ nanoindentation experiments. Examined material was a metastable austenite phase steel with a composition of Fe-0.04C-5Mn-12Cr (wt.%). The austenite-to-martensite transition was systematically analyzed with the indentation load-displacement data and the TEM images. Additionally, we compared the result of nanoindentation tests with that of macro uni-axial test and investigated the size effect of phase transformation behavior.

W-68: Investigation of the Polymer Composite Materials Reinforced by Hybrid Carbon and Basalt Fibers: *Nikoloz Chikhradze*¹; *Guram Abashidze*¹; *Levan Japaridze*¹; ¹Mining Institute/Georgian Technical University

Carbon fiber reinforced plastics are considered as high-costly materials. This circumstance highly decreases an economic efficiency of large-dimensional, materials consuming items and structural elements, including the blades of wind turbines, produced from these materials. To solve this problem in the paper the possibilities of the partial replace of the carbon fibers in the plastics by basalt fibers of local (Country Georgia)

production is considered. The basalt reinforcing elements was prepared from raw material with chemical composition: SiO₂ – 15,3%, CaO – 10,8%, Fe₂O₃ – 12,1%, CaO – 10,8%, Na₂O – 4,2%, MnO – 0,7%, TiO₂ – 0,7%. The strength on tension and compression, elasticity modulus and Poisson ratio of the composites prepared by the use of proposed hybrid reinforcing means and by various technologies were determined. In the work the results of the composites testing on bending, shift and fatigue are presented.

W-69: Laboratory Testing Results of Kinetics And Processing Technology of the Polymetallic Sulphide Concentrate Blagojev Kamen - Serbia: *Milorad Cirkovic*¹; *Željko Kamberovic*¹; *Vlastimir Trujic*¹; ¹Mining and Metallurgy Institute Bor

This work presents the laboratory testing results of kinetics the oxidation process and sample processing of the sulphide polymetallic concentrate Blagojev Kamen. Characterization of this raw material is based on the chemical analyses, XRD results, DTA analysis, etc. For these investigations, the sulphide concentrate with the following content was used, in %: Cu – 2.3; Fe – 19.8; S – 27.19; Zn – 9.13; As – 0.167; Pb – 15.63; SiO₂ – 17.93; CaO – 0.97; Al₂O₃ – 1.43; Ag – 480 g/t; Au – 659 g/t. Kinetic investigations of oxidation processes were carried out under isothermal conditions within the range of temperature from 400 to 625°C. Pyrometallurgical treatment of this type of polymetallic concentrate, in the laboratory conditions, was carried out using the oxidative roasting and then the reduction smelting was done in the Taman's furnace.

W-70: Manufacturing and Macroscopic Properties of Cold Sprayed Cu-Ga Coating Material for Sputtering Target: *Kee-Ahn Lee*¹; *Young-Min Jin*¹; *Byeong-Cheol Choi*¹; *Dong-Yong Park*²; *Hyung-Jun Kim*³; ¹Andong National University; ²Tae-Kwang Tech.; ³RIST

This study attempted to manufacture a Cu-Ga coating via the cold spray process and to investigate the applicability of the layer as a sputtering target material. Changes made to the microstructure and properties of the layer due to annealing heat treatment were also evaluated. The results showed that Cu-20%Ga coating layers could be manufactured via cold spray process. With the coating layer, the \149; -Cu and Cu₃Ga were found to exist inside the layer regardless of annealing heat treatment. With thermal treatment ongoing, the porosity and hardness tended to drop dramatically. A sputtering test was actually conducted using the sputtering target Cu-Ga coating layer (~ 2 mm thickness). It was confirmed that the cold sprayed Cu-Ga coating layer may be applied as a sputtering target material. [supported by “the program for the Industrial Strategic Technology Development” and “The Program for the Training of Graduate Students in Regional Innovation”, Korea]

W-71: Material Characterization of TRISO Particles Using Nanoindentation: *Jenny Martos*¹; ¹UC Berkeley

The mechanical properties of Tristructural Isotropic (TRISO) coated fuel particles, which are used in High Temperature Gas Cooled Reactors (HTGR), are being explored with the use of nanoindentation. The silicon carbide layer of the TRISO particle is considered to be the most important since it acts as a pressure vessel in order to contain gaseous and solid fission products and therefore must withstand high stresses during irradiation. Nanoindentation techniques are being explored to measure Young's modulus and hardness of the different layers in the TRISO particles. In addition, fracture toughness of the silicon carbide layer is measured using nanoindentation techniques. TRISO particles subjected to various processing parameters and sample treatments are being explored in order to investigate the effect on the mechanical properties.

W-72: Mechanical Properties of Nanocomposites Based on PA6 Blends: *Pankaj Agrawal*¹; *Gustavo Brito*¹; *Bartira Cunha*¹; *Shirley Nobrega*¹; *Edcleide Araújo*¹; *Tomás Mélo*¹; ¹Federal University of Campina Grande - UFCG

Nanocomposites based on Polyamide 6 (PA6) blends were developed using an organically modified clay (organoclay) and a compatibilizer. The nanocomposites were prepared in two steps. First, PA6 was pre-mixed



with the organoclay in an internal mixer forming a concentrate. In the second step, this concentrate was diluted in either PA6, PA6/EG or PA6/HDPE blends in a twin screw extruder. The degree of dispersion of the clay in the polymer was evaluated through X-Ray Diffraction (XRD) and Scanning Electron Microscopy (SEM). XRD Results indicated that for PA6/EG/CL20A and PA6/EG/HDPE/CL20A nanocomposites, a partially exfoliated structure was obtained. SEM analysis results showed that the organoclay is well dispersed in the polymers. The presence of the compatibilizer improved the impact strength of the blends and the nanocomposites.

W-73: Mechanical Behavior of Porous NiAl Fabricated by Unidirectional Solidification: *Ji-Woon Lee*¹; Soong-Keun Hyun¹; Mok-Soon Kim¹; Takuya Ide²; Hideo Nakajima²; ¹Inha University; ²Osaka University

Porous NiAl with porosity of 32.3% was fabricated by unidirectional solidification. The mechanical behavior of porous NiAl was investigated under compression tests at temperatures of 298K, 673K and 873K. Nonporous NiAl exhibited brittle behavior at temperature up to 673K. Porous NiAl, however, exhibited ductile behavior even at 673K. All specimens showed ductile behavior at temperature of 873K. Different behavior between porous and nonporous NiAl with regard to temperature can be attributed to crack tip blunting and dislocation escape through pores. Anisotropic mechanical properties between parallel and perpendicular solidification directions to the compressive direction were also shown in both porous and nonporous NiAl. This behavior is due to inherent anisotropy of NiAl and orientation of cylindrical pores especially in the case of porous NiAl. Crystallographic orientation of each solidification direction to the compressive direction was confirmed by electron backscattered diffraction.

W-74: Microstructural Characterization of Aged MAR-M247(Nb) Nickel-Based Superalloy: *Renato Baldan*¹; Carlos Nunes¹; Gilberto Coelho¹; Paulo Ricardo Azevedo Silva¹; ¹USP - University of São Paulo

MAR-M247 superalloy has excellent mechanical properties and oxidation resistance. The aim of this work is to evaluate microstructural changes in the MAR-M247(Nb) superalloy (10.2 wt % Co; 10.2 W; 8.5 Cr; 5.6 Al; 1.6 Nb; 1.4 Hf; 1.1 Ti; 0.7 Mo; 0.15C; 0.06 Zr; 0.02 B; Ni balance) due to different aging heat treatments. The samples were submitted to solution heat treatment at 1260°C for 8 hours and aging in single and double steps at 780, 880 and 980°C for 5, 20 and 80 hours. The materials in the as-cast condition as well as those from the heat treatments were characterized with SEM-FEG with EDS and DTA experiments. The results have shown that solution heat treatment at 1260°C for 8h dissolves the gamma/gamma prime eutectics and precipitates small gamma prime particles during the cooling from the heat treatment to room temperature whilst aging heat treatment grows the gamma prime phase.

W-75: Microstructure and Property Modifications in Mould Steels Treated by Pulsed Electron Beam: *Kemin Zhang*¹; ¹Shanghai University of Engineering Science

Surface modifications on AISI H13 and D2 mould steels generated by the low energy high current pulsed electron beam (LEHCPEB) treatments have been investigated. From the observations of SEM, XRD and electron back scattering diffraction (EBSD) determinations, the microstructure modifications were studied in details. It is found that the formation of the metastable microstructures in the surface layer are related to the very rapid heating, melting, solidification and cooling induced by the LEHCPEB irradiation. After the LEHCPEB treatment, the wear resistance of the mould steels can be effectively improved. This can be mainly attributed to the higher hardness of the ultra fine structures formed on the top surface and the hardened subsurface layers after treatment.

W-76: Modeling Cyclic Creep Relaxation in Fiber-Reinforced Gasketing Materials: *James Williams*¹; Ali Gordon¹; ¹University of Central Florida

Gasket materials, which are applied as seals in bolted connections, are generally subject to step loading as a part of normal operation. The time-dependent response of fiber-reinforced gasket materials is strongly dependent on factors such as flange detail, lubricity, mechanical load history, etc. Characterizing the time- and history-dependence of these materials has been identified as a technique by which materials selection and mechanical load history can be designed. Using a multi-scale experimental setup, the mechanical response of a white glass reinforced Teflon is characterized. A constitutive model for the load history of the material is developed. The research is applicable to support the design and selection of materials used in flanges such as the Ground Umbilical Carrier Plate as a part of the Shuttle Transportation System.

W-77: Modeling of Al/W Granular Porous Composites during Dynamic Deformation: *Karl Olney*¹; Vitali Nesterenko¹; David Benson¹; ¹UCSD

Aluminum/Tungsten granular composites are materials which combine high density and strength with the ability to undergo bulk distributed fracture of Al matrix into small particles under impact or shock loading. They are processed using cold and hot isostatic pressing of W particles/rods in the matrix of Al powder. The presentation will describe modeling of these materials under dynamic conditions simulating low velocity high energy impact in drop weight test (10 m/s) and behavior during explosive shock loading. It will be demonstrated that morphology of W component and bonding between Al particles dramatically affects their strength, shear localization and mode of fracture of Al matrix. The support for this project provided by the Office of Naval Research Multidisciplinary University Research Initiative Award N00014-07-1-0740.

W-78: Morphology of Nanocrystalline ZnO Prepared from Aqueous Solutions: *Eguberto Galego*¹; Marilene Serna¹; Lalgudi Ramanathan¹; ¹CNEN-IPEN/SP

Zinc oxide (ZnO) has been used in a variety of applications, because of its electrical, optical, and acoustic characteristics. This material has been also used as electrodes in thin film type or dye sensitized solar cells. The morphology of nanocrystalline ZnO is vital to obtain an ideal surface for use in these applications. In this study, nanostructured ZnO was prepared by sequentially dipping the substrate in several chemical baths. Experiments were conducted with a special rig in which the time, temperature, and extent of agitation of the baths were controlled by a microcomputer. Use of this rig along with control of solution pH and concentration enabled fabrication of ZnO nanorods and nanograins. Comparison of micrographs of the deposits indicated that pH and temperature have a marked influence on morphology.

W-79: Nanocomposite of Platinum Particle by Liquid Chemical Phase Reduction: *Jin Ho Lee*¹; Jin Woo Kim¹; Se Hoon Kim¹; Young Do Kim¹; ¹Hanyang University

Platinum (Pt) has been widely used such as catalyst of fuel cell and exhausted gas clean system due to high catalytic activity. In this study, we synthesized Pt nano particle by using polyol process which is one of liquid chemical phase reduction method. It is known that liquid chemical phase reduction is one of the high yield processes and could control size and shape during synthesis. $H_2PtCl_6 \cdot 6H_2O$, used as a precursor, was dissolved in diethylene glycol and $AgNO_3$ is added as metal salt in order to form particular shape of platinum nano particle. Also, we added polyvinylpyrrolidone (PVP) as capping agent for reducing the size and dispersed the particles. We made comparison of synthesized platinum particles depending on temperature and time during synthesis using particle size analyzer (PSA). And Transmission Electron Microscopy (TEM) is used to analyze morphologies and patterns.

W-80: Organic Coatings to Prevent Molten Aluminum Water Explosions in Aluminum Plants: *Alex Lowery*¹; Joe Roberts²; ¹Wise Chem LLC; ²Pyrotek Inc.

It was over 60 years ago; the first reported molten metal explosion from a bleed-out during direct chill casting in an aluminium mill was reported. Soon thereafter testing was performed to determine the root cause of the explosion. Upon determination of the root cause, an investigation to determine if any preventive measures could be instituted to prevent the explosions was conducted. Results found that a specific organic coating (e.g., Tarsel Standard) prevented molten metal explosions, whereas some specific organic coatings initiated the explosions. Fifteen years ago the U.S. Department of Energy in conjunction with the Aluminum Association reinvestigated the root cause of the molten metal explosions. Testing revealed that an initiation or trigger had to be present for a molten metal explosion to occur. Testing identified three additional coatings that could afford protection.

W-81: Oxidation Resistances of Al₂Ca Added Al-5Mg Alloy: *Shae K. Kim*¹; Gun-Young Oh¹; Young-Ok Yoon¹; ¹KITECH

Al-Mg alloys have attracted considerable attention for a wide range of applications due to excellent corrosion resistance, formability and weldability in automotive industry. However, the heat treatment of the Al-Mg alloys is limited under an ambient atmosphere at high temperatures because of their poor oxidation resistance. The continuous oxidation during heat treatment leads to alloy damage by the formation of thick oxide layer on the surface. The oxide layer may have undesirable effects on the production and performance of the alloys. A study has been performed to improve the oxidation resistance of Al-Mg mainly by Be addition. However, it is difficult to be handled and should be limited due to its toxicity. The aim of this study is to investigate the effect of Al₂Ca and Al₂Ca added Mg contents on the behavior of the oxidation resistances of Al-5Mg alloy. The oxidation test was carried out with thermogravimetric analysis (TGA).

W-82: Phase Decomposition in Isothermally-Aged Fe-Cr Alloys: *Victor Lopez-Hirata*¹; Erika Avila-Davila²; Hector Dorantes-Rosales¹; Maribel Saucedo-Muñoz¹; ¹Instituto Politécnico Nacional (ESIQIE); ²Instituto Tecnológico de Pachuca

Phase decomposition was studied during aging of Fe-32 and 40 at.%Cr alloys by means of TEM, hardness and the numerical solution of the nonlinear Cahn-Hilliard differential partial equation using the explicit finite difference method. Results of the numerical simulation permitted to describe appropriately the mechanism, morphology and kinetics of phase decomposition during the isothermal aging of these alloys. The growth kinetics of phase decomposition was observed to be very slow during the early stages of aging and it increased considerably as the aging progressed. The morphology of decomposed phases consisted of an interconnected irregular shape with no preferential alignment for short aging times and a further aging caused the change to a plate shape of the decomposed Cr-rich phase aligned in the <110> directions of the Fe-rich matrix. The increase in hardness seems to be associated with the coherency and nanometer size of the spinodally-decomposed phases in the aged alloys.

W-83: Physical Modeling on the Effect of Nozzle Clogging on Mold Flow: *Suzhou Wu*¹; ¹Wuhan University of Science and Technology

SEN clogging often occurs during continuous casting of low carbon Al-killed steel. Clogging materials remain in the nozzle are likely to cause bias flow of molten steel in mold, which will lead to slag entrapment. At the same time, in order to remove clogging materials, method of the rapid opening and closing stopper to flush the nozzle outlet was used. This situation will result in serious fluctuation of mold level and then could lead to breakout. In current study, effect of two states of nozzle clogging on mold flow was modeled through physical water modeling. 'Recovery time' is used to describe the mold flow status from the 'non-state' to the 'steady-state' process due to nozzle clogging being washed away from nozzle. Effect of nozzle outlet angle and casting speed on the recovery time will be discussed.

W-84: Plasticity and Fracture of Vintage Steel under Varying Stress-States, Strain Rates and Temperatures: *Ruth Hidalgo-Hernandez*¹; Paul Allison¹; Mark Horstemeyer²; Kennan Crane¹; Vince Charito¹; ¹US ARMY Corps of Engineers -ERDC; ²Mississippi State University

The use of vintage materials in the nation's infrastructure presents a problem determining the state of structures built from these aging systems and how to properly protect the systems from loading conditions such as seismic activity. Researchers are investigating the microstructure and mechanical response of vintage steels under varying stress-states, strain-rates, and temperature effects. The material response under tension, compression, and torsion examines stress-state effects. While quasi-static and dynamic experiments provide strain rate response data, and the elevated temperature experiments elaborates on how the material behaves under different temperature conditions. The investigation allows an understanding of the mechanical behavior of vintage steel alloys and compares them to modern steels. The microstructure and mechanical property data is being used to calibrate an internal state variable (ISV) plasticity-damage model developed for cast materials, and adapted to wrought, powder metals, and extruded materials, for the prediction of material behavior under varying loading conditions.

W-85: Polaritons in Photonic Crystal at THz Frequency Range: *Umberto Fulco*¹; Eudenilson Albuquerque¹; ¹Universidade Federal do Rio Grande do Norte

We study polaritons modes arising from the propagation of a phonon-polariton excitation at the THz frequency range, in periodic and quasiperiodic (Fibonacci type) photonic structure comprised of alternating layers of both positive and negative refractive index materials. The choice of the THz frequency range is justified because current THz modulators based on semiconducting structures have the desirable property of being broadband, relevant to THz interconnects. Therefore, further improvement of the performance characteristics are welcome for practical applications, and in fact a possible application of the present model is an efficient active device that can be engineered to operate at THz frequencies. We make use of a theoretical model based on a transfer matrix treatment to simplify the algebra. We present also a quantitative analysis of the results, pointing out the distribution of the allowed photonic bandwidths for high generations, which gives a good insight into their localization and power laws.

W-86: Porosity Characterization of Surrogates for Oxide Nuclear Fuels: A Statistical Analysis of Correlations among Grain Boundary Misorientation, Pore Distribution and Processing Conditions: *Robert McDonald*¹; Karin Rudman¹; ¹Arizona State University

Porosity plays an important role in oxide fuel performance because of its influence on microstructure reconstruction, i.e., recrystallization is known to initiate at large lenticular pores interacting with grain boundaries. Porosity also affects the rate of fission gases release, i.e., they act as vacancy sources for nucleating gas bubbles. A relationship between local microstructure (crystallography, geometry and topology) and porosity (size, distribution, shape, location) is needed as input for microstructurally explicit mesoscale simulations to model these phenomena. Therefore, samples of d-UO₂ manufactured under different conditions and oxygen stoichiometries were studied using Scanning Electron Microscopy to collect statistical data on porosity for several samples. These data were compared to electron backscattering diffraction maps to find correlations between grain boundary misorientation, pore character and pore location for different processing conditions. Results are discussed in terms of grain boundary and pore interactions and their potential effects on grain boundary mobility during microstructural evolution.

W-87: Potential Fiberboard Material from Cow Manure and Disposable Water Bottle: *Boon-Chai Ng*¹; Marlene Murray¹; Craig Bradfield¹; Roy Pritchard¹; ¹Andrews University

In this pilot project readily available solid cow manure from the nearby Andrews University dairy farm was rinsed to remove any feces, dried, and then tested for any life bacteria. This fiber material is then blended with shredded disposable plastic water bottle to form a "green" composite



material. This composite material was placed in a cylindrical mold and heated to various temperatures to allow bonding of the thermoplastics to the fiber. The heated composite material was subsequently compacted with a 10,000 lbs. load using the universal tensile tester. Results showed that the composite material heated to a temperature of 250 C for an hour before compacting with a 10,000 lbs. load produced a well bonded fiberboard

W-88: Preparation of Pb Free Solder (Cu–Ag–Sn) Particles by Ultrasonic Spray Pyrolysis and Hydrogen Reduction (USP-HR)
Method: Çigdem Toparli¹; Burcak Ebin¹; Sebahattin Gürmen¹; ¹Istanbul Technical University

Electronic industry has been striving to find suitable material replaced Sn-Pb solder paste due to environmental concerns of using lead. Cu-Ag-Sn solder alloy is the most promising candidate as lead free solders due to low cost, low melting point, good mechanical properties and superior solderability. Nanocrystalline Pb free solder Cu–Ag–Sn alloy particles were synthesized by ultrasonic spray pyrolysis and hydrogen reduction method. Stoichiometric amount of copper, silver and tin salts were used to prepare precursor solution in desired concentration. Particles obtained by hydrogen reduction of the aerosol droplets of the precursor solution under constant H₂ flow rate at 1000°C. Shape morphology, size, chemical composition and crystal structure of the particles were investigated by scanning electron microscope (SEM), energy dispersive spectroscopy (EDS) and X-ray diffraction (XRD). The results show that nanocrystalline Cu-Ag-Sn ternary alloy particles were prepared in submicron size range with spherical morphology.

W-89: Processing and Characterization of NiTi-MAX Phase Composites Prepared by Spark Plasma Sintering: Ankush Kothalkar¹; Liangfa Hu¹; Francesco Schaff¹; Sandip Basu¹; Miladin Radovic¹; Ibrahim Karaman¹; ¹Texas A&M University

Herein we report the fabrication of shape memory alloy (SMA) – MAX phase composites by spark plasma sintering (SPS) of equiatomic NiTi and Ti₃SiC₂ or Ti₂AlC powders at temperatures in the range of 960-1000°C under 100 MPa uniaxial load. The microstructure and phase composition along the interfaces of these two-phase composites were studied using Scanning Electron Microscopy (SEM) and Energy-Dispersive Spectroscopy (EDS). The phase evolution near the interfaces in SPSed composites depends significantly on sintering temperature, because of the formation of Ni-Ti liquid phase at temperatures higher than 980°C. Differential Scanning Calorimetry (DSC) has been carried out to confirm the martensitic phase transformation, and estimate the volume fraction of transforming NiTi phase in the SPSed composites. Thermo-mechanical properties of the composites are also discussed, along with practical implications of the results on inducing compressive stresses in ceramic MAX phases through phase transformations in SMA.

W-90: Processing of c-BN Film from B4C Target Using R.F. Magnetron Sputtering: Seungkeun Oh¹; Youngman Kim¹; ¹Chonnam National University

The cubic boron nitride (c-BN) film has unique physical and chemical properties such as extreme hardness next to diamond, excellent chemical inertness, high thermal conductivity, and thermal stability. In this study, c-BN thin films were processed on WC substrates using B4C targets in R.F. magnetron sputtering system as a function of substrate bias voltage. The morphology and thicknesses of the deposited films were observed. Fourier transform infrared microscopy (FT-IR) were used to analyze the bonding characteristics of c-BN. Intensity of absorption band of FT-IR corresponding to B-C and C-N bond were increased with increasing the substrate bias voltages. Possible mechanisms for the formation of c-BN films were also discussed.

W-91: Reciprocal Space Configurational Kinetics of Amorphous SystemsW: Volodymyr Bugaev¹; Mariya Rasshchupkyna¹; Alexander Udyansky²; Miguel Castro-Colin¹; Peter Wochner¹; ¹Max Planck Institute for Intelligent Systems; ²Max Planck Institute for Iron Research GmbH

We propose a reciprocal-space kinetic approach for inhomogeneous systems, based on the correlation correction algorithm (CCA) [1] and atomic density functional theory [2]. This concept deals with cooperative reciprocal-space atomic density modes and takes into account coupling in effective atomic interaction modes. The set of dominant modes, corresponds to the minimal negative value of the Fourier component of the renormalized effective pairwise interaction potential $V_{eff}(q)$. It is visualized that interference of the dominant modes leads to long-living structural states, e.g. clusters with discernible symmetries, recently revealed by the X-ray cross-correlation analysis [3] from coherently scattered X-rays.[1] V.N.Bugaev, A.Udyansky, O.Shchyglo, H.Reichert, H.Dosch, Phys. Rev. B. 74, 024202-1 (2006).[2]Y.M.Jin, A.G.Khachatryan, J. App. Phys. 100, 013519-1 (2006).[3]P.Wochner, C. Gutt, T.Autenrieth, T.Demmer, V.N.Bugaev, A.D.Ortiz, A.Duri, F.Zontone, G.Gruebel, H.Dosch, P. Natl. Acad. Sci. USA. 106, 11511 (2010).

W-92: Refinement of Ligaments of Nanoporous Ag Ribbons by Controlling the Surface Diffusion of Ag: Tingting Song¹; Yulai Gao¹; Zhonghua Zhang²; Qijie Zhai¹; ¹Shanghai University; ²Shandong University

Nanoporous silver (NPS) with different nanoporosity was manufactured by chemical dealloying of rapid solidified Al-Ag ribbons consisting of two distinct phases of a-Al(Ag) and Ag₂Al. The as-dealloyed samples were characterized by X-ray diffraction (XRD), scanning electron microscopy (SEM), and energy dispersive X-ray (EDX) analysis. It has been found that the width of the average ligaments can be dramatically decreased and be more homogeneous when surfactants were added to the H₂SO₄ solution, which would definitely increase the specific area of NPS and is pretty desirable for certain applications, such as catalyst, absorption, etc. The finer ligaments were attributing to the hindered surface diffusion of Ag atoms by surfactants, and the surface diffusion coefficient (Ds) of Ag was decreased from the order of 10-14 to 10-16 m²/s as a result of surfactants. This simple method to reduce the ligament width of NPS is also anticipated to prepare the other related nanoporous metals.

W-93: Relationship between Heat Input and Microstructure and Mechanical Properties of Laser Beam Welded Superalloy Inconel 718: Akin Odabasi¹; Necip Ünlü²; Gültekin Göller²; M. Niyazi Erusu²; E. Sabri Kayali²; ¹Firat University; ²Istanbul Technical University

Autogenous butt, laser beam welds were carried out using Inconel 718 alloy sheets (2.1 mm thick). The relationship between heat input laser beam welding (LBW) and the microstructural and mechanical properties of superalloy Inconel 718 were investigated. Nine different heat inputs in the range of 61.29–90.09 Jmm⁻¹ were applied to evaluate the geometry of weld seams. Full penetration was achieved in all weld experiments. Optical and field emission scanning electron microscopy and microhardness tests were performed. Test results indicate that increasing the amount of heat input from 61.29 Jmm⁻¹ to 90.09 Jmm⁻¹ presented solidification rates between 1.27x10⁶ and 1.46x10⁶ °Cs⁻¹. The hardness property of the weld samples decreased with the increasing the heat input.

W-94: Role of Work Hardening during Sliding Wear of Heat Treated 2024 Al Alloy: Yong-Suk Kim¹; Hyuk Woo Kwon¹; Gonam Kim¹; ¹Kookmin University

In the present study, the role and effect of strain hardening during dry sliding wear of 2024 Al alloy was investigated. Dry sliding wear tests were performed on the naturally aged (T4), artificially aged (T6) and solution treated 2024 Al alloy using a pin-on-disk wear tester at various loads and for differing sliding distances. Alumina balls were employed as a counterpart. Wear rates of the alloy with various microstructures due to different heat treatments were compared; and related with work hardening during the wear, which varied greatly with the microstructure. The work hardening was evaluated by measuring cross-section hardness

as a function of distance from the worn surface. Work-hardening at the wearing surface affected the wear of the Al alloy significantly by forming a surface-deformation layer, which was closely connected with wear-particle generation. The hardened layer also acted as a protecting layer that resists further progress of wear.

W-95: Silver Uptake from Dilute Cyanide Solution Using Activated Charcoal: *Bihter Zeytuncu*¹; Onuralp Yucel¹; ¹Istanbul Technical University

The adsorption of silver cyanide on activated charcoal from dilute cyanide solution of 200 ppm has been investigated. The effects of different adsorption parameters on the silver adsorption percentage are reported in detail. The percent of silver adsorption increased with a raising amount of adsorbent, as well as with increasing retention time and temperature. Additionally, the experimental rate data is explained by use of a kinetic equation. The characterization of activated charcoal was analyzed by X-Ray Diffraction (XRD).

W-96: Structural and Electrical Characteristics of Ba2DyNbO6: *Suharto Chjatterjee*¹; Koushik Biswas²; Mukul Pastor²; Mukul Pastor²; ¹Ace Calderys Ltd; ²Indian Institute of Technology, Karagpur, India

The electro ceramic material Ba2DyNbO6 has been prepared by a standard solid-state reaction technique. Structural analysis was performed with XRD in which dominant (98%) cubic perovskite phase was found. The tolerance factor of the sample was found to be 0.891 suggesting that the sample is stable. The FTIR analysis showed good bond strength in the sample. The experimental results of impedance spectrum indicate that the material exhibits (i) electrical resistance due to bulk material up to 5750C (ii) negative temperature coefficient of resistance (NTCR)-type behaviour and (iii) temperature-dependent relaxation phenomena up to 500oC. The behaviour of the modulus spectrum is suggestive of temperature-dependent ion hopping mechanism for electrical conduction (charge transport) in the system. The AC conductivity spectrum was found to obey Jonscher's universal power law. Conductivity phenomenon has been explained with respect to thermal activation resulting in mobile charges.

W-97: Study of Stacking Fault Formation Probability under Loading in High Manganese Steels: *Mihyun Kang*¹; Wanchuck Woo¹; Vyacheslav Em¹; Yong Kook Lee²; Eunjoo Shin¹; Back-Seok Seoung¹; ¹KAERI(Korea Atomic Energy Reserch Institute); ²Yonsei University

Since the reason of the excellent mechanical properties of the high manganese steels has been known to the twinning induced plasticity (TWIP) phenomenon, stacking faults and twinning formation have been extensively studied under deformation. We measured diffraction of (111) and (222) during tensile loading up to ~800MPa stopped at 7 different loading steps using neutron diffraction. Difference of the peak shifts between the two reflections increases as the loading increases even though the peak shifts should be same when considering the elastic strain with crystallographic point of view. The difference was correlated to the stacking fault probability (SFP) based on the Warren's analysis of twin faulting and peak shifts. The analyzed results can suggest quantitative variations of SFP as a function of loads in TWIP steels.

W-98: Synergistic Extraction and Solvent Extraction of Uranium from Sulfate Solutions – A Comparative Study: *Rajesh Kumar Jyothi*¹; Chul-Joo Kim¹; Jin-Young Lee¹; Joon-Soo Kim¹; Ho-Sung Yoon¹; ¹Korea Institute of geoscience and Mineral Resources (KIGAM)

Energy consumptions growing vigorously throughout the world in new millennium, this fact drive the researchers towards energy related research and development areas. The present scientific study focused on uranium extraction from sulfate solutions by using amine based extractants as promising reagents. The present efforts made on two different extraction methodologies such as solvent extraction process and synergistic solvent extraction process for uranium. For the extraction phenomena the following conditions are fixed: the temperature (25oC), time (30 min), aqueous: organic phase ratios (A:O = 1:1) for all experiments. Synergistic extraction process tested the ability of the extractants to

recover the title metal with amines as extractants as well as synergists and organophosphorus reagents used as synergists with amines. For the uranium analysis in aqueous solutions ICP-OES used as analytical instrument.

W-99: Synthesis and Characterization of Metallic Oxides: *Eduardo Brocchi*¹; Rodrigo Souza¹; Marina Doneda²; Jose Campos³; Ana Cristina Wimmer¹; Rogério Navarro¹; ¹PUC-Rio; ²VALE; ³CBPF

Due to recent great interest on nanostructured materials this work is related to an alternative synthesis method as compared to the already established aqueous phase precipitations and gaseous species reactions. It deals with the pyrolysis of Fe, Cu, Ni, Zn and Al nitrates, including a theoretical thermodynamics decomposition approach and the corresponding experimental characterizations of the products, by XRD and SEM. The thermodynamics have shown that these decompositions can start in the temperature range between 150°C and 550°C and the XRD patterns have confirmed the formation of Fe2O3, CuO, NiO, ZnO and Al2O3. SEM indicates the occurrence of a typical particles agglomerated structure for Fe, Cu and Ni oxides while the two others are formed either as faceted crystal (ZnO) or in the pancake shape (Al2O3). Further analysis by the Rietveld method proved that this methodology can be used to produce oxides with nanosized particles content.

W-100: Synthesis and Characterization of Nacre-Inspired Nanocomposites: *Omar Rodriguez-Negron*¹; Carlos Morales-Del Valle¹; Ruth Hidalgo-Hernandez²; Robert Moser²; Paul Allison²; Mei Chandler²; Charles Weiss²; Philip Malone²; ¹UPRM/ ARMY ERDC; ²US ARMY ERDC

The U.S. Army Engineer Research and Development Center (ERDC) is currently synthesizing and characterizing bioinspired nanocomposites utilizing the multi-layered hierarchical design principles found in nacre. Electrophoretic electro transport deposition and hydrothermal hot pressing are methods currently being investigated in order to synthesize nacre's hierarchical structure. Both methods are intended to provide the ability to control the crystallographic form, crystal size and crystal location within a polymer matrix. Calcium acetate and ammonium carbonate are the chemical compounds employed with the purpose of replicating calcium carbonate biomineralization. The influence over precipitate mineralogy of different reactants concentrations as well as the presence of magnesium acetate or strontium acetate was also investigated. X-ray diffraction is employed in characterizing the crystal structures being synthesized while scanning electron microscopy is used in determining the size and shape of the crystal structures forming. Initial results suggest the approach may produce useful new composites.

W-101: Synthesis and Electrochemical Performance of LiMnBO3 as a Novel Li-Ion Battery Materials: *Hyukjae Lee*¹; Yong-Suk Lee¹; ¹Andong National University

As a new cathode material for Li-ion batteries, LiMnBO3 is prepared by solid state reaction using Li2CO3, H3BO3, and MnCO3. At lower calcination temperatures, less than 600°C, monoclinic phase is obtained, while hexagonal phase is obtained at higher calcination temperature, above 800°C. To improve the electronic conductivity, LiMnBO3/C composites are also prepared using a carbon black or organic carbon precursor. The electrochemical measurements show that the monoclinic LiMnBO3 has the higher capacity than hexagonal counterpart and the enhanced electrochemical performance from the LiMnBO3/C.

W-102: Synthesis of SiC Nanoparticles for Ink-Jet Printing: *Jong-Woong Kim*¹; Young-Sung Kim²; Sung-Jei Hong¹; Hyun-Min Cho¹; ¹Korea Electronics Technology Institute; ²Seoul National University of Science & Technology

SiC has been known for high hardness, wear resistance and good resistance to oxidation, thermal shock, and corrosion. More importantly, it has good thermal conductivity, which makes it possible for applications in fabrication of micro hotplates. Here we intended to fabricate various SiC patterns for use as micro hotplates by ink-jet printing. For application



of the ink-jet printing to fabricate SiC micro patterns, ink composed of SiC nanoparticles, solvent and additives are needed. In order to achieve uniform thin film from the ink, fine sized SiC nanoparticles less than 100 nm has to be uniformly dispersed. In this study, we employed a mechanical milling method that is called as the ultra apex mill (UAM). The SiC nanoparticles were synthesized by the UAM and SiC ink was formulated with ethylene glycol based solution. The patterns were made by ink-jetting, then a high temperature annealing was followed to fabricate the micro hotplates.

W-103: Synthesis, Characterization and Application of Core-Shell Oxide Nanoparticles: *Yuanbing Mao*¹; Suresh Alaparthi¹; ¹University of Texas-Pan American

Miniaturization in various industries has led to the requirement for multifunctionality. Here we have developed some core-shell nanostructures with strong interfacial couplings. These nanostructures have at least three advantages: (i) to realize multifunctionality, (ii) to provide novel functions not available in single-component materials or structures, and (iii) to achieve enhanced properties and breaking the natural constraints of single-phase materials. These nanoparticles are thoroughly characterized by x-ray diffraction, scanning electron microscopy, (high resolution) transmission electron microscopy, selected area electron diffraction, and energy-dispersive x-ray spectroscopy, as well as ultraviolet-visible, Fourier transform infrared and Raman spectroscopies to delineate their structure and composition. Their luminescent and magnetic properties have been systematically studied. The aimed applications of these core-shell nanoparticles mainly include: (1) national security, such as core-shell nanoparticles for gamma-ray radiation detection; and (2) information storage, such as multiferroics and exchange-biased magnetic materials.

W-104: TEM Study of Crystal Defects in Laves Phase Alloys: *Ke Wang*¹; Kwo Young²; Leonid Bendersky¹; ¹NIST; ²Energy Conversion Devices

Transmission Electron Microscopy (TEM) was employed to investigate the crystal defects in AB₂ type Nickel Metal Hydride (NiMH) battery alloys. A high density of stacking faults and micro twins were found within the cubic C15 Laves phase. In contrast, high density dislocations appeared in the hexagonal C14 Laves phase. A typical grain boundary structure was observed between C14 and C15 phases. The orientation relationship between two Laves structures was determined to be {111}<110>C15//{0001}<11-20>C14. These results reveal that the stacking fault energies (SFE) of C14 and C15 Laves phases are very different. These crystal defects in the material are believed to play an important role in the hydrogen absorption/desorption behavior during electrochemical process for hydride electrode alloys.

W-105: The Effect of Die-Shape and Die Parameters in ECAP on the Microstructure and Flow Properties of Some 2-Phase Alloys: *Nithyanand Prabhu*¹; B Kashyap¹; P Hodgson²; Rahul Kulkarni¹; Pabitra Palai³; V Srinivas⁴; ¹Indian Institute of Technology Bombay; ²Deakin University; ³Tata Steel; ⁴Vizag Steel Plant

Equi-channel angular pressing (ECAP) of a Pb-Sn eutectic alloy up to six passes in a T-shaped die, rather than a conventional L-shaped die, was studied for grain refinement. Microstructure predominately changed in the early part of the ECAP process and became equiaxed and uniformly distributed in both the longitudinal and the transverse sections after four passes. There occurred substantial softening over the first two passes & ductility increased drastically. Various tensile properties and concurrent microstructural evolution were used to develop a mutual relationship among them. The effects of die channel angle (θ) in hot (~623 K) ECAP on microstructure, and tensile and compressive flow properties of AZ80 Mg alloy were investigated at room temperature. Flow stresses in tension and compression are found to increase with decreasing value of die angle. There appears flow asymmetry between tension and compression with the latter exhibiting greater flow stress and strain to failure.

W-106: The Effect of High Superheat on the Solidification Structure and Carbon Segregation of Ferrite-Based Alloy: *Honggang Zhong*¹; *Yi Tan*¹; *Huigai Li*¹; *Xinping Mao*²; *Qijie Zhai*¹; ¹Shanghai University; ²Guangzhou Zhujiang Iron and Steel Co., Ltd.

The Ferrite-based alloy was melted and poured in-situ to investigate the effect of high superheat on the solidification structure and macrosegregation of permanent mold casting. The alloy solidified horizontally from the chill wall in a furnace, which be shut down after the alloy liquid be poured. The coarse equiaxed dendritic grains, which diameters are more than 5mm, are observed with high superheat (80-120 K), and the secondary dendritic arm spacing increases with superheat increasing. However, the degree of carbon macrosegregation K(C), which is defined as the ratio of concentration of solute (C_i) to average concentration of solute (Cave), are less than 1.2, which indicate the fluctuations of carbon concentration are small.

W-107: The Effect of Oxygen Vacancies on the Stability and Reactivity on Rutile TiO₂ (110) and Its Reconstructions: *Jackelyn Martinez*¹; *Tzu-Ray Shan*¹; *Susan Sinnott*¹; *Simon Phillpot*¹; ¹University of Florida

Rutile TiO₂ (110) is often used as the base surface for heterogeneous catalysts for many important metal nano-clusters. To better understand reactivity of the surface, a computational study of this surface was carried out using an empirical, variable charge potential for Ti and TiO₂ based on the charge-optimized many body (COMB) framework. The surface energies of the pristine (110) surface along with reconstructed and stepped surfaces were determined, and compared to literature results. The effect of oxygen vacancies on the surface energy of the differing (110) rutile surfaces was also explored. In addition, the defect energies of surface and subsurface oxygen defects were calculated. The defect formation energy depends on the distance below the surface which suggests that sub-surface vacancies should have little or no effect on the reactivity of this surface. This work is supported by NSF (DMR-1005779).

W-108: The Formation and Characterization of Al Metal Matrix Composite Reinforced by Ni₆₀Nb₂₀Zr₂₀ Amorphous Powders: *Pee-Yew Lee*¹; ¹National Taiwan Ocean University

The Ni₆₀Nb₂₀Zr₂₀/Al metal matrix composite powders with 10~50 wt% Ni₆₀Nb₂₀Zr₂₀ amorphous powders were prepared by high energy ball milling of the corresponding amorphous and pure Al powders. The Ni₆₀Nb₂₀Zr₂₀/Al metal matrix composite powders were then consolidated into bulk discs by vacuum hot pressing methods. The DSC result shows that the melting temperature of Al matrix was shift to lower temperature with increasing of milling time. The Vicker's microhardness of bulk samples can be promoted by increasing the amount of Ni₆₀Nb₂₀Zr₂₀, milling time and hot pressing time. The corrosion behavior of 40 wt % Ni₆₀Nb₂₀Zr₂₀/Al metal matrix composite discs in four different corrosive media was studied using the potentiodynamic method. The resultant polarization curves indicated the Ni₆₀Nb₂₀Zr₂₀/Al-based metal matrix composite has poor corrosion resistance either in strong acid or strong alkaline solutions. However, it is noted the alloy exhibits the best corrosion resistance in 3.5wt. % NaCl.

W-109: The Formation of an Eutectic Mixture for Predicting the Ideal Solubility of Thermally Stable and Unstable Compounds: *Rodolfo Pinal*¹; *Ryan McCain*¹; ¹Purdue University

The melting properties of organic compounds are critical to the solubility behavior of APIs (active pharmaceutical ingredients). Solubility of poorly water soluble APIs is one of the largest challenges in formulation development. Estimating solubility by means of the melting temperature and heat of fusion is a widely established practice. However, a common problem in drug development is that some APIs are thermolabile and undergo chemical decomposition before melting. This situation makes the essential melting parameters experimentally inaccessible. Eutectic microcrystalline mixtures offer the potential advantage of increased dissolution rates at lower temperatures without changing the selected crystalline form of the API. Eutectic mixtures also offer a means to overcome the hurdles imposed by thermal limitation. The purpose of this

work was to develop and test a thermodynamic model for estimating the enthalpy of fusion of thermolabile compounds, based on the entropy of fusion, thus enabling further prediction of their ideal solubility.

W-110: The Importance Role of Sulfur in Autogenous Copper Smelting Technology: *Ljubisa Mistic*¹; *Vlastimir Trujic*¹; *Tatjana Trujic*¹; ¹Mining and Metallurgy Institute

There are many reasons why sulfur represents one of the most important question in the copper pyrometallurgical processes. The most of the copper sulfide concentrates contains approximately 1 to 1.5 ton of sulfur (2 \8722 3 t SO₂) per each ton of the produced copper. Sulfur has chemical, technological, energy and ecological importance in the copper smelting processes. In the last decades, energetical and ecological aspects of sulfur is the most considerable and the best solution of its are incorporated in the autogenous copper smelting processes.

W-111: The Solid-State Sn/Ni Interfacial Reaction Under Three-Point Bending: *Chih-Ming Chen*¹; *Wen-Kai Liao*¹; ¹National Chung Hsing University

Effect of strain on the Sn/Ni interfacial reaction annealed at 200 oC is investigated. A bi-layer of Sn/Ni deposited on a Si substrate is subjected to tensile or compressive strain by virtue of a three-point bending apparatus. Enhanced growth of the Ni₃Sn₄ phase formed at the Sn/Ni interface is observed under both tensile and compressive strains. The Ni layer subjected to strains exhibits significant microstructure evolution, which is suggested to play a crucial role for the enhanced growth of the Ni₃Sn₄ phase.

W-112: The Study of Thermal Properties and Devitrification Behaviors of Al-RE-TM Amorphous System: *Song-Yi Kim*¹; *Gwang-Yeob Lee*¹; *Min-Ha Lee*¹; ¹Kitech

Al-based amorphous with minor additions of rare earth elements and transition metals were technical interest, because of their extraordinary high strength. Recently, amorphous with high glass forming ability with wide supercooled liquid region which defined by temperature range between glass transition temperature (T_g) and crystallization temperature (T_x) have been reported in many alloy systems. Various kinds of techniques have been tried to promise potential process obtaining a fast densification without crystallization during the consolidation of amorphous. In this study the effect of RE addition on the Al-based amorphous was evaluated and the structure and property of Al-RE-TM (transition-metal) were investigated by various techniques. Thermal and physical properties of the Al-based amorphous were characterized using DSC and XRD. Crystallization kinetics of Al-based amorphous was analyzed by applying modified Johnson-Mehl-Avrami equation from the isothermal annealing results of Al-based amorphous at various temperatures.

W-113: The Variability of Small Crack Growth in Notched Bars of IN100: *D'Anthony Ward*¹; *Andrew Rosenberger*²; *Dennis Buchanan*³; ¹University of Dayton ; ²Air Force Research Laboratory; ³University of Dayton Research Institute

Small crack growth appears to be the critical link to predict the minimum fatigue life using fracture mechanics. The present study builds upon our current understanding of small crack initiation and growth in smooth bars and assesses the growth of small cracks in fracture critical locations associated with areas of high stress concentrations, e.g. bolt holes, fillets, balance flange scallops, etc. Results indicate that the same initiation mechanisms are operable in smooth and notched bars. Generally the same small crack growth mechanisms exist in the two conditions, however, the concentrated stress in the notched geometry promotes the formation of additional cracks ahead of the main crack such that the effects of crack merging must be considered. Furthermore, replicate notch fatigue tests indicate that the minimum fatigue life can be discovered even when interrogating only the small volume of material at the notch.

W-114: Thermal Analysis of the Composition of Poly(Acrylic Acid)/Carboxymethylstarch Used as a Polymeric Binder: *Beata Grabowska*¹; *Mariusz Holtzer*¹; *Sonja Eichholz*²; *Krzysztof Hodor*²; *Ewa Olejnik*¹; ¹AGH University of Science and Technology; ²Applications Laboratory Thermal Analysis, NETZSCH-Gerätebau GmbH

Samples of poly(acrylic acid)/carboxymethylstarch used as a binding agent in molding sands were investigated. Methods of thermal analysis were applied to assess the thermal stability of the investigated polymer sample by estimation of temperature and thermal effects of transformations occurring during its heating. In the temperature range -100-1000°C none polymorphic transformations were found. It was established that the degradation process starts at a temperature app. of 130°C. On the bases of the analysis of volatile products of the polymer decomposition performed by means of the IR spectral method and the thermo gravimetric method coupled 'on-line' with the mass spectrometry the signals for low molecular masses were found in the temperature range: 300-400°C. This indicates that the degradation process occurs, polymer chains are undergoing fragmentation and low molecular compounds are formed. At the higher temperature range compounds and alkyl radicals of higher mass numbers are formed.

W-115: Thermal Radiation Spectra in Photonic Crystals: *Luciano da Silva*¹; *Manoel Vasconcelos*¹; ¹Universidade Federal do Rio Grande do Norte

In this work we investigate the behavior of a light beam normally and obliquely incident on a one-dimensional multilayer photonic structure, composed of a positive refractive index material (SiO₂) and a polaritonic metamaterial (LiTaO₃), arranged in a periodic and quasiperiodic (Fibonacci) fashions. Their emission spectra are determined by means of a theoretical model based on Kirchoff's second law, together with a transfer matrix formalism. We discuss the radiation spectra for both the ideal case, where the negative refractive index material can be approximated as a constant in the frequency range considered, as well as the more realistic case, taking into account the frequency dependent magnetic permeability and the electric permittivity characterized by a polaritonic dielectric function. Our main result shows that the quasiperiodic structure presents a more rich thermal radiation spectrum than observed in the periodic case, pointing it as a good candidate for designing efficient negative index refraction filter.

W-116: Thermographic Defects Evaluation of Railway Bogies: *Jeongguk Kim*¹; ¹Korea Railroad Research Institute

The lock-in thermography was employed to evaluate the defects in railway bogies. Prior to the actual application on railway bogies, in order to assess the detectability of known flaws, the calibration reference panel was prepared with various dimensions of artificial flaws. The panel was composed of structural steel, which was the same material with actual bogies. Based on the defects information, the actual defect assessments on railway bogie were conducted with different types of railway bogies, which were used for the current operation. In summary, the defect assessment results with thermography method showed a good agreement as compared with the conventional inspection techniques. Moreover, it was found that the novel infrared thermography technique could be an effective way for the inspection and the detection of surface defects on bogies since the infrared thermography method provided rapid and non-contact investigation of railway bogies.

W-117: Thermographic Monitoring of Braking in Railway Brake Shoe: *Jeongguk Kim*¹; *Sung-Cheol Yoon*¹; ¹Korea Railroad Research Institute

The damage evolution due to generation of hot spots and/or thermal bands on railway brake shoe has been considered the main degradation mechanism in brake shoe. Therefore, the understanding of the formation of hot spots and/or thermal bands is important for a better understanding of material design as well as enhancement of materials properties in railway brake shoe. In this investigation, during braking up to maximum speed of 300 km/h, the thermographic temperature analysis of railway brake shoe



TMS 2012

141st Annual Meeting & Exhibition

was quantitatively performed to investigate the degradation mechanism of brake shoe. The analysis of surface temperature changes on railway brake shoe was conducted using a high-speed infrared camera. Through the analysis of thermographic monitoring images, the temperature evolution with different braking speeds was qualitatively evaluated. In this investigation, the qualitative investigation results on the temperature evolution of railway brake shoe was summarized and presented.

W-118: Titania Based One-Dimensional Nanomaterials for Lithium Ion Batteries: *Hyukjae Lee*¹; Young-Jun Kim²; Jong-Hwan Park¹; ¹Andong National University; ²Korea Electronics Technology Institute

Recently, TiO₂ based materials are drawing much attention as anode materials for lithium ion batteries due to its safety, abundance in nature, chemical stability, and non-toxicity. However, their low lithium ion diffusivity and electronic conductivity deteriorate reversible capacity and high rate performance. To overcome this, nanostructuring of TiO₂ has been exploited to reduce transporting path for lithium ions and electrons. Of particular interest is 1D- nanostructures since their interesting size, shape related properties. In this study, various titania and lithium titanate 1D-nanostructures are prepared and their lithium electrochemical performances are compared. Further, the effects of the surface treatment and doping are investigated.

W-119: Toxic Metals in Ash Residue from Electronic Waste Dismantling and Incineration Practices: *Kathleen Hibbert*¹; Oladele Ogunseitan¹; ¹University of California, Irvine

This research investigates the toxic metals and chemicals in residual ash after burning of electronic waste (e-waste). These toxins can leach into soil and water systems, and can be dispersed widely in the environment; thus creating a public health risk to populations. Currently, e-waste is the fastest growing form of solid waste, yielding over 2 million tons of material generated annually in just the United States. Approximately 90% of e-waste is discarded, with incineration recognized as a common procedure for recycling and disposal globally. We investigated the chemical residues in ash generated from incinerated cell phone components divided into four categories: screens, plastics, circuit-boards and batteries. Results from ash residue analysis that have raised initial concern have revealed seventeen metals including beryllium, cadmium, copper, lead, nickel and zinc. Results have also identified PCBs, PBDEs and furans.

W-120: Wettability and Interfacial Microstructure of Pb-Free Sn_{3.5}Ag Alloy Powders on Cu Substrate: *Jin Zhao*¹; Weipeng Zhang²; Tingting Song²; Yulai Gao²; Qijie Zhai²; ¹Shanghai university; ²Shanghai University

Sn_{3.5}Ag powders in different sizes were prepared by arc technique. Powders in different sizes mixed with Rosin Mildly Activated (RMA) fluxes were soldered on pure Cu substrate. The contact angle is a critical parameter to affect the quality of solder joints. Presently the Pb-free Sn_{3.5}Ag solder has been widely applied in industry. However, its wettability on Cu substrate is not good enough, and the contact angle of commercial Sn_{3.5}Ag solder paste is about 26°. In contrast, the contact angles of the Sn_{3.5}Ag solder paste prepared in the present study are 16.1°, 13.9°, and 21.4° respectively, depending on the specific characteristics of the powders. So good wettability was obtained attributing to the novel technique to prepare Sn_{3.5}Ag powders. In addition, the intermetallic compounds (IMCs) were observed by optical microscope and scanning electron microscope, and the results showed that continuous intermetallic compounds layer formed, confirming the validity of the packaging.

Biological Materials Science Student Poster Contest: Poster Session

Sponsored by: The Minerals, Metals and Materials Society, TMS Structural Materials Division, TMS: Biomaterials Committee Program Organizers: Nima Rahbar, University of Massachusetts Dartmouth; Candan Tamerler, Istanbul Technical University; Po-Yu Chen, National Tsing Hua University; Molly Gentleman, Texas A&M University

Monday PM
March 12, 2012

Room: Atlantic Hall
Location: Dolphin Resort

Session Chairs: Nima Rahbar, University of Massachusetts Dartmouth; Po-Yu Chen, National Tsing Hua University; Candan Tamerler, University of Maryland Baltimore County

I-1: Addition of Apatite Microparticle to Cell Cultures- Effects on Differentiation: *Amanda Farley*¹; Laura Datko¹; Marian Kennedy²; Delphine Dean¹; ¹Clemson Bioengineering; ²Clemson Materials Science and Engineering

Recent studies show that hard particles added to suspensions of cell growth media can stimulate bone marrow stem cells (BMSCs). This study looks at the response of dental pulp stem cells (DPSCs) and Osteoblasts to 40µm diameter Hydroxyapatite (HA) and Fluorapatite (FA) particles for cranial reconstruction applications. BMSCs were also studied to compare to the previous results of other research groups. Cells were given 24hrs to adhere in individual wells and then a 10mg/mL suspension of either HA or FA microparticles were added to 2/3 of the wells, with remaining wells left as a control. ALP and BCA assays were run on days 1,3,5 and 14. Antibody stains and confocal imaging were done for collagenI and osteocalcin. In general, the control cells produced more protein, osteocalcin, and collagenI, and had higher levels of ALP specific activity than cells cultured with microparticles. The authors would like to acknowledge funding from NIH (Award number:092228).

I-2: Adhesion and Interfacial Fracture Toughness between Hard and Soft Materials: *Nima Rahbar*¹; Sina Youssefian¹; ¹Umass Dartmouth

To quantify adhesion between the drug-eluting layer and a Parylene C primer, Brazil nut sandwich specimens were prepared mimicking the layers of drug-eluting stent coating. These samples were stressed to fracture, and the resulting initial cracks at the Parylene C/drug and Steel interface were used to measure the dependence of interfacial fracture energy of mode mixity. The mating fracture surfaces were then analyzed using scanning electron microscopy (SEM) and energy dispersive x-ray spectroscopy (EDX). The interfacial energy release rates were obtained over a wide variety of mode mixities. Adhesion and fracture mechanics models were used to estimate the mode mixity dependency of interfacial fracture toughness. Fracture toughness was found to be larger under higher mode mixity than that under lower mixity and the analytical model showed close agreement with experimental results. The experimental adhesion results between the Parylene C and Stainless Steel are later verified using a Molecular Dynamics simulation.

I-3: Cellulose-based Nanocomposite as a Potential Scaffold in Cardiovascular Tissue Engineering: *Parisa Pooyan*¹; Rina Tannenbaum¹; Hamid Garmestani¹; ¹Georgia Institute of Technology

Cellulose nanowhiskers (CNWs) with its renewable and environmentally benign nature, and its abundance and excellent biocompatibility could potentially open a new avenue in cardiovascular tissue engineering for small caliber grafts. Inspired by this bioapplication, we have designed a fully bio-based nanocomposite of aligned CNWs embedded in a matrix of cellulose acetate possessing a controlled biodegradability, 3D porosity, and non-acidic byproducts as opposed to degradable PLA/PGA. To ensure uniform distribution, CNW were delicately extracted from a multi-stage process and dispersed in a solvent of choice prior to mixing with the matrix to inhibit whiskers flocculation. Comparable to Carbon Nanotubes

or Kevlar, CNWs imparts significant strength and directional rigidity to the composite even at 0.2 wt% yet doubles that within a controlled magnetic field of only 0.3T. We believe our fibrous porous aligned nanocomposite could have ground-breaking features withstanding the physiological pressure and mimicking the topographical texture of the native extracellular graft.

I-4: Comparison of Composites with Biological or Synthetic Hydroxyapatite Scaffolds: *Steve Lee*¹; Ekaterina Novitskaya¹; Antoni Tomsia²; Po-Yu Chen³; Joanna McKittrick¹; ¹University of California, San Diego; ²Lawrence Berkeley National Laboratory; ³National Tsing Hua University

Most bone substitute materials are primarily based on hydroxyapatite. Their shortcomings include low strength due to the porosity required for osteointegration and difficulty of fabrication. We have developed new polymer/hydroxyapatite composite that is porous, strong as natural bone and is easy to fabricate. The designs use scaffolds from either biological or synthetic hydroxyapatite. The biological hydroxyapatite scaffold was formed by deproteinizing samples of cancellous bovine femur bone and the synthetic hydroxyapatite scaffold was formed by freeze casting. Both scaffolds have 25-40 vol.% mineral, inside the range of natural bone. The scaffolds were filled with biocompatible polymers such as PMMA and various epoxies. The composites have an order of magnitude higher compressive strength than that of bovine femur bone. Composite materials based on these fabrication methods could potentially find use in prostheses where low weight and good strength are required. This work is supported by NSF, Ceramics Program Grant DMR1006931.

I-5: Effects of Heat Treatment and Moisture on Mechanical Properties of Bamboo: *Peter Kotowski*¹; Nima Rahbar¹; ¹Umass Dartmouth

This talk presents experimental and numerical studies on the deformation mechanisms of bamboo in torsion, bending, and fatigue. The microstructure of bamboo can be considered as a material composed of non-uniformly distributed longitudinal fibers that are segmented by nodes. Using specially designed fixtures, samples of kiln dried bamboo were cut and tested in torsion with varying moisture to determine the effects on the torsional strength of bamboo. Finite element simulation was also used to study the torsional strength and bending of bamboo. The toughness of bamboo was studied for each case. Also, simple four point bending tests with strain gauges on 5-inch strips of bamboo determined the variation of the elastic modulus in culm segments. This data was integrated into conducting fatigue testing and obtaining an S-N curve. The results are presented to reflect how heat treatment and moisture along with bending and fatigue affect the mechanical behavior of bamboo.

I-6: In Vitro Restoration of Tooth Root via Protein-Derived Mineralization Peptides: *Mustafa Gungormus*¹; Ersin Oren¹; Hanson Fong¹; Jeremy Horst¹; Malcolm Snead²; Ram Samudrala¹; Martha Somerman¹; Candan Tamerler¹; Mehmet Sarikaya¹; ¹University of Washington; ²University of Southern California

In the quest for developing biomimetic restoration protocols, we describe here remineralization of hydroxyapatite (HAP) microlayer on the root of mammalian tooth using peptides designed by similarity analysis of natural mineral-binding proteins and biocombinatorially selected peptides. The bioinformatics approach provides, e.g., amelogenin-derived peptides (ADPs) with various functions (surface affinity, mineralization or rate control) We demonstrate case studies where ADPs are used to remineralize artificial tooth root lesions. When treated with ADPs, exposed dentin remineralizes in a relatively short time, and the mineral is mechanically well-integrated with dentin and withstands clinically relevant stresses. Furthermore, in vitro cytocompatibility assays demonstrate that the newly formed mineral creates an environment to promote adhesion and proliferation of periodontal ligament cells. The designed mineralization peptides offer great potential for clinical applications leading to development of effective biomimetic therapies for root caries. The research was supported by GEMSEC, an NSF-MRSEC (DMR# 0520567) at the UW.

I-7: Kinetics of Phosphate Ion Cerium Oxide Nanoparticle Interaction and Effect on Redox Activity of Bare and Functionalized Cerium Oxide Nanoparticles: *David Letter*¹; Amit Kumar¹; Vanessa Moosavifazel¹; Soumen Das¹; William Self¹; Sudipta Seal¹; ¹AMPAC

Cerium oxide nanoparticles (CNPs) have drawn interest in biomedical science due to their superoxide dismutase and catalase mimetic activity. However recent studies have indicated that these activities can be altered by the presence of phosphate ions. It is necessary to understand the kinetics of the CNP phosphate ion interaction. The purpose of this study is to elucidate the CNP and phosphate ion interaction at different pH(6-8). Bare and functionalized CNPs with poly-ethylene glycol and dextran were used to do time-based assay using UV-Vis and photoluminescence spectroscopy. To evaluate whether the surface change is temporary or permanent in the buffer, the bare and functionalized CNPs were washed and characterized. Moreover, superoxide dismutase and catalase mimetic activity will be estimated to find bare and functionalized CNPs redox activity after exposure to phosphate ions. These experiments should give insight to how phosphate can affect CNPs catalytic function in biological systems.

I-8: Nanotechnology For Drug Formulation: Improving Solubility of Insoluble Drugs: *Aeriel Murphy*¹; Dennis Leung²; ¹University of Alabama; ²Merck Sharp & Dohme Corporation Inc.

Many of the marketed drugs we use today are practically insoluble. Nanomaterials science is being studied to improve the solubility of these drugs. Nanosize particles are ideal because they cover more surface area which improves exposure and bioavailability and they have faster dissolution rates in the body. Nanoparticle stability is a major issue because Van der Waals forces cause the particles to aggregate and clump together and Ostwald Ripening causes the particles to increase in size over time. Because of the stability issues polymer/surfactant stabilizers are being studied to help prevent aggregation and recrystallization. In this experiment, drug nanosuspension formulations were created using three model compounds and five different stabilizers. Each drug/stabilizer combination was tested for particle size, zeta potential, solubility, and chemical stability. The purpose of this experiment is to understand why certain drug/stabilizer combinations are more efficient than others by analyzing what properties make each combination unique.

I-9: Molecular Modeling of Adhesion Between Hydrogels and Polyurethane Fibers: *Hossein Salahshoor*¹; Nima Rahbar¹; ¹University of Massachusetts Dartmouth

Nano-scale modeling of hydrogels will lead to better understanding of their mechanical properties. Agrawal et. al. have previously reinforced hydrogels with polymer fibers to enhance their mechanical properties. In this study, both fibers and hydrogel are modeled using molecular dynamics (MD) framework using Condensed-Phased Optimized Molecular Potential (COMPASS) as the force field for the simulations. The hydrogel is modeled as a cross-linked polymer with Polyethylene Glycol Diglycidyl Ether (PEGDGE) as epoxy and Jeffamines as the curing agents. Hydrogel is constructed by mixing both chemicals in the presence of water followed by curing at 60-70° C. Mechanical properties of both hydrogel and fibers are studied and verified separately. Finally, the interface between hydrogel and polymer is studied. Interfacial energy is estimated by summation of the kinetic, non-bonded and potential energies. The interfacial energy per unit area of contact is computed and compared as a measurement of the interface strength.

I-10: Cortical Bone Fractures Initiate at Fatigue Microcracks Located Near Elevated Intracortical Porosity but not Elevated Mineralization:

*Travis Turnbull*¹; Ryan Roeder¹; ¹University of Notre Dame

The hypothesis that intracortical porosity provides stress concentrations for fracture initiation at pre-existing fatigue microcracks has been overlooked due to an inability to nondestructively measure intracortical porosity and large attention given to microcracks that predominately form within more



highly mineralized tissue. Post-mortem investigations of these microcracks are inherently limited to cracks that did not lead to fracture and may be misleading with respect to understanding fracture risk. Therefore, the spatial correlation between intracortical porosity, mineralization levels, and fatigue microdamage within specimens subjected to cyclic uniaxial compression followed by a tensile overload was measured for the first time using registered images in micro-computed tomography. Fatigue microcracks that subsequently acted as fracture initiation sites were spatially correlated with elevated levels of intracortical porosity, but not mineralization. This suggests that clinical fracture risk assessment could be improved by measuring intracortical porosity which is now clinically feasible due to recent advances in computed tomography.

EMPMD 2012 Technical Division Student Poster Contest

Sponsored by: The Minerals, Metals and Materials Society, TMS Electronic, Magnetic, and Photonic Materials Division

Monday PM
March 12, 2012

Room: Atlantic Hall
Location: Dolphin Resort

SP-1: Vertically Aligned Carbon Nanotubes as Active Electrodes for Metal Substrate Supercapacitors: *Radu Reit*¹; Justin Nguyen¹; William Ready¹; ¹Georgia Tech Research Institute

The aim of this project is to create dense growths of vertically aligned carbon nanotubes on various conductive substrates. Vertically aligned carbon nanotubes present a larger pore size as compared to activated carbon or nonaligned carbon nanotubes, increasing the motility of the ions contained in the electrolyte separating the two electrodes. By utilizing various combinations of a diffusion barrier layer and catalyst support layers, vertically aligned nanotube growth can be controlled to alter height and density. Current testing has produced samples on Inconel substrates with specific capacitance values of 51.1 ± 14.7 F/g and samples on aluminum substrates with specific capacitance values of 321.1 ± 86.1 F/g. With further optimization of the spatial distribution of vertically aligned carbon nanotubes, as well as the addition of pseudocapacitive elements to the current configuration, more powerful supercapacitors can be designed with potential applications in hybrid energy vehicles.

SP-2: Controlling Phase Evolution in Thin Film PZT by Switching pO₂ during Crystallization: *Patrick Wanninkhof*¹; Sung Wook Min¹; Jacob Jones¹; ¹University of Florida

As devices have decreased their power consumption, piezoelectric ambient vibration energy harvesting has become an attractive alternative to batteries. Thin film Lead Zirconate Titanate (PZT) can be easily integrated into MEMS devices and micro sensors using established semiconductor fabrication technology. This study explores phase evolution during the crystallization of these thin films. We used time-resolved in-situ XRD and SEM to investigate the effects of switching pO₂ during annealing. Previous studies observed that an intermetallic compound PtxPb forms at the interface of PZT thin film and platinum electrode between 300 and 450 C; in this experiment the atmosphere was switched from oxidizing to reducing at intermediate temperatures during annealing, 350, 400, and 450 C. The pO₂ during the dwell at 600 C influences the texturing of the perovskite structure, which affects the piezoelectric coefficient and energy conversion efficiency of the thin films.

SP-3: Correlation between Multi-scale Microstructure and Creep Properties of Micron Scale Coarse Grained Solder Interconnects: *Subhasis Mukherjee*¹; ¹University of Maryland, College Park

The mechanical properties of SnAgCu solder are controlled by their multiscale coarse grained microstructure. A secondary creep model has been proposed which captures two homogeneous lower length scales of the solder joints – nano scale Ag₃Sn IMCs dispersed in Sn-Ag eutectic

region and micron scale Sn dendrites embedded in Sn-Ag silver eutectic phase reinforced with micron scale Cu₆Sn₅ IMCs. Several morphological characteristics such as radius and volume fraction of dispersoids and reinforcements, size of Sn dendrites, distribution of IMCs in the matrix have been investigated and incorporated into a multiscale mechanistic creep model of dislocation climb and detachment to capture the dominant strengthening mechanisms. Theoretical insights into the influence of anisotropy of Sn on the viscoplastic properties of coarse grained solder interconnect are provided. The model is capable of effectively capturing the effect of alloy composition on SAC solders thereby helping in optimization of the viscoplastic behavior of SAC alloys.

SP-4: Effect of Doped Atom Magnetism On electronic Transport through C₅₉X and C₆₉X(X = B and N) Molecular Junctions: *Hamidreza Vanaie*¹; Mojtaba Yaghobi²; Zahra Sedaghat³; ¹Islamic Azad University; ²Islamic Azad University; ³Tehran University of Medical Sciences

In this paper, a theoretical study of spin-polarized quantum transport through a C_nX molecular junction is presented applying the Keldysh non-equilibrium Green's function formalism. The effects of contacts, doped atom and cage type and the gate and bias voltages on spin-polarized quantum transport through the C_nX molecular junction are considered in calculations. The calculations indicate that the spin-dependent local density of states of the C_nX molecules is the cause of magnetic moment on every carbon atom in the vicinity of the doped atom. Also, the spin polarization can reach as high as about 100% with proper selection of bias and gate voltages.

SP-5: Fabrication and Design of a Thin Film Triode Type Carbon Nanotube Field Emitter as an Electron Source: *Graham Sanborn*¹; Jud Ready¹; Stephan Turano¹; ¹GT

Electron sources are commonly used in many technological fields for applications ranging from space propulsion, display technologies, X-ray sources and vacuum electronics. Considering the advancements in electronics in recent times, the electron source has not significantly changed. Carbon nanotubes have shown favorable properties for field emission and performance as electron sources. The objective of this work is to optimize and understand CNT electron emission in a compact and lightweight design. This work presents the fabrication of a carbon nanotube field emission device using a Spindt type cathode design, which incorporates arrays of etch pits into a thin film substrate. Several process improvements were made to maintain electrical isolation of the gate, a single point failure. These improvements resulted in a unique cathode design that incorporates substrate etching to form pits containing bundles of carbon nanotubes. In addition, the carbon nanotube synthesis methods are presented.

SP-6: Improving Charge Transfer Characteristic of Graphene for Triiodide Reduction in Dye-Sensitized Solar Cells: *Santanu Das*¹; P Sudhagar²; Ved Verma¹; Dong Hoon Song²; Eisuke Ito³; S. Y. LEE³; Yong Soo Kang²; Wobong Choi¹; ¹Florida International University; ²Hanyang University; ³RIKEN-ASI

Graduate Student. We report the fabrication and functionalization of large scale graphene and its electrocatalytic properties towards iodine reduction in the dye sensitized solar cell (DSSC). The as grown graphene film, contained few layers of monolayer graphene sheet as confirmed by Raman spectroscopy and HRTEM. Further, the graphene film was reacted with CF₄ reactive ion plasma and fluorine ions were successfully doped in graphene as confirmed by XPS and UV-photoemission spectroscopy. From AFM and Raman spectroscopy, we confirm that the fluorinated graphene shows no structural deformations compared to the pristine graphene except an increase in surface roughness. Electrochemical measurements reveal that the enhancement of catalytic activity of graphene for iodine reduction with increasing plasma treatment time, which was attributed to an increase of graphene's catalytically active sites for charge transfer. Furthermore, the fluorine doped graphene was characterized as a DSSC counter electrode showing ~2.56% photon to electron conversion

efficiency with ~11mAcm⁻² current-density.

SP-7: Mechanical Behavior of DGEBA-DAPSONE Epoxy Networks from Molecular Dynamics Simulations: *Abhishek Kumar*¹; Veera Sundararaghavan¹; ¹Aerospace Department

Simulations were performed to study high strain and high strain rate mechanical behavior of epoxy-amine (Di-Glycidyl Ether of Bisphenol A cured with diamino diphenyl sulfone) cross-linked polymer networks through the entire stress - strain profile before fracture (elastic regime, plastic regime, yield point) under both glassy and rubbery conditions relevant for energy-dissipating light-weight composite materials. Approaches were developed to compute the phonon dispersion curves from MD simulations using velocity-velocity autocorrelation function in reciprocal space and non-local averaging kernels in Fourier space from the phonon dispersion curves. We did research on epoxy failure using atomistic techniques and non-local theory. The approaches developed here allow one to predict the strain at which failure will occur in an ideal structure even before synthesis of the epoxy polymer, using only the knowledge of the chemical structure.

SP-8: Nanotechnology and Its Applications: *Abhijeet Gaikwad*¹; ¹JBIMS

Nanotechnology is the projected ability to make things from the bottom up, using techniques and tools that are being developed today to place every atom and molecule in a desired place. If this form of molecular engineering is achieved, which seems probable, it will result in a manufacturing revolution. Presently our handling of the molecular manufacturing process is very crude, we move atoms around in great heaps and pile them together, but we lack the ability to snap them together in a meaningful way. With nanotechnology, we'll be able to snap together the fundamental building blocks of nature easily, inexpensively and in almost any arrangement that we desire. In this paper the author presents the basic concept of Nanotechnology with a focus on Nanocomputing. Further this paper takes a review of applications of nanotechnology in the fields of transportation, data storage, space exploration, national security, energy and information systems.

SP-9: New Numerical Method to Calculate the True Optical Absorption of Hydrogenated Nanocrystalline Silicon Thin Films and Solar Cells: *Fatiha Besahraoui*¹; ¹Oran University

The enhanced optical absorption measured by Constant Photocurrent Method (CPM) of hydrogenated nanocrystalline silicon thin films is due mainly to bulk and/or surface light scattering effects. A new numerical method is presented to calculate both true optical absorption and scattering coefficient from CPM absorption spectra of nanotextured nanocrystalline silicon films. Bulk and surface light scattering contributions can be unified through the correlation obtained between the scattering coefficient and surface roughness obtained using our method.

SP-10: Surface Morphology and Phase Distribution of Zn and Zn-Co Alloy Coatings, Obtained by Direct Current: *Meysam Heydari Gharahcheshmeh*¹; Ahmed Touhami²; ¹University of Texas at Brownsville; ²University of Texas at Brownsville

Zn and Zn-Co alloy coatings were electrodeposited on AISI 1018 steel specimens from weakly alkaline Glycine solutions by using direct current. The surface morphology, chemical composition and phase distribution of coatings were investigated using SEM, EDS and XRD. The results showed that increasing current density during deposition, increases cobalt content of the alloy coatings. It was also shown that increasing current density, up to 15 mA cm⁻², decreases the grain size and further increase in current density increases the grain size of the deposit. XRD results showed that Zn-Co alloy coatings with 1.95 and 3.34 wt.% Co are consisted of two phases (η and γ), but Zn-Co alloy coatings with lower cobalt content have single phase structure (η -phase).

SP-11: The Temperature and Excitation Intensity Effects on the Photoluminescence Spectra of InAs/InP Quantum Dots: *Fatiha Besahraoui*¹; ¹Oran University

The optoelectronics properties of InAs /InP quantum dots (QDs)

are investigated by means of photoluminescence (PL) measurements. The mechanisms of electron-heavy/light hole recombination which is responsible of the PL peaks appearance are explored in this study. The electron-hole recombinations are influenced by the temperature and the laser excitation intensity. The PL signal and its yield are reduced with the increase of temperature. Especially, in high energies range. The PLE measurements are very sensitive to the excitation intensity. From an appropriate value of Laser excitation, the energies levels will be saturated, which favors the light emission. The bands filling is translated by a widening in the PL spectrum towards the high energies range.

SP-12: Towards Ultra-thick Battery Electrodes: Aligned Carbon Nanotube - Enabled Architecture: *Kara Eyanoff*¹; Javed Khan²; Alexander Balandin²; Alexandre Magasinski¹; W. Jud Ready¹; Thomas Fuller¹; Gleb Yushin¹; ¹Georgia Institute of Technology; ²University of California

Increasing the specific capacity of Li-ion battery electrodes and minimizing the relative weight and volume of inactive components by increasing the electrode thickness are important for further improvements of Li-ion technology. Conventional electrodes contain active particles mixed with conductive additives and a polymer binder in a mixture typically limited by thickness and homogeneity, porosity control, tortuous diffusion paths, and high electrical and thermal resistances. We report the fabrication of ultra-thick (1 mm) electrodes composed of vertically aligned carbon nanotubes uniformly coated with Li-alloying materials (here, silicon) through vapor deposition techniques. The electrodes demonstrate a specific capacity much larger than standard graphitic anodes, high Coulombic efficiency, and stable performance for 250 cycles. With thermal conductivity >400 W•m⁻¹K⁻¹, the electrode provides a significantly lower thermal resistance than a densely packed nanoparticle-based electrode of similar thickness. Since most degradation processes in Li-ion batteries are temperature-dependent, the achieved results are of great practical significance.

SP-13: Applying Taguchi Method for Optimization of Pulsed TIG Welding Process Parameters of AZ31 Magnesium Alloy Weldments: *Alireza Amirkhani*¹; Alireza Ebrahimi²; Rasool Azari Khosroshahi²; ¹Tekin Joosh Asia Company; ²Sahand University of Technology

In this research, Taguchi method with an orthogonal array of L9 (34), was used for optimizing the parameters of pulsed TIG welding to obtain optimum mechanical properties (UTS) of AZ31 Magnesium alloy weldments. On this basis, the main parameters of pulsed TIG welding, including peak current (80-120 A), base current (20-40 A), pulse frequency (1.6-5 Hz), and welding speed (200-300 mm/min), each in three levels, were investigated. Then, the effect of each parameter on ultimate tensile strength (UTS) was evaluated. In addition, to choose a proper set of parameters, results were analyzed by variance analysis (ANOVA).

EPD 2012 Technical Division Student Poster Contest

Sponsored by: The Minerals, Metals and Materials Society, TMS, TMS Extraction and Processing Division

Monday PM
March 12, 2012

Room: Atlantic Hall
Location: Dolphin Resort

SP-14: Aluminum-zinc Dealloying: A Comparative Analysis of Processing Methods for Porous Metals: *Rafael Soler-Crespo*¹; Elvin Estremera¹; Ulises Barajas-Valdes¹; Amarilis Declat¹; Oscar Suarez²; Arturo Hernandez-Maldonado¹; ¹University of Puerto Rico - Mayaguez

Dealloying is the removal of a metallic element in a binary alloy by means of controlled corrosion processes. Due to its chemical nature, we selected aluminum-zinc binary alloys system as suitable candidates for dealloying using free or electrochemical corrosion. The application of an electrochemical potential with a galvanic cell aids in breaking the



natural passivation on the surface of the alloy. Therefore, we prepared highly porous substrates from these distinct routes controlling various parameters. Aluminum-zinc alloys were specially cast and dealloyed using both pathways; varying composition, processing time and solidification rate upon alloy processing. Optical microscopy, scanning electron microscopy and image analysis permitted the microstructure characterization of the resulting porous material. Hardness measurements were performed to understand the behavior of the substrate, according to the processing technique used. The results show that alloy composition and cooling rate have a prominent effect in the properties of the obtained porous substrate.

SP-15: Delaminating and Recycling of Printed Circuit Boards using Supercritical Carbon Dioxide: *Mariela Robledo¹; ¹Arizona State University*

Currently, traditional metallurgical processes are being used for the recycling of printed circuit boards which require high energy input, provide limited economic returns, and are environmentally harmful. The objective is to test a new, exciting technology using carbon dioxide, which is abundant and environmentally benign, in supercritical conditions to delaminate and recycle PCB. Recent experimental results show successful delamination of the printed circuit board using the supercritical carbon dioxide process, in addition to being non-hazardous for the environment. Future work includes integrating other processes to this approach to understand the polymer degradation mechanism and identify previous components of contamination threats.

SP-16: A Novel Synthesis Method for Titanium Dioxide Pigment – Eliminating Direct CO₂ Emissions: *Scott Middlemas¹; Z. Zak Fang¹; Peng Fan¹; ¹University of Utah*

Titanium dioxide (TiO₂) has been widely used as pigment in paints, paper and cosmetic products, as well as high-tech applications such as PV Cells, semiconductors, biomedical devices and air purification. TiO₂ pigment is primarily produced by the high temperature chloride process, resulting in considerable CO₂ emissions. A novel hydrometallurgical process for making TiO₂ pigment without CO₂ emission is investigated. The new method promises to eliminate direct CO₂ emissions, consume significantly less energy, and produce minimal environmental waste. The novel process involves molten salt roasting of titania slag, with subsequent leaching, solvent extraction, hydrolysis, and calcination stages, resulting in high-purity anatase or rutile pigments while realizing significantly reduced environmental impacts. Pigment whiteness is critically sensitive to trace amounts of discoloring impurities such as iron and chromium. Several methods for reducing the levels of these impurities are investigated. Energy consumption and emission models are also developed.

SP-17: Dielectric and Magnetic Losses of Iron Oxides in Microwave Ironmaking: *Zhiwei Peng¹; ¹Michigan Technological University*

Dielectric and magnetic losses of iron oxides in the microwave ironmaking process were evaluated based on the characterizations of microwave absorption properties of hematite, magnetite and wüstite. The equations for determining the losses were first derived from Maxwell's equations. It was subsequently followed by the microwave permittivity and permeability measurements of the oxides using the cavity perturbation technique. The calculation of the losses shows that microwave ironmaking strongly depends on the dielectric losses of hematite and wüstite as well as the magnetic loss of magnetite.

SP-18: Dimethyl Sulfoxide: An Alternative to NMP for Electrochemical Performance of Cathode Active Materials in Lithium Ion Battery: *Oluwatosin Bankole¹; Lixu Lei¹; ¹Southeast University,*

The effect of extracting and doping cathode active material of lithium ion battery, LiMn_{1/3}Ni_{1/3}Co_{1/3}O₂ with dimethyl sulfoxide (DMSO) instead of the commonly used N-methylpyrrolidone (NMP) on the electrochemical performance of the battery has been investigated. Observation shows that doping the cathode materials with DMSO will increase the conductivity

of the battery especially for the LiMn_{1/3}Ni_{1/3}Co_{1/3}O₂ calcined with the discharge capacity of 210 mAhg⁻¹ and 152 mAhg⁻¹ at 0.1C rate in the third and twenty-one cycles with approximately 70% and 61% discharge-charge efficiencies respectively. The X-ray diffraction patterns obtained revealed that LiMn_{1/3}Ni_{1/3}Co_{1/3}O₂ has been successfully recycled by DMSO used. The results of the electrochemical performance show that NMP could be replaced with relatively cheap DMSO on the basis of its effective battery conductivity and also being environmentally safe according to the Data Safety Sheet.

SP-19: Electrochemistry of Enargite: Reactivity in Alkaline Solutions: *Robert Gow¹; Courtney Young¹; Hsin Huang¹; Greg Hope²; Yasushi Takasaki³; ¹Montana Tech; ²Griffith University; ³Akita University*

The presence of enargite (Cu₃As₃S₄) is problematic in gold processing as it is refractory, increasing cyanide and oxygen consumption, and environmentally hazardous. Selective leaching and treatment of the arsenic would prove advantageous to conventional gold leaching methods. The reactivity of enargite samples from Montana, US and Quiruvilca, Peru were studied under alkaline conditions, pH range of 8-13, using a cyclic voltammetry corrosion cell setup. Raman spectra of the surface were taken during and after cycling to compare surface species against theoretical predominance diagrams. Under slightly oxidizing conditions, covellite (CuS) peaks were found on the surface in a short matter of time, above ~0V vs SHE for pH 9-13, suggesting arsenic leaching, but for longer conditioning times, elemental sulfur peaks were also found, which created a passivating surface layer. By operating above pH 12, under reducing conditions, ~-0.500V vs SHE, arsenic can be leached as a thioarsenate (AsS_(4-x)O_x³⁻), without sulfur formation.

LMD 2012 Technical Division Student Poster Contest

Sponsored by: The Minerals, Metals and Materials Society, TMS Light Metals Division

Monday PM
March 12, 2012

Room: Atlantic Hall
Location: Dolphin Resort

SP-20: Feasibility Study of the Fabrication of a Niobium Diboride/Aluminum Composite: *Jose Moreno Quiles¹; Neshma Lopez¹; ¹University of Puerto Rico - Mayaguez*

Despite the low density of ceramics, an appealing characteristic for aerospace applications, diboride compounds cannot be used in critical applications due to their brittle nature. The purpose of this research was to study physical properties of niobium diboride specimens containing different levels of aluminum. In the fabrication of the new composite, different homogenization techniques were used, including jar milling and high energy ball milling. Powder samples are shaped into green bodies using a cylindrical chamber pressed to 7500 psi. The samples were sintered at 600°C for two hours in a vacuum capsule to avoid oxidation. It was found that boride particles size reduction by fragmentation is the key to highly homogeneous samples and that ball milling is an effective method to homogenize the dispersed phase distribution in the composite. Also, percentages of aluminum ranging from 25 to 40 wt % were found to be more effective in the sintering process.

SP-21: Mechanical Behavior of Cast Mg AZ31-B Alloy Produced by Magnetic Suspension Melting Process: *Paige Boehmcke¹; Nagy El-Kaddah¹; Aerial Murphy¹; ¹Univ of Alabama*

This poster describes the mechanical behavior Mg AZ31-B alloy produced via the Magnetic Suspension Melting (MSM) technique at a low superheats. In comparison to the dendritic structures observed in conventionally cast alloys, it was found that casting via MSM at low superheat produced a fine globular grain structure. In the MSM cast alloy, the Mg17Al12 phase formed mainly at the grain boundaries, in contrast

to conventional castings which exhibited dendritic entrapment within the grains. Charpy impact energies for the MSM castings were equivalent to published values for Mg-Al-Zn alloys. Conventional castings exhibited large regions of quasi-cleavage decohesion and microshrinkage voids whereas in the MSM castings the cleavage facets were smaller and less numerous, and the percentage of microvoids was higher, suggesting a higher potential for plastic deformation.

SP-22: Effect of Precipitates on Shear Banding during Deformation of Mg Alloys: *Frank Sapienza¹; Zachary Bryan¹; Michele Manuel¹; ¹UF*

Magnesium alloys that contain reinforcing particles exhibit increased strength, but have decreased ductility due to extensive shear banding and void nucleation. Research in steels and aluminum alloys has shown that altering the particle volume fraction affects the homogeneity of plastic flow and can increase the propensity for shear band formation. To improve the ductility of magnesium alloys, the connection between particles and shear band formation must be elucidated. The effect of varying precipitate volume fraction on the deformation behavior of Mg-Al alloys under shear loads at strain rates of 10^{-4} to 10^{-2} mmsec⁻¹ and temperatures of 25°C and 300°C has been characterized. The formation and propagation of shear bands under these deformation conditions was examined in relation to the initial microstructure. These experiments highlight the role of precipitates on the shear deformation and shear banding behavior of magnesium alloys. This research is supported by the National Science Foundation (Award#: DMR-0845868).

SP-23: The Effect of Scandium Additions on the Degradation Behavior of Magnesium in Simulated Body Fluid: *Nancy Nguyen¹; Harpreet Brar¹; Michele Manuel¹; ¹University of Florida*

With advances in health care and technology, the human life expectancy has increased and the need for bioabsorbable orthopedic and cardiac implants is following suit. So far research has shown that magnesium is a good candidate for biodegradable implant applications. It has high specific strength, high fracture toughness, and an elastic modulus that is comparable to that of human bone. Additionally, Mg and its corrosion products are non-toxic. However, the application of pure magnesium in implant applications is limited by its low ultimate strength and high corrosion rate. Addition of alloying elements has shown to alleviate this problem by improving both strength and corrosion resistance. This paper analyzes the effect of scandium additions on the degradation behavior of magnesium in Hank's solution. Hydrogen evolution measurements were used to determine the rate of degradation while the microstructure and corrosion products were analyzed using optical and electron microscopy.

SP-24: Evaluation of the Mechanical Response of a Bcc Mg-Li-Al/C Composite: *Ryan Hooper¹; Zachary Bryan¹; Michele Manuel¹; ¹University of Florida*

Mg alloys with more than 11 weight percent Li exhibit a bcc crystal structure that has been documented to give greatly improved ductility; however, these alloys possess limited strength. The addition of secondary phases via precipitation or ex-situ addition has shown great promise in the strengthening of these alloys. In this study C was added to a Mg-Al-Li alloy due to its potential to react with Al to form Al₄C₃, which would strengthen the bcc matrix. Microscopy and x-ray diffraction were used to determine the extent of the Al-C reaction. The composite was then tested in tension and the results were compared to the monolithic matrix, specifically looking for increases in strength while retaining the desirable ductility of the alloy. This study provides insight into a method of in situ synthesis of a potential strengthening phase in Mg alloys. This work was funded by National Science Foundation Grant#: DMR-0845868.

SP-25: Experiments and Modeling of Low-Cycle Fatigue of Extruded 6061 Aluminum Alloy: *Andrew Brammer¹; J Jordan¹; ¹The University of Alabama*

In this study, we reveal the micromechanics of fatigue damage with respect to microstructure in an extruded 6061 aluminum alloy. Low-cycle fatigue tests were conducted in strain control at room temperature and

relative humidity. Scanning electron microscopy observations were made on the fracture surfaces to distinguish the three stages of fatigue damage. Fatigue cracks were found to initiate primarily from intermetallic particles at or near the surface. In the microstructurally/physically small crack growth regime, the fracture surface displayed a rough and brittle like fracture along the propagation direction. Striation spacings were measured and were found to vary across grain boundaries. In the long crack regime the striation spacings became more uniform, indicating that crack growth was less influenced by microstructure. Finally, a multistage fatigue model based on the relative microstructural sensitive features quantified in this study was employed to capture the fatigue damage experimentally observed in this alloy.

SP-26: Application of Computational Thermodynamics and Precipitation Kinetics to Light Weight Al Alloy Design: *Danielle Belsito¹; Richard Sisson¹; ¹Worcester Polytechnic Institute*

The U.S. Military needs structural materials for air and land transportation vehicles that provide superior mobility as well as protection from the impact of improvised explosive devices (IEDs) and projectile artillery to increase soldier survivability. To meet that need, new high strength, high toughness, light weight alloys are being developed. This project focuses on an effort to develop an alloy to be applied for a cold spray application. Initial efforts involve the development of multi-component phase diagrams, isotherms, and isopleths using thermodynamic and kinetic software, Thermo-Calc, Pandit and TC-PRISMA®, to predict the microstructure and performance of this alloy and therefore performance. Precipitation and dispersion hardening will be investigated, including the effect of potential cohesive precipitate-forming elements. Additional factors affecting process results will also be examined, including the process control agents and cryomilling process parameters. Finally, characterization of the powders and coatings will be performed using TEM, SEM, XRD, and SIMS.

SP-27: A Study of Biodegradable Mg-Ca-Sr Alloys: *Ida Berglund¹; Harpreet Brar¹; Malisa Santinoranont¹; Benjamin Keselowsky¹; Michele Manuel¹; ¹University of Florida*

Magnesium (Mg) has properties like high specific strength and an elastic modulus comparable to that of bone, and it is non-toxic and also susceptible to dissolution. It is therefore an ideal candidate for biodegradable orthopedic implant applications. The low corrosion resistance and yield strength of pure Mg is, however, a major limitation that needs to be addressed in the fabrication of these materials. One approach to increase the mechanical properties and corrosion resistance of Mg is by adding alloying elements. For this study, calcium and strontium were chosen as alloying elements for their biocompatibility, strengthening potential and grain refining properties. Different compositions of the Mg-Ca-Sr system were fabricated and their degradation rate in Hanks' solution was established. The microstructures of the alloys were also characterized before and after immersion. It was shown that Mg-1.0Ca-0.5Sr has good potential for orthopedic implant applications.

SP-28: New Numerical Method to Calculate the True Optical Absorption of Hydrogenated Nanocrystalline Silicon Thin Films and Solar Cells: *Fatima Besahraoui¹; ¹Oran University*

The enhanced optical absorption measured by Constant Photocurrent Method (CPM) of hydrogenated nanocrystalline silicon thin films is due mainly to bulk and/or surface light scattering effects. A new numerical method is presented to calculate both true optical absorption and scattering coefficient from CPM absorption spectra of nanotextured nanocrystalline silicon films. Bulk and surface light scattering contributions can be unified through the correlation obtained between the scattering coefficient and surface roughness obtained using our method.



TMS 2012

141st Annual Meeting & Exhibition

SP-29: Oxidation Behavior of Zr56Al16Co28 Metallic Glasses: *Wenhuan Cao*¹; *Jiliang Zhang*¹; *Chan Hung Shek*¹; ¹City University of Hong Kong

The oxidation behavior of Zr56Al16Co28 bulk metallic glass was studied in synthetic air over the temperature range of 673–923 K. The oxidation kinetics of the metallic glass follows a two-stage or single parabolic rate law from 673K to 923K. Cobalt oxides precipitated on the topmost oxide layer of the metallic glass during oxidation. The observations on their morphologies show that the size and amount of these precipitations both increased with elevated temperature. A high resistance against oxidation in Zr56Al16Co28 bulk metallic glasses was observed below crystallization temperature: Only about 2 μ m-thickness scale formed after oxidation for ten hours at 773K. The oxidation is accelerated dramatically at 823K. However, the oxidation resistance was enhanced at a further increased temperature, 923K, which was likely attributed to the formation of large amounts of Al₂O₃ and m-ZrO₂.

SP-30: Sensitivity Analysis of Crack Initiation Life of a 2-grain Model of Ti-6Al-4V: *Daniel Sparkman*¹; *Harry Millwater*¹; *Somnath Ghosh*²; ¹University of Texas at San Antonio; ²John Hopkins University

Crack initiation in Ti-6Al-4V has been observed to occur in a grain with a hard orientation for basal slip neighboring a grain with a soft orientation. A crystal plasticity model of 2 grains was exercised considering the Schmid Factor of the soft grain, the misorientation angle between the two grains, and the soft grain size as random variables. A probabilistic sensitivity analysis of the time-to-crack-initiation was employed to ascertain the relative importance of the random variables. It was found that the Schmid Factor had the largest effect on the variance of the crack initiation life and that grain size and misorientation angle had little effect. A local sensitivity analysis found larger Schmid Factors result in smaller mean life and larger variance.

SP-31: Effects of Pulsed Magnetic Annealing on the Grain Boundary of Primary Recrystallized Microstructure in the Grain-Oriented Silicon Steel: *Junjun Huang*¹; *Lihua Liu*¹; *Xin Xia*¹; *Xiang Jiang*¹; *Lijuan Li*¹; *Qijie Zhai*¹; ¹Shanghai University

In this work, the effects of pulsed magnetic field applied during the annealing of grain-oriented silicon steel on the grain boundaries in the primary recrystallized microstructure were investigated. Samples of cold rolled grain-oriented silicon steel were annealed under pulsed magnetic field with the maximum strength 1T from three different directions-rolling direction, transverse direction and normal direction at the temperature of 700 \square for 16 minutes. Electron Backscattering Scattering Diffraction (EBSD) technology was used to measure grains for texture determination, and software called Channel 5 was used to calculate the messages of boundaries. Results show that pulsed magnetic field can influence the development of grain boundaries. It is found that the frequency of the low angle boundaries increases when pulsed magnetic field is applied, especially from the rolling direction. Compared to the ordinarily annealed sample, the frequencies of CSL boundaries vary in samples annealed with pulsed magnetic field in different directions.

SP-32: The Role of Solute Nature on the Deformation Behavior and Texture Evolution in Magnesium Alloys: *Zachary Bryan*¹; *Ryan Hooper*¹; *Michele Manuel*¹; ¹University of Florida

Rare earth solutes alter the basal-dominated texture exhibited by conventional magnesium alloys during recrystallization and lead to increased ductility. The unique texture component that arises has been attributed to shear band nucleation and solute drag effects. The rare earth solute characteristics that are needed for texture modification, however, remain unclear. This work systematically varied solute size and stacking fault energy through alloy selection to determine their individual and combined effects on the mechanical properties and annealed texture. Mechanical tests were performed at temperatures from 100 to 350 \square C and strain rates from 10⁻³ to 10⁻¹ s⁻¹ to elucidate the effect of dynamic strain aging on texture evolution. This research ultimately evaluates the role of solute size and stacking fault energy on the rare earth texture evolution.

This work is supported by the National Science Foundation (Award#: DMR-0845868) and the Department of Energy Office of Science Graduate Fellowship (Contract#: DE-AC05-06OR23100).

SP-33: The Temperature and Excitation Intensity Effects on the Photoluminescence Spectra of InAs/InP Quantum Dots: *Fatiha Besahraoui*¹; ¹Oran University

The optoelectronics properties of InAs/InP quantum dots (QDs) are investigated by means of photoluminescence (PL) measurements. The mechanisms of electron-heavy/light hole recombination which is responsible of the PL peaks appearance are explored in this study. The electron-hole recombinations are influenced by the temperature and the laser excitation intensity. The PL signal and its yield are reduced with the increase of temperature. Especially, in high energies range. The PLE measurements are very sensitive to the excitation intensity. From an appropriate value of Laser excitation, the energies levels will be saturated, which favors the light emission. The bands filling is translated by a widening in the PL spectrum towards the high energies range.

SP-34: X-Ray Radiography of Magnesium MMCs Processed by Electromagnetic Acoustic Transduction: *Hunter Henderson*¹; *Zachary Bryan*¹; *Orlando Rios*²; *Alexander Melin*²; *Gail Ludtka*²; *George Lopp*¹; *Yu-Min Su*¹; *Michele Manuel*¹; ¹University of Florida; ²Oak Ridge National Laboratory

Magnesium (Mg)-based alloys reinforced with ceramic nanoparticles have attained interest for their improvement in strength and ductility, compared to traditional Mg alloys. A specialized technique known as Electromagnetic Acoustic Transduction (EMAT), magnetically induced sonication, is evaluated with regard to the dispersion of several particle types in Mg. This technique potentially offers several advantages over traditional melt sonication, including non-contact, higher intensity, and smoother energy distribution. The present study investigates a pure Mg and Mg-Li alloys with and without ceramic nanoparticle reinforcement. Radiography investigating the macroscale distribution of particles and the associated causes is presented. The authors would like to acknowledge the support of the National Science Foundation (DMR 0845868), National High Magnetic Field Laboratory User Program, and Department of Energy's Energy Efficiency and Renewable Energy Industrial Technologies Program.

MPMD 2012 Technical Division Student Poster Contest

Sponsored by: The Minerals, Metals and Materials Society, TMS Materials Processing and Manufacturing Division

Monday PM
March 12, 2012

Room: Atlantic Hall
Location: Dolphin Resort

SP-35: Novel Three-Dimensional Printing Technology for Advanced Modeling and Casting of A356 Impeller: *Blake Whitley*¹; ¹The University of Alabama

Metal casting is one of the earliest known materials manufacturing methods, and has been employed for millennia for the creation of metal formation into desired forms. In this study, an analytical approach was taken in order to optimize the casting process through conditions of material selection, vent placement, riser placement and dimensions, mold filling orientation, superheat, and pouring rate. Through careful analysis of each of these conditions, we have taken steps to model and simulate the casting of an A356 impeller with optimal physical, microstructural, and mechanical properties. Advanced casting modeling software and mold printing technologies were employed for the creation of the ideal mold for the casting of the desired impeller. Through this systematic casting study, properties of near-net shape castings have been optimized for intricate and complex forms in three dimensions.

SP-36: Processing of Aluminum Wires and Its Effect on Their Electrical Properties: *Grace Rodriguez*¹; ¹University of Puerto Rico

The present study focuses on the fabrication of aluminum wires by adding NbB₂ particles into an aluminum matrix. These particles were obtained by fragmentation in a high energy ball mill, mixing aluminum powder with NbB₂. The product obtained was then compacted in a hydraulic press at 119.7 KPa and sintered at 600°C for two hours. Then the sintered pellets were incorporated into molten aluminum. After solidification the ingot was cold rolled to obtain 1mm diameter wires. The treated specimens were mechanically tested and their electrical resistivity was measured and compared with pure aluminum wires. The highest electrical resistivity measured in aluminum wires containing 1 wt.% of NbB₂ was 3.509•10⁻⁰⁸ Ω•m compared to 3.061•10⁻⁰⁸ Ω•m of pure aluminum wires cold-drawn under similar conditions. Our results evinced the feasibility of improving the mechanical properties of the material without significantly affecting its electrical resistivity.

SP-37: Frequency and Temperature Dependent Dynamic Mechanical Properties of Metal Matrix – Barium Titanate Composites: *Jack Tilka*¹; Zachary Bryan¹; Jacob Jones¹; Michele Manuel¹; ¹University of Florida

Ferroelastic reinforced metal matrices have exhibited anomalous dynamic mechanical properties that are believed to be caused by mechanical coupling between the metal matrix and the frequency-dependent ferroelectric reinforcement. To examine this unique behavior, powder metallurgy was used to fabricate a composite consisting of a copper matrix and ferroelastic barium titanate particles. Dynamic mechanical analysis of the storage and loss moduli as a function of frequency and temperature was completed on the composite, as well as the individual copper and barium titanate constituents. These studies are used to determine if there are mechanical properties that extend beyond those predicted by traditional mixing rules or superposition. Ultimately, this reveals details about the unique interaction of constrained ferroelastic particles in a damping matrix. This research was funded by NSF Grant #CMMI-0824352.

SP-38: Novel Manufacturing Processes for Ultra-fine Grained Microstructure in 9310 Steel: *Thomas Kozmel*¹; ¹Illinois Institute of Technology

Novel manufacturing processes that induce the formation of an ultra-fine grained microstructure may improve the wear resistance and performance of 9310 steel parts currently in use for gears, rotors and shafts. By inducing large amounts of strain during the hot deformation and carefully controlling the deformation temperature, dynamic recrystallization can assist in achieving a very fine grain size throughout the material. Results from preliminary studies investigating the dynamic recrystallization response of 9310 in double cone specimens are presented and discussed.

SP-39: Automatic Combination of Multi-tile EBSD Datasets: *Adam Shiveley*¹; Adam Pilchak²; Paul Shade²; Jay Tiley²; Donna Ballard²; ¹Southwestern Ohio Council for Higher Education; ²United States Air Force

Electron backscatter diffraction (EBSD) has found extensive use in the field of materials science. Faster acquisition speeds has led to the creation of large datasets using combinations of beam scans and automated stage movements. Stage positioning inaccuracies often lead to missing or duplicated data at tile boundaries. Thus, functions have been implemented to identify grain and phase boundaries in each scan and correlation functions to determine the appropriate offset between adjacent tiles. The advantages and limitations of the method are discussed.

SP-40: Electro-Chemical Mechanical Polishing (ECMP) For Electron Microscopy: *Kevin Shiveley II*¹; Jay Tiley²; Adam Shiveley³; Gopel Viswanathan⁴; Christopher Crouse⁴; ¹Universal Technology Corporation; ²United States Air Force; ³Southwestern Ohio Council for Higher Education; ⁴Universal Energy Systems

Surface preparation is a vital component when characterizing materials.

Surface or subsurface damage of the material can adversely impact data quality captured by backscatter electron imaging and electron backscatter diffraction (EBSD) techniques. To address these issues, a low-stress automated polishing device was developed. The system uses pulsed electrochemical reactions within an alkaline electrolyte to generate a thin passivation layer on the surface of the sample, which is removed by the mechanical vibration of the system. Results indicate that applied cyclic electrical potentials remove material faster than typical removal techniques. In addition, electron back scatter diffraction data showed a decrease in subsurface damage using the developed electrochemical–mechanical process compared to standard mechanical polishing techniques. The system design and the application of electrical potentials will be discussed.

SP-41: Synthesis and Characterization of Nacre-inspired Nanocomposites: *Omar Rodriguez-Negron*¹; Carlos Morales-del Valle²; Ruth Hidalgo-Hernandez; Paul Allison³; Robert Moser³; Mei Chandler³; Charles Weiss³; Phillip Malone³; ¹UPRM/ ARMY ERDC; ²UPRM; ³ARMY ERDC

The U.S. Army Engineer Research and Development Center is currently synthesizing and characterizing bioinspired nanocomposites utilizing the multi-layered hierarchical design principles found in nacre. Electro transport deposition and hydrothermal hot pressing are methods currently being investigated in order to synthesize nacre's hierarchical structure. Both methods are intended to provide the ability to control the crystallographic form, crystal size and crystal location within a polymer matrix. Calcium acetate and ammonium carbonate are the chemical compounds employed with the purpose of replicating calcium carbonate biomineralization. The influence over precipitate mineralogy of different reactants concentrations as well as the presence of magnesium acetate or strontium acetate was also investigated. X-ray diffraction is employed in characterizing the crystal structures being synthesized while scanning electron microscopy is used in determining the size and shape of the crystal structures forming. Initial results suggest the approach may produce useful new composites.

SP-42: Synthesis and Properties of Bulk Graphene NanoPlatelets Consolidated by Spark Plasma Sintering: *Andy Nieto*¹; ¹Florida International University

Graphene nanoplatelets (GNP) are consolidated as a bulk structure by spark plasma sintering (SPS) to study the feasibility of the structure retention at extreme processing conditions. Structural characterization of the sintered GNP pellet is performed using Raman Spectroscopy, X-ray diffraction and scanning electron microscopy. Mechanical and tribological properties are evaluated through nanoindentation and ball on disk wear testing. It is shown that bulk GNP structures can be successfully synthesized through SPS processing at an extreme temperature of 1850 °C and a pressure of 80 MPa. GNPs survived the processing with minimal damage to the structure. Energy dissipation mechanisms are observed in the form of bending and sliding of the platelets. The results indicate the potential for GNP to be successfully used as a reinforcing phase in ceramic and metal matrix composites synthesized by SPS.



TMS 2012

141st Annual Meeting & Exhibition

SMD 2012 Technical Division Student Poster Contest

Sponsored by: The Minerals, Metals and Materials Society, TMS Structural Materials Division

Monday PM

Room: Atlantic Hall

March 12, 2012

Location: Dolphin Resort

SP-43: Characterization and Quantification of X65, X80, and X100 Pipeline Steels for Statistical Microstructural Analysis: *Elisa Duesing*¹; Elizabeth Rust²; Brian Welk¹; Dan Huber¹; John Sosa¹; Hamish Fraser¹; ¹Center for the Accelerated Maturation of Materials; ²The Ohio State University

Currently, there are no quantitative databases available relating mechanical properties to microstructural features for pipeline steels. The work to be presented focused on determining the feasibility of collecting data for such a database using stereology to objectively quantify scanning electron micrographs. Specifically, three different pipeline steel samples, X65, X80, and X100, were examined. Based upon the microstructural features present in the various steels, quantitative analysis was performed on bainite, martensite, pearlite, and ferrite. Images were analyzed to obtain quantitative values for ferrite grain size, as well as the volume fraction of each phase. Finally, the data collected was used to display the statistical variance of the microstructure within a given sample, as well as between the various pipeline steels. Materials Image Processing and Automated Reconstruction (MIPAR) software developed within the Center of Accelerated Maturation of Materials (CAMM) at The Ohio State University was used for sample analysis.

SP-44: Analysis of Hafnium Addition Effects to Microstructural and Mechanical Properties in the Nickel-Titanium-Hafnium System for Shape-Memory Optimization: *Blake Whitley*¹; ¹The University of Alabama

Shape-memory alloys have emerged as a smart material of interest to materials scientists in recent years due to their unique physical properties which stem from characteristic microstructural features. Such alloys have become of particular interest for applications in the automotive, aerospace, telecommunications, and robotics industries where their unique material characteristics have seen the greatest potential. In this study, the Nickel-Titanium-Hafnium ternary alloy system has been selected for detailed analysis. The primary concern has revolved around the addition of hafnium to the system, and its effects on both microstructure and physical properties. After heat treatment in an evacuated system, alloys of varying hafnium content were analyzed on the basis of microhardness using Vickers hardness measurements. Changes in microhardness were subsequently correlated with microstructural changes through the employment of optical microscopy in order to monitor phase and precipitate formations.

SP-45: Design of pH and Thermal Sensitive Hydrogels for Catheter Based Minimally Invasive Heart Surgery: *Min Zhang*¹; James Bush¹; Travis Busbee¹; Zhenqing Li¹; Jianjun Guan¹; ¹Ohio State Univ

A family of injectable and pH-sensitive hydrogels was developed to deliver cardiosphere-derived progenitor cells (CPCs) to infarcted heart by a minimally invasive approach. The hydrogels were based on N-isopropylacrylamide (NIPAM), propylacrylic acid (PAA) and hydroxyethyl methacrylate-poly(trimethylene carbonate) (HEMA-PTMC). The hydrogels were injectable at physiological pH (7.4), but quickly gelled at pH similar to that in the infarct heart (6.5–6.8). This makes it possible to inject the hydrogels through catheters used for heart injection, and ensure sufficient cell retention after delivery. The hydrogels are also biocompatible. No significant cell death was observed. Furthermore, gel mechanical properties can be tuned to mimic the biomechanics of native heart muscle by alternating molar ratio of NIPAM, PAA and HEMA-PTMC. These results demonstrate that the developed hydrogels can potentially be used to deliver cells using minimally invasive approach.

SP-46: Serial Sectioning and 3D Reconstruction of Grains to Obtain Metric and Topological Properties: *Amy Adams*¹; David Rule¹; Veena Tikare¹; Burton Patterson¹; Robert DeHoff¹; ¹University of Florida

Grain size and the grain growth process have a significant impact on mechanical and other properties of materials. Just how the grain volume distribution and related topological properties evolve throughout grain growth is still not understood. These distributional characteristics of the grain structure cannot be obtained from normal 2D images and require 3D analysis to obtain. This poster presents serial sectioning at different stages within the grain growth process and the development of 3D reconstruction methods. The initial grain structures were synthesized via powder processing to have wide and narrow initial grain size distributions to compare their evolution throughout grain growth. Metric properties include distribution of grain volumes, surface areas, faces, and integral mean curvatures per face class. Topological properties include the distributions of the grain volume and numbers of faces. It is intended to later compare these experimental results with 3D Monte Carlo grain growth simulations.

SP-47: Atomistic Prediction of Precipitate Strengthening in Nanoscale Metallic Multilayers: *Niaz Abdolrahim*¹; Ioannis Mastorakos¹; Hussein Zbib¹; ¹washington state university

Nanoscale metallic multilayer's (NMM) can play a leading role in the future micromechanical devices due to their high structural stability, mechanical strength, high ductility, toughness and resistance to fracture and fatigue. The design of better NMMs can be achieved by properly tailoring the nanostructure using appropriate materials-by-design algorithms. However, before those materials are put into service in any significant applications, many important fundamental issues remain to be understood. Among them, the role of the second phase particles on the strengthening properties of the nanocomposite materials. The purpose of this work is to address the question if the second phase particles can strengthen the nanoscale materials in the same manner as in bulk crystalline solids. In this view, Cu/Nb thinfilms with spherical Nb particles inside the Cu layer were examined using molecular dynamics simulations and show to exhibit a significant improvement on their mechanical behavior, compared to similar structures without particles.

SP-48: A Review of First-Principles Investigations of Iron Based Alloys Using DFT: *Krista Kalac*¹; Julia Medvedeva¹; ¹Missouri S&T

First principles investigations of the behavior of metallic solids have become more widely used as computational power increases. Density Functional Theory (DFT), a commonly used quantum based modeling technique, is used to investigate electronic structures of multi-component systems. DFT provides high accuracy calculations using the plane wave basis for solid state systems. Iron based alloy design has been a continual subject of interest due to the large market and wealth of experimental data. Immediate results of the calculations provide optimum atom positions for various structures, cell parameters, and atom size, as well as the magnetic moment for a given structure. Calculated total energy values and forces on atoms can be used in a wide array of applications, leading to advanced understanding of structural properties, such as the stability of an inclusion or intermetallic phase and their impact on fracture toughness.

SP-49: Characterization of Transformation Toughening in Shape Memory Alloy Reinforced Composites: *Fatmata Barrie*¹; Michele Manuel¹; ¹University of Florida

Materials capable of undergoing martensitic phase transformations have been shown to inherently increase the fracture toughness of monolithic and composite materials in a process known as transformation toughening. The toughness behavior has been extensively researched for certain classes of transforming materials such as stabilized zirconia, however not for shape memory alloys (SMAs). Therefore, a fundamental understanding of the martensitic phase transformation on SMA embedded composites is needed to further the development of SMA embedded

composites. A comparative J-integral fracture toughness study was performed using nickel-titanium (NiTi) SMAs and non-transforming aluminum reinforcements embedded within an epoxy matrix. The NiTi was used in the as-received and heat-treated conditions to change the stress that the martensitic transformation was induced. The fracture toughness results will be used to explain the effects of the SMA martensitic transformation on SMA embedded composites. The authors gratefully acknowledge support from the National Science Foundation under grant number CMMI-0824352.

SP-50: Creep Deformation Mechanisms in Grade 91 Steel: *Triratna Shrestha*¹; Indrajit Charit¹; Mehdi Basirat¹; Gabriel Potirniche¹; Karl Rink¹; ¹University of Idaho

Grade 91 (modified 9Cr-1Mo) steel is a candidate material for the pressure vessel of the Very High Temperature Reactor (VHTR). The creep behavior of this steel was studied in the temperature range of 873 K to 1023 K and at a stress range of 35 to 350 MPa. Threshold stress correction of the creep data in the higher stress regime yielded a true stress exponent of 5, indicating the operation of high temperature climb-controlled creep. The estimated threshold stresses displayed strong temperature dependence. The origin of the threshold stress was explained in terms of particle-dislocation attractive interaction. Creep tests in the lower stress regime resulted in a stress exponent of 1, indicating the operation of a Newtonian viscous creep mechanism. Furthermore, the rate-controlling creep mechanisms in both the stress regimes were elucidated with the help of transmission electron microscopy (TEM).

SP-51: Crystal Structure and Disorder of Refractory High-Entropy Alloys: *Soumyadiptra Maiti*¹; Walter Steurer²; ¹ETH Zurich ; ²ETH Zurich

The refractory HEA contains metals like W, Mo, Ta, Nb, V, Zr, Hf etc in high proportion and could have potential high temperature applications. Equiatomic WMoNbTa alloy was prepared from powder through arc melting in argon atmosphere. The alloy was annealed and heat-treated at different temperature inside tantalum ampules starting from 1800°C. X-Ray diffraction of both powder and single crystals were performed. SEM-EDX was done to investigate grain sizes and compositional variance of annealed sample. Analysis shows grain size of 80-150 micron and the compositional variance within 2% from expected value. The materials were annealed for long time at intermediate temperature (900-1000\176C, 1-3 weeks) but no significant ordering from BCC structure could be found. The peak broadening analysis from diffraction indicates crystallite domain size of 50nm, which appears unexpected from 100micron grains. This could be explained by grains forming nano-domains and atoms having high atomic displacement parameter.

SP-52: Design of Aluminum-Based Metal Matrix Composite with Self-Healing Capabilities: *Charles Fisher*¹; Michele Manuel¹; ¹University of Florida

In order to advance to the next generation of smart structural materials, metal-matrix composites with the ability to self-heal are currently under development. Self-healing has the potential to greatly increase the life-cycle of specific components, especially for processes involving multiple cycles as within the aerospace industry. However, designing new alloy systems which possess the appropriate processing-structure-property relationships for self-healing, however, can be a difficult undertaking. The multifaceted interaction across multiple length scales yields a very complex issue for composite development. To combat this issue, a systems design approach governed by thermodynamics and empirical models was utilized to aid in the selection of materials with potential for self-healing. This study will present the alloy selection process for an Al-based alloy utilizing shape-memory alloy wire reinforcements to aid in self-healing in addition to initial characterization of the composite. Support for this project comes from the National Science Foundation under grant number CMMI-0824352.

SP-53: Analysis of Serrated Flow in Ni-10Pd during High Temperature Instrumented Microindentation: *Bin Gan*¹; Sammy Tin¹; ¹Illinois Institute of Technology

Instrumented microindentation tests were carried out on a Ni-10Pd(wt.%) alloy from room temperature to 450°C with loading rates spanning from 62.5 to 1000mN/s. When this single phase, substitutional solid solution was tested at temperatures above 337.5°C, the loading segment of the load-depth curve that was initially smooth became serrated after reaching a critical load. For the same loading rate, increasing the testing temperature from 350 to 450°C resulted in an earlier appearance of the serrated flow with a lower load threshold. At a constant temperature (450°C), increases in the loading rate resulted in an earlier occurrence of the serrated flow with a higher load threshold. A modified cavity expansion model that accounts for the reconfiguration of dislocation substructure as well as the interactions between solute atoms and forest dislocations was developed and used to elucidate the mechanisms responsible for the serrated flow behavior.

SP-54: High Temperature Deformation of Ti-Al-Nb-Cr-Mo Alloys: *Glenn Bean*¹; Fereshteh Ebrahimi¹; Hans Seifert²; Michele Manuel¹; ¹University of Florida; ²Karlsruhe Institute of Technology

Titanium aluminides with $\gamma+\alpha_2$ microstructure have been shown to exhibit good mechanical properties below 700°C, but it is desirable to increase high temperature properties. Limited research has been conducted towards the development of alloys with $\gamma(\text{TiAl})+\sigma(\text{Nb}_2\text{Al})$ microstructure, and alloys with over 0.5 V_f σ -phase have exhibited excellent high temperature properties up to 1000°C. However, these alloys are brittle at room temperature, prompting the study of alloys with less than 0.5 V_f σ -phase which has led to improvements in room temperature properties. To determine the high temperature performance of these alloys with below 0.5 V_f σ -phase, a series of alloys in the TiAlNb(CrMo) system have been developed, characterized, and tested at elevated temperatures ($\approx 700^\circ\text{C}$). The performance of these alloys has been evaluated at strain rates ranging from 10^{-2} to 10^{-5} s^{-1} and relationships between chemistry, microstructure, and the resulting mechanical properties were investigated. This work has been supported by NSF/AFOSR (DMR-0856622).

SP-55: Influence of Austenite Stability on Steel Low Cycle Fatigue Response: *Greg Lehnhoff*¹; Kip Findley¹; ¹Colorado School of Mines

Materials containing metastable austenite, such as multiphase transformation induced plasticity (TRIP) steels, demonstrate exceptional combinations of strength and ductility that allow utilization of thinner automobile structural components for weight reduction purposes. Both the monotonic and fatigue properties of these steels have been shown to depend strongly on the stability of austenite with respect to deformation induced martensite formation. To properly design steel compositions and processing schedules for components subjected to complex loading histories, a fundamental understanding of the factors governing austenite stability is critical. The current work focuses on the effects of austenite composition, namely aluminum and silicon alloying, on resulting austenite properties such as stacking fault energy in fully austenitic steels. These properties will then be correlated to austenite stability and mechanical response during strain-controlled fatigue testing using a modeling approach based on the underlying physical mechanisms of deformation induced martensite nucleation.

SP-56: Mechanical Characterization of Hierarchical Biological Structures: *Rogie Rodriguez*¹; Wayne Hodo²; Paul Allison²; Mei Chandler²; Jen Seiter²; Aimee Poda²; Mark Chappell²; Brandon Lafferty²; ¹UPRM/US Army ERDC; ²US ARMY ERDC

Research on biological systems such as abalone shell, turtle shell, and human bone revealed carefully arranged multilayered systems. Each layer comprises unique subscale structures resulting in properties far superior to any man-made materials and systems. Understanding such structures will enable pathways to improved bioinspired materials for many applications such as human body armor and high-energy absorbent materials. Therefore, this investigation was focused on studying the



mechanical and chemical properties of multilayer biological structures, specifically the alligator gar (*Atractosteus spatula*) fish scales. Scanning electron microscopy on the fish scale cross-section revealed a three-layer arrangement with distinct differences in their morphologies. X-ray fluorescence (μ -XRF) was performed to determine the elemental distribution within the fish scale existing layers. Atomic force microscopy (AFM) was performed on the cross-section for micro and nanostructural characterization. Mechanical testing based on nanoindentation revealed a functional gradient on the elastic modulus, increasing from the inner to the outer layer.

SP-57: New Numerical Method to Calculate the True Optical Absorption of Hydrogenated Nanocrystalline Silicon Thin Films and Solar Cells: *Fatiha Besahraoui*¹; ¹Oran University

The enhanced optical absorption measured by Constant Photocurrent Method (CPM) of hydrogenated nanocrystalline silicon thin films is due mainly to bulk and/or surface light scattering effects. A new numerical method is presented to calculate both true optical absorption and scattering coefficient from CPM absorption spectra of nanotextured nanocrystalline silicon films. Bulk and surface light scattering contributions can be unified through the correlation obtained between the scattering coefficient and surface roughness obtained using our method.

SP-58: Recycling of the Alloy AZ91D Departing from Scrap in the Shape of Shavings Contaminated with Mineral Oil: Roberto Lucci¹; Roger López Padilla¹; ¹Universidad Tecnológica Nacional Facultad Regional Córdoba

In this paper we present the results of experiments carried out for recycling melting AZ91D alloy, departing from scrap in the shape of small shavings contaminated with mineral oil, which come from machining centers of automotive industry. Due to the large surface exposed and contamination of the shavings, these were upgraded prior to their fusion. Later, the recycling was realized using a device designed for the fusion of the shavings under protective atmosphere of gas argon with mixtures salts. The results showed an average yield of 80% metal recovery. Jointly presented some results of metallographic, mechanical and chemical alloys obtained.

SP-59: Rheological Performance and Compressive Strength of Superplasticized Mortar Cements with SiO₂ Nanoparticles Additions: *Luis Zapata*¹; Genock Portela¹; O. Marcelo Suárez¹; Orlando Carrasquillo²; ¹University of Puerto Rico, Mayagüez; ²US Army Corps of Engineers

This paper aims to study the effects nanoparticles of SiO₂ (nS) employed in type I Portland cement (PC) mortars at w/b=0.35 and 0.40 (cement:sand ratio=1:3) under various dosages of superplasticizer (SP). Stage I presents Marsh cone tests (MCT) to estimate the rheological parameters of the SP grouts at w/b=0.35 and 0.40. Stage II presents factorial experiments at w/b=0.35 to evaluate the flow area (A~), fresh density (UW) and air content (AC) in the fresh mortar state. The variables analyzed were statistically significant with respect to nS and SP following nonlinear relationships. Stage III studies the 90 days compressive strengths (Sc) of mortar cubes at w/b=0.35, where the nS content seems to be the noteworthy parameter. The maximum strength was obtained at 1.0 wt%. In all cases, the oversaturation for A~, UW, and AC was defined positive. SEM examinations show that Sc was controlled by densification of the ITZ.

SP-60: Atom Probe Tomography of Simulated Fission Product Segregation in CeO₂: *Billy Valderrama*¹; Hunter Henderson¹; In-Wook Park²; Jianling Lin²; John Moore²; Clarissa Yablinsky³; Todd Allen³; Michele Manuel¹; ¹University of Florida; ²Colorado School of Mines; ³University of Wisconsin-Madison

To improve the performance of nuclear fuel, one must understand the irradiation induced defects that lead to the decrease in fuel performance at an atomic scale. Irradiation induced defects, specifically fission gas bubble formation and nucleation, fission product segregation to grain boundaries and clustering, are of interest in this investigation. Characterization

techniques, like atom probe tomography (APT) provides the capability to spatially resolve these features at an atomic scale. This study investigates the segregation behavior of fission products (Xenon and Lanthanum) in surrogate nuclear fuel material (CeO₂) using APT. The Xe doped CeO₂ samples analyzed were ion implanted with 400 keV Xe⁺ ions and annealed to induce clustering. The La doped CeO₂ sample analyzed was irradiated with 1.8 MeV Kr⁺ ions to simulate irradiation induced diffusion of fission products. Commentary will also be provided on the advantages and challenges in using APT to study nuclear fuel. DOE Contract No. DE-AC07-05ID14517.

SP-61: The Development of Nanostructured In₂O₃ Oxide by Electron Stimulated Oxidation on InP and InSb Surfaces: *Fatiha Besahraoui*¹; ¹Oran University

We have used the Auger Electron Spectroscopy (AES) and Electron Energy Loss Spectroscopy (EELS) as an appropriated methods of surface characterization to study the effect of the electrons beam on the morphology of InP and InSb surfaces. The electronic bombardment of InP and InSb surfaces leads to the creation of In₂O₃ nanostructures. The explored AES and EELS spectra of InP and InSb compounds demonstrate the development of In₂O₃ oxide of small size on the irradiated InP and InSb areas. We have developed these experimental results by using a simulation methods based on the electron-matter interaction process. The CASINO simulation method used in this study shows that the distribution mode of In₂O₃ nanostructures on InSb surface is most clear than on InP one. This behavior is due to the good stability and the high compactness of InSb compounds compared to the InP one.

SP-62: The Temperature and Excitation Intensity Effects on the Photoluminescence Spectra of InAs/InP Quantum Dots: *Fatiha Besahraoui*¹; ¹Oran University

The optoelectronics properties of InAs/InP quantum dots (QDs) are investigated by means of photoluminescence (PL) measurements. The mechanisms of electron-heavy/light hole recombination which is responsible of the PL peaks appearance are explored in this study. The electron-hole recombinations are influenced by the temperature and the laser excitation intensity. The PL signal and its yield are reduced with the increase of temperature. Especially, in high energies range. The PLE measurements are very sensitive to the excitation intensity. From an appropriate value of Laser excitation, the energies levels will be saturated, which favors the light emission. The bands filling is translated by a widening in the PL spectrum towards the high energies range.

- A**
- Aagesen, L 108, 248, 326
Aarhaug, T 224, 378, 380, 381
Aashuri, H 538
Abashidze, G 571
Abbaschian, R 539
Abbasipour, B 55
Abdalla, P 190
Abdalla, M 563
Abdelaziz, M 56
Abdeljawad, F 384
Abdelkader, H 56
Abdolrahim, N 542, 586
Abdolvand, H 421
Abdulla, S 302
Abdul-Latif, A 136
Abedrabbo, S 492, 522
Abe, E 196
Abe, F 409
Abernathy, D 346, 391, 487
Abernathy, H 313
Abolghasem, S 367, 558
Abraham, P 94
Abrahams, H 437
Abreu, A 460
Abu-Farha, F 404
Abuomar, O 360
Abu Samk, K 116
Abuzaid, W 94, 96
Acchar, W 157, 158
Achar, S 47
Acharya, R 309
Acicbe, B 124
Acoff, V 495, 496
Acosta, A 335
Adachi, H 289
Adams, A 463, 586
Adams, B 535
Adams, D 263
Adams, T 31, 92
Adham, K 103
Adlakha, I 241, 412
Afonso, C 17
Agaliotis, E 233
Agarwal, A 13, 16, 65, 68,
81, 115, 138, 141, 142, 169, 215, 218,
294, 297, 374, 375, 383, 453, 485
Agarwal, K 73
Ager III, J 34
Aghvami, M 41
Agirseven, O 354
Agnew, S 196, 197, 274, 317, 434
Agrawal, A 22, 152, 282, 529
Agrawal, P 216, 565, 567, 571
Ågren, J 303
Aguilar, J 214
Aguilar, M 62
Ahli, N 301
Ahluwalia, R 44, 237
Ahmad-Bitar, R 389, 497
Ahmadzadegan, A 459
Ahmed, K 475
Ahmed, M 378
Ahmed, T 210, 470
Ahmed, Y 249
Ahn, J 355, 356
Ahn, K 522
Ahn, S 105
Aichi, T 209
Aich, S 138, 430
Aidhy, D 352
Aindow, M 129
Aitken, Z 414
Ajmani, S 458
Akasheh, F 543
Akhmetov, S 302
Akhtar, K 124
Akhtar, R 164
Akhtar, S 28, 144, 199, 376
Akin, I 124, 125, 529
Akmmetov, S 301
Akpa, O 523
Akpinar, I 526
Akram, M 530
Aksoy, M 150
Aktas, B 388
Al-Abbas, F 530
Alabi, T 295
Alamdari, H 318, 319, 394
Alam, M 329
Alankar, A 187, 547
Alaparathi, S 576
Al Aswad, K 302
Al-Aswad, K 302
Alava, M 360
Albagnac, M 111
Al Bedour, F 527
Albe, K 281, 338
Albuquerque, E 562, 573
Alcorn, T 226
Alderman, M 37
Alexander, D 177, 246, 501
Alexandre, A 319
Alex, T 70
Alfano, J 138
Alfantazi, A 89
Algarin Amaris, P 215
Al Halwachi, H 379
Al-Jallaf, M 147
Al-Jassim, M 202, 493, 522
Al kahtanid, S 73
Alkahtani, S 72
Alkan, M 68, 296, 562
Allahar, K 255, 280
Allano, B 147
Allanore, A 39, 88, 107, 165, 166, 181, 244,
259, 320, 539
Allard, B 243
Allart, M 340
Allen, A 116, 117, 190
Allen, B 481
Allen, S 271
Allen, T 177, 254, 265, 277, 278, 300, 333,
351, 352, 408, 415, 424, 476, 478,
516, 551, 588
Allison, J 96, 238, 326, 472
Allison, P 20, 573, 575, 585, 587
Alliston, T 34
Allyson, B 94
Al-Mazouzi, A 518
Almeida, A 460
Almer, J 151, 347, 383, 487
Almutairi, D 539
Alonso, A 498
Alonso, E 173
Alonso-Falleiros, N 399
Alpas, A 331
Al Sayed, W 302
Altamirano, A 556
Altenhof, W 331
Althouse, C 569
Altieri, A 392
Altinordu, O 296
Alvarado, L 498
Alvarado-Orozco, J 142
Alvear Flores, G 174
Alves, A 315
Alvi, F 419
Al Zarouni, A 147, 301, 302
Al-Zarouni, A 302
Amani Hamedani, H 466
Amargier, R 437
Amato, K 82
Ambai, H 93
Ambard, A 158
Ambrosek, J 333
Amer Abdelmegeed, A 56
Amini, S 234, 539
Aminossadati, S 53
Amiri, F 430
Amirkhani, A 534, 581
Amodeo, J 519
Amoozeaei, M 534
Ananthanarayanan, D 238
Anasori, B 471
Anbukarasu, P 560
An, C 355
Anderegg, J 42
Anderhalt, B 235
Anderoglu, O 45, 113, 187, 265, 341, 415
Anderson, I 50, 118, 122, 192, 197, 198, 255,
270, 349, 422, 423, 424, 491, 550
Anderson, J 115
Anderson, K 97, 406
Anderson, M 333
Anderson, P 185, 261, 269, 326, 414, 469, 487
Anderson, T 252
Andersson, D 38, 282, 352
Ando, D 538
Ando, T 198
Andren, H 167
Andrén, H 90
Andrews, R 98
Andriese, M 140, 181, 376
Anento, N 475
An, G 269
Angoua, B 465
Angré, A 427
An, K 86, 92, 152, 163, 180, 241, 317, 348,
349, 393, 487, 488, 532
Ankem, S 340, 341
Anopuo, O 25
Anselmo, G 554
Antico, F 470
Antila, O 253
Antipov, E 379
Antolin, N 314
Antonou, A 412
Antozzi, A 89
Antrekowitsch, H 222, 223
Antretter, T 63
Antropov, V 424
Anumandla, N 486



TMS 2012

141st Annual Meeting & Exhibition

An, X	135, 210, 377	Au, D	28	Ballato, J	344
Anyalebechi, P	260	Augustine, S	231	Balle, F	371, 442, 443
Apak, B	124, 427	Au, M	30, 31, 92, 168, 247, 321, 395, 465, 510	Ballinger, R	333
Apata, A	82	Aune, R	144, 199, 231, 376, 383, 452	Balogh, L	188, 268, 288, 343, 517
Apelian, D	99, 162, 173, 174, 392	Aussel, J	224	Balogh, Z	433
Apisarov, A	127, 379	Austin, P	81	Baltrus, J	295
Appolaire, B	130, 530	Avallone, J	96, 566	Baltuch, E	380
Aqeel Ali Mohd, S	380	Averback, R	128, 129, 236, 281	Baltuch, S	380
A, R	334	Averty, X	415	Balzar, D	268, 269
Arai, T	109	Avila-Davila, E	438, 573	Bambach, M	72, 173, 361
Ara, K	525	Aydin, U	532	Bamberger, M	329
Arakere, N	94	Azari, K	318	Bandaranayake, A	437
Arangi, S	170	Azari Khosroshahi, R	534, 581	Bandaru, P	66
Arao, R	190	Azevedo Silva, P	572	Bandegani, H	530
Araujo, A	375	Azimi, G	139, 296, 466	Bandyopadhyay, D	200
Araujo, E	548, 565	B		Banerjee, R	57, 68, 207, 247, 267, 286, 348, 381
Araújo, E	375, 567, 571	Baars, D	357	Banerji, A	331
Araujo, O	134	Babakhani, A	555	Baney, R	342
Arazaghi, M	500	Babbitt, C	450	Bang, A	459
Arbizu, C	208	Babu, S	18, 75, 148, 149, 226, 303, 381, 478	Baniassadi, M	283
Ardell, A	56, 57	Bach, M	143	Bankole, O	582
Arellano, B	552	Backe, D	443	Bannerjee, A	445
Arenas Arrocena, M	567	Backhouse, N	242	Bannister, L	389
Ares, A	74, 233, 259	Badakhshan, A	12	Banobre, A	522
Arey, B	91	Badinier, G	58	Bansal, R	309
Arfaei, B	50, 350	Badowski, M	308	Bao, J	504
Argade, G	324, 538	Bae, D	267, 537, 548	Bao, L	70, 321
Ariharan, S	68	Bae, G	558	Bao, M	115, 297
Armstrong, D	342, 357, 480	Bae, J	107, 275	Bao, S	308
Armstrong, L	189, 370	Baek, Y	194	Bao, Y	374, 486
Arnberg, L	28, 75	Baggash, I	301, 302	Barabash, R	48, 112, 116, 190, 263, 268, 345, 347, 419, 420, 486, 549
Arnold, C	372	Bagot, P	91, 247, 518	Baracho, M	138, 375
Arola, D	77, 227, 228	Bahadir, A	157	Barajas-Valdes, U	373, 581
Aromaa, J	244, 365	Bahari, A	524	Barakat, M	356
Aronov, M	108	Bahmanpour, H	370, 440	Barashev, A	187, 342
Arora, H	290	Bahr, D	13, 184, 203, 263, 338, 401, 412, 545	Barati, M	202, 376
Arroyave, R	26, 83, 158, 160, 235, 237, 312, 314, 315, 390, 462, 530	Bai, C	24, 66, 81, 156, 157, 233, 310, 388, 459, 461, 498, 508, 555	Barat, P	340
Arruffat, R	500, 559	Bai, G	297	Barbaro, F	246
Arsenlis, A	188	Bai, H	468, 512	Barbato, C	70
Arsenlis, T	412	Bailey, C	450	Barbee, T	116, 172
Arslan, S	143	Baillot, P	224	Barbier, D	58
Aruga, Y	247	Bain, K	32, 335	Barbosa, A	460
Arzpeima, M	383, 452	Baird, J	101	Barbosa, N	45, 113, 114, 187, 265, 341, 415
Asadi, M	107	Bai, X	37, 351, 352, 494	Barcelos, F	157
Asai, T	51	Baiyong, Z	71	Barekar, N	230
Asavavisithchai, S	199	Bakai, A	505, 506	Barik, R	243
Aschauer, U	563	Bakai, S	506	Barker, E	472
Asgharzadeh, H	369	Baker, I	16, 544	Barlat, F	130
Ashe, C	326	Bakken, J	144, 376	Barnes, E	445
Ashida, M	558	Bakonyi, I	332	Barnes, M	450
Ashkenazy, Y	128, 281	Bakshi, S	16, 68, 141, 142, 218, 297	Barnett, M	274, 329
Ashrafi, H	524	Balandin, A	581	Barney, E	152
Ashraf, R	534	Balani, K	68, 375, 427	Baró, M	455, 457, 529
Askari, H	535	Balasubramanian, B	123	Barpanda, P	30
Aslan, S	71	Balch, D	325	Barrales-Mora, L	433
Asle Zaeem, M	239, 406	Baldan, R	572	Barrat, J	454
Asselin, E	88, 89, 165, 244, 320, 321	Baldock, R	98	Barr, C	342
Assis, W	315	Baldo, P	342	Barreau, N	168
Assoufid, L	419	Baldwin, J	342	Barreiro, J	379
Assuncao, M	243	Baldwin, K	547	Barreto, L	158
Asta, M	26, 27, 83, 158, 160, 235, 237, 240, 303, 312, 314, 326, 390, 462, 494, 530	Bale, H	34, 469	Barrie, F	470, 586
Asthagiri, A	129	Balk, T	93	Barrioz, E	147
Asthana, A	30, 480	Ballard, D	585	Barriuso, S	462
Atlas, S	57	Ballarini, R	451	Barron, M	458
Atodaria, I	96, 363			Barrón, M	556
Atzmon, M	229			Barsoum, F	170, 249

Barsoum, M.	469, 471, 518	Belharouak, I.	30, 92	Bhattacharya, J.	158
Bartel, T.	284	Bellet, M.	232	Bhattacharya, M.	340
Bart, F.	516	Bellon, P.	128, 129, 236, 281	Bhattacharya, S.	83
Barthelat, F.	540	Bellot, J.	80	Bhattacharyya, D.	56, 477
Barthe, M.	517	Belova, I.	236, 313, 463	Bhattacharyya, S.	26
Barth, H.	34	Belsito, D.	583	Bhavsar, R.	446
Bartolo, L.	326	Belt, C.	467	Bhoi, B.	144
Bartolucci, S.	55	Belton, D.	304	Bhowmick, S.	339, 529
Barton, N.	435	Belyakov, S.	120, 121	Bian, M.	274, 403, 538
Barton, T.	103	Benaduce, A.	383	Bichler, L.	514
Barto, R.	428	Benafan, O.	49	Bieler, T. 50, 51, 112, 264, 271, 357, 420, 437,	491
Baruj, A.	45	Benard, F.	89	Biermann, D.	437
Basargan, T.	382	Bendersky, L.	576	Bigelow, G.	35, 393, 563, 570
Basavaraj, V.	289	Bendert, J.	78	Bijlsma, R.	449
Bashiri, M.	512	Benes, O.	277	Billet, B.	257
Bashyal, B.	558	Ben Hadid, H.	233	Billia, B.	183, 260, 337
Basirat, M.	46, 240, 334, 406, 587	Benitez, R.	565	Bindal, C.	150
Baskaran, R.	294	Benitez, S.	24	Biner, B.	37, 38, 282, 406
Baskes, M.	38	Benkirane-Jessel, N.	453	Bingert, J.	164, 234, 353, 358
Basnayaka, P.	189, 419	Bennett, J.	288, 336	Bing, P.	447
Bass, R.	485	Benson, D.	572	Bin, L.	536
Basu, B.	449	Benzerga, A.	251	Birnie, D.	169
Basu, S.	367, 443, 538, 558, 565, 574	Ben-Zion, Y.	384	Biro, A.	34
Bateman, T.	386	Beraldo, L.	17	Birol, Y.	298
Bathias, C.	372	Berbenni, S.	101	Birosca, S.	363, 436
Batista, E.	224	Bergeon, N.	183, 337	Birringer, R.	362
Batista, V.	399	Berglund, I.	452, 583	Biswas, A.	69, 128
Batson, R.	25	Bergman, S.	491	Biswas, K.	229, 474, 575
Battaile, C.	251, 252	Bergström, T.	232	Biswas, S.	400
Battezzati, L.	109	Beringov, S.	202	Bjarnø, O.	224
Battle, T.	35, 98, 174, 253, 327, 401, 428	Berkmortel, R.	533	Björling, G.	383, 452
Baudin, T.	560	Berla, L.	421	Blacketter, J.	39
Bauer, E.	501	Berlin, M.	257, 258	Blackwood, V.	266
Baumann, A.	34	Berman, T.	274, 472	Blais, A.	148, 394
Baumbach, T.	119	Bermudez, K.	330, 405	Blanchet, T.	16
Baumert, E.	443	Bernal, R.	13	Blankenhorn, M.	73
Baumgarten, M.	540	Bernardi, J.	271	Blasques, J.	147
Baumgart, H.	545	Bernazzani, P.	489, 490	Blawert, C.	533
Bau, N.	329	Bernhard, C.	162, 239	Bleck, W.	173, 179, 233
Baxter, R.	154	Bernier, J.	159, 420, 433	Blendell, J.	112, 422, 423
Bayandorian, I.	330	Bernstorff, S.	191	Bloch, J.	570
Baygul, M.	71, 143, 526	Bertetta, G.	20	Blosse, A.	202
Baygül, M.	220	Berthel, B.	437	Blue, C.	124
Bayles, R.	163	Bertino, M.	459	Blumenthal, W.	44, 113
Bayliss, C.	11, 380, 467	Bertolino, G.	45	Bochvar, N.	561
Bazoune, A.	527	Bertram, M.	467	Bodde, S.	529
Bealing, C.	160	Beryerlein, I.	281	Boeckels, H.	286
Beall, G.	489, 490	Besahraoui, F.	14, 169, 581, 583, 584, 588	Boeckl, J.	12
Bean, G.	393, 587	Besmann, T.	38, 92	Boeck, T.	181, 387
Beaugnon, E.	122	Besser, M.	455	Boehlert, C.	102, 112, 420, 437
Bechade, J.	518	Besson, R.	128	Boehmcke, P.	330, 582
Becker, D.	146	Bettles, C.	132	Boehm, R.	445
Beckermann, C.	41, 84, 162, 260	Beuth, J.	412	Boerio, F.	432
Beckman, S.	170	Bevitori, A.	460, 498, 556	Boesenberg, A.	424
Bedel, M.	232	Beyerlein, I. 44, 110, 111, 112, 261, 282, 341,	366, 414, 482	Boetcher, S.	182
Bednarski, T.	365	Beygi, H.	444	Bogno, A.	337
Beeler, B.	38	B, G.	430	Bohlen, J.	102
Behera, F.	23, 361	Bhajun, S.	87	Bojarevics, V40, 109, 182, 260, 261, 337, 387,	410, 540
Behera, R.	38, 425	Bhamare, S.	170	Boles, S.	184
Beheshti, R.	199	Bhame, S.	175	Bolfarini, C.	17, 151
Behrens, B.	259	Bhanu Sankara Rao, K.	291, 370, 561	Bolind, A.	478
Beidaghi, M.	322	Bharadawaj, M.	410	Boller, C.	443
Bei, H.	413, 506, 507	Bhaskar, P.	298	Boller, R.	438
Bejinariu, M.	232	Bhatia, M.	111, 393	Bölling, R.	467
Beladi, H.	487	Bhat, S.	262	Bonakdar, A.	323
Belak, J.	159, 433	Bhattacharjee, D.	100	Bond, G.	188
Belassel, M.	488	Bhattacharjee, T.	196		
Belaygue, P.	94				



TMS 2012

141st Annual Meeting & Exhibition

INDEX

Bonnen, J.	300	Breyner, S.	99	Burns, D.	362
Bonneville, A.	397	Brice, C.	18	Burns, J.	280, 323
Bonollo, F.	85, 316	Brillo, J.	109, 541	Burton, B.	391
Bonora, N.	77, 416	Bringa, E.	184, 483, 543	Busbee, T.	586
Bon, P.	301	Brinkman, K.	516	Busby, J.	334, 407, 409
Bonville, L.	180	Brisset, F.	239, 560	Busch, J.	392
Booker, J.	451	Brito, G.	565, 567, 571	Bushby, A.	250, 412
Boom, R.	127	Brito, M.	180	Bush, J.	586
Boothby, R.	167	Broad, R.	188	Bush, P.	235
Booty, M.	493	Brocchi, E.	575	Busse, B.	34
Borbely, A.	268	Brockman, R.	436	bussmann, K.	446
Boresevich, A.	29	Broderick, T.	59, 207	Buta, D.	303
Borgenstam, A.	26, 149, 303, 381	Brodie, R.	98	Butler, B.	125, 212
Borges, A.	143	Broek, S.	11	Butler, T.	563
Borgesén, P.	50, 350	Broido, D.	395	Butt, D.	114, 255, 280, 357
Borges, J.	143	Brokmeier, H.	132, 489	Bu, X.	496
Bor, H.	479	Brommer, T.	198	Buxmann, K.	467
Borkar, H.	515	Bronkhorst, C.	341, 416	Buzunov, V.	302, 318
Borkar, T.	267	Bronsch, A.	67	Buzzi, D.	552
Bornapour, M.	452	Brooks, G.	309, 401	Byer, C.	546
Borodiak, M.	300	Brosi, J.	248	Byler, D.	278, 417, 484
Borovikov, V.	494	Brown, A.	417, 484	Byrd, D.	197
Bor, S.	452	Brown, C.	123	Byrne, C.	231
Borysenko, V.	505	Brown, D.	49, 188, 268, 269, 343, 346, 469, 517, 567	Byun, K.	270
Borzone, G.	194	Brown, E.	346	Byun, T.	265, 415
Bose, A.	54	Browne, D.	231, 240, 260, 541		
Botelho, F.	397	Browning, J.	188	C	
Botta, W.	17	Brown, T.	295	Caballero, F.	168, 227
Botton, G.	19, 148	Broz, P.	121	Caballero-Flores, R.	332
Bouaziz, O.	58, 116	Bruce, T.	304	Cabana, J.	93
Bouche, C.	87	Bruder, E.	212, 560	Caceres, C.	102
Bouhabila, E.	74	Bruening, R.	61	Cáceres-Díaz, L.	142
Bourell, D.	353	Brüggenmann, T.	71	Caddeo Johansson, S.	427
Bourgeois, L.	17, 75, 223	Bruhís, D.	163	Cadel, E.	168
Bourke, M.	478	Brundidge, C.	442	Cady, C.	242
Boussaa, R.	233	Bryan, Z.	55, 393, 482, 583, 584, 585	Caffarey, M.	451
Bo, W.	299	Brynjulfssen, T.	157	Cahill, D.	161
Bowen, P.	132, 452, 553, 563	Buchanan, D.	96, 252, 577	Cai, F.	218
Bower, A.	400	Buchanan, K.	18, 257	Cai, J.	367
Bowers, M.	261	Buchheit, T.	251, 342	Cai, L.	92, 180
Bowles, A.	153, 308	Buchholz, A.	232	Caillard, D.	42, 129, 205, 262
Boyce, B.	33, 95, 96, 171, 172, 250, 252, 264, 324, 400, 468	Buchholz, E.	414, 544	Cai, M.	15, 24, 81, 156, 233, 310, 388, 459, 461, 508
Boyce, D.	59	Buchovecky, E.	400	Cairney, J.	246
Boyer, R.	59	Buchovska, I.	202	Cairns, E.	93
Boyle, J.	426	Buckner, B.	96	Cairong, C.	244
Boyne, A.	315	Budai, J.	419, 420, 421	Cai, S.	488
Boysen, D.	166	Budenkova, O.	232, 233	Cai, W.	78, 481
Bozin, E.	347	Budiman, A.	262, 270, 421, 547	Cai, Z.	496, 509, 513, 532
Bradfield, C.	573	Buehler, M.	20, 33, 46, 396	Cak, M.	432
Bradley, J.	400	Bufford, D.	172, 544	Calvert, K.	59
Brady, M.	336, 409	Bugaev, V.	313, 345, 574	Calvert, P.	382, 529
Brammer, A.	201, 583	Bührig-Polaczek, A.	146	Campbell, A.	96, 341, 516
Branagan, D.	264	Bulatov, V.	159, 315, 433, 463	Campbell, B.	346
Brandes, M.	45, 276, 363, 364, 436	Bulent, G.	90	Campbell, C.	235
Brandl, C.	44, 186, 263	Bülöw, E.	570	Campbell, J.	27, 400
Brar, H.	452, 583	Bummer, J.	98	Campelo, N.	356
Brasileiro, M.	356, 548	Bunin, I.	81, 156	Campos, D.	375
Brassard, M.	394	Bunn, J.	347	Campos, J.	575
Bras, W.	118	Burba, M.	95, 394	Campos, K.	569
Bratberg, J.	106, 222, 350	Burek, M.	262	Camposo Pereira, A.	459
Bräuer, D.	541	Burger, J.	177	Canales, A.	377
Braun, C.	362	Burger, S.	443	Candia, A.	74
Bray, S.	132	Burgos, B.	254	Cang, D.	468, 512
Brechet, Y.	303	Burheim, O.	467	Cannova, F.	319
Breen, A.	246	Burke, P.	165, 535	Cantonwine, S.	469
Brennan, S.	330, 405, 514	Burkes, D.	105	Cantwell, P.	465
Breschi, D.	448	Burks, G.	266		

Cao, B	186	Cerrone, A	32	Chemezov, O	127
Cao, H	317	Certain, A	478	Chen, C	51, 52, 53, 119, 120, 193, 194, 195, 221, 242, 248, 272, 273, 349, 395, 417, 423, 435, 492, 550, 577
Cao, L	361	Ceschini, L	85, 378	Chen, D	447
Cao, S	532	Cetlin, P	62	Chen, E	364
Cao, W	107, 545, 547, 584	Chada, S	271	Chen, F	67
Cao, X	147, 182	Chae, H	521, 537	Chen, G	92, 273, 362, 465
Cao, Y	472, 557	Chaffron, L	477	Cheng, C	195, 351
Cao, Z	527	Chai, D	301	Cheng, G	188, 555
Capdevila-Montes, C	227	Chai, G	371, 409	Cheng, I	373
Caplovic, L	85	Chai, L	447, 503, 525	Cheng, J	532, 534, 536
Capolungo, L	101, 135	Chai, Y	79, 121	Cheng, K	496, 558, 559
Capozzi, A	540	Chaka, A	42, 263	Cheng, P	535
Capps, N	266	Chakkathara Janardhanan Nair, D	180	Cheng, S	264, 446, 481, 483
Capuano, G	337	Chakoumakos, B	317	Cheng, T	84
Caram, R	528	Chakraborti, N	283	Chenguang, B	376, 447, 512
Caramto, R	270	Chakraborty, M	430	Cheng, W	333
Caratini, Y	147	Chakravarty, J	289, 435	Cheng, X	461
Cardona, N	161	Chalasanani, D	404	Cheng, Y	119, 129, 152, 182, 385, 397, 465, 507
Carlson, B	17	Champel, B	301	Chen, H	149, 202, 317, 383, 493, 534
Carmack, J	177	Chan, D	50	Chen, I	77
Carmo, M	79	Chandia, M	153	Chen, J	69, 156, 157, 186, 258, 297, 375, 441, 500, 520, 524
Caro, A	44, 187, 203, 204, 266, 312, 547	Chandler, M	20, 575, 585, 587	Chenjuan, W	226
Caron, A	506	Chandola, N	87	Chen, K	192
Carozzani, T	232	Chandra, D	438, 459, 507, 566	Chen, L	26, 31, 54, 55, 67, 84, 119, 125, 129, 141, 146, 158, 237, 238, 259, 337, 377, 526, 534, 550
Carpenter, A	404	Chandrasekaran, N	294	Chen, M	151, 193, 230, 321, 447, 534
Carpenter, J	24, 81, 113, 156, 233, 261, 310, 366, 388, 414, 459, 461, 508	Chandrasekar, S	59, 102, 211, 441, 560	Chen, P	20, 33, 76, 77, 149, 227, 228, 304, 382, 383, 451, 493, 528, 578, 579
Carpenter, K	246	Chandross, M	481	Chen, Q	106, 222, 350
Carpenter, M	374	Chang, C	53, 202	Chen, S	107, 120, 121, 142, 193, 273, 417, 512
Carpus, E	355	Chang, S	568	Chen, T	242, 439
Carrado, A	489, 492	Chang, T	192, 259	Chen, W	15, 27, 51, 124, 254, 277, 278, 279, 322, 350, 352, 422, 423, 551
Carrasquillo, O	588	Chang, W	445	Chen, X	22, 45, 97, 108, 140, 193, 224, 296, 297, 304, 355, 376, 503
Carr, D	268, 477	Chang, Y	25, 107, 120, 173, 492, 524	Chen, Y	28, 39, 60, 115, 136, 159, 186, 193, 216, 361, 424, 426, 455, 513
Carreiro, R	460, 461, 498	Chan, K	33, 96, 265	Chen, Y 478	
Carreño, C	499	Chan, L	32, 235	Chen, Z	28, 102, 222
Carreon, H	462	Chanturiya, V	156	Chernatynskiy, A	351, 353, 425
Carrez, P	206, 519	Chan, Y	383, 493	Cherng, S	248
Carrillo-Abad, J	567	Chao, C	529	Cherskikh, I	302
Carr, J	215	Chaojian, M	71	Cherukara, M	189
Carroll, J	94, 96	Chao, Z	219	Cheruvathur, S	334, 555
Carroll, L	45, 46, 254	Cha, P	214, 215	Cheung, C	504
Carroll, M	45, 254, 357	Chapdelaine, D	449	Cheung, K	71
Carsley, J	18	Chapman, K	117	Chew, S	81
Cartas, A	342	Chapman, M	233, 285	Chiang, A	120
Carter, J	401, 404, 472, 514	Chapman, N	81, 422	Chiang, F	116
Carter, M	426, 452	Chappell, M	587	Chiang, T	351
Carter, W	282, 326, 469	charette, o	448	Chiang, Y	282
Carvajal, M	112	Charit, I	46, 255, 280, 334, 357, 477, 587	Chiba, A	218, 229, 238, 324, 360, 528
Carvalho, M	569	Charito, V	573	Chichester, H	106
Case, S	201	Chartrand, P	225, 378	Chichuk, E	302
Casperson, M	96	Chason, E	68, 139, 422	Chien, W	86, 241, 393, 438, 459, 507, 566
Cassir, M	165	Chaswal, V	170	Chi, F	375, 520
Castano, C	255, 403	Chatterjee, A	131, 432	Chikashi, H	217
Castillo, T	460	Chattopadhyay, A	96, 363	Chikhradze, M	368, 370
Castro-Colin, M	313, 345, 574	Chaudhari, G	126, 292, 410, 509, 563	Chikhradze, N	370, 571
Castro, R	548	Chaudhary, R	457	Chi, M	92, 511
Castro, W	554	Chaudhary, S	215, 216, 294	Chimani, C	300
Caton, M	95, 252, 394	Chaudhary, U	169	Chin, B	79, 488
Catorceno, L	404	Chaudhuri, S	36	Chinella, J	163
Cavalcanti, S	565, 567	Chaudhury, Z	443, 444		
Cavalu, S	529	Chavali, S	491		
Cavanaugh, D	122, 424, 521	Chavarriaga, E	157		
Çavusoglu, H	557	Chavez, T	343		
Cazacu, O	87	Chawla, N	50, 52, 81, 95, 96, 169, 264, 323, 420, 422, 442		
Celikel, B	143	Chefai, S	321		
Çelikel, B	220	Chellali, M	433		
Cerezo, A	29, 90	Chemam, R	560		
Cerreta, E	82, 186, 241, 416, 483, 484, 519				



TMS 2012

141st Annual Meeting & Exhibition

INDEX

Chinellato, A	460	Cinar Sahin, F	124, 427	Cortez Suarez, V	298
Ching, W	384	Cirkovic, M	570, 571	Cortie, M	162
Chirdon, W	48	Cizek, J	269	Coryell, J	400
Chisholm, B	445	Cížek, J	290	Cosin, S	311, 552
Chisholm, C	413	Cizek, L	292	Costa, A	158
Chiu, T	273	Clark, C	178	Costa, F	225
Chiu, Y	58, 241	Clarke, A	149, 226, 246	Costanza, G	526
Chjatterjee, S	474, 575	Clarke, K	177, 246	Coté, J	148
Chockalingam, K	37, 38	Clark, M	124	Cotts, E	350
Cho, D	180	Clark, S	118	Cottura, M	530
Choe, H	325	Clark, W	206	Coughlin, D	35
Choe, K	562	Clausen, B	49, 197, 268, 469	Counts, W	256
Cho, H	14, 486, 570, 575	Clémendot, F	518	Couper, M	101, 162, 387
Choi, B	222, 415, 571	Clemens, H	256, 257, 358	Coursol, P	148, 161
Choi, C	151	Clemente, C	77	Courtenay, J	231, 308
Choi, D	119	Cloue, J	518	Couvrat, M	477
Choi, H	64, 125, 126, 273, 318, 325	Clouet, E	111, 206	Couvy, H	441
Choi, I	543, 547, 567, 571	Cloutier, B	74	Couzinie-Devy, F	168
Choi, J	180, 194, 197, 273, 528	Cocalia, V	365	Covarrubias-Alvarado, O	499
Choi, M	294	Cochran, C	427	Coward, R	515
Choi, P	168, 226, 424, 554	Cochrane, C	488	Cowen, C	336
Choi, S	569	Cockcroft, S	28, 131, 162	Cowgill, D	188
Choi, W	12, 64, 65, 159, 294, 361, 524, 580	Cocke, D	489, 490	Cox, B	469
Choi, Y	318, 365	Cockeram, B	265, 477	Cox, W	27
Cho, J	146, 338, 472, 527	Coelho, G	572	C, P	164
Cho, K	209, 290, 472, 514, 533, 538	Coen, G	114	C. Pissolati, N	343
Chollier-Brym, M	319	Cohen, F	59	Craievich, A	190
Chona, R	94, 96	Cohen, L	331	Crane, K	573
Chong, L	504	Cohen, S	480	Cranford, S	20, 46
Chong, Z	447	Cola, G	149	Creber, D	88
Choo, H	21, 78, 151, 229, 305, 384, 453, 455, 504, 506	Colakoglu, C	217, 562	Cremasco, A	528
Chookajorn, T	212	Colas, K	158	Cremer, B	277
Chopde, I	508	Colby, D	260	Cremer, M	442
Chopra, N	12, 13, 63, 65, 66, 137, 138, 213, 215, 216, 293, 294, 372, 374, 375, 445, 523	Cole, J	98, 176, 255, 280, 477, 517	Crétinon, L	422
Choudhuri, D	50	Coleman, P	398	Crimp, M	112, 264, 420, 437
Choudhuri, S	260	Coleman, S	494	Crocce Romano Espinosa, D	498
Choudhury, S	359	Colle, J	277	Croell, A	541
Chou, K	142, 143	Collins, P	107, 206, 207, 234, 286	Croft, N	309
Chou, M	180	Collins, S	82	Cröll, A	541
Chou, Y	14	Colon-Mercado, H	92	Cromwell, M	515
Christ, H	371, 436, 442	Colorado, H	46, 255, 427	Crosby, S	490
Christianson, R	257, 258	Combaz, E	242	Cross, M	309
Christien, F	340, 341	Combeau, H	23, 80, 154, 232, 309, 387, 457	Crouse, C	188, 585
Christ, K	305	Companhoni, M	440	Crudden, D	98
Christman, M	302	Compton, C	357	Crundwell, F	244
Chrzan, D	315	Conde, A	332	Cruz, E	87
Chuang, A	306, 454, 487, 505	Conduit, B	335	Cruz Perez, J	567
Chuang, C	152, 306, 454, 488	Conduit, G	335	Cruz, R	511
Chuang, H	192, 193, 351	Connolley, T	162, 488	Csernica, C	188
Chu, H	111, 414	Connolly, G	364	Cuadra, J	94
Chu, J	202, 230, 306, 307, 445, 455	Conrad, T	150	Cubero-Sesin, J	440
Chu, L	530, 555	Conry, T	31	Cui, B	123
Chulliparambil, M	449	Constanti-Carey, K	103	Cui, J	73
Chu, M	241	Constantinides, S	424	Cui, Q	511
Chumbley, S	316	Contescu, C	348	Cui, X	322
Chung, B	165, 194	Contieri, R	528	Cui, Y	139
Chung, C	307	Conway, J	496	Cullen, R	231
Chung-Kai, C	518	Conway, P	192, 271	Culler, M	234
Chung, M	272	Cook, R	411, 493	Cummings, J	338
Chung, Q	270	Cooksey, M	450	Cunha, B	571
Chun, T	67, 447, 448, 503	Coppa, A	570	Cunha, L	490
Chun, Y	544	Cora, O	471	Cunlong, W	539
Ciftja, A	126, 202	Cordeiro Morais, A	356	Cunningham, N	247
Cifuentes, G	133	Cordier, P	206, 519	Cutrim, A	116
Cilz, N	445	Cordill, M	341		
		Cornelius, T	263		
		Cornide, J	168, 227		
		Cortes, V	26		
				D	
				Dabkowska, H	129

Dabrowski, J	163	Dayeh, S	338, 480	Denoual, C	484
da Costa Caldas, T	356	Daymond, M	343, 408, 416, 421, 488	Denton, G	36
Dadfarinia, M	265, 325	De Abreu, A	243	Deo, C	38, 187, 425
Daehn, G	45	Dean, D	304, 578	De Oliveira Campos Neubauer, P	164
Dahmen, K	384	De Andrade, R	11	De, P	559
Dahmen, U	27, 93, 494	De Angelis, R	211	De Pascale, F	337
Dahotre, N	69, 182	de Araújo, C	554	Derakhshandeh Haghi, R	125
Dai, C	174	Debacker, A	158	Derezinski, S	103
Daigle, A	424	deBarbadillo, J	392	Derin, B	68, 296
Dai, J	496	Debierre, J	183	Derlet, P	454
Dai, L	156, 157	de Boer, M	412	de Rosset, W	125
Dai, S	92, 511	Decamps, B	518	Derrick, A	244
Daisuke, Y	405	Décamps, B	517	D'Errico, F	513, 514, 515
Dai, X	392, 397	de Carlan, Y	478	Deschamps, A	345
Dai, Y	328, 513	De Carlan, Y	266	Desgardin, P	517
Dalili, N	272	De Cicco, M	56	Deshmukh, V	200
Dal Martello, E	127	Decker, R	274, 470, 472, 501	Désilets, M	394
Daly, S	371	Declet, A	373, 581	Despina, L	385
Damm, E	108	Dedyukhin, A	379	Despinasse, S	148, 448
Damoah, L	202, 218, 308	Deemyad, S	484	Detsi, E	264
D'Amours, G	310	De Felice, V	80	Deurling, J	34
Danaie, M	198, 466	de Gelas, B	467	Deutchman, H	284, 401
Danczyk, S	12	de Geuser, F	345	Devanathan, R	38, 277, 351, 352, 424, 551
Dandekar, D	242, 417	Deheri, P	175	Devaraj, A	57, 91, 167, 207
Dando, N	74	Dehm, G	41, 251, 261, 341, 421	de Vasselot, A	224
Daniels, J	445	Dehoff, R	124	Devine, B	129
Daniil, M	176, 276, 295	DeHoff, R	463, 586	Devlin, E	376
Danoix, F	227, 245, 246	De Hosson, J	231, 264, 522	Dewan, M	309
Dan, S	299	de Ita, A	458	Dewei, L	388
Dantas, L	116	de Jong, M	27	Dhage, S	427
Dao, M	33	Dekich, A	180	Dhakar, B	354
Daoud, I	80	Dekker, R	471	Dhindaw, B	290
Darbandi, P	357, 491	De la Garza Garza, M	141	Dhobe, M	508
Darlapudi, A	240	de la Garza, M	479	Dhumal, M	170
Darling, K	211, 212, 213, 368, 370, 505	Delaire, O	391	Diak, B	346, 421
Darmstadt, H	242	Delannoy, Y	203	DiAntonio, C	343
Das, D	389	De Leon, N	205	Diao, J	140
Dasgupta, A	83	del Mastro, N	460	Dias, A	490
Dash, R	144	DeLorme, R	290, 514, 533, 538	Dias, O	397
Dashti, S	89	DelRio, F	493	Dias, R	351
da Silva, I	460	Delsante, S	194	Diaz, D	180
da Silva, L	567, 577	Delshad Khatibi, P	198, 411	Díaz de la Rubia, T	100
da Silva, M	399	DeLucas, R	357, 431, 552	Diaz, F	556
da Silva-Valenzuela, M	524	DeMarco, J	462	Diaz-Michelena, M	275
Das, S	11, 17, 65, 72, 145, 169, 189, 222, 295, 296, 300, 304, 309, 377, 384, 396, 449, 467, 511, 524, 526, 579, 580	Demchyshyn, A	476	Dibelka, J	201
Datko, L	578	de Melo, R	399	DiCecco, S	331
Dattelbaum, D	346	Demenet, J	481	Dichiaro, S	416
Datye, A	150	Demetriou, M	22, 305, 307	Dick, A	86, 160, 314
Dauskardt, R	33, 95, 171, 250, 324, 400, 468	DeMint, A	105	Dickerson, C	265
Davenport, B	61	Demiray, Y	67	Dickerson, R	340, 390
David-Pur, M	12	Demirci, G	103	Dickert, H	173
Davidsen, J	99	Demir, E	420	Dickey, M	264
Davidson, C	162, 309	Demir, G	143, 220, 526	Dickson, J	408
David, W	237	Demirkol, N	150	Dickson, R	223
Davies, C	292	Demirtas, T	507	Diefenbach, A	540
Davies, R	451	Demkowicz, M	57, 203, 204, 340	Diercks, D	90
Davis, B	37, 226, 290, 464, 514, 533, 538	Demkowicz, P	106	Dieringa, H	403, 470
Davis, M	402	De Moor, E	149, 167	Diethold, C	181
Davis, R	91	Demura, M	257	Digonnet, H	232
Davis, S	257, 258	Demuth, M	397	Dikovits, M	509
Davydov, A	339, 411	Deng, B	351, 353, 425	Di Lisa, D	165
Davydov, V	347	Deng, G	367, 559	Dillon, Jr., O	534
Dawson, P	420	Deng, H	281	Dillon, O	561
Dawson, S	300	Deng, Q	67, 68, 554	Dimiduk, D	58, 106, 111, 113, 129, 205, 284, 362, 363, 434
Dayal, P	339, 477	Deng, S	479	Dinda, G	83
Dayananda, M	491	Deng, X P	516	Ding, B	397
		Dennis, K	122, 176, 423, 424	Ding, J	473
		Dennis-Koller, D	416, 417		



TMS 2012

141st Annual Meeting & Exhibition

INDEX

Ding, X	76, 205, 494	Dubey, M	495	Edwards, L	242, 318, 477
Ding, Y	68	Dubey, S	475	Efe, M	59, 102, 441
Dinsdale, A	121	Dubuisson, P	415	Eftink, B	185, 186
Dion, M	242	Du, C	217	Egami, T	49, 151, 152, 306, 345
Dirras, G	136, 369	Duchesne, C	511	Egeland, G	177, 475
Di Sabatino, M	28	Dudney, N	92, 511	Eghbalnia, M	320, 321
Dispinar, D	28, 162, 231, 233, 310, 532	Dudzik, M	428	Egry, I	110
Divine, B	446	Dudzinski, D	171	Eguchi, K	179
Divinski, S	211	Duesing, E	586	Ehm, L	517
Dixit, M	355	Duffie, N	55	Eichholz, S	577
Dixit, P	138	Duffy, M	20	Eick, I	450
Dixit, V	206	Dufour, G	74	Eidem, P	99
Dixon, D	320, 321	Dugdale, H	480	Eiffler, D	371, 442, 443
Djambazov, G	239, 457	Duh, J	195, 307, 351, 383, 491, 493	Eikerling, M	510
Dmowski, W	152, 306, 345, 488	Du, J	444, 464	Einarsrud, K	450
Dobatkina, S	291, 561	Du, L	93	Eisenbach, M	161
Dobosz, R	63	Dumas, B	319	Eisenlohr, P	112, 420
Dobra, G	145	Dunand, D	124, 281, 487	Eivani, A	522
Doeff, M	31	Dunn, J	450	Ekiz, E	128
Dogan, O	257, 358	Dunstan, D	250, 412	Eksteen, J	99
Doherty, K	378	Dupon, E	164	El-Awady, J	111, 205
Doherty, R	462	Dupuis, M	148, 503	El Azab, A	475
Dolan, M	507	Dupuy, A	123	El-Azab, A	251, 351, 352, 475
Domack, M	18	Dupuy, L	206	El-Bealy, M	386
Dominguez, O	511	Du, Q	83	El Desouky, A	124
Donahue, R	97	Durdu, S	536	El-Desouky, A53, 123, 197, 278, 353, 426, 552	
Donald, K	252	Durham, D	142	Elfimov, I	237, 303
Donaldson, I	172	Durygin, A	258, 520	Elineni, K	305
Donchev, A	495	Du, S	499	El-Kaddah, N 23, 80, 154, 232, 309, 330, 387, 388, 457, 582	
Donchev, V	571	Duscher, G	139, 373	El Kadiri, H	101, 102, 405, 406
Doneda, M	575	Du Terrail, Y	232	Elkholy, A	539
Dong, A	60, 431	Dutkiewicz, J	292	Ellingsen, M	305
Dong, P	297	Dutler, S	310	El Mahallawi, I	56
Dong, Q	136, 211	Dutrizac, J. 61, 133, 208, 287, 365, 438, 439, 497, 498, 554		Elmer, J 50, 118, 192, 270, 349, 422, 491, 550	
Dong, S	387	Dutta, A	340	El Metwally, M	249
Donlon, W	238, 274, 472	Dutta, I	193, 491	Elmustafa, A	305, 543, 545, 546
Doñu Ruiz, M	298	Dutta, P	232	Elorfi, S	276
Doorenbos, Z	189	Duvah Pentiah, S	154	Elsayed-Ali, H	543, 545
Dorantes-Rosales, H	573	Duval, D	448	Elsayed, M	248
dos Santos, M	399	Duval, H	80	Elsener, H	194
Dost, S	40	Du, Y	222	Emadi, R	524
Dou, S	247	Dwaraknath, S	516	Embury, D	116
Dou, Z	70	Dwarknath, S	515	Embury, J	58
Dowding, J	384	Dwivedi, D	354, 378	Em, V	575
Dowling, W	81	Dwyer, C	75	EM, V	269
Downey, J 35, 40, 98, 109, 174, 182, 253, 257, 258, 260, 327, 337, 401, 410, 540		Dye, D	364, 408	Enayati, M	372, 524
Downing, C	341	Dyer, L	321	Ener, S	191
Doyle, F	156, 321, 344	E		Engel, E	164
Draper, R	69, 189	Earthman, J	96, 372	Engl, T	308
Drautz, R	128, 160, 432	East, D	78	England, J	271
Dravid, V	389	Easter, S	261	English, C	167
Drchal, V	431	Easton, M	162, 196, 309, 387	Engstrom, A	321, 350
Dreisinger, D	245	Eaves, L	261	Engström, A	106, 222
Dreizin, E	568	Eberl, C	443	Enikeev, N	63, 212
Drelich, J	366, 452, 497	Ebin, B	574	Enloe, C	382, 554
Drera, S	266	Ebner, T	222	Enomoto, M	303, 381
Drezet, J	162, 386	Ebrahimi, A	534, 581	Epstein, E	338
Droz, V	258, 520	Ebrahimi, F	587	Erasmus, D	244
Drumby, L	344	Echeverri Restrepo, S	553	Ercius, P	93
D, S	164	Eckenrode, J	271	Erdem, E	156, 295
Duan, C	226	Ecker, L	267, 517	Erden, F	126
Duan, D	15, 502	Eckerlebe, H	269	Erden, I	157
Duan, H	112	Eckert, J	22, 229, 230, 307, 506, 529	Erdmann, R	40, 183
Duan, J	28	Edalati, K	291, 501	Erdogan, M	126, 556
Duan, X	540	Edmondson, P	477	Ergül, E	126
Dua, R	150			Ergun, C	157
Dubey, D	20			Eric, R	67, 327

Ertugral, S 71
 Eruslu, M. 574
 Erzi, E 142, 219
 Esawi, A 353
 Escande, A. 147
 Escobedo-Diaz, P 416
 Escobedo, J 82, 186, 416, 484
 Esen, Z 452
 Esfahani, S 376
 Eshraghi, M. 238
 Eskin, D. 154
 Esparza, N. 552
 Esper, F 116
 Espinosa, D. 199, 200, 280, 311, 451, 552
 Espinosa, H. 13
 Espinoza, R. 320
 Esposito, L 77
 Essadiqic, E. 471
 Essadiqi, E. 330, 331, 405, 515
 Estremera, E 373, 581
 Estrin, Y 292, 437
 Etay, J 109, 110
 Etienne, A 422
 Eufinger, J 85
 Evanoff, K. 581
 Evans, B 276
 Evans, C 408
 Evans, J 323, 504
 Evans, K. 143
 Everett, R 132
 Evteev, A. 313
 Ewh, A 408

F

Fabregue, D. 218
 Facca, S. 453
 Facco, G 407
 Fafard, M. 318, 319, 394
 Fahrman, M. 106, 178, 256, 334, 409, 478
 Fampiou, I. 510
 Fan, C 52
 Faney, T. 313
 Fang, C 22
 Fang, H 77, 288, 310
 Fang, Y 193, 397
 Fang, Z 53, 278, 287, 582
 Fanisalek, H 302, 512
 Fan, J 15
 Fanning, J 59
 Fan, P 287, 582
 Fan, R 73
 Fan, W 510
 Fan, X 14, 140, 296, 297, 376, 503
 Fan, Z 330
 Farahany, S 527
 Farbaniec, L 136
 Fardeau, S 301
 Farha, A. 543
 Farhangdoust, S. 528, 530
 Faria, R 311
 Farkas, D. 45, 111, 483
 Farley, A 578
 Farrokhzad, M. 115
 Farrow, A. 484
 Farzadfar, A. 405, 471, 515
 Faure, L. 559
 Fautrelle, Y 40, 233, 387

Favel, N. 147, 448
 Favre, J 218
 Fazarinc, M. 146, 217
 Feaugas, X. 206, 518
 Fecht, H. 109, 506, 542
 FECHT, H. 131
 Fehrenbacher, A 55, 125
 Fei, H 50
 Felicelli, S. 238
 Felon, L. 170
 Feng, G 334, 395, 462
 Feng, J 432
 Feng, K 402
 Fenglu, Z. 71
 Feng, N 449
 Feng, Q 106, 178, 256, 307, 334, 335, 409, 478, 506, 554
 Feng, S 273
 Feng, X 430
 Feng, Y 208, 450
 Feng, Z 348, 376
 Fensin, S 484
 Fergus, J 179, 180, 257, 335
 Ferguson, I 418
 Ferracane, J 229
 Ferrante, M 210
 Ferraris, M. 255
 Ferraro, S. 85, 316
 Ferre, A 437
 Ferreira, A. 461
 Ferreira, G 343
 Ferre, R 437
 Ferron, J 365
 Ferry, M. 537
 Feuvrier, J 250
 Fidler, B 70, 562
 Fiedler, T. 463
 Field, D 37, 145, 417, 535
 Fielden, D 317
 Field, F 173
 Fielding, R. 177, 178
 Field, R 246, 501
 Fields, K 46
 Fife, J 85
 Figueiredo, R 62, 135, 290, 441, 500, 557, 560
 Filho, J 143
 Fillery, S 344
 Fillon, A. 354
 Filzwieser, A 133
 Findeisen, A. 336
 Findley, K 114, 382, 554, 587
 Finel, A 130, 158, 239, 530
 Fiona, D. 156
 Fioretti, F. 453
 Fiory, A 493, 522
 Fiot, L 301
 Fiot, N 165
 Firoozbakht, M 55
 Firouzdor, V 177
 Firrao, D 24, 81, 156, 233, 310, 388, 438, 459, 461, 508
 Fischerauer, S 191
 Fischer, F. 63, 239
 Fischer, M. 233
 Fischer, W 164
 Fisher, C 35, 587
 Fisher, F 485
 Fitchorov, T. 424

Fitzka, M. 371
 Flanagan, T 507
 Flater, P. 211
 Flender, R 25
 Fletcher, M 514
 Florando, J. 349, 435
 Flores, J. 310
 Flores, K. 22, 151, 152, 228, 282, 385, 454
 Flores, L 511
 Flores, M. 157, 310
 Fluch, R. 323
 Fluss, M. 415
 Flynn, D 98
 Foiles, S. 434, 494
 Foley, D. 212, 439, 533
 Fonda, R 132
 Fong, H 304, 529, 579
 Fontes Vieira, C. 356
 Foreman, R 177
 Forest, S 263, 530
 Fornell, J. 457, 529
 Forsén, O. 244, 365
 Forsmann, B 515
 Forsmark, J 256
 Fortini, O. 148
 Fortner, J. 105
 Foulk, J 250, 252
 Fouvry, S. 94, 164, 437
 Fox, E 92
 Fagner, W. 223
 Fragoso, E 527
 Franco, V. 332
 Frandsen, B 346
 Frary, M. 357
 Fraser, H 21, 32, 57, 95, 106, 107, 206, 207, 284, 286, 348, 355, 364, 381, 586
 Fredriksson, H. 240
 Free, M 61, 88, 133, 134, 165, 208, 244, 287, 320, 365, 438, 497, 498, 554
 Freeman, A 432, 547
 Frenette, H. 74
 Fressengeas, C. 135
 Friak, M. 86, 314
 Friedrich, C. 151
 Friedrich, R. 164
 Frieslich, C 570
 Friis, J 75
 Frincu, B 276
 Frint, P 440
 Frisk, K 314, 427
 Fritsch, S. 59, 300
 Fritze, H 109
 Fritzen, C. 436
 Fritzsche, H. 198, 466
 Frizorger, V. 302
 Froehlich, T. 181
 Frommert, M. 25
 Frosta, O 319
 Frost, D 540
 Fu, B 64, 497
 Fuchs, G 563
 Fu, E 415
 Fuerst, J. 426, 452
 Fu, G 297
 Fugetsu, B 55
 Fu, H 539
 Fujda, M 289
 Fujieda, S 365, 366



TMS 2012

141st Annual Meeting & Exhibition

INDEX

Fujikawa, T	323	Ganter, M	450	Genzel, C	192
Fujino, N	109	Gao, B	104, 319, 379	Geoffroy, O	276
Fujita, K	78, 506	Gao, F	38	George, E	362, 413, 436
Fujita, T	365, 366	Gao, G	111	Georges, E	362
Fujiyoshi, M	119	Gao, H	262, 454	George, T	276
Fukuda, H	55	Gao, J	23, 78, 261	Gerberich, W	250, 263, 545
Fukuda, T	260	Gao, M	257, 313, 358, 385	Gerzszak, T	516
Fukunaga, K	525	Gao, N	135, 208, 367, 441, 562	Gerdes, K	313
Fukunaka, Y	411	Gaona, A	511	Germann, T	43, 186, 263, 282, 482
Fukuoka, T	243	Gao, Q	338	German, R	53, 54, 410
Fulco, U	562, 573	Gao, S	165, 169	Gerogiorgis, D	80, 361
Fuller, B	124	Gao, T	228, 423	Gershenson, M	74
Fuller, T	581	Gao, W	311	Gesing, A	533
Fullwood, D	535	Gao, Y	19, 21, 62, 78, 151, 173, 196, 229, 305, 339, 373, 384, 453, 455, 473, 487, 504, 506, 507, 551, 574, 578	Geslin, P	130
Fultz, B	48, 116, 190, 268, 345, 346, 347, 390, 391, 419, 486, 519, 549	Garay, J	123, 266, 267	Getty, H	452
Funami, K	405, 471, 514	Garces Plaza, G	515	Geveci, A	502
Fundenberger, J	500, 559	García-Antón, J	564	Ghahremaninezhad, A	320
Furnish, T	172, 545	García-Caballero, F	462	Ghamarian, I	207
Furrer, D	97	García, E	326	Gharghour, M	275, 317
Furuhara, T	18, 75, 148, 149, 226, 227, 303, 381, 382	García-Gabaldón, M	567	Ghasemi-Nanesa, H	560
Furu, J	232	García-García, J	243	Ghassemi, H	30, 480
Furusaka, M	346	García, H	139	Ghazisaeidi, M	495
Furu, T	153, 231, 308, 386	García-Herrera, J	142	Ghisleni, R	481
Furuta, T	42, 291	García, M	401	Ghodrat, S	249
Fu-Zhi, D	19	García-Mateo, C	168	Ghonem, H	32
		García-Sanchez, E	288, 289	Ghoniem, N	251
G		Gardner, M	346	Ghorai, S	200
Gabay, A	123	Garg, A	35, 81	Ghosh, D	390
Gaertner, H	381	Gargac, J	34	Ghosh, S	200, 430, 584
Gage, T	177	Gargarella, P	230	Ghaasiaan, S	18
Gaggero-Sager, L	294	Garg, R	87, 88	Gianola, D	262, 411
Gagne, J	74	Garimella, N	287, 492	Gibson, J	357
Gaies, J	17, 18, 357	Garimella, S	148, 511	Gibson, M	21, 78
Gaikwad, A	581	Garlea, E	114, 567	Giddings, D	90
Gaines, L	450	Garlea, O	268	Gierlotka, W	122
Galán, L	379	Garmestani, H	150, 283, 465, 578	Gigineishvili, A	370
Galego, E	565, 572	Garmetani, H	248	Gihleengen, B	198
Gallagher, M	212	Garner, F	114	Gilbon, D	518
Gallant, N	305	Garrett, G	346	Gilchrist, M	231
Gall, D	16	Garrido, F	70	Gill, A	248, 408, 435, 484, 488
Gallego, N	347, 348	Garvin, K	451	Gillard, A	300
Galliez, K	516	Gasior, W	550	Gilles, R	269
Gallo, J	220	Gaston, D	37	Gill, P	150, 513
Gallops, S	95	Gatepin, M	469	Gill, S	267, 517
Gallup, K	316	Gaulin, B	129	Gill, V	166
Galmarini, S	553	Gaustad, G	174, 450	Gin, A	64
Galvão Dantas, L	116	Gautam, A	93	Ginatta, M	88
Gamarra, M	483	Gavras, A	97	Giordano, E	151
Gambone, J	309	Gavrilov, S	114	Girard, J	441
Gamsjäger, E	239	Gayathri, N	340	Girault, G	448
Gamweger, K	15	Gaytan, S	82, 461	Giri, A	340
Ganapathysubramanian, B	215	Gbur, J	171, 529	Giribaskar, S	557
Gan, B	43, 469, 545, 587	Geathers, J	371	Gittard, S	445
Gancarz, T	550	Gebert, A	307, 474, 520	Giuranno, D	194
Gandin, C	232, 260, 337	Gee, S	295	Giust, F	143
Ganeev, A	212	Geiler, A	424	Glavicic, M	59, 130
Gan-Feng, T	299	Gelbaugh, J	452	Gleason, K	257, 258
Gangloff, R	169, 323, 324	Geldenhuys, I	36	Gleason, W	257, 258
Gangolu, S	200	Genc, M5	07	Gleeson, P	271
Gangopadhyay, A	78, 139, 373	Geng, H	426	Glensk, A	160
Gang, Z	329	Genin, X	165	Glicksman, M	41, 239
Gan, J	104, 277, 278, 351, 424, 551	Genma, Y	404	Glockner, S	232
Ganley, J	180	Gentils, A	478, 517, 518	Glover, J	283
Gan, M	296, 297, 376, 503	Gentleman, E	305	Gluck, T	245
Gantan, I	438, 459	Gentleman, M20, 76, 149, 227, 304, 305, 382, 451, 528		Gludovatz, B	305, 400
				Glukhov, D	379
				Gobin, D	232

Goddard, W. 466
 Godfrey, A. 370, 440
 Godlewski, L. 256
 Goerigk, G. 49
 Gogia, A. 207
 Gogte, C. 508
 Göken, M. 439
 Göksu, O. 556
 Golden, P. 252
 Goldenstein, H. 227
 Goldfine, N. 97
 Goldman, J. 452
 Gollapudi, S. 164, 207
 Goller, G. 124, 125, 427, 529
 Göller, G. 574
 Golosker, I. 349
 Golovoshchenko, S. 300
 Golubov, S. 187, 342
 Golumbfskie, W. 17, 18, 300
 Gomes, A. 490
 Gomes, J. 489, 490
 Gomez, H. 142, 419
 Gong, P. 456
 Gong, X. 136
 Gong, Y. 182
 González-Carrasco, J. 462
 Gonzalez-Escarcega, A. 499
 Gonzalez, S. 151
 González, S. 457, 529
 Gooch, J. 105
 Goodman, B. 260
 Goossens, D. 345
 Gopagoni, S. 68, 247
 Gopal, P. 236
 Gorbunov, V. 144
 Gordon, A. 47, 201, 462, 497, 572
 Göring, E. 410
 Gorman, B. 177
 Gorny, A. 72
 Goroshin, S. 411, 540
 Gorti, S. 269, 279, 317
 Gosselin, L. 511
 Gosselin, S. 148
 Goswami, M. 200
 Goswami, R. 163, 223, 446
 Gottstein, G. 71, 433
 Gou, J. 47
 Gouma, P. 13
 Gouné, M. 227, 303
 Gourlay, C. 120, 121, 487
 Goutière, V. 308
 Gouvêa, D. 549
 Govender, G. 301
 Gower, L. 150
 Gow, R. 320, 582
 Goyal, A. 353, 521
 Goyal, D. 351
 Grabowska, B. 564, 577
 Grabowski, B. 160, 161
 Gracio, J. 130
 Graff, J. 293
 Graham, B. 220
 Gramegna, N. 85, 316
 Gram, M. 414
 Gramss, M. 181
 Grande, T. 394, 395
 Grandfield, J. 27, 309
 Gratz, E. 166, 513

Gray, G. 241, 242, 417, 428, 483, 484
 Gray III, G. 82, 186, 484
 Gray-Weale, A. 67
 Greaves, G. 118
 Greene, J. 115
 Greene, R. 95
 Greenfield, S. 484
 Green, N. 309
 Greenwood, M. 381
 Greer, A. 229
 Greer, J. 41, 43, 110, 183, 261, 262, 307, 338,
 411, 413, 414, 480, 542, 545
 Gregurek, D. 99, 443
 Grewal, H. 81
 Grewer, M. 362
 Greytak, A. 13
 Griffin, D. 383
 Griffith, B. 492
 Grillo, F. 199, 200
 Grimes, M. 553
 Gripenberg, H. 231
 Groh, J. 409
 Groschner, C. 275
 Grosinger, W. 421
 Grossman, J. 169
 Grovenor, C. 341
 Gruan, C. 217
 Gruber, P. 184, 362
 Gruebel, G. 345
 Gruen, G. 308
 Grugel, R. 183, 427
 Grundy, D. 97
 Grunlan, J. 418
 Gu, A. 383
 Guan, C. 226
 Guang, B. 513
 Guangchun, Y. 462
 Guan, J. 586
 Guan, X. 536
 Guan, Z. 12
 Guardino, M. 24
 Guay, D. 464
 Gubiza, J. 290
 Gu, C. 292
 Gu, D. 545
 Gudipati, P. 60
 Guduru, R. 92, 322
 Guenes, J. 170, 408
 Guennec, B. 371
 Guerin, R. 183
 Guerra, E. 208, 321
 Guerrero, M. 479
 Guerrero Mata, M. 141, 527, 568
 Guest, G. 231
 Guest, J. 451, 452
 Gu, G. 90
 Gu, H. 98, 343
 Guibao, Q. 376, 512
 Gui, L. 542
 Guillen, D. 396, 467, 511
 Guimaraes, M. 243
 Gui, T. 499
 Gu, J. 337
 Guldogan, Y. 526
 Guler, K. 126
 Gulsoy, E. 410
 Gumbsch, P. 43
 Gundakaram, R. 544

Gunderov, D. 136
 Gunduz Akdogan, N. 123
 Gunes, G. 157
 Gungormus, M. 579
 Günther, B. 410
 Guo, B. 81
 Guo, F. 51, 120, 324
 Guo, G. 315
 Guo, H. 462
 Guo, J. 46, 115, 119, 188, 189, 266, 343, 344,
 418, 465, 485, 548
 Guo, L. 439, 540
 Guo, M. 227, 423, 447
 Guo, Q. 413
 Guo, R. 65
 Guo, S. 288, 362, 439
 Guo, W. 223, 306
 Guo, Y. 14, 15, 67, 132, 296, 297, 382, 483,
 560
 Guo, Z. 524
 Guozhi, L. 67, 70, 217, 218, 299, 526
 Gupta, A. 449, 535
 Gupta, G. 427
 Gupta, M. 277, 329, 430
 Gupta, N. 46, 47, 266, 312, 547
 Gupta, S. 295, 445
 Gupta, V. 189, 374
 Gu, R. 235
 Gürmen, S. 574
 Guruprasad, P. 251
 Guruswamy, S. 175, 331, 332, 473, 474
 Gu, S. 147
 Gusberti, V. 503
 Gusev, A. 379
 Gutfleisch, O. 122, 176, 332, 520
 Güth, K. 122, 520
 Guthrie, R. 386
 Gutierrez, A. 552
 Gutierrez, J. 271
 Gutierrez-Urrutia, I. 340
 Gutiérrez-Urrutia, I. 102
 Gutschick, D. 326
 Gutt, C. 345
 Gutu, T. 12
 Gu, X. 204, 413
 Guyer, J. 215, 326

H

Haarberg, G. 225, 379
 Haataja, M. 158, 238, 384, 521
 Habib, A. 276
 Habibi-Parsa, M. 560
 Haboub, A. 469
 Hachani, L. 233
 Hackenberg, R. 149, 227
 Hackett, M. 333, 407
 Hackley, V. 190
 Hackney, S. 474
 Hadadzadeh, A. 330
 Hadian, R. 148
 Hadian, S. 19
 Hadjikhani, A. 524
 Hadjipanayis, G. 123
 Haertling, C. 516
 Hafley, R. 131
 Hafsås, J. 153
 Hagihara, K. 196, 360, 531



TMS 2012

141st Annual Meeting & Exhibition

INDEX

Hagio, Y	512	Hardin, R	84	Henager, C	83, 167, 255
Ha, H	479	Hardman, W	249	Henderson, H	55, 584, 588
Hahn, H	128	Hardy, M	98, 335	Henderson, J	254
Haibei, W	61	Hariharaputran, R	313, 390, 391	Henein, H	40, 109, 182, 198, 260, 337, 410, 411, 540, 550
Haider, H	451	Harimkar, S	13, 16, 65, 68, 138, 141, 142, 182, 215, 218, 267, 294, 297, 374, 505	Henke, T	361
Haider, M	489	Harlow, D	306, 398	Hennayaka, H	247
Haifei, X	88	Harlow, G	398	Hennies, W	116
Haines, C	189, 370	Harmer, M	56, 547	Hennig, R	160, 282, 360, 416, 483, 519
Hai-Yan, Y	299	Harmon, J	485	Henry, J	92, 415
Hakonsen, A	386	Harrell, J	64	Hensmann, M	253
Håkonsen, A	153	Harrigan, W	200	Heo, T	26, 158
Halbedel, BA	181	Harrison, G	201, 301, 527, 560	He, Q	171, 528
Halep, A	146	Harrison, R	477	Hequet, A	148, 448, 449
Hales, J	37	Harris, B	211	Herbig, M	554
Haley, B	47, 326	Harris, V	424	Héripéré, E	206
Haley, D	30	Hartfield-Wunsch, S	17	Herlach, D	260, 337
Halim, M	287	Hartfield-Wünsch, S	18	Hernandez-Avila, J	438
Halle, T	440	Hartley, C	435	Hernández, I	24
Hallstadius, L	426	Hartmann, T	177, 475	Hernandez, J	82, 310, 461
Hallstedt, B	314	Hartshorne, M	128	Hernandez-Maldonado, A	581
Halse, K	153	Hartwig, K	416, 439, 533	Hernández Muñoz, G	568
Hals, T	560	Haruyama, O	506	Hernández, R	556
Hamaguchi, M	243	Hashemi Oskouei, R	171	Hernandez-Rodriguez, M	289
Hamann, E	246	Hashida, T	508	Herráiz-Cardona, I	564
Hamed, E	228	Hashimoto, A	254, 512	Herrera-Romero, O	444
Hamhuis, R	90	Hassan, A	352	Herzer, G	424
Hamilton, J	514	Hatano, H	243	He, S	296
Hamilton, R	162	Hathaway, R	126	Hesaraki, S	528, 530
Hammen, J	521	Hatkevich, S	242	Hess, A	541
Hammen, R	521	Hattar, K	342	Hetherly, J	204
Hammer, J	233	Hattori, M	471	Heuser, B	277, 425, 487
Hammerschmidt, T	160, 432	Hauch, B	177, 254	He, W	479
Hammond, K	266, 359, 531	Hauser, A	355	Heximer, M	209
Hammond, V	125, 439, 533	Hawk, J	84, 179, 257, 335, 336	He, Y	325
Hamouda, A	329	Haxhijaj, A	540	Heydari Gharahcheshmeh, M	581
Hampton, M	180	Haxhijaj, B	540	Hibbard, G	69, 116
Han, B	249	Hayashi, S	287	Hibbert, K	578
Hanbo, Z	217	Hayashi, T	501	Hibiya, T	182
Handwerker, C	50, 422, 423, 522	Hayes, S	106, 177	Hickel, T	160, 161, 236, 237, 314, 532
Hanein, Y	12	Hayward, E	187	Hickman, R	342
Han, G	376	Haywar, E	38	Hidalgo-Hernandez, R	573, 575, 585
Hangen, U	251	Hazeli, K	94	Hiebert, R	257, 258
Hang, Y	297	Hazra, S	412	Higashida, M	93
Han, H	318, 502	Hebert, R	291, 292, 307, 507	Higashi, K	86
Hanhold, B	149	Hector Jr, L	400, 470	Higgins, A	411
Han, J	119, 136, 197, 255, 318	Hector, L	87, 197, 404	Hilbrunner, F	181
Han, K	246, 249	Hedström, P	26	Hildeman, G	126, 202
Han, L	153	Hefferan, C	420, 421	Hilerio, I	26, 458, 556
Hanlon, T	487	Hefti, L	60	Hill, E	170, 249
Han, M	243	He, G	468	Hillert, M	303
Hannemann, U	331	He, H	220	Hill, L	429
Hannon, A	152	Hehui, Z	450	Hill, M	252
Hannoyer, B	495	Heidary Moghadam, A	279	Hill, R	261
Han, Q	144, 153, 378	Heidloff, A	197	Hinojosa, B	129
Han, S	107, 466, 547	Heilmaier, M	363	Hinoki, T	255
Hansen, N	62, 186, 211, 212, 213, 370, 440	Heinicke, C	181	Hintsala, E	250
Hansen, P	177	Heinrietz, A	84, 85	Hinz, B	305
Hanusiak, W	125	Heinz, N	75	Hinze, B	234
Han, W	186, 261, 340, 482	Heinz, S	442	Hirano, T	257
Han, X	41, 425, 507	He, J	297, 480	Hiroki, K	103
Han, Y	66, 67, 347	He, L	24, 277, 315, 348, 531	Hirosawa, S	91
Han, Z	240	Helfen, L	119	Hirse Korn, S	443
Hänzi, A	191	Helfen, T	443	Hirt, G	72, 361
Haque, M	122	Helle, S	464	Hirth, J	18, 434
Haque, N	103	Helmi, E	524	Hiskey, B	133
Hara, M	567	Hemker, K	42, 43, 362, 429, 434, 435	Hiura, F	102
Hara, Y	156, 467	Hemphill, M	487	H.J., A	563
Harcuba, P	286				

Hjelen, J	136	Horstemeyer, M	76, 239, 405, 406, 573	Hu, C	52
Hjelm, R	346	Horstemeyer, S	101, 405	Hudak, N	544
Hnilova, M	304, 529	Horst, J	579	Huda, M	401
Hoagland, R	43, 56, 203, 204, 340	Hort, N	36, 97, 101, 103, 328, 330, 402, 403, 404, 470, 472, 513, 514, 533	Huffman, P	170
Hoang, T	315	Hosemann, P	114, 478, 517	Hufnagel, T	151
Ho, C	52, 491	Hosseinian, E	481	Hu, G	242
Hochrainer, T	352	Hosseini, V	538	Huggett, P	162
Hockauf, M	209, 300, 439, 440, 560	Hossenlopp, J	489	Hu, H	331, 535
Hodge, A	116, 172, 373, 545	Hosson, J	506	Huh, J	194
Hodges, J	276	Hou, J	446	Hui-Lan, S	299
Hodgson, P	487, 537, 576	Houlachi, G	88, 165, 244, 320	Hui, X	22, 312, 508, 533
Hodor, K	577	Houltz, Y	337	Huizenga, R	226
Hodo, W	20, 587	House, J	209, 211	Hu, L	456, 565, 574
Hoelzer, D	409, 415, 478	Hovanski, Y	37	Hulett, M	249
Hofer, C	517	Hovestädt, E	155	Hull, L	483
Hofer, M	515	Howe, B	115	Hu, M	498
Hoff, A	418	Howe, J	18, 75, 148, 226, 303, 381	Humadi, H	159, 303
Hoffman, E	518	Howell, R	209, 290, 533, 538	Humphreys, N	309
Hoffman, M	339, 468	Hoyt, J	159, 237, 303, 462, 463, 494	Hunger, P	177
Hoffmann, A	400	Hrabe, N	130	Hunger, S	300, 560
Hofman, G	105	Hrabe, R	496	Hung, F	31, 259, 377, 513, 534
Hofmann, D	22, 183, 305, 455	Hrkac, G	176	Hunter, J	235, 236, 538
Hofmann, M	269	Hryn, J	226	Hunt, W	99
Hofmeister, W	18	Hsiao, H	52, 195	Huo, Q	375
Höglund, L	303	Hsiung, L	177, 203, 415, 435	Hu, P	173
Höglund, T	170	Hsu, C	120, 193	Hu, R	257
Ho, H	423	Hsu-Chi, C	301	Huron, E	335
Hohenwarter, A	291	Hsu, D	164	Hurtado, J	175
Hohl, B	87	Hsu, E	356	Hurwitz, E	418
Ho, L	493	Hsueh, H	259	Hu, S	83
Holdsworth, S	348	Hsu, H	120	Huskins, E	368
Holec, D	314	Hsu, K	479	Hussain, R	530
Holleis, B	397	Hua, F	118	Husseini, N	442
Hollingsworth, J	137	Hua, H	462	Hutchinson, C	148, 256, 303
Holm, E	251, 358, 434, 479	Hua, J	189	Hutchinson, N	152, 454
Holmgren, H	253	Huang, C	140, 408, 431, 447	Huth, J	473
Holt, C	510	Huang, D	389, 493	Hutson, A	96
Holt, R	408	Huang, E	94, 248, 349, 454, 518	Hu, X	104, 126, 315, 379
Holtzer, M	577	Huang, G	116	Hu, Y	14, 195, 404
Holtz, R	163, 223, 323	Huang, H	320, 351, 518, 582	Hwang, B	479
Holywell, G	88	Huang, J41, 110, 148, 183, 184, 185, 186, 214, 215, 250, 261, 274, 338, 339, 360, 411, 413, 471, 472, 480, 509, 525, 542, 544, 566, 584	116	Hwang, I	429
Hölzel, M	269	Huang, K	43, 105, 281, 446, 499, 556	Hwang, J14, 24, 61, 66, 68, 81, 133, 139, 140, 156, 181, 208, 217, 233, 247, 267, 287, 296, 310, 365, 366, 376, 388, 389, 438, 439, 446, 453, 459, 461, 497, 498, 502, 507, 508, 554, 565	100, 270, 355, 356
Homayonifar, M	251	Huang, L	488, 506, 546	Hyde, J	167
Homer, E	434	Huang, M	288	Hyde, T	177
Homma, T	197	Huang, Q	141, 447	Hyers, R40, 109, 182, 260, 337, 338, 410, 540, 541	541
Honda, T	222	Huang, R	66	Hyland, M	74, 380
Hong, C	183	Huang, S	110, 209, 242, 338, 339, 472, 487, 520, 542, 544	Hyllander, G	253
Hong, H	552	Huang, T	119, 136, 211	Hynowska, A	529
Hongliang, Z	219, 450	Huang, X	62, 134, 136, 140, 157, 181, 183, 186, 209, 211, 212, 213, 218, 288, 291, 297, 339, 366, 368, 370, 419, 439, 440, 499, 544, 555, 557	Hyun, S	294, 568, 572
Hong, M	353, 391	Huang, Y	194, 195, 259, 290, 330, 343, 376, 454	I	
Hong, S	249, 258, 267, 521, 527, 528, 552, 575	Huang, Z	192, 193, 270, 377, 503	Iannitti, G	416
Hong, W	422, 551	Huan, W	220	Ibrahim, R	171
Hong, X	402	Hu, B	200	Ide, T	221, 572
Hong, Y	32, 93, 295	Hubbard, C	347	Idrees, Y	416
Hon, K	318	Hubbard, D	266	Idris, M	527
Honkimäki, V	362	Hubbard, J	18	Idrobo, J	66
Hono, K	90, 196, 328, 423	Huber, D	32, 107, 207, 286, 586	Idzikowski, B	331
Hood, R	161	Huber, L	237	iio, Y	221
Hooper, R	393, 583, 584	Huber, N	132	Iizuka, A	287
Ho, P	120			Ikeda, M	207
Hope, G	320, 582				
Höppel, H	62, 371, 439				
Horikawa, S	79				
Horita, T	179, 180, 257, 335				
Horita, Z	135, 291, 440, 501, 557, 558				
Horky, J	370, 440, 501				
Hormozi-Nezhad, M	525				
Hornbuckle, B	164, 176, 393, 563				



TMS 2012

141st Annual Meeting & Exhibition

INDEX

Ikeda, T	75, 120	Jamaly, N	162	Jiang, X	376, 446, 502, 503, 554
Ikehata, H	381	Jame, S	490	Jiang, X	93, 509, 566, 584
Ikhmayies, S	126, 202, 389, 459, 497	James, A	389	Jiang, Y	85
Ilavsky, J	117, 118, 190	James, B	496	Jiang, Z	117
Ilbagi, A	337, 411	James, R	257, 258	Jianping, P	104, 147, 226, 299
Ilhan, S	499, 555	Jamison, L	516	Jian, X	464
Imam, M	432	Janardhanan, J	449	Jianzhong, L	430
Imhoff, S	151	Jana, S	37	Jiao, C	382
Imrich, P	41, 421	Janas, A	564	Jiao, S	60, 166, 217, 281
Inaba, A	100	Jandhyala, S	64, 524, 525	Jiao, Z	476
Inácio, W	459	Janecek, M	212, 286, 290, 534	Jia, W	447
Inal, K	87	Jang, D	229, 262, 307	Jia, X	539
Inatomi, H	179	Jang, J	455, 543, 547, 558, 567, 570, 571	Jia, Y	255, 398
Inden, G	226	Jankowski, A	210, 470	Jicheng, H67, 70, 217, 218, 219, 299, 388, 504	
Ingole, S	142, 372, 373	Janotti, A	285	Jie, L	226, 450
Ingraffea, A	32	Janousch, T	164	Jimenez, F	175
Inoue, A	22, 78, 151, 171, 306, 307, 457	Jansen, H	461	Jin, C	445
Inoue, J	413, 509	Janssen, A	277	Jin, F	447
Inoue, T	210, 472	Janssen, M	249	Jinfu, X	297
Instone, S	308	Jansto, S	173	Jing, Y	112, 299
Inui, H	58, 129, 205, 284, 360, 362, 434, 531	Japaridze, L	571	Jin, H	114, 262, 303
Ipser, H	50	Jaquerod, C	386	Jin-Kyu, L	564
Iqbal, A	475	Jaques, B	114, 280	Jin-Long, H	464
Iqbal, K	390	Jaramillo, E	47	Jin, Q	85
Iqbal, S	549	Jaramillo, L	157	Jin, S	194, 270
Irons, G	39	Jardy, A	80, 154	Jinwoo, H	455
Irukuvarghula, S	105	Jareankieathbovorn, N	199	Jin, X	113, 482
Irving, D	43, 44	Jarvis, I	264	Jin, Y	27, 474, 571
Irwin, G	489	Jasiuk, I	228	Jin, Z	43, 350
Isac, M	386	Jassim, A	147	Jira, J	252
Isakov, A	127	Javadi, T	258	Ji, Y	76
Isasti, N	553	Jawahir, I	534, 561	Ji, Z	297, 376
Ishida, K	334	Jayaganthan, R	17, 219	Jobic, S	516
Ishikawa, T	109	Jayaraman, T	115, 175, 389	Johannessen, J	88
Ishiyama, C	259	Jayaram, V	16, 400	Johanns, K	362
Islamgaliev, R	213	Jayasankar, K	144	Johansen, I	153, 308
Islam, M	490, 530, 549	Jebaraj, P	182	Johansen, S	450
Issa, A	533	Jee, S	453	Johansson, S	488
Isshiki, M	288	Jekl, J	533	John, R	95, 96, 252
Ito, E	580	Jeltsch, R	244	Johnson, A	463
Ivanisenko, J	212	Jemian, P	117	Johnson, D	126, 309
Ivanisenko, Y	367	Jenabali Jahromi, A	125	Johnson, F	175, 331, 473
Iveland, T	386	Jeng, R	445	Johnson, J	302
Ivey, D	198, 272, 322	Jennerjohn, S	412	Johnson, O	108
Iwahori, S	253	Jennings, A	110	Johnson, W	21, 22, 305, 307, 455
Iwaoka, H	557	Jennings, H	117	Johnston, A	448
Iwasaki, J	316	Jensen, B	176	Johnston, S	202
Iwashita, T	151, 152	Jeong, H	440, 562	Johto, H	327
Iwata, N	350	Jeong, K	214, 523, 525	Jolly, M	27, 28, 84, 162, 239, 316, 392, 396, 397, 467, 511
Iwata, S	426	Jeong, S	561	Joly, L	80
Izatt, N	61	Jeon, H	64, 195, 273, 294	Jones, I	241
Izatt, S	61	Jeon, J	25	Jones, J	95, 371, 442, 472, 482, 580, 585
		Jewel, S	543	Jones, L	521
J		Jha, A	156, 396, 467, 511	Jones, N	275, 364
Jablonski, D	97	Jha, G	319	Jones, R	36
Jablonski, P	336	Jha, M	396, 467	Jones, S	467, 496
Jackson, J	98	Jha, P	23, 458	Jones, W	274
Jacob, A	67	Jha, S	32, 95, 96, 252, 363, 394, 436	Jóni, B	367
Jacobsen, A	469	Jhon, M	20, 411	Joost, W	341
Jacon, M	448	Jhu, W	192	Joo, U	528
Jadhav, N	139, 422	Jian, D	181	Joo, Y	270
Jagadish, C	338	Jiang, B	330, 556	Jordan, B	470
Jain, V	21	Jiang, F	393	Jordan, H	320
Jakes, J	453	Jiang, H	50	Jordon, J	201, 470, 583
Jakkali, V	420	Jiang, J	14, 132, 365, 456, 500	Josell, D	215
Jakobsson, L	327	Jiang, K	61, 208, 288	Joseph, B	189
Jalli, J	295	Jiang, L	238, 334, 335, 464, 487, 525	Joseph, C	184
		Jiang, T	14, 15, 66, 67, 139, 217, 296, 297,		

Joseph Vijay, S 126
 Joshi, S 544
 Jouen, S 495
 Jou, H 106, 179, 256
 Jung, D 384
 Jo, Y 272
 Juan, P 101
 Juan, Z 219
 Juárez, J 157
 Juarez-Lopez, G 438
 Judge, C 517
 Jue, J 104, 105, 278
 Ju, H 487
 Ju, J 229
 Junca, E 311
 Jung, B 14
 Jung, H 403
 Jung, I 272, 327, 331, 403, 405, 471, 515, 537
 Jung, J 25
 Jung, M 272
 Jung, S 523
 Jung, W 90
 Jung, Y 537
 Junhua, Q 79
 Junichi, N 103
 Jun, Z 464
 Juping, Z 298
 Ju, s 104
 Ju, S 221, 288, 439
 Juslin, N 313, 531
 Juul Jensen, D 419
 Jyothi, R 575

K

Kabir, A 405, 537
 Kabirian, F 471
 Kaboli, S 405
 Kabra, S 268, 487
 Kacher, J 185, 187
 Kad, B 543
 Kado, Y 287
 Kaftelen, H 295
 Kahleel, M 38
 Kahofer, S 440
 Kahruman, C 142, 499, 555, 557
 Kai, J 518
 Kail, B 137
 Kainer, K 330, 404
 Kainuma, R 268
 Kaiser, R 240
 Kaïtasov, O 478
 Kajdas, C 139
 Kajihara, M 194
 Kakkar, B 302
 Kakpovbia, T 530
 Kalaantari, H 539
 Kalac, K 586
 Kalay, E 316, 453, 507
 Kalay, I 453
 Kalay, Y 455
 Kale, A 67
 Kalidindi, S 60, 285, 286, 462
 Kalisvaart, P 198, 466
 Kalita, S 20, 142, 201, 509
 Kalkan, K 374
 Kalokhtina, O 477
 Kalpakli, A 499, 555

Kalyanaraman, R 139, 373, 570
 Kamado, S 197
 Kamali, R 512
 Kamal, T 388
 Kambara, M 127
 Kamberovic, Ž 571
 KAMBEROVIC, Ž 570
 Kamble, N 69
 Kambli, V 201, 527
 Kamfjord, N 377
 Kamikawa, N 382
 Kamineni, P 404
 Kamisetty, V 438
 Kanbur, H 124, 427
 Kandasamy, K 533, 538
 Kaneko, S 512
 Kaneko, T 273
 Kane, R 150
 Kaner, R 432
 Kanetake, N 222
 Kaneta, Y 426
 Kang, B 408
 Kang, C 65, 294
 Kang, D 357
 Kang, F 535
 Kang, H 537, 548
 Kang, I 272
 Kang, J 316, 539
 Kang, K 44
 Kang, M 575
 Kang, P 369
 Kang, S 50, 118, 146, 181, 192, 213, 270, 318,
 349, 350, 422, 472, 491, 550, 563
 Kang, U 559
 Kang, Y 331, 580
 Kan, H 466
 Kanno, N 410
 Kano, S 544
 Kant, M 114
 Kant, S 458
 Kanzawa, Y 260
 Kao, A 338
 Kao, C 53, 119, 192, 193, 350
 Kao, P 209
 Kaoumi, D 476
 Kao, W 274
 Kaplan, M 563
 Kapoor, D 55, 188, 189, 368, 370
 Kapp, M 421
 Kapusta, J 531
 Karakaya, I 103, 126, 218, 556
 Karalis, K 376
 Karaman, I 315, 439, 443, 499, 533, 565, 574
 Karcher, C 181, 387
 Kareh, K 487
 Karewar, S 312, 547
 Kargl, F 40
 Karhausen, K 71, 72, 144, 221
 Karki, K 338
 Karl, J 462
 Karlsson, S 383, 452
 Karma, A 110, 183, 260, 337
 Karpenkov, A 332
 Karube, Y 227
 Kasahara, H 243
 Kasala, J 85
 Kaschner, G 43
 Kashaev, N 132

Kashinath, A 203
 Kashyap, B 200, 537, 576
 Kasinath, R 137
 Kasisomayajula, V 493
 Kasprzak, W 73
 Kassegne, S 124
 Kasuga, T 528
 Katakam, S 69
 Katgerman, L 154
 Kato, C 243
 Kato, H 453
 Katoh, Y 255
 Katou, N 121
 Kato, Y 39
 Katragadda, S 499
 Katsman, A 318, 329
 Katsukiyo, M 388
 Katti, D 20
 Katti, K 20
 Kauffman, D 137
 Kaufman, J 462
 Kaufman, M 81, 90
 Kaufmann, H 223
 Kaune, V 561
 Kavanagh, A 28
 Kawabata, H 404
 Kawamura, K 180
 Kawamura, S 180
 Kawamura, Y 196, 328, 514
 Kawasaki, A 454
 Kawasaki, M210, 368, 441, 500, 543, 558, 559
 Kawauchi, H 182
 Kayaci, M 220
 Kayali, E 150, 574
 Kaya, M 280
 Kaya, S 241
 Kazakov, V 298
 Kazanski, B 218
 Keckes, J 263, 421
 Keeskes, L 153, 209, 210, 212, 213, 274, 368,
 439, 473, 505, 533
 Kedron, J 292
 Keefer, E 12
 Keiji, N 388
 Keiser, D 37, 104, 105, 176, 254, 278, 333, 405,
 407, 475, 476, 515, 517
 Keizer, J 90
 Ke, J 119
 Kekki, A 244
 Kelleher, B 333
 Kelly, P 19
 Kelly, S 484
 Kelly, T 29
 Kelton, K 78, 109, 182, 541
 Kemper, T 429
 Kennedy, A 20
 Kennedy, J 176, 177, 178
 Kennedy, M 144, 304, 376, 401, 402, 578
 Kennedy, R 105, 177
 Kennerknecht, T 443
 Kent, P 161
 Keralavarma, S 251
 Kerber, M 191, 370, 440
 Kercher, A 271
 Kern, C 179
 Kernion, S 276, 473
 Kerr, M 45, 113, 187, 265, 341, 415



TMS 2012

141st Annual Meeting & Exhibition

INDEX

Kers, J	280	Kim, K	21, 249, 272, 414, 523, 565, 566	Koc, M	471
Keselowsky, B	452, 583	Kim, M	214, 565, 568, 572	Kodali, H	215
Keshri, A	68, 142	Kim, N	107, 275, 328, 329, 440, 564, 569	Kodambaka, S	546
Keskinkilic, E	502	Kim, S	181, 187, 199, 274, 294, 333, 414, 451, 453, 479, 507, 515, 534, 551, 564, 565, 566, 569, 570, 572, 573, 577	Koehler, J	127
Kesselheim, B	461	Kim, T	214, 521, 537, 562	Koenig, T	266
Kessler, J	168	Kimura, Y	121, 140	Koenraad, P	90
Kestens, L	249	Kim, W	82, 294, 453, 509	Koepsell, L	451
Ketkar, S	418	Kim, Y	47, 105, 184, 187, 214, 222, 273, 329, 333, 334, 416, 418, 478, 514, 523, 525, 533, 543, 546, 547, 548, 566, 567, 569, 571, 572, 574, 575, 578	Koermann, F	314
Ketov, S	474	King, A	211, 419, 463	Koerner, H	344
Ke, X	238	King, B	510	Koester, P	436
Keylin, V	473	King, R	360	Kohnert, A	266, 476
Khabarova, I	156	Kingsbury, D	96	Koh, S	12, 63, 137, 213, 293, 372, 445, 523
Khabashesku, V	266	Kingstedt, O	186	Kohse, G	518
Khachatryan, A	26, 159	Kinney, C	118	Koide, J	243
Khalaf, A	18	Kinoshita, M	426	Koike, J	16, 538
Khaleel, M	83, 472, 535, 537	Kinsel, K	206	Koizumi, Y	218, 229, 238, 324, 360, 531
Khalilpasha, M	524	Kipouros, G	535	Kolbeinsen, L	40, 327, 467
Khamsuk, S	289	Kirchain, R	173, 174, 198	Kolesnikov, A	348
Khan, J	581	Kircher, R	130	Kolesnikov, Y	181
Khanna, S	455	Kirchheim, R	204, 433	Kolitsch, A	495
Khan, R	264	Kirchlechner, C	41, 421	Kollo, G	369
Khan, T	115	Kiriyama, T	512	Kolluri, K	204
Khan, Z	372	Kirk, M	277, 278, 342, 405	Kolmakov, A	420
Kharicha, A	155, 232, 310	Kirschen, M	443	Kolmskog, P	149
Khatayevitch, D	529	Kirschman, D	170	Kolpak, A	169
Khater, H	434, 476	Kish, D	163	Komarasamy, M	559
Khatibi, G	50, 271	Kishida, K	284, 531	Komatsu, N	243
Khawaled, S	329	Kishimoto, H	180	Komiya, A	548
Khew, W	492	Kish, J	404, 471	Komiyama, S	16
Khodadad, R	238	Kiss, L	332, 379	Komiya, Y	91
Khondaker, S	384	Kitahara, T	180	Kompatscher, A	63
Khorami, M	528, 530	Kitayama, K	130	Konca, E	218
Khoshnevis, B	279	Kito, M	222	Konda Gokuldoss, P	424
Khosravani, A	535	Ki, W	550	Kondo, D	291
Khounsary, A	419	Kjar, A	221	Kondoh, K	55, 131, 473
Khraisheh, M	470, 501	Kjar, T	298	Koneru, S	367
Khvostenko, D	229	Kjellqvist, L	222	Konetschnik, S	133
Kiani, S	546	Kjelstrup, S	467	Kong, C	496
Kickinger, R	191	Kjos, O	224	Kong, L	520
Kidmose, J	211, 440	Klafehn, G	412	Kong, Y	569
Kieffer, G	443	Klaumünzer, D	455	Konings, R	277
Kiener, D	114, 251, 362	Klausner, J	511	Konishi, H	126
Kiga, T	51	Kleinfeldt, B	277, 352, 551	Konitzer, D	142
Kiggans, J	124	Klein, R	181	Kontsevoi, O	432, 547
Kikuchi, N	243	Klem, M	137	Kontsos, A	93, 94
Kilicaslan, M	258, 527	Kliauga, A	291	Koo, D	562
Killmore, C	246	Klier, E	212	Koo, J	528
Kim,	428	Klimentenok, G	144	Koporulina, E	156
Kim, B	24, 81, 156, 233, 270, 310, 388, 459, 461, 508, 569	Kline, J	127	Koppes, J	423
Kim, C	51, 195, 354, 428, 429, 492, 521, 575	Klut, P	164	Koratar, N	47, 55
Kim, D	35, 61, 64, 87, 114, 133, 134, 137, 187, 208, 265, 275, 287, 293, 312, 318, 365, 422, 438, 453, 478, 497, 498, 551, 554, 565	Knabl, W	358	Korcak, A	170
KIM, D	563, 570	Knapp, J	188	Korenaga, A	544
Kim, G	115, 426, 574	Knezevic, M	130	Körmann, F	160, 314
Kim, H	62, 64, 82, 107, 134, 137, 146, 166, 209, 211, 273, 288, 291, 294, 366, 368, 369, 414, 439, 440, 486, 499, 500, 514, 521, 528, 533, 546, 557, 558, 562, 565, 566, 568, 571	Knipling, K	132, 176, 295, 433	Kornegay, S	445
Kiminami, C	17	Knobbe, H	436	Kosaka, Y	60
Kim, J	12, 13, 25, 35, 63, 64, 65, 87, 100, 137, 138, 213, 214, 215, 247, 293, 294, 328, 372, 374, 445, 459, 523, 524, 525, 550, 551, 562, 565, 566, 567, 571, 572, 575, 577	Knödler, P	439	Kosch, K	259
		Knori, K	114	Kosec, G	232
		Knox, S	32, 233, 285, 348, 381	Koseki, T	413, 509
		Kobasko, N	108	Koshikawa, N	109
		Kobayashi, K	124	Koskelo, A	417, 484
		Ko, C	122	Kos, L	383
		Koch, C	274, 369, 370, 440	Koslowski, M	62, 361, 480, 545
		Kochergin, V	545	Kossenko, A	218
				Kostorz, G	48, 116, 117, 190, 268, 345, 347, 419, 486, 549
				Kothalkar, A	443, 574
				Kotowski, P	579
				Koury, D	475

Kou, S	408	Kuhn, J	356	Lachanary, J	357
Kovac, J	331	Kühn, U	230	Lach, C	131
Kovalev, A	156	Kuhr, S	95	Lach, T	128
Ko, Y	429, 501, 537, 551, 558, 559	Kui, H	229, 508	Ladanov, M	215
Koyama, T	306	Kukimoto, Y	51	Lados, D	34, 97, 172, 251
Koza, J	307	Kuksenko, S	477	Lafferty, B	587
Kozar, R	406	Kulczyk, M	366	Laflamme, F	148
Koziatek, P	454	Kulkarni, N	235, 236, 405, 538	Lagrange, T	159, 433
Kozikowski, P	191	Kulkarni, R	537, 576	Laha, T	443
Kozmel, T	585	Kulkarni, S	470, 501	Lahiri, D	115, 297, 375, 383, 453
K, R	182	Kulovits, A	54, 185, 234, 407	Lahiri, I	64, 65, 294
Kraaijveld, B	127	Kulshreshtha, P	202	Lahlouh, B	522
Kraft, O	184, 262, 362, 443	Ku, M	377	Lahoda, E	277, 351, 424, 426, 551
Kraft, S	497	Kumar, A	142, 147, 189, 215, 232, 352, 388, 418, 419, 442, 458, 570, 579, 581	Lai, B	49
Krajewski, P	37, 404	Kumar, G	79, 230	Lai, G	530, 555
Kral, M	18, 249, 257	Kumar, M	159, 417, 420, 433, 435	Laikhtman, A	480
Král, R	534	Kumar, N	209, 324, 533, 538, 559	Lai, M	395
Kramer, M	42, 122, 255, 275, 423, 424, 453, 455, 507, 521	Kumar, P	21, 23, 193, 201, 378, 458, 491, 527	Lai, Q	53
Krane, M	80, 155, 239, 309, 392	Kumar, R	70	Laird, B	303
Kranjc, K	228	Kumar, S	262, 357, 401, 414	Lai, W	52
Kranzmann, A	335, 336, 570	Kumar, V	53	Lai, Y	119
Krasienapibal, S	413	Kumbhat, N	270	Lakshmanan, L	287
Krasnov, D	387	Kundu, A	395, 547	Lamant, D	448
Krasovitskiy, A	224	Kundu, T	458	Lamas, D	190
Kraus, L	289	Kunn, E	148	Lambertin, D	516
Krauss, G	29, 90, 167, 245	Kuntzel, H	127	Lamb, J	566
Kraus, T	191	Kunz, M	118, 192, 262, 270, 362, 421	Lambotte, G	225
Krautz, M	332	Kuo, C	356, 479	Lambros, J	94, 96, 186
Krebs, T	271	Kuo, M	192, 193	Lampke, T	440
Kreitz, K	510	Kuo, T	52	Lamsal, C	522
Kremer, U	461	Ku, P	248	Lance, M	92
Kretz, R	300	Kuper, J	536	Landa, A	161, 391, 475
Krichlechner, C	263	Kuramoto, S	42, 291, 567	Landi, B	450
Kridli, G	535	Kuribayashi, K	410	Landry, M	319
Krill, C	84	Kurmanaeva, L	367	Lan, G	119
Krill III, C	159	Kuroda, K	403	Lang, A	177
Krings, D	308	Kurosu, S	238, 324	Langdon, T	62, 134, 135, 209, 210, 211, 288, 290, 291, 366, 368, 439, 441, 499, 500, 543, 557, 558, 559, 560, 562
Krins, N	92	Kurtz, R	83	Langenfeld, G	97
Krishna, K	426	Kurumadalli, K	271	Langer, K	170, 248
Krishnamurthy, R	521	Kurumaddali, K	271	Langlais, J	308
Krishnan, K	417, 484	Kurzydowski, K	63	Lang, Y	239
Krishnapisharody, K	39	Kusada, K	139	Lan, P	39, 317
Krishna, R	301	Kushima, A	338, 339, 544	lan, R	67
Kristiansen, L	380	Kutbay, I	150	Lan, S	229, 508
Kroupa, A	121	Kuwayama, M	512	Lan, X	98
Krug, M	281	Ku, Y	77	Lapidus-Lavine, G	208, 498
Krumdick, G	450	Kuyucak, S	333	Lapovok, R	291, 292, 437
Kruml, T	129	Kuzel, R	211, 212, 269	Lapusta, Y	443
Krupp, C	165	Kužel, R	286, 347	Lara Mendoza, A	141
Kruse, N	91	Kuzmin, O	231	Laroche, D	319
Kruzic, J	33, 35, 95, 171, 229, 250, 306, 324, 400, 468	Kvello, J	378	Laros, T	143
Krylyuk, S	339, 411	Kvithyld, A	231, 308	Larsen, J	95, 96, 252, 436
Krystad, E	127	Kwakernaak, C	76	Larson, B	190, 191, 251
Krzywosinski, K	305	Kwak, H	36	Larson, D	29, 90
Kuan, B	103	Kwak, J	246	Larsson, H	303
Kuba, M	75	Kwalela, S	175	LaSalvia, J	519
Kubena, I	129	Kwiryn, D	70	Laughlin, D	122, 275, 276, 423
Kubin, L	130	Kwong, K	288, 336	Lauhon, L	13, 137, 216
Kuchibhatla, S	91, 167, 352, 478	Kwon, H	569, 574	Lau, M	229, 508
Kucukaragoz, C	67	Kwon, J	114, 436	Launey, M	33, 305
Kucukgok, B	418	Kwon, S	459	Lauridsen, E	419, 463
Kuder, R	271	Kwon, Y	563	Laurinavichute, V	379
Kudrnovsky, J	431	L		Lau, Y	390
Kuebel, C	362	Labat, S	263	Lavender, C	537
Kuehmann, C	179, 256, 428	Lacaze, J	40	Lavender, E	537
Kugler, G	146, 217			Lavernia, E	34, 134, 135, 197, 213, 242, 274,



TMS 2012

141st Annual Meeting & Exhibition

INDEX

... 290, 353, 368, 369, 372, 441, 446, 453, 483, 499, 536, 561	Leitner, H 168, 358	Li, H 23, 76, 92, 112, 132, 135, 147, 218, 223, 288, 374, 375, 379, 382, 420, 437, 468, 498, 511, 512, 540, 576
Lavoie, D 148	Lei, Z 61	Lihao, G 342
Lavvafi, H 171, 529	Lekakh, S 241, 310	Li-Hui, C 301
Lawrence, B 354	Lenski, H 40	Li, J 24, 25, 27, 31, 77, 185, 203, 205, 228, 254, 263, 281, 285, 301, 333, 338, 339, 364, 413, 435, 456, 465, 482, 507, 508, 544, 546
Lawrence, S 263	Leong, Z 159	Lijuan, J 297
Lazarev, N 245	Leonhardt, T 357, 431, 552	Lijun, F 88
Leary, A 473	Leoni, M 268	Li, L 115, 181, 185, 208, 216, 269, 322, 487, 509, 526, 566, 584
LeBeau, S 470, 501	Lescoat, M 478	Lill, J 240
Lebensohn, R 130, 164, 187, 547	Leslie, S 271	Lillkung, K 365
Lebeuf, M 394	Lessing, P 515	Li, M 24, 81, 238, 256, 316, 384, 405, 447, 472, 503, 534, 536
Lebon, B 457	Letter, D 579	Lima, A 569
Lebon, C 206	Letzig, D 102	Lima, H 143
Le Bot, C 232	Leung, D 374, 579	Lim, H 278, 426, 534, 564
Le Bouar, Y 239, 530	Leung, N 249	Lim, K 453
Le Breton, J 354	Levchenko, E 313	Li, N 110, 185, 203, 415, 421, 468
Le Brun, P 386	Leventis, N 459	LINA, A 422
Lech, A 432	Levine, L 42, 48, 116, 117, 118, 190, 263, 268, 345, 347, 412, 419, 486, 549	Linares, X 118
Leclerc, F 154	Levin, I 411	Lin-Bo, L 464
Lederer, M 50	Levitas, V 62, 159	Lin, C 53, 195, 272, 526, 550
Ledford, K 83, 234	Lewandowska, M 63, 366	Lin, D 312
Ledonne, J 113	Lewandowski, J 171, 248, 417, 529	Lind, J 420, 421
LeDonne, J 261, 281	Lewis, A 433	Lindley, T 364, 408
Leduc Lezama, L 568	Lewis, N 45	Lindsay, S 74, 221
Leduc, M 74	Leyman, P 496	Lindvall, M 253
Lee, A 50, 119, 491	L'Heureux, S 308	Lindwall, G 314
Lee, B 195, 229, 273, 312	Li, A 375	Ling, C 158
Lee, C 249, 306, 500, 527, 544, 550, 551, 558, 562	Liaaw, P 487	Ling, Y 349
Lee, D 562, 565	Liang, C 92	Lin, H 52, 214, 395
Lee, E 453	Liang, D 78, 108	Lin, J 335, 474, 588
Lee, G 137, 214, 262, 523, 525, 577	Liang, H 141	Lin, K 51, 273, 350
Lee, H 14, 64, 137, 195, 214, 247, 272, 273, 293, 294, 312, 334, 486, 523, 525, 559, 561, 564, 566, 575, 578	Liang, J 142	Linli, W 461, 462
Lee, J 14, 35, 42, 51, 64, 66, 120, 194, 230, 267, 272, 273, 307, 338, 396, 397, 479, 485, 486, 493, 544, 559, 572, 575	Liang, L 140	Lin, M 52
Lee, K 94, 118, 181, 230, 249, 537, 563, 565, 569, 571	Liang, R 541	Lin, R 165
Lee, L 248	Liang, T 129, 312, 397, 407	Lin, S 51, 83, 120, 121, 194, 272
Lee, M 22, 35, 87, 137, 185, 214, 215, 523, 525, 563, 565, 577	Liang, W 156, 338	Lin, T 122, 195
Lee, N 12, 64	Liang, Y 119, 474, 550	Lin, W 65
Lee, P 85, 162, 239, 392, 487, 576	Liangying, W 376, 447	Lin, Y 52, 77, 350, 368
Lee, S 55, 77, 94, 107, 137, 214, 215, 273, 281, 283, 317, 355, 356, 455, 523, 525, 543, 552, 558, 579	Lian, L 298, 299	Lin, Z 480
LEE, S 580	Lianxu, S 67	Li, P 32, 221, 398
Lee, T 50, 51, 118, 192, 195, 270, 349, 422, 479, 491, 550	Liao, C 395	Liping, N 67, 217, 218
Lee Voigt, H 359	Liao, H 73	Lipin, V 298
Lee, W 112, 242, 501	Liao, W 457, 577	Li, Q 13, 20, 26, 86, 163, 169, 205, 241, 305, 317, 339, 384, 393, 435, 468, 527, 532, 546, 554
Lee, Y 87, 222, 230, 544, 550, 551, 568, 575	Liao, X 62, 91, 135, 242, 289, 338, 367, 526, 557, 558	Li, R 79, 182, 306, 385
Leff, A 553	Liao, Y 116, 307	Li, S 32, 52, 79, 162, 218, 315, 420, 421, 461, 531, 539
Le, G 370	Liaskovskiy, O 202	Liss, K 49, 268, 486, 487
Le Gall, R 340	Liaw, P 21, 31, 48, 78, 93, 116, 151, 169, 170, 171, 190, 229, 248, 268, 305, 306, 307, 317, 323, 345, 347, 349, 384, 385, 398, 419, 421, 453, 454, 455, 483, 486, 487, 488, 504, 505, 506, 549	Li, T 91
Legendre, F 477	Li, B 101, 102, 104, 155, 274, 366, 393, 405, 449, 464	Littrell, K 488
Legris, A 158, 478	Li, C 15, 48, 52, 141, 193, 230, 307, 346, 374, 391, 482, 549	Liu, B 240, 375, 532, 536, 556
Legros, M 41, 42, 43, 58, 110, 183, 261, 262, 338, 411, 480, 542	Lichao, D 430	Liu, C 44, 53, 54, 78, 113, 142, 164, 171, 195, 217, 234, 271, 273, 488, 508, 556
Lehner, T 35, 98	Lickova, M 85	Liu, D 208, 270, 328, 513
Lehnhoff, G 587	Li, D 12, 38, 95, 157, 293, 362, 386, 445, 468, 472, 533, 537	Liu, F 91, 147, 223, 270, 504
Lei, C 432	Liddicoat, P 91, 366, 367	Liu, G 187
Leikvang, B 224	Liebl, D 357	Liu, H 19, 119, 157, 196, 344, 350, 473, 513, 520, 527, 549
Lei, L 545, 582	Liebl, M 462	Liu, J 122, 123, 132, 169, 175, 275, 331, 332, 379, 423, 431, 473, 489, 491
Leinenbach, C 194	Lienert, U 48, 420, 421, 488	Liu, K 50, 51, 195, 297, 299, 317, 491, 534
Lei, T 502	Li, F 69	
	Lifer, A 183	
	Li, G 14, 15, 376, 502, 525	
	Ligda, J 210, 544, 561	

Liu, L 219, 362, 396, 446, 539, 556, 566, 584
 Liu, M 255, 288, 398, 429
 Liu, P 497
 Liu, Q 25, 136, 226, 272, 275, 311, 536
 Liu, R 412, 457, 538
 Liu, S 66, 120, 222, 288, 360, 497, 553
 Liu, T 194
 Liu, W 25, 112, 148, 255, 420, 421
 Liu, X 15, 22, 56, 78, 96, 110, 128, 157, 179, 203, 204, 254, 257, 281, 282, 335, 338, 339, 352, 354, 358, 367, 433, 441, 468, 488, 494, 498, 508, 539, 542, 544, 553, 554
 Liu, Y 32, 39, 70, 72, 113, 144, 145, 172, 180, 186, 203, 276, 338, 444, 464, 465, 488, 523, 526, 542, 544
 Liu, Z 19, 26, 27, 83, 92, 106, 146, 153, 158, 160, 220, 235, 237, 312, 314, 385, 390, 402, 462, 480, 504, 506, 530, 533, 569
 Livescu, V 358
 Li, W 56, 123, 220, 224, 297, 301, 376, 504, 524, 556
 Li, X 54, 55, 56, 72, 76, 93, 125, 126, 140, 145, 147, 200, 261, 262, 321, 338, 394, 429, 524
 Li, Y 38, 39, 50, 55, 75, 83, 118, 134, 136, 150, 165, 192, 203, 230, 238, 240, 242, 270, 284, 298, 299, 312, 317, 324, 328, 349, 351, 368, 369, 372, 390, 396, 412, 422, 446, 447, 466, 483, 491, 508, 534, 550, 560
 Li-Yuan, C 447
 Li, Z 255, 324, 398, 468, 586
 L. Jones, T 473
 Llobet, A 151, 258
 Llorca, J 102
 LLorca, J 264
 Lob, A 28
 Lobkis, O 285
 Loeblich, H 85
 Loewer, Y 271
 Löffler, J 191, 455
 Lograsso, T 424
 Lohmar, J 72
 Lohmiller, J 184, 362
 Lohoefer, G 541
 Lohöfer, G 109
 Lokshin, K 152
 Lo, L 195
 Lolla, T 149
 Longazel, T 163
 Longfield, C 446
 Long, G 117, 118
 Long, S 17, 424
 Long, X 464
 Long, Z 17, 31, 72, 93, 145, 169, 222, 248, 300, 323, 377, 398, 526
 Lookman, T 494
 Lopes, E 528
 Lopes, F 461, 498
 Lopez-Hirata, V 508, 573
 Lopez, M 77, 241, 383
 Lopez, N 582
 López Padilla, R 588
 Lopez Perrusquia, N 298
 Lopp, G 55, 584
 Lordi, V 177, 391

Loretto, M 284
 Lorich, A 358
 Lösch, S 410
 Lotfian, S 264
 Löth, K 337
 Louca, D 151, 305, 384
 Loucif, A 560
 Lou, J 104
 Louzguine, D 457
 Lovato, M 44, 113
 Lowery, A 386, 573
 Lowe, T 62, 134, 209, 211, 288, 291, 366, 368, 439, 499, 500, 557
 Lowry, M 413
 Lozano-Perez, S 480
 Luan, B 429
 Luan, Z 188
 Lubin, M 318
 Lu, C 53, 367, 496, 543, 558, 559
 Lucas, M 277, 343, 344, 345, 346, 391, 519
 Lucas, R 81
 Lucci, R 588
 Lucero, A 214, 523
 Lucey, T 162
 Ludtka, G 276, 549, 584
 Ludwig, A 183, 232, 443
 Ludwig, W 419, 463
 Lugovskoy, A 218
 Lu, H 147, 355, 468, 496, 527
 Lui, T 31, 119, 259, 377, 513, 526, 534
 Lu, J 71, 245, 246, 446, 466, 545
 Lu, K 43, 134, 135, 183, 213, 292
 Lukáš, P 347
 Lukin, M 302
 Lukitsch, M 102, 142
 Lukyanov, A 136
 Lu, L 135, 162, 310, 440
 Lu, N 418, 485, 486
 Lund, A 256
 Lundgren, M 253
 Lun, N 20
 Luo, A 36, 54, 125, 163, 200, 240, 256, 514
 Luo, H 511
 Luo, J 57, 354, 385, 428, 492, 521
 Luo, S 132, 186, 417, 482, 484
 Luo, T 499
 Luo, W 60
 Luo, Y 28, 163
 Lu, S 439
 Lus, H 126
 Lusk, M 284
 Lü, T 549
 Lutomski, P 233
 Lutterotti, L 49
 Lu, W 12
 Lu, X 254, 385, 468
 Lu, Y 60, 255, 317, 398, 431, 539
 Luyima, A 280
 Lu, Z 22, 23, 78, 152, 265, 508, 526
 Lv, G 70
 Lv, X 66, 141, 157, 461, 498, 555
 Lyprendi, A 239
 Lyubina, J 331

M
 Ma, A 499, 500
 Maalekian, M 478

Maass, R 43, 413, 455
 Maaß, R 262, 545
 Ma, C 55, 125
 MacCuspie, R 190, 493
 MacDowell, A 469
 Macedo, E 397
 Macêdo, E 199
 Machado, B 82
 Machado, F 343, 356
 Machai, C 437
 Macias, A 527
 Maciejewski, K 32
 Maciel, T 399
 Mackey, P 161
 Mackiewicz-Ludtka, G 55
 MacKinnon, R 96
 Macrander, A 419
 Ma, D 152
 Maddala, D 507
 Maddela, S 403
 Maddox, B 543
 Madec, R 130, 285
 Madison, J 108
 Ma, E 42, 152, 171, 185, 205, 230, 264, 339, 385, 413, 435, 507, 508, 536, 546
 Maeda, M 245, 438, 512
 Maezawa, Y 190
 Magalhães, E 199
 Magasinski, A 581
 Magdefrau, N 129
 Magerl, A 49
 Ma, H 51, 195
 Mahadevan, P 321
 Mahadevapuram, R 215, 216
 Mahadik, S 459
 Mahaffey, P 443
 Mahajan, S 274
 Mahapatra, M 23, 181, 458
 Mahapatra, R 432
 Mahato, N 375
 Mahdak, K 247
 Mahdavi Shahri, M 170
 Mahendiran, R 331
 Mahmood, S 457
 Mahmoudi, R 471
 Mahon, M 89
 Mahurin, S 92
 Maich, A 156
 Maier, B 254
 Maier, H 499
 Maier, P 25, 403
 Mai, J 127
 Majjer, D 27, 28, 131, 145
 Mainard, D 453
 Maire, E 218
 Maiti, S 587
 Maiwald, D 165
 Mai, Y 160, 338
 Ma, J 416, 464, 523
 Majcenovic, C 443
 Majeed, T 302
 Majidi, B 318
 Maj, J 419
 Majkut, M 421
 Major, R 263, 339, 545
 Ma, K 369
 Makas, A 96
 Makhlouf, M 153



TMS 2012

141st Annual Meeting & Exhibition

INDEX

Makino, A	22	Mariz, F	138	Matsui, N	93
Makino, T	93	Markov, V	96	Matsui, T	179
Ma, L	45, 51, 120, 408, 412	Marks, J	380	Matsumoto, H	93, 229, 238, 324
Malanik, K	292	Markström, A	222, 350	Matsumoto, S	548
Malard, T	74	Marouf, N	94	Matsushita, T	253
Malek, K	510	Marquis, E	91, 128, 247, 381, 495, 518	Matteis, P	438
Mallaiah, S	460	MARQUIS, E	478	Mattern, N	152, 506
Mallesham, B	389	Marquis, F	53, 123, 197, 278, 353, 426, 552	Matthews, G	215
Mallick, A	388	Marshall, D	469	Matthews, W	335
Mallik, U	82	Marshall, M	134	Mausewicz, R	401
Malone, M	208	Marshall, U	134	Mauger, L	391, 519
Malone, P	575, 585	Martha, S	92, 511	Maung, K	372
Maloney, C	384	Marthinsen, K	232	Maupin, H	212
Maloney, J	282	Martin, A	175	Mauro, N	78
Maloy, S45, 113, 114, 187, 188, 265, 341, 415, 416, 517		Martin-Aranda, M	227	Ma, X 1	26
Maltais, J	74	Martin-Cortés, G	116	Maxwell, K	115
Mamontov, E	348	Martin, D	189	Ma, Y	14
Mamun, M	543, 545	Martineau, P	74	Mayer, H	95, 371
Mamutov, A	300	Martineau, R	37	Mayer, J	56
Ma, N	199, 310	Martinez Alvarez, O	567	Mayer, S	256, 257
Manchiraju, S	261	Martinez-Alvarez, O	569	Mayevsky, E	505
Manga, V	236	Martinez, D	82, 484	Mazar Atabaki, M	532
Mangelinck, N	260	Martinez, E	23, 82, 266, 312, 418	Maziasz, P	336, 409
Mangler, C	63	Martinez, J	82, 576	Mazumder, J	83
Manilay, Z	77, 529	Martinez-Jimenez, E	208	McAlexander, W	516
Mani, S	449	Martinez-Saez, E	204	McAllister, D	83
Mankidy, B	189	Martinez-Saez, E	44	Mcallister, J	134
Mannava, S	170, 248, 408, 435, 484, 488	Martinez-Villafañe, A	499	McAllister, J	134
Mann, V	302	Martin, M	190, 325	McBride, D	309
Man, O	347	Martin, O	74, 147, 224, 225, 301, 378, 380, 448, 449, 503	McCabe, R	43, 113, 130, 283
Manoj Kumar, B	219	Martins, L	460, 530, 555	McCain, R	375, 576
Mansfield, C	201	Martin, T	445	McCallum, B	423
Mansikkaviita, H	253, 512	Martis, V	118	McCallum, R	122, 176, 424
Mansoor, B	470, 501	Martos, J	114, 571	McCallum, T	365
Mantha, D	467	Marus, L	359	McCarter, M	474
Mantineo, F	526	Maruyama, B	115	McCartney, G	68
Mantz, Y	313	Maruyama, S	287	McClellan, K	254, 278, 426, 484
Manuel, M	35, 55, 164, 241, 265, 277, 351, 393, 402, 424, 452, 470, 482, 551, 583, 584, 585, 586, 587, 588	Maruyama, T	180	McCloskey, J	257, 258
Manzato, C	360	Ma, S	67, 68	McCormack, R	384, 570
Mao, H	520	Maser, J	49	McCulloch, R	154
Mao, L	539	Mashimo, T	215	McDeavitt, S	105
Mao, S 41, 110, 183, 184, 185, 186, 250, 261, 338, 339, 411, 480, 507, 542, 544		Maslyk, D	271	McDermid, J	404, 471
Mao, X	576	Mason, D	112, 264	McDonald, R	278, 426, 573
Mao, Y	214, 418, 576	Mason, P	106, 222, 326, 350	McDonald, S	121, 349
Ma, P	227	Masset, P. 14, 66, 67, 139, 140, 217, 296, 376, 446, 502		McDougall, I	99
Mapar, A	357	Massih, A	407	McDowell, D	251, 281, 436
Ma, Q	102, 405	Mastorakos, I	542, 586	McElroy, R	235
Maqsood, A	390	Matej, Z	212	McGinnis, A	342
Mara, N 43, 110, 112, 113, 185, 186, 261, 263, 281, 338, 340, 366, 413, 482, 547		Mathaudhu, S	36, 62, 101, 102, 103, 134, 196, 209, 210, 211, 212, 213, 274, 288, 291, 328, 330, 366, 368, 402, 404, 439, 470, 472, 499, 513, 514, 533, 536, 557	McGowan, K	231
Marathe, G	292	Matheus, J	440	McGuffin-Cawley, J	326, 529
Marcantoni, G	72	Mathevon, R	448	McHenry, M	122, 275, 276, 423, 473
Marcellin, P	448	Mathew, K	160	Mckittrick, J	529
Marchwica, P	533	Mathew, R	89	McKittrick, J. 33, 77, 124, 197, 228, 383, 579	
Marcin, J	331	Mathew, S	224	McLean, M	483, 547
Mardon, J	518	Mathiesen, R	337, 541, 560	McLeod, A	249
Marelle, V	425	Matlock, D	167	McMeeking, R	324
Margarido, F	450	Matranga, C. 13, 65, 137, 138, 215, 216, 294, 374		McNaney, J	435
Margem, F	460	Matson, D	40, 109, 182, 235, 260, 337, 338, 410, 540, 541, 542	McTrusty, S	487
Mariani, R	104, 176, 177, 178, 266, 515	Matsuda, M	564	McWhinney, H	489
Marian, J	188, 315	Matsuhira, H	207	McWilliams, B	125, 200
Marichal, C	184, 268			Md. Raihanuzzaman, R	552
Marin, E	405			Meacham, B	264
Marino, J	318			Medeiros, B	552

Medvedev, P	104, 177, 278	Mikkelsen, Ø	174	Moats, M	61, 88, 133, 165, 244, 320
Mehrraram, P	536	Militzer, M	178, 237, 303, 304, 326, 478	Mo, C	550
Mehrotra, S	70	Millán, J	226	Modarres-Razavi, S	439, 533
Mehta, N	188	Miller, B	45, 106, 278, 477	Modi, M	325
Meier, M	88, 164	Miller, M	29, 45, 78, 90, 167, 168, 227, 245, 246, 266, 420, 477, 488	Modi, O	427
Meijer, M	449	Miller, P	445	Moelans, N	159, 238, 553
Meilong, H	376	Miller, S	167	Mogeritsch, J	183
Meintjes, G	147	Miller, V	274, 472	Mogonye, J	68
Meirbekove, R	225	Millett, J	241	Mohajeri, N	180
Meisner, R	511	Millett, P	37, 38, 84, 282, 352, 405, 406	Mohamed, A	73
Mei, Z	533	Millitzer, M	381	Mohamed Al-Jallaf, M	302
Mejia-Rodriguez, G	35	Mills, K	189	Mohamed, F	172, 372, 446, 499
Mekala, P	438	Mills, M	35, 45, 83, 205, 261, 284, 285, 364, 401, 406, 436	Mohamed, M	251
Melgarejo, Z	453	Mills, R	180, 317, 348	Mohame, F	136
Melin, A	55, 276, 584	Millwater, H	584	Mohammadi, F	89
Melnichenko, Y	348	Milshstein, J	166, 513	Mohammadi, R	432
Melo, T	548	Mimoto, T	131	Mohan, A	451, 535, 559
Mélo, T	565, 567, 571	Mimura, K	288	Mohanty, H	23
Mendelev, M	42, 384, 464	Minarik, P	534	Mohanty, P	92, 322, 388
Mendez, C	259	Minchenya, V	387	Mohapatra, B	144
Mendis, C	196	Mingo, N	395	Mohles, V	71
Menezes, R	356	Mingyang, L	143	Mohney, A	12
Meng, F	180	Min, J	472, 514	Mohri, M	354
Meng, J	180, 499, 534	Minor, A	185, 250, 251, 362, 413, 483	Mohri, T	391
Meng, X	316	Min, S	580	Mohseni, H	68, 234
Meng, Z	173	Minter, L	276	Moitra, A	111, 241, 393, 412
Menictas, C	504	Minville, R	74	Mo, K	46
Menifee, D	83	Minyi, Z	430	Mokkelbost, T	379
Menushenkov, V	474	Miracle, D	152, 432, 455, 504	Molaei, M	397
Merah, N	527	Mirgizoudi, M	271	Molina-Aldareguia, J	264
Meredith, C	267	Mirihanage, W	260, 541	Molina, G	139, 249
Mérot, J	239	Miroux, A	154	Moller, H	301
Mert, F	330	Mirsepasi, A	560	Mølån, H	402
Meshi, L	480	Mishra, A	438, 459	Molotnikov, A	292, 437
Meskers, C	99	Mishra, B	99, 144, 173, 266, 530	Momeni, K	480
Mesquita, A	380	Mishra, C	144, 299	Mompou, F	42, 43, 184, 262
Messadeq, N	453	Mishra, L	301	Monadal, C	301
Metelva-Fischer, Y	127	Mishra, R	34, 36, 87, 102, 209, 256, 290, 324, 477, 483, 533, 535, 538, 559	Monden, K	508
Meyer, A	40, 380	Mishra, S	99, 400, 458	Mönig, R	184
Meyer, J53, 123, 197, 198, 278, 353, 426, 552		Misic, L	577	Monirvaghefi, S	55
Meyer, L	209	Misiolak, W	353	Monlevade, E	227
Meyer, M	74	Misra, A56, 110, 185, 203, 204, 246, 256, 263, 264, 267, 281, 340, 342, 390, 415, 421, 477, 482, 547, 554		Monnet, G	476
Meyers, M33, 77, 101, 184, 279, 383, 483, 543		Missori, S	526	Monsegue, N	337
Meyyappan, M30, 92, 168, 247, 321, 395, 465, 510		Mitarai, K	501	Monson, T	343
Meza, L	43	Mitchell, J	229, 309	Montalvo, F	377
M. Ferreira, A	343	Mitchel, W	12	Monteiro-Riviere, N	445
M'hamdi, M	232	Mitlin, D	137, 198, 322, 466, 510	Monteiro, S101, 388, 459, 460, 461, 498, 530, 555, 556	
M'Hamdi, M	387	Mitsui, J	365	Montero, S	24, 81, 156, 233, 310, 388, 459, 461, 508
Miao, J	95	Miura-Fujiwara, E	528	Montgomery, R	37
Miao, S	496	Miura, H	279	Montiel, D	534
Miao, Y	277, 352, 551	Miwa, A	563	Moodley, S	67
Michael, N	354, 428, 429, 492, 521	Miwa, K	222	Moody, M	246
Micha, J	421	Miyahara, Y	254	Moody, N	263, 545
Micha, B	425	Miyamoto, G	149, 227, 382	Moon, B	533
Michel, F	425	Miyamoto, H	323	Moon, K	124
Michels, H	146	Miyaoka, M	349	Moon, M	64, 181, 563
Michiel, M	119, 454	Mizuguchi, T	291	Moore, J	332, 351, 588
Michler, j	481	Mizuguchi, Y	51	Moore, K	341
Mickael, P	146	Mizuno, A	182	Moore, M	122
Middlemas, S	287, 582	Mizuno, H	381	Moore, T	209
Mignanelli, P	335	Mizuta, Y	253	Moosavifazel, V	304, 579
Miguras, M	111	Mladenov, G	571	Mora-García, A	142
Mihaila, B	130	Moat, R	454	Moral, C	311
Mihaylov, I	208			Morales-del Valle, C	585
Mihelich, M	97			Morales-Del Valle, C	575
Mikhail, J	171			Morales-Estrella, R	142
Mikhailovskij, I	506				



TMS 2012

141st Annual Meeting & Exhibition

Morales Garza, E	470	Müller, S	403	Nakai, Y	305, 306
Moran, K	162	Mulligan, C	16	Nakajima, H	221, 567, 572
Moras, A	74	Mullis, A	532	Nakamura, T	100, 287
Mordehai, D	543	Müllner, P	63, 191	Nakamura, Y	371
Mordi, G	64, 524, 525	Munetoh, S	501	Nakanishi, N	131
More, K	335	Munir, Z	334	Nakano, J	288, 336
Moreno Quiles, J	582	Munitz, A	90	Nakano, T	284, 360, 531, 567
Morgan, D	406	Munoz, D	301	Nakashima, K	139
Moriarty, G	418	Munoz, J	346, 391, 519	Nakata, K	509
Mori, G	323	Muñoz, J	26	Nakawaki, S	197
Mori, M	528	Muñoz-Morris, M	289, 292	Nakayama, H	124
Morimitsu, M	88, 244, 563, 564	Muñoz-Saldaña, J	142	Nalwa, K	215
Morita, K	39, 244	Munroe, N	150, 513	Na, M	453
Morley, T	89	Munro, M	20	Namavar, F	451
Morrall, J	237, 238, 476	Murai, K	182	Namavar, R	451
Morreale, B	396	Murakami, K	109	Namboothiri, S	449
Morrell, J	567	Murakami, T	382	Nambu, S	509
Morri, A	85, 378	Murakami, Y	51, 222, 325	Nam, H	214
Morris, D	288, 289, 292, 412	Muralidharan, G	37, 50, 118, 192, 269, 270, 271, 317, 336, 349, 409, 422, 491, 550	Nam, N	403
Morris, J	118, 250, 385	Muralidharan, S	238	Nam, S	537
Morris, Jr., J	42	Murali, S	169	Nam, W	559, 561
Morris, T	133, 134	Muramatsu, M	209	Nanda, J	66
Morrow, B	406	Murashkin, M	63, 86, 91, 288, 289, 291, 367	Nandasiri, M	91
Morsi, K	53, 123, 124, 197, 278, 353, 354, 426, 552	Murayama, M	337	Nandwana, P	286
Mortensen, A	242	Murch, G	236, 312, 313, 463	Nandy, T	164, 207
Morton, A	196	Murcia Santanilla, A	399	Nanstad, R	45
Morton, D	45	Murdoch, H	213	Napolitano, R	260
Mosbrucker, P	188, 265, 517	Muroyama, H	179	Narayan, R	354, 428, 445, 492, 521
Moscoso, W	59, 102, 441	Murphy, A	330, 374, 541, 579, 582	Narita, H	566
Mosecker, L	179	Murray, M	573	Na, S	64, 273
Moser, R	575, 585	Murr, L	82, 461	Nascimento, D	498
Moshkovich, A	480	Murty, K	477	Nascimento, J	138, 569
Mosler, J	251	Murugan, N	126	Naser, J	401
Moss, S	118	Muth, T	37, 124	Nash, P	39
Mostaghel, S	253	Mutnick, D	501	Nasiatka, J	469
Motta, A	158, 476, 478	Mutter, N	201	Nasir, A	445
Mottura, A	245, 285, 335	M, V	555	Nastac, L	23, 80, 154, 155, 232, 309, 310, 387, 457
Motz, C	41, 421	Myrhaug, E	377	Nastasi, M	204
Moura, E	460, 556	Myung, W	523	Nasun-Saygili, G	311, 382
Moura, T	158			Natarajathinam, A	295, 445
Mourer, D	285, 335			Natesakhawat, S	295
Moutanabbir, O	545			Nathalie, B	146
Moxnes, B	301			Nathal, M	529
Mponda, E	99			Nath, M	388
M, R	544			Nath, S	126, 292, 410, 563
Mrutyunjay, P	287			Navarra, A	531
Mubarak, A	307			Navarro Chávez, O	294
Muci-Küchler, K	305			Navarro, L	133, 134
Mu, D	121, 351			Navarro, R	138, 575
Muddle, B	17, 75, 223			Navessin, T	510
Mudryy, R	310			Nawrocki, J	564
Mueller, C	560			Nayak, A	69
Mueller, J	290			Nayyeri, G	317
Muftu, S	383			Nazarian, H	528
Mughrabi, H	42, 58, 129, 205, 284, 362, 434			Nazarov, R	237
Muhlstein, C	172			Nazmutdinov, R	379
Muijsenberg, E	402			Ncapayi, V	523
Mu, K	296			Neale, K	102
Mukai, T	101, 328, 472			Nebebe, M	251
Mukerjee, P	144			Need, R	501
Mukherjee, A	42			Neelamegham, N	36, 88, 101, 103, 328, 330, 396, 402, 404, 467, 470, 472, 511, 513, 514, 533
Mukherjee, S	79, 580			Neibecker, P	230
Mukherji, D	269			Neil, D	123
Mukhopadhyay, N	287			Neilsen, M	479
Mula, S	369, 440			Neishi, Y	93
Mulay, R	434				
Müller, C	561				

Neithardt, T.	262	Nolle, D.	410	Ohodnicki, P.	137, 215, 216, 276, 295, 473
Neklyudov, I.	506	Nonaka, I.	371	O'Holleran, T.	176, 177, 178, 515
Nelson, A.	254	Nonon, C.	425	Ohriher, E.	357
Nerikar, P.	352	Noordhoek, M.	265, 407	Oh, S.	546, 568, 574
Neri, M.	499	Nordheim, E.	143	Ohsawa, Y.	144
Nesbit, P.	89	Nordmark, A.	28, 231	Ohtomo, T.	238
Nesterenko, V.	572	Norton, G.	203	Okabe, T.	365
Neugebauer, J.	86, 160, 161, 237, 314, 532	Nose, K.	365	Okada, J.	109
Neuhaus, J.	191	Nose, Y.	287	Okamoto, N.	284
Neuhaus, P.	40	Nouranian, S.	239	O'Keefe, M.	403
Neves, G.	356	Nouri, A.	203	Okido, M.	403
Neves Monteiro, S.	356	Novak, B.	394	Oktar, F.	150
Newaz, G.	443, 444	Novakovic, R.	194	Okuda, H.	190
Ngan, A.	32, 93	Novitskaya, E.	77, 228, 529, 579	Okuniewski, M.	38
Ng, B.	573	Novotny, M.	269	Okura, T.	253
Ngo, E.	548	Novotny, P.	128	Okuyama, N.	243
Ng'uni, C.	217	Nowak, M.	73	Oldfield, B.	165
Nguyen, A.	70	Nowell, M.	395, 493	Olejnisk, E.	564, 577
Nguyen, J.	453, 580	Nowicki, C.	511	Olesen, F.	401
Nguyen, K.	28	Nukala, P.	360	Olevsky, E53, 54, 77, 123, 197, 278, 279, 353,	410, 426, 552
Nguyen, N.	583	Nunes, C.	572	Oliveira, J.	199, 200, 311, 552
Nguyen-Thi, H.	260, 337	Nunn, S.	124	Oliveira, M.	460
Niarchos, D.	123	Nuo, J.	208	Oliveira, R.	556
Nibur, K.	325	Nychka, J.	20	Oliveira, S.	315
Nicholason, D.	549	Nylese, T.	235	Olivetti, E.	174, 198
Nicholson, D.	49, 161			Olmsted, D.	434, 494
Nicola, L.	553	O		Olney, K.	572
Nicolella, D.	33	Oaks, A.	277, 278, 352, 475, 551	Olsen, B.	349
Niebur, G.	34	Obadele, B.	108	Olsen, J.	24
Nie, J.	18, 19, 75, 78, 148, 196, 226, 274,	Oba, Y.	346	Olson, D.	266, 530
	303, 328, 381, 473	OBA, Y.	191	Olson, G.	29, 90, 167, 178, 245, 246, 326, 547
Nie, K.	126	Oberdorfer, B.	63	Olson, L.	333
Niendorf, T.	499	Oberson, G.	45, 113, 187, 265, 341, 415	Olsson, E.	253
Nieto, A.	585	O'Brien, C.	240	Olubambi, P.	108
Niewczas, M.	59, 102, 129	O'Brien, J.	211	Oluwatobi, O.	523
Nie, Z.	270	O'brien, M.	357	Omdal Tveito, K.	232, 387
Niezgoda, S.	43, 283, 285	O'Bryan, G.	545	Omori, T.	268
Niinomi, M.	528, 567	Ocakoglu, K.	295	Omraei, M.	468
Nikolenko, S.	138	Ochiai, S.	190	OMURA, A.	153
Nili Ahmadabadi, M.	431	Odabasi, A.	574	Omurzak, E.	215
Nili-Ahmadabadi, M.	233, 354, 560	Odbadrakh, K.	276	Onck, P.	264
Ningileri, S.	72, 145	Oddershede, J.	130, 419, 421	Onimus, F.	187, 206, 518
Niroumand, B.	55	Odegard, G.	480	Ono, T.	323
Ni, S.	135	Odenthal, H.	155	Ooki, S.	333
Nishikawa, A.	227	Odette, G.	46, 129, 247	Oosthuizen, T.	60
Nishikawa, H.	350	Odqvist, J.	303	Opeka, M.	357
Nishimura, T.	121, 349, 350	Oehring, M.	132	Ophus, C.	27, 494
Nishino, N.	404	Ofan, A.	267, 517	Oppedal, A.	405
Nishitani, S.	273	Offerman, S.	226	Orangi, S.	394
Niu, H.	60	Ofori-Opoku, N.	237, 381	Oren, E.	579
Niu, L.	228	Ogata, S.	111	Orler, B.	346
Nixon, M.	211	Oguma, N.	253	Orsborn, J.	207
Nix, W.	421, 481, 543	Ogunseitan, O.	578	Ortega, E.	564, 567
Ni, Y.	65	Ogura, T.	91	Ortiz, A.	460, 556
Nkosi, S.	327	O'Hare, E.	105	Ortiz, C.	46
N. Mathaudhu, S.	473	Oh, C.	422, 551	Ortiz-Cuellar, E.	289
Nminibapiel, D.	545	Oh, G.	564, 573	Ortiz-Merino, J.	142
Noble, M.	286	Oh, I.	181, 524, 568, 569	Osborne, W.	203
Nobrega, M.	548	Oh, J.	413, 523, 563	Osen, K.	380
Nobrega, S.	571	Oh, K.	318	Ose, S.	224
Nochovnaya, N.	59	Ohkubo, T.	90, 196, 328	Osetskiy, Y.	188
Noda, M.	405, 471, 514	Ohlhausen, J.	250	Osetsky, Y.	495
Noebe, R.	35, 49, 81, 393, 563, 570	Oh, M.	294	Oskuie, A.	399
Nogita, K.	121, 349, 350, 351	Ohmura, T.	571	Ossa, A.	77
Nogueira, B.	460	Ohnuma, I.	51, 120, 194, 272	Oster, N.	122
Nogueira, C.	450	Ohnuma, M.	191, 346	Ostrovski, O.	127
Nogués, J.	457	Ohnuma, S.	346	Otomar, H.	71
Nolan, T.	408				



TMS 2012

141st Annual Meeting & Exhibition

INDEX

Ott, E	300	Pan, J	67, 447, 448, 502	Pavlina, E	108
Otte, A	112	Pan, K	120	Pawlek, R	394
Ott, R	42, 455, 521	Panov, A	144	Pearman, B	180
Oubram, O	294	Pan, T	37, 403	Peaslee, K	23
Ou, J	131	Pant, B	481	Pech-Canul, M	443, 444
Ourdjini, A	527	Pantelides, S	66	Pedrazas, N	358
Outerio, J	561	Pantleon, W	48, 419	Pei, F	139, 422
Ouvarov-Bancalero, V	464	Pantuso, D	238	Pei, Y	231, 522
Ouyang, F	120, 192, 429	Pan, W	344	Peker, A	21
Owashi, A	86	Pan, X	315	Pekguleryuz, M	452, 515
Oxley, M	66	Pan, Z	420, 473	Pelletier, J	230
Øye, H	319	Panzenböck, M	323	Pellicer, E	457, 529
Oyler, K	188	Pao, P	163, 323	Pemmasani, S	544
Ozaki, K	124	Papangelakis, V	208	Peng, B	447, 465, 503, 525
ÖZALP, G	258	Papanikolaou, S	159, 361	Pengfei, X	226
Oza, S	486	Papesch, C	515	Peng, J	104, 156, 157, 221, 288, 362, 439, 447, 459, 530, 540, 555, 556
Ozawa, S	182	Papi, P	16	Peng, N	447, 503
Ozaydin, F	372, 373	Parada, R	161	Peng, P	555
Ozcan, O	375	Paradowska, A	488	Peng, R	488
Özdemir, A	330	Paramadhayalan, T	23	Peng, S	89
Ozen, B	71	Parameswaran, S	126	Peng, Y	472
Ozer, G	126	Páramo López, V	141	Peng, Z	15, 140, 181, 254, 376, 389, 446, 508, 582
Ozkan Zayim, E	124, 354	Paramo, P	479	Penner, L	89
Ozolins, V	38, 160, 161	Paramore, J	212	Pennycook, S	66, 139
P		Paranjape, H	469	Pennumadu, D	114, 347, 444, 446
Pacheco, M	420	Paras, J	55, 368	Peralta, P	96, 278, 363, 417, 426, 484
Pachla, W	366	Pardo, J	243	Perea, D	168
Packard, C	412	Pareige, C	477	Perederiy, I	208
Padalkar, S	137, 216	Pareige, P	168, 422, 477, 517, 518	Pereira, A	460
Padap, A	292	Parga, J	280	Pereira, L	157
Padhi, P	23, 361, 388	Parish, C	271, 477, 478	Perepezko, J	151
Padilha, A	404	Pär, J	388	Perez-Bergquist, A	186
Padilla, E	420	Park, B	178	Perez-Bergquist, S	241, 415
Padilla, H	172	Park, C	83, 90, 246	Perez, D	94
Padilla, R	14, 66, 139, 217, 296, 376, 446, 502	Park, D	571	Perez, E	104
Padron, I	522	Park, E	79	Pérez-Herranz, V	564, 567
Padula, S	49, 529	Parker, C	145	Perez-Labra, M	438
Paes, M	300	Park, H	246, 524, 528, 543, 568	Perez, M	354
Paglieri, S	507	Park, I	588	Pérez, M	157, 310
Paital, S	69, 182	Park, J	249, 269, 420, 566, 578	Perez-Prado, M	102
Pajunen, P	365	Park, K	500, 544, 566	Perfilyev, V	480
Palai, P	576	Park, L	500	Pericleous, K	110, 239, 261, 338, 387, 397, 457
Pal, B	137	Park, M	565	Perroud, O	263
Palchoudhury, S	374, 486	Park, N	214	Perruchoud, R	88
Paliwal, M	331	Park, S	272, 279, 453, 514, 533, 562	Perry, C	304
Pal, J	200	Park, Y	105, 418, 542	Perus, I	146, 217
Palkowski, H	107, 489, 492	Parra, R	161	Peter, I	392
Palmu, L	244	Parson, N	387	Péter, L	332
Pal, N	507	Parthasarathy, T	111, 205	Peterlechner, M	63
Pal, U	166, 513, 536	Parveen, A	460	Petersen, E	510
Palukuri, N	289, 558	Pasciak, M	345	Peters, J	20
Paluri, R	142, 372, 373	Pasebani, S	255	Peterson, B	83
Panahi, D	303	Paspaliaris, I	80, 361	Peter, W	37, 124, 279
Pan, C	141, 157	Pastor, M	474, 575	Petford-Long, A	29
Panchal, J	318	Patel, D	485	Petre, M	145
Pancholi, V	292, 509	Patel, M	397, 457	Petrenec, M	347
paNDA, D	361	Pathak, S	413	Petric, A	258
Pande, C	112	Patiño, F	157, 310	Petrov, I	115
Pandey, A	229, 429	Pati, S	80, 103, 166, 396, 467, 511, 513	Petrov, R	249
Pandolfelli, V	220	Patout, L	239	Petrusenko, Y	504, 505, 506
Pan, F	461	Patra, B	243	Petry, W	191
Pan, H	531	Patrick, L	111, 483	Pettifor, D	160
Panias, D	80, 361	Patterson, B	54, 164, 234, 463, 484, 586	Pettit, R	97
Panichas, C	325	Paulino, L	225	Pfefferkorn, F	55
Panigrahi, S	290, 533, 538	Paul, R	476	Pfeifer, H	155, 467
Panishev, N	14	Paulus, R	243	Pfennig, A	570
		Pauly, S	230		
		Pautrat, A	240		

Pham, Q. 484
 Phani, P. 362, 436
 Pharr, G. 362, 414, 436
 Philip, E. 445
 Philippon, S. 559
 Phillion, A. 85, 162
 Phillips, J. 178
 Phillips, L. 13
 Phillips, P. 284, 285
 Phillipot, S. 129, 265, 312, 351, 353, 391, 397,
 407, 414, 425, 446, 553, 576
 Phongphisutthinan, C. 144
 Picard, D. 319, 394
 Pickard, C. 519
 Picraux, S. 168, 480
 Picraux, T. 338
 Pierce, C. 188
 Pierer, R. 162, 239
 Pierre, L. 146
 Pierre-Olivier, B. 146
 Pierron, O. 443, 481
 Pietrzyk, S. 225
 Pikhovich, V. 126
 Pilchak, A. 59, 130, 132, 206, 207, 285, 286,
 363, 364, 436, 495, 585
 Pillai, K. 201
 Pili, S. 37
 Pilshchikov, V. 14
 Pimpalgaonkar, H. 23
 Pinal, R. 375, 576
 Pineau, F. 310
 Pinheiro, F. 300
 Pinisetty, D. 47
 Pinson, G. 257, 258
 Pinto, A. 440
 Pippan, R. 213, 289, 291, 323, 400, 559
 Pirker, S. 300
 Pirling, T. 386, 489
 Piskazhova, T. 224
 Pistorius, P. 253, 327
 Piertsev, N. 302
 Plaut, R. 71
 Pleitt, J. 255
 Ploger, S. 106
 P, N 290
 Poda, A. 587
 Podgorodetskiy, G. 144
 Poehl, C. 358
 Po, G. 251
 Pogatscher, S. 222
 Poirier, D. 183
 Pokor, C. 517, 518
 Polesak, F. 197, 317
 Poletti, C. 509
 Poling, W. 45, 114
 Pollock, T94, 95, 196, 274, 284, 285, 316, 335,
 442, 472
 Polt, G. 191
 Polyakov, A. 500
 Polyakov, P. 224
 Pomrehn, G. 392
 Pomykala, J. 198, 280, 355, 430, 520, 552
 Ponscak, S. 379
 Pond, R. 18, 75, 340, 434
 Ponge, D. 168, 226, 554
 Pontes, L. 375, 569
 Poole, G. 330, 388
 Poole, W. 275, 317, 404, 478

Pooyan, P. 150, 578
 Popa, N. 269
 Popovic, M. 146
 Poret, J. 188, 189
 Portela, G. 588
 Porter, D. 98, 106, 266
 Porter, L. 91
 Porter, W. 96
 Portman, J. 326
 Porto, G. 375
 Possato, L. 151
 Post, E. 70, 562
 Potesser, M. 397
 Potirniche, G. 46, 334, 406, 587
 Potomati, F. 151
 Pougis, A. 500, 559
 Poulsen, H. 48, 419
 Poulsen, S. 463
 Pourboghra, F. 357, 491
 Pournaderi, S. 502
 Pouryazdan, M. 128
 Poveda, R. 47
 Povirk, G. 333
 Powell, A23, 80, 103, 154, 166, 232, 309, 387,
 457, 513
 Powell, B. 36, 200, 256
 Powell, C. 396
 Powell, J. 108
 Pozuelo, M. 274
 Prabhakaran, R. 37, 104, 105, 176, 254, 277,
 333, 351, 405, 407, 424, 475, 476,
 477, 515, 517, 551
 Prabhu, N. 200, 537, 576
 Pradhan, S. 20
 Prakash, S. 17
 Prange, M. 66
 Pranger, W. 63
 Prangnell, P. 259
 Prasad, M. 401
 Prasad, R. 170
 Prasad, Y. 404
 Pratt, J. 42
 Pratt, T. 207
 Prentice, L. 103
 Presley, T. 286
 Presoly, P. 239
 Presser, V. 469
 Primig, S. 358
 Prinsloo, N. 244
 Pritish, R. 573
 Proffen, T. 345
 Prosa, T. 91
 Proudhon, H. 263
 Proulx, A. 164
 Provatas, N. 159, 237, 381, 534
 Provazi, K. 451
 Przybyla, C. 436
 Przybysz, M. 366
 P, S 496
 Pstrus, J. 550
 Pubill Melsió, A. 531
 Puddu, V. 304
 Pugno, N. 20
 Puleo, D. 534, 561
 Pullen, S. 487
 Pulugundla, G. 387
 Pulugurtha, R. 270
 Puncreobutr, C. 85, 162

Punzhin, S. 264
 Purcek, G. 499
 Purdy, D. 336
 Purdy, G. 19, 148, 303
 Puttinger, S. 300
 Pu, Z. 534, 561
 Pyshkin, S. 344

Q

Qassab, H. 380
 Qian, D. 170, 248, 408, 435, 484, 488
 Qian, G. 489, 490
 Qiang, Z. 67, 447, 448, 502, 503
 Qian, M. 53, 132, 196
 Qian, X. 544
 Qian, Z. 430
 Qiao, J. 230, 454
 Qiao, L. 398
 Qiao, X. 367
 Qi, C. 503
 Qi, J. 543
 Qing, J. 241
 Qin, L. 447
 Qiu, A. 13, 545
 Qiu, D. 19
 Qiu, G. 15, 67, 68
 Qiu, J. 548
 Qiu, S. 301
 Qiu, X. 534
 Qiu, Y. 151
 Qiuyue, Z. 67, 219, 504, 526
 Qi, X. 448, 449
 Quaglia, G. 85, 316
 Quaresma, D. 199
 Quaresma, J. 199
 Qu, D. 558
 Quek, S. 44, 237
 Queyreau, S. 188
 Quinn, T. 130
 Qu, J. 92, 511
 Qu, M. 282
 Qu, R. 456
 Qu, T. 513
 Qu, X. 360, 553
 Qvist, S. 478

R

Raabe, D. 86, 168, 226, 340, 424, 554
 Raabe, G. 127
 Raab, G. 86, 500
 Raahauge, B. 70, 143, 219, 298, 526
 Raaness, O. 127
 Rabaça, A. 143
 Rabbi, F. 465
 Rabenberg, E. 114
 Rabe, U. 443
 Rabier, J. 58, 481
 Rabkin, E. 543
 Rack, H. 285, 286
 Radetic, T. 146, 494
 Radhakrishnan, B. 235, 236, 269, 317
 Radiguet, B. 477, 517, 518
 Radmilovic, V. 27
 Radovic, M. 443, 565, 574
 Raesisinia, B. 98
 Rafiee, J. 55



TMS 2012

141st Annual Meeting & Exhibition

INDEX

Rafiee, M.	55	Ready, J.	99, 399, 428, 580	Riley, J.	13
Rahbar, N20, 76, 149, 227, 304, 382, 429, 451,	528, 529, 578, 579	Ready, W.	580, 581	Rima, R.	329
Rahimi, R.	431	Rebak, R37, 104, 176, 254, 333, 405, 407, 475,	476, 515, 517	Rimkus, N.	330
Rahman, M.	249, 463, 490	Rebeyrolle, V.	154	Ringdalen, E.	327
Rahneberg, I.	181	Reboredo, F.	161	Ringer, S. 29, 90, 91, 135, 222, 246, 289, 367,	557, 558
Raihan, R.	465	Reddy, R 13, 65, 138, 166, 215, 294, 374, 396,	467, 511	Ringuette, D.	319
Rajan, K.	29	Redin, E.	14	Rink, K.	46, 334, 587
Rajulapati, K.	291, 370, 544, 561	Redkin, A.	379	Rios, G.	208
Rakha, K.	487	Redner, P.	188	Rios, O.	55, 276, 549, 584
Ramachandran, K.	270	Reed, B.	159, 420, 433	Rios, P.	283, 315
Ramachandran, M.	138	Reed, R.	98, 245, 381	Ritchie, R.	22, 33, 34, 305, 469
Ramakrishna, K.	427	Reedy, E.	250, 252	Ritter, C.	224
Ramakrishnan, G.	170, 488	Regis, S.	529	Rivera, C.	77
Rama, M.	540	Reiche, H.	317	Rivera, I.	310
Ramamurthi, M.	547	Reichert, P.	34	Rivera, L.	315
Ramanathan, L.	565, 572	Reid, D.	189, 510	Rivoaland, L.	394
Ramanathan, M.	332, 474	Reid, M.	162	Rivoirard, S.	122, 275, 276
Ramanathan, S.	465	Reifsnider, K.	465	R, J.	289, 290, 558
Ramanujan, R.	175, 331, 473	Reilly, C. 27, 28, 84, 131, 162, 239, 316, 392	337	Roberts, A.	505
Ramasse, Q.	57	Reinhart, G.	337	Roberts, J.	386, 573
Ramasubramaniam, A.	510	Reip, C.	25	Robertson, D.	36
Ramaswamy, S.	150	Reit, R.	580	Robertson, I.	185, 186, 187, 265, 325
Ramesh, K. 76, 125, 242, 368, 417, 435, 546		Remennik, S.	318	Roberts, S.	342, 357, 455, 480
Ramesh, P.	228	Remington, B.	184, 543	Robin, P.	443
Ramiere, I.	425	Renaud, J.	35	Robinson, A.	104, 278
Ramirez, A.	337, 399	Ren, C.	142, 332, 474	Robinson, H.	545
Ramirez, D.	82	Ren, N.	462	Robinson, T.	88, 244
Ramirez, L.	280	Ren, X.	65, 76, 86, 312	Robison, J.	36
Ram, M.	189, 215, 418, 419	Ren, Y.	143, 270, 306, 561	Robledo, M.	582
Ramprasad, R.	359, 554	Ren, Z.	273	Robson, J.	274
Rana, N.	17	Resagk, C.	181	Rocha, A.	141
Ranck, H.	183	Ressler, A.	99	Rodney, D.	58, 454
Randall, N.	383	Rest, J.	278	Rodrigues, A.	138, 356, 548
Randman, D.	37	Restrepo, O.	157, 314	Rodriguez, C.	74, 259
Rangari, V.	460, 556	Rettberg, L.	94	Rodriguez, G.	585
Rangel, V.	433	Reuter, M.	14, 98, 401	Rodriguez, M.	188
Ranjan, S.	336	Revard, B.	184	Rodriguez-Negron, O.	575, 585
Rantala, A.	133	Reveles, J.	455	Rodriguez, R.	20, 460, 587
Rao, A.	200	Reverdy, M.	225, 301, 302	Rodriguez-Santoyo, H.	567
Rao, H.	470	Revil-Baudard, M.	154	Rodriguez-Santoyo, H.	569
Rao, M.	502	Reyes, I.	157, 310	Roeder, R.	34, 149, 150
Rao, S.	111, 205, 363	Reyes, M.	157	Roesler, J.	234
Rao, W.	159	Reynolds, M.	203	Rogal, J.	128
Raphael, J.	170	Reynolds, W.	337	Rogers, J.	109
Rapoport, L.	480	Rhadigan, J.	452	Rogl, G.	501
Rapp, D.	70	Rhamdhani, M.	309	Rogl, P.	501
Rashchi, F.	89, 431, 554, 555	Rhee, H.	76, 360	Roha, D.	80, 174
Rashid, Y.	37	Rhee, K.	199, 451	Rohrer, G.	216, 358
Rashkeev, S.	38	Rhoads, M.	409	Rokhlin, S.	285, 364
Rasmussen, C.	221	Rhodes, N.	204, 481	Rokkam, S.	475
Rasschupkyna, M.	345	Riad, M.	311	Rollant, H.	74
Rasschupkyna, M.	313, 574	Ribis, J.	266, 478	Rolle, J.	318
Rastegar, V.	24	Ricci, E.	109	Rollett, A.	32, 113, 281, 284, 421
Rathmayr, G.	559	Richard, D.	448	Romero, I.	210
Ratke, L.	40	Richard, M.	263	Romero-Serrano, A.	438
Ratvik, A.	319, 379, 381, 394, 395	Richardson, T.	31, 92	Romero, T.	415
Rauch, E.	129, 130	Richards, V.	241, 310	Romhanji, E.	146
Rauter, W.	162	Riches, S.	271	Rondinella, V.	277
Ravindra, N.	354, 428, 492, 493, 521, 522	Richter, G.	184	Rongguang, X.	219, 220
Ravines, P.	235	Ricker, R.	398	Rong, L.	346
Rawlings, M.	487	Riedler, M.	436	Rong, Y.	24
Ray, S.	426	Rieken, J.	197, 198, 255	Roorda, S.	118
Razavihesabi, Z.	248	Riesenkamp, M.	449	Roosz, A.	40
Razavi, Z.	247	Riesterer, J.	106	Rørvik, S.	395
Read, D.	114	Rieth, M.	357	Rosado Cruz, D.	298
Read, J.	121, 349, 350	Rigg, P.	483	Rosalie, J.	17, 223, 328
Read, W.	133, 134			Rosa, N.	460, 530, 555

Rosário, D	549	Sachdev, A	36, 240, 256, 290	Samuel, F	72, 73
Rosén, A	452	Sadagopan, S	262	Samuelsson, C	253
Rosenberg, E	257, 258	Sadangi, R	54, 370	Samuha, S	480
Rosenberger, A	95, 96, 252, 577	Sadasiva, S	238	Sanborn, G	580
Rosenberger, M	74, 233	Sadayappan, K	162	Sanchez, G	511
Rosenkilde, C	308, 380	Sadeghi Nik, A	524	Sanchez, J	452
Roset, G	98	Sadekar, A	459	Sanchez, N	417
Rösler, J	269	Sadic, E	375	Sander, P	542
Rösner, H	211	Sadiq, M	147	Sanders, D	60
Ross, F	14	Sadler, B	319	Sanders, P	183
Rossinyol, E	457	Sadoway, D	165, 166, 326	Sandlöbes, S	86
Rossi, T	77	Sadrameli, S	468	Sandström, R	170
Rosso, M	392	Saeed-Akbari, A	179	Sane, S	238
Roth, D	198	Saevarsdottir, G	225	Sangid, M	31, 94
Rotstein, S	452	Safarian, J	40, 202	Sanin, V	296
Rott, A	71	Safarik, D	186, 258	Sanjari, M	405, 471, 515
Rottler, J	237, 381	Sagapuram, D	59, 102, 441	San Marchi, C	235, 325
Rotundo, F	378	Sagdic, S	125	Sano, T	200, 378
Roué, L	464	Saha, B	332, 474	SanSoucie, M	109
Roven, H	136, 288, 557, 560	Saha, D	348	Sansoz, F	110, 396
Roy, B	100	Saha, J	458	Santafé Júnior, H	459
Roy, I	172, 446, 451, 499	Saha, R	115	Santana, L	356
Roy, M	145	Sahaym, U	46, 203	Santanilla, A	498
Roy, R	287	Saheet, H	219	Santella, M	37, 403, 409
Roy, S	45, 70	Sahin, F	124, 125, 427	Santhanam, P	568
Rozak, G	357, 431, 552	Sahin, Y	526	Santodonato, L	385, 505
Rozas, J	48	Sahoo, N	69	Santos, N	460
Rozenak, P	346	Saida, J	190, 455	Santos, R	70
Rozgonyi, G	202	Saigal, A	235, 459	Santos, T	143
R, S	207	Saimoto, S	346	Sanusi, K	60
Ruan, F	402	Saini, D	305	Sapienza, F	583
Ruan, S	78	Saint-Lebes, F	535	Saraf, S	69, 294
Ruan, Y	148	Saito, J	525	Saraf, V	59
Ruan, Z	448	Saito, N	139, 403	Saralaya, R	94
Ruban, A	391	Sajjadi, S	444	Saraloglu Guler, E	218
Rubinstein, A	451	Sajjad, M	526	Sargent, G	206
Rubitschek, F	499	Sakaguchi, N	387	Sargin, I	260
Rückert, A	155	Sakai, M	243	Sarikaya, M	149, 529, 579
Ruda, M	45	Sakai, T	371, 471	Sarkar, A	289, 435
Rudin, S	258	Sakala, J	175	Sarkar, R	207
Rudman, K	278, 426, 573	Sakurai, H	51, 514	Sarkar, S	27
Rudy, D	34	Salajka, M	292	Sarma, V	363
Ruggiero, A	416	Salama, I	353	Sarntinoranont, M	452, 583
Ruixin, M	298	Salas Zamarripa, A	527	Sarobol, P	422, 423
Ruiz-Luna, H	142	Salazar, T	315	Saroja S	334, 555
Rule, D	463, 586	Salazar-Villalpando, M	396, 467, 511	Sartori, M	556
Rumball, J	321	Saldana, C	211	Sasaki, H	245, 438
Ruppert, M	439	Saleeb, H	353	Sasaki, T	176, 196, 328, 393
Rust, E	586	Salehinia, I	184, 401	Sasikumar, J	175
Rusz, S	292	Saleh, M	412	Sastry, G	287
Ruth, T	89	Saleh, T	415	Satapathy, B	144
Rutkevych, P	313	Salem, A	59, 60, 285, 286	Satish, S	82
Ryan, M	331	Salem, H	112	Satko, D	285, 462
Ryan, S	180	Salinas, E	310	Sato, H	253
Rybalchenko, O	291	Salinas-Rodriguez, E	438	Sato, R	209
Ryu, I	481	Salisbury, T	257, 258	Satoshi, O	253
Ryu, J	137, 568	Salje, E	494	Sato, T	91, 144
S		Salman, O	158	Satoyama, D	42
Saada, G	58, 129, 205, 284, 285, 362, 434	Salman, S	388, 403	Sattari, M	408
Saadi, B	233, 387	S. Almeida, F	343	Saucedo-Muñoz, M	508, 573
Saal, J	533, 569	Salston, M	46	Saue, N	88
Sabatini, J	188	Salvador, P	216	Sauermann, H	541
Sabau, A	23, 80, 154, 232, 279, 309, 387, 457	Samaniego-Benitez, E	142	Sauter, D	389
Sabbaghianrad, S	559	Samimi, P	207	Sauvage, X	63, 212, 354, 495, 562
Sabirianov, R	451	Sami, P	25	Sava, I	145
Sachan, R	139, 373	Sampaio, J	70	Savic, V	400
		Samudrala, R	579	Savvides, N	339
		Samuel, A	72	Sawada, H	506



TMS 2012

141st Annual Meeting & Exhibition

INDEX

Sawatzki, S	122	Schvezov, C	74, 233, 259	Serrano de Caro, M	478
Saxena, A	494	Schwabe, J	173	Serruys, Y	477
Saxey, D	167	Schwaiger, R	262	SERRUYS, Y	478
SAYGILI, G	461	Schwam, D	171, 529	Sethna, J	159, 360, 361
Scardi, P	347	Schwartz, E	94	Setman, D	369, 370, 440, 501
Scattergood, R	369, 370, 440	Schwarz, B	506	Seto, K	167
Scavino, G	438	Schwarz, M	141, 155, 296, 402	Setyawan, A	455
Schablitzki, T	128	Schwarz, P	450	Severo, D	503
Schaedler, T	469	Schwen, D	128	Seyedhosseini, E	525
Schäfer, J	281	Scorsone, M	305	Seyed Vakili, S	233
Schaffer, G	53, 132	Scott, C	354	Shaber, E	178
Schaffer, P	89	Scott, J	209, 439	Shade, P	113, 363, 436, 585
Schaff, F	574	Scott, D'Antuono, D	18	Shae K., K.	564
Schafner, E	191, 367, 501	Screnci, A	513	Shaffer, J	285, 462
Schafrik, R	428	Scwedt, A	56	Sha, G	90, 222, 289
Schaible, E	34	S. Dantas, M	343	Shahani, G	502
Scharf, T	68, 234	Seal, J	437	Shahbazian Yassar, R	30, 92, 168, 247, 321, 395, 465, 510
Schatte, J	358	Seal, S	69, 115, 180, 294, 304, 352, 384, 510, 570, 579	Shahbazian-Yassar, R	30, 92, 168, 247, 321, 395, 465, 480, 510
Scheck, C	86	Sears, J	124, 288, 336, 426, 428, 452	Shahnazi, A	431
Scheel, M	454	Sebastian, J	179, 246	Shahrabi, T	399
Scheibe, T	397	Sedaghat, Z	580	Shahriari, A	399
Schembri, P	325	Sediako, D	73, 514	Shamma, M	469
Schemmel, T	461	Sedlmayr, A	184, 262	Shamsuzzoha, M	73, 341, 434
Schlesinger, M	36	Seetala, N	266	Sham, T	46
Schloth, P	363	Seetharaman, S	109	Shang, C	93, 100, 178
Schmetterer, C	51, 66, 67, 120, 140, 194, 272	Sefta, F	531	Shangina, D	561
Schmid, A	15	Segatz, M	147	Shang, J	53, 119, 169, 242, 305, 400
Schmid-Fetzer, R	196	Seguchi, T	404	Shang, S	312, 533, 569
Schmidt, C	439	Seguin, D	223	Shanholtz, E	519
Schmidt, D	27	Sehitoglu, H	31, 94, 96	Shankar, M	366, 367, 538, 558
Schmidt, H	219, 220	Seidel, A	40, 109, 182, 260, 337, 410, 540	Shankar, R	60
Schmidt, M	128	Seidman, D	29, 56, 128, 203, 281, 358, 433, 494, 553	Shankar, S	18, 72
Schmidt, S	419	Seifeddine, S	84, 85	Shankar, V	341
Schmidt, T	94	Seifert, H	587	Shan, M	155
Schmitt, W	271	Seifi, M	248	Shan, T	312, 407, 553, 576
Schmitz, G	56, 128, 203, 281, 358, 433, 494, 553	Seim, S	327	Shanthraj, P	112
Schmoelzer, T	257	Seiser, B	160	Shan, Z	43, 112, 185, 205, 263, 339, 340, 413, 435, 482, 507, 508, 536, 546, 547, 553
Schmoll, R	308	Seiter, J	587	Shao, L	153, 415, 416, 456
Schneider, A	362, 448	Seixas, D	70	Sharma, A	21, 374
Schneiderbauer, S	300	Self, W	384, 579	Sharma, C	378
Schneider, I	552	Sellers, R	333	Sharma, G	289, 435
Schneider, M	165	Sellmyer, D	123, 276	Sharma, H	226
Schneider, S	540	Selvadorai, P	249	Sharma, J	486
Schneider, W	27	Selyshev, P	406, 476	Sharma, K	460
Schneller, M	224	Semenova, I	500	Sharma, S	354, 458
Schnitzler, M	467	Semerau, B	177	Sharon, J	42, 43
Schoenfeld, B	190	Semiatiin, L	59, 206	Sharp, J	304, 451
Schoenung, J	369, 441	Semiatiin, S	60	Sharypov, N	224
Schoeppner, R	545	Sencer, B	105, 114	Shash, Y	56
Scholz, A	346	Sen, I	444, 446, 481	Shassere, B	276, 549
Schönbauer, B	95	Senk, D	28	Shaw, L	279
Schreiber, D	29, 168	Senkova, S	432, 504	Shechtman, D	318
Schroers, J	21, 79, 230	Senkov, O	152, 432, 504	Sheedy, M	365
Schuh, C	78, 212, 213, 256	Sen, S	118	Shehata, L	56
Schuller, R	371	Seo, J	564, 569	Sheikh-Ali, A	434
Schulte, A	278	Seok, M	543, 547, 567	Sheikhzeinoddin, T	287
Schultz, A	216	Seol, J	246	Sheiretov, Y	97
Schultz, J	16	Seong, B	347	Shek, C	584
Schultz, L	307, 332, 474, 520	Seoung, B	575	Shekhar, S	367
Schultz, P	188	Seo, Y	273	Shekhawat, A	360
Schulz, M	109	Seppi, K	346	Shen, B	240
Schulz, S	570	Sercombe, J	425	Shen, G	71
Schumacher, J	387	Sergueeva, A	263, 264	Shengfu, Z	376, 447
Schuster, B	209, 210, 544, 561	Serizawa, A	91	Shen, H	52
Schuster, J	560	Serna, M	565, 572	Shen, J	473, 558
Schuster, S	253	Serra, A	434, 475, 476		
Schütze, M	495				

Shenoy, R	18	Shukla, A	31, 92, 93	Slattery, D	180
Shen, S	253, 473	Shukla, P	38, 425	Sloof, W	76
Shen, Y	81, 113, 454, 482	Shukla, V	219	Sluiter, M	27
Shepherd, J	321	Shull, R	399, 428	Smilauerova, J	286
Sherek, P	404	Shunmugasamy, V	47	Smith, C	265, 302
Sherman, V	77	Shutao, X	143	Smith, D	42
Shet, S	493, 521, 522	Shute, C	116	Smith, G	30, 91, 167, 247, 518
Shevchenko, D	309	Shutthanandan, V	352, 478	Smith, H	346, 519
She, X	66	Shvindlerman, L	433	Smith, J	139
Shibasaki, K	109	Sickafus, K	129	Smith, L	138, 270
Shibata, E	287	Sidelkheir, O	202	Smith, S	321
Shield, J	115, 123, 175	Sidhu, R	491	Smith, T	36, 99
Shigang, Z	104	Siegel, A	443	Smugeresky, J	278
Shi, H	280	Siegel, D	128	Smyrak, B	570
Shih, D	36	Sietsma, J	76, 226, 249	Snead, L	477
Shih, W	192	Si, G	539	Snead, M	579
Shi, J	383, 500	Siham, A	146	Snell, R	471
Shi, L	528	Sili, A	526	Sniadecki, Z	331
Shi, M	202	Sillekens, W	36, 101, 103, 328, 330, 402, 404, 470, 472, 513, 514, 533	Snow, C	188
Shimada, T	381	Silva, C	227	Snyder, G	75, 120
Shim, M	275, 329	Silva, F	70	Soares Tenorio, J	498
Shimonosono, T	180	Silva, G	343	Sobota, A	85
Shinagawa, K	291	Silva, I	498, 556	Soboyejo, W	228
Shina, L	298	Silva, F	552	Sobrinho, A	138, 375, 548, 569
Shin, C	114	Silva, V	556	Sobrinho, V	199
Shin, D	38, 429, 501, 537, 558, 569	Simakov, D	379	Soderlind, P	161
Shindo, P	82	Simard, C	319	Söderlind, P	391, 475
Shin, E	347, 575	Simard, L	319	Soderstrom, M	365
Shin, G	565	Simchi, A	369	Soellner, W	109, 337, 540
Shin, H	63, 213, 270	Simoes, T	243	Soffa, B	122, 275, 423
Shin, J	267, 479, 548, 566	Simonassi, N	459, 461	Soffa, W	423
Shin, K	274, 293, 312, 403, 429, 538	Simon, D	12	Sofronis, P	265, 325
Shin, M	565	Simon, D	12	Sohn, I	64
Shinoda, K	365, 366	Simonelli, M	131	Sohn, J	199, 451
Shin, S	107, 537, 548	Simon, V	529	Sohn, S	107
Shi, P	350	Simpson, J	83, 133	Sohn, Y	104, 105, 235, 236, 330, 405, 408, 462, 514, 538
Shipway, P	68	Sinclair, C	275, 304, 354, 381	So, J	264
Shi, Q	146	Sindelar, R	518	Sokalski, V	423
Shi, R	206, 207, 473	Singh, A	101, 142, 287, 295, 328, 410, 472, 505	Sokolov, M	45, 357
Shirani, A	372	Singh, B	187	Sokolowski, J	533
Shirato, N	139, 373, 570	Singh, D	200	Solanki, K	111, 204, 241, 393, 412, 481
Shi, S	71, 84	Singh, H	81, 219, 290	Sole, K	244
Shishino, J	249	Singh, J	245, 288, 289, 409, 435, 458	Soler-Crespo, R	581
Shivaram, P	23	Singh, M	346	Soler, R	373
Shiveley, A	233, 285, 348, 585	Singh, N	332	Solheim, A	224, 225, 378
Shiveley II, K	585	Singh, R	370	Solheim, I	15, 377
Shivpuri, R	73	Singh, S	384	Solis-Marcial, O	498
Shi, W	13, 65	Singh, T	219	Soloiu, V	249
Shi, X	57	Singh, U	486, 570	Somekawa, H	101, 328, 472
Shi, Y	151, 384, 385	Singh, V	69, 115, 384	Somerday, B	324, 325
Shi, Z	75, 104, 319, 379	Sinnot, S	129, 265, 312, 351, 353, 391, 397, 407, 414, 425, 429, 446, 544, 553, 576	Somerman, M	579
Shofner, M	46, 115, 188, 266, 343, 418, 485, 548	Siriruk, A	114	Sommerseth, C	380
Shokoohfar, A	372	Sisneros, T	188, 517, 567	Somnard, B	87
Shokuhfar, T	151	Sisson, R	24, 107, 315, 531, 583	Sone, M	259
Short, M	333	Sitaraman, S	270	Song, C	25
Shoukry, S	311	Siyahjani, F	495	Songca, S	523
Shreff, T	176	Skinner, J	545	Song, D	500, 580
Shrestha, S	246	Skocic, M	116	Song, G	163, 402, 534
Shrestha, T	46, 334, 587	Skokov, K	332, 506	Song, H	432, 463, 494
Shuaib, A	527	Skomski, R	123, 276	Song, J	153, 181, 552
Shuai, H	329	Skorpenske, H	317	Song, K	82, 230, 389, 509, 539
Shuai, L	430	Skorvanek, I	122, 275, 331, 423	Songqing, G	219
Shuai, Y	450	Skovron, J	47	Song, S	455, 566
Shubakov, V	474	Skybakmoen, E	224, 394, 395	Song, T	373, 551, 574, 578
Shuchan, W	219, 504	Skyllas Kazacos, M	504	Song, W	73, 152
Shu Hui, W	524	Skyllas-Kazacos, M	503	Song, X	98, 257, 288, 336, 358
Shu Jing, Z	311	Slamovich, E	465	Song, Y	294



TMS 2012

141st Annual Meeting & Exhibition

INDEX

Son, H	82, 270	Stan, T	129	Subbarayan, G	50, 491
Sonmez, S	296	Stanzl-Tschegg, S	95, 371	Subbarayan, S	557
Sönmez, S	296	Starink, M	222, 366, 367	Subbarayan-Shastri, G	238
Sordelet, D	22	Staron, P	132	Subhash, G	94, 342, 390
Sordi, V	210	Stauffer, D	263, 339, 545	Subramanian, G	201, 527, 560
Sorensen, J	148	S.T. Ciminelli, V	343	Subramanian, K	50, 119, 491
Sorhuus, A	99, 224, 380, 448	Steen, I	386	Subramanian, S	170
Sorhuus, A	380	Steenkamp, J	402	Su, D	296, 297
Soria, A	460	Steen, P	392	Suder, W	488
Sorlie, M	87, 164, 242, 318, 394, 464	Stegall, D	543, 546	Sudhagar, P	580
Sorokin, S	224	Steinbach, S	40	Suenaga, S	121
Sort, J	457, 529	Stein, C	32	Sueptitz, R	307, 474, 520
Sosa, J	107, 286, 586	Steiner, G	63	Sugakov, V	406
Sotiriou-Leventis, C	459	Steinfeld, A	396	Suganuma, K	51
Soto, A	365	Steinhardt, P	118	Sugiyama, K	506
Soucy, G	394	Stender, P	433	Su, H	445, 539
Southwick, L	174	Stenzel, C	40, 109, 540, 541	Suharto, J	559
Souza, J	199, 397	Stephens, M	510	Suh, B	275
Souza, R	575	Stergar, E	46, 247, 517	Suh, D	303, 543
Souza, V	311	Sterner, G	106	Suh, J	267, 548
Spangenberg, J	226, 355, 430	Stets, W	84, 85	Suh, M	270
Spanring, A	99, 443	Steurer, W	587	Su, J	405, 537
Sparkman, D	584	Stevens, K	249	Sujata, M	496
Sparks, C	357	Stevenson, J	180	Sukenaga, S	139
Spataru, C	57	Stewart, D	395	Suk, M	568
Spathis, D	223	Steyskal, E	63	Su, L	367, 418, 558, 559
Spealman, T	260	Stickler, R	358	Sulaiman, D	87, 88
Spear, J	530	Stieben, A	233	Suleman, J	170
Spearot, D	56, 128, 203, 267, 281, 358, 433, 494, 553	Stiles, D	17	Sulger, P	164
Specht, E	348	Stinson, J	452	Sullivan, C	305
Specht, P	482	StJohn, D	162, 196	Sullivan, E	238
Speer, J	108, 149, 382, 554	Stocia, A	549	Sullivan, J	338, 450, 542
Spencer	302	Stock, S	383	Summers, E	424
Spencer, D	302	Stoen, L	378	Summerville, L	66
Sperlink, K	289	Stoica, A	152, 269, 317, 348	Sun, A	454
Spieckermann, F	191	Stoica, G	152, 269, 317, 348	Sun, C	32, 77, 415, 416
Spolenak, R	184, 191	Stoica, M	230	Sun, D	69, 303
Spoljaric, D	397	Stokes, D	496	Sundaram, N	560
Spowart, J	46, 115, 188, 266, 343, 418, 485, 548	Stollberg, D	12, 63, 137, 213, 214, 293, 372, 445, 523	Sundaram, V	270
Sprengel, W	63	Stoller, R	187, 188, 191, 342, 357, 495	Sundararaghavan, V	283, 581
Squires, L	515	Stone, D	453	Sundararaman, M	245, 291, 409
Srba, O	212	Stone, H	335	Sundarraj, S	23, 388
Sreelatha, K	561	Stone, I	330	Sundqvist Ökvist, L	253
Srichaiyaperk, A	199	Stone, M	152, 346, 391	Sun, E	129, 234
Sridharan, K	177, 254, 333, 516	Støre, A	395	Sun, G	447
Sridhar, R	287	Stormvinter, A	26	Sung, M	136
Sridhar, S	336	Stoudt, M	18	Sung, S	249
Srikanth, V	561	Strachan, A	47, 189, 282, 326, 482, 542, 546	Sung, W	423
Srinath, T	182	Stráský, J	286	Sun, H	317, 458, 466
Srinivasan, B	391	Straszheim, W	521	Sun, J	185, 205, 339, 413, 435, 507, 508, 536, 546
Srinivas, V	576	Stratton, D	231	Sun, N	392, 431
Srivastava, N	126	Straub, T	443	Sun, P	60, 209, 306
Srivilliputhur, S	236, 266, 312	Strehle, M	277	Sun, Q	108
Srolovitz, D	44, 411, 463	Strehl, G	440	Suntharampillai, T	167
Stach, E	14, 465	Strömberg, E	452	Sun, X	38, 83, 225, 389, 472, 537, 553, 559
Stadler, F	223	Strunz, P	269, 347	Sun, Y	126, 193, 258, 290, 294, 496
Stafford, G	422	Stuart, J	515	Sunyer, A	208
Stafslien, S	445	Stubbins, J	46, 277, 278, 352, 475, 551	Sun, Z	247, 445, 535
Staicu, D	277, 424	Stukowski, A	412	Su, P	422, 423
Stair, P	389	Stumpf, W	301	Suresh, K	191
Stål, J	98	Sturz, L	260	Suresh, S	33
Stanek, C	37, 278, 352, 359, 426	Styman, P	167	Suri, J	279
Stanescu, C	145	Suarez, C	11, 71, 143, 220	Suriñach, S	457, 529
Stanescu, M	355	Suarez, J	101	Suri, P	353
Stanford, N	274, 329	Suarez, O	373, 581	Suter, R	234, 420, 421
Stan, G	411, 493	Suárez, O	588	Sutou, Y	16, 538
		Su, B	240	Suvaci, E	11

Su, X 43, 81, 256
 Su, Y 55, 584
 Su, Z 220
 Suzuki, A. 106, 178, 256, 334, 335, 409, 478
 Suzuki, K. 275, 333
 Suzuki, S. 229, 238, 333, 365, 366
 Svens, K. 208
 Svensson, I. 85
 Svoboda, J. 239
 Swan, J. 564
 Sweatman, K. 121, 349, 350
 Sweet, L. 162, 387
 Swenson, C. 501
 Swenson, D. 183
 Syed Asif, S. 413
 Syuy, N. 138
 Syvertsen, F. 28, 233
 Szczepanski, C. 59, 130, 206, 252, 285, 363, 394, 436, 495
 Szlufarska, I. 43, 112, 113, 185, 263, 340, 406, 413, 482, 547
 Szpara, S. 132
 Szymanski, P. 248

T

Tabereaux, A. 503
 Tabouris, S. 376
 Tada, S. 153, 222
 Tafaghodi Khajavi, L. 202
 Tahanpesarandezfuly, N. 279
 Taheri, M. 17, 18, 128, 342, 465, 515, 553
 Tai, K. 281
 Takada, T. 109
 Takagi, K. 54, 124
 Takagi, Y. 291
 Takahashi, H. 209
 Takahashi, S. 182
 Takahashi, Y. 423
 Takamiya, H. 381
 Takamori, S. 144
 Takasaki, Y. 207, 320, 582
 Takashima, S. 78
 Takashi, Y. 103
 Takata, N. 410
 Takayama, N. 149
 Takebe, H. 253
 Takemoto, T. 350
 Takesue, N. 567
 Takeuchi, I. 423
 Takeyama, M. 179, 409, 410
 Takigawa, Y. 86
 Takla, M. 467
 Talbot, J. 197
 Talebanpour, B. 193
 Taleff, E. 357, 358, 404, 431, 552
 Talekar, A. 507
 Talja, J. 253, 512
 Tallman, D. 518
 Tamerler, C. 20, 76, 149, 227, 304, 382, 451, 528, 529, 578, 579
 Tamirisakandala, S. 125
 Tamura, N. 192, 262, 270, 362, 421
 Tanaka, K. 381
 Tanaka, M. 566
 Tanaka, Y. 268, 291
 Tan, E. 28, 233, 310, 532
 Tane, M. 567

Tang, C. 194, 195, 403
 Tang, F. 411
 Tang, G. 474
 Tang, J. 31
 Tang, K. 127, 308
 Tang, L. 165
 Tang, M. 159, 416, 433
 Tang, N. 324
 Tang, S. 34
 Tangstad, M. 14, 40, 99, 127, 157, 174, 202, 308, 327, 402
 Tang, T. 47
 Tang, W. 122
 Tang, X. 48, 293, 346, 418, 494
 Tang, Y. 184, 483
 Tang, Z. 505
 Tan, H. 519
 Taniguchi, K. 215
 Tan, L. 334, 407, 409, 415
 Tannenbaum, R. 150, 578
 Tan, P. 40, 259, 438
 Tan, T. 395
 Tan, Y. 203, 540, 576
 Tao, J. 296
 Tao, N. 134, 135, 183
 Tao, S. 198, 466, 512
 Tapily, K. 545
 Tarakanova, A. 20
 Tarakci, A. 310
 Tarakcilar, A. 28, 532
 Tarascon, J. 30
 Tarcy, G. 224
 Tarigan, I. 409
 Taskinen, P. 327, 328
 Taspinar, O. 375
 Tassios, S. 103
 Tata, M. 526
 Taupin, V. 135
 Tavares de Moraes, V. 498
 Tavazza, F. 42, 263
 Tavsanoglu, T. 354
 Ta, Y. 512
 Taylor, A. 79, 341
 Taylor, J. 162, 387
 Tazoe, K. 501
 Teague, M. 177
 Teider, B. 220
 Teixeira, C. 332
 Tekeli, S. 388
 Telang, A. 408, 435
 Telila, H. 57
 Telles, V. 199
 Tello, K. 81
 Tenorio, J. 199
 Tenório, J. 199, 200, 280, 311, 451, 552
 Terada, D. 289
 Tercelj, M. 146, 217
 Tesfaye, F. 328
 Tesmer, J. 516
 Tessier, J. 224
 Tewari, A. 553, 563
 Tewari, R. 432
 Tewari, S. 183
 Tewari, V. 219
 Teysseyre, S. 98
 Tezuka, H. 144, 333
 Thadhani, N. 279, 482, 484
 Thakur, S. 445

Thanh Hung, D. 103
 Thawabi, H. 332
 Theisen, E. 392
 Thess, A. 181, 387
 Thevuthasan, S. 91, 352
 Thevuthasan, T. 168
 Thian, D. 159
 Thibault, P. 148
 Thiele, G. 451
 Thiele, H. 277
 Thielsch, J. 122
 Thijsse, B. 542, 553
 Thomas, B. 23, 27, 80, 84, 154, 162, 232, 239, 309, 316, 387, 392, 457
 Thomas, J. 117
 Thomas, M. 269
 Thomas, O. 263
 Thomas, S. 169
 Thompson, G. 64, 164, 176, 393, 563, 570
 Thompson, H. 167
 Thompson, J. 410
 Thompson, R. 216
 Thonstad, J. 225
 Thornton, K. 83, 158, 248, 326
 Threrujirapapong, T. 131
 Thron, A. 359
 Thuinet, L. 128, 158, 476
 Thula, T. 150
 Thuss, J. 471
 Tian, L. 507
 Tian, S. 217, 503
 Tian, T. 119, 192
 Tian, W. 71
 Tian, Y. 115, 147, 210, 441, 461, 513
 Tien, N. 64
 Tietböhl, J. 570
 Tieu, A. 496
 Tieu, K. 367, 496, 558, 559
 Tijani, Y. 84
 Tikare, V. 463, 586
 Tikasz, L. 154
 Tiley, J. 57, 60, 68, 95, 115, 207, 233, 247, 267, 285, 286, 348, 381, 585
 Tilka, J. 482, 585
 Tilson, W. 180
 Timelli, G. 85, 316
 Timmons, A. 249
 Timokhina, I. 487
 Ting'an, Z67, 70, 217, 218, 219, 299, 504, 526
 Tingaud, D. 368, 369
 Tin, S. 43, 469, 545, 587
 Tippey, K. 445
 Tipton, W. 160
 Tirumalasetty, G. 76
 Tischler, J. 191, 420, 421
 Titomanlio, D. 337
 Titus, M. 335
 Tiwari, S. 281, 400
 Tiwary, P. 313
 Tjahyono, N. 380
 Tkacheva, O. 226, 379
 Tlustochowicz, M. 354
 T.N, P. 334, 555
 T.N, R. 82
 Toader, O. 518
 Tobash, P. 258
 Tober, G. 25
 Tobo, H. 512



TMS 2012

141st Annual Meeting & Exhibition

INDEX

Todaka, Y	207	Tsang, E	91	Uhlemann, M	307, 474, 520
Todeschini, P	518	Tsao, W	119, 550	Uhlig, V	541
Tohji, K	209	Tschöpe, K	394, 395	Uhl, J	384
Toihara, T	16	Tschopp, M	204, 241, 393, 412, 481	U, K	334
Tokas, R	69	Tschulik, K	474, 520	Ullal, V	267
Tolbert, S	432	Tsekenis, G	384	Ulrich, O	421
Toledo, R	311	Tselev, A	420	Umakoshi, Y	284
Toloczko, M	415	Tseng, C	195	Umeda, J	55, 131
Tolpygo, V	429	Tseng, Y	513	Umpierre, A	343, 356
Tolvanen, A	338	Tsesmelis, K	143	Ungar, T	317
Tomar, M	374	Tse, Y	131, 436	Ungár, T	288, 367, 487
Tomar, V	20, 35, 47	Tsirlina, G	379	Unlu, M	427
Tomassi, K	234	Tsiros, J	223	Ünlü, N	574
Tombouliau, B	541	Tsuchida, N	210	Upadhaya, A	427
Tome, C	43, 101, 130, 187, 268, 283	Tsuchiya, K	116, 506	Upadhaya, A	427
Tomé, C	130	Tsui, T	262, 547	Upadhyay, M	135
Tomiya, S	51	Tsuji, N	289	Uppal, R	446
Tomlinson, P	275	Tsukihashi, F	155	Uranga, P	553
Tomomasa, O	103	Tuck, C	131	Urata, N	504
Tomsia, A	579	Tucker, G	281, 414	Urbanczyk, K	489, 490
Tondel, P	153	Tucker, J	32, 50, 266, 358, 408	Urones-Garrote, E	227
Tong, C	24	Tucker, M	164, 234	Usselman, R	137
Tong, P	151	Tucker, S	103	Usta, M	150
Tong, Y	152	Tudela, A	501	Ustundag, E	283
Tong, Z	298, 299	Tugcu, K	289	Utsunomiya, H	471
Tonks, D	186, 358	Tuggle, J	538	Uysal, O	526
Tonks, M	37, 38, 282, 352, 406, 475	Tu, K	14, 119, 192	Uzun, O	258, 527
Toorani, M	88	Tulenko, J	342		
Toparli, Ç	574	Tumey, S	415	V	
Topbasi, C	476	Tummala, R	92, 270, 322	Vahidi, E	89, 431, 555
Topkaya, Y	502	Tunncliffe, M	89	Vaia, R	344
Topping, T	213, 242, 353, 368, 369, 372, 441, 453, 536, 561	Turan, A	15	Vaidyanathan, R	49
Torquato, S	118	Turano, S	580	Vaikuntam, L	396, 467, 511
Tort, M	443	Turbini, L	518, 192, 270, 349, 422, 491, 550	Vaithiyalingam, S	91, 167
Toth, L	500, 559	Turchi, P	177, 391, 431, 475	Valderrama, B	588
Touhami, A	581	Turhan, S	316	Valdes Leon, K	289
Tournadre, L	518	Turnbull, T	34	Valdevit, L	469
Tourret, D	110, 183, 337	Turner, C	432	Valega Mackenzie, F	542
Towne, W	97	Turner, D	285	Valenza, F	194
Tracy, S	519	Turner, K	305	Valenzuela Diaz, F	552
Tran, D	490	Tveit, H	377	Valenzuela-Diaz, F	524
Tranell, G	24, 126, 127, 202	Tylsar, S	292	Valenzuela-Díaz, F	116
Trapaga-Martinez, G	142	Tymiak, N	250	Valenzuela, J	280
Trápala, N	310	Tympel, S	387	Valiev, R	62, 63, 86, 91, 134, 136, 209, 211, 212, 213, 242, 288, 289, 291, 366, 367, 368, 372, 439, 499, 500, 557
Tremblay, D	308	Tytko, D	29	Vallejo, E	520
Trice, R	80, 155	U		Valletti, K	544
Trinkle, D	87, 197, 236, 237, 240, 282, 359, 360, 416, 483, 487, 495, 519	Uberuaga, B	38, 187, 204, 352, 358, 359, 494	Valone, S	43, 57, 358, 484
Tripathi, A	458	U, C	207	Vanaie, H	580
Tritt, T	293, 418	Ucar, H	275	Van Aken, D	75
Trivedi, P	485	Uchic, M	111, 113, 205, 363, 401	van Benthem, K	359
Trivedi, R	183, 337	Uchikoshi, M	288	Vance, A	545
TROCELLIER, P	478	Ucisk, A	150, 536	Van den Bosch, J	114
Trochez, A	266	Uda, T	287	van der Giessen, E	553
Troubat, L	448	Udofot, B	373	van der Ven, E	235
Truan-Sheng, L	301	Udovic, T	487, 488	Van der Ven, A	158, 236, 326
Trubaki, N	180	Udyansky, A	313, 314, 532, 574	van der Zwaag, S	303
Trujic, T	577	Ueda, M	180, 207	Van Der Zwaag, S	149, 178
Trujic, V	571, 577	Ueji, R	291	Van de Sanden, R	522
TRUJIC, V	570	Ueno, A	371	van de Walle, A	313, 390, 391, 392
Trujillo, C	82, 186, 241, 416, 484	Ueno, S	566	van Dijk, N	420
Trumble, K	59, 102, 126, 441	Uenoya, T	323	Van Ende, M	403
Trung, T	64	Ueshima, M	492	Van Hoose, J	183, 427
Truskinovsky, L	158	Uesugi, T	86	Van Huis, M	76
Tsai, M	292, 505	Ufuktepe, Y	543	VanLeeuwen, B	213
Tsai, S	518	Uggowitz, P	191, 222, 223	Van Petegem, S	184, 268, 269, 348, 363, 487
Tsai, T	455	Uheida, E	60		

van Peteghem, B 164
 van Rooyen, I 106
 Van Steenberge, N. 529
 Van Swygenhoven, H . 44, 184, 268, 269, 347,
 348, 363, 487
 Van Swygenhoven-Moens, H 284
 Van Tyne, C. 108
 Van Vliet, K. 282
 Vanvoren, C. 11
 Van Weert, G. 365
 Varam, S 370
 Varanasi, K 139, 296, 466
 Vargas, C. 133
 Vargas, H. 311
 Vargas, J 24
 Vargas, T 320
 Varga, T. 167
 Varma, S 433, 552
 Vartiainen, A 175
 Vasconcelos, M. 567, 577
 Vasconcelos, P. 380
 Vassileva, V. 571
 Vassiliev, S 379
 Vasudevan, V46, 170, 248, 408, 416, 432, 435,
 483, 484, 488, 519
 Vattré, A. 57, 484
 Vaughan, G 419
 Vaxelaire, N. 263
 Vedula, R. 326
 Velasco, E 377
 Velasco, M. 44
 Velázquez, A 275
 Vempati, U 151
 Vemuri, V 167
 Venancio, L. 199, 397
 Venkataraman, D. 168
 Venkataraman, M 370
 Venkatesh, P 200
 Venkatesh, V . 59, 60, 97, 130, 206, 285, 363,
 436, 495
 Ventura, T 349
 Venturini, G. 282
 Venturumilli, R 23
 Ventzke, V 132
 Venuturumilli, R 23
 Verga, A. 337
 Verhelst, D. 209
 Verma, A 245, 409
 Verma, N. 16
 Verma, R 17, 404, 472, 514, 535
 Verma, V 580
 Veron, M 129
 Véron, M. 434
 Veshchunov, M 425
 Vetterick, G 342
 Veyssiére, P. 58, 285
 Vian, C 153
 Vianco, P. 479
 Vichytil, C. 323
 Vieira, A 490
 Vijaya Kumar, M. 410
 Vilenkin, A 434
 Villa, E 283
 Villalba, P 189, 215
 Villanueva, M 445
 Villarreal, T 363
 Viñals, J. 208
 Vincent, L 206

Vinci, R. 483, 547
 Vincze, G. 130
 Vinson, D 518
 Viray, J 228
 Virieux, F 74, 87, 165, 231
 Virzi, D 142
 Vishnu, K 189
 Visileanu, E. 355
 Viswanathan, G32, 57, 95, 206, 233, 285, 348,
 381, 585
 Vitek, V 284
 Vitos, L 391
 Vittoria, C 424
 Vlasenko, T 202
 Vodnick, D 251
 Voevodin, A. 115
 Vogel, S 49, 269, 317, 366, 567
 Voglewede, D 433
 Voigt, P 84
 Voit, W 12
 Volgin, A 517, 518
 Volinsky, A 305
 Volkman, T 337
 Vollmer, J 333
 Vo, N 128
 von Kaenel, R. 448
 von Pezold, J. 532
 von Schweinichen, P. 28
 Voorhees, P 83, 410, 463
 Vo, P 405, 537
 Vora, H 182
 Voss, D 40, 109, 182, 260, 337, 410, 540, 541,
 542
 Voter, A 494
 Voyles, P 453, 455, 507
 Vrátná, J 290
 Vrestal, J 121
 Vue, V 346
 Vurpillot, F 30
 Vutova, K 571

W

Wachs, D 105, 278
 Wade, A 483
 Waeckerle, T 276
 Wagner, G 371, 442
 Wagner, M. 59, 209, 300, 440, 481, 560
 Wagoner, R 87
 Waite, P 308
 Waitz, T 63
 Waldera, B. 201
 Walker, L. 336
 Wallace, R. 63
 Wallis, R 59
 Wall, M 177
 Walmsley, J. 136
 Wanderka, N 245, 409
 Wang, B. 176, 201, 205, 297
 Wang, C. 39, 52,
 91, 107, 147, 167, 181, 216, 259, 295,
 322, 338, 447, 507, 508, 513, 539, 542
 Wang, D 56, 86, 376, 421, 451
 Wang, F 155, 180, 449, 474
 Wang, G . 13, 21, 24, 78, 151, 152, 171, 225,
 228, 229, 305, 306, 307, 339, 349,
 384, 385, 453, 455, 504, 505, 506
 Wang, H 42, 52, 53, 58, 67, 68, 102, 137, 172,

186, 208, 317, 322, 415, 464, 479, 544
 Wang, I 195
 Wang, J 26, 39, 43, 44, 66, 67, 79, 81,
 110, 111, 112, 117, 140, 141, 185, 194,
 195, 204, 215, 221, 238, 261, 263,
 273, 282, 338, 340, 341, 351, 377,
 402, 413, 414, 421, 447, 477, 480,
 482, 503, 535, 538, 544, 547, 562
 Wang, K 431, 500, 576
 Wang, L67, 112, 292, 293, 355, 374, 419, 420,
 497, 510, 520, 549
 Wang, M 16, 335, 378, 535
 Wang, N 217, 498
 Wang, O 365
 Wang, P 47, 72, 101, 145, 200, 239, 405
 Wang, Q 15, 73, 165, 296, 317
 Wang, S . 27, 61, 88, 133, 134, 165, 208, 244,
 287, 320, 322, 365, 438, 445, 497,
 498, 554, 555, 556
 Wang, T 316, 465, 467
 Wang, W 230, 511, 530, 533, 556
 Wang, X 14, 48, 116, 126, 146, 152, 166, 181,
 190, 224, 233, 268, 269, 305, 317,
 345, 347, 348, 387, 396, 419, 450,
 466, 483, 486, 488, 540, 549
 Wang, Y19, 26, 27, 48, 52, 59, 83, 84, 86, 107,
 111, 116, 135, 140, 158, 160, 173,
 190, 196, 206, 207, 218, 235, 237,
 238, 243, 255, 268, 270, 284, 288,
 312, 314, 315, 338, 345, 347, 385,
 390, 403, 415, 416, 419, 421, 439,
 456, 462, 473, 478, 483, 486, 488,
 504, 516, 530, 533, 549, 557, 558, 569
 Wang, Z32, 104, 185, 291, 292, 305, 319, 339,
 379, 413, 435, 446, 450, 508
 Wan, H 113
 Wan, K 383
 Wanninkhof, P. 580
 Warchomicka, F 509
 Ward, A 395
 Ward, C 428
 Ward, D 577
 Ward, L 22, 282, 385
 Ward, M 239
 Ware, T 12
 Warmack, R. 236
 Warnken, N 334
 Warren, J26, 83, 158, 160, 235, 237, 312, 314,
 390, 428, 462, 530
 Warren, O 413
 Was, G 341, 342, 476, 516
 Wasik, L 89
 Waske, A 506
 Watanabe, H 86
 Watanabe, M. 109, 182, 483, 510
 Watanabe, T. 38
 Watanabe, Y 528
 Watkins, T 37, 549
 Watson, A 121, 194
 Wayne, L 417
 Weaver, B 432
 Weaver, M. 138, 393, 563, 570
 Webb, J 342, 357
 Weber, W. 277
 Webster, T 157
 Webster, V 82
 Weck, A. 354
 Wedde, G. 99, 224, 380, 448



TMS 2012

141st Annual Meeting & Exhibition

INDEX

Weertman, J.	116	Whittington, W.	405	Woo, K.	181, 563, 569
Wegfrass, A.	181	Wicaksono, A.	304	Woo, W.	94, 269, 575
Wegst, U.	177	Wicker, R.	82, 461	Woracek, R.	347, 444
Wehrs, J.	269	Widener, C.	496	Wright, C.	305, 543, 545
Wei, B.	208	Widom, M.	276, 313	Wright, J.	177, 246, 256, 419
Wei, C.	161, 235, 279, 479	Wiebeck, H.	524	Wright, R.	45, 46, 65, 98, 254
WEI, C.	15	Wienczek, T.	105	Wu, A.	50, 118, 122, 192, 194, 195, 270, 349, 422, 491, 550
Wei, D.	285, 335	Wiezorek, J.	54, 185, 234, 284, 407	Wu, C.	31, 153, 385, 550
Weigand, S.	118	Wilde, G.	211	Wu, D.	60, 158, 159, 284, 313, 390, 464, 522, 523
Weih, T.	362, 482	Wiley, B.	139	Wu, G.	143, 421
Weiland, H.	54	Wilford, K.	167	Wu, H.	120, 237, 535
Weiler, J.	473	Wilhelm, H.	191	Wuhrer, R.	162
Weinberg, A.	191	Wilkerson, L.	242	Wu, J.	66, 214, 216, 360, 375, 389
Weinberger, C.	110, 184, 186, 251, 414, 481, 546	Wilkie, W.	438	Wu, K.	84, 126, 465
Wei, Q.	56, 153, 209, 210, 473, 483, 544, 561	Wilkinson, A.	342, 357, 480	Wu, L.	467
Wei, R.	303	Wilks, G.	46, 115, 188, 266, 343, 418, 455, 485, 548	Wu, M.	232
Wei, S.	189, 343, 344, 418, 485, 486	Willard, M.	176, 276, 295	Wu, M.	109, 110, 131, 506, 542
Weiss, A.	362	William, G.	311	Wu, P.	102, 305, 317
Weiss, B.	50, 271	Williams, C.	242, 247, 417, 518	Wuppermann, C.	155
Weiss, C.	575, 585	Williams, E.	71, 144, 221	Wu, R.	393
Weisser, M.	348, 363	Williams, F.	220	Würschum, R.	63
Weissmüller, J.	262	Williams, J59, 81, 246, 323, 363, 364, 422, 572	422	Wurster, S.	400
Wei, W.	322, 468	Williams, M.	240	Wu, S.	135, 203, 210, 273, 349, 385, 573
Wei, Y.	107, 531	Williamson, K.	177	Wu, W.	52, 59, 60, 170, 317, 349, 487
Wei, Z.	156, 524	Williams, R.	57, 107, 207, 286, 355, 364	Wu, X.	62, 132, 134, 209, 211, 274, 288, 291, 366, 368, 439, 499, 544, 557
Wejdemann, C.	48	Williams, S.	488	Wu, Y.	22, 23, 46, 78, 115, 129, 140, 152, 247, 398, 423, 424, 426, 455, 490, 526
Welberry, R.	48, 345	Williams, T.	167	Wu, Z.	192, 492
Welch, B.	503, 504	Williard, M.	122	Wyatt, Z.	341
Welch, C.	346	Willnecker, R.	540	Wynne, B.	378
Welk, B.	21, 207, 586	Wilson, L.	177		
Weller, T.	418	Wilson, R.	132	X	
Wells, M.	330, 536	Wimmer, A.	575	Xakalash, B.	202
Wells, P.	247	Wimpor, R.	489	Xayasenh, A.	80
Wen, C.	193	Windl, W.	22, 152, 282, 314, 358, 385	Xenidis, A.	376
Wendhausen, P.	332	Winiarski, B.	428, 454	Xia, G.	180
Weng, W.	67	Winkler, C.	553	Xia, H.	556
Weng, Y.	100	Winter, S.	59	Xia, J.	222
Weng, Z.	156	Winther, G.	130, 370, 440	Xia, K.	132
Wen, H.	213, 561	Wirth, B37, 188, 266, 313, 315, 334, 359, 405, 476, 531	476, 531	Xianchao, C.	79
Wen, L.	361	Wisner, C.	459	Xiang, F.	462
Wenlong, J.	328	Wiss, T.	277	Xiangli, N.	299, 526
Wen, W.	32, 93, 163	Witezak, Z.	152	Xianyao, K.	70
Wen, X.	46, 72, 145, 223	Withers, P.	48, 400, 428, 454	Xiaobing, Y.	143
Wen, Y.	84	Withey, E.	42	Xiao, C.	28, 163
Wenyuan, W.	521, 537	Wittig, J.	168	Xiaohui, F.	297
Wenzhong, C.	71	Witt, P.	103	Xiao, J.	36
Wenzl, C.	133	Wixom, R.	188	Xiao, J.	316
Werlitz, T.	570	Wochner, P.	313, 345, 574	Xiao, J.	316
Werner, J.	342	Wolf, D.	352	Xiao, J.	104
Werner, M.	181	Wolf, M.	442	Xiao, J.	104
Wertz, T.	84	Wolk, J.	132	Xiao, J.	104
Wessels, V.	191	Wollants, P.	238	Xiao, J.	104
Wesstrom, B.	134, 365	Wolverton, C.	27, 128, 533	Xiao, J.	104
West, E.	45, 113, 187, 265, 341, 415	Wong, A.	6	Xiao, J.	104
Westendorf, N.	74	Wong, C.	65	Xiao, J.	104
Westfall, L.	346	Wong, D.	380	Xiao, J.	104
West, G.	436	Wong, D.	380	Xiao, J.	104
Wetzlich, S.	570	Wongsa-Ngam, J.	441	Xiao, J.	104
Weyland, M.	75	Wong, Y.	477	Xiao, J.	104
Wheeler, R.	436	Won-Seok, Y.	564	Xiao, J.	104
White, C.	174, 223	Woo, C.	347	Xiao, J.	104
White, J.	35, 98, 174, 253, 327, 401	Woodcock, T.	122, 176	Xiao, J.	104
Whitfield, A.	17	Woodfield, A.	207	Xiao, J.	104
Whitfield, D.	302	Woodford, W.	282	Xiao, J.	104
Whitfield, R.	345	Wood, J.	473	Xiao, J.	104
Whitis, D.	106, 178, 256, 334, 335, 409, 478	Woodward, C.	32, 95, 111, 205, 240, 363, 432, 462, 504	Xiao, J.	104
Whitley, B.	584, 586			Xiao, J.	104

Xie, J 402
 Xie, K 246
 Xie, L 169, 503
 Xie, M 432, 479
 Xie, R 118
 Xie, W 293, 418
 Xie, Y 70, 480
 Xinghua, H 311
 Xing, Q 424
 Xingyuan, H 220
 Xinqin, L 71
 Xin, W 288
 Xin, X 220
 Xin, Y 275
 Xiong, H 192
 Xiong, Y 218, 536
 Xiujin, Z 226
 Xiuju, L 220
 Xiuqin, T 447
 Xiu, Y 499
 Xi, W 311
 Xi, Y 539
 Xu, B 32, 328, 513
 Xu, C 153, 341, 342
 Xu, D 58, 266, 315, 405, 469, 476
 Xue, B 521, 537
 Xue, F 193, 335
 Xue, G 310, 439, 497
 Xue, J 39, 217, 221, 226, 243, 299, 394, 464
 Xue, L 69
 Xue, Q 66, 67, 377
 Xue, S 522
 Xuewei, L 512
 Xue, X 446
 Xu, F 119
 Xu, G 51, 120, 218
 Xu, H 51, 92, 195, 255, 429, 511
 Xuhua, Z 70
 Xu, J 54, 55, 125, 171, 293, 453, 454, 468, 527, 528, 532
 Xu, L 219, 362
 Xuling, C 297
 Xu, M 310, 337
 Xu, P 277, 278, 351, 424, 426, 516, 551
 Xu, Q 532, 555
 Xu, R 72, 145, 421
 Xu, S 276, 400
 Xu, T 12, 63, 137, 213, 293, 372, 445, 523
 Xu, W 178, 500, 537
 Xu, X 136, 436
 Xu, Y 257, 315, 374, 486, 489
 Xu, Z 32, 76, 93, 169, 360, 397, 473, 489, 490

Y

Yablinsky, C 177, 277, 278, 588
 Yacob, B 148
 Yacout, A 278
 Yadavali, S 139, 373
 Yadav, S 554
 Yadav, V 159, 553
 Yafeng, D 71
 Yaghobi, M 580
 Yahyazadehfar, M 228
 Yakovlev, A 59
 Yamada, R 454
 Yamada, S 528

Yamaguchi, K 140
 Yamaji, K 180
 Yamamoto, Y 124, 273, 279, 336, 409
 Yamanaka, K 528
 Yamane, L 280
 Yamanis, J 129
 Yamasaki, M 196
 Yamasaki, T 78, 506, 528
 Yamaura, Y 109
 Yamazaki, T 360
 Yan, B 458
 Yan, F 148, 202
 Yang, B 41, 171, 255, 328, 375, 513, 520
 Yang, C 160, 486, 513
 Yang, D 225, 377, 500
 Yang, E 423
 Yang, F 24, 86, 104, 163, 241, 317, 319, 355, 393, 411, 480, 532
 Yang, G 146
 Yang, H 339, 441, 446, 548
 Yang, J 12, 19, 28, 31, 46, 60, 224, 255, 257, 274, 301, 311, 495, 503, 546
 Yang, K 102, 429
 Yang, L 161, 180, 220, 317, 468, 549
 Yang, M 223, 315, 531
 Yang, N 57
 Yang, Q 218
 Yang, R 25, 58
 Yang, S 24, 28, 39, 104, 214, 228, 319, 523, 525, 534, 561
 Yang, T 119, 192, 193
 Yang, W 77, 520, 529
 Yang, X 75, 148
 Yang, Y 12, 14, 15, 78, 112, 127, 132, 254, 265, 300, 303, 408, 415, 473, 554
 Yang, Z 88
 Yan, K 268
 Yanke, J 80, 155, 309
 Yankov, R 495
 Yan, L 67, 70, 217, 218, 219, 299, 504, 526
 Yan, M 104, 122
 Yano, T 567
 Yanqing, L 226, 450
 Yan, Y 493, 522
 Yao, D 119
 Yao, G 444, 464, 523, 527, 534, 536
 Yao, K 456
 Yao, T 223
 Yaowu, W 147, 226, 299
 Yao, Z 416, 517
 Yap, Y 30, 480
 Yardley, R 174
 Yaron, D 326
 Yasi, J 87, 197
 Yasuda, H 260
 Yatsuk, S 202
 Yavari, A 78
 Yazdan Parast, S 101
 Yazici, H 304
 Yazzie, K 50, 264, 442
 Ye, B 277, 352, 551
 Ye, F 456, 474
 Ye, G 253
 Yeh, F 273
 Yeh, H 214, 395
 Yeh, J 292, 505
 Yeh, Y 505
 Yen, C 125, 200, 378

Yen, H 19
 Yen, Y 51, 120, 194, 195, 272
 Yeo, S 293, 312
 Ye, Q 156, 157
 Yeung, M 432
 Yeung, W 162
 Ye, X 262, 541
 Yeyu, H 226
 Ye, Z 338, 542
 Yi, J 414
 Yi, L 377, 554
 Yildirim, H 15
 Yildirim, S 219
 Yilmaz, D 446
 Yilmaz, F 258, 527
 Yilmaz, S 68, 142, 219
 Yim, C 514, 533
 Yin, D 538
 Yin, G 361
 Ying, L 173
 Ying, Y 388
 Yinhe, C 88
 Yin, J 220
 Yin, L 50, 350
 Yin, W 153, 473
 Yin, Z 108, 182, 220
 Yip, Y 229, 508
 Yi, S 88, 102
 Yi, X 148
 Yoda, S 548
 Yodoshi, N 454
 Yokokawa, H 180
 Yokoyama, Y 78, 151, 152, 171, 306, 307, 506
 Yolisa, L 523
 Yonezawa, T 254, 333
 Yoo, B 567, 571
 Yoo, J 168
 Yoo, K 355, 356
 Yoo, M 181
 Yoon, E 440, 562
 Yoon, H 459, 575
 Yoon, J 269
 Yoon, K 216
 Yoon, O 64
 Yoon, S 429, 459, 537, 562, 567, 577
 Yoon, Y 564, 569, 573
 Yoo, S 550, 551
 Yoozbashizadeh, M 279
 Yorioka, K 222
 Yoshida, T 61, 127
 Yoshikawa, T 39
 Yoshiya, M 260
 You, B 329, 514, 533
 You, J 79, 456, 506
 Young, C 320, 582
 Young, G 266, 408
 Young, J 535
 Young, K 576
 Young, M 171, 529
 Young, S 446
 Youn, H 524, 568
 Youn, J 222
 Yousefiani, A 372
 Yousefian, S 429, 529, 578
 Yousef, K 202, 274, 369
 You, Z 15
 Ystgaard, J 88
 Yu, A 81



TMS 2012

141st Annual Meeting & Exhibition

INDEX

Yuan, D	65, 295, 296	Zaunbrecher, K	202	388, 389, 441, 444, 456, 464, 488,
Yuan, H	554	Zavattieri, P	470	523, 530, 539, 555, 556, 574
Yuan, L	168, 296, 503	Zbib, H	535, 542, 586	Zhanhu Guo, J
Yuan, Q	457	Zbib, M	203	188, 343
Yuan, R	325	Zebarjad, S	444	Zhao, A
Yuan, W	538	Zedan, Y	72	32
Yuan, X	53	Zehetbauer, M	134, 191, 209, 211, 288, 291,	Zhao, B
Yuan, Y	93, 147	366, 367, 368, 369, 370, 439, 440,	499, 501, 557	Zhao, C
Yuanzheng, Y	79	Zeisler, S	89	141, 447, 565
Yu, B	69, 273	Zemanova, A	121	Zhao, D
Yu, C	209, 418	Zeng, B	392, 397	147, 223
Yucel, O	14, 15, 66, 68, 124, 125, 139, 217,	Zeng, J	221, 296	Zhao, F
296, 354, 376, 427, 446, 502, 575	Zeng, K	508	464	Zhao, J
Yücel, O	67, 217, 296, 562	Zeng, Q	25	106, 161, 165, 178, 235, 236, 256,
Yu, D	447	Zeng, X	18, 200	257, 334, 381, 409, 478, 502, 524,
Yue, G	320	Zeng, Z	217, 275	532, 536, 549, 551, 578
Yuehong, Z	226	Zeqiri, I	540	Zhao, K
Yuelin, Q	376, 512	Zeytuncu, B	575	53
yue, s	405	Zhai, L	384	Zhao, L
Yue, S	405, 471, 515, 537	Zhai, Q	25, 108, 182, 373, 509, 522, 551, 566,	73, 468
Yuezhong, D	104, 147, 299	574, 576, 578, 584	574, 576, 578, 584	Zhao, M
Yu, F	147, 223	Zhai, T	17, 31, 32, 72, 93, 145, 163, 169, 222,	465
Yuge, K	360, 531	248, 300, 323, 377, 398, 526	248, 300, 323, 377, 398, 526	Zhao, P
Yu, H	37, 158, 315	Zha, M	560	235, 456, 531
Yu, J	192, 200, 278, 352, 378, 539, 548,	Zhan, C	192	Zhao, Q
551, 565	Zhancheng, G	219, 220	165, 504	Zhao, S
Yujie, X	450	Zhang, B	61, 104, 221, 461, 539	25, 531
Yu, K	416	Zhang, C	60, 107, 112, 140, 141, 169, 217, 297,	Zhao, T
Yukhvid, V	296	437, 453, 535	437, 453, 535	429
Yuki, I	471	Zhang, D	14, 502, 534	Zhao, W
Yuksel, B	298	Zhang, F	107, 117, 118	225
Yu, M	359	Zhang, G	127, 303, 562	Zhao, X
Yun, D	278	Zhang, H	14, 39, 73, 95, 213, 304, 532	147, 528
Yun, H	214, 523, 525	Zhang, j	584	Zhaoxia, L
Yun, J	566, 569	Zhang, J	25, 28,	220
Yunnen, C	430	39, 143, 145, 163, 217, 223, 305, 317,	393, 402, 458, 461, 502, 539, 543	Zhao, Y
Yu, Q	483	Zhang, K	450, 517, 572	46, 86, 135, 210, 240, 242, 247, 353,
Yurko, J	88, 165, 166, 244, 320	Zhang, L	23, 28, 37, 39, 53, 67, 80, 104, 107,	372, 435, 483, 496
Yushin, G	30, 581	137, 154, 158, 181, 202, 218, 221,	222, 232, 240, 259, 280, 284, 288,	Zheng, B
Yusufoglu, I	499, 555, 557	308, 309, 322, 338, 387, 406, 431,	439, 457, 476, 496, 497, 510, 520,	134, 274, 536
Yu, T	211, 212	525, 531, 539, 540, 542, 556, 569	525, 531, 539, 540, 542, 556, 569	Zheng, G
Yu, X	217, 357, 398	Zhangli, L	430	447
Yu, Y	254, 379	Zhang, M	19, 156, 393, 447, 496,	Zheng, H
Yu, Z	14, 297, 348, 520, 549	497, 508, 586	497, 508, 586	184, 186, 338, 522, 544
		Zhang, N	466, 497	Zheng, J
		Zhang, P	210	55, 398
		Zhang, Q	236, 394, 396	Zheng, L
		zhang, R	555	487
		Zhang, R	39, 238, 282, 482, 522	Zheng, M
		Zhang, S	69, 127, 309, 338, 339, 472, 488, 544,	126, 406
		547	547	Zheng, S
		Zhang, T	22, 66, 70, 79, 88, 306, 385, 506	340, 402, 568
		Zhang, W	18, 19, 22, 75, 148, 204, 226, 303,	Zheng, W
		348, 381, 430, 431, 551, 578	348, 381, 430, 431, 551, 578	25, 333, 404
		Zhang, X	30, 42, 62,	Zheng, X
		71, 102, 120, 129, 140, 141, 172, 186,	343, 393, 415, 416, 418, 440, 449,	161
		464, 485, 535, 536, 544, 557	464, 485, 535, 536, 544, 557	Zheng, Y
		Zhang, Y	14, 15, 18, 32, 37, 42,	207, 286
		67, 135, 170, 216, 217, 230, 261, 282,	293, 301, 330, 362, 376, 391, 394,	Zheng, Z
		406, 454, 455, 457, 477, 502, 505	406, 454, 455, 457, 477, 502, 505	430
		Zhang, Z	32, 41, 65, 131, 135, 140, 152, 181,	Zhen, X
		210, 261, 312, 348, 369, 373, 374,	210, 261, 312, 348, 369, 373, 374,	141
				Zhihe, D
				67, 70, 217, 218, 299
				Zhijian, S
				388
				Zhilyaev, A
				62
				Zhiqi, Z
				218
				Zhi, W
				219, 220
				Zhiwei, X
				79
				Zhong, H
				71, 108, 576
				Zhong, L
				338, 339
				Zhongliang, T
				226
				Zhou, B
				50, 51, 271, 383, 491
				Zhou, C
				111, 341, 414
				Zhou, D
				148, 180
				Zhou, F
				38
				Zhou, G
				14, 66, 139, 217, 296, 376, 446, 502
				Zhou, H
				324, 474, 539
				Zhou, J
				39, 148, 193, 465, 489, 490, 504
				Zhou, L
				288, 495, 536
				Zhou, M
				555
				Zhou, N
				57, 83, 107, 284
				Zhou, R
				85
				Zhou, S
				468
				Zhou, W
				66
				Zhou, X
				22, 31, 60, 255, 398, 447
				Zhou, Y
				134, 274, 453, 502, 536
				Zhou, Z
				248, 435
				Zhuang, Y
				462
				Zhuang, Z
				339
				Zhu, C
				115, 246, 500
				Zhu, D
				67, 95, 447, 448, 502
				Zhu, G
				339
				Zhuge, J
				47
				Zhu, H
				156, 157, 165, 166, 217, 281, 359,

..... 376, 446, 496, 499, 556
 Zhu, J 39, 189, 226, 243, 335, 343, 344, 394,
 418, 423, 485
 Zhu, M 524
 Zhu, P 219
 Zhu, Q 119, 534
 Zhu, R 315
 Zhu, T 41, 110, 183, 261, 338, 411, 480, 542,
 544
 ZHu, T 339
 Zhu, Y .62, 86, 116, 135, 196, 242, 274, 372,
 414, 439, 446, 557
 Zhu, Z 477
 Ziegler, D 318, 319, 394, 449, 511
 Zifer, T 545
 Zikry, M 112
 Zilberstein, V 97
 Zimmerman, J 281
 Zimmerman, M 459
 Zimmermann, A 173
 Zimmermann, E 34
 Zimmermann, G 40, 260, 337
 Zimmermann, J 184, 268, 269, 363
 Zimmermann, M 371, 442
 Zindel, J 256
 Zin, E 429
 Zinigrad, M 218
 Zinkicheva, T 379
 Zinkle, S 409
 Zink, P 536
 Zografidis, C 376
 Zolotoyabko, E 118, 359
 Zoofan, B 364
 Zou, X 208, 288
 Zou, Y 31, 255, 398
 Zrnik, J 288, 289
 Zschack, P 421
 Zue, G 497
 Zu, F 539
 Zu, G 72, 145, 444, 534, 536
 Zulli, P 81
 Zuo, L 147, 223
 Zuo, X 67
 Zuo, Y 51, 330
 Zupan, M 86
 Zurco, M 259
 Zurecki, Z 107
 Zurek, E519
 Zurob, H 18, 75, 116, 148, 226, 227, 303, 381

Thanks! to our Corporate Sponsors

Platinum Sponsors



HYDRO

Silver Sponsors



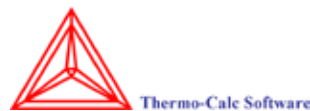
Bronze Sponsors



Gold Sponsors



Friends of TMS



H	He
Li	Ne
Na	Ar
K	Kr
Rb	Xe
Cs	Rn
Fr	Uuo
Be	F
Mg	Cl
Ca	Br
Sr	I
Ba	At
Ra	Uus
B	O
Al	S
Ga	Se
In	Te
Tl	Po
Uut	Uuh
C	N
Si	P
Ge	As
Sn	Sb
Pb	Bi
Uuq	Uup
Zn	Cd
Cu	Ag
Au	Hg
Rg	Cn
Ni	Pd
Pt	Ds
Co	Rh
Ir	Mt
Fe	Ru
Os	Hs
Mn	Tc
Bh	
Cr	Mo
Sg	
V	Nb
Ta	
Ti	Zr
Hf	
Rf	
Sc	Y
La	
Ac	
Y	
Zr	
Nb	
Mo	
Tc	
Ru	
Rh	
Pd	
Ag	
Cd	
In	
Sn	
Sb	
Te	
Bi	
Po	
Uup	
Uuq	
Uuh	
Uuo	

Ce	Lu
Pr	Yb
Nd	Tm
Pm	Er
Sm	Ho
Eu	Dy
Gd	Tb
Yb	Lu
Th	No
Pa	Md
U	Fm
Np	Es
Pu	Cf
Am	Bk
Cm	Cf
Bk	Lr

Now Invent.TM



The World's Manufacturer of
Engineered & Advanced Materials

photovoltaics Nd:YAG
shape memory alloys

catalog: americanelements.com

© 2001-2011. American Elements is a U.S. Registered Trademark.

